XII DBMC
International Conference on Durability of Building Materials and Components
PORTO - PORTUGAL, April 12th-15th, 2011

Meeting Today's and Future Requirements for the Life Expectancy of Building Functions and Products

Christer Sjöström [1]

ABSTRACT

Those engaged in research, development and the connecting innovation processes focussing on the longevity of building functions, and the systems and products providing these services have probably never operated in an atmosphere as favourable as the one occurring today. How can this be stated when most of us, in for example academia who are also attempting to address this R&D area, experience the daily struggle to survive and to fi-nance our research?

This introduction to the 12DBMC, the very latest of this distinguished series of conferences, attempts to contrib-ute an explanation to this statement, and to underpin it with some examples.

The series of DBMC conferences started in 1978. From the outset, the ambition was to harmonise the area of "durability R&D", and to raise its scientific level. To a large extent the first six conferences focussed on the chal-lenge of harmonising service life prediction methodologies, and the conferences thereafter have gradually come to more explicitly address "durability" and "R&D and Innovation" in an engineering context. A shift may be ob-served towards making research on service life and performance over time really useful in answering today's and tomorrows requirements and expectations on building.

The European R&D project "Smart-ECO" (Sustainable Smart ECO-buildings in the EU) concluded during the second half of 2010. The project established a Vision of ECO-buildings up to 2030, in which a comprehensive survey of several existing innovations was completed and subsequently evaluated from which the most promis-ing schemes and approaches, that could possibly help carry the vision through, were retrieved from the "R&D and Innovation" society. All of this project process was supported by an international stakeholder group, broadly representing the building and construction community, which scrutinised the project observations and helped set priorities. Interestingly enough – but maybe not so surprising to me – the stakeholder group ranked life cycle perspectives in building design, management, operation, and refurbishment as being the top issue in striving to create

[1] Materials Technology, KTH Research School, University of Gävle, Gävle, SWEDEN, christer.sjostrom@hig.se

Sustainable and Smart Eco-buildings for 2030. The Smart-ECO project is presented in more detail during the Conference.

A glimpse at the direction taken by within European directives and legislation for the built environment supports and thereby further underwrites the above prioritisation of the Smart-ECO stakeholders.

International and European standardisation on sustainability, resource conservation, life cycle assessment, and products environmental impacts creates instruments for the market and such efforts help move building and con-struction practice in the same direction.

In short, environmental concerns and the environmental movement have ranked our research area as top priority.

This key note lecture will address the above. Starting with the Smart-ECO project analyses and the prioritisation of objectives for sustainable building, the focus is then on the development and innovation processes needed to take us there. New materials and technologies, innovative adaptation and use of established products and sys-tems, and all this paired with the necessary life cycle analyses of materials, products and systems. Apart from the Smart-ECO project examples are given on new insulation technologies, and on the emerging increase in re-quirements for indoor air quality. The examples are primarily chosen from contributions that will be presented more in depth during the 12DBMC.

XII DBMC
International Conference on Durability of Building Materials and Components
PORTO - PORTUGAL, April 12th-15th, 2011

Building Physics and Durability

Hartwig M. Künzel [1]

ABSTRACT

The durability of building materials and components depends to a large extent on phenomena belonging to the realm of building physics. Impacts from natural weathering and building operation are important degradation pa-rameters for building envelope systems. While some well-known loads such as UV-exposure of exterior surface materials depend only on the local climate conditions, other parameters are strongly influenced by the construc-tion itself. Especially the hygrothermal response of building envelope systems is governed by transport and stor-age characteristics. E.g., thin exterior surface layers of well insulated components show much greater tempera-ture and humidity fluctuations than massive façade structures. Also, the occurrence of extreme values depends on external loads and the component's physical properties. Solar radiation may be absorbed or reflected; rain-water may be absorbed or drained away. Hygrothermal inertia helps to prevent overshooting temperature and humidity conditions.

It is a widely accepted fact that temperature and moisture peaks may cause failure when safe limits are exceeded. However, extreme values are not limited to the envelope's surfaces where they can easily be measured or con-trolled. Shading devices or other radiation absorbing or reflecting layers within a glazing unit may cause the highest temperatures in the interior space of the unit. Materials exposed to wind-driven rain often show the maxi-mum in water content at some distance from the exterior surface making that zone vulnerable to frost damage. Therefore, investigating the hygrothermal behaviour of building envelope systems in response to environmental impacts may help to understand degradation processes and opens the door for more accurate durability assess-ment procedures and ultimately more durable building products.

To achieve that goal necessitates thorough knowledge of the dominant ageing and degradation processes of all building materials. While relevant research results are still scarce, there is growing awareness that modelling has to play an important part in this. Today, hygrothermal building envelope simulation models are recognized as useful tools for moisture control design of new and existing buildings. The models which have been experimen-tally validated predict the transient temperature, relative humidity and water content distributions in building ma-terials and envelope systems under

[1] Fraunhofer-Institute for Building Physics (IBP), Holzkirchen, GERMANY, hartwig.kuenzel@ibp.fraunhofer.de

different indoor climate and outdoor exposure conditions. Comparing the re-sults with specific threshold values (e.g. critical water content of 20% by mass for wood and wood based materi-als) is the first step to safeguard durability. However, many degradation processes depend on a variety of parameters and elude simple interpretations. There is a need for new approaches that use hygro¬thermal simulation results in order to obtain durability relevant information. They may be based on long-term experience or involve the design of accelerated weathering tests. The ultimate goal of building physics related durability research should be the development of material specific degradation models.

1 COMPARATIVE DURABILITY ASSESSMENT

Globalization produces demand for export of well-established building systems from one country to another. While there may be long-term track records and detailed durability related experience in the country of origin, successful transfer of envelope components to another climate cannot be guaranteed without further investiga-tion. By employing climate analysis and hygrothermal simulation it is usually possible to compare the system's climate dependent behaviour. If the overall hygrothermal performance as well as the peak loads, under the new climate conditions, are similar to those in the country of origin, it is very likely that the system can be transferred without causing unexpected durability problems. If they differ, especially if the temperature and humidity ex-tremes are greater under the new climate conditions, further investigations become necessary.

2 ACCELERATED TEST TAILORING

The development of accelerated test cycles concentrates on the peak loads without exceeding real life extremes (amplified extremes may provoke reactions that will never occur under practice conditions). This approach is empirical and requires only little insight into the real ageing and degradation processes. It is based on the as-sumption, that peaks in temperature and humidity or water content are the main factors for material degradation. That means periods with moderate conditions can be cut out of the annual hygrothermal simulation results leav-ing only those periods where the extremes occur. Ideally, this should cut the real life cycle short by at least a fac-tor of 10 without resorting to unrealistic extremes. The resulting transient temperature and moisture conditions should be analysed and somewhat simplified before they can serve as boundary conditions for an accelerated test cycle. The advantage of this procedure is its simplicity; the disadvantage is the necessity of doing artificial weathering tests and the limited reliability of the acceleration factor. Verifying the accelerated test result by comparison with field tests and practical experience is imperative.

3 DEGRADATION MODELS

A degradation model should be based on the physical, chemical or biological material reactions to the ambient temperature and humidity conditions. Many ageing and degradation processes in the construction sector are somehow related to moisture and temperature, such as:

- chemical reactions like corrosion, carbonation or hydration
- biological processes like rot, mould growth and algae formation
- physical damage to the microstructure due to frost or salt crystallization

Apart from models that predict mould formation and rot, there is still a lack of sophisticated and validated degradation models. The challenge is to simulate chemical reactions (e.g. corrosion) or mechanical micro-damage processes (e.g. damage by freeze-thaw or hygrothermal dilatation) occurring in building materials as a function of environmental conditions. The output of such models could be for example loss of mass or loss of compressive strength. The period of time elapsing until relevant material properties drop below a predefined threshold represent the end of service life of a certain building component under the consid-ered exposure conditions.

XII DBMC
International Conference on Durability of Building Materials and Components
PORTO - PORTUGAL, April 12th-15th, 2011

Study of Decay of Historic Masonry Due to Salt Crystallization: A Systematic Approach

Luigia Binda [1]
Giuliana Cardani [2]
Elsa Garavaglia [3]

ABSTRACT

The literature concerning the chemical-physical decay and processes of decay of natural building stones subject to aggressive environments is very broad and substantially developed at both the macro and micro structural level. Whereas research carried out on the durability of masonry as a composite material and on the mutual influence of its components (mortar, brick or stone) is much less abundant or advanced and in the 1980's it was even less developed. The results of research in recent decades have shown that in order to study and understand the decay phenomena due to salt crystallisation and freeze-thaw action, experimental accelerated ageing tests should be carried out on masonry specimens and not on single components. Since the end of the 1970s a Research Unit of the Polytechnic of Milan's Department of Structural Engineering (DIS) has followed a systematic methodology for the study of damage caused to masonry by salt crystallisation. The decay of masonry is highly influenced not only by aggressive environments but also by the choice and combination of constituents within masonry. Within the DIS group research was initiated by G. Baronio and L. Binda in 1980 [Baronio *et al.* 1982].

During the initial phase of the research a crystallisation experiment was undertaken, on the basis of state diagrams of the most diffused and harmful salts to masonry components, from which a cyclic ageing test for single masonry components was developed; the experiment had two different aims: (i) ability to study the decay of slender elements such as columns and decorations by total immersion in a salt solution; (ii) study of decay in structural elements having large dimensions by capillary rise of salt solutions where solutions could not typically reach the core of the element. In these experimental studies the specimens were exposed to selected temperature and relative humidity conditions over specified periods of time following uptake of the solution causing decay. The conditioning cycles were repeated until damage to specimens reached a given level [Binda *et al.* 1985, 1987]. In this manner, the first accelerated ageing tests by capillary rise of salt solutions were proposed for brick and stone.

[1] Department of Structural Engineering, Politecnico di Milano, Milano, ITALY, binda@stru.polimi.it
[2] Department of Structural Engineering, Politecnico di Milano, Milano, ITALY, cardani@stru.polimi.it
[3] Department of Structural Engineering, Politecnico di Milano, Milano, ITALY, garava@stru.polimi.it

Several tests were carried out with different types of salts and different thermo-hygrometric conditions and as well, different duration of conditioning cycles (Fig. 1a, b) [Binda, Charola *et al.* 1985]. From these studies it was determined that sodium sulphate solution was the most aggressive to brick and stone masonry components over the shortest test duration.

Salts	Type of cycle
NaCl MgSO Na_2SO_4	A. t_1 = 2 h t_2= 46 h (50% RH) B. t_1 = 2 h t_2= 94 h (50% RH) C. t_1 = 2 h t_2= 166 h (50% RH) D. t_1 = 2 h t_2 = 46 h (50% RH) t_3 = 120 h (60° C) E. t_1 = 2 h t_2 = 46 h (50% RH) t_3 = 120 h (100° C)

a)

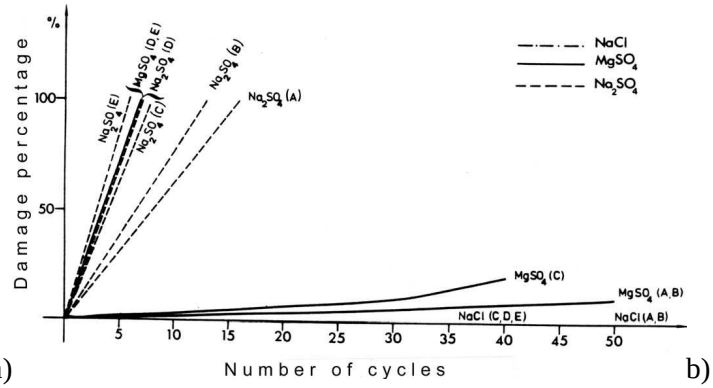

b)

Figure 1. (a)-Different thermo-hygrometric conditions used for different crystallisation cycles; (b)-Percentage of damage refers to the external surface of brick specimens, due to different crystallisation cycles caused by various types of salt solution.

A survey of surface decay on monuments located in Milan has been carried out in which photographs of the surface have been acquired every three to six months since 1981. The natural environment was also studied from which results acquired over 10 years by the Brera Observatory in Milan were evaluated and since 1990 the onsite micro-environment was also monitored near model masonry structures. The data compared with the equilibrium curve of sodium sulphate showed that the formation of its two phases, thenardite and mirabilite, could occur in Milan every month of the year and several times a month with an average duration of 48 hours.

Since a non destructive technique was required to measure the on-going process of material decay, the research revealed that decay started from the external surface of the material and proceeded, cycle by cycle, toward the interior, the decay often manifesting itself as a delamination (Fig. 2a, b) [Binda *et al.*1987]. Furthermore it was found that the material characteristics below the decayed surface remained unaltered (Fig. 2c). Measurements of surface decay were first carried out with gauges applied to the external surface [Binda *et al.* 1992]. Thereafter, a laser profilometer was adopted as it was determined from studies to be the best tool to precisely measure decay over time (Fig. 3), [Binda *et al.* 1992].



a)



b)



c)

Figure 2. (a)-Decay of historic masonry exposed to the synergetic effects of different decay actions; (b)-Fatigue damage behind brick external surface before delamination; (c) Penetration of decay is shown as only a few millimetres behind external surface damage.

The mutual influence of masonry components on surface damage was first studied on masonry prisms damaged by salt crystallisation [Binda *et al.* 1985]. From these initial results the decision was then

taken to build full-scale models and subject these to the environmental conditions prevalent of a polluted area of Milan [Baronio *et al.* 1993]. In order to accelerate the damage process, a sodium sulphate solution was injected into the building foundation so that the ageing could occur by capillary rise of the solution to the masonry structure.

The different types of decay caused to brick masonry by salt crystallisation were defined from work carried out within a European Community (EC) study [Van Balen *at al.* 1997] and thereafter collected in a "Damage Atlas". A product of the same study was an expert system (MDDS) on the decay and diagnosis of brick masonry prepared with the aim of helping non expert professionals in the interpretation of decay mechanisms of masonry structures [Van Balen *at al.* 1997]. Currently, the laboratory crystallisation test that is carried out on masonry prisms forms part of a RILEM recommendation for testing as proposed by the TNO-Delft and the results have been calibrated in three EC studies in which other partners have also participated [RILEM 1998].

A more sophisticated device was introduced to measure surface decay: the laser profilometer. This device uses a laser beam that scans the surface of the materials and is thus able to characterise the variation in surface profile of a material. A suitable data acquisition system transforms these measurements to surface roughness profiles that in turn can be modified to describe the decay as a function of time and space (Fig. 3). The values of the chosen parameter measured over time can constitute the input data for a deterministic or probabilistic mathematical model in which material behaviour and durability of surface treatments in the presence of different soluble salts and exposed to salts of different concentration can be studied [Cardani *et al*. 2002]. The high degree of randomness associated with acquiring the material characteristics and their level of decay when subjected to natural ageing conditions suggests that the deterioration process may be defined, for example, by a function L(t,ℓ); hence this is a stochastic process having random variables ℓ and t, where ℓ is the loss of material at the surface in time t (Fig. 4) [Garavaglia *et al.* 2002].

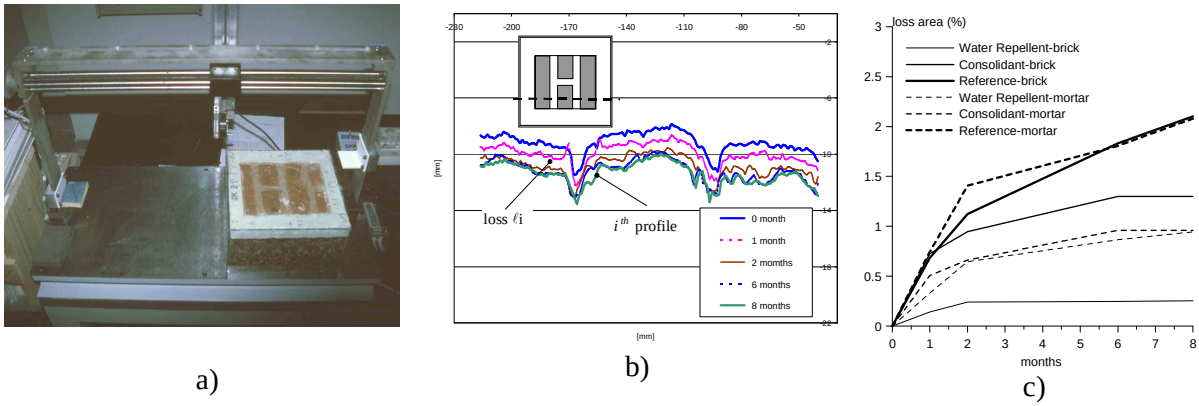

a) b) c)

Figure 3. (a)-Laser profilometer used in laboratory; (b)-Profiles measured on a masonry specimen over time during different cycles; (c)-Damage curves on a masonry specimen obtained during a salt crystallisation test with solutions of 2,5% $Na_2 SO_4$.

In order to model this decay function of material loss, a log-normal probability density function was chosen. Whereas, the deterioration process can be treated as a reliability problem in which the time to achieve a specified, yet significant degree of damage ℓ is determined and as well, the variation in time needed to exceed it. In this way, for different damage levels ℓ it is possible to develop a vulnerability to decay curve for each degree of damage ℓ (Fig. 4c). A vulnerability to decay curve describes the probability of reaching or exceeding a given damage ℓ over time. In order to model the vulnerability to decay curves obtained experimentally, a Weibull distribution was chosen as in fact, this type of distribution appears to provide a good interpretation of the physical phenomenon. This approach was used not only to model decay mechanisms, but also to reduce the time required in completing ageing

tests and thus prevent the occurrence of decay, particularly when using surface treatments and material substitutions. The results of these research studies can help in making choices of appropriate repair and protection techniques for external surfaces of historic masonry buildings.

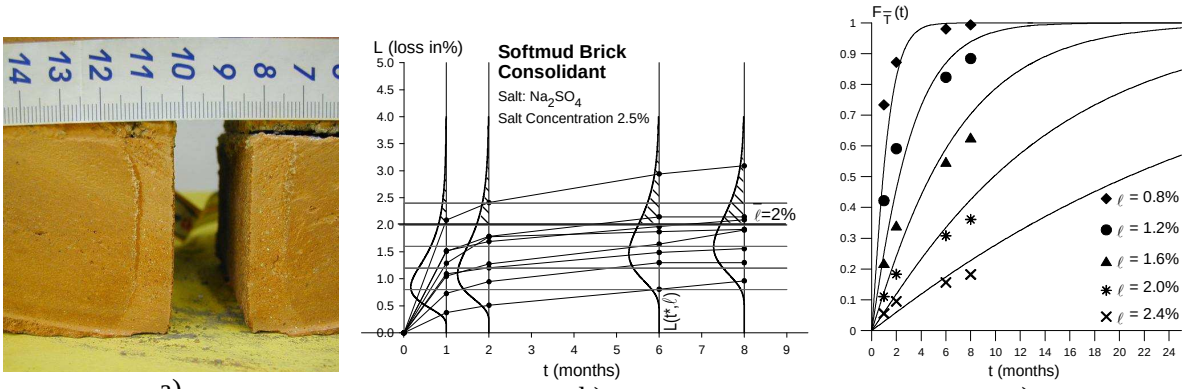

a) b) c)

Figure 4. (a)-Brick specimen treated with water repellent and damaged by crystallisation test with a concentration of 2.5% of Na_2SO_4 after cut; (b)-Interpolation of the curve loss area/time for modelling of the decay process L(t*,ℓ); (c)-Vulnerability to decay curves for same masonry specimen.

REFERENCES

Baronio G., Binda L., 1982, Sulla durabilità dei laterizi in ambiente aggressivo, Proc.6° IBMaC, Ed. ANDIL, Roma, pp. 1554-1566.

Baronio G., Binda L., Cantoni F., Rocca P. 1993, 'Durability of stone and brickwork protectives and consolidants: experimental research on full-scale models', 6th Int. Conf. on Durability of Building, Materials and Components, Omiya, Vol.2, pp. 824-833.

Binda L., Baronio G. 1985, 'Alteration of the Mechanical Properties of Masonry Prisms due to Aging', 7th IBMaC, Melbourne, Australia, Vol. 1, pp. 605-616.

Binda L., Baronio G. 1987, Mechanisms of masonry decay due to salt crystallization, *J. Durability of Buildings Materials*, N.4, Elsevier, Amsterdam, pp. 227-240.

Binda L., Baronio G., Squarcina T. 1992, 'Evaluation of the durability of bricks and stones and of preservation treatments', 7th Int. Congr. on Deter. and Conserv. of Stone, Lisbona, pp. 753-761.

Binda L., Charola A.E., Baronio G. 1985, 'Deterioration of porous materials due to salt crystallization under different thermohygrometric conditions', 5th Int. Conf. on Deterioration and Conservation of Stone, Lausanne, Suisse, pp. 279-288.

Cardani G., Tedeschi, C., Binda L., Baronio G. 2002, 'Crystallisation Test on Treated Brick/Stone Masonry Specimens for Damage Evaluation', Proc. Int. Conf. 9th Durability of Building Materials, 17-20/03/2002, Brisbane, (Australia), CD-ROM, paper 039.

Garavaglia E., Lubelli B., Binda L. 2002, Two Different Stochastic Approaches Modelling the Decay Process of Masonry Surfaces Over Time, *Materials and Structures*, Vol. 35, n.248, pp. 246-256.

RILEM MS. A.1 1998, Determination of the resistance of wallettes against sulphate and chloride, *Materials and Structures*, 31, pp. 2-19.

Van Balen K., Mateus, J., Binda L., Baronio G. 1997 Scientific background of the Damage Atlas and the Masonry Damage Diagnostic System, Expert System for the Evaluation of the Deterioration of Ancient Brick Structures, EC Contract EV5V-CT92-0108, Final Report.

XII DBMC
International Conference on Durability of Building Materials and Components
PORTO - PORTUGAL, April 12th-15th, 2011

An Overview of the Degradation Process and Estimation of the Long Term Performance of Polymer Films

Stuart G. Croll [1]

ABSTRACT

It is not practical to test a candidate material in each of its likely application environments for periods of its likely service. In normal laboratory accelerated testing the best that can be achieved is the identification of materials with a weakness, then it is frequently difficult to identify which of the remaining candidates would be the most cost-effective in the real world. Trends deduced by curve-fitting large sets of exposure data, no matter how rigorously applied, are not useful outside that dataset. This overview attempts a predictive scheme for how the deterioration in physical properties of a material may linked to the physical and chemical processes of degradation.

Degradation of any material in its service environment is caused by huge numbers of energetic photons, or abrasive particles, or aggressive molecules. The arrival time of photons or grains of sand is random, as is the exact location where they strike and only chance determines whether a permanent change is effected by individual events. The stochastic nature of degradation allows us to calculate the accumulation of degradation in two ways:

1) Monte Carlo computer simulations
2) Using the Central Limit Theorem to gain simplified algebraic models

If a link can be made between the chosen service property and the amount of damage then there is a pathway to predicting how a material's properties decay and thus its service lifetime. If one can link more than one end-use property to the damage, then one property might be used to predict the fate of another. In the case of polymer coatings, for which these ideas were developed, properties such as gloss and corrosion protection may be related to physical and chemical properties of the materials, e.g. toughness, modulus, surface energy.

Monte Carlo mapping of degradation events across the surface or within the bulk of a material represented by a grid of locations stored in a computer allows the modelling of material loss and/or property changes. The consequent roughness, thickness changes, or property changes can then be translated into physical properties as described later. The Central Limit Theorem applied to the

[1] North Dakota State University, Fargo, USA, Stuart.Croll@ndsu.edu

repeated, nominally identical, degradation events allows the use of Gaussian statistics and provides algebraic equations that may be more rapidly used than Monte Carlo simulations. Photo- or other degradation of a polymer starts and is concentrated at its surface, which usually becomes rougher where material is volatilized and lost. Important physical properties are determined by surface roughness, by the thickness of coating remaining to protect the substrate or by changes to the chemical composition of the remaining material.

If a homogenous coating surface is degraded by ultraviolet radiation where the process is independent of location and does not change as material is ablated, i.e. zero order chemical kinetics:

$$\frac{dN(t)}{dt} = \phi.A.Q \qquad (1)$$

where $dN(t)/dt$ is the average number of fragments being removed at points across the coating or the flux of photons X absorption probability X probability of damage occurring, $N(t)$ is the number of damaging events/area, t is the exposure time, ϕ is the photon flux, A is the probability of adsorption (cross-section) and Q is the 'quantum efficiency' or yield for damage occuring.

Although the equation is for photodegradation, a similar equation could be developed for chemical or abrasive attack. If suitable, one could apply autocatalytic or first order kinetics, instead of the simpler equation above. All the quantities on the right hand side of the equation are constant in a stable environment, thus we may calculate $N(t)$. If a characteristic fragment size is known, then this equation gives the mass or volume lost as a function of exposure time. If the exposure consists of repeated cycles then this simple integration will be valid provided the overall period is much longer than one cycle. This will apply to natural weathering if the exposure is long enough. The Central Limit Theorem applied to the repeated, nominally identical, degradation events allows the use of Gaussian statistics, so we can calculate the standard deviation in material lost, across the bombarded surface, from the mean. This standard deviation can be used to calculate roughness, and flaw size produced by degradation. Assumed here is that degradation is at the surface of the material, but similar ideas could be used to describe degradation within the bulk material, if required.

The output from either the Monte Carlo or algebraic approaches can be used to calculate the physical properties that are used to determine the utility of the material. Surface roughness (standard deviation in material lost) determines largely the gloss of a coating via models that have been used for a long time [Bendler et al. 1998]. Changes in surface roughness also have a large effect on contact angle via the Wentzel [1936] equation. Flaw size, from the standard deviation again, determines crack resistance via the Griffith [1921] equation which is important in many protective uses of a polymer film. Corrosion protection of a barrier film depends on coating thickness, its roughness and its crack resistance. These models for deterioration also require knowledge of physical properties, such as modulus or surface energy... How these properties change can be measured, but the equations match exposure data well when only thickness or roughness change with exposure. An example will be presented of an attempt to use gloss loss in a coating to predict deterioration in corrosion protection.

One can never predict, in an absolute sense, how long something will last. However, this approach, that links well-established models of physical properties with a stochastic model for damage, gives one more confidence for relative comparisons, and indicates the material parameters that determine how a chosen property deteriorates. Different or more exact ideas can be added as requirements dictate. Variables in the environment are included in the equation above. Chemistry of degradation can be included via the fragment size and kinetics of degradation and how the properties may change as the material remaining changes. The approach identifies the physical consequences of degradation which clarifies why chemical damage indices, often measured by spectroscopy, do not correlate directly with deterioration in service properties. In fact, this approach helps elucidate how service lifetime can be (seemingly) arbitrarily sensitive to small differences in exposure and why accelerated weathering of coating films does not often correlate with natural exposure.

REFERENCES

Bendler, J.T., Feldman, S.F., Hatti, H. & Hobbs, S.Y., 1998, 'Approximate model of diffuse reflectance from rough polymer surfaces', *J. Appl. Phys*., **83**[2], 998-1004.

Griffith, A.A., 1921, 'The Phenomena of Flow and Rupture in Solids', *Phil. Trans. Roy. Soc. Lond.A,* **221**, 163-198.

Wenzel, R.N., 1936, 'Resistance of solid surfaces to wetting by water', *Ind. Eng. Chem.*, **28**, 988-994.

XII DBMC
International Conference on Durability of Building Materials and Components
PORTO - PORTUGAL, April 12th-15th, 2011

Sustainable Construction, Innovation and Durability: Trends and Research Needs

Vanderley M. John [1]

ABSTRACT

Sustainable development is a major opportunity and challenge to engineers: it requires rethinking of the entire industrial sector to such an extent that the environmental impacts on the life cycle of goods are reduced by a factor of five, whilst simultaneously increasing both economic gains for the industry as well as social benefits. This cannot be achieved without radical change in business operations and the adoption of innovations in all industrial sectors [Crul & Diehl 2007; Eppinger & Hopkins 2010].

The construction industry is considered to be a priority in order to achieve global sustainability. The sector has the highest intensity material usage of the entire economy, consuming from 40 to 75% of the total value of materials extracted and accounts for up to 15% of the GDP. Along its supply chain, waste generation is proportional to the total value of materials consumed. Likewise, following a life cycle assessment of construction products consisting primarily of buildings and roads, it became apparent that these are responsible for a significant share of total energy consumption. Buildings themselves in the "in-use" phase are responsible for about 25% of total CO_2 gas emissions –, resulting from the production of energy [Price et al. 2006]. The production of cement generates about 5% of total anthropogenic CO_2 emissions, and the proportion is growing [United Nations Environment Programme 2007]. The social aspects of sustainability must not be ignored; this will also require the construction industry to become increasingly heedful to its responsibility in respect to quality of life and social welfare. If current business practices and technological solutions are not changed it is certain that the construction industry's share of contributions to environmental loads will steadily grow in the future.

The relationship between sustainability and that of service life planning and durability has already been addressed in several DBMC conferences. The major aim of this paper is to explore the research needs in the field of service life planning and durability of building materials as posed by innovation for sustainable construction. Despite the important social implications, the discussion here will be focused on the environmental and economic dimensions of sustainability.

[1] Polytechnic School, University of São Paulo, São Paulo, SP, Brazil, john@poli.usp.br

1 SUSTAINABLE CONSTRUCTION & DURABILITY

Most of the current available green building certification schemes and green building construction manuals do not mention durability or service life issues or, if mentioned, take it "without further analysis" [Haapio & Viitaniemi 2008]. This fact is somewhat surprising since even the "business eco-efficiency" theory [DeSimone & Popoff 2000; Allwood et al. 2011] has established that sustainable development and durability are linked by the fact that the larger the service-life of a product is, the higher resource productivity will be and, the lower the environmental impact. The reason why almost all green building tools ignore durability issues must be debated.

This link between environmental loads and durability is valid in cases were an increase of durability, can be achieved without significantly increasing construction environmental loads, as demonstrated by reinforced concrete structures [John et al. 2002]. Another possible limitation for this rule is obsolescence of construction [John et al. 2002], which can be a result of changes in user needs or urban development or decaying and, sometimes, due to unsustainable marketing strategies.

Despite being almost ignored by green building tools, enhancing and prolonging the service life of infrastructures has long been recognized as having considerable benefits. This is very important for public infrastructure [Mirza 2006] and also, for buildings, although the latter having a greater propensity for obsolescence. Efforts to overcome such limitations have produced concepts of adaptive or flexible design [Vakili-Ardebili & Boussabaine 2010] as well as design for deconstruction or disassembling [Burak et al. 2010]. In order to successfully design for longer service life a far deeper knowledge is needed of the degradation of materials and components and also the factors and mechanisms contributing to obsolescence. However, flexible design and design for deconstruction might require some degree of "over engineering" such as, for example, dismantling loads must be considered and additional loads might be applied to account for unknown future applications.

Therefore, increasing the durability of design solutions may not always be eco-efficient: all environmental and economic benefits must be quantitatively measured and expressed on a *per year* basis, using as a basis of comparison, tools such as life cycle assessment [LCA] and life cycle costing [LCC]. This may be self-evident, but frequently ignored by most authors. Of course, LCA and LCC cannot be performed without first estimating the service life of all system components. To facilitate the application of such methods, more sophisticated and user-friendlier service-life planning methods than current knowledge allows, including clear strategies to deal with uncertainty associated to long term forecasts [Hans & Chevalier 2005], are needed.

2 ENVIRONMENTAL BUILDING ASSESSMENT AND DURABILITY

Despite LCA being considered a unique tool for undertaking a rational decision making process based on environmental performance [Erlandsson & Borg 2003; Chevalier et al. 2009], its practical application to construction is still limited. The currently available "green building" labelling schemes are not LCA based and therefore do not give consistent results [Wallhagen & Glaumann 2011]. The introduction of LCA based construction design and assessment methods is presently an international priority.

A combination of simplified LCA methods [Malmqvist et al. n.d.; Eppinger & Hopkins 2010] and building information modelling tools are being devised to make LCA usable in actual construction projects. However, without simple and reliable service life planning methods the accuracy of LCA will be reduced.

Nowadays, almost everything published on the LCA of construction assets does not include consistent estimates of the actual service life or, assess the effect of inaccurate service life estimates on the environmental loads. The crucial roles of project details, construction practices, material quality, maintenance standards and the actual environmental and user loads established at the project level

when defining the service life of a given product – and therefore its LCA and LCC - are rarely considered. With few exceptions, like the French HQE system [Chevalier et al. 2009; Hans & Chevalier 2005] the "green building" movement ignores service life planning. One possible reason is the lack of adequate tools to quantify these effects, even for traditional building materials: we must recognise that there are few models which can be used by construction professionals to estimate service life in their "day to day" design activities. Without further developments and the dissemination of existing service life planning knowledge and methodologies, the introduction of a LCA approach for construction will not succeed.

3 INNOVATION & DURABILITY

It is certain that dissemination of the already available, more eco-efficient construction technologies can allow for a significant reduction in the environmental impacts resulting from construction. However, reducing the environmental loads by a factor of five and maximizing social welfare by offering the poor citizens of the developing world an adequate built environment, with the available financial resources, will require reinventing construction by introducing both incremental [Eppinger & Hopkins 2010] and radical innovative solutions [Crul & Diehl 2007].

The process of innovation in construction is just beginning to accelerate, but progress is already visible. The more radical innovations will introduce new functions for construction components. One approach is to embed sensors which help users or asset managers to better operate and manage building systems or track degradation [Song et al. 2006] in so-called "smart" buildings, bridges and roads. The data produced by these sensors, if collected in a standardized way and shared, might allow a much better understanding of building in-service behaviour, user interference and local environment degradation. A protocol for such databases is an interesting opportunity for the research community.

Another approach is the production of active construction systems, which are able to react to environmental changes or have better control over the environmental factors. Photo and electrochromic glazing [Benito et al. 2004], phase change materials [Baetens et al. 2010], self-healing components [Williams et al. 2008] or magneto-rheological fluids [Wang et al. 2005] are good examples of such innovations. These are much more complex solutions, most of them, produced in the industrial sector where requirements for service life are much shorter. For each system it would be useful to develop a set of performance indicators that also take into account possible interference with the entire building assembly.

A significant part of the innovation is dedicated to the aspects of energy usage. Many of these solutions are based on advanced engineering of surfaces. Cool-paints [Uemoto et al. 2010] are an efficient way to cut down solar energy loads and even reduce heat islands [Synnefa et al. 2008], but simple dust deposition or mould growth, which are very dependent on building location, can reduce their performance in a short period of time [Prado & Ferreira 2005; Cheng et al. 2011]. Self-cleaning surfaces [Parkin & Palgrave 2005; Chen & Poon 2009], including the super-hydrophobic lotus effect methodology and titanium dioxide photocatalysis [Fujishima et al. 2000] can be a solution but their service life is also not proved [Gould 2003; Maury & De Belie 2010]. There is little actual experience on surface degradation phenomena. It is probably fast and very sensitive to local conditions. Modelling these environmental aspects is certainly a challenge.

Zero-net energy [Kornevall 2007] or even energy positive buildings are becoming part of public policy in Europe and will most probably become economically viable within the next 10 years [Kolokotsa et al. n.d.]. This may be achieved by a combination of measures related to improved energy efficiency including, e.g., cool paints and phase change materials - with local production of energy. Most likely, this will require the transformation of a significant fraction of building surface area into solar energy collection. Thus, building design, construction and operation will become a much more complex activity. Service life planning for such a mixture of electronic and traditional

materials will require more complex models. These difficulties can be anticipated due to the fact that the service life of the crucial components of conventional photovoltaic systems is still not well established for all climates [Dunlop et al. 2005] and most of the published data on LCA uses a standard service life of 25 or 30 years [Sherwani et al. 2010]. The degradation mechanisms and factors that affect the service life of these complex systems, when integrated with actual construction, and in different use conditions, still needs to be understood not only from the point of view of estimating service life, but also to help improve their design.

The introduction of incremental innovation of conventional materials and products will also require assessment of their durability. For example, the replacement of CCA by less toxic biocides is ongoing but their long term performance needs to be better assessed [Przewloka et al. 2008] because the benefits of reducing toxicity can be lost if indeed the service life is reduced. The environmental impact of concrete is largely dependent on the binder content. Many standards do establish minimum binder contents in order to ensure durability, the hypothesis being disputed by recent results [Dhir et al. 2006; Wassermann et al. 2009]. Preliminary results show that it is possible to reduce binder content as low as 5 $kg.MPa^{-1}.m^{-3}$ [Damineli et al. 2010], which would allow structural concretes with binder contents below 150kg/m³ of concrete resulting in significant reductions of CO_2 emissions. The long term performance of such low binder content formulations must be carefully reviewed to allow transition to a safe standard.

As previously discussed, the environmental and economic performance of such innovations cannot be demonstrated without reliable estimates of their service life frequency distribution under different in-use conditions. However, because they are essentially new, and might include totally new materials, service life estimates should/must not be made on the basis of previous experience. Hence, a in depth understanding of degradation factors and mechanisms affecting the deterioration of components and the likely influence of the local environment and construction practices on service life are not at all trivial. In this respect, there is an urgent need for the dissemination of the methodology presented in ISO15686 and also the development of reliable methodologies to establish service life density functions.

At the moment, most of the papers published on the durability of construction products are still devoted to the traditional materials, such as concrete, paints and metals. There is a great need to enlarge the scope of research to encompass new materials and technologies.

Finally, the increase of demand for innovation in construction will benefits if the existing service life planning methodology was adapted specifically to assist R&D activities in maximizing service life. It is worth mentioning that in manuals which support industry innovation, such as UNEP´s Design for Sustainability [Crul & Diehl 2007], durability is only mentioned incidentally. Perhaps developing dedicated tools in partnership with other organizations can be a strategy to accelerate dissemination of methodologies for estimating the service life of products, and help identify ways of upgrading such products.

4 CONCLUSION

In conclusion, the sustainability of a solution cannot be demonstrated nor achieved in a practical sense without first estimating its service life. LCA and LCC tools, which are basic for sustainable design and assessments, require estimation of service life density functions of traditional and innovative solutions. However, the green building movement incorporates little of the available knowledge on durability and service life planning.

Sustainability is bringing innovation to the construction industry, increasing the complexity of construction products. The durability of such innovative products must be not only estimated but also improved in the design phase.

In consequence, there is a great need for the dissemination of existing knowledge and for advanced research in the field of service life planning and durability, including the development of using friendly dedicated tools.

REFERENCES

Allwood, J.M. et al., 2011. Material efficiency: A white paper. *Resources, Conservation and Recycling*, 55[3], pp.362-381.

Andersson, Å.C. & Strömvall, A., 2001. Leaching of Concrete Admixtures Containing Thiocyanate and Resin Acids. *Environmental Science & Technology*, 35[4], pp.788-793.

Baetens, R., Jelle, B.P. & Gustavsen, A., 2010. Phase change materials for building applications: A state-of-the-art review. *Energy and Buildings*, 42[9], pp.1361-1368.

Benito, R. et al., 2004. Characterization of novel all-plastic electrochromic devices: Electro-optic and voltammetric response. *Optical Engineering*, 43[12], pp.2967-2975.

Burak, R., Hall, B. & Parker, K., 2010. Designing for adaptability, disassembly, and deconstruction. *PCI Journal*, 55[3], pp.40-43.

Burkhardt, M. et al., 2007. Biocides used in building materials and their leaching behavior to sewer systems. *Water Science & Technology*, 56[12], p.63.

Chen, J. & Poon, C., 2009. Photocatalytic construction and building materials: From fundamentals to applications. *Building and Environment*, 44[9], pp.1899-1906.

Cheng, M. et al., 2011. Chemical and microbial effects of atmospheric particles on the performance of steep-slope roofing materials. *Building and Environment*, 46[5], pp.999-1010.

Chevalier, J. et al., 2009. Integrated environmental and health assessment of construction products and buildings: French context. In *3rd CIB Conference on Smart and Sustainable Environments*. SASBE2009. Delft: CIB.

Crul, M. & Diehl, J., 2007. *Design for Sustainability: a practical approach for Developing Economies*, UNEP.

Damineli, B.L. et al., 2010. Measuring the eco-efficiency of cement use. *Cement and Concrete Composites*, 32[8], pp.555-562.

DeSimone, L.D. & Popoff, F., 2000. *Eco-Efficiency: The Business Link to Sustainable Development*, MIT Press.

Dhir, R.K. et al., 2006. Role of cement content in specifications for concrete durability: aggregate type influences. *Proceedings of the ICE - Structures and Buildings*, 159[4], pp.229-242.

Dunlop, E., Halton, D. & Ossenbrink, H., 2005. 20 years of life and more: where is the end of life of a PV module? In *Photovoltaic Specialists Conference, 2005. Conference Record of the Thirty-first IEEE*. Photovoltaic Specialists Conference, 2005. Conference Record of the Thirty-first IEEE. pp. 1593-1596.

Eppinger, S.D. & Hopkins, M.S., 2010. How Sustainability Fuels Design Innovation. *MIT Sloan Management Review*, 52[1]. Available at: http://www.ptc.com/WCMS/files/117883/en/

MIT_Eppinger_interview.pdf.

Erlandsson, M. & Borg, M., 2003. Generic LCA-methodology applicable for buildings, constructions and operation services--today practice and development needs. *Building and Environment*, 38[7], pp.919-938.

Fujishima, A., Rao, T. & Tryk, D., 2000. Titanium dioxide photocatalysis. *Journal of Photochemistry and Photobiology C: Photochemistry Reviews*, 1[1], pp.1-21.

Gould, P., 2003. Smart, clean surfaces. *Materials Today*, 6[11], pp.44-48.

Haapio, A. & Viitaniemi, P., 2008. A critical review of building environmental assessment tools. *Environmental Impact Assessment Review*, 28[7], pp.469-482.

Hans, J. & Chevalier, J., 2005. Sustainable tools and methods for estimating building materials and components service life. In *10th International Conference on Durability of Building Materials and Components*. 10DBMC. Lyon: CSTB / CIB. Available at: http://www.cstb.fr/fileadmin/documents/publicationsScientifiques/DOC00004700.pdf.

John, V.M., Agopyan, V. & Sjostrom, C., 2002. Durability In The Built Environment And Sustainability In Developing Countries. In *9th Int. Conf. on Durability of Building Materials and Components*. 9th DBMC. Brisbane: CIB, CSIRO, pp. 11-1-11-7.

Kolokotsa, D. et al., A roadmap towards intelligent net zero- and positive-energy buildings. *Solar Energy*, In Press, Corrected Proof. Available at: http://www.sciencedirect.com/science/article/B6V50-515RHM1-1/2/f09661295676f42f83e502d38c776ce8 [Accessed January 24, 2011].

Kornevall, C., 2007. *Energy Efficiency in Buildings Business realities and opportunities*, Conches-Geneva: WBCSD.

Malmqvist, T. et al., Life cycle assessment in buildings: The ENSLIC simplified method and guidelines. *Energy*, In Press, Corrected Proof. Available at: http://www.sciencedirect.com/science/article/B6V2S-4YW3788-3/2/bb7983a4a25dfcc39dc6c7178ffe95e2 [Accessed January 24, 2011].

Maury, A. & De Belie, N., 2010. Estado del arte de los materiales a base de cemento que contienen TiO₂: propiedades auto-limpiantes. *Materiales de Construcción*, 60[298], pp.33-50.

Mirza, S., 2006. Durability and sustainability of infrastructure - a state-of-the-art report. *Canadian Journal of Civil Engineering*, 33[6], pp.639-649.

Müller, F. et al., 2007. Self-Cleaning Surfaces Using the Lotus Effect. In *Handbook for Cleaning/Decontamination of Surfaces*. Amsterdam: Elsevier Science B.V., pp. 791-811 (Available online).

Parkin, I.P. & Palgrave, R.G., 2005. Self-cleaning coatings. *Journal of Materials Chemistry*, 15[17], p.1689.

Prado, R.T.A. & Ferreira, F.L., 2005. Measurement of albedo and analysis of its influence the surface temperature of building roof materials. *Energy and Buildings*, 37[4], pp.295-300.

Price, L. et al., 2006. *Sectoral Trends in Global Energy Use and Greenhouse Gas Emissions*, Berkeley: LBNL.

Przewloka, S.R. et al., 2008. Assessment of biodeterioration for the screening of new wood

preservatives: Calculation of stiffness loss in rapid decay testing. *Holzforschung*, 62[3], pp.270-276.

Sherwani, A., Usmani, J. & Varun, 2010. Life cycle assessment of solar PV based electricity generation systems: A review. *Renewable and Sustainable Energy Reviews*, 14[1], pp.540-544.

Song, G. et al., 2006. Health monitoring and rehabilitation of a concrete structure using intelligent materials. *Smart Materials and Structures*, 15[2], pp.309-314.

Synnefa, A. et al., 2008. On the Use of Cool Materials as a Heat Island Mitigation Strategy. *Journal of Applied Meteorology and Climatology*, 47[11], pp.2846-2856.

Tiruta-Barna, L., Imyim, A. & Barna, R., 2004. Long-term prediction of the leaching behavior of pollutants from solidified wastes. *Advances in Environmental Research*, 8[3-4], pp.697-711.

Uemoto, K.L., Sato, N.M. & John, V.M., 2010. Estimating thermal performance of cool colored paints. *Energy and Buildings*, 42[1], pp.17-22.

United Nations Environment Programme, 2007. BUILDINGS AND CLIMATE CHANGE - Status, Challenges and Opportunities. Available at: http://www.unep.org/sbci/pdfs/ BuildingsandClimateChange.pdf.

Vakili-Ardebili, A. & Boussabaine, A.H., 2010. Ecological Building Design Determinants. *Architectural Engineering and Design Management*, 6[2], pp.111-131.

Wallhagen, M. & Glaumann, M., 2011. Design consequences of differences in building assessment tools: a case study. *Building Research & Information*, 39[1], p.16.

Wang, J. et al., 2005. Magneto-rheological tuned liquid column dampers [MR-TLCDs] for vibration mitigation of tall buildings: Modelling and analysis of open-loop control. *Computers and Structures*, 83[25-26], pp.2023-2034.

Wassermann, R., Katz, A. & Bentur, A., 2009. Minimum cement content requirements: a must or a myth? *Materials and Structures*, 42[7], pp.973-982.

Williams, H., Trask, R. & Bond, I., 2008. Self-healing sandwich panels: Restoration of compressive strength after impact. *Composites Science and Technology*, 68[15-16], pp.3171-3177.

XII DBMC
International Conference on Durability of Building Materials and Components
PORTO - PORTUGAL, April 12th-15th, 2011

Control of Moisture Safety Design by Comparison between Calculations and Measurements in Passive House Walls Made of Wood

S. Olof Hägerstedt [1]
Lars-Erik Harderup [2]

ABSTRACT

The use of passive house technique has been used in a new wood framed building in Sweden. Besides the positive effect of reduced energy need, highly insulated wooden houses often have a higher risk of moisture and mould problems. The reason is that critical positions is more exposed to higher relative humidity compared to ordinary houses with thinner insulation. To investigate if an external wall has been correctly designed and constructed it has been investigated both with hourly measurements and by calculations with WUFI 5.0.

The aim of this study is to investigate the result of the moisture design process and the way changes in the design influence the moisture safety with real climate conditions. The study also investigates if WUFI 5.0 is a reliable tool to use in the construction design process. This was investigated by comparisons between measured and calculated relative humidity and temperature in different positions in an exterior wooden wall from April 2009 to October 2010.

In the original design the outer wooden studs have no protecting layer from the ventilated air gap behind the façade. Results from calculations with WUFI 5.0 shows that it is sufficient with a thin protecting thermal insulation on the outside of outer studs to considerably improve the moisture conditions in the outer parts ot the wall. If we never want the relative humidity to be above the critical level, at least 87 mm of insulation have to be applied on the outside of the wooden studs.

Comparisons between measurements and calculations show that WUFI 5.0 can be a reliable tool in moisture design of highly insulated wood framed walls. To get safe results it is important to use reliable climate and correct assumption about the air flow in the air gap behind the façade material.

KEYWORDS

Moisture, Measurements, WUFI, Comparisons, Mould.

[1] Faculty of Engineering at Lund University, Lund, SWEDEN, olof.hagerstedt@byggtek.lth.se
[2] Faculty of Engineering at Lund University, Lund, SWEDEN, lars-erik.harderup@byggtek.lth.se

1 INTRODUCTION

1.1 Background

The use of passive house technique in new wood framed buildings increases in Sweden. Besides the positive effect of reduced energy need passive house often have a higher risk of moisture and mould damages. The reason is that critical positions with organic material in the frame becomes more exposed to higher relative humidity compared to ordinary houses with thinner insulation. In order to minimize risk for moisture damages in a new passive house made of wood experts were given the opportunity to implement moisture design and suggest changes throughout the design phase of a major wood build project. This paper show possibilities to use the one dimensional heat and moisture calculation program WUFI 5.0 [WUFI] in the moisture design process and the effects it could result in concerning moisture safety.

1.2 Aim

The aim of this study is to use real climate conditions and show how changes in the design will influence the moisture safety, and consequences if no changes are made. Another aim is to investigate if WUFI 5.0 is a reliable tool to use in the moisture design process. This is demonstrated with comparisons between measured and calculated relative humidity and temperature in different positions in a highly insulated exterior wooden wall in an apartment building in Sweden, in 2009.

1.3 Limitations

The limitations in this study are primarily related to conditions for the measurements. Project schedule, production plan, construction type and building location only admit data for one design in one location. The limited duration of the measurements also affects the reliability of the results. The study does not include detailed information about parameters and functions used in the calculations.

2 METHOD

During the moisture design process [Mjörnell, K. 2007] a number of calculations was carried out for an initial proposal of wall construction, shown as “Initial wall” in Fig. 1. One challenge in the moisture design process was to protect the outside of the wood studs, position B, from mould growth. This was made by adding a insulation board on the outside of the wood studs, shown in “Build wall” in Fig. 1. Conditions in the design phase limited the thickness of the insulation board to 17 mm. To study moisture conditions in the wall and to compare with results from WUFI 5.0, measurements have been carried out in positions B to E in the modified wall, shown as “Build wall” in Fig. 1.

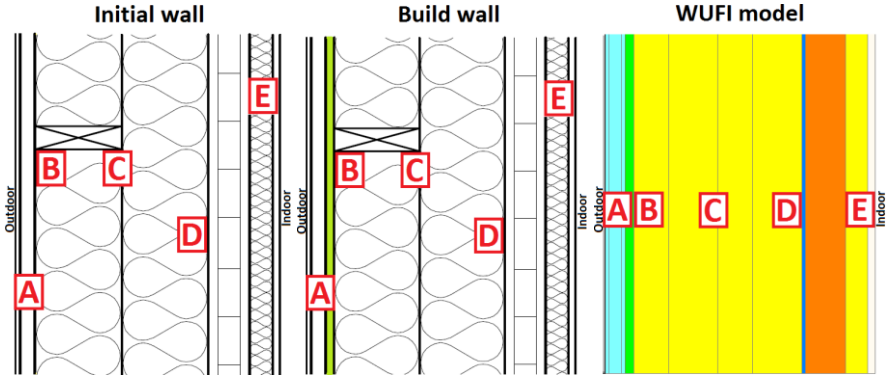

Wall from outside:
8 mm Concrete board[1]
30 mm Air gap 40 ACH[2]
(17 mm Insulation board)[3,4]
170 mm insulation/studs[3,4]
170 mm insulation/studs[3,4]
1 mm Vapour retarder[2]
82 mm Massive wood[2]
45 mm Insulation/studs[3,4]
13 mm Gypsumboard[5]

Figure 1. Initial wall without insulation board and Build wall with insulation board (green). Air gap A and measuring positions B to E. Calculation model with insulation board, air gap A and calculated positions B to E. [1. Hedenblad, G. 1996, 2. IBP, 3. IEA Annex 24, 4. Paroc, 5. Krus, M. 1996].

As a first case conditions for positions B to E in the initial wall were calculated in WUFI 5.0 with real climate as boundary conditions. To get a similar model to the wall that was built, a 17 mm insulation board was added, as shown as "WUFI model" in Fig. 1, and calculations in position B to E were repeated. Calculated results from the initial wall and the built wall were analysed. Since 17 mm of board was not enough to avoid critical relative humidity levels a number of calculations were carried out to investigate the minimum thickness of the board to avoid critical relative humidity levels.

To validate the calculations and show the possibilities to use WUFI 5.0 in the design process calculations of relative humidity and temperature for position B to E are compared with measured values. The comparisons are blind, i.e. measured results have not been available until calculations were completed. Calculations and measurements have been carried out and compared hour by hour. The agreement between measured and calculated relative humidity and temperature are presented and analysed.

Measurements are carried out at sixth floor in the north façade at different distances from the outside, shown as position B to E in Fig. 1. The north façade is supposed to be the most critical regarding the risk of moisture related problems. It is also less exposed to short wave radiation, which is excluded in the calculations. Measuring sensors have been applied during the production at the same time as constructions were controlled for deviations to drawings. Measurements of temperature and relative humidity have been carried out every hour using a wireless Protimeter Hygro Trac system [Sandberg, K. et al. 2011; GE Sensing 2006]. Measurements in position B to E started 2009-05-01 and are still running.

Boundary conditions and a model for the calculations are shown in Fig. 1 as "WUFI model" and set to match build wall and measured conditions. The house is built under a tent so no initial construction moisture is added in the calculations. According to the height and earlier studies the air flow in the air gap, position A, are set to 40 air changes per hour [Hägerstedt & Arfvidsson 2010]. Used outdoor boundary conditions are taken from SMHI, Swedish meteorological and hydrological institute, at a climate station nearby [SMHI]. All indoor boundary conditions are based on measurements from October 2009 to October 2010. The apartment, where the indoor climate is measured, has not been inhabited during the measurement period. Lack of in- and outdoor climate conditions are replaced with relevant data [Hägerstedt O. 2010, A, in press]. Periods with lack of outdoor climate data are shown in the top of Figs. 4 to 8. Lack of temperature and relative humidity are shown separated because of its impact.

A complete detailed method description with defined sources of error is given in a separate report [Hägerstedt, O. 2010, in press].

2.1 Sources of error

The main sources of error can be summarized as follow: Lack of measured boundary conditions for parts of the time and lack of some material data. Possible defects in WUFI´s physical model, convergence errors and bad correspondence between material data used in calculations and real material is also treated as possible errors. In the one dimensional model wooden beams have been neglected, as shown in Fig. 1, which is a simplification. The use of field measurements both as boundary conditions and as a part of the comparison also creates unknown possible sources of error.

3 RESULTS - MOISTURE DESIGN

In this report only results from the most moisture critical position on the outside of the wall studs, position B, is presented. Other positions, C to E, are not so exposed to moisture critical conditions. Complete results for all positions are shown on the webpage www.framtidenstrahus.se.

A critical relative humidity limit, as a function of temperature [Zedlbauer, K. 2001], is shown as a green line for the initial wall in Fig. 2 and for a test calculation with 87 mm board in Fig. 3. Difference between the critical and calculated relative humidity at specific times for each case are shown in the bottom of Figs. 2 and 3. The level of critical relative humidity as a function of temperature [Sedlbauer, K. 2001] for one studied case is also added in Figs. 2 and 3. Specific time and difference between critical and actual relative humidity is also shown.

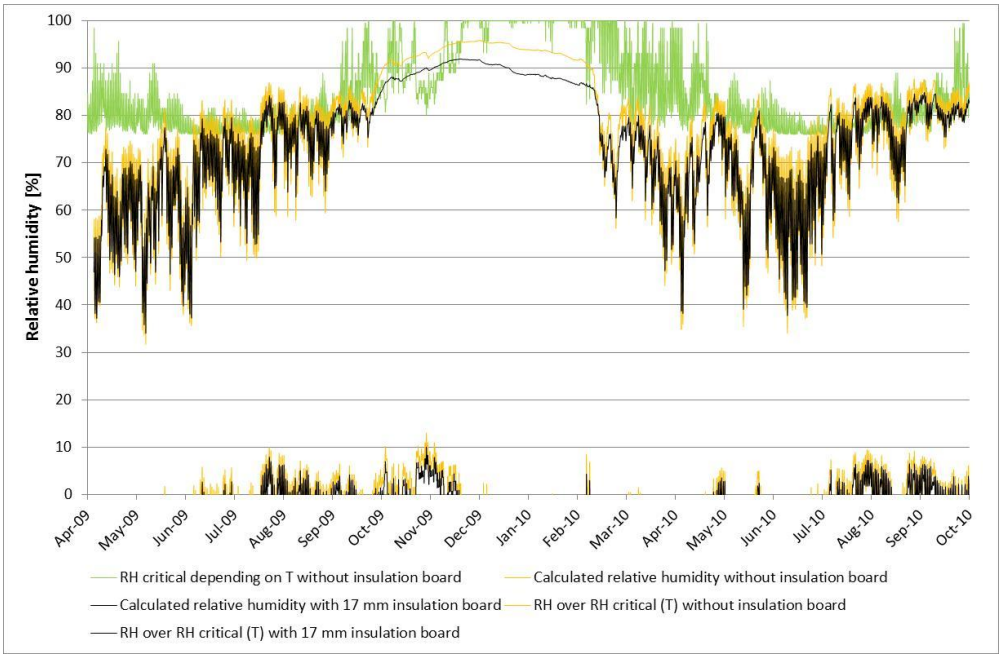

Figure 2. Position B. Calculated RH without insulation board and exceeded to critical RH (yellow). Critical RH level as a function of temperature for calculated RH without insulation board (green). Calculated RH with 17 mm insulation board and exceeded to critical RH (black).

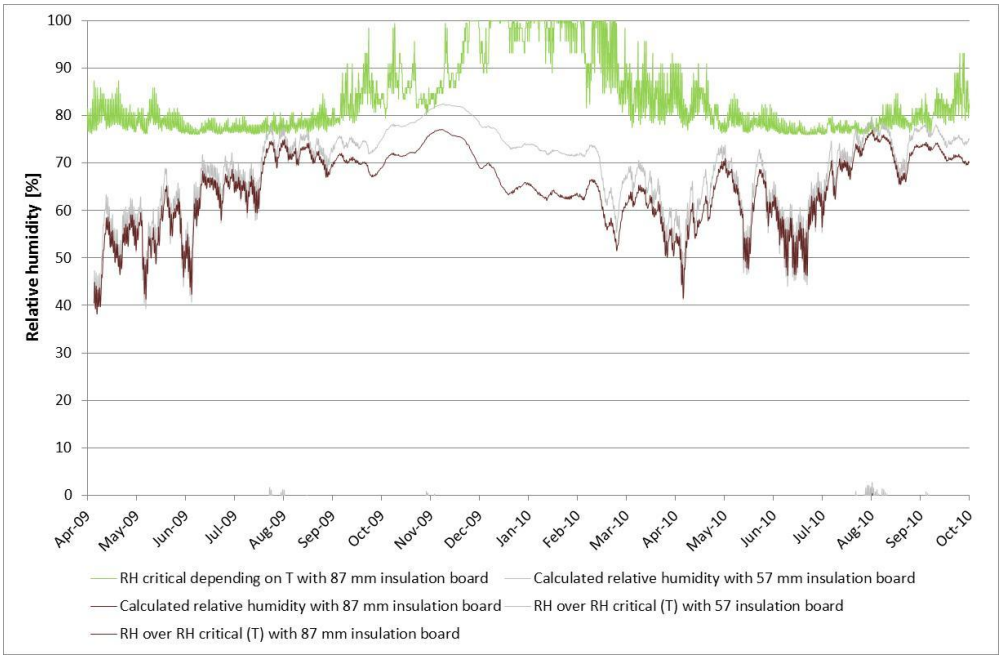

Figure 3. Position B. Calculated RH with 57 mm insulation board and exceeded to critical RH (grey). Critical RH level as a function of temperature for calculated RH with 87 mm insulation board (green). Calculated RH with 87 mm insulation board and exceeded to critical RH (dark red).

4 RESULTS - VALIDATION OF CALCULATIONS

Comparison between calculated and measured relative humidity and temperature are presented.

4.1 Position B - Outside of the wood studs

Comparison between calculated and measured relative humidity and temperature are show in Fig. 4. In Fig. 5 a more detailed comparison from March 2010 to June 2010 is shown.

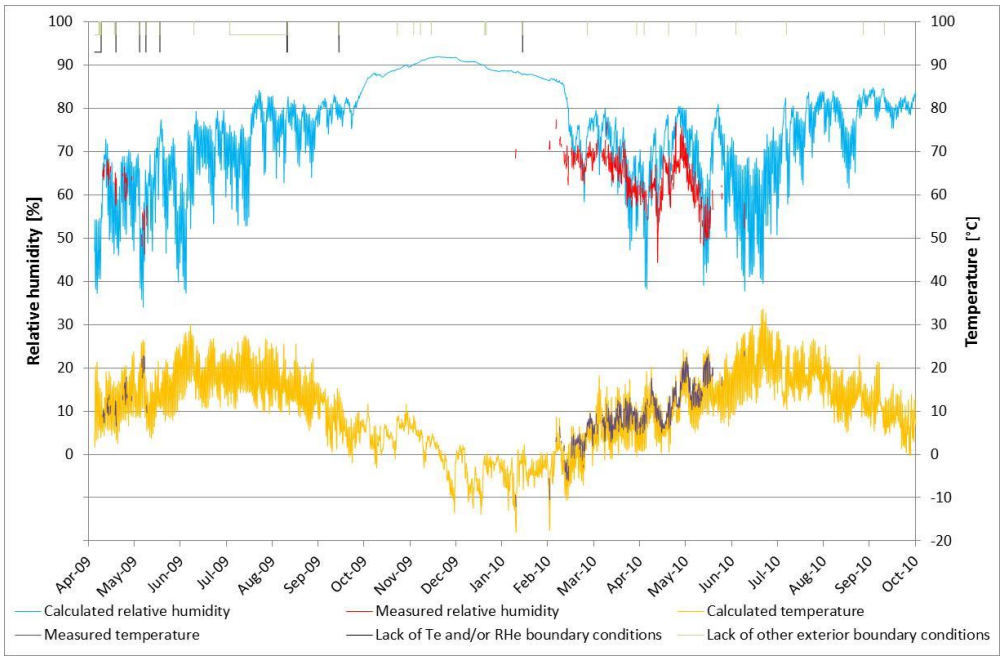

Figure 4. Position B - Outside of the wood studs. Relative humidity: Calculated (blue), measured (red). Temperature: Calculated (yellow) measured (purple). Lack of boundary condition (green/black).

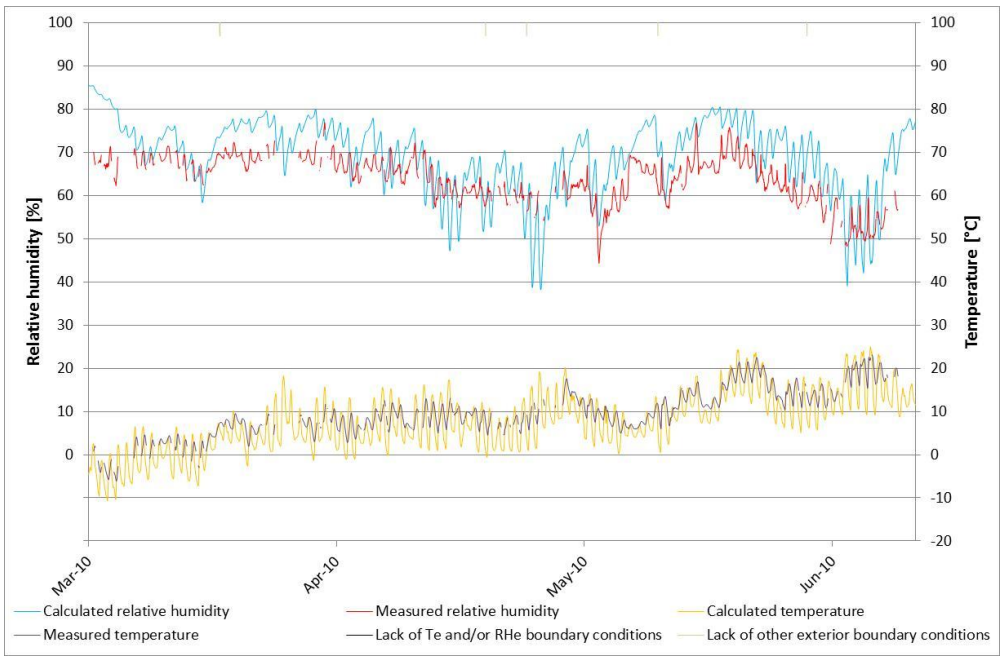

Figure 5. Position B - Outside of the wood studs. Relative humidity: Calculated (blue), measured (red). Temperature: Calculated (yellow) measured (purple). Lack of boundary condition (green/black).

4.2 Position C - In the middle of insulation

Comparison between calculated and measured relative humidity and temperature are show in Fig. 6. Unfortunately there is an extensive lack of measurements in position C.

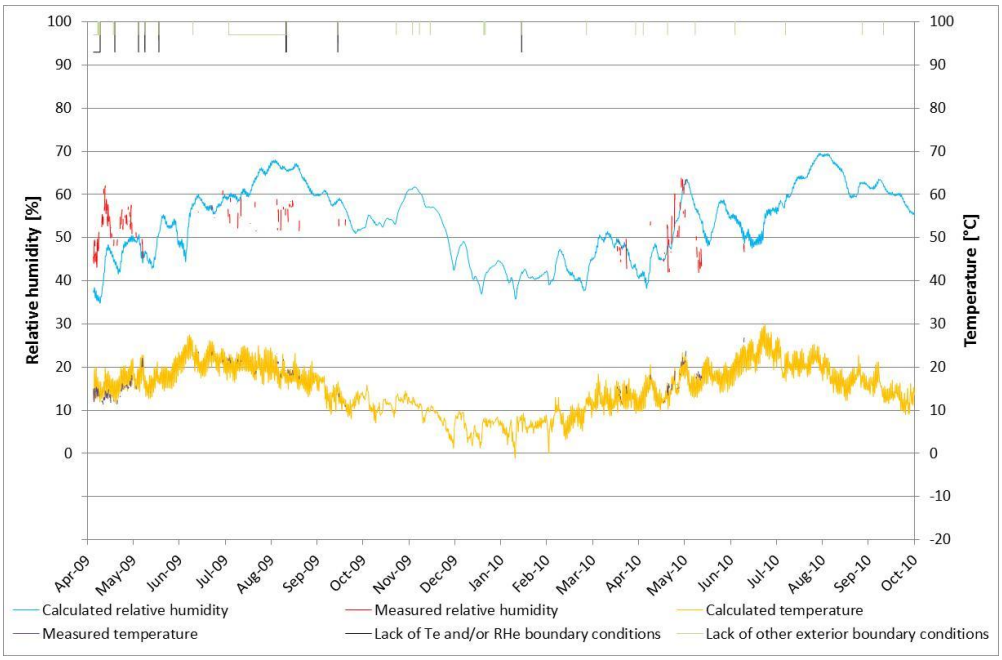

Figure 6. Position C - The middle of insulation. Relative humidity: Calculated (blue), measured (red). Temperature: Calculated (yellow) measured (purple). Lack of boundary condition (green/black).

4.3 Position D - Cold side of the vapour retarder

Comparison between calculated and measured relative humidity and temperature are show in Fig. 7.

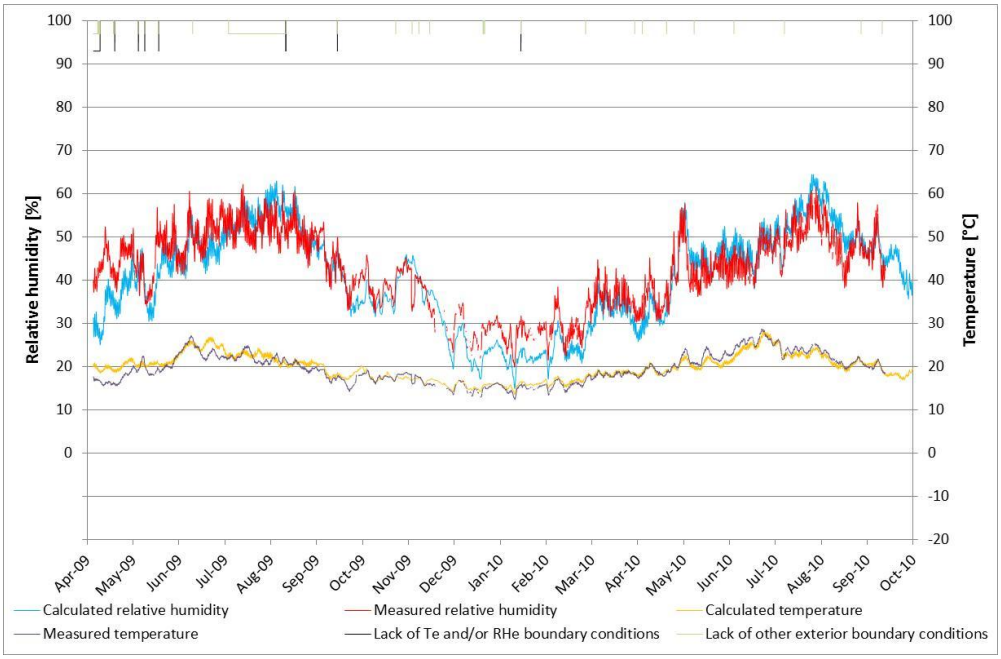

Figure 7. Position D - Cold side of vapour retarder. Relative humidity: Calculated (blue), measured (red). Temperature: Calculated (yellow) measured (purple). Lack of boundary condition (green/black).

4.4 Position E - Installation layer on the warm side of the vapour retarder

Comparison between calculated and measured relative humidity and temperature are show in Fig. 8.

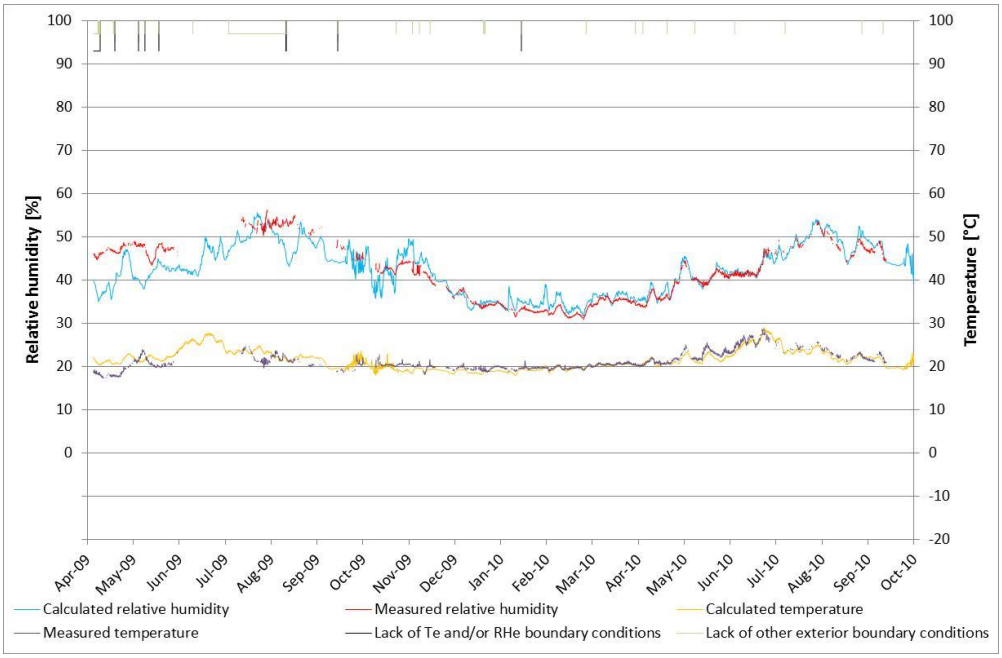

Figure 8. Position E - Installation layer on the warm side of the vapour retarder. Relative humidity: Calculated (blue), measured (red). Temperature: Calculated (yellow), measured (purple). Lack of boundary condition (green/black).

5 ANALYSIS

The evaluation, as shown in Fig. 1, shows that an extra 17 mm insulation board improves the moisture conditions in position B. However, the evaluation also shows that 17 mm is insufficient to protect the exterior part of the wooden studs from moisture damages.

Calculations in Fig. 3 shows that an 87 mm thick insulation board is needed to prevent mould growth on the outside of the wooden studs. Fig. 3 also shows that 57 mm thick insulation board reduces the risk of mould growth significantly. Not presented initial calculations with standard climate data shows a need of about 65 mm insulation board. Today the building system allows 80 mm insulation board.

The results in Figs. 2 and 3 shows that August is the most critical period although critical conditions occur in other parts of the year to. Because of defective measurements no moisture critical conditions have been measured. For all that we have to assume that mould growth on the studs may occur.

The comparison between calculated and available measured values of relative humidity and temperature in Figs. 4 to 8 shows a considerable convergence witch validates the use of WUFI 5.0. Deficiencies in measurements make positions C impossible to use and position B weaker in analyze.

Divergence in position D and E from April to October 2009 can be explained by the indoor boundary conditions. During this period the indoor boundary conditions are based on the following April to October 2010.

The amplitude of daily calculated values for both relative humidity and temperature are bigger compared to available measured ones in position B and C during the warm period. Daily amplitude of calculated and measured values in position D and E shows agreement throughout the whole period. As

shown in a previous study the daily amplitude is low during the winter (Hägerstedt & Arfvidsson 2010). All used measurement sensors are located close to solid wood. In the calculation model it is only possible to take account of the solid wood structure near position D and E. The fact that calculated daily amplitude in position D and E converges with measured when solid wood is close supports the theory that nearby wood reduce the daily amplitude (Hägerstedt & Arfvidsson 2010). In the calculations model the solid wood is separated from position C by a vapour barrier. This means that the heat capacity of the wood that affects the daily amplitude but not the moisture capacity.

6 CONCLUSIONS

The first conclusion of this study is that the moisture design process has both exposed bad design and improved moisture conditions in critical positions. Unfortunately the modifications in the construction do not seem to be good enough to ensure that no moisture or mould damages will occur.
Today the wall manufacturer has change the design that will allow 80 mm thick insulation board.

The second conclusion is that WUFI 5.0 can be used as a tool in the moisture design process of passive wood framed houses with an open air gap behind the façade material. When using WUFI 5.0 in those cases it is of great importance that proper assumptions, materials, models and boundary conditions are used. The importance of accurate climate data has been shown. The study also shows that it is reasonable to believe that wooden material reduces the daily amplitude inside the wall.

REFERENCES

GE Sensing 2006, 'Protimeter HygroTrac, Wireless environmental monitoring'.

Hedenblad 1996, 'Moisture safety in buildings. Materialdata for Moisture Calculations'. In Swedish. Byggforskningsrådet, T19:1996, Stockholm, Sweden.

Hägerstedt, O. 2010, 'Calculations and field measurements method in wood framed hoses', Department of Building Physics, Lund University, Report TVBH-XXXX, 2010, In press.

Hägerstedt, O. & Arfvidsson J. 2010, B, 'Comparison of Field measurements and Calculations of relative humidity and Temperature in Wood Framed Walls', Thermophysics 2010 – Conference proceedings, Bruno University of Technology, Faculty of Chemistry 2010.

IBP. Fraunhofer Institute for Building Physics. http://www.ibp.fraunhofer.de.

IEA Annex 24 1996, 'Heat air and moisture transfer through new and retrofitted insulated envelops'.

Krus, M. 1996 'Moisture Transport and Storage Coefficients of Porous Mineral Building Materials', Fraunhofer IRB Verlag.

Mjörnell, K. 2007 'ByggaF' Method for moisture proof building process. In Swedish.

Paroc, 2002, 'Product information - Construction book' Produktinformation - byggboken. In Swedish.

Sandberg, K., Pousette, A. & Dahlquist, S. 2011, 'Wireless in situ measurements of moisture content and temperature in timber constructions'. XII DBMC – Conference proceedings, Porto, Portugal 2011.

SMHI, Swedish meteorological and hydrological institute, Climate data, Klimatdata www.smhi.se.

Zedlbauer, K. 2001 'Vorhersage von Schimmelpilzbildung auf und in Bauteilen', Uni. Stuttgart, Dis.

WUFI 5.0, IBP Softwaer, www.wufi.com.

XII DBMC
International Conference on Durability of Building Materials and Components
PORTO - PORTUGAL, April 12th-15th, 2011

PCM Incorporation into Building Envelope Masonry Walls

Tiago Silva [1]
Romeu Vicente [2]
Nelson Soares [3]
Victor Ferreira[4]

ABSTRACT

The storage capacity of latent energy by incorporating phase change materials (PCMs) into building envelope solutions allows the building industry to become more sustainable, reducing environmental costs and increasing the energy efficiency levels and overall durability. In the present paper, a parametric numerical simulation was carried out to analyse the potential of PCM macro encapsulated and incorporated into an envelope masonry wall solution. The external conditions were imposed using climatic data for Portugal. The final results reveal the optimized quantity of PCM incorporated, in order to control thermal insulation and increase storage capacity. This model shows a good thermal and energy performance, combining latent heat storage capacity with the reduction or delaying the energy transmission, resulting in an improved thermal inertia, minimizing the fluctuations of indoor temperatures.

KEYWORDS

Phase change material, PCM, Thermal inertia, Latent heat, Energy efficiency.

[1] University of Aveiro (UA), Aveiro, PORTUGAL, tiagomsilva@ua.pt
[2] University of Aveiro (UA), Aveiro, PORTUGAL, romvic@ua.pt
[3] University of Aveiro (UA), Aveiro, PORTUGAL, nsoares@ua.pt
[4] University of Aveiro (UA), Aveiro, PORTUGAL, victorf@ua.pt

1 INTRODUCTION

The use of Phase Change Materials (PCMs) in building construction components is a growing tendency. For a review, see [Sharma *et al.* 2009], [Tyagi & Buddhi 2007], [Zalba *et al.* 2003] and [Alawadhi 2008]. Their potential is unquestionable, on account of their high latent heat storage capacity and their role in systems employing endogenous energies, such as solar thermal energy. The use of a latent heat storage system incorporating PCM benefits also from the isothermal nature of the phase change process.

The incorporation of PCMs into building components is contributing to increase thermal efficiency of sustainable solutions. Other authors [Maruoka & Akiyama 2003] have revealed good results on the durability of PCMs cyclic heating and cooling.

This paper presents the numerical thermal analysis of a typical fireclay brick containing macro encapsulated PCM to be used in Mediterranean climate. According to Castell *et al.* [2009] the integration of such a system into building envelope walls provide a higher thermal inertia that combined with the thermal insulation effect can reduce the energy consumption of the building.

As Kuznik *et al.* [2008] explain when the temperature of PCM increases the material changes phase from solid to liquid. As this physical reaction is endothermic, the PCM absorbs heat. When the temperature decreases the material changes phase from liquid to solid. As this reaction is exothermic the PCM releases heat. The main problem lies in how to incorporate PCM into building envelope walls to satisfy comply with *U*-value of the wall defined in the Portuguese thermal code. The imposed *U*-value is different for winter and summer seasons as well as the climate conditions, mainly the solar radiation and the ambient temperature. The behaviour of the wall under different conditions must be studied to evaluate the potential of PCM during winter and during summer seasons.

In the scope of this work, a parametric study was conducted to optimize the brick wall system during the winter season and to assess the effect of different designs parameters, such as the PCMs quantity and the thickness of the heat exchanger container material – capsule.

2 SYSTEM DESCRIPTIONS

2.1 System configuration

A fireclay brick incorporating PCM has been idealised to enhance the solar heat gain by absorbing the thermal energy in the wall through the melting process of the PCM leading to provable extra inertia behaviour. The scheme of the system is shown in Fig. 1.

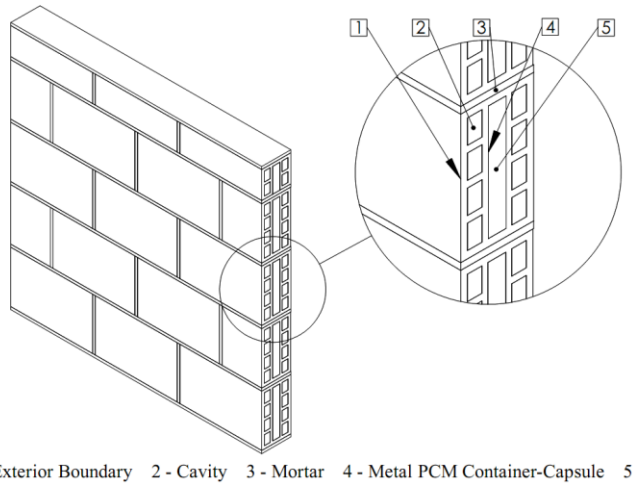

Figure 1. Schematics of the latent heat storage system – PCM-Brick.

The system consists of a horizontal perforated fireclay brick (0.11 × 0.20 × 0.30 m). The metal sheet PCM container – capsule – is located at the centre void of the bricks. The metal liner will help to enhance the rate of heat transfer to the PCM. Due to the low thermal conductivity of PCMs, they have an inherent disadvantage of slow heat transfer during the charging and discharging processes. The incorporation of a high-conductivity material as the heat exchanger material will improve the thermal effectiveness of the proposed brick wall solution. The thickness of the metal liner must be optimized as well the PCMs quantity. The metal encapsulation of the PCMs enables the long-term durability and heat transfer rate of the material (Paraffin).

2.2 General assumptions

The chosen PCM for this simulation is Rubitherm® RT18. The thermo physical properties of this PCM are given in Table 1 and the properties of the heat exchanger material are given in Table 2.

Table 1. Thermo physical properties of the PCM – Rubitherm® RT18 [Rubitherm Tech. 2010].

Latent heat of fusion (J kg^{-1})	134000
Density (kg m^{-3})	756
Specific heat (J kg^{-1} °C^{-1})	2000
Melting temperature (°C)	18
Thermal conductivity (W m^{-1} °C^{-1})	0.2

Table 2. Thermo physical properties of the container material – steel.

Density (kg m^{-3})	7832
Specific heat (J kg^{-1} °C^{-1})	434
Thermal conductivity (W m^{-1} °C^{-1})	63

The main outdoor conditions are external air temperature and solar radiation. According to Kuznik *et al.* [2008] these conditions are taken into account using the equivalent temperature, T_{eq}, calculated using:

$$T_{eq} = T_e + \frac{\alpha S}{h_e} \tag{1}$$

with T_e the exterior air temperature, S the total solar radiation calculated for a vertical oriented South wall, α the solar absorption coefficient of the surface and h_e the exterior convective heat transfer (h_e =25 W m^{-2} C^{-1}). The values given for the temperature cycle in Figure 2 represent the temperatures for a south-faced oriented wall surface. Figure 2 shows the polynomial evolution of the equivalent temperature, T_{eq}, considered for numerical simulations during a complete 24 h day cycle. T_{eq} evolution was calculated considering the average values of the equivalent temperature for a number of Portuguese cities in January, according to the climate data SOLTERM®.

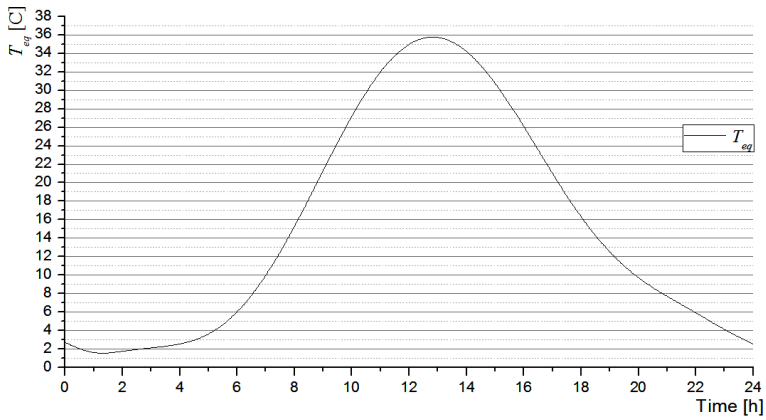

Figure 2. Polynomial evolution during a 24 h day cycle of the equivalent temperature, T_{eq}, considered for numerical simulation climate data determined from SOLTERM®.

3 MODELLING AND METHOD

The optimization process of the PCM volume and the metal thickness layer is performed with the help of numerical simulations. The computational modelling domain is shown in Fig. 3.

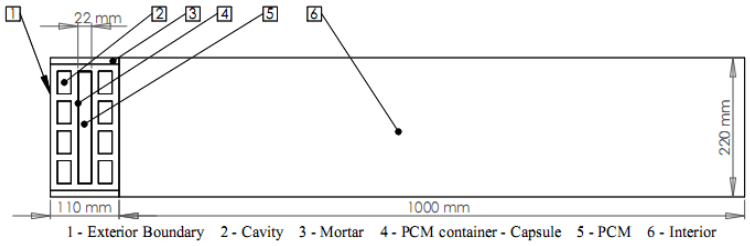

Figure 3. Schematic of the computational domain.

In order to find the optimal thickness for the heat exchanger material (metal layer of the capsule), a set of numerical experiments was held using four metal thicknesses: e_{caps} = 1.0 mm, e_{caps} =1.5 mm, e_{caps} = 2.0 mm and e_{caps} = 2.5 mm. For each metal thickness considered, a set of numerical experiments was held changing the volume of the PCM, to find the optimal PCM quantity to incorporate in the brick. Four PCM layer thicknesses were considered: e_{PCM} = 19 mm, e_{PCM} =22 mm, e_{PCM} = 25 mm and e_{PCM} = 28 mm. Figure 4 sketches the sixteen numerical experiments that had been carried through to quantify the influence of the PCM quantity and the metal exchanger thickness in the indoor temperature swing.

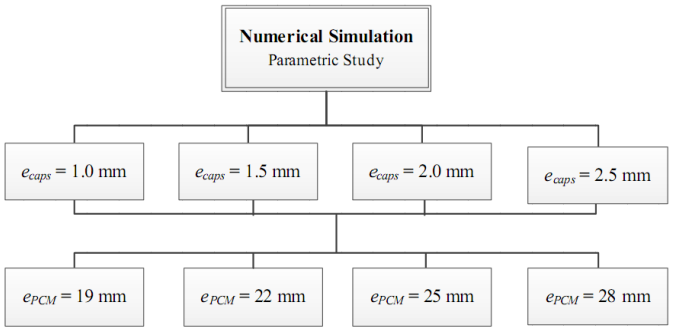

Figure 4. Organogram of the 16 numerical simulations carried through to quantify the influence of the PCM quantity and the metal exchanger thickness in the indoor temperature swing.

The model to simulate the thermal behaviour was developed using a finite element program. Quadrilaterals and tetrahedrons elements were used to mesh the computational domain. In order to ensure that a mesh independent solution was obtained, several finite elements models were examined with different number of elements until the convergence was obtained.

Figure 5 illustrates the computational domain and the finite element mesh. The minimum element size in the mesh is $1x10^{-3}$ m and the maximum size is $1x10^{-2}$ m.

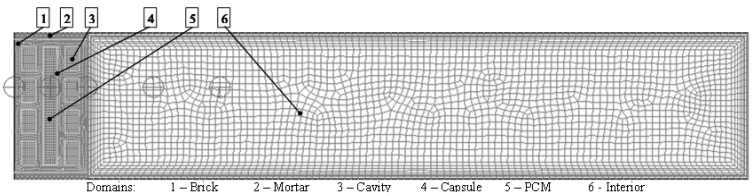

Figure 5. Computational domain and the finite element mesh.

The Fig. 6 shows the different control points.

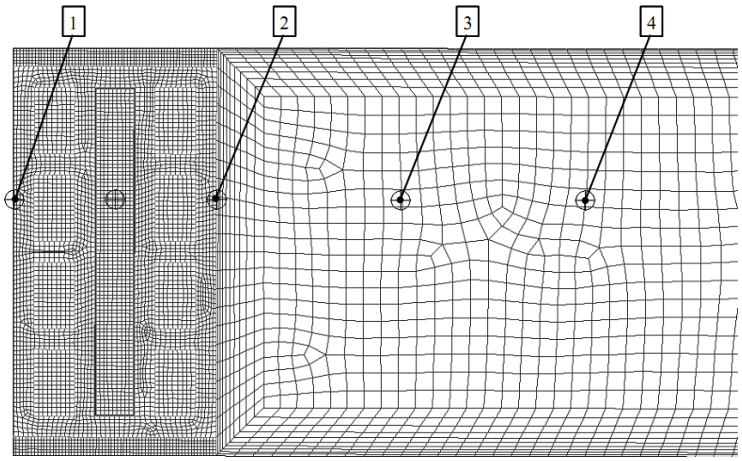

Points: 1 – Exterior boundary 2 – Brick/Interior boundary 3/4 - Cavity Interior

Figure 6. Numerical model with extended mesh.

The temperature in the interior cavity was obtained considering the average of the temperatures obtained for the control points 2, 3 and 4. The temperature at the control point 1 was used to compare with external temperature imposed in the numerical studies.

The numerical simulation of the wall system was carried out using a developed code based on the enthalpy formulation. The simulations were performed for a transient regime. The computing method for the spatial discretization of the convection resourced to the Least Squares Cell Based algorithm and for the convection-diffusion, the energy flow equations are handled by second order upwind discretization, because with the non-aligned mesh this option leads to better convergence and results.

The relaxation factors used in calculations were 0.3 for the pressure, 0.7 to the momentum, 0.9 for the liquid fraction, and 1 for the total energy.

4 RESULTS

Figure 7 shows the result of a parametric analysis evaluating the influence of the PCM volume and the metal thickness in the average interior cavity temperature calculated.

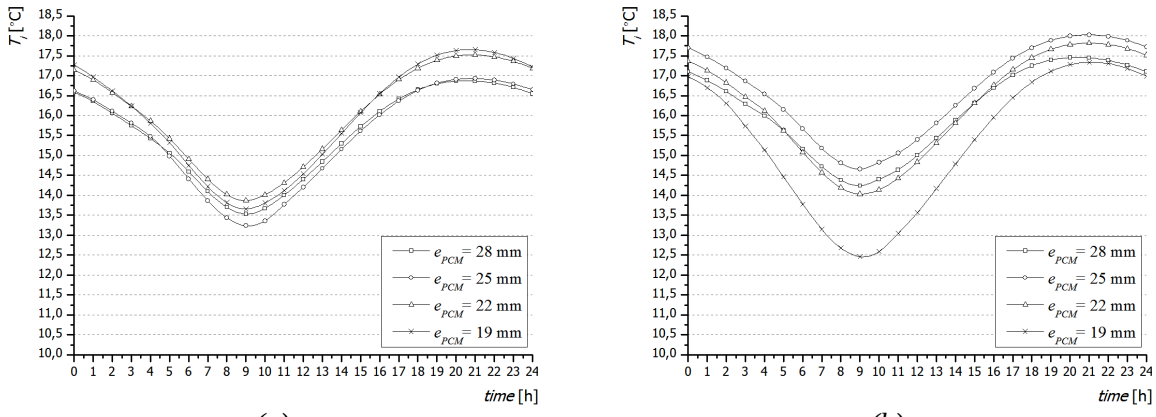

(a) *(b)*

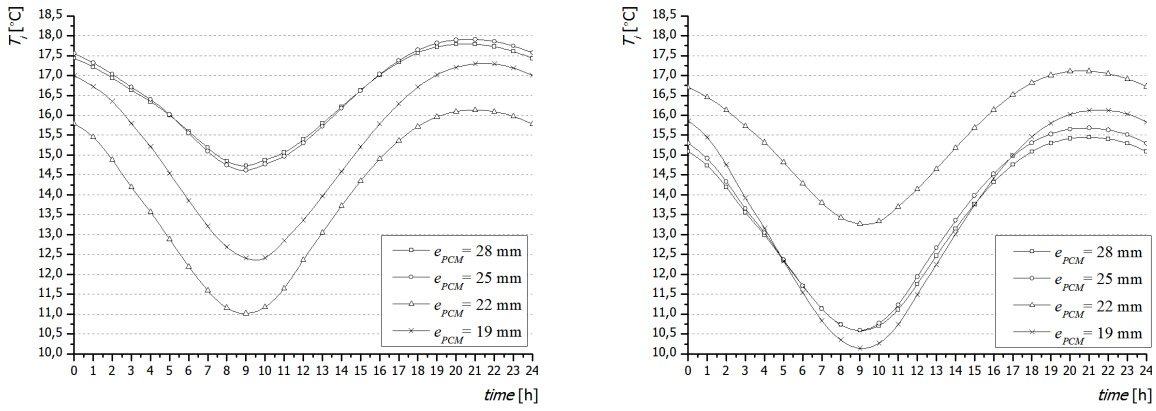

(c) *(d)*

Figure 7. Parametric analysis of the influence of the PCM quantity in the indoor temperature swing considering: (a) e_{caps} = 1.0 mm; (b) e_{caps} = 1.5 mm; (c) e_{caps} = 2.0 mm; (d) e_{caps} = 2.5 mm.

Increasing the thickness of the metal liner of the capsule increases the thermal amplitude in the interior cavity. The temperatures obtained for the smallest metal liner thickness, Fig. 7(a), have smaller thermal amplitude compared with those obtained for the largest metal liner thickness, Fig. 7(d). In this model, the increase of PCM volume influences directly the temperature in the interior of the cavity. The optimal PCM quantity changes according to the thickness of the metal liner capsule. To choose the best model, the best results in each case of Figure 7 were chosen.

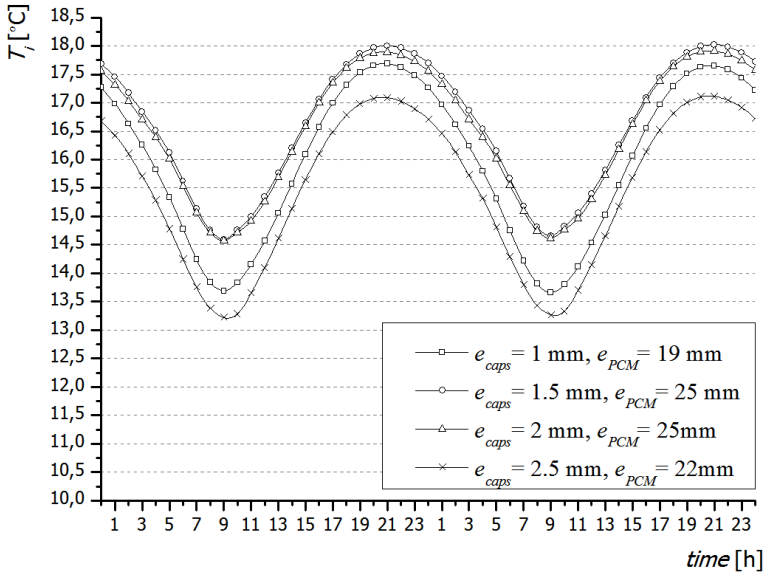

Figure 8. Comparison between the 4 best numerical models.

Figure 8 shows the selected results. Two of the models correspond to same PCM volume (25 mm) and the other two correspond to 19 mm and 22 mm PCM volume. Table 3 displays the detailed numerical results obtained in each case.

Table 3. Comparison between temperature values of four numerical models.

Model	*Thermal Amplitude* [°C]	*Max.* T_i [°C]	*Min.* T_i [°C]
e_{caps} = 1.0 mm, e_{PCM} = 19 mm	3.9	17.6	13.7
e_{caps} = 1.5 mm, e_{PCM} = 25 mm	3.3	18	14.7
e_{caps} = 2.0 mm, e_{PCM} = 25 mm	3.3	17.9	14.6
e_{caps} = 2.5 mm, e_{PCM} = 22 mm	3.9	17.1	13.2

All models present similar results, however with different characteristics in terms of PCM and metal capsule thickness. The best results are for the two cases for which the thickness of PCM is 25mm and the capsule thickness is 1.5 and 2.0mm. The other two cases with a smaller thickness of PCM revealed higher thermal amplitude of about 0.6ºC.

From the results shown above, the model with e_{caps} = 1.5 mm and e_{PCM} = 25 mm presents the lowest thermal amplitude. Since the numerical simulations were carried out for a typical winter season day cycle, this model was chosen for further discussion, presenting the higher values for the minimum and maximum temperature, T_i (see Table 3). As intended, this model has the lowest fluctuation in the interior cavity temperature, therefore a lower energy loss during the temperature fall of the night.

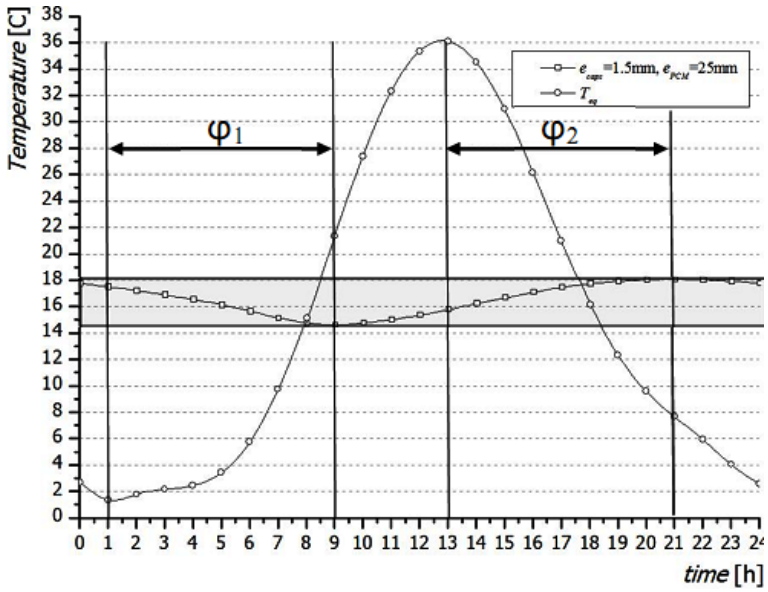

Figure 9. Comparison between the model 5 and the curve imposed in the exterior boundary.

Figure 9 represents a comparison between the model selected and the equivalent external temperature imposed for a last 24 hour day cycle. A delay of 8 hours between the external imposed temperature profile and the temperature inside the in interior cavity is shown in Figure 9 (assigned as φ_1 e φ_2). This value is rather high, however if considered the superficial interior temperature of the wall (point 2) this value decreases. This delay allows the minimal temperature to be obtained in the interior cavity domain at the ninth hour (see Figure 9). For that instance (t=9 hours) the equivalent temperature imposed is higher than the PCM fusion temperature (18 ºC), allowing the system to recharge while the temperature in the interior cavity fluctuates very little. The resulting thermal amplitude is 3.3 ºC which proves the thermal regulative nature of the PCM as an insulation layer through the creation of a thermal inertia capacity of the pseudo-adiabatic boundary condition.

5 CONCLUSIONS

Typically external envelope walls are not single leafed masonries in the European countries. However the recent trends assume that in the future thicker single leaf masonries are a reality. Thus the incorporation of PCM´s into external wall solutions is a potential development from two points of view: energy accumulation and thermal insulation.

The thickness of the PCM, as expected, influences the obtained results, more PCM does not mean better results. The optimized quantity of PCM is influenced by the metal capsule thickness.

The numerical simulations carried out, have shown that the model with e_{caps} = 1.5 mm and e_{PCM} = 25 mm attain the best results. The thermal amplitude of this model is relatively low (3.3 ºC)

which represents a 90% reduction of the 35ºC thermal amplitude of the equivalent temperature profile imposed. The maximum temperature attained in the selected model is 18 ºC and the minimum 14.7 ºC, values that are below the comfort temperature requirement, defined as 20 ºC in the present national thermal code.

This aspect is not a limitation, since the on-going research will study the addition of a conventional thermal insulation layer, as well as an optimization of the thermo physical properties of PCM, particularly the melting point temperature, that has a strong influence on the energy storage capacity of the system.

REFERENCES

Rubitherm Technologies. 2010. *EEC - Safety data sheet Rubitherm® RT18*, Sperenberger, Berlin.

Tan, F.L., Hosseinizadeh, S.F., Khodadadi, J.M. & Fan L. 2009, 'Experimental and computational study of constrained melting of phase change materials (PCM) inside a spherical capsule', *International Journal of Heat and Mass Transfer*, 52, 2009, pp. 3464-3472.

Tyagi, V.V. & Buddhi, D. 2007, 'PCM thermal storage in buildings: A state of art', *Journal of Renewable and Sustainable Energy Reviews*, 11, 2007, pp. 1146-1166.

Zalba, B., Marín, J.M., Cabeza, L.F. & Mehling, H., 2003, 'Review on thermal energy storage with phase change: materials, heat transfer analysis and applications', *Journal of Applied Thermal Engineering*, 23, 2003, pp. 251-283.

Sharma, A., Tyagi, V.V., Chen, C.R. & Buddhi D. 2009, 'Review on thermal energy storage with phase change materials and applications', *Journal of Renewable and Sustainable Energy Reviews*, 13, pp. 318-345.

Alawadhi, E.M., 2008, 'Thermal analysis of a building brick containing phase change material', *Journal of Energy and Buildings*, 40, 2008, pp. 351-357.

Kuznik, F., Virgone, J. & Noel, J., 2008, 'Optimization of a phase change material wallboard for building use', *Journal of Applied Thermal* Engineering, 28, 2008, pp. 1991-1298.

Maruoka, N. & Akiyama, T., 2003, 'Thermal Stress of PCM Encapsulation for Heat Recovery of High Temperature Waste Heat', *Journal of Chemical Engineering of Japan*, 36, 2003, pp. 794-798.

XII DBMC
International Conference on Durability of Building Materials and Components
PORTO - PORTUGAL, April 12th-15th, 2011

A Study on the Carbonation Progress of Concrete Concerning the Influence of Deterioration of the Coating Material for Textured Finish

Lee Youngran [1]
Masuda Yoshihiro [2]

ABSTRACT

A coating material for textured finish is effective for the carbonation suppression of concrete. However, the carbonation suppressive effect decreases when the polymer of the coating material is deteriorated by ultraviolet rays, wind, rain, etc. This paper analyzes and proposes a prediction formula for the carbonation progress of concrete, in which the coefficient of diffusion of the coating material increases and the carbonation resistance decreases with time. It is based on an analysis model expressing that carbon dioxide moves according to an approximation of a steady state of diffusion and the carbonation progresses. When the deterioration of the coating material is considered, the carbonation progress is expressed by Equation (13). The carbonation progress is simulated using data from a previous experiment about the increase in the diffusion coefficient and the decrease in the carbonation resistance according to the deterioration of the coating material. At the beginning of simulation, the carbonation progress is similar to concrete with a coating material that is not deteriorated. As the simulation progresses, the carbonation progress becomes similar to concrete with a coating material that is deteriorated. At the end of the simulation, the value of carbonation depth converges with the value of carbonation depth of non-finished concrete.

KEYWORDS

Coating material for textured finish, Carbonation suppression of concrete, Carbonation resistance, Deterioration, Carbon dioxide diffusion.

[1] Department of Architecture Engineering of Utsunomiya University, Utsunomiya, JAPAN, leeyr@cc.utsunomiya-u.ac.jp
[2] Department of Architecture Engineering of Utsunomiya University, Utsunomiya, JAPAN, masuday@cc.utsunomiya-u.ac.jp

1 INTRODUCTION

Coating materials for textured finish of concrete are expected to suppress carbonation [Japan Institute of Consturction Engineering 1986 and Architectural Institute of Japan 2004]. However, their carbonation-suppressing effect is gradually lost over time due to the deterioration of polymers under ambient conditions including ultraviolet rays and weather. Izumi [Japan Institute of Consturction Engineering 1986] and Hasegawa et al.[2002] have reported on the progress of carbonation in concrete coated with finishing materials over time based on exposure tests. In these reports, however, the carbonation-suppressing effect of finishing materials is evaluated by determining the ratio between the carbonation depths with and without finishing (hereafter referred to as 'carbonation ratio') at the end of the tests. The progress of carbonation in concrete coated with a finishing material in this manner is expressed by Eq. (1) using the carbonation ratio, *s* [Japan Institute of Consturction Engineering 1986 and Architectural Institute of Japan 2004], but the value of *s* changes over time. The carbonation-suppressing effect of the material can therefore be properly evaluated only at the point of measurement.

$$C = As\sqrt{t} \tag{1}$$

where C : carbonation depth (mm)
A : coefficient of carbonation speed (mm/year$^{1/2}$)
s : ratio of carbonation
t : time(years)

Baba et al.[1987] has expressed the progress of carbonation in concrete coated with a finishing material by Eq. (2) using the carbonation resistance, R. The authors [Kono et al. 2008] derived the same equation based on analysis. This analysis was conducted by applying equations expressing a phenomenon in which CO_2 diffuses through the finishing material and carbonated concrete, following Fick's law, and instantaneously reacts with $Ca(OH)_2$, which is present at the boundary between carbonated and uncarbonated regions in concrete, thereby sequentially shifting the boundary inward.

$$C = A\left(\sqrt{t + R^2} - R\right) \tag{2}$$

Where R : carbonation resistance (years$^{1/2}$)

Equation (2) is capable of predicting the carbonation depth of concrete at a certain time when the finishing material becomes deteriorated, provided the ultimate carbonation resistance of the material at that time is determined, but cannot calculate the degree of carbonation at an arbitrary age of concrete.

The authors intend to widen the application of the model to cover the case where the finishing material is deteriorated, changing the carbonation resistance, so as to investigate the resulting carbonation-suppressing effect and carbonation progress.

2 CONCEPT OF CARBONATION PROCESS CONSIDERING THE DETERIORATION OF THE COATING MATERIAL FOR TEXTURED FINISH

2.1 A Carbonation Process Model Of Concrete Based On The Approximation Of Steady State Of Diffusion

In a thermo-hygrostatic environment with a constant CO_2 concentration, the carbonation of concrete having a homogeneous quality from the surface through the core proceeds in proportion to the square root of time. A rationale for this √t rule is explained as follows [Architectural Institute of Japan 2004]: Figure 1 schematically shows the steady diffusion of CO_2 through carbonated concrete and the progress of carbonation. Strictly speaking, the diffusion of CO_2 in concrete is unsteady, but in this study it is approximately regarded as being steady and subject to Fick's law. Assuming the coordinate of the concrete surface is zero and carbonation reaches a depth of x at an age of t, Eq. (3) expresses ΔCO_2, the amount of CO_2 reaching a depth of x from the concrete surface through a plane perpendicular to the depth direction with an area of S during time Δt. Also assuming that CO_2 diffusing through concrete instantaneously reacts with $Ca(OH)_2$, which is present at the boundary with

a thickness of Δx between the carbonated and uncarbonated regions, Eq. (4) expresses ΔCO_2, the amount of CO_2 consumed in the reaction.

$$\Delta CO_2 = D \cdot \frac{C}{x} \cdot S \cdot \Delta t \tag{3}$$

$$\Delta CO_2 = H \cdot S \cdot \Delta x \tag{4}$$

where x : carbonation depth (mm)
t : time (years)
C : CO_2 concentration at concrete surface
D : diffusion coefficient in carbonation region of concrete (mm^2/year)
S : area (mm^2)
H : amout of $Ca(OH)_2$ per unit volume of concrete
Δx : thickness of boundary region
Δt : time increment

From Eqs. (3) and (4), $x\frac{\Delta x}{\Delta t} = \frac{D \cdot C}{H}$

Assuming that Δt approaches zero, the following differential equation is obtained: $x\frac{dx}{dt} = \frac{D \cdot C}{H}$

By integrating both members, $\frac{1}{2}x^2 = \frac{D \cdot C}{H}t$

From this equation, Eq. (5) is obtained as a carbonation speed equation for concrete.

$$x = \frac{\sqrt{2}\sqrt{D}\sqrt{C_0}}{\sqrt{H}} \cdot \sqrt{t} \tag{5}$$

Among equations expressing the carbonation-suppressing effect of finishing materials, Eq. (1) incorporating the carbonation ratio corresponds to Eq. (5) when the microstructure of concrete is dense with a low diffusion coeffient or when the CO_2 concentration at the concrete surface is low. Since the microstructure of concrete is the same, it is necessary for validating Eq. (1) to keep the CO_2 concentration at a low level at the interface between the finishing material and concrete. However, this requires small changes in the ratio of the diffusion coefficient of the finishing material to that of concrete as carbonation proceeds, being paradoxical. For this reason, the carbonation-suppressing effect of finishing mateirals is hereafter investigated based on Eq. (2).

2.2 Carbon Dioxide Diffusion And Reaction With Carcium Hydroxide In The Coating Material For Textured Finish And Concrete

Figure 2 schematically shows the steady diffusion of CO_2 through the finishing material and carbonated concrete, causing carbonation to proceed.
When carbonation proceeds to a depth of x from the concrete surface at an age of t, Eq. (6) expresses ΔCO_2, the amount of CO_2 diffusing in the finishing material through a plane perpendicular to the depth direction with an area of S to the concrete surface during time Δt. Similarly, Eq. (7) expresses ΔCO_2, the amount of CO_2 reaching the depth of x from the concrete surface during time Δt. At the depth of x in concrete, CO_2 is consumed by reaction with $Ca(OH)_2$. The CO_2 concentration at this depth is therefore zero. Equation (8) expresses ΔCO_2, the amount of CO_2 consumed by reaction with $Ca(OH)_2$ in the boundary region.

$$\Delta CO_2 = D_i \cdot \frac{C_0 - C}{d} \cdot S \cdot \Delta t \tag{6}$$

$$\Delta CO_2 = D \cdot \frac{C}{x} \cdot S \cdot \Delta t \tag{7}$$

$$\Delta CO_2 = H \cdot S \cdot \Delta x \tag{8}$$

Where C_0 : CO_2 concentration at the surface of the finishing material
C : CO_2 concentration at the boundary between the finishing material and concrete
D_i : diffusion coefficient of the finishing material at time t ($T_i \le t \le T_{i+1}$) (mm^2/year)
D : diffusion coeffieint of the carbonated region of concrete (mm^2/year)

S : area (mm^2)
d : thickness of the finishing material (mm)
Δx : thickness of the boundary region
Δt : time increment

From Eqs. (6) and (7), $\frac{C}{x} = \frac{D_i \cdot C_0}{D_i \cdot x + D \cdot d}$

From Eqs. (7) and (8), $D \cdot \frac{C}{x} \cdot \Delta t = H \cdot \Delta x$, $\left(D_i \cdot x + D \cdot d\right)\frac{\Delta x}{\Delta t} = \frac{D \cdot D_i \cdot C_0}{H}$

Assuming that Δt approaches zero, the following differential equation is obtained:

$$\left(D_i \cdot x + D \cdot d\right)\frac{dx}{dt} = \frac{D \cdot D_i \cdot C_0}{H}$$

By integrating both members, $\frac{1}{2} D_i x^2 + D \cdot d \cdot x = \frac{D \cdot D_i \cdot C_0}{H} t + I$ (I: integration constant)

$$x^2 + \frac{2D \cdot d}{D_i} x - \frac{2D \cdot C_0 \cdot t}{H} = I' \quad (\text{where } I' = \frac{2I}{D_i}) \tag{9}$$

By putting $A = \sqrt{\frac{2D \cdot C_0}{H}}$ and $R_i = \sqrt{\frac{H \cdot D \cdot d^2}{2D_i^2 \cdot C_0}}$, $A \cdot R_i = \sqrt{\frac{2D \cdot C_0}{H} \cdot \frac{H \cdot D \cdot d^2}{2D_i^2 \cdot C_0}} = \frac{D \cdot d}{D_i}$ (10)

By substituting Eq. (10) into Eq. (9), Eq. (11) is obtained.

$$x^2 + 2A \cdot R_i \cdot x - A^2 \cdot t = I' \tag{11}$$

Assuming $x=X_i$ ($i=0, 1, 2\ldots$) when $t=T_i$, $I' = X_i^2 + 2A \cdot R_i \cdot X_i - A^2 \cdot T_i$

Eq. (11) is solved by substituting I' as:

$$x = -A \cdot R_i + \sqrt{A^2 \cdot R_i^2 + A^2 \cdot t + I'} = A\left(\sqrt{t + R_i^2 + \frac{I'}{A^2}} - R_i\right) = A\left(\sqrt{t + R_i^2 + \frac{1}{A^2} X_i^2 + \frac{2R_i}{A} X_i - T_i} - R_i\right) \tag{12}$$

Equation (12) expresses the carbonation depth when carbonation proceeds to a depth of X_i at time t ($T_i \le t \le T_{i+1}$).

2.3 A MODEL OF CARBONATION PROGRESS CONSIDERING THE DETERATION OF THE COATING MATERIAL FOR TEXTURED FINISH

The diffusion coeffieint of CO_2 in a finishing material changes over time as shown in Fig. 2. At time t ($T_i \le t \le T_{i+1}$), the diffusion coefficient is assumed to be D_i.

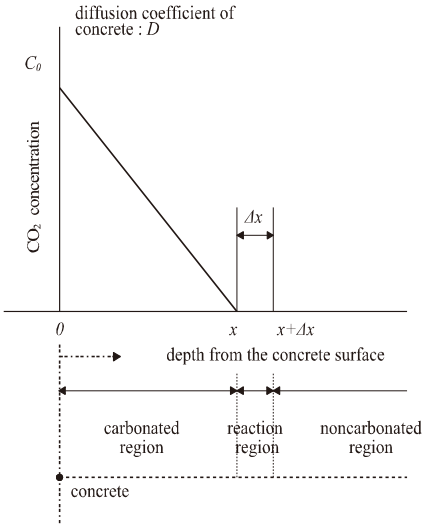

Figure 1. Model of CO_2 diffusion in concrete.

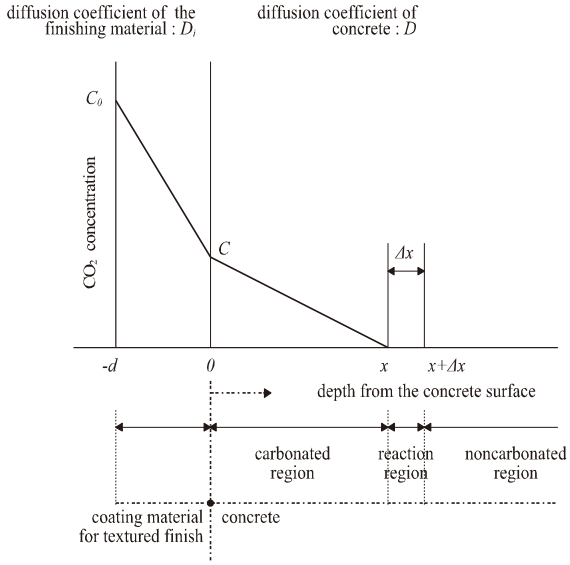

Figure2. Model of CO_2 diffusion in concrete with a coating material for textured finish.

(1) When $i=0$, $T_0 \le t \le T_1$, $T_0=0$, and $X_0=0$. Therefore, Eq, (12) is rewritten as

$$x = A\left(\sqrt{t + {R_0}^2} - R_0\right) \tag{13}$$

$$R_0 = \sqrt{\frac{H \cdot D \cdot d^2}{2{D_0}^2 \cdot C_0}}$$

When $t=T_1$, $x=X_1$. Therefore, $X_1 = A\left(\sqrt{T_1 + {R_0}^2} - R_0\right)$

By transposing $A \cdot R_0$, squaring both members, and rearranging, $\frac{1}{A^2}{X_1}^2 = T_1 - \frac{2R_0}{A}X_1$ (14)

(2) When $i=1$, $T_1 \le t \le T_2$. Therefore, Eq, (12) is rewritten as

$$x = A\left(\sqrt{t + {R_1}^2 + \frac{1}{A^2}{X_1}^2 + \frac{2R_1}{A}X_1 - T_1} - R_1\right) \tag{15}$$

By substituting Eq. (14) and rearranging , Eq. (16) is obtained.

$$x = A\left(\sqrt{t + {R_1}^2 + \frac{2}{A}(R_1 - R_0)X_1} - R_1\right) \tag{16}$$

When $t=T_2$, $x=X_2$. Therefore, $X_2 = A\left(\sqrt{T_2 + {R_1}^2 + \frac{2}{A}(R_1 - R_0)X_1} - R_1\right)$

This is rewritten as $\frac{1}{A^2}{X_2}^2 = T_2 - \frac{2R_1}{A}X_2 + \frac{2}{A}(R_1 - R_0)X_1$ (17)

(3) When $i=2$, $T_2 \le t \le T_3$. Therefore, Eq. (12) is rewretten as

$$x = A\left(\sqrt{t + {R_2}^2 + \frac{1}{A^2}{X_2}^2 + \frac{2R_2}{A}X_2 - T_2} - R_2\right)$$

By substituting Eq. (17), the following equation is obtained:

$$x = A\left(\sqrt{t + {R_2}^2 + \frac{2}{A}\{(R_2 - R_1)X_2 + (R_1 - R_0)X_1\}} - R_2\right)$$

(4) When $i= i$, $T_i \le t \le T_{i+1}$. Following the same procedure,

$$x = A\left(\sqrt{t + {R_i}^2 + \frac{2}{A}\{(R_i - R_{i-1})X_i + (R_{i-1} - R_{i-2})X_{i-1} + \cdots + (R_1 - R_0)X_1\}} - R_i\right) \tag{18}$$

3 SIMULATION USING PAST EXPERIMENTAL RESULTS

3.1 OUTLINE OF EXPERIMENT

The authors have conducted accelerated carbonation tests of concretes coated with finishing materials, which were deteriorated using an accelerated weathering tester having carbon-arc lamps (hereafter referred to as a "weathermeter"), and have reported that the carbonation-suppressing effect of a finishing material is weakened by weathering [Kono et al. 2004 & 2008]. This experment included irradiation of specimens with the weathermeter for 1,500 or 3,000 h to accelerate the deterioration of finishing materials. The carbonation resistance of these finishing materials, R, is as given in Table 1 [Kono et al. 2004]. These irradiation periods are equivalnet to 6 and 12 years, respectively, by outdoor exposure testing. The finishing materials were also subjected to acelerated deterioration using a xenon lamp weathermeter to measure the amount of CO_2 permeating through these materials using a double-chamber diffusion coefficient meter. The CO_2 diffusion coefficinets, D, of these materials were thus determined experimentally from the permeation time and changes in the CO_2 concentration as given in Table 2. These measurements practically validated Eq. 11 expressing the relationship between D and the carbonation resistance, R [Kono et al. 2008].

Table 1 gives the measured carbonation resistance of the finishing materials at different stages of deterioration. In order to determine the carbonation resistance at arbitrary periods, these values were applied to Eq. (21) to determine the coefficients by least squares. Coefficients *a* and *b* in Eq. (21) were determined as given in Table 3, which are shown as a diagram in Fig. 4. The three finishing materials consisted of multi-layer coating E (AT), waterproof exteiror film coating E (SE), and waterproof mult-layer coating E (ET). Only the standard thickness (s) of these materials was examined in this study.

$$R_t = a \cdot e^{-bt} \qquad (21)$$

Also, the relationship between the carbonation resistance, R, determined by Eq. (21) and the diffusion coefficient of finishing materials, *D* [Kono et al. 2008], is shown in Fig. 5. Since the approximation equation was determined by least squares, it is found to roughly approximate to theoretical Eq. (10).

3.2 RESULTS OF CARCULATION

Figure 6 shows the progress of carbonation in concrete finished with different materials as the materials are gradually deteriorated, with the carbonation resistance values *R* decreasing as shown in Fig. 4. This figure also shows the carbonation curves when the carbonation resistance is fixed at the values of the finishing materials at the beginning (R_0) and deteriorated after 6 and 12 equivalent years (R_6 and R_{12}) based on Eq. (19). Assuming concrete with slightly low qualities, the carbonation depth after 25 years and the coefficient of carbonation speed were set at 30 mm and 6 mm/year$^{1/2}$, respectively. A time step length of 1 year was selected for time history analysis.

These figures reveal that the carbonation of concrete coated with a finishing material porgresses following the initial carbonation resistance of the material, but the carbonation speed progressively increases, approaching the carbonation curves of deteriorated materials. The curve then crosses the curves of detriorated materials, approaching the carbonation curve of exposed concrete. It is also found that the carbonation curve with a gradually deteriorated finishing material crosses the curves with finishing materials deteriorated for 6 and 12 years at points later than 6 and 12 years, respectively.

When concrete is finished with the standard thickness of waterproof multi-layer coating E (ETs) and the coating is assumed to be gradually deteriorated, it takes 36 years for carbonation to reach a depth of 30 mm, which is longer than the time required in exposed concrete, 25 years. This curve is found to

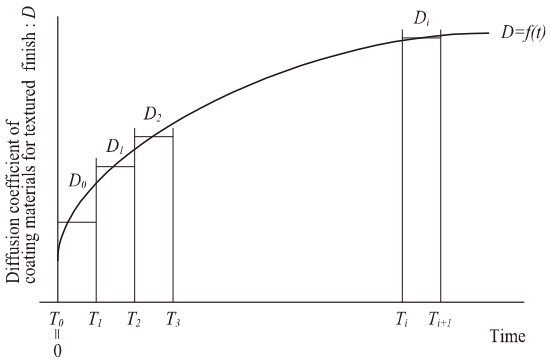

Figure 3. Changes in diffusion coefficients of coating materials for textured finish over time.

Table 1. Measured carbonation resistance R.

		Carbonation resistance R (√years)		
Radiation time (hours)		0	1500	3000
Equivalent time by exposure test (years)		0	6	12
Coating materials for textured finish	Multi-layer coating E (AT)	1.09	0.57	0.31
	Waterproof exterior film coating material E (SE)	10.69	0.76	0.78
	Waterproof multi-layer coating E (ET)	21.15	2.40	1.12

Table 2. Measured diffusion coefficient of coating materials for textured finish.

		Diffusion coefficients of coating materials for textured finish D (×10^{-7}cm^2/sec)		
Radiation time (hours)		0	1500	3000
Equivalent time by exposure test (years)		0	6	12
Coating materials for textured finishes	AT	7.7	8.6	27.0
	SE	2.4	7.1	22.2
	ET	12.8	24.8	23.9

Table 3. Values of coefficients a and b

Coating materials	a	b
AT	1.09	0.11
SE	10.70	0.26
ET	21.15	0.27

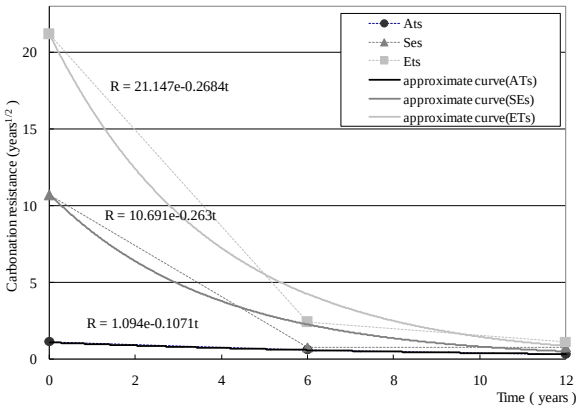

Figure 4. Measured carbonation resistance and approximate curves of ATs, SEs and ETs.

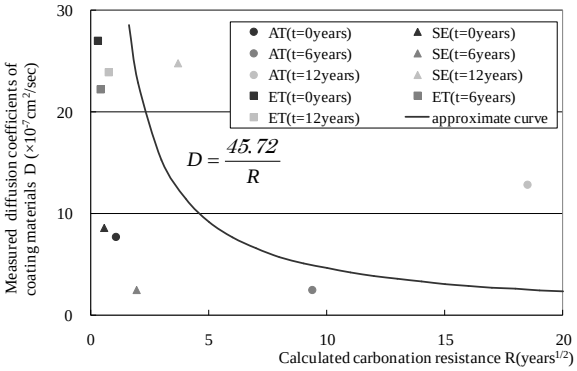

Figure 5. Relationship between calculated and measured diffusion coefficients of coating materials.

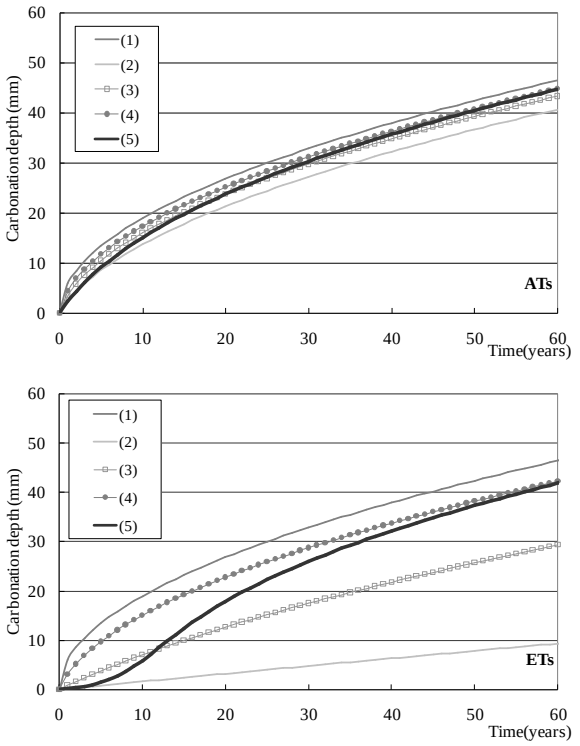

(1) $A\sqrt{t}$ non-finished

(2) $A\left(\sqrt{t+R_0^2}-R_0\right)$ R_0: initial carbonation resistance

(3) $A\left(\sqrt{t+R_6^2}-R_6\right)$ R_6: carbonation resistance at 6 years

(4) $A\left(\sqrt{t+R_{12}^2}-R_{12}\right)$ R_{12}: carbonation resistance at 12 years

(5) $A\left(\sqrt{t+R_i^2+\frac{2}{A}\left\{\left(R_i-R_{i-1}\right)X_i+\left(R_{i-1}-R_{i-2}\right)X_{i-1}+\cdots+\left(R_1-R_0\right)X_1\right\}}-R_i\right)$

Figure 6. Progress of carbonation.

coincide with the curves assuming deterioration periods of 6 and 12 years at ages of around 12 and 60 years, respectively.

4 CONCLUSIONS

The results of this study are summarized as follows:

(1) When the effect of a finishing material in suppressing carbonation of concrete is expressed by Eq. (2) using carbonation resistance, *R*, the carbonation of concrete progresses following Eq. (12) on the assumption that the carbonation resistance of the finishing material is gradually deteriorated over time and that the transfer of CO_2 follows approximate steady diffusion.

(2) The carbonation of concrete coated with a finishing material proceeds with the gradual deterioration of the finishing material, initially following the progress of the case with a sound

finishing material, but the carbonation curve then approaches the curve with a deteriorated finishing material, and finally converges with the carbonation curve of exposed concrete.

REFERENCES

Japan Institute of Consturction Engineering 1986, 'Durability improvement technology of Reinforced Concrete buildings', Gihodoshuppan, pp.279-282.

Architectural Institute of Japan 2004, 'Recommendations for Durability Design and Construction Practice of Reinforced Concrete (Draft)', pp97-107 .

Hasegawa Takuya, Senbu Osamu, Baba akio & Watanabe Tsugumichi 2002, '**A** study on the carbonation protection effects of surface finishing materials using a model building at the age of eleven years', Journal of structural and construction engineering. Transactions of AIJ (555), pp.37-43.

Baba Akio & Senbu Osamu 1987, 'Prediction model of carbonation depth in concrete with srface layeres', Summaries of technical papers of JCI annual convention, Vol.9, No.1, pp.333-338.

Kono Masanori, Masuda Yoshihiro, Okihashi Takanori & Nakamura Yusuke 2008, 'Study on the prediction of carbonation progress of concrete consideringthe aging of coating materials for textured finishes on diffusion theory', Cement Science and Concrete Technology No. 63, pp.318-325.

Kono Masanori, Masuda Yoshihiro,Ochiai Ryota & Karasawa Tomoyuki 2004, 'Study on the carbonation suppressive effects of concrete considering the aging of coating materials for textured finishes', Journal of structural and construction engineering. Transactions of AIJ (584), pp.15-21.

XII DBMC
International Conference on Durability of Building Materials and Components
PORTO - PORTUGAL, April 12th-15th, 2011

Watertightness of Masonry Walls: An Overview

Nathan Van Den Bossche [1]
Michael Lacasse [2]
Arnold Janssens [3]

ABSTRACT

Masonry walls are commonly used in a range of different climates and there has emerged over the years a consensus amongst building practitioners that, if correctly installed and adequately maintained, masonry walls clearly achieve adequate long-term performance. Two key features of masonry walls contribute in providing acceptable performance by mitigating the effects of wind-driven rain: the evident capacity of the exterior masonry to absorb and store rainfall; an open cavity behind the exterior masonry cladding to drain infiltrated water. Recent European trends in respect to energy conservation have building practitioners considering applying spray-in-place insulation to fill the open cavity in walls. As well, there is an emerging interest in low energy wood frame construction for moderate climates such as those of North-western Europe. Such construction would incorporate brick veneer cladding with reduced space behind the cladding. Knowing the degree of water infiltration of brick masonry walls might help provide a useful estimate of moisture loads behind the cladding and hence improve HAM-simulations of these new concepts. Extensive research has been carried out over the years to assess the performance of masonry walls systems with regards to watertightness. This paper offers an overview of research on water infiltration through brick masonry walls. Assessment protocols and test methods are discussed and where possible test data amongst the different methods compared.

KEYWORDS

Watertightness, Masonry, Test protocols, HAM-simulations

[1] Department of Architecture and Urban Planning, Faculty of Engineering, Ghent University , Ghent, BELGIUM, nathan.vandenbossche@ugent.be
[2] Institute for Research in Construction, National Research Council Canada, Ottawa, CANADA, michael.lacasse@nrc-cnrc.gc.ca
[3] Department of Architecture and Urban Planning, Faculty of Engineering, Ghent University , Ghent, BELGIUM, arnold.janssens@ugent.be

1 INTRODUCTION

Since the beginning of the 20th century, masonry walls were increasingly constructed as a two layer system. The cavity that separates the inner and outer masonry leaf provides significantly better watertightness and thermal performance as compared to single leaf systems. Since the Second World War, it has been common to fill the cavity to improve thermal performance, however, it is eivdent this may also introduce additional risk concerning water management in the wall. Over the preceding two decades less research has been published on the watertightness of brick masonry walls. However, due to the recent evolution in numerical simulation software to model the hygrothermal behaviour of materials, building components and whole buildings, there is a renewed interest in the watertightness of masonry walls. Furthermore, since cavities between brick wythes are increasingly being completely filled with insulation, the drying response of a wall may be significantly altered, and as well, the effects of solar driven moisture on the hygrothermal response should also be considered. Other drying effects can cause increased salt efflorescence from the brick and a higher risk to deterioration due to frost action. Salonvaraa and Karagiozis [1998] have likewise demonstrated that rain penetration in masonry brick walls due to wind driven rain has a significant effect on their hygrothermal behaviour; they helped demonstrate that recent advances in hygrothermal simulation software and its application to resolving moisture management issues offers an interesting approach to the development of new or enhanced construction methods. Although there has been very promising research on water transport in (cracked) porous materials [Roels et al., 2006], most hygrothermal models can not accurately simulate water infiltration due to wind driven rain [Janssen et al., 2006]. Hence, these models typically assume that 1% of the wind driven rain deposited on the wall will infiltrate behind the cladding and perhaps into the assembly [ASHRAE 160-2009]. For example, simulations by Künzel et al. [2010] on EIFS systems were used to determine that the annual average water content of a clay brick structure can be doubled by incorporating 1% rain water infiltration into the wall assembly. This indicates that the effect of water infiltration can be significant and thereby dominate the hygrothermal behaviour of the wall assembly. Consequently, to obtain a useful understanding of the hygrothermal response of wall systems a correct estimation of the water ingress into walls is necessary. In this paper, a review of test standards is first provided since the relation of the standardized test conditions with actual weathering conditions must be made explicit in order to allow a reliable performance assessment. Thereafter, a broader review of literature on the results of watertightness testing of masonry using both standard methods and in-situ evaluations is offered.

2 TEST STANDARDS

To the knowledge of the authors, there is only one standard that describes an experimental test method to assess the water penetration through masonry walls, namely ASTM E 514-09 "Standard Test Method for Water penetration and Leakage through Masonry". A few other test methods are described by Chew [2001], but are not widely used and typically only qualitative in nature. The basis for the ASTM E 514-09 test standard was developed by Fishburn [1938], and he explicitly stated that the test conditions were more severe than natural exposures. The ASTM E514 standard provides extensive details concerning the test setup. The samples should be representative of current construction practice, and after fabrication the samples should be stored for 7 days in an impervious plastic wrap, and then cured for at least 7 days at lab conditions. e.g., Research undertaken by the Portland Cement Association [1992] showed lower water infiltration if walls were cured in humid conditions. The applied water spray rate is 138L/h-m², and if no pressure difference is specified the specimen should be tested at 500Pa pressure difference (water supply and pressure difference are to be maintained for at least 4 hours). Note that the standard specifies that at least three test samples should be tested, but no publications have been found where this rule was applied.

The standard does not provide an absolute criterion, but specifies which aspects should be recorded during testing, namely: the area of dampness on the back of the wall, time of appearance of dampness and first visible water, and the amount of water collected during the total test period. The validity of the boundary conditions for the E514-09 test method was discussed by Monk [1982]. Based on U.S. Weather Service rainfall intensity maps for 25, 50 and 100 recurrence years, it was concluded that the

rainfall intensity could be well above the test value of 138L/h-m² for 15-minute rain events (for 5-minute rain events values up to 250L/h-m² were recorded), whereas it is typically lower for longer averaging periods: below 100L/h-m² for 30-minute values and below 76 L/h-m² for hourly values. Consequently, the applied spray rate is unrealistically high compared to reality for all locations in the U.S. It is noted that the effect of the spray rate is negligible once the entire exterior surface of the porous wall cladding is saturated and covered with a thin film of water; however, no relation is made to the depth of the thin water film in terms of spray rate intensity. In respect to test pressures at which specimens are subjected, ASTM C1601-10 provides a formula to relate wind speeds to wind pressure: $P_0 = \rho v^2/2$. Where P_0: air pressure [Pa], v: wind speed [m/s] and ρ: mass density [kg/m³]. This is simply the wind velocity pressure and consequently, a 500Pa pressure difference across the specimen corresponds to a wind speed of 28.5m/s. Monk [1982] reports that this wind speed does occur according to U.S. Weather Service wind speed maps for 25, 50 and 100 recurrence years, but only for short durations, and "whether winds of this intensity occur simultaneously with the suggested rainfall intensity is difficult to say". A comprehensive methodology to determine boundary conditions for watertightness testing was offered by Cornick and Lacasse [2009]. According to this analysis, the test conditions in the E514 standard can only occur at specific locations, and corresponds to very low probabilities (e.g. a return period of about 400 years for Miami).

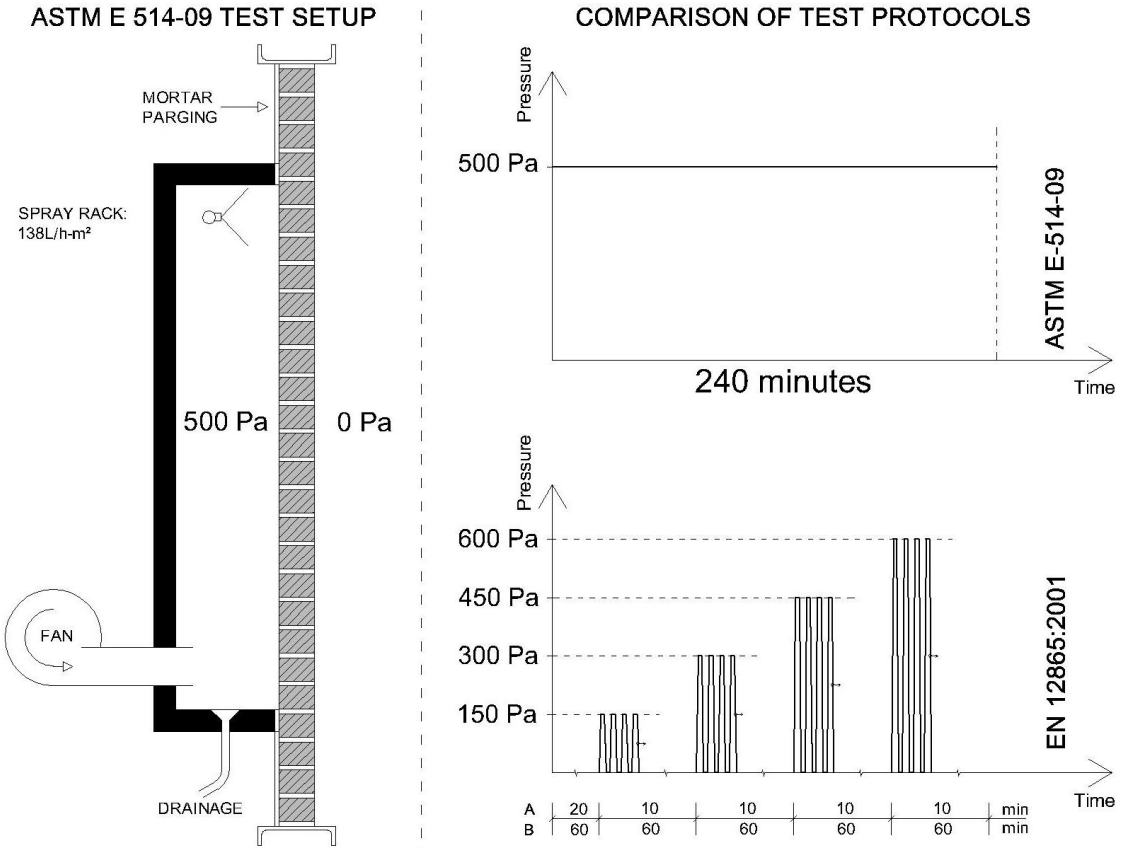

Figure 1. *E514-09 test setup and comparison of E514-09 and EN 12865:2001 test protocol.*

The European standard EN 12865:2001 describes a test protocol to determine the resistance of external wall systems to driving rain under pulsating air pressure. According to this standard, water is prayed at two locations: 72l/h-m at the top as run-off, and 90L/h-m² on the whole area to simulate direct wind driven rain. The pressure difference is applied in a step-wise approach to determine at which level water entry occurs. Furthermore, the standard offers two procedures: one for qualitative testing (A - steps of 10 minutes after 20 minutes of initial wetting), and quantitative testing (B - steps of 60 minutes). Contrary to the ASTM E514-09 test, the pressure difference is not a constant value, but is applied in a pulses with a cycle of 15 seconds: going from 0Pa up to the maximum pressure level is that step (see figure 1). Unfortunately, no papers have been found with published results using these test protocols. The standard does not relate explicitly to realistic boundary conditions or return

periods, and does not offer information on the interpretation of the results. This test standard is very similar to standards that have been published in Europe, US and Japan to test window frames.

3 LITERATURE REVIEW

Table 1 provides an overview of the infiltration rates of single-wythe masonry brick walls as obtained from literature. A short description of the relevant test parameters and protocols is summarized in sections 3.1 and 3.2. Based on these results, a number of conclusions can be drawn. First of all, infiltration through mortared masonry brick walls at 500Pa pressure difference covers a wide range, from 0% up to about 20% of the applied water spray rate, with 2 median values well below 1%, and 3 reported values well above 1%. At lower pressure differences, the median infiltration was 1.3% (0Pa) and 0.223% (25Pa). Secondly, very high infiltration rates were found for mortared concrete brick walls, with a median value of 31.7% [Brown, 1982]. Finally, very high infiltration rates are reported for glued masonry brick veneer walls (up to 64.34%), with a median value of 47.04% [Hens et al., 2004].

Table 1. Infiltration rates for single-wythe brick walls expressed as percentage of applied spray rate.

Reference	Pressure difference	Spray rate	Number of walls	Type of walls	min. and max. infiltration	median infiltration
	[Pa]	[L/m²-h]	[-]	[-]	[%]	[%]
ASTM C1715- 2010	0	138	X	X*	X	1.2
ASTM C1715- 2010	500	138	X	X*	X	3.3
Chiovitti - 1999	500	138	6	MMBW	3.4 – 8.0	X
Brown - 1982	479	140	6	MMBW	0.04 – 0.18	0.06
Brown - 1982	479	140	6	MCBW	20.4 – 52.3	31.7
Ghosh et al. - 1991	500	138	8	MMBW	< 0.005	< 0.005
Rathbone - 1982	500	150	22	MMBW	0 – 19.6	1.16
Hens et al. - 2004	25	40	9	MMBW	0.0065 – 6.0	0.223
Lacasse et al. - 2003	0 - 400	51 - 204	4	MMBW	0.47 – 1.23	0.83
Hens et al. – 2004	8.5	3.8-6.4	8	GMBW	0.0007 – 64	47.04

X: not specified; X*: not specified, but MMBW can reasonably be assumed; MMBW: mortared masonry brick wall; MCBW: mortared concrete brick wall; GMBW: glued masonry brick wall

3.1 Mortared masonry brick walls

ASTM standard C1715-10 provides a test procedure for the water leakage performance of masonry wall drainage systems, and offers details on historical data according to E514 and C1601: a median penetration rate of 4.5L/h-m² is reported at 500Pa (3.3% of the applied 138L/h-m² water spray rate), and 1.7L/h-m² without pressure difference (1.2% of water spray rate). Chiovitti et al., [1999] tested 6 masonry walls, of which 5 were treated with water repellents. Initial tests on the walls prior to installation of the water repellent showed a range of water leakage rates: the water infiltration ranged from 5.176 to 12.265 L/h-m² (3.4% up to 8% of the applied water spray rate). By applying water repellents, the water penetration was initially reduced between 44 and 99%, although additional tests showed that the effect decreased significantly over time.

Brown [1982] tested 12 walls to analyze the effect of coatings, with a pressure difference of 479Pa and water spray rate of 140L/m²-h throughout 72h. Six uncoated single wythe brick masonry walls showed peak infiltration rates after 120 up to 420 minutes (240 minutes on average), whereas all six concrete brick walls showed peak infiltration rates within 20 minutes. Three walls were constructed with masonry cement mortar, and showed significantly lower peak infiltration rates compared to the walls constructed with Portland cement-line mortar, although this effect is less clear for longer averaging periods. Conversely, concrete brick walls showed higher infiltration rates with Portland cement-line mortar. Average infiltration rates ranged from 0.05L/h (0.04%) to 0.246L/h (0.18%) for the masonry brick walls (median: 0.06%), and from 28.5L/h (20.4%) to 73.2L/h (52.3%) for the concrete brick walls (median: 31.7%). Note that the ASTM E514 dating back from 1972 did require a test period of

72h, which was only changed to 4h in the 1986 version of the standard. Furthermore, Grimm – author of several papers and literature reviews on masonry performance – made recommendations for masonry construction types as a function of the driving rain index as indication of the actual rain load [Grimm, 1982], but does not relate this to the ASTM E514 test method. ASTM standard C1601-10 (field test of watertightness of brick walls) offers a method to shorten the E514 test procedure, based on a paper by Galitz and Whitlock [1999]. However, the formulas presented by Galitz and Whitlock [1999] are perhaps speculative, given that no validation is reported and none of the references provided in this paper help confirm the formulas or the underlying assumptions in the theory.

Ghosh and Melander [1991] tested 8 walls at 0 and 500Pa pressure difference, with both continuous as intermittent spraying (half hourly intervals). It was demonstrated that intermittent spraying results in infiltration rates about 3 times lower for the test without pressure difference, and 6 times lower for the tests with pressure difference. Consequently, this underlines the sensitivity of the results to the test method, particularly regarding the spraying protocol. Note that all walls leaked less than 0.005% of the applied water spray rate. Furthermore, depending on the sorptivity (range 0.3 up to 3 $mm/min^{1/2}$) masonry brick walls can absorb quite a volume of water before runoff occurs. It has been shown that for a sorptivity of $3mm/min^{1/2}$ and a moderate spray rate of 5L/h, the wall will become saturated after 13h of spraying, whereas it would take only 8 minutes if the sorptivity were $0.3mm/min^{1/2}$ [Hall and Kalimeris, 1982]. A high sorptivity allows rapid moisture transport by which the surface layer does not become quickly saturated. For high rainfall intensities however, such as the typical spray rates in test standards, the surface becomes saturated in a few minutes (i.e. < 15min). These calculations omit the effect of local deficiencies. Cracks are the primary source of water infiltration, but also increase the volume of water that can be stored in a short period of time before runoff occurs.

Rathbone [1982] reported water infiltration rates for 31 wall panels, for varying pressure differences (0 to 600Pa with 100Pa increments) and water spray rates (2, 3, 4, 5 and 6 $L/h/m^2$). These tests showed that nearly all walls leaked without pressure difference. For 9 panels, very high leakage rates were reported (41 - 95% of the applied water spray rate) but this can be attributed to the specific brick types. For the other 22 wall panels, the infiltration ranged from 0% to 19.6%, with a median value of 1.16%. The water infiltration was not very sensitive to changes in water spray rate above a threshold of about $60L/h\text{-}m^2$ (contradicting the theory by Galitz and Whitlock). The pressure difference has a more significant effect, as the infiltration rate steadily increased with increasing pressure loads. Furthermore, it was reported that the performance ranking of the 31 wall panels could likewise be achieved through the use of either the water infiltration or air leakage tests, although the extent of the differences in performance between panels was dependent upon the test type.

Lacasse et al. [2003] conducted watertightness tests on four masonry wall assemblies to determine the gross amounts of water leakage to the cavity behind the masonry veneer cladding and as well, provide estimates of water entry through deficiencies at windows, ventilation ducts and electrical outlets located in the wall assembly. Tests were conducted at spray rates of 51, 102 and 204 $L/h\text{-}m^2$ and at pressures ranging between 0 and 400 Pa over a 50 minute period; the average pressure applied across the assembly during the 50 minute test sequence was 185 Pa. For those walls having water collected behind the cladding, the range of values obtained for the rate of water collection in relation to the degree of water deposition on the wall were the following: 0.50 to 1.23% at 51 $L/h\text{-}m^2$; 0.78 to 1.18 at 102 $L/h\text{-}m^2$; 0.47 to 0.80% at 204 $L/h\text{-}m^2$. Dynamic tests were reported and yielded results that showed less water entry at given mean pressures as compared to those obtained for testing under static loads.

3.2 Glued masonry brick walls

Hens et al. [2004] compared water leakage though mortared brick veneer walls and glued brick veneer walls. Glued brick veneer walls typically have open head joints, which may facilitate higher water infiltration into the cavity. The mortared walls were tested with 0 and 25Pa pressure difference and a water deposition rate of $40L/m^2\text{-}h$, whereas the glued veneer walls were subjected to a pressure difference of 0 and 8.5Pa and a water spray rate between $3.8L/m^2\text{-}h$ and $6.4L/m^2\text{-}h$ (because a higher leakage rate was expected). The test period was between 4 and 6 hours. The infiltration rate for the

mortared brick veneer wall ranged from 0.0065% to 5.97%, with a median value of 0.223% (based on results with and without pressure difference). The effect of the pressure difference on the leakage rate was not significant, but the leakage did correlate with the air permeability of the walls. The tests on the glued veneer walls with open head joint showed much larger quantities of water infiltration: between 0.0007% and 64.36% (median value: 47.04%) of the water that was sprayed at top of the wall. Field tests were also conducted in which 5 masonry walls of 2.8m high by 1.8m wide were subjected to realistic exterior conditions (length of test period is not reported). Remarkably, these results contradict the lab results: the field test showed higher infiltration rates for the mortared brick veneer walls. First of all, the field test allowed pressure equalisation in the cavity due to an airtight inner wall, lowering the driving forces on the runoff water. The glued veneer with open head joint allowed rapid local pressure equalisation, whereas the mortared joints only allowed an average relief with local pressure differences due to pressure gradients acting on the outer leaf. However, the conclusion from these laboratory tests that suggest glued brick veneer walls are more susceptible to water entry is in fact confirmed from the findings of a major European brick manufacturer that most of the watertightness problems around the window-wall interface are found in buildings with glued brick veneer walls [Meuleman, 2010].

4 DISCUSSION

It is important to stress that all results were obtained during several hours of testing. During the tests extremely high water spray rates were applied on the walls. Although these conditions may occur in reality, very high rainfall intensities and high wind speeds will not often happen simultaneously. Cornick and Lacasse [2009] analyzed wind speeds and rainfall intensities in 5 US cities, and the maximum hourly wind pressure with a 20 year return period never exceeded 500Pa. The maximum wind driven rain on a building facade (with the same return period) was below 60L/h-m² for 4 out 5 locations, but reached 206L/h-m² at one location. This indicates that the combination of 138L/h-m² and 500Pa – the test conditions in ASTM E514 – are very extreme and the combination will probably never occur at most locations throughout a full hour. The literature review showed that the highest infiltration rates were only reached after a few hours of testing, and depending on the sorptivity of the brick wall and the wind driven rain on the facade, it can take between minutes and over 10 hours before the exterior brick face is saturated and runoff occurs. On the other hand, a masonry brick wall when subjected to outdoor weather conditions and relative humidities that might occur during winter in some European locations can remain very wet for long periods of time due to low solar radiation and high relative humidities. Furthermore, the ASTM E514-09 standard requires a constant pressure difference, whereas the European EN 12865 standard describes pulsating pressure difference to test the performance. Note that the European standard is generic, as it was not specifically designed to test masonry walls. Next to that, Lacasse et al. [2003] found lower infiltration rates during cyclical testing.

The amount of water infiltrating the cavity will in particular depend on the wetting and drying spells, essentially the succession of rain showers during windy conditions that wet the cladding surface interspersed with periods where drying occurs. It will also depend on the boundary conditions (temperature, relative humidity, solar irradiation), and the hygric properties of the wall components. The only paper that reports measured values of walls subjected to actual weather conditions in a field test [Hens et al., 2004], shows 18 rain events with a wind driven rain intensity above 1kg of water/m²-day (the test period is not specified). Of those 18 events, the infiltration rate was below 1% for 14 cases, and between 1% and 3.4% for the remaining events. These results are significantly higher than the reported values from laboratory test, but are only based on a limited number of walls for a restricted period of time.

The MEWS project [Kumaran, 2000] offers an interesting approach to convert infiltration data into a practical tool. The hygrothermal response of four different types of walls (i.e. brick masonry, stucco, EIFS and hardboard siding) to simulated wind driven rain conditions was achieved through laboratory watertightness testing of full-scale wall assemblies. Consequently, water entry functions were developed for each wall type that provided an estimate of water entry to the interior of the wall assembly. This information was thereafter modelled as a moisture source placed at a specific location in the wall so that the consequences of water infiltration into the wall assembly could then be determined.

5 CONCLUSIONS

The current test methods are somewhat incomplete, because no relation is made with actual weather conditions. Although ASTM E514 explicitly states that the results should only be used for comparison, it is not certain that comparison based on the extreme boundary conditions would be representative of actual performance in the field. Several authors have reported that the current test period of 4 hours is too short to obtain steady state conditions that would then allow a useful comparison between different wall assemblies, but neither do these test methods relate to actual weather conditions. Future laboratory tests should focus on different combinations that affect water infiltration, taking into account alternative wetting and drying effects for realistic conditions. The European standard EN 12865 prescribes cyclical pressure pulses, but no published results have been found for brick walls, and the relation with actual weather conditions is unclear.

Water infiltration into brick cavity walls can have a significant effect on the hygrothermal response of the assembly and its long-term performance. Advanced simulation models should include the effect of wind driven rain on building facades, but currently use a simplified method to account for water leakage. ASHRAE guideline 160-2009 assumes that 1% of the wind driven rain infiltrates into the wall. The literature review of laboratory results has shown that the actual infiltration in walls having an exterior brick veneer covers a wide range of values for infiltration (between 0% and 20%, median values between 0% and 5%) whereas the results of some confined field tests have shown infiltration rates between 0% and 3.4%. Consequently, assuming 1% of infiltration of brick masonry veneer walls appears to be a reasonable estimate of infiltration rates. Based on the literature review, three recommendations can be made for future research:

(1) When conducting hygrothermal simulations, the sensitivity of the results to water infiltration should always be verified, with infiltration rates between 0% and 10% for brick veneer walls. (2) These limits can only be confined by means of experiments with brick veneer walls subjected to realistic boundary conditions over longer periods of time. (3) The simplified approach – applying a percentage of the wind driven rain directly into the construction - can be omitted by incorporating advanced models that simulate water transport through fractured porous media.

However, the type of data required for hygrothermal simulations will depend on the goal of the study. Some studies target average performance (e.g. for energy use calculations, efflorescence, and some aspects of durability) whereas other simulations are focused on risk analysis during extreme events (e.g. condensation, durability). The analysis of average hygrothermal behaviour should use infiltration rates at low pressure differences. The literature reports values between 0.0065% and 5.97%, with median values of 0.223% and 1.3% for single wythe mortared masonry brick walls.

REFERENCES

ASHRAE 160-2009. Criteria for moisture-control design analysis in buildings. American Society of Heating, Refrigerating and Air-Conditioning Engineers, Atlanta, US.

C1601 – 10, 2010. Standard test method for field determination of water penetration of masonry wall surfaces. American Society for Testing and Materials, Philadelphia, US.

C1715 – 10, 2010. Standard test method for evaluation of water leakage performance of masonry wall drainage systems. American Society for Testing and Materials, Philadelphia, US.

Chew M.Y.L., 2001. A modified on-site water chamber tester for masonry walls. Construction and Building Materials 15: 329-337.

Chiovitti D., Gonçalves M., Renzullo A., 1999. Performance evaluation of water repellents for above grade masonry. *Durability of Building Materials and Components* 8: 561-570. Institute for Research in Construction, Ottawa, Canada.

Cornick S.M., Lacasse M.A., 2009. An investigation of climate loads on building facades for selected locations in the US. *Journal of ASTM International*, 6, No 2: 1-17.

E514/E514M – 09, 2009 Standard test method for water penetration and leakage through masonry. American Society for Testing and Materials, Philadelphia, US.

EN 12865:2001. Hygrothermal performance of building components and building elements – determination of the resistance of external wall systems to driving rain under pulsating air pressure. CEN Brussels.

Fishburn C.C., Watstein D., Parsons D.E., 1938. Water permeability of masonry walls. Building *Materials and Structures Report*, BMS 7; Report IRN 13094555. Washington, US.

Galitz C.L., Whitlock A.R., 1999. Simulating design storms with water chamber testing. *Water problems in building exterior walls: evaluation, prevention, and repair, Third Volume*. ASTM STP1352. American Society for Testing and Materials, Philadelphia, US.

Ghosh S.K., Melander M., 1991. *Air content of mortar and water penetration of masonry walls*. Masonry Information, Portland Cement Association.

Grimm C.T., 1982. A driving rain index for masonry walls. *Masonry: materials, properties, and performance.* ASTM STP 778: 171-177. American Society for Testing and Materials, Philadelphia, US.

Hall C., Kalimeris A.N., 1982. Water movement in porous building materials – V. Absorption and shedding of rain by building surfaces. *Building and Environment*, Vol. 17, No 4: 257-262.

Hens H., Roels S., Desadeleer W., 2004. Rain leakage through brick veneer walls, built with concrete blocks. CIB W40 Meeting, 31 August – 3rd September 2004, Glasgow, UK. International Council for research and innovation in building and construction.

Janssen H., Blocken B., Carmeliet J., 2006. Conservative modelling of the moisture and heat transfer in building components under atmospheric excitation. *Intl. J. of Heat and Mass Transf.* 50: 1128-1140.

Künzel H.M., Zirkelbach D., Radon J., 2010. Hygrothermal consequences of rainwater leaks investigated for different wall structures with exterior insulation. Proceedings: 209-213. Central European Symposium on Building Physics, 13-15 September, 2010, Cracow, Poland.

Kumaran, M.K.; Mukhopadhyaya, P.; Cornick, S.M.; Lacasse, M.A.; Rousseau, M.Z.; Maref, W.; Nofal, M.; Quirt, J.D.; Dalgliesh, W.A. (2003), An Integrated methodology to develop moisture management strategies for exterior wall systems, 9th Canadian Conference on Building Science and Technology (Vancouver, B.C. 2003-02-27), pp. 45-62.

Lacasse, M.A.; O'Connor, T.; Nunes, S.C.; Beaulieu, P., 2003. Report from Task 6 of MEWS Project : Experimental Assessment of Water Penetration and Entry into Wood-Frame Wall Specimens - Final Report , Research Report, Vol. 133, NRC Institute for Research in Construction, Ottawa, Canada

Meuleman R., 2010. Internal communication with a major European brick manufacturer.

Monk C.B., 1982. Adaptations and additions to ASTM test method E514 (water permeance of masonry) for field conditions. *Masonry: materials, properties, and performance.* ASTM STP 778: 237-244. American Society for Testing and Materials, Philadelphia, US.

Portland Cement Association, 1992. *Water Penetration Tests of Masonry Walls*. IS219.03M. Masonry Information, 02/1992. Illinois, USA.

Rathbone A.J., 1982. *Rain and air penetration performance of concrete blockwork*. Technical report 553. Cement and Concrete Association.

Roels S., Moonen P., De Proft K., Carmeliet J., 2006. A coupled discrete-continuum approach to simulate moisture effects on damage processes in porous materials. *Computer methods in applied mechanics and engineering*. Vol. 195: 7139-7153.

Salonvaara M.H., Karagiozis A.N., 1998. The influence of waterproof coating on the hygrothermal performance of a brick façade wall system. *Water leakage through building facades*. ASTM STP 1314. American Society for Testing and Materials, Philadelphia, US.

XII DBMC
International Conference on Durability of Building Materials and Components
PORTO - PORTUGAL, April 12th-15th, 2011

Hygric Performance of Different Interior Insulation Systems: an Experimental Comparison

Evy Vereecken [1]
Staf Roels [2]

ABSTRACT

This article compares the hygric performance of single leaf wall assemblies provided with different interior insulation systems. To do so, small test walls are placed in a hot box – cold box. At regular time steps, the moisture distribution within the components is investigated using the X-ray projection method and the total moisture increase in the walls is measured. Special attention is paid to the difference between capillary active insulation systems, which have the capacity to redistribute liquid moisture, and the more standard non capillary active insulation systems.

KEYWORDS

Interior insulation, Hygrothermal performance, Interstitial condensation, X-ray radiography, Capillary active insulation.

[1] Division of Building Physics, Catholic University of Leuven (KUL), Leuven, BELGIUM, evy.vereecken@bwk.kuleuven.be
[2] Division of Building Physics, Catholic University of Leuven (KUL), Leuven, BELGIUM, staf.roels@bwk.kuleuven.be

1 INTRODUCTION

Rising energy prices, limited energy sources and increasing climate and environmental changes, have placed energy issues centre stage world-wide. A large potential to decrease our energy use, can be found in the building sector. After all, in a lot of countries the largest part of the existing building stock is built before the first energy crises and hence often bad or hardly insulated. Increasing the thermal performance of single leaf masonry walls – the common construction method for exterior walls in several European countries until the Second World War – can be achieved by adding exterior or interior insulation. The latter forms the most risk full technique due to potential thermal bridges, the risk of interstitial condensation, frost damage, mould, etc. [Straube & Schumacher 2007; WTA 6-4]. Though, in cases of historical buildings with worth-preserving façades [Häupl et al. 2003; Grunewald et al. 2006] or buildings in the urban environment restricted to a strict road building line, interior insulation is often the only possible solution to improve the thermal resistance [Hens 1998].
Interior insulation changes the hygrothermal behaviour of the wall significantly. During the heating season, the temperature in the masonry wall will be strongly reduced. When the temperature at the interface between masonry wall and insulation drops below the dew point and the insulation system is vapour open, interstitial condensation can occur. To avoid this, often vapour tight insulation, like XPS or cellular glass or a vapour open system in combination with a vapour retarder, is recommended. Though, by using these systems, a drying out of the masonry wall towards the inside is excluded. Consequently, especially when the wall is exposed to wind-driven rain, a moisture increase in the masonry wall will be obtained. To overcome this problem, nowadays some innovative systems, e.g. the use of a smart vapour retarder [Künzel 1999] or hydrophilic mineral wool [Pavlik & Cerny 2009] or capillary active insulation systems, are suggested. The latter system enables, due to capillary forces, moisture redistribution. Consequently, according to e.g. Scheffler & Grunewald [2003] the risk on interstitial condensation can be reduced in cases of a good contact between masonry wall and insulation system. Besides, since the system is vapour open, drying out of the masonry wall remains possible.

In this paper, the hygric performance of different interior insulation systems exposed to a winter condition is compared. To do so, small test walls are placed in a hot box – cold box. Approximately every three weeks, walls are taken out of the box to investigate the moisture distribution in the walls, using X-ray tomography [Roels and Carmeliet 2006]. In addition, the walls were weighted to follow up the total moisture increase. In a first section of this paper, the investigated wall assemblies and the hot box – cold box setup will be shown. The next section reiterates the main principles of the X-ray projection method. After this, the measurement results will be shown and main conclusions will be drawn.

2 EXPERIMENTAL SETUP

2.1 Test walls

The hygrothermal performance of different wall assemblies with interior insulation was studied based on an experiment on small test walls of 30 cm high and 3 cm thick (Figure 1a), where the latter dimension was choosen to enable an investigation of the moisture distribution using the X-ray projection method. To obtain 1D vapour transport, plexiglass was glued at all sides except the inner and outer surface. Between the different material layers, temperature (T-) and relative humidity (RH-) sensors were placed at approximately one third height of the test wall to keep the middle and upper part free for the X-ray measurements. Since contact between materials can be of crucial importance when looking at moisture transport [de Freitas 1996; Scheffler & Grunewald 2003], an air space between the materials at the middle and the upper part of the walls is avoided by embedding the sensors in a narrow groove in the insulation (Figure 1b, c and d). The composition of the different test walls can be found in Table 1. To obtain a good contact between (capillary active) insulation and masonry wall, glue mortar was used. An exception to this can be found in case of wall G, which makes an investigation of the effect of the glue mortar possible. Test wall L is constructed as a wall

with exterior insulation. This to compare the vapour resistance of the masonry wall obtained by a cup test at brick and mortar separately with the resistance determined using the method described in [Hens 2006]. However, latter measurement is out of the scope of this article.

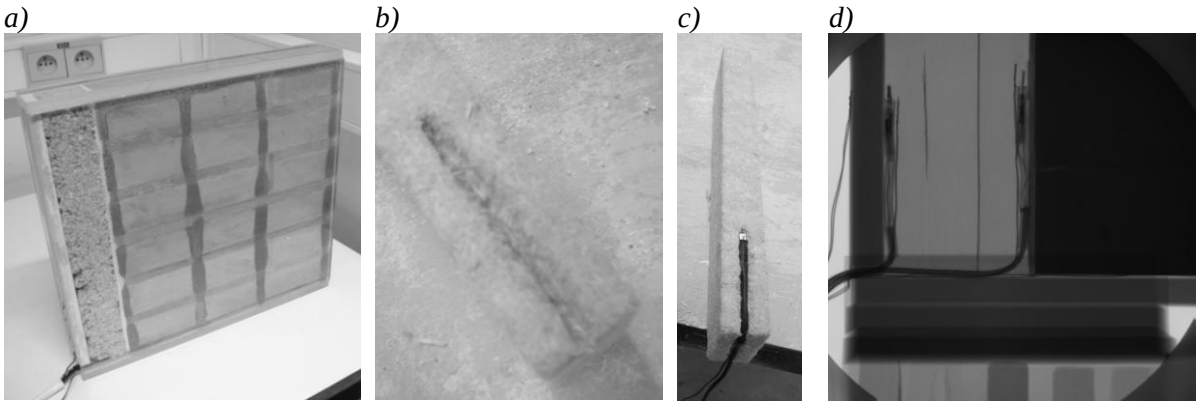

Figure 1. a) One of the test walls, b, c, d) RH- and T-sensors are embedded in the material.

Table 1. Overview of the different test wall compositions. The insulation thickness was 5 cm, except for Foamglas and Pavadentro (6 cm).

A	OUTSIDE	Masonry wall (+/- 29 cm)	Glue mortar			Gypsum board (1.25 cm)	INSIDE
B			Mineral wool				
C			Mineral wool		Vapour retarder		
D			Glue mortar	XPS			
E			Glue mortar	Foamglas			
F			Glue mortar	Multipor			
G			Multipor				
H			Glue mortar	Calcium silicate			
I			Glue mortar	Pavadentro (EP 1 900 884 A1)			
J			Glue mortar	Cellulose			
K			Glue mortar	Cellulose	Vapour retarder		
L		Plexiglass	Calcium silicate		Mineral wool	Masonry wall	

2.2 Hot box - cold box

The different test walls were placed in a hot box – cold box (Figure 2). Saturated salt solutions were used to control the relative humidity. The relative humidity in the hot box (Figure 3c) and cold box (Figure 3a) was respectively +/- 85% (KCl) and +/- 45% ($Mg(NO_3)_2.6H_2O$ and $MgCl_2.6H_2O$). In the cold box a temperature of +/- 2°C was implemented, using a cooling unit. In the hot box, infrared bulbs were used to obtain a temperature of 35°C. Obviously, these conditions do not confirm with realistic boundary conditions, but were choosen to obtain at a short time spam a clearly detectable increase in moisture content using the X-ray projection method. Between hot box and cold box a connecting part was fixed (Figure 3b), in which the test walls were positioned with the gypsum board and the brick towards the hot box and cold box respectively. To obtain 1D heat transport, XPS insulation was placed between the different test walls. Air leaks, and consequently heat and vapour leaks, were minimized by taping all the edges between test walls, XPS-insulation boards and connecting part.

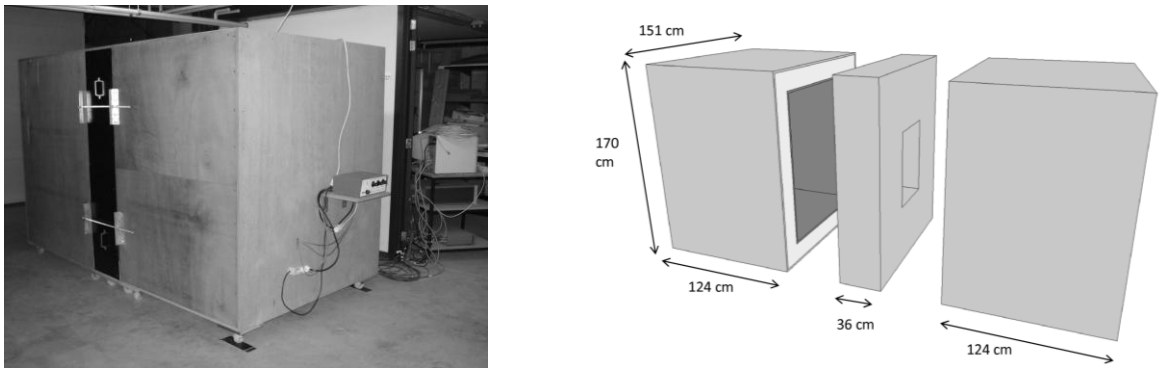

Figure 2. Real view and shematic view of the hot box – cold box.

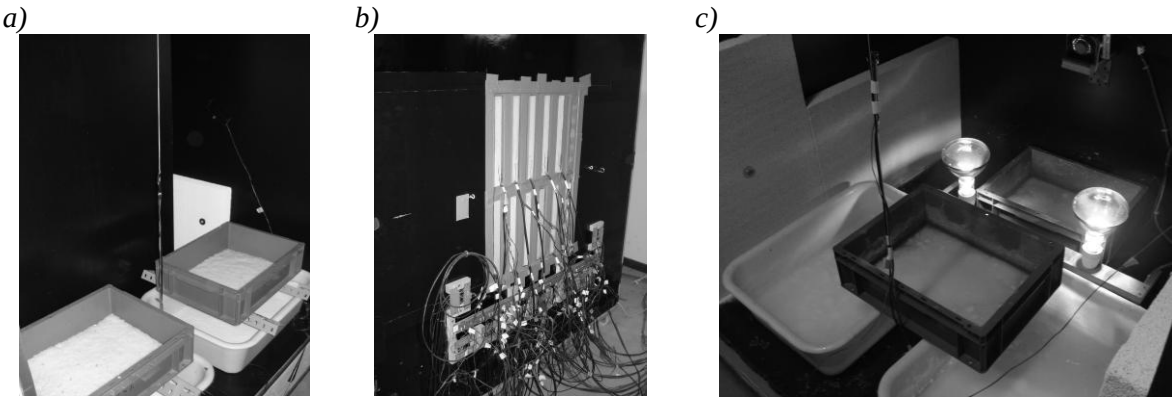

Figure 3. a) Cold box, b) connecting part with the different test walls, c) hot box.

3 X-RAY PROJECTION METHOD

3.1 Methodology

X-ray radiography is a technique, evolved from medical science, which enables a non-destructive analysis of the inside of materials. Roels and Carmeliet [2006] showed the X-ray projection as an accurate technique to measure the moisture content in materials. In this paragraph, the crucial elements of the technique are reitterated.

The X-ray projection method is based on the attenuation of materials. When X-ray beams are sent through a material, the beams will be attenuated according to Beer's law:

$$\frac{I}{I_0} = \exp\left(-\mu d\right) \tag{1}$$

with I_0 and I respectively the incident and attenuated intensity and μ (-) and d (m) respectively the attenuation coefficient and the thickness of the material. Using Eq.(1), the attenuated intensity through a dry (I_{dry}) and a wet (I_{wet}) sample can be respectively given by:

$$I_{dry} = I_0 \exp\left(-\mu d\right) \tag{2}$$

$$I_{wet} = I_0 \exp\left(-\mu d - \mu_w d_w\right) \tag{3}$$

with μ_w (-) and d_w (m) respectively the attenuation coefficient and the thickness of a fictitious water layer in agreement with the moisture content in the material. The moisture content w (kg/m³) is given by:

$$w = \frac{\rho_w V_w}{V} = \frac{\rho_w d_w}{d} \tag{4}$$

with V (m³) the volume of the sample, V_w (m³) the volume of the water and ρ_w the density of water (1000 kg/m³). Using Eq.(2) and (4), Eq.(3) can be rewritten as:

$$I_{wet} = I_{dry}.\exp\left(-\frac{\mu_w w d}{\rho_w}\right) \tag{5}$$

which can in his turn be rewritten as:

$$w = -\frac{\rho_w}{\mu_w d}\ln\left(\frac{I_{wet}}{I_{dry}}\right) \tag{6}$$

$$= -\frac{\rho_w}{\mu_w d}\left(\ln\left(I_{wet}\right) - \ln\left(I_{dry}\right)\right)$$

Consequently, Eq.(6) shows that the moisture content distribution in a sample can be determined based on the X-ray projection of a reference (dry) sample and the examined (wet) sample.

3.2 X-ray projection of the test walls

Before starting the hot box – cold box experiment, X-ray projections of the test walls were made to determine the reference images or I_{dry}-values. After the start of the measurement, X-ray images were made approximately every three weeks. The measurements were performed on an AEA Microfocus CT. A shematic view of the setup can be found in Figure 4a. The used X-ray energy was 85 keV. The detector was a CCD 12-bit camera (4096 intensity levels). The intensity levels were visualized as grayscales. To reduce noise, the average of 256 frames, made at a speed of 25 frames/s, was used. A dummy-construction (Figure 4b) was used to charge the time instability of the X-ray source (Figure 4c). This construction was stored in an oven between the different X-ray measurement times, so the moisture content of the different dummy's could be assumed identical during the different measurements. By use of a correction function (Figure 4d) the different images could be scaled. To visualize a whole test wall separated images were made and afterwards combined. An example of a combined image is shown in Figure 4e.

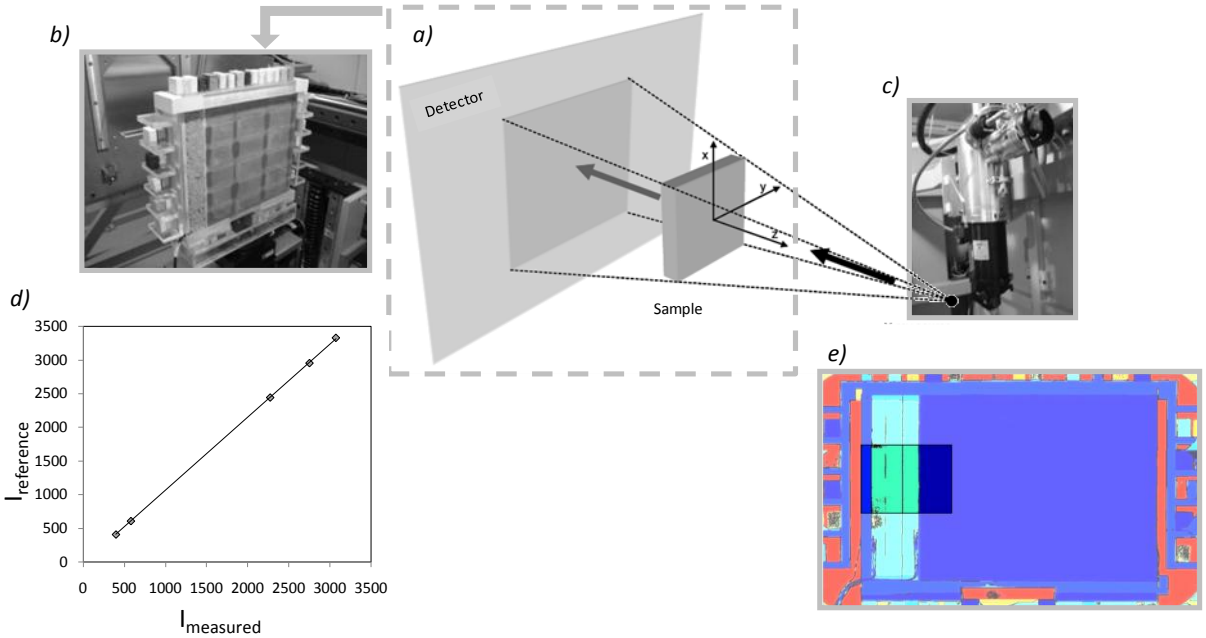

Figure 4. a) Schematic view of the X-ray measurement setup, b) a test wall with dummy-construction is placed before the X-ray screen, c) X-ray source, d) example of a correction function, e) X-ray view of a total test wall with dummy-construction. The dark coloured rectangle indicates the investigated part of the walls shown in Figure 5.

4 RESULTS

4.1 Moisture distribution

Figure 5 shows the moisture content profiles, obtained by use of the X-ray projection method, for wall A, B, F, H, I and J (for the composition see Table 1). The figures show only a part of the total test wall (seeFigure 4e). From left to right gypsum board, insulation (except in case A) and a part of the masonry wall can be observed. In cases of wall A, F, H, I and J a glue mortar was used to stick the insulation material or the gypsum board to the masonry wall. The moisture content of this mortar glue highly increased. The horizontal board in the part of the masonry wall is a mortar joint, showing a higher moisture accumulation than found in the bricks. Figure 5a shows an important moisture increase in the gypsum board of the uninsulated wall, due to a lower surface temperature. In cases of the wall with mineral wool (b), the moisture content in the mineral wool stays negligible and no moisture content profiles are found. In the Multipor insulation (c), a small increase in moisture content nearby the glue mortar is observed. However, this increase could be partially due to the presence of some Multipor pores filled with glue mortar. A more clear increase in moisture level is found in the calcium silicate (d), Pavadentro (e) and cellulose (f). The Pavadentro exists out of three layers of 2 cm wood fibre board. The two wood fibre layers towards the inside are glued to each other and are separated from the third layer by a vapour barrier, which is called the functional layer. The moisture content at the functional layer has been increased and the moisture is partly redistributed towards the room side. The wood fibre board at the right of the functional layer shows some moisture content profiles at the side of the mortar glue. In cases of the four capillary active systems (c, d, e, f) the moisture at the interface between brick and insulation is captured by the glue mortar. However,

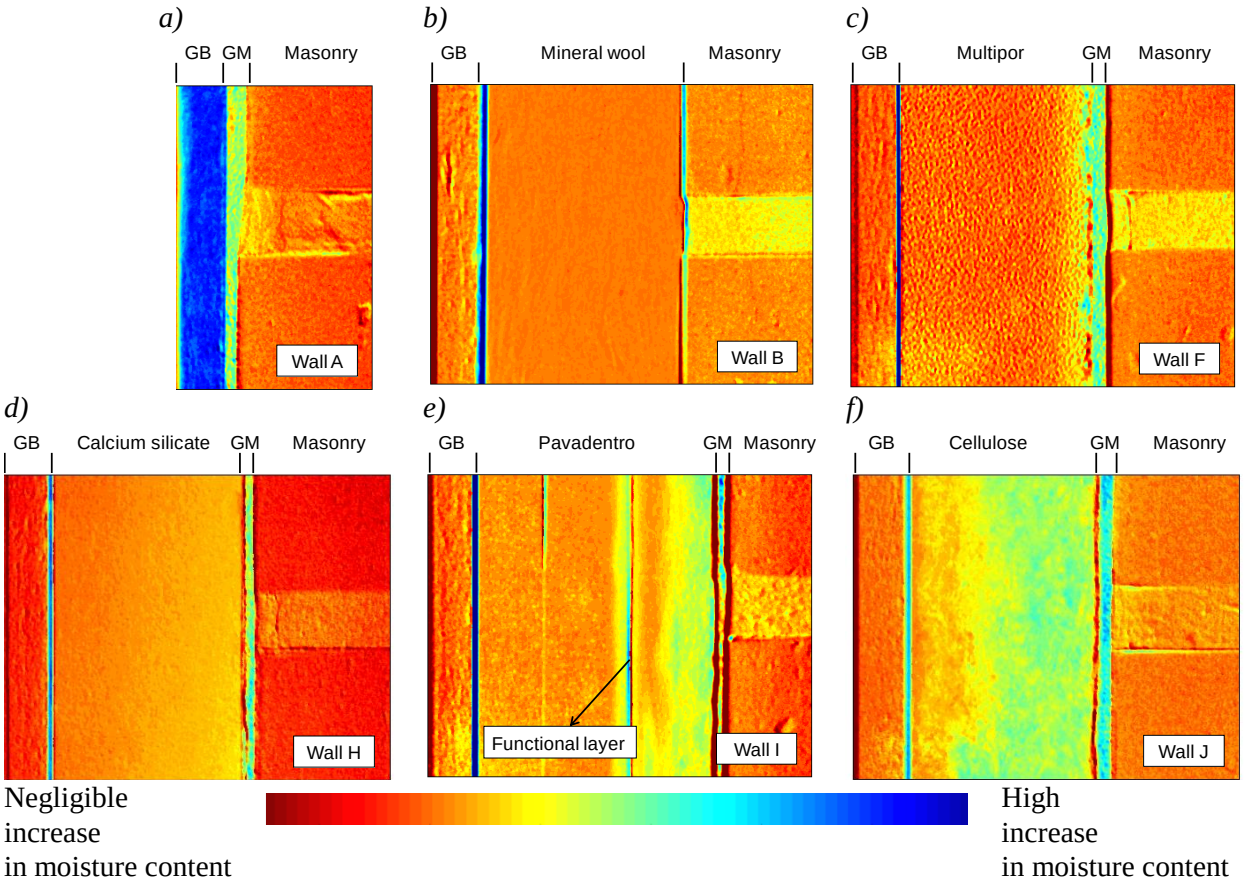

Figure 5. X-ray views of the moisture content in the wall assemblies (see Table 1 for the different test wall compositions) after six weeks in the hot box – cold box. At the figure gypsum board (GB) – insulation – glue mortar (GM) and masonry wall are plotted.

these preliminary results indicate also a possible redistribution towards the masonry wall. A correct match of the material properties (especially liquid permeability) of the glue mortar and insulation will be of crucial importance to obtain a secure insulation system. Note also that in some cases at the interfaces (e.g. between insulation and gypsum board) an unexpected line indicating an apparent increase or decrease in moisture content can be found. This can be due to a small shifting of the wet image compared to the dry image caused by an expansion of the materials during the experiment.

4.2 Weight increase

Each time the box was opened for the X-ray measurements, the test walls were weighted. The measured moisture increase in the entire wall is plotted in Figure 6a. As can be seen, a subdivision based on the different systems can be made. The weight increase of the wall without insulation (×) and the wall with the vapour open, non capillary active mineral wool (□) is the highest. A lower moisture increase can be found in cases of the capillary active systems (◊). However, the moiture increase of these systems is higher than the moisture increase found for the vapour tight systems (o) (XPS, Foamglas, systems with a smart vapour retarder). Note also that at the beginning of the experiment, hygric buffering can play a major role. At the end of the measurement, the different material layers were seperately weighted. The moisture content of the different glue mortar layers at the end of the measurement is given in Figure 6b. As can be seen, the moisture content of the glue mortar in cases of the walls with a capillary active insulation system is higher than in cases of the vapour tight systems. Both results gives a first indication of the need of a more in depth study of the behaviour of capillary active systems.

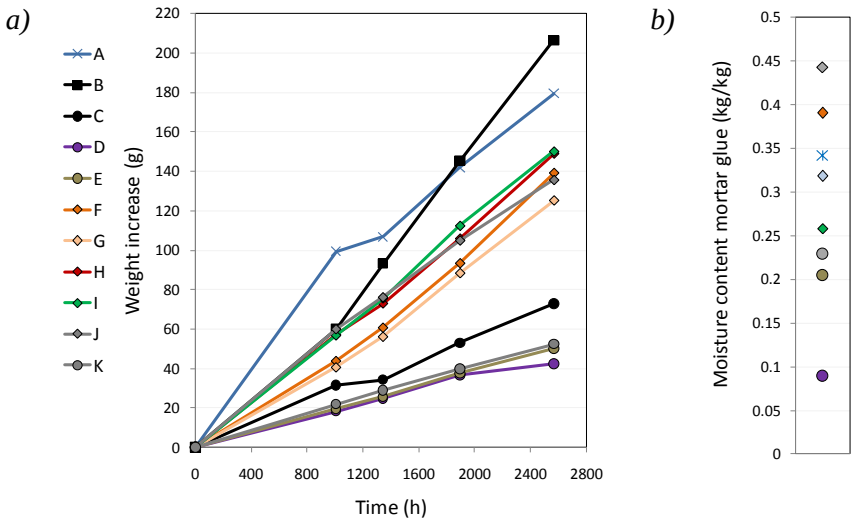

Figure 6. a) Total weight increase of the different walls, b) moisture content of the glue mortar at the and of the experiment (see Table 1 for the different test wall compositions).

5 CONCLUSIONS

Although interior insulation forms the most risky insulation technique, in a lot of cases it offers the only possibility to increase the thermal resistance of existing walls. In this article, the phenomena of interstitial condensation occuring in these composed wall systems has been investigated based on a hot box – cold box experiment. The moisture distribution was analysed using the X-ray projection method, which is shown to be a useful technique to investigate the working principle of insulation systems. In cases of the capillary active systems, moisture content profiles in the insulation were found. The glue mortar, which was used to stick the insulation to the masonry wall, was found to become wet. In this study the moisture distribution is investigated qualitatively. However, also a

quantitative analysis is possible, as described in 3.1. Furthermore, the weight increase of the walls with a capillary active insulation system is found to be lower than in cases of a vapour open non capillary active system or the wall without insulation. However, a larger moisture increase of the entire wall and the glue mortar was obtained compared to the vapour tight insulation systems. Latter results indicate the need of a more in depth study of the behaviour of capillary active insulation systems. In a further study the X-ray results will be combined with the temperature and relative humidity course obtained by the sensors.

ACKNOWLEDGMENTS

The results in this paper have been partially obtained within IWT 3E90050 'Global performance approach and economic analysis of interior insulation with regard to renovation projects' funded by the Flemish Government and KUL OT/09/23 'Towards a reliable application of interior insulation for the retrofit of existing buildings' funded by the K.U.Leuven. These financial supports are gratefully acknowledged. The measurements with the X-ray radiography equipment were performed at the Department of Metallurgy and Materials Engineering of the K.U.Leuven. We would like to thank Prof.dr.ir. M. Wevers and her co-workers for the fruitful collaboration.

REFERENCES

EP 1 900 884 A1 Europäische petentanmeldung, Holzweichfaserplatte für die raumseitige Dämmung, 19.03.2008 Patentblatt 2008/12.

de Freitas, V.P., Abrantes, V., Craussen, P. 1996, 'Moisture migration in Building Walls – analysis of the interface phenomena', *Building and Environment,* 31, 99-108.

Grunewald, J., Ruisinger, U., Häupl, H. 2006, 'The Rijksmuseum Amsterdam – hygrothermal analysis and dimensioning of thermal insulation', in *Research in Building Physics and Building Engineering,* eds. Fazio, Ge, Rao, Desmarais, Taylor & Francis group, Londen, pp. 345-352.

Häupl, P., Jurk, K., Petzold, H. 2003, 'Inside thermal insulation for historical facades', in *Research in Building Physics,* eds. Carmeliet, Hens, Vermeir, Lisse: A.A. Balkema Publishers, pp. 463-469.

Hens, H. 1998, 'Performance predictions for masonry walls with inside insulation using calculation procedures and laboratory testing', *Journal of Thermal Envelope and Building Science,* 22, 32-48.

Hens, H. 2006, 'The vapour diffusion resistance and air permeance of masonry and roofing systems', *Building and Environment*, 41, 745-755.

Künzel, H., 1999, 'Flexible vapour control solves moisture problems of building assemblies – Smart retarder to replace the conventional PE-film', *Journal of Building Physics*, 23, 95-102.

Pavlik, Z., Cerny, R. 2009, 'Hygrothermal performance study of an innovative interior thermal insulation system', *Applied Thermal Engineering,* 29, 1941-1946.

Roels, S. & Carmeliet, J. 2006, 'Analysis of moisture flow in porous materials using microfocus X-ray radiography', *International Journal of Heat and Mass Transfer*, 49, 4762-4772.

Straube, J., Schumacher, C. 2007, 'Interior insulation retrofits of load-bearing masonry walls in cold climates'. Building Science Digest 114.

Scheffler, G. & Grunewald, J. 2003, 'Material development and optimisation supported by numerical simulation for a capillary-active inside insulation material', in *Research in Building Physics*, eds. Carmeliet, Hens, Vermeir, Lisse: A.A. Balkema Publishers, pp. 463-469.

WTA Merkblatt 6-4 Ausgabe 05.2009/D. Innendämmung nach WTA I. Fraunhofer IRB Verslag 2009.

XII DBMC
International Conference on Durability of Building Materials and Components
PORTO - PORTUGAL, April 12th-15th, 2011

Thermal Diffusion of Water Vapour in Porous Materials: a Critical Review

Hans Janssen[1]

ABSTRACT

The reliable evaluation of moisture transfer in porous materials is essential in many engineering applications, also in building science. One key aspect is a correct description of moisture flow phenomena and their transport potentials. While several issues can be debated in that respect, thermal diffusion – vapour diffusion in response to temperature gradients – currently stands out due contradicting findings on the topic. Several studies corroborate that vapour pressure is the only significant transport potential for water vapour diffusion, while other investigations suggest that temperature gradients may similarly yield notable water vapour diffusion.

This paper resolves that contradiction. A critical analysis of the investigations supporting the occurrence of thermal diffusion reveals that all are flawed. A correct reinterpretation of the measurements allows concluding that no consistent nor significant thermal diffusion can be noted. This brings these investigations in line with their original opponents. This observation also agrees with the thermodynamics, confirming the actual existence of thermal diffusion, but also indicating is negligible magnitude. It can in conclusion be stated that thermal diffusion is of no importance for building science applications, leaving vapour pressure as the only significant transport potential for diffusion of water vapour.

KEYWORDS

Vapour diffusion, Fick's law, Soret effect, Thermal diffusion, Vapour pressure.

[1] Department of Civil Engineering, Technical University of Denmark, Kgs. Lyngby, DENMARK, haj@byg.dtu.dk

1 INTRODUCTION

Reliable assessment of moisture transfer in porous materials is crucial to arrive at sustainable, durable, healthy and comfortable buildings. A central aspect therein is the correct description of moisture flow phenomena and their transport potentials. While many issues can be discussed in that respect, thermal diffusion – diffusion of water vapour in response to temperature gradients – currently stands out due to contradicting findings on the matter.

Most research on 'thermal diffusion in porous materials' is experimental and all studies apply the same measurement concept. The vapour diffusion flow through a material layer under combined gradients of vapour pressure and temperature is measured, and compared to the respective isothermal diffusion flow. Some studies [Kumaran 1987, Dahl *et al*. 1996, Galbraith *et al*. 1998, Stephenson 2003, Peuhkuri *et al*. 2008] note substantial thermal diffusion. These thermal diffusion proponents thus maintain that both vapour pressure and temperature are significant transport potentials for vapour diffusion:

$$j_v = -\delta_p \nabla p_v - \delta_T \nabla T = j_p + j_T \tag{1}$$

where j [kg/m^2·s] is the diffusion flow, δ_p [kg/m·s·Pa] is the permeability for vapour pressure gradients, δ_T [kg/m·s· K] is the permeability for temperature gradients, and subscripts $_{v/p/T}$ indicate the total/standard/thermal diffusion flows. Typically, the deduced thermal permeabilities δ_T are positive – indicating thermal diffusion from high to low temperature – and one to two orders of magnitude higher than their standard counterparts δ_p. Other studies [Galbraith *et al*. 1998, Thomas 1999, Glass 2007, Baker 2009] however use similar principles and conditions but find no consistent nor significant thermal diffusion evidence. These thermal diffusion opponents hence assert that vapour pressure is the sole significant transport potential for diffusion.

While vapour diffusion is of course surpassed in magnitude by capillary transport of liquid, or advective transport of vapour, it still forms a notable moisture transfer mechanism. Water vapour diffusion is essential in the assessment of moisture buffering by interior enclosures, evaporative cooling of roofs or interstitial condensation in building parts. And in these, the (non)occurrence of thermal vapour diffusion may have a substantial impact, as illustrated by a simple interstitial condensation example. The construction consists of 3 layers: 200 mm ceramic brick (1.00 W/m·K & $1.3 \cdot 10^{-11}$ kg/m·s·Pa), 100 mm mineral wool (0.04 W/m·K & $1.6 \cdot 10^{-10}$ kg/m·s·Pa) and 10 mm gypsum board (0.20 W/m·K & $33 \cdot 10^{-11}$ kg/m·s·Pa) (exterior to interior; values between the brackets are thermal conductivity & standard permeability). The exterior and interior conditions are -10 °C & 200 Pa and 20 °C & 1200 Pa, with exterior and interior surface resistances respectively 0.04 m^2·K/W & $6.7 \cdot 10^6$ m^2·s·Pa/kg and 0.13 m^2·K/W & $5.0 \cdot 10^7$ m^2·s·Pa/kg.

First, the vapour pressure profile and the vapour diffusion flows are quantified with standard diffusion only, thus solely driven by vapour pressure gradients. Results can be found in Table 1. A condensation plane exists in the brick-insulation interface, with a resulting condensation flow of 75.6 g/m^{2}day. In a second quantification, the thermal permeability for each material is assumed equal to 30 times its standard permeability, an average value derived from the 'thermal diffusion proponent' studies. Such inclusion of thermal vapour diffusion dramatically increases the condensation flow in the brick-insulation interface to 149.1 g/m^{2}day, roughly doubling the original result.

Table 1. Vapour pressure profiles and vapour condensation flows with(out) thermal diffusion.

	temperature (°C)	vapour pressure (Pa) $\delta_T = 0$	vapour pressure (Pa) $\delta_T = 30 \cdot \delta_p$
exterior environment	-10.00	200.0	200.0
interf. exterior - brick	-9.62	200.1	188.8
interf. brick - min. wool	-7.75	339.7	339.7
interf. min. wool - gypsum	18.31	883.8	628.4
interf. gypsum - interior	18.78	1155.8	1149.6
interior environment	20.00	1200.0	1200.0
		$j_{condens}$ (g/m^2·day)	$j_{condens}$ (g/m^2·day)
		75.6	149.1

The application example above clearly illustrates that a correct assessment of thermal diffusion is required to reliably evaluate moisture transfer in porous materials and all related durability issues. This paper hence aims at reconciling the currently contradictory findings.

2 SIGNIFICANT THERMAL DIFFUSION ?

While various studies find no consistent nor significant evidence of thermal diffusion, other studies do present such evidence, even while applying the same measurement principles and conditions. Below however the flaws in each of those are demonstrated, and corrected where possible. It will then become clear that their initial support of thermal diffusion no longer holds.

2.1 Kumaran 1987

2.1.1 Authors' measurements

Kumaran used a heat flow apparatus to indirectly measure vapour diffusion in glass fibre insulation. A sample was wetted at one surface and sealed in a plastic wrap. With the sample's wet side on the warm plate, the liquid evaporates and diffuses to the cold plate, where it condenses again. Measurements of sensible and latent heat flows during and after evaporation allow determination of the vapour flow.
In the most cited publication, Kumaran [1987] measures on glass fibre with a thickness of 8.55 cm and a density of 17 kg/m^3, with temperature differences ranging from 28 K to 39 K, and on glass fibre with a thickness of 5.47 cm and a density of 30 kg/m^3, with temperature differences from 21 K to 39 K.

Linear regression of the obtained vapour flows with the imposed vapour pressure differences yielded a positive non-zero intercept, an indication of a diffusion flow not attributable to vapour pressure gradients. These observations led the author to conclude that 'even in the absence of a vapour pressure gradient, moisture transfer may exist. A driving force other than vapour pressure is also responsible for the moisture transport. The obvious choice for the second potential in the present experimental investigation is the temperature.' An alternative linear regression, applying vapour pressure and temperature as transport potentials finally gave the thermal permeabilities δ_T. These were positive, a sign of diffusion from high to low temperature, and in magnitude 17 and 36 times bigger than their δ_p (for the 17 kg/m^3 and 30 kg/m^3 glass fibre respectively).

2.2.2 Additional analysis

The analysis discussed above is the first in a series of heat flow experiments on wet glass fibre insulation [Kumaran & Mitalas 1987; Hokoi & Kumaran 1993; Kumaran 1994]. In these, measurements on glass fibre samples with various thicknesses (2.5 to 15.4 cm) and densities (45 to 117 kg/m^3) are reported. Figure 1 presents the results from the in total 17 measurement series, showing the vapour flow in function of the vapour pressure difference. The convention in this paper is that vapour flows are taken positive if flowing from the warm environment to the cold environment. For the figure, each measurement has been recalculated to a sample with unit thickness. Additionally, linear regressions are given.

The positive δ_T's as reported by Kumaran [1987] are essentially based on a positive intercept at a 0 Pa vapour pressure difference. In Fig. 1 it can be noted that the signs of the intercepts are not consistent: positive and negative values of similar magnitudes are obtained.

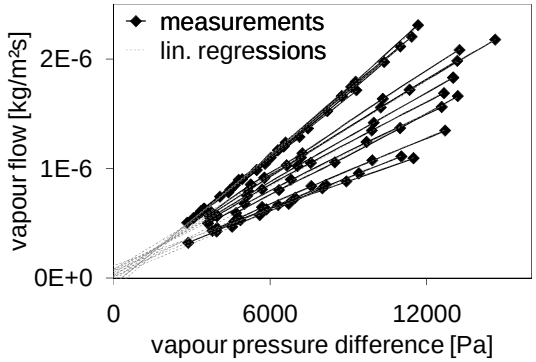

Figure 1. Overview of measured vapour flows and their linear regressions for all of Kumaran's measurements. Their 0 Pa intercepts are not consistent in sign and can thus not be an indication of thermal vapour diffusion.

This implies that the earlier positive conclusion on the occurrence of thermal diffusion [Kumaran 1987] is not generally valid, and probably a mere consequence of the restricted accuracy of the measurement technique. It seems that such also recognised by the author, as the last publication [Kumaran 1994] no longer refers to "thermal diffusion": the whole vapour diffusion flow is instead accepted to result from vapour pressure differences only. Conclusively it has to be stated here that the analysis by Stephenson [2003], using data from [Kumaran 1987], is thus similarly disproved.

2.2 Galbraith *et al.* 1998

2.2.1 Authors' measurements

Galbraith et al. performed non-isothermal vapour diffusion measurements on two materials: 19.5 mm plasterboard and 25 mm polystyrene insulation. They used the common cup set-up with the humidity regulator in the cup and the cup placed in a climate chamber. A temperature gradient was imposed by use of a heater mat, heating up the top surface of the samples (via radiation and convection). Applied temperature differences ranged from 5 °C to 20 °C.

Measurements at different temperature gradients allowed the authors to determine a relation between the vapour flow and the temperature gradient (see Fig. 2, excluding the 'expected isothermal flows'). They observed 'a direct relationship between the measured total moisture flux and the imposed temperature gradient', and deduced that 'measurable thermal diffusion does exist for both materials.' They derived positive values for δ_T, about 30 and 55 times bigger in magnitude than their δp (for the plasterboard and insulation respectively).

2.2.2 Additional analysis

Figure 2 portrays the measured diffusion flows and the imposed temperature gradients, but confronts those with the expected isothermal flows. It is clear that these isothermal flows totally disturb the earlier link of diffusion flow and temperature gradient. A consistent relation between vapour diffusion and temperature gradient can no longer be detected, and the authors' support for thermal diffusion can hence not be maintained. Unfortunately no clear explanation for the observed behaviour can be given.

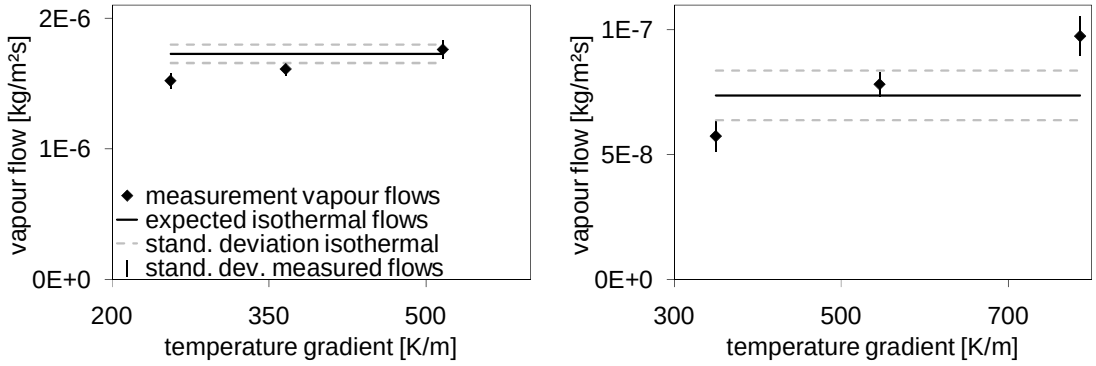

Figure 2. Measured non-isothermal and expected isothermal vapour diffusion flows, and the respective standard deviations, for plasterboard (left) and polystyrene insulation (right).

2.3 Peukhuri *et al*. 2008

2.3.1 Authors' measurements

Peuhkuri *et al*. measured on six materials: five insulation materials (glass fibre, mineral fibre, cellulose, flax, perlite) and cellular concrete. A built-to-purpose set-up was used: the Megacup is essentially a small climate chamber with a large-size sample forming its horizontal top. A normal climate chamber imposed the other set of conditions. The Megacup was usually held at 12-13 °C, while the climate chamber was at 17-21 °C. A number of different vapour pressures were imposed, yielding 4 to 9 measurement sets for each material.

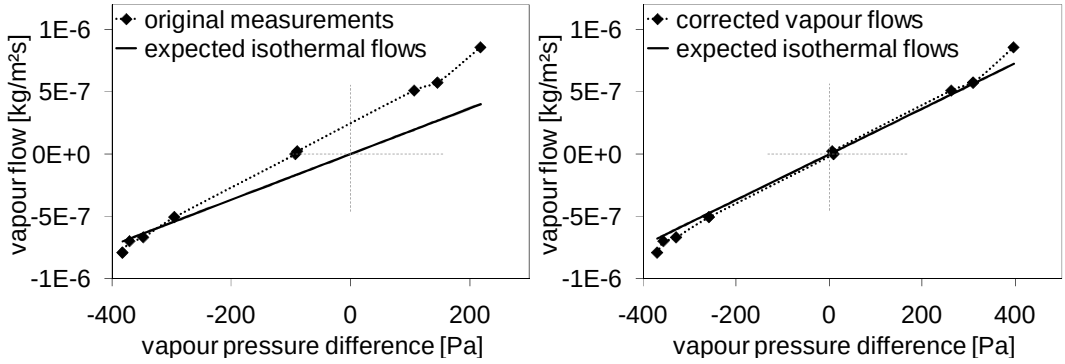

Figure 3. Measured non-isothermal and expected isothermal vapour diffusion flows (left) and corrected non-isothermal and expected isothermal vapour diffusion flows (right) for glass fibre insulation.

The measured sets of vapour pressure difference and vapour diffusion flow demonstrated positive non-zero intercepts at 0 Pa vapour pressure difference. Positive should be understood in view of the reference scheme used in this paper: flows and differences are positive if from the warm to the cold chamber. This led the authors to infer that 'there must exist other transport mechanisms than the water vapour pressure-driven one alone', and that 'the temperature gradient itself is driving the moisture from the warm towards the cold side.'

The measured flows were approximated with a moisture transfer model taking vapour pressure, temperature and capillary pressure as transport potentials. The measured moisture flows were thus considered combinations of liquid and vapour, the latter driven by gradients in vapour pressure and temperature. This modelling allowed determination of thermal vapour permeabilities δ_T: these were primarily positive (except for perlite insulation), and in magnitude about 5 to 50 times bigger than their δ_p. It should be noted however that significant liquid transport had to be included to reliably approximate all moisture flow measurements.

2.3.2 Additional analysis

Liquid transfer

Such inclusion of liquid transport is the Achilles heel of the entire analysis. Since measurements took place with RH's from 40 % to 90 %, a liquid flow contribution is plausible: at higher humidities liquid islands may form in the pores and facilitate moisture transfer by 'liquid transfer shortcuts'. When considering vapour diffusion, this is usually accounted for by a rise in vapour permeability with relative humidity. However, Table 4 in [Peukhuri *et al.* 2008] states that the vapour permeabilities applied in the approximation are already wet-cup values, measured between 50 % and 93 % RH, and consequently representative for the applied measurement range. Such wet-cup values already comprise the liquid moisture transfer facilitation. Moreover, the used wet-cup values coincide with the dry-cup values, except for the cellular concrete (permeabilities are given in Appendix A of [Peukhuri 2003]). For the five insulation materials, the equality of the dry-cup and the wet-cup values implies that the facilitation by liquid islands must be negligible. This does imply of course that liquid transports can not be called upon for explaining purposes.

RH sensor flaws

The measurement results on glass fibre insulation are shown in Figure 3, complemented with expected isothermal flows. The measured and expected flows obviously disagree, and the measured 'vapour flow - vapour pressure difference' relations do moreover not go through the origin. Both observations are attributed to thermal diffusion by the authors. It is also evident however that the deviation between measured and expected flows is not even: the largest deviation is found for the positive pressure differences (high RH in megacup, low RH in room), whereas the deviations at negative pressure differences (intermediate RH in megacup, intermediate RH in room) appear to fade out. With liquid transport ruled out above, it would be likely that thermal diffusion gives a constant deviation between the measured and expected flows.

Such observation focuses the attention on the RH-sensors that were used to determine the conditions at both surfaces of the specimen. The 'negative flow' measurements have similar RH levels in the Megacup and in the chamber. A systematic deviation in the RH sensors would affect both sides similarly, with a small global effect on the vapour pressure difference. The 'positive flow' measurements on the other hand have high RH in the Megacup and low RH in the chamber. A progressive RH error would strongly influence the vapour pressure difference and consequently the final analysis. Figures 6.9 and 6.10 in [Peukhuri 2003] are partially reproduced in Figure 4: they imply that the RH sensors are not very accurate. In a comparison with dew-point sensors, the deviations were fairly large:

- *low RH*: Figure 4 (right) shows that the dew-point sensors yield 49-54%, while the RH sensors give roughly 49%: a probable underestimation with 2.5% (in absolute RH terms).
- *high RH*: Figure 4 (left) shows that the dew-point sensors give 91%, while the RH sensors give roughly 84%, Figure 4 (right) shows 87-91% for the dew-point sensors and 72-75% for the RH-sensors: a probable underestimation with 7% and 15% respectively. Here 10% is accepted as representative value.

This evidently represents a progressive error: small at small RH's, larger at larger RH's; such progressive relation is quite common. To correct the reported RH-values, the deviations of 2.5% at 49% RH and of 10% at 74% RH are linearly related:

$$RH_{act} = RH_{mea} + 2.5 + 7.5\left(\frac{RH_{mea} - 49}{74 - 49}\right) \qquad (2)$$

where $RH_{mea/act}$ is the measured/actual (corrected) RH [%]. Correction of the measured RH's via Eq. (2) transforms the dependence between vapour pressure differences and vapour diffusion flows (Fig. 3, right). The corrected curve for glass fibre insulation now virtually coincides with the expected isothermal curve, hence nullifying all thermal diffusion. This observation is also valid for the other materials involved. While all the original results show positive intercepts and slopes higher than expected from wet-cup permeabilities, the corrected results reveal both positive and negative intercepts and slopes in far better agreement with the wet-cup permeabilities. The corrected results do however no longer support the authors' positive conclusion on the occurrence of thermal diffusion.

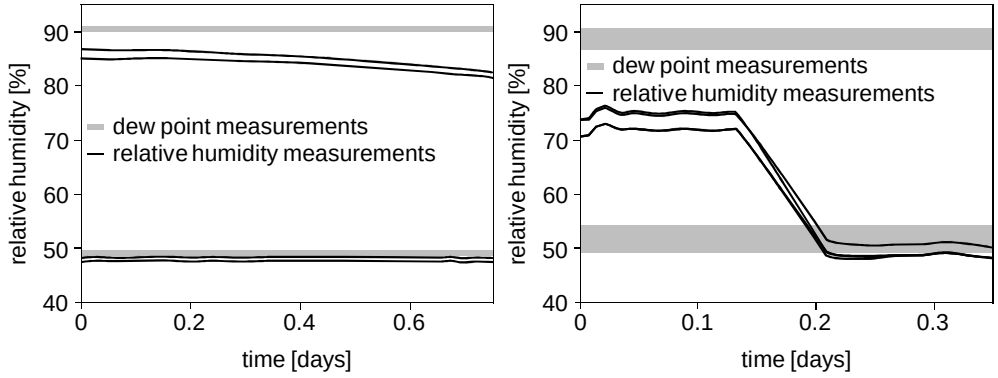

Figure 4. Comparison of relative humidity sensor measurements with dew point sensor measurements, reproduced from [Peukhuri 2003].

3 DISCUSSION

The studies reanalysed in the previous paragraph originally supported thermal diffusion, by observing consistent and significant deviations from isothermal diffusion. All of them were shown to be flawed though. The positive '0 Pa' intercept in [Kumaran 1987] was shown to not be generally present. The perceived relation between vapour diffusion flows and temperature gradients in [Galbraith *et al*. 1998] was virtually annulled by introducing the expected isothermal flows. All deviation between measured and expected flows in [Peuhkuri *et al*. 2008] disappeared by correcting the measured RH. The results of [Dahl *et al*. 1996] have not been explicitly analysed here, but can similarly be shown to be invalid.

Reinterpretation of their results brought them in line with other studies [Galbraith *et al*. 1998, Thomas 1999, Glass 2007, Baker 2009] that already upheld that no consistent nor significant thermal diffusion is to be detected. A more detailed analysis of the reliability of the latter investigations' results cannot be included here for reasons of conciseness, but can be retrieved in [Janssen 2011]. The investigation here has hence succeeded in reconciling the earlier contradiction to ultimately come to the convergent conclusion that no consistent nor significant thermal diffusion in porous materials can be detected.

In most measurements however, vapour pressure gradients were one to two orders of magnitude larger than temperature gradients, possibly masking occurrence of thermal diffusion, while for measurements with small vapour pressure gradients, on the other hand, the limited accuracy of the experiments is the restricting factor. To complement the experimental findings on thermal diffusion, the phenomenon is further analysed on thermodynamic grounds in [Janssen 2011]. The thermodynamic elaboration there shows that both vapour pressure and temperature are actually transport potentials for vapour diffusion, but also that the thermal vapour permeabilities are in magnitude only amounting to about the standard permeabilities. The elaboration moreover shows the thermal permeabilities to be negative, thus a sign of diffusion from low to high temperatures. This once again confirms the flawed nature of the studies that originally supported thermal diffusion, as they all obtained positive thermal permeabilities, which were furthermore far larger in magnitude than their standard counterparts. This equally indicates that the imposed vapour pressure and temperature differences were inappropriate to attain any evidence of thermal diffusion.

The experimental and thermodynamic findings thus all conclude only minimal amounts of thermal diffusion are to be expected. This of course implies that the quantification of 'interstitial condensation with thermal diffusion' as shown in the introduction (see Table 1, case '$\delta_T = 30 \cdot \delta_p$') is unrealistic, as it applies a thermal diffusion with a highly overestimated magnitude and an incorrect direction. When repeating the calculation with $\delta_T = -1 \cdot \delta_p$, an average value derived from the thermodynamic analysis, the condensation flow decreases some 3 % relative to the 'standard diffusion only' flow, hence indicating the negligible impact of thermal diffusion.

4 CONCLUSIONS

Reliable evaluation of moisture transport in porous materials requires a correct description of moisture flow phenomena and their transport potentials. In that respect, thermal diffusion of water vapour is an important topic of discussion: several studies [Galbraith *et al.* 1998; Thomas 1999; Glass 2007; Baker 2009] demonstrate that vapour pressure is the sole transport potential, whereas other studies [Kumaran 1987; Dahl *et al.* 1996; Galbraith *et al.* 1998; Stephenson 2003; Peuhkuri *et al.* 2008] imply that temperature gradients also yield significant water vapour diffusion.

The latter five studies, originally supporting thermal diffusion of water vapour in porous materials, have been scrutinised in this paper, and all of them were shown to be flawed. These studies formed the main support for thermal diffusion in porous materials. Reinterpretation of their results brings them in line with the four other studies that already supported the vapour pressure as the only significant transport potential for vapour diffusion. Essentially, all studies had the same aim: to assess the significance of thermal diffusion of water vapour in porous materials. The examination here has succeeded in reconciling their previously contradictory findings, to arrive at one convergent conclusion: no consistent nor significant thermal diffusion can be detected. This, in the end, does not come as a surprise. While the thermodynamic elaboration points to the vapour pressure and temperature as possible transport potentials, the phenomenological coefficients suggest that only a minimal negative thermal diffusion is to be expected. In the measurements analysed above, temperature differences were generally two orders of magnitude below the vapour pressure differences. With a standard and thermal vapour permeability of comparable size, thermal diffusion can only contribute minimally, remaining undetectable with current measurement accuracy. The measurements with the minimal vapour pressure differences, on the other hand, similarly lead to undetectably small diffusion flows.

This conclusion is more generally valid for vapour diffusion in building science applications: often vapour pressure differences over a construction are far larger than temperature differences, with resultantly a negligible role for thermal diffusion. It can hence cautiously be concluded that thermal diffusion of water vapour in porous materials can be considered insignificant, and that vapour pressure is the sole significant transport potential for diffusion of water vapour in porous materials.

ACKNOWLEDGMENTS

Thank you very much to Gregor A. Scheffler, for our initial discussions on the topic.

REFERENCES

Baker, P.H., Galbraith, G.H. & McLean, R.C. 2009, 'Temperature gradient effect on moisture transport in porous building materials', *Building Services Engineering Research and Technology*, **30,** 37-48.

Dahl, S.D., Kuehn, T.H., Ramsey, J.W. & Yang,, C.-H. 1996, 'Moisture storage and non-isothermal transfer properties of common building materials', *HVAC&R Research*, **2**, 42-58.

Galbraith, G.H., McLean, R.C., Gillespie, I., Guo, J. & Kelly, D. 1998, 'Nonisothermal moisture diffusion in porous building materials', *Building Research & Information*, **26**, 330-339.

Glass, S.V. 2007, 'Measurements of moisture transport in wood-based materials under isothermal and non-isothermal conditions', in proceedings of *Thermal Performance of the Exterior Envelopes of Whole Buildings Buildings X*, Clearwater Beach, Florida, United States.

Hokoi, S. & Kumaran, M.K., 1993, 'Experimental and analytical investigations of simultaneous heat and moisture transport through glass fiber insulation', *Journal of Thermal Insulation and Building Envelopes*, **16**, 263-292.

Janssen, H., 2011, 'Thermal diffusion of water vapour in porous materials: fact or fiction ?', *International Journal of Heat and Mass Transfer*, **54**, 1548–1562.

Kumaran, M.K. 1987, 'Moisture transport through glass fiber insulation in the presence of a thermal gradient', *Journal of Thermal Insulation*, **10,** 243-255.

Kumaran, M.K. & Mitalas, G.P. 1987, 'Analysis of simultaneous heat and moisture transport through glass fibre insulation', in proceedings of *ASME/AIChE National Heat Transfer Conference*, Pittsburgh, Pennsylvania, United States.

Kumaran, M.K. 1994, 'Temperature dependence of water vapour permeability of glass fiber insulation from heat flow meter measurements', in proceedings of *1st ISHMT-ASME Heat and Mass Transfer Conference*, Bombay, India.

Peuhkuri, R. 2003, *Moisture dynamics in building envelopes*, PhD thesis Technical University of Denmark, Kgs. Lyngby, Denmark.

Peuhkuri, R., Rode, C. & Hansen, K.K. 2008, 'Non-isothermal moisture transport through insulation materials', *Building and Environment*, **43**, 811-822.

Stephenson, D.G. 2003, 'Thermal diffusion of water vapour through glass fiber insulation', *Journal of Thermal Envelope and Building Science*, **27**, 31-48.

Thomas, W.C. 1999, *Moisture transfer in porous materials exposed to combined humidity and temperature gradients*, Final Report ASHRAE 810-RP.

XII DBMC
International Conference on Durability of Building Materials and Components
PORTO - PORTUGAL, April 12th-15th, 2011

Influence of Under-Cooling on the Wetting and Drying of Rainscreen Walls in Cold and Humid Climates

Hua Ge [1]
Wendy Y. Simpson[2]

ABSTRACT

Undercooling is a phenomenon that results from the radiant heat exchange between a surface and the terrestrial environment and the sky. The anisotropic radiation by the sky, i.e. absorptivity of 1 but emissivity lower than 1, causes the exterior surface temperature to drop below the air temperature and sometimes below the dew-point of outside air. Previous research has indicated that undercooling induced condensation may cause durability issues i.e. metal corrosion in well insulated ventilated roofs and increased freeze and thaw cycles in veneer walls in humid climates. Significant amounts of undercooling induced condensation have been observed on facades in the coastal climate of British Columbia during the sunny periods in the winter, spring and fall. Whether undercooling induced condensation would significantly impact the hygrothermal performance of ventilated rainscreen walls was studied. Six test walls were installed on a two-storey building envelope test facility. The test parameters include cavity depth, top vent sizes, and initial moisture loads. Four test walls have plywood sheathing with high initial moisture content of 38 - 41% while the other two have plywood sheathing with a low initial moisture content of about 7%. The preliminary results show that under-cooling induced condensation on cavity surfaces is observed, which elevates the MC in initially dry plywood sheathing and restricts the drying of initially wet plywood during the winter period.

KEYWORDS

Rainscreen walls, Hygrothermal performance, Field measurements, Undercooling, Wood-frame construction.

[1] Faculty of Engineering, Architecture and Science, Ryerson University, Toronto, CANADA. huage@ryerson.ca
[2] Research assistant, Building Science Centre of Excellence, British Columbia Institute of Technology. Wendy_ye@bcit.ca

1 INTRODUCTION

To provide a reliable moisture management and prevent rainwater penetration, the British Columbia Building Code (BCBC, 2006) now mandates the use of rainscreen walls in the wet regions of BC. The provision of an air cavity behind cladding not only provides a capillary break and a drainage path for any accidentally entered rainwater but also promotes drying if top vents exist. Previous research studying the effect of cavity ventilation on drying concluded that cavity ventilation is beneficial for wet panel cladding during summers to alleviate solar-driven inward vapour diffusion, however, the drying provided in winter is minimal (Bassett and McNeil 2005; Davidovic 2004; Hazleden and Morris, 2002; Mukhopadhyaya, et al., 2003; Onysko, 2000; Rousseau and Dalgliesh, 2004; Shi and Burnett, 2006; Stovall and Karagiozis, 2004).

The coastal climate of British Columbia is characterized by a long rainy winter with mild wind (<2m/s on average), low rainfall intensity (<2mm/hr), and high humidity (>80%). The statistical analysis of historical wind and rain data showed that in December on average it rains 17 days per month and 8 hours per day. With low solar radiation and high humidity during the winter months, cavity ventilation in rainscreen walls may introduce wetting if outdoor air is moister than the air in the cavity, which occurs when a rainy period is followed by a few sunny days. During the sunny period, the temperatures on the exterior surface of the cladding and sometimes even the interior surface of cladding may fall below the outdoor air dry-bulb and dewpoint due to the night clear sky radiation. Under this situation, condensation may form on both the exterior surface and the cavity surface of the cladding when cavity ventilation brings moist outdoor air into the cavity. Significant amounts of condensation have been observed on facades in the coastal climate of British Columbia during the sunny periods in the winter, spring and fall. Previous research has indicated that undercooling induced condensation may cause durability issues i.e. metal corrosion in well insulated ventilated roofs and increased freeze and thaw cycles in veneer walls in humid climate. Whether the clear-sky radiation has any significant impact on the hygrothermal performance of rainscreen walls has not been studied or reported.

Within the framework of a comprehensive study on the influence of cavity ventilation on the hygrothermal performance of rainscreen walls, the impact of undercooling on the wetting and drying of rainscreen walls is studied. Six test walls clad with fiber cement panels were installed on a two-storey building envelope test facility and the indoor conditions were maintained at typical indoor conditions and the test walls were exposed to local climatic conditions. This paper presents the experiment setup and test results.

2 EXPERIMENT SETUP

2.1 Building Envelope Test Facility

The experimental study was carried out at the BCIT Building Envelope Test Facility (BETF) (Photo shown in Figure 1). Six test walls were installed on the southeast side of the façade, as shown in Figure 2. The research facility is designed to evaluate the hygrothermal performance of full-scale building envelope assemblies under simulated indoor and real climatic outdoor conditions. The 44' x 28' two-story structure can accommodate in total 62 1.2 m by 2.4 m (4' x 8') panels. Two mechanical systems are fitted within the facility allowing the separation of interior spaces into two conditioned horizontal zones, thus allowing control of the indoor boundary conditions, namely, temperature and relative humidity, at the desired values. Each system can maintain indoor temperature within the range of 18–26ºC, with a precision of ±2ºC, and relative humidity within the range of 40–80%, with a precision of ±5%. The facility is equipped with a data acquisition system with over 600 channels, allowing for the monitoring of hygrothermal conditions within wall assemblies including temperature, relative humidity, moisture content, heat flux, air velocity, wind-induced pressure, and incidence of condensation and rain penetration. The facility is also equipped with a weather station mounted on the rooftop of the facility to measure the outdoor boundary conditions

including wind speed, wind direction, solar radiation on both horizontal and vertical surfaces, and horizontal rainfall. Driving rain on wall surfaces is also collected. More information about this facility can be found in (Ge, et al., 2008).



Figure 1. Building Envelop Test Facility (BETF) at the Burnaby Campus of BCIT.

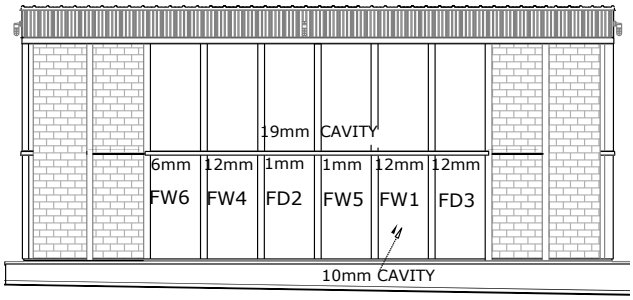

Figure 2: Test wall location on SE façade of BETF.

2.2 Test walls and instrumentation

All of the six fibre cement walls had dimensions of 1.22m by 2.44m and an identical 2x6 wood-frame back wall assembly as, from interior to the exterior:

- 12mm unpainted gypsum board with a vapour barrier of 6 mil polyethylene
- 38mm x 140mm wood frame with R20 fibreglass batt insulation
- 12mm plywood (Douglas fir) sheathing
- Spun bonded polyolefin (SBP) sheathing membrane

Five of the six fibre cement walls have an air cavity depth of 19 mm and one has a 10 mm air cavity. The bottom vents are all 12 mm high continuous slot vents with an insect screen. The top slot vents vary in height, i.e. 1mm, 6mm and 12mm, also with insect screen. The location of test walls on the test facility is shown in Figure 2. To evaluate the drying and wetting provided by the cavity ventilation, two levels of moisture loads were introduced into the plywood sheathing. Four walls were pre-wetted to a high initial moisture content of 38% to 41% to represent a construction situation where the plywood sheathing is wetted by rainwater during construction; these are the "wet wall" configurations, denoted as "high" in Table 1. The other two walls have a low initial moisture content of about 7% to 8%, which is the equilibrium moisture content level inside the test facility and is denoted as "low" in Table 1. The vent configurations and variables are summarized in Table 1.

Table 1. Vent configurations of test walls.

Wall Label	Continuous slot vent height (mm)		Air cavity depth (mm)	Initial moisture content in plywood
	Bottom vent	Top vent		
FW1	12	12	10	high
FD2	12	1	19	low
FD3	12	12	19	low
FW4	12	12	19	high
FW5	12	1	19	high
FW6	12	6	19	high

The hygrothermal state of each test wall was monitored including temperature, moisture content, and relative humidity. The moisture content (MC) of plywood, stud and bottom plate was monitored by both gravimetric samples and electric moisture pins. Each test wall had seven gravimetric samples on the plywood sheathing, two gravimetric samples on the stud and two on the bottom plate. The gravimetric samples on the plywood were round disks of 51mm (2") diameter. The edges of the samples were sealed with tuck tape to limit two-dimensional moisture transport. The gravimetric

samples on the stud and bottom plate were cubes of 19mm (3/4") length. For the purpose of comparison, a pair of resistive MC pins made of stainless steel screws was installed close to each gravimetric sample. All electronic sensors and gravimetric samples were installed in the central bay of each test wall. The other two 400mm-stud spaces were used as guard bays. In total 84 thermocouples, 14 relative humidity transducers, 60 pairs of moisture pins were installed in the test walls. The typical layout of the sensors in each wall component is presented in Figure 3.

The measurements of on-site weather conditions include air temperature and relative humidity, wind speed, wind direction, horizontal solar radiation, horizontal rainfall, and wind-driven rain. The indoor conditions were controlled at 22 ºC and 55 % RH. Data from the test walls was recorded every 5 minutes for moisture content, temperature, and relative humidity. Data from the weather station were sampled at one-minute interval. The gravimetric samples were weighed weekly.

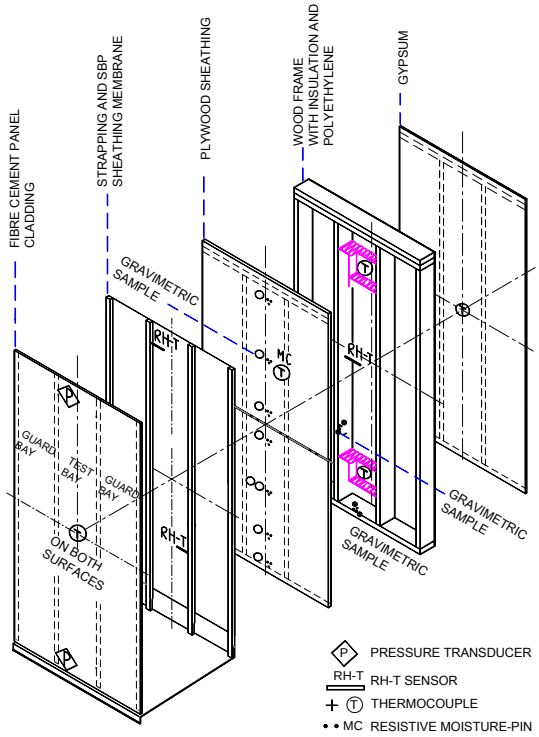

Figure 3:.Typical layout of the sensors in a wall specimen.

3 RESULTS AND DISCUSSION

In this paper the results and discussion focus on analyzing the frequency of occurrence of undercooling and its impact on the wetting of test walls during the period from December, 2007 to June 2008. The change of moisture content in the plywood was used as an indicator to evaluate the effect of cavity ventilation on the wetting and drying of rainscreen walls.

3.1 On-site weather conditions

The recorded temperature and relative humidity for the period from December 2007 to June 2008 are shown in Figure 4. The daily average RH remained in the range of 80 - 98% from December 2007 to March 2008 with low fluctuations. After March 2008, the relative humidity decreased gradually with higher fluctuations, which is an indication of higher daily temperature range and stronger solar radiation.

Figure 5 shows the monthly average temperature, relative humidity and horizontal rainfall. The temperatures were more or less constant with an average of 2ºC during the months of December and January and with an average of 4.5 ºC during the months of February and March. Starting from April, the temperature gradually increased.

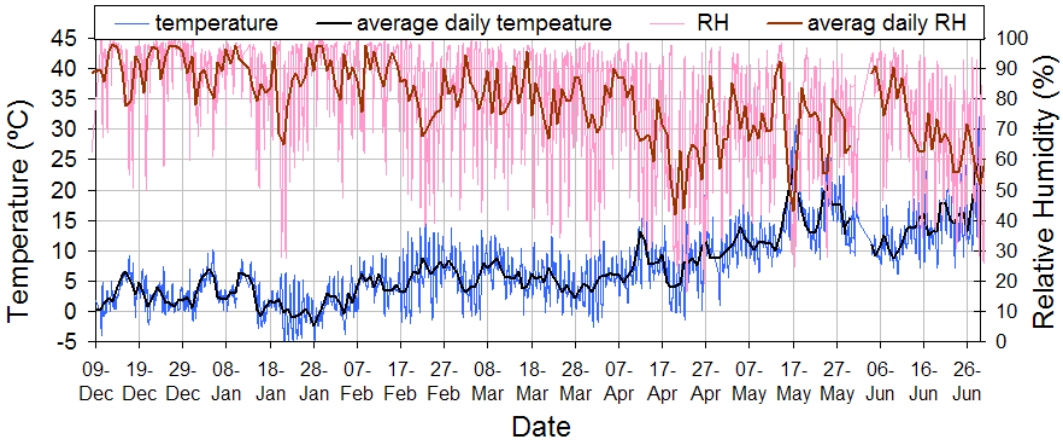

Figure 4. On-site temperature and relative humidity during test period from December 07 to June 08.

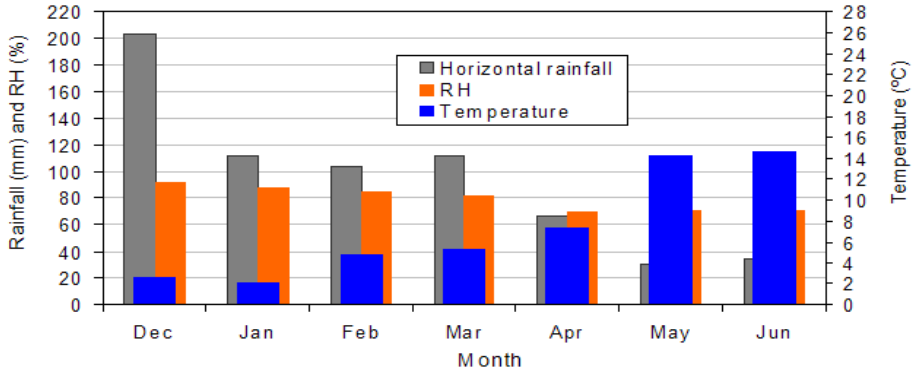

Figure 5. Average horizontal rainfall, temperature and RH recorded by the weather station on the roof of the test facility from Dec. 07 to June, 08.

The total amount of rainfall received horizontally was 662 mm for the seven months from December 2007 to June 2008. The highest rainfall received was in December 2007 with a monthly total of 203mm and the amount of rainfall received from January to March 2008 was more or less the same with a total of about 110mm in each month. Starting from April, the rainfall amount starts to decrease significantly. The amount of horizontal rainfall was 67mm in April, 30mm in May, and 35mm in June.

Figure 6 shows the solar radiation and the accumulative rainfall over the test period. The almost linear increase of cumulative rainfall with time indicates a constant rainfall during the winter season from December to April with two sunny periods, one in January and the other in February.

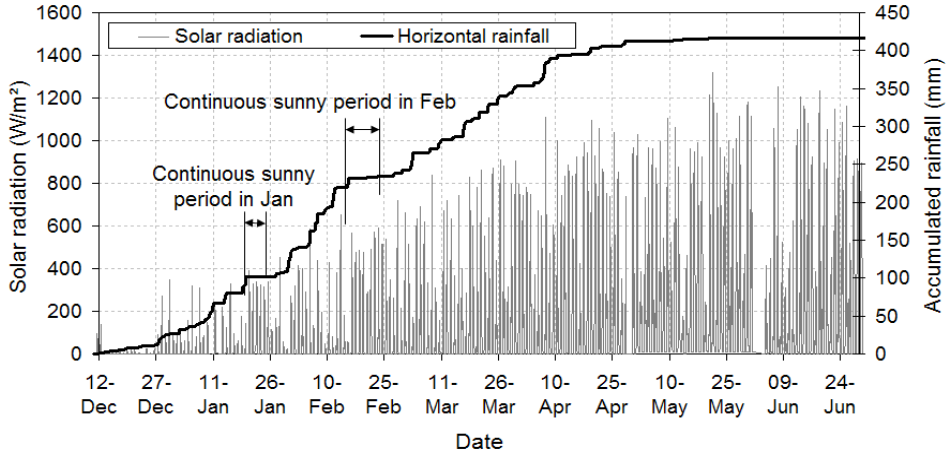

Figure 6. Solar radiation with rainfall accumulation during test period from Dec. 12, 07 to Jun. 30, 08.

Weather data collected on site during the test period showed a typical winter season for this region: mild temperatures, high relative humidity and constant rainfall.

3.2 Frequency of undercooling effect

The clear sky radiation may lower the cladding surface temperature to below the outdoor air dry-bulb temperature and even below the dewpoint. For the less thermally massive cladding (8mm fiber cement), the clear sky effect may also lower the cladding cavity surface temperature below outdoor dry-bulb or dewpoint, which will consequently increase the relative humidity of the cavity or condensation may occur on the cladding cavity surface when cavity ventilation brings in moist outdoor air into the cavity. A slightly reduction of surface temperature due to undercooling may generate condensation on the exterior and cavity surface of the cladding given that the outdoor air relative humidity is often greater than 90% during the winter, as shown in Figure 1. Since only the undercooling effect and condensation potential within the air cavity have an effect on the wetting of the plywood sheathing due to cavity ventilation, the undercooling effect and condensation potential is analyzed on the cladding cavity surface, i.e. the interior surface of the cladding instead of the exterior surface.

The frequency of undercooling effect on the cladding cavity surface, i.e. when the cladding cavity surface temperature is lower than outdoor air dry-bulb temperature, is analyzed and shown in Figure 7. For all test walls, the cladding cavity-surface temperatures are often lower than the outdoor air temperature due to the clear-sky effect combined with their smaller thermal storage capacity. The high frequency of under-cooling effect occurs in the winter months from December to February and in May with the highest frequency in February. This is probably due to the sunny period observed in February, as shown in Figure 6.

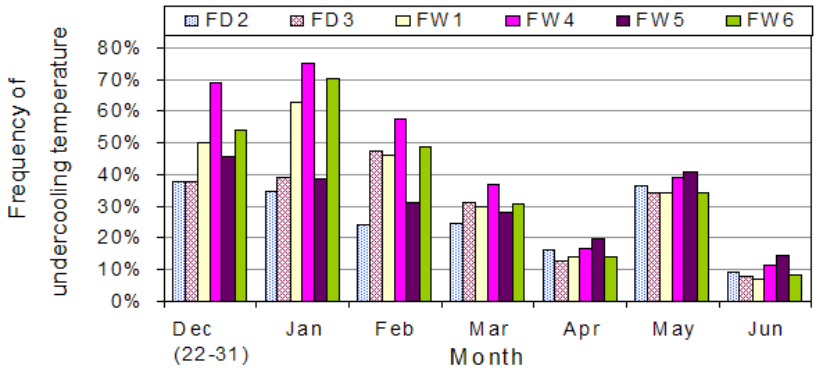

Figure 7. Frequency of under-cooling effect on the cavity-surface of fibre cement cladding for all test walls from December 07 to June 08. FD2 with 1mm top vent, FD3 with a 12mm top vent, FW1 with a 12mm top vent but 10mm cavity depth, FW4 with 12mm top vent, FW5 with 1mm top vent and FW6 with 6mm top vent.

The vent configuration of the test walls seems to influence the under-cooling frequency and the higher cavity ventilation achieved by a larger top vent or a wider cavity depth seems to result in a higher frequency of undercooling during the winter months. For walls with low initial moisture levels, FD2 and FD3, the under-cooling frequency of test wall FD3 (with a 12mm top vent) is twice that of test wall FD2 (with 1mm top vent) in February. With a high initial moisture level in the plywood sheathing, FW4, which has a 12mm top vent, the highest under-cooling frequency of 75% was in January whereas FW5 with a 1mm top vent had an under-cooling frequency of only 39%, and FW6 with a 6mm top vent had the second highest under-cooling frequency of 70%. The wall FW1, with a 10mm air cavity and 12mm top vent had the third highest under-cooling frequency of 63%. In the spring, the difference in under-cooling frequency became quite small amongst all test walls; this was a result similar to that observed for test walls having low initial moisture levels in the plywood sheathing.

The hour in a given day in which the occurrence of undercooling on the cladding cavity surface (i.e. when the cladding cavity surface temperature is lower than outdoor air temperature) was observed was analyzed as shown in Figure 8. It can be seen that undercooling occurs mostly during the night time from 21:00pm to 6:00am with the peak between midnight to 5:00am. The undercooling effect also exists during the daytime although the frequency of occurrence is quite low.

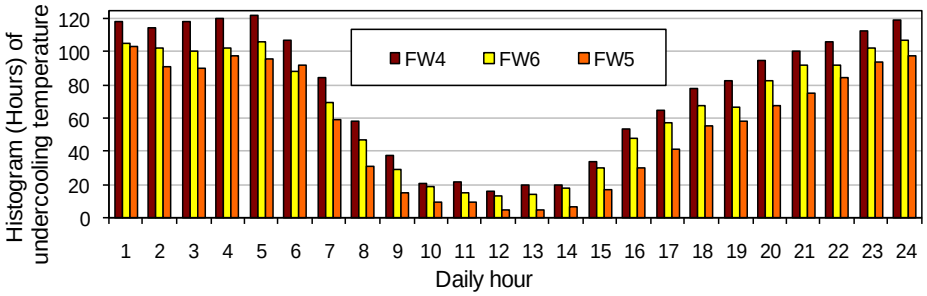

Figure 8. Daily distribution time at which undercooling occurred on the cladding cavity surface for walls with high initial moisture content in plywood sheathing during test period of December 2007 to June 2008 (203 days). FW4 with 12mm top vent, FW5 with 1mm top vent and FW6 with 6mm top vent.

The frequency of condensation on the cladding cavity surface is also analyzed by comparing the cavity surface temperature to the outdoor air dewpoint temperature. Figure 9 shows the daily condensation hours, i.e. the number of hours with condensation on the cladding cavity surface, in FD2 and FD3. Three peak periods for FD2 include: late December, January 21 – 30, and from February 29 to March 12 while a constant condensation period for FD3 occurred from mid-January to beginning of March. The condensation that occurred during the first two periods had a significant effect on the moisture content in the plywood.

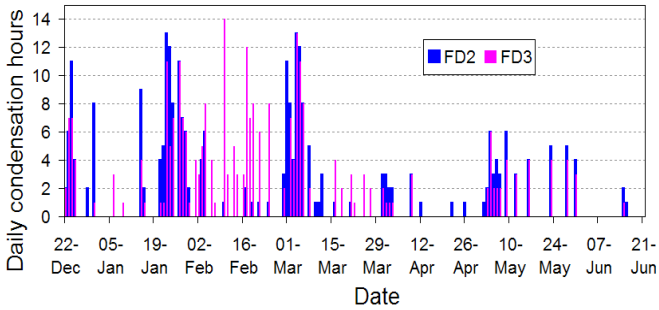

Figure 9. Daily condensation hours on cavity-surface of the fibre cement cladding for dry walls of FD2 and FD3.

As shown in Figure 10, the plywood sheathing in dry walls FD2 and FD3 went through a wetting process first from the beginning of test period to January 20, 2008. During this period, the moisture content of plywood sheathing in both walls increased gradually and reached their maximum level in 38 days, a moisture content level just below 19% and afterwards both walls went through a drying process. Test wall FD3 with a larger top vent (12mm) seemingly had a slightly higher wetting rate than test wall FD2, having the smaller 1mm top vent. During the drying period, the MC level in FD3 remained slightly higher than FD2. The higher frequency of condensation on the cladding cavity surface in FD3 may have contributed to the slightly faster wetting. The similar values for drying rate observed during the drying period was an indication that cavity ventilation wetting also occurred, which may counter-balance the higher drying rate that should have been achieved for FD3 that had a larger top vent and thereby a higher expected cavity ventilation rate. The preparation stage shown in Figure 10 refers to the period during which the test walls were fabricated inside the facility, the gravimetric samples were inserted into the plywood sheathing, and test walls were installed on the test facility. The average moisture content level in the plywood of test walls FD2 and FD3 gained about 7%, reaching a MC level of 14% from an initial of 7%.

For walls with a high initial MC in the plywood sheathing, the vent configurations have a significant influence on the occurrence of condensation on the cladding cavity surface. As shown in Figure 11, the daily hours for condensation in FW4 (12mm top vent) reached a maximum of 18 hours at the end of December 2007 and varied from 3 to 16 hours per day from January to the beginning of March 2008. However, the frequency of condensation in FW5 (1mm top vent) from December to March was much less than that in FW4, within 1 – 13 hours due to small ventilation rates and slightly higher cavity-surface temperatures. The difference in total condensation hours between FW4 and FW5 is 217 hours.

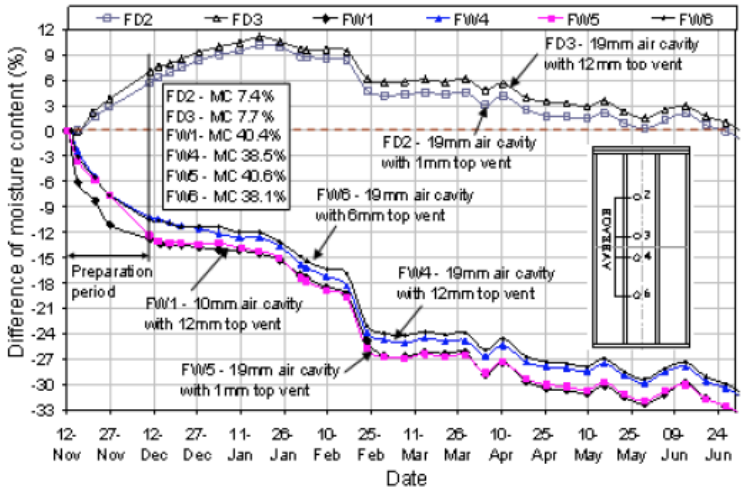

Figure 10: Changes of average moisture content in plywood of test walls during the test period.

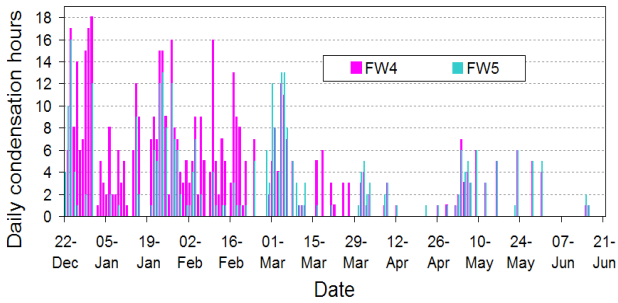

Figure 11. Daily condensation hours on cavity-surface of walls FW4 (12mm top vent) and FW5 (1mm top vent).

Compared with FW4 (12mm vent - 19mm cavity depth), the days of condensation and daily condensation hours on the cladding cavity-surface of FW1 (12mm vent-10mm cavity depth) were slightly less during the entire test period, as shown in Figure 12. The difference in condensation hours between FW4 and FW1 is 148 hours during the entire test period.

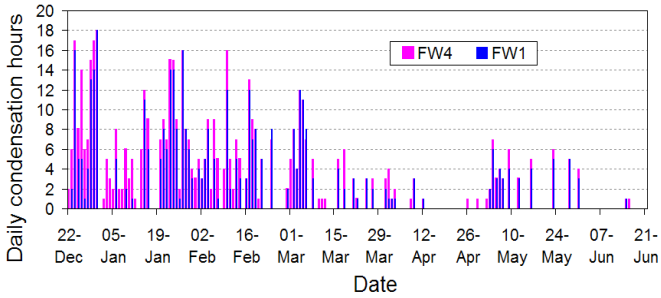

Figure 12. Daily condensation hours on cavity-surface of walls FW1 (10mm cavity) and FW4 (19mm cavity).

The undercooling effect on the cladding cavity surface seems to have a significant effect on the drying of wet plywood in test walls FW1, FW4, FW5 and FW6 ("wet walls"). Due to the differences in terms of top vent sizes and cavity depth, walls with larger vent sizes and wider cavity depths are supposed to provide greater drying rates if indeed cavity ventilation assists drying. However, as shown in Figure 10, although the difference in drying rates is quite small (<1% MC) among "wet test" walls, FW1 (12mm vent-10mm cavity) and FW5 (1mm vent-19mm cavity) have slightly higher drying rates as compared to walls FW4 (12mm vent-19 mm cavity) and FW6 (6mm vent-19mm cavity). The higher occurrence of cavity condensation in FW4 probably contributed to a slightly lower drying rate. The undercooling effect reduced the drying of wet panels during the winter months. The net result is that the difference amongst the "wet test" walls is negligible indicating that the size of the slot at the top vent has an insignificant effect on the drying of fibre cement clad walls given that the higher cavity ventilation rate also increased the wetting to the cavity components.

CONCLUSIONS

Within the framework of a comprehensive field study on the influence of cavity ventilation on the wetting and drying of rainscreen walls in the coastal climate of British Columbia, the impact of under-cooling on the moisture performance of fiber cement rainscreen walls was evaluated. Results show that the undercooling effect and resulting condensation occurs on the cavity-surface of fibre cement cladding every month during the test period and condensation occurs more frequently in the winter as compared to the spring due to the higher outdoor air RH in the winter.

The difference in the frequency of occurrence of condensation on the cladding cavity surface is insignificant for "dry test" walls FD3 and FD2 although FD3 had a slightly higher frequency of occurrence of condensation due to its wider top vents. For "wet test" walls, the larger vent size seems to have caused more condensation and under this climate, cavity ventilation becomes an additional moisture source that in fact restricts the drying of wet plywood sheathing. Therefore, taking into account both benefits provided by larger vents in assisting drying during sunny periods and the wetting introduced during the undercooling period, it can be concluded that cavity ventilation assists rainscreen wall systems to dry in the cold and humid winter climates of coastal BC when the initial moisture level is high, however, the wall with smaller top vent and a 19mm cavity may perform better in terms of reducing cladding surface condensation and ensuring its long-term durability. In general, the effect of vent configurations on the hygrothermal performance of rainscreen walls is not significant for fiber-cement clad panel type rainscreen walls.

ACKNOWLEDGMENTS

The authors are grateful for the financial support provided by the British Columbia Institute of Technology, the Natural Sciences and Engineering Research Council of Canada, and the British Columbia Housing Commission Management.

REFERENCES

Bassett, M.R. & S. McNeil. 2005. Drained and vented cavity walls – measured ventilation rates. IRHACE Conference. Institution of Refrigeration, Heating and Air Conditioning Engineers, Nelson, New Zealand.

BCBC. 2006. British Columbia Building Code. Ministry of Forests and Range and Minister Responsible for Housing.

Davidovic, D. 2004. Convective drying potential of ventilated wall cavity systems in building enclosures. Master thesis, The Pennsylvania State University, Pennsylvania, USA.

Ge, H. Krpan, R. Fazio, P. and Ye, Y. 2008. A two-storey field station for investigation of building envelope performance in the coastal climate of British Columbia. Proceedings of the symposium in Building Physics. Leuven, Belgium, October.

Hansen, M., Nicolajsen, A., and Stang, B. 2002. On the influence of ventilation on moisture content in timber framed walls. Proceedings of the 6th Symposium on Building Physics in the Nordic Countries.

Hazleden, D., and Morris, P., 2002. The Influence of Design on Drying of Wood-Frame Walls Under Controlled Conditions. Thermal Performance of Building Envelopes VIII 2002. Clearwater Florida.

Mukhopadhyaya, P.; Kumaran, K.; Tariku, F.; VanReenen, D. 2003. Final Report from Task 7 of MEWS Project at the Institute for Research in Construction: Long-Term Performance: Predict the Moisture Management Performance of Wall Systems as a Function of Climate, Material Properties, etc. Through Mathematical Modelling. IRC-RR-132.

Onysko, M. D. 2000. Drying of walls with ventilation: a parametric analysis. Research report-Housing Technology Series, Canada Mortgage and Housing Corporation.

Rousseau, M.Z. and W. A. Dalgliesh. 2004. Selected findings of an IRC study of the wetting and drying potentials of wood-frame walls exposed to different climates. CIB 2004 World Building Congress, Toronto, Ontario. pp.1-9.

Shi, X. and E. Burnett. 2006. Ventilation drying in walls with vapor impermeable claddings. Proceedings of the 3rd international conference in Building Physics and Building Engineering. p. 395-402. Montreal, Canada.

Stovall, T.K., and Karagiozis, A. 2004. Airflow in the ventilation space behind a rainscreen wall. Performance of Exterior Envelopes of Whole Buildings IX International Conference, ASHRAE, December, Florida.

XII DBMC
International Conference on Durability of Building Materials and Components
PORTO - PORTUGAL, April 12th-15th, 2011

Zinc Roofs. Pathology and Rehabilitation

Isabel Torres [1]
J. Mendes da Silva [2]
Carla Mauricio [3]

ABSTRACT

Zinc roofs are not standard solutions in Portugal. However their outstanding characteristics of durability, image and adaptability to more complex forms had motivated the architects to introduce this material in their projects. Today, the number of buildings that integrate external zinc layers on their roofs are quite significant, what means that they are reaching a new role in the architectural language. The application of this material does not happen only in new buildings; it is also used in many rehabilitation projects that seek materials with higher lifetime. However, as it is not a traditional building material in Portugal, the application techniques are not fully known, either by designers or by installers. The number of zinc works and installers has been increasing, creating a greater probability of pathologies in this kind of roofs.

The condensation phenomenon in zinc roofs is an important factor for their performance. Glaser method is a simplified hygrothermal method, with which we can predict and calculate the condensation phenomena inside the building elements. Using the calculation program CONDENSA - and in order to make clear which are the variables that might influence the phenomenon of condensation and to identify behavioural differences between ventilated roofs and compact roofs face to condensation - we have performed various simulations on different types of coverings. In this article we present and discuss the results obtained in these simulations.

KEYWORDS

Zinc roofs, Rehabilitation, Glaser method.

[1] Department of Civil Engineering - University of Coimbra, Coimbra, PORTUGAL, itorres@dec.uc.pt
[2] Department of Civil Engineering - University of Coimbra, Coimbra, PORTUGAL, raimundo@dec.uc.pt
[3] Department of Civil Engineering - University of Coimbra, Coimbra, PORTUGAL, carla.mauricio@netcabo.pt

1 INTRODUCTION

Zinc is not a very common element on earth, and being only the 23rd item, the more abundant. Most of all the zinc used today comes from recycling of zinc products in end of life. Although uncommon, zinc is a metal widely used. Manipulated by man zinc has wide application in various metal alloys, such as construction element or protective element of other metals from corrosion. Zinc is widely used in construction as part of a waterproof coating for roofs. Its plastic properties make their use greatly appreciated, for its easy moulding and application. This element also combines a good rate cost / longevity, which makes it an election material.

When we speak about zinc roofs it is inevitable talking about Paris due to the high number of roofs zinc visible when we reach some specific places of the city (Figure 1). The use of zinc as coating of roofs of Paris dates to the period of Napoleon III at the beginning of the industrial revolution.
The large avenues replaced the medieval streets and buildings owned a new materiality, in which we can detach the mansards and the zinc roofs. Actually we estimate that zinc roofs in the centre of Paris represent about 85% of total coverings.

In Portugal the number of zinc roofs is very small, but, nowadays this number is growing and zinc roofs are reaching more notoriety. "Pavilhão Atlântico" is one of the examples that contrast for its unusual shape. The choice of this material for the coating was essential to recreate a symbolic volume, the shape of an inverted hull.



Figure 1. Geral view of Paris.



Figure 2."Pavilhão Atlântico", Lisbon.

Old buildings with zinc roofs are very unusual in Portugal. However there are several buildings whose original covering was in zinc and that suffered rehabilitation works.
The dome of the actual Faculty of Economics of the New University of Lisbon is one of the examples of a zinc roof that as been recently rehabilitated. The building was founded in 1858. The dome had great problems of rainwater infiltrations. When it was rehabilitated it was notorious the degradation of the wood structure as well as the zinc sheet. The anomalies observed were deformations, drilling and open joints. After the reinforcement of all the structure the coating of the dome was renewed with zinc sheets.

2 ZINC ROOFS

Zinc roofs can be grouped into two major groups: ventilated roofs or compact roofs. Traditionally, zinc roofs were ventilated and the compact solution is relatively recent. Ventilated roofs (cold coverage) differ from compact roofs (hot coverage) by the existence of the ventilation layer. Within each of these two groups there is a wide variety of solutions, with multiple options for the membranes, insulation, supports and application of zinc. The type of solution adopted can significantly affect the coverage in its performance, durability, cost and visual impact.

2.1 Zinc ventilated roofs

Zinc ventilated roofs comprise three distinct levels of layers and each level corresponds to a distinct function: exterior layer (A, B e C), intermediate layer (D) and interior layer (E, F, G e H).

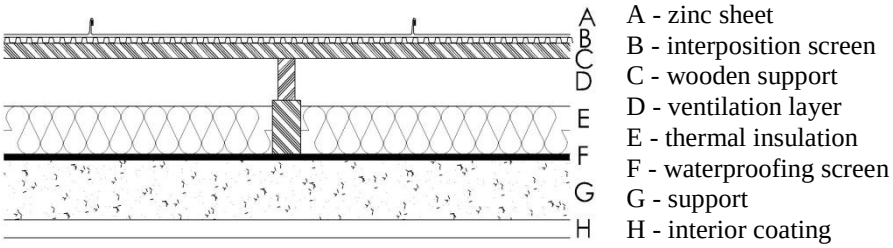

Figure 3 – Simplified scheme of zinc ventilated roof.

The outer layer corresponds to the zinc sheet that behaves as a waterproofing layer. The high malleability of this material requires rigid support, which must either be made of a compatible wood or have an intervening barrier. Screens create a separation between the zinc and the adjacent layer, allowing water to run off without damaging the adjacent layer or the zinc. This top layer has no important physical influences, because it is not subject to large differences in water vapour temperature or pressure. The intermediate level between the two extremes is the space that distinguishes ventilated roofs. This layer has the function of ventilation, reducing potential condensation on the underside of the sheet and its corrosion. This layer is associated with holes located at the lowest and the highest levels allowing for the inflow and outflow of air respectively. The inner layer is composed of the support structure and insulation and may also have a vapour barrier. The support structure can be of two distinct types, light or heavy and it influences, also, the hygrothermal calculation.

2.2 Zinc compact roofs

The growth in the number of compact zinc roofs is notorious. Besides architectural issues, the reasons for this growth are clearly economic. With the absence of the ventilation layer moisture becomes trapped inside the roof having difficulty to get out. Due to the high resistance of the zinc to water vapour, moisture that enters the building element may condense and remain within the coverage. This condensation can cause severe corrosion on the underside and tends to aggravate if it occur in cycles giving the cover a short and unacceptable shelf life. So it will be necessary to control humidity by two distinct ways: create ways to quickly evacuate it and avoid its entrance to the interior of the building element. Figure 4 represents a simplified scheme where A - zinc sheet, B - interposition screen, C - wooden support (may not exist); E - thermal insulation; F - waterproofing screen (may not exist), G - support; H - liner.

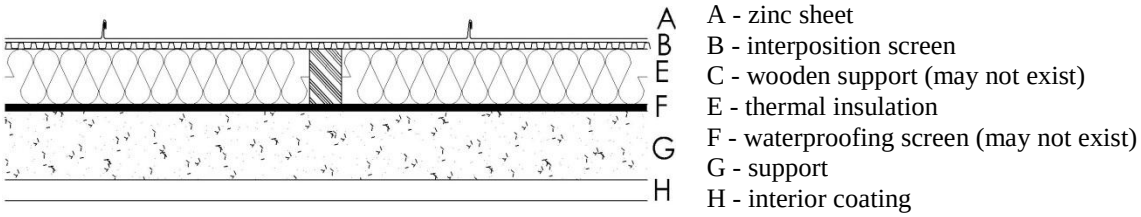

Figure 4 – Simplified scheme of zinc compact roof.

2.3 Comparison between zinc ventilated roofs and zinc compact roofs

The advantages of zinc ventilated roofing include: it has been subject of more research; there is more experience in its application; ventilation allows for evacuation of the humidity from the inside the cover; condensation is more easily controlled; there is less chance of corrosion on the underside of the sheet of zinc.

The advantages of non-ventilated zinc roofing are: it is the cheapest solution requiring less equipment and less labour; it impedes the entry of external moisture into the coverage and, therefore, under cooling is less likely (Hens, 2002). Architecturally, we can take advantage of the loft; and finally it is greener in cases where chemical wood protection becomes unnecessary

2.4 Deterioration and causes

Some of the main types of deterioration recorded in zinc roofs are listed below.
Deterioration recorded in the zinc:
- Loss of brightness or the whitening of zinc sheet can be considered as an anomaly although it is debatable.
- Other changes include discoloration; stains; runoffs; perforations; loss of thickness; changes in mechanical properties; cracks or fractures; warping; corrosion; and the loosening of tiles due to wind.

Deterioration recorded in the fasteners and metal support:
- Use of less costly materials for the setting without proper isolation can cause metal corrosion, the loosening of fasteners;
- Corrosion.

More important than analysing the anomalies, is understanding the causes and developing mechanisms to control them. The causes of anomalies are: deficiencies in geometry due to errors in design or construction/assembly; moisture provoked by rain and/or water vapour; and corrosion. Repairing the problem without eliminating the source does not prevent its recurrence.

Moisture is one of the main causes of the anomalies of zinc roofs, affecting the maintenance of the building, its durability, its energy efficiency, its comfort and human health. Moisture may have different origins: precipitation, rising damp, construction, hygroscopicity, accidental causes and condensation. Moisture is not static and develops mechanisms that trigger its migration. Moisture that penetrates to the interior and remains there during a significant period may have consequences: condensation; activation of zinc incompatibility with other materials, reduction in thermal performance; biological attack on the elements of wood, corrosion in the metal structure and/or zinc sheets. The main problem of zinc roofs is the condensation that emerges on the inferior face of the zinc sheet. The anomalies created by the condensation are not easily detected and can have serious results and even lead to its ruin.

It is of extreme importance that we can predict end avoid the occurrence of internal condensations in zinc roofs.

3 NUMERICAL SIMULATIONS

3.1 Glaser Method

The theoretical study of heat and moisture transfer in non-saturated porous media and in particularly in construction elements and materials has been object of important investigation. The first models based in the fluid mechanics and using the laws of the mass diffusion (Darcy's law for the liquid phase and Fick law for the vapour phase) and of heat (Fourrier's law) appeared at the decade of fifty. We can state the works carried out by Glaser, Krischer, Vos, Luikov and Philip and DeVries.

The Glaser Method based on the principle that in a construction element subjected to a gradient of temperatures and pressures, the saturation pressure will change from point to point, analysis the risk of occurrence of internal condensations in that element.

The condensations will occur at any point within the construction element, whenever vapour pressure at this point is equal to the saturation pressure. Thus, if the "curve" of installed pressures generated by the boundary conditions, intersects the "curve" of saturation pressures condensation will occur, otherwise we will have no occurrence of condensation in the building element.

Applying this method involves the consideration of some simplifications that lead to the condensate flows are calculated by excess. Those simplifications are:
- Moisture moves inside the element only by water vapour transfer;
- Vapour transfer is only due to diffusion and follows Fick's law;

- Heat transfer is only due by conduction and under steady state;
- Materials are not hygroscopic;
- Construction elements are airtight and have their faces flat and parallel;
- Water vapour permeability coefficients and thermal conductivity coefficients are constant;
- There is no movement of the condensed water vapour.

3.2 Simulation program

The simulation program used was "CONDENSA", that allows the easy calculation of the "curves" of the installed pressures in a constructive element and their "curves" of saturation pressures.
It is based in Fick's law, which gives us the water vapour flux through a building element consisting of homogeneous elements and that is governed by the following equation:

$$g = \sum_j \frac{\pi_j}{e_j}\left(P_i - P_e\right)$$

Where: g – water vapour diffusion flux per unit area [kg/(m^2 s)]; π_j – water vapour permeability coefficient of the layer [kg/(m s Pa)];e_j – thickness of the layer [m]; P_i, P_e –partial water vapour pressure inside and outside, respectively [Pa].
And in Fourrier's law, which gives us the heat flux according to the following equation:

$$q = \sum_j \frac{\lambda_j}{e_j}\left(t_i - t_e\right)$$

Where: q – heat flux per unit area [W/m^2]; λ_j – thermal conductivity coefficient of the layer [W/(m ^{o}C)]; t_i, t_e –interior and exterior temperatures respectively [^{o}C].
Thus, knowing the weather conditions inside and outside, the material properties, its thickness and the thermal resistance of the surface, we can determine the "curves" of the installed pressures, the "curves" of the saturated pressures and then verify the probability of the occurrence of internal condensations.

3.3 Performed simulations and obtained results

One of the most important issues that we intent to study with the continuation of this work is the comparison of the results along the year, with regard to condensation, for many distinct situations.
These situations are somewhere between two extremes: on the one hand, a dynamic simulation with a detailed evolution of the weather conditions throughout the year and on the other hand, a completely static analysis, with the average monthly climatic values.

Between these two extreme cases there are a wide variety of intermediate situations to be assessed in order to identify the degree of uncertainty or error and evaluate the effort for its implementation.
This article reports to an initial phase of this work where we considered the minimum monthly values for temperature, that influence, as starting conditions, the following month.. We are now developing work to find an optimization procedure whose results will be timely disclosed.

The adopted temperatures were the minimum values for the city of Coimbra, according to data provided by "Instituto de Meteorologia" (table 1).

Table 1. Values of minimum temperatures in Coimbra.

Month	Jan	Feb	Mar	Apr	May	Jun	Jul	Aug	Sept	Oct	Nov	Dec
Temp. min	-4.9	-4	-3.3	11.5	2	4.1	6.8	6	2	-2.6	-3.1	-2.8

Simulations performed program Condensa varied according to the solutions presented in Table 2. Among all the studied solutions only 3 had high hygrometry (solutions 2, 15 and 16) the remaining 13 had low hygrometry.

We evaluated different combinations of layers of zinc roofs, so we can compare results and draw some conclusions regarding their performance
From all of the studied solutions, 14 are of compact roofs and just two are of ventilated roofs. This fact is basically due to:
- The lack of studies on the compact covers;
- The lack of practical results in compact roofs, as they are newer solutions;

Table 2. Studied solutions for zinc roofs.

Layers	Material		Solution															
			1	2	3	4	5	6	7	8	9	10	11	12	13	14	15	16
Exterior protection	Zinc sheet				X	X				X	X	X	X	X	X	X	X	X
	Fibrocement								X									
Layer of air caused by the non solidarization screen	Air				X	X		X	X		X	X	X	X	X	X	X	X
Non solidarization screen	Polyethylene screen piton				X	X	X	X	X		X	X	X	X	X	X	X	X
Thermal insulation	Extruded polystyrene	3 cm										X						
		5 cm	X	X	X	X	X	X	X	X				X	X	X	X	X
		7 cm											X					
Vapour barrier	PVC sheet															X		X
Resistant structure	Reinforced concrete	15 cm												X				
		20 cm	X	X	X	X	X	X	X	X	X	X	X			X	X	X
		40 cm													X			
Interior coating	Plaster and stucco		X	X	X	X	X	X	X	X	X	X	X	X	X	X	X	X

Table 3. Characteristics of the constituent materials of the roofs.

Layers	Material	Thickness (m)	Thermal conductivity (λ) [w/m ºC]	Water vapour permeability coefficient (π) [g/(m.h.mmHg]
External protection	Zinc sheet	0.0012	110	0
	Fibrocement		0.65	$180x10^{-5}$
Layer of air caused by the non solidarization screen	Air	0.008	0.025	$9000x10^{-5}$
Non solidarization screen	Polyethylene screen piton	0.0006	0.5	$0.12x10^{-5}$
Thermal insulation	Extruded polystyrene	0.05	0.035	$50x10^{-5}$
Vapour barrier	PVC sheet	0.0008	1.75	$0.88x10^{-5}$
Resistant structure	Reinforced concrete	0.2	1.75	6.3
Interior coating	Plaster and stucco	0.02	1.3	$180x10^{-5}$

Solutions 1 and 2 represent zinc ventilated roofs. In their simulations only the layers below the layer of ventilation were contemplated. Making this simplification in zinc ventilated roof we are considering that all water vapour transported by diffusion through different materials, from the inside,

will be totally conducted to the exterior through the ventilation layer. As it was expected there are no condensations in any of the layers of both solutions.
Simulation 3, which refers to a compact roof, allowed us to conclude that there is always condensation on the underside of the zinc sheets. In the intervals 11 and 12, which correspond to lower temperatures and a relative humidity of 90%, we could also notice condensation on the underside of the screen python.

The results of solution 4 were similar to those of solution 3. In solution 5 the zinc sheet was removed and the simulation reproduced a roof whose exterior coating would be screen piton. In this case, the condensation risk appeared, in all time intervals, at the screen piton.

In an attempt to understand what the effect of zinc sheet is, solution 6 (purely theoretical) was simulated. In this simulation, similar to solution 4, the zinc sheet was removed and the air layer resulting from the screen piton maintained. This simulation allowed us to conclude that a small air layer (t=0.008m), that we considered non-ventilated, changes the results and leads to a solution without condensations in any of the time intervals.
With simulation 7 we pretended to do a comparison of the zinc sheet with another coating material. The zinc sheet was replaced by a fibrocement sheet and all the other layers remained according base solution (solution 4). The values of the water vapour permeability coefficient of the fibrocement, which is quite different from the one of the zinc sheet, change the results and we obtained a solution without any condensations at any time.

Solution 8 reproduces a compact zinc roof without screen piton, the obtained results are the expected one, and there is risk of condensations between the zinc sheet and the thermal insulation
Solutions 9, 10 and 11 were performed in order to understand how the thickness of the thermal insulation or its absence could influence the results. In solution 9, which is a solution without thermal insulation, condensations will occur at the inferior face of the zinc sheet. Changing the thickness of the thermal insulation, in solutions 10 and 11 showed the influence of the thermal insulation in the system. The study shows that when we increase the thicknesses of the thermal insulation the risk of condensations in the inferior face of the screen piton also increases.

Comparing simulations 4, 12 and 13 we can conclude that variations in the thickness of the layer of reinforced concrete are not determinants in the evaluation of the internal condensations risk.
Solution 14 is the base solution (solution 4) with a PVC vapour barrier and we can say that the observed changes are basically for the lower temperatures. The introduction of a PVC sheet under the thermal insulation reduced the points of possible condensations. Condensations will occur only at the inferior face of the zinc sheet.

Table 4. Results about fluxes and condensates in solution 1.

ΔT [h]	Σ ΔT [h]	Tint [ºC]	Text [ºC]	Hyint [g/m3]	HRext [%]	Fterm [W/m²]	Fent [mg/(m².h)]	Fsaida [mg/(m².h)]	Fcond [mg/(m².h)]	Fcond/Fent [%]	HUM TOT [g]
744	744	20	-4,9	2,5	80	14,662	13,591	13,591	0,000	0,0%	0,000
672	1416	20	-4	2,5	80	14,132	13,538	13,538	0,000	0,0%	0,000
744	2160	20	-3,3	2,5	80	13,720	13,498	13,498	0,000	0,0%	0,000
720	2880	20	-1,5	2,5	80	12,660	13,395	13,395	0,000	0,0%	0,000
744	3624	20	2	2,5	80	10,599	13,256	13,256	0,000	0,0%	0,000
720	4344	20	4,1	2,5	80	9,363	13,211	13,211	0,000	0,0%	0,000
744	5088	20	6,8	2,5	90	7,773	12,993	12,993	0,000	0,0%	0,000
744	5832	20	6	2,5	90	8,244	12,989	12,989	0,000	0,0%	0,000
720	6552	20	2	2,5	90	10,599	13,056	13,056	0,000	0,0%	0,000
744	7296	20	-2,6	2,5	90	13,308	13,282	13,282	0,000	0,0%	0,000
720	8016	20	-3,1	2,5	90	13,602	13,314	13,314	0,000	0,0%	0,000
744	8760	20	-2,8	2,5	90	13,426	13,295	13,295	0,000	0,0%	0,000

Simulations 15 and 16 refers to compact zinc roofs have a high hygrometry. Those were the simulations were we could observe more significant values, proving that hygrometry class is determinant for the occurrence of condensations in a zinc roof. In those solutions we have the occurrence of condensations in two distinct points, in the inferior face of the zinc sheet and between thermal insulation and the screen piton even for positive values of temperature.

The results of these simulations allow underlining the importance of the hygrometry in the presented solutions for different buildings.

The calculation program Condensa beyond allowing us the easy calculation of the "curves" of the installed pressures in a constructive element and their "curves" of saturation pressures, gives us the values of the several fluxes. It gives us the in flux, the out flux and the condensed flux in the constructive element.

As an example we can see in table 4 and 5 the obtained results for simulation of the solutions 1 and 16. In first case we can verify that there is no risk of condensations by observing column "Fcond" (condensed flux) in the second one we can see that the risk is high.

Table 5. Results about fluxes and condensates in solution 16.

ΔT [h]	Σ ΔT [h]	Tint [ºC]	Text [ºC]	Hyint [g/m3]	HRext [%]	Fterm [W/m²]	Fent [mg/(m².h)]	Fsaida [mg/(m².h)]	Fcond [mg/(m².h)]	Fcond/Fent [%]	HUM TOT [g]
744	744	23	-4,9	7,5	80	13,547	4,744	0,056	4,688	98,8%	3,488
672	1416	23	-4	7,5	80	13,110	4,684	0,060	4,624	98,7%	3,107
744	2160	23	-3,3	7,5	80	12,770	4,638	0,064	4,574	98,6%	3,403
720	2880	23	-1,5	7,5	80	11,896	4,526	0,074	4,452	98,4%	3,205
744	3624	23	2	7,5	80	10,197	4,253	0,096	4,157	97,8%	3,093
720	4344	23	4,1	7,5	80	9,177	4,070	0,110	3,959	97,3%	2,851
744	5088	23	6,8	7,5	90	7,866	4,486	0,066	4,419	98,5%	3,288
744	5832	23	6	7,5	90	8,255	4,518	0,063	4,455	98,6%	3,315
720	6552	23	2	7,5	90	10,197	4,712	0,048	4,664	99,0%	3,358
744	7296	23	-2,6	7,5	90	12,430	4,913	0,034	4,879	99,3%	3,630
720	8016	23	-3,1	7,5	90	12,673	4,931	0,032	4,899	99,3%	3,527
744	8760	23	-2,8	7,5	90	12,528	4,920	0,033	4,887	99,3%	3,636

4 CONCLUSIONS

The calculations performed have confirmed the advantages of ventilated roofs. The risk of condensation in zinc roofs is higher in compact solutions than in ventilated ones. The risk of condensation is influenced by the thickness of the thermal insulation. The study shows that for higher thicknesses of thermal insulation beyond the risk of condensations in the inferior face oh the zinc sheet we have an increase of the condensations in the screen piton. With the introduction of the vapour barrier the observed changes are basically in the lower temperatures. With the introduction of a PVC sheet under the thermal insulation the points of condensation have just been registered on the underside of the zinc sheet. However what most affects the system is the hygrometric class. When we have buildings with high hygrometric class the risks of condensation is very high and we must proceed to additional studies.
Glasser method allows us to determine in which points of the roof we will have risk of occurrence of condensations. Thus it is possible to determine the right solution for each case.

REFERENCES

Freitas, V. P. de; P. Pinto - *Caracterização de Barreiras Pára-Vapor e sua Aplicação,* Construção 2001- Congresso Nacional de Construção, IST;Volume II, 2001.

Freitas, Vasco Freitas, Marília Sousa - *Degradação do Revestimento em Chapa de zinco de uma Cobertura em Terraço não Acessível*, www.patorreb.com.

Greff, Alain - *Corrosion de Feuilles de Zinc en Couverture*, www.smabtp.fr.

Hens, Hugo - *Metal Constructions: all Hygrothermal Problem Cases?*, CIB2004, 2004, Toronto.

Hens, Hugo, R. Zheng, Carmeliet - *The influence of Roofing Systems on the Corrosion Zinc*, Research in Building Physics, Leuven.

Mauricio, Carla - *Coberturas de zinco – Anomalias e Soluções de Reabilitação*, Msc Thesis, FCTUC, Coimbra 2009.

XII DBMC
International Conference on Durability of Building Materials and Components
PORTO - PORTUGAL, April 12th-15th, 2011

Reducing the Risk of Microbial Growth on Insulated Walls by PCM Enhanced Renders and IR Reflecting Paints

K. Sedlbauer [1]
M. Krus [2]
C. Fitz [3]
H.M. Künzel[4]

ABSTRACT

Staining of façades due to microbial growth has been on the rise in recent years. Especially walls with external insulation systems are affected because low thermal mass of the exterior render combined with high thermal resistance of the insulation layer leads to frequent overcooling of the render's surface by long-wave radiation exchange with the sky. Condensation forming on the overcooled façade is of major importance for microbial growth. Therefore, the best way to prevent growth is to reduce the frequency of condensation by limiting the periods of overcooling. This could be achieved by increasing the thermal inertia of the exterior render through the addition of phase change materials (PCM) or by applying low IR emissivity (Low-E) paint coats. The performance of novel rendering systems including PCM additives and/or Low-E coating has been investigated by field tests as well hygrothermal simulations. The results show that Low-E coats may be more effective than PCM additives because the latent heat of phase change is only beneficial when the surface temperature coincides with PCM's melting temperature range.

KEYWORDS

Microbial growth, Phase change materials, Low-E coating, Exterior condensation.

[1] Fraunhofer-Institute for Building Physics (IBP), Valley, GERMANY, klaus.sedlbauer@ibp.fraunhofer.de
[2] Fraunhofer-Institute for Building Physics (IBP), Valley, GERMANY, martin.krus@ibp.fraunhofer.de
[3] Fraunhofer-Institute for Building Physics (IBP), Valley, GERMANY, cornelia.fitz@ibp.fraunhofer.de
[4] Fraunhofer-Institute for Building Physics (IBP), Valley, GERMANY, hartwig.kuenzel@ibp.fraunhofer.de

1 INTRODUCTION

Due to the enhancement of the thermal insulation of external building components the probability is increased that higher surface humidity, even condensation, can occur on the external surfaces of façades. As a result, humidity being the most important basis for microbial growth on walls has increased [Blaich 1999], [Venzmer 2001]. The consequences are most severe for external thermal insulation composite systems (ETICS), since they possess only a low thermal storage capacity compared to monolithic constructions. Only a small part of the energy of the solar radiation during daytime can be stored so that the long-wave radiation during the night frequently causes a reduction of the surface temperature below the dew point temperature of the ambient air. Fig. 1 shows a façade with the typical microbial growth of fungi and algae. The surface above the tilted window clearly shows that even the ventilation behaviour of the residents can have an influence on the microbial growth. The effect of thermal bridges is also clearly visible. The slightly higher surface temperature causes an interruption of the massive fungal growth above the window. The surface below the window shows predominantly the growth of algae.

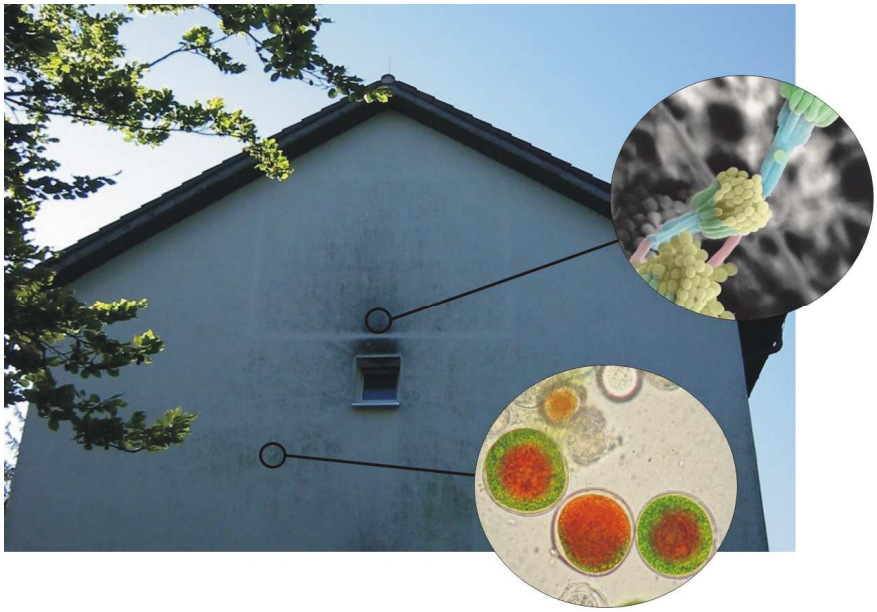

Figure 1. Growth of algae on a façade with external thermal insulation composite system (ETICS) and fungal growth above the window.

Since biocidal finishing of surfaces should be an extraordinary solution for environmental reasons and due to the temporary efficiency, new possibilities must be found to avoid the growth of algae or fungi preferably by physical measures. For this purpose, comprehensive analyses of façade surfaces are conducted on the outdoor testing site of the Fraunhofer Institute for Building Physics (IBP). The whole variety of interesting variations, however, cannot be studied by field tests. Calculations can be carried out by the hygrothermal programme WUFI® modified for this purpose. It allows after validation the rapid and cost-efficient assessment of numerous further variations to evaluate the influence of different factors, e.g. orientation, thickness of thermal insulation layers or enhancement of the thermal storage capacity by using phase change material (PCM) effects.

2 COMPUTATIONS OF PREVENTION STRATEGIES

Computations are carried out by means of the computation programme WUFI® [Künzel H.M. 1994], which was developed by IBP and meanwhile received multiple validations. To allow the comparison of the computed results (surface temperature and surface humidity) of individual wall constructions with measured data, calculations are carried out on the basis of the boundary conditions of the exterior climate recorded in the same period of time. Therefore all following results refer to the

climate in Holzkirchen. The most critical season for biological growth on external walls are autumn and spring. Winter and summer do not offer any optimal climate for the growth of algae and fungi [Hofbauer et al. 2006].

There are principally two different physical approaches to reduce condensation on the external surfaces of ETICS. By enhancing the thermal storage capacity close to the exterior surface for example with phase change materials (PCM), it is possible to store the heat from the daily solar warming of the building component to avoid the lowering of temperature below the dew point temperature. In addition, the daily warming of the façade can be enhanced by applying paint with a short wave-higher absorption factor. The drop in temperature at night can be reduced by means of applying paint with a reduced long-wave emissivity (IR paints). A possible criterion to assess the results and the risk of growth is the duration of condensation and the intensity of the dew point temperature undercut.

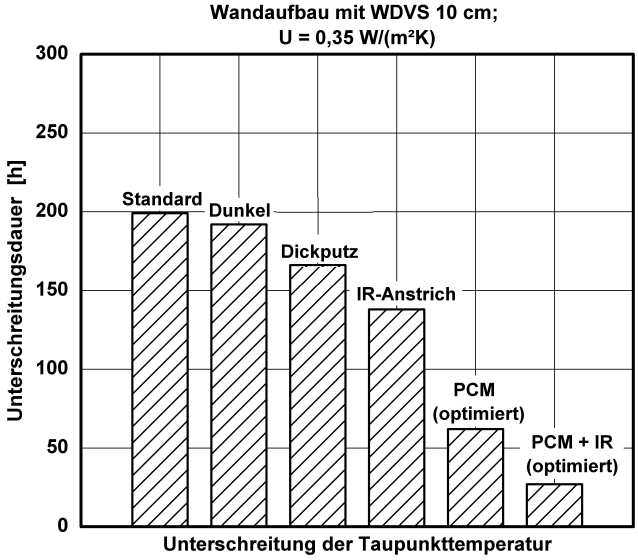

Figure 2. effects of various measures on the duration of the dew point temperature undercut in the period from September to October.

Figure 2 shows the diagram, which summarizes the effects to be expected of different measures. It can be clearly seen that the application of darker façade paint with regard to avoiding condensation does not yield any noteworthy result. Nevertheless, a tinted paint can be advantageous, since it conceals slight growth as well as entails higher temperatures from time to time, which may be lethal to micro-organisms. A thicker external plaster with a high thermal mass can reduce dew point temperature undercut by a maximum of 20 %, IR paint by almost 30 %, and a latent thermal storage layer even by 70 %. The combination of both measures (PCM + IR) can further reduce the duration of dew point temperature undercut, as an extreme case. It must, however, be taken into consideration that in case of applying phase change materials (PCM) the desired effect will only occur, if the melting point of the PCM is adjusted to the climate boundary conditions, which is expressed by the additional term “optimized” in Fig. 2. Microcapsules filled with paraffin as phase change material is mostly used, which is available for this purpose with different melting point between 5 °C and 15 °C. The melting heat amounts to about 200 kJ per kg paraffin.

3. FIELD TESTS

Temperature profiles on the external surfaces of the wall assemblies were measured during outdoor tests to determine by comparison with the measured ambient air dew point temperature the duration and intensity of condensation. Fig. 3 shows western oriented (right) and a northern oriented (left) façade being tested.



Figure 3. Photos with the view of the western oriented (right) and the northern oriented (left) façade.

To show that the impact of condensation is lower on monolithic systems, the measured results of massive walls are also taken into consideration (Fig. 4). Compared to ETICS they clearly show shorter condensation times. As the calculations already showed, the grey colour only yielded a negligible improvement.

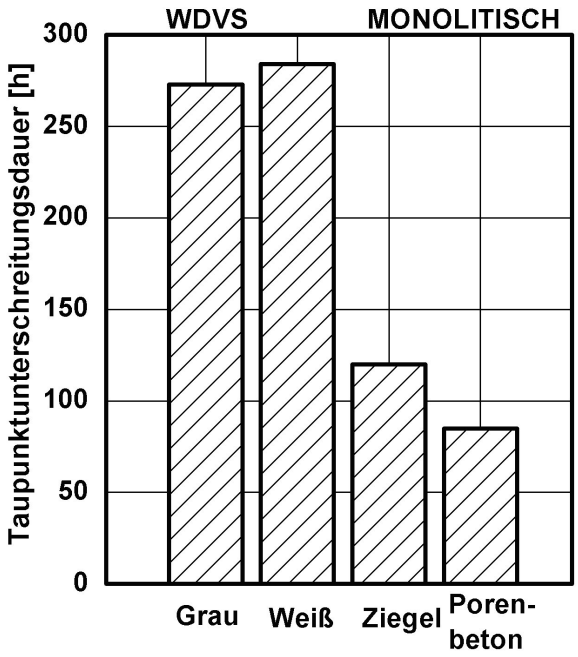

Figure 4. Summarized condensation times for various wall constructions and paints for the most important period of growth in autumn.

The advantage of innovative materials, e.g. IR paints, PCM plasters and the combination of PCM and IR paint can be proven by measurement (see Fig. 5, from the northern façade of Fig. 3). Since temperatures are too low for microbial growth in winter, autumn (as general observations confirm) is the main period of microbial growth. If the measured condensation times are observed for this period of time, the effectiveness of PCM is clearly visible in the first autumn, although measurements could only be started in October. In comparison to a white thin plaster duration of condensation was reduced by approx. 30 % for thick plaster with PCM additives. When comparing with the calculated results for PCM in Fig. 2 it must be taken into consideration that only half the quantity of PCM was added so that the measured duration of condensation tends to show good compliance with the calculation result.

The façade with IR paint, which only achieved a emissivity value of 0.74 instead of 0.6 in contrast to the calculations, shows a decrease of the condensation times by approx. 15 %. As was expected, the combination of PCM plaster and IR paint achieves a reduction of the exterior condensation of almost 50 %, clearly a higher reduction than the results with PCM additive and IR paint alone.

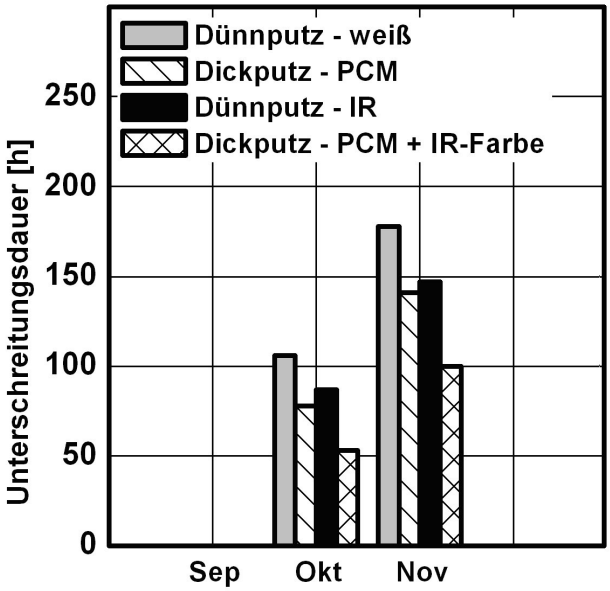

Figure 5. Duration of condensation for the ETICS without and with PCM and IR paint for the first autumn of the measurement period.

Besides the duration and quantity of condensation the actual amount of surface water is decisive to assess the risk of microbial growth, since only the water on the surface of a façade is available for micro-organisms. Therefore, the surface humidity on a western façade without PCM plaster was determined by dabbing. Fig. 6 shows the results of a morning after a clear night. Almost double the amount of water was measured on the surface of a standard ETICS with white paint than on the surface of a white thick plaster. It must, however, be taken into consideration that these results are dependent on the hygric material properties of the plaster and paint to a very large extent. More condensation is penetrating through the thick plaster beneath the surface. The best result is achieved by the surface with IR paint (variant with an emission coefficient of approx. 0.6). Almost no water could be measured on the surface this morning. Unfortunately, the IR paints available at present are not yet sufficiently weather resistant. This could be seen by the fact that for the investigated paints aluminium flakes, which were used to reduce long-wave emission, appeared on the surface due to the impact of weathering after a relative short period. The result is a metallic glaze of the paint. The measurements, however, show that it would be beneficial to further develop IR paints to adjust weathering resistance to present requirements.

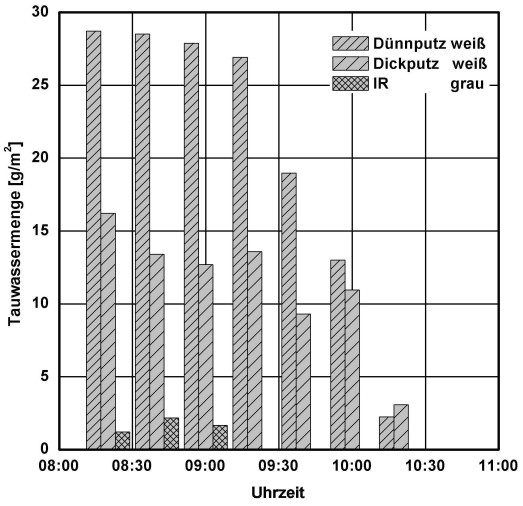

Figure 6. Courses of surface humidity of western oriented walls with various ETICS.

The measurements on the northern façade of Fig. 3 were continued. Fig. 7 shows the results for the successive 2 periods in autumn. Surprisingly, the façade with PCM additives shows no or only a slight reduction of the condensation times in contrast to the first period in autumn. The reason is not the stability but the melting temperature of the PCM used, which amounts to 6 °C. Whereas the mean ambient air temperature was 5 °C in the autumn of the first year of investigations, it amounted to approx. 10 °C in the following years. Therefore, no latent heat could be released. The façade with IR paint, however, shows a continuous and constant lowering of condensation times. An interesting aspect is the fact that the combination of PCM plaster and IR paint shows a clearly higher reduction of the condensation production during the total period of measurements than the IR paint alone, although the PCM additive alone did not yield any improvement from time to time.

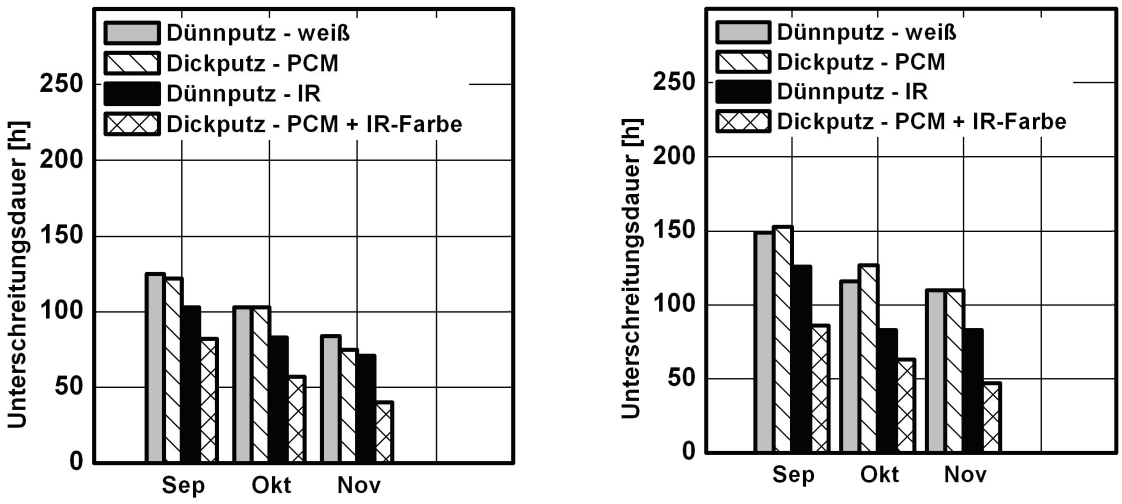

Figure 7. Duration of condensation on the surface of the ETICS without and with PCM and IR paint of the second autumn (left) and the third autumn (right) of the period of measurements.

4 SUMMARY

In the last decades, the level of thermal insulation was clearly increased especially for new buildings. The improvement of the standard of thermal insulation resulted in a clearly higher risk of microbial growth on external façades by mould and algae. The essential criterion for the risk of microbial growth on façades is the availability of sufficient humidity. Condensation at night caused by nocturnal long-wave emission is of special importance, since it is the only explanation for the observed increase

in microbial growth on the northern façade with only little driving rain. To assess the risk of microbial growth condensation on the surface is thus a good criterion. The direct comparison of monolithic walls e.g. made of aerated concrete or bricks, with walls with ETICS shows that they are more at risk. But to improve the thermal insulation of already existing buildings the application of ETICS is the most practicable way in most cases. Therefore possible solutions against microbial growth are investigated for these systems. Calculations as well as field test measurements were conducted for this purpose. If we consider the problem of undesired microbial growth on façades, we must notice that the majority of ETICS is without any damage. Only a minor percentage shows microbial growth. This is the reason why the authors suggest that already the reduction of the time of condensation by 25 % could avoid most problems. But there are always special circumstances, for example a shaded wall in the vicinity of a forest or water, where the application of chemical agents is inevitable.

A possible solution to reduce nocturnal condensation is to use latent heat effects by adding so-called PCM (phase change materials) in external façades. Paraffin for example, which is available with various melting point ranges, can serve as PCM. The optimization of the temperature for the phase change is essential to reduce the condensation by applying PCM. The problem, however, is its application. The optimization of the phase change point is calculated by applying test reference years. Yet, the differences of the climate conditions in successive years are so immense that not even this kind of optimized PCM can be continuously effective. This example, however, also shows that calculations alone do not reflect practical reality despite correct calculation results, since parameters are neglected from time to time, which can only be revealed by outdoor testing, in this case over a period of several years.

In case of IR paints the emission coefficient for long-wave radiation could be reduced from more than 90 % to approx. 60 %. Higher maximum temperatures during the day as well as a reduction condensation are achieved by reduced thermal emission. This is the method, which is most simply practicable in already existing buildings. Unfortunately, IR paints, which are sufficiently resistant to weathering, are not yet available.

REFERENCES

Blaich, J. 1999. *Außenwände mit Wärmedämm-Verbundsystem, Algen- und Pilzbewuchs*. (Facades with ETICS, algae and mould growth) Deutsches Architektenblatt 31, H.10, S.1393 - 1394.

Venzmer, H. 2001. *Grüne Fassaden nach der Instandsetzung durch WDVS? Nicht bestellt und dennoch frei Haus (Green Facades after renovation with ETICS? Not ordered but delivered freely)*. 3. Dahlberg-Kolloquium.

Künzel H.M. (1994). *Simultaneous heat and moisture transport in building components. One- and two-dimensional calculation using simple parameters*. PhD Thesis, University of Stuttgart.

Hofbauer, W.; Fitz, C.; Krus, M.; Sedlbauer, K.; Breuer, K.: *Prognoseverfahren zum biologischen Befall durch Algen, Pilze und Flechten an Bauteiloberflächen auf Basis bauphysikalischer und mikrobieller Untersuchungen (Assesment procedure for microbial growth of algae and mould on the basis of physical and biological investigations)* . Hrsg.: Fraunhofer-Institut für Bauphysik –IBP-, Holzkirchen; Bauforschung für die Praxis Band 77 (2006). IRB-Verlag. ISBN 978-3-8167-7102-9.

XII DBMC
International Conference on Durability of Building Materials and Components
PORTO - PORTUGAL, April 12th-15th, 2011

Investigation of a Multi-Layer Latent Heat Solar Thermal Energy Storage System with PCMs

Nelson Soares [1]
Romeu Vicente [2]
António Samagaio [3]
José Costa[4]

ABSTRACT

Thermal energy storage techniques incorporated into the building's envelope are receiving increasing attention due to their importance in energy saving, in the new building's dynamic physics approach and in building's durability. The use of a latent heat storage system incorporating Phase change Materials (PCMs) benefits from their high-energy storage density and from the isothermal nature of the phase change process.

A multi-layer latent heat storage system incorporating a PCM that based on solar thermal energy for heating building spaces during the winter was designed. The system is associated with a southward façade window storing solar thermal energy during the day and releasing that energy during the night. This system was optimized numerically using a two-dimensional simulation model, based on the enthalpy formulation. The main goal is to quantify the energy storage/release capacity of the shading element structure designed during a typical day cycle and to compare it with that of other current building materials. Additionally the goal is to optimize the melting temperature of the PCM.

The results show the high-energy storage capacity of the PCM. They also show that an optimal system can be designed for any given location and climatic data during the winter. Besides the external boundary conditions, the optimum system is strongly affected by the thermophysical properties of the PCM and by the internal boundary conditions imposed, particularly by the convection heat transfer rate on the inner side of the shading element during the night.

KEYWORDS

Phase change materials (PCM), Latent heat, Enthalpy formulation, Energy storage.

[1] Civil Engineering Department of the University of Aveiro, Aveiro, PORTUGAL, nsoares@ua.pt
[2] Civil Engineering Department of the University of Aveiro, Aveiro, PORTUGAL, romvic@ua.pt
[3] Environment and Planning Department of the University of Aveiro, Aveiro, PORTUGAL, samagaio@ua.pt
[4] ADAI – Mechanical Engineering Department of the University of Coimbra, Coimbra, PORTUGAL, jose.costa@dem.uc.pt

1 INTRODUCTION

Solar energy resources are abundant in the winter season in the Mediterranean climates. This is a great advantage, from the point of view of energy-saving, for the integration of PCMs into buildings construction. An interesting feature is that they can store latent heat energy as well as sensible energy. The storage of thermal energy as latent heat has attractive features over that of sensible heat due to its high storage density and isothermal nature of the changing phase process at the PCM's melting temperature. For a review, see [Sharma *et al.* 2009], [Tyagi & Buddhi 2007], [Zalba *et al.* 2003].

The volume of melted PCMs depends on the extension of the sunshine period and the amount of solar radiation. It must be optimized because if it is too large, the time needed for the heat to penetrate the PCM becomes larger than the total number of available sunshine hours and the storage process cannot be complete during a day. Also due to a low thermal conductivity of PCM, these systems have an inherent disadvantage of slow heat transfer during the charging and discharging processes.

The improvement of the thermal performance of the building due to the incorporation of PCM in a building envelope system depend on the climate conditions, mainly on the solar radiation and ambient temperature, on the thermal properties of the materials, on the design parameters such as shading, configuration and orientation of the system, but also on the amount and type of PCM. Therefore, these systems require a complex thermal behaviour simulation to account for all these features.

The problem of predicting the behaviour of phase change is difficult due to its nonlinear nature at the moving interface and, in addition, to the fact that the two phases have different thermophysical properties. When the PCM undergoes a phase change, both the solid and the liquid phases are present and are separated by a moving interface between them. The difficulty in solving a phase change problem is the presence of a moving boundary or region on which heat and mass balance conditions have to be met. One of the methods to solve the moving boundary problem is the enthalpy formulation proposed and studied by various authors: Swaminathan and Voller [1993], Costa *et al.* [1998], Brousseau and Lacroix [1998], Chen and Sharma [2006], Sharma *et al.* [2006], Chen *et al.* [2008]. According to Costa *et al.* [1998] and Chen and Sharma [2006] by introducing an enthalpy formulation, the phase change problem becomes much simpler.

In this paper, a latent heat storage system with PCM has been numerically designed and optimized, using a two-dimensional simulation model based on the enthalpy formulation in order to take advantage of the solar thermal energy for buildings space heating during the winter season in Coimbra, Portugal. The numerical simulation aims to demonstrate the true potential of incorporating PCMs in structural cells of shading elements in the building envelope, especially when associated to southward façade windows. The numerical simulation of the system is performed with a code specifically developed for this purpose. The main goal of this work is to quantify the energy stored in and released by the system during a complete day cycle and to optimize the melting temperature of the PCM for the volume of material considered and for the boundary conditions imposed.

2 SYSTEM DESCRIPTION

2.1 System configuration

A system incorporating PCM has been idealised to store the solar energy in the form of thermal energy during the winter period. The scheme of the system is shown in Fig. 1. The system consists of a battery of several aluminium rectangular containers for the PCM. The thickness of the aluminium used in the container is 0.002 m, which coincides with the thickness of the black aluminium liner. These are supposed to act as a fin and help to enhance the rate of heat transfer to the PCM. Due to the low thermal conductivity of PCM, the use of metal fins in a latent storage system to enhance the heat transfer, were studied by Chen and Sharma [2006], Sharma *et al.* [2006], Chen *et al*. [2008]. The total width of the metal PCM container plus the black metal liner is 0.03 m which is the overall thickness

of the system used in the numerical calculation, considering the boundary in contact with the insulation material as adiabatic. The volume of PCM with which the container can be filled represents 40 % of the total volume of the system. The insulation material layer is essential to enable the control of the direction of the heat flow transfer, especially during the discharging of the system.

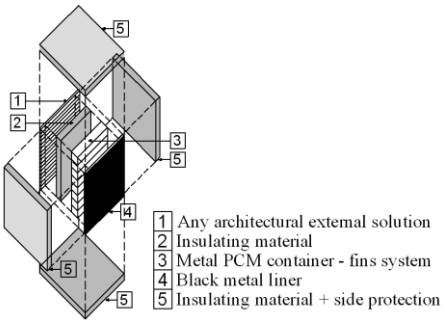

Figure 1. Schematics of the latent heat storage system.

The schematics of the functioning of the system during the winter can be seen in Fig. 2. The system must be opened during the daytime and closed during the night. It operates cyclically, reflecting the ongoing cycles of phase change of the PCM (from solid to liquid and *vice versa*), and at the same time enabling the storage and release of thermal energy. It is designed to enable the control of the direction of heat transfer most suited to the time of day and to increase the thermal resistance of the glass area during the periods in which it is important to minimize the heat losses of the enclosure.

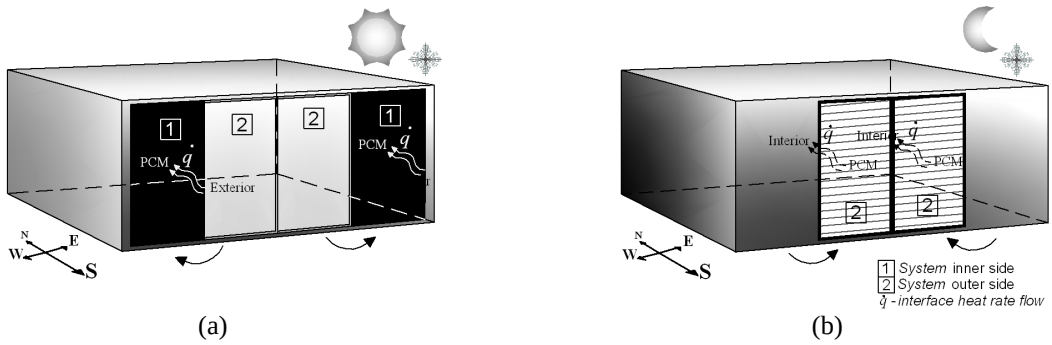

(a) (b)

Figure 2. Schematics of the functioning of the latent heat storage system during de winter during: **(a)** the day – PCM charging; **(b)** the night – PCM discharging.

During the winter, the goal is to maximize the solar thermal energy intake. Therefore shutters should remain open during the daylight periods. In this way it is possible to get viable solar intakes from the windows and simultaneously charge the system with thermal solar energy storage. By exposing the inner surface of the system – black surface – to solar radiation it is possible to trigger the phase change from solid to liquid and store thermal energy. During the night, the shutters should be closed so that thermal energy can be released to the inner space via the phase change from liquid to solid. Closing the shutters ensures a greater thermal resistance of the glass façade during the night and simultaneously imposing the desired direction of the heat transfer.

2.2 General assumptions

The chosen PCM for this simulation is similar to a n-Octadecane. The thermophysical properties of this PCM are given in Table 1 as well as the properties of the heat exchanger material - aluminium. One uses all of n-Octadecane's thermophysical properties but that of its melting temperature which shall be considered lower than that of n-Octadecane and nearer to inner comfort temperature during the winter.

Table 1. Thermophysical properties of the n-Octadecane - CH3(CH2)16CH3 and of the aluminium.

	n-Octadecane	Aluminium
Latent heat of fusion (J kg^{-1})	243500	-
Melting temperature (ºC)	20	-
Density – solid (kg m^{-3})	865	2707
Density – liquid (kg m^{-3})	780	-
Specific heat – solid (J kg^{-1} ºC^{-1})	1934	896
Specific heat – liquid (J kg^{-1} ºC^{-1})	2196	-
Thermal conductivity – solid (W m^{-1} ºC^{-1})	0.358	204
Thermal conductivity – liquid (W m^{-1} ºC^{-1})	0.148	-

The main outdoor conditions are external air temperature and solar radiation. Figure 3 shows the sinusoidal evolution of the exterior air temperature, T_e, and the solar radiation, q_{rad}, calculated for a vertical wall in Coimbra in January, according to the climate data of SOLTERM® during the time when the system is opened – from 9 am until 5 pm. The exterior convection heat transfer coefficient considered is h_e = 25 W m^{-2} ºC^{-1}.

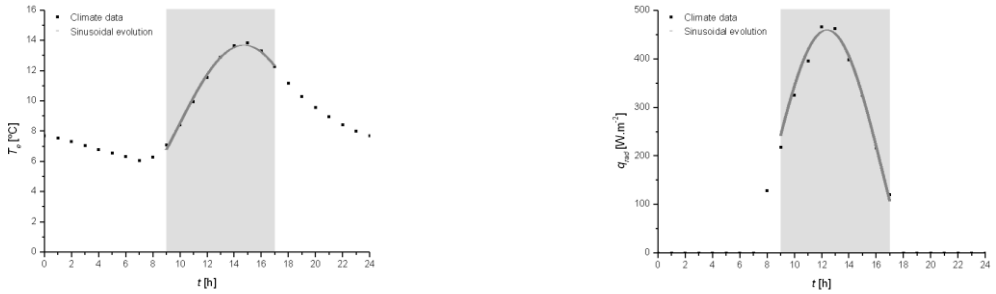

(a) (b)

Figure 3. Sinusoidal evolution, during the time when the system is opened, of the: **(a)** external air temperature; **(b)** solar radiation calculated for a vertical wall. Climate data determined from SOLTERM® – conditions in Coimbra in January.

The indoor air temperature, T_i, is influenced by outdoor conditions, internal loads and the buildings envelope constitution. During the time when the system is closed – from 5 pm until 9 am – the average indoor air temperature is considered fixed and equal to 15 ºC. The interior convection heat transfer coefficient can vary according with the model chosen for its determination.

3 NUMERICAL SIMULATION

The following assumptions are made to analyse the latent heat storage system as suggested by Costa *et al.* [1998], Brousseau and Lacroix [1998], Chen and Sharma [2006] and Sharma *et al.* [2006]: *(i)* thermophysical properties of the PCM and fin material are independent of temperature, but they are different for solid and liquid phases of PCM; *(ii)* PCM is initially in solid phase; *(iii)* PCM is homogeneous and isotropic; *(iv)* for two-dimensional simulation, the mode of heat transfer is conduction only. Phase change problems are usually solved with finite difference or finite element techniques in accordance with the numerical approach. The enthalpy formulation is one of the most popular fixed-domain methods for solving the Stefan problem. According to Chen and Sharma [2006] by introducing an enthalpy formulation, the phase change problem becomes much simpler and has the following advantages: the governing equation is similar to the single phase equation; there is no condition to be satisfied at the solid-liquid interface, as it automatically obeys the interface condition; and the enthalpy formulation allows a mushy zone between the two phases. To introduce the formulation, an enthalpy function *h* is defined as a function of temperature and the equation is applied over the whole fixed domain.

As suggested by Costa *et al.* [1998], Brousseau and Lacroix [1998], Chen and Sharma [2006] and Sharma *et al.* [2006], for a material undergoing a phase transformation, the conservation of energy for constant thermophysical properties can be expressed as:

$$\frac{\partial H}{\partial t} = \nabla(k_k(\nabla T)) \tag{1}$$

where H is the total volumetric enthalpy is the sum of sensible and latent heat of the PCM

$$H(t) = h(t) + \rho_l f(t) L \tag{2}$$

where

$$h = \int_{T_m}^{T} \rho_k c_k \mathrm{d}T \tag{3}$$

In case of isothermal phase change, the liquid fraction of melted PCM is given by:

$$f = \begin{cases} 0, & \text{if } T < T_m \quad \text{(solid)} \\ ]0,1[, & \text{if } T = T_m \quad \text{(mushy)} \\ 1, & \text{if } T > T_m \quad \text{(liquid)} \end{cases} \tag{4}$$

Following Eq. (2) and (3), the enthalpy of PCM is:

$$H = \int_{T_m}^{T} \rho_s c_s \mathrm{d}T = h \qquad \text{(solid, } T < T_m \text{ and } h < 0\text{)} \tag{5a}$$

$$H = \rho_l f L \qquad \text{(mushy, } T = T_m \text{ and } h = 0\text{)} \tag{5b}$$

$$H = \int_{T_m}^{T} \rho_l c_l \mathrm{d}T + \rho_l L = h + \rho_l L \qquad \text{(liquid, } T > T_m \text{ and } h > 0\text{)} \tag{5c}$$

Equation (5a) represents the sensible enthalpy from the initial temperature, T, to the melting temperature, T_m. Solving the Eq. (5) for the PCM temperature, one obtains:

$$T = T_m + \frac{H}{\rho_s c_s} \qquad \text{(solid, } T < T_m \text{ and } H = h < 0\text{)} \tag{6a}$$

$$T = T_m \qquad \text{(mushy, } T = T_m \text{ and } h = 0\text{)} \tag{6b}$$

$$T = T_m + \frac{H - \rho_l L}{\rho_l c_l} = T_m + \frac{h}{\rho_l c_l} \qquad \text{(liquid, } T > T_m \text{ and } h > 0\text{)} \tag{6c}$$

Figure 4 sketches the present enthalpy formulation.

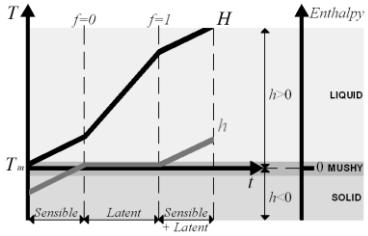

Figure 4. Sketch of the enthalpy formulation.

Using Eqs. (2) and (3), an alternative form of Eq. (1) for heat transfer in the PCM two-dimensional domain can be obtained as (where S_h represents the source term):

$$\frac{\partial h}{\partial t} = \frac{\partial}{\partial x}\left(\alpha \frac{\partial h}{\partial x}\right) + \frac{\partial}{\partial y}\left(\alpha \frac{\partial h}{\partial y}\right) - \rho_l L \frac{\partial f}{\partial t} + S_h \tag{7a}$$

And for the fins (heat exchanger container material) it is given as:

$$\frac{\partial h}{\partial t} = \frac{\partial}{\partial x}\left(\alpha \frac{\partial h}{\partial x}\right) + \frac{\partial}{\partial y}\left(\alpha \frac{\partial h}{\partial y}\right) + S_h \tag{7b}$$

4 NUMERICAL SOLUTION

To obtain the algebraic equations using the control volume technique developed by Patankar [1980], it is necessary to divide the domain into elementary control volumes and then integrate the equation in these control volumes over time and space. Equation (5a) is solved using a fully implicit finite difference solution method. The discretization of Eq. (7a) leads to the scheme proposed by Patankar [1980].Equation (8) represents the discretization equation:

$$a_P h_P = a_E h_E + a_W h_W + a_N h_N + a_S h_S + b \tag{8}$$

where

$$a_E = \frac{\alpha_e \Delta y}{\delta x_{EP}} \tag{9a}$$

$$a_W = \frac{\alpha_w \Delta y}{\delta x_{PW}} \tag{9b}$$

$$a_N = \frac{\alpha_n \Delta x}{\delta y_{NP}} \tag{9c}$$

$$a_S = \frac{\alpha_s \Delta x}{\delta y_{PS}} \tag{9d}$$

$$a_P^{\,0} = \frac{\Delta x \Delta y}{\Delta t} \tag{9e}$$

$$a_P = a_E + a_W + a_N + a_S + a_P^{\,0} - S_P \Delta x \Delta y \tag{9f}$$

$$b = S_U \Delta x \Delta y - \rho_l L \left(f_P - f_P^{\,0} \right) a_P^{\,0} + a_P^{\,0} h_P^{\,0} + S_{Ucorr} \tag{10}$$

Equation (8) has been solved using a tri-diagonal matrix algorithm (TDMA). Here, $h_P^{\,0}$ and $f_P^{\,0}$ refer to the enthalpy and the melt fraction, respectively, from the previous time step. The S_{Ucorr} term refers to the under or over correction that comes from the iterative estimation of the melt fraction term f in each node. S_U and S_P terms come from the linearization of the source term of the Eq. (7). The central feature of the present enthalpy technique is the source term b (Eq. (10)). It keeps track of the latent heat evolution and its driving element is the melt fraction f. Its value is determined iteratively from the solution of the enthalpy equation. On the node points where $0 \leq f_P \leq 1$ the phase change is occurring. As one can see in Fig. 4, the liquid fraction update can then be obtained by setting $h_P = 0$ in Eq. (8). Rearranging it, one obtains:

$$f_P^{\,k} = f_P^{\,0} + \frac{a_E h_E + a_W h_W + a_N h_N + a_S h_S}{\rho_l L a_P^{\,0}} + \frac{h_P^{\,0}}{\rho_l L} + \frac{S_{U,corr}^{k-1}}{\rho_l L a_P^{\,0}} \quad \text{and} \quad f_P = \begin{cases} 0, & \text{if } f_P^{\,k} < 0 \\ 1, & \text{if } f_P^{\,k} > 1 \end{cases} \tag{11}$$

The superscript k stands for the kth iteration of f at node P and the superscript 0 stands for the values from the previous time step. The S_{Ucorr}^{k-1} term is evaluated in the previous iteration and stands for the correction that we need to make to the value of h_P whenever the melt fraction f in the control volume of P, as calculated by Eq. (11), reaches unrealistic values (negative or >1). Equation (11) is used at each node, along with under/over correction. Further details concerning the numerical implementation of present enthalpy methods may be found in the work of Costa *et al.* [1998].

4 RESULTS AND DISCUSSION

In order to demonstrate the potential of the integration of PCMs into the building envelope, the total energy stored during the day and released to the interior during the night per linear meter by the 0.03 m system, considering the total high of the system to be 1.5 m, was quantified and is shown in Fig. 5. The total energy stored and released by the system during a complete day cycle is compared

with that of 0.03 m of other building materials under the same operating conditions. In the results showed in Fig. 5 one considered T_m = 20 ºC and h_i = 25 W m^{-2} ºC^{-1}.

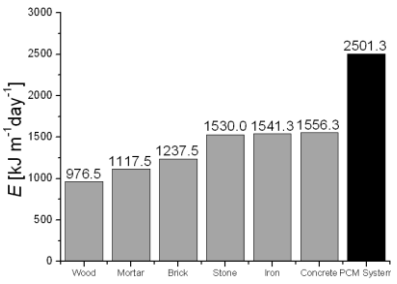

Figure 5. Total energy stored by PCM during the day-time and released to the interior during the night in a complete day cycle and compared it with that of 0.03 m of other building materials under the same operating conditions.

The total energy stored in and released by the system is strongly influenced by the melting temperature of the PCM, T_m. When it is lower than the optimum T_m, the charging process is faster and less time is needed to complete it, thereby melting all the PCM mass. On the other hand, if the difference between T_m and T_i is very small, the discharging process of the system is compromised and the time needed to complete it is larger than the time for which the system is closed. When T_m is higher than the optimum temperature, the discharging process is more efficient. However, the charging process does not finish in the time specified by operating conditions. Figure 6 (a) illustrates the influence of T_m in the E value.

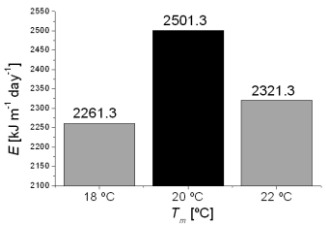

(a)

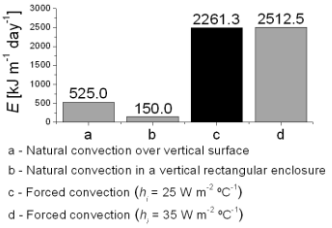

(b)

Figure 6. (a) Influence of T_m in the E value under the same operating conditions. **(b)** Influence of h_i in the E value under the same operating conditions.

In order to evaluate the influence of the interior heat transfer coefficient, h_i, in the E value, four models to determinate h_i were studied under the same operating conditions, for T_m = 18 ºC. The results are show in Fig. 6 (b). The discharging of the system is strongly influenced by the value of h_i. To enhance the discharging of the PCM, a ventilator must be adjoined to the inner side to increase the interior heat transfer coefficient.

5 CONCLUSIONS

In conclusion, an optimal latent heat storage system, with an optimal melting point temperature for the PCM, can be designed for any given location and characteristic climatic data during the winter season. The results for stored and released energy in a complete day cycle, using a 0.03 m thick layer of different materials, enable to show the enhancement of thermal inertia of the wall obtained by using the system described.

The convection heat transfer rate on the inner side of the shading element during the night plays an important role for the PCM solidification and has a strong effect on energy release. To enhance the discharging of the PCM a ventilator must be adjoined to the inner side to increase the interior heat transfer coefficient. The thermophysical properties of PCM, particularly the melting point

temperature, have a strong influence on the energy storage capacity of the system. In this paper calculations were made to optimize the melting point temperature of PCM in 20 ºC.

ACKNOWLEDGMENTS

The authors gratefully acknowledged the financial support of FCT, under the contract no. PTDC/ENR/68224/2006.

NOMENCLATURE

c	*specific heat* ..... $J\ kg^{-1}\ ºC^{-1}$	*Greek letters*	
dx, dy	*length of control volume* ..... m	α	*thermal diffusivity* ..... $m^{-2}\ s^{-1}$
E	*total energy stored and released by the system during a day cycle per linear meter* ..... $kJ\ m^{-1}\ day^{-1}$	δx , δy	*space increment* ..... m
		Δx , Δy	*space increment* ..... m
		ρ	*density* ..... $kg\ m^{-3}$
f	*liquid fraction of melt* ..... [ ]	*Subscripts*	
H	*total volumetric enthalpy* ..... $J\ m^{-3}$	e	*exterior*
h	*sensible volumetric enthalpy* ..... $J\ m^{-3}$	i	*interior*
h_e	*ext. heat transfer coefficient* .... $W\ m^{-2}\ ºC^{-1}$	k	*phase*
h_i	*int. heat transfer coefficient* ..... $W\ m^{-2}\ ºC^{-1}$	l	*liquid*
k_k	*thermal conductivity phase k* ... $W\ m^{-1}\ ºC^{-1}$	m	*melting*
L	*latent heat of fusion* ..... $J\ kg^{-1}$	s	*solid*
$\dot{q}_{rad}$	*solar radiation* ..... $W\ m^{-2}$	N,E,P,W,S	*North, East, Central, West, South*
t	*time* ..... h	n,e,p,w,s	*North, East, Central, West, South*
T	*temperature* ..... $ºC$	*Superscripts*	
T_m	*PCM melting temperature* ..... $ºC$	k	*iteration number*
		0	*a value at the previous time step*

REFERENCES

Brousseau, P. & Lacroix, M. 1998, 'Numerical simulation of a multi-layer latent heat thermal energy storage system', *International Journal of Energy Research*, **22**, 1-15.

Chen, C.R. & Sharma, A. 2006, 'Numerical investigation of melt fraction of PCMs in a latent heat storage system', Journal of Engineering & Apllied Sciences, 1[4], 437-444.

Chen, C.R., Sharma, A., Tyagi, S.K. & Buddhi, D. 2008, 'Numerical heat transfer studies of PCMs used in a box-type solar cooker', Renewable Energy, 33, 1121-1129.

Costa, M., Buddhi, D.& Oliva, A. 1998, 'Numerical simulation of a latent heat thermal energy storage system with enhanced heat conduction', Energy Conversion and Management, 39[3/4], 319-330.

Patankar S.V. 1980, Numerical heat transfer and fluid flow, Hemisphere Publishing Corporation, Washington.

Sharma, A., Sharma, S.D., Buddhi, D. & Won L.D. 2006, 'Effect of thermo physical properties of heat exchanger material on the performance of latent heat storage system using an enthalpy method', International Journal of Energy Research, 30, 191-201.

Sharma, A., Tyagi, V.V., Chen, C.R. & Buddhi D. 2009, 'Review on thermal energy storage with phase change materials and applications', Renewable and Sustainable Energy Reviews, 13, 318-345.

Swaminathan, C.R. & Voller, V.R. 1993, 'On the enthalpy method', International Journal of Numerical Methods for Heat & Fluid Flow, 3, 233-244.

Tyagi, V.V. & Buddhi, D. 2007, 'PCM thermal storage in buildings: 'A state of art'', Renewable and Sustainable Energy Reviews, 11, 1146-1166.

Zalba, B., Marín, J.M., Cabeza, L.F. & Mehling, H. 2003, 'Review on thermal energy storage with phase change: materials, heat transfer analysis and applications', Applied Thermal Engineering, 23, 251-283.

XII DBMC
International Conference on Durability of Building Materials and Components
PORTO - PORTUGAL, April 12th-15th, 2011

Development of a Risk Assessment Procedure Applied on Building Physics: Part One; Model Development

Pär Johansson [1]
Simon Pallin [2]
Mohammad Shahriari [3]

ABSTRACT

Although it is highly appreciated and asked for by the practitioners there is a lack of tools to perform proper risk assessment and risk management procedures in the area of building physics. Many of the influential parameters, such as outdoor temperature and indoor moisture supply, have stochastic variations, which make a general approach for risk assessment complicated. The aim of this study is to present a risk assessment model to be used in building physics. The study is based on hazard identification tools used in process industry, such as What-if, HAZOP, FMEA and VMEA. The tools are compared and used in the modeling process which leads to identification of influential variables during design, construction and service life. The influential variables are called hazards and safeguards which in turn are influenced by noise factors. By combining the hazards and safeguards in a scenario, together with Monte Carlo simulations of the noise factors, give results with a spread dependent on the variability of the noise factors. Subsequently, the risk is defined by comparing the result of the scenario to an allowed level of consequence. By implementing risk management into building physics design, it is possible to indentify critical points to avoid extra unwanted costs. In addition, risks concerning indoor climate, health and durability are clarified. The risk assessment model developed here is used in an applicability study in part 2.

KEYWORDS

Risk assessment model, Hazard identification, Stochastic variations, Building physics.

[1] Department of Civil and Environmental Engineering, Chalmers University of Technology, Gothenburg, SWEDEN, par.johansson@chalmers.se (Corresponding author)
[2] Department of Civil and Environmental Engineering, Chalmers University of Technology, Gothenburg, SWEDEN, simon.pallin@chalmers.se
[3] Department of Product and Production Development, Chalmers University of Technology, Gothenburg, SWEDEN, mohammad.shahriari@chalmers.se

1 INTRODUCTION

The European Union has agreed to reduce its greenhouse gas emissions by 20% from 1990 to 2020 and up to 30% with an international agreement. Since the energy used in buildings account for 40% of the total final energy use, a large part of the existing buildings in the EU need measures of thermal retrofitting to reach the target. This may result in an increased insulation thickness in the building envelope, which might lead to problems with moisture damages in the buildings [Pallin 2010]. The Swedish National Board of Housing, Building and Planning estimates that approximately 66% of all Swedish buildings are damaged in some way; 45% of the damages that have been discovered happen because of moisture damages, mostly in crawl and attic spaces. The moisture damages might affect the durability and the indoor climate of the buildings [Boverket 2009].

This paper aims to develop a risk assessment model and tool which can be used during the design process in order to reduce the vulnerability of failures in the construction and minimize the effects of failures. The model is based on hazard identification and risk assessment with consideration to the building's lifetime. Buildings are complex systems where the use of deterministic data limits the possibilities to make simulations for a proper risk analysis. A large part of the parameters varies stochastically which demands data produced during stochastic conditions. Figure 1 shows an example of how a parameter may vary when performing a large number of simulations. The impact of influencing parameters such as weather, building materials, indoor moisture sources and ventilation can be studied using stochastic data in the simulation.

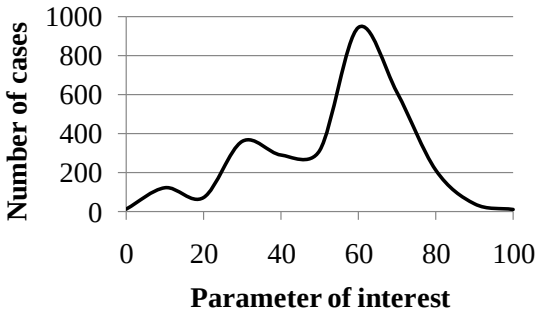

Figure 1. The distribution of the studied parameter has to be taken into consideration when performing a risk analysis. Example of a frequency curve from a large number of observations.

2 RISK MODELLING

In order to create a risk assessment model, one has to define the system structure and system behavior, but also the standards and targets that the system outcome should fulfill. Information is needed on how the parts of the system are put together and how the system develops over time. Basically the model should be a representative of reality, broken down in manageable pieces which each describe a part of the system behavior. When the model is put in place, simulations can be performed to study the outcome when different data in the system are varied.

There are numerous hazard identification tools developed, such as what-if, HAZOP, FMEA and VMEA. The outcome when using one of these tools is possible scenarios, or failure modes, that can lead to loss or damage. The scenarios might need to be validated, for instance by the opinion of experts in the studied field, in order to reduce the uncertainties and also to ensure that all major and credible scenarios have been targeted. Each of the scenario is then connected to a probability for a consequence and the probability can be evaluated and compared to the acceptable level of loss or damage as specified by targets or standards. If the risk is higher than what is an acceptable level, measures have to be taken in order to lower the risk of that consequence.

3 HAZARD IDENTIFICATION TOOL COMPARISONS

The first method discussed is the what-if method, which aims to analyze the consequences of different scenarios based on a brainstorming process performed by an experienced expert team. The results from the what-if analysis usually suggest solutions to specific hazards [Shahriari 2010]. Questions asked during the process for building physics might be of the type "What if the indoor moisture supply in the building reaches critical levels?". The consequences and recommendations to the scenario are based on the knowledge and experience of the expert team [Davidsson *et al.* 2003].

HAZOP, HAZard and OPerability study, is another tool for hazard identification which was developed for the processing industry. The method is a detailed review of a system for identifying possible hazards, failures and operability problems. This method requires a team of experienced experts that discuss every part of the system with help of different guidewords that describe different parameters that can deviate from normal operation. The purpose of the HAZOP is not primarily to solve potential problems, but to identify possible problems [Davidsson *et al.* 2003].

Another method that can be used in building physics to analyze risks is the FMEA (Failure Modes and Effects Analysis) which is a method that evaluates the way equipment can fail and the effects these failures can have on the system. Each individual failure is considered to be an independent event with no connection to other parts of the system, except for following failures caused by the original failure. The FMEA identifies single failure modes in the system and determines the consequences the failure might cause on a small scale and on the system as a whole. A grading system is used to find the worst failure modes and effects, for which recommended solutions are proposed [Shahriari 2010]. Nielsen [2002] used FMEA on moisture problems in buildings with the three failure modes "liquid water in the building", "surface condensation" and "internal condensation in the structure". The failure modes are then divided down to fifth level to find the root cause of the failure modes. Nielsen finds it to be a seldom case that the root causes are found and that we often are able to go more into detail with the causes, something that proves to be very time demanding.

A recently introduced hazard identification method is the VMEA (Variation Mode and Effect Analysis). Instead of concentrating on failure modes, the VMEA method looks for noise factors with excessive variation, affecting the system outcome. The goal of the analysis is to find and rank noise factors that have effect on the variation of the final product. By conducting four steps in the VMEA, done by an experienced team, a VRPN (Variation Risk Priority Number) is calculated for the noise factors, ranking the most influential noise factors highest [Chakhunashvili *et al.* 2004]. In this paper, the VMEA method is used, since it treats the variations of the many noise factors found in the field of building physics.

4 DEFINITION OF RISK

There is a difference between the definitions of reliability and risk which can be found in the field of reliability engineering. Kaplan and Garrick [1981] discuss risk as something involving both uncertainty and some kind of received loss or damage. According to this definition risk is an uncertainty connected to a bad consequence that should be avoided. This definition of risk would require some kind of quantified consequence that gives a percentage or level for how large the risk is compared to other risks. Haldar and Mahadevan [2000] define reliability as the probability of a process to successfully satisfy some performance criteria and risk as a measure of the probability of failure, hence risk and reliability are complementary terms. This way of describing risk and reliability is not possible in the field of building physics since there is always a risk of failure. The part of a consequence not leading to failure is instead called a safe consequence, see Fig. 2. A safe consequence is not necessarily part of a reliable system, based on the previously described definitions of risk and reliability. Therefore it is hard to further develop reliability models in building physics. In

this paper risk and safe consequences are separated by some grading of the scenario's consequence, compared to the allowed consequence.

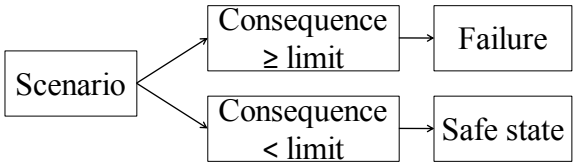

Figure 2. A scenario leads to a defined consequence which either result in failure or may be considered safe.The safe state is the residual value of the probability of failure. The consequence evaluation can be based on design standards or expert's opinions.

There are some basic components that have to be defined in order to discuss the concept of risk. In this paper, the noise factors are considered to be at the lowest level of influence in the risk assessment model. They influence the outcome of different events or activities that hereafter are called hazards and safeguards, see Fig. 3.

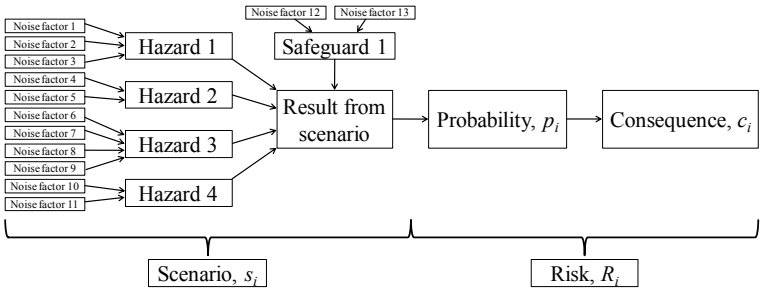

Figure 3. Risk assessment model with a scenario sample, s_i, composed of a number of hazards and safeguards. The noise factors influence the hazards and safeguards which define the distribution of the result. The consequence, c_i, and probability, p_i, are based on the results from the scenario which altogether give the risk, R_i.

Hazard is a potential energy; a condition or source of danger that have the potential of resulting in some kind of event; mold growth in the bathroom or condensation in an exterior wall. Risk is defined as the probability that a scenario composed of a number of different hazards and safeguards will cause failure or damage to the system. Therefore hazard is the source of a potentially dangerous event and risk is connected to the probability of that event leading to loss or damage. It is possible to use safeguards in order to reduce the risk for a hazard to result in a specific consequence, but it is not possible to make the risk zero. Awareness of a hazard means that safeguards can be put in place to minimize the risk, thus awareness of risk reduces risk [Kaplan & Garrick 1981].

The Greek word "stochos" means uncertain and create the base of the word stochastic, which means a random process [Haldar & Mahadevan 2000]. Most engineering tasks involve some degree of stochastic variables that influence the outcome of a given problem, e.g. the number of occupants in a randomly chosen apartment will influence the moisture production in the apartment. Another example is measurements which will give different results for different test specimens, caused by stochastic variations of the physical properties of the test specimen and changes in the measuring device. These variations are here called noise factors which are defined as variations that cannot be controlled, or are very difficult to control. When designing a system, it is crucial to take the noise factors into account in order to design a system free of unwanted events. Risk is then the probability of a defined system or scenario to result in a specified consequence. Kaplan and Garrick [1981] discuss this matter as the "Set of Triplets Idea" which can be described by the following Equation:

$$R_i = f(s_i, p_i, c_i) \qquad i = 1,2,...,n \tag{1}$$

where R_i is the risk of a scenario sample, s_i is the scenario sample, which have to be a subset of the whole scenario, p_i is the probability of the sample leading to c_i, the consequence of the sample. i is the scenario sample number from 1 to n. In order to calculate the total risk for a specified consequence, the risk for all scenario samples leading to that consequence should be added:

$$R_{tot} = \sum_{i=1}^{n} R_i \tag{2}$$

5 HAZARDS, SAFEGUARDS AND NOISE FACTORS IN BUILDING PHYSICS

The field of building physics involves many hazards that can result in scenarios ending in unwanted consequences. Some of the major influential parameters are outdoor climate, indoor moisture production, indoor heat supply, material and surface properties, air tightness and air exchange rate, see Fig. 4. These parameters are usually included in simulations using heat, air and moisture simulation tools, but they do not consider the deviations caused by stochastic variations in reality. During the hazard identification process, the main scenarios leading to an unwanted consequence are presented and evaluated in order to identify the most significant hazards. Examples of the scenarios and consequences in building physics are; household equipment used in a bad way leading to failure (water leakage), the relative humidity in a building part exceeds the critical relative humidity for mold growth initiation or a building material fails to satisfy the expected level of thermal resistance.

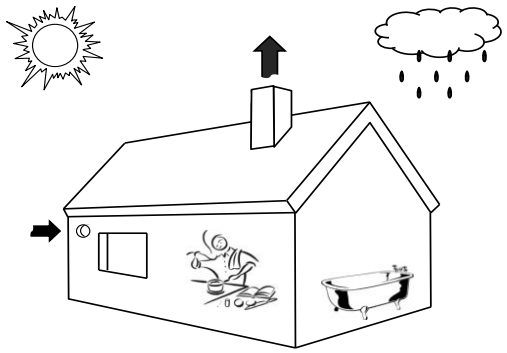

Figure 4. Schematic figure of some of the hazards and safeguards which have to be taken into consideration in the risk assessment model; climate, indoor heat and moisture production and ventilation.

The number of noise factors and hazards influencing the final simulation grows rapidly and therefore the risk assessment model is not adapted for hand calculations. Because of the large number of noise factors affecting the system, use of computer software is recommended. In the applicability study, in part 2, Monte Carlo simulations are performed in the Microsoft Excel software add-in @Risk in order to produce a distribution of the indoor moisture production based on stochastic variations.

5.1 Hazard and Safeguard Ranking using VMEA

The indoor moisture supply in a bathroom has been chosen as an example to demonstrate how the VMEA method works, see Fig. 5. Identification of hazards have revealed that bathing, showering, laundry appliances and floor mopping give an additional moisture production and the ventilation can be used as a safeguard in order to reduce the effect of these hazards on the resulting indoor moisture supply.

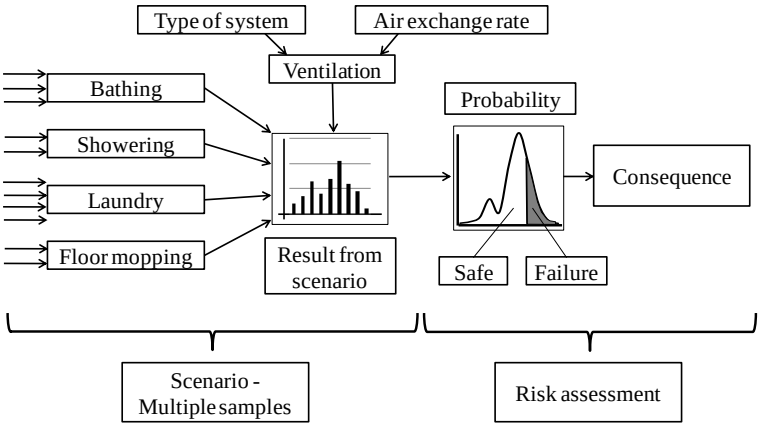

Figure 5. The risk assessment model for a scenario of the indoor moisture supply in a bathroom with the hazards bathing, showering, laundry appliances, floor mopping and the safeguard ventilation. Simulations of multiple samples of a scenario give the distribution of the indoor moisture supply.

According to Chakhunashvili *et al.* [2004] the hazards should be given a weight index 1-10 depending on their influence on the final scenario results. Four hazards and one safeguard have been identified and weighted as shown in Table 1.

Table 1. Example of weighting according to the VMEA method of four hazards and one safeguard identified for the scenario indoor moisture supply in bathroom [Chakhunashvili *et al.* 2004].

#	*Hazard and safeguard*	*Weighting*
H1	*Bathing*	*3*
H2	*Showering*	*5*
H3	*Laundry*	*8*
H4	*Floor mopping*	*2*
S1	*Ventilation*	*7*

A higher weighting index on the scale 1-10 gives a larger probability that the hazard in question will influence the result of the scenario. In the weighting performed in Table 1, laundry and showering are considered to have the largest probability to influence the variability of the indoor moisture supply in the bathroom. Bathing and floor mopping are not considered to be major contributors to the variability of the indoor moisture supply. The safeguard ventilation is assumed to be a large contributor to the variation of the moisture supply in the bathroom.

5.2 Noise Factor Ranking using VMEA

The next step of the VMEA process is to identify and assess the noise factors that influence the different hazards and safeguards. Weighting of the noise factors is performed on a scale 1-10 for their variability and 1-10 for their sensitivity for influencing the hazard or safeguard. To evaluate the variability of the noise factors, identification of the different influential variables have to be carried out. For the case with indoor moisture production three major influential variables have been identified; time (at what time of the day is the moisture source active?), duration (during how long time is the source in progress?) and level (how much moisture is generated and with how much variance?). Each of the noise factors have been weighted according to their variation in time, duration and level, see Table 2. The weighting is a subjective process which is dependent on the experience of the team performing the evaluation of the noise factors. Not included here are the important noise factors of how common a certain hazard is in any random household (the incidence factor I_f) and the correlation between different noise factors which can enhance or decrease their effects.

Table 2. Example of noise factor weighting for the indoor moisture supply in a bathroom according to the two criteria's presented by Chakhunashvili *et al.* [2004]. The size of the variability of a noise factor is weighted on a scale 1-10 which is also done for the sensitivity of a hazard or safeguard.

H or S #	*Noise factor*	*Size of variation of noise factor*	*Sensitivity of H or S to noise factor*
H1	*Bathing duration*	*6*	*7*
	Water temperature	*2*	*1*
	Saturation vapor pressure	*5*	*3*
H2	*Shower duration*	*4*	*6*
	Water temperature	*3*	*2*
	Saturation vapor pressure	*5*	*3*
H3	*Tumble drier system*	*7*	*8*
	Weight of excess water	*6*	*4*
	Drying duration	*4*	*6*
H4	*Area of floor*	*3*	*6*
	Amount of water used	*1*	*4*
S1	*Type of system*	*9*	*10*
	Air exchange rate	*6*	*7*

5.3 Variation Risk Priority Number for Moisture Supply

When all the exemplified noise factors have been evaluated, the VRPN (Variation Risk Priority Number) can be calculated. This is performed by multiplying each weighting number from the three previously described weightings. The higher VRPN, the higher is the risk that the noise factor influences the total performance. The VRPNs of the indoor moisture supply in a bathroom are presented in Table 3.

Table 3. Variation Risk Priority Number, VRPN, for the indoor moisture supply in a bathroom.

#	*Weigh-ting*	*Noise factor*	*Size of variation in noise factor*	*Sensitivity of H or S to noise factor*	*VRPN (NF)*	*VRPN (H/S)*
H1	*3*	*Bathing duration*	*6*	*7*	*126*	*177*
		Water temperature	*2*	*1*	*6*	
		Saturation vapor pressure	*5*	*3*	*45*	
H2	*5*	*Shower duration*	*4*	*6*	*120*	*195*
		Water temperature	*3*	*2*	*30*	
		Saturation vapor pressure	*3*	*3*	*45*	
H3	*8*	*Tumble drier system*	*7*	*8*	*448*	*1072*
		Weight of excess water	*6*	*9*	*432*	
		Drying duration	*4*	*6*	*192*	
H4	*2*	*Area of floor*	*3*	*6*	*36*	*44*
		Amount of water used	*1*	*4*	*8*	
S1	*7*	*Type of system*	*9*	*10*	*630*	*924*
		Air exchange rate	*6*	*7*	*294*	

The result of the VMEA is that the hazard laundry is the largest contributor to the variation of the indoor moisture production, followed by showering. For the hazard with the highest VRPN, safeguards should be implemented in order to lower the variance of that hazard. Examples on safeguards are recurring inspection of the technical appliances, installation of moisture sensors or air dehumidifiers and usage of specified checklists during construction.

6 DISCUSSION AND CONCLUSION

This paper compares the hazard identification tools what-if, HAZOP, FMEA and VMEA in order to find a risk assessment model for the field of building physics. A difficulty when using the hazard identification tools is recognized by Nielsen [2002] where he recommends to keep the analysis on a higher level and not go into too much detail. The introduced method uses VMEA which does not study failure modes, but the underlying noise factors. As an example on how the method works, it is applied on the indoor moisture supply in a bathroom. In future studies a validation may be performed in order to confirm the results of the example.

In building physics related problems, it is usually difficult to evaluate all hazards affecting the behavior of the building and indoor climate. It is also difficult to evaluate the interaction between different hazards, since they might influence different parts of the building's characteristics; e.g. energy consumption, moisture durability and need of repair work. The model defined and described in this paper is an approach of how to treat the noise factors in building physics on a structured and transparent way that allows us to take all variations into consideration. In part 2, a system analysis is performed of the moisture supply in an apartment in a Swedish multi-family dwelling in order to apply the model on a real case.

7 ACKNOWLEDGMENTS

The work is supported by FORMAS – the Swedish Research Council for Environment, Agricultural Sciences and Spatial Planning.

8 REFERENCES

Boverket 2009, *Så mår våra hus - redovisning av regeringsuppdrag beträffande byggnaders tekniska utformning m.m.*, Boverket, Karlskrona, Sweden.

Chakhunashvili, A., Johansson, P., & Bergman, B. 2004, 'Variation Mode and Effect Analysis', Paper presented at the Annual Reliability and Maintainability Symposium, Los Angeles, CA.

Davidsson, G., Postgård, U., & Hardestam, P. 2003, *Handbok för riskanalys*, Statens räddningsverk, Karlstad, Sweden.

Haldar, A. & Mahadevan, S. 2000, *Probability, reliability and statistical methods in engineering design*, Wiley, New York.

Kaplan, S. & Garrick, B. J. 1981, On The Quantitative Definition of Risk, *Risk Analysis*, **1**[1], 11-27.

Nielson, A. 2002, 'Failure Modes and Effects Analysis (FMEA) used on Moisture Problems', Paper presented at the 9th International Conference on Indoor Air Quality and Climate, Monterey, California, USA.

Pallin, S. 2010, 'Potential risks when combining experienced retrofitting measures with newly developed techniques', Paper presented at the Central European Symposium on Building Physics, Cracow, Poland.

Shahriari, M. 2010, *Risk Management and Safety*, [Unpublished PowerPoint slides], Department of Product and Production Development, Chalmers University of Technology, Gothenburg, Sweden.

XII DBMC
International Conference on Durability of Building Materials and Components
PORTO - PORTUGAL, April 12th-15th, 2011

Concrete Durability: Review of Rapid Chloride Permeability Testing For Durability Compliance

Kribanandan Gurusamy Naidu [1]

ABSTRACT

This paper examines the applicability of the widely-adopted ASTM C1202-97 "Electrical indication of concrete's ability to resist chloride ion penetration", which is also AASHTO T277-83 "Rapid chloride permeability test" for the evaluation of the resistance of concrete to chloride ion penetrability. Particular reference is made to the first infrastructure project in Malaysia where the RCPT testing was specified for compliance.

The original correlation established using the AASHTO 90-day salt-ponding test, for ranking concretes in terms of their chloride ion penetrability using the RCPT results has various limitations. This is especially so for concretes incorporating chemical and mineral admixtures. This review attempts to develop a rational approach to a judgment on chloride penetrability of concretes. An overview of RCPT is made and possible alternative options for compliance testing considered.

KEYWORDS

Corrosion of reinforcement, Chlorides, Carbonation, Permeability, RCPT, Durable construction and Life cycle assessment.

[1] JTK Consult Sdn Bhd, Kuala Lumpur, MALAYSIA, drkribangn@jtkconsult.com.my

1 INTRODUCTION

The Butterworth Viaduct is a pre-stressed cable stayed road bridge and it was the first project in Malaysia where the RCPT test was specified as a requirement for concrete compliance (see JTK report r7026). The specification called for three types of concrete, OPC, OPC/PFA and OPC/PFA/SF. All exposed surfaces of the concrete were to be coated with an anti-carbonation coating. Three of the piers are within the tidal estuary and hence exposed to chlorides via splash or direct contact. The rest of the structure is exposed to wind borne chlorides.

Considering the importance placed on achieving long term durability, there was no specified design life (intended working life – BS 8500-1, 2006), or a definition of what constitutes the end of the service life.

2 EXPOSURE CONDITIONS

2.1 Marine Exposure Conditions

Deterioration of marine concrete structures is mainly due to the ingress of chloride ions into the concrete, leading to corrosion of the embedded steel reinforcement. This potentially leads to a shortening of the service life and increasing the maintenance costs of these concrete structures. Durability of such structures is a particular concern in the hot wet tropical environment in Malaysia and the use of low permeability concretes is key method adopted in ensuring serviceability.

As the bridge was to be built over a tidal estuary it can be safely assumed that the structure will be exposed to chlorides. The exposure regimes can be divided into areas where wind borne chlorides will predominate, a splash zone area, a tidal zone and a submerged area below the low water tide level (exposure classes, XS1, XS2 and XS3 – BS EN 206-1: 2000).

2.2 Carbonation

The carbonation process is very susceptible to moisture content of the concrete. Either side of 65% RH the carbonation rate diminishes rapidly. Thus in areas where the concrete is saturated, such as below ground or water, carbonation is not a concern (exposure classes, XC1, XC2, XC3 and XC4 – BS EN 206-1: 2000).

At higher levels, above the splash zone, the threat of carbonation will be greater. However with the type of concrete provided (Grade 60) and particularly as the segments are required by specification to be well cured, carbonation was not thought to be a durability issue of concern. To add to this the application of an anti-carbonation coating as required by the contract will improve the resistance of the concrete.

2.3 Chloride Ion Resistance Testing

2.3.1 Background

Steel in concrete is normally stable due to the formation of a passive iron oxide film on the steel surface. Corrosion initiation due to the presence of chloride ions is thought to be the primary mechanism leading to a loss of durability over time. Once chloride ions reach a critical concentration at the reinforcement surface, the passive iron oxide film breaks down and corrosion is initiated.

One of the aspects to consider during the design of a reinforced concrete structure for a service environment where chloride ions are present is therefore the chloride ion (CI) resistance of the concrete. This can be utilized to determine the maintenance free period with respect to corrosion. Similarly, for the repair and/or protection of a chloride contaminated structure (or structure in a

chloride environment) the CI resistance of the repair materials and surface coating/penetrant systems is a very important performance parameter.

Chloride ion diffusion, penetration and permeability tests have therefore been developed so as to establish the Cl resistance of concretes, cementitious/polymeric repair materials and surface coating/penetrant systems.

2.3.2 Test Methods

Various durability tests have been developed for the evaluation of the resistance of concretes to chloride ion penetration. The tests can be broadly grouped into ponding/immersion/salt spray tests, concentration driven diffusion tests and voltage driven accelerated diffusion/permeability tests. These tests include long-term soaking tests such as the AASHTO T259 "90-day salt-ponding test" which aims to simulate the actual marine exposure environment and rapid tests such as the ASTM C1202-97 "Electrical indication of concrete's ability to resist chloride ion penetration", generally known as the rapid chloride permeability test (RCPT).

Environmental chloride contamination of concrete structures occurs via the following transport mechanisms:

Diffusion, associated with Cl concentration gradients (eg. tidal and atmospheric zones of a marine structure).

Dispersion and diffusion. Dispersion of Cl takes place when bulk flow of saline water occurs, eg. water sorptivity. The splash zone of a marine structure is an example of where dispersion (ie. high surface build-up of C1 occurs due to absorption of water borne chlorides) and diffusion of C1 occurs.

Hydrostatic pressure gradient (eg. water borne chloride transport in the submerged zone of a marine structure).

The ponding, immersion, concentration driven diffusion and voltage driven diffusion tests enable determination of Cl diffusion resistance (via measurement of a Cl diffusion coefficient).

The voltage driven diffusion methods were developed because of the sometimes impractical test duration (i.e. months to years) of the concentration driven methods. The conventional long-term soaking tests take a long time, resulting in the increasing usage of the RCPT as a rapid means of assessing concrete permeability.

Neither a Cl diffusion or penetration coefficient is obtainable from the ASTM C 1202-97/AASHTO T 277-831 rapid permeability test. The total charge passed, in coulombs, determined from this test is related to chloride ion penetration resistance. A Table of Charge Passed versus Chloride Ion Penetrability is provided in the standards where Cl penetrability is stated qualitatively as either "negligible", "very low", "low", "moderate" or "high".

In essence, the RCPT measures the total amount of charge (in coulombs) that passes through a standard cylindrical test specimen during the test duration of 6 hours. Based on the total amount of charge passed, the concrete is given a chloride ion penetrability ranking using the general correlation (Table 1) in ASTM C1202 (1997) established by Whiting (1981) using the 90-day salt ponding test.

Table 1. Chloride ion penetrability based on charge passed.

Charge Passed (Coulombs)	Chloride Ion Penetrability	Type of Concrete
> 4,000	High	High W/C
2,000 to 4,000	Moderate	0.4-0.5 W/C
1,000 to 2,000	Low	W/C < 0.4
100 to 1,000	Very Low	Latex modified Concrete
< 100	Negligible	Polymer concrete

Note: W/C = water-cement ratio

Limitations

Critical aspects related to the in-service chloride ion resistance of a concrete mix include:

i) chloride binding capacity of a cementitious binder
ii) tendency towards development of a high surface chloride build up of a cementitious binder
iii) pore size, continuity and tortuosity of the cementitious paste
iv) threshold chloride content of a cementitious binder type to initiate reinforcement corrosion

The ASTM C 1202-97/AASHTO T 277-831 rapid Cl permeability test provides only an indication of aspect iii). In fact, the widely-adopted RCPT has been criticized by many researchers to be non-reflective of concrete permeability. The test is based on the principle that the electrical resistivity of concrete decreases with increasing free chloride ion concentration. As such, this test would reflect the electrical resistivity of the concrete being tested rather than the resistance of the concrete to chloride ion penetration (Wee et al 1999) (3). The electrical resistivity of concrete is affected by the paste volume of the concrete (Wee et al 1999) and the chemistry of the pore solution (Buenfeld and Newman 1987) (3). Arup et al (3) already stated in 1993 that "the information provided by a rapid chloride permeability test or an ASTM C 1202-97/AASHTO T 277-831 test is – at the most – equivalent to that which can be obtained by measuring the resistivity of the water –saturated sample and can not be taken as measure of C1 diffusion resistance, unless the conductivity of the porewater in that particular type of concrete and in that particular hydration state is known and the appropriate correction made." Andrade (1993) also confirmed that the total amount of charge passed during the test accounts for the total current due to the flow of all the different ions present in the electrolyte solution of the concrete and not only that corresponding to the flow of chloride ions further adding to the uncertainty of the result.

The scope of ASTM C 1202-97 state that this method is applicable to concretes in which a correlation has been established between the coulomb value and long term Cl ponding tests such as AASHTO T 259-80. Pfeifer et al (4) stated that "based on the documents referenced in ASTM C 1202, it is concluded that reliable and proper correlations do not exist between the rapid test procedure results and 90-day ponding test results. The ASTM C 1202 or AASHTO T 277 test procedures should not be used in specifications without proper correlation to long term tests. It is recommended that the table relating chloride penetration to coulomb values in these test procedures be removed since it is inaccurate and can be misleading".

Pfeifer et al (4) also stated that "selection or rejection of concrete based solely on ASTM C 1202 can result in improper decisions and the rejection of concrete known to be durable".

"The studies reviewed show that virtually impermeable conventional concretes can be produced with very low water-cement ratios of 0.30 to 0.32, even though their coulomb values may range from 1000 to 5000".

It is clear that a wide school of research and study has come to the conclusion that while a useful tool the usage of RCPT as a sole test for durability compliance is not advisable.

3 REVIEW OF AVAILABLE DATA

3.1 Overview of Approach

As part of the compliance requirements beam elements of size 750 x 150 x150 were prepared by the concrete supplier at the time of casting and cured either at the pre-cast yard or at a designated Laboratory. Four (4) beams were cast for every segment. These were cured prior to testing as follows:

As soon as the beam is cast, concure was sprayed on the open face followed by a 50 mm saturated foam. Over this a saturated hessian was laid which was kept moist by a water drip system. Demoulding took place between 14 and 24 hours and the samples were immediately stored in a water bath until testing. Cores were taken from the beam samples at the designated test ages (28, 60 or 90 days) and the samples subjected to the RCP test. The compliance criteria according to the contract are summarized in the table below. An allowance for further testing at 90 days is provided for if the 60 day results are 500 to 575 coulombs and 1000 to 1150 coulombs for the pre-cast and in-situ elements respectively.

Table 2. RCPT Compliance Criteria.

Element Type	Compliance Criteria	Maximum Coulombs at 28 Days	Maximum Coulombs at 60 Days	Maximum Coulombs at 90 Days
Pre-cast Elements	Primary Compliance	575	500	
Pre-cast Elements	Further Testing Permitted at 90 Days if 60 day result >575		500 - 575	500
In-situ Elements	Primary Compliance	1150	1000	
In-situ Elements	Further Testing Permitted at 90 Days if 60 day result >1150		1000 - 1150	1000

It should be noted that these compliance requirements are onerous and do not allow for any measurement uncertainty which is inherent in the RCP test. The specified value, e.g. 1000 Coulombs may be treated as the characteristic value. Assuming 30 % expected variability of test results as the margin, the target value is therefore 700 and an extreme value of 1300 accepted as the uppermost limit with not be more that 5 % above 1000. The precision statements in ASTM C1202-97 in fact states that “the single operator coefficient of variation is 12.3% indicating that the results of two properly conducted tests by the same operator on concrete samples from the same batch and of the same diameter should not differ by 42%.

3.2 Concrete Segment details

The concrete mix supplied for this project is summarised below:

Table 3. Concrete mix design details.

	Precast	In-Situ
Mix Type	TM14	TM4
OPC (kg/m3)	210	270
Masscrete (kg/m3)	270	180

Silica Fume (kg/m3)	38.5	27
20 mm Aggregates (kg)	1000	1040
Sand (Kg)	650	755
Water content (Liters)	145	150
Daracem liters per 100 kg cement	9.12	9.06
Daratard 40 liters per 100 kg cement	1.20	1.24
PFA %	14	10
Silica Fume %	8	6
W/C Ratio	0.280	0.314
RCP Criteria (Coulombs)	500	1000
Trial RCPT	488, 491 (At 40 Days)	741, 759 (At 36 Days)

Approximately four segments were cast per day at the pre-cast yard with concrete volume per segment varying from 31 cu m to 50 cu m. The cover to reinforcement is as low as 26 mm for the pre-cast elements and 45 mm for the in situ elements.

3.3 Review of Results

The RCPT results are summarized below and based on this the project consultants deemed the concrete to be non-compliant. The results are presented sequentially for concrete cast between 12 Jan 2002 to 17 Nov 2002. RCPT results at 28 days were available up to 21 Sept 2002. The equivalent data at 56 days and 90 Days were available up to 26 Aug 2002 and 3 Aug 2002 respectively.

There is quite a variation in the RCP results particularly at 28 days. However the coefficient of variation of results at all ages is less than 30%. In general as concrete hydrates there would have been an expected decrease in permeability and resistivity of concrete but there are several instances (5 out of 41 results) when the RCPT results in fact increase in value between 56 and 90 days. This is also reflected in the higher mean results. It should however be noted that the ASTM C1202-97 standard concludes that the results of two properly conducted tests by the same operator on concrete samples from the same batch and of the same diameter should not differ by more than 42%. These results should therefore be viewed in the light of the fact that they are within the expected variability of individual test results and may not represent a real increase in permeability at all. It was the view of the author that rejection of the concrete purely based on the RCPT tests without taking into consideration the variability of the test itself was not defensible

Table 4. Summary of RCP results for the precast concrete (TM14).

TM14	28D Strength	56 D Strength	28 RCP	56RCP	90 Day RCP
Max	88.2	88.2	1149	830	803
Min	61.9	68.5	353	219	367
No	357	160	153	134	41
Mean	76.1	79.0	638	496	512
Std Dev	4.3	4.5	182	111	91
COV	5.6	5.7	28	22	18

4 COMPLIANCE TESTING

The original development of the RCP test in 1981 was based on a correlation to the 90–day ponding test. Several researchers have examined this further and found that the correlation between the tests rather less convincing particularly with modern concretes with additives. Pfeifer et al. (1994) for example found that they obtained inconsistent test results when comparing the salt ponding test and the RCPT procedure. McGrath and Hooton (1999) also found that due to the partially saturated condition of the ponding test specimens, other processes such as wicking, adsorption and carbonation are involved and these effects are difficult to account for in a laboratory environment. Furthermore, the methods of analysis of the 90-day salt ponding test data are all based on apparent diffusion, which is a factor derived from the actual penetration. It should also be noted that the original tests were undertaken primarily for OPC concretes and polymer modified concrete. These reasons probably account for the difficulties encountered by researchers when trying to reproduce the linear relationship between the results generated from the RCPT and the 90-day salt ponding test (Goh et al, 2002). Scanlon and Sherman (1996) also reported a substantial conflict between the two test procedures and stated that the generalized relationship found by Whiting was not valid if silica fume, fly ash, blast furnace slag or superplasticizer was used. It should however be noted that some of these variations are associated with the general variability of the test itself and the associated variability of concrete.

As noted above the classification of the chloride ion penetrability of concrete based on the RCPT results and the chloride ion penetrability rankings set forth in ASTM C1202-97 specifications was originally based on the ponding test (ASSHTO-T227).. This test is not meant to provide a correlation to RCPT as it is already well established that any such relationship is difficult to establish even in controlled laboratory trials. The ASSHTO test should be used merely to check on the variability of concrete from a penetrability point of view.

5 CONCLUSIONS AND RECOMMENDATION

The ASTM C 1202-97 rapid chloride permeability test (RCPT) is a durability tests based on voltage driven diffusion which has been developed for the evaluation of the resistance of concretes to chloride ion penetration. Voltage driven methods were developed because of the sometimes impractical test duration (i.e. months to years) of the concentration driven methods. This test has often been specified as the primary compliance requirement for concrete durability.

A wide school of research and study over several years has come to the conclusion that while a useful tool, the usage of RCPT as a sole test for durability compliance is not advisable. The test provides an indication of pore size, continuity and tortuosity of the cementitious paste and more a measure of electrical resistivity rather than the resistance of the concrete to chloride ion penetration.

Despite the concerns for durability which were apparently raised based solely on the RCPT results it was the opinion of the Author that given the concrete of mix design and the triple blend OPC/PFA/SF concrete specified and the consistent achievement of normal quality control parameters and the fact that additional coatings were applied to the structure any concerns for durability based solely on ‘non-compliance’ to RCPT requirements in this contract were unfounded.

REFERENCES

Arup, H, Sorenson, B, Frederiksen, J and Thaulow, N 1993, ‘*The rapid chloride penetration test – an assessment*’, NACE Corrosion 93, New Orleans, LA, March 7-12.

Andrade C. 1993, ‘*Calculation of Chloride Diffusion Coefficients in Concrete from Ionic Migration Measurements*,’ Cement and Concrete Research, Vol. 23, pp. 724-742.

ASTM C1202 1997, '*Standard Test Method for Electrical Indication of Concrete's Ability to Resist Chloride Ion Penetration*', Annual Book of ASTM Standards, Vol. 04.02, American Society for Testing and Materials, West Conshohocken, 6 pp.

Buenfeld, N.R. and Newman, J.B. 1987, '*Examination of three methods for studying ion diffusion in cement pastes, mortars and concrete*,' Materials and Structures, Vol. 20, No.115, pp. 3-10.

Goh G C, Ho D W S, Tam C T 2002, '*Applicability of ASTM C1202-97 in assessing chloride penetration*' Journal, Institution of Engineers, Singapore, pp17-22.

JTK Report 1201/02 /7026, 2002 '*Review of Rapid Chloride Permeability Testing for Durability Compliance, Butterworth Bridge, Prai'* Pioneer Concrete Sdn Bhd.

McGrath, P.F. and Hooton, D.R. 1999, '*Re-evaluation of the AASHTO T259 90-day salt ponding test*' Cement and Concrete Research, Vol. 29, pp. 1239-1248.

Pfeifer, D.W., McDonald, D.B. and Krauss, P.D. 1994, '*The rapid chloride permeability test and its correlation to the 90-day chloride ponding test*,' PCI Journal, Vol. 41, No. 4, pp. 82-95.

Pfeifer, D W, McDonald, D B and Krauss, P D 1994, '*The rapid chloride permeability test and its correlation to the 90-day chloride ponding test*', PCI Journal – February, pp 38-47.

Wee, T.H., Arvind, K. Suryavanshi and San San Tin, 1999, '*Influence of aggregate fraction in the mix on the reliability of the rapid permeability test*,' Cement and Concrete Composites, Vol. 21, pp. 59-72.

Wee, T.H., Arvind, K. Suryavanshi and San San Tin, 2000, '*Evaluation of rapid chloride permeability test (RCPT) results for concretes containing mineral admixtures*,' ACI Materials Journal, Vol. 97, No. 2, pp. 221-232.

Whiting D 1981, '*Rapid Measurement of the Chloride Permeability of Concrete*,' Report No. FHWA/RD-81/119.

XII DBMC
International Conference on Durability of Building Materials and Components
PORTO - PORTUGAL, April 12th-15th, 2011

Experimental Determination of Liquid Transport Properties on Salt-Contaminated Porous Stone

Roel Hendrickx [1]
Staf Roels [2]
Hilde De Clercq [3]
Yves Vanhellemont [4]

ABSTRACT

The presence of salts is one of the major causes of decay of porous building materials. In order to be able to model the transport and phase changes it is essential to have reliable material parameters. This contribution deals with the experimental determination of the liquid transport parameters of Euville limestone and ceramic brick laden with NaCl, $NaNO_3$ or Na_2SO_4 at several concentrations. The water transport parameters for liquid and vapour were determined according to well-established methods. In the presence of crystalline salts there are two penomena changing the solid matrix and thereby the transport properties: firstly the salts precipitated on the pore wall cause a decrease in pore size, and secondly the crystallisation pressure causes dilation of the pores and possibly introduces new pores due to cracking. Other factors affecting tranport parameters are liquid density and liquid viscosity, surface tension and contact angle of the liquid.

Mercury intrusion porosimetry (MIP) measurements were done to characterise the pore system. Liquid transfer was studied by investigating a simple capillary uptake experiment, which was monitored using X-rays radiography. A methodology was developed to use a non-polar organic liquid in the speciments loaded with salts, so that there is no interaction between the absorbed liquid and the present salt crystals. Results reveal a strong dependence of the liquid transport properties on the type of salt.

KEYWORDS

Salt, Liquid transport, Porous stone.

[1] Building physics section, Katholieke Universiteit Leuven, Leuven, BELGIUM, roel.hendrickx@bwk.kuleuven.be
[2] Building physics section, Katholieke Universiteit Leuven, Leuven, BELGIUM, staf.roels@bwk.kuleuven.be
[3] Royal Institute for Cultural Heritage (KIK-IRPA), Brussels, BELGIUM, hilde.declercq@kikirpa.be
[4] Belgian Building Research Institute (BBRI), Brussels, BELGIUM, yves.vanhellemont@bbri.be

1 INTRODUCTION

The presence of soluble salts is one of the most important and widespread causes of damage to historical buildings [Doehne 2002]. Transport of dissolved salt ions in porous building materials occurs through the combined action of diffusion and advection, sometimes also through the presence of an electric field [Poupeleer 2007]. Phase changes of salts are the cause of damage and they also affect considerably the state of the porous medium and its transport properties. These changes can be: crystallisation and dissolution, hydration and dehydration, deliquescence and freezing. Phase changes and the rate at which they occur are influenced by the transport properties (liquid and vapour), which vary in place and time due to:

1. changes in liquid properties: viscosity and density increase;
2. changes in interface equilibrium: liquid-vapour equilibrium, liquid-gas surface tension and solid-liquid surface energy;
3. changes in the solid matrix: decrease of porosity due to precipitation of crystals, clogging of certain pores and thereby reduction of pore connectivity, dilation due to crystallisation pressure and crack formation due to crystallisation pressure.

It may be clear from this list that it is not evident to incorporate this behaviour in numerical models for the analysis of hygrothermal phenomena in porous building materials because both the liquid retention curve and the permeability curve may be different in every point and time step. They are influenced by a series of variables. As an example: an existing state-of-the art simulation code applies correction factors or functions to accounting for the volumetric crystalline salt content, however without reference to the actual physical mechanisms or experimental data [Nicolai 2008].

This paper describes the results obtained from the following liquid transport experiments: uptake of a salt solution by an initially salt-free porous material, and uptake of an organic liquid in a the same building materials containing a known amount of precipitated salts. Both phenomena are not influenced by diffusion. The liquid uptake experiments – monitored in an X-ray setup – were related to results of MIP measurements on samples of the same materials.

Some preliminary assumptions can be made based on the literature. MIP and helium pycnometry measurements on limestones contaminated with sodium sulphate in an absorption-drying experiment revealed that the distribution of salt crystals can be assumed – as a first approximation – uniform over all the pores [Angeli, Benavente et al. 2008]. Hence it can be expected that porosity decreases, that all pores decrease in size, and subsequently the liquid suction (capillary pressure) should increase while the permeability decrease for a comparable level of liquid saturation. Previous research has revealed that the air permeability of Tuffeau, Sireuil or Richemont limestones drops up to two and a half orders of magnitude in case salts were introduced, but the behaviour depends largely on the stone type [Birginie 2000].

When the crystallisation pressure is large enough and/or the modulus of the stone low enough, the solid dilates and pore sizes and porosity increase again. Measurements performed by [Lubelli 2006] on lime-cement mortar laden with sodium chloride showed a dilation of the material up to 0.4 mStrain during the crystallization process, part of which was irreversible and thus linked to the formation of micro-cracks. Further ESEM investigation illustrated that the crystals formed a regular thin layer adhering to the binder and partially filling the larger pores.

The ceramic brick used in this article has a porosity comparable to the limestones and mortar studied in the cited references, but a relatively low strength and modulus, so effects of both dilation and pore narrowing can be expected.

2 MATERIALS AND METHODS

The tested porous materials are a ceramic brick, type 'Spanish red' produced by Wienerberger (Belgium), and the french Euville limestone. Most of the tests were performed on the brick, some on the Euville. The brick has a rather high total and capillary porosity and corresponding high absorption coefficient and permeability [Table 1]. The brick has relatively low strength (10.2 MPa) and Young's modulus (1025 MPa).

Table 1. Properties of the tested porous materials. Coefficients of variance are given between brackets if known.

	Ceramic brick	*Euville*
Porosity [vol fraction]	0.323 (0.7%)	0.152 (0.5%)
Capillary water content [kg/m³]	206.7 (0.1%)	81.3 (3.7%)
Median pore diameter [micron]	1.7	3.08
Dry bulk density [kg/m³]	1786 (0.2%)	2260 (0.3%)
Capillary absorption coefficient [$kg/m^2s^{0.5}$]	0.534 (8.2%)	0.067 (10.7%)
Cap. saturated permeability [s]	5.52E-8	1.04E-9

The porous materials are laden with salt solutions of NaCl, $NaNO_3$ and Na_2SO_4 at different concentrations [Table 2]. Salt contamination was performed by free capillary uptake in dry specimens, until capillary saturation. After this, the specimens were wrapped in plastic foil and kept at 20°C during 24 h in order to obtain an equal distribution of the solution. The bricks were then dried at 105°C during 48h. As expected, an important part of the salt crystallises on the surface as efflorescence. The salt distribution within the specimens was controlled through conductivity measurements on the water extract of slices of the dry specimens. It proved that some 30% of the original amount of salt remained more or less uniformly distributed over the volume of the brick. The outer 10 mm of the brick specimens, which are enriched with salts, were cut off and were not used for the experiments.

Table 2. Overview of the salt solutions used in the experiments on brick specimens.

Salt	*NaCl*	*$NaNO_3$*	*Na_2SO_4*
Solubility 20°C [mol/kg]	6.14	10.26	1.4
Concentration [mol/kg]	1-3-5	2-4-6	0.5-0.75-1
Code brick specimen	A-B-C	D-E-F	G-H-I

Porosimetry measurements (MIP) in a Micromeritics Autopore IV were performed on all specimens. Each test consists of a low (up to 345 kPa) and a high pressure run (up to 228 MPa). Two samples per type of specimen were tested.

Liquid uptake tests were performed using 3 types of liquids: water, for the measurement of normal hygric properties, a highly concentrated NaCl solution and decane. Decane is a hydrocarbon with the chemical formula $CH_3(CH_2)_8CH_3$ which is immiscible with water and can not act as solvent for salts. Its nonpolar properties render it suitable for testing liquid transfer in salt-contaminated materials without affecting the salt. Table 3 gives an overview of the relevant properties of the liquids and shows that the density and surface tension of water increases when salts are dissolved in it. Surface tension is much lower in case of decane. The assumption of a zero contact angle is usually made for contact between aqueous liquids and stone or brick, but it cannot be made for decane, which has a considerably larger measured contact angle in reported experiments using glass and siliceous powders.

Monitoring of the uptake process was done by taking consecutive images of an initially dry sample during liquid uptake. Figure 1 shows the schematic setup of this experiment, which can be conducted

with the different liquids. Details on the procedure and the calculation method of the liquid content are published in [Roels 2006]. Two samples were cut from each specimen and used in the measurements (sample size depth x width x height = 15x30x60 mm).

Table 3. Overview of liquids used in capillary uptake experiments.

	Water	*NaCl brine*	*decane*
Density [kg/m³]	998	1278	730
Surface tension [mN/m)]	72.75	85.05	23.83
Contact angle [°]	~0	~0	22-43*
Viscosity [mPas]	1	1.93	0.92

*[Siebold, Nardin et al. 2000], others based on [Lide 2000]

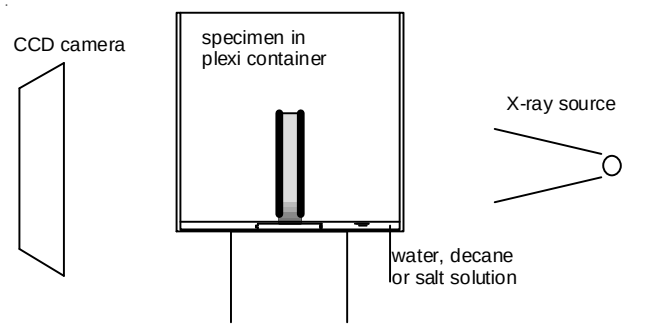

Figure 1. Schematic setup for a liquid uptake experiment in an X-ray station.

3 POROSITY, PORE SIZE DISTRIBUTION AND DILATION

In the overview of measured porosities for all brick specimens [Fig. 2] it appears that the three salts have a very different effect. Specimens laden with sodium nitrate follow quite a linear effect of salts filling the pores and hence little dilation. The opposite is found for the other salts, in which at first a decrease of the porosity at low salt content is noticed followed by an increase and an important dilation. This effect is most remarkable for sodium sulphate.

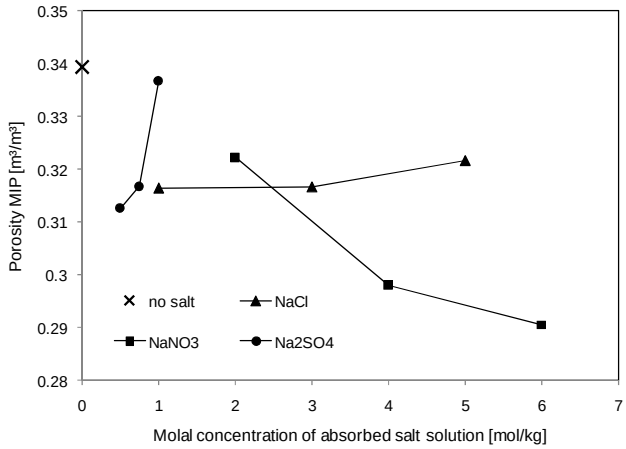

Figure 2. Measured porosities of brick samples containing various amounts of salts.

While $NaNO_3$ is in general characterised by hygroscopic properties but not considered as a destructive salt, sodium chloride and sulphate are known to cause higher crystallisation pressure and hence severe damage. The pore size distribution confirms this statement: a shift of the curve towards smaller pore radius is noticed, which is most clearly pronounced in the range of the small pores (1 to 10 micron). The shift is larger for a contamination with sodium nitrate than for the other salts, and increases with the salt content. The similar shape of the curves suggests that the salt forms a more or

less continuous layer and not in one specific range of pore sizes. There is no clear indication of the formation of micro-cracks of a certain width.

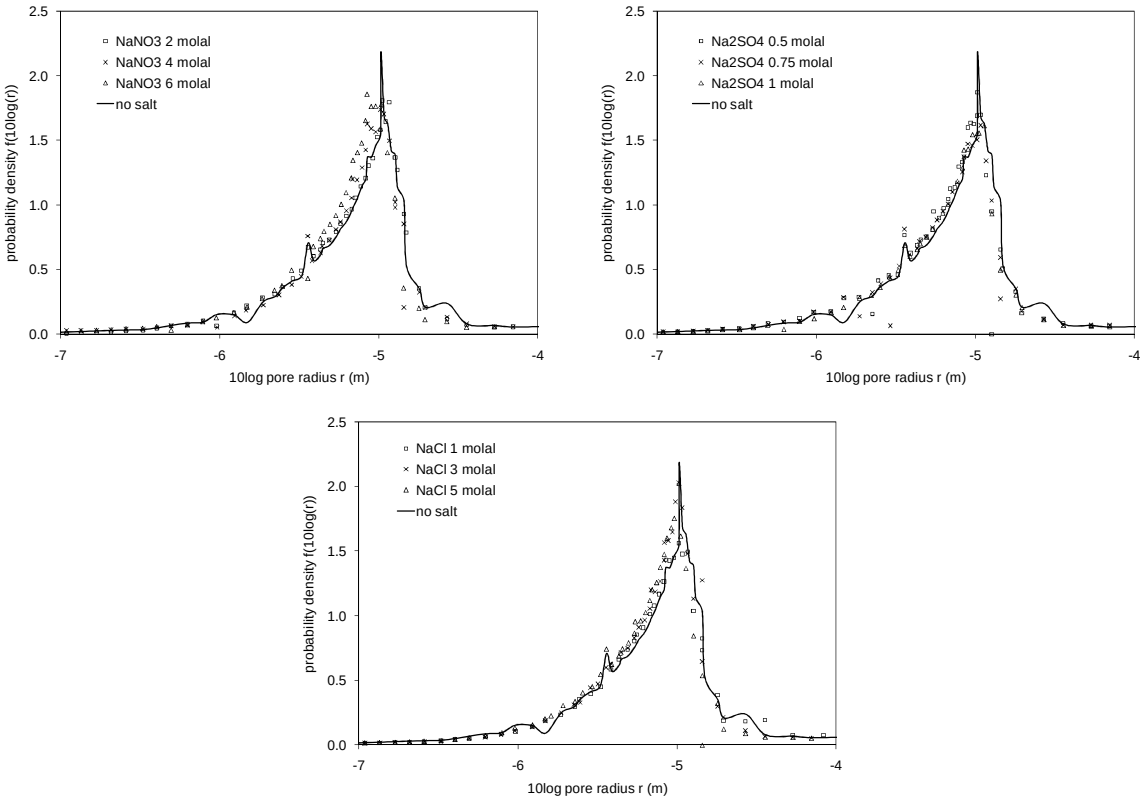

Figures 3. Pore size distributions for brick specimens without salts (solid line) versus those laden with various salt contents (expressed as concentration of absorbed salt solution).

In case the solid matrix is assumed to be incompressible, the total volume increase of the material (cubic volumic strain e) equals the increase in pore volume. The volume filled by salt crystals in the pores is also known. From these considerations an estimation of the linear strain ε can be made based on the MIP results. For a cubic sample ε approaches 3e [Hibbeler 2005]. The $NaNO_3$ laden samples have dilations below 0.9%, whereas the NaCl ones lead to a maximum of 2.3% and the Na_2SO_4 to 3.9%.

The MIP data can be used together with those of the contact angle and the surface tension to draw the liquid retention curves, using Laplace's law. These calculated results are not further discussed in this paper.

4 DIFFUSIVITY AND PERMEABILITY

4.1 Data treatment

The data of absorption tests were processed to quantify liquid permeabilty of the materials. This gives a good approximation of the permeability near capillary liquid saturation, but should be complemented with other experiments (e.g. drying) to have more precise data over a larger range. Permeability is assessed indirectly by using a diffusivity method as described in [Carmeliet, Hens et al. 2004]. The moisture profiles obtained from X-ray measurements are transformed ('Boltzmann-transformation') and recalculated to a liquid diffusivity curve. Figures 4 and 5 demonstrate the results for one particular specimen.

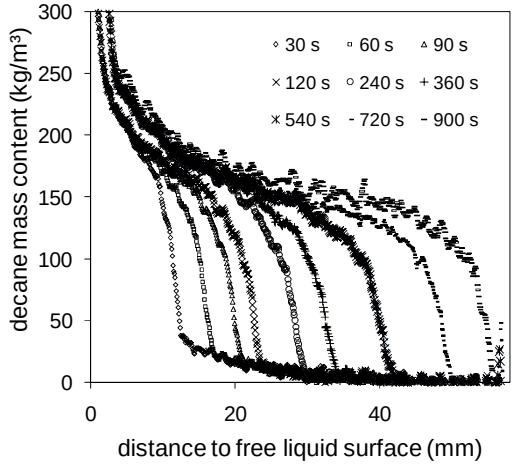

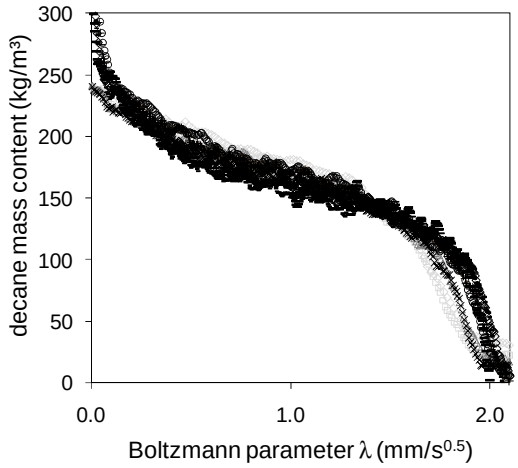

Figures 4 and 5. Liquid uptake curves for decane in brick specimen C (laden with a 5 molal NaCl salt solution): liquid content as a function of distance to free liquid surface at different times (left, Fig. 4) and transformed curves used for the calculation of diffusivity (right, Fig. 5).

4.2 Permeability for a salt solution in a salt(crystal)-free material

From the considerations above it can be expected that the liquid retention curve for a salt solution is not very different from that for water, apart from the density difference between both when expressed in mass terms. Hence, it can be expected that permeabilty is the most important parameter influencing the liquid transport. As the solid matrix remains unchanged, so does the intrinsic permeability. If K_{sol} is the mass permeability of the salt solution in [s] and K_w the permeability of water in the same material, K_{sol} can theoretically be calculated from K_w as:

$$K_{sol} = \frac{\eta_w}{\eta_{sol}} \frac{\rho_{sol}}{\rho_w} K_w \tag{2}$$

with η_{sol} and η_w the (dynamic) viscosities of solution and water and ρ their densities. This statement can be validated by comparing uptake tests with water and with a NaCl solution. The test with water was used to build the permeability curve $K_w(p_c)$ according to [Carmeliet, Hens et al. 2004] which was further rescaled to $K_{sol}(p_c)$ using Eq. (2). Based on this rescaled permeability curve and the original water retention one, a salt solution uptake experiment was simulated in Delphin 5. The results are presented in Figure 6 which shows a good correspondence between the theoretical curve and the one based on experimental X-ray data.

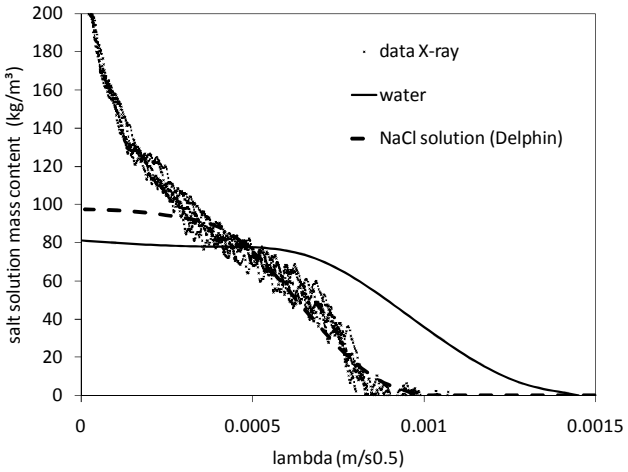

Figure 6. W-λ curves for water (fitted measured spline curve), and simulated curve for a NaCl solution (6.1 molal, dotted) compared to experimental results for Euville limestone.

The liquid content profiles of the salt solution lag behind the ones of water due to the reduced permeability and are scaled in the direction of the y-axis, when expressed in mass terms, due to the higher density of the salt solution. In terms of volume the capillary moisture content remains constant. Similar results were obtained for another limestone (Savonnières) which are not shown here limestone.

4.3 Permeability of decane in salt-loaded material

The data of the capillary uptake tests of decane were treated for bricks laden with NaCl and with $NaNO_3$. As expected after MIP measurements, capillary absorption coefficient and capillary saturation content decrease progressively for an increasing salt crystal content with $NaNO_3$ (Figs 7-8). This is however not the case for specimens laden with NaCl: absorption proceeds slower, but the amount of absorbed liquid is larger and less correlated to the salt content. The shape of the uptake curve changes in a systematic way for increasing $NaNO_3$ content [Fig. 9]: compared to the salt free specimen the position slope of the front slightly decreases and it recedes with respect to the x-axis for increasing salt content. for Again such a trend was not observed for NaCl-contaminated specimens: the measured w-λ profiles closely resemble the one for the salt-free specimen regardless the salt content.

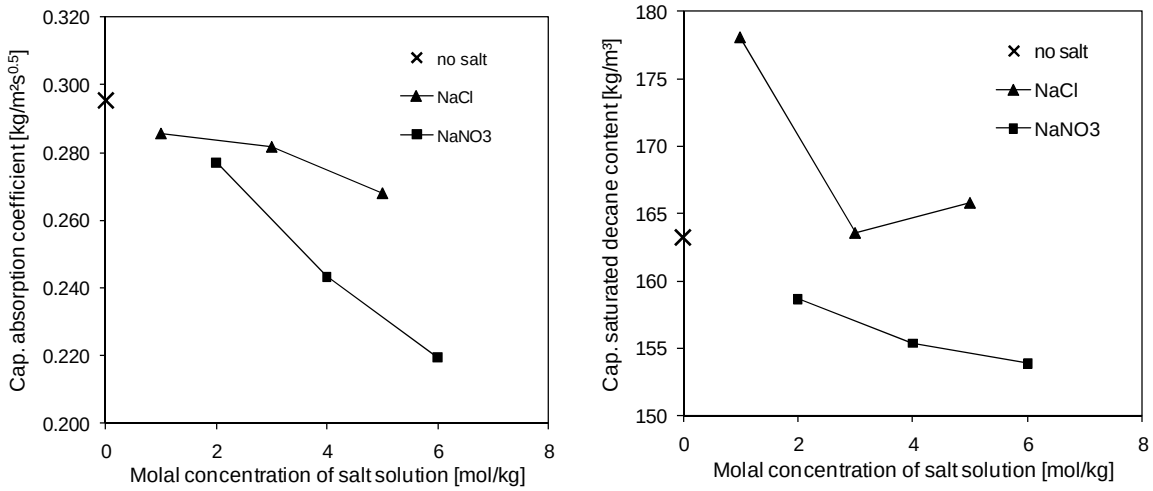

Figures 7 and 8. Capillary absorption coefficient (Fig. 7, left) and capillary saturated liquid content (Fig. 8, right) for decane on ceramic brick laden with different concentrations of NaCl and $NaNO_3$.

5 SUMMARY AND CONCLUSIONS

From the presented research, the influence of the type and amount of salts on the liquid transport properties of porous materials is demonstrated. As long as no salt crystals are precipitated, the intrinsic permeability remains unchanged and can be predicted for a given salt solution by scaling the water permeability with density and viscosity data available in literature. In case of salts crystallisation, the effect on the liquid tranport properties is strongly dependent on the type of salt. All tested salts result in a reduction of pore sizes. In case of NaCl and Na_2SO_4 this reduction in pore size is compensated by a dilation of the material and subsequent increase of porosity, due to the crystallisation pressure. The effect is strongest for sodium sulfate, which is known to be the most destructive salt in many situations [De Clercq 2008a; De Clercq 2008b; De Clercq 2008c]. Experiments with decane as non-polar organic liquid showed to be suitable to investigate the capillary liquid uptake in salt-contaminated porous materials since they do not interact with the present salt. It was demonstrated that the absorption proceeds slower and goes to a lower saturation content for increasing $NaNO_3$ content. This statement was not confirmed for NaCl. In this case it is supposed that the permeability is not reduced, because the effect of dilation and/or crack formation compensates the effect of pore size reduction.

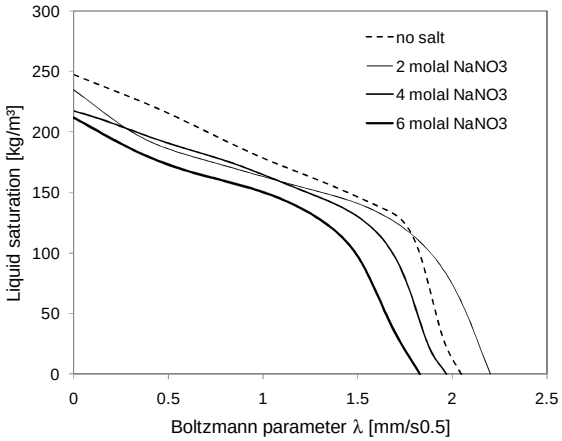

Figure 9. w-λ profiles for decane uptake in brick loaded with $NaNO_3$ at different concentrations.

Decane permeability curves as a function of liquid saturation and solid salt content (using a decane liquid retention curve) can be built up based on data from capillary uptake experiments. They can further be converted into curves for water or a salt solutions at any concentration. Future investigations will include treatment of the data with Na_2SO_4 and calibration of decane permeability curves with drying experiments. Another point of interest is to check to what extent the permeability changes are reversible, i.e. when the crystalline salt is dissolved again: does the permeability go back to the salt-free value? Finally it should be noted that the results are only valid for the tested building materials: the salt - porous material interaction depends strongly on the moduli of the building material and will probably differ in case of high strength and low porosity.

ACKNOWLEDGMENTS

Grants of IWT project ‘Collectief onderzoek 399 576’ of the Flemish government are acknowledged.

REFERENCES

Angeli, M., & D. Benavente, & J. Bigas, & B. Menendez, & R. Hebert, & C. David 2008. 'Modification of the porous network by salt crystallization in experimentally weathered sedimentary stones'. *Materials and structures*, **41**[6], 1091-1108.

Birginie, J. M. 2000. 'Changes in the permeability to gas of calcareous stone core samples exposed to salt spray'. *Materials and structures*, **33**[5], 331.

Carmeliet, J., & H. Hens, & S. Roels, & O. Adan, & H. Brocken, & R. Cerny, & Z. Pavlik, & C. Hall, & K. Kumaran, & L. Pel 2004. 'Determination of the liquid water diffusivity from transient moisture transfer experiments'. *Journal of Building Physics*, **27**[4], 277.

De Clercq, H. 2008a, 'Performance of limestone contaminated with binary mixtures of sodium sulphate and treated with a water repellent'. *Hydrophobe V, Fifth International Conference on Water Repellent Treatment of Building Materials*, Brussels, 15-16 April 2008, 107-116.

De Clercq, H. 2008b, 'The effect of other salts on the crystallization damage to stone caused by sodium sulphate'. *Int. Conference on Salt Weathering on Buildings and Stone Sculptures*, Copenhagen, 22-24 Oct., 307-317.

De Clercq, H. 2008c. 'Behaviour of Limestone Contaminated with Binary Mixtures of Sodium Sulphate and Treated wit a Water Repellent'. *Int. Journal for the Restoration of Buildings and Monuments*, **14**[5], 357-364.

Doehne, E. 2002. 'Salt weathering: a selective review'. *Geological Society special publication*, **205**[1], 51.

Hibbeler, R. 2005, *Mechanics of materials*, Prentice Hall, New York.

Lide, D. R. 2000, *CRC handbook of chemistry and physics*, CRC, London.

Lubelli, B. 2006, 'Sodium chloride damage to porous building materials', TUDelft. PhD.

Nicolai, A. 2008, 'Modeling and numerical simulation of salt transport and phase transitions in unsaturated porous building materials'. Dresden, TUDresden. PhD.

Poupeleer, A.-S. 2007, 'Transport and crystallization of dissolved salts in cracked porous building materials'. *Building physics laboratory*. Leuven, KULeuven. PhD.

Roels, S. 2006. 'Analysis of moisture flow in porous materials using microfocus X-ray radiography'. *International journal of heat and mass transfer*, **49**[25-26], 4762.

Siebold, A., & M. Nardin, & J. Schultz, & A. Walliser, & M. Oppliger 2000. 'Effect of dynamic contact angle on capillary rise phenomena'. *Colloids and Surfaces A: Physicochemical and Engineering Aspects*, **161**[1], 81-87.

XII DBMC
International Conference on Durability of Building Materials and Components
PORTO - PORTUGAL, April 12th-15th, 2011

Moisture Transport through Nano-based Treated Wood Exposed to Transient Climatic Conditions

Selamawit Mamo Fufa [1]
Per Jostein Hovde [2]
Bjørn Petter Jelle [3]
Goce Talev [4]

ABSTRACT

Moisture is one of the weathering factors which affect the durability of wood. Protection against degradation due to moisture is a key factor for exterior wooden claddings. The objective of this work is to present the moisture transport in nano-based surface treated and impregnated spruce and pine wood species. Both treated and untreated specimens were exposed to weekly cyclic step changes between 75 % relative air humidity (RH) and 40 % RH for a total of six weeks. The temperature was kept constant at 23 ºC. Experimental analysis identifies the variation of moisture content of the specimens as a function of the relative humidity cyclic step change. The results from the measured transient climate in this test have been compared with WUFI 5 simulations. Hygroscopic material properties of the specimens obtained from sorption and cup measurements were used as input data during the WUFI 5 calculations.

KEYWORDS: Nano-based coatings, Material properties, WUFI.

[1]Norwegian University of Science and Technology (NTNU), Department of Civil and Transport Engineering, Trondheim, Norway, selamawit.fufa@ntnu.no
[2]Norwegian University of Science and Technology (NTNU), Department of Civil and Transport Engineering, Trondheim, Norway, per.hovde@ntnu.no
[3]SINTEF Building and Infrastructure, Department of Material and Structures, Trondheim, Norway bjorn.petter.jelle@sintef.no and Norwegian University of Science and Technology (NTNU), Department of Civil and Transport Engineering, Trondheim, Norway, bjorn.petter.jelle@ntnu.no
[4]Norwegian University of Science and Technology (NTNU), Department of Civil and Transport Engineering, Trondheim, Norway, goce.talev@ntnu.no

1. INTRODUCTION

Wood has a natural affinity to water and always contains significant quantities of moisture. Wooden claddings subjected to different climate conditions are exposed to water and exhibit moisture movement to and from the surface. Moisture is one of the most important factors that play a vital role in physical and mechanical properties of wood. Understanding the moisture transport in wooden cladding is crucial from the point of view of predicting the long term performance of buildings.

Since long various treatments have been used for wood towards overcoming its behaviour that leads to degradation (Hill 2006). The growing interest towards improving the durability and sustainability of wood used in buildings urges the development of new wood treatment technologies. Nano-based surface treatments are new approaches used in current wooden buildings (Fufa & Hovde 2010). Coatings help to control dimensional changes and degradation caused by rapid change in moisture content. The coatings do also protect towards the solar radiation exposure. However, it should be noted that coated wood can also be degraded. Hence, it is crucial to investigate the performance of newly developed paints under the influence of climate conditions before their applications.

Experimental data are required to study this issue but such experiments are either time consuming, have lot of uncertainties or are expensive. Numerical models are therefore good alternatives to solve such kind of problems. Recently, major progress has been made worldwide in development of different hygrothermal modeling tools as described in Canada Mortage and Housing Corporation (CMHC 2003). The models differ in the way of simplifying different parameters including moisture transfer dimension (one, two or three), type of flow (steady state or dynamic), quality and availability of information (Karoglou et al. 2007).

WUFI, a one dimensional heat and moisture transfer simulation tool, is used to calculate the hygrothermal performance of building envelopes. WUFI is used to predict the combined heat and moisture transfer in multilayered constructions under transient conditions (WUFI 5 Pro 2009). It is used to validate the experimental data and assess the performance of wooden claddings coated with new paints before their real application.

Material properties are the main input parameters for the simulation. However, not all material properties affect the overall moisture response at the same rate. Water vapour resistance factor (WVRF) and sorption isotherms have been proved to be the two most important material properties (Kwiatkowski et al. 2009; Mukhopadhyaya et al. 2002). WVRF describes the moisture transport property while the dependence of equilibrium water content on the relative air humidity (RH) level is illustrated by the sorption isotherm. Both WVRF and sorption isotherm properties are dependent on the RH.

In this work the influence of nano-based coatings and coatings modified with nanoparticles on moisture transport of wooden claddings exposed to cyclic climate conditions is presented. The experimental measurements were divided into two parts. In the first part WVRF and adsorption isotherms of the specimens were measured. The measurement of moisture uptake of specimens with step change in the RH was carried out in the second part. Finally, the measured material properties were used as input data for WUFI in order to simulate the moisture performance.

2. EXPERIMENTAL

2.1 Overview of the overall study

The results presented in this paper are part of ongoing research work where some key properties of two types of wood species (Norway spruce and Scots pine) modified with surface treatment and impregnation under varying climate conditions is studied. The objective is to investigate the performance of the two treatments modified with clay and titanium nanoparticles on durability and

reaction to fire wood properties. Stain, water based paints (WBP) and preservatives were mixed with the nanoparticles. Specimens were treated with either coatings or impregnation. After measuring the material properties of treated specimens, they were exposed to (40 ± 3) % RH and (75 ± 3) % RH and temperature of (23 ± 0.5) ^{0}C in weekly step cycles for a total of 6 weeks. The experimental values were validated with WUFI simulation. In a previous paper (Fufa et al. 2010), the influence of two commercially available transparent nano-based coatings (which were labelled as SPN and SPf) on spruce moisture transport was assessed. In this paper, only the results from spruce coated with SPN, WBP and WBP modified with nanoparticles are presented; the remaining results will be presented elsewhere.

2.2 Test specimens

Norway spruce (*Picea abies*) without knots and defects were selected in the experimental work. Specimens were coated with SPN (purchased from Kalin & Co. AG), WBP (obtained from Jotun AS) and WBP modified with titanium dioxide nanoparticles (labelled as WBNT) and nanoclay (labelled as WBNC). An overview of the type of specimens and surface treatments used is given in Table 1 below.

Table 1. List of specimens used in this study.

No.	Treatment type	Abbreviation
1	Uncoated spruce	US
2	Spruce coated with 2 coats of SPN	S+SPN
3	Spruce coated with 2 coats of WBP × 1 coat of primer	S+WBP
4	Spruce coated with 2 coats of WBNT × 1 coat of primer	S+WBNT
5	Spruce coated with 2 coats of WBNC × 1 coat of primer	S+WBNC

The specimens with size of (100.0 ± 0.5) mm x (100.0 ± 0.5) mm x (20.0 ± 0.5) mm (width × length × thickness) were prepared for the sorption and transient tests. Circular specimens with a diameter of (73.0 ± 0.5) mm and thickness of (5.0 ± 0.5) mm were used for the cup test. All specimens were preconditioned before running the test. For the transient test, edges and the back side of the specimens were sealed with aluminium foil before exposure to approximate one dimensional transport process.

3. MODEL DESCRIPTION

In this study WUFI was used to calculate the transient heat and moisture transport behaviour of building components exposed to different climate conditions. Material properties, initial and boundary conditions are important input parameters to simulate real world situation. Material properties required for the WUFI simulation are: bulk density, porosity, specific heat capacity, thermal conductivity, adsorption and WVRF. In the WUFI database, the properties of different materials tested in different countries are available.

3.1 Material properties

Based on the literature data and preliminary simulation performed, sorption isotherm and WVRF were the main properties which determine the moisture content of the specimens. Therefore, sorption isotherm and WVRF were measured while other properties were utilized directly from the WUFI database. These two properties were experimentally determined based on ISO standards (ISO 12571 2000; ISO 12572 2001).

For the adsorption test, dried specimens were exposed to (40 ± 3) % RH, (50 ± 3) % RH, (75± 3) % RH and (94 ± 3) % RH in increasing order. The moisture content was determined when the specimen reaches in equilibrium with the surrounding environment. The amount of moisture adsorbed into the specimen per unit surface area in each RH is expressed in the adsorption curve. While, WVRF was determined using the well known cup method (Söderström 1998). Specimens were sealed into the

mouth of the aluminium cups containing a vapour pressure regulator which was either distilled water or lithium chloride (LiCl). Specimens were exposed to different RH of (11/50 ± 3) % RH, (100/50 ± 3) % RH and (100/75 ± 3) % RH inside and outside the cup respectively in order to create a water vapour flow either into the cup or out of the cup. The WVRF of the specimens were determined from the test. The experimental results of the sorption isotherm and WVRF are presented here in Figure 1 and Figure 2, respectively.

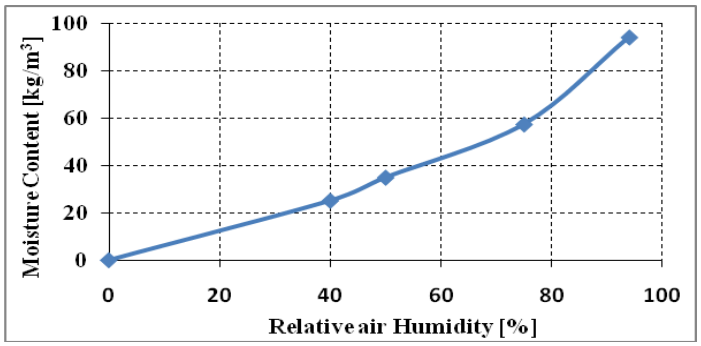

Figure 1. Adsorption isotherm experimental data for untreated spruce.

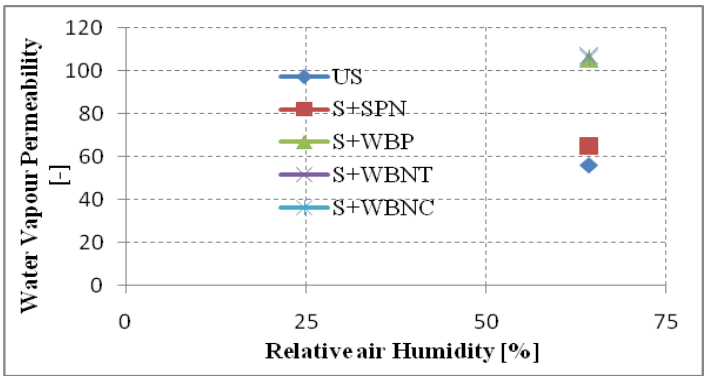

Figure 2. Water vapour resistance factor determined from cup test experimental data.

Likewise, the transient tests were conducted to investigate the efficiency of the treated materials exposed to different RH. The results of both coated and uncoated specimens exposed to weekly cycles between (75 ± 3) % RH and (40 ± 3) % RH for a total of six weeks. Due to the lengthy experimental process, only the results from two weeks of exposure are presented in Figure 3.

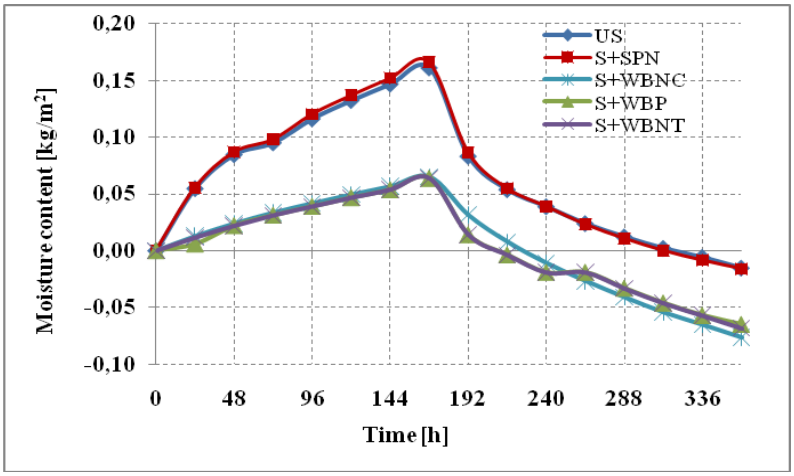

Figure 3. Moisture content of wood specimens exposed to transient test**.**

3.2 Simulation methodology

Water vapour resistance (WVRF) and sorption isotherm properties obtained from the experimental work were used as input parameters for the simulations. All other material properties were taken from the WUFI database *Scandinavian Spruce transverse direction II*. The parameters used for the simulations are presented in Table 2 and Table 3.

Table 2. Common parameters from the WUFI database *Scandinavian spruce transverse direction II*.

Parameters		Amount	Unit
Basic data (Material properties)	Bulk density	420	kg/m^3
	Porosity	0.75	m^3/m^3
	Heat capacity	1 600	J/(kg K)
	Thermal conductivity	0.13	W/(m K)
Surface transfer coefficients	Exterior surface heat resistance	0.0588	m^2K/W
	Interior surface heat resistance	0.125	m^2K/W
	Interior surface equivalent air layer thickness (s_d) value	10 000	m
Initial conditions	RH	50	%
	Temperature	23	ºC

Table 3. Modified parameters from the experimental data applied in the simulations.

Parameters		Source of data
Basic material data	Water vapour permeability	Figure 1
Optional material data	Moisture storage function	Figure 2

Initial conditions of 23 ºC and 50 % RH were set to match with experimental conditions. In this study a thin layer (20 mm) of only one wall component made of wood was considered.

4. RESULTS AND DISCUSSION

From the transient test results shown in Figure 3, specimens coated with WBP and WBP modified with nanoparticles show significant reduction in the moisture transport. The paint used as vapour barrier limits the moisture transport significantly. However, the degree of the transport resistance depends on the type of paint applied or treatment method used.

There are two features that can be recognized from Figure 3, i.e. poor performance of SPN and almost similar effect of WBP with that of WBP modified with nanoparticles (WBNT and WBNC). But as described by Fufa and Hovde (Fufa & Hovde 2010), there have been several studies showing good performance of nano-based coatings. From these results, the type, particle size and the degree of the dispersion of nanoparticles applied may be parts of the reason for the observed low moisture inhibition properties of the nanocoatings. In addition, the coating application method may also be the cause for poor performance.

In order to obtain a clear image of the moisture content (MC) of the different treatments, the simulation results are presented in Figure 4 and Figure 5.

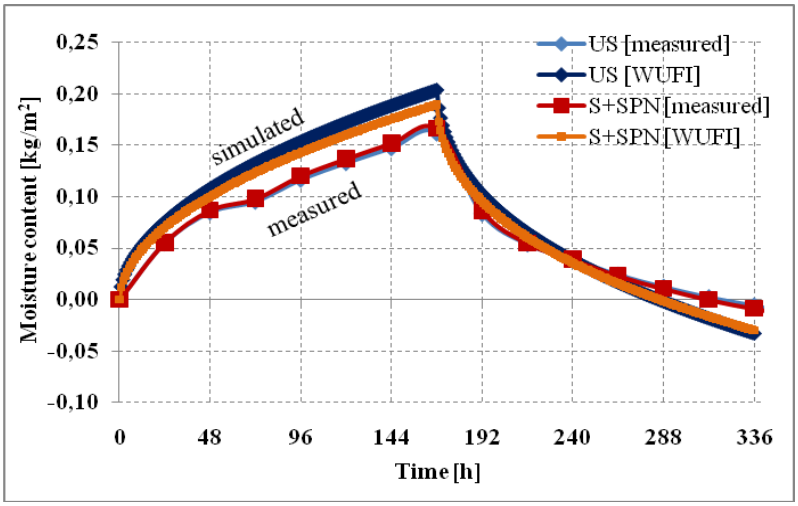

Figure 4. Moisture content comparison of transient test results of US and S+SPN with WUFI simulations.

Both Figure 4 and Figure 5 show rather good agreement between the simulated and measured data with some discrepancies. Especially the US and S+SPN measured and simulated values show good agreement. The deviation for the coated specimens (Figure 5) may be due to the assumed material properties taken directly from the WUFI database. Additionally, utilization of too long time steps in the simulations may be the cause for the divergence of the simulation value with the experimental one.

For both coated and uncoated specimens significant deviations in adsorption than in desorption have been observed. This can be due to a hysteresis effect (difference between absorption and desorption curves). In WUFI only the adsorption isotherm is considered by neglecting any hysteresis effect. Hysteresis in the sorption process affects the relation between both water vapour permeability and moisture content with RH (Kwiatkowski et al. 2009). Neglecting the hysteresis effect might lead to underestimation of the risk of moisture related damage in building envelopes.

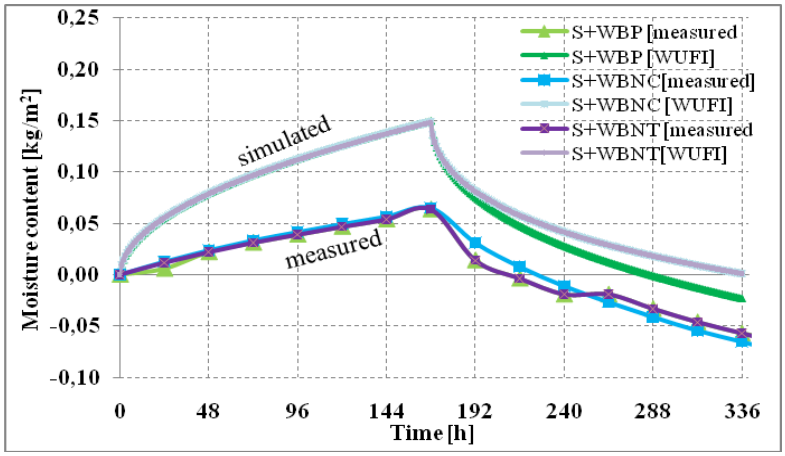

Figure 5. Moisture Content comparison of transient test results of S+WBP, S+WBNC and S+WBNT with WUFI simulation.

As a natural material, the moisture storage capacity of wood varies even within the same tree. The variation in the pore structure of the wood may be the main cause for the variation of the results. The experimental uncertainty in the measured material properties might also cause significant variation of the measured data from the simulations. These include accuracy in the cup measurements, precision of RH and temperature of the climate room, accuracy of the salt solution used for adjusting RH levels and some other measurement errors.

5. CONCLUSIONS

In this study the influence of nano-based treated wood on the transient moisture transport was studied both experimentally and numerically. The preliminary results show poor performance of spruce coated with both commercially available and modified nanopaints. The commercially available nanopaint shows almost no improvement when compared to the uncoated spruce. While specimens coated with modified WBP shows good improvement than uncoated but the degree is almost similar with that of unmodified WBP. The moisture distribution was studied based on the data obtained from the simulation carried out by using WUFI. The simulation from WUFI shows good correlation with the experimental results, though with some discrepancies.

ACKNOWLEDGMENTS

The authors would like to acknowledge Moelven Wood and Jotun AS for providing materials and many helpful discussions; Erik Larnøy, Adreas Treu and Britta Witt of the Norwegian Forest and Landscape Institute for their support in impregnation and to Ole Aunrønning for assistance with various laboratory tasks. The financial support by the Research Council of Norway is also gratefully acknowledged.

REFERENCES

CMHC 2003, *Review of hygrothermal models for building envelope retrofit analysis*,Mortage and Housing Corporation , Technical series 03-128, Ottawa, December.

Fufa, S.M. and Hovde, P.J. 2010, 'Nano-based modifications of wood and their environmental impact: Review', World Conference On Timber Engineering, Riva del Garda, Trentino, Italy, 24-26 June 2010, 1093-1094.

Fufa, S.M., Hovde, P.J., Talev, G. and Jelle, B.P. 2010, Nano-based coatings and the influence on the hygroscopic properties of wood, Espoo, Finland,27-29 September 2010.

Hill, C. 2006, *Wood Modification: Chemical, Thermal and Other Processes*. John Wiley & Sons Ltd, Atrium/Southern Gate/Chichester.

ISO 12571 2000, Hygrothermal performance of building materials and products- Determination of hygroscopic sorption properties. International Organization for Standardization, Geneve, Swizerland.

ISO 12572 2001, Hygrothermal performance of building materials and products-Determination of water vapor transmission properties. International Organization for Standardization, Geneve, Swizerland.

Karoglou, M., Moropoulou, A., Krokida, M.K. and Maroulis, Z.B. 2007, A powerful simulator for moisture transfer in buildings. Building and Environment, 42: 902-912.

Kwiatkowski, J., Woloszyn, M. and Roux, J.-J. 2009, Modelling of hysteresis influence on mass transfer in building materials. Building and Environment, 44: 633-642.

Mukhopadhyaya, P., Goudreau, P., Kumaran, K. and Reenen, D.V. 2002, 'Influence of material properties on the moisture response of an ideal stucco wall: results from hygrothermal simulation', Sixth Nordic Building Physics Symposium, Trondheim, Norway, 17-19 June 2002, 611-618.

Söderström, O. 1998, On Analysis of Cup Method Measurements on Hygroscopic Materials with Surface Coatings. Nordic Journal of Building Physics.

WUFI 5 Pro 2009, Transient Heat and Moisture Transport, Holzkirchen, Germany.

XII DBMC
International Conference on Durability of Building Materials and Components
PORTO - PORTUGAL, April 12th-15th, 2011

Full-Range Modelling of Heat and Moisture Transfer Coefficients in Damaged Building Materials

Simon Rouchier [1,2]
Monika Woloszyn [1]
Geneviève Foray [2]
Jean-Jacques Roux [1]

ABSTRACT

The reduction in energetic consumption of existing buildings not only includes the conception of new isolating materials, but also requires a complete understanding of the transport processes at every scale of observation. While the combined heat and moisture transfer in building components has been the subject of numerous numerical and experimental studies in the latest years, current simulation codes usually do not include the effects of material aging, although moisture permeability can be significantly increased in the presence of macroscopic fractures or microcracks in cementitious materials.

The transport equation for the conservation of mass and energy are to include transfer coefficients which reflect the microscopic structure of the investigated material. In the present work, a model based on resistor networks is proposed, which accounts for the presence of microscopic or macroscopic cracks in a porous media and allows the calculation of its water vapour diffusion factor as well as equivalent thermal conductivity.

The computations are compared with detailed simulations and experimental measurements of the moisture uptake of damaged mortar. Fracture networks are generated by uniaxial tension in the samples, which are then brought to fluctuating climatic conditions in hygroscopic range while their mass uptake is measured with a dynamic weighing system.

KEYWORDS

Moisture transfer, Porous media, Diffuse damage.

[1] Centre de Thermique de Lyon (CETHIL), UMR CNRS 5008, Université Claude Bernard Lyon 1, FRANCE, simon.rouchier@insa-lyon.fr
[2] MATEIS, UMR CNRS 5510, INSA Lyon, France

1 INTRODUCTION

The study of moisture transfer inside building materials is an important issue in building physics, as it influences the durability and thermal performance of the inner and outer walls. Since the first questionings on the subject, various methods were developed for the experimental determination of the equilibrium moisture content and permeability of these materials and for the numerical simulation of coupled heat and moisture transfer at the scale of entire buildings.

However, the material description in simulation tools is often based on hypothesis such as anisotropy and constant transfer properties of the materials. This can be an important source of calculation errors, especially in the case of damaged building materials, which permeability can change as their microstructure presents defaults and fractures. Fractures in cementitious materials can be caused by various phenomena: compressive and tensile mechanical loading and fatigue phenomena, imbibition/drying cycles and periodic variations of the capillary pressure, transport of reacting chemicals such as chloride ions, thermal cycles...

Studies in the field of durability of building materials tend to describe the degradation of semi-brittle materials such as concrete in two phases [Mazars and Pijaudier-Cabot 1996] : damage mechanics [Bazant & Oh 1983] for the description of diffuse microcracking and fracture mechanics for the growth of macroscopic cracks.

Recent studies [Pijaudier-Cabot *et al.* 2009] have shown the consequences of diffuse micro-cracking on the intrinsic permeability of concrete during mechanical loading or after unloading. The liquid and gaseous conductivity of cementitious materials can be significantly increased before the formation of a macrocrack. However, moisture transport in building materials is not only caused by the displacement of a continuous liquid phase which can appear in case of rain [Janssen *et al.* 2007], but also by water vapour gradients and sorption processes in the hygroscopic range.

2 NUMERICAL MODELLING

2.1 Moisture Transfer in Porous Media

The conservation equation for the water content w includes terms for moisture transport in both gazeous g_v and liquid g_l phases, which are usually expressed separately, and driven respectively by a gradient of water vapour pressure p_v or capillary pressure p_c.

$$\frac{\partial w}{\partial t} = -\nabla \cdot \left(\vec{g}_v + \vec{g}_l \right) = -\nabla \cdot \left(-\delta_p \nabla p_v - K_l \nabla p_c \right)$$

where δ_p and K_l are respectively the water vapour permeability and liquid conductivity of the material. As the latter has been the subject of experimental and numerical studies showing its evolution with both diffuse microcracking and seepage through macroscopic discrete fractures, we focus this study on the diffusion of moisture in gaseous phase.

2.2 Permeability of a Fracture Network

An expression of the effective diffusivity of a fractured porous media can be proposed, based on the representation of the crack network inside the material as overlapping resistor networks.

$$\delta_p = \frac{1 - a/2}{\dfrac{a}{2\delta_{p,f}} + \dfrac{1 - a/2}{\delta_{p,0}}} + \frac{a}{2}\delta_{p,f}$$

where $\delta_{p,f}$ and $\delta_{p,0}$ are respectively the water vapour diffusivity inside a fracture and in the porous matrix and a is the relative volume occupied by fractures in an representative elementary volume. See

[Shah and Choi 1999] for a review of nondestructive techniques usually applied for the measurements of such geometrical properties of the fracture network.

3 DYNAMIC MEASUREMENTS OF MOISTURE UPTAKE

3.1 Experimental Setup

A full experimental setup was established, which covers the entire process of generating and observing crack growth as well as measuring the resulting water vapour permeability.

The material used for all tests is a newly developed mortar with a water/cement ratio of 0.8 and reinforced with glass fibers, so that progressive diffusive cracking will occur and develop during mechanical loading before the formation of a main macroscopic fracture. Plates of dimensions 300x100x10 mm are loaded at uniaxial tension. The specimens are loaded beyond their limit of elasticity then the loading is interrupted before a macroscopic fracture can be observed, and their diffuse damage is characterised by a single scalar value *D*, which is measured as the relative change in their Young modulus [Mazars & Pijaudier-Cabot 1989].

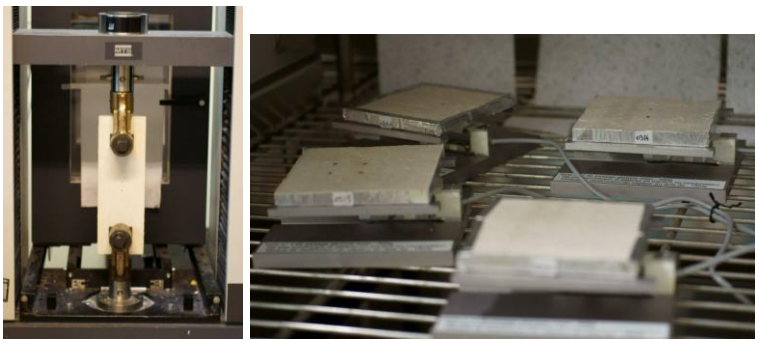

Figure 1. Left: specimen placed in the mechanical loading device; right: display of samples placed on weighing systems inside the climatic chamber after loading.

The central part (100x100x10 mm) of each plate is then insulated from moisture on all sides but one, so moisture transfer are close to unidimensional, then placed in a climatic chamber with fluctuating ambient humidity following the Nordtest protocol [Rode 2003]: the chamber recreates hygric cycles alternating high (75%RH during 8 hours) and low (33%RH during 16 hours) relative humidity steps at a constant temperature of 23°C. The weight of up to 8 samples can be continuously measured during the climatic simulations.

3.2 Effusivity and Permeability Estimation

The transfer properties of the mortar samples are compared in terms of hygric effusivity b_m. This property is defined similarly to the thermal effusivity as an indicator for the instantaneous water vapour transfer at the surface of a sample in response to a step change in ambient humidity:

$$b_m = \sqrt{\frac{\delta_p \xi}{p_{sat}}}$$

where ξ is the slope of the water retention curve and p_{sat} is the saturation pressure of water vapour. In order for b_m to be considered a property of the material, the role of the convective mass transfer coefficient at the boundary has to be neglected in comparison to the material's internal resistance to moisture diffusivity [Rode *et al.* 2005]. This hypothesis is assumed to be accurate in the present study.

After a step in ambient relative humidity, a fairly accurate approximation is to consider the instantaneous mass uptake rate in a specimen g_m proportional to the effusivity divided by the square root of the time which has elapsed since the start of the humidity step :

$$g_m \propto \frac{b_m}{\sqrt{t}}$$

Integration of this relation allows to link directly the mass measurements from the weighing systems to the transfer properties δ_p and ξ of the material:

$$\frac{\Delta m}{S} = \int_0^t g_m d\tau \propto \sqrt{\frac{\delta_p \xi}{p_{sat}}} \sqrt{t}$$

where Δm is the registered mass uptake in a sample of exposed surface S since the start of the humidity step. This relation allows to compare the hygric effusivity of all the samples simultaneously placed in the chamber as it is proportional to the slope of the mass uptake plotted versus the square root of time. If the hypothesis is made that the sorption isotherm in not influenced by the presence of fractures, the permeability δ_p can be considered proportional to the square of the mass measurements. Although δ_p can not be directly calculated, its ratio between two or more samples can. Simultaneously placing several samples in different damage states therefore allows to estimate the impact of damage on the permeability.

4 RESULTS AND DISCUSSION

Two series of samples were first loaded as described above then repeatedly placed in the climatic chamber for hygric cycles. The value of the scalar damages reached with tensile loading span from 0 (samples kept intact) to 0.6 (before peak stress). No macroscopic crack propagation was observed on any of the samples used in this study. The ratio of the measured mass uptake during the last humidity step to the square root of time is then obtained by linear fitting as shown on Fig. 2. This figure illustrates the increase in the sorption rate with higher damage values.

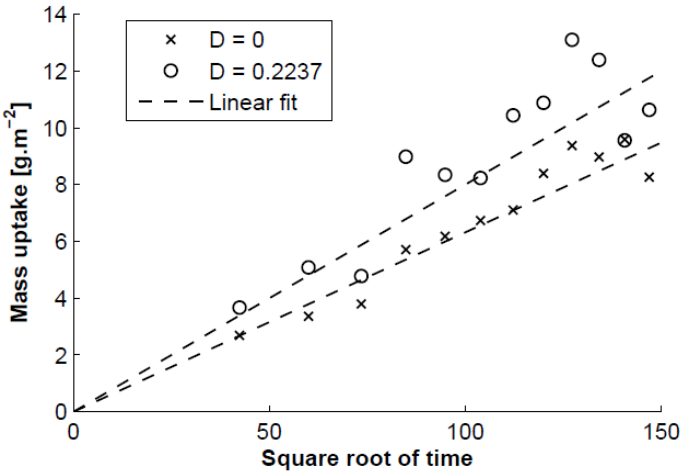

Figure 2. Mass uptake during a high humidity step in the climatic chamber versus square root of time shown on two examples of samples with different damage values.

The square of the slopes being proportional to the permeability, we can estimate the effects of damage by comparing loaded samples with intact ones, as several are simultaneously subject to the same humidity cycles. Results on these two series of samples are shown on Fig. 3. Each sample has been subjected to several humidity cycles as to obtain a mean value of its relative permeability. The permeability of samples with no applied damage has been set to 1.

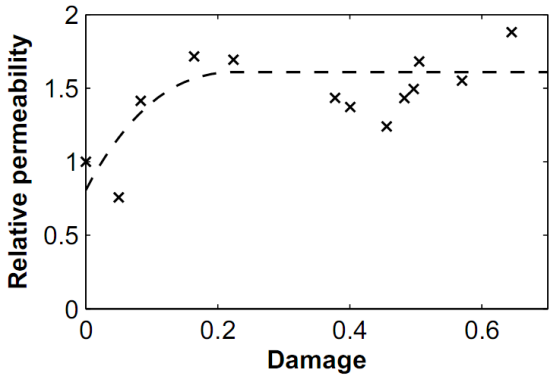

Figure 3. Relative evolution of water vapour permeability with tensile damage applied on the sample prior to its hygric characterization (dots), and approximation (line).

It can be noticed that the water vapour permeability shows an immediate increase as microscopic defaults start to appear in the material. This increase then tends to stop for medium values of *D*, although this tendency needs confirmation with additional measurements on new series of samples. However a high standard deviation is to be expected with such measurements for both high and low damages, as microcracks already start to develop during the maturation and hydratation processes in Portland cement [Elaqra *et al.* 2007].

5 CONCLUSION

This characterization of δ_p as a function of a scalar damage value, along with studies on the evolution of the liquid phase conductivity [Pijaudier-Cabot *et al.* 2009] can allow the numerical simulation of moisture transfers in existing building with an additional variable *D* which can also be considered an intensive physical property. By expressing the thermal conductivity as a function of the liquid phase saturation in the porous medium [Carson *et al.* 2005], one can run coupled heat and moisture transfer taking into account the diffuse microcracking gradually occuring in building materials.

Further studies on the subject are to be lead, in order to relate models for the formulation of the effective permeability of fractured porous media to experimental measurements. Further characterization of the studied samples is necessary for quantitative measurements of the fracture network geometry.

6 ACKNOWLEDGEMENTS

The work presented in this paper was achieved within the RENOVBAT project supported by the Energy Research Cluster of the Rhône-Alpes region, which the authors would like to thank for its financial support through the project.

REFERENCES

Bazant, Z. & Oh, B. 1983, 'Crack band theory for fracture of concrete' *Materials and Structures*, vol. 16, pp. 155-177

Carson, J. K., Lovatt, S. J., Tanner, D. J. & Cleland, A. C. 2005, 'Thermal conductivity bounds for isotropic, porous materials' *International Journal of Heat and Mass Transfer*, vol. 48, pp. 2150-2158

Elaqra, H., Godin, N., Peix, G., R'Mili, M. & Fantozzi, G., 'Damage evolution analysis in mortar, during compressive loading using acoustic emission and X-ray tomography: Effects of the sand/cement ratio' *Cement and Concrete Research*, 2007, vol. 37, pp. 703-713

Janssen, H.; Blocken, B. & Carmeliet, J. 2007, 'Conservative modelling of the moisture and heat transfer in building components under atmospheric excitation' *International Journal of Heat and Mass Transfer*, vol. 50, pp. 1128-1140

Mazars, J. & Pijaudier-Cabot, G. 1989, 'Continuum damage theory - application to concrete', *Journal of Engineering Mechanics*, vol. 115, pp. 345-365

Mazars, J. & Pijaudier-Cabot, G. 1996, 'From damage to fracture mechanics and conversely: A combined approach', *International Journal of Solids and Structures*,vol. 33, pp. 3327-3342

Pijaudier-Cabot, G., Dufour, F. & Choinska, M. 2009, 'Permeability due to the increase of damage in concrete: from diffuse to localized damage distribution', *Journal of Engineering Mechanics*, vol. 135, pp. 1022-1028.

Rode, C. 2003, *Workshop on Moisture Buffer Capacity – Summary report. Report R-067.* Department of Civil Engineering, Technical University on Denmark

Shah, S. & Choi, S., 'Nondestructive techniques for studying fracture processes in concrete, *International Journal of Fracture*, 1999, vol. 98, pp. 351-359

XII DBMC
International Conference on Durability of Building Materials and Components
PORTO - PORTUGAL, April 12th-15th, 2011

Simulation Study of Building Envelope Performance with High Resolution Meteorological Data

Wai Ki Wu [1]
Miljana Horvat [2]

ABSTRACT

One of the goals of conducting combined heat, air and moisture (HAM) analysis is to calculate both the temperature and water content of components of which the building envelope is comprised. A previous study showed that brick cladding could accrue up to thirty times more moisture when different weather data sources are used. In addition, other studies suggest that weather data having a 10 minute resolution would be required to complete a useful analysis. In order to pursue further this idea, the study described in this paper has investigated the effect of time resolution of meteorological data on HAM results and wind driven rain analysis for a typical residential wood frame construction in Toronto, Canada. Five minute weather data used in this study was collected from the Ryerson University Weather Network. An hourly dataset was constructed from an arithmetic average of 5 minute data. It was found that the averaging had little effect on the temperature but had an extreme effect for WDR loads. The averaging eliminated all south wind whereas there were only minor differences on the north side. By utilizing HAM Tools and Matlab for the simulation of 5 months of data, it was determined that WDR loads so derived drives the water content of brick layer to saturation at similar times in the WDR analysis. The moisture can dry out in a reasonably short period of time and the rest of the wall structure has similar average water content in either cases. The extreme result from averaging has a significant effect on the wind driven rain load and minimal effects on the overall moisture content in the structure.

KEYWORDS

Heat, air and moisture (HAM) transfer, HAM-Tools, Building envelope, Performance simulation, Wind driven rain (WDR), Driving rain.

[1] Faculty of Engineering and Architectural Science, Ryerson University, Toronto, CANADA, waiki.wu@ryerson.ca
[2] Faculty of Engineering and Architectural Science, Ryerson University, Toronto, CANADA, mhorvat@ryerson.ca

1 INTRODUCTION

The use of inappropriate weather data can lead to under-estimating moisture accumulation and drying potential of building envelopes, which directly influences the durability of buildings. For example: in 1998, Salonvaara and Karagiozis found the difference in moisture accumulation in brick cladding up to 30 times more when employing WYEC (Weather Year for Energy Calculation) data than with weather data by NOAA (National Oceanic and Atmospheric Administration) in their calculations [Salonvaara & Karagiozis, 1998]. Correspondingly, wind-driven rain (WDR) on building façades is not only one of the main moisture sources for building envelopes, but also an important factor in the dry and wet deposition of pollutants, façade surface soiling and façade erosion.

Both HAM (Heat, Air and Moisture) and WDR calculations require data records of wind speed, wind direction and horizontal rainfall intensity as inputs. Studies show that the accuracy of the HAM simulation and calculated WDR amounts and intensities results are, to a large extent, determined by the time resolution of the meteorological input data [Blocken & Carmeliet, 2007; B. Blocken *et al*, 2007]. The same authors highly recommend that high-resolution data (e.g. 10-min data) be used for more accurate simulation results in the guidelines that they developed for WDR [Blocken & Carmeliet, 2008]. However, the effect on HAM analysis on the building envelope when higher resolution data is used as compared to, for example, hourly data is not provided. Ryerson University has established a local weather station network to measure weather data at five minute intervals. These data are valuable if one wishes to compare the effects of data resolution from the HAM analysis of the building envelope.

It is acknowledged that previous work on the quantification of WDR has been extensively covered by Blocken. However, the research of those effects on hygrothermal performance of the building envelope is very limited. This study attempts to investigate the effects of high resolution data on HAM transfer across the building envelope. The result from this study will reveal whether there is a significant difference in terms of moisture management performance and energy performance of the building envelope. This can subsequently show if results from previous studies mentioned above apply to the Toronto area.

2 HIGH RESOLTION WEATHER DATA

Currently most of weather stations across the world provide arithmetically averaged hourly dataset for HAM software, commercial or research based [Blocken & Carmeliet, 2008]. These hourly data are averaged from the "raw data" from higher time resolution at the weather station. The WYEC dataset provided by Environment Canada (EC) is also an hourly dataset. However, since a raw dataset could not be obtained from EC, an alternative source was needed to obtain high resolution weather data.

2.1 Ryerson University Weather Network

The Ryerson University Weather Network was established in 2009 across the campus to collect meteorological data for scientific research and analysis. The data is collected in 5 minute interval and includes the following parameters: dry bulb temperature, dew point, wind direction, wind speed and rain. In this study, these pieces of data were used to formulate the hourly data set and were then compared to the 5 minute raw data.

2.2 Construction of Weather Dataset

In order to complete a heat, air and moisture (HAM) analysis for a wall structure, additional parameters missing in Ryerson Weather Network were required from other sources. These parameters included global radiation, diffuse radiation, normal direct radiation, and long wave radiation. In the Ryerson Weather Network the weather stations do not include solar radiation sensors. Hence the radiation data was appended from another source.

The radiation data was obtained from EC since they have a weather station in Toronto at very close proximity to the Ryerson Weather Network. According to EC, weather station 04714 is located about 2 km north of the Ryerson campus [*Canada's national climate archive*.]. The WYEC dataset of that station was used as provides a summary of weather data for 30 years. Since the radiation data was recorded hourly in units of energy, the radiation power (in watts) was calculated by dividing by the time. The radiation power in watts was then applied to each 5 minute data for that hour. In reality, the radiation power will be different from the beginning of the hour to the end of the hour. However, this approach was nonetheless used because it was determined that to linearly interpolate each line of the 5 minute data for the solar radiation would be too resource intensive. Also, it was judged that the overall effect on the building envelope loads would be very minor as radiation solely contributed to temperature and is not interconnected to other climate parameter as is, for example, wind-driven rain which consist of wind speed, direction, rainfall rate. Therefore, a linear interpolation of solar radiation data to develop a 5 minute data set was not performed. The radiation power was assumed to be equal from the beginning of the hour to the end of the hour and the calculated power was used in each 5 minute data record for that hour.

The hourly dataset was constructed by arithmetically averaging the 5 minute data. Special attention was required for averaging wind direction. If a true mathematical average method is used, the angle of the wind would normally be added together and thereafter divided by the number of instances of occurrence of wind in that direction. However, the angular value is not a monotonically increasing value; i.e., when it reaches 360 degrees it returns to zero. Therefore, regular arithmetical averaging was not applicable in this instance. Instead a vector average was used in the analysis which is also the method commonly used by the Nation Oceanic and Atmospheric Administration [*NDBC*]. Using this technique the wind direction angle is broken down into cosine and sine components. . The hourly wind direction was then calculated by the above method from the 5 minute wind direction in that specific hour.

The final hourly and 5 minute dataset then went through a quality check for each line of the climate record. It was also observed that at time data was missing from the data record (e.g. March 13, 2010 2:00am) , likely due to miscellaneous issues on the data acquisition process. In this instance the data record was interpolated from the previous and following time steps. The importance of having a continuous weather data record is self-evident; otherwise, a HAM analysis using such a record would be erroneous. If the software cannot find the weather data at the specific time step, the calculation will be halted.

3 WEATHER DATA ANALYSIS

The weather data from January 2010 to May 2010 was obtained from the Ryerson Weather Network. The completed weather dataset was analysed before a HAM analysis of a building envelope was performed. The preliminary analysis can reveal the significance of differences between the hourly and 5 minute weather data record. This could allow further correlation with the HAM analysis results. Figure 1 shows the temperature the 2 sets of data and it is noticed that the difference is minimal between the hourly and 5 minutes data. The hourly average temperature seems to be lagging the 5 minutes data, which is normal in arithmetic technique. The effect of the time resolution is relatively minor.

3.1 Wind Driven Rain Analysis

The wind driven rain load is the combined effect of wind and rain deposition on a wall surface. The result is essentially one of the boundary conditions for completing a HAM analysis of a wall. Physical measurements of wind-driven rain is very time consuming and prone to error [Blocken & Carmeliet, 2006]. There are different approaches to obtaining WDR data from meteorological data. According to Blocken and Carmeliet [2010], the most common and frequently used methods are:

1. Semi-empirical model taken from the ISO Standard for WDR [ISO, 2009]
2. Semi-empirical model by Straube and Burnett [Straube, 1998]
3. CFD model by Choi [Choi, 1999], extended by Blocken and Carmeliet [Blocken & Carmeliet, 2002; Blocken & Carmeliet, 2007]

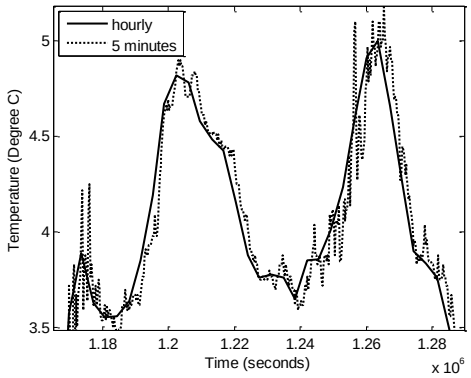

Figure 1: Temperature comparison between hourly and 5 minute data.

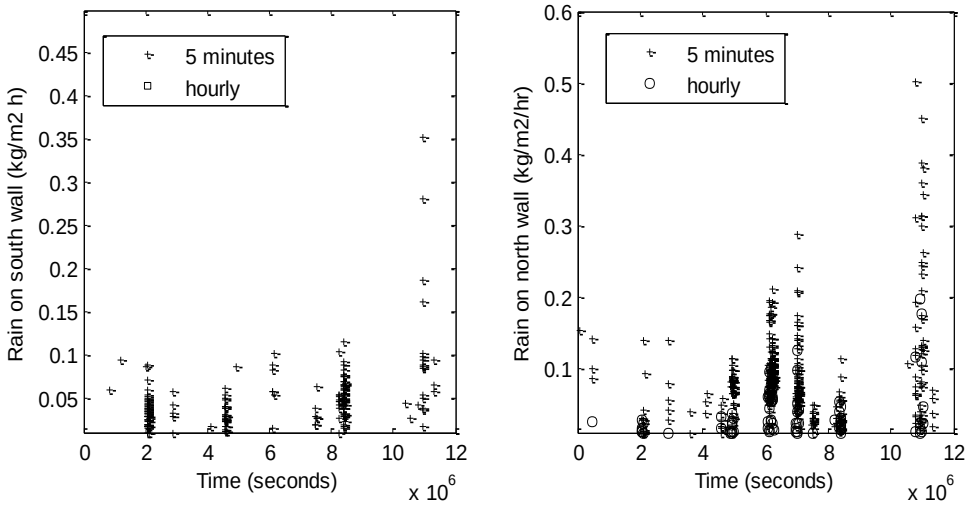

Figure 2: WDR comparison on south and north wall.

ASHRAE Standard 160 [ASHRAE 2009] *"Criteria for Moisture-Control Design Analysis"* is a standard which includes calculating the wind driven rain load on a wall based on the wind speed, direction, and normal rain load. The standard describes the design rain loads for a wall exposed to rain and is a semi-empirical model which is comprised of factors very similar to that of found in the ISO standard [Wu & Horvat, 2010].

In this study, the use of the CFD model proposed by Choi [1999] was not considered as it was deemed beyond the scope of resources available to the project. It was felt that the Straube and Burnett model [Straube 1999] would have required further investigation on the power-law function for which currently there is no specific information available [Blocken & Carmeliet, 2010]. Since ASHRAE S160P is a North American standard, it was considered more suitable for this study as Toronto is the location of interest and it was also used in a previous study by Wu & Horvat [2010].
Based on the above empirical model, the wind-driven rain for a south façade and north façade of a building located in Toronto are shown in Fig 2. It was observed from the results of these calculations that there was a significant difference in terms of wind driven rain deposited on the wall. For the south facing wall, it was evident that, there was no driving rain that occurred if hourly average data was used. Upon further investigation, it was found that there was no south wind if using the hourly

averaging data. This observation is in accord with the general weather condition during that period of time. North winds were dominant during the month from winter to spring. For the north facing wall, it was observed that the rain events seem to be in close proximity time frame. However, the quantity of the rain deposited is noticeably different. The significance of this difference will be further analysed in the HAM analysis.

4 HAM ANALYSIS

The HAM analysis of the wall was carried out using HAM-Tools in MATLAB Simulink. HAM Tools is a library of the MATLAB Simulink model blocks that can be configured to analyze different building cases [Kalagasidis et al., 2007]. The blocks themselves are very flexible and allow different customization. One of the most significant advantages is the flexibility of time resolution of weather data and time step in the analysis, which is not commonly allowed with most simulation software. These two parameters are independent of one another. The user can provide hourly data and perform the analysis in minutes. The time step resolution usually does not affect the speed of the analysis. In this study, the time step for the weather data was provided as hourly and 5 minute steps. Both analyses were performed in a second time step so that the difference from the time step was eliminated.

4.1 Wind Driven Rain Module

HAM Tools does not incorporate any wind-driven rain module as part of the model blocks. Therefore, a ASHRAE S160P wind-driven rain module was devised and added to the model blocks as shown in Figure 4.

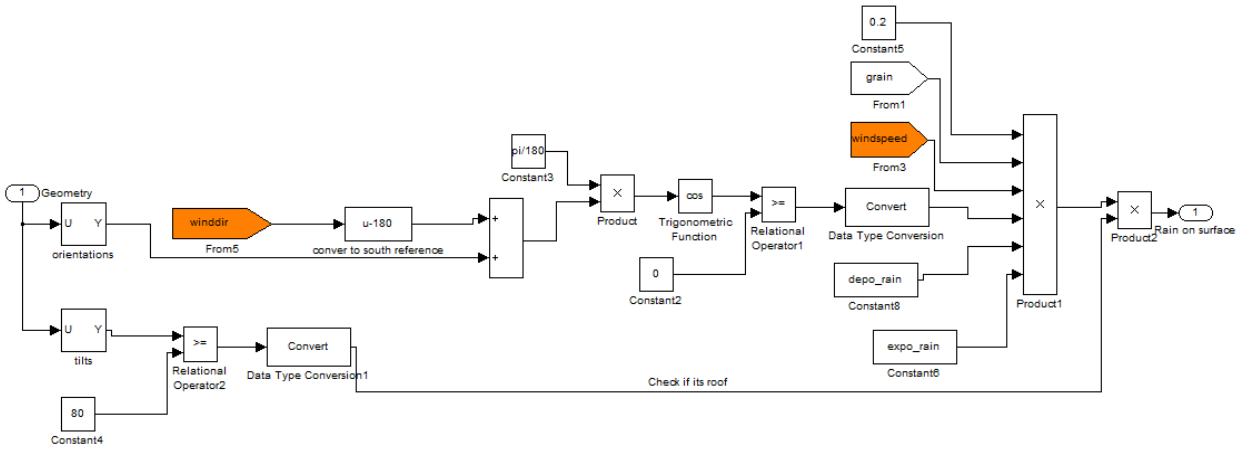

Figure 3: ASHRAE 160P wind driven rain module created in HAM-Tools.

4.2 Wall Construction

The wall construction analysed in this study is typical of residential wood frame construction in North America. The material thickness of each wall component are given in Table 1. HAM Tools requires detail material properties for the moisture transfer analysis including, sorption curve at different water contents, thermal conductivity at variable water contents and moisture dependence of temperature. In this study, the material properties were collected from WUFI and the ANNEX 41 final report.

Table 1: Wall construction.

Material (outdoor to indoor)	*Thickness*
Exterior brick veneer	105mm
Air space (ventilation gap)	25mm
60 min building paper (weather barrier)	0.1mm
OSB sheathing	12.5mm
Fiberglass insulation	140 mm
Polyethylene vapour retarder (6 ng/s m^2 Pa)	0.15mm
Gypsum board	12.5mm

4.3 Boundary Conditions

The exterior climate was based on the weather dataset prepared from information described in the previous sections. The indoor climate was that specified in standard EN15026 which provides a definition of the indoor temperature and relative humidity throughout a year; this is also one of the standard indoor climate conditions available in HAM Tools. In this study, it was assumed that the building is a "townhouse" in a row of similar houses, and hence only the north and south facing walls are subject to exterior climate conditions. The North direction wind was the dominant direction in the Toronto area during the period of study.

5 RESULTS

The analysis was performed from January 2010 to May 2010. The temperature profiles of the wall construction are very similar between the hourly and 5 minute data. The overall amount of water in the wall was also found to be very similar. The only major differences that occurred on the brick layer where the amount of wind driven rain that was deposited most on the wall. Figures 4 and 5 show the water content in the brick layer of the wall.

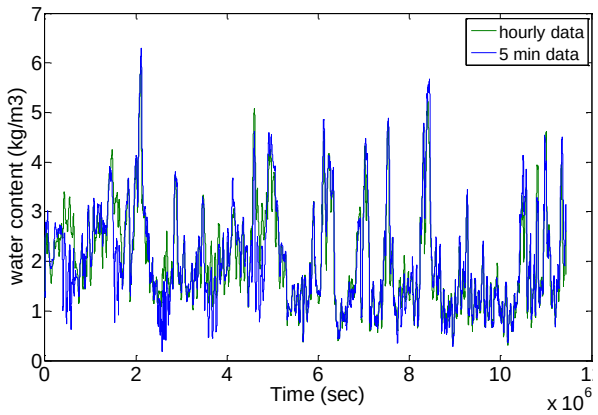

Figure 4: Average water content in brick layer, south facing wall.

Figure 4 shows the water content of the brick layer of the south facing wall . It is evident that the 5 minute data provides slightly higher water content to the brick layer as compared to that offered using the hourly data. These results coincide with the results obtained from the wind driven-rain study. However, the magnitude of the difference is much smaller than that obtained from the WDR analysis. Although not shown in the graph, it was noticed that the other layers of the wall section have a minimal variation in terms of water content throughout the study period.

Figure 5 shows the water content at the north facing wall. It is noticed that both hourly and 5 minute data generate similar results in terms of water content. The 5 minute data created peaks which were higher than those observed from the analysis using hourly data. In terms of timing and occurrence, these results closely matches that derived from the wind driven rain analysis described in the previous

section (Figure 2, north facing wall). However, it does not match in terms of percentage: the quantity of wind-driven rain that falls on the brick layer calculated from use of the 5 minute data set is almost 200% higher than that obtained using the hourly data. Nonetheless, in Figure 5, it is shown that the water content in the brick layer is about the same in the two sets of data. This could be explained by the absorption rate of the brick. The brick can only absorb a certain amount of water over a given time frame and excess water will run off.

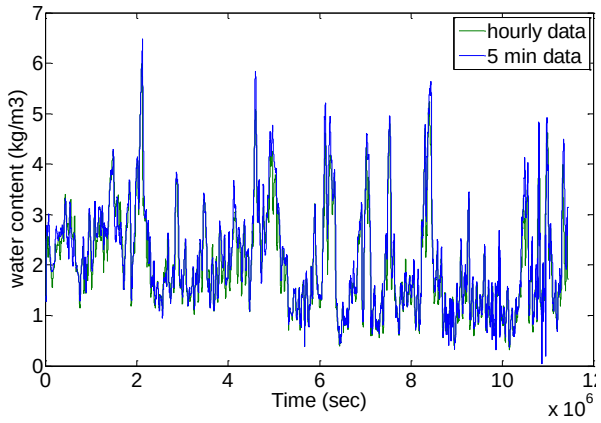

Figure 5: Average water content in brick layer, north facing wall.

From this analysis, it was found that use of averaging weather data can result in two extremes. In the case of south facing wall, the averaging technique completely eliminated the wind driven rain effect for the hourly data. However, on the north side, the average weather data had minimal effect compared to the 5 minute data. Since wind-driven rain is one of the major sources of moisture (water) to the wall, this revealed that the averaging of weather data can result in large variability in the results of HAM analysis of wall assemblies. This follows the result from previous work by Blocken and many others.

However, it is noticed that the water content of the brick layer and the rest of wall structure is relatively similar on both the south and north facing walls, within 10% of the calculated average. This could be explained by the rain absorption rate of the brick and also the number of rain events in Toronto. Toronto has only about 650 mm of rain in a year so it could provide sufficient time for the bricks to dry. With, for example, 1200 mm of rain in Vancouver, this analysis may render different results; therefore, further studies are required. However it may perhaps be concluded that for moderate rain events, hourly average data would be sufficient to obtain useful results from a HAM analysis of the wall assembly.

6 CONCLUSIONS

In this study the effects of using high resolution weather data for HAM and WDR analysis on the building envelope was investigated by using 5 minute data collected from the Ryerson University Weather Network and hourly data, developed using an arithmetic average. For the wind-driven rain analysis, it was found that the average technique completely eliminated south facing rain deposition on walls. For the north direction, the averaging affected the amount of wind-driven rain occurring on the wall surface by a factor of 2. The rain events on both hourly and 5 minute data occurred over a similar time and location.

From the HAM analysis of a typical North American wood frame wall, it was observed that there were only minor differences in both the south and north facing walls in terms of water content, despite the significant differences obtained from the wind-driven rain analysis. There were local peaks that occurred during the time of the study, however, the overall water content of the brick masonry wall and as well the remainder of the wall structure was fairly similar. This indicates that the averaging of weather data could nonetheless have a significant effect on the quantification of WDR, as stated in the

previous study by Blocken & Carmeliet [2008)]. However, the effect on the hygrothermal properties of the building envelope could be limited for wood frame residential structures in the Toronto area. For locations where high resolution weather data is not available, the use of hourly data would likely be acceptable if the climate at the location provides for moderate rain events.

REFERENCES

ASHRAE (2009), ANSI/ ASHRAE Standard 160-2009, Criteria for Moisture-Control Design Analysis in Buildings, ASHRAE, 16 p.

Blocken, B., & Carmeliet, J. (2002). Spatial and temporal distribution of driving rain on a low-rise building.

Blocken, B., & Carmeliet, J. (2006). On the accuracy of wind-driven rain measurements on buildings. *Building and Environment, 41*(12, pp. 1798-1810), December.

Blocken, B., & Carmeliet, J. (2008). Guidelines for the required time resolution of meteorological input data for wind-driven rain calculations on buildings. *Journal of Wind Engineering and Industrial Aerodynamics, 96*(5), 621-639.

Blocken, B., & Carmeliet, J. (2010). Overview of three state-of-the-art wind-driven rain assessment models and comparison based on model theory. *Building and Environment, 45*(3), 691-703.

Blocken, B., & Carmeliet, J. (2007). On the errors associated with the use of hourly data in wind-driven rain calculations on building facades. *Atmospheric Environment, 41*(11), 2335-2343.

Blocken, B., Roels, S., & Carmeliet, J. (2007). A combined CFD–HAM approach for wind-driven rain on building facades. *Journal of Wind Engineering and Industrial Aerodynamics, 95*(7), 585-607

Canada's national climate archive. Retrieved 4/2/2010, 2010, from http://www.climate.weatheroffice.gc.ca/climateData/canada_e.html

Choi, E. C. C. (. (1999). Wind-driven rain on building faces and the driving-rain index. *Journal of Wind Engineering and Industrial Aerodynamics, 79*(1-2, pp. 105-122), January.

ISO. (2009). ISO 2009, 15927-3 *Hygrothermal performance of buildings – calculation and presentation of climatic data – part 3: Calculation of a driving rain index for vertical surfaces from hourly wind and rain data,* International Organization for Standardization, Geneva, SW.

Kalagasidis, A. S., Weitzmann, P., Nielsen, T. R., Peuhkuri, R., Hagentoft, C. E., & Rode, C. (2007). The international building physics toolbox in simulink. *Energy and Buildings, 39*(6), 665-674.

NDBC. Retrieved 10/7/2010, 2010, from http://www.ndbc.noaa.gov/wndav.shtml

Salonvaara, M. H., & Karagiozis, A. N. (1998). Influence of waterproof coating on the hygrothermal performance of a brick facade wall system. *Proceedings of the 1996 Symposium on Water Leakage through Building Facades.*

Straube, J. F. (1998). Moisture control and enclosure wall systems. , Dissertation Abstracts International, vol. 59-09B.

Wu, W. K., & Horvat, M. (2010). Simulation study of building envelope performance using microclimatic meteorological data. *1st International High Performance Buildings Conference at Purdue - proceedings,* Purdue University, July 12-15th, 2010, West Lafayette, Indiana, US.

XII DBMC
International Conference on Durability of Building Materials and Components
PORTO - PORTUGAL, April 12th-15th, 2011

Performance of PVA and Cellulose Reinforced Fiber Cement in Different Brazilian Climates

Cleber Marcos Ribeiro Dias [1]
Vanderley M. John [2]

ABSTRACT

This work evaluates the effects of natural aging on the microstructure and mechanical performance of asbestos-free fiber cement. Four-point bending tests were performed to accompany the evolution of modulus of rupture (MOR), limit of proportionality (LOP), modulus of elasticity (MOE) and toughness of asbestos-free fiber cement specimens along 3.5 years of exposition in four different Brazilian climates. SEM with EDS analyzes and mercury intrusion porosimetry (MIP) were performed to evaluate the aging effects on the microstructure of the specimens. The results show that the effect of the aging on the mechanical performance of fiber cement is a result of a balance of positive and negative effects. The experiments also show that the velocity of deterioration is related to the climate condition. Embrittlement of the composite was the main effect in natural aging as a result of vegetable fiber deterioration and enhancement of the bond between PVA fibers and the cementitious matrix.

KEYWORDS

Asbestos-free fiber cement, natural aging, mechanical performance, microstructure.

[1] University of São Paulo, São Paulo, SP, Brazil, cleber.dias@poli.usp.br
[2] University of São Paulo, São Paulo, SP, Brazil, vanderley.john@poli.usp.br

1 INTRODUCTION

The use of asbestos-free fiber cement technology is relatively recent in many countries, including Brazil where some industries have used poly (vinyl alcohol) (PVA) or polypropylene fibers combined with cellulose fibers in the manufacture of fiber cement roofing components. Since users expect long service life for such components, durability becomes an important parameter to be considered by both producers and users.

In a situation where a building component, developed with a new technology, must be placed immediately on the market, the use of accelerated aging tests to evaluate the durability is essential to reduce risks to premature failure. However, such kind of aging tests are only valid when reproducing the primary mechanisms of deterioration expected under normal in-use conditions. A set of accelerated aging tests has been developed to help forecast long-term performance of cementitious products. Most of these tests are variations of wetting and drying cycles or carbonation combined with wetting and drying cycles [Mohr *et al*. 2005] [Mohr *et al*. 2006] [Gram 1988] [Agopyan 1991] [Soroushian & Marikunte 1992]. In these tests, most researchers have adopted mechanical properties as indicators of deterioration. Subjecting specimens to natural aging conditions, in turn, provides aging conditions more closely resembling the real in-use conditions. This is usually undertaken with small-size specimens, which are exposed to the elements in the same environment where the products will be exposed. It is a relatively inexpensive test, but responses can only be obtained after long periods of exposure time.

The purpose of the present study is to evaluate the effects of natural aging on the performance of asbestos-free fiber cements. The effects of aging were studied through a methodology that involves the characterization of the microstructure, chemical and mineralogical composition, and the mechanical properties of un-aged specimens and specimens exposed to natural aging conditions. In this study, we particularly present the effects on the microstructure and mechanical properties of asbestos-free fiber cements that were exposed to the elements for 3.5 years in different Brazilian cities: São Paulo, Pirassununga, Belém and Rio Grande.

2 EXPERIMENTAL

2.1 Materials and Specimen Preparation

Fiber cement pads with dimensions of 200 x 200 mm² and a thickness of about 6.0 mm were produced with the following materials: a) Portland cement (PC) with density of 3.12 g/cm³ and BET surface area of 1.39 m²/g; b) limestone filler with density of 2.74 g/cm³ and BET surface area of 1.25 m²/g; c) silica fume with specific surface of 22.5 m^2/g and Chapelle reactivity equal to 814 mgCaO/g; d) Kuraray PVA fibers with a nominal length of 6 mm, average diameter of 14.85 μm and density of 1.27 g/cm³ and; e) short bleached cellulose fibers. The pads were produced with the formulations shown in Table 1. The main feature that differentiates them is the PVA fiber content.

Vacuum dewatering method, similar to that employed by Savastano *et al.* [2005] was used for moulding the pads. The five materials were mixed in a container with a capacity of 3 L, using a mixer Fisaton model 722D with speed equal to 2000 rpm. First, the cellulose fibres were dispersed in 1 L of water for 10 min. Then, the PVA fibres and another 1 L of water were added and the dispersion continued for another 2 min. Silica fume was added and the materials were mixed for 1 min. Finally, the cement and limestone filler were added and mixed for 2 min. Part of water of the mixture was drained and the green pads were pressed with a pressure of 3.2 MPa for 5 min. The pads were placed in sealed plastic bags where they remained for two days. Shortly after, the curing was performed in water for five days, followed by air-curing at room temperature until completion of 28 days. The specimens used in the aging tests were extracted from the pads, cut with dimensions roughly equal to 160 mm long and 40 mm wide using a rotary saw.

Table 1. Fiber cement specimens formulations.

Material	*Weight content (w/w%)*		
	PVA14	*PVA20*	*PVA30*
Portland Cement	75.20	75.20	74.00
Limestone filler	12.72	12.72	13.50
Silica fume	6.68	6.08	5.00
PVA fibers	1.40	2.00	3.00
Cellulose fibers	4.00	4.00	4.50

2.3 Natural Aging

Forty five specimens per series were produced with the formulations PVA14, PVA20 and PVA30 and exposed to the elements in four different cities of Brazil: São Paulo, Pirassununga, Belém and Rio Grande. Table 2 presents the characteristics of these cities. The specimens were installed in mounting brackets so that the surfaces exposed to the elements stay oriented to the true north and inclined at an angle of approximately 45 degrees with the local zenith. These specimens were characterized before and after one and three and a half years of exposure with the exception of those exposed in Rio Grande that were not evaluated after one year. In this work, particularly the reporting of results, the aging stations of São Paulo, Pirassununga, Belém and Rio Grande have been identified as SP, PG, BE and RG respectively.

Table 2. Characteristics of the cities.

City	*Code*	*Geographic coordinate**	*Annual rainfall (mm)*	*Mean annual Temperature (°C)*	*RH** (%)*	*Environment*
São Paulo	SP	23°33'S, 46°43'W, 725 m.	1500	19.5	78	Urban, inland
Pirassununga	PG	21°57'S, 47°27'W, 610 m.	1300	23.0	73	Rural, inland
Belém	BE	1°28'S, 48°27'W, 8 m.	3000	26.0	87	Urban, inland
Rio Grande	RG	32°12'S, 52°10'W, 2 m.	1160	17.6	80	Urban, Ocean

*Longitude, latitude and altitude.
**RH = mean relative humidity.

2.4 Characterization of the specimens

Fiber cement specimens were submitted to SEM/EDS analysis. A LEO Leika S440 microscope with an acceleration voltage of 20 kV and current of 150 mA was used to examine the fractured section, the polished cross-section and the surface of specimens. Cross-sectional surfaces of samples for evaluation by backscattering electron image analysis (BSEI) and SEM, were vacuum (200 mbar) impregnated with epoxy resin and air cured for 24 h before grinding with silicon carbide and polishing with diamond paste (3, 1 and 1/4 μm respectively). All samples received carbon coating before SEM examination.

Four-point bending tests (15 specimens/sample) were conducted with an INSTRON 5569 using bending spans of 135 mm. Displacement ratio was controlled (1.5 mm/min) and deflection measured with a LVDT positioned under the specimens in the middle of the span. Modulus of rupture (MOR), limit of proportionality (LOP), modulus of elasticity (MOE) and toughness of specimens were evaluated. All specimens were soaked in water for 24 h before bending tests.

3 RESULTS

3.1 Natural Aging Effects on the Microstructure

SEM images of the fractured and polished sections of PVA14 unaged specimens and specimens exposed to the elements in São Paulo city for 1 year are shown in Figure 2. Once the specimens exposed in the others cities presented similar behaviour we decide to show only the images of the specimens from São Paulo. The images of fractured sections of unaged specimens show that cellulose fibers are mostly pulled out of the matrix when the composites are fractured (Figure 2a). Figure 2b shows the existence of a gap between cellulose fibers and cement matrix. This was already registered by Savastano and Agopyan [1999]. Vegetable fibers are extremely hydrophilic and expand when absorb water during mixing and shrink after the composite is dry, leaving the gap which reduces the adhesion bond strength facilitating the pull-out energy dissipation.

After 1 year of exposure to natural aging, rupture of cellulose fibers became predominant when the composite was fractured. Figure 2d shows that the interface between cellulose fibers and cement matrix became more compact than in the unaged ones (Figure 2b). This figure also shows unaged specimens in which cellulose fibers presents empty lumens. However it can be clearly observed that the cellulose lumens of aged specimens became filled with calcium-rich phases (Figure 2d) (Figure 2e and Figure 2F). The calcium-rich phase also impregnated the walls of the cellulose fibers. Alkaline attack and mineralization are the main mechanisms of deterioration of cellulose fibers embedded in the Portland cement matrix. These mechanisms act simultaneously. The deterioration by alkaline attack occurs mainly by the action of alkaline water in the pores of the matrix in contact with lignin and cellulose compounds [Gram 1983]. Alkaline water broke the link between individual cells of fibers causing weakening of fibers and reducing its reinforcement capacity. Mineralization or petrification is a mechanism similar to fossilization and it occurs by filling the pores of fibers and impregnating the walls. Therefore, the change on the fracture mode of cellulose fiber from pull-out to rupture is a result of both the deterioration of the fibers by mineralization and alkaline attack as well as of interface densification.

The interface between PVA fibers and the matrix shows no gap for both unaged and aged samples (Figure 2b and 2b) and fibers are predominantly pulled out in both unaged and aged specimens (Figure 2a and 2c). It was possible to identify broken PVA fibers in the matrix of the aged specimens (Figure 2c). Therefore, the increase on the fiber-matrix adhesion resulting from hydration and carbonation – indirectly expressed by the increase of the limit of proportionality (LOP) during aging – was not sufficient to make the pull-out force surpass the tensile strength of the fiber. A review of literature shows no results in which a considerable decrease in strength of PVA fibers when embedded in Portland cement paste is evident (Kalbskopf *et al*. 2002).

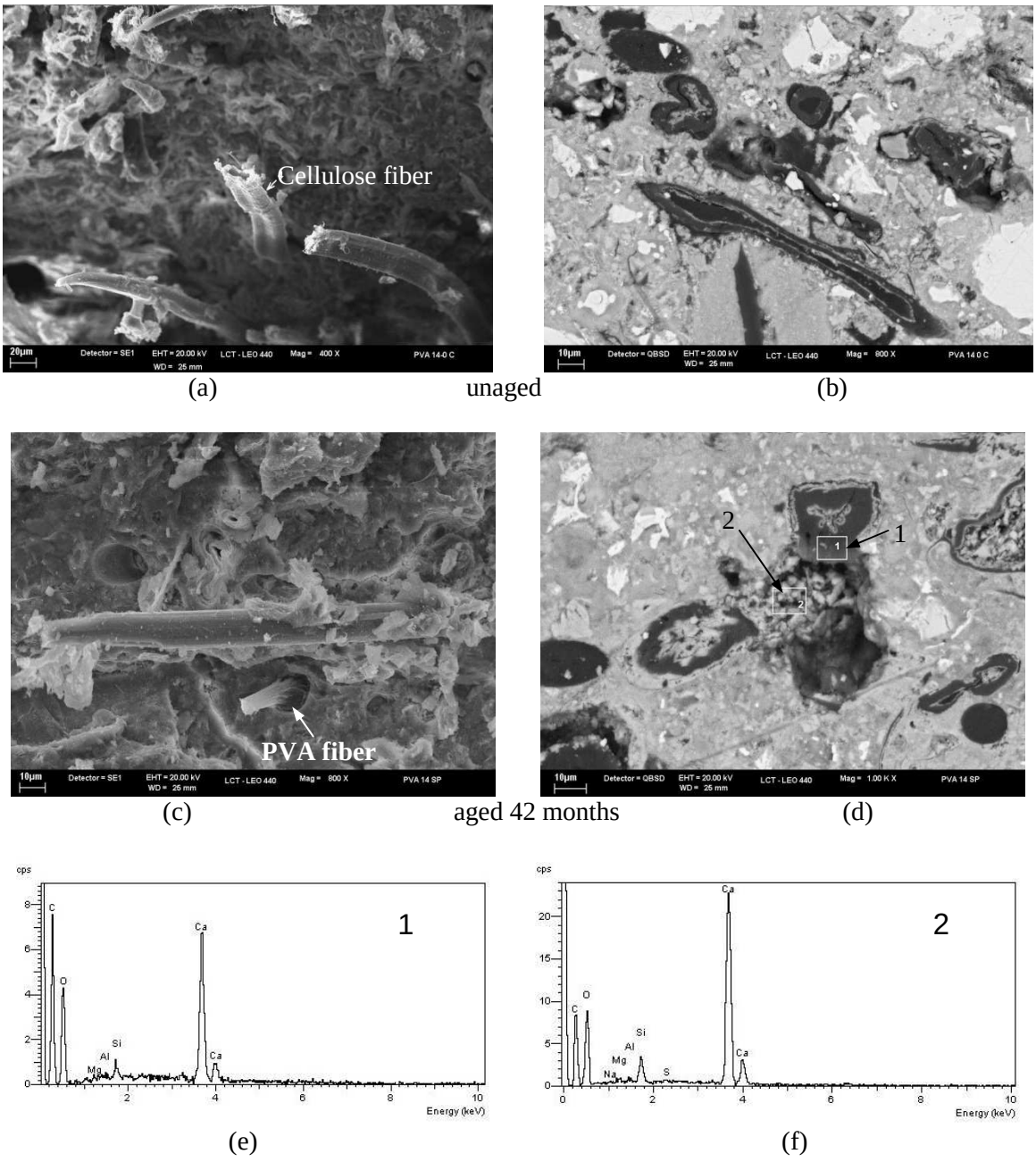

Figure 1. Micrographs of PVA14 specimens: a) fracture section of an unaged specimen – SE image; b) polished section of an unaged specimen showing hollow cellulose fibers; c) fracture section of a 1-year exposed specimen from São Paulo; d) polished section with cellulose fibers completely filled with cement compounds; e) EDS of region 1 Figure 2d and; f) EDS of the region 2 of the Figure 2d.

3.2 Mechanical Performance

The results obtained with the mechanical characterization are summarized in Table 3 and 4. The results show that LOP and MOE of unaged specimens slightly decrease when the PVA fiber content increase from 1.4% to 3.0%. Conversely, MOR and the specific energy of the unaged specimens, shown in Table 4, are strongly dependent on the fiber content. One of the reason for this is that fibers interfere more expressively on the post-cracking properties of the composites.

LOP and MOE significantly increased with natural aging. As an example, for PVA14 specimens, LOP increases from 10.2 MPa to about 17.5 MPa after 1 year of exposition to the elements in São Paulo and this property remain constant up to 3.5 years. MOE increases from 15.0 GPa to about 19.0

GPa after 1 year and remain constant up to 3.5 years. Improvement on the LOP and MOE is related to the enhancement of the matrix with hydration and carbonation. The cement hydration generates stronger compounds and reduces the porosity of the matrix. Carbonation also presents positive effects once it reduces the alkalinity and porosity of the matrix [Gram 1988] [Tolêdo Filho *et al*. 2003]. Negative effects of carbonation are reduction of the solubility of hydrated cement compounds, which facilitates the mineralization of fibers and, according Bentur and Akers [1989], contributes to the embrittlement of the composite. The less expressive increase in LOP and MOE was observed in specimens exposed to the elements in Belém.

Modulus of rupture increased significantly with natural aging (Table 4). The MOR of the composites increased considerably after natural aging in specimens exposed in all cities and it is also related to the improvement of the composite after hydration and carbonation of the matrix. In this case, improvement of the PVA fibers-matrix adhesion bond strength could be contributed to the increase of MOR. The specimens from Belém seem to have been subjected to the worst condition. The MOR did not increase as much as the modulus of rupture of specimens exposed to the elements in Sao Paulo and Pirassununga. Hydration of the matrix does not seem to explain this behaviour, since the results of thermogravimetric analysis, do not present in this paper, did not show a significant difference in the degree of hydration. It is likely that the porosity of the composite, which is higher for specimens from Belém compared to Sao Paulo, has an important function in the mechanical strength of the composite. Maybe, damage in the interface zone between fibers and matrix might be the cause of both porosity and mechanical strength.

Embrittlement was the main negative effect of aging on the mechanical performance of the composite: fracture toughness decreased by a factor of ~2 in the 24 months and by a factor ~3 in 42 months of aging. Embrittlement means loss of toughness (specific energy) and is related to the deterioration of cellulose fibers and also probably due to a reduction of pull out energy of PVA fibers due to the increase of the number of broken PVA fibers. The results show that PVA fibers present an important role on the final toughness of the composite and the toughness is greater for composites with higher PVA contents (Table 4).

Table 3. LOP and MOE of the specimens.

	LOP (MPa)			*MOE (GPa)*		
Series	*PVA 14*	*PVA 20*	*PVA 30*	*PVA 14*	*PVA 20*	*PVA 30*
Unaged	10.1 ± 1.0	9.3 ± 1.6	9.0 ± 1.1	15.0 ± 1.6	13.8 ± 1.4	14.2 ± 1.5
SP_1-year	17.6 ± 2.8	16.9 ± 2.4	16.8 ± 1.2	18.9 ± 1.5	18.1 ± 1.3	17.7 ± 1.6
SP_3.5-year	17.7 ± 2.8	16.1 ± 2.0	14.8 ± 1.8	19.9 ± 2.4	18.6 ± 1.2	18.6 ± 1.0
PG_1-year	16.2 ± 1.8	15.0 ± 2.9	16.3 ± 2.0	19.5 ± 1.1	16.6 ± 2.4	17.0 ± 2.1
PG_3.5-year	18.8 ± 2.2	16.6 ± 1.8	16.6 ± 2.1	18.5 ± 1.3	16.8 ± 1.3	15.8 ± 1.5
BE_1-year	14.1 ± 1.9	11.7 ± 1.5	11.2 ± 0.7	18.2 ± 1.8	17.8 ± 2.1	14.5 ± 2.3
BE_3.5-year	15.5 ± 1.5	12.4 ± 2.1	11.4 ± 2.4	17.4 ± 1.0	15.2 ± 1.7	14.3 ± 3.0
RG_3.5-year	16.3 ± 2.0	13.5 ± 2.6	13.4 ± 2.5	18.8 ± 0.8	15.7 ± 1.3	15.0 ± 1.6

Table 4. MOR and specific energy of the specimens.

Series	*MOR (MPa)*			*Specific energy (kJ/m²)*		
	PVA 14	*PVA 20*	*PVA 30*	*PVA 14*	*PVA 20*	*PVA 30*
Unaged	12.7 ± 1.1	13.6 ± 1.5	16.6 ± 1.3	1.73 ± 0.38	2.77 ± 0.49	5.83 ± 1.15
SP_1-year	17.9 ± 2.8	18.7 ± 1.8	19.6 ± 2.1	0.87 ± 0.19	1.47 ± 0.19	2.55 ± 0.67
SP_3.5-year	17.8 ± 2.7	17.3 ± 2.0	17.9 ± 1.5	0.57 ± 0.11	1.03 ± 0.10	2.21 ± 0.97
PG_1-year	16.5 ± 1.5	16.1 ± 2.1	19.2 ± 1.7	0.89 ± 0.15	1.42 ± 0.36	2.64 ± 0.52
PG_3.5-year	18.8 ± 2.2	17.0 ± 1.8	18.5 ± 1.0	0.54 ± 0.09	0.77 ± 0.10	1.95 ± 0.64
BE_1-year	14.5 ± 1.9	13.5 ± 1.4	14.4 ± 0.9	0.92 ± 0.16	1.31 ± 0.26	2.78 ± 0.89
BE_3.5-year	15.5 ± 1.5	13.7 ± 1.1	15.5 ± 2.0	0.54 ± 0.14	0.98 ± 0.26	2.87 ± 1.03
RG_3.5-year	16.7 ± 1.8	14.9 ± 1.7	16.9 ± 2.0	0.63 ± 0.06	1.01 ± 0.26	2.18 ± 0.80

3 CONCLUSIONS

The main effects of natural aging on the microstructure and mechanical performance of PVA and cellulose reinforced cement exposed to different Brazilian climates were: a) deterioration of cellulose fibers; b) filling of the lumens of the cellulose fibers by calcium-rich compounds; c) enhancement of the matrix with hydration and carbonation and; d) embrittlement of the composite as a result of cellulose fiber deterioration and probably PVA-matrix interface modification.

Natural aging significantly changed the mechanical properties of the fiber cements. However, there was not significant change of mechanical properties after 1 to 3.5 years of exposure to the elements in all cities in which specimen were exposed, except in respect to changes in toughness.

ACKNOWLEDGMENTS

The authors would like to thank Fundação de Amparo à Pesquisa do Estado de São Paulo (FAPESP), CNPq, Financiadora de Estudos e Projetos (FINEP, HABITARE Program), INFIBRA and IMBRALIT for their financial support.

REFERENCES

Mohr B.J., Nanko, H., Kurtis, K.E. 2005. *Durability of kraft pulp fiber–cement composites to wet/dry cycling*. Cement & Concrete Composites 27, pp. 435–448.

Mohr, B.J., Biernacki, J.J., Kurtis, K.E. 2006. *Microstructural and chemical effects of wet/dry cycling on pulp fiber–cement composites*. Cement and Concrete Research 36, pp. 1240–1251.

Gram, H-E. 1988. *Natural fibre concrete roofing*. Concrete Technology and Design 5: natural fibre reinforced cement and concrete, Glasgow and London.

Agopyan, V. 1991. *Fibrous materials for building construction in development countries: the use of vegetal fibers* [Thesis of Polytechnic school of University of São Paulo]. São Paulo. In Portuguese.

Soroushian, P., Marikunte, S. 1992, *Long-term durability and moisture sensitivity of cellulose fiber reinforced cement composites*. In: Fibre Reinforced cement and concrete [Edited by R. N. Swamy]. RILEM. London.

Savastano Jr., H., Warden, P G, Coutts, R S P. 2005, *Microstructure and mechanical properties of waste fibre–cement composites*. Cement and Concrete Composites; 27(5), pp 583-592.

Savastano, H.; Agopyan, V. 1999. Transition zone studies of vegetable fibre-cement paste composites. Cement and Concrete Composites, V21, N1, pp. 49-57.

Kalbskopf, R.; De Lhoneux, B.; Van Der Heyden, L.; Alderweireldt, L. 2002. Durability of fiber-cement roofing products. In: Inorganic-Bonded Wood and Fiber Composite Materials V8. Sun Valley.

Tolêdo Filho, R.D.; Ghavami, K.; England, G.L.; Scrivener, K. 2003. Development of vegetable fibre-mortar composites of improved durability. In: Cement and Concrete Composites 25, pp. 185-196.

Bentur, A.; Akers, A.S. 1989, *The microstructure and ageing of cellulose fibre reinforced cement composites cured in a normal environment*. In: The International Journal of Cement Composites and Lightweight Concrete vol 11, N2.

XII DBMC
International Conference on Durability of Building Materials and Components
PORTO - PORTUGAL, April 12th-15th, 2011

Influence of Additives on the Weatherability Behaviour of Glass Reinforced Concrete (GRC) Prefabricated Façade Panels

J.M. Pastor [1]
R. Zangroniz [2]
J.Martínez [3]
J. Peña[4]

ABSTRACT

GRC (Glass fiber reinforced) is a thin, high strength concrete with many applications in construction, being one of the most versatile building materials available to architects and engineers. GRC composite materials consist of high strength glass fiber embedded in a cementitious matrix. In addition to the main components – cement, sand and special alkali resistant glassfibres – GRC may contain additional filler materials, pozzolanic aditives and admixtures. In this sense, polymer emulsions have been included in GRC formulations in order to improve the fluidity of the slurry, the curing procedure, the strain capacity of the hardened product, and, ultimately, the long-term weatherability of the composite.

GRC panels containing different percentages (<10%) of several commercial additives were prepared in collaboration with SEIS (ACS group). In order to simulate the behavior of these materials as a function of time and climatic conditions and to envisage the possible appearance of efflorescences, the so obtained composites are environmentally exposed or aged in a climatic chamber under a cyclic weathering test (humidity/drying/ temperature) that can be extrapolated to natural weathering during 10 to 20 years. The results of these test programs, with a particular focus on the aged flexural strain to failure behaviour of these aged composites, are reported in this work. In addition, the evolution of the porosity is examined by means of a Hg intrusion porosimeter. The variation on the pore size, distribution and percentage plays a decisive role on the mechanical performance of the GRC panels as well as on the emergence of efflorescences which, in turn, determine the long-term weatherability of the composite.

KEYWORDS

Efflorescences, Porosity, Durability, Natural and accelerated ageing tests.

[1] Escuela Politécnica de Cuenca (EUPC), UCLM, Campus Universitario s/n, Cuenca, SPAIN, JoseManuel.Pastor@uclm.es
[2] Escuela Politécnica de Cuenca (EUPC), UCLM, Campus Universitario s/n, Cuenca, SPAIN, Roberto.zangroniz@uclm.es
[3] Escuela Politécnica de Cuenca (EUPC), UCLM, Campus Universitario s/n, Cuenca, SPAIN julio-wolv@hotmail.com
[4] Escuela Politécnica de Cuenca (EUPC, UCLM, Campus Universitario s/n, Cuenca, SPAIN juan.pena@uclm.es

1. INTRODUCTION

Glass fiber reinforced (GRC) composite materials consist of high strength glass fiber embedded in a cementitious matrix. In this form, both fibers and matrix retain their physical and chemical identities, yet they encompass a combination of properties that cannot be achieved with either of the components acting alone. Generally speaking, fibers are the main load-carrying members, while the surrounding matrix keeps them in the desired locations and orientation, acting as a load transfer medium between them, and protects them from environmental damage. In fact, the fibers provide reinforcement for the matrix and other useful functions in fiber-reinforced composite materials [Glassfibre Reinforced Concrete Association].

Commercially, GRC is used to make large, lightweight panels that are often used as façades. These panels are considered non-structural, in that they are designed to support their own weight plus seismic and wind loadings, much in the way glass window curtain walls are designed. The panels are considered lightweight because of the thinness of the material, not because GRC concrete has a significantly lower density than normal concrete. Façade panels are normally bonded to a structural steel frame which supports the panel and provides connection points for hanging. GRC does not replace reinforced concrete when true load carrying capacity is required. It is best used for complex, three dimensional shells where loads are light [Van Gemert D. At al, Gartshore at al, Hollaway L.C. at al, Kim G.B. et al].

Different admixtures are used in GRC production. The most common admixtures are those that reduce the water demand and/or improve fluidity. These improve the dispersion of cement and are generally referred to as plasticizers with the early forms being based on lignosulfonates. Recently, a new range of products has been launched based on polycarboxylate ether chemistry. Increasingly, plasticizers are used with VMAs (viscosity modifying admixtures), which improve cohesion. They are added mainly to prevent segregation and bleeding when a highly fluid mix is required. In addition to the above, there are a number of other admixtures that are frequently used for concrete such as set retarders for hot weather, accelerators for cold weather and water-repellent/antiefflorescence chemicals [Fowler D.W. et al, Bijen, J. et al].

For the last 30 years polymers have been used with GRC and their use in all forms of concrete and cement-based blends is growing [Majumdar et al, Bartos P. J. at al]. For GRC, the following are some of the reasons:

- The elimination of wet curing while still achieving good 7- and 28 –day strengths.
- Greatly improved workability and application even without the use of other admixtures.
- To improve the long-term mechanical properties of GRC, particularly the aged flexural strain to failure.
- Harder, denser surface with no “dusting” and less crazing
- Reducing the water content and curing the GRC correctly, efflorescence is kept to a minimum.

The polymers used are white latex, usually acrylic emulsions with approximately 50% solid content. The polymer must be resistant to alkali and UV stable. They function by forming a network of flexible polymer bridges between the brittle mineral ingredients, helping to bind them together. The polymer forms a film, which traps in the water preventing premature evaporation and sealing the surface. The outcome is a harder surface, which also reduces moisture ingress with special incidence on the rate of water penetration. The prevention or reduction of water evaporation from the surface contributes to minimize the efflorescence formation [Purnell P. et al].

2. MATERIALS AND METHODS

Panels with dimensions 50 x 80 cm were prepared according to the compositions shown in table 1. An alkali-resistant fibre at a percentage of 3% was employed. The quantity of water varied as a function of the environmental conditions and the components' requirements. Different compositions were prepared by combining two plastifiers and two additives. The plasticizers were commercially available products, one of them has been traditionally employed in the GRC industry while the second can be described as belonging to the policarboxylate family and have been termed for this work as samples T and P; these admixtures were added at a percentage of 1% by weight of cement. The two additives employed, also commercially available products, could be described according to their composition: an acrylic suspension (A) or with a ceramic nature (C). The dosage employed was 3% by weight of cement.

Table 1. Compositions employed to prepare the panels.

	WATER	PLASTIFIER		ADDITIVE		SAND	CEMENT
		T	P	A	C		
T-control	16-21 L	0,5 Kg	-----	-----	-----	50 Kg	50Kg
P-control		-----	0,5 Kg	-----	-----		
T-C		0,5 Kg	-----	-----	2,5 Kg		
P-C		-----	0,5 Kg	-----	2,5 Kg		
T-A		0,5 Kg	-----	2,5 Kg	-----		
P-A		-----	0,5 Kg	2,5 Kg	-----		

The casting of the panels was carried out by spray up; the concrete is sprayed out of a gun-like noozle that also chops and sprays a separate stream of fibres. The concrete and fibres mix upon hitting the mould surface. Glass fibre is fed off of a spool in a continuous thread into the gun, where blades cut it just before it is spayed. The fabrication process took place in the SEIS factory in Chiloeches (Guadalajara) and is shown in figure 1.

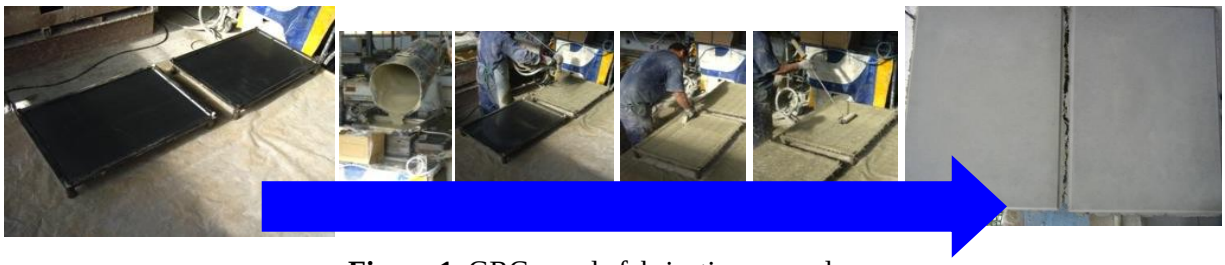

Figure 1. GRC panels fabrication procedure

The so obtained panels were demoulded after 24 hours and cured at ambient temperature inside the factory. One of the panels of each sample was cut and divided in test specimens in accordance with the standards of UNE-EN_1170-5.

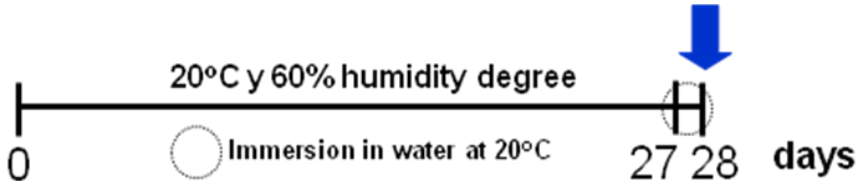

Figure 2. Storage and analysis conditions for 28 days samples.

Other panels were subjected to a cyclic weathering type test proposed by the European Committee for Standardization (UNE-EN_1170-8). This test incorporates the main ageing parameters which a glass-fibre reinforced concrete will have to withstand under natural exposure conditions: humidity, drying, temperature, and corresponds to natural weathering during 10 to 20 years. The test conditions are schematized in figure 3.

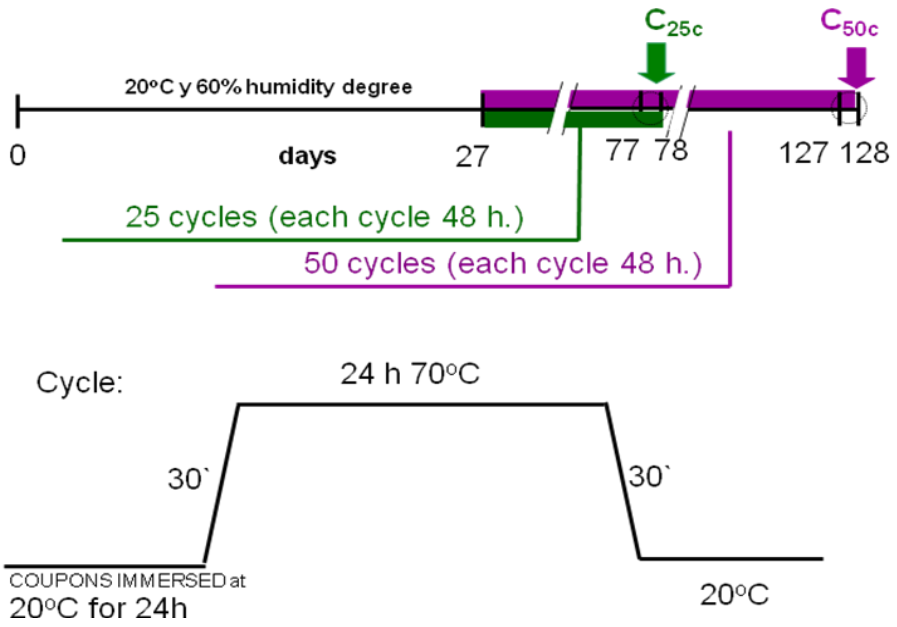

Figure 3. Cyclic weathering test conditions

A third series of panels are being environmentally exposed for one year as shown in figure 4.

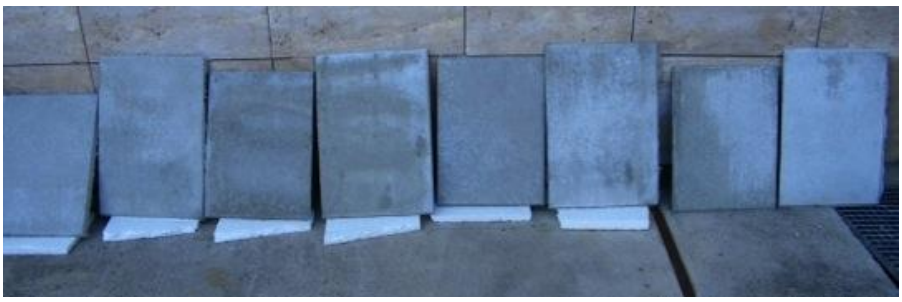

Figure 4. Environmentral exposure of the test boards for 1 year.

The so obtained materials were characterized by Hg-intrusion porosimetry, strength testing and optical microscopy. Additionally, the emergence of efflorescences has been photographically documented.

3 RESULTS AND DISCUSSION

In this work a comparison between samples with different admixtures aged in a climatic chamber or environmentally exposed have been carried out. The results shown and discussed focus on accelerated ageing in a chamber following the cyclic weathering type test proposed by the European Committee for Standardization. The effects on naturally aged test boards have been only photographically documented, although a complete characterization of these panels is pending to be carried out after one year of exposure.

The presence of the admixtures does generally improve the mechanical performance, exceptuating the combination of the traditional plasticizer and the ceramic additive where a slight decrease is observed.

In any case the ageing during 25 or 50 cycles causes a minor decrease on the flexural ultimate values as can be observed in figure 5.

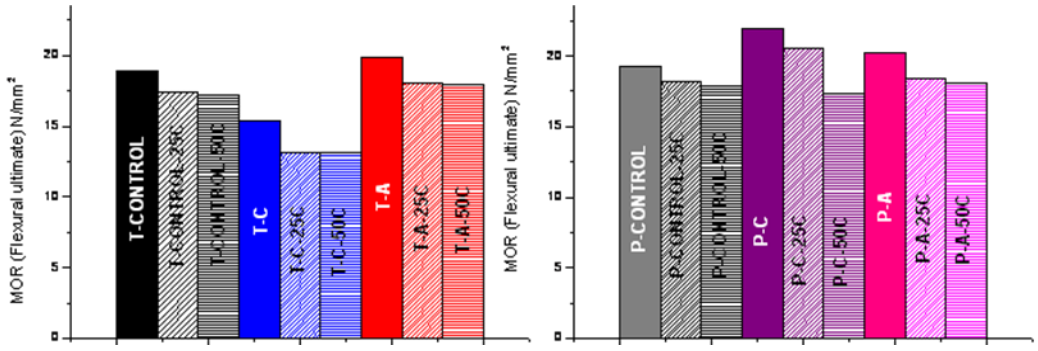

Figure 5. MOR (flexural ultimate) values of samples after 28 days and 25 or 50 cycles of weathering test.

A closer examination of the fiber as well as of the fiber/cementitious matrix allows to discard a serious concern of GRC materials: the etching of the glass fiber by hydration products, such as calcium hydroxide cystals. No evidences of this effect or the degradation of the fiber has been detected as can be observed in micrographs collected in figure 6. These photographs indicate that the fiber is still in excellent condition within the aged composite.

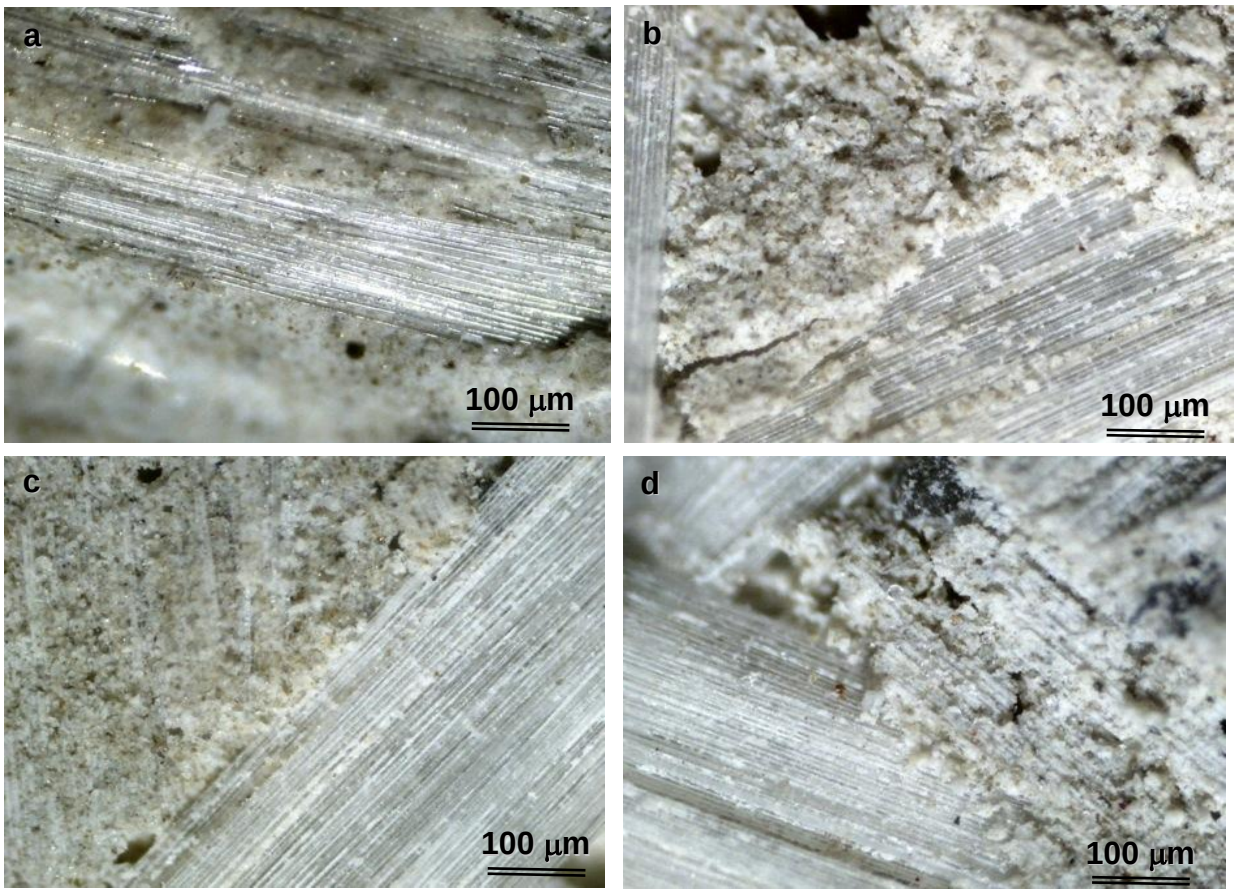

Figure 6. Microscopy photographs of samples (a) P-C and (c) P-T, unexposed, and (b) P-C-50c and (d) P-T-50c, after being exposed to 50 weathering cycles.

The porosity of the panels was determined by Hg intrusion porosimetry in order to try to establish a relationship between pore size and distribution with the permeation of water through the material, considering its crucial role on the efflorescence arising. Figure 7 shows the different pore size distributions obtained as a function of the additive and plasticizer employed, before and after being aged in the climatic chamber for 50 cycles. In the case of unexposed boards, the presence of the ceramic component seems to induce the generation of a second pore distribution at higher sizes (around 1 micron) in addition to that below 0,1 μm observed in control samples (without additions). The presence of the acrylic suspension induces a wider pore size distribution between 1 and 0,01 μm. Despite these differences in pore size distribution no differences have been observed in terms of porosity percentages (between 15-20%) or skeletal density (around 2,5 g/mL). The examination of the 50-cycle aged samples shows no remarkable differences neither on the pore size distributions nor on the porosity percentages or skeletal densities.

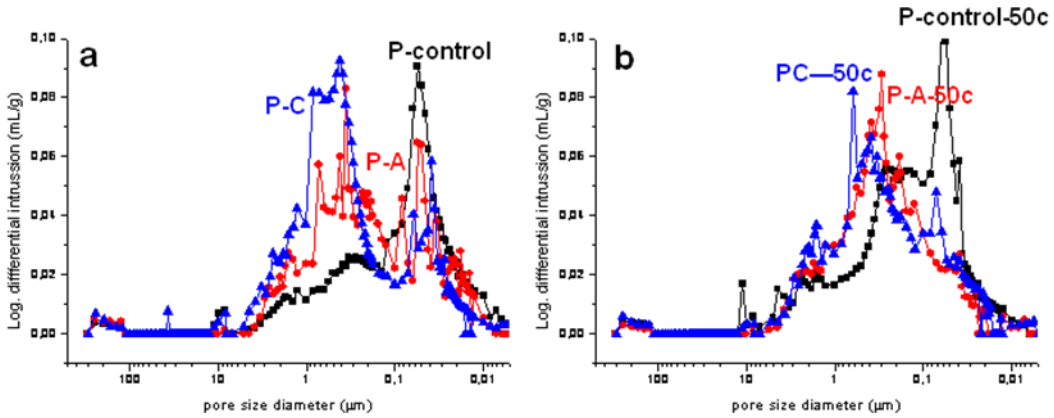

Figure 7. Pore size distributions of test boards obtained with the P plasticizer unexposed (a) and after being exposed to 50 weathering cycles (b).

This different pore size distribution has a decissive role on the interaction of the material with water. Bigger pores seem to have a critical role in the faster soaking behavior of panels containing the ceramic additive. On the contrary the absence of ceramic induces a more hydrophobic behaviour that contributes to the formation of droplets onto the surface of the panels. However, a clear relationship has not been established yet between the pore characteristics, the interaction of the panels with water and the generation of efflorescences.

In all cases the examinations of the panels after being exposed for two months under severe rainfalls show the arising of efflorescences (fig. 8). However, the presence of the admixtures seems to minimize the efflorescence generation. This may be caused by the different interaction of the panel with water or with the specific action that these components have against the efflorescence generation. Independently on the possible reactions that may minimize the salt precipitation and crystallization, the control of the pores/channels that determine the water migration inside the material should have a critical role on the possible prevention of efflorescences.

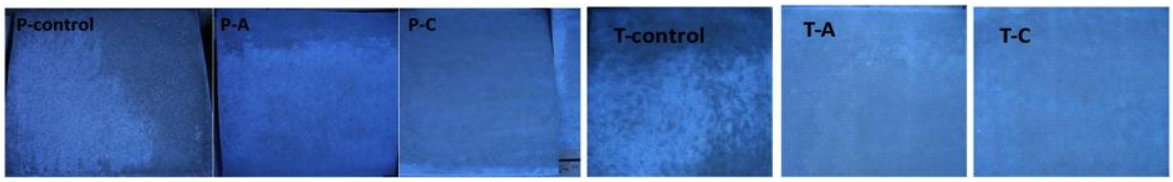

Figure 8. Photographs of the panels environmentally exposed for two months

4 CONCLUSIONS

- ✓ The inclusion of polymeric or ceramic admixtures does not have noticeable negative effects on the mechanical performance of the composites prepared.

- ✓ The ageing in a climatic chamber according to a European standard does not induce remarkable changes on the mechanical properties or porosity percentage and pore size distribution. In addition, the fiber seems not to be affected within the aged composite.

- ✓ This work contributes to connect porosity, water migration inside the material and efflorescence occurrence, although the correlation with the efflorescence arisen cannot yet be ascertained in all its extent.

- ✓ In all cases this research constitutes a milestone in a long term project, in collaboration with SEIS (ACS group), which aims mainly to minimize the appearance of efflorescence in prefabricated panels through the inclusion of additives of different nature.

ACKNOWLEDGMENTS

This work was supported by the Ministerio de Industria, Comercio y Turismo through a project (UCTR080273) in collaboration with SEIS (Soluciones de Edificación Integrales y Sostenibles) and by the Ministerio de Ciencia e Innovación, Spain (project BIA2009-10225). The authors would like to thank to all the personnel in SEIS for their valuable assistance in the fabrication of the GRC panels.

REFERENCES

Bartos P. J. M., Zhu W. (1996) Effect of Microsilica and Acrylic Polymer Treatment on the Ageing of GRC, *Cement & Concrete Composites* **18**, 31-39.

Bijen, J. (1990) Improved Mechanical Properties of Glass Fibre Reinforced Cement by Polymer Modification *Cement & Concrete Composites*, **12**, 95-101.

Fowler D.W. (1999) Polymers in concrete: a vision for the 21st century Cement & Concrete Composites **21** 449-452.

Gartshore, Gavin, A Recent Development for GRC Composites, *The Review, Design & Architecture,* Stoudgate Publications, Ltd., London, 1991, 147.

Hollaway L.C. (2003) The evolution of and the way forward for advanced polymer composites in the civil infrastructure, *Construction and Building Materials* **17**, 365–378.

Kim G.B., Pilakoutas K., Waldron P. (2008) Thin FRP/GFRC structural elements, *Cement & Concrete Composites* **30**, 122–137.

Majumdar, A.J. Singh, B. West, *(1987)* Properties of GRC modified by styrene-butadiene rubber latex, *Composites* **18**, 61-64.

Purnell P., Beddows J. (2005) Durability and simulated ageing of new matrix glass fibre reinforced concrete, *Cement & Concrete Composites* **27**, 875–884.

Specification for the manufacture, curing and Testing of GRC products, 2nd Ed 2006, International Glassfibre Reinforced Concrete Association.

Van Gemert D., Czarnecki L., Maultzsch M., Schorn H., Beeldens A., Łukowski P., Knapen E. (2005) Cement concrete and concrete–polymer composites: Two merging worlds. A report from 11th ICPIC Congress in Berlin, 2004, *Cement & Concrete Composites* **27**, 926–933.

XII DBMC
International Conference on Durability of Building Materials and Components
PORTO - PORTUGAL, April 12th-15th, 2011

Probabilistic Analysis of Hygrothermal Conditions and Mould Growth Potential in Cold Attics. Impact of Weather, Building System and Construction Design Characteristics

Carl-Eric Hagentoft[1]

ABSTRACT

Problems with high humidity levels and mould growth in cold attics have been increasing over the last few years. A recent Swedish study showed that as many as up to 60 – 80 % of the single-family houses in Västra Götaland (largely, the Gothenburg region) are showing significant mould growth and thereby risk developing serious moisture problems. The high humidity levels are to a large extent a consequence of the increasing demand on energy efficiency. Houses are frequently retrofitted with additional attic insulation, which leads to a colder attic space and hence a higher humidity. Furthermore, furnace heating is often replaced in favour of heat pumps or district heat. This may alter the air-pressure balance of the house, resulting in an increased thermal pressure on the ceiling with subsequent air-leakage up to the attic. Also newly built attics have problems. The probability density function of the mould growth potential is modelled using the Monte Carlo method and a simplified deterministic calculation tool. The risk of failure due to attic design and building system differences is compared.

KEYWORDS

Mould growth, Probabilistic, Risk, Weather, Attics.

[1] Chalmers University of Technology, Gothenburg, Sweden, carl-eric.hagentoft@chalmers.se

1 INTRODUCTION

Problems with high humidity levels in cold attics have been remarkably increasing in Sweden over the last decade. Beside clear evidence – the significant mould growth on the wooden parts of cold attics, which is recently confirmed in about 60-80 % single-family houses in Västra Götaland region (largely, the Gothenburg region; Ahrnens C & Borglund E, 2007.), mould odours in indoor air seem to be one of the most frequent side effects. Thus, cold attics are together with crawl spaces singled out as the two worst constructions in existing Swedish buildings with large existing and future mould problems.
The high humidity levels are to a large extent a consequence of the increasing demand on energy efficiency. Houses are frequently retrofitted with additional attic insulation, which leads to a colder attic space and hence a higher humidity (Hagentoft 2008). Leaks of indoor air up to the attic through the attic floor, and the under cooling of the roof due to sky radiation, increase the problem (Holm and Lengsfeld 2006, Sanders et. al 2006, Essah et. al 2009). The moist air might condensate at the underlay and small droplets of liquid water can build up. The water will then be absorbed and accumulated in the surface area. High moisture content can even lead to rot.
Another important moisture source influencing the attic hygrothermal condition is the water vapour in the surrounding outdoor air. The advice given to the building sector in Sweden today is to have a not too high or not too low ventilation rate, by outdoor air, of the attic. A too high ventilation rate, in combination with under cooling, results in high relative humidity (Sasic 2004). Too low ventilation is also risky in case of construction damp or leaky attic floor (Arfvidsson and Harderup 2005, Sanders 2006, Essah 2009). The optimal air exchange rate varies with the outdoor climate, and fixed ventilation through open eaves and/or gable and ridge vents are not always the best choice (Hagentoft et. al 2008, 2010).

2 PROBABILISTIC ANALYSIS

The probabilistic model of attic performance presented in this paper uses deterministic models for the heat and moisture transfer. Simplified transient models will be used, but in principle, more advanced models can of course be used as well. The yearly variations in the attic will be calculated based on measured full year weather data. The Monte Carlo method will be used to calculate the probability distribution for the mould growth potential, se Section 5 below. One of 30 weather data years (1961-1990) with hourly values will be selected randomly for each simulation. The air exchange rates (1/h) for the attic ventilation by exterior air, n_e, and the fraction of the indoor ventilation rate that flows up to the attic, f_{ia}, will have a fixed value for each yearly simulation. Normally distributed random numbers are assumed.

$$n_e = N(\mu_{ne}, \sigma_{ne}) \quad f_{ia} = N(\mu_{fia}, \sigma_{fia}) \qquad n_e \geq 0.1 \;\; f_{ia} \geq 0 \tag{1}$$

The indoor moisture supply (kg/m^3) will vary randomly each hour according to:

$$\Delta v = N(\mu_{\Delta v}, \sigma_{\Delta v}) \tag{2}$$

These random numbers are limited to the minimum physically realistically values shown in (1).

3 THERMAL MODEL OF ATTIC

In the modelled attic the roof underlay consists of 0,015 m thick wooden boards with a water and moisture tight membrane facing the exterior. The attic floor is thermally insulated with varying airtightness towards the living space underneath.

The attic is ventilated through openings at the gables. The model assumes a common resultant attic air temperature. The heat capacity is located in the roof underlay; i.e. the remaining heat capacity of materials in the attic is neglected. The attic temperature is determined by the heat exchange with the outdoor air through ventilation and indoor air through air leakage and heat transmission through the attic floor. The temperature, *T*, of the underlay is determined by the heat exchange with the attic air temperature, the exterior equivalent temperature and the heat storage by the material itself. In this

simple model differences due to the two different oriented sides of the roof are neglected. Basically this corresponds to a low sloped roof.

The indoor temperature is T_i, the exterior temperature T_e and the equivalent temperature for the roof is T_{eq}.

Using thermal conductances K (W/K), the following ordinary differential equation can be found for the wooden roof underlay temperature:

$$A\, d\rho c \frac{dT}{dt} = \left(T_{res} - T\right)\cdot K'_{res} + \left(T_{eq} - T\right)\cdot K^e \tag{3}$$

Here

$$T_{res} = \frac{K_v^e \cdot T_e + K_{floor}\cdot T_i + K_v^i \cdot T_i}{K_{res}} \qquad K_{res} = K_v^e + K_{floor} + K_v^i \tag{4}$$

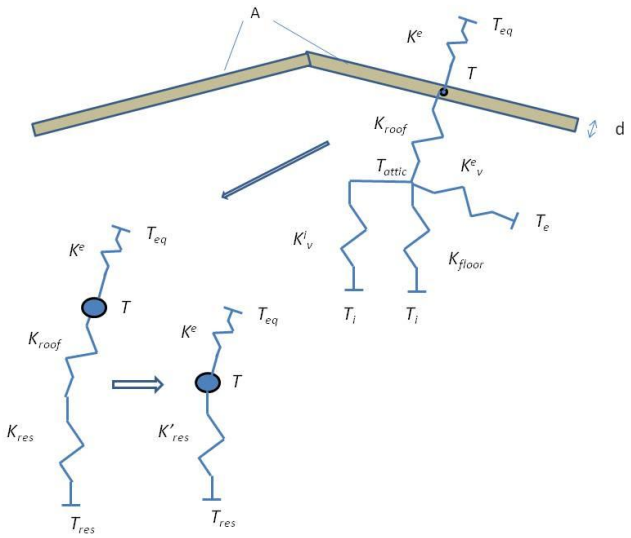

Figure 1. Thermal network of attic using thermal conductances K (with the unit W/K) and a node representing the heat capacity (J/K) of the wooden roof underlay. The second and third network (down left) shows reduced networks.

Here, d (m) represents the thickness of the wooden roof underlay layer, ρc (J/m^{3}K) the volumetric heat capacity of wood, and A (m^2) is the total roof surface area. Reduction of two serial coupled conductances gives (Hagentoft 2001):

$$1/K'_{res} = 1/K_{res} + 1/K_{roof} \tag{5}$$

The conductances (W/K) are given by the following expressions:

$$K_{floor} = A_{floor}\cdot U_{floor}$$
$$K_v^e = \rho_a c_{pa}\cdot R_a^e \qquad K_v^i = \rho_a c_{pa}\cdot R_a^i \tag{6}$$
$$K^e = \frac{A}{1/(\alpha_c+\alpha_r) + d/2/\lambda_{roof}} = \frac{A}{R_{se} + d/2/\lambda_{roof}} \qquad K_{roof} = \frac{A}{R_{si} + d/2/\lambda_{roof}}$$

Here, R_a refers to the ventilation flow rate (m^3/s) and the indices refer to if it is air from the exterior, *e*, or the interior, *i* (air leakage from the room below). The volumetric heat capacity of air, at constant pressure, is denoted $\rho_a c_{pa}$ (J/m^3K). The thermal conductivity of wood is denoted λ_{roof} (W/mK). The heat transfer coefficients for long wave radiation and convection are denoted α_r and α_c (W/m^2K) respectively. The total surface resistances at the interior and exterior side of the roof are denoted R_{si} and R_{se} (m^2K/W) respectively.
Expressed as air exchange rates per hour (1/h) we can write the expression as:

$$R_a^e = V_{attic} \cdot \frac{n_e}{3600} \quad R_a^i = V_{room} \cdot \frac{n_i}{3600} \cdot f_{ia} \tag{7}$$

The latter express the indoor air leakage to the room as a fraction, f_{ia}, of the room air ventilation rate.

Rewriting (3) we get:

$$\begin{aligned} &\frac{dT}{dt} = -T_{factor} \cdot T + T_{e,factor} \cdot T_e + T_{eq,factor} \cdot T_{eq} + T_{i,factor} \cdot T_i \\ &T_{factor} = \frac{1}{A_{floor} d\rho c}\left(K'_{res} + K^e\right) \quad T_{e,factor} = \frac{1}{A_{floor} d\rho c} K_v^e \frac{K'_{res}}{K_{res}} \\ &T_{eq,factor} = \frac{K^e}{A_{floor} d\rho c} \quad T_{i,factor} = \frac{1}{A_{floor} d\rho c}\left(K_{floor} + K_v^i\right) \cdot \frac{K'_{res}}{K_{res}} \end{aligned} \tag{8}$$

This general way of writing the differential equation will be handy when using our mathematical solver.

The attic air temperature is given by:

$$T_{attic} = \frac{K_{roof} \cdot T + K_{res} \cdot T_{res}}{K_{roof} + K_{res}} \tag{9}$$

The underlay surface temperature is:

$$T_{surf} = T + (T_{res} - T) \frac{K'_{res}}{A_{roof}} \frac{d}{2\lambda} \tag{10}$$

The external equivalent temperature is determined by the exterior air temperature, T_e, the global solar radiation, I_g (W/m^2) and the long wave radiation, I_{lw} (W/m^2).

$$T^{eq} = T_e + R_{se} \cdot \left(I_g \cdot \alpha_{sol} + \alpha_r \cdot (T^r - T_e)\right) \quad T^r = \sqrt[4]{\frac{I_{lw}}{\sigma}} - 273.15 \quad (°C) \tag{11}$$

Here, T^r represents the apparent sky temperature, and σ is the Stefan-Boltzmann constant. The solar absorptance of the roof surface is denoted α_{sol}.

4 MOISTURE MODEL OF ATTIC

The moisture model assumes that the whole moisture storage capacity of the roof is within the roof underlay material and that the roof surface is perfectly moisture tight. The diffusion of moisture through the attic floor is neglected. The only way for moisture to come in to the attic is by ventilation and air leakages.

The mass balance of the underlay, assuming no condensation at the roof underlay surface, gives:

$$\frac{dM}{dt} = K_{res}^v (v_{res} - v) = K_{res}^v \left(\frac{v_i \cdot R_a^i + v_e \cdot R_a^e}{R_a^i + R_a^e} - v \right) = K_{res}^v \cdot \frac{v_i \cdot R_a^i}{R_a^i + R_a^e} + K_{res}^v \cdot \frac{v_e \cdot R_a^e}{R_a^i + R_a^e} - K_{res}^v \cdot v \tag{12}$$

Here, M (kg), is the total moisture weight of the roof underlay and, v (kg/m^3), is its humidity by volume.

$$R_{a,res} = R_a^i + R_a^e$$

$$v_{res} = \frac{v_i \cdot R_a^i + v_e \cdot R_a^e}{R_a^i + R_a^e} \quad 1/K_{res}^v = \frac{1}{R_{a,res}} + \frac{1}{A/Z} \quad Z = Z_{si} + \frac{d}{2\delta_v} \tag{13}$$

Here, Z (s/m), is the vapour resistance between the air and the centre of the underlay layer and δ_v (m^2/s) is the vapour permeability of wood. The interior and exterior humidity by volume are denoted v_i and v_e (kg/m^3) respectively.

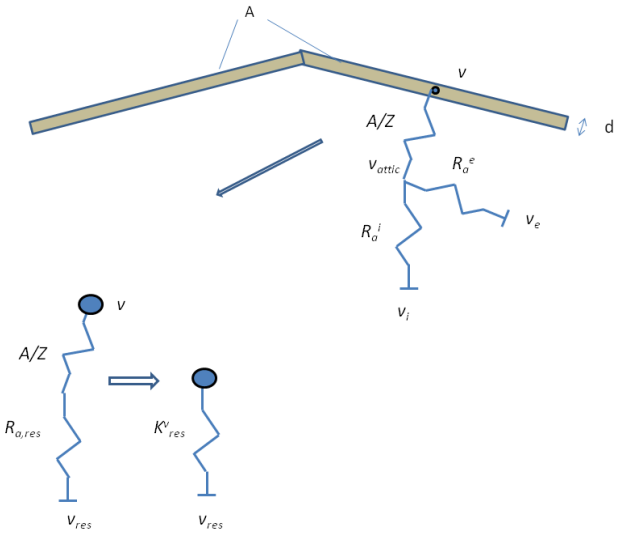

Figure 2. Moisture network of attic using vapour transfer conductances (with the unit m^3/s) and a node representing the moisture capacity of the wooden roof underlay. The second and third ones show reduced networks.

For the case of condensation we get:

$$\frac{dM}{dt} = \overline{K}_{res}^v \cdot (v_{res} - v_{sat}(T_{surf})) \qquad v_{res} - v_{sat}(T_{surf}) \geq 0$$

$$\frac{dM}{dt} = \overline{K}_{res}^v \cdot \frac{v_i \cdot R_a^i}{R_a^i + R_a^e} + \overline{K}_{res}^v \cdot \frac{v_e \cdot R_a^e}{R_a^i + R_a^e} - \overline{K}_{res}^v \cdot v_{sat}(T_{surf}) \tag{14}$$

$$1/\overline{K}_{res}^v = \frac{1}{R_{a,res}} + \frac{1}{A/Z_{si}}$$

Here, v_{sat}, denotes the humidity at saturation. We assume that the condensed water on the surface of the underlay is absorbed by the layer. Assuming a known slope, $\xi(\varphi)$ (-), of the sorption isotherm $w(\varphi)$ (kg/m^3) we can write:

$$\frac{dM}{dt} = A_{roof} d\xi \frac{d\varphi}{dt} \qquad \xi = \frac{dw}{d\varphi} \tag{15}$$

Combining it with (12) and using the definition of relative humidity we have for the case with no condensation:

$$\frac{d\varphi}{dt} = \left(-\varphi_{factor} \cdot v_{sat}(T) \cdot \varphi + v_{i,factor} \cdot v_i + v_{e,factor} \cdot v_e\right)\frac{1}{\xi} \qquad v_{res} - v_{sat}(T_{surf}) < 0$$

$$\varphi_{factor} = K_{res}^v \frac{1}{A_{roof} d} \quad v_{i,factor} = K_{res}^v \frac{R_a^i}{R_a^i + R_a^e} \frac{1}{A_{roof} d} \quad v_{e,factor} = K_{res}^v \frac{R_a^e}{R_a^i + R_a^e} \frac{1}{A_{roof} d} \tag{16}$$

, and with condensation:

$$\frac{d\varphi}{dt} = \left(-\bar{\varphi}_{factor} \cdot v_{sat}(T_{surf}) + \bar{v}_{i,factor} \cdot v_i + \bar{v}_{e,factor} \cdot v_e\right)\frac{1}{\xi} \qquad v_{res} - v_{sat}(T_{surf}) \geq 0$$

$$\bar{\varphi}_{factor} = \bar{K}^{v}_{res}\frac{1}{A_{roof}d} = \frac{\bar{K}^{v}_{res}}{K^{v}_{res}} \cdot \varphi_{factor} \quad \bar{v}_{i,factor} = \frac{\bar{K}^{v}_{res}}{K^{v}_{res}} \cdot v_{i,factor} \quad \bar{v}_{e,factor} = \frac{\bar{K}^{v}_{res}}{K^{v}_{res}} \cdot v_{e,factor} \tag{17}$$

The exterior humidity by volume, v_e, is obtained from weather data. The interior one comes from:

$$v_i = v_e + \Delta v. \tag{18}$$

Here, the second term represents the moisture supply, which will be a random variable, see (2).

5. MOULD GROWTH MODEL

A fundamental uncertainty lies in how to evaluate the calculations for the temperature and the relative humidity. What we really want to do is to estimate the probability or risk for mould growth in the attic. There are several studies on this subject. However, there is no standardized or widely accepted method for the evaluation of the mould growth risk. Here, we will base the risk assessment on the method developed by (Hukka, Viitanen,1999). As a measure of the mould risk, a mould growth potential *m* has been used in this paper, which is simply the relative humidity divided by the critical relative humidity for mould growth to start according to the reference:

$$m = \frac{RH}{RH_{crit}} \qquad RH_{crit} = \begin{cases} 100\%, \; T \leq 0°C \\ -0.00267T^3 + 0.160T^2 - 3.13T + 100.0, \; 0°C \leq T \leq 20°C \\ 80\%, \; T > 20°C \end{cases} \tag{19}$$

Theoretically, mould growth is possible only when $m > 1$. Hence, the development over time of *m* represents an indicator of risk for the development of mould. By using this parameter different attic designs can be compared.

6. RESULTS

The "ode45" Matlab solver for coupled ordinary differential equations (8), (16) and (17) has been used to calculate the hourly value for a whole year for the attic temperature and relative humidity. By combining this with the model for mould growth potential the probability density function can be calculated.

The following data have been used in the simulation:

Weather: Gothenburg, Sweden, A=100 m^2, d=0.015 m,

V_{attic}=100 m^3, V_{room}=250 m^3, n_i=0.5 1/h, δ_v=2·10^{-6} m^2/s, R_{si}=0.13 m^{2}K/W, R_{se}=0.04 m^{2}K/W, Z_{si}=360 s/m, α_r=4 W/m^{2}K, α_{sol}=0.7, T_i=20 ° C, φ_{start}=0.8, λ_{roof}=0.14 W/mK, ρc=750 000 J/m^{3}K.

The sorption isotherm for the wood (IEA, Annex 14, 1992) is given by:

$$w(\varphi) = \frac{\varphi}{-0.027\varphi^2 + 0{,}027\varphi + 0.0089} \tag{20}$$

The indoor moisture supply is the same for all scenarios:

$$\Delta v = N(0.004, 0.002) \quad (\text{kg/m}^3) \tag{21}$$

For well and less ventilated attics we have the alternatives:

$$n_e = N(7{,}5) \quad n_e = N(2{,}1) \; (1/\text{h}) \tag{22}$$

For tight, less tight and leaky attic floor we have:

$$f_{ia} = 0 \quad f_{ia} = N(0.1, 0.1) \quad f_{ia} = N(0.2, 0.1) \; (-) \tag{23}$$

The attic floor insulation is thick, 0.50 m, or thin, 0.05 m, giving:

$$U_{floor} = 0.08 \; \text{W/m}^2\text{K} \; U_{floor} = 0.8 \; \text{W/m}^2\text{K}$$

The air exchange rates are constant for each yearly simulation. The indoor moisture supply for each hour of the year is calculated before the actual dynamic simulation for a year starts. The calculation time is approximately 25 seconds per sample i.e. one year's simulation, on a PC (Intel Core 2 Duo CPU, P9400 @ 2.40 GHz).

Figure 3 shows the cumulative distribution for different samples i.e. number of yearly simulations. The scenario with an attic floor having thick insulation is less air tight and where the attic is less ventilated is simulated. The results for the probability of exceeding the mould growth potential of one is given in Table 1 as a function of number of yearly samples.

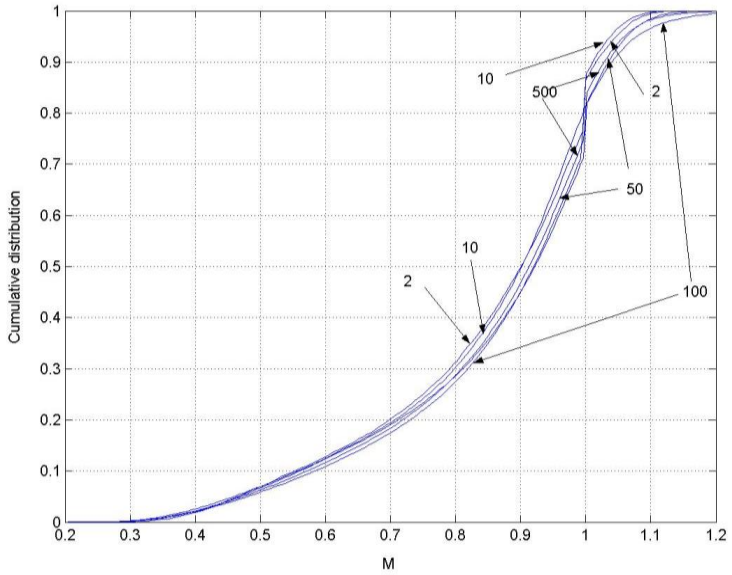

Figure 3. The cumulative distribution for the mould growth potential of the underlay wooden surface. The scenario with an attic floor having thick insulation is less air tight and where the attic is less ventilated is simulated. The number of samples, i.e. yearly simulations, varies from 2 to 500.

Table 1. The probability of exceeding a mould growth potential of one for the underlay wooden surface. The scenario with an attic floor having thick insulation is less air tight and where the attic is less ventilated is simulated. The number of samples, i.e. yearly simulations, varies from 2 to 500.

Number of yearly samples	2	10	50	100	500
Probability	13,5%	13,9%	17%	18,5%	19,6%

Table 2. The probability of exceeding a mould growth potential of one for the underlay wooden surface. The scenario for the attic floor insulation, the attic floor tightness varies. The attic is *well ventilated.*

	Leaky attic floor	Less tight attic floor	Tight attic floor
di=0,05 m	14%	12 %	6%
di=0,5 m	23%	20 %	13%

Table 3. The probability of exceeding a mould growth potential of one for the underlay wooden surface. The scenario for the attic floor insulation, the attic floor tightness varies. The attic is *less ventilated*.

	Leaky attic floor	Less tight attic floor	Tight attic floor
di=0,05 m	13%	11 %	2%
di=0,5 m	26 %	17 %	9%

Table 2 and 3 shows the probability of exceeding the mould growth potential of one for the specified scenarios using 50 yearly samples.

DISCUSSION AND CONCLUSIONS

The paper shows a tool that can be used in the performance risk assessment of cold attics. The construction is known for moisture related problems such as mould growth. In order to decide on less risky design alternatives the demonstrated Monte Carlo based method is an alternative. The paper gives results accounting for the random variation in yearly weather, indoor moisture supply, ventilation rates and air leakages. The results show greater risk for mould growth when using well insulated attic floors. It is also shown that a lower ventilation rate of the attic is benificial except for the case with a leaky attic floor and well insulated attic floor (0,5 m).

The purpose of the paper is to demonstrate the methodology and not covering all random phenomenons. For more detailed analyses, the variations in indoor temperature, indoor moisture supply, air flow rates, and surface resistance should depend on the actual time of the year and weather condition. Then, simulations require state dependent factors in the expression of the ODE. This is not in principle more complicated to model but a bit more time consuming. Also more detailed HAM-models can be used to improve the accuracy of the deterministic calculation results accounting for a more detailed moisture and heat transfer in the attics and its components.

REFERENCES

Ahrenens, C., Borglund E. 2007. Fukt på kallvindar. Master thesis 2007:11. CTH, Building Physics.
Alexandersson, H., 2006. Klimat i förändring: En jämförelse av temperatur och nederbörd 1991-2005 med 1961-1990. Faktablad i Meteorologi nr 29 Oktober 2006. SMHI, SE-601 76 Norrköping, Sweden, 8 pp.

Arfvidsson, J. and Harderup, L-E. 2005. Moisture Safety in Attics Ventilated by Outdoor Air. 7th Symposium in Building Physics, Reykjavik, Island.

Essah, E.A. 2009. Modelling and measurements of airflow and ventilation within domestic pitched roofs. Doctoral thesis. Glasgow Caledonian University, Scotland, UK.

Hagentoft C E 2001, Textbook: Introduction to Building Physics. Studentlitteratur, ISBN 91-44-01896-7.

Hagentoft C.E., Sasic Kalagasidis A., Nilsson S.F., Thorin M. Mould growth control in cold attics through adaptive ventilation. 8th Symposium on Building Physics in the Nordic Countries, Copenhagen, Denmark, June 2008.

Hagentoft C-E, Sasic Kalagasidis A. Mould Growth Control in Cold Attics through Adaptive Ventilation. Validation by Field Measurements. 12th International Conference on Performance of the Exterior Envelopes of Whole Buildings, 2010, Clearwater Beach, Florida.

Holm, A., Lengsfeld, K. 2006. Hygrothermal performance of unfinished attics (ventilated roofs) – an experimental study. Research in Building Physics and Building Engineering. Proceedings from the third International Building Physics Conference, Montreal, Canada.

Hukka E., Viitanen H.A., 1999. A mathematical model of mould growth on wooden material. Wood Science and Technology 33, Springer-Verlag.

Samuelson, I. 1995. Hygrothermal performance of attics. In Swedish. SP Report 1995:68, Sweden.

Sanders, C.H. 2006. Modelling condensation and airflow in pitched roofs – Building Research and Establishment (BRE) information paper, IP 05/06. BRE Press, Garston, Watford – UK. ISBN 1-86081-912-5, pp. 1-7

Sasic Kalagasidis A. 2004. HAM-Tools. An Integrated Simulation Tool for Heat, Air and Moisture Transfer Analyses in Building Physics. Doctoral thesis. Chalmers University of Technology, Sweden.

IEA, Annex 14. Condensation and Energy, Catalogue of Material Properties Vol 3, IEA-ECBCS. K.U Leuven, Belgium 1992.

XII DBMC
International Conference on Durability of Building Materials and Components
PORTO - PORTUGAL, April 12th-15th, 2011

Study of Marine Aerosol Salinity in Brazilian Coast – Relationship with Concrete Durability and Proposal of Aggressiveness Subzones

Gibson Rocha Meira [1]
Carmen Andrade [2]
Mª Cruz Alonso [3]

ABSTRACT

Corrosion of reinforcement in concrete structures is influenced by salt concentration in marine aerosol inland. This work analyses the behaviour of marine aerosol salinity in marine atmosphere zone in Brazilian coast and its interaction with concrete structures. Marine aerosol salinity was monitored on chloride concentration in marine aerosol by the wet candle method and chloride concentrations in concrete were periodically monitored by chloride profiles analysis. Results show a strong decrease in airborne salinity with the distance from the sea as well as in chloride penetration into concrete structures. However, this does not take pace at the same rate. Numerical extrapolations of chloride profiles in concrete over time, which took into account environmental and material data, show that chloride deposition rate on the wet candle can be used as an environmental indicator, helping to set different marine aggressiveness subzones in the studied region, with different material requirements for a required service life.

KEYWORDS

Chloride deposition, Concrete durability; Marine atmosphere zone, Wet candle.

[1] Federal Institute of Education, Science and Technology of Paraíba and Urban and environmental Engineering Postgraduate Programme, João Pessoa, BRAZIL, gibsonmeira@yahoo.com; gibson.meira@ifpb.edu.br
[2] Eduardo Torroja Construction Research Institute, Madri, SPAIN
[3] Eduardo Torroja Construction Research Institute, Madri, SPAIN

1 INTRODUCTION

Chloride aggressiveness in marine atmosphere zone has its origin in aerosol production, which can take place either in the surf zone or in the open sea [Gong *et al.* 1997]. This mechanism, which is strongly influenced by wind characteristics [Fitzgerald 1991], is more effective in seashore due to the breaking waves movement. After being produced, marine aerosol is transported inland by wind. During this transport, particles that compose marine aerosol settle after having covered a certain distance from the sea, which depends on their weight, wind characteristics and obstacles present in aerosol trajectory [Lovett 1978, Fitzgerald 1991, Morcillo *et al.* 2000]. As a consequence, a strong decrease tendency of salt concentrations in atmosphere takes place in the first meters away from the sea [Feliu *et al.* 1999].

Studies that show the relationship between aerosol salinity and concrete durability are still scarce. Some efforts done in this way show that, as in aerosol salinity, there is a similar decrease tendency for the total amount of chlorides that penetrate into concrete structures built in marine atmosphere zone [Mustafa & Yusof 1994, Meira *et al.* 2007]. These studies, which were carried out under field exposure, observed decreases up to 70% in chloride penetration into concrete in the first hundred meters from the sea. However, long-term data and service life analyses were not incorporated to these analyses.

Chlorides from marine aerosol deposit on concrete surface and from that penetrate into bulk concrete. Corrosion of rebar in concrete structures exposed to marine environment start only after that a certain level of chloride content is exceeded at the rebar surface. This chloride content is known as chloride threshold for starting corrosion [Glass and Buenfeld 1997]. Its behaviour is directly related to service life analysis of concrete structures.

Taking into account the lack of studies connecting environmental characteristics with durability performance of concrete structures, the aim of this paper is to analyse the relationship between chloride deposition rate on the wet candle device and chloride accumulation into concrete, concerning the critical chloride advance in concrete. This analysis was used as a basis to propose different chloride aggressiveness subzones in marine atmosphere zone. Curves representing the relationship of this environmental indicator with chloride threshold advance in concrete in marine atmosphere zone are presented. Long-term data and service life analysis were also incorporated in this paper.

Modelling of chloride penetration into concrete has been traditionally done by the use of Fick's second law, assuming as constants the surface chloride concentration and the diffusion coefficient [Crank 1975]. Advances have been obtained on this modelling considering the effect of variables like time [Mangat & Molloy 1994], temperature [Saetta et al. 1993], saturation degree of concrete [Almenar 2000], etc, on chloride transport. Taking into account the multiple influence of variables on chloride transport into concrete, numeric models have been proposed to represent these phenomena. This way, finite difference method has been used in some approaches [Tang & Nilsson 1996, Nielsen & Geiker 2003] and finite element method has been used in more sophisticated models [Pérez 1999]. This work used the finite difference method with some simplifications described in section 4.

2 EXPERIMENTAL WORK

An environmental characterization was carried out considering climatic and sea-salt data. Climatic data were collected by a Brazilian Government weather station located in the region where the research took place and it was done on temperature, relative humidity, and wind speed and wind direction. The UTC (coordinated universal time) references were followed on these measurements.

Sea-salt data was measured by the wet candle device, according to the specifications established in the ASTM standard G140 [2002]. These devices were placed at places located at 10, 100, 200 and

500 meters from the sea. Samples from the wet candle device were collected monthly and analysed by potentiometric titration throughout the research period.

Prismatic concrete specimens of 0.15 x 0.15 x 1.40 m were cast using a Brazilian cement CPIIF (Filler-modified Portland). Water to cement ratios were set at 0.50, 0.57 and 0.65, representing materials with a large range of porosity characteristics and composing the mixtures C1 – C3 (Table 1). Compressive strength, concrete slump and mercury intrusion porosimetry were also measured to characterize the concretes (Table 1).

Table 1. Concrete mixtures and properties.

Concrete	C1	C2	C3
Cement (kg/m^3)	406	356	320
Sand (kg/m^3)	769	812	840
Aggregate (kg/m^3)	947	947	947
Plasticiser (kg/m^3)	1,22	1.06	-
w/c ratio	0.50	0.57	0.65
Slump (mm)	8 ± 1	8 ± 1	8 ± 1
Compressive strength (MPa) – 28 days	31.0	27.0	20.3
Total porosity (mercury intrusion porosimetry –180 days) – (%vol.)	13.0	13.7	15.7

The specimens were cured in a wet chamber for 7 days before being placed at locations 10, 100, 200 and 500 m away from the sea, at the same monitoring stations used for measuring chloride deposition. The specimen faces not perpendicular to the predominant winds were waterproofed with a polyurethane coating to simulate the unidirectional transport of chlorides into concrete.

After six, ten, fourteen, eighteen and forty-six months of exposure, samples were extracted from the specimens to obtain chloride profiles in concrete. The first step in obtaining the samples was to remove (by drilling), from the prismatic specimens, 7.0 cm diameter cores. The first millimetre of each core was powdered and was used as a surface sample. Additional samples, also powdered, were taken up to the depth of 30 or 35 mm, depending on the exposure time. For each sample the total chloride content was determined by potentiometric titration, following the procedures of the International Union of Laboratories and Experts in Construction Materials, Systems and Structures - RILEM [2002].

Measurements of the saturation degree of concrete porous network were also done along the observation period using a methodology based on mass measurements of concrete specimens over time and comparisons with saturated mass of these specimens [Guimarães & Helene 2005]. This methodology is not discussed here, but the behaviour of this variable for the concretes studied in this paper is incorporated to the numeric approach used in section 4. Detailed data of this variable and methodology can be seen in Meira [2004].

3 RESULTS

The local temperature in the region chosen for the experimental work shows little variation, ranging roughly from 20 to 30 degrees Celsius. The relative humidity stays usually between 60 and 80 %, with higher values during longer rain periods. Winds are usually from S-SE-E directions and their speeds are typically low and stay in the range between 1.0 and 4.0 m/s daily average.

The results of chloride deposition on the wet candle device show a clear reduction of airborne salinity in the first 200 m (Fig. 1). This reduction demonstrates that chloride aggressiveness reduction is stronger in the first land zones. After this distance from the sea, there are also differences on measured data, but they are less accentuated.

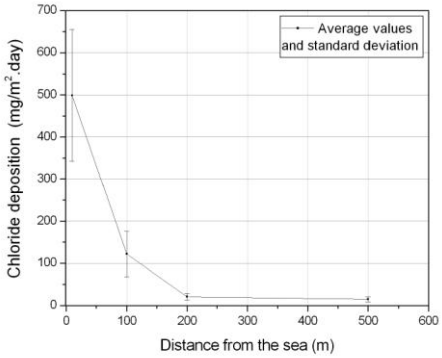

Figure 1. Chloride deposition on the wet candle device.

During the experimental study, dozens of chloride profiles were obtained. Profiles show that there is a clear increase in chloride content over time, as a consequence of a continuous exposure to marine aerosol (Fig. 2a). Chloride profiles also show lower chloride penetration into concrete with the distance from the sea, as a consequence of the availability of chlorides in atmosphere at each exposure site (Fig. 2b). A typical decrease in chloride content with w/c decrease is also presented, which is related to materials porosity (Fig. 2c). Profiles behaviour is the basis for the analysis done in the next section, where simulations for 50 years of field exposure are incorporated.

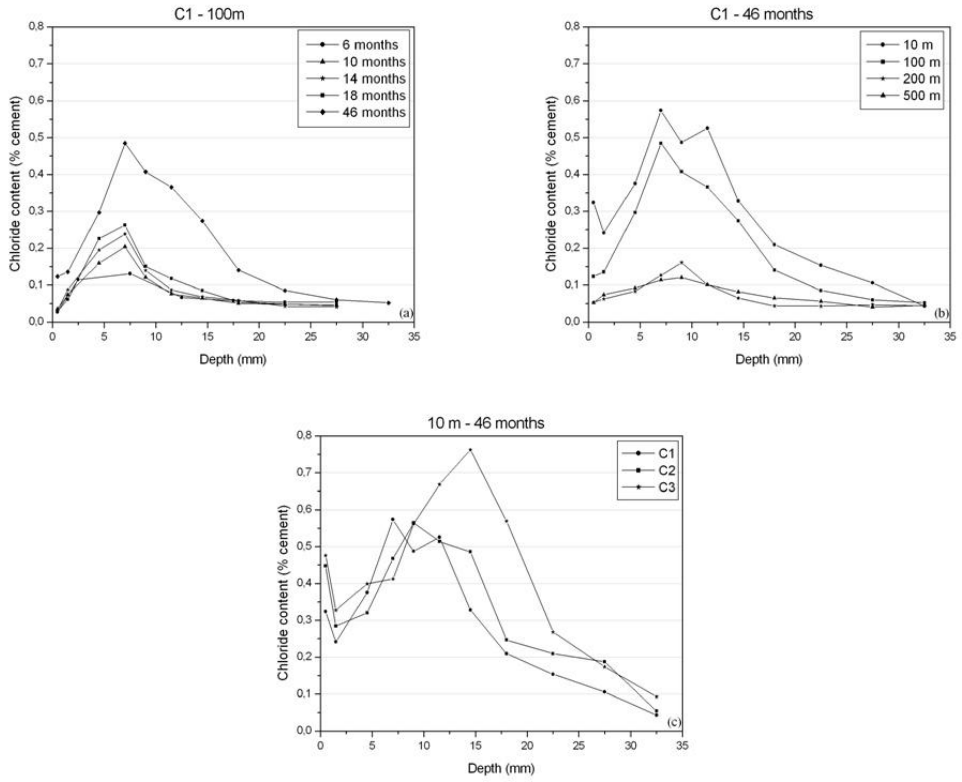

Figure 2. Chloride profiles in concrete – influence of exposure time (a), distance from the seashore (b) and concrete characteristics (c).

4 SERVICE LIFE ANALISYS AND PROPOSAL OF AGGRESSIVENESS SUBZONES

One way to set relationships between chloride deposition rate on the wet candle and concrete structures performance is through service life analysis. This was done here by numeric extrapolations over 50 years of exposure, considering chloride profiles during the first 46 months of exposure,

environmental and concrete characteristics influence on chloride transport and 0.4 % of cement mass as total chlorides threshold [Glass & Buenfeld 1997]. The procedures adopted are resumed below in three steps, which consider the rescaling of chloride profiles, the numerical obtaining of transport parameters and numerical extrapolations and proposal of aggressiveness subzones.

4.1. Rescaling of Chloride Profiles

When concrete structures are subjected to wetting and drying cycles, which is the case of concrete structures in marine atmosphere zone, chloride profiles tend to be two-zone profiles, with a maximum chloride concentration a few millimetres inside [Tuutti 1993, Pérez 1999]. In accordance with this behaviour, chloride profiles obtained in this study are two-zone profiles with an external zone, where wetting and drying cycles take place and favour to capillary sorption and an inner zone, where the humidity remain at higher levels and the transport of chlorides can be attributed mainly to diffusion [Pérez 1999, Castro *et al*. 2001, Meira *et al.* 2007].

In this study, only the diffusion zone was considered. A rescaling of chloride profiles starting from the end of convection zone was used [Nilsson *et al.* 2000]. The maximum chloride concentration in the interface between convective and diffusion zones ($C_{máx}$), which means the surface chloride content of the rescaled profile, was represented by Eq. 1, where, C_0 is the initial chloride content in concrete, $k_{cmáx}$ is a material and environmental dependant coefficient and D_{ac} is the accumulated deposition of chlorides on the wet candle.

$$C_{máx} = C_0 + k_{cmáx}\sqrt{D_{ac}} \tag{1}$$

4.2. Numerical Obtaining of Transport Parameters

Using the finite difference method, least-squares fitting [Hornbeck 1982] and computational routines, a numerical simultaneous fitting was done to each set of chloride profiles representative of each concrete and exposure station to obtain the parameters of the model: D_0 and m, which are detailed along this section. Equation 2 corresponds to the finite difference representation of Fick's second law of diffusion and it is complemented by Eq. 3 that represents the dependence of diffusion coefficient on some variables. In these equations, $C_{i,j}$ is the chloride concentration at the depth i and time j, Δx is the depth variation, Δt is the time variation, D_{ap} is the apparent diffusion coefficient, D_0 is a referential diffusion coefficient and $f(t)$, $f(T)$ and $f(SD)$ represent, respectively, the influence of time, temperature and water saturation degree of concrete on apparent diffusion coefficient [Mangat & Molloy 1994, Almenar 2000, Nielsen & Geiker 2003, Boddy *et al.* 1999].

$$C_{i,j+1} = \frac{(C_{i+1,j} - 2C_{i,j} + C_{i-1,j})}{\Delta x^2}.\Delta t.D_{ap} + C_{i,j} \tag{2}$$

$$D_{ap} = D_0.f(t).f(T).f(SD) \tag{3}$$

The influence of temperature was not considered in this study, due to its low influence on the apparent diffusion coefficient in this specific case. As a result, Eq. 3 was rewritten as Eq. 4, where t_0 is a reference time (1 s), t is the variable time, m is a time dependant coefficient and SD is the water saturation degree of concrete porous network. The structure of $f(t)$ and $f(SD)$ terms was based on previous works that consider the concrete hydration over time [Mangat & Molloy 1994, Boddy *et al*. 1999] and the influence of water content in concrete porous network in chloride transport [Almenar 2000]. The behaviour of water saturation degree of concrete over time was represented by Eq. 5, where SD_{max} and SD_{min} are, respectively, the maximum and the minimum saturation degree observed.

$$D_{ap} = D_0.f(t).f(SD) \Rightarrow D_{ap} = D_0.\left(t_0 \big/ t\right)^m.e^{4.6(SD-1)} \tag{4}$$

$$SD = \frac{SD_{\max} + SD_{mim}}{2} + \frac{SD_{\max} - SD_{mim}}{2} \sin\left(2\pi \frac{(t - t_0)}{365}\right) \quad (5)$$

4.3. Numerical Extrapolations and Proposal of Aggressiveness Subzones

Simulations of $C_{máx}$ were done, considering average chloride depositions on the wet candle of 500, 120 and 15 mg/m^2.day, which are close to average values for the studied region. Numeric extrapolations of chloride profiles were done for 50 years also using finite difference method. From these profile extrapolations, the advance of chloride threshold was obtained and represented in Fig. 3.

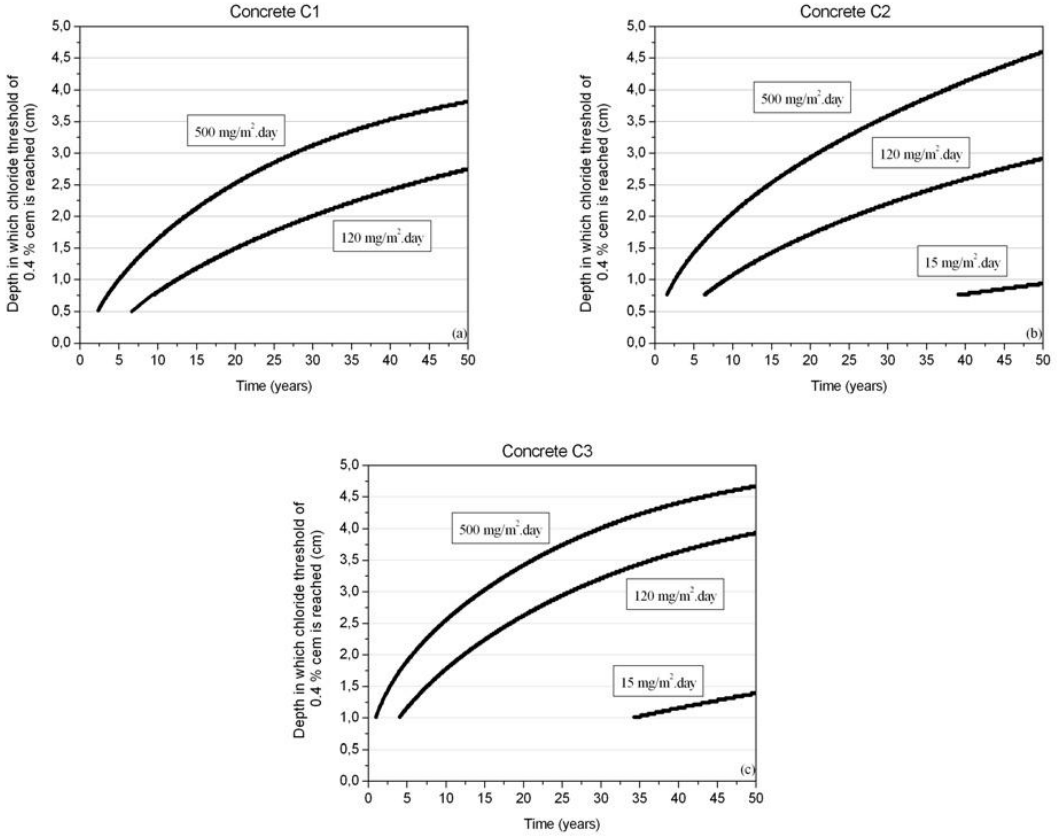

Figure 3. Simulations of chloride threshold advance in concretes C1 (a), C2(b) and C3(c).

Simulations done in Fig. 3 show that, considering service life as the time for chloride threshold to be reached at the rebar surface, it is possible to observe different situations about service life, depending on chloride deposition rate. For example, after 50 years, concrete structures with w/c 0.5 – C1 (Fig. 3a) and located at sites with 15 mg/m^2.day average chloride deposition rate did not present 0.4 % of cement mass at any depth. For sites with 120 mg/m^2.day chloride threshold takes place at 27.5 mm depth and for sites with 500 mg/m^2.day it takes place at 38.0 mm depth, indicating that if reinforcement was placed at 30 mm depth, structures subjected to 500 mg/m^2.day had already reached their service life. For concretes with w/c 0.57 – C2 (Fig. 3b), these depths after 50 years were 9, 29 and 46 mm, respectively, which indicates that more than 45 mm of reinforcement cover are necessary for concrete C2 to reach a service life close to 50 years at sites with 500 mg/m^2.day. A similar analysis can also be done for concrete C3 (Fig. 3c).

Chloride penetration into concrete in marine atmosphere zone is closely related to the availability of chlorides in atmosphere. Simulations done here show that chloride deposition rate on the wet candle device can be used as an environmental indicator for concrete durability study in marine atmosphere zone, helping to set minimum durability requirements for concrete structures depending on the deposition level expected. For the studied region, the reference of distinct chloride deposition levels

on the wet candle lead to different combinations of w/c ratios and concrete cover requirements, considering 50-year service life, which can be represented in different aggressiveness subzones and concrete requirements, as presented in Table 2. To compose the presented ranges in Table 2, chloride penetration into concrete was assumed as the main reason for reinforcement depasivation. This was supported by the low rates of concrete carbonation observed in this experiment. Furthermore, some interpolations were done using curves from Fig. 3, as well as a minimum concrete cover of 30 mm was adopted.

Table 2. Proposal of aggressiveness subzones.

Aggressiveness subzones		**Maximum water to binder ratio**	**Minimum concrete cover (mm)**	**Distance from the sea for the studied region (m)**
Aggressiveness level	**Chloride deposition rate (mg/m^2.day)**			
High	Higher than 100	0.50	40	Less than 100
Moderate	Between 100 and 10	0.55	35	Between 100 and 750
Depreciable	Less than 10	0.60	30	More than 750

5 CONCLUSIONS

The use of chloride deposition on the wet candle as an environmental indicator for service life analysis can be done thorough simulated curves of chloride threshold advance for each level of chloride deposition on the wet candle. From an expected chloride deposition level for a given environment and the characteristic curves of chloride threshold advance for each concrete it is possible to preview the expectancy of service life for different concrete structures, considering different concrete covers or, in another way, to suggest a minimum concrete cover depth for a required time of service life.

Taking into account that marine atmosphere zone can assume different extensions depending on aerosol characteristics, wind regime, land surface, etc., the proposal of aggressiveness subzones for marine atmosphere zone considering ranges of chloride deposition rates seems to be suitable. As a consequence, concrete structures in marine atmosphere zone should have different durability requirements depending on the chloride deposition level expected.

ACKNOWLEDGMENTS

The authors thank the Brazilian Government Agency for the Improvement of Graduated Professionals and Eduardo Torroja Construction Research Institute for partially supporting this research. The authors also thank the Bazilian National Institute of Meteorology for providing climatic data.

REFERENCES

Almenar, G V. 2000. Chloride ingress into concrete: analyse methods, non-destructive detection and transport modelling under a limited first approach. PhD. thesis Alicante: Alicante University (in Spanish).

American Society for Testing Materials, ASTM G-140, 2002. Standard test method for determining atmospheric chloride deposition rate by wet candle method. Annual Book of ASTM Standards. Philadelphia, USA: ASTM.

Boddy, A.; Bentz, E.; Thomas, M. D. A.; Hooton, R. D. 1999, 'An overview and sensitivity study of a multimechanistic chloride transport model', Cement and Concrete Research, 29, 827-837.

Castro, P.; Rincón, O. T.; Pazini, E. J. 2001, 'Interpretation of chloride profiles from concrete exposed to tropical marine environments', Cement and Concrete Research, 31, 529-537.

Crank, J. 1975, The mathematics of diffusion, 2nd ed., Oxford University Press, Oxford.

Feliu, S.; Morcillo, M.; Chico, B. 1999. 'Effect of distance from sea on atmospheric corrosion rate', NACE, 55 (9), 883-891.

Fitzgerald, J. W. 1991, 'Marine aerosols: a review', Atmospheric Environment, 25A, 533-545.

Glass, G. K.; Buenfeld, N. R. 1995, 'Chloride threshold levels for corrosion induced deterioration of steel in concrete', in International RILEM Workshop on Chloride Penetration into Concrete, eds L. O. Nilsson, J. P. Ollivier, RILEM, Paris, pp. 429 – 440.

Gong, S. L.; Barrie, L. A.; Blanchet, J. P. 1997, 'Modelling sea-salt aerosols in the atmosphere – 1. Model development', Journal of Geophysical Research, 102, 3805-3818.

Guimarães, A. T. C.; Helene, P. R. L. 2005, 'Chloride diffusion and the influence of the saturation degree of the concrete', in. Third RILEM Workshop on Testing and Modelling the Chloride Ingress into Concrete, eds C. Andrade, J. Kropp, RILEM, Madrid, pp. 237-256.

Hornbeck, R. W. 1982, Numerical methods, Quantum Publishers, New York.

International Union of Testing and Research Laboratories for Materials and Structures, RILEM TC 178-TMC 2002, 'Analysis of total chloride content in concrete', Materials and Structures, 35, 583-585.

Lovett, R. F. 1978, 'Quantitative measurement of airborne sea salt in the North Atlantic' Tellus, 30, 358-364.

Mangat, P. S.; Molloy, B. T. 1994, 'Prediction of long term chloride concentration in concrete', Materials and Structures, 27, 338-346.

Pérez, B. M. 1999, Service life modelling of R. C. highway structures exposed to chlorides, PhD thesis. University of Toronto ,Toronto.

Morcillo, M.; Chico, B.; Mariaca, L.; Otero, E. 2000, 'Salinity in marine atmospheric corrosion: its dependence on the wind regime existing in the site', Corrosion Science, 42, 91-104.

Meira, G. R. 2004, Chloride aggressiveness in marine atmosphere zone connected with corrosion problems in reinforced concrete structures, PhD Thesis, Federal University of Santa Catarina, Florianópolis (In Portuguese).

Meira, G. R.; Andrade, C.; Alonso, C.; Padaradtz, I. J.; Borba Jr, J. C. 2007, 'Chloride penetration into concrete structures in the marine atmosphere zone – relationship between deposition of chlorides on the wet candle and chlorides accumulated into concrete', Cement and Concrete Composites, 29, 667 – 676.

Mustafa, M. A.; Yusof, K. M. 1994, 'Atmospheric chloride penetration into concrete in semi-tropical marine environment', Cement and Concrete Research, 24(4), 661 - 670.

Nielsen, E. P.; Geiker, M. R. 2003, 'Chloride diffusion in partially saturated cementitious material', Cement and Concrete Research, 33, 133-138.

Nilsson, L. O.; Andersen, A.; Tang, L.; Utgenannt, P. 2000, 'Chloride ingress data from field exposure in a Swedish road environment' in. 2nd International RILEM Workshop on Testing and Modelling Chloride Ingress into Concrete, eds. C. Andrade C, J. Kröpp, RILEM, Paris.

Saetta, A. V.; Scotta, R. V.; Vitaliani, V. 1993, 'Analysis of chloride diffusion into partially saturated concrete', ACI Materials Journal, 90, 441-451.

Tang, L.; Nilsson, L. O. 1996, 'Service life prediction for concrete structures under seawater by a numerical approach', in Durability of Building Materials and Components, ed. Sjöström, E & FN Spon, London, pp. 97-106.

Tuutti, K. 1993, 'The effect of individual parameters on chloride induced corrosion', in Chloride Penetration into Concrete Structures, ed. L O Nilsson, Göteborg, Sweden.

XII DBMC
International Conference on Durability of Building Materials and Components
PORTO - PORTUGAL, April 12th-15th, 2011

Wireless in Situ Measurements of Moisture Content and Temperature in Timber Constructions

Karin Sandberg[1]
Anna Pousette [2]
Simon Dahlquist[3]

ABSTRACT

The aim of this article is to report on experience from a continuous wireless in situ measuring system. Today more than 600 sensors have been installed in wooden structures (beams, posts) and buildings at several sites for various research projects in Sweden. In order to measure a large amount of data, a wireless monitoring system was chosen with gateway connected to a GSM modem that sends the information to an Internet-connected computer database from whence it is transferred to the users. A wireless system is a comparatively cheap system and is easy to install, since there is no need of wires. When the plans for continuous measurements started, this was a relatively untested system, and experience from large scale measurements was limited. The purpose of the measurements is to verify models for prediction of long-term durability of wooden structures and wooden buildings based on periods of surface wetting, on moisture conditions related to climatic loads, coatings, wood processing and design and from the position inside walls or floors. With wireless HygroTrac sensors, relative humidity can be measured in the range of 10% to 90% ±2.5%, temperature can be measured with an accuracy of ±0.5°C at 25°C and moisture content in the range of 8% to fiber saturation point (FSP) ±1%. After nearly two years of measuring with the wireless system, the following experience was gained: the sensors was easy to set up and build in, some problems with the operation of the devices and the need for restarts after power failures; the effective range from the gateway to the sensors needs to be depends on the individual building construction.

KEYWORDS

E Wireless sensors, Temperature, Moisture content, Relative humidity, In situ measurements.

[1] SP Technical Research Institute of Sweden (SP Trätek), Skellefteå, SWEDEN, karin.sandberg@sp.se
[2] SP Technical Research Institute of Sweden (SP Trätek), Skellefteå, SWEDEN, anna.pousette@sp.se
[3] SP Technical Research Institute of Sweden (SP Trätek), Skellefteå, SWEDEN, simon.dahlquist@sp.se

1 INTRODUCTION

Service-life assessments and life cycle costs are becoming gradually more important in the investment and planning of construction works. Durability is consequently essential for all outdoor structures where a long life is preferred to control costs. The ability of a construction to resist degradation depends on its materials and design, on maintenance and on the surrounding environment. For wooden structures in outdoor environments, such as bridge beams and columns, it is important for safety reasons to be able to determine when they can no longer carry the intended load and when actions are needed to repair damage. Decay reduces strength and is thus a factor to consider, but such other factors as cracks also influence service life. Large cracks can hold water and dirt that are favorable for the growth of microorganisms. A field test with beams and columns studies the effect of cracks and the prolongation of the life of structures [Pousette & Sandberg 2010].
There have been many attempts to make models to predict durability from different points of view. For instance, there are models based on laboratory tests to predict mould growth [Viitanen 1997a,] or decay [Viitanen 1997b]. Brischke & Rapp [2008] have a dose-response model based on fungal decay in field test sites above ground. To examine how geographic locations affect the construction, there are models that take climate data and exposure conditions into consideration as well [Isaksson *et al.* 2009, Viitanen *et al.* 2010, Häglund *et al.* 2010]. Van de Kuilen [2005] has made service-life predictions from existing structures. Foliente [2002] gives an overview of different approaches to durability design in wood construction and describes an Australian approach to developing an engineering tool as a method for durability design.

Woodbuild is the name of a research program in Sweden with the goal of developing engineering tools that can be used in the planning and design of timber structures with regard to service life. These tools will be based on computational models. The long-term durability of wooden structures depends mainly on moisture conditions in combination with temperature and exposure time. Climatic data and exposure conditions will be used as input in the models to calculate moisture content and risk of decay. The purpose of the in situ measurements is to verify such models for many different situations based on the duration of surface wetting, moisture conditions dependent on climatic loads, coatings, wood processing and design and the position inside walls or floors.
To verify models or provide a basis for assumptions, measurements on real test items may be necessary. In situ measurement tends to be difficult and expensive. For the purpose of making numerous measurements, a wireless system can be an alternative because it is cheap and the test objects can be transported with the probe inside, thus avoiding a tangle of wires. The disadvantages are that these systems have not been thoroughly tested on a large scale, nor is it certain how well the technologies withstand weather conditions and use. Today, more than 600 sensors have been installed in wooden structures (beams, posts) and buildings at several sites for different research projects in Sweden. In order to cover as many parameters as possible, there will be many measurements. In order to capture a large amount of data, a wireless system was chosen. To keep track of all the data, they are registered in a database. This is the first time this system has been used on this scale, which would have been impossible just a few years ago. But the developments of sensors together with access to GSM and internet have changed that. The aim of this article is to share experiences and solutions to difficulities that might arise during continuous measurement of moisture content (MC), relative humidity (RH) and temperature (T) with a wireless on-site measuring system.

2 MATERIAL AND METHODS

For continuous measurement of moisture content (MC,%), relative humidity (RH,%) and temperature (T,°C) in wood constructions, wireless sensors and the OmniSense Facility Monitoring System (FMS**)** [OmniSense 2010] were used. The sensors send measured values to a gateway connected to a broadband socket or GSM modem that sends the information further to an Internet-connected

computer database. Through a website, data were transferred to a private database, and then measured data were compensated for wood species and temperature and transferred to the researchers or users.

2.1 Sensor

Protimeter HygroTrac sensors S-900-1 from General Electric [General Electric 2010] were used for registering MC, RH and T. The sensor dimensions are length 60 mm, width 30 mm and height 60 mm. The sensors have a lithium battery with 15 years' nominal battery life when reporting hourly. Transmission frequency was 868 MHz (EU). All sensors were delivered with a unique ID number for identification in the database.

The sensors measure relative humidity (RH) from 0% to 100% (noncondensing) with an accuracy of ±2.5% in the range of 10% to 90%. The range of temperature measurement is from -40°C to 85°C, with an accuracy of ±0.5°C at 25°C. In this case, the sensors have been controlled by OmniSense [OmniSense 2010] using an ESPEC LTU-112 humidity chamber and a General Eastern Optica chilled mirror reference. The sensors have been tested at 25°C and RH 50% and 85% to verify that they meet or exceed their specified accuracy of RH ±2.5%. The measurement range for moisture content was from 8% to fiber saturation point (FSP) with an accuracy of ±1%. The values are not correct for wood species, but are for temperature. Above FSP, there are values that showed some dissolution, but these have not been calibrated.

Measurements have been performed at the surface and at depths of 5 mm and 15 mm into the wood. To make it possible to measure the moisture content at different depths, the original screws were replaced with stainless steel nails (see Fig 1a). These nails were provided with shrink tubing as insulation to mimic the much more expensive gauge used with hand-held electrical moisture meters. The nails used were 35 mm long and had a diameter of 2.5 mm. The tip design was similar to the special measuring gauges and the tip had a depth of contact of 3 mm.

The sensors for surface moisture measurements have been equipped with ring terminals that have been attached to the surface with plastic clamps (see Fig.1b).



a)

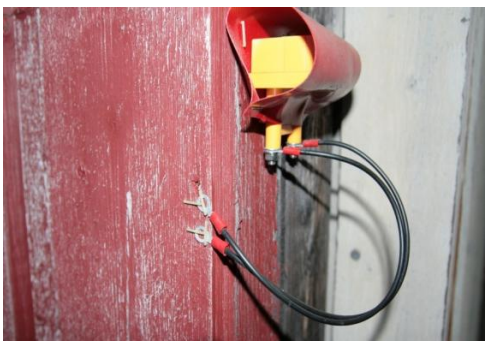

b)

Figure 1. a) HygroTrac sensor nail b) Ring terminals that have been attached to the surface with plastic clamps.

2.2 Data Transmission

In this work, each measurement point contained three values: T, RH, MC. The sensors were activated once an hour, and they sent data to a gateway FMS G-900-E from General Electric [General Electric

2010]. The distance between sensors and the data acquisition gateway was about 50 to 100 m. Fig. 2 shows the data distribution system used.

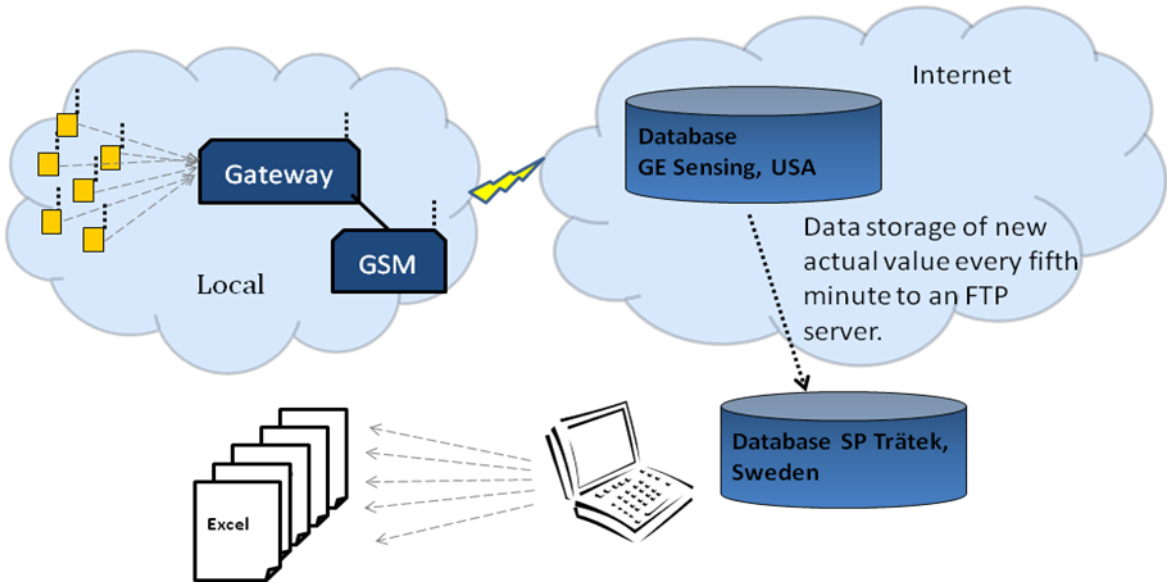

Figure 2. Data distribution schema. Data were transferred from wireless sensors to a gateway that collected and sent data to GE Sensing database through GSM. From the central database, data were sent to a local database where measured data were compensated for wood and temperature and sent via email to the user.

The data-acquisition gateway buffered data from the HygroTrac sensors and delivered measurements to a database provided by the manufacturer via local area network (LAN) when online. The LAN was connected to the Internet via Option GlobeSurfer X.1 Wi-Fi Cradle [Dustin 2010] using the 3G mobile connection standard. The sensors entered energy-saving mode between each transmission. Every 5 minutes, new measurements were exported as an xml file to an FTP server provided by SP. Data from these xml files were inserted into a private database specially developed by SP Trätek (SP Technical Research Institute of Sweden). In the SP Trätek database, additional parameters such as wood species, measurement depth, the four cardinal points, placement in wall, system of beams, floor, roof, *etc.*, were specified for each sensor. The sensors are searchable in the database due to these different parameters. Moreover, it is possible to attach drawings and photos to sensor data that show the orientation and location of the sensors.

When measured data were exported from the SP Trätek database to a user (researcher), each wood humidity value was compensated for wood species, *i.e.*, pine (*Pinus sylvestris*) and spruce (*Picea abies*) and for temperature according to Samuelsson [1990]. The values from surface moisture measurements were not compensated for wood species.

3 RESULTS AND DISUSSION

3.1 Assembly

The data transmission includes a chain of events as shown in Fig. 2. The wireless sensors offer great benefits during installation and make it possible to easily set up and follow the construction sets during manufacturing. Since there are no wires, the sensors can be built into and transported within the wall, and there is no need to have wires through the weatherproofing layer or the surface coat. **Fig. 3a** shows a sensor installed inside a wall at the factory on a wall stud under an opening for window. Fig. 3b shows installation of sensors on a roof joist at a building site.

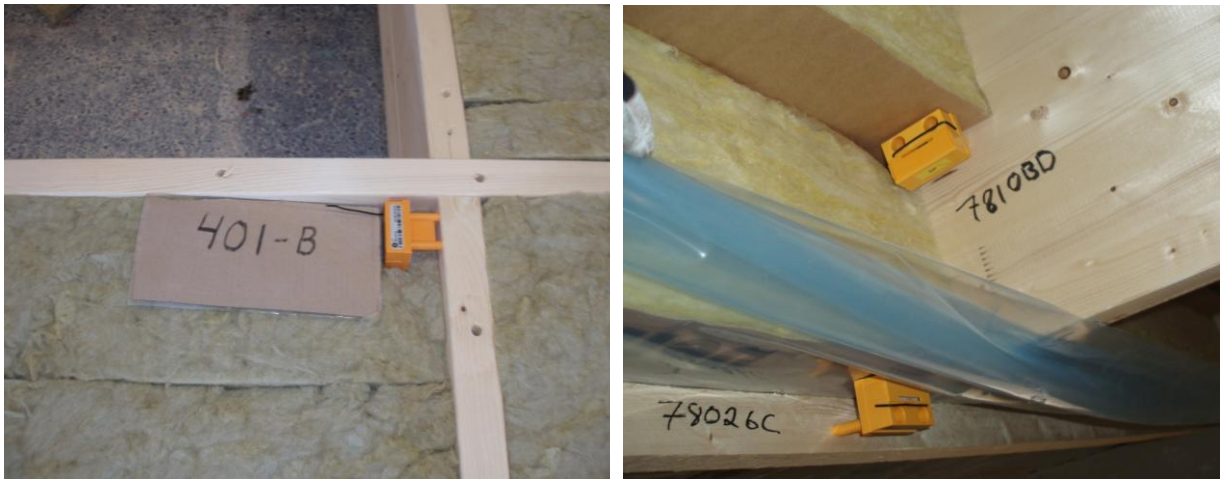

Figure 3. a) Installation of a sensor inside wall b) Installation of two sensors in a roof.

Measurement in situ requires careful planning and flexibility. There are many factors to take into account: changes in planning schedules on the building site or at the house factory; accessibility people with the expertise to install the sensors; the place to put the sensor might be available only for a short time before it becomes closed in or the scaffold moved so that the location for installation of a sensor becomes impossible to reach; sensor installation might be forgotten due to misunderstanding or time pressure in the production; *etc*.

3.2 Sensors

A reference block for electric moisture meter was used to control the sensor reliability. The block consists of four resistors that correspond to the resistance of spruce at different MC. These are MC 10.8%, MC 16.1%, MC 19.8% and 25.9% MC. Fig 4 shows sensors measured resistances for each MC during three months.

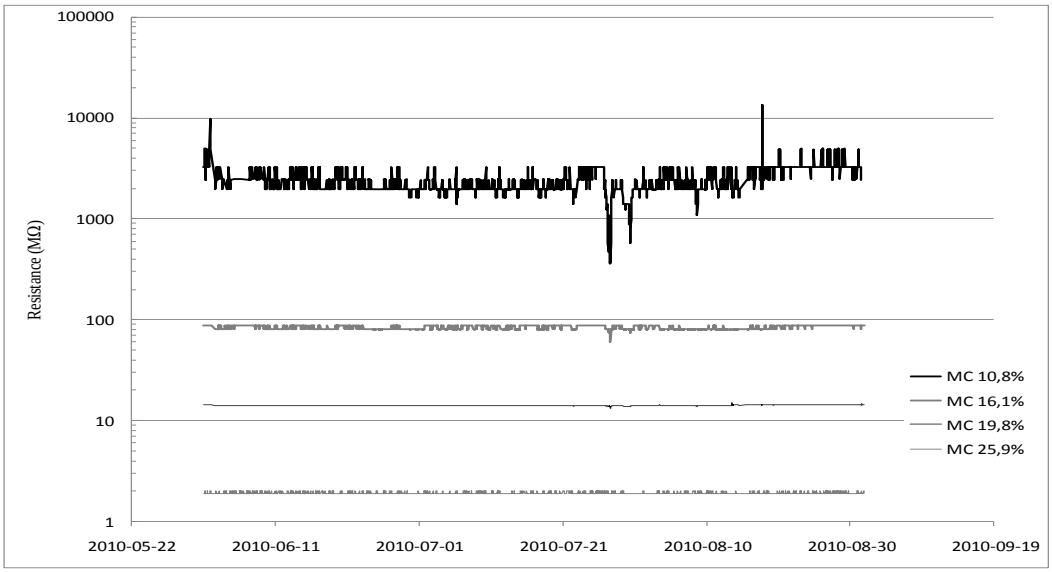

Figure 4. Resistance measured at reference block for spruce at MC 10.8%, 16.1%, 19.8% and 25.9%.

3.3 Loggers and Antennas

After installation of the system, signals from some sensors were not picked up by the gateway, *i.e.*, the range was limited by certain building structures. The problem was solved by using more loggers and /or additional antennas. One must also consider where to place the gateway (practicability of location, availability of power, *etc*.) which may not always coincide with the optimal location to reach sensors. By replacing the original antenna to a splitter with two antennas, horizontal and vertical polarization of the signals from the sensors can be caught up in a better way. The variable polarization is due to the fact that the issue of antennas in the installation was not addressed in terms of final position in the design.

3.4 Reliability of Service

As long as the gateways have power, they collect and store data from the sensors, but the collection of logged data is dependent on the GSM network and the Internet working. They are, unfortunately, not completely stable and may require visits to the site to reboot the system. Continuous follow-up of data collection will, however, minimize this. Usually data were retrieved once a month, which means that losses due to communication dropouts could be up to 4 weeks. When the Internet is not accessible, data cannot be retrieved, and the modem must be restarted manually on site. A timer, FailureGlobe Surfer, that restarts automatically once every 24 hour was used to minimize the need for visits to the location to manually restart the logger.
Power supply to the measuring system can be affected by thunderstorms, which can disrupt communications gateways, and data can be lost if the power goes off. At the building sites, when the houses were constructed, power failures were common. Also, disconnection of the logger due to builders' need for power outlets occurred, after which the logger might not be plugged in again.
Battery failure of sensors might occur, especially for the ones installed on outdoor constructions exposured to large changes in temperature compared the ones installed within walls where the temperature changes are smaller. If the sensors are accessible, the battery can be replaced. Fig. 5a shows sensors that failed after cold and snowy weather. For installation on facades, beams, *etc*., the yellow sensors were protected and hidden behind sheet metal or plastic covers painted in the same color as the specimen.



Figure 5. a) A beam with sensors after cold and snowy weather. b) Installation on a façade, sensor behind sheet metal painted in the same color as the wall.

3.5 Future Work

Future work is to calibrate and verify the moisture measurements above FSP.

4 CONCLUSIONS

Wireless sensors can be used for measuring MC, RH and T in the field even when the number of measuring points is large. This technology has never been used to such a large extent before, and therefore new experiences were gained. This means that we have discovered flaws in the system and taken care of them. The positive aspects of this wireless system are:

• It is easier to set up many wireless sensors than it is to set up wired sensors.
• It is possible to build in sensors for measurements inside constructions (balcony, joist, beam, post, *etc*.) without any damages on weatherproofing layer and surface coat.
• Sensors can be installed inside walls during their construction at house-building factories and transported to the building site without any additional installation needed on site.
• Measurement at mobile constructions is possible.

Difficulties that may occur:

• Temporary data losses may occur (power down, wireless connection blocked, sensor-battery failure, lighting damage, *etc*.).
• Unsecure power supply at building sites.
• Equipment demands manual service on site.
• Hard outdoor climate puts higher demands on the equipment.

ACKNOWLEDGMENTS

This project is part of WoodBuild, a research program within the Sectoral R&D Program 2006-2012 for the Swedish forest-based industry. This Program is jointly funded by the government, industry and other stakeholders with interests related to the Swedish forest-based industry.

REFERENCES

Brischke, C. Rapp, A.O. 2008, Dose-response relationships between wood moisture content, wood temperature and fungal decay determined for 23 European field test sites, Wood Science and Technology 42:507–518.

Dustin 2010, http://www.dustin.se

Foliente, G.C., Leiceste, R.H., Wang, C., Mackenzie, C., Cole, I.,2002. 'Durability design for Wood Construction', Forest Products Journal, Vol 52. No 1.

General Electric 2010. http://www.ge.com

Häglund, M. Isaksson, T. Thelandersson, S. 2010. Onset of mould growth-the effect of climate variability and different geographic locations. IRG paper IRG/WP 10-20446 .

Biaritz. France 9–13 May, 2010.

Isaksson, T. Thelandersson, S. Ekstrand-Tobin A. Johansson P. 2009. 'Critical conditions for onset of mould growth under varying climate conditions, Building and Enviroment 45 (2010):1712–1721.

OmniSense 2010. http://www.omnisense.com, E-mail: info@omnisense.com

Pousette A. Sandberg K. 2010. 'Outdoor tests of timber beams and columns', Proc. International Conference on Timber Bridges, ICBT2010, Lillehammer, Norway, 12-15 September, 2010, pp 169-178.

Samuelsson, A. 1990. Resistanskurvor för elektriska fuktkvotsmätare, TräteknikCentrum, Rapport L 9006029, Stockholm.

van de Kuilen J-W G. 2005. 'Service life modelling of timber structures', Materials and Structures, DOI 10.1617/s11527-006-9158-0.

Viitanen, H 1997a. 'Modelling the time factor in the development of mould fungi in wood - the effect of critical humidity and temperature conditions', Holzforchung 51 (1):6–14.

Viitanen, H. 1997b.'Critical time of different humidity and temperature conditions for the development of brown rot decay in pine and spruce', Holzforchung 51 (2):99–106.

Viitanen, H, Toratti, T, Makkonen, L, Peuhkuri, R. Ojanen, T. Ruokolainen, L.& Räisänen J. 2010. 'Towards modelling of decay risk of wooden materials', European Journal of Wood Product 68:303–313., DOI 10.1007/s00107-010-0450-x.

XII DBMC
International Conference on Durability of Building Materials and Components
PORTO - PORTUGAL, April 12th-15th, 2011

Corrosion of Nails in Weathered Timbers

Zhengwei Li [1]
Nick Marston [2]
Mark Jones [3]

ABSTRACT

This study investigated the influence of natural weathering on the aggressivity of timbers treated with copper-containing preservatives towards metals. Nails made of mild steel and hot dip galvanised steel were inserted into timbers that had been exposed at the BRANZ's Judgeford exposure site for one and two years. The assemblies were then exposed to an atmosphere of 49°C and 90% RH for 30 days. Corrosion rate, expressed as thickness reduction (mm/year), was derived from mass loss measurements. It was found that the corrosivity of the weathered timbers was related to both the natural weathering time and the preservative retention level. No simple correlation of corrosivity change with time was observed. The underlying mechanisms are briefly discussed.

KEYWORDS

Corrosion, Timber, Weathering.

[1] BRANZ Ltd, Judgeford, Porirua City, Wellington, New Zealand, Zhengwei.Li@branz.co.nz
[2] BRANZ Ltd, Judgeford, Porirua City, Wellington, New Zealand, Nick.Marston@branz.co.nz
[3] BRANZ Ltd, Judgeford, Porirua City, Wellington, New Zealand, Mark.Jones@branz.co.nz

1 INTRODUCTION

Timber is used extensively in the building industry despite competition from ceramic, metallic and polymeric materials. Timber and metal are compatible in most construction. However, susceptible timber-metal interfaces can be attacked by corrosion and lose their integrity, leading to premature failure of structures. Moisture in timber is fundamental to corrosion. Above the critical level, 18-20%, appreciable corrosion of chemical and/or electrochemical natures will be initialised. Chemicals used for timber preservation could be another corrosion hazard [Baker 1987]. Most water-borne preservatives do increase the aggressivity of timbers because their chemically active metallic ions can act as an added oxidizer for galvanic corrosion. Preservatives and natural chemicals in timber act synergistically to create a unique corrosive environment.

Copper chromate arsenic (CCA) has been the most widely used water-borne preservative [Preston 2000]. Its primary drawback is the perceived human health issues associated with arsenic and hexavalent chromium [Hingston *et al*. 2001]. Non-chrome and non-arsenic alternatives to CCA, such as alkaline copper quaternary (ACQ) and copper azole (CuAz), have then been developed [Freeman & McIntyre 2008]. The major concern however is their considerably higher copper contents compared with CCA, which contribute to higher corrosion risk of metallic components [Kear *et al*. 2009].

When exposed to the weather, timbers will suffer from slow degradation induced by biological, chemical, mechanical and/or photochemical factors [Illston & Domone 2001]. These will result in color change, surface fibre loss and erosion, wood structure degradation, checking and raised grain development [Williams 2005]. More importantly, wetting and drying cycles will affect the state of the water soluble components of the preservatives. Since timbers represent a unique micro-climatic environment for corrosion, a clear understanding of the potential effects of weathering on the performance of metallic components would be helpful in rational selection of materials for retrofit and establishment of property maintenance schemes. In this work, the corrosivity of several treated timbers was tested after one and two years of atmospheric exposure using embedded nails and an accelerated testing methodology. The objective was to understand how natural weathering processes will affect the aggressivity of the timbers treated with copper-containing preservatives, e.g. CCA, CuAz and ACQ at H3 and H4 levels.

2 EXPERIMENTAL

An embedded fastener test developed by other workers was used in this study [Kear *et al*. 2005]. This methodology aims to create an aggressive environment that can provoke corrosive interactions between the fastener, the high humidity atmosphere and the treated timber. The weathered timbers were collected from the structures exposed at the BRANZ's Judgeford site. Another set of timbers were stored in the lab at constant temperature and humidity. These timbers were cut into blocks of 40×40×90 mm with the longest dimension parallel to the wood grain. The blocks were moisture equilibrated at 49°C and 90% RH for 30 days. Mild steel and hot dip galvanised nails were then manually hammered into the timber blocks through pre-drilled guide holes. The assemblies were immediately returned to the environmental chamber at 49°C and 90% RH for another 30 days.

After exposure, the surfaces of the retrieved nails were characterised using visual and microscopic techniques. Removal of corrosion products was achieved following ASTM G1 recommendation [ASTM G1]. The mass losses were measured to calculate corrosion rate.

3 RESULTS

3.1 Timber Moisture Content

The moisture contents for a selected range of timbers after moisture equilibration at 49°C and 90% RH for 30 days were measured according to the recommendations of AS/NZS 1080.1:1997 [AS/NZS 1080]. The results are shown in Fig. 1. The timbers after one-year weathering had a higher moisture

content than those stored in the lab, this trend was not reproduced by timbers after two years of natural exposure or lab storage. Natural weathering appeared to decrease the ability of timbers to absorb moisture since current measurements showed that the timbers exposed for two years had a slightly lower moisture content than those exposed for one year. However the difference of moisture content between these timbers was not large, typically ranging from 0.3 to 2.2%.

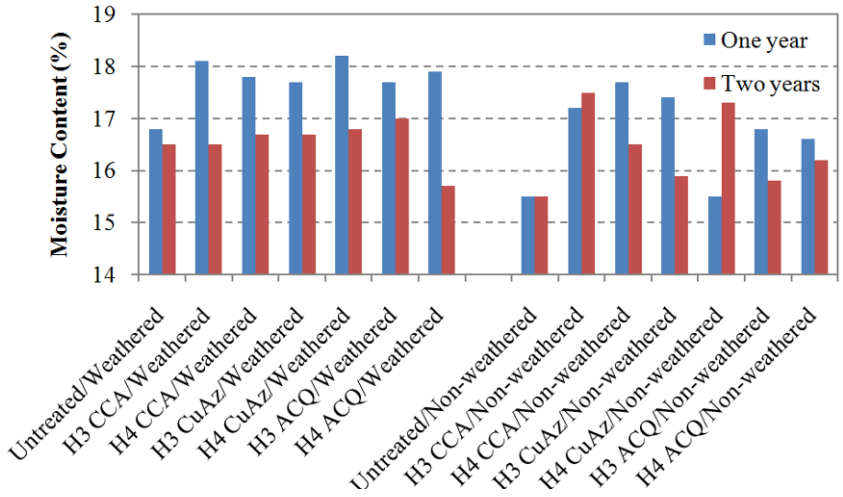

Figure 1. Moisture content of timber blocks after equilibration at 49°C and 90% RH for 30 days.

In addition, no noticeable trend of moisture content as a function of preservative type and hazard level was found in present study.

3.2 Corrosion Test

3.2.1 Mild steel nails

In the weathered timbers, the change in the corrosion rate of mild steel nails with natural exposure time was related mainly to the preservation hazard level (Fig. 2). At an H3 level, the nails inserted into the treated timbers after two-year weathering had a lower corrosion rate than those in the timbers after one-year weathering. The corrosion rates in CCA, CuAz and ACQ treated timbers exposed for two years were 41%, 70% and 37% of those for timbers exposed for one year, respectively. At an H4 level, the corrosion rates in the timbers exposed for two years were similar or slightly higher than those for timbers after one-year exposure. The nails in the untreated timbers after two years weathering had a much lower corrosion rate than those in the timbers after one-year weathering.

The experimental observations also demonstrated that timbers treated with ACQ to an H4 level were more aggressive than CCA treated timbers after two-year natural exposure. This is similar to the findings from tests using freshly treated timbers (after 1-3 months of fixation). However the corrosivities of the timbers treated with CCA and CuAz were not very different after weathering.

For timbers stored in the constant climate lab, the effect of storage time on their corrosivity was straightforward. Mild steel nails in all timbers (treated and untreated) after two years storage had a lower corrosion rate than those in the timbers after one-year storage (Fig. 3).

A comparison was also made between the aggressivities of the weathered and non-weathered timbers towards mild steel fasteners. The nails inserted into the one-year weathered timbers generally had a lower corrosion rate compared with those inserted into the timbers stored in the lab (Fig. 4). The only exceptions were the untreated and H4 CuAz treated timbers. It appeared that weathering increased their aggressivity towards mild steel. The nails inserted into the naturally weathered, untreated timber were measured to have a corrosion rate that was about ten times higher than those in the timber stored in the lab of constant climatic conditions.

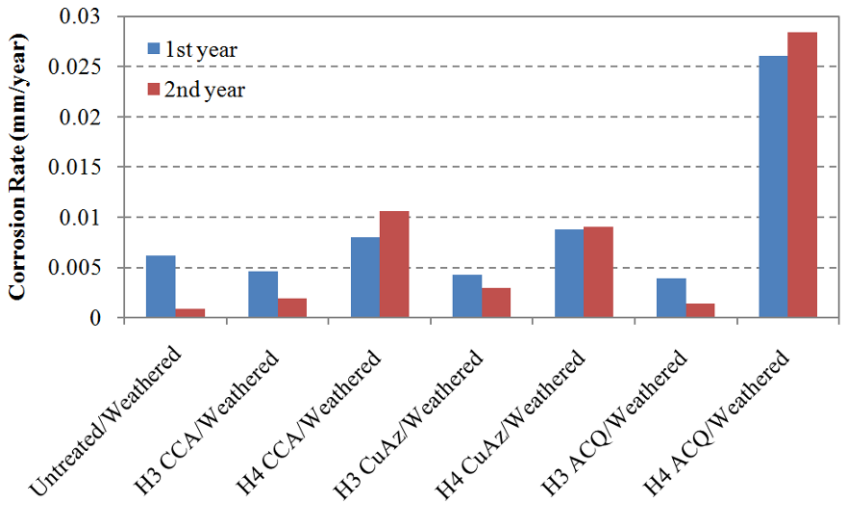

Figure 2. Corrosion of mild steel nails in timbers after one and two-years natural exposure.

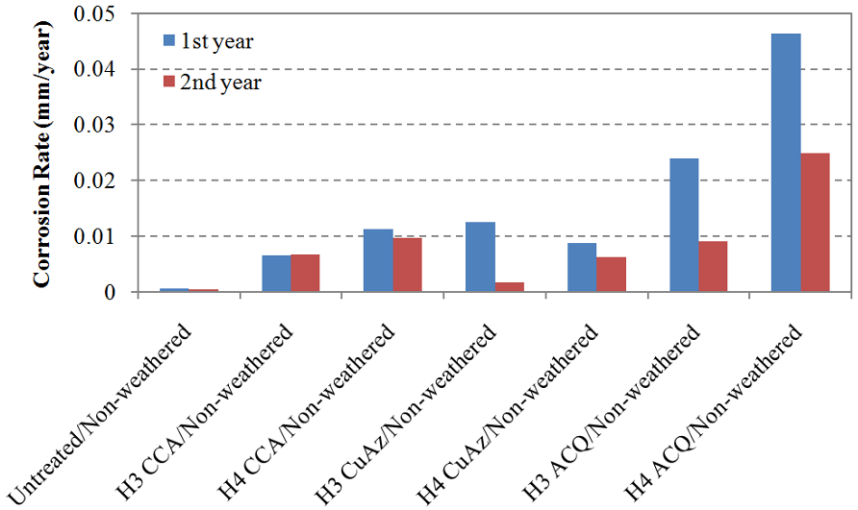

Figure 3. Corrosion of mild steel nails in timbers after one and two-years storage in the lab.

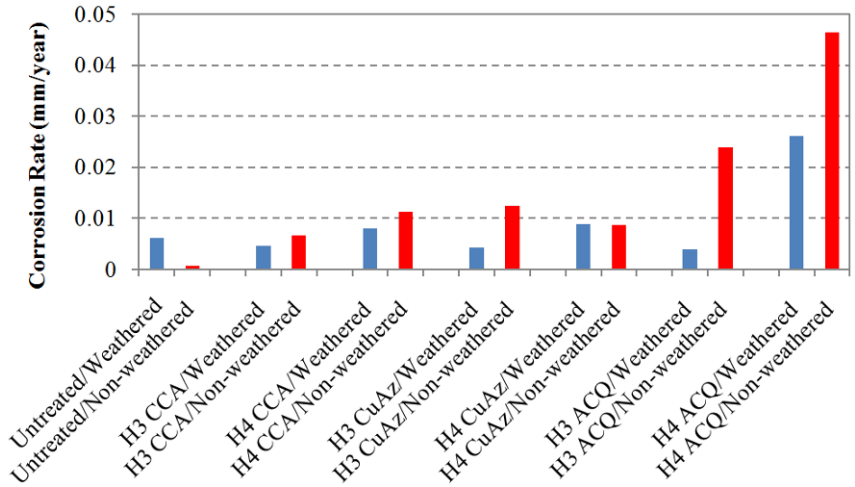

Figure 4. Corrosion of mild steel nails in timbers after one-year storage in the lab or after one-year weathering.

After two years, the comparative aggressivity of the weathered and stored timbers was variable (Fig. 5). For H3 CCA and H3 ACQ treated timbers, mild steel nails inserted into the weathered blocks exhibited a lower corrosion rate than those inserted into the lab stored blocks. For all other timbers, the opposite trend was observed, i.e. a higher corrosion rate was observed on the nail inserted into the weathered blocks. As for timbers after one-year exposure or lab storage, mild steel nails inserted into the weathered, untreated timber had a higher corrosion rate than those in the non-weathered, untreated timber under identical testing conditions. However, the corrosion rate in the weathered, untreated timber was only twice as high as that in the non-weathered untreated timber. This is much lower than that observed in the one-year test.

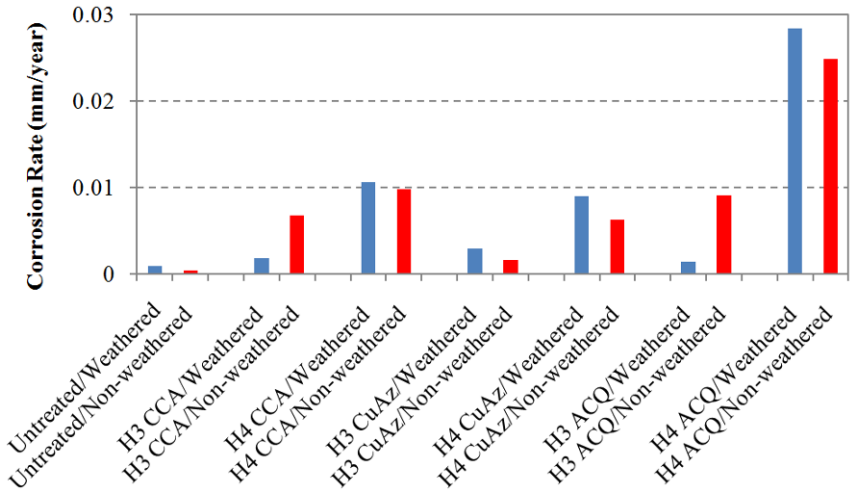

Figure 5. Corrosion of mild steel nails in timbers after two-years storage in lab or weathering.

3.2.2 Hot dip galvanised nails

The corrosion rate of the galvanised nails in the treated timbers was related to the weathering time and also to the preservation hazard level. This behaviour is similar to that observation in the tests using mild steel nails.

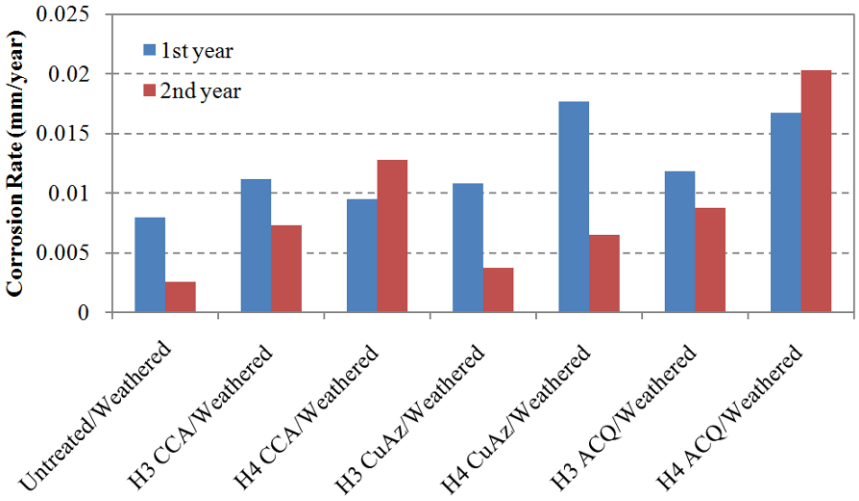

Figure 6. Corrosion of hot dip galvanised nails in timbers after one and two-years natural exposure.

At an H3 level, the corrosion rate in all two year weathered timbers was lower than that in timbers after one-year weathering. At an H4 level, the corrosion rate in CCA and ACQ treated timbers after two-years exposure was slightly higher than that found after only one-year exposure (Fig. 6). Within

this test regime, natural weathering processes decreased the aggressivity of the untreated timbers toward galvanised steel nails, evidenced by the lower corrosion rate obtained from the nails embedded into the timbers experienced two-years natural weathering. This was also similar to that observed with mild steel nails.

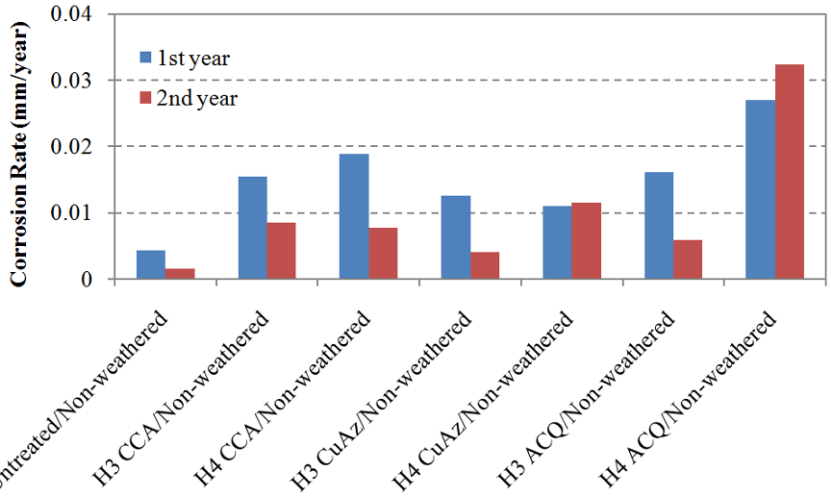

Figure 7. Corrosion of hot dip galvanised nails in timbers after one and two-years storage in the lab.

In most cases, the aggressivity of the treated timbers stored in the constant climate lab towards galvanised fasteners was decreased with storage time (Fig. 7). Lower corrosion rates were measured for the nails inserted into H3 CCA, H3 CuAz, H3 ACQ and H4 CCA. However, H4 CuAz and ACQ treated timbers stored for two-years, gave slightly higher corrosion rates (1.05 and 1.2 times).

One year natural weathering, decreased the aggressivity of most timbers compared with lab storage. This trend was much the same as that found with mild steel nails. The only exception was the H4 CuAz treated timbers. After two years, galvanised nails in most weathered timbers also exhibited a lower corrosion rate than those in the lab stored timber blocks. The exceptions were those timbers treated to H4 CCA and H3 ACQ.

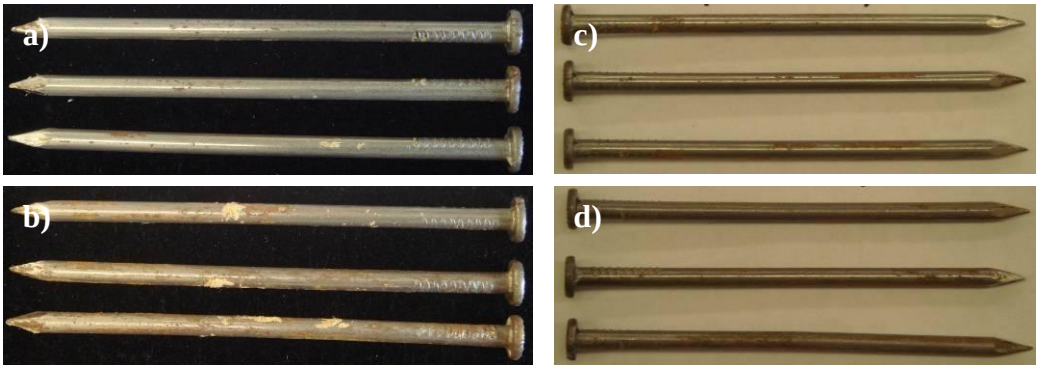

Figure 8. Surface morphology of mild steel nails in weathered (a, c) and non-weathered (b, d) H3 CuAz treated timbers. (a-b) after one-year expsoure and (c-d) after two-year exposure.

The weathering time and preservative retention have been found to be two important factors governing the corrosivity of the treated timbers. Since storage in a constant environment decreased the corrosivity of timbers, the comparative corrosivity of the weathered and non-weathered timbers was variable. This was supported by surface morphological characterisation. As shown in Fig. 8, iron-rich red rust covered a large portion of the surface of the mild steel nails inserted into the non-weathered H3 CuAz treated timbers while the nails in the weathered timbers showed limited rust formation and most of the surface was still metallic and glossy. After two years, the opposite was observed.

4 DISCUSSION

4.1 Untreated Timber

In the untreated timbers, contact corrosion by acids released from the hydrolysis of wood cellular structures is likely to be the governing mechanism. Exposure to ultra-violet light in solar radiation would degrade lignin, the photo-sensitive component in the middle lamella of the wood structure. Consequently, the hemicelluloses become more vulnerable to hydrolysis [Williams 2005]. Natural weathering also produces cracks and checks that provided easy pathways for the ingress of moisture [Evans *et al*. 2008]. Actually, the weathered, untreated timbers had a higher moisture content than the untreated timbers stored in the lab. A higher moisture content in the timber would promote corrosion through accelerated hydrolysis and increased conductivity. However, the amount of the photo-sensitive components in timber will decrease with time, gradually slowing down hydrolysis process and decreasing acid concentration. This in turn will lead to a lower aggressivity towards metals. This interpretation agreed well with the experimental finding which showed that steel in the timbers of exposure for two years had a lower corrosion rate than that in the timber exposed for one year.

4.2 Treated Timber

The present study demonstrates that long-term storage in a constant environment will decrease the corrosivity of the treated timbers studied. During storage in a dry atmosphere, volatile chemicals can escape and chemical/physical reactions are completed [Faherty & Williamson 1997]. This results in a higher degree of preservative fixation, thus a lower content of active components for corrosion.

However, the corrosivity of the weathered, treated timbers is governed by the exposure time and also the original preservative retention level in the timber. This behavior is believed to be mainly related with the dissolution, migration and loss of preservative components from the timbers. In the initial stage of natural exposure, the non-fixed components, especially those on the timber surface, would be washed away, lowering corrosivity. In extended exposures, physical defects would be generated, facilitating moisture ingress. This would change the state of the components of the complexed preservation chemicals and result in their hydrolysis/dissolution, diffusion and re-distribution in the treated timber [van der Sleet *et al*. 1997]. Wetting-drying cycles induced by precipitation and solar heating could drive some dissolved active species from the interior of the timber to the timber-metal interface. This would supply more materials for the corrosion process. However, some chemical species moved to the exterior surface would be lost, lowering the corrosion rate.

Obviously, the preservation retention can affect the dissolution and migration of chemicals in the treated timbers. A higher original content in timber gives a larger reservoir of the active species that can be dissolved and supplied during a longer period of exposure. This was partially supported by the observation that nails in the timbers treated to an H4 level and exposed natually for two years exhibited a higher corrosion rate than those in the timbers weathered for only one year. Thus the long-term corrosivity of the weathered, treated timbers will be largely determined by several processes in competition: mobilisation, diffusion and loss of the originally fixed preservative components.

5 CONCLUSIONS

Natural weathering decreased the corrosivity of untreated timbers and this is hypothesised to be mainly due to the gradual consumption of photo-sensitive components. However, weathered timbers exhibited a higher aggressivity towards steels than timbers stored in the lab since the weathering processes produced more physical defects for moisture ingress. A longer period of storage in a dry environment decreased the corrosivity of the treated timbers; this was mainly a result of enhanced fixation of preservation chemicals. The long-term corrosivity of the treated timbers was relatively complex and was controlled by the weathering time and also by the original preservative retention. Several competitive processes, appeared to be involved including dissolution, diffusion and loss of the preservation components originally fixed to the cellular structure.

The experimental results from this study offer some insight into the sensible selection of fastening materials for retrofit of already weathered timber structures. However, BRANZ believes that further research is required to achieve a better understanding of the corrosion behaviors of metals in weathered timbers. This will allow robust advice to be given to the New Zealand building industry for work involving retrofitting and renovating.

ACKNOWLEDGMENTS

This work was supported by New Zealand Building Research Levy.

REFERENCES

AS/NZS 1080.1:1997, Timber – Methods of Test, Method 1: Moisture content, Standards Australia, Sydney, NSW 2001, Australia; Standards New Zealand, Wellington 6020, New Zealand.

ASTM G1-03, Standard Practice for Preparing, Cleaning, and Evaluating Corrosion Test Specimens, ASTM International, United States.

Baker, A. 1987, 'Corrosion of metals in preservative-treated wood', Proceedings 47358: Wood protection techniques and the use of treated wood in construction, 28-30 October 1987, Memphis, TN. Madison, WI: Forest Products Research Society, pp. 99–101.

Evans, P., Urban, K. & Chowdhury, M. 2008, 'Surface checking of wood is increased by photodegradation caused by ultraviolet and visible light', *Wood Science and Technology*, **42**, 251–265.

Faherty, K. & Williamson, T. 1997, *Wood Engineering and Construction Handbook* (3rd ed.), McGraw-Hill, USA.

Freeman, M. & McIntyre, C. 2008, 'A comprehensive review of copper-based wood preservatives', *Forest Products Journal*, **58**[11], 6–27.

Hingston, J., Collins, C., Murphy, R. & Lester, J. 2001, 'Leaching of chromate copper arsenic wood preservatives: A review', *Environmental Pollution*, **111**, 53–66.

Illston, J. & Domone, P. 2001, *Construction Materials: Their nature and behavior* (3rd ed.), Taylor & Francis Group, London, New York.

Kear, G., Jones, M. & Haberecht, P. 2005, 'Corrosion of mild steel, HDG steel and 316 stainless steel in CCA, CuAz and ACQ treated pinus radiata', Proceedings of the 16th International Corrosion Congress, Beijing, China, 19-24 September 2005.

Kear, G., Wu, H. & Jones, M. 2009, 'Weight loss studies of fastener materials corrosion in contact with timbers treated with copper azole and alkaline copper quaternary compounds', *Corrosion Science*, **51**, 252–262.

Preston, A. 2000, 'Wood preservation', *Forest Products Journal*, **50**[9], 12–19.

Van der Sleet, H., Heasman, L. & Quevauviller, Ph. 1997, 'Harmonization of leaching/extraction tests', *Studies in Environmental Science*, **70**, 209–226.

Williams, R. 2005, 'Weathering of wood', in *Handbook of Wood Chemistry and Wood Composites*, ed. R.M. Rowell, Taylor & Francis, Boca Raton, London, New York, Singapore, pp. 139–185.

XII DBMC
International Conference on Durability of Building Materials and Components
PORTO - PORTUGAL, April 12th-15th, 2011

Study of Preconditioning Procedures for Absorption and Permeability of Concrete

J.P. Castro-Gomes [1]
D. Wang [2]
L. Pereira de Oliveira [3]
R.M. Ferreira [4]

ABSTRACT

The permeability and ability for capillary absorption of concrete are usually served as criteria for assessing the long-term performance (durability) of concrete. In order to know the long-term performance (durability) of concrete, the permeability or capillary absorption test is usually required. However, a long term preconditioning procedure prescribed in RILEM TC 116-PCD is unavoidable if one wants to carry out the permeability or capillary absorption tests. An attempt is made in this paper to address the possibility of simplifying the RILEM preconditioning procedure. The RILEM preconditioning method and a simplified preconditioning procedure were carried out on several sets of specimens which were cut from the same concrete slab. Thereafter, capillary absorption and gas permeability tests were carried out on these same specimens. Results of these two tests were compared between RILEM procedure and the simplified procedure and the results indicate that the two procedures provided similar results and as thus comparable to one another.

KEYWORDS

Capillary absorption, Gas permeability, RILEM preconditioning, Concrete durability.

[1] C-MADE Centre of Materials and Building Technologies, Department of Civil Engineering and Architecture, University of Beira Interior (UBI), Covilhã, PORTUGAL, castro.gomes@ubi.pt
[2] Department of Civil and Environmental Engineering, University of Macau, Macau SAR, China, astetndong@gmail.com
[3] C-MADE Centre of Materials and Building Technologies, Department of Civil Engineering and Architecture, University of Beira Interior (UBI), Covilhã, PORTUGAL, luiz.oliveira@ubi.pt
[4] University of Minho, Department of Civil Engineering, Campus de Azurém, 4800-058 Guimarães, Portugal, Phone +351 253 510 200/494, Fax +351 253 510 217, rmf@civil.uminho.pt

1 INTRODUCTION

According to the procedure given in RILEM TC 116-PCD, before carrying out gas permeability and capillary absorption tests, concrete specimens should first reach an intermediate average moisture concentration; this can be achieved by placing it in an environment of 75±2% RH and 20±1ºC, so that a uniform distribution of the evaporable water in the test specimens can be formed. The preconditioning procedure itself consists of a pre-drying step and a subsequent moisture redistribution phase and may take up to 35 days. Thus, it consists of a longer term conditioning period and offers a relatively complex preconditioning procedure. This however is unavoidable if a uniform moisture distribution in the concrete specimen is sought, as is specified prior to undertaking concrete absorption and gas permeability tests. [RILEM 1983].

An attempt is made in this paper to address the possibility of simplifying the RILEM preconditioning procedure. In this study, the RILEM TC 116-PCD and a simplified preconditioning procedure were carried out on several groups of concrete specimens cut from concrete slabs, of C20/25 compressive strength class, having aged 1 and 6 months. Capillary absorption and gas permeability tests were then carried out on these specimens [LNEC 1993], [LNEC 1993a], [Pereira et al. 2009]. Results of the capillary absorption and gas permeability carried out on groups of samples preconditioned according to the RILEM procedure and the simplified procedure were compared to determine if any differences were evident in the results when using either preconditioning method.

2 RILEM PRECONDITIONING PROCEDURE

2.1 Total Evaporable Water Content

According to the method given in RILEM TC 116-PCD, a specimen of each group should first be dried in an oven at 105ºC until the weight loss between two 24-hour intervals is less than 0.5g. The evaporable water content is then obtained as follows:

$$W_e = m_0 - m_d \tag{1}$$

Where W_e is the total evaporable water content [g], m_0 is the mass of specimen before the drying process [g], m_d is the mass of specimen after oven drying [g]. Then the evaporable moisture concentration w_e is calculated by:

$$w_e = W_e / m_d \tag{2}$$

2.2 Intermediate Equilibrium Moisture Concentration

After the specimen had been dried according to 2.1, it was then placed in a chamber (desiccator) and conditioned at of 75±2% relative humidity (RH) and 20±1ºC, until moisture equilibrium in the specimen was reached. The 75±2% RH condition was produced by a saturated solution of sodium chloride (NaCl) with excess solid salt in the solution. Equilibrium moisture conditions in the concrete was assumed when the difference between weights of specimens at two 24-hour intervals was less than 0.1g. The intermediate equilibrium water content at 75±2% RH, $W_{e,75}$ is given by:

$$W_{e,75} = m_{e,75} - m_d \tag{3}$$

Where $W_{e,75}$ is the mass of concrete at equilibrium with 75±2% RH [g],and m_d is the dry mass of concrete [g]. The intermediate equilibrium moisture concentration $w_{e,75}$ is calculated by:

$$w_{e,75} = W_{e,75} / m_d \tag{4}$$

to accelerate the drying and moisture absorption process and thus to hasten the procedure for determining the equilibrium moisture concentration of the specimen, the specimen was crushed into smaller pieces (with particle size less than 5 mm) [RILEM 1983].

2.3 Weight Loss for Each to-be-Tested Specimen During Pre-Drying

After obtaining w_e and $w_{e,75}$, one can then calculate the necessary weight loss for each specimen to be tested by:

$$\Delta m = \left(\frac{w_e - w_{e,75}}{1 + w_e} \right) m_0 \tag{5}$$

where m_0 is the mass of each specimen to be tested [g].

Attention should be paid to ensure that the small crushed pieces of specimen and the specimens to be tested should come from the same concrete slab, so one can assume that every specimen has the same initial water content. As well, during the process of determining the total evaporable water content of the specimen (2.1) and the intermediate equilibrium moisture concentration (2.2), the specimens to be tested should be sealed so that the same water content before pre-drying can be assured.

2.4 Pre-drying for Specimens to be Tested

All the specimens to be tested must be dried under a temperature of 50ºC in a ventilated oven until the difference between observed mass loss and the calculated mass loss (from 2.3) is less than 5%:

$$\frac{\Delta m_{obs} - \Delta m_{cal}}{\Delta m_{cal}} < 5\% \tag{6}$$

where Δm_{obs} is the observed mass loss during the drying process for specimens to be tested, and Δm_{cal} is the calculated mass loss to reach 75±2% RH in the specimens.

2.5 Moisture Redistribution

After the pre-drying phase, the evaporable water in the test specimen was the same amount as that in an environment of 75±2% RH, but the moisture content was not considered evenly distributed in the specimens. To achieve an even redistribution of moisture in the specimens to be tested, the specimens were sealed and then put in an oven at 50ºC for two weeks. Following this two week period, and after the specimens had cooled to room temperature, the gas permeability or capillary absorption test were carried out on the preconditioned specimens.

3. SIMPLIFIED PROCEDURE FOR ABSORPTION TEST

The RILEM procedure may provide an accurate moisture content which is the same as moisture under the environment of 75±2% RH in the specimens (actually, it is really hard to assure the specimens are really sealed during moisture redistribution period, mass loss can always be observed during moisture redistribution). However, the time to complete this process can be really long. For instance, cutting the specimens and natural drying for specimens can take 2 days. Then determining the intermediate equilibrium moisture concentration can take 4 or 5 days. Pre-drying for the specimens to be tested can take 3 or 4 days. Moisture redistribution will take two weeks. So totally, the conditioning for specimens needs 3 to 4 weeks or so. And, as obviously, long time of conditioning can reduce the

efficiency of research studies. Thus, several simplified procedures were applied in this study. Then the results of capillary absorption and gas permeability tests were compared to evaluate the possibility to use the simplified procedures as alternative to RILEM procedure.

3.1 Comparison Between Samples Preconditioned According to RILEM Procedure and Samples Without any Preconditioning.

Before carrying out the simplified procedures, a comparison between the samples preconditioned according to RILEM procedure and the samples without any preconditioning were made. The purpose of this comparison was to see whether there was an obvious difference in results if no preconditioning was carried out. Tests were carried out on concretes that had been aged for 1 month and 6 months, respectively. Results of capillary absorption tests, for a group of six specimens, are shown in Figures 1 and 2. From the information given in these two figures, it can be observed that the specimens which had been preconditioned have a higher capillary absorption than those without any conditioning. As well, concrete aged for 1 month has higher capillary absorption than concrete aged6 months. However, in the RILEM procedure, during the moisture redistribution period, an amount of 15 g and 11 g moisture loss were observed for the concrete aged 1 month and 6 months, respectively. So the absorption results may be affected by this loss of water.

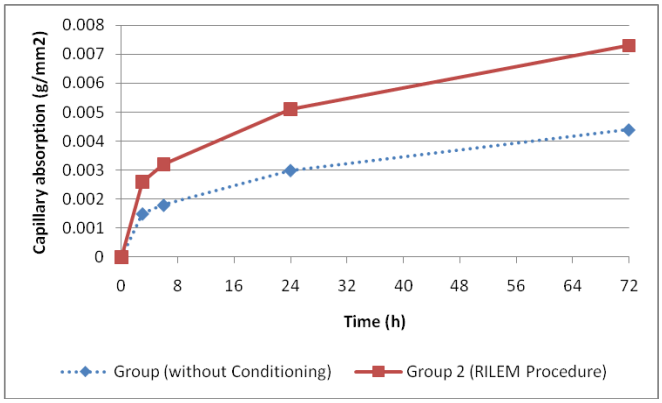

Figure 1. Capillary absorption test comparison between 1 month concrete with conditioning and without conditioning

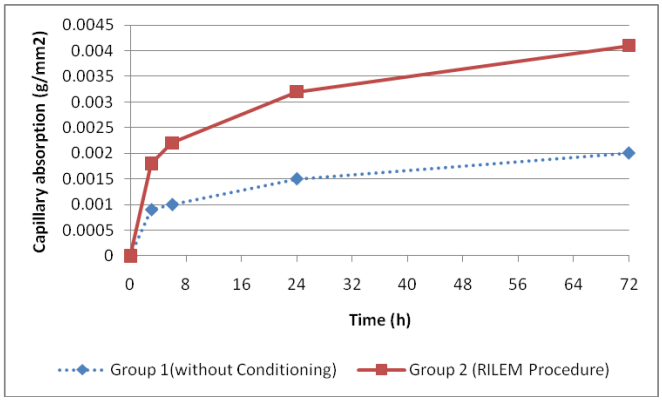

Figure 2. Capillary absorption test comparison between 6 months concrete with conditioning and without conditioning

3.2 Comparison Between RILEM Procedure and Simplified Procedure

Because too much moisture was lost during completing the procedures in section 3.1, a test was redone on the same specimens that had aged 6 months. This test was carried out after one month from those tested in 3.1. The results are shown in 3.2.1.

3.2.1 Simplified Procedure 1

After the specimens were placed in the laboratory for one month, the specimens that were not conditioned in 3.1 were put in a sealed box with 75±2% relative humidity for two weeks. And for the specimens that were pre-conditioned by RILEM procedure, they were immersed in water for half an hour and then dried until the mass reaches to the calculated pre-drying mass. And then they were sealed and put into oven with 50ºC, moisture redistribution for two weeks. Results of capillary absorption tests on these two groups of specimens are shown as in Figure 3. From this figure, one can see the capillary absorption for two groups are similar to each other, and the group with RILEM procedure has slightly higher absorption ability. However, the specimens pre-conditioned according to simplified procedure had been espoused in laboratory for one month. This is quite a long time. So new specimens were made and new tests were carried out on 6 months aging concrete as in 3.2.2 and 3.2.3.

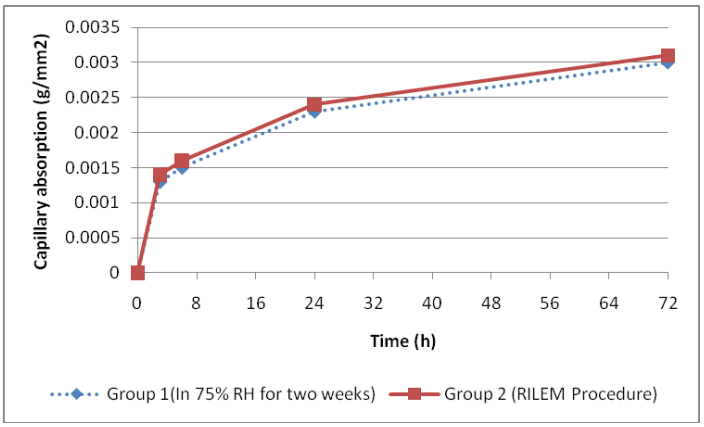

Figure 3. Capillary absorption test comparison between 6 month concrete for group 1: natural dried in laboratory for one month and then put in sealed 75%HR box for two weeks. Group 2:RILEM Procedure

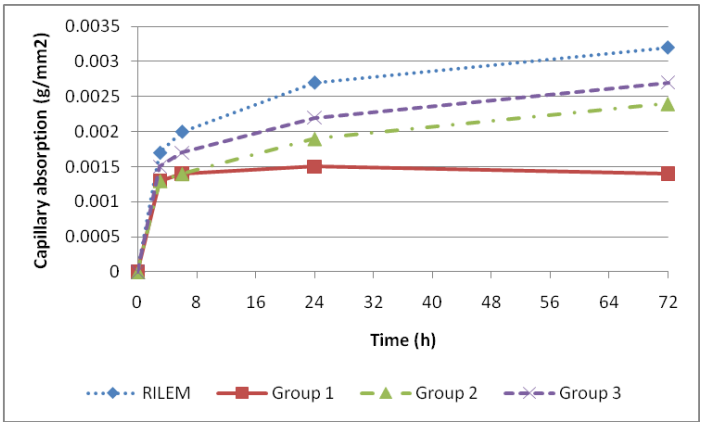

Figure 4. Capillary absorption test comparison between 6 month concrete for RILEM: conditioning according to RILEM procedure. Group 1: natural drying two days, 24 hours oven drying, 1 week 75% RH box, open space absorption test. Group 2: natural drying two days, 24 hours oven drying, 1 week 75% RH box. Group 3: 24 hours oven drying after cutting from concrete slab, 1 week 75% RH box.

3.2.2 Simplified Procedure 2

In this simplified procedure, specimens were naturally dried for 2 days after cutting from the concrete slab. Then they were put in a 50ºC ventilated oven drying for 24 hours. Then they were put in a sealed box with 75% RH for one week. Absorption test was carried out in an open space and in a sealed box, respectively. Specimens in the test carried out in an open space were denoted by group 1, and

specimens in the test carried out in a sealed box were denoted by group 2. In this study, all the absorption tests were carried out in a sealed box except for group 1 in this part.

3.2.3 Simplified Procedure 3

This procedure is similar to 3.2.2, except that the specimens were directly dried in the oven after cutting. That is, specimens were put in a 50ºC ventilated oven drying for 24 hours after cutting from the concrete slab, when it was totally wet. Then they were put in a sealed box with 75% RH for one week. Then absorption test was carried out. Specimens treated by this procedure were denoted by group 3. Capillary test results of these three groups and their comparison to RILEM procedure are shown in Figure 4.

Form Figure 4, we can see the capillary absorption ability of group 1 increases in the first 24 hours, then it decrease from 24 hours to 72 hours. Attention should be paid that the absorption test of group 1 was carried out in an open space (the laboratory) which has a RH about 50%. The mass of sample decreases from 24 hours to 72 hours might be due to the moisture that absorbed is slower than the moisture evaporate from the specimens. Considering the relative humidity in each laboratory is different, carrying out the absorption test in the sealed box is preferred.

Results of group 2 and group 3 have similar pattern to the result of RILEM procedure. But the specimens pre-conditioned according to RILEM procedure still have higher absorption ability. And group 3, in which specimens were put into oven immediately after cutting, has higher absorption ability than group 2, in which samples had been naturally dried for two days. This may due to the capillary effect in the void of concrete, if there is water in the surface of concrete, when it is dried in the oven, the evaporated water in the surface can form a negative pressure so that the inner surface water is attracted to the outer surface. Then much more water is evaporated, and higher absorption ability can be expected.

3.3 Summary

The absorption test should be carried out in a sealed box rather than in an open space because the relative humidity in each place can be different, and this variable environment can change the results obtained from the absorption test. The simplified procedure can provide similar results to RILEM procedure. However, a difference still exists. If the simplified procedure is to be used, the following one is suggested: the samples should be placed in a ventilated oven at 50ºC for 24 hours immediately after cutting the specimen from the slab (or immersed in water for half an hour if the samples were cast). The specimens should then be placed in a sealed box with 75% RH for one week. The absorption test can then be carried out in a sealed box. The absorption results with samples conditioned by this procedure can be smaller than the specimens conditioned by RILEM procedure. However, a coefficient of 1.18 can be multiplied so that the results by simplified procedure can match the results by RILEM procedure. However, further study for the value of the coefficient is still needed.

4. SIMPLIFIED PROCEDURE FOR GAS PERMEABILITY TEST

After comparing the absorption test results derived from specimens tested using the simplified procedure and the RILEM procedure, a similar comparative study was carried out for the gas permeability test.

Specimens for the gas permeability test were cut from a concrete slab that had been aged for 6 months. A column of concrete of 5 cm diameter was first cut and thereafter three samples of 4cm height were cut from this column. Hence, each sample had dimensions of 5 cm diameter by 4 cm high. The gas permeability of six groups of samples prepared in this manner was then tested and a comparison was made amongst the results obtained for the different groups. For each of the six groups

of specimens, three samples were located, respectively, in the upper, the middle, and the lower part of the concrete slab. After one day in natural drying conditions, the 6 groups of specimens were further conditioned as follows:

Table 1. Simplified conditioning procedure for gas permeability test of different specimen groups.

Specimen set	Designation*	Conditioning method	
		Drying	Moisture redistribution
Group 1	1T, 1M and 1B	RILEM procedure	RILEM procedure
Group 2	2T, 2M and 2B	24 hours in 50ºC ventilated oven	sealed container for one week at 75% RH and 25ºC
Group 3	3T, 3M and 3B	24 hours in 50ºC ventilated oven	sealed container for 2 weeks at 75% RH and 25ºC
Group 4	4T, 4M and 4B	24 hours in 50ºC ventilated oven	sealed container for 3 weeks at 75% RH and 25ºC
Group 5	5T, 5M and 5B	No oven drying	sealed container for one week at 75% RH and 25ºC
Group 6	6T, 6M and 6B	No oven drying	sealed container for 2 weeks at 75% RH and 25ºC

*T; M; B denote top, middle, and lower samples respectively

Each specimen was tested under an absolute pressure of 2.4 bars, and the time for a bubble traveling 10 cm in a graduated pipette was recorded [Pereira et al. 2009]. The permeability of the specimen was calculated by the following equation:

$$K = \frac{4.04vL*10^{-5}}{A(P_1 - 1)} \tag{7}$$

where υ is the flow, which can be read from the pipette [m^3/s], L is the specimen height [m], A is the cross section area of the specimen [m^2], p_1 is the test pressure [Pa].

The results of the 6 groups of specimens are shown below in Table 2. From Figure 5, one can see that there is a greater difference between the groups without oven drying (Group 5 and Group 6) and the RILEM procedure than the groups with 24 hours of oven drying. As well, for the groups that had been dried in an oven for 24 hours, given that the time for redistribution of moisture increases, the higher the expected permeability of the specimens. It can be seen from a comparison of results from group 2 to group 4, that the permeability of the specimens gets closer to that of the specimens in group 1, the group 1 specimens having been conditioned according to the RILEM TC 116-PCD procedure. In this instance, one can use the simplified procedure, as was demonstrated for group 4, to replace the RILEM procedure when testing the permeability of concrete samples. However, a coefficient of 1.08 is nonetheless needed to calibrate the results thus making the results from the different procedures comparable.

Table 2. Permeability results for each specimen [m^2].

Group / No. / Sample location	1	2	3	4	5	6
T	1.06×10^{-17}	3.20×10^{-18}	5.52×10^{-18}	6.07×10^{-18}	1.89×10^{-18}	1.90×10^{-18}
M	8.76×10^{-18}	3.25×10^{-18}	6.31×10^{-18}	5.73×10^{-18}	3.82×10^{-18}	2.61×10^{-18}
B	5.73×10^{-18}	3.48×10^{-18}	5.47×10^{-18}	1.14×10^{-18}	3.20×10^{-18}	2.76×10^{-18}
Average	8.36×10^{-18}	3.31×10^{-18}	5.77×10^{-18}	7.73×10^{-18}	2.97×10^{-18}	2.42×10^{-18}

From Table 1, one can see that permeability is related to the conditioning procedure and the location of the samples. However, the average permeability of each group can still be made to permit a comparison amongst the different conditioning methods and how these procedures would affect the permeability results. Hence the average permeability of each group was also calculated; results are shown in Figure 5.

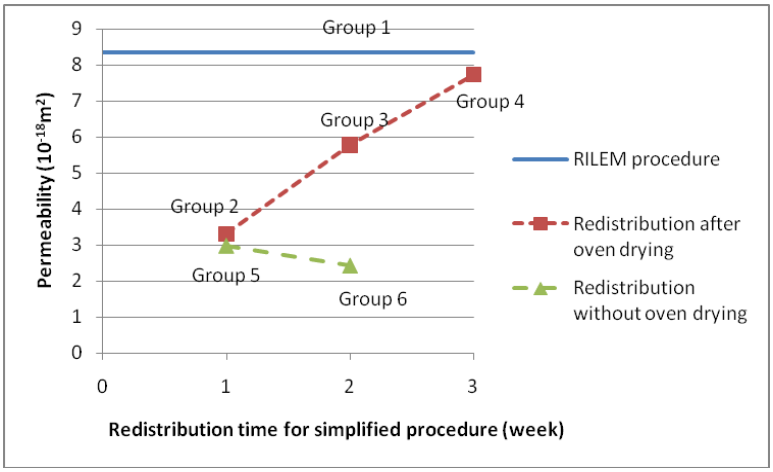

Figure 5. Permeability results for group 1: RILEM procedure. Group 2: Drying in oven for 24 hours, 1 week redistribution in 75% RH. Group 3: Drying in oven for 24 hours, 2 weeks redistribution in 75% RH. Group 4: Drying in oven for 24 hours, 3 weeks redistribution in 75% RH. Group 5: 1week redistribution in 75% RH without oven drying. Group 6: 2 weeks redistribution in 75% RH without oven drying.

5 CONCLUSIONS

In the study described in this paper, simplified procedures were sought for the pre-conditioning of specimens prior to undertaking standard concrete absorption and gas permeability tests. The samples for the simplified procedure and which had been dried in a ventilated 50ºC oven, and thereafter placed in a sealed box having 75% RH, showed similar values for concrete absorption and gas permeability to those specimens which had been conditioned according to procedure given in RILEM TC 116-PCD. For the absorption test, if the conditioning time is limited, one can condition the specimens according to the simplified procedure, which only takes two weeks, and then multiply the results by a coefficient, as provided in this study, to match the RILEM results. For the permeability test, one can condition the specimens as follows: drying in a ventilated 50ºC oven for 24 hours, then moisture redistribution in a sealed box having 75% RH for three weeks. Results of specimens conditioned by these respective procedures are comparable to results obtained using RILEM procedure.

REFERENCES

RILEM 1999, *RILEM TC 116-PCD, Permeability of Concrete as a Criterion of its Durability*, Materials and Structures/Materiaux et Constructions, Vol. 32, April, pp 174-179.

LNEC 1993, *E392, Concrete: Determination of the permeability to oxygen*, LNEC specification, Portuguese National Laboratory of Civil Engineering. Lisbon.

LNEC 1993a, *E393, Concrete: Determination of the absorption of water through capillarity*, LNEC Specification, Portuguese National Laboratory of Civil Engineering. Lisbon.

Pereira, C.N.G. & Oliveira, L.A.P. & Castro-Gomes, J.P. 2009, *Influence of natural coarse aggregates size, mineralogy and water content on the permeability of structural concrete*, Construction and Building Materials, Volume 23, Issue 2, February, Pages 602-608.

XII DBMC
International Conference on Durability of Building Materials and Components
PORTO - PORTUGAL, April 12th-15th, 2011

Effects of Ageing and Moisture on Dynamic Thermal Performance of ETICS Cladding

Bruno Daniotti [1]
Fulvio Re Cecconi [2]
Riccardo Paolini [3]

ABSTRACT

In this paper, we discuss the influence of ageing and increase of moisture content – achieved with accelerated laboratory exposure – on the thermal performances of External Thermal Insulation Composite Systems with rendering (ETICS).

We propose herein two types of dynamic test methods (non-standard methods), which were designed to assess time shift and decrement factor. With a first type of test, the exterior surface of the cladding, facing a climatic chamber, is exposed to a 24 h sinusoidal temperature forcing, while the conditions in the laboratory are stable. In a second test, the solicitation reproduces the sol-air temperature, to check the influence of temperature on time shift. Then, we discuss limits and improvements needed in the test method, and we present early results. Finally, we study the influence of uncertainty in values of material properties – namely thermal conductivity, density, and specific heat capacity – on time shift, decrement factor, and periodic thermal transmittance.

We note that, with ageing, the studied building component offered higher water absorption capability and, thus, the thermal resistance presented a decreasing trend, while an increasing trend was observed for heat capacity, and time shift. We conclude that a standard test procedure is necessary, including information about the duration of draining periods.

KEYWORDS

ETICS, Thermal admittance, Time shift, Decrement factor, Moisture.

[1] Politecnico di Milano, Building Environment Science & Technology Dept., Milano, ITALIA, bruno.daniotti@polimi.it
[2] Politecnico di Milano, Building Environment Science & Technology Dept., Milano, ITALIA, fulvio.rececconi@polimi.it
[3] Politecnico di Milano, Building Environment Science & Technology Dept., Milano, ITALIA, ric.paolini@gmail.com

1 INTRODUCTION

Exterior insulation cladding systems are a very common building technology – since the 1960s – both in Continental Europe (where they are usually applied to a masonry substrate and are called ETICS), and in North America (where they are usually applied on a wood frame and are called EIFS). Despite differences in terminology, and more relevantly, different building materials, exterior insulation cladding systems offer similar durability issues. The most relevant reported degradation modes are: mould growth, cracking over joints of insulation boards and blistering due to summer thermal shock, water absorption [Künzel et al. 2006; Hens & Carmeliet, 2002; and Daniotti & Paolini, 2005], and air leakages combined with wind driven rain; the latter is true especially for EIFS [Sahal & Lacasse, 2005]. In synthesis, the most relevant problems occur in presence of water (by itself or in synergy with other agents). Furthermore, increase in moisture content in the insulator affects all hygro-thermal performances.

Given the importance of moisture influence on degradation and hygro-thermal performances, several Heat and Moisture Transport (HMT) numerical studies have been performed to assess the response to moisture of exterior insulation cladding systems [e.g. Beaulieu et al., 2002; Zirkelbach et al., 2005]. However, software models are normally not able to cope with some phenomena (e.g. gravity), or they adopt simplifications, such as assuming a coefficient describing the percentage of water hitting the façade that does not bounce away from the surface (for walls, often assumed equal to 0.7). Sometimes, constraints are given by the lack of input data, for instance driving rain, especially with a sampling time shorter than one hour, or properties of interfaces between layers – relevant in heat and moisture transfer [de Freitas et al., 1996] – or of singular points. Actually, building details are the main points of penetration of rain in EIFS [Bronski, 2005]. Especially for ETICS, the main moisture flow takes place, beyond connections with other building components (e.g. windows), through joints between insulation boards [Barreira & de Freitas, 2005; Daniotti & Paolini, 2008b].

In the laboratory, with accelerated ageing and testing, we assessed ETICS cladding durability [Daniotti & Paolini, 2008a,b], comprising the survey of both degradation of the finishing system and evolution of the thermal performances. Early results, namely loss in thermal resistance, are offered in Daniotti & Paolini [2008b]. We introduce herein two types of test methods for assessing time shift and decrement factor, we discuss limits and improvements needed in the testing procedure, and we present results. Finally, we discuss the influence of uncertainty in thermal conductivity, density, and specific heat capacity on time shift, decrement factor, and periodic thermal transmittance (according to ISO 13786), later identified, respectively as φ, f_a, and Y_{12}.

2 THERMAL PERFORMANCE EVOLUTION WITH ACCELERATED AGEING

We performed, in the laboratory, accelerated ageing exposure on a 1 m^2 sample (Tab. 1) of an ETICS over masonry wall, including UV, freeze-thaw, and summer thermal shock cycles, grouped in macro-cycles as detailed in Daniotti et al. [2008]. Before ageing, and at each macro-cycle, we monitored degradation, and evolution of performances: thermal resistance; time shift (sine temperature curve forcing); thermal constants (solicitation: +20°C, +70°C, +20°C, each for 24 h); and a moisture response cycle (RH: 20%, 50%, 80%, then, rain; each step for 2 h).

2.1 Measurement of Thermal Resistance and Derived Moisture Content in Layers

Thermal resistance was measured, by means of ISO 9869 method, of main section profile, for the entire specimen, for substrate, and for ETICS. Data in table 1 and 2 refer to the sample non-aged (T0), and after exposure to two macro-cycles (T1, and T2). Condition T2+ concerns ageing time T2 after a rain cycle (1 lt m^{-2} h^{-1} for 2 hours). With a correction to the mean heat flow rate (using the storage effect method described in ISO 9869), we took into account for each layer both the thermal capacity when dry (labelled as *dry*) and the total thermal capacity, including moisture contribution (labelled as

wet). Then, we derived thermal resistance and water content of each layer from a numerical solution starting, from an estimate of moisture and thermal gradient in the sample.

Table 1. Estimated water content (w) and thermal conductivity (λ_{wet}) - derived considering water content - of the tested sample not aged (T0), after ageing (T1, T2, and T2+). In the calculation, we subdivide EPS in six layers of 1 cm.

n° Layer	*t [m]*	w_c *T0* [kg m^{-3}]	w_c *T1* [kg m^{-3}]	w_c *T2* [kg m^{-3}]	w_c *T2+* [kg m^{-3}]	$\lambda_{wet\ T0}$ [W m^{-1} K^{-1}]	$\lambda_{wet\ T1}$ [W m^{-1} K^{-1}]	$\lambda_{wet\ T2}$ [W m^{-1} K^{-1}]	$\lambda_{wet\ T2+}$ [W m^{-1} K^{-1}]
1 Gypsum	0.005	4.35	3.59	5.46	4.09	0.208	0.207	0.210	0.208
2 Plaster	0.015	33.53	29.92	39.28	29.96	0.913	0.901	0.932	0.901
3 Masonry	0.12	25.00	29.11	33.72	52.36	0.375	0.413	0.415	0.431
4 Plaster	0.015	49.38	61.56	54.72	66.3	0.966	1.007	0.984	1.023
5 Binder	0.003	62.52	61.56	54.72	66.35	1.010	1.007	0.984	1.023
6 EPS 1	0.01	5.00	5.00	5.00	5.00	0.0339	0.0335	0.0337	0.0337
7 EPS 2	0.01	7.50	10.00	15.00	20.00	0.0335	0.0334	0.0338	0.0339
8 EPS 3	0.01	10.00	15.00	20.00	37.50	0.0332	0.0365	0.0358	0.0382
9 EPS 4	0.01	12.50	17.50	25.00	40.00	0.0358	0.0371	0.0392	0.0435
10 EPS 5	0.01	15.00	20.00	27.50	42.50	0.0360	0.0374	0.0396	0.0435
11 EPS 6	0.01	23.59	22.36	29.83	43.04	0.0380	0.0378	0.0399	0.0436
12 Base coat	0.005	43.71	39.05	47.45	30.00	0.947	0.931	0.960	0.901
13 Top coat	0.0015	13.17	8.37	16.36	3.98	0.870	0.870	0.870	0.870

Table 2. Thermal performances of the tested sample not aged (T0), after ageing (T1, and T2), and at ageing time T2 after a rain cycle (T2+)

Thermal Performance		*T0 dry*	*T0 wet*	*T1 dry*	*T1 wet*	*T2 dry*	*T2 wet*	*T2+ dry*	*T2+ wet*	*unit*
Substrate resistance	$R_{cd,12}$	0.374	0.376	0.349	0.346	0.345	0.344	0.335	0.334	[m^2 K W^{-1}]
ETICS resistance	$R_{cd,23}$	1.716	1.725	1.699	1.684	1.642	1.640	1.556	1.553	[m^2 K W^{-1}]
Conductive resistance	$R_{cd,T}$	2.090	2.100	2.048	2.030	1.986	1.984	1.891	1.887	[m^2 K W^{-1}]
Conductance	Λ	0.479	0.476	0.488	0.493	0.503	0.504	0.529	0.530	[W m^{-2} K^{-1}]
Tot resistance	R_T	2.260	2.270	2.218	2.200	2.156	2.154	2.061	2.057	[m^2 K W^{-1}]
Transmittance	U	0.443	0.440	0.451	0.455	0.464	0.464	0.485	0.486	[W m^{-2} K^{-1}]
Substrate heat capacity	C_{12}	145.0	162.9	145.0	165.4	145.0	168.0	145.0	177.5	[kJ m^{-2} K^{-1}]
ETICS heat capacity	C_{23}	15.7	18.7	15.7	19.0	15.7	19.9	15.7	21.3	[kJ m^{-2} K^{-1}]
Tot heat capacity	C_T	160.6	181.6	160.6	184.5	160.6	187.8	160.6	198.8	[kJ m^{-2} K^{-1}]
Time shift SINa	ΔT	n.a.		10h 48’		6h 34’		n.a.		[h]
Time shift SINb	ΔT	n.a.		11h 07’		5h 54’		n.a.		[h]

2.2 Unsteady Thermal State Test Procedure

The sample was exposed (for two days to achieve harmonic periodic stabilised regime) to two types of tests to measure φ and f_a, namely:

- A sine wave reproducing the outdoor air temperature (SINa in fig. 1a) for Milano (Italy) the 21st July (peak yearly condition); and
- A curve reproducing the sol-air temperature with absorbance of the finishing coat set as 0.6 (SINb in fig. 1b).

Results for T0 (non-aged sample) are not available, since these tests were introduced only later. For high insulated samples, we acknowledge some issues in the measurement procedure, namely:

- With a low sinusoidal temperature wave (min 20°C, max 30°C) it is difficult to read φ, and f_a, since the very small thermal gradient between laboratory (20 ± 2°C) and climatic chamber;
- A non perfectly sinusoidal temperature wave representing the sol-air temperature has a higher maximum, but the same minimum value in solicitation, and the same problem in measuring f_a;
- Adopting higher values for the temperature waves, to enhance readability of the test, would alter the thermal properties of water, and the overall hygro-thermal response; and
- For well-insulated samples, it is difficult to measure f_a, since the error in estimation of results is of the same magnitude of the heat-flowmeter resolution. In our case, we could not read f_a.

Since these constraints, we adopted the selected testing solicitations, despite issues in readability of results. However, we stress upon the need of standardisation in terms of sensors resolution, laboratory conditions, curing time between tests, and complementary side tests to check the main measurement.

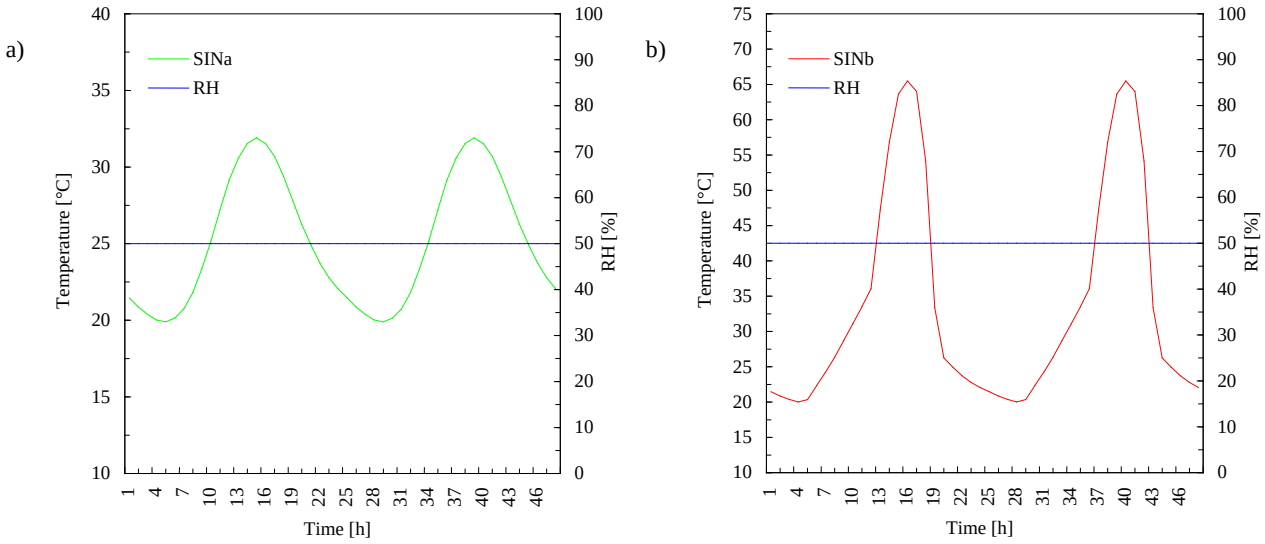

Figure 1. Test forcing for SINa (on the left) and SINb (on the right). Each sine solicitation is repeated for two days, so as to reach harmonic periodic stabilised regime

3 ERROR RISK ANALYSES

Given the risk of uncertainty in measurement results, and the risk of error in the calculation of dynamic performance due to uncertainty in input, we performed a risk analysis.

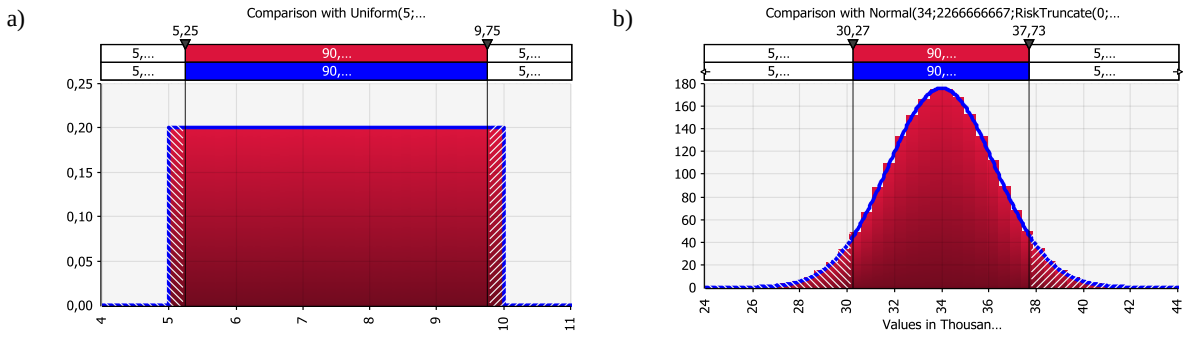

Figure 2. On the left, the probability distribution assigned to surface heat resistance. On the right, the normal probability distribution assumed for material properties (here for EPS thermal conductivity).

We assumed a probability distribution (Gauss) for thermal conductivity, density, and specific heat capacity of each layer. Then, for each parameter, we considered that a variability comprised between -20% and +20% (centred on a value selected as average or most probable) should represent the 99.7% of all the possible case (±3σ). Only for surface heat resistances (Fig. 2a), we assumed a flat probability distribution - any value has the same probability to be correct - since they are not the result of an industrial process, and may assume diverse values for the same building component. As centre value for surface heat resistances we assumed 0.17 m^2 K W^{-1} (estimated in the lab). For all other layers, instead, we assumed a normal probability distribution (Fig. 2b).

3.1 Risk analysis – Three Moisture Content Conditions

We computed Y_{12}(Fig. 3a), f_a (Fig. 3b), and φ (Fig. 4a) for three conditions of moisture content:

- Case A – all layers are dry;
- Case B – all layers present the typical moisture content for their class of material; and
- Case C – all layers present the moisture content in condition of free saturation.

Results are displayed versus cumulative distribution functions (by percentile), to assess the stochastic reliability of computed thermal performances.

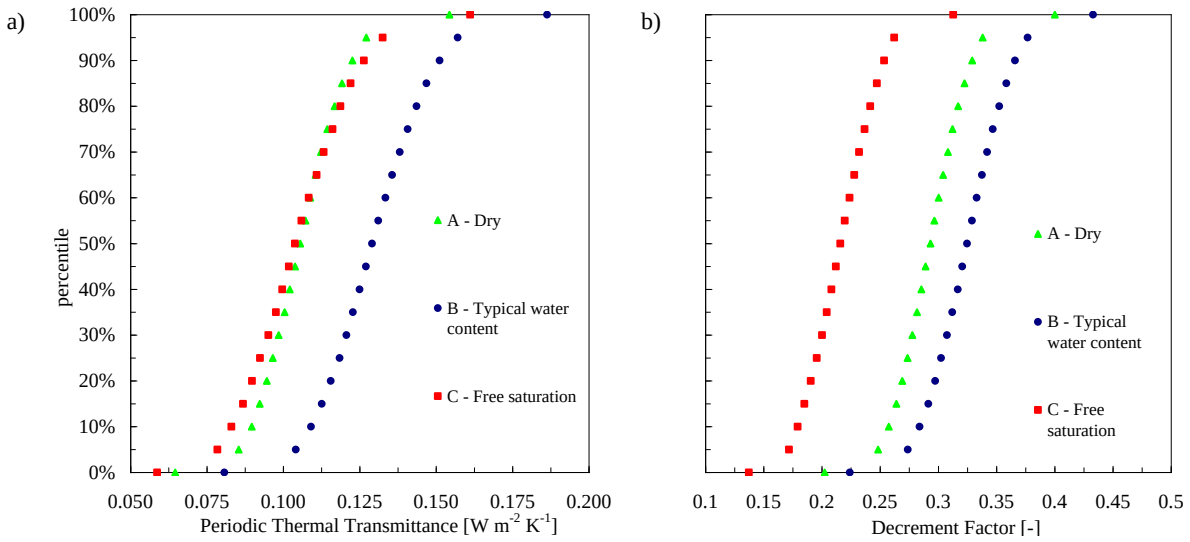

Figure 3. a) Periodic Thermal Transmittance; b) Decrement Factor.

For the materials employed for the aged sample, we did not measure the moisture storage function, the moisture diffusivity, and thermal conductivity depending on moisture content, but we assumed - as trial values for the stochastic risk analysis - the curves given in the literature [IEA, 1991; Künzel, 1995]. We adopted this approach since we note that, for many materials, properties may be highly influenced by laying conditions. For instance, a plaster may offer different properties when applied to a masonry substrate or by itself, manufacturing a small laboratory sample. We also note that, as yet, there is no test method to measure these properties depending also on temperature. In this work, we focus on dynamic parameters; other studies analyse on the influence of variability of hygro-thermal parameters values on moisture content, and they confirm the large influence that these parameters have on the result [Salonvaara et al., 2001].

3.2 Risk Analysis – Laboratory Testing and Stochastic Monte Carlo Simulation

We performed a second error risk analysis, with the same procedure, assuming as central values the thermal conductivities, specific heat capacities, and densities that we measured (and derived

depending on the moisture content computed as discussed in § 2.1) for the ageing conditions T0 (non aged), T1, T2, and T2+ (i.e. T2 immediately after a rain cycle).

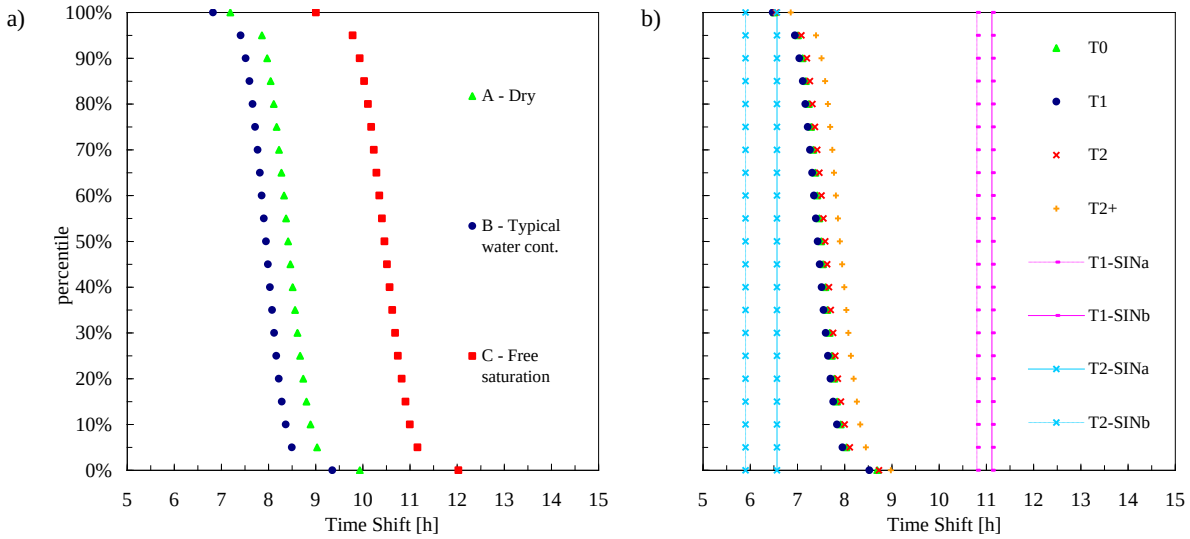

Figure 4. a) Time shift for conditions A - dry materials, B - with typical moisture content, and C - with maximum moisture content in free saturation (typical and maximum moisture content according to Künzel [1995]); b) Time shift for ageing times: measured (lines) and modelled (plots).

4 DISCUSSION

With reference to periodic solicitation, the dynamic thermal response (Y_{12}, φ, f_a) of building components – according to ISO 13786 – can be related to the periodic penetration depth δ (where $\delta = (\lambda T \pi^{-1} \rho^{-1} c_p^{-1})^{0.5}$, with T the period of solicitation in seconds), and hence to thermal conductivity, and the product of heat capacity and density. These quantities depend on water content (and temperature); thus, moisture has a dual effect: it decreases the thermal conductivity of a layer, and it increases the heat capacity and density of the layer. The risk analysis (Figs. 3, and 4a) highlights that with typical moisture content (case B), in comparison with the dry condition (case A), φ decreases (at 50%-ile from 8h 25' in case A, to 7h 57' in case B), while increase both Y_{12} (at 50%-ile from 0.106 W m^{-2} K^{-1} in case A, to 0.129 W m^{-2} K^{-1} in case B) and f_a (at 50%-ile from 0.29 in case A, to 0.32 in case B). Then, for high water contents (free saturation, case C) φ reaches the maximum (at 50%-ile 10h 28'), while Y_{12} and f_a show the minimum values (at the 50%-ile respectively 0.19 W m^{-2} K^{-1}, and 0.22).

In our experiment, we observed a loss in thermal resistance (Tab. 2), with increasing moisture content due to rain penetration occurred during ageing cycles, and decrease in time shift (from roughly 11 h at T1, to about 6 h at T2). We explain the decrease in time shift, considering that the increase in moisture content in the insulation board caused a reduction of the thermal resistance, more influent than the increase of the heat capacity for the same layer. Moreover, we did not observe a relevant increase in moisture content in the masonry substrate (except at T2+), meaning that the most of water penetrated and concentrated in the thermal insulator (Tab. 1).

Comparing measurement results with computer simulations, we observed that with laboratory testing we obtain a larger variation in time shift for the same moisture contents: with tests, φ is 10 h 48' at T1, and 6 h 34' at T2, while with calculations φ varies (at the 50%-ile) from 7 h 26' (T1) to 7 h 35' (T2). We explain this noting that the moisture content was derived for the main section, while the most relevant rain penetration occurs through the joint between insulation boards. In addition, we note that the time shift measured at T1 (10h 48'), corresponds, roughly, to that computed for free saturation condition (10h 28', curve C – 50%-ile, Fig. 4a). Furthermore, water is subject also to draining forced by gravity, and we expect the largest moisture content to be at the base of the sample.

Moreover, we note a large influence on results of the surfaces heat resistances, which are difficult to characterise in the laboratory and may vary test by test (depending on the sample and the thermal gradient).

5 CONCLUDING REMARKS

We monitored the hygro-thermal performances of a sample of an ETICS over masonry wall subject to accelerated ageing. We observed decreasing thermal resistance – almost only for the ETICS – due to increase of water content caused by rain penetration. Then, performing dynamic tests with sinusoidal temperature solicitation, a decrease in time shift was observed. We also computed the time shift (together with decrement factor and periodic thermal transmittance) for the sample with moisture content derived at each ageing time. We observed large differences in values of computed and measured time shift. We impute these differences to the fact that we measured the moisture content for the main profile section, while we estimate (thanks to IR thermography) that most relevant water penetration occurs through the joint between insulation boards.

We conclude that ageing, and moisture, whose content within layers is increased by ageing, affect dynamic thermal performances. Moreover, we argue that considering the main section profile is not sufficient to capture hygro-thermal dynamic performances of ETICS. Moreover, we point out the need of standardisation of un-steady state thermal performance testing methods.

ACKNOWLEDGMENTS

We acknowledge the Italian Ministry of Research (MIUR) for the initial funding of the experimental programme. We also want to thank for their precious help the BSc and MSc students: M. Tansi, F. Rotella, F. Caimi, A. Fumagalli, and I. Ferrara.

REFERENCES

Barreira, E. , de Freitas, V. P. 2005, 'Importance of Thermography in the Study of ETICS Finishing Coatings Degradation due to Algae and Mildew Growth', Proc. 10th International Conference on Durability of Building Materials and Components, Lyon, France, 17-20 April 2005.

Beaulieu, P., Bomberg, M., Cornick, S., Dalgliesh, A., Desmarais, G., Djebbar, R., Kumaran, K., Lacasse, M., Lackey, J., Maref, W., Mukhopadhyaya, P., Nofal, M., Normandin, N., Nicholls, M., O'Connor, T., Quirt, D., Rousseau, M., Said, N., Swinton, M., Tariku, F., van Reenen, D. 2002, "Final Report from Task 8 of MEWS Project (T8-03) - Hygrothermal Response of Exterior Wall Systems to Climate Loading: Methodology and Interpretation of Results for Stucco, EIFS, Masonry and Siding-Clad Wood-Frame Walls", Institute for Research in Construction, National Research Council Canada, Ottawa, ON, Canada, November 2002.

Bronski, M.B. 2005, 'Wall Cladding System Durability Lessons Learned from the Premature Deterioration of Wood-Framed Construction Clad with Exterior Insulation and Finish Systems (EIFS) in the U.S.', Proc. 10th International Conference on Durability of Building Materials and Components, Lyon, France, 17-20 April 2005.

Daniotti, B., Paolini, R. 2005, 'Durability Design of External Thermal Insulation Composite Systems with Rendering', Proc. 10th International Conference on Durability of Building Materials and Components, Lyon, France, 17-20 April 2005.

Daniotti, B., Lupica Spagnolo, S., Paolini, R. 2008, 'Climatic Data Analysis to Define Accelerated Ageing for Reference Service Life Evaluation', Proc. 11th International Conference on Durability of Building Materials and Components, Istanbul, Turkey, 11-14 May 2008, Vol. 3, pp. 1343 – 1350.

Daniotti, B., Paolini, R. 2008a, 'Experimental Programme to Assess ETICS Cladding Durability', Proc. 11th International Conference on Durability of Building Materials and Components, Istanbul, Turkey, 11-14 May 2008, Vol. 3, pp. 1195 – 1204.

Daniotti, B., Paolini, R. 2008b, 'Evolution of Degradation and Decay in Performance of ETICS, Proc. 11th International Conference on Durability of Building Materials and Components, Istanbul, Turkey, 11-14 May 2008, Vol. 4, pp. 1523 – 1530.

de Freitas, V.P., Abrantes, V., Crausse, P. 1996, 'Moisture Migration in Building Walls – Analysis of the Interface Phenomena', *Building and Environment*, **31**, [2], 99-108.

Hens H., Carmeliet, J. 2002, 'Performance Prediction for Masonry Walls with EIFS Using Calculation Procedures and Laboratory Testing', *Journal of Thermal Envelope and Building Science,* **25**, 167-186.

Holm, A., Künzel, H.M. 1999, 'Combined Effect of Temperature and Humidity on the Deterioration Process of Insulation Materials in ETICS', Proc. 5th Symposium Building Physics in the Nordic Countries, Göteborg, Sweden, pp. 677-684.

IEA - International Energy Agency 1991, Condensation and Energy, Catalogue of Material Properties, Report Annex XIV, Volume 3.

ISO 9869: 1994 – Thermal insulation – Building elements – In-situ measurements of thermal resistance and thermal transmittance.

ISO 13786: 2007 – Thermal performance of building components – Dynamic thermal characteristics – Calculation methods.

Künzel, H. M. 1995, Simultaneous Heat and Moisture Transport in Building Components (One- and two-dimensional calculation using simple parameters), IRB-Verlag, Stuttgart.

Künzel, H., Künzel, H.M., Sedlbauer, K. 2006, Long-term Performance of External Thermal Insulation Systems (ETICS), *Acta Architectura*, **5**, [1], 11–24.

Sahal, N., Lacasse, M.A. 2005, 'Water entry function of a hardboard siding-clad wood stud wall', *Building and Environment*, **40**, 1479–1491.

Salonvaara, M., Karagiozis, A., Holm, A. 2001, 'Stochastic Building Envelope Modeling – The Influence of Material Properties', Proc. VIII Conference of Performance of Exterior Envelopes of Whole Buildings, 2-7 December 2001, Clearwater Beach, Florida, USA.

Zirkelbach, D., Holm, A., Künzel, H.M. 2005, 'Influence of Temperature and Relative Humidity on the Durability of Mineral Wool in ETICS', 10th International Conference On Durability of Building Materials and Components, Lyon, France, 17-20 April 2005.

XII DBMC
International Conference on Durability of Building Materials and Components
PORTO - PORTUGAL, April 12th-15th, 2011

The Durability Experimental Evaluation of Photocatalytic Cement-Based Materials

Bruno Daniotti [1]
Sonia Lupica Spagnolo [2]
Rosanna Galliano [3]

ABSTRACT

Photocatalytic cement-based materials for building applications represent one of the most interesting developments in the construction field in the last few years. In order to study their performances at international level, they have already been object of many research programmes: their application, in fact, allows to obtain performances such as the removal of some air pollutants, the dirtiness prevention or the anti-bacteria and deodorization actions. Thanks to their capability to exploit luminous energy (solar or artificial) for activating chemical reactions of oxidation, which can neutralize the adsorbed pollutants.

As for every innovative material, besides the study of their initial performances, it is necessary to know their behaviour in the long run and to define their Service Life: with this aim, an experimental programme for monitoring the photocatalytic activity over time for such materials was undertaken at Politecnico di Milano.

The idea is to use a photocatalytic plaster for the refurbishment of "Torre Velasca". For that, several experiments were commissioned to the laboratory of "Durability Building Components" of BEST since April 2010. These experiments are aimed to study accelerated ageing of representative samples of new rendering, in order to evaluate durability as integrity, colorimetric variations and photocatalytic performance over time.

The paper describes the designed experimental methodology and the main results after accelerated ageing tests.

KEYWORDS

Photocatalytic, Experimental evaluation, Accelerated ageing, Torre Velasca.

[1] Politecnico di Milano, BEST Department, Milan, ITALY, 20133, piazza Leonardo Da Vinci 32, Phone +39 0223996002, Fax +39 0223996020, bruno.daniotti@polimi.it
[2] Politecnico di Milano, BEST Department, Milan, ITALY, 20133, piazza Leonardo Da Vinci 32, Phone +39 0223996052, sonia.lupica@polimi.it
[3] Politecnico di Milano, Milan, ITALY, 20133, piazza Leonardo Da Vinci 32, rosanna.galliano@mail.polimi.it

1 INTRODUCTION

Photocatalytic materials possess properties that make them extremely interesting in construction, particularly because, if used as finishing layers they maintain colour, a characteristic that in contexts of strong pollution permits aesthetic benefits and considerable savings of maintenance costs (to restore its original appearance), and on the other hand allow a reduction of pollution itself, resulting in a positive environmental impact. Many studies have investigated the photocatalytic activity levels of different materials with the addition of titanium dioxide, in different terms of use, considering especially the characterizations performance at time zero. It is however important to assess whether the photocatalytic activity remains constant in the long run, or if it tends to decrease with the natural ageing of building products. Moreover, with regard to innovative materials, it is useful to examine, in similar conditions of use and solicitation, how the photocatalytic materials behave in the long run, what mechanisms of degradation they are subjected to and whether they are more or less durable than traditional materials.

Some studies have demonstrated how the photo-activity depends on micro-structural and environmental factors; cement products are especially suitable for incorporating TiO_2 particles through their porosity, that turns out to be one of the most significant parameters for pollution purposes. A more porous material contains more TiO_2 and absorbs more pollutants and photocatalysis products. With the exposure to climatic conditions, more porous materials are subject to abrasion, losing a part of the incorporated TiO_2, but keeping generally good values of photo-activity [Maury *et al.* 2009].

Photocatalytic activity decreases with the maturation of the dough. During the hydration period a decrease of porosity is generated because of the formation of hydration products that could inhibit the reaction of the TiO_2, by blocking both the absorption of reagents and the transport of photons. This occurred also to specimens subject to an accelerated carbonation presenting a photocatalytic activity loss with respect to samples in normal conditions, measuring NOx removal through several stages of maturation. The correlation between the increase of carbonation level and photocatalytic efficiency loss is due to the change of microstructure in the conversion of $Ca(OH)_2$ to $CaCO_3$. This transformation in fact, leads to an increase of solid volume of 11%, and a reduction of the total porosity, therefore the deposition of $CaCO_3$ pores causes a negative effect on the degradation of NOx [Chen & Poon 2009]. In relation to the microclimatic context, environmental parameters such as temperature, relative humidity, irradiance, pollutant concentration, the presence and direction of the wind affect photocatalytic efficiency. Optimal conditions for photocatalytic activity levels are represented by high temperatures and low relative humidity [Hungher M. *et al*. 2009].

In July 2007 the Durability Group of Politecnico di Milano, BEST department, in collaboration with CTG s.p.a. – Italcementi Group, performed an experimental evaluation on construction products manufactured with photocatalytic cements: different products were subjected to accelerated ageing in a climatic chamber in order to identify the strongest ones and assess their performance and decay modes of physical degradation. Through such experiments both photocatalytic properties such as reduction of pollutants (in particular NOx), self-cleaning (through rhodamine test), and physical characteristics of specimens object of the study were monitored over a period of time, evaluating not only the integrity but also the colour variation, both characteristics that can compromise the same photocatalytic effect [Daniotti *et al*.2007].

Torre Velasca (studio BBPR, 1956-1958) [Fiori & Prizzon 1982] is an historic building of Milan which needs to be brought back to its optimal aesthetic and structural conditions. It presents disseminated cracks (many of them were sealed in the past) and the risk of the detachment of the finishing layer. It was necessary to perform various diagnostic analyses to quantify the causes and the extension of the degradation and to evaluate which operation was the most appropriate. [Ronca P. *et al.* 2009][Bertolini *et al*. 2009]. After surveying all the relative structural and architectural elements it was suggested that the coating of the structural elements be restored, a solution that was composed of two layers of plaster, where the finishing layer presents photocatalytic capability. Before specifying the executive process, the Durability Group of BEST was requested to subject representative samples

to accelerated ageing tests to evaluate durability of the new rendering. This experimental activity began in April 2010 and gave the possibility to better characterize photocatalytic cement-based products in view of that application and made it possible to make a comparison with the traditional pre-existing plaster on Torre Velasca.

2 EXPERIMENTAL ACTIVITY

The experimental work began in April 2010 and had the purpose of assessing the durability of photocatalytic plaster that could be used as a covering for the refurbishment of Torre Velasca.

This assessment was carried out by subjecting samples to accelerated ageing tests in a climatic chamber, in order to analyse their behaviour and to evaluate decay of performance as photocatalytic efficiency and physical features due to the action of weathering conditions. The samples are representative of the plaster and concrete layers of the structural elements of Torre Velasca and they are of three types, one is made of traditional plaster similar to that running exists and two with plaster to which TiO_2 is added. Specifically the types are:

- photocatalytic plaster applied on substrate with reinforcement mesh (type "A+R");
- photocatalytic plaster applied on substrate without reinforcement mesh (type "A");
- plaster similar to the existing one (type "B").

2.1 Set-up of the Climatic Chamber



Figure 1. Experimental set-up and positioning of test samples.

The climatic chamber used for testing allows setting the values within the desired temperature and relative humidity and radiating the specimens in it by inserting a special UV lamp. The ageing cycle hypothesized was divided into two sub-cycles [Table1, Table 2] to avoid a drastic reduction of UV lamp life, due to the exposure to low temperatures.

Table 1. Specification of sub-cycles "A".

n.	*Phase*	T_{air} [°C]	T_{H20} [°C]	*RH* [%]	*Duration* [min]
1	Rain	20	15-20	---	60
2	Freeze	-20	---	---	90
3	Humid heat	55	---	95	60
4	Dry heat without UV	70	---	40	80

Table 2. Specification of sub-cycles "B".

n.	*Phase*	T_{air} [°C]	T_{H20} [°C]	*RH* [%]	*Duration* [min]
1	UV	30	---	40	80

A structure, for the vertical positioning of the samples subjected to the ageing cycle, was designed: the structure, connected to the walls (n.2 lateral and no. 1 front) of the climatic chamber, allowed the insertion of No. 4 samples per side, for a total of No. 12 specimens at once inside the chamber.

To avoid the stagnation of water at the base of the sample and the consequent absorption for the capillary rise, the specimens were placed on a horizontal raised grid relative to the base of the compartment by C profiles, as shown in Fig. 2. The average size of these samples, previously agreed upon in function of the internal useful area of the climate chamber and the expected stratigraphy, is (40x20x10) cm. During the manufacturing phase of the samples, a waterproofing of the areas not exposed to ageing was provided, in order to avoid water absorption along the edges.

2.2 Sections of the Climatic Chamber

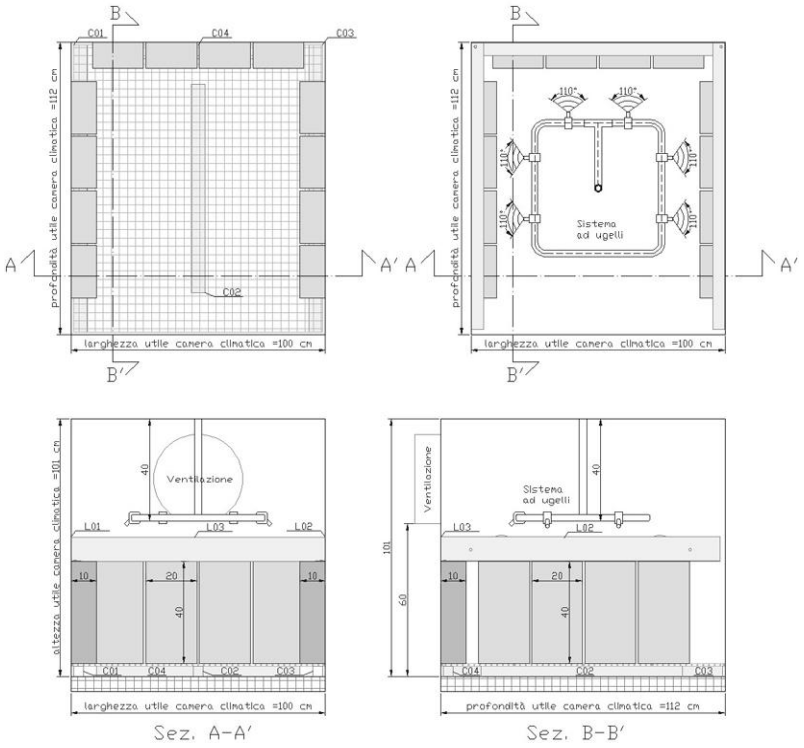

Figure 2. Horizontal sections (figure above) and vertical sections (figure below) for the schematization of experimental set-up.

Every type of specimen was subjected to a maximum of 300 cycles of exposure in the climatic chamber; samples of each type were taken from the climatic chamber to assess the state of deterioration and decay of performance at: t_1= 50 cycles; t_2= 100 cycles; t_3= 200 cycles; t_4= 300 cycles.

3 EVALUATION OF THE DURABILITY OF PHOTOCATALYTIC PLASTER FOR TORRE VELASCA

Characterization tests on both the samples not aged (time zero) and samples subjected to ageing cycles for the assessment of degradation were performed:

- Photographic survey to assess the level of degradation and colour changes;
- Measurement of residual photocatalytic efficiency using NOx removal test;
- Colorimetric analysis with the CIELab method to measure the colour variation.

3.1 Analysis of Degradation Through Photographic Surveying

Visual analysis and photographic survey reveal that the samples with photocatalytic capability do not show significant degradation up to 200 ageing cycles; at 300 cycles a rather uniform yellowing on the surface can be seen. This yellowing occurred after 200 cycles and was clearly visible at 250.
Representative samples of the existing plaster present a first significant deterioration at 100 cycles with the crystallization of the salts, cracks and localized surface discoloration; a detachment of the layer of plaster occurred with rupture of waterproofed side at their edges. At 150 cycles the total detachment of the layer of plaster from the substrate was found, which was generated by the disintegration of the plaster in the lower part of the sample; for the third sample this happened at around 225 cycles.

In summary the experimentation on accelerated ageing showed that:

- in all samples tested water absorption resulted higher at the bottom of the samples themselves, visible after a long time from the end of ageing cycles ;
- photocatalytic plasters, meant for the new covering of Torre Velasca (types "A+R" and "A") do not show any cracks or an increase of surface roughness, but after 200 cycles show a yellowing visible on all three samples submitted to 300 cycles of ageing;
- all samples belonging to types "B" (current plaster) showed obvious physical deterioration already in the early stages of ageing, probably due to high water absorption at the bottom of the sample during rain and the expanding action of the water detained during the next phase of frost, reaching the end of service life between 150 and 200;
- considering the only physical degradation, the photocatalytic samples behaved overall better with respect to samples that reproduce existing plaster;
- the yellowing necessitated a quantitative feedback using colorimetric survey.

3.2 Colorimetric Test

Measurement tests were performed to evaluate the variation of colour and brilliance of the topcoat of the samples following the accelerated ageing. These measurements are based on CIE L*a*b* model:

- L* describes the lightness, if L* = 0 no light is reflected, if L* = 100 the whole incident light is reflected;
- a* indicates a value between the red (+ a) and the green (-a);
- b* indicates a value between the yellow (+b) and the blue (-b).

These three values represent the Cartesian axes of a solid that allow the definition of each gradation of colour uniquely through three coordinates in a three-dimensional system. In Figure 3 relative measurements of the three parameters of the photocatalytic samples are represented in order to make the evolution of the deviations from the values measured before ageing more visible.

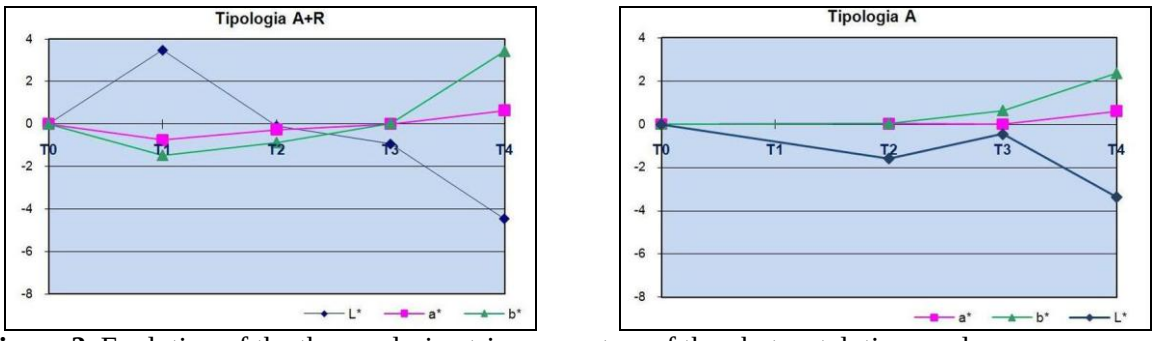

Figure 3. Evolution of the three colorimetric parameters of the photocatalytic samples.

The graphs shows how, besides a slight decrease in lightness (L *), after 200 cycles an increase of the parameter b * occurs and moves towards positive values; this indicates a yellowing of the samples as found in the photographic survey.

3.3 Photo-Activity Test

Photo-activity tests, performed by the method described in standard UNI 11247, were conducted on sample sections 8x8x2cm to evaluate the capability of removing NOx (NO_2 + NO).

The results of these tests have shown at time 0 values of removal of 22%, after 100 cycles that value has declined to 12%, and eventually to about 11% and it stabilizes around this value in the following ageing step. It can therefore be said that in this case a decay of performance concerning the photocatalytic capacity equal to 50% of initial value occurred.

3.4 Comparison Between Photocatalytic Plaster and Traditional Plaster Pre-Existing on Torre Velasca

In the accelerated ageing experimental activities that were carried out on the representative samples of the new coating of Torre Velasca (in comparison with the existing representative samples of plaster) it was discovered how well the photocatalytic plaster responds to weathering, since there has been no physical degradation (no increase of roughness, no cracking or disintegration). This plaster is also resistant to the action of frost-thaw, representing one of the most burdensome factors for the durability of a cement-based coating. The only problem encountered is the yellowing, that occurs between 200 and 300 ageing cycles; it represents an aesthetic degradation but it can be considered performance if one of the primary goals in the refurbishment is to ensure the unchanging colour over time.

Representative samples of plaster currently existing on Torre Velasca, subjected to the same cycle of ageing, showed a significantly different behaviour compared to the first one. In fact from the early stages they showed signs of physical degradation such as stains, salt deposit and cracks, up until the breakup of the plaster and the total detachment from the support. That which occurred with the accelerated ageing is comparable to degradation phenomena found on the coating of the structural elements of Torre Velasca, namely the formation of cracks distributed on the surface and the first detachments that occurred already at the end of 1970s.

We must consider that on the set plaster there are other factors that could not be taken into account in accelerated ageing, for example, during the climatic chamber experiment it would be impossible to evaluate how the disposition and corrosion of reinforcements in concrete support affect formation of cracks. By conducting a comparative analysis between the findings from surveys carried out on Torre Velasca and from the experimental results, it is possible to formulate hypotheses in relation to alleged long service-life of the photocatalytic plaster with regards to the service life of the traditional one.

Representative samples of existing traditional plaster, during the tests of accelerated ageing, have reached the end of service life within 150 cycles, breaking-up and detaching from the support. Investigations and surveys performed on Torre Velasca show that the plaster, coating structural elements, showed more noticeable signs of degradation, even before the 1990s, about 25 years after the construction of Torre Velasca, that period may be taken as the term of service life. In broad terms it is thought that 150 cycles can represent about 25 years of ageing under field conditions. Durability of photocatalytic plaster was instead of at least 300 cycles, twice as much at traditional plaster; this means, always with the necessary approximations, that this plaster can have a service life of at least 50-60 years.

4 COMPARISON BETWEEN THE RESULTS OF THE EXPERIMENTS

It is possible to make a comparison between the new results and those related to experimentation in 2007, taking as reference the sample of plaster in thickness made with photocatalytic mortar (INT-M). In this experiment, by correlating the levels of degradation with the decrease in the time of photocatalytic activity it was possible to evaluate how the degradation affects efficiency. To make the correlation between the level of deterioration and decay of photocatalytic activity (from its initial value T0, considered as a reference), values have been shown in percentage as shown in Fig. 4.

4.1 Relative level of Performance of Pollution Removal Capability

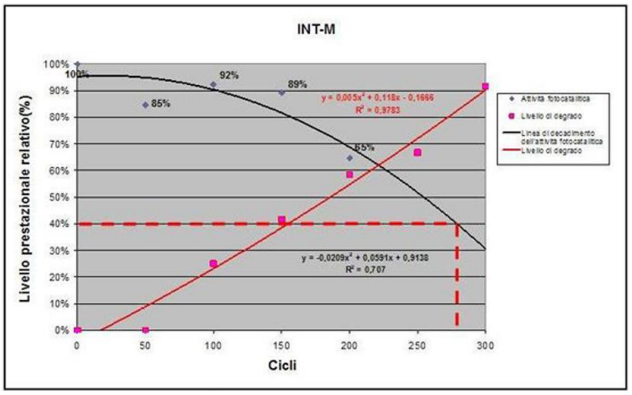

Figure 4. Comparison between decay of the photocatalytic activity and the levels of degradation of the samples of plaster in thickness subjected to accelerated ageing cycle.

Developments of decay of performance of samples in two testing are comparable, because the ageing cycle which they have undergone is analogous. The results obtained are quite similar in the photocatalytic pollution removal capability, less with regards to physical degradation. Based on the line of the decay of photocatalytic efficiency for sample INT-M, at 300 cycles photocatalytic power decrease 70% compared to the initial value, greater than the value obtained in the second experiment. With regards to the physical degradation, while the sample INT-M reaches the end of service life at 300 cycles, the representative sample of the new rendering of Torre Velasca exceeds this number. This distinction is mainly due to the difference size between samples, the specimen INT-M is 8x8x1cm and it is therefore more susceptible to weathering stages.
In relation to colorimetric variation in testing in 2007, in addition to a lightness variation (L *), a yellowing (b *) occurred for various types of samples, as shown in fig 5, due to the presence of certain additives.

4.2. Colorimetric Variation

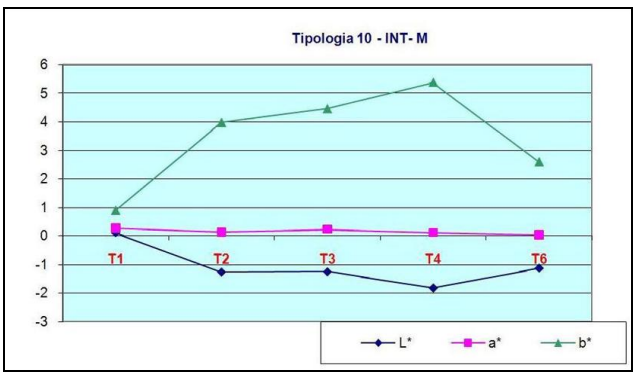

Figure 5. Evolution of the variation of the colorimetric parameters for the sample INT-M.

5 CONCLUSIONS

The developed experimental research allowed the owner of Torre Velasca, a very important Milan Building, to control durability of the proposed solutions for innovative photocatalytic facade rendering.

The accelerated ageing test developed by Politecnico di Milano during last decade in this case was useful to compare the degradation and performance decay in time, of the innovative solutions, developed by some of the most important mortar producers in Italy, with traditional rendering.
In order to evaluate Service Life, new research is needed to compare these results with outdoor exposure or with the actual time behaviour of the old rendering of Torre Velasca.

Other tests are being developed to evaluate bond strength decay within the mortar rendering layers, with and without metal mesh reinforcement, which will give us other important information about mechanical durability.

REFERENCES

Bertolini L., Lollini F. & Redaelli E., 2009 *Corrosion assessment of structural and decorative reinforced concrete of Torre Velasca in Milan*, PROHITECH.

Chen J. & Poon C.-Sun, 2009, *Photocatalytic Cementitious Materials: Influence of the Microstructure of Cement Paste on Photocatalytic Pollution Degradation,* Environmental Science & Technology, Vol. 43, No.23.

Daniotti B., Guerrini G.L. & Lupica Spagnolo S., 2007, *La durabilità di prodotti cementizi fotocatalitici: analisi del comportamento del tempo mediante prove di invecchiamento accelerato.*

Daniotti B., *La valutazione della durabilità di pareti perimetrali verticali non portanti*, Ed. Editecnica, Palermo, 2006.

Daniotti B. & Lupica Spagnolo S., 2008 *Service Life Prediction Tools for buildings' design and management, proceedings of the conference* "11DBMC International Conference on Durability of Building Materials and Components", Istanbul, Turkey.

Fiori L. & Prizzon M., 1982, *BBPR, La Torre Velasca: Disegni e progetto*, Editrice ABITARE Segesta, Milano.

Hungher M., Hüsken G. & Brouwers H.J.H., 2009, *Photocatalytic degradation of air pollutants - From modelling to large scale application* , Building and Environment, ELSEVIER .

Maury Ramirez A., Demeestere K., De Belie N., Mäntylä T. & Levänen E., 2009, *Titanium dioxide coated cementitious materials for air purifying purposes: Preparation, characterization and toluene removal potential*, Building and Environment, ELSEVIER.

Ronca P., Crespi P., Franchi G. & Zichi A., 2009, *Il Patrimonio architettonico del moderno: conservazione e durabilità per Torre Velasca*, CIAS.

UNI 11247, 2007 *Determinazione dell'attività di degradazione di ossidi di azoto in aria da parte di materiali inorganici fotocatalitici*, Dicembre.

XII DBMC
International Conference on Durability of Building Materials and Components
PORTO - PORTUGAL, April 12th-15th, 2011

Ecological Behaviour of Mineral Mortars and Plasters

Christian R. Scherer [1]
Regina Schwerd [2]
Christoph Schwitalla [3]
Florian Mayer [4]
Klaus Breuer [5]

ABSTRACT

CEN TC 351 WG1 is working on release scenarios for dangerous substances from building materials into the soil and groundwater. Therefore, different laboratory methods for the estimation of substance release are being discussed. In the evaluation scheme proposed by the German Working Group on Water Issues (Bund/Länder Arbeitsgemeinschaft Wasser, LAWA), concentration values are given for organic and inorganic substances, which are considered as non-critical for the groundwater. Results of laboratory leaching experiments are commonly used as input values for this evaluation scheme. The scope of these experiments is focussed on building elements in direct contact with the groundwater. To date no long-time real-climate surveys of irrigated façade materials regarding the leaching of organic and inorganic matter have been published. In a 3 three year experiment, test specimens of mineral plasters and mortars were exposed to real climate conditions. The concentrations of selected organic and inorganic compounds in the run-off rain water were measured after nearly each rainfall. Comparing concentrations or release rates measured for a single rainfall with the insignificance threshold values, shows that there is no simple way of evaluating the release behaviour of façade coatings using the values derived from building elements in direct contact with the groundwater. The release mechanisms of façade coatings under real climatic conditions are, due to the intermittent water contact, quite different. Concentrations and release rates determined in the exposition experiment give important information about the leaching characteristics of plasters and mortars.

KEYWORDS

Mortar, Plaster, Leaching, Ecological properties, Inorganic cations, Inorganic anions, TOC.

[1] Fraunhofer-Institute for Building Physics (IBP), Valley, GERMANY, christian.scherer@ibp.fraunhofer.de
[2] Fraunhofer-Institute for Building Physics (IBP), Valley, GERMANY, regina.schwerd@ibp.fraunhofer.de
[3] Fraunhofer-Institute for Building Physics (IBP), Valley, GERMANY, christoph.schwitalla@ibp.fraunhofer.de
[4] Fraunhofer-Institute for Building Physics (IBP), Valley, GERMANY, florian.mayer@ibp.fraunhofer.de
[5] Fraunhofer-Institute for Building Physics (IBP), Valley, GERMANY, klaus.breuer@ibp.fraunhofer.de

1 INTRODUCTION

In 1988 the European Commission (EC) passed the European Construction Products Directive (CPD) [EC 1988]. The CPD introduced a new essential requirement for building product regulations, as well as for the standardisation of building products. This new essential requirement No. 3 (ER 3) "hygiene, health and the environment" has to be considered when setting up horizontal standards for building products. Building products and buildings made thereof are not allowed to compromise neither human health nor the environment. The first generation of horizontal product standards did not consider ER 3. Now these standards have to be revised. Therefore, in 2005 the EC gave the mandate M /366 "Horizontal complement to the mandates for the development of horizontal standardised assessment methods for harmonised approaches relating to dangerous substances under the construction products directive (CPD)" to CEN [M /366 CEN]. On behalf of this mandate, CEN established the technical committee TC 351 to set up scenarios for the release of dangerous substances under the CPD. Working group 1 (CEN TC 351 WG1) describes release scenarios for the release of dangerous substances into the soil and groundwater and develops or adapts laboratory test methods for this purpose. The results of product testing according to this horizontal testing method, may be interpreted by each European member state in accordance with national regulations and thresholds. In 2010 the idea of emission classes was raised for discussion, which means that the EU establishes a classification system for emissions from building products. The member states can then decide where, building products with a certain emission class, may be used. In Germany the Federal Institute for Civil Engineering (Deutsches Institut für Bautechnik, DIBt) set up regulations for the evaluation of the impact of building products on soil and groundwater. Insignificance threshold values (IT) for the impact of building materials on the groundwater were derived by the Working Group of the Federal States on Water Issues [LAWA 2004]. Hohberg [2003] examined and modelled the substance release from cementitious products. Brameshuber et al. [2005] performed calculations using the insignificance thresholds to re-evaluate the ecological behaviour of concrete. All this work was completed under the assumption that the building product which has to be evaluated is permanently in direct contact with the ground water. In 2010 Vollpracht and Brameshuber [2010] investigated the release of cations from façade coatings under laboratory conditions and compared these values with results from tank tests. In modern architecture, buildings without roof overhang are en vogue, a design feature which can lead to problems regarding the run-off water of irrigated façades. In areas like southern Bavaria where driving rain is quite common, even façades of buildings with roof overhang are often exposed to rainwater. Actual façade coatings like mortars and plasters consist, either of mineral compounds with organic additives or of resin-based materials. Mineral mortars and plasters are deemed as products which only release small amounts of dangerous substances into the soil and groundwater. There were however, not sufficient data available to decide whether these façade coatings show a long-term substance release under real climatic conditions. This gap should be closed by a 3-year study. 15 different mineral mortars and plasters were exposed to natural climatic conditions and the substance release into run-off water was determined.

2 MATERIALS AND METHODS

15 different façade coating materials were exposed to real climatic conditions in Valley (Germany) over a period of three 3 years. Valley is located approx. 30 km south of Munich on a plateau at 680 m above sea level, north of the Bavarian Alps. Frequent warm wind periods from the south (Foehn) are common for this geographical location. The warm Foehn wind descending from the Alps consequently leads to summer-like temperatures, even in February. Due to the thermal radiation, it can however even freeze during the night. The climatic conditions are characterised by a) temperature differences which can reach up to 35 K within 24 h, and b) heavy thunderstorms in summer with wind driven rain from western directions. During the experimental period the average precipitation was 106 mm m^{-2} M^{-1} (range 17 mm m^{-2} M^{-1} – 336 mm m^{-2} M^{-1}, median = 86 mm m^{-2} M^{-1}, n = 37). The seasonal distribution of the precipitation during the exposition period is depicted in Fig. 1. Due to the altitude

the thermal radiation at night is high, resulting in cold nights. The temperatures at night often fall below the dew point. Thus thawing on façade materials is quite common.

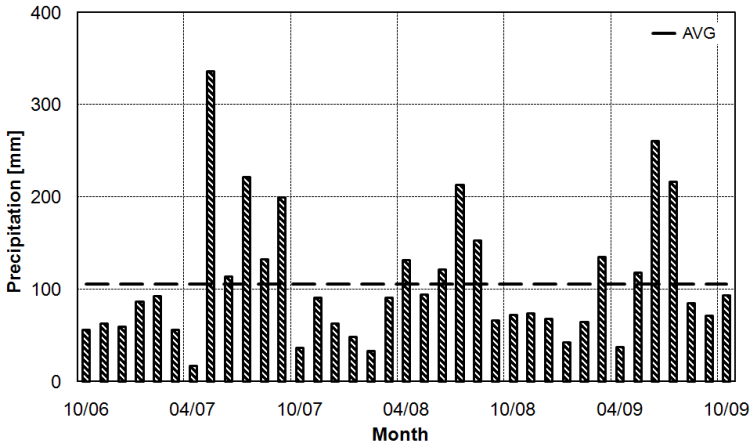

Figure 1. Precipitation during the exposition period.

2.1 Plasters and Mortars

13 Plasters (7 single layer, 5 double layer, 1 triple layer) and 2 mortars (1 single layer, 1 double layer) were filled into sample holders made of laboratory glass, as shown in Fig. 2. Empty sample holders were used to collect blanks for chemical analysis. Plasters and mortars were compounded as worst-case mixtures, implying that ingredients regarded as possibly critical, concerning their release of dangerous substances, were used in higher amounts than usual. In accordance to real-life products, test specimens were made as single-layer (8), double-layer (6) or triple-layer (1) render. The surface of a test specimen was 0.04 m². Samples were allowed to dry for at least 2 weeks under standard conditions (23 °C, 50 % r. h.) before being mounted on the test rig.



Figure 2. Sample on the test stand.

2.2 Sampling and Chemical Analysis

The run-off water of nearly each rainfall was collected, resulting in a total of 101 samples being taken within an exposition period of 1111 days. Sampling was suspended during the frost period. Different bottles were used to collect water for cation (PP), anion and sum parameter (glass) analysis. When necessary, water samples were stabilized and stored at 4 °C prior to analysis. Cation concentrations were determined by ICP/MS (Agilent 7500 CE, Agilent Technologies Deutschland GmbH, Böblingen, Germany). Al, B, and Be were measured in the normal mode. Ba, Cd, Cr, Cu, Mo, Mn, Ni, Pb, Sb, Sr, Tl, V and Zn were measured in the collision mode. Helium was used as collision gas at a flow rate of 5 mL/min. Se and Sn were measured in the reaction mode using hydrogen as reaction gas at a flow rate of 4 mL/min. Sc, In, Lu and Bi (SPEX CertiPrep®, HORIBA Jobin Yvon GmbH, Munich, Germany) were used as internal standards at a concentration of 1 mg/mL. Sc and In were measured in all three operation modes. Analysis of Lu and Bi was conducted in collision and normal modes. Calibration curves were linear in the range of 0 – 500 ppb. Anions, Cr(VI) and TOC were analyzed by an external laboratory.

3 RESULTS

Samples of 101 rainfalls were analysed. The volumes collected were between 2 mL and 615 mL. In 9 cases the volume of the run-off water exceeded that of the bottles. Sample volumes of one rainfall could differ up to 405 mL, depending on render properties and wind direction. With the exception of sum parameters, pH and electrical conductivity (EC) results were calculated as substance release rates. The cation release rates which are determined are already corrected, as a consequence of the cation content of the pure rain water. Due to long frost periods in the winter and also some longer dry periods in the spring and summer, a correlation of release vs. exposition time does not seem to make sense. It was established, that the time between two rainfalls has a significant influence on substance release. This coincidentally verifies the work of Schießl [1995], who postulated three release mechanisms for facade coatings from laboratory experiments: initial wash-off, stripping from the surface and diffusion from inside to the surface of the render.

3.1 Sum Parameters

Rain water had a pH between 4.6 and 7.7 (mean 6.17, median 6.18, n = 97). Run-off water of the test specimen had significantly higher pH values up to 11.6 [Fig. 3]. EC of pure rain water was between 4 µS cm^{-1} and 150 µS cm^{-1} (mean 14 µS cm^{-1}, median 11 µS cm^{-1}, n = 97). The EC values of the run-off water were between 17 and 923 µS cm^{-1}. Total organic carbon (TOC) concentrations ranged from 0.9 mg L^{-1} to 11 mg L^{-1} (mean 4.2 mg L^{-1}, median 4.3 L^{-1}, n = 35). Single-layer coatings showed TOC releases up to 809 mg m^{-2}, whereas the maximum release of multi-layer renders was about 307 mg m^{-2} [Table 1]. TOC measurement was stopped after one year because of visible microbial growth on the samples. This led to a sudden rise of the TOC.

Table 1. Ranges of sum parameters.

Sample	*pH* [-]	*EC* [µS cm^{-1}]	*TOC* [mg m^{-2}]
Blank	4.6 – 7.7	4 - 150	7 - 80
Single layer coatings	7 - 11	17 - 923	2 - 809
Multi layer coatings	7 – 11.6	23 - 810	2 - 307

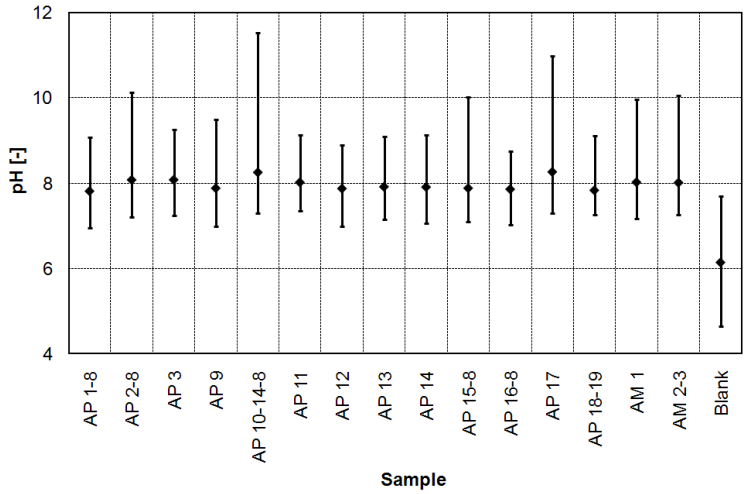

Figure 3. pH of the run-off water.

3.2 Cations

Cations could be divided into three groups: a) Be, Hg, Tl and Bi which could not be determined, b) Mn, Co, Ni, Cu, As, Cd, Sn, Sb, Ba and Pb which appeared sporadically and c) B, Al, V, Cr, Zn, Se, Sr and Mo which were detected frequently and in relatively high amounts. Release rates of group c) are given in Table 2. Cumulated chromium release from two single-layer (AP 3 and AP 9) and two multi-layer renders (AP 15-8 and AP 18-19) are depicted in Fig. 4. It can be seen that the number of layers does not have any influence on the substance release rates. The shapes of the curves of AP 9 and AP 15-8 indicate that chromium release decreases. AP 3 and AP 18-19 do not show such behaviour.

Table 2. Ranges of cation release rates.

Sample	*B* [mg m^{-2}]	Al [mg m^{-2}]	*V* [mg m^{-2}]	*Cr* [mg m^{-2}]	*Zn* [mg m^{-2}]	*Se* [mg m^{-2}]	*Sr* [mg m^{-2}]	*Mo* [mg m^{-2}]
Single layer coatings	0 – 17.9	0 – 21.6	0 - 0.39	0 - 0.99	0 - 1.7	0 - 0.05	0 - 3.58	0 - 0.19
Multi layer coatings	0 – 12.0	0 – 5.9	0 - 0.94	0 - 0.68	0 - 2.1	0 - 0.04	0 - 4.42	0 - 0.08

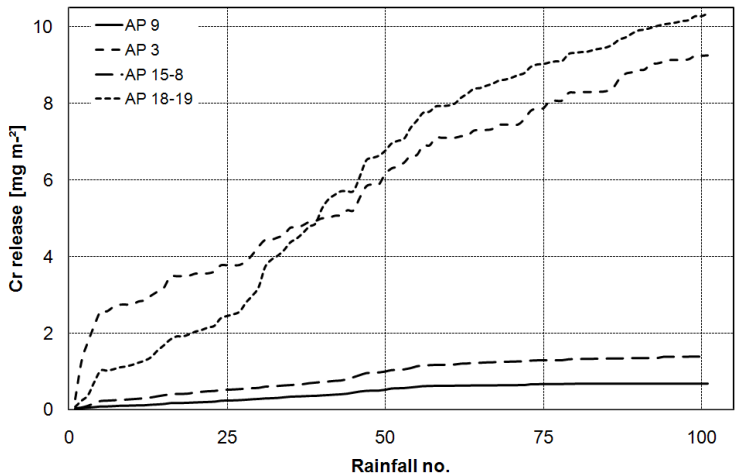

Figure 4. Comparison of cumulated total chromium release from two single-layer and two multi-layer renders.

3.3 Anions

Sulphate and chloride were determined frequently. Fluoride and acetate were detected sporadically. Nitrate release rates were mostly in the range of pure rain water. Only multi-layer coatings showed significantly higher nitrate release rates than pure rain water [Table 2]. Cumulated sulphate release rates of the four renders AP 3, AP 9, AP 15-8 and AP 18-19 are shown in Fig. 5.

Table 2. Ranges of anion release rates.

Sample	*Sulphate* [mg m^{-2}]	*Chloride* [mg m^{-2}]	*Nitrate* [mg m^{-2}]	*Acetate* [mg m^{-2}]
Blank	0 - 66	0 - 27	0 – 45	0 - 11
Single layer coatings	0 - 1792	0 - 819	0 - 57	0 - 260
Multi layer coatings	3 - 1912	0 - 279	0 - 175	0 - 297

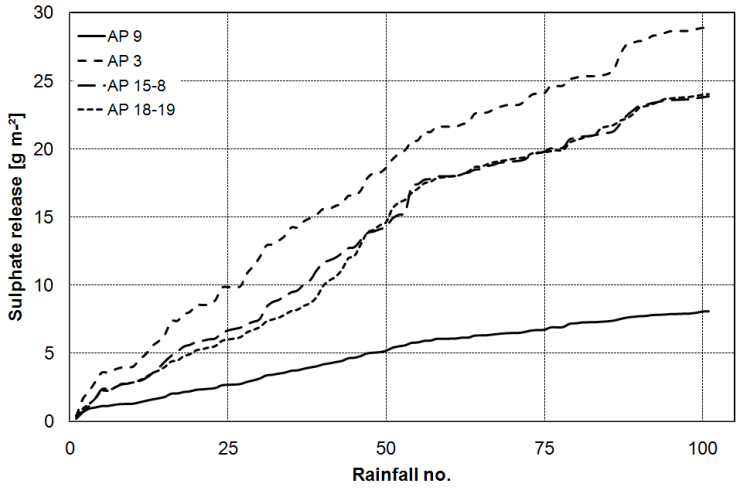

Figure 5. Cumulated sulphate release from two single-layer and two multi-layer renders.

In contrast to chromium release only AP 9 shows a decay of sulphate release. The slope of the release curves of AP 3, AP 15-8 and AP 18-19 does not show a tendency toward lower release rates.

4 DISCUSSION AND CONCLUSIONS

A broad variation of all parameters examined was observed. Shown was that the assumption of a short-term decay of substance release from mineral mortars and plasters is not generally valid. In fact, the ecological behaviour of these building products is much more complex and depends on the individual composition of each product (e. g. water repellent equipment, capillary water adsorption properties and organic additives), the frequency and duration of rainfall as well as the drying process between subsequent rainfalls. Therefore, comparing the concentrations of substances of concern, e.g. those with ITs, in the run-off water with the corresponding ITs, seems inappropriate for the ecological evaluation of irrigated building materials. Accumulation of leachable compounds on the surface is responsible for the compound concentration in the leachate in the case of short rainfall. Following the first flush, bulk material has to be soaked to enable mass transport from the interior of the material to the surface, for further leaching. Drying after rainfall (evaporation of water) also causes mass transport to the surface. These compounds deposited on the surface are leached in the first minutes of the next rainfall. In contrast, mass transport to the surface is the dominating release mechanism in

materials with continuous contact with water. A laboratory test method for ecological evaluation of irrigated materials has to take these mechanisms influencing substance release, into consideration. When release scenarios are set up for risk assessment or ecological issues, it also has to be taken into account that run-off water from irrigated building surfaces passes chiefly through soil layers which may have different adsorption capabilities e. g. for metals or inorganic anions and that the leachate may be diluted by additional rainwater. These facts must also be taken into account when setting up limits or thresholds for the release of dangerous substances under the CPD from building materials exposed to rain.

ACKNOWLEDGMENTS

This work was funded by IWM Industrieverband WerkMörtel e. V. and its industrial partners.

REFERENCES

Brameshuber, W. & Vollpracht, A. 2005, *Modellrechnungen zur Untersuchung der Auswirkungen der neuen LAWA-Regelungen auf die Bewertung der Umweltverträglichkeit von Beton.* Research Report: RWTH Aachen, Institut für Bauforschung, F 909, Aachen.

Council Directive of 21 December 1988 on the approximation of laws, regulations and administrative provisions of the Member States relating to construction products (89/106/EEC), Official Journal of the European Communities, No. L 40/12 of 11.02.1989, Mended by the Council Directive 93/68/EEC of 22 July 1993 (OJ L 220, 30.8.1993).

Development of horizontal standardised assessment methods for harmonised approaches relating to dangerous substances under the construction products directive (CPD); M /366 EN, 16th March 2005.

Hohberg, I. 2003, Charakterisierung, Modellierung und Bewertung des Auslaugverhaltens, umweltrelevanter, anorganischer Stoffe aus zementgebundenen Baustoffen. In: *Schriftenreihe des Deutschen Ausschusses für Stahlbeton*, Vol. 542, Beuth, Berlin.

Schießl, P.; Hohberg, I.; Rankers, R. 1995, *Umweltverträglichkeit von Baustoffen für Außenfassaden.* Research Report: RWTH Aachen, Institut für Bauforschung, F 415, Aachen.

Vollpracht, A. & Brameshuber, W. 2010, Investigations on the leaching behaviour of irrigated construction elements. *Environmental science and pollution research*, **17**[5], 1177 – 1182.

Working Group of the Federal States on Water Issues (Länderarbeitsgemeinschaft Wasser, LAWA) 2004, *'Determination of insignificance thresholds for groundwater'*, Kulturbuch-Verlag, Berlin.

XII DBMC
International Conference on Durability of Building Materials and Components
PORTO - PORTUGAL, April 12th-15th, 2011

Accelerated Ageing Tests of Clay Roofing Tiles under Salt Mist Atmosphere

Cláudio Cruz [1]
Maria do Rosário Veiga [2]
Victor M. Ferreira [3]

ABSTRACT

Clay roof tiles are largely used in traditional construction in Portugal and other countries. Due to the exposition to a salt mist atmosphere, some cases of accelerated decay have been affecting the ceramic roofing tiles durability in coastal zones.

This paper presents two types of accelerated weathering tests of clay roofing tiles in a climatic chamber. In both of these tests the specimens are subjected to an atmosphere of salt mist produced by a NaCl solution spray.

The first is a simple cyclic test with each cycle consisting of a salt mist period and a drying period. The second is a composite test consisting of several phases. Each phase consists of several simple cycles followed by a large drying period. In each phase the specimens are subjected to cleaning and wetting operations.

The results obtained were discussed and compared. Accelerated ageing tests can cause different levels of alteration and degradation of the same types seen in natural exposed ceramic tiles. The composite test induced more degradation on the specimens than the simple cyclic test. Hydrophobic surface tiles may resist longer to salty mist but they can suffer higher damage than non-hydrophobic tiles. Some parameters as the raw materials and the firing temperature can influence the behaviour of the tiles under salt mist. Characteristics as the water absorption under vacuum and the porous structure may give some information about the relative durability of different types of tiles.

KEYWORDS

Clay roofing tiles, Accelerated weathering tests, Salt mist atmosphere, Durability.

[1] National Laboratory of Civil Engineering (LNEC), Buildings Department, Lisboa, PORTUGAL, ccruz@lnec.pt
[2] National Laboratory of Civil Engineering (LNEC), Buildings Department, Lisboa, PORTUGAL, rveiga@lnec.pt
[3] University of Aveiro (UA/CICECO), Civil Engineering Department, Aveiro, PORTUGAL, victorf@ua.pt

1 INTRODUCTION

Clay roof tiles are largely used in traditional construction in Portugal. In coastal zones some cases of accelerated decay have been affecting the roofing tiles durability, apparently due to the exposition to a salt mist atmosphere.

The crystallization of soluble salts is considered one of the main causes for the degradation of porous construction materials [Rodrigues and Gonçalves 2006]. In spite of NaCl crystallization can cause severe damages in service situations, it has been difficult to obtain the same level of degradation in artificially accelerated laboratory weathering tests, as noted by several authors [Gonçalves 2007, Lubelli 2006, Goodie & Viles 1997], which present some reasons that can explain that discrepancy.

To evaluate the performance of the clay roofing tiles subjected to a sea environment, an experimental study was carried out [Cruz 2010] based on artificial accelerated weathering tests. The study includes the development of accelerated weathering tests and aims at reproducing the pathology mechanisms observed in real conditions.

The study of the accelerated weathering tests of several kinds of tiles also aims at identifying the parameters having a higher contribution to the decay of roofing tiles.

2 MATERIALS AND METHODS

2.1 Test Specimens

The specimens were prepared through transversal cuts of the tiles. Specimens cut from the mid transversal area of the roofing tiles were preferentially used, having the width of the tile and circa 9 cm length (Fig. 1). The cut faces of the specimens were sealed with epoxy resin. Roofing tiles of two manufacturers (F1 and F2) were used. From manufacturer F1 three types of tiles of the same model 1 were used: F1 NH - model 1, non-hydrophobic red tiles; F1 B - model 1, non-hydrophobic white tiles and F1 H - model 1, hydrophobic red tiles. From manufacturer F2 five types of tiles of three models were used: F2 NH - model 1, non-hydrophobic red tiles; F2 B - model 1, non-hydrophobic white tiles; F2 H - model 1, hydrophobic red tiles; F2 T2 NH - model 2, non-hydrophobic red tiles and F2 T3 NH - model 3, non-hydrophobic red tiles. The tiles were fired at a maximum temperature between 950 ºC and 1050 ºC, with thermal cycles of 15 hours to 48 hours. They have thicknesses of 10 mm to 14 mm.



Figure 1. Specimens before and during tests

2.2 Artificial Accelerated Weathering Tests

Two types of tests were designed based on the European Norm EN 14147:2003 and adapted to what was thought to be realistic conditions for this product [Cruz et al, 2007]. These tests were carried out

in a climatic chamber where the specimens are subjected to sets of cycles of wetting under salt mist atmosphere and subsequent drying. Salt mist is produced by spraying a salt solution into the chamber with a concentration of 110g of sodium chloride per litre of de-ionised water.

The first type of test is a simple cyclic test – simple weathering test – consisting of several 24 hours cycles (8 hours of salt mist + 16 hours of drying) with the temperature in the chamber maintained at 35ºC. For each type of tiles, one or two specimens were subjected to 10 cycles, another one or two to 20 cycles and three or four to 30 cycles [Cruz et al., 2008]. Since the degradation development stopped in the last salt mist/drying cycles, other operations rather than continue with more cycles should have been done to obtain higher degradation levels.

So, a second type of test – composite weathering test – was developed, taking into account the results of the previous simple test and designed to simulate different weathering actions, in several phases. Only specimens from the non-hydrophobic tiles (F1 NH, F1 B, F2 NH, F2 B, F2 T2 NH and F2 T3 NH) were subjected to the second type of test.

In the composite weathering test the cycles have the same 24 hours (8 hours of salt mist + 16 hours of drying) of the simple cyclic test. The temperature in the chamber was raised from 35ºC to 50ºC to obtain a higher level of drying in each cycle. The composite test consists of four phases of several 24 hours cycles followed by a large drying period, intended to promote the increase of degradation in the subsequent cycles. In some phases the specimens were subjected to cleaning with a dry brush to simulate the wind effect on the roofs. In one phase the specimens were subjected to a water spray followed by cleaning with a wet brush to simulate the rain and wind effect on the roofs.

So, the composite test was constituted by four phases with the following constitution and sequence of operations:

Phase 1:
- 13 cycles of 24 hours in the climatic chamber at 50ºC (8 hours of salt mist + 16 hours of drying)
- 10 days of drying in the climatic chamber at 50ºC

Phase 2:
- 10 cycles of 24 hours in the climatic chamber at 50ºC (8 hours of salt mist + 16 hours of drying)
- Dry cleaning with a brush
- 11 days of drying in the climatic chamber at 50ºC

Phase 3:
- 11 cycles of 24 hours in the climatic chamber at 50ºC (8 hours of salt mist + 16 hours of drying)
- Dry cleaning with a brush
- Wetting with water and cleaning with a wet brush
- 20 days of drying in the climatic chamber at 50ºC

Phase 4:
- 15 cycles of 24 hours in the climatic chamber at 50ºC (8 hours of salt mist + 16 hours of drying)
- 44 days of drying in the chamber at 50ºC
- Dry cleaning with a brush
- 30 days of drying in the climatic chamber at 50ºC

3 RESULTS

3.1 Visual Assessment

Visual inspection results (Table 1, Table 2, Table 3 and Fig. 2) demonstrate different types and levels of degradation caused on the specimens by the weathering tests. Alterations and degradations are of the same types seen in natural exposed ceramic tiles.

In the cyclic test hydrophobic specimens didn't show immediate defects but some of them suffered huge degradation following the access of the salty solution to the material under the protected surface. Hydrophobic tiles from manufacturer 2 seem to be more resistant to weathering than those from manufacturer 1.

In the cyclic test non-hydrophobic tiles, both red and white, showed low to medium degradation levels characterized mainly by pitting, some disaggregation and peeling, with a slightly higher level in the white ones.

In the composite test all of the specimens tested (only the non-hydrophobic ones) suffered higher degradations levels than in the cyclic test. Regarding F2 B specimens, they showed lower level of pitting, granular disaggregation and peeling than in the cyclic test, but they had other types of degradation that are localized and are potentially more severe.

Table 1. Alteration and degradation examples of manufacturer 1 specimens.

Specimens	*Cyclic test*	*Composite test*
F1 NH		
F1 B		
F1 H		Not tested
F1 H		Not tested

Table 2. Alteration and degradation examples of manufacturer 2 specimens.

Specimens	*Cyclic test*	*Composite test*
F2 NH		
F2 B		
F2 H	None	Not tested
F2 T2 NH		
F2 T3 NH	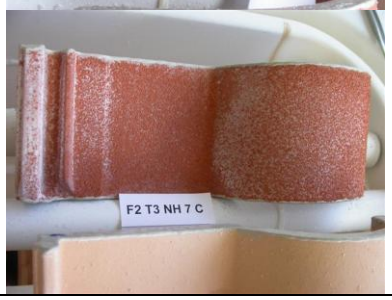	

Figure 2 shows some examples of a higher degradation level (Delamination) and of localized degradations (Fissure/Fracture/Spalling) caused by the composite test.

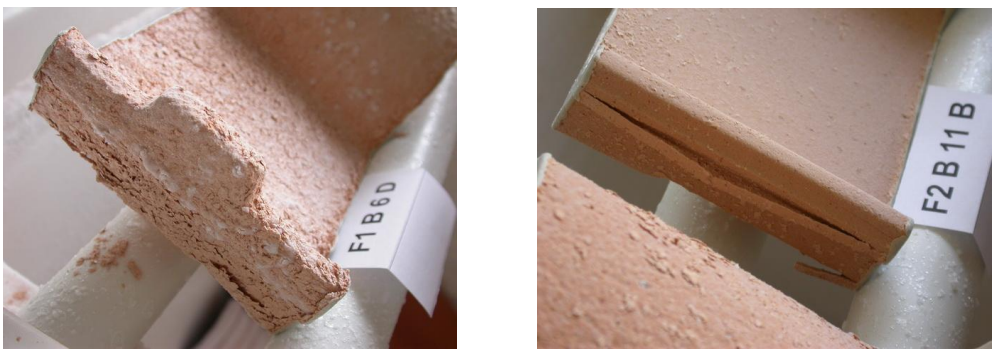

Figure 2. Delamination and Fissure/Fracture/Spalling caused by the composite test

Table 3. Alteration and degradation forms caused by the weathering tests.

Specimens	*Cyclic test*	*Composite test*
F1 NH	Pitting Granular disaggregation	Pitting Granular disaggregation Peeling Fissure / Fracture / Spalling
F1 B	Pitting Granular disaggregation Peeling	Pitting Granular disaggregation Peeling Fissure / Fracture / Spalling Delamination or Flaking
F1 H	None Fissure Bowing Plaquettes	Not tested
F2 NH	Pitting Granular disaggregation	Pitting Granular disaggregation Peeling Fissure / Fracture / Spalling
F2 B	Pitting Granular disaggregation Peeling	Pitting Granular disaggregation Peeling Fissure / Fracture / Spalling
F2 H	None	Not tested
F2 T2 NH	Pitting Granular disaggregation Peeling	Pitting Granular disaggregation Peeling Bowing Plaquettes Fissure / Fracture / Spalling
F2 T3 NH	Pitting Granular disaggregation Peeling	Pitting Granular disaggregation Peeling

4 RESULTS AND DISCUSSION

Visual inspection results demonstrate different types and levels of degradation caused by the two types of weathering tests on the specimens. As seen in the simple cyclic test, hydrophobic specimens don't show immediate defects but they can suffer huge degradation if the solution can pass through the protected surface. Hydrophobic tiles from manufacturer 2 seem to be more resistant to weathering than those from manufacturer 1.

In the simple cyclic test non-hydrophobic tiles, both red and white, show low to medium degradation levels, with a slightly increased level in the white ones. With the changes and new operations introduced in the composite test it was possible to achieve higher levels of degradations.

With the increase of the chamber temperature from 35ºC to 50ºC a higher level of drying was obtained in each cycle. As a consequence a higher level of degradations in the majority of the

specimens was visible in the cycles of the first phase. The 50ºC temperature is consistent with summer conditions, where temperatures on coloured exposed surfaces may easily reach those values, or even higher.

The degradation development stopped in the last salt mist/drying cycles of the several phases of the composite test, just as it had happened in the last cycles of the cyclic test. The introduction of a large continuous drying period between the cycles of phases 1 and 2 allowed the reduction of the level of humidity of the specimens. In consequence, in salt mist/drying cycles of the phase 2, an increase of degradation was observed again. The long drying period is also a realistic action, correspondent to warm dry periods in summer.

With the cleaning with a dry brush, to simulate the wind effect, and the water spraying of the specimens and the cleaning with a wet brush, to simulate the rain and wind effect, the surfaces of the specimens were washed out and a degraded and cleaned surface was subjected to new cycles of salt mist/drying. The particles resulting from the degradation in these cycles had smaller dimensions than the materials resulting from the degradation on the previous phases. So, it was possible to observe different behaviour between the superficial and the internal materials of the specimens under the salt mist/drying cycles.

With the continuation of the composite test new forms of degradations were obtained, such as localised degradations beginning with fissures that evolve to fractures and spalling. These defects, despite being localized, can be of higher consequences, as they can reach the thickness of he tiles and have an effect on the water tightness of the tiles and of the roof.

Regarding F1 B specimens, the continuation of the composite test caused delamination or flaking. This is a progressive loss of material in the form of thin blades that can reach, as the localised degradations, all the thickness of the tile.

The composite test shows the influence of weathering changes, in particular high temperatures and of driven rain, on the durability of ceramic tiles. It simulates a sequence of weather actions commonly occurring in coastal zones of Portugal, where salt mist, high temperatures, wind and rain happen in natural cycles.

5 CONCLUSIONS

Artificially accelerated weathering tests composed of cycles of wetting with a salty mist and subsequent drying can be used to cause different levels of artificial weathering alteration and degradation to different ceramic roofing tiles. These defects are of the same types seen in natural exposed ceramic tiles.

In the composite test the degradations obtained were of the same types of the obtained in the simple cyclic tests, in many cases reaching a level of higher degradation, and also other defects of more critical types. For that it will have contributed the increase of the temperature of operation of the climatic chamber and the increase of the number of cycles salt mist/drying.

The introduction of long drying periods between the cycles in the composite and the dry and wet cleaning of the surfaces contributed to the continuation of degradation development. These operations try to reproduce the effects of natural events as wind, rain and long periods of dry weather.

The study [Cruz, C. 2010] allowed the identification of some characteristics and properties that can influence in the durability of the ceramic tiles subjected to marine atmosphere.

Hydrophobic tiles may resist longer to salty mist but they can suffer high damage if there is some penetration of salty solution.

White tiles showed higher levels of degradation than the non-hydrophobic red ones, so the raw materials (higher CaO contents in the white tiles) can influence in the durability. White tiles have higher absorption of water under vacuum and higher porosity than the red ones of the same manufacturer, although not always show higher absorption of water by immersion.

An accelerated ageing test of clay roofing tiles under salt mist atmosphere was thus obtained and validated, permitting to evaluate the durability of ceramic tiles on a comparative basis. The influence of some climatic conditions was assessed, making it possible to identify particularly risky conditions. This test will also make possible the realization of parametric studies to evaluate the influence of several parameters of composition and manufacture in the durability of roofing tiles under salt mist atmosphere.

ACKNOWLEDGMENTS

The authors thank the manufacturers of the roofing tiles and CTCV (Centro Tecnológico da Cerâmica e do Vidro) for the specimens and information delivered and acknowledges the collaboration of the Materials Department of LNEC and its personnel, where the tests have been done.

REFERENCES

Cruz, C. 2010, *Comportamento e durabilidade de telhas cerâmicas em ambiente marítimo (Behaviour and durability of clay roofing tiles under salt mist atmosphere)*, PhD thesis, University of Aveiro, Portugal.

Cruz, C., Veiga, M. R. & Ferreira, V. M. 2007, 'Evaluation of Durability of Clay Roofing Tiles', Materiais 2007, XIII Conference of Sociedade Portuguesa de Materiais - IV International. Materials Symposium – A Materials Science Forum, Porto, Portugal, 1-4 April 2007.

Cruz, C., Veiga, M. R. & Ferreira, V. M. 2008 'Durability of Clay Roofing Tiles under Salt Mist Atmosphere', Proc. 11 DBMC International Conference on Durability of Building Materials and Components, Istanbul, Turkey, 11-14 May 2008, vol. 3, pp. 1081-1088.

Gonçalves T.D. 2007, *Salt crystallization in plastered or rendered walls*, PhD thesis, Instituto Superior Técnico (IST), Technical University of Lisbon, Portugal.

Goudie, A. & Viles, H. 1997, *Salt Weathering Hazards*, John Wiley & Sons, Ltd, Chichester, UK.

Lubelli, B. 2006, *Sodium chloride damage to porous building materials*, PhD thesis, Technical University of Delft, The Netherlands.

Rodrigues J. D. & Gonçalves T.D. 2006, 'Sais solúveis nas construções históricas. Introdução e relato sumário (Soluble salts in historic constructions. Introduction and summary)'. in Sais solúveis em argamassas de edifícios antigos. Danos, processos e soluções, CS 32, LNEC, Lisboa, 2006, pp. 1-13.

XII DBMC
International Conference on Durability of Building Materials and Components
PORTO - PORTUGAL, April 12th-15th, 2011

The Role of Moisture and Temperature Variations in the Accelerated Weathering Cycles for Durability Studies of Cellulose-Cement Composites

Conrado de Souza Rodrigues [1]
Mariana Arruda Pereira [2]

ABSTRACT

Cellulose-cement components are already produced in large scale in some world regions for more than 30 years. In spite of that, durability aspects are still addressed in recent investigations, in which the use of accelerated weathering cycles is the main approach to establish the deterioration mechanisms and the efficiency of treatment methods. Once moisture transport is the main agent leading to the deterioration of cellulose-cement composites, the accelerated ageing tests are commonly based on wet-drying cycles with a combination of temperature and moisture changes. Both variables result in dimensional changes of the samples, leading to interfacial abrasion and the progressive decrease in composites' toughness. To investigate the effects of each of these variables, the weathering tests were performed in an environmental chamber considering each variable separately using two setups for the ageing cycles. In the first one, the changes in moisture, from dry to saturated condition, occur at a constant 25°C. In the second setup, the temperature variation between 20°C and 60°C, occur at a constant 50% RH. The effects of the weathering cycles on the cellulose-cement composites were established based on physical and mechanical parameters. Part of the samples was instrumented with strain gauges, allowing the determination of the composites' expansion-shrinkage behaviour during ageing cycles. Also, the use of rice husk ash (RHA) as a supplementary cement material as a treatment approach is investigated. These weathering tests have shown that moisture variations result in higher dimensional changes than a varying temperature. Consequently, composites toughness is more affected by moisture than temperature changes. Concerning the use of RHA as a treatment approach, it was observed that it was successful, as far as the composites with RHA maintained the bending strength after the weathering cycles, while the strength of the reference composites decreased.

KEYWORDS

Agricultural wastes, Asbestos-free fibrocements, Cellulosic pulp, Mineral admixture, Rice husk ash.

[1] Civil Engineering Department (CEFET-MG), Belo Horizonte, BRASIL, crodrigues@civil.cefetmg.br
[2] Civil Engineering Department (CEFET-MG), Belo Horizonte, BRASIL, marianaarrudapereira@yahoo.com.br

1 INTRODUCTION

1.1 The Deterioration of Cellulose-Cement Composites and the Matrix Modification as a Treatment Approach

Plain and corrugated cement-based composites sheets play an important role in building construction, providing low cost roofing and dry wall systems. The worldwide application of thin fibrocement sheets was established based to a great extent, on the performance of asbestos-cement that has high strength, durability and low cost [Studinka, 1989]. Driven by the need to replace asbestos fibers in fibrocements due to health issues, alternative reinforcements have being tested since the early 70s – with cellulosic fibers being considered a viable option [Studinka, 1989]. With all the different fibers investigated since that time, it has been shown that by only replacing the asbestos fibers does not result in composites with properties fully compatible to asbestos-cement; the main differences being observed in porosity, composite structure and fiber-matrix interaction. Altogether, these changes lead to decreased strength and durability. Therefore, besides the fiber replacement, changes in matrix composition and in the production process must take place for a cement composite presenting adequate performance [Studinka, 1989].

Environmental effects due to moisture and heat variations, combined with cement hydration products, activate a range of mechanisms in the high alkalinity environment of the cementitious matrix that modify the properties of the cellulose-cement composites, impairing their long term performance. These mechanisms are described in detail in the literature [Macvicar et al., 1999; Toledo Filho et al., 2003] and specifically concern the composite's strength loss due to:
a) Interfacial debonding resulting from expansion-shrinkage cycles of fibers and matrix subjected to temperature and moisture changes;
b) Fiber embrittlement due to the migration of hydration products to the fibers' pores and lumen;
c) Alkali attack through dissolution of the cellulosic chain by some hydration products, leading to fiber deterioration.

An inherent property of cellulose fibers is their high water absorption, with high volume changes associated to their moisture content. Therefore, when the cellulose-cement composites are subjected to saturation-dying cycles, the different expansion coefficient of matrix and fibers result in a progressive interfacial abrasion. This probably takes place well before the other ageing mechanisms. The deterioration mechanisms are all strictly related to the moisture movement through the porous network of composites. Therefore, durable cellulose-cement composites can be obtained at low matrix alkalinity and reduced porosity and permeability of the matrix and interfaces, which can be achieved by matrix modification through partial replacement of ordinary Portland cement (OPC) by finely ground reactive mineral admixtures with high silica content. Both the pozzolanic reaction and the filler contribute to a denser matrix and interface, resulting in significant improvements in strength and durability [Rodrigues et al., 2010].

In this context, rice husk ash (RHA), an agricultural waste largely produced worldwide, has been investigated for more than three decades. The availability, high ash yield and high silica content make RHA a potential source of pozzolanic material for high performance cement-based materials [Bui, 2001]. However, the effects of RHA in cementitious materials strongly depend on its chemical and physical characteristics which, in turn, are derived from the burning process when rice husks are rendered to ash [James and Subba-Rao, 1986]. When applied as a supplementary cementitious material for cellulose-cement production, highly reactive RHA provided composites with decreased porosity and permeability [Rodrigues et al., 2006], improved bending [Rodrigues et al., 2010] and interfacial adhesion strength [Rodrigues et al., 2009]. Altogether, these observations strongly indicate that RHA can improve the durability of cellulose-cement composites, considering the main deterioration mechanisms in these materials.

1.2 The Durability of Cellulose-Cement Composites

The durability of cellulose-cement composites are typically investigated through accelerated ageing tests, although few studies describe the material behaviour under the natural environment, as in Akers and Studinka [1989]. A range of different test setups to deteriorate the composites are described in the literature [Akers and Studinka, 1989; Bentur and Akers, 1989; Macvicar et al., 1999; Toledo Filho et al., 2003; Mohr et al., 2007; Silva et al., 2009] and in standards [ASTM, 1999]. The degradation of the composites is mainly addressed in terms of their mechanical properties from bending or tensile tests, with the main effect of cellulose-cement composites deterioration being the decrease in toughness. Complementarily, changes in the chemical composition and in composites' structure are also reported.

The main deterioration mechanisms of cellulose-cement composites are all based on moisture movement within their pore structure, hence the different experimental setups to deteriorate these products, and reported in the literature, are based on saturation-drying cycles. However, although the basic aspects of such tests are essentially the same, the way they are developed involve differences such as the period of each cycle as well as other variables including : water soaking and drying temperatures, environment with controlled CO_2 concentration, UV radiation and convection drying under controlled wind velocity.

The simplest saturation-drying cycles comprise saturation at room temperature and drying in an electric oven at a higher temperature, typically from 50 to 80 ^{o}C. The thermal shock resulting from the temperature difference from the saturation to the drying process can cause excessive microcracking, leading to a sharp decrease in composites´ toughness only after few ageing cycles. To avoid such an extreme deterioration, the more recent studies involve drying temperatures not higher than 60 ^{o}C, sometimes with a transition step between the saturation and drying stages [Mohr et al. 2007; Silva et al. 2009].

1.3 Research Significance

Even in a simple saturation-drying cycle for the evaluation of durability of cellulose-cement composites the effects of moisture and temperature variations are mixed. Therefore, the efficiency of applying RHA as a treatment approach for cellulose-cement composites was investigated by means of ageing cycles in which each variable (temperature and moisture) was varied separately. This is accomplished by establishing two setups for the accelerated ageing cycles: changing moisture content at a constant temperature and; varying temperature at constant relative humidity. The gradual deterioration of the composites is reflected not only by the changes in the mechanical properties, but also by the overall dimensional changes of the composite. To investigate this correlation, composite samples were instrumented with electrical strain gauges, providing data on the expansion-shrinkage behaviour during the weathering cycles.

2 METHODOLOGY

2.1 Raw Materials and Composite Production

The raw materials employed in the composite matrix were: ordinary Portland cement (OPC), carbonate filler and RHA, whose chemical composition and physical properties are related in Table 1. Concerning the composition of the RHA, its carbon content of almost 21% can be considered high for its use as mineral admixture. A more adequate burning process would have allowed a sharp decrease in the carbon content, with a correspondent increase in SiO_2 and an improved reactivity of the RHA [Rodrigues et al., 2010]. However, in large scale burning of biomass for energy cogeneration, the resulted ash typically presents high carbon content. This motivated the use of RHA without any other processing for reducing its carbon content.

Kraft eucalyptus pulp was used as reinforcement at a fixed 5% related to the composite volume (corresponding to approximately 8% wt). The composites were produced by the slurry mix-vacuum

dewatering-compaction method that simulates on a laboratory scale one of the methods for fibrocement production in the industry [Rodrigues et al., 2006]. In the reference composite (thereafter referred to as REF), the matrix was composed of a combination of cement and carbonate filler in equal amounts (wt.). In the composites with RHA, the mineral admixture partially replaces cement and carbonate filler, with cement, carbonate filler and RHA contents being 35%, 35% and 30% wt., respectively. The composites were produced as square plates of 160mm x 160mm, with thickness varying from 6 mm to 8 mm. For the three point bending tests, the plates were sawed in three samples of 40mm x 160mm. For the determination of the expansion-shrinkage behaviour, linear strain gauges were fixed on the square plates, as shown in Figure 1. The instrumented composites were hung from the shelf of the chamber without any restriction to their dimensional changes.

Table 1. Major chemical composition and physical parameters of RHA, carbonate filler and OPC.

Major chemical components (%)	*RHA*	*Carbonate filler*	*OPC*
L.O.I.	20.78	42.60	3.60
SiO_2	75.22	0.66	18.86
Al_2O_3	0.90	0.17	5.29
Fe_2O_3	0.53	0.28	2.91
CaO	0.39	54.98	63.44
Physical Parameters			
S_{BET} (m^2/g)	125.23	1.61	1.89
Average particle size (μm)	5.2	36	10.27

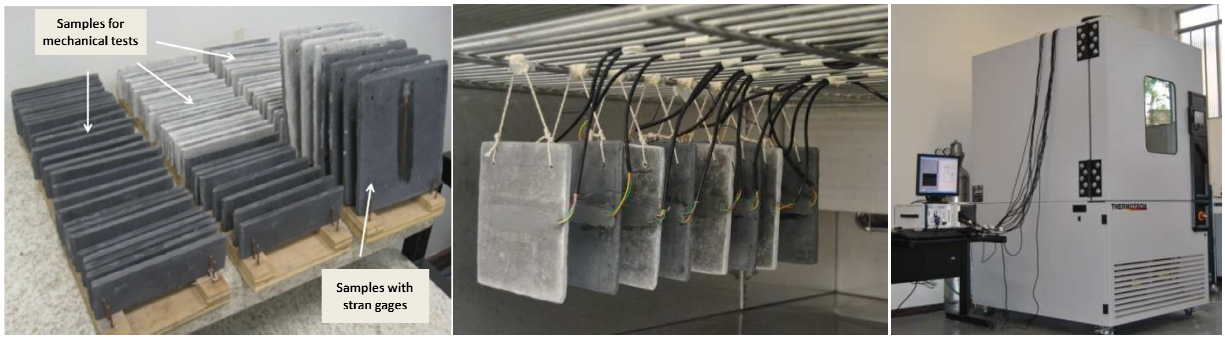

Figure 1. Composites samples prepared for the durability tests, instrumented samples arranged in the environmental chamber and the general test setup with the data acquisition system.

2.2 Weathering Cycles and Composite Testing

To establish the role of temperature and moisture on the deterioration mechanisms of cellulose-cement composites, two test setups for the accelerated ageing cycles were performed in the environmental chamber. In the first test setup (type A), the composite samples were submitted to saturation and drying at a constant 25ºC. Each saturation-drying cycle took 24 hours with 3 hours saturation in water followed by 21 hours drying at 20% RH. For the second test setup (type B), similar composites were submitted to a constant 50% RH with temperature varying from 20ºC to 60°C. The temperature changes occurred at a constant 1ºC/min, always followed by a 2 hours stabilization stage, as indicated in Figure 4. In the two test setups, 50 cycles were applied. At intermediate stages during the cycles, samples were collected for physical and mechanical characterization. The details of the three point bending tests and the determination of the mechanical parameters, as well as porosity, density and water absorption, can be found in Rodrigues et al. (2010).

3 RESULTS AND DISCUSSION

3.1 Weathering Cycles Type A (varying moisture content at a constant 25°C)

Figure 2 presents expansion-shrinkage behaviour of RHA and REF composites after the first and 50th weathering cycles. The curves show the expansion of the composites due to the water absorption and their shrinkage during the drying stage. It can be seen that composites with RHA usually present more expansion than the reference composites. Also, a maximum expansion of about 800 με in the first cycle remains somehow constant up to the 50th cycle. The more remarkable difference after 50 cycles can be observed in REF composites, with their average 500 με reduced to about 250 με.

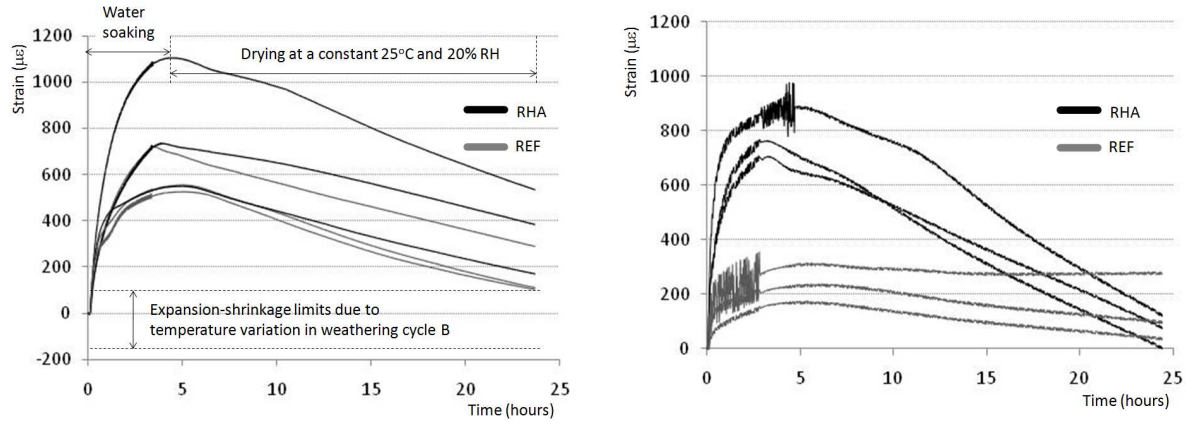

Figure 2. Expansion-shrinkage behaviour of composites after the 1st and 50th weathering cycles type A

The hygroscopic behaviour of the cellulose reinforcement and its dimensional changes due to moisture variation are the main responsible for the dimensional changes of cellulose-cement composites. Therefore, the reduced expansion and shrinkage behaviour of the REF composites may be due to deterioration of the fibre-matrix interface. Also, fibre embrittlement and its deterioration by the cement alkalis may have contributed to the changes in REF composites. In a previous study involving high carbon content RHA, it was observed that it resulted in composites with lower interfacial adhesion strength [Rodrigues et al., 2009]. Therefore, the looser bond between fibres and matrix has likewise less restriction on the dimensional changes.

At specific stages during the weathering cycles, samples were collected for physical and mechanical tests. Among the properties established from the three point bending tests, Figure 3 shows the results of bending strength (Modulus of Rupture, MOR) and the strain energy absorption (bending toughness). The latter is determined in terms of the Specific Energy – the ratio between the area under the load-deflection curve and the cross sectional area of the samples. In these cement-based composites, with short and low modulus reinforcement, the bending strength reflects mainly the matrix behaviour, while bending toughness is related to the fibre-matrix interaction.

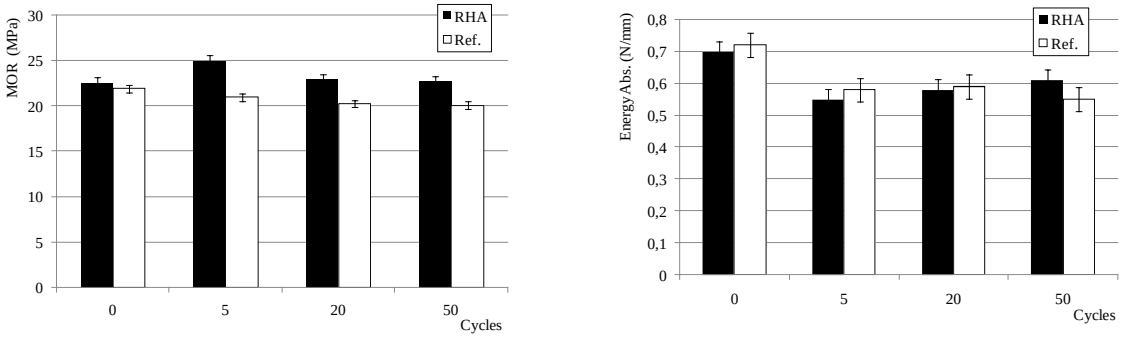

Figure 3. Effects of RHA and the weathering cycles type A on strength and toughness of composites

It can be observed in Figure 3 that REF and RHA composites presented similar mechanical behaviour before the weathering test. This can be considered a very positive aspect, once one considers the high amount of an agricultural waste incorporated in the composite matrix. In all intermediate stages during the type A watering cycles, RHA composites presented higher bending strength than REF composites. While the MOR of RHA composites remained almost constant during the cycles, the strength of REF composites presented a slight decrease just after 5 cycles, after that the strength remained constant up to the 50th cycle. Considering that the bending strength of cement based composites reinforced by low modulus fibres is governed by the matrix, it can be concluded that the introduction of RHA results in significant changes to the matrix structure that contribute to its higher strength. These changes are even more relevant if one considers that in RHA composites less cement is applied when compared to the reference composites formulation.

The energy absorption behaviour of REF and RHA composites are similar. There is a decrease in specific energy after 5 weathering cycles and the values remain without significant changes up to 50 cycles. This indicates that significant damage to the composites occurs during the first saturation-drying cycles. Probably, this is interfacial damage resulting from the high volume changes of the fibres due to their high capacity for water absorption.

Concerning the apparent porosity and water absorption, significant changes were not observed with the weathering cycles. RHA composites present higher apparent porosity, about 70%, and water absorption, circa 30%, as compared to the reference composites, which presented apparent porosity and water absorption of 45% and 18%, respectively. The high specific surface area of RHA (125 m^2/g) indicates that the particles have a highly porous surface. The introduction of RHA in the cement matrix thus incorporates additional pores in the matrix, leading to the increased overall porosity of RHA composites. When these physical properties are compared to the expected mechanical parameters, the higher strength of RHA composites seems to be incompatible with its higher porosity. This perhaps reflects the high degree of reactivity of RHA, resulting in the formation of additional calcium silicate hydrates through the pozzolanic reaction, and therefore contributing to improved bending strength, in spite of the increase in porosity of the composite.

3.2 Weathering Cycles Type B (varying temperature at a constant 50% RH)

In Figure 4 it can be evaluated the effects of the varying temperature under a constant 50% RH on the dimensional changes of the composites after the 1st and 50th weathering cycle. Different from cycle type A, 50 cycles type B did not result in significant modifications in expansion and shrinkage behaviour of both RHA and REF composites. Also, the dimensional changes occur within narrower limits when compared to cycle A. Once the composites presented expansion sometimes higher than 1000 με during saturation in cycle A, the temperature changes in cycle B resulted in expansion and shrinkage of up 100 με and 150 με, respectively, as indicated in Figure 2.

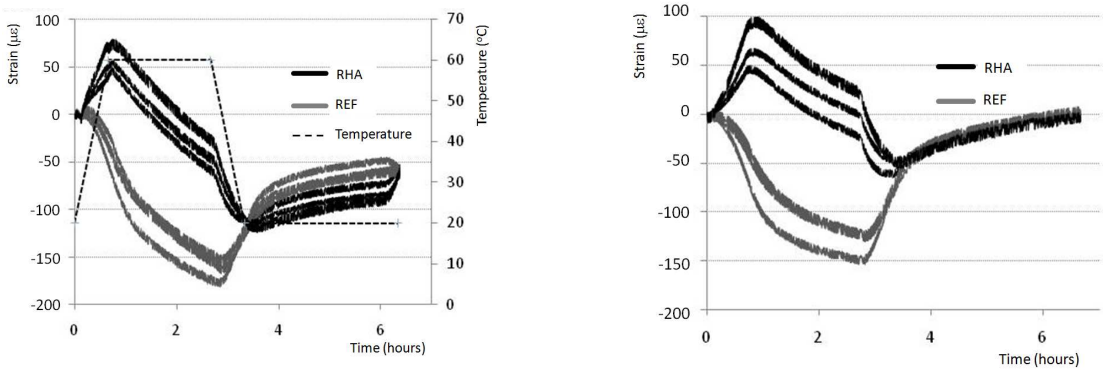

Figure 4. Expansion-shrinkage behaviour of composites after the 1st and 50th weathering cycles type B

The dimensional changes of RHA and REF composites are quite different under the temperature changes during the cycle B; being not exactly what would be expected in principle. Instead an expected expansion during the higher temperatures and shrinkage during the lower ones, the curves representing the dimensional changes show a more complex behaviour. As the temperature rises from 20°C to 60°C, REF composites shrink, while RHA composites expand. During the 2 hours stabilization period at 60°C both composites behave similarly, presenting shrinkage. When the temperature decreases from 60°C to 20°C, the composites present opposite behaviour again, with shrinkage of RHA and expansion of REF composites. In the final stage, with 2 hours stabilization at 20°C, the dimensional changes of RHA and REF became very similar, sometimes with coincident curves in the graphic.

The general aspect of the dimensional changes and the differences between RHA and REF composites can be explained in terms of the heat transport mechanisms through the composites' thickness and the fact that curves in Figure 4 only reflects the strain on the surfaces of the samples. Also, the fact that RHA composites present a higher porosity (70%) than REF composites (45%) is an important factor. After the expansion of RHA composites during the temperature rising, during the stabilization stage their surfaces lose heat to the inner parts of the composites samples. The rate at which this heat transfer occurs (heat conduction) is higher than that of the heat transfer from the environment to the surface (heat convection). So, the surface of the samples shrinks during the temperature stabilization stage. During the temperature decrease, the surface of RHA composites shrinks at a higher rate. Finally, when the temperature of the chamber stabilizes at 20°C, as the core of the composite became more hot than the surface, the migrates to the outer parts of the composites and the surface expands.

The differences between REF and RHA composites are observed mainly during the temperature rising and decrease. Here, the denser and less porous structure of REF composites play an important role. During the temperature increase, the heat is readily transferred from the surface to the core of the plates through heat conduction. As the surface loses heat, it shrinks. On the other hand, when the temperature of the chamber decreases, the same mechanism is responsible to bring the heat from the inner part of the plate to its surface, which expands.

The effects of the weathering cycles B on the mechanical behaviour of the composites are shown in Figure 5. Although the dimensional changes observed in weathering cycles type B are much smaller than those in cycles type A, they were enough to cause a strength decrease of REF composites. The more pronounced strength decrease occurs just after the first five cycles and may be due to matrix microcracking. In RHA composites, there were not significant changes in strength due to temperature variation. Their bending strength remained about 20% higher than that of REF composites during the weathering process. Concerning the composites toughness, Figure 5 shows that no noticeable changes result from the type B cycles.

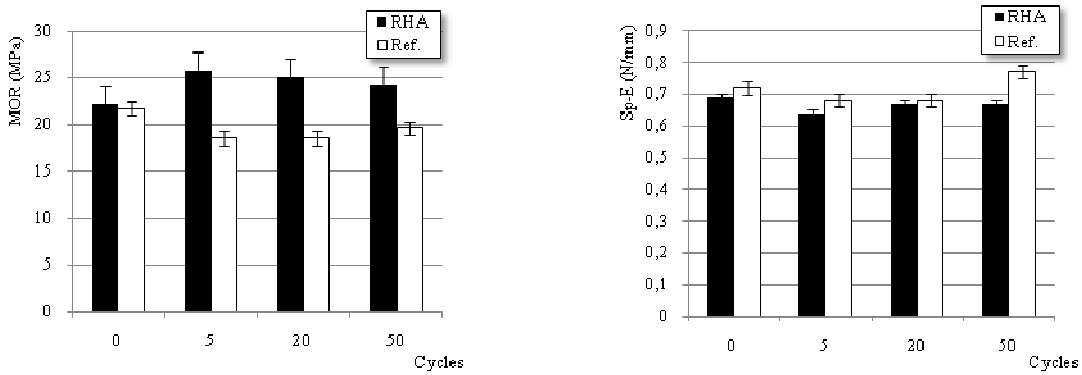

Figure 5. Effects of RHA and the weathering cycles type B on strength and toughness of composites

5 CONCLUSIONS

Once the main tests for durability of cement composites relay on a varying moisture and temperature, this study provided useful information on the role of each of these agents. The higher dimensional changes were observed in cycles with saturation-desorption at a constant 25°C, in which the expansion of the composites could reach 1000 με during saturation. The role of temperature variations on dimensional changes obtained by electrical strain gauges is more complex, being dependent on the heat transport through the composites' thickness and, therefore on the pore structure of the samples. Both weathering cycles applied resulted in decreased bending strength of the reference composites (without the use of rice husk ash, RHA, as a mineral admixture), while the composites with RHA maintained the bending strength along with the weathering cycles. Therefore, the use of RHA can be regarded as a proper strategy for obtaining high performance cellulose-cement composites. Usually, the more pronounced effect of cellulose-cement deterioration is the toughness loss. It was observed that this effect is due to the moisture variations during the ageing process, as far as there were no noticeable changes when only temperature variation was applied (at a constant 50% RH). Finally, the use of an environmental chamber for setting the two different weathering tests has resulted in valuable data on the role of moisture and temperature on the deterioration process of cellulose cement composites. This will be helpful in studies on the synergetic effects of these variables in weathering cycles in which they are combined.

ACKNOWLEDGMENTS

The authors would like to thank CAPES for the financial support of this project through the *Pró-Engenharias* program. Also, the support from the FAPEMIG, CNPq and CEFET-MG is also acknowledged.

REFERENCES

Akers, S.A.S., Studinka, J. B. 1989, 'Ageing behaviour of cellulose fibre cement composites in natural weathering and accelerated tests'. *The International Journal of Cement Composites and Lightweight Concrete*, 11[2], p. 93-97.

American Society for Testing and Materials (ASTM). 1999 C 1185 – *Standard Test Methods for Sampling and Testing Non-Asbestos Fiber-Cement Flat Sheet, Roofing and Siding Shingles, and Clapboards*.

Bentur, A., Akers, S.A.S. 1989, 'The microstructure and ageing of cellulose fibre reinforced cement composites cured in a normal environment'. *The International Journal of Cement and Lightweight Concrete*, 11[2], p. 99-109.

Bui, D.D. 2001, *Rice husk ash as a mineral admixture for high performance concrete*, Delft Univ. Press, Delft.

James, J., Subba-Rao, M. 1986, 'Reactivity of rice husk ash'. *Cement and Concrete Research*, 16, 296-302.

Luxán, M.P.; Madruga, F.; Saavedra, J. 1989, 'Rapid evaluation of pozzolanic activity of natural products by conductivity measurement'. *Cement and Concrete Research*. 19, pp. 63-68. USA.

MacVicar, R., Matuana, L.M., Balatinecz, J.J. 1999, 'Aging mechanisms in cellulose fiber reinforced cement composites'. *Cement and Concrete Composites*, 21, 189-196.

Mohr, B.J.; Biernacki, J.J.; Kurtis, K.E. 2007, 'Supplementary cementitious materials for mitigating degradation of kraft pulp fiber-cement composites'. *Cement and Concrete Research*, USA, 37, p.1531-1543.

Rodrigues, C.S., Ghavami, K., Stroeven, P. 2006, 'Porosity and water permeability of rice husk ash-blended cement composites reinforced with bamboo pulp'. *Journal of Materials Science*, 41, 6925-6937.

Rodrigues, C.S., Stroeven, P., Ghavami, K. 2009, 'Assessment by law of mixtures approach of interfacial adhesion strength in cellulose-cement composites'. In: Brandt, A.M., Olek, J., Marshall, I.H. (ed). *Procceedings of the Ninth International Symposium on Brittle Matrix Composites - BMC*9. Warsaw,p.71-80.

Rodrigues, C.S.; Ghavami, K., Stroeven, P. 2010, 'Rice husk assh as a supplementary raw material for the production of cellulose-cement composites with improved performance'. *Waste and Biomass Valorization*, 1[2], p.241-249.

Silva, F. A. ; Mobasher, B.; Toledo Filho, R.D. 2009, 'Cracking Mechanisms in Durable Sisal Fiber Reinforced Cement Composites'. *Cement & Concrete Composites*, 31, p. 721-730.

Studinka, J. B. 1989, 'Asbestos substitution in the fibre cement industry'. *The International Journal of Cement Composites And Lightweight Concrete***,** 11[2], p. 73-78.

Toledo Filho, R.D., Ghavami, K., England, G.L. 2003, Scrivener, K. 'Development of vegetable fibre-mortar composites of improved durability'. *Cement & Concrete Composites*, 25, 185-196.

XII DBMC
International Conference on Durability of Building Materials and Components
PORTO - PORTUGAL, April 12th-15th, 2011

Corrosion of Fasteners in Treated Timber Field Exposure Testing

Zhengwei Li [1]
Nick Marston [2]
Mark Jones [3]

ABSTRACT

Past research by BRANZ has found that under laboratory conditions timber treatments using alkaline copper quaternary (ACQ) and copper azole (CuAz) preservatives cause more corrosion of hot dip galvanised (HDG) fasteners than copper chrome arsenate (CCA) treatments. Field exposure tests are underway at BRANZ' site, in the Wellington region of New Zealand, to confirm whether these observations apply under natural weathering conditions for HDG coated steel, mild steel and stainless steel components.

Assessments completed after the first and second year field exposures have confirmed that CuAz and ACQ treated timbers have an increased aggressivity towards metals in comparison with CCA treated timbers under identical conditions. Consequently, HDG and mild steel nails and screws embedded into timbers treated with CuAz and/or ACQ, particularly at higher treatment levels, showed significant corrosion. Unsurprisingly, components made of austenitic stainless steel exhibited excellent performance in all timbers, no signs of corrosion were observed after a two year exposure.

The increased corrosivity of CuAz and ACQ treated timbers suggests that corrosion rate increases with initial copper content in the treated timbers. This implies that copper ions are being reduced by active steel components. However, it is believed that other mechanisms are also contributing to deterioration of the metallic components..

KEYWORDS

Corrosion, Timber, Preservation, Field test.

[1] BRANZ Ltd, Judgeford, Porirua City, Wellington, New Zealand, Zhengwei.Li@branz.co.nz
[2] BRANZ Ltd, Judgeford, Porirua City, Wellington, New Zealand, Nick.Marston@branz.co.nz
[3] BRANZ Ltd, Judgeford, Porirua City, Wellington, New Zealand, Mark.Jones@branz.co.nz

1 INTRODUCTION

Timber retains its prime importance within the building industry because of its diversity, sustainability, versatility and aesthetic properties [Falk 2009]. However when exposed to the environment, timber deteriorates due to biological, chemical, mechanical, photochemical and thermal effects [Illston & Domone 2001]. To combat these effects, preservation treatments are commonly applied to enhance its durability [Archer & Lebow 2006].

Most timbers are aggressive towards metals due to the hydrolysis of acetyl radicals to acetic acid in the presence of moisture. Preservation chemicals can also be a potential corrosion hazard. It is well-known that water-borne preservatives could cause accelearted degradation for susceptible metals because they provide added oxidisers for corrosion. As a result the corrosivity of timbers treated with copper chrome arsenate (CCA) alternatives, e.g., copper azole (CuAz) and alkaline copper quaternary (ACQ), has become a concern due to their considerably higher copper retention [Simpson Strong Tie 2006].

The performance of metallic components in timbers is critical to the durability and stability of timber structures. Despite a lack of fundamental understanding of metal corrosion in timber, there have been several attempts to create rapid, quantitative testing techniques to evaluate the corrosion performance of metal in contact with timber. The American Wood-Preservers' Association (AWPA) standard, E12, is a popular methodology used by timber preservers and fastener manufactures to addresses corrosion of metal in contact with treated timber [AWPA 2004]. However the results obtained must be interpreted carefully since the testing conditions are not representative of common exterior corrosion environments. The corrosion rate derived cannot be extrapolated to all possible scenarios because it is not possible to correlate the corrosion of metal in timber exposed to high temperature and high humidity environments to the corrosion rate under real service conditions.

The simplest way to evaluate the corrosion performance of a metal in contact with a specified timber is to expose the metal-timber assembly directly to the environment of interest. Hence, outdoor exposure is the most reliable method to evaluate the degradation behaviour of metal in timber and has been widely used to provide useful information for the development of preservatives, timber based construction materials and timber-metal structures. Although short-term, accelerated test results on corrosion of metals in ACQ and CuAz treated timbers are available [Kear *et al*. 2005 & 2009], there is a lack of long-term and reliable exposure data in the public domain. Therefore, BRANZ has completed field exposure testing of the degradation of typical fasteners in Pinus radiata treated with CCA, CuAz and ACQ. This paper reports the findings from the intital stage of this exposure study.

2 EXPERIMENTAL

2.1 Timber and Preservation Treatment

Rough-sawn kiln-dried Pinus radiata sapwood with nominal cross-sectional dimensions of 100×100 mm and 100×50 mm was custom-treated with CCA (oxide), CuAz (CA-B containing tebuconazole) and ACQ (ACQ-B containing didecylthyl ammonium chloride for H3.2 and ACQ-C containing alkylbenzyldimethyl ammonium chloride for H4). Post treatment, the timbers were stored at 25°C and 55% RH for one month and then cut to the required size with their longest dimension running in parallel to the wood grain. Gate-shaped structures were constructed to incorporate mild steel, galvanised steel (hot dip galvanising and mechanical plating) and stainless steel (AISI 304 & 316) nails and screws in a quasi-realistic application. These were then exposed at BRANZ' natural weathering site on the Judgeford campus in the Wellington region of New Zealand.

2.2 Corrosion Tests

After exposure, a set of the metallic components were retrieved. Surface morphology was examined visually and microscopically. Corrosion products were then removed using the procedures

recommended by ASTM G1. The consequent mass loss enabled corrosion rates to be quantified for various combinations of steel, preservative and hazard class.

3 RESULTS AND DISCUSSION

3.1 Timber Moisture Content

The moisture content of the timber blocks of the gate-shaped structures was monitored periodically using an electrical resistance type moisture meter to probe the moisture content variation with rainfall and season. Determined moisture contents ranged from 10 to 30% in CCA treated timbers and 13 to 50% for CuAz/ACQ treated timbers. However, due to the shallow penetration depth of moisture meter probes and non-uniform wetting of the timber these results should be regarded as indicative.

3.2 Corrosion Morphology

3.2.1 One-year exposure

After one year, mild steel fasteners suffered relatively uniform corrosive attack across all of their surfaces. However, fasteners in contact with untreated and CCA treated timbers were in very much better condition than those removed from ACQ and CuAz treated timbers (Fig. 1).

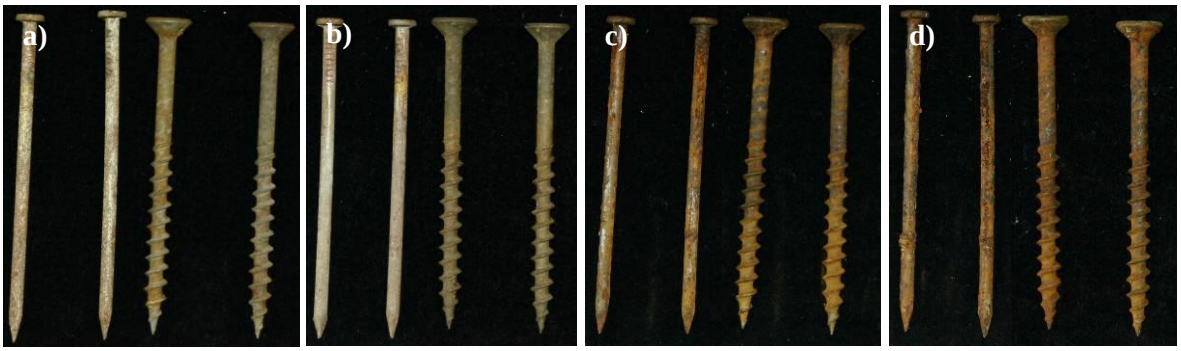

Figure 1. Surface morphology of mild steel fasteners embedded into timbers exposed at Judgeford, NZ for one year. (a) Untreated, (b) H3 CCA, (c) H3 CuAz and (d) H3 ACQ.

Unsurprisingly, hot dip galvanised nails performed better than mild steel nails in all timbers. The zinc coating on the head of the nails was still in relatively good condition. No obvious corrosion failures were observed. Instead, corrosion was mainly localised to the shaft and tip areas. This performance difference probably relates to the corrosivity difference betwen the atmosphere and the micro-environment inside the timber and to damage caused by the nail hammering process.



Figure 2. Surface morphology of and zinc coated fasteners embedded into timbers exposed at Judgeford, NZ for one year. (a) H4 CCA, (b) H4 CuAz, (c) H3 ACQ and (d) H4 ACQ.

Patterns of material degradation on the zinc coated screws are more complex. The heads of the screws remained basically sound, though a small number showed partial failures along the margin and at the bottom of the square drive mortise. The spiral sections appeared to be the most susceptible to corrosion. Corrosion of the underlying steel substrate, shown as red iron-rich rust, could be easily observed even for those embedded into untreated timber. This suggests stresses associated with the driving-in process have partially damaged the zinc coating, leaving more structural defects.

The quantity of corrosion products formed was strongly related to the timber treatment, both with respect to preservative type and hazard class. Corrosion was more extensively developed for nails embedded in the CuAz and ACQ treated timbers, particularly, at the H4 treatment level. In comparison, nails in CCA timber were in much better condition, as may be seen by comparing the respective images in Fig. 2. Screws in ACQ and CuAz treated timbers, even at the H3.2 preservative level, were extensively rusted on the bodies. Some screws embedded into the H4 ACQ timbers were, in fact, so corroded that they could not be extracted intact. The results clearly indicate that ACQ and CuAz treated timbers are more corrosive than CCA treated timber.

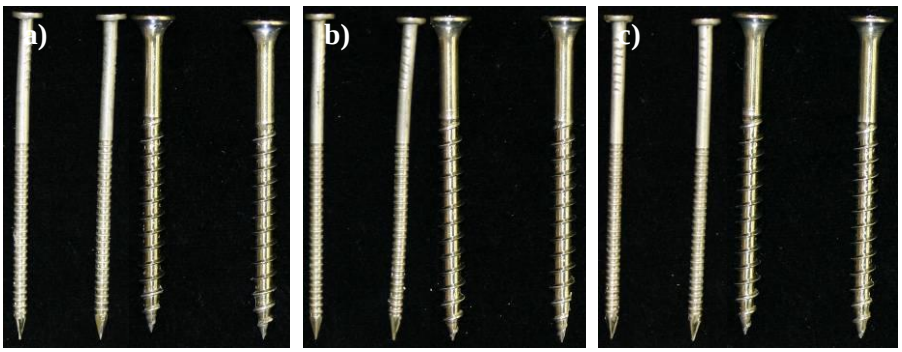

Figure 3. Surface morphology of stainless steel fasteners embedded into timbers exposed at Judgeford, NZ for one year. (a) H4 CCA, (b) H4 CuAz and (c) H4 ACQ.

Stainless steel nails and screws performed very well in all combinations of preservative type and hazard class. No obvious sign of corrosion was observed on their body sections (Fig. 3). Occasionally very limited iron-rich rust could be observed on heads where directly exposed to the atmosphere. This is likely the result of partial damage to the passive film and/or iron contamination from the hammer when the fastener was driven into the timber.

3.2.2 Two-year exposure

On some mild steel nails inserted into CuAz or ACQ treated timbers, degradation of the metal was very serious, leading to observable thickness reduction in some areas after two years of exposure to the atmosphere. On mild steel screws, serious corrosion was again mainly found in the thread areas. Small pits were also found on the shank areas.

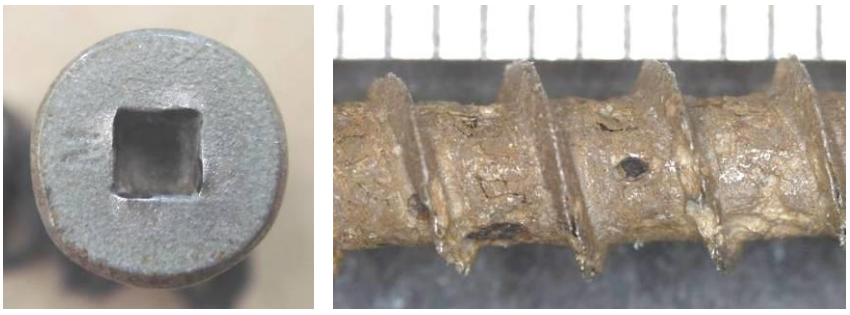

Figure 4. Morphologies of head and thread of a zinc coated screw retrieved from H4 ACQ treated timber exposed at Judgeford, NZ for two years.

There was still limited red rust formation on the galvanised nails embedded into untreated timbers and timbers treated to an H3 level with CCA, CuAz and ACQ. This indicates that most areas were still protected by zinc. In timbers treated to an H4 level, in particular those treated with CuAz and ACQ, rust formation was quite obvious. Rust was more pronounced on the zinc coated screws, even in timbers treated with H3 CCA. It was noted that there was a marked difference in the condition of the head and the body of the zinc coated nail/screws after two years of exposure (Fig. 4). This makes the identification of any pre-mature failure of fasteners more difficult using non-invasive techniques.



Figure 5. Morphologies of head and body section of stainless steel fasteners retrieved from H4 ACQ treated timber exposed at Judgeford, NZ for two years.

Stainless steel fasteners performed very well in all timbers (Fig. 5). A comparison between the rust formed after one and two years indicated that this corrosion was progressing extremely slowly.

3.3 Estimation of Corrosion Rates

3.3.1 Corrosion rate derived from the first year of exposure

For the purpose of calculations, densities of mild steel and zinc were assumed to be 7.86 g/cm^3 and 7.14 g/cm^3 respectively. As observed from morphological characterisations, the zinc coatings on some fasteners were completely consumed. As a result, the corrosion products included both zinc and iron-bearing constituents and the mass loss recorded reflected an indeterminate combination of both the zinc coating and the steel substrate. This complicated calculating an unambiguous corrosion rate. Therefore, it was simply assumed that the mass loss of zinc coated fasteners was due to the loss of zinc alone. Hence, the corrosion rates derived from the mass loss measurements presented here on severely corroded fasteners can only be used as an indication of the corrosivity of the timber and the degradation of fastener. The mass loss was expressed as mm/year and a standard deviation was calculated for five replicate specimens removed from each timber treatment variant (Figs 6 and 7).

Corrosion rate of fateners in CCA (H3.2 & H4) treated timbers was relatively low and did not differ greatly from that of those embedded in untreated timber. In contrast, CuAz and ACQ treatments promoted markedly increased corrosion rates. For example, the mild steel nails had a corrosion rate of 6.63×10^{-2} mm/year in H4 ACQ treated timber, while the equivalent corrosion rates in H4 CCA and untreated timbers were 1.87×10^{-2} mm/year and 2.66×10^{-2} mm/year, respectively. Zinc coating provided enhanced protection, reflected in lower mass losses in all timbers (the only exception is the zinc coated screw in H4 CuAz treatment). However, corrosion acceleration by CuAz and ACQ treatments was more obvious. For instance, the corrosion rates of galvanised nails in H4 CuAz and H4 ACQ treated timbers were 6.2 and 7.4 times greater, respectively, than that of the nails in H4 CCA.

The mass loss of the stainless steel fasteners was extremely limited and very close to, or lower than the value of the error associated with the measurement technique. Hence, it is impossible to determine the potential influence of timber preservation treatment on their performance. As a result, their corrosion rates will not be reported in this paper. This again indicates that they had a very favorable level of corrosion resistance when in contact with all types of timbers used in this testing.

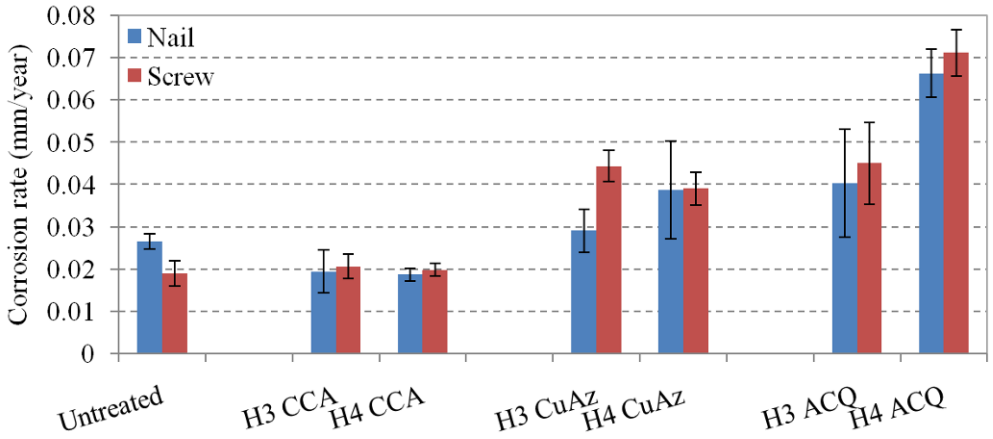

Figure 6. Corrosion rates of mild steel fasteners in timbers exposed at Judgeford, NZ for one year.

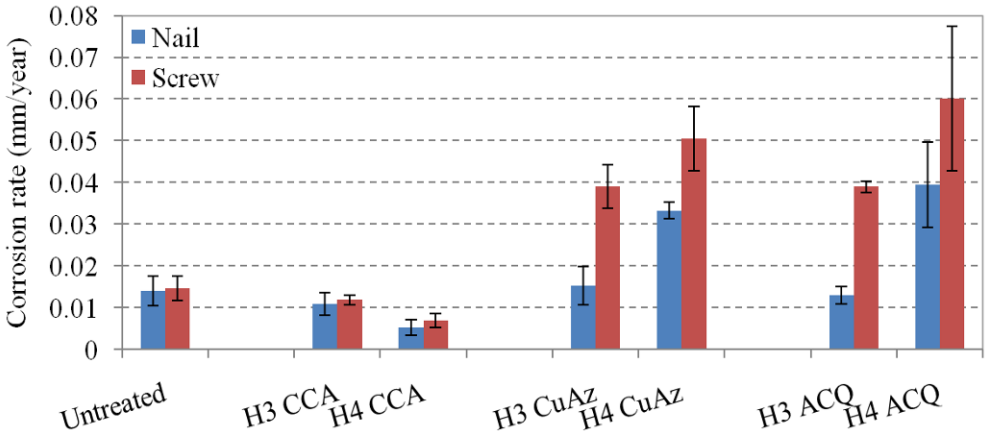

Figure 7. Corrosion rates of galvanised fasteners in timbers exposed at Judgeford, NZ for one year.

3.3.2 Correlation between corrosion rate and copper retention

CCA, CuAz and ACQ all contain copper as the principal fungicidal component. The retention levels of copper for each are quite different at the same NZS 3640 hazard class [NZS 3640]. The present results indicate that a specific grade of metallic component perform quite differently in timber treated with each of the preservatives. Corrosion of metal in treated timber is a complex process and is not well understood. One explanation widely cited is the reduction of copper ions by active metallic constituents in steel, such as iron or zinc [Baker 1980]. According to this hypothesis, a higher corrosion rate would be observed when steel is embedded in a timber with a higher copper content.

Figures 8 and 9 present the correlation between retained copper content in the treated timber and the experimentally-measured corrosion rate of nails in this study. It can be seen that:

- The corrosion rates of mild steel fasteners in H3 & H4 CCA treated timbers are approximately equal despite the retained copper in H4 being virtually double that in the H3.2 grade;

- Fasteners in CuAz and ACQ treated timbers have a higher corrosion rate than those in CCA treated timber. On average, CuAz and ACQ treated timbers have a higher copper content than CCA treated timber. The copper retention ratio of H4 CCA, CuAz and ACQ is 1:2.05:3.32 while the corrosion rate ratios are 1:2.07:3.55 for mild steel nail and 1:6.24:7.40 for hot dip galvanised nails;

- An increase of hazard level from H3.2 to H4 in CuAz and, particularly, in ACQ treated timbers will increase corrosion rate. The copper content in H4 ACQ treated timber is about 3 times as high as the content in H3 ACQ treated timber, however the corrosion rate in H4 ACQ treated timber is only about 1.6 times as high as the rate in H3 ACQ treated timber.

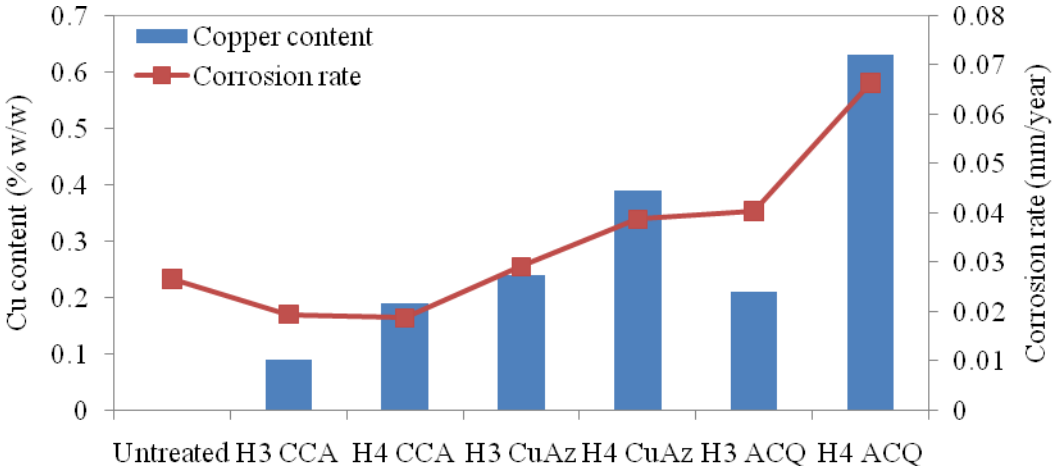

Figure 8. Correlation between mean copper retention measured in the unexposed timber and corrosion rate of mild steel nails embedded in the timbers exposed at Judgeford, NZ for one year.

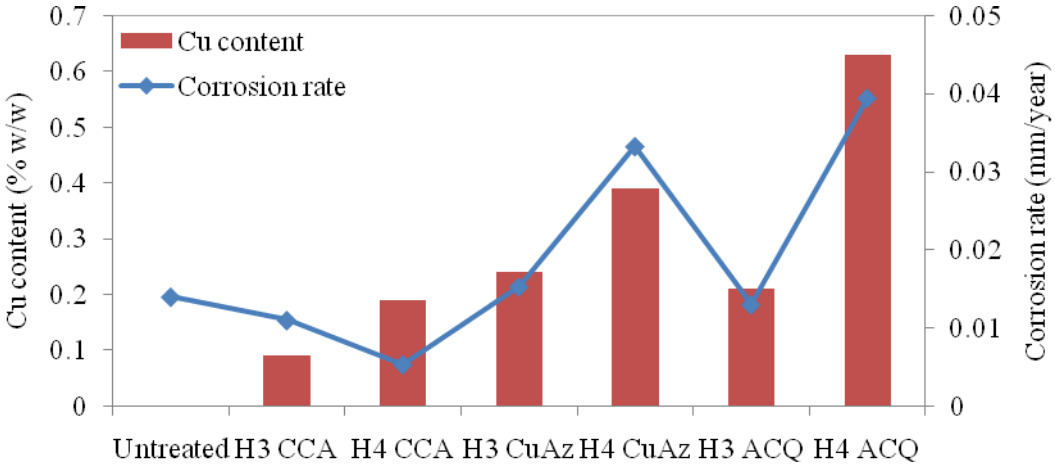

Figure 9. Correlation between mean copper retention measured in the unexposed timber and corrosion rate of hot dip galvanised nails embedded in the timbers exposed at Judgeford, NZ for one year.

These observations indicate that copper retention has a degree of correlation with corrosion performance of steel fasteners embedded into the treated timbers. However, copper ion reduction is unlikely to be the only mechanism actively responsible for the enhanced corrosion rates seen [Zelinka *et al*. 2008]. The moisture content of the timbers exposed at Judgeford, NZ was then monitored semi-continuously using an electrical-resistance moisture meter. The results showed that CuAz and ACQ treated timbers normally had a higher moisture content than CCA treated timbers. On the other hand, the hexavalent chromium, Cr^{6+}, in CCA, can potentially act as a corrosion inhibitor, and the arsenic may also confer corrosion resistance [Murphy 1998]. These factors may contribute to the complex corrosion phenomena observed.

To more fully understand the corrosion mechanism, the micro-environments created by the interactions between preservatives and wood components would need to be better understood together with the influences of climatic conditions on the hydrolysis, migration and loss of preservation chemicals.

4 CONCLUSION

This paper confirms the hypothesis that both CuAz and ACQ treated timbers are capable of greatly accelerating the corrosion of mild steel and zinc coated steel fasteners relative to both untreated and CCA treated timbers. Given that mean corrosion rates of mild steel and zinc coated items measured could be three to eight times higher in timber treated with ACQ or CuAz preservatives than CCA, the use of either AISI 304/316 grades of stainless steel or durable equivalents such as silicon bronze are recommended for timber structures that require long-term durability and would frequently get wet during service.

ACKNOWLEDGMENTS

This work was supported by New Zealand Building Research Levy.

REFERENCES

Archer, K. & Lebow, S. 2006, Chapter 9: Wood preservation, in *Primary Wood Processing: Principle and Practice*, 2nd Edition, ed J.C.F. Walker, Springer, Dordrecht.

ASTM G1-03, Standard Practice for Preparing, Cleaning, and Evaluating Corrosion Test Specimens, ASTM International, United States.

AWPA E12, 2004, Standard Method of Determining Corrosion of Metal in Contact with Treated Wood, American Wood Preservers' Association, Selma.

Baker, A. 1980, 'Corrosion of metal in wood products', in *Durability of Building Materials and Components*, ASTM STP 691, eds. P.J. Sereda and G.G. Litvan, American Society for Testing and Materials, pp. 981–993.

Falk, B. 2009, 'Wood as a sustainable building material', *Forest Product Journal*, **59**, 6–12.

Illston, J. & Domone, P. 2001, *Construction Materials: Their nature and behavior* (3rd ed.), Taylor & Francis Group, London, New York.

Kear, G., Jones, M. & Haberecht, P. 2005, 'Corrosion of mild steel, HDG steel and 316 stainless steel in CCA, CuAz and ACQ treated pinus radiata', Proceedings of the 16th International Corrosion Congress, Beijing, China, 19-24 September 2005.

Kear, G., Wu, H. & Jones, M. 2009, 'Weight loss studies of fastener materials corrosion in contact with timbers treated with copper azole and alkaline copper quaternary compounds', *Corrosion Science*, **51**, 252–262.

Murphy, R. 1998, Chromium in timber preservation, The Chromium File, No.5, http://www.icdachromium.com.

NZS 3640, 2003, Chemical Preservation of Round and Sawn Timber, Standards New Zealand, Wellington 6020, New Zealand.

Simpson Strong Tie, 2006, Preservative treated wood, Technical Bulletin T-PTWOOD06, Simpson Strong Tie, http://www.strongtie.com.

Zelinka, S., Rammer, D. & Stone, D. 2008, 'Electrochemical corrosion testing of fasteners in extracts of treated wood', *Corrosion Science*, **50**, 1251–1257.

XII DBMC
International Conference on Durability of Building Materials and Components
PORTO - PORTUGAL, April 12th-15th, 2011

Accelerated Laboratory Ageing of Vacuum Insulation Panels

Erlend Wegger [1]
Bjørn Petter Jelle[1,2]
Erland Sveipe[1]
Steinar Grynning[2]
Arild Gustavsen[3]
Jan Vincent Thue[1]

ABSTRACT

A vacuum insulation panel (VIP) represents a high performance thermal insulation material solution. With thermal conductivities as low as 4.0 mW/(mK) it offers a solution of how to meet future requirements for thermal efficiency of buildings, while retaining slim building envelopes.

VIPs consist of a porous core, usually fumed powder silica (SiO_2), which is sealed in a gas and vapour tight envelope maintaining vaccum in the core. During the lifetime of VIPs, air gases and water vapour permeate through the barrier envelope, reducing the thermal performance. This process is highly dependent upon the external climate factors of the panel. To better evaluate the performance of VIPs over time, and to study how the external climate affects VIP ageing, accelerated ageing test are necessary. Hence, a theoretical and experimental study into accelerated ageing have been performed.

The external factors found theoretically to contribute most to the ageing of VIPs are temperature, moisture and pressure. Utilizing these theoretical relationships, accelerated ageing experiments are designed to test the theoretical predictions and evaluate the ageing effects on VIPs. Within this study, thermal conductivity is employed for evaluation of VIP performance.

KEYWORDS

Accelerated ageing, Vacuum insulation panel, VIP, Thermal insulation.

[1] Department of Civil and Transport Engineering, Norwegian University of Science and Technology (NTNU), NO-7491 Trondheim, Norway
[2] Department of Materials and Structures, SINTEF Building and Infrastructure, NO-7465 Trondheim, Norway
[3] Department of Architectural Design, History and Technology, Norwegian University of Science and Technology (NTNU), NO-7491 Trondheim, Norway

1 INTRODUCTION

For several decades, thermal insulation has been the preferred way to improve the energy efficiency of buildings, and the thermal insulation requirements have increased steadily. Increasing wall thicknesses and amounts of insulation are a challenge both for architects and engineers in building aesthetically, economically and in accordance with sound building physical principles.

Vacuum insulation panels (VIPs) might offer a solution to this problem. VIPs consist of a solid, porous core which is sealed with an airtight and watertight laminate maintaining a vacuum in the core. VIPs have thermal conductivities that are 5-10 times lower than for traditional thermal insulation. Thus, it will be possible to reduce the thickness of the building walls, and at the same time retain or even increase the thermal resistance.

As an innovative material solution, special concern is given to the performance of VIPs during time. The thermal performance will decrease over time, as air gases and water vapour penetrate through the barrier envelope. To evaluate the performance and ageing effects of VIPs, accelerated ageing experiments are vital for such investigations to be carried out within a limited timeframe. As no standardized methods exist at the moment, a variety of ageing experiments are tested to evaluate their suitability as accelerated ageing methods for VIPs.

The ageing of VIPs depend both on the core material of the panels, and on the materials used for envelope barrier. The most common core material for VIPs are pressed fumed silica or pyrogenic silica (SiO_2), which is a fine powdered, highly porous, silica based material with low solid state conductivity. This low solid state conductivity combined with low gas conduction in the vacuum pores lead to the high thermal performance of VIPs.

As envelope barriers the most common materials are so called multilayer (MF) foils, which consist of several layers of aluminum-metalized polyethylene terephthalate (PET) or polypropylene (PP) sheets sealed on the inside with a polyethylene (PE) layer. This provides sufficient gas and vapour tightness and a minimal thermal bridge at the panel edges. A variety of foil configurations are shown in Figure 1.

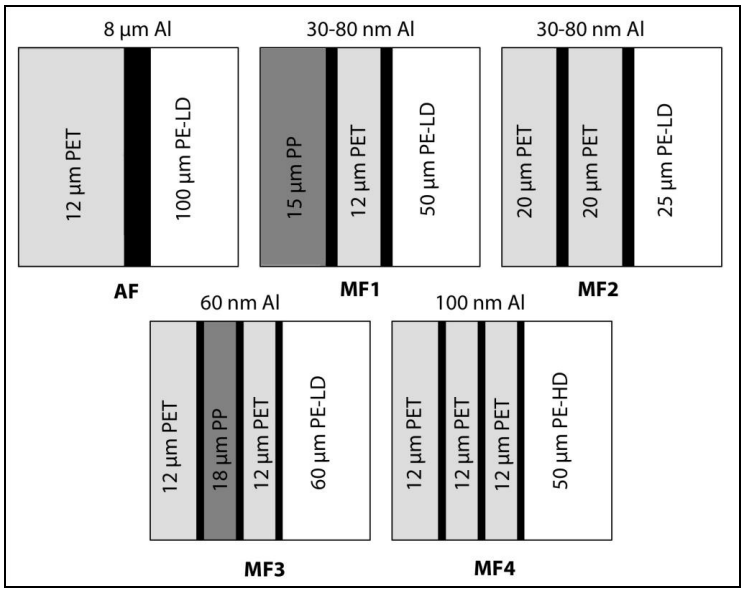

Figure 1. Cross-sections of various envelope solutions for application in VIPs. The drawing is not to scale.

2 BACKGROUND

The ageing of VIPs is dependent upon the gas and vapour diffusion through the envelope barrier into the core. This will only be summarized briefly here. A comprehensive review of most VIP aspects can be found in Baetens *et al.* (2010).

The total center-of-panel thermal conductivity of VIPs (λ_{tot}) is considered as a sum of the contributions from solid conductivity (λ_{cd}), gaseous conductivity (λ_g), radiative thermal conductivity (λ_r), and conduction due to air and moisture convection in the pores (λ_{cv}). In addition a coupling term (λ_{coup}) is added to account for the interaction between the gas molecules and the pore walls [Brodt 1995].

$$\lambda_{tot} = \lambda_r + \lambda_{cd} + \lambda_g + \lambda_{cv} + \lambda_{coup} \tag{1}$$

As gas and water vapour penetrate the barrier foil, the gas pressure and water content of the core increases, leading to an increased gaseous and solid thermal conductivity. The increase in thermal conductivity over time may be calculated as [Tenpierik 2009]:

$$\begin{aligned} \Delta\lambda_c &= \frac{\partial\lambda_c}{\partial p_g}\Delta p_g + \frac{\partial\lambda_c}{\partial p_{wv}}\Delta p_{wv} + \frac{\partial\lambda_c}{\partial u}\Delta u \\ &\approx \frac{\partial\lambda_c}{\partial p_g}\, p_{g;e}(1-e^{-(t-t_{get})/\tau_g}) + \frac{\partial\lambda_c}{\partial p_{wv}}\, p_{wv;e}(1-e^{-(t-t_{des})/\tau_w}) + \frac{\partial\lambda_c}{\partial u}\frac{du}{d\varphi}\varphi_e(1-e^{-(t-t_{des})/\tau_w}) \end{aligned} \tag{2}$$

where

p_g = pore gas pressure (Pa)

$p_{g,e}$ = atmospheric gas pressure (Pa)

$p_{wv,e}$ = partial water vapour pressure outside the VIP (Pa)

φ_e = relative humidity of the air outside the VIP (-)

u = water content of the core material (-)

t = time (days)

t_{get} and t_{des} = time shifts due to getters and desiccants (s)

τ_g and τ_w are time constants according to:

$$\tau_g = \frac{\varepsilon V}{GTR(T,\varphi)} \cdot \frac{T_0}{p_o T} \tag{3}$$

$$\tau_w = \frac{\rho_{dry} V}{WVTR(T,\varphi)} \cdot \frac{1}{p_{sat}(T)} \frac{du}{d\varphi} \tag{4}$$

GTR and WVTR are the empirically found *gas transmission rate* and *water vapour transmission rate* for VIPs, respectively. Graphical plots for thermal conductivity for constant climatic conditions up to 100 years can be found in Baetens *et al.* [2010] and Wegger *et al.* [2011]. To be able to accelerate the ageing of VIPs, it is necessary to increase the permeation of water vapour and air gases through the envelope barrier. In Wegger *et al.* [2011] it is found that temperature, moisture and pressure are the external factors contributing most to ageing of VIPs. These external factors are all elements in the thermal conductivity formula in eq. 1.

3 EXPERIMENTAL

Four different ageing methods have been performed in this study, based on existing methods and knowledge on ageing. The following ageing methods have been used:

- Temperature ageing according to CUAP 12.01/30
- Cyclic climate ageing according to NT Build 495
- Moisture and temperature ageing
- Pressure ageing

A summary of the procedure for each of these methods can be found in Table 1.

Table 1. Summary of ageing procedures conducted on vacuum insulation panels.

Method	**Procedure**	**Conductivity Measurement Periods**
CUAP 12.01/30	• Cycling in alternating climate (8 cycles) o 8 hours at (80 ± 3) °C o 16 hours at (-15 ± 3) °C Temperature ageing for 180 days at (80 ± 3) °C	• Initial • After cycling • 90 days • Final (180 days)
NT Build 495	VIPs mounted in vertical climate simulator. Two panels used, one fully exposed and one protected by a ventilated timber frame. Rig consists of the following successive climate strains: o UV-radiation (UVA = 33 W/m^2, UVB = 2.4 W/m^2) and IR-radiation giving a black panel temperature of (63 ± 5) °C o Wetting with a spray of water o Freezing at -20 ± 5°C o Thawing at laboratory climate One hour in each position for a total of 180 days.	• Initial • Two intermediate measurements • Final (180 days)
Moisture and Temperature	VIP stored in plastic envelope with water container inside a heating cabinet. Stored at 70°C, giving a RH of between 90 and 100%.	• Initial • Every 30 days • Final
Pressure Ageing	VIPs stored at elevated pressures to evaluate the change in thermal conductivity. The following procedure was employed: • Pressurizing to 8 bar overpressure using pressurized air o 1 panel tested for new thermal conductivity o 2 panels stored for 30 days at 8 bar before determination of new thermal conductivity • Comparison between panel pressurized to 8 bar and not stored, and those stored for 30 days to evaluate any relative change of thermal conductivity.	• Initial • After Pressurizing

The VIPs used in the experiments presented in this paper are of the type va-Q-vipB from the producer va-Q-tec (2009). Va-Q-vipB consists of a core of amorphous silicon dioxide and an inorganic opacifier. The panel is sealed with a high barrier film which is again covered on the exterior with a black fire protection fleece. The high barrier film consists of three layers of metalized polyethylene

terephthalate (PET) with polyethylene (PE) as a sealing layer on the inside. Total thickness is approximately 100 µm. The panel dimensions are 100 cm x 60 cm x 2 cm. One VIP sample is used for each procedure. The VIPs used for pressure testing were somewhat smaller than the rest due to limitations on equipment. Dimensions for these panels were 20 cm x 12 cm x 2 cm. These smaller panels were not covered by fire protection fleece.

To evaluate the change in thermal conductivity of VIPs, a heat flow meter apparatus (HFM) has been used. All measurements are performed in accordance with current versions of ISO 8301 and NS-EN 12667.

4 RESULTS AND DISCUSSION

During the experiments physical alterations could be observed on some of the VIPs. The panel exposed to the CUAP procedure swelled approximately 2 mm. This corresponds to 5-10% increase in thickness for the panel. In addition the fire protection fleece covering the VIP loosned from the substrate. This was also observed on the exposed VIP in the vertical climate simulator. The latter VIP also experinced curving towards the exposed side in the simulator quite early into the experiment. Neither of these changes had any notable effect on thermal properties of the VIPs. Failure of VIPs occurred in two of the experiments, the temperature and moisture VIP and the protected VIP in the climate simulator both failed. The reason for this is judged to be some external factor like mechanical damage and should not be attributed to accelerating effects.

The VIPs exposed to increased pressure all experinced a significant decrease in thickness of approximately 10-15%.

Results from the measurements of thermal properties are shown in the figures below. Figures 2 and 3 show the thermal conductivity and thermal reisistance, respectively, for all experiments except the pressure ageing resuls which is shown in Figure 4.

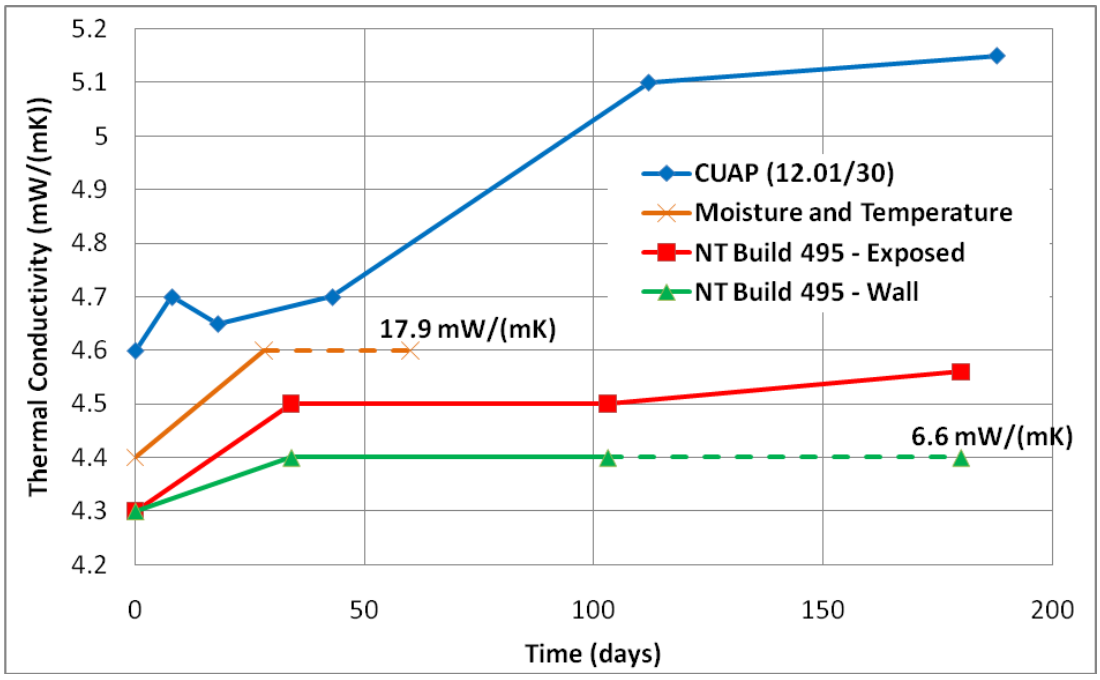

Figure 2. Thermal Conductivity of VIPs exposed to various ageing experiments. The time periods for total exposure vary somewhat depending on the method.

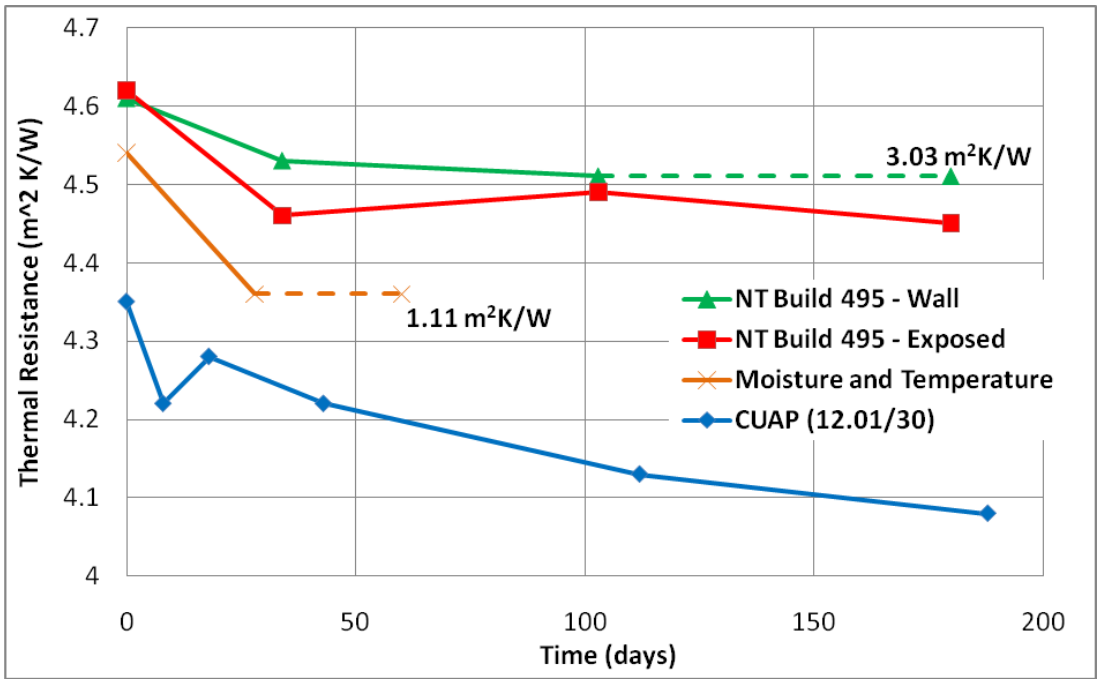

Figure 3. Thermal resistance of VIPs exposed to various ageing experiments. The time periods for total exposure vary somewhat depending on the method.

For the thermally aged VIP (CUAP 12.01/30) it can be seen that the relative change in thermal conductivity is far higher than the change in thermal resistance. This is due to the increased thickness of the VIP that occurred as a result of swelling during the experiment. The insulating capacity is therefore best represented by the thermal resistance, as this value incorporates the geometrical changes of the VIP. For the moisture and temperature aged VIP and the protected VIP in the climate simulator, increases in thermal conductivity was higher than can be explained by ageing effects alone, and some failure must have occurred. This is marked with dotted lines for the relevant VIPs in the above figures.

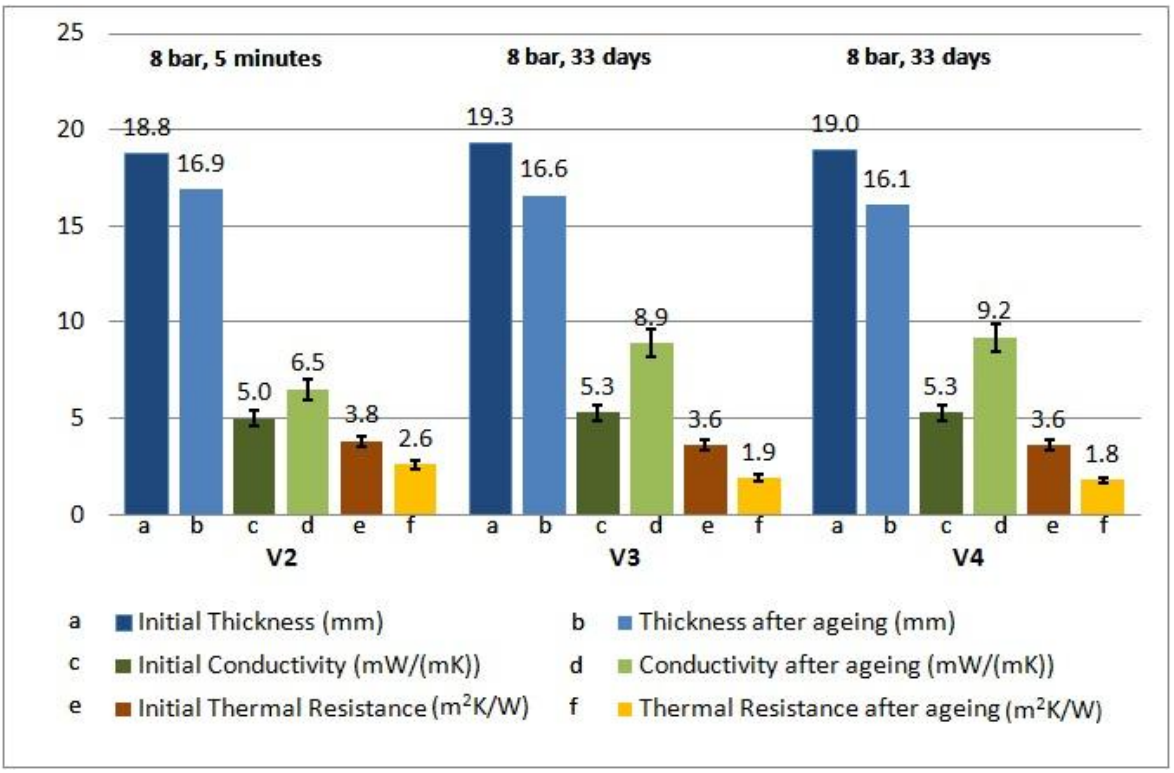

Figure 4. Thickness and thermal conductivity for VIPs exposed to elevated pressures (8 bar), before and after exposure.

From Figure 4 it can be seen that all VIPs exposed to elevated pressure experinced a reduction in thermal resistance. Some of this is likely due to collapsed pore structure in the VIP core. The change is higher for the panels exposed for a longer period of time, however, which could indicate increased diffusion of air molecules through the barrier.

For all ageing procedures the changes in thermal conductivity and resistance are small, compared to the overall performance of VIPs. This shows that the VIPs have a relatively high robustness to severe climatic loads. This is in agreement with prediction curves for the ageing of VIPs under constant climatic conditions. For a VIP with MF2 foil and size 100 cm x 100 cm x 2 cm, the predicted thermal conductivity after 100 years is ≈ 8.5 mW/(mK). This represents a total increase of 4.5 mW/(m K), or less than 0.05 mW/(mK) each year. In other words, a relatively low increase in thermal conductivity should be expected if the predictions are correct.

The changes in thermal properties for the pressure tested VIPs can not be interpreted in terms of theoretical predictions for accelerated gas diffusion due to increased external pressure. Whatever the reason, it is considered significant that the thermal properties of the VIPs continued to degrade over time at elevated pressures, despite the geometrical reductions remaining comparatively constant. The mechanisms leading to increased thermal conductivity over time is difficult to ascertain, but is assumed to be a combination of increased solid conductivity due to collapsed pores and some unknown effect on the core or envelope due to the high external pressure.

5 CONCLUSIONS

Miscellaneous ways to perform accelerated climate ageing of vacuum insulation panels (VIP) have been investigated. Results indicate that VIPs have a high resistance to external climatic loads. The change in thermal conductivities were small and in the range that could be expected from theoretical

predictions. The acceleration method using elevated pressure gave a significant change in thermal properties. This should be investigated further to acertain the reason for the change and to evaluate the suitability of the method.

Two of the VIPs failed during experiments, most likely due to some mechanical damage. This demonstrated that despite the high resistance of VIPs to climatic loads, the VIPs represent a fragile material solution.

ACKNOWLEDGMENTS

This work has been supported by the Research Council of Norway and several partners through the SINTEF and NTNU research project "*Robust Envelope Construction Details for Buildings of the 21st Century*" (ROBUST) and "*The Research Centre on Zero Emission Buildings*" (ZEB). The company va-Q-tec, by Roland Caps, is acknowledged for supplying the vacuum insulation panel test samples. Ole Aunrønning (NTNU), Per Christian Moe (SINTEF) and Egil Rognvik (SINTEF) provided valuable help during various experimental tasks.

REFERENCES

Baetens, R., Jelle, B.P., Thue, J.V, Tenpierik, M.J., Grynning, S., Uvsløkk, S. & Gustavsen, A., 2010, 'Vacuum insulation panels for building applications: A review and beyond', *Energy and Buildings*, **42**, 147-172.

Brodt, K., 1995, 'Thermal insulations: cfc-alternatives and vacuum insulation', PhD thesis, Delft University of Technology, Delft.

CUAP 12.01/30, 2009, 'Factory made vacuum insulation panels'.

EN 12667, 2001, 'Thermal performance of building materials and products. Determination of thermal resistance by means of guarded hot plate and heat flow meter methods. Products of high and medium thermal resistance'.

ISO 8301, 1991, 'Thermal insulation - Determination of steady-state thermal resistance and related properties - Heat flow meter apparatus'.

Nordtest Method, NT Build 495, 2000, 'Building materials and components in the vertical position: Exposure to accelerated climatic strains'.

Tenpierik M., 2009, 'Vacuum insulation panels applied in building constructions (VIP ABC)', PhD thesis, Technische Universiteit Delft, Delft.

Wegger, E., Jelle, B.P., Sveipe, E., Grynning, S., Gustavsen, A., Baetens, R. & Thue, J.V., 2011, 'Ageing effects on thermal properties and service life of vacuum insulation panels', In press in *Journal of Building Physics*.

XII DBMC
International Conference on Durability of Building Materials and Components
PORTO - PORTUGAL, April 12th-15th, 2011

Accelerated Test Procedure to Assess the Microbial Growth Resistance of Exterior Finishes

Hartwig M. Künzel [1]
Martin Krus [2]
Cornelia Fitz [3]
Wolfgang Hofbauer [4]
Christian Scherer [5]
Klaus Breuer [6]

ABSTRACT

Rising incidents of microbial growth on façades show the downside of energy efficiency. In cold and moderate climates, well-insulated façade systems are more prone to elevated surface moisture than traditional walls and therefore provide better growing conditions for algae and fungi. While it is difficult to alter the exterior moisture loads, the resistance of finish systems to microbial growth may be enhanced by eliminating potential nutrients, adding biocides or optimizing the material characteristics. Since progress of microbial growth under natural conditions is too slow to keep up with industrial product development schedules, an accelerated test would be beneficial. As a result of extensive exposure tests at different locations in Germany the autumn months have been identified as major growth period. Therefore, an artificial exposure chamber has been devised that simulates the conditions representative for a typical autumn day. Special lamps reproduce the effect of sunlight and wind-driven rain is imitated by weekly spray-wetting. Finish samples are installed in the climate simulator which reiterates the climate cycle including night-time surface condensation until microbial growth is detected. To provide reproducible conditions a cocktail composed of typical algae and fungi is periodically applied to the tested samples. Compared to microbial growth in real life the new test is supposed to accelerate the biological processes by a factor of three to four.

KEYWORDS

Microbial growth on façades; Algae; Fungi; Accelerated testing; Exposure chamber.

[1] Fraunhofer-Institute for Building Physics (IBP), Holzkirchen, GERMANY, hartwig.kuenzel@ibp.fraunhofer.de
[2] Fraunhofer-Institute for Building Physics (IBP), Holzkirchen, GERMANY, martin.krus@ibp.fraunhofer.de
[3] Fraunhofer-Institute for Building Physics (IBP), Holzkirchen, GERMANY, cornelia.fitz@ibp.fraunhofer.de
[4] Fraunhofer-Institute for Building Physics (IBP), Holzkirchen, GERMANY, wolfgang.hofbauer@ibp.fraunhofer.de
[5] Fraunhofer-Institute for Building Physics (IBP), Holzkirchen, GERMANY, christian.scherer@ibp.fraunhofer.de
[6] Fraunhofer-Institute for Building Physics (IBP), Holzkirchen, GERMANY, klaus.breuer@ibp.fraunhofer.de

1 INTRODUCTION

Current building energy regulations in Europe require high levels of thermal insulation of external walls. As a consequence the façade surface temperature gets colder and external condensation may appear which increases the likelihood of microbial growth [Künzel & Sedlbauer 2001]. Recent German court rulings have confirmed a defects liability period of 5 years for façade systems which includes staining by microbial growth. According to ETICS manufacturers up to 5% of all installed **E**xternal **T**hermal **I**nsulation **C**omposite **S**ystems show such defects. Innovations such as photo catalytic or extremely water repellent paints have done nothing to reverse this trend [Hofbauer et al. 2006]. It is therefore evident that further system improvements are essential. However, assessing the resistance of a façade system against microbial growth is challenging because in practice it can take a couple of years before microbial growth may be detected. The fast development on the market forces producers of coatings to establish faster methods for evaluating the resistance of products against microbial infestation. While tests with exaggerated ambient conditions may produce faster microbial growth they are not necessarily representative for the situation in real life. Therefore, an accelerated test method has been developed that simulates the biological and hygrothermal conditions on façades in practice. The principles of this new method and first results demonstrating the potential acceleration of microbial growth are presented in this paper.

2 TEST PRINCIPLE

The tests are carried out in an exposition chamber that allows establishing realistic climate conditions at the investigated façade samples including surface condensation processes connected with long-wave radiation to the sky. Additionally also the course of daylight and rain are provided. The whole procedure is completed by inoculation of the samples with a mixture of certain microorganisms. The aim is to devise a test method that discriminates the growth resistance of façade products according to their real life performance only 3 to 4 times faster. Simple breeding tests in incubators that will produce rapid and indiscriminate growth on every material unless it contains large amounts of biocides won't do the job. While it is important to determine the comparative growth resistance this is not sufficient because manufactures also need to know how their products will perform in practice. In order to avoid liability the façade has to stay free of microbial stains for at least 5 years.

2.1 Development of the Test Climate

Previous studies show that the development of growth on outside building surfaces shows a cyclic pattern with the most intense phase in autumn/winter [Hofbauer et al. 2006]. This corresponds to findings in [Künzel & Sedlbauer [2001] that after winter which is too cold for growth, autumn is the season with the highest incidence of exterior surface condensation. Driving rain loads, also a frequent cause for growth [Künzel 2007], may not peak in autumn. However, the time of wetness at the façade surface can still be higher than in spring and summer because evaporation slows down when the ambient humidity rises. Analysing and averaging the climate data of the 3 autumn months (Sep. – Nov.) recorded by the meteorological station at the field test site in Holzkirchen has resulted in typical diurnal cycles shown in Fig. 1. Since progress of microbial growth depends on humidity as well as on temperature the diurnal cycle of September is selected as basis for the test cycle. This choice is also confirmed by the annual growth pattern in Fig. 2 showing that the most rapid progress has been detected during early autumn [Hofbauer et al. 2006]. However, a high humidity is not enough to provoke microbial growth on external surfaces. Long-term observations indicate that sporadic surface wetting by liquid water either from exterior condensation or driving rain is generally necessary to start and sustain growth on façades. Therefore natural wetting cycles must be part of the test climate. While the effect of driving rain may be simulated by periodic spray-wetting, reproducing exterior condensation, caused by façade temperature drops below the ambient dewpoint (as a result of night-time long-wave radiation to the sky), is rather challenging.

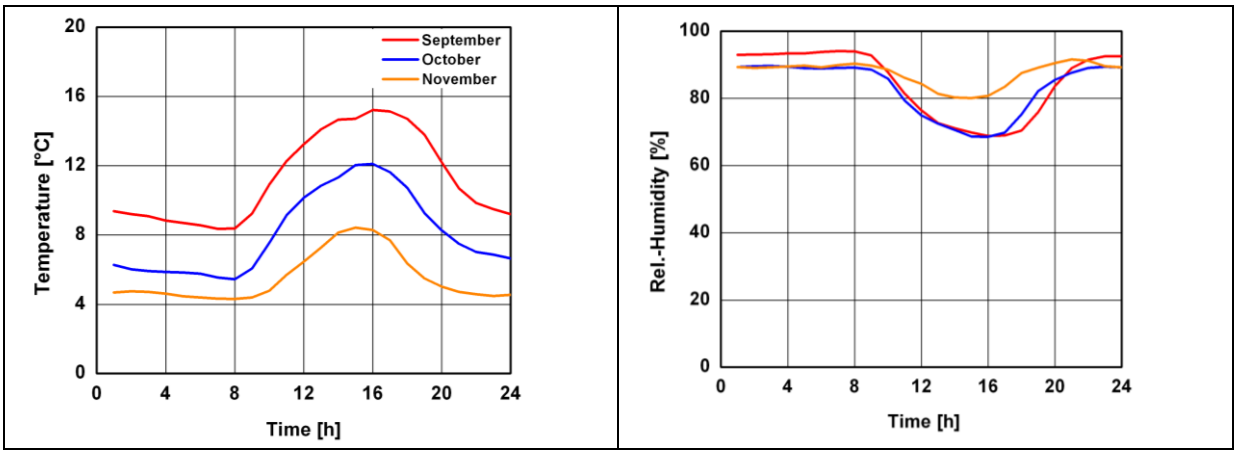

Figure 1. Average diurnal cycles of ambient air temperature (left) and humidity (right) representative for the 3 autumn months at the IBP field test site in Holzkirchen (foothills of the Alps).

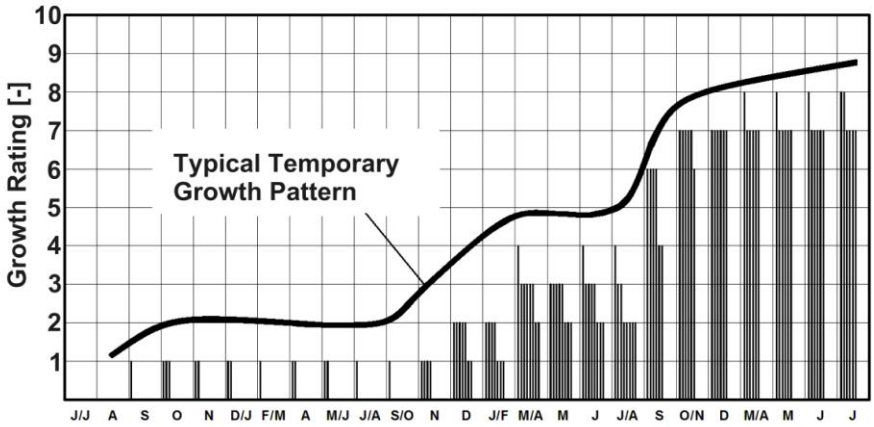

Figure 2. Temporal microbial growth pattern on insulated façade systems determined by field investigations in Germany. The growth rating is described in [Hofbauer et al. 2006] and may be interpreted in a simplified way as follows: 1-3 microscopic growth, hardly visible; 4-5 growth visible with naked eye; 6-10 severe staining.

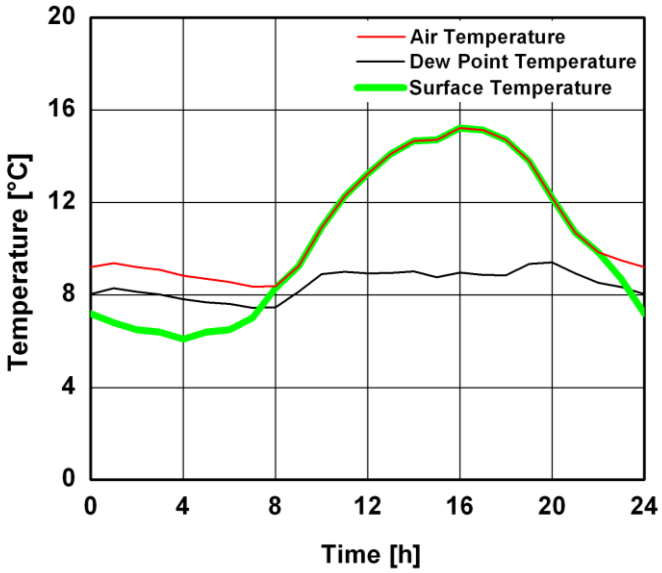

Figure 3. Average diurnal cycles of ambient air temperature and dew-point compared to the surface temperature likely to occur on a well-insulated façade with standard ETICS in Holzkirchen.

Since it is impossible to simulate long-wave radiation to the sky in a climatic chamber an alternative solution had to be devised that produces the same surface cooling effect responsible for condensation of ambient air humidity. Based on measured façade temperatures correlated to meteorological data and validated hygrothermal simulations [Krus et al. 2006] diurnal cycles of the ambient conditions in the climatic chamber and on the surface of the investigated façade samples have been selected (Fig. 3). These conditions are representative for the month of September at the IBP field test site in Holzkirchen. They may be modified to reproduce the conditions at different locations by feeding the respective meteorological data into a validated hygrothermal model.

2.2 Assembly of the Test Facility

The test facility depicted in Fig. 4 consists of a stainless steal chamber whose rear wall can be chilled. This feature provides the possibility to cool down the attached façade samples so that their surface temperature gets in line with the real conditions outdoors under the influence of the long-wave radiation to the sky. Through evenly distributed slots in the side walls of the chamber the air conditioned according to the September cycles in Fig. 1 is recirculated. Rainwater (decalcified tap water) from a separate container may be spayed upon the samples from the front by special nozzles providing droplets whose size is close to that of real rain. In order to prevent cross-contamination the rainwater running of the samples is collected by small gutters beneath them. Daylighting which is important for the growth of algae occurs by 2 lamps integrated into the front doors of the chamber. They provide approximately 650 lx to the samples during 12 h/d. The size of the testing chamber allows concurrent weathering of up to 50 façade samples with a size of 100 cm². A special software is controlling the specified cycles of the chamber conditions within ± 0.5 K and ± 2% RH within the range of 5 – 25 °C res. 65% – 93% RH.



Figure 4. Photograph of the running test facility for accelerated microbial growth on façade samples.

2.3 Inoculation Procedure and Visible Growth Assessment

In previous investigations the most abundant primary colonizers of exterior building surfaces in Germany resp. Central Europe and connections to material properties were revealed [Hofbauer et al. 2003], [Hofbauer et al. 2006], [Hofbauer 2007]. Further recent studies also considering ecophysiological features of microbial colonization on building surfaces confirm and extend these results (e.g. [Rindi & Guiry 2004], [Escadeillas et al. 2007], [Grbić et al. 2009], [Macedo et al. 2009], [Uher 2010]). The special challenge is to provide an adequate inoculation mixture which is suitable for many different coatings together with an appropriate method for inoculation of the coated surfaces. All used strains originate from microbial investigations of colonized surfaces [Hofbauer 2007] and are taken from our own collection of building relevant microorganisms (Table 1). They were selected according to their abundance as primary colonizers of buildings, if they show good growth in culture in order to provide enough spore material for the inoculation procedures. Whereas

the green algae *Chlorella trebouxioides*, *Diplosphaera chodatii* and *Stichococcus bacillaris*, and the fungi *Alternaria alternata*, *Cladosporium cladosporioides* and *Ulocladium chartarum* comprise very abundant microorganisms involved in the disfigurement of masonry the fungi *Epicoccum purpurascens* and *Phoma* sp. were added after they became conspicuous on some of the investigated coatings exposed in outdoor tests for comparison issues. As it turned out, that in course of driving rain incidents microorganisms are transported very effective onto building surfaces [Hofbauer 2007] we decided to use a wet inoculation method. For the inoculation suspension different cultures adjusted to a density of 10^5-10^6 spores per millilitre aqueous suspension were mixed together. In order to provide a homogenous inoculation for all investigated surfaces a special brush is used. For the first tests the inoculation was performed in a two weeks cycle.

Table 1. Strains which are used for the inoculation procedure with strain number from the culture collection of building relevant microorganisms at the Fraunhofer-IBP and with affiliation to higher taxonomic categories.

Microorganism	*Strain number*	*Additional information*
Chlorella trebouxioides	HOKI A 39	Alga, Trebouxiophyceae
Diplosphaera chodatii	HOKI A 315	Alga, Trebouxiophyceae
Stichococcus bacillaris	HOKI A 281	Alga, Trebouxiophyceae
Alternaria alternata	HOKI F 189	Fungus, Dematiaceae
Cladosporium herbarum	HOKI F 190	Fungus, Dematiaceae
Epicoccum purpurascens	HOKI F 224	Fungus, Dematiaceae
Phoma sp.	HOKI F 246	Fungus, Coelomycetes
Ulocladium chartarum	HOKI F 95	Fungus, Dematiaceae

Parallel to the investigations with the new accelerated test procedure additional samples are exposed to natural conditions (field tests) for comparison purposes. For the assessment of the development of biological growth on the investigated surfaces an 10-stage semi-quantitative rating scale was used, that was developed during previous investigations [Hofbauer et al. 2003], [Hofbauer et al. 2006], [Hofbauer 2007]. The lower categories of this rating scale provide a minute resolution of the first colonization whereas the upper categories follow strictly the percentage of coverage by growth. Ratings between 0 and 3 will be hardly recognized by an untrained person, because there is very little visible growth. Ratings from 6 to 10 are recognizable as severe unacceptable staining also by laymen. Ratings 4 and 5 describe visible scattered growth which may already be a cause for complaints. The assessment of growth intensity was done on a weekly or fortnightly basis during the accelerated test procedure in the climatic chamber resp. on a monthly or two-monthly basis for the field tests.

3 FIRST RESULTS

After calibrating the test facility, test climate, inoculation procedure and frequency of inoculation, the first parallel (accelerated and natural weathering) investigations were carried out. Recordings of the diurnal climate cycle in the test chamber and at the rear wall which controls the surface temperature of the tested samples are compared to the set-point conditions in Fig. 5. The correspondence for climate conditions in the chamber is quite good. There is a slight overshoot in the recorded rear wall temperature towards the end of the diurnal cycle which will, however, not affect the sample temperature a great deal because it lasts only a few minutes and is therefore dampened by the thermal inertia of the samples.

The assessment of the evolution of biological growth on the investigated samples in the new test facility is shown for two samples with different coatings in Fig. 6. In both cases the threshold of

visible growth (Rating > 3) has been reached within 12 – 13 weeks. Compared to general observations in the field, e.g. in Fig. 2 (the results from the parallel exposure of identical samples under natural conditions are not available yet) where visible growth is usually not detected during the first year of exposure the acceleration of growth in the new test facility amounts approximately to a factor of 4. More precise information on the acceleration will be available as soon as the parallel running natural exposure tests have been evaluated. Although the first results are very promising the new and accelerated testing procedure will be refined. Especially the assessment frequency will be increased in order to get a better resolution of the course of the colonization. Further tests are currently under way.

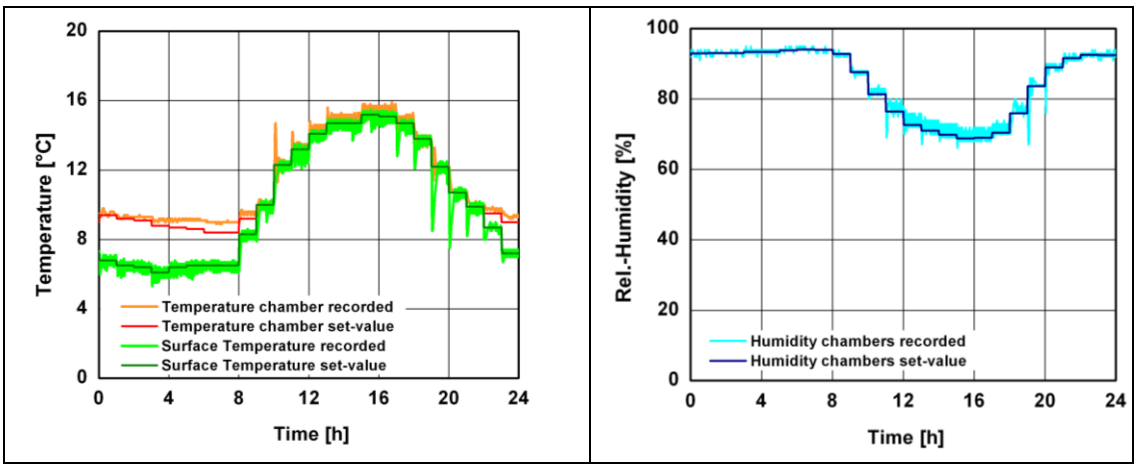

Figure 5. Comparison between the set values for temperature and humidity compared to the recorded actual conditions in the test chamber.

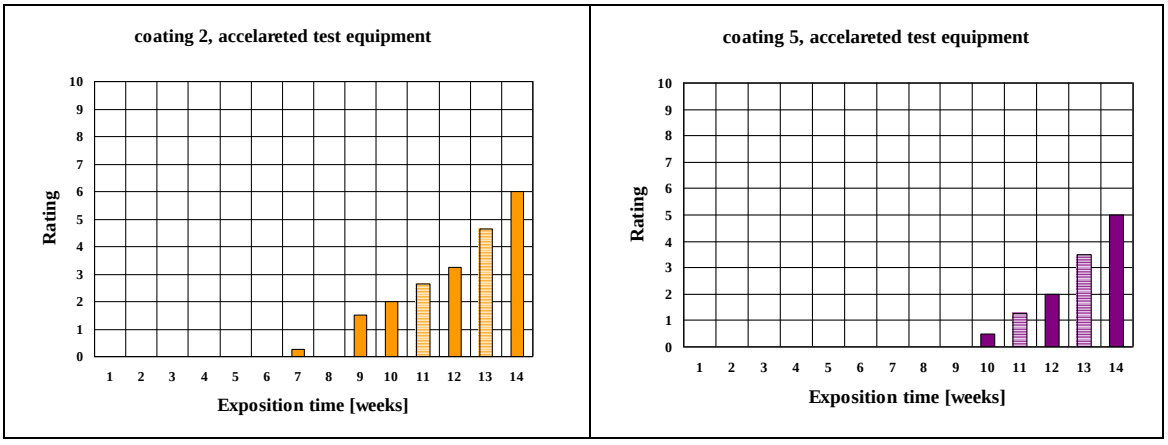

Figure 6. Development of growth on 2 different coatings on rendering samples in the test chamber (broken bars indicate estimated values).

4 DISCUSSION AND CONCLUSIONS

The accelerated test procedure shows promising first results. It is obvious that an acceleration of biological colonization compared to the development under natural conditions can be achieved. Since the natural exposure tests with samples having the same variety of coatings as the samples in the new test facility are not finished yet, it is impossible to judge whether the acceleration factor is comparable for all tested materials. If this is not the case it will be difficult to use the test to identify the real growth resistance of coatings. However, if the new test shows a good correlation with natural exposure, it may be adapted to other climate zones by simply analysing the meteorological data with the help of a validated hygrothermal model such as WUFI®. While it is obvious that a different climate necessitates a change in test conditions, different exposure conditions (e.g. orientation,

building geometry) in the same climate zone may also require some modifications. If the driving rain load is negligible the test could be done without spray-wetting. This would be beneficial for the effectiveness of common biocides which are less likely to be washed out during the test. In order to test the performance of photo catalytic additives the lamps in the test facility may have to be replaced by special UV-lamps.

Other comparable laboratory test procedures which are used to investigate the sensitivity of exterior building coatings to unwanted growth of microorganisms (compare e.g. [Guillitte & Dreesen 1995], [Barberousse 2007], [De Muynck et al. 2009], [Escadeillas et al. 2009], [Wiktor et al. 2009]) lay more emphasis on a comparison of the material characteristics under very severe and maybe not real practical conditions and/or are more time consuming and sometimes require more complicated machinery for assessment of growth compared to the new test method described here. The proposed setup is unique for two reasons: First, it simulates realistic environmental loads and their dynamic behaviour within a broad range of possible climatic impacts including surface condensation. Second, potential colonization of the investigated surfaces by microorganisms is facilitated under realistic conditions by use of strains that are already well known as primary colonizers from building coatings.

ACKNOWLEDGMENTS

The presented research was sponsored by the Bundesministerium für Wirtschaft und Technologie of the Federal Republic of Germany and partners from industry.

REFERENCES

Barberousse, H., Ruot, B., Yéprémian, C., Boulon, G. 2007, 'An assessment of fac-ade coatings against colonisation by aerial algae and cyanobacteria', *Building and Environment* **42**, pp. 2555-2561.

De Muynck, W., Maury, A., De belie, N., De Bock, J., Verstraete, W. 2009, 'Evaluation of anti-fouling strategies on aerated concrete by means of an acceöerated algal growth test', in *Concrete Repair, Rehabilitation anRetrofitting*, eds M.G. Alexander, H.-D. Beushausen, F. Dehn, P. Moyo, 2nd International Conference on Concrete Repair, Rehabilitaion and Retrofitting 2008, ISBN 0415468507: pp. 253-259.

Escadeillas, G., Berton, A., Blanc, P., Dubosc, A. 2007, 'Accelerated testing of biological stain growth on external concrete walls. Part 1: Development of the growth tests' *Materials and Structures* **40**, pp. 1061-1071.

Escadeillas, G., Berton, A., Ringot, E., Blanc, P., Dubosc, A. 2009, 'Accelerated testing of biological stain growth on external concrete walls. Part 2: Quantification of growths', *Materials and Structures* **42**, pp. 937-945.

Grbić, L., Subakov-Simić, G., Kricmanić, J., Lađić, V. 2009, 'Cyanobacterial, algal and fungal biofilm on sandstone substrata of Eiffel´s Lock in Bečij (Serbia)', *Botanica Serbica* **33**(1), pp. 101-105.

Guillitte, O. & Dreesen R. 1995, 'Laboratory chamber studies and petrographical analysis as bioreceptivity assessment tool of building materials', *The Science of the Total Environment* **167**, pp. 365-374.

Hofbauer, W. 2007, *Aerophytische Organismen an Bauteiloberflächen*, Ph.D. Thesis, Innsbruck University (Austria).

Hofbauer, W., Breuer, K., Sedlbauer, K. 2003, 'Algen, Flechten, Moose und Farne auf Fassaden', *Bauphysik* **25**(6), pp. 383-396.

Hofbauer, W., Fitz, C., Krus, M., Sedlbauer, K., Breuer, K. 2006, *Prognoseverfahren zum biologischen Befall durch Algen, Pilze und Flechten an Bauteiloberflächen auf der Basis bauphysikalischer und mikrobieller Untersuchungen*, Bauforschung für die Praxis Vol. 77, Fraunhofer IRB Verlag, Stuttgart, Germany.

Krus, M;. Rösler, D; Sedlbauer, K..: New model for the hygrothermal calculation of condensate on the external building surface. Proceedings of the Third International Building Conference, Concordia University, Montreal, Canada, 27.-31. August 2006. S. 329 – 333. ISBN 0-415-41675-2.

Künzel, H.M. & Sedlbauer, K. 2001, 'Biological Growth on Stucco' Proc. Buildings VIII Conference, ASHRAE Publications, Atlanta.

Künzel, H.M.: Factors Determining Surface Moisture on External Walls. Proceedings Buildings X, ASHRAE, Atlanta 2007, 6p.

Macedo, M.F., Miller, A.Z., Dionísio, A., Saiz-Jimenez, C. 2009, 'Biodiversity of cyanobacteria and green algae on monuments in the Mediterranean Basin: an overview', *Microbiology* **155**, pp. 3476-3490.

Rindi, F. & Guiry, M.D. 2004, 'Composition and spatial variability of terrestrial algal assemblages occuring on the bases of urban walls in Europe', *Phycologia* **43**(3), pp. 225-235.

Sedlbauer, K., Krus, M., Hofbauer, W., Breuer, K., Fitz, C. 2006, 'Neue Erkenntnisse zum mikrobiellen Bewuchs auf Außenoberflächen', WKSB 56, pp. 10-18.

Uher, B. 2010, *Cyanobacteria and algae as significant actors of biodeterioration*, Lambert Academic Publishing, Saarbrücken, Germany.

Wiktor, V., De Leo, F., Urzi, C., Guyonnet, R., Grosseau, P., Garzia-Diaz, E. 2009, 'Accelerated laboratory test to study fungal biodeterioration of cementitious matrix', *International Biodeterioration & Biodegradation* **63**(8), pp. 1061-1065.

XII DBMC
International Conference on Durability of Building Materials and Components
PORTO - PORTUGAL, April 12th-15th, 2011

The Effect of Concrete Composition on the Possibilities of Accelerated Testing: Carbonation Example

Jeanette Visser[1]

ABSTRACT

At the design stage of a concrete structure, decisions have to be made on how to fulfil the required service life and consequently, what concrete composition to use. With respect to the durability, no tailor made design rules are yet available. Hence, the service life of a certain concrete composition has in general to be proven by 'design-by-testing'. When limited time is available for testing, accelerated tests often are performed. If there is no good insight in the underlying principles of the effect of the acceleration, some serious mistakes in the service life designs will be made.

In this paper, an example of accelerated testing is shown for carbonation. Accelerated carbonation tests at 2 % CO_2 and normal carbonation tests at ambient CO_2-level have been executed. Based on the results, the resistance against carbonation have been calculated. Since this resistance is a material property, it should be similar in both tests. For two of the tested concrete compositions this proved to be the case, a third type of concrete made with fine cement did however not. It was speculated that this was due to the high water formation during the carbonation in combination with low capillary pore content. This makes the drying out at the carbonation front dominant over the ingress of CO_2. A new simple model was derived for this case. The modelling gave similar resistance of carbonation when this change in carbonation mode was taken into account.

KEYWORDS

Accelerated testing, Modelling, Carbonation, Moisture, Pore structure.

[1] Department of Civil Engineering, TNO Built Environment and Geosciences, Delft, The Netherlands, jeanette.visser@tno.nl

1 INTRODUCTION

At the design stage of concrete structures, decisions have to be made on how to fulfil the required service life and, consequently, what concrete composition to use. With respect to the durability, design rules to select a suitable concrete composition are not available, thus a selection is generally made based on testing.

The available period of testing at the design stage is often limited hence accelerated tests are preferred. Accelerating can be performed in two ways: increasing the driving force of the degradation process (e.g. concentration, temperature) or compressing time (e.g. using shorter freeze thawing or drying/wetting cycles). Acceleration can however lead to several unwanted effects. Among others, a different degradation process or parameter in the process may become dominant. There thus is often a maximum on the possible acceleration rate. Complicating things even more, concrete itself is an ageing material. Especially at young age, its properties have not yet been developed fully. This can also give rise to results that are not compatible with the long-term behaviour at normal test conditions and result in serious errors in the service life predictions.

One of the most important degradation mechanisms of reinforced concrete structures that seems to be easy to accelerate is carbonation. For many very large infrastructural works requiring long service life, this test is prescribed due to their importance or high costs. In a brief research to investigate two concrete compositions for a new Dutch tunnel required to have a service life of 100 years, both accelerated (at 2% CO_2) and normal (at ambient CO_2) were performed in order to investigate whether also for concrete with supplementary materials (fly ash and blast furnace slag) accelerated was suitable. For comparison, also an OPC-concrete was tested. In this paper, these results are presented and discussed in light of the chosen acceleration parameters. In section 2, firstly the theoretical background of testing for service life design, the carbonation modelling and possibilities for accelerated carbonation test are discussed. In section 3, the experiments and the results are presented. Discussion of the results with respect to the chosen acceleration and its possible influence is given in section 4. Section 5, finally, givens the conclusions.

2 SERVICE LIFE DESIGN FOR CORROSION DUE TO CARBONATION

2.1 The Carbonation Reaction and Service Life Design

The most widespread degradation mechanism in reinforced concrete structures is without doubt corrosion of the reinforcement. Corrosion is initiated when the passivation layer on the reinforcement steel is broken. This can be brought about by carbonation of the surrounding concrete, which results in a drop in the surrounding pH, from the usually very high alkaline environment (pH about 13) to about 9 (e.g. Glass and Page [1991]).

A good overview of the chemical reactions in the carbonation process can be found, among others, in Thiery *et al*. [2007] and Maekawa *et al*. [2003]. To recapitulate it very briefly: carbonation starts from the surface of the concrete, by penetration of CO_2. After diffusion of the gas into the concrete, it dissolves in the pore water as carbonic acid H_2CO_3 that dissociates in HCO_3^-ansd CO_3^{2-}, the concentrations depending on the pH of the pore water, the ambient CO_2 concentration and the other species in the pore water, most notably the alkalis. The dissociation decreases pH of the pore water since it also produces H_3O^+.The dissolved Ca^{2+} reacts with the CO_3^{2-} to solid $CaCO_3$, which precipitates in the pore space. Both the reduction in pH after dissociation of CO_2 and the decrease in calcium concentration after precipitation of the calcium carbonates are drivers for the dissolution of the $Ca(OH)_2$, restoring the pore water concentrations again. In addition to the calcium hydroxide, calcium is dissolved from other calcium bearing cement phases as CSH, ettringite (AFt) and monosulphate hydrated (AFm). With progressive consumption of calcium from the easily dissolving compounds of the cement stone and precipitation of the almost insoluble calcium carbonate,

ultimately there will be compounds that are no more easily dissoluble. At this moment, the pH cannot increase anymore and a new equilibrium at about pH = 9 is set. In this chemically reaction process, water is required to dissolve the CO_2 but also liberates water that previously was held in the solid $Ca(OH)_2$.

In most situations, there exists a narrow reaction layer in which the bulk of the carbonation reaction is located and which progresses from the surface of the concrete inwards. At the back, the concrete is fully carbonated while in front, the concrete is unaffected. Since the existence of a very narrow carbonation zone has been proven for a whole range of experimental conditions [see e.g. Peter et al. 2008 and references therein], the carbonation zone is usually modelled as a jump change of the concentration of the CO_2 in this zone. This is because the carbonation reaction consumes any new CO_2 molecule arrives at a not fully carbonated spot. Thus, all carbonatable matter must be consumed first before the carbon dioxide molecules can penetrate further. For convenience sake, and because of the fact that the measuring method consists of spraying of phenaftholeine which changes colour at a pH of 9, this narrow zone is usually modelled as a sharp front and is called the carbonation front. Variations in this carbonation front are often found to be solely due to variations in microstructure of the cement stone (local variations in amount of consumable matter, degree of saturation, micro cracks facilitating diffusion etc.).

The time, which it takes the carbonation front to reach the reinforcement bars and breaks, their passivation layer, is called the (corrosion) initiation time. For a service life design, it is usually required that the time of corrosion initiation due to carbonation is longer than the required service life. Although carbonation itself does not any harm, the following stage of corrosion of the reinforcement can be very fast and the consequences of possible failure due to undetected corrosion can be huge and necessary repairs costly. Hence, the service limit state then states that the probability that the carbonation front reaches the reinforcement within the expected service life must be lower than some predefined probability: $P\{t_{ini}<T\}<P(\Phi(\beta))$.

2.2 Modelling Carbonation Ingress

According to Meier et al. [2006], experimental evidence has shown that the dissolution and precipitation reactions are very fast in comparison to the ingress of CO_2. The ingress takes place under diffusion under (according to Fick's law) if the pore diameters are larger than the mean free path [Arandigoyen and Alvarez 2006].Therefore, the carbonation rate is in general modelled by a simplified equation for the CO_2-flux q in the concrete specimen is given by a linear decline of the concentration over its carbonation depth, i.e.:

$$q = -D\nabla c = DA(c_{out} - c_{in})/x \qquad (1)$$

with
- q= flow rate of CO_2 [kg/m^2s]
- D = diffusion coefficient [m^2/s]
- c = CO_2 concentration at the outside (out) and at the front (in) [kg/m^3]
- A = area through which the transport is taking place [m^3]
- x = the location of the front [m]

Based on the assumption that the carbonation front cannot move on except when all carbonatable matter has reacted within a reference volume Adx, the total mass of CO_2 that has to be transported to the carbonation front to transform this matter a, thereby progressing the carbonation front by dx, is given by:

$$dM = aAdx \qquad (2)$$

Since this is similar to the flux that goes through this reference volume in a reference time dt to move from dx forward, substituting the above equation in the simplified form of Fick's first law then gives:

$$[DA(c_{out} - c_{in})]/x = aAdx/dt \qquad (3)$$

Solving this by integration results in:

$$x_c = \sqrt{2Dc_s t / a} \quad (4)$$

This square-root time relation ship is well known and seems to be reasonably applicable. Rewriting eq. (4) to the time in which the carbonation front reaches the reinforcement at cover depth d_c:

$$t_{ini} = R_{carb} d_c^2 / 2c_s t \quad (5)$$

In which the resistance of the concrete to carbonation $R_{carb} \equiv a / D$.

2.3 Acceleration of the Carbonation Ingress

The simplest way of acceleration is to increase the CO_2 concentration (c_s) of the ambient air. By Henry's law, the concentrations of the CO_2 in the pore water are directly related to the concentration of the CO_2 in the pore air. Since then more CO_2 molecules arrive at the carbonation front within a certain time period, dissolve and dissociate, more calcium can react to calcium carbonate, increasing the dissolution rate of the calcium form the cement stone constituents. Thus, the calcium supply that can react is depleted faster and the carbonation front progresses. According to eq. (4), the degradation rate is accelerated by an amount equal to the ratio of accelerated concentration divided by the normal concentration. E.g. using a concentration of 2% whereas normal CO_2-concentration is about 0.04 % thus increases the degradation 50-fold. As a result, the carbonation process can be accelerated as much as one wish by increasing the concentration accordingly.

Based on the simple model in eq. (4), there are no other driving forces than the concentration. However, there are more possibilities of accelerating, i.e. by increasing the pressure of the air (Al-Kahdhimi et al. [1996]. Since these driving forces are not modelled, rescaling to 'normal' exposure condition is not possible based on eq. (4). As such and for the sake of this paper, they are therefore neglected.

3 Experiments

3.1 Materials

Three different types of concrete were cast for the investigation, in which only the type of cement was varied. One concrete contained 100% Ordinary Portland Cement (OPC), the others contained either fly ash (FA) or blast furnace slag (BFS) as clinker replacement (see Table 1). The slag was added by mixing BFSC with OPC while FA was added as a pure component to the OPC. All FA and BFS were taken into account as binder. The concrete composition of all mixtures had a water-binder ratio (wbr) of 0.45 and a binder content of 340 kg/m^3. River sand and gravel was used as aggregate, with a maximum diameter of 32 mm.

Table 1. Concrete compositions used in the carbonation tests, with slag and fly ash percentage as OPC replacement.

name in this paper	binder	slag (%)	fly ash (%)
fine OPC	CEM I 52.5 R	0	0
FAC	CEM I 52.5 R – fly-ash	0	30
BFSC	CEM III/B 42.5 – CEM I 52.5 R	50	0

3.2 Carbonation Test

Both Natural Carbonation (NC) and Accelerated Carbonation (AC) tests have been performed on the three types of concrete, as given in Table 1. For each type of concrete, six concrete prisms (300 mm x 100 mm x 100 mm) were cast. After one day, the specimens were demoulded and stored in a fog room. At an age of seven days, the specimens were placed in a 20/65 climate room (temperature 20 ^{o}C and relative humidity 65%), at natural carbon dioxide concentrations (approximately 0.037 (V/V) % CO_2). At an age of 28 days, three concrete prisms were placed in a climate room with a CO_2 concentration of 2 % (V/V) but once again at a temperature of 20 ^{o}C and relative humidity of 65%. The other three specimens remain in the 20/65 climate room with a natural CO_2 concentration.

In the accelerated carbonation test, the carbonation depth is determined after 28, 62 and 152 days of accelerated carbonation at 2 (V/V) % CO_2. For the specimens at the natural carbonation test, the carbonation depth has been measured after 6 months, one year and three years of exposure, in the same way as for the accelerated test. The carbonation depth is determined according to point 4.2 of RILEM CPC-18: 'Measurements of hardened concrete carbonation depth' [Rilem, 1988].

3.3 Results

The results of the natural and accelerated carbonation tests are given in Figure 1. Both tests show the same order in resistance against penetration: Portland cement concrete, blast furnace slag cement concrete and fly ash concrete. Note the difference in carbonation depth in the NC and AC test.

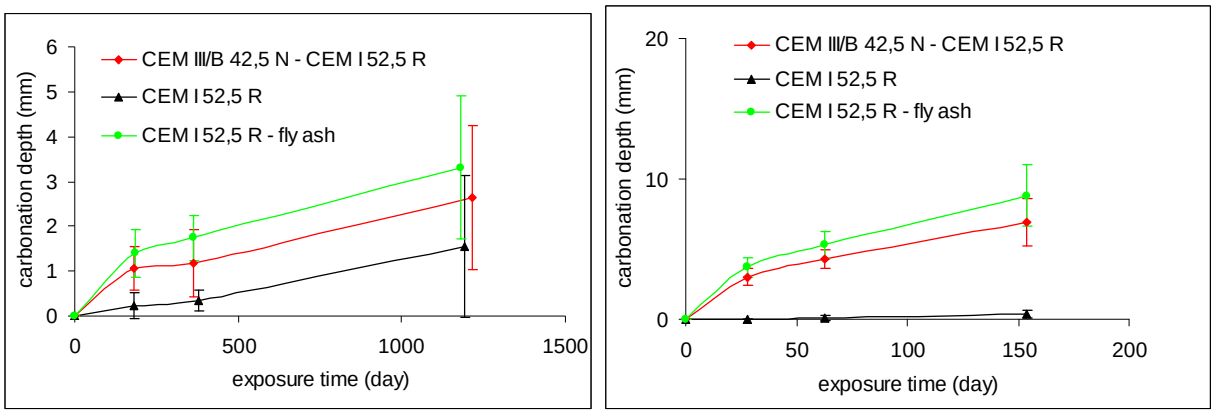

Figure 1. Carbonation depths after exposure under natural carbonation (left) and accelerated carbonation (right)

From Polarization and Fluorescence Microscopy (PFM) analysis of the carbonated specimens after exposure in the AC test for 180 days, it was observed that the porosity of the fine OPC was changed from 0.45 to 0.40. In addition, the degree of hydration of the non-carbonated concrete was high. For the BFSC and the FAC, an increase of the porosity was observed, raising the apparent wcr in the carbonated zone from 0.45 to 0.50, with medium hydration.

4 DISCUSSION

4.1 Comparing Carbonation Resistance Under Normal and Accelerating Conditions

In Figure 2, the results of the normal and accelerated tests are compared as a function of the concentration-independent variable $\sqrt{}_{2cst}$. On account of equations (4) and (6):

$$x_c = \sqrt{1/R_{carb}}\sqrt{2c_s t} \qquad (6)$$

The curves should become straigth lines with a tangent being similar to $\sqrt{1/R_{carb}}$. Since this is a material variable, the curves for the accelerating and normal carbonation tests should be similar, and the resistance against carbonation should be the same. It can be seen in Figure 2 that the carbonation depths of concrete made with BFSC and FAC agree very well. For OPC, there is less agreement between the AC and NC test results. Moreover, the curves deviate from the expected straight line.

The carbonation resistance, R_{carb}, can be determined by means of least-square approximation of eq. (7) to the data. The results are given in Table 2.

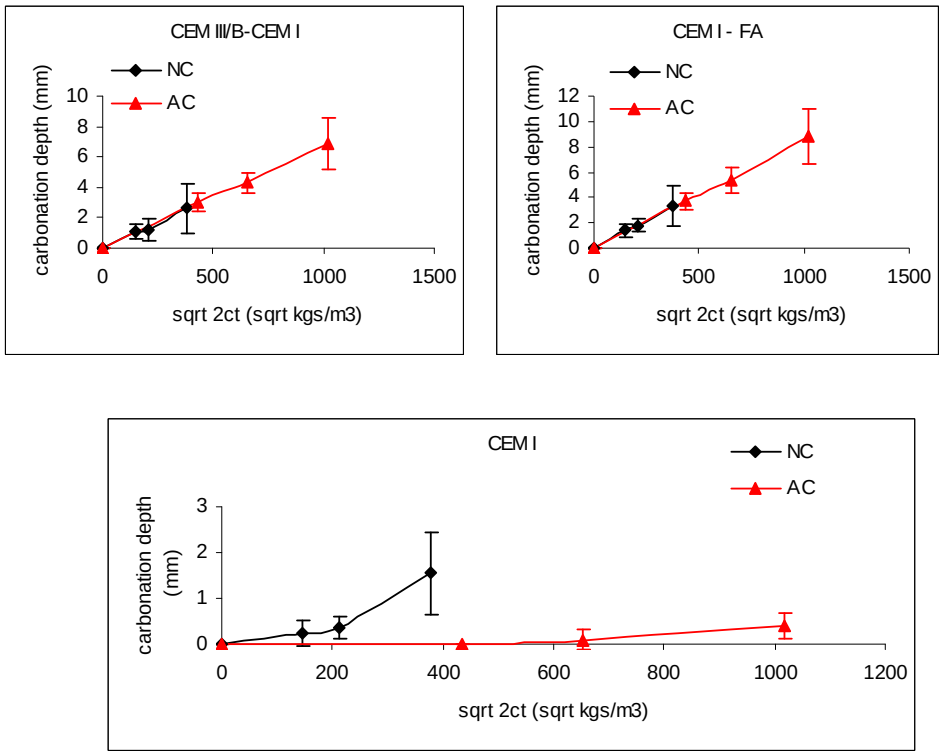

Figure 2. Comparing normal and accelerated carbonation test

Table 2. R_{carb} (in kg/m^3/yr/mm^2) determined by means of least square approximation to equation (4), for the normal carbonation test (NC) and accelerated carbonation test (AC).

concrete	binder	NC	AC
fine OPC	CEM I 52.5 R	[1.2 10^{-2}] (*)	--(**)
coarse OPC	CEM I 32.5 R	n.a.	1.2 10^{-3}
FAc	CEM I 52.5 R - fly-ash	4.2 10^{-4}	4.5 10^{-4}
BFS	CEM III/B 42.5 – CEM I 52.5 R	6.8 10^{-4}	7.0 10^{-4}

(*) the least square fitted profile mostly ignores the last data point since the standard deviation of the measurement is high, profile on two data points

(**) the least square procedure is unstable, since the form of the data curve is different from that of the model

The resistance against carbonation for both the FAC and BFSC is small, indicating the ease with which the concrete carbonates. On the other hand, the resistant of the OPC is, as far as could be estimated from the NC-test, two order of magnitudes higher. For the AC-test of the fine OPC concrete, no stable results were found for the LSQ-modelling.

Figure 3 shows that there is hardly any difference in carbonation rate in the normal and accelerating test for the fine OPC concrete. For comparison, a coarse OPC concrete (CEM I 32.5 R) with the same composition as the fine OPC concrete (CEM I 52.5 R) has been tested in acceleration as well, up to an age of three year. This concrete has the desired square root t behaviour and thus fits the model very well. The results of the LSQ-modelling are also given in the table above.

4.2 Possible Causes of Mis-Modelling and Testing

The PFM analysis of the thin sections indicate a noticeable difference in the pore structures of the fine OPC concrete and the concretes with supplementary cementing materials in the carbonated zone. The porosity of the FAC and BFSC were seen to have increased from 0.45 to 0.50 while that of the OPC was decreased from 0.45 to 0.40. This is generally attributed to the fact that the high $Ca(OH)_2$ content in the OPC forms a large amount of $CaCO_3$ that has about 11% larger volume than the calcium hydroxide and therefore clogs up the pore space, reducing its porosity. However, there is sufficient evidence that also the other hydration phases carbonate [Castellote et al. 2009, Anstice et al. 2005, Borges et al 2010], leading to a shrinkage of the CSH. For the FAC and BFSC, the content of $Ca(OH)_2$ is much lower than for OPC. Firstly less calcium hydroxide is formed because the fraction of the clinker is reduced (the total binder content was kept constant). Secondly, especially the fly ash consumes calcium hydroxide in its hydration. The carbonation of the other hydration phase is for these concrete compositions therefore dominant: a coarsening of the pore space is observed.

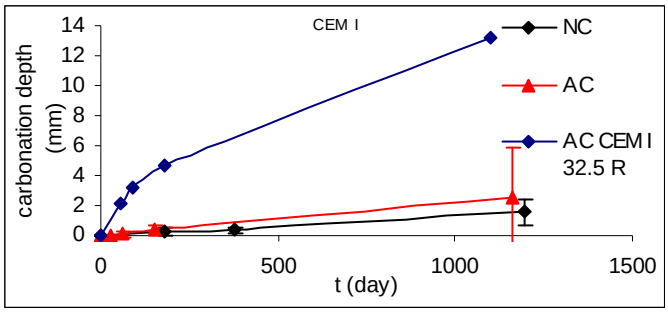

Figure 3. Comparing fine OPC in normal and accelerated carbonation tests and course OPC (CEM I 32.5 R) in accelerated test

Meier et al [2007] and Peter et al. [2008] found from their numerical modelling that the rate of carbonation of the other constituents (CSH etc.) in carbonation was dependent on the relative reaction rates of all constituents. Since that of $Ca(OH)_2$ is much faster, this phase dominates the progress of the carbonation front. The others were found to be of only of secondary effect and hardly influencing the carbonation depth. If the largest effect of ageing is an increase in calcium hydroxide content and a reduction of capillary pores, it is thus expected that these effects would be seen in a thin section. This was however not the case. Moreover, if ageing due to ongoing hydration would cause a significant effect, it is expected that the fly ash and the slag concretes were showing the largest influence. Both hydrate at a later age than the OPC clinkers [see e.g. Neville 2003] and have been observed to have only medium degrees of hydration at an age of 180 days.

In the modelling of the carbonation process by Meier et al. [2006], there is another effect of the carbonation illustrated: the formation of water at the dissolution of $Ca(OH)_2$. The combination of having a very small amount, if any, capillary pores left after carbonation, combined with a very high content of $Ca(OH)_2$, producing the double amount of water at the carbonation front, makes it possible that the evaporation of the pore water at the carbonation front dominates the carbonation process in the AC-test. For the coarse OPC, the degree of hydration will be much lower, having given rise to less $Ca(OH)_2$ and thus less water production and therefore would follow the expected square root t behaviour of eq. (4). Possibly, also the porosity is somewhat coarser, resulting in a higher saturation

degree at which the pore water becomes a continuous phase and does not allow gas transport to the carbonation front [Bear and Bachmat, 1991]. Since diffusion of CO_2 in water being a factor 10^4 lower [Thiery *et al*., 2007] this mode is still not considered as driving force.

If the above explanation is correct, the carbonation process cannot go further until the pores are sufficiently dried out to allow for diffusion of CO_2 through the vapour phase [Maekawa *et al.* 2003]. Since carbonation is still going on, it is likely that a fully saturated thin zone exists at the carbonation front. In the limit that this drying out is very slow, the diffusion of CO_2 (in the accelerated test at least) might be completed and a constant CO_2 concentration in the carbonated zone will exists. As a first order model, assuming this constant CO_2 concentration throughout. The flux is equal to:

$$q = DA(c_{out} - c_{in}) \quad (7)$$

(First order approach of Fick's law over a membrane). Since the amount of carbonatable matter remains the same, as is the condition for the movement of the front, equation (3) becomes instead

$$[DA(c_{out} - c_{in})] = aAdx/dt \quad (8)$$

Solving this by integration results in:

$$x_c = Offset + Dc_s t/a = Offset + c_s t/R_{carb} \quad (9)$$

From least square modelling of this equation to the data, it was found that the integration constant (offset) could not be excluded. The fit resulted in a calculated carbonation resistance of 1.2 10^{-02} kg/m^3/yr/mm^2. This value is the same as calculated for the normal carbonation test.

5 CONCLUSIONS

Accelerated testing of carbonation in only possible if the processes of carbonation in the concrete are not changed. The square root t-model usually applied for both natural carbonation tests and accelerated test is found not always applicable. On the basis of the observed change in porosity in the thin sections and the results of the numerical modelling of Meier et al. [2006], it is speculated that the carbonation of very dense concrete with a high content in carbonational matter may not follow the square root –t behaviour because there is so much water produced which needs to evaporate first before carbonation becomes possible and the carbonation front can move on. Since the porosity in the carbonated zone is small, this is a slow process compared to the diffusion of carbon dioxide into the concrete.

A very simple analytical model has been derived taking as condition that the progress of the carbonation front is no longer the slowest step in the whole reaction process. Instead, it is the progress of the drying front. Therefore, the concentration of the CO_2 in the carbonated concrete is assumed constant and similar to the applied CO_2-concentration. Then the progress of the carbonation front can be described as linearly progressing. Least square modelling gives a resistance to carbonation that is similar to that from the modelling of the natural carbonated sample.

REFERENCES

Al-Kadhimi, T.K.H., Banfill, P.F.G., Millard, S.G. and Bungey, J.H. 1996, 'An accelerated carbonation procedure for studies on concrete', *Adv.Cem.Res.* **30[8]**: 47-59.

Arandigoyen, M. and Alvarez, J.I. 2006,Carbonation process in lime pastes with different water/binder ratio *Mater.Construcc*. **56 [281]:** 5-18 (ISSN 0465-2746).

Bear, J. and Bachmat, Y. (1991), *Introduction To Modelling Of Porous Materials*, Kluwer Ac. Press

Borges, P., Costa, J. et al. 2010 'Carbonation of CH and C-S-H in composite cement pastes containing high amounts of BFS', *Cem.&Concr.Res*. **40**: 284-292.

Castellote, M., Fernandez, L., Andrade, C. and Alonso, C. 2009, 'Chemical changes and phase analysis of OPC pastes carbonated at different CO_2 concentrations', *Mat&Struct*. **42**: 515-525.

Glass, G.K. and Page, C.L. and Short, N.R. 1991, 'Factors affecting the corrosion rate of steel in carbonated concrete', *Corros.Sci*. **32**: 1283-1294.

Maekawa, K. Ishida, T. and Kishi, T. 2003, Multi-scale modelling of concrete performance. Integrated material and structural mechanics, *J.Adv.Concr.Techn*. **1[2]:** 91-126.

Meier, S.A., Peter, M.A., Muntean, A. and Bohm, M. 2007, 'Dynamics of the internal reaction layer arising during carbonation of concrete', *Chem.Engrg.Sc*. **62**: 1125-1137.

Neville, A.M. 1993, *Properties of Concrete*, Pearson / Printice Hall.

Peter, M.A., Muntean, A., Meier, S.A. and Bohm, M 2008, Competition of several carbonation reactions in concrete: a parametric study, *Cem&Concr.Res*. **38**: 1385-1393.

Sisomphon, K. and Franke, L. 2007, 'Carbonation rates of concretes containing high volume of pozzolanic materials', *Cem&Concr.Res*. **37**: 1647-1653.

Thiery, M., Villian, G., Dangla, P. and Platret, G., 2007 'Investigation of the carbonation fron shape on cementitious materials: effect of the chemical kinetics. *Cem&Concr.Res*. **37**: 1047-1058.

XII DBMC
International Conference on Durability of Building Materials and Components
PORTO - PORTUGAL, April 12th-15th, 2011

Outdoor Paint Ageing of Brazilian Paints - Part two

Kai Loh [1]
Edson Luís Cardoso [2]
Neide Matiko Nakata Sato [3]
Marcia Shirakawa [4]
Vanderley Moacyr John[5]

ABSTRACT

The main objective is to discuss the appearance changes in acrylic latex paints after seven years of outdoor exposure. The results after one-year exposure were already presented (Uemoto et al, 2005). In the study, acrylic latex paint, produced by two major Brazilian architectural paint manufacturers, were collected from the City of São Paulo retail market. The paint samples presented different resin content resulting in differences in gloss finish (semi-gloss, silk and matt). The natural aging was performed on painted mortar specimens, produced with cement, lime and aggregate, volume proportion of 1:2:9. The outdoor exposure testing was conducted according to ASTM G-7 on three sites located in São Paulo state, in areas subject to urban, marine and rural environments. The appearance changes of exposed specimens were evaluated by visual inspections and instrumental measurement (color), before and after high pressure water cleaning. The results obtained were discussed and compared with those in the literature.

KEYWORDS

Paint, Acrylic latex paint, Weathering, Outdoor exposure, Pathology.

[1] Escola Politécnica, University of Sao Paulo (USP), BRAZIL, kai.loh@poli.usp.br
[2] Escola Politécnica, University of Sao Paulo (USP), BRAZIL, cardosoeds@yahoo.com
[3] Nove de Julho University (UNINOVE), BRAZIL, neide.sato@uninove.br
[4] Escola Politécnica, University of Sao Paulo (USP), BRAZIL, marcia.shirakaw@usp.br
[5] Escola Politécnica, University of Sao Paulo (USP), BRAZIL, vanderley.john@poli.usp.br

1 INTRODUCTION

Paintings present two major functions: substrate protection from the environment and decorative effects. The outdoor exposure causes visual disfigurement due to various effects being the more common staining, cracking, dirt deposition, biological colonization [Gaylarde & Gaylarde, 2005], often resulting from combined effects. The phenomenon of building facade soiling and darkening, common in industrial and marine atmospheres, results from the deposit of atmospheric pollution from the troposphere and microbiological development due to algal and fungal growth [Bagda 2004], changing the building appearance. This contamination is considered one of the most significant problems throughout the world [Sedlbauer *et al* 2002]; [Becker & Putterman 2002], especially in sub-tropical and tropical regions [Uemoto *et al* 2008]; [Sato *et al* 2008]; [Chew & Ping 2003] [Shirakawa *et al* 2010] with high impact on the quality of the urban environment and life cycle cost of the buildings.

The coatings for facades should provide long-term weather resistance. To avoid a faster disfigurement in the appearance of building facades, it is important to select paints with higher resistance against the effects of the outdoor environment. The rate and extension of the change in appearance depend on the painting performance and on the severity of the exposure conditions. Durability tests must be designed to be as similar as possible to the intended end-use of the material in order to provide a more realistic exposure. It is thus important to test the paint at many different sites, each with its own particular set of influencing factors [Hicks & Crewdson 1995]. Our main objective of the paper is to discuss the appearance changes of acrylic latex paints after seven years of outdoor exposure in three sites located in São Paulo state, in areas subject to urban, marine and rural environments. The results after one-year exposure were already presented [Uemoto et al 2005].

2 THE EXPERIMENT

2.1 Paint Samples

Eight architectural acrylic latex paints, produced by two major Brazilian manufacturers, were collected from the City of São Paulo retail market. For each manufacturer, three conventional products with different pigment volume content (PVC) and an elastomeric paint were selected. PVC controls the gloss and permeability of the paint film and corresponds to different formulations [Uemoto et al, 2008]. The collected samples were identified as A1, A2, A3 and A4 for manufacturer A and B1, B2, B3 and B4 for manufacturer B. Table 1 presents the samples studied, their identification, appearance, PVC and permeability.The appearance and the elastomeric grade (crack bridging properties) designation are information presented in the packaging. PVC and water permeability data are based in literature according to appearance [Uemoto et al., 2008).

Table 1. Paint formulations associated with gloss levels.

Samples	Appearance/Finishing	Estimated PVC
A1	Low sheen or “matt”	35-45
A2	Sheen or “silk”	30-35
A3	Semi-gloss	15-30
A4	Low sheen (100% elastomeric grade)	35-45
B1	Low sheen or “matt”	35-45
B2	Sheen or “silk”	30-35
B3	Semi-gloss	15-30
B4	Semi-gloss (800% elastomeric grade)	15-30

2.2 Natural Weathering Test [Uemoto *et al* 2005]

To allow better simulation of in-service condition, the paints were applied on mortar specimens (1:2:9 v/v cement:lime:sand), measuring approximately 20cm X 10cm X 3 cm, cured in laboratory conditions for more than two months. A set of unpainted mortars was used as reference. The latex paints were applied in two coats according to the manufacturers' instructions with a nylon brush on one face of the mortar specimens and stored at 25 ± 2°C and 50 ± 5% RH for two weeks prior to exposure.
The painted and unpainted specimens were exposed at an angle of 45 degrees to the horizontal, facing North and 0.45 m above the ground, in three locations (ASTM G 7-97): a) Urban atmosphere: Sao Paulo weathering site is located on the campus of Sao Paulo, University of Sao Paulo, Department of Civil Construction Engineering, b) Rural atmosphere: Pirassununga weathering site is located on the campus of Pirassununga, University of São Paulo, Faculdade de Medicina Veterinária e Zootecnia, c) Marine atmosphere: Ubatuba weathering site is located on the Marine Base of the Oceanographic Institute of the University of São Paulo. The grounds at Pirassununga and Ubatuba sites are grass and in São Paulo the site is placed on a rooftop so the ground is concrete. The annual weather summary data at the sites is presented in Table 2.

Table 2. Climate summary data at the sites.

Site	Latitude	Longitude	Temperature (°C)			Rainfall
			Average	Maximum	Minimum	(mm)
Pirassununga [Uemoto, 2005]	21°58'S	47°27'W	19.1	30.1	9.5	1298
Ubatuba [Barbosa, 2006]	23°26'S	45°04'W	22.4	27.0	17.7	2653
São Paulo [Barbosa, 2006]	23°32′ S	46° 38′W	20.2	25.0	15.3	1475

The appearance of the specimens was evaluated periodically by visual inspection and instrumental measurement of color. Only the seven-year exposure evaluation is shown herein.

2.3 Evaluation of Weathering Effects

The appearance is a critical attribute for paintings because the service life for users is often determined by changes in apperance. Specimens after exposure were evaluated by color, visual inspection and qualitative analysis of microorganisms.

2.3.1 Color measurements

The most used colorimetric measurement technique is based on the CIE Lab System (**CIE L*a*b*)**. It consists of two axes a* and b* which are at right angles and represent the hue dimension or color. The third axis is lightness L* and is perpendicular to a*b* plane. The color is established in terms of difference between sample color and a reference sample color rather than absolute values. The change in color ΔE*, is commonly used to to represent the color difference according the equation:

$\Delta E^* = \sqrt{(\Delta L^*)^2 + (\Delta a^*)^2 + (\Delta b^*)^2}$. In this study, the color was expressed in absolute values, measured according to ASTM D 2244/89 before exposure, after exposure and after cleaning procedure, using a Byk-Gardner color-guide (45/0 geometry).

2.3.2 Visual inspection

Although visual inspection is subjective and qualitative, it is important because the user's perception is determined by the change in appearance. For paintings, the evaluations can be carried out with the naked eye based on ASTM standards of coating defects, using a rating system (ASTM D 662 and ASTM D 661). The changes are rated by intensity of the common possible defects, such as chalk, blistering, cracking, erosion, mildew, dirt retention, adhesion etc. Here, only loss of adhesion, erosion, dirt retention and biological growth was considered, using a rating system varying from 1 to 5 based on pictorial (photographic) standards. All areas of the film where the substrate is visible, failures such as loss of adhesion and erosion were considered detachments and areas where dirt retention and

biological growth were observed were considered darkening. Fig.1 presents the photographic reference standards of detachments and darkening.



Reference standards					
0	1	2	3	4	5

Legend
0 - No failure in an exposed painted mortar specimen
1 - Less than 10% of detachments/darkenings
2 - Between 10% and 30% of detachments/darkenings
3 - Between 30% and 50% of detachments/darkenings
4 - More than 50% of detachments/darkenings
5 - Approximately 100% of surface with detachments/darkenings

Figure 1. Photographic degrees of detachments and darkenings proposed by the main author

2.3.3 Qualitative analysis of microorganisms

Samples of the painted and unpainted surface of the specimens were collected with a special device [Shirakawa et al, 2010]. After sampling, each one was pressed on 2Sabouraud Dextrose Agar 4% (Merck) plates and incubated at 25° C for 3 days for fungal analysis. Phototroph analyses were realized according to Gaylarde and Gaylarde [2005].

3 RESULTS AND DISCUSSION

3.1 Color Change After Weathering

Table 5 presents the color measurements on the specimens, exposed at the three sites, before and after 7 years exposure and after high pressure water cleaning procedure. According to the measurements all the painted specimens showed a very high change in color after the natural weathering.

The paints A1 (ΔE = 66) and A4 (ΔE=59), exposed in Ubatuba site, are products that showed the highest color change and this change according to item 3.3 is caused by the development of biological microorganisms. The measurements show that after high pressure water cleaning procedure the appearance is partially recovered.

The paints B2 and B3, exposed in Pirassununga site, are products that showed change to reddish that is caused by the deposition and impregnation of micro particles like clay present near the Pirassununga site. The measurements show that after high pressure water cleaning procedure the redden color observed in B2 and B3 was not eliminated showing that the micro particles were impregnated in the porous matrix of the paint films.

Table 5. Color measurements of specimens exposed at the three sites before and after 7 years exposure and after high pressure water cleaning procedure

		Before exposure			After 7 years exposure				After cleaning			
Paint	Site	L	a	B	L	a	b	ΔE	L	A	b	ΔE
A1	Ubatuba	93	-1	4	28	2	8	66	72	1	8	22
	São Paulo	93	-1	4	58	1	8	35	79	-1	6	14
A2	Ubatuba	94	-2	2	67	1	6	26	82	1	6	13
	São Paulo	94	-2	2	63	1	10	33	83	0	7	13
A3	Ubatuba	94	-2	2	65	1	6	29	81	0	6	13
	São Paulo	94	-2	2	64	2	10	31	89	-1	6	6
A4	Ubatuba	93	-1	3	35	6	7	59	76	5	7	18
	São Paulo	93	-1	3	68	1	7	25	80	0	5	13
B2	Pirassununga	93	-1	4	68	5	17	29	83	2	11	13
	São Paulo	93	-1	4	62	1	9	30	81	-1	6	13
B3	Pirassununga	93	-2	4	71	4	17	28	83	2	12	14
	São Paulo	93	-2	4	67	1	7	32	77	-1	7	16
B4	Pirassununga	94	-1	3	56	2	8	39	79	0	9	16
	São Paulo	94	-1	3	28	1	3	28	82	0	4	13

3.2 Visual Inspection

Tables 3 and 4 present the qualitative evaluation conducted on the specimens exposed at the three sites before cleaning procedures and after high pressure water cleaning. The rating of detachments and darkenings observed in the specimens is carried out according the photographic degrees presented in Fig. 1. Fig. 2 presents the appearance of the specimens after 7-year exposure in São Paulo, Ubatuba and Pirassununga sites before and after high pressure cleaning procedure. Part of the specimens was lost during the exposure in the sites. The cleaning procedure was performed only in one specimen of each paint sample because other tests were programmed to continue this study.

Table 3. Qualitative evaluation of detachments and darkenings of specimens after 7 years, before cleaning.

Specimens	Darkenings São Paulo	Darkenings Ubatuba	Detachments São Paulo	Detachments Ubatuba
A1	2	4	2	4-5
A2	1	2	0-1	1-2
A3	1	2	0-1	1-2
A4	1	4-5	0	0-1
Unpainted	5	5	Unpainted	unpainted
	São Paulo	Pirassununga	São Paulo	Pirassununga
B2	1	1	0	1
B3	1	2	0-1	1
B4	2	2	0-1	1
Unpainted	5	5	Unpainted	unpainted

Table 4. Qualitative evaluation of detachments and darkenings of specimens after 7 years, after high pressure water cleaning procedure.

Specimens	Darkenings São Paulo	Darkenings Ubatuba	Detachments São Paulo	Detachments Ubatuba
A1	0-1	0-1	3-4	5
A2	0-1	0-1	0-1	3
A3	0-1	0-1	0-1	3
A4	0	0-1	0	1
	São Paulo	Pirassununga	São Paulo	Pirassununga
B2	0-1	0-1	2	1
B3	0	0-1	3	1-2
B4	1	0-1	1-2	2

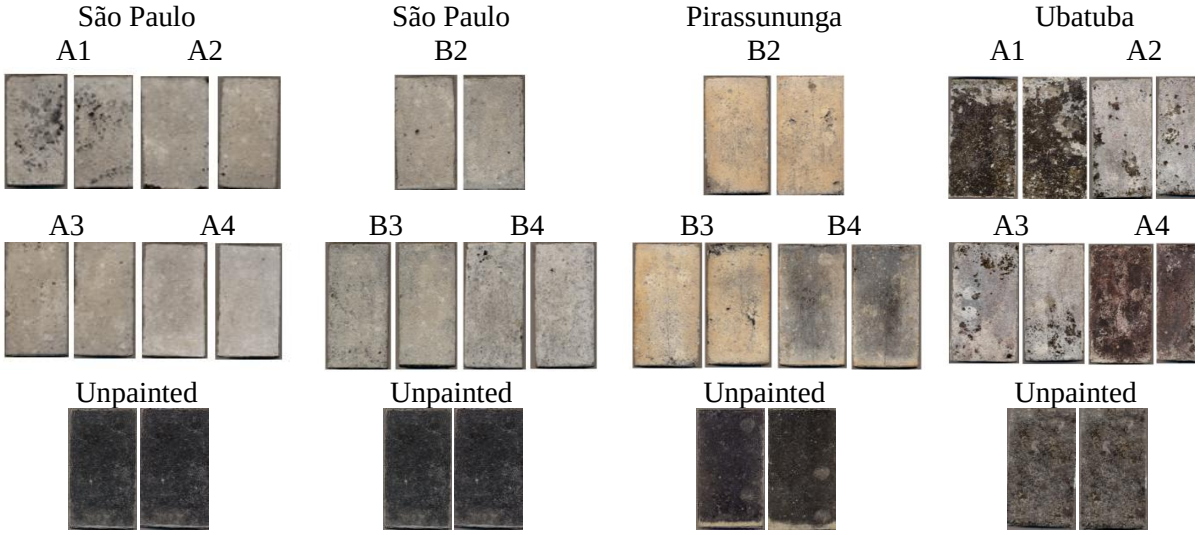

a)

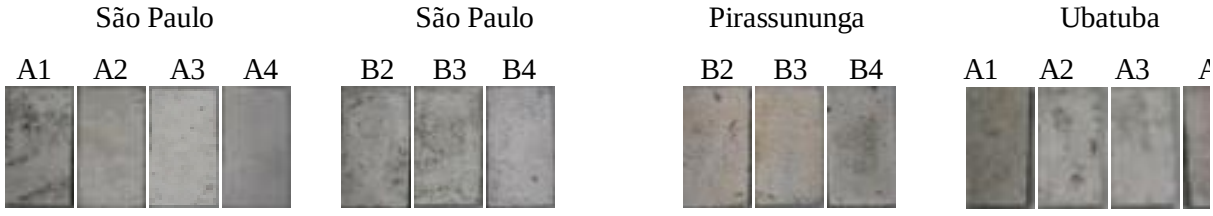

b)

Figure 1. Appearance of the specimens after 7 years exposure in São Paulo, Ubatuba and Pirassununga, a) uncleaned, b) after cleaning.

In **São Paulo site** the specimens painted with B2 and B3, presented the same degree of darkening and detachment as A2 and A3, probably because both have similar PVC and water permeability. On the other hand, B4 and A4 did not present the same result. The paint B4 is semi-gloss and 800% elastomeric grade, with higher resin content than A4 matt finish and 100% elastomeric grade.

Generally elastomeric paints are formulated with low Tg (glass trasition temperature) resin resulting in more tacky films and resulting in higher dirt retention. In this case, the higher is the resin content (B4), the higher is the dirt retention. The high pressure water cleaning part of the darkening observed on the painted specimens was removed and the initial appearance was partially recovered. However, the same was not observed for detachments; the painted surfaces A2, A3, A4 were maintained and for A1, B2 and B3 detachments higher than degree 2, except for paint B4 (degree 1-2), were observed.

In **Pirassununga site** the specimens painted with B2, B3 and B4 presented darkening degree between 1 and 2 and detachment degree 1. The darkening observed in the specimens painted with B2 and B3 was a change to reddish, caused by the deposition of red clay present in an area near the site. However, the specimens painted with B4 did not change to reddish but to grey, different from of B2 and B3. The painted specimens, after water cleaning, recuperated part of the initial appearance but specimens painted with B2 and B3 continued reddish and B4 with a light grey color (degree 1 and 2).

In **Ubatuba site** the paints A1 and A4 showed more than 50% of darkening (degree 4 and 4-5) but presented different degree (4-5 and 0-1) of detachments. The exposure showed that the elastomeric resin used in A4 presented higher resistance in marine environment than A1. However, the higher tackyness of A4 the film presented a higher staining and lower detachment. In Ubatuba site paints A1 and A4 presented a much higher darkening than São Paulo and Pirassununga sites. Qualitative analysis of microorganism showed that the darkening is caused by biological growth (fungi and phototrophs). The paints A2 and A3 showed more than 10% failures (darkening degree 2 and detachments 1-2) and after cleaning procedure the darkening was partially removed, but the detachments increased (degree 3) showing the low resistance of the film in environments with high humidity.

In the three sites all the unpainted specimens (reference) showed 100% of darkening (degree 5). The exposure tests showed that the paints can reduce the darkening caused by biological growth, besides high PVC formulations, as A1 and B1, result in films with high porosity so they do not protect porous substrate so well against water penetration. The high humidity of the marine site create an environment especially favorable for the development of these organisms.

3.3 Microorganism Development

In Pirassununga all painted specimens presented greatest colony diversity in Sabouraud Dextrose Agar than São Paulo and Ubatuba. In Pirassununga the fungal genera identified were: *Alternaria*, the most abundant, *Pestalotia, Cladosporium, Curvularia, Epicoccum, Fusarium, Paecilomyces, Pithomyces*. In Ubatuba a brown non sporulating fungi was the most commom followed by *Cladosporium* and *Pestalotia*. In São Paulo *Cladosporium* was the most frequent confirming data obtained by Shirakawa et al (2010). The occurrence of phototrophs was also detected in all sites, Ubatuba being with most abundant presence of these organisms.

4. CONCLUSION

The study showed that the environment and climatic conditions are the main factors that affect the deterioration of the paints and the importance of testing the materials at different environments because each of them has its particular set of influencing factors (Uemoto et al., 2005). The exposures were realized in sites with similar insolation but in Ubatuba with higher rainfall. The development of fungi and phototrophs in different environments was already studied by Shirakawa (2010). Besides, short exposure periods do not permit prediction of differences observed after seven-year exposure in the three different environments. According to visual inspection and color measurements, paints of different PVC levels present different performance.

The weathering tests showed that the products A2 silk and A3 semi-gloss, from manufacturer A, both present similar performance; small differences in appearance were observed after seven-year exposure in the three sites, before and after cleaning procedures. The same result was observed for products B2 silk and B3 semi-gloss, from manufacturer B, for equivalent products. Products A2 silk, A3 semi-

gloss, B2 silk and B3 semi-gloss can be recommended for exterior application, for example in facades of tall buildings. The same result is not observed for low gloss product, A1 matt, that presents much lower performance, with high degrees of detachments and darkening, independent of the exposure site. These products are recommended for interior applications. The results obtained permit us to conclude that products presenting silk and semi-gloss appearance are less susceptible to weathering, showing less differences in appearance, such as detachment, darkening, cracking or change in color.

ACKNOWLEDGMENTS

The authors would like to acknowledge the financial support granted by FAPESP (The State of Sao Paulo Research Support Foundation) for this research project.

REFERENCES

Bagda, E. 2004, Exposed to the forces of nature. Farbe & Lack No.12, pp 60 – 65

Barbosa, J. 2006, Utilização de método de interpolação para análise e espacialização de dados climáticos: o sig como ferramenta. In. Caminhos de geografia - revista on line. 9 (17) pp. 85 - 96. http://www.ig.ufu.br/revista/caminhos.html. ISSN 1678-63431.

Becker, R.; Putterman, M. 2002, Patterned mould growth on rendered facades in Israel – A consequence of substrate thermal insulation'. In: *The 6th Symposium on Building Physics in Nordic Countries. Trondheim. Proceedings*... Norway, pp.17-19.

Chew, M.Y. L.; Ping, T. P. 2003, 'Staining of facades'. Singapore.

Gaylarde, P. M.; Gaylarde, C. C., 2005, A comparative study of the major microbial biomass of biofilms on exteriors of buildings in Europe and Latin America, In: *International Biodeterioration and Biodegradation* 55, pp. 131–139

Hicks, L.S.; Crewdson, M. J. 1995, Natural weathering, In: *Paint and Coating Testing Manual Fourteenth Edition of the Gardner-Sward Handbook*, ASTM manual series; MNL 17, ed J. V. Koleske, Ann Arbor, Michigan, pp.619-642.

Sato, N.; Shirakawa, M.; Uemoto, K; John, V. 2008, Influence of thermal properties of materials in condensation and microorganism growth of building façades. In. *11th International Conference on Durability of Building Materials and Components*. Istanbul Turkey, May, pp. 1405-1412.

Sedlbauer, K.; Krus, K.; Zillig, W. 2002, Prediction of mould growth by hygrothermal calculation. In: The 6th Symposium on Building Physics in Nordic Countries 2002. Trondheim. Proceedings... Norway, June, pp. 17-19.

Shirakawa, M. A.; Tavares, R. G., Gaylarde, C. C., Taqueda, M. E. S., Loh, K., John, V. M., 2010. Climate as the most important factor determining anti-fungal biocide performance in paint films. Science of the Total Environment. 408, pp.5878-5886.

Uemoto, K, Ikematsu, P., Agopyan, V. 2005, Comparative Evaluation Between Accelerated and Outdoor Ageing of Brazilian Paints - Part one. 10DBMC International Conférence On Durability of Building Materials and Components. Lyon, France pp. 17-20.

Uemoto, K, Sato, N., John, V. 2008. Influence of the mix proportion of mortars and paint formulation on the behaviour of the mortar/coating system in water transport phenomena. In. 11th International Conference on Durability of Building Materials and Components. Istanbul Turkey, May, pp. 11-14.

XII DBMC
International Conference on Durability of Building Materials and Components
PORTO - PORTUGAL, April 12th-15th, 2011

Natural Ageing Tests to Study in-Service Water Resistance of Pre-Mixed One-Coat Rendered Walls with Hydrophobic Agents

Luís Silva[1]
Inês Flores-Colen[2]
Nuno Vieira[3]
Ana Barros Timmons[4]

ABSTRACT

In situ testing is a precious auxiliary mean to reduce the subjectivity of visual inspections, leading to a more accurate characterization of existing degradation mechanisms of the materials and buildings systems. Inspections in natural conditions along the time can increase the knowledge of in-service behaviour and can contribute also to a better correlation between accelerated and natural ageing tests.
This paper presents a field experimental campaign applied on several test-rendered walls, during a period of 6 years after their construction, in order to study the water resistance of renders in real conditions. This analysis focus on the study of the influence of the hydrophobic agent (in this case, salts of fatty acids) on the behaviour of the renders during that time, in terms of surface condition (aesthetics' problems assessment through field evaluation) and water penetration (assessment through Karsten tube on the walls and capillary tests on samples collected on-site). Additionally, lab tests on the performance of several hydrophobic agents are also presented and discussed, in order to improve the in situ results interpretations.

KEYWORDS

Natural ageing tests; Rendered walls; In situ testing; Water resistance; Hydrophobic agents.

[1] Saint Gobain Weber Portugal, Aveiro, PORTUGAL, luis.silva@saint-gobain.com
[2] IST, Department of Civil Engineering and Architecture, Technical University of Lisbon, PORTUGAL, ines@civil.ist.utl.pt
[3] Saint Gobain Weber Portugal, Aveiro, PORTUGAL, nuno.vieira@saint-gobain.com
[4] CICECO, Department of Chemistry, University of Aveiro, Aveiro, PORTUGAL, anabarros@ua.pt

1 INTRODUCTION

Aesthetics and waterproofing are the main functions that a facade's cladding must fulfil during its service life. The observation of facades along the time of exposure to environmental conditions suggests, furthermore, that aesthetic is strongly conditioned by the behavior that a cladding system has in the presence of water and its effective capacity to prevent the penetration and promote the elimination of this degradation agent. In the particular case of a pre-mixed one-coat render, which consists of applying a colored layer of pre-mixed mortar, can show a good level of waterproofing when this product has itself adequate waterproofing characteristics, when doesn't crack and also when its adherence to the support is good [ANFAPA 1990].

The ability that a pre-mixed one-coat render has to resist to the penetration of water is expressed by the coefficient of water absorption by capillarity, which measures the speed that the material absorbs water by this mechanism. The requirements for resistance to water penetration are defined in EN 998-1:2003 through three classes, namely, W0 when not specified; W1 when the value is between 0.2 and 0.4 $kg/m^2.min^{1/2}$ and W2 when the value appears less than 0.2 $kg/m^2.min^{1/2}$. For durability testing, the same standard covers this issue in the case of one-coat mortars, recommending, beyond the study of adhesion, resistance to penetration of liquid water after exposure to climate cycles with a maximum requirement of $1ml/cm^2$, after 48 hours of testing [CEN, 2003]. However, as mentioned by Quintela [2006] these tests may not correspond to significant variations that can express changes in terms of real in-service behavior.

To ensure the minimum requirements recommended by the previous mentioned standard, the one-coat render is formulated with hydrophobic agents, whose mechanism of action is to decrease the surface tension of the solid with the water, leading to an increased contact angle between the two surfaces. Among these are metallic soaps such as salts of oleic or stearic acid, which by their ratio efficiency / cost are, to date, compounds commonly used to guarantee the hydrophobicity of a render. In this context, any mortar which incorporates concentrations of 0.2% to 0.5% on these compounds will show coefficients of water absorption by capillarity well below the maximum levels allowed by standard requirements. On the other hand, for the last decade, silanes were being introduced as well. Silanes are silicon chemicals that possess a hydrolytically sensitive centre that can react with inorganic substrates to form stable covalent bonds and possess an organic substitution that alters the physical interactions of treated surfaces [Tanford 1979]. Their action is to modify the surface energy or wettability of substrates. The latest results with silanes have shown a potential use of these compounds as an improvement of hydrophobic behaviour of mortars in order to achieve better water resistance and longer effect [Lanzón & Garcia Ruiz 2008].

The widespread observation of facades indicates that a mortar classified as W2, by EN 998-1:2003, class that corresponds to the higher ability to resist to water penetration, is not necessarily equivalent to a higher durability, although it is often admitted. In fact, the field observation of facades indicates signs (dirt, discolouration, among others) of a possible degradation or leaching of water repellent agents after the first year. This is evidenced by the higher wettability of the facades, indicating a decrease of contact angle, probably due to the increase of surface tension of the solid, suggesting the presence of water for longer periods of time. In fact, it is common the confusion between efficiency and durability of water repellent agents, which leads, for example, to the use of materials of different composition, such as silicon powder, without maintaining the desired effect over time. In fact, some work on the long-term durability of concrete with silanes and siloxanes demonstrate the need for additional care and use of higher concentrations, to adoption the best ratio mortar / type of molecule, drying conditions and application among others, clearly showing the need for further research studies in this field [Raupach & Wolff, 2005].

Considering the need for more knowledge about the real durability of these hydrophobic solutions and on the interpretation of the mechanisms that lead to the decrease of the efficiency of these solutions in time, this paper intends to give an input on in situ performance of a colored one-coat render when

exposed to normal in-service degradation agents, in terms of its ability to resist penetration of liquid water and, by extension, in terms of the waterproofing contribution of hydrophobic agents such as conventional metallic soaps. Additionally, this paper presents a set of experimental methods that allow the correlation between laboratory tests and in situ techniques that can characterize the slow degradation mechanisms in field conditions (natural ageing).

2 EXPERIMENTAL CAMPAIGN

2.1 Aplication and Evaluation in Rendered Walls Exposed to Natural External Conditions

The experimental work was the application of one-coat render, with salts of stearic acid and oleic hydrophobic agents and classified as a W2 by EN 998:1 [LNEC 2004], through a machine for discontinuous projection on masonry walls (brick 11 cm), exposures with the North, South, East and West. Specifically, in the north direction, the mortar was applied and subjected to a different finish, ie float finish / sanded unlike all other cases where it took place a scraped finish. Table 1 shows, briefly, the relationship between the orientations of the walls and the parameters of the study.

Table 1. Relation between orientations of the rendered walls and parameters of the study.

Wall orientation	*Color*	*Finishing*
North	Red (“brick”)	Float finish / sanded
South	Red (“brick”)	Scraped
East	Red (“brick”)	Scraped
West	Red (“brick”)	Scraped

After applying the mortar, a series of inspections for each year of service with the aim of analyzing various characteristics of the one-coat renders were performed. Therefore, assessments of adherence by perpendicular tensile tests (pull-off tests) and of render inherent capacity to resist to liquid water penetration were performed. In this context, the following tests were included within inspections:

a) After the pull-off test, samples were collected from the rendered walls and prepared with 4 * 4 cm^2 (thickness equals to mortar applied in case of adhesive tensile strength, or smaller, in the case of cohesive rupture in this test), according to figure 1 a). In this context, it should be noted that, in any case, the thickness obtained was never less than 1 cm; absorption coefficient of water by capillarity was also determined for the collected samples, according to EN 1015: 18 [CEN 2002].
b) Penetration tests of liquid water under pressure, known as pipe method or Karsten test, were conducted on tested-walls; this technique consists in the measurement of water volume absorbed by the mortar’s surface in a given area and for an estabilished period of time. The technical procedure uses a graduated tube, pipe-shaped, with a circular cross-section, 5.7cm^2 along surface contact with mortar; the total height of the water column applied is 9 cm (see Figure 1 b)). The results for this analysis are expressed in terms of accumulated values of absorbed water after 180 minutes.
c) Finally, the resulted samples from the adherence test were also tested for the determination of open porosity by hydrostatic weighing method with immersion in water, in order to investigate possible changes in the internal structure of mortars which may, by changing the structure of pores, contribute to possible variations of capillarity and water absorption [Flores-Colen 2009].

2.2 Laboratory Testing

The laboratory testing campaigns consisted in the assessment of hydrofobicity capacity under the following conditions:

1. Preparation of test circular pieces of one-coat with a) metallic soaps (0.5%) and b) silanes (0.5%), with 2 cm thickness and diameter of 13 cm subject to curing conditions 22ºC, 55% RH, for 28 days (t0);
2. After the period mentioned in the test specimens, determination of the coefficient of absorption of water by capillarity, absorption of water under pressure from Karsten tube and contact angle of one drop applied on the surface of the samples (the last one, just in case t0 and t1) were performed; the static contact angle was measured with an instrument (coupled to a camcorder) that measures the surface energy, developed at the University of Brno, Czech Republic, according to figure 1 c).
3. Further study of the previous properties was performed after samples were subjected to leaching/drying cycles - different times of immersion in water (t1: 24 hours, t2: 7 days and t3: 14 days) with subsequent drying to 70ºC until constant weight.

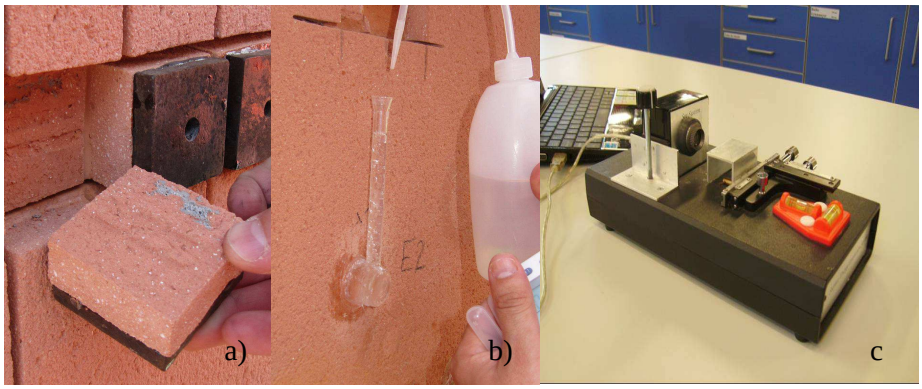

Figure 1. a) The perpendicular tensile adhesion test with consequent sampling for the determination of the coefficient of absorption of water by capillarity; b) Karsten tube test; c) equipment for the evaluation of contact angle.

3 RESULTS

3.1 Aplication and Evaluation in Rendered Walls Exposed to Natural External Conditions

The results for the water absorption by capillarity test and water absorption by application of Karsten tube, after 6 years of exposure to environmental conditions, are sintetized in table 2 and figure 2. Additionally, the graphs in figure 3 show the variation of the results of the absorption coefficient of water by capillarity, C, and the water absorption after 180 minutes, through Karsten pipe, over time, of rendering walls with the orientations already mentioned. The initial value (zero year) corresponds to the measurement in the laboratory.

Table 2. Results of the coefficient of absorption of water by capillarity and water absorption after 180´ for various walls' orientations, after 6 years of exposure to environmental conditions.

Facade	*C* [kg/m^2.min^{½})]	*Absorption of water under pressure 180´* [ml]
North	0.011	0.48
South	0.012	3.40
East	0.013	0.45
West	0.011	2.33

Figure 4 shows the results on the determination of adhesion (pull-off test) and open porosity for samples collected from the various walls' orientations in the study. It is the determination of these properties that allows the characterization of the loss of resistance to penetration of liquid water due exclusively to the behaviour of hydrophobic agents, because this compounds will help the elimination of factors due to possible internal structural changes resulting from the dynamics of hydration of cement of mortar.

3.2 Laboratory Testing

The results related to the tests of capillarity, Karsten tube and measurement of the angle of contact on circular pieces of one-coat mortar with metallic soaps and silanes are shown in figures 5, 6, 7, 8 and table 3. The figure 7 represents the variation of the absorption coefficient of water by capillarity and water absorbed during 180 minutes, using Karsten pipe method, depending on the number of leaching/drying cycles performed.

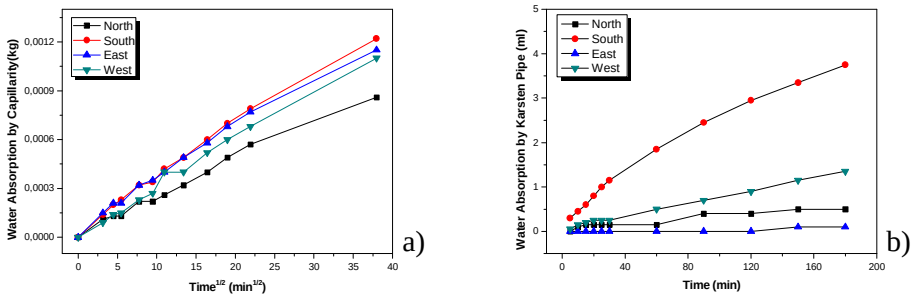

Figure 2. Results after 6 years of diferent exposure conditions for a) water absorption by capillarity; b) water absorption by Karsten tube method.

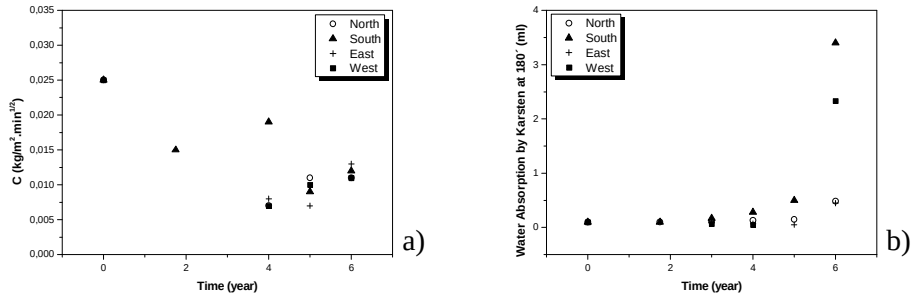

Figure 3. Results after 6 years of diferent exposure conditions on time for a) capillarity coefficient; b) water absorption by Karsten tube.

4 DISCUSSION

Figure 2 and table 2 don´t show significant differences to the absorption coefficient of water by capillarity between the various walls' orientations studied, after 6 years of exposure to environmental conditions. Additionally, according to figure 3, the values obtained are very different between the years of study (field inspections assessments), especially up to 3 years, but always below the reference value (year zero) measured in the laboratory. On the other hand, between 4 and 6 years, there is a potential tendency to increase in the several exposure walls' orientations studied.

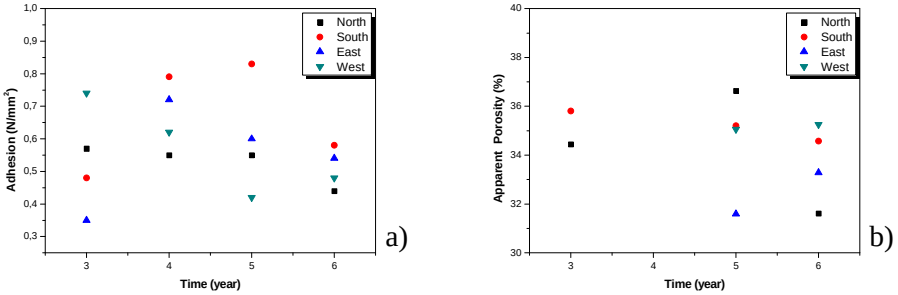

Figure 4. Variation of the a) pull-off adhesion test and b) open porosity, for the rendered walls orientations evaluated, according to the time of exposure to environmental conditions.

The results of water absorption obtained by Karsten tube method, express in table 2 and figures 2 and 3 show that the facades exposed to the South and West have less resistance to water penetration. In fact, the water absorption values are substantially higher for these orientations and the difference concerning other walls orientations is still incremented over the years of service. The analysis of figure 3 also shows a trend to increase water absorption for all orientations evaluated, especially from the 5th year of exposure to environmental conditions. For specific cases to South and West, the value given at 6 years highlights a "rupture point" since the amount absorbed is significantly higher in all cases.

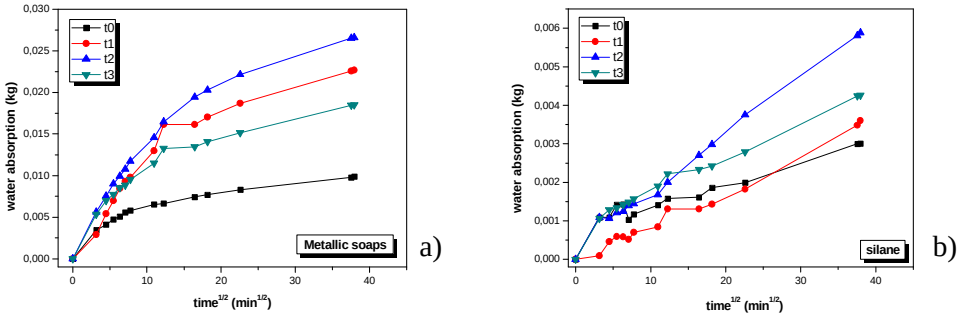

Figure 5. Capillarity curves of one-coat mortar with a) metallic soaps and b) silane, depending on curing time at normal conditions (t0) and after lixiviation/drying cycles (t1, t2 and t3).

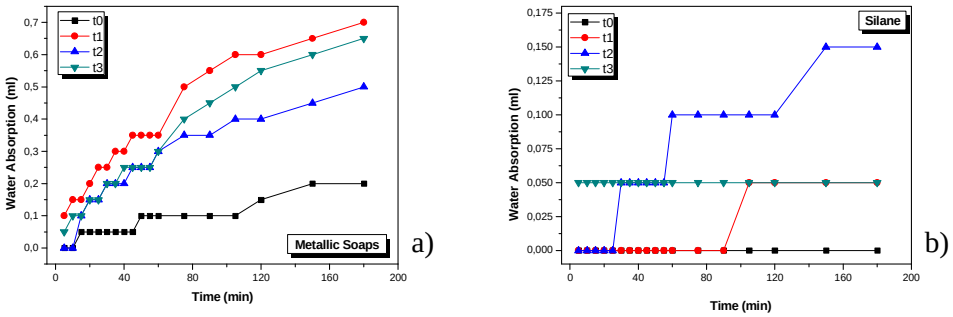

Figure 6. Karsten pipe test graphs of one-coat mortars with a) metallic soaps and b) silane, depending on curing time at normal conditions (t0) and after lixiviation/drying cycles (t1, t2 and t3).

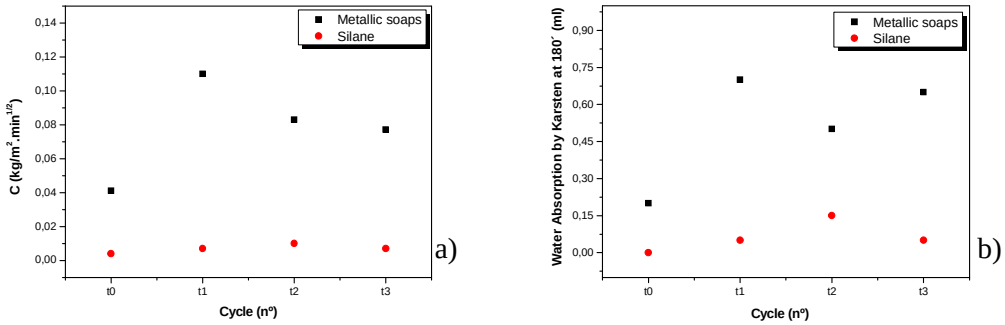

Figure 7. Variation of a) coefficient of capillarity and b) water absorption by Karsten pipe method, depending on the number of leaching/drying cycles.

The analysis of figure 3 also shows that the absorption of water, determined by Karsten tube method, is more affected over years of exposure than the coefficient of absorption of water by capillarity. In fact, this test presented a significant change after 5 years of exposure and, for two specific orientations, the values obtained raise doubts about the current capacity of mortar to resist to the penetration of water and to ensure waterproofing. It is assumed that mortar will continue to fulfil waterproofing function by considering that the coefficient of capillarity is not superior to standard values considered as a guarantee of efficiency at this level (water absorption with suction mechanism). On the other hand, results from Karsten tube can complement the interpretation of aesthetic variation occurred in rendered walls. With effect from 4 years it was observed higher concentration of fungi in rendered walls which can derive greater concentration of moisture on the mortar surface, clearly evidenced by the increase of water absorption values at 180´.

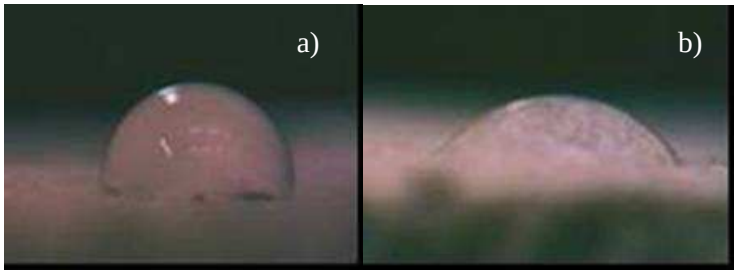

Figure 8. Contact angle images after t0; a) silane; b): metallic soap.

Data of open porosity of mortar, showed in Figure 4, suggest a slight decrease trend over the years of exposure, therefore this parameter can´t contribute to the interpretation of results related to the variations of the absorption coefficient of water by capillarity and water absorption by Karsten tube method. The variation of adhesion corroborates the previous statement because the results haven´t also shown any direct relationship with this parameter and the hydrothermal properties evaluated.

Table 3. Capillary coefficient, water absorption after 180´ (Karsten pipe) and contact angle measurements.

Facade		*C* [kg/m^2.min ^{½})]	*Absorption of water under pressure 180´* [ml]	*Contact angle* [º]
Silane	t0	0.004	0	89.70
	t1	0.007	0.05	---
	t2	0.010	0.15	---
	t3	0.007	0.05	84.30
Metallic Soap	t0	0.041	0.2	45.96
	t1	0.11	0.7	---
	t2	0.083	0.5	---
	t3	0.077	0.65	46.94

Laboratory tests reveal, as expected, significant differences in the behavior of mortar when protected with metallic soaps or with silanes. As noted by figure 5 and table 3, the values of absorption of water by capillarity are much lower when silanes are added. Figure 7 shows a value of capillarity increment after the first cycle of leaching/drying (t1) although the stability is reached for subsequent cycles. An attempt of correlation between the results shown in this context with the results relating in situ tests, expressed in figure 3, allows the consideration of a "pseudo-trend", mentioned at the beginning of this discussion, can indeed be true, but this can only be proven with further testing with more years of evaluation.

Also, the absorption of water by Karsten tube test is significantly lower when the mortar presents the silane as hydrophobic agent, as revealed by the results show in table 3 and figure 6. The data in figure 7 shows, especially for the mortar with metallic soaps, that its resistance to penetration of water decreases shortly after the first cycle of leaching/drying. Analysis of values obtained indicates that, although not reaching values as high, can make an interesting correlation with the values obtained by in situ tests, as shown in figure 3, and assume that this action of leaching/drying causes an action equivalent to a range around 5 to 6 years for in situ conditions assessed. For mortar with silane, the variation is not so evident, especially because it is considered that absorbance values are substantially lower. Nevertheless, the leaching action causes a change in resistance of mortar to penetration of liquid water, since it also register the increase in the value of water absorption. The analysis of table 3 and figure 8, on the assessment and measurement of the angle of contact of mortars studied, reveals a peculiar behavior, since increase for the case of metallic soaps and a decrease in case of silanes which leads to the difficulty to relate directly this property with measurements of coefficient of capillarity and absorption of water by Karsten pipe. Again, data analysis show the biggest potential of silanes in ensuring the hydrofobicity of mortars, since these compounds have lead to contact angle values significantly higher.

5 CONCLUSIONS

Field testing, such as the determination of the coefficient of absorption of water by capillarity and Karsten tube, revealed behavior changes in the ability of an one-coat render to resist to the penetration of liquid water. Despite the mortar still present values below the limits recommed by the standard, it is concluded that situations more exposed to climatic conditions begin a process of degradation after 6 years of service. The results obtained for the render indicates that conventional water repellents agents as metallic soaps, allow the resistance to penetration of water, ensuring the ability of waterproofing mortar for long periods considerably. However, its superficial effect lacks durability resistance, which can contribute to the progressive aesthetic degradation of the render. Has not been demonstrated, unequivocally, that the mechanism responsible for this loss of efficiency, can derive from leaching or chemical degradation. These degradation factors may also be decisive in the efficiency of other hydrophobic agents, such as silanes; the laboratory leaching tests showed also a loss of efficiency though less pronounced, since these compounds presented a resistance to penetration of water considerably higher. Leaching tests conducted in laboratory promotes, with reasonable approximation, a correlation tests in situ by the adoption of a 24 hour cycle can be considered equal to more severe exposure conditions for a period significantly long.

6 ACKNOWLEDGEMENTS

The authors would like to thank to the students Lisendra Marbelia and Xuan Binh from Erasmus Mundus EMMS - European Masters in Materials Science.

7 REFERENCES

ANFAPA, 1990, *Nuevos Revestimientos de fachada: Los morteros monocapa*.

CEN, EN 998-1, 2003, *Specification for mortar for masonry*.

CEN, 1015:18, 2002, *Methods of test for mortar for masonry- Part 18: Determination od water absorption coefficient due to cappilary action of hardened mortar*, Brussels.

Flores-Colen, I., 2009, "Metodologia de avaliação do desempenho em serviço de fachadas rebocadas na óptica da manutenção predictiva", PhD Thesis, IST, Lisboa.

Lanzón, M. & Garcia-Ruiz, P.A., 2008, "Effectiveness and durability evaluation of rendering mortars made with metallic soaps and powdered silicone", *Construction an Building Materials*, **22**, 2308-15.

LNEC, Relatório 427/05, 2004, *Homologação do revestimento de paredes monocamada, weber.pral classic*, Lisboa, 2004.

Quintela, Marisa A., 2006, "Durabilidade de revestimentos exteriores de parede em reboco monocamada", MS. SC. Thesis, FEUP, Porto.

Raupach, M, Wolff, L., *Long term durability of hydrophobic treatment on concrete*, Institute for Building Materials Research of the Technical University, Aachen, Germany, 2005.

Tanford, C., 1979, *The hydrophobic effect*, Wiley.

XII DBMC
International Conference on Durability of Building Materials and Components
PORTO - PORTUGAL, April 12th-15th, 2011

Evaluation of Building Products by Conducting Accelerated Climate Ageing in the Laboratory

Bjørn Petter Jelle [1]

ABSTRACT

Miscellaneous building materials, components and structures have to fulfil many functional demands during the lifetime of a building. Therefore it is important require satisfactory durability of these building products. However, experience tells that the building products too often do not satisfy the various specified requirements after a relatively short period of use, i.e. the expected service life is considerably shorter than foreseen. The result is increased and large costs due to increased maintenance, extensive replacements of the specific building products, any possible consequential building damages and potential health hazards. In order to avoid this the solution is to apply building products which have properly documented adequate and satisfactory long-term durability. That is, building products which have been subjected to appropriate accelerated climate ageing in the laboratory.

This work examines the main climate exposures and how these may be reproduced in the laboratory in various ways. Hence, crucial properties of building products and their durability towards climate strains may be investigated within a relatively short time frame compared with natural outdoor climate ageing. Examples of miscellaneous climate ageing laboratory apparatuses, ageing methods and building product properties to be tested before, during and after ageing are given. A simplified yet versatile calculation method for estimating acceleration factors is also demonstrated. The choice of reference frames and values for comparison are very important for these accelerated ageing calculations.

KEYWORDS

Accelerated climate ageing, Building, Material, Component, Structure.

[1] SINTEF Building and Infrastructure, Department of Materials and Structures, NO-7465 Trondheim, Norway, and Norwegian University of Science and Technology (NTNU), Department of Civil and Transport Engineering, NO-7491 Trondheim, Norway, bjorn.petter.jelle@sintef.no

1 INTRODUCTION

Building materials, building components and building structures have to fulfil many functional demands during parts of or during the whole lifetime of a building. Hence, these building products must possess a satisfactory durability with respect to several properties. However, the experience is that many building products all too often do not satisfy the various requirements after a relatively short time of use. Lack of durability results in large and increased costs caused by increased need of maintenance, extensive replacements of the specific building products and any possible consequential building damages. Failure in the building products may also lead to increased health hazards with respect to both health risks, i.e. the chance of a health hazard to occur, and health consequence, i.e. the impact of the health hazard if it occurs. Thus, it is important to select building products which have proven and properly documented adequate and satisfactory long-term durability. Documentation is achieved either by already carried out natural outdoor long-term climate exposure or by performing appropriate accelerated climate ageing in the laboratory. The purpose of this work is to investigate and present the main climate exposures and how these may be reproduced and applied in the laboratory in various ways. Hence, crucial properties of building products and their resistance and durability towards climate strains may be studied within a relatively short time frame compared with natural outdoor long-term climate ageing. Selected examples of various climate ageing laboratory apparatuses, ageing methods and building product properties to be tested before, during and after ageing are given. Finally and importantly, a calculation method for estimating acceleration factors is also demonstrated and discussed. That is, this study addresses durability of building materials, components and structures and the versatile and powerful application of accelerated climate ageing.

2 CLIMATE EXPOSURE FACTORS

Buildings are daily and throughout the whole year subjected to large and changing climate strains (e.g. see Fig.1), which may be divided into the following climate exposure factors:

- Solar radiation, i.e. ultraviolet (UV), visible (VIS) and near infrared (NIR) radiation.
- Ambient infrared (IR) heat radiation (the resulting elevated temperature increases the rate of chemical degradation reactions and the growth rate of rot and fungus up to limiting temperatures).
- High and low temperatures.
- Temperature changes/cycles (relative temperature movements between different materials, number of freezing point passes during freezing/thawing).
- Water, e.g. moisture, relative air humidity, rain (precipitation) and wind-driven rain.
- Physical strains, e.g. snow loads.
- Wind.
- Erosion (also from above factors).
- Pollutions, e.g. gases and particles in air.
- Microorganisms.
- Oxygen.
- Time (determining the effect for all the factors above to work).

Several and varying combinations of the climate exposure factors will occur, and the total climate strain may be substantially larger than the added sum of the single exposure factors. During selection of building products it is of great importance to choose the ones which will endure the climate strains they will be subjected to during their anticipated service life. So how should this be accomplished without having to test the materials and components throughout their whole lifetime? The solution is to carry out accelerated climate ageing in the laboratory. Hence, one will obtain results within a much shorter time frame than a natural outdoor climate ageing. In addition, in the laboratory one may in principle control all the chosen climate exposure factors, which of course is not possible in a natural outdoor environment, i.e. we do not control the (natural) weather. Nevertheless, it should be noted that climate exposure in the laboratory does not cover all exposures and their interactions which take place in a natural outdoor climate ageing with real weather conditions. Therefore, care has to be taken when performing accelerated climate ageing in the laboratory, both with respect to the actual test

procedures and the interpretation of the results. Concerning photodegradation of polymers it is referred to more general literature by Kumar et al. [2009], Pospíšil et al. [2006], Rånby and Rabek [1975] and Rabek [1995, 1996]. Furthermore, an extensive survey report on accelerated laboratory test procedures has recently been carried out by Daniotti and Cecconi [2010].



Figure 1. Buildings are subjected exposed to large and changing climate strains throughout their lifetime. Photos: Samfoto (left) and Scanpix (right) [Lisø and Kvande 2007].

3 SOLAR RADIATION

Solar radiation, one of the main climate exposure factors, at the earth's surface is roughly located between 290 nm and 3000 nm (0.29 μm and 3.0 μm, respectively). The ultraviolet (UV) radiation has wavelengths below 380 nm, the visible (VIS) light lies between 380 nm and 780 nm and the near infrared (NIR) radiation ranges between 780 nm and 3000 nm. Almost half of the solar energy is located in the NIR region. The UV radiation is further divided into the three subregions UVA (320-380 nm), UVB (280-320 nm) and UVC (100-280 nm), where the actual wavelength borders may have small variations in the literature. Above 3000 nm, and not part of the direct solar radiation, lies the thermal radiation called infrared (IR) radiation, which all materials radiate above 0 K (peak at around 10 μm at room temperature).

Building materials, and then especially organic materials, may deteriorate as the chemical bonds are being broken by the more high-energy parts of the solar spectrum, i.e. UV radiation and short wave visible light. The photodamage in materials ranges from discolouration to loss of mechanical integrity. Solar degradation of organic materials may include chemical, physical or biological reactions resulting in bond scission of organic materials with subsequent chemical transformations. These processes may involve molecular branching and crosslinking, fragmentations of molecular main chain leading to changes in molecular weight, alterations due to splitting off low molecular weight species, unsaturated carbon double bonds (C=C) and oxygenated groups. The photodegradation mechanism is influenced by thermal degradation, mechanochemical degradation, physical ageing and oxidation processes. If the single photon energy E of the solar radiation given by

$$E = h\nu = hc/\lambda \quad (1)$$

where h denotes the Planck constant ($6.63 \cdot 10^{-34}$ Js), ν the photon frequency, λ the photon wavelength and c the light velocity ($3.00 \cdot 10^{8}$ m/s), is larger than the chemical bond energy of the specific material, then photodegradation processes may start. Further details and various photodegradation reactions are given in work by Tylli et al. [1989], Gerlock et al. [1998], Croll and Skaja [2003], Jelle et al. [2007, 2008] and the comprehensive studies by Rånby and Rabek [1975] and Rabek [1995, 1996]. Note that UV radiation with shorter wavelengths than exist in natural solar radiation at the earth's surface is not to be applied in accelerated climate ageing apparatuses, as the short wave UV radiation may induce degradations and chemical reactions that would never occur in nature.

4 ELEVATED TEMPERATURES

The solar radiation may initiate a photodegradation and the chemical degradation processes which then are started will have exponentially increasing kinetic reaction rates with respect to increasing temperatures (see e.g. Fig.2). A higher ageing temperature is therefore causing a higher reaction rate

for the ageing processes and thus leading to an acceleration of the climate ageing. A high acceleration factor does then imply a shorter test period. However, it is important to not expose test samples towards conditions or strains, in this case temperatures, which may induce reactions which never will take place during natural outdoor climate ageing. For ageing of various polymers accelerated ageing temperatures are therefore often chosen between 60ºC to 70ºC.

5 FREEZING/THAWING CYCLES, WATER AND WIND-DRIVEN RAIN

Repeated freezing and thawing of building materials and components containing water may cause large degradations due to frost weathering and cracking during water to ice volume expansion, both at a macro and micro scale. Especially in climates like e.g. the Nordic climate, which experience extremely many freezing point passes during freezing and thawing, it is of uttermost importance to test the resistance towards these freezing/thawing cycles. Water in its various states, e.g. free water, relative air humidity, water condensation, precipitation and wind-driven rain, will often take part in the degradation of the building materials and components. Both dissolution reactions and dilutions, mechanical degradations and erosion, freezing/thawing cycles, temperature gradients and similar may contribute to this degradation.

6 ACCELERATION FACTOR

As to estimate the required ageing time in the climate ageing apparatus, i.e. relating the accelerated climate ageing to the desired service lifetime of the product, one may calculate acceleration factors. The higher UV intensity (W/m^2) and total energy (kWh/m^2) in the ageing apparatus, the higher acceleration factor for the climate ageing. The UV acceleration factor AF_{uv} may be calculated as directly proportional to the ratio between the total UV energy in the laboratory ageing apparatus Φ_{lab} and the natural outdoor ageing Φ_{nat} for a given time period:

$$AF_{uv} = \Phi_{lab} / \Phi_{nat} \tag{2}$$

The above Eq.2 is is valid as long as one may assume that all the UV radiation contributes to initiate degradation reactions, in addition to an equal spectral distribution for artificial and natural UV radiation, which naturally is never completely fulfilled. The chemical degradation processes increase exponentially with increasing temperature (Arrhenius equation). A temperature acceleration factor AF_{temp} may then be calculated as the ratio between the reaction rate in the laboratory ageing apparatus k_{lab} and the natural outdoor ageing k_{nat}:

$$AF_{temp} = k_{lab} / k_{nat} = \frac{C_{lab} e^{-E_{lab}/(RT_{lab})}}{C_{nat} e^{-E_{nat}/(RT_{nat})}} \approx \frac{e^{-E_{lab}/(RT_{lab})}}{e^{-E_{nat}/(RT_{nat})}} \tag{3}$$

where T_{lab} and T_{nat} denote the temperature in laboratory ageing apparatus and the natural outdoor ageing, respectively. $R = 8.314$ J/(Kmol) is the gas constant. It is here assumed that the pre-exponential factor C is temperature independent which gives $C_{lab} \approx C_{nat}$. Furthermore, it is also assumed that the activiation energy E is temperature independent and set to $E_{lab} = E_{nat} = 70$ kJ/mol, which example value is applied in the graphical plots in Fig.3.

In a simplified model one may assume that the total acceleration factor AF_{tot} equals the product of AF_{uv} and AF_{temp}:

$$AF_{tot} = AF_{uv} \cdot AF_{temp} = \frac{\Phi_{lab}}{\Phi_{nat}} \cdot \frac{e^{-E_{lab}/(RT_{lab})}}{e^{-E_{nat}/(RT_{nat})}} \tag{4}$$

which is visualized in Fig.3 where $AF_{uv} = 2$ is chosen as an example. These calculations are of course a strong simplification. The other climate factors as mentioned above, e.g. water, will influence AF_{tot}. The acceleration factor is strongly dependent upon the chosen reference level, i.e. the natural outdoor ageing comparison exposure level, e.g. T_{nat}. In order to determine the real AF_{tot} one may strictly not base the calculations upon annual or daily values for Φ_{nat} and T_{nat} (k_{nat}), on the contrary rather perform calculations with short time intervals which hence are integrated. It is important to note that a natural

outdoor exposure time period at a high temperature and an equal natural outdoor exposure time period at a low temperature will result in a substantially higher reference temperature than the average temperature due to the exponentially increase in reaction rate with increasing temperature (Eq.3 and Fig.2). Nevertheless, the simplified model may be applied for various mutual comparisons by accelerated climate ageing in the laboratory. Laboratory results should also be compared with outdoor tests in natural climate. Typical calculated values for AF_{tot} are often ranging between 5 to 250.

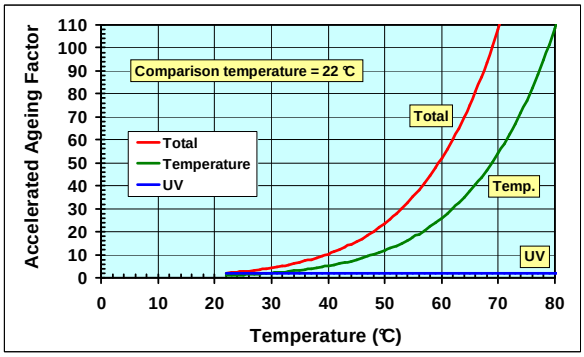

Figure 2. Calculated UV, temperature and total acceleration factor vs. temperature (Eqs.2-4).

7 ACCELERATED CLIMATE AGEING APPARATUSES AND METHODS

Miscellaneous accelerated climate ageing apparatuses, which are subjecting test samples with various climate exposures, are utilized in the laboratory according to different ageing methods and standards. The building products have to withstand these climate exposures in order to endure the naturally occuring climate strains, and thus be able to avoid building damages in prospective applications. Some of these ageing apparatuses and methods will be mentioned within this context to illustrate their possibilities.

Accelerated climate ageing of wooden samples with various surface treatments in a vertical climate simulator according to Nordtest Method NT Build 495 [2000] is shown in Fig.3, including a principial drawing of the apparatus. In this test equipment the samples are subjected in turns to four different climate zones, that is, one UV and IR irradiation zone (black panel temperature of 63ºC), one water spray zone (15 $dm^3/(m^2h)$), one freezing zone (-20ºC) and thawing in one indoor laboratory climate zone. Depending on the choice of type of UV tubes, the UV intensity may be chosen at different levels, e.g. for one specific set of UV tubes the UVA and UVB intensities are averaged to 15 W/m^2 and 1.5 W/m^2, respectively. The exposure time is 1 hour in each climate zone in the above given sequence. For further details it is referred to the test method [NT Build 495, 2000]. Note that this specific vertical climate simulator is a special non-commercial accelerated climate ageing apparatus fulfilling the requirements of a specific ageing method, i.e. NT Build 495 [2000].

Various commercial climate ageing apparatuses are also available, e.g. QUV apparatus (UV tubes) Weathering Tester Horizontal Option with Ponding and Water Spray (The Q-Panel Company, Cleveland, Ohio, USA), Atlas SC600 MHG Solar Simulator (metal halide global lamp) and Atlas Suntest XXL+ (xenon lamp), which may be run according to different test methods and standards. The choice of light source for the accelerated climate ageing tests may be crucial. Various UV tubes with energy peaks shifted towards lower or higher wavelengths in the UV region may be purchased and applied. Metal halide (MH) lamps simulate the solar spectrum at the earth's surface, with the global version (MHG) closest to the solar spectrum. Xenon lamps are reckoned as the lamps able to closest simulate the solar radiation at the earth's surface. For example, if a photovoltaic solar cell is subjected to accelerated climate ageing with simultanously measurements of the solar cell characteristics (e.g. open circuit potential, short circuit current, maximum output power, fill factor and efficiency), xenon or metal halide global lamps have to be used, i.e. UV tubes can not be applied in

such a case. For some applications special filters are employed, e.g. in order to simulate solar radiation through window glass panes.

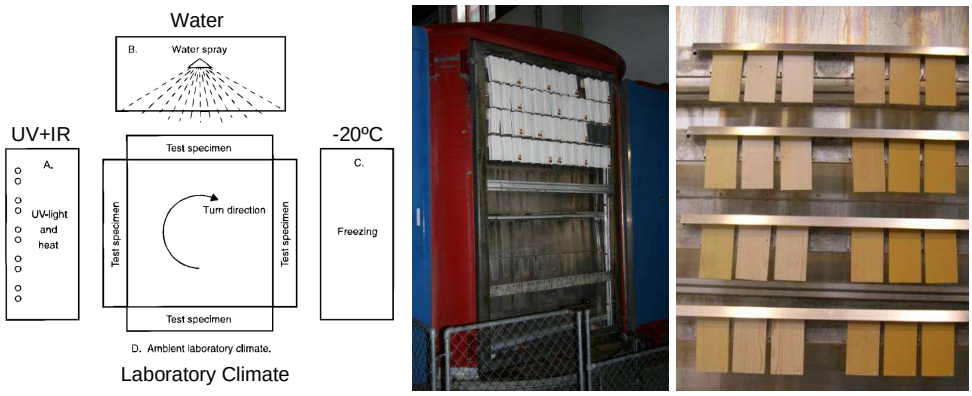

Figure 3. Accelerated climate ageing of wooden samples with various surface treatments in a vertical climate simulator according to Nordtest Method NT Build 495 [2000] with a principial drawing of the apparatus to the left.

Several weathering or accelerated climate ageing methods and standards exist, e.g. ASTM G23-81 [1981], ASTM G24-87 [1987], ASTM G26-84 [1984], ASTM G53-84 [1984], EN 927-3 [2000], EN 927-6 [2006], EN 1296 [2001], EN 1297 [2004], EN ISO 4628-1 [2003], EN ISO 4892-1 [2000], EN ISO 4892-2 [2006], EN ISO 4892-3 [2006], EOTA [2004], NT Poly 161 [1993], NT Build 216 [1982], NT Build 228 [1992], NT Build 229 [1989] and NT Build 495 [2000]. Due to space limitations most of the above referred standards and methods are not repeated in the reference list.

8 EVALUATION BEFORE, DURING AND AFTER ACCELERATED CLIMATE AGEING

Selected properties of the building materials and components should be tested and evaluated before, during and after completed accelerated climate ageing. Specific requirements are chosen for these properties in order to avoid building damages. Examples of various properties to be evaluated may be visual evaluation, colour measurements, various mechanical tests (e.g. tensile strength, shear strength, elongation, resistance towards impact), adhesive strength, water tightness, water vapour permeability, flexibility at low temperature and material characterization by FTIR analysis. The development of a given property with time may be difficult or impossible to predict in advance. Both large and small changes in properties may occur in the start, during and at the end of the ageing time, and the development may follow different courses and curve shapes, e.g. both linear and exponential. That is, if a property is measured only before and after ageing, valuable information about the ageing resistance might be lost. For example, if the measurements after ageing, corresponding to e.g. 10 years of natural outdoor ageing, demonstrate that the material or component has failed, one does not know if the product failed after only 2 years or if it in fact showed almost no degradation up to 9 years, whereas thereafter it failed rapidly. Depending on the required service life, it may also be of great interest to know how well above a given failure level a property is able to be throughout the desired lifetime. Hence, it is concluded that in addition to measurements before and after ageing, it may also be beneficial to perform different tests during the accelerated climate ageing.

9 FTIR ANALYSIS

Material characterization by Fourier transform infrared (FTIR) analysis before, during and after an accelerated climate ageing may give information about both the extent of the ageing and which degradation mechanisms are taking place. This information may then be utilized to prevent building damages. In Fig.4 the FTIR analysis reveals that an oxidation of polypropylene occurs during an accelerated climate ageing with UV exposure at 50ºC in QUV apparatus, where the absorbance peak

around 1732 cm^{-1} is attributed to carbonyl (C=O) stretching, see further details by Jelle and Nilsen [2011]. In addition, quantitative results from a FTIR analysis may be correlated to other tests performed during an accelerated ageing experiment, e.g. tensile strength measurements. Thus, FTIR analysis may represent a powerful and insightful evaluation tool during accelerated climate ageing.

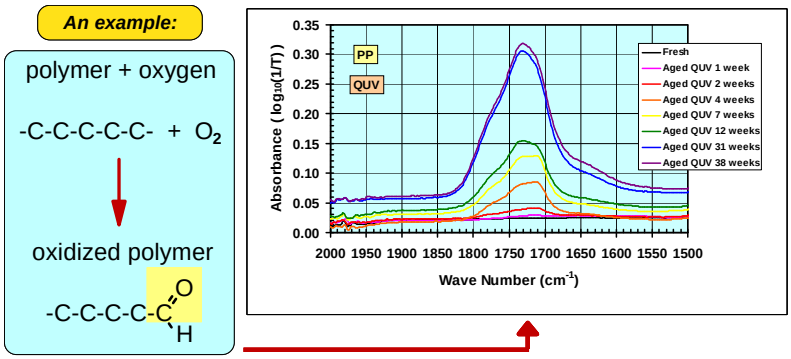

Figure 4. Accelerated climate ageing of polypropylene and corresponding FTIR analysis, also depicting the oxidation of the polymer.

10 ACCELERATED CLIMATE AGEING OF NEW MATERIALS AND SOLUTIONS

As new materials and solutions, some of them applying nanotechnology, are being developed, there arises a need to carry out extensive testing of their ability to withstand long-term climate exposure with satisfactory durability of several crucial properties. Conducting accelerated climate ageing studies will be of vital importance for materials science and engineering advances during development, characterization and testing of these new materials and solutions. These advances will not represent a real progress in materials science unless a satisfactory performance with respect to climate ageing durability has been demonstrated. An example of such new materials and solutions is building integrated photovoltaics (BIPV), where the developed solar cell materials and systems may beneficially be implemented into a building's exterior climate screen envelope. A BIPV system then also has to fulfil the requirements of a building envelope versus the different climate exposure factors, e.g. rain, air and wind tightness and various building physical aspects like heat and moisture transport. Various properties of the solar cell materials and systems have to be tested before, during and after the accelerated climate ageing, e.g. solar cell open circuit potential, short circuit current, maximum output power, fill factor (FF), efficiency, different mechanical properties and any chemical changes. The development of the new high performance thermal insulation materials and solutions represent another group of building products which need to be tested with respect to climate ageing and different building physical properties (e.g. moisture transport and the risk of condensation) during their service life. The low thermal conductivity is a key property for these materials. The high performance thermal insulation materials and solutions include vacuum insulation panels (VIP), gas-filled panels (GFP), aerogels, phase change materials (PCM), vacuum insulation materials (VIM), gas insulation materials (GIM), nano insulation materials (NIM) and dynamic insulation materials (DIM) [Baetens et al. 2010a, Jelle et al. 2010]. Smart windows, e.g. electrochromic windows, represent yet another new building product which need to withstand the various climate strains. Electrochromic windows allow a dynamic control of daylight and solar energy in buildings, where commercial products are available [Baetens et al. 2010b]. Important properties to be evaluated before, during and after accelerated climate ageing are visible solar transmittance modulation, solar transmittance modulation, solar reflectance modulation, colouration efficiency, cycling lifetime, switching time and memory effect among others.

11 CONCLUSIONS

The main climate exposures and the reproduction and application of these in the laboratory have been studied. Hence, crucial properties of building materials, components and structures and their durability towards climate strains may be investigated within a relatively short time period compared to natural outdoor ageing. Examples of various climate ageing laboratory apparatuses, ageing methods and building product properties to be tested before, during and after ageing are given. A calculation method for estimating acceleration factors is demonstrated and discussed. An extension is drawn towards the need for testing of new materials and solutions. It is concluded that accelerated climate ageing should be carried out in order to avoid building damages, either at a material, component or structural level. Accelerated climate ageing will pay off with respect to time, costs and reputation, ensuring that advances within materials science and engineering satisfy the durability requirements.

ACKNOWLEDGMENTS

This work has been supported by the Research Council of Norway, AF Gruppen, Glava, Hunton Fiber as, Icopal, Isola, Jackon, maxit, Moelven ByggModul, Rambøll, Skanska, Statsbygg and Takprodusentenes forskningsgruppe through the SINTEF and NTNU research project "*Robust Envelope Construction Details for Buildings of the 21st Century*" (ROBUST).

REFERENCES

Baetens, R., Jelle, B.P., Thue, J.V., Tenpierik, M.J., Grynning, S., Uvsløkk, S. & Gustavsen, A., 2010(a), *Energy and Buildings*, **42**, 147-172.

Baetens, R., Jelle, B.P. & Gustavsen, A., 2010(b), *Solar Energy Materials & Solar Cells*, **94**, 87-105.

Croll, S.G. & Skaja, A.D., 2003, *Journal of Coatings Technology*, **75**, 85-94.

Daniotti, B. & Cecconi, F.R., 2010, 'Accelerated laboratory test procedures and correlation between laboratory tests and service life data', CIB W080: Test methods for service life prediction, CIB Publication 331.

EOTA Technical Report, 2004, 'Exposure procedure for artificial weathering', TR 010, Edition May 2004.

Gerlock, J.L., Smith, C.A., Cooper, V.A., Dusbiber, T.G. & Weber, W.H., 1998, *Polymer Degradation and Stability*, **62**, 225-234.

Granqvist, C.G., 2005, *Journal of the European Ceramic Society*, **25**, 2907-2912.

Jelle, B.P., Gustavsen, A., Nilsen, T.-N. & Jacobsen, T., 2007, *Solar Energy Materials & Solar Cells*, **91**, 342-354.

Jelle, B.P., Rüther, P., Hovde, P.J. & Nilsen, T.-N., 2008, 'Attenuated total reflectance (ATR) Fourier transform infrared (FTIR) radiation investigations of natural and accelerated climate aged wood substrates', *Proc. of the 11th International Conference on Durability of Building Materials and Components*, Volume 2, pp. 665-672, Istanbul, Turkey, 11-14 May, 2008, Cenkler Matbaacilik Tic. Ltd. Şti., Istanbul.

Jelle, B.P., Gustavsen, A. & Baetens, R., 2010, *Journal of Building Physics*, **34**, 99-123.

Jelle, B.P. & Nilsen, T.-N., 2011, *Construction and Building Materials*, **25**, 2122-2132.

Kumar, A.P., Depan, D., Tomer, N.S. & Singh, R.P., 2009, *Progress in Polymer Science*, **34**, 479-515.

Lampert, C.M., 2004, *Materials Today*, pp. 28-35, March 2004.

Lisø, K.R. & Kvande, T., 2007, 'Klimatilpasning av bygninger' (Climate adaption of buildings) (in Norwegian), SINTEF Byggforsk.

Nordtest Method NT Build 495, 2000, 'Building materials and components in the vertical position: Exposure to accelerated climatic strains'.

Pospíšil, J., Pilař, J., Billingham, N.C., Marek, A., Horák, Z. & Nešpůrek, S., 2006, *Polymer Degradation and Stability*, **91**, 417-422.

Rabek, J.F., 1995, 'Polymer photodegradation. Mechanisms and experimental methods', Chapman & Hall.

Rabek, J.F., 1996, 'Photodegradation of polymers. Physical characteristics and applications', Springer-Verlag.

Rånby, B. & Rabek, J.F., 1975, 'Photodegradation, photo-oxidation and photostabilization of polymers. Principles and applications', John Wiley & Sons.

Tylli, H., Olkkonen, C. & Forsskåhl, I., 1989, *Journal of Photochemistry and Photobiology, A: Chemistry*, **49**, 397-408.

XII DBMC
International Conference on Durability of Building Materials and Components
PORTO - PORTUGAL, April 12th-15th, 2011

The Experimental Evaluation of Parameters Contributing to the Durability of Coating Materials for Colouring and Protecting External Plastered Surfaces

Paolo Gasparoli [1]
Chiara Livraghi [2]
Matteo Scaltritti [3]

ABSTRACT

Building components and products durability is a high topical issue for the evaluation of built systems efficiency. It's also relevant about the theme of durability certification and constructions insurability. From the market comes the need to promptly determinate the performances of new products, often innovative, which are not testable through observations on site in real-time.

The paper reports a performances evaluation test of outdoor coating materials based on accelerated aging processes on natural and artificial samples.

The test, 3 years long, was directed to the evaluation of durability of 7 different systems, polymer-based, normally found on the market, applied on expressly prepared supports.

Physical durability tests, after different intervals of time, consisted in water absorption, steam permeability, adhesion, colorimetric values tests and surfaces observation at macro and micro scale of the products.

Experiment evaluated not only the tested systems behavior but also some critical aspects of the artificial ageing processes in weather chamber, mainly due to excessive severity of the cycles.

Natural ageing outdoors has produced good results showing general good performances of the tested systems.

KEYWORDS

Durability, Varnishes, Artificial ageing, Outdoor coating materials.

[1] Politecnico di Milano, Dept. BEST, paolo@gasparoli.it
[2] Politecnico di Milano, Dept. BEST, chiara.livraghi@polimi.it
[3] Politecnico di Milano, Dept. BEST, matteo.scaltritti@polimi.it

1 INTRODUCTION

The longevity of components and products for the construction industry is a highly topical issue for the role it plays in the overall assessment of the reliability of systems built in relation to the theme of insurability of the works, and then increasingly in the interests of producers and users.
Durability of a product in construction means the ability to maintain the levels of performance and functional requirements over time (i.e. those planned) under the impact of foreseeable actions [1].

The evaluation of the behaviour of materials based on time has become an established and shared tradition just like the measurement or observation tools and methods. However, it still needs to be appropriately adjusted to the unique characteristics of each product and their use in specific environmental conditions.

In a market with constant product development, the assessments of durability provide reliable results only when performed over long periods of time and when based on statistically significant samples. Thus, the need to respond to the question of performance assessments in a decidedly more content remains strictly because of rapidly changing technology industry. From the market comes the need to promptly determine the behaviour of new products to commercialize. Based on their innovative nature, it is not possible to observe their functional behaviour in real-time.
For this reason, methods have been introduced to evaluate the performance of products over time. These methods are based on accelerated aging processes in natural or artificial environment. The tested samples are adequately prepared in order to simulate the main critical conditions due to exposure or use.

2 THE EXPERIMENT

The surface protection systems for surfaces plastered on buildings are generally made of polymer-based paints and varnishes (p.v.). It is well known that the aging and subsequent degradation of these systems are caused by water permeability, defects in adhesion and embrittlement of the polymer film upon exposure to UV.

To evaluate the durability of the p.v. it is possible to use outdoor exposure methods with accelerated natural aging and testing with accelerated aging in a weather chamber.
The experiment presented here was carried out in the experimental laboratory in the BEST [2] department of the Politecnico of Milan. Both of the abovementioned methods were activated also to verify if there is a significant possibility of comparison.

The experiment involved the evaluation of the durability of seven different systems normally found on the market[3]:
- System 01A - ACRYLIC PAINT
- System 02A - ACRYLIC QUARTZ PAINT
- System 01B – SILOXANE PAINT
- System 02B - SILOXANE PAINT
- System 02C – ELASTOMETRIC SYSTEM
- System 02D – HYDROPAINT
- System 02E – PLASTER FINISH[4]

2.1 Exposure to accelerated natural aging conditions

The experimental evaluations, the parameters of exposure of the samples to the outdoors that maximize the action of the weather agents using the most critical conditions in terms of where, how and when they are exposed were identified. The criteria defined by UNI 2810[5] provide that at our

latitude, the samples should be placed on a stand with an inclination of 45° from horizontal plane and are oriented towards the south. These criteria increased the degradation rate of material by 4-6 times in the experimental tests. In fact, this method maximizes solar radiation, which is the main case of degradation of products with polymer-based coatings, just like those covered by this experiment. Furthermore, it is clear that the climatic and weather conditions of the exposure period directly influence the ageing results, and that is why an exposure period of at least 3 years is considered sufficient. The rate of air pollution in the area where the exposure takes place and local conditions are other parameters that significantly affect the exposure effects.

7 systems were tested and for each of these systems 2 samples were produced. The samples were made up of brick tables (100 x 25 x 6 cm) that were plastered on one of the two main facades and on the two long sides. This allowed to also evaluate the behaviour of the product at the corners. This is especially critical because of the reduced thickness of the protective film that is inevitably linked to the application technique.

The samples were exposed to the outside, on a galvanized steel support specifically designed and protected above by a steel flashing to prevent water seepage from the upper edge.
The exposure was based on normal parameters and started from the summer solstice of 2006 on the flat cover of a building of the Politecnico of Milan (Fig. 1). From an exposure and concentration of polluting agents point of view, this is a particularly stressed area. The evaluation of the performance behaviour of the samples was carried out through direct observations to consider the changes in surface characteristics and possible colour change of systems with colorimetric measurements.
In regards to the evaluation of surface characteristics, visual observations were made with optical instruments at different zoom factors.



Figure 1. The exposure of the samples on the flat cover of a building of the Politecnico of Milan.

The samples were then photographed with a macro lens at a close range, with a magnification factor of approximately 2:1 and with detailed photos with the help of an optical digital microscope (Fig. 2), able to record images with magnification factors of 50 x, 100 x and 200 x. The use of this sophisticated instrument allowed us to observe and document the evolution of the morphological characteristics of the surface of the samples.

The variations in the chromatic characteristics were registered with the use of a reflectance colorimeter[6]. To make the measurements taken with this instrument as reliable as possible. 20 measurements were taken for each sample, within a defined area of 25 $cm^{2,}$ to avoid the risk non-significant local conditions for the whole sample.

The observations were performed on samples each year for 4 consecutive years and with intermediate readings (every six months) during the first and second year to evaluate the most significant variations that could be verified during the most critical period corresponding to the break-in period.



Figure 2. Observation by the optical digital microscope.

2.2 Outdoor exposure: results of the experiment

Following the colorimetric measurements, it was possible to observe how all the products had responded well to the aging process. In fact, all of them had undergone a normal surface greying process and yellowing of the colour trend caused by the exposure to UV rays that at the storage of atmospheric particles accumulated over time. These results, which were predicted because of the environmental characteristics of the exposure area, can be traced back to physiological degradation products.

Compared to the average behaviour, only one product (02D) showed to be more stable while, for some other products after the initial overall chromatic variation, the colour tended to be closer to the original. Thus, we can hypothesize that there is a kind of physiological colour change in the first phase of product life during the first year. In some cases this tends to stabilize at lower lees than those registered at the first threshold measurement. In this regard, an important variable with respect to the results of the observations is that of the effect of weather and rain in particular. In fact, if the observations and the colorimetric measurements are carried out after a rainfall, it is possible that this is removed due to the washing effect. On the contrary, if the observations are carried out after a long dry spell, the accumulation of dirt on the sample surface could be greater.

The chromatic variations of the surface, especially regarding the greying phenomenon, are reflected in the observation of microscopic samples. In fact, the gradual deposit of atmospheric particles and the consequent appearance of dark spots are visible with high magnification factors (superior to 50x). These phenomenon, which are almost invisible to the naked eye, contribute to the overall darkening of the surface. The use of the microscope allows us to fully appreciate the phenomena that contribute to the greying of the surface. In some cases, it has been seen that localized spots tend to form in areas where dirt particles accumulate on a small scale. In other cases, brown spots interpreted as oxidation of iron particles probably deposited from atmospheric dust have been observed.
The use of the microscope also allowed for very efficient observations on the surface morphology of the tested products. Some of these products (01A, 01B, 02A and 02B) showed a change in the surface at the microscopic level. This change was caused by the large number of micro-cracks and varying pore sizes (Fig. 3).

A micro erosion phenomenon of the product's binder component highlighted the aggregated granules of the product. This micro degradation was very clear and in particular on sample 02E, which was already characterized by a particularly pronounced physiological graining. The sequence of observations allowed to evaluate the progressive dynamics of this phenomenon that led to put more light on the granular structure of the aggregate. If the surface covered with the binder component of the product was uniformly covered at the beginning of the observation, after 3 years of exposure the angular grains of the aggregate were apparent.

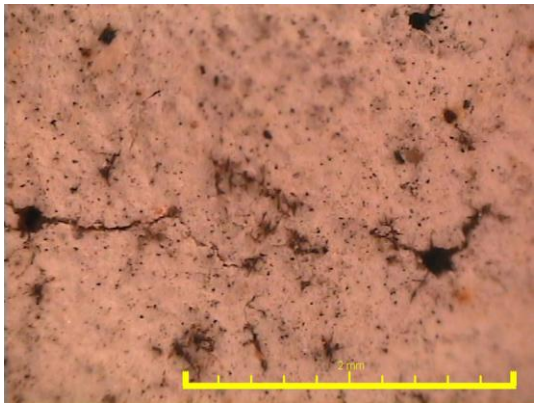

Figure 3. The surface morphology observed by the microscope (200x) after 2 years.

It is believed that these surface decay phenomena may only impair the functionality of the tested system only after very prolonged exposure.

2.3 Exposure in accelerated aging conditions in a weather chamber

In parallel, other samples of the same products were subjected to a process of accelerated aging in a weather chamber [7].

The samples destined for the weather chamber were made up of small tiles (40 X 25 X 3 cm). Only the tops of these tiles were covered with plaster and they were suitably protected on the backside with a siloxane water repellent product and sealed on the edges with the application of a epoxy resin based coating.

The correct preparation of samples is critical for the success of the experiment. In fact, treatment in a weather chamber could subject the samples to very harsh stress and thus making it crucial to protect all of the weak points that could distort the result. In fact, if the samples were not well sealed on the back and on the sides, infiltration may occur between the layers constituting the substrate. This infiltration would cause obvious consequences.

As is known, the weather chamber is an apparatus capable of simulating the main agents of weather and climate such as rain, solar radiation, frost, dry and humid climate and cold and hot climate:

- The relative temperature and humidity of the air inside the climatic chamber can be respectively regulated between -40 and +180 °C and between 10% and 98% RH;
- The facility that simulates the rain has four full-cone spray tips that are radially oriented at 90° intervals and with a spray angle of 120° able to create a round cover jet and with uniform distribution.

Based on previous experience, the equipment was programmed with the following sequence of agents, duration of action and number of cycles:

- precipitation stage: duration of 60 minutes, the test samples are uniformly hit by a water jet with a temperature of 20°C. The air within the compartment is constantly kept at a temperature of 20°C and a relative humidity equal to 95%.
- 30 minutes to pass from 20 °C to -16 °C
- frost phase: duration of 60 minutes, the wet samples and the air of the compartment are kept at 16°C for the whole duration of this phase.
- hot and humid climate phase: duration of 60 minutes, the air within the compartment is kept at a constant temperature of 55°C and 95% of relative humidity. This phase is preceded by a

transitional period lasting 80 minutes required to adjust the temperature from -20 °C of the earlier stage to 55 °C of this phase.

- Hot dry climate phase: duration of 80 minutes, the air of the compartment is at a temperature of 30°C and at a relative humidity equal to 35%.

During the exposure to ageing, the operation data of the equipment was measured according to defined methods and time intervals in order to monitor the proper performance of the test procedure. The use of the weather chamber to accelerate the ageing processes of the test pieces has the advantage of significantly reducing the experiment times but results in some very critical issues. The first thing to consider is the difficulty in compare the relationship between the natural aging, in normal operating conditions and the accelerated ageing in the weather chamber; secondly, as already mentioned, the sharp acceleration of the processes of atmospheric agents submit the samples to stresses that may be too stressful. Test criteria that are truly effective in relation to the nature and size of the weather chamber and that enable an effective assessment of the durability of products and systems still have to be developed.

In the case presented here, the test samples were forced into a horizontal position in the weather chamber. The result of the thermal cycles led to the stagnation of a film of water on the surface that plays an important mechanical action on the tested product. Additionally, this position is insignificant compared to the most common operating conditions for these systems that are used to protect vertical wall surfaces.

The fact that a protective product requires application to a support during testing is also worth consideration. During the test phase, this support is also stressed by the weather conditions and this has a more or less significant impact on the overall performance of the system (product + support). Surely, the more efficient the protective action of the tested product, the more contained the phenomenon, but the complexity of the data related to the characteristics of the support inevitably introduce variables that must be taken into account.. Therefore, in this sense, the support should be simplified (characteristics, functional layering) with the aim of limiting the possible disturbance factors on the test results.

Before introducing the samples in the weather chamber, characterization tests of physical performance were carried out on the comparison samples (T_0). These tests were designed to assess the degree of vapour and liquid water absorption and the ability to adhere to the support. As for permeability of liquid water, it is carried out by measuring the degree of capillary absorption of the protective systems in question.

The tests were carried out on cylindrical test pieces (Ø 50 mm) obtained by coring. These were protected on the lateral edges with an epoxy resin based varnishing product; the upper surface of the core is immersed in water and subsequently the test pieces are weighted with a digital scale every 10 minutes, 20 minutes, 1 hour, 2 hours, 3 hours, 4 hours and 24 hours. The obtained data is processed and systematized in appropriate tables containing the partial Δt values calculated for the samples of each test piece (Fig. 4).



Figure 4. The cylindrical test pieces immersed in water for permeability of liquid water test.

Subsequently, the amount of water absorbed (Kg) in one square meter of surface (W) and the coefficient of liquid water permeability, in kilograms per square meter and on the square root of the hour (w) were calculated. Both of these were calculated after a period of 6 and 24 hours[8].

The assessment of behaviour in terms of permeability to water vapour[9] was carried out on three test pieces with a diameter of 100 mm obtained with the use of coring. The test was carried out by applying the disk test piece obtained by coring, like a cap, to an special capsule containing a volatile liquid (Fig. 5). The capsule was then weighed at predetermined time intervals. The weight change is indicative of the amount of vapour that goes through the test piece[10].



Figure 4. A capsule for the test of permeability to water vapour.

The adhesion test is carried out by applying an axial traction to a plaque affixed to the sample surface. Its aim is to calculate the tensile strength value (adhesion to the support) and the break point of the tested system.

Based on legislation, three test areas with a diameter of 50 mm were delimited through milling. These three areas were delimited for each product and round metal plates were applied with the use of an epoxy for testing. We were able to record the tension value measured at the time of the break and the point in the test when rupture happened.

In the majority of the test pieces, the fracture of the test piece happened within the occurred within the mortar plaster of the support state. Even though this does not provide a tensile strength value indicative of the adhesion of the product to the support, this shows that the latter exceeds the tensile strength of the mortar. The tests described above were repeated on test pieces after exposure in the weather chamber.

3 CONCLUSIONS

In conclusion, it may be noted that the tests conducted on samples that naturally aged outdoors have provided intriguing indications on the ageing mechanisms. Over all, these mechanisms showed superior performance of the tested systems in terms of durability. On the contrary, the process of artificial ageing in the weather chamber demonstrated several critical points due primarily to the severity of the cycles. In this case, it was impossible to determine the correlations between the accelerated natural ageing and artificial ageing in the weather chamber.

Furthermore, from the findings of this and other trials it does not seem possible to define standardized ageing cycles in the weather chamber. In fact, we believe that the specifications of these cycles must be evaluated each time (probably with a distinctive pre-experimental phase) and calculated based on the risk factors of each system or, at least, risk factors that are specific to uniform system categories.

---

[1] Regulation UNI 11156-1:2006 Evaluation of the longevity of construction components. Part 1: Terminology and definition of evaluation parameters

[2] Building Environment Science and Technology (B.E.S.T.)

[3] All by applicator technicians of the manufacturer with a plain white colour in order to replicate the actual conditions of use on construction sites as closely as possible. The supports were carried out by technicians commissioned by the BEST and under the supervision of the researchers in order to have a uniform support for all systems using widely available commercial products and applied in accordance with normal construction practices.

[4] System 01A - ACRYLIC PAINT: 1 layer of cement mortar component, fibreglass mesh, 1 coat of acrylic primer diluted in water, 1 layer of acrylic CONTINUOUS APPLICATION PLASTIC COATING, 2 coats of acrylic resin, quartz flour and pigmented based paint. System 01B - SILOXANE PAINT: 2 layers of mono-component cement mortar, 1 coat of siloxane primer diluted in water, 1 layer of siloxane CONTINUOUS APPLICATION PLASTIC COATING. System 02A – ACRYLIC QUARTZ PAINT: 1 coat of Pigmented solvent-based fixative, 1 coat of an acrylic base coat, 2 coats of acrylic resin, quartz flour and pigmented based paint. System 02B - SILOXANE PAINT: 1 coat of Impregnating siloxane-acrylic binder based primer, 1 coat of siloxane-acrylic binder and quartz flour based fixative base, 2 coats of mineral, organic and aggregate mixed matrix acrylic and siloxane based paint. System 02C - ELASTOMETRIC SYSTEM: 1 coat of Pigmented solvent-based fixative, 2 coats of acrylic resin, quartz flour and pigmented based paint. System 02D – Hydro-pliolite based mural hydropaint: 1 base coat of product diluted with 10% water, 1 top coat of white coloured product diluted with 10% water. System 02E – PLASTER FINISH: 1 coat of xiloxane-acrylic binder based Impregnating primer, 1 coat of siloxane-acrylic binder and quartz flours based primer.
2 layers of acrylic-siloxane resin, balance grained quartz flour and special lamellar filler based top coat.

[5] Regulation UNI EN ISO 2810:2005 Paints and varnishes. Natural aging of coatings. Exposure and evaluation.

[6] CR200 Minolta Colourimeter, able to detect and store three pieces of information: the L component, luminosity or light components, the "a" value that varies from green to red and the "b" value that varies from blue to yellow. In terms of the application field, the formulas and the CIELAB colour difference, reference was made to regulation UNI 8941-3:1987 "Coloured surfaces – Colourimetry, Calculation of colour difference".

[7] For the record, an Angelantoni Industrie CH 1200 model weather chamber was used at the Experimental Technical Laboratory at SUPSI (University of Applied Sciences and Arts of Southern Switzerland) in Lugano

[8] Classification of the degree of liquid water transmission kg/($m^2 \cdot \sqrt{h}$): I [high] if > 0.5; II [medium] from 0.1 to 0.5, III [low] if< 0.1 Refer to UNI EN 1062-3:2001 Paints and varnishes – Varnishing products and systems for external brick and concrete works - Determination and classification of the degree of transmission of liquid water (permeability)

[9] According to UNI EN ISO 7783-1:2001

[10] Classification of the degree of water vapour transmission according to EN 1062-1 g/($m^2 \cdot d$): I [high] if> 150, II [medium] from 15 to 150, III [low] if< 15

XII DBMC
International Conference on Durability of Building Materials and Components
PORTO - PORTUGAL, April 12th-15th, 2011

New Insights into the NT Build 492 Rapid Chloride Migration Test

P. Spiesz [1,*]
M. M. Ballari [2]
H. J. H. Brouwers [3]

ABSTRACT

In this study a new theoretical model is developed for the popular Rapid Chloride Migration test (NT Build 492). This model can in a proper way predict the transport of chlorides due to application of the electrical field.
In order to improve the traditional chloride transport model, the non-linear binding of chlorides and non-equilibrium between free- and bound- chlorides are introduced. The new system of equations is solved numerically and applied to experimental data obtained elsewhere. From these simulations several parameters are obtained, namely: the effective chloride diffusion coefficient, the non-linear binding constants and the chloride mass transfer coefficient. This opens the new possibility of obtaining the effective chloride diffusion coefficient (usually derived from long-term, laborious techniques) from the short-term migration tests. The obtained binding constants are in line with experimental data found in literature. The chloride mass transfer coefficient shows a tendency to decrease in time during the application of electrical field, which can give evidence of changes in the microstructure and/or in the pore solution of concrete.

KEYWORDS

Concrete; Chloride; Diffusion; Accelerated test.

* Corresponding author
1 Department of Architecture Building and Planning, Eindhoven University of Technology, The Netherlands, p.spiesz@tue.nl
2 Department of Architecture, Building and Planning, Eindhoven University of Technology, The Netherlands, j.brouwers@tue.nl
3 Department of Architecture, Building and Planning, Eindhoven University of Technology, The Netherlands, m.ballari@tue.nl

1. INTRODUCTION

Deterioration of concrete elements and structures being in contact with chloride-bearing solutions (e.g. seawater or de-icing salts) in majority of cases is caused by the chloride-initiated corrosion of steel rebars reinforcing concrete. The rebars are passivated as long as the chloride concentration at their level does not reach the critical threshold value. Once the critical concentration of chloride ions is reached, the corrosion process is triggered and leads in time to the deterioration of concrete. The cover layer (the bulk of concrete between its surface and the reinforcing steel) is the barrier against the chloride source. Nevertheless, in concrete, being a porous material, the transport of chlorides takes place due to capillary suction and diffusion processes. Thus, the critical chloride concentration at the level of steel reinforcement will be reached, and this is only a matter of time. However, this time, being related to the service lifetime of concrete, is dependent on the quality (rate of chloride diffusion) and quantity (distance that chlorides have to penetrate) of concrete. Hence, the chloride ingress speed (usually expressed as the chloride diffusion coefficient in concrete) and the thickness of the cover layer of concrete are usually employed in service life design models of concrete structures. In order to determine the diffusion coefficient, a number of laboratory measurement techniques have been developed over years, among which the NT Build 492 - Rapid Chloride Migration test (also termed as the CTH or RMT test) is nowadays becoming more and more popular. The importance of this technique increased when its output value was included in the European DuraCrete Project for the service life design of concrete. Although the test is commonly accepted and performed, this paper addresses some issues to its theoretical model. In this model, the binding of chlorides by cement hydrates is assumed to be linear and in instantaneous equilibrium, however, it is known that the binding is non-linear and certain duration of the exposure to free- chlorides is necessary in order to reach the equilibrium. Hence, it is demonstrated that the currently adopted chloride transport model is oversimplified, which explains the origin of big differences between the theoretical and measured chloride concentration profiles in concrete after application of the electrical field. This difference shows that the output value of the migration test is incorrect, thus should not be used in service life models.

As presented in this paper, the transport model for the chloride migration in concrete is modified by including the non-linear chloride binding isotherm and non-equilibrium conditions between free- and bound- chlorides. As the result of implementation of this new theoretical model, the chloride concentration profiles in concrete can be predicted in a good way. From application of the model to the experimental data, several parameters can be obtained (e.g. effective diffusion coefficient of chlorides, binding parameters).

2. RAPID CHLORIDE MIGRATION TEST (NT BUILD 492)

The Rapid Chloride Migration (RCM) test developed by Tang [1996], is a non-steady-state test, based on the ionic migration induced by an external electrical voltage applied across a concrete specimen saturated in $Ca(OH)_2$-saturated water solution. Due to the potential difference applied between the electrodes, chloride ions move from the upstream solution, through the concrete specimen, towards the downstream solution, for a certain time. Afterwards, the specimen is split open and sprayed with $AgNO_3$ – a colorimetric indicator for chlorides. Finally, the chloride penetration depth is measured and based on its value the non-steady-state chloride diffusion coefficient (D_{RCM}) is calculated from a model based on the Nernst-Planck equation. This model reads as follows [Tang 1996]:

$$\frac{\partial c}{\partial t} = -\frac{\partial J_0}{\partial x} = \frac{D_0}{1+\frac{\partial c_b}{\partial c}}\left(\frac{\partial^2 c}{\partial x^2} - \frac{zFE}{RT}\frac{\partial c}{\partial x}\right) = D_{RCM}\left(\frac{\partial^2 c}{\partial x^2} - \frac{zFE}{RT}\frac{\partial c}{\partial x}\right) \quad (1)$$

where: c – concentration of chlorides in the pore solution, t – time, J_0 - total flux of chlorides through a unit area of solution, x – distance, D_0 – diffusivity of chlorides in pore solution of concrete, c_b – concentration of chlorides bound in concrete, z – ion valence, F – Faraday constant, E – electrical

field, R – universal gas constant, T – temperature, D_{RCM} – non-steady-state chloride diffusion coefficient.
Eq. (1) is further simplified and solved for D_{RCM} [Tang 1996]:

$$D_{RCM} = \frac{RT}{zFE} \times \frac{x_d - \alpha\sqrt{x_d}}{t_{RCM}} \tag{2}$$

where: x_d – chloride penetration depth indicated by a colorimetric indicator, α – laboratory constant and t_{RCM} – duration of the test.

3. A NEW MODEL OF CHLORIDE TRANSPORT DUE TO MIGRATION IN CONCRETE

3.1 Verification of the Traditional Model

In Fig. 1 the theoretical chloride concentration profile, representing the solution of Eq. (1) is shown. On the other hand, an example of the experimental chloride concentration profile from Stanish [2002] is given in Fig. 2. Similar experimental profiles for chloride migration tests can be also found e.g. in Yuan [2009], Castellote *et al.* [1999] or Gruyaert *et al.* [2009].

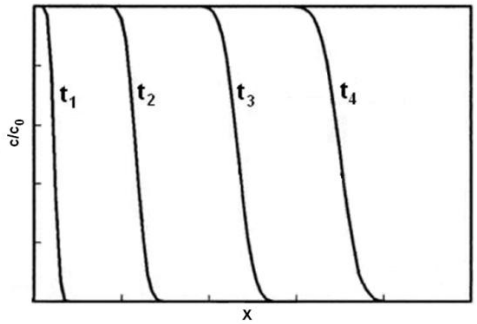

Figure 1. Theoretical chloride concentration profile (Eq. 1) [Tang 1996].

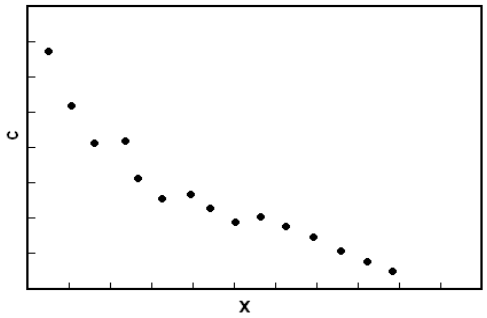

Figure 2. Experimental chloride concentration profile [Stanish 2002].

As can be deduced from Figs. 1 and 2, the chloride transport model, governed by Eq. (1), cannot predict in the proper way the behaviour of chlorides migrating into concrete due to the electrical field. Thus, the value of D_{RCM} calculated from Eq. (2) is incorrect.

3.2 Non-linear Chloride Binding in Non-Equilibrium

It is worth to emphasize that the chloride binding, introduced in the constant term of $\partial c_b / \partial c$ (see Eq. 1), is assumed to be linear ($c_b = \beta \times c$, where β is a constant). Nevertheless, as presented e.g. in Tang [1996] and Zibara [2001], the amount of bound chlorides increases non-linearly with an increase of the free-chlorides amount. The linear chloride binding isotherm does not predict in a proper way the relation between bound and free-chlorides and it can be applicable only within a limited range of free-chlorides concentration [Tang 1996].
Tang [1996] shows experimentally that the chloride binding in concrete obeys the Freundlich isotherm in free-chloride concentrations in the range of 0.01 - 1 [mol/dm^3] and the Langmuir isotherm at low Cl^- concentrations (< 0.05 [mol/dm^3]). The Freundlich isotherm is given as follows:

$$C_b = K_b c^n \tag{3}$$

where: C_b – concentration of bound chlorides, K_b – chloride binding capacity of concrete and n – binding intensity parameter.

The chloride binding data presented in Zibara [2001] shows that even for higher chloride concentration (up to 3 [mol/dm^3]), the Freundlich equation describes the binding correctly. During the RCM test, the concentration of chlorides in the bulk solution yields 2 [mol/dm^3], thus the Freundlich isotherm can adequately represent the chloride binding for this test. Considering the fact that the binding of chloride is non-linear, the assumption of constant $\partial c_b / \partial c$ in Eq. (1) is incorrect, thus the value of D_{RCM} calculated from Eq. (2) should be treated with scepticism.
When chloride ions are transferred from one phase (liquid) to another (solid) across an interface that separates the two, the resistance to mass transfer causes a concentration gradient in each phase. Due to these limitations in the mass transfer, usually a certain time is required in order to achieve the equilibrium between the concentrations in liquid and solid. From literature it is known that the equilibrium for chloride sorption in concrete can be achieved after 7 days [Tang 1996] or 10 - 14 days [Theissing *et al*. 1978] of exposure. For long-term diffusion tests, the assumption of equilibrium is acceptable since the chloride exposure period is sufficiently long. However, the duration of the RCM test usually amounts to 24 hours, and only sometimes varies from 6 hours (for poor quality concrete) up to 4 days (for very good quality concrete). Thus, during the migration process, equilibrium between free- and bound- chlorides cannot be achieved, which implies a necessity of the application of the Cl^- mass transfer rate. The mass transfer rate of chlorides from the pore solution, through the liquid-solid interface and towards the solid, is considered to be induced by a concentration gradient in these phases.

3.3 New Chloride Transport Model for the RCM Test

The main idea of the new model proposed in this paper is based on the introduction of the non-linear chloride binding isotherm and non-equilibrium between free- and bound- chlorides concentrations in the system based on the Nernst-Planck equation. The simplified Nernst-Planck equation is commonly used to describe ionic transport in porous medium due to combined actions of migration and diffusion. However, as presented in Narsilio *et al*. [2007], when a sufficiently large electrical voltage (U) is applied across the concrete specimen, the flux of ions due to electrical migration dominates over the diffusion flux due to concentration gradients. The fact that during the RCM test U = 10 - 60 [V] allows neglecting the flux of chloride ions due to the gradient of concentrations.

The binding of chlorides takes place instantaneously at the surface of the active solid, but there is a resistance to the mass transfer through the liquid-solid interface. This limitation in the mass transfer rate of chlorides is responsible for the non-equilibrium conditions in the system and is governed by the mass transfer coefficient – k. Therefore, r, being the mass transfer rate, reads:

$$r = k\left(c - c_s\right) \tag{4}$$

where: c_s – chloride concentration in liquid at liquid-solid interface.
Calculating c_s from Eq. (3) and inserting into Eq. (4) gives [Brouwers 1999]:

$$r = k\left[c - \left(\frac{C_b}{K_b}\right)^{1/n}\right] \tag{5}$$

When considering the total volume of concrete (solid state and pores completely saturated with liquid), the reaction term in the total chloride mass balance in concrete yields 0, because the rate of the disappearance of chlorides in the liquid phase is equal to the rate of chlorides increment in the solid phase. However, when considering liquid and solid phases separately, there will be non-zero reaction term as shown in Eq. (5). Thus, assuming that the chloride transport due to diffusion is neglected and applying Eq. (5) and the Nernst-Planck equation, the chloride mass balance, for liquid and solid respectively, reads:

$$\varphi\frac{\partial c}{\partial t}+u\frac{\partial c}{\partial x}=-k\left[c-\left(\frac{C_b}{K_b}\right)^{1/n}\right] \tag{6}$$

$$(1-\varphi)\rho_s\frac{\partial C_b}{\partial t}=k\left[c-\left(\frac{C_b}{K_b}\right)^{1/n}\right] \tag{7}$$

where: φ – porosity of concrete, ρ_s – density of the solid state of concrete and u – ionic migration velocity, $u = DzF/RTE$, D – diffusion coefficient.
During the migration of chlorides a penetration front can be localized. The position of the front $\psi(t)$ is governed by the following equation:

$$\psi(t)=\frac{ut}{\varphi} \tag{8}$$

The boundary and initial conditions pertaining to Eqs. (6) and (7) read:

$$\begin{aligned} &c(x=0,t)=c_0\\ &C_b(x=\psi,t)=C_{bi}\end{aligned} \tag{9}$$

where: C_{bi} - the initial bound chloride concentration prior to migration test.
The D_{RCM} coefficient (see Eq. 1) is the apparent diffusion coefficient, because its value is depending on the binding term. As can be seen in Eqs. (6) and (7), the diffusion coefficient D, applied in the new model, is an independent constant, thus its value is related only to the diffusivity of chlorides in free liquid and the pore system in concrete (considering constrictivity and turtuosity). Hence, the D is representing the effective diffusion coefficient in concrete – D_{eff}.

3.4 Numerical Solution of the New Chloride Transport Model

In order to obtain the numerical solution of Eqs. (6) and (7) a forward discretization is performed, and reads as follows:

$$\varphi\frac{c_{(i+1,\,j)}-c_{(i,\,j)}}{\Delta t}+u\frac{c_{(i+1,\,j+1)}-c_{(i+1,\,j)}}{\Delta x}=-k\left[c_{(i+1,\,j)}-\left(\frac{C_{b(i+1,j)}}{K_b}\right)^{1/n}\right] \tag{10}$$

$$(1-\varphi)\rho_s\frac{C_{b(i+1,j)}-C_{b(i,j)}}{\Delta t}=k\left[c_{(i,\,j)}-\left(\frac{C_{b(i,j)}}{K_b}\right)^{1/n}\right] \tag{11}$$

where: Δt – interval of time, i – position in time, i = 1.. $t/\Delta t$, Δx – interval of distance, j – distance in concrete and j = 1.. $L/\Delta x$.
Solving Eqs. (10) and (11) for $c_{(i+1,j+1)}$ and $C_{b(i+1,j)}$ respectively, gives:

$$c_{(i+1,\,j+1)}=c_{(i+1,\,j)}-\frac{\Delta x}{u}\left(\varphi\frac{c_{(i+1,\,j)}-c_{(i,\,j)}}{\Delta t}+k\left(c_{(i+1,\,j)}-\left(\frac{C_{b(i+1,j)}}{K_b}\right)^{1/n}\right)\right) \tag{12}$$

$$C_{b(i+1,j)}=C_{b(i,j)}+\frac{\Delta t}{\rho_s(1-\varphi)}k\left(c_{(i,\,j)}-\left(\frac{C_{b(i,j)}}{K_b}\right)^{1/n}\right) \tag{13}$$

With the initial and boundary conditions:

$$c_{(i,\ j\ =1)} = c_0$$
$$C_{b(i=1,\ j)} = C_{bi} \tag{14}$$

4. APPLICATION OF THE NEW MODEL TO EXPERIMENTAL DATA

A wide database of total chloride concentration profiles obtained for concrete tested using the RCM test is presented in Stanish [2002], therefore it has been used for further investigations presented in this paper. The experimental data of Stanish [2002] is summarized in Table 1. The measured profiles are representing the total chloride concentration in concrete, which can be represented as follows:

$$C_t = \frac{\varphi c + (1-\varphi)\rho_s C_b}{\rho_c} \tag{15}$$

where: C_t – total concentration of chlorides in concrete and ρ_c – total density of concrete.

Table 1. Testing conditions and properties of concrete [Stanish 2002].

Concrete	OPC 0.35	c_0	70.9 [g/dm^3]	w/c	0.35
t_{RCM}	6, 9 and 18 [h]	T	296.5 [K]	cement	418 [kg/m^3]
ρ_c	2557 [g/dm^3]	L	0.05 [m]	water	146 [kg/m^3]
ρ_s	2601 [g/dm^3]	φ	0.113	coarse aggregates	1025 [kg/m^3]
U	60 [V]	C_{bi}	0.5×10^{-3} [g/g]	fine aggregates	695 [kg/m^3]
Concrete	OPC 0.45	c_0	70.9 [g/dm^3]	w/c	0.45
t_{RCM}	6, 9 and 18 [h]	T	296.5 [K]	cement	362.5 [kg/m^3]
ρ_c	2553 [g/dm^3]	L	0.05 [m]	water	163 [kg/m^3]
ρ_s	2606 [g/dm^3]	φ	0.143	coarse aggregates	1025 [kg/m^3]
U	60 [V]	C_{bi}	0.5×10^{-3} [g/g]	fine aggregates	698 [kg/m^3]

Based on the data shown in Table 1and the experimental total chloride concentration profiles, the values of k, K_b, n and D_{eff} are optimized by using Microsoft Excel Solver tool and applying Eqs. (12), (13) and (15). The optimized values of these parameters and the corresponding simulated chloride profiles are shown respectively in Table 2 and Figs. 4 and 5.

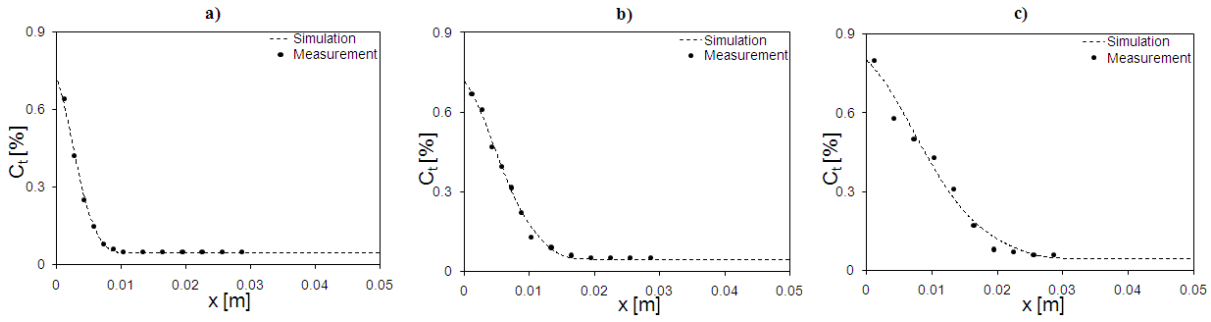

Figure 4. Optimized total chloride concentration profiles, Concrete OPC 0.35 (Table 1). a) 60V, 6h; b) 60V, 9h; c) 60V, 18h.

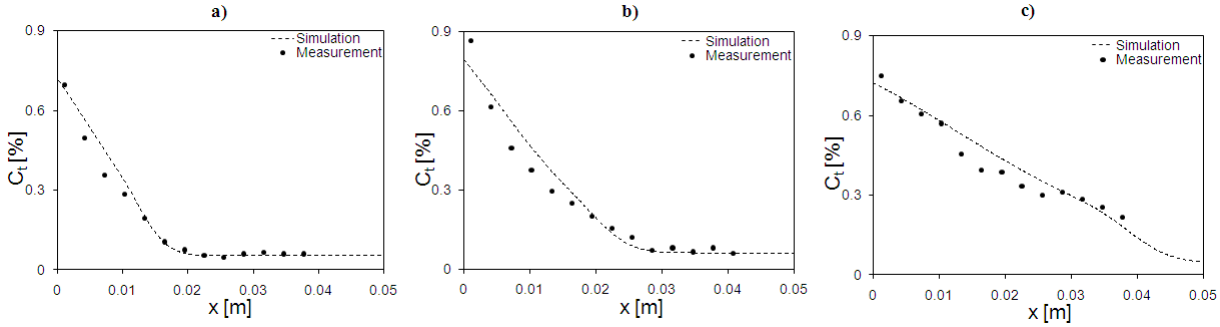

Figure 5. Optimized total chloride concentration profiles, Concrete OPC 0.45 (Table 1), a) 60V, 6h; b) 60V, 9h; c) 60V, 18h.

Table 2. Optimized model parameters.

OPC 0.35					OPC 0.45				
t_{RCM} [h]	k [$\times 10^{-6}$ s^{-1}]	K_b [$\times 10^{-3}$ dm^{3n}/g^n]	n -	D_{eff} [$\times 10^{-12}$ m^2/s]	t_{RCM} [h]	k [$\times 10^{-6}$ s^{-1}]	K_b [$\times 10^{-3}$ dm^{3n}/g^n]	n -	D_{eff} [$\times 10^{-12}$ m^2/s]
6	10.54	0.55	0.53	0.85	6	5.58	0.52	0.52	2.04
9	7.45	0.57	0.51	1.08	9	5.32	0.60	0.55	2.15
18	4.55	0.61	0.54	0.96	18	2.10	0.56	0.52	1.92

When analyzing the binding capacity K_b, it can be noticed that the values obtained from the numerical model are in line with experimental values presented in Tang [1996] and Zibara [2001], taking into consideration that these experiments were performed on cement pastes, thus, in concrete, due to lower paste content, the binding capacity must be respectively lower. The binding capacity K_b, which determines the upper limit of bound chlorides, is dependent on the w/c ratio, hence is related to the degree of hydration and connectivity to the cement hydration products. Hence, in the case of concrete with a higher w/c ratio the value of K_b should also be increased, and this trend can indeed be observed in Table 2. The optimum value of n, describing the intensity of binding and the maximal amount of bound chlorides, is found to be in the range of 0.51 – 0.55, which is also in line with the experimental data presented in Tang [1996] and Zibara [2001].

The effective chloride diffusion coefficient in concrete - D_{eff}, is retrieved from the simulations. This coefficient, which is independent from the binding of chlorides and refers only to the pore system in concrete, so far has been obtained only from time consuming and laborious steady-state tests. These values of D_{eff} presented in Table 2 are in line with the values presented in literature [Tang 1996], for concrete with similar w/c ratios.

In none of the analyzed experimental chloride concentration profiles the maximal total chloride concentration was achieved except for the surface layer of concrete. This confirms validity of the assumption of non-equilibrium in the new chloride transport model. In order to account for this phenomenon, k, being the mass transfer coefficient, was introduced. The values of k are showing a tendency to decrease during the migration process, which can be observed in Table 2. One can find in Figs. 4 and 5 that the value of k is playing deciding role on the shape of each profile. When the chloride mass transfer coefficient is larger, equilibrium between c and C_b can be reached faster, which results in a sharp chloride profile (e.g. see in Fig. 4a). However, when the value of k becomes smaller, the mass transfer rate of chlorides becomes the limiting step and the profile is characterized by a more flattened shape such as in Figs. 4c and 5c. The diminishing chloride mass transfer rate in concrete needs further investigations, since it plays an important role in the case of chloride migration in concrete, and has not been studied yet.

5. CONCLUSIONS

As shown is this paper, the currently adopted mathematical model for the Rapid Chloride Migration test is oversimplified, so the theory cannot satisfactorily predict the chloride behaviour in concrete during the migration process. For this reason, the chloride diffusion coefficient (D_{RCM}) being the output value of the test, has a doubtful meaning and should not be used for service life models of concrete. In order to improve the migration model of chlorides in concrete, non-linear chloride binding and non-equilibrium between free- and bound- chlorides concentrations are proposed in this paper. The new chloride transport model is solved numerically and applied to experimental chloride concentration profiles. The values of the non-linear binding parameters (K_b and n) extracted from the new model are in good agreement with experimental data presented in literature.
Due to the limitations in chloride mass transfer through the liquid-solid interface, the equilibrium between free- and bound- chlorides concentration cannot be achieved during the relatively short-term migration test. It is shown that the mass transfer coefficient, represented by k, plays a deciding role on the chloride transport process, hence also on the shape of the chloride concentration profile in concrete. It is found that the value of k tends to decrease in time during the migration process, thus the shape of each analyzed chloride profile changes from sharp in the beginning to flatten at the end of the migration test. This phenomenon has to be further analyzed, since no research has been carried out in this field yet.
The effective diffusivity of chlorides can be derived by using the new theoretical model. This reveals a new possibility of application of the short-term non-steady-state migration test in order to obtain the effective chloride diffusivity (so far being only obtained by laborious and long-term techniques), which is related only to the pore structure in concrete and is not influenced by binding.

REFERENCES

Castellote, M., Andrade, C., Alonso, C. 1999, 'Chloride-binding isotherms in concrete submitted to non-steady-state migration experiments', *Cement and Concrete Research*, **29**, 1799 – 1806.

Brouwers, H. J. H. 1999, 'Transport model for desorption from natural soils packed in flushed columns', *Water Resources Research*, **35**, 1771 – 1780.

Gruyaert, E., Van den Heede, Ph., De Beile, N. 2009, 'Chloride ingress for concrete containing blast-furnace slag, related to microstructural parameters', *Proceedings of the 2nd International RILEM Workshop on Concrete Durability and Service Life Planning*, 440-448, Haifa, Israel.

Narsilio, G. A., Li, R., Pivonka, P., Smith, D.W. 2007, 'Comparative study of methods used to estimate ionic diffusion coefficients using migration tests', *Cement and Concrete Research*, **37,** 1152 – 1163.

Stanish, K.D. 2002, 'The migration of chloride ions in concrete', *PhD Thesis*, University of Toronto, Toronto, Canada.

Tang, L. 1996, 'Chloride transport in concrete – measurement and prediction', *PhD Thesis*, Chalmers University of Technology, Gothenburg, Sweden.

Theissing E.M., Hest-Wardenier, P.v., de Wind, G. 1978, 'The combining of sodium chloride and calcium chloride by a number of different hardened cement pastes', *Cement and Concrete Research*, **8**, 683 – 692.

Yuan, Q. 2009, 'Fundamental studies on test methods for the transport of chloride ions in cementitious materials', *PhD Thesis*, University of Ghent, Ghent, Belgium.

Zibara, H. 2001, 'Binding of external chlorides by cement pastes', *PhD Thesis*, University of Toronto, Toronto, Canada.

XII DBMC
International Conference on Durability of Building Materials and Components
PORTO - PORTUGAL, April 12th-15th, 2011

Durability of Biocidal Agents in Facade Coatings and their Release Under Real Climatic Conditions

Regina Schwerd [1]
Christian Scherer [2]
Florian Mayer[3]
Martin Krus [4]
Cornelia Fitz [5]
Klaus Breuer[6]
Klaus Sedlbauer[7]

ABSTRACT

Growth of algae and fungi is a well known phenomenon on exterior building surfaces. Modern façade coatings, especially coatings based on organic resins, therefore contain antimicrobial agents. The biocides are meant to inhibit or at least to delay microbiological growth significantly. Visible microbiological activity in the form of coloured spots is accepted as deficit in German prevailing law cases. Besides juristic aspects the leaching of biocidal ingredients from coatings may also have environmental effects and points out the necessity for product optimisation to minimize the impact of biocides on water and soil.
In a four year outdoor study the behaviour of façade coatings equipped with different biocidal agents was examined. Special test specimen based on external thermal insulation composite systems (ETICS) were designed and furnished with different façade coatings. The coatings contained four different mixtures of biocides. In sum, 20 different types were exposed to real climatic conditions at two locations in Germany. At defined times the biocide content of the coatings was analyzed by high performance liquid chromatography/tandem mass spectrometry (LC/MS-MS). Additionally, the run-off water from the specimen was collected and analyzed. In all coatings the concentrations of the active ingredients declined depending on the type of the ingredient and the matrix. In the run-off water the highest concentrations were found within the first three months of exposure. The results show clearly that the decrease of the antimicrobial ingredients in the coatings can not only be explained by leaching. Other ways of release are also possible, as well as the formation of transformation or degradation products.

KEYWORDS

Façade coatings, microbiological growth, antimicrobal agents, weathering-experiment, run-off water

[1] Fraunhofer-Institute of Building Physics (IBP), Valley, GERMANY, regina.schwerd@ibp.fraunhofer.de
[2] Fraunhofer-Institute of Building Physics (IBP), Valley, GERMANY, christian.scherer@ibp.fraunhofer.de
[3] Fraunhofer-Institute of Building Physics (IBP), Valley, GERMANY, florian.mayer@ibp.fraunhofer.de
[4] Fraunhofer-Institute of Building Physics (IBP), Valley, GERMANY, martin.krus@ibp.fraunhofer.de
[5] Fraunhofer-Institute of Building Physics (IBP), Valley, GERMANY, cornelia.fitz@ibp.fraunhofer.de
[6] Fraunhofer-Institute of Building Physics (IBP), Valley, GERMANY, klaus.breuer@ibp.fraunhofer.de
[7] Fraunhofer-Institute of Building Physics (IBP), Valley, GERMANY, klaus.sedlbauer@ibp.fraunhofer.de

1 INTRODUCTION

The design of building façades shows a wide variety related to regional habits and changes permanently due to technological reasons and fashionable trends. For the choice of the coatings the substrate and the potential appearance have to be considered. This results in different requirements for the preservation of the coatings [Lindner 2005].

Modern coating materials show reduced amounts of heavy metals, many components are bio-degradable, and biogene ingredients are used. Because of this, microbiological growth can develop more easily than in former days. There are different antimicrobial agents applied in organic bound façade coatings. In general they are added to the coating as an appropriate formulation, i. g. as a powder, solution or dispersion. For the protection against microbiological growth in the wet state of a coating in-can preservatives are used. Dry film preservatives are applied for the protection of the finished coatings. Both types of conservatives should possess a broad spectrum of activity and a convenient cost effectiveness as well as being easy to handle. They must not interact with other ingredients of the coatings or influence the workability. Additionally, they must be stable at pH-values up to 13 which is important for example in silicate-based paints. Generally, in-can preservatives should have a high water solubility, i. e. a low partition coefficient pKow and a rapid way of action. In contrast, dry film preservatives should show low water solubility and high partition coefficients. Dry film preservatives have to be stable under the influence of weathering conditions and show a long lasting activity against microorganisms. Therefore, low volatility and water solubility are important aspects concerning the durability of the protection. Common dry film preservatives generally are organic molecules with molecular masses between 200 and 500 g/mol, water solubilities from 2 to 300 mg/L and partition coefficients from log 2,5 bis log 4 [Lindner 2000]. Normally combinations of several active ingredients are used because of the specific way of action of most biocides.

2 MATERIALS AND METHODS

In a four year outdoor study the behaviour of façade coatings equipped with different biocidal agents was examined. Two plasters with inorganic binders and three plasters with organic binders were selected. A lime cement plaster, a silicate plaster and three plasters with organic binders based on styrene acrylate, terpolymer and silicone resin were used. Dispersion type silicate paint, an emulsion paint (styrene acrylate based) and a silicon resin based paint were also examined. The renders were applied without a paint coating. The paints were applied on different biocide free plasters. All coatings were special, but realistic formulations. One of four different biocide combinations was added to every coating. Every mixture consisted of three active ingredients: terbutryne (CAS 886-50-0), OIT (CAS 26530-20-1) and a third ingredient which was either carbendazim (CAS 10605-21-7), DCOIT (CAS 64359-81-5), IPBC (CAS 55406-53-6) or zinc-pyrithione (CAS 13463-41-7) (Table 1). The biocide combinations were added in concentrations of 0.5 mass-% to the plasters and 1.0 mass-% to the paints.

Approximately 350 test specimen based on external thermal insulation composite systems (ETICS) were exposed to real climatic conditions at two locations in Germany, most of them in Holzkirchen, located approx. 25 km south of Munich in Upper Bavaria on a plateau at an altitude of 680 m above sea level. The climate is characterized by three main factors: at foehn conditions, when warm winds from the south blow over the Alps, temperature differences within one day may reach up to 35 K. Radiation at night causes surfaces temperatures to fall below the dew point frequently. Especially in summer heavy thunderstorms with intense rainfalls occurs which lead to high exposure to driving rain.

At defined times the biocide content of the coatings was analyzed by high performance liquid chromatography/tandem mass spectrometry (LC/MS-MS). Additionally, the run-off water from the specimen was collected and analysed.

Table 1. Properties of the biocides used in the study.

active ingredient (CAS-numberr)	*substance category*	*properties*
IPBC (55406-53-6)	carbamate	broad spectrum of activity, fungicide, unstable under UV-radiation, high pH-values and presence of catalysts (metalls like Co)
carbendazime (10605-21-7)	benzimidazole-derivative	fungicide, high activity (but not against *Alternaria*), chemically stable
OIT (26530-20-1)	isothiazolinone	broad spectrum of activity, high water solubility and mobility
DCOIT (64359-81-5)	isothiazolinone	broad spectrum of activity, high volatility, unstable, hydrolysis at pH-values > 8,5
zinc-pyrithione (13463-41-7)	pyridine-derivative	very broad spectrum of activity, fungicide and algicide, in alkaline systems possiblity of complexation with calcium, possibility of discolouration with other metalls, hydrolysis at pH-values > 9
terbutryne (886-50-0)	triazine-derivative	algicide, high activity, sublimation possible, dependent on the microorganism partly high concentrations necessary, otherwise metabolizable and possibilty of fomation of resistances

3 RESULTS

3.1 Biocide contents in coatings

The active ingredients show strong differences in their durability within the examined façade coatings. Depending on the type of the coating, recoveries can be widely spread (Figure 1). The upper limit of the range corresponds to the highest found recovery, the lower limit to the minimal found recovery within all examined coatings. It becomes obvious that the biggest loss of active ingredients takes place within the first year of exposition.

The biocide carbendazime possesses a high durability in all coatings. In some coatings there is no decrease of the content detectable within the observation period. Partly concentrations above 100 % are found. This probably is due to migration within the coating. Terbutryne also shows high recoveries. In the worst case observed, the terbutryne content drops below the analytical detection limit after three years. For IPBC, OIT, DCOIT and zinc-pyrithione this is the case already after one year. IPBC and OIT are very similar concerning their durability. Recoveries of DCOIT are little lower. After one year, Zinc-pyrithione can be found only in one coating with a very low recovery.

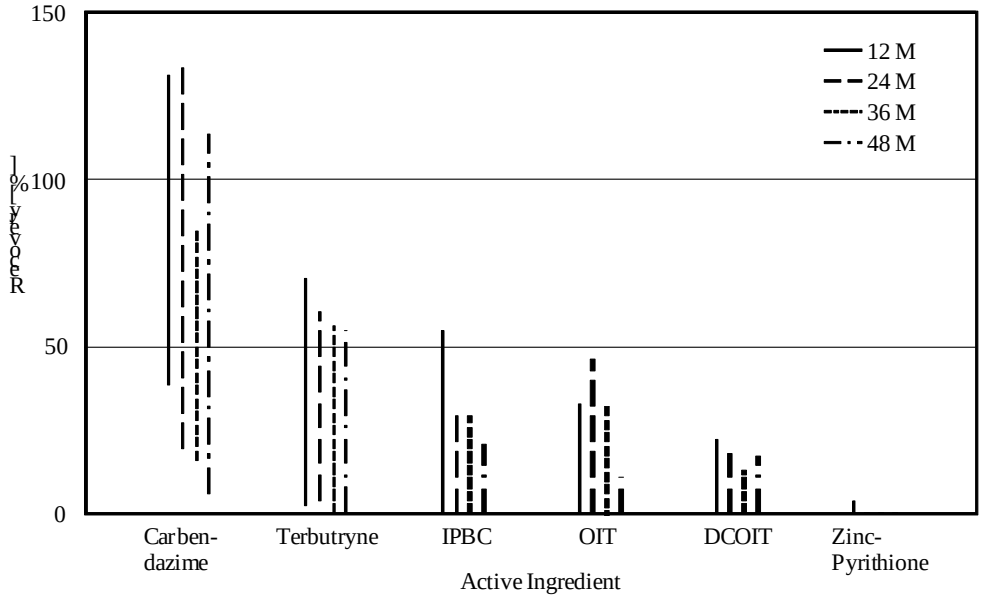

Figure 1. Durability of the biocides in the coatings. Ranges of recoveries within all examined coatings after 12, 24, 36 and 48 months of exposition.

3.2 Biocide contents in run-off water

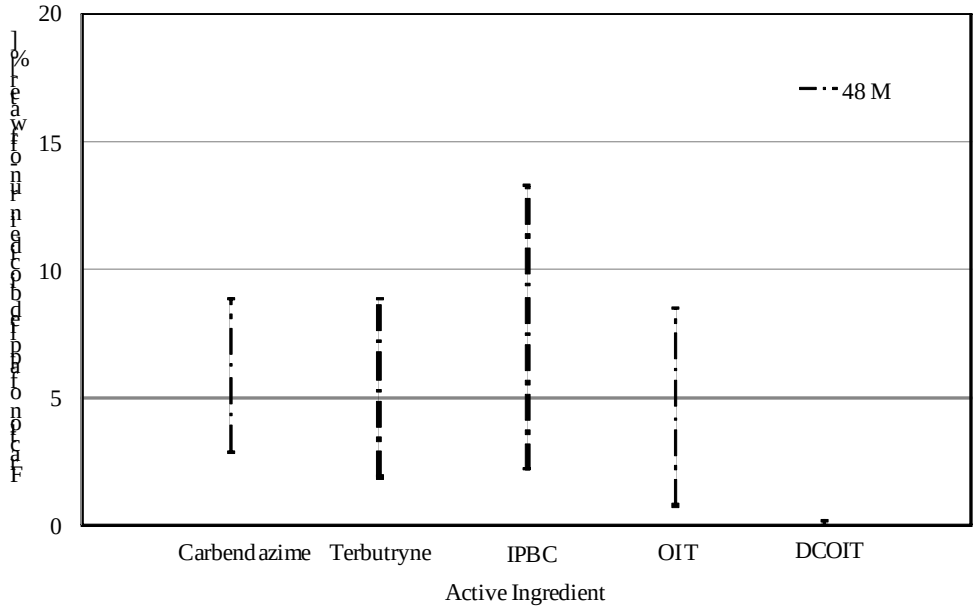

Figure 2. Accumulated amounts of the biocides originally applied in the coatings which is found in run-off water within 48 months of exposition. Ranges of recoveries over all examined coatings.

The active ingredients may be released from the coatings because of the influence of driving rain. In this context mainly the first months of the exposition are relevant. The highest contents of biocides (OIT, IPBC, DCOIT, terbutryne) in run-off water are measured within three months after application of the coatings. In the following, no changes in the total amounts are observed. Carbendazime is washed off significantly for six months and shows permanently small release in the ongoing time.

In sum there were fractions between maximum 0.2 % (DCOIT released from terpolymer based plaster) and 13.3 % (IPBC released from silicone resin based paint applied on lime cement plaster) of the originally used biocides released by rain water after four years (Figure 2).
Analysis of zinc-pyrithione in water is not conducted due to its high reactivity and its short half-life.

3.3 Biocide content in the coating vs. content in run-off water

Considering the applied amounts of biocides, the contents in the coating and the release by run-off water partly very high gaps of balance appear (Figure 3). In the case of carbendazime the largest range of a possible gap is found. In some coatings like the styrene acrylate based plaster or the silicate plaster no reduction of the carbendazime content is observable whithin four years, at the same time only small amounts are measured in the run-off water. This results in an equalized balance (gap of balance 0 %). In the lime cement plaster the carbendazime content has decreased down to 6 % after four years. At the same time no significant release by run-off water could be measured. This leads to a gap of balance of 85 %. For terbutryne, the gap of balance lies between 46 % and 95 %, IPBC shows a gap of balance between 75 % and 93 %. The isothiazolinones OIT and DCOIT show gaps of 83 % to 99 % and 100 %, respectively. This means that in some cases there is no biocide measurable after four years and at the same time also is not released with water.

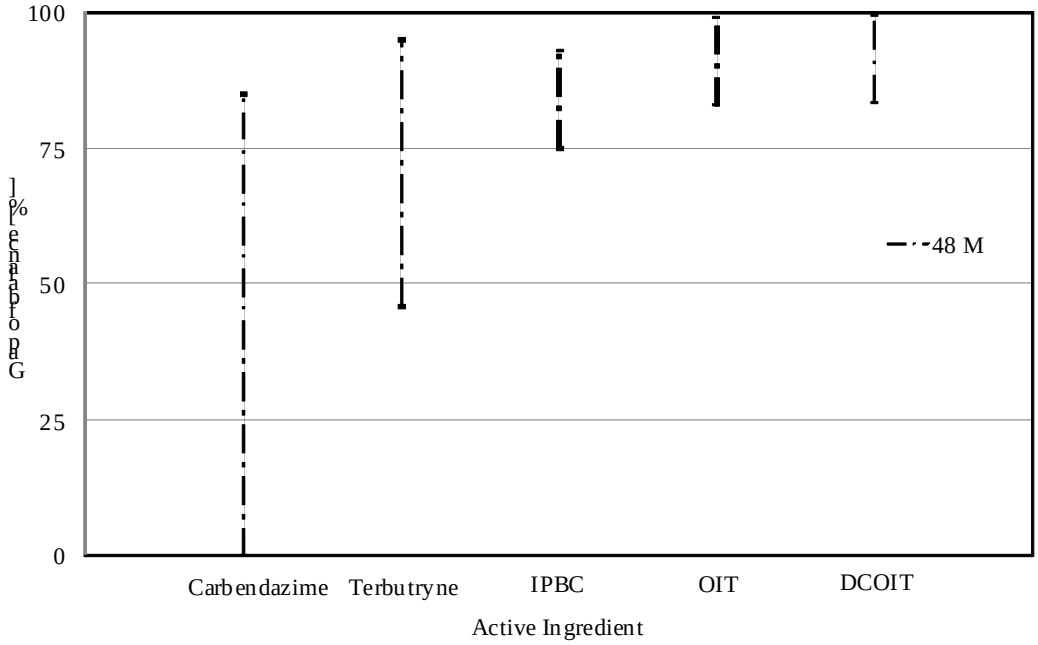

Figure 3. Gap of balance of the biocides in the coatings. Ranges within all examined coatings after 48 months of exposition.

4 CONCLUSION

The biocides show strong differences concerning their durability in façade coatings. In relation to the type of the coating, the recovery rates spread over a wide range. Carbendazim is very consistent in the coatings, followed by terbutryne. IPBC and OIT are less durable but they show recovery rates higher than those of DCOIT. After one year zinc-pyrithione can be detected only in one coating (terpolymer based plaster), in the following years the ingredient can not be determined any more.

The type of the binder has strong influence on the durability of the biocide. Carbendazim is very consistent in all coatings apart from the lime cement plaster. The other active ingredients show high contents in the styrene acrylate and the terpolymer based plaster, followed by the silicate plaster. For

the silicon resin plaster the recovery rates are significantly lower. The lowest recovery rates are found for the lime cement plaster.

The substrate influences the durability of the biocides in the applied paint. Within the paints the emulsion paint applied on styrene acrylate based plaster shows the highest recovery rates. Applied on lime cement plaster, the same paint has significantly lower recovery rates. The recovery rates of the silicon resin base paints and the dispersion type silicate paint are even lower.

The active ingredients of façade coatings can be released by run-off water. The highest concentrations of biocides in water are found within the first six months of weathering. Only carbendazime shows a continued release of small percentages during the entire observation time of four years. The minimum cumulated fraction of biocide after four years is found for DCOIT with 0.2 %, the maximum for IPBC with 13.3 %.

The results show that the decrease of the antimicrobial ingredients in the coatings can not only be explained by leaching. In some cases there exist gaps of balance of over 90 %, meaning that over 90 % of the originally applied biocides are neither found in the coating nor in the run-off water. This becomes especially significant for the active ingredients OIT and DCOIT plus the silicon resin plaster. This means that for the decrease in the coatings, additional mechanisms have to be taken into account. On the one hand, other ways of release like sublimation are also possible, as well as migration of ingredients in deeper layers of the facades. On the other hand, the formation of transformation or degradation products under the influence of high temperatures, UV-radiation, oxidation or hydrolysis in the complex matrix of a coating has to be considered. Mechanisms like these may lead to potent metabolits which possess antimicrobial activity themselves, so that the coating may be protected against microorganism in spite of the decrease of the parent biocide. The biocide content is not alone decisive for the susceptibility to development of biological growth on a coating.

ACKNOWLEDGMENTS

This work was funded by a grant (grant no. 0329663G) of the German Federal Ministry of Economics and Technology due to a resolution of the german parliament.

REFERENCES

Lindner, W. 2000, ‘Zur Chemie der Biozide an Fassaden’, in *Biozide in Bautenbeschichtungen*, ed E. Bagda, ExpertVerlag, Renningen, pp. 53-76.

Lindner, W. 2005, ‘Surface coatings’, in *Directory of Microbicides for the Protection of Materials*, ed W. Paulus, Springer, New York, pp. 347-348.

XII DBMC
International Conference on Durability of Building Materials and Components
PORTO - PORTUGAL, April 12th-15th, 2011

Durability Assessment of New Generation Coated Steel Technologies for use in Building and Construction: Methodology and a Case Study

Rob Scott [1]

ABSTRACT

Coated sheet steel is widely used in roofing, cladding, framing and rain water goods, with proven field performance in a number of environments. In recent years, a range of coating developments has been brought to market to extend the product life or reduce the overall cost of corrosion.

The development of the new generation of metallic coatings provides a challenge in determining whether the benefits seen in accelerated testing are delivered in the field. Determining the expected field life is critical for all stakeholders, in terms of addressing warranty offers, Standards and Building Code certification, life cycle analysis and so on.

BlueScope Steel has been active in the research, development and commercialisation of coating technologies over many years, including both metallic and polymer coatings. This has led to the development of expertise in assessing and understanding accelerated and long-term coated steel performance and durability, and the relationship between these assessments.

This paper discusses the approach taken to the assessment of new generation coatings, and in particular the scale-up from accelerated testing to service life assessment. The critical nature of this work in ensuring that commercial building products meet the durability requirements expected of them is discussed, along with the recent case study around the development of the next generation aluminium-zinc-magnesium (AM) metallic coating for the building market.

KEYWORDS

Durability, Steel, Metallic coatings, Buildings.

[1] BlueScope Steel Product Research and Development. Robert.scott@bluescopesteel.com

1 INTRODUCTION

The durability of coated steel is infleunced by a number of environmental factors, including:

- the rate of deposition of corrosive media, such as marine salts and industrial pollutants,
- the rate of removal (or washing) of corrosive media, and
- micro and macro climactic influences, such as humidity, condensation and temperature.

Galvanized steel has been widely used since the 1830s [Roberge 2000], providing an understanding of the product's durability and the impact of environmental factors. Over the years, coatings have been developed to prolong the durability of steel. A number of these coatings technologies, such as the Galvalume® steel 55%Al-Zn coating, Galfan® 95%Zn-Al, Aluminised 90%Al-Si and Terne have been around for decades, allowing study of their outdoor performance in a range of environments.

A suite of new technologies, summarised in Table 1 (Shedden [2010]), has recently been brought onto the market. These technologies combine zinc, aluminium and magnesium in the metallic coating, with the bulk of the coating being zinc. A study by Prosek *et al.* [2009] of these types of coatings showed that "… (t)he corrosion stability of Zn-Mg and Zn-Al-Mg coatings strongly depended on the exposure conditions. Although it was superior to zinc reference materials under all experimental conditions, improvements from low tens of per cent up to 10-fold drop in corrosion rate were observed". Given this range, the durability of these new generation coatings requires thorough assessment, to determine suitability for various applications in the construction industry.

Table 1. Summary of some of the recently introduced metallic coated steel technologies.

Composition	*Brand*	*Manufacturer*	*Reference*
Zn-6%Al-3%Mg	ZAM®	Nisshin Steel	De Bruycker [2006]
Zn-11%Al-3%Mg-0.2%Si	SuperDyma®	Nippon Steel	De Bruycker [2006]
Zn-5%Al-0.8%Mg	ECOGAL®	JFE Steel	Fujisawa *et al.* [2009]
Zn-1.5%Al-1.5%Mg	MagiZinc™	Corus Group	Vlot *et al.* [2006]
Zn-1.5%Al-1%Mg	ZMg EcoProtect™	ThyssenKrupp Steel	Lamprecht [2009]
Zn-2%Al-2%Mg	Corrender™	voestalpine	voestalpine [2010]

2 DURABILITY EXPECTATIONS OF COATED STEEL IN BUILDING APPLICATIONS

The current widespread use of coated steel is in part due to the market confidence in the durability of these products. In developing new coated steel technologies, it is important to highlight the durability expectations, to allow an understanding of whether the new techologies are able to deliver against these expectations. Without meeting the expectations, the technologies may not be widely accepted.

2.1 Building Code of Australia

The Australian Guidelines on Durability in Buildings [Australian Building Codes Board 2003] provide an indication on the design aspirations for various components of buildings in Australia (Table 2). Apart from the Guidelines, the Building Code of Australia does not provide direct indications of durability requirements. However, for metallic coated steel, specific coating masses are required to meet the Deemed to Satisfy provisions of the Code. The implication of this is that the coating masses referred to have been proven over the years to provide adequate performance to meet consumer expectations. A comparison to incumbent products is therefore a starting point for the introduction of new coating technologies, with testing aligned to the applications covered in the Code.

Table 2. Extract from the Australian Guidelines on Durability in Buildings.

Design Life of buildings (dl) (years)		*Design Life of components or sub-systems (years)*		
		Category		
Category	*Number of years*	*Readily accessible and economical to repair*	*Moderate ease of access but difficult or costly to replace or repair*	*Not accessible or not economical to replace or repair*
Short	1 < dl < 15	5 or dl (if dl<5)	dl	dl
Normal	50	5	15	50
Long	100 or more	10	25	100

2.2 Durability Warranties

Under Australian Law, there are two forms of warranties – contractual and statutory. The former is an explicit statement outlining the warranty a manufacturer provides for the product, given certain requirements (terms and conditions) are met. The latter is provided by legislation, and provides consumers protection that the product is of merchantable quality and is fit for purpose.

Contractual warranties for coated steel in Australia vary in duration. BlueScope Steel, for example, provides warranties ranging from 10 years to 50 years, under certain conditions. The widespread acceptance and market application for these warranties provides a baseline level of durability expectation.

The duration of the statutory warranties for coated steel in Australia has not been fully tested. They are based on what a reasonable consumer would expect, which in part will be influenced by past performance, technical data and marketing communications. While of importance, they have a maximum duration of 10 years from the date of purchase of the product.

3 DETERMINING FIT WITH DURABILITY EXPECTATIONS

In order to understand whether new generation coated steel technology will provide the required durability, which, depending on the current warranty, code or other expectation, may be in excess of fifty years, a range of product assessments is essential.

3.1 Accelerated Testing Alone

While accelerated testing provides a comparison of corrosion performance, it can be limited in direct application. GalvInfo [2009] stated that "…(f)or an accelerated corrosion test to be truly useful, a prime requirement is that the results correlate with performance in the real world, something that has never been demonstrated with the salt spray test (one of the key accelerated tests). This has led many researchers to conclude that the test has no relevance, and should be discontinued". Shedden [2010] similarly found limited evidence for the correlation between a range of accelerated tests and real world corrosion performance.

In general, accelerated testing relies on the corrosion mechanisms and relative kinetics for the new coatings being similar to the corrosion mechanisms for the coatings being compared to. This is not necessarily the case. The relative kinetics of corrosion in the accelerated test can be quite different to washed outdoor exposure. As an example, in salt spray testing, Zn-6%Al-3%Mg coated steel (ZAM®) has shown 10-20 times the life of galvanised steel, while in outdoor testing after 7 years, the ZAM® coated steel has a projected life in a washed environment of 3-4 times galvanised steel [Nisshin Steel Corp 2008].

3.2 Washed Outdoor Testing of Panels Alone

Washed outdoor testing of panels are more likely to experience corrosive environments, mechanisms and kinetics similar to real world full scale buildings. However, there are shortfalls. The kinetics of washed outdoor corrosion can be quite different to sheltered outdoor exposure. In sheltered exposure, the build-up of corrosive salts continues without any washing to remove these salts. Such a situation occurs in open buildings (e.g. walkways, carports, sheds, hangars), on the top surface of roofs under ridge capping, and inside roof cavities. Kimata *et al.* [2007] showed that in sheltered exposure, three metallic coatings on steel showed significantly greater corrosion than in washed exposure.

Interactions occur in buildings that may not be seen on panels. In an application such as roofing, there are interactions with fasteners, battens and flashing. An example of the flashing issue is evident where lead was used for flashing roofs. The interaction between lead and Galvalume® coated steel caused accelerated corrosion of the Galvalume® steel [NSW Heritage Office 2004]. Similarly, the replacement of galvanised steel with Galvalume® coated steel for roofing increased the purity of the rain water running off roofs and into gutters; the result was an inert catchment affect, where the corrosion of galvanised steel gutters was rapidly accelerated [Tyler 2008].

4 A SCALE-UP APPROACH FOR ASSESSING COATED STEEL PRODUCTS

A scale-up approach allows assessment of various factors that can affect the life of coated steel in buildings in a way that mitigates risk and progressively develops confidence in a coated steel product. Such an approach involves the use of various test methodologies, including

- standard accelerated tests,
- standard panels in outdoor exposure in various environments,
- sophisticated panels in outdoor exposure in various environments,
- various different laboratory-scale application assessments,
- multiple ‘installed sites’, with small volumes of product in real-world assessment, and
- full-scale buildings in various sites.

The approach is shown schematically in Fig. 1. Examples of each stage of the product assessment are shown in Table 3. The progressive increase in confidence assists in determining the ‘real world’ durability, leading to development of performance statements, warranties, building practices, LCA durability inputs, and meeting of Building Codes and Standards.

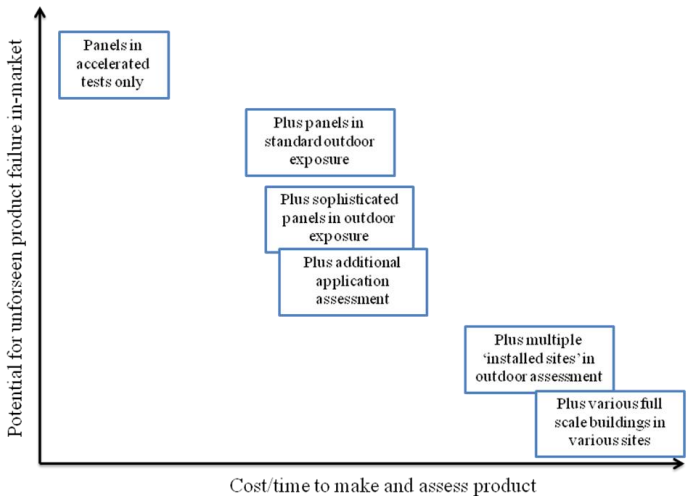

Figure 1. Schematic indicating the progressive reduction in risk as the investment in the scale-up approach for coated steel assessment progresses.

Table 3. Examples of tests performance at each stage of assessment in a scale-up appraoch.

Stage	*Assessment Examples*	
1. Accelerated testing	 a) Panels in QFog cyclic corrosion test.	 b) Panels in the Salt spray test.
2. Standard outdoor	 a) Marine outdoor assessment site (Bellambi Point in Australia).	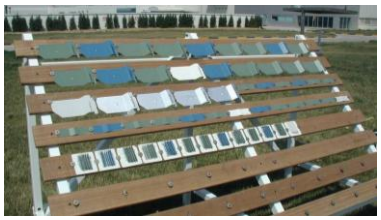 b) Acid rain outdoor assessment site (Cheng Du in China).
3. Sophisticated panels, including interaction assessment	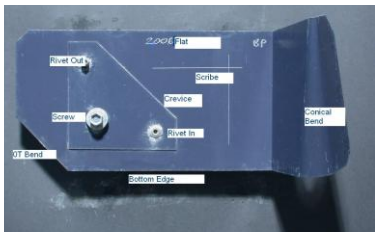 a) Sophisticated panel, incorporating rivets, screw, overlap panel and a 0T bend, allowing interactions and other factors to be assessed.	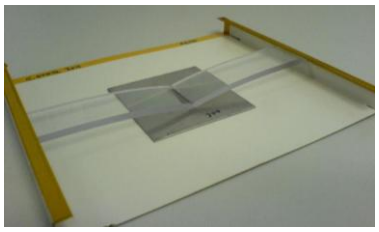 b) Dissimilar metals panel, with one metal held in contact with the coated steel and then assessed outdoors.
4. Laboratory / small scale, including interaction assessment	 a) Assessment in a guttering (inert catchment) application, while also assessing the run-off.	 b) Assessment of product immersed in concrete.
5. Installed applications	 a) Assessment Hut comprising various building components.	 b) Shed door on Surf Life Saving Club, located at ocean beach.

4.1 Case Study: The Development of Al-Zn-Mg Coating Technology

Table 1 indicated that recent developments in coated steel have been based on zinc, with additions of aluminium and magnesium. By comparison, BlueScope Steel has focused on using the aluminium-zinc (or AZ) (Standards Australia 2010) coating as a starting point, and identified the factors which could improve the overall durability of coated steel in building applications. The resulting product

has been optimised, through the range of testing, to produce the aluminium-zinc-magnesium (or AM) (Standards Australia 2010) coating. The following section details the history of the development of this composition, testing results and discusses the comparative findings at the different stages.

4.1.1 History of the development of the Al-Zn-Mg coating

Work at BlueScope Steel commenced in the early 1990s, with small panels produced with a range of compositions. This included various different levels of magnesium addition to the AZ coating. Over the subsequent two decades, the scale-up approach was applied to optimise the composition, and determine the performance in a range of applications and environment. This is summarised in Fig. 2.

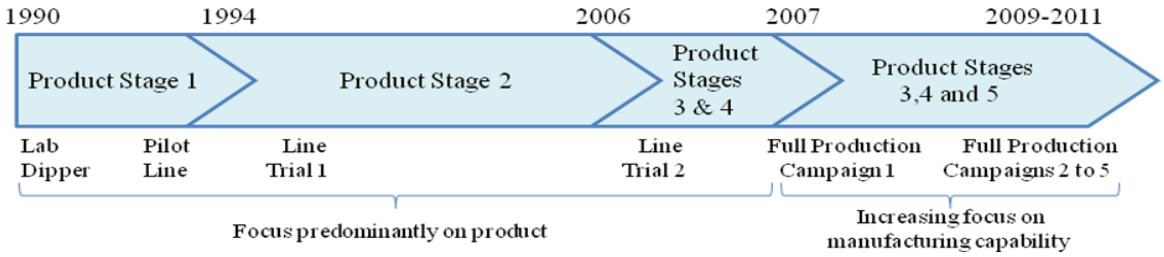

Figure 2. Timeline for the development of Al-Zn-Mg coating technology

4.1.2 Test methods discussed in this paper

The scale-up approach employed a broad range of tests. The tests (Table 4) and results presented in this Case Study focus on the key understandings elucidated from this approach.

Table 4. Selected tests from the development of the AM coating that gave greatest range of learnings and highlighted the benefit of the scale-up approach.

Stage	*Test Method*
1. Accelerated testing	a. Cyclic Corrosion Test (CCT): CCT-1, or Cycle E from AS2331.3.13. b. Neutral Salt Spray: ASTM B117
2. Standard outdoor	a. Outdoor mass loss: Method as per Townsend and Zoccola (1979). b. Outdoor general corrosion assessment of surface, edges and bends: Formed panel with a scribe and 3T and 5T bends, facing north installed at 45° at various test sites in Australia.
3. Sophisticated panels	Outdoor general corrosion assessment of surface, edges, bends, laps, around rivets and screws a. Standard panels with the addition of a lap, rivets and screws. b. Sheltered panels incorporating a conical bend ranging from 10T to 20T, a 0T bend, a lap with rivets and screws. c. New panel with side-by-side bends ranging from 0T to 6T.
4. Lab scale, including interaction assessment	a. Run-off simlulation of catchment and gutter, as shown in the guttering (inert cathcment) example in Table 3. b. Sets of standard panels inserted in various types of concrete, with the concrete broken open for inspection of panels after 1 month, 1 year or 3 years.
5. Installed applications	Assessment Huts comprising roofing, walling, fencing, rain water goods, framing, garage doors and gutter guards in 5 different corrosive environments in Australia. Water run-off captured and analysed for elemental content.

4.1.3 Selected results and discussion around the Scale-Up Approach

Stage 1 and 2 comparison: Unpainted AZ and AM coated steel samples were assessed in the accelerated tests, with the AM product outperforming the AZ product (Table 5). However, for

painted AM product, certain paint systems in salt spray testing exhibited unusual blister formation commencing from the cut edge. By comparison, the accelerated cyclic corrosion testing and the Stage 2 outdoor assessment did not show this behaviour, but rather exhibited standard blistering appearance. Further, the rate of edge corrosion on the AM coating was around ½ of that on the AZ coating in both the accelerated cyclic corrosion test and outdoor assessment. Having the Stage 1 and 2 product available allowed assessment of corrosion mechanisms, indicating that the salt spray assessment, by keeping the corrosion product continuously wet, did not allow the drying and barrier protection mechanism form that occurs in either the 'real world' or the accelerated cyclic corrosion test.

Table 5. Amount of corrosion as measured by surface metallic coating mass loss (g/m^2) for the AZ and AM coated steel samples after 5 weeks in CCT-1 (Cycle E or QFog) cyclic corrosion testing. The samples were as-metal coated, i.e. no passivation.

Edges protected	*AZ coating*	*AM coating*	*Reduction in corrosion rate*
Yes	50	35	30%
No	105	70	33%

Stage 1 to 5 comparison: The AM coating is harder and less ductile than the AZ coating. For tight bends, this leads to a greater number of microcracks in the coating. Intuitively, this may have an impact on the bend corrosion performance. Stage 1 accelerated testing on unpainted product did not show this, however, for painted product there was a higher propensity for white corrosion product to be visible on tight bends. The differing nature of the corrosion process was highlighted in the comparison to the Stage 2 outdoor assessment; after 9 years exposure in a marine environment, the corrosion level on the bends of the painted product was statistically no different between the AZ and AM coatings. Extended outdoor exposure in Stage 2, assessment of product with tight bends in Stages 3 and 5, and understanding the performance when in contact with brick cleaning acid in Stage 4 allowed confidence to be developed that the observations in the accelerated test were an artefact of the methodology, and do not correspond to the 'real world' performance of the product.

Stage 4: The performance of the AM coating in ponding (with a reduced level of surface discoloration on unpainted product), in concrete (less corrosion at the air-concrete interface), and in overall powder coated performance (reduced corrosion rate of the powder coated product), amongst other areas, has shown a marked improvement, not otherwise apparent in the other types of tests. Assessment of water run-off has furthered the understanding of the overall corrosion mechanisms, and helped with the development of corrosion physical models.

5 CONCLUSION

The development of new metallic coating technology opens opportunities to improve the durability of coated steel in current building applications, create the possibility for the use of coated steel in new building applications, and/or reduce the environmental load of coated steel. In understanding these new technologies, a scale-up approach allows a thorough performance profile to be developed and confidence to be delivered to all stakeholders around the durability in 'real world' applications. The importance of understanding different mechanisms between accelerated and 'real world' performance, interactions with other building components, and unwashed conditions, cannot be overstated.

ACKNOWLEDGMENTS

A number of BlueScope Steel personnel contributed to the development and review of this paper, including Tahnee Lowe, Ross Smith, Bryan Shedden, Jacob Thomas, Sean Wong and David Varcoe.

REFERENCES

Australian Building Codes Board 2003, *Guideline on Durability in Buildings*, Australian Building Codes Board, Canberra Australia.

De Bruycker, E. 2006, *Zn-Al-Mg Alloy Coatings: Thermodynamic Analysis and Microstructure-Related Properties*. Doctoral Thesis. University of Ghent

Fujisawa, H., Kaneko, R. & Ishiwaka, H. 2009 "Hot-Dip Zn-5%Al Alloy-coated Steel Sheets JFE ECOGAL®", JFE Technical Report No.14, Dec 2009, pp. 41-45.

GalvInfo 2009, *GalvInfoNote 3.4 – The Salt Spray Test, Rev 1.0*, International Zinc Association. Sourced from http://galvinfo.com/ginotes/GalvInfoNote_3_4.pdf, 8 October 2010.

Kimata, Y., Takahashi, A. & Asai, K. 2007, 'Corrosion Resistance of Zn-11%Al-3%Mg-0.2%Si Coated Steel Sheet after Sheletered Outdoor Exposure Test in Miyakojima', Proc. 7th International Conference on Zinc and Zinc Alloy Coated Steel Sheet (Galvatech 2007), Iron and Steel Institute of Japan, Osaka, Japan, 19-22 November 2007, pp. 586-591.

Lamprecht, M. 2009 "ZMg EcoProtect® A new galvanised product for the building industry", Advancements for Metal Buildings, EPAQ Congress, 12-13 Nov 2009, Helsinki.

Nisshin Steel Corp 2008, *Nisshin Steel Quality Products - ZAM*. http://www.nisshin-steel.co.jp/nisshin-steel/english/product/ecatalog/pdf/R15-10.pdf. 8 October, 2010.

NSW Heritage Office 2004, *The Maintenance Series Information Sheet 4.1 - Corrugated Roofing*,

Prosek, T., Nazarov, A. & Thierry, D. 2009, "Role of magnesium in corrosion performance of Zn-Mg and Zn-Al-Mg alloy coatings in atmospheric conditions", Abstract from 216th Electrochemical Society (ECS) Meeting - Vienna, Austria, 4-9 October, 2009.

Roberge, P. 2000, *Handbook of Corrosion Engineering*, McGraw Hill Books, New York.

Scott, R., Buxton, D. & Smith, R. 2008, internal BlueScope Steel report.

Shedden, B. 2010, internal BIEC publication.

Standards Australia 2010, *DR AS 1397: Continuous hot-dip metallic coated steel sheet and strip - Coatings of aluminium, zinc and magnesium*, Draft for Public Comment Australian Standard

Townseand, H. E. & Zoccola, J. C. 1979, "Atmospheric Corrosion Resistance of 55%Al-Zn Coated Steel Sheet: 13 Year Test Results", *Materials Performance* 18 [10] 13-20.

Tyler, J. 2008, *GALVALUME® The BIEC Journey*, BIEC International Inc, Vancouver WA USA.

Vlot, M., Bleeker, R., Maalman, T. & van Perlstein, E. 2006 "MagiZinc™: A new generation of hot-dip galvanised products", Galvanized Steel Sheet Forum, 30-31 May 2006, Dusseldorf, Germany.

Voestalpine 2010, "Hot-dip Galvanized Steel Strip: Corrender Coated - innovative coating systems for the highest degree of corrosion resistance", http://www.voestalpine.com/, 10 October, 2010.

XII DBMC
International Conference on Durability of Building Materials and Components
PORTO - PORTUGAL, April 12th-15th, 2011

Durability of Materials used in the Two-by-Four Residential Buildings

Shiro Nakajima [1]
Yukio Tsujimura [2]
Tomonori Murakami [3]
Hideki Matsumoto [4]
Akira Seino [5]
Masao Nakajima [6]

ABSTRACT

Almost 40 years has past since the North American wood frame (two-by-four) construction method became one of the common construction methods for the wooden residential buildings in Japan. The durability of this North American style construction method was one of the strong interests for the designers, engineers and researchers. Particularly the durability of the relatively small cross section size of the framing members, the sheathing materials and the steel connectors such as common nails were in discussion. The information on the strength properties of the structural materials of the existing building that have be served for a certain period will help to further confirm the affordablity of the durability of the wood frame construction method. The object of this research is to evaluate the performance of the shear walls at certain stages of the buildings' service life and review the "Reduction Factors" that are commonly used in the structural design of the buildings of wood frame construction. The sheathing panels and nails were extracted from wooden existing buildings of certain ages and the extracted sheathing panels and nails were tested for their strength properties. A calculation method to estimate the strength properties of the shear walls from the strength data of the joints composed of lumbers, sheathing panels and nails was discussed to prepare a methodology that can help reevaluating the "Reduction Factors".

KEYWORDS

Two-by-four construction, Structural materials, Durability, Strength property, Reduction factor.

[1] Building Research Institute, Tsukuba, JAPAN, nakajima@kenken.go.jp
[2] Japan 2X4 Home Builders Association, Tokyo, JAPAN, tsujimura@2x4assoc.or.jp
[3] Mitsui Home Co.Ltd. Tokyo, JAPAN, t-murakami@mitsuihome.co.jp
[4] Japan 2X4 Home Builders Association, Tokyo, JAPAN, h-matsu@kenken.go.jp
[5] Mitsui Home Co.Ltd., Tokyo, JAPAN, a-seino@mitsuihome.co.jp
[6] Kanto-Gakuin University, Yokohama, JAPAN, mnaka@kanto-gakuin.ac.jp

1 INTRODUCTION

The durability of the wooden materials and metal connectors affect on the strength and stiffness properties of the structural elements such as shear walls and diaphragms of the wooden structures. In most cases the strength and stiffness properties of the structural elements are evaluated from the test results of the test specimens that have no deterioration or no damage. Wooden materials and metal connectors that compose the joints and the shear walls of wooden structures have a possibility to deteriorate during the service life of the buildings. And the long term performance of the structures will be governed by the long term performance of the wooden materials and metal connectors composing the structures.

The simplest way to evaluate the performance of the shear walls at certain stages of the buildings' service life is to conduct racking tests on the shear walls extracted from buildings of a certain age. But in reality it is quite difficult to extract a full size shear wall from the existing buildings and subject them to racking tests. For this reason it will be quite helpful if we can estimate the performance of the shear walls from the test results of the composing materials and joints partially extracted from existing buildings.

The object of this research is to evaluate the performance of the shear walls at certain stages of the buildings' service life and review the "Reduction Factors" that are commonly used in the design of the wood frame buildings. Sheathing panels and nails were extracted from wooden existing buildings of certain ages and the extracted sheathing panels and nails were tested for their strength properties. A method to estimate the strength properties of the shear walls from the charasteristics of the nail joints were developed to provide a techinical tool that can help reviewing the currently used "Reduction Factors".



Figure 1. The elevation of the wood frame house.

Note: The areas noted with alphabets shows the location where the wall test specimens and roof test specimens were extracted.

2 EXTRACTIONS OF STRUCTURAL ELEMENTS FROM AN EXISTING BUILDING

Figure 1 gives the elevation of the house that the test specimens were extracted. The house is a wood frame construction single detached house owned by one family and was built in 1979. The test specimens were extracted in 2009 and this means that all the materials extracted have been used for 30 years.

The areas noted with alphabets in Fig. 1 indicate the location where the elements were extracted from the house. Seven exterior walls and two interior walls were extracted from the first floor and six exterior walls, one interior wall and two floor elements were extracted from the second floor. The elements of the attic were also extracted. The sizes of the extracted elements were approximately 840x1500mm or 800x800mm for the wall elements and floor elements and 840x1500mm for the roof elements.

The extracted elements were delivered to the laboratory of the Building Research Institute with care so that the elements would not be damaged during the delivering process. Test specimens for the lateral nail resistance test, nail pullout test and the nail bending test were produced from the extracted elements. In general four test specimens for the lateral nail resistance test and four test specimens for the nail pullout test were produced from one extracted element. And all the nails existing in the extracted elements were removed carefully to test for their bending properties.

3 TESTING METHOD

3.1 Lateral Nail Resistance Test

Figure 2(a) shows the testing method of the lateral nail resistance test. The sheathing materials were cut into the size of 150x75mm. And a nail was nailed at 12mm edge and center of the sheathing materials. The nail was pulled laterally at a loading speed of 1mm/min. The combinations of the type and condition of the sheathing materials and the nails are summarized in Table 1.

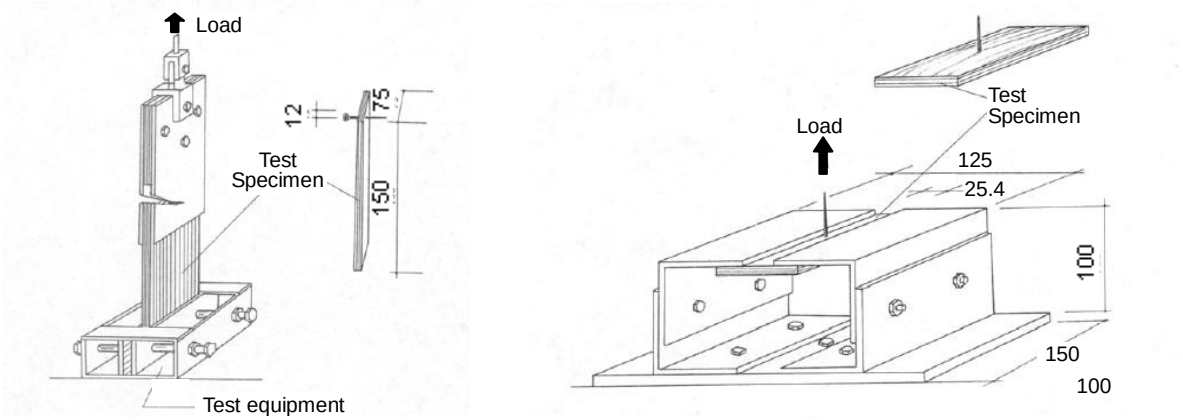

(a) Lateral nail resistance test (b) Nail pullout test

Figure 2. Testing methods for the lateral nail resistance test and the nail pullout test. [Building Research Institute 1975].

3.2 Nail Pullout Test

Figure 2(b) shows the testing method of the nail pullout test. The sheathing materials were cut into the size of 150x75mm. And a nail was nailed at the center of the sheathing materials. The nail was pulled at a loading speed of 1mm/min. The combinations of the type and condition of the sheathing materials and nails are summarized in Table 1.

Table 1. The condition and type of the sheathing materials and nails being tested.

Sheathing materials	Nails
Plywood [1] (Extracted)	CN50 [3] (Virgin)
Plywood [1] (Virgin)	CN50 [3] (Extracted)
Plywood [1] (Virgin)	CN50 [3] (virgin)
Gypsum board [2] (Extracted)	GN40 [4] (Virgin)
Gypsum board [2] (Virgin)	GN40 [4] (Extracted)
Gypsum board [2] (Virgin)	GN40 [4] (Virgin)

Note1: 9mm thick softwood plywood Grade S-2 stipulated in the Japan Agricultural Standard.
Note2: 12mm thick gypsum board (18N/mm^2) stipulated in the Japan Industrial Standard.
Note3: Common nail for wood frame construction stipulated in the Japan Industrial Standard.
Note4: Gypsum board nail stipulated in the Japan Industrial Standard.

3.3 Bending Test of the Nails

The bending properties of the nails were evaluated by the three points bending test. The span of the test was set as 20mm and the loading speed was controlled to 1mm/min. The load and the deflection of the nails were measured. The extracted and virgin nails were tested.

4 TEST RESULTS

4.1 Lateral Nail Resistance Test

The test results of the lateral nail resistance tests are summarized in Table 2 and Table 3. Table 2 gives the test results for the test specimens composed of plywood and nail CN50 and Table 3 gives the test results of for the test specimens composed of gypsum board and nail GN40.

The test results for the test specimens composed of plywood and CN50 can be summarized as follows:
(1) The aged plywood led approximately 20% reduction in the lateral nail resistance.
(2) The aged nails led approximately 15% reduction in the lateral nail resistance.
(3) The stiffness was not reduced either by the aged plywood or the aged nails.

The test results for the test specimens composed of gypsum board and GN40 can be summarized as follows:
(1) The lateral nail resistance and the stiffness were both not reduced by the aged gypsum boards.
(2) The aged nails led 30% reduction in the lateral nail resistance and 35% reduction in the stiffness.

Table 2. The results of the lateral nail resistance test (Plywood and CN50).

Condition of nails Condition of plywood	Virgin Virgin	Virgin Aged		Aged Virgin	
Pmax (N)	1321	1029	(0.78)	1133	(0.86)
Standard Deviation (N)	79.9	108.9		167.5	
COV (%)	6.1	10.6		14.8	
Stiffness (N/mm)	1306	1543	(1.18)	1523	(1.17)
Standard Deviation (N/mm)	176.5	181.6		298.5	
COV (%)	13.5	11.8		19.6	

Note: The values in the parenthesis are the reduction ratio.

Table 3. The results of the lateral nail resistance test (Gypsum board and GN40).

Condition of nails / Condition of gypsum board	Virgin / Virgin	Virgin / Aged		Aged / Virgin	
Pmax (N)	425	425	(1.00)	289	(0.68)
Standard Deviation (N)	33.3	51.3		12.3	
COV (%)	7.8	12.1		4.3	
Stiffness (N/mm)	528	578	(1.09)	337	(0.64)
Standard Deviation (N/mm)	160.5	69.6		45.9	
COV (%)	30.4	12.0		12.6	

Note: The values in the parenthesis are the reduction ratio.

4.2 Nail Pullout Test

The test results of the nail pullout tests are summarized in Table 4 and Table 5. Table 4 gives the test results for the test specimens composed of plywood and CN50 and Table 5 gives the test results of for the test specimens composed of gypsum board and GN40.

Table 4. The results of the nail pullout test (Plywood and CN50).

Condition of nails / Condition of plywood	Virgin / Virgin	Virgin / Aged		Aged / Virgin	
Pmax (N)	1658	1330	(0.80)	1438	(0.87)
Standard Deviation (N)	152.3	106.6		237.5	
COV (%)	9.2	8.0		16.5	
Stiffness (N/mm)	619	651	(1.05)	346	(0.56)
Standard Deviation (N/mm)	88.8	119.7		78.9	
COV (%)	14.4	18.4		22.8	

Note: The values in the parenthesis are the reduction ratio.

The test results for the test specimens composed of plywood and CN50 can be summarized as follows:

(1) The aged plywood led approximately 20% reduction in the nail pullout resistance.
(2) The aged nails led approximately 15% reduction in the nail pullout resistance.
(3) The stiffness was not reduced by the aged plywood.
(4) The aged nails led approximately 40% reduction in the stiffness.

Table 5. The results of the nail pullout test (Gypsum board and GN40).

Condition of nails / Condition of gypsum boards	Virgin / Virgin	Virgin / Aged		Aged / Virgin	
Pmax (N)	337	629	(1.67)	352	(0.93)
Standard Deviation (N)	38.7	46.7		42.6	
COV (%)	10.3	7.4		12.1	
Stiffness (N/mm)	498	484	(0.97)	318	(0.64)
Standard Deviation (N/mm)	91.4	42.2		125.7	
COV (%)	18.3	8.7		39.6	

Note: The values in the parenthesis are the reduction ratio.

The test results for the test specimens composed of gypsum board and GN40 can be summarized as follows:
(1) The aged gypsum boards led approximately 65% increase in the nail pullout resistance.
(2) The aged nails led approximately 5% reduction in the nail pullout resistance.
(3) The stiffness was not reduced by the aged gypsum boards.
(4) The aged nails led approximately 35% reduction in the stiffness.

As it is commonly known that the physical properties of the gypsum board has changed in these 20 years and the currently produced products are rather weaker than the products produced in the past. This may be one reason for the 65% increase in the nail pullout resistance of the aged gypsum boards.

4.3 Nail Bending Test

The test results of the nail bending tests are summarized in Table 6. The test results of the nail bending test can be summarized as follows:
(1) The yield bending strength of the aged plywood nails (CN50) was almost equivalent to that of the virgin nails.
(2) The yield bending strength of the aged gypsum board nails (GN40) was approximately 25% less than that of the virgin nails.
(3) The bending stiffness of the aged plywood nails and the aged gypsum board nails were 2% to 6% less than that of the virgin nails.

Table 6. The results of the nail bending test.

Nail type	CN50			GN40		
Condition of nails	Virgin	Aged		Virgin	Aged	
Py (N)	612.4	618.6	(1.01)	333.4	247.6	(0.74)
Standard Deviation (N)	17.0	17.3		14.0	29.0	
COV (%)	2.8	2.8		4.2	11.7	
Bending stiffness (N/mm)	2046	1924	(0.94)	914	893	(0.98)
Standard Deviation (N/mm)	265	201		103	13.6	
COV (%)	13.0	10.5		11.3	9.8	

Note: The values in the parenthesis are the reduction ratio.

5 SIMULATION OF THE STRENGTH REDUCTION OF SHEAR WALLS DUE TO THE DETRIORATION OF COMPOSING MEMBERS

5.1 Simulation Model and Calculation Method

Several model and calculation methods [for example Tuomi 1978] are developed to predict the strength properties of the shear walls from the strength properties of their composing members. To predict the reduction of the yield strength and stiffness of the deteriorated shear walls the model and calculation method proposed by Hirai [Hirai et.al. 1999] was refered. The simple illustration of the model used for the simulation is given in Fig. 3. In this model the shear deformation of the sheathing panels is considered to be very small and negligible. And the shear deformation of the shear walls is considered to be equivalent to the shear deformation produced by the slip of the nail joints.

The load-slip relationship of the nail joints reported by Nakajima [Nakajima, 2002] was used in the calculation. Figure 4 gives a typical load-slip curve of the CN50 nail joints with no deterioration. A formula that can be generally expressed by Equation 1 was given to model the load-slip curve of the CN50 nail joints. The modeled load-slip curve is shown in Fig. 4 by the broken line. Both the stiffness and the yield strength of the nail joints were reduced to 80% to represent the effect of the

deterioration. The dotted line in Fig. 4 gives the load-slip curve for the deteriorated nail joints. The 80% reduction of the yield strength and stiffness were roughly determined by taking account the test results of the lateral nail resistance tests and the nail pullout tests.

$$P = k_1 \times \ln(1 + d \times k_2) \qquad \text{-----(1)}$$

Where P is load,
d is displacement,
k_1 and k_2 are given constants.

The strength properties of the shear walls were calculated for three different level of deterioration. Level 1 is a deterioration level that the nail joints of the bottom plates are deteriorated. Level 2 is a deterioration level that the nail joints of the bottom plates and bottom half of the studs are deteriorated. And level 3 is a deterioration level that the nail joints of the whole wall are deteriorated. The deterioration levels are illustrated in Fig. 3.

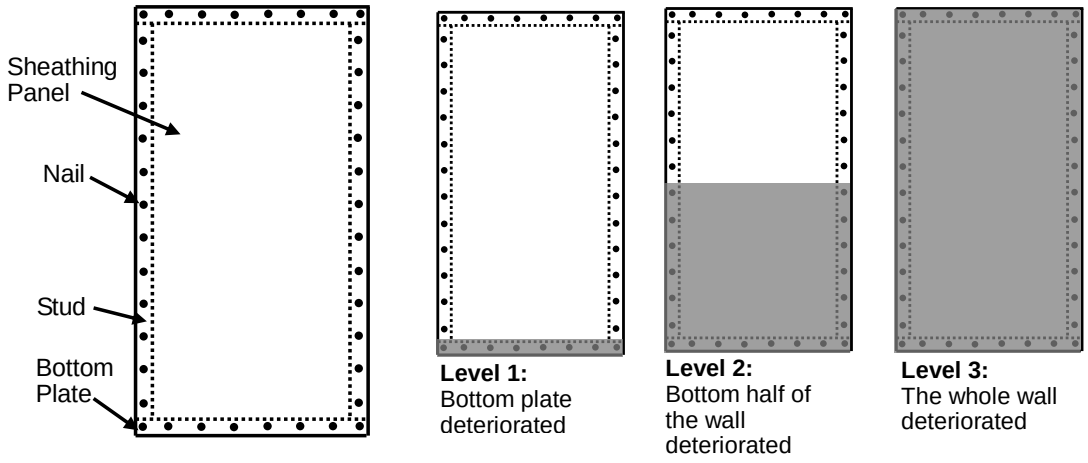

(a) Calculation model. (b) Deterioration levels.

Figure 3. Modeling for the shear walls and the deterioration level.

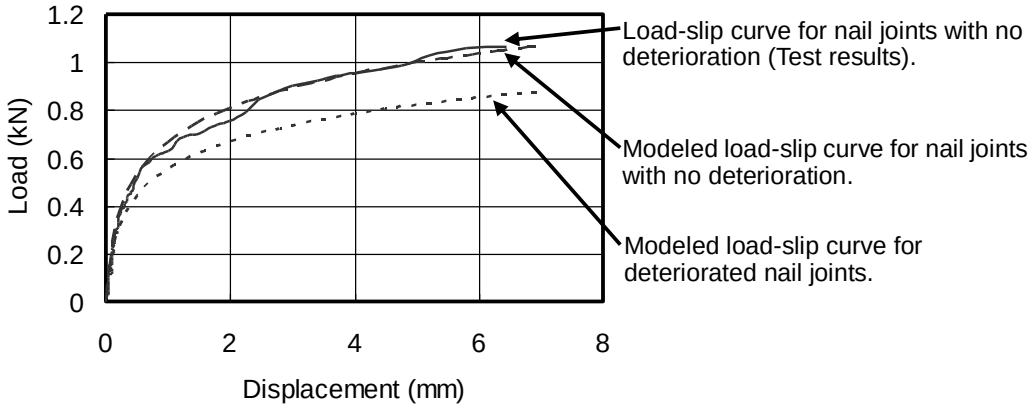

Figure 4. Load-slip curve of the nail joints (CN50).

5.2 Results of the Simulation

The simulated results of the yield strength (*Py*) are summarized in Table 7. The results of the simulation indicates that the deterioration of the bottom plate will cause almost 2% reduction in the yield strength. And the simulation results also indicates that the deterioration of bottom half of the wall will cause almost 10% reduction and the whole deterioration of the wall will cause almost 20%

reduction in the yield strength. It can be said that the proposed model can well estimate the effect of the deterioration of the composing members on the yield strength of the shear wall.

Table 7. Results of the simulation.

	With no deterioration	Deteriorated		
		Level 1	Level 2	Level 3
Py (kN)	5.88 (1.00)	5.78 (0.98)	5.38 (0.91)	4.91 (0.83)

Note: The values in the parenthesis are the reduction ratio.

6 CONCLUSIONS

The sheathing panels and the nails were extracted from a wood frame existing building. The extracted sheathing panels and nails were tested for their strength properties. Some strength properties were reduced by the deterioration of the materials. A calculation model to estimate the strength properties of the shear walls from the strength data of the nail joints were proposed. The calculation model could well represent the effect of the deterioration of the composing members on the yield strength of shear walls. The calculation method can technically support the process of reevaluating the "Reduction Factors" currently used in the structural design of the buildings of wood frame construction. The calculation model can also be a powerful tool for the policy makers when they have to decide the design criteria for the wood frame buildings.

ACKNOWLEDGMENTS

Some of the tests were conducted by Yoshiyasu SHIMIZU a graduated student of Shibaura Industrial University.

REFERENCES

Building Research Institute MOC. 1975, '*Annual Report of the General Technology Development Project – Development of the Construction Methods for the Small Scale Wooden houses*', Building Research Institute MOC.

Tuomi, R.L. and McCutcheon, W.J. 1978, '*Racking strength of light-frame nailed walls*', J. Struct. Div. ASCE. 104[ST7], pp.1131-1140.

Hirai, T. Zhang, T.W. Irie, Y. and Wakashima, Y. 1999, '*Lateral resistance of nailed timber joints with structural wooden panels*', Journal of Japan Wood Science Society, 45[2], pp. 120-129.

Nakajima, S. 2002, '*Evaluation and estimation of the performance of the shear walls in humid climate*', Proceedings of CIB-W18/35-15-3.

XII DBMC
International Conference on Durability of Building Materials and Components
PORTO - PORTUGAL, April 12th-15th, 2011

Hygrothermal Behaviour Testing of External Thermal Insulation Composite Systems with Rendering in Nordic Climate

Toni Pakkala [1]
Jommi Suonketo [2]

ABSTRACT

Finnish weather conditions differ a great deal in contrast to e.g. Central Europe and thus they are very demanding considering building structures. One of the most considerable issues is freeze-thaw cycles which can occur all year round. The biggest problems with freeze-thaw cycles occur while at the same time ambient conditions are wet. That is common in Finland during autumn and spring time when the daytime temperature is slightly above 0 °C and by night below it. Same problems occur on warm winter days.

External thermal insulation composite systems with rendering (ETICS) have been the one of the most used façade structures in Central Europe for decades, nowadays also in Finland when building new residential buildings or renovating old ones. The Guideline for European Technical Approval of External Thermal Insulation Composite Systems with Rendering (ETAG 004) covers a rather wide variety of tests to be used when assessing the fitness of system. However, it does not include any significant frost attack. Instead, frost durability requirements are presented in the form of absorption properties and it also instructs a method for testing hygrothermal behaviour. The latter test includes segregated heat-rain and heat-cold cycles for the wall structure and between those two steps the wall, in practice, dries. That is, however, not a functional method in Finnish weather conditions where freeze-thaw cycles often include wet structures and moist ambient air caused by rain or melting snow. Thus Tampere University of Technology has developed an accelerated weather testing method which includes harder stress cycles than suggested by ETAG 004.

KEYWORDS

Hygrothermal behaviour, Accelerated weather test, External thermal insulation composite systems with rendering, Freeze-thaw durability with moist ambient air.

[1] Structural Engineering, Faculty of Built Environment, Tampere University of Technology (TUT), Tampere, FINLAND, toni.pakkala@tut.fi
[2] Structural Engineering, Faculty of Built Environment, Tampere University of Technology (TUT), Tampere, FINLAND, jommi.suonketo@tut.fi

1 INTRODUCTION

The frost durability of façade structures and materials is very important factor in durability issues especially in countries on cold weather region, such as Finland. Therefore the separate freeze-thaw – tests of single material components and the full-scale rig tests with harsh weather conditions have been commonly conducted when developing new structure types or using new kind of materials in façades.

ETAG 004 recommends testing the Hygrothermal Behaviour (§ 5.1.3.2.1) of external thermal insulation composite systems (ETICS) with rendering after selecting suitable coatings by the Water Absorption test (§ 5.1.3.1). The Hygrothermal Behaviour test is done for a test wall, referred here as a rig, which has a normal rendered external thermal insulation wall structure with a substructure, insulation material and rendering. The minimum dimensions of the rig are specified as 2.50 m wide and 2.00 m high, yet the total surface should be at least 6.00 m². [Anon 2008]

The test includes two different cycles: heat–rain and heat–cold. The heat–rain cycle is repeated 80 times and after at least 48 hours of subsequent conditioning (10 – 25 °C; 50% RH) the heat–cold cycle is repeated 5 times. In the heat–rain cycle the surface of the rig is subjected to a treatment which comprises the following phases:

- h
  eating to 70 ± 5 °C (rise for 1 hour) and maintaining for 2 hours (total of 3 hours)
- s
  praying water (15 ± 5 °C) for 1 hour
- 2
  hours of drainage

Following the heat–rain cycles and the subsequent conditioning, the heat–cold cycle comprises of the following phases:

- h
  eating to 50 ± 5 °C (rise for 1 hour) and maintaining for 7 hours (total of 8 hours)
- c
  ooling to - 20 ± 5 °C (fall for 2 hours) and maintaining for 14 hours (total of 16 hours)

Thus, the test lasts a minimum of 27 days. During the test observations must be done frequently, and any cracking, blistering or peeling of the surface should be recorded. [ETAG 004 2008]

As can be seen the heat–rain and heat–cold cycles are segregated and between them the rig, in practise, dries. In Finland the weather conditions during autumn, winter and spring often include freeze-thaw cycles, sometimes even a few times a day. At the same time with freeze-thaw cycles the structures are often wet because of rain, snow or humidity, thus the wall structure is heavily subjected to frost weathering.

As shown in the Fig. 1, freeze–thaw cycles have occurred between 11 and 38 times (in average 27) annually between 1961 and 2006 based on the data from the Meteorological Institute of Finland. The data includes every occasion when the temperature has dropped below 0 °C not more than three days after raining. Thus the test methods suggested by ETAG 004 are not functional methods in Finnish weather conditions.

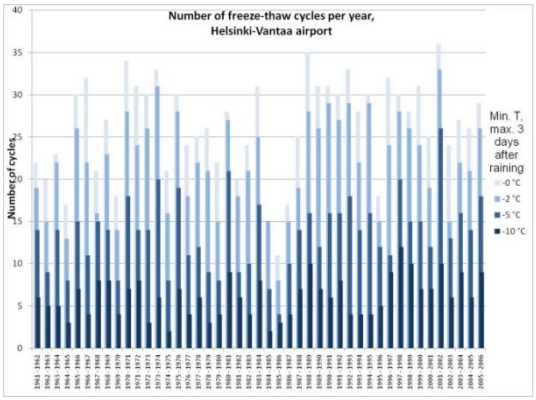

Figure 1. Annual freeze-thaw cycles in Finland between years 1961-2006. The annual data of freeze-thaw cycles contains data between September and April whereupon each bar in the chart is cited with two years.

During last decade most of ETICS systems in Finnish markets have been tested in a Structural Engineering laboratory of Tampere University of Technology with harsh weathering tests, where repeated 8 hour long cycles include freezing to -20°C temperature, fast heating to 60°C and wetting the façade surface with spraying. This 'standardized' Finnish test method includes 100 cycles and the judgment of the tested structure is based on occurred damages and strength tests before and after weathering. The new Finnish national instructions for ETICS will be published shortly. The instructions will involve the requirements of frost durability testing for rendering materials and full façade systems.

Quite often ETICS, especially imported systems, have already been tested according ETAG 004 requirements. However, in some cases the tested structures still have failed and major frost damages have occurred. This paper will present the new Finnish testing instructions and compilation of test results and examples of occurred failures mechanisms.

2 COMBINED HEAT- RAIN AND FREEZE-THAW CYCLES

Department of Civil Engineering at Tampere University of Technology (TUT) has developed a test which includes heavier stress cycles than the test suggested by ETAG 004. In the TUT test heat, rain and cold phases are merged, which is the main difference compared to the ETAG 004 version.

2.1 Stress Cycles

The limit temperatures of the stress cycles are selected to cover normal temperature ranges in Finnish climate conditions: the sun warms the surfaces of houses rarely over 65 °C and at the temperature of -20 °C, the smallest capillary pores in the plaster freeze [Pigeon & Pleau 1995]. The stress cycles have three phases as shown in Fig. 2:

- s
  praying water (15 ± 5 °C) for 1 hour
- c
  ooling to - 20 ± 5 °C as fast as possible and maintaining, total 4 hours
- d
  irect heating to 65 ± 5 °C as fast as possible and maintaining, total 3 hours

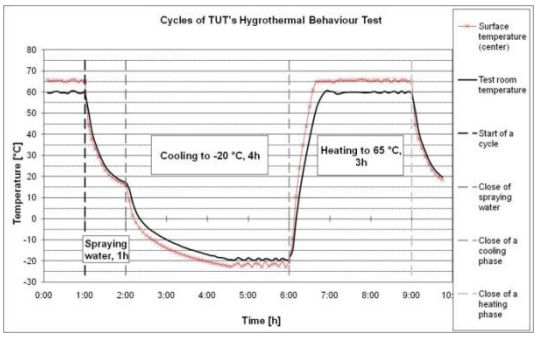

Figure 2. The chart demonstrates a progress of a cycle of the TUT Accelerated Weather Test. When the warm phase of the former cycle ends cools the sprayed water the rig surface near 15 °C.

The rendering of the rig is usually made by the manufacturer of the render product or other qualified worker so that the quality of the work is ensured. The external structure of the rig can also be bisected in the middle so that both sides have a different coating, e.g. different render products. If a fault situation is aspired to be studied, a self-imposed discontinuity, e.g. a horizontal crack can be made on the coating. That should be done to be on the safe side because outcome of the rendering work is rarely perfect throughout a whole building. The discontinuity should be made at the bottom part of the rig, therefore the other parts will not sustain damages.

2.2 Weather Test Apparatus

The test apparatus is 3 m wide, 6 m long and 2 m high box which has EPS insulation. The rig is positioned in the middle so that an outdoor condition and an indoor condition rooms are equal. Within 1 m from the rig are positioned 16 water nozzles and 6 infrared heaters as can be seen in the Fig. 3. They are directed so that the nozzles spray water all over the surface of the rig and the heaters could warm the surface as evenly as possible.



Figure 3. The water nozzles and infrared heaters photographed from the rig. A cooling cell can be seen hanging from the ceiling.

3 SURVEILLANCE DURING THE CYCLES AND FINAL TESTS

Observation methods and final testing of the test rig are basically the same as ETAG 004 [Anon 2008] suggests.

3.1 Observations During the Test

The rig should be examined visually each working day and the progress of visual cracks should be recorded. The rendered surface can be inspected more thoroughly at least once a week e.g. by knocking the rendered surface with hard and light object avoiding to cause damages to find out if rendering has peeled.



Figure 4. The damages on the rendered surface may vary between barely visible cracks and large scale blistering.

In Fig. 4 the failure in the left picture was caused by insufficient work with reveal of a window which necessitated peeling of the rendering. On the right picture is shown blistering of rendering, diameter of 50 mm, outlined with marker. Blistering was caused by large-scale temperature deformation of an insulation material in contrast to rendering.

3.2 Observations After the Test

As the test has come to an end the rig is left to dry for a week in normal room conditions. The rig may be studied more closely during drainage. E.g. an extent of frost weathering of the rendering may not always appear during the test as shown in Fig. 5. After the drying, sections containing cracks or blistering can be removed to observe better water penetration i.e. penetration depth of cracks in rendering.

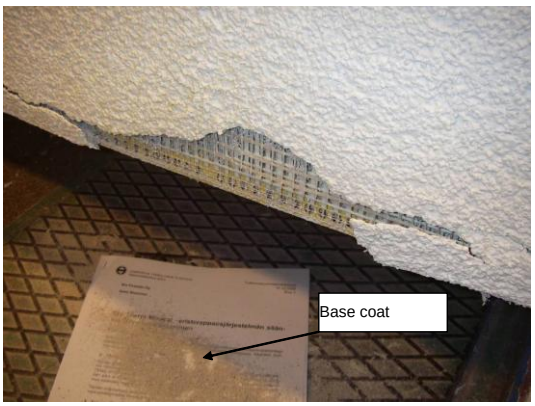

Figure 5. The base coat underneath the fairly good looking finishing coat had pulverized and fell down as the finishing coat was tapped with fingers.

3.3 Final Tests on the Rig

Final tests include bond strength test (§ 5.1.4.1. on ETAG 004) and impact resistance test (§ 5.1.3.3.1. on ETAG 004) [Anon 2008]. For both tests it is recommended to have non-stressed comparison specimens which should have the same structure as the rig.

3.3.1 Bond strength test

Bond strength test after the stress cycles determines the bond between a base coat and an insulation material. Number of tests is usually 6 per structure and test places should locate on undamaged area. However, if needed more tests can be made and locations vary e.g. near the self-imposed discontinuity cracks. Thus, the effect of water penetration in contrast to an undamaged surface can be determined.



Figure 6. Bond strength testing machine. The wooden tensile pieces are glued on the surface with two-component polyurethane glue.

3.3.2 Impact resistance test

The impact resistance is tested by hard body impact tests with a steel ball. The 3 and 10 joule impact tests are conducted for each structural variation (6 impacts / series / structure). The results of individual impacts are assessed visually on the basis of cracks appearing on the surface. In unclear cases a section of the thin rendering is removed and the backside is inspected for damage. The degree of the damage is divided in three categories I, II and III. Demands of each category are specified in ETAG 004 [Anon 2008].



Figure 7. An example of an unsatisfactory result on impact resistance test.

3.4 Experiences

It should be noted that the Accelerated Weather Test is very demanding for the ETICS with rendering. Thus, Experiences during the last 25 years of accelerated weather testing have shown that in Finnish climate conditions the heavy stress testing method is needed to assure frost resistance of ETICS. Often the system may have passed the requirements of ETAG 004 yet still have failed relatively fast on the real outdoor climate. Figures 8, 9 and 10 show typical failures that have occurred with ETICS in Finland.



Figure 8. Large scale frost damage and blistering on the wall of a three years old building with ETICS.



Figure 9. Heavy frost weathering on the base coat after a TUT test.

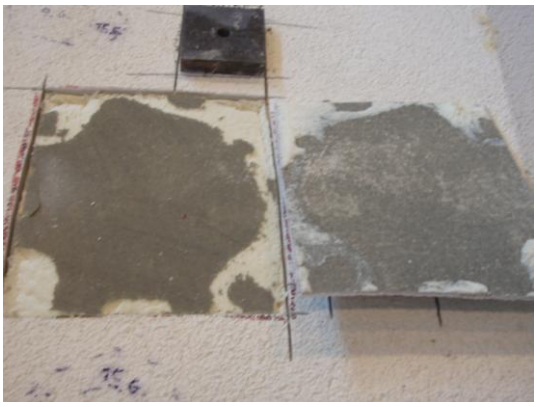

Figure 8. Different temperature deformation rates between a rendering and rigid insulation may also be critical for bond and thus cause blistering while temperature can vary annually between -30 – 65°C. On the picture is shown bond failure between primer and base coat under a blister.

4 CONCLUSIONS

The ETICS tested according ETAG 004 has failed in several cases within few years after construction in Finland. The failures have occurred due to harsh climate conditions in Nordic weather region which has not been taken into account on the testing guidelines for the ETICS given in ETAG 004. The most significant issue is that it does not include any significant frost attack. Instead, frost durability

requirements are presented in the form of absorption properties. Thus the methods described on ETAG 004 give insufficient proof of durability for ETICS used in Nordic climate.

Tampere University of Technology has developed an accelerated weather test to substitute the Hygrothermal Behaviour and Water Absorption tests to cover the both frost durability and hygrothermal testing at the same time. The accelerated weather test is done for a wall which has 6 m² surface area. The test includes 100 repeated 8 hour lasting cycles. Every cycle consist of spraying water on the surface of the wall for an hour, rapid exposure to freezing temperature (-20 °C) for 4 hours and heating to 60 °C for 3 hours. In consequence long-term frost durability combined with hygrothermal behaviour of the wall structures can be assured.

Due the problems especially with the frost durability of the ETICS in Finland, they should always be tested with the full scale tests. Therefore in presently forthcoming new Finnish guideline for ETICS both the accelerated weather test and direct freeze-thaw test for mortars are required.

REFERENCES

ETAG 004 2008, 'Guideline for European Technical Approval of External Thermal Insulation Composite Systems With Rendering'. European Organisation for Technical Approvals, Brussels. June 2008, 144 p. + app. 29 p.

Pigeon, M. & Pleau, R. 1995. 'Durability of Concrete in Cold Climates'. London, E & FN Spon, 244 p.

XII DBMC
International Conference on Durability of Building Materials and Components
PORTO - PORTUGAL, April 12th-15th, 2011

Durability of Nano-based Treated Wood Exposed to Accelerated Weathering

Selamawit Mamo Fufa [1]
Per Jostein Hovde [2]
Bjørn Petter Jelle [3]
Per Martin Rørvik[4]

ABSTRACT

Wood is a widely used material for the building and construction industries due to a number of its favorable qualities. However, wood is also sensitive to weathering factors which cause degradation. Nano-based modifications are new approaches aiming to overcome the drawbacks of wood and extend its service life, especially when it is used for outdoor applications. The unique properties of nanomaterials derived from their small size and high surface area have a great potential to improve important wood properties. In this study, spruce and pine wood species were treated with nano titanium dioxide and nanoclay based coatings and impregnation. The specimens were exposed to various accelerated weathering tests and the surface changes were investigated by colour measurements, and Fourier transform infrared characterization methods. From the test results, the durability of nano-based treated wood used in exterior claddings was assessed.

KEYWORDS:

Wood, Exterior claddings, Nanotechnology, FTIR, Accelerated weathering tests, Colour measurement.

[1]Norwegian University of Science and Technology (NTNU),Department of Civil and Transport Engineering, Trondheim, Norway, selamawit.fufa@ntnu.no
[2]Norwegian University of Science and Technology (NTNU), Department of Civil and Transport Engineering, Trondheim, Norway, per.hovde@ntnu.no
[3]SINTEF Building and Infrastructure, Department of Material and Structures, Trondheim, Norway bjorn.petter.jelle@sintef.no and Norwegian University of Science and Technology (NTNU), Department of Civil and Transport Engineering, Trondheim, Norway, bjorn.petter.jelle@ntnu.no
[4] Norwegian University of Science and Technology (NTNU), Department of Materials Science and Engineering, Trondheim, Norway, per.martin.rorvik@sintef.no

1. INTRODUCTION

Wood is composed of natural polymeric materials, including cellulose, hemicelluloses, lignin and extractives, which are subject to changes undergoing during its exterior application. Different environmental factors such as rain, solar radiation and temperature are ageing mechanisms that contribute to physical and chemical changes in wood; described as weathering. Weathering initially leads to fast colour change followed by large chemical modification and breakdown of the surface layer [Rosu et al. 2010]. In addition to the weathering conditions, the rate of degradation can also be dependent on the type of wood (soft or hardwood) [Anderson et al. 1991a; Anderson et al. 1991b].

There have been different studies which give an overview of the mechanisms of wood weathering [Anderson et al. 1991b; Colom et al. 2003; Pandey 2005; Rowell 2005].They clearly described that decrease in lignin content and chemical modification due to bond breakage in cellulose occur as a consequence mainly due to the combination effect of sunlight (UV radiation) and water. The colour and chemical changes were commonly identified by using colour measurements and FTIR analysis, respectively.

Wood treatments have a long history of use towards overcoming wood degradation from weathering when exposed to harsh exterior environments [Hill 2006]. However, these treatments may only be effective over the short term effect or contain hazardous chemicals. The growing interest towards improving the durability and sustainable utilization of wood in buildings urges the development of new wood treatment technologies. Nanotechnology becomes one of those treatment options widely used in current wooden buildings [Fufa and Hovde 2010]. The unique properties of nano-based materials derived from their small size and high surface area have a great potential to improve wood properties.

In order to investigate the performance of the treatments, wooden claddings should be subjected either to natural outdoor exposure or accelerated weathering tests prior to their utilization. Accelerated ageing has advantages over natural exposure as it is reproducible, controllable and may simulate the rate of degradation and long term effect of treatments within a short time period.

Fourier transform infrared (FTIR) spectroscopy is a very useful tool for obtaining information about the structure of wood constituents and chemical changes taking place in wood due to various treatments. Several studies have been carried out on identification of colour and chemical changes in wood caused by weathering [Jelle et al. 2008; Pandey 1999; Rosu et al. 2010; Temiz et al. 2007]. The effect of weathering at the surface of treated wood samples has been studied and it is observed that better performances of modified specimens are obtained as compared to untreated ones.

In this study, conventional and nano titanium dioxide and nanoclay based impregnated wood specimens used for exterior claddings were tested. The changes undergone by the treated specimens were studied upon exposure of the specimens to an accelerated ageing test. The colour and structural changes that take place due to different treatments and environmental exposure conditions were characterized by colour measurements and FTIR spectroscopy.

2. EXPERIMENTAL

2.1 Overview of the Overall Study

The results presented in this paper are part of an ongoing and broad study where the effect of nano-based treatments on exterior wooden claddings exposed to artificial weathering is being assessed. Spruce and pine wood species were treated with a commercially obtained water based coating, stain and preservatives both alone and modified with nanoclay (hydrophilic bentonite) and titanium dioxide nanoparticles (rutile type). The effects of weathering on treated specimens were tested in laboratory using a vertical accelerated climate simulator and an Atlas SC600 MHG Solar Simulator. In the Atlas Solar Simulator, the specimens were exposed to solar radiation and water spray. The exposure

condition can be determined based on the required test. Detail description of this apparatus is given in section 2.3 below. Here, only the results from impregnated spruce aged in the Atlas Solar Simulator are presented, the remaining results will be presented elsewhere.

2.2 Test Specimens

Norway spruce (Picea abies) with planed surface was used for easy measurement of the colour and gloss of the specimens. Before finishing, the test specimens are sawn to 10 cm width × 20 cm length × 1 cm thickness. All specimens were preconditioned at (20 ± 2) ^{o}C and (65 ± 5) % relative humidity (RH) based on ISO 554 standards. In addition to the reference untreated specimens, specimens were impregnated with preservative (labeled as Wnt) modified with 1% nano titanium dioxide , 1% nanoclay and a combination of nano titanium dioxide and nanoclay each with 1% . Treatments were mixed with 1% of the nanoparticles in order to see the performance of low concentrated nanoparticles on the overall wood properties. Each type of treated wood was represented by three series specimens. An overview of types of treatments is given in Table 1 below.

Table 1. Type of treatments used to modify spruce in this study

No	Treatment type	Abbreviation
1	Untreated	U
2	Wnt	W
3	Wnt modified with nanoclay	WNC
4	Wnt modified with nano titanium dioxide	WNT
5	Wnt modified with both nano clay and nano titanium dioxide	WNCT

2.3 Accelerated Ageing Tests in Atlas Solar Simulator

Accelerated ageing laboratory test was performed in Atlas SC600 MHG Solar Simulator with 2500 W metal halide global (MHG) lamp giving a solar radiation intensity at the specimen surface 55 cm below the climate chamber glass ceiling at 100% lamp power (applying no external lamp filters). The exposure was performed by cycles of 20 h solar radiation at 63 ^{o}C and 50 %RH followed by 4 h water spray at 10 ^{o}C and 100 % RH. The water nozzles located at each side of the apparatus sprayed a total of 1 l/h. In every 24 h cycle, the exposure duration consisted of 4 ageing cycles each with 5 h solar radiation and 1 h water spray. Colour and chemical changes of the specimens were monitored by taking out the specimens at regular intervals. The results from up to 336 h exposure are presented in this paper.

2.4 Colour Measurements

Colour changes of the specimens were easily determined by using CIEL*a*b* colour scale method. The *L**, *a** and *b** colour parameters of the specimens before and after ageing were recorded using Mercury 3000 colorimeter with D65/10° light source. The two numbers in D65/10° describe the angle of illumination and method of view or the angle at which the detector receives the reflected light. The measurements were taken at three points for each of the parallels and the average values are presented in this paper.

The *L**, *a** and *b** parameters are also used to determine the total colour change, ΔE, as a function of irradiation time, using the following equation:

$$\Delta E = \sqrt{(L_2^* - L_1^*)^2 - (a_2^* - a_1^*)^2 - (b_2^* - b_1^*)^2} \quad (1)$$

where L_1*, a_1* and b_1* are the colour coordinates of the specimens before ageing and L_2*, a_2* and b_2* are values after ageing. The *L* parameter stands for lightness where the value of the change in ($\Delta L^* = L_2^* - L_1^*$) vary from 0 (black) to 100 (white). For the chromatic coordinates, a positive value of

$\Delta a^* = a_2^* - a_1^*$ shows a red shift, and a negative value shows a green shift on the green-red scale, while positive value of $\Delta b^* = b_2^* - b_1^*$ illustrates yellow shift and a negative value shows a blue shift on the blue-yellow scale.

2.5 FTIR Spectroscopy

FTIR spectroscopy of the specimens was performed with a Thermo Nicolet 8700 FTIR spectrometer equipped with a horizontal attenuated total reflectance (ATR) accessory designed for single reflection. The ATR crystal is made of diamond due to the high refractive index and the excellent chemical and physical properties of diamond. Smaller wood specimens (chips) can be put into intimate contact with the sampling area through high pressure clamping. This yields high quality and reproducible spectra in the wavelength range from 4000 cm^{-1} to 400 cm^{-1} at spectral resolution of 4 cm^{-1} and 32 scans. Three FTIR spectra per each specimen were documented to increase the accuracy of the results by getting a satisfactory contact between the ATR diamond crystal and the specimen. The bands in the FTIR spectra of the specimens were assigned based on data available in literature [Pandey 1999; Pandey and Pitman 2003; Rowell 2005; Temiz et al. 2007].

3. RESULTS AND DISCUSSION

The colour changes of the specimens following the accelerated weathering process reflect the chemical changes that occurred in wood components due to photodegradation. Lignin is the wood component that is most susceptible for photodegradation due to its good light absorbing properties [Pandey 2005]. The colour of both treated and untreated wood changes rapidly during the first 100 h of exposure and is then reduced with an increase in exposure time. This is indicated in Figure 1, showing the lightness change (ΔL^*), green-red coordinate (Δa^*) and blue-yellow coordinate (Δb^*) upon exposure.

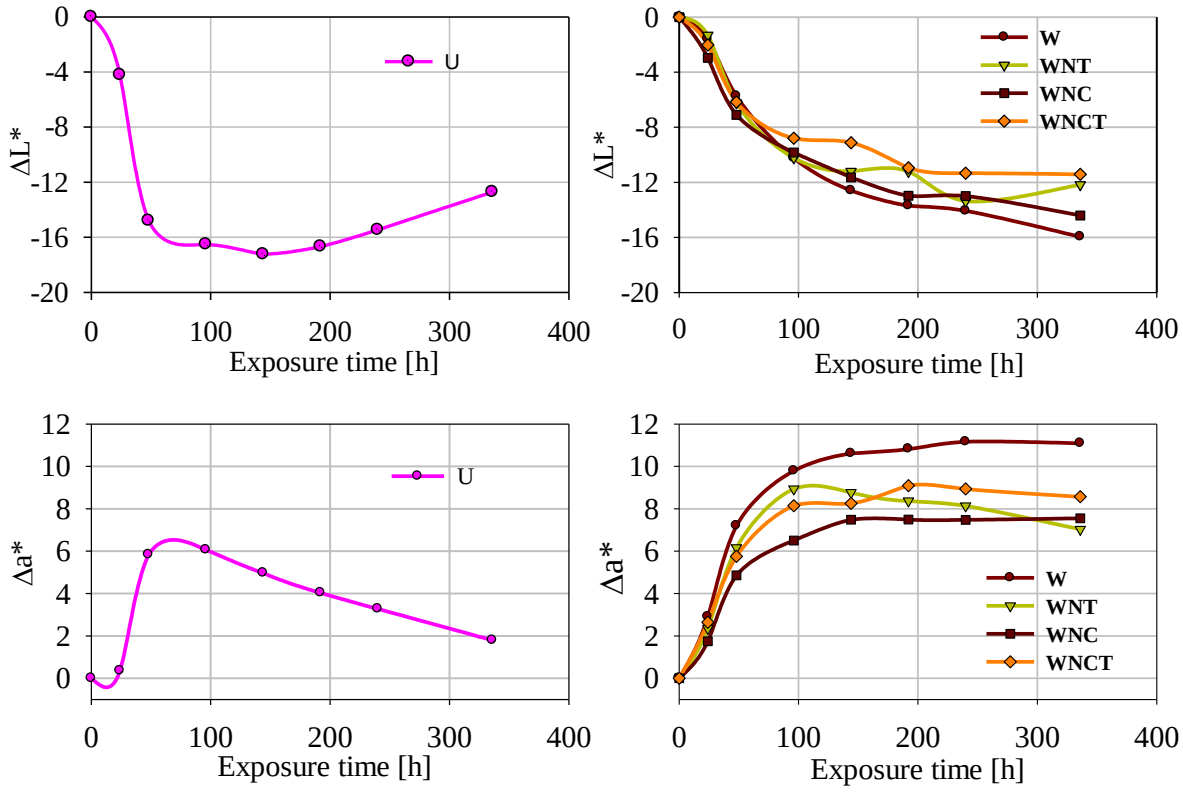

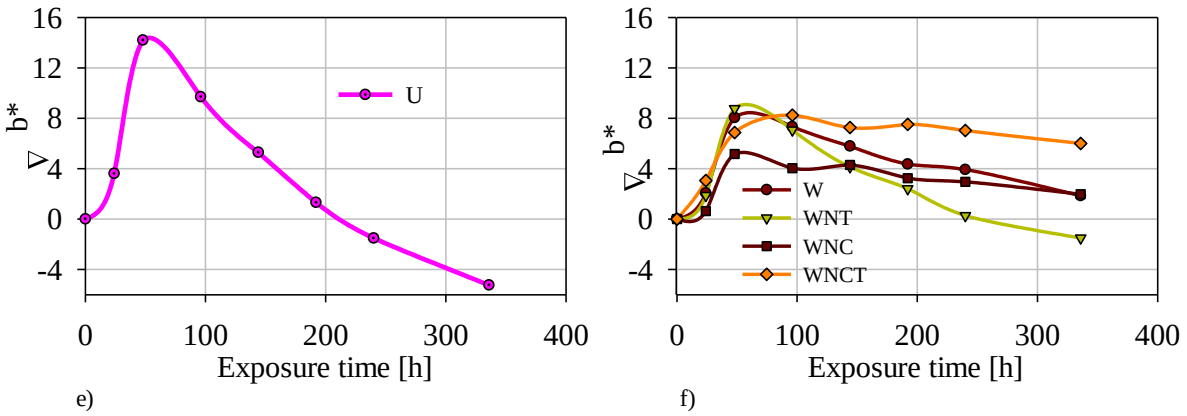

Figure 1. Colour coordinates Δ*L** (a & b), Δ*a** (c & d) and Δ*b** (e & f) for untreated and impregnated specimens aged in Atlas Solar Simulator.

During artificial weathering, the colour of the surfaces changes rapidly from light to dark represented by decrease in the value of Δ*L** and increase in Δ*b** and Δ*a** values upon exposure. Initially, Δ*b** (yellowness) increases much more quickly than Δ*a** (redness) with exposure time. After attaining the maximum value, Δ*b** decreases again to lower values than for Δ*a**.The negative value of Δ*L** shows that surface becomes darkened with increase in exposure and this can be due to degradation of lignin.

For both treated and untreated wood the lightness changes were rapid in the first 48 h of exposure while all impregnated specimens reduce the change by about a half during the same period of exposure. For untreated specimens, the rapid reduction in the change of lightness continued up to 144 h and then the lightness increased significantly through the rest of the exposure. However, the colour of the untreated specimens changed appreciably and faded. For the treated wood the lightness decreased with increasing exposure. For two of the specimens exposed for 336 h the lightness even decreased to below the value for untreated specimen. For specimens treated with nanoparticles combined with preservative the colour change is delayed more than for the ones treated with preservative alone.

The total colour change illustrates the colour change upon exposure due to the modification of wood constituent polymers (mainly lignin). Table 2 shows the total colour change *(*Δ*E*) of both treated and untreated wood specimens during the short time of exposure to high intensity irradiation. Although Δ*E* decreases with increasing of exposure period for both untreated and treated wood, the highest discoloration rate was observed in untreated wood in the early exposure period. Untreated wood shows higher increase at the initial stage of exposure followed by reduction with increase in exposure time. Treated specimens show significant colour change reduction.

Table 2. Overall colour change *(*Δ*E*) of aged specimens at different exposure period.

Treatment	Exposure time [h]						
	24	**48**	**96**	**144**	**192**	**240**	**336**
U	6.40	20.9	20.5	18.5	17.3	15.8	13.2
W	3.90	12.2	16.0	17.5	18.0	18.4	19.5
WNT	3.29	12.4	15.3	14.8	14.2	15.7	14.1
WNC	3.50	10.0	12.5	14.5	15.3	15.3	16.4
WNCT	4.52	10.9	14.6	14.3	16.1	16.1	15.5

FTIR spectra of untreated and treated specimens exposed to the Atlas Solar Simulator before and after artificial weathering are presented in Fig. 2-6. In these figures only the results from the "finger print" regions, 1800-800 cm^{-1}, are presented, as most of the changes occur in this region due to the presence of various functional groups. Photo-induced degradation causes changes in the chemical composition of the functional groups mainly at transmittance peaks located around 1740 cm^{-1} (arise from C=O stretching in hemicelluloses), 1620 cm^{-1} (due to stretching of conjugated C=C attributed to lignin), 1508 cm^{-1} (due to C=C stretching of lignin) and 1261 cm^{-1} (C-O stretching vibration in lignin and hemicelluloses) [Jelle et al. 2008; Pandey 1999; Pandey 2005; Pandey and Pitman 2003; Temiz et al. 2007]. Most of these bands probably have contributions from cellulose, hemicelluloses or lignin.

Although the above mentioned peaks also appear in the result of this study, the peaks around 1510 cm^{-1} shows significant change and are thus presented here. The reduction in the absorption peak around 1510 cm^{-1} arises from C=C stretching frequency shows the formation of carbonyl groups and lignin degradation [Prakash and Mahadevan 2008]. The rate of degradation of untreated specimens is greater than that of treated specimens in this region. Specimens treated with WNT and WNC show delay in the reduction of this degradation. Note that the ageing process decreases the absorbance peak around 1510 cm^{-1} which may be partly masked or hidden by some of the treatments, i.e., especially the WNCT treatment as shown in Fig. 6. As a result it is difficult to describe the spectra of these treatments, i.e. compare the fresh (non-aged) absorbance peaks at around 1510cm-1 for all five samples (Figs. 2-6). Since the nanoparticles are small they can easily disperse into the wood structure and thereby strengthen the mechanical stability and hinder cracking, and thus reduce the degradation of wood components. Additionally, the titanium dioxide nanoparticles can absorb and reflect the incoming light, preventing light to degrade, for instance, lignin. Further studies are in progress to understand the effect of the nanoparticles on the wood properties.

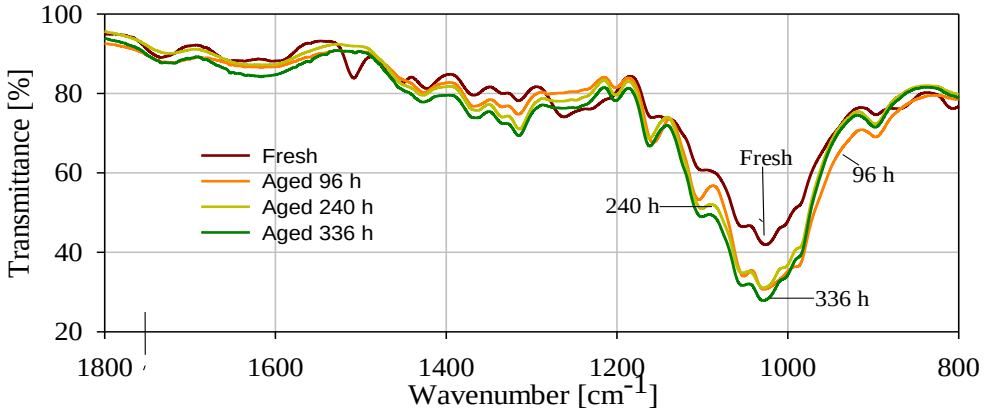

Figure 2. FTIR spectra of untreated spruce before and after exposure in Atlas Solar Simulator

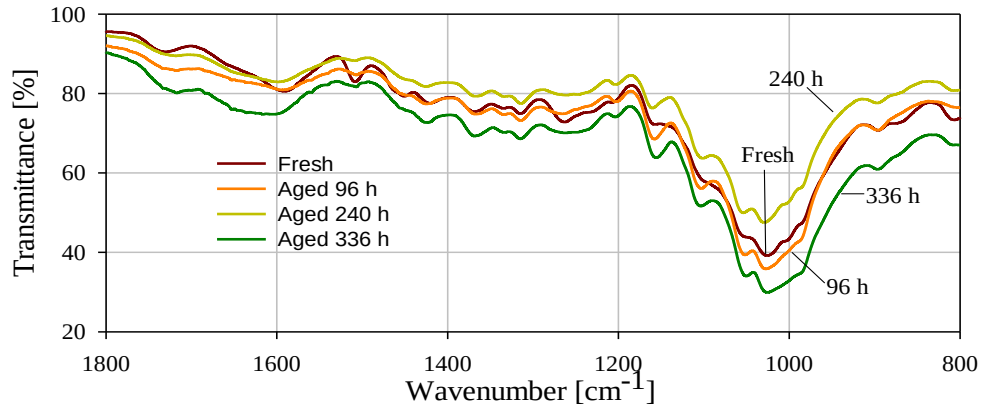

Figure 3. FTIR spectra of spruce impregnated with preservative (W) before and after exposure in Atlas Solar Simulator

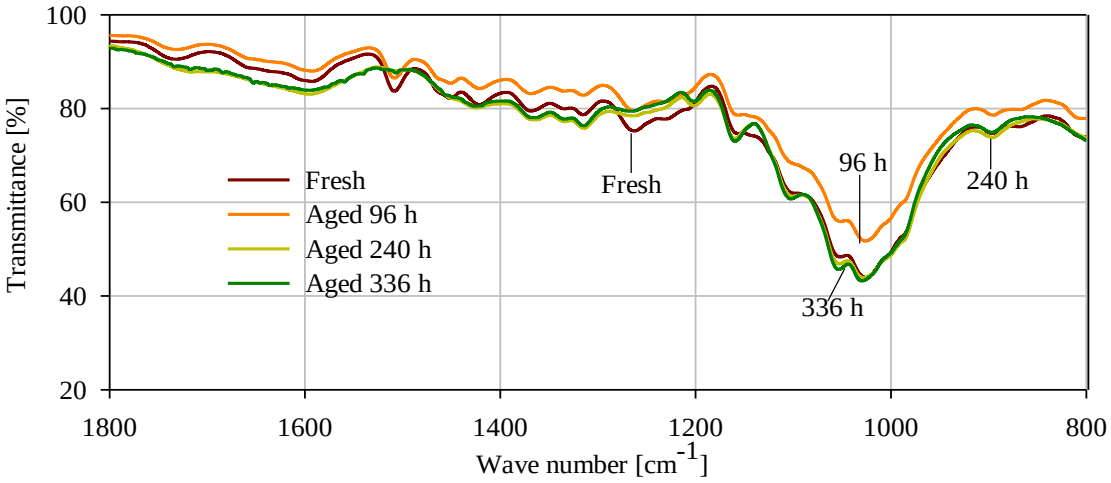

Figure 4. FTIR spectra of spruce impregnated with preservative and nano titanium dioxide (WNT) before and after exposure in Atlas Solar Simulator

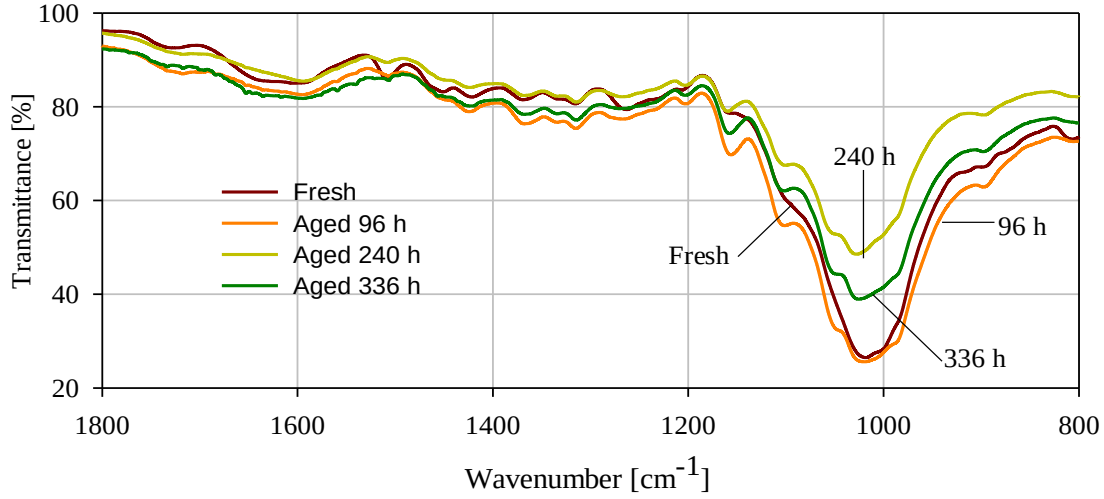

Figure 5. FTIR spectra of spruce impregnated with preservative and nanoclay (WNC) before and after exposure in Atlas Solar Simulator.

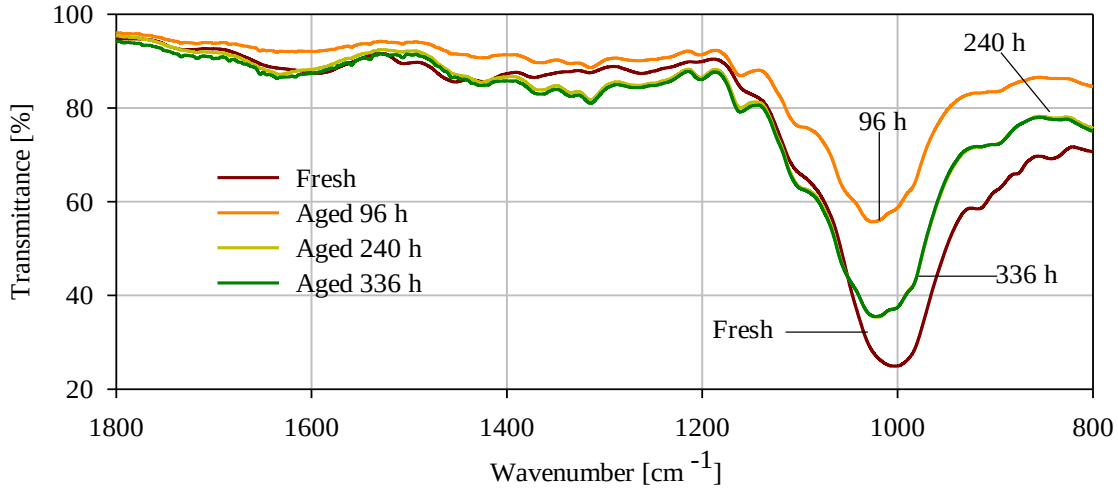

Figure 6. FTIR spectra of spruce impregnateda mixture of preservative, nano titanium dioxide and nanoclay (WNCT) before and after exposure in Atlas Solar Simulator.

4. CONCLUSION

Accelerated ageing tests are useful to assess the degradation of wooden claddings coated with new types of paint before their real application. In this work, the effects of weathering on both untreated and treated specimens were studied. The results of colour measurements illustrate significant colour changes of untreated specimens especially at initial stages of exposure. Although the colour of treated specimens is also changed with increase in the exposure period, the treatments help to delay the colour changes significantly. FTIR analysis also confirmed that the effect of weathering on lignin degradation is less pronounced in treated wood specimens than that of untreated specimens. Specially, specimens treated with a preservative containing nano titanium dioxide and nanoclay show better protection of the specimens against weathering effects.

ACKNOWLEDGEMENTS

The authors would like to acknowledge Moelven Wood and Jotun AS for providing materials and many helpful discussions; Erik Larnøy, Andreas Treu and Britta Witt of the Norwegian Forest and Landscape Institute for their support in impregnation and to Ole Aunrønning for assistance with various laboratory tasks. The financial support by the Research Council of Norway is also gratefully acknowledged.

REFERENCES

Anderson, E.L., Pawlak, Z., Owen, N.L. & Feist, W.C. 1991a, Infrared studies of wood weathering. Part II: Hardwoods, *Applied Spectroscopy*, 45, 648-652.

Anderson, E.L., Pawlak, Z., Owen, N.L. & Feist, W.C. 1991b, Infrared studies of wood weathering.Part I: Softwoods, *Applied Spectroscopy*, 45, 641-647.

Colom, X., Carrillo, F., Nogués, F. & Garriga, P. 2003, Structural analysis of photodegraded wood by means of FTIR spectroscopy, *Polymer Degradation and Stability*, 80, 543-549.

Fufa, S.M. & Hovde, P.J. 2010, Nano-based modifications of wood and their environmental impact: Review, World Conference On Timber Engineering, Riva del Garda, Trentino, Italy, 24-26 June 2010, pp 1093-1094.

Hill, C. 2006, *Wood Modification: Chemical, Thermal and Other Processes*, John Wiley & Sons Ltd, Atrium/Southern Gate/Chichester.

Jelle, B.P., Ruther, P., Hovde, P.J. & Nilsen, T.-N. 2008, Attenuated Total Reflectance (ATR) Fourier Transform Infrared (FTIR) Radiation Investigations of Natural and Accelerated Climate Aged Wood Substances, Istanbul,Turkey.

Pandey, K.K. 1999, A study of chemical structure of soft and hardwood and wood polymers by FTIR spectroscopy, *Journal of Applied Polymer Science*, 71, 1969-1975.

Pandey, K.K. & Pitman, A.J. 2003, FTIR studies of the changes in wood chemistry following decay by brown-rot and white-rot fungi, *International Biodeterioration & Biodegradation*, 52, 151-160.

Pandey, K.K. 2005, Study of the effect of photo-irradiation on the surface chemistry of wood, *Polymer Degradation and Stability*, 90, 9-20.

Prakash, G.K. & Mahadevan, K.M. 2008, Enhancing the properties of wood through chemical modification with palmitoyl chloride, *Applied Surface Science*, 254, 1751-1756.

Rosu, D., Teaca, C.-A., Bodirlau, R. & Rosu, L. 2010, FTIR and color change of the modified wood as a result of artificial light irradiation, *Journal of Photochemistry and Photobiology B: Biology*, 99, 144-149.

Rowell, R.M. 2005, *Handbook of Wood Chemistry and Wood Composites*, CRC Press, Florida.

Temiz, A., Terziev, N., Eikenes, M. & Hafren, J. 2007, Effect of accelerated weathering on surface chemistry of modified wood, *Applied Surface Science*, 253, 5355-5362.

XII DBMC
International Conference on Durability of Building Materials and Components
PORTO - PORTUGAL, April 12th-15th, 2011

Minimum Criteria for Durability Evaluation of Unplasticized PVC Building Products, for Outdoor Applications

Vera Fernandes Hachich[1]
Vahan Agopyan [2]

ABSTRACT

A method is proposed for durability evaluation of unplasticized PVC building products in use for outdoor applications. The method relies on accelerated weathering of PVC specimens in a fluorescent ultraviolet-condensation apparatus (QUV). The procedure is validated by comparison of 3000 h of QUV exposure to five years of outdoor exposure in Piracicaba, SP. Physical and chemical properties of nineteen compounds were compared. Impact modifiers, stabilizers and pigment content (titanium dioxide) varied among those base formulations. Analysis of the influence of each of these variables, for both weathering conditions, led to quantitative criteria for rejection of inadequate compounds, based upon the initial value and the rate of decrease of the Charpy impact strength, as determined after 2000 h of QUV exposure.

KEYWORDS

PVC; Plastics, Durability; uPVC profiles; PVC formulation.

[1] Technical Manager, TESIS – Tecnologia e Qualidade de Sistemas em Engenharia S/C Ltda; PhD in Civil Engineering, Polytechnic School of the University of São Paulo - EPUSP, 1999; MSc, EPUSP, 1991; Civil Engineer, EPUSP, 1984 São Paulo, SP, BRASIL, vera@tesis.com.br

[2] Provost for postgraduate studies, since 2009; Director of Polytechnic School of University of São Paulo, 2002-2006; Professor of materials, EPUSP, 2000; Associate Professor of building Materials, 1998; PhD in civil engineering by University of London, 1982; MSc, EPUSP, 1979; Civil engineer, EPUSP, 1974. vahan.agopyan@poli.usp.br

1 INTRODUCTION

The use of rigid, unplasticided, PVC (uPVC) profiles for windows and external sidings is just starting in Brazil. Lack of information on the material behaviour during its lifetime when subjected to solar radiation and temperatures prevalent in Brazil, is one of the main factors that has hindered the commecial growth of uPVC in the construction market. This study helps address this issue.

2 METHODOLOGY

2.1 Experiment Planning

Durability of white extruded uPVC was assessed by means of results from Charpy impact resistance tests. Samples were cut from uPVC profiles and were exposed to natural weathering conditions, at an angle of 45 degrees north, in accordance with the ASTM D1435 Standard (1994) for periods of up to five years. The natural weathering station is located in the city of Piracicaba, State of São Paulo, Brazil (lat. 22º43' South, long. 47º25' West; 580 m a.s.l.).

In order to reduce statistical uncertainty, tests were performed on ten specimens for a given set of conditions and the average value was calculated to represent the measured properties (BS 7413, 1994 and ASTM D256, 1984). Thus, the value of the Charpy impact resistance of a given formulation, after a given exposure period, for example, is the average of the breaking energy of ten specimens.

2.2 Selection of Formulations to Natural Weathering

The resistance to aging due to weathering effects and in particular those as a result of solar radiation is central to the long-term performance of PVC windows. Resistance of a compound formulation to the effects of weathering is therefore an extremely relevant property to predict. White profiles were selected for the experiment because, being pigmented with titanic dioxide, they usually exhibit better durability irrespective of weather conditions. Four different impact modifiers, then in use in Brazil (1988), were used in the experiment. These were: acrylic (ACR), chlorinated polyethylene (CPE), acrylonitrile-butadiene-styrene (ABS), and metacrylate-butadiene-styrene (MBS). Some of those modifiers are still (2010) the most widely used in Brazil. Four different sets of thermal stabilizers were analyzed: a complex of lead, barium and cadmium (Pb/Ba/Cd), lead (Pb), a complex of barium and cadmium (Ba/Cd), and tin (Sn).

Due to the high cost of titanium dioxide, the experiment was conducted for three additivation levels: 3 (combined with anti-UV additives), 5 and 10 phr (parts per hundred resin). The titanium dioxide (TiO_2) pigment promotes opacity and protection to the PVC resin against degradation due to ultraviolet (UV) radiation.

For practical reasons, related primarily to the extrusion process, not all possible combinations of these factors were tested: only 19 out of a possible 37 compound formulations could be exposed to natural weathering. Table 1 shows all compound formulations that were processed and those that were tested. Codes used to identify the compounds are summarized in Table 2.

Climatic variables were measured several times per day during the 5-year period of the experiment (January, 1989 – December, 1993): global solar radiation (cal/cm².day), hours of sunlight (hours/day), rain (mm), relative humidity (%), wind velocity - maximum, minimum and average (m/s), temperature – maximum, minimum and average (°C). The yearly values of meteorological data for the weathering station were presented by Fernandes-Hachich (2005).

Table 1. Compound formulations processed/studied.

	Pb/Ba/Cd	*Pb*	*Sn*	*Ba/Cd*	*Number of compounds processed/studied*
Acrylic	4 / 2[(1)]	6 / 2[(1)]	2 / 0	5 / 3	17 / 7
CPE	3 /3	3 / 3	7 / 0	[(3)]	13 / 6
ABS	3 / 3[(2)]		1 / 0		4 / 3
MBS	3 / 3[(2)]				3 / 3
Total	13 / 11	9 / 5	10 / 0	5 / 3	37 / 19

(1) Only compounds with 3 and 10 phr of TiO_2 were exposed to weathering.
(2) In this case, since ABS and MBS impact modifiers reduce weathering resistance of the final compounds, only one thermal stabilizer was used, to permit comparasion of the mechanical properties of products using other impact modifiers.
(3) CPE impact modifiers were not combined with Ba/Cd thermal stabilizer due to difficulties very determining the correct lubrification.

Table 2. Compound coding.

Impact modifiers 2 letters		*Thermal Stabilizer 1 letter*		*Additive (phr of TiO_2)*
LL		L		N
AC	ACR (acrilyc)	P	Pb	3
CP	CPE	S	Sn	5
AB	ABS	B	Ba/Cd	10
MB	MBS	C	Pb/Ba/Cd	

- Example: ABC5: Compound with ABS impact modifier, thermal stabilizer Pb/Ba/Cd and 5 phr of TiO_2.

2.3 Selection of Formulations to Artificial Weathering

In order to minimize costs and time, only 10 phr TiO_2 formulations were selected for accelerated weathering, after preliminary analyses of properties changes – primarily loss of impact resistance – caused by natural weathering, as shown in Fernandes-Hachich (2008) and presented in Table 3.

Table 3. Formulations exposed to accelerated weathering.

Formulation code	Impact modifiers	Thermal Stabilizer	TiO_2 (phr)	% of loss of impact resistance after 5 years of natural weathering
MBC10	MBS	Pb-Ba-Cd	10	75,2%
ABC10	ABS	Pb-Ba-Cd	10	53,2%
CPP10	CPE	Pb	10	12,6%
CPC10	CPE	Pb-Ba-Cd	10	25,4%
ACC10	ACR	Pb-Ba-Cd	10	17,0%
ACB10	ACR	Ba/Cd	10	7,4%

3 MINIMUM CRITERIA FOR DURABILITY EVALUATION OF UNPLASTICIZED PVC BUILDING PRODUCTS, FOR OUTDOOR APPLICATIONS

3.1 Values to Evaluation

To define how to eliminate inadequate formulations in relation to impact resistance (assumed measure of durability of product) it was necessary to select a limiting value for loss of impact resistance

following exposure to natural weathering conditions. The equivalent value in artificial weathering will establish the desirable criteria.

In this choice it is convenient to use all uPVC formulations in natural weathering, not only the six utilized in artificial weathering because the natural decay of resistance will define the criteria and it will be better to use all the available data (see Table 1).

3.2 Establishment of quantitative criteria

In analyzing the results of resistance of nineteen formulations subjected to natural aging it was observed that the patterns of variation of impact strength were even more different from each other than those observed in the six formulations chosen for the experiment accelerated aging, and as was shown by Fernandes-Hachich, (2008) linear variation models were inadequate to help predict the behavoir of aged products). Therefore, a decision was taken for the purpose of setting a threshold rate of decrease in resistance, use only the initial resistance (t = 0) and final strength (t = 5 years) of natural aging, calculating the a fee from them "nominal" to decrease resistance. Adopted this procedure, it was necessary to discard the formulation CPP5 because this formulation was not available for the outcome of resistance after 5 years of natural exposure (Fernandes-Hachich,1999). Table 4 gives the values of decrease in resistance after 5 years expsoure in natural weathering conditions and the nominal rate of decrease in resistance used in the analysis

.

Table 4. Decrease of resistance of 18 formulations subjected to natural aging.

Formulation	Decrease of resistance after 5 years of natural aging	Nominal fee of decrease resistance (year $^{-1}$)
MBC3	71,6%	14,3%
MBC5	68,1%	13,6%
MBC10	75,2%	15,0%
ABC3	67,9%	13,6%
ABC5	57,4%	11,5%
ABC10	53,2%	10,6%
CPP3	26,6%	5,3%
CPP10	12,6%	2,5%
CPC3	56,8%	11,4%
CPC5	40,6%	8,1%
CPC10	25,4%	5,1%
ACP3	62,2%	12,4%
ACP10	9,3%	1,9%
ACC3	24,3%	4,9%
ACC10	17,0%	3,4%
ACB3	13,5%	2,7%
ACB5	5,6%	1,1%
ACB10	7,3%	1,5%

The histogram of Figure 1 summarizes the distribution of rates of decrease of resistance found in the eighteen formulations.

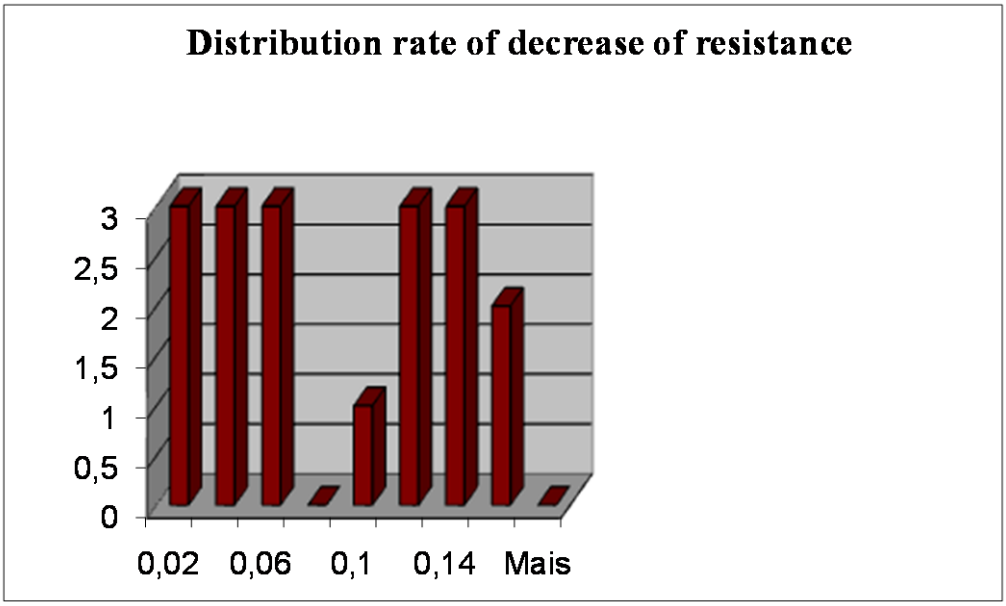

Figure 1. Histogram of the rate of decrease of resistance of 18 formulations subjected to natural aging.

The histogram of Figure 1 suggests the existence of two distinct populations. We conducted an analysis of variance (ANOVA) to test the hypothesis that this sample have been generated by a single population. The results of this test, summarized in Table 5, clearly indicates that the probability that this set of results was obtained from a single population. i is very small (i.e. about 10^{-8}). It could then be considered that this result allowed the subdivision of the rate of decrease of resistance in two groups, one of which could be considered "acceptable" and the other "unacceptable."

Table 5. Analysis of variance of resistance rates of decrease of 18 formulations subjected to natural. aging

Anova:single factor		Comparison of mean values of 2 groups of 9 each		
SUMMARY				
Group	Score	Sum	Average	Variance
Column 1	9	0.2829978	0.0314442	0.0002579
Column 2	9	1.10626	0.1229178	0.0004583

ANOVA						
Source of variation	SQ	gl	MQ	F	value-P	F critical
Between groups	0.0376534	1	0.0376	105.15	1,934E-08	4.49
Inside of groups	0.0057293	16	0.000358			
Total	0.0433827	17				

The nominal rate of decrease of resistance observed in 18 formulations subjected to natural weathering conditions for 5 years are provided in Table 6, and are grouped into sets of “acceptable” and “unacceptable” rates of resistance decrease.

Table 6. Rates of decrease of resistance acceptable and unacceptable observed after 5 years of natural exposure of 18 formulations.

Formulations	Acceptable rates	Formulations	Unacceptable rates
ACB5	1,1%	**CPC5**	8,1%
ACB10	1,5%	**ABC10**	10,6%
ACP10	1,9%	**CPC3**	11,4%
CPP10	2,5%	**ABC5**	11,5%
ACB3	2,7%	**ACP3**	12,4%
ACC10	3,4%	**ABC3**	13,6%
ACC3	4,9%	**MBC5**	13,6%
CPC10	5,1%	**MBC3**	14,3%
CPP3	5,3%	**MBC10**	15,0%
Average	3,1%	Average	12,3%
Standard deviation	1,6%	Standard deviation	2,1%

This analysis confirms that from all the compounds selected for the experiment of accelerated aging (i.e., those with 10 phr of TiO_2), the ABC10 and MBC10 were the only compounds to show poor behavior under natural weathering conditions (Table 6).

By having the data in Table 6 (including means and standard deviations) can be predicted for any choice of limit rate of decrease of resistance, the probability of a compound acceptable to exceed this limit and the probability of a compound unacceptable not exceed it . For this, we used the t-test sampling distribution. The results for various choices of limit rate of decrease of resistance, are presented in Table 7.

Table 7. Probabilities of rejecting a suitable compound and accepting an inappropriate compound for various limit rates of decrease of impact resistance

Limit value for rates of decrease of impact resistance	Probability of rejecting a suitable compound	Probability of accepting an inappropriate compound
0,05	14,1%	0,5%
0,06	5,7%	0,9%
0,07	2,2%	1,9%
0,08	0,8%	4,0%
0,09	0,3%	8,1%
0,10	0,1%	15,8%
0,11	0,1%	28,1%

Figure 2 presents the data given in Table 7, with probabilities and natural logarithmic scale.

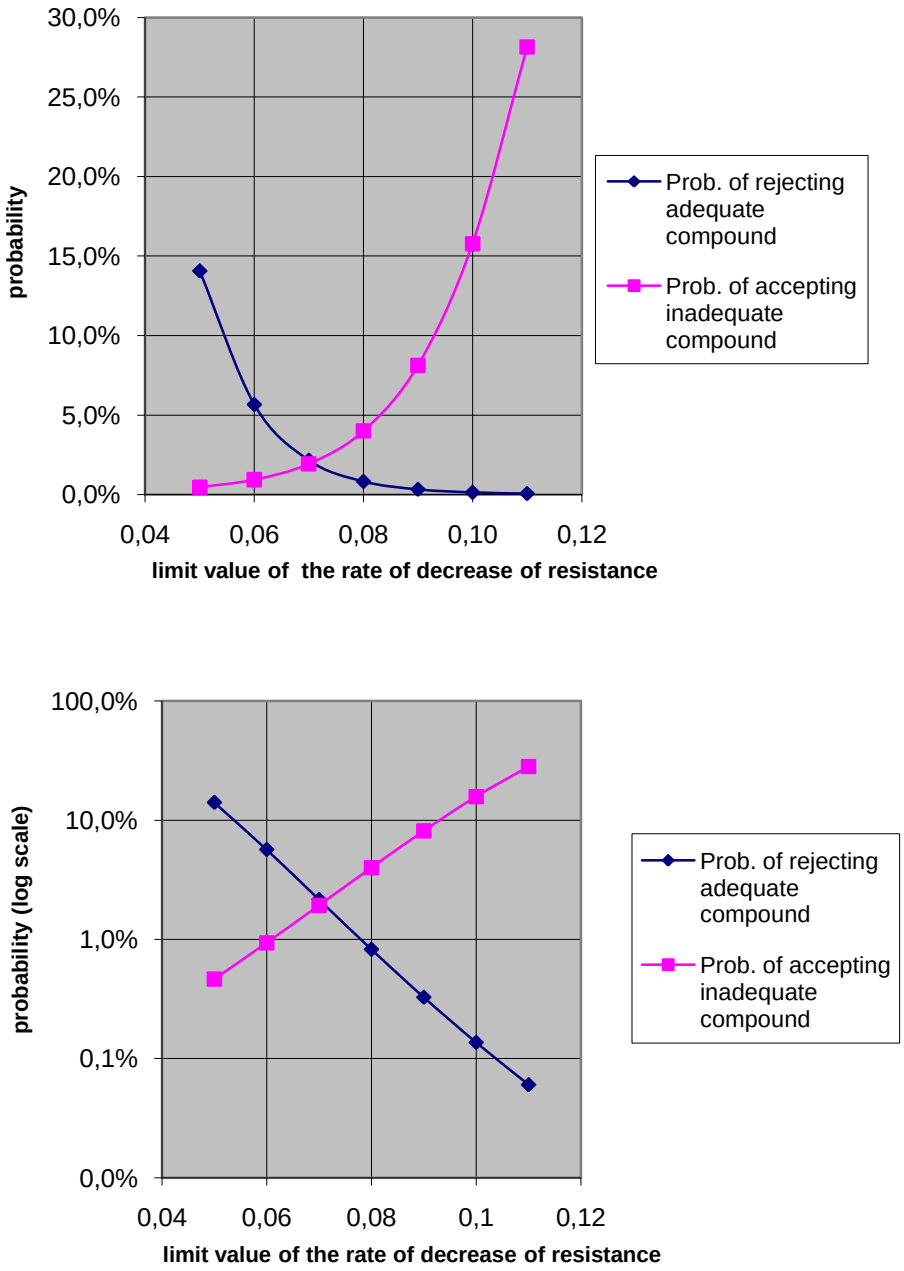

Figure 2. Probabilities of errors in the expedite classification of compounds, for various limit values of the rates of decrease of resistance.

With this information it becomes possible to choose a value in a reasoned manner to limit the rate of decrease of resistance, which separates the acceptable from unacceptable compounds in natural aging. Using the regression of Figure 2 it is then possible to set the corresponding limit rate of decrease of resistance in accelerated aging, which will be the criteria for quantitative evaluation of products when subjected to accelerated aging tests.

At present, in Brazil, it seems more appropriate to establish a criteria that divides the risks, that is, the risk of rejecting a good formulation should be similar to the risk of accepting a bad one. Thus, the assessment is balanced, without neglecting the international awareness of the product but without leaving the end user unprotected. The value of the rate of decrease is, therefore, the point of intersection of the curves presented in Figure 2: 7% per year.

This rate is equivalent, as can be seen in Figure 2, at a rate of 14.8% x 10^{-3}/hour or 0.015%/ hour of exposure in the ultraviolet chamber. Futher analysis of the tests have shown that the rate of reduction must be calculated from the determining the impact resistance at at least four points (i.e., original, 500, 1,000 and 2,000 hours). As well, it has been shown that the impact resistance at each exposure time should be the average of at least ten samples taken from the outer surface of rigid PVC profiles for windows, according to the test methods described in this work.

The initial value of BS7413 (1994) and EN 13245-2 (2008) - Charpy impact strength greater than or equal to 12 KJ/m2 for the unplasticized PVC - will be adopted as a benchmark because it was shown to be adequate. Only the formulations with titanium dioxide content of less than or equal to 5 phr and therefore potentially unacceptable, showed non-compliance with this requirement (MBC3; ABC3; ABC5 and ACC3).

ACKNOWLEDGMENTS

The authors wish to thank the help received from: Braskem S/A, IPT – Instituto De Pesquisas Tecnologicas De Sao Paulo, and TESIS - Tecnologia de Sistemas em Engenharia S/C Ltda.

REFERENCES

American Society For Testing And Materials. *Standard Test Methods for Determining the Pendulum Impact Resistance of Notched Specimens of Plastic*;. ASTM D256. Philadelphia, 1984.

____. *Standard Practice for outdoor weathering of plastics*; ASTM D1435. Philadelphia, 1994.

____. *Standard Practice for Operating Light and Water Exposure Apparatus (Fluorescent UV Condensation Type) for Exposure of Nonmetallic Materials*; ASTM G53. Philadelphia, 1991.

British Standard Institute – BSI. *Specification for white PVC-U extruded hollow profiles with heat welded corner joints for plastic windows: materials type A*. BS 7413. London, 1994.

European Standard – CEN. *Plastics - Unplasticized poly(vinyl chloride) (PVC-U) profiles for building applications – Part 2: PVC-U profiles and PVC-UE profiles for internal and external walls and ceiling finishes*. EN 13245-2. Brussels, 2008.

Fernandes-Hachich, V.C., 1999. *Minimum criteria for evaluation of Rigid Poly (Vinyl Chloride) (PVC) products for exterior use in buildings*. São Paulo. PhD Thesis – Polytechnic School of University of São Paulo.

Fernandes-Hachich, V.C., Agopyan, V., 2005. '*Influence of Composition of uPVC on the Impact Resistance of Window Profiles Exposed to Weathering*'. 10DBMC International Conférence On Durability of Building Materials and Components. Lyon, France, 17-20 April.

Fernandes-Hachich, V.C., Agopyan, V., 2008. '*Influence of Composition of uPVC on Mechanical Properties of Window Profiles Exposed to Weathering*'. Journal Of Materials In Civil Engineering © ASCE / March 2008.

Fernandes-Hachich, V.C., Agopyan, V. 2008. *'Comparison Between Accelerated and Natural Weathering of uPVC Window Profiles in Brazil'.* 11DBMC International Conférence On Durability of Building Materials and Components. Istambul, Turkey, 11-14 May.

XII DBMC
International Conference on Durability of Building Materials and Components
PORTO - PORTUGAL, April 12th-15th, 2011

Modelling Durability of Timber Structures Based on Dose-Response Functions for Decay

Christian Brischke [1]
Boris Lauenstein
Maik Bilstein
Andreas O. Rapp [2]

ABSTRACT

Scots pine sapwood (*Pinus sylvestris* L.) and Douglas fir heartwood (*Pseudotsuga menziesii* Franco) specimens were exposed in double layer field trials at 24 different European test sites under different exposure conditions (in total 28 test sets). The material climate in terms of wood moisture content (MC) and wood temperature was automatically recorded over a period of up to eight years and compared with the progress of decay.

The overall aim of this study was to establish dose-response relationships between climate factors and decay as a basis for service life prediction of wooden components. The material climatic parameters MC and wood temperature were modelled to obtain feasible dose-response functions, which turned out to be a useful basis for service life prediction.

They permit estimating the moisture and temperature induced decay potential for any wooden building component and exposure, and thus the service life to be expected. Long-term moisture recordings were applied to different wooden commodities, e. g. fence posts, pickets, decking, and facades. Furthermore, the impact of orientation, distance to the ground, and driving rain load on facade panels was studied. First results from the various studies including preliminary service life estimation for various components are also presented.

KEYWORDS

Detailing, Exposure, Material climate, Moisture content, Wood protection by design.

[1] Leibniz University Hannover, Faculty of Architecture and Landscape Sciences, Institute of Vocational Sciences in the Building Trade, Hannover, GERMANY, brischke@ibw.uni-hannover.de
[2] Leibniz University Hannover, Faculty of Architecture and Landscape Sciences, Institute of Vocational Sciences in the Building Trade, Hannover, GERMANY, rapp@ibw.uni-hannover.de

1 INTRODUCTION

Consolidated knowledge about the interrelationship between the intensity of fungal degradation over time and the numerous decay-influencing factors is needed to estimate the service life to be expected for wooden components in outdoor applications. In principal, there are three different sources providing information about decay processes. 1. Laboratory experiments, 2. Field trials, and 3. Surveys on structures in service (in-service performance). Laboratory tests allow setting up exactly defined conditions, e. g. in terms of moisture, temperature, and organisms involved. On the other hand it is difficult to mimic real life conditions in the lab, because many factors occurring in the field are not reproducible or are even unknown. Field tests are more time-consuming compared to lab tests, but closer to reality [Hedley 1993, Nilsson and Edlund 1995, Augusta 2007]. While the test set up may be identical, the local climate conditions vary from one trial to the other in dependence of time and site. As a matter of course most realistic conditions appear on real buildings and building components. Surveys on such structures in service are therefore a very important data source [Ross Gobakken et al. 2008, Brischke and Rolf-Kiel 2010]. However, in most cases they suffer from long exposure times until decay occurs or the lack of information about their history (initial protection measures, environmental conditions during exposure, and maintenance intervals). The establishment of dose-response functions as described by Brischke and Rapp [2010] allows to overcome the drawback of long exposure times needed for field trials. Once the interrelationship between the most important decay influencing factors wood moisture content and wood temperature (dose) and fungal decay (response) is determined in long-term field experiments (dose-response functions), the impact of further decay factors may be quantified in terms of dose-time functions. To determine dose-time functions medium-term-recordings (2-3 years) of moisture content and temperature will be sufficient, because it is no longer necessary to await the onset of decay. This study aims on quantifying the impact of material, exposure, and design detailing on the expected service life of wooden components. Therefore various field trials including automated moisture and temperature recordings were set up considering different wood species, typical outdoor commodities, vertical and horizontal exposure situations as well as differently oriented facades. The test set up and preliminary results will be presented.

2 EXPERIMENTAL

2.1 Field Trials

This study approaches service life prediction of wooden components by using dose-response functions. Coming from results of long-term field trials a mathematical relationship was established between moisture and temperature induced dose and a response in terms of fungal decay. A detailed description of the experimental set up, the field test results and the modelling of dose-response functions are given by Brischke and Rapp [2010]. Dose-time functions and resulting service life estimations are based on the following functions:

MC induced daily dose d_{MC}:

$$d_{MC} = 6.75 \cdot 10^{-10} MC^5 - 3.50 \cdot 10^{-7} MC^4 + 7.18 \cdot 10^{-5} MC^3 - 7.22 \cdot 10^{-3} MC^2 + 0.34MC - 4.98 \quad ; \text{if } MC \geq 25\% \qquad (1)$$

MC = daily moisture content

Temperature induced daily dose d_T:

$$d_T = 1.8 \cdot 10^{-6} T^4 + 9.57 \cdot 10^{-5} T^3 - 1.55 \cdot 10^{-3} T^2 + 4.17 \cdot 10^{-2} T \quad ; \text{if } T_{min} > -1°C \text{ and } T_{max} < 40°C \qquad (2)$$

T = daily average wood temperature
T_{min}= daily minimum temperature
T_{max}= daily maximum temperature

Daily dose d:

$$d = ((a \bullet d_T) + d_{MC}) / (a + 1) \quad ; \text{ if } d_T > 0 \text{ and } d_{MC} > 0 \qquad (3)$$

a = 3.2 (weighting factor of temperature induced daily dose component d_T)

Dose response function:

$$\text{Decay rating} = y = 4 \bullet EXP \bullet (-EXP(1.7716-(0.0032 \bullet D))) \qquad (4)$$

D = Total dose

The dose response function (4) was determined for Scots pine sapwood and Douglas fir heartwood and will further on be used for all wood species.

2.2 Automated Recordings of Wood Moisture Content (MC) and Wood Temperature

The measurement system applied in this study was described in an earlier publication [Brischke 2007] and can be summarized in brief as follows: Electrodes of polyamide coated stainless steel cables were conductively glued in the specimens or wooden commodities respectively. The electrodes were connected to a small data logger (‘Materialfox Mini’, Scanntronik Mugrauer GmbH, Zorneding, Germany), that recorded the electrical resistance of the wood. The data loggers were calibrated in a range between 15% and 50% MC [Brischke 2007]. Measurements above fibre saturation were increasingly inaccurate, but still indicated a tendency within the calibration range. Minimum and maximum temperatures were recorded using ‘Thermofox Mini’ data logger and used to calculate the average daily temperature. The logging intervals differed between the studies.

2.3 Wooden Commodities

Dose-time functions were recorded on typical wooden commodities for outdoor use. Therefore long-term moisture and temperature recordings were carried out on fence posts, pickets and terrace decking. The assemblies were made from Scots pine sapwood, Norway spruce, and Douglas fir, afterwards instrumented and exposed on the IBW test site in Hannover-Herrenhausen (Figure 1). The fence posts were buried directly in the ground; the decking elements were placed on pavers. The whole test field was covered with a water-permeable horticultural foil to protect the test devices from growth of grass and other plants.

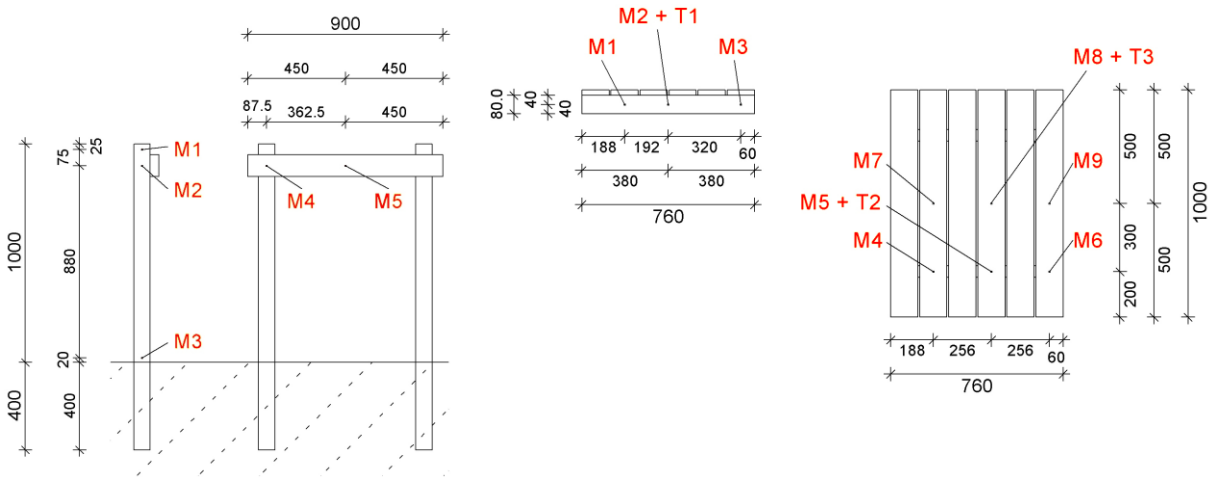

Figure 1. Position of measurement points. Left: M1 – M5 for daily wood moisture content recordings in fence elements. Right: M1 – M9 for daily wood moisture content and T1 – T3 wood temperature recordings in decking elements. Dimensions in mm.

2.4 Test House

The impact of wall orientation and of the distance to the ground on the moisture induced decay risk was studied on the claddings of a test house, which was built in Hannover-Herrenhausen in December 2008 (Figure 2). The house had a quadratic floor plan of 3 x 3 m² and a total height of 3.18 m. The four facades were exactly aligned to the cardinal points of the compass. The stud frame, which was made from Norway spruce, carried a board-on board cladding and a pyramidal broach roof. The roof overhang was minimized to a width of 7.5 cm including the gutter. Five test boards of Norway spruce, Scots pine sapwood and Douglas fir were mounted on each side of the building. The spaces in between were filled with so-called blind boards made from Norway spruce.

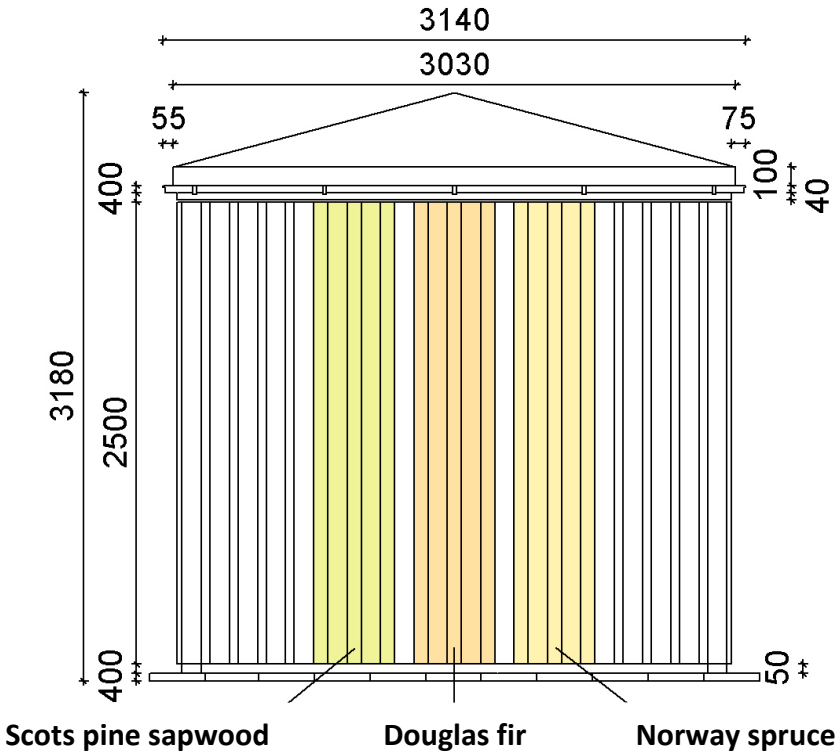

Figure 2. Position of test boards from different wood species in the board-on-board cladding of the test house (dimensions in mm).

For measuring the wood moisture content electrodes were installed at seven different heights: 5, 10, 20, 40, 80, 160, and 240 cm from the bottom end of the boards. Three measurement points per wood species, height and wall orientation were set, which means in total 252 pairs of electrodes. The electrodes were glued in from the back side of the cladding, two pairs in the central cover boards, and one pair in the central base board. In addition 84 temperature sensors were installed, one for each parameter combination. Temperature and wood moisture content were recorded every two hours.
Additionally, driving rain gauges were installed on each facade. Each driving rain event as well as the driving rain sum for each day was recorded automatically. Corresponding data on total precipitation, wind speed, and wind direction were taken from the Institute of Meteorology and Climatology, which is located 300 m from the test house.

3 PRELIMINARY RESULTS AND DISCUSSION

3.1 In and Above Ground Exposure of Wooden Commodities

After one year of exposure (September 2008 till August 2009) the expected service life of the different wooden commodities was estimated. In Table 1 the sum of the daily dose components d_{MC}

and d_T as well as the sum of the total daily dose d are listed. The dose differed significantly between wood species, commodities, and differently severe exposed positions on the assemblies. Douglas fir featured least dose; pine sapwood - the most permeable species - had the highest dose. The dose differences between the wood species were more pronounced for those details, where re-drying of the assembly was allowed, e.g. the terrace board and picket centres. Furthermore the results clearly indicated the higher decay risk for those components, which suffered from hindered drying such as the contact face between picket and post or between terrace board and bearing. So far the data show, that the experimental set ups are working as expected. Numeric calculation and quantification of decay risk will follow, when enough data for serious calculations have been collected.

Table 1. Sum of daily dose components d_{MC} and d_T and total daily dose D_a of different wooden decking assemblies determined for the exposure interval September 2008 till August 2009.

Wood species	*Commodity*	Σd_{MC}	Σd_T	$D_a = \Sigma d$
Douglas fir	Terrace board centre	35.8	123.9	13.1
	Terrace board at contact face	96.9	117.8	23.3
	Bearing	51.9	140.1	23.0
Scots pine sapwood	Terrace board centre	198.7	123.8	82.1
	Terrace board at contact face	217.0	121.0	88.2
	Bearing	178.1	141.4	67.4
Norway spruce	Terrace board centre	114.8	129.1	43.1
	Terrace board at contact face	122.0	110.4	32.3
	Bearing	108.9	140.0	42.6
Douglas fir	Picket close to post	2.0	110.9	3.5
	Picket centred	0.2	115.5	0.5
	Post above picket	55.7	130.3	19.9
	Post close to picket	8.7	139.2	7.7
	Post close to ground	3.5	155.4	7.0
Scots pine sapwood	Picket close to post	134.4	110.7	56.1
	Picket centred	81.6	017.1	30.2
	Post above picket	136.5	128.9	48.0
	Post close to picket	96.7	141.9	36.5
	Post close to ground	142.9	152.2	104.0
Norway spruce	Picket close to post	2.0	108.8	13.1
	Picket centred	2.2	107.2	3.5
	Post above picket	69.3	128.9	21.0
	Post close to picket	51.7	139.8	22.7
	Post close to ground	88.6	145.1	67.9

For a first and very preliminary service life prediction of the assemblies a critical dose was determined according to the dose-response function in Figure 3. The following assumptions were made: A mean decay rating = 2, corresponding to moderate fungal decay, was set as limit state. Any decay rating above this limit state means that the serviceability is not longer given. According to Equation 4 a critical dose $D_{crit} = 670$ is needed to be summed up to reach the limit state. Finally in the following the expected service life was considered to be the quotient of the critical dose D_{crit} and the annual dose D_a for the first year of exposure.

For the decking elements service lives between 8 years (Scots pine sapwood) and 29 years (Douglas fir) were estimated (Table 2), which coincides with expectations from practice. The service life of well ventilated pickets was estimated to be much higher, 22 years for pine sapwood and even more for spruce and Douglas fir, whereby the expectation for Douglas fir (1340 years) seemed to be not plausible so far, but did well indicate the extremely low risk of fungal decay for this application.

An unexpectedly high dose was determined for the fence posts' upper ends, corresponding with predicted service lives between 14 and 34 years. Through setting the measurement points only 25 mm below the open and unprotected end grain of the posts, an easy water uptake as well as re-drying was allowed. However, with respect to the comparatively high moisture-induced dose (Table 1), in this case the moisture uptake seemed to have a dominating effect.

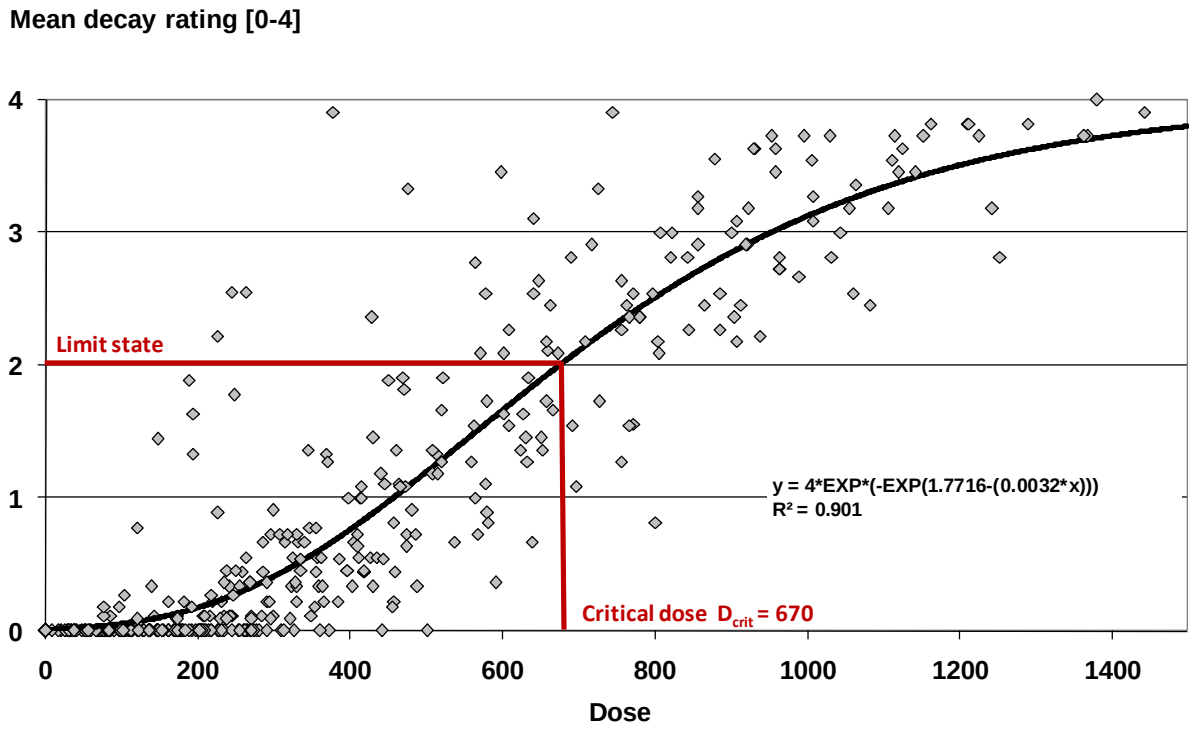

Figure 3. Determination of critical dose D_{crit} based on dose-response function for service life estimation of wooden components. Limit state: Mean decay rating = 2 (moderate decay).

Table 2. Preliminary estimation of service lives for different wooden fence and decking assemblies based on dose-response functions.

	Estimated service life [a]		
	Douglas fir	*Scots pine sapwood*	*Norway spruce*
Terrace board centre	51	8	16
Terrace board at contact face	29	8	21
Bearing	29	10	16
Picket close to post	191	12	51
Picket centred	1340	22	191
Post above picket	34	14	32
Post close to picket	87	18	30
Post close to ground	96	6	10

3.2 Facade Orientation and Distance to Ground

Moisture and temperature data from the test house facades were analysed in analogy to the decking and fence assemblies. As expected, these invariably vertically exposed components showed less dose and thus longer service lives were predicted. The sum of total daily dose D_a and the corresponding service life estimations can be seen from Table 3. For many combinations of wood species, orientation and height above ground the service life to be expected was far above one century or even unlimited. At first view this seemed to be illegitimate, but was finally the result of no or at least very little measureable dose. Consequently, the results have to be interpreted as "snapshot" of the water-uptake behaviour at the present state. Ongoing weathering, staining, and decay will change that and

lower the extremely high service life estimates. For future modelling the altering moisture behaviour might be extrapolated.

On the other hand, significant differences between the four test house walls were found. The West facade revealed the highest dosages for all wood species, leading to minimum service life estimations between 76 and 83 years. As South-west is the weather side in Hannover and solar irradiation is most intensive on the South side, it seems plausible that decay hazard is highest on the West facade. For the remaining three orientations no clear decay hazard ranking was indicated: Least severe exposure for Douglas fir was found in the North and East, for pine sapwood in the East and South, and for spruce on the North facade. In contrast, the impact of the distance to the ground on the decay potential became apparent in most cases: The highest dose was determined close to the ground (5-10 cm).

Table 3. Sum of total daily dose D_a of facades in dependence of orientation and height above ground determined for the exposure interval January 2009 till December 2009. In brackets: Corresponding preliminary estimation of service lives based on dose-response functions.

Wood species	*Orientation*	*Height above ground [cm]*						
		5	*10*	*20*	*40*	*80*	*160*	*240*
Douglas fir	North	0.00	0.00	0.00	0.12	0.00	0.00	0.00
		(∞)	(∞)	(∞)	(5583)	(∞)	(∞)	(∞)
	East	0.00	0.00	0.00	0.00	0.00	0.00	0.00
		(∞)	(∞)	(∞)	(∞)	(∞)	(∞)	(∞)
	South	1.36	5.94	0.44	0.00	0.00	0.00	0.00
		(493)	(113)	(1523)	(∞)	(∞)	(∞)	(∞)
	West	4.84	6.71	5.33	8.09	7.76	6.90	6.70
		(138)	(100)	(126)	(83)	(98)	(97)	(99)
Scots pine sapwood	North	6.13	4.44	4.03	2.25	3.75	0.82	0.00
		(109)	(151)	(166)	(298)	(179)	(817)	(∞)
	East	0.00	0.93	0.00	0.15	0.17	0.00	0.00
		(∞)	(720)	(∞)	(4467)	(3941)	(∞)	(∞)
	South	0.00	0.00	0.00	0.00	0.00	0.35	3.02
		(∞)	(∞)	(∞)	(∞)	(∞)	(1914)	(222)
	West	5.30	8.87	5.90	5.48	6.05	4.65	4.55
		(126)	(76)	(114)	(122)	(111)	(144)	(147)
Norway spruce	North	1.38	0.73	0.00	0.41	1.51	0.43	0.00
		486	(918)	(∞)	(1634)	(444)	(1558)	(∞)
	East	2.88	4.20	5.58	4.44	0.47	0.89	0.00
		(233)	(160)	(120)	(151)	(1426)	(753)	(∞)
	South	7.47	1.72	0.69	0.00	0.00	0.00	0.00
		(90)	(390)	(971)	(∞)	(∞)	(∞)	(∞)
	West	8.77	8.88	7.90	5.20	6.45	1.32	1.32
		(76)	(76)	(85)	(129)	(104)	(508)	(508)

4 CONCLUSIONS

The impact of material and exposure conditions on the service life of wooden components as well as the effectiveness of different protective measures by design was found to be quantifiable through determination of dose-time functions. The impact is hereby indicated as service life number in years or alternatively as factor between two options.

After only one year of exposure, the results certainly need to be considered as preliminary. The annual dose D_a is most likely influenced by climatic variations between one year and the other. Therefore the annual dose should be calculated as mean average for at least three years. Reference years in terms of local climate should be identified. Furthermore one can expect that the moisture sorption behaviour of

wood is influenced by weathering, e. g. through cracking, greying, and staining. Thus, the annual total dose may increase with exposure time.

For future studies further commodities and detailing need to be included in order to piece the puzzle together. On this matter a couple of studies were initiated to consider also the influence of roof overhangs, contact to ground and metal joints, covering, and coatings.

ACKNOWLEDGEMENTS

The authors are grateful for financial support of the project „Service life prediction of wooden components in outdoor use based on dose-response functions" by the Leibniz University Hannover in the frame of the funding program "Access to Research II".

Furthermore the authors express their special thanks to Prof. Gilbert Lösken, Institute of Landscape Architecture, for providing the land for the test house and his technical support.

REFERENCES

Augusta, U. 2007, ‚*Untersuchung der natürlichen Dauerhaftigkeit wirtschaftlich bedeutender Holzarten bei verschiedener Beanspruchung im Außenbereich*' Doctoral thesis, University of Hamburg, Hamburg

Brischke, C. 2007 *'Investigation on decay influencing factors for service life prediction of exposed wooden components'* Doctoral thesis, University of Hamburg, Hamburg

Brischke, C. & Rapp, A.O. 2010, '*Service life prediction of wooden components – Part 1: Determination of dose response functions for above ground decay'* Document IRG/WP 10-20339. International Research Group on Wood Protection, Stockholm, Sweden

Brischke, C. & Rolf-Kiel, H. 2010 *'Durability of European oak (Quercus spp.) in ground contact – A case study on fence posts in service'* European Journal of Wood and Wood Products **68**: 129-137.

Hedley, M.E. 1993, '*Comparison of performance of wood preservatives in laboratory and field tests and in service tests of treated commodities'* Document IRG/WP 93-20010. International Research Group on Wood Protection, Stockholm, Sweden

Nilsson, T. & Edlund, M.-L. 1995, '*Laboratory versus field tests for evaluating wood preservatives: A scientific view'* Document IRG/WP 95-20076. International Research Group on Wood Protection, Stockholm, Sweden

Ross Gobakken, L., Mattson, J. & Alfredsen, G. 2008, '*In-service performance of wood depends upon the critical in-situ conditions. Case studies*' Document IRG/WP 08-20382. International Research Group on Wood Protection, Stockholm, Sweden

XII DBMC
International Conference on Durability of Building Materials and Components
PORTO - PORTUGAL, April 12th-15th, 2011

Biological Defacement of ETICS - A Risk Assessment Methodology

Eva Barreira [1]
Vasco Peixoto de Freitas [2]

ABSTRACT

External Thermal Insulation Composite Systems – ETICS are nowadays often used in Europe. Despite its thermal advantages, low cost and ease of application, this system has serious problems of microbiological growth causing the cladding defacement. Recent studies allowed to understand the physical phenomenon causing the ETICS defacement and made it possible to develop mathematical models simulating its performance. However, no simple process has yet been developed to predict the risk of ETICS defacement, which may be used by designers and by the building industry.

This paper presents a methodology to assess the risk of biological growth, based on the definition of indices, which combine the effect of surface condensation, wind-driven rain and drying process, three of the most prevalent parameters influencing the surface moisture content. The proposed indices were calculated using data collected during a one year "in situ" test campaign, which provided information about the exterior climate conditions and about the surface temperature and wind-driven rain on four façades covered with ETICS facing the cardinal directions. The indices were compared with the results of the surface relative humidity measured simultaneously that allowed the validation of the methodology. An example of the practical use of this methodology is also presented in this paper, with the definition of hazard classes of biological defacement of façades covered with ETICS located in the Portuguese territory.

KEYWORDS

Biological defacement, Hygrothermal behaviour, ETICS.

[1] Faculty of Engineering of the University of Porto (FEUP), Porto, PORTUGAL, barreira@fe.up.pt
[2] Faculty of Engineering of the University of Porto (FEUP), Porto, PORTUGAL, vpfreita@fe.up.pt

1 INTRODUCTION

External Thermal Insulation Composite Systems – ETICS are often used in Europe since de 70's, both in new buildings and in retrofitting. Despite its thermal advantages, low cost and ease of application, this system has serious problems of microbiological growth, causing the cladding defacement. Although no changes occur in the thermal and mechanical performance of the system, biological defacement has an enormous aesthetic impact, which gathers the building's dwellers disapproval and restricts the full implementation of this technology (Fig. 1).



Figure 1. ETICS defacement due to biological growth.

Studies carried out during the last decade allowed understanding the physical phenomena that promote microbiological growth on ETICS [Blaich 1999, Kunzel & Sedlbauer 2001, Becker 2003, Venzmer *et al.* 2008]. They pointed that microbiological growth is due to high values of surface moisture content, which results from the combined effect of four parameters: surface condensation, wind-driven rain (WDR), drying process and properties of the exterior layer.

Exterior surface condensation occurs mostly during the night, when the exterior surface temperature is lower than the dew point temperature, as a result of long wave radiation exchange between the surface and the atmosphere. During clear nights, the atmosphere's emitted radiation decreases considerably and the radiation emitted by the surface is greater than the one that reaches the surface, causing a loss of radiation towards the sky. This negative balance on the surface is maintained until heat transport by convection and by conduction compensate for the loss by radiation [Holm et al. 2004].

WDR results from the combination of rain and wind. Its intensity depends on the building geometry and environment topology, position on the building façade, intensity of rainfall through a horizontal plane, wind speed and wind direction. The most used semi-empirical model says that WDR intensity is proportional to the product of the wind speed normal to the façade and the intensity of rainfall through a horizontal plane [Nore et al. 2007].

The drying process allows the evaporation of the liquid water accumulated on the surface due to the surface condensation and WDR. Evaporation from the wet surface occurs whenever the saturation pressure at the surface is greater than the vapour pressure of the ambient air [Hagentoft 2001]. If the drying process is not sufficiently fast, the surface moisture content remains high for long periods and increases the risk of microbiological growth [Krus et al. 2006].

Several authors refer to the importance of the properties of the exterior layer in the biological growth. Concerning the thermal properties, emissivity is referred as the most relevant as it rules the emission of radiation by the surface. For lower values of emissivity the heat loss during the night reduces and the surface temperature increases. The risk of surface condensation is therefore lower [Krus et al.

2006]. Also some hygric properties are referred as having capital influence on the surface moisture content, namely water absorption of the external coating. Lower water absorption allows longer availability of liquid water on the surface as less water is absorbed by the plaster system following WDR and surface condensation [Blaich 1999, Becker 2003, Venzmer *et al.* 2008]. Barberousse *et al.* [2006] assessed the influence of the coating roughness in the biological growth and stated that it could promote or restrict the adhesion process of the spores and the liquid water retention on the surface.

2 HYGROTHERMAL MODEL TO ASSESS THE RISK OF BIOLOGICAL GROWTH

The knowledge gathered during the last decade made it possible to develop mathematical models simulating ETICS performance, considering different conditions of use [Kunzel *et al.* 2002]. However, no simple process has yet been developed to predict the risk of ETICS defacement. Considering the work already done for mold growing on interior finishes [Adan 1994], the relative humidity of the surface or the time of wetness obtained from the surface humidity, might be the better criterion for assessing the risk of biological growth. Nevertheless, the comparison of simulated values with the results of "in situ" tests performed on a façade covered with ETICS showed that there is no go agreement between the simulated and the measured values of the relative humidity, especially when WDR is taken into account [Barreira 2010].

The use of surface relative humidity as a criterion for the risk assessment is, therefore, restricted. The next paragraphs present an alternative methodology to assess the risk of biological growth, based on the definition of indices, which combine the effect of surface condensation, wind-driven rain and drying process, three of the most prevalent parameters influencing the surface moisture content. The effect of the exterior layer properties is not taken into consideration explicitly in the model.

2.1 Assessing Exterior Surface Condensation

Exterior surface condensation can be analyzed using psychrometry principles. When water vapour partial pressure of the air is greater than the water vapour saturation pressure at the surface, condensation will occur [Hagentoft 2001]. According to Zheng *et al.* [2004] the difference between the water vapour partial pressure in the air ($P_v(air)$, in Pa) and the water vapour saturation pressure on the surface ($P_{sat}(surface)$, in Pa) may be called Condensation Potential (*CP*, in Pa), which implies condensation for positive values. *CP* can be understood as the amount of water vapour that is available to condensate.

$$CP = P_v(air) - P_{sat}(surface) \tag{1}$$

The same author refers that to evaluate the amount of condensation, both positive *CP* and its lasted time should be considered. The product of positive *CP* ($CP_{(>0)}$, in Pa) by its lasted time ($\Delta t_{CP(>0)}$, in h) may be called Condensation Potential Equivalent (*CPE*, in Pa) and allows estimating the amount of condensated water. To estimate the risk of condensation for a certain period of time *CPE* must be accumulated in time (CPE_a).

$$CPE = CP_{(>0)} \cdot \Delta t_{CP_{(>0)}} \tag{2}$$

2.2 Assessing *WDR*

The humidification of a façade due to *WDR* may be assessed, for a certain period of time, through the *WDR* Potencial Equivalent ($WDRPE_a$, in kg/m^2), which is obtained by integrating in time the intensity of *WDR* (in kg/(m^2·s). $WDRPE_a$ shall be multiplied by 100 in order to reach values that are comparable with CPE_a values.

$$WDRPE_a = 100 \cdot \int_0^t WDR \; dt \tag{3}$$

2.3 Assessing the Drying Process

As condensation also the drying capacity of a wet surface can be analyzed using psychrometry principles [Hagentoft 2001]. By analogy, it is possible to establish the concept of Drying Potential (*DP*, in Pa), as being the difference between the water vapour saturation pressure on the surface ($P_{sat}(surface)$, in Pa) and the water vapour partial pressure in the air ($P_v(air)$, in Pa), which implies evaporation for positive values. *DP* can be understood as the amount of water vapour transferred to the air, considering that the surface remains permanently wet.

$$DP = P_{sat}(surface) - P_v(air) \tag{4}$$

To evaluate the maximum ability to dry out, the product of positive *DP* ($DP_{(>0)}$, in Pa) by its lasted time ($\Delta t_{DP(>0)}$, in h) shall be considered and may be called Drying Potential Equivalent (*DPE*, in Pa). To estimate this ability for a certain period of time, *DPE* must be accumulated in time (DPE_a).

$$DPE = DP_{(>0)} \cdot \Delta t_{DP_{(>0)}} \tag{5}$$

It must be stated that DPE_a is not useful as a parameter for modeling the real drying capacity of a wet surface, as it is not permanently saturated. After some time, the liquid water evaporates and the vapour pressure at the surface depends not only on the surface temperature, but also on its relative humidity. However, to avoid the use of relative humidity and to simplify the parameters used in the drying process assessment, DPE_a can be employed as an overvalued drying capacity.

2.4 The model BIO.MOD

The model BIO.MOD defines three indices that relate the surface humidification, by condensation (CPE_a), due to WDR ($WDRPE_a$) or due to the sum of the two, with the maximum drying capacity (DPE_a).

$$BIO.MOD1 = \frac{CPE_a}{DPE_a} \cdot 10^3 \qquad \left[\frac{\text{Pa}\cdot\text{h}}{\text{Pa}\cdot\text{h}}\right] \tag{6}$$

$$BIO.MOD2 = \frac{WDRPE_a}{DPE_a} \cdot 10^3 \qquad \left[\frac{\text{kg/m}^2}{\text{Pa}\cdot\text{h}}\right] \tag{7}$$

$$BIO.MOD3 = \frac{CPE_a + WDRPE_a}{DPE_a} \cdot 10^3 \qquad \left[\frac{\text{Pa}\cdot\text{h} + \text{kg/m}^2}{\text{Pa}\cdot\text{h}}\right] \tag{8}$$

3 VALIDATION OF THE MODEL BIO.MOD

3.1 Setting Up the Test

To validate the proposed indices an "in situ" test campaign was carried out during one year (from March 2009 to February 2010). Instruments were set up on the façades covered with ETICS of a building located in the University of Porto campus, whose walls face the four cardinal directions. The devices provided information about the surface temperature (T-type thermocouples), wind-driven rain (WDR gauges) and surface relative humidity (humidity and temperature probes) on the four façades

(black dots on Fig. 2). They were coupled to a data acquisition system, collecting data every 10 minutes. At the same time, climate parameters (temperature and relative humidity) were also collected, every 10 minutes, by the Building Physics Laboratory – LFC weather station, located near the building under study (Fig. 2).

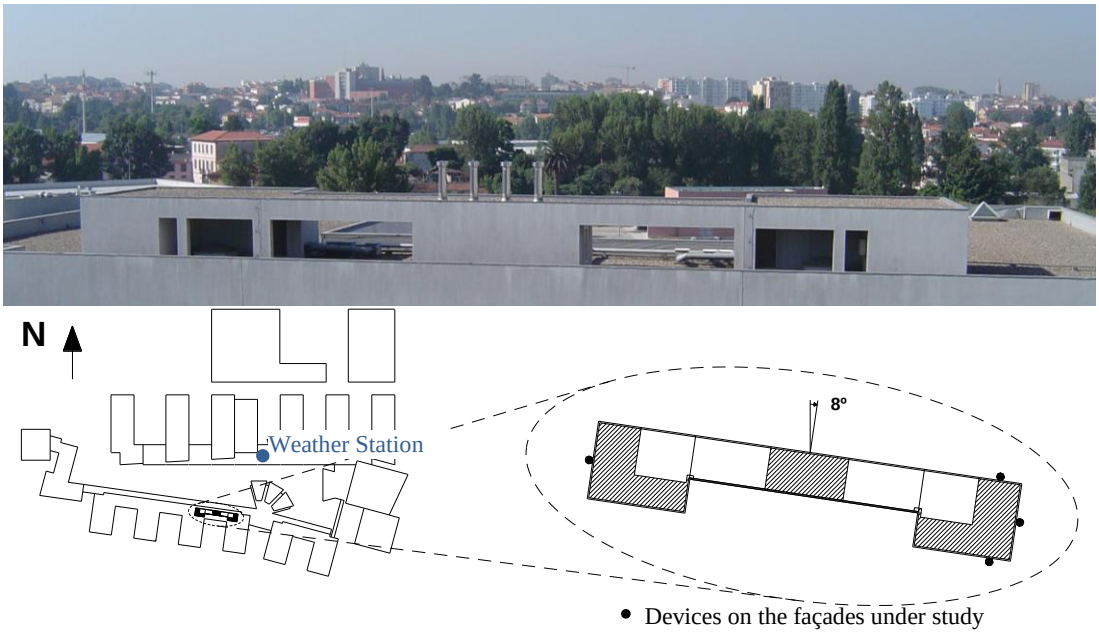

Figure 2. Building under study and layout with the devices and weather station locations.

3.2 Results – Validation of the model and Discussion

Using the data collected during the "in situ" campaign, CPE_a, $WDRPE_a$, DPE_a and the three indices of BIO.MOD were calculated in annual bases (Figs. 3 and 4). Figure 5 shows that there is a go agreement between the index *BIO.MOD3*, which combines surface condensation with the effect of WDR and "quantifies" the risk of defacement due to biological growth, and the accumulated hours of the surface saturation (relative humidity equal to 100%), measured simultaneously. This good agreement allowed the validation of the model. On the other hand, there is also a good relation between the façades defacement per orientation and the annual values of *BIO.MOD3*, as the West and North façades present more colonization by microorganism than the East and South façades that don't have any biofilm on its surface.

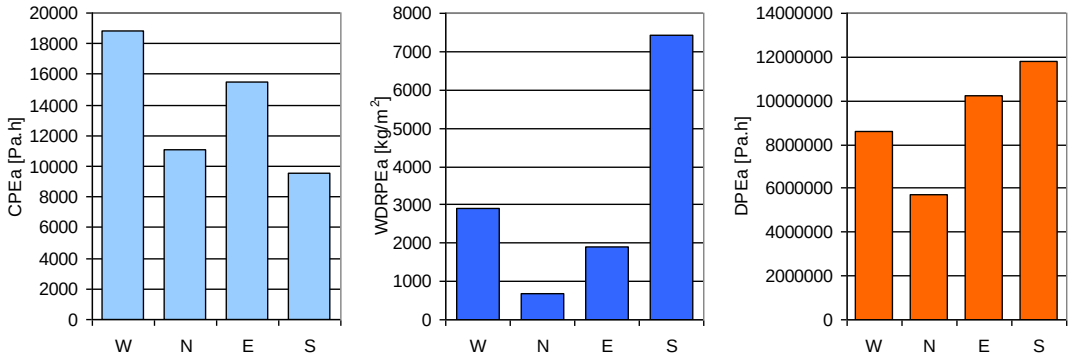

Figure 3. CPE_a, $WDRPE_a$ and DPE_a per orientation (annual values).

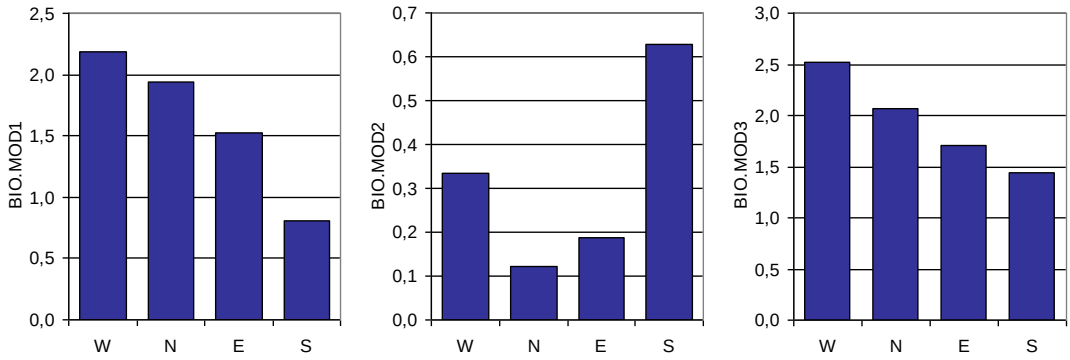

Figure 4. Indices of BIO.MOD per orientation (annual values).

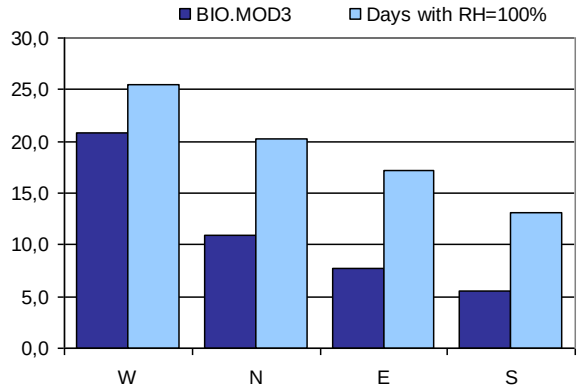

Figure 5. Index *BIO.MOD3* and days with RH=100% per orientation (November 2009).

The risk of surface humidification due to condensation (*BIO.MOD1*) is greater for the West façade, followed by the North, East and South façades. It depends mostly on the drying process, which is quite clear for the North façade that didn't had high values for surface condensation (CPE_a) but had the lowest drying capacity (DPE_a) and, consequently, the highest risk of humidification by condensation (*BIO.MOD1*). The East façade, with one of the highest amount of condensation (CPE_a), didn't present very high risk of humidification by condensation (*BIO.MOD1*) due to the drying capacity (DPE_a).

The risk of surface humidification due to WDR (*BIO.MOD2*) is greater for the South façade, followed by the West, East and North façades. The risk is related with the intensity of WDR ($WDRPE_a$) on each façade and there is no clear influence of the drying capacity (DPE_a), although it had slightly reduced the risk in the South façade.

The risk of defacement due to biological growth (*BIO.MOD3*) is strongly dependent on surface condensations (*BIO.MOD1*), as both indices follow the same trend. The influence of the WDR is not very relevant although it slightly increases the risk of biological growth. However, it must be stated that this model doesn't takes into account the water run-off along the surface neither its accumulation, which may increase the influence of WDR in the risk of microorganisms colonization.

4 RISK MAP OF BIOLOGICAL DEFACEMENT IN PORTUGAL

As an example of the practical use of the model BIO.MOD, it was defined hazard classes of biological defacement of façades covered with ETICS located in the Portuguese territory. A risk map was created using the index *BIO.MOD3*, on annual bases, calculated with the results of numerical

simulation for the same wall, facing North and South, and located in main towns of Portugal. The simulation was performed considering generated climatic data for each town and the interior conditions were assumed to be identical.

The hazard classes were established considering three classes of risk, having as top limit the highest value of *BIO.MOD3* obtained: Low Risk, considering values lower than 1,5, Medium Risk, for values between 1,5 and 3,0, and High Risk for values higher than 3,0. Figure 6 displays the risk of biological defacement on façades facing North and South.

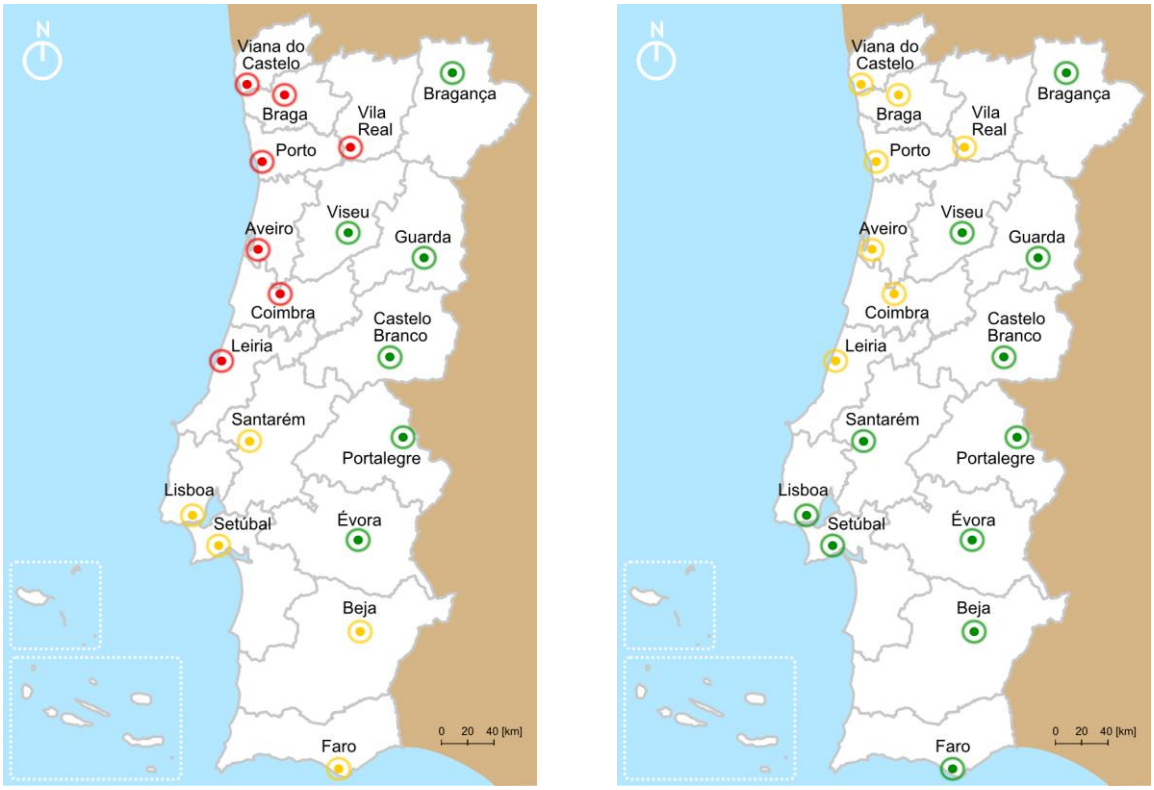

Façades facing North Façades facing South

Figure 6. Risk of biological defacement on façades facing North and South (Green – Low Risk, Yellow – Medium Risk and Red – High Risk).

The results show that façades facing North have higher risk of defacement and the towns located in the North West of Portugal present more risk than the ones located in the North country side. In the South of Portugal, the risk is intermediate. The results also showed that the towns with higher risk are Coimbra, Porto and Aveiro and the ones with lower risk are Portalegre, Guarda and Castelo Branco.

5 CONCLUSIONS

It was developed and validated a methodology to assess the risk of biological defacement. This model is based on the definition of indices that relate humidification, by surface condensation and due to WDR, with the drying capacity. The main advantage of this methodology is related with the simplicity of the parameters used and with the ability of knowing the real load of surface condensation, WDR and drying capacity in the façade surface moisture content.

Using the model BIO.MOD it was possible to say that the drying process is the most relevant parameter and that surface condensation has more impact than WDR. It was also possible to establish a risk map for walls covered with ETICS located in Portuguese territory.

ACKNOWLEDGMENTS

The authors would like to thank the financial support of FCT – Fundação para a Ciência e Tecnologia that allowed the necessary conditions to carry out this study.

REFERENCES

Adan, O. 1994, *On the fungal defacement of interior finishes*, PhD Thesis, Eindhoven University of Technology, The Netherlands.

Barberousse, H., Lombardo, R., Tell, G. & Couté, A. 2006, 'Factors involved in the colonisation of building façades by algae and cyanobacteria in France', *Biofouling*, 22[2], 69–77.

Barreira, E. 2010, *Biological defacement of façades covered with external thermal insulation systems due to hygrothermal behaviour*, PhD Thesis, FEUP, Portugal.

Becker, R. 2003, 'Patterned staining of rendered facades: hygro-thermal analysis as a means for diagnosis', *Journal of Thermal Envelopes and Building Science*, 26[4], 321–341.

Blaich, J. 1999, *La détérioration des bâtiments – Analyse et prévention*, EMPA, Suisse.

Hagentoft, C.-E. 2001, *Introduction to building physics*, Studentlitteratur, Sweden.

Holm, A., Zillig, W. & Kunzel, H. 2004, 'Exterior surface temperature and humidity of walls – Comparison of experiment and numerical simulation', *Proc. Performance of Exterior Envelopes of Whole Buildings IX*, ASHRAE, Clearwater Beach, Florida, December 2004.

Krus, M., Rosler, D. & Sedlbauer, K. 2006, 'New model for the hygrothermal calculation of condensate on the external building surface', *Proc. Third International Building Physics Conference – Research in Building Physics and Building Engineering*, Concordia University, Montreal, Canada, 27 31August 2006, 329-333.

Kunzel, H. & Sedlbauer, K. 2001, 'Biological growth on stucco', Proc. Performance of Exterior Envelopes of Whole Buildings VIII: Integration of Building Envelopes, ASHRAE, Clearwater Beach, Florida, December 2001.

Kunzel, H., Schmidt, Th. & Holm, A. 2002, 'Exterior surface temperature of different wall constructions – Comparison of numerical simulation and experiment', Proc. 11th Symposium of Building Physics, Technische Universitat Dresden, Dresden, Germany, 26 30 September 2002, vol. 1, pp. 441–449.

Nore, K., Blocken, B., Jelle, B., Thue, J. & Carmeliet, J. 2007, 'A dataset of wind-driven rain measurements on a low-rise test building in Norway', *Building and Environment*, 42, 2150–2165.

Venzmer, H., von Werder, J., Lesnych, N. & Koss, L. 2008 'Algal defacement of façade materials – Results of long term natural weathering tests obtained by new diagnostic tools', Proc. 8th Symposium on Building Physics in the Nordic Countries, DTU, Copenhagen, Denmark, 16 18 June 2008, vol. 1, pp. 277–284.

Zheng, R., Janssens, A., Carmeliet, J., Bogaerts, W. & Hens, H. 2004, 'An evaluation of highly insulated cold zinc roofs in a moderate humid region – Part I: Hygrothermal performance', *Construction and Building Materials*, 18[1], 49–59.

XII DBMC
International Conference on Durability of Building Materials and Components
PORTO - PORTUGAL, April 12th-15th, 2011

Application of Fracture Mechanics in Reliability Analysis of Corrosion Affected Cast Iron Water Mains

Hamed Mohebbi [1]
Chun Qing Li [2]

ABSTRACT

Time dependent defects such as localised corrosion in cast iron water mains are the primary cause of the failure of in-service pipes. Although it is impossible to predict when a pipe will fail, due to stochastic nature of corrosion process, it is feasible to estimate whether it is sufficiently deteriorated for the failure to be likely. In this paper therefore a probabilistic risk assessment method for application to the time-dependent defect (corrosion pits) associated failure of the cast iron trunk mains is developed. This work assesses the structural reliability of the pipes by comparing their state behaviour as a function of time to a limit sates that is based on the fracture mechanics. A power law corrosion deterioration model from tests on specimens taken from an ex-service pipe and tested in the laboratory is developed. A numerical example is provided to illustrate the proposed method with a view to predict the failures of the pipes during their service life. The proposed methodology can help the management with their network rehabilitation programme on the basis of targeted replacement to ensure the safe and serviceable operation of the pipes.

KEYWORDS

Microstructure, Material, Probability of failure, Corrosion rate, Stress intensity factor, Fracture toughness.

[1]School of Engineering, University of Greenwich, UK, mh45@gre.ac.uk
[2]School of Engineering, University of Greenwich, UK, c.q.li@sgre.ac.uk

1. INTRODUCTION

Cast iron is a material that still has significant usage in the water industry. In the context of the United Kingdom, although cast iron pipes are being phased out of distribution and mains systems, a significant portion of current pipe networks are comprised of an aging cast iron infrastructure that can be up to 150 years old. This includes 335,000 km of mains of which more than 60% is estimated to be cast iron pipes. This cast iron infrastructure is deteriorating at different rates, e.g. [Rajani and Makar 2000; Atkinson *et al.* 2002], which are linked to the geology and other localised conditions. The problem is complicated further by the diversity in production quality as well as the range of diameters and wall thicknesses used. This ageing network requires maintenance and targeted replacement. Trunk mains are large diameter pipes which take water from the reservoirs to major settlements and then smaller diameter distribution mains carry the water to individual properties. When a trunk main fails, a large amount of water is lost with the potential for major flooding and even the loss of life is a possibility. Therefore, for the water industry the ability to predict a situation in which a catastrophic failure may occur is of great importance. In order to develop a rehabilitation or replacement strategy for the industry, it is important to develop an assessment strategy for the asset management.

It is a common practice to assess the reliability of pipes based on the condition of pipes. It is accepted that the failure is likely to occur when the structural integrity of a pipe has been compromised by the defects. Corrosion pits are the most prominent defects as they become worse over time, decreasing the remaining wall thickness of the pipes and compromising the ability of pipes to withstand the service-loading. Many studies have been carried out to investigate the structural reliability of the underground pipes using deterministic or probabilistic models. Some research has used deterministic methodology, the main drawback of which is the fact that it relies entirely on the historical data, which in most cases is unknown. On the other hand, some research has modelled the structural reliability of the in-service pipes using probabilistic approach. Most of these probabilistic studies are based on the consideration that the residual strength of pipes reduces as a result of corrosion process and take into account the corrosion pit induced changes in the structural capacity. [Ahammed and Melchers 1997; Rajani and Makar 2000; Sadiq *et al.* 2004]. The probabilistic models, on the other hand, address some of the shortcomings of deterministic studies, such as need of the historical data, measurement of pit depth and the effects of the uncertainties on the prediction of the remaining life of the water main. However, the main shortcoming with deterministic methods is that there are not much documented studies to validate the two phase corrosion models used.

Based on the examination of service failures of trunk mains, most cast iron water mains failure is of the wall fracture type failure as a result of growth of a crack and subsequent breakage of the pipe, as opposed to corrosion wall pin holing in material such as steel and ductile iron [Marshall 2001]. Moreover, taking into account that the time dependant defects are defects that can become worse in service, it is important to understand the performance of pipes in the presence of growing defects. In the light of this, for the estimation of the future performance of the in-service pipes, Linear Elastic Fracture Mechanics has been used as the core principle. The present paper intends to formulate the problem of the time dependent reliability of in-service pipes and tries to integrate deterministic fracture mechanics with probabilistic analysis in a consistent manner to facilitate remaining life evaluation.

2. THEORETICAL INVESTIGATION

2.1 Formulation of Service Life Prediction

Service life of a pipe or structure in general is a time period at the end of which the pipe stops performing the functions it is designed and built for. To determine the service life for the pipe, a performance-based assessment criterion should be established. In reliability theory, this criterion is expressed in the form of a limit state function as follows:

$$G(L,S,t) = L(t) - S(t) \tag{1}$$

where $S(t)$ is the action (load) or its effect at time t and $L(t)$ is the acceptable limit (resistance) for the action or its effect. With the limit state function of Equation (1), the probability of pipe (structural) failure, p_f, can be determined by the probability of the attainment of this limit state. Making the assumption that both the applied load, S and the pipe resistance R are normally distributed, the probability of failure P_f of the concrete in-service pipe is directly obtained from

$$P_f = \Phi\left[\frac{-(\mu_R - \mu_S)}{\left(\sigma_S^2 + \sigma_R^2\right)^{1/2}}\right] = \Phi(-\beta) \tag{2}$$

where β is defined as the safety index, μ is mean and σ is standard deviation. P_f has to be smaller than an acceptable limit to eliminate undue risk of collapse. With this constraint, the expected service life can be roughly determined by assuming that the service life of the pipe is reached when P_f is equal to the acceptable limit.

To apply Equation (2) to practical structures, the main effort lies in developing a model of action process S(t). For underground pipes subjected to external corrosion, the action process is mainly related to stress intensity at the defects, i.e., pits of corrosion. For this problem, two performance criteria of interest to utility engineers will be considered in the paper: (i) leak-before-break which is a serviceability limit state in reliability theory, and (ii) structural collapse [Shreir *et al.*], which is an ultimate limit state.

2.2 Stress Intensity Factor

Cast iron is brittle material and its failure can be characterised by fracture. According to the theory of fracture mechanics, when a structural element such as a pipe, under a nominal stress contains a sharp crack, e.g., corrosion pit, the stress field ahead of the sharp crack can be related to a single parameter K, known as stress intensity factor. The stress intensity factor K is a function of far-field stress level σ_{ij}, the size of the crack/defect, a, the shape and orientation of the crack/defect, and dimensions of the element where the crack occurs. This relationship can be expressed as follows [Hertzberg 1996].

$$K = \frac{\sigma_{ij}}{\left(\frac{1}{\sqrt{2r}}\right) f_{ij}(\theta)} \tag{3}$$

Where, r and θ are the crack tip polar coordinate and $f_{ij}(\theta)$ is the correction factor. Exact equations for the stress intensity factor vary and depend on the mode of the deformation and geometry of the specimen. In this paper, only mode I, or opening mode, is considered since mode I is thought to be the dominant cracking condition in under normal service loading, i.e., a crack plane is perpendicular to the direction of the stress incurred (Marshal 2000). If K_c is defined as the critical stress intensity factor beyond which the pipe wall cannot sustain the defect, the probability of the pipe failure can be determined as follows:

$$p_f(t) = P[K(t) \geq K_c] \tag{4}$$

Evidently for different performance criteria, i.e., limit state, the values of K_t are different. In practical application of Equation (4), the main effort lies in developing a model of action process $K(t)$, since K_c is the material constant, which is related to a number of factors in particular the geometry and the microstructure of the pipe material and can be determined according to [ASTM-E1820-01 2001]. For

this paper reliability of the buried pipes with only external surface crack pits subjected to service loading are investigated. For stresses, two states will be considered; (i) hoop stress that causes longitudinal crack (perpendicular to stress direction); and (ii) normal stress that causes transverse crack (also perpendicular to stress direction).

2.2.1 Case 1 External surface pit under hoop stress.

The typical example of this case is a pipe under internal pressure and subjected to external corrosion. Figure 1 shows an idealised section of a pipe with external pitting corrosion which is assumed to be semi-elliptical.

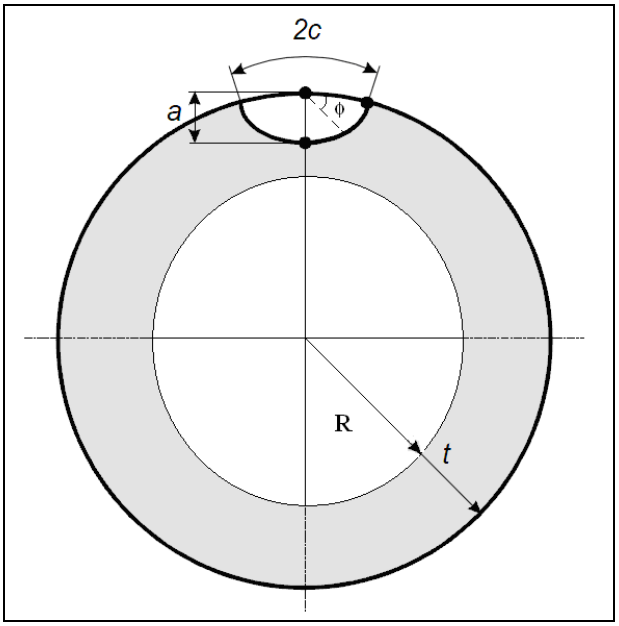

Figure 1. External semi-elliptical surface crack of a pipe.

In Fig. 1, *2c* is the width of the semi-elliptical pit, *a* corresponds to the depth of the pit through the pipe wall and the angle ϕ is used to describe the position around the semi-elliptical pit which varies between $0 \le \phi \le \pi$. The stress intensity factor K_1 for a semi-elliptical external surface pit under an internal pressure can be determined as follows [Newman and Raju 1982]

$$K_{I1} = \sigma_{hoop}\sqrt{\pi \frac{a}{Q}} F_e\left(\frac{a}{t}, \frac{a}{c}, \frac{t}{R}, \phi\right) \tag{5}$$

where, *c* is the surface length of the defect, *a* is radial depth of the defect, *R* is inner diameter, *t* is the thickness, ϕ is the parametric angle of the semi-elliptical crack, and F_e is the boundary correction factor for a semi-elliptical surface crack (pit) located outside an internally pressurised pipe and can be determined from

$$F_e = \frac{t}{R}\left(\frac{R_o^2}{R_o^2 - R^2}\right)\left[2G_0 + 2\frac{a}{R}G_1 + 3\left(\frac{a}{R}\right)^2 G_2 + 4\left(\frac{a}{R}\right)^3 G_3\right] \tag{6}$$

where, G_j is the influence coefficient for *j*th stress distribution on crack surface. The values of G_0, G_1, G_2 and G_3 for a semi-elliptical external surface crack for a/c=1 condition are obtained from an earlier study [Newman and Raju 1982]. Also in Equation (5) *Q* is semi-elliptical defect correction and can be determined from

$$Q = 1 + 1.464\left(\frac{a}{c}\right)^{1.65} \tag{7}$$

2.2.2 Case 2 External surface pit under normal stress.

This is the case when a pipe is subjected to external corrosion pits and under normal stresses, e.g. bending and tensile stresses. In this case, the stress intensity factor for a semi-elliptical external surface pit can be determined by modified version of Newman [Newman and Raju 1979] as follows:

$$K_{I2} = (\sigma_t + H\sigma_b)\sqrt{\pi \frac{a}{Q}} F(\frac{a}{t}, \frac{a}{c}, \frac{c}{R}, \phi) \tag{8}$$

Where F and H are defined as boundary correction factors for tensile σ_t and bending stress σ_b and are determined from:

$$F(\frac{a}{t}, \frac{a}{c}, \frac{c}{R}, \phi) = \left[1.040 + 0.201\left(\frac{a}{t}\right)^2 - 0.106\left(\frac{a}{t}\right)^4\right] \times \left[\sec\left(\frac{a\pi}{2R}\sqrt{\frac{a}{t}}\right)\right]^{0.5} \tag{9}$$

$$H = 1 - 1.34\left(\frac{a}{t}\right) - 0.03\left(\frac{a}{t}\right)^2 \tag{10}$$

For the present paper conservative assumptions and simplified form of Equations (5)-(10) is used to measure a lower (conservative) value for K_I, where the stress intensity factor for the deepest point of the crack, ($\phi = 90°$), is considered. In Equations (5)-(10) it is also assumed that *c*, the surface length, and *a*, the radial depth of the semi-elliptical surface flaw, are equal. This comes from the assumption that a semi-elliptical surface crack tends to grow more rapidly in a direction parallel to the minor axis of the ellipse and the stress intensity factor has been ($\phi = 90°$) until the flaw approaches a semicircular configuration [Hertzberg 1996]. These modified equations give mode *I* stress intensity factor, K_I, at the deepest points on the periphery of a semi-elliptical crack.

2.3 Fracture toughness

The material property pertinent to the present fracture mechanics analysis is the plane strain fracture toughness which is a function of material thickness[Hertzberg 1996]. The method predicts that crack instability (fast fracture) occurs when the stress intensity factor reaches a critical value called fracture toughness K_{Ic}. The value of stress intensity factor K_I can increase only when the applied load is increased; the defect/crack length is increased, or the thickness of the plate is decreased. Under an assumption that the buried pipes experience a constant service loading, then the value of K_I can only increase and reach to its critical value, K_{Ic}, when the defect/s grow to a critical length a_c.

As indicated, defects in buried cast iron pipes could be generated during installation or arise in service amongst which the time dependent defects e. g. corrosion pits are the most prominent ones. Taking into account that the time dependant defects are defects that can become worse in service, it is important to understand the performance of pipes in the presence of growing defects. That is, understanding the rate at which a corrosion pit will perforate the pipe wall and reaches a critical size that cannot to be sustained by the pipe anymore is of particular importance for the method of the calculation of the reliability proposed in this paper.

3. CORROSION PROPAGATION

Since the purpose of this paper is to predict the service life of water mains subjected to external corrosion defects that grows in time, the loads that pipes are incurred over the service life are assumed to be constant. Under this assumption the key to determine the stress intensity factor and hence the probability of a pipe failure is to determine the depth of corrosion pit, *a*. The corrosion rate of in-service cast iron pipes is believed to slow down over time as corrosion is a self-inhibiting process [Shreir *et al.* 1994]. Corrosion of cast iron pipes is a complex process and can occur both internally and externally. The external corrosion of the buried pipes is considered to be aqueous, but the condition can range from fully immersed solution to atmospheric, depending on the soil compactness and the water content and can range from rapid to almost negligible [Chacker and Palmer 1989]. A number of models have been proposed to estimate the depth of corrosion pit based on the corrosion rate of the buried pipes. These models have been subject to debates as to whether the corrosion rate has been assumed linear or otherwise. The loss of pipes wall thickness has been the subject of debate [Kucera and Mattsson 1987; Sadiq *et al.* 2004]. In this paper a power law corrosion rate has been introduced based on Kucers model [Kucera and Mattsson 1987] to address the effect of the type of pipe material/microstructure in the reliability performance of them. The modification to Kucera model in this paper was done to incorporate materials coefficients in the formula. This modification is appropriate as Kucera models does not take into the account the impact of the microstructure of cast iron on the corrosion rate [Lunarska 1996].

$$a_t = \alpha t^{\beta n} \tag{11}$$

Where, *a* is the loss of wall thickness (depth of corrosion pit) at time *t*, and α and β are pipe's material constant.

In the present paper an experimental work was carried out on specimens from a 32" diameter cast iron trunk main, which was previously failed in service, in order to determine the corrosion rate of the pipe. Plates from the pipe was cut in to bars and then machined and cut into samples of nominal size of 35x25 mm x the thickness of the pipe, which were 22 mm. Six specimens from Pipe B were subjected to laboratory corrosion test over a period of 15 months. The specimens were exposed to an aerated tap water solution. Information regarding the micro-structural analysis and fracture properties of the pipe can be found in an earlier study [Mohebbi *et al.* 2010]. The samples were washed using 50% acetone, dried prior to the exposure to the aerated flowing tap water. The specimens were placed on knife edge nylon bars in a tray, exposed to flowing water pumped from reservoir tanks, containing tap water. For this experiment 25 litres of solution was required (15 litres in the specimen tray plus 10 litres of the solution held in the reservoir tank), where water was pumped from a 10 lit reservoir tank with a flow rate of $0.3mm^3/s$. Electrochemical measurements were carried out using a computer controlled Gamry PCI4750 potentiostat. The study was conducted in a temperature controlled environment (23±1 ºC). A saturated calomel electrode and a carbon rod were used for reference and auxiliary electrodes respectively. The corrosion rates of the specimens were calculated after 12 and 15 months of the commencement of the test using Electrochemical Frequency Modulation (EFM) technique. The value of α and β, material constants of Equation (11), was then calculated by differentiating the Equation (11) and using the regression analysis with three data points. The values of α and β reflect the differences in the microstructure ,e.g. pearlite content and the graphite morphology in the corrosion rate of the cast iron samples respectively.

4. WORKED EXAMPLE

In this worked example, information obtained from the experimental procedure of the corrosion rate (loss of wall thickness) and fracture toughness is used in the investigation of structural reliability of Pipe B. For this, four types of service loading stresses are considered; (i) internal pressure; (ii) point load due to poor bedding condition (iii) bending loads; and (iv) axial loads due to temperature

variation. For the calculation of the stresses the worst case scenario has been assumed, where pipes are buried about 0.9 m depth under the main road condition. The stresses imposed by thermal contraction of pipes has been assumed to be 18 MPa [Marshall 2001]. The calculation of the stresses was done according to BSEN1295.

Figure 2 (P_f vs. time) present the probability of the failure of Pipe B based on the worst case scenario service loading and laboratory modelled corrosion rate for a given perlitic microstructure and calculated with Equations (2) and (4). Figure 3 (P_f vs. time for various thickness) illustrates that he expected life of an in-service cast iron can vary depending on the thickness, service loading regime and condition.

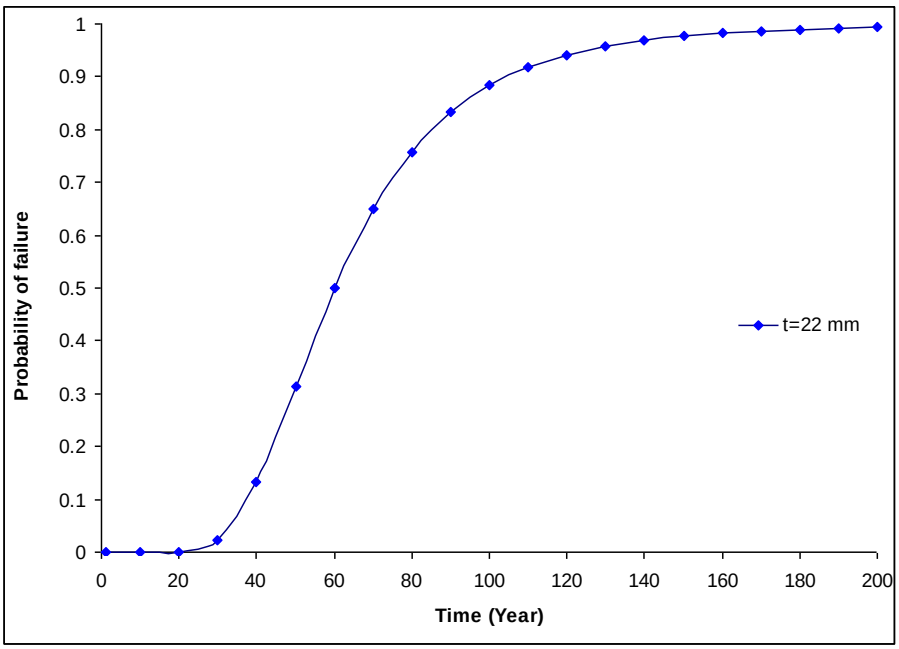

Figure 2. Probability of failure vs. Time.

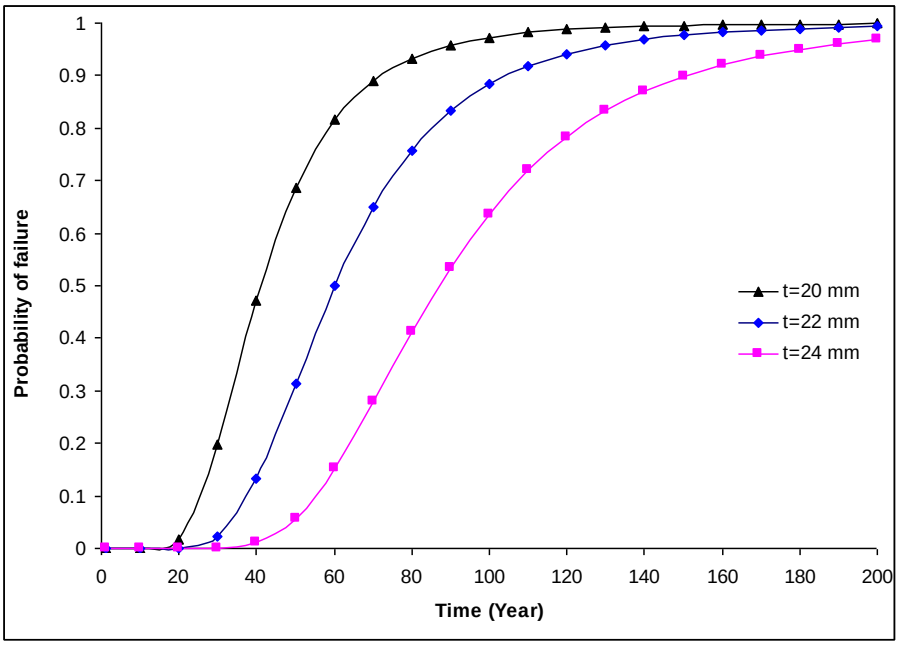

Figure 3. Probability of failure vs. time for various thicknesses.

From Fig. 2 it is seen that the structural reliability of buried water mains remains relatively constant only for a small period of time and then it suffers a steep decline. The time when this steep decline starts depends mainly on the thickness of the pipe, the extent of corrosion defect and in the case of the small diameter pipes the size of the unsupported length of the pipe. Once significant decline in structural reliability starts its rate depends mainly on corrosion rates and occurrence rates of the intermittent loads. From Fig. 3 it is seen that as the thickness of the pipes decreases, the ratio of a_c/t (thickness of the wall) gets larger. This means that the increase in the thickness of the same diameter pipes decreases stresses imposed by internal pressure and point load.

6. CONCLUSION

The variation in the corrosion rate and the thickness of different diameter pipes used in the study indicated that a considerable portion of the networks may not be far from the point where the steep decline in their structural reliability starts. The use of fracture mechanics in implementation of a probability-based reliability method represents an approach that has shown to be both useful and practical.

Further work needs to be done to improve or develop a corrosion pit growth as a function of microstructure and environment. Furthermore, it is important to take into account the effect of the internal corrosion pits on the life predication of the pipes.

REFERENCES

Ahammed, M. and R. E. Melchers (1997). "Probabilistic analysis of underground pipelines subject to combined stress and corrosion." *Engineering Structures* **19**(12): 988-994.

ASTM-E1820-01 (2001). Standard Test Method for Measurement of Fracture Toughness, ASTM international.

Atkinson, K., J. T. Whiter, M. J. Mulheron and P. A. Smith (2002). "Failure of Small Diameter Cast Irion Pipes " *Urban Watter* **4**: 263-271.

Chacker, V. and J. D. Palmer, Eds. (1989). *Effect of soil characteristic on corrosion*. ASTM special technical publication, Ann Arbor.

Hertzberg, R. W. (1996). *Deformation and Fracture Mechanics of Engineering Materials*. Chichester, Wiley.

Kucera, V. and E. Mattsson (1987). Atmospheric Corrosion. *Corrosion Mechanics*. E. Mansfeld. New York, Marcel Dekker Inc.

Lunarska, E. (1996). "Effect of Graphite Shape on the Corrosion of Grey Cast Iron in Phosphoric Acid." *Materials and Corrosion* **47**: 539-544.

Marshall, P. (2001). The residual structural properties of cast iron pipes- Structural and design criteria for lining for water mains *Pipeline innovation*.

Mohebbi, H., D. Jesson, M. J. Mulheron and P. A. Smith (2010). "The fracture and fatigue properties of cast iron used in the water industry." *Materials Science and Engineering a-Structural Materials Properties Microstructure and Processing* **527**: 5915-5923.

Newman, J. C. and I. S. Raju (1979). "Analysis of surface cracks in finite plates under tension or bending loads ".

Newman, J. G. and I. S. Raju (1982). "Stress-Intensity Factors for Internal and External Surface Cracks In Cylindrical Vessels." *Journal of Pressure Vessel Technology* **Vol. 104**: 293-298.

Rajani, B. and J. Makar (2000). "A Methodology to Estimate Remaining Service Life of Grey Cast iron Water Mains." *Canadian Journal of Civil Engineering* **27**(6): 1259-1272.

Sadiq, R., B. Rajani and Y. Kleiner (2004). "Probabilistic risk analysis of corrosion associated failures in cast iron water mains." *Reliability Engineering & System Safety* **86**(1): 1-10.

Shreir, L. L., R. A. Jarman and G. T. Burstein (1994). *Corrosion*, Butterworth Heinemann.

XII DBMC
International Conference on Durability of Building Materials and Components
PORTO - PORTUGAL, April 12th-15th, 2011

Mould Growth Modelling to Evaluate Durability of Materials

Hannu Viitanen [1]
Tuomo Ojanen [2]
Ruut Peuhkuri [3]
Juha Vinha [4]
Kimmo Lähdesmäki [5]
Kati Salminen [6]

ABSTRACT

This paper presents the latest findings of mould growth and the modelling of these factors on different materials. Expected risk and durability of materials to mould growth can be predicted by solving a numerical value, so called mould growth index, by using the dynamic temperature and relative humidity histories of the subjected material surfaces. An improved mould growth model has been developed by taking into account different materials and the effect of seasonal, long period dry or cold periods that do not allow growth. The laboratory and field results show that the sensitivity of mould growth index level may vary in a large range depending on materials and the boundaries of materials. Different mould sensitivity classes of materials have been found varying from resistant to very sensitive.

KEYWORDS

Mould fungi, Modelling, Moisture, Temperature, Building materials.

[1] Technical Research Centre of Finland , VTT, Espoo, FINLAND, hannu.viitanen@vtt.fi
[2] Technical Research Centre of Finland , VTT Expert Service Ltd, Espoo, FINLAND, tuomo.ojanen@vtt.fi
[3] Technical Research Centre of Finland , VTT, Espoo, FINLAND, ruut.peuhkuri@vtt.fi
[4] TUT, Tampere University of Technology, FINLAND, juha.vinha@tut.fi
[5] TUT, Tampere University of Technology, FINLAND, kimmo.lahdesmaki@tut.fi
[6] TUT, Tampere University of Technology, FINLAND, kati.salminen@tut.fi

1 INTRODUCTION

There are several biological processes causing aging and damage to buildings. Partly this is due to natural ageing of materials (like gray surface of wood in outdoor conditions), and partly it is caused by excess moisture (damage during use). The critical factors for these processes are water and temperature. Mould typically affects the quality of the adjacent air space with volatile compounds and spores (Airaksinen et al 2004). The next stage of moisture induced damage, the decay development, forms a serious risk for structural strength depending on moisture content, materials, temperature and time. The worst decay damage cases in North Europe are found in the floors and lower parts of walls, where water accumulates due to different reasons. For mould development, the minimum (critical) ambient humidity requirement is shown to be between RH 80 and 95 % depending on other factors like ambient temperature, exposure time, and the type and surface conditions of building materials (Clarke et al. 1998, Sedlbauer 2001, Viitanen 1996). For decay development, the critical humidity is above RH 95 % or wood moisture above 25 – 30 %, depending on temperature (Viitanen 1996).

2 CRITICAL CONDITIONS FOR THE ACTIVITY OF ORGANISMS AND DAMAGE

In the table 1, general overview on the critical humidity or moisture conditions for decay activity of some organisms are shown. We know that the mould fungi are often the first colonizers microbes on building materials. On the exterior surfaces, growth of mould fungi, algae and even lichens is a normal part of the reaction to outdoor climate.

On indoor surface, the growth of mould fungi or bacteria should be avoided, and the modern life style where people spend more time indoors and are more exposed to indoor air sets higher demands for the reliable function of the whole building system. The economical consequences of the humidity and microbial growth related problems in buildings are remarkable. E.g. poor indoor air quality in schools or in working places has been shown to interfere with learning or working activities and can cause discomfort, irritation, and various short- and long-term health problems. This is especially acute in Nordic countries, where the climate is colder and the air ventilation through open window is not suitable during cold winter periods.

With very sensitive building materials, like pine sapwood, the relative humidity level of 80 % RH is typically considered to be the lowest possible to allow growth during long exposure time. Even lower levels of relative humidity has been used (75 % RH), but mainly for other than building materials. With more resistant materials the required growth condition is obviously higher or, at least, the required exposure time is much longer.

Modelling of mould growth and mould development based on humidity, temperature, exposure time and material will give new tools for the evaluation of durability of different building materials and structures. The models make it possible to evaluate the risk and development of mould growth and to analyse the critical conditions needed for the start of mould growth. It is also a tool to measure the progress of mould development under different conditions on the structure surfaces.

3 MODELLING OF MOULD GROWTH

3.1 Original mould growth model based on the work with untreated pine and spruce sapwood

The first version of the mould growth model was based on large laboratory studies with pine sapwood (Viitanen and Ritschkoff 1989). The mould growth intensities were determined at the constant conditions. In the later stages, studies in varied and fluctuated humidity conditions were performed and based on these studies, mould growth model (equation 1) was presented by Hukka and Viitanen 1999.

$$\frac{dM}{dt} = \frac{1}{7 \cdot \exp(-0.68 \ln T - 13.9 \ln RH + 0.14W - 0.33SQ + 66.02)} k_1 k_2 \quad (1),$$

where the factor k_1 represents the intensity of growth (Equation 3), W is the timber species (0 = pine and 1 = spruce) and SQ is the term for surface quality (SQ = 0 for sawn surface, SQ = 1 for kiln dried quality). For other materials than wood the value SQ = 0 is used, which omits this factor. Numerical simulation is typically carried out using one hour time steps (climate data intervals) and hours are used in the equations instead of days.

$$k_1 = \begin{cases} 1 & \text{when } M \le 1 \\ \dfrac{2}{t_{M=3} / t_{M=1} - 1} & \text{when } M > 1 \end{cases} \quad (2).$$

In this equation (2) the factor $t_{M=1}$ is the time needed to start the growth (M = 1, Table 2), and $t_{M=3}$ the time needed to reach level M =3. The factor k_2 (Equation 3) represents the moderation of the growth intensity when the mould index (M) level approaches the maximum peak value in the range of 4 < M < 6.

$$k_2 = \max[1 - \exp[2.3 \cdot (M - M_{max})], 0] \quad (3),$$

where the maximum mould index M_{max} level depends on the current conditions (Equation 4):

$$M_{max} = 1 + 7 \cdot \frac{RH_{crit} - RH}{RH_{crit} - 100} - 2 \cdot \left(\frac{RH_{crit} - RH}{RH_{crit} - 100} \right)^2 \quad (4).$$

In Equation 5 RH_{crit} is the limit RH level to start the mould growth.

3.2 Models for the mould growth on other building materials

Mould growth model was improved in a project carried out at VTT (Technical Research Center of Finland) and Tampere University of Technology. This project included large sets of steady-state and dynamic laboratory experiments for typical building materials: Spruce board (with glued edges), concrete (K30, maximum grain size 8 mm), aerated concrete, cellular concrete, polyurethane thermal insulation (PUR with paper surface and with polished surface), glass wool, polyester wool and expanded polystyrene (EPS) (Salminen et al. 2009). Pine sapwood was used as a reference material. The results of these experiments were used to improve the existing numerical model for mould growth. Based on the experimental data, new mould growth threshold value could be set for some, more resistant materials to 85 % RH.

The mould growth intensities were determined from the constant condition. The idea was to compare the mould growth of different materials to that of the pine sapwood. These correlations could be used to generate such factors that could be applied in the original model for different materials.

3.2.1 Growth intensity factors for other materials

The factors presented in equations (1) – (5) were determined for different new materials using the experimental results. The growth intensity factor k1 was determined using the time needed for the mould index to change from level M = 1 to level M = 3. The original moudl index scale was adjusted for the other building materials (Table 1).

Table 1. Mould Index for Experiments and Modeling. New determinations for index levels 3 and 4 are presented using bold fonts.

Index	Description of the growth rate
0	No growth
1	Small amounts of mould on surface (microscope), initial stages of local growth
2	Several local mould growth colonies on surface (microscope)
3	Visual findings of mould on surface, < 10 % coverage, or, **< 50 % coverage of mould (microscope)**
4	Visual findings of mould on surface, 10 - 50 % coverage, or, **>50 % coverage of mould (microscope)**
5	Plenty of growth on surface, > 50 % coverage (visual)
6	Heavy and tight growth, coverage about 100 %

The new mould growth intensity factors are presented as relative values compared to those of the reference material pine by using Equations (5) and (6).

$$k_1 = \frac{t_{M=1,pine}}{t_{M=1}} \quad \text{when M < 1} \tag{5}$$

$$k_1 = 2 \cdot \frac{\left(t_{M=3,pine} - t_{M=1,pine}\right)}{\left(t_{M=3} - t_{M=1}\right)} \quad \text{when M} \geq 1 \tag{6}$$

where $t_{M=1}$ is the time needed for the material to start the growth (Mould index reaches level M = 1), and $t_{M=3}$ the time needed for the material to reach level M =3. The subscript $_{pine}$ refers to the value with the reference material pine

Table 2 represents the tested materials, whose resulting mould indexes were used for the determination of k_1 for the respective classes. The k_1 classes were determined by using expert estimation for most suitable values.

Table 2. Mould growth sensitivity classes and some corresponding materials in the research. The figure in table illustrates the predicted mould growth for the established sensitivity classes for constant conditions at 97 % RH and 22 C.

Sensitivity class	Materials
Very sensitive	Pine sapwood
Sensitive	Glued wooden boards, PUR with paper surface, spruce
Medium resistant	Concrete, aerated and cellular concrete, glass wool, polyester wool
Resistant	PUR polished surface

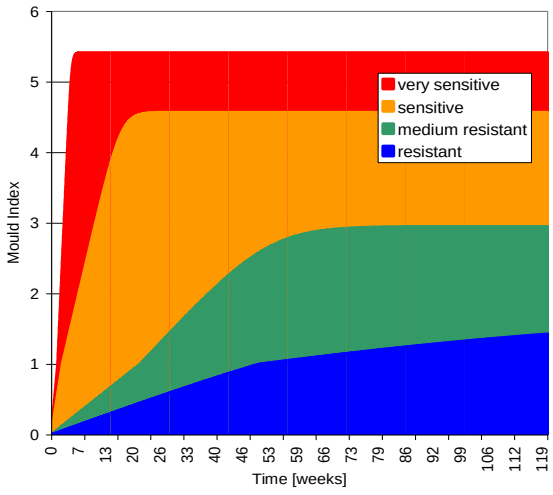

The mould growth maximum values set restrictions for the growth and limit the index to realistic levels. For the new set of materials the equation of the maximum mould index level was written in form (Equation 7):

$$M_{\max} = A + B \cdot \frac{RH_{crit} - RH}{RH_{crit} - 100} - C \cdot \left(\frac{RH_{crit} - RH}{RH_{crit} - 100} \right)^2 \quad (7)$$

In this equation the coefficients A, B and C can have values that depend on the material class. The new M_{max} has an effect on the factor k_2 (Equation 3) and it contributes to the simulation results. Table 4 presents the maximum levels of mould index values for different materials under different conditions. These results were classified to material sensitivity groups, presented both for growth intensities and maximum mould index levels. Table 3 gives the values for the growth intensity parameter k_1 classes and for the coefficients of the maximum mould index factors M_{max} and k_2. The factor RH_{min} represents the minimum humidity level for starting mould growth for each material group.

Table 3. Parameters for the sensitivity classes of the updated mould model.

			k_2 (M_{max})			RH_{min}
Sensitivity class	**M<1**	**M≥1**	**A**	**B**	**C**	**%**
very sensitive, vs	1	2	1	7	2	80
sensitive, s	0.578	0.386	0.3	6	1	80
medium resistant, mr	0.072	0.097	0	5	1.5	85
resistant, r	0.033	0.014	0	3	1	85

The factors presented in Table 5 form the new basis for numerical simulation of mould growth on different material surfaces. These values will be applied in the following studies where the model performance will be evaluated.

3.2.2 The decline of the mould growth and mould index caused by frost or dry condition

As living organisms mould fungi need water and suitable temperature to grow. When conditions are unfavorable for fungi, activity of mould fungi will be inactivated depending on the extent of the frost or dryness and the time periods of unfavorable conditions, see
Figure 1.

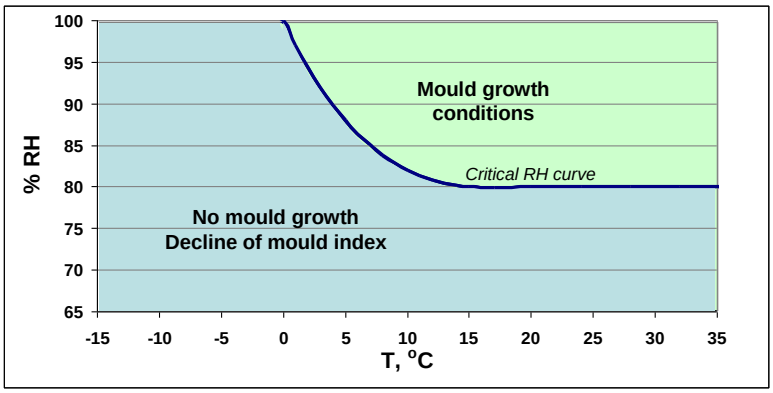

Figure 1: Illustration of the regimes for the favaourable and unfavourable conditions for mould growth**.**

The degradation of mould on wooden surface has been modeled based on cyclic changes between two humidity conditions (Equation 8).

$$\frac{dM}{dt} = \begin{cases} -0.00133, \text{when } t - t_1 \le 6\,\text{h} \\ 0, \text{when } 6\,\text{h} \le t - t_1 \le 24\,\text{h} \\ -0.000667, \text{when } t - t_1 > 24\,\text{h} \end{cases} \quad (8),$$

where M is the mould index and t is the time (h) from the moment t_1 when the conditions on the critical surface changed from growth to outside growth conditions.

Under long period seasonal variations of humidity conditions the decline of mould index may e differ from that presented in Equation 8. Also the material may have a significant effect on the decline process. The decline of mould index for other materials was presented using a constant, relative coefficient for each material (Equation 9).

$$\frac{dM}{dt}_{mat} = C_{mat} \cdot \frac{dM}{dt}_{0} \quad (9),$$

where $(dM/dt)_{mat}$ is the mould decline intensity for each material, $(dM/dt)_0$ is that for pine in the original model (Equation 9), and C_{mat} is the relative coefficient for mould index decline used in the simulation model. The original decline model for wood could be applied using these additional factors.

The decline of mould intensity on materials under unfavorable mould growth conditions could be presented as decline classes (Table 4). This classification is based on few measurements with relatively large scattering and it should be considered as the first approximation of these classes.

Table 4. Classification of relative mould index decline.

C_{eff}	**Description**
1.0	Pine in original model, short periods
0.5	Significant Relevant decline
0.25	Relatively low decline
0.1	Almost no decline

4 USING THE MODELS TO PREDICT THE EFFECT OF EXPOSURE CONDITIONS ON DURABILITY OF BUILDING MATERIALS

Mould growth is one of the first signs of biological deterioration caused by excess of moisture, and therefore mould growth can be used as one of the best hygrothermal performance criteria of building structures. Mould does not deteriorate the material, but it is a sign of too high moisture content and it represents a risk for other moisture caused problems, like decay. This has been one of the main motivations to develop and use numerical models for mould growth.

When evaluating the performance and durability of the building constructions with the mould growth model, the results from dynamic hygrothermal simulations can be easily post processed with the presented mould growth model. For more serious damage to develop, decay development model should be used (Viitanen et al. 2010).

One of the basic outputs from the dynamic heat and moisture simulations are the hourly temperature and relative humidity conditions in a specific location of the construction. These locations depend strongly on the studied construction type. For the assessment purpose of the performance, a set of

hygrothermal simulations with parameter variations can be created in such way that a potential trend of solutions will be revealed. The issue to investigate could be e.g. what effects the insulation thickness or a specific insulation material or exterior finish or if a non-ventilated construction have on the hygrothermal performance of the construction. In Figure 2 there is an example on the mould modelling calculations of such an investigation

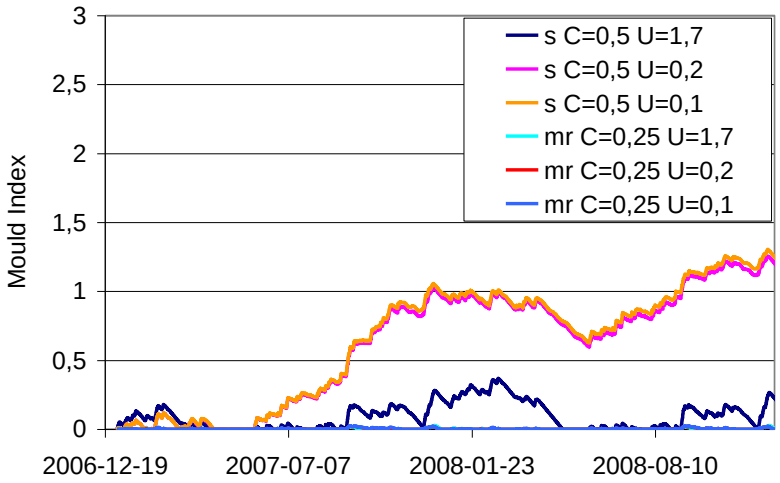

Figure 2: Calculated mould index on the extetior surface of a wall. Effect of different U-values (U=0,1 -1,7 W/m2K) and assumptions for sensitivity classes (s= sensitive and mr = medium resistant) including decline (C=0,5 and C=0,25).

If the assumptions for the presented mould growth calculation were that the material of the exterior surface is moderate resistant to biological growth, i.e. inorganic material, there will be no risk for mould growth. But if the surface contains organic material, there will be a risk of mould growth both moderately and very well insulated constructions.

It must be emphazied that the results of mould modelling calculations must be seen in relation to other solutions and not as absolute values. Often the most important information from the calculations is, however, if the modelled mould growth is increasing from year to year - or not. For the example case, this makes the hygrothermal conditions of this construction risky if the surface includes organic material. On the other hand, mould spores are naturally everywhere and therefore hard to avoid especially on the exterior part of the building constructions. In addition, the conditions of the exterior parts of the building envelope are close to exterior weather conditions, which in many climate regions are favourable for mould growth.

DISCUSSION AND CONCLUSION

The presented numerical mould growth model is based on experimental results from several research projects. It is suitable for post-processing temperature and humidity data from any numerical simulation of hygrothermal conditions in building constructions. However, it must be kept in mind when performing the assessment that there are a great uncertainty coupled to this kind of analysis:
the variation of the material sensitivities is high, estimation of a product sensitivity class is difficult without testing, the surface treatments may enhance or reduce growth potential, different mould species have different requirements for growth and the evaluation of the actual conditions in the critical material layers may include uncertainties.

Nevertheless, the motivation to use and develop numerical mould growth models and application of them is to give tools for better prediction and evaluation of the risks for biological growth on structure surfaces and to find the best solutions to ensure safe performance for the building and the indoor

climate. The best way to use the predicted mould growth as an assessment tool is to compare different solutions with each others: The solution with the lowest risk for the mould growth would most probably also have least other moisture related problems.

ACKNOWLEDGMENTS

This paper is a part of the project "Modelling of mould growth" financed by Tekes, Industry and VTT.

REFERENCES

Airaksinen M; Kurnitski J; Pasanen P; and Seppänen O. 2004 Fungal spore transport through a building structure, Indoor Air, 14: 92-104.

Clarke, J.A. Johnstone, C.M. Kelly, N.J. Mclean, R.C. Anderson, J.A., Rowan N.J. and Smith, J.E. 1998. A technique for prediction of the conditions leading to mould growth in buildings. Building and Environment 34 pp 515-521.

Hukka, A, and Viitanen, H. 1999. A mathematical model of mould growth on wooden material. Wood Science and Technology. 33 (6) 475-485.

Salminen, K., Viitanen, H., Paajanen, L., Lähdesmäki, K., Strander, T., Vinha, J., Iitti, H., Ojanen, T., Peuhkuri, R. 2009. Mould growth on building materials in laboratory and field experiments(in Finnish). Rakennusfysiikka 2009. Symposium Proceedings. Tampere 2009. pp.219 -228.

Sedlbauer, K. 2001. Prediction of mould fungus formation on the surface of/and inside building components. University of Stuttgart, Fraunhofer Institute for building Pgysics, Thesis. Stuttgart. Germany.

Viitanen, H. 1996. Factors affecting the development of mould and brown rot decay in wooden material and wooden structures. Effect of humidity, temperature and exposure time. The Swedish University of Agricultural Sciences. Uppsala, 1996.

Viitanen, H. & Ritschkoff, A. 1991. Mould growth in pine and spruce sapwood in relation to air humidity and temperature. Uppsala. The Swedish University of Agricultural Scienses, Department of Forest Products. Report no 221. 40 p.

Viitanen, H; Vinha, J; Salminen K; Ojanen, T; Peuhkuri, R. Paajanen, L; Lähdesmäki, K. 2010. Moisture and bio-deterioration risk of building materials and structures. Journal of Building Physics. 33 (3) 201-224.

XII DBMC
International Conference on Durability of Building Materials and Components
PORTO - PORTUGAL, April 12th-15th, 2011

Material Specific Isopleth-systems as Valuable Tools for the Assessment of the Durability of Building Materials Against Mould Infestation – The "Isopleth-traffic Light"

Klaus Sedlbauer [1]
Wolfgang Hofbauer [2]
Nicole Krueger [3]
Florian Mayer [4]
Klaus Breuer [5]

ABSTRACT

Information on the resistance of building materials against microbiological infestation is of great interest in material development/optimization for the construction of new buildings or for remediation since humidity and mould have been recognized as important health hazards. A valuable tool for the comparative durability assessment of materials against mould infestation is the so-called material specific isopleths system. It specifies the combinations of temperature and relative humidity under which it is infestation tolerant or not. If a certain material is characterized according to its resistance against unwanted growth of mould, the range of environmental conditions in which it can be used is clearly defined. In a practical approach the material specific isopleths systems can be used as a mould resistance indicator system analogue to a "traffic light". It is possible to distinguish between a range of conditions under which mould growth is likely to occur ("red"), and another range under which mould growth cannot be completely excluded ("yellow"), as well as finally a range under which no growth is to be expected ("green"). Not only different materials and constructions can be compared by means of this isopleths system but also different methods against fungal infestation can be evaluated, e.g. the use of biocides. The data acquired provide for product development an additional and new tool and also give planners and users additional security.

KEYWORDS

Mould resistance, Isopleth system, Microorganisms, Building materials, Indoor environment.

[1] Fraunhofer-Institute for Building Physics (IBP), Valley, GERMANY, klaus.sedlbauer@ibp.fraunhofer.de
[2] Fraunhofer-Institute for Building Physics (IBP), Valley, GERMANY, wolfgang.hofbauer@ibp.fraunhofer.de
[3] Fraunhofer-Institute for Building Physics (IBP), Valley, GERMANY, nicole.krueger@ibp.fraunhofer.de
[4] Fraunhofer-Institute for Building Physics (IBP), Valley, GERMANY, florian.mayer@ibp.fraunhofer.de
[5] Fraunhofer-Institute for Building Physics (IBP), Valley, GERMANY, klaus.breuer@ibp.fraunhofer.de

1 INTRODUCTION

Dampness and mould indoors are recognized as important risks to health (e.g. [Bonnefoy et al. 2003], [Bornehag et al. 2004], [Mudarri & Fisk 2007], [Heseltine & Rosen 2009], [Klich 2009]). Therefore information on the resistance of building materials against microbiological infestation is of great interest in material development and optimization for the construction of new buildings or for remediation purposes. Material compounds, constructions and whole buildings behaviour can be assessed theoretically mathematically, simulation tools are constantly increasing. Also energy flows and consumption can be modelled, as well as the hygrothermal conditions within a material or a complete wall structure. With special models it is even possible to calculate temperature and humidity conditions in the cross section of a building part or in a room to predict mould growth, if the climatic environment parameters and the hygrothermal features of the employed materials are known (e.g. [Viitanen 1994], [Rowan et al. 1997], [Viitanen 1997], [Hukka & Viitanen 1999], [Sedlbauer 2001], [Sedlbauer 2002]). Still these models indicate the possibility of unwanted growth quite general. In order to describe the specific reaction of growth or germination of the different mould species to different combinations of temperature and relative humidity and water activity, respectively, there was established a so called "isopleth-system" (e.g. [Snow 1949]; [Ayerst 1969]; [Smith & Hill 1982], [Mangan & Lacey 1984]). The original investigations were made by using nutrient rich culture media and quite some species have been characterized in this way until now. Recently this kind of isopleth system was found to be suitable also for describing the relation of mould fungi to environmental conditions within the building situation (e.g. [Rowan et al. 1997], [Rowan et al. 1999], [Sedlbauer 2001], [Sedlbauer 2002]). Data of many building part relevant species have been collected and used to define a "lowest isopleth for mould" (LIM 0), which describes the border conditions for any mould growth at optimal media [Sedlbauer 2001]. Actual growth of mould on a special material not only depends on suitable environmental conditions but also on its chemical and physical characteristics. Many materials that are used for building parts and constructions can not be regarded as optimal media for growth of moulds. Therefore different border conditions for different classes of materials have been evaluated. Apart from LIM 0 further border lines for different groups of materials can be defined as seen in figure 1 [Sedlbauer 2001; Sedlbauer et al. 2001]). Substrate class I and LIM I describe materials that are easy degradable, but do not contain nutrients as much as optimal media. Substrate class II and LIM II indicate materials with very low amount of nutrients. Finally substrate class III and LIM III stand for materials without nutrient, biologically inert. Substrate group III is not shown because there growth of fungi is only to be expected if additional nutrients are brought in by contamination. This grouping is still rather general and there is a need to know more exact data for building materials, for material specific isopleth systems. The follwing describes a special experimental setup with which more accurate and comparable measurements can be performed and whose data are used to define material specific isopleth systems.

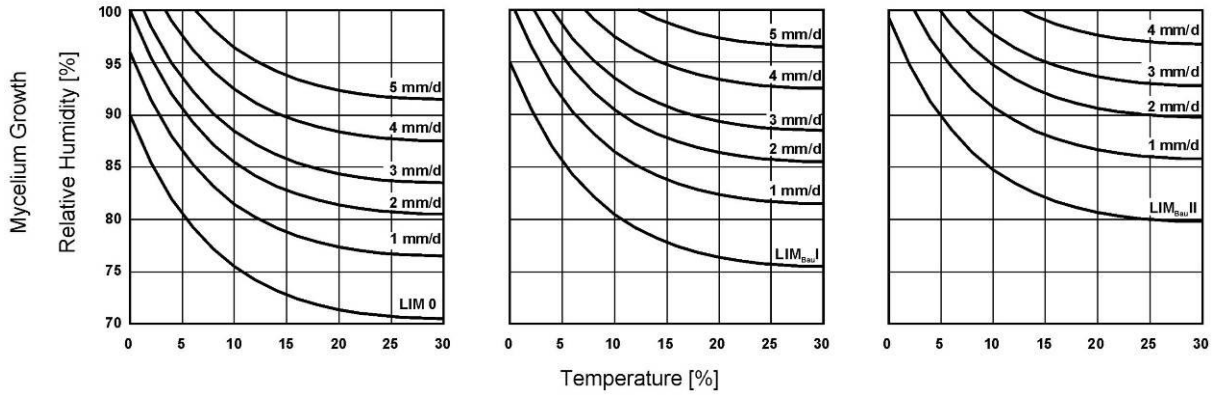

Figure 1. Generalized isopleth systems for mycelial growth on different substrates. The left graph describes the behaviour on optimal substrate; the centre for substrate group I and the right for substrate group II.

2 METHODS

For detailed investigations a special experimental set up was developed and many different materials have been characterized so far. The underlaying principle is a connection of a dew point bath and an incubator [Hofbauer et al. 2005a]; [Hofbauer et al. 2005b]; [Hofbauer et al. 2008]. Controlled by a flow meter air flows through an inlet filter and through a water bath and is thus saturated with water at temperature t_1. Then this water saturated air is conducted into an incubator and further into an incubation unit where it is warmed up to temperature t_2. Heating to t_2 results in a relative humidity which is defined by law of nature and can be taken from the corresponding Mollier diagrams or be calcultated by the Magnus formula. By constantly recording t_1 and t_2 the whole system is controlled on line. Additionally lighting can be empoyed and therefore also the behavior of photosynthetic organisms like algae and lichens on the surface of building materials can be assessed. For experiments 12 different incubation units with different combinations of temperature and humidity are used. Measurements are conducted for 100 days because afterwards germination of originally inoculated spores is not to be expected. Test specimen are checked for beginning of mould growth until the end of the measurements. Growth and condition of fungi is recorded and documented by taking photographs. The different test conditions, combinations of temperature and relative humidity, are selected in order to enclose situations in old buildings with rather low surface temperatures as well as insulated new buildings [Hofbauer et al. 2005a]. An example of typical test climates which are used during measurements is shown in table 1. The test climates can be altered in order to refer to special conditions or materials. For the investigation of materials used in a bath room, for instance, the conditions may be altered to higher levels.

Table 1. Test climates set up in the different incubation units.

Number of incubation unit	*relative humidity* [%]	*temperature* [°C]
1	85	10
2	88	10
3	90	10
4	93	10
5	95	10
6	97	10
7	75	25
8	78	25
9	81	25
10	84	25
11	87	25
12	90	25

Special test specimen have to be produced from the materials which are investigated. Therefore a square piece of the size of 5 x 5 cm² is cut out of the material. If the material for investigation is loose it is kept in containers made of wire mesh of the same outline. Before inoculation with a mixture of spores the test specimen are sterilized by gamma radiation in order to avoid additional spore contamination. For the experiments well known building material related fungi are inoculated as a mixture (tabel 2). Since different materials can be colonized by different species of mould the choice of fungi is very important and depends on the investigated materials. For instance testing of products which are derived from animals (e.g. wool) with fungi which are known from plant substrates only (e.g. wood, hemp) is not feasible. The fungi mentioned in table 2 are common in indoor environments and may grow on a wide range of substrates including animal matter like leather. In order to investigate more extreme ecologies, which could be assumend for wet and hot rooms like a bathroom, partly other fungi would be used which are more adapted to the proposed conditions and materials, e.g. *Phialophora* spp. or *Exophiala* spp. or other fungi capable of hot and amphibic conditions.

Table 2. Example for fungal species used in the measurements.

species of mould	*special characteristic*
Eurotium chevalieri	drought tolerant
Penicillium chrysogenum	drought tolerant
Wallemia sebi	drought tolerant
Acremonium strictum	prevalent after water damage
Chaetomium globosum	prevalent after water damage
Scopulariopsis brevicaulis	prevalent after water damage
Alternaria alternata	frequent air germ
Aureobasidium pullulans	frequent air germ
Cladosporium cladosporioides	frequent air germ
Mucor racemosus	frequent air germ

3 RESULTS

The data which are gained with the special set up show clearly when and to which extent mould growth happens on the test specimen within the investigation time. On the surface of the test specimen it can be distinguished between the inoculation zone and the original material surface. Since spores do contain some nutrients for germination and because also very little traces of adhering nutrients at the washed spores from growth media or parts from mycelia might provide additional source of nutrients usually the area of inoculation is excluded for results. Regarding mould resistance of certain building materials the results of the measurements are expressed in a so called isopleth system. Using data of twelve different test climates a range can be given in which the material specific border isopleth is found. That means below this range no mould growth is to be expected whereas above the range mould growth will occur within 100 days.

As a practical approach the isopleth-diagrams presented can be used as a mould resistance indicator system analogous to a traffic light (fig. 2). In the center area of the diagram mould growth is possible ("yellow", means attention). In the upper range mould growth will occur ("red") and the material is absolutely not suitable for those climatic conditions. In the lower area there is no mould growth to be expected ("green").

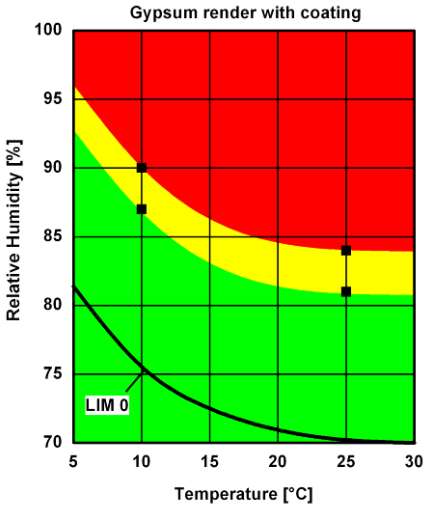

Figure 2. Practical approach to the isopleth system with the colours of a traffic light for a material with average resistance. Whereas the green area marks conditions under which the material is safe against mould infestation the yellow area shows the possibility for growth of mould and conditions under which mould growth is expected are red. LIM 0, lowest isopleth for mould, is marked.

As already expected materials on a mineral basis with very low content of nutrients show a rather high resistance against mould. Further investigations of different building materials with a high content of organic matter revealed only partly a lower resistance against growth of mould. Surprisingly some organic products, such as a hemp mat for insulation, showed profiles indicating a high resistance against mould, which was not expected. With the measured data different profiles can be assigned to the three substrate classes mentioned before (figure 3, 4 and 5). Measurements presented are all conducted under steady conditions. With the experimental set up also dynamic tests can be carried out. Further measurements are currently under way.

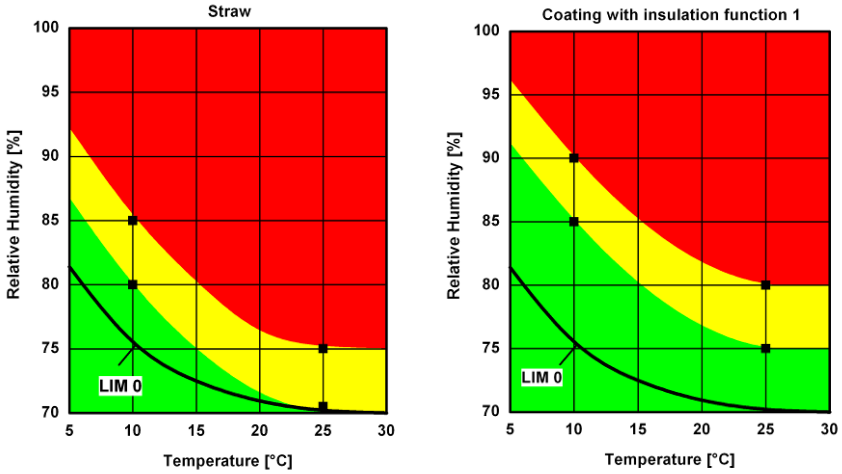

Figure 4. Isopleth systems of wheat straw and a special insulation coating. These isopleth systems represent substrate class I. LIM 0, lowest isopleth for mould, is marked.

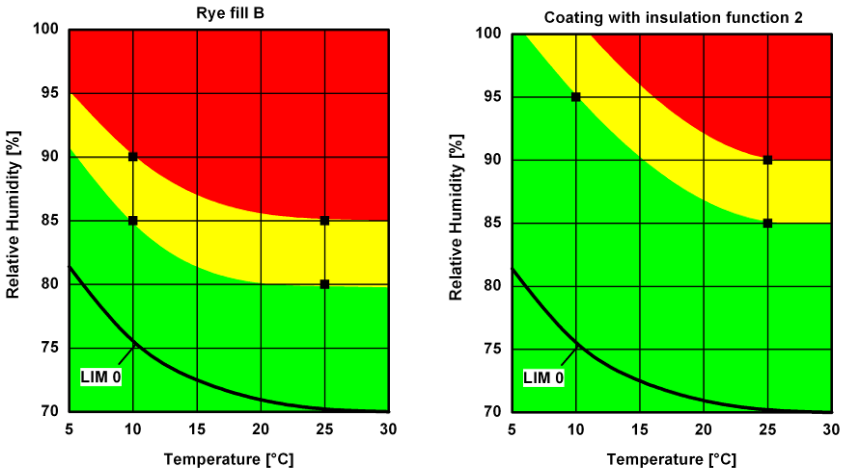

Figure 5. Isopleth systems of a rye fill and another insulation coating. They show material characteristics of substrate class II. LIM 0, lowest isopleth for mould, is marked.

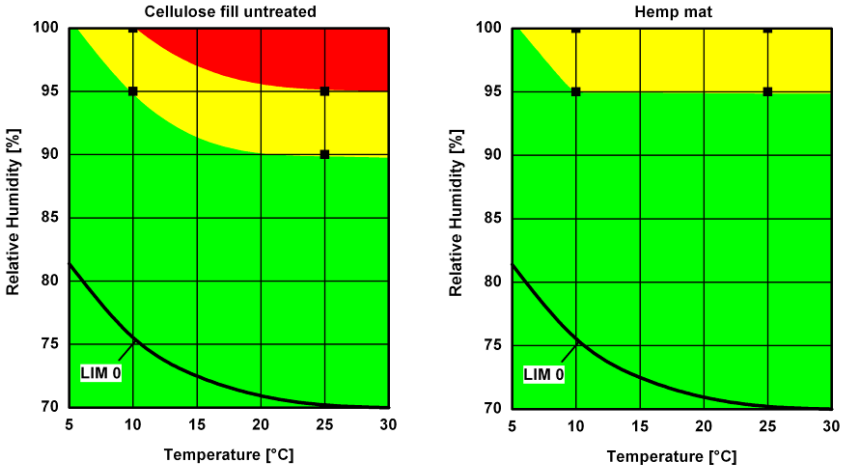

Figure 6. Two different materials, cellulose fill and hemp mat, that are very resistant against mould colonization. The second material, hemp mat, is almoust reaching substrate class III. LIM 0, lowest isopleth for mould, is marked.

4 DISCUSSION

The isopleth ranges presented are based on measurements performed and are the closest approximation according to the already established LIM curves. Additional measurements with different combinations of temperature and relative humidity than used so far would provide further data to narrow down the given ranges until a single curve can be established for each material. Measurements are performed with real material relevant fungal agents. In comparison to models or other quick test methods [Viitanen, 1994]; [Li et al., 2005] not regarding the real behavior of mould on a building material in a practical time scale the data gained here with an admittedly elaborate investigation method are much more reliable and material specific. In a different approach by Nielsen et al. [2004] also controlled humidity and temperature were applied. Assessment of fungal growth was done in a different way and the used fungal isolates were different. The results were shown as course diagrams, therefore the material properties can be compared for the measured data whereas our model allows some extrapolation. The presented data can be used in different ways. At first they give an easy and clear overview on the conditions under which the investigated material itself is suitable for application. Furhter they can be used for some improvements of the material or they indicate if additional measurements are necessary in order to prevent damage (e.g. use of biocidal agents, alteration in the construction, additional heating). And eventually they are essential for mathematical calculations within the building situation and for compound constructions. In the recent years some experience with material specific isopleth ranges was made [Hofbauer et al. 2005a],[Hofbauer et al. 2005b], [Hofbauer et al. 2008]. Some effort is already made for experimental material characterization in a dynamic environment [Sedlbauer 2002], [Cziesielski & Belaschk 2004], [Karlström 2004], [Isaksson et al. 2010]. Althoug very elaborated methods for measurements and experimental concepts in defining the relation of microbial growth and material properties have been used there are still problems in transfering the gained knowledge into practice, to detatch it from the exactly defined experiments and to use it in the random environment of a real building. The isopleth traffic light allows to compare the resistance against microbial infestation of different materials directly and forms an important baseline for future dynamic concepts.

5 CONCLUSIONS

The experimental set up presented is very suitable to characterize building materials according to the isopleth system. Each material has its own profile which enables classification into one of three different substrate classes of building materials. Furthermore, if a certain material is characterized

according to its resistance against unwanted growth of moulds the range of environmental conditions in which it can be used is clearly defined. Thus the measurements give planners and users of buildings a better security in choosing suitable materials for every circumstance. Besides characterization of different materials and compounds against mould colonization investigations on growth conditions of certain mould species or investigations at dynamic conditions can be performed by use of this multifunctional experimental tool that is presented here. Data according to the "isopleth traffic light" form a baseline for further dynamic experiments.

ACKNOWLEDGEMENTS

Thank is due to Xella Technologie- und Forschungsgesellschaft mbH, Gips-Schüle Stiftung, Deutsche Bundesstiftung Umwelt and Fachagentur Nachwachsende Rohstoffe e. V. for support.

REFERENCES

Ayerst G. 1969, 'The Effects of Moisture and Temperature on Growth and Spore Germination in some Fungi', *J. stored Prod. Res*. **5**, pp. 127-141.

Bonnefoy X.R., Braubach M., Moissonnier B., Monolbaev K., Röbbel N. 2003, 'Housing and Health in Europe: Preliminary Results of a Pan-European Study', *American Journal of Public Health* **93**(9), pp. 1559-1563.

Bornehag C.G., Sundell J., Bonini S., Custovic A., Malmberg P., Skerfving S., Sigsgaard T., Verhoeff A. 2004, ' Dampness in buildings as a risk factor for health effects, EUROEXPO: a multidisciplinary review of the literature (1998–2000) on dampness and mite exposure in buildings and health effects', *Indoor Air* **14**(4), pp. 243-257.

Cziesielski E. & Belaschk H. 2004, 'Rechnerische Methoden zur Erfassung von Wärmebrücken im Hinblick auf einen möglichen Schimmelpilzbefall', Bauphysik **26**, pp. 347-352.

Heseltine E. & Rosen R. (eds.) 2009. *'WHO guidelines for indoor air quality: dampness and mould*', World Health Organization.

Hofbauer W., Breuer K., Tschaikner A., Krus K., Sedlbauer K., Schoch T. 2004a, 'Vergleichende Untersuchungen zum Schimmelpilzwachstum auf verschiedenen Baustoffoberflächen – materialspezifische Wachstumsisoplethen', *IBP Mitteilung* **32**(457): 2 pp.

Hofbauer W., Breuer K., Krueger N., Sedlbauer K. 2005, 'Toxic mould versus façade-jungle – a comparison of undesirable biological growth on indoor surfaces and outer building coatings', Proceedings of the 10th International Conference on Indoor Air Quality and Climate – Indoor Air 2005, Beijing, Vol. 2, pp. 2450-2454.

Hofbauer W., Krueger N., Breuer K., Sedlbauer K., Schoch T. 2008, 'Mould resistance assessment of building materials - Material specific isopleth-systems for practical application', in Proceedings of the 11th International Conference on Indoor Air Quality and Climate, eds P. Strøm-Tejsen, B.W. Olesen, P. Wargocki, D. Zukowska, J. Toftum, Indoor Air 2008, August 17-22 2008, Copenhagen, Denmark.

Hukka A. and Viitanen H.A. 1999, 'A mathematical model of mould growth on wooden material', *Wood Science and Technology* **33**, pp. 475-483.

Isaksson T., Thelandersson S., Ekstrand-Tobin A., Johansson P. 2010, 'Critical conditions for onset of mould growth under varying climate conditions', *Building and Environment* **45**, pp. 1712-1721.

Karlström P. 2004, 'Soft Heating and Cooling in Humid Climates', Haster Thesis, Royal Institute of Technology (Sweden).

Klich M.A. 2009, 'Health effects of *Aspergillus* in food and air', *Toxicology and Industrial Health* **25**(9-10), pp. 657-667.

Li Y., Wadsö L., Bjurman J. (2005), 'Using measurements of fungal activity by isothermal microcalorimetry as a base for modelling fungal growth in buildings', Proceedings of the 10th International Conference on Indoor Air Quality and Climate – Indoor Air 2005, Beijing, Vol. 2, pp. 2439-2443.

Mangan N. & Lacey J. 1984, 'Effect of Temperature and pH on Water Relations of Field and Storage Fungi', *Trans. Br. Mycol. Soc.* **82**(1), pp. 71-81.

Mudarri D. & Fisk W.J. 2007, 'Public health and economic impact of dampness and mold', Indoor Air 17(3), pp. 226-235.

Nielsen K.F., Holm G., Uttrup L.P., Nielsen P.A. 2004, 'Mould growth on building materials under low water activities. Influence of humidity and temperature on fungal growth and secondary metabolism', *International Biodeterioration & Biodegradation* **54**, pp. 325-336.

Rowan N.J., Anderson J.G., Smith J.E., Clarke J.A., McLean R.C., Kelly N.J., Johnstone C.M. 1997, 'Development of a Computer Programme for the Prediction and Control of Mould Growth in Buildings Using the ESP-r Modelling System', *Indoor and Built Environment* **6**, pp. 4-11.

Rowan N.J., Johnstone C.H., McLean R.C., Anderson J.G., Clarke J.A. 1999, 'Prediction of Toxigenic Fungal Growth in Buildings by Using a Novel Modelling System', *Applied and Environmental Microbiology* **65**(11), pp 4814-4821.

Sedlbauer K. 2001, *'Vorhersage von Schimmelpilzbildung auf und in Bauteilen*', Ph.D. Thesis, Stuttgart University (Germany).

Sedlbauer K. 2002, 'Prediction of Mould Growth by Hygrothermal Calculation', *Journal of Building Physics* **25**, pp. 321-336.

Sedlbauer K., Zillig W., Krus M. 2001, 'Isoplethensysteme ermöglichen eine Abschätzung von Schimmelpilzbildung', *IBP-Mitteilung* **28**(388), 2 pp.

Smith S.L. and Hill S.T. 1982, 'Influence of temperature and water activity on germination and growth of *Aspergillus restrictus* and *A. versicolor*', *Trans. Br. mycol. Soc*. **79**(3), pp. 558-560.

Snow D. 1949, 'The germination of mould spores at controlled humidities' *Ann. appl. Biol*. **36**, 1-13.

Viitanen H. 1994, 'Factors affecting the development of biodeterioration in wooden constructions', *Materials and Structures* **17**(172), pp. 483-493.

Viitanen H. 1997, 'Modelling the Time Factor in the development of Mould Fungi - the Effect of Critical Humidity and Temperature Conditions on Pine and Spruce Sapwood', *Holzforschung* **51**, pp. 6-14.

XII DBMC
International Conference on Durability of Building Materials and Components
PORTO - PORTUGAL, April 12th-15th, 2011

Artificial Neural Networks for Predicting Drying Shrinkage of Concrete

Lyes Bal [1,2]
François Buyle-Bodin [2]
Said Kenai [3]

ABSTRACT

Concrete is the most used material in construction for a century. Concrete after its casting and setting, shows various dimensional physical and mechanical evolutions of which drying. Drying accompanies the hardening of concrete and leads to significant dimensional changes that appear as pre judiciable cracks, which influence in turn the durability of the civil engineering works.

This study aims to show the application of a nonparametric approach called Artificial Neural Networks (ANN) in order to predict effectively spontaneous dimensional variations type drying shrinkage.Using this approach allows us to develop models for predicting this shrinkage. These models use a multi layer back propagation. They also depend on a very large database of experimental results obtained in the literature (RILEM Data Bank) and an appropriate choice of architectures and of used learning process. These models take into account the different parameters of concrete preservation and making which affect drying shrinkage of concrete as: Relative humidity (RH), Cure Period, volume to surface area ratio (V / S), water to cement ratio (W / C) and sand to aggregates ratio (S / A). In order to better appreciating the validity of our models, we have compared it with other existing models in the literature as: B3, ACI 209, CEB and GL2000.

In these comparisons, it seems that our models are correctly adapted to describe the evolution within time of drying shrinkage.

KEYWORDS

Concrete, Drying shrinkage, Modelling, Prediction, Artificial neural network.

[1] Laboratory of Geo-Materials, University SAAD DAHLAB of Blida (USDB), Blida, ALGERIA, lyes.bal@polytech-lille.fr
[2] Laboratory Mechanical of Lille, University of Lille1 (USTL), Lille, FRANCE, francois.buyle-bodin@univ-lille1.fr
[3] Laboratory of Geo-Materials, University SAAD DAHLAB of Blida (USDB), Blida, ALGERIA, sdkenai@yahoo.com

1 INTRODUCTION

Concrete is submitted to delayed deformations which develop without external loading, inducing a volume reduction named shrinkage. This variation is caused by evaporation of a part of the mixing water, resulting by reduction in volume of cement paste. Its prediction is of great importance regarding the aptitude for long-term operation of concrete structures. It depends on several parameters related to the composition of the concrete, the quality of its components, and the elements size as well as the external conditions of conservation. The paper focuses on the drying shrinkage. It appears at the end of the setting, due to the loss of a large part of the mixing water.

During 50 last years, various formulations of shrinkage were proposed as American Concrete Institute 209 [ACI 209], Comite Europeen du Beton (CEB) selected for Eurocode 2, B3 [Bazant & Baweja 2000]; [Bazant 1998], Atlanta [Gardner & Zhao 1993] and GL2000 [Gardner & Lockman 2001]. The results of these models of phenomenological type will be compared with those which ANN technique will give.

2 DATABASE

Data sets from experiments carried out in various laboratories, including 176 tests, supplemented of 123 tests extracted from the RILEM database are used. Various concretes made with various types of cement are considered. The modelling parameters choice is based on their effect on the shrinkage of the concrete and their availability in the databases, as the mix proportions, the relative humidity, the ratio of the volume of the sample on its surface exposed to drying, the age at which the wet cure is stopped, the average compressive strength at 28 days and the elasticity modulus at 28 days. To conduct the research a database structured under management system (DBMS) is developed.

3 NEURAL NETWORKS

Neural network (NN) is a functional abstraction of the biological neural structure of the central nervous system. Artificial neural network ANN consists of an interconnected group of artificial neurons and processes information using a connectionist approach. In most cases an ANN is an adaptive system that changes its structure based on external or internal information that flows through the network during the learning phase, usually used to model complex relationships between inputs and outputs.

The ANN elements (formal neurons) are strongly connected to each other by weights of connections which treat data input to produce the desired exits. The most basic system presents three layers, the first layer with input neurons sending via synapses data to the second layer of neurons, and then via other synapses to the third layer of output neurons. Knowledge is acquired by the network through a learning process. Connections between neurons (synaptic weights) are used to store knowledge.

The more used ANN is the multi-layer perceptron MLP with back propagation for minimizing error [Lippmann 1987]; [Rumelhart & al 1986]; [Najjar & Zhang 2000]; [Basheer & Hajmeer 1997]; [Senthil Kumar & al. 2004]. The network includes input layer, one or more hidden layers and output layer. The optimization is conducted using the minimization of the mean-squared error. The back propagation algorithm is used for learning process.

The input data are divided into three parts. 70% for the learning process, 15% for test phase and 15% for validation phase. The test phase consists in checking the network issued from the learning process on data not yet used. The validation phase is carried out on the last part of the data.

4 NEURAL NETWORKS TECHNIQUE APPLICATION

In a first stage the matrix of inputs and output are standardized. Secondly the learning process is engaged by the initialization of the correlation coefficients used for the three phases (learning, test and

validation), then of the number of neurons per hidden layer, testing first one hidden layer, then two hidden layers. The construction of the neural network passes by the use of a transfer function for each layer and of a learning algorithm which uses the technique of back Levenberg-Marquardt propagation. Table 1 presents the parameters and their range of variation.

The number of hidden layers and of neurons per hidden layer is determined by digital simulations with various network architectures. Table 2 presents different architectures.

Table 1. Used parameters – variation range.

Parameters Type	Description	Variation range
Input	***V/S*** : Volume / Surface exposed to air	$18mm \le V/S \le 200mm$
	HR : Relative Humidity	$20\% \le HR \le 75\%$
	t_c : Age at start of drying	$t_c \ge 1$ day
	t : Age of onset of shrinkage measurement	$t \ge t_c$ day
	Cement Type	Cement Type I, II et III
	C : Cement	$250kg/m^3 \le C \le 564kg/m^3$
	W : Water	$129kg/m^3 \le W \le 293kg/m^3$
	a : Aggregates	$1661kg/m^3 \le a \le 1985kg/m^3$
	S/a : Sand / Aggregate	$0.357 \le S/a \le 0.77$
	f_{cm28} : Average compressive strength at 28 days	$11.4MPa \le f_{cm28} \le 119MPa$
	E_{cm28} : Modulus of elasticity at 28 days	$12537MPa \le E_{cm28} \le 53200MPa$
Output	Drying Shrinkage ***S***	Shrinkage $(\mu m/m)$

Table 2. Effect of the hidden layers number.

Neural Network	Transfer Function	Number of Itération	Performance
NN 11- 8 - 4- 1	Tansig-Tansig-Purelin	47	0.0021
NN 11- 8 - 6- 1	Tansig-Tansig-Purelin	45	0.0091
NN 11- 9 - 4- 1	Tansig-Tansig-Purelin	25	0.0353
NN 11- 9 - 6- 1	Tansig-Tansig-Purelin	39	0.0031

Table 3. Performance of MNNPS Model (11-8-4-1).

ANN Model	Learning		Test		Validation	
	R^2	*MSE*	R^2	*MSE*	R^2	*MSE*
***MNNPS* (11-8-4-1)**	0.9788	0.0019	0.9820	0.0037	0.9740	0.0033

The performance of the network NN 11-8-4-1 is the best. This network is selected for the predicting model of drying shrinkage. The architecture of this network is presented in Figure 1. Table 3 presents

the quality of the model for the 3 phases and Figure 2 presents the comparison between experimental and calculated output for the 3 phases.

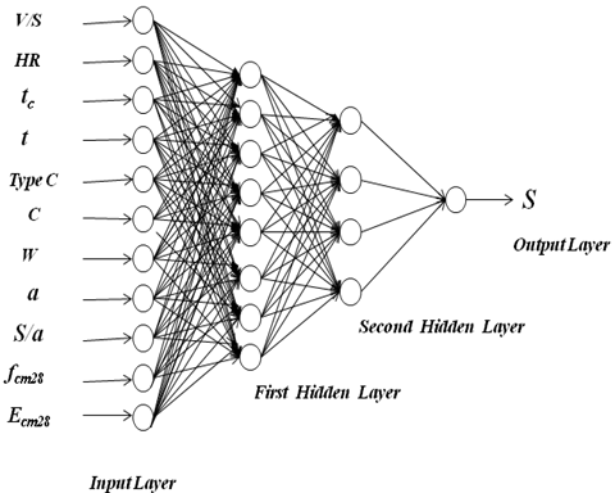

Figure 1. Selected architecture for prediction of drying shrinkage.

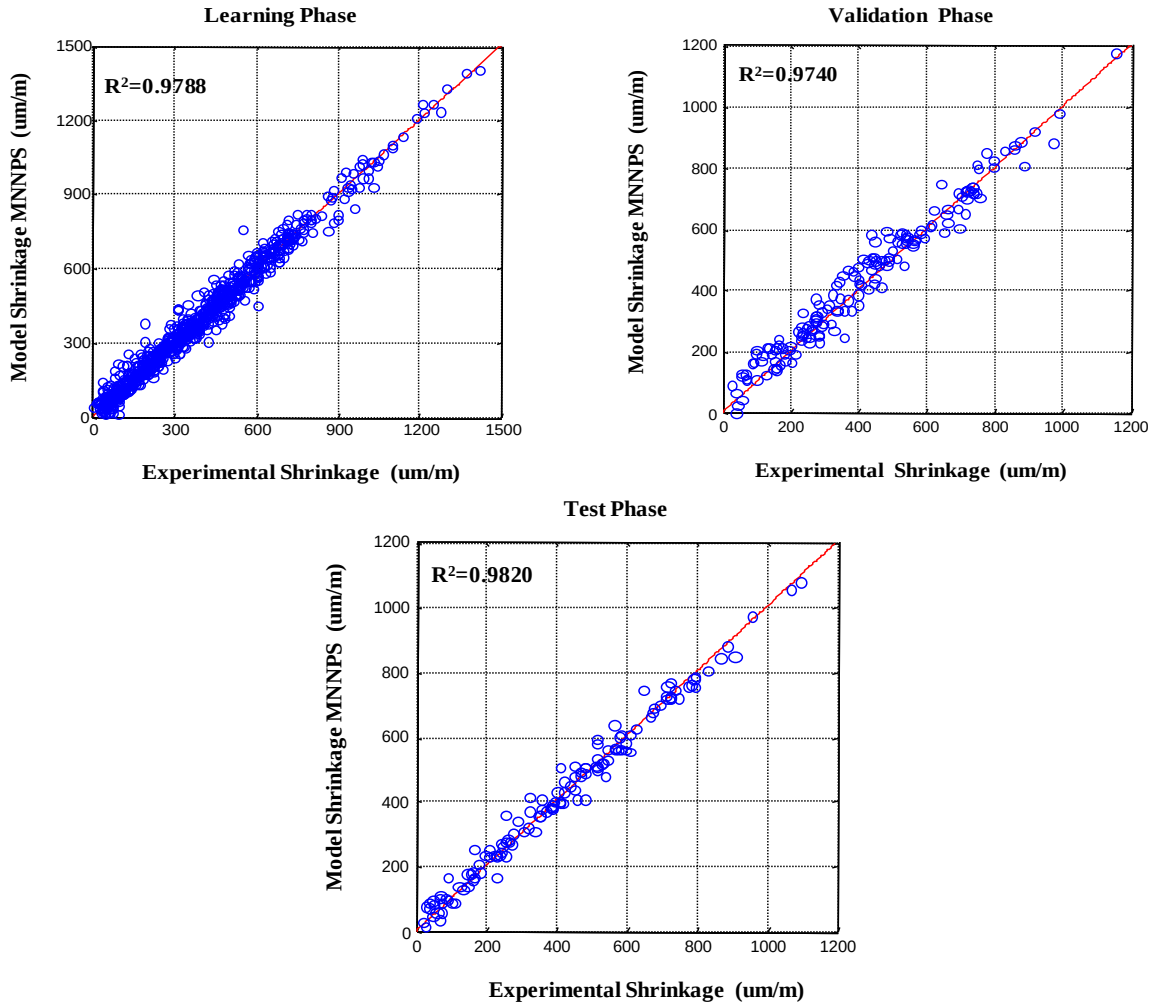

Figure 2. Performance of MNNPS Model.

5 COMPARISON BETWEEN THE PREDICTION GIVEN BY MNNPS MODEL AND OTHER MODELS.

Table 4 presents the comparison of the correlation coefficients between experimental values and those provided by the models MNNPS, ACI, CEB, GL 2000, B3 and ATLANTA.
MNNPS Model gives the best correlation, followed by B3, GL2000 and CEB.
Figure 3 presents the comparison between experimental results and calculated predictions.

Table 4. Comparison of the correlation coefficients between various models.

Models	correlation coefficients	
	R	***R*²**
MNNPS Model	0.9834	0.9672
ACI Model	0.7842	0.6149
CEB Model	0.9076	0.8238
GL2000 Model	0.9277	0.8606
B3 Model	0.9390	0.8818
ATLANTA Model	0.8993	0.8088
S.B3 Model	0.8887	0.7898

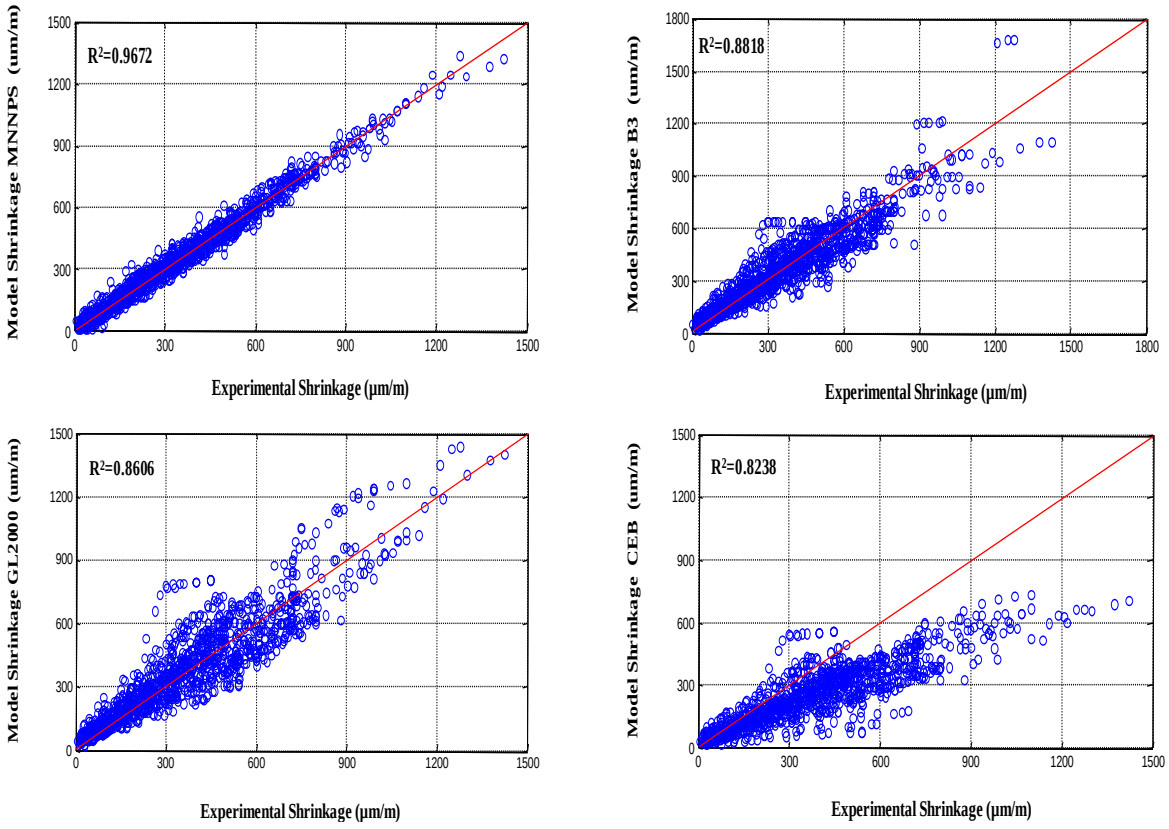

Figure 3. Comparison between experimental and calculated output issued from the models MNNPS, B3, GL 2000 and CEB.

6 CONCLUSIONS

The model based on the artificial neural network gives the best prediction of the drying shrinkage, compared to traditional models. It requires less computing time. It is not limited by the number and the nature of the input parameters.
In first approach, it seems now possible by increasing the number of these parameters to extend the model to any type of concrete, with additions, new cements etc.
More, by adding a principal component analysis, it should be possible to reduce the number of these parameters to those identified as dominant and then limit the necessary laboratory tests to predict the drying shrinkage for new formulations of concrete.

REFERENCES

ACI Committee 209, 'Guide for Modeling and Calculating Shrinkage and Creep in Hardened Concrete (ACI 209.2R-08)', *American Concrete Institute*, May 2008, 44 p.

Basheer I.A., Hajmeer M.N.,'Artificial neural network : Fundamentals, Computing Design, and Application', *Journal of Microbiological Methods*, N° 34, 1997, pp. 3-31.

Bazant Z.P.,'Criteria for Rational Prediction of Creep and Shrinkage of Concrete', Department of Civil Engineering, Northwestern University, Structural Engineering Report 98-7/B675c, Evanston, Illinois, USA, 1998, 25 p.

Bazant Z.P., Baweja S., **'**Creep and Shrinkage Prediction Model for Analysis and Design of Concrete Structures : Model B3', ACI International SP-194-1, Editor Akthem Al-Manaseer, Farmington Hills, Mitchigan, SP-194, 2000, pp. 1-83.

Gardner N. J., Lockman M. J., 'Design Provisions for Drying Shrinkage and Creep of Normal Strength Concrete', *ACI Materials Journal*, Vol. 98, N° 2, Mar.-Apr. 2001, pp. 159-167.

Gardner N. J., Zhao J.W., 'Creep and Shrinkage Revisited', *ACI Materials Journal*, N° 90-M26, May-June 1993, pp. 236-246.

Lippmann R.P.,'An Introduction to Computing with Neural Nets', *IEEE ASSP Magazine*, April 1987, Vol. 4, N° 2, pp. 4-22.

Najjar Y., Zhang X.,'Characterizing the 3D Stress-Strain Behavior of sandy Soils: A Neuro-Mechanistic Approach', In Numerical Methods in Geotechnical Engineering, ASCE *Geotechnical Special Publication*, N° 96, Filz G. and Griffiths D. (Editors), 2000, pp. 43-57.

Rumelhart, D.E., Hinton, G.E. and Williams, R.J.,'Learning internal representations by error propagation', In Rumelhart, D.E., McClelland J.L., (Eds),'Parallel Distributed Processing: Explorations in the microstructures of cognition', 1986, Vol. 1, pp. 318-362.

Senthil Kumar A.R., Sudheer K.P., Jain S.K., and Agarwal P.K.,' Rainfall-runoff modelling using artificial neural networks : Comparison of network types', *Hydrological Processes*, 2004.

XII DBMC
International Conference on Durability of Building Materials and Components
PORTO - PORTUGAL, April 12th-15th, 2011

Improving the Durability and Service Life of Wooden Components in Outdoor Applications: the French Approach

Magdalena Kutnik [1]
Marc Jequel[2]
Serge Le Nevé[3]

ABSTRACT

The European Standard EN 335 gives general definitions of Use Classes in different service situations and recommendations for their application to solid wood and wood-based products.Accurate assignment of a wooden commodity to a particular Use Class is often critical in actual practice, especially in the case of outdoor applications. Exposing an unprotected (untreated) wooden commodity to environmental factors, such as high humidity and biological agents, may result in its premature degradation. The main objective of the French project "Durability of Wooden Components" is to highlight how improving the design of wooden structures meant for outdoor applications can reduce the impact of local moisture conditions, and thus also the wood's susceptibility to fungal decay. Field experiments are currently being conducted in four different climatic areas on wooden commodities manufactured using six different untreated timber species and both traditional and improved designs. The ongoing research is strongly related to the desire of the French standardization committee to bring into compatibility different approaches to the service life of wood that are applied according to the current French and European standards and technical guidelines. As an outcome of this study, the range of timber species that could be used without any wood preservative treatment will be hopefully widened and the lifespan (or service life) of outdoor wooden commodities will be extended.

KEYWORDS

Wood durability, Service life, Use classes.

[1] Technological Institute FCBA, Laboratory of Biology, Bordeaux, FRANCE, magdalena.kutnik@fcba.fr
[2] Technological Institute FCBA, Laboratory of Biology, Bordeaux, FRANCE, marc.jequel@fcba.fr
[3] Technological Institute FCBA, Laboratory of Biology, Bordeaux, FRANCE, serge.leneve@fcba.fr

1 INTRODUCTION

Because of its inherent chemical structure, wood is susceptible to biological decay. Its natural durability to biological agents varies depending on the timber species, geographical origin, age and growth conditions of the tree, and the presence of heartwood or sapwood and their relative proportions.
The service life of wooden commodities, which means how long a product is expected to perform under specific environmental conditions, depends on many factors, which include both the material's inherent characteristics and environmental factors. Exposing wooden commodities to harsh outdoor conditions such as rain, wind and sun highly increases the risks of the material being damaged by biological organisms such as xylophageous insects and decay fungi. Therefore, proper design and protection of wooden products for outdoor use is crucial to ensure the best service life for them as expected by the market and final users.
The main biological agents that may damage wood when used outdoors under the conditions of Use Classes 3 and 4 (see the European standard EN 335-1 for the definitions) are:

- moulds and stains which are wood colonising fungi that do not cause decay but aesthetically damage the wood, thus lessening the commercial value of the product
- decay fungi, divided into brown rot, white rot and soft rot fungi, which cause severe mass and strength losses to wood
- xylophageous insects and termites, which feed on different wood compounds (starch, cellulose) and thus cause significant damage

Biological organisms usually attack the outer layers (sapwood), which constitute the non-durable portion of wood. Unlike sapwood, heartwood exhibits natural durability, which may vary from "highly durable" (Durability Class 1, see the European standard EN 350-2) to "non-durable" (Durability Class 5), depending on the timber species and its growing conditions. In order to ensure the best service life, non-durable wood must be treated according to a carefully chosen wood preservation procedure (surface application or impregnation with biocidal products, wood modification, physical protection, etc.). The choice of a particular wood protection technology should be dictated by the wood's natural durability (= the durability class), its susceptibility to preservative treatments (= the impregnability) and its exposure to environmental parameters (= the use class). However, assigning a wooden commodity to a specific Use Class is often difficult and controversial. Additionally, current knowledge about what the reference lifespan (or “life in service”) of outdoor timber structures should be is still limited. As a consequence, biological damage (mainly fungal decay) is frequently reported, chiefly caused by inappropriate use of building materials, poor design and bad maintenance generating water traps and increasing the moisture content of the wood. This is particularly true about such common wooden commodities used outdoors as decking, cladding, log houses, and exterior carpentry, which are at constant risk of being prematurely damaged.
The idea for the "Durability of Wooden Components" research project arose from the combined desire of the French public authorities and of wood industry professionals to optimize today's quasi-systematic use of biocidal preservatives meant for wood products used outdoors in response to the general bad knowledge regarding proper design and use and design, and to value the natural durability of selected French timber species. The general aim of this project is to improve the life expectancy of commodities made with untreated wood and used outdoors under different conditions of exposure and weathering.

2 EXPERIMENTAL SET UP

The current test methods used to evaluate the durability of wood species do not very well correspond with the ways of evaluating service life of finished wooden products, therefore more work is needed to improve and refine these methods. Field tests are more time-consuming compared to laboratory tests, but they render results which more closely reflect real-life condtitions (Nilsson and Edlund 1995, Brischke and Rapp 2010). The aim of the experimental phase of the project, initiated in 2009, is to work out an experimental protocol which will make it possible to estimate, in terms of service life,

the performance in a real-life situations of a range of currently used wooden commodities made of different timber species, This will involve quantifying the impact of material, climate, exposure, and design on the expected service life of selected outdoor wooden components.

2.1 The timber species

Six timber species with different levels of natural durability which are of economic importance for the construction industry in France were chosen for the study. Only the heartwood (or at least the most inner parts of the sawn logs when heartwood was not possible to distinguish from sapwood) were used.
One softwood species – Norway spruce (*Picea abies*) – and one hardwood species – poplar (*Populus sp.*) - were specifically chosen because they are non-durable and thus subject to attacks by insects and fungal decay (durability class 5, i.e. non-durable according to the European Standard EN 350-2). Including non-durable species in the experiment will allow us to evaluate the impact of design on fungal decay's kinetics after a short period of time (2-3 years), which would certainly not be the case with durable species. It should be noted, however, that in reality spruce and poplar are rarely used without any preservative treatment for outdoor applications.
Three softwood species – Douglas fir (*Pseudotsuga menziesii*), Maritime pine (*Pinus pinaster*) and larch (*Larix decidua*) – are commonly used in manufacturing outdoor commodities, mainly claddings and terrace deckings. Their natural fungal durability ranges from 3 (moderate durability) to 4 (low durability), and all three are resistant to wood boring beetles (class D) but susceptible to termite attacks (termite class S).
The last species, a hardwood one – oak (*Quercus robur*) - is classified as durable to fungal decay (class 2), durable to wood boring beetles (D) and moderately durable to termites (M).

2.2 The experimental sites

Climatic parameters such as heat, rain, wind and UV radiation strongly affect the esthetic durability and susceptibility to fungal decay of wood used for outdoor purposes. While the test set-up may be identical, climate conditions vary from one trial to another.
In order to compare the lifespan of wooden commodities under different climatic conditions, four experimental sites were selected in France as follows (see Fig. 1): Montpellier - mediterranean, Charrey sur Saône - continental, Bordeaux - oceanic, and Kourou (French Guyana) - tropical. Prior to initiating this experiment, climatic data were collected over the previous ten years at the selected sites and then analyzed.

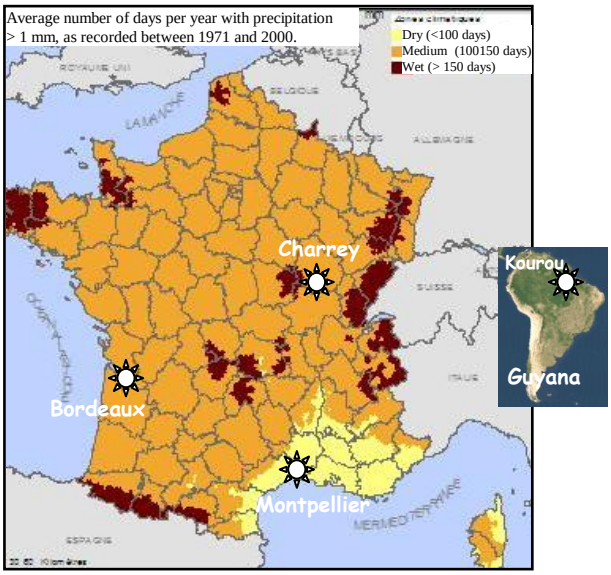

Figure 1. Locations and climatic data from the experimental sites.

2.3 The wooden commodities

Deficiencies in current practices used in designing outdoor commodities made of wood often result in the wood's excessive or abnormal moistening of wood. Wood products can contain zones where rainwater may accumulate, stagnate in a quasi-permanent way, and generate so-called “spots of insalubrity," which are generally places where biological (particularly fungal) attacks occur. Mistakes made at the conception stage often lead to a switch of the in-service situation of the wood: wooden elements initially meant for Use Class 3 are finally exposed to a level of biological risk that is higher than expected in this Use Class, such as soft rot fungi which develop more frequently on wood in Use Class 4. As a result, in situations where wooden components are not in ground contact but may permanently accumulate water due to their design or surface deposits, it may be necessary to consider that these situations are equivalent to contact with the ground or fresh water and thus require a higher level of natural or preservative-based protection.

To estimate the decay potential of different wood species under various exposure situations, various wooden commodities typically meant for outdoor use were manufactured. Identical sets of commodities were made with spruce and poplar (the less durable species) on one side (set of commodities No. 1) and with oak, larch, Douglas fir and maritime pine (the more durable species) on the other side (set of commodities No. 2) (Fig. 2).

Set No. 1 (spruce and poplar) includes:
- A horizontal structure made of six elements (decks) that are fixed on concrete blocks;
- A house-like metallic structure with different vertical (clads, logs, posts) and inclined elements (posts) attached to it by screws. The orientation of the two sides of the structure was specifically chosen in order to have one side severely exposed to wind-driven rain and one side with less severe exposure. Both sides are comprised of exactly the same wooden elements.

Set No. 2 (oak, larch, Douglas fir and maritime pine) includes:
- A horizontal structure made of two elements (decks) that are fixed on concrete blocks;
- A wall-like metallic structure with different vertical (logs and posts) elements attached to it by screws. The chosen orientation maximizes the exposure of the wooden elements to wind-driven rain.

A total of two No. 1 sets and four No. 2 sets were exposed on each of the four selected experimental fields.

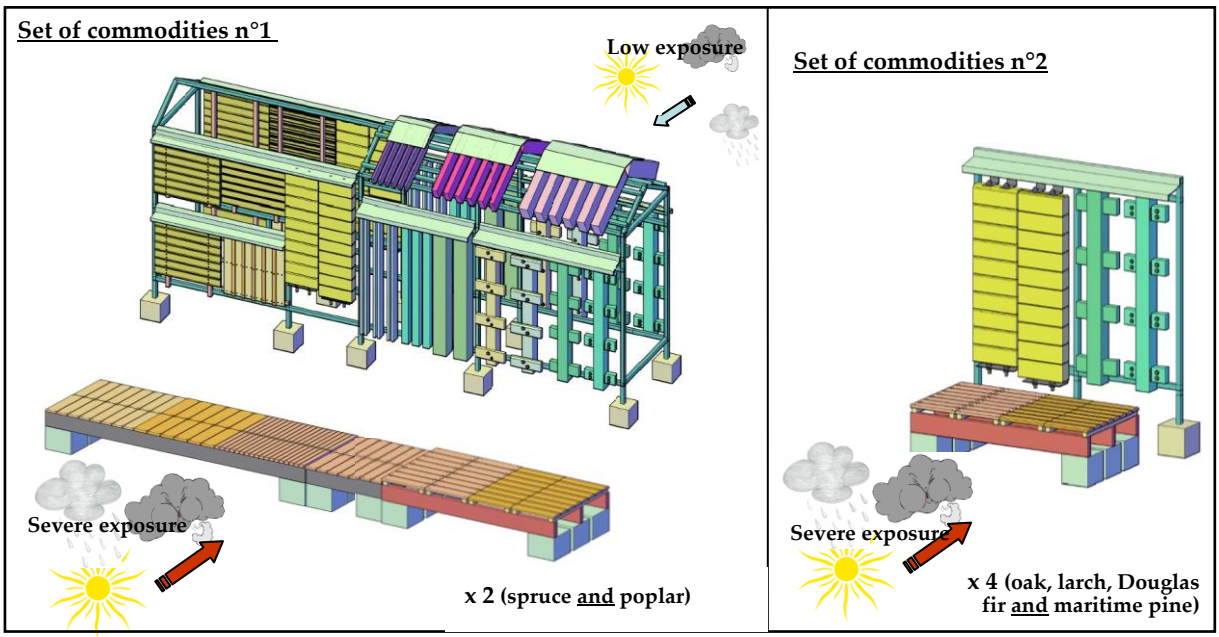

Figure 2. General presentation of the test devices installed on each experimental site.

Identical sets of experimental devices have been so far installed in Montpellier, Charrey sur Saône, and Bordeaux. Installation is still under way in Guyana.

2.4 The selected designs

For each family of commodities, different designs were selected in order to progressively decrease the risk of water being entrapped in the wood.

Decks: Horizontal structures are regarded as the most severely affected by weathering because of the possibility of rain-water accumulation and stagnation on the wood's surface. Six different designs were chosen, the main differences between them being the thickness (22 or 30 mm) and the width (5 or 12 cm) of the boards, their shape (plain or slope-shaped), the way of screwing them on the joists (top or bottom screwing), and the number of wood-to-wood contact zones generating water traps (direct contact between boards and joists or insertion of nylon or rubber joints, boards overhanging the joists or not).

Six different deck units (squares of 1 m x 1 m) were made of spruce and six of poplar, only two (with the worst and the best designs, as presented in Fig. 3) with the four other species.

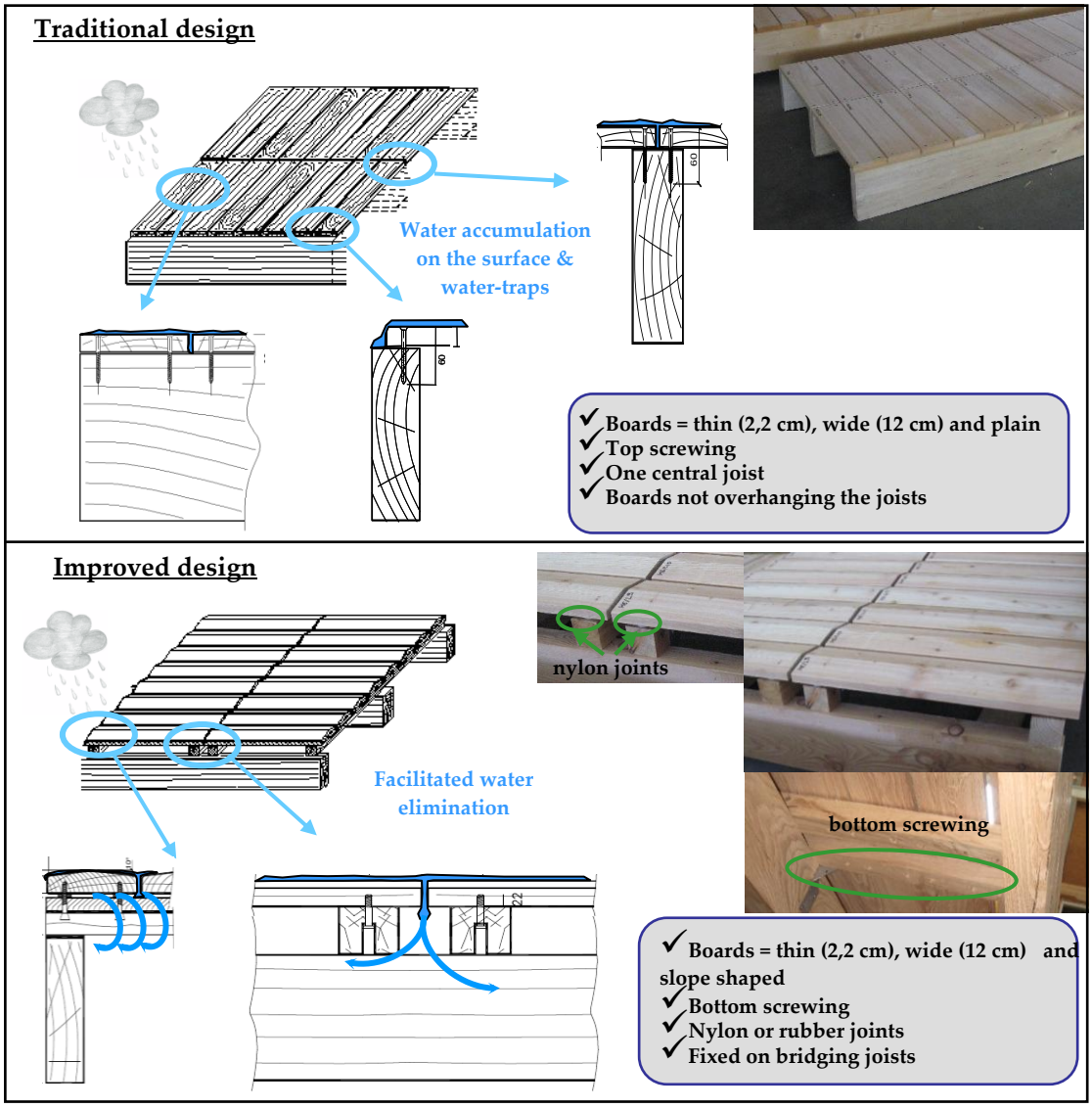

Figure 3. Examples of traditional and improved designs that have been chosen to represent the worst-case and the best-case scenario of exposure for terrace decking.

Cladding: facade elements were built after choosing four different designs, the main differences between them being the thickness (20 or 30 mm) of the test boards, the way of assembling and screwing them on the battens (tongue and groove boards with visible nails or lap joint boards with hidden nails), and the orientation of the wood's fibers (three horizontal and one vertical cladding). Each selected design was applied to manufactured cladding units of 1m x 1m.
Eight facade elements were made of spruce and eight of poplar. The same set of elements (four elements made of spruce and four elements made of poplar) was installed in situations that either allow or prevent their direct exposure to driven rain. The end-grain of the vertically exposed boards was protected from rainwater by stainless steel sheets.

Log walls: two different designs were chosen, the main differences being the shape of the logs and thus their ability to facilitate water drainage. Identical sets of log walls were installed in situations that either allow or prevent their direct exposure to driven rain.
Two different walls 2 meters high and 50 cm wide were made with each of the timber species selected for the study.

Posts: the durability of wooden posts is being tested along their incline (vertical or semi-horizontal with a 10% slope) and their thickness (from 3 to 25 cm). The initial assumption is that thicker posts may be more sensitive to deformation that can generate shrinks and cracks and thus water-traps. The end-grain of the posts was protected from rainwater by stainless steel sheets.

Posts connected to beams: different kinds of joinery are being tested which are representative of traditional carpentry: the mortise and tenon joint, which has been used for centuries around the world to connect wooden elements, mainly when the adjoining pieces connect at an angle of 90°, and the cross lap joint, which occurs in the middle of two elements being at right angles to each other.
Two innovative types of joint are also being tested, both including the use of stainless steel connectors which reduce the wood-to-wood contact zones and allow for efficient water drainage from the two connected elements.
The posts were screwed to the metallic frames. Their end-grain was protected from rainwater by stainless steel sheets.

3 EVALUATION OF THE BEHAVIOUR OF THE WOODEN COMPONENTS WITH REGARD TO BIOLOGICAL AND PHYSICAL DEGRADATION

The test specimens are exposed in different configurations producing a decay risk corresponding either to Use Class 3 or 4. The cumulated impact of the type of wood, exposure conditions and effectiveness of different protective measures by design on the service life of wooden components can be quantified through the quotation of biological and physical degradation. The progress of molds, blue stain, fungal decay as well as UV aging and the appearance of shrinks, cracks, swelling and all kinds of mechanical defects is monitored once a year, starting in 2010. Because differences between exposure sites, wood species and different designs are expected to begin to manifest themselves only after a couple of years, the experiment will be conducted over a period of ten years.

The specimens are evaluated yearly by rating the extent and distribution of molds and blue stain according to XP X 41-549 (1999) as: 0 (0% of the sapwood), 1 (<5%), 2 (6 to 25%), 3 (26 to 50%) or 4 (>50%), and of decay according to EN 252 (1989) as: 0 (sound), 1 (slight attack), 2 (moderate attack), 3 (severe attack), or 4 (failure).

After the first year of exposure, all the specimens were rated 4 for blue stain and 0 for decay in Bordeaux and Charrey. No significant differences in termes of durability were found between the different species or design details. However, big differences were reported with regard to the

mechanical behaviour of the exposed wood, swelling and shrinking strongly affecting the wooden elements exposed in Charrey (the colder area). However, after only one year of exposure, the results need to be considered as preliminary.

4 EXPECTED ISSUES FOR THE TIMBER CONSTRUCTION MARKET

The French and European standards provide keys to proper selection of timber species (EN 350-2), understanding of the biological risks associated with their use (EN 335) and proper treatment if necessary (EN 599). However, the timber construction industry needs practical guidelines that will explain how to improve the expected service life of wooden products by taking into account parameters such as climate, exposure and design details. Moreover, only informed designers are able to correctly interpret the existing standards and handle complex cases where the implementation of wooden products can turn out delicate.

One practical goal of the work being done within the framework of the "Durability of Wooden Components" project is the publication of two technical guidebooks. The results of the present field experiments will be included in the first guidebook, a collaborative effort of the FCBA and FIBC (Memento «Durability of the Works made with Wood ") and will also be used in another one, which will present « healthy » constructive solutions designed to reduce biological hazards as compared to the current practices. The first guidebook will explain the rules of assigning use classes to wooden products or components of larger structures and provide a review of different durability hazards that are commonly encountered. The second one will review the traditional designs as commonly applied for outdoor commodities and outline some recommended technical practices that architects, engineers, contractors and others can use to create long-lasting wooden structures. These technical rules will be consistent with the technical standards currently being prepared by the French Standardization Office for Wood, which aims to harmonize with one another the recommendations given in the different French standards and building specifications referring to the durability of wooden components. They are be summarized in Fig. 4.

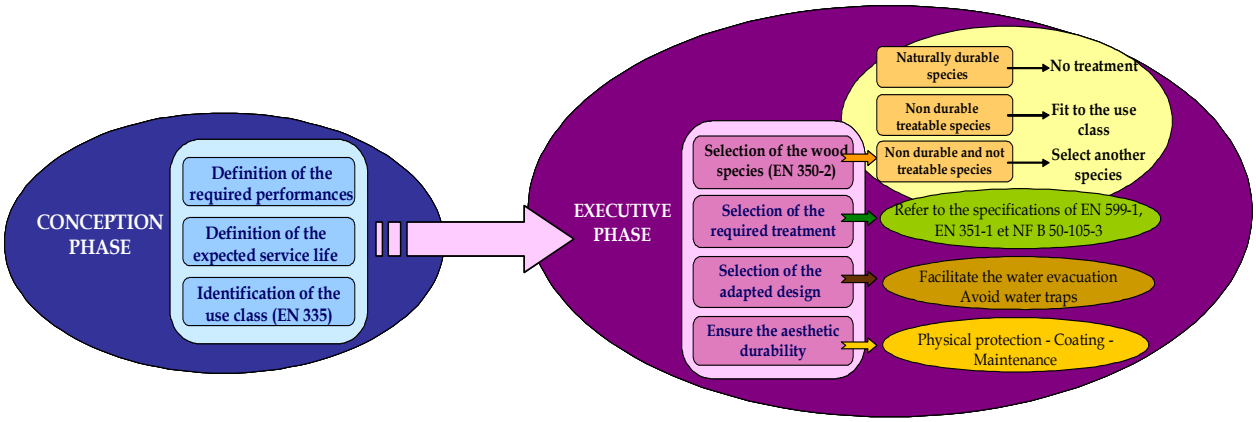

Figure 4: The decisionnal rules for propoer use of wooden components

5 CONCLUSIONS

The durability of wood is either natural or a result of appropriate treatment. Whether natural or preservative-based, it needs to be adapted to the end use of particular wooden products, commodities or structures, as their service life depends so strongly on their design and exposure to physical and biological agents. The research project presented here contributes to the knowledge of how to extend the service life of commodities made with untreated wood and increase the quality and value of timber and different wooden products.

ACKNOWLEDGMENTS

We are grateful to the French Ministry of Agriculture and Forestry (DGFAR) for the financial support given to the „Durability of wooden commodities" project. Our thanks also go to France Douglas, CRPF Champagne-Ardenne and ADIB for their help in supplying the wood, and to Lycée du Bois de Mouchard for the great job they made manufacturing and installing the experimental devices.

REFERENCES

EN 335-2 (2007) Durability of wood and wood-based products - Definition of use classes — Part 2: Application to solid wood

EN 350-2 (1994) Durability of wood and wood-based products - Natural durability of wood — Part 2: Guide to natural durability and treatability of selected wood species of importance in Europe

XP X 41-549 (1999) Wood preservatives - Evaluation of fongicide efficacy to temporary wood protectives for green sawn timber – Site method.

EN 599-1 (2006) Durability of wood and wood-based products - Effectiveness of preventive wood preservatives as determinated by biological tests – Part 1 : Specifications according to use class

Brischke, C. & Rapp, A.O. 2010, "Service life prediction of wooden components – Part 1: Determination of dose response functions for above ground decay", Document IRG/WP 10-20439. International Research Group on Wood Protection, Biarritz, France.

Nilsson, T. & Edlund, M.-L. 1995, 'Laboratory versus field tests for evaluating wood preservatives: A scientific view', Document IRG/WP 95-20076. International Research Group on Wood Preservation, Stockholm.

Ross Gobakken, L., Mattson, J. & Alfredsen, G. 2008, 'In-service performance of wood depends upon the critical in-situ conditions. Case studies', Document IRG/WP 08-20382. International Research Group on Wood Protection, Stockholm.

XII DBMC
International Conference on Durability of Building Materials and Components
PORTO - PORTUGAL, April 12th-15th, 2011

Salt and Moisture Transport in Non-Isothermal Condition Considering the Kinetics of Salt Phase Change

Marcin Koniorczyk [1]
Piotr Konca [2]

ABSTRACT

Water and salt are wildly recognized as major factors of porous materials damage, therefore a lot of experimental and theoretical studies are devoted to them. One of the most adverse phenomenon which is related to the salt and moisture presence in the pore system of building materials is salt crystallization. The experimental setup was constructed to measure the changes of temperature due to the crystallization/dissolution process. The mathematical model of salt, moisture and energy transport was derived and based on it the computer code was developed. The salt phase change kinetics is taken into account while modelling. The crystallization process itself changes the internal structure of porous medium e.g. porosity, permeability, which must be taken into account while modelling the transport phenomena. Additionally the heat is released or consumed during the crystallization/dissolution process. To solve the set of governing, differential equations the finite element and finite difference methods are used. Salt phase change was calculated using three different rate laws. The comparison of experimental data and numerical results is presented for cooling-warming of brick containing sodium sulphate.

KEYWORDS

Salt, Moisture, Energy transport, Kinetics, Crystallization.

[1] Faculty of Civil Engineering, Architecture and Environmental Engineering, Łódź, POLAND, marcin.koniorczyk@p.lodz.pl
[2] Faculty of Civil Engineering, Architecture and Environmental Engineering, Łódź, POLAND, piotr.konca@p.lodz.pl

1 INTRODUCTION

One of the most adverse phenomenon which is related to the salt and moisture presence in the pore system of building materials is salt crystallization. Salt crystallization during drying using NMR was recognized by Pel et al.[2004]. The equation for maximum stress caused by crystals growth was firstly derived by Correns and Steinborn [Flatt et al. 2007]:

$$P = \frac{RT}{V_m} \ln S \tag{1}$$

where P is the crystallization pressure, R is the gas constant, T is the absolute temperature, V_m is the molar volume of salt and S is the solution supersaturation. There are different ways of defining the supersaturation of the solution: a ratio of concentration, solute activities, etc. Equation (1) was modified many times and extended for particular cases, e.g. porous materials with different structure etc. [Scherer 1999; Flatt 2002; Coussy 2006]. Generally there exist two kinds of approaches which might be used for calculation of the dissolved and precipitated salt concentration: equilibrium and non-equilibrium approach, Koniorczyk [2010]. The first one might be employed when considering the long lasting processes related with diffusion and adsorption but it can not be used to calculate the supersaturation ratio. In order to predict correctly the amount of crystallizing salt the non-equilibrium kinetic approach must be applied. In such model one does not know the explicit relation between the dissolved salt concentration and the amount of the precipitated salt. The only relation which might be derived from the experiment describes the increment of salt crystals as a function of solution supersaturation. There are two kinds of experiments that might be utilized for determining the rate laws: the first one might be applied only for salts whose solubility depends on the temperature-cooling-warming experiment, [Espinosa et al. 2008]; the second one is drying experiment which is employed for the other kind of salts. In the first group of experiments the heat which is released during crystallization or consumed during salt dissolution is measured.

The paper consists of two parts: the experimental and theoretical investigation of mass and energy transport considering salt phase change. In the experimental part the results concerning thermal effects of salt crystallization are analyzed. The experimental setup was constructed. It consists of two brick samples, one saturated with pure water and the other with sodium sulphate solution, whose saturation strongly depends on the temperature. The samples were put into the climatic chamber, they were cooled and then warmed. The temperature was measured in the same places in both samples. The difference of temperature between the samples is the result of the additional heat source/sink, which is related with crystallization/dissolution process. In the theoretical part the mathematical model describing heat, moisture and salt transport and its numerical solution is shortly described. The kinetics of salt phase change is taken into account. Using the developed software the above described experiment was simulated. In such an experiment one can observe the salt crystallization due to the cooling and the dissolution of salt crystals due to the warming. The computer simulations were carried out by means of the HMTRA_SALT software [Koniorczyk and Gawin 2008], which was appropriately extended. In order to take into account the kinetics of salt phase change the additional state variable describing the amount of the precipitated salt had to be introduced.

2 EXPERIMENTAL RESEARCH

To perform the experiment the bricks saturated with pure water and with 28% sodium sulphate in water solution were prepared. The bricks were placed in polystyrene thermal insulation of 10 cm thick. The heat flux was possible only in one direction - along the longest edge of the brick. Before the test cycles were started the samples had been stored for 24 hour at 30°C. The temperature in a climatic chamber changed according to the testing cycle (Fig. 2 - chamber):
- cooling from temperature 30 º C down to 11 º C within 16 hours,
- constant temperature of 11 º C for 16 hours,

- heating temperature from 11 º C up to 30 º C for 16 hours,
- constant temperature of 30 º C for 16 hours.

Two such cycles were investigated. Dimensions of samples, insulation and places of sensors are presented in Fig. 1.

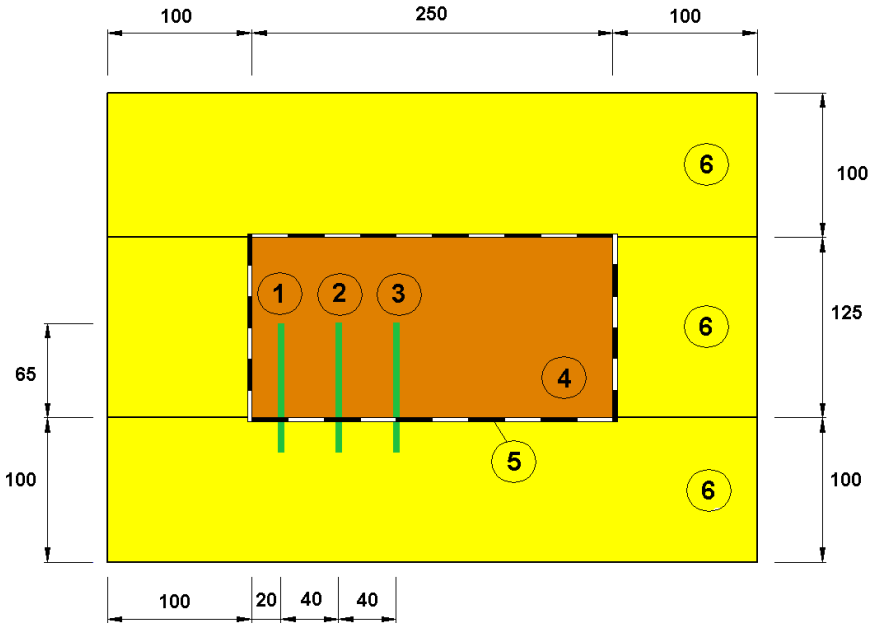

Figure 1. Location of the sensors in the samples: 1,2,3 –temperature sensor; 4 – brick; 5 – moisture barrier; 6 – expanded polystyrene.

A periodically changing temperature is shown in Fig. 2. The data collected by three selected temperature sensors are shown: one sensor in place 3 in brick containing pure water, one in the same place but in brick containing sodium sulphate solution and the last one in the climate chamber - boundary conditions.

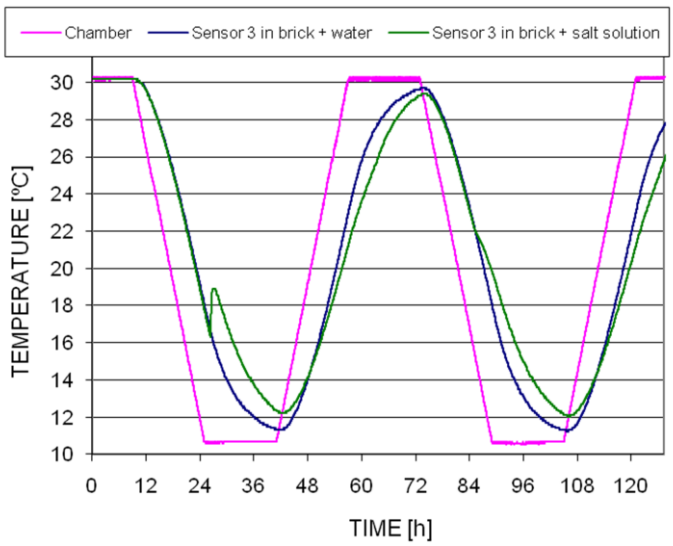

Figure 2. Measured temperature in samples and in a climate chamber.

In the first period of cooling there is no change between the temperature measured in the brick saturated with pure water and the one with sodium sulphate solution. Even when the supersaturation

ratio is greater than one there is no additional heat source due to crystallization. Only when the supersaturation ration approaches ap. 1.7 crystals grow suddenly. It manifests in the temperature difference peak. When the temperature raises the crystals dissolute. This process consumes heat which reveals in the reduction of the temperature in comparison with the temperature measured in the brick saturated with pure water. About 76th. h. whole crystals are dissolved and the temperature measured in both bricks is the same. The secondary crystallization starts at higher temperature, when supersaturation ratio is close to 1.0.

3 MATHEMATICAL MODEL

The mathematical model is an extension of the formulation proposed by Lewis and Schrefler [1998] and then modified by Gawin and Schrefler [1996], describing heat and moisture transport in porous building materials, with salt transport and its influence on thermal and hygral processes. A porous material consists of the following phases: solid skeleton, liquid water (salt solution), water vapour and precipitated (crystallized) salt. It is assumed that only one salt is dissolved in the solution. The voids in the skeleton are filled partly with a liquid phase consisting of water and dissolved salt, partly with a gaseous phase consisting of dry air and water vapour, and partly with the precipitated salt. The liquid phase consists of bound water, which is present in the whole range of water content, and capillary water, which appears when water content exceeds the upper limit of hygroscopic region – S_{ssp}. The liquid content is described by the water saturation degree – S_w. Salt appears in two phases: the former is the salt dissolved in the liquid phase, described by the mass concentration – ω, the latter is the precipitated salt, which is described by the degree of pore saturation with the precipitated salt – S_p. The degrees of saturation with all phases of the material follow the formula $S_g + S_w + S_p = 1$. It is assumed that the solution is ideal and the gas is perfect gas. The chosen primary variables of the model are: $p^g(\mathbf{x}, t)$, $p^c(\mathbf{x}, t)$, $T(\mathbf{x}, t)$, $\omega(\mathbf{x}, t)$ and $S_p(\mathbf{x}, t)$ is internal variable of the model.

The mathematical model consists of four governing equations: moisture mass conservation, dry air mass conservation, salt mass conservation and energy conservation as well as the evolution equation describing salt precipitation-dissolution kinetics.

3.1 Governing Equations

The mass conservation equation of dry air includes both diffusive (the third term on the left hand side) and advective (the last term on the left hand side) components of the mass flows, an influence of the precipitated salt on the gas saturation degree is also considered:

$$\phi \frac{\partial}{\partial t}(S_g \rho^a) + \mathrm{div}(\mathbf{J}_g^a) + \mathrm{div}(\phi S_g \rho^a \mathbf{v}^{gs}) = 0 \tag{2}$$

where t is time, ϕ is porosity, ρ^π is the density of π-phase ($\pi = w, a, g, s, p$ – liquid, dry air, gas, solid skeleton, precipitated salt), $\mathbf{v}^{gs}$ is the velocity of gas relative to solid skeleton.

The mass conservation of moisture was obtained by summing together the liquid water mass balance and the water vapour mass balance equations. Evaporation of water determines the sink term for liquid water and on the other hand it constitutes the source term in water vapour mass balance equation. After summing up the liquid and vapour water mass balance equations the following moisture mass conservation equation was obtained:

$$\phi \frac{\partial}{\partial t}(S_w \rho^w + S_g \rho^v) + \mathrm{div}(\mathbf{J}_g^v) + \mathrm{div}(\phi S_w \rho^w \mathbf{v}^{ws}) + \mathrm{div}(\phi S_g \rho^v \mathbf{v}^{gs}) = 0 \tag{3}$$

where $\mathbf{J}_g^v$ is diffusive flux of water vapour, $\mathbf{v}^{ws}$ is the velocity of liquid relative to solid skeleton.

It is assumed that salt influences the water density, dynamic viscosity and water retention characteristic [Koniorczyk and Wojciechowski 2008]. The sources or sinks of dissolved salt influence

the saturation degrees of water and gas due to the physical constraint, $S_g + S_w + S_p = 1$. The mass conservation of the salt dissolved in the fluid phase and precipitated (crystallized) salt is expressed as:

$$\phi \frac{\partial}{\partial t}(\rho^w \omega S_w) + \phi \rho^p \frac{\partial S_p}{\partial t} + \mathrm{div}(\phi S_w \omega \rho^w \mathbf{v}^{ws}) + \mathrm{div}(\mathbf{J}^{dysp}) = 0 \tag{4}$$

where $\mathbf{J}^{dysp}$ is the dispersive flow of salt.

The enthalpy conservation equation of the multiphase medium, obtained by summing the appropriate balance equations of the constituents, includes the heat effects due to phase change of water and heat released during the salt crystals grow (the terms on the right hand side), as well as the heat convection and conduction:

$$\begin{aligned}&(\rho C_p)_{ef} \frac{\partial T}{\partial t} + (\rho^w C_p^w \mathbf{v}^{ws} + \rho^g C_p^g \mathbf{v}^{gs}) \cdot \mathrm{grad}\, T - \mathrm{div}(\chi_{ef}\, grad\, T) = \\ &- \dot{m}_{vap}\, \Delta H_{vap} - \dot{m}_{prec} \Delta H_{prec}\end{aligned} \tag{5}$$

where ΔH_{prec} is enthalpy of crystallization per unit mass, χ_{ef} is effective thermal conductivity. The latent heat transport is considered in the above equation by adding the product of water sink-source term due to evaporation-condensation, $\dot{m}_{vap}$, and the water phase change enthalpy, ΔH_{vap}. The precipitated salt mass source, $\dot{m}_{prec} = \dot{S}_p \phi \rho^p$, is obtained from the evolution equation (6) describing the salt precipitation-dissolution process.

3.2 The Kinetics of Salt Crystallization-Dissolution

In the presented paper the kinetic model of salt phase change is applied. It assumes that there are no salt crystals in pores until the solution saturation limit ω_{sat} (i.e. the salt mass concentration of the saturated solution at a current temperature) is exceeded. After exceeding the maximum salt concentration the solution is supersaturated. The supersaturation ratio (i.e. current concentration / concentration at saturation), *S*, is the driving force of the salt crystallization, which starts when the solution supersaturation ratio is greater than one. The first crystals are formed on the crystallization nuclei, which are usually built by dust or other contaminations. There exists no equilibrium between dissolved salt and salt crystals, therefore the relation between the increment of salt crystals mass and solution supersaturation is often called as a non-equilibrium isotherm [Bear and Bachmat 1991]. An increase of solid salt mass is calculated on the basis of the supersaturation ratio, according to the following equation [Bear and Bachmat 1991]:

$$\frac{dS_p}{dt} = \begin{cases} S_w K(\omega - A'\omega_{sat})^p, & \omega \geq A'\omega_{sat} \wedge S_p < 1 \\ -S_w K \mid \omega - A'\omega_{sat} \mid^p, & \omega < A'\omega_{sat} \wedge 0 < S_p < 1 \end{cases} \tag{6}$$

The process order, *p*, and coefficient *K* depend on the properties of a porous body and a kind of the salt (Espinosa et al. 2008). For primary crystallization the supersaturation parameter $A' \geq 1$, and when the first salt crystals appear in the pores further crystallization proceeds at $A' = 1$. The equation (6), known as the rate law [Atkins and Paula 1999], is also valid for the dissolution of crystals. In this case there exist salt crystals in the pore system and the solution supersaturation is lower than one. Therefore the right hand side term in (6) is negative and the left hand side is likewise. Hence an increase of the mass of solid salt is also negative – which physically means dissolution of salt crystals. Assuming the kinetic (non-equilibrium) model of salt phase change it is not possible to calculate directly the saturation degree with the precipitated salt but only its increment. The solution saturation depends on the temperature for some kinds of salts, e.g. Na_2SO_4. Hence during cooling the crystallization process could be observed. An additional heat is released or consumed during the phase change of salt. The change in temperature for two pore solutions: one - pure water (no thermal effects related to crystallization), the other - sodium sulphate solution (additional heat sources caused by crystal growth) was measured. On the basis of that and solving the appropriate inverse problem

modelling the performed experiment, we obtained all necessary material parameters. The enthalpy of crystallization of sodium sulphate solution depends on temperature [Marliacy et al. 2000].

All material parameters and properties which are needed to complete the mathematical model (densities, dynamic viscosity, sorption isotherms etc.) depend on the primary variables. They are not introduced here because of the lack of available space, and can be found in the appropriate literature [Koniorczyk and Gawin 2008, Koniorczyk 2010]. The model is strongly nonlinear and the proper numerical methods must be applied in order to solve the set of governing equations.

3.3 Numerical Solution

The mathematical model consists of the set of partial parabolic differential equations. In order to solve them both initial and boundary conditions are needed. Initial conditions constitute the values of the primary variables assigned to all points of the analysed domain at the beginning of the process $t = 0$. The boundary conditions might be of three types: Dirichlet (the values of primary variables), Neumann (fluxes related to the primary variables), Robin (linear combination of two previous types). They must be assigned to the boundary during the whole time, $t \in (0, t_{\max}]$.

The spacial derivatives were calculated by means of the finite element method and time integration is done using the finite difference method (implicit Euler method). The Green's theorem was employed in order to weaken the requirements for shape functions and to consider the boundary condition in the explicit form. The Newton scheme was applied for the linearization of the problem. The developed computer code allows to calculate 2D problems. It was verified against some experimental data for fully and partly saturated state in non-isothermal conditions assuming the equilibrium between the dissolved and precipitated salt [Koniorczyk and Gawin 2008].

4 NUMERICAL SIMULATIONS

Using the developed software the experiment described in paragraph 2 was simulated. The porous brick was modeled as a 2D domain by means of 100 isoparametric eight-nodded finite elements of equal size – Fig. 3. The boundary conditions are listed in Table 1.

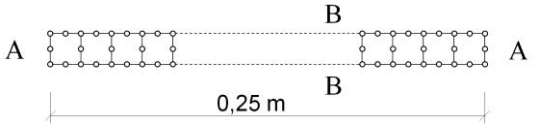

Figure 3. Geometry and boundary conditions for numerical simulations.

Table 1. The boundary conditions.

Side	Variable	Cooling-warming	
		Values and coefficients	BC type
A	p^c	$\mathbf{q}^v = \mathbf{0}$ $\mathbf{q}^w = \mathbf{0}$	II
	p^g	$p^g = 101325$ Pa	I
	T	T change - chapter 2. $\alpha_c = 23\ \mathrm{W/m^2K}$	III
	ω	$\mathbf{q}^\omega = \mathbf{0}$	II
B	p^c	$\mathbf{q}^v = \mathbf{0}$ $\mathbf{q}^w = \mathbf{0}$	II
	p^g	$\mathbf{q}^a = \mathbf{0}$	II
	T	$\mathbf{q}^T = \mathbf{0}$	II
	ω	$\mathbf{q}^\omega = \mathbf{0}$	II

4.1 Numerical Results

The following brick properties were assumed: ϕ = 0.20, intrinsic permeability k = 3.0 10^{-16} m^2, specific heat C_p = 880 J/(kg·K), thermal conductivity λ = 0.77 W/(m·K), density ρ = 1700 kg/m^3.Two kinds of experiments were modelled. Firstly the brick was saturated with pure water, secondly with sodium sulphate solution. The initial conditions are as follows: p_o^g = 101325 Pa, S_{wo} = 1.0, T_o = 303.15 K (30°C), ω_o = 0.0 kg/kg (1st case) ω_o = 0.28 kg/kg (2nd case). For the second case the initial dissolved salt concentration is lower than the solution saturation and no solid salt is initially present in the pores system, $S_{p,0}$ = 0. The ambient temperature changes from 30^{0}C to 10^{0}C then it remains constant at 10^{0}C, then rises up to 30^{0}C and lastly it remains constant at 30^{0}C. Each stage lasts 16 hours. The whole temperature loop takes 64 hours. During the simulations two loops were investigated. The material parameters appearing in equation 6 were obtained by comparing the temperature difference for experimental data, assuming pure water and salt solution, with the temperature difference obtained in numerical simulations for the corresponding assumptions. The calculated results for different values of materials parameters were analyzed. Three different rate orders were tested: p=1.5, p=2.5, p=3.5. Parameter A influences the point and the height of the first peak in the temperature difference graph – Fig. 4a. The best agreement between the experimental data and the calculated results was obtained for, p=1.5 and A=1.7, see Fig. 4a for sensor 3. One can notice a sudden peak of temperature difference after 20 h when the salt crystallization starts and the crystallization heat is released. The second peak is observed about 80th h. but this one is smoother. This difference is related with the primary (after 20 h.) and the secondary (about 80 h) crystallization. Crystal growth starts from the surface, where the temperature decreases firstly and the solution becomes supersaturated – Fig. 4b. During the increase of temperature one can observe the dissolution of salt crystals due to the fact that the solution solubility increases – Fig. 2, 4a, what manifests the temperature decrease.

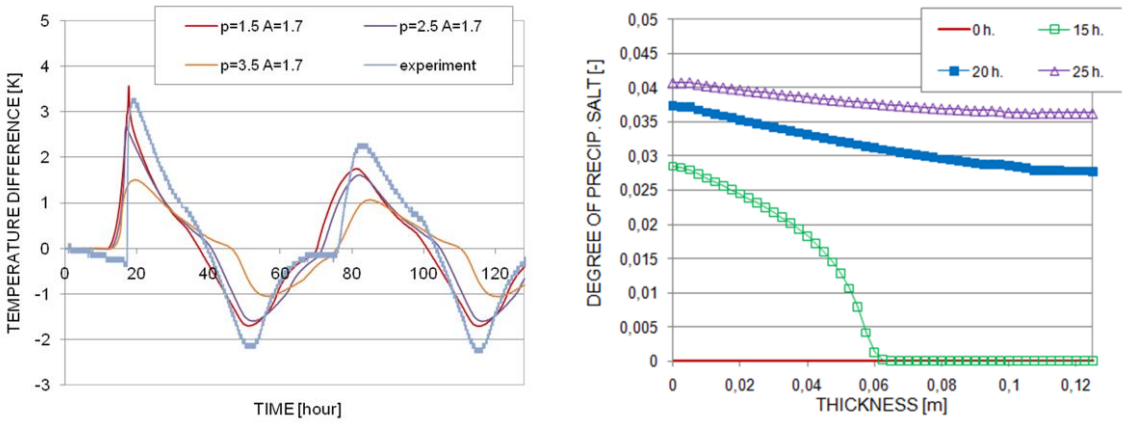

Figure 4. a) the comparison of temperature difference between problems without and with salt in sensor 3 obtained in the experiment and in the computer simulations assuming various material parameters, **b)** the profiles of the saturation degree with the precipitated salt.

CONCLUSIONS

The experimental setup, which can be used to measure the kinetics of salt crystallization and dissolution, was constructed. It is based on the measurement of the temperature difference, therefore only the salt whose solubility depends on temperature can be analyzed.

The mathematical model of salt moisture and energy transport considering the salt phase change kinetics was proposed. The crystallization heat is taken into account while considering the energy transport. Based on it the computer code was developed and verified against the obtained experimental data. By solving the inverse problem all materials parameters appearing in equation 6 might be estimated.

ACKNOWLEDGMENTS

Scientific research has been carried out as a part of the Project "Innovative recourses and effective methods of safety improvement and durability of buildings and transport infrastructure in the sustainable development" financed by the European Union from the European Fund of Regional Development based on the Operational Program of the Innovative Economy.

REFERENCES

Atkins, P., de Paula, J., 1999, *Atkins' Physical Chemistry*, 6th edition, Oxford University Press, Oxford.

Bear, J., Bachmat, Y. 1991, *Introduction to Modeling of Transport Pheneomena in Porous Media*, Kluwer Academic Publishers, The Netherlands.

Coussy, O. 2006, 'Deformation and brittle fracture from drying-induced crystalisation of salts', *J Mech Phys Solids*, **54**, 1517-1547.

Espinosa R.M., Franke L., Deckelmann G. 2008, 'Phase changes of salts in porous materials: Crystallization, hydration and deliquescence', *Construction and Building Materials*, **22**, 1758–1773.

Flatt, R.J. 2002, 'Salt damage in porous materials: how high supersaturations are generated' *J Crystal Growth*, **242**, 435-454.

Flatt, R.J., Steiger, M., Scherer, G.W. 2007, 'A commented translation of the paper by C.W. Correns and W. Steinborn on crystallization pressure', *Environ Geology*, **52**, 187-203.

Gawin, D., Schrefler, B.,A., 1996, 'Thermo-hydro-mechanical Analysis of Partially Saturated Porous Materials', *Engineering Computations*, **13**, 113–143.

Koniorczyk, M, Gawin, D. 2008, 'Heat and moisture transport in porous building materials containing salt', *J Build Phys*., **31**, 279–300.

Koniorczyk, M., Wojciechowski, M. 2009, 'Influence of salt on desorption isotherm and hygral state of cement mortar – Modelling using neural networks', *Construction and Building Materials*, **23**, 2988-2996.

Koniorczyk M. 2010, 'Modelling the phase change of salt dissolved in pore water – Equilibrium and non-equilibrium approach', *Construction and Building Materials*, **24**, 1119–1128.

Lewis, R. W., Schrefler, B.A. 1998, *The finite element method in the static and dynamic deformation and consolidation of porous media*, John Wiley & Sons, Chichester.

Marliacy P., Solimando R., Bouroukba M., Schuffenecker L. 2000, 'Thermodynamics of crystallization of sodium sulphate decahydrate in H_2O-NaCl-Na_2SO_4: application to Na_2SO_4 $10H_2O$-vased latent heat storage materials', *Thermodynamica Acta*, **344**, 85-94.

Pel L., Huinink H., Kopinga K., van Hees R.P.J., Adan O.C.G. 2004, 'Efflorescence pathway diagram: understanding salt weathering', *Construction and Building Materials*, **18**, 309–313.

Scherer, G.W. 1999, 'Crystallization in pores', *Cement and Concrete Research*, **29**, 1347–1358.

XII DBMC
International Conference on Durability of Building Materials and Components
PORTO - PORTUGAL, April 12th-15th, 2011

Prediction of Time-variant Probability of Failure for Concrete Sewer Pipes

Kong Fah Tee [1]
Chun Qing Li [2]
Mojtaba Mahmoodian [3]

ABSTRACT

Millions of dollars are being spent worldwide on the repair and maintenance of sewer networks and wastewater treatment plants. Approximately 40% of the damage in concrete sewers can be attributed to biogenous sulphuric acid attack, which causes severe structural deterioration and ultimate structural collapse. In some cases, it is difficult or not cost effective to design a sewer pipeline system that will be free of sulphide problems. It is then useful to know what levels of deterioration of sewer pipe can be expected during its service life. The major determining factors for sulfide build-up are temperature, biochemical oxygen demand (BOD), pH and stream velocity. The rate of corrosion of a concrete sewer can be calculated from the rate of production of sulphuric acid on the pipe wall, which is in turn dependent upon the rate that hydrogen sulphide is released from the surface of the sewage stream. This paper presents a detailed analysis of structural failures of corrosion affected concrete sewer pipes during their service lives. Stochastic models for pipe deterioration are developed and the associated risks of pipe collapse are quantified. A numerical example will be provided to illustrate the proposed method with a view to prevent unexpected failures of the structure during its service life. The proposed methodology can help the management in making correct decisions concerning the intervention to ensure the safe and serviceable operation of the pipes. This will, in turn, result in better asset and capital utilization.

KEYWORDS

hydrogen sulphide, Concrete sewer pipe, Probability of failure, Corrosion.

[1] School of Engineering, University of Greenwich, UNITED KINGDOM, k.f.tee@gre.ac.uk
[2] School of Engineering, University of Greenwich, UNITED KINGDOM, c.q.li@gre.ac.uk
[3] School of Engineering, University of Greenwich, UNITED KINGDOM, mm12@gre.ac.uk

1 INTRODUCTION

The UK has one of the largest sewerage networks in Europe, with an asset value of about £110 billion [Hau *et al*. 2005]. It is also known to be one of the oldest sewerage systems in the world, with more than 40% of its network constructed prior to 1945 [Read & Vickridge 1997]. The Water Services Regulation Authority estimates that the cost of replacing this entire infrastructure requires £200 billion [OFWAT 2002]. With such high stakes, this highlights the urgent need to develop methods to predict the time-variant probability of failure and innovative solutions to the optimal management of aging sewerage infrastructure. In England and Wales, the economic regulator imposes a duty on the privatised water companies to maintain the condition and serviceability of this asset.

Most of the maintenance strategies rely on the reliable data about the pipe's physical attributes, for example wall thickness, strength, bending modulus, etc and its failure or performance history. With incomplete sewerage databases this can place significant restrictions on the decision of the most suitable maintenance strategy. Various frameworks have been proposed to model the behaviour of underground pipelines with different types of material, using reliability-based concept. Ahammed & Melchers [1997] developed a nonlinear limit state model for the analysis of underground pipelines subjected to combined stresses and corrosion. The reliability model was assumed to be a function of 20 independent random variables in order to study their effects. Li *et al*. [2009] presented a methodology for predicating corrosion remaining life of underground pipelines with a mechanically-based probabilistic model by taking into account the effect of randomness in pipeline corrosion. Monte Carlo simulation was employed to calculate the remaining life and its cumulative probability distribution function.

It has been known that the degradation of concrete sewer systems can be primarily attributed to concrete corrosion induced by biogenous sulfuric acid attack, which causes severe structural deterioration and ultimate structural collapse. Such problems are rarely brought to the attention of the public until a catastrophic failure occurs. Hydrogen sulphide (H_2S) related corrosion is among the most challenging problems regarding sewer operation and maintenance because sewer systems suffering from H_2S corrosion generally require costly replacement or rehabilitation of pipes. Study on sulphide formation and its corresponding modelling as well as its effects on concrete corrosion has been performed for many years [Pomeroy 1976]. Recently, new findings of a long-term study of H_2S gas adsorption and oxidation on concrete and plastic sewer pipe surfaces have been reported [Nielsen *et al*. 2009]. The processes have been studied using a pilot-scale setup designed to replicate conditions in a gravity sewer located downstream of a force main. The kinetic data obtained in the pilot-scale experiments can be used for prediction of concrete corrosion in real sewer systems based on H_2S measurements from a conventional gas detector.

The mechanism of H_2S in material degradation has been reasonably understood. What is less understood, however, are the factors that affect and control the process of concrete corrosion. Furthermore, little is known, in particular quantitatively, on the effect of concrete corrosion on the remaining safe life of the pipes. Without knowing this, rational decisions on maintenance and rehabilitation of the pipes are not possible and more importantly, unexpected failures of the pipes cannot be prevented during the lifetime. Therefore, the main objective of this paper is to present a method to predict the time-variant probability of failure and the expected life for concrete sewer pipes.

2 FAILURE MECHANISM OF CONCRETE SEWER PIPELINES

Sewer pipes are deteriorating slowly or fast depending on specific local conditions and not determined by age alone. There have been numerous cases of severe damage to concrete pipes, where it has been necessary to replace the pipes before the attainment of the designed life. There are many cases in which sewer pipes designed to last 50 to 100 years have failed due to H_2S corrosion in 10 to 20 years. In extreme cases, concrete pipes have collapsed in as few as 3 years [Pomeroy 1976]. The most corrosive agent that leads to the rapid deterioration of concrete pipelines in sewers is H_2S. Approximately 40% of the damage in concrete sewers can be attributed to biogenous sulphuric acid

attack. Sulphide corrosion, which is often called microbiologically induced corrosion, has two distinct phases as follows:

1) The conversion of sulphate in wastewater to sulphide, some of which is released as gaseous hydrogen sulphide
2) The conversion of hydrogen sulphide to sulphuric acid, which subsequently attacks susceptible pipeline materials.

The surface pH of new concrete pipe is generally between 11 and 13. Cement contains calcium hydroxide, which neutralizes the acids and inhibits formation of oxidizing bacteria when the concrete is new. However, as the pipe ages, the neutralizing capacity is consumed, the surface pH drops, and the sulphuric acid-producing bacteria become dominant. In active corrosion areas, the surface pH can drop to 1 or even lower and can cause a very strong acid attack. The corrosion rate of the sewer pipe wall is determined by the rate of sulphuric acid generation and the properties of the cementitious materials. As sulphides are formed and sulphuric acid is produced, hydration products in the hardened concrete paste (calcium silicon, calcium carbonate and calcium hydroxide) are converted to calcium sulphate, more commonly known by its mineral name, gypsum [ASCE 1989].

Gypsum does not provide much structural support, especially when wet. It is usually present as a pasty white mass on concrete surfaces above the water line. As the gypsum material is eroded, the concrete loses its binder and begins to spall, exposing new surfaces. This process will continue until the pipeline fails or corrective actions are taken. Sufficient moisture must be present for the sulphuric acid-producing bacteria to survive, however; if it is too dry, the bacteria will become desiccated, and corrosion will be less likely to occur.

3 FORECASTING SULPHIDE BUILD-UP AND RATES OF CONCRETE CORROSION

3.1 Forecasting Sulphide Build-Up

In some cases, it is difficult or not cost effective to design a sewer pipeline system that will be free of sulphide problems. It is then useful to know what levels of sulphide can be expected. The major determining factors for sulphide build-up are oxygen, temperature, pH, stream velocity, BOD, organic nutrients and sulphate. The sulphide concentrations in a partly filled sewer will approach a limiting level S_{lim} as follows [ASCE 2007]

$$S_{lim} = \frac{0.0005[BOD](1.07)^{T-20}}{(su)^{3/8}} \times \frac{P}{b} \quad (1)$$

where [BOD] is biochemical oxygen demand concentration (mg/l), T is sewage temperature (^{0}C), s is the slope of the pipeline, u is the velocity of the stream (m/sec) and P/b is the ratio of wetted perimeter of the pipe wall (P) to the surface width of the stream (b).

3.2 Forecasting Concrete Corrosion Rate

The rate of corrosion of a concrete sewer can be calculated from the rate of production of sulphuric acid on the pipe wall, which is in turn dependent upon the rate that H_2S is released from the surface of the sewage stream. The moisture on the pipe wall with oxidizing bacteria is very efficient in converting all of the H_2S to sulphuric acid. Under most conditions, very little of the H_2S escapes entirely from the sewer. The average flux of H_2S to the exposed pipe wall is equal to the flux from the stream into the air multiplied by the ratio of the surface area of the stream to the area of the exposed pipe wall, which is the same as the ratio of the width of the stream surface (b) to the perimeter of the exposed wall (P'). The average flux of H_2S to the wall is therefore calculated as follows [ASCE 2007]

$$\Phi = 0.7(su)^{3/8} j S_{\lim}(b/P') \quad (2)$$

where j is pH-dependent factor for proportion of H_2S. Concrete pipe is made of cement-bonded material, or acid-susceptible substance, so the acid will penetrate the wall at a rate inversely proportional to the acid-consuming capability (A) of the wall material. The acid may partly or entirely react. The proportion of acid that reacts is variable (k), ranging from 100% when the acid formation is slow, to perhaps 30% to 40% when it is formed rapidly. Thus, the average rate of corrosion (mm/year) can be calculated as follows

$$c = 11.5 k \Phi (1/A) \quad (3)$$

where k is the factor representing the proportion of acid reacting, to be given a value selected by the judgement of the engineer and A is the acid-consuming capability, alkalinity, of the pipe material, expressed as the proportion of equivalent calcium carbonate.

4 PROBABILITY OF FAILURE AND EXPECTED SERVICE LIFE

To predict the probability of failure for sewer pipes, a performance-based assessment criterion should be established. In reliability theory, this criterion is expressed in the form of a limit state function as follows

$$G(S,R,t) = S(t) - R(t) \quad (4)$$

where G( ) is termed the 'limit state function', S(t) is the load effect in the pipe at time t, and R(t) is the resistance of the pipe. The pipe will be considered to have failed if its resistance R is less than the load effect S in the pipe. The probability of pipe failure is determined by the probability of a limit state violation. With the limit state function of Equation (4), the probability of pipe (structural) failure, P_f, can be obtained by

$$P_f(t) = P(R \le S) = P[G(S,R,t) \le 0)] \quad (5)$$

For a structural member with a known distribution function $F_R(t)$ of ultimate strength R and density function $f_S(t)$ for load effect S, the probability of failure in Equation (5) can be written in a single integral form as follows:

$$P_f(t) = \int_{-\infty}^{\infty} F_R(t) f_S(t) dt \quad (6)$$

For a Gaussian distribution of R and S, it is possible to integrate the convolution integral in Equation (6) analytically. When both the load effect (S) and the pipe resistance (R) are normal random variables with means μ_R and μ_S and variances σ_R^2 and σ_S^2 respectively, the safety margin of Equation (4) is

$$Z(t) = R(t) - S(t) \quad (7)$$

which has a mean and variance given by well-known rules for addition /subtraction of normal random variables:

$$\mu_Z = \mu_R - \mu_S \quad (7a)$$

$$\sigma_Z^2 = \sigma_R^2 + \sigma_S^2 \quad (7b)$$

Equation (5) then becomes:

$$P_f(t) = P(R \le S) = P(R - S \le 0) = P(Z \le 0) = \Phi(\frac{0 - \mu_Z}{\sigma_Z}) \tag{8}$$

where $\Phi()$ is the standard normal distribution function (zero mean and unit variance). By replacing (7a) and (7b) in Equation (8), the probability of pipe failure P_f can be determined from [Melchers 1999]:

$$P_f(t) = \Phi(-\frac{\mu_R - \mu_S}{\sqrt{\sigma_R^2 + \sigma_S^2}}) = \Phi(-\beta) \tag{9}$$

where $\beta = \mu_Z / \sigma_Z$ is known as the safety index or reliability index. If either of the variances σ_R^2 and σ_S^2 or both are increased, the term in brackets in Equation (9) will become smaller and P_f will increase, as it is expected. Likewise by reducing the difference between the mean of the load effect and the mean of the resistance, P_f increases.

4.1 Resistance of Underground Concrete Pipes

The resistance of a pipe is the strength against the operational loads which are field specific and can be determined for a given field or site. The load acting on a pipe can be determined based on Marston load theory as follows:

$$W_d = C_d \gamma B_d^2 \tag{10}$$

Therefore the resistance (strength) of a pipe would be (Moser and Folkman 2008):

$$R = \left(\frac{W_d}{B_F}\right) \times \frac{1}{D} \tag{11}$$

where

R	= Resistance of the pipe (N/m^2)
C_d	= Load coefficient
γ	= Unit weight of backfill material (N/m^3)
B_d	= horizontal width of the ditch at top of conduit (m)
B_F	= Bedding factor, which is defined as the ratio of total field load to equivalent three-edge bearing load that causes the same bending moment at the invert of the pipe.
D	= Inner diameter of the pipe (m)

Due to the corrosion of concrete in a sewer pipe, the wall thickness of concrete pipe will reduce with a rate presented in Equation (3). Consequently the resistance of the pipe decreases with time, which can be determined as follows

$$R(t) = \left(\frac{C_d \gamma B_d^2}{B_F}\right) \times \frac{1}{(D + 2ct)} \tag{12}$$

where

$R(t)$	= Resistance of the pipe at time t (N/m^2)
c	= corrosion rate (mm per year)
t	= time in years

and the other variables are as previously defined.

4.2 Maximum Design Load in an Underground Pipe

Since the emphasis of the paper is to demonstrate how to predict the service life of sewer pipes, the maximum affordable design load of the pipe will be determined from load tests for easy practical applications. One widely used test in practice is the equivalent three-edge bearing load test. From this test, the design load for an underground concrete sewer pipe is [Moser & Folkman 2008]:

$$F_{3-edge} = \frac{F_{earth} + F_{live} + F_{water}}{B_F} \tag{13}$$

where F_{3-edge} is the applied load in three edge bearing test, $F_{earth} + F_{live} + F_{watee}$ are different types of loads that need to be considered for the pipe in the field as indicated by subscripts.

ASTM C497 (2003) defines the design load D_{load} as the three edge bearing load that produces a 0.01 inch maximum crack width in the pipe. The D_{load} is measured by the three edge bearing load per meter of inner diameter so that it provides a strength classification of pipes independent of their diameters as provided by manufacturers. In practice, it is convenient to express the maximum allowable stress of reinforced concrete pipes in terms of the design load D_{load} (American Concrete Pipe Association 2007).

Considering the D_{load} of a pipe as its maximum allowable stress (S) of Equation (13) and the resistance of the pipe (R) of Equation (12), the time-variant probability of pipe failure can be determined from Equation (9). Obviously, P_f has to be smaller than an acceptable limit to eliminate undue risk of collapse. With this constraint, the expected service life can be approximately determined by assuming that the service life of the pipe is reached when P_f is equal to the acceptable limit as shown in the example below.

Alternatively, the expected service life of the pipe can also be calculated easily based on the criterion of non-exposure of reinforcing steel, which can be simply determined by dividing the concrete cover by average rate of corrosion, i.e., Equation (3).

5 WORKED EXAMPLE

A reinforced concrete sewer pipe with a diameter of 2286 mm, wall thickness of 216 mm and concrete cover of 45 mm is laid at a gradient of 1 in 667 (0.0015). The flow is half full at a velocity of 0.60 m/sec. The sewage temperature in the pipe is 22°C and the BOD is 250 mg/l. The pH of the sewage is 7.4 (taken from Table 1 of Pomeroy [1976], where j is 0.28 for pH=7.4). The pipe is made of concrete having an alkalinity equal to 0.20 of calcium carbonate. In this study, the coefficient k which represents the proportion of acid reaction, is selected to be 0.5. The statistics of the loading W_d acting on the concrete sewer pipe are estimated to be N(400 kN/m, 10). The strength in the pipe is decreasing with respect to time due to corrosion induced reduction of the wall thickness. The maximum allowable stress by the pipe based on its D-load design value is S = 200 kN/m^2.

With above given values, the limiting level of sulphide concentration in the pipe is 3.12 mg/l and the average rate of corrosion is 0.81 mm/year which are determined using Equations (1) and (3). From this, the probability of the pipe failure can be determined using Equations (9) and (13), the results of which are shown in Figure 1 (P_f vs. time) and Figure 2 (P_f vs. thickness).

From Figure 1 it is clear that the probability of pipe failure increases with time which makes sense both theoretically and practically. It is important to note that the shape of the probability of failure curve is similar to the well known “bath-tub” from which it can be seen that year 25 seems to be the critical turning point. Also from Figure 2, it can be seen that after the wall thickness of the pipe reduces to about 170 mm the probability of pipe failure increases sharply. This again makes sense both theoretically and practically as observed in the real world.

If the acceptable probability of failure is 0.1, the expected life for the concrete pipe subjected to corrosion is 52 years (Figure 1), where the remaining thickness is 173 mm, i.e. 20% reduction of thickness (Figure 2). On the other hand, the expected life of the concrete pipe is 55 years if the criterion of non-exposure is adopted. Despite different criteria for predicting the expected service life results from both criteria are in good agreement. It is important to note that the calculated rate of corrosion is conservative because it is based on limiting value of sulphide concentrations.

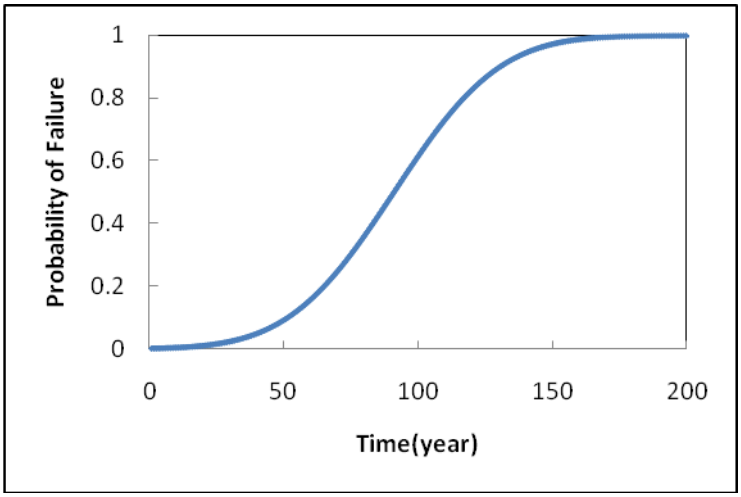

Figure 1 Probability of failure vs. time.

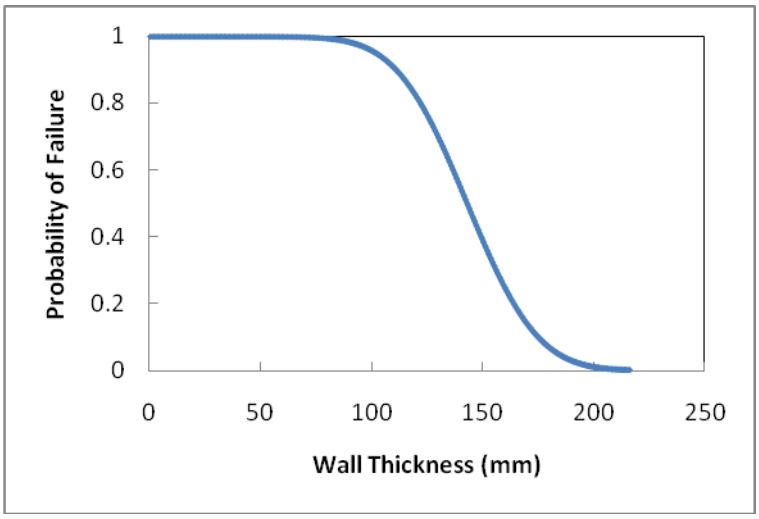

Figure 2 Probability of failure vs. thickness.

6 CONCLUSION

A widely used reliability method is presented to predict the time-variant probability of failure for concrete sewer pipes, based on the forecasted sulphide build-up and concrete corrosion rate. The major determining factors for sulfide build-up are temperature, biochemical oxygen demand (BOD), pH and stream velocity. The rate of corrosion of a concrete sewer can be calculated from the rate of production of sulphuric acid on the pipe wall, which is in turn dependent upon the rate that hydrogen sulphide is released from the surface of the sewage stream. It has been found that the expected service life of concrete sewer pipes can be determined through average rate of corrosion either based on safety criterion or non-exposure of reinforcing steel. It can be concluded that the method presented here can

predict the expected life of concrete pipes subjected to hydrogen sulphide-induced corrosion with reasonable accuracy.

REFERENCES

Ahammed, M. & Melchers, R.E. 1997, 'Probabilistic analysis of undergroud pipelines subject to combined stresses and corrosion', *Engineering Structures*, **19**[12], 988-994.

ASCE Manuals and Reports of Engineering Practice No. 60, 2007, *Gravity Sanitary Sewers*, 2nd edition, American Society of Civil Engineers, New York, USA.

ASCE Manuals and Reports on Enginering Practice No. 69, 1989, *Sulfide in Wastewater Collection and Treatment Systems*, American Society of Civil Engineers, New York, USA.

ASTM C497-03a, 2003, *Standard Test Methods for Concrete Pipe, Manhole Sections, or Tile*. American Society for Testing and Materials.

American Concrete Pipe Association, 2007, *Concrete Pipe Design Manual*.

Hau, Y., Clarke, B., Howes, C., Cunningham, R. & Mathews, M. 2005, 'Defects in sewer pipe joints and water tests', Proc. Institution of Civil Engineers, Water Management 158, Issue WM3, September 2005, pp. 119-125.

Li, S.X., Yu, S.R., Zeng, H.L., Li, J.H. & Liang, R. 2009, 'Predicting corrosion remaining life of underground pipelines with a mechanically-based probabilistic model', *Journal of Petroleum Science and Engineering*, **65**[3-4], 162-166.

Melchers, R. E. 1999, *Structural Reliability Analysis and Prediction*, 2nd edition, John Wiley and Sons, Chichester.

Meyer, W.J. 1980, Case study of prediction of sulphide generation and corrosion in sewers', *Journal Water Pollution Control Federation*, **52**[11], 2666-2674.

Moser, A.P., and Folkman, S. 2008, *Buried Pipe Design*, 3rd edition, Mc Graw Hill.

Nielsen, A.H., Jensen, H.S., Hvitved-Jacobsen, T. & Vollertsen, J. 2009, 'New findings in hydrogen sulfide related corrosion of concrete sewers', Proc. Int. Conf. on Pipeline: Infrastructure's Hidden Assets, ASCE, San Diego, USA, 15-19 August 2009, vol. 1, pp. 344-353.

OFWAT. 2002, *Maintaining Water and Sewerage Systems in England and Wales, Our Proposed Approach for the 2004 Periodic Review*, London.

Pomeroy, R.D. 1976, *The Problem of Hydrogen Sulphide in Sewers*, Clay Pipe Development Association.

Read, G. & Vickridge, I. 1997, *Sewerage. Rehabilitation and New Construction, Repair and Renovation*, Arnold, London.

XII DBMC
International Conference on Durability of Building Materials and Components
PORTO - PORTUGAL, April 12th-15th, 2011

Numerical Model Based on Fuzzy Logic for Predicting Penetration of Chloride Ions into the Reinforced Concrete Structures – First Estimates

Wellington Mazer [1]
Maryangela Geimba de Lima [2]

ABSTRACT

The action of aggressive agents on the concrete induces its degradation, showing as main symptoms cracks, crumbling, and stains, where the Chloride ions are one of the major causes of degradation of reinforced concrete. To determine the service life of a reinforced concrete structure exposed to the action of Chloride ions, it is necessary to determine the chloride concentration existing within the mass concrete, next to the reinforced barr. Many models are based on Fick's laws to determine the penetration profile of Chloride ions in concrete structures. However, such models consider the diffusion coefficient of Chloride ions constant and that this fact is not valid for concrete, as variations occur in the diffusion coefficient of Chlorides according to environmental parameters and the structure of concrete itself. In order to model the penetration profile of Chloride ions, we proposed a model based on Fuzzy Logic to determine the diffusion coefficient of Chloride ions using environmental parameters. The results indicate good prospects for the use of Fuzzy Logic for the estimate of the diffusion coefficient of Chlorides.

KEYWORDS

Chloride ions, Fuzzy logic, Concrete structures.

[1] Federal Technological University of Paraná (UTFPR), Curitiba, BRAZIL, mazer.eng@gmail.com
[2] Technological Institute of Aeronautics (ITA), São José dos Campos, BRAZIL, magdlima@ita.br

1 INTRODUCTION

The corrosion of reinforcement due to the action of chloride ions is a major cause of degradation of reinforced concrete structures. Chloride ions, on contact with the reinforcement at higher levels in a quantity called the critical concentration, they begin a process of reinforcement corrosion, which initially manifests itself in spots from the iron oxide. In a second stage, due to the feature expansive products of corrosion, cracking may occur one of the concrete followed by its breakdown [Martin-Perez et al, 2000].

Chloride ions can penetrate into the concrete in several ways; among them one can cite the use of additives containing chlorides in its composition, impurities in the aggregate, per share of chemicals, the marine environment, among others. Once present in the mass of concrete, chloride ions can be combined with compounds of cemente, physically adsorbed on the surface of the capillary pores or the free pores of the concrete where free ions that can reach the reinforcement and start a corrosive process shorten the life of the structure [Isaia, 2005].

To determine the life of a reinforced concrete structure exposed to the action of chloride ions, it is necessary to determine the chloride concentration levels that exist within on concrete and preferably in close proximity to the reinforcement. Some authors [Vu & Stewart, 2000][Andrade & Dal Molin, 2001][Troconis de Rincon et al, 2004] have used models based on Fick's laws to determine the profile of penetration of chloride ions in concrete structures. However, other authors [Chaterji, 1995][Halamicova et al, 1995][Nugue & Ollivier, 2004] argue that the Fick's 2nd law, which considers the diffusion coefficient of chloride ions constant does not in fact apply in this case, because there are variations in the diffusion coefficient of chlorides according to the depth of penetration, the degree of hydration of cement, and the temperature and pH of the concrete.

In search of a better "shape" to chloride ions penetration profile, many researchers [Andarde et al, 1997][Shin & Kim, 2002][Lounis, 2003] have proposed deterministic or probabilistic models to describe the process of diffusion of chloride ions in concrete, and some of these models consider the influence of environmental parameters.

2 MATHEMATICAL MODELLING

The proposed mathematical model is divided into two parts, (i) a first part based on Fuzzy Logic and relates to the coefficient of diffusion of chlorides through concrete, taking into consideration specific parameters such as water/cement ratio, compressive strength and concreting temperature. At this stage, the model undertakes the process of *fuzzification*, based on a "Rules Map" within the model that defines the relevant "membership" functions of the output variable and will determine the degree of membership (contribution) of each of the input parameters (i.e. water/cement ratio, compressive strength and concreting temperature) such that a subsequent process of *Defuzzification*, can occur. Following the *Defuzzification* process a chlorides diffusion coefficient referred to as D_{fuzzy} is defined. membership functions represent the degree of belonging to a variable in the different possible classifications of the parameter being analyzed.
(ii) In a second part, of the depth of penetration of chloride ions by using the Fick's 2nd law, is modelled in which the chloride ions concentration at various depths is defined.

2.1 Definition of the Diffusion Coefficient of Chloride ion using Fuzzy Logic

2.1.1 Water/cement ratio

For a definition of membership functions and the extent of coverage of the values of water/cement ratio (a/c), this work was based on the Brazilian standard NBR-6118 - Design of Concrete Structures

[ABNT, 2003]. The maximum values of water/cement ratio as a function of aggressive environment class to which the structure is exposed were, determined as shown in Table 1.

Table 1 - Water / cement according to environmental aggression.

Concrete	Type	Agressive Environmetal Class			
		I	II	III	IV
The water / binder	CA	<= 0.65	<= 0.60	<= 0.55	<= 0.45
	CP	<= 0.60	<= 0.55	<= 0.50	<= 0.45

Note: CA - concrete; CP - prestressed concrete. (Source: ABNT - NBR 6118/2003).

Based on values established in the Brazilian standard, and noting that a structure subject to the action of chloride ions have a Class III Environmental aggressiveness, but can be dosed to a specific Class IV Environmental aggressiveness by region of exposure, and considering the relationship linear observed by [Pereira, 2001] between the water/cement ratio and the diffusion coefficient of chlorides, outlined the membership functions to this variable as shown in Figure 1.

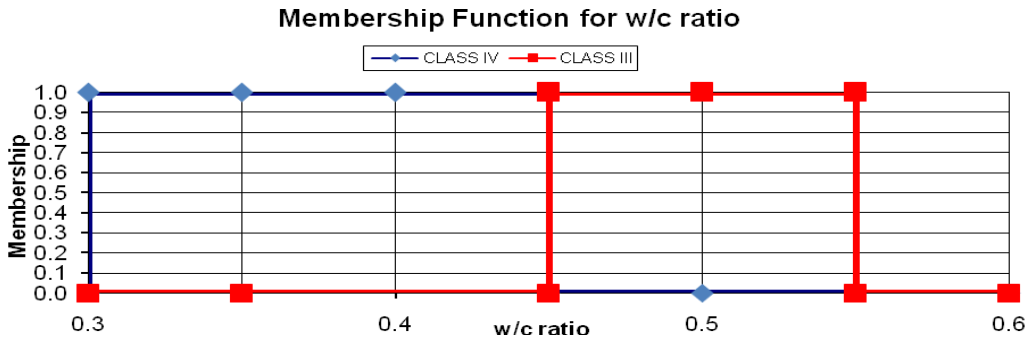

Figure 1 – Membership Functions to the variable water / cement ratio.

In Figure 1 the existence of two curves are shown in which are defined the membership functions to the values of water/cement ratio of permissible doses for Classes Aggressive Environmental referring to the attack of the concrete by chloride ions. The curves were limited in the lower end of 0.3 due to the difficulty of casting the concrete with water/cement relations below that level without the use of additives which can influence the process of penetration of chloride ions in mass of concrete, which is also water-cement relations very low are used to produce concrete of high strength above 50MPa, and such concrete is not covered by the NBR 6118 [2003], used as a parameter for defining the membership functions. At the upper end was limited to the value of the water / cement ratio of 0.6 because this is the maximum allowed for Class II Environmental aggressiveness, in which case it would not meet the conditions of exposure of sample.

2.1.2 Compressive Strength

Just as the NBR 6118 [ABNT, 2003] provides values for the water/cement ratio, it also sets minimum values of compressive strength depending on the Agressive Environmetal Class indicated in Table 2.

Table 2 - Compressive strength as a function of environmental aggression.

Concrete	Type	Agressive Environmetal Class			
		I	II	III	IV
Class of concrete	CA	> = C20	> = C25	> = C30	> = C40
	CP	> = C25	> = C30	> = C35	> = C40

Note: CA - concrete; CP - prestressed concrete. (Source: ABNT - NBR 6118/2003).

Whereas the minimum standard set out in [Truc et al, 2000] for Aggressive Environmental Classes III and IV, and studies [Pereira, 2001][Andrade, 2001], outlined the membership functions to the variable resistance to axial compression shown in Figure 2. The curves represent the concrete classes defined in NBR 6118/03 because of aggressiveness environmental correspondent to the action of chloride ions.

In developing the membership functions considered the possibility that up to 5% of the resistance values may be below the specified value, as provided in rule. For this reason, the membership functions have a slight tail to the left. Also the limiting value of concrete is no higher than 50MPa because this is the maximum value of compressive strength for conventional concrete as regulated by the NBR 6118 [ABNT, 2003]; concrete having values of resistance to compression above this are considered high-strength concrete. It is observed that the membership functions defined in this study are similar to the functions defined by [Anoop et al, 2002]. The chart can be used as input for the characteristic compressive strength (f_{ck}) defined in the project as the 28 day strength or in the case of existing structures results of tests for resistances to axial compression may be used.

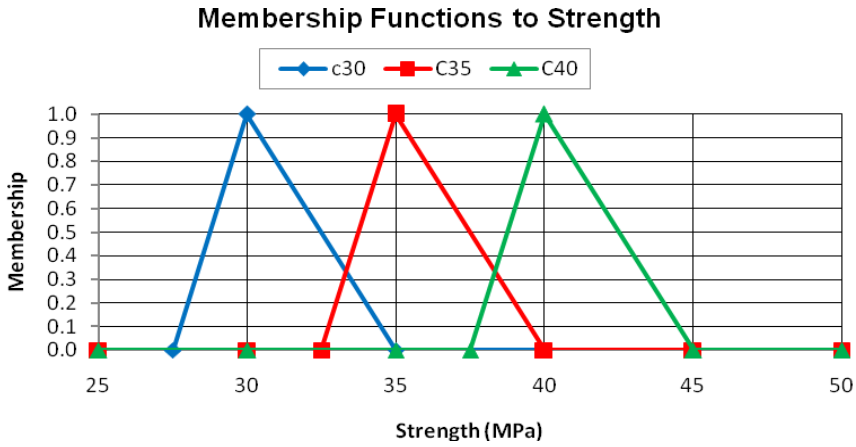

Figure 2 – Membership Functions to the variable strength.

2.1.3 Concreting Temperature

To define the limits of study for the cure temperature, it was considered as the lower limit value recommended by the British Cement Association (BCA) as the minimum temperature to make a concrete pour is 5°C, it is advisable to make an concreting at temperatures below 5°C by the fact that the reactions of cement hydration are very slow, damaging the properties of concrete. For the upper limit we adopted the value used by [Anoop et al, 2002] because most of the cast concrete works site is subject to a cure at environmental temperature and the values adopted by the author cover normal temperatures in Brazil. Figure 3 shows the membership functions used for concreting temperature.

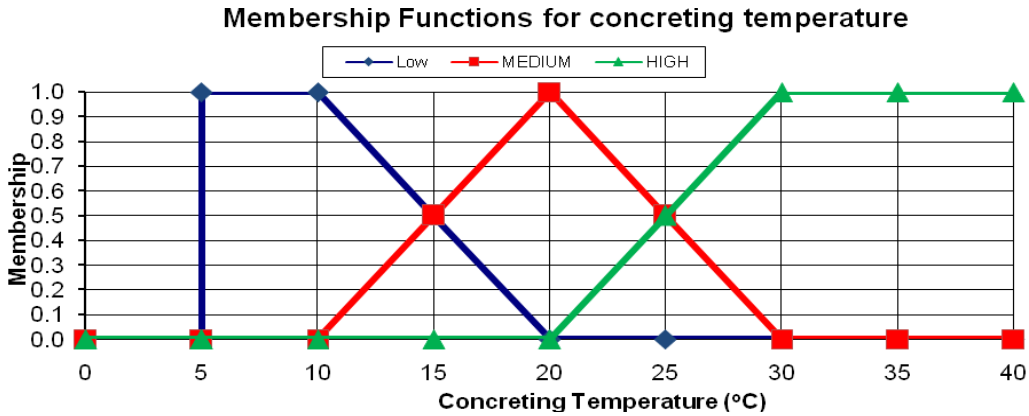

Figure 3 – Membership Functions to the variable cure temperature.

Based on the input variables of the system and the possible combinations between them, we defined the Map of Rules and System Membership Functions of Variable Output System. For a definition of inference rules we adopted the operation of conjunction and therefore for the whole case, will always set a water / cement ratio and compressive strength, and will always be possible to determine a temperature for the process cure the concrete, so that set the rules set out in Table 3, so that the inference rules took the form showed in Equation 1:

If *Fa / c* and *T* and then f_{ck} *Da* (Eq. 1)

where *Fa/c* represents the water/cement ratio; f_{ck} is the characteristic compressive strength of concrete in MPa, and *T* is the curing temperature of concrete in ^{o}C.

Table 3 - Map of inference rules of fuzzy variables.

Fa / c	Operation conjunction	f_{ck}	Operation conjunction	T		Da
III	AND	C30	AND	B	THEN	A
III	AND	C30	AND	M	THEN	A
III	AND	C30	AND	A	THEN	A
III	AND	C35	AND	B	THEN	A
III	AND	C35	AND	M	THEN	A
III	AND	C35	AND	A	THEN	N
III	AND	C40	AND	B	THEN	N
III	AND	C40	AND	M	THEN	N
III	AND	C40	AND	A	THEN	B
IV	AND	C30	AND	B	THEN	A
IV	AND	C30	AND	M	THEN	N
IV	AND	C30	AND	A	THEN	N
IV	AND	C35	AND	B	THEN	N
IV	AND	C35	AND	M	THEN	B
IV	AND	C35	AND	A	THEN	B
IV	AND	C40	AND	B	THEN	B
IV	AND	C40	AND	M	THEN	B
IV	AND	C40	AND	A	THEN	B

In the Map of Rules on Table 3, the water/cement ratio is indicated by the aggressiveness of Class III or IV Environmental, the compressive strength is represented by the Class of Concrete, C30, C35 or

C40, the cure temperature and may take the linguistic values: Low (B), Medium (M) or High (A). The combinations of the various possibilities of these variables lead to a qualification of the Diffusion Coefficient of Chloride, which can take qualifications: Down (B), Medium (M) or High (A), and this classification was based on values of diffusion coefficient obtained in tests carried out by several authors [Anoop et al, 2002][Truc et al, 2000][Thomas & Bemforth, 1998][Calçada, 2004][Kropp & Hilsdorf, 1995]. Fig. 4 illustrates the membership functions of the output variable of the system, the Coefficient of Diffusion of Chloride (Da).

To perform the defuzzification initially determined the vectors for the fuzzy input variables f_{ck}, T and w/c, then identifies which of the possible rules are applied, according to the statement of rules, whereas the operators diffuse used are the conjunction *and*, we use the MAX-MIN inference to obtain the composition of output variable of fuzzy system. Finally, determine the coefficient of diffusion of chlorides through the defuzzification method of Center High, which is a weighted average of the maximum of membership functions of output variable encompassed in the composition of output fuzzy system.

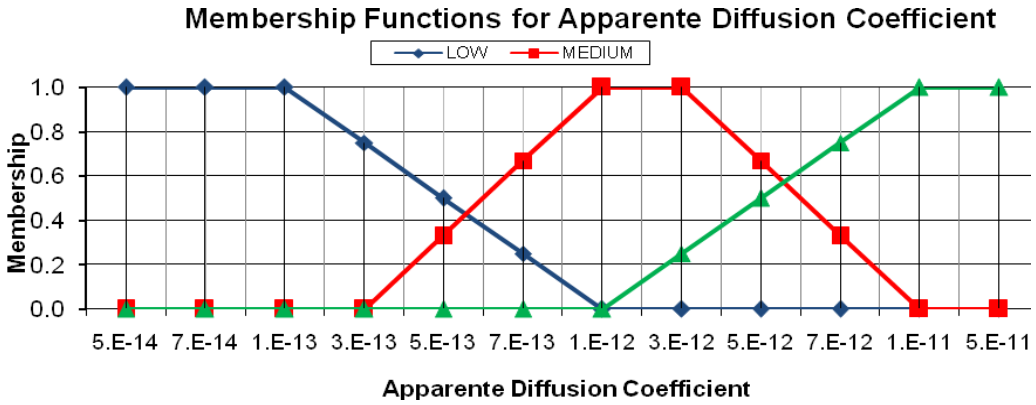

Figure 4 – Membership Functions for the variable apparent diffusion coefficient.

3 RESULTS AND ANALYSIS

To evaluate the performance of the mathematical model for the various situations studied in the laboratory, it was necessary to consider the parameters set for the concrete surface and the concentration of chloride ions, as indeed occurred in laboratory tests, namely:

- Resistance characteristic of concrete = 30MPa;
- Temperature of concreting = 22°C;
- Water-cement ratio = 0.55;

When using the mathematical model, we analyzed the various possible combinations with variations in environmental parameters, a total of 180 simulations. The values of environmental parameters used are:

- Exposure time: 6 months, 12 months and 18 months;
- Ambient Temperature: 15 °C, 20 °C, 25 °C and 30°C;
- Depth of analysis: 1mm, 2mm, 3mm, 4mm, 5mm;
- Area of exposure: 1 - Salt spray (N), 2 – Splash zone (V) and 3 – Submerged (S).

The values for mean error for the prediction of chloride concentration given by the model are presented in Table 4:

Table 4 – Mean error of Chloride concentration.

Depth (mm)	ERROR (%)
1	9,88
2	23,81
3	34,09
4	48,47
5	83,52

Area	ERROR (%)
N	42,91
V	22,10
S	54,85

4 CONCLUSIONS

It was observed that the age of 6 months of analysis of exposure, the submerged region showed higher concentrations of chloride ions in all depths, but for other ages of analysis has already happened a balance between the values of concentration of chloride ions in the regions submerged and change in water level and and the region of fog reached this equilibrium concentration at 18 months of exposure. Due to the short exposure time of 18 months, and the small height of the specimens used in evidence, only 50cm, it was not possible to identify the real influence of each region in the penetration of chloride ions in concrete.

The determination of the concentration of chloride ions using the model developed for estimating the coefficient of diffusion of chlorides and Fick's 2nd law for determining the concentration of chloride ions showed good results, with prediction errors below 40% on average, so that this model has good potential for use.

ACKNOWLEDGMENTS

The Technological Institute of Aeronautics, the Federal Technological University of Paraná and CAPES are acknowledged for the funding of the research presented in this paper.

REFERENCES

ABNT - *NBR 6118 - Design of concrete structures,* São Paulo, 2003.

Andrade, J., Dal Molin, D., *Probabilistic concepts in service life prediction of reinforced concrete structures inserted in saline environments***,** II Workshop on Durability of Constructions, Sao Jose dos Campos, 2001.

Andrade, MC, Diez, JM, Cruz Alonso, M., Mathematical modeling of the concrete surface "Skin Effect" on chloride diffusion in contaminated media. *Advanced Cement Based Materials,* vol. 6, pp. 39-44, 1997.

Andrade, JJO, Contribuição à previsão da vida útil das estruturas de concreto armado atacadas pela corrosão de armaduras: Iniciação por cloretos. *Tese de Doutorado,* UFRGS, Porto Alegre, 2001.

Anoop, MB; Rao, KB; Rao, TVSRA, Application of fuzzy sets for estimating service life of reinforced concrete structural members in corrosive environments. *Engineering Structures*, 2002.

Calçada, LML, Estudo da eficácia do ensaio de migração em condições de fluxo não estacionário na previsão da penetração de cloretos em concreto. *Tese de Doutorado*, UFSC, Florianópolis, 2004.

Chaterji, S., On the applicability of Fick's Second Law to chloride ion migration through Portland cement concrete. *Cement and Concrete Research*, vol. 25, No. 2, pp. 299-303, 1995.

Halamickova, P.; Detwiler, RJ; Bentz, DP; Garbocz, EJ, Water permeability and chloride ion diffusion in Portland cement mortars: Relationship to sand content and critical pore diameter. *Cement and Concrete Research*, vol. 25, no. 4, pp. 790-802, 1995.

Isaia, GC, *Concrete - Teaching, Research and Achievements***,** São Paulo, Brazilian Institute, 2005.

Kirkpatrick, TJ, Weyers, RE, Anderson-Cook, C., Sprinkel, MM, Probabilistic model for the chloride-induced corrosion service life of bridge decks. *Cement and Concrete Research*, vol 32, pp 1943-1960, 2002 .

Kropp, J. Hilsdorf, HK, Performance Criteria for Concrete Durability, *Rilem Report 12*, London, 1995.

Lounis, Z., probabilistic modeling of chloride contamination and corrosion of concrete bridge structures. *ISUMA'03,* Canada, 2003.

Martin-Perez, B., Zibara, H., Hooton, RD, Thomas, MDA, A study of the effect of chloride binding on service life prediction. *Cement and Concrete Research***,** vol. 30, pp. 1215-1223, 2000.

Nugue, F., Lorente, S., Ollivier, JP, Basis for the prediction of chloride ingress into cement-based materials. *E-Mat - Journal of Science and Technology of Construction Materials*, vol. 1, No. 1, pp. 10-21, 2004.

Pereira, VGA, Avaliação do coeficiente de difusão de cloretos em concretos: Influência do tipo de cimento, da relação água/cimento, da temperatura e do tempo de cura. *Dissertação de Mestrado*, UFRGS, Porto Alegre, 2001.

Shin, CB, Kim, EK, Modeling of chloride ion ingress in coastal concrete. *Cement and Concrete Research*, vol. 32, pp 757-762, 2002.

Thomas, MDA, Bamforth, PB, Modelling chloride diffusion in concrete – Effect of fly ash and slag. *Cement and Concrete Research*, vol. 29, pp. 487-495, 1998.

Troconis de Rincon, O., Castro, P., Moreno, EI, Torres-Acosta, AA, Moron de Bravo, O., Arrieta, I., Garcia, C., Garcia, D., Martin-Madrid , M., Chloride profiles in two marine structures - meaning and some predictions. *Buildng and Environment*, vol. 39, pp. 1065-1070,2004.

Truc, O., Ollivier, JP, Nilsson, LO, Numerical simulation of multi-species transport through satured concrete during a migration test – MsDiff code. *Cement and Concrete Research*, vol. 30, pp. 1581-1592, 2000.

Vu, KAT, Stewart, MG, Structural reliability of concrete bridges incluiding improved chloride-induced corrosion models. *Structural Safety***,** vol. 22, pp. 313-333, 2000.

XII DBMC
International Conference on Durability of Building Materials and Components
PORTO - PORTUGAL, April 12th-15th, 2011

Material Aging Simulation by Modelling Interaction of Micro-Environment Stress and Material Performances

Pierre Zurbrügg [1]

ABSTRACT

This paper presents a method and a simulation tool that are based on research undertaken from 1990 to 1997 by the EPFL-LCC Building Pathology Service in collaboration with the ARIA-Laboratory of the Ecole Nationale Supérieure d'Architecture de Lyon and developed from 2005 to 2010 in a PhD work. The tool permits simulation of material aging processes related to environmental stresses by computing variations of performance over time for the different material layers of multi-layer components.

On one hand, this allows for the tracking of the components' performance evolution over time. On the other, by comparing specific performances with failure criteria, it is possible to recognise indications of technical obsolescence and to estimate service life.

To demonstrate the potential of the method and the tool, aging behaviour related to stress for currently used building materials such as wood, stone, concrete, paints, glass, etc, has been modelled and integrated into the software-tool. This allows testing of various types of components and construction systems.

A case study presents the application of the simulation method as well as different computation result interpretations such as performance over time curves, failure events tables and service life estimation.

KEYWORDS

Service life prediction, Simulation, Construction materials, Degradation, Durability.

[1] Laboratoire de Construction et de Conservation - EPFL, Lausanne, SWITZERLAND, pierre.zurbruegg@epfl.ch

1 INTRODUCTION

Blachère [1969] has highlighted the importance of durability both as an economic performance and as a specific domain of science (science of durability). Nowadays, the evolution of IT capabilities offers the opportunity to approach the question of predicting the durability of building components with new methods and software tools. These would allow the checking of service life requirements of new buildings at the design stage and they would be helpful in planning for the maintenance of existing construction.

This paper presents an approach to modelling the aging behaviour of multi-layer components exposed to various stress agents. The first work on this method was undertaken from 1990 to 1996 by the EPFL-LCC Building Pathology Service (François Iselin) in collaboration with the ARIA-Laboratory of the Ecole Nationale Supérieure d'Architecture de Lyon (UMR CNRS n°694 MAP, Hervé Lequay, see Iselin and Lequay, 1994) .The research was resumed in a PhD work form 2004 to 2010 [Zurbrügg, 2010]. The present text gives a brief description of the simulation method as well as an illustration of its application in a case study.

2 METHOD

The simulation method takes into account that the tool is designed with Object Orientated Programming (OOP) and that the different parts work as independent modules linked to each other. Three parts can be distinguished: the *computing of the performance curves*, the *initialisation of surface stress levels* and the *detection of failures*. Figure 1 is a simplified representation of the main model and illustrates the relationships between the different parts described hereafter.

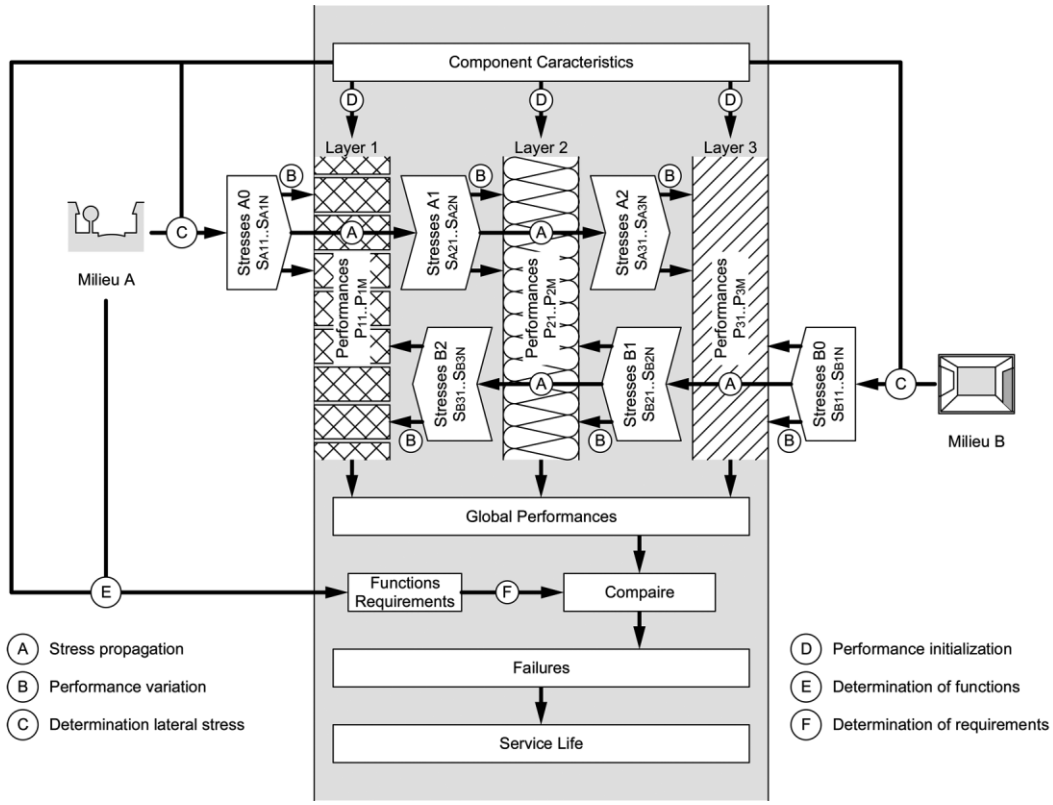

Figure 1. Schematic illustration of the simulation model layout
(Circled letters refer to the text).

2.1 Computing Performance Curves

The core of the simulation model is designed to compute the evolution over time of a construction element's performances, taking into account the interaction of two types of vertices: stress agents and material performances.

2.1.1 Stresses

The first vector, the stresses, represents degradation factors as they have been enumerated in ISO 6241 [1984]-Table 4 and the EOTA guidance document GD003 [1999]-Appendix B. Table 1 shows the stresses used in the model classified by the type of agent.

Table 1. Stresses provoking material modification that have been selected for the model

Agent type	**Agents**	**Stress**	**Scale**
1. Mechanical	Hail, moving actions	Shocks	0…10
	Moving actions, internal and external shocks	Stabs	0…10
	Abrasion, friction	Mechanical wear	0…10
	Running water	Wash out	0…10
	Wind	Air speed / wind	0…10
2. Electromagnetic	Sun	Solar radiation	0…10
3. Thermal	Warming, thermo-shock	Temperature	°C
	Frost	Frost	0…10
4. Chemical	Precipitation, surface water, ground water, projected water, water infiltration	Wetness	0…10
	Air humidity, condensation	Moisture	Pa
	Acids, bases, concrete medium	pH	pH
	Carbon dioxide	CO_2-concentration	g/m^3
	Dust, soot	Pollutants	0…10

2.1.2 Performances

The second vector, the performances, is used to define specific material properties used in the simulation method. Table 2 illustrates the basic performances used in all material layer models.

Table 2. Basic performances with their scales

Performance	scale
Thickness / width	mm
Shock-absorption	0...10
Static strength	0...10
Wear Resistance	0...10
Resistance to shocks	0...10
Resistance to stabs	0...10
Resistance to corrosion	0...10
Resistance to wash out	0…10
Water tightness	0...10
Air tightness	0...10
Light tightness	0...10
Surface appearance	0...10
Surface flatness	0...10
Thermal conductivity	W / m K
Moisture conductivity	mg / h m Pa
CO_2-Tightness	mm^2/a
pH-Value (Alkalinity)	pH

2.1.2 Interaction of Stresses and Performances

The interaction of these two vertices is based on two considerations. The first is the fact that each construction element is exposed to various types of stress agents resulting from environment conditions on each side of the component. The propagation of these stresses through the multi-layer component depends on the specific performances of each layer. For instance, penetration of water depends on water-tightness, propagation of wind on air-tightness, conduction of heat on thermal conductivity, etc. We call this type of interaction *stress propagation* (A, see Fig. 1). The second consideration concerns the durability of materials. In a general way, one can say that degradation of building materials depends on the type and intensity of the stress agents to which they are exposed. These physical, chemical or biological degradations lead normally to a variation of one or more performance aspects. Water infiltration can for example provoke loss of thermal conductivity, loss of stability and modification of visual aspects. This kind of interaction is called *performance variation* (B). Figure 2 illustrates the data flow of these two interactions.

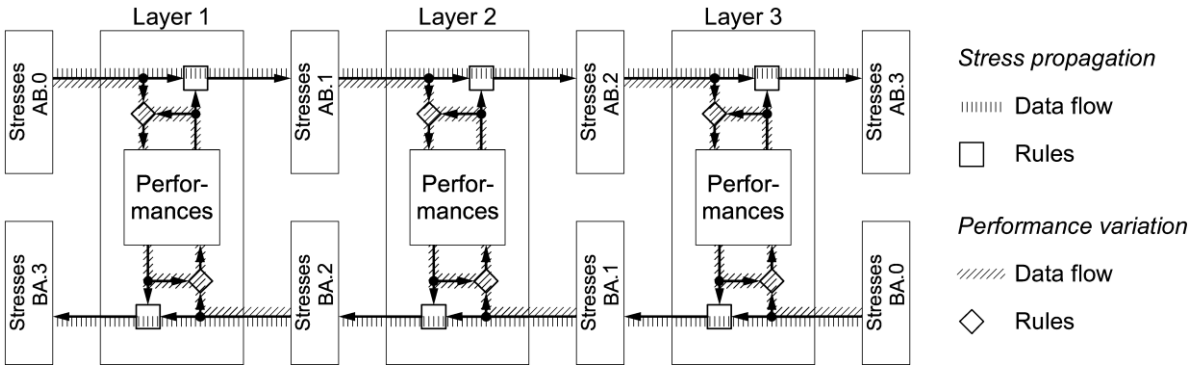

Figure 2. Illustration of stress propagation and performance variation.

2.1.3 Simulation Sequences

The performance evolution over time is computed by an iterative cycle as shown in Figure 3. The initialisation step consists of creating the simulation model by assembling the different material layer-objects according to the user-defined component composition. This permits that every material layer has its own performances and rules of *performance variation,* i.e. it acts like an independent sub-model. All modelled materials are stored in a material-class library. Also defined during initialisation are the stresses intensities on the surface (C, see paragraph 2.2) and parameters of the failure detection (E and F, see paragraph 2.3).

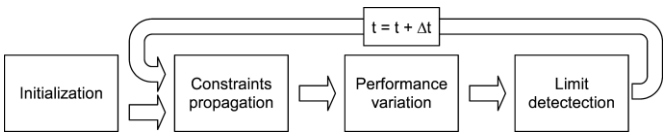

Figure 3. Iteration cycle.

The principal tasks within the cycle are the computation of the *stress propagation* algorithm and the *performance variation* rules. At the end of each cycle some other tasks are executed such as the generation of alarms for signal failure (see paragraph 2.3). Before starting a new cycle, the time variable is incremented by the duration of the time step, usually one year.

2.2 Definition of Surface Conditions

In analogy to definition of the microclimate being "the meteorological variables in the absolute proximity of a material surface" [Jernberg et al., 2004], the stress agents that affect a component on its surface can be seen as a micro-environment that includes not only climatic parameters but also

stresses due to occupation. In contrast, the meso-environnement or *milieu* describes the general conditions of the larger environment.

To estimate the nature and intensity of the stresses, one has to take into account the conditions of the milieu as well as attributes of the component such as orientation, slope, distance from ground, type of element, protection from direct sunlight or from rain etc. The reason for this can be illustrated with the example of a room. In this kind of configuration it is obvious that climatic and occupation conditions are equal but the floor, walls or the ceiling will be affected in different ways. For instance, while the floor is regularly subject to mechanical abrasion and shocks, due mainly to persons walking on it, the walls are exposed to such actions only from time to time and the ceiling only very rarely and with much less intensity. Similar considerations can be made for outdoor environments where the surface conditions depend on orientation, slope etc.

In the simulation tool, due to the big difference between outside and inside conditions, two types of milieu have been introduced: inside-milieu and outside-milieu. The estimation of the stress agents on the surface is made by rules that take into account the description of the milieu and the component's attributes. This is computed in the initialisation stage.

2.3 Failure and End of Life Detection

The computation of the performance evolution normally produces a huge amount of data and gives no direct information about failure and service life. Therefore it was necessary to add a module able to process performance data and detect the component's failure.

Viewed from a technical point of view, bi-dimensional components such as slabs, facade elements, roofs etc. are supposed to fulfil different specific functions in a building. They have to guarantee the stability of the construction, respond to esthetical values and, in a general way, protect one milieu from the undesired agents of the other, i.e. they are used to separate the two different milieus. These function requirements can be achieved if the component presents certain performance characteristics. For instance, to prevent an interior environment from outside weather conditions, the component must have minimal levels of water-tightness, air-tightness and thermal insulation. This way the serviceability of a component can be monitored by comparing some of its key performances to minimal values. This principle is also used in the Performance Limits Method (PLM) presented by Daniotti and Lupica Spagnolo [2008] and the Failure Modes and Effects Analysis (FEMA) presented by Talon [2008]. Detecting failures and end of service life by surveying the evolution of the component's performances over time requires identification of critical functions and fixing key performances as well as minimal performance requirements. The definition of these parameters is made during the initialisation of the model.

The failure detection is processed at the end of each time step by comparing the key performances to their threshold-values. Where the limit is passed, the module generates a specific failure event, including the nature as well as the date of failure. This method permits surveying the evolution of the degradation and generating alarms of different levels.

2.4 Stochastic Simulation

Methods for durability estimation must deal with the uncertainty of the model parameters. This is due to the fact that degradation processes depend on various hazardous parameters and on errors introduced by modelling and simplification of the processes. In order to introduce these uncertainties into the model and to obtain results in form of cumulative distribution functions (CDF), the tool was completed with an extra module, able to proceed to a Monte-Carlo simulation. Therefore, probability density functions (PDFs) instead of discrete values are used to initialise performance and stress parameters. For each alarm event, the variation of the failure age is used to draw CDFs.

3. CASE STUDY

In order to illustrate the working of the simulation tool, a south orientated masonry wall with external insulation and timber cladding has been chosen. The façade element separates a courtyard on ground floor level (milieu A) from a living room (milieu B). Figure 4 represents the component's layer assembly and the material attributes.

Index	Layer	Material	Additional characteristics	Width [mm]
1	Cladding	Coniferous Wood	Tongue & groove assembly	20
2	Sub-construction	Coniferous Wood		60
3	Insulation	Glass Fibre Wool Mat		100
4	Wall	Brick	Cement joints	180
5	Plaster	Gypsum		10
6	Paint	Dispersion	Clear colour	3 coats
	Total			370

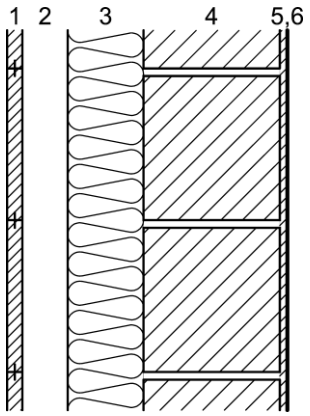

Figure 4. Wall composition - Left : Table with materials and widths, Right: Wall Section.

The evolution of different width-performances over the first 100 years computed with discrete simulation is shown in Fig. 5. One can see for instance that the degradation of the sub-construction (2) starts when the cladding layer (1) is strongly affected.

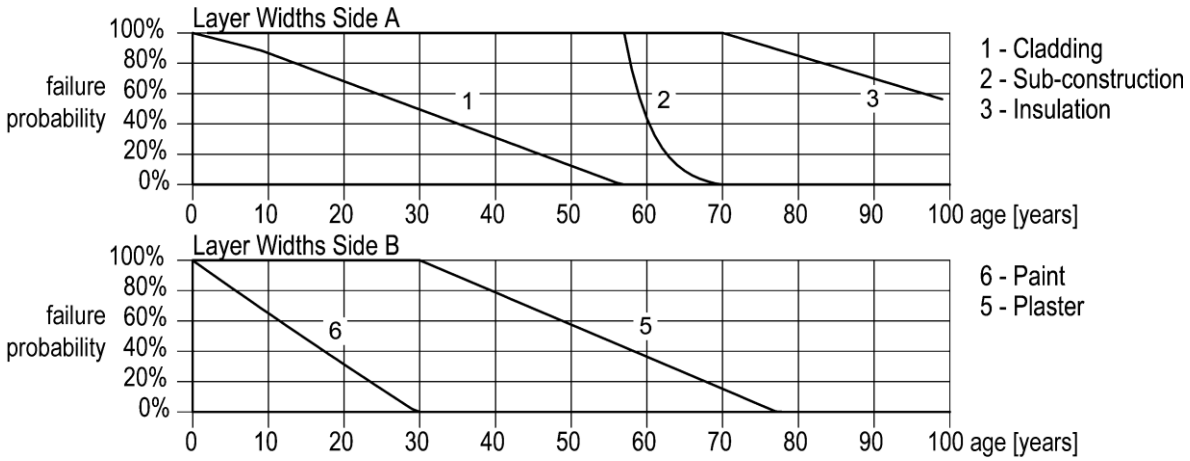

Figure 5. Evolution of width-performances in percent of original width

The alarm event list in Table 3 enumerates the various warnings generated by the failure detection module. The first four columns on the left indicate event index, alarm level, concerned element and type of failure. The columns on the right present numerical results in years from a stochastic simulation with 1000 trials. The failure probability is expressed either in mean values and standard deviation or in values at specific reliability levels (20%, 50%, 80%).

Table 3. Alarm event list with event dates in years.

Ind.	Al.	Element	Text	Mean	Std Dev.	Failure Probability		
						20%	50%	80%
I	5	Dispersion Paint	Layer strongly affected	30.6	6.7	24	29	35
II	5	Cladding	Layer strongly affected	56.6	3.1	53	56	59
III	4	Sub-Construction	Exposed to water (risk of rot).	57.6	3.1	54	57	60
IV	3	Insulation	Light Glass Wool Board – Humidification.	57.6	3.1	54	57	60
V	2	Ventilated Facade	Important decrease of thermal insulation.	60.2	3.1	57	60	62
VI	5	Sub-Construction	Layer strongly affected	69.6	3.1	66	69	72
VII	5	Plaster	Layer strongly affected	77.6	10.1	68	78	88

Stochastic simulation results cans also be presented as CFDs. Figure 6 shows these graphs for level 5 alarm events.

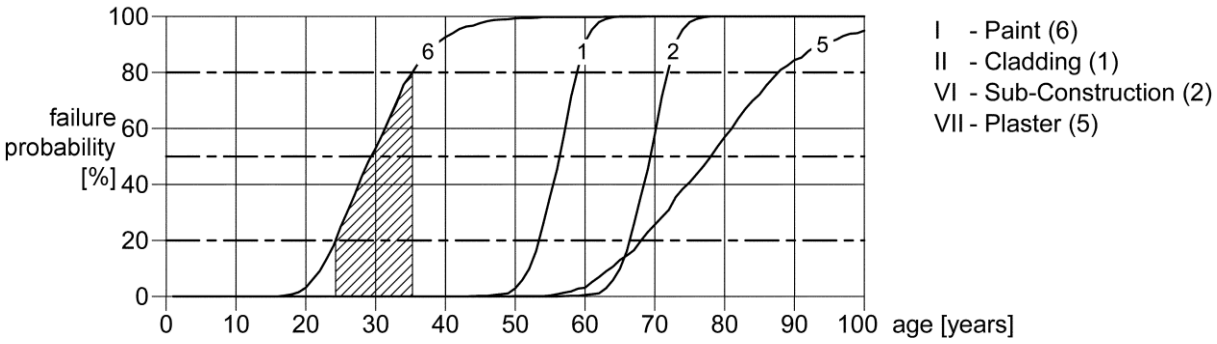

Figure 6. Cumulative distribution functions for level 5 alarm events; service life distribution of paint-layer is highlighted.

4. CONCLUSIONS AND OUTLOOK

Simulating deterioration phenomena on a layer level rather then on a component level is a promising way to estimate durability and service life of construction elements and gives various advantages:

- Even if the number of available building materials is increasing continuously, it is much less than the number of potential building components in use. Collecting specific data for one material allows for the simulation of many components.
- If materials data is available, the service life of new component assemblies can immediately be estimated, even without field experience.
- The fact that the performance curves are computed by iteration over time makes it very easy to integrate maintenance actions.
- The principle of surveying performance and stress levels allows detection of various changes in the component and a detailed analyse of its aging behaviour.
- The use of object oriented programming permits easy upgrading of material-models without changing the basic model-structure. The very simple degradation rules currently used can be gradually refined with the progress of knowledge.

On the other hand, there are important challenges and difficulties that must be faced up to. These include:

- Homogeneous levels for stress agents must be defined as must rules allowing determination of stress intensities on the surface from milieu and component characteristics.
- Known material properties must be transposed to model compatible performance scales.

- Many currently unknown material properties must be determined by measurements, observation or estimation.
- Dose-response functions for each degradation mechanisms and each material must be determined.

Currently, the rules for simulating constraint propagation and performance variation are very simple and the corresponding parameters have been determined for about 40 materials based on research and experience from the EPFL-LCC Building Pathology Service. Further investigations must be carried out in order to model missing materials and to refine the existing material models.

REFERENCES

Blachère, G., 1969. *Savoir bâtir, Habitabilité - Durabilité - Economie des bâtiments*. Paris: Ed. Eyrolles.

Daniotti, B. & Lupica Spagnolo, S., 2008. *Service Life Prediction Tools for buildings' Design and Management*. In: 11dbmc, Istambul, T72-191.

Iselin, F., Lequay, H. & Bercioux, H., 1994. *AMB: Analyse et Modélisation du Bâtiment*. In: Colloque "Pathologie du Bâtiment", Symposium CIB WS94, 30. sept. 1994. CIB WS94: Varenna (Italy).

ISO 6241:1984. *Performance standards in building - Principles for their preparation and factors to be considered*. Genève: International Standard Organisation (ISO).

Jernberg, P., Lacasse, M.A., Haagenrud, S.E. & Sjöström, C., 2004. *Guide and Bibliography to Service - Life and Durability Research for Building Materials and Components*. Rotterdam: CIB, n°295.

Talon, A., 2005. *Temporal quantification method of degradation scenarios based on FMEA*. In: 10dbmc, Lyon, France 17-20 april 2005. CSTB: Lyon, France, TT4-139.

Zurbrügg P., 2010. *Simulation des phénomènes de dégradation d'éléments de construction, Application d'une méthode basée sur la modification des performances de matériaux et la propagation des contraintes*. PhD thesis, Ecole Polytechnique Fédérale de Lausanne (EPFL), Lausanne.

XII DBMC
International Conference on Durability of Building Materials and Components
PORTO - PORTUGAL, April 12th-15th, 2011

An Analytical Study on the Carbonation Progress of Concrete Depending on the Quality of the Surface Layer

Sato Sachie [1]
Lee Youngran [2]
Masuda Yoshihiro [3]

ABSTRACT

This paper theoretically examines and proposes simple computational methods of predicting the carbonation progress of concrete when the qualities of the surface layer and internal concrete are not the same but cementitious materials have been combined at the surface layer of concrete. It is based on the model that carbon dioxide moves at a steady rate of diffusion according to Fick's law; reacts instantaneously with calcium hydroxide ($Ca(OH)_2$) at the boundary between carbonated and noncarbonated regions; and the boundary moves inward sequentially. The carbonation progress is simulated using data from previous papers.

KEYWORDS

Quality of the surface layer of concrete, Carbon dioxide diffusion, Simulation of carbonation progress.

[1] Department of Architecture of Tokyo City University, Tokyo, JAPAN, s-sato@tcu.ac.jp
[2] Department of Architecture Engineering of Utsunomiya University, Utsunomiya, JAPAN, leeyr@cc.utsunomiya-u.ac.jp
[3] Department of Architecture Engineering of Utsunomiya University, Utsunomiya, JAPAN, masuday@cc.utsunomiya-u.ac.jp

1 INTRODUCTION

In a thermo-hygrostatic environment with a constant CO_2 concentration, the carbonation of concrete having a homogeneous quality from the surfaces inward is known to progress in proportion to the square root of time, following the so-called rule of √t [Japan Institute of Consturction Engineering 1986]. This is theoretically explained by the solution of a model expressing a phenomenon in which CO_2 steadily diffuses through a carbonated region of concrete and instantaneously reacts with $Ca(OH)_2$ at the boundary between the carbonated and noncarbonated regions, thereby progressively shifting the boundary deeper inward [Architectural Institute of Japan 2004]. This hypothethis has also been virtually validated by accelerated tests under thermo-hygrostatic conditions with a constant CO_2 concentration. Moreover, it has been proven to be practically valid by analyses based on unsteady diffusion [Maeda 1989, Fukushima 1991 & Masuda et al. 1991]. The progress of carbonation can therefore be expressed by Eq. (1).

$$C = A\sqrt{t} \tag{1}$$

where C : carbonation depth(mm)
t : time(years)
A : coefficient of carbonation speed(mm/year$^{1/2}$)

The coefficient of carbonation speed may also be expressed by Eq. (2) as a coefficient determined by the effects of various factors [Architectural Institute of Japan 2004].

$$A = \alpha\beta\gamma\delta \tag{2}$$

where α : coefficient for environmental conditions (CO_2 concentration, temprature, humidity, etc.)
β : coefficient for concrete qualities (W/C, srength, cement type, etc.)
γ : coefficient for defects related to placing (cracking, degree of honeycombs, etc.)
δ : coefficient for finishing material (gas permeation resistance, type, etc., of finishing material)

The quality of the surface region of architectural concrete in actual buildings is said to be rougher than that of internal concrete due to the effect of drying [Ohta Tatsumi et al. 2003 & Yuasa et al. 1998]. The quality of concrete is also made inhomogeneous from the surface along the depth by the use of water-permeable forms [Ishihara et al. 1987] or the application of an inorganic impregnant to densify the microstructure of surface concrete. When the quality of surface concrete is altered from that of internal concrete in this manner, it is not clear whether or not the progress of carboantion can be appropriately expressed by putting the coefficent for concrete quality in Eq. (2) as $\beta<1$ or $\beta>1$.

When applying finishing mortar or using cementitious stay-in-place forms [Baba et al. 2001], the carbonation of core concrete may progress after such mortar or forms have been carbonated, if they are monolithically integrated. Investigation has also been insufficient as to whether or not the progress of concrete carbaontion can be appropriately expressed by putting the coefficient for the finishing material in Eq. (2) as $\delta<1$ or $\delta>1$.

Meanwhile, Baba et al.[1987] proposed a method of estimating the carbonation depth of concrete having various surface layers including a finishing material, and several analyses have been conducted using the proposed equations [Kawanishi et al. 2006 & Kono et al. 2006]. The equations proposed by Baba et al. were derived by schematically solving the problem while introducing the concept of equivalent time.

In this study, the authors investigated the progress of concrete carbonation when the quality of surface concrete differs from that of internal concrete and when a cementitious material is monolithically integrated with base concrete. This was carried out theoretically using a model that expresses a phenomenon in which CO_2 steadily diffuses through the finishing material and concrete, obeying Fick's law, and instantaneously reacts with $Ca(OH)_2$, which is present at the boundary between carbonated and noncarbonated regions. This causes the boundary to progressively shift deeper inward. This paper propses a simple method of calculating such progress of carbonation. Note that the diffusion of CO_2 through mortar and concrete is assumed to be steady, though it is actually unsteady.

2 ANALYSIS

2.1 Subjects Of Analysis

The following two cases are investigated as subjects of analysis:
Case 1: Where finishing mortar is applied to concrete surfaces. A cementitious material in contact with concrete surfaces (e.g., stay-in-place forms) can be similarly dealt with.
Case 2: Where the microstructure near the surfaces is altered from that in internal concrete. This includes denser surfaces due to modification and rougher surfaces due to deterioration.
These two are basically similar, because in both cases a cementitious material having qualities different from internal concrete forms the surface layer, which is carbonated prior to the carbonation of internal concrete. The difference is that in Case 2 the depth of the surface cementitious layer is included in the cover depth whereas in Case 1 it is not.
Note that the case where a polymeric finishing material or coating is applied to concrete surfaces should be investigated separately, as carbonation of such finishing is irrelevant. Such a case is therefore not dealt with in this paper.

2.2 Case 1 (where finishing mortar is applied to concrete surfaces)

2.2.1 Mortar Carbonation Phase
Figure 1 shows a pattern diagram expressing the diffusion of CO_2 and its reaction with $Ca(OH)_2$ in mortar in the phase of carbonation within finishing mortar. Assuming the coordinate of a concrete surface and the thickness of finishing mortar to be *0* and *d*, respectively, the coordinate of the surface of finishing mortar is *–d*. Putting the coordinate of the carbonation depth of finishing mortar as *x*, the amount of CO_2 reaching a depth of *x* during time Δt through a plane with an area of *S* perpendicular to the depth direction from the surface of finishing mortar, ΔCO_2, is expressed by Eq. (3). If CO_2 reaching the depth of *x* instantaneously reacts with $Ca(OH)_2$, then the amount of CO_2 consumed is expressed by Eq. (4).

$$\Delta CO_2 = D_m \cdot \frac{C_0}{x-(-d)} \cdot S \cdot \Delta t \tag{3}$$

$$\Delta CO_2 = H_m \cdot S \cdot \Delta x \tag{4}$$

where x : carbonation depth of finishing mortar ($-d \le x \le 0$, mm)
t : time(years)
C_0 : CO_2 concentration at the surface of finishing mortar
D_m : diffusion coefficient of carbonated region in finishing mortar (mm^2/year)
S : surface area(mm^2)
H_m : $Ca(OH)_2$ content per unit volume of finishing mortar
Δx : thickness of boundary region
Δt : time increment

By rearranging Eqs. (3) and (4), $(x+d)\frac{\Delta x}{\Delta t} = \frac{D_m \cdot C_0}{H_m}$

Assuming that Δt approaches zero, the following differential equation is obtained:

$$(x+d)\frac{dx}{dt} = \frac{D_m \cdot C_0}{H_m}$$

Both members are integrated as follows: $\frac{1}{2}x^2 + d \cdot x = \frac{D_m \cdot C_0}{H_m} t + I_1$ (I_1: integration constant)

When t=0, x=-d. Therefore, $I_1 = -\frac{1}{2}d^2$

$$\frac{1}{2}x^2 + d \cdot x - \frac{D_m \cdot C_0 \cdot t}{H_m} + \frac{1}{2}d^2 = 0$$

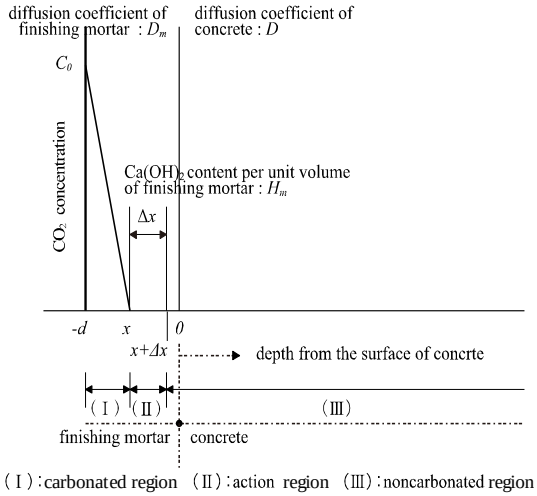

Figure 1. Model of CO_2 diffusion and reaction with $Ca(OH)_2$ while carbonation of finishing mortar is in progress.

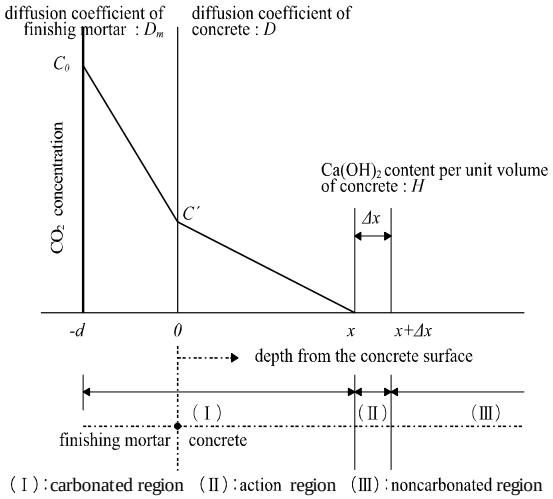

Figure 2. Model of CO_2 diffusion while carbonation of concrete is in progress.

By solving this, $x = \sqrt{\frac{2D_m \cdot C_0 \cdot t}{H_m}} - d$ (5)

By putting $\sqrt{\frac{2D_m \cdot C_0}{H_m}} = A'$, Eq. (5) can be summarized as follows:

$$x = A'\sqrt{t} - d \quad (6)$$

Also, when finishing mortar is entirely carbonated, i.e., when $x=0$, $t = \frac{H_m}{2D_m \cdot C_0} d^2$

2.2.2 Concrete Carbonation Phase

Figure 2 shows a pattern diagram expressing the diffusion of CO_2 while concrete carbonation is in progress after the finishing mortar has been entirely carbonated. Assuming that carbonation has progressed to a depth of x from the concrete surface at an age of t, Eq. (7) expresses ΔCO_2, the amount of CO_2 that diffuses through the finishing mortar layer and reaches the concrete surface during time Δt through a plane with an area of S, which is perpendicular to the depth direction. Similarly, Eq. (8) expresses ΔCO_2, the amount of CO_2 reaching a depth of x from the concrete surface during time Δt. CO_2 diffusing to the depth of x is consumed by reaction with $Ca(OH)_2$. The amount of CO_2 consumed by this reaction, ΔCO_2, is expressed by Eq. (9), and then the CO_2 concentration becomes zero.

$$\Delta CO_2 = D_m \cdot \frac{C_0 - C'}{d} \cdot S \cdot \Delta t \quad (7)$$

$$\Delta CO_2 = D \cdot \frac{C'}{x} \cdot S \cdot \Delta t \quad (8)$$

$$\Delta CO_2 = H \cdot S \cdot \Delta x \quad (9)$$

where x : depth of concrete carbonation ($0 \le x$, mm)
C' : CO_2 concentration at the boundary between finishing mortar and concrete
D : diffusion coefficient of CO_2 in carbonated concrete (mm^2/year)
H : $Ca(OH)_2$ content per unit volume of concrete

From Eqs. (7) and (8), $C' = \frac{D_m \cdot x}{D_m \cdot x + D \cdot d} C_0$ (10)

From Eqs. (8) and (9), $\frac{\Delta x}{\Delta t} = \frac{D \cdot C'}{H \cdot x}$ (11)

By deleting C' from Eqs. (10) and (11) and assuming that Δt approaches zero, the following differential equation is obtained:

$$\left(x + \frac{D}{D_m} d \right) \frac{dx}{dt} = \frac{D \cdot C_0}{H}$$

By integrating both members,

$$\frac{1}{2} x^2 + \frac{D \cdot d}{D_m} x = \frac{D \cdot C_0}{H} t + I_2 \text{ (I_2: integration constant)} \quad (12)$$

Because $t = \frac{H_m}{2 D_m \cdot C_0} d^2$ when $x=0$, $I_2 = -\frac{D \cdot H_m \cdot d^2}{2 D_m \cdot H}$

By substituting I_2 into Eq. (12), $\frac{1}{2} x^2 + \frac{D \cdot d}{D_m} x - \frac{D \cdot C_0}{H} t + \frac{D \cdot H_m \cdot d^2}{2 D_m \cdot H} = 0$ (13)

By solving Eq. (13), $x = \sqrt{\frac{2D \cdot C_0}{H}} \left(\sqrt{\left(t - \frac{H_m \cdot d^2}{2 D_m \cdot C_0} \right) + \frac{H \cdot D \cdot d^2}{2 D_m{}^2 \cdot C_0}} - \sqrt{\frac{H \cdot D \cdot d^2}{2 D_m{}^2 \cdot C_0}} \right)$ (14)

By putting $\sqrt{\frac{2D \cdot C_0}{H}} = A$, $\sqrt{\frac{H \cdot D \cdot d^2}{2 D_m{}^2 \cdot C_0}} = R$, and $\frac{H_m \cdot d^2}{2 D_m \cdot C_0} = T$, Eq. (14) can be summarized as follows: $x = A\left(\sqrt{(t - T) + R^2} - R \right)$ (15)

Also, $A \cdot R = \frac{D \cdot d}{D_m}$

Equation (15) is the same as the equation proposed by Baba et al. when $T=R^2$, i.e., when $H_m \cdot D_m = H \cdot D$.

2.3 Case 2 (where the microstructure of surface concrete is altered from that of internal concrete)

2.3.1 Surface concrete carbonation phase

Figure 3 shows a pattern diagram expressing the diffusion of CO_2 and its reaction with $Ca(OH)_2$ while carbonation proceeds in surface concrete. The coordinate of concrete surface and the thickness of surface concrete are assumed to be zero and d, respectively. The amount of CO_2 that diffuses through concrete and reacts with $Ca(OH)_2$ at the broundary between carbonated and noncarbonated regions, ΔCO_2, is expressed similarly to Case 1.

$$\Delta CO_2 = D_s \cdot \frac{C_0}{x} \cdot S \cdot \Delta t \quad (16)$$

$$\Delta CO_2 = H_s \cdot S \cdot \Delta x \quad (17)$$

where x : carbonation depth of surface concrete ($x \le d$, mm)

D_s : diffusion coefficient for the carbonated region in surface concrete (mm^2/year)

H_s : $Ca(OH)_2$ content per unit volume of surface concrete

This is solved as $x = \sqrt{\frac{2 D_s \cdot C_0 \cdot t}{H_s}}$ (18)

By putting $\sqrt{\frac{2 D_s \cdot C_0}{H_s}} = A''$, Eq. (18) can be summarized as follows: $x = A'' \sqrt{t}$

Also, when surface concrete is entirely carbonated, i.e., when $x=d$, $t = \frac{H_s}{2 D_s \cdot C_0} d^2$

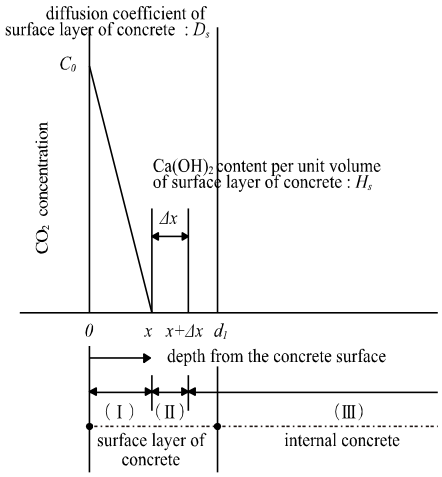

Figure 3. Model of CO_2 diffusion and reaction with $Ca(OH)_2$ while carbonation of surface concrete is in progress.

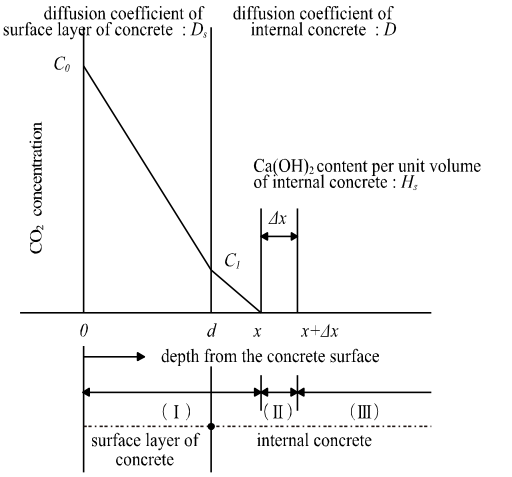

Figure 4. Model of CO_2 diffusion while carbonation of internal concrete is in progress.

2.3.2 Internal concrete carbonation phase

Figure 4 shows a pattern diagram expressing the diffusion of CO_2 in the phase in which carbonation proceeds in internal concrete after surface concrete has been entirely carbonated. The amount of CO_2 that diffuses through surface and internal concretes and reacts with $Ca(OH)_2$ at the boundary between carbonated and noncarbonated regions, ΔCO_2, is expressed similarly to Case 1.

$$\Delta CO_2 = D_s \cdot \frac{C_0 - C'}{d} \cdot S \cdot \Delta t \tag{19}$$

$$\Delta CO_2 = D \cdot \frac{C'}{x - d} \cdot S \cdot \Delta t \tag{20}$$

$$\Delta CO_2 = H \cdot S \cdot \Delta x \tag{21}$$

where x : carbonation depth of internal concrete (d≤x, mm)

C' : CO_2 concentration at the boundary between surface and internal concrete

D : diffusion coefficient of CO_2 in the carbonated region of internal concrete (mm^2/year)

H : $Ca(OH)_2$ content per unit volume of internal concrete

From Eqs. (19) and (20), $C' = \dfrac{D_s(x-d)}{D_s x + (D - D_s)d} C_0$ (22)

From Eqs. (20) and (21), $\dfrac{\Delta x}{\Delta t} = \dfrac{D \cdot C'}{H(x-d)}$ (23)

By deleting C' and assuming that Δt approaches zero in Eqs. (22) and (23), the following differential equation is obtained:

$$\left\{ x + \frac{(D - D_s)d}{D_s} \right\} \frac{dx}{dt} = \frac{D \cdot C_0}{H}$$

By integrating both members, $\dfrac{1}{2} x^2 + \dfrac{(D - D_s)d}{D_s} x = \dfrac{D \cdot C_0}{H} t + I_3$ (I_3: integration constant) (24)

Because $t = \dfrac{H_s}{2 D_s \cdot C_0} d^2$ when $x=d$, $I_3 = \dfrac{(2D \cdot H - D \cdot H_s - D_s \cdot H) d^2}{2 D_s \cdot H}$

By substituting I_3 into Eq. (24), $x^2 + \dfrac{2(D - D_s)d}{D_s} x - \dfrac{2D \cdot C_0}{H} t - \dfrac{(2D \cdot H - D \cdot H_s - D_s \cdot H) d^2}{D_s \cdot H} = 0$ (25)

By solving Eq. (25), $x = \sqrt{\frac{2D \cdot C_0}{H}} \left\{ \sqrt{\left(t - \frac{H_s \cdot d^2}{2D_s \cdot C_0} \right)} + \frac{H \cdot D \cdot d^2}{2{D_s}^2 \cdot C_0} - \sqrt{\frac{H \cdot D \cdot d^2}{2{D_s}^2 \cdot C_0}} \right\} + d$ (26)

By putting $\sqrt{\frac{2D \cdot C_0}{H}} = A$, $\sqrt{\frac{H \cdot D \cdot d^2}{2{D_s}^2 \cdot C_0}} = R$ and $\frac{H_s \cdot d^2}{2D_s \cdot C_0} = T$, Eq. (26) can be summarized as follows: $x = A\left(\sqrt{(t - T) + R^2} - R \right) + d$ (27)

Also, $A \cdot R = \frac{D \cdot d}{D_s}$

Equation (27) is the same as the equation proposed by Baba et al. when $T=R^2$, i.e., when $H_s \cdot D_s = H \cdot D$.

3 EXAMPLE OF NUMERICAL CALCULATION

In this section, a simulation of carbonation progress is attempted by substituting specific values into the above-mentioned analysis results where finishing mortar is applied to concrete surfaces. Table 1 gives the calculation conditions. Figures 5 and 6 show the progress of carbonation in concretes finished with mortars with a W/C of 50% and 60%, respectively.

With a W/C of 50% (Fig. 5), carbonation of exposed concrete reaches a depth of around 21 mm after 50 years. When covered with a rich mortar mixture, carbonation reaches the bottom of the mortar layer after 44 years. With a W/C of 65% (Fig. 6), the carbonation depth in exposed concrete is 30 and 40 mm after 14 and 25 years, respectively. When covered with a lean mortar mixture, the carbonation depth in concrete is 30 and 40 mm after 33 and 48 years, respectively. When a rich mortar mixture is aplied, carbonation remains within the mortar layer up until 44 years.

When comparing the calculations by Baba's equation and the present equation proposed by the authors, their differences are small regarding concrete covered with a rich mortar mixture, because of the slow progress of carbonation. With a lean mortar mixture, however, both equations lead to different results, as carbonation progresses in proportion to the square root of time by Baba's equation, whereas the present equation incorporates the effect of CO_2 permeation through carbonated mortar. With a W/C of 50%, for instance, it takes 35 years for carbonation to reach a depth of 10 mm by Baba's equation, whereas the present equation calculates this as 22 years. Thus the differences between both equations are found to be large in regard to a lean mortar mixture.

Table 1. Calculation conditions

Concrete		Mortar coating		*T*	*R*
W/C	*A*	*d*	*A′*		
50	3	20	8	6.25	0.63
		20	3	44.44	4.44
65	8	20	8	6.25	1.67
		20	3	44.44	11.85

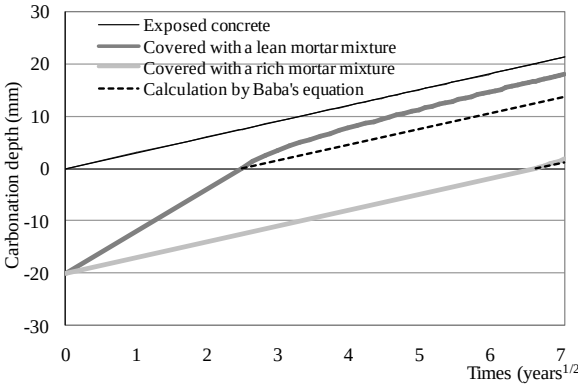

Figure 5. Carbonation progress (W/C 50%).

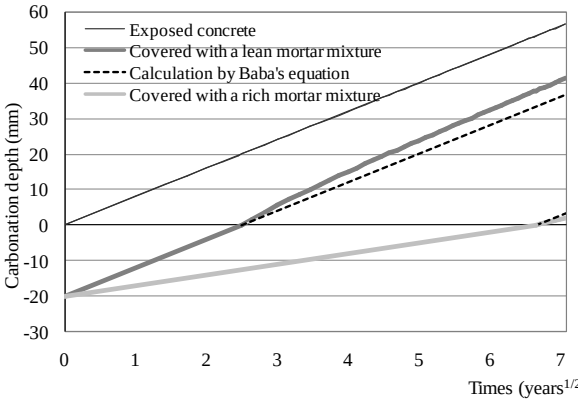

Figure 6. Carbonation progress (W/C 65%).

4 CONCLUSION

The progress of carbonation in concrete in which the quality of the surface region differs from that of internal concrete was theoretically investigated based on pseudo steady diffusion. A method of calculating such progress was proposed, and carbonation was simulated. The results are summarized as follows:

(1)After carbonation of the surface layer is completed, carbonation in internal concrete proceeds according to the equations below respectively when finishing mortar or a cementitious material is applied to the concrete surface (Eq.15) and when the microstructure of surface concrete differs from that of internal concrete (Eq.27).
(2)The equations proposed by the authors led to results slightly different from those proposed by Baba et al., as the present equations incorporate the effect of CO_2 permeation through carbonated mortar or surface concrete. These are valid when assessing the effect of the quality of finishing materials and surface concrete.

REFERENCES

Japan Institute of Consturction Engineering 1986, *Durability improvement technology of Reinforced Concrete buildings*, Gihodoshuppan, pp.279-282.

Architectural Institute of Japan 2004, *Recommendations for Durability Design and Construction Practice of Reinforced Concrete (Draft)*, pp97-107.

Maeda Koichi 1989, 'Study on a numerical analysis for carbonation of concrete', Journal of structural and construction engineering. Transactions of AIJ (402), pp.11-19.

Fukushima Toshio 1991, 'Theoretical predictive methods and numerical analysis for the progress of neutralization of concrete:Prediction of service lives of external vertical walls of reinforced concrete buildings (Part 1)', Journal of structural and construction engineering. Transactions of AIJ (428), pp.1-15

Masuda Yoshihiro & Tanano Hiroyuki 1991, 'Prediction model of carbonation progress in concrete', Concrete Research and Technology Vol. 2 No. 1, pp.125-134.

Ohta Tatsumi, Yamazaki Nobuyuki & Masuda Yoshihiro 2003, 'An experimental study on properties of cover concrte', Journal of structural and construction engineering. Transactions of AIJ (572), pp.1-8.

Yuasa Noboru, Kasai Yoshio & Matui Isamu 1998, 'Inhomogeneous distribution of the moisture content and Porosity from the surface layer to internal parts of dried concrete', Journal of structural and construction engineering. Transactions of AIJ (509), pp.9-16.

Ishihara Seiichiro & Tatematsu Kazuhiko 1987, 'Study of durability at the surface layer in concrete using excess water and air permeable form', Proceedings of the Japan Concrete Institute Vol.13, No.1, pp.531-566.

Baba Akio, Ishii Katuyuki, Senbu Osamu, Mori Akiko & Watanabe Tsuqumichi 2001, 'A predictive method on carbonation lifespan of reinforced concrete buildings with cementitious casting form', Summaries of technical papers of Annual Meeting Architectural Institute of Japan. A-1, Materials and construction 2001, pp.469-470.

Baba Akio & Senbu Osamu 1987, 'Prediction model of carbonation depth in concrete with srface layeres', Proceedings of the Japan Concrete Institute Vol.9, No.1, pp.333-338.

Kawanishi Taichiro, Hamasaki Hitoshi & Masuda Yoshihiro 2006, 'Analysis on the carbonation of concrete based on investigation of existing buildings', Journal of structural and construction engineering. Transactions of AIJ (608), pp.9-14.

Kono Masanori & Masuda Yoshihiro 2006, 'Verifiction of the carbonation suppressive effects evaluation method of concrete considering the aging of coating materials for textured finishes using the exposure data, Journal of structural and construction engineering. Transactions of AIJ (609), pp.9-14.

XII DBMC
International Conference on Durability of Building Materials and Components
PORTO - PORTUGAL, April 12th-15th, 2011

Development of a Risk Assessment Procedure Applied on Building Physics. Part Two - An Applicability Study

Simon Pallin [1]
Pär Johansson [2]
Mohammad Shahriari [3]

ABSTRACT

Risk assessment procedures are essential in order to ensure durable construction techniques that must withstand the changing climate and the standards of the future. An evaluation of the techniques that are least costly, most durable and least hazardous demands an identification of the most important noise factors and the risk caused by them. Based on existing risk assessment procedures in the field of product and production development, a risk assessment model was developed, which is described in part 1. This paper aims to apply the developed risk assessment model in an applicability study where the moisture supply in an apartment in a Swedish multi-family dwelling is studied. The procedure is based on Monte Carlo simulations of noise factors that influence hazards and safeguards, as defined in part 1. Simulations of the moisture production in the apartment is used together with air flow calculations in CONTAM for evaluating the spreading of excess indoor moisture. Distributions of plausible real-life hygrothermal parameters, useful when performing heat, air and moisture simulations are produced. The simulations also show which parameters that are the most influential and has the largest risk of causing damages to the construction. The simulated indoor moisture production shows good agrrements with *in situ* measurements. Strengths and weaknesses of the risk assessment model is discussed and evaluated.

KEYWORDS

Applicability study, Multi-family dwelling, Indoor moisture production, Ventilation, @Risk.

[1] Department of Civil and Environmental Engineering, Chalmers University of Technology, Gothenburg, SWEDEN, simon.pallin@chalmers.se (Corresponding author)
[2] Department of Civil and Environmental Engineering, Chalmers University of Technology, Gothenburg, SWEDEN, par.johansson@chalmers.se
[3] Department of Product and Production Development, Chalmers University of Technology, Gothenburg, SWEDEN, mohammad.shahriari@chalmers.se

1 INTRODUCTION

The Greek word "stochos" means uncertain and create the base of the word stochastic, which means a random process [Haldar & Mahadevan 2000]. Most engineering tasks involve some degree of stochastic variables that influence the outcome of a given problem, e.g. the number of occupants in a randomly chosen apartment will influence the moisture production in the apartment. These variations are called noise factors which are defined as variations that cannot be controlled, or are very difficult to control.

This paper uses the indoor moisture production in an applicability study. The rates of moisture generation from various moisture sources, also referred to as moisture loads, are essential inputs [Yik *et al.* 2004]. To be able to estimate the total daily moisture load, the incident frequencies are needed [Christian 1994]. The moisture loads will also vary on weekly basis due to the variations of user behavior of the residents during weekdays and weekends. It is also important to define variations for longer period of time since seasonal variations could be expected [Kalamees *et al.* 2006].

The aim of this paper is to apply the risk assessment model developed in part 1 in a case study. Simulations of the moisture production are based on the special conditions of this studying object, literature study of the indoor moisture production and time user surveys as presented in [Johansson *et al.* 2010]. The software @Risk uses multiple Monte Carlo simulations based on the distribution of the indoor moisture sources and provide statistical analysis tools. In addition, the resulting distribution of indoor moisture production is used in an apartment in a Swedish multi-family dwelling. The software CONTAM is used to simulate the air flows between the rooms of the apartment in order to obtain the distribution of the moisture supply in each room.

2 INDOOR MOISTURE SOURCES

In order to identify realistic and useful properties for each moisture source, a general model have been defined in part 1. The model serves as a template when identifying and gathering the noise factors and their variations over time. Three general noise factors in the model are time (at which time of the day that the moisture source is ongoing), duration (the time that the moisture source is in progress) and level (the rate of moisture generation). In addition to these general noise factors, other factors also influence the distribution depending on the hazard. Several of the specified moisture sources are not present in every household which must be taken into consideration by the incidence factor, I_f. Also correlations between different noise factors might be relevant in order to define a complete distribution of the moisture production over time. The entire input data collection and hazard discription can be found in [Johansson *et al.* 2010], where the definitions of the given noise factors is based on surveys and measurements made in the field of building physics, as well as on information from manufactures.

3 STUDYING OBJECT

The risk assessment model developed in part 1 is applied on a retrofitted building. The building is located in Märsta, north of Stockholm in Sweden. It has load bearing walls made of concrete and wall panels made of non-bearing timber. During 2009 the building was retrofitted with 70 mm mineral wool and the supplementary insulation was mounted on the interior side of the external walls. The original windows were kept, but the internal glass pane was replaced with a two glass pane system filled with argon gas. The building is monitored in a research project at Lund University and some preliminary results and more information on the building can be found in [Stein 2010]. The plan drawing for the chosen apartment is defined in Fig 1.

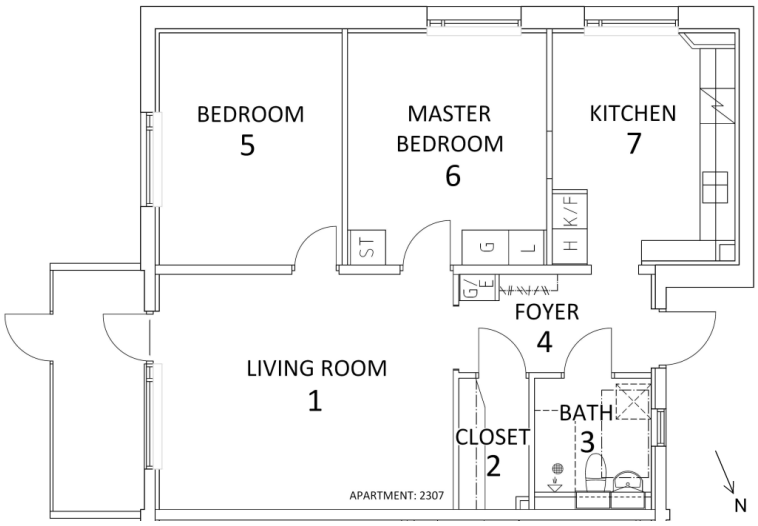

Figure 1. Plan drawing of the apartment located in Märsta, Stockholm. The total residential floor area is 70.9 m^2. Supply air devices for the ventilation are placed in the bedrooms and living room (1, 5, and 6) and extract air devices are located in the bathroom (3) and kitchen (7).

The total residential floor area of the apartment is 70.9 m^2 which is divided into rooms according to Fig. 1. The ventilation air flows in the different rooms are provided by the building services engineer and represent the design values, see Table 1. No measurements of actual air flows have been performed. According to the design values, there is an unbalanced air flow in the apartment which can be seen when summarizing the ventilation rates of the different rooms in Table 1. The supply air flow is in total 23 l/s and the extract air flow is 27 l/s. Not included in these numbers is the air flow through the kitchen fan which, when operating, adds up to 50 l/s on the total extract air side.

Table 1. Residential floor area and ventilation rates in the rooms of the apartment. The roof height is 2.4 m in all rooms of the apartment.

#	*Space*	*Ventilation rate*	*Room area*
1	Living room	Supply 8 l/s	25.7 m^2
2	Closet	-	-
3	Bathroom	Extract 16 l/s	3.9 m^2
4	Foyer	-	-
5	Bedroom	Supply 7 l/s	12.4 m^2
6	Master bedroom	Supply 8 l/s	13.5 m^2
7	Kitchen	Extract 11 l/s and kitchen fan	11.9 m^2

The defined moisture sources must be placed in the rooms where they are most likely to exist. This approach is essential in order to make real life simulations of the indoor moisture supply in each room of the apartment. Table 2 presents where each moisture source is assumed to be operating.

Weather data for Stockholm of the year 2000 is used in the simulations of the indoor moisture supply. The average outdoor temperature for the year is 7.6°C with a maximum temperature of 21.3°C and minimum of -15.4°C. The average wind velocity is 3.0 m/s and the dominating wind direction is from southwest. In CONTAM, the building divided into 5 zones (living room, master bedroom, second bedroom, kitchen and bathroom). The foyer is treated as a part of the living room and the closet is treated as a closed space. The studied contamination is the excess vapor content in the air which is

produced inside the different rooms of the apartment where the distribution for each room is obtained from @Risk simulations of moisture production.

Table 2. The location of the moisture sources in each room of the apartment. The moisture source caused by floor mopping is present in all the rooms of the apartment.

#	*Space*	*Moisture sources*
1	Living room	Humans, pets, aquarium, plants, ironing.
2	Closet	-
3	Bathroom	Bathtub, tumbler drier, humans, showering, bathing.
4	Foyer	Humans, pets.
5	Bedroom	Humans, pets, ironing, plants.
6	Master bedroom	Humans, pets, ironing, plants.
7	Kitchen	Dishwashing machine, humans, food preparation, hand dishwashing, plants.

4 RESULTS

The subsequent simulations are based on measurements, statistical data and qualified assumptions of the hazards involved in the indoor moisture production as defined in [Johansson *et al.* 2010]. The results are presented in diagrams showing the distribution of the indoor moisture production in Swedish single and multi-family dwellings. CONTAM is used to study the airflows between the different zones of the studying object in order to obtain the moisture supply in each room.

4.1 Indoor Moisture Production

Figure 2 presents the moisture production rate when making simulations of household compositions in Swedish multi-family dwellings. The results are based on the mean production rate per hour and year of a simulated family. 10,000 iterations have been performed where every iteration represents a plausible family with statistical variation of the incidence factors, residential floor area and number of members in the household. According to the data presented in Fig. 2, about 35% of Swedish households in multi-family dwellings have an average moisture production rate between 110 to 140 grams per hour, which corresponds to 2.6 to 3.3 kg per day.

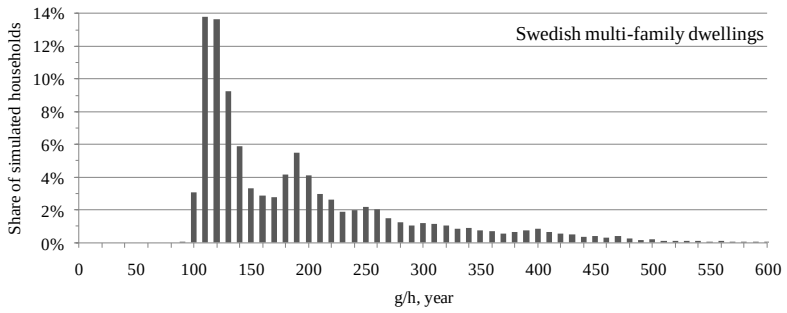

Figure 2. Simulated moisture production in Swedish multi-family dwellings, average rate per hour on yearly basis.The result is obtained from 10,000 iterations where each iteration represents the yearly mean indoor moisture production from a simulated household in a Swedish multi-family dwelling.

The histogram in Fig. 2 seems to peak at several intervals of moisture production rates. The main reason to the shape of the distribution is the number of household members. This relation is clarified

in Fig. 3 which show results from simulations with a fixed family size of one, two and three members. Except from the fixed number of household members, all other inputs remain varying.

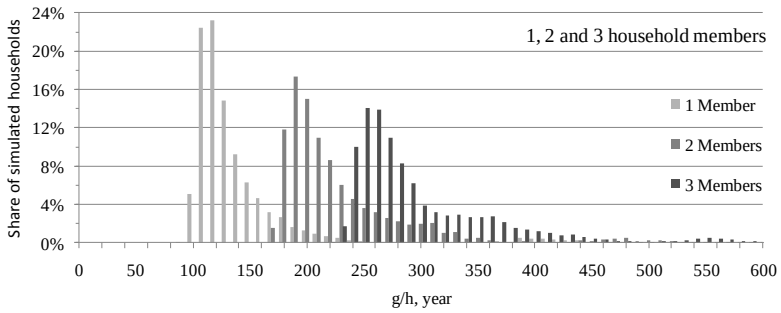

Figure 3. Simulated moisture production in Swedish multi-family dwellings with a fixed number of household members on one, two or three; consequently three different distributions are presented. The peaks from the three simulations corresponds with the peaks in Fig. 2 where the number of household members varies according to statistical data.

A comparison with field measurements performed in Swedish dwellings shows good correspondence with the simulation results of the indoor moisture production presented in this paper. Figure 4 shows the results from a Swedish measurement study from the early 1990s. The yearly mean value of moisture production per day was measured to 5.8 kg for multi-family dwellings and with a confidence interval of 95% [Tolstoy *et al.* 1993; Norlén & Andersson 1993].

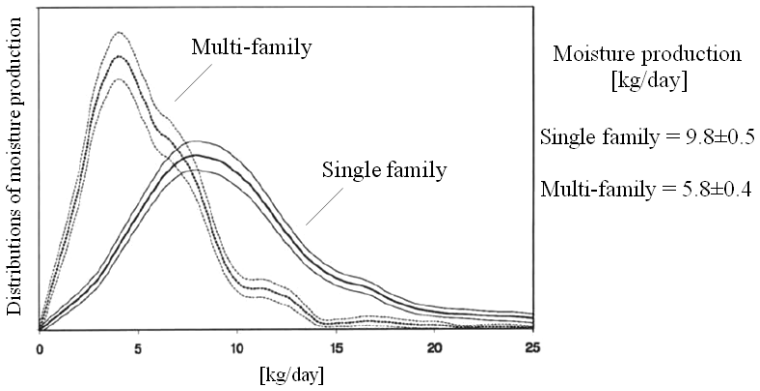

Figure 4. The two distributions represents the variation of moisture production based on measurements made in 1,100 dwellings in Sweden between 1991-1992 [Norlén & Andersson 1993]. The graph to the left shows the the daily average moisture production on yearly basis in Swedish multi-family dwellings with 95% confidence interval.

A recent measurement study by the National Board of Housing, Building and Planning in Sweden presented results from measurements in 1,800 buildings [Boverket 2009]. The levels of moisture production in this study are lower than what was found in the previous study from the early 1990s. According to informations given by Mattsson [2010], the mean value of the indoor moisture production was measured to be 2.4 kg/day. Consequently, the daily mean value of the indoor moisture production varies between 2.4 and 5.8 kg for the Swedish studies and the corresponding mean value from simulations is 4.7 kg/day. A measurement study made in Finland on 101 single family dwellings present an yearly average moisture production of 5.9 kg per day. Maximum averages per day based on received data during one week and during the winter season was 18.6 kg and 12.7 kg respectively [Kalamess *et al.* 2006].

4.2 Indoor Moisture Supply

The distributions of the indoor moisture supply was obtained by CONTAM calculations of air flow rates trough the living room, master bedroom and kitchen in the studying object. These distributions are presented in Fig. 5. The intervals of the moisture supply are changing between the different rooms because of the different moisture production and air flow rates between them. The moisture supply is higher in the kitchen compared to the bedroom and the living room. As is shown in Fig. 5, the moisture supply varies largely between the different rooms. The figure is based on minimum, maximum and nine deciles obtained from simulations of the indoor moisture production, thus corresponding with 11 cases. The distributions in Fig. 5 are obtained by assuming linear interpolation of values between these 11 points.

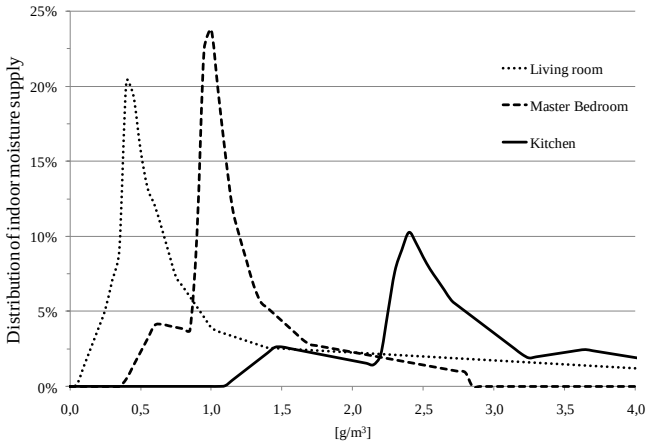

Figure 5. Distributions of indoor moisture supply based on simulations of moisture production and air flow calculations in CONTAM for the living room, master bedroom and kitchen. The moisture supply in the kitchen is much higher than in the living room and bedroom, mainly due to a higher level if moisture production.

A comparison of the simulation results with the measurements [Boverket 2009] performed in Swedish multi-family dwellings shows good agreement. Figure 6 shows the results of the measurements made in living rooms and bedrooms during October, 2007 to May, 2008. The values in [Boverket 2009] are similar to the values obtained in the simulations of indoor moisture supply in the living room and the bedroom. Since no measurements were performed in the kitchen, the simulated indoor moisture supply cannot be validated in this room .

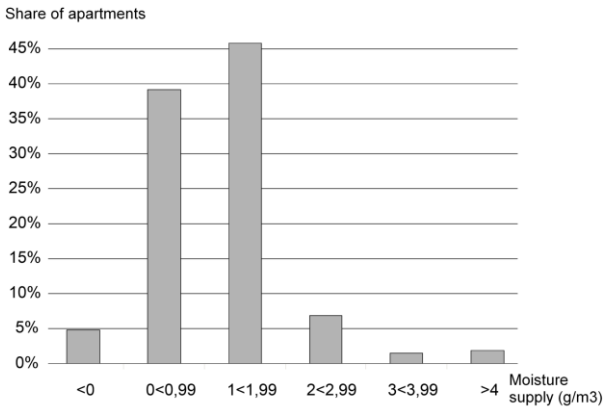

Figure 6. Indoor moisture supply in Swedish multi-family dwellings [Boverket 2009]. Measurements performed in the living room and bedroom. A comparison with Fig. 5 shows good agreement between the simluated and measured values in these rooms.

5 DISCUSSIONS AND CONCLUSION

The simulated moisture production is both lower and higher compared to the two Swedish studies made in the early 1990s and late 2000s [Tolstoy *et al.* 1993; Boverket 2009]. There are some important aspects to consider when comparing the moisture production rates from the field measurements with the ones simulated in this study. The sensors which measure the relative humidity in the measurement studies are placed in the bedrooms and the living room. If the ventilation system works as intended, activities which involve moisture production in areas such as bathrooms and kitchens will have low influence on the measuring devices.

The results from the simulations of the moisture production show great similarity with the measurements presented in Fig. 4. The reason behind the multiple peaks of the simulated curves was discovered to be influenced by the number of family members. Similar peaks are visible from the measurements of the moisture production in single and multi-family dwellings in Sweden [Norlén & Andersson 1993].

A disadvantage with the approach of simulating the indoor moisture production is the dependence of accurate input data. In this study, no verification has been made regarding the validity of the results from measurements or statistical surveys. Qualified assumptions have been made of the shapes of distributions when no such information was found. The uncertainties depend on the input data and vary greatly between different measurement studies and measuring equipments. In many statistics the 95% confidence interval is applied, although lower levels of confidence intervals are not uncommon. If improvements are to be made on the simulation model, a more directed statistical survey would be of interest.

The time between the measurements is an important factor to consider, since there are activities which exists for a short period of time but with a high moisture production rate. Examples of such activities are food preparation and showering. Their total influence on the moisture production may theoretically be underestimated if only measuring once every hour, as for the case of the Finnish study [Kalamess *et al.* 2006]. In the Swedish study BETSI [Boverket 2009], the sensors received data every fifteen minutes which is probably more sufficient in order to measure the moisture production over time. The disadvantage of the Swedish study in comparison with simulation results is that the measurements were performed during a period of two weeks between October, 2007 and April, 2008. Some of the defined moisture sources are considered to have seasonal variations; hence annual averages will not give satisfying results for these variations. Since measuring during the heating season means that the ventilation rate, thus the effect on the indoor moisture supply, is assumed to be higher due to increased stack effect.

6 FUTURE RESEARCH

Simulations of moisture production are performed with hourly resolution and the air flow calculations can also be performed with this definition. With a network model, the moisture supply in the studied zone can be produced for each hour. Higher resolution of the simulations makes it possible to in detail study the changes in moisture supply between day and night as well as annual variations.

Many of the recommended moisture production rates are based on measurements performed during more than 25 years and therefore their relevance needs to be investigated and in some cases, new measurements might be required.

7 DISCLAIMER

This document presents results drawn from the Harmonised European Time Use Survey (HETUS) database and table generating tool, but the interpretation of it and other views expressed in this text are those of the author. This text does not necessarily represent the views of the team behind the

HETUS database or any national statistical institute which has contributed data to the HETUS database. The author bears full responsibility for all errors and omissions in the interpretation of the output of the HETUS database and table generating tool.

ACKNOWLEDGMENTS

The work is supported by FORMAS – the Swedish Research Council for Environment, Agricultural Sciences and Spatial Planning. Johan Stein at Lund University, Vahid Nik at Chalmers University of Technology, Mikael Molén and Anders Kraftling at the Economic Welfare Statistics Unit of Statistics Sweden and the staff at Sigtunahem are acknowledged for their cooperation. Axel Berge, teaching assistant at Chalmers University of Technology, performed the CONTAM simulations.

REFERENCES

Boverket, 2009, *Så mår våra hus – Redovisning av regeringsuppdrag beträffande byggnaders tekniska utformning m.m., (Swedish), Boverket, Karlskrona, Sweden.*

Christian, J.E. 1994, 'Moisture sources', in *Moisture control in buildings*, ed. H.R. Trechsel, ASTM, Philadelphia, PA, pp. 176-182.

Haldar, A. & Mahadevan, S. 2000, *Probability, reliability and statistical methods in engineering design*, Wiley, New York.

Johansson, P., Pallin, S. & Shahriari, M. 2010, *Risk Assessment Model Applied on Building Physics: Statistical Data Acquisition and Stochastic Modeling of Indoor Moisture Supply in Swedish Multi-family Dwellings*, Working Report, IEA/ECBCS-Annex 55, Copenhagen meeting.

Kalamees, T., Vinha, J. & Kurnitski, J. 2006, *Indoor humidity loads and moisture production in lightweight timber-frame detached houses*, Journal of Building Physics 2006:29 pp. 219-246, Tampere/Helsinki Finland.

Mattson, B. 2010 *Extract of raw data from the measurements in BETSI-study.* Boverket, Karlskrona, Sweden.

Norlén, U. & Andersson, K. 1993, *Bostadsbeståndets inneklimat – ELIB-rapport nr 7,* Statens institut för byggnadsforskning, Gävle, Sweden.

Stein, J. 2010, *Preliminary results from moisture measurements in a Swedish multi-family dwelling retrofitted with interior insulation*, Paper presented at the International Conference on Building Envelope Systems and Technologies, ICBEST 2010, Vancouver, Canada.

Tolstoy, N., Borgström, M., Högberg, H. & Nilsson, J. 1993, *Bostadsbeståndets tekniska egenskaper – ELIB rapport nr 6,* Statens institution för byggnadsforskning, Gävle, Sweden.

Yik, F.W.H. Sat, P.S.K. & Niu, J.L. 2004, *Moisture Generation through Chinese Household Activities*, Indoor and Built Environment 2004:13 pp. 115-131, Hong Kong, China.

XII DBMC
International Conference on Durability of Building Materials and Components
PORTO - PORTUGAL, April 12th-15th, 2011

Using the Statistics of Random Processes to Predict the Deterioration in End-Use Properties of Polymeric Coatings

Stuart G. Croll [1]
Brian R. Hinderliter[2]

ABSTRACT

Any attempt to be truly predictive of a material's service lifetime must rely on physical and chemical parameters related to its composition, not on empirical curve-fitting. If one accepts that weathering degradation events are many, e.g. ultraviolet photons, acid molecules, etc. and that they occur at random and create random features as the material is degraded, then one can use the Central Limit Theorem to calculate the consequences. The approach given here calculates the likelihood of physical defects being formed by degradation processes. Degradation leads to an increase in surface roughness and reduction in thickness of a polymeric coating. The number or size of those defects, when used in well-known models of physical properties, calculate how properties such as gloss, toughness, corrosion barrier properties etc. change during exposure. In fact, these ideas are not specific to polymers but could be applied to other types of materials. This approach calculates properties in terms of a material's physical and chemical characteristics, the initial state of the coating and the environment. It provides scientifically based, well-behaved functions for extrapolation if one seeks to estimate a service lifetime. Indeed, this approach establishes connections between the deterioration in different properties via their common causes, and results from one, e.g. gloss loss, can be used to calculate how other properties might decrease. Although modeling decrease in performance during weathering seems to be a formidable task, this modeling provides a basis for future progress.

KEYWORDS

Coatings, Corrosion, Durability, Weathering, Statistics.

[1] North Dakota State University, Fargo, USA, Stuart.Croll@ndsu.edu
[2] Virginia Commonwealth University, Richmond, USA, bhinderliter@vcu.edu

1. INTRODUCTION

Attempts to predict service lifetime directly from the chemistry of a construction or engineering material will fail without understanding of how chemistry and physical properties are linked. Degradation of any material in its service environment is caused by a myriad of energetic photons, or abrasive particles or aggressive molecules. Within the overall exposure interval, the arrival time of photons or grains of sand is random and there is nothing that determines which molecule they will strike. Further, only chance determines whether a permanent change is effected by the energy that photons or grains of sand deposit on the target. If a link can be made between the chosen service property and the amount of damage then there is a pathway to predicting how a material's properties decay and thus its service lifetime. If one can link more than one end-use property to the damage, then the properties should be linked. If the model which calculates damage is based on physical or chemical parameters, then there is linkage to composition, which is one of the objectives of the ideas presented here. The approach presented here is not specific to any particular degradation chemistry but is intended to provide a useful link between the chemistry of degradation and the effect on the physical, end use properties that is based on physics, not *ad hoc* curve fitting.

2. DAMAGE ACCUMULATION DUE TO STOCHASTIC EVENTS.

Photo- or other degradation of a polymer starts and is concentrated at its surface, which usually becomes rougher and is where material is volatilized and lost. The simplest situation is degradation of an homogenous coating surface by ultraviolet radiation where the reaction kinetics are independent of location and do not change as material is ablated, i.e. zero order chemical kinetics:

dN(t)/dt = Average number of fragments being removed at points across the coating
= Flux of photons x Absorption probability x Probability of damage occurring (quantum efficiency)

$$\frac{dN(t)}{dt} = \phi.A.Q \qquad [1]$$

where $N(t)$ = number of damaging events/area; t = exposure time; ϕ = photon flux; A = probability of adsorption (cross-section); Q = 'quantum efficiency' or yield for damage occuring.

Although the equation is couched in terms of photodegradation, a very similar equation would describe chemical or abrasive attack. All the quantities on the right hand side of equation 1 will be constant for a given material in a constant environment,

$$N(t) = \phi AQ.t \qquad [2]$$

If a characteristic fragment size is known from the degradation chemistry, then this equation gives the mass or volume lost as a function of exposure time, which would be important in most protective functions. If the exposure consists of repeated cycles then this simple integration will be valid provided the overall period is much longer than one cycle. This will apply to natural weathering if the exposure is long enough. In this work the implication is that degradation is initiated at the surface of the material, but similar ideas could be used to describe degradation within the bulk material if driven by a different mechanism.

2.1. Stochastic Calculation of Surface Roughness

The Central Limit theorem allows that the outcome of a sufficiently high number of equivalent events can be modeled by a Normal distribution. i.e. a Gaussian function. An important result of such statistics is that the standard deviation is essentially given by the square root of the mean:

Standard deviation = (number of events)$^{1/2}$ [3]

These are the same statistics that determine the outcome of a random walk, e.g. the radius of gyration of a randomly coiled polymer. Surface roughness is often quantified using the standard deviation in the height or thickness, σ. Equation (2) is a calculation of the number of fragments being removed, on average, thus it is simple to extend that to calculate roughness. There may be initial surface roughness due to application or some intrinsic property of the formulation, but if $\Delta\sigma(t)$ is the additional surface roughness due to degradation, it must increase as the square root of $N(t)$:

$$\Delta\sigma(t) = \varepsilon\sqrt{N(t)} = \varepsilon\sqrt{\phi AQ.t} = \sqrt{k.t} \qquad [4]$$

Here, ε = characteristic dimension of a fragment that leaves the coating. The parameter k combines, for convenience, the quantities that are considered constant here. If there is a distribution in fragment sizes then there will be a summation instead of the single ε parameter, but otherwise the relationship would be the same. If pigments are present, the characteristic fragment size will change at some exposure time from being a polymer fragment to the size of a pigment particle. If the starting surface has a roughness, $\sigma_{initial}$, that is also Gaussian, then the effect combined with degradation can be calculated by summation of the variances:

$$\sigma^2(t) = \sigma^2_{initial} + \Delta\sigma^2(t) = \sigma^2_{initial} + \varepsilon^2 N(t) = \sigma^2_{initial} + k.t \qquad [5]$$

This is an algebraic expression for surface roughness, which would start at zero for an initially smooth surface.

Autocatalytic behavior is sometimes seen in polymers under degradation. In this case, the degradation rate increases as the extent of degradation proceeds, but eventually the supply of material for degradation dwindles. For example, one could envision a free radical process that multiplied the degradation, or degradation producing chromophores that absorbed yet more radiation, and so on. In this case the kinetics follow:

$$\frac{dN(t)}{dt} = \phi.A.Q.N(t)\left[1 - \frac{N(t)}{L}\right] \qquad [6]$$

L represents a limit in the number of fragments that may be lost, and N_0 is the starting concentration of labile moieties. The solution is given by the Logistic (Verhulst) equation. In extreme cases L might represent all the material, so it is very large and Malthusian (exponential) growth would be a good approximation of the behavior. The solution, giving the number of fragments that may be lost is:

$$N_{Lost}(t) = \frac{L}{1 + \left(\frac{L}{N_0} - 1\right)\exp(-\phi AQ.t)} - N_0 \qquad [7]$$

Degradation accelerates exponentially early in the exposure then slows down as the process or material is depleted. In practical situations, one might see only the Malthusian increase since one would not be interested in the properties of a coating after it is severely depleted. In other cases the limit, L, may not be much greater than N_0 and the loss reaches a plateau and the overall behavior resembles first order kinetics or one could decide that 1st order kinetics apply and develop a simpler expression for $N(t)$ and $\sigma(t)$.

Stabilizers to absorb ultraviolet radiation or to inhibit degradation chemistry change the degradation kinetics. These materials have a useful life of their own, over which they limit the degradation rate. Regardless of whether they limit degradation by absorbing some fraction of the ultraviolet flux, or whether they are anti-oxidants and limit the reaction rate (quantum efficiency in equation 1), they slow the kinetics of degradation according to:

$$\frac{dN(t)}{dt} = \phi AQ\left(1 - a.e^{-t/\tau}\right) \qquad [8]$$

Now τ represents the exponential life of the ultraviolet absorber/anti-oxidant and a is a measure of its efficiency (<1). The solution to this equation is very straightforward and contains a term $t.\left(1 - a.e^{-t/\tau}\right)$ instead of only t. This additional factor may be included when the situation demands and permits solutions for the properties explored later. Unfortunately, while the more complicated expressions for degradation kinetics offer more possibilities to match real exposure data, they require knowledge of parameters that are seldom considered, or known, so much of the discussion here will be limited to the approximation of 'zero order' kinetics.

If there is a need to model a material in detail, for example, systems that have heterogenous composition or more than one degradation processes, then a computer simulation can be made wherein the loss of material, and other changes, at each location in the material may be deduced using Monte Carlo techniques [Croll & Hinderliter 2005]. The Monte Carlo approach uses the same statistical ideas as presented here but can be programmed to incorporate details that are limited only by the computing resources available.

The degradation rate, $k = \varepsilon^2 \phi AQ$, uses parameters from the material and its environment. Parameters ε, A and Q are determined by the material and may, for example, depend on temperature and other environmental aspects. The flux of aggressive events, ϕ, clearly depends on the environment and if it is the flux of ultraviolet photons, it will depend on the latitude, altitude and weather at a geographical location. At this stage we have expressions for damage accumulation assuming it occurs due to random events and it proceeds via simple kinetics. Now we use well known expressions for physical properties. Some very practical properties may be linked either to the amount of material lost, or the roughness of the surface.

3. PROPERTIES

3.1 Mass Loss

The most direct test of ideas presented above is to measure $N(t)$ directly, i.e. via weight or thickness loss and compare results to equation (2). A linear progression of weight loss models results found in several, different studies [Hollande & Laurent 1999; Hoffman & Saracz 1972; Monney *et al.* 1999] and thus equation (2) and zero order kinetics are reasonable approximations. Other data shows how systems may show an increase in roughness (square root of $N(t)$) that proceeds with the square root of exposure period, as indicated by equation (5) [Yang & Croll 2004].

3.2 Gloss and Corrosion Protection

Gloss is a very important aspect of appearance; it may determine service life and is a common, facile and quantitative parameter to measure as weathering proceeds. Gloss is the specular reflectance of the coating surface compared to the reflectance of a standard glass. The effect of surface roughness is most simply modeled by an approximation due to Bennett and Porteus [1961] which amounts to the

leading term in the Kirchhoff approach [Bourlier *et al*. 2002] where the reflectance is reduced exponentially according to the variance in the height (thickness) of the surface. By including how the variance in surface height changes with exposure, from equation 5, a very simple expression for this leading term can be deduced [Hinderliter & Croll 2005].

$$R_s(t)/R_s(0) = \exp\left[-\left(\frac{4\pi\cos\varphi}{\lambda}\right)^2 kt\right] \qquad [9]$$

Where:
$R_s\ (t)$ = specular reflection of the rough surface as it changes with exposure
$R_s\ (0)$ = reflection of the surface prior to exposure,
φ = 'specular' angle,
λ = wavelength of the illumination

Refraction index and the comparison to the reflectance of the gloss standard are effectively eliminated in equation 9 by calculating the gloss lost relative to its starting value. Fitting the Kirchhoff expression to data allows the contribution of the first term to be deduced especially at high gloss angles, and thus a value of *k*,. fig. 1.

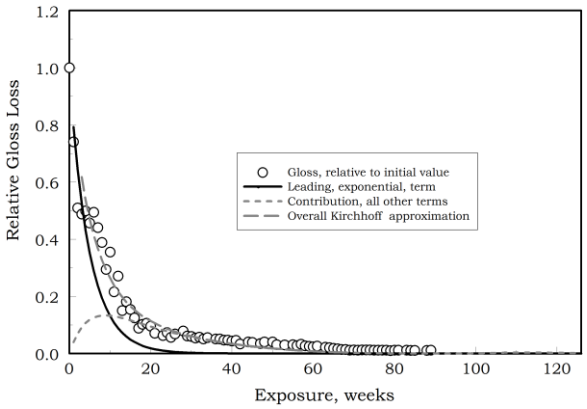

Figure 1. Loss in gloss of an unstabilized polyurethane topcoat, measured at 20°. The curves show how the Kirchhoff approximation is used.

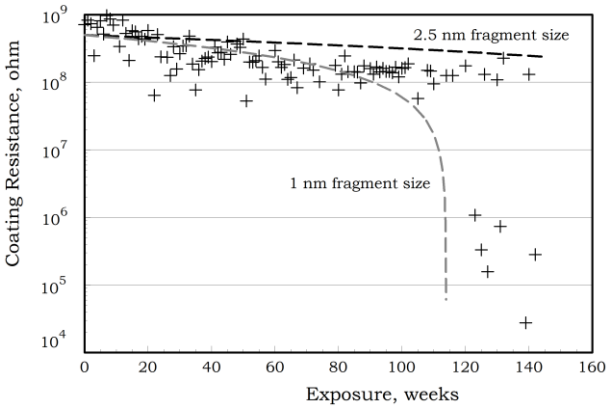

Figure 2. Coating Resistance from electrochemical impedance spectroscopy, of the same material in figure 1.

If one defined service life in terms of a gloss loss, one could use early data to find the trend and extrapolate to the exposure time when that loss in gloss would be likely. If one assumes that the electrical resistance of a coating, and thus its corrosion protection ability during degradation, is governed by its resistivity [Grundmeier *et al*, 2000] via its remaining thickness, then one can use equations (2) and (4) to calculate the deterioration in resistance (thickness), and thus corrosion protection. This is shown in fig. 2 for the same coating as in fig. 1. The fragment size, ε, has to be specified separately in this calculation [Hinderliter & Croll, 2010], but the range shown here, between 1 nm and 2.5 nm (maintaining the overall value of *k*, taken from the gloss measurements) is very reasonable for the degradation fragment size and clearly, one could fit the data to deduce a value that matches all the data well. Thus this approach provides a link between two properties, provided that both are determined by the same degradation process.

Many properties are thought of as representing the properties of an extensive coated area, but are really properties produced by singular and microscopic effects. For example, most protective properties rely on the mechanical integrity of a coating against cracking. Such cracks may be sparsely distributed across a painted surface. The statistical approach outlined above may be applied to these circumstances but with the interest being in the largest defect in the distribution.

3.3 Toughness

Coatings' properties change with degradation and they become brittle as they degrade. Even when a coating is fresh and at its most flexible, the strain rate at a crack tip would be very high and so one can reasonably use linear elastic fracture mechanics to describe the failure of crosslinked polymeric coatings via Griffith's equation:

$$Stress_G = \sqrt{\frac{2EG}{\pi a}} = Stress_{External} + Stress_{Internal} \qquad [10]$$

E = Young's modulus,
G = fracture energy per unit area,
a = half length of the initiating crack (assuming coin-shaped cracks)
$Stress_G$ = Griffith fracture stress, the critical stress above which a crack propagates, which will comprise of internal stresses due to curing shrinkage and external, environmental stresses.

Inevitably the modulus and fracture energy change due to the chemical changes during degradation. The assumption here is that the changes in modulus and fracture energy are much less than the effect of defects being introduced by degradation. If the deepest degradation defect provides the initiating crack and there is no internal stress:

$$Stress_G = \sqrt{\frac{2EG}{\pi n \sqrt{\sigma_{initial}^2 + \Delta\sigma^2(t)}}} \qquad [11]$$

The factor, n, multiplies the standard deviation in the surface topography so that the equation uses a large and infrequent value in the distribution of surface roughness as the flaw size. In a Monte Carlo simulation one could track progress and use the deepest flaw generated at any stage. It is very difficult to measure fracture stress of a coating on a substrate and there is very little published data with which to test this equation, but it predicts, reasonably, that coatings that are applied badly, or have an inconsistent structure, i.e. a high value of $\sigma_{initial}$, will have diminished toughness and any coating that degrades quickly (large k) will fail rapidly, even if it was applied well.

A simple expression is possible if fracture stress is expressed relative to the value for the unexposed material. For the simple, zero order kinetics:

$$\left[\frac{Stress_G(t)}{Stress_G(0)}\right]^{-4} = 1 + \frac{\Delta\sigma^2(t)}{\sigma_{initial}^2} = 1 + \frac{kt}{\sigma_{initial}^2} \qquad [12]$$

Figure 3(a) shows examples of how the zero order and the Logistic equation kinetics behave in equation 12, together with the effect of stabilization. Figure 3(b) shows how zero order and Malthusian kinetics model data from Nicols [Nicols & Peters 2002] on an automotive coating with and without stabilization. Data published on the deterioration in tensile strength of poly(ethylene terephthalate) [Fechine *et al.* 2002] is very reminiscent of behaviour in fig 3(a). In principle one could measure a value of k from loss of gloss with exposure, and then calculate the change in toughness in equation 12, if we knew $\sigma_{initial}^2$. There is so few data in the literature that it is difficult to distinguish between the different kinetics offered here so one has to say that zero order kinetics is a plausible representation of the data in any case. In other work on the fracture of ABS pipes [Davis & Burn 2004] the authors calculated an equivalent notch depth based on impact strength measurements which they fitted to a 3 parameter equation for the trend with exposure time.

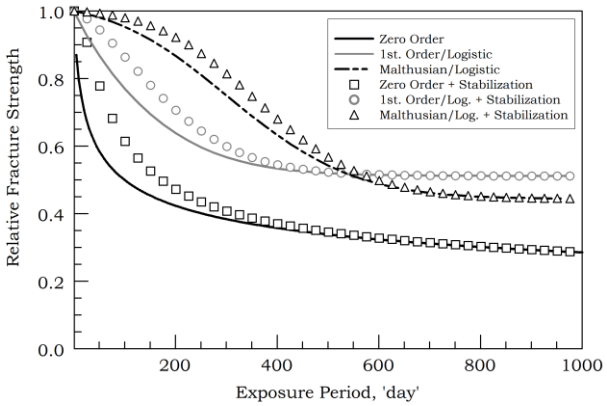

Figure 3(a). Examples of the trends possible in fracture strength with exposure by using different kinetics of degradation in the stochastic calculation of damage accumulation.

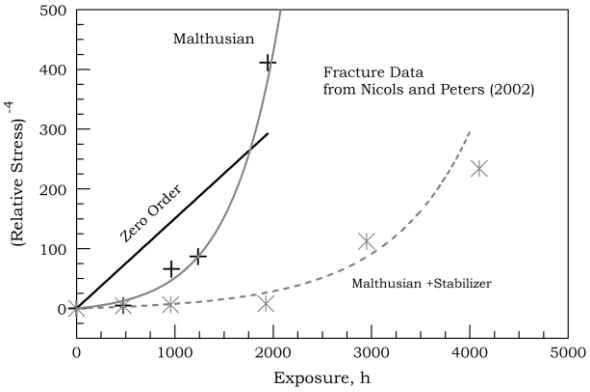

Figure 3(b). Comparison of model with data from Nicols and Peters [] of an unstabilized and stabilized automotive coating. Here the data is plotted so that zero order kinetics in equation 12 gives a linear trend with exposure.

The stochastic model with the simple zero order kinetics, equation 5, gives the progress of flaw size with the square root of exposure time which models that data at least as well as the authors' model.

4 CONCLUSIONS

Assuming damage is stochastic permits simple relationships to be derived for its accumulation with exposure, together with its standard deviation. In the simplest, and possibly most useful, case all the material is assumed to be equally likely to suffer the chemical or mechanical environmental processes and so the degradation follows zero order kinetics, and simple algebraic equations can be deduced. Other kinetics can be included if there is sufficient supporting evidence. Accumulation of damage as material loss, or its standard deviation (roughness), can be inserted in well-established physical models to model the deterioration in end-use properties, e.g. gloss, toughness, corrosion protection. Such properties are measures of performance whose deterioration depends on the same damage and thus must be correlated. The quantities used in the models are physical and chemical parameters of the environment or the material, thus enabling *a priori* comparisons. When the material is not homogenous or when the degradation processes are more complicated, the stochastic nature of the degradation can be simulated by in Monte Carlo computer calculation to provide the input for the same models to calculate the physical properties of the coating.

The ideas here provide equations whose parameters are based on the physics and chemistry of the environment and the material under consideration. One should hesitate to use these equations to predict a time of failure since it is difficult to know enough about either an environment or a material; they are probably most useful in comparative studies and providing the intellectual framework for understanding how the physics and chemistry of degradation and a material's performance in service are connected.

ACKNOWLEDGMENTS

The authors would like to acknowledge the support of the US Army Research Laboratory and the US Air Force Office of Scientific Research during the course of their research.

REFERENCES

Bennett H. E., Porteus J. O. 1961, 'Relation Between Surface Roughness and Specular Reflectance at Normal Incidence,' J. Opt. Soc. Am., **51**[2], 123.

Bourlier C., Berginc G., Saillard J. 2002, 'One- and Two-Dimensional Shadowing Functions for any Height and Slope Stationary Uncorrelated Surface in the Monostatic and Bistatic Configurations,' IEEE Trans. Antennas Prop., **50**[3], 312 – 324 .

Croll S. G., Hinderliter B. R. 2007 'Estimating Service Lifetimes In Weathering: An Optimistic View,' J. Coat. Technol. Res., **4**[3], 217 – 230.

Davis B. E. P., Burn L.S. 2004, 'The effect of photo-oxidative degradation on fracture of ABS pipe resins,' Polym. Degrad. Stab., **84**, 233-242.

Fechine G. J. M., Rabello M. S., Souto-Maior R. M. 2002, 'The effect of ultraviolet stabilizers on the photodegradation of poly(ethylene terephthalate),' Polym. Deg. Stab., **75**(1), 153-159.

Grundmeier G., Schmidt W., Stratmann M. 2000 'Corrosion protection by organic coatings: electrochemical mechanism and novel methods of investigation,' Electrochemica Acta, **45** 2515 – 2533.

Hinderliter, B. & Croll, S. (2005), 'Monte Carlo approach to estimating the photodegradation of polymer coatings', *J. Coat. Tech. Res.* **2**(6), 483-491.

Hinderliter B. R., Croll S. G.2010 'Predicting Coating Failure using the Central Limit Theorem and Physical Modelling,' ECS Transactions Volume: **24(1)**, 1- 26 .

Hoffman E., Saracz A. 1972 'Weathering of paint films: IV. Influence of the radiation intensity on chalking of latex paints,' J. Oil. Col. Chem. Assoc., **55**, 101 – 113.

Hollande S., Laurent J-L.1999 'Degradation Process of an Industrial Thermoplastic Elastomer Polyurethane-Coated Fabric in Artificial Weathering Conditions,' J. Appl. Polym. Sci., **73**, 2525 – 2534.

Monney L., Dubois C., Chambaudet A. 1999 'Evolution of the thin photo-oxidation layer of an epoxy matrix during artificial photo-aging,' Ang. Mak. Chemie, **273**[4593], 6 – 11.

Nicols M. E., Peters C. A. 2002 'The effect of weathering on the fracture energy of hardcoats over polycarbonate,' Polym. Deg. Stab., **75**[3], 439 – 446.

Yang X, Croll, S.G. 2004, 'Accelerated exposure of pigmented anti-corrosion coating systems,' Surf. Coatings Int. Part B: Coatings Transactions, **87**[B1], 7 – 14.

XII DBMC
International Conference on Durability of Building Materials and Components
PORTO - PORTUGAL, April 12th-15th, 2011

Development of Service Life Model for Wooden Structures

Hannu Viitanen [1]
Tomi Toratti [2]
Lasse Makkonen [3]

ABSTRACT

In this paper, attempts to model the service life of wood structures is developed by utilising earlier durability experiments and relating the decay models to a hygrothermal analysis of building physics. The model is also used in connection with the ERA-40 weather observations in Europe to assess the geographical dependence on service life related to durability. These studies provide new tools to evaluate the durability and service life of wooden commodities and a preliminary European wood decay map, is presented in this paper. A further enhancement of the model, which is currently under development, is the assessment of the effects of the various structural choices (e.g. protection to driving rain, coatings, etc.) and other parameters (e.g. geographical location and orientation) on the durability of wooden structure.

KEYWORDS

Timber, Ageing, Moisture, Lifespan, Durability.

[1] Technical Research Centre of Finland , VTT, Espoo, FINLAND, hannu.viitanen@vtt.fi
[2] Technical Research Centre of Finland , VTT, Espoo, FINLAND, tomi.toratti@vtt.fi
[3] Technical Research Centre of Finland , VTT, Espoo, FINLAND, lasse.makkonen@vtt.fi

1 INTRODUCTION

In the future, the life time expectations and analyses of different building products will need more data on the durability of products, service life and resistance against mould and decay, not only data on wood material itself. Also the effect of other factors, like solar radiation, surface erosion, mechanical impact has a role for the durability of wood.

The first step to evaluate the exposure conditions is to find the macroclimate conditions. The driving rain, moisture, temperature and also the solar radiation are the most important factors. The long term durability of building structures depend typically on several factors, but the first stage for evaluation of durability and service life consist on evaluation of the exposure conditions [ISO 15686-1]: e.g. climate, type of local environment, building type and orientation, design and details of the structure.

For wood material, the microbes play often a key role on the durability, especially in high humidity conditions. The microbial activity is often highest in the tropical and subtropical climate and lowest in the boreal and arctic climate. There are several climatic approaches for biological activity. Koeppen's climate classification was originally developed for the botanical and agricultural use, but it will give an overview on the world macro-climate mapping for environmental biological activity. A new version of the climate classification was presented by Kottek et al [2006]. For evaluation of the effect climate on decay development, the Scheffer index was developed [Scheffer 1971], and it has long been used for mapping the decay hazard areas in the USA.

The microclimatic means the climate conditions close the materials and structure, and it is a result of several simultaneous factors: macroclimate (rainfall, temperature, humidity, air pressure conditions etc.), and meso-climate (location of the building, structural details and the materials used). The micro-climate conditions are the basic level for building physical and microbial activity evaluations.

The mould and decay models can be incorporated with climatic and building physic models to evaluate the effect of different exposure conditions on the durability and service life of wooden products. These models can be used to support the service life evaluation of building and building components. A basic method for service life evaluation is the factor method presented in the standards ISO 15686. For wooden components, the most important factors are wood material and coatings, design and execution of structure, exposure conditions of environment and maintenance of the wood structure and surface.

2 USE CONDITION OF WOOD AND WOOD BASED PRODUCTS

According to standard EN 335-1, the use conditions of wood products are classified based on the eventual activity of different biological agents. The classification is however, very general, and in reality the details are often more important for the durability and service life of the structure. Under a dry condition, as wood in indoor conditions (UC1), bio-deterioration risk is only related to accidents or building errors. When wood is under an outdoor and sheltered condition (UC2), condensation of water on the surface of the wood products may occur (risk of mould growth). In condition UC 3 wood is above ground and exposed to the weather, in UC 3.1 for only limited periods under wet conditions and in condition UC 3.2, the time of wetness may be prolonged. In the condition UC 4 the exposure is a direct contact with ground and/or fresh water. In this case the bio-deterioration risk is high.

For damages to develop, several different organisms can be involved (Figure 1). In the accelerated laboratory tests, however, the worst case scenario is often simulated and tests will be very hazardous for materials compared to the intended use conditions above ground (Brischke and Rapp 2007). The intended use conditions should be kept in mind when evaluating the needed durability of wood products, this applies especially for use class 2 and 3.1 (claddings) situations.

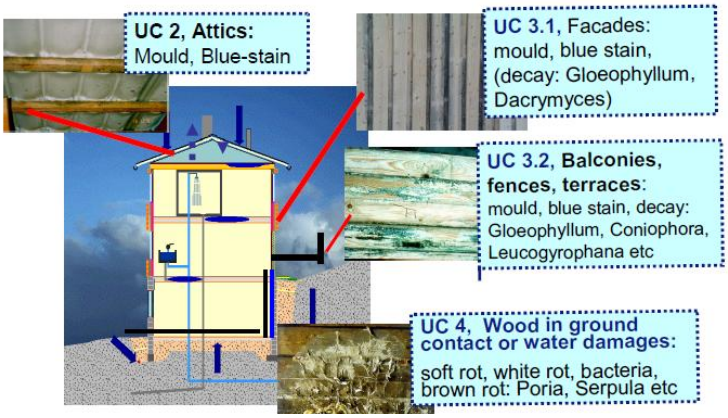

Figure 1. Example of the fungi causing damage in different parts of buildings and the different use classes (UC 2 – UC 4).

The damage cases in cladding are mainly caused by the excess of water by malfunction of the structure. The high exposure conditions, however, exist for wood in decking, dock or wood in ground contact, when more aggressive test conditions are needed. The most critical parts of the cladding and decking are details where water can be accumulated and decay will be started. The risk is lower in Nordic Countries than that in Atlantic Climate area where unprotected and uncovered decking is more exposed to weather and decay [Viitanen et al 2010]. In these use conditions, more durable materials and products are needed, and the classification of natural durability of heartwood of different wood species is presented in the standard EN 350-2.

3 MODELLING THE DECAY DEVELOPMENT IN WOOD

There is always a wide variation within the growth conditions of different fungul species, and an overall evaluation of the growth activity and decay development of a "typical" example fungi (mixture of mould/blue-stain fungi) or typical decay fungi (e.g. *Coniophora puteana* or *Gloeophyllum sepiarium*) is needed. VTT has done comprehensive research in mould and decay growth and their numerical modelling on timber [Viitanen et al 2003]. This paper shows results on the updated decay model and an overview of the decay risks on timber structures under different climate zones.

Using the decay model and the climatic exposure we can get information on the hazard zones of Europe. The model is based on pine sapwood, but in the future stages, a modification of this model also for other materials should be studied. For other wood products, as well as for coated or treated or modified wood, the critical values and parameters may be different. For example, UV light deteriorates the outer surface of wood, especially when liquid water is available. Greyish colour of wood surface and aging of coated wood is caused by the combination of actions: water, UV light and micro-organisms (mould and blue-stain fungi).

The present model is developed from the work presented in references Viitanen and Ritschkoff [1991], Viitanen [1996], and Viitanen [1997]. In these references, the decay growth of brown rot in spruce and pine sapwood is studied experimentally in different constant relative humidity and temperature conditions. In the present model, only the data of pine sapwood is considered. Based on the experimental findings, a model for variable conditions is proposed. This model is a time stepping scheme. The development of decay is modelled with two consecutive processes:

a) Activation process:

This is termed as α parameter, which is initially 0 and gradually grows depending on the air conditions to a limit value of 1. This process is able to recover in favourable conditions (dry air) at a given rate (although no experimental evidence of recovery is available).

b) Mass loss process:
This occurs when the activation process has fully developed (α=1) otherwise it does not occur. This process is naturally irrecoverable.

In this model, these processes only occur when the temperature is 0..30 ^{0}C and the relative humidity is 95% or above, as other temperatures were not tested. Outside these condition bounds, the activation process may recover, but the mass loss process is simply stopped. The activation process is as given in Equation 2. The recovery time (i.e. α recovers from a value of 1 back to 0) is assumed to be 17520 hours (2 years). Recovery takes place when the conditions are outside the bounds of the decay growth.

$$\text{Activation process } \alpha = 0..1$$

$$\alpha(t) = \int_0^t d\alpha = \sum_0^t (\Delta\alpha) \text{ , where} \qquad (1)$$

$$\Delta\alpha = \frac{\Delta t}{t_{crit}(RH,T)} \text{ or (in favorable conditions of decay)}$$

$$\Delta\alpha = -\frac{\Delta t}{17520} \text{ (in unfavorable conditions of decay)}$$

$$t_{crit}(RH,T) = \left[\frac{2.3T + 0.035RH - 0.024T \times RH}{-42.0 + 0.14T + 0.45RH}\right] \times 30 \times 24 \quad \text{[hours]}$$

The mass loss process proceeds the activation process, when α has reached 1(Eq. 2).

$$\text{Mass loss process when } \alpha \geq 1 \qquad (2)$$

$$ML(t') = \int_{t\,at\,\alpha=1}^{t'} \frac{ML(RH,T)}{dt} dt = \sum_{t\,at\,\alpha=1}^{t'} \left(\frac{ML(RH,T)}{dt} \times \Delta t\right)$$

$$\frac{ML(RH,T)}{dt} = -5.96 \times 10^{-2} + 1.96 \times 10^{-4} T + 6.25 \times 10^{-4} RH \text{ [\%/hour]}$$

3.1 Evaluation the Exposure Conditions in Different Part of Europe

The empirical wood decay model was run using the ERA-40 data for air temperature, humidity and precipitation at 6 hour intervals. ERA-40 is a massive data archive produced by the European Centre of Medium-Range Weather Forecasts (ECMWF). The reanalysis involves a comprehensive use of a wide range of observational systems including, of course, the basic synoptic surface weather measurements. The ERA-40 domain covers all of Europe and has a grid spacing of approximately 270 km. The nature of the data and the reanalysis methods of ERA-40 are described in detail in Uppala et al. [2005].

The evaluation of decay development in the model is based on the mass loss caused by the decay fungus. Within specified limitations, the mass loss is an applicable variable for evaluating the decay development in wood. The decay development model will give a general assumption of the effect of humidity, temperature and exposure time on the start and progress of the decay.

The resulting modelled mass loss in 1961-1970 at the calculation points of the ERA-40 grid were analyzed by a chart production software producing a maps of wood decay in Europe (Figure 2a). A modification of the weather data was made so that the humidity of air was set to 100% during precipitation (at non-freezing temperatures) as this is thought to result in a full saturation in the wood surface. The solar radiation was evaluated based on the climatic data of Europe, 30 years average of solar radiation (Figure 2b).

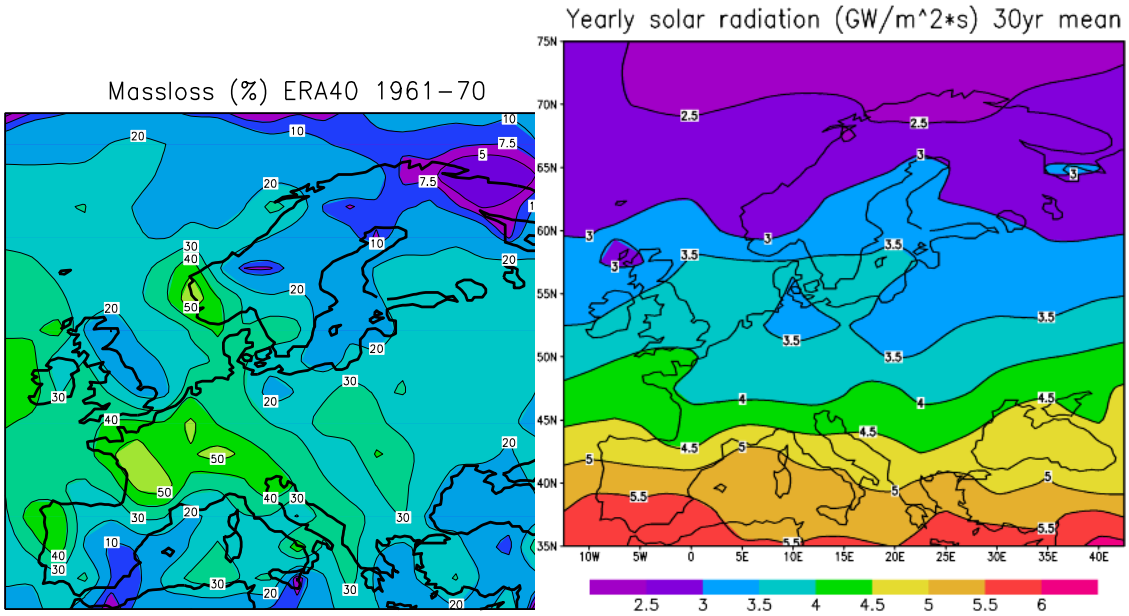

Figure 2. a) Modelled mass loss (in %) of small pieces of pine wood that are exposed to rain in 10 years in Europe (from [Viitanen et al. 2010]). **b)** Solar radiation in Europe. The exposure means structure exposed direct to weather (rain and solar radiation). For sheltered structure, the mass loss values and figures are different.

4 SERVICE LIFE EVALUATION OF WOOD PRODUCTS AND COMPONENTS

The long term durability of building structures depend on several factors. The ISO 15686 standard identifies a wide range of parameters which are important to Service Life Prediction (Figure 3). This factor method uses factors as:

A= Quality of components e.g. wood natural durability, treatment and coatings
B = Design level e.g. protection by design
C= Work execution e.g. joints and details
D= Indoor environment, e.g. temperature., RH, condensation
E= Outdoor Environment e.g. climate, driving rain, shadow
F= In use conditions e.g. wear, mechanical impacts
G= Maintenance level e.g. repair, revisions, repainting

The exposure conditions in different regions of Europe can be used as an outdoor environment factor needed for the durability and service life estimation of a wood structure (Figure 4). For wood materials and components, the factors B, C, E and G are obviously the most important [Vesikari et al 2001, Viitanen 2005, Englund 2010]. The values of these parameters could be determined regionally, taking into account the local effects of the external factors considered to be important. The quality of components signifies here the different wood species, including sapwood and heartwood parts. Wood based products include different impregnated and modified products which make possible the use of wood products in more severe use conditions. For service life evaluation, a relative value of each factor can be given based on the data from results or from experience. This value is depends on the importance of the factor, and as a first step, the most important factors may be set as: quality of the components, design level, main climate conditions and maintenance level. In a further step, more factors could be included.

For normal use conditions in Nordic Countries, coated spruce boards and paint base film coated birch plywood have been used for long time in exterior conditions without any significant durability problems when best practices are followed [Viitanen et al 2008b]. For decking, the effect of wood material is more important than that for cladding. For decking material, most often impregnated or modified wood is used.

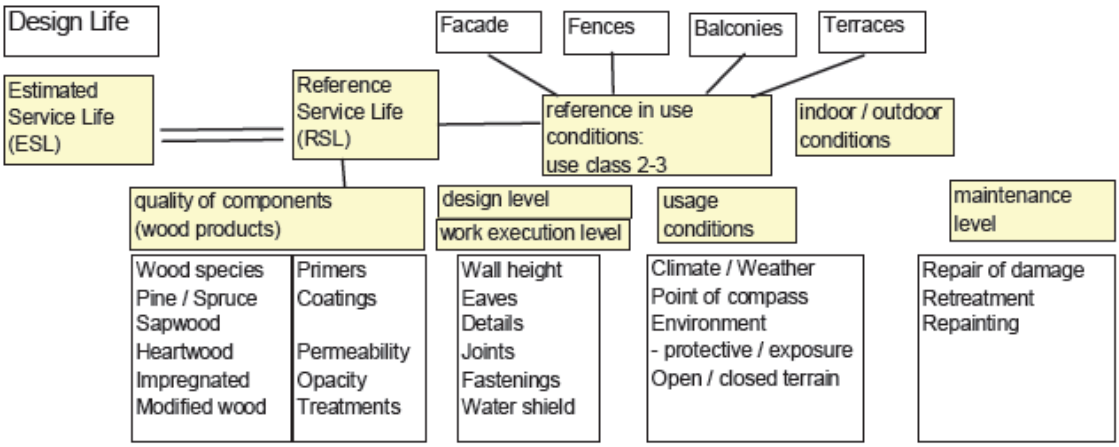

Figure 3. The overall picture on the different factors dealing with the durability and service life of different wooden structure.

European macroclimate, humidity (Map 1)	D1
Nordic climate zone, North	0,50
Nordic climate zone, South	0,80
Continental Europe climate zone	1,00
Atlantic climate zones, North	1,50
Atlantic climate zones, Middle	2,00
Atlantic climate zones, South	2,50
Mediterranean climate zone 1 (wet)	1,50
Mediterranean climate zone, 2 (dry)	0,80

European macroclimate, solar radiation (Map 2)	D2.1
Nordic zones, North	0,70
Nordic zones, South	0,85
Middle Europe, North	1,00
Middle Europe, South	1,14
Southern Europe	1,30
Southern Europe, Southern parts	1,60

Figure 4. The factors for outdoor exposure in different regions of Europe (based on the maps shown in figure 2) to be used for the evaluation system shown in figure 5.

In Finland, an evaluation and calculation system for acceptable exposure conditions for service life of wooden cladding has been developed (Figure 5). The service life evaluation draft model of EnnusPuu [Viitanen 2005] developed at VTT is based on the factors shown in Figure 3. This evaluation system was built on the factor method based on the ISO 15686, and the method assesses the service life of wooden claddings. In the woodexter project, this method was further developed to evaluate different exposure factors.

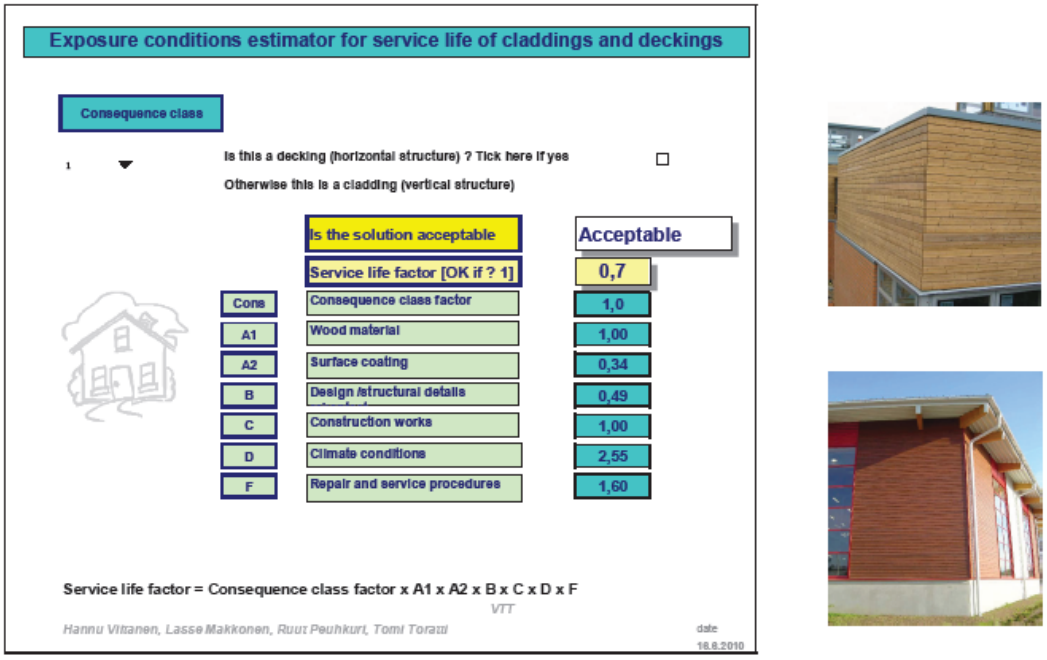

Figure 5. An example on a calculation method to evaluate the exposure conditions and service life of wooden cladding and decking. Method is based on previous "EnnusPuu" VTT programme (a first version presented by Viitanen 2005).

5 CONCLUSION

New attempts have been made to develop calculation methods for service life estimations for different exposure conditions. It still remains to be verified with field experience. So far the comparison of the method result to practice has been encouraging.

ACKNOWLEDGMENTS

The authors gratefully acknowledge the financial support of WoodWisdom-Net and the wood industry partnership Building with Wood for funding the research work within project "WoodExter". The "WoodExter" research partners are thanked for their cooperation and collaboration in this project. ECMWF ERA-40 data used in this study have been provided by ECMWF.

REFERENCES

Brischke, C. and Rapp, A.O. 2007. *Dose-response relationships for service life prediction of wood*. Wood Science and Technology (In Brischke C. 2007).

Englund, F. 2010. *Standardisation related to Service Life Planning*. State-of-the-art. SP report 2010-37. SP Technical Research Institute of Sweden.

ISO 15686-1. 2006. *Building and construction assets - Service life planning - Part 1: General principle*

Kottek, M.J., Grieser, C., Beck, B.R. and Robel, F. 2006. *World map of the Köppen-Geiger climate classification updated*. Meteorol. Z 15, 259-263.

Räisänen, J., Hansson, U., Ullerstig, A., Döscher, R., Graham, L.P., Jones, C., Meier, M., Samuelsson, P., Willén, U., 2004. *European climate in the late 21st century: regional simulations with two driving global models and two forcing scenarios*, Climate Dynamics, 22, 13-31.

Scheffer TC (1971) *A climate index for estimating potential for decay in wood structures above ground*. Forest Prod J 21(10):25-31

Uppala, S.M., Kållberg, P.W., Simmons, A.J., Andrae, U., da Costa Bechtold, V., Fiorino, M., Gibson, J.K., Haseler, J., Hernandez, A., Kelly, G.A., Li, X., Onogi, K., Saarinen, S., Sokka, N., Allan, R.P., Andersson, E., Arpe, K., Balmaseda, M.A., Beljaars, A.C.M., van de Berg, L., Bidlot, J., Bormann, N., Caires, S., Chevallier, F., Dethof, A., Dragosavac, M., Fisher, M., Fuentes, M., Hagemann, S., Hólm, E., Hoskins, B.J., Isaksen, L., Janssen, P.A.E.M., Jenne, R., McNally, A.P., Mahfouf, J.-F., Morcrette, J.-J., Rayner, N.A., Saunders, R.W., Simon, P., Sterl, A., Trenberth, K.E., Untch, A., Vasiljevic, D., Viterbo, P., and Woollen, J. 2005: *The ERA-40 re-analysis*. Quarterly Journal of the Royal Meteoroogical Society, 131, 2961-3012.

Vesikari, E., Rautiainen, L., Häkkä-Rönnholm, E., Silvennoinen, K.; Salonvaara, M. Viitanen, H. *Julkisivujen ja katteiden käyttöiän ennakointi*. Service life prediction of facades and roofs. Espoo, VTT Rakennus- ja yhdyskuntatekniikka, 2001. 158 s. VTT Julkaisuja - Publications; 850 (In Finnish, English abstract).

Viitanen, H. 1996. *Factors affecting the development of mould and brown rot decay in wooden material and wooden structures. Effect of humidity, temperature and exposure time*. Doctoral Thesis. Uppsala. The Swedish University of Agricultural Sciences, Department of Forest Products. 58 p.

Viitanen, H. 1997. *Critical time of different humidity and temperature conditions for the development of brown rot decay in pine and spruce*. Holzforschung 51 (2): 99-106.

Viitanen, H. & Ritschkoff, A. 1991. *Brown rot decay in wooden constructions. Effect of temperature, humidity and moisture*. Uppsala. Swedish University of Agricultural Scienses, Department of Forest Products. Report no 222. 55 p + appendix 2 p

Viitanen, H., Ritschkoff, A-C, Ojanen, T., Salonvaara, M. 2003. *Moisture conditions and biodeterioration risk of building materials and structure*. Proceedings of the 2nd International Symbosium ILCDES 2003. Integrated Lifetime Engineering of Buildings and Civil Infrastructures, Kuopio, 1-3 Dec. 2003 RIL, VTT, RILEM, IABSE, ECCE, ASCE. Espoo (2003), 151 – 156.

Viitanen, H. 2005. *Tests of resistance and durability of wooden products; an example of evaluation of service life for wooden façade*. COST Action E37. Sustainability through new technologies for enhanced wood durability. Workshop. Service life prediction: The contribution to Sustainability. Oslo 19th - 21th June 2005. WG2 Performance Seminar - "Service Life Prediction Tools".

Viitanen, H, Toratti, T. Makkonen, L. Peuhkuri, R. Ojanen, T. Ruokoloainen, L. and Räisänen , J. 2010. *Towards modelling of decay risk of wooden materials*. Eur. J. Wood Prod. 68: 303-313.

XII DBMC
International Conference on Durability of Building Materials and Components
PORTO - PORTUGAL, April 12th-15th, 2011

Estimation and Validation of Concrete Strength and Service Life Using Software Packages based on Predictive Models

V.G. Papadakis [1]
S. Demis [2]

ABSTRACT

Despite the high level of research and the significant advances achieved in concrete technology, issues of unsatisfactory durability of structures are a major concern of the international engineering community. The observed deterioration of concrete structures in service may be perceived as the result of the joint action of mechanical and environmental effects. Corrosion of steel reinforcement is recognised as the most serious outcome of these actions, impairing not only the appearance of the structure, but also its strength and safety. A correct selection of the raw building materials, a systematic construction process but most importantly a thorough durability design process that identifies the influence of the harmful environmental agents, in a way that the designer can take all the appropriate measures (in advance) to mitigate their influence, is the only way to safeguard a prolonged service-life of any type of structure. On this note, a significant step forward is the development of appropriate software packages, based on predictive models, for the estimation of concrete strength and service life.

In this study, a step by step procedure, previously developed (in full compliance with the European Standards EN 197 for cement and EN 206 for concrete), based on analytical mathematical models for the estimation of concrete service life and strength, is briefly presented. Validation of the estimated strength and service life results is taking place using a wide range of data collected throughout the recently published literature and from field observations and existing structures. It is hoped that the focus of this study will initiate a wider acceptance of software based predictive models in achieving a feasible and durable solution, possible by incorporating them in next generation standards.

KEYWORDS

Predictive models, Concrete strength, Service life, Carbonation, Durability.

[1] Associate Professor, Department of Environmental and Natural Resources Management, University of Ioannina, Agrinio, Greece, vgp@psp.org.gr
[2] Civil & Structural Engineer (Ph.D., MSc.Eng) Durability Consultant, Patras Science Park, Patras, Greece, demis@psp.org.gr

1 INTRODUCTION

While recognising the problem of premature structural deterioration of reinforced concrete (RC) structures as a combined effect of mechanical and environmental actions (diffusion of carbon dioxide from the atmosphere, ingress of chlorides), emphasis is given from a durability point of view on the effect of the latter, in understanding the physiochemical processes and mechanisms leading to the reduction of an RC element service life. However, approaches on modelling the deterioration mechanisms, presented so far, are usually limited to complicated mathematical models not widely applicable in practice. What is missing is a set of toos that will aid the designer in identifying the influence of the harmful environmental agents, in order to take all the appropriate measures (in advance) to mitigate their effect, in safeguarding a prolonged service-life of any type of structure.

Considering that on the European Standard for concrete EN 206 [2000] durability is approached either through the definition of limiting parameters on the cement and concrete composition (w/c ratio, cement content, etc.) or through the continuation and development of performance-related methods, a significant step forward could be the development of appropriate software for the estimation of concrete service life, based on the principles of these methods, using reliable mathematical proven models and strengthened by adequate experimental data. A performance-related method considers each relevant deterioration mechanism, the service life of the structure, and the criteria which define the end of this service life, in a quantitative way. Such a method may be based on data derived from established performance test methods for each relevant mechanism, or on the use of proven predictive models. Bearing in mind that in reinforced concrete, the most serious deterioration mechanisms are those leading to corrosion of the reinforcement, it is therefore necessary, if a long service life is required, the modelling attempts to focus on these mechanisms and chemical attack processes.

In this study, a simulation tool, based on proven predictive models developed by Papadakis et al. [1981; 1992; 2007] well published and awarded by the ACI, for estimation of concrete service life and strength (according to in performance-related methods of EN 206 for assessing durability) is briefly presented and verified. Its structure is illustrated in Fig. 1.

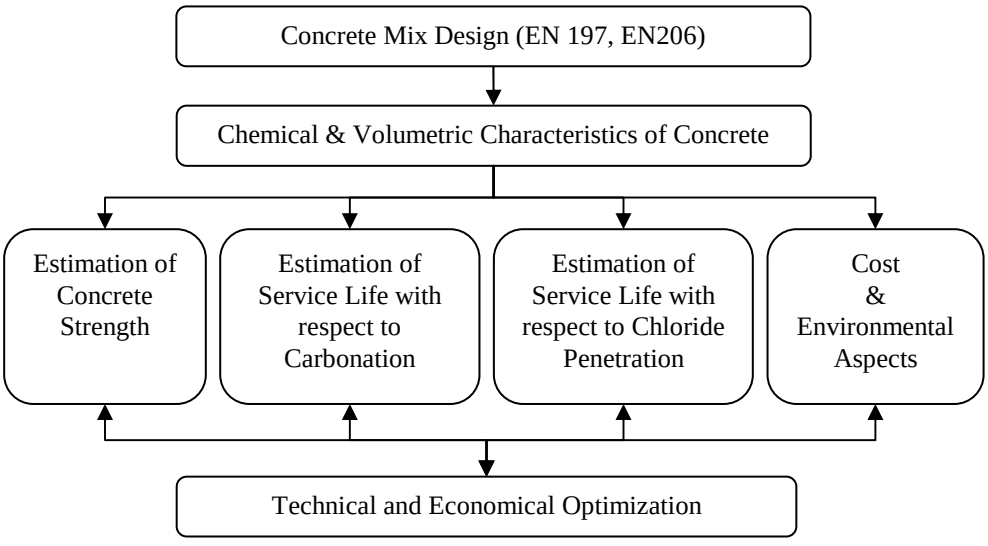

Figure 1. Logic tree of software for estimation of concrete service life and strength.

After the definition of the concrete mix design and the calculation of the main chemical and volumetric characteristics of concrete (chemical composition of hydrated cementitious materials, porosity and related characteristics) the compressive strength is estimated, introducing a new

approach based on the cement strength class, using a modified version of Feret's formula. By taking into account the environmental conditions where the structure will be exposed, the concrete service life is reliably predicted using fundamental mathematical models that simulate the basic deterioration mechanisms of reinforced concrete, such as carbonation and chloride penetration. Principles of chemical and material engineering have been applied to simulate the physicochemical processes [Papadakis et al. 1989]. Finally, cost and environmental aspects on concrete composition are analysed.

2 COMPRESSIVE STRENGTH AND SERVICE LIFE ESTIMATION

In this section the thoughts behind the compressive strength and service life estimation, for carbonation exposure, are briefly presented. The reader should bear in mind that these attempts have been published extensively elsewhere [Papadakis et al. 1981; 1992; 2007; Papadakis, 2000].

2.1 Compressive Strength Estimation

Usually most of the equations found in the literature relating compressive strength to the concrete constituents are of an empirical nature, and can not be applied in general. Furthermore, considering that the effect of each component of hydrated cement on strength is not just additive, as well as bearing in mind their dependence on age and curing conditions and their various interactions, it becomes apparent that a generally applicable strength prediction is not possible. On this note, but more important due to the lack of experimental results, the cement strength class can be used to estimate a safe lower limit of concrete strength. The European Standard EN 197-1 [2000] prescribes a compressive strength test for cement on mortar specimens of fixed composition. By incorporating the information mentioned in the Standard to Feret's formula (the most well recognised strength equation relating compressive strength to concrete characteristics), since it contains only one adjustable parameter a safer approximation of the minimum compressive strength class of concrete (at 28 days) can be derived for different values of W/C, C or ε_{air} as:

$$f_c \geq 7.84\, S_c / [1 + (W/C)\,(d_C/d_W) + \varepsilon_{air}\,(d_C/C)]^2 \quad (1)$$

where C and W are the cement and water contents in concrete (kg/m^3 concrete), d_C and d_W the densities of cement and water respectively (kg/m^3), ε_{air} the air content in concrete, and S_c is the standard strength class (at 28 days) of cement (MPa).

If a strength result from the above mentioned mortar specimens is known at another age (2, 7, or 90 days), it can be used in the above equation as S_c, in order to estimate the compressive strength at the same age and for other W/C values. In this way, the strength development can be predicted. In the case of SCM-concrete, the pozzolanic action of the addition is taken under consideration (since it generates strength components) using the concept of the SCM efficiency factor. The latter (or k-value) is defined as the part of the SCM that can be considered equivalent to portland cement (CEM I), providing the same concrete properties (k=1 for portland cement) [Papadakis, 2000]. In this way, the compressive strength can be estimated as:

$$f_c \geq 7.84\, S_c / \{1 + [W/(C+k_F F_{ACT}+k_S S_{ACT})]\,(d_C/d_W) + \varepsilon_{air}\,[d_C/(C+k_F F_{ACT}+k_S S_{ACT})]\}^2 \quad (2)$$

where F_{ACT} and S_{ACT} are the active contents of concrete additions fly ash and silica fume (kg/m^3), having an efficiency factor k_F and k_S respectively.

2.2 Estimation of Service Life for Carbonation Exposure

Based on reaction engineering principles, a system of non-linear differential equations, developed by Papadakis et al. [1989; 1991] models in a quantative way the processes leading to concrete carbonation (diffusion of CO_2 in the gas-phase of pores, its dissolution in the aqueous film of these

pores, the dissolution of solid $Ca(OH)_2$ in pore water, its ultimate reaction with the dissolved CO_2, and the reaction of CO_2 with CSH). The solution of the set of differential equations permits the calculation of the carbonation depth x_c, at a given time t, as well as the estimation of the critical time, $t_{cr,carb}$, required for the carbonation front to reach the reinforcement located at a distance c (concrete cover to reinforcement), for both portland and blended cements, as well as when additions of SCM are used separately in concrete:

$$x_c = \sqrt{\frac{2D_{e,CO2}(CO_2/100)t}{0.33CH + 0.214CSH}}\ ,\ t_{cr,carb} = \frac{(0.33CH + 0.214CSH)c^2}{2D_{e,CO2}(CO_2/100)} \quad (3)$$

where, CO_2 is the CO_2-content in the ambient air at the concrete surface (%), $D_{e,CO2}$ the effective diffusivity of CO_2 in carbonated concrete (m^2/s), *CH* and *CSH* the contents of calcium hydroxide and calcium-silicate-hydrate, respectively, in concrete volume (kg/m^3). In this way the service life of a concrete structure, regarding corrosion of reinforcement induced by carbonation, is at least $t_{cr,carb}$.

3 EXPERIMENTAL VERIFICATION

3.1 Verification of Compressive Strength Predictions

As far as strength estimation is concerned, a two step verification process took place, based on data collected from ready-mix plants and from the literature. Characteristic examples of these sets of data, as well as their overall comparison with the compressive strength values, calculated using the equations described above, are presented in this section.

3.1.1 Comparison with experimental results from ready-mix plants

The experimental results gathered, concern strength measurements of CEM I and CEM II/B-M specimens of compositional studies from various worksites and ready-mix factories throughout Greece. Depending on the w/c ratio, various cement contents have been used (from 200 to 500 kg/m^3) without any active additions (fly ash, silica fume, etc.). Crushed aggregates of a maximum grain size of 31.5 mm were used, and a mean air-content of 1.2 % (representative in most cases) was assumed. As shown in Fig. 2a, an excellent agreement is observed between strength measurements and predictions, based on the previously described Equation (1), for the CEM I / 42.5 cement type. The cement strength class for these specimens (i.e., the S_c parameter of Equation 1) was 42.5.

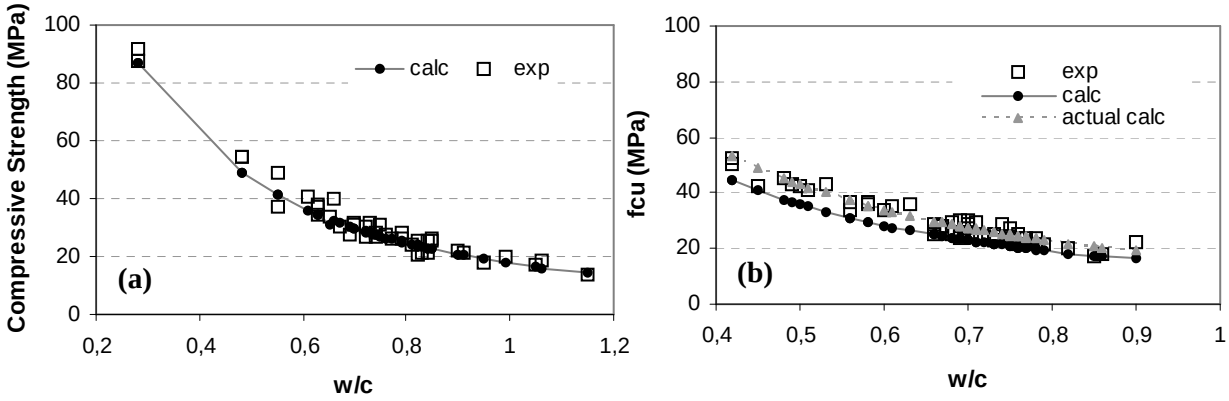

Figure 2. Comparison between predictions of the 28 days-compressive strength and experimental measurements of CEM I / 42.5 and CEM II/ 32.5 type of cements.

In the case of CEM II/32.5 type of specimens (Fig. 2b), a first quick observation can be translated as a slight underestimation, especially for the range of w/c ratios from 0.4 to 0.62 (even though it is not far from the aim of this study in estimating a safe lower limit of concrete strength). The reason that these predictions constitute a safe lower bound, is that the real cement strength is higher than the nominal cement strength class (the Greek cement factories usually, for this type of cement, produce higher

cement strength than the nominated one due to underestimation of active additions of the cement). Bearing the latter in mind, and based on the real mortar strength at 28 days (39 MPa, instead of 32.5 MPa), the previously mentioned "safe lower limit" or compressive strength can be re-calculated to approach in a more accurate way the compressive strength of concrete at 28 days. It can be seen that the "actual" values of the estimated concrete compressive strength of the CEM II / 32.5 samples are in a very good agreement with the experimental results (Fig. 2b).

3.1.2 Comparison with literature-based data

At the second verification stage of the compressive strength estimation, validation using data obtained from the literature was achieved. A significant amount of experimental data were collected concerning CEM I type of cements, CEM I with Type II additives (silica fume, fly ash), CEM II and III type of cements. The chemical composition of each type of cement (where given) and Type II additive (where used) were incorporated in the calculations. In cases where the air content was not given, it was calculated based on the maximum grain size of aggregates, using linear interpolation between the air content values of aggregate sizes of 31.5 mm, 16 mm and 8 mm, as 1.5 %, 2.3 % and 3.5 % respectively. A wide range of w/c ratios was covered (from 0.3 to 0.9). Representative sets of data and the corresponding results are given in Table 1.

Table 1. Characteristic compressive strength estimation sets of data obtained from the literature.

Reference	Cement Type	S_c	C *(kg/m^3)*	F *(kg/m^3)*	w/c	ε_{air} *(%)*	f_c exp *(MPa)*	f_c calc *(MPa)*
Kockal & Turker, 2007	CEM I	42.5 N	340	-	0.45	1.8	50.9	49.9
Liu, 2010	CEM I	42.5 N	245	105	0.83	1.5	31.4	30.4
Kockal and Turker, 2007	CEM II/B-M	32.5 R	340	-	0.41	1.8	45.2	42.2
Climent et al., 2002	CEM II/A-L	32.5 R	350	-	0.6	3.3	27.9	25.1
Tsivilis et al., 2003	CEM II/B-L	32.5 R	333	-	0.62	2.3	26.5	25.3

f_c exp, f_c calc are the compressive strength values from the literature and those calculated from the model

The comparison for every type of cement used between the estimated and the experimental compressive strength values is illustrated in Fig 3. A mean variation of 6.0 % was observed for the CEM I, CEM I with Type II additives and CEM II sets of data. Overall the new proposed method for estimation of the concrete compressive strength, based on cement strength class (S_c), offers an accurate prediction on any type of cement used, incorporating or not Type II additives.

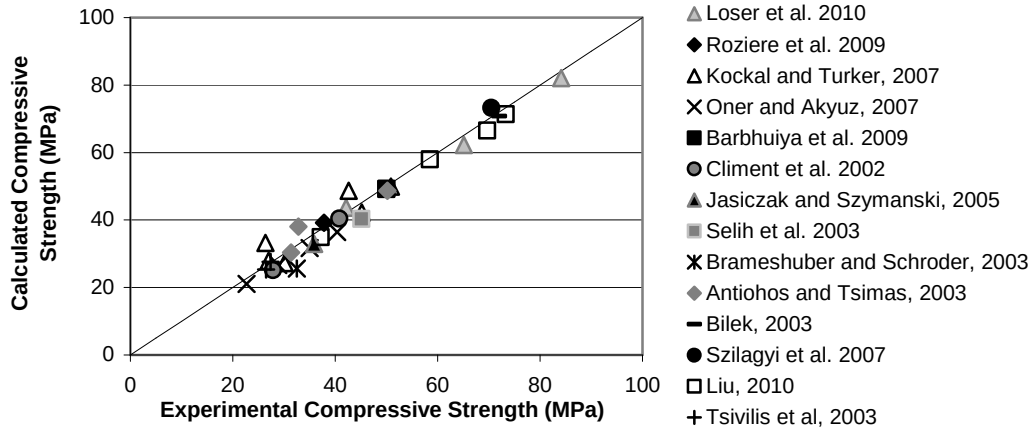

Figure 3. Comparison of experimental with calculates values of concrete compressive strength data.

3.2 Verification of Service Life Prediction for Carbonation Exposure

Carbonation depth results were collected from the recent published literature, under either accelerated conditioning or natural ageing, for different exposure times. Parameters as cement type, mix design characteristics, chemical composition of the clinker and pozzolanic materials, levels of relative

humidity and carbon dioxide concentration (where the reinforced concrete element was exposed) were recorded and inserted into the model developed by Papadakis et al. [1991; 2007]. The calculated carbonation depth values were compared with the corresponding values taken from the literature (Fig. 4). A very good correlation was observed (an average variation of 7.6 % was calculated).

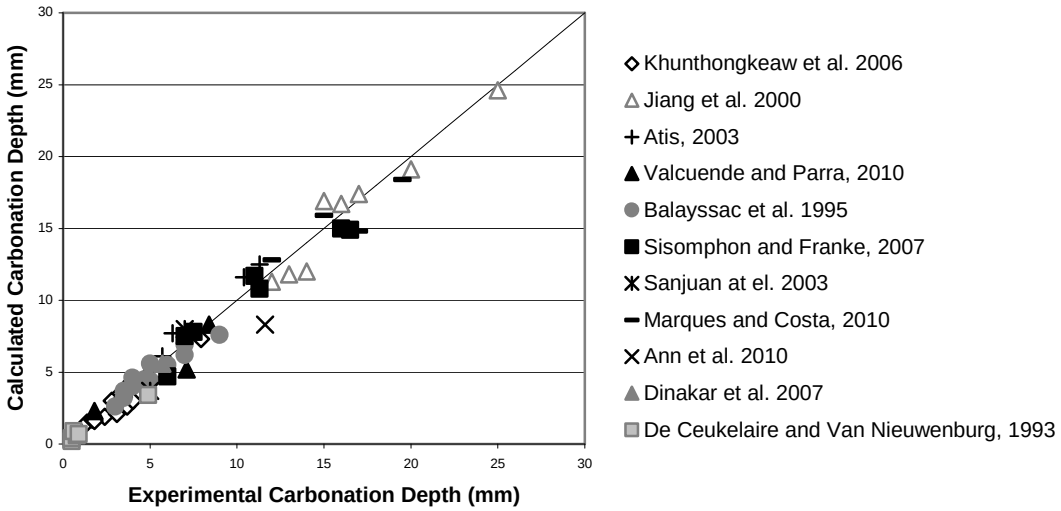

Figure 4. Comparison of calculated to experimental carbonation depth values.

From the characteristic data given in Table 2 it can be seen that the model yields very accurate predictions for a range of both accelerated (up to 1 year) and natural exposure times (up to 18 years, where considering the experimental value of 11.62 mm with a standard deviation of 2.45, the 8.3 mm calculated is a very good approximation) and for different cement and concrete compositions.

Table 2. Characteristic Estimated Carbonation Depth Values.

.

Reference	*Cement type*	*w/c*	*RH* (%)	CO_2 (%)	*Exp.* X_c (mm)	*Calc.* X_c (mm)	*Exposure Time*
Khunthongkeeaw et al. 2006	CEM I	0.67	72.5	0.0625	5.68	5.30	2 year
Sisomphon & Franke 2007	CEM I + fa	0.68	65.0	3	7.50	7.80	4 weeks *
Sisomphon & Franke 2007	CEM I + fa	0.68	65.0	3	11.0	11.7	9 weeks *
Ann et al. 2010	CEM I	0.45	60.0	0.08	11.62 (2.45)	8.30	18 years
Valcuente & Parra, 2010	CEM II/B-M	0.55	60.8	0.035	3.50	3.80	9 months
Valcuente & Parra, 2010	CEM II/B-M	0.55	60.8	0.035	8.40	8.30	42.5 months
Balayassac et al. 1995	CEM II/B-L	0.48	60.8	0.035	3.00	2.60	6 months
Balayassac et al. 1995	CEM II/B-L	0.48	60.8	0.035	3.50	3.70	12 months
Balayassac et al. 1995	CEM II/B-L	0.48	60.8	0.035	4.00	4.60	18 months
Marques and Costa, 2010	CEM II/A-L	0.60	65.0	5	15.0	15.9	42 days *
Dinakar et al. 2007	CEM II/A-V	0.54	65.0	5.0	5.71	5.6	1 year *
Sisomphon, 2007	CEM III/B	0.60	65.0	3	16.00	15.0	9 weeks *
Marques and Costa, 2010	CEM IV/B	0.55	65.0	5	19.50	18.4	42 days *

* denotes accelerated exposure

In Fig 5, just as a representative example, an excellent agreement between calculated and experimental values is observed, for a longer natural exposure time (up to 4.5 years) and for different w/c ratios.

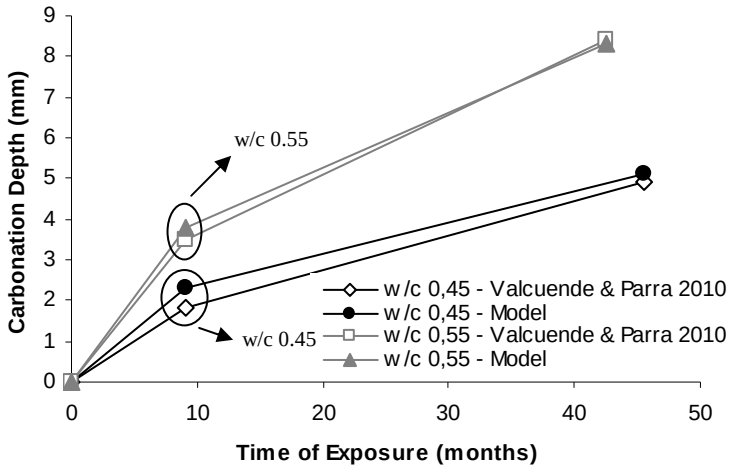

Figure 5. Calculated and experimental carbonation depth values for different w/c ratios of a CEM II/B-M type of cement.

4 CONCLUSIONS

The increasingly observed reduction of reinforced concrete structures service life, necessitates the need for a more robust durability approach implemented on the design stages of a project. Considering that on the European Standard for concrete [EN 206-1, 2000] durability is also defined through performance-related methods, based on proven predictive models, a significant step forward could be the development of appropriate software packages, according to the principles previously mentioned, for the estimation of concrete strength and service life. Such a prediction tool developed by Papadakis et al., for compressive strength and service life estimation, is briefly presented and validated in this study. A rather simple (yet accurate) equation for compressive strength prediction has been developed based on cement strength class. By using the concept of k-value (efficiency factor) of any active addition, the prediction formula is extended in the cases of incorporation of these supplementary cementing materials in concrete. By simulating the physicochemical processes in concrete in a quantative way and by taking into account deterioration models for carbonation and chloride exposures, developed by Papadakis et al, the concrete service life can be reliably predicted.

The validation for compressive strength and service life estimation for carbonation exposure, using a variety of experimental results from the literature and worksite specimens, for a wide range of w/c ratios, cement contents, type of cements and exposure conditions, illustrate a generally excellent agreement, proving thus the validity of the proposed method. It is hoped that the focus, the results and the proven soundness of the predictive tools presented in this study, will pave the way for the adaptation of valid software prediction models as a tool of paramount importance in achieving a soundproof level of durability on a reinforced concrete structure.

REFERENCES

Ann, K.Y., Pack, S.W., Hwang, J.P., Song, H.W. & Kim, S.H. 2010, 'Service life prediction of a concrete bridge structure subjected to carbonation', *Construction and Building Materials*, **24**, 1494–1501.

Antiohos, S. & Tsimas, S. 2003, 'Chloride Resistance of Concrete Incorporating two types of fly ashes and their intermixtures. The effect of the active silica content', Proc 6th CANMET/ACI International Conference on Durability of Concrete, Thessaloniki, Greece, 2003, pp. 115-129.

Atis, C.D. 2003, 'Accelerated carbonation and testing of concrete made with fly ash', *Construction and Building Materials*, **17**, 147-152.

Balayssac, J.P., Detriche, C.H. & grandet, J. 1995, 'Effects of curing upon carbonation of concrete', *Construction and Building Materials*, **9**[2], 91-95.
Barbhuiya, S.A., Gbagbo, J.K., Russell, M.I. & Basheer, P.A.M. 2009, 'Properties of fly ash concrete modified with hydrated lime and silica fume', *Construction and Building Materials*, **23**, 3233-3239.

Bilek, V. 2003, 'Investigation of long-term mechanical properties of High Strength Concrete', Proc. 6th CANMET/ACI International Conference on Durability of Concrete, Thessaloniki, Greece, 2003, pp. 211-223.

Liu, M. 2010, 'Self-compacting concrete with different levels of pulverized fuel ash', *Construction and Building Materials*, **24**, 1245-1252.

Brameshuber, W. & Schroder, P. 2003, 'Influence of the hydration age on frost and de-icing salt resistance of concrete with blast furnace slag cement', Proc 6th CANMET/ACI International Conference on Durability of Concrete, Thessaloniki, Greece, 2003, pp. 99-113.

Climent, M.A., De Vera, G., Lopez, J.F., Viqueira, E. & Andrade, C. 2002, 'A test method for measuring chloride diffusion coefficients through non saturated concrete – Part I. The instantaneous plane source diffusion case', *Cement and Concrete Research*, **32**, 11136-1123.

De Ceukelaire, L. & Van Nieuwenburg, D. 1993, 'Accelerated carbonation of a blast-furnace cement concrete', *Cement and Concrete Research*, **23**, 442-452.

Dinakar, P., Babu, K.G. & Santhanam, M. 2007, 'Corrosion behaviour of blended cements in low and medium strength concretes', *Cement & Concrete Composites*, **29**, 136–145

Jiang, L., Lin, B. & Cai, Y. 2000, 'AA model for predicting carbonation of high-volume fly ash concrete', *Cement and Concrete Research*, **30**, 699-702.

Jasiczak, J. & Szymanski, P. 2005, 'Influence of different kinds of cement on early shrinkage of concrete', Proc International Conference on Cement Combinations for Durable Concrete, Dundee, Scotland, 2005, pp. 399-406.

Khunthingkeaw, J., Tangtermisirikul, S. & Leelawat, T. 2006, 'A study on carbonation depth prediction for fly ash concrete', *Construction and Building Materials*, **20**, 744-753.

Kockal, N.U. & Turker, F. 2007, 'Effect of environmental conditions on the properties of concretes with different cement types', *Construction and Building Materials*, **21**, 634-645.

Marques, P.F. & Costa, A. 2010, 'Service life of RC structures: Carbonation induced corrosion. Prescriptive vs. performance-based methodologies', *Construction and Building Materials*, **24**, 258–265.

Oner, A. & Akyuz, S. 2007, 'An experimental study on optimum usage of GGBS for the compressive strength of concrete', *Cement & Concrete Composites*, **29**, 505-514

Papadakis, V.G., Vayenas, C.G. & Fardis, M.N. 1989, 'A Reaction Engineering Approach to the Problem of Concrete Carbonation', *American Institute of Chemical Engineers Journal*, **35**[10], 1639-1650.

Papadakis, V.G., Vayenas, C.G. & Fardis, M.N. 1991, 'Fundamental Modeling and Experimental Investigation of Concrete Carbonation', *ACI Materials Journal*, **88**[4], 363-373.

Papadakis, V.G., Fardis, M.N. & Vayenas, C.G. 1992, 'Effect of Composition, Environmental Factors and Cement-Lime Mortar Coating on Concrete Carbonation', *Materials and Structures*, **25**, 293-304.

Papadakis, V.G. 2000, 'Effect of Supplementary Cementing Materials on Concrete Resistance against Carbonation and Chloride Ingress', *Cement and Concrete Research,* **30**[2], 291-299.

Papadakis, V.G., Efstathiou, M.P. & Apostolopoulos, C.A. 2007, 'Computer-Aided Approach of Parameters Influencing Concrete Service Life and Field Validation", *Computers & Concrete,* **4**[1], 1-18.

Sanjuan, M.A., Andrade, C. & Cheyrezy, M. 2003, 'Concrete carbonation tests in natural nad accelerated conditions', *Advances in Cement Research*, **15**[4], 171-180.

Selih, J., Tritthart, J. & Strupi-Suput, J. 2003, 'Durability of Portland limestone powder-cement concrete', Proc 6th CANMET/ACI International Conference on Durability of Concrete, Thessaloniki, Greece, 2003, pp. 147-161.

Sisomphon, K. & Franke, L. 2007, 'Carbonation rates of concretes containing high volume of pozzolanic materials', *Cement and Concrete Research,* **37**, 1647-1653.

Szilagyi, H., Ioani, A. & Corbu, O. 2007, 'Self compacting concrete with silica fume – procedure for mix design', Proc 3rd Central European Congress on Concrete Engineering, Visegrad, Hungary, 2007, pp. 167-172.

Tsivilis, S., Tsantilas, J., Kakali, G., Chaniotakis, E. & Sakellariou, A. 2003, 'The permeability of Portland limestone cement concrete', *Cement and Concrete Research*, **33**, 1465-1471.

Valcuende, M. & Parra, C. 2010, 'Natural carbonation of self-compacting concretes', *Construction and Building Materials*, **24**, 848–853.

European Standard EN 206-1, 2000, *Concrete - Part 1: Specification, Performance, Production and Conformity*, CEN, Brussels.

European Standard EN 197-1, 2000, *Cement - Part 1: Composition, Specifications and Conformity Criteria for Common Cements*, CEN, Brussels.

XII DBMC
International Conference on Durability of Building Materials and Components
PORTO - PORTUGAL, April 12th-15th, 2011

Durability of Interior Renderings in Schools: Optimization of Envelope Insulation for Mitigation of Mould Growth Risk

Nuno M.M. Ramos [1]
Isabel M. Ribeiro [2]
Patricia Santos [3]
João M.P.Q. Delgado [4]
Vasco Peixoto de Freitas [5]

ABSTRACT

A high standard education is, now a day, a clear objective for any modern society. In Portugal, the retrofit of educational buildings has an enormous relevance as demonstrated by the "Program for Retrofit and Upgrade of High Schools". Educational buildings specific characteristics such as high occupancy rates and high amount of time children spend in classrooms make them a special case compared to other buildings. Mould growth on envelope surfaces is frequently observed in these buildings, reducing the expected durability of renderings and coatings.

The present work consisted of two main lines of research: one of simulation and other of optimization. The simulation part included modelling, using the Energy-Plus software, of Interior Surfaces Temperature, Indoor Air Temperature and Relative Humidity variation, before and after a hypothetical retrofit process.

Optimization techniques were applied in the definition of insulation thickness to be numerically tested in the "after retrofit" scenario. The objective was to minimise insulation thickness in each building element of the envelope. The constraints were derived from the control of surface temperature values that would result in mould growth risk.

KEYWORDS

Building retrofitment; Hygrothermal behaviour; Mould; Optimization.

[1] Faculty of Engineering of the University of Porto (FEUP), Porto, PORTUGAL, nuno.ramos@fe.up.pt
[2] Faculty of Engineering of the University of Porto (FEUP), Porto, PORTUGAL, iribeiro@fe.up.pt
[3] Faculty of Engineering of the University of Porto (FEUP), Porto, PORTUGAL, ec05149@fe.up.pt
[4] Faculty of Engineering of the University of Porto (FEUP), Porto, PORTUGAL, jdelgado@fe.up.pt
[5] Faculty of Engineering of the University of Porto (FEUP), Porto, PORTUGAL, vpfreita@fe.up.pt

1 INTRODUCTION

A high standard education is, now a day, a clear objective for any modern society. In Portugal, the retrofit of educational buildings has an enormous relevance as demonstrated by the "Program for Retrofit and Upgrade of High Schools" (PMEES [2007]). The retrofit of the first 205 schools will represent an investment of 2500 million Euros, intending for them to respond to present demands namely energy efficiency, comfort, indoor air quality (IAQ) and functional organization (SCE [2006] and RSECE [2006]).

Educational buildings specific characteristics such as high occupancy rates and high amount of time children spend in classrooms make them a special case compared to other buildings (Grimsrud *et al*. [2006]). Therefore, the retrofit process should take into account the high internal heat gains due to high occupancy rates, the high solar gains due to glazing and the demanding needs for ventilation and IAQ (Holm *et al*. [2008] and Freitas [2009]).The regulations adopted in recent years were thought for new buildings and not for the retrofit of existing ones. Therefore their implementation may not lead to intended objectives. On the other hand, the costs for satisfying the demands are so high and imply such intrusive interventions that justify a careful technical reflexion.

Durability issues are also of main importance when looking at intensively used buildings. In this work, the focus was put on degradation of inside surfaces due to mould growth. This is a common problem in some existing Portuguese buildings due to the combination of a mild humid climate, discontinuous heating, adventitious ventilation and low quality envelope.

The objective of this work is to find the optimal insulation thickness to be added to envelope components regarding mould growth mitigation. Two major constraints were elected to conduct the optimization process. The resulting thermal resistance of walls and ceiling should prevent mould growth by avoiding surface condensation and contribute to the increase of minimum indoor temperature admitting no additional heating is available. It should be taken into account that due to high internal gains in classrooms and mild climate Portuguese conditions it may be possible, in some cases, to avoid additional heating. Also, due to economic restraints, adequate heating regarding comfort may not be implemented. The result of this optimization process should therefore be regarded as a safety net for the envelope, rather than the ideal solution for a properly operated building.

The demand for energy efficiency and IAQ has lead to solutions where the passive behaviour of the building becomes of minor importance when compared to systems. But for technical or economic reasons the full operation of the systems may be impossible and therefore the evaluation of the building performance for that scenario must be investigated.

The present work consisted in two main lines of research: one of simulation and other of optimization. The simulation was focused on the hygrothermal behaviour of a classroom using a simplified model developed by the authors. The Energy-Plus software (Energy Plus Manual [2009] and Crawley *et al*. [2000]) was used to simulate the same scenarios, providing results for comparison. The optimization process was adapted to the simplified model since it uses linear functions.

2 DESIGN PROBLEM

Figure 1 presents a 3D model of the studied building, which is part of a school built on the late 1970's. This specific building holds two classrooms that have simultaneous occupation and can therefore be approximated with a one zone model.

The building envelope (Figure 2) is composed of 15 cm concrete walls, single glazed aluminium frame windows and a flat roof composed by a 25 cm concrete slab protected by cement-fibre plates. No thermal insulation was originally applied in the envelope opaque elements.

The building is located in Porto, in the so-called Warm-Summer-Mild-Winter zone. The exterior temperature will not drop below 0 ºC and may reach 30 ºC in the summer. The average temperature in January is 7.5 ºC. For simulation purposes, the TMY format weather file for Porto, available on the Energy Plus web page, was used.

The occupation of the two classrooms corresponds to a total of 50 persons with a metabolic rate of 70 W/m^2 (ISO 7730 [2005]), in a schedule 8.30-13.00 and 14.00-18.30. No mechanical ventilation was applied in the original classrooms, therefore relying on adventitious ventilation and window opening by users. But since the new regulations (RSECE [2006]) demand 30 m^3/h per person, it was admitted in all calculations that, when occupied, an ach = 2.2 h^{-1} would prevail and, in the remaining periods, ach would drop to 0.6 h^{-1}.

The difference between the scenarios of pre or post retrofit was the insulation thickness added to the envelope elements. In this exercise, XPS (0.035 W/(m^2.ºC)) was considered as insulation material, applied on interior surfaces.

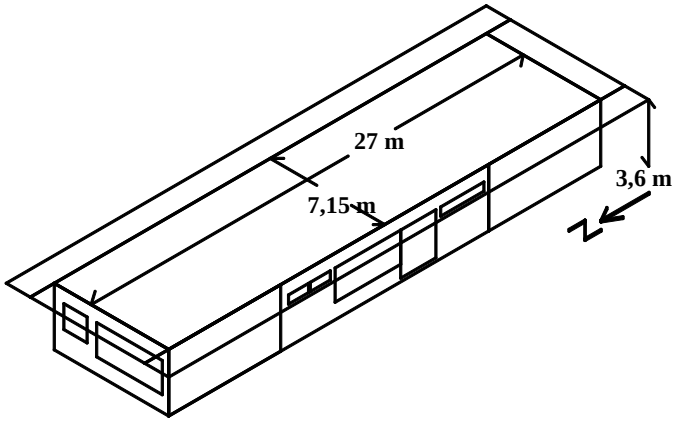

Figure 1. Sketch of the building analyzed.



Figure 2. School building's East façade.

3. NUMERICAL AND OPTIMIZATION MODEL

For these calculations an energy simulation needs to be performed to solve the design optimization problem described above. Energy-Plus, a building energy analysis tool, was used to simulate the hygrothermal behaviour of the building. The differential equation that define the energy balance of a room is (Energy Plus Manual [2009])

$$C_z \frac{dT_z}{dt} = \sum_{i=1}^{sl} Q_i + \sum_{i=1}^{Ns} h_i A_i \left(T_{si} - T_z\right) + \sum_{i=1}^{Nzones} m_i C_p \left(T_{zi} - T_z\right) + m_{\inf} C_p \left(T_\infty - T_z\right) + Q_{sys}$$

where Q is the internal gains by convection, $C_z(dT_z/dt)$ is the total energy stored in the air in each thermal zone, $h_i A_i \left(T_{si} - T_z\right)$ is the heat transfer by convection to the surface of the elements, $m_i C_p (T_{zi} - T_z)$ is the heat transfer due to outside air infiltration, $m_{\inf} C_p \left(T_\infty - T_z\right)$ is the heat transfer between different thermal zones and Q_{sys} is the heat transfer by the building outlet air.

The above differential equation is solved numerically in Energy-Plus using an explicit finite difference scheme, resulting in equation (1) for the energy balance.

$$T_z^t = \frac{\sum_{i=1}^{sl} Q_i^t + \sum_{i=1}^{Ns} h_i A_i T_{si}^t + \sum_{i=1}^{Nzones} m_i C_p T_{zi}^t + m_{\inf} C_p T_\infty^t + m_{sys} C_p T_{\sup}^t - \left(\frac{C_z}{\delta t}\right)\left(-3T_z^{t-\delta t} + \frac{3}{2}T_z^{t-2\delta t} - \frac{1}{3}T_z^{t-3\delta t}\right)}{\left(\frac{11}{6}\right)\frac{C_z}{\delta t} + \sum_{i=1}^{Nsurf} h_i A_i + \sum_{i=1}^{Nzones} m_i C_p + m_{\inf} C_p + m_{sys} C_p} \quad (1)$$

The inside superficial temperature is given by

$$\frac{\rho C_p \Delta x\left(T_{i,t} - T_{i,t-\delta t}\right)}{\delta t} = \frac{\lambda\left(T_{i-1,t} - T_{i,t}\right)}{\Delta x} + \frac{\lambda\left(T_{i+1,t} - T_{i,t}\right)}{\Delta x} \tag{2}$$

The aim of this study is to optimize the thickness of thermal insulation to be added in the retrofit process of the building envelope. The model seeks an optimal solution corresponding to the minimum use of the thickness of the different elements (concrete, glass and insulation) so that, without additional climatization, the indoor air temperature throughout the whole occupation period is between the recommended values of comfort: $T_{com} \le T_z^t \le 25^o C$, if $\sum_{i=1}^{sl} Q_i^t > 0$ with *t=1,..Nt*, and the occurrence of surface condensation is not allowed: $T_{si}^t \ge T_{dp}^t$ with *i=1,.., Ns* and *t=1,..Nt*. Thus the objective function takes the form: $\sum_{i=1}^{Np} A_i \left(x_i^{ins} + x_i^{con}\right) + \sum_{j=N_p+1}^{Ns} A_j x_j^{glas}$, where *Np* is the number of opaque walls, $x_i^{ins} ... x_i^{con}$ and x_i^{glas} are the thicknesses of insulation, concrete and glass.

Since each interface between materials (concrete, glass and insulation) is a node with a predictable heat flow, it is necessary to include equations for its calculation. These equations result from Eq. (2) with the necessary modifications to the conditions of the school built. In this model, some simplifications have been taken into account. One such simplification is related to the thickness of the elements. In this study, the thickness of concrete and glass surfaces are given, while for each opaque surface the optimized thickness of thermal insulation takes the same value.

The gains associated with solar radiation, an important factor of energy balance, were not included in the model. Thus, the energy balance obtained during the optimization process will only be adequate for colder days, usually associated with cloudy skyes and rain, in which solar gains are negligible. The last simplification is the consideration of the internal gains by convection as an average value throughout the year, i.e., the values of the gains due to occupancy and lighting are considered as an average value during periods with occupation. All these considerations lead into the following formulation of the model under study in this paper:

Minimize:
$$\sum_{i=1}^{Np} A_i \left(x_i^{ins} + x_i^{con}\right) + \sum_{j=N_p+1}^{Ns} A_j x_j^{glas} \tag{3}$$

subject to

$$T_z^t = \frac{\sum_{i=1}^{sl} Q_i^t + \sum_{k=1}^{Ns} h_k A_k T_{sk}^t + \dot{m}_{\inf} C_p T_\infty^t - \left(\frac{C_z}{\delta t}\right)\left(-3T_z^{t-\delta t} + \frac{3}{2}T_z^{t-2\delta t} - \frac{1}{3}T_z^{t-3\delta t}\right)}{\left(\frac{11}{6}\right)\frac{C_z}{\delta t} + \sum_{k=1}^{Ns} h_k A_k + \dot{m}_{\inf} C_p} \tag{4}$$

$$\rho^{con} C_p{}^{con}\left(x_i^{con}\right)^2 x_i^{ins}\left(T_{coni}^t - T_{coni}^{t-\delta t}\right) = \left[\lambda^{con} x_i^{ins}\left(T_\infty^t - T_{coni}^t\right) + \lambda^{ins} x_i^{con}\left(T_{si}^t - T_{coni}^t\right)\right]\delta t \tag{5}$$

$$\rho^{ins} C_p{}^{ins}\left(x_i^{ins}\right)^2\left(T_{si}^t - T_{si}^{t-\delta t}\right) = \left[\lambda^{ins}\left(T_{coni}^t - T_{si}^t\right) + h_i x_i^{ins}\left(T_z^t - T_{si}^t\right)\right]\delta t \tag{6}$$

$$\rho^{glas} C_p{}^{glas}\left(x_j^{glas}\right)^2\left(T_{sj}^t - T_{sj}^{t-\delta t}\right) = \left[\lambda^{glas}\left(T_\infty^t - T_{sj}^t\right) + h_j\left(T_z^t - T_{sj}^t\right)\right]\delta t \tag{7}$$

$$T_{si}^t \ge T_{dp}^t;\ \ T_{com} \le T_z^t \le 25^o C, \text{ if } \sum_{i=1}^{sl} Q_i^t > 0 \tag{8}$$

$$x_i^{ins} \ge 0, \quad x_i^{con} \ge 0, \quad x_j^{glas} \ge 0 \quad (\text{with } i=1, \ldots, Np \text{ and } j=Np+1, \ldots, Ns) \tag{9}$$

where N_t is the number of time intervals analyzed, Q_i^t is the internal gains at time *t*, *Np* is the number of opaque elements, N_j is the number of glass elements, N_s is the number of surface (*Ns=Np+Nj*), δt is the time interval considered, h_l is the transfer coefficient of the surface *l*, A_l is the area of surface *l*,

m_{inf} is the infiltrated air mass, T_{∞}^{t} is the outside air temperature at time t, $C/\delta t$ is the total amount of energy in the air during δt, $T_z^{t-\delta t}$ is the average air temperature inside the 1st instant before the instant t, $T_z^{t-2\delta t}$ is the average air temperature inside the 2nd instant before the instant t, $T_z^{t-3\delta t}$ is the average air temperature inside the 3rd instant before the instant t, ρ^k is the density of material k, c_{pm} is the specific heat capacity of material k, x_i^k is the thickness of material k (concrete or glass) of surface i, T_{dp} is the dew point temperature, T_{com} is the comfort temperature, λ^k is the thermal conductibility of material k, T_z^t is the indoor air temperature at time instant t, x_i^{ins} is the thickness of thermal insulation of opaque element i and T_{sk}^t is the indoor superficial temperature of surface k at time instant t.

The optimization problem described by the Eqs. (3-9) consists of minimizing a linear function on a set of linear and bilinear constraints. So the solver Minos of the commercial software Gams has been used to solve this problem (Broke *et al*. [1998]). In this case Gams/Minos employs a project Lagrangian algorithm, based on a method due to Robinson [1972] (Murtagh and Saunders [1987]). This involves a sequence of major iterations, each of which requires the solution of a linearly constrained subproblem. Each subproblem contains linearized versions of the nonlinear constraints, as well as the original linear constraints and bounds.

4. RESULTS AND DISCUSSION

The simulation of the building in the pre-retrofit scenario, using Energy Plus, provided a portrait of its hygrothermal behaviour. Figure 3 presents the indoor temperature variation in January. The existence of heat gains due to users and lighting as well as solar gains, provide a rather small difference between indoor and outdoor temperature. This is caused by the very high ventilation rate considered.

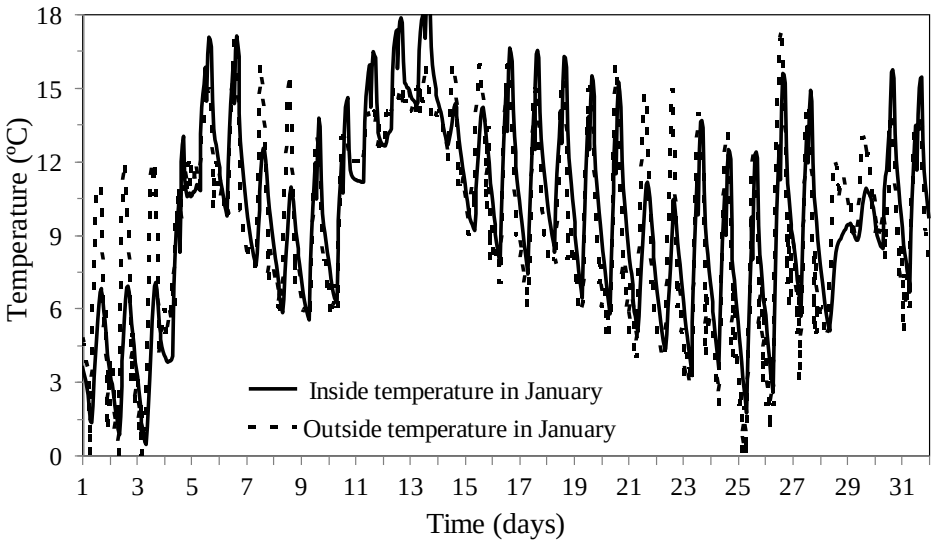

Figure 3. Temperature variation during January in the pre-retrofit scenario.

The application of the Optimization Programme (O.P.) to this specific case provided results at different levels. Not only the optimal insulation thickness was spotted but also the evolution of indoor temperature and inside surface temperature was defined by hourly values. As it was possible to have the same temperature values simulated in Energy Plus, using the spotted insulation thickness, the temperature variations obtained in both models could be compared.

One of the days targeted for analysis was January 4, since it was one of the coldest days with occupation.The Optimization Program was run using the two criteria separately. Applying the first

criterion, corresponding to the increasing of the inside temperature during winter, O.P. determined an insulation thickness of 4.5 cm. But with this insulation level the increase of indoor temperature for that day was less than 2ºC. For higher increments of temperature the problem is infeasible. Using the second criterion for optimization, corresponding to the elimination of surface condensation, the O.P. returned an insulation thickness of 2.4 cm.

The overall conclusion would be that relying only on indoor heat gains and passive behaviour, reaching hygrothermal comfort would be impossible. But the control of surface condensation, however, would be possible, using less than 3 cm insulation.

The results of the hourly values of temperature obtained in O.P. and Energy Plus were also compared, as presented in Figure 4. The modelling of January 4 using O.P. provided excellent results, when comparing with the more complete modelling using Energy Plus. The quality of the simulation using O.P. cannot of course be achieved for days where high solar radiation prevails. That was the case for January 13 and, as it is presented in Figure 5, the difference between O.P. and E.P. results is rather large. But winter days with high solar gains present a much lower risk of condensation.

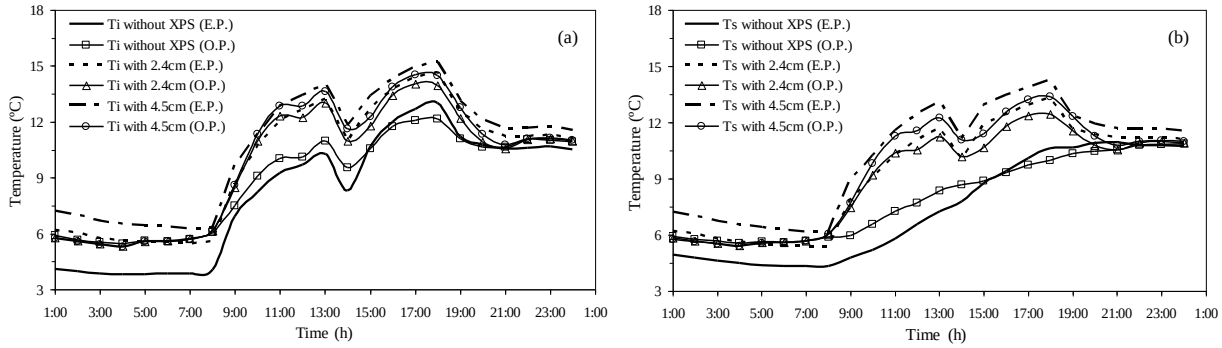

Figure 4. Evolution of the (a)-indoor temperature and (b)-superficial indoor temperature on north façade, obtained by the optimization program (O.P.) and Energy-Plus (E.P.) with different insulation thicknesses, on January 4.

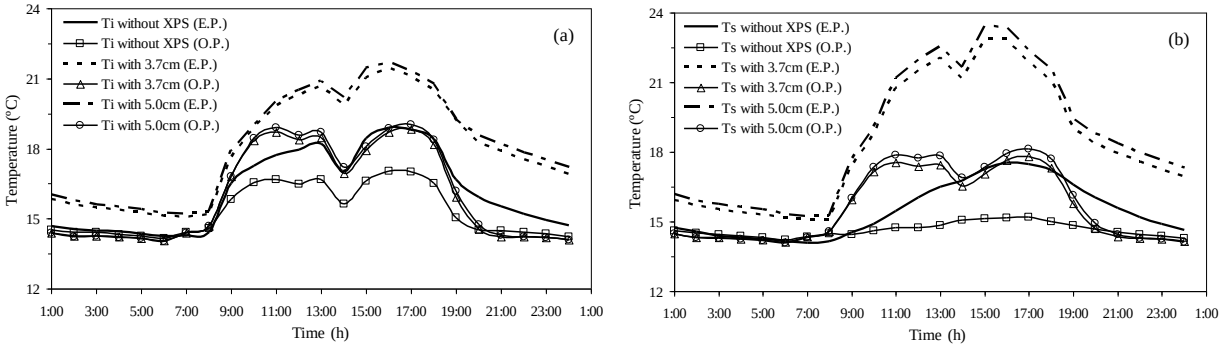

Figure 5. Evolution of the (a)-indoor temperature and (b)-superficial indoor temperature on north façade, obtained by the optimization program (O.P.) and Energy-Plus (E.P.) with different insulation thicknesses, on January 13.

To understand how far the results of O.P. could be interesting for the determination of the optimal insulation thickness regarding surface condensation control, the building was simulated in E.P. for several thickness values until condensation was eliminated. The results of that simulation are presented in Table 1. The results can be considered in agreement with the ones returned by O.P. if December 29 is disregarded. The comparison for that day is presented in Figure 6. The graph shows that certain days can lead to an exaggerated value of insulation thickness due to specific hygrothermal behaviour with low overall significance.

Table 1 – Results of Energy-Plus simulations with different thicknesses of thermal insulation.

Insulation thickness (cm)		**0**	**1**	**2**	**3**	**4**	**5**	**6**	**7**	**8**	**9**
T_{min}		0.4	1.6	2.3	2.9	3.3	3.7	4.0	4.2	4.4	4.6
T_{max}		30.7	33.1	34.6	35.5	36.3	36.8	37.3	37.6	37.9	38.1
Results for an annual simulation	$P_{5\%}$	7.5	8.8	9.7	10.2	10.6	10.9	11.2	11.4	11.6	11.7
	T_{ave}	15.8	17.5	18.5	19.2	19.7	20.1	20.4	20.6	20.8	21.0
	$P_{95\%}$	23.6	26.0	27.4	28.3	29.0	29.5	29.9	30.3	306	30.8
Nº of days with superficial condensations on the walls		33	12	4	2	1	1	1	1	1	0
Nº of days with superficial condensations on the ceiling		126	22	4	4	1	1	1	1	1	0

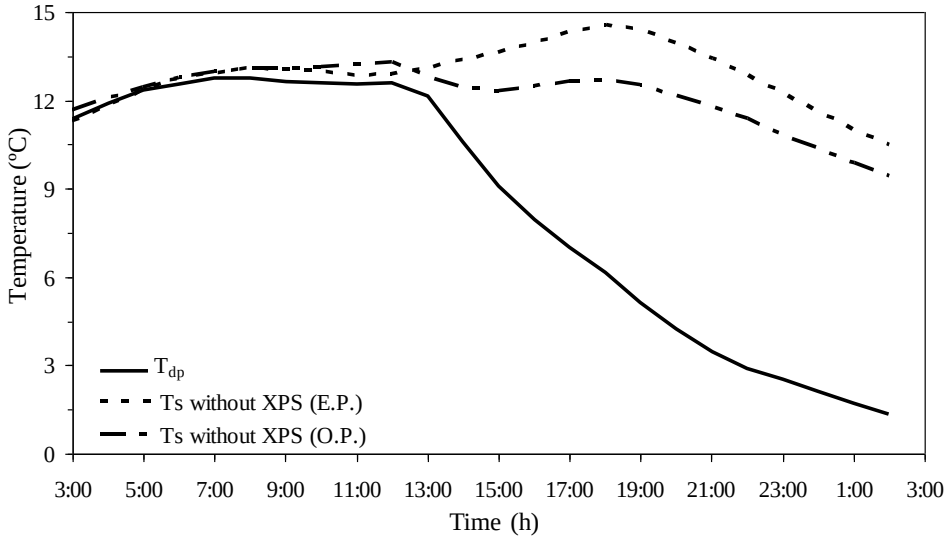

Figure 6. Evolution of the superficial indoor temperature on north façade, obtained by the optimization program (O.P.) and Energy-Plus (E.P.), on December 29.

5. CONCLUSIONS AND FUTURE DEVELOPMENTS

Thermal comfort, energy efficiency, indoor air quality and durability must be analysed in depth for sensitive buildings of which schools are an example. The scenario analysed in this example puts in evidence that a detailed analysis of the hourly hygrothermal behaviour can be very important. If a detailed analysis is available, the decision on using additional insulation will be based not only on energy efficiency vs. comfort but also on durability aspects that can depend, for instance, on avoiding defacement caused by mould due to surface condensation.

In this specific case, it was shown how 3 cm additional insulation would be sufficient to reduce the risk of severe mould growth.

The optimization problem, consisting of minimizing a linear function on a set of linear and bilinear constraints, using the solver Minos of the commercial software Gams proved to be an interesting aid for retrofit processes analysis. The limitations of the O.P. are linked to the fact that it doesn't yet include solar gains, but this component will be introduced in a next step.

A set of aspects must be added, however, so that a complete design methodology can be of use, providing a complete risk anakysis scheme. Especially the stochastic nature of the hygrothermal

processes must be included, leading to a non deterministic approach. The authors believe that the developed optimization program will be useful due to the linear functions adopted on simulation.

REFERENCES

Broke, A., Kendrick, D., Meeraus, A. & Raman, R., 1998, *GAMS a User's Guide*, GAMS Development Corporation, New York.

Crawley, D.B., Lawrie, L.K., Winkelmann, F.C. & Pedersen, C.O., 2000, 'Energy-Plus: Energy Simulation Program', *ASHRAE Journal*, **42**[4], 49-56.

SCE, 2006, *Sistema nacional de certificação energética e da qualidade do ar interior nos edifícios*, DL nº 78/2006, Diário da República, I Série-A, Abril, Lisboa. (in Portuguese)

Energy-Plus, 2009, *Engineering reference*, in EnergyPlus Documentation Main Menu.

Freitas, V.P., 2009, 'Educational building retrofitting', Proc. 3rd International Symposium on Building Pathology, Durability and Rehabilitation-PATORREB 2009, Porto, Portugal.

Grimsrud, D., Bridges, B. & Schlte, R., 2006, 'Continuous measurements of air quality parameters in schools', *Building Research and Information*, **34**[5], 447-458.

Holm, A. & Hellwig, R. & and Sedlbauer, K., 2008, 'Retrofitting of a school with an integral aspect', Proc. 8th Nordic symposium of Building Physics, Copenhagen, Denmark.

ISO 7730, 2005, *Ergonomics of the thermal environment analytical determination and interpretation of thermal comfort using calculation of the PMV and PPD indices and local thermal comfort criteria*, Switzerland.

Murtagh, B.A. & Saunders, M.A., 1987, '*MINOS 5.1 User's Guide'*, Report SOL 83-20R (Revised), Department of Operations Research, Stanford University.

PMEES, 2007, *Programa de Modernização das Escolas do Ensino Secundário*, Resolução do Conselho de Ministros nº1/2007, Lisboa, Portugal. (in Portuguese)

Robinson, S.M., 1972, 'A quadratically-convergent algorithm for general nonlinear programming problems', *Mathematical Programming*, **3**[1], 145-156.

RSECE, 2006, *Regulamento dos sistemas energéticos de climatização dos edifícios*, DL nº 79/200Diário da República, I Série-A, Abril, Lisboa. (in Portuguese)

XII DBMC
International Conference on Durability of Building Materials and Components
PORTO - PORTUGAL, April 12th-15th, 2011

Hygrothermal Simulation and Service Life Prediction of Selected AAC-based Building Envelopes

Václav Kočí[1]
Jiří Maděra[2]
Jaroslav Výborný[3]
Robert Černý[4]

ABSTRACT

Computational prediction of hygrothermal conditions in three types of innovated AAC-based building envelopes is presented. The mathematical model of heat and moisture transport is solved using the Galerkin finite element approach, and a computational implementation is performed. The computations are accomplished using the computer code HEMOT, which was developed at Department of Materials Engineering and Chemistry, Faculty of Civil Engineering, Czech Technical University in Prague. Climatic data corresponding to the test reference year for Prague are used as boundary conditions, so that cyclic wetting and drying occurs in the envelope. The results of computer simulations of moisture and temperature fields are then utilized in the subsequent service life analysis. On the basis of changes of moisture and temperature, particularly the number of wetting-drying cycles and frost cycles the durability of the AAC envelopes is assessed.

KEYWORDS

Computational analysis, Hygrothermal performance, Service life, AAC-based building envelopes.

[1] Department of Materials Engineering and Chemistry, Faculty of Civil Engineering, Czech Technical University in Prague, Prague, CZECH REPUBLIC, vaclav.koci.1@fsv.cvut.cz
[2] Department of Materials Engineering and Chemistry, Faculty of Civil Engineering, Czech Technical University in Prague, Prague, CZECH REPUBLIC, madera@fsv.cvut.cz
[3] Department of Materials Engineering and Chemistry, Faculty of Civil Engineering, Czech Technical University in Prague, Prague, CZECH REPUBLIC, vyborny@fsv.cvut.cz
[4] Department of Materials Engineering and Chemistry, Faculty of Civil Engineering, Czech Technical University in Prague, Prague, CZECH REPUBLIC, cernyr@fsv.cvut.cz

1 INTRODUCTION

Autoclaved aerated concrete (AAC) is a structural material which is commonly used around Europe, particularly as it combines ease of construction with excellent combination of its mechanical and thermal properties. However, the empirical principles employed in construction design until now have led in many countries to a series of failures which began to have serious consequences for the practical applications of the material. In the current durability assessment of AAC-based building envelope systems a complex view is often missing. Precise and serious analyses of hygro-thermal performance of the new AAC technologies based on sound scientific knowledge are not performed very frequently. However, AAC-based building envelopes should be designed as a system consisting of AAC, internal and external finishes and possibly also thermal insulation layer, and in this design process, the details have to be solved using suitable methods.

2 COMPUTATIONAL ANALYSIS

2.1 Computer Code and Mathematical Models

The computational analysis was accomplished by computer code HEMOT, which was developed at the Department of Material Engineering and Chemistry, Faculty of Civil Engineering, Czech Technical University in Prague on the basis of the general finite element package SIFEL [Černý 2010]. As basic input parameters of the mathematical model, material parameters of used materials, construction detail, initial and boundary conditions and time specification of simulation were required. Description of all input parameters in more detail is given later.

In the computer simulations we focused on a comparison of hygrothermal behavior of several building envelopes based on AAC. Particularly it was building envelope provided with different external thermal insulation and building envelope with external and internal finishes only.

Künzel's mathematical model of heat and moisture transport [Künzel 1995] was used in the simulations which can be formulated as

$$\frac{d\rho_v}{d\varphi}\frac{\partial\varphi}{\partial t} = div\left[D_\varphi grad\varphi + \delta_p grad\left(\varphi p_s\right)\right] \tag{1}$$

$$\frac{dH}{dT}\frac{\partial T}{\partial t} = div\left(\lambda gradT\right) + L_v div\left[\delta_p grad\left(\varphi p_s\right)\right] \tag{2}$$

where ρ_v is the partial density of moisture, φ relative humidity, δ_p permeability of water vapour, p_s partial pressure of saturated water vapour, H enthalpy density, L_v heat of evaporation, λ thermal conductivity and T temperature,

$$D_\varphi = D_w \frac{d\rho_v}{d\varphi} \tag{3}$$

is liquid moisture diffusivity coefficient, D_w capillary transport coefficient.

2.2 Scheme of Construction Detail

Three variations of building envelope based on AAC were chosen for simulation, in order to analyze the consequences of different material combinations. As a start-up building envelope we chose AAC only with Baumit MVR Uni plaster, which is universal plaster recommended for AAC structures. This

material combination is marked as Var. 1. In the next simulation we provided the AAC block with expanded polysterene with lime-cement external finish, which is marked as Var. 2. In the further step we assumed hydrophobic mineral wool provided with lime-cement plaster as well. This combination is marked as Var. 3. On the material interface between thermal insulation and AAC an adhesive mortar layer was placed. Description of used materials in more detail is given in next subsection. Scheme of construction detail including the dimensions of each layer is shown in Figure 1. In all investigated variations we focused on the hygrothermal conditions at a point within the AAC layer just 2 mm under its external surface which can be considered as characteristic position from the point of view of possible frost damage. At the same time, hygrothermal conditions of exterior plaster 2 mm under external surface were assessed as well.

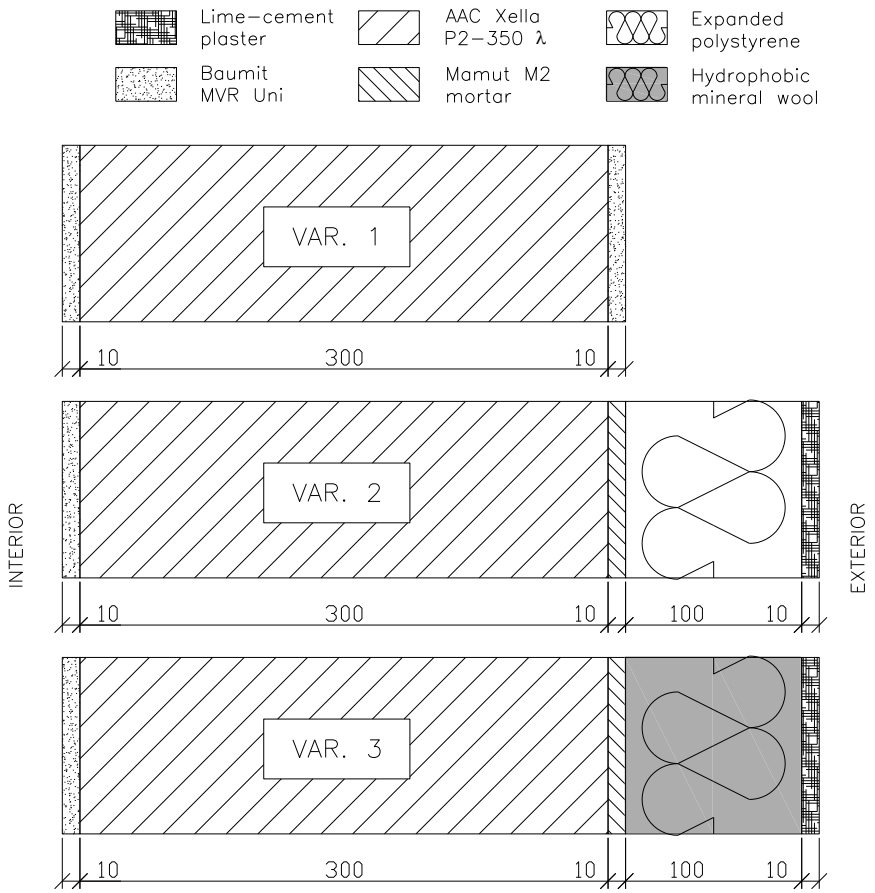

Figure 1. Scheme of analyzed construction details.

2.3 Material Parameters

Autoclaved aerated concrete P2-350 λ produced by Xella Czech Republic, Ltd. was under consideration in this paper [Výborný 2009a]. As material for exterior and interior renders we used Baumit MVR Uni Plaster, which is single-layer plaster for exterior and interior surfaces especially recommended for AAC [Jerman *et. al.* 2010]. And further we used common lime cement plaster [Maděra *et. al.* 2009]. As the thermal insulation we assumed hydrophobic mineral wool [Jiřičková and Černý 2006] and expanded polystyrene [Grunewald 2000]. For adhesive layer between AAC and thermal insulation material we used Mamut M2 mortar.

All the material parameters were measured in laboratory of transport processes at the Department of Materials Engineering and Chemistry, Faculty of Civil Engineering, Czech Technical University in Prague and are summarized in Table 1. Data for Mamut M2 mortar were measured by M. Jerman and

have not been published yet. We used these symbols: ρ – bulk density [kg m^{-3}], ψ – porosity [%], c – specific heat capacity [J kg^{-1} K^{-1}], μ – water vapour diffusion resistance factor [-], w – moisture content by volume [m^3 m^{-3}], λ – thermal conductivity [W m^{-1}K^{-1}], κ_{av} – average moisture diffusivity [m^2 s^{-1}].

Table 1. Basic material characteristics.

	AAC Xella P2-350 λ	*Mamut M2 mortar*	*Hydrophobic mineral wool*	*Expanded polystyrene*	*Baumit MVR Uni plaster*	*Lime-cement plaster*
ρ [kg m^{-3}]	367	1430	270	50	1402	1550
ψ [%]	81.6	42.6	88.0	97.0	44.4	40.0
c [J kg^{-1} K^{-1}]	1160 - 1450	1020	630	1300	1020 - 1780	1200
μ [-]	3.3 – 12	12.4	2.1 – 3.7	50.0	4.5 – 12.4	7.0
λ_{dry} [W m^{-1} K^{-1}]	0.083	0.481	0.045	0.040	0.443	0.700
λ_{sat} [W m^{-1} K^{-1}]	0.746	2.022	0.246	0.560	1.380	2.400
κ_{av} [m^2 s^{-1}]	2.48e-9	1.07e-9	2.51e-10	2.10e-11	1.59e-9	7.30e-7
w_{hyg} [m^3 m^{-3}]	0.021	0.201	0.007	0.001	0.042	0.040

2.4 Initial and Boundary Conditions

Initial and boundary conditions should be as realistic as possible. This was the reason why we used climatic data in the exterior in the form of Test Reference Year for Prague which contained average data for 30 years. On the interior side we used constant value of relative humidity 55% and temperature 21°C (see Fig. 2). The simulation started on 15th July and took 4 years. The final results show data during the last year.

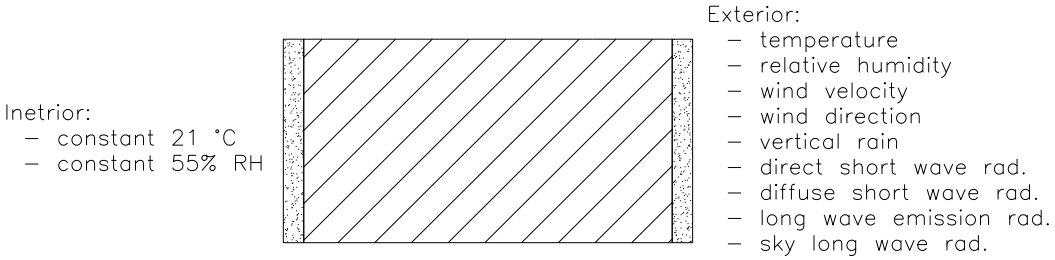

Figure 2. Boundary conditions.

3 COMPUTATIONAL RESULTS

The results of computational simulations are summarized in a set of figures which describe hygric and thermal performance of studied material of building envelope during a reference year. In all figures we focused on moments when moisture content and temperature reached certain limits simultaneously. In case of moisture content this limit was the value of hygroscopic moisture content (see Tab. 1), in case of temperature the freezing point of water. When these two conditions are fulfilled, contained liquid moisture is getting frozen. This leads to consequent damage of material.

The materials capability to resist to freezing of contained water is characterized by its freeze-thaw resistance which can be measured under laboratory conditions [ČSN 2007]. This was accomplished for AAC and its freeze-thaw resistance was set to 25 cycles [Výborný 2009b]. Durability of AAC can

be then calculated as quotient of freeze-thaw resistance and number of freezing cycles appearing in the material in building envelope during a year.

3.1 AAC Building Envelope Provided with External and Internal Finishes

Hygric and thermal performance of AAC building envelope provided only with external and internal finishes are shown in Figs. 3 and 4, where 0 on the distance axis means the interior side.

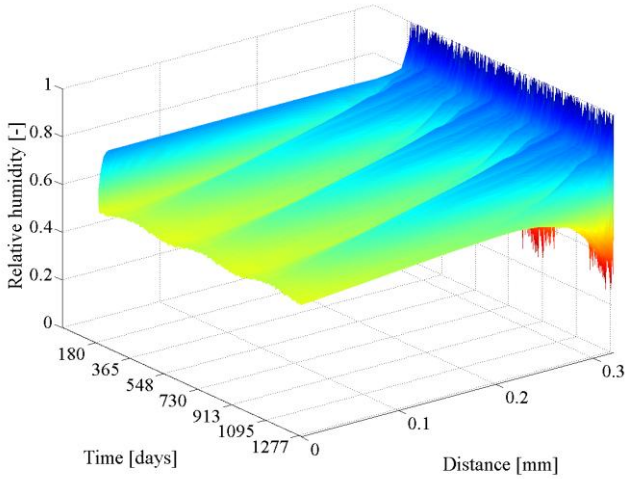

Figure 3. Moisture field across AAC building envelope – Var. 1.

As it is obvious, moisture content in external finish is very variable in contrast to internal plaster, where the moisture content is almost stable. This can be applied on whole envelope, that means the closer to the exterior the more variable the moisture content is.

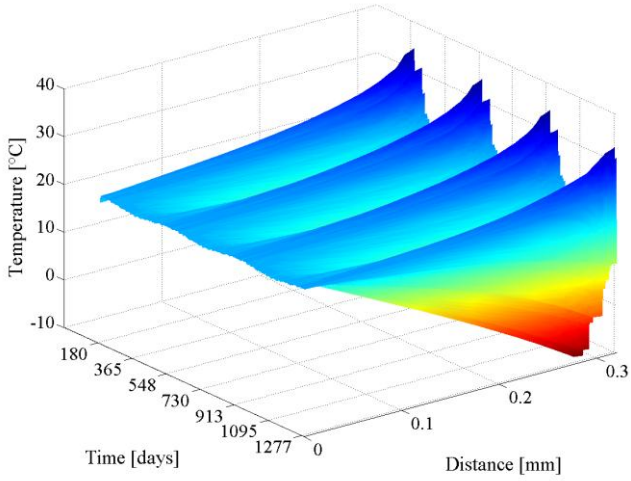

Figure 4. Temperature field across AAC building envelope – Var. 1.

The same conclusions can be drawn also for the temperature field. Temperature on the interior side is almost stable, while on the exterior side the differences are very apparent.

In Figs. 5 and 6, the evaluation of hygrothermal performance of AAC and external plaster is shown.

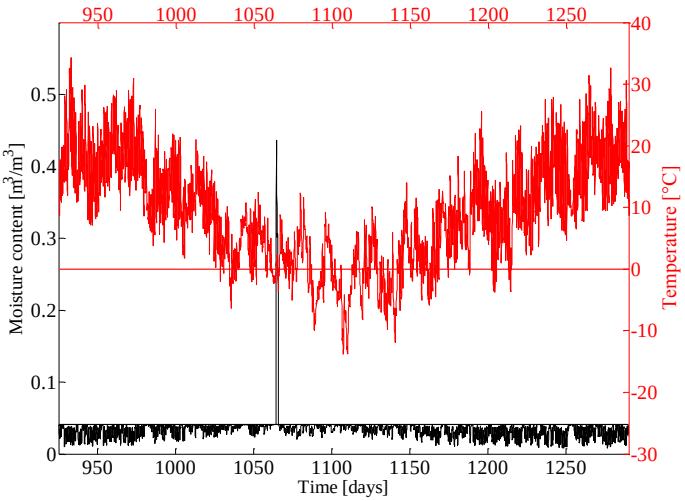

Figure 5. Hygrothermal performance of Baumit plaster – Var. 1.

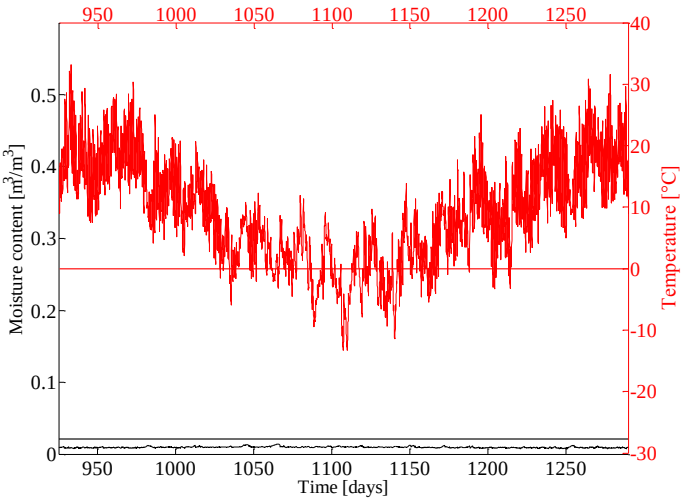

Figure 6. Hygrothermal performance of AAC – Var. 1.

As we can see, the durability of AAC building envelope depends on the protection capabilities of applied plaster, because its main objective is to protect AAC against high moisture income. According to Fig. 6, this was reliably fulfilled. But on the other hand, the moisture content in the plaster is higher and very close to overhygroscopic range, which can be crossed many times during the reference year (see Fig. 5).

3.2 AAC Building Envelope Provided with External Insulation and with External and Internal Finishes

As external insulation, hydrophobic mineral wool and EPS were assumed. The results of distribution of moisture and temperature field differ only very little, so it will be further presented together.

External lime-cement plaster applied on thermal insulation is exposed to substantial straining due to climatic conditions, as it is evident from Fig. 7, while hygrothermal performance of AAC is satisfactory (Fig. 8).

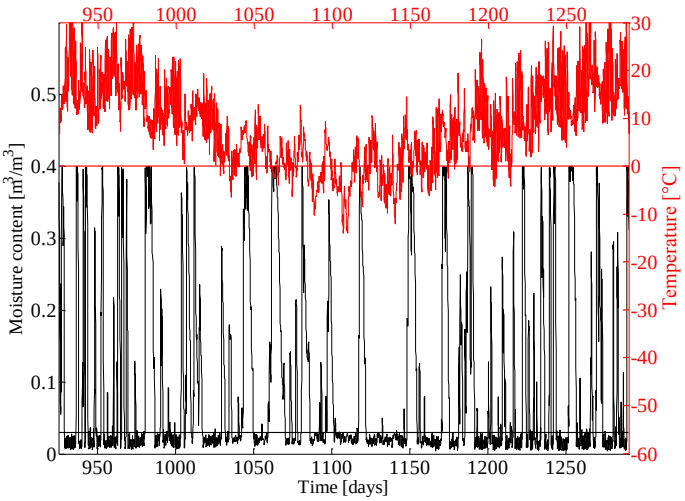

Figure 7. Hygrothermal performance of lime-cement plaster – Var. 2.

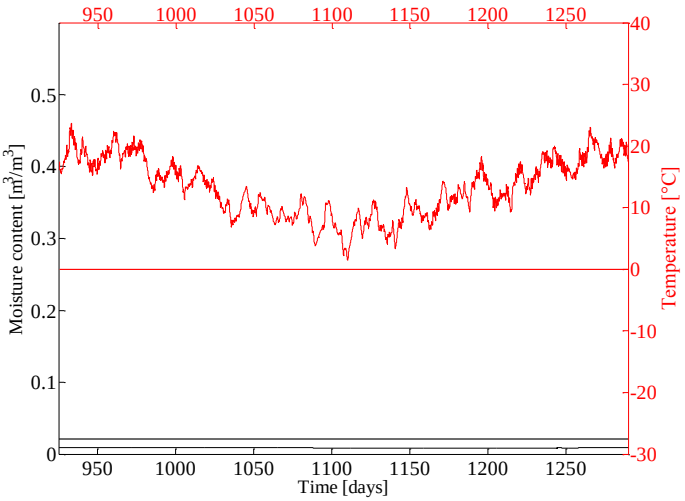

Figure 8. Hygrothermal performance of AAC – Var. 3.

4. DISCUSSION

Comparing the Figs. 5-8, it can be declared, the service life of AAC block from point of view of frost resistance is higly dependent on the material combination, namely on the surface layers applied on it.

There are two ways how to prevent freezing of water contained in AAC block. We can keep the moisture content of AAC under hygroscopic range using suitable external finish (Fig. 6) or we can keep the temperature inside the AAC block above zero (Fig. 8). Anyway, meeting the second condition brings along with meeting the first condition at the same time so this could be perceived as the best solution. However, we must focus then on service life of external finish applied on the thermal insulation, which is exposed to abnormal environmental load (Fig. 7).

The investigated building envelopes give following results. In case of Var. 1, there are not any freezing cycles appearing in AAC, however in Baumit MVR Uni plaster, we counted one freezing cycle per a reference year. Variations 2 and 3 did not bring any freezing cycles inside AAC block, but in the plaster applied on expanded polystyrene, there were 28 freezing cycles counted and inside the plaster applied on mineral wool 33 freezing cycles.

According to the results, durability of AAC was not be the limiting factor for service life of studied building envelopes, because there was not any single freezing cycle counted inside it in any variation. So first failures during building envelopes' service life will appear in plasters.

Baumit MVR Uni plaster is classified as lime-cement plaster, which freeze thaw resistance was set to more than 103 cycles [Maděra *et. al.* 2009]. Durability of this plaster is then limited by its freeze-thaw resistance to more than 100 years (Var. 1). In the case of variations 2 and 3, the durability of plasters can be estimated to 3-5 years.

5. CONCLUSIONS

The computational simulations of temperature and moisture fields in building envelopes based on AAC showed that using the plaster developed specifically for AAC constructions or, in general, plaster with low value of moisture diffusivity is a viable solution for contemporary buildings, from the points of view of both hygrothermal performance and service life. However, with respect to the expected increasing requirements on energy savings, application of thermal insulation will be in most cases unavoidable, in the near future. In this case it is necessary to consider the reduced service life of external finish, when first signs of damage can appear after 3-5 years if mineral wool or expanded polystyrene are used as thermal insulation.

ACKNOWLEDGEMENTS

This research has been supported by the Czech Science Foundation, under grant No. 103/09/0016.

REFERENCES

Černý, R. (ed.) 2010, *Complex System of Methods for Directed Design and Assessment of Functional Properties of Building Materials: Assessment and Synthesis of Analytical Data and Construction of the System*, Prague: CTU. pp. 192-201.

ČSN EN 15304. 2007, Determination of the freeze – thaw resistance of autoclaved aerated concrete. Prague: Czech Standards Institute.

Grunewald, J. 2000, DELPHIN 4.1 – Documentation, Theoretical Fundamentals, TU Dresden, Dresden.

Jerman, M., Kočí, V., Maděra, J., Výborný, J., Černý, R. 2010, Water and Heat Transport Parameters of Materials Involved in AAC-based building envelopes. In: *Proceedings of the 1st Central European Symposium on Building Physics 2010*. Lodz: Technical University of Lodz, pp. 39-46.

Jiřičková, M., Černý, R. 2006, Effects of Hydrophilic Admixtures on Moisture and Heat Transport and Storage Parameters of Mineral Wool. *Construction and Building Materials* 20, pp. 425-434.

Künzel, H. M. 1995, Simultaneous Heat and Moisture Transport in Building Components, Ph. D. Thesis. IRB Verlag, Stuttgart.

Maděra, J., Kočí, V., Vejmelková, E., Černý, R., Rovnaníková, P. et al. 2009, Influence of material characteristics of concrete and thermal insulation on the service life of exterior renders. *In: Fourteenth International Conference on Computational Methods and Experimental Measurements*, Algarve, Portugal. Southampton: WIT PRESS, p. 13-23.

Výborný, J. 2009a, Stanovení tepelných parametrů a smrštění při vysychání vybraných pórobetonových tvárnic firmy H+H Česká republika s.r.o. a Xella CZ. *In: Proceedings of the International Conference 15th Construmat 2009*. Praha: České vysoké učení technické v Praze, pp. 449-461.

Výborný, J. 2009b, Testing of the Drying Shrinkage and Freeze - thaw Resistance of Autoclaved Aerated Concrete. *In: XII International scientific conference Technická zařízení staveb a energie budov.* Brno: Akademické nakladatelství CERM, pp. 215-218.

XII DBMC
International Conference on Durability of Building Materials and Components
PORTO - PORTUGAL, April 12th-15th, 2011

Thermal Performance Degradation of Foam Insulation in Inverted Roofs Due to Moisture Accumulation

Daniel Zirkelbach [1]
Beate Schafaczek [2]
Hartwig Künzel [3]

ABSTRACT

A normal roofing membrane is exposed to various mechanical and climatic impacts which can reduce durability and the service life of the membrane. In so called inverted roofs the membrane is situated beneath the insulation layer - which is ballasted with gravel or vegetated substrate. Thus, the sealing is protected versus the above mentioned damaging influences. Drawback of this solution is the direct exposure of the insulation to the outdoor climate. Therefore only materials with a high vapour diffusion resistance shall be used to minimize the entry of water into the insulation. However, the long term experience shows that also XPS boards experience some moisture accumulation especially in case where the cover layer remains humid most of the time. This slows down the drying process towards the top compared to gravel ballasted roofs. Based on long term field tests of green roofs this paper provides new approaches to simulate the hygrothermal conditions in inverted roofs. The model includes the simulation of the moisture behaviour of the substrate and an estimation of the amount of rainwater remaining at the interface between the sealing membrane and the insulation boards. Applying this model allows to asses the moisture accumulation in the insulation and the subsequent increase in the material's thermal conductivity over the life time of the roof. Considering the long-term moisture behaviour helps to specify the thickness of the insulation layer required to maintain the aspired level of thermal resistance over the whole service life of the roof.

KEYWORDS

Inverted roof, Foam insulation, XPS boards, Vegetated roof, Moisture accumulation.

[1] Fraunhofer Institute for Building Physics, GERMANY, daniel.zirkelbach@ibp.fraunhofer.de

[2] Fraunhofer Institute for Building Physics, GERMANY, beate.schafaczek@ibp.fraunhofer.de

[3] Fraunhofer Institute for Building Physics, GERMANY, hartwig.kuenzel@ibp.fraunhofer.de

1 INTRODUCTION

Flat roofs may accumulate precipitation moisture due to leakages in the sealing layer which impairs their thermal performance. As the sealing layer – normally a roofing membrane – is exposed directly to the outdoor conditions degradation due to ageing or mechanical damage caused by the operation hold significant risks for defects and leakages. Changing the sequence of the construction layers by placing the insulation above the sealing membrane is one approach to improve the situation. In the so called inverted roof the membrane is well protected against both climate loads and mechanical impacts.

In Germany protected membrane (inverted) roofs have a long track record showing excellent durability of the sealing layer. However, the protection of the roofing membrane comes at the expense of higher loads for the insulation layer. Therefore water repellent and diffusion retarding insulation materials should be chosen. Predominantly extruded polystyrene boards (XPS) with high compression strength and a diffusion resistance factor of more than 100 are used. Initially it was assumed that the high vapour diffusion resistance would prevent moisture absorption or accumulation in the insulation boards. However, field tests and inspections of existing roofs showed a certain and sometimes continuous moisture accumulation of the boards especially in case of cover layers involving vegetation or pavers. The precipitation water which penetrates the insulation at the board joints results in a water film at the interface between the insulation and the roofing membrane which can hardly dry out in regions with higher precipitation loads. The water film on the warm side of the insulation leads to high water vapour pressure causing a diffusion flux into the boards and condensation during winter time.

If fast drying gravel serves as cover layer, the moisture in the insulation dries through the top side of the boards during dry summer periods - this compensates the moisture entry from the bottom side. In case of more water retaining cover layers like growth media for vegetated roofs or sand and split beneath concrete pavers, towards the top becomes impossible and moisture accumulation can occur. The moisture level in the insulation boards affects also the thermal conductivity, which has to be considered for the definition of the thermal resistance of the roof. Since the insulation layer of inverted roof lies beyond the water and vapour control layer of the construction its thermal resistance cannot be considered for energy performance calculations in Germany unless a technical approval for the roof system has been issued. In order to obtain such an approval it is necessary to check and prove the moisture content in the boards by long term field and in-situ tests. The paper shows that the long term water content in the boards can also be determined by the help of hygrothermal simulations depending on outdoor climate, building operation and the specific material properties of the insulation boards. Important factors for the reliability of the calculation results are the realistic modelling of the cover layers and their moisture behaviour as well as of the water film beneath the insulation board.

2 FIELD TESTS – MEAUSREMENT AND SIMULATION

2.1 Vegetated Roofs at the Field Test Site of the IBP in Holzkirchen

The reported investigations were carried out at the field test site of the Fraunhofer IBP in Holzkirchen, which is located on a plateau close to the Bavarian Alps in the south of Germany at 680 m above sea level. On the concrete slab sized of 12 by 12 m of a flat roof above a heated laboratory inverted roof structures with different composition have been installed. [IBP-Report 1993]. The individual test fields had a size of 3x3 m² - allowing parallel investigation of 8 different roof systems. The first tests started in 1985 - the last ones were finished in 2004. Table 1 shows the different insulation thicknesses and cover layers above the sealed concrete ceiling for three of the eight roof systems. The longest investigation period lasted approx. 20 years.

Table 1. Test roof assemblies on the top of the 120 mm concrete slab with vapor diffusion tight roofing membrane.

Roof (meas. period)	*Assembly*
Roof 1 (1985 – 2004)	80 mm growth medium 50 mm drainage layer (gravel, expanded clay) Filter fleece 100 mm XPS insulation Type A
Roof 2 (1985 – 2004)	80 mm growth medium 50 mm drainage layer (gravel, expanded clay) Filter fleece 100 mm XPS insulation Type B
Roof 3 (1985 – 2004)	80 mm growth medium Filter fleece Drainage and water retention boards (EPS) 80 mm XPS insulation

The focus of the investigations was the hygrothermal behaviour of the insulation layer, i.e the water content in the insulation boards and its influence on the thermal conductivity of the material. Therefore samples of the boards were regularly (in the main test period once or twice a year) taken from the roof and the water content of the boards was measured in the laboratory. To determine the hygrothermal conditions beneath the vegetated substrate – which is necessary to model the conditions in the cover layer later on - the temperature and humidity directly on top of the insulation was measured. For this purpose temperature (PT100) and dew point sensors (intermittently heated LiCl sensors) have been installed in the middle of the test fields as illustrated in Fig. 1 [IBP-Report 1996].

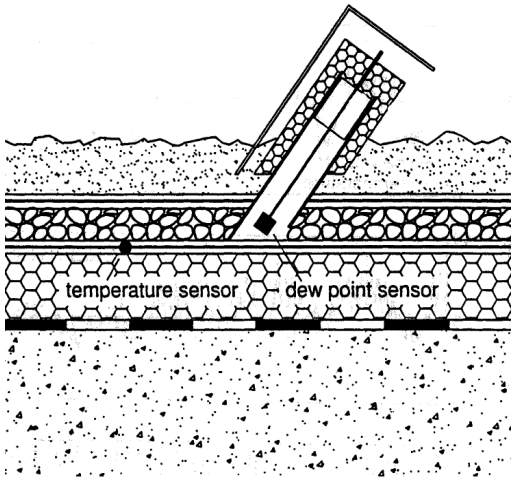

Figure 1. Schematic figure showing the positions of the temperature and dew point sensors in the drainage layer of the green roof.

The main test period lasted from autumn 1985 to summer 1992. Before disassembling the roofs in 2004 detailed moisture probing by weighing of the insulation boards was performed. The measured

water contents are listed in Table 2 as average of normally two individual probings per year. The moisture content in all different test roofs showed a more or less continuous increase over the years. Depending on the different cover layers and material properties of the XPS boards the water content in the insulation boards varied between 4.8 and 8.7 Vol.-% (48 to 87 kg/m³) after 19 years. The increase in water content is a function of the vapour diffusion resistance of the insulation material and the humidity conditions beneath and above the boards. In roof 2 the XPS Type B with lower vapour diffusion resistance reached a higher moisture content (8.7 Vol.-%) after 19 years than XPS Type A in roof 1 (4.8 Vol-%). In roof 3 with EPS drainage boards the water content at the end of the test period reached 7.0 Vol.-%.

Table 2. Measured moisture content during the test period [Vol.-%].

Roof	*1986*	*1987*	*1988*	*1989*	*1990*	*1992*	*1996*	*2004*
Roof 1	0.29	0.59	0.85	1.26	1.83	2.22	-	4.79
Roof 2	-	1.28	1.86	1.74	2.19	2.62	5.18	8.70
Roof 3	0.60	0.84	1.20	1.13	1.68	2.16	-	7.01

As consequence of the rising moisture content, the thermal conductivity of the insulation material increases by approximately 2.8 % per Vol.-% (water content) according to [Zehendner 1979]. That means that at the end of the test period the heat conductivity of the XPS boards reaches between 113% and 125% of the dry state. This increase in conductivity should therefore be considered at the design stage to allow correct U-value assumption and evaluation of the long term heat losses through such roof assemblies.

2.2 Hygrothermal Modelling of Inverted Roofs Including the Cover Layers

By the help of modern hygrothermal simulation tools it is possible to simulate the performance of inverted roofs. While past calculations used constant humidity conditions above the insulation boards [Künzel & Kießl 1997], the following simulations include a new approach to model the hygrothermal performance of the cover layers (gravel or vegetated substrate) and the water films beneath the insulation boards. The new cover layer model includes all relevant effects such as moisture storage, latent heat of fusion and evaporation and in case of vegetation the reduced solar radiation absorption by partial shading provided by the plant cover. The following calculations are performed with the hygrothermal simulation tool WUFI® (Wärme und Feuchte instationär – transient heat and moisture) which has been developed at Fraunhofer IBP for the past 15 years and validated by numerous laboratory and field tests [Künzel 1995].

Table 3. Optimized material properties for a gravel cover layer.

Material property	*Value*
Bulk density	1400 [kg/m³]
Heat capacity	1000 [J/kgK]
Heat conductivity (dry)	0.7 [W/mK]
Vapor diffusion resistance factor	1 [-]
Free water saturation w_f	50 [kg/m³]

The hygrothermal material properties of a gravel layer are not so complex and could be adapted by previously done comparisons with field tests (not presented in this paper). Table 3 shows the optimized material properties of the gravel. In the gravel layer there is no capillary transport only drainage – therefore the rainwater is not absorbed at the surface but introduced over the thickness of the whole layer modeled by rain dependent moisture sources.

Table 4. Optimized material properties for a green roof growth medium.

Material property	*Value*
Bulk density	1500 [kg/m³]
Heat capacity	1500 [J/kgK]
Heat conductivity (dry)	0.9 [W/mK]
Vapour diffusion resistance factor	5 [-]
Liquid transport coefficients	
DW0, DWS, DWW	1E-10, 1E-6, 1E-7 [m²/s]
Free water saturation w_f	300 [kg/m³]

The material properties for the growth medium of an extensive green roof are listed in Table 4. The vegetated substrate will absorb rain water by capillary action. However, because the precipitation water cannot be absorbed fast enough in case of intense rainfalls, part of the rain water would be shed by the model originally designed to simulate the effect of driving rain; i.e. it would be assumed that it drains off the roof's surface the same way as driving rain drains of an exposed wall. To avoid this effect which hardly occurs in practice (the water will normally run off through the growth medium and not above it) a moisture source is introduced once again which deposits 40 % of the precipitation water directly into the bottom section of the growth medium. The above mentioned moisture film beneath the insulation boards is also accounted for by a moisture source in a 1 mm fleece layer which deposits 1 % of the precipitation water (limited to the free saturation of this layer).

Applying this model to a vegetated substrate layer under the climate of Holzkirchen with its high precipitation load, results in humidity conditions beneath the insulation which remain above 99 % RH all the year round. Due to the manufacturing process (extrusion of the polymer-gas mixture) the XPS boards have on both surfaces dense skins with significantly increased vapour diffusion resistance. In the laboratory a 10 mm thick surface layer of the boards was cut off (thinner layers are difficult to cut) to determine the different diffusion resistances of the core material and the skin. In reality the extrusion skin is much thinner but with the assumption of a 1 mm thick extrusion skin with a very high and a core with constant lower resistance a good agreement between the measured and simulated data could be achieved.

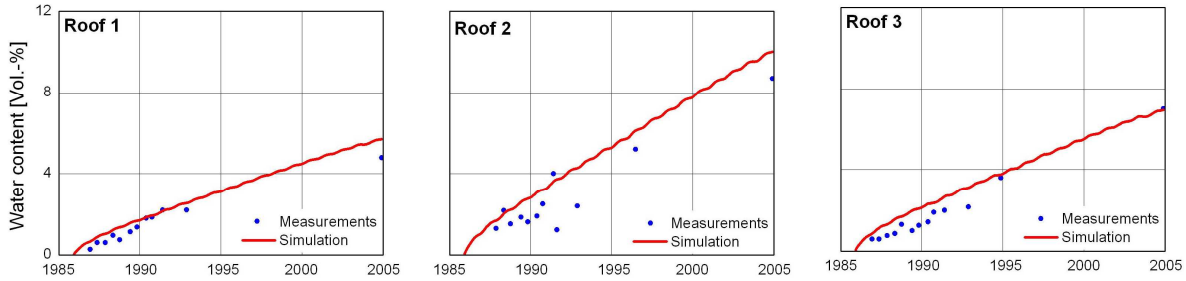

Figure 2 **Figure 3** **Figure 4**

Measured and simulated water contents in the three test roofs at the IBP in Holzkirchen over the test period of approximately 20 years.

Figures 2 to 4 compare the measured and simulated water content in the XPS boards of the three different vegetated roofs at the field test site in Holzkirchen. The overall agreement is quite satisfying and the simulation as well as the field tests show a slow but continuous increase of the moisture content in the boards. The comparison of the model with further field investigation of inverted roofs at different locations in Germany, Switzerland and Austria confirmed the reliability of the approach

and its transferability to locations with different precipitation loads. The mentioned investigations cannot be disclosed yet and will be published at a later stage.

3 LONG TERM BEHAVIOUR OF INVERTED ROOFS

The optimization of the simulation approaches showed the following main influencing factors for the moisture content in the XPS boards: the type of the cover layer, the diffusion resistance of the insulation material (skin and core), the outdoor climate and the temperature level below the roof. Therefore simulations with different outdoor climate, indoor temperature levels and cover layers are performed. As roof construction serves the same assembly as in the field tests in Holzkirchen with 120 mm concrete slab, a vapour diffusion tight roofing membrane and 100 mm XPS insulation boards beneath the cover layers. As outdoor climate, weather files of the locations Espoo (close to Helsinki in Finland), Lisboa (Portugal) and Holzkirchen (Germany) are chosen to represent cold, moderate and warm European climate regions. For the three locations indoor climate conditions for residential buildings according to EN 15026 are derived from the local outdoor conditions. In Holzkirchen additionally a variation of the indoor temperature level (18 °C, 22 °C and 26 °C (e.g. swimming pool) constant over the whole year) is performed to check the temperature influence on the water content in the boards.

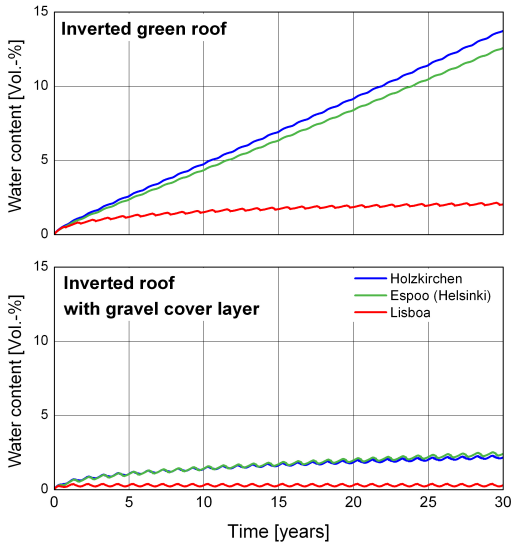

Figures 5 (top) and 6 (bottom). Simulated water content of the insulation boards in inverted roofs with vegetation (green roof Fig. 5) and gravel cover layer (Fig. 6) at Holzkirchen (Germany), Espoo (Helsinki, Finland) and Lisboa (Portugal) over a period of 30 years.

Figure 5 shows the water content in the insulation boards of an inverted green roof at the three different locations. While the water content only increases moderately in Lisboa to about 2 Vol.-% after 30 years, the increase is much higher in colder regions with 12 Vol.-% in Holzkirchen and 13 Vol.-% in Espoo. In Holzkirchen and Espoo the diffusion flux from the water film beneath the insulation layer penetrates the boards from the bottom side and can hardly dry out to the top into the permanently humid growth medium. In Lisboa the temperature gradient over the insulation layer is smaller due to the milder winter conditions and the growth medium can temporarily dry out during the hot and dry summer period. Both effects together lead to a significantly slower moisture uptake of the boards compared to the locations Holzkirchen and Espoo. The water content in the boards beneath the gravel roof (Fig. 8) are with less than 1 Vol.-% in Lisoba and around 2.5 Vol.-% in Holzkirchen and Espoo. The gravel cover layer having only little water retention can also dry out in Espoo and

Holzkirchen during periods with minor precipitation and thus allows also some dry out of the moisture in the insulation boards.

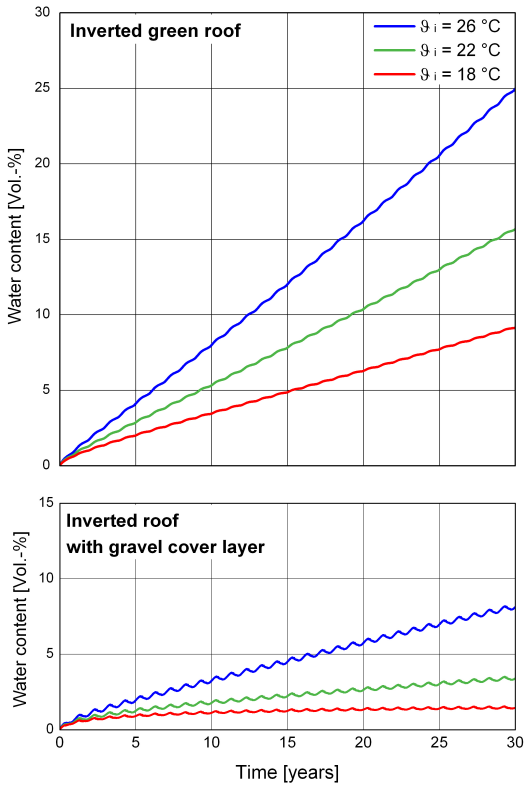

Figures 7 (top) and 8 (bottom). Simulated water content of the insulation boards in an inverted roof with vegetation (Fig. 7) and gravel cover layer (Fig. 8) at Holzkirchen with different indoor temperature levels of constant 18, 22 and 26 °C.

The temperature level below the concrete slab is mainly responsible for the vapour pressure in the water film beneath the insulation boards and thus for the diffusion flux into the XPS material. Figure 7 shows the water content in the insulation boards of green roofs in Holzkirchen for constant indoor temperatures of 18, 22 and 26 °C. While the 18 °C lead to approx. 10 Vol.-% after 30 years the values increase to 16 Vol.-% at 22 °C and even 25 Vol.-% at 26 °C. Again the conditions beneath the gravel covering are much more favourable with only 1.5, 3 and 8 Vol.-% for the three temperature levels.

4 CONCLUSIONS

Inverted roofs are well proven and reliable roof systems which provide a high durability of the sealing layer as the insulation boards protect the roofing membrane from climatic and mechanical impacts. However the insulation boards are exposed to the outdoor weathering with high humidity and precipitation water. The field tests show high humidities or even water films with more than 10 mm thickness beneath the insulation boards as a result of penetrating precipitation water being retained due to the usual unevenness of the underground. Thus a vapour diffusion flux into the boards cannot be avoided. Cover layers which can dry out during periods with little precipitation allow some drying of the boards towards the top of the roof which usually keeps the water content of the insulation low. For cover layers which remain humid most of the time like those of vegetated (green) roofs, moisture may accumulate in the insulation layer at different rates depending on outdoor climate, indoor temperature and material properties. The paper shows that hygrothermal simulations can be applied

successfully to predict the long term water content in the boards and its influence on the thermal resistance of building assemblies. Due to the wide range of measured data and many uncertainties concerning for example the unevenness of the underground care has been taken to assure that the simulation model provides results which remain a little bit on the safe side.

Gravel covering shows a more favourable behaviour during drying periods which leads to only minor moisture accumulation in the boards even in case of colder outdoor climate. Only in combination with high indoor temperatures in winter, for example in swimming pools or buildings with industrial operation, the high vapour pressure beneath the boards results in a steeper increase of the insulation water content. Inverted roofs with vegetation experience significant moisture accumulation except in climates with warm and dry summer periods and mild winters. Under moderate and cold climate conditions especially in combination with higher temperatures beneath the roof the increase of moisture cannot be neglected and the influence on the thermal conductivity has to be accounted for. Insulation materials with a higher diffusion resistance show smaller water contents than more permeable materials. The simulation allows an evaluation of the different influencing factors material properties, cover layers and boundary conditions and help to maintain the aspired level of thermal resistance of the roof by adapting the insulation layer thicknesses.

REFERENCES

Künzel, H.M. and K. Kießl. 1997. *Moisture Behaviour of Protected Membrane Roofs with Greenery*. CIB W40 Proceedings, Kyoto, Japan, 1997.

Zehendner, H. 1979. *Einfluss von Feuchtigkeit auf die Wärmeleitfähigkeit von Schaumkunststoffen im Bereich von -30 bis +30 °C.* Kunsstoffe im Bau 14 (1979), H.1: 18-22.

Künzel H.M. 1995: *Simultaneous Heat and Moisture Transport in Building Components. - One- and two-dimensional calculation using simple parameters.* IRB Verlag (1995).

IBP-Report RB-17/1993: *Langzeituntersuchungen an begrünten Umkehrdächern (Longterm behavior of vegetated inverted roofs),* Holzkirchen, Germany, 1993.

IBP-Report HTB-2/1996: *Feuchverhältnisse in Umkehrdächern mit verschiedenen Deckschichten (Moisture conditions in inverted roofs with different cover layers),* Holzkirchen, Germany, 1996.

XII DBMC
International Conference on Durability of Building Materials and Components
PORTO - PORTUGAL, April 12th-15th, 2011

Durability of Marine Concrete in Libya – Field Study on Five Seaports

Abdalla O. Elshukry [1]
Adel M. Gilani [2]

ABSTRACT

The construction practice of marine concrete structures is of a great concern, considering the severe conditions that this concrete is subjected to. These conditions may lead to the relatively rapid deterioration of concrete of marine structures in case of inappropriate specifications or poor practice. This issue is of more importance in the hot-humid climates such as the case of Libyan Coast, North Africa.

In view of the above, this study is aimed to conduct a detailed survey on five major commercial and industrial seaports along the coast of Libya. The quality of concrete in the surveyed parts was evaluated thoroughly, including visual inspections and conducting several field and laboratory concrete tests.

The study concluded that the concrete structures in all the ports suffer from serious durability problems, especially those related to steel corrosion due to the electro–chemical activity in all tested elements, in addition to high percentage of chloride ions concentrations penetrated through the concrete. Furthermore, it was found that the compressive strength in two of the surveyed ports was below the minimum limits specified in the related specifications.
The study discusses the possible causes that led to this situation, and suggests a series of practical procedures that ensure better design for durable marine concrete with the minimum need to maintenance through its service life.

KEYWORDS

Libya, Marine Concrete, Steel Corrosion, Compressive Strength, Durability.

[1] Bonyan Consulting Engineers, Tripoli, LIBYA, bonyan@bonyan-ce.com
[2] Civil Engineering Department, Alfateh University, Tripoli, LIBYA, adelgilani@hotmail.com

1 INTRODUCTION

Marine concrete durability is becoming an increasingly important issue due to growing need for concrete coastal structures in developing countries. Massive quantities of concrete were poured in the Libyan port projects during the last three decades, in order to meet the rapidly growing demand for port facilities due to increase in the oil exports and the country's imports needed for development. Although concrete structures in marine environment are designed to last for a considerable life span with minimum maintenance, natural deterioration of reinforced concrete components in particular can occur in the following forms: alkali aggregate reaction, frost attack, sulphate attack, chloride attack and carbonation. Good quality concrete may eliminate some or all of the factors influencing deterioration, starting from the proper choice of constituent materials and their proportioning, to the workmanship at site in the form of mixing, casting, compacting and curing. The objective of this paper is to present a case study of concrete deterioration of some major marine structures in arid and semi arid climates of Libya, showing and stressing the importance of drafting and implementing the proper specifications for the works throughout.

2 MARINE CONCRETE DURABILITY

It has been proved in practice that concrete structures can remain serviceable, with little or no maintenance, for 50 years or more in a marine environment. One of the main characteristics influencing the durability of concrete is its permeability. With strong dense aggregate, a suitable low permeability is achieved by having a sufficiently low water/cement ratio, by ensuring complete compaction of the concrete and by using proper curing methods to ensure complete hydration of the cement and crack-free surfaces. The cement content should be sufficient to provide adequate workability with a low w/c ratio so that the concrete can be completely compacted with the means available. Construction and supervision must be such as to ensure a consistently high standard of workmanship [FIP 1985]. The durability of reinforced concrete structures is, in general terms, affected by three parameters under the control of designer: cover, crack widths and concrete quality. The principal factors influencing concrete durability in arid and semi-arid environment are water/cement ratio, reinforcement cover, curing, type of cement and cement content.

3 CONCRETE SPECIFICATIONS OF LIBYAN PORTS

A review of the concrete specifications used in different ports along the Libyan coast is made. The study ports from west to east are Abukammash, Tripoli, Misurata Commercial, Misurata LISCO and Brega Industrial Port (Fig.1). The specifications differ according to the design and construction aspects. Presented below are some of the mostly adopted specifications [Elwefati and Barony 1988].



Figure 1. Location of the ports on the Libyan coast

3.1 Mixing of Concrete

In addition to the common specifications, admixtures were prohibited in the case of Tripoli port, while for the other ports a reference was made to the minimum cement content, minimum concrete strength, and maximum w/c ratio. These limits, however, varied from one port to another as shown in Table 1.

3.2 Curing

Curing compounds were specified in Tripoli port, while only water curing was allowed in other ports. No reference to any specific curing procedure was made in the other ports.

3.3 Reinforcement Cover

While no reference is made in any of the specifications to the reinforcement cover, the tolerance from what is given in the working drawings was stated.

3.4 Precautions during inclement weather

All specifications considered cases of windy, rainy and cold weather conditions, while no reference to hot weather concreting was made, which was interesting because of the long hot/dry summer season.

3.5 Concrete production

Beside the common specifications for mixing, transporting, placing, compacting and curing of concrete, some of the specifications made no reference to minimum concrete strength, and the requirements for the mix design and quality control. Table 1 shows some of the given concrete specifications as well as the produced concrete characteristic cube strength and the corresponding standard deviation in the investigated port projects.

Table 1. Deviations from specifications in some selected Libyan ports

Port	W/C		Cement Content (Kg/m^3)		Compressive Strength (MPa)		
	Specified	Actual	Specified	Actual	Specified	Characteristic	St. Deviation
Tripoli (TP)	0.5	0.5	-	300	-	33.2	15.7
Benghazi	0.5	0.48	370	360	37.5	42.7	5.2
Brega (BIP)	0.5	0.51	370	370	37.5	44.1	7.0
Misurata (MP)	0.5	0.43	370	380	40	46.2	9.2

4 CASE STUDIES

Arid desert climate prevails as in the case of Brega port, with maximum temperature from 40ºC to 45ºC during summer, extending up to six months. Winter months, on the other hand, can experience a drop of temperature down to slightly above zero coupled with an increase in humidity up to 75%. Winter months, also, are characterized with some violent storms and modest rainfall with mean annual precipitation of 150 mm all occur during winter. Appreciable fluctuation in both temperature and humidity occurs between day and night all year round.

The semi-arid, also known as semi- Mediterranean climate in other four ports offers relatively more temperate conditions as regard to both temperature and humidity, while sea storms are violent as well. Annual rainfall in the Tripoli area is around 350 mm, while in Misurata commercial and LISCO ports are is around 280 mm, most of which fall during the winter months from December to February

[National Atlas of Libya 1978]. Hot and generally dry winds called 'Ghibli' are active in summer. This is usually accompanied by dust and sand. The two major types of deterioration inflected upon the concrete of the above ports are salt weathering and reinforcement corrosion, Fig. 2. Apart from appearance, salt weathering of concrete surfaces is not considered a problem for the structural concrete. Its formation is only limited to the outer few millimeters and was likely to have been caused by the increase in the concentration of salts in the pores of the hardened cement paste during the cycles of wetting and drying. In the following, a brief description of each of the studied ports is presented.



Figure 2. Samples of corrosion deterioration in the investigated ports

4.1 Abukammash Port

Abukammash port is located about 150 km west of Tripoli, Fig.1. Its main purpose is to import the raw materials needed to run Abukammash petrochemical complex, and to export the products of the complex. The main component is a 1100 m long and 3.5 m wide R.C. Jetty. The structural elements consist of precast slabs, steel trusses, capping beams, 800 mm steel piles and R.C. abutment. The visual inspection and field tests showed that the precast concrete slabs and beams suffer from medium to severe corrosion which led to spalling of concrete cover and considerable losses in the reinforcement and concrete cross-sectional areas.

4.2 Tripoli Port

Tripoli port is considered as one of the oldest ports in the southern coast of the Mediterranean from the point of continuous existence and commercial use. The present major development consists of two rubble mound breakwaters constructed in two stages, the first stage was built during 1973-1977, with a length of 2190 m, and in the second stage, a further 2520 m length was completed during 1976-1980. The main breakwater has suffered from so many distressing effects leading to cross-sectional failure and heavy structural damages. Further investigations recommended a new design and rehabilitation of the breakwater. Repairs and rehabilitation of Tripoli port constitutes a major reconstruction through change in the ruble mound cross-section as well as casting new wave wall on top of the old one. This was required due to the increase of significant wave height (H_S) to almost double of its original value [Barony et al. 1987]. The change of H_S from 4.0 m to 7.5 m is currently being considered as design parameter for maritime structures on the Libyan coast.

4.3 Misurata Commercial Port

Misurata commercial port is located about 210 km east of Tripoli, Fig. 1. It consists of two rubble mound breakwaters and berthing and storage facilities. The main breakwater was constructed in the first stage at 1987, with a length of 1200 m for north part, and 1800 m for east part, while the berths were constructed in two stages, the first stage was built at 1978, with a length of 1120 m, and second stage with a length of 1520 m. Corrosion deterioration in the form of cracks of the rubble mound breakwater wall was observed. These are generally following the reinforcement bars. There are also

signs of an abrasion on the surface of the walls leaving the aggregate exposed. For berths, no signs of serious deterioration were noticed. However, the berths suffered also from differential settlement.

4.4 Misurata Industrial Port (LISCO)

This port has been established to serve the Libyan iron and steel company (LISCO) to receive ships carrying raw materials. It is located about 5 km east of Misurata Commercial Port. The first stage was built during 1983-1995 consisting of rubble mound breakwater with a length of 1650 m, and berth structure is distinguished by 12 modules, each module has a dimension of 32 m×36 m separated from each other by expansion joints. On each module there are 25 prefabricated transverse beams and 24 prefabricated longitudinal beams. A major type of deterioration, observed at 1993, is the spalling of concrete at soffits of the beams and spalling of concrete at 15 cm height along the sides of the beams. Cracking and cover delamination of some of breakwater walls observed. These deteriorations have been caused by the corrosion of the reinforcement.

4.5 Brega Industrial Port

Brega Industrial Port is located in the gulf of Sirte, Fig. 1, about 800 km east of Tripoli and 250 km west of Benghazi. The port development consists of the main breakwater and berthing facilities which was carried out as an extension of an old oil terminal. The breakwater starts at the shore as rubble mound type then changes to caisson type. The superstructure consists of a roadway slab supported by cross beams and short columns. The north side of the slab rests on a wave wall. This port represents a classical example for concrete deterioration, where the main detrimental factors combined together causing rapid and severe deterioration of concrete within few years of the port service life. In fact, deterioration of concrete was reported early in 1979, only one year after completion of construction which was carried out between 1974 -1978. SRPC was specified and used throughout the port except for a small part of the roadway slabs for which BFSC was used.
The extent of damage inflicted upon the different concrete elements varied widely. The caissons, prefabricated in much better conditions than other components of the project, suffered almost no damage. The cast-in-situ cover slabs were however badly damaged. Elements exposed to direct sunlight and cycles of wetting and drying, such as the super structure of the caisson breakwater, the jetties, and urea berth were badly deteriorated also. Protected surfaces of some of the above elements were less deteriorated. Due to the fact that most of the concrete elements of Brega Industrial Port showed high chloride contamination levels well beyond the rebars, it was suggested that repairs for these elements would be difficult and expensive to undertake and yet questionable as regard to their effectiveness in the long run [Elwefati and Barony 1988].

5 INSPECTION, TESTING AND ANALYSES

Based on the findings of the visual inspection, a field and laboratory testing program was implemented at locations representing the elements subject of this investigation.

5.1 Field Testing Works of R.C. Elements (Corrosion Assessment)

These works comprise a number of the R.C. elements, covering the structural elements.The tests listed below aim to provide information to evaluate the general status of corrosion deterioration.

5.1.1 Rebar Location and Cover Thickness Measurements
According to BS 1881: Part 204: 1988 [British Standard Institution 1988].

5.1.2 Half-Cell Potential Measurements
According to recommendations of ASTM C 876 [American Society for Testing and Materials 1985].

5.1.3 Core Extraction
Thirty one Concrete cores were extracted from a number of the ports structural elements.

5.1.4 Depth of Carbonation
Measured by the classical method of phenolphthalein spraying immediately after extraction.

5.1.5 Dust Extractions
A drill pit of 12 mm was used for dust extractions every 25 mm up to 75 mm, i.e. behind rebars.

5.2 Laboratory Tests

5.2.1 Compressive Strength Testing
All cores were capped with sulpher compound. Core preparation and consequent testing were undertaken with reference to BS 1881: Part 120, 1983 [British Standard Institution 1983].

5.2.2 Chloride Analyses
The objective of this test was to evaluate the chloride penetration profile of concrete to verify possible chloride attack, the dominant factor influencing R.C. corrosion deterioration. Chloride analysis was performed on concrete dust and core samples according to the recommendations of BS 1881: Part 124:1988 [British Standard Institution 1988]. The result of this analysis is useful in assessing the status of concrete durability for both visually defective and sound concrete. Results are also essential in the process of choosing the suitable type of repair scheme.

6 DISCUSSION OF RESULTS

Table 2 shows samples of the conducted tests. Based on the obtained results from the field & lab tests and analyses, the following remarks and discussions are presented.

6.1 Compressive Strength

Table 2 summarizes the average values of compressive strength for the cores taken from the investigated ports, and the specification requirements. It is clear from this table that the compressive strength of Tripoli and Brega ports didn't meet the specification requirements. The results indicate also the inconsistency of concrete strengths possibly due to inconsistent concrete practice.

6.2 Rebars Corrosion Rates

a. The results of half cell potential test were in conformity with the findings of visual inspection, where it indicated a high activity of electro-chemical corrosion reactions in all tested elements when compared to the limits of ASTM C876 [American Society for Testing and Materials 1985]. The readings exceeded -300 m.v. in most of the elements.
b. The results of chemical analysis of dust samples revealed that the chloride contents in the concretes of all ports exceeded the limits of chloride content by mass of concrete specified in concrete society technical report no. 26 [Concrete Society 1994]. This was a clear indication of chloride attack extension to beyond steel rebars.

6.3 Carbonation

Slight carbonation was recorded in all tested specimens, 10 to 20 mm carbonation depth in all ports except Misurata Commercial Port in which the concrete showed even less carbonation of only 2 to 5 mm. Keeping in mind that the concrete cover in all tested elements ranged from 50 to 140 mm, which is higher than the measured values of carbonation, led to the conclusion that carbonation was not a reason for the high levels of rebar corrosion.

Table 2. Summary of test results.

Port	Element	Specimen ID	Concrete Cover (mm)	Half- cell Potential (mmv-)	Equivalent Cube Compressive Strength (MPa)	Carbonation Depth (mm)	Chloride content Weight/ weight of concrete (%)					
							0~25 (mm)	25~50 (mm)	50~75 (mm)	75~100 (mm)	100~125 (mm)	125~150 (mm)
Abukam-mash port	Abutment	AB-3	25	200~312	53	15	0.37	0.26	0.32	0.13	-	-
	Precast Slabs	S3	50	109~199	52	10	0.49	0.37	0.06	-	-	-
		S7	50	128~280	58	10	1.12	0.74	0.33	-	-	-
		S50	70	195~321	57	-	0.64	0.56	0.33	0.02	-	-
Tripoli Port	Break-water Wall	WT1	65	365~447	29	20	0.87	0.65	0.50	0.36	0.25	0.17
		WT3	65	431~663	29	10	0.95	0.86	0.65	0.51	0.32	0.15
		WT4	65	417~501	42	10	0.38	0.29	0.20	0.12	0.08	0.07
	Berth	WT5	65	445~605	14	10	1.39	0.37	0.35	0.21	0.14	0.08
		ST6	65	406~515	21	20	0.42	0.31	0.22	0.12	0.09	0.07
		ST7	65	415~465	19	20	0.34	0.29	0.21	0.15	0.06	0.04
Misurata Comm. Port	Break-water Wall	WM1	50	297~465	68	2	0.54	0.45	0.26	0.13	0.13	0.12
		WM2	50	316~475	58	5	0.50	0.45	0.31	0.20	0.15	0.14
		WM3	50	316~475	45	5	0.35	0.26	0.21	0.15	0.14	0.13
	Berth	SM1	140	336~369	61	2	0.08	0.07	0.06	0.04	0.03	0.02
		SM2	140	336~369	60	2	0.42	0.41	0.34	0.21	0.15	0.11
LISCO	Break-water Wall	W34	100	198~310	53	15	0.46	0.41	0.32	0.21	0.10	0.04
		W70	100	344~421	56	15	0.38	0.33	0.28	0.24	0.23	0.21
		W90	100	340~471	48	15	0.30	0.27	0.24	0.20	0.12	0.10
		W99	60	269~391	62	20	0.38	0.35	0.30	0.25	0.17	0.16
		W106	115	294~392	43	15	0.47	0.40	0.33	0.29	0.20	0.15
		W214	105	343~511	52	20	0.47	0.45	0.37	0.26	0.21	0.15
Brega Industrial Port	Break Water wall	WB1	91	475~501	35	10	0.47	0.31	0.16	0.11	0.09	0.08
		WB2	91	420~451	31	10	0.45	0.38	0.33	0.25	0.22	0.20
		WB3	55	415~477	30	10	0.45	0.39	0.25	0.14	0.11	0.09
		WB4	50	458~501	24	20	0.51	0.34	0.19	0.14	0.11	0.09
	Slab	SB1	100	496~566	31	15	0.51	0.40	0.31	0.23	0.15	0.09
		SB2	100	498~556	22	10	0.61	0.53	0.41	0.34	0.31	0.29
		SB3	90	425~485	19	10	0.45	0.35	0.29	0.23	0.15	0.09
		SB4	90	460~501	38	10	0.52	0.45	0.42	0.39	0.36	0.33
		SB5	71	295~385	22	10	0.63	0.59	0.45	0.32	0.25	0.19

7 CONCLUSIONS

There are many reasons for deterioration of the concrete of the investigated ports. The main causes are related to using inappropriate materials, poor practice and inadequate project specifications, which led to chloride attack to most of the elements and hence, corrosion of reinforcement bars. For example, reviewing the documents and field investigation led to the following:

a. Project specifications were mainly prepared by consulting firms from north Europe based on their experience of the concreting in cold and mild climate of Europe, instead of the hot /humid environment of the Libyan coast.
b. Continuous change of sources and types of constituent materials led to non-homogenous concrete.
c. High porosity of concrete in spite of the relatively high compressive strength.
d. Insufficient concrete cover and poor control of w/c which reached 0.7 in some cases.
e. Insufficient curing and using sulphate resistant cement which is not suitable for corrosive environments.
f. Absence of surface protection to rebars or concrete surfaces.

8 RECOMMENDATIONS

In view of the findings of the study, some practical recommendations can be taken in consideration regarding construction of marine concrete in similar hot/humid climates. Here are some of the most important recommendations:

a. Preparing a local standard for marine concrete depending on local environmental conditions of the Libyan coast.

b. Lowering w/c to less than 0.4 using superplasticizers.
c. Using blended cements such as blast furnace slag cements.
d. Proper practice, particularly, a special care must be given to compaction and curing.
e. Cement content should be 400kg/m^3 at least.
f. Using carbon fibers instead of steel reinforcement if possible.
g. Avoiding thin sections and horizontal surfaces.
h. Providing protective coatings to steel rebars and concrete surfaces.

ACKNOWLEDGMENT

The authors are deeply grateful to professor Adel Elwefati, Alfateh University for his valuable guidance and comments throughout the study.

REFERENCES

American Society for Testing and Materials. 1985, 'ASTM C 876: Standard Test Method for Half – Cell Potentials of Reinforcing Steel in Concrete', Annual Book of ASTM Standards.

Barony, S.Y., Mallick, D.V. and Sehery, F. 1987, 'Tripoli Harbour NW Breakwater new design criteria and long term solution', Proceedings of. 2nd Int. Conference on Coastal and Port Engineering in Developing Countries, Beijing, China.

British Standards Institution (BSI) 'BS 1881: Part 120:1983, Method for Determination of the Compressive Strength of Concrete Cores', London.

British Standards Institution (BSI) 'BS 1881: Part 124:1988, Testing Concrete, Methods for Analysis of Hardened Concrete', London.

British Standards Institution (BSI) 'BS 1881: Part 204:1988, Testing Concrete, Recommendations on the Use of Electromagnetic Covermeters', London.

Concrete Society Technical Report No. 26, 1994, 'Repair of Concrete Damaged by Reinforcement Corrosion', UK.

Elwefati, A.M. and Barony, S.Y. 1988, 'Durability of Structural Concrete on the Mediterranean Coast of Libya', Proceedings of The 2nd Int. Conf. on Performance of Concrete in Marine Environment, Supplementary Papers, St. Andrews, New Brunswick, Canada.

FIB 1985, 'Design and Construction of Concrete Sea Structures', 4th Ed., London.

National Atlas of Libya, 1978.

XII DBMC
International Conference on Durability of Building Materials and Components
PORTO - PORTUGAL, April 12th-15th, 2011

Service Life and Maintenance Needs of Corrugated Steel Roofing in Iceland- Case Study

Björn Marteinsson [1, 2]

ABSTRACT

Galvanized corrugated steel claddings, usually painted, are by far the most common roofing material in Iceland. It is well known that corrosion speed of mild steel and zinc (small specimens) varies in different environments, but it is of greater interest to record if and how service life and maintenance need of the roofing materials depend on environmental loads. The paper presents results from a study of 250 roofs on privately owned homes, based on questionnaires answered by the owners, in two different areas of Iceland. About half of the answers are from homes in the capital city Reykjavik, located in a coastal area that is both wet and windy and therefore time of wetness and chlorides content in air is high. A comparison is made with a small city on the north coast of the island, a location in a deep fjord, relatively shielded and dry in comparison with Reykjavik. The comparison shows a significant difference in service lives of metal claddings, even though both locations are classified as corrosivity class 2-3 according to ISO 9223.

KEYWORDS

Corrosion of metals, metal roofing, service life, maintenance needs.

[1] University of Iceland, Faculty of Civil and Environmental Engineering, 101 Reykjavik, Iceland, Phone +354 525 4651, Fax 552 1331, bjomar@hi.is
[2] Innovation Center Iceland, 112 Reykjavik, Iceland, Phone +354 522 9000, Fax 522 9111, bjorn.m@nmi.is

1 INTRODUCTION

Roofs and roofing are a very important part of the building enclosure and are expected to function properly in often a very severe environment. The requirements on safety against leakage are high and as a result the building and maintenance cost of roofs is a considerable part of the total cost of buildings.

In estimating life cycle cost (LCC) and life cycle assessment (LCA) it is needed to know what service life (SL) of the component may be expected to be, depending on actual maintenance and environment. In the factor method of ISO 15686 it is proposed that based on a known reference case (with known SL, environment and maintenance) the SL for a new case may be predicted based on appropriate assumptions regarding environment and maintenance for the new location.

In an effort to study service life of metal claddings in Iceland and actual maintenance needs of roofing's, a case study was carried out at two environmentally different locations, the municipalities of Reykjavik and Akureyri. Environmental information was gathered from different locations where the State Meteorological Institute is an important actor, and some own measurements on corrosion and amounts of aerosols were carried out.

2 THE HOUSING INVENTORY AND SAMPLE OF HOUSES IN THE STUDY

This study is a part of a larger research project where the effect of various parameters on degradation and need for maintenance will be considered. The main parameters studied are: climate, age of buildings, type of building materials and earlier maintenance actions.

Information was gathered from two different municipalities: Reykjavik, the capital city of Iceland, and Akureyri, the main city on the north coast of Iceland. Reykjavík has about 110,000 inhabitants and Akureyri, a little more than 15,000. The two communities have considerably different climates. Reykjavik has a shore climate, typical of islands: wet, windy and temperate, whereas Akureyri has a more continental climate, with a greater difference between summer and winter temperatures, as well as being drier and less windy. The two places were chosen exactly for this reason, that is, to get a comparison between two different climatic locations.

The research is largely based on a questionnaire. The recipients of the survey were chosen by statistical methods from all house owners in the two municipalities, such that the chosen lot would be statistically representative for the houses in general, regarding type, age, owners and location. It was realised from the beginning, that the response ratio would be low, and the results, therefore, would not be statistically representative for all houses in the municipalities. In total 1,850 houses were chosen from houses built after 1950 and having a maximum of three flats in each house. The restriction on the sample regarding building period was made because the average age of houses in Iceland is less than 30 years, and it was seen as necessary that at least 10 houses be in each age group of ten years in order to get comparable data amounts between age groups. In earlier works of similar nature it was difficult to get reliable information on refurbishment and maintenance for bigger houses, since no specific person had the responsibility of gathering the necessary information.

It is most customary for Icelanders to own their own homes, and at least until now, it is customary for the owner to personally participate in the maintenance and refurbishment work. The owner therefore often is knowledgeable about what has been done and even the materials chosen. The questionnaire was posted early spring 2006 and the bulk of answers came early winter 2006 and a few as late as summer 2007.

3 FACTORS AFFECTING SERVICE LIFE OF ROOFING MATERIALS OF METAL

By far the most frequently used roofing material in Iceland is of metal, and the metal coverings discussed here are mostly hot dip galvanised steel, aluminium coatings are a minor part of the whole. The coverings can be with or without a coating, coverings coated with organic coatings beeing by far the most usual case, other types of coatings are very scarce. The coating may be applied on site or in the factory.

All metals are imported to the country, metal for covering imported as coated or uncoated metal strip and then profiled by a roll forming process in domestic factories. The most numerous coatings in Iceland for the time period studied are;

Painted on site: Oil based paints, and in later year's acrylic paints.

Factory coated: PVC-plastisol, PVDF, silicon modified polyester and acrylic paints.

There are some instances of coverings without organic coating, these are amost always either aluzinc coated steel claddings or aluminium claddings. Factory coated metal roofing came first onto the Icelandic market in 1981 (plastisol), these types of coatings have less than half of the coated roofing market. Today a noticeable part of the market is taken by aluzinc coated steel to be painted on site or left unpainted.

The metal covering and coating is thus usually a combination of layers and the degradation process therefore not so simple or easy to evaluate. The degradation of metal coverings on roofs can be described as three steps:

A – degradation of organic coating (if any). This degradation can be a purely aesthetical one such as gloss or colour change, or directly affecting the corrosive protecting ability of the coating e.g. delamination (peeling) or corrosion from edges can begin.

B- corrosion of a protective metal layer of zinc or aluzinc on steel.

C- corrosion of the metal substrate.

From information gathered from specialists and the market the main reason for repainting seems to be (in order of decreasing importance);

- Corrosion from cut edge
- Corrosion at or around fasteners
- Delamination of coating (peeling)
- Colour change

These failures are rather typical for metal claddings as discussed by Ryan *et al.* [1994].

The main reason for replacement of roofing material seems to be when repainting needs to be done to frequently, compared to others in the neighbourhood. This typically happens when a widespread corrosion of substrate metal is visible. For spot corrosion the substrate metal may be patched,even when the metal is corroded through, as a temporary repair (sometimes lasting years) so long as the main surface keeps the paint well enough.

The factors that are likely to affect the SL of the cladding in one way or another, and also considered by ISO 15686, are; inherent performance, design, workmanship, environment, in use conditions, maintenance. Most of these factors may be considered to be on average similar in each age group of buildings and for the two locations (same tradition, similar training, same materials). Environment though will be different and due to this so also will be the maintenance.

<u>Environment</u>

Degradation of organic coating will most likely be affected by outdoor air temperature, windspeed, UV, precipitation (and moisture in general) and probably aerosols.

Corrosion speed of metals depends mainly on temperature, surface moisture and aerosols.

Table 1. Environment and measured corrosion speed in Reykjavik and Akureryri

	Reykjavik	*Akureyri*	*Ratio*	*Comments*	
Air temperature, average (°C)	4.53	3.51	1.29	Years 1961-2006	2)
.. air temperature one year period (°C)	4.6	4.1		Year 1999-2000	2)
Precipitation (mm/year)	817	505	1.62	Years 1961-2006	2)
Air humidity, average (%RH)	78.4	79.5	0.99	Years 1961-2006	2)
.. air temperature one year period (°C)	78.3	75.9		Year 1999-2000	2)
TOW, average sum (hours/year)	3903	2301	1.70	Year 1999-2000	1,2)
Wind speed, average (m/s)	5.61	4.24	1.32	Years 1961-2006	2)
.. wind direction from sea (ratio)	0.15	0.10	1.5	Year 1999-2000	2)
Sunshine (hours/year)	1292	1046	1.24	Years 1961-2006	2)
Chlorides, deponated Cl^- (mg/m^2,day)	10-50			Years 1974-2000	2)
NO_2 in air, average (µg/m3)	36			Years 1993-1998	4)
SO_2 in air, average (µg/m3)	3.55	1.95	1.72	Rvk: years 1993-1998 AK: year 2004-2005	4)
Zinc corrosion (µm/first year)	2.3	1.6	1.44	Year 1999-2000	1,3)
Carbon steel corrosion (µm/first year)	20.7	5.5	3.76	Year 1999-2000	1,3)

Notes:

1) An average year for Reykjavík but a rather hot and dry year in Akureyri compared to the average, a more usual ratio is probably nearer to 1,5. The calculated TOW for Akureyri is probably unusually low measured and measured corrosion probably unusually low too.
2) Data from Icelandic Meteorological Station
3) [Marteinsson & Sigurjónsson 2002], the measurement period is from start of July 1999 to end of June 2000
4) [Benjaminsson, 1999]

In table 1 measured values for the two locations are shown, together with a calculated ratio showing the difference in values. Time of wetness (TOW; conditions when simultaneously θ_{air}>0°C and φ_{air}>80%RH as defined by ISO 9223) is shown as an indicator of the combined effect of temperature and moisture on corrosivity of environment.

The environment in Reykjavik is clearly warmer, wetter, more windy and with higher content of aerosols, the degradation effect on almost any material will be bigger in Reykjavik than in Akureyri. When corrosivity of metals is considered, the main agents in Iceland are considered to be the combined effects of temperature, moisture (precipitation) and chlorides as content of SO_2 in air is low [Marteinsson & Sigurjónsson]. The corrosivity of both locations is classified as 2 - 3 according to ISO 9223.

Maintenance

Information from specialists and the market indicate that only a small part of houseowners plan maintenance based on a fixed interwall. Most owners just wait until they consider that the degradation has gone far enough and then make repairs. This maintenance strategy is not considered to be different between the two locations, and so the maintenance frequency may be considered as a measure of degradation effects in both places.

4 RESULTS AND DISCUSSIONS

In the study, the house owners/users were asked to answer a questionnaire with 48 questions regarding their houses and earlier maintenance and refurbishment.
The questions of interest to the paper presented are as follows:

- The building period and type of house

- How long the present owner/user has been living in the house
- What refurbishment and maintenance actions have been done on roofs and roofing to the knowledge of present owner/user, which year and why.

Information on occupation duration [Marteinsson 2008] shows that the answers represent opinion of both long-term and short-term residents, and the distribution in occupation time spans a very broad range, or often almost the entire service time of each building age category.

It is clear from the answers that in some cases the roofs have been rebuilt due to leakage, and then the roofing material replaced. In these cases it is not the durability of the cladding that decides the SL but rather some other factors, e.g. faulty design or workmanship. In most cases though it seems that degradation of the material is the main deciding factor for the SL of the cladding. Driving force for maintenance of roofs seems to be mainly that to protect the roofing and the building component in whole against harmful degradation rather than to keep aesthetical values at top score.

The data is sorted into age groups of 10 years, for both the age of the buildings and of material when replaced with new, to get representative numbers for comparisons between age groups.

4.1 Service life of surface treatment

The results regarding SL of surface treatment of metal claddings in Reykjavik and Akureyri are shown in table 2. The table shows repainting or replacement ratio of coatings, e.g. for factory coatings in Reykjavik; three have been replaced and of these one (33.3%) in 16-20 years old buildings and ten are still in uses of which three (30%) are in buildings of that age. Generally surface treatments keep longer in Akureyri, and this is especially noticeably for both surfaces without coatings and factory coated surfaces. It should also be noted that factory coated surfaces are more numerous in Akureyri; 22 answers compared to a total of 13 in Reykjavik.

There are some examples on factory coated surfaces that already have a SL of more than 20 years at both locations, and in Akureyri none of the coatings have needed repainting so far even in the oldest group with age more than 20 years. Generally the factory coatings prove to be more durable than has been assumed until now in Iceland.

Table 2. Service life ratio (% of total in each group) of surface coatings on metal claddings

		Cases	*Agegroup (years)*				
		total	*6-10*	*11-15*	*16-20*	*21-25*	*26-*
Reykjavik							
Painted	Replaced	19	31.6	0.0	31.6	15.8	21.1
	In use						
Unpainted	Replaced						
	In use	1	0.0	100.0	0.0	0.0	0.0
Factory coated	Replaced	3	0.0	33.3	33.3	0.0	33.3
	In use	10	0.0	30.0	30.0	40.0	0.0
Akureyri							
Painted	Replaced	27	11.1	11.1	18.5	22.2	37.0
	In use						
Unpainted	Replaced	0					
	In use	6	16.7	33.3	33.3	0.0	16.7
Factory coated	Replaced	0					
	In use	22	22.7	22.7	18.2	36.4	0.0

Repainting on site is done at very different times, but clearly more frequently in Reykjavík than in Akureyri. It is rather common in Reykjavik to repaint each 6-10 years, or in 31.6% of all, but similar figure for Akureyri is only 11.1%. There are examples at both locations of painting in situ with a SL of more than 25 years, whereas the general rule of thumb on the market has been to repaint on average each 12-15 years (Reykjavik).

4.2 Service life of roof claddings

In table 3 the number of buildings in each age group and replacement ratio of roofing materials for different age groups (houses and materials) for Reykjavik and Akureyri is shown. The notes following the table describe the two different ways the data can be considered; the probability that roofing will need replacement in a building of certain age can be seen and also the service life distribution of the roofing can be worked out. In table 2 it may e.g. be seen that in Reykjavik for buildings from the period 1967-76 a total of 42.1% of roofing materials has been replaced or 42.9% of all metal claddings. Of the replaced metal claddings 14.3% where replaced at age 20-29 years and 28.6% when 30-39 years old. Reading the bottom line it can be seen that of all metal claddings in Reykjavik 5.6% where replaced in the age interwall 10-19 years and 5.9% at age 20-29 years. From table 3 it may be assumed that some replacements must have been done already in the older house groups (when compared to replacements in younger house groups) but the owners of these houses have not known about this (change of owners in the meantime). It is clear that the information from the owners is not complete in all instances, but hopefully gives a correct enough picture of typical service lives.

The longest known SL of galvanized steel roof cladding in Reykjavik is a little more than 100 years, but the study now shows only younger buildings and cases of very long SL are not visible. The data can though be ordered such that average SL and even some estimate on how frequently very high SL figures may be expected. Based on the assumption that factors affecting SL have not changed over time a cumulative frequency graph for replacement of materials vs. age can be based on the data at bottom of table 3 (see Note C), see figure 1. The difference between SL of metal roofing at the two locations is noticeable. If the 50% (average) SL is taken for comparison it can be seen that the average SL of metal roofing material in Reykjavik is about 38 years and in Akureyri 49 years. Earlier studies on the SL of metallic roofing materials in Reykjavik lead to a SL of 45-50 years [Jónsson & Marteinsson 1999]. That result was based on information regarding only if roofing material on houses had been replaced, but not when the replacement had been done (at which age of the building). The two methods will give different results, as can easily be seen from table 3, the earlier study giving an overestimate of the SL. The ratio between SL in the two locations is about 1.3. This ratio cannot be explained by better maintenance in Akureyri as maintenance actions (repainting) are less frequent there than in Reykjavik. Factory coatings are more frequent in Akureyri and this certainly is one of the reasons for the longer SL of claddings there. This is only a part of the explanation though, as factory coated surfaces are only about 20% of all claddings, even in Akureyri.

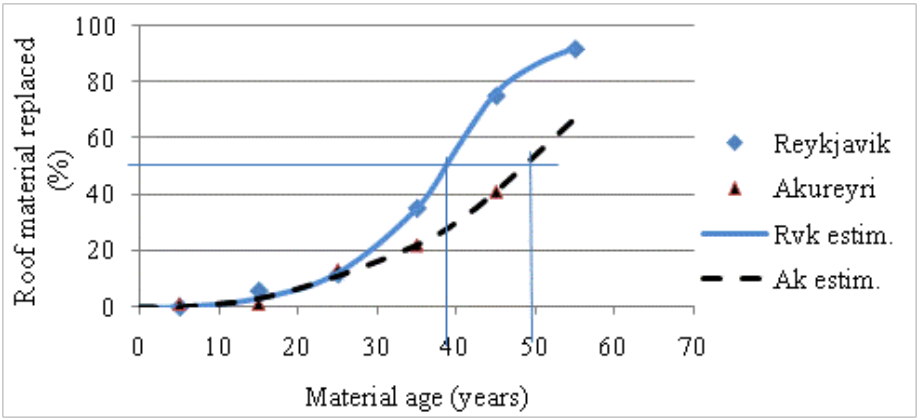

Figure 1. Cumulative replacement ratio of metal roofing vs. material age for Reykjavik and Akureyri.

The longer SL of claddings in Akureyri than in Reykjavik is most certainly due to a better environment; and partly due to better surface coatings of a very limited part of the claddings. There is clearly a difference in the environments and measured corrosion is different, table 1.

Table 3. Service life of metal roof claddings in Reykjavik and Akureyri, depending on age of buildings

Building year	*Age group of houses*		*Answers*		*Replaced materials (% of useable answers)*						
	(yrs)	*Mat. type*	*total*	*useable*	*total*	*Agegroup of material (years) when replaced*					
						<10	*10-19*	*20-29*	*30-39*	*40-49*	*50-59*
Reykjavik											
1947-56	50-59	All	9	7	71.4					42.9	28.6
		Metal cl.	7	5	60.0					40.0	20.0
1957-66	40-49	All	24	18	66.7				22.2	44.4	
		Metal cl.	19	14	78.6				28.6	50.0	
1967-76	30-39	All	23	19	42.1		5.3	15.8	21.1		
		Metal cl.	16	14	42.9			14.3	28.6		
1977-86	20-29	All	27	18	16.7		16.7				
		Metal cl.	26	18	16.7		16.7				
1987-96	10-19	All	14	12	0.0						
		Metal cl.	13	12	0.0						
1997-06	<10	All	17	16	0.0						
		Metal cl.	14	14	0.0						
Total		All	115	91							
		Metal cl.	96	78	***30.8***		***5.6***	***5.9***	***23.6***	***45.0***	***16.7***
Akureyri											
1947-56	50-59	All	5	3	33.3					33.3	
		Metal cl.	5	3	33.3					33.3	
1957-66	40-49	All	34	28	53.6		3.6	14.3	25.0	10.7	
		Metal cl.	24	18	33.3			5.6	11.1	16.7	
1967-76	30-39	All	36	22	59.1		9.1	40.9	9.1		
		Metal cl.	18	13	46.2			38.5	7.7		
1977-86	20-29	All	28	24	4.2			4.2			
		Metal cl.	28	24	4.2			4.2			
1987-96	10-19	All	18	14	7.1	7.1					
		Metal cl.	17	14	7.1	7.1					
1997-06	<10	All	36	36	0.0						
		Metal cl.	33	33	0.0						
Total		All	156	127							
		Metal cl.	126	106	***14.3***	***1.0***	***0.0***	***12.1***	***8.8***	***19.0***	

Notes to table 3:

A The left part of the table shows age groups of buildings, number of houses and number of useable answers.

B The right part of the table shows calculated replacement ratio (%) of materials in each age group of buildings (reading the table horizontally).

C The last two lines at bottom for each location are calculated replacement ratios (%) for each age group of materials (reading the table vertically), in each case calculated as a ratio of total number of answers at that age or older.

The degradation effect on the cladding is based on two different processes; first a degradation of surface coating and then corrosion of metal in the final stage of the SL. The protective effect of the coating is thus an important factor but what the difference is for the two locations can't be decided on by the data presented here. For the second stage of degradation the corrosion speed of metal (here zinc) can be used. Ratio of corrosion speeds for the two locations can be used, either as a measured or a calculated value based on dose response functions. The calculated value from measurements is here 1.44 (table 1 and note 3) but is probably too high and compared with the estimated difference in SL of 1.3 in fig 1 seems to indicate a little to high a ratio in SL's of the roofings for the two locations. In lack of better the corrosion speed alone can be used to estimate difference in degradation between reference and design case, but will then give an overestimation of the difference.

5 CONCLUSIONS

Service life of metal claddings and coatings on metal claddings are shown to be different by as much as 30% between two locations that according to ISO are classified as corrosivity environment 2-3. Service life of a coated metal cladding depends first on the protective effect of the coating and then on the corrosive speed of the metal. The two stages in degradation are dependent on different degradation mechanisms and it is difficult to estimate the combined effect. In this study it is therefore difficult to evaluate an environmental factor to use in the factor method of ISO 15686 to predict SL in design case based on a known reference case. Using the ratio of corrosion speeds for the two locations gives an idea of the ratio of SL's, but possibly overestimates the difference in environments somewhat.

ACKNOWLEDGEMENTS

The research project presented is funded in part by RANNÍS – the Icelandic Centre for Research and also Íbúðalánasjóður- The State Housing Board, whose financial support is gratefully acknowledged.

REFERENCES

Ryan, P.A. , Wolstenholme, R.P. and Howell, D.M. 1994, *Durability of Cladding – a state of the art report*, Thomas Telford services Ltd, London.

ISO 9223:1992 Corrosion of metals and alloys – Corrosivity of atmospheres – Classification

ISO 15686 Buildings and constructed assets- Service life planning.

Jónsson B. and Marteinsson B. 1999, *Viðhaldsþörf húsa á Íslandi*, Sérrit Rb nr. 77, Rannsóknastofnun byggingariðnaðarins, (in Icelandic).

Benjaminsson, J. 1999, 'Air pollution in Reykjavik the capital of Iceland' in *Air pollution VII*, eds C.A. Brebbia, M. Jacobson, and H. Power, WIT Press, Boston.

Marteinsson B. 2008, 'Homes in Iceland-flexibility and service life fulfilment of functional needs', Proc. 11DBMC International Conference on Durability of Building Materials and Components, ISTANBUL-TURKEY May 11-14th, 2008, pp. 1485-1490.

Marteinsson B. and Sigurjónsson J. 2002, 'Corrosion of metals-mapping of the environment in Iceland', Proc. 9th International Conference on Durability of Building Materials and Components, Australia, 17-21 March 2002, paper 029, 6p.

XII DBMC
International Conference on Durability of Building Materials and Components
PORTO - PORTUGAL, April 12th-15th, 2011

Moisture Conditions in Coated Glulam Beams and Columns During Weathering

Karin Sandberg [1]
Anna Pousette [2]
Lars-Olof Nilsson [3]

ABSTRACT

Service-life assesment and life-cycle cost are becoming more and more important in investment and planning of construction work. Woodbuild is the name of a Swedish research programme with the goal of developing engineering tools based on models that can be used in the planning and design of timber structures with regard to improved service life.The purpose of the full-scale test is to verify models for prediction of wetting periods on wood surfaces and of moisture conditions dependent on climate loads, finishes, wood processing and design. The objective of the present work was to show results on moisture conditions in glued laminated timber (glulam) beams of Scots pine (*Pinus Sylvestris*) and Norway spruce *(Picea abies)* and glulam columns of spruce to demonstrate differences that can be ascribed to different coating types and colours and the influence of the varying positional orientation (north/south), up or down at columns and measurement depth. The glulam beams were 315 mm high, 140 mm, 215 mm or 90 mm wide and 2 m long. The columns had 100 x 100-mm cross-sections. Moisture content, relative humidity and temperature were measured using wireless sensors, measurement depth 5 mm and 15 mm. MC measurements of the beams' undersides show small fluctuations over the time irrespective of temperature and measurement depth. MC measurements on the south and north sides of the beams fluctuated more compared to underside. The beam with oil treatment, follow climate changes more quickly compared to the painted ones'. MC show small difference depending on the height of the columns.

KEYWORDS

Wireless sensors, Temperature, Moisture content, Relative humidity, outdoor exposure

[1] SP Technical Research Institute of Sweden (SP Trätek), Skellefteå, SWEDEN, karin.sandberg@sp.se
[2] SP Technical Research Institute of Sweden (SP Trätek), Skellefteå, SWEDEN, anna.pousette@sp.se
[3] Div. of Building Materials, Lund Institute of Technology, Lund, SWEDEN, Lars-Olof.Nilsson@byggtek.lth.se

1 INTRODUCTION

Durability is essential to minimize life-cycle costs for outdoor structures. Degradation of wood is a complex process involving interaction between wood, microorganisms, climate and moisture content, exposure time, surrounding environment, irradiation, temperature, surface treatment, *etc.* Especially the presence of water in wood causes many problems, since it affects dimensional change through shrinking and swelling, which in turn influence crack formation, decay and strength reduction. To prevent water uptake, and thus reduce dimensional change, wood can be painted. A number of investigations show the importance of protection of endgrain with sealers and paint to reduce moisture uptake [Sell 1982; Öqvist 1988; Boxhall *et al*. 1992; Elowson *et al.* 2003]. However, after some year's exposure, the initial effect of protective coatings declined on sapwood. Generally, paint cannot make sapwood as durable as heartwood [Boxhall *et al*. 1992; Rydell *et al.* 2005]. Grüll [2010] found that degradation of paint led to decreasing moisture protection from less durable coating systems over time exposure. This means that paint not only protects wood, it might also cause problems if the moisture balance in wood is interfered with or if the painted surface cracks and water gets in, but not out.

Outdoor constructions of wood, such as posts, beams and columns, often crack or delaminate, which can result in damage to the coating film and disturbances in the moisture balance of the wood, which in turn can lead to damaged wood and reduced service life. High moisture content can occur locally at and around cracks (Ekstedt 2002).

Decay reduces strength and is thus a factor to consider, but other factors such as cracks also influence service life. Large cracks can hold water and dirt that are favorable for the growth of microorganisms. A field test with beams and columns is examining the effect of cracks on the prolongation of the life of structures [Pousette & Sandberg 2010], and this paper reports on a part of that study.

Woodbuild is the name of a research program in Sweden with the goal of developing engineering tools that can be used in the planning and design of timber structures with regard to service life. These tools will be based on computational models. Climatic data and exposure conditions will be used as input in the models to calculate moisture content and risk of decay. The purpose of the in situ measurements being done over time is to verify such models for many different situations based on the duration of surface wetting, on moisture conditions dependent on climatic loads, coatings, wood processing and design and on the position of the object inside walls or floors.

To verify models or provide a basis for assumptions, continuous measurements are performed on real test items. Moisture content (MC), relativ humidity (RH) and temperature (T) are monitored continuously using a wireless in situ measuring system. In order to measure a large amount of data, a wireless monitoring system was chosen with a gateway connected to a GSM modem that sends the information to an Internet-connected computer database from whence it is transferred to the users [Sandberg *et al.* 2011].

The objective of this paper is to show results on moisture conditions in glued laminated timber (glulam) beams and columns with different materials and paint coatings, and the influence of the different directional orientations (north/south, up/down) and measurement depth.

2 MATERIAL AND METHODS

Measurements were performed on glulam beams and columns under natural weathering conditions in the northeast of Sweden. Moisture content (MC, %), relative humidity (RH, %) and temperature (T, °C) were registered every hour with wireless electric resistance sensors and loggers [Sandberg *et al.* 2011] along with climate data. Associated with these data were measurement depth and orientation (north-/south-/underside).

2.1 Testing ground

The glulam beams and columns were placed on the testing ground in Bygdsiljum (Lat. 64°20′57″N, Long. 20°30′14″E) in the county of Skellefteå in northern Sweden in August–September 2007 and are part of a larger test described in Pousette & Sandberg [2007] and Pousette & Sandberg [2010]. For continuous measurements of MC, RH and temperature, glulam beams were chosen from the field and the measurement started in January 2009. Climate, temperature and humidity at the test site were measured with a weather station at the test field.

The beams were placed on supporting frames at various heights, with the lowest beam approximately 1 m above the ground (see Fig. 1). Five beams were placed on each frame. Beams were placed with one side facing south to receive the warmth of the sun and the other to the shaded and cooler north. The top surface was covered with a sheet of metal that was mounted in such a way as to prevent water from penetrating into the beam from above. Beam faces were exposed to rainfall, sunlight and the surrounding environment. The frames were placed so that they did not shade each other. The columns were fastened to a concrete foundation (see Fig. 1).



a) b)

Figure 1. a) Measurements at the middle of the glulam beams two meters long, one meter from the ground in the lowest row. Meaurments on the south side, north side and underneath. b) Measurment on the top and bottom of columns two meters heigh. Top surfaces are covered with sheet metal.

2.1 Sample preparation

2.1.1 Glulam Beams

Glulam beams of pine (*Pinus Sylvestris L.*) and spruce *(Picea abies* (L). Karst.) were studied. MC, RH and T were measured. The sizes of the beams were chosen in order to facilitate computer tomograpy (CT) scanning. They can easily be lifted and transported from the test site to the Luleå University of Technology, Campus Skellefteå. Beam width may be relevant to cracking and moisture content, and therefore widths of 90 mm and 215 mm were included as well. Surface treatments were chosen similar to what is used today for many timber bridges in Sweden. The painting was done at the glulam manufacturer. The amount of paint should correspond to a dry-film thickness of 60 µm according to the Swedish standards for construction of wooden bridges, TK Bro [Anon. 2009].

The surface treatments were

- oil (raw linseed oil with aliphatic naphta as thinner).
- Paint system 1: priming oil + two layers of water-based, alkyd oil-acrylic latex hybrid opaque glazing paint. All surfaces were treated with a water based priming oil, biocide Class 3, before painting.
- Paint system 2: priming oil + primer + two layers of topcoat. All surfaces were treated with a solvent-based based priming oil, biocide Class 3, before painting. The primer was solvent-based, semigloss modified alkyd oil.

The orginal trial consisted of 35 beams, but for this paper, seven beams were chosen for measurement of MC, RH and temperature. Table 1 shows the characteristics of the specimens.

Table 1. Characteristics of glulam beams 2 meters long placed one meter above ground.

Name	*Material/dimensions (width x hight)* [mm]	*Surface treatment/ Thinner*	*Colour*
H59	Pine, pressure treated/140 x 315	Oil/solvent based	-
H63	Pine, pressure treated/140 x 315	Paint system 1/water based	White
H69	Pine, pressure treated/140 x 315	Paint system1/ water based	Red
H73	Spruce/140 x 315	Paint system 1/ water based	Red
H76	Spruce/140 x 315	Paint system 2/ solvent based	Red
H81	Spruce/90 x 315	Paint system 1/ water based	Red
H86	Spruce/215 x 315	Paint system 1/ water based	Red

2.1.2 Columns

Five columns (H51, H52. H53 H54, H55) of solid spruce (*Picea abies* (L). Karst.) 100 mm x 100 mm, length two meters, were included in the test. The columns were documented with tomographs through the cross section and scanning of the side surfaces before they were placed on the test site. All columns were covered with sheet metal or wood on top. The columns were painted with the same system that was used for the beams, paint system 1 (opaque glazing), red colour.

2.2 Measurement system

Documentation at the start included dimensions of beams and columns, visual inspection, measurement of moisture content, measurement of dry paint-film thickness, CT scannning (Siemens SOMATOM AR.T) through the cross-section and scanning image of the surfaces. The specimens were scanned in an SP Trätek laboratory in Skellefteå with a camera equipped with a sensor line for the best colour reproduction. An LED (light emitted diod) ramp was used to minimize the need to calibrate for uneven illumination. White balance was calibrated against a gray card.

Colour was measured with a Minolta Chroma Meter CR-310 to quantitatively describe colour by measuring the reflected colour of the surfaces. The Chroma Meter illuminates the surface and measures the colour of an area of diameter 50 mm. The chosen colour coordinates were expressed in the L * C * h colour space, where L is lightness from 0 (black) to 100 (white), C is the chroma from 0 (grey) to more saturated colour the higher value, and h is the hue angle where 0º is red, 90º is yellow, 180º is green and 270º is blue. The measurements were done on the north and south sides of the specimens.

Dry paint-film thickness was measured using a paint thickness gauge, DeFelsko Model 200, that measures with high frequency ultrasound to reflect from surfaces with different densities, in this case the layer between paint and wood. The measurements were done on the norh and south sides of the specimens.

Beams and columns were inspected every year during the summer using non-destructive methods. Visual inspections were done of cracks, biological attacks and other visible defects. Measurements of colour and paint thickness were made once a year in the field at the same spot (area). Width, length and depth of cracks were measured, but are not shown in this work. For continuous measurement of MC (%), RH (%) and T (°C), wireless sensors and the OmniSense Facility Monitoring System (FMS**)** [OmniSense 2010] were used. The sensors send measured values to a gateway connected to a broadband socket or GSM modem that sends the information on to an Internet-connected computer database. Through a website, data were transferred to an SP Trätek (SP Technical Research Institute of Sweden) database. Measured data were then compensated for wood species and temperature [Samuelsson 1990] and transferred to the researchers. The system is decsribed in [Sandberg *et al.* 2011].

MC, RH and T were measured in the middle of the glulam beams, on the north and south surfaces and on the underside. The measurements were made at the three depths—on the surface and 5 mm and 15 mm below the surface—at 49 measurement points.
Continuous measurements of MC, RH and T were performed on the top and bottom on the south sides of the columns on the surface and 5 mm and 15 mm below the surface at 22 measurement points.

3 RESULTS AND DISCUSSION

3.1 Materials

The beams' mean MC at the start in 2007 was 13.4 %±1.4. Mean dry paint-film thickness was measured at the start in 2007 and then once a year. The mean dry paint-film thickness was 77 ±7.7, 73 ±5.9 and 77 ±8.2 and 70 ±4.4 µm respectively for the years 2007 to 2010. The beam with alkyd paint had a somewhat grainy surface.

The columns had a mean MC of 15.3% ±0.9 at the start in 2007 (mean value of four measured points on five columns). The mean dry paint-film thickness was 69 ±17.7, 59 ±7.7 and 60 ±6.9 µm respectively for 2008, 2009 and 2010. Table 2 shows the mean value of colour coordinates before and after three years of exposure.

Table 2. Mean value of colour coordinates measured on south and north sides. L is lightness, C is chroma, h is the hue angle.

No. of specimen	L_{start}	C_{start}	H_{start} *[°]*	*L*	*C*	*H [°]*
Oiled (1)	56.75 ±0.13	28.20 ±0.26	79.80 ±0.28	55.59 ±0.34	20.66 ±1.93	76.60 ±2.97
White (1)	91.43 ±0.19	6.63 ±0.57	104.50 ±0.71	90.38 ±0.03	4.07 ±0.89	103.80 ±0.14
Red (5)	37.05 ±0.21	20.84 ±0.31	30.86 ±0.73	36.42 ±0.96	20.99 ±1.25	31.15 ±0.42

The results show a small average decrease in paint film thickness and change in colour coordinates during the three years. The method for measuring paint-film thickness can suffice as a method for comparison between the years. The increased value for film thickness on the beams in 2009 may be related to the fact that a different person did the measurements that year.

3.2 MC glulam beams during exposure

Fig 2. shows moisture conditions in one glulam beam (H69) during outdoor exposure. Under the beam, the MC condition are rather even during the measured time.

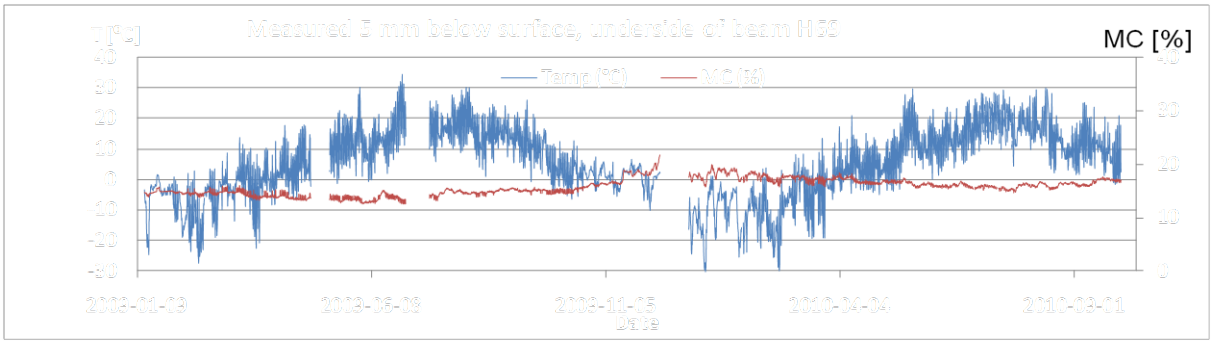

Figure 2. MC measured at 5 mm depth on the underside of beam H69. Values measured every hour. The gaps in the graph correspond to values missing as a result of malfuncion of the measuring system.

Fig. 3 shows measurements on the south side of beam H59. There are larger variation over the year compared to Fig. 2. The beam is an impregnated beam with oil treatment, and it follows climate changes rather quickly. There is a crack about 10 mm below the measured point that may influence the measurements.

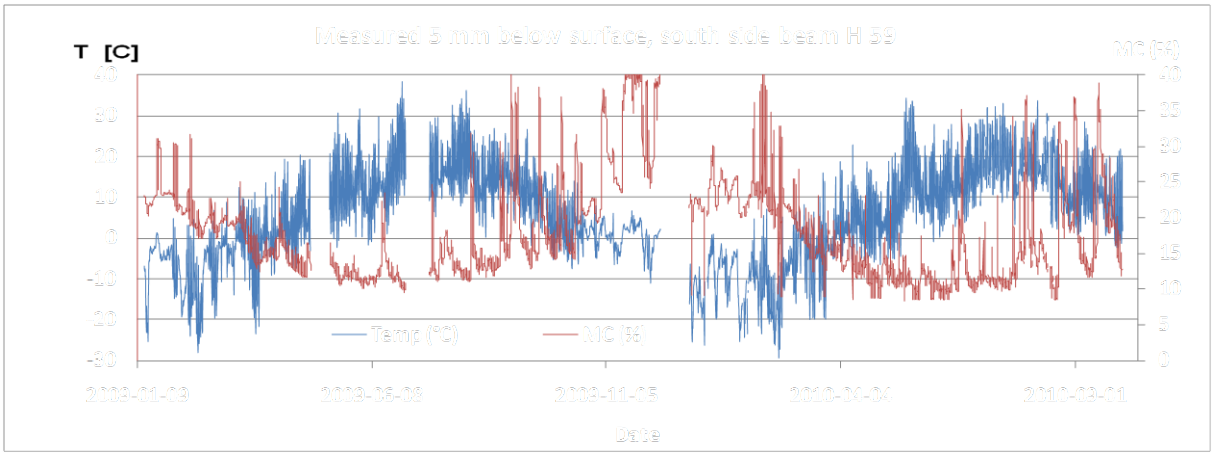

Figure 3. MC variations over a year in a beam H59 measured once every hour. Gaps in the graph correspond to values missing as a result of malfuncion of the measuring system.

Above fiber saturation point (FSP), there are values that showed some dissolution, but these have not been calibrated. Over time, the MC measurements show fluctuations that can be difficult to explain without a thorough investigation. For example, there were very high MC values in December in a winter climate. It was found that for a couple of days, the temperature was above freezing point, and probably the sun melted the snow or frost on the surface for a few hours during those days. After that, the weather turned cold again. Some sensors registered MC above 26% during a long period when temperature was around or below zero, which can be seen in Table 3, footnot 2. Unexpected high MC were found during this period. A possible reason might be measuring failure due to condensation or snow on the device. If there is a natural reason for high MC values during periods with low temperatures or measuring failure must be further investigated.

Cracks and delamination occur in the beams and columns during the first year and then increase. There are differences between the beams. For beam H59, the sensor is placed approximately 10 mm under a delamination gap showing on both the north and south sides. On beam H69, the sensor is placed approximately 10 mm above a crack on south side. On beam H86, the sensor is placed approximately 10 mm above a crack on the south side.

In this case the cracks break the paint coat and therfore the paint gives limited protection.

3.3 MC in different orientations and measurement depths

As shown in Fig. 3, there are fluctuations over the year. The data was treated in the following way. MC below 11% and above 50% have been regarded as errors in measurements or as a result of the sensors not working. These values have been excluded from the statsitics. MC values within the range of 12% and 26% are used in mean-value calculation and standard deviation based on measurements made at night (from 01:00 to 03:00) to avoid influence from the sun. Values above FSP (>26% and <50%) are shown as percent of total measured values. Table 3 shows data from January 2009 until October 1, 2010.

Table 3. Mean value of MC measurement (depth 5 mm and 15mm) on glulam beams and columns. Measured from January 2009 until October 1, 2010. Measured every night for three hours.

		H59	*H63*	*H69*	*H73*	*H76*	*H81*	*H86*
South	Mean (%)	19	14	20	16	14	16	16
5 mm	SD	5	1	5	3	2	3	3
	>FSP (%)	13[2]	0	24[1]	1	0	0	0
North	Mean (%)	20	21	20	17	16	17	18
5 mm	SD	5	3	3	2	2	2	2
	>FSP (%)	0	0	0	0	0	0	0
Under	Mean (%)	16	18	16	16	16	18	15
5 mm	SD	2	1	2	2	1	2	1
	>FSP (%)	0	0	0	0	0	0	0
South	Mean (%)	17	15	15	14	13	14	15
15 mm	SD	3	1	3	2	2	2	2
	>FSP (%)	0	0	0	0	0	0	0
North	Mean (%)	21	18	16	14	15	16	17
15 mm	SD	4	1	1	1	1	2	3
	>FSP (%)	17[2]	0	0	0	0	0	1
Under	Mean (%)	16	18	18	17	20	18	15
15 mm	SD	2	1	2	1	5	2	1
	>FSP (%)	0	0	0	0	33[2]	0	0
		H51	*H52*	*H53*	*H54*	*H55*		
Down	Mean (%)	19	17	16	17	17		
5 mm	SD	3	3	2	3	4		
	>FSP (%)	1	0	0	0	4		
Upper	Mean (%)	18	17	15	16	14[3]		
5 mm	SD	3	3	3	2	1		
	>FSP (%)	3	0	0	0	0		

[1]H69 appeared to have developed a resin pocket next to the sensor, which may have influence measurements made after the summer of 2009. [2] MC >26% for a long time during winter when wood is frozen, maybe due to snow or condensation.
[3] Many values are missing due to malfunction of the measuring sensor.

It should be noted that several of the beams are impregnated and that measurements made using resistive moisture-quotient meters do not compensate for this fact. The only way to measure moisture quotient in impregnated timber is to use the dry-weight method, which is not possible in the present application. Therefore, the measured values can be seen as a comparison of moisture changes over time, rather than absolute values.

4. CONCLUSIONS

Exposure of beams and columns outdoors show that MC measurements;
- of the beams' undersides had small fluctuations over the time irrespective of temperature and measurement depth (5 mm or 15 mm).
- on the south and north sides of the beams have larger fluctuations than underside.
- on the same beam can differ between the south and north side.
-show small difference depending on the height of the columns.
Some peaks or deviations were difficullt to explain and can be due to condensation, sensor malfunction, the influence of sunshine, cracks, resin, etc. Future work is to calibrate and verify

moisture measurements above FSP.

ACKNOWLEDGMENTS

This project is part of WoodBuild, a research programme within the Sectoral R&D Programme 2006–2012 for the Swedish forest-based industry. This Programme is jointly funded by government, industry and other stakeholders with interests related to Swedish forest-based industry. A thanks to TCN (Wood Centre North) for supporting the work.

REFERENCES

Anon. 2009. *TK Bro*. Publikation Vägverket 2009:27, July 2009. ISSN 1401-9162. (*Technical Requirements for Bridges*. In Swedish).

Boxhall, J., Carey, J. K. and Miller, E. R. 1992. The effectiveness of end-grain sealers in improving paint performance on softwood joinery, Part 3.: Influence of coating type and wood species on moisture content and fungal colonization. *Holz Roh. Werkst*. 50:227–232.

Ekstedt, J. 2002. *Studies on the barrier properties of exterior wood coatings*. Doctoral thesis, KTH-Royal Institute of Technology Department of Civil and Architectural Engineering Stockholm, Sweden, Thesis No. TRITA-BYMA 2002:5.

Elowson, T., Bergström, M. and Hämäläinen, M. 2003. Moisture dynamics in Norway spruce and Scots pine during nine years of outdoor exposure above ground in relation to different surface treatments and handling conditions. *Holzforschung* 57:219–229.

Grüll, G. Truskaller, M. Podgorski, L. Bollmus, S. De Windt, I. and Suttie, E. 2010. Moisture conditions in coated wood panels during 18 months natural weathering at five sites in Europe. *Proceedings 7th Woodcoatings Congress 2010*, PRA Hampton, Amsterdam

OmniSense 2010. http://www.omnisense.com, E-mail: info@omnisense.com

Pousette, A. and Sandberg, K. 2007. *Träbalkar och stolpar i utomhusförsök planering och utplacering*. SP Rapport 2007:35, SP Technical Research Institut of Sweden (*Beams and columns in outdoor tests, planning and placement*. In Swedish).

Pousette, A. and Sandberg, K. 2010 Outdoor tests of timber beams and columns. *Proc. International Conference on Timber Bridges*, ICBT2010, Lillehammer, Norway, 12–15 September, 2010, pp 169–178.

Rydell, Å. Bergström, M. and Elowsson, T. 2005. Mass loss and moisture dynamics of Scots pine (*Pinus sylvestris L.*) exposed outdoors above ground in Sweden. *Holzforschung* 59:183–189.

Samuelsson, A. 1990. *Resistanskurvor för elektriska fuktkvotsmätare*. TräteknikCentrum, Rapport L 9006029, Stockholm. (Resistance *curves of electrical moisture-quotient meters*. In Swedish).

Sandberg, K, Pousette, A. and Dahlquist, S. 2011. *Wireless in situ measurements of moisture content and temperature in timber constructions*. XII DBMC, Porto, PORTUGAL, 12–15 April, 2011 (not yet published).

Sell, J. 1982. Untersuchungen zur Optimerung des Oberflächeneschutzes von Holzbauteilen, Teil 1: Bewitterungsversuche mit Fensterrahmen-Abschnitten. *Holz Roh. Werkst*. 40:225–232.

Öqvist, H. 1988. *Utomhusvirkets beständighet. Fältförsök: Ovanjordexponering av Träpaneler*. Sveriges lantbruksuniversitet, Institutionen för virkeslära, Rapport nr 204. Uppsala: Sveriges lantbruksuniversitet.

XII DBMC
International Conference on Durability of Building Materials and Components
PORTO - PORTUGAL, April 12th-15th, 2011

Effect of Urbanization on Chinese Residential Building Energy Consumption: Comparative Study in Yangtze River Basin

Lizhen Huang [1]
Rolf Andre Bohne [2]
Per Jostein Hovde [3]

ABSTRACT

In the past 2 decades, China has experienced rapid economic growth, urbanization and increase in household energy use. Rapid urbanizing of the Chinese population and economic growth, is expected to strongly influence both the family structure and behaviour, which in turn will have an effect on dwelling size and energy consumption. Using statistical data from the on demography and energy from three main regions in the Yangtze River basin, a comparative analysis of the effect of urbanization on residential energy consumption in China is provided. The results show that the effect of urbanization on residential energy consumption depends on the degree of urbanization. Urbanization decrease total residential energy consumption, but increase the consumption of commerical energy, while non-commerical energy are still the main energy resource in the rural households.

KEYWORDS

Urbanization, Residential energy consumption, Lifestyle, Yangtze River basin

[1] Department of Civil and Transport Engineering, NTNU, NORWAY, lizhen.huang@ntnu.no
[2] Department of Civil and Transport Engineering, NTNU, NORWAY, rolf.bohne@ntnu.no
[3] Department of Civil and Transport Engineering, NTNU, NORWAY, per.hovde@ntnu.no

1 INTRODUCTION

The proportion of people living in urban areas rose dramatically from 13% in 1900, to 29% in 1950, to 49% in 2005 world wide, and it is expected to reach 60% living in urban areas in 2030 [UN 2005]. The Architecture, Engineering and Construction (AEC) industry, which supplies shelter to people who move from rural to urban area, plays a significent role in the urbanization process by concentration of wealth and consumption of large amounts of energy and materials simultaneously. Energy use in buildings includes embodied energy and operating energy in a broad sense. While embodied energy accounts for less than 20% of the total energy use of the service life of buildings [Sartori & Hestnes 2007], operational energy use in dwellings, residential energy, was responsible for 24% of total world energy consumption in 2008[IEA 2010]. Residential energy is the integrated outcome of buildings, climate and occupants behaviour. Occupant behaviour is a function of their socio-economic-cultural situation, such as income, household size, tradition culture, religion, etc. However, no uniform cross-country relationship between energy requirements and occupants' socio-economic-cultural situation is found.

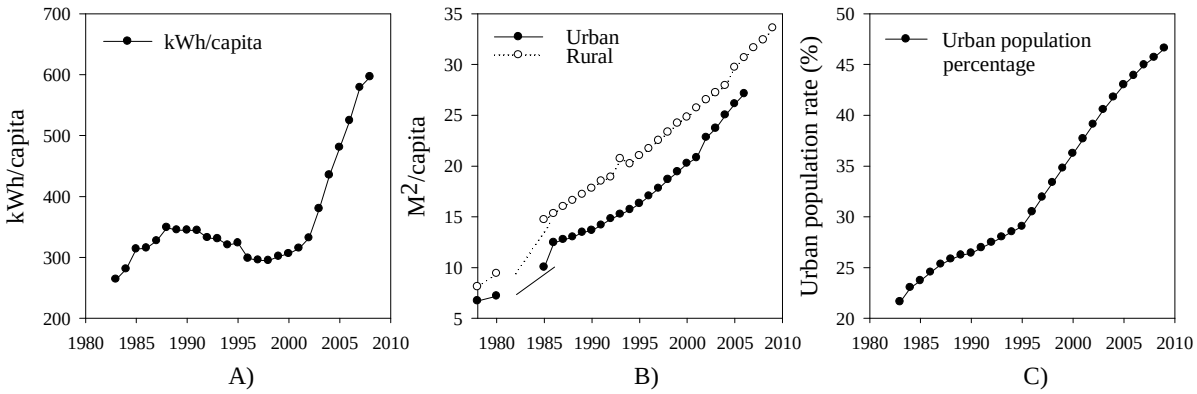

Figure 1. A) Residential energy use in China. B) Dwelling size per capita in China. C) Urbanization in China.

When moving from rural to urban areas, occupants change their lifestyle due to the change of surroundings, income, access to appliances and energy. Evidence from developed countries has shown that urban households exhibit a lower energy intensity than rural households. [Herendeen 1978; Herendeen *et al* 1981]. However, even the per capita energy concumtion is still lower than developed countires', urbanization has led China into a critical energy situation, especially in buildings [Li *et al* 2006; Li & Yao, 2009]. Per capita commercial energy consumption in the residential sector has been doubled in past nearly three decades, and especially boomed after 2000, see 'Fig. 1'. Simultaniously, since 1995 China has experienced a rapid urbanization. In addition, the per capita dwelling space in urban and rural areas both have been doubled over past two decades. Furthermore, residential commercial energy consumption in Urban is 800 kWh/capita while the value in rural is 421 kWh/capita. Thus the rural demand for commercial energy, is half of urban consumption at the end of 2008. Considering the huge Chinese population and rapid urbanizing coupling with emerging economy, this will create a great pressure upon energy supply and climate change if China is striving for an equal energy comsumtion pattern as developed countries. Together with urbanizing and enhanced standards of living, commercial energy use in the operation of dwellings has become more important for both energy supply and energy security in China, as well as the rest of the world. To realize sustainable development in China, the relationship between urbanization and residential energy use should not be ignored. Two questions may be raised: Is urbanization increasing per capita residential energy consumption in China? And how will urbanization affect total residential energy consumption in China? To answer these questions, residential energy consumption in urban and rural families in provinces and municipalities in the middle and lower reaches of Yangtze River is

investigated. The selected areas are in different stages of urbanization, but share the same climate and cultural situation.

2 DESCRIPTION OF YANGTZE RIVER BASIN

The Yangtze River basin is the home to one-third of China's population and generates more than 40% of Chinese GDP. The middle and lower reaches of the Yangtze are known as China's 'home of rice and fish'. From Chongqing which is main center of the "west developing strategy" to Shanghai which is the most developed region in China, Yangtze River drains Hubei, Hunan, Anhui, Jiangxi, Jiangsu, and Zhejiang, then flows into the East China Sea at Shanghai. The prosperous Yangtze River Delta generates as much as 20% of China's GDP. The Yangtze River basin experiences different economic developing stages from east to west. The Yangtze River is important to the cultural origins of southern China. The residents are deeply influenced by local culture traditions. The climate zone of Yangtze River middle and lower basin is typically a zone of warm temperate climates with hot summer [it is classified as hot summer and cold winter zone in the code for building thermal design in China]. Due to similar culture tradition and local climate situation, there are few differences in the building type, material and occupants behaviour between regions in the middle and lower reaches of the Yangtze. There are six provinces and two municipalities from Chongqing to Shanghai. The socio-economic conditions of middle China in Yangtze River basin such as Hubei, Hunan, Anhui and Jiangxi are silimar and Wuhan, which is the capital of Hubei province, is the center of middle China. Jiangsu and Zhejiang are similar to Shanghai. Therefore, Shanghai, Hubei and Chongqing is chosen, and will be used as examples and symbols to east, middle and west, respectively, and also the different developing stages of urbanization.

3 DATA AND METHOD

The supply system of dwellings in Chinese urban areas was reformed in 1998. Before 1998, urban habitants could get an apartment directly from the organization they work for. After reformation, they had to buy dwelling from market, with some finance aid from their organization. The real estate market started its booming after 1998. And rich rural residents started to buy their own dwelling in urban areas and became reisdnets in urban due to the developing of real estate market. Furthermore, it could be found that urbanization also started its rapid stage from 1995, see 'Fig 1'. In another hand, Chongqing became the No.4 municipality due to the strategy of west developing in April 1997, and the scope of data in Chongqing statistics year book started to change because its administrative region changed. To decrease the noise of data in comparing the situation between east, middle and west in the Yangtze river area, most information discussed here starts from 1998. Thus, all residential energy consumption data in this paper were collected from Chinese energy statistics year book from 1998 to 2008. The tme series of non commerical energy use would be from 1998 to 2007 due to the lack of information of rural non commerical energy use in 1997 and 2008. Data concerning population, urbanizaion , income, appliances ownership and so on were got from Chongqing, Hubei and Shanghai local statistics year book from 1997/1998 to 2009. Information of the degree of urbanization of the whole country was collected from Chinese statistics year book 2010.

Data collection and comparation are main study mothods in this paper. Because residential energy in energy balance sheets in Chinese energy statistics includes energy use for private cars and motors, the value of gasoline and diesel oil from this paper is excluded. Furthermore, biomass which is still the main energy resource in China and is not included in energy balance sheets, shoud be combined. Units standard value biomass energy data in China are 10^4 ton coal equialent. Provincial data of commericial energy used for household from Chinese energy statistics year book are based on physcial units. So all these data were transferred to same unit (kWh) and combined here. Comparation study of residential energy use and resoureces were used here to show the relationship between urbanization and residential energy consumption. Field studies of life style, building style and material were introduced to discuss the effect of urbanizaion on housebold energy use. Moreover, because of its climate conditions with hot summers and warm winters and residents' hot food preference, cooking is one of the most important end use of energy in Chinese households along the Yangtze river. According to Li

et al [2009], cooking is responsible for 29% of total end use of energy while appliances occupied 33% in Shanghai. Energy use for cooking is directly affected by household size and cooking times. Then residential energy per capita should be used as a main indicator for comparing energy here.

4 RESULTS AND DISCUSSION

4.1 Residential energy use in urban and rural households

Residential energy per capita in rural households is some less than residential energy per capita in urban households of Shanghai, see 'Fig.2[4]'except in year 2007 and 2008. And the average residential energy use per capita in urban areas is higher than in rural areas in Shanghai. Shanghai is the most urbanized region in Yangtze river area. However, in lower urbanization regions such as Hubei and Chongqing, residential energy per capita in rural households is higher than for urban household , see 'Fig.2'. This information is quite interesting. That means, it could not be concluded whether the urbanization has positive or negative effect on operating energy use in dwellings. However, there is no biomass use for residents in Shanghai and the commercial energy consumption in rural households in middle and west of Yangtze river area are quite low. If only commercial energy is calculated in residential energy, the residential energy per capita in rural households is much lower than for their urban neighbours.

Residential energy consumption per capita in urban households decreased geographically from east to middle and then west. GDP per capita also followed the same pattern. Also, residential energy per capita increased during the past decade in both urban and rural households. Consumption in rural households raised more quickly than in urban households in Shanghai and Chongqing except Hubei.

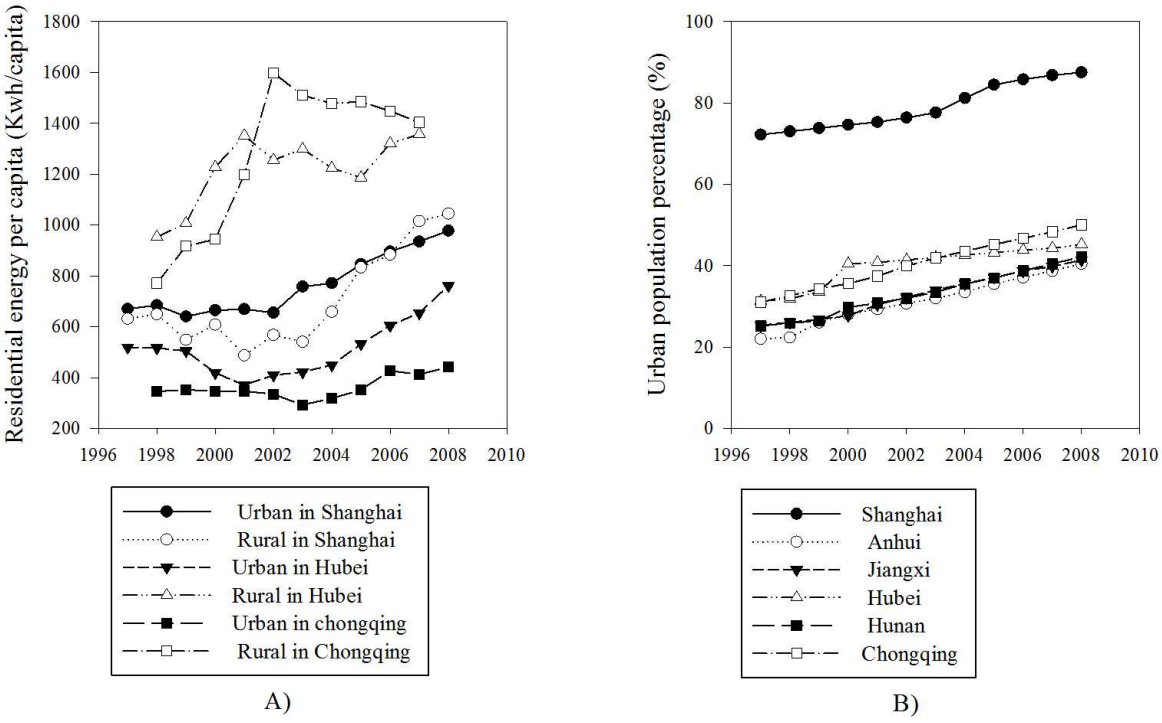

Figure 2. A) Residential energy per capita in selected region in Yangtze River basin; B) Urbanization in selected region in Yangtze River basin.

[4] In Chinese energy statistics book series, the stalks consumption in Chongqing was 15055.8 KTCE in 2006, which was much higher than in 2005 and 2007. The use of firewood was 6714.1 KTCE in 2005 and much higher than the figures of 2004 and 2006. These two data would not be trusted and the value of the consumption would be estimated as the average value of pre-year and the data of late year.

4.2 Energy resources for dwellings

During the past decade, the percentage of raw coal which is the biggest problem of pollution was decreasing, while electricity became more and more important in the residential energy supply system in Shanghai, Hubei and Chongqing, see 'Fig.3, 4 and 5'. At the end of 2008, 84% of energy used in urban households and 43.5% of energy used in rural households in Shanghai was electricity. Another energy source for rural households in Shanghai are PLG. The percentage of PLG in rural Shanghai households increased from 11.26 % to 40.71 % from 1997 to 2008. In the rural households in Hubei and Chongqing, biomass is still the main sourse of residential energy. The rate of biomass in this rural residential energy did not change vey much in the past and was 75% at the end of 2007. Main biomass used in rural households in Yangtze River basin are firewood, stalks and biogas, while biogas is not as popular as firewood and stalks due to local indirstial structure. For example, biogas is rich and used for lighting and cooking in Jiangxi where pork indirsty are well developed. More than 70% of biomass used in Anhui rural households, and more than 50% in Hubei rural households and 50% in Chongqing rural households are stalks. Around 55% -70% of biomass used in Hunan and Jiangxi rural households is firewood. Stalks and firewood are main resources of NO_X emission, while stalks are main resources of total suspended particulate (TSP) emmision [Yu, J.P. *et al* 2008]. Raw coal, which is another main energy use in rural households, is responsible for SO_2 emissions. SO_2, NO_X and TSP are related to respiratory system diseases which is one of main causes of local peasants' death. Rural habitants use raw coal, stalks and firewood for cooking and heating. There are few electirc heating systems in rural households. Then increasing the heating efficiency in buildngs and access to more clean energy in rural households in Yangtze River basin are very important for human health and energy consumption in the future.

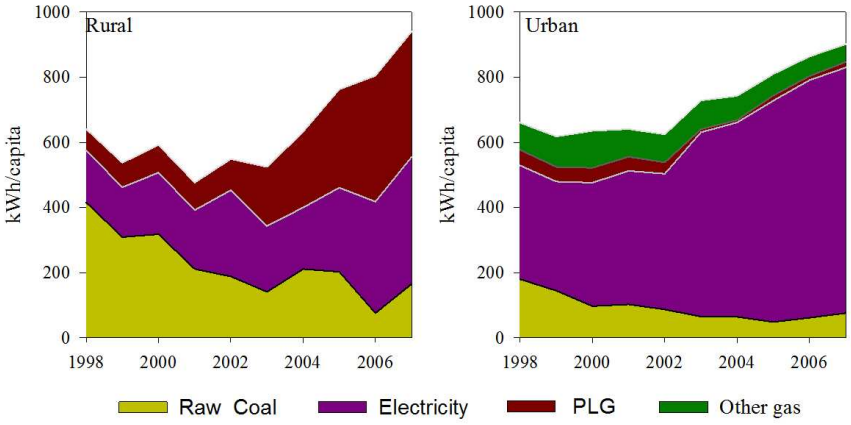

Figure 3. Main resources of household energy use in Shanghai 1998-2007: Rural (left) & Urban (right).

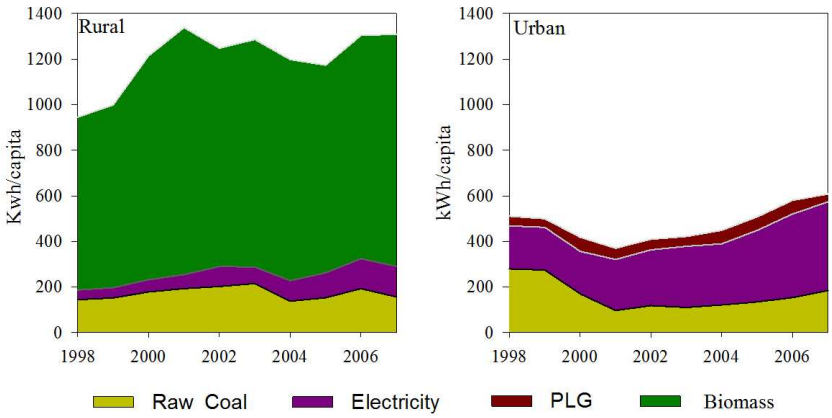

Figure 4. Main resources of household energy use in Hubei 1998-2007: Rural (left) & Urban (right)

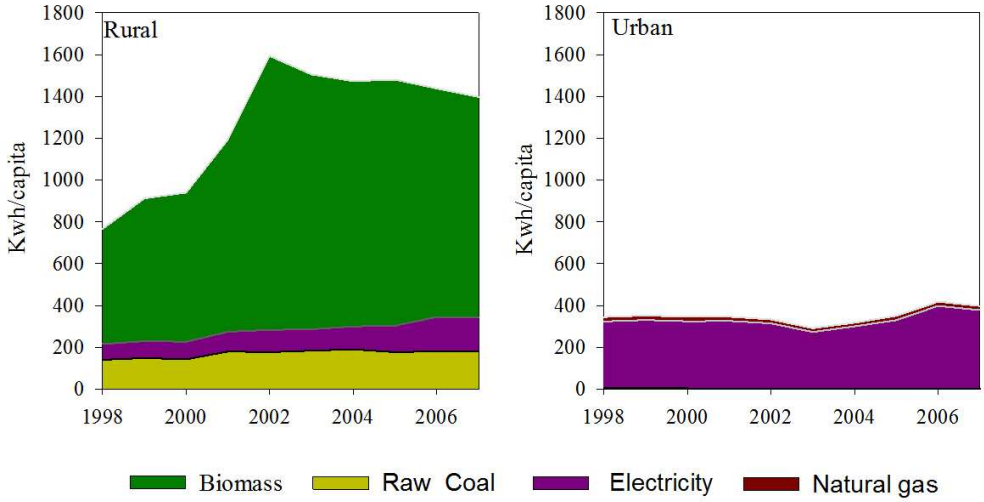

Figure 5. Main resources of household energy use in Chongqing 1998-2007: Rural (left) & Urban (right).

4.3 Building types and materials

Due to high population density in Chinese urban areas, typical dwellings in such areas are multi-floor or high-rise buildings with concrete and steel structures. The satification for local occupants regarding cooling and heating are mainly relying on air conditioners. And cooling in hot summer is more important than heating in cold winter. Energy use for cooling and heating is mainly depent on occupants' behaviour, outdoor temperature and efficency of buildings and appliances. Typical dwellings in rural regions are detached or chain buildings. Building materials and floors changed very much in the past three decades in Yangtze River basin rural region. Main material use before 1990 in rural areas were natural soil and wood. Most dwellings built before 1990s have not more than 2 floors and were fully constructed by human power. So, the embodied energy is very low. This type of dwellings has around 30-40 cm thick walls and is cool in summer but warm in winter. However, this low energy dwellings are not popular after 1990s, see 'Fig.6'. With the increased access to concrete, steel and bricks, and the fact that richer people would like to show their family status, more and more commercial materials are used for dwellings. At the same time, dwellings became higher and higher while household sizes were decreasing due to family birth control policy in China.



Dwellings built before 1990. And most of them are occupied by low income rural families.The left one was renovated with lime and ceramic tile to protect the earth wall after 2000.

Dwellings built after 1990. There is no protector of wall which is normally occupied by middle income rural families.

Dwellings built after 1990 which is normally occupied by high income rural families. And they started to use Solar energy for hot water after 2005.

Dwellings built in new small towns after 2000.

Figure 6. Typical dwellings built in different time periods.

4. 4 Lifestyle change during urbanization

While climate and efficiency of buildings and technical systems are key factors for energy consumption in buildings, the role of occupants should also be considered. Lifestyle of local people determine occupants' behaviour, and lifestyle is more determined by cultural tradition than by other factors, such as income, in China [Zhang, S. *et al* 2010]. Ocupants with different life style due to

various cultural, social and economical background could consume different amounts of energy when living in the same house with same technical system. Especially, with more and more low energy technology introduced into the building sector, the occupants behavior becomes more important. There are several common characteristics of people who live in Yangtze River basin and south China: 1) they use energy when they are in the room and they are in need for heating/cooling and lighting; 2) cooling is more important than heating, preferences to wear warm clothing in rooms during winter; 3) drying clothes with sunlight instead of electric driers; 4) prefer cooling/ heating of one room in the house and the whole family stay together. The life style of living in rural or urban areas will be some different, but their behaviour with respect saving culture is the same.

On the way towards urbanization, the habitants will change their life style due to the change of income, dwelling type/size, access to appliances and commerical energy. Firstly, the sourecs of energy will shift from biomass to commercial energy such as electricity. Families moving from rural areas to towns will not continue to use biomass due to the lack of access to stalks or firewood in towns. Secondly, Chinese people will use more appliances when they become residents in towns. In Yangtze River basin, air conditioner which is mostly used for cooling will play a key role in this change because of the climate situtation. In rural areas, few residents will use air conditioner for cooling. Since they have bigger houses and more outdoor space, they tend to cool their homes by natural ventilation and electric fans. They would like to buy meat in the closest local market, pick up vegetables in their own garden when needed, and cook by biomass, thus the need for refrigerators and ovens is less. Also they use to take showers with room temperatured water in summer and hot water only in cold winter. Rural people would like to wash clothes by hand and not by machine. Even if they have washing machine, they would like to use it only in cold winter for thicker clothes. 'Figure. 7' shows the big difference of ownership between urban households and rural households. It could be found that nearly every family have air conditioner in urban areas, while less than 5% of rural households own air conditions. Thirdly, people in towns are busier than when they lived in rural areas. For people who live in rural areas, the time is more flexible, and then their lives are less relying on appliances and they will be cooking more in their homes. There are also some different working time schedules between Shanghai and other urban areas in Yangtze River basin. In Shanghai, normal working time is from 9:00 am to 5:00 pm with a short lunch break, and people will not return home for lunch. In the middle and west, working time would be from 8:00 am to 5:00 pm with a long lunch break, and people prefer to return home for cooking. However, when urban areas become bigger and bigger, fewer and fewer people would like to return home for cooking during lunch time because their homes are not as close to their offices as before due to the expansion of the urban.

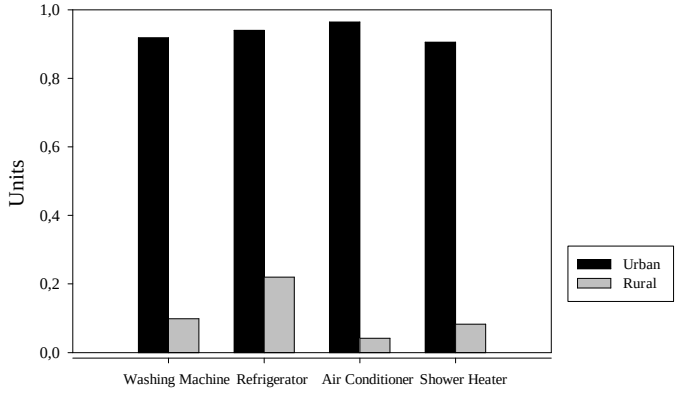

Figure 7. Ownership of major appliances per 100 households in Jiangxi 2008.

5 CONCLUSIONS

By comparison of different urbanization stages of regions with the same climate and cultural tradtions, the paper reveals that: 1) There is a negtive relationship between the degree of urbanization and residential energy use in less urbanized areas. Urbanization would decrease total energy and bio-mass

consumtion, but increase per capita commerical energy consumtion in the residential sector. However, per capita residential energy use in rural areas will be less than in urban areas with a higher level of urbanization. 2) The non commerical energy still plays a key role in China's rural household energy use, which is the main source of pollution related to health of local residents' respiratory system and with lower energy efficiency. Urbanization can decrease such hidden health danger and increase energy efficiency by using more commerical energy. 3) The change of lifestyle coupled with urbanizing plays an important role in residential energy comsumption. However, occupants' behaviour is locked in their strong saving culture.

The impact of urbanization on residential energy consumption is notable in China. And finding a way to meet the strive for a better life with less energy use is a key problem in urbanization in China today, which should be further studied.

ACKNOWLEDGMENTS

This paper has been written within the ongoing project "Knowledge base and tools for development and management of a sustainable infrastructure", which is funded by the Research Council of Norway.

REFERENCES

Herendeen, R. 1978, 'Total energy cost of household consumption in Norway, 1973', *Energy*, 3[5], 615-630.

Herendeen, R. A., Ford, C., & Hannon, B. 1981, Energy cost of living, 1972–1973', *Energy*, 6[12], 1433-1450.

International Energy Agency 2010, 'Energy balance of NON-OECD country 2010', Paris, France

Li, B., Liu, M., & McKinnell, K. G. 2006, 'Impact of urbanization on building energy consumption and the role of BEE design codes in China: A position statement', *Property Management*, 24[3], 354-364.

Li, B., & Yao, R. 2009, 'Urbanisation and its impact on building energy consumption and efficiency in China', *Renewable Energy*, 34[9], 1994-1998

Li, Z., Sun, J., &Yoshino, H. 2009, 'Field measurement and analysis of the residential energy consumption structure of Shanghai', *Tongji Daxue Xuebao/Journal of Tongji University*, 37 [3], 384-389 [in Chinese]

Sartori, I. & Hestnes, A. G. 2007, 'Energy use in the life cycle of conventional and low-energy buildings: A review article', *Energy and Building*, 39[3], 249–257

United Nations 2005,World Urbanization Prospects: The 2005 Revision, Pop. Division, Department of Economic and Social Affairs, UN
http://www.un.org/esa/population/publications/WUP2005/2005wup.htm.

Zhang, S., Yang, X., Jiang, Y., & Wei, Q. 2010, 'Comparative analysis of energy use in China building sector: Current status, existing problems and solutions', *Frontiers of Energy and Power Engineering in China*, 4[1], 2-21.

Yu, J.P., Cui P., & Wang, W.Y. 2008, 'Estimation on SO_2 , NO_x and TSP emissions from energy consumption for non production purpose in rural areas of China', *Geographical Research*,127[13],547-555 [in Chinese]

XII DBMC
International Conference on Durability of Building Materials and Components
PORTO - PORTUGAL, April 12th-15th, 2011

Retrofitting of Timber Frame Walls by Application of Vacuum Insulation Panels and Investigations of Moisture Robustness

Erland Sveipe[1]
Bjørn Petter Jelle[1,2]
Erlend Wegger[1]
Sivert Uvsløkk[2]
Jan Vincent Thue[1]
Steinar Grynning[2]
Arild Gustavsen[3]

ABSTRACT

Many older buildings with timber frame walls are ready to be retrofitted. To carry out this retrofitting in a durable and robust way is important to make the solution economic and environmental in a long-term perspective. Application of vacuum insulation panels (VIPs) can make it easier to improve the thermal insulation in building walls with a minimal additional thickness. Retrofitting of buildings using VIPs may therefore be done without large changes to the building. Additionally, U-values low enough to fulfil passive house standards or zero energy building requirements may be achieved. Thus, contribute to a reduction of the energy use and CO_2 emissions within the building sector. This work investigates the moisture robustness of two different ways of retrofitting timber frame walls, one with VIPs on the cold side and one with VIPs on the warm side. A wall module containing four different fields was built and tested between two climate rooms with indoor and outdoor climate, respectively. The module consisted of one reference field representing a timber frame wall built according to regulations in the 1970s in Norway, and three fields representing different ways of improving the thermal insulation of the reference field with VIPs. As VIP is a vapour tight barrier, the fields were tested with respect to condensation risk. The results of the experiment show that this method of retrofitting may be acceptable in certain structures within limited climate zones, humidity classes, and building envelopes.

KEYWORDS

Retrofit, Moisture, Condensation, Timber frame wall, Vacuum insulation panel.

[1] Department of Civil and Transport Engineering
Norwegian University of Science and Technology (NTNU), NO-7491 Trondheim, Norway
[2] Department of Materials and Structures, SINTEF Building and Infrastructure, NO-7465 Trondheim, Norway
[3] Department of Architectural Design, History and Technology,
Norwegian University of Science and Technology (NTNU), NO-7491 Trondheim, Norway

1 INTRODUCTION

A large amount of the buildings in Norway is built after the Second World War, especially many in the 1970s [Statistics Norway 2009]. The building tradition in Scandinavia implies that a large amount of these buildings have timber frame walls and are now ready to be retrofitted. The building regulations today are sharper, the allowed energy loss through a wall structure is close to halved in the past 40 years. If these old buildings are retrofitted properly, they have a potential of saving energy. The durability of the chosen solution of retrofitting is important for the long-term economic and environmental results. Therefore addressing the moisture robustness of the solution is important.

Vacuum insulation panel (VIP) is a high performance thermal insulating material solution with thermal conductivity in the order of 0.004 W/(mK). The VIP is built up of a fumed silica core enclosed by a high barrier envelope to maintain the vacuum. More information on the VIP's build-up may be found in e.g. Baetens et al. [2010]. The ageing of VIP is mainly caused by increased moisture content and a reduction of vacuum over time, a thorough description of the ageing effects is found in e.g. Wegger et al. [2011] and Baetens et al. [2010]. A major challenge using VIP is the risk of puncturing. A punctured panel has about 5 times higher thermal conductivity than an intact, i.e. increases to about 0.02 W/(mK) [Binz et al. 2005]. A puncture may be crucial with regard to condensation in the structure, and hence the risk of decay. Use of VIPs can make it easier to improve the thermal insulation in walls with a minimal additional thickness. Retrofitting of buildings using VIPs may therefore be done without large changes to a building, e.g. extension of the protruding roof and fitting of windows. At the same time, low U-values that fulfil the passive house standard may be achieved.

Traditional advices for retrofitting timber frame walls, are adding insulation on the outside of the existing wall. This prevents moisture problems because the temperature in the old wall structure rises. In addition, the thermal bridges in the old wall structure become insulated. However, this way of improving thermal insulation cannot uncritically be implemented using vapour tight VIPs. Introducing a vapour tight layer on the cold side of a wall increases the risk of condensation inside the wall. However, VIPs have very good insulating properties and the temperature at the warm side of the VIPs might therefore be high enough to avoid condensation. SINTEF Building Research Design Sheets [SINTEF 523.002, 2008] allow installing the vapour barrier 50 mm inside a 200 mm thick wall of regular mineral wool, e.g. ¾ of the total amount of insulation must be located on the cold side of the vapour barrier. VIPs applied on the cold side may be compared with such a case. Due to the differences in thermal conductivity, a thin layer of VIP on the outside of a mineral wool wall may still represent ¾ or more of the total thermal resistance of the wall.

This work investigates two different ways of retrofitting timber frame walls, one with VIPs on the cold side and one with VIPs on the warm side. A wall module containing four different fields was built and tested between two climate rooms with indoor and outdoor climate, respectively. The moisture and temperature conditions in the wall were logged and analysed.

2 EXPERIMENTAL

A full size realistic laboratory test may provide different results than a numerical analysis because of complex mechanisms that a numerical model may not handle. Figure 1 illustrates the test module and the four fields in 3D, seen from the bottom.

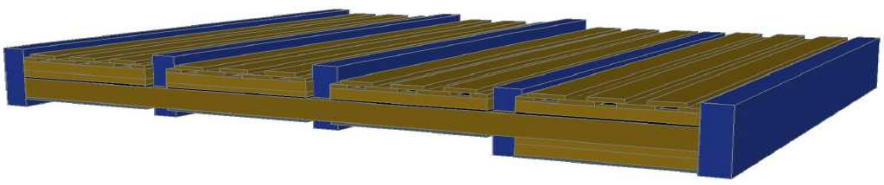

Figure 1. The test module in 3D view, seen from the bottom.

2.1. Description of Test Fields

The test module contains four fields seen in Figure 1 - 3. Field 3 (F3) is built without VIPs and represents the original structure before retrofitting, i.e. a timber frame wall from the 1970s. The three other fields (F1, F2 and F4) represent three different ways of improving thermal insulation of the reference field (Figure 2):

- F1: Outside 30 mm VIP
- F2: Outside 20 mm VIP
- F3: Reference field
- F4: Inside 30 mm VIP

The four fields are separated by plastic film and extruded polystyrene (XPS), i.e. separated with respect to moisture and heat transport. Field 1 and Field 4 have an initial U-value about 0.12 W/(m^{2}K) with VIPs in their pristine condition.

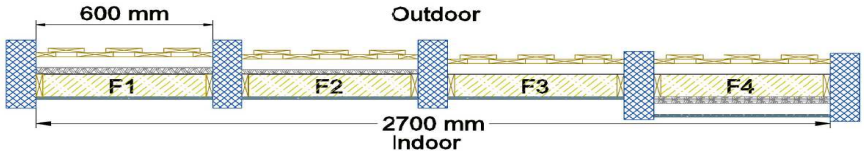

Figure 2. Horizontal cross-section of the test module. Note that the fields have no vapour barrier.

The build-up of Field 2 from outdoor to indoor (Figure 2 and Figure 3):

- Vertical weather boarding
- Furring strip (attached with an alternative fastener, not shown here)
- VIP, joint not taped (attached with the same alternative fastener)
- Wind barrier (bitumen-impregnated paper)
- Mineral wool
- Plasterboard

Normally, the wall should have a vapour barrier as well but this was omitted due to a short timeframe for the experiment. Not installing a vapour barrier represents a conservative modification and might be considered as a worst-case scenario, but may nevertheless be a realistic case too.



Figure 3. Vertical cross-section of the test module. Note that the field has no vapour barrier, only the vapour tight VIPs at the cold exterior side (F2, see Figure 2).

The vacuum insulation panels used in the experiments in this work are of the type Vacupor NT - B2 from the producer Porextherm. Vacupor NT – B2 is a micro porous insulation material and consists of inorganic oxides. The main constituent is fumed silica. Other components are: opacifiers for minimizing infrared radiation, and silicates. The panel is heat sealed with a high barrier film to maintain the vacuum [Porextherm 2009].

2.2. Temperature and Moisture Measurements

Thirty six sensors of three different types were used in experiment:

- Thermocouple
- Air humidity sensor including thermocouple (two logging channels)
- A tailor-made moisture sensor (seen in Figure 5)

The thermocouple consists of a cable with two separate conductors (copper and constantan). The air humidity sensors were of the type “VAISALA Humidity and temperature transmitter TYPE HMP233”, which here are abbreviated as *RH air sensors*. These sensors were calibrated over a water

solution of NaCl, i.e. at 75.36 % RH at 23 °C. The calibration was later re-examined by measuring the RH over a water solution of KNO3 (94.0 % RH at 23 °C). The three different sensors are depicted in Figure 4.

An alternative tailor-made moisture sensor was used in the experiment. The background was that the point of measurement using regular air-humidity sensors might be eccentric from the surface of the material-layer where the measurement is wanted. Condensation might therefore occur on a cold material surface while the air-humidity sensor shows a RH below 100 %. The idea was therefore to measure the electrical resistance on a thin material taped on the respective surface, this way the measurement could come as close to the material surface as possible. The build up of the sensor was of double-sided tape, electrodes and copy paper The wetness sensor is to be considered as an indicator of RH and condensation, and must be further verified. The principle and calibration of the sensor is not further explained here, but the result chapter shows some of its properties. The moisture sensor is henceforth called the *wetness sensor* and may be seen in Figure 4 (marked C).

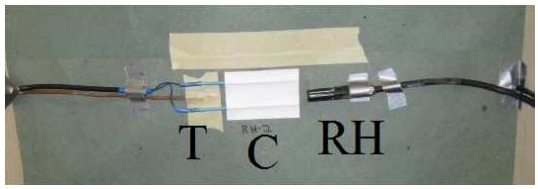

Figure 4. From the left: Thermocouple (T), tailor-made wetness sensor (C), and RH air sensor (RH) was installed on the wind barrier before the mineral wool was installed.

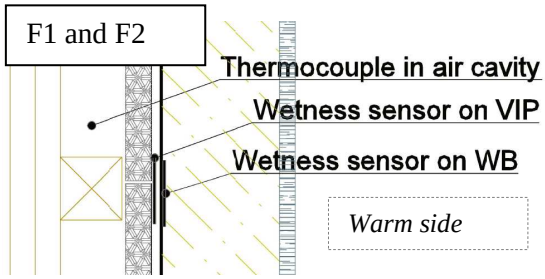

Figure 5. F1 and F2 had a wetness sensor both on the wind barrier and on the VIPs joint at the middle of the fields. The thermocouple in air cavity is also depicted.

The most critical location for condensation was considered to be on the warm side of the VIPs in Field 1 and 2 (Figure 2), and at the warm side of the wind barrier at the reference field (F3). The thermal resistance of the wind barrier is marginal and the type of wind barrier used has a small water vapour resistance so condensation was expected to occur at the wind barrier as well as on the VIP surface. Hence, for practical reasons and the desire of having the sensors at the same locations for all four fields most of the sensors in the experiment were located at the warm side of the wind barrier. However, there were also sensors at other locations in the wall. A wetness sensor was glued directly over the VIPs joint in F1 and F2 as shown in Figure 5, i.e. F1 and F2 had wetness sensors on both sides of the wind barrier located in the middle of the field. There were thermocouples in all four ventilated air cavities, located as seen in Figure 5. In addition, air temperature and RH were measured in both climate rooms.

Vertically locations of sensors were at the top, middle and bottom of the fields. The sensors at the top and the bottom are located 100 mm from the sills where convection in the mineral wool is considered to have the largest influence. The sensors at the middle were located directly within the joints of the VIPs, i.e. 1200 mm above the bottom sill.

2.3. Data Logging

The 36 sensors gave a total amount of 42 logging channels because of six combined Humidity and temperature (RH air) sensors. Three different logging systems were used in the experiment. Because of the large number of sensors, the thermocouples and the air humidity sensors were logged by two systems; *Solartron 35951C I.M.P.* connected to *Orchestrator 1.4.7* software, and *FLUKE Hydra data logger 2625A* with appurtenant software, respectively. The new moisture sensors required a separate logging system. This was a logger made by SINTEF and contained a *Greisinger GMH 830 Material moisture meter*. The logger was connected to a computer via *LabVIEW8.6* and the result logged to a data file.

2.4. Procedure

The test module was built between two climate rooms in the laboratory. The outdoor temperature was − 18 °C. The relative humidity in the outdoor climate was not controlled, but was in the order of RH ~ 60 %. The relative humidity in the indoor climate was adjusted in steps of 10 % while the temperature was held constant at 20 °C:

1. RH 30 % (Internal moisture excess ~ 4 g/m^3)
2. RH 40 % (Internal moisture excess ~ 6 g/m^3)
3. RH 50 % (Internal moisture excess ~ 8 g/m^3)
4. RH 60 % (Internal moisture excess ~ 10 g/m^3)

These moisture levels are henceforth called *climate steps*. The term *internal moisture excess* [EN ISO 13788, 2001] represents the difference in moisture content (g/m^3) from the indoor to the outdoor air. The term is often used in practical condensation calculations and divides different type of buildings into *humidity classes* from humidity class 1 (< 2 g/m^3, e.g. a warehouse) to humidity class 5 (> 8 g/m^3, e.g. a swimming pool), see EN ISO 13788 [2001] for further details.

3 RESULTS AND DISCUSSION

In the following note that the value of the wetness sensor goes beyond 100 in the plots of the results. This is because of certain errors concerning use of a wood moisture sensor (measuring the wetness sensor) and is not further commented here. The values below 100 are equivalent with percent air RH. The values above 100, however, indicate condensation at the sensor. Calibration results have shown that values above 105 are to be considered as condensation, this includes a small safety margin, i.e. free water on the surface leads to low electrical resistance and thus the RH equivalent may peak far above 100 % (above calibration range), e.g. as in Figure 7 and Figure 8. Thus, the ordinate axes of Figure 6 to Figure 9 have not been denoted as percentage RH. The climate room on the cold side had problems keeping the temperature at -18 °C any longer than about 5 days. Further details from these experiments may be found in Sveipe et al. [2011].

None of the fields experienced condensation during step 1 or 2 (described in the procedure), with a RH of ~ 30 % and ~ 40 %, respectively. Hence, day 1 to day 15 of the experiment are only plotted for Field 2, see Figure 6. The alternation of RH in the climate room might be seen in Figure 6. The variation is up to 25 % from the lowest to the highest value. This problem was however reduced past test day 15, when a different humidifier was installed. In climate step 3 and 4 condensation was measured in Field 1 and 2 as shown in Figure 7 and Figure 8. The RH inside the climate room is shown in the lower plot of the figures, and has a variation of about 10 % from the lowest to the highest value.

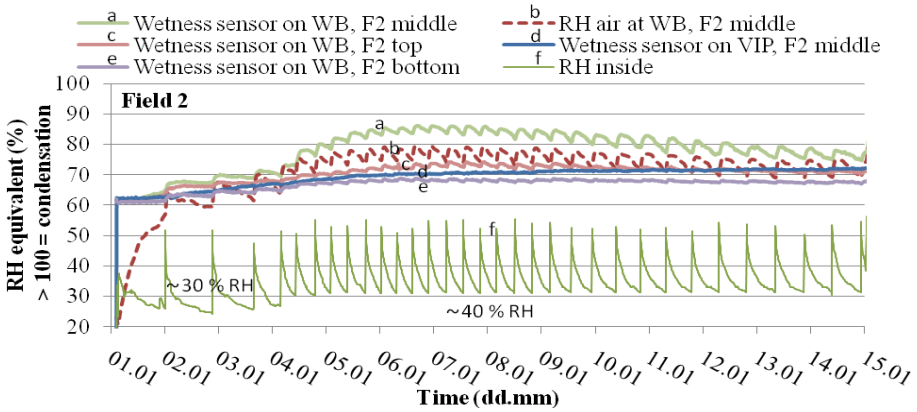

Figure 6. Moisture sensors in Field 2 during climate step 1 and 2. The RH equivalent values of the four wetness sensors and the RH air sensor are shown. The location of sensors is depicted in Figure 5. The climate room RH was ~ 30 % from day 1 to 4, and ~ 40 % from day 4 to 15 (lower plot).

Figure 7 shows Field 1 that has 30 mm VIP on the outside, during the two climate steps with RH ~ 50 % and ~ 60 %. The field showed condensation at RH ~ 50 %, which was not expected for this climate step compared to numerical simulations, at least not after that short period of exposure. This might be caused by the alternations in RH inside the climate room. The moisturising at the RH peak is possibly larger than the exsiccating at the RH bottom. Small air leakages in the structure might also contribute to the measured condensation.

The wetness sensor shows condensation (value of 105) when the RH air sensor shows about 95 % RH. A possible explanation is that the RH air sensor is located about 5 mm from the wind barrier. Moreover, the wetness sensor is more influenced by condensed water on the vapour barrier than the RH air sensor. The wetness sensor located on the VIP joint has lower values than the wetness sensor on the wind barrier. Assuming that both sensors have the same temperature, condensation may be caused by the small vapour resistance of the wind barrier. The wetness sensor on the VIP (behind the wind barrier) then becomes moisturised by the wet wind barrier, which causes the sudden increase at the wetness sensor on the VIP. Another factor is the convection over the VIP joints (about 2 mm opening) that might dry the sensor somewhat. A third aspect may be time delay due to the small vapour resistance of the wind barrier, but this should not result in a sudden increase.

The wetness sensors at the top and the bottom showed different development at the end of climate step 3. A possible explanation is that the wetness sensor at the top experiences a lower RH caused by an increase in the outdoor temperature. The increase at the wetness sensor at the bottom may be condensed water that runs down the vapour barrier and moisturises the sensor.

Figure 8 shows Field 2 that have 20 mm VIP on the outside, during the two climate steps with RH ~ 50 % and ~ 60 %. In accordance with numerical simulations, the field had condensation at both climate steps 3 and 4. However, an interesting difference between Field 1 and 2 is the wetness sensors on the VIPs. In Field 1 this sensor (on the VIPs) measures condensation at both climate steps. In Field 2 however, the sensor measures condensation only for climate step 4 even if this field is less insulated (only 20 mm VIP). The temperatures measured at the warm side of the wind barrier (not plotted here) show that the wetness sensor at Field 1 has a higher temperature than the wetness sensor in Field 2. This is according to what one should expect, so the reason why the wetness sensor at the VIP joint in Field 2 does not show condensation is unclear. It might be caused by difference in workmanship of the wall. The stiff wind barrier was hard to fit properly and this might cause air cavities between the VIP and the wind barrier that is different from Field 1 to Field 2. Another unexplainable occurrence is the sudden drop at the wetness sensor at the VIP joint in Figure 8. What might have caused this is not investigated.

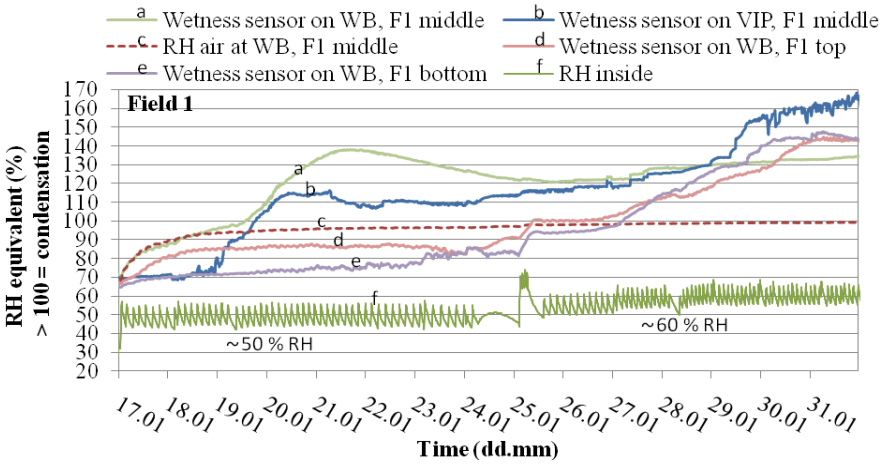

Figure 7. Moisture sensors in Field 1 during climate step 3 and 4. The RH equivalent values of the four wetness sensors and the RH air sensor are shown. The location of sensors is depicted in Figure 5. The climate room RH was ~ 50 % from day 17 to 24, and ~ 60 % from day 26 to 32 (lower plot).

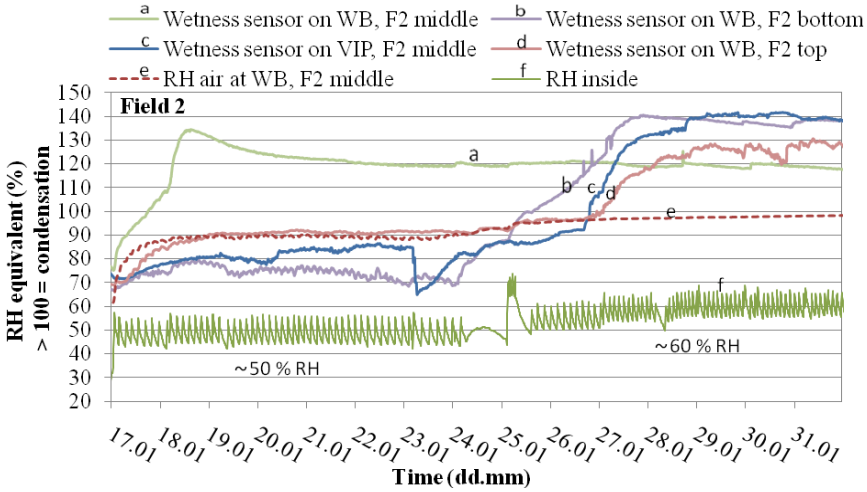

Figure 8. Moisture sensors in Field 2 during climate step 3 and 4. The RH equivalent values of the four wetness sensors and the RH air sensor are shown. The location of sensors is depicted in Figure 5. The climate room RH was ~ 50 % from day 17 to 24, and ~ 60 % from day 26 to 32 (lower plot).

Figure 9 shows the reference field (F3) during the two climate steps 3 and 4. None of the sensors shows condensation. The wetness sensors are not tested for temperatures below 0 °C and are therefore less trustworthy in Field 3. It is reasonable that the electrical resistance increases at low temperatures. Therefore, the values from the wetness sensors in this field are lower than the RH air sensor.

Condensation might be present in the reference field (F3) without being measured because the sensors were placed at a location on the cold side where the temperature was below zero degrees Celsius (measured between – 6 ºC to – 14 ºC for Field 3). The outside temperature was in addition increasing from the start of the climate step to the end (the cooling unit was manually de-iced for each climate step). This contributed to hold the RH air sensor on the wind barrier stable, as seen in Figure 9. Field 4 performed well during the entire test, i.e. no condensation occurred. RH at the middle of the wind barrier was around 50 %, thus far from the risk of condensation. The results from this field are therefore not shown in graphical plots.

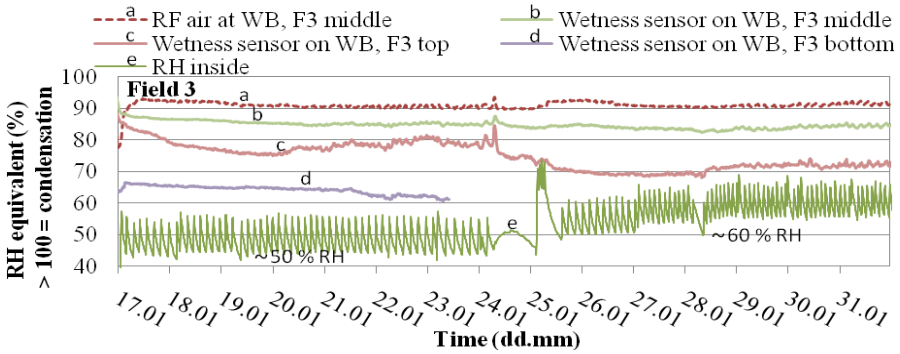

Figure 9. Moisture sensors in Field 3 during climate step 3 and 4. The RH equivalent values of the three wetness sensors, as well as the RH air sensor are shown. The wetness sensor at the bottom was to dry and stopped giving reliable outputs. The location of sensors is depicted in Figure 5. The climate room RH was ~ 50 % from day 17 to 24, and ~ 60 % from day 25.5 to 32 (the lower plot).

The results of the experiment show that 20 mm and 30 mm VIPs may be used at the outside of a 100 mm mineral wool wall and be robust enough against condensation. Provided that the building has an internal moisture excess less than 6 g/m^3 and do not experience exterior climate conditions more severe than - 18 °C/RH 60 %, and interior climate conditions more severe than 20 °C (RH ~ 40 % with 6 g/m^3 internal moisture excess). Consequently, this method of retrofitting requires limitations to climate zone, humidity class, and the building envelope of a structure. Note that these results might

not be valid for aged or punctured VIP with higher thermal conductivity (and as earlier noted the experiments were run without a vapour barrier).

4 CONCLUSIONS

Experimental work has been carried out on a test module consisting of four fields. One reference field representing a timber frame wall built according to regulations from the 1970s in Norway, and three fields representing different ways of improving the thermal insulation of the reference field by application of vacuum insulation panels in durable and moisture robust ways. The results of the experiment show that this method of retrofitting may be acceptable with respect to condensation risk in certain structures within limited climate zones, humidity classes, and building envelopes.

ACKNOWLEDGMENTS

This work has been supported by the Research Council of Norway and several partners through the SINTEF and NTNU research project *"Robust Envelope Construction Details for Buildings of the 21st Century*" (ROBUST) and *"The Research Centre on Zero Emission Buildings*" (ZEB). Franco Bløchlinger from Metallplan and the manufacturer Porextherm are acknowledged for supplying the test samples of vacuum insulation panels.

REFERENCES

Baetens, R., Jelle, B.P., Thue, J.V., Tenpierik, M.J., Grynning, S., Uvsløkk, S. & Gustavsen, A., 2010, 'Vacuum insulation panels for building applications: A review and beyond', *Energy and Buildings*, **42**, 147-172.

Binz, A., Moosmann, A., Steinke, G., Schonhardt, U., Fregnan, F., Simmler, H., Brunner, S., Ghazi, K., Bundi, R., Heinemann, U., Schwab, H., Cauberg, J.M., Tenpierik, M.J., Johannesson, G., Thorsell, T., Erb, M. & Nussbaumer, B., 2005, 'Vacuum insulation in the building sector. Systems and applications (Subtask B)', Final report for the IEA/ECBCS Annex 39 HiPTI-project.

EN ISO 13788, 2001, 'Hygrothermal performance of building components and building elements - Internal surface temperature to avoid critical surface humidity and interstitial condensation - Calculation methods'.

Porextherm, 2009, 'Vacupor NT – B2, data sheet', http://www.porextherm.com/web/pdfdownload.htm?ID=255&doctype=PDF_EN&lang=en&externeswindow=2&ts=1270722658 (Retrieved 08.04.2010).

SINTEF 523.002, 2008, SINTEF Building Research Design Sheets no. 523.002, 'Yttervegger over terreng. Egenskaper og konstruksjonsprinsipper. Krav og anbefalinger' (Exterior walls above ground. Properties and construction principles. Requirements and recommendations), SINTEF Building and Infrastructure, Norway.

Statistics Norway, 2009, 'Boliger, etter bygningstype og byggeår (K)', (Buildings, ranged by type of building and year of construction), Table 06266.

Sveipe, E., Jelle, B.P., Wegger, E., Uvsløkk, S., Grynning, S., Thue, J.V., Time, B. & Gustavsen, A., 2011, 'Improving thermal insulation of timber frame walls by retrofitting with vacuum insulation panels – Experimental and theoretical investigations', Accepted for publication in *Journal of Building Physics*.

Wegger, E., Jelle, B.P., Sveipe, E., Grynning, S., Gustavsen, A., Baetens, R. & Thue, J.V., 2011, 'Ageing effects on thermal properties and service life of vacuum insulation panels', In press in *Journal of Building Physics*.

XII DBMC
International Conference on Durability of Building Materials and Components
PORTO - PORTUGAL, April 12th-15th, 2011

Service Life Prediction of Surface Finishing Coating Systems Based Upon Markov Chain Model

Kei Matsuda [1]
Kei-ichi Imamoto [2]
Manabu Kanematsu [3]
Takumi Ota [4]
Kenji Motohashi [5]
Takashi Nıreki [6]

ABSTRACT

It is becoming increasingly important for us to maintain and manage buildings using more rational methods, and the degradation of finishing material is significant in this regard. However, because many factors contribute to degradation, it can be difficult to analyze them quantitatively. For this reason, the service life of finishing materials typically remains unclear, which creates problems in maintenance and management. To address this problem, we surveyed actual buildings in order to better understand the degradation of finishing material. In the three areas we investigated, we focused on five degradation phenomena: gloss level, colour difference, chalking, cracking, and the coefficient of air permeability. The results of our survey of the external walls of these buildings showed that cracking was correlated with the age of deterioration, and the gloss level and coefficient of air permeability tend to deteriorate with age. We also simulated the future progress of degradation using a Markov chain model; by putting only the present condition in the Markov chain model, we are able to predict the future condition, without reference to the past condition. The simulation model thus enables us to establish a rational renovation program for existing buildings.

KEYWORDS

service life prediction, building survey, external coatings, markov chain analyses, degradation

[1] Tokyo university of science, Tokyo, JAPAN, kei19corona@gmail.com
[2] Tokyo university of science, Tokyo, JAPAN, imamoto@rs.kagu.tus.ac.jp
[3] Tokyo university of science, Tokyo, JAPAN, manabu@rs.noda.tus.ac.jp
[4] Tokyo university of science, Tokyo, JAPAN, aozora1ba@yahoo.co.jp
[5] Shibaura institute of technology, Tokyo, JAPAN, motoken@shibaura-it.ac.jp
[6] Center for Better Living, Ibaraki, JAPAN, nireki@tbtl.org

1 INTRODUCTION

In this study, we discuss how to determine the service life of buildings based upon a survey of multi-family flats by focusing on finishing materials. The Factor method which estimates the service life is described in ISO[1], originated from the Japanese Guide[2]. In this method, the service life multiplies the Reference Service Life by a number of factors (coefficient of environment, workmanship, direction, age, etc.) that degrade the finishing materials. The quantification of these factors, however, is difficult because they are numerous and because the building data in Japan is insufficient. These problems combine to make it difficult to manage the maintenance of buildings. For this reason, we are needed to provide a database which could help for the rational way to estimate service life of building materials and components.

2 DETALS OF SURVEY

2.1 Objective Buildings:

Use: Publicly owned Multi-family high-raised dwellings
Structure: Reinforced Concrete construction
Location: In three different areas, all are within the Greater Tokyo Metropolitan zone.
under rather close to pastoral environment. Building age: shown in Table 1.

2.2 External Coating Systems

Three types of Multi－layer rendering coatings*
*one of the widely applied surface coating for concrete, cement mortar, inorganic sidings in Japan. This system is often consisted of primer, under coat, main layer and top coating by applying spray and troweling. Typical surface texture can be observed in Fig.1

2.3 Gloss Level Retention

We measured gloss levels using a gloss checker. A section of a building that has been unaffected by rain and sun is defined as the initial value. The relative values of gloss level retention are then evaluated based on this initial value (Table. 2).

2.4 Color Difference

A colour system was applied on CIE L*a*b*. The colour phase, brilliance, and chroma of finishing materials were measured with a colour-difference meter. By comparing these values with other initial values, as was done with gloss level retention, the colour difference is calculated (Table. 2).

2.5 Chalking

In order to investigate chalking, powders on the surface walls were gathered using vinyl tape (5×10cm). Chalking is examined in terms of area and density (Table.2).

2.6 Cracking

Cracking is a degradation phenomenon that is easily evaluated by visual investigation. Conditions of crack degradation were categorized from level 0 to level III (Table. 2).

2.7 Coefficient of Air Permeability

Air permeability is measured by a Torrent permeability tester; the tester system is shown in Fig. 2. Air permeability is measured by changes in pressure in the inner chamber of the tester. All the excess air

flowing into the outer chamber is evacuated, so the air flow into the inner chamber is basically unidirectional and is unaffected by unwanted ingress of air along the building skin. [6]

Table 1. Survey Buildings

Area Name	Age (Year)
A area	9
	12
	16
B area	11
	14
	16
C area	5
	7
	9

Table 2. Measurement of Degradation

Degradation	Value	Method
Gloss Reduction	Gloss Level Retention	JIS K 5600-47(1999) JIS Z 8741(1997)
Discoloration	Color Difference	JIS Z 8722(2009)
Chalking	Peel off tape method	JIS K 5600-8-6(1999)
Cracking	Visual observation	
Permeability Performance	Coefficient Of Air Permeability	

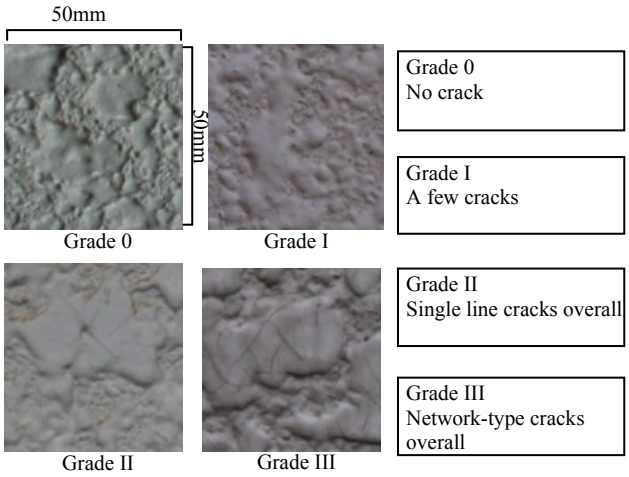

Fig. 1 Classification of Crack Degradation

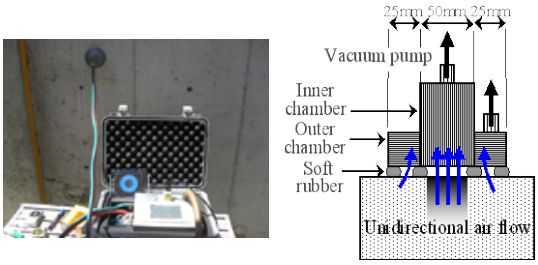

Fig. 2 Left: Measuring Device; Right: Principle of Torrent Method

3 SURVEY RESULTS

3.1 Gloss Level Retention

Figs. 3 and 4 show histograms of the B and C area. The closer the gloss level retention value is to 0%, the more the finishing material has degraded. The survey results show that the measured values of a 14-year-old building in B area display the worst Gloss Level Retention. Thus, a tendency toward aging degradation is not noticeable. The degradation of each surface in C area proceeds according to the order of building age during the period from 5 to 9 years old, which indicates that an aging degradation can be distinguished. Therefore, it can be estimated that the degradation of the gloss level can reach its peak in about 10 years.

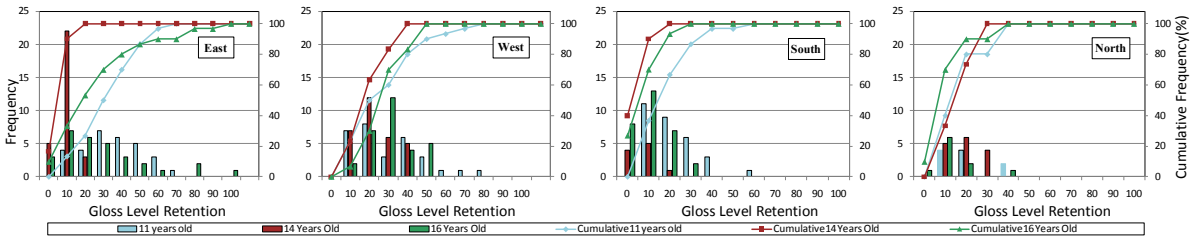

Fig. 3 B area - Gloss Level Retention

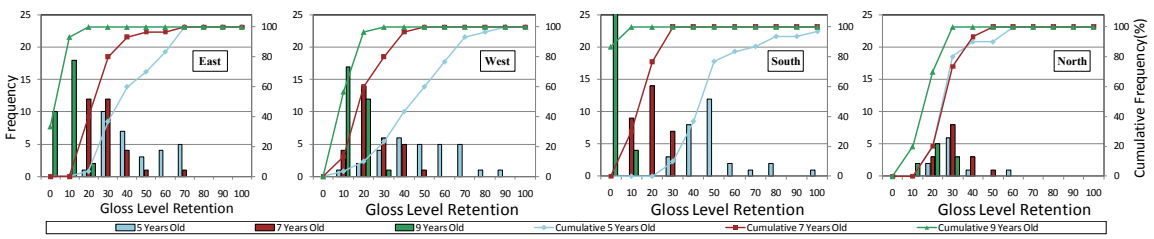

Fig. 4 C area - Gloss Level Retention

3.2 Colour Difference

Fig. 5 and 6 show histograms of colour difference obtained from our examination of the A and C area. The greater the colour difference, the more severe the degradation. At the A area, the degradation on the west and north sides is the most severe in the youngest building (which is 9 years old). At the C area, the middle building (7 years old) shows a tendency toward the most severe degradation. Therefore, in terms of colour difference, it seems that the factors that most influence degradation are craftsmanship, solar radiation, and rain exposure, rather than aging.

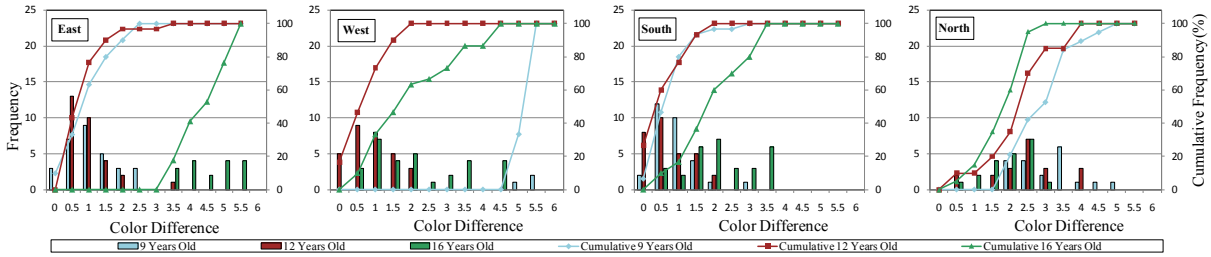

Fig. 5 A Area - Colour Difference

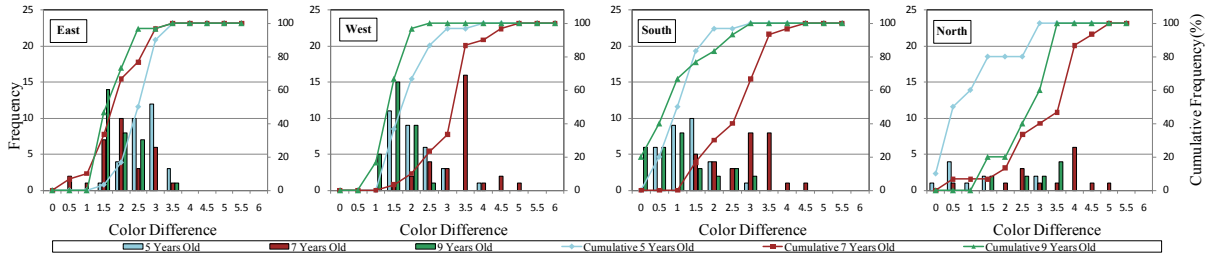

Fig. 6 C Area - Colour Difference

3.3 Chalking

Figs. 7 and 8 show the histograms of chalking for the B and C areas. In the B area, the 11-years-old building displays the most severe degradation. In the C area, chalking proceeds as the building gets older. These results suggest that chalking is related to aging, and the younger area has the greater tendency toward aging degradation.

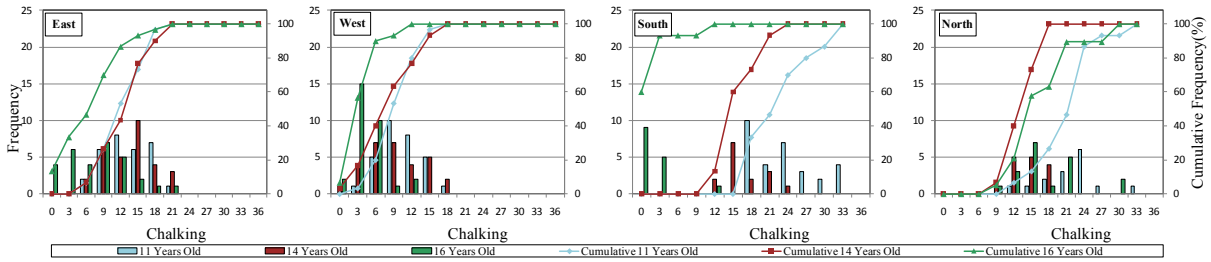

Fig. 7 B Area - Chalking

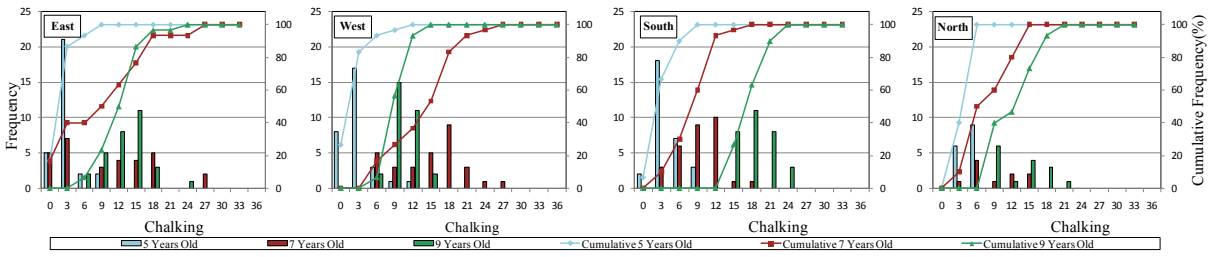

Fig. 8 C Area - Chalking

3.4 Cracking

Figs. 9, 10, and 11 show the results of our evaluation of the degrees of cracking in the A, B and C areas. In all three areas, the north side displayed the most severe degradation. In particular, the A and C areas showed the most pronounced tendency toward aging degradation. There are differences between the north and other sides in terms of solar radiation and relative humidity. Despite the fact that the solar radiation on the south side is different from that on the east and west sides, the effect of solar radiation is not conspicuous. This suggests that humidity (moisture) is the factor that is most responsible for cracking. Further, research would be needed to determine the relationship between cracking and humidity.

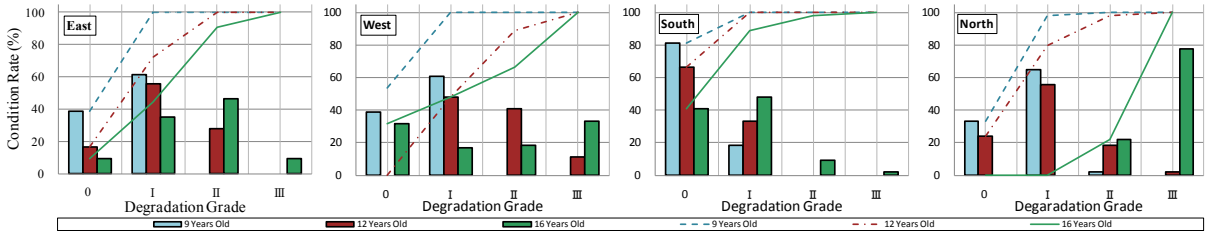

Fig. 9 A Area - Cracking

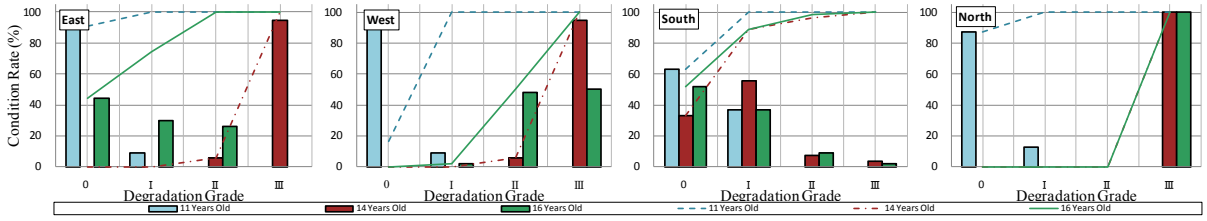

Fig. 10 B Area - Cracking

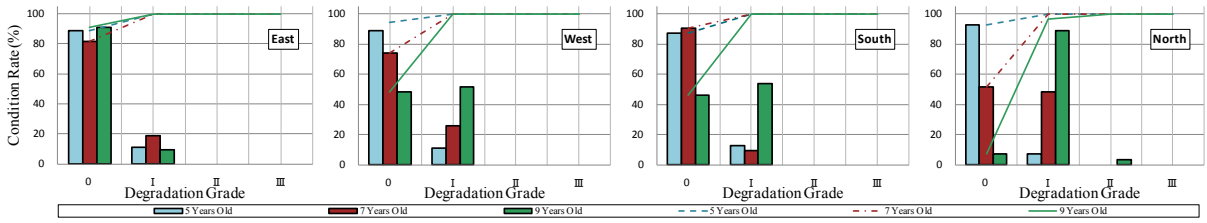

Fig. 11 C Area - Cracking

3.5 Coefficient of Air Permeability

Table 3 shows the condition of the insolation and exposure to rain in each member. Figs. 12, 13 and 14 present the results of permeability testing in each area. In the A area, there is no conspicuous tendency toward aging degradation.

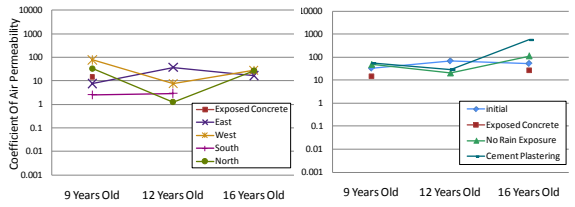

Fig. 12 A Area - Coefficient of Air Permeability

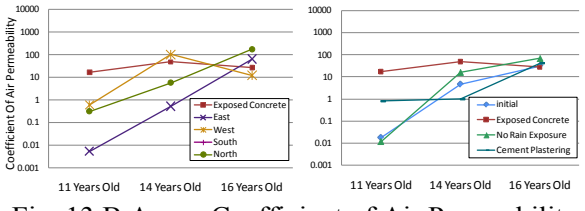

Fig. 13 B Area - Coefficient of Air Permeability

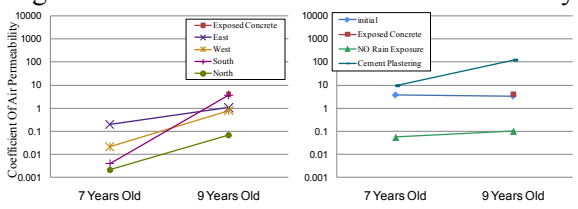

Fig. 14 C Area - Coefficient of Air Permeability

Table 3. Condition Of Member

Member / Condition	Initial	Exposed Concrete	No Exposure to Rain	Outer Wall	Fundation (Cement Plastering)
Insolation	×	×	○	○	○
Rain	×	×	×	○	○

Moreover, because the permeability of each member is equivalent to that of exposed concrete, the performance of the finishing material in protecting the building frame is low from the point of view of permeability. In the B area, there are changes in permeability except on the west side, which indicates a conspicuous tendency toward aging degradation. In the 16-year-old building, because the permeability on each side is equivalent to that of an exposed concrete member, the service life of the finishing material is estimated to be about 16 years, in terms of resistance to carbonation. In the C area, there is aging degradation on each side. The permeability of the cement plastering is greater in all the housing estates, which suggests that this kind of plastering is not effective at improving permeability. Incidentally, there is very little correlation between the two degradation categories of cracking and permeability.

3.5.1 Evaluation of Permeability of Finishing Material

Fig. 15 shows the histograms for each are in terms of the coefficient of air permeability. The relationship between the accelerated carbonation depth and the coefficient of air permeability is plotted along with an approximated curve. The coefficient of air permeability is evaluated on a scale ranging from Very good to bad. In the A area, the total frequency value from Normal to Bad exceeds 60%. In the B area, it generally ranges from Very good to Good. In the C area, which also ranges from Very good to Good, it is estimated that this area is in an almost healthy condition.

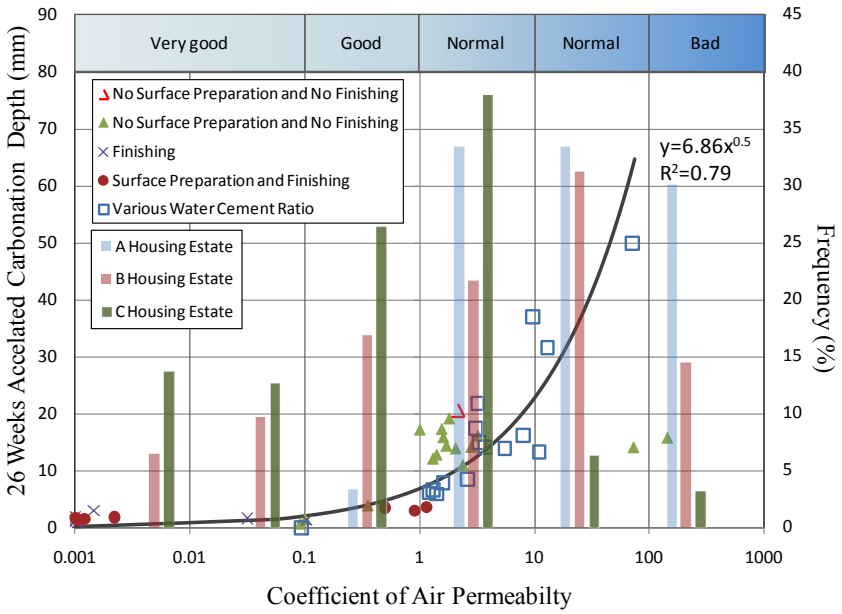

Fig. 15 Permeability Evaluation

4 MARKOV CHAIN MODEL

The Markov Chain Model is a probability theory model in which a future condition is decided only by the present condition, unrelated to past conditions. This model is employed in cases in which the mechanisms and factors at work are not clearly defined, such as in pier maintenance and as a management tool in civil engineering. Fig. 16 presents a conceptual diagram of this model, in which two definitions can be seen. First, there are 4 grades of degradation, ranging from 0 to III. Second, Xn is the probability of transition from one grade to the next grade after any time (t) passes. Using this model (Fig. 17), it is possible to simulate aging degradation. In this study, Xn is derived from the survey results for each area.

4.1 Simulation of Degradation

Each condition of degradation is subdivided into each of the grades (Table 4), and the transition probabilities are calculated in accordance with the principles that all degradation grades are present. Figs. 18 - 23 show the results of the simulation based on the Markov Chain Model. The building ages used are shown in the parentheses. Here, we assume that the service life of the finishing material is the time it takes for II+III to reach 80% in each degradation phenomenon (gloss level retention, colour difference, and chalking), except for cracking, for which we assume a value of 60%. Based upon these assumptions, the estimated service life is 10 years for gloss level retention (Figs. 18, 19), 12 years for colour difference (Fig. 20), 17 years for cracking (Fig. 21), and 23-28 years for chalking (Figs. 22-23). Thus, we are able to construct a rational maintenance tool when we have gathered sufficient data for multiple kinds of finishing materials.

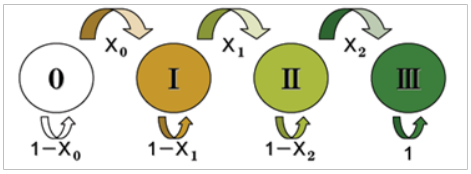

Fig. 16 Conceptual Diagram of Markov Chain Model

$$\begin{pmatrix} 0 \\ I \\ II \\ III \end{pmatrix} = \begin{pmatrix} 1-x_0 & 0 & 0 & 0 \\ x_0 & 1-x_1 & 0 & 0 \\ 0 & x_1 & 1-x_2 & 0 \\ 0 & 0 & x_2 & 1 \end{pmatrix}^t \begin{pmatrix} 1 \\ 0 \\ 0 \\ 0 \end{pmatrix}$$

Fig. 17 Determinant Representation of Markov Chain Model

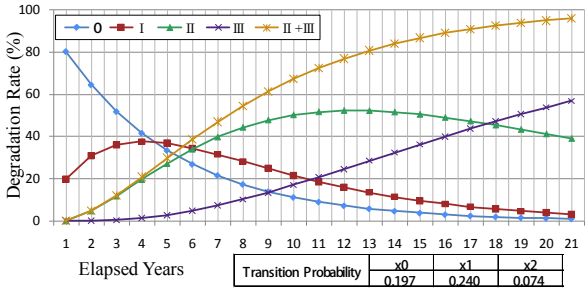

Fig. 18 B Area - Gloss Level Retention (16 Years Old)

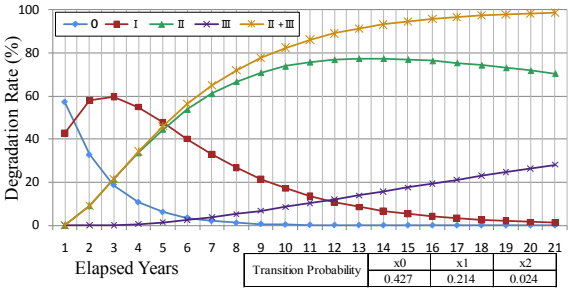

Fig. 19 C Area - Gloss Level Retention (5 Years Old)

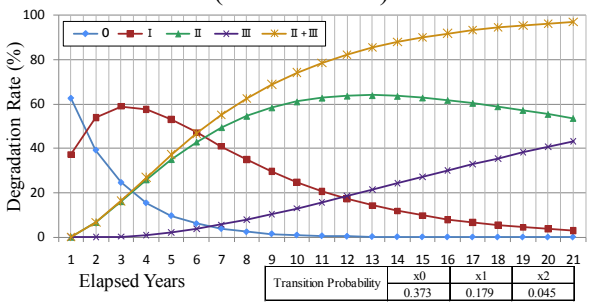

Fig. 20 A Area - Colour Difference(5 Years Old)

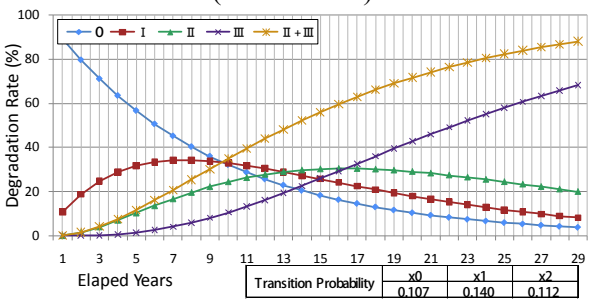

Fig. 21 A Area - Cracking (16 Years Old)

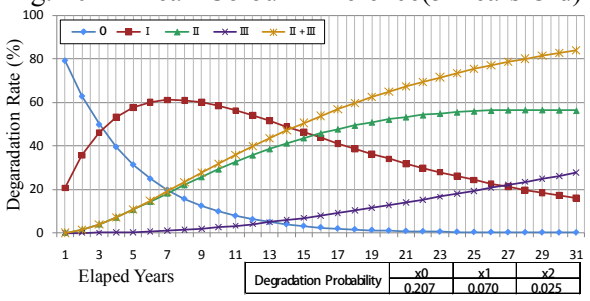

Fig. 22 A Area - Chalking(9 Years Old)

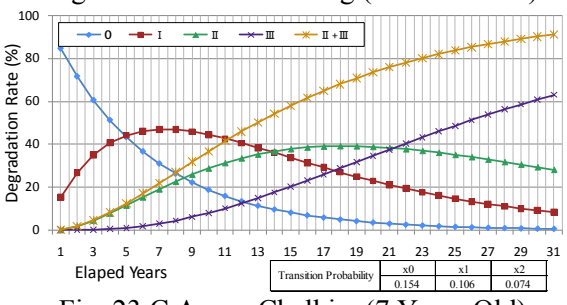

Fig. 23 C Area - Chalking(7 Years Old)

Table 4 Classification of Degradation Grade

Survey Items \ Degradation Grade	0	I	II	III
Gloss Level Retention	80 - 100	50 - 80	20 - 50	0 - 20
Color Difference	0 - 1,5	1,5 - 3	3 - 4,5	4,5 -
Chalking	0 - 9	9 - 18	18 - 27	27 -

5 CONCLUSIONS

Based upon this study it is that the Markov Chain Model could decide the service life of the finishing material in various degradations.

Gloss level retention and chalking has a little tendency of the aging degradation.

Color difference can't indicate the aging deterioration. It would be that local contaminations such as rainfall and dust strongly affect the color difference more than aging deterioration.

Cracking has a remarkable correlation with aging degradation, in particular, when the north side degradation is severe.

In terms of permeability, younger finishing materials protect the building frame, though the degree of permeability degrades across the different ages. Cement plastering does not offer effective long-term protection of the building frame.

ACKNOWLEDGEMENT

This Survey project is carried out in conjunction with the activities of the Sub-Committee 'Reference Service Life' in the Architectural Institute of Japan (AIJ).

REFERENCE

ISO 15686-8 Buildings and constructed assets-Service life planning Part 8 Reference service life and service life estimation

Architectural Institute of Japan, The English Edition of Principal Guide for service Life Planning of Buildings, 1993

JIS K 5600 (1999) Testing methods for paints

Akio Tanaka et al. 2009, 'Air permeability and its relation to Carbonation resistance of finished concrete' *Concrete Engineering Series* 87, pp 129-134

Kei-ichi Imamoto et al. 2009, 'State of the art on on-site air permeability test' *Concrete Engineering Series* 87, pp 340

Torrent, R. 1992 'A two-chamber vacuum cell for measuring the coefficient of permeability to air of the concrete cover on site' Materials and Structures, v.25, n.150, pp 358-365

XII DBMC
International Conference on Durability of Building Materials and Components
PORTO - PORTUGAL, April 12th-15th, 2011

Deterministic and Stochastic Prediction Models For the BuildingsLife Platform

Pedro Vaz Paulo [1]
F. A. Branco [2]
Jorge de Brito [3]

ABSTRACT

Managing a building throughout its whole life cycle requires being able to plan maintenance actions that will be necessary long before they are actually needed. To achieve this level of planning, it is vital to know the service life of the materials and components incorporated in buildings. The BuildingsLife platform was developed to estimate best plan maintenance, standing as a building life cycle management tool that acts as a decision support system. This platform is an information technology answer to the issues presented by the life cycle management of buildings, such as the definition of the buildings' characteristics, monitoring of the buildings' conditions and degradation states, characterization of key environmental agents, service life forecasting for the vital materials and components incorporated and elaborating maintenance plans that optimize building performance versus intervention costs. This paper will present the architecture of the prediction model in terms of deterministic and stochastic models used to estimate the levels of degradation for different considered defects.

KEYWORDS

Predictive models, Risk analysis, Markov chains, deterministic models.

[1] Instituto Superior Técnico (IST), Lisboa, PORTUGAL, ppaulo@civil.ist.utl.pt
[2] Instituto Superior Técnico (IST), Lisboa, PORTUGAL, fbranco@civil.ist.utl.pt
[3] Instituto Superior Técnico (IST), Lisboa, PORTUGAL, jb@civil.ist.utl.pt

1 INTRODUCTION

Efficient management of constructed assets over their life cycle is an issue that has gained relevance in the last decades. Mostly this can be related to political and social pressures to steer the construction industry towards a goal of "sustainable development" [Pearce, 2003]. In achieving this goal, the construction industry in its broadest definition must place a greater emphasis on proper maintenance and refurbishment works, so as to valorise constructed heritage, which has been considered in bridge management in the last decades and in building management in the last years.

Improvement in this area largely depends on the availability of data. In fact, to optimize efforts undertaken to maintain constructed building heritage it is vital to be able to plan maintenance actions throughout the building's life cycle. To do so, building managers need to have data regarding materials and components incorporated in the building, environmental agents that might accelerate their degradation, and their expected service life under those exposure conditions [Daniotti et al., 2008]. In this task, the use of information technology in the form of databases and decision support tools would be of great interest. In fact, a need for broader use of information technology in the construction industry has been referred by various authors [Martin et al., 1994; Pearce, 2003; Kohler, 2006].

The BuildingsLife platform was developed to address these problems, standing as a building life cycle management tool that acts as a decision support system. This platform is an information technology answer to the issues presented by the life cycle management of buildings, such as the definition of buildings' characteristics, monitoring of buildings' conditions and degradation states, characterization of key environmental agents, service life forecasting for vital materials and components incorporated and preparation of maintenance plans that optimize building performance *versus* intervention costs.

2 SERVICE LIFE PREDICTION METHODOLOGIES

2.1 Overview

Managing a building throughout its life cycle requires being able to plan maintenance actions long before they are actually needed. To achieve this level of planning, it is vital to know the evolution of the service life of the materials and components incorporated in buildings [Daniotti, 2008].

The subject of service life prediction has been discussed by many authors, and various methodologies have been presented to perform such forecasts [Masters and Brandt, 1987; Masters and Brandt, 1989; Martin et al., 1994, Martin, 1999]. During the last decade, the standards in the ISO 15686 series have attempted to harmonize the various methodologies, presenting a comprehensive guide to this subject.
In essence, service life prediction methodologies can be divided into two stages: *data collection* and *data analysis*. For each of these stages there are many different approaches that can be used, as illustrated in Figure 1. The data collection stage is characterized by undertaking observations, tests, local inspections and measurements in order to gather information about materials or components and their degradation mechanisms over time. On the other hand, the data analysis stage is when the collected information is processed and used to model the evolution of degradation phenomena, so that service life forecasts can be made.

2.2 Data collection

Data collection can be made through several methods. These usually consist on the exposure of materials or components to degradation agents and evaluation of the degradation caused by those agents. Such methods can rely on observations and measurements obtained from [ISO, 2000]:

- Long-term degradation under in-use conditions (long-term exposure);
- Short-term degradation under exposure conditions designed to accelerate the degradation effects of agents causing degradation (short-term exposure).

In a long-term exposure test the material or component is actually exposed to the degradation agents in full strength, over a time period similar to its expected service life. To obtain data regarding long-term

degradation under in use conditions there are many possible approaches, such as field exposure tests, inspection of in-service buildings, experimental buildings or in-use exposure. An example of this sort of methodology can be found in the work of Larsen et al. [2008], where the durability of various surface protection systems for concrete in harsh marine environments was assessed through the incorporation of such systems in actual in-use concrete bridges.

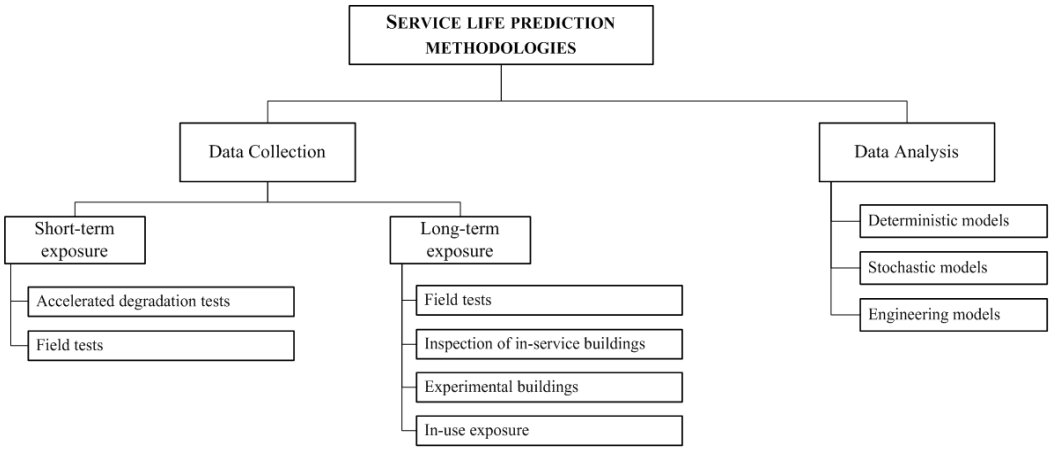

Figure 1. Service life prediction methodologies

For a short-term testing methodology, two types of tests can be used: accelerated degradation or aging tests and field exposure tests. Accelerated degradation tests are carried out over a time period considerably shorter than the expected service life of the material or component, but usually employ a much higher intensity in the degradation agents that act during that period than would be expected in real exposure. As for field exposure tests, even though they can be used for long-term degradation (as mentioned above), they are usually used as a short-term exposure methodology. In these tests, a number of test specimens are placed under natural exposure, generally at sites recognized as having an especially aggressive environmental agent, with environmental conditions regularly monitored and registered. Short-term exposure tests are broadly used [Roy et al., 1996; Jacques, 2000; Perrin et al., 2001; Fekete et al., 2005; Giacardi et al.. 2008; Motohashi, 2008], since they represent a great economy in time. They also allow the isolation of degradation agents acting on the tested materials or components, thus being useful to relate specific degradation mechanisms to the agents that cause them, however, the correlation between the results and period since last maintenance is frequently difficult to achieve.

2.3 Data analysis

In the data analysis stage, collected data can be used to create degradation models and forecast service life. These degradation models can generally be fitted into one of three types:

- Deterministic models;
- Stochastic models;
- Engineering models.

The most commonly accepted example of a deterministic model is the *factor method*, which is proposed by ISO 15686 standard [ISO, 2000]. Other types of deterministic models can be obtained through the use of mathematical laws, which can be shaped to model the degradation behaviour of materials and components, such as Gompertz laws or Weilbull curves. Stochastic models often use Markov chains to provide results with associated probabilities of occurrence. In these models, degradation is regarded as a stochastic process, and for each property during each time period, a probability of deterioration is defined [Cecconi, 2004].

Engineering models intend to be easily used at the design stage of buildings, while still preserving the ability to describe as correctly as possible the actual degradation processes that affect the buildings' materials and components. The application of engineering models to the service life prediction subject must ensure that the methods obtained have the same degree of complexity and depth of other

common design tasks in building physics [Cecconi, 2004]. A possible approach to service life prediction engineering models, adopted by many authors [Aarseth et al., 1999; Hovde, 2002; Moser et al., 2002; Cecconi, 2004], consists on the adaptation of the factor method by considering its seven factors as random variables with associated probability density functions.

2.4 Service life prediction within the BuildingsLife platform

The BuildingsLife platform (a management system to support building decisions with the best maintenance plan, according to individual or global criteria) was developed, initially as a tool to assist in the study of the durability of materials and components incorporated in the façades of traditional buildings. The service life prediction methodology adopted in BuildingsLife follows this *two-stage* approach. In the data collection stage, the inspection of in-service buildings was used to gather information regarding their characteristics, the characteristics of materials incorporated in their façades, and the degradation state of those materials. In the data analysis stage, deterministic and stochastic models were applied: Gompertz laws and Markov chains, respectively.
This software, called BuildingsLife, was developed under web programming, to be accessed by every computer with an internet connection, all over the world. Its architecture (www.buildingslife.com) consists, basically, in relationships between design functionalities and software workflows (Table 1).

Table 1. Software scheme

Software BuildingsLife	
Design functionalities	**Software workflow**
• Table and form design. • Platform design. • Menu design. • Functions. • Methods.	• User definition. • Relation between tab menus. • Report information.

Adopting a data collection methodology based on the inspection of in-service buildings presents several advantages (initially the database contains results from more than 800 buildings' inspection). The most obvious advantage is that the data it provides is directly related to the actual degradation processes and mechanisms that occur in real buildings, under concrete exposure conditions. By inspecting a large enough group of buildings with given characteristics, under well known exposure conditions, it is possible to draw conclusions regarding the service life of buildings with similar characteristics and under similar exposure conditions. This means that the methodology must include the determination of those characteristics, and also the characterization of the relevant exposure conditions. Another advantage presented by this methodology, is that by implementing an inspection routine that can be applied to real buildings, and using the collected data to perform service life estimates for the materials and components of those buildings, the obtained results can be fed back to the building managers, in an advantageous cooperation between research and practice.

3. DEFECT SEVERITY ASSESSMENT BASED ON DEFECT QUANTIFICATIONS

Defect assessment and classification in civil engineering infrastructures is a common practice during building inspections [de Brito et al., 1997; Walter et al., 2005; Flores-Colen et al, 2008; Silvestre et al, 2009; Lima et al., 2009]. Nevertheless, this type of qualitative rating of defects has currently the limitation of being conditioned by inspector's experience, i.e. it is a subjective measure of degradation. Instead of using qualitative assessments of building degradation, in the BuildingsLife database a quantification of defects provides a more reliable and absolute form of defect measurement, producing comparable results from different inspectors. An example of defect quantification in civil engineering structures can be found in the work of Lemaire et al. [2005], where an image analysis process is used to evaluate defects in non-coated concrete surfaces.

Gaspar et al. [2008] also proposed a defect assessment methodology based on defect quantifications, applied to cement-rendered façades. These concepts can be illustrated with the example of mortar cracking in façade renders. For this defect, the extension could be the area of the façade that is affected, the intensity could be given by the average width of the cracks, and the relative importance would be a factor that accounts for how significant the cracking defect is to the rendering in its ability to perform its functions when compared to other defects, such as staining or spalling.

BuildingsLife has been used to quantify several defects based in measurable parameters, concerning colour information pixels, length or area information. Table 2 presents an example of quantification methodology used in BuildingsLife.

Table 2. Chalking paint quantification severity defect.

<table>
<tr><th>Image</th><th colspan="5">Description</th></tr>
<tr><td></td><td colspan="5">Consists in a powering on the paint surface and is usually due to insufficiently sealed porous surfaces. Chalking occurs when ultraviolet rays cause the paint binder to disintegrate. It can happen when interior paints are used for exterior surfaces. UV light, oxygen, and chemicals degrade the coating, resulting in chalk. This can be corrected by providing an additional topcoat with the proper UV inhibitor.</td></tr>
<tr><td colspan="6">Degradation unit</td></tr>
<tr><td colspan="6">Percentage of non white pixels (NWP)</td></tr>
<tr><td colspan="6">Quantification method</td></tr>
<tr><td colspan="6">Chalking is removed from the coating under testing by the use of an adhesive tape. Chalking adhering to the tape is examined against a contrasting white background and the degree of chalking is assessed with reference to a rating scale [ISO 4628-6, 2007]. PhotoColour was used to classify the defects, according to the above ratings, by measuring the white pixels and the sum of different grey scale pixels.</td></tr>
<tr><td colspan="6">Quantification formula</td></tr>
<tr><td colspan="6">$NWP = \frac{\sum_{j=1}^{n} Pj}{\sum_{i=1}^{m} Pi}$</td></tr>
<tr><td colspan="6">NWP - Percentage of non white pixels; m – number of total pixels; n – number of non white pixels</td></tr>
<tr><td colspan="6">Degradation level</td></tr>
<tr><td>DL 0</td><td>DL 1</td><td>DL 2</td><td>DL 3</td><td>DL 4</td><td>DL 5</td></tr>
<tr><td>0% < NWP < 15%</td><td>0% < NWP < 15%</td><td>15% < NWP < 21%</td><td>21% < NWP < 34%</td><td>34% < NWP < 49%</td><td>NWP > 49%</td></tr>
</table>

4. BUILDINGSLIFE METHODOLOGY

The BuildingsLife management system supports 6 main modules namely: Building data (to register any building event); Degradation level (to quantify and classify defects); Environmental agents (to characterize the several degradation agents due to meteorological and atmospheric pollution agents); Service life deterministic and stochastic models (to predict the service life according to materials performance and environmental agents) and management system (to estimate best maintenance plan).

4.1 Building data

The methodology used in BuildingsLife is supported by real buildings' degradation and data which makes the task of information collection critical to the success of the achieved prediction service life methods; it was based on in situ inspection and on documents archived in City Council.

The historic maintenance plan (81% of buildings have such information) is described in those documents or by people who live in the buildings (19% of buildings only have this information). A record sheet was created to enter data on the site, to minimize the inspection time and to ensure regular information collection (this sheet had 4 versions and was tested for 2-3 months). All these data were recorded in BuildingsLife using the same form (Table 3).

Table 3. Building data scheme.

Building data	
***In situ* building façade inspection**	**City council buildings data**
• Building design. • Street design. • Traffic information. • Environmental information. • Climate information.	• Historic maintenance plan. • Architecture design data.

4.2 Degradation levels

One of the major challenges was to develop methods to quantify the different façade defects to ensure that equal results would by obtained by different specialist observers (Table 4). They were developed in BuildingsLife based on the composition and perspective correction of all images of a façade. In addition, 6 different levels were created for each defect, based on standards and fitting the results obtained, to group the results (to simplify analysis and to prepare the data for the Markov chains).

Table 4. Degradation level scheme.

Degradation levels	
Level definition	**Defect quantification**
• System based on 6 degradation levels. • Levels based on standards (ISO, ASTM or NZ). • Assure representative levels according to the samples. • Levels fitting and validated by results.	• Develop uniform methods. • Composition and perspective correction of façade images. • *PhotoMeasure* model to quantify areas or lengths. • *Photo Colour* model to quantify colour changes.

4.3 Materials performance

Materials/constructive elements analysis depends on their durability properties as a function of several degradation agents (Table 5). There are many reports in scientific papers of materials with different properties performing differently, but few of them indicate the real influence on their durability. For example, a textured coating showed better resistance to cracking than a smooth coating but what is this difference in terms of durability gain? To be able to answer this and other questions some destructive and non-destructive tests had to be carried out to verify the materials' properties. It was again important to define ranges for different properties of the materials.

Table 5. Materials performance scheme.

Materials performance	
Sample collection	**Tests**
• Defect analysis. • Collect paint sample. • Collect mortar sample. • Record samples' façade location.	• *In situ* tests. • Laboratory tests. • Establish range for properties of materials.

4.4 Environmental agents

To complete the input data to ensure a correct interpretation of the service life methods the external agents such as, rain, wind, solar radiation, driving rain and pollutant emissions had to be modelled (Table 6). Scientific methods adapted to the particular façade were used. The results for each model were compared to the real data for those degradation agents, as far as possible. Finally, ranges had to be created to group different results. In BuildingsLife it was possible to define 4 ranges. However, to analyse the durability results with the combination of degradation agents and materials performance, the information increases directly with the number of ranges considered (e.g. if a defect is influenced by one material property and two degradation agents and if each of them is characterized in three ranges, then 27 combinations have to be analysed).

Table 6. Degradation agents' scheme.

Environmental agents	
Range definition	**Modelling actions**
• Ensure representative ranges according to the samples. • Fitting ranges and validation with results.	• Create models for each degradation agent • Validation of models with some real results. • Micro-scale definition models (façade or street scale).

4.5 Service life methods

Degradation estimation is based on two possible approaches: deterministic and stochastic (Table 7).

Table 7. Degradation agents scheme.

Service life methods	
Deterministic model	**Stochastic model**
• Level histogram. • Degradation ageing law – Gompertz curve. • Sample best fitting. • Degradation factors' combination.	• Distributions (Normal and Kernel) for each degradation level. • Estimation of historic degradation. • Transition matrices – Markov chains. • Degradation tables, vectors and Markov maps.

4.6 Management system

To achieve its main goal a Building management system must be able to estimate the best maintenance plan in order to minimize the total costs in a certain period (Table 8). The BuildingsLife program uses a genetic algorithm to solve the multiple solutions and find the best combination. The user can introduce a limit to an acceptable degradation level and the period, to analyse the best solution. The type of maintenance (BuildingsLife allows the introduction of 10 types, maximum) can be introduced for each defect and it can be characterized according to the degradation factor. The genetic algorithms were supported by results obtained by Markov chains for each degradation factor. However, Markov chains require huge volumes of data to be able to produce the transition matrices so that, with the collected information, it is possible to use Markov chains in a first degradation factor combination.

Table 8. Degradation agents scheme.

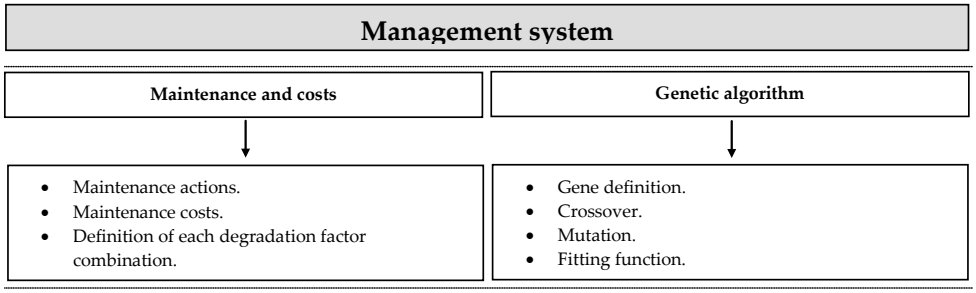

5. CONCLUSIONS

In summary, it has been demonstrated that the BuildingsLife model allows:

- To collect regular data (design, street, environment and degradation) related to several building façades and register it into web platform;
- To model and quantify the materials' performance;
- To model and quantify the degradation factors (climatic and environmental);
- To analyze degradation factors affecting service life;
- To model and quantify degradation levels;
- To develop a deterministic method to predict service life;
- To present degradation laws;
- To develop a stochastic method to predict service life;
- To compare the results with real degradation during service life;
- To estimate the best plan and calculate maintenance costs.

This research is thus intended to provide building managers who have to maintain their buildings assets more efficiently, with a software platform (Building Management System - BdMS) that can optimize the short and long-term maintenance and rehabilitation costs and indicate the optimal maintenance planning actions based on an expected maintenance budget, or determine the budget required to maintain the building at a minimum acceptable level of performance.

REFERENCES

Aarseth, L. I., Hovde, P. J. (1999), *A stochastic approach to the factor method for estimating service life*, 8th DBMC International Conference on Durability of Building Materials and Components, Vancouver; Canada, pp. 1247-1256.

Cecconi, F. (2004), *Engineering method for service life planning: the evolved factor method*, Building for the Future: 16th CIB World Building Congress, Toronto, Canada.

Daniotti, B., Spagnolo, S. L. (2007), *Service life prediction for buildings' design to plan a sustainable building maintenance*, SB07 Lisbon - Sustainable Construction, Materials and Practices: Challenge of the Industry for the New Millenium, Delft University Press.

de Brito, J., Branco, F. A. (1997), *An expert system for concrete bridge management*, Engineering Structures, 19(7), pp. 519-526.

Fekete, E., Lengyel, B. (2005), *Accelerated testing of waterborne coatings*, Progress in Organic Coatings, 54(3), pp. 211-215.

Flores-Colen, I., de Brito, J., de Freitas, V. P. (2008), *Stains in façades' rendering – Diagnosis and maintenance techniques' classification*, Construction and Building Materials, 22(3), 211-221.

Gaspar, P. L., de Brito, J. (2008), *Quantifying environmental effects on cement-rendered façades: A comparison between different degradation indicators*, Building and Environment, 43(11), 1818-1828.

Giacardi, A., Morra, L. (2008), *Outdoor wall painting semi-natural test*, 11th DBMC International

Conference on Durability of Building Materials and Components, Istanbul, Turkey.

Hovde, P. J. (2002), *The factor method for service life prediction: From theoretical evaluation to practical implementation*, 9th DBMC International Conference on Durability of Materials and Components, Brisbane, Australia.

ISO, International Organization for Standardization (2000), *Buildings and constructed assets – service life planning – part 1: general principles*, ISO 15686-1:2000.

Jacques, L. F. E. (2000), *Accelerated and outdoor/natural exposure testing of coatings*, Progress in Polymer Science, 25(9), pp. 1337-1362.

Kohler, N. (2006), *A European perspective on the Pearce Report: policy and research*, Building Research and Information, 34(3), 287-294.

Larsen, C. K., Østvik, J.-M. (2008), *Durability of surface protection systems in harsh marine climates*, 11th DBMC International Conference on Durability of Building Materials and Components, Istanbul, Turkey.

Lemaire, G., Escadeillas, G., Ringot, E. (2005), *Evaluating concrete surfaces using an image analysis process*, Construction and Building Materials, 19(8), 604-611.

Lima, J. M., de Brito, J. (2009), *Inspection survey of 150 expansion joints in road bridges*, Engineering Structures, 31(5), 1077-1084.

Martin, J. W., Saunders, S. C., Floyd, F. L., Wineburg, J. P. (1994), *Methodologies for predicting the service lives of coating systems*, NIST Building Science Series 172, Gaithersburg, MD, USA.

Martin, J. W. (1999), *A systems approach to the service life prediction problem for coating systems, service life prediction of organic coatings: A systemic approach*, Vol. 722, pp. 1-20, ACS Symposium Series, American Chemical Society.

Masters, L. W., Brandt, E. (1987), *Prediction of service life of building materials and components*, RILEM Technical Committee, Materials and Structures, 20(1), pp. 55-77.

Masters, L. W., Brandt, E. (1989), *Systematic methodology for service life prediction of building materials and components*, RILEM Technical Committee, Materials and Structures, 22(5), pp. 385-392.

Moser, K., Edvardsen, C. (2002), *Engineering design methods for service life prediction*, 9th DBMC International Conference on Durability of Materials and Components, Brisbane, Australia.

Motohashi, K. (2008), *Durability evaluation of newly developed water-based paint systems for buildings*, 11th DBMC International Conference on Durability of Building Materials and Components, Istanbul, Turkey.

Paulo, P. V. (2009), *A building management system (Buildingslife) – application of deterministic and stochastic models with genetic algorithms to building façades*, PhD thesis, Lisbon. Portugal, 443 p.

Pearce, D. (2003), *The social and economic value of construction – The construction industry's contribution to Sustainable Development*, CRISP, London, UK.

Perrin, F. X., Irigoyen, M., Aragon, R., Vernet, J. L. (2001), *Evaluation of accelerated weathering tests of three paint systems: a comparative study of their aging behavior*, Polymer Degradation and Stability, 72(1), pp. 115-124.

Roy, S. K., Thye, L. B., Northwood, D. O. (1996), *The evaluation of paint performance for exterior applications in Singapore's tropical environment*, Building and Environment, 31(5), pp. 477-486.

Silvestre, J. D., de Brito, J. (2009), *Ceramic tiling inspection system*, Construction and Building Materials, 23(2), 653-668.

Walter, A., de Brito, J., Lopes, J. G. (2005), *Current flat roof bituminous membranes waterproofing systems – inspection, diagnosis and pathology classification*, Construction and Building Materials, 19 (3), 233-242.

XII DBMC
International Conference on Durability of Building Materials and Components
PORTO - PORTUGAL, April 12th-15th, 2011

Survival Analysis Methodology for Service Live Prediction and Building Maintenance

Carles Serrat [1]
Vicenç Gibert [2]

ABSTRACT

This paper deals with, on one hand, the introduction of survival analysis techniques for being used in building maintenance and, on the other hand, the application of this methodology for analyzing a large building stock in order to obtain information for maintenance strategies and/or prevention policies. In particular, in this contribution the description of the time to the event when the event of interest is some damage (or some level of degradation or extent) on the building façade is the main goal to reach.

For the time being, building follow-up is based on inspections. However, data coming from building inspections are always not completed, but censored, due to the fact that, at each inspection time, the event of interest is already happened, or not yet. In order to solve this problematic, the existing methodology for fields like medicine, biology, industrial engineering or event history analysis is adapted, and routines in S-PLUS for a numerical and graphical systematic analysis are implemented. Estimates for non-parametric durability and hazard functions are derived.

The possibilities of the proposed methodology will be illustrated with its application to the building façades in Hospitalet de Llobregat, the second most important city in population in Catalonia (Spain), where more than 14.000 buildings have been inspected. The analysis of the results allows technicians to detect different zones and levels of intervention to be applied in the city.

KEYWORDS

Censored data, Durability, Maintenance, Nonparametric estimator, Survival analysis.

[1] Escola Politècnica Superior d'Edificació de Barcelona of Universitat Politècnica de Catalunya-BarcelonaTECH, Barcelona, SPAIN, carles.serrat@upc.edu
[2] Escola Politècnica Superior d'Edificació de Barcelona of Universitat Politècnica de Catalunya-BarcelonaTECH, Barcelona, SPAIN, vicenc.gibert@upc.edu

1 INTRODUCTION

The management of building maintenance is increasingly an important topic around the world, especially in recent decades, with the incorporation of tools to automate the tracking information and potential follow-up. From the social point of view it is illogical to leave without controlling the building stock. Moreover, if we take into account the high cost that the non-maintenance of buildings in appropriate good service conditions represents.

The primary objective of the study presented in this paper is that of establishing building maintenance policies based on maintenance criteria from which director plans are created that allow defining the which way maintenance actions are affected the built assets; no matter if the actions are at macro or micro urban level. This will allow establishing more consistent decisions in accordance with the findings of analytical reliable studies.

Throughout this process an important issue must not be overlooked: the methodology should enable generating a base of information and results on the historical evolution of the facades of buildings and their most relevant elements. This fact underlines the crucial role of future interventions and actions to be implemented with a scientific supported base. The sample size in this study was sufficiently large to contain all data needed to achieve the proposed targets to analyze the results and assess its impact without necessarily having to apply not provided corrective actions (what saves the corresponding extra costs that they represent).

2 STATE OF THE ART

In respect to buildings, the use of survival analysis techniques based on the statistical approach of a large sample size does not exist in the literature. First contributions dealing with building or civil maintenance issues appeared in the nineties and they are basically devoted to the prediction of the service life of materials of construction [Frohnsdorff 1996].

One of the first statistical approaches is the one proposed by Flourentzou *et al.* [2000]. They introduce MEDIC as a method for predicting residual service life and refurbishment investment budgets. Predictions are based on the combination of prior probability coming from the experience from a large number of previous investigations/refurbishments and the current state of the subject (building) under study. The goal is to obtain a conditional probability of changing (to worse) between states, given the current state. However a drawback of this methodology is the fact that the deterioration process is described by stratifying it in four states, what is impossible to determine if we do not know the (a priori) true distribution of the time to deterioration. The relevance of having information about the survival functions of buildings or building elements have already pointed out by Buergel-Goodwin *et al.* [2005].

A different approach is found in Gaspar and de Brito [2003 & 2005]. The authors propose identification techniques for durability factors in order to predict service life of buildings or civil infrastructures. The same authors remark in the convenience of working with field data recollection techniques in order to assess the degradation level of a building element (in a facade, for example) in real life service conditions, in order to capture the effect on the deterioration process of the full complexity of the environmental context. In their work the estimation process at each time is based on an overall degradation level defined as a weighted average of specific degradation levels in several points in the moment of inspection, and performing a less squares cubic regression. It is obvious that this approach assumes that the time to event coincides with the inspection time; this is an unfeasible assumption. In fact, the resulting estimates for the deteriorating times are positively biased in an unknown quantity.

European guidelines for life time design and management of buildings can be found, among others, in the Project Cluster Lifetime by Sarja *et al.* [2005]. On the other hand, North American standards and

advanced methodologies for predicting service life of building materials and components can be found, for instance, in the references of the Institute for Research in Construction (Montreal, Canada) [Lacasse 2008]. In all these cases, guidelines represent relevant information in order to define the severity of the injuries, the states in the initiation and progression of the deteriorating process and the transitions between them.

3 INSPECTION AND ANALYSIS METHODOLOGIES

In what follows the methodology that has been used for the inspection process is introduced as well as the survival analysis techniques used for the data analysis.

3.1 Inspection Methodology

The systematic inspection of façade elements is aimed at detecting risk factors for façades in order to later evaluate their condition and likely time to repair and refurbishment. To develop an inspection methodology and obtain homogeneous results for further analysis, criteria based on a standardization of the most significant indicators were established. In this sense a classification of buildings, building elements that make up the façades and their materials was completed, as well as a cataloguing of defects that may affect the façades, the severity of the defects and, finally, the extent, as follows:

- The characterization of the buildings was carried out by the location of the building, year of construction, construction typology, and so on.
- The characterization of the constructive elements of the façades was done by subdividing the body into two parts: corps of the façade and corps outgoing. Within them the elements that the façade may contain have been identified. For example, in the case of the body of the façade we find cladding, voids, coatings and deck railings, and for example, within the voids we find lintels, jambs and parapets. Finally, we have defined the materials that can be used for each element.
- The definition of defect has been established to include the most common defects that can affect façade elements. In particular, the following eight defects have been considered: breach, fissure, material degradation, deformation, dampness, oxidation, desunity (incompatibility?) and detachment.
- The classification of the severity of defects has been established in terms of the action that is necessary to remove the risk that it may represent for people. After taking into account the term of the corresponding preventative action the following apply: 0 = “low severity”, 1 = “intermediate severity” and 2 = “high severity”.
- The definition of the extension of the defects has been established according to the proportion of the inspected element that it is affected by the defect: punctual (when the defect affects an element less than a 25%), local (affects element between 25% and 50%) and general (when the affected zone is greater than a 50% of the element).

The model that systematizes the inspection process allows encoding and entering data in a computer application for the assessment and the management of the results, with an interface similar to the field sheets used in data collection. Fig. 1 shows two screens available from the application.

By using this software application, several descriptive indicators can be obtained, referred to the inspected sample that the user wishes to consult for the analysis. For example, the software allows obtaining, among others, the following descriptors:

- List of maximum severities affecting the façades of the sample.
- Location of elements affected by defects of a certain severity.
- Number of detected defects by specific type of construction element, for a particular choice of type of defect and severity.

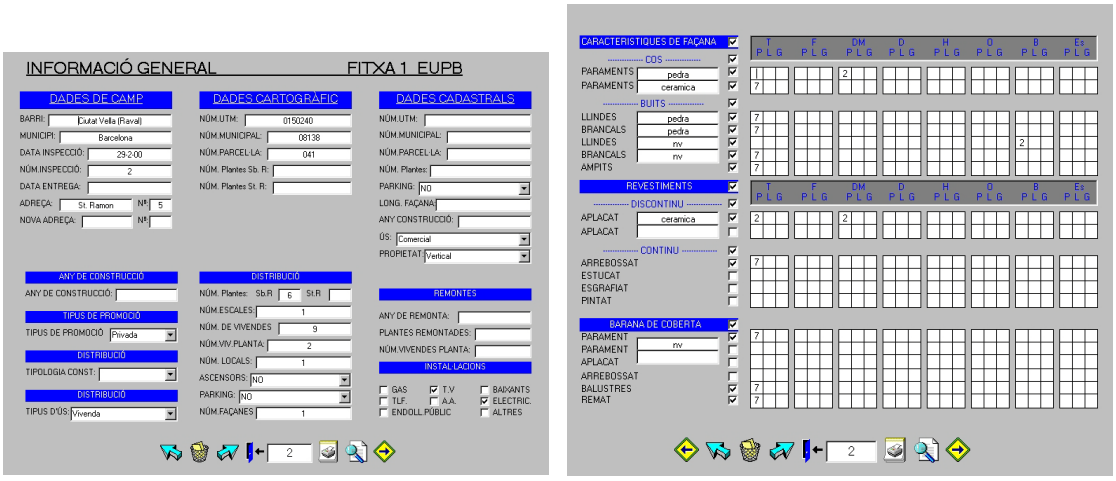

a) b)

Figure 1. Screens that allow a) the introduction of parameters of the inspected buildings and b) definition of materials for façade building elements and severity and extent of each type of defect.

3.2 Analysis Methodology

In this subsection, basic definitions of durability, the censorship mechanism issue and the non-parametric approach are introduced that were subsequently used for statistical analysis of data. Among many possible references, the primary reference on reliability and survival analysis used in this study was the work by Klein and Moeschberger [1997].

3.2.1 Fundamental Concepts in Survival Analysis

Three basic concepts in durability analysis (survival in the bio-medical field, reliability in the industrial-technologic field or event history analysis in the social field) are the failure, the durability function and the hazard function, that are defined as follows.

Definition 1: *failure* is an event of interest in which we are concerned about.

According to the International Organization for Standardization (ISO), quality is the set of properties and characteristics of a product that enable it to satisfy the requirements for whom it has been defined. In this sense, let T be the time from the beginning of the follow-up (time zero) until the failure (the event of interest) happens. The time T is a random variable and of interest in its distribution, such that in order to compute probabilities of occurrence under its density $f(t)$ or to obtain statistics like, for instance, the quantiles of the distribution. This will allow us to estimate the time until a proportion of damaged buildings in the population or, in the reverse sense, the proportion of damaged buildings at certain time for a particular defect. In the maintenance setup, time zero will mean the date that the building is built and by failure it is understood the successive grades of severity defects or successive grades of the extent of defects.

Definition 2: The *durability function* for the random variable T, $R(t)$, is the complement to one of the distribution function of T:

$$R(t) = 1 - F(t) = 1 - P(T \le t) = P(T > t) \tag{1}$$

Definition 3: The *mean hazard rate* in the interval $[t_1, t_2]$ is defined as

$$h(t_1, t_2) = \frac{R(t_1) - R(t_2)}{(t_2 - t_1) R(t_1)}, \tag{2}$$

where the durability, $R(t_1)$, is the proportion of survivors at the moment t_1 and $\left[R(t_1)-R(t_2)\right]/R(t_1)$ represents the proportion of elements that, have not yet failed at time t_1, but fail in the interval of time $[t_1,t_2]$. When t_2 tends to t_1 the *(instantaneous) hazard function* at time t_1 is given as: $h(t_1)=\lim_{t_2\to t_1} h(t_1,t_2)$. It can be shown that $h(t)=f(t)/R(t)$ and, in this sense, the hazard function measures the propensity to failure of the elements or statistical subjects as a function of time. If the cumulative hazard function, $H(t)$, is defined as $H(t)=\int_0^t h(s)\,\mathrm{ds}$, then the relationship between the durability function and the cumulative hazard function is:

$$R(t)=e^{-H(t)} \tag{3}$$

3.2.2 Censorship Mechanism

If *T* is the true time until failure occurs and C_1 denotes the time of an inspection event, then at time C_1 there are two possibilities: that failure has already occurred and thus $T<C_1$, or; failure has yet to occur and $T>C_1$. So, as a consequence, for each object of interest on which an inspection is performed the exact time at which *T*, is observed is not likely possible, hence only a part of the information is obtained upon inspection.

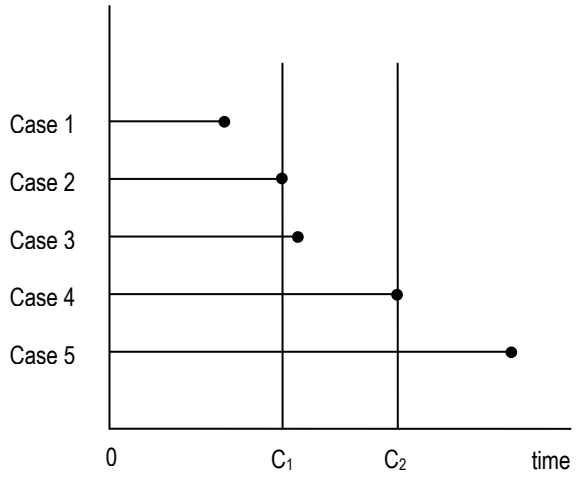

Figure 2. Illustration of the censorship mechanism: a) At time C_1, case 1 is left censored, case 2 is exact observation and cases 3, 4 and 5 are right censored observations. b) With a second inspection time C_2, case 1 is left censored, cases 2 and 4 are exact observations, case 3 is interval censored and case 5 is right censored.

In fact, if $T<C_1$, we only know that the true value of *T* is in the interval $(0,C_1)$, in this case the variable *T* is *left censored* and denote the observation by C_1^-. Otherwise, if $T>C_1$, $P\left(T\in(C_1,\infty)\right)=1$ and that *T* is *right censored* and denote the observation by C_1^+. This is usual approach taken to categorise failure data in "durability" studies, and in this instance all data are either left or right censored. This is referred to as *current status data*. Note that if there is a second inspection time, C_2, with $C_1<C_2$, then the observed data would be left, right or interval censored as illustrated in Fig. 2. . In the current study only one inspection time was considered and so only left or right censored observations are dealt with.

Concerning to the censorship mechanism it is important to assume a non-informative hypothesis, which is that the inspection time *C* is independent on the random variable of interest *T*. In general, when *C* is defined by design the non-informative hypothesis can be assumed.

3.2.3 A Non-Parametric Approach

Since there are no references on the distributions of failure times for the different defects and elements it follows that the durability function and the hazard function should be estimated non-parametrically. That is, estimates were only based on the data and no hypothetical (and non-testable)

distributions were assumed for the unknown density f of T. Kaplan and Meier [1958] proposed a non-parametric estimator, called product limit estimator, for the durability function in the case of right censored data. Turnbull [1976] extended the Kaplan-Meier estimator to the case of interval censored data. The Turnbull's estimator is an iterative algorithm that maximizes the non-parametric likelihood function

$$L = \prod_{i \in O} \left(F(o_i) - F(o_i^-) \right) \prod_{i \in R} \left(1 - F(r_i) \right) \prod_{i \in L} F(l_i) \prod_{i \in I} \left(F(r_i) - F(l_i) \right), \quad (4)$$

where O, R, L and I are, respectively, the subsets of exact, right-censored, left-censored and interval-censored observations. Turnbull's algorithm identifies the intervals where probabilistic mass can be estimated and the resulting durability and hazard functions derived.

3.2.4 Implementation of the Analysis Methodology

We have developed all the durability analysis methodology; a library containing routines and procedures for obtaining estimates for failure probabilities, durability and hazard functions and summary statistics tables, have been implemented in S-PLUS® (Insightful®).

4 ILLUSTRATION

4.1 Scope of the Project

The project and methodology presented in the previous section have been applied in several cities and locations, not only nationally in Spain but also internationally. Table 1 shows the location of inspections and the number of inspected façades.

Table 1. Scope of the project to date

Country	*City*	*Location*	*Number of façades inspected*
Spain	Barcelona	Ciutat Vella	2631
		L'Eixample	2736
	L'Hospitalet de LLobregat	Whole city	13193
France	Toulouse	Old Town	80
México	México DF	Casco Antiguo	525
Chile	Valparaíso	Zona de los Cerros	396
	Santiago de Chile	Casco Antiguo	1403

As an illustration of these techniques some results are presented of the software application to the inspection of L'Hospitalet de Llobregat (hereafter L'Hospitalet) in the metropolitan area of Barcelona.

4.2 About L'Hospitalet de Llobregat and the Dataset

L'Hospitalet has 266,973 inhabitants (Institute of Statistics of the city, 31 December, 2008). In Catalonia, it is the city having the second largest population and is among the twenty most populated cities in Spain. The municipality covers an area of 12.5 square kilometres between the towns of Barcelona, Esplugues, Cornellà and El Prat. Administratively L'Hospitalet is divided in 7 districts and 12 sectors.

4.3 Univariate and Multivariate Analyses by Severity and by Extent

Univariate analyses were first performed on failure times for all the defects according to the severity and extent criteria. Thereafter, multivariate analyses were performed. In this paper only the univariate analysis is presented.

With the aim of illustrating the capabilities of the software system and the merit of our proposal, a small sample of graphical and numerical results taken from a severity analysis is presented in this section. The durability function for jambs for which defects are characterised by the presence of fissures along the jamb is given in Fig. 3 and Table 2. Among other conclusions, one can determine that after 10 years, 5.2% of jambs will suffer a punctual fissure of low severity and 1.6% and 0.1% of jambs punctual fissures of intermediate and high severity, respectively.

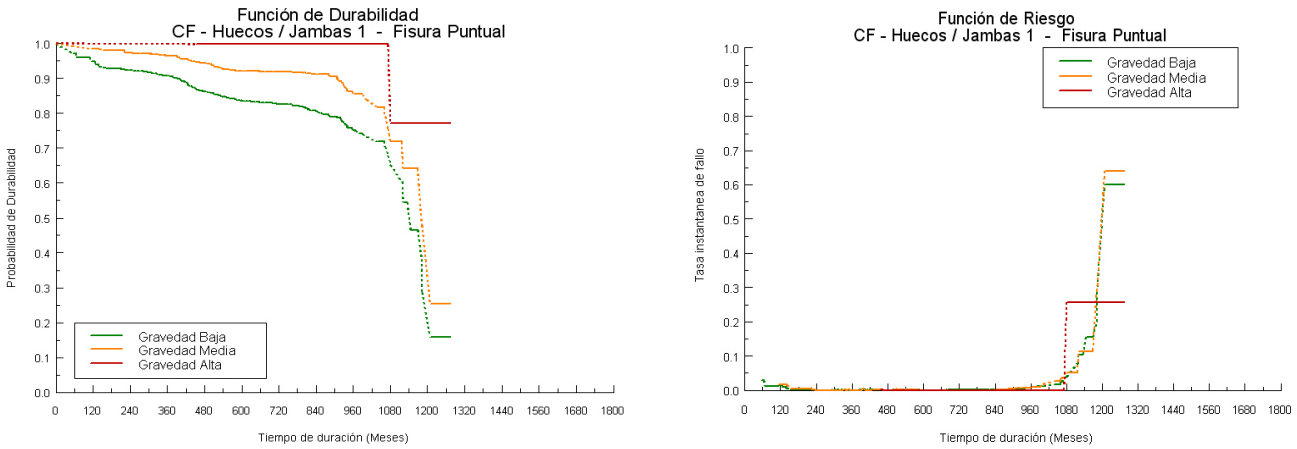

Figure 3. Durability and hazard functions for punctual fissure on the jambs (by severity level)

Table 2. Numerical results of the graphical analysis in Fig 3.

Number at risk	% of censoring		Estimated % of injuries Initial		Final		Years until a % of cumulative injuries				Cumulative % of injuries across the years			
	Left	Right	Years	%	Years	%	10%	25%	50%	75%	10	25	50	100
2960	12.4	87.6	4.7	2.8	106.1	84.3	32.6	80.7	95.1	99.2	5.2	8.3	16.4	79.8
2960	5.3	94.7	9.5	1.6	106.1	74.7	75.7	89.5	98.4	--	1.6	3.0	7.9	66.9
2960	0.1	99.9	37.8	0.2	106.1	22.8	89.7	--	--	--	0.1	0.2	0.2	22.8

5 DISCUSSION AND FUTURE WORK

We have introduced a proposal for the use of "survival techniques" for building maintenance. As a probabilistic technique it allows estimating the failure distributions for all defects which may be of interest to a maintenance manager. Moreover, those characteristics which play (or not) a significant role in the product deterioration process can be tested. All this knowledge now allows an understanding of how the elements of the building envelope system functions, as well as how failures should be anticipated in service conditions as a consequence of aging, and especially how if indeed failures are anticipated, what preventive actions can be taken in-service. As well, it permits a viewpoint on what decisions need be taken at the design stage to help reduce anticipated defects and thus ensure the long-term performance (durability) of the building envelope.

The analysis platform that was developed and implemented becomes the basis for a continuous analysis in the future that will allow not only the design of maintenance strategies and prevention policies, these being based on economic and safety criteria, but also permit on-line decisions to be made.

We would like to provide information on two aspects for future development on which we are now working. Firstly, development of programming to achieve a more accurate inspection schedule. This will allow improvement of the quality of the data by reducing the proportion of censoring required or

replacing left or right censoring by interval censoring, the latter method being the preferred approach. Secondly, the interest of adjusting the resulting distributions to the covariates of interest in the sense we mentioned in Section 4.3, when we referred to the multivariate analysis. In many cases, the failure distribution will be sensitive to building conditions. It is the belief of the authors that both these development items will make the building maintenance strategy more efficient.

ACKNOWLEDGMENTS

This work has been partially supported by the School of Building Construction of Barcelona (EPSEB-UPC), by the Building Laboratory at EPSEB and by the Spanish Ministry of Science and Innovation under grant MTM2008-06747-C02-01. Special thanks are due to the City Hall and to the inhabitants of L'Hospitalet de Llobregat for their collaboration in data collection, to the authors of several Graduation Final Projects for their contribution to this work, and to the members of the IEMAE for their valuable comments and suggestions.

REFERENCES

Buergel-Goodwin E., Ferrara C. & Bradley PE. 2005, "Survival functions of buildings and building elements", in Proceedings of the 10DBMC International Conference On Durability of Building Materials and Elements. Lyon, France.

Flourentzou F., Brandt C. & Wetzel C. 2000, "MEDIC, A method to predicting residual service life and refurbishment investment budgets", *Energy and Building* **31,** 167-170.

Frohnsdorff GJC. 1996, "Predicting the Service Lives of Materials of Construction", in Proceedings of the Fourth Materials Engineering Conference. Chong KP. (ed), 38–53, American Society of Civil Engineers (ASCE), Washington, DC, USA.

Gaspar PL. & de Brito J. 2005, "Assessment of the overall degradation level of an element, based on field data" in Proceedings of the 10DBMC International Conference On Durability of Building Materials and Elements. Lyon, France.

Gaspar PL. & de Brito J. 2003, "Service Life Prediction: Identifying Independent Durability Factors", in Proceedings of the Second International Symposium for Integrated Lift-time Engineering of Buildings and Civil Infrastructures. 319–324, ILCDES Kuopio, Helsinki, Finland.

Kaplan EL. & Meier P. 1958, "Nonparametric estimation from incomplete observations", *Journal of the American Statistical Association*, **53**, 457-481.

Klein JP. & Moeschberger ML. 1997, *Survival Analysis. Techniques for Censored and Truncated Data.* Springer, New York, USA.

Lacasse MA. 2008, "Advances in service life prediction - an overview of durability and methods of service life prediction for non-structural building components" in Proceedings of the Annual Australasian Corrosion Association Conference. Wellington, New Zealand.

Sarja A., Bamforth, Caccavelli and Chevalier JL. 2005, *European Guide for life time design and management of civil infrastructures and buildings*, Project Cluster Lifetime

Turnbull BW. 1976, "The empirical distribution function with arbitrarily grouped, censored and truncated data", *Journal of the Royal Statistical Society, Series B,* **38** (3), 290-295.

XII DBMC
International Conference on Durability of Building Materials and Components
PORTO - PORTUGAL, April 12th-15th, 2011

A Probabilistic Approach to Performance-Based Durability Engineering

Madeleine Flint [1]
Sarah Billington [2]

ABSTRACT

It is proposed to apply the methodology and lessons learned in the recent development of a performance-based earthquake engineering (PBEE) framework to structural deterioration. The development of PBEE by, for example, the Pacific Earthquake Engineering Research Center (PEER) has led to increased collaboration among research institutions to develop robust methods of implementing the framework, the improvement of analysis tools, and the propagation of research results into simplified methods for practicing engineers. PBDE as presented here utilizes the concept of separating the analysis of deteriorating structures into four stages, and passing a few variables between each phase of analysis. Definitions of the four stages, models used, and variables passed between models are presented. This approach allows for generality and flexibility in modeling, comparison between the results of models, and the output of information useful to decision makers. Comparisons to existing frameworks and methodologies are made, and existing models and data to be used in the framework are discussed. Sufficient models and data exist to begin simulation for testbed structures for chloride-induced corrosion in reinforced concrete structures, especially bridges. In implementing this approach, the goal is to emulate the positive impacts that PBEE is having on the research and design communities.

KEYWORDS

Reliability, corrosion, chloride, reinforced concrete

[1] Graduate Student in Civil and Environmental Engineering at Stanford University, Stanford, CA, USA, flint@stanford.edu
[2] Faculty of Civil and Environmental Engineering at Stanford University, Stanford, CA, USA, billington@stanford.edu

1 INTRODUCTION

Designing durable and efficient structures has always been a goal of the structural engineering community. Recent interest in life cycle costs and environmental impacts has led to increased interest in improving the accuracy of models of structural deterioration. Recently developed models, detailed in section 2, have the potential to predict the onset and propagation of deterioration for structures of varying geometry, material, and exposure. While these predictions are valuable, their implementation in a probabilistic framework extending to information useful to owners has not been carried out systematically and is expected to provide enhanced utility.

1.1 Background

Recognition of the positive impacts of the development of performance-based earthquake engineering (PBEE) on the research and practicing engineering communities motivates the application of the methodology to structural deterioration. In developing the PBEE guidelines, the Pacific Earthquake Engineering Research Center (PEER) set out to bring a probabilistic and transparent methodology to evaluating structural risk and reliability, and has succeeded in developing the models necessary for making more rational choices in structural design and renovation [Hamburger 2006]. While analysis tools for nonlinear seismic behavior and fragility curves for building components had not yet been fully developed at the time of the methodology's proposal, testbed studies identified areas in which modeling uncertainty had the greatest impact on the decision variables. These areas became the focus of intensive research efforts that succeeded in reducing model uncertainty. These efforts were then incorporated into simplified methods for practicing engineers.

The methodology developed by PEER for performance-based earthquake engineering is an extension of the probabilistic frameworks developed for nuclear risk simulation [Deierlein *et al.* 2003]. The PBEE framework links together the results of different areas of earthquake-related research (hazard, structural simulation, and risk analysis), allowing calculation of recurrence rates and mean values for variables at four stages of the analysis. Hazard analysis determines the intensity measure, structural analysis determines the engineering demand parameter and damage measure, and risk analysis predicts the decision variable. While the four stages of analysis can be complex, only a few "pinch point" variables are passed between stages. This framework allows for flexibility of modeling within each realm, as each sector of analysis is decoupled.

1.2 Motivation

Concurrent interest in optimizing design of structural durability and the adoption of PBEE in the engineering community suggest the use of a similar framework for durability. Although the details must differ, the method of using analysis "pinch points" where a few variables can be passed from one model to another can be used to develop an analogous framework.

Environmental deterioration occurs due to a variety of interacting mechanisms, which makes the selection of a "testbed" mechanism necessary to develop an example application of the framework. The mechanism chosen should be of interest to both decision-makers as a threat to safety or cause of large maintenance costs, and to researchers developing deterioration models. Deterioration of transportation infrastructure, caused by scour, deck pounding, and corrosion in reinforced concrete, meets these constraints. The availability of a variety of degradation models led to the selection of the corrosion of steel reinforcement in structural concrete as the testbed mechanism for this research. Predicting the onset of corrosion and its propagation is a complex challenge, and its effect on structural safety and behavior are similarly difficult to determine. The combination of complexity and large economic loss due to corrosion make it an important trial mechanism for PBDE.

As a proposal for one type of PBDE, this paper outlines the major models, variables, and pinch points needed to develop a chloride-induced corrosion framework. Stages of modeling are defined, and

existing models that could be used for a testbed simulation are referenced. If the chloride-induced corrosion integrated framework is deemed feasible, it should be possible to extend the framework to other causes of corrosion, such as carbonation, and then to other degradation mechanisms, such as scour, pounding, freeze-thaw degradation in concrete and masonry, or rot in timber structures.

1.3 Existing Deterioration Frameworks

Existing frameworks for corrosion-related structural deterioration fall into three main categories: reliability analysis for safety and serviceability failures; design criteria that attempt to predict performance or service life; and maintenance optimization methods.

1.3.1 Reliability Frameworks

Enright and Frangopol [1998], Vu and Stewart [2005], and Li and Melchers [2005], among many others, performed reliability assessments of corroding concrete structures. Some reliability analyses have also undertaken sensitivity analysis to determine which input variables have the largest impact on the analysis. Corrosion rate, steel yield strength, and cover depth have large impacts on the reliability assessment for all models. Spatial correlation of these variables was found by Vu and Stewart [2005] to have a large effect on the analysis, which is neglected by many studies. While the details of the type of reliability analysis performed (FORM, Monte Carlo), characterization of stochastic variables, and determination of end-of-service life vary between the frameworks, some generalizations about these approaches can be made. The framework results are only as robust as the models they employ to track chloride ingress, corrosion initiation, and propagation. The use of effective Fickian diffusion, constant, uniform corrosion rate, and other assumptions may lead to inaccurate predictions of service life [Angst *et al.* 2009, Bamforth 1999]. Furthermore, while a probabilistic distribution of predicted service life aids is useful, information on repair costs, or phenomenon such as crack width or corrosion current at a point in time is not always incorporated and would be helpful to owners for decision making.

1.3.2 Design Frameworks

The need to design durable structures has led to the creation of several frameworks for performance-based design for durability. These include RILEM's DuraCrete model [Siemes & Edvarsen 1999], fib *Bulletin 34 Model Code for Service Life Design* [2006], ACI Life-365 [Violetta 2002], and work by JSCE-331 [Shimomura *et al.* 2006]. A new SEI-ASCE Technical Council on Life-Cycle Performance, Safety, Reliability and Risk of Structural Systems also intends to develop guidelines for durability. Many frameworks use empirical degradation models and output service life predictions. The limitation of these methods is the user's inability to replace parts of the model with their own preferred analysis tools. Additionally, the outputs may be difficult to assess within a PBDE framework.

1.3.3 Maintenance Optimization Methods

Maintenance optimization is a well-developed field, and there are many techniques to determine optimal repair timing to reduce costs for a given desired level of performance. Bridge Management Systems (BMS) such as Pontis track inspections of commonly recognized "CoRe" elements and predict deterioration based on environmental condition using Markov models [Guerre *et al.* 2007]. NCHRP Report 590 presents a multi-objective optimization method for BMS [Patidar, *et al.* 2007]. The optimization schemes used can be very sophisticated. However, Markov models may not be appropriate for all environments, and their implementation in Pontis is limited with regard to risk analysis and fragility updating.

1.3.4 Summary of Existing Methods and Limitations Addressed by this Research

Reliability, design, and optimization methods share several of the same limitations. The limitations are lack of generality caused by assumptions made in analysis, the inability to replace models, and difficulty in producing output data that is fully inclusive of the sort of information useful to decision

makers. Complexity is an additional limitation of both the existing and the proposed frameworks, but the proposed methodology does offer a comprehensive approach, transparency, and clear, practical decision information. As ATC 58 uses more advanced research efforts to develop a simpler design approach to PBEE, it is hoped that a simplified and perhaps deterministic framework (at least from the user's point of view) could be developed for PBDE. The methodology presented here is expected to complement existing methods for analyzing and predicting structural deterioration and durability.

1.4 Overview of Proposed Probabilistic Framework

The PBDE framework encompasses four phases of analysis, shown in Figure 1. The first is exposure analysis to determine the environmental variables and loading as exposure conditions (EC). The next phase, deterioration analysis, may be broken down into sub-models, but essentially relates the EC to a suite of damage measures (DM) by tracking chloride ingress, corrosion propagation, and resulting damage. These DM's are used in repair analysis to predict necessary repair actions (RA), which can in turn be linked to repair costs and downtime for repair. The integration over possible repair actions and associated consequences is termed impact analysis, and results in a characterization of decision information (DI). The structural capacity calculated in the second phase can also be used to develop reliability predictions as a third type of DI.

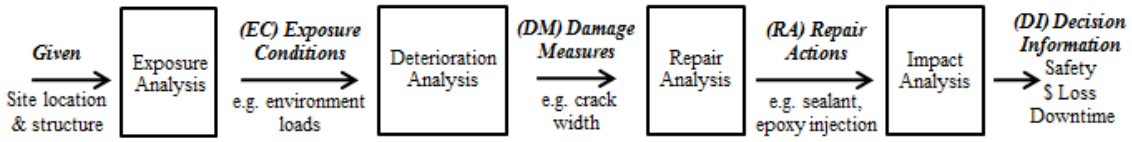

Figure 1. PBDE framework showing four stages of analysis and "pinch point" variables.

The stages will be discussed in more detail in the following sections in terms of what models exist and are ready to implement in the framework. Advantages and disadvantages of various models are presented. Implementation and analysis of results is ongoing.

2 FRAMEWORK STAGES

Before analysis can begin, the structure needs to be divided into elements (preferably tied to CoRe elements) and spatially discretized. As analysis flows from exposure to impact, these discretizations are used to determine the extent of deterioration. At the end of the analysis it is possible to characterize annual mean values of the decision information variables, expected values over the lifetime of the structure, or full exceedence curves. Exceedence curves at interim stages can also be computed.

2.1 Exposure Analysis—Determining the Location-Based Environmental Conditions (EC)

For chloride-induced corrosion, the goal of exposure analysis is to develop surface chloride concentration, temperature, humidity, and live load profiles as a function of location of or on the structure, and time. There are four main sources of surface chlorides in structures: marine air, immersion in salt water or chloride-contaminated soil, exposure to salt spray in a splash zone, and deicing salts. These four categories have a range of temporal and spatial variation, and some structures will experience two or more exposure sources. In the simplest of cases, the profiles might assume full correlation over all the affected surfaces of the structure, with variance reflecting seasonal changes in exposure as a frequentist component to the uncertainty. A more refined model might explicitly account for the seasonal periodic shift in the mean or median exposure, and in the change in variation as a periodic function of time. The most complex model would take into account periodic changes in the stochastic descriptors as well as spatial variation and correlation due to the geometry of the structure considered. Depending on the chloride ingress and propagation models used in deterioration analysis, information about surface moisture or temperature may not be required.

Exposure analysis additionally needs to consider loading on the structure. In most cases live load due to truck and other vehicle traffic is the main load considered, although seismic, wind, or flood loads could also be studied. The live load can be measured as a non-stationary random variable based on projected future traffic conditions, and is needed in order to accurately determine the stress state for the deterioration analysis. Reliability analysis would more likely use extreme value distributions to compare degrading capacity with peak live loads.

2.1.1 Existing Exposure Models and Data Sources

Most existing data on chloride profiles comes from surveys of existing structures. Many papers provide useful profiles and diffusion data for a variety of exposure categories, such as Bamforth [1999] and Meira, *et al.* [2008], among others. While the existing data is not fully comprehensive of all exposure types, it is sufficient to run trial simulations, and ongoing research projects in Brazil, and Japan, among others, will improve the volume and quality of data available. These data sets can be used to develop general exposure categories (from mild to severe) or they may be used as detailed stochastic descriptors.

2.2 Deterioration Analysis—Determining Structural Capacity and Damage (DM)

With exposure conditions available, the next step is to model chloride ingress and the initiation and propagation phases of corrosion, as well as the resulting structural damage. Concrete properties, structural geometry, exposure history, and load history are well-known to influence the ingress of chloride ions and initiation and propagation of corrosion, requiring modeling of all variables to achieve the most robust prediction of corrosion. This robust form of deterioration analysis will require numerical modeling of chloride, oxygen, and water ingress, changes in concrete properties, electrochemistry at the rebar surface, and concrete stress and strain, including in cracked or damaged regions. In some cases it would be advantageous to allow swapping of sub-models for transport, initiation, propagation, material degradation, and structural behavior. The use of sub-models would also allow a variety of damage measures (DM) to be calculated as the analysis proceeds. DM's could include chloride concentration profiles (cores are frequently taken as part of inspections), corrosion rate (measurable using nondestructive corrosion monitoring techniques), and crack width or spalling (commonly recorded as part of inspections). While all of these sub-models can be combined in a finite element approach, it is also possible to use empirical or other analytical models in each category. Depending on the complexity of the analysis, mean values of material properties and geometry can be used to take a deterministic approach, with uncertainty incorporated at the end of the analysis using FORM or response surface methods, or full Monte Carlo or importance sampling methods can be used following the reliability analyses of section 1.3.1.

2.2.1 Existing Structural and Damage Models and Data Sources

DuCOM [Maekawa *et al.* 2009] is an example of an "all-in-one" finite volume concrete model for transport, electrochemistry, material degradation and structural deterioration. However, as noted by its authors, DuCOM is currently limited to uniform corrosion, and makes other assumptions that may limit its accuracy under certain conditions. Another approach is to break the analysis down into sub-models, as shown in Figure 2. Each of the sub-models discussed makes its own set of simplifying assumptions, limiting the range of applicability. Again, ability to select a model for a given situation and to assess impacts on results is a benefit of the framework proposed here.

(1) If the methodology of sub-models is selected, transport could utilize several numerical models for diffusion of chlorides and other ions, some including coupling with moisture transport, for example Kemper *et al.* [2010]. Other transport models, such as those used in the reliability analyses cited in section 1.31, are based on effective Fickian diffusion, and may account for changes in stress state, chloride concentration, or diffusion coefficient.

(2) Corrosion initiation has generally been modeled by use of a "critical chloride concentration" or "chloride threshold" expressed as a ratio to cement or binder, concrete weight, or hydroxyl concentration [Angst *et al.* 2009] The validity of this assumption has been contested, but using separate sub-models side-steps this issue by allowing the use of stochastic parameters. Additionally, the Nernst equations or a Pourbaix diagram could be used to determine the likelihood of initiation. This would require knowledge of the electropotential, which could be modeled as a random variable or a field variable following Kranc and Sagüés [2001]. Furthermore, the rust products formed and their density are dependent on the concentrations and electropotential at the anode. Most models assume a distribution of rust density a priori. If the pertinent molecular concentrations are modeled at the anode it may be possible to determine a distribution of products based on a Pourbaix diagram.

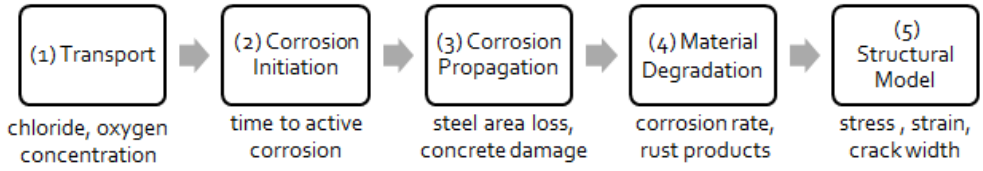

Figure 2. Use of sub-models within deterioration analysis phase of assessment.

(3) Corrosion propagation is similarly uncertain and difficult to model. In addition to solving the Maxwell equations, there are empirical models for corrosion rate based on those typically found for a given exposure condition, such as those given in Roberts *et al.* [2002].
(4) There are a variety of models for continuum damage and cracking in concrete. In a finite element formulation, continuum models incorporating physico-chemical damage could be used to determine change in stiffness and diffusion coefficient due to damage caused by the expanding rust [Bangert *et al.* 2003]. The Liu and Weyers [1998] and other similar models for cracking are based on thick-walled cylinder assumptions and could be used in a cross-section-based fiber-type analysis.
(5) While much of the focus here has been on finite element or finite volume methods, these are not the only choices for modeling structure-level behavior. Fiber analysis, discretized over a cross section, could be used to assess structural reliability. Concentrated plasticity frame models could be used to assess seismic performance of a deteriorating structure. If the more advanced finite element model is selected, the effects of deterioration including rebar area loss, cracking, and bond loss could be modeled. Models for bond loss are available in Fang, *et al.* [2006], among others.

2.3 Repair Analysis—Determining Appropriate Repairs for Given Damage (RA)

Repair analysis is comprised of two challenges. The first is to develop an inventory of realistic repair actions (RA), and the materials, equipment, and time taken to complete these repairs for later use in impact analysis. Due to the generally slow rate of corrosion deterioration in reinforced concrete structures it will not be trivial to build a sufficiently large dataset to accurately characterize the distributions of for example, materials and methods, for a repair type. The second challenge is to link specific DM's to RA's in a fragility curve, and inspection data is being analyzed for this.

This analysis phase is hypothesized to be the most variable between operators. In the US for instance, states and even local maintenance operators within states vary in the repair timing and action favored. This phase of the analysis will be adjusted for each application to match stakeholder preferences with the eventual goal of having a general repair action inventory that can then be customized.

2.3.1 Existing Repair Models and Data Sources

Markovian deterioration and repair schemes, briefly reviewed in section 1.3.3, are examples of repair models for maintenance optimization. For this research. data sources provided by the California Department of Transportation, Caltrans, are being reviewed. The Caltrans Bridge Inspection Records Information System (BIRIS) contains inspection reports, including reports based on CoRe elements from 1997 onward, and can be searched to retrieve information on bridges with a certain level of

recorded deterioration. The set of all bridges with records of interest, e.g. advanced deterioration of element "Reinforced Concrete Open Girder," is being studied to determine which damage measure instigated the repair process as well as repair details. While, as noted in Thompson & Johnson [2005], this is likely to provide a rather small data set, it should demonstrate the feasibility of this approach, and can be improved with access to more inspection records. Additionally, the national adoption of AASHTO Bridge Element Inspection Manual 5 will provide more robust and specific data to link damage with repair [2010].

2.4 Impact Analysis—Determining Impacts of Repairs to Optimize Decisions (DI)

The inventory created in repair analysis is used directly in impact analysis. Loss curves, similar to those developed for PBEE, link the repair of an element to the distribution of cost for the repair. Downtime curves provide an analogous link for determining closure time associated with repair.
Structural reliability is one type of decision information that is not determined from repair actions but rather from the capacity calculated in deterioration analysis. This field is very well established (section 1.3.1). Here, the PBDE framework will be used to systematically compare reliabilities calculated with a variety of models in the four analysis phases.

2.4.1 Existing Impact Models and Data Sources

In addition to project plans, specifications, and bids for individual repair or rehabilitation projects, sources used for cost and schedule estimation provide additional data for the development of loss and downtime curves. These include references such as Caltrans contract cost data [2009]. These general sources should be sufficient if the desired outcome of the PBDE analysis is selection of a lower-impact alternative, i.e. relative performance is of interest. If an extremely accurate cost or downtime assessment is required the operator would need to develop their own curves and repair inventory.

3 CONCLUSIONS

A performance-based durability engineering framework is proposed based on recent successful implementation of a performance-based earthquake engineering framework by PEER. This approach differs from existing frameworks for durability in its use of separate analysis stages and "pinch point" variables. The use of separate stages allows for flexibility in modeling, which can be used to assess the impacts of model choice and to model a variety of structures and exposures. The inclusion of impact analysis allows the framework to predict distributions of decision information useful to owners and operators. The existing models and datasets discussed here allow for testbed simulation of PBDE for chloride-induced corrosion. Future work on testbed simulation will demonstrate how the framework is implemented for archetype problems. It is hoped that the further development of this framework will lead to new research and design methods, replicating the effects of the introduction of PBEE.

ACKNOWLEDGMENTS

This research is being conducted under the support of a National Science Foundation Fellowship, a Stanford Graduate Fellowship, and the John A. Blume Earthquake Engineering Center. The authors thank Michael Johnson and Pete Whitfield at Caltrans for their generous sharing of expertise and data.

REFERENCES

AASHTO 2010, *Bridge element inspection manual 5*, Draft, 1st Ed.

Andrade, C., Alonso, C., & Molina, F.J. 1993, 'Cover cracking as a function of bar corrosion: Part I-Experimental test,' *Materials and Structures*, **26**[8], 453-464.

Angst, U., Elsener, B., Larsen, C., & Vennesland 2009, 'Critical chloride content in reinforced concrete--A review,' *Cement and Concrete Research*, **39**[12], 1122-1138.

Bamforth, P. 1999, 'The derivation of input data for modelling chloride ingress from eight-year UK coastal exposure trials,' *Magazine of Concrete Research* **51**, 87-96.

Bangert, F., Grasberger, S., Kuhl, D., & Meschke, G., 2003, 'Environmentally induced deterioration of concrete: physical motivation and numerical modeling,' *Engineering Fracture Mechanics*, **70**[7-8], 891-910.

Caltrans, 2009. *2009 Contract cost data*, State of California, Department of Transportation.

Deierlein, G.G., H. Krawinkler, & Cornell, C.A. 2003, 'A framework for performance-based earthquake engineering,' Proc. Pacific Conference on Earthquake Engineering, New Zealand.

Enright, M., & Frangopol, D. 1998, 'Probabilistic analysis of resistance degradation of reinforced concrete bridge beams under corrosion,' *Engineering Structures*, **20**[11], 960-971.

Fang, C., Lundgren, K., Plos, M., & Gylloft, K. 2006, 'Bond behaviour of corroded reinforcing steel bars in concrete,' *Cement and Concrete Research* **36**[10], 1931-1938.

fib, 2006, 'Bulletin 34: Model Code for Service Life Design,' fib, Lausanne.

Guerre, J., Robert, W., & Fraher, M., 2007, 'Framework for Using Pontis Bridge Management System to Support Development of Bridge Programs,' 86th Annual Transportation Research Board Mtg.

Hamburger, R., 2006, 'The ATC 58 Project: Development of next generation performance based earthquake engineering design criteria for buildings,' Proc. Structures Congress, St Louis, ASCE.

Kemper, M., Timothy, J. J., Kruschwitz, J., and Meschke, G., 2010, 'Modeling of Chloride and CO2 transport in intact and cracked concrete in the context of corrosion predictions of RC structures,' Proc. EURO-C 2010, Austria, 503-512.

Kranc, S., & Sagüés, A., 2001, 'Detailed modeling of corrosion macrocells on steel reinforcing in concrete,' *Corrosion Science*, **43**[7], 1355-1372.

Li, C. Q. and Melchers, R.E., 2005, 'Time-dependent reliability analysis of corrosion-induced concrete cracking,' *ACI Structural Journal*, **102**[4], 543-549.

Liu, Y. & Weyers, R. 1998, 'Modeling the time-to-corrosion cracking in chloride contaminated reinforced concrete structures,' *ACI Materials Journal* **95**[6], 675-681.

Maekawa, K., Ishida, T., & Kishi, T. 2009, *Multi-scale modeling of structural concrete*, Taylor & Francis Group, New York.

Meira, G., Andrade, C., Alonso, C., Padaratz, I., and Borba, J., 2008, 'Modelling sea-salt transport and deposition in marine atmosphere zone,' *Corrosion Science*, **50**[9], 2724-2731.

Roberts, M., Atkins, C., Hogg, V., & Middleton, C., 2002, 'A proposed empirical corrosion model for reinforced concrete,' *Structures & Buildings*, **152**[1], 79-82.

Patidar, V., Labi, S., Sinha, K., & Thompson, P. 2007, *Multi-objective optimization for bridge management systems, NCHRP Report 590*, Transportation Research Board.

Shimomura, T., Miyazato, S., Yamamoto, T., Kobayashi, K., Sato, T., Saito, S., Kamiharako, A., & Akiyama, M., 2006, *Report of Research Project on Structural Performance of Deteriorated Concrete Structures by JSCE-331*, Japan Society of Civil Engineers.

Siemes, T., & Edvardsen, C., 1999, 'Duracrete: service life design for concrete structures,' Proc. 8 DBMC, Vancouver, 1343-1356.

Thompson, P., and Johnson, M., 2005, 'Markovian bridge deterioration: developing models from historical data,' *Structure and Infrastructure Engineering*, **1**[1], 85-91.

Violetta, B. 2002, 'Life-365 service life prediction model,' *Concrete International* **24**[12], 53-57.

Vu, K. A. T. & Stewart, M. G. 2005, 'Predicting the likelihood and extent of reinforced concrete corrosion-induced cracking,' *Journal of Structural Engineering* **131**, 1681-1689.

XII DBMC
International Conference on Durability of Building Materials and Components
PORTO - PORTUGAL, April 12th-15th, 2011

Moisture Risks Assessment Related to Energy Retrofitting of Existing Buildings: Method and Case Studies

Julien Chorier [1]
Charlotte Abele [2]
Julien Hans [3]
Manuel Bazzana [4]

ABSTRACT

Several surveys have revealed that most of the existing French buildings are still poorly insulated. The current rate of retrofitting is low (1%) but it is tending to accelerate to reach the announced objectives. The problem of internal moisture requires special attention during retrofitting operations. In strongly insulated and poorly ventilated buildings internal condensation can leads to the development of micro-organisms, materials degradations, discomfort and potentially health issues. The aim of the Humirisk project was to propose a renovation methodology in order to limit the moisture risks related to the building modifications. This paper describes a method that has been developed and discuses the results obtained from six case studies. The method is based on assessment of the building initial state according to several parameters (construction system, condition of housing units, behaviour of inhabitants, temperature, relative humidity, air permeability and diagnostic through infrared camera). The building is then split into several sub-systems and studied through a simplified Failure Modes and Effects Analysis (FMEA) in order to emphasize potential failure modes that would result from the retrofitting step. This modeling approach allows representing easily different configurations of buildings. Results of the different FMEAs can then be compared in order to propose a suitable retrofitting solution that takes into account the risks related to moisture.

KEYWORDS

Risks assessment,FMEA, energy retrofitting, moisture

[1] Centre Scientifique et Technique du Bâtiment (CSTB), Saint Martin d'Hères, FRANCE,
[2] Centre Scientifique et Technique du Bâtiment (CSTB), Champs sur Marne, FRANCE, charlotte.abele@cstb.fr
[3] Centre Scientifique et Technique du Bâtiment (CSTB), Saint Martin d'Hères, FRANCE
[4] Centre Scientifique et Technique du Bâtiment (CSTB), Saint Martin d'Hères, FRANCE, manuel.bazzana@cstb.fr

1 INTRODUCTION

Products and innovative systems are and will be designed to achieve the ambitious goals of reducing energy consumption in buildings. Their levels of performance will thus be particularly high, and they must be maintained over time to ensure the durability of the works and in compliance with essential requirements "for a reasonable economically service life " as stated in the Construction Products Directive.

So, the failure criteria of these retrofit packages must be studied with new eyes. What was previously assessed as minor degradation (less critical failures) will be most serious malfunctions of tomorrow regarding the new energy performance requirements. We must also take into account interactions between the different systems and products used in a retrofitting.

Failure Mode and Effect Analysis (FMEA) is a method that aims to identify the combination of events leading to the failure of a product. Previous works have shown that this approach is interesting for durability assessment of building systems [Talon, 2006]. The literature reports several approaches presenting guidelines for FMEA integration in the building sector as well as case studies [Talon et al., 2006]. For instance [Hans & al. 2007] used a common FMEA workflow involving products and method experts to assess durability of several inovative building systems.

The HUMIRISK [Abele & al. 2010] project aims to assess the consequences of a renovation on heat and moisture transfer and intend to demonstrate that a risk free renovation is possible. This requires to integrate the issue of durability and risk management at early conception stage.

In this objective, the FMEA approach has been adapted to include several components of building. Indeed the system has been defined to collect the various renewal actions (establishment of a ventilation system , change of windows, installation of insulation ...) and to list the events leading to a degradation both on the element themselves but also on others parts of the buildings. From this analysis failures scenarios have been highlighted. This study was managed by CSTB attended by several partners (ALDES, Saint-Gobain Isover).

The study is divided into different steps:

- Definition of functional generic block (wall, interior insulation, ventilation system,…)
- The selection of blocks and interfaces for defining housing in the initial state;
- The selection of blocks and interfaces for defining the unit after renovation;
- The definition of links between blocks;
- The definition of the functions of each of these blocks (functional analysis) and study of possible damage;
- The list of the final degradation related to the renovation for each block;
- Analysis of critical points related to the renovation;

2 SYSTEM ANALYSIS

The analysis of the system deals with the description, characterization and modeling of the studied product and its components. For our study the system which was studied was the building before renovation.
In this analysis we have defined the structural composition of the building (system boundaries, components, interfaces, binding modes), its environment, functions and errors, omissions, negligence suffered by the product during its construction process that can cause damages or failures during its operational phase.
This first step gives information about the structural condition of the building during its operational phase (before renovation) and its behavior in response to environmental contrains.

To meet the expectations of the study, that is to say to have a method to effectively assist innovation in the renovation with the problematic of moisture, we propose a new FMEA methodology.

The FMEA method requires a large investment for each new study as it is necessary to redefine the system with all its component. To be able to model and study more easily a building, we have split the building into different "generic blocks ". The 13 blocks created (ventilation system, heating system, interior insulation, ...) are showned in the system structural analysis. This simplification of the FMEA method allows to reuse these blocks without having to conduct a study on every detail of the building structural decomposition.

Each block is representing a portion of the building and is initially studied independently.

The blocks are the following:

- Ventilation system;
- Heating System;
- Technical jacket;
- Interior insulation;
- External insulation;
- External vertical walls;
- Roofing;
- Floor;
- Balcony / loggia / window sill;
- Window;
- Door;
- Outdoors;
- Service Parts;
- Living areas

3 DETERMINATION AND CHARACTERIZATION OF INTERFACES

The interfaces are modeled as mechanical connections (glued, welded, bolted, attached or single contact) between system components (e.g. The window is connected to the vertical wall with screws).

3.1 Functional analysis of blocks and bonds

The goal of functional analysis is to determine the overall system functions and the functions performed by its components and interfaces.

For this, key features of each block are identified, thus leading to the creation of a functional model of the studied building. This model will be used as a basis for failure effect identification. Indeed if one of the function is no more maintened the impact on the component and the system could be immediately identified trough relations between functions.

This step is crucial, but still difficult to carry out. Indeed the definition of the overall system functions gives the boundaries of the study and the determination of relevant failure modes is strongly depend on the quality of the functional description.

In our approach, functions are attibuted to the generic blocks previsouly defined, but also at the interface between blocks.
The table below shows the functions of blocks and their connections (table 1).

Table 1. Exemple of functions

Block 1	Block 2	Connection function
Ventilation system	**Heating system**	
extract the house contaminated air	to be safe (user safety)	
bring fresh air	to be safe (user safety)	
Ventilation system	**outside wall**	
Distribute air flow	stop air flow	remain in position
Distribute air flow	limit weathering flow	remain in position
limit outside noise	control noise flow	remain in position
be silent	control noise flow	remain in position
reduce heat losses	limit heat flow	remain in position
Distribute air flow	Esthetic	remain in position
Distribute air flow	limit noise flow	limit noise flow
Ventilation system	**Roofing**	
extract contaminated air	control weathering flow	limit weathering flow
provide fresh air	control weathering flow	limit weathering flow
Ventilation system	**under the window**	
Distribute air flow	stop air flow	remain in position
Distribute air flow d	limit weathering flow	remain in position
limit outside noise	control noise flow	remain in position
be silent	control noise flow	remain in position
reduce heat losses	limit heat flow	remain in position
Distribute air flow	being aesthetic	remain in position
Distribute air flow	limit noise flow	limit noise flow
Ventilation system	**window frame**	
Distribute air flow	stop air flow	remain in position
Distribute air flow	limit weathering flow	remain in position
limit outside noise	control noise flow	remain in position
be silent	control noise flow	remain in position
reduce heat losses	Limit heat flow	remain in position
Distribute air flow	being aesthetic	remain in position

4 QUALITATIVE ANALYSIS THROUGH FMEA

FMEA allows the identification and description of degradations modes and product failures.
For each block and its associated functions we seek to identify all potential degradations, their causes and consequences. This process is iterative and ends when all the failure scenarios are known.
The first step summarizes the damage caused by construction process, stage 1 corresponds to the initial state at the beginning of the exploitation phase which is not necessarily a stage without damage since it can integrate those due to errors in the construction process. The following steps identify the sequence of degradations, that is to say the scenarios of system failures. Examples of results obtained are presented in table 2 bellow.

Table 2. Excerpt from FMEA results.

	Function	Component	Cause	direct effect	indirect effect
1	air distribution	Ventilation system	airflow not or partially insured	Insufficient air turnover	Insufficient air quality / humidity
2	limiting outside noise	Ventilation system	noise	obstruction of the ventilation system	back 1
3	limiting functional noises	Ventilation system	noise	obstruction of the ventilation system	back 1
4	limit heat loss	Ventilation system	cold air / energetic losses feeling	obstruction of the ventilation system	back 1
5	extract the house contaminated air	Ventilation system	airflow not or partially insured	Insufficient air turnover	Insufficient air quality / humidity
6	provide fresh air (focuses on people)	Ventilation system	airflow not or partially insured	Insufficient air turnover	Insufficient air quality / humidity

5 FAILURES GRAPH

FMEA identifies all possible failure scenarios in a table. Therefore the table quickly becomes very large and make it difficult to visualize the scenarios.
To overcome this problem, results are ussully represented as failure event graphs. The graphs represent event-failure sequence and / or the concomitant degradation of components over time that lead to product failure (see figure 1).

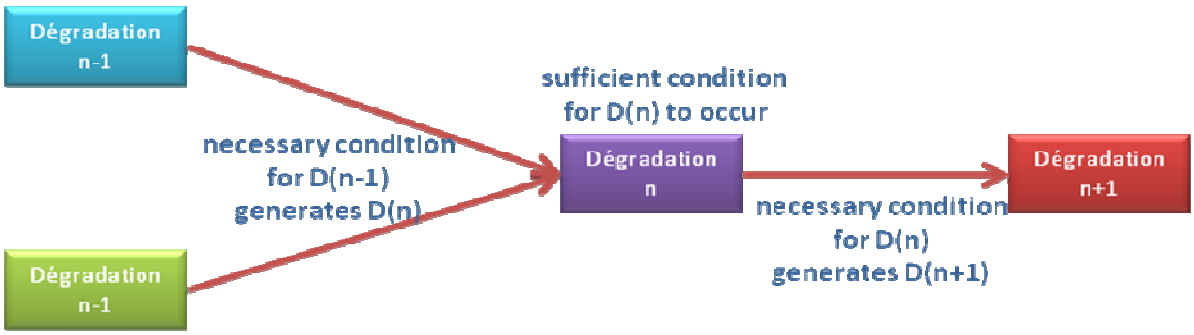

Figure 1. Convention adopted for reading failure graphs

The failures graphs construction is based on the same principle as the iterative development of the matrix of failure modes and effects analysis. They are composed of nodes and edges.
Nodes define : the name of the component or interface, the functions provided by this component or the interface and their modes of deterioration.

In addition, to support damage diagnosis, failures graphs can be useful for the analysis of potential malfunctions during the design phase, and the quality control provided for the different stages of the process (implementation, maintenance) or implemented for an existing product (operation, retrofitting).

6 MODELING THE CONFIGURATION AFTER RETROFITTING

Using the generic blocks presented earlier, we can modelize the initial configuration of the building before the renovation.
Changes related to the renovation are then integrated as, for instance an exterior insulation or the installation of a ventilation system.

The risk analysis shows that the presence of a balcony or loggia or window sill may create a thermal bridge if the area is not properly treated. Figure 4 show that this failure should creat the Loss of overall thermal performance.

The photo below shows that the insulation does not return on the window sill, this is leading to the presence of a thermal bridge. Cracking of the coating can also create points of water infiltration (see Fig 2).



Figure 2. Treatment of windowsills in a renovation

This thermal bridge itself can cause a cold spot. The realization of a thermal imaging confirms this degradation and the presence of cold spot at the junction outside wall / floor. The two zones are surrounded on the figure below.

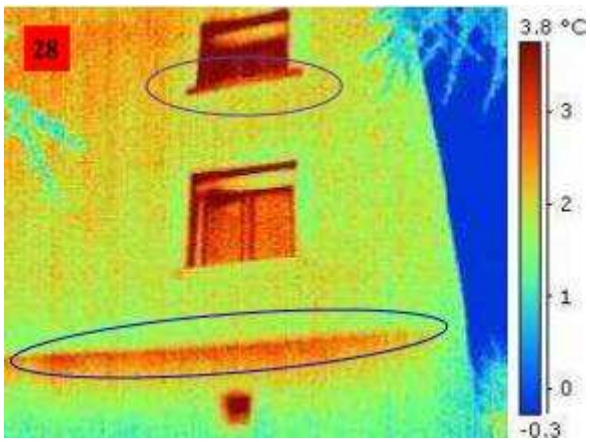

Figure 3. Infrared thermography performed after the renovation

Figure 4 bellow shows one of the failure event graph developed from FMAE study. The analysis of this graph allows us to identify the consequences of these cold spots and water infiltration.

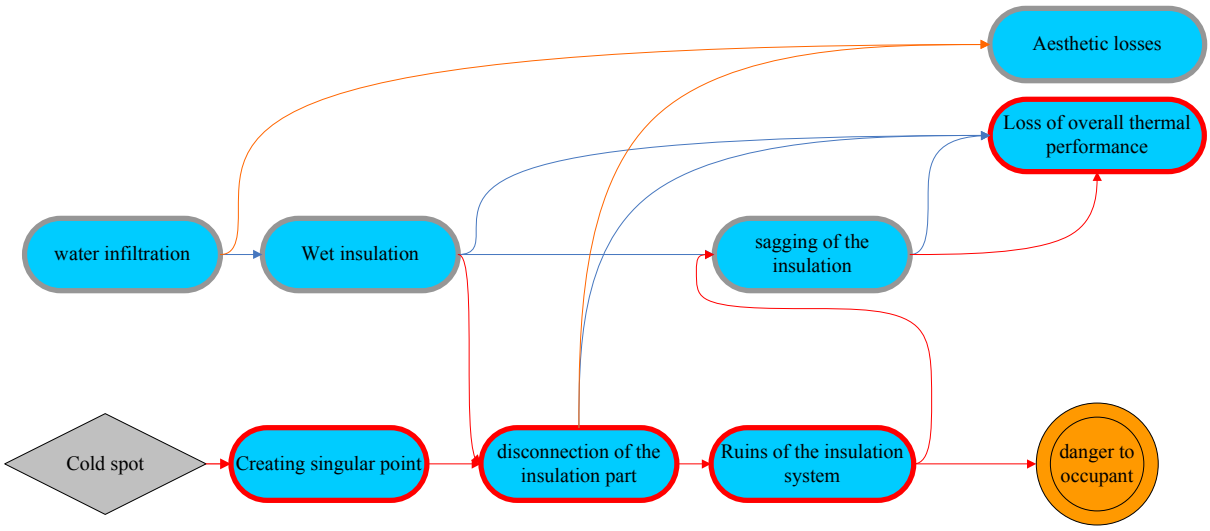

Figure 4. Failure event graph of deterioration of the External insulation renovation

We note that the consequences can be of 3 types:

- Aesthetic losses;
- Loss of thermal performance;
- Destruction of the structure and therefore potentially dangerous to people.

To be complete, the probability of occurrence of the different events has been taken into acount.Results shown that the ruin of the insulation system remains very unlikely. In contrast some water infiltration may create aesthetic losses without too serious consequences.

7 CONCLUSIONS

The proposed approach, through simplified FMEA allowed us to evaluate the consequences of a renovation on the expected functions of a building (transfer of moisture, thermal performance, indoor air quality, structural stability, occupant safety). Several potential failure modes related or caused by retrofiting have been identified.

FMEA at macroscopic scale is quite innovative and allows to reuse the work done to any building or building renovation and open the way to Risk analysis from component to building scale.
Furthermore, this approach may serve as decision helping tool for project owner involved in renovation projects.

To complete this study, it is still important to work to determine the occurrence and severity and thereby define an criticality assesment of the identified defects .

In addition, incorporation of a time scale in the degradation phenomena will also helps to identify priorities for action or further feasibility studies.

ACKNOWLEDGMENTS

This study has been supported by the ADEME (French Environment and Energy Management Agency)

REFERENCES

Talon, A. Boissier, D. Hans, J. Lacasse, MA. Chorier, J. 2008, 'FMECA and Management of building components', Proc. 11th Durability of Building Materials and Components (11th DBMC), Istanbul, Turkey, 11-14 May 2008.

Hans, J. Chorier, J. Morlot, R. Boddaert, s. Proisy B, & Boulanger, B. 2007, *Durabilité des équipements énergétiques et de composants d'enveloppe du bâtiment*. CSTB – Internal report.

Abele, C. Chorier, 2010, *HUMIRISK Renforcement de l'Isolation dans l'Existant - Evaluation des Risques liés à l'Humidité*. CSTB – Internal report.

French agency for quality in construction, 2005, Qualité progressions ensemble 1995-2005, Report of the AQC.

Talon, A. Hans, J. Chevalier, J.-L., Hans, J. 2006, Failure Modes Effects and Criticality Analysis Research for and Application to the Building Domain, CIB Punlication n°310, Working commission 80, 246 p. Rotterdam.

Talon, A., Boissier, D., Chevalier, J.-L., Hans, J., 2004, A methodological and graphical decision tool for evaluating building component failure. In Proceeding of CIB World Building Congress 2004, Toronto, Canada, 2 7 may 2004.

Talon, A., 2006, Evaluation of the construction products degradations scenarios. PhD Report, CSTB, University Blaise Pascal, Clermont 2.

XII DBMC
International Conference on Durability of Building Materials and Components
PORTO - PORTUGAL, April 12th-15th, 2011

Characterization of the Conservation State of the Façade of Teatro Nacional de S. João, Porto

Ana Luísa Velosa[1]
Fernando Rocha[2]
Aníbal Costa[3]
João Coroado[4]
Ana Fragata[5]
Esmeralda Paupério[6]

ABSTRACT

Teatro Nacional de S. João (TNSJ), in the city of Porto, is a building from 1918, with richly decorated façades. The decorative elements, of a variable size, depicting floral elements, faces and simple patterns, are made of mortar and some contain an underlying steel frame that provides a basis for the complex shapes. Although the architecture is current for the age, there was some innovation in the choice of building materials, as possibly cement and not traditionally used air lime was employed.

Although this building has had various interventions, there was evident degradation of the façades and specifically of the ornaments. Therefore the ornamental structures of TNSJ were inspected and samples were taken from each façade in order to characterize constituents and proportions, identify differences in materials brought about by previous interventions and determine the extent and causes of degradation. The analytical procedures comprised XRD, XRF, PLOM, binder/agregate proportion estimation by hot acid dissolution and determination of particle size distribution.

In depth carbonation and large presence of salts, associated to sea fog promoted the oxidation of the metallic elements and consequent degradation of surrounding mortars. This shoud be mitigated in order to avoid the continuous degradation. An intervention of conservation and restoration should consider the desalination of existent mortars, the passivation of metalic elements and the reconstruction of the decorative volumetries and/or the reposition of the gaps with new compatible mortars.

KEYWORDS

Mortars, characterization,conservation.

[1] Department of Civil Engineering, Geobiotec, University of Aveiro, 3810-193 Aveiro, Portugal. avelosa@ua.pt
[2] Department of Geological Engineering, Geobiotec, University of Aveiro, 3810-193 Aveiro, Portugal, tavares.rocha@ua.pt
[3] Department of Civil Engineering, University of Aveiro, 3810-193 Aveiro, Portugal. agc@ua.pt
[4] Department of Art, Conservation and Restoration, Polythecnic Institute of Tomar, 2300 Tomar, Portugal, jcoroado@ipt.pt
[5] Department of Civil Engineering, University of Aveiro, 3810-193 Aveiro, Portugal / National Laboratory of Civil Engineering (LNEC), 1700-066 Lisboa, Portugal,. afragata@lnec.pt
[6] Instituto da Construção, FEUP, University of Porto, Portugal, pauperio@fe.up.pt

1 INTRODUCTION

The building of Teatro Nacional de S. João (TNSJ) ended its construction in 1918, after the destruction by a fire of the previous theatre in the same location. The project, by Architect José Marques da Silva didn´t have a noticeably modern architecture but the use of materials was more audacious. At the beginning of the 20th Century, in Portugal and specifically in the region of Porto, traditional construction prevailed, with load-bearing stone (granite) walls and air lime mortars. However, the use of hydraulic binders and especially of cement, that had started in England and France, had widespread throughout Europe [Callebaut *et al* 2000, Suponitski *et al* 2001] and the architect chose this material for the execution of the external ornaments, work of the well known mason António Baganha Pai. These elaborate ornaments are extremely varied in shape and size, depicting floral arrengements, geometric patterns or the human figure and were built around a steel frame that was used as a basis for the various forms.

TNSJ is built at a high spot in Porto, near the river Douro but some distance inwards from the sea. However, the city is frequently prone to fog and the weather is also characterised by the predominance of rainy spells.

Almost one century after its construction, TNSJ has had a few maintenance interventions that have introduced some transformations in terms of the external renders and ornaments, the last of which was carried out in 1994. However, in 2009 the state of the mortar ornaments was precarious, with severe cracks and material loss. This paper describes the study of mortars from these ornaments by the use of analytical techniques and attempts to explain the reasons of such severe degradation. A complete set of analysis and tests was carried out in order to characterize these mortars and enable the develoment of compatible mortars for restoration purposes.

2 SAMPLING AND ANALYSIS

2.1. Sampling

A total of 18 samples was collected from the ornaments present in 3 façades (east, west and north) of the TNSJ building, taking into account different ornamental structures as those shown in Figures 1 and 2. Sampling was quite extensive due to the current state of the building, providing enough material for a more criterious anlysis. Sampling also took into account differences in mortars that could indicate a latter execution, possibly linked to a conservation intervention.



Figure 1. Sampling from an ornament depicting a face in the western façade



Figure 2. Sampling from a circular ornament in the western façade

2.2. Testing Procedures

Mortars were characterized in terms of their composition and in terms of physical and mechanical characteristics. The mortar/steel frame interface was also analysed.The employed methodology took into account current methods for the testing of historical mortars [Alvarez *et al* 1999, Gleize *et al* 2009, Maravelaki-Kalaitzaki *et al* 2003, Middendorf *et al* 1999, Velosa *et al* 2010]. In order to characterise the sampled mortars, the following analytical methods and tests were used:

- X-Ray Fluorescence (XRF) for the determination of the chemical composition
- X-Ray Diffraction (XRD) for the determination of the mineralogic composition
- Acid dissolution to evaluate aproximate binder/aggregate ratio
- Particle size analysis of the aggregate
- Observation of thin sections and polished surfaces by Polarized light optical microscopy
- Determination of water absorption by capillary action
- Determination of mechanical strength
- Determination of carbonation depth

Acid dissolution was performed in order to dissolve the binder fraction and create a residue composed by the aggregate fraction. Hot hydrochloric acid was used to guarantee a residue composed by siliceous sand. Results give an approximate value of binder/aggregate ratio, as the used acid dissolution technique dissolves carbonates and partially dissolves soluble silica. The obtained residue was dried until constant mass was achieved. Particle size distribution by dry sieving was performed on the residue obtained from acid dissolution according to standard NP EN 993-1.

X-Ray Fluorescence (XRF) allows the detection of elements present in the samples, by X-ray excitation of the sample. Sample preparation followed the procedure used for XRF and a Panalytical Axios Dispersive XRF Spectrometer was used.

X-Ray Diffraction (XRD) provides qualitative information on the crystalline mineral phases existent in the samples. For this analysis, mortars were crushed and dried at a low temperature. This anaysis was performed on the total mortar sample and on the fraction below 75µm in order to allow a more thorough analysis of the binder. The equipment used was a Panalytical X-Pert Pro X-Ray Diffractometer.

The observation of thin sections and polished surfaces by optical microscopy provides further information on the mortar structure and in this case also on the mortar/steel frame interface. Thin sections and polished surfaces were prepared by impregnation in epoxy resin and observed with an transmited and reflected polaraized ligth optical microscope Nikon Optiphot.

Mechanical strength was determined on 30mmx30mm cubes and the determination of carbonation depth was performed by the spraying of phenolphtalein on freshly cut surfaces and evaluating colour change.

3 RESULTS AND DISCUSSION

3.1. Mortar composition

Mortar chemical composition characterized by XRF is shown in Table 1, taking into account representative mortars from different façades and types of ornaments. From the analysis of Table 1 it is clear that generally there is a similarity between the analysed mortars independent of their origin. Mortars with a weight ratio of 3:7 (WF3 and NF1) display a higher percentage of silica due to the higher content of siliceous sand in comparison with mortars with a 4:6 weight ratio (WF2 and NF2). Mortar WF1 was classified as a renovation mortar. In this case, there is a clear increase in binder content shown by the percentage of CaO, that is in agreement with the rich 1:1 weight ratio that was the result of acid dissolution.

Table 1. XRF analysis of representative mortars.

Sample	*West Façade Renovation Mortar (WF1)*	*West Façade Human Figure – Face (WF2)*	*West Façade Geometric Ornament (WF3)*	*North Façade Rim (NF1)*	*North Façade Rim (NF2)*
SiO_2	19,53	28,06	34,60	34,41	28,60
Al_2O_3	5,36	4,59	5,14	5,10	5,63
Fe_2O_3	2,76	2,52	1,97	2,27	2,24
MnO	0,05	0,03	0,05	0,04	0,04
MgO	0,81	0,96	0,81	1,07	0,55
CaO	53,92	36,99	32,27	36,32	36,36
Na_2O	n.d.	n.d.	n.d.	n.d.	n.d.
K_2O	0,13	0,99	1,47	1,40	1,68
TiO_2	0,33	0,24	0,29	0,28	0,23
P_2O_5	0,19	0,08	0,08	0,44	0,77
LOI	17,30	25,71	23,38	18,73	23,92

XRD results of the fraction below 75µm revealed the presence of calcite and quartz in all samples and the presence of feldspars and/or kaolinite in some cases. In most samples there is an indication of the presence of a hydraulic binder. All samples displayed the presence of soluble salts, namely gypsum, halite, nahcolite and natron, although there was no evidence of efflorecence in any of the samples. The presence of salts, sometimes quite meaningful, reveals that mortars are quite altered from their original composition. The presence of kaolinite, due to the alteration of feldspars, is also another indicator of the degree of alteration of these mortars. The presence of natron and nahcolite is usually related to their formation in concrete under the action of sodium carbonates [Haynes *et al* 2010]. Current studies have revealed that the action of sodium carbonate usually results in salt crystallization inside voids in the mortar matrix while the action of suphates may be more destructive, often promoting concrete delamination [Haynes *et al* 2010].

Acid dissolution of mortars [Alvarez *et al* 1999, Middendorf *et al* 1999] resulted in approximate binder/aggregate proportion in weight, taking into account that siliceous sand was used as an aggregate. Two main weight ratios were identified, 3:7 and 4:6, but there is no relation between different ratios and different types of ornaments or different façades. A singular case of a weight ratio of 1:1 was encountered in a specific mortar withdrawn from an ornament in the western façade, with a

clearly distinctive appearance, probably from a past intervention. Acid dissolution of this particular mortar created saponifiction which may be due to the presence of water repelent agents.

Particle size distribution of aggregates showed a great variation, suggesting that sand from different proveniences may have been used. Although there is no relation between particle size distribution of the aggregates and different mortar compositions or ratios, mortar WF1 displays a distinctive aggregate mainly composed of fine sand (Figure 3) in comparison to the river sand aggregate used in the other mortars (Figure 4).



Figure 3. Renovation Mortar Aggregate



Figure 4. Typical mortar aggregate

3.2. Mortar characteristics

Mortar testing for compressive strength implied the execution of 30mmx30mm cubes from the extracted samples as this was the maximum size possible. However, it was only possible to test two samples due to the irregular shape of most of the mortar samples.

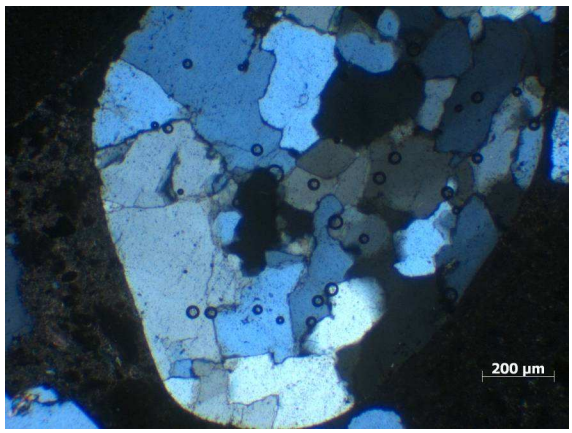

Figure 5. Quartzitic paticle in binder matriz taken from arm of human figure (North façade) visualised in + nicols under transmitedPLOM

Compressive strength values for a sample withdrawn from a feminine face on the western façade and from a geometric ornament in this same façade resulted in values of 16,6MPa and 38,9MPa, respectively. These high values are only compatible with mortars with a hydraulic binder, but seem to indicate that, although the mortars have been affected by the action of soluble salts, this did not affect their mechanical strength. This fact is further justified by the analysis of thin sections on the transmited PLOM (Figure 5) showing a quartzitic particle in a compact binder of the mortar. The salts encountered were mainly gypsum, nahcolite and natron and they may have filled an initially porous mortar structure.

The determination of carbonation depth was done on site, as the mortars were extracted, and in the laboratory, on freshly cut mortar surfaces. On site spraying of a phenolphtalein solution on surfaces

next to the steel structure, immediately after mortar extraction, showed complete carbonation. Laboratorial tests measured a carbonation depth of up to 7cm corresponding to the maximum mortar thickness over the steel structure. In depth carbonation of concrete and mortar may be caused by environmental contact [Bertolini *et al* 2008] and is quite typical of mortars that have endured extensive exposure. A porous structure and weather conditions such as rain and fog are favourable to this reaction.

3.3. Mortar/steel frame interface

Polished surfaces of the steel/mortar interface were viewed under the optical microscope to evaluate the effect of corrosion. Figure 6 depicts the lack of cohesion between mortar and steel and the corrosion of the steel frame.

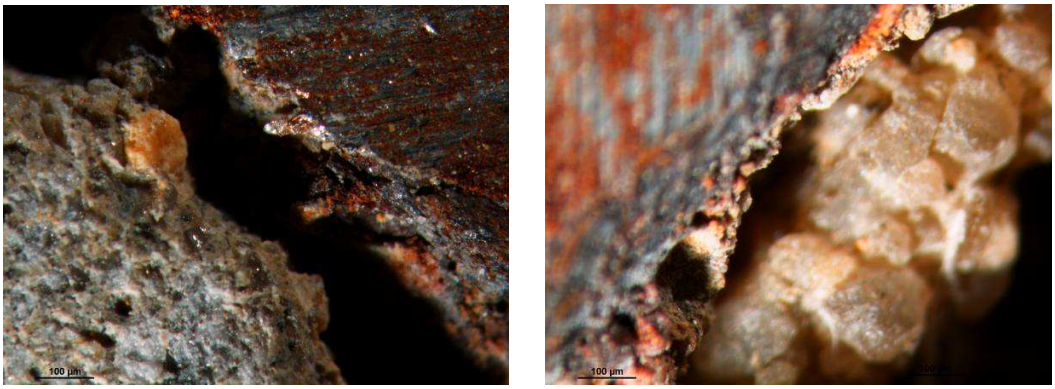

Figure 6. Steel structure/mortar interface showing strong discontinuity and steel corrosion

Mortar carbonation was extensive, reaching the steel frame, due to environmental action and possibly porous mortars. This led to steel depassivation and consequent corrosion and expansion of the steel frame. This fact created the main problems in the various ornaments in TNSJ façades, as stresses produced by the volume increase of the steel frame created generalized cracking in mortars and lack of cohesion between the mortar and the steel. Mortars over the steel frame are almost loose and prone to detach with time.

4 CONSERVATION ISSUES

The conservation state of the ornamental figures is generally poor, mainly caused by the extensive corrosion of the steel frames. Although mortars have a high salt content, they display a compact structure and high compressive strength. Cracking of mortars and consequent detachment was promoted by the expansion of the steel frames due to long-term environmental exposure to a salty atmosphere and humidity and irregular mortar thickness over the frames.

Conservation and restoration actions must take into account the current state of the ornaments upon which the choice of repair or replacement should be based. Desalination and consolidation of existent mortars should be considered. In the cases in which there is a need for restoration of the gaps or reconstitution of the original elements, these actions must be guided by conceptual, functional and technical requirements [Van Balen *et al* 2005]. The use of mortars for these purposes must take into account compatibility requirements - aesthetic, mechanical, physical and chemical - and should be based on the analysis of the existent mortars. The passivation of the frames and the use of mortars that protect these frames (high pH, low permeability, low cracking susceptibility) will ensure the durability of the restoration action.

5 CONCLUSIONS

External ornaments mortars of TNSJ were mostly made using a hydraulic binder, possibly cement, and a siliceous aggregate. Two main binder/aggregate weight ratios were encountered, 3:7 and 4:6, but the

aggregate grading was varied, suggesting different provenience. A different mortar, with fine sand and a 1:1 weight ratio, possibly incorporating a water repelant, was used on a previous intervention on the façade.

Analysis performed on the mortar samples revealed the strong presence of soluble salts: gypsum, nahcolite, natron and more seldom, halite. This fact is the result of long-term exposure to pollution and sea fog. However, salt content did not negatively affect the mortars' mechanical characteristics and could instead have contributed towards a more compact structure by salt crystallization inside mortar voids. Undoubtedly carbonation also increased mortar compactness and all analysed mortars were completely carbonated at a depth corresponding to the position of the steel structure.

Mortars were moulded around steel frames that acted as a basis for shape, but the mortar thickness over the steel structure was extremely varied, ranging from barely a few milimeters to 6 to 7 centimeters. This fact in itself promoted steel degradation but depassivation also occured by extensive carbonation of the mortars after a long exposure to external conditions. The steel structure is profoundly affected and its volume increase by corrosion created widespread cracking in the external ornaments, promoting further degradation.

Therefore, the conservation and restoration intervention of the TNSJ ornamental structures implies special care and may include desalination and consolidation of existing mortars, the passivation of the frames or in cases of losses, their replacement. The volumetric reconstitution and the gaps restoration should be done with mortars with mechanical, physical and chemical properties that must be compatible with the original materials.

REFERENCES

Alvarez, J.I., Martín, A., García Casado, P.J., Navarro, I., Zornoza, A. 1999, 'Methodology of validation of a not hydrochloric acid attack' *Cement and Concrete Research*, **29** (7), 1061-1065.

Bertolini, L., Carsana, M., Redaelli, E. 2008, 'Conservation of historical reinforced concrete structures damaged by carbonation induced corrosion by means of electrochemical realkalisation', *Journal of Cultural Heritage*, **9**, 376-385.

Callebaut, K., Elsen, J., Van Balen, K., Viaene, W. 2000, 'Nineteenth century hydraulic restoration of mortars in the Saint Michael's Church (Leuven, Belgium). Natural hydraulic lime or cement?', *Cement and Concrete Research*, **31**, 397-403.

Gleize, P.J.P., Motta, E.V., Silva, D.A., Roman, H.R. 2009 'Characterization of historic mortars from Santa Catarina (Brazil)' *Cement and Concrete Composites* **31** (5), 342-346.

Haynes, H., O'Neill, R., Neff, M., Mehta, P. K. 2010, 'Salt Weathering of Concrete by Sodium Carbonate and Sodium Chloride' *ACI Materials Journal*, **107** (3), 255-266.

Maravelaki-Kalaitzaki, P., Bakolas, A., Moropoulou, A. 2003 'Physico-chemical study of Cretan mortars' *Cement and Concrete Research* **33** (5), 651-661.

Middendorf, B., Baronio, G., Callebaut, K., Hughes, J. 1999 'Chemical-mineralogical and physical-mechanical investigations of old mortars' in *Historic Mortars: Characteristics and Tests, Proceedings of the International Rilem Workshop*, eds P. Bartos, C. Groot, J.J. Hughes, RILEM Publications S.A.R.L., France, pp. 53-59.

Souponitski, S.Z., Sniatkov, S.V., Grigoriev, S.E. 2001, 'Early reinforced concrete constructions in Russia: specific faults and causes of failure', *Engineering Failure Analysis*, **8**, 201-212.

Van Balen, K., Papayianni, I., Van Hees, R., Binda, L., Waldum, A., 2005, 'Introduction to requirements for and functions and properties of repair mortars', *Materials and Structures* **38** (8), 781-785.

Velosa, A.L., Veiga, R., Coroado, J., Ferreira, V.M., Rocha, F. 2010, 'Characterization of ancient mortars from Roman times to the nineteenth century' in *Compatibility issues of new mortars with substrates and ancient mortars, Materials, Technologies and Practice in Historic Heritage Structures*, eds Bostenaru Dan, Maria; Prikryl, Richard; Török, Ákos, Springer, Berlin, pp. 235-257.

XII DBMC
International Conference on Durability of Building Materials and Components
PORTO - PORTUGAL, April 12th-15th, 2011

The Sloterhof Complex in Amsterdam an Example of Exposed Concrete

Hielkje Zijlstra[1]
Herdis Heinemann[2]

ABSTRACT

Sloterhof in Amsterdam is a neighbourhood in Amsterdam in the Slotermeer and Slotervaart section of the Algemene Uitbreidingsplan (General Expansion Plan) for Amsterdam of 1939, which was implemented under C. van Eesteren (1897-1988). In 1954 Architect J.F. Berghoef (1903-1994) started on the design for the area and completed it in 1960. Berghoef was used to traditional building methods. Sloterhof was one his first major commissions after the Second World War. During the war he joined a research group developing industrial housing. The modernist philosophy and the human approach were combined in an economical approach to architecture. The buildings looked modern and the building services had high specifications, including central heating and running hot water. Sloterhof has not yet been listed as a monument, however, it is on the top 100 list of potential listed monuments in Amsterdam. TNO (research institute) and TU Delft (University of Technology) investigated the qualities of the project and how to make this neighbourhood more sustainable. The main conclusions were that this complex is worth preserving. Fortunately it has not changed much during its lifetime. It belongs to our recent cultural heritage and it needs a durable protection instead of a zero CO2 approach. Sloterhof can be refurbished to make it more sustainable, while at the same time respecting its architecture.

KEYWORDS

post war, refurbishment, prefabrication, exposed concrete, monument, durability, ABCD research method

[1] Faculty of Architecture, dep. ®MIT of the Delft University of Technology, Delft, NETHERLANDS, h.zijlstra@tudelft.nl
[2] Faculty of Architecture, dep. ®MIT of the Delft University of Technology, Delft, NETHERLANDS, h.a.heinemann@tudelft.nl

1 INTRODUCTION

Sloterhof was investigated using the ABCD research method which was modified to suit this case and covered three levels of scale: town planning, architecture and construction engineering [Zijlstra 2009]. Technology provided me with the inspiration to develop a comprehensive research method to assess buildings: Analysing Buildings from Context to Detail in time: ABCD research method. Providing information on practice is a key element in construction engineering, which is a learning process. We are not solely concerned with the end result. Changes are made during the life of a building, and they might be made differently if the history and technical aspects of the building were studied in greater detail. Both maintenance and changes require us to understand the building concerned.

2 THE ABCD RESEARCH METHOD

The first part of the study concerns the context. It analyses the contextual aspects (brief, site, architect, typology, and design process), one after another, over all periods. The information provided by observation is sifted to obtain the contextual information which is or was relevant to the design, creation, existence and decay or future existence of the building. Where typology is concerned we should not only consider a functional or chronological order of buildings, based on building types. Instead, the buildings should be analysed primarily on the basis of a spatial typology, as the spatial conditions will remain, or may have to change when the function of the building is changed.

The second part of the study considers the building in greater detail and initially considers the following periods: creation, existence and decay/continued existence. The building is then analysed on the basis of the following aspects: space (interior and exterior); structure (load-bearing structure and elements which determine the structure); materials (the definition of space by materials, determined by: light, colour, texture, surface, sound, radiation, smell, dimensions and weight); building services (plant and installations to support climate control, comfort, maintenance and communications).

Analysing the four elements at the three levels (periods) leads to a matrix at the level of the whole building: the Analysing Building Construction in time matrix, or ABC matrix. When this matrix is combined with the considerations based on the contextual factors it forms the regenerative conclusion of the ABCD study of the building.

With Sloterhof the levels town planning, architecture and construction engineering were considered from two time perspectives: during the process of creating of the building (through to the handover) and how it expired after completed(from the handover to the present, and a look towards the future).

3 TOWN PLANNING - CREATION

This paper concerns the Sloterhof complex of dwellings, shops and commercial spaces in Amsterdam, on the Comeniusstraat in the Slotervaart district. Cornelis van Eesteren worked on the Amsterdam General Expansion Plan (AUP) from 1928 and the plan was approved in 1939 [Gemeente Amsterdam 1985]. It provided for Amsterdam a expansion from 4,608 to 12,052 hectares, around 120 km². The Garden City Committee appointed in 1923 had a major impact on these plans. The plan aimed to provide both housing and services with a series of buildings set within a green landscaped setting rather than designing separate satellite towns, the plan extended the edge of Amsterdam, with a fair degree of independence and open design [Van der Velde 1968]. The Slotervaart expansion plan was developed as part of the AUP, following these principles. In 1954, architect J.F. Berghoef was commissioned to design Sloterhof, part of the district of Slotervaart Fig. 1. When the design was completed in 1960, it included 668 dwellings, 21 shops, 2 service stations, lock up garages, a bank and a pub/restaurant. [Fischer 1968].

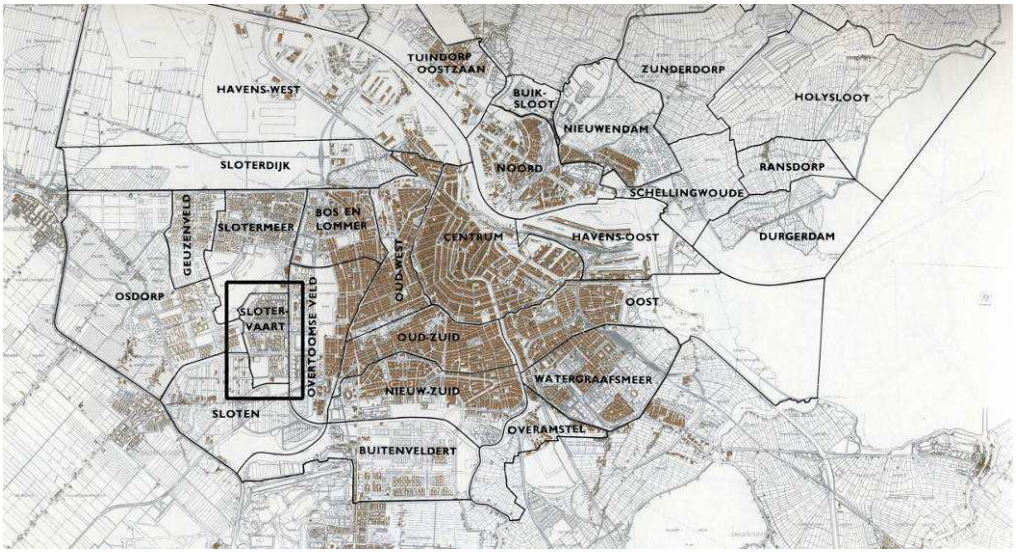

Figure 1. Sloterhof located in Sloterhof in the city of Amsterdam [Van der Velde 1968].

3 TOWN PLANNING - EXPIRED

In 2001Sloterhof was assessed in particularly positive terms by Hereijgers and Van Velzen [2001]. In 2001 Sloterhof was described also as a "pearl" within the framework of Park City 2015 [Gemeente Amsterdam 2006]. It was also identified as a potential listed building in the study undertaken early in 2008 by Steenhuis & Urban Fabric. In May 2009 it was included among the Top 100 potential new monuments to be listed in Amsterdam [Bureau Monumentenzorg Amsterdam 2009]. The comments note that the objects are protected as "cherished rarities" and express surprise that Sloterhof, with its 900 dwellings, was not included among the national Top 100 of state listed monuments in the Netherlands [Van Santen 2007].

Current town planning concepts such as those outlined in Parkstad 2015 offer new opportunities to appreciate the original qualities of the Slotervaart district in Amsterdam. The aim is to provide a positive residential and work environment, with a diversity of residents and uses. The spaces for the provision of services could be used effectively again, and the public areas should be maintained and repaired to return them to their original condition, after which they might be further optimised. For example, the playgrounds designed by Aldo van Eijck are still there, but better use could be made of them. The potential redevelopment of Slotervaart should be guided by concepts such as the ranking of maximum house rents related to income, residents from different socioeconomic groups, affordability and the garden city concept.

4 ARCHITECTURE - CREATION

Sloterhof was built between 1958 and 1960 although the design work started in 1954. Working closely with H. van Saane, director of the Nederlandse Maatschappij van Volkshuisvesting (Nemavo), Berghoef applied the Airey-Nemavo system (NA system) in several projects like Populierenweg (1950, 300 dwellings) and Amstelhof (1952, 350 dwellings and general services). Although he had his doubts about prefabricated structures, he used them shortly after the Second World War. In his view, industrial production restricted architectural expression. Berghoef emphasised the importance of the urban context - public areas had to be incorporated in the design in order to offer a pleasant residential environment [Berghoef 1981]. His designs, which were realised using system construction, tempted to strike the right balance between tradition, new technology and public spaces. Based on those principles, his practice, which previously used traditional construction methods, started using system construction. He made a real effort to ensure that the human scale was still paramount in this

form of architecture. The mixed uses, carefully designed greenery, playing areas, covered playing galleries, craft rooms, lock up garages and small business units all underline his philosophy.

For Berghoef, the cohesion of the whole provided the basis of design for Sloterhof. Along Lelylaan, there are seven blocks to the left, and nine to the right, grouped around Huizingalaan at their centre Fig. 2. The tall blocks(M) extend into the water, they mark the division and frame the development. During the development of the design the tall block envisaged on the Hemsterhuisstraat side was replaced by a square tower block (T) of twelve storeys, which broke the symmetry with a striking final chord. The recessed five-storey blocks (B) flank internal courtyards which are shielded from Comeniusstraat by blocks of lock-up garages (g) and shops at the ends. Huizingalaan forms the centre, with an urban variation of the low blocks (B) accessed by stairwells. Near Huizingalaan there are two blocks of shops (W) and two service stations (s). On the water side the internal courtyards have pergolas. The courtyards have playing areas for children. All shops have a dwelling for the shop owner. Near the tower there was space for four houses with artist's studios (A). An octagonal pavilion, for a bank, was built on the extensive paved area along Huizingalaan. The restaurant was accommodated in the block on the east side of Huizingalaan, near Lelylaan. Berghoef also designed the electricity substations, using the same precast concrete system. The prefabricated system imposed a pattern of concrete slabs with dimensions of 625 x 375 x 40 mm. Within this pattern variation was provided through the use of materials, detailing and colour. The lower blocks and shops had light grey as the dominant colour, while the taller blocks and the tower were black with prominent white concrete surrounds Fig. 3.

The garages, electricity substations and dwellings over the shops were striped, dark and light grey, while the houses with the studios were brick red. The two service stations stand out with their gull wing roofs. The dwellings were finished to a high standard for the time: central heating, hot water, fitted Bruynzeel kitchens, fitted wardrobes, central waste disposal and lifts in the taller buildings. The initial rents ranged from EUR 75 to EUR 84 per month, including maintenance and heating. This was rather expensive that time (1960).

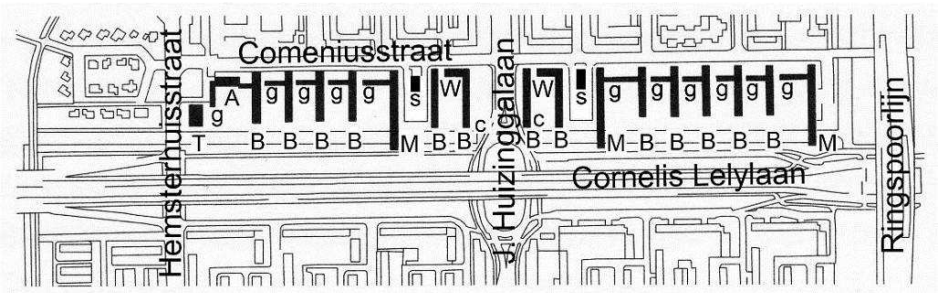

Figure 2. Sloterhof and its realized program [Hereijgers & Van Velzen 2001].



Figure 3. The blocks on the Comeniusstraat [Messcheart 2004].

5 ARCHITECTURE – EXPIRED

Sloterhof still has a plan based on the division of the plots into strips. The dwellings still have the original layouts and the local services are effective. Berghoef was fully aware of the duality of the brief. Hence he designed the dwellings so they face two directions. Berghoef [1951] commented as follows on the Airey-Nemavo system: "*Strictly speaking, once the width and depth have been chosen, based on the module of the wall slabs, you are free to design the layout. The windows were designed in series: the width and height of each window are a multiple of the wall slab dimensions. There was complete freedom in placing the apertures, as long as the window frames were aligned with the joints in the wall slabs. One of the difficulties is that the elevations are flat, and the building looks like a cardboard cut-out. The recesses at the front doors, a few balconies and the protruding chimneys at the end of the blocks help, but the plasticity is still limited. There are two options for dealing with this: changes, preferably clear ones, in the building line and the introduction of plastic elements in the street profile: posts, hedges, shrubs and trees. Trees, with their colour and irregular shapes, are particularly effective in combination with these light, unfussy houses. The porches associated with the storey levels are essential to create a plastic rhythm in the extended facades. It is clear that the street layout, building lines, division into plots and the greenery, i.e. all town planning aspects, are essential to the nature and character of the Nemavo-Airey complexes.*" Berghoef used these elements effectively in the Sloterhof development, and they govern its present quality.

6 CONSTRUCTION ENGINEERING - CREATION

In 1925 H. van Saane set up a construction company in Amsterdam. He specialised in designing and building social housing, rather like project developers these days. His plans for Amsterdam were inspired by residential construction projects in Germany and Austria after the First World War. Before the Second World War, he built Geuzenhof (1933) and Muzenhof (1939), both designed by Berghoef [Fischer 1968].

In 1946, the Dutch Reconstruction Committee asked him to study prefabricated housing systems in the UK and in 1947 Van Saane founded the Nederlandse Maatschappij voor Volkshuisvesting (Nemavo; Dutch Housing Company). The Dutch government subsidised prefabricated construction as there were shortages of materials and trained workers. Van Saane opted for the system developed by Sir Edward Airey in Leeds and decided to adapt it for the Dutch market. He asked architects Berghoef and H.T. Zwiers to work with De Vries Robbé in Gorinchem (steel structures and windows) and N.V. Betondak in Arkel (concrete roofs) to prepare the system "industrially and architecturally" for series production in the Netherlands, under the name Nemavo-Airey system. However, it never went into real series production and the money subsidised by the goverment was subject to inconsistent government policies. The municipality of Amsterdam decided to use the Nemavo-Airey system in Slotermeer and Watergraafsmeer.

The British Airey system was adapted for use in the Netherlands [Priemus & Van Elk 1970]. The Nemavo-Airey system was based on a table structure. The table top was formed by a wooden floor nailed to steel lattice girders which were rigidly connected to a steel ring beam. The legs of steel were secured to the corners to form a rigid and stable table. Centre beams with legs could be used to obtain a greater span. The advantages over the British system was that the columns could be placed anywhere relative to the horizontal members. There were no restrictions related to the floor joists and the columns could be installed anywhere to obtain reasonably large openings for doors and windows. For multi-storey buildings the tables were placed on top of each other and a steel frame was added inside the construction .

The exterior walls comprised a precast reinforced concrete load-bearing structure of columns connected by steel ring beams at each storey height. Precast concrete panels were used as the outer cladding and insulating boards were used for the inner cladding and could be finished with gypsum-

concrete units Fig. 4. Berghoef [1951] commented on the window openings: *"At first, the steel window frames were incorporated in special concrete uprights and cills. However, these elements were difficult to produce and heavy and unwieldy during installation on site. After eighteen months we found a solution, by securing a special profile to standard steel window frames. This was an improvement in structural engineering terms. However, aesthetically it was a major disadvantage as the white surround between the grey wall and the steel window frame was lost. This presented the architects with a serious problem: the facades were already flat and now the last bit of plastic expression around the windows as well the added colour were lost. The only compensation was that they now had much more freedom than before in placing the windows."* However, in Sloterhof we see that Berghoef continued to use an obvious white surround, now made of concrete, into which a steel window frame was fitted in the factory.

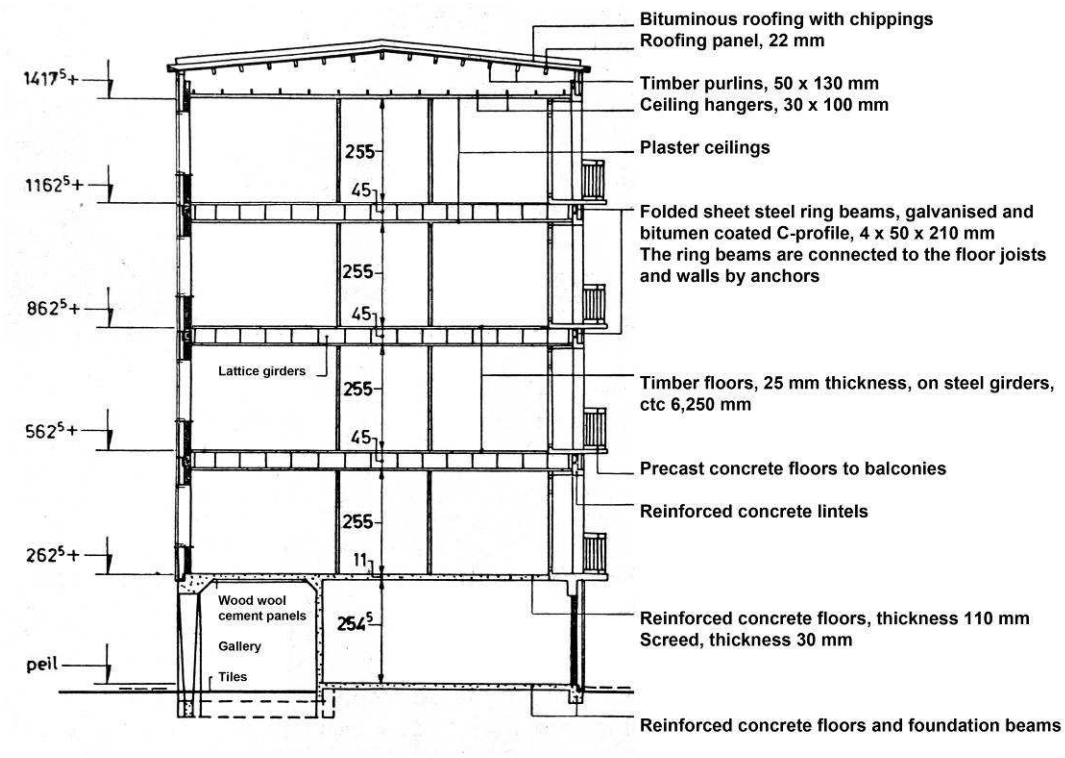

Figure 4. Construction of the Sloterhof B blocks [Polytechnisch tijdschrift 1959].

7 CONSTRUCTION ENGINEERING - EXPIRED

During Sloterhof's existence there have been few construction engineering changes. The surface colours of the smooth concrete elements such as the columns and surrounds of the balconies and window frames have changed several times. Concrete components affected by spalling have been repaired. In some areas the facade panels have been damaged, cracked or broken off. Furthermore, holes have been made in the panels for gratings, cables, and so on.

The recessed window frames of the balconies and porches are made of timber and are easily replaced where necessary. The flush window frames feature the concrete surrounds and have steel frames and steel opening lights. The same construction was used for the window and door frames in the end elevations of the B blocks. These frames have now been replaced by aluminium units fitted to the concrete surround. The original fenestration pattern was lost as a result. Replacement of the steel windows will be difficult, and is architecturally undesirable. They are integral with the concrete surrounds. The walls have 20 mm of insulation in the cavity and the air cavity is 120 mm. The design drawings for the tower block show that the architect considered the use of double glazing. This could

still be installed, in the existing frames. However, in that case the overall building physics balance of the wall will need to be considered.

8 CONCLUSIONS

The Sloterhof complex, designed by Berghoef in the 1950s, is a surprisingly well preserved complex, in a favourable location relative to the centre of Amsterdam. Many of the building details have also been preserved Fig. 6. Elsewhere complexes of this type have been redeveloped architectonical and technical unsuccessfully. The existing qualities of the complex of Sloterhof can be strengthened and used to their best advantage. It should be redeveloped as a whole, rather than be split in different parts in order to conserve its integrity as a complex. There are many reasons, at different levels of scale (town planning, architecture and construction engineering) for treating the complex respectfully, from context through to detail. The quality and value of Sloterhof is determined by its details, or the sum of its parts and shows us an example of durability with the use of traditional materials Fig. 5.

Hence, Sloterhof deserves a comprehensive well considered refurbishment plan: first from small to large and then from large to small, as Berghoef intended. Hence, the future development of the complex should preserve the town planning, architectural and construction engineering qualities of the complex. In essence this means that the current appearance of the facades should be maintained and that the complex should continue to provide affordable rented housing, for which there is a high demand. This means that it should also be possible to improve the complex. Although some intervention is required, any structural and building physics measures should not detract from its appearance. The measures could add to the complex: restoring the original colour scheme, repairing facade panels and concrete surrounds, fitting internal insulation to exterior walls, installing thermal glazing, insulating the roof and basement and providing energy-efficient building services plant for the whole complex.



Figure 5. Present day details of exposed concrete and steel in Sloterhof Amsterdam.



Figure 6. Present day environmental situation of Sloterhof Amsterdam.

ACKNOWLEDGMENTS

The research has been worked out together with TNO Building and Surface, Delft.

REFERENCES

Bureau Monumentenzorg Amsterdam 2009, *Top 100 jonge monumenten*, Gemeente Amsterdam.

Berghoef, J.F. 1951, 'De N.A.-woningen', in: *Forum*, [10], 266-278.

Berghoef, J.F. 1981, 'Architectuur en stedebouw: Spiegel van de samenleving', in: *Wie is er bang voor nieuwbouw*, H. de Haan and I. Haagsma, Intermediair Amsterdam, pp. 49-78.

'De systeembouw in Nederland' 1959, in: *Polytechnisch Tijdschrift (B)*, [13], 110b-121b.

Fisher, E. 1968, *H. van Saanen, Bouwen en wonen. Aspecten 40 jaar volkshuisvesting*, Van Saane N.V. Amsterdam.

Gemeente Amsterdam 1985, *Algemeen Uitbreidingsplan Amsterdam*, Stadsdrukkerij Amsterdam.

Gemeente Amsterdam 2006, *Richting Parkstad 2015*, Gemeente Amsterdam.

Hereijgers, A. and E. van Velzen 2001, De Naoorlogse stad een hedendaagse bouwopgave, NAi Rotterdam.

Messchaert, Z., et al. 2004, *Pracht in Prefab. Het Nemavo Airey-systeem in Amsterdam*, Amsterdamse raad voor de Monumentenzorg Amsterdam.

Priemus, H. and R. van Elk 1970, *Niet-traditionele woningbouwmethoden in Nederland*, Samsom Alphen aan de Rijn.

Santen, J. van, et al. 2007, *Monumenten van herrezen Nederland*, RACM Amersfoort.

Van der Velde, J.J. 1968, *Stadsontwikkeling van Amsterdam 1939-1967*, Scheltema Amsterdam.

Zijlstra, H. 2009, *ABCD℗ research method*, IOS Press/DUP Amsterdam.

XII DBMC
International Conference on Durability of Building Materials and Components
PORTO - PORTUGAL, April 12th-15th, 2011

Characterisation of Damages of Ceiling Joists Caused By Wood-damaging Fungi

Jiri Frankl [1]

ABSTRACT

Experimental description of the extent of damage of timber joists (embedded in walls) has been carried out in order to provide their damage typology. The studied joists, or rather their end parts, originally formed parts of ceiling structure of historic house in Prague built in the 19th century. The ends of joists were damaged by the activity of wood-damaging fungi up to 0.3 to 0.6 metres distance from the joist head. The end parts of approximately 0.7 m long were divided by cutting following a regular mesh to standard test specimens with dimensions of 20x20x30 mm. Compressive strength tests along and across fibres were carried out in the tangential direction of the specimens. The measured values were divided into six groups according to the relative decrease in their strength compared to the strength of healthy wood. The relative strength values were depicted according to the position of the specimen in the joist in all three dimensions. By this method, degradation profiles of the elements in different modular positions (30mm) along the joist have been determined. Such spatial description of damage serves as a basis for a typological description of typical wooden joists degradation caused by fungi in connection with the construction details. This could eventually serve as a basis for an assessment of residual load bearing capacity of joists and a prediction of service life of ceiling structures in relation to the type of biological damage.

KEYWORDS

Wood, Timber, Wood-damaging Fungi, Degradation Profiles

[1] Institut of Theoretical and Applied Mechanics, v.v.i., Academy of Sciences of the Czech Republic, Prague, Czech Republic, frankl@itam.cas.cz

1 INTRODUCTION

Durability and reliability of wooden structures and individual structural elements are, to a large extent, affected by the activities of a number of destructive biological agents. In wood incorporated in structures, among the most significant biological pests are wood-damaging fungi. The information about the activities of wood-damaging fungi, their destructive effects on wood and about the changes in the mechanical properties of wood under laboratory conditions is available in literature. Relatively little is known about the impact of wood-damaging fungi and changes in mechanical properties of wood under real conditions of actual structures [Reinprecht & Tiralova 2000, 2001; Reinprecht 2008; Frankl 2009]. The objective of this contribution is to create a "degradation profile of structural elements" - a graphic representation of changes in selected mechanical properties of wood - caused by the activities of wood-damaging fungi under the conditions of an actual structure, in individual parts of the damaged elements.

2 DEGRADATION PROFILES OF WOODEN STRUCTURAL ELEMENTS

For the experiment, wooden (spruce) beams from the ceiling structure of the second floor of a historical building in the centre of Prague were selected. According to the ascertained data, the ceiling structure comes from the period of 1866 – 1868 when the last known reconstruction was taking place. The ceiling structure of a residential room on the second floor consisted of seven ceiling beams - carrying, on their upper surfaces, a wooden plank filler block, clay filling and floor boarding and six soffit joists - carrying, on their bottom surfaces, wooden boards, reed mats and ceiling plastering. Both the ceiling beams and the soffit joists were placed in pockets in the support walling with the overlapping of approx. 20 centimetres, Fig. 1.

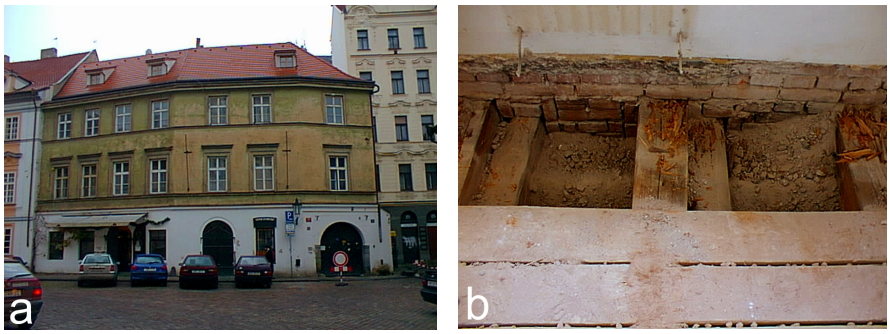

Figure 1: a) building, b) view of the ceiling structure above the 2nd above-ground floor

All the ceiling beams and soffit joists had their ends and parts resting on the load-bearing masonry along the street-facing perimeter load-bearing wall damaged. The beams and joists were damaged by wood-damaging fungi (brown rot) and ligniperdous insects. The damage sustained by wooden elements was old, it originated in the past, apparently shortly after the elements were built in the structure. At the time when the ceiling was opened (spring 2010), all the biological pests were in a non-active stage. For the experiment, three ceiling beams were selected from the damaged elements (or rather their parts ST 1, 2 and 3) in which the damage was caused only by wood-damaging fungi, specifically species of the genera Serpula, Coniophora and Gloeophyllum, Fig. 2. Parts of the beams separated for experimental tests were 70 centimetres long with the cross-section of 18 by 24 centimetres (width x height). The damage by wood-damaging fungi observable with the naked eye covered the distance of 30 to 60 centimetres from the ends of the elements. In all beams, the first 5 to 15 centimetres of length from the end were completely destroyed and mouldered to dust and tiny fragments of wood.



Figure 2: removed parts of the ceiling beams, a) side surface of ST 3, b) end of ST 1, c) side surface of ST 1

The objective of the experiment was to ascertain the change in mechanical properties of wood (compression strength in the direction of the fibres and perpendicular to fibres in the tangential direction) as a result of damage caused by wood-damaging fungi in individual parts of the element. With regards to the requested size of test samples (30 x 20 x 20 mm) and dimensions of the taken parts of the ceiling beams, it was decided that they would be divided into a regular network of 14 x 6 x 8 segments of the size of 50 x 30 x 30 millimetres. Test samples of the required size were then made from individual segments. The difference in the dimensions covered losses originated during the processing, made it possible to partly compensate the natural defects of wood (knots, fissures) and to maintain a similar orientation of growth rings in the samples with clearly given tangential and radial surfaces. The division of parts of the beams by transverse and longitudinal cuts into individual segments and the production of test samples is clear from Fig. 3. Due to extensive damage of some parts of the beams and to the defects of wood it was not possible, despite this measure, to prepare test samples from some segments, Fig 4.

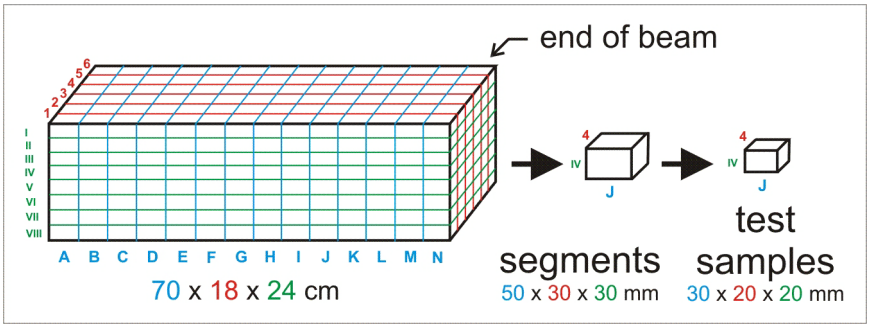

Figure 3: division of parts of the beams into individual segments, their marking and the scheme of the production of test samples

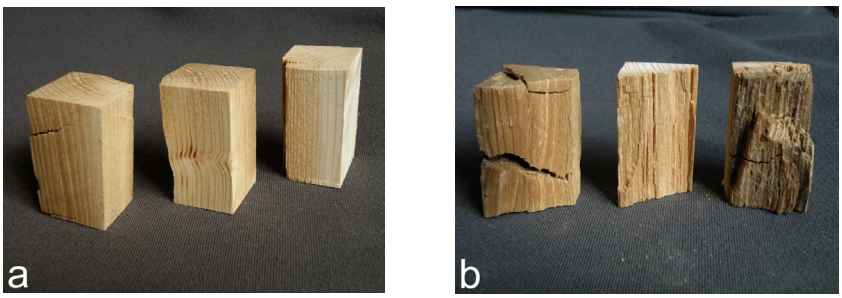

Figure 4: examples of segments originated by cutting beams before the production of exact test samples, a) segments with the potential to produce a test sample, b) segments with no opportunity to produce a test sample

In test samples prepared from individual segments of parts of the ceiling beams ST 1 and ST 2, a test of the limit of compression strength was performed across the fibres in a tangential direction. In test samples prepared from part of the beam ST 3, a test of the limit of compression strength in the direction of fibres was performed. The tests were performed using the Testatron load testing apparatus as per the CSN 490110 and CSN 490112 Czech national standards. Before the tests, humidity of test samples was adjusted in a climatic chamber to the prescribed 12 %. The testing apparatus and examples from the tests of the samples are shown in Fig. 5.

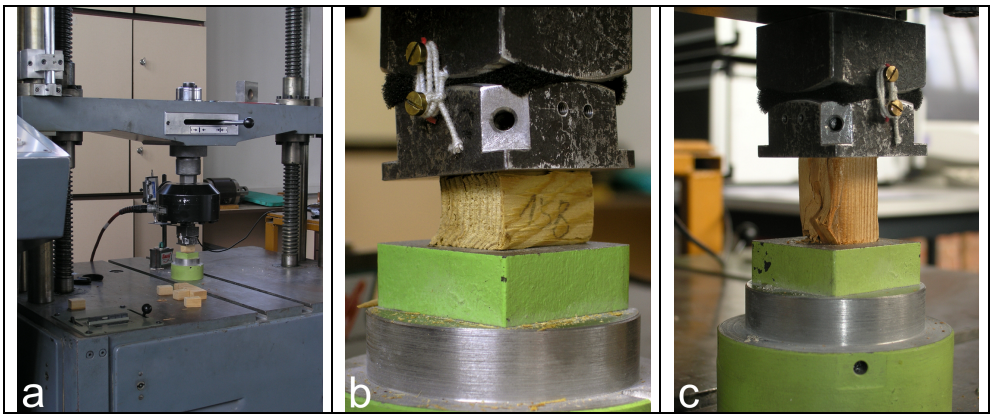

Figure 5: tests of mechanical properties of the wood, a) testing equipment, b) tests of compression strength across the fibres in the tangential direction, c) test of the compression strength in the direction of fibres

The force at the limit of strength was measured using the load testing apparatus (Fmax). The compression strength was then calculated using a formula (1), whereby σ is compression strength, $\mathbf{F_{max}}$ is the force at the strength limit and **a**, **b** are dimensions of the loaded surface.

$$\sigma = \mathbf{F}_{max} / \mathbf{a} * \mathbf{b} \quad (1)$$

In test samples prepared from individual segments of parts of the ceiling beams ST 1 and ST 2, the limits of compression strength of the wood across the fibres in a tangential direction were ascertained as ranging from 8.2 to 0.6 MPa (ST 1) and from 8.6 to 0.8 MPa (ST 2). In test samples prepared from individual segments of parts of the ceiling beam ST 3, the limits of compression strength of the wood in the direction of the fibres were ascertained as ranging from 36.3 to 2.7 MPa. Intervals of values of strength limits for individual tests were, for simplification purposes and in order to provide a graphic depiction of the degradation profiles of elements, divided into four groups according to the degree of damage or rather the size of the change in the monitored mechanical property. The division into groups is clear from Table 1.

Based on this division, degradation profiles were prepared for individual beams, i.e. the graphic depiction of the changes in the wood strength due to degradation by wood-damaging fungi in individual parts of the ceiling beams. Examples of drawing of degradation profiles in some transverse and longitudinal cuts through the beams (in the previously chosen network of 14 x 6 x 8 segments) are shown in Fig. 6. and 7.

Table 1: division of the damage of the elements by wood-damaging fungi into four groups depending on the change (drop) in the monitored mechanical property

		ceiling beam ST 1	*ceiling beam ST 2*	*ceiling beam ST 3*
	decrease in property (tentative)	*limit in compression strength across fibres*	*limit in compression strength across fibres*	*limit in compression strength in the direction of fibres*
	[%]	[MPa]	[MPa]	[MPa]
sound	0 – 10	8.2 – 7.5	8.6 – 7.5	36.3 – 33.0
damaged	10 – 40	7.5 – 5.0	7.5 – 5.0	33.0 – 22.0
strongly damaged	40 – 70	5.0 – 2.5	5.0 – 2.5	22.0 – 11.0
completely damaged	70 – 100	2.5 – 0	2.5 – 0	11.0 – 0

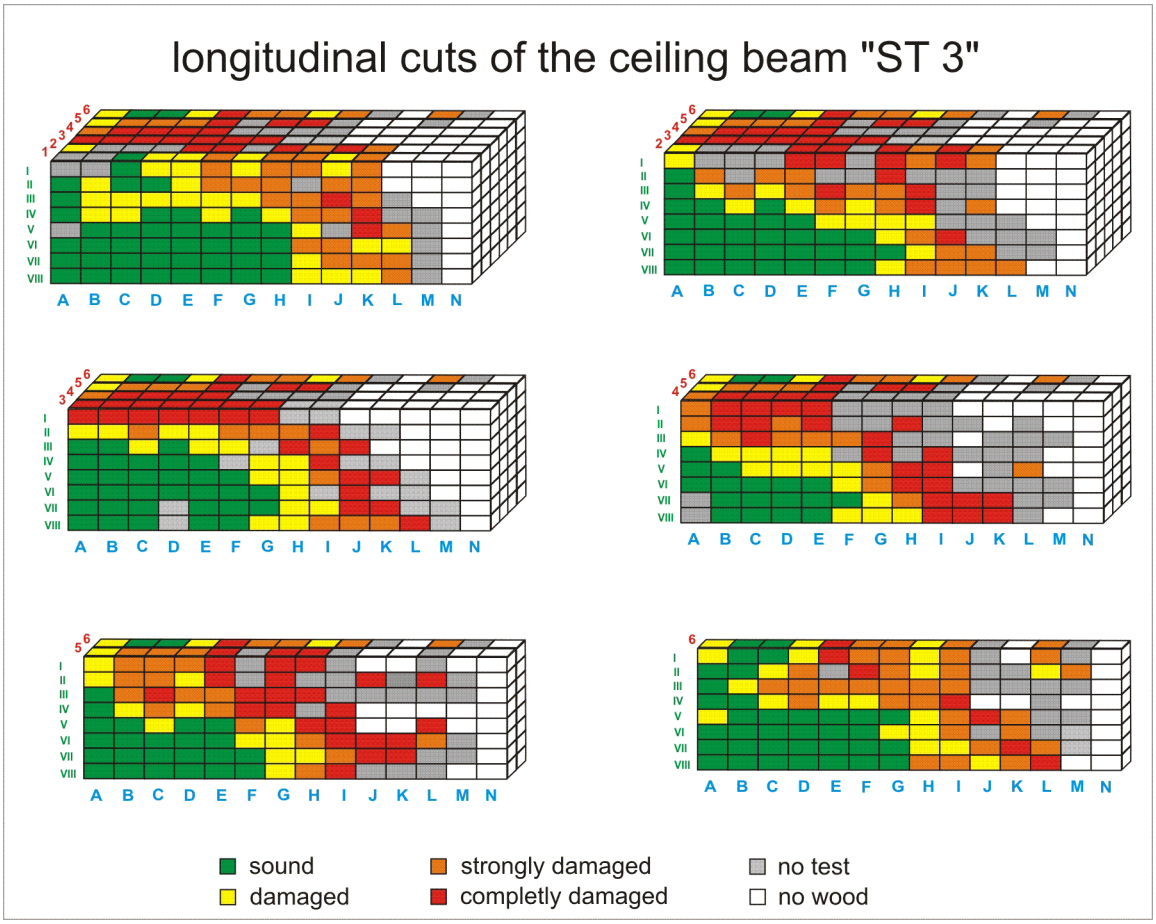

Figure 6: examples of drawing of degradation profiles in longitudinal cuts through the ceiling beams ST 3

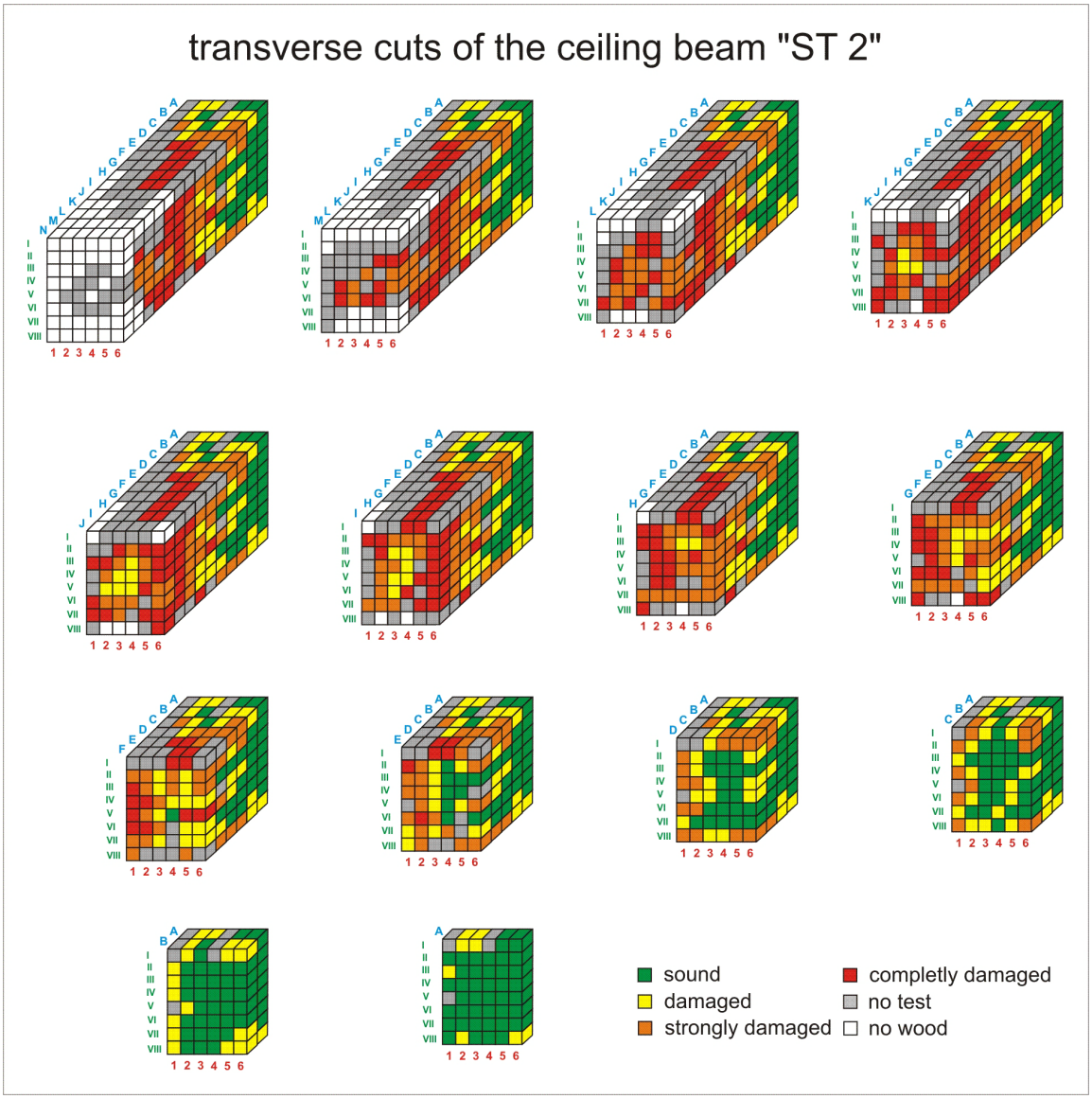

Figure 7: examples of drawing of degradation profiles in transverse cuts through the ceiling beams ST 2

3 CONCLUSION

The experiment performed proved a considerable effect of the destructive activity of wood-damaging fungi on mechanical characteristics of the attacked wood From the results of the tests of compression strength of wood and from the processed degradation profiles of individual beams, what is clear is a significant spread of values of strength of wood in individual segments of beams under review. This spread corresponds to the macroscopically observable accompanying phenomena of destruction caused by cellulosevorous wood-damaging fungi (darkening of wood, fissures, disintegration into minuscule particles). From the results, it is clear that the transition zone between strongly damaged wood (with the decrease in strength by more than 50%) and sound wood is relatively narrow and is in the order of millimetres. In the beams under review, a phenomenon was observed whereby the upper surface and the core of the element were damaged while in the lower and, especially, both side surfaces, there remained a thin (0.5 – 1.5 cm) surface layer of undamaged wood. This phenomenon is related to the manner of how humidity gets into wood, condensation of water vapours and leaking of rain water from the upper surface at the place where beams are deposited in the walling. Degradation profiles of damaged elements have clearly proved changes in shape and considerable decrease in the

effective cross-section (of sound wood) in bearing elements at the place they were deposited on the bearing masonry. Spatial descriptions of degradation profiles of elements may serve as a basis for assessing the residual bearing capacity and determining the life of structures in relation to the type of biological damage.

ACKNOWLEDGMENTS

This contribution was made with support from GAČR P105/11/P628 and La 09008.

REFERENCES

Reinprecht, L. & Tiralova, Z. 2000, *Spruce wood decay due to individual and combined action of selected brown-rot fungi,* in: Ochrona drewna, 20th International symposium, Rogow, Poland, 2000, pp. 43 - 49

Reinprecht, L. & Tiralova, Z. 2001, *Susceptibility of the sound and the primary rotten wood decay by selected brown-rot fungi. Wood research, 46, (1), pp. 11 – 20*

Reinprecht, L. 2008, *Ochrana dreva, Technicka univerzita vo Zvolene, Zvolen, Slovakia, 2008,*

Frankl, J. 2009, *The changes in compression strength of wood along and across grain caused by an impact of damage to wood by wood-damaging fungi,* in: Engineering Mechanics 2009, International conference, Svratka, Czech Republic, pp. 261 – 272

XII DBMC
International Conference on Durability of Building Materials and Components
PORTO - PORTUGAL, April 12th-15th, 2011

Assessment of Structural Conditions for an Old Fortification in Tallinn, Estonia

Karl Õiger [1]

ABSTRACT

The fortified naval complex was erected in 1828-40 on the shore of the Finnish Gulf, in Tallinn by the Tsarist Russia. Today it is an item of cultural (industrial) heritage, composed of quite large and heavy limestone blocks. The building is 247 m long and was a main defense fortress housing cannon. The front walls have a thickness of 1.8 m and flanking walls of 0.8 – 1.6 m. The main fortifications had holes in the ceilings to let out cannon smoke.

From 1864 the complex was used as a barrack. After the Russian Revolution and Estonia's independence in 1920, the complex was retrofitted as a prison. It has been used for this purpose also during Nazi occupation through 1944, Soviet occupation until 1992 and after Estonia's second independence until 2007. This notorious prison building is now under cultural protection, presently used as a museum of horrors. Because of its notoriety it is perhaps psychologically unsuitable as a public or residential building. As well, no interest in renovation work has begun. Five years ago our team examined the complex's condition for damage, with renovation in mind as a museum, or hotel, etc. Our measurements included moisture content and its distribution in thick walls, salt content and its crystallisation in or on wall surfaces, deformations, cracks, conditions of the foundation, and mold growth on wall surfaces was measured. The results of our examinations and proposals for renovation are described in this article. To conclude, renovation of this building with its thick stone walls and cross-vaulted ceilings for normal use - will be a costly and serious challenge.

KEYWORDS

Technical condition of an old fortification, cultural heritage, limestone building, moisture and salt damages, mold, fungus.

[1] Chair of Building Physics and Architecture of Tallinn University of Technology, ESTONIA, karl.oiger@ttu.ee

1 INTRODUCTION

The massively strong limestone complex (Figure 1) consists of a 247 m curved main defense fortress facing the sea (1). There are as well the adjacent wings (2) and (3), and an intermediate building (4), and a separate multi-storey building (5). The whole building complex consists of more than five hundred rooms. It could be renovated for use as an attractive hotel, an office building, or a museum with cafes or restaurants as a tourist attraction.

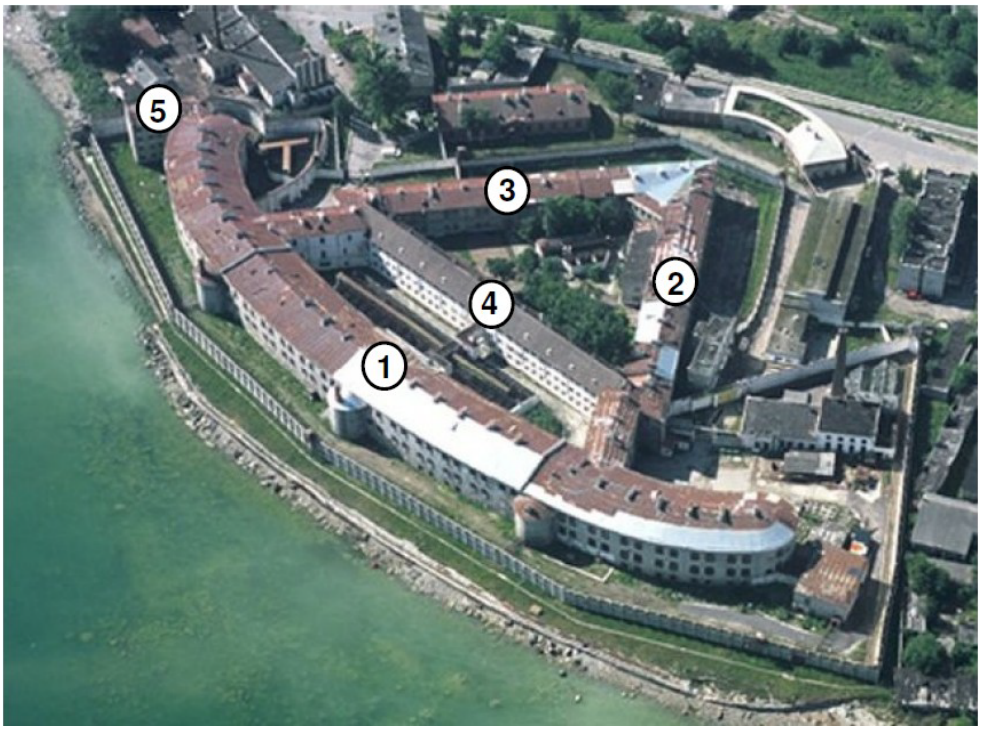

Figure 1 View from above.

2 2. GENERAL DESCRIPTION OF THE STRUCTURE AND TECHNICAL CONDITION OF THE BUILDINGS

The limestone exterior walls of the main fortress building (1) are 1.8 m thick. Outer wall thickness of the adjacent building (2) and (3) is 0.8 – 1.6 m. The thickness of the limestone outer walls of in-between building (4) and a separate building (5) is 0.8 m. The external walls of the intermediate building and the courtyard-side of the main body (1) are plastered. Currently the condition is poor. The outer surface of limestone or ceramic walls are damaged by moisture and frost. Plaster and painting is spalling, and in some parts the internal walls are covered with salts or with mold (Figure 8 and 11). Currently there is no proper heating (not known to be properly heated in recent years), or proper ventilation. The basement walls are water saturated, especially in the sauna and kitchen rooms. The main reasons for damages are leaking roofs, broken rainwater pipes, leaking windows, and the lack of hydro-isolation between the foundation and the walls.

Walls in much of the main building (1) used as former prison cells are covered with a thick dust, dirt and mold. The same condition prevails in flanking buildings (2) and (3) and in building (4). Most of the rooms lack ventilation. In very rare places, some rooms have undergone proper repairs. Altogether there are about 300 rooms in the complex with substantial moisture and other damage. Roofs of the main building (1) and adjacent wings are constructed from sheet metal or from roof tiles that are not watertight (Figures 12 and 13). For this reason timber rafters and roof battens have considerable decay. Because of the lack of proper maintenance of roofs, stone cornices (Figure 4), and chimney heads have been compromized by water and have deteriorated.



Figure 2 Façade of main building (1)



Figure 3 Façade of adjacent buildings (2) and (3)



Figure 4 Hazardous cornices.



Figure 5 Building (4).



Figure 6 Limestone vaults.



Figure 7 Moisture damages on vaults.



Figure 8 Mold on the inner surface of walls.



Figure 9 Dry rot in ceiling beams.



Figure 10 Moisture damages.



Figure 11 Salt crystallisation on the inner surface of walls.



Figure 12 Roof from metal sheets.



Figure 13 Roof from tiles.

In buildings (1), (2), and (3), the floor-bearing structures are limestone vaults, with the load bearing capacity sufficient for a hotel, apartments or offices. At present the floors supported on the vaults have timber, cement, or quarry tile flooring, which are widely worn. Structure of the attic floor consists of timber beams that are downward covered with boarding or plates. There is no special thermal insulation. Because of roof leakage the timber elements in the attic floor have moisture damage and are partly deteriorated by fungi. In one of the regions clearly developed dry rot (Serpula lacrymans, Figure 9) is present.

The inner surface of the external walls of building (4) are extensively water-damaged, and are covered with mold (Figure 8). The supporting structure of the floors is composed of steel beams, and between the beams, cast concrete slabs. In certain places, especially on the first floor, steel beams are heavily corroded. Overall, the extensively damaged ceiling structures should be demolished and replaced. Roof coverings from tiles and its carrying timber structure is worn, and light shines through in places and needs to be replaced (Figure 13). Defects in the roof and rainwater system, and also poor ventilation are the main reasons for high building moisture, and resulting damages.
It would be possible to improve the condition of this building by the addition of external thermal insulation if not for historical limitations. On the internal surfaces, all damaged and wet plaster should be removed, then for a period time the walls allowed to dry out, and finally new finishing can be installed. No significant damages of the foundations were observed.

The external walls, concrete ceilings and foundations of building (5) are in relatively good condition. The roof is from metal sheets and needs to be replaced with a new one. Because of leaking of the roof and poor ventilation of the walls are water-damaged and inner surfaces are covered with mold and salts.

The foundations were dug out in three places of the main building (1) and wing (2). The ground water level was observed at building (1) at a depth of 2.55 m from the surface, and at building (2) at a depth of 1.15 m from the surface. It was observed that no substantial damage had been caused by capillary rise to the exterior surface of walls, however, at ground level, moisture damage was obvious on inner wall surfaces.

3. MOISTURE DETERMINATION OF STRUCTURES

3.1 The humidity of the inner air, wall moisture and its distribution along the walls

Results of the indoor air temperature, humidity, and moisture content of the inner surface of walls are as follows: in September (outside air t^o = 17.1°C, RH 61.5 %) air humidity, temperature, moisture of the wall surface were optionally measured in different rooms (mainly rooms with walls of moisture damages or with damp air). The indoor air humidity (RH) in five different buildings was 55 - 75 %, wall inside surface temperature - 13-15°C (approximately the same as indoor air temperature), and limestone wall weight humidity was 1.8–7%. In building (4) walls were covered with heavy mould (Figure 14).

3.2 Moisture content of drilled test cylinders (core samples) of limestone external walls (outer surfaces)

Limestone masonry moisture content was quite different at different core depths: close to the wall surface it was lower than at the deeper core depth. Along the length of the drilled test cylinder it ranged from 5.4 to 16.6 %. Differences in average moisture content taken from different places in the walls ranged from 1.8 to 12.2 %. The measurements were carried out (MSc Lembit Kurrik) using microwave reflection measuring equipment of MOIST 200. Available frequency was 2.45 GHz. Depth of the sensor MOIST-P was up to 30 cm, and uncertainty of measurement was 1…2 %, measuring range - 0%< W < 400% (as compared with a dry material). MOIST 200 collects data in a matrix, through COM port transfer, for further computerized processing of measurement results. To reduce random errors an average of three measurements were used. Measurements were carried out

for buildings (1), (3), (4) and (5). Below, for example, are the results of building (4) with widespread moisture damage (Figure 14).

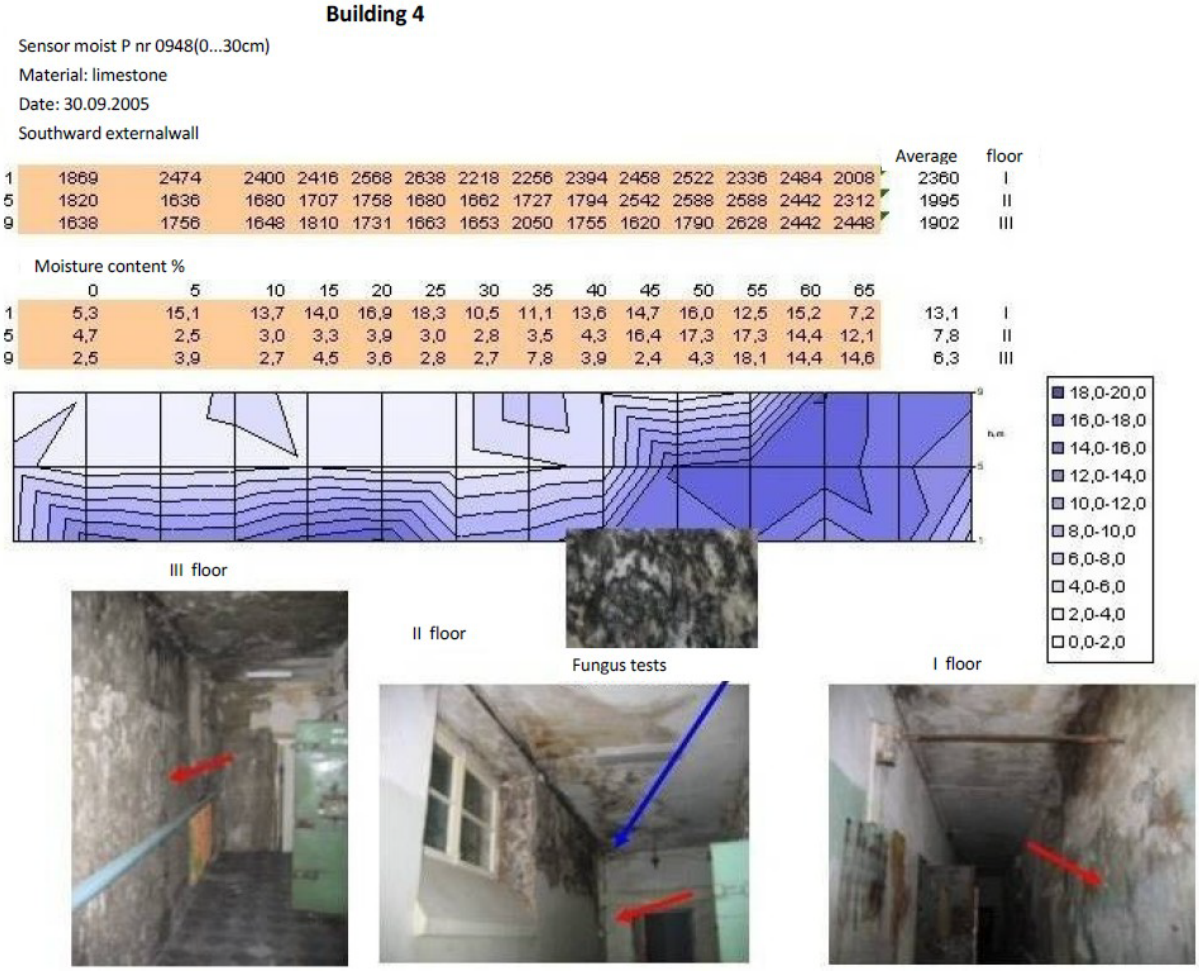

Figure 14 Moisture damages of the limestone external wall. Mold is on the inside wall surface.

As shown in the results, the moisture content of the masonry varies greatly. The measurements of north and southward facing external walls of the whole length of building (4) is particularly expressive of the situation. These are largely influenced by the leaking roofs, damaged cornices and downpipes. This situation is worsened with the heating turned off in the month of May. As outside spring air warms quickly, an intense amount of moisture then collects from condensation on cold wall surfaces - causing further saturation of walls.

4. MOISTURE, MOLD AND FUNGUS DAMAGE OF STRUCTURAL ELEMENTS

Examples of moisture and mold damage are given in Figures 6, 7, 8, 13. In addition, higher moisture saturation of inner wall surfaces is also caused by salts, as salt absorbs moisture from the surrounding air.

According to the investigations in the labratory of Professor Urve Kallavus at Tallinn University of Technology, timber floors of buildings (1), (2), and (3) mainly contain wet rot (Coniophora puteana) and ceilings of buildings (1) and (2) contain white rot. At least in one place of the attic ceiling of buildings (2) and (3), a dangerous microorganism of dry rot (Serpula lacrymans) was found. Therefore during renovation the whole timber structure in this region should be replaced with a new one and also stone walls need to be treated with fungicide accordingly.

5. DETERMINATION OF SALTS IN STONE WALLS AND REPAIR POSSIBILITIES

The limestone masonries of the old buildings may have been exposed to high salt deposition for decades. Such masonry is usually damp and the surface is either partially or fully decayed or crumbled. Currently, there are no known methods that can be used for immediate or short-term salt removal from masonry, especially if the walls are quite thick [Maier. 2002, p.203-210, Reul. 2001].

According to the investigations of Professor Urve Kallavus, the masonry plaster and jointing mortar of this building contains mainly natural calcium carbonates. There are also Na, Ca and Mg sulphides salts - for example, gypsum. Drilled cores (6 samples of stone and mortar) on the marine side of the external walls (main building) showed that small amounts of sulphates are present. Chlorides could be found only in a thin surface layer. Therefore, salt damage of the external surfaces is relatively small. The following is an example of one diffraction pattern (Figure 15) of a sample taken from an inner surface of the wall near a window opening.

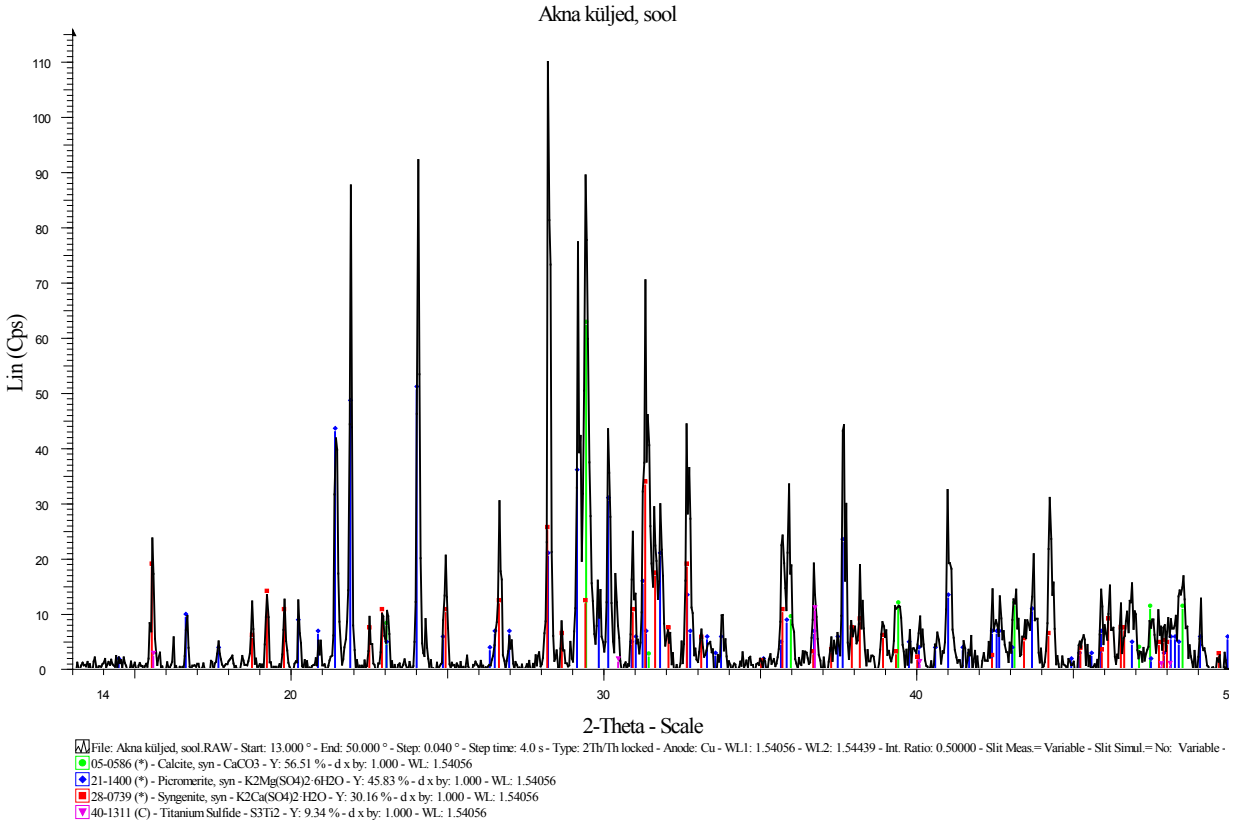

Figure 15 Diffraction pattern of test sample of building (1).

6. PROPOSALS FOR PREVENTION OF DAMAGE ADVANCEMENT FOR THE FUTURE

The main surfaces under consideration are external walls and attic ceilings. The first step is to improve the current situation of the roofs, and build a proper heating and ventilation system. The complex of the buildings is presently equipped with a on-site piped water central heating system. The heat source is an on-site non-functional gas boiler. The soil level around the outer walls must be lowered to decrease saturation of the lower part of the walls. Initially, installing temporary heating and ventilation equipment may be considered to reduce the moisture content of thick limestone walls as early as possible.

At the same time it should be stressed that renovation of buildings (1), (2) and (3) with thick limestone walls and cross-vaulted ceilings for the purposes mentioned above is a serious challenge. After a series of initial problem-solving actions has been undertaken, one of the more serious tasks is then to reduce heating costs. Historically the building is under preservation of Estonian antiquities and changing the façade is not an option. Therefore, the addition of exterior insulation to the façade walls is not an option, except in building (4). According to building physics, insulating the walls from the inside is risky and causes further difficulties in moisture content of the walls. Therefore for such historic buildings it seems more logical to insulate other exterior structures such as windows, doors, and roofs as efficiently as possible rather than consider the additon of wall insulation. This will - to some extent - compensate high heating consumption costs caused by massive stone structure. For example, we can assume that heat conductivity of a 1.8 m thick limestone wall is 3.7 times higher than modern walls ($U=0.25$ W/m^{2}K). However, the thermal bridges around old windows, doors, and roofs cause heat losses that are almost tenfold. Attic ceilings need a vapour barrier and effective thermal insulation to create an envelope for increased thermal resistance.

Keeping the temperature inside the building, even in the range of + 8°C ... +17°C and continous ventilation in all rooms (these requirements depend largely on the function of the rooms: a museum, office, hotel, etc., however, it is not clear yet) should also be ensured. When housing people in winter a comfortable indoor air temperature at +18-+19°C and inside surface temperatures of 15° for external walls should be maintained. To minimize structural damage and maintain comfort for people a RH should be in the range of 50-55 %. However, there is a contradiction yet to be solved – indoor temperature should be kept as low as possible, at the same time, indoor temperature should satisfy the visitors' convenience.

No strengthening works are needed for the foundations and load-bearing walls.
It must be emphasized that there is no working hydro isolation on the outside surface of the foundation walls or between the foundation walls, and the first-floor walls.

7. MEASURES FOR FINISHING SURFACES

Firstly the water-damaged (damp) plaster, covered or filled with salts and mould, down to a clean limestone wall surface, must be removed from the inner surfaces of the walls. Also, it is necessary to clear joints from damaged mortar up to the depths of 2 cm. Next, a decision must be made whether there is any need for special finishes. Further, the question of removing salt covering the surfaces has to be solved. At the same time, plasters that can withstand salt deposits without spalling should be used.

8. CONCLUSION

Renovation of the old complex of buildings is possible for use as a museum, offices, cafes, and restaurants, or for a tourist attraction however it will not be fully compliant with today's comfort standards. Renovation will take at least two or three years and have a rather high cost. Unfortunately during last 6-7 years no potential investor has been found. There has been no restoration work begun and structural building damages continuously grow.

REFERENCES

Maier Josef. 2002. `Handbuch Historisches Mauerwerk. Untersuchungsmethoden und Instandsetzungsverfahren`, Brikhäuser Verlag. Basel. Boston. Berlin, p. 168 – 256.

Reul Horst. 2001. `Handbuch Bautenschutz und Bausanierung, Schadenursachen, Diagnoseverfahren, Sanierungsmöglichkeiten`, 4. Auflage, Verlags-gesellschaft Rudolf Müller GmbH & Co. KG, Köln, p.171-196.

XII DBMC
International Conference on Durability of Building Materials and Components
PORTO - PORTUGAL, April 12th-15th, 2011

Non/Minor Destructive Methods for Investigating Concrete Durability of National Museum of Western Art, Japan

Kei-Ichi Imamoto [1]
Akio Tanaka [2]
Yuji Umezu [3]
Manabu Kanematsu [4]
Yoshiyuki Yamana [5]

ABSTRACT

The National Museum of Western Art (NMWA), designed by Le Corbusier and constructed in 1959, is an important cultural landmark of Japan. A working group (Chairman: Prof. Hiroyuki Suzuki, Aoyamagakuin Univ.) established under the Architectural Institute of Japan, assessed the condition of the structural concrete of this building, with the aim of devising a maintenance strategy in order to register the building as a national heritage site. This paper reports on the phenomenon responsible for the degradation and deterioration of the structural concrete members in the NMWA building, such as the excessive deflection of slab and corrosion risks due to carbonation. Both non-destructive test methods and those that inflict only minor damage to the structure (NDT/MDT) were used in the study. Non destructive test (NDT) methods were employed for measuring the air permeability of the concrete cover and the cover thickness in order to assess the steel corrosion risk due to carbonation. The results showed that half of the slabs exhibited excessive deflection. The carbonation depths varied from 5 to 35 mm. Furthermore, the results of the non destructive tests indicated that corrosion rate is 6% at present and will gradually increase. Half the steel bars will have corrode within 60 years. It is assumed that many historical reinforced concrete buildings worldwide suffer from such degradation. For such buildings whose authenticity must be maintained, non/minor destructive test methods (NDT/MDT), which do not damage the structure of the building, will be effective for assessing the condition of the building.

KEYWORDS

National Museum of Western Art, Concrete, Carbonation, Steel corrosion risk, Non destructive test

[1] Faculty of Engineering, Tokyo University of Science, Tokyo, JAPAN, imamoto@rs.kagu.tus.ac.jp
[2] Faculty of Engineering, Tokyo University of Science, Tokyo, JAPAN, at2862@yahoo.co.jp
[3] Faculty of Engineering, Tokyo University of Science, Tokyo, JAPAN, yumezu@rs.kagu.tus.ac.jp
[4] Faculty of Science and Engineering, Tokyo University of Science, Tokyo, JAPAN, manabu@rs.noda.tus.ac.jp
[5] Faculty of Engineering, Tokyo University of Science, Tokyo, JAPAN, atelieryamana@hotmail.co.jp

1 INTRODUCTION

The National Museum of Western Art (NMWA), designed by Le Corbusier and constructed in 1959, is an important cultural landmark of Japan. A working group (Chairman: Prof. Hiroyuki Suzuki, Aoyamagakuin Univ.) established under the Architectural Institute of Japan, assessed the condition of the structural concrete of this building with the aim of devising a maintenance strategy in order to register the building as a national heritage site. This paper reports on the phenomenon responsible for the degradation and deterioration of the structural concrete members in the NMWA building, such as the excessive deflection of slab, presence of cracks, and corrosion risks due to carbonation. Both non-destructive test methods and those that inflict only minor damage to the structure (NDT/MDT) were used in the study. Non destructive test (NDT) methods were employed to determine the air permeability of a concrete cover in order to assess the steel corrosion risk due to carbonation. In this paper, the significant degradation that these historical reinforced concrete structures will face has been explained; thus, a reasonable repair method that will also maintain the authenticity of these strucures will be required in the near future. It is believed that many historical reinforced concrete buildings worldwide might suffer from different types of degradation. For such buildings, whose authenticity should be maintained, non/minor destructive test methods (NDT/MDT), which do not damage the structure, will be effective for assessing the condition of the building. NDTs should prove to be effective for determining the air permeability of concrete cover and the cover thickness in order to evaluate the steel corrosion risk faced by structural members in the near future.

2 THE NATIONAL MUSEUM OF WESTERN ART

The NMWA (Photograph 1 and Figure 1) was constructed in 1959 with a concrete design strength of 18 MPa. Further details of the building and specifications of the concrete mixture are listed in Table 1 and 2, respectively. Round bars with a yield strength of 235 N/mm^2 were used for reinforcement.



Photograph 1. Appearance of the NMWA

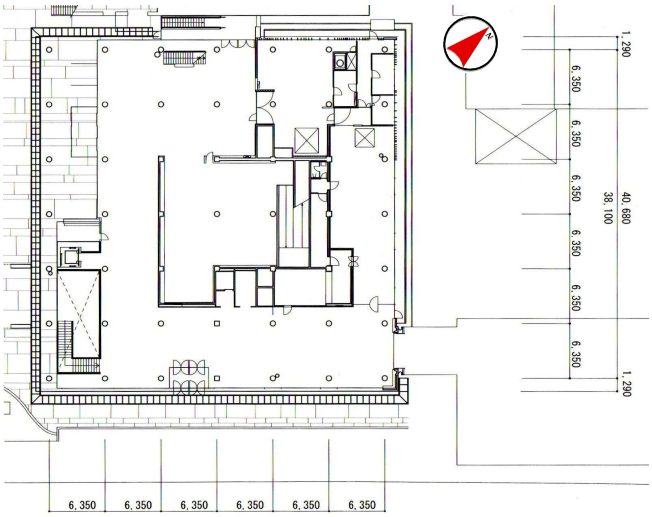

Figure 1. Plan of 1st floor

Table 1. Details about NMWA

Location	Ueno Tokyo
Completion	29 May 1959
Designer	Le Corbusier
Assistant designer	Junzo SAKAKURA, Kunio MAEKAWA, and Takamasa YOSHIZAKA
Structural design	YOKOYAMA structural design office
Contractor	SHIMIZU Corporation
Ground area	1,587 m^2
Total floor area	4,353 m^2
Height	11.46 m
Type of structure	Reinforced concrete 3 stories

Table 2. Concrete composition

Materials		Unit content
Water	-	204 kg/m^3
Cement	Ordinary Portland cement	340 kg/m^3
Sand	Sagami/Koito River	921 kg/m^3
Gravel	Crushed stone (Futo) Max.20 mm	829 kg/m^3
Admixture	Air entrained agent	-

3 PREVIOUS SURVEYS

In 1979, the first survey of the NMWA was conducted for investigating the cracks of the cantilever beams present on the second floor, which are supported by a Precast concrete panel (see photograph 2). In 1986, a second survey was conducted to study the spalling of the decorative stone from the PCa panel. In 1995, from the viewpoint of retrofitting the building, detailed surveys were conducted on the core compressive strength, carbonation progress of the cover thickness, cracks on the strucural concrete, and steel corrosion. The test results of the core compressive strength are listed in table 3.

Table 3. Test result of core compressive strength

1979			1986					
BF1			BF1			1F		
24.9	25.1		20.6	33.1	21.4	22.6	19.8	23.8
1F			2F			3F		
30.4	23.6	27.2	29.0	22.9	25.2	25.1	26.8	28.7



Photograph 2. Precast concrete panel of north-side wall

4 PRELIMINARY VISUAL INSPECTION

In 2009, preliminary visual investigations of the building were carried out; in these investigations, cracks were observed in several places. Photograph 3 shows cracks under the 1st floor and photographs 4 and 5 show cracks on the walls along steel bars. The cracks shown in photograph 2 are probably caused by the excessive deflection of the slab; and those shown in photographs 4 and 5 by carbonation-induced steel bar corrosion.



Photograph 3. Cracks under 1st floor



Photograph 4. Cracks on walls



Photograph 5. Steel corrosion

4.1 Investigation areas

According to the results of the preliminary investigations, a detailed investigation on the deflection of the slab and the carbonation progress of concrete was carried out. The National Museum of Western Art (NMWA) is an important cultural landmark of Japan. In order to maintain the authenticity of the building, a non/minor destructive test method (NDT/MDT) was performed. A combination of a small core sampling test and a non destructive on-site air permeability test [Torrent 1992] was performed to determine the carbonation progress of the concrete structures and also to minimize the impact on the concrete appearance.

4.1.1 On-site air permeability test

The method described here is known as the 'Torrent Permeability Tester' and was developed in Switzerland. In this test, the pressures in the outer and inner chambers are always maintained at the same value. Thus, the outer chamber acts as a 'guard-ring', providing a controlled, unidirectional flow of air into the inner chamber (see Figure 2). The latest report by RILEM TC NEC [RILEM TC NEC 2007], mentioned two advantages of this system: (1) The spurious air entering through preferential paths (e.g. microcracks or extremely porous outer skin) is absorbed by the outer chamber, and thus, it does not affect the measurements, and (2) because of the well-defined air-flow path, the coefficient of permeability kT [m^2] can be easily calculated by means of a theoretical model.

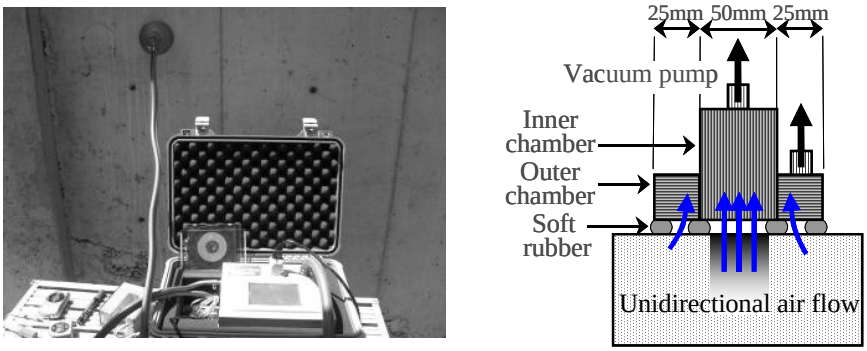

Figure 2. Schematic description of Torrent permeability tester

4.1.2 Small core sampling

Small core specimens with a diameter of 20 mm were drilled in the structure in order to determine the relationship between the air permeability coefficient (kT) and the carbonation progress of concrete. The carbonation progress was measured, as shown in Photographs 6 and 7. After the core drilling, grout was injected into the hall and the sliced surface of the core was installed back into the concrete member structure (see Figure 3). This process enables the impact of the core drilling to be invisible as shown in photo 8.



Photograph 6 Core drilling

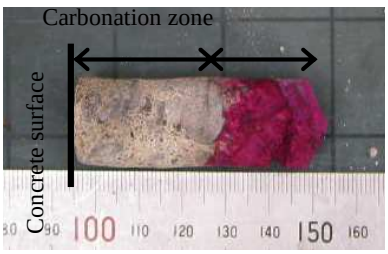

Photograph 7 Carbonation of specimens

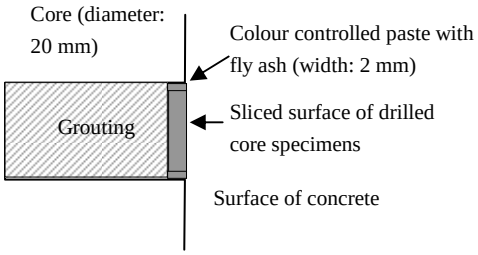

Figure.3. Schematic description of repair of drilled hole

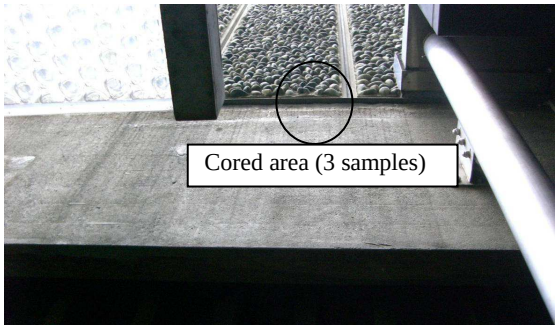

Photograph 8 Impact of core drilling after repair (shown in Fig.3)

4.1.3 Radar test

The cover depth and the steel bar arrangement was measured with a radar device shown in Photograph 9. This method utilizes the reflection of the radar onto a steel bar installed in a concrete member. The radar released from the device reflects on the steel bar and turn to concrete surface. The receiver measures the round trip time, from which the position of the steel bar can be detected based on the relationship between the velocity and time of radar in concrete.



Photograph 9 Radar test device

5 RESULTS AND DISCUSSION

5.1 Deflection of slab

The deflection of the slab was measured using level surveys. The results are shown in Figures 4 and 5. According to the guidelines for structural design proposed by the Architectural Institute of Japan, the deflection per short span of slab should be limited to less than 1/250th of the span. Hence, a greater value of deflection per span implies excessive deflection. It can be seen that half of the slabs exceed this criterion, and thus, these slabs will require further strengthening in the near future.

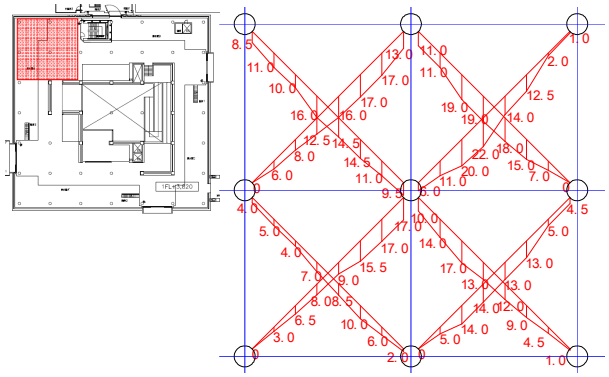

Figure 4. Example of measured deflection of slab

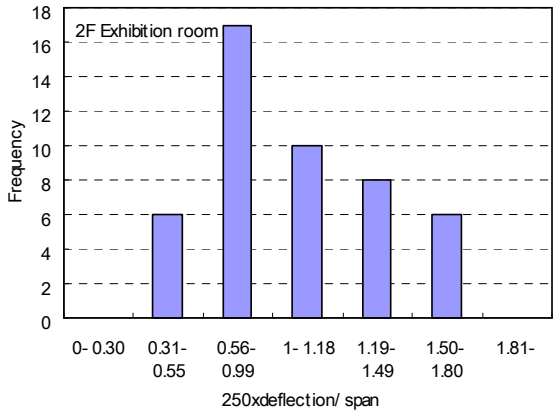

Figure 5. Deflection of slab

5.2 Carbonation progress

The carbonation progress was measured by conducting small core sampling tests at several places in the NMWA. Figure 6 shows the carbonation progress of concrete; carbonation gradually progresses with time and varies from 5 to 35 mm at the present age of 50 years (2010). On the exterior wall, carbonation reaches up to 40 mm, and half of the steel bars face the risk of corrosion (the corrosion rate being 50%) 55 years hence; this rate is measured assuming that the cover thickness of the exterior wall is 40 mm.

Figure 7 shows the relationship between the carbonation velocity and the air permeability coefficient (kT) of concrete. It can be seen that agreement is obtained and the air permeability tester can be considered to be a suitable tool for estimating the carbonation progress of concrete in a non destructive manner. Based on this finding, the carbonation depth of the north-side exterior wall was evaluated in detail (see Photograph 2). Figure 8 shows the distributions of carbonation depth, estimated through the air permeability test, and the cover thickness of the steel bar, measured through the radar test at 122 points. Assuming that the steel bar would corrode if the carbonation depth exceeds the cover thickness, the corrosion rate of the steel bars in the north-side exterior wall can be evaluated. Figure 9 shows the progress of the corrosion rate of the steel bars in the exterior wall. It can be observed that the present corrosion rate is 6% and that this rate is increasing gradually. Thus,

the steel bars will have corroded by half within 60 years. This value almost agrees with the value obtained by the core sampling test and the square root time theory that is widely used to estimate the progress of concrete carbonation. Hence, a non destructive on-site air permeability test and radar test (to locate the steel bar position) will be useful for estimating the carbonation of the RC building at present.

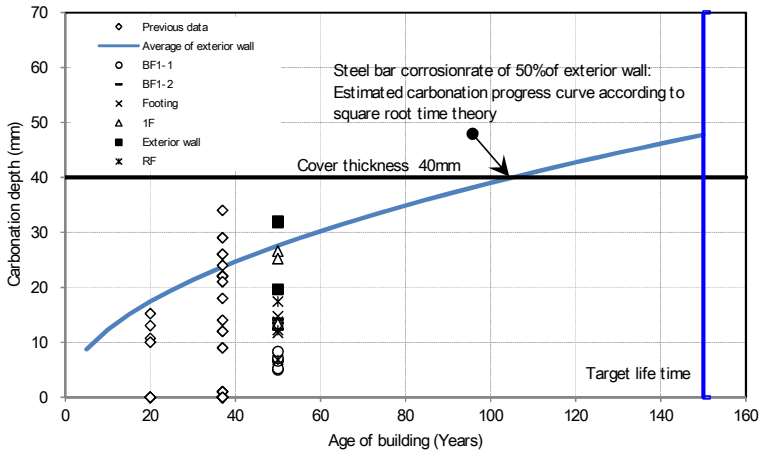

Figure 6. Carbonation progress of concrete by small core sampling test

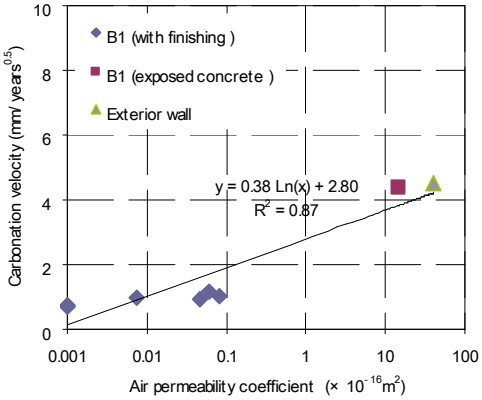

Figure 7 Carbonation and air permeability

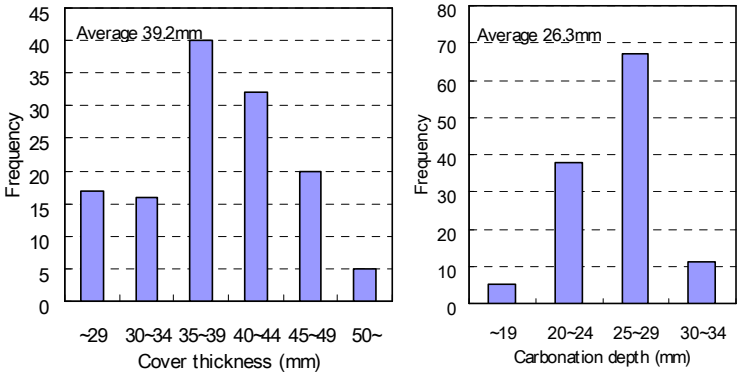

Figure 8 Distribution of cover thickness and carbonation depth

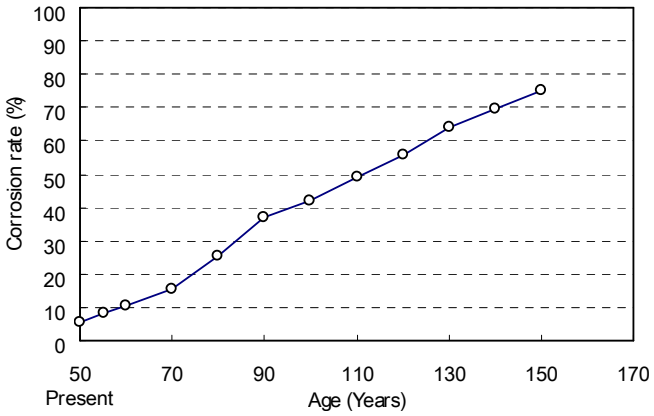

Figure 9. Progress of steel bar corrosion rate in exterior wall

6 CONCLUSION

The National Museum of Western Art is an important cultural landmark of Japan, and it is over 50 years old. The deflections of the slab and the concrete carbonation depths of this building were investigated using non/minor destructive methods (NDT/MDT). It was found that deflections of the slab and concrete carbonation can lead to significant risk. A non destructive method, on-site air permeability test, and steel bar radar test were useful for assessing the risk of steel bar corrosion. The development of a suitable repair method will be required in the near future to maintain the authenticity of the building.

REFERENCES

Ministry of Construction: *Report on Retrofitting of the National Museum of Western Art*, 1996.8.

RILEM Report 40: Non-Destructive Evaluation of the Penetrability and Thickness of the Concrete Cover, State of the Art Report of RILEM Technical Committee TC 189-NEC "*Non-Destructive Evaluation of the Concrete Cover*", Edited by R. Torrent and L. Fernandez Luco, 2007.

Torrent, R.: *A two-chamber vacuum cell for measuring the coefficient of permeability to air of the concrete cover on site*, Mater. & Struct. , Vol.25, No.150, pp.358-365, July 1992.

XII DBMC
International Conference on Durability of Building Materials and Components
PORTO - PORTUGAL, April 12th-15th, 2011

Environmental Factors Affecting Corrosion of Steel Inserts in Ancient Masonry

Luca Bertolini [1]
Maddalena Carsana [2]
Bruno Daniotti [3]
Eleonora Marra [4]

ABSTRACT

Steel inserts are often present in ancient masonry in order to improve the structural behaviour of buildings or to prevent the propagation of cracks. Though, the presence of inserts embedded in the materials of the masonry (e.g. mortar, bricks) may be harmful for the durability of the whole structure, since their corrosion may produce deleterious expansive phenomena leading to cracking and detachment of the covering materials. Inserts may have a complex corrosion behaviour, which depends on the material they are in contact and its moisture content. Starting from this problem, the paper shows the preliminary results of a study on the corrosion behaviour of steel inserts embedded in masonry. The effect of temperature and moisture on corrosion rate of steel and resistivity of mortar and brick specimens exposed in a climatic chamber to cycles of temperature (20-40°C) and relative humidity (65-80-95%) are discussed. In order to extend the results obtained on small-scale specimens to case studies that should consider the effect of the real hygrothermal conditions on corrosion of steel inserts in ancient masonry, numerical simulations have been also performed. The results obtained have shown that corrosion rate is negligible in specimens exposed to 65-80% RH (even at 40°C), whereas it has reached high values in wet environments or in the presence of water suction. A correlation between electrical resistivity of embedding materials and corrosion rate of steel has been observed. The validation of these data by means of a bi-dimensional HMT model is now in progress.

KEYWORDS

Corrosion, steel inserts, ancient brick masonry, hygrothermal conditions, electrical resistivity

[1] Politecnico di Milano, CMIC Dep, Milano, ITALY, luca.bertolini@polimi.it
[2] Politecnico di Milano, CMIC Dep, Milano, ITALY, maddalena.carsana@polimi.it
[3] Politecnico di Milano, BEST Dep, Milano, ITALY, bruno.daniotti@polimi.it
[4] Politecnico di Milano, BEST/CMIC Dep, Milano, ITALY, eleonora.marra@chem.polimi.it

1 INTRODUCTION

Steel inserts are often present in ancient masonry, either due to an original design choice or as the result of later restoration works. They may have different aims, e.g. improving the structural behaviour of buildings (chains and ties) or preventing the propagation of cracks, and they may be applied externally or embedded in the materials of the masonry (mortar, bricks, stone blocks, etc.). In the latter case, the presence of these elements may be harmful for the durability of ancient masonry, since their corrosion may produce deleterious expansive phenomena leading to the detachment of the covering materials [Bertolini *et al.* 2009, Lourenco 2006, Straube & Schumacher 2006].

It is important to make a distinction between steel inserts dated to the creation of the original structure, normally embedded in the structural elements, and those fixed later during restoration phases (most often applied externally). While externally applied steel inserts are directly exposed to the action of the atmosphere (either inside or outside the building), inserts embedded in the masonry may have a complex corrosion behaviour, which depends on the material they are in contact (e.g. bricks, hydraulic mortars, gypsum) and its moisture content. Microstructure of these materials and chemical composition of the solution contained in their pores will influence the corrosion behaviour of steel. For example, the nearly neutral pH of some types of mortar can cause the corrosion process on the steel surface as soon as they are wet; conversely, in the case of alkaline mortars that promote passivity of the steel, corrosion can only take place after carbonation of the mortar cover has occurred. The corrosion rate will also depend on the availability of water and oxygen in the pores of the embedding material near the steel surface, hence it will be a function of environmental conditions. Temperature and humidity of the environment influence the electrical resistivity of the mortar or bricks and the corrosion rate of the embedded steel insert. As instance, a mortar with very high moisture content (that is near saturation, e.g. due to wetting or water condensation) is characterized by low resistivity, but, if saturation conditions are maintained for long time, the oxygen content at the steel surface may be low due to the low diffusivity through the water-filled pores. Conversely, in the case of masonry characterized by lower water content, although oxygen is available at the steel surface, the resistivity is high and it increases as the moisture content decreases.

Concerning masonries, rarely condition of permanent saturation are reached, thus oxygen is available at the steel surface and the corrosion rate depends on the resistivity of the materials in contact with steel; in general, the lower the moisture content, the higher the electrical resistivity of these materials and the lower the corrosion rate of steel. Nevertheless, a large number of parameters, related to both the environment and the materials, may have a complex role, which makes any prediction of the actual corrosion behaviour of steel inserts quite difficult. As matter of facts, the study of the dependence of resistivity of masonry and corrosion rate of steel insert on the environmental conditions is a subject of great interest in relation to optimising restoration methods and promoting a durability approach for historical buildings. Improving the understanding on corrosion of steel embedded in masonry could provide a tool for the design, of repair works which are not merely aimed at the remediation of corrosion damages, but also at the control of the corrosion rate necessary to fulfil conservation requirements of preserving as much as possible the original materials.

This paper shows the preliminary results of a study on the corrosion behaviour of steel inserts embedded in brick masonry. The first part of this study deals with the assessment of the corrosion behaviour of low carbon steel embedded in mortar, brick and composite brick and mortar samples, exposed to several environments. The effect of temperature and humidity on corrosion rate of steel and resistivity of specimens exposed in a climatic chamber to cycles of temperature (20-40°C) and relative humidity (65-80-95%) are discussed. In order to extend the results obtained on small-scale specimens to case studies that should consider the effect of the real hygrothermal conditions on corrosion of steel inserts in ancient brick masonry, numerical simulations have been performed. Although different types of mortars (based on several types of binders: gypsum, lime, or blends of gypsum-lime, lime-pozzolana and lime-cocciopesto) have been considered in the study; only

preliminary results concerning fired brick and a mortar based on gypsum-lime blend will be considered in this paper.

2 CORROSION OF LOW CARBON STEEL EMBEDDED IN BUILDING MATERIALS

2.1 Experimental procedure

2.1.1 Materials and specimens description

In order to study the behaviour of steel embedded in a masonry made of fired bricks and a blended lime-gypsum mortar, different sets of specimens have been manufactured: mortar specimens (LG), composite brick and mortar specimens (B+LG) and, finally, brick specimens (B). In 80x90x30 mm^3 lime-gypsum mortar samples, two carbon steel bars (6 mm in diameter) and two stainless steel wires (AISI 304, 2 mm in diameter) have been inserted. Brick specimens have a size of 55x120x60 mm^3, in order to obtain many samples from the same brick; in two of these specimens two carbon steel bars (6 mm in diameter) have been inserted in two holes and the space between the bar and the brick has been filled with lime-gypsum mortar; in the other specimen bars have been forced in direct contact with the brick. A sketch of specimen geometry is shown in Fig. 1. The blended lime-gypsum mortar has been prepared using the following mix proportions (kg/m^3): lime 212, gypsum 430, sand 769 and water 404, resulting in a 0.63 water/binder ratio and a 30% flow measured on the flow table (D_m = 130 mm). Concerning brick samples, reused fired masonry bricks have been used. Finally, as far as steel bars are concerned, a low carbon steel (C 0.04%, Si 0.041%, Mn 0.285%, S 0.012% and P 0.012%) and ferritic microstructure (grains size of about 20 μm) and little pearlitic inclusions, has been used.

2.1.2 Environmental conditions

Mortar specimens have been cast in PVC moulds and demoulded after 5 days, following the procedure described in the EN 1015-11 standard. Every sample has been cured for 28 days in a climatic chamber (7 day at 95% RH and 21 days at 65% RH, 20°C T). At the end of the curing time all the specimens have been kept in a carbonation chamber (0.2% CO_2, 65% RH and 20°C), until complete carbonation has been achieved (14 and 28 days respectively for the composite brick and mortar and for the mortar specimens), as shown by tests with an alcoholic solution of phenolphthalein. At the end of curing, specimens have been exposed to several environments.

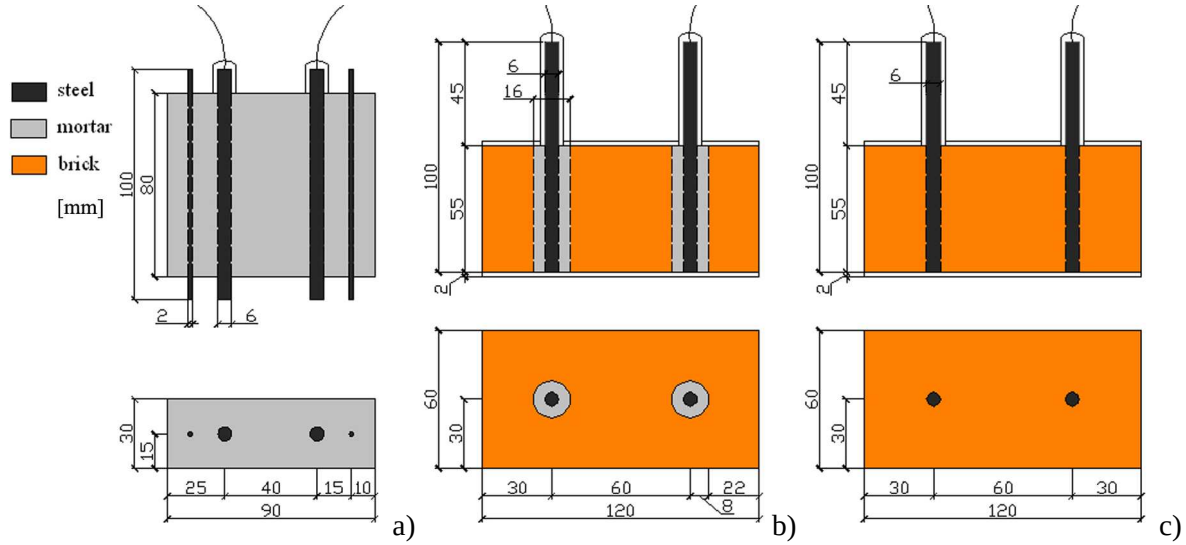

Figure 1. Longitudinal section (up) and cross-section (low) of the specimens manufactured in the laboratory: a) blended lime-gypsum mortar sample (LG) with 2 low carbon steel bars and 2 stainless steel wires; b) composite brick and mortar sample (B+LG) with 2 low carbon steel bars embedded in a 5 mm mortar layer; c) fired brick sample (B) with 2 low carbon steel bars. Dimensions in mm.

Brick and composite brick and mortar specimens have been exposed to three moisture conditions, keeping constant the temperature at 20°C: 95% RH (C1), water (C2), and again 95% RH (C3). In the case C2, only 10 mm of the samples has been put in water, to allow water uptake towards steel bars placed at 20 and 60 mm from the water surface. As far as mortar specimens are concerned, instead, they have been exposed to six different environments, varying relative humidity (65-80-95%) and temperature (20-40°C). Each condition has been kept for at least 28 days, apart from the storage in water (7 days). Finally, one of the three mortar samples has been further exposed to the moisture conditions (C1, C2 and C3) undertaken by the brick-based specimens (though, storage in C2 has been kept only for 1 day, maintaining steel bars at 20 and 80 mm form the water surface).

2.1.3 Corrosion measurements

Corrosion behaviour of specimens has been investigated by monitoring electrical resistivity of the mortar or brick (ρ, Ωm), corrosion potential (E_{corr}, mV vs Ag/AgCl) and corrosion rate (i_{corr}, mA/m^2) on the steel bars. Resistivity measurements could provide information about the moisture content of specimens and their porosity. Electrical conductance (G, mS) has been measured with a conductivitymeter and converted in resistivity by using the relationship: $\rho = K / G$ (where K is the cell constant that considers the specimen geometry, which was determined with a FEM model); these measurements have been carried out using pairs of stainless steel wires (in the case of LG samples) or carbon steel bars (in the case of B and B+LG specimens), linked to the conductivitymeter. Corrosion potential has been measured versus an external reference electrode (Ag/AgCl) using a high impedance voltmeter. Finally, corrosion rate has been measured with the polarisation resistance R_p method, by imposing potential steps of $\Delta E = \pm 10$ mV versus the corrosion potential and measuring the resulting current density (i, mA/m^2); corrosion rate has been calculated as: $i_{corr} = B / (\Delta E/i)$, considering B = 26 mV [Bertolini *et. al.*, 2004]. With regard to the measurement of corrosion rate on LG samples, stainless steel wires have been used as counters electrodes; carbon steel bars have been utilized in turn as counter electrode or working electrode in the case of B and B+LG specimens.

2.2 Results and discussion

Figure 2a shows corrosion potential (empty symbols) and corrosion rate (filled symbols), as a function of time, of different specimens (LG, B and B+LG) in three different moisture conditions (at 20°C): humid environment at 95% RH (C1), wet (C2), and again humid (C3). Red, green and blue curves represent an average of the measurements performed respectively on different replicate bars. Corrosion potential values corresponding to -200 mV vs Ag/AgCl (suggesting negligible corrosion) have been registered only on brick-based specimens (B and B+LG) in the 95% RH condition (C1), while in all the other cases corrosion potential falls to -400÷-600 mV showing active corrosion. These observations are supported by the corrosion rate measurements: indeed, only in brick-based samples (B and B+LG) in humid condition (C1) negligible corrosion rate have been measured (being the threshold conventionally fixed at 1 mA/m^2, which is equal to 1.17 μm/year, assuming uniform corrosion); in the other situations, moderate (2 mA/m^2 on LG sample, in environment C1) or even high (10÷100 mA/m^2 on every other sample, in C2) corrosion rates have been observed. Table 1 shows the average values and standard deviations of steady state measurements in each exposure condition (C3 condition has been excluded since steady values have been not reached). In this table, for condition C2, separate values are reported for corrosion potential and corrosion rate of bars at different distance from the water uptake surface (20 and 60÷80 mm). Lower bars, at 20 mm that experienced a higher water content have shown higher corrosion rate, though, LG specimen was more affected by this phenomenon.

Corrosion behaviour of steel can be correlated to results of electrical resistivity measurements. Indeed, Fig. 2b shows the resistivity, as a function of time, of the specimens. Extremely high values of resistivity have been achieved in C1 condition by B+LG specimens (red curve represents an average of two replicate specimens). This could be attributed to the presence of a discontinuity between the brick and the mortar layer; though, further investigations are required for a full comprehension of such an aspect. Lower resistivity is shown by LG (blue curve, about 1100 Ωm) and especially B

(green curve, about 500 Ωm) specimens, the latter being more porous than the former. In wet condition (C2) these differences tend to become negligible (values roughly 10÷40 Ωm), whereas in the final condition (C3) there is a progressive recover of the initial differences. Comparing the wetting process with the drying one, it is possible to notice the differences in the kinetic of the hygrometric pattern: in the former case (C1-C2 boundary) the transient is very short (constant curve is reached in few hours), while in the latter (C2-C3 boundary) is slower (resistivity returns to its first range value in more than 10 days). Moreover, the drying process seems to be quicker in the B+LG specimens, followed by the B sample and by the LG one.

Since electrical resistivity measurements can provide information about the water content of specimens and their porosity, it could be used as a corrosivity index in the different environments. In general, the lower the resistivity of the embedding material, the higher the corrosion rate of inserts. This can be clearly observed in Fig. 3a, where the relationship between electrical resistivity and corrosion rate in the specimens is presented, hence allowing an evaluation of the influence of different hygrothermal conditions on such parameters. As a matter of fact, in the B+LG samples (red curve) the safest condition has been achieved (highest resistivity and lowest corrosion rate), if compared to that reached in the B specimen (green curve) and in the LG one (blue curve).

Also in the case of the LG mortar specimens, it could be useful to analyse the relationship between electrical resistivity and corrosion rate (Fig. 3b). Each of them has been stored at a fixed relative humidity, just varying the temperature (blue curve refers to 20°C and red one to 40°C). As far as corrosion rate is concerned, it is below 1 mA/m^2 for samples stored at both 65% RH (empty symbols) and 80% RH (filled symbols), whatever the temperature is. At 95% RH (bold symbols), instead, corrosion rate increases up to 10 mA/m^2. With regards to electrical resistivity values, they decrease as the moisture level increases; this happens at any temperature, even though this is more evident at 40°C. Concerning the role of temperature, it can be also observed that in dry environment (65% RH) an increase in temperature enhances drying out hence reducing the corrosion rate of bars (below 0.01 mA/m^2); as relative humidity raises (80% RH), this effect is reduced to the point of being negligible. Indeed, at 95% RH the increase in the kinetic of the corrosion process is the key factor, so corrosion rate is higher at 40°C (10 mA/m^2) than at 20°C (3 mA/m^2). In Table 2, average values and standard deviation of resistivity, corrosion rate and corrosion potential values, measured on LG mortar, are reported.

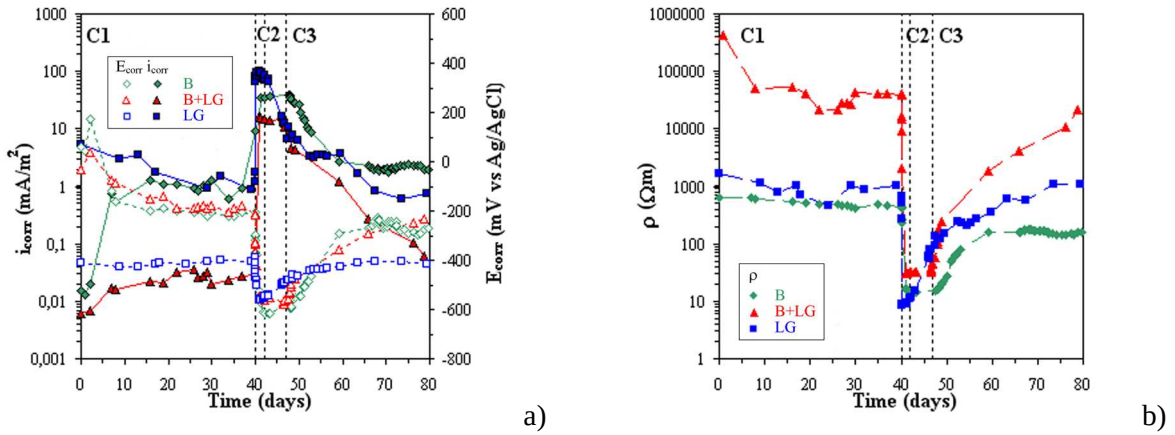

Figure 2. a) Corrosion potential E_{corr} and corrosion rate i_{corr}, as a function of time, of steel bars embedded in different materials, in three exposure conditions at 20°C (C1 and C3 refer to 95% RH, while C2 refers to wet environment). Green, red and blue symbols refer respectively to brick (B), composite mortar and brick (B+LG), mortar samples (LG); empty symbols refer to E_{corr} values, filled ones to i_{corr} values. b) Electrical resistivity ρ, as a function of time (same specimens and exposure conditions). Average values of replicate specimens (4 bars for LG, and 2 bars for B and B+LG).

Table 1. Mean value μ and standard deviation σ of electrical resistivity ρ, corrosion potential E_{corr} and corrosion rate i_{corr} measured on brick (B), brick and blended lime-gypsum mortar (B+LG), blended lime-gypsum mortar (LG), exposed to different environmental conditions.

Environmental condition	*Material*	*ρ* [Ωm]		*E_{corr}* [mV vs Ag/AgCl]		*i_{corr}* [mA/m^2]	
		μ	*σ*	*μ*	*σ*	*μ*	*σ*
T 20°C RH 95% (C1)	B+LG	36532	14001	-197	77	0.03	0.01
	B	482	51	-201	32	0.97	0.22
	LG	1072	535	-415	10	2.06	1.65
T 20°C in H_2O (C2)	B+LG	39	2	-510 (a)	76 (a)	3.53 (a)	0.55 (a)
				-587 (b)	9 (b)	9.95 (b)	1.15 (b)
	B	16	3	-545 (a)	20 (a)	33.72 (a)	1.65 (a)
				-579 (b)	55 (b)	35.25 (b)	5.01 (b)
	LG	9	0	-472 (a)	54 (a)	64.93 (a)	9.84 (a)
				-494 (b)	60 (b)	118.93 (b)	16.65 (b)

(a) bars at 60÷80 mm, (b) bars at 20 mm from the water uptake surface

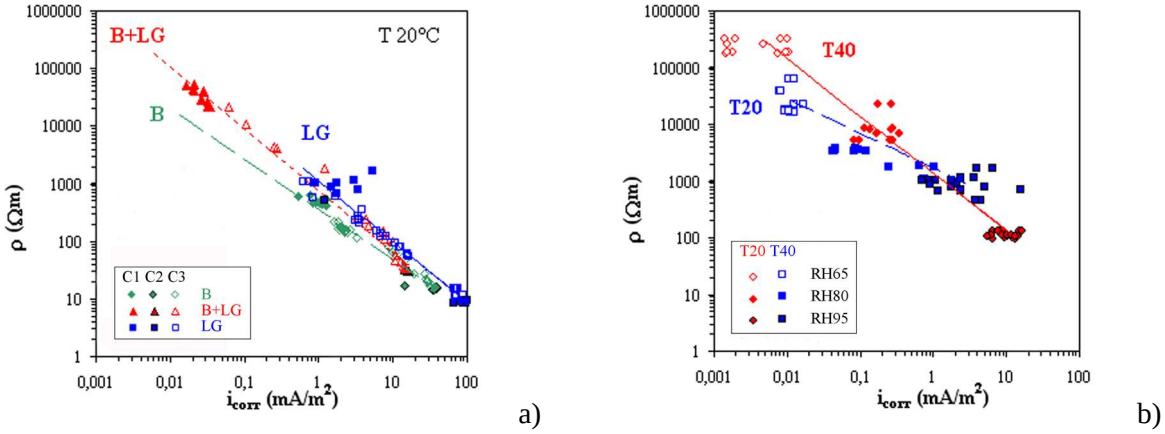

Figure 3. a) Relationship between electrical resistivity ρ and corrosion rate i_{corr} in different materials during the exposure to various RH conditions (T constant at 20°C). Green, red and blue symbols refer respectively to brick (B), composite mortar and brick (B+LG), mortar samples (LG). Filled symbols refer to 95% RH (C1), bold ones to water uptake (C2), empty ones to drying at 95% RH (C3). b) Relationship between electrical resistivity ρ and corrosion rate i_{corr} in blended lime-gypsum mortar samples (LG) during the exposure to different hygrothermal conditions. Red and blue symbols refer to 40°C and to 20°C; empty symbols refer to 65% RH, filled ones to 80% RH, bold ones to 95% RH.

Table 2. Mean value μ and standard deviation σ of electrical resistivity ρ, corrosion potential E_{corr} and corrosion rate i_{corr} measured on blended lime-gypsum mortar (LG), exposed to different environmental conditions.

Environmental condition		*ρ* [Ωm]		*E_{corr}* [mV vs Ag/AgCl]		*i_{corr}* [mA/m^2]	
		μ	*σ*	*μ*	*σ*	*μ*	*σ*
T 20°C	RH 65%	28096	10339	-241	28	0.01	<0.00
	RH 80%	2567	1685	-360	39	0.39	0.36
	RH 95%	935	475	-415	10	3.17	2.59
T 40°C	RH 65%	239199	155042	-219	34	0.01	<0.01
	RH 80%	9235	10683	-413	23	0.21	0.12
	RH 95%	113	44	-359	25	10.24	3.25

3 HYGROTHERMAL SIMULATIONS

Laboratory trials have highlighted the key role of temperature, relative humidity and water (rising damp, condensation or rainwater) on the corrosion behaviour of steel bars embedded in masonry materials. Though moisture and temperature conditions within a brick masonry wall consist of a complex set of parameters (e.g. material properties, indoor and outdoor environmental conditions), taking into account for all these variables could be done by means of hygrothermal models. Indeed, heat and moisture transfer (HMT) models and tools have had a great spread in the last two decades [Straube, J & Burnett, E.F.P. 2001], and have shown a good aptitude in predicting moisture and temperature conditions with a reasonable degree of accuracy [Künzel 1995]. Therefore, in order to extend the results obtained in the laboratory on small-scale specimens, numerical simulations have been performed: temperature, relative humidity and water conditions at the interface between the metal inserts and the materials in which they are embedded have to be analysed. By now, an effort to do the first steps in the definition of the kind of analysis requested (steady or unsteady state) and in the selection of the input data (defining geometry, material characteristics and environmental conditions) for the hygrothermal simulations have been done. Moreover, a preliminary assessment of thermal and hygrometric behaviour of brick masonries exposed to Milan clime and to several laboratory climatic chambers conditions has been performed.

3.1 Simulation models

As far as preliminary assessment is concerned, two series of simulations have been performed, both considering mono-dimensional geometries and implementing a finite difference algorithm: the first one studies only the temperature field; the second one analyses the simultaneous effects of temperature and relative humidity. In particular, concerning temperature and relative humidity variations, the behaviour of a typical ancient brickworks (consisting of non-hydraulic mortar and fired bricks, width 380 mm) has been studied by means of different hygrothermal boundary conditions, which are steady state ones (20°C T, 50% RH) and dynamic sinusoidal ones (48, 24, 12, 6 and 3 hours periods, mean value and maximum variation respectively of 20°C and 5°C for T, 50 and 15% for RH). Moreover, two further series of situations have been modelled. The first one simulates again traditional brick masonries (width 380 mm), assuming as external boundary condition a reference year in the geographic area of Milan, whereas as internal boundary condition constant temperature and relative humidity (20°C T, 50% and 65% RH) has been considered. In order to validate the experimental data obtained in the laboratory, instead, the second one reproduces brick blocks (width 120 mm) subject to the hygrothermal fluctuations laboratory tests conditions: temperature steps have been imposed (20-40°C), keeping constant the relative humidity (65-80-95%); in addition, relative humidity steps have been fixed (65-80-95%), keeping constant the temperature (20-40°C).

3.2 Results and discussion

The simulations results have shown that an unsteady state analysis is needed for a consistent evaluation of the thermal behaviour of the brick masonries considered (Fig. 4a), whereas a steady state approach is enough to describe the hygrometric behaviour inside the domain, apart from the boundary zone (Fig. 4b): while the thermal fluctuations involve the whole samples thickness, the relative humidity variations are limited to the very first centimetres from the interface with the environment. The simulations of the experimental laboratory tests, confirming such results, have highlighted a very fast thermal response (24 hours are enough to reach the equilibrium with the environment) and a slower hygrometric one (asymptotic values are not reached in the core region). Finally, since these results have to be validated by the experimental laboratory data concerning the corrosion behaviour of steel inserts, an attempt to consider bi-dimensional HMT models is in progress.

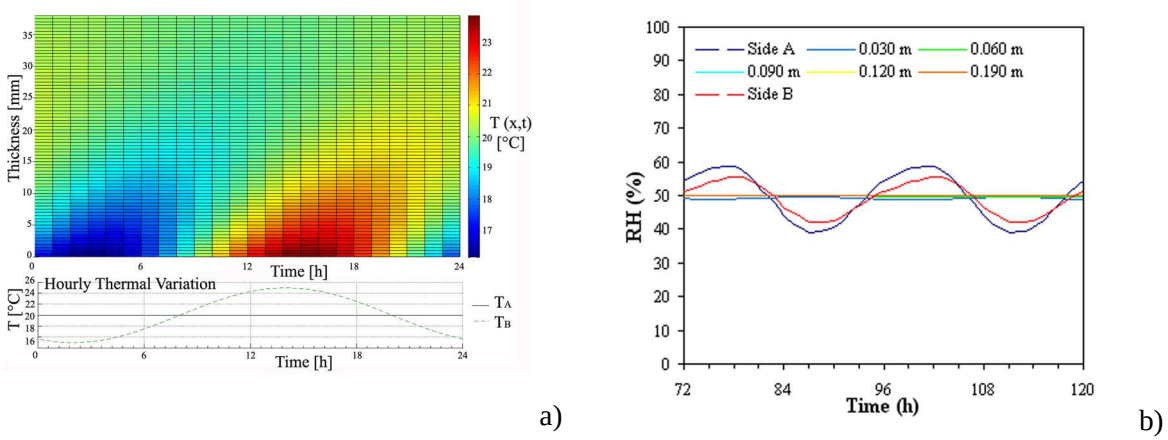

a) b)

Figure 4. a) Thermal response of a 380 mm brick masonry wall to a sinusoidal variation, 24 hours period on side A (down), constant on side B (up). b) Hygrometric response of the same wall to a sinusoidal variation, 24 hours period on side A (blue curve), constant on side B (red curve).

4 CONCLUSIONS

This study has shown the key role of temperature, relative humidity and water on the corrosion behaviour of low carbon steel inserts embedded in masonry materials. Tests in specimens with blended lime-gypsum mortar and fired brick have shown that corrosion rate is strongly related to the moisture content of the embedding material. Corrosion rate was negligible in specimens exposed to relative humidity of 80% and 65%, even at 40°C. Conversely, in wet environments or in presence of water suction, corrosion rate has reached high values. A clear correlation between electrical resistivity of embedding material and corrosion rate of steel has been observed. Moreover, with the aim to extend the results obtained on small-scale laboratory specimens to case studies that should consider the effect of the real hygrothermal conditions on corrosion of steel inserts in ancient brick masonry, numerical simulations have been performed. Concerning this, an attempt to define a bi-dimensional HMT model, which can predict corrosion behaviour of inserts as a function of the hygrothermal conditions, is now in progress.

REFERENCES

Bertolini, L., Carsana, M. & Marra, E. 2009, 'Degradation of mortars and steel inserts from the ciborium of the medieval abbey of San Pietro al Monte', in *Special Topics on Materials Science and Technology – An Italian Panorama*, Brill Publisher.

Bertolini, L., Elsener, B., Pedeferri, P. & Polder, R. 2004, *Corrosion of steel in concrete*, Wiley-VCH.

Künzel, H.M. 1995, *Simultaneous Heat and Moisture Transfer in Building Components*, IBP Verlag.

Lourenco, P.B. 2006, 'Recommendations for restoration of ancient buildings and the survival of a masonry chimney', *Construction & Building Materials*, 20, 239–251.

Straube, J. & Burnett, E.F.P. 2001, 'Overview of hygrothermal (HAM) analysis methods', in *ASTM Manual Series MNL 40 – Moisture analysis and condensation control in building envelopes*, ed. H.R. Trechesel, Philadelphia, pp. 81–89.

Straube, J. & Schumacher C. 2006, 'Assessing the durability impacts of energy efficient enclosure upgrades using hygrothermal modelling', *WTA-Journal*, 2, 197–222.

XII DBMC
International Conference on Durability of Building Materials and Components
PORTO - PORTUGAL, April 12th-15th, 2011

Is It Possible to Reutilize a Brick Masonry Structure after a Fire According to UNE EN 1996-1-2:2005?

María Eugenia Maciá Torregrosa [1]
Antonio Rolando Ayuso [2]

ABSTRACT

Due to the consideration that masonry elements have a good behaviour at high temperatures, the methods of calculation established in UNE EN 1996-1-2:2005 are not developed enough to assess the masonry compression strength at high temperatures. By thermometric analyses it is possible to determine the temperature a masonry element has been submitted and, therefore, it is possible to calculate the loss of strength in that section.

The target of this study consists of determining which is the relation between the masonry compression strenght at ambient temperature and at high temperatures in order to determine the masonry loss of resistance at different steps of temperature.

The development of this research includes the analysis of the thermomechanic characteristics of the brick masonry components, the construction of the masonry wallets, the development of a procedure of testing and an experimental device to combine thermal and mechanical action, and the manufacturation of the compression strength tests to ambient and high temperatures.

The relation established in UNE EN 1996-1-2:2005 between the masonry element compression strength to ambient temperature and the masonry element compression strength to high temperatures is defined experimentally by means of a coefficient c. It is clear from analysis that the estimation of the coefficient c in the calculations carried out by several authors is a little penalizing as it has been demonstrated in this research.

KEYWORDS

Fire resistance, masonry, heat transmission, compression strength, high temperatures, experimental test

[1] Escuela Politécnica Superior de la Universidad San Pablo CEU (EPS-San Pablo CEU) , Madrid, SPAIN, memacia@ceu.es
[2] Escuela Técnica Superior de Arquitectura de la Universidad Politécnica Madrid (ETSAM-UPM), Madrid, SPAIN, antonio.rolando@upm.es

1 INTRODUCTION

The study of compressive strength after a fire of a brick masonry wall in the normal direction has been traditionally necessary to study the behaviour of the brick masonry, at least until recent introduction of the numerical methods for brick masonry structures. There are different authors who establish particularities on the way of carrying out uniaxial compression strength tests for piled up elements under ambient temperature (1) (2) (3). They all show uncertainties, cautions and observations about the obtaining of some parameters for every type of test. There is a greater acceptance on the values given from the RILEM test, but this test is relatively long and cost executing. Provided that other authors (4) (5) establish small prisms for the masonry elements analysis, it is proposed to use this typology of sample test to carry out the uniaxial compression tests under high temperatures.
It is possible this way to determine the compressive strength of a masonry element affected by high temperatures after cooling.

2 OBJECTIVE

Although the masonry structures have a good behaviour when they are submmited to high temperatures it is necessary to calculate the compression strength reduction of a masonry element that has been affected by a fire. This is the way we could know if it is possible to reutilize a brick masonry structure element after that accidental action.

The determination of fire resistance of a masonry element is a complex question that only can be approached throught numerical and experimental analysis. The masonry stress-strength analysis at high temperatures is a particular thermo mechanical problem.

The main objective of this research is to obtain results about the residual compression resistance of masonry elements submitted to high temperatures in order to observ which is the mechanical behaviour of those elements previously submitted to different thermal situations and posterior cooling.

3 EXPERIMENTAL PROGRAM

To develop the experimental program an experimental device has been designed that allows submitting the samples to a stationary and uniform evolution of temperatures. The whole sample has been warmed up by means of refractary heater plates and has been left cooling down to temperature ambient. Finally the element is subjected to ultimate load and breakage.

A new device for the experiments and 48 tests have been carried out in order to analyze the thermo-mechanic behavior of the masonry elements to different steps of temperature and to validate the test protocol.

Formal aspects related to the material properties, specimens preparation, heat transference device, geometry, instrumentation and test arrangement, and series of test realized have been summarized here.

3.1 Material Properties

The masonry elements have been built with clay bricks and Portland mortar. They are described as follows (Figure 1).

a) Bricks

A one-faced perforated clay brick, dimensions 240x114x48 mm without nonabsorbent treatment and fired at temperatures near 900ºC is used.

Table 1. Physical brick properties

Characteristics	Value	Standard
Density	1810Kg/m^3	UNE EN 772-13:2003
Thermal conductivity	0,34W/mK	UNE EN 1745: 2002
Compressive strength	20 N/mm^2	UNE EN 772-1:2002
Hollows	<45%	

b) Mortars

The mortar made was a M7,5 pre-proportioned for conventional use. The mortar was mixed by a conventional mixer; the minimal time of mixing was approximately five to seven minutes. The water was progressively added to the mass, in order to reach a suitable workability. The water retention of the mortar was considered to be correct in its execution; mortar did not show quick losses of water content in its disposal and was very workable.

Table 2. Physical mortar properties

Characteristics	Value	Standard
Density	1950+-50 Kg/m^3	UNE EN 1015-10:2000
Thermal conductivity	0,52-0,65 W/mK	UNE EN 1745: 2002
Compressive strength	7,5N/mm^2	UNE EN 1015-11:2000



Figure 1. Stock up materials at the EPS Materials Laboratory

3.2 Specimens preparation

The masonry test samples have been built following the Eurocode (6) recommendations relatively to the preparation, confection and hardening.

The test samples have been made on a smooth horizontal surface and measures have been taken in order to avoid the drying of the specimens during the first days after construction. After that they have been left in a laboratory environment. A thin end joint of plasterwork flat and parallel between them (with higher strength than mortar of the test samples) have been used in order to assure the load will be right applied.



Figure 2. Masonry samples plasterwork process

3.3 Heat transference device

After the plasterwork process the masonry samples have been warmed up to certain temperatures using the Fouriers´s equation. A heat transference device is designed (Figure 3) in order to guarantee every thermal step to which the material is going to be submitted to obtain reliable results.

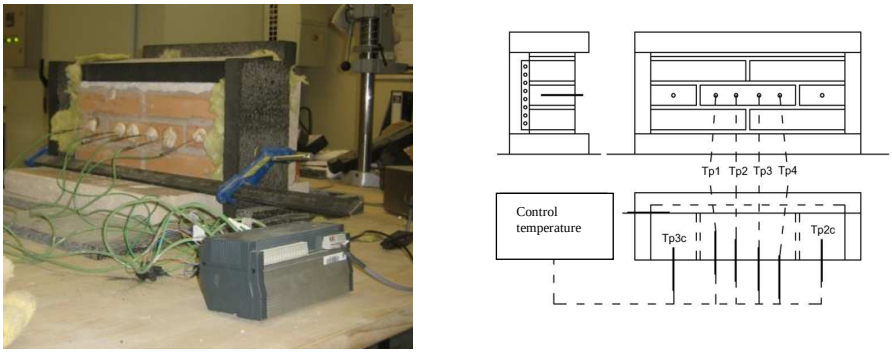

Figure 3. Refractary clay heater plates to assure heat transfer to the specimen in the tests

3.4 Geometry and test arrangement

Provided that it does not exist a specific test to obtain information on the residual compression strength of masonry elements submitted to high temperatures and cooling later to ambient temperature, a device is designed for such an effect.
According to the Eurocode (6) for making a masonry element compression test it is necessary a Universal press that allows to apply such a load on a test sample with uniform displacements on the loaded surfaces. As the plates of the test machine are minor that the test masonry element, distribution beams with a major length that the test specimen and a bigger or equal thickness than the length between the edge of the plates; must be used (Figure 4).

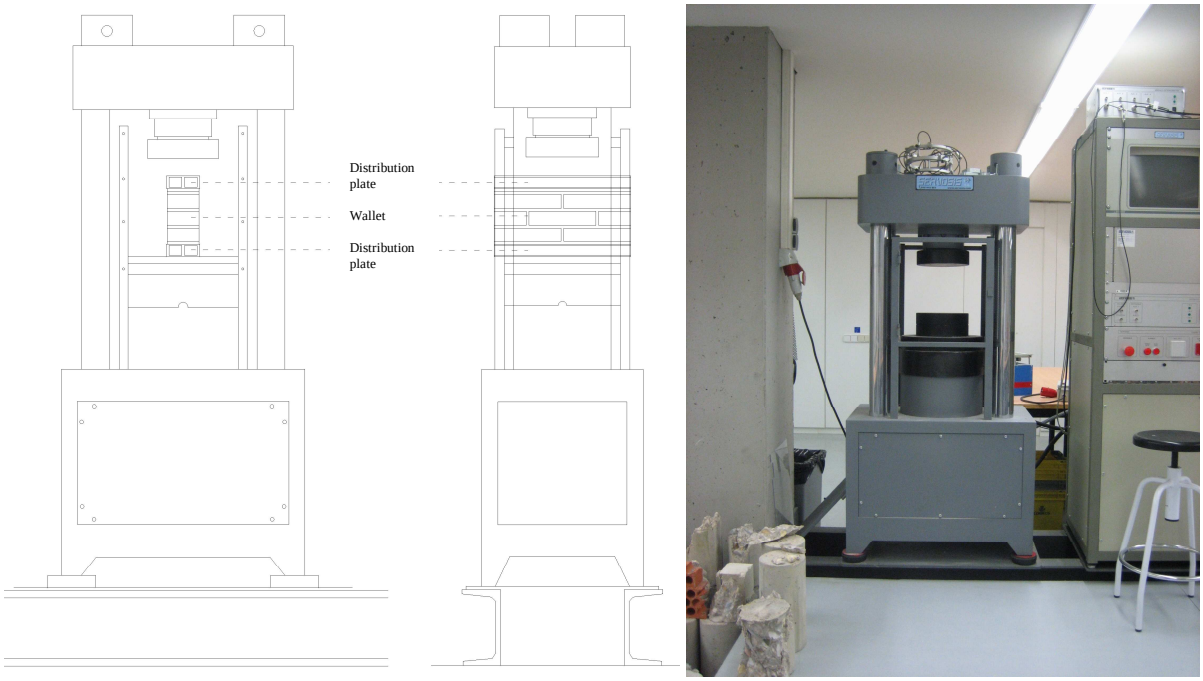

Figure 4. Design of the experimental device. Universal press.

Due to Universal press had cilindrical plates for the load distribution it was built two special pieces to guarantee a correct load distribution (Figure 5).

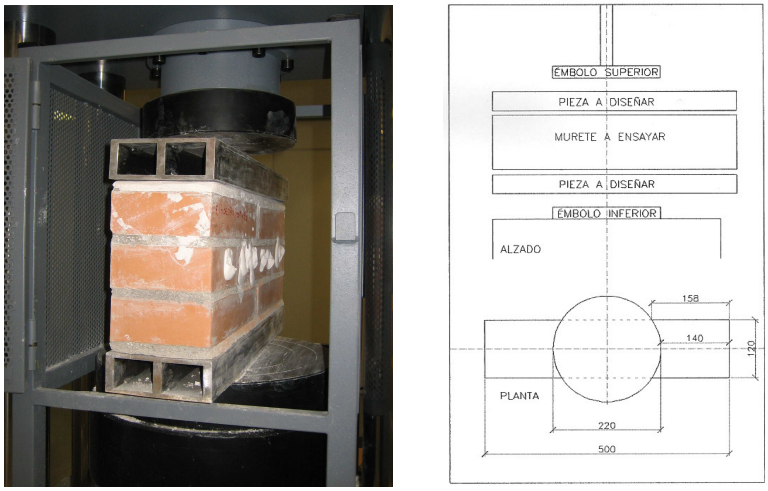

Figure 5. Universal press with load distribution plates.Distribution plates design.

3.5 Instrumentation and test procedure.

In order to evaluate the residual compression strength of the masonry samples the instruments used for this proposal were:

- Universal press machine Mod. IBERTEST (600 KN) (Figures 4 and 6).
- Analysis control software PCD-2K for static and dynamic tests (Figure 6).
- Special pieces designed to homogeneous sample load distribution (Figure 5).



Figure 6. Equipment view from the Laboratory of Materials of the Technical Upper School of the San Pablo CEU University. Control and measurement test progress.

In order to carry out the tests one of the designed load distribution plates was placed onto the lower Universal press cilindrical plate. The sample was placed onto the lower distribution plate and finally the other distribution plate was placed on the upper Universal press cilindrical plate.

3.6 Test series

Six series of wallets for every step of temperature has been carried out. These series had been submitted to high temperatures along periods over 210 minutes to obtain temperature profiles.

The masonry wallet had been subjected to eight temperature steps (from 50ºC to700ºC) before-being placed at the device. Six brick masonry wallets for every step of contemplated temperature have been tested.

The tests to know the compression strength in masonry elements submitted to high temperatures temperature were carried out in the Laboratory of Materials of the Technical Upper School of the San Pablo CEU University during July, 2009.

4 RESULTS

After the obtaining of the experimental results f_i it has been calculated the characteristic compression strength f_K of the masonry element to different steps of temperature (from 50 to 700ºC) as it is indicated in Table 3.

Table 3. Determination of characteristic compression strength at 700ºC

Characteristic compression strength			$f_K = f_{media} - Ks$	
i	F_i	$f_i = \frac{F_i \cdot 10^3}{115 \cdot 490}$	f_{media}	$[f_i - f_{media}]^2$
Sample	(KN)	(N/mm^2)	(N/mm^2)	
1	252,2	4,47	5,08	0,36
2	287,8	5,10		0
3	256,3	4,54		0,28
4	315,2	5,59		0,26
5	321,2	5,70		0,38
6	285,3	5,06		0
$\sum (f_i - f_m)^2$				1,29
n-1				5
$\frac{\sum (f_i - f_m)^2}{n-1}$				0,25
$s = \sqrt{\frac{\sum (f_i - f_m)^2}{n-1}}$				0,50
$f_k =$				
5,08-2,01x0,50= 4,05 (N/mm^2)				

In order to enable the use of the simplified method of design proposed at Eurocode 6 (6) trought the formula of minoration of the characteristic compression strength of a masonry wall submitted to high temperatures and cooled down afterwards ($f_{d\theta 2} = c \cdot f_{d\theta 1}$) values of Coefficient *c* of this formula obtainned in this research are shown as follows (Table 4).

Table 4. Constant *c* obtained from stress-strain tests at elevated temperature

θ	20ºC	50ºC	100ºC	200ºC	300ºC	400ºC	500ºC	600ºC	700ºC
$f_{k\theta}$ (N/mm^2)	5,81	5,32	5,59	5,66	5,29	4,98	4,66	4,27	4,05
c	1	1	1	1	0,94	0,89	0,83	0,76	0,72

In the simplified calculation method the remaining loadbearing capacity is determined by boundary conditions on residual cross section of the masonry for stated periods of fire exposure using the load at ambient temperature.

5 CONCLUSIONS

The experimental study presented in this work clearly demonstrated that obtaining the coefficient of minoration of the resistance to high temperatures it is possible to know instantly which is the loss of resistance of a masonry element submitted to the fire action. The use of technologies like petrographic examinations (non destructive test, test without contact, rapid, precise, easy to operate …) allows the identification of the temperature reached in the zones affected by a fire and therefore it is possible to know easily its loss of resistance.

Up to date the design of a masonry structure in a fire situation was calculated using the simplified method established in the Eurocode 1996-1-2:2005 in absence of information about coefficient *c* (values of the coefficient *c* do not exist in any document). After this study it is possible to contribute results on the values of the coefficient *c* bearing in mind the loss of resistance of the element while it is acting the thermal action (concomitant with the mechanical action) as when the cooling of the factory has taken place.

Values of coefficient *c* obtained from this research demostrate that values obtained by others authors (7) are exceedingly penalizing.

The information obtained could be important in the editing of design guides or standards because the value of constant *c* to be used in each Country may be found in its National Annex.

REFERENCES

Instituto Eduardo Torroja: "Piet 70, Obras de fábrica. "Prescripciones del Instituto Eduardo Torroja, Madrid, 1971.

Wesche, K. and Ilantzis, A. General recommendations for methods of testing load bearing walls, Materials and Structures, RILEM 433-445, 1980.

Mann, W. and Betzler, M. “Investigations on the effect of different forms of test samples to test the compressive strength of masonry”, Proc. 10th Int. Brick and Block Masonry Conf., Calgary, Alberta, 1305-1313, 1994.

Lourenço, P.B. (1996): Computational strategies for masonry structures. Tesis doctoral, Delft University of Technology. I.S.B.N: 90-407-1221-2

Pina-Henriques J.L (2005): Masonry under compression: Failure analysis and long-term effects. Tesis Doctoral. Universidad do Minho. I.S.B.N: 972-8692-24-2

EN 1996-1-2:2005. Design of masonry structures. Part 1-2: General rules. Structural fire design.

Villagrá, C. (2005): Cálculo de estructuras de fábrica en caso de incendio según el Eurocódigo 6. Caso práctico. Jornada Técnica: Eurocódigos Estructurales. Comportamiento de la estructura en caso de incendio. IETcc-CSIC. I.S.B.N: 84-931709-3-3. pp: 123-136.

XII DBMC
International Conference on Durability of Building Materials and Components
PORTO - PORTUGAL, April 12th-15th, 2011

Application of the "Moisture Buffering" Approach to Improve the Durability of Historical Wooden Elements

Marco D'Orazio [1]
Enrico Quagliarini [2]

ABSTRACT

We report the results of a research study aimed at developing a new strategy for the conservation of wooden structural elements which are present in historical buildings, based on moisture regulating systems. The idea is to develop systems based on the ability of some highly hygroscopic materials to buffer the peaks in relative humidity. In order to experimentally verify this possibility using current, low cost and easy handling building materials, five bentonites were laboratory processed to improve their adsorbing properties.

KEYWORDS

Moisture buffering, wood, masonry, building, cultural heritage

[1] Università Politecnica delle Marche, DACS department, via di Brecce Bianche 60131 Ancona, m.dorazio@univpm.it
[2] Università Politecnica delle Marche, DACS department, via di Brecce Bianche 60131 Ancona, m.dorazio@univpm.it

1 INTRODUCTION

This research paper reports the first results of a more general study which involves the use of bentonites as a moisture regulating system in building applications. Recent research studies, in fact, have shown that relative humidity (RH) control is an important environmental issue not only for humans but also for artefact preservation and that passive systems (mostly hygroscopic materials) have some potential in controlling indoor RH [Osanyintola, 2006]. Thus materials that adsorb and release moisture could be positively used to reduce the extreme values of RH into the micro-climate, for example between wooden elements and masonry. This moisture buffer performance will obviously depend on the moisture buffer capacities of each combination of materials together with the moisture production and air exchange rate and the ratio between the surface area of the material and the involved air volume.
Bentonite shows some interesting hygroscopic properties and it is used in civil engineering, for oil drilling, for some pharmaceutical and cosmetic applications and also in the food industry. No applications of bentonite as an adsorbent of water vapour in preserving artefacts are known. Hence it is our opinion that bentonite could be used for its adsorbing capacity, or more generally as a moisture regulating system, to preserve historical wooden elements.

2 MATERIALS AND METHODS

Bentonites were all obtained through Laviosa Chimica Mineraria (Livorno, Italy). The samples came from different locations: Greece (samples AK and RR), Turkey (STP), Morocco (M) and Italy (RP). All samples (about 3 kg each, sealed in plastic bags) were already sieved for the same average particle dimension (200 mesh). Bentonite is a mineral material with a defined crystalline clay-like structure. The mineral is made up of silica and alumina sheet-like units, bound together; water can enter between the sheets separating them and hence bentonites can be readily dispersed in water in extremely small particles [Grim, Giiven, 1978]. A generic bentonite is always unbalanced, with a net negative charge which can be balanced with adsorbed cations such as sodium or calcium; these cations determine the ease of separation and to some extent, the quantity of adsorbed water. In fact, raw bentonite materials are industrially treated under appropriate conditions with sodium carbonate in order to obtain products at different degrees of ion substitution, hence enhancing their adsorbing capacity.
In order to experimentally verify the use of bentonite as a moisture regulating system, 5 bentonite samples were laboratory processed. In order to enhance their adsorbing properties by means of cation exchange, sodium carbonate (Na2CO3, Carlo Erba Reagents, Milan, Italy) at three different concentrations (2%, 3% and 4% by weight) and distilled water (30% by weight) were added to them and mechanically mixed with a blender for 2 h. After this treatment, the samples of bentonites were dried in a thermostatically controlled oven at 120°C until constant weight was reached; dried samples were milled by means of a rotary ball grinder (Retsch RMO, Milan, Italy) and finally passed through a 200 mesh sieve. The effectiveness of the cation exchange treatment on bentonites was controlled by measuring the swelling volume. Exactly 2 g of dried bentonite were introduced into a graduated glass cylinder filled with 100 ml of distilled water. After 2 h the swelling volume of bentonite, expressed in millilitres, was measured. All the samples (n = 15) were firstly tested for their hygroscopic properties [Stazi et al., 2002]. Their adsorption isotherms were made following the static method as described by Spiess and Wolf [1990]. 8 desiccators containing, respectively, silica gel, 6 different saturated salt solutions ([Rockland ,1960]; [ASTM E 104-85,1985]) and bi-distilled water were used to control RH at 25°C. Each sample of bentonite was put inside the first desiccator (dried silica gel, RH = 2%) and maintained until constant weight was reached; it was then transferred to the second one (LiCl, RH = 12%) and so on until the last desiccator at UR ≈ 100% (bi-distilled water). The change in the weight of the samples was measured by means of an analytical balance (Gibertini E42, Modena, Italy) in order to evaluate the water content M. The desiccators and the analytical balance were kept in a room at a controlled temperature of 25°C. In order to evaluate the hysteresis phenomenon, after the adsorption period, for some bentonite samples, desorption was carried out, starting at RH ≈ 100% and moving downward to lower values.

These experimental data were compared with those of some historical materials such as spruce and brick.
In order to evaluate the dynamics of moisture exchange between materials (bentonite, masonry and spruce wood) we used the Delphin code [Grunewald, 2005]. The simulations were carried out by isolating the masonry-wood node (Fig. 1), lying the masonry on the external environment and the wood beam on the internal environment and considering as acceptable (with respect to the simulation time) its reduction to a bi-dimensional case (that is to say, the gradient perpendicular to the section analysed was considered null).

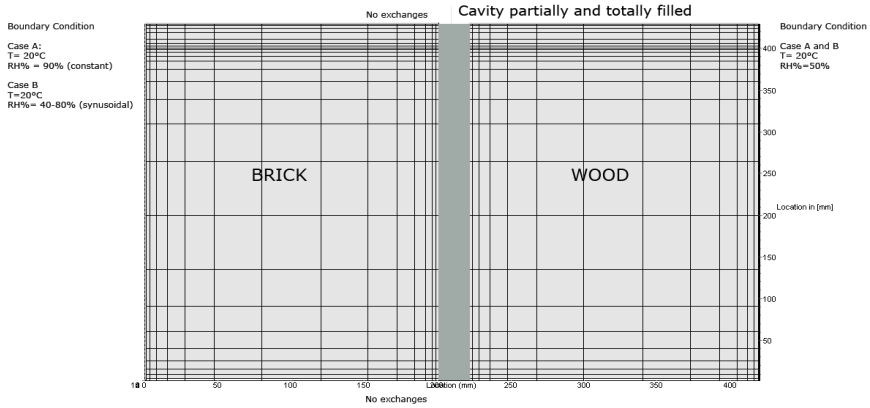

Figure 1. Numerical simulations: boundary and geometric conditions for each set-up. Mesh were increased at the internal and external boundary.

The simulations were carried out considering three numerical set-ups: - empty interspace between the wooden beam and the masonry (air cavity 20 mm); this is the most common arrangement used in historical building; - interspace between the wooden beam and the masonry partially filled (20%) with bentonite; this set-up corresponds to the hypothesis of putting small bags containing the adsorbing material into the cavity. This should reduce the RH of the cavity without making all the wooden element getting in touch with the bentonite; - interspace between the wooden beam and the masonry completely filled with bentonite; this set-up corresponds to the hypothesis of completely filling the cavity with the adsorbing material so as to reduce the amount of humidity into the wood thanks to the direct contact between two materials which have different hygroscopic capacities. Two types of hygrometric boundary conditions were arranged for each of these set-ups, at constant T = 20°C (see Fig. 1): Static (case A): 90% RH was fixed for the external boundary condition of the masonry and 50% for the internal boundary condition of the wood (spruce); Dynamic (case B): a sinusoidal daily variation of the environmental RH (average 60% RH ; amplitude 20% RH) was fixed for the external boundary of the masonry while a constant value of 50% RH was fixed for the wood (spruce). Initial conditions were set to T = 20°C and 50% RH for each of the previous set-up. Table 1 and Fig. 2 show the characterisation data for the materials used in the simulations carried out. One of the lowest hygroscopic values' bentonite in the hygroscopic range considered in terms of maximum water content and adsorption rate has been used, thus considering the worst case for simulation.

Table 1. Dry matter vapour diffusion resistance factor μ_{dry} for materials used with the Delphin code.

Material	μ_{dry} ***[-]***
Wood (spruce)	40
Bentonite	1
Brick	10

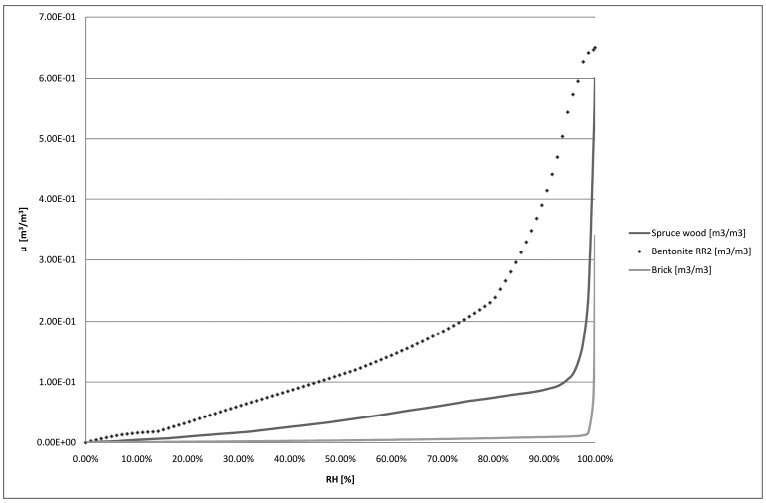

Figure 2. Isothermal adsorption curves for brick, spruce wood and RR2 bentonite used for numerical simulations.

3 RESULTS AND DISCUSSION

3.1 Swelling volume and adsorption isotherms of bentonites

Because the hygroscopic properties of the raw materials were one order of magnitude lower than the sodium carbonate treated samples [Barbanti et al. 1996], in this paper we will refer only to the data on treated bentonite samples. In Table 2 the swelling volume for all bentonites as a function of the percentage of Na2CO3 is reported. The cation exchange (sodium in, calcium out) increased the distance between the sheet structures of bentonite, hence allowing water to enter. As a consequence, the volume of all bentonites rose with an increasing percentage of Na2CO3. However, due to the different original structures, bentonites showed very different swelling volume changes; in fact, the lowest values were about +22-23% (RR3 and M3), while the highest (AK4 and RP4) were around +90-94%. Fig. 3 shows the adsorption isotherms for the RP2, RP3 and RP4 samples; the isotherms are almost superimposed, regardless of the degree of ion substitution and a similar behaviour was also observed for the other bentonites. Some differences were measured in terms of the maximum M value, which ranged from 0.26 for STP samples to 0.34 for RP sample.
A complete comparison of the adsorption isotherms of all bentonites is reported in Fig. 4. In these cases, even if the shape of the curves is substantially the same, some differences are evident. RP samples, at any RH value, show the highest values of M for each percentage of sodium carbonate treatment while the corresponding RR and STP samples have always the lowest value.
In order to compare the adsorption range between bentonites, masonry and wood, the adsorption isotherm of RR2 sample has been reported together with the isotherms of a sample of historical wood (spruce) and brick [Grunewald, 2005], as shown in Fig. 3. The u values of RR2 bentonite are greater than those of the selected materials, especially during the hygroscopic range. Hence the bentonite, for its low cost and for the ease of handling, under appropriate conditions could be used as buffer material. Nevertheless, it was not possible to compare bentonite and the selected materials in terms of the water adsorption kinetics because for these last ones there was no data as a function of time. Thus numerical simulation were made as reported in paragraph 6.3.

Table 2. Swelling volumes and percentage of swelling volumes (samples treated at 2% with sodium carbonate used as references) for all bentonites.

Bentonite	***% of Na_2CO_3***	***Abbreviation***	***Swelling volume (ml)***	***Swelling volume increase (%)***
AK	2	AK2	21	-
	3	AK3	35	+66
	4	AK4	40	+90
RR	2	RR2	22	-
	3	RR3	27	+22
	4	RR4	31	+41
STP		STP2	17	-
		STP3	22	+29
		STP4	24	+26
M		M2	38	-
		M3	47	+23
		M4	48	+26
RP		RP2	18	-
		RP3	25	+38
		RP4	35	+94

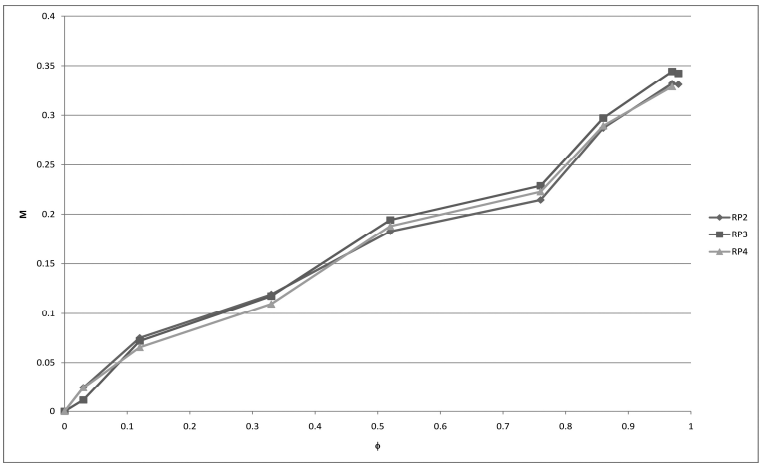

Figure 3. Adsorption isotherms (at 25°C) of type RP bentonites.

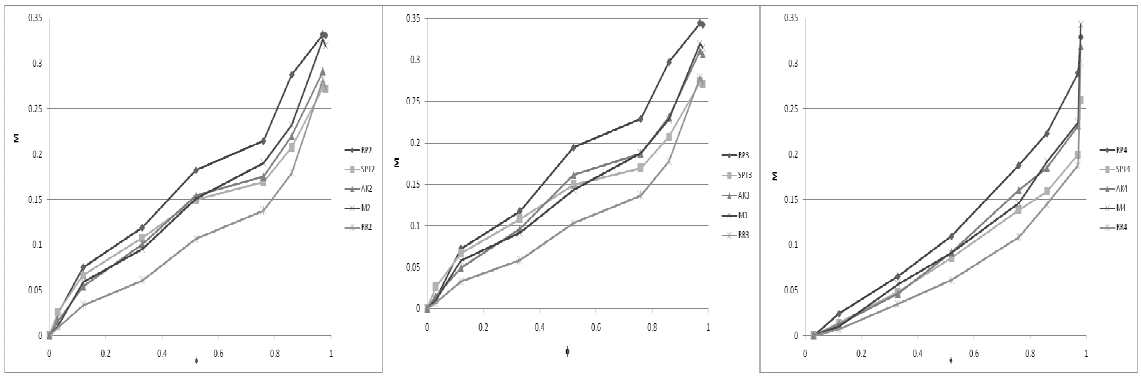

Figure 4. Adsorption isotherms (at 25°C) of type RP, STP, AK, M and RR bentonites treated with sodium carbonate at 2% (left),3%(middle),4% (right) by weight.

3.2 Kinetics of water adsorption

If the M data of the adsorption isotherms are expressed as weight increase percentage as a function of time, the kinetics of water adsorption are obtained. Fig. 5 reports the kinetics for bentonite samples. It can be observed that the bentonite kinetics varied considerably from one sample to another. A substantial difference can be observed between the RP and the other samples; the weight increase of this bentonite reaches about 20% in 20 days, while the other samples needed from 32 to 40 days to reach the same value. In this case, the different bentonite kinetics could be used in order to buffer the quantity of adsorbed water in a period of time, in a hypothetical wood-bentonite-masonry system.

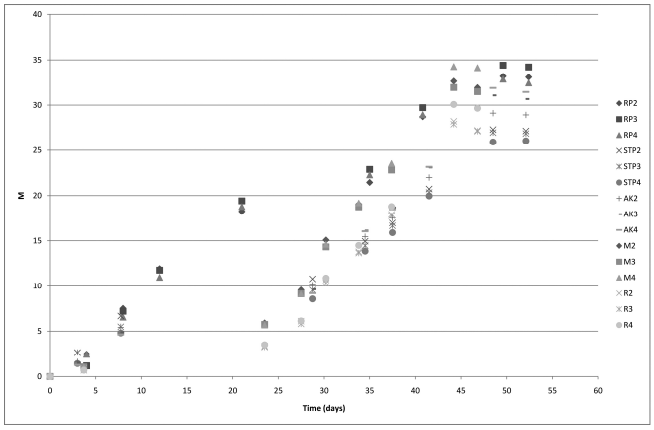

Figure 5. Kinetics of water adsorption for bentonites.

3.3 Dynamics of the processes of moisture exchange (bentonite between wooden and masonry)

In order to evaluate the dynamical process of moisture exchange between bentonite, wooden element and masonry, a series of numerical analyses were carried out using the Delphin software for thermo-hygrometric analysis. During the numerical assessment the RR2 type of bentonite has been used, in order to consider an unfavourable situation. Fig. 6 (left) illustrates the comparison of the results of the simulations carried out in order to show the dynamics of the accumulation processes in the wood element with or without the presence of bentonite for the first type of boundary conditions (Static conditions – Case A). It is possible to underline that the presence of bentonite in the air cavity tends, as expected, to reduce the hygroscopic loads borne by the wood at the interface with the masonry. The u difference after 60 days of simulation is of about 20% between the two extreme situations: only air and air cavity totally filled with bentonite. It is therefore clear that the adsorbent material is able to retain part of the water which would otherwise have been adsorbed by the wood leading to very severe damage over a long exposure time. Even the partial filling of the cavity leads to a reduction in the hygroscopic content of the wood, although in this case it is much less noticeable. Fig. 6 (right) shows the comparison of the results of the simulations carried out to understand the effect of the adsorbent material in the cavity with a sinusoidal cyclic variation in the RH (Dynamic boundary conditions - Case B). This set-up could be considered as analogous with typical daily variations. The results appear to be similar to those previously indicated. The only apparent change is the scale for the water content in the wood. Fig. 7 (left) shows the curve for the water content in the wooden beam with respect to the distance from the wood/cavity interface for the Static boundary conditions. It can be seen that the reduction in water content in the wood involves a portion of the wooden structure which is of about 60 mm. This size is one order of magnitude greater than the "effective depth of penetration", as described in [Keresteciogl u A., et al., 1988], indicated as the thickness of the material which is able to follow the daily variations in the water content according to variations in the RH.
Finally, Fig. 7 (right) shows the variation in the water content into the wooden element with or without bentonite keeping the boundary conditions constant and verifying that the equilibrium

condition has been reached (increase in the water content <0.005 m3/m3). It seems to be clear that about 3 years are needed to reach this equilibrium condition. Moreover the presence of bentonite tends to significantly reduce the final water content in the interface of the wood, preventing the equilibrium of the water threshold at 0.075 m3/m3 from being reached. This value corresponds to a water content equilibrium which is reached by exposing this wood type to an environmental RH of 80%. This value is a conventional threshold beyond which the start of a decay process in the wooden structures is assumed to be inevitable [Johansson,2005].

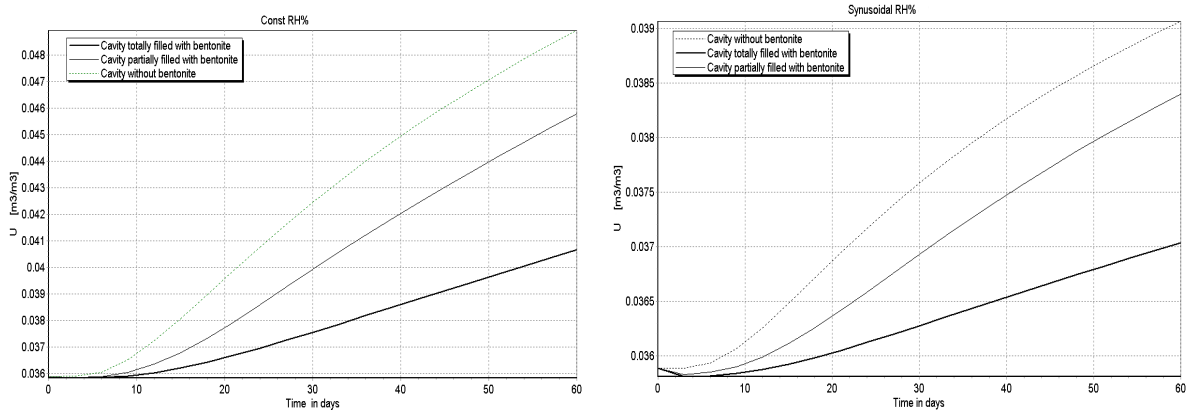

Figure 6. Wood moisture content for the (case A) static (left) and (case B) dynamic (right) boundary conditions as a function of time into the first two millimetres of wooden thickness from the cavity.

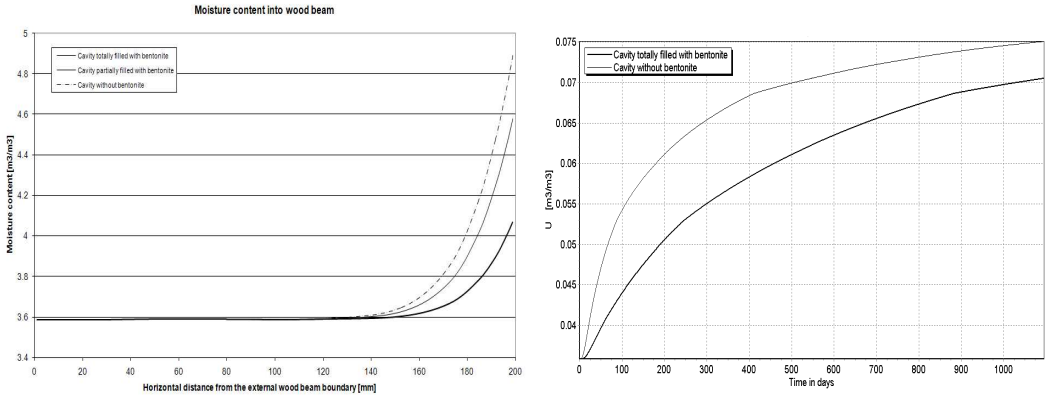

Figure 7. Static boundary conditions (case A). On the left: curves for moisture content in spruce wood as functions of the distance from the external environment (left) to the cavity (right); On the right: dynamics of water adsorption in spruce wood with and without bentonite

4 CONCLUSIONS

This initial study of some hygroscopic properties of bentonites clearly illustrates the potential use of this mineral material as a moisture regulating system in historical structures.
In particular, using this material as a hygroscopic regulator it can be pointed out that:
- The hygroscopic properties of these bentonites, after the ion substitution treatment, are mainly related to their geographical origin;
- An increase in the degree of ion substitution from 2% to 4% modified the hygrometric properties of bentonites to different extents;
- The u values of the adsorption isotherms of treated bentonite samples are always greater than the ones of the selected historical materials, that is spruce and brick; thus, it should be possible to use

bentonites as hygrostatic regulating systems, because of the different maximum adsorbing capacities and also the different adsorbing velocities.
Moreover, the isothermal numerical simulations, carried out both in stationary and dynamic hygrometric conditions, and ignoring at this initial stage the hysteretic behaviour of desorption, showed that the hygrometric characteristics of the RR2 bentonite tend to considerably reduce the water content into the wood, thereby favouring its conservation over time. These characteristics prevent the conventional water content threshold balance from being reached. Beyond this threshold the start of a decay process in the wooden structures is assumed to be inevitable.
Results show that it seems to be possible to use bentonites as a moisture buffering material in order to reduce moisture content in wooden beams at least during their adsorption phase. It remains to investigate their actual desorption phase (hygroscopic hysteresis) and their behaviour if they be in a saturation condition. Further simulations are currently being carried out in order to process the desorption stage of the hygroscopic material, with the possibility of introducing "preferential pathways" which favour the release of moisture into the indoor environment by exploiting the hygroscopic properties of bentonite.

REFERENCES

Osanyintola O. F., Simonson C. J., 2006, Moisture buffering capacity of hygroscopic building materials: Experimental facilities and energy impact, *Energy and Buildings*, 38, 1270–1282.

Grim R. E., Giiven N., 1978, Bentonites, geology, mineralogy, properties and uses. In *Developments in sedimentology*, ed. R. E. Grim and N. Guven. Elsevier, Amsterdam.

Spiess W. E. L., Wolf W. (1990). Critical evaluation of methods to determine moisture sorption isotherms. In Water Activity: Theory and Application to Food, eds L. Rockland and L. Beuchat. Marcel Dekker, New York.

Rockland L. B. (1960). Saturated salt solutions for static control of relative humidity between 5 and 40°C. Anal. Chem., 32, 1375-1376.

ASTM E 104-85. Standard Practice for Maintaining Constant Relative Humidity by Means of Aqueous Solutions. The American Society for Testing and Materials. Philadelphia, 33-34, 637(1985).

Grunewald J. (2005). Documentation of the numerical simulation program Dim 3.1; vol.1 theoretical Fundamentals; vol2. user's guide (electronic internal print).

Barbanti D., Galassi S., Pietracaprina A., Potentini G. (1996). Impiego della bentonite nel settore alimentare. Nota 1 Controllo dell'umidita relativa. Industrie Alimentari, 35, 258-262.

Keresteciogiu A., Swami M., Dabir R., Razzaq N., Fairey P., 1988, Theoretical and Computational Investigation of Algorithms for Simultaneous Heat and Moisture Transport in Buildings, FSEC-CR-191-88, Florida Solar Energy Center, Cape Canaveral, FL.

Johansson, P., Samuelson, I., Ekstrand-Tobin, A., Mjörnell, K., Sandberg, P.I., Sikander, E., Microbiological growth on building materials – critical moisture levels. State of the art. Extracts from the report SP Rapport 2005:11, SP Swedish National Testing and Research Institute.

Stazi A., D'Orazio M., Quagliarini E., 2002, In-life prediction of hygrometric behaviour of buildings materials: an application of fractal geometry to the determination of adsorption and suction properties, *Building and Environment* 37, 733 – 739.

XII DBMC
International Conference on Durability of Building Materials and Components
PORTO - PORTUGAL, April 12th-15th, 2011

Repair Mortars for Rammed Earth Constructions

Maria Idália Gomes [1]
Paulina Faria [2]

ABSTRACT

Rammed earth buildings, with resistant and monolithic walls, often have constructive pathology. A survey on more than thirty rammed earth buildings, mainly in Alentejo region (South Portugal), was conducted. As a result, it was found that surface deterioration of the walls seemed to be an usual problem.

Many rammed earth buildings are deteriorating due to lack of maintenance and rehabilitation, but also due to incorrect repairs. Several of them were repaired by applying cement-based mortars in the attempt to overcome the general decay, of the walls that could or not be deep.

This paper presents the most common pathology: problems due to water ingress and low drying capacity; salt transport and contamination; construction technology like voids left from the formworks; biological attack; different mechanical behaviour between the walls and the repair mortars - mechanical incompatibility.

An intervention methodology for repair the degradation of exterior surface, including anomalies diagnosis and application of these repair mortars, is proposed. The support samples preparation - laboratorial rammed earth blocks with surface deterioration - is also described. Finally, an experimental campaign foreseen for the development and application of earth-based mortars for repair rammed earth walls is presented.

KEYWORDS

Rammed earth walls, pathology, causes, laboratory wall samples, repair mortars.

[1] Lisbon Engineering Superior Institute, Polythecnic Institute of Lisbon (ISEL), Lisboa, PORTUGAL, idaliagomes@dec.isel.ipl.pt
[2] Nova University of Lisbon, PORTUGAL, paulina.faria@fct.unl.pt

1 INTRODUCTION

Earth buildings are nowadays redrawing the attention of professional and scientific communities due to peculiar characteristics of earth materials. They are environmentally friendly, recyclable, low cost, accessible, incombustible, provide good acoustic and thermal insulation and thermal inertia. Rammed earth - earth compacted between formworks - is among the oldest and most widespread building techniques in the world. In recent years, this technique has seen a revival and new developments. In Portugal, it has been used in new constructions and also in old rammed earth buildings rehabilitation.

For build with earth it is necessary to understand the main construction methods, the characteristics of the materials used and their mechanisms of degradation. This knowledge is also needed in order to hold proper rehabilitation and/or conservation interventions. When those factors are not taken into account it may lead to errors and premature anomalies appearance in buildings. The development of suitable repair methods for rammed earth is therefore necessary. Indeed, many old buildings are still deteriorating due to lack of maintenance or rehabilitations works, what leads to the need of deep interventions. Because the knowledge on rammed earth building techniques is still far from being consolidated, new buildings often present problems. This is related with the fact that this type of construction was not used for a long period of time and the investigation about it ceased with the appearance of new building materials, such as steel and concrete.

The anomalies are usually caused not only by one but by a combination of different agents. However, water is probably the main decay agent - moisture reduces the internal cohesion and mechanical strength of the material, increments the destructive action of soluble salts and favours biological development. The result is often the walls surface degradation. One of the major difficulties in rehabilitation works regards the correct use of repair mortars. Sometimes the repairs are inadequate due to the use of incompatible materials. The use of mortars based on hydraulic binders, as cement, is a bad example of an attempt to overcome degradation.

2 PATHOLOGY AND CAUSES OF DEGRADATION

Old earth buildings are considered vernacular architecture but, in the last decades, many new earth constructions have been built in Portugal and in other countries. In some of these countries the industrialization and regulation of this kind of buildings is becoming a reality, like the German reference, Lehmbau Regeln [2009]; however, the Code and Standard support is still not enough developed in Europe, unlike countries like New Zealand, Australia, New Mexico and USA. The preservation and conservation of these buildings, carried out by the owners, is often very weak or inexistent.

Most rehabilitation interventions, or even new constructions, do not take into account the specific characteristics of the raw material or the specificity of the construction system, leading to errors and premature appearance of anomalies in buildings. According to several authors [Guettala *et al.* 2006, Atzeni *et al.* 2008, Hall & Allinson 2009] it is important not only to understand the materials and techniques of these constructions, but also their behavior when exposed to natural agents. Surface coatings, renders and plasters have a very important function in protecting the wall against such actions as climatic - mainly water, moisture and wind -, mechanical actions or environmental contamination. They also contribute to improve thermal and acoustic comfort, namely indoors, to hide wall imperfections and to change building aesthetics. Because exterior surface coatings - paint layers and renders - are exposed to many potentially destructive actions, these elements are more prone to degradation in constructions.

Analyzing the most frequent anomalies in earth constructions, several deterioration agents can be identified, namely water which is the main degradation agent that causes the most important and frequent anomalies. When combined with other agents, water can cause serious damage to the materials. After analysing, *in situ*, over than thirty rammed earth buildings - old and new ones -

recurrent anomalies were detected in the exterior surface of the walls in a significant number of buildings.

2.1 Exterior surface pathology and causes of degradation

The pathology can range from a simple alteration to severe degradation. The main anomalies found in the exterior surface of walls are: surface deterioration - loss of cohesion, cracking, appearance of salt deposition, detachment, patch repair poorly made, dust and dirt. The main causes are: structural strain, lack of ductility, continued acess of water, salt contamination, low drying capacity, lack of adhesion to substrate and lack of rendering. They can be due to: inappropriate conception, inappropriate construction technique, the use of inappropriate materials, sloppy application, aging of materials and lack of maintenance. In many cases the exterior surface of the wall was never rendered and was not protected, the coating no longer exists or is already detached, endangering wall integrity (Fig. 1).

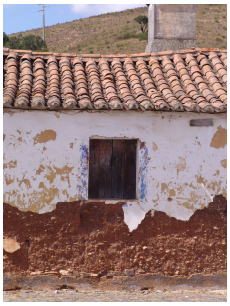

Figure 1. Rammed earth house in Bemposta, Odemira. Detachment of the coatings due to capillary rising and problably hygroscopic salts, with degradation of the wall.

In rammed earth walls is usual to detect anomalies due to the application of incompatible renders. The renders should be made of mortars with similar physical, mechanical and chemical properties with the walls where they are supposed to be applied, but often this does not happen. The main problem with renders is ensuring the long-term integrity of bond between the render and the earth substrate; this characteristic is very important but also difficult to achieve.

There are many anomalies with respect to exterior surface of walls but in this paper only the most frequent will be discussed. It is usual to observe coatings detachments, with different depths, causing wall degradation. This kind of pathology is due to different anomalies which may be, or not, associated with each other. It is usual to find very brittle coatings, with very low cohesion, that easily begin to disintegrate. This defect leads to the appearance of recesses and degradation with different depths that may even reach the support. It is mainly caused by the loss of the binder from the mortar, washed by water. On unrendered or unmaintained walls it can happens on the surface of the support. These anomalies occur mainly in more exposed areas of the wall surface like corners [Houben and Guillaud 1994].

Render cracking is another common anomalie in wall coatings, that often accelerates its rate of failure and increase the risk of water penetration. Cracks may be few but wide open or very numerous with small aperture. Microcracks may evolve into larger cracks over time. If the mortars of the new render are too stiff and cannot support the wall movements because of the incompatibility between materials - mortar and substrate -, the adherence between them can be very weak and the render may crack; the stiff and strong render can also induce the wall to break within its superficial thickness.

After the application of a mortar it will tend to shrink due to evaporation of the water contained; this shrinkage is restrained by the adhesion to the substrate and it will lead to the development of tensile stresses in the coating which may tend to crack. This shrinkage will also develop shear stresses in the plane of contact between the coating and the support, which may leads to their detachment.

Crazing is a network of fine cracks on the surface of a material; they are in infinite number very thin and linked. If the mortar is less rich in binder and applied in a thin layer, cracks are usually less deep, less spaced and the stress levels are smaller. By contrast, in a mortar with very rich binder, for example containing a high clay fraction and which is quite active, the cracks tend to be fairly wide, separated from each other but quite deep.

Salt crystallization commonly occurs near the interface between the support and the render, and it may accelerate the coatings decay and detachment. That crystallization usually produces crystalline or amorphous deposits of alkali or alkaline salts: carbonates, chlorides, sulphates and nitrates, causing usually small white or gray colourful halos in the walls surface. According to Faria Rodrigues [2005] and many other studies, the movement of salts is due to the moisture flow inside the wall that tends to carry them in its dissolved state to the surface - depending on the drying capacity of the different layers -, where they accumulate. It often occurs with problems of water penetration - as it can be the case due to capillary rising (Fig. 1). Sucessive cycles of drying/hydration of the salts produce tensions which induces loss of cohesion in the material close to the salt deposit [Gonçalves *et al.* 2007].

It is important to repair these anomalies in order to prevent the continuous deterioration of the wall and to restore its protection. For a proper intervention a right combination of the repair mortar and the substrate is needed. It may be necessary to do a quite deep repair, which may lead to multiple mortar layers. For this type of intervention compatible repair mortars need to be developed and the effect of shrinkage of the new mortars on the rammed earth walls is very important and should be taken into special account.

3 DIAGNOSIS

To achieve a reliable diagnosis for the rehabilitation of a rammed earth building it is necessary to know it beyond what is in sight. It is essential to understand: the materials used and their conservation condition, the building's structural typology, the building's current uses and the surrounding environment. The building and its surroundings are in an equilibrium that may be disturbed by the implementation of any construction works. According to Guillaud [2008], there is a "golden rule" that should be applied whenever conservation and rehabilitation interventions are needed. This rule defines the following course of action:

- observe and document the baseline condition of the building;
- minimize the intervention, with compatible materials and techniques;
- assure the reversibility of interventions;
- document the interventions;
- make a regular inspection and maintenance.

Before any intervention it will be necessary to determine which degradation processes occur and if the circumstances which led to the deterioration are complex or combined. In most cases the "domino effect" is rather drastic: one problem creates another problem, which in turn generates another and so on. The diagnosis should be sought to address the causes and origins of the anomalies found in the building. No intervention should be held while the causes and origins of the anomalies are not yet properly addressed and resolved.

4 INTERVENTION METHODOLOGIES

Mortars need to be formulated and tested in order to be applied in repair interventions. There is a premise in all mortars application, especially for those with common binders: the first layer applied should not be stronger than the substrate and the binder content should not increase along the coating thickness from the inside to the outside, avoiding the creation of tensions that could lead to craking or peeling of the upper layer. As said before, also the materials used for repairs must be compatible with the original material. These characteristics are similar between any repair mortars, being them earth-based mortars or not. Whenever possible, materials for earth-based mortars should be collected from

the same place as those originally used. It is necessary to check if the materials are suitable for the objective set and how the mortars can be further improved.

Repair mortars for total or partial replacement of renders and thickness reconstitution of the walls shall contribute to the protection of those walls being durable and without contributing to their degradation. Compressive and flexural strength and elasticity modulus should be compatible to the original support materials. The resistance to the pullout should not be higher than the tensile strength of the support. The capillary absorption should not be high but particularly the drying capacity of the new mortars can not be lower than those of the support and interior layers.

Taking into account all the characteristics mentioned, an intervention methodology based on the use of earth-based mortars is proposed, supported by an experimental campaign for the development and application of repair mortars for rammed earth walls. A variety of repair mortars will be characterized for the most critical properties - dimensional stability, mechanical resistance, adherence, water absorption and drying, durability to ambiance factors - and tested on different rammed earth laboratory blocks - samples that intend to reproduce different rammed earth walls with common anomalies.

It is necessary to choose the most promising mortars. According to Moropoulou & Bakolas [1998] the selection process of a mortar composition should be an iterative process, idea that is accepted by other authors [Válek *et al.* 2000, Veiga *et al.* 2001, Papayianni 2008]. This process should contain the following steps:

1. determination of the approximate constitution and the physical and mechanical characteristics of the original mortar;
2. preparation of a mortar similar in terms of constitution and appearance, with similar aggregates, preferably local;
3. testing to verify minimum requirements and the similarity of the main features;
4. corrections to the formulation tested in order to approximate the characteristics;
5. repetition of steps 2 through 4 until reaching a reasonable likeness of the fundamental characteristics and therefore expected proper behavior;
6. realization of experimental panels at work site;
7. again, if necessary, carry out adjustments in the formulation tested.

4.1 Rammed earth blocks

Before the execution of experimental panels at work site, and in order to develop and evaluate different repair mortars, some rammed earth blocks were manufactured. The material used was obtained from non deteriorated walls of rammed earth buildings. Ten rammed earth blocks were produced with three different compositions of soil. Each material composition represents a material gathered in a diferent building. They were particularly chosen in an attempt to represent different soils usually used for rammed earth technique in Portugal - with different grain size distribution, type of clay and colour. In order to obtain similar dry mass to the existing building wall, it was conducted a test based on LNEC Specification E205 by measuring the weight and volume of undisturbed samples, that were collected directly from the building wall. Through the values obtained in the test it was extrapolated the value of the mass needed for the volume of the each block, with dimensions 30cm $\times$20cm$\times$28cm.

Two types of anomalies, most currently found in the exterior surfaces of rammed earth walls, were recreated on the sample blocks: superficial irregularity with loss of cohesion and deep voids (Fig. 2). The block samples are being kept in a controlled ambiance - 20ºC and 50% RH. The repair mortars will be applied over the two types of anomalies, in order to verify the compatibility between the substrate and the repair mortars and the applicability and effectiveness of the intervention.

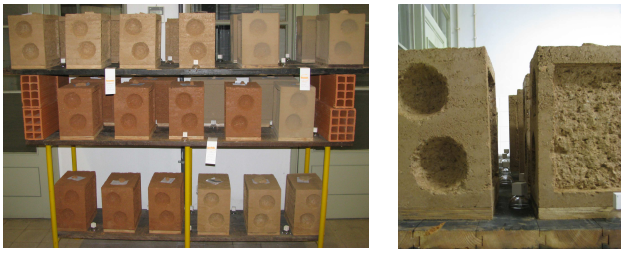

Figure 2. Rammed earth laboratory blocks with different soils and with two types of surface degradation - deep voids and superficial irregularity with loss of cohesion.

4.2 Constituents for repair mortars

Rammed earth has a relatively weak surface and cannot tolerate strong renderings. There are some recomendations in the literature for the composition of mortars for rammed earth walls: Delgado & Guerreiro [2006] recommend the use of earth-lime mortars; Ashurst & Ashurst [1995] recommend a lime/sand composition of 1:2.5/3 prepared with lime putty; Gernot [2006] refers that an earthen render should contain 5-12% of pure clay.

All earth-based mortars have a binding agent that can be only clay or added lime or cement. In the twentieth-century most of the references on conservation of earth construction, in order to improve the waterproofing properties of renders, recommended the addition of Portland cement. However some other studies refer that this component is not recommended for the repairs [Ashurst & Ashurst 1995], which may be a problem and represents a colossal mistake when used in unstabilised earth constructions [HB 195 2001, Guelberth & Chiras 2008]. Cement wicks moisture into the interior of walls causing deterioration. Also Delgado & Guerreiro [2006] do not agree with the use of cement-rich renders to cover unstabilised walls. Figure 3 shows an unrendered rammed earth house with a cement mortar in a localized repair; it is possible to see biological agents of degradation underneath the repair.



Figure 3. Rammed earth market house in S. Luís, Odemira. Left, repair with hard cement; and right, agents of degradation namely insects underneath the repair.

These recommendations can be used as a starting point but not as a rigid solution. It is well known that all cases are different (soil change from region to region) and is therefore necessary to assess which features exist in the building and try to get the best solution for a repair mortar.

The repair mortar to be used in earth buildings must have the following features: suitable workability and adherence to the support, ecological sustainability - this should be consistent with the rammed earth walls -, effectiveness as repair and protective systems. The final quality of repair mortars depends on the proportions but also on the quality of each component. It is necessary to understand the main characteristics introduced by each component. Although these recommendations, cement will be used in some compositions in order to show its problems and the results will be evaluated and compared with other ecological mortars that will be optimized, for efficient and protective repair applications.

In this study four types of components will be used for the repair mortars: clay soil, sand, eventually a binder - lime or cement - and hemp fibbers. The amount of water used will be strictly the one needed to make the mortar workable and adhesive. Also a composition for a standard soil to use for repair mortars will be pursuit. Different earth-base mortar compositions will be characterized and the most promising will be tested in the three different types of rammed earth blocks.

5 DISCUSSION

Rammed earth construction is an old traditional method but most of their characteristics and properties still remain poorly investigated. The shortage of training courses and the lack of specific specialists and researches in this area do not allow the updating of knowledge; in this field the know-how lies on elderly people that have experience (in terms of construction practices or even maintenance) but they are disappearing. However, since the last decades, the interest on earthen architecture, both nationally and internationally, raised awareness for the important gains of this construction technique, as well as for the need of its conservation and preservation.

The maintenance of this type of buildings is fundamental. If the exterior drainage of the wall base is assured, if the roof is properly functioning, if the walls are protected and if the interior ventilation of the dwellings is assured, the longevity of the building is guaranteed. In order to assure the superficial protection of the exterior walls, at least when needed, they must be rendered and painted. The paint should be compatible with the render and the render with the wall - mechanically, physically and chemically - and, for the time being, that can easily be assured with traditional and ecological materials: lime paints for finishing layers and lime mortars, earth-lime mortars or earth mortars for renders or for deterioration repair.

Lime paints and lime mortars have been investigated by many researchers all over the world; not many studies have been held for earth-based mortars. The aim of the continuity of this study, in the frame of the first author PhD, intends to contribute for a better knowledge on this type of mortars and for the possibilities of applications in order to repair two very common types of degradation that occurs in the exterior surface of rammed earth walls. As said before it is fundamental that repair mortars for this type of application must fullfill specific requirements and present specific characteristics, including compatibility with existing elements (in order to effectively protect the taipa walls) and durability.

ACKNOWLEDGMENTS

This work was carried out at LNEC, Lisbon. M. I. Gomes was supported by a doctoral grant from the Portuguese Foundation for Science and Technology (FCT). The authors are grateful to the many people from the Materials Department of LNEC, in particular to Eng. Teresa Diaz Gonçalves for her valuable collaboration in this study; also thankful to the technicians that collaborated on the experimental work, João Júnior, José Costa and João Ribeiro.

REFERENCES

Atzeni, C.; Pia, G. & Sanna, U. 2008, 'Surface wear resistance of chemically or thermally stabilized earth-based materials', *Materials and Structures*, 41, 751-758.

Ashurst, J. & Ashurst, N. 1995, *Pratical building conservation - brick, terracotta & earth, English Heritage Technical Handbook*. Gower Technical Press, volume 2, Hampshire, England.

Delgado, M. C. J. & Guerrero, I. C. 2006, 'Earth building in Spain', *Construction and Building Materials*, 20, 679-690.

Faria Rodrigues, P. 2005, 'Rendering of earth walls', in *Earth Architecture in Portugal*, Argumentum, Lisbon, 68-73.

Gernot, M. 2006. *Building with earth, design and technology of a sustainable architecture*, Birkhäuser, Publishers for Architecture. Berlin, Germany.

Gonçalves, T. D.; Pel, L. & Rodrigues, J. D. 2007, 'Drying of salt-contaminated masonry: MRI laboratory monitoring', *Environ. Geol*, 52, 249-258.

Guelberth, C. R. & Chiras, D. 2008, *The natural plaster book, earth, lime and gypsum renders for natural homes*, New Society Publishers.

Guettala, A., Abibsi, A. & Houari, H. 2006, 'Durability study of stabilized earth concrete under both laboratory and climatic conditions exposure', *Construction and Building Materials*, 20[3], 119-127.

Guillaud, H. 2008, 'Characterization of earthen materials', in *Terra Literature Review - An overview of research in earthen architecture conservation*. Avrami, E.; Guillaud, H.; Hardy, M. (ed.), The Getty Conservation Institute, Los Angeles, United States, 21-31.

Hall, M. & Allinson, D. 2009. 'Assessing the effects of soil grading on the moisture content-dependent thermal conductivity of stabilised rammed earth materials', *Applied Thermal Engineering*, 29[4], 740-747.

HB 195: Walker, P. & Standards Australia, 2001. '*The Australian earth building handbook*', Standards Australia, Sydney, Australia.

Houben H. & Guillaud H. 1994, *Earth construction: a comprehensive guide*. Intermediate Technology Publications, London.

Lehmbau Regeln. Begriffe; Baustoffe; Bauteile. Dachverband Lehm e.V. (Hrsg.), Germany: Vieweg & Teubner, 3, überarbeitete Auflage. Praxis, 2009.

Moropoulou, A. & Bakolas, A. 1998, Range of acceptability limits of phisical, chemical and mechanical characteristics deriving from the evaluation of historic mortars, Proceedings of the Worshop *Compatible Materials Recommendations for the Preservation of European Cultural Heritage*, Athens.

Papayianni, I. 2008, Criteria and methodology for manufacturing compatible repair mortars and bricks. Proceedings of the Workshop *Compatible Materials Recommendations for the Preservation of European Cultural Heritage*, Athens.

LNEC Specification E 205:1967. Determination of "in situ" dry density by the displaced water volume method (in Portuguese). LNEC, Lisbon.

Válek, J., Huges, J. J. & Bartos, P. J. M. 2000, Compatibility of historic and modern lime mortars, Proceedings of the *12th International Mansory Conference*, Madrid.

Veiga, M. R., Aguiar, J., Silva, A. S. & Carvalho, F., 2001, Methodologies for characterization and repair of mortars of ancient buildings, *International Seminar Historical Constructions*, University of Minho, Guimarães, Portugal.

XII DBMC
International Conference on Durability of Building Materials and Components
PORTO - PORTUGAL, April 12th-15th, 2011

The Influence of Slaking Time on Lime Putty

Maria Goreti Margalha [1]
António Santos Silva [2]
Maria do Rosário Veiga [3]
Jorge de Brito [4]

ABSTRACT

A new interest in the preservation of mortars, plasters and decorative finishings in façades has emerged in certain European countries in the past thirty to forty years, with a view to understanding how they have evolved throughout History. There is a growing interest in learning about the composition and execution techniques of original surfaces and a number of Heritage Institutions have encouraged the systematic application of conservation in this area.

Up to the XX century, limes were often used in work as lime putty. After the transformation of quicklime into lime putty the latter was stored to maintain its characteristics. Tanks or large pits were used to store the lime putty, always covered with water in order to prevent its carbonation. The quality of the material was guaranteed for many years with this process.

The evolution of the storage processes for materials has led to a change in this procedure and in most cases binders are now used as powders.

The influence of the maturation time of lime putty has been studied. The aim of this paper is to present the physical and microstructural changes on lime putty due to the effect of ageing, focusing on the particle size of the portlandite crystals and on the reorganization of the internal structure.

KEYWORDS

Mortar, air lime binders, lime putty, slaking time

[1] Municipality of Beja (CMB), Beja, PORTUGAL, goreti.margalha@cm-beja.pt
[2] National Laboratory of Civil Engineering (LNEC), Lisbon, PORTUGAL, ssilva@lnec.pt
[3] National Laboratory of Civil Engineering (LNEC), Lisbon, PORTUGAL, rveiga@lnec.pt
[4] DECivil-IST, Technical University of Lisbon (IST), Lisbon, PORTUGAL, jb@civil.ist.utl.pt

1 INTRODUCTION

The fine conditions in which many ancient mortars still are today proves beyond doubt that the binder preferably used for centuries, lime, has high quality.

Slaked lime putty stored with excess water guaranteed the material's quality for many years. As an example Duquesnay [1883] refers that in Landsberg, near Meiningen in Germany, a lime pit 300 years old was found with lime putty carbonated only to a few centimeters of depth, the rest remaining in good conditions even if a bit dry.

There are references to the need for the slaking period of the lime to be extended to guarantee its quality. Plinius for example stood for a three-year delay before lime were used [Millar, 1897].
Plasticity gained during this slaking time has been empirically known for a long time. Nowadays this property is attributed to the morphology and dimensions of the portlandite crystals and to the water retention capacity [Rodrigues -Navarro, 1998, Margalha, 2010].

The improvement of lime mortars quality, based on quality factors involving its constituent materials, namely lime, the aggregate or the addition of other components, is important for them to acquire proper characteristics with the usual resource to hydraulic binders such as Portland cement.

It is necessary to know all the potential of lime for its use to be reactivated in adequate conditions. Since this binder was used for centuries as putty with large slaking periods in mortars that are still in a good conservation state, it is important to understand the factors that have contributed to that.

2 EXPERIMENTAL WORK

2.1 Techniques

The set of tests selected mainly aimed at understanding the physical and microstructural changes of lime putties due to the effects of aging.

The thermo gravimetric and differential thermal analyses, TGA-DTA, are both thermal techniques of materials characterization that allow measuring continuously the mass and temperature variations, as a function of the temperature imposed and of time, in samples that are heated (or cooled) at a constant rate.

The microstructure of lime putty was analyzed in an environmental scanning electron microscope (ESEM) complemented by an x-ray microanalysis spectrometer (EDS). The ESEM analysis allowed visualizing the damp samples, at amplifications of 8000x and 10000x, and verifying microstructural changes with time. These observations were complemented with the use of a high-resolution ionic beam microscope (FIB), at amplifications of 15000x and 25000x, which emits a beam of ions of varying energy and allows the observation in depth of the microstructure of materials.

2.2 Materials

The industrial slaked lime putty used (CL90) is produced from Alcanede limestone. The chemical characteristics of the limestone and corresponding lime are presented in Table 1.

Table 1. Chemical composition of Alcanede limestone and lime (mass %)

Sample	*CaO*	*Fe_2O_3*	*Al_2O_3*	*SiO_2*	*MgO*	*SO_3*	*Fe_2O_3*	*K_2O*	*MnO*	*CuO*	*LOI**
Alcanede limestone	52.3	0.1	0.7	0.4	1.5	0.2	0.1	0.8	0.06	0.06	44
Alcanede lime	71.9	-	0.1	0.2	-	0.2	0.03	-	-	-	27.6

* Loss of ignition determined by ATG-ATD in the range 20 ºC to 1000 ºC

The TGA-DTA tests were performed on limes with maturation times of 1 month, 1, 3 and 5 years. Using ESEM the initial extinction phase was observed for 20 minutes and after approximate maturation times of 4 and 24 hours, 1, 8 and 9 months and 5 years. Using FIB limes aged lime putties were observed with 4 months and 5 years.

3 RESULTS AND DISCUSSION

3.1 TGA-DTA analysis

Lime putty incorporates water in different ways. Part of this water is chemically unbound and is easily separated from lime through drying, at 100 ºC, being identified as free water or capillary water. Water may also be adsorbed linked to lime particles by physical forces, only to be released at higher temperature, of 350 ºC. Finally, chemically combined water present within $Ca(OH)_2$ is released between 350 ºC and 600 ºC.

By drying limes at 100 ºC a direct relationship was established between lime slaking time and amount of free water incorporated (Table 2). In the older lime putties, from 3 years upwards, the amount of free water is kept practically constant and close to 50%. In the intermediate lime putty, 1 year, a higher amount of free water was registered, i.e. 58%, by weight. In the more recent putties, with slaking time of 48 hours and 1 month, the amount of free water incorporated in the putty is even higher, around 64%.

Table 2. Determination of mass loss of lime putties when heated at 100 ºC

	Slaking time				
	48 hours	*1 month*	*1 year*	*3 years*	*5 years*
Lime putty left to dry (g)	42.06	50.09	39.36	36.97	40.49
Dried lime (g)	15.12	18.10	16.65	19.06	19.90
Free water within the sample, by weigtht (%)	64.05	63.87	57.69	48.44	50.85

In limes putties dried at 40 ºC (Table 3) the greatest percentage of free water incorporated in the putty is lost, even though further loss is reported when heating at 100 ºC. The most recent putties, 1 month or less old, contain more free and adsorbed water in their composition. Slightly higher values of water chemically bound were also registered in these limes. During lime maturation the paste gradually becomes more compact, i.e. the same percentage of calcium hydroxide takes up less volume.

Table 3. Water (in %, by weight) within limes with different slaking times previously dried at 40 ºC

Samples (slaking time)	*Temperature range (ºC)*		
	25→350	*350→600*	
	Free and adsorbed water	*Chemically bound water*	*Total loss*
1 month lime	3.5	21.5	25
1 year lime	0.8	20.8	22
3 years lime	0.7	17.2	18
5 years lime	0.9	19.2	20

In the TGA/DTA readings (Figure 1) of limes dried at 40 ºC it is clear that most free water has already been eliminated since low mass losses are registered in the 25-200 ºC temperature range. The main differences found are in the most recently slaked lime (1 month) where a higher intensity peak around 100 ºC is found, corresponding to loss of free water. Since this is the lime putty with the shortest maturation time it is also the one that loses the most water at low temperatures. The percentage of $CaCO_3$, corresponding to the mass loss between 550 ºc and 850 ºC, is higher in the limes with the longer

maturation time (5 and 3 years) and lower in the 1 month lime. This is due essentially to the greater carbonation rate of the older limes that can be related to the size of the calcium hydroxide crystals.

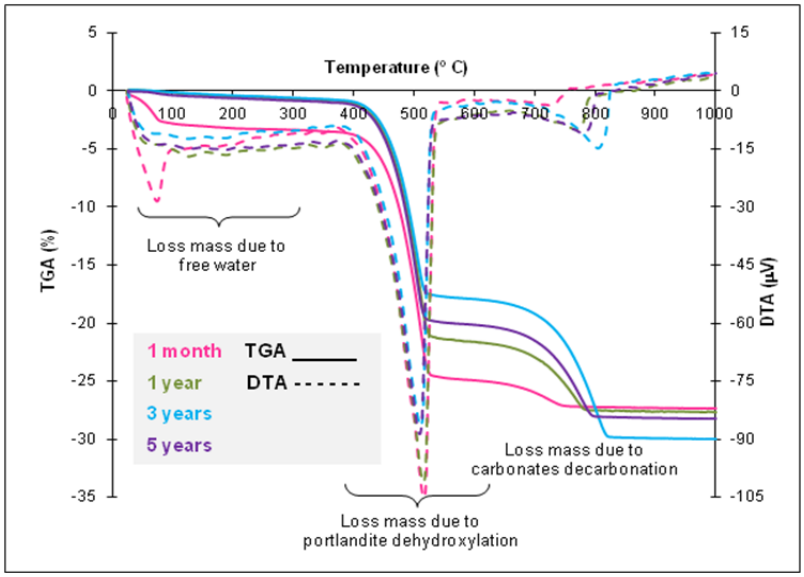

Figure 1. TGA/DTA chart of the 1 month, 1, 3 and 5 years, lime putty previously dried at 40 ºC

3.2 ESEM and EDS analyses

The observations made with ESEM aimed at analyzing lime putty, with no previous drying, at different slaking stages and also at observing a lime whose slaking occurred within the chamber for a 20 minute period. The initial slaking stage of the quicklime was observed by letting water inside the chamber.

An Electroscan 2020 ESEM with a Peltier stage was employed. The sample was introduced into the chamber and imaged using the standard procedure at 733 kPa. The sample was then cooled to 5°C and the chamber pressure increased to 1040 kPa. Water was allowed to condense on the surface of the sample holder sufficient to just cover the calcium oxide particles. The pressure was then adjusted manually to maintain the desired water film thickness. Following the reaction of calcium oxide with water, the pressure decreased to 733 kPa and the sample temperature increased to 15°C. The procedure described above was repeated at intervals allowing the sample to be imaged after total exposure times to the water film of 5, 10 and 20 minutes.

The condensation of water became visible on the sample surface after the chamber pressure had been increased to 1040 kPa with the sample at 5 °C. The water shows up as dark patches on the sample which grow during the sequence. igures 2 and 5 show sets of images taken at exposure times of 0, 5, 10 and 20 minutes respectively. Each set of images contains typical structures viewed at magnifications of 8000x.

Changes in the morphology of the sample throughout the experiment were observed. Figure 2 shows the morphology of the calcium oxide before hydration in water. The angular nature of these crystals suggests that sintering has not occurred and burning has been efficient. Figure 3 shows the structure of the calcium oxide after 5 minutes in water. Small crystals are visible on the surface of the oxide particles in Figure 3. The structure after 10 minutes is shown in Figure 4. A dramatic change in morphology is observed. A complex structure, shown in Figure 4, was observed in material adjacent to the aluminum stub. Figure 4 shows a crystal with edges resembling portlandite. After 20 minutes in contact with water the recognizable hexagonally angled facets of portlandite plates are clearly visible in Figure 5. These crystals are particularly noticeable in the centre of the image in Figure 5. The crystals range in size up to approximately 5 microns. The calcium oxide was successfully hydrated in situ within the ESEM. Crystals clearly resembling portlandite are shown after 20 minutes.

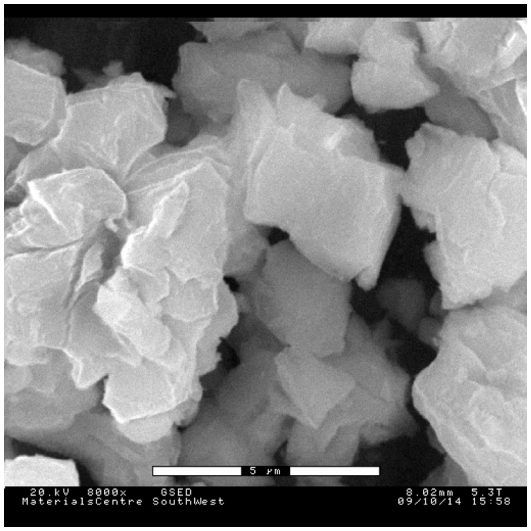

Figure 2. Un-hydrated calcium oxide after immediate insertion into ESEM (8000x)

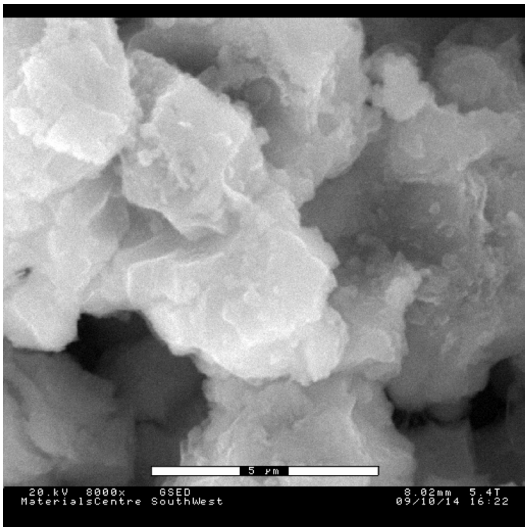

Figure 3. ESEM image of calcium oxide after 5 minutes of hydration (8000x)

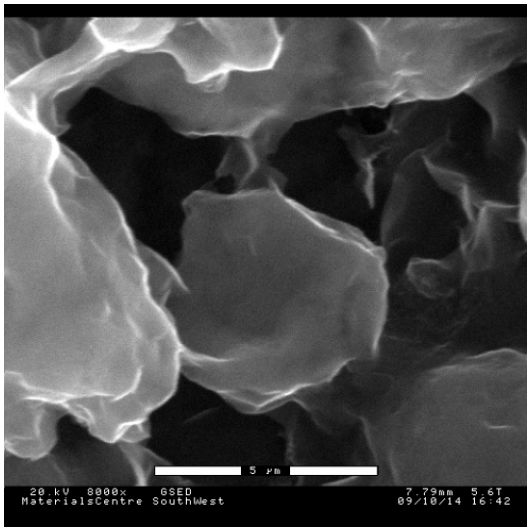

Figure 4. ESEM image of calcium oxide after 10 minutes of hydration (8000x)

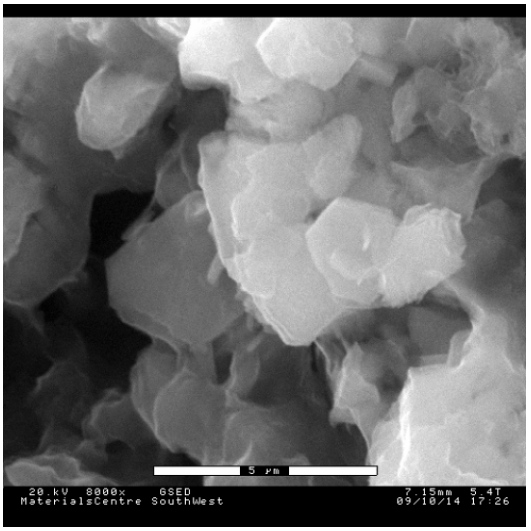

Figure 5. ESEM image of calcium oxide after 20 minutes of hydration (8000x)

Limes observed with 24 hours, 1 and 8 months and 5 years of slaking time were previously kept for a few seconds under a water surface because it would not be viable to keep them inside the chamber for very long periods. Lime putties with 24 hours and 1 month have a less defined structure than older lime putties with 8 months and 5 years (Figures 6 to 9). A densification of the putty that becomes less porous with aging time is visible. There is a change in size of the crystals within the lime putty. The lime putty with 24 hours has an incipient structure made of prisms. After 1 month the structure is still ill-defined but start the formation of hexagonal portlandite crystals packed in layers. In the 8 month aged lime these crystals are already well defined and started to separate into finer crystals. The 5 year putty compared with the 8 month putty shows separated finer crystals, with a great decrease in particle size generally with a diameter on the hexagonal surface smaller than 1.3 µm.

According to some authors [Rodriguez-Navarro et al., 1998; Cazalla et al., 2000; ELERT et al., 2002; HANSEN et al., 2008], who observed fresh and aged lime putties with 2 months, 1 year and 14 years, the portlandite crystals change their shape over time from prisms to thin plate-like crystals.
Hansen et al. [2005], who have studied two limes from distinct origins, industrial and traditional, concluded that 1 year maturation changed the size of the crystals and their morphology, and using DRX they registered a reduction of the prismatic particles and an increase of the small plates.

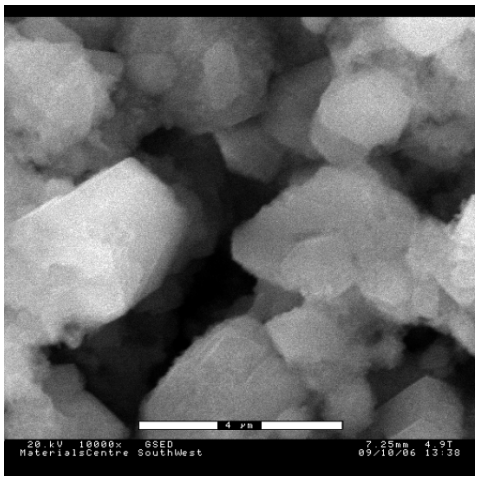

Figure 6. ESEM image of a lime putty after 24 hours (10000x)

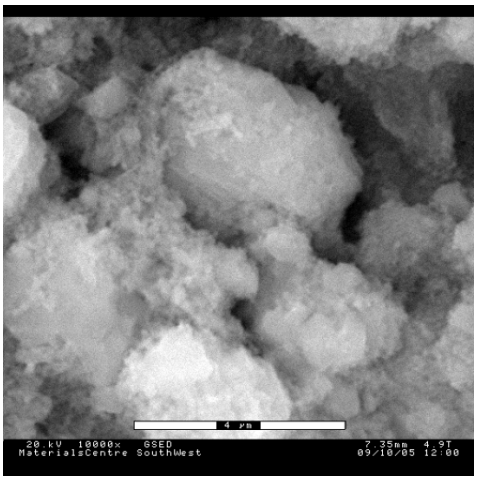

Figure 7. ESEM image of a lime putty after 1 month (10000x)

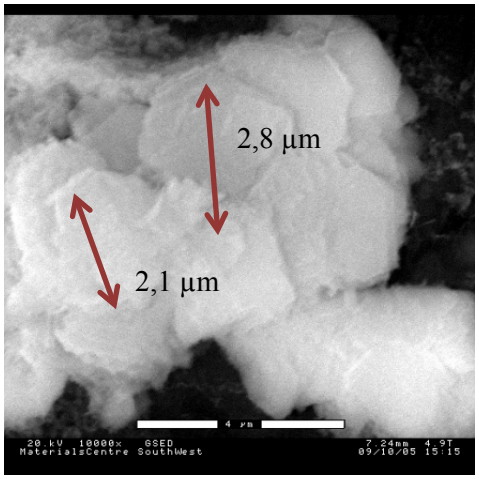

Figure 8. ESEM image of a lime putty with 8 months (10000x)

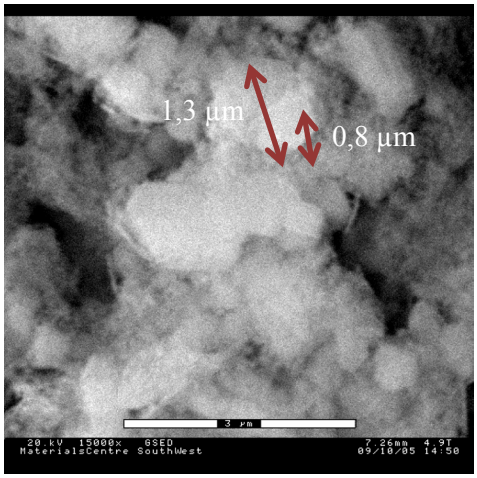

Figure 9. ESEM image of a lime putty with 5 years (10000x)

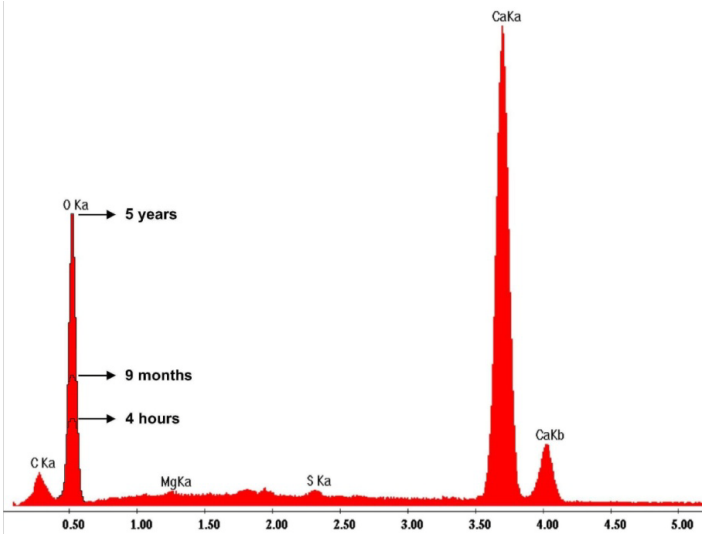

Figure 10. EDS spectrum of a lime putty after 4 hours, 9 months and 5 years

Lime putty gets more compact and takes up less space as the maturation time increases in agreement with the results obtained in the TGA-DTA observations where it was found that aged lime putties con-

tained smaller amounts of free water. The EDS analysis of limes with 4 hours, 9 months and 5 years (Figure 10) show that oxygen content increases with maturation time, which correlates well with the greater percentage of $Ca(OH)_2$ in the aged lime putties.

3.4 Observations in FIB

Visualizing the samples in FIB revealed a dense structure of the 5 year lime putty and a more open structure of the 4 month lime putty. The hexagonal shaped portlandite crystals are not completely visible but the shape can be glimpsed underneath the carbonated skin, with much finer dimensions in the 5 year lime (Figures 11 to 14).

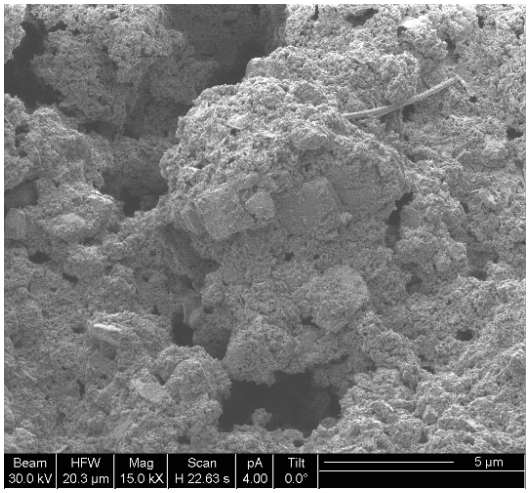

Figure 11. FIB image of a lime putty with 4 months : 15000x

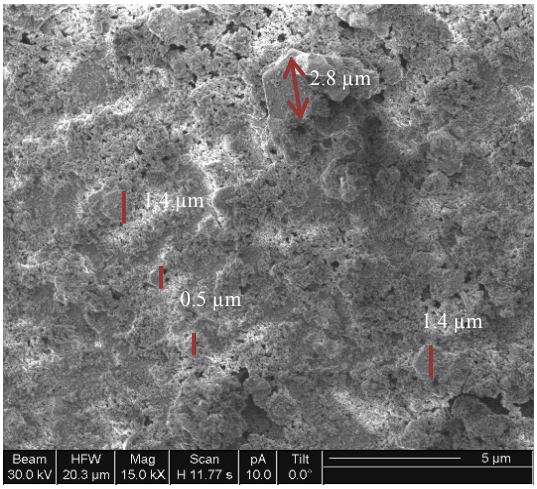

Figure 12. FIB image of a lime putty with 5 years: 15000x

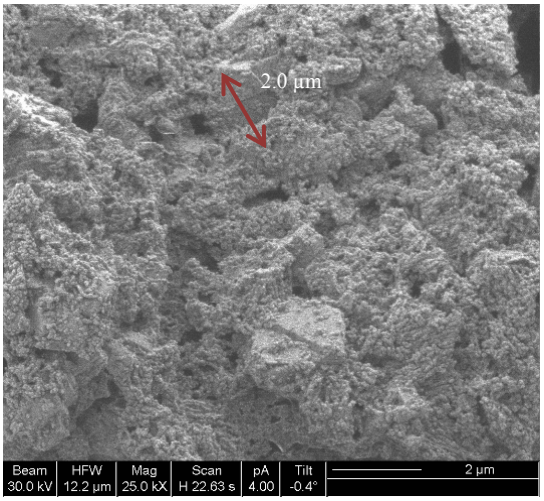

Figure 13. FIB image of a lime putty with 4 months: 25000x

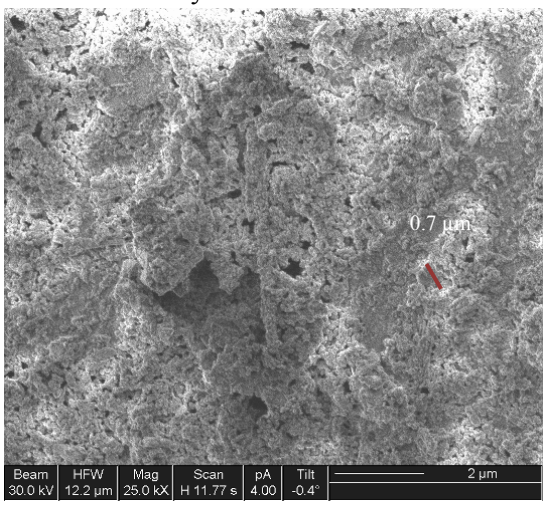

Figure 14. FIB image of a lime putty with 5 years: 25000x

The observations in ESEM and FIB allow concluding that portlandite particles decrease in size as maturation time increases and, also according to the preliminary TGA tests, free water separates itself from the putty with aging and a densification of the crystalline structure.

4 CONCLUSIONS

Slaking lime putty has the great advantage of not loosing qualities with storing since water is a slow diffuser of carbon dioxide and therefore stops lime from carbonating, thus remaining indefinitely as calcium hydroxide. Lime putties with a shorter aging time contain more free water that those with a longer time. It was found that the greater part of this mass is lost by drying at 40 ºC.

The various techniques of analysis used allowed confirming the change of physical and microstructural characteristics of lime putty with aging time.

The crystals of calcium hydroxide mostly hexagonal shaped are smaller in the aged lime putties (5 years), mostly < 1.4 μm, with a great quantity of particles near 0.5 μm, while in the 8 and 4 month putties these sizes range from 2.0 μm to 2.8 μm. This small dimension of the calcium hydroxide particles in the aged lime putties seems to justify the greater reactivity they usually display [Cazalla et al., 2000; Margalha, 2010].

Lime and particularly lime putty has played a unique role in construction throughout History and its use must be reactivated mostly when the intention is to preserve or restore ancient buildings, since it is the binder most securely compatible with the materials that make up ancient walls.

ACKNOWLEDGMENTS

The authors thankfully acknowledge the support of the National Laboratory of Civil Engineering, in Lisbon, where the experimental work presented here was performed, of the ICIST Research Institute from IST, Technical University of Lisbon and of the Interface Analysis Centre, University of Bristol. They also thank the support of the Portuguese Foundation for Science and Technology (FCT) which partially financed this research, within Research Project PTDC/ECM/100234/2008 - Conservation and durability of historical renders: compatible techniques and materials and of the Portuguese Foundation Calouste Gulbenkian that supported the PhD scholarship of the first author.

REFERENCES

Cazala, Olga, Rodriguez-Navarro, Carlos, Sebastian, Eduardo, Cultrone, Giuseppe, De La Torre, Maria José 2000, *Aging of lime putty: effects on traditional lime mortar carbonation*, Journal of the American Ceramic Society 83(5), pp. 1070-1076.

Duquesnay, M. 1883, *Encyclopédie chimique - calcaires, chaux, ciments, mortier*, Dunod, Paris, France, 47 p.

Elert, Kerstin, Rodrigues-Navarro, Carlos, Pardo, Eduardo Sebastian, Hansen, Eric, Cazalla, Olga 2002, Lime mortars for the conservation of historic buildings, Studies in Conservation, 47, pp. 62-75.

Hansen, E.F., Balen, K. Van, Rodriguez-Navarro, C. 2005, *Variations in high-calcium lime putty and mortar and properties resulting from the use of freshly-slaked quicklime and commercial dry hydrated lime*, International Building Lime Symposium, Orlando, USA, CD.

Hansen, E.F., Rodriguez-Navarro, C. Balen, K. van 2008, *Lime putties and mortars. Insights into fundamental properties*, International Studies in Conservation 53, pp. 9-23.

Margalha, Maria Goreti 2010, *Mineral air binders, The influence of slaking process and curing time on their quality (in Portuguese)*, PhD Thesis in Civil Engineering, Instituto Superior Técnico, Technical University of Lisbon, Portugal.

Millar, William 1897, *Plastering. Plain and decorative*, Donhead, London, UK.

Moropoulou, Antonia, Bakolas, A., Moundoulas, P., Aggelakopoulou, E., Anagnostopoulou, S. 2005, *Strength development and lime reaction in mortars for repairing historic masonries*, Cement & Concrete Composites 27(2), pp. 289-294.

Rodriguez-Navarro, Carlos, Hansen, Eric, Ginell, William S. 1998, *Calcium hydroxide crystal evolution upon aging of lime putty*, Journal of American Ceramic Society 81(11), pp. 3032-34.

XII DBMC
International Conference on Durability of Building Materials and Components
PORTO - PORTUGAL, April 12th-15th, 2011

Investigation the Effects of Fire Precautions on Durability of Building Materials

Nuri Serteser[1]

ABSTRACT

Historic buildings on which have to be taken special considerations are the most important cultural heritage of nations. Although many of historic buildings have somehow protection measurements against fire unfortunately every year hundreds of them are destroyed partially or completely in case of fire accidentally or deliberately.

Fire is still one of the biggest threatening factors for the historic buildings which can cause destruction of them and its contents in only a few hours. Not only the building itself but also the irreplaceable work of arts have been seriously damaged or lost due to destructive nature of it.

Historic museums can be present much more hazardous conditions for fire. Highly combustible contents like extremely dried wood surface linings, draperies, furniture with easy flammable surface materials poses critical fire situations. A dilemma can possibly be happen when we decide to establish fire precaution hardware on the building like detectors, sprinkler heads, fire hoses etc. in the domain of the building while saving the architectural and historic character of it. Especially the techniques which do not diminish the durability of the original material properties have to be used in application.

Dolmabahce Palace which is one of the magnificent historic buildings in Turkey's history is investigated in respect to the fire precaution effects on durability of material properties.

KEYWORDS

Fire fire precautions historical buildings material durability

[1] Faculty of Architecture of the Istanbul Technical University (I.T.U.), Istanbul, TURKEY, serteser@itu.edu.tr

1 INTRODUCTION

A big part of our duty as a human in our life is responsibilty not only for the human being but also for the buildings that compose our cultural heritage. They constitutes a strong bridge with their past and future of the communities which belongs to. Historic buildings shall be considered by the societies that the work of previous generations is an important part of their culture. They are a valuable part of our environment. Due to the features that they have like age, history, appearance, materials, and craftsmanship all combine to make each one a unique, non-renewable resource [Watts Jr. 2001]. When we look at over the last 40 years, it is clear there has been considerable technical development and philosophical change regarding the preservation and repair of older and historic buildings. Additionally new requirements have been placed on the performance of buildings, like the improvements on fire safety area [Simith & Elefante 2009].

Fire, may be, the most dangerous phenomena for buildings when the effects are compared with the other threatening factors like degradation, decomposition or dampness. It is the most hazardous one amongst them due to its rate and destructive effect. Fire protection can be defined as a sophisticated balance between the needs of the building, its user and its use [Taylor]. Historic buildings have long been under served by the architectural and engineering professions related to fire safety. They have suffered from inadequate attention and protection, given the difficulties and costs involved in retrofitting them to meet current standards. Due to their historic nature professionals who have responsibilities in taking care of them worry about the aesthetic impacts and limited access to concealed spaces. Many curators fear that unproper installations will destroy a building's historic character, or that water discharge from a suppression system will destroy rare collections. Additionally historic buildings do not conform to the generic construction model on which modem codes and fire protection systems are based. Generally fire codes for new construction focus on life safety whereas historic buildings present an additional challenge that of protection of the property itself [Kaplan & Watts 1997].

The function of an existing building may be changed during its lifetime and can be assigned to completely diffirent function than before. This kind of function change may affect the level of fire safety degree of the building. There is a delicate balance between preserving the economic viability of reusing existing buildings and avoiding intrusive alterations to or demolition of significant architectural features . Moreover there should be more concern for preserving our built heritage from destruction by fire [Watts, 2003].

2 CONSIDERATION FOR LIFE SAFETY AND/OR BUILDING PROTECTION

2.1 Role of Fire Codes and Regulations

EU has been conducted and supported several researchs about historic buildings and importance of their fire safety. The research of "Position of Fire Safety of Cultural Heritage in the Regulatory System in Various European Countries" which has been printed on February, 2005 is directly related to this issue. According to the report of the commission named "Fire Risk Evaluation to European Cultural Heritage-FIRE-TECH" founded for identification of priorities and rehabilitation on fire safety strategies there would not being mentioned the term "cultural heritage" on the fire regulation of 10 of 13 countries which participated into the researh. There are only three countries which have separate regulations for fire safety of cultural heritage are Italy, Switzerland and Portugal. However other countries have similar sanctions for fire safety of buildings on their fire regulations they have not any distinct regulations for saving their historic buildings against fire demolition.

In Turkey, despite there is no specific sanction for the fire safety of historic buildings on the National Fire Regulation, 2002 but only some rules exist for the buildings having historic attributes that has subjected to functional change. While implementing of these rules as it is mentioned on the regulation

for the fire-safety installation on the buildings which has been registered as a cultural heritage for saving it is necessary to have the remark of the commission assigned [Serteser & Ozgunler 2006].

It can be taken the advantage of the other codes accepted the validity worldwide like NFPA. According to NFPA 5000 (Building Construction and Safety Code**)** buildings shall be designed and constructed to reasonably preserve the original quality or character of a historic building, structure, or site [NFPA 2006]. In another code of NFPA, 914 (Code for Fire Protection of Historic Structures) requirements for protection of historic structures from fire while protecting the elements, spaces and features that make these structures historically or architecturally significant are provided [NFPA 2001]. NFPA 909 (Code for the Protection of Cultural Resource Properties-Museums, Libraries and Place of Worship) is a kind of guide sequencing the least common requirements for saving historic and cultural buildings like museums, libraries and place of worship [NFPA 2005].

2.2 Team Working for Succesfull Design

Adapting lots of code provisions to an historic building is generally more difficult while modern buildings are designed from the outset to allow the occupants to leave quickly and easily in the event of a fire without any harm. Primarily two desing factors must be considered: either the people living, working or visiting the premises or the building fabric and its contents will be protected against fire. In case of the building concerned is also used for the public visiting, the life safety measures will have a greater importance. Law concerns only the provision for life safety and adequate means for escape, not the protection of property. Whereas conservationists are primarily concern with preserving the building fabric without the intrusive effects and loss of fabric that are the inevitable consequences of most standard fire precaution measures [Forrest 1996].

Working in historic buildings require to set up a professional group initially. As a part of the group the fire protection specialist needs to work closely with the historical preservationist to determine what aspects of the building are of historical significance. Then an approach is determined together to come up with the acceptable level of fire safety sollution for the building [Koffel 2010] It must be understood well that the historic features are uniqe and irreversible for a historic building and to ensure a proper installation of systems the system designer and installation contractor must work closely with the preservation architect [Artim 2003].

There would be two type of approaches to follow for the design team members: fire protection and fire prevention. The former is related mostly to technology and the other is related to mangement of fire strategies. Sometimes it is also possible to make a selection from the elements of fire-protection and fire prevention strategies that incorporate both together. The best thing to achieve fire safety is a considered interaction of management and technical solutions. At the same time to integrate the design sollutions on the context of the historic building the best way is to provide involvement of the broadest number of stakeholders like design professionals, preservation professionals, building owners etc. [Kaplan 2003].

The nature and science of fire can be understood easier with the fast developments on recent years. Despite these kind of develoments in building technolgy a specifier does not need to rely on the prescribed standards for the design. Instead a specific tailored solution which gives more advantages for the existent building can be derived. Risk assesment which is featured in the comprehensive fire safety of the building have a key role in determination of the total risks for life and property safety. Satisfying life safety issues and property protection requirements have to be balanced in a concious design by describing identified and quantified fire risks [Forrest 1996].

2.3 Fire Safety Measures

As a requirement of safety issues on buildings new facilities and renovation projects need to be designed and equipped with efficient, cost-effective passive and active fire protection systems. The purpose of the installation of these systems are to detect a fire in its preliminary stage, to provide containment, controlling and/or extinguishing a fire effectively before it spreads out. Integrated systems approach enables the designer to analyze all of the building's elements as a part of whole building's fire protection plan. This kind of analysis requires more than code compliance or meeting the minimum legal responsibilities for protecting a building. The role of building and fire codes are to protect building users against loss of life and limit fire impact on the community. To achieve a balaced design that gives a satisfying level of safety it is necessary to creatively and efficiently integrate code requirements with other fire safety measures as well as other design strategies like evacuation, recovery, smoke discharge etc. [WBDG 2010].

Mostly the automatic sprinkler systems assigned to protect the property against fire hazards. If this kind of suppression systems can not be applied due to the appearance of sprinkler heads on inner surfaces time lag for detection is very important in a closed environment. Before developing a fire in its initiated location and suppress and extinguish it is a vital process for the buildings having a sprinkler system. If it is not ensured to put a permanent officer in the building there have to be provide a 24-hour attendance who is skilled to detect a fire, can use fire fighting facilities and can cope with a fire in early stage. Providing a continuous attendance means early detection and intervention on time by fire brigade [Forrest 1996]. Effective fire prevention measures such as staff training and smoke detection systems are often relied on as an alternative to fire suppression. But on the other hand this kind of early detection systems by smoke detectors do even not submit a gurantee situation in fire conditions with automatic dialling [Gibbon & Forbes 2001].

Advances in fire-safety installations make better sollutions possible in future in terms of penetrating the historic building fabric with less effect than the available technology. It will be possible to use piping with smaller diameters and more flexible, will be used wireless technology in detection systems instead hard-wired cabling and moveable equipment providing interim detection and suppression will be available. The design must be carried out with less impact on the fragile fabric of historic building and it might be anticipate that the next generation of the fire-safety installation will be less invasive by taking into account the life expectancy of the installation may be less than 25 years [Kaplan 2003]. In ideal, all piping and cabling should be concealed in the domain of the building. But this may not possible in every building due to its specific design, architectural details, structural system and other obstructions. Concealment of the elements of installations makes the design expensive. So each space have to be determined by system designer and preservation architect whether it will have installation elements remained exposed or concealed.

Consequently it is not possible to design and apply an excellent system without intrusing to the fabric of the historic building. The important thing is to which degree it intruces to the fabric and to what degree the safety plan will be succesfull [Artim 2003].

3 FIRE PRECAUTIONS IN DOLMABAHCE PALACE

The Palace of Dolmabahçe, completed in 1856, is the third largest Ottoman palace in Istanbul. It embodies, in its very form the social and cultural structure of the period, of which is stylstically typical. Dolmabahce was a prestigious addition to the urban silhouette of Istanbul built on a prominent site at the entrance to the Bosphorus. It stands at a focal point in the fast groving 19'th century city and was built at a time of increasing enthusiasm for all things occidental.

The style of the palace has, in fact, been variously interpreted by different sources of the period. It was the product of eclecticizm. The plan bears both Occidental and Turkish features, while the

ornamentation both inside and out reveals Baroque, Roccoco and Empire features which have been skillfully amalgamated in one building by the Ottoman architects.

The palace contains a total of 285 rooms, 43 halls, 6 terraces and 6 hamams (Turkish bath) over a total area of 14.595 m^2. The façades are pierced by 1427 windows and there are 25 doors to the palace, each with a different function, giving access from the shore and gardens. The walls of the palace are stone with brick infill-frame and faced with ashlar. They support a roof of timber surfaced with lead. Over the Muayede Salon the timber sloping roof acts as a most unusual outher membrain for the dome covering the wall, while the crystal staircase in the Mabeyn-I Humayun vaulted over with a glass roof. The interior structure-walls, ceilings etc. wood. Various kinds of sandstone were used on the façades along-side stone from Marseille and Trieste. The structural timbers are mainly pine and oak, together with some African and Indian woods. Some of the ceilings are casetted, each casette bearing different decorations.

Much of the palace is covered with parquet flooring, some of which is intricate. The doors, of mahogany and walnut are also decorated with marquetry. Some furniture were made by order for the palace while it was under construction, while other pieces were gifts from other European countries, and far eastern countries such as China, India and Egypt. Turkish fabrics were used throughout for the furnishings, mainly pure silks woven on the imperial looms at Hereke [National Palaces 2008].

The Palace is full of flammable objects which consistute high fire load for the building. Evacuation is provided by using the 16 of emergency exits located inside the palace. These exit doors belong to the original plan arrangement and have not been added after the completion of the construction. They were used by the building staff previously but now serve to the visitors in emergency situations. Therefore all of them sealed with a weak wire preventing visitors not to use them except emergency.

Smoke discharge neither passive nor active ways couldn't be provided due to the historic nature of the palace. Although it is crucial issue letting the smoke goes out in case of fire but the original structure and architectural composition of the building does not allow to apply this kind of system on the fabric.

A permanent 24-hour attendance by fire brigade that consists of well educated staff to detect and intervene to an initiated fire immediately has been provided. They provide a regular attendance and control in certain locations with pre-determined intervenes. They also monitor the detection system electronically by using computers in the control center where the fire control panel is located. The palace has been divided into fire zones and each zone has been equipped with detector heads which are sensitive to heat, smoke and smell effectively. Each zone has a certain amount of detector heads and all of them connected to the central detection panel by cables. Cables serving to the detectors has been concealed into the context of the ceiling surface coating in the rooms that have special importance. The concelament of cables gives less impact on the surfaces that pass through. An application of the detector head can be seen in Fig.1.



Figure 1. Detector head located on a ceiling of a room having special importance

On the other hand the detector heads located on the ceiling of the rooms having less importance have been equipped with exposed cable lines. Fig.2 shows this kind of application in its palace.



Figure 2. Detector head located on a ceiling of a room having less importance

When the detectors detect an unusual effect from the inner space that they protect, it is addressed by signals electronically and devices giving light and sound are also triggered simultaneously.

Automatic sprinkler system does not assigned in the palace for suppression purposes. Instead wet-pipe type fire hose cabinets having hard-round fire hoses have been located at the distances according to the limits allowed by National Fire Regulation. All the pipeline supplying water to the cabinets has been located into the passageways that has been built below the ground floor level. Therefore it is not possible to see any kind of pipeline in the rooms which has great importance. But on the other rooms having less importance the pipes bring water for the hose cabinets can be visualized easily. Fig.3 shows one of the fire hose cabinet left exposed to the inner space.



Figure 3. A fire cabinet and the pipeline serving to it left exposed

All pipeline of the fire-safety installation had been moved into that passageway 6-7 years ago as a design strategy. Application of this design desicion supports the durability and lifetime of building materials in a better way allowing less penetration and invasion to the historical fabric.

As a fire-safety strategy to extinguish fires nearly 1500 portable extinguishers of ABC type including monamonium phosphate has been positioned in different locations of the palace. Additionally some other devices having halocarbon and CO_2 for the rooms containing electronics have been utilised for fire fighting. Morover 6 fire cupboards having some type of equipments used for immediate intervention to a fire has been placed distictly in some critical places for fire.

There is a pump location on the garden having one diesel and one electric power pumps and both connected to a water tank of 240.000 lt on the ground for emergency.

It is prohibited to use any kind of device that produces flame or sparks while operating without having permission of fire brigade office of the palace. It can be allowed only by taking some special cares and having a staff from fire brigade office who accompanies to that issue.

4 CONCLUSION

Fire protection in historic buildings is an important subject and needs to have much more consideration than the buildings newly designed or constructed.

It requires a group of professionals working close each other in consistency and each member of the group must be aware of the importance of the fire safety apporoach for a historic building having special importance. The level of safety agains fire must be determined by working of that group and it involves participation of each stakeholders simultaneously.

Building fabric in historic buildings is more vulnarable than the others. It is obvious that it is impossible to achieve succesfull integration of the fire-safety measures within building without invasion to the fabric. But the level of that invasion is the key point for a succesfull integration.

Dolmabahce Palace is one of the paramount historic heritage of Istanbul and it has been protected with active and passive fire-protection measures. Existency of a permanent 24-hour fire brigade attendance is a great importance for it. Every room is monitored by a computer system regularly and the palace has been equipped with portable extinguishers in quantified numbers. Permanent fire-hose cabinets provide water for extinguishment fires in the building domain. All the pipelines travels throughout the passageways under the building. Therefore application of this fire-safety strategy supports the durability of the building materials while permitting less invasion to the historic fabric.

REFERENCES

Artim, N. 2003, 'Automatic Fire Suppression for Historic Structures: Options and Applications', *APT Bulletin*, **34**[4], 35-40.

Forrest, R. 1996, 'Strategic Fire Protection in Historic Buildings' , (available from: http://www.buildingconservation.com/articles/fire/fire.htm).

Gibbon, D. & Forbes, I. 2001, 'Fire Suppression in Historic Buildings', (available from: http://www.buildingconservation.com/articles/firesup/firesup.htm).

Kaplan, M. & Watts, Jr. J.M. 1997, 'Development of a Prototypical Historic Fire Risk Index to Evaluate Fire Safety in Historic Buildings', *APT Bulletin*, **12**, 11-17.

Kaplan, M.E. 2003, 'Considering Fire-Safety Improvements to Historic Buildings', *APT Bulletin*, **34**[4], 10-17.

Koffel, E, W. 2010, 'Fire Protection Engineering in Existing Buildings: From Rehabilitation Codes to Performance-Based Design', (available from: http://www.fpemag.com/archives/article.asp?issue_id=53&i=439).

Serteser, N. & Ozgunler, M. 2006, 'Integrated Design Precautions in Protecting of Historic Buildings Agains Fire' 3. Ulusal Yapı Malzemesi Kongresi ve Sergisi: TMMOB Mimarlar Odası İstanbul Büyükkent Şubesi Bildirileri Taşkışla-İstanbul, 15-17 Kasım, pp. 324-32.

Smith, B.M. & Elefante, C. 2009, 'Sustainable Design in Historic Buildings: Foundations and the Future and Source', *APT Bulletin* , **40**[3/4], 19-26.

NFPA 909, 2005, Code for the Protection of Cultural Resource Properties-Museums, Libraries and Place of Worship, Quincy, MA.

NFPA 914, 2001, Code for Fire Protection of Historic Structures, Quincy, MA.

NFPA 5000, 2006, Building Construction and Safety Code, Quincy, MA.

Taylor, A, 'Going to Blazes: Fire Prevention in Historic Buildings', (available from: http://www.ihbc.org.uk/ context_archive/47/alantaylor.htm).

TBMM National Palaces 2008, 'Dolmabahce Palace', (available from: http://www.dolmabahce.gov.tr/ source.cms.docs/dolmabahce.gov.tr.ce/dolmabahce.html).

Watts, Jr. J.M. 2001, 'Fire Protection Performance Evaluation for Historic Buildings', *Journal of Fire Protection Engineering*, **11**, 197.

Watts, Jr. J.M. 2003, 'Fire-Risk Indexing: A Systemic Approach to Building-Code "Equivalency" for Historic Buildings', *APT Bulletin*, **34**[4], 23-28.

WBDG 2010, 'Plan for Fire Protection', (available from: http://www.wbdg.org/design/ fire_protection.php)

XII DBMC
International Conference on Durability of Building Materials and Components
PORTO - PORTUGAL, April 12th-15th, 2011

Influence of Curing Conditions on Lime and Lime-Metakaolin Mortars

Paulina Faria [1]
Ana Martins [2]

ABSTRACT

Air-lime mortars with or without pozzolanic components were largely used in historic buildings. Due to natural or accidental degradation it is often necessary the application of repair mortars, durable and compatible with the masonries of historic buildings.

Within this context and associating the improvement of mortars characteristics to the necessity of sustainable construction practices, some mortars formulated with lime and the addition of pozzolans have been studied. In previous papers, the influence of some types of air-lime (powder hydrated lime or lime putty) and the addition of metakaolin in lime mortars have been presented. Each type of mortar presents its specificities. In pure lime mortars the setting occurs by carbonation and in lime-metakaolin mortars it occurs both by carbonation and hydration. A crucial question in order to optimize the characteristics of the mortars (and its applicability) is related with the curing conditions.

This article describes an experimental campaign with different pure air lime mortars and lime-metakaolin mortars, cured under different conditions of relative humidity and CO_2 content.

Properties of the mortars, mainly in terms of mechanical behaviour and open porosity, capillary water absorption and drying capacity, are obtained, compared and discussed. The benefits in some properties revealed by the different mortars are correlated with the laboratorial curing conditions and with *in situ* applications possibilities.

KEYWORDS

Air lime, metakaolin, mortar, curing condition, characterization.

[1] Faculty of Science and Technology, *Nova* University of Lisbon, PORTUGAL, paulina.faria@fct.unl.pt
[2] Barreiro School of Technology, Polythecnic Institute of Setubal, PORTUGAL, ana.martins@estbarreiro.ips.pt

1 INTRODUCTION

Air lime-based mortars are present in all Portuguese old buildings, in different types of applications. The most common types of applications in old buildings are as renders, plasters and masonry mortars. As the name implies, these mortars are composed by air lime - as unique or at least main binder -, sand and sometimes pozzolans. They are ecological mortars, in comparision with mortars with hydraulic binders, because air lime is obtained by calcination at lower temperature than the one needed for hydraulic binders production. Air lime can be purchased and used as a hydrated power - after hydration of quicklime with a minimum of water - or as putty - obtained by hydration of quicklime with excess of water [Faria *et al*. 2008]. The hydration of the quicklime occurs with rising temperature and traditionally can be held together with the addition of vegetal or animal fat, for water repellence of the air lime. The pozzolans, fine materials rich in silicates or aluminates in amorfous form, can parcially substitute the air lime. In the presence of water, the pozzolans react and combine with the calcium hydroxide of the air lime, developing calcium silicate and calcium aluminate hydrates that confer hydraulic properties to the mortars [Charola *et al.* 2005] and can also increment the mortar durability - but generally maintaining its compatibility with old masonry materials [Faria 2009]. Pure air lime mortars harden by carbonation, while air lime-pozzolan mortars harden by carbonation but also cure by hydration. The carbonation process occurs by combination of $Ca(OH)_2$ with CO_2 from the environment and depends on the presence and transport of CO_2 through the mortar. The pozzolanic reaction is a slow process as well; depends on the presence of uncarbonated $Ca(OH)_2$, on the reactivity of the pozzolan - which also depends on its specific surface - and on the presence of water. The presence of water, as moisture, is then important for the CO_2 transport for carbonation and for the hydration of compounds by pozzolanic reaction.

Since the begining of the 20th century and until nowadays air lime mortars have been replaced in old buildings, mainly in renders, by cement mortars and since then, the thousands of years knowledge of lime mortars craftsmen abruptly decreased. In the last decades, the origin of many defects that appeared in old buildings was attributed to the new cement mortars that have been applied. Since then, many researches, all over the world, have been trying to fundament the advantages of air lime--based mortars when compared with cement-based mortars. Fortunately also the knowledge of lime mortars craftsmen tends to be regained.

The main problems of cement mortars when applied as substitution renders in old buildings are their mechanical, chemical and physical incompatibility with the masonries and with other old mortars. In fact, cement mortars are much stiffer and stronger than the old masonry walls, inducing stresses in the interface with those walls and, later on, tend to break by the wall, that the render was supposed to protect. Often the cement mortar releases salts, namely sulphates that contaminate those walls they were supposed to protect. Also often the old walls have access to water - for instance by capillary rising from the ground, by problems in the roofs, by migration of the rain water through the porous structure of the exterior layers of the walls, by water vapour generated inside the building that migrate through the thickness of the walls and its protective layers towards the exterior. The water can transport salts from the outside and also salts that were already inside the walls. When the water front faces a layer that is much less permeable to water vapour in comparision to the wall materials - some paint layers or some substitution mortar layers, for instance -, the water and eventual dissolute salts concentrate in the previous layers, often the exterior surface of the original walls, weaker than the impermeable layers. In cold climates that water can originate problems of freeze/thaw, weakening the surrounding material. When salts are involved, they can go through cyclic crystallization/dissolution processes, involving stresses that also weaken the old materials. Even if the exterior rendering seems in good conditions, behind its thickness often there are big voids, due to material without cohesion. Later on the apparently good substitution render detaches, showing a huge degradation in the wall. Nevertheless air lime mortars also have disadvantages mainly regarding actual construction constrains. In fact, in construction sites rapid construction schedules and fast resistant gains are often pursuit and these are not easily achieved with pure air lime mortar renders. Often no one cares if cement renders will behave properly and if they will really protect the walls; but everyone should

remark the fact that lime renders need different application procedures. Some of those different procedures are: the air lime-based mortars should be applied with low water content compared with cement mortars; the lime render have to be applied in separate layers, with about a week between them to achieve some carbonation; each lime mortar layer should be re-tight over the base after suffering initial shrinkage to achieve better compactness.

The characteristics of the walls where the mortars are applied alter significantly the properties of the mortar and that should also be taken in to account when formulating a mortar. But in the study that is presented here, the main focus is on the different properties obtained in air lime-based mortars cured in different relative humidity conditions and CO_2 content. In face of the results, several conclusions can be taken in order to optimize *in situ* curing conditions of pure air lime mortars and of air lime-metakaolin mortars. Those results are obtained within researches held in projects FCT LIMECONTECH and METACAL.

2 EXPERIMENTAL CAMPAIGN

2.1 Preparation of the Material and of the Mortar Samples

For the preparation of mortars two washed sands were used as aggregates: a coarser sand 0/4 and a finer sand 0/2. Two air limes were used as binder in the different mortars: a powder air lime CL90 commercialized by Lusical (AL); a water repellent lime putty CL 90 commercialised by Fradical (PL). A metakaolin was used as a pozzolan (MK) produced from thermal and granulometric treatment of Portuguese kaolin. All mortar volumetric compositions were 1:3, 1 volume of air lime - or air lime+metakaolin - and 3 volumes of sand - 1 volume of finer sand and 2 volumes of coarser sand. By the dried weight of a specimen of lime putty and its apparent density it was possible to assure that the content of air lime in the lime putty mortars was higher than the one in mortars with powder air lime. In air lime-metakaolin mortars, 20% of the mass of the air lime volume was replaced by metakaolin. In mortars with lime putty, once the volume of air lime was heavier - compared with the same volume of powder air lime -, the content in metakaolin was higher. Four different mortars were prepared: mortar AL with powder air lime; mortar AL+MK with powder air lime and 20% of metakaolin; mortar PL with lime putty; PL+MK with lime putty and 20% of metakaolin (Table 1). By weight the mortars composition was 1:12 for AL mortars and 1:3,5 for PL mortars.

The mixture of the mortar components was mechanical and always identical: the water was added in the mechanical mixer tank, followed by the air lime and the sand (previously hand homogenized); mechanical mixture at low speed for 30 seconds; another 30 seconds to scrape the material inside the tank and mechanical mixture for three minutes at high speed. The procedure was based on EN 196-1 [CEN 2005] and EN 1015-2 [CEN 1998] but the period of mixture was enlarged because the one defined in the standard was considered inadequate for air lime-based mortars. In lime putty mortars PL no water was added and only a little amount was added for PL+MK mortars; the other constituents were mixed similarly. The mortar samples were mechanically compacted in two layers inside prismatic metallic moulds 40 mm x 40 mm x160 mm. The samples of each mortar were subjected to four types of curing conditions until the age of test - 60 days or 120 days -, at 20ºC temperature, inside conditioned chambers: 50% relative humidity (RH) - cure identified by D; 65% RH – standard cure identified by S; 65% RH and 5% carbon dioxide – cure identified by C; 95% RH – cure identified by H (Table 1). Six samples of each mortar undergone each curing conditions.

2.2 Testing Program and Results

For each type of mortar multiple mixings were made, due to the mechanical mixer capacity and the quantity of mortar samples required for the experimental campaign. For each type of mortar, when needed, always the same quantity of water was added. All mortars seemed to provide good workability for application in real conditions. The influence of the amount of water in the fresh

mortars was evaluated by the consistency flow table test [CEN 1999a]. For all mortars preparation a comparable consistency flow of 153 mm ± 3 mm was always reached (Table 2).

The mortars shrinkage inside the moulds was evaluated, with 6 samples of each mortar/curing condition, before demoulding, at the age of 7 days, except for mortars cured inside the carbonation chamber (cure C) that could only be demoulded - without registering any visual shrinkage - at the age of 21 days. At the age of 7 days those samples were almost as soft as at the moment of moulding; at the age of 14 days the problem persisted and only at the age of 21 days, with particular care, they could be demoulded. A possible justification for this occurrence was a possible saturation of carbonate ions at the only exterior surface of the mortar samples, inside the moulds, forming a solution rich in hydrogen carbonates - from the reaction of carbon dioxide with water - that diminished the carbonation velocity or even stopped the carbonation front in the mortar sample exterior face. It showed that confined rich CO_2 environments are not adequate for laboratory initial curing of lime-based mortars. Nevertheless and except for mortars C, shrinkage inside the moulds of the different mortar submitted to diverse curing conditions was registered, showing that shrinkage evaluation since moulding - and not only after demoulding - is important to lime-based mortars.

The carbonation velocity intended to be evaluated by the phenolphthalein method. A phenolphthalein solution at 0,5% in alcohol was applied in fresh cutting surfaces - 2 cm thickness - of 3 samples of each type at the ages of 30, 60, 90 and 120 days. It was obvious that mortar C achieved complete carbonation during the test; for the other cure conditions, carbonation were very slow, generally a little faster in mortars D and S, and a little slower in those in cure H.

At 60 days of age, 3 samples of each mortar and cure were dried in an oven at 60ºC until constant mass - weight variation in 24 h not higher than 0,1%. They were used to dynamic modulus of elasticity determination by fundamental resonance frequency [CEN 2004], and three points bending flexural strength determination [CEN 1999b]. One half of each specimen from the flexural test were used to compressive strength determination at 60 days [CEN 1999b]. The other half were kept in interior environment at medium temperature of 30 ± 3 ºC and 50 ± 5% RH. Those conditions were not particularly beneficial for the lime-based mortars curing, due to the lack of moisture for carbon dioxide transport and for pozzolanic reaction. At 120 days the half samples were used to compressive strength determination and afterwards the tops of those half samples - which were perfectly undamaged - were used for open porosity determination by vacuum and hydrostatic weighing [RILEM 1980, CEN 1999c].

At 120 days, the half of 3 samples of each mortar and cure, resulting from the ones used before for the carbonation determination, were dried in an oven at 60ºC until constant mass. After cooling in dry environment, they were used for capillary water absorption determination (capillary coefficient in terms of initial capillary absorption velocity and capillary absorption in terms of total adsorbed water) [CEN 2002, CEN 2009]. The lateral faces of the samples were not watertight and the test was held inside a box with saturated environment; the samples were over a geotextil with 2 mm water high. When completely saturated by capillary water, the samples were used for the drying index determination [C.Normal 1991, Brito 2009]. During drying they were kept in environmental conditions of 20 ± 3ºC temperature and 50 ± 5% RH.

3 RESULTS

Test results of mechanical characteristics and internal structure are presented in Table 1; flow table consistency and physical characteristics are presented in Table 2.

3.1 Mechanical Characteristics and Internal Structure

Mortars with powder air lime AL present higher dynamic modulus of elasticity E than mortars with lime putty PL, what may induce a higher deformability of lime putty mortars due to the decrease of

portlandite crystal dimensions of the putty when compared to powder air lime [Hansen *et al.* 1999]. Mortars with metakaolin AL+MK and PL+MK present higher E than similar mortars without metakaolin AL and PL - except in the case of mortars with powder air lime cured with high CO_2 content AL+MK_C, with a very high standard deviation. With regard to mortars of each type (mortar and curing), the higher E is always registered by samples C cured with high CO_2 content; the following values of E are registered by samples cured at 50% or 65% RH (cure D or S) for mortars without metakaolin and by samples cured at 95% RH (cure H) for mortars with metakaolin.

Table 1. Test results (average values and standard deviation) of dynamic modulus of elasticity, flexural and compressive strength and open porosity of mortars and curing

Mortar	*Mortar/Curing*	$E_{(60d)}$	*StDv*	$R_{f\,(60d)}$	*StDv*	$R_{c\,(60d)}$	*StDv*	$R_{c\,(120d)}$	*StDv*	*Open Poros.*	*StDv*
[ID]	*[ID]*	*[Mpa]*		*[Mpa]*		*[Mpa]*		*[Mpa]*		*[%]*	
AL	AL_D	2671	10	0,2	0,1	0,4	0,1	1,0	0,0	30	0,2
	AL_S	2627	42	0,2	0,0	0,5	0,0	0,9	0,0	30	0,3
	AL_C	5028	227	0,8	0,1	1,4	1,0	1,2	0,2	29	0,4
	AL_H	2412	98	0,2	0,0	0,4	0,1	0,9	0,1	31	0,3
AL+MK	AL+MK_D	3023	123	0,3	0,0	0,5	0,2	1,1	0,1	30	0,1
	AL+MK_S	2822	71	0,3	0,1	0,4	0,2	1,0	0,0	30	0,2
	AL+MK_C	3691	504	0,7	0,1	1,2	0,3	1,2	0,2	29	0,3
	AL+MK_H	3194	76	0,3	0,0	0,7	0,3	1,3	0,0	29	0,2
PL	PL_D	1529	29	0,2	0,0	0,3	0,1	0,6	0,0	35	0,4
	PL_S	1455	4	0,2	0,0	0,3	0,0	0,6	0,0	35	0,1
	PL_C	4587	179	0,7	0,1	1,3	0,4	1,7	0,2	35	0,3
	PL_H	1232	43	0,2	0,0	-	-	0,5	0,0	35	1,0
PL+MK	PL+MK_D	2153	52	0,3	0,1	0,5	0,0	0,9	0,0	34	0,1
	PL+MK_S	2132	61	0,2	0,0	0,5	0,1	0,9	0,1	35	0,1
	PL+MK_C	4518	147	0,8	0,0	1,6	0,1	1,9	0,2	35	0,4
	PL+MK_H	2167	86	0,4	0,1	0,7	0,0	1,0	0,0	35	0,1

Regarding the flexural strength at 60 days of age, mortars with lime putty generally register a slight increase comparatively with mortars with powder air lime. Except for mortar AL+MK_C, mortars with MK register slightly higher values of flexural strength. In what concerns each type of mortar with different type of cure, as for the case of E, also mortars cured with high content of CO_2 register the higher results. Respecting the compressive strength, an increase of the results generally occurs from 60 to 120 days of age of the mortars, although the environmental condition where the samples were kept meanwhile. At 120 days mortars with powder air lime AL register higher values than those with PL (except for mortar with lime putty PL cured with a higher content of CO_2). Mortars with MK generally register an increase of compressive strength compared to the similar ones without MK. In what concerns each type of mortar with different types of cure, as for the case of E and R_f, also mortars cured with high content of CO_2 register the highest results of R_c, except for AL+MK_C; as happened before for E, the following values of R_c are registered by mortars cured at 50% or 65% RH (cure D or S) among mortars without metakaolin and by mortars cured at 95% RH (cure H) among those with metakaolin. In what relates to open porosity, it is higher for mortars with lime putty PL compared with mortars with powder air lime AL; those last mortars are then denser than the previous. Results of similar mortars with or without MK are almost the same. Regarding each type of mortar with different types of cure, only mortars with powder air lime AL cured with high content of CO_2 present a lower open porosity and a higher compactness; that can be related to rapid carbonation evolution. Results of open porosity can justify some of the mechanical characteristics obtained but also underline the particularly different internal structure that may occur in mortars with lime AL compared with lime PL.

Table 2. Test results (average values and standard deviation) of flow consistency, maximum values of capillary absorption, capillary coefficient and drying index of mortars and curing

Mortar	*Flow*	*StDv*	*Mortar/Curing*	*Capillary Absorp.*	*Capillary Coef.*	*Drying Index*
[ID]	*[mm]*		*[ID]*	*[kg/m^2]*	*[kg/m^2.min.^{0,5}]*	
AL	155	3	AL_D	13,21	1,14	0,25
			AL_S	13,90	1,20	0,23
			AL_C	12,42	1,17	0,24
			AL_H	14,40	1,32	0,23
AL+MK	154	3	AL+MK_D	13,85	1,07	0,15
			AL+MK_S	14,47	1,12	0,21
			AL+MK_C	16,91	0,96	0,13
			AL+MK_H	13,33	0,92	0,24
PL	151	5	PL_D	4,08	0,09	0,35
			PL_S	3,27	0,03	0,33
			PL_C	1,54	0,01	0,27
			PL_H	3,28	0,05	0,42
PL+MK	152	1	PL+MK_D	4,11	0,13	0,56
			PL+MK_S	2,74	0,13	0,47
			PL+MK_C	6,49	0,03	0,25
			PL+MK_H	4,40	0,07	0,51

3.1 Physical Characteristics

Regarding the capillary coefficient, there is a strong difference of capillary coefficient between mortars with powder air lime AL and with lime putty PL; the last mentioned mortars are much less absorbent than the others due to the water repellent natural product incorporated in the lime putty - an olive oil by-product. Capillary coefficient of mortars with air lime AL is lower for mortars with metakaolin; for mortars with lime putty PL, capillary coefficient is a little higher when metakaolin partially substitutes the lime. Regarding each type of mortar with different types of cure, generally mortars cured with high content of CO_2 register the lower results - only mortar with powder lime with metakaolin cured in humid conditions AL+MK_H present a slightly lower value compared to AL+MK_C. But these results should be analysed toghether with the capillary water absorption. In what concerns the capillary water absorption, also the mortars with lime putty PL register very low absorption compared with those with AL. Comparing mortars with lime AL, there is an increase of water absorption when metakaolin is used, except with mortar with metakaolin and humid cure AL+MK_H. These last mentioned mortar present the best behaviour in terms of capillary absorption, among the ones with AL+MK and particularly in terms of capillary coefficient among mortars with lime AL; mortar AL_C present the best behaviour among the ones with AL without MK, in terms of capillary absorption, and one of the best concerning capillary coefficient. Comparing mortars with lime PL, the best behaviour in terms of capillary absorption is registered by mortar PL_C. Among mortars with PL+MK, the mortar with lower capillary coefficient register the highest values of total absorption and the mortar with lower capillary absorption register the higher capillary coefficient.

Results of capillary absorption must be analysed toghether with the drying capacity of mortars, fundamental for the elimination of water, once absorbed. Mortars with lime AL generally register lower values of drying index compared to mortars with lime PL, what means the moisture can be easily and faster eliminated from AL mortars than from PL mortars. Among mortars with lime AL, mortars with metakaolin present lower values; between mortars with lime PL, mortars without metakaolin present lower values - except for mortar C cured with high CO_2 content, with similar values. All mortars AL cured in different conditions present very similar values; among mortars with

the same lime but with metakaolin, mortar AL+MK_D and AL+MK_C register the lowest values, and humid cured mortar H present the highest drying index. Among mortars with lime PL, also mortar C present the lowest value and mortar H the highest value; among mortars with metakaolin PL+MK, a low drying index is register by mortar C while the other mortars present the highest values.

4 DISCUSSION AND CONCLUSIONS

The experimental campaign highlighted several aspects: the good workability of air lime-based mortars, even with relatively low flow table consistencies; the difficulty but the need on evaluating shrinkage since moulding; the phenolphthalein test inadequacy to evaluate lime-metakaolin carbonation due to changes registered on PH by pozzolanic reaction; the increase of mechanical characteristics when lime was partially substituted by metakaolin - although the metakaolin that was used was not very reactive and the lime-metakaolin proportion was not optimized; the good deformability, expressed in terms of the dynamic modulus of elasticity, evidenced by all mortars but particularly by mortars with lime putty, with similar flexural strength results; the higher porosity of mortars with lime putty compared to powder air lime mortars, but with similar mechanical resistances when metakaolin replacement occurred; the low capillary water absorption of analyzed lime putty mortars - this lime had a water repellent product - but also the greater difficulty to dry of these mortars - while lime without water repellent mortars absorbed rapidly and more quantity of capillary water but could release that moisture more easily; an improvement of the behavior of powder air lime mortars to initial water capillary absorption and drying capacity when metakaolin was added and the inverse situation for lime putty with water repellent mortars.

Regarding the influence of different curing conditions, the most important aspects that were detected were: the initial difficulty of hardening of lime-based mortars when exposed to high levels of CO_2; the increase of carbonation evolution and on mechanical characteristics, after the initial hardening, when the cure occurred with high level of CO_2. Although that cure situation is not reproducible on site applications, the acceleration of cure of pure air lime mortars that, after initial hardening and demoulding, are submitted to higher CO_2 environments during a defined period of time, can help in the preparation of lime mortar samples to be tested and characterized. Accordingly this study is being extended to the characterization of mortar samples submitted to other curing conditions, combining some of the previous and different ones. The aim is to define cure conditions that potentiate pure lime mortars characteristics, in order to prepare laboratory specimen to be used as support to other products, but also trying to optimize curing conditions that can be reproduced *in situ*. For the time being and from the obtained results of conditions reproducible on site, curing at 65% RH seemed to be the most appropriate for pure air-lime mortars.

For lime-metakaolin mortars, and although the general improvement registered in the mortars characteristics by the partial substitution of lime, the authors think that a substantial improvement can yet be achieved with the use of a more reactive metakaolin and a better defined proportion between each type of lime and metakaolin. In this type of mortars the amount of calcium hydroxide must be able to react with the silicates and aluminates of the metakaolin but also to carbonate. It is important to be aware of the kinetic of both the pozzolanic reaction and the carbonation process, in order to potentiate the best conditions during mortar formulation and curing. Anyway, from the analyzed results, and although not reproducible *in situ*, curing with high level of CO_2 generally potentiated the lime-metakaolin mortar characteristics. Among the curing conditions that can be closer to *in situ* situations, humid curing can potentiate lime-metakaolin mortars characteristics. Humid curing seems fundamental both for the continuity over time of the hydration - the pozzolanic reaction - and the CO_2 transport - for the carbonation process. In most Portuguese exterior environmental conditions cycles occur, between night and day, ranging from very humid to dryer conditions. Nevertheless a geotextile covering frequently wetted could be recommended to be applied *in situ* over lime-metakaolin renders during the first ages. For interior plastering of old walls in very humid environments, the application of lime-metakaolin mortars should be advantageous.

ACKNOWLEDGMENTS

The authors acknowledge the support of the Polytechnic Institute of Setubal where the experimental work was conducted, the availability of limes Lusical and Fradical, the financial support from the Portuguese Science and Technology Foundation to projects LIMECONTECH (PTDC/ECM/100234/2008) and METACAL (PTDC/ECM/100431/2008) and the fruitful discussions with colleagues from the project teams and with Cristiana Gonilho Pereira.

REFERENCES

Brito 2009, 'Influence of wall paints on drying of the substrate' (in Portuguese). MSc thesis. Lisbon, *Nova* University of Lisbon and National Laboratory of Civil Engineering.

CEN 1998, Methods of test for mortars for masonry. Part 2: Bulk sampling of mortars and preparation of test mortars. Brussels, EN 1015-2: 1998/A1:2006.

CEN 1999a, Methods of test for mortars for masonry. Part 3: Determination of consistency of fresh mortar (by flow table). Brussels, EN 1015-3: 1999/A1: 2004/A2: 2006.

CEN 1999b, Methods of test for mortars for masonry. Part 11: Determination of flexural and compressive strength of hardened mortar. Brussels, EN 1015-11: 1999/A1:2006.

CEN 1999c, Natural stone test methods. Determination of real density and apparent density, and of total and open porosity. Brussels, EN 1936: 1999.

CEN 2002, Methods of test for mortars for masonry. Part 18: Determination of water absorption coefficient due to capillary action of hardened mortar. Brussels, EN 1015-18: 2002.

CEN 2004, Natural stone test methods. Determination of the dynamic modulus of elasticity (by measuring the fundamental resonance frequency). Brussels, EN 14146: 2004.

CEN 2005, Methods of testing cement. Part 1: Determination of strength. Brussels, EN 196-1: 2005.

CEN 2009, Conservation of cultural property. Test methods. Determination of water absorption by capillarity, Brussels, EN 15801: 2009.

Charola, E., Faria Rodrigues, P., McGhie, A., Henriques, F. 2005, 'Pozzolanic components in lime mortars: correlating behaviour, composition and microstructure', Restoration of Buildings and Monuments, 11 [2],111-118.

Commissione Normal 1991, Misura dell´indice di asciugamento (drying index), Roma, CNR/ICR, Doc. 29/88.

Faria Rodrigues, P. 2009, 'Resistance to salts of lime and pozzolan mortars', RILEM Proc. PRO 067: Repair Mortars for Historic Masonry, Delft, The Nederlands, February 2005, pp. 099-110.

Faria Rodrigues, P., Henriques, F., Rato, V. 2008, 'Comparative evaluation of aerial lime mortars for architectural conservation', J. Cultural Heritage, 9 [3], 338-346.

Hansen, E., Tagle, A., Erder, E., Baron, S., Connell, S., Rodríguez-Navarro, C., Van balen, K. 1999, 'Effects of ageing on lime putty', RILEM Proc. PRO 012: Historic Mortars. Characteristics and Tests, Paisley, Scotland, pp. 197-207.

RILEM Commission 25 PEM 1980, 'Essais recommendés pour mesurer l´alteration des pierres et évaluer l´efficacité des methods de traitment'. Matériaux et Constructions, 13 [75].

XII DBMC
International Conference on Durability of Building Materials and Components
PORTO - PORTUGAL, April 12th-15th, 2011

Damage in Architectural Historic Patrimony - An Approach on "Stucchi" of Facades

Rosilena Martins Peres [1]
Luis Carlos Bonin [2]

ABSTRACT

In any construction, the coverings of facades are the most exposed elements to the environmental action or of pathological agents. Of easy perception, for the character wrapper and protecting of the constructions, it becomes necessary and of fundamental importance the maintenance. For the best understanding of the damage in the coverings of walls, it is important the knowledge of the materials and techniques constructive used, of the which, in most of the historical buildings, registrations that make possible the correct diagnosis don't exist for the effectiveness of the conservation and restoration decision-making. Besides, it is important the knowledge of the environmental interferences or of the users, that happened during the life of the construction. This publication try to explain that any pathological manifestation is the result of a complex process, that involves agents or causes, mechanisms and the own degradations as links of a chain that can generate other chains and, it depends directly on the materials, constructive techniques, environmental conditions and on users' interventions. A classification of the pathological manifestations was elaborated for the coverings of walls with their possible causes, so that it serves as tool in the systemization of other analyses of damages in historical buildings.

KEYWORDS

Building heritage, pathological manifestations, building pathology.

[1] Instituto Federal de Educação, Ciência e Tecnologia Sul-Rio-Grandense (IFSUL); Universidade Federal de Pelotas (PROGRAU-UFPel), Pelotas, BRASIL, rosimperes@gmail.com
[2] Universidade Federal do Rio Grande do Sul (PPGEC-UFRGS), Porto Alegre, Brasil, luis.bonin@ufrgs.br

1 INTRODUCTION

The development of any product, and it wouldn't be different with the buildings, is subject to several basic criteria, such as longevity, cost-benefit, quality, among others. And for the performance of any product is considered satisfactory, it is necessary that their properties to enable them to fulfill the functions that was proposed, when subjected to the actions or uses for a certain specified time. About the buildings, the use of these concepts requires that we take into account not only the characteristics of the building, but also its production process, from design until the waste disposal. When the approach is intervention in historic buildings, the scale of analysis increases because the architectural design reflects the materials and construction process of a period, including technics and "know-how" - without register of a workmanship devoid of regular academic and of fundamental importance for the understanding of the product built. And these are the real heritage historical documents to be analyzed.

When we encounter any building, the first impact is the external image, with volumetry, the appearance of the wall's coatings and construction details of the facades. These aspects are always important, but the particular importance in the built heritage is because they reveal, at first sight, the repair and maintenance needs of the building. The wall covering influences on the image perceived by the observer and shows the performance of the constructive element - wall, mainly about the functionality of protective covering of the internal spaces. In intervention's case studies in historic buildings is common to find buildings that are maintained for several years with their protections intact or with only some minor damage but without missing or outstanding.

Mainly, this occurs because the building being "in use" even were few initiatives of maintenance or protection (replacing tiles, repairing gutters, painting etc..), this remains secured from destruction. Once empty and abandoned, then there, it becomes vulnerable to a range of pathogens that causes triggering mechanisms of disease processes more complex. To be able to review any damage in historic building's wall covering, as well as in buildings of any age, it's necessary to deep in knowledge of used materials, of application's methods, of environmental conditions submitted, of the user's interference by using or intervention, whether for maintenance, conservation or changes.

2 PATHOLOGICAL MANIFESTATIONS IN HISTORIC BUILDINGS

One of the first steps in planning interventions in heritage is diagnosis, which allows broad view of conditions in which the object is located. At this stage, in the historic buildings, is very common to encounter several numbers of pathological manifestations that result from different origins and are caused by one or more types of agents, acting with or without simultaneity. The understanding of building pathology requires above all a systemic view that considers the pathological manifestations as the result of a complex process, involving agents or causes, mechanisms and their own degradation as if they were links in a chain, which must be perceived in all and in its parts before applying any therapy for solution of problems and actions to be chosen for preservation or restoration work.

In the case of buildings that are part of heritage to be preserved, the scope of the analysis increases the complexity in the characterization of materials, the characterization of the technique for use, in physical, chemical and/or mechanical phenomenon that is occurring. Another important factor to be considered is the action of man on the building and should be investigated all the interventions that have occurred, whether maintenance, renovation or any attempt to solve problems. It should also be part of the search data in the life of the building, those natural macro phenomenon that may have occurred as windstorms, floods, fires or any occurrence of short duration but high-impact or even destructive actions of vandalism. For a better understanding of how a process occurs in pathological manifestation with agents and mechanisms acting with or without simultaneity, resulting in deteriorated appearance, one can observe the example of efflorescence type 1, on plaster, commonly found in historic buildings whose materials were of high porosity, the foundations were often of clay bricks and there were no film-waterproof at the interface foundation-walls [Table 1].

Table 1. Efflorescence type 1 – causes, mechanisms and appearance

Efflorescence type 1		
Agents or causes	*Mechanisms probably acting with or without simultaneity*	*Appearence resultant*

• Water circulating from
  ◦ soil
  ◦ materials (mixing water, aggregates, binders)
• Presence of salts
  ◦ materials
  ◦ into the soil where move the groundwaters
	• Physical – rise of water by materials capillarity
	• Chemical – crystallization of salt in water evaporation
	• Physical – increased volume in the crystalization causing chalking of the coating
		• White powder soluble in water accumulated on coating's outer surface

It is recommended to study Uemoto (1985), Guimarães (2002) and Cincotto (1983), which approach the processes of plasters decay by efflorescence and other types of events widely found in wall coverings.

3 WALL COVERINGS

For millennia until the beginning of twentieth century, external coverings were characterized by plastering with lime mortar, becoming an effective protection system of masonry and structures, besides being used as ornamental elements of the facades.

The Romans gave to this type of coating the generic term of stucco, which can be originated from the ancient lombard word *stuhhi*, that indicated crust or skin. According Arcolao (1998), the term referred to the plaster based on lime and marble dust used both in filling empty or cracks in the surface and to create decorative elements in relief, or simply to give a finish plain wall. Traditionally, the surface finishes of plaster could be substantially obtained in two ways: extending over the last layer of plaster, a layer of dye or extending a thin plaster colored paste with varied composition and surface finish. The dyeing plaster could be performed on fresh or dry with the technique of *scialbo*, in other words, a coating of lime past and colors.

Initially the term stucco was used only to lime and marble dust mortar; only from the second half of the sixteenth century it was employed indifferently to mortars based on lime or gypsum. Treaties relating to the older practice of building - *De architectura* by Vitruvius and *Naturalis Historia* by Plinio, both Romans, show the technique of stucco, whose recommendation for surface coatings was that there was the splendor and brightness of the marble, being advised against the use of gypsum, because they are easily perishable and thus less durable. Only after the Renaissance, the use of stucco as finishing coat was new impulses, being employed in order to reinvoke the image of ancient architecture, using as well to the crust, that seemed marble or to model the various architectonic elements (cornices, pilasters, capitals, corbels or *cassetoni per soffiti* - decorative boards of ceiling).

Only in the baroque and rococo period, in Europe, particularly in Italy, the use of gypsum stucco was consolidated as fundamental material for complex plastic decorations. It was the exaggerated period of ornamentation through the use of formal elements such as flowers, leaves, angels, scrolls, shells, human figures and other decorative shapes that stand out from the walls as real sculptures applied on the facades. Decorative painting with golden can also be found in these ornaments. And it is in the eighteenth century that the technique of stucco seems to find through the work of true and proper artist dynasties, the most interesting technical variations. These active families, especially in northern Italy, transmit as secrets, numerous technical tricks, but it was rarely founded in hadbooks of this time.

The coatings of lime were usually employed with the technique of *multilayer*. On the wall regularization layer, were applied three or more layers, the first being in general, composed of lime and aggregates with a higher granulometry or, alternatively, using additives such as *cocciopesto* (dust of crushed brick or tile) or pozzolan, to increase the hydraulicity of mortar. Then two more layers of lime and sand. And finally, a layer of marble dust (can be composed by three fine layers of lime paste and marble dust).

Other additives were often used in general to provide specific and varied properties to the mixed such as impermeability, adhesion capacity, hydraulicity, retardation of carbonation, plasticity, stability. It is common to find in the manuals, specifications of organic materials such as milk, glue, oil, animal grease, vegetable resins, tartar of wine and fig.

According to Veiga et al (2004), techniques and finishing materials, could provide the walls of a variety of aesthetic and illusionistic effects (fresh; semi fresh; *graffito* - incision through punctures or other instruments in the lime coatings; *sgraffito* - removal of material to allow the chromatic contrast of the different layers; simulaters - paintings simulating the noblest materials like wood and stone, *trompe-l'oeil* - decorative painting simulating architectural elements in perspective).

From the second half of the nineteenth century, the technique of stucco reduces to a semi-industrialized practice. Prefabricated decorative elements replace traditional ones. In manuals of this period, in fact, the gypsum mortars begin to appear predominantly in the chapters devoted to bastard mortars, so called, mixtures of two different ligands and in particular, those formed with common lime mortar which is added some amount of gypsum or, especially way of the century end, the cement dust and other additives intended to accelerate the setting time and reduce the working time of manufacture. These mortars are recommended in place of traditional mortars used in decor and finish work inside the buildings, to the plaster walls and ceilings (Arcolao, 1998).

4 RESEARCH ON WALL COVERINGS

According Feiffer (2000), historical studies were prepared some geographical areas, allowing a very accurate classification, in the ways of implementation of employed materials, identifying them in different areas and eras. It was also possible to deep in building typologies, materials used, capture areas, transportation, cultural features of wide spectrum of colors and ways applied on surfaces. It is significant the fact that the historical study of plaster was conducted, first through direct and indirect historical sources, using archival sources through original chapters etc.. and on the other side directly analyzing the historical plasters still present in buildings and once perfectly preserved, then getting old description parameters, and historical prescriptions based on reality.

Scientific research have analyzed not only the intrinsic qualities of materials, the pathological manifestations of damage, the technical problems of consolidating, but also the factor "quality" of pre-industrial products. The extraordinary longevity of many historic plasters has been carefully investigated and it was verified that this is a consequence, wether by care of the ancient builders in the supply of basic materials (lime matured or employed "hot" just burned, sifted sand, natural additives etc..) wether by attention put into the preparation (many layers applied carefully in succession, many hours of manual labor etc..) wether by the maintenance techniques that have used similar and compatible materials.

Analysing wall coverings of historic buildings, it is essential not only to deep the physicochemical data, but also enhance the desired quality and durability, which today has little consideration in traditional materials production, being more surveyed the materials intended for new buildings. This opens an important research sector on existing materials analysis on site, time-tested, and new materials, produced today, in which little can be seen in relation to the durability and compatibility with the historic materials.

5 PATHOLOGICAL MANIFESTATIONS IN WALL COVERINGS

The pathological manifestations in buildings can be divided into three large groups, according Ioshimoto (1994): humidity, fissures and cracks and, coating detachment. The causer agents of pathological manifestations can be the most diverse and are distributed according to the type of event. Thus, with respect to humidity problems, according to Perez (1988), the main manifestations of humidity are: efflorescence, mildew and blistering with detachment. These symptoms may be caused by seepage, condensation, accidental, building remaining activities, and absorption by capillary rise. The fissures and cracks can be caused by structural problems, like repression, shrinkage or movement structural. In wall coverings other problems may also occur in fissures and cracks due to mooring failure and thermal or hygrometric expansion. The detachment of the coating can also be caused by several factors, such as structural moves, unsuitable materials, lack of adherence, environmental action, expansion, among others. The detachment by loss of adhesion between the plaster and the substratum on which it was applied or between plaster layers and can occur in three phases: detachment, bulge and layer detachment. The first stage is characterized by the removal of plaster from its substratum and can be identified by hollow sound when impacted with a the knock of fingers. The plaster is bulged when it is possible to perceive convexity on portion or on all surface. Finally, the detachment is characterized by a lack of portion or total wall covering. Dirt is a very common manifestation perceived as characterized by the cover over the coating with dust, soot and other particle pollutants in atmospheric air. The causer agents of this type of event usually occur together. The rough texture with protrusions and shares into the surface favors the particle's deposition and the rain action enhanced by wind, with longer contact on the surfaces causing droppings stains. The wind also acts as a carrier agent of the pollutant particles to the wall's surface.

The table below shows the classifications described above, by type of manifestation and the main possible causes of degradation. These causes act with or without simultaneous and are caused by several factors, such as execution errors, use of inappropriate materials to function, poorly designed projects, errors in previous interventions and lack of maintenance, the latter being found more frequently.

Table 2. Pathological manifestations and its causes

MANIFESTATION PATHOLOGICAL TYPES	CAUSES
HUMIDITY – Eflorescence – Mildew – Blistering with detachment	– seepage – condensation – accidental – building remaining activities – absorption – capillary rise
FISSURES AND CRACKS	– repression – shrinkage – movement – thermal or hygrometric expansion – mooring – overload
COATING DETACHMENT	– structural moves – unsuitable materials – lack of adherence – environmental action – expansion
DIRT	– surface texture of the plaster – building elements (protusions, shares into, ongoing plans) – rain and wind action – atmospheric pollutant

In general, it is possible to find many pathological manifestations originated by maintenance lack or incompatible material use in interventions over the life of the property. The negligence on historic building, which is not concerned with its maintenance and conservation has been the main origin of damage. Or, attempts to maintain, if not used rigorous criteria for the biological, chemical, physical and mechanical or morphological identifications and used incompatible materials with the originals, have resulted in new pathological problems.

From another focus, Lersch (2003) considers the climatic agents, biological agents and the man action as the main causes for buildings damage of cultural heritage. The main degradation mechanisms of these buildings are the phenomena caused by solar radiation, temperature variation, humidity action, winds and air constituents, beyond those caused by biodegradation, mainly insects and microorganisms.

The activities of these factors or agents depends first on materials characteristics, their properties and function, and second, the presence of one or more degradation agents. Also the exposure conditions can vary for the same material or component. Moreover, various types of pathologies that occur in buildings can have more than one cause. In addition, an agent can act on another, chain, generating one or more manifestations. The below graphic scheme clarifies, by example, how the pathologic manifestations can occur causing others deteriorative process more complex.

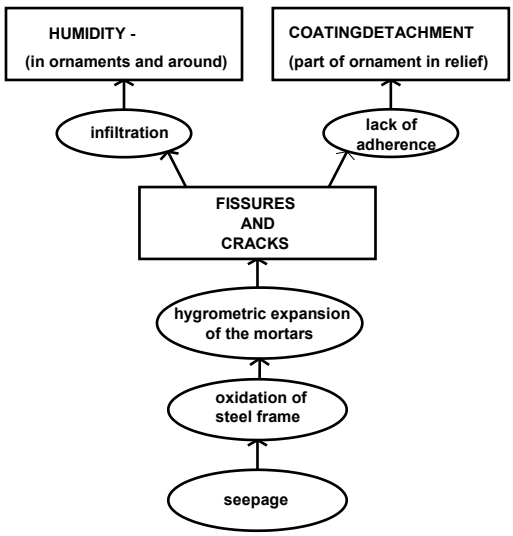

Figure 1. Graphic scheme in chain of causes and damage

6 DAMAGE IN *STUCCHI* OF FACADES

Examples of pathological manifestations or damages to the facade coatings or *stucchi* presented below is restricted to coating mortars, whether plasters done with lime mortar, whether that ornaments in relief done with lime plaster and marble dust.

It is recommended that a particular study of the pathological manifestations in paintings on the facades of historic buildings, whose execution, though with a lime mortar, uses others naturals pigments and dditives through various application techniques, and thus requiring a search of the origins of materials for better understanding the damages and corrects interventions for its restoration. Mortars coating of walls flat surfaces can show several pathological manifestations caused by incorrect interventions, using mortars whose materials are incompatible with the original. (Fig. 2) Also, it is common to find efflorescence caused by capillary rise, since the walls of historic buildings not used film waterproofing against waters of soil and, often, the presence of salt provides the mortar crumbling (Fig. 3).



Figure 2. Recuperation of *stucco* in north facade of public library in Pelotas/RS



Figure 3. Eflorescence in north facade of public library in Pelotas/RS



Figure 4. Covering detachment by expansion due oxidation of methalic element in Clube Caixeiral in Pelotas/RS



Figure 5. *Stucchi* with dirt in south facade of Clube Comercial in Pelotas/RS

In general, the centenarians buildings have their ornaments in relief in good condition. Most are well adhered to the walls, just with only dirt manifestations. Examples of other damage are large ornaments sets attached by metal – wires, boards, hangers and frames. These, when in oxidation process, expand and cause the detachment of part or all decoration (Fig. 4). The protusions and shared into forms are retainers of atmosphere dust and favor the proliferation of biological agents enhanced by rain and winds (Fig. 5). Unlike, small ornament sets usually are well adhered to the wall, due to be fixed on lime mortar, which, due to its high plastic properties, support the thermal and hygrometric movements, ensuring their adherence to the wall.

7 FINAL CONSIDERATIONS

The study of pathological manifestations in historical buildings has a special dimension for the witness that this building represents in relation not only to materials that were employed in it, but also the mode of production of architecture. As regards, more specifically, to wall's coatings of the historic buildings, the research must be understood according to each specific case, with diverse influences as the source of technique and materials used. Although the coverings have been, mostly, mortar, there are variations, such as stucco coatings, composed of lime, applied in several layers and use of organic or mineral additives, whose behavior of damages are not widely known . In addition, special techniques for finishing the walls of providing aesthetic and illusionistic effects reinforce the

need for prior studies of these materials and techniques for posterior understanding the pathological manifestations and, thereafter, be proposed repairs or restorations.

REFERENCES

Arcolao, C. 1998, '*Le ricette del restauro – malte, intonaci, stucchi dal XV al XIX secolo'*. Marsilio Editori, Venezia.

Büchli, R. 2003, 'Crescimento microbiológico em fachadas', in: *2nd Simpósio Internacional sobre Patologia, Durabilidade e Reabilitação de Edifícios*, CIB, Lisboa.

Cincotto, M. A. 1983, '*Patologia das argamassas de revestimento e recomendações'*. Monografia 8. IPT, Instituto de Pesquisas Tecnológicas do Estado de São Paulo. São Paulo.

Feiffer, C. 2000, **'***La conservazione delle superfici intonacate – Il metodo e le techniche*'. Skira editore, Milano.

Guimarães, J. E. P. 2002, '*A cal*: *fundamentos e aplicações na engenharia civil*'. Pini, São Paulo.
Ioshimoto, E.1994, '*Incidência de manifestações patológicas em edificações habitacionais'*. IPT, São Paulo, Publicação 2182.

Lersch, I. M. 2003, '*Contribuição para a identificação dos principais fatores e mecanismos de degradação em edificações do patrimônio cultural de Porto Alegre'*. Dissertação (Mestrado em Engenharia) Curso de Pós-Graduação em Engenharia Civil, Universidade Federal do Rio Grande do Sul, Porto Alegre, 181 f.

Peres, R. M. 2004, '*Manifestações patológicas em edificações'*. Ed. da UFPel, Pelotas.
Perez, A. R. 1988, 'Umidade nas edificações', in _____. *Tecnologia das edificações.* Pini/IPT, São Paulo.

Uemoto, K. 1985, 'Patologia: danos causados por eflorescência', in *A Construção*: Região Sul, São Paulo, n.198, pp.29-32.

Veiga, M.do R., Aguiar, J., Silva, A. S.; Carvalho, F. 2004, '*Conservação e renovação de revestimentos de paredes de edifícios antigos'*. LNEC, Lisboa.

XII DBMC
International Conference on Durability of Building Materials and Components
PORTO - PORTUGAL, April 12th-15th, 2011

Building Details of a *Tabique* Dwelling in *Trás-os-Montes e Alto Douro* Region

Rui Cardoso [1]
Anabela Paiva [2, 3]
Jorge Pinto [2, 4]
António Murta [2]
Humberto Varum [5]
Lina Nunes [6]
Luís Ramos [2]

ABSTRACT

Tabique is one of the main Portuguese traditional building techniques which use earth as a building material. In general, a *tabique* building component is formed by a simple timber structure covered by an earth based mortar on both sides. The mortar has an important role in this system because it protects the internal timber structure as well as it is a coating. *Trás-os-Montes and Alto Douro*, is the northeast region of Portugal and it is rich in terms of *tabique* heritage construction. Meanwhile, previous research works have shown that the existing *tabique* constructions, in this region, show a generalized advanced stage of deterioration. This aspect associated to the fact that there is still a lack of scientific studies done in this field motivated this research work, which its main objective is to identify and to understand the structural system of *tabique* dwellings. A two storey *tabique* dwelling located in *Lamego* Municipality, near *Douro* River, in the UNESCO classified heritage area, is used as reference in this study. Building details of the original applied structural system solutions are shown and described. The adopted connection solutions between structural components are some of the above building details which are introduced and described. Finally, the conservation stage of these elements is also analysed.

KEYWORDS

Tabique, building detail, raw materials, traditional building techniques, EC5

[1]Coimbra Polytechnic Institute, Oliveira do Hospital Technology and Management Superior Scholl, Oliveira do Hospital, PORTUGAL, rui.cardoso@estgoh.ipc.pt, http://www.estgoh.ipc.pt.
[2]Trás-os-Montes e Alto Douro University, Vila Real, PORTUGAL, apaiva@utad.pt, tiago@utad.pt, lramos@utad.pt. http://www.utad.pt.
[3]C-MADE, University of Beira Interior, Covilhã, Portugal
[4]Associated Laboratory I3N, 3810-193 Aveiro, Portugal
[5]Aveiro University. Aveiro, PORTUGAL, hvarum@ua.pt, http://www.ua.pt.
[6]Núcleo de Estruturas de Madeira, Laboratório Nacional de Engenharia Civil (LNEC), Lisboa, PORTUGAL, linanunes@lnec.pt.

1 INTRODUCTION

A *tabique* building component such as a wall, is formed by a timber structure covered by an earth-based mortar on both sides, equivalent to wattle and daub in England or *torchis* in France, Minke [2006] and Torgal & Jalali [2009]. Previously research works Pinto *et al.* [2010] and Cardoso *et al.* [2010], for instance, focused on the study of the *tabique* building technique in *Trás-os-Montes e Alto Douro* region, indicate that a *tabique* wall may have a structural function apart of only being a partition element. According to Pinto *et al.* [2009], it was concluded that the most common building materials used in this context are the *pinus pinaster* for the timber structural elements, a sandy-clayed based mortar for the filling and coating, and steel nails for the connection between timber elements. This research work is part of a study of the *tabique* building technique used in the region of *Trás-os-Montes e Alto Douro*. This region is the northeast part of Portugal. There is a significant incidence of this traditional Portuguese building technique in this region, Carvalho *et al.* [2008] and Martinho *et al.* [2009]. Until early XX century, before the massive introduction of the reinforced concrete, this building technique was very relevant. In this region, there are several examples of *tabique* dwellings that have stone masonry as exterior walls at the ground floor level, and *tabique* exterior walls at the first floor, Cepeda *et al*. [2010]. This paper intends to describe building structural details adopted in a *tabique* dwelling located in *Lamego* Municipality which was considered as a reference of the above feature. This information may contribute for a better understanding of this traditional Portuguese building technique and, therefore, may give guidance for future rehabilitation building processes. This paper is structured as follows: Firstly, the location of the *tabique* dwelling used as reference is done; Secondly, a brief description of this building is delivered and also the description of the adopted overall main structural system solution; Thirdly, some used building details solutions are introduced and described. Finally, the main conclusions are drawn. During this sequence, the level of conservation of the different structural elements is commented.

2 LOCATION OF THE *TABIQUE* DWELLING

As it was stated above, a *tabique* dwelling was used as a reference of a *tabique* dwelling of two floors which has exterior *tabique* walls at the first floor level. This is one of the most common solution types in this region. The other common solution type is a *tabique* dwelling of two floors, having exterior stone masonry walls and *tabique* partition (or interior) walls. The *tabique* dwelling used as reference is located in this region, in the *Douro* North Valley Municipalities Association, in the *Lamego* Municipality and according to Fig. 1. The GPS coordinates of the precise location are: latitude of N 41º 09.230’ and longitude of W 7º 47.117’.

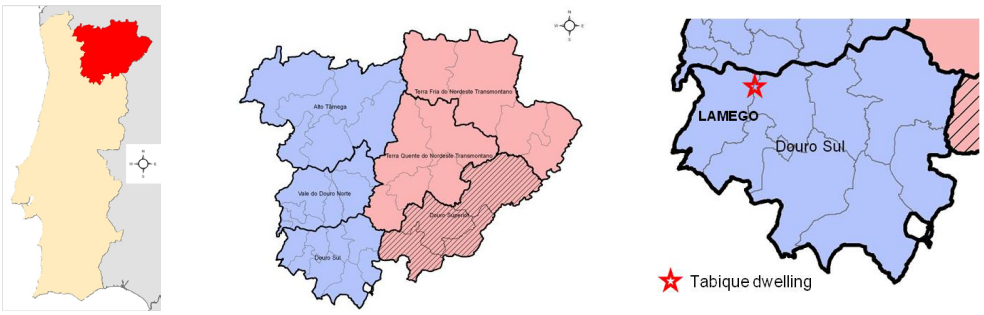

Figure 1. *Tabique* dwelling location

3 OVERALL STRUCTURAL SYSTEM SOLUTIONS

The frontal view of the studied *tabique* dwelling is shown in Fig. 2. Its age is over 100 years old. It is a two floors dwelling (ground and first floors), having an attic. The exterior walls are stone masonries and *tabique* at the ground and the first floors, respectively. All the interior walls are *tabique*. From

Fig. 3 it is noticed that there is no interior *tabique* wall at the ground floor level, this is a common building solution among the *tabique* building already studied. It is evident from Fig. 2 that this dwelling presents an advanced level of deterioration. This fact is in accordance with the results reported in previous works Cepeda *et al*. [2010] which highlight for the urgency of conservation demand that this type of buildings are requiring.



Figure 2. *Tabique* dwelling used as reference

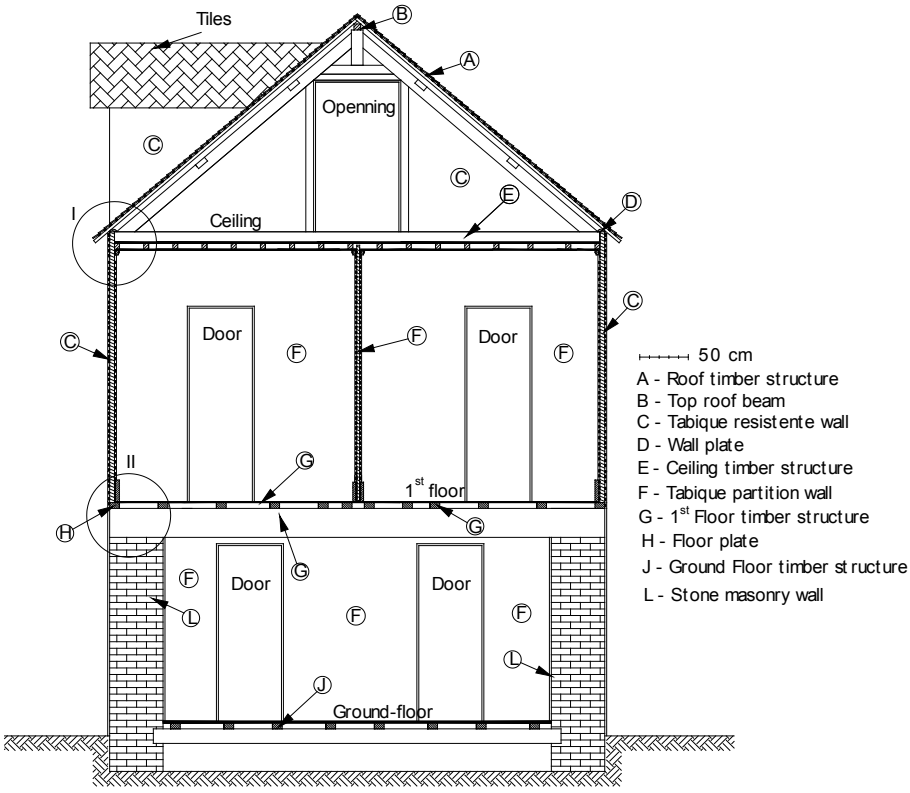

Figure 3. Cross section

The main structural solution is formed by exterior stone masonry walls located at the ground floor level (detail L, Fig. 3) which support timber beams which are part of the timber structural system solution of the 1st floor, (detail G, Fig. 3). This floor also includes boards or secondary beams and the flooring, (detail G, Fig. 3). Meanwhile, exterior *tabique* walls are supported on the beams of the 1st floor (detail II, Figs 3 and 12 c)), at the 1st floor. The floor of the ceiling has a similar timber structural

solution as the 1st floor but inverted, (detail E, Figs 3 and 4 b)). The timber structural solution of the roof is beam type (i.e. 3 hinged arch), detail A of Fig. 3, this structure supports on the beams of the ceiling floor. There is also a timber paving at the ground floor level (detail J, Fig. 3) which its structural solution is similar to the one adopted in the 1st floor pavement. This structure is not in direct contact with the ground, as Fig. 3 illustrates.

The adopted building detail solutions are introduced and described in the next section. This description is done from the top to the bottom. Therefore, building details concerning the solution applied at the roof and ceiling levels are delivered followed by the description of building details related to the *tabique* walls. These building details related to the *tabique* walls are the connections between the exterior walls and the ceiling and the roof, the connection between the exterior wall and the 1st floor and the exterior masonry wall, the orthogonal junction between exterior and exterior walls, and the orthogonal junction between an interior and an exterior wall. Finally, building details related to the timber floors are also introduced.

4 BUILDING DETAILS

4.1 Roof and ceiling level

The roof structural system is shown schematically in Fig. 4 a). The ceramic tiles (A1) are supported on the tile batten (A2) and these ones are supported on the rafter (A3). On the other hand, these last ones are supported at the bottom edge on the wall plate (D) and at the top edge on the top roof beam (B). Two primary timber roof beams, in the same cross section alignment form the 3 hinged arch mentioned above. Meanwhile, Figs 4 b) and 4 c) illustrate the building connection detail between the roof structural system and the external timber walls located at the first floor level.

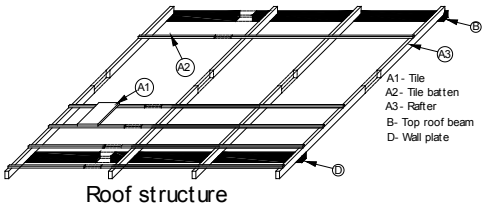

a) Roof structural system

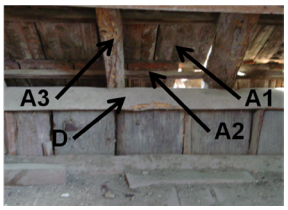

b) Detail I.1

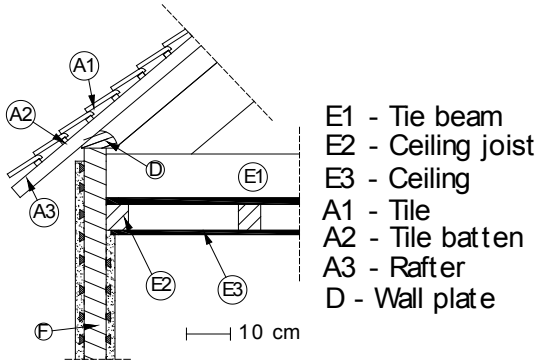

c) Detail I.2

Figure 4. Roof structural system solution

4.2 *Tabique* walls

The exterior and interior *tabique* walls (C and F of Figs 3 and 5) of this dwelling have as timber structural solution vertical elements connected by horizontal ones (i.e. laths), Fig. 5, the horizontal laths helps to support and hold in place the earth based mortar and are used as structural element. This

is precisely the most common timber structural solution used for *tabique* building components in this region, Pinto *et al.* [2010]. From Fig. 5, it is also noticed that these timber elements present a very good level of conservation which contrast with the overall building that is almost reaching the collapse as Fig. 2 shows. We strongly believe that the earth based mortar which completely covers the timber structural elements of the *tabique* walls is able to protect the timber structure. Furthermore, in the interior of the *tabique* walls it was found small peaces of wood which probably resulted from the building process of the main timber structure. This building waste was used to fill the existing gap between the vertical timber elements and as Fig. 5 b) highlights in detail III.



a) Exterior b) Interior

Figure 5. *Tabique* walls

The shape of the cross section (detail IV) and its respective average dimensions of the laths of an exterior wall is shown in Figs 6 a) and b), respectively. Meanwhile, the endings of the laths are mismatched among them as Fig. 6 c) indicates along the vertical direction. This aspect is interesting because it suggests that a *tabique* component may fulfil the conditions prescribed by the EN1995-1-1 [2004] for a load-carrying capacity of systems in which the horizontal timber elements may work as a load distribution system.

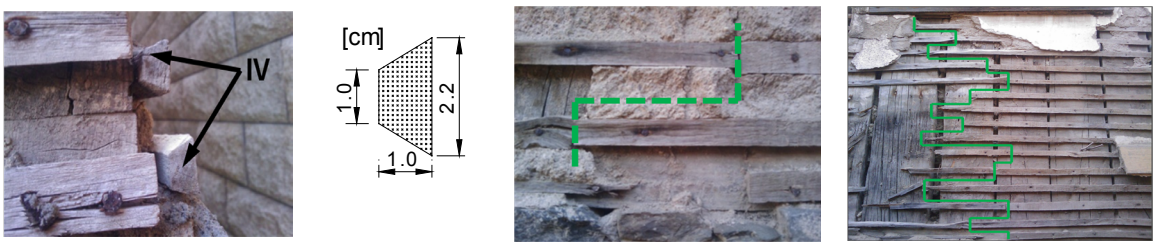

a) Cross section shape b) Dimensions c) Mismatched of the endings

Figure 6. Lattice work of the *tabique* walls

The building connection between *tabique* walls, exterior (C) and exterior (C), and exterior (C) and interior (F) details are presented schematically in Figs 7 a) and b), respectively. The last vertical timber element of each exterior walls connect directly, the horizontal timber elements (i.e. laths) are intercalated. In order to figure out these details it was necessary to remove the coating of earth based mortar locally as Fig. 7 shows. This aspect and the very bad conservation level of the building (unsafe fieldwork), were the main reasons because it was not possible to collect data related to all the building details.

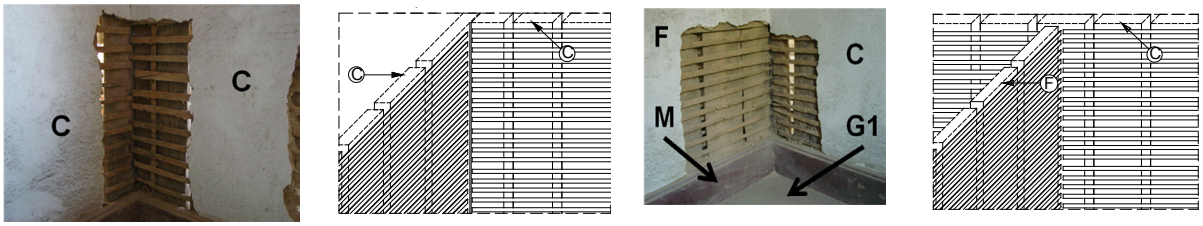

a) Exterior (C) and exterior (C) b) Exterior (C) and interior (F)

Figure 7. Connection between walls

In Figures 6 a) and c) it is noticed that the connection between vertical and horizontal timber elements are materialised by metal nails which correspond to the most common solution as already reported in Pinto *et al.* [2010]. It was also stated there that usually it is used steel nails. In this paper, we are presenting in Fig. 8 a building solution detail of the connection between an exterior *tabique* wall and the floor. The vertical timber elements of the external *tabique* wall are connected to the floor plate or wall plate (H) by metal nails (V) and according to the detail delivered in Fig. 8.



Figure 8. Connection between external *tabique* wall and the floor

4.3 Floors

As it was stated above, in general, the timber floors and, in particular, the first floor has the following structural solution: the main or the principal beams are directly supported on the masonry walls; the boards or the secondary beams are supported on the previously ones; the flooring boards are supported on the secondary beams; the floor plates are supported on the principal beams and, on the other hand, support the exterior *tabique* walls.

The main timber floor beams, G3 in Fig. 9, are simple supported directly to the top edge of the exterior masonry walls. The support length corresponds to the thickness of the wall and as Fig. 12 documents. In this particular case, it corresponds to a 0.60 m average thickness.

Fig. 9 b) and c) also gives guidance to realise how the connection between exterior *tabique* wall and the pavement is done (detail II of Fig. 3) and complements the description done related to Fig. 11. In Fig. 9 b) the main timber floor, the floor plates and the vertical timber elements of the wall are clearly identified as well as, their disposition among them. The outer face coating of the walls have completely deteriorated and disappeared in this part of the walls and this is the reason because the main timber beam top surface is exposed to the outside, Fig. 9 b). In normal conditions, it should be covered and protected with the earth based mortar.



(a) The beam



(b) The support

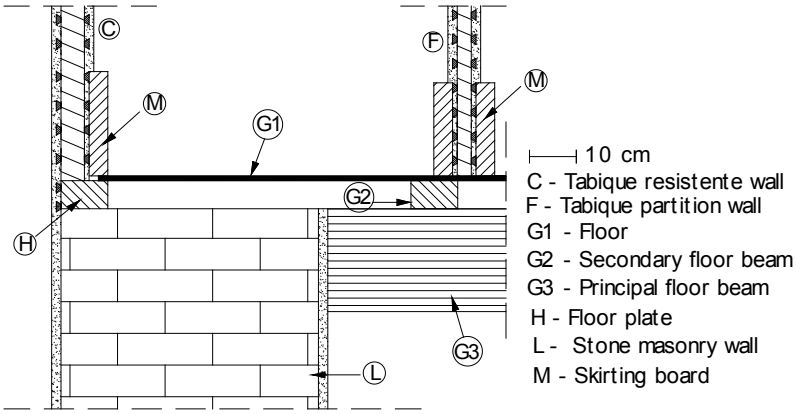

(c) Detail II

Figure 9. The main timber floor beams

5 CONCLUSIONS

The main structural system solution of an ancient *tabique* dwelling located in *Lamego* was presented and described. This system comprises exterior stone masonries walls, *tabique* exterior and interior walls, timber pavements and roof. The usage of timber structural elements is very expressive. These elements were used basically in the upper floors avoiding the direct contact with the ground.
Some building details specific of this dwelling were presented and described throughout this paper. These details were essentially focused on the connection between components. For instance, the connection between the roof structure and the exterior *tabique* wall, the connection between the exterior *tabique* wall and the floor, the connection between the floor and the exterior stone masonry walls were presented.

Furthermore, details of *tabique* walls were also delivered and compared with the results of previously reported research works done in this subject. It was concluded that there is a consistence in this aspect. This paper also highlights the fact that a *tabique* component may guaranty the prescribed conditions by the EN1995-1-1 [2004] for a load-carrying capacity of systems in which the horizontal timber elements may work as a load distribution system.

These details also show a sustainable building procedure which consists on reusing timber waste for the filling of the *tabique* walls. It was noticed that the dwelling used as reference presents an alarming deterioration level almost reaching the ruin. However, it was simultaneously noticed that the timber elements located in the inside and, in particular, the ones still covered by the earth based mortar present a very good level of conservation. The safety conditions for performing the field work were not the convenient ones. This fact hugely limited the data collecting task.

REFERENCES

Cardoso, R., Damião, C., Pinto, J., Paiva, A. & Varum, H. 2010, 'Caso de Estudo de Aferição do Potencial da Aplicação de Terra Local na Reabilitação de Construções de Tabique' , Proc. VII Congreso Internacional de Arquitectura de Tierra, Tradición e Innovación. Cuenca de Campos, Valladolid, 25-26 de Setembro de 2010.

Carvalho, J., Pinto, J., Varum, H., Jesus, A., Lousada, J. & Morais, J. 2008, 'Construções em Tabique na região de Trás-os-Montes e Alto Douro' CINPAR 2008 – 4th International Conference on Structural Defects and Repair. Civil Engineering Department – University of Aveiro. Portugal. 25-28 June 2008. Editors: Humberto Varum, Francisco Carvalho, Aníbal Costa, Alexandre Bertini, Petr Stepánek. ISBN: 978-989-95695-3-9.

Cepeda, A., Murta, A., Lousada, A., Vieira A., Pinto, J., Fernandes, L., Tavares, P., Silva, P. & Varum, H. 2010, 'Tabique construction in Alto Tâmega'. Book of abstracts of the 1st International Conference on Structures and Architecture (ICSA2010). Ed. Paulo Cruz. CRC Press, Taylor & Francis Group. London. ISBN 978-0-415-49249-2. pp. 397-398

EN 1995-1-1: 2004. Eurocode 5: design of timber structures – part 1.1: general rules and rules for buildings. European Committee for Standardization, Brussels, Belgium, (E).

Martinho, J., Gonçalves C., Magalhães, F., Lousada, J., Vieira, J., Varum, H.; Tavares, P. & Pinto, J. 2009, 'Construção de Tabique no Vale do Douro Sul'. CD do VIII Seminario Iberoamericano de Construcción com Tierra (VIII SIACOT) e do II Seminario Argentino de Arquitectura y Construcción com Tierra (II SAACT). Editor: CRIATIAC – FAU – UNT. Tucumán, Argentina, Junho de 2009, pp. 514 - 521.

Minke, G. 2006, *Building with Earth, Design and Technology of a Sustainable Architecture*. Birkhäuser – Publishers of Architecture, Basel-Berlin-Boston. ISBN 13: 978-3-7643-7477-8.

Pinto, J., Varum, H., Cruz, D., Sousa, D., Morais, P., Tavares, P., Lousada, J., Silva, P. & Vieira, J. 2010, 'Characterization of Traditional Tabique Constructions in Douro North Valley Region'. *Journal WSEAS Transactions on Environment and Development,* ISSN 1790-5079, **2**, pp. 105-114.

Pinto, J., Varum, H., Cruz, D., Sousa, D., Morais, P., Tavares, P., Lousada, J., Silva, P. & Vieira, J. 2009, 'Tabique Construction Characterization in Douro North Valley, Portugal: A First Step to Preserve this Architectural Heritage', 2nd WSEAS International Conference on Urban Rehabilitation and Sustainability (URES'09) - Environmental Science and Sustainability - Proceedings published by WSEAS Press (printed and in CD), Editors: Manoj Jha, Charles Long, Nikos Mastorakis, Cornelia Aida Bulucea, ISBN 978-960-474-136-6, ISSN 1790-5095, Baltimore, USA, 7-9 de Novembro de 2009, pp. 48-53.

Torgal F. Pacheco, Jalali Said *et al*. 2009, *A construção em Terra*. Ed. TecMinho. Universidade do Minho, Guimarães 2009. ISBN 978-972-8692-40-7.

XII DBMC
International Conference on Durability of Building Materials and Components
PORTO - PORTUGAL, April 12th-15th, 2011

Influence of Grain Size of Aggregate in Freeze/thaw Cycles of Lime Mortars

Sandro Botas [1]
Vasco M. Rato [2]
Paulina Faria [3]

ABSTRACT

Mortars are porous materials used in several types of applications in construction. Like any other building material, it is necessary to have a good understanding of their behaviour to fulfil the requirements that are defined in each case. When the use of cement became generalized, the lime-based mortars fell into disuse and the knowledge of centuries was progressively lost. It is therefore necessary to resume and further deepen this knowledge in order to create the conditions for the use of lime-based mortars, not only in conservation and rehabilitation, but also in new buildings.

The objective of this paper is to evaluate the influence of the grain size of aggregate in freeze/thaw cycles of lime based mortars. Twelve mortar compositions were prepared by varying the type of binder (air lime, hydraulic lime and air lime + cement), sand grain size and the use of an air entraining agent. These mortars were tested for mechanical strength, open porosity, capillary water absorption and resistance to freeze/thaw cycles, in order to evaluate their performance particularly in cold climates.

Through the analysis of the results some conclusions were drawn, namely about the aggregate grain size, the use of an air entraining agent and the influence of different types of binders. The open porosity depends mainly on the particle size of the sand and the mechanical strength depends on the type of binder used. These two properties have a great influence on the resistance to freeze/thaw cycles and consequently in its adequability to cold climates.

KEYWORDS

Mortar, lime, aggregate, resistance to freeze/thaw

[1] National Laboratory for Civil Engineering (LNEC), Lisbon, PORTUGAL, sandro_botas@hotmail.com
[2] ISCTE – University Institute of Lisbon, DINAMIA-CET, Lisbon, PORTUGAL, vasco.rato@iscte.pt
[3] Faculty of Science and Technology, *Nova* University of Lisbon, PORTUGAL, paulina.faria@fct.unl.pt

1 INTRODUCTION

Lime-based mortars were, in the past, commonly used in buildings and are now a frequent option in conservation. The good condition of some built heritage shows the quality of this material in terms of durability. For centuries, air lime was the widely used binder.

The rise of cement and cement mortars has changed sharply the use of lime mortars. In a short period of time, there was an excessive use of cement in new construction and, later, in rehabilitation. Lime mortars fell therefore into disuse and the knowledge of centuries was lost. Decades later, it was noted that the total replacement of lime mortars by cement mortars, common practice in conservation and rehabilitation, was a very serious mistake.

Cement mortars have mechanical, physical and chemical incompatibilities with old building materials; for instance, they are too stiff and strong and too much impermeable to water vapour, when compared with old masonry walls, and soluble salts are released during the hardening process. Generally, cement mortars also have a shorter service life when compared to old lime-based mortars. Instead of protecting old walls, cement-based mortars contribute to their deterioration. A strong research is needed, and is on-going by many researchers, in order to optimize the behaviour of mortars based in lime.

The durability factor is very important in mortars for building construction. Mortars have greater durability when a better resistance to deterioration is obtained. Deterioration agents may vary depending on regional and climatic characteristics. Arid, sunny and cold climates are propitious to have, respectively, deterioration agents such as wind, sun and freeze/thaw cycles [Botas 2009]. The presence of water, one of the main deterioration agents of mortars, increases the effect of freeze/thaw cycles in cold climates. Freeze/thaw is a cyclic process during which a change in volume occurs as water crystallizes within the mortar during freezing prior to its liquefaction during melting. The durability of mortars to freeze/thaw cycles is dependent on their ability to resist water penetration and to lose water quickly - to prevent freezing inside the mortar - and also on a porous structure that is able to resist the strain caused by the increased volume of freezing water in successive cycles [Coutinho 1997].

Sand, as an aggregate, has a significant role in the properties of mortars. Therefore, the variation of its type is one of the most effective ways to induce changes in the mortar microstructure when the objective is to evaluate and compare the response to a specific external action. The sand is like the "skeleton" of the mortar, gaining cohesion by the connection of its particles to the binder. The quality of the aggregate is therefore essential to the mortar volume stability, durability and structural performance.

Based on the previous assumptions, a research program was developed aiming at the study of freeze/thaw cycles in lime-based mortars. The type of binder, the use of an air entraining agent and the grain size of sand were the variation factors used to induce different properties in the hardened mortars. In this paper, the relationship between the mortar microstructure - resulting from the use of different sands - and their behaviour to freeze/thaw cycles is presented and analysed.

2 EXPERIMENTAL CHARACTERIZATION OF MORTARS

The standards, when available and considered adequate, were the base of the experimental procedures. Mortar test standards are sometimes not adequate for the assessment of lime-based mortars because they were not specifically prepared to this type of material. Mortar test specifications [Henriques 1999] developed by the research team at the Faculty of Science and Technology of *Nova* University of Lisbon (UNL) were used for complementing the standard test specifications.

2.1 Mortar Materials

The materials used in the experimental campaign were a commercial hydrated air lime (CL90 from Lusical), a commercial hydraulic lime (NHL5 from Secil), Portland cement (CEM I / BL 32.5 N from Secil), a commercial current washed river sand, two grain size controlled sands (AGS 1/2 – coarse sand and FPS120 – fine sand), public drinking water and an air entraining agent (AER5 from Sika). The air entraining agent, when used, was applied following the commercial recommendations and the same quantity was always added. Figure 1 presents the grain size distribution of sands.

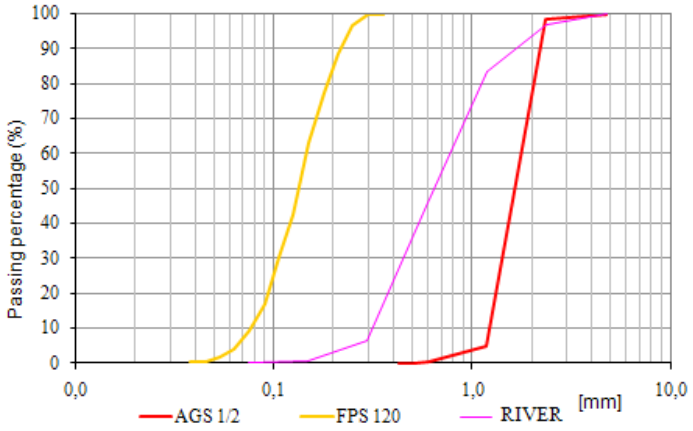

Figure 1. Grain size distribution of sands

2.2 Mortar Preparation and Test Program

Twelve mortars were prepared as described in Table 1. The general procedure used in the mortars mixing was based on the European Standard EN 1015-2:1998 [CEN 1998] with indications from the test card Fe 19 [Henriques 1999]. The mortars were mechanically mixed in a laboratory mixer using a standard sequence of operations. Compaction in the moulds was mechanically performed by twenty falls for each of two layers. Impermeable metallic moulds (40mm x 40mm x 160mm) were used with a minimum of grease to assure removal. Once moulded, the samples were kept in controlled conditions at 20±2 ºC and 65±5 % relative humidity. Curing time was 90 days for the air lime mortars without an air entraining agent and 60 days for the remaining mortars.

The testing program included the determination of the consistency of fresh mortars, mechanical properties - flexural and compressive strength -, open porosity, capillary water absorption and the resistance to freeze/thaw cycles of hardened mortar samples.

2.3 Fresh Mortar Characterization

Flow table consistency tests were performed based on EN 1015-3:1999 [CEN 1999a]. The mortar average diameter after 15 shots of the flow table in 15 seconds was registered. In the case of mortars without an air-entraining agent, the amount of water used in the mixing was dependent on the flow value using 175 mm as reference. For air-entrained mortars, water quantity was the same as the respective mortars without the admixture.

2.4 Hardened Mortar Characterization

The open porosity of the mortars was determined following the test specification Fe 02 [Henriques 1999], based on hydrostatic weighing after vacuum immersion [RILEM 1980, CEN 1999c].

Mechanical properties were evaluated by the three points bending flexural strength procedure and by a common compressive strength testing. Tests were performed using an universal tensile machine according to EN 1015-11:1999 [CEN 1999b].

Water absorption by capillary test was conducted according to Fe 06 [Henriques 1999] and similar to EN 15801:2009 [CEN 2009] and EN 1015-18:2002 [CEN 2002].

Tests to assess the resistance to freeze/thaw cycles specifically in lime-based mortars are not addressed in any current standard. The existing standards related to freeze/thaw test methods are specific to concrete, ceramic materials or natural stone. These procedures were considered too aggressive for lime mortars, mainly due to the fact that each cycle considers the immersion of the samples. A different and original testing method was adopted - based on the method described by Konow [2005] - with the objective of measuring specimen mass loss and their visual aspect during the deterioration process; a qualitative and a quantitative assessment of the damage over time were established.

The mortar samples were immersed in water until constant weight was obtained - less than 1% weight variation in 24h. They were then placed inside sealed airtight bags to retain their moisture conditions and placed inside an environmental chamber programmed to simulate freeze/thaw cycles. The environmental chamber was scheduled to carry out two cycles per day with a temperature interval of -10 °C to 10 ºC.

Stagnation time in each extreme temperature was defined in two hours. The samples were weighed every 24 hours after two hours of rising temperature. The test was concluded when a substantial disintegration of the sample occurred - percentage of weight loss greater than 30 % of the original mass of the sample - with a limit of 40 cycles. Three comparative index corresponding to the percentage of weight lost at 10 (i10), 20 (i20) and 40 cycles (i40) were established.

The test is easy to carry out with simple equipment. A critical aspect that can be pointed out is that it does not take in to account the different drying capacity of mortars between freeze/thaw cycles.

3 RESULTS AND DISCUSSION

This chapter presents the results of the experimental campaign and a relational analysis seeking to identify the characteristics of a mortar that produce the most promising resistance to freeze/thaw cycles. Table 1 presents the constituents of each mortar, the volumetric ratio of binder:aggregate and the results of porosity tests, capillary absorption – water capillary coefficient and asymptotic value of capillary absorption -, compressive and flexural strength. Table 2 includes the percentage of weight lost after 10, 20 and 40 freeze/thaw cycles. Some mortars disintegrated between the 20th and the 40th cycle.

3.1 Open porosity

Mortars with sand AGS1/2 have the lower open porosity values. The higher open porosity of mortars with sand FPS120 was expected, since a finer grain size leads to greater specific surface and a great amount of pores. The binder that leads to greater difference in porosity values was hydraulic lime (with sand AGS1/2 - 29%; with sand FPS120 - 39%). The air entraining agent increased the open porosity of river sand mortars, also as expected.

3.2 Capillary absorption

Two opposite trends are identified when analysing hydraulic binder mortars and air lime mortars. In air lime mortars, capillary absorption coefficient decreases with decreasing particle size of sand,

whereas in mortars with hydraulic binder the coefficient increases with the reduction of the aggregate particle size. This different behaviour can be explained taking into account the great interconnectivity of pores in air lime mortars. The absorption coefficient depends on the pore size and the connectivity of the porous network. In air lime mortars, the connectivity that determines the absorption coefficient depends mainly on large pores. In mortars with lower porous connectivity "the absorption coefficient depends of open porosity. In this case, the water access only to large pores through the binder matrix fractions; since the size magnitude of small pores is very uniform and the water absorbed depends on the pore volume available, the absorption coefficient is greater in mortars with bigger porosity" Rato [2006]. All mortars show a clear trend towards greater volume of capillary water absorption with decreasing particle size of sand.

Tab1e 1. Mortar constituents and test results

Material			Binder: aggregate ratio(vol.)	Por.	Capillary absorption		C.S.	F.S.
Binder	Sand	A.E.		[%]	C.C. [kg/m^2.s^{0,5}]	A.V. [kg/m^2]	[MPa]	[MPa]
al	AGS1/2	-	1:2	31	0,39	33,98	0,46	0,17
	River	-	1:2	34	0,26	36,31	1,01	0,30
	FPS120	-	1:2	38	0,24	38,75	2,23	0,58
hl	AGS1/2	-	1:3	29	0,41	36,50	0,53	0,11
	River	-	1:3	32	0,43	42,70	0,43	0,13
	FPS120	-	1:3	39	0,63	53,14	0,79	0,34
alc	AGS1/2	-	1:1:6	30	0,28	31,60	3,95	0,76
	River	-	1:1:6	30	0,30	38,26	4,89	1,05
	FPS120	-	1:1:6	37	0,42	50,32	5,00	1,35
al	River	yes	1:2	35	0,27	36,21	1,04	0,26
hl		yes	1:3	34	0,36	37,74	0,52	0,11
alc		yes	1:1:6	32	0,28	36,65	5,13	0,93

Binder: al - air lime, hl - hydraulic lime, alc - air lime+cement.
Sand: AGS1/2, river, FPS120. A.E. – yes when air entraining agent is used.
Tests: Por.- open porosity, C.C.- capillary coefficient, A.V.- Asymptotic value of capillary absorption, C.S.- compressive strength, F.S.- flexural strength.

Table 2. Resistance to freeze/thaw cycles

Freeze/thaw cycles – weight loss [%]	Sand type											
	al			hl			alc			al	hl	alc
	AGS	River	FPS	AGS	River	FPS	AGS	River	FPS	River+A.E.		
i10	1,1	0,6	2,3	0,4	0,2	5,0	0,7	0,8	0,9	0,6	0,8	0,7
i20	19,2	2,4	5,9	1,9	3,4	6,0	2,6	1,8	2,1	2,4	4,3	1,8
i40	-	7,5	-	4,6	6,4	9,5	28,9	4,4	3,2	10,5	6,5	29,3

Sand type: AGS - AGS1/2, FPS - FPS120, River+A.E. - mortar with river sand and air entrained agent
Binders: al - air lime, hl - hydraulic lime, alc- air lime+cement
Coefficients: i10, i20 and i40 - percentage of weight loss after 10, 20 and 40 freeze/thaw cycles

3.3 Compressive and flexural strength

There is an increase of mechanical resistance - flexural and compressive strength - when particle size of aggregate decreases. Reddy & Gupka [2008] presented different results, stating that in finer sand mortars the connection binder-aggregate is weaker than in coarser sand mortars. The explanation for the observed trend seems to be the mortars curing time. Stefanidis and Papayianni [2005], in an aggregates study for lime mortars, indicate that, in the long term, coarse aggregates are advantageous

for the mechanical strength of mortars. With 90 days curing time in air lime mortars with fine aggregate, the larger pores and cracks are located in the lime matrix, and in lime mortars with coarse aggregates the larger pores and cracks are located at the boundary aggregate-binder. With an extended curing time (730 days) the cracks are blocked by coarser grain aggregates.

The work presented here studied mortars with 90 days cure time and finer aggregate mortars presented in fact higher mechanical strength. The only exception to this evident trend occurred with mortar with hydraulic lime and sand AGS1/2 for compression strength. It is thought that this difference is not significant.

In the case of mortars with an air entraining agent compressive strength results were not as expected. The use of this component increased the compressive strength in all mortars. The fact that the results of this test do not follow the trend of flexural resistance is also quite unexpected. The air entraining agent may have unknown plasticizers properties.

3.4 Resistance to freeze/thaw cycles

Air lime mortars presented different behaviour to freeze/thaw cycles depending on their other components. Mortars with AGS1/2 and FPS120 had similar behaviour among themselves, with a lower resistance to freeze/thaw. These mortars did not complete 40 freeze/thaw cycles and it was not possible to identify any clear trend. The explanation to this performance may be the pore size distribution and the pore structure properties. FPS120, being a very fine sand, may create small pores which decrease the resistance to freeze/thaw cycles [Powers cited by Chaterji 2003]. AGS1/2 is made of large particles that probably lead to wide drying/shrinkage cracks and the hardened material loses cohesion [Lanas & Alvarez 2003]. Air lime mortar with a currently used river sand presented acceptable results even after 40 cycles.

In hydraulic lime mortars it was identified a general trend of worse behaviour to freeze/thaw cycles with the decreasing particle size of aggregate. This type of mortar has presumably less shrinkage cracks when compared to lime mortars. The porosity seems to assume great importance in the behaviour of these mortars; with finer sands, porosity increases but the smaller pore sizes could justify this behaviour. Hydraulic lime mortars had a weight loss between 5% and 10% after 40 cycles, meaning they are mortars with a homogeneous behaviour.

Lime + cement mortars present different behaviour with extreme grain size aggregates. FPS120 (finer sand) mortars are the ones with a better resistance to freeze thaw/cycles and mortars with AGS1/2 (coarser sand) are those with the poorest performance. Despite the good performance after 20 cycles, this mortar loses a great amount of material after 40 cycles. The rate of deterioration decreases with an increasing open porosity. This may be explained with the mechanical strength. The increasing of freeze/thaw resistance is associated with higher mechanical strength. Cement does increase the mechanical strength of mortars and therefore the lime + cement mortar analysed do has a better resistance to freeze/thaw cycles.

4 CONCLUSIONS

This work compared 12 mortars compositions to study the influence of grain size of aggregate in the microstructure of mortars in order to assess the resistance to freeze/thaw cycles.

In air lime mortars, capillary absorption coefficient decreases with decreasing particle size of sand, probably due to their large pores and better connected porous structure. In hydraulic mortars, the capillary coefficient increases with decreasing sand particle size; the amount of pores and the less significant connectivity seem to have greater importance. Generally, the mechanical strength of mortars increases with decreasing particle size of aggregate.

In face of freeze/thaw cycles, air lime mortars with AGS1/2 and FPS120 sands had similar behaviour, with a low resistance to this type of action and did not complete 40 freeze/thaw cycles. Hydraulic lime mortars show a general trend of a worse behaviour with the decreasing particle size of aggregate. In air lime + cement mortars the rate of deterioration decreases with an increasing open porosity. In this type of mortars, an increasing resistance to freeze/thaw is associated with higher mechanical strength, when compared to lime mortars.

The use of an air entraining agent led to unexpected and inconclusive results. Further studies should be developed varying the quantity of this admixture and the curing time of mortars.

The freeze/thaw test developed in this study led to reliable and conclusive results with this type of mortars. Its little destructive nature - when compared with other freeze/thaw tests - allows the evaluation of mechanically weaker mortars like lime based mortars.

ACKNOWLEDGMENTS

The authors are greatly acknowledged to the section of Building Materials at the Department of Civil Engineering (DEC) of *Nova* University of Lisbon (UNL) where the experimental campaign was performed and the financial support from the Portuguese Science and Technology Foundation to projects LIMECONTECH – PTDC/ECM/100234/2008 and AZULEJAR – PTDC/ECM/101000/2008.

REFERENCES

Botas, S. 2009, '*Testing the behaviour of mortars in cold climates*' (in Portuguese). MSc thesis in Civil Engineering, Nova University of Lisbon.

Chatterji, S. 2003, *Freezing of air-entrained cement-based materials and specific actions of air-entraining agents*. Cement and Concrete Research 25, pp. 759-765.

CEN 1998, *Methods of test for mortar for masonry. Part 2: Bulk sampling of mortars and preparation of test mortars*. Brussels, EN 1015-2:1998/A1:2006.

CEN 1999a, *Methods of test for mortar for masonry. Part 3: Determination of consistence of fresh mortar (by flow table)*. Brussels, EN 1015-3:1999/A1:2004/A2:2006.

CEN 1999b, *Methods of test for mortar for masonry. Part 11: Determination of flexural and compressive strength of hardened mortar*. Brussels, EN 1015-11:1999.

CEN 1999c, *Natural stone test methods. Determination of real density and apparent density, and of total and open porosity*. Brussels, EN 1936:1999.

CEN 2002, *Methods of test for mortar for masonry. Part 18: Determination of water absorption coefficient due to capillary action of hardened mortar*. Brussels, EN 1015-18:2002.

CEN 2009, *Conservation of cultural property. Test methods. Determination of water absorption by capillarity*. Brussels, EN 15801:2009.

Coutinho, A. Sousa 1997, '*Manufacture and properties of concrete*' (in Portuguese). Vol I, 3ª ed.. Lisboa, LNEC. ISBN 972-49-0326-5.

Henriques, FMA 1999, Test cards Fe 02, Fe 06, Fe 19, Fe 25 e Fe 27 (in Portuguese). FCT/UNL.

Konow, T. Von 2005, *Theory transformed in practice and the results from practice distorting theories. Experiences from masonry restoration at the Fortress of Suomenlinna in Finland*. Repair Mortars for Historic Masonry. RILEM Workshop. Delft University of Technology.

Lanas, J. & Alvarez, J.I. 2003, *Masonry repair lime-based mortars: Factors affecting the mechanical behaviour*. Cement and Concrete Research 33, pp. 1867-1876.

Rato, Vasco M. 2006, *Microstructure morphology influence on mortars behaviour* (in Portuguese). PhD thesis in Civil Engineering, Nova University of Lisbon.

Reddy. B. V. & Gupka, Ajay 2008, *Influence of sand grading on the characteristics of mortars and soil-cement block masonry*. Construction and Building Materials 22, pp. 1614-1623.

Stefanidou, M. & Papayianni, I. 2005, *The role of aggregates on the structure and properties of lime mortars*. Cement and Concrete Composites 27, pp. 914-919.

RILEM Commission 25 PEM 1980, Essais recommendés pour mesurer l´alteration des pierres et évaluer l´efficacité des methods de traitment. Matériaux et Constructions, 13 [75].

XII DBMC
International Conference on Durability of Building Materials and Components
PORTO - PORTUGAL, April 12th-15th, 2011

Water and Chloride Transport Properties of Renovation Plasters Developed for Historical Masonry

Zbyšek Pavlík [1]
Lukáš Fiala [2]
Milena Pavlíková [3]
Robert Černý [4]

ABSTRACT

Water and water-soluble salts represent harmful substances that critically affect materials' durability and service life. Therefore, for the durability improvement of buildings, it is necessary to study water and salt transport properties of materials used in the building structures. Especially in historical buildings, several degradation mechanisms of water and water soluble salts can be usually recognized. On that account, investigation of properties of two types of newly developed mortars that should find application in restoration of masonry of historical buildings is presented in the paper. Within the performed experiments, measurements of chloride binding isotherms, moisture and salt concentration profiles are done. Determination of moisture and chloride concentration profiles is done in the conditions of one-sided water or sodium-chloride-in-water solution uptake. Experimentally determined concentration profiles are then used for identification of chloride diffusion coefficient and moisture diffusivity on the basis of inverse analysis using the diffusion-advection model. These material parameters represent necessary information for assessment of materials' durability from the point of view of possible water and salt induced damage. The obtained results can find use also in the computational modelling of material performance even in the long time period and exposure to harmful climatic conditions.

KEYWORDS

Renovation mortars, moisture and chloride trasnport, salt accumulation, historical buildings

[1]Czech Technical University, Prague, CZECH REPUBLIC, pavlikz@fsv.cvut.cz
[2]Czech Technical University, Prague, CZECH REPUBLIC, fialal@fsv.cvut.cz
[3]Czech Technical University, Prague, CZECH REPUBLIC, milena.pavlikova@fsv.cvut.cz
[4]Czech Technical University, Prague, CZECH REPUBLIC, cernyr@fsv.cvut.cz

1 INTRODUCTION

In the investigation of effect of harmful environmental factors on materials and buildings, one must take into account that the deterioration process is a complex interplay of the effects of climate and local meteorological characteristics, of biological processes and of compex chemical reactions and processes resulting from the impact of environmental pollutants and natural constituents from the surrounding environment. The most of decay processes are usually result of temperature, moisture, solar radiation, wind, air pollutants, water soluble salts and biological organisms' action. According to Mocmanová [2007], the main deterioration mechanisms include erosion, volume change of material and the volume changes in material porous structure, dissolution of a material and the associated chemical changes, and biological processes.

Since the salt weathering is considered by many authors as a major decay mechanism in a wide range of materials and environments [Thorborg von Konow 2006], [Antonova *et al.* 2006], we have focused on this problem in the presented work. There are many ways in which the building materials and structures become contaminated with salts. Probably air pollution is a major source of sulphates and nitrates. Other salt source includes subsoil, from which salts may be carried into the masonry by rising damp. The salts can be also blown by the wind from the sea or the deserts. Another significant source of salt is represented by deicing salts and incompatible building materials [Price, 1996].

The salt related durability problems are observed above all in historical and older buildings, however, for example in highway construction, the harmful salt action is important also in newly built structures, as bridges and highways. On that account, the salt action, mechanism of their transport, crystallization, and accumulation, represent highly actual topic for researches coming from culture heritage and monuments restoration area as well as from areas dealing with design of new building structures. One must take into account also the fact that the salt action is coupled with the liquid water transport and possible water vapour evaporation. Therefore, the process of salt and water transport must be studied together [Pavlík 2009].

Within the salt damage and weathering research, many conservation and redevelopment treatments have been developed for the consolidation and protection of porous building materials affected by salt weathering. However, these methods commonly do not stop the further development of salt damage [Price, 1996]. Protection efforts may even enhance salt damage by preventing the migration of saline solutions towards the material/air interface, thereby inducing subflorescence growth when salts are already present in the pores or when they are supplied by capillary rise. On the other hand, current desalination methods are mainly inefficient in some ways (e.g. poulticing, reverse osmosis). Hence, there is a need for the development of new conservation treatments, which can preferably be applied both for preventing salt damage development, and for obtaining effective desalination. The better understanding to the coupled moisture and salt transport mechanism is needed as well, especially for the optimisation of the conservation and reconstruction treatments, and for the damage assessment of buildings and their inbuilt materials.

The main objective of the presented work is to contribute to the explanation of the process of water salt solution transport in the inner structure of porous building materials. It should be beneficial for practical application of materials, their restoration, protective treatments, as well as for computational analysis of durability problems of existing buildings and estimation of their service life. Also the formulation of experimental and computational approach for the assessment of water and salt properties of building materials that is presented in the paper represents significant contribution to the investigation of salt related problems of buildings and inbuilt materials.

2 EXPERIMENTAL

In the experimental part of the paper, measurement of moisture and chloride concentration profiles was done in the conditions of one-sided 1-D suction experiment. Also the measurement of chloride

binding isotherms was realised. These measurement were done in order to get necessary input data for computational assessment of material parameters characterising the coupled water and chloride ions transport in the inner structure of investigated materials.

2.1 Studied materials

As the chemical analyses of many plasters from historical buildings show, the past centuries external plasters that are preserved until today contain products formed by lime reaction with pozzolanic or hydraulic admixtures. Pozzolanic admixtures appeared to have positive effect on properties of lime binder and the pozzolanic compounds are the cause of the plasters resistance against environmental conditions and in this way of the durability of these plasters [Cabrera & Rojas 2001], [Pernicová *et al.* 2008], [Fiala *et al.* 2010]. On that account, our research focused on the development of lime-based mortars with addition of pozzolanic admixtures. Within the intensive research, applicability of several pozzolanas was tested, among them, metakaolin, milled ceramic brick, and different types of mudstone were the most in detail studied admixtures.

In this paper we studied two lime plasters (denoted S53P and S54P) modified with pozzolana based on calcined kaoline mixed with milled mudstone. This pozzolana material is formed within the calcination of raw kaoline in rotation kiln at temperature close to 750°C and consequent milling in rotation silo. To this "metakaolin" is then added milled mudstone and the mixture is homogenized. The final material is highly fine having specific surface area 14.56 m^2/g and D_{50} 4.09 μm. The chemical composition of used pozzolana measured by X-ray fluorescence analysis is presented in Table 1.

Table 1. Chemical composition of the used pozzolana (in mass %).

SiO_2	52.4
Al_2O_3	41.3
Fe_2O_3	1.19
TiO_2	1.77
CaO	0.14
MgO	0.15
K_2O	0.79
Na_2O	< 0.01
P_2O_5	0.07
ZrO_2	0.03
V_2O_5	0.05
F	< 0.01
Cr_2O_3	0.03
SO_3	0.10

Compostion of the studied plasters is given in Table 2. Lime hydrate is product of the lime kiln Čertovy schody, Inc., Czech Republic, whereas the silicious sand is coming from sand-pit Hlavačov, Czech Republic. Looking at Table 2, one can see that the studied plasters differ in amount of pozzolana only. The water/dry substances (w/d) ratio was then slightly modified in order to keep the workability of fresh mixtures on the same level.

Table 2. Composition of studied plasters.

Plaster	*Lime hydrate* [kg]	*Pozzolana* [kg]	*Sand 0 – 4 mm* [kg]	*w/d ratio* [-]
S53P	200	50	750	0.23
S54P	150	100	750	0.21

The basic properties of studied plasters are given in Table 3. We can see that both developed plasters exhibit high total open porosity what is promising feature, as for their application in historical buildings.

Table 3. Basic properties of renovation plasters.

Plaster	*Bulk density* [kg/m^3]	*Matrix density* [kg/m^3]	*Total open porosity* [-]
S53P	1688	2560	0.341
S54P	1694	2582	0.344

2.2 Experimental Determination of Moisture and Chloride Concentration Profiles

For determination of moisture diffusivity and chloride diffusion coefficient of studied plasters, the measurement of moisture and chloride concentration profiles was necessary. In the transport experiments, coupled water and chloride transport was investigated in the conditions of one-sided water or sodium-chloride-in-water solution uptake. For this purpose, rod-shaped samples with the dimensions of 20 x 40 x 290 mm were used for the determination of moisture and chloride concentration profiles. Epoxy resin was employed for water and vapour proof insulation on the lateral sides to assure 1-D water and salt solution transport. In the determination of moisture and chloride concentration profiles, the specimens were put in contact with distilled water and 1M NaCl solution, whereas the measurements were realised in the vertical setup. After chosen time intervals (1h, 2h, 24h) the samples were cut into several pieces 20 mm thick, and the moisture content was determined in each piece by gravimetric method. The chloride concentration was measured in each piece by means of ion chromatography.

2.3 Measurement of Chloride Binding Isotherms

Within the salt transport, part of salt ions is accumulated in the porous structure of materials and bonded on the pore walls. This process is realised both on physical as well as on chemical principle. For the description of material capacity do bound salt ions, the salt binding isotherms are measured as complex parameter taking into account physically as well as chemically bonded ions. The binding isotherm represents dependence of the amount of bound ions C_b [kg/m$^3_{(sample)}$] in the material on the free ions concentration C_f [kg/m$^3_{(solution)}$] in the pore solution in equilibrium conditions. In this work, the chloride binding isotherms of studied plasters were measured using modified adsorption method [Jiřičková & Černý 2006]. For the measurement, samples having dimensions of 40 x 40 x 10 mm were used. Experimental procedure is quite simple. Within the measurement, the samples are put into water salt solution of specific known concentration until the equilibrium is reached. Then, the salt concentration in particular sample is measured and point wise function $C_b=C_b(C_f)$ is determined. In this paper, the salt concentration in the analysed solutions was measured using pH/ION 340i device with utilization of ion selective electrode. On the basis of measured concentrations, the content of bound chlorides was obtained by calculating the difference between the concentration of the initial solution and the concentration after certain period of exposure, when the equilibrium is reached.

3 Computational Assessment of Moisture Diffusivity and Chloride Diffusion Coefficient

Moisture diffusivity and chloride diffusion coefficient as main parameters characterising the materials' capability to transport water and salt were calculated using inverse analysis of measured moisture and salt concentration profiles. For the inverse analysis, there is crucial to formulate optimised and reliable mathematical model that describes coupled moisture and salt transport. Here we assumed diffusion-advection mechanisms of chloride ions transport [Bear & Bachmat 1990], whereas the partial chloride binding was taking into account as well. In model formulated by Bear and Bachmat [1990] the chloride mass balance is expressed by the following equation

$$\frac{\partial(wC_{fCl})}{\partial t} = div(wDgradC_{fCl}) - div(C_{f\,Cl}\vec{v}) - \frac{\partial(C_{bCl})}{\partial t}, \quad (1)$$

where C_{fCl} [kg/m^3] is the concentration of free chlorides in water, C_{bCl} [kg/m^3] the concentration of bound chlorides in the whole porous body, D [m^2/s] the chloride diffusion coefficient, $\vec{v}$ [m/s] the Darcy's velocity, and w [m^3/m^3] the volumetric moisture content measured for salt solution penetration.

The water mass balance is expressed by equation

$$\frac{\partial w}{\partial t} = div(\kappa(w)\, gradw), \quad (2)$$

where κ [m^2/s] is the moisture diffusivity dependent on moisture content determined for transport of salt solution (in our case for penetration of 1M NaCl water solution).

For calculation of $D(C_{Cl})$ and $\kappa(w)$ functions, inverse analysis of concentration profiles using an extension of the Boltzmann-Matano treatment was performed. We have assumed constant initial conditions and Dirichlet boundary conditions on both ends of the specimen for both moisture content and salt concentration, where one of the Dirichlet boundary conditions was equal to the initial condition. For details on inverse analysis procedure and final formulas for determination of chloride diffusion coefficient and moisture diffusivity see Pavlík *et al.* [2006].

4 RESULTS AND DISCUSSION

The ion binding isotherms measured for NaCl water solution by modified adsorption method are presented in Fig. 1.

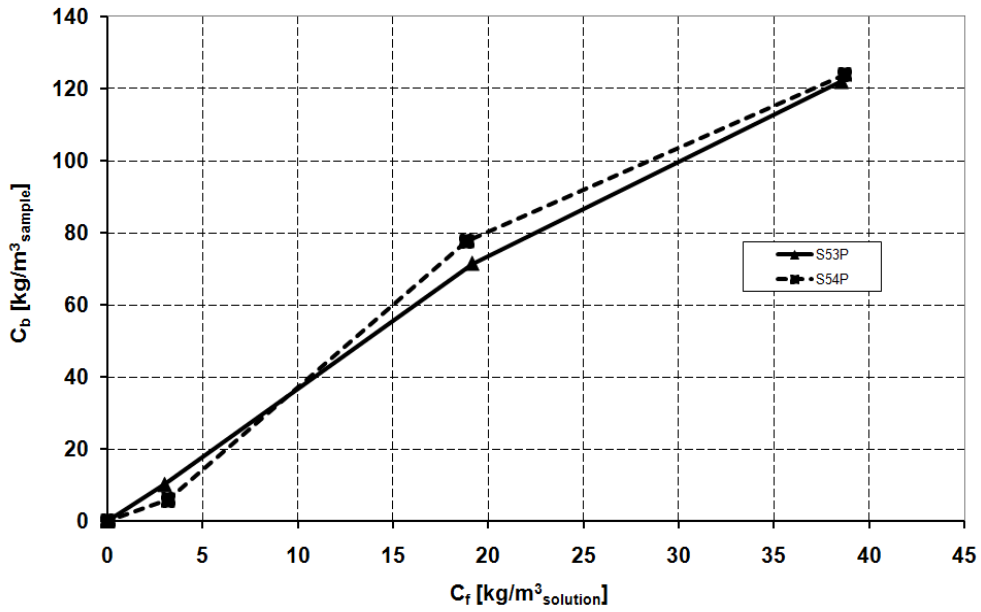

Figure 1. Chloride binding isotherms of studied plasters.

This data gives information on binding capacity of studied plasters and represents the highest possible value of steady state bound salt concentration at specific concentrations of NaCl water solution. Looking at this data one can see that the measured binding isotherms are for both studied materials almost similar and exhibit two specific slopes of the measured linear dependence of bound chloride concentration in material on free chloride concentration at solution.

The moisture diffusivity coefficients as functions of moisture content calculated for penetration of 1M NaCl water solution as well as for pure distilled water are presented in Fig. 2.

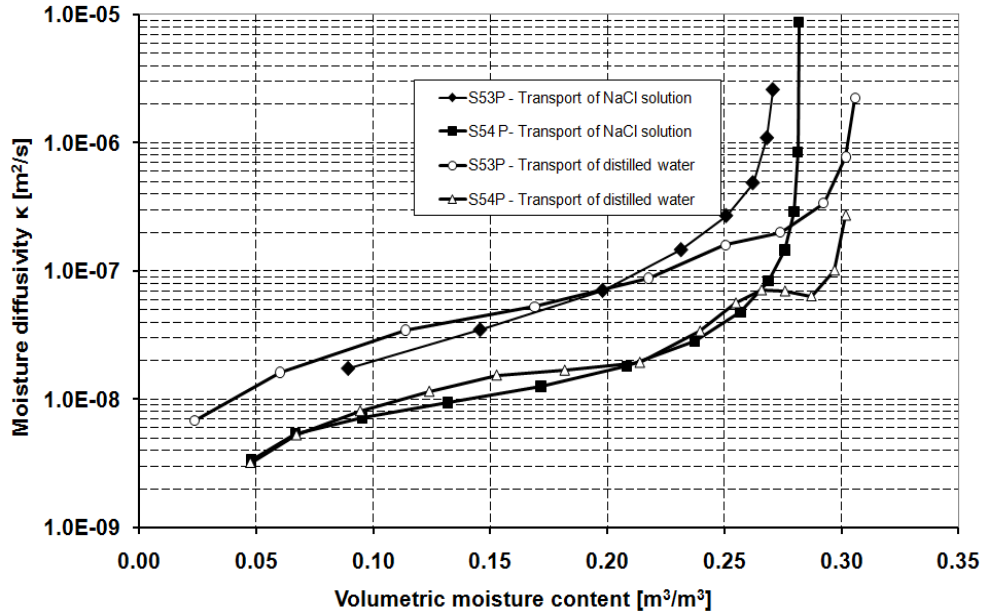

Figure 2. Moisture diffusivity of studied plasters.

This data characterizes the capability of plasters to transport liquid water and salt solutions. The moisture transport was in both studied cases faster for plaster denoted S53P although the total open porosity was found to be more or less the same for both materials. However, this finding is in agreement with pore size distribution measurement that showed for SP53P higher amount of capillary pores having the pore diameter range 0.1 – 1 μm.

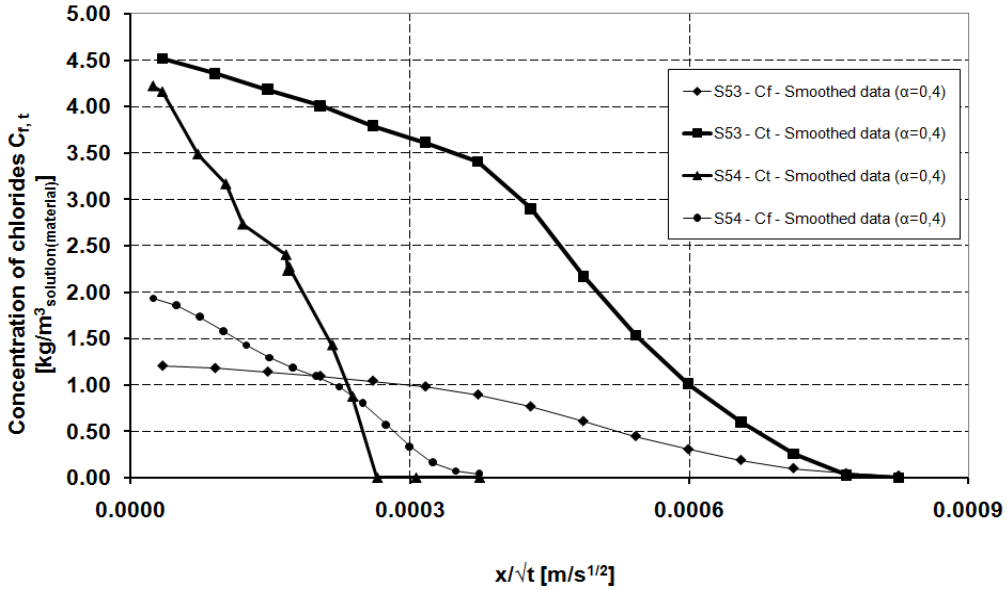

Figure 3. Chloride concentration profiles.

From the comparison of moisture diffusivities measured for distilled water and 1M NaCl water solution penetration, two different features can be distinguished. In lower moisture contents, typically up to 0.2 m^3/m^3, the moisture diffusivities calculated for 1M NaCl penetration were lower and the moisture transport was in this case slower in comparison with transport of pure distilled water. This

finding we assign to the differences in bulk density and viscosity of penetrating media. On the other hand, in higher moisture contents, the moisture transport was for 1M NaCl penetration faster than for pure distilled water and calculated moisture diffusivities were for 1M NaCl water solution transport higher. This can be explained by acceleration of moisture transport by electrochemical forces formed by material interaction with Na^+ and Cl^- ions.

Smoothed concentration profiles of total chloride concentration as well as of free chloride concentration used for calculation of chloride diffusion coefficient are plotted in Fig. 3. We can see slower chloride transport in plaster S54P than in material S53P. These results are also in agreement with pore size distribution measurement as well as with determined moisture diffusivities.

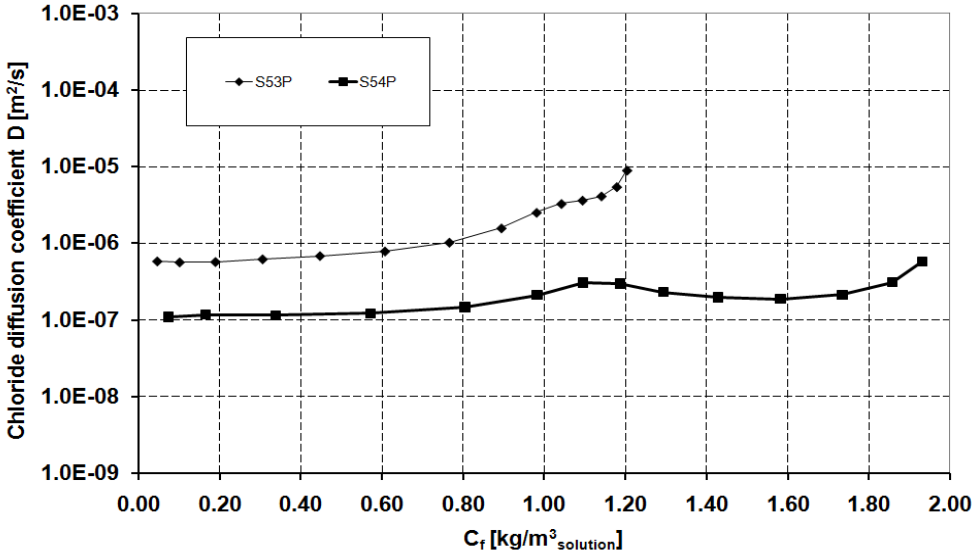

Figure 4. Chloride diffusion coefficients of studied plasters.

Dependences of chloride diffusion coefficient upon its concentration are shown in Fig. 4. We can see systematically lower values of *D(C)* function of renovation plaster S54P in comparison with plaster 353P. On that account we can conclude, the addition of higher amount of pozzolana admixture had positive effect on reduction of moisture and chloride transport in plaster S54P. When we compare the obtained data with chloride diffusion coefficient measured for reference lime plaster [Fiala *et al.* 2010] we can summarize that application of pozzolana was proved to be beneficial for both studied plasters, especially from the point of view enhanced durability of developed materials that is in clear relation with limited moisture and salt transport.

Looking at the results from the quantitative point of view, the calculated chloride diffusion coefficients in plasters were higher at least by two orders of magnitude than in water solution by itself. It indicated that the chloride transport was accelerated by electrochemical interactions of ions with the pore walls and possibly also by osmosis and surface diffusion. Since we have assumed in our calculations only the diffusion-advection-based model of salt solution transport, no other electrochemical analysis is possible on the basis of calculated data.

5 CONCLUSIONS

Moisture diffusivities, chloride diffusion coefficients and chloride binding isotherms of two types of newly developed renovation plasters were studied in the paper. The studied plasters differed in composition, especially in the amount of used pozzolana admixture.

Water and chloride water solution transport properties of both studied materials are in comparison with usually used pure lime plaster much lower, what makes good prerequisites for their application within the restoration of historical buildings' facades even in the case of salt laden materials. On the basis of obtained data, one can assume higher durability of the both studied plasters as compared to the traditional pure lime plaster.

ACKNOWLEDGMENTS

This research was supported by the Czech Science Foundation, under grant No. 103/09/0780.

REFERENCES

Antonova, E., Postnikova, O. & Zachorova, A. 2006, *Proceedings of the ARCCHIP Workshops*, European Research of Cultural Heritage, **5**, 295-300.

Bear, J. & Bachmat, Y. 1990, *Introduction to Modelling of Transport Phenomena in Porous Media*, Vol. 4, Kluwer, Dordrecht.

Cabrera, J. & Rojas, M. F. 2001, 'Mechanisms of hydration of the metakaolin-lime water system'. *Cement and Concrete Research*, **31**, 177-182.

Fiala, L., Pavlíková, M., Pavlík, Z., Keppert., M., Pernicová, M. & Černý, R. 2010, 'Chloride accumulation and transport in renovation plasters', Proceedings of 1st Central European Symposium on Building Physics, Lodz: Technical University of Lodz, 127-133.

Mocmanová, A. 2007, *Environmental deterioration of materials*, Chapter No. 1 - Environmental factors that influence the deterioration of materials, WIT Press, Southampton.

Jiřičková, M. & Černý, R. 2006, 'Chloride Binding in Building Materials', *Journal of Building Physics*, **29**, 189-200.

Pavlík, Z. 2009, *Identification of parameters describing the coupled moisture and salt transport in porous building materials*, Habilitation thesis, CTU Press, Prague.

Pavlík, Z., Jiřičková, M., Fiala, L. & Černý, R. 2006, 'Inverse Modeling of Salt Diffusion and Advection in Building Materials', Research in Building Physics and Building Engineering, Taylor and Francis, London, 155-160.

Pernicová, R., Pavlíková, M. & Černý, R. 2008, 'Durability Properties of Innovative Plasters for Renovation of Historical Buildings', Proceedings of Durability of Building Materials and Components 11. Istanbul, Cenkler Matbaacilik Tic. Ltd., 1267-1274.

Price, C., 1996, *Stone conservation, an Overview of Current Research*, The Getty Conservation Institute, Los Angeles.

Thorborg von Konow, 2006, *Proceedings of the ARCCHIP Workshops*, European Research of Cultural Heritage, **5**, 213-223.

XII DBMC
International Conference on Durability of Building Materials and Components
PORTO - PORTUGAL, April 12th-15th, 2011

Durability of Glass, Polypropylene and Steel Fiber Reinforced Concrete

Tara Rahmani [1]
Behnam Kiani [2]
Farzaneh Sami [3]
Bastam Najafi Fard [4]
Yaghoob Farnam [5]
Mohammad Shekarchizadeh [6]

ABSTRACT

This paper investigats the effects of addition of polypropylene, glass, and steel fibers on durability properties of fiber reinforced concrete. The properties include compressive and flexural strengths, electrical resistivity, water penetration, gas permeability, and scaling resistance to deicing chemicals. Fibers are added at volume fractions of 0.125%, 0.125%, and 0.5% respectively. The results show that polypropylene and glass fibers improve the electrical resistivity by 61.9% and 11.9% respectively. Moreover, the water penetration and gas permeability of steel fiber reinforced concrete are increased compared to plain concrete. In addition, the scaling resistance also is improved more for steel fiber reinforced concrete.

KEYWORDS

Durability, fiber reinforced concrete, electrical resistivity, water penetration, gas permibility, and scaling resistance

[1] University of Tehran, School of Civil Engineering, Tehran, Iran 34469, Phone +98 21 88973631, Fax +98 21 88959740, Tara_rahmani@ut.ac.ir
[2] University of Tehran, School of Civil Engineering, Tehran, Iran 34469, Phone +98 21 88973631, Fax +98 21 88959740, cmi@ut.ac.ir
[3] University of Tehran, School of Civil Engineering, Tehran, Iran 34469, Phone +98 21 88973631, Fax +98 21 88959740, cmi@ut.ac.ir
[4] University of Tehran, School of Civil Engineering, Tehran, Iran 34469, Phone +98 21 88973631, Fax +98 21 88959740, cmi@ut.ac.ir
[5] University of Tehran, School of Civil Engineering, Tehran, Iran 34469, Phone +98 21 88973631, Fax +98 21 88959740, Bayas3@yahoo.com
[6] University of Tehran, School of Civil Engineering, Tehran, Iran 34469, Phone +98 21 88973631, Fax +98 21 88959740, shekarch@ut.ac.ir

1 INTRODUCTION

Experimental research results have been showed considerable improvement in the post-cracking behavior of concretes containing fibers. Therefore, compared to plain concrete, fiber reinforced concrete is much tougher and more resistant to impact [Mehta & Monteiro 2001]. In addition to strength chracteristics, concrete should have adequate durability to perform in accordance with its intended level of functionality and serviceability over an expected or predicted life cycle. Durable concrete must potentially have the ability to withstand expected exposed deteriorative conditions.

In terms of deterioration of concrete due to physical or chemical causes, the penetration of fluids or gases through the concrete are nearly always involved. The overall susceptibility or penetrability of concrete structures, especially when compounded by additional environmental or exposure challenges, is the key to its ultimate serviceability and durability [Mindess et al. 2002].

According to Balaguru and Ramakrishnan [1986], steel fiber reinforced concrete had lower water absorption and lower permeability than plain concrete. Miloud [2005], however, found that addition of steel fiber to concrete increases water and gas permeability, irrespective of the fiber amount or fiber length. Balaguru and Shah [1992] indicated that permeability of polymeric fiber reinforced concrete and plain concrete are also increased. Hoseini *et al.* [2009] reported that fiber reinforcement results in a drop in the permeability of concrete under mechanical stress. This was likely due to a change in the crack profile in the presence of fibers whereby a multitude of closely spaced microcracks form instead of appearance of a few large cracks.

The objective of the present study is to investigate the effect of fibers on durability properties of concrete. To achieve this goal, polypropylene, glass, and steel fibers by volume fractions of 0.125%, 0.125%, and 0.5%, respectively, were studied. The effect of these fibers on compressive and flexural strength, electrical resistivity, water penetration, gas permeability, and scaling resistance to deicing chemicals were investigated.

2 MATERIALS AND MIX PROPORTIONS

The cement used in all mixes was ordinary Portland cement which complies with ASTM type II. The W/C ratio for all mixtures is equal to 0.47. Natural siliceous sand with a maximum nominal size of 4.75 mm was used as fine aggregate in mix proportions. Fine aggregate had a fineness modulus of 3.31 and specific gravity value of 2.62 gr/cm^3. Two sizes of crushed natural stone with maximum nominal size of 9 mm and 19 mm were used in this study as coarse aggregate. Specific gravity of coarse aggregates was 2.66 and 2.67 respectively. Three different types of fibers were used to investigate the effect of fibers on durability characteristics of concrete. The properties of fibers are shown in Table 1.

Table 1. Properties of the different fibers used

Property	*Polypropylene*	*Steel*	*Glass*
Length (mm)	12	35	15
Diameter (mm)	0.022	0.55	0.012
Aspect ratio (*l/d*)	545	64	1250
Specific gravity	0.91	8	2.74
Tensile strength (MPa)	300-400	1100	2450
Geometry	Fibrillated	Hooked	Fibrillated

In this study, four mixture proportions were considered; polypropylene, glass, and steel fiber reinforced concrete mixtures together with control mixture were prepared. Results are compared with control mixture results, which proportioned without any fibers. The details of mixture proportions are presented in Table 2. Volume fractions of various fibers used in the mixtures are also given in Table 3.

Table 2. Mix proportions for all mixtures

Cement (kg/ m^3)	*Fine aggregate* (kg/ m^3)	*Coarse aggregate* (kg/ m^3)		*Water* (kg/ m^3)
		12.5 mm	19 mm	
400	1044	261	435	188

Table 3. Dosage of different fibers

Mixture No.	*Fiber type*	*Volume fraction* (%)	*Fiber dosage* (kg/ m^3)
C0	-	0	0
PF	Polypropylene	0.125	1.14
SF	Steel	0.5	39
GF	Glass	0.125	3.5

2.1 Mixing Procedure

All mixtures were mixed in a conventional pan mixer with a capacity of 150 lit. At First, the coarse aggregate, fine aggregate, and 20 percent of mixing water were placed in the mixer. After 1 min of mixing, the mixer was stopped for 1 min. Then, the remainder of the mixing water and also cement were added and mixed for 2 min. Finally, fibers were dispersed by hand to achieve a uniform distribution throughout the concrete and mixed for 2 min. In the case of steel fibers, to help fiber dispersion, the fibers were saturated with 1-2 litres of mixing water for about 10 min. After mixing, the workability of concrete was determined using slump and inverted slump tests.The freshly mixed fiber reinforced concrete was placed in the moulds and consolidated by a vibrating table. Then, each of the specimens was allowed to stand for 24 h before demoulding, afterward stored in water at 23 ± 1 ºC until the time of testing.

3 MECHANICAL PROPERTIES

3.1 Compressive Strength

Compressive strength test was carried out according to BS-1881. For each type of fiber, three 150 mm cubic specimens were tested at the age of 3, 7, and 28 days. The average results are shown in Fig. 1. The reduction in compressive strength of polypropylene and glass fiber reinforced concretes can be attributed to the fact that larger specific surface area of these fibers increases the air content in concrete which can reduce the compressive strength [Wu & Wenhui 2006].

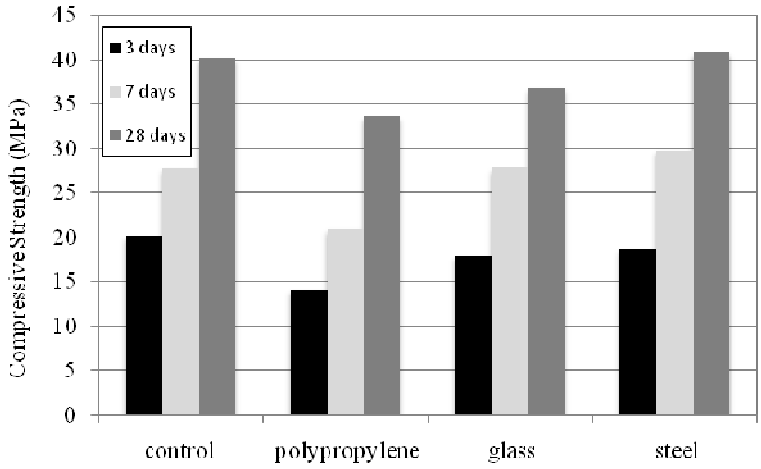

Figure 1. Compressive strength of concrete specimens

3.2 Flexural Strength

Flexural strength test was performed on prismatic specimens with dimensions of 100×100×500 mm using the third point loading procedure according to ASTM C1018. Three specimens per mix were tested at the age of 28 days. The average results are presented in Fig. 2. According to the results, the flexural strength of concrete improved with addition of polypropylene, glass, and steel fibers, achieving 9.8%, 10.3%, and 27.3% improvements, respectively.

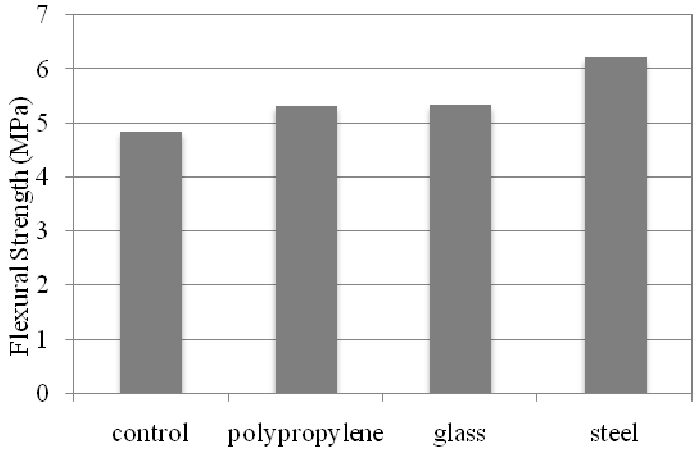

Figure 2. Flexural strength of concrete specimens

4 DURABILITY PROPERTIES

4.1 Electrical Resistivity

The electrical resistivity of concrete is being increasingly used to indirectly evaluate concrete characteristics such as the chloride ion diffusivity, the degree of concrete resistivity to severe environments, and its aggressiveness. This parameter may also provide useful information regarding the rebar corrosion performance in concrete. The electrical resistivity of the specimens was measured based on AC Impedance Spectrometry (ACIS) method in this study. In this method, a fresh cement paste (R~0) was used in order to provide the proper electrical connection between copper plate and concrete specimen.

The test was carried out on 100 mm cubic specimens at the age of 3, 7 and 28 days. The avearage values obtained over three specimens are reported as electrical resistivity of concrete. The electrical resistivity results of three diffrent fiber reinforced concrete are presented in Fig. 3.

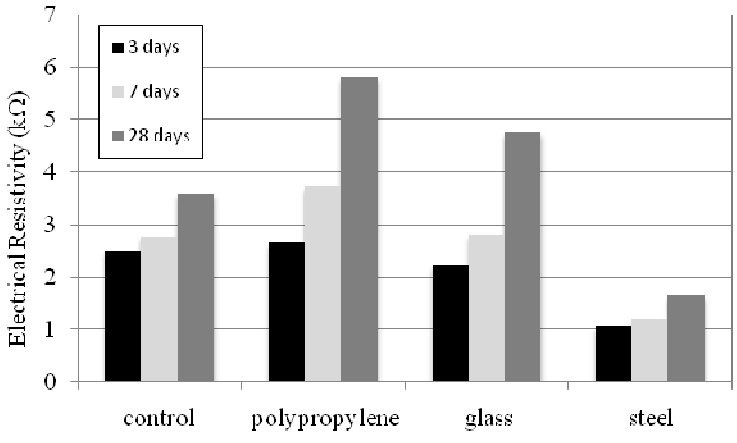

Figure 3. Electrical resistivity of concrete specimens

The results show that polypropylene fiber reinforcing improves resistivity, or reduces conductivity. Although being significant at an early age itself, the improvements in resistivity appear to be more pronounced at later ages. In addition, it is seen that hydration has a negative effect on conductivity [Banthia *et al.* 1992]. As we expected, steel fiber presence extremely decreased resistivity due to high electrical conductivity of steel fibers. Lower conductivity of polypropylene and glass fibers in comparison with steel fiber leads to increasing electrical resistivity of concrete.

4.2 Water Penetration Depth

Water permeability test was done according to DIN-1048 Part I. The test was carried out on cylindrical specimens with 300 mm height and 150 mm diameter at the age of 28 days. Specimens were kept at water pressure of 1, 3, and 7 atmosphere bar for duration of 48, 24, and 24 hours sequentially. The water penetration depth was determined by splitting the cylinder and measuring the average depth of discoloration (due to wetting) taken as equal to the depth of penetration. Results are shown in Fig. 4.

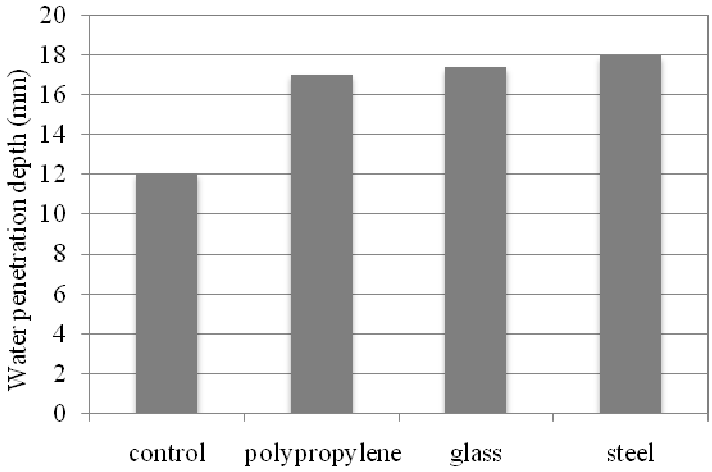

Figure 4. Water permeability of concrete specimens

The results show that water penetration depth of polypropylene, glass and steel fiber reinforced concretes increases by 41%, 45%, and 51%, respectively, over plain concrete. This could be the consequence of several reasons. In fiber reinforced concrete, presence of fibers and their wall effect leads to increasing capillary effect. Indeed, fibers play the role of channels and conduct the water in concrete. Hence, water penetration depth increases. This phenomenon is more considerable about steel fibers because they have a stronger wall effect in comparison with other fibers [Liu *et al.* 2010]. Also, fibers act as a bridge and facilitate the interconnection between pores so that water permeability is increased [Miloud 2005].

4.3 Oxygen Gas Permeability

Permeability of concrete largely depends on the ease with which fluids, both liquids and gases, can migrate through the hardened concrete mass. Consequently, measurement of permeability provides an indicator of concrete durability so that permeability called as the key to durability [Neville 1995]. In this study, permeability of concrete to oxygen was determined by a method developed by Cembureau. In this method, the underlying principle is the Hagen-Poiseuille relationship for laminar flow of a compressible fluid through a porous body with small capillaries under steady-state condition. The relationship proposed by Hagen-Poiseuille for determining specific permeability coefficient can be written as Equation 1.

$$K = \frac{2Q.p_a.L.\eta}{A(p^2 - p_a^2)} \quad (1)$$

Where Q is volume flow rate of the gas (m^3/s); A is cross-sectional area of the specimen (m^2); L is thickenss of the specimen in the direction of flow (m); □ is dynamic viscosity of the fluid at test temperature ($N.s/m^2$); p is the absolute value of inlet pressure (N/m^2); p_a is outlet pressure, assumed to be equal to atmospheric pressure (N/m^2).

By using oxygen as a gas and standard reference specimen with 50 mm thickness and 150 mm diameter, the relationship can be simplified to Equation 2.

$$K_{oxygen} = \frac{1.14\times10^{-4}Q.p_a}{(p^2 - p_a^2)} \quad (2)$$

For each type of fiber, three specimens were tested at the age of 28 days. Oxygen permeability coefficient of the specimens would be obtained by evaluating the mean value of five pressure stages. The average results of gas permeability tests are presented in Fig. 5.

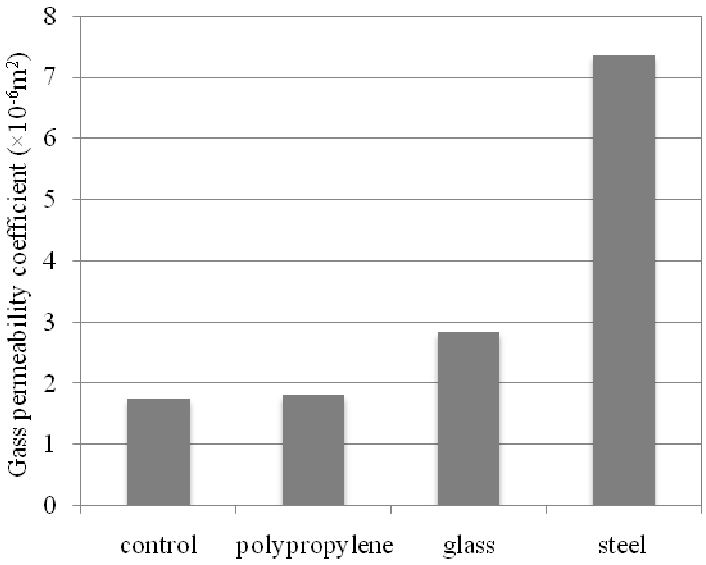

Figure 5. Gas permeability coefficient of concrete specimens

From the results, it can be drawn that the coefficient of gas permeability increases with adding fibers especially for steel fibers. The average value permeability coefficient for plain concrete is 1.75×10^{-16}, while that of steel fiber reinforced concrete is 7.34×10^{-16}. To explain such increase in gas permeability of fiber reinforced concrete, it may be assumed that permeability is determined more by matrix properties than the fibers. In particular, the matrix-fiber interface has the largest content of pores and micro cracks that affect overal permeability. Also it is very important to mention that fibers act as ties between pores so that interconnections are created which allow gas flow to penetrate more easily inside the concrete structure [Miloud 2005].

4.4 Scaling Resistance to Deicing Chemicals

The deicer scaling resistance test was performed in accordance with ASTM C672. For each type of fiber, two specimens of 250×200×100 mm were tested. The specimens were placed in moist storage for 14 days and stored in air for 14 days. Then, the surface of each specimen was covered with approximately 6 mm of a solution containing 4% calcium chloride. The specimens were exposed to

this solution under a single cycle of freezing (for 16 to 18 hours) and thawing (for 6 to 8 hours) per day. Every five cycles the solution was changed, the surface of each test specimen was visually evaluated, and the surface mass loss was measured. The test was stopped when the visual rating reached 5. Visual rating of 5 is related to the specimens exhibited severe scaling such that coarse aggregates would be visible over entire surface. The average results are summerized in Table. 4.

Table 4. Deicer scaling resistance of concrete specimens

No.	*Mass loss* (kg/m^2)				
	5C	10C	15C	20C	25C
C0	16.6				
PF	0.6	9.1	13.2		
GF	0	0	0.7	6.1	10.4
SF	0	0	0.3	5.6	8.7

It can be clearly seen that the deicer scaling resistance of fiber reinforced concretes are improved especially for steel fiber reinforced concrete. The reason for improvement is mainly that the concretes with fibers have much higher air content than those without fibers and therefore have much lower spacing factor [Quanbing & Beirong 2005].

5 CONCLUSION

Based on the results presented and discussed, following conclusions may be drawn:

- The flexural strength of the three fiber reinforced concretes considered in this study, were found to be 10-30% higher than plain concrete.
- The compressive strength of polypropylene and glass fiber reinforced concretes reduced due to an increasing in the air aontent of concrete.
- Polypropylene fiber reinforced concrete had the highest electrical resistivity compared to other types of fibers, at 28 days. Electrical resistivity of steel fiber reinforced concerte decreased significantly at all ages.
- The water penetration and gas permeability of concrete both increased with adding fibers due to increasing porosity. Steel fiber reinforced concrete had the highest gas permeability among the various types of fibers. Scaling resistance of all fiber reinforced concretes improved especially for steel fibers.

REFERENCES

Balaguru, P. & Ramakrishnan, V. 1986, 'Freeze-thaw durability of fiber reinforced concrete', *ACI Journal,* Vol. **83**, 374–382.

Balaguru, P.N. & Shah, S.P. 1992, *Fiber-Reinforced cement composites,* McGraw-Hill, New York.

Banthia, N., Djeridane, S. & Pigeon, M. 1992, 'Electrical resistivity of carbon and steel micro-fiber reinforced cements', *Cement and Concrete Research,* Vol. **22**, 804–814.

Hoseini, M., Bindiganavile, V. & Banthia, N. 2009, 'The effect of mechanical stress on permeability of concrete: A review', *Cement and Concrete Composites,* Vol. **31**, 213–220.

Liu, X., Chia, K.S. & Zhang, M.H. 2010, 'Water absorption, permeability, and resistance to chloride-ion penetration of lightweight aggregate concrete', *Construction and Building Materials,* Vol. **25**, 335–343.

Mehta, P.K. & Monteiro, P.J.M. 2001, *Concrete: Microstructure, Properties and Materials,* McGraw-Hill, New York.

Miloud, B. 2005, 'Permeability and porosity characteristics of steel fiber reinforced concrete', *Asian Journal of Civil Engineering*, Vol. **6**, 317–330.

Mindess, S., Young, J.F. & Darwin, D. 2002, *Concrete*, Prentice-Hall, New Jersy.

Neville, A. 1995, *Properties of Concrete*, Wiley & Sons, New York.

Quanbing, Y. & Beirong, Z. 2005, 'Effect of steel fiber on the deicer-scaling resistance of concrete', *Cement and Concrete Research*, Vol. **35**, 2360–2363.

Wu, Y. & Wenhui, Z. 2006, 'Effect of polypropylene fibers on the long-term tensile strength of concrete', *Journal of Wuhan University of Technology*, Vol. **22**, 52–55.

XII DBMC
International Conference on Durability of Building Materials and Components
PORTO - PORTUGAL, April 12th-15th, 2011

Hygrometric Kinetics and Microstructure of Building Materials

Maria Karoglou [1]
Antonia Moropoulou [2]
Magdalini K. Krokida [3]
Zacharias B. Maroulis [4]

ABSTRACT

One of the main factors effecting durability of building materials is water in all forms. The deteriorating effect occurs during the moisture movement to and from the building materials. Both drying and capillary rise are the dominant mechanisms which take place during the moisture transport to and from the building walls. The scope of the present work is to propose a simplified model for short cut calculations predicting all the related hygrometric properties of the building materials, based on the average pore radius. The proposed quasi-mechanistic model is summarized as follows: capillary rise phenomenon is described by a first order kinetic model, where both the time constant and the moisture equilibrium height are functions of the average pore radius of the material. The drying phenomenon is described also by a first order kinetic model, where both the time constant and the equilibrium moisture content are functions of the average pore radius of the material. And the environmental factors, such as air temperature, air humidity, and air velocity are also included in the proposed model. The model was validated using a large set of experimental data, which refer to the drying and capillary rise phenomena as well as to their corresponding equilibrium states. The proposed mathematical model permits the prediction of hygrometric properties of various building materials, which is very useful in cases that experimental data are not available.

KEYWORDS

Average pore radius, drying kinetics, capillary rise kinetics, sorption isotherms

[1] Faculty of Chemical Engineering of the National Technical University of Athens (NTUA), Athens, GREECE, margo@central.ntua.gr
[2] Faculty of Chemical Engineering of the National Technical University of Athens (NTUA), Athens, GREECE, amoropul@central.ntua.gr
[3] Faculty of Chemical Engineering of the National Technical University of Athens (NTUA), Athens, GREECE, mkrok@central.ntua.gr
[4] Faculty of Chemical Engineering of the National Technical University of Athens (NTUA), Athens, GREECE, maroulis@mail.ntua.gr

1 INTRODUCTION

Moisture problems are detrimental to buildings sustainability and human health. The moisture movement to and from the wall assembly, under variations of environmental factors, such as relative humidity, temperature, rainfall and solar radiation, is influenced by the basic hygrothermal properties of the component materials [Mukhopadhyaya, et. al. 2002].

On the other hand, the deterioration action of moisture depends strongly on the materials microstructure [Meng, 1992]. Thus, interconnecting moisture, as expressed by the hygrometric properties of materials with their microstructural characteristics, could contribute significantly in understanding and even predicting materials durability.

Significant progress has been reported in the literature in modelling and simulating moisture transport phenomena in building components [Mendes & Philippi, 2004]. Less work has been reported in which both laboratory experimentation and modelling are combined [Maref, et. al. 2002]. Moreover, the main models treat separately the various transport processes involved such as sorption, evaporation and suction, depending on the environmental conditions. A more general approach is needed, which depends mainly at the materials involved, including also the environmental conditions, based on real measurement data.

In this direction, a power law model is proposed, which describes the water content of materials as a function of relative humidity. The building materials microstructure is described in fractal terms [Stazi, et. al. 2002].

In this study, a quasi-mechanistic simplified model is proposed for predicting all the related hygrometric properties of the building materials, based on the average pore radius. Although today there are numerous models and softwares (like those based on EN 15026), the development of simplified models, which are based on time experimental data, is a useful alternative solution for the user. The main advantage of using this simplified model is that it is proper for short cut calculations.This gives to the user the advantage of a quick study concerning building materials properties such as drying kinetics under various environmental conditions.

2 MATERIALS AND METHODS

Three categories of building materials were studied: bricks, plasters and stones. For each category various materials were selected, having different microstructural characteristics and therefore different hydroscopic behaviour.

The total porosity and the average pore radius r(μ) of samples were measured using a mercury intrusion porosimetry (POROSIMETER 2000, FISONS Instruments).

For the study of water transport phenomena, three kinds of tests were performed: assessment of materials water sorption isotherms, study of materials drying kinetics and study of materials capillary rise kinetics.

Water sorption analysis (CISORP, CI Electronics Ltd) was used to estimate the water adsorption-desorption isotherms of the samples. Water uptake and release was determined gravimetrically, i.e. by weighing the sample during the process. The samples weighed about 0.5 g. The isotherms were estimated at three temperatures (15°C, 25°C, and 35°C), while the relative humidity was controlled ranging from 10 to 90%, using a 10-scale step, at ambient pressure. Data were recorded and saved automatically during the experiments.

Experiments to determine the drying kinetics were performed in a convective air dryer, under constant drying conditions, namely air temperature, air humidity and air velocity. The drying experiments were carried out on sample size of 3x3x3cm for each material, at four levels of air-temperature (20°, 30°

and 35°C and 40°C), three levels of air velocity (1, 3 and 8 m/s) and 5 levels of relative humidity of the air (30 to 80%). Before the start of the experiment, the samples were saturated with water through immersion in distilled water.

In order to assess the capillary rise kinetics, the materials capillary moisture content versus time was recorded for each sample using Italian standard Normal 11-85.

3 MATHEMATICAL MODELS

Karoglou et al (2005a, b) proposed first order empirical equations to describe drying and capillary rise kinetics (eq. 1 & 2).

$$\frac{dX}{dt} = -\frac{1}{t_{cd}}\left(X - X_e\right) \tag{1}$$

$$\frac{dH}{dt} = -\frac{1}{t_{cr}}\left(H_e - H\right) \tag{2}$$

Where $\frac{dX}{dt}$ and $\frac{dH}{dt}$ are the drying and capillary rise rates,
X_e, and H_e are the equilibrium values for moisture content and height ,
t_{cd}, t_{cr} are the drying and the capillary rise time constants.

The equilibrium material moisture content *Xe* depends on air temperature *T* and water activity a_w. Various empirical or semi-theoretical models have been proposed in the literature, but a modified Oswin model proved to be the most appropriate in process design calculations (Karoglou, et. al. 2005c):

$$X_e = b_o \exp\left(\frac{b_1}{T}\right)\left(\frac{a_w}{1 - a_w}\right)^{b_2} \tag{3}$$

where, b_o, b_1, b_2 are adjustable empirical constants.

Equilibrium capillary height for vertical water rise is related to average pore radius *r* of materials through the Darcy law:

$$H_e = \frac{2\gamma}{\rho g r} \tag{4}$$

where, γ is the surface tension of water (dyn/cm)
g is the acceleration gravity force (cm/s^2)
ρ is the water density (g/cm^3)

The drying time constant t_{cd} depends on air conditions, i.e. air velocity *u*, temperature *T* and water activity a_w and material microstructure, average pore radius *r*.

$$t_{cd} = c_o T^{c_1} \alpha_w^{c_2} u^{c_3} \tag{5}$$

where, c_o , c_1, c_2, c_3 are adjustable empirical constants.
The main advantage of the above model is that all the empirical constants are related to experimental conditions and material characteristics. More specifically c_o, b_o and t_{cr} depend on material microstructure, as described by average pore radius. New simple power equations (eqs. 6, 7, 8) are used to correlate c_o, b_o and t_{cr} with material average pore radious:

-For drying:

$$c_o = c_o' r^{-c_r} \quad (6)$$

-For equilibrium moisture content:

$$b_o = b_o' r^{b_r} \quad (7)$$

-For capillary rise, the drying rise constant t_{cr}:

$$t_{cr} = d_o' r^{d_r} \quad (8)$$

where, $c_o', c_r, b_o', b_r, d_o', d_r$ are constants.

The effect of the average pore radius on moisture equilibrium height has already been taken into account through Darcy law (eq. 4).

The above mathematical model is summarized in Table 1, while the information flow diagram of the above model is described in Fig. 1.

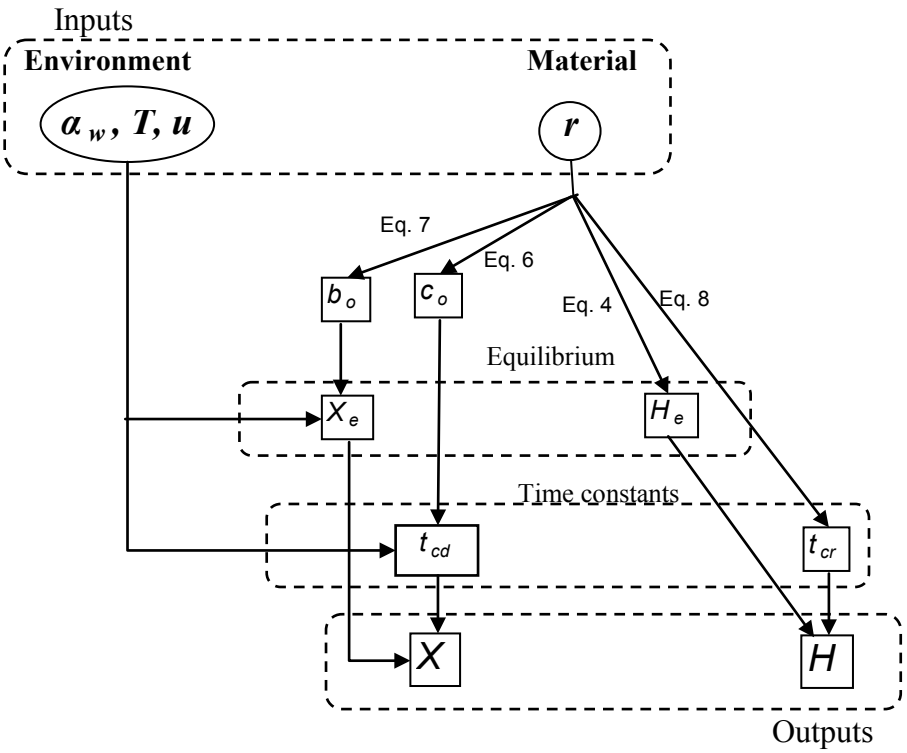

Figure 1: Model information flow diagram

Table 1. Mathematical model

Properties

H	capillary rise height	(m)
X	moisture content	(kg/kg db)

Factors

Material

r	average pore radius	(μ)

Environment

a_w	water activity	(-)
T	air temperature	(^{o}C)
u	air velocity	(m/s)

Properties equations

Drying

$$\frac{dX}{dt} = -\frac{1}{t_{cd}}\left(X - X_e\right)$$

Capillary rise

$$\frac{dH}{dt} = -\frac{1}{t_{cr}}\left(H_e - H\right)$$

Time Constants

t_{cd} drying time constant (h)

$$t_{cd} = c_o\, T^{\,c_1}\ \alpha_w{}^{c_2} u^{\,c_3},\ c_o = c_o' r^{-c_r}$$

t_{cr} capillary rise time constant (d)

$$t_{cr} = d_o' r^{d_r}$$

Equilibrium values

X_e equilibrium moisture content (kg/kg db)

$$X_e = b_o\, exp\left(\frac{b_1}{T}\right)\left(\frac{a_w}{1 - a_w}\right)^{b_2},\ b_o = b_o' r^{b_r}$$

H_e equilibrium capillary height (m)

$$H_e = \frac{2\gamma}{pgr}$$

3 RESULTS AND DISCUSSION

Materials average pore radious are summarized in Table 2. All materials presented average pore radious ranging from 0.4 to 4.9, except PEM and SRH which had average pore radious 33.2 and 39.8 respectivelly.

Table 2. Materials microstructure as described by average pore radius (r)

Code	*Material*	*Average pore radius r(μ)*
BRI	Brick	0.45
BRM	Brick	2.01
PEM	Plaster	33.2
PMP	Plaster	2.42
PRL	Plaster	0.87
PTI	Plaster	1.46
PTR	Plaster	0.53
PZN	Plaster	0.51
SCY	Stone	4.86
SRH	Stone	39.8
SRY	Stone	2.83
SRW	Stone	4.45

The above experimental pore radius values were fitted to eqs. 6, 7, 8 in order to estimate c_o, b_o and t_{cr} respectively.
Figure 2a shows the correlation of parameter b_o to the average pore radius r of the material. Although the standard deviation between experimental and calculated values is about 20%, this estimation can be used for the estimation of the equilibrium moisture content values (eq. 3) for all the examined building materials.
Figure 2b demonstrates that the equilibrium moisture content of a material can be predicted with satisfactory precision, knowing its pore radius. The equilibrium moisture content values decreases significantly with the average pore radius increment.

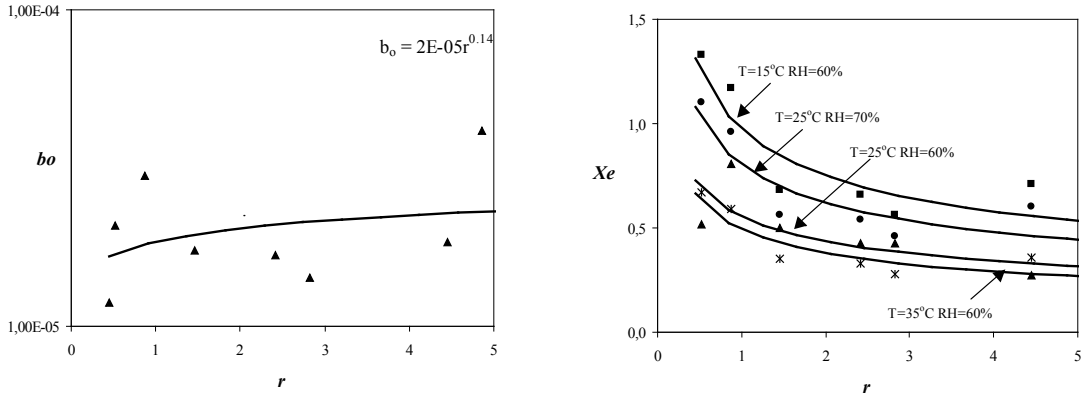

Figure 2a,b. Equilibrium moisture content prediction through average pore radius

Figure 3a shows the correlation of parameter c_o to average pore radius r (eq. 6) of the material. The fitting of the proposed model to the experimental data is considered satisfactory (standard deviation is 10%). The other three parameters of eq 5, c1, c2 and c3, which show the effect of temperature, cwater activity and air velocity where found to be constants for all the examined conditions. Consequently, time drying constant depends mostly on material pore radius.

Figure 3b shows the dependence of time drying constant on the materials average pore radius. It must be noted that the increment of average pore radius leads to significant time drying constant increase, corresponding to quicker drying.

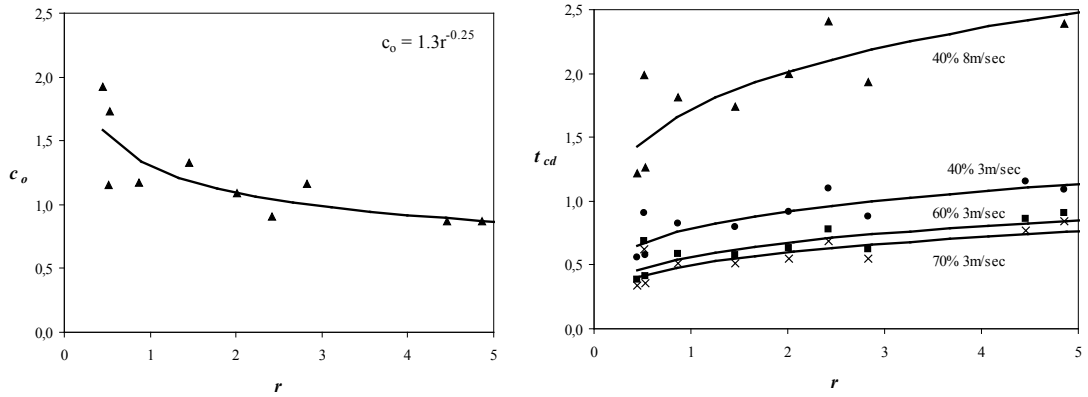

Figure 3 a,b. Drying kinetics prediction through average pore radius

Figure 4 shows the prediction of capillary rise time constant for a measured average pore radius. An average pore radius increment leads to a significant reduction of the capillary time constant.

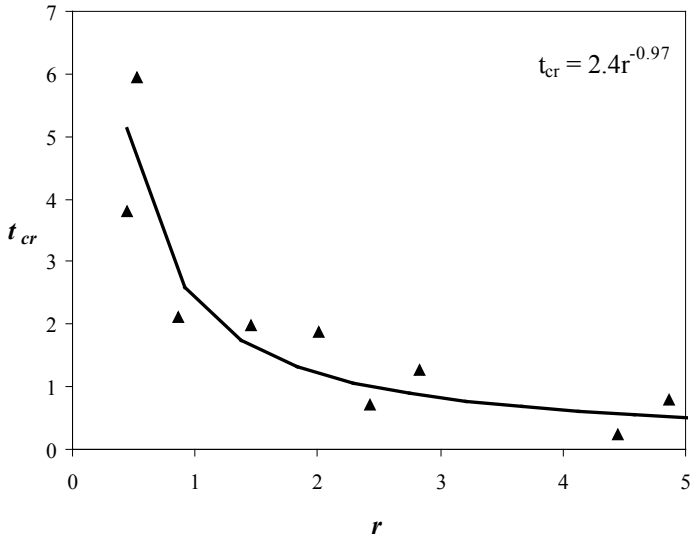

Figure 4. Capillary rise kinetics prediction through average pore radius

The estimation of the corresponding parameters of the mathematical model are shown in Table 3.

Table 3. Parameters estimation

Code	*Material*
Sorption	b_o'=2E-05 b_r=0.14
	b_1=3.00 b_2=0.36
Drying	c_o'=1.3 c_r=-0.25
	c_1=0 c_2=0.75
	c_3=-0.8
Capillary rise	d_o'=2.4 d_r=-0.97

4 CONCLUSIONS

A short cut prediction of drying time constant, capillary rise constant and equilibrioum moisture constant was based on the material average pore radius. This simplified mathematical model permits the prediction of hygrometric properties of various building materials based on materials average pore radius when experimental data are not available. Moreover, it can be embodied to simulators, which can predict the moisture content of masonries, constructed with various materials under different environmental conditions.

REFERENCES

Mukhopadhyaya, P., Goudreau, P., Kumaran & M. K. van Reenen, D. 2002, 'Influence of material properties on the moisture response of an ideal stucco wall: results from hygrothermal simulation', Proc. 6th Symposium on Building Physics in the Nordic Countries, Trondheim, Norway, 17-19 June 2002, pp. 611-618.

Meng, B. 1992, 'Moisture-transport relevant characterisation of pore structure', Proc. 7th International Congress on Deterioration of Stone, Lisbon, 15-18 June 1992, Portugal, vol.I, pp.387-396.

Mendes N. & Philippi P.C. 2004, 'A method for predicting heat and moisture transfer through multilayered walls based on temperature and moisture content gradients', in *International Journal of Heat and Mass Transfer*, **48**[1], 37-51.

Maref, W., Lacasse, M., Kumaran, M. K. & Swinton, M. C. 2002, 'Benchmarking of the advanced hygrothermal model hygIRC with mid scale experiments', Proc. Canadian conference on building energy simulation, Montreal, 11th - 13th September 2002, Canada, pp.171-176.

Stazi A., D'Orazio M. & Quagliarini E. 2002, 'In-life prediction of hygrometric behaviour of buildings: application of fractal geometry to the determination of absorption and suction properties', *Building and Environment*, **37**, 733-739.

ICR, Italian Normal 11/85, Assorbimento d' acqua per capillarità – Coefficiente di assorbimento capillare: water absorption coefficient by capillarity – water absorption coefficient.

Karoglou M., Moropoulou A., Krokida M.K. & Maroulis, Z.B. 2005a, 'Drying Kinetics of some building materials', *Drying Technology*, **23**[1-2], 305-315.

Karoglou M., Moropoulou A., Giakoumaki, A. & Krokida M.K., 2005b, 'Capillary rise kinetics of some building materials', *Journal of Interface and Colloid Science*, **284**[1] 260-264.

Karoglou M., Moropoulou A., Krokida M.K. & Maroulis, Z.B. 2005c, 'Sorption Kinetics of some building materials', *Drying Technology*, **23**[1-2] 289-303.

XII DBMC
International Conference on Durability of Building Materials and Components
PORTO - PORTUGAL, April 12th-15th, 2011

Degradation Control of Walls with Rising Damp Problems: Numerical and Mathematical Analysis of the Evaporative Process

Ana S. Guimarães [1]
J.M.P.Q. Delgado [2]
Vasco Peixoto de Freitas [3]

ABSTRACT

Degradation in walls of Historical Building with rising damp is a complex problem to solve, due to the thickness and heterogeneity of those walls. The traditionally treatment techniques used (such as watertight barriers, injection of hydrofuge products, etc.) show, sometimes, to be ineffective, justifying the need to find a new approach. Experimental studies validate the effectiveness of a new treatment technique applied to the walls of old buildings – wall base ventilation system.

Building Physics Laboratory of the Faculty of Engineering, University of Porto is developing a model of this technique. The sizing of the treatment system is based on knowledge of the characteristics of the wall, of the geometry of the ventilation system and of the building being dealt with.

In this paper it is described the moisture transfer process between the moving air flux, inside the system, and the wall. A mathematical solution of a partial differential equation describing moisture conservation gave the concentration field near the wall surface and the mass transfer flux was integrated to give values of the Sherwood number as a function of Peclet number. Experimental results were used to validate the mathematical solution and the values obtained are practically the same. It is possible to get a relation between the flux of evaporation inside the system and some sizing parameters which is crucial to control the damp front level.

KEYWORDS

Rising damp treatment; Wall base ventilation system; Moisture transfer.

[1] Faculty of Engineering of the University of Porto (FEUP), Porto, PORTUGAL, anasofia@fe.up.pt
[2] Faculty of Engineering of the University of Porto (FEUP), Porto, PORTUGAL, jdelgado@fe.up.pt
[3] Faculty of Engineering of the University of Porto (FEUP), Porto, PORTUGAL, vpfreita@fe.up.pt

1 INTRODUCTION

The mechanisms underlying the moisture transport through buildings are complex. In the vapour phase diffusion and convection have the main important role, while, in the liquid phase, capillary action, gravity and the pressure gradient effect control the moisture transfer.
In practice, moisture transport occurs in the liquid and vapour phases simultaneously, being dependent of several parameters such as temperature, relative humidity, precipitation, solar radiation, wind effect, atmospheric pressure (which define the boundary conditions) and the characteristics of building materials used.

Rising damp coming from the grounds that, by capillarity, climb through the porous materials constitutes one of the main causes of old buildings degradation, especially, its thick walls with heterogeneous composition. Once there are identify the special characteristics of those buildings, it is important to recognize the limitations of traditionally used technologies and to study new solutions for the rising damp phenomenon in historic buildings.

In Building Physics Laboratory (LFC), at Faculty of Engineering of University of Porto (FEUP), has been developed important experimental research about rising damp problems. In recent years, has been validated and experimentally characterized the operation principle of a treatment technique called "Wall Base Ventilation System to Treat Rising Damp - HUMIVENT" that consists on circulating air on the base of buildings walls with high thickness and heterogeneity in its constitution, with a saturation distant relative humidity. Wall base ventilation increases evaporation, which leads to a reduction in the level achieved by the damp front. This is possible only when the groundwater is lower than the base of the wall (see Colombert [1975]).

In previous studies it was possible to conclude, after experimental results analysis, that the wall base ventilation system reduces the level achieved by wet front. Following this work, experimental campaigns were carried out to explore the boundary conditions, geometry, speeds engine, etc., and it was possible to observe that a hygro-regulated system is essential to control the possibility of condensations occurrences in the interior of our system. A hygro-regulated system is a mechanical scheme controlled by probes placed at the inlet and outlet. These probes, in accordance with a pre-programmed criterion, will induce the system to turn on/off.

As a first step, it would be interesting to understand the behaviour of air within the conduct and to calculate the water flow removed from the wall. Therefore, this paper intends to develop a mathematical/numeric model that describes and characterizes the water vapour transport phenomena over the conduct and between the wall and the conduct. The experimental results of the present study are also useful to validate the proposed model and this is illustrated in the section on comparison with mathematical and numerical results.

2 ANALYTICAL AND NUMERICAL ANALYSE

In terms of analysis we consider a wall base ventilation system along which air is flowing, close to the saturated wall ($0<z<L$). Air flow will be taken to be steady, with uniform average velocity u, and if the concentration of water vapour in the air fed to the channel is c_0 and the water vapour saturation in the solid wall is c^*, a moisture transfer boundary layer will develop, across which the water vapour concentration drops from $c=c^*$, at $y=0$, to $c \rightarrow c_0$, for large y.

As there are basically two different forms of boundary layer flows: laminar and turbulent. In laminar flow, the transport of moisture, temperature and momentum across the boundary layers are controlled by molecular diffusion. The Reynolds number, $\mathrm{Re}=uL/\nu$, may be interpreted as the ratio of the flow destabilizing forces (inertia, u) to the stabilizing forces (viscosity, ν). Stable laminar flow is thus

characterized by low values of Re. Laminar flow is found for Reynolds number less than approximately 3×10^5 (see Incropera and deWitt [2002]). In our study the $Re<10^5$, for all experiments.

If we restrict our analysis to those situations for which the moisture transfer boundary layer is thin and if a small control volume is considered, inside this boundary layer, with side lengths δz, δy and unity (perpendicular to the plane of the figure), a steady state material balance on the solute leads to

$$u\frac{\partial c}{\partial z} = D_{\mathrm{m}}\frac{\partial^2 c}{\partial y^2} + D_{\mathrm{m}}\frac{\partial^2 c}{\partial z^2} \tag{1}$$

where D_{m} is the molecular diffusion coefficient, in the cross stream and in the stream wise directions and c is the concentration of water vapour.

2.1 Analytical solution

Noting that the surface y=0, 0<z<L, is a surface of constant concentration, along which $\partial^2 c/\partial z^2 = 0$, it may be shown that the last term on the right hand side of (1) will be negligible, for a boundary layer which is thin in comparison with the length of the saturated wall. Equation (1) reduces then to the equation of diffusion in one dimension (Hall *et al*. [1984])

$$u\frac{\partial c}{\partial z} = D_{\mathrm{m}}\frac{\partial^2 c}{\partial y^2} \tag{2}$$

and for the situation sketched in Fig. 1, Eq. (2) is to be solved with

$$c = c_0 \qquad z = 0 \qquad y > 0 \tag{3a}$$

$$c = c^* \qquad z > 0 \qquad y = 0 \tag{3b}$$

$$c \to c_0 \qquad z > 0 \qquad y \to \infty \tag{3c}$$

The first condition states that the leading edge of the saturated wall is approached by “fresh air” with the bulk concentration of water vapour, c_0. Condition (3b) states that the air is in equilibrium with the saturated water vapour at the wall surface (see Cussler [1997]). Condition (3c) states that the channel is wider (in the y direction) than the boundary layer. For constant u and D_{m}, the solution is

$$\frac{c - c_0}{c^* - c_0} = \mathrm{erfc}\left(\frac{y}{2\sqrt{D_{\mathrm{m}} z/u}}\right) \tag{4}$$

and the flux of evaporation at the saturated wall surface may be obtained from (4) as

$$N = -D_{\mathrm{m}}\left(\frac{\partial c}{\partial y}\right)_{y=0} = \left(c^* - c_0\right)\left(\frac{D_{\mathrm{m}}}{\pi\, z/u}\right)^{1/2} \tag{5}$$

The total rate of evaporation may be calculated taking the width b along the saturated wall surface, perpendicular to the flow direction

$$n = \int_0^L N\, b\, dz = \left(c^* - c_0\right) bL\left(\frac{4D_{\mathrm{m}}}{\pi L/u}\right)^{1/2} \tag{6}$$

and it is useful to define the coefficient

$$k = \frac{n}{(bL)\,(c^* - c_0)} = \left(\frac{4D_{\mathrm{m}}}{\pi L/u}\right)^{1/2} \tag{7}$$

2.2 Numerical solution

In order to integrate numerically Eq. (1) it is convenient to define the following dimensionless variables:

$$C = \frac{c - c_0}{c^* - c_0} \quad (8a)$$

$$Y = \frac{y}{L} \quad (8b)$$

$$Z = \frac{z}{L} \quad (8c)$$

$$\mathrm{Pe} = \frac{uL}{D_\mathrm{m}} \quad (8d)$$

where Pe represents the Peclet number (based on the length, L). In terms of dimensionless variables, Eq. (1) may then be rewritten as

$$\mathrm{Pe}\frac{\partial C}{\partial Z} = \frac{\partial^2 C}{\partial Z^2} + \frac{\partial^2 C}{\partial Y^2} \quad (9)$$

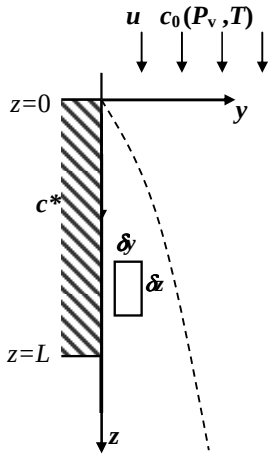

Figure 1. Moisture transfer boundary layer.

and the appropriate boundary conditions are

$$\mathrm{C} \to 0 \qquad \mathrm{Z} \to -\infty \qquad \forall \mathrm{Y} \quad (10a)$$

$$\mathrm{C} = 1 \qquad 0 \le \mathrm{Z} \le 1 \qquad Y = 0 \quad (10b)$$

$$\frac{\partial \mathrm{C}}{\partial \mathrm{Y}} = 0 \qquad \mathrm{Z} < 0 \vee \mathrm{Z} > 1 \qquad Y = 0 \quad (10c)$$

$$\mathrm{C} \to 0 \qquad \forall \mathrm{Z} \qquad \mathrm{Y} \to +\infty \quad (10d)$$

$$\mathrm{C} \to 0 \qquad \mathrm{Z} \to +\infty \qquad \mathrm{Y} \ge 0 \quad (10e)$$

Equation (9) is to be solved numerically, subject to the boundary conditions (10a-e), over a large range of Pe of practical interest.

2.2.1 Discretisation

Equation (9) was solved numerically, using a finite-difference method in a non-uniform grid. The method is similar to that described in detail by Alves *et al.* [2006]. A second-order central differencing scheme was adopted for the discretisation of the diffusive terms on the right hand side of Eq. (9) and the convective term, on the left hand side of Eq. (9), was discretised using the CUBISTA high-resolution scheme of Alves *et al.* [2003], which preserves boundedness and higher-order accuracy, even for highly advective flows.

The discretised equation resulting from the finite-difference approximation of Eq. (12) reads:

$$\mathrm{Pe}\frac{C_{i+1/2,j} - C_{i-1/2,j}}{(\Delta Z_i + \Delta Z_{i+1})/2} = \frac{C_{i+1,j}(\Delta Z_i) - C_{i,j}(\Delta Z_i + \Delta Z_{i+1}) + C_{i-1,j}(\Delta Z_{i+1})}{\Delta Z_i\, \Delta Z_{i+1}\, (\Delta Z_i + \Delta Z_{i+1})/2} + \frac{C_{i,j+1}(\Delta Y_j) - C_{i,j}(\Delta Y_j + \Delta Y_{j+1}) + C_{i,j-1}(\Delta Y_{j+1})}{\Delta Y_j\, \Delta Y_{j+1}\, (\Delta Y_j + \Delta Y_{j+1})/2} \quad (11)$$

It is important that the $C_{i+1/2,j}$ and $C_{i-1/2,j}$ values are adequately interpolated from the known grid node values in order to preserve boundedness of the solution. The CUBISTA high-resolution scheme (Alves *et al.* [2003]) was therefore adopted, since it gives numerical stability and good precision. Details on the application of the CUBISTA scheme to evaluate the $C_{i-1/2,j}$ and $C_{i+1/2,j}$ face values are given in Alves *et al.* [2006].

The resulting system of linear equations was solved iteratively using the straightforward successive over-relaxation method (Ferziger and Peric [1996]. The implementation of the boundary conditions was as described in previous papers (e.g. Alves *et al.* [2006]). For the situation under study, an orthogonal mesh is adequate and care was taken to ensure proper refinement in the regions where the highest concentration gradients were expected.

The converged solution obtained in each grid yields values of $C_{i,j}$, from which the overall moisture-transfer rate from the saturated wall, *n*, was calculated. The total rate of evaporation may be calculated taking the width *b* along the saturated wall surface, perpendicular to the flow direction,

$$n = -\sum_i b(z_{i+1} - z_i) D_{\mathrm{m}} \left(\left.\frac{\partial c}{\partial y}\right|_{i,1} + \left.\frac{\partial c}{\partial y}\right|_{i+1,1} \right) \Big/ 2 \tag{12}$$

and the value of n was used to obtain the average Sherwood number,

$$\mathrm{Sh} = \frac{kL}{D_{\mathrm{m}}} = \frac{n}{bL\,(c^* - c_0)} \frac{L}{D_{\mathrm{m}}} \tag{13}$$

which in dimensionless discretised form reads

$$\mathrm{Sh} = -\sum_i (Z_{i+1} - Z_i) \left(\left.\frac{\partial C}{\partial \mathrm{Y}}\right|_{i,1} + \left.\frac{\partial C}{\partial \mathrm{Y}}\right|_{i+1,1} \right) \tag{14}$$

3 EXPERIMENTAL STUDY

The "HUMIVENT" technique consists of ventilating the base of the walls using a natural ventilation process or by installing a hygro-regulated mechanical ventilation device. The experiments were designed to show how these walls are affected by rising damp in view of different boundary conditions.

In our laboratory, LFC-FEUP, the relative humidity profile of 20 cm thick and 2 m length stone (limestone) walls was measured. In order to assess the effect of the insertion of a wall base ventilation system, a ventilation channel was placed on both sides. The ventilation box outlines the wall and as a 20cmx30cm section. A mechanical ventilator was placed at one end of a tube, leaving the other end free. This ventilation system functioned continuously throughout the testing period, so as to ensure that the temperature and relative humidity within the system were similar to the conditions inside the laboratory. The air velocities used were between 0.08 m/s and 0.63 m/s to avoid turbulence and consider that a low speed is adequate.

To assess moisture transfer inside the walls, probes were inserted at different heights and depths to measure relative humidity and temperature. The range of temperature and relative humidity's obtained were 9.6ºC-24.8ºC (wall), 9.2ºC-28.8ºC (inlet), 8.9ºC-28.5ºC (outlet) and 94.2%-95.2% (wall), 20.4%-85.3% (inlet), 22.7%-87.6% (outlet). These probes were then connected to a data acquisition and recording system.

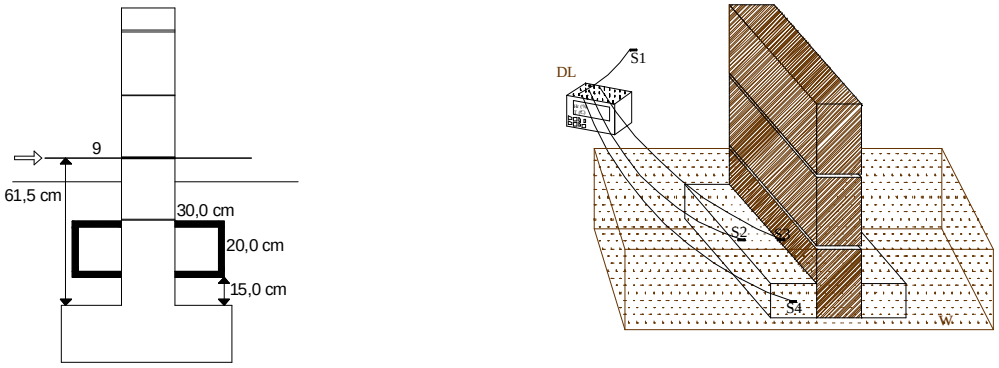

Figure 2. (a)-Relative damp variation at Level 9 and (b)-Physical model and location of probes (Freitas and Guimarães [2008]).

The configuration used is schematically represented in Fig. 2a, as are the relative humidity profiles in the section located at Level 9, 61.5 cm above the base of the wall (see Torres and Freitas [2007]). The boundary condition with system waterproofing was used. Probes were placed to obtain readings of the temperature and relative humidity at the entrance and exits of the ventilation systems (see Fig. 2b).

4. RESULTS AND DISCUSSION

4.1 Numerical results

The numerical solution of Eq. (9) gives the concentration field and from it, the instant rate of evaporation of the saturated wall, *n*, is obtained integrating the diffusion/dispersion flux over the whole saturated wall. This integral may be evaluated numerically, for each set of conditions, from the discretised concentration field that is obtained through the numerical solution of Eq. (9). It is convenient to express the rate of evaporation in terms of the Sherwood number, $\mathrm{Sh} = kL / D_{\mathrm{m}}$, where $k = n/[A(c^* - c_0)]$ is the moisture transfer coefficient for the saturated wall and *A* is the exposed area.

For the range of Peclet numbers numerically analysed the plot of Figure 3 reveals two asymptotes:

$$\mathrm{Sh} \to \left(\frac{2}{\pi}\right)^{1/2} (\mathrm{Pe})^{1/8} \qquad \text{for } \mathrm{Pe} \to 0 \tag{15}$$

and

$$\mathrm{Sh} \to \left(\frac{4}{\pi}\right)^{1/2} (\mathrm{Pe})^{1/2} \qquad \text{for } \mathrm{Pe} \to \infty \tag{16}$$

The numerical solution obtained is

$$\mathrm{Sh} = \left[\frac{2}{\pi}\mathrm{Pe}^{1/4} + \frac{4}{\pi}\mathrm{Pe}\right]^{1/2} \tag{17}$$

and the numerical values do not deviate by more than 3% from the value given by Eq. (17), over the entire range of values of Pe. Figure 3 shows that for Peclet numbers greater than 50 the numerical and analytical solutions do not deviate by more than 1%; and it is not surprising, since for thin concentration boundary layer, the asymptote given by Eq. (15) is not a relevant parameter.

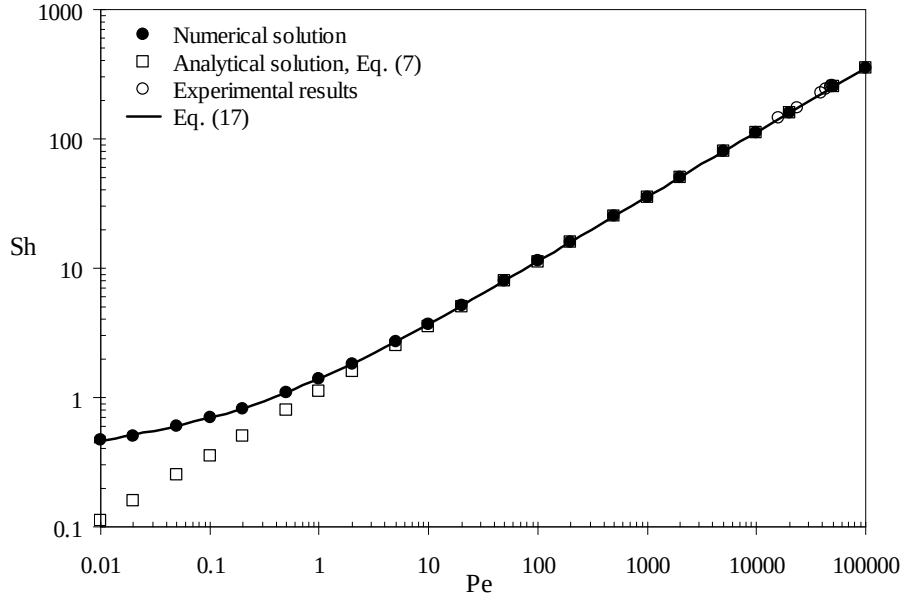

Figure 3. Dependence of Sh on Pe.

4.2 Experimental results

An example of experimental values of Sherwood numbers obtained for seven different air velocities are plotted as a function of Peclet number in Fig. 4. The values of Sh obtained are in good agreement with the numerical predictions, given by Eq. (17), with an error lesser than 4%. The water vapour concentration in the outlet stream, c_{out}, was continuously measured by data loggers, and when steady state was reached, the evaporation rate of the saturated wall could be found from:

$$n = Q(c_{out} - c_0) \tag{18}$$

where Q is the measured air volumetric flow rate. From Eq, (18) with Eq. (17) and $n = kA(c^* - c_0)$, the following equation is obtained

$$c_{out} = c_0 + \frac{D_m}{Q} b(c^* - c_0)\left[\frac{2}{\pi}\left(\frac{uL}{D_m}\right)^{1/4} + \frac{4}{\pi}\left(\frac{uL}{D_m}\right)\right]^{1/2} \tag{19}$$

and if we used the analytical solution (Eq. 7), instead Eq. (17), the following equation is obtained

$$c_{out} = c_0 + \frac{D_m}{Q} b(c^* - c_0)\left(\frac{4}{\pi}\frac{uL}{D_m}\right)^{1/2} \tag{20}$$

For our values of air velocity the Peclet numbers were between 6000 and 50000. In this range of Pe values the Eqs. (19) and (20) given practically the same results, which show that the effect of axial molecular diffusion can be negligible compared with transverse molecular diffusion. In Fig. 4 it is possible to see that the agreement between the theoretical and experimental results is excellent over the entire range.

During the five months of experimental research the new treatment technique extract approximately 80 kg of water. Actually, our group are studying if these values can cause bad consequences in terms of long-term deterioration of the wall materials. As we know the salts dissolved on water and the behaviour of these salts in terms of crystallization/dissolution aspect, the target, in the future, will be sizing the new system of rising damp treatment to avoid crystallization/dissolution problems.

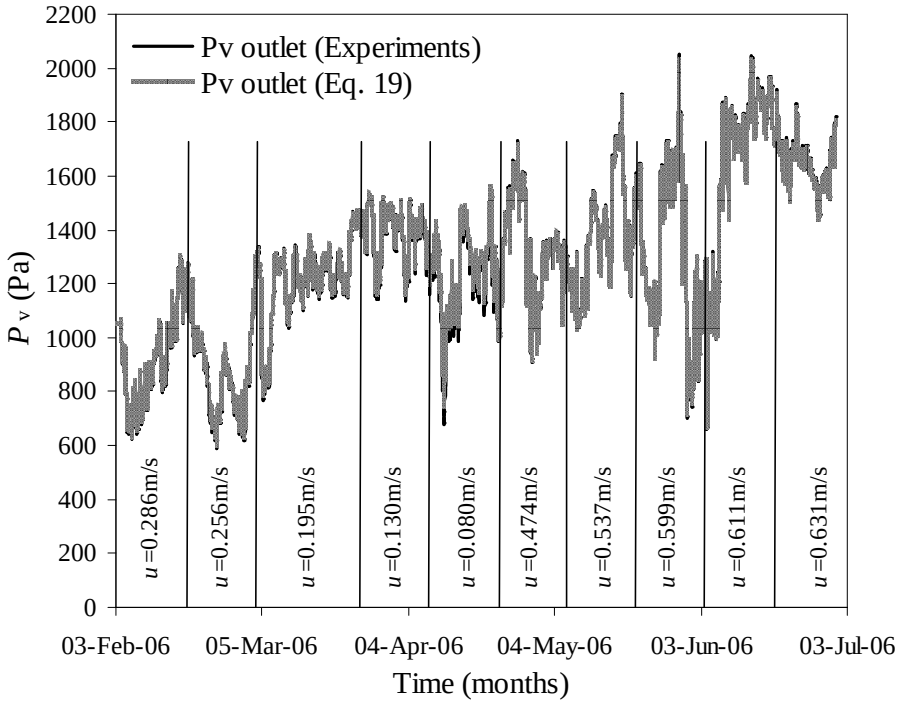

Figure 4. Comparison between the experimental values of water vapour in the outlet stream and the prevision given by Eq. (19).

5. CONCLUSIONS

The mechanisms of moisture transfer are complex, particularly regarding with rising damp in historic buildings. Once, the rising damp is one of the main causes of degradation of these buildings, it became important to study the factors related to this phenomenon. The placement of vapour-impermeable layers on the wall surface increases the level reached by rising damp.

Wall base ventilation is a simple technique that has a great practical potential and the experimental results performed at LFC-FEUP have shown that the placement of a wall base ventilation system on both side of the wall reduces the rising damp level.

The problem of moisture transfer between a saturated wall surface and the air flowing along it, lends itself to a simple full theoretical analysis, under an appropriate set of conditions. The elliptic equations resulting from differential moisture balance has been solved numerically over a wide range of values of the relevant parameters. It was found that the resulting Sherwood numbers are accurately represented by the equations presented above, Eq. (17).

REFERENCES

Alves, M.A., Delgado. J.M.P.Q. & Guedes de Carvalho, J.R.F., 2006, 'Mass transfer from cylinders and plane surfaces buried in packed beds in alignment with the flow direction', *Chemical Engineering Science*, **61**[4], 1174-1183.

Alves, M.A., Oliveira, P.J. & Pinho, F.T., 2003, 'A convergent and universally bounded interpolation scheme for the treatment of advection', *International Journal for Numerical Methods in Fluid*s, **41**[1], 47-75.

Colombert, R. 1975, *L'Humidité des Bâtiments Anciens; Causes et effets; Diagnostic et remèdes*, Editions du Moniteur, Paris.

Cussler, EL., 1997, *Diffusion: Mass Transfer in Fluid Systems*, 2nd edition, Cambridge University Press.

Ferziger, J.H. & Peric, M., 1996, *Computational Methods for Fluid Dynamics*, Berlin, Springer-Verlag.

Freitas, V.P. & Guimarães, A.S., 2008, 'Characterization of a hygro-regulated wall base ventilation system for treatment of rising damp in historical buildings', Proc. 8nd Nordic Symposium on Building Physics, Copenhagen, Denmark, pp. 911-919.

Hall, C., Hoff, W.D. & Nixon, M.R., 1984, 'Water movement in porous building materials-VI. Evaporation and drying in brick and block materials', *Building and Environment*, **19**[1], 13–20.

Incropera, F.P. & deWitt, D.P., 2002, *Fundamentals of Heat and Mass Transfer*, Third edition, John Wiley and Sons, USA.

Torres, M.I.M. & Freitas, V.P., 2007, 'Treatment of rising damp in historical buildings: wall base ventilation', *Building and Environment*, **42**[1], 424-435.

XII DBMC
International Conference on Durability of Building Materials and Components
PORTO - PORTUGAL, April 12th-15th, 2011

Water Behaviour of Old and New Tiles – A Contribution Towards the Conservation of Ceramic Façades

Ana Luísa Velosa [1]
Rosário Veiga [2]
Gilberto Martins [3]

ABSTRACT

Throughout Portugal there is a dissemination of buildings with ceramic façades, with a special incidence on 19th Century buildings, when this technique became quite popular accompanying an increase in production capacity of ceramic tiles. This specific heritage, characteristic of Portugal, Brazil and ancient colonies (India, Cape Verde) has an urgent need for intervention, due to lack of maintenance and difficulty to apply adequate conservation actions. This complex system, composed by sustaining walls, mortar and glazed ceramic tiles often displays detachment of panels and/or lack of tiles that are often replaced by mortars or by different tiles, creating a heterogeneous, degraded effect. Recently, attempts to replace these tiles by replicas have generated an improvement in the conservation of these façades, particularly when it is associated to the use of traditional lime mortars. However, actual glazed tile production materials and techniques differ from those of the 19th Century creating possible differences in the behaviour of old and new materials. For this study, both ancient and recent tiles were tested in terms of water absorption to evaluate differences and possible impacts of their application.

KEYWORDS

Glazed ceramic tiles, conservation, capillary water absorption.

[1] Department of Civil Engineering, Geobiotec, University of Aveiro, 3810-193 Aveiro, Portugal. avelosa@ua.pt
[2] National Laboratory of Civil Engineering, Avenida do Brasil, 101, 1700-066, Portugal. rveiga@lnec.pt
[3] Department of Civil Engineering, University of Aveiro, 3810-193 Aveiro, Portugal. gjfm1972@iol.pt

1 INTRODUCTION

The cladding of façades with ceramic tiles became a popular practice in Portugal, during the 19th century, conjugated with the semi-insustrialization of glazed ceramic tile production. A vast number of patterns were produced by factories situated mainly in the areas of Porto, Lisboa and Aveiro, that used different production materials and methods. Façades all throughout the country became richly decorated with patterns displaying varied colouring and providing a distinctive visual display.

Nowadays, glazed ceramic tile façades still characterize city centres throughout Portugal, with a special emphasis in the cities of Porto and Lisboa, that used tiles from different factories and therefore display distinct sets of patterns. The city of Ovar, due to the concentration and variety of tiles in the city centre, is considered the Museum City of Glazed Tiles. However, this unique heritage is disappearing at a fast rate due to the inevitable degradation of the tile/mortar system and lack of maintenance. Difficulties in pursuing adequate conservation actions due to lack of knowledege and/or lack of the adequate materials have accelerated the disapearance of this type of façades, that are being replaced by rendered façades that are easier to execute and maintain and easy to integrate with external insulation, complying with actual building requirements.

In order to contribute towards adequate conservation actions, there is definite need for a thorough study of the building materials used in the 19th century in order to use compatible materials for the conservation of these façades. As part of a project dedicated to the study of these materials, this paper focuses on the behaviour in terms of water intake of old tiles from different factories, replicas and new tiles. This information is a first step towards the study of mortar/glazed tile interface as water absorption, linked to porosity, interferes with mortar/glazed tile adhesion. Results show differences between 19th cetury tiles of different origin, and between old tiles, replicas and new tiles and may be used as an indicator towards an adequate choice of materials.

2 SAMPLING AND ANALYSIS

2.1. Sampling

Sampling was performed taking into account three different types of tiles: original tiles from the 19th or early 20th centuries, industrial tiles especially produced for use in old buildings and industrial tiles that have been used as a basis for the execution of replicas in conservation actions. Tiles that had previously been applied in buildings in Ovar that were undergoing conservation actions were tested prior to re-use as façade claddings. They were considered ‘original tiles’(Figures 1 to 3). Industrial tiles produced specifically as restoration materials were used and named as ‘restoration tiles’ (Figures 4 and 5). Industrial tiles that have been used as a basis for the creation of replicas were considered ‘new tiles’(Figure 6 and 7).



Figure 1. Tile from Factory José Pereira Valente e Filhos (OT1).

The tile from Figure 1 (OT1) is from the 19th to early 20th century, produced in Vila Nova de Gaia in the factory of José Pereira Valente e Filhos. Its dimensions are 14x14x0,9cm and the tile execution was performed using a transfer print technique, resulting in a monochromatic pattern.



Figure 2. Tile from Devesas Factory (OT2).

Figure 2 depicts a tile (OT2) from the well known factory of Devesas, in Vila Nova de Gaia, also from the late 19th century or beginning of the 20th century, with dimensions of 14x14x0,9cm, that was brush painted using a stencil technique. The factory of Devesas produced a great ammount of tiles with a diversity of patterns, that are very frequent in the façades in the north and centre of Portugal.



Figure 3. Tile from Sacavém Factory (OT3).

'Fábrica de Louça de Sacavém' also produced a great quantity of glazed tiles, used mainly in the south of the country and with different materials, due to English ownership and influence. This tile (OT3) (Figure 3), also from the same period, has dimensions of 14x14x1cm, and was glazed over motif obtained by a mechanical press. The base is made from stone dust basis and not from the traditional mixture of clays that characterize the tiles above.



Figure 4. Renovation tile 1 (RT1).

Figures 4 and 5 show the renovation tiles (RT1 and RT2) used in this study, of current production and replicating ancient patterns, with a size of 14x14x1cm.



Figure 5. Renovation tile 2 (RT2).

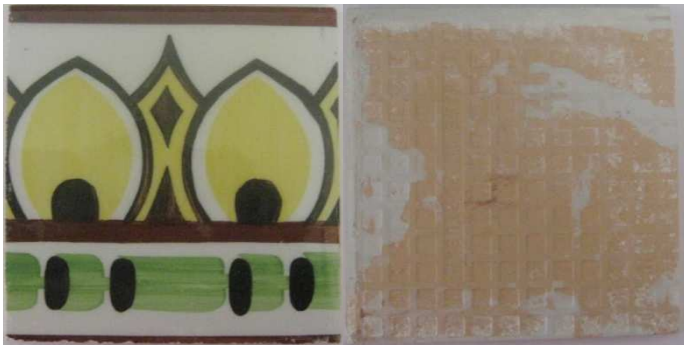

Figure 6. Insutrial tile with galzing replicating ancient tile (NT1).



Figure 7. Insutrial tile with galzing replicating ancient tile (NT2).

Industrial tiles from 2 different producers have been used for the production of replicas in conservation actions. The tile from Figure 6 (NT1) has dimensions 13,5x13,3x0,8 and the tile from Figure 7 (NT2) has dimesions of 14x14x0,7, revealing a lower thickness of these tiles in comparison to ancient or renovation tiles.

2.2. Testing Procedures

Samples were tested for water absortion by capillary action following the procedure used for conservation mortars developed by LNEC and other european partners [Veiga et al 2004, LNEC 2005, Veiga 2005]. This procedure implies the evaluation of water absorption over time through the ceramic's unglazed surface placed on a geotextile to avoid errors by loss of friable particles. Two samples were used for each capillary water absoption test.

3 RESULTS AND DISCUSSION

3.1. Water Behaviour of 19th Century Tiles

Capillary absorption behaviour of original tiles is shown in Figure 8 and reveals a great variation, both in terms of initial absoption speed and of total water absorption. OT3 from Sacavém Factory, based on different raw materials has the highest absorption and also the highest capillary coefficient (10,72 kg/m^2.h$^{1/2}$). The tile from the Devesas Factory (OT2) has the lowest capillary coefficient (4,21 kg/m^2.h$^{1/2}$) but absorbs more water in the long run than the tile from the factory of José Pereira Valente e Filhos (OT1) with a capillary coefficient of 6,35 kg/m^2.h$^{1/2}$. This different behaviour may be due to use of different raw materials and/or production techniques that create distinct porous structures. There may be some impact from ageing but this must be further evaluated.

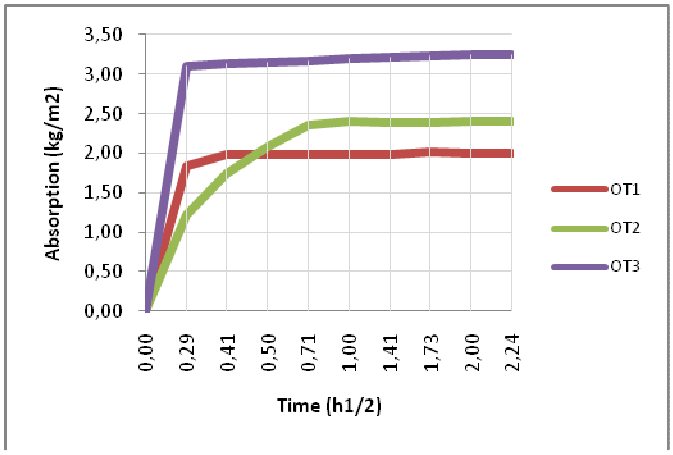

Figure 8. Water absorption of original 19th Century tiles.

3.2. Water Behaviour of Replicas and New Tiles

Generally replicas (RT1 and RT2) absorb more water than new tiles (NT1 and NT2) as shown in Figure 9. This may be explained by a different porous structure but also by the decrease in thickness of new tiles in comparison to other tested tiles. However higher absorption coefficients of replicas (8,27 kg/m^2.h$^{1/2}$ and 7,03 kg/m^2.h$^{1/2}$, respectively) compared to new tiles (6,64 kg/m^2.h$^{1/2}$ and 5,16 kg/m^2.h$^{1/2}$, respectively) reinforces the hypothesis of a differentiated pore structure.

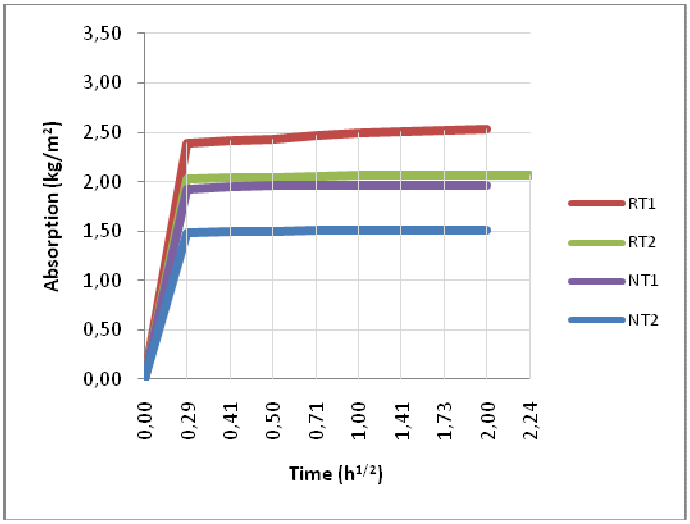

Figure 9. Water absorption of replicas and new tiles.

3.3. Comparative Water Behaviour and Choice of Tiles

Figure 10 reveals the water absoption behaviour of glazed tiles from different origins in comparison to tiles that are frequently used in conservation actions of façades. There is no replica that simulates the high absorption characteristics of OT3, from Sacavém and produced with a stone dust basis. However renovation tile RT2 and new tile NT1 have a very similar behaviour to the tile from the José Pereira Valente e Filhos factory (OT1), that is also expressed in terms of capillary water absoprtion coefficients (Figure 11). The tile from the Devesas factory (OT2) is characterised by a very low water absorption coefficient, although total water absoprtion is similar to that of RT1.

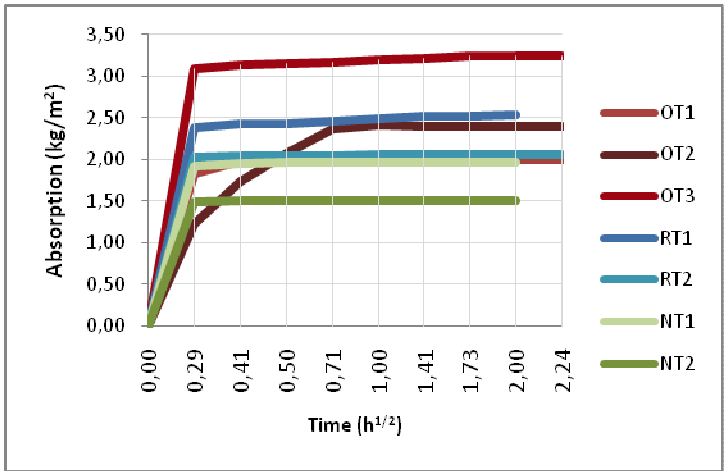

Figure 10. Comparative water absorption of glazed tiles.

Taking into account data from Figures 10 and 11, it may be stated that there is a great variety in terms of water absorption of original tiles from different production centres, that is reflected both in terms of initial absorption rate and total water absorption. Renovation tiles have higher capillary water absorption coefficients than new tiles and generally present a water absoption behaviour that is more approximate to that of original tiles.

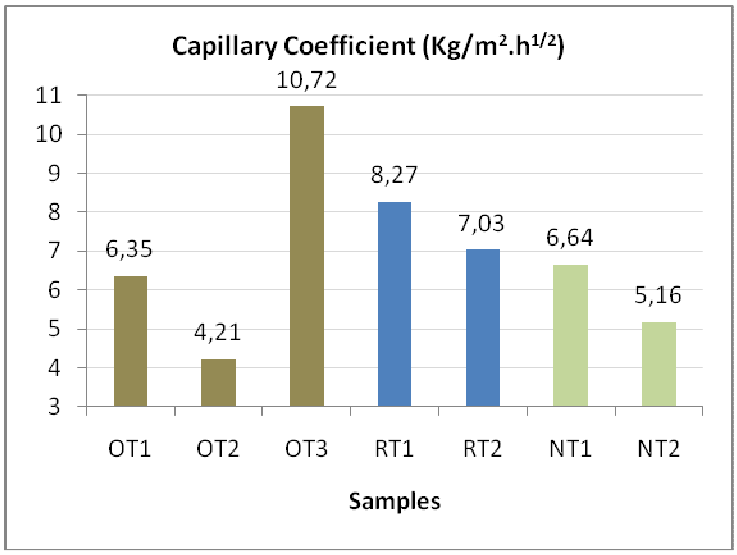

Figure 11. Capillary coefficient of glazed tiles.

4 CONCLUSIONS

The determination of capillary water absoprtion of glazed tiles is only the first step towards the adequate choice of tiles to be used in conservation actions and must be complemented with further testing incorporating water vapour permeability, visualization by scanning electron microscopy (SEM) and the determination of porosimetry and adhesion between tiles and mortars, among others. However, it is an initial indicator of the adequacy of tiles for this particular use.

The capillary water absorption of old glazed tiles is also an important characteristic to determine the choice of mortars to be used for their reapplication.

Results of capillary absorption tests on original tiles from three different production centres revealed that for the case of the Factory José Pereira Valente e Filhos, renovation tiles and new tiles used for conservation purposes may be found with similar water absoprtion characteristics, rendering them possibly adequate for use in glazed tile façade conservation practice. However, no renovation or new tiles showed similar behaviour to the other original tiles. This is especially noticeable in the case of the tile from the Sacavém Factory.

A more complete study of 19th century tile characteristics will increase the knowledge of their composition and behaviour, enabling the production of replicas that may be used in façades as compatible materials.

ACKNOWLEDGMENTS

FCT- Portuguese Foundation for Science and Technology for its support through the Project PTDC/ECM/101000/2008 – AZULEJAR – Conservation of glazed ceramic tile façades.

REFERENCES

Veiga, Maria do Rosário 2005, Characteristics of repair mortars for historic buildings concerning water behaviour. Quantification and requirements. In Workshop Repair Mortars for Historic Masonry, TC RMH. Delft, RILEM, 25-28.

LNEC Fe Pa 40.1 2005, Revestimentos de paredes. Ensaio de absorção de água por capilaridade para amostras irregulares e friáveis, MOPTC, LNEC, NRI.

Veiga, M. R., Magalhães, A., Bosilikov, V. 2004, 'Capillarity tests on Historic mortar samples extracted from site. Methodology and compared results.', *Proceedings of 13th International Masonry Conference*, Amsterdam.

XII DBMC
International Conference on Durability of Building Materials and Components
PORTO - PORTUGAL, April 12th-15th, 2011

An Old Roof and a New Function

Ana-Maria Dabija [1]

ABSTRACT

The roof is part of the envelope and therefore, the functions of the roof are the same as the functions of the envelope. However, historically, each function was "acquired" in a specific period. Initially the roof was supposed to protect against water, wind and snow and later, against fire and noise. Then the protection against excessive sun was required, or a better ventilation of the space under the roof. As requirements for thermal comfort increased, the insulated 'blanket' found its way on top of the building, with all the corresponding layers that ensured the proper functioning of both the thermal insulation and the waterproof / water resistant system. In the midst of an energy crisis, of the traditional fuel crisis, scientific research was oriented towards developing and using new and effective energy sources. In an attempt to save the planetary environment, buildings play an important role: they have to integrate and function with nature, not against it. This is the context in which the roof of the building is acquiring two new and important functions: the energetic function of preserving and producing energy and the environmental function, of decreasing urban pollution. The paper presents an experimental project of a BIPV system installed on the roof of a historic building in Bucharest, Romania.

KEYWORDS

Roof, rehabilitation, solar energy, natural light.

[1] 'Ion Mincu' University of Architecture and Urbanism, Bucharest, Romania, am.dabija@iaim.ro

1 INTRODUCTION

The volume under the roof represents a potential extra space, considering that it was not given a specific function when the building was designed. In some European countries the designers took advantage of this space; in others, like in Romania, it was a technical space, used for instance for drying and smoking food (not as a metaphor but literally, as it can be seen in Figure 1).



Figure 1. An example of a traditional Romanian village house; in the upper part, the traces of smoke show what the roof was used for: smoking food in order to preserve it from winter to spring.

Within a roof rehabilitation this space may be given a new function (other than a technical function) while the roof can also represent a means of saving or producing energy. In order to turn the roof from a technical space into a liveable space and to accommodate the new function, the whole structure of the roof has to be upgraded. The roof traditionally protects against water and snow, wind and dust (with the biological components that come along: pollen, seeds, bees, birds etc), fire, sun and noise. It ensures natural light and ventilation, through the provided openings. It also offers hygrothermal protection for the space beneath. Recently, the roof started being seen as an opportunity to accommodate systems that save or produce energy. Therefore it is natural that, in the case of such interventions, the overall performances of the roof should be updated and the new functions mentioned above (saving and / or producing energy) should be included.

2 (BRIEF) PRESENTATION OF THE BUILDING

The Old School of Architecture is a historic building in the centre of Bucharest, with an interesting story: built in 15 years, between 1912 and 1927, with many interruptions (due to the difficulty of expropriating the whole site, to the lack of funding, and due to the World War I when, for some years, all work was interrupted). The long period of construction and the discontinuity of funding are the main reasons for the diversity of the constructive systems of the building, as well as for the huge differences between finishes: from the monumental part of the facade, with columns covered in stone lace, to a very simple stone cladding on the opposite side; from a rich interior marble staircase, to simple terrazzo floor finishing; from painted decorated beams inside the Hall of the Amphitheatre to very simple plastered walls. The building had to withstand five earthquakes, two of them (1940 and 1977) catastrophic, with thousands of dead and injured and immense material loss.



Figure 2. Image of the Old School of Architecture, Bucharest, Romania

For some years now, the 'Old School' – as it is also known - is subject of a holistic process of consolidation, conservation and modernization, for the first time since it was built. The main objective is to ensure that the building, a monument but also a public institution, is structurally sound. However the process includes the upgrade of the installations (sanitation, HVAC, electrical) and the equipment so that they respond to the education requests of the 21st century. Knowing that the action of structural consolidation will imply ample interventions, as mentioned above, we took the opportunity to increase the functional space of the building as well, by retrofitting some of the spaces, including the attic - previously a cold space with no particular use – that was transformed into a mansard, with offices and seminar rooms, lined up on both sides of the space beneath the roof, separated by a median corridor (and with the correspondent facilities and equipment).

Initially with a heavy structure of wooden trusses (which were cut to provide an emergency escape during World War II, as seen in Figure 3), the attic was structurally remodelled by replacing the original structure with a slimmer, metallic one, which allowed for the space beneath to be used.



Figure 3. The original structure of the attic, including the corridor that was cut in the trusses in order to provide an emergency escape during the war.

The new structure is presented in Figure 4. As can be seen, the space resulting from the replacement of the old structure is very generous. Roof windows were designed for the natural lighting of the

rooms, while the resulting dark central corridor was provided with artificial lighting, by means of the lamps placed on the gypsum board ceiling and on the lateral walls. At least this was the first proposal.



Figure 3. The new, slim roof structure during the execution stage.

3 NEW INTERVENTIONS FOR ENERGY SAVINGS IN A PILOT PROJECT

3.1 General Considerations

The initial idea of placing lamps on a dark corridor, which would be lit all day long, thus using conventional energy, seemed, on second thought, an outdated proposal so we adopted a better solution: the use of solar tunnels. The new proposal was made in order to improve the quality of the space and to save energy, by bringing natural light onto the ceiling of the central corridor of the mansard (see Figure 4). The changes of the initial design were not major, on the contrary, the line of lateral light sources (placed on the walls) was eliminated, the current solution (of including lamps within the tubes) being more elegant.

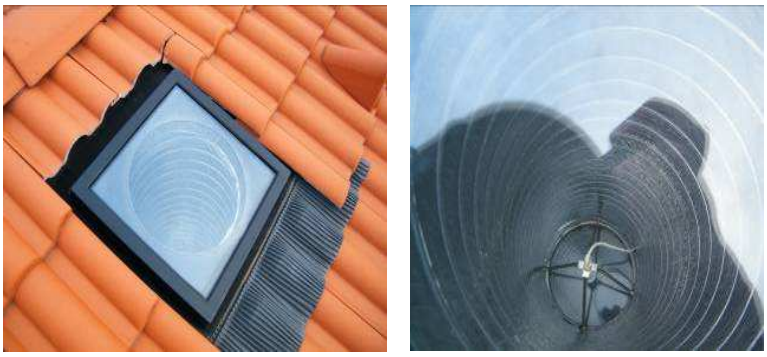

Figure 4. Solar tunnels at the 'Ion Mincu' University (the left hand side image represents the tunnel on the southern slope and the right hand side image represents an interior photo where the electricity supply system of the light source inside the tube can be seen)

Solar tubes are systems which allow natural light to enter in 'blind' areas (hallways, closed offices, toilets, etc.), or in areas with low natural lighting (deep rooms, etc.). They can bring natural lighting in many interior spaces. They are considered the best solution for different types of buildings, from houses and residential complexes, to office buildings, schools, hospitals, shopping centres, industrial

warehouses and gymnasiums [Dabija & Gheorghe, 2010]. The system includes a light diffuser that is installed in the ceiling of the building and a super reflective tube that is installed on sloped or flat roofs.

We took advantage of the possibility of installing an artificial light source within the tube, so it is no longer necessary to provide other artificial lighting. This solution is implicit, requiring an appropriate design and connections. On the other hand it is a very elegant solution in terms of interior space, as can be seen in Figure 5.



Figure 5. An image of the central corridor, lit by the solar tunnels

Besides the consolidation activity, in the last three years a research project was carried out in our University regarding the use of BIPV. As the consolidation works were carried out in the historic building, we made a proposal for integrating the panels within one of the slopes of the roof of the Old School. As this is a historic monument, the insertion could only be made on the slopes facing the interior courtyard. Fortunately, the orientation of these slopes is appropriate: South.
In order to decide on the location of the solar panels, we carried out a study of sun-light.

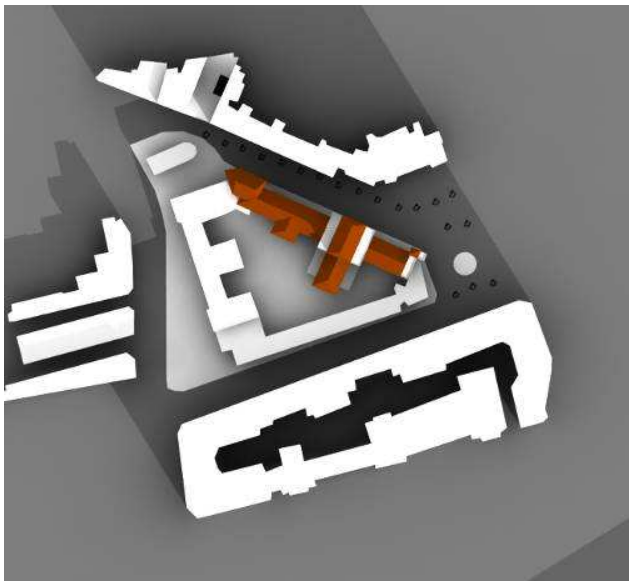

Figure 4. Off-print of the sun-light study (December 22, at 3 p.m.) carried out in order to decide where to install the experimental BIPV system

The aim was to evaluate which slope is not affected by shade at the most disadvantageous moment of the year: the winter solstice. Two possibilities for the installation of the panels were considered, taking into account the ease of installation, accessibility and – very important – what the energy provided by the panels will be used for. The installation of the solar tunnels and the fact that they provide a 'green' solution led us to the decision of placing the BIPV on the same slope as the solar tunnels and use the energy produced by the panels to feed the batteries that are connected to the artificial light provided within the solar tubes. This way the two systems work together, achieving an altogether 'green' solution: daylight by means of the solar tunnels, night light provided by the solar energy accumulated in the batteries.

3.2 Technical Data

3.2.1 Solar Tunnels

With an inner surface of 98% reflective mirror, the solar tube captures, focuses and reflects natural light, and then distributes it evenly through a microprismatic diffuser. Once installed, it can illuminate any interior space at no cost. Solar tubes offer a great advantage as they receive, besides direct sun light, sky diffuse light as well, so that they illuminate any interior space in any weather conditions.

The tunnels at the 'Ion Mincu' University of Architecture are placed on the southern slope, facing the inner courtyard. They have the following characteristics:

- Outside capture cover allows the passage of unaltered interior day light, having a high transparency of 97 - 98%. It is made of weatherproof material.
- Super-reflective tube is designed to reflect the captured light and transfer it inside. In the case of the system used at the University, the tube has a diameter of 50cm.
- Diffuser is designed to collect the reflected light rays in the super reflective tube and send them to the inner side, for uniform illumination.

Transmitted light has an average power of 13,000 lumens and can reach 20,000 lumens. For the night lighting, the system is equipped with an economical electric lamp, consuming 5 times less energy than a traditional one. The saving may be of 100% during the day and may go up to 80% during a 24-hour operation, depending on the conventional lighting system that is used (the producers boost). In order to feed the light sources with electric power at night, we chose to install a stand-alone solar photovoltaic panel system.

3.2.2 Building Integrated Photovoltaic System

Insofar as photovoltaic systems are concerned, there are two choices: grid-connected systems (used in areas with electricity) and stand-alone systems (used in areas without power or where the network connection is difficult). Stand-alone systems are generally grouped into professional applications for telecommunications, pumping systems, lighting, etc. or applications for rural areas without electricity. The major advantage is the system independence, but this independence has a relatively high cost due to the maintenance of the energy storage system (batteries and accumulators controller).The grid-connected system is more economically effective since, due to the elimination of the energy storing system (batteries), the costs due to the relatively short life-cycle of batteries and general maintenance are reduced. However, we chose to use the stand-alone system, because it can be better monitored for this pilot project. The BIPV system used at the 'Ion Mincu' University is composed of four monochrystalline panels of PV cells, which provide a maximum power of 1kWp. The panels were installed on a slope of 32° with a south – south-west orientation. Although the optimal tilt of the panels in Bucharest would have been, for the given orientation, 44°66', the need to integrate the panels into the existing roof led to the acceptance of a lower slope, the same as the roof slope. However, the decrease in the efficiency of the photovoltaic panels is, in this case (according to the charts), less than 5%. The electrical system is set in a technical space, accommodated in a space under the panels. It houses the charge controller, the batteries, and the AC / DC.



Figure 7. Installation of the PV system, by displacing the corresponding area of roof tiles

4 CONCLUSIONS

The pilot project is the result of a research project in which the 'Ion Mincu' University of Architecture and Urbanism was a partner in a consortium led by a national research institute - IPA - and four University Centres. The idea to combine two systems, one that saves energy and one that produces energy, is an objective beyond the research project. The results are being monitored and we expect to be able to offer more information on the performance of the BIPV in the future.

REFERENCES

Dabija, A-M *et al.* 'Possibilities of Integrating PV Panels on an Existing Roof; A Case Study of a Building in Bucharest, Romania', in Proceedings of the SASBE (Smart and Sustainable Building Environment) International Conference, Delft, The Netherlands, June 2009

Dabija, A-M & Gheorghe, S, "Licht, Mehr Licht'. The Use of Natural Light in Dark Spaces; A Case Study', in Proceedings of the World Energy System Conference, Targoviste, Romania, 2010

Sandia National Laboratories – Stand-alone Photovoltaic Systems – A handbook of recommended Design Practices – March 1995, available from National Technical Information Service, US Department of Commerce

Terry Galloway Solar House: A Guide for the Solar Designer, Architectural Press, an Imprint of Elsevier Limited, 2004

XII DBMC
International Conference on Durability of Building Materials and Components
PORTO - PORTUGAL, April 12th-15th, 2011

Current Problems Involving the Dismantle of Asbestos-Cement Sheets in Buildings. The Case of Central Market in Alicante

Cesar Daniel Sirvent Pérez [1]
Beatriz Piedecausa García [2]
Mónica Mateo García [3]
Carlos Pérez Carramiñana [4]

ABSTRACT

The project and the works described in this article mainly deal with the removal of the current asbestos-cement covering of the roof of the Central Market in Alicante and its replacement with zinc diamond-shaped scales, similar to the originals which were implemented in 1921 when the building was put into service.

These upgrades were necessary to avoid the causes (and consequences) of rainwater infiltration, as described in an earlier report in 2006, also drafted by the author of this article.

The article illustrates the difficulties involving the practical application of spanish Code RD 396/2006 (minimum safety and health requirements for work with risk of exposure to asbestos) in a complex case such as this, especially with regard to aspects such as economic (increasing costs), technical (increased difficulty of implementation), and the total duration of the work (total increase in duration due to interference with other trades).

KEYWORDS

Asbestos-cement, chrysotile, roof deconstruction, zinc.

[1] Architectural Construction Department. University of Alicante. SPAIN, sirvent@ua.es
[2] Architectural Construction Department. University of Alicante. SPAIN, piedecausa@ua.es
[3] Architectural Construction Department. University of Alicante. SPAIN, monica.mateo@ua.es
[4] Architectural Construction Department. University of Alicante. SPAIN, c.perez@ua.es

1 INTRODUCTION

Since its opening in 1921, the Alicante Central Market building (Fig. 1) has undergone two significant changes: first, in 1938, when it was badly damaged as a result of the bombings during the Spanish Civil War (May 25, 1938) [Perez 2007], and second, in 1987, when it underwent significant reforms, affecting almost all of its functional elements [Navarro 1987]. Since then, the building had presented a clinical picture that included, among other problems, a series of leaks that presented themselves whenever it rained.

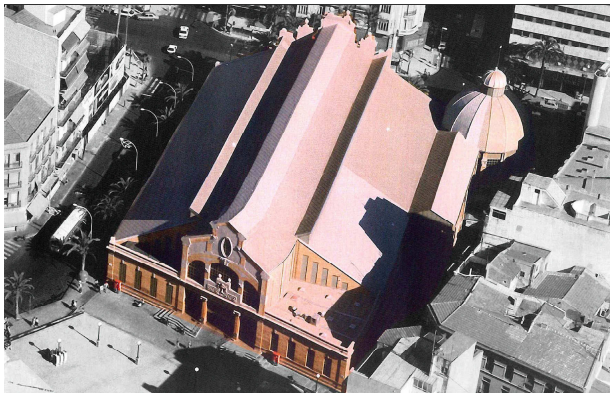

Figure 1. Central Market (Alicante).

2 BACKGROUND

2.1 Description Of The Cover System

The roof is supported by a combination of metal pillars (interior), small brick pillars (east and west facades), and load-bearing walls (north and south facades) which support long-span steel trusses, in two orthogonal directions. The substructure of the roof, which consists of large and small slats of wood, is supported by metal profiles. The outermost layer of the roof cover consists of asbestos-cement plates that are nailed over the little slats(Fig. 2).

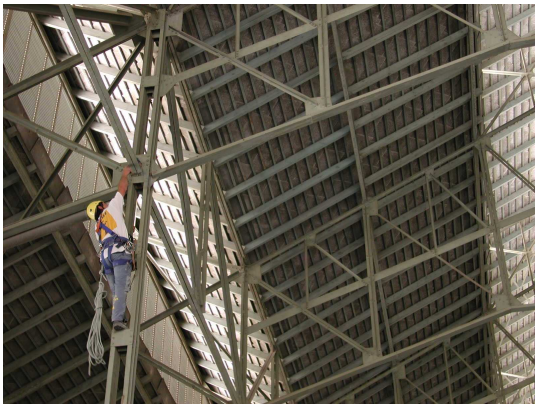

Figure 2. Partial view of the inside of the cover (photos taken during the inspection work "in situ" for drafting the injury report, 2006).

To each specific function we can assign a main material; in this way we have:

- Steel, which is used for the main load-bearing structure (brackets, trusses, and support straps)
- Wood, which is mainly used for the substructure (small slats and supports)
- Asbestos-cement, which, together with zinc, is the finishing material

The outer layer of the roof is composed of plates of different shapes and materials, depending on their location:

- Inclines: asbestos-cement squares 6 mm
- Top: asbestos-cement squares 3 mm
- Lantern of the dome: diamond-shaped zinc scales

2.2 Damage To The Items Covered

A technical study in 2006 identified the following risks associated with and deficiencies in each of these materials [Sirvent 2006]:

The steel, although relatively acceptable, had at various points begun to corrode, which manifested itself in the form of surface pitting (the profiles had not lost structural integrity).

Many of the wooden items remained undamaged, but we found some specific elements that had become unusable due to them having broken, or because they had begunto show symptoms of decay.

Finally, the main problem that we found with the topcoat was that it contained leaks in various locations. Before the renovation, a large surface of asbestos-cement square plates had received several additional layers of waterproofing paint with a base of chlorinated rubber and fiberglass mesh.

As a result of this study, we concluded that the most technically viable solution would involve the deconstruction of the existing roof, finished in asbestos-cement boards to proceed with the implementation of a new deck that guarantees a certain level of durability and waterproofing.

2.3 Restoration Concept: Historical Research

As a preliminary to the drafting of the project for replacement of the deck, we reviewed the original project report (written in 1914 by the City Architect, sr. Fajardo, along with Engineer, sr. Lafarga), in order to better understand the materials and systems that were used in the original building. Various sections of the report [Fajardo & Lafarga 1914] described different parts of the roof structure as follows: "*The main spaces [...]. Knives are placed on the belt and above them the galvanized sheet metal and galvanized which serves as the cover. The roof of the dome and lantern are coated with zinc diamond pieces*."

The second part of the report, “Calculation of the Elements of the Market”, states: "*We propose the use of corrugated and galvanized sheet metal for the covers, and zinc pieces for the remaining areas*."

Using this data, with the fundamental criterion being to restore the original image of the building, we proposed the use of diamond-shaped pieces of zinc, using current materials and techniques that ensure adequate waterproofing and durability, while respecting the original image.

3 THEORETICAL DATA (Investigations Prior to Commencement of the Renovation)

3.1 Asbestos

The term "asbestos" designates a series of fibrous minerals composed of silicates of iron, aluminum, magnesium and calcium among others, according to the internationally accepted registration of chemicals provided by the Chemical Abstract Service (CAS). There are two main types of asbestos: chrysotile and amphibole.

Chrysotile (white asbestos, CAS No. 12001-29-5) is a hydrated magnesium silicate (40% Si, 38% Mg, 2% Fe), white or greenish, with fibers in multiple vertical streaks.

The main health risk associated with asbestos is the airway inhalation of microscopic fibers, which requires special caution in activities that involve the release of fibrous particles into the environment. The two main illneses that one can develop by exposure to asbestos are malignant mesothelioma (pleural or peritoneal), and asbestosis (pulmonary fibrosis).

The spanish national legislation regarding minimum safety and protection of workers from health risks arising from asbestos exposure at work is the RD 396/2006 of March 31, 2006. The current European standard is the Directive 2009/148/EC of the European Parliament and the Council, November 30, 2009, on the protection of workers from risks related to asbestos exposure at work.

3.2 Asbestos Identification Tests Performed in Alicante Central Market

In order to unequivocally characterize the material composure of the sheets of Alicante Central Market roof, we obtained a sample from each type (thicknesses of 3 mm and 6 mm). They were transported to the laboratory at the Department of Building Materials at the University of Alicante, where they underwent analysis by optical microscopy. The presence of chrysotile (white asbestos) was discovered in each sample (Fig. 3).



Figure 3. Chrysotile (micrograph of a sample of the roof of the Central Market, corresponding to a square plate of thickness 3 mm).

3.3 Description of the Works

The renovation of the Central Market building [Sirvent, 2007] included the work leading to the removal of the current coat of asbestos-cement, restoration of the steel structure and substructure of wood, and the installation of a new layer of zinc plates.

It also included the placement of various types of interior and exterior scaffolds, lifelines, and temporary protection to ensure safe work practices. The most significant project items were:

- Fall protection safety net (2,850 m2).
- Double protective plastic membrane (3,010 m2).
- Removal of asbestos cement plates (3,475 m2).
- Cleaning and treating steel structure (1,515 m2).
- Replacement and painting of the wooden substructure (2,780 m2).
- New roof finished with diamond scales of zinc (3,475 m2).

4 EXPERIMENTAL (Execution of the Works)

4.1 Requirements of the Asbestos Spanish Law RD 396/2006 and Its Application

The demands arising from the implementation of the RD 396/2006, together with the need to protect the interior of the market from weather elements, required a carefully planned intervention. Following are some of the requirements of the RD 396/2006, which helped determine the project planning:

Section 8: Personal Protective Equipment. "*The use of personal respiratory protective equipment shall not be continuous, and its usage time for each worker, [...]shall in no case exceed 4 hours a day.*" This article is quite limiting on the speed of the renovation, since the process of replacing the deck must begin with the removal of the existing asbestos-cement plaques.

Section 7: Organizational Measures. Paragraph d) -2 º indicates that "*the places where such activities are conducted [...] shall not be accessible to persons not pertaining to the asbestos removal job.*" This section requires us to create different shifts so that the removal of the asbestos cement sheets does not coincide with work in other trades.

Section 6: Preventive Measures. Paragraph a) states that "*the working procedures must be designed so as not to produce asbestos fibers, if that proves impossible, the release of asbestos fibers into the air must be avoided.*" This requirement necessitates the use of measures that complicate the project´s execution, as will be apparent in later sections.

4.2 Initial Work-Planning & Organization

The project plan [Sirvent 2007] was developed as a result of combining the above basic premises. City authorities added a final condition: the market must be kept open to the public during the renovation.

The first phase involved installing guards on the exterior of the building (a perimeter of tubular scaffolding) and on the interior a system of multidirectional scaffolding that created a platform for ongoing security and lifeline nets anchored to the trusses (Fig. 4).

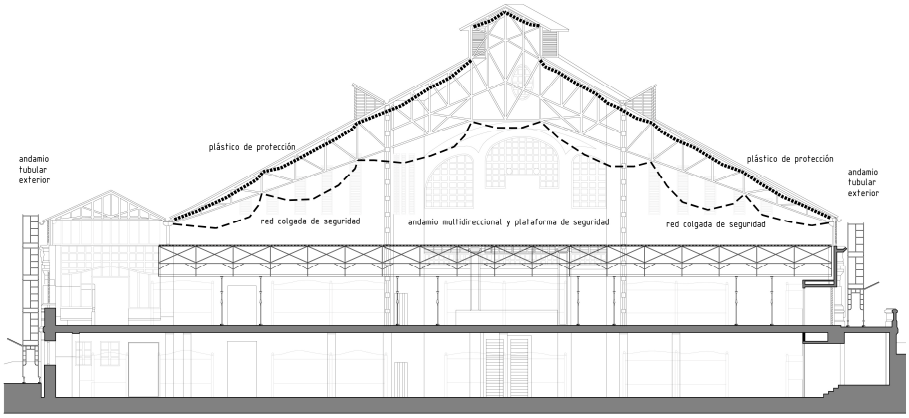

Figure 4. Section Deconstruction Project (2007).

The second phase involved placement of two plastic protective membranes under the roof and above the net (the lower membrane was impermeable, and was used as protection in case of rain, and the higher, thinner membrane was used to collect and encapsulate the asbestos dust; *section 6 RD 396/2006*).

The third phase involved the removal of the asbestos-cement plates, performed by specialists in handling asbestos [Sanjuán 2007]. Their work was coordinated with three other teams (steel, wood, zinc) so as not to coincide in the use of space and/or time, since their activity is harmful to the other workers (*section 7 RD 396/2006*).

4.3 Changes: The Difficulty of Implementation of Some Requirements

The first problem that arose during the execution of the works concerned *Section 7: Organization*. It was impossible to coordinate the performance of three teams of different trades, so that all could work simultaneously on a small portion of the roof (during different hours of the day) in order to avoid exposure of large areas of the roof to rain.

From a technical standpoint, an ideal situation would involve each team working only the hours required to perform their tasks in a small area of the roof (*Section 8*). In reality, this conflicts with economic considerations of both the owner of the building (longer duration of the project) and of the companies (limiting hours each working day is less profitable).

Another change to the plans was the elimination of the dual plastic membrane system under the current cover (*Section 6*) due to the difficulty of removal of asbestos collected in the plastic. It was replaced by a different extraction system (allowed by law). However, practice showed that this new system would not allow the removal of small and medium asbestos pieces, which were deposited on plastic or metal sections of the trusses (Fig. 5). We subsequently needed to measure fiber concentration in accordance with regulations.



Figure 5. Chunks of asbestos is not removed by exhaust systems deposited on the metal structure.

5 CONCLUSIONS

The RD 396/2006 has clear requirements for workers at risk of exposure to asbestos, so we assumed that specialists in these tasks would understand and apply these rules.

However, the problem arises in renovations in which other trades outside of asbestos handling share the same space and/or schedule. In these cases, we must try to avoid this simultaneity because of the health risks to these other workers, who usually have neither the adequate training nor equipment to protect themselves from these risks. Article 7 d) -2 º explicitly prohibits this simultaneity.

In any case, before granting access to other workers not specialized in asbestos to areas where there has been manipulation of asbestos (simultaneity in space but not in time), the work environment must be assessed and controlled according to the prescriptions made in Article 5 of the code, to ensure that the thresholds set out in Article 4.1 are not exceeded.

The same procedure should be applied in cases where there is simultaneity in time but not in space, for example, in the case where several trades agree on the same shift schedule but in different areas of the jobsite. We should indicate that this scenario is worse than the previous one, because handling asbestos may cause ruptures that generate a substantial amount of airbore fibers that are easily carried by the wind (when working outdoors), affecting other non-specialized workers.

Finally, we should say that the capture of fibers in the vicinity of the emitting source with extraction systems is suitable only for very tiny particulates, but does not remove pieces of small and medium size. Thus, deconstruction by breaking of pieces should be avoided, or, at the very least, an additional means of collecting these pieces (eg, encapsulated by plastic) should be provided to prevent fibre deposition in other parts of the jobsite.

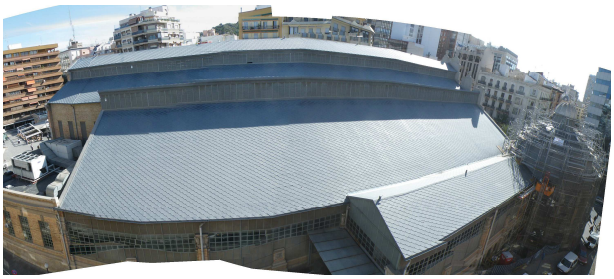

Figure 6. Final appearance of the new cover of zinc pieces (March 2010).

REFERENCES

Egea, L. (2007). Packaging and waste management. Applicable requirements for the removal of elements that contain asbestos. Proc. Technical Conference: requirements for the removal of items that contain asbestos. INVASSAT, Alicante.

Fajardo, Lafarge. (1914). Descriptive Report and Calculation of the elements of the market. Project (consulted the Municipal Archives).

G. Gilson C. (1989). Asbestos. ed. Parmeggiani L. Madrid.

Ministry of Health. (1999). Specific health surveillance protocols: Asbestos. Health Surveillance, Public Health Commission.

Navarro, A. (1987). Implementation Project: Rehabilitation of Central Market in Alicante. (consulted at City Hall).

Perez, M. A. (2007). May 25, the forgotten tragedy. ed. ECU. Alicante.

Royal Decree 396/2006 of 31 March, laying down minimum safety and health requirements for work involving the risk of exposure to asbestos.

Sanjuán, J. (2007). Removing asbestos cement roofing. Proc. Technical Conference: requirements for the removal of items that contain asbestos. INVASSAT, Alicante.

Sirvent, C.D. (2006). Current state of the roof of the Central Market. Technical Report.

Sirvent, C.D. (2007). Complete replacement of the roof and waterproofing Central Market Total Market Square. Basic Project and Execution.

XII DBMC
International Conference on Durability of Building Materials and Components
PORTO - PORTUGAL, April 12th-15th, 2011

Hygric Properties of Lime Based Mortars used for Restoration Interventions on Historic Structures

Eleni Aggelakopoulou [1, 2]
Asterios Bakolas [3]
Antonia Moropoulou [4]

ABSTRACT

In this research work, four syntheses of lime mortars were prepared by using hydrated lime (powder or putty) and sand (quartz or calcite), in order to be used in restoration interventions of historic structures. The microstructure characteristics were estimated by using Mercury Instrusion Porosimetry (MIP) in time evolution from the production till 18 months of curing. At the period of 36 months, water capillary rise and immersion tests were applied to mortars in order to estimate the total cumulative volume accessible to water and the capillary rise coefficient. The microstructure characteristics and the hygric properties of lime mortars are correlated and compared to the ones of traditional structural materials in order to ensure the compatibility and the durability of the restoration interventions.

KEYWORDS

Lime mortars, hygric properties, microstructure, capillary rise, immersion

1 Directorate for Technical Research on Restoration of the Hellenic Ministry of Culture, Athens, GREECE, eaggela@gmail.com
[2] School of Chemical Engineering of the National Technical University of Athens (NTUA), Athens, GREECE, laggela @central.ntua.gr
[3] School of Chemical Engineering of the National Technical University of Athens (NTUA), Athens, GREECE, abakolas@mail.ntua.gr
[4] School of Chemical Engineering of the National Technical University of Athens (NTUA), Athens, GREECE, amoropul@central.ntua.gr

1 INTRODUCTION

Lime mortars and plasters have been used in structures since 7000 BC [Malinowsky and Grafinkel 1991] till nowadays covering different usages such as joint mortars between masonry units, supporting or decorative materials (pavements, mosaics, frescoes), binders for waterproof linings (cisterns, reservoirs, baths). Although they present a rather vulnerable behaviour when they are exposed to sulphur compounds [Karatasios et al 2007] and chemical degradation, lime mortars have been proved to be well compatible to the historic building materials and long lasting under severe mechanical and environmental loads [Moropoulou, 2000].

By the middle of the 19th century, the production technology of lime has changed. By using oil, gas and carbon dust as fuel in limekilns, the dissociation temperature was exceeded and the produced lime was over-burnt [Wingate 1985], resulting to produce lime mortars of low quality. At the same time, cement mortars first appeared promised to be stronger, more consistent, quicker setting and more durable than lime mortars. Their use on historic structures proved to be extremely damaging, since there are too hard, brittle, impervious, with high concentration of salts for historic masonries [Fassina and Borsela 1993, Baccaro et al 2000]. Hence, the architectural conservation community has recently paid attention in the reengineering of lime mortars, presenting similar characteristics with the historic ones for conservation interventions on historic structures. Several studies have been published up to now regarding the quality of hydrated lime [Moropoulou et al, 2001] used as a binder in restoration mortars, physicomechanical characteristics of lime mortars, [Faria et al 2008, Lanas and Alvarez 2003, Lanas et al 2006] the carbonation process and its effect on mortars characteristics [Lawrence et al 2007, Cazalla et al 2000, Cultrone et al 2005].

In this research work, it was evaluated the effect of lime (putty or powder) and of aggregates nature (quartz or calcitic) to lime mortars produced. Furthermore, the microstructural and hygric properties of lime based mix designs are evaluated and correlated.

2 MATERIALS AND TECHNIQUES

Two types of hydrated lime with similar chemical composition were used for mortars production; a powder commercial hydrated lime (L) (CaO Hellas) and a lime putty (LPu). LPu was produced by calcinating a limestone with high percentage of $CaCO_3$, followed by slaking the produced quicklime for 15 years. Table 1 reports DTA-TG results of the two types of lime used for the mortars preparation. The free water present in the slurry of LPu is about 43%. The two types of hydrated lime were used in order to evaluate the effect of different type of lime (powder or putty) in the final microstructuarlal and hygric characteristics.

Moreover, in order to study the effect of aggregates chemical composition to mortars characteristics two types of sand with similar grain size distribution was used; a standard siliceus sand (Sq, EN 196-1) and a quarry sand of calcitic nature (Sc). Both sands exhibit grain size in the range of 0-2mm. Fig. 1 presents the grain size distribution of the two types of sand used.

Table 1. DTA/TG analysis results for hydrated limes used for lime mortars preparation

Lime	$Ca(OH)_2$ (%)	$CaCO_3$ (%)	$Mg(OH)_2$ (%)
L	89.10	5.98	-
LPu	91.02	7.13	1.45

Table 2 reports the mortars mix design. The difference in the mixing percentage of hydrated lime in mix designs has been done with intention of having almost the similar percentage of $Ca(OH)_2$ finally

in all mix designs, when the free water will be dehydrated. A mixer was used for stirring the materials used with the appropriate amount of water. The stirring procedure lasted 15 minutes. The mix designs produced exhibited a similar consistence measured by flow table (EN 1015-Part 3), in the range of 15.6-15.9cm. The characteristics of fresh mortars were determined according to EN 1015. The apparent density measured for all mix designs is in the range 1.83-1.70 g/cm^3, the percentage of retained water is about 87.8-88.5% and the air contained in the mix is in the range 2.0-2.9%.
The amount of added water in the case of lime putty mortars is calculated without considering the amount of free water already present in the lime putty.

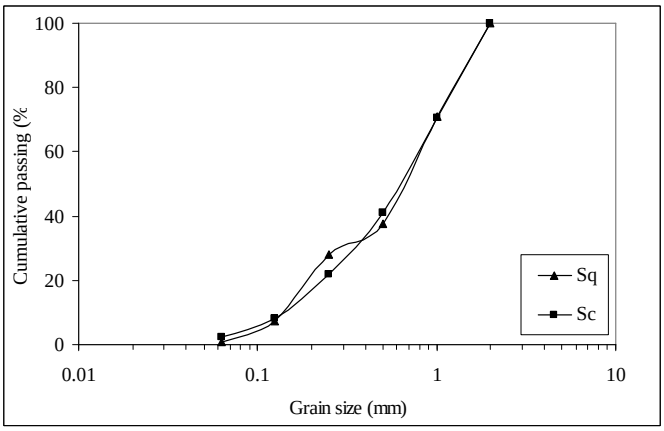

Figure 1. Grain size distribution of the two types of sand.

Table 2. Mortars mix design-Materials as percentage per weight.

	Mix design (%p.w.)				
Code	*L*	*LPu*	*Sq*	*Sc*	*W/L*
L	30		70		0.88
LPu		40	60		0.16
LCal	30			70	0.95
LPuCal		40		60	0.20

W/L: water to lime ratio (p.w)

The mortars were casted in prismatic moulds of 4x4x16cm. Lime mortars were stored in moist curing chamber (RH=95±5%, T= 20±2°C) for the first two days and then they were cured at standard conditions chamber (RH=65±5%, T= 20±2°C) till the testing date. They were demolded the 9th day after their preparation. Lime mortars chemical and physicomechanical characteristics were evaluated by using the following techniques:

- Mercury Intrusion Porosimetry (MIP, Fisons, Porosimeter 2000) for the evaluation of microstructural characteristics (open total porosity (%), bulk density, pore radius average, total cumulative volume, specific surface area) at 1, 3, 6, 12 and 18 months of curing time. The samples were taken from the core of the specimen.
- Capillary rise tests for the determination of capillary rise coefficient (C.R.C., mg/cm^2.sec$^{1/2}$), total cumulative volume of absorbed water per sample mass (TCVw.c., mm^3/g), open total porosity accessible to water through capillaries ($\varepsilon_{w.c}$.%) (UNI-10859) after 36 months of curing time when the the carbonation is completed. The test was carried out on three cubic samples of dimensions 4x4x4cm for each of the mix design.
- Water immersion test for the determination of absorbed water percentage or percentage of water immersion test (WIT%), total cumulative volume accessible to water by immersion (TCVw.im., mm^3/g), total porosity accessible to water by immersion test ($\varepsilon_{w.im}$.%) (Normal 07/81).

Capillary rise and water imersion tests carried out on three cubic samples of dimensions 4x4x4cm for each of the mix design, in 36 months of curing time after the completion of carbonation.

3 RESULTS AND DISCUSSION

3.1 Mercury Intrusion Porosimetry (MIP)

Table 3 reports the microstructural characteristics for lime mortars (mean values of three measurements) at 1, 3, 6, 12 and 18 months of curing time. It could be observed that the total cumulative volume (TCV) and the open total porosity (OTP) for all mix designs are decreasing with time evolution. Thus, it could be said that the carbonation evolution results to the reduction of TCV and OTP values. The final values of TCV and OTP reported are similar for all mix designs (~186 mm^3/g and ~32%, correspondingly) except LCal mix design that exhibits higher values (TCV: 219 mm^3/g, OTP: 37%).

Concerning the specific surface area, for all mortars syntheses the values are decreased in time. The final values of specific surface area (As) reported at 18 months are in the range of 2.13-3.52 m^2/g. Regarding the bulk density values, all mix designs present an increasing trend from 1 to 18 months. The final values of bulk density are in the range of 1.70-1.76 g/cm^3. The main difference in microstructural characteristics by using lime putty or lime powder is PRA final values (Table 3) and the pore size distribution of mix designs (Fig. 2). It is measured PRA final value in ranges of 0.58-0.72μm and 14-19μm for lime powder and lime putty mix designs, respectively. In addition, lime powder mortars present an increase in PRA in time while lime putty mortars exhibit a slight decrease of PRA in time evolution.

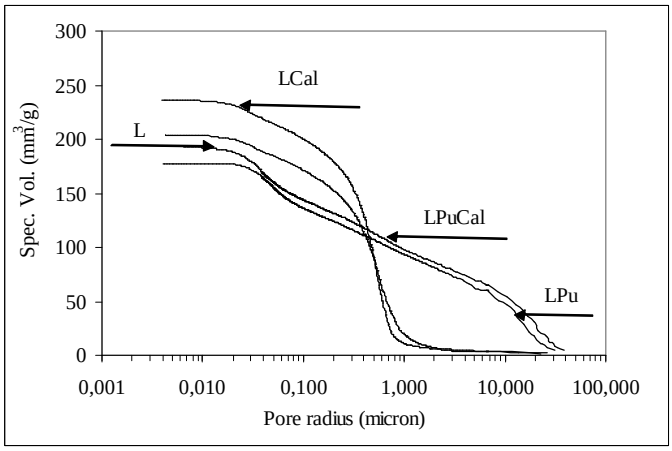

Figure 2. Distribution of specific volume (mm^3/g) to the pore radius

Figure 2 presents the distribution of specific volume (mm^3/g) to the pore radius of lime powder and lime putty mix designs. Table 4 exhibits the total volume distribution in specific ranges of pore size for L and LPu mix designs. From the results reported in Fig. 2 and Table 4 it could be said that lime putty produce lime mortars with higher percentage of coarse pores compared to lime powder mortars. Furthermore, lime powder mix designs exhibit a concentration of pores in the range 0.1-1.0μm that is coming up to 75.27%. On the other hand, lime putty mix designs exhibit a regular and broad distribution of specific volume in the pores range 0.01-50.00μm, as it is observed in Table 4 (~25% for each pore radii range). The pore size distribution of lime putty mortars is similar to the one reported for historic lime based mortars [Schafer and Hilsdorf 1993] fact that assures the microstructural compatibility between the historic and the restoration mortar.

Therefore, it is concluded that the type of lime (powder or putty) affects mainly the pore radius distribution of mortar. At the same time there is no significant effect in other microstructure characteristics, by using different types of lime (powder or putty) or aggregates (quartz or calcitic) for all mix designs except for LCal mix design that presents higher values of OTP nad TCV. This could be attributed to the higher amount of water used for LCal mix preparation respect to the others (Table 2). This higher amount of water used is detected to the consistence measured by flow table that in the case of LCal mix design is 15.9cm respect to the rest mix designs that present a consistence equal to 15.6cm.

Table 3. Microstructural characteristics of lime mortars in time evolution (MIP results).

Mix Design		*T.C.V. (mm3/g)*	*As (m^2/g)*	*P.R.A. (μm)*	*dbulk (g/cm^3)*	*O.T.P. (%)*
L	1	237.56	4.82	0.61	1.59	37.85
	3	222.16	3.52	0.58	1.64	36.35
	6	222.61	4.25	0.56	1.65	36.65
	12	207.20	3.37	0.59	1.70	35.22
	18	186.23	2.13	0.72	1.74	32.38
LPu	1	204.68	6.10	15.97	1.69	34.58
	3	191.18	4.20	12.71	1.71	32.69
	6	190.20	3.71	14.77	1.73	32.90
	12	189.35	3.65	14.63	1.75	33.14
	18	187.89	3.52	14.01	1.75	32.85
LCal	1	245.25	5.34	0.46	1.56	38.17
	3	229.65	3.37	0.52	1.65	37.81
	6	225.20	3.35	0.53	1.66	37.44
	12	220.83	3.33	0.58	1.69	37.32
	18	218.89	2.88	0.58	1.70	37.20
LPuCal	1	203.53	5.23	20.74	1.68	34.18
	3	193.76	3.15	17.85	1.75	33.91
	6	184.96	3.11	18.11	1.75	32.42
	15	183.94	3.09	15.64	1.77	32.56
	18	186.73	2.69	9.12	1.76	32.85

T.C.V.: Total Cumulative Volume (mm^3/g), As: Specific Surface Area (m^2/g), P.R.A.: Pore Radius Average (μm), dbulk: Bulk Density (g/cm^3), O.T.P.: Open Total Porosity (%)

Table 4. Total volume distribution in specific ranges of pore size for L and LPu mix designs.

Pore radius range (μm)	*Percentage of specific pore volume (%)*	
	L	*LPu*
0.01-0.1	15.78	23.45
0.1-1.0	75.27	24.33
1.0-10.0	8.46	26.06
10.0-50.0	0.99	26.16

3.2 Capillary rise and Immersion tests results

Table 5 present the capillary rise and the immersion tests results for lime based mix designs at 36 months of curing time. By observing the results of capillary rise tests, it could be drawn that two group of mix designs are produced. Lime powder mix designs present lower values of C.R.C and higher values of $T.C.V._{w.c.}$ and $\varepsilon_{w.c.}$ compared to the mix designs of lime putty.

This fact indicates that lime powder mortars (L, LCal) are absorbing the water with lower rate but the final amount of absorbed water per sample weight is higher compared to the second group of mortars (LPu, LPuCal). The values of capillary rise coefficient detected are ~29 $mg/cm^2.s^{1/2}$ and ~33-34 $mg/cm^2.s^{1/2}$ for lime powder and lime putty mix designs respectively. On the other hand, the values of porosity accessible to water though capillaries reported are ~31-33% and ~25% for lime powder and lime putty mix designs correspondingly. By combining the MIP results with the capillary rise tests results it could be said that for lime mix designs tested in this research, the higher the pore radius average of mortar the higher the rate of absorbing water (C.R.C.) and the lower the final amount of absorbed water.

The immersion tests results present a similar trend, taking into consideration that lime powder mix designs exhibit higher values of T.C.V.w.im. and $\varepsilon_{w.im.}$ than lime putty mix designs. Comparing the accurate values of T.C.V. and open porosity calculated by mercury intrusion porosimetry, immersion test and capillary rise test it could be observed that the highest values are reported by MIP measurements followed by immersion and finally by capillary rise tests, as it is shown in Fig. 3. This fact is attributed to the presence of small pores in mortars that could be measured only by using MIP.

Table 5. Capillary rise and immersion tests results for lime mix designs.

Mix Design	*Water capillary rise test*			*Water immersion test*		
	C.R.C ($mg/cm^2.s^{1/2}$)	*T.C.V.w.c.* (mm^3/g)	$\varepsilon_{w.c.}$ *(%)*	*W.I.T (%)*	*T.C.V.w.im.* (mm^3/g)	$\varepsilon_{w.im.}$ *(%)*
L	29.15	179.15	31.17	18.26	182.89	31.82
LPu	33.43	142.13	24.87	15.39	154.13	26.97
LCal	29.75	196.94	33.48	20.26	202.89	34.49
LPuCal	34.38	139.66	24.58	15.75	157.71	27.77

C.R.C.(mm^3/g): Capillary Rise Coefficient, T.C.V.w.c. (mm^3/g):Total cumulative volume of absorbed water through capillaries per sample gram, $\varepsilon_{w.c.}$%: Open total porosity accessible to water through capillaries, W.I.T.% (Weight Immersion Test): Percentage of absorbed water, T.C.V.w.im. (mm^3/g):Total cumulative volume of absorbed water per sample gram , εw.im.%: Open total porosity accessible to water by immersion test.

At the same time all mix designs present sufficient microstructural and hygric characteristics compared to traditional structural materials (Moropoulou and Bakolas 1998, Moropoulou et al. 2003, Maravelaki-Kalaitzaki et al. 2005), assuring the compatibility and the durability of the restoration interventions and the historic structures.

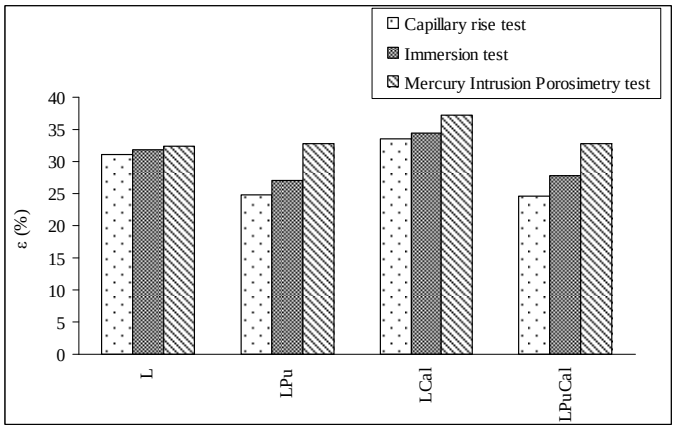

Figure 3. Open total porosity for lime based mix designs measured by capillary rise, immersion and mercury intrusion porosimetry test.

4 CONCLUSIONS

From the obtained results the following conclusions could be drawn:

- Lime powder mix designs present different microstructure compared to lime putty one in terms of pore radius average and pore size distribution. More specifically, it is measured PRA final value in ranges of 0.58-0.72μm and 14-19μm for lime powder and lime putty mix designs respectively. Regarding the pore size ditsribution lime powder mix designs exhibit a concentration of pores in the range 0.1-1.0μm that is coming up to 75,27%. On the other hand, lime putty mix designs exhibit a regular distribution of specific volume in the pores range 0.01-30.00μm (~25% for each pores size range). Except pore size distribution, no significant effect in other microstructural characteristics studied is observed by using different types of lime (powder or putty) or aggregates (quartz or calcitic).
- Lime powder mix designs are absorbing the water with lower rate but the final amount of absorbed water per sample weight is larger compared to the lime putty mix designs. The values of capillary rise coefficient detected are ~29 $mg/cm^2.s^{1/2}$ and ~33-34 $mg/cm^2.s^{1/2}$ for lime powder and lime putty mix designs respectively. The values of porosity accessible to water though capillaries reported are ~31-33% and ~25% for lime powder and lime putty mix designs correspondingly.
- The highest values of open total porosity measured by mercury intrusion porosimetry (MIP), immersion and capillary rise test is reported for MIP measurements followed by immersion and finally by capillary rise tests. This fact is attributed to the presence of small pores in mortars that could be measured only by using MIP.
- All lime based mix designs present sufficient microstructural and hygric characteristics compared to traditional structural materials, assuring the compatibility and the durability of the restoration interventions and the historic structures.

REFERENCES

Baccaro M.L.P., Balzi S., Del Chiaro L., Vannucci S., 'The Effects of the Strong Use of Cements in Restoration: The Case of Barga Duomo (Northern Tuscany)', Proceedings of the 9th International Congress onDeterioration and Conservation of Stone, Venice, vol. 2, 2000, pp. 3–12.

Cazalla O., Rodriguez-Navarro C., Sebastian E., Cultrone G., 'Aging of lime putty: effects on traditional lime mortar carbonation', J. American Ceramic Society 83 (5) (2000) 1070– 1076.

Cultrone G., Sebastian E., Ortega Huertas M., 'Forced and natural carbonation of lime-based set mortars with and without additives: Mineralogical and textural changes', Cement and Concrete Research 35 (2005) 2278– 2289.

Faria P., Henriques F., Vasco Rato V., 'Comparative evaluation of lime mortars for architectural conservation', Journal of Cultural Heritage 9 (2008) 338-346

Fassina, S. Borsela, 'The Effects of Past Treatments on the Accelaration of Weathering Processes in the Statues of Prato Della Valle', Intern. UNESCO-RILEM Congress on the Conservation of Stone and other Materials, Paris, 1993, Proc. pp. 129

Karatasios I., Kilikoglou V., Colston B., Theoulakis P., Watt D., 'Setting process of lime-based conservation Wingate mortars with barium hydroxide', Cement and Concrete Research 37 (2007) 886-893.

Lanas J., Alvarez J. I., 'Masonry repair lime-based mortars: Factors affecting the mechanical behaviour', Cement and Concrete Research 33 (2003) 1867–1876.

Lanas J., Sirera R., Alvarez J.I., 'Study of the mechanical behavior of masonry repair lime -based mortars cured and exposed under different conditions', Cement and Concrete Research 36 (2006) 961–970.

Lawrence R. M., Mays T. J., Rigby S. P., Walker P., D' Ayala D., 'Effects of carbonation on the pore structure of non-hydraulic lime mortars', Cement and Concrete Research 37 (2007) 1059-1069

Malinowsky R., Grafinkel Y., Prehistory of Concrete, Concrete International (1991) 62-68.

Maravelaki-Kalaitzaki P., Bakolas A., Karatasios I., V. Kilikoglou, 'Hydraulic lime mortars for the restoration of historic masonry in Crete', Cement and Concrete Research 35 (2005) 1577-1586.

Moropoulou A., Bakolas A., Aggelakopoulou E., Pineli T., Prasianakis I., 'Estimation of elastic constants of stones, used in historic monuments, using ultrasound techniques and mechanical tests. Correlation of the mechanical characteristics to the microstructure', In: Hellenic Society for NDT (Eds.), 3rd International Conference on Non-Destructive Testing, Chania, 2003, pp. 242-245.

Moropoulou A., Bakolas A., Aggelakopoulou E., 'The effects of limestone characteristics and calcination temperature to the reactivity of quicklime', Cement and Concrete Research 31 (2001) 633-639.

Moropoulou A., Bakolas A., 'Range of Acceptability limits of Physical, Chemical and Mechanical Characteristics deriving from the Evaluation of Historic Mortars', In: Biscontin G., Moropoulou A., Erdik M. and Rodrigues J.D., (Eds.), Compatible Materials for the Restoration of European Cultural Heritage, Pact 56, 1998, pp.165-178

Moropoulou A., 'Reverse Engineering to discover traditional technologies: A proper approach for compatible restoration mortars', In: Moropoulou A., Biscontin G., Rodrigues J.D., Erdik M., Siotis I. and Zoppi S. (Eds.), Compatible Materials for the Restoration of European Cultural Heritage, Pact 58, 2000, pp. 81-103.

Schafer J., Hilsdorf H. K., 'Ancient and new lime mortars-The correlation between their composition, structure and properties', Conservation of Stone and Other Materials, ed. by M. J. Thiel, RILEM-UNESCO, E&FN SPON, Chapman & Hall, Paris, Vol. 2, 1993, p. 605-612.

Wingate M., 'Small-scale lime burning: a practical introduction', Intermediate Technology Publications, London, 1985.

XII DBMC
International Conference on Durability of Building Materials and Components
PORTO - PORTUGAL, April 12th-15th, 2011

Field Study of Hygrothermal Performance of Log Wall with Internal Thermal Insulation

Endrik Arumägi [1]
Simo Ilomets [2]
Targo Kalamees [3]
Tanel Tuisk [4]

ABSTRACT

The energy efficiency of old wooden apartment buildings built before the Second World War need to be improved to save energy and increase thermal comfort. According to the regulations no changes outside the external wall on the facade are permitted. Internal insulation is a possible solution when the external style has a high value and must be preserved. Internal insulation consists high hygrothermal risks. This paper analyzes the measurement results of the temperature and RH of an internally insulated log wall. Six different solutions were used to insulate the log wall: three different insulation materials together with and without air/vapour barrier were used. According to the measurement results there is a high risk of condensation and mould growth inside the wall in dwellings with high humidity load. In the studied case the durability of the renovation solutions is questionable because the measurement results show inadequate hygrothermal performance of the internally insulated log wall. Based on the mould growth model, in all the cases the temperature and RH level inside the wall between the insulation layer and the log layer exceeded the temperature and relative humidity conditions favouring initiation of mould growth more than 75% of the time. To use the internal insulation it is recommended to lower the vapour pressure inside the wall by reducing the moisture excess inside the room by installing a mechanical ventilation system or increasing the vapour resistance by adding vapour retarding foil to the warm side of the insulation layer.

KEYWORDS

Hygrothermal performance, mould growth, internal insulation, wooden apartment building.

[1] Chair of Building Physics and Architecture of Tallinn University of Technology, ESTONIA, endrik.arumagi@ttu.ee
[2] Chair of Building Physics and Architecture of Tallinn University of Technology, ESTONIA, simo.ilomets@ttu.ee
[3] Chair of Building Physics and Architecture of Tallinn University of Technology, ESTONIA, targo.kalamees@ttu.ee
[4] Chair of Building Materials of Tallinn University of Technology, ESTONIA, tanel.tuisk@ttu.ee

1 INTRODUCTION

The wooden apartment building was the prevalent building type before World War 2 in the suburbs of many towns in Estonia. Currently these areas are listed as milieu or culturally valuable areas with specific planning and building regulations set to preserve the existing environment. The majority of old wooden apartment buildings have massive log (thickness typically 12-15 cm) walls without any additional thermal insulation. Walls are covered with external wooden cladding and internal plaster layers. Thermal transmittance of these types of walls is U_{walls}≈0.6…0.7 W/(m^2·K). The average air leakage value of the building envelope is n_{50}≈17 h^{-1}.

Estonian (57…59 N; 22…28 E) climate is characterized by cold and humid winters and warm summers with the average annual temperature +5.6 °C. The annual average number of heating degree-days tin S for indoor balance temperature of +17°C is 4249 days. Due to cold climate buildings are heated during winter.

In view of the fast increasing energy prices, living in buildings with low energy efficiency can become a very expensive ”pleasure”. By improving the building envelope with additional insulation, it is possible to save energy and increase thermal comfort.

Due to the regulations no changes outside the external wall on the facade are allowed to be done. Internal insulation is a possible solution when the external style has a high value and must be preserved. Internal thermal insulation may cause hygrothermal risks and special requirements for the properties of other material layers. The low temperature of the log layer has an effect on the partial vapour pressure conditions and can cause moisture risks on the log layer [Ojanen 2007]. It is possible to eliminate the problem of moisture diffusion with vapour retarder, but the problem with moisture convection may stay still [Ojanen and Simonson 1995]. External thermal insulation is a hygrothermally much safer solution compared to internal thermal insulation.

Nevertheless, many studies [Stopp, et al. 2001, Maděra 2003, 2003, Häupt et al. 2004, Juhart et al.2005, Toman et al. 2009] have analysed the possibilities to use the internal thermal insulation for improving external wall structures. Even if the risks and solutions of internal thermal insulation are presented, most of these studies are concentrated on stone walls, as a typical wall structure in Central Europe, but many to the log walls. Saarimaa et al. 1985 and Koski et al. 1997 have analysed hygrothermal performance of additionally insulated log walls in Finland by visual inspection and mostly by momentary measurement of moisture content. It is possible to study many buildings with momentary measurement, but it is not clear if the measurement period is sufficiently critical over the whole year. Therefore long-term measurements are needed. Comparison of different materials and envelope solutions is necessary because they affect hygrothermal performance in different ways.

In this study six solutions of internal thermal insulation for the log wall are analysed based on follow-up field measurements. Hygrothermal performance is analysed based on the temperature and relative humidity measurements in the wall. Durability of refurbishment solutions is assessed in terms of the risk for mould growth and condensation inside the wall.

2 METHODS

2.1 Studied Wooden Apartment Building

The measurements were carried out in a typical wooden apartment building called “Lenderi Maja”, situated in a milieu valuable area in Tallinn. The building originates from the beginning of the 20th century. The building has two floors and a cellar, apartments are heated by stove and electrical radiators. There is a natural passive stack ventilation system in apartment with mechanical exhaust

fans in the toilets (not permanently used). The test wall was situated in apartment 1 (on the first floor) on north-facing wall of the main bedroom.

The apartment building was studied under a larger national research project focused on the technical condition and service life of Estonian wooden apartment buildings. The building was under renovation and occupants decided to insulate walls with internal mineral wool insulation. After discussion, the occupants promised to conduct the follow-up measurements about the hygrothermal performance of the wall with internal insulation.

2.2 Studied Test Walls

The initial log wall construction consisted of a 140 mm log sealed with a tow and covered externally with sheathing paper and 20-mm wooden cladding.

Six different insulation solutions were analysed. The size of the analysed wall section was 60×60cm. All wall sections faced to the same wall of the bedroom. Test walls were separated by metal battens and polyurethane foam tightening. The solutions differed in the insulation materials and air barriers that were used, see Figure 1.

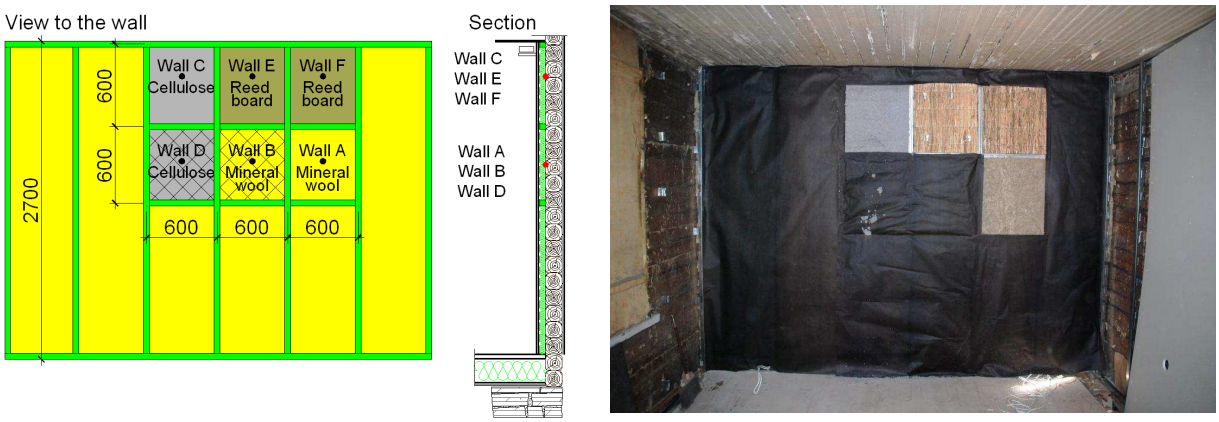

Figure 1. Temperature and relative humidity sensor positions on the log layer before the added insulation material (left) and a view of the insulated wall before the finishing layer (right).

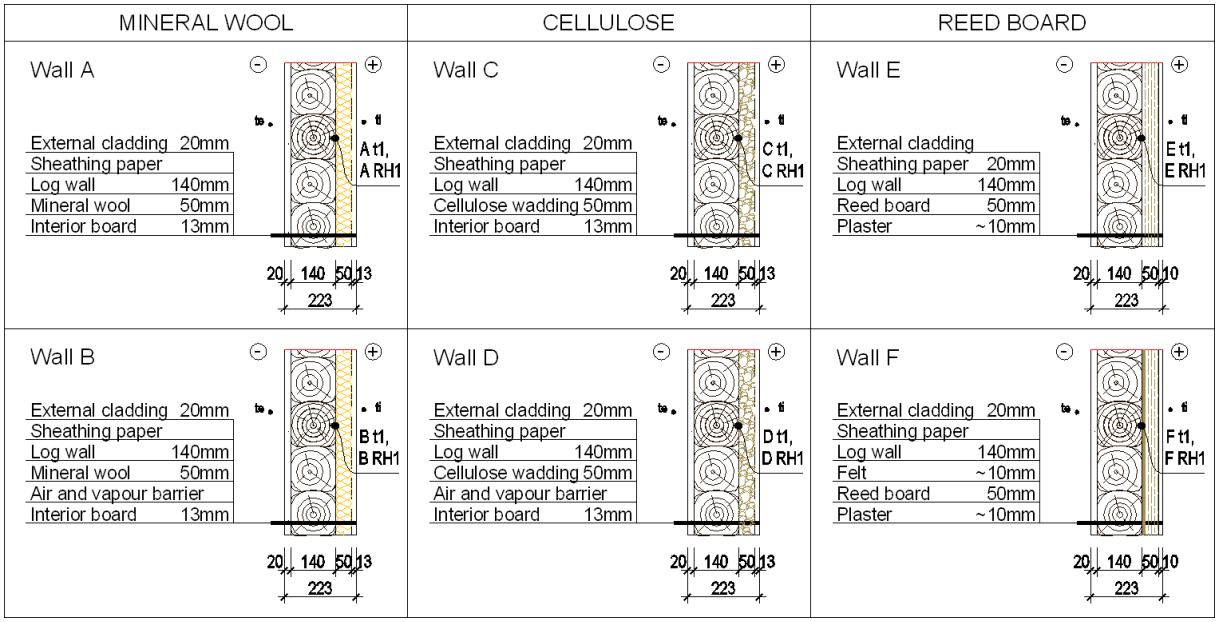

Figure 2. Sections of the studied test walls.

Altogether three different insulation materials were used: reed insulation mat (λ_{reed}≈0.054 W/(K·m)), cellulose insulation ($\lambda_{cellulose}$≈0.045 W/(K·m)), and mineral wool (λ_{mv}≈0.040 W/(K·m)). Insulation materials were used with and without air barrier and were finished inside the room with gypsum board or render. Air barrier paper impregnated with bitumen (Z_p $0.6 \cdot 10^9$ m^2sPa/kg) was used as an air barrier between the inside sheathing and the insulation material. Sections of the insulated log wall are shown in Figure 2.

2.3 Measurements

The values of temperature and relative humidity (RH) were measured with Ø 5mm sensors (Rotronic Hygroclip SC05; measurement range: –30 °C…+100 °C, 0…100 % RH with accuracy ±0.3 °C, ±1.5 % RH) inside the wall between the additional thermal insulation layer and the log layer (see Figure 2) and saved with a data logger. Temperature and RH inside the bedroom and outside the building were measured with data loggers (Hobo U12-013; measurement range -20…+70 °C; 5…95% RH, with an accuracy of ±0.35 °C; ±2.5% RH). All the measurements were taken at a one-hour intervals. The indoor data logger was placed in the middle of the bedroom and an outdoor temperature data logger was placed on the north facade of the building, protected from direct solar radiation.

2.4 Assessment of risk for mould growth

The risk of mould growth assessed according to the experiments reported in [Hukka & Viitanen 1999] suggest that covering the temperature range of 5-40°C the boundary curve for the risk of mould growth on a wooden material can be described by a polynomial function:

$$RH_{crit} = \begin{cases} -0.00267 \cdot t^3 + 0.160 \cdot t^2 - 3.13 \cdot t + 100 & ,when\ t \le 20°C \\ 80\% & ,when\ t > 20°C \end{cases}$$

The time of the temperature and RH conditions favourable for mould growth during the measurement period was calculated.

3 RESULTS

3.1 Climate Condition

Hourly temperature and RH's data measurements were taken and collected through out a near one-year period: 12.12.2009…6.10.2010. Outdoor temperature during the measurement period varied between -21.5°C…+33.6°C and RH between 22%...100%. During winter the average temperature was -7.4°C (min. -21.5°C, max. +4.2°C) and RH 89% (min. 62%, max. 100%). The annual indoor temperature in the bedroom varied between +13.5°C…+27.5°C and RH between 43%...83%. During winter months the average temperature was +17.4°C (min. +13.5°C, max. +24.5°C) and RH 64% (min. 43%, max. 74%).

Figure 3 left shows the dependence of the indoor temperature on the outdoor temperature. Each dot represents the measured value corresponding to the outdoor temperature. The indoor temperature depends quite linearly on the outdoor temperature. This indicates to problems with sufficient heating power of the heating system. The average indoor temperature stays below the lowest category of thermal comfort 50 % of the time during winter due to low indoor temperatures.

It is important to know the humidity load to assess the hygrothermal performance of the wall. Humidity loads are presented as internal moisture excess that shows the difference between the indoor and outdoor air humidity by volume. Dependence of the moisture excess on the outdoor temperature is shown in Figure 3 right. From this data, the 90 % critical level [Sanders, 1996] was

calculated (black dotted line). This level means that hygrothermal loads higher than the determined critical value should not exceed 10% of the cases. During cold periods the weekly average internal moisture excess is between +7 g/m^3. Based on earlier studies in Estonian dwellings [Kalamees 2006], the studied apartment may be classified as a dwelling with a very high humidity load. The humidity load was high due to low ventilation (natural ventilation), higher occupancy (23 m^2/pers.), and possible drying out of structural moisture.

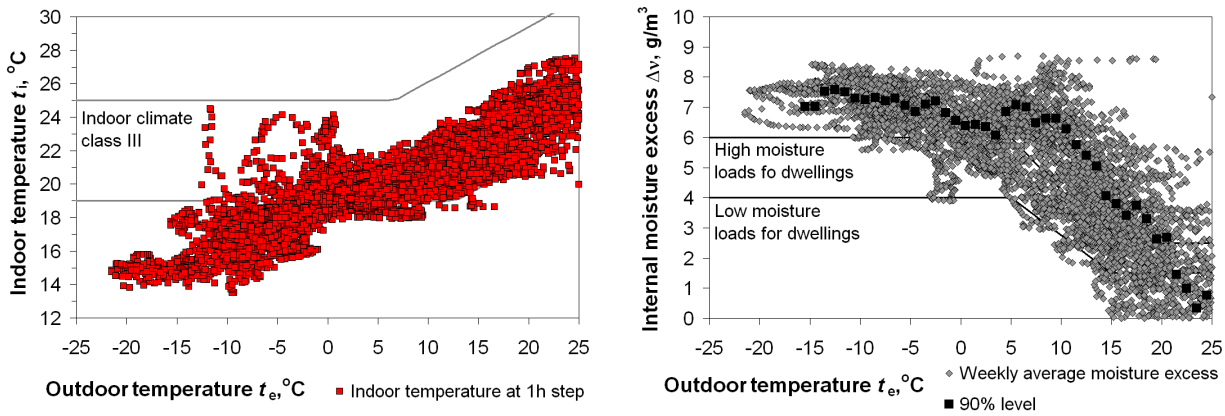

Figure 3. Dependence of the indoor temperature and moisture excess on outdoor temperature.

Due to low temperature and high humidity loads, indoor RH was high during cold period, Figure 4. The indoor RH stays above the criteria for indoor RH during winter in Estonia (RH 25…45%) most of the time.

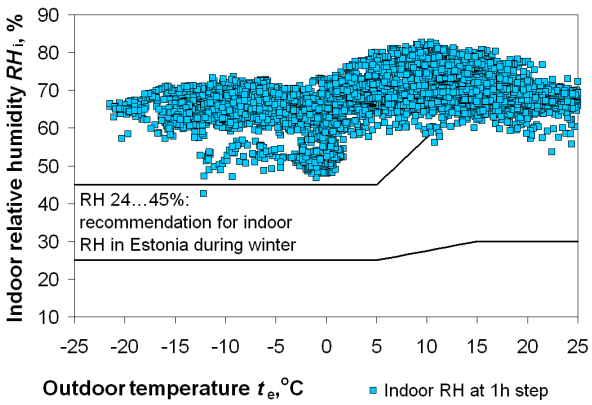

Figure 4. Dependence of the indoor RH on the outdoor temperature.

3.2 Hygrothermal Condition Inside the Wall

Reference point to assess the hygrothermal performance of the internally insulated wall was between the original log and the internal insulation.

Indoor and outdoor temperature as well as temperatures inside the wall between the insulation material and the log layer is shown in Figure 5 left. Steady-state distributions of temperature during February are shown in Figure 5 right. During the measurement period, the lowest temperature on the internal surface of the log was observed in the case of mineral wool insulation. This corresponds also well to the lowest thermal conductivity of this insulation material.

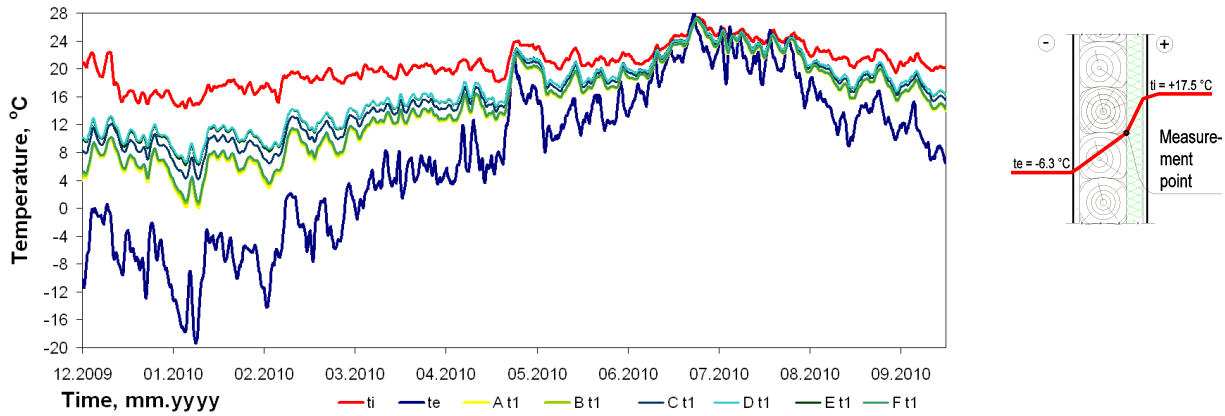

Figure 5. Measured daily running-average temperatures (left). The distribution of average temperature during February (right).

RH was high through out the winter-spring period, Figure 6. RH was close to the upper measurement limit, indicating possible moisture condensation to the inner surface of the log. Also, the calculated steady-state vapour distribution in the wall indicated possible moisture condensation in the wall between the insulation material and the log layer. The RH was highest in test walls with mineral wool insulation. On the other hand, test walls with mineral wool insulation dried more quickly than the wall with cellulose or reed insulation mat during summer period.

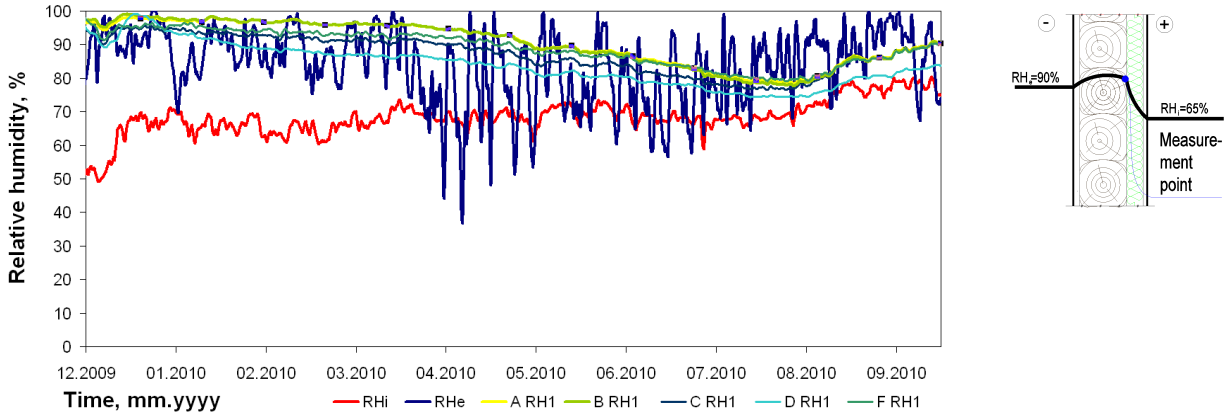

Figure 6. Measured daily running-average RH (left). The distribution of average RH during February (right).

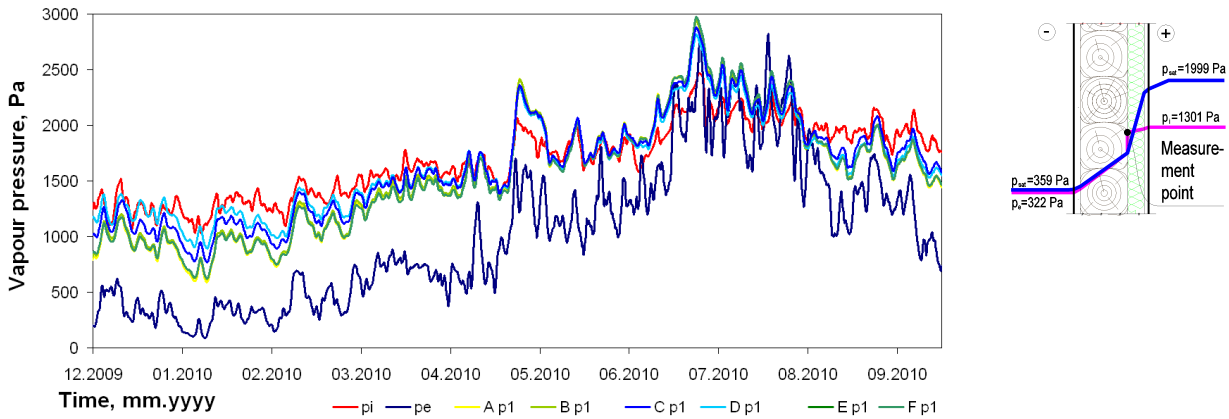

Figure 7. Measured daily running-average water vapour pressures (left). The distribution of average water vapour pressure during February (right).

Water vapour pressure on the indoor and outdoor air as well as inside the wall between the insulation layer and the log layer are presented in Figure 7. During the spring-summer period the air vapour pressure inside the wall was higher than the air vapour pressure in the bedroom, indicating the drying of the wall to the indoor air. Water vapour pressure was higher in the test walls with hygroscopic thermal insulation.

As the air pressure difference across the structure was ±2…3 Pa the main moisture transport mechanism is assumed water vapour diffusion.

The RH on the inner surface of the log wall stays at the high level during the whole measurement period. Based on the mould growth model [Hukka and Viitanen 1999] in all the cases, the temperature and RH level inside the wall exceeded the temperature and relative humidity conditions favouring initiation of mould growth on wooden materials, see Figure 8.

In the case of the mineral wool insulation temperature and RH conditions are favourable for mould growth more than 88% of the time. With cellulose insulation the risk for mould growth is higher in walls without air- and vapour barrier (84 % of measured time length) than with air- and vapour barrier (75 % of measured time length). With the reed insulation mat more than 93% of the time is favourable for mould growth.

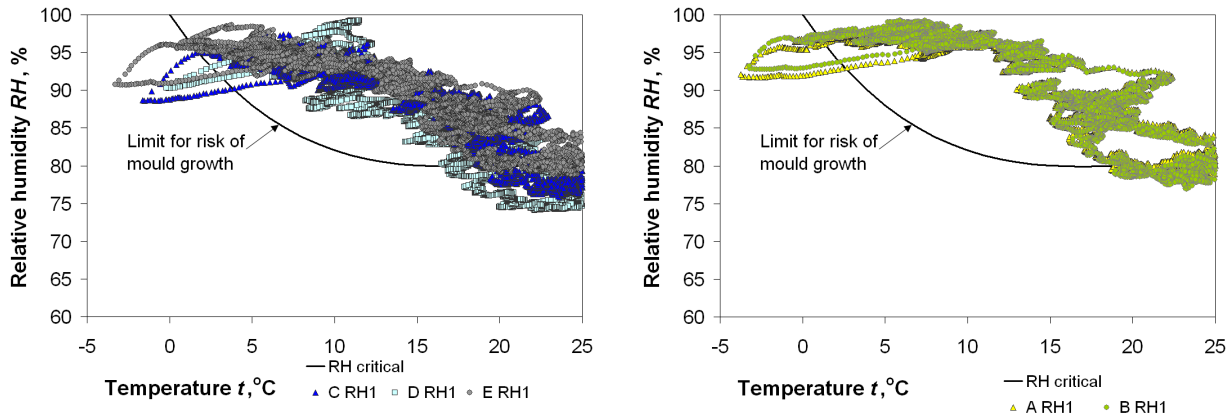

Figure 8. Temperature and RH conditions are favourable for mould growth for "green" insulations (left) and for mineral wool (right).

According to the mould growth assessment, there should be a high risk for mould growth. Nevertheless, the wall was not opened for examination. No visual inspections were done and no mould could be observed.

4 DISCUSSION

Field measurements showed a high humidity level in the internally insulated log wall. Hygrothermal conditions on the inner surface of the log wall were favourable for mould growth in all test walls. Insulation material (hygroscopic or not) did not significantly lower the risk for mould growth. Different test walls were separated by metal battens and polyurethane foam tightening to prevent diffusion and conduction between the test walls. Although there may have been some minor leaks between the test walls, the potential for the diffusion and conduction was low and possible heat and moisture movement between the test walls was probably minor.

Some earlier studies carried out in wooden buildings in cold climate conditions have shown the possibilities to assemble additional insulation layer inside a log wall without a vapour barrier [Saarimaa *et al.* 1985; Koski *et al.* 1997]. According to Saarimaa [1985] it is possible to use internal insulation without vapour barrier but there were too many uncertainties to be convinced that the measurement results assure it. According to Koski [1997] no hygrothermal problems occurred with log walls with internal insulation. Neither was there great differences discovered between the log wall

with a vapor barrier and without a vapor barrier. The main reason for that was the internal sheeting. The internal sheeting proved to have a rather high vapor resistance compared to the sheeting used in this study. The internal sheeting had about five times higher vapour resistance than a gypsum board. Nevertheless the results obtained in the studies referred to were not based on many long-term measurements in dwellings with high humidity loads. To work out viable renovation solutions critical boundary conditions should be obtained.

The test walls studied were located in apartments with high humidity loads. This was caused mainly due to low air change rate (natural ventilation) because the ventilation system was not renovated. Therefore, to guarantee good indoor climate and energy efficiency of buildings, the following three components must be maintained in the process of renovation:

- hygrothermal performance of building envelope;
- performance of ventilation;
- performance of heating systems.

5 CONCLUSION

The measurement results of the temperature and RH of the internally insulated log wall were analysed. All the test walls with different thermal insulation resulted in high humidity levels that were favourable for mould growth on wooden material more than 75%...80% of the time. It was found that the vapour permeable air barrier paper mounted between the insulation material and the finishing layer has very low impact on the RH levels inside the wall and has no impact on temperature. High RH levels between the insulation material and the log layer correspond to the calculated steady-state winter conditions where the partial vapour pressure in the wall between the insulation material layer and the log layer exceeds the saturation pressure level. The internal insulation of the log wall could be used if the vapour pressure inside the wall is lowered. Thus the moisture excess inside the room by installing a mechanical ventilation system is reduced or the diffusion resistance by adding vapour retarding foil to the warm side of the insulation layer is increased.

Even the internal thermal insulation seems to be a possible solution when the external style has a high value and must be preserved, the solution should be carefully calculated in order to prevent occurrence of hygrothermally critical conditions. In the studied case the durability of the renovation solutions is questionable because the measurement results show inadequate hygrothermal performance of the internally insulated log wall. In addition, the high risk of mould growth can lead to mould problems that can cause health problems for the inhabitants of the apartment.

ACKNOWLEDGMENTS

The financial support of the Credit and Export Guarantee Fund KredEx and Tallinn University of Technology are gratefully acknowledged.

REFERENCES

Häupl, P., Fechner, H., Petzold, H. 2004. ‘Interior retrofit of masonry wall to reduce energy and eliminate moisture damage: Comparison of modelling and field performance’, Thermal Performance of the Exterior Envelopes of Buildings IX, Florida.

Hukka, A., and H. Viitanen. 1999. ‘A mathematical model of mold growth on wooden material’, Wood Science and. Technology 33(6):475–85.

Juhart, J., Seiler, A. et al. 2005. ‘Product- and system development for an inside thermal insulation construction of historic houses using magnesite bonded wood wool panels’, Final Report-Building of Tomorrow within the program on technologies for sustainable development, Spittal an der Drau.

Kalamees, T.2006. 'Indoor Hygrothermal Loads in Estonian Dwellings', In: The 4th European Conference on Energy Performance & Indoor Climate in Buildings. 20-22 November. , 2006, 541 - 546.

Koski, T., Lindberg, R. & Vinha, J. 1997, 'Lisäeristettyjen hirsiseinien kosteustekninen kunto', Tamperen Teknillinen Korkeakoulu, Rakennustekniikan osasto, Julkaisu 78

Maděra, J. 2003. 'Computational analysis of optimal thermal and hygric properties of materials and systems for interior thermal insulation of historical buildings', Ph.D. Thesis, Czech Technical University in Prague, Prague, 2003.

Ojanen, T. 2007, 'Low Energy Log Walls Under Cold Climate Conditions', Proc. Thermal Performance of the Exterior Envelopes of Whole Buildings X International Conference, Clearwater Beach, Florida, paper nr. 224.

Ojanen, T., and C. Simonson. 1995. 'Convective moisture accumulation in structures with additional inside insulation', Proceedings of the Thermal Performance of the Exterior Envelopes of Buildings VI Conference, Florida.

Saarimaa, J., Krankka, J. & Sevon, J. 1985,'Ulkoseinien lisälämmöneristäminen. Lisäeristettyjen rakenteiden kenttäseuranta.', VTT, research notes 420.

Said, M.N.; Demers, R.G.; McSheffrey, L.L. 2003. 'Hygrothermal performance of a masonry wall retrofitted with interior insulation'. 2nd International Building Physics Conference (Leuven, Belgium 2003-09-14) pp. 445-454. 2003-09-01

Sanders, C. 1996. International Energy Agency, Annex 24 Heat, Air and Moisture Transfer in Insulated Envelope Parts (HAMTIE), Final Report: Environmental conditions, 2: 2: Laboratorium Bouwfysica, K.U.–Leuven.

Stopp, H., Strangeld, P., Fechner, H., Häupl, P. 2001. 'The hygrothermal performance of external walls with inside insulation', Thermal Performance of the Exterior Envelopes of Buildings VIII, Clearwater Beach, Florida.

Toman, J., Vimmrová, A., Černý, R. 'Long-term on-site assessment of hygrothermal performance of interior thermal insulation system without water vapour barrier', Energy and Buildings, Volume 41, Issue 1, January 2009, Pages 51-55.

XII DBMC
International Conference on Durability of Building Materials and Components
PORTO - PORTUGAL, April 12th-15th, 2011

Old Current Architecture Heritage: Assessment of Buildings in use, after Interventions - Work in Progress

Fernanda Corrêa Giacomini [1]
Rui H. C. Fernandes Póvoas [2]

ABSTRACT

In this paper, we aim to present an on-going PhD research, whose main goal is to analyse the interventions carried out in "old current architecture buildings" located in the so called "historical centres" through a qualitative approach, assessing the performance of this settings in use .

The different practical solutions suggested and consolidated over time by the usage of the rehabilitated buildings constitute the bases for a new debate grounded on (and related to) reality. Their analysis may contribute to promote better solutions in the future, presupposing a better balance between the built structure's resistance, the habitability of the available spaces, the sustainability of the technological options and the increase or decrease in value of the heritage reference of each building, and its ensemble, after the interventions.

Porto, Évora and Guimarães were defined as case studies. In each of them, specific buildings were selected, and will be subjected to a more or less intense visual diagnosis, along with a survey to be answered by its inhabitants.

In this context, we argue here that the characteristics of this type of building requires specific attention to technical, political and architectural proposals, and the analysis of the results of these proposals also need a specific treatment. A proposed approach was developed and applied in form of pre-test on a small sample of the survey universe. The perception of the difficulties and potentialities of the instruments (now under review) must serve for the discussion and redirection of ongoing research.

KEYWORDS

Old Current Architecture, Post-Occupancy Evaluation; Historical Center; Research Methodology

[1] Doc. Student; Faculty of Architecture of the University of Porto (FAUP), Porto, PORTUGAL, fcgiacomini@gmail.com
[2] Orient. Prof. Dr. Faculty of Architecture of the University of Porto (FAUP), Porto, PORTUGAL, rpovoas@arq.up.pt

1 INTRODUCTION

In this paper we aim to present a PhD research under way that, from a qualitative approach for assessing the performance of the environments in use, wants to do a critical analisys of the interventions made in ancient buildings of current architecture, in so-called "historic centers". This paper seeks to disseminate the work in progress, highlighting the importance of the aproached topic in the context of building interventions, and facilitating the discussion about aspects of a conceptual and methodological questions that accompany and restrain this type of investigations.

The current old buildings have been treated as an ensemble (ex.: amount of isolated buildings spread through the city) or as urban composition (ex.: block, street), and are evaluated according to specifically technical aesthetic, or typological criteria. Now, however, it has been perceived that the existence of the set depends on the individualized care of each building, and on the interrelation of knowledge and skills techniques. In this same context, it has been noted a lack of knowledge and of analysis of trends and strategies that were used (and have been used) for their rehabilitation. The guidelines for building interventions, materialized in safeguarding plans and in restoration and upgrading works, create positive or negative results that may be serving as models for new projects, although their implications for the medium and long term have not been sufficiently recorded and analysed[3].

Some methodological approaches to researches in the architectural field indicate that, after some years of use, we can check the conditions of sustainability, ownership and maintenance of buildings, in order to reorient new project proposals, and new technical or management solutions. However, an assessment with this type of approach becomes different and potentially more complex than the assessment so far conducted in groups of recent buildings or in old isolated buildings. The accumulation of the restrictive features in buildings that comprise the historic sites, such as the variability of ages, constructive characteristics, and condictions of conservation, along with the occupation of these areas seems to be related to social exclusion problems and economic and touristic strategies. These specific conditions of analysis, so far, have been little discussed.

Considering this framing we seek here to (1) draw attention to the peculiarities of the current old buildings that contribute to restrict the proposals of intervention and, therefore, the proposals for evaluation of those interventions; (2) present the methodological decisions for the research in course, emphasizing the criteria for delineation of the universe and sample for the survey, and the instruments to obtain data that will enable the verification of their hypothesis; and 3) introduce the cases in which will be tested the proposed assessment instruments. The results of these tests (currently in the process of analysis), will make viable the assessment and the discussions about the viability of the proposed methodology and redirect the instruments previously outlined.

2 CURRENT ARCHITECTURE

In present time, the current architecture buildings, treated as a whole, emerges as representative heritage, as an urban monument formed by many individual and interrelated parts, and places new issues to the practice and to the theory of intervention[4]. They belong to a kind of heritage in which every object has no "intrinsic importance" to justify a special legal protection, but that "takes interest

[3] Vazquez [2004] emphasizes the importance of this problem by presenting the trend of an accelerated speculation and indiscriminate use of the cultural heritage in contemporary society. The author presents the consequences of the current vulgarization of that concept, questioning projects that reproduce uncritically, in cities, the claims of tradition and of local identities, often in forms of pastiches and imitations, which mask the value of existing assets, building new empty references.

[4] There is a tendency to consider the "rehabilitation of edifices", especially housing, as a common problem for old and new buildings, as can be seen in Paiva et al [2006]. The same happens with the "urban regeneration", in which new and old areas are treated as problems not equivalent, but at least similar, as in Fernandes and Cannatá [2009], so that the specific problem of the old habitational buildings is mixed with other issues and approaches.

in terms of urban or rural environment, or quality of life"[5]. It isn't known how much they are monuments, built reserves, or cultural and historical references. They are different from the monumental buildings, the "author's buildings", and the vernacular architecture, not only in its constructive characterization but also in how they receive treatment in cases of intervention[6]. They are, thus, on the threshold between cultural heritage buildings and common buildings, and don't have even a statute that allows appropriate interventions for their situation, even if they're valued as an important asset to maintain the identity of each city.

The term "current architecture"[7] can be applied in both new buildings and old buildings, and is related to the functional and constructive strategies of them, to the limitations involved in its design and construction, as well as to how they are available for society. Implanted in urban lots, the common or current buildings are constructed following existing models and typologies, reasonably consolidated. These works are anonymous and/or constructed in series, without singularity, and undertaken by entrepreneurs and technical teams wich answer literally the housing market requirements.

These buildings are usually built for own use or for rent (residential, commercial or mixed) with materials of controlled cost, and compartmentalization that makes a better use of the urban terrain in which it is deployed. They add various housing units in the same building or even in a urban block, and are frequently changed, depending on the needs of users (which evolve according to the demands of society in each period), and on the exchange of users in each housing throughout the lifecycle of the building.

2.1 Old Current Buildings

The old current buildings are constructed according to a different economic, structural, material, compositional and distributive logic in relation to the recent buildings. They have a pre-industrial base, which impart specific characteristics that should be considered in case of interventions, and also to evaluate these interventions. The vast majority of buildings which have survived in the cities are composed by various strata, replaced and/or accumulated[8]; recycled materials in new settings; new expansions in upper floors; replacements of facades to keep up with new fashions and urban norms; new superficial materials on ancient structures, and so on[9].

Its architectural logic combines, over time, aspects that relate the aesthetic urban framework, the form the lot occupancy, the choice of certain materials and building systems, and the organization of internal spaces. Guidelines and legal restrictions were gradually incorporated in these buildings to

[5] As suggested in the Convention for the Protection of the Architectural Heritage of Europe, art. 10, paragraph 4 .In: Correia and Lopes [2004], p. 208.

[6] Of monumental they differ especially for don't having the artistic and memorial repository value, originated from the purposeful to mark an event, a period, or an artistic or stylistic landmark . They are also different from the "author's buildings", whose designers are known by "name" and whose projects aim at the theoretical development of the disciplinary field, or the consolidation of certain values or dominant theories, usually associated with artistic and qualitative values of exception. In turn, they are different from the vernacular buildings, although this type of building also takes advantage of materials and traditional building techniques and of the local users or mutual-aid community actions. Currently the vernaculars building are more common in non-urban areas, or at least in urban areas of low population density. Sometimes, though, they represent the basis for the present buildings of current architecture, which by successive substitutions and modifications have come to nowadays. There may be current buildings which, as well as other types, that gain monumentality through the use. These ones are treated based on the same guidelines used to the monumental ones, with similar procedures.

[7] Term used, among others, by Fernandes [1999], to approach the changes and continuities in Porto´s houses and Coelho [1994], to display characteristics of social housing buildings.

[8] Authors such as Fernandes [1999] show how changes and sedimentation processes were slow in the city; Kluber [2004] shows the transitions of the forms in time from their series, continuities and transitions; Frampton [1999] emphasizes the materiality of the transitions, and Freitag [2004] points out that the synthesis of the material representation of society is dynamic, varying in time.

[9] The situations that orient these changes differ from city to city, from country to country, depending on their specific historical constraints. Here are defined the broad terms of which this type of building is subjected, and which can be filled with examples of various cities, relativized in each context.

respond to new demands of comfort, hygiene, security and accessibility[10]. Also has been slow the infrastructural changes, according to the new requirements of each period. Although the spatial configuration of each building have been guided according to similar formal characteristics, there are in some sets a wide variety of design, organization, structure and volume[11].

We have to consider that these constructions, passed from generation to generation, are the repository of the accumulated experience and memory of what it should be convenient, possible and accepted as appropriate and recognizable by each community. They are houses (and are therefore linked to the specific demands of each function in contemporary society), but also a cultural reference (and thus are linked to subjective values of identity, authenticity and apropriation).

2.2 Trends of Intervention and Recovery

The interventions in older current buildings are not simple, either by the intrinsic characteristics that distinguish them from the new ones, either by the social component of temporary or permanent relocation of families (rooted or not) who occupy these buildings, or by the (re)vitalization intended for the concerned areas, and its use by local and foreign public, or even by the external values of visual expressiveness and the notions of quality of life and livability imported from other contexts[12].

However, the present evaluation of the current architecture buildings as cultural heritage shows not only an added value in terms of cultural interest or beauty, but also a capacity to generate new business and to attract new economic investments. It follows that one of the most evident problems in the intervention processes in this type of immobile is the need for financial valorization of the property subject to works. The formal solutions found for these situations emphasize the visibility of the work, with the recovery of the facades without concerns the quality of the interior and/or the general destruction of their internal compartments, rebuilding then along new lines, responding to the market requests by spaces like the new ones. At the same time, there is no record that such transformations actually configure a qualitative contribution to increase the building durability or sustainability, their habitability and security, or even to maintain their cultural qualities valued.

Once known and analyzed the implications for the lifetime of buildings in use caused by the interventions previously made is possible to generate a new moment of criticism, to propose more appropriated solutions to the reality, and avoid frequent changes and interferences.

The development of such type of research, meanwhile, presuppose the collect of data on the conditions of maintenance of buildings and on the perceptions of users about the advantages and difficulties in dealing with that type of built. The justified selection of buildings to evaluate, and the establishment of a coherent methodology with the development of operational hypothesis that enable the collection of field data are conditioned, among others, by the peculiarities of the buildings, the social conditions of its occupants, the conditions of the registers, the confinement of the scientific disciplines related to the theme, even more specialized in specific topics in their field of expertise.

[10] Usually such laws were (and still are) prepared according to generic landmarks, little related to local or regional features. Some effects of such legislation in the actual city can be evaluated Giacomini [2005].

[11] In the same set buildings can be both a ground floor or a high rate of occupancy, in five or more floors. Each one may be recessed from the street or the backyard and away from the side neighbours; or aligned with the street and with neighbours, in lots of different size fronts and depths, with different arrangements of openings and ornamental details.

[12] The replacement of the ancient materials by industrialized materials in current processes of intervention, for example, can lead to pathologies in constructive level (application of plaster, cement, plastic paint, and other non-hygroscopic materials, such as thermal and acoustic insulation), mischaracterize and change its original constructive logic. On the other hand, new technologies for enhancing and matching gives benefits for the longevity, at least structural, for the buildings that threaten to ruin.

3. REFLECTIONS FOR METHODOLOGICAL APPROACH OF THE PROBLEM

Departing from previous research that tested technical features (such as anomalies and guidelines for interventions in buildings), sociological issues (such as the impact on the social space caused by interventions in cities), theoretical aspects (such as the architectural strategies for the recovery of ancient buildings in the broad context of cultural heritage) and methodological proposals (such as post-occupancy evaluation of recent current buildings in sets or old monumental buildings isolated), the aim is, with this research, a combined treatment of the complementary instruments and methodologies[13].

3.1 Guidelines

The hypothesis to investigate, in the case of this research, considers that a joint evaluation of the material results and the appropriation of space by the user allow to generate data that contribute to new architectural project guides that seek cultural appreciation of this type of building, highlighting positive and negative aspects that would not be observed in only technical or social analysis. Within this purpose it seeks to ascertain: 1) how viable conditions of buildings' preservation have been made, from the application of new techniques and materials, 2) how the appropriation of habitational spaces by their users has been enabled, either due to ease of use and occupation, or to legibility of the building as urban heritage.

For this purpose it was developed a matrix of eighteen guidance cards distributed among four sets, which deal with the 1) prospecting, mapping and selection of buildings, 2) characterization of the context, 3) documentation and characterization of the chosen buildings (preparatory for the implementation of field work) and finally, 4) evaluation of buildings-case (from which are obtained field data for characterization and analysis of its use and occupation).

The fourth set, because of their characteristics, is a synthesis of the strategies presented in previous researches, adjusted to the specific reality of the old current buildings, placed in historical center, intervened and in use. The buildings will be analyzed unit by unit (considered as architectural object) to allow to evaluate the institutional proposals for the set formed by them (the object of safeguarding plans).

We seek to compare trends of intervention that contributed to better or worse solutions, considering four categories of analysis: "materiality, sustainability, livability and representativity" (the latter one is proposed here as a novelty, because it is not normally present in other similar research), covered for surveys and observations.

[13] As well as in other areas of knowledge there is a long-term monitoring of experimental methods results, or of new materials application (such as in Medicine or Engineering), also Architecture, along to Sociology, has sought to evaluate built project hypotheses over time in various types, specially through the Post Occupancy Evaluation. In the international field, the POE has been used by U.S. environmental psychologists for 40 years. In Europe there is the International Association for People-Environment Studies (IAPS), while in the U.S. exist the Environmental Design Research Association (EDRA), created in 1969 (in which stand out as personalities as Richard Wener, Wolfgang Preiser, Christopher Alexander, Claire Cooper Marcus, Amos Rapoport, Robert Sommer, Denise Lawrence). In Brazil, this research strategy is also well developed, with researches and publications coming especially from the NUTAU (Center for Research in Technology of Architecture and Urbanism, University of São Paulo) and ProLUGAR (Group Quality of Place and Landscape, Postgraduate Program, Federal University of Rio de Janeiro). In Portugal we highlight the works of LNEC (National Laboratory of Civil Engineering), many of them developed in collaboration with Brazilian researchers. For a State of the art on the subject see, among others, Roméro and Ornstein [2003], p. 26-54.

3.2 Basis and Methodological Guidance

The research adopts the "embodied observation" [14] as posture for field work. The understanding of the environment will be then openly local and situated, but always creative (as cognitive act), and will seek to defy the supposed intrinsic efficiency of the operational and instrumental recognized aspects.

It is developed through qualitative view and uses the non-parametric statistics (the statistical significance of samples in relation to the universe of research did not main the point of departure) and case studies to guide field surveys and analysis comparative data. While the qualitative approach allows the acquisition of a substantial amount of information in a limited time (is extensive, horizontal), the quantitative approach enables a deeper understanding of some of the investigated aspects (is focused, vertical).

Are used as research tools: prospecting in Historic Archives; Library researchs; Sketches; Photographic records, Surveys[15], POE (Post Occupancy Evaluation), Walkthrough, Analysis of Scale, Visual Selection[16], Thick Description[17], Drifting (*Dérive*) [18], Visual Analysis and Non-intrusive Diagnosis[19]. For analysis and synthesis are used the SPSS (Statistical Package for the Social Sciences) and the Matrix of Discovery[20].

3.3 Case Selection

The historical centers of Porto, Évora and Guimarães (the three cities classified by UNESCO as World Heritage Site in Portugal) are case studies, where buildings are building-cases to allow the application of the research tools for further comparison. Considering the amount and variability of buildings in the three historical centers were established composite samples in each city. Buildings should be selected according to the guidelines 1) pathways with observation[21]; 2) pathways with surveys; 3) suggestion by technicians, 4) selection of the awarded works; and 5) existence of previous documentation. These criteria will highlight a better way to choose the series of isolated buildings which should be organized into groups based on the overlap of features, in sets of streets and blocks.

4 TEST SAMPLING

Since the proposed strategy to assess the interventioned buildings constitutes a methodological novelty, and considering the presence of specific questionnaires as an instrument of work, it was necessary to provide a stage of pre-test, for evaluation of the applicability of the instruments selected and redesigned for this purpose.

Considering only the case of Porto, around 1,8000 buildings can be identified that must be maintained. This case is the broader and most diverse of all, and was chosen as the starting point of

[14] Reinghantz, Del Rio and Duarte [2002].
[15] Hill and Hill [2009].
[16] The last four ones are detailed in Ornstein, Bruna and Romero [1994].
[17] The Thick Description is one that explains not just the behavior, but its context as well, such that the behavior becomes meaningful to an outsider. http://en.wikipedia.org/wiki/Thick_description.
[18] The concept to Drift was first noted in French language with the term *dérive*, meaning an aimless walk of a drifter who follows the whim of the moment. The original concept was the exploration of a built environment without preconceptions, to discuss the reality of actually inhabiting the environment. http://en.wikipedia.org/wiki/Drifter_%28person%29.
[19] Acording, among others, Appleton [2003].
[20] Ornstein, Bruna and Romero. Op. cit.
[21] The term Pathway and your significance was drawn by Kevin Lynch, to comprehending the "city image". After that, the concept evolved, and have been used in some researches as a instrument for perception of space and selection of cases for studies. More in Ornstein, Bruna and Romero. Op. cit.

research. The existence of data in the Municipal Archive led to the choice of one set of edifices in two contiguous blocks in Miragaia (Figure 1) for a first research tools application. The feasibility of this prior choice was confirmed after the place's visit.

The buildings chosen were combined into two blocks and the street between, in order to incorporate a significant variability of buildings to explore. Thus, was generated a similar context to the classified area, but that did not interfere directly in the data generated for that territory.

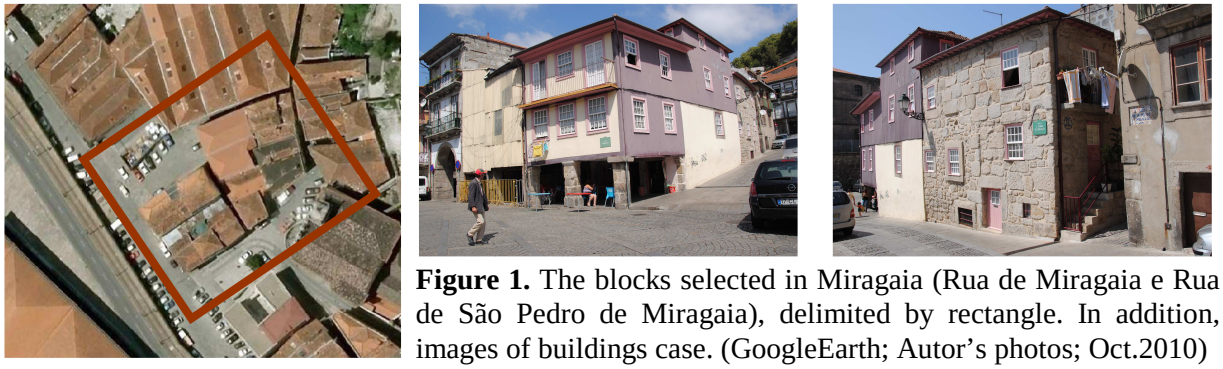

Figure 1. The blocks selected in Miragaia (Rua de Miragaia e Rua de São Pedro de Miragaia), delimited by rectangle. In addition, images of buildings case. (GoogleEarth; Autor's photos; Oct.2010)

The conditions for selecting these blocks were conditioned by the own characteristics of the old current architecture and by the methodological choices entailed. They represent a choice that allows us to observe the technical issues of conservation and maintenance, as well as the conditions for the apropriation of different buildings wich have similar features, compatible with the application of proposed tools in the research.

5 FINAL CONSIDERATIONS

In this ongoing research is considered essential the role of architectural project, included in the safeguard plans, as rudder for solutions that coordinate and equilibrate the increase of the quality of life levels, the sustainability and the durability of the building, without losing sight the need to protect the representativeness of the properties subject to intervention as cultural heritage. Also accounts that after executed, the project is appropriate and modified by users according to their real needs. This attitude may be often incompatible with the project itself, and in some cases, if added to the design choices, may be potentially contrary to material, sustainable and habitational characteristics or to the cultural heritage values that they want to preserve. Consider the specificities of this type of buildings is the first step to understand the problem lineate for the interventions that they are subject, and the perception of these differences also enables to select representative samples for analysis to check the longevity of the solutions implemented under the guidance of safeguarding plans.

The urban blocks chosen in Miragaia allows the application of questionnaires and technical diagnostic roadmaps in form of test, for posterior application in classified area of the Historic Centre of Porto (and, later, in Évora and Guimarães), The preliminary results of these tests are under development and will be available soon, but we consider esssencial enable their release and discuss them in the scientific community in order to facilitate a better understanding of this type of research.

ACKNOWLEDGMENTS

FCT- Fundação para a Ciência e a Tecnologia de Portugal – Individual Doctoral Scholarship

REFERENCES

Appleton, J. A. S. 2003, *Reabilitação de edifícios antigos: patologias e tecnologias de intervenção*, Alfragide, Orion.

Coelho, A. J. M. B. 1994, *Análise e avaliação da qualidade arquitectónica residencial* [Tese de Doutoramento em Arquitectura apresentada à FAUP], Porto, FAUP. 3 Vol.

Fernandes, F. B. 1999, *Transformação e permanência na habitação portuense:* as formas da casa na forma da cidade, 2ª Ed, Porto, FAUP-Publicações.

Fernandes, F. e Cannatá. M. 2009, *Territórios Reabilitados,* Casal de Cambra, Caleidoscópio.

Frampton, K. 1999, *Estudios sobre cultura tectónica:* poéticas de la construcción en la arquitectura de los siglos XIX y XX, Madrid, Akal.

Freitag, M. 2004, *Arquitectura e Sociedade,* Lisboa, Dom Quixote.

Giacomini, F. C. 2005, *Além das palafitas: espacialidade de edificações em encosta e sua relação com a legislação de Belo Horizonte* [Dissertação de Mestrado], Belo Horizonte, UFMG.

Hill, M. M.; Hill, A. 2009, *Investigação por questionário*, Lisboa, Sílabo.

Kubler, G. 2004, *A forma do tempo: observações sobre a história dos objeto,* Lisboa, Veja.

Lopes, F.; Correia, M. B. 2004, *Património arquitectónico e arqueológico*: cartas, recomendações e convenções internacionais. Lisboa, Livros Horizonte.

Paiva, J. V.; Aguiar, J. e Pinho, A. 2006, *Guia Técnico de Reabilitação Habitacional* – Volumes I e II, Lisboa, LNEC.

Ornstein, S.W.; Bruna, G.; Roméro, M. 1994, *Ambiente Construído e Comportamento: A Avaliação Pós-Ocupação e a Qualidade Ambiental,* São Paulo, Studio Nobel/ FUPAM/ FAU-USP.

Reingantz, P.; Del Rio, V.; Duarte, C. S. 2002, *Cultural factors: a needed category for post-occupancy evaluation.* In: Proceedings of EDTA 33, Pennsylvania, EDRA.

Roméro, M.de A.; Ornstein, S. W. 2003 *Avaliação Pós*-Ocupação*: métodos e técnicas aplicados à habitação social*, Porto Alegre, ANTAC. (Coleção Habitare) Acesso em 30 de Agosto de 2008. Disponível em: <http://www.habitare.org.br/publicacao_colecao1.aspx>

Vazquez, C. G. 2004, *Ciudad hojaldre: visiones urbanas del siglo XXI*, Barcelona, Gustavo Gilli, p. 7-53 (La visión culturalista de la ciudad).

XII DBMC
International Conference on Durability of Building Materials and Components
PORTO - PORTUGAL, April 12th-15th, 2011

Case Studies: Preliminary Investigation on Diagnosis and Repair Measures to Prevent Capillary Water Rise in Historical Buildings

Ana Fragata [1]
Maria do Rosário Veiga [2]
Ana Luísa Velosa [3]
Martha Lins Tavares [4]

ABSTRACT

In Portugal, interventions on monuments and historical centers, have been assuming increasing relevance. Most of these buildings have renders based on lime, usually with good cohesion and adhesion to the background, although the gradual use of Portland cement since the beginning of the 20th century leaded to the disuse and consequent loss of knowledge about properties, characteristics and execution of lime renders. In old buildings interventions the most current anomaly is usually due to humidity that penetrates in the walls from external sources such as: rising ground water, sea-salt spray, sea-flooding, etc. In one side, lime renders should be preserved and repaired; when there is a high degree of degradation and their substitution is needed, the application of new compatible renders is required; on the other side, the present requirements of habitability and aesthetic appearance, without de-characterization, in conservation interventions, should guarantee the maintenance of buildings integrity and durability. In order to achieve both goals, it is necessary to implement compatible renders, durable and adequate to the surrounding conditions. In the present work, several case studies with capillary water rise are compiled. The diagnosis methodology to define the probable causes of this anomaly and to evaluate the conservation state is presented, as well as the main measures adopted for the repair, based on control of causes and on the minimization of their effects.

KEYWORDS

Case studies, conservation, lime renders, capillary water rise.

[1] National Laboratory of Civil Engineering, 1700-066 Lisbon, Portugal, afragata@lnec.pt / Department of Civil Engineering, University of Aveiro, 3810-193, Aveiro, Portugal
[2] National Laboratory of Civil Engineering, 1700-066 Lisbon, Portugal, rveiga@lnec.pt
[3] Department of Civil Engineering, Geobiotec, University of Aveiro, 3810-193 Aveiro, Portugal. avelosa@ua.pt
[4] National Laboratory of Civil Engineering, 1700-066, Lisbon , Portugal, marthal@lnec.pt

1 INTRODUCTION

An ineffective rehabilitation and/or conservation intervention using inadequate renders solutions, due to the lack of knowledge about the materials, conservation techniques, maintenance principles and particular surrounding conditions (humidity conditions, presence of soluble salts, ventilation conditions), are factors that can promote the premature degradation.

In conservation action, the priority is to achieve compatibility and optimize the durability and adequate protection to water of the whole building [Magalhães *et al.* [2006]; Veiga *et al.* [2009-1]] and some solutions do not match this goal. For example, an impermeable mortar keeps the water inside masonry or forces its transport through the more permeable old mortar and masonry. Besides, they should not have high contents of salts, to avoid the increase of salt contamination into the walls. Some studies [Charola [2000]; Gonçalves [2007]] refer a synergetic effect of chlorides and sulphates that imply an aggravation of salt attack when both are present, so the contamination with sulphates (present in cement and some kinds of hydraulic limes) may be particularly harmful in buildings close to sea.

In the present work a compilation of twelve Portuguese case studies since the XV century, is made. These case studies have renders and plasters with several types of anomalies due to the exposition to humidity from different sources (rising capillary water, infiltrations due to damaged roof and salt mist). The case studies are located in Portugal: three in the North, in the towns of Porto and Aveiro; six in the centre of Portugal, around Lisbon; and three in the South of Portugal, in Évora, Tavira and Estói.

In this work, the application to those case studies of a methodology to define the possible causes of the anomalies is described, as well as the main anomalies and the measures adopted for their repair are defined, for an adequate intervention, in each case. The diagnosis methodology adopted allowed to identify the distribution and localization of the humidity in the renders and plasters, as well as to evaluate the origin of the humidity and to establish if it is still active or not. The quantification of the effects was also made, leading to an adjusted definition of a set of repair recommendations.

2 METHODOLOGY OF DIAGNOSIS

The adopted methodology of diagnosis was based on visual observation of the main anomalies as well as on non-destructive *in situ* tests (portable humidimeter and strip salt tests). The tests were carried out in several internal and external walls.

2.1 Visual Observation of the Main Anomalies

The description of the main anomalies based on visual observations for each case study is present in Tables 1 to 3. The case studies are divided in three groups depending on the source of humidity and on the time of occurrence: continuous rising damp and/or moisture from damaged roof – anomalies starting before the intervention; continuous rising damp and/or moisture from damaged roof – anomalies starting after intervention; salty mist and sea sparkles.

Table 1. Case studies - rising damp or moisture from damaged roof (anomalies before intervention).

Case studies	*Main anomalies*
Case 1: National Theatre in Porto (beginning of the XX century).	   Loss of cohesion of the paint, biological colonization, presence of soluble salts
Case 2: Old Convent in Aveiro (XVI century).	   Dark moisture stains, detachments of plasters and paints, salt efflorescences, biological colonization
Case 3: Old Convent belonging to the Foreign Affairs Portuguese Office in Lisbon (XVII century).	   Detachments of the plasters, loss of cohesion and adhesion of the plasters and paints, salt efflorescences
Case 4: Building in Lisbon with "Valmor prize" (beginning of the XX century).	   Detachments of the renders, biological colonization, dark moisture

Case studies with cement, lime and cement, and hydraulic lime renders, could present severe anomalies after interventions, when there is continuous rising damp and/or moisture from damaged roof. When the intervention is needed, the choice of compatible renders (lime based renders specially designed for each case) for old buildings becomes crucial for the success of the intervention.

Based on visual observations it could be seen that the main anomalies could be due to humidity problems, because the main observed anomalies were mainly dark moisture, loss of adhesion and cohesion of the renders and plasters, associated with the presence of salts in most of the cases.

Table 2. Case studies - rising damp or moisture from damaged roof (anomalies after intervention).

Case studies	*Main anomalies*
Case 5: Old Monastery converted into a museum in Aveiro (XV century). Intervention in 2008/2009.	   Dark moisture stains along the plasters, efflorescences, detachments of the paint
Case 6: Old Convent converted into a luxurious housing building in Lisbon (XVII century). Intervention 2008/2009.	   Detachments of the plasters, loss of cohesion and adhesion of the plasters and paints, salt efflorescences
Case 7: Old Palace converted into a luxurious housing building in Lisbon (XVIII/XIX centuries). Intervention 2008.	   Dark moisture stains along the renders and plasters, loss of cohesion of the paint
Case 8: Old Palace in Évora used as a public institution office. (XVII century). Intervention on the second half of XX century	   Dark moisture stains along the external mortars, detachments of mortars due to salt efflorescences, loss of cohesion and adhesion and biological colonization
Case 9: Old Convent adapted to a Charming Hotel in Tavira. (XVI/XVII centuries). Intervention 2006.	   Detachments of mortars due to salt eflorescences, loss of cohesion and adhesion of the mortars, detachments of the paint
Case 10: Old Palace adapted to a Charming Hotel in Estói. (XVIII century). Intervention 2009.	   Dark moisture stains along the external mortars

Table 3. Case studies with salty mist and sea sparkles near Lisbon (Fortresses on the coast between Lisbon and Cascais)

Case studies	*Before intervention*	*After intervention*	*Intervention*
Case 11 - Fortress in the coast of Lisbon (XVII century)	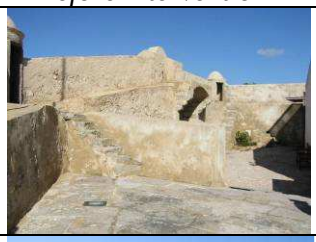		Substitution renders composed by mortars with air lime and metakaolin
Case 12 - Fortress in the coast of Lisbon (XVIII century)			Substitution renders composed by mortars with air lime and low content in cement, and silicate paint

2.2 Non-destructive *in situ* tests

2.1.1 Portable humidimeter – evaluation of moisture content

A portable humidimeter was used to evaluate the superficial moisture content in the walls [Veiga *et al.* [2009-1]; Massari & Ippolito [1993]; Henriques [2001]]. This test was performed in several internal and external walls, at different heights - between 0.10 m and 1.80 m from the pavement – and in some case studies at two different periods – dry weather and after a rainy week – in order to determine the possible origin of the water. This equipment presents a range of values from 0 to 6.9, corresponding to a dry and very wet render, respectively. Values between 0 and 2 correspond to dry zones; 2 to 4 correspond to slightly humid zones, 4 to 6 humid zones and from 6 to 6.9 to very humid zones [Veiga *et al.* [2009-2]; Magalhães & Veiga [2009]].

Depending on the values obtained and the distribution of the humidity it was possible to establish the origin of humidity. When wet or very wet zones were concentrated on the lower parts of the walls the probability was that the causes were rising damp or infiltration of superficial water due to the lack or inefficient drainage. When moisture symptoms were localized on the upper parts of the walls, the probable origin of the water could be the damaged roofs or damaged or ineffective roof drainage systems. If there is humidity in the vaults and roofs the moisture was probably inside the walls due to infiltrations by a damaged roof.

2.1.2 Strip tests - salts identification

The strip tests for the semi-quantitative identification of salts give information on the type of salts present as well as on the degree of contamination, based on semi-quantitative determination of ions associated with the type of salts [Veiga *et al.* [2009-1]; Borrelli [1999]].

The presence of sulphates can be associated to the presence of cement or some kinds of hydraulic limes in the mortars as well to the atmospheric pollution, marine environment (sea spray), ground water, contaminated soils or to the presence of old materials (stones, bricks or mortars). The presence of nitrates can be due to contamination with organic products, namely from animals and the presence of chlorides can be due to proximity of sea or to the presence of these salts in other wall materials such as sand. Salts can be transported in a porous material only if dissolved in water, thus their presence indicates water transport through the walls [Lubelli [2006]]. In spite of the lower dissolution rate of sulphates, when compared with the other salts present, the circulation of water in the walls can promote their dissolution and dissemination [Otossen *et al.* [2008]].

3 CAUSES OF THE ANOMALIES

Both visual observations and *in-situ* tests help on the evaluation of the origin, localization and distribution of the moisture in the walls. With the analysis of the results obtained with the adopted *in situ* methodology it was possible to identify the causes of the anomalies. In most of the cases they were mainly a consequence of the high accumulation of water in the walls and ceilings. The evaluation of the distribution and localization of the humidity allowed the identification of the origin of the water (Table 4).

Table 4. Source of humidity in each case study

Case studies	*Source of the water/humidity*
2, 5, 6, 8, 9, 10,	A. Capillary rising water from the underground through foundations and walls
2, 5, 6, 7, 8, 9, 10	B. Capillary rising water from the surface, due to the accumulation of the rain water near the base of external walls and/or due to the absence or disability of rain drainage systems
3, 6, 9	C. Water infiltrations from the exterior with saturation of the walls and ceilings due to the absence or inability of the roof during a long period before the intervention
1, 4, 6, 7, 8, 10	D. Localized infiltrations in some areas of the exterior walls
11, 12	E. Capillary rising ground water associated with sea-salt spray and sea-flooding

4 ADOPTED REPAIR MEASURES

Before an intervention of rehabilitation and/or conservation the repair of anomalies should be preceded, if possible, by the elimination of their causes. If that approach is not possible, it is necessary to minimize the effects of those causes and control the related symptoms [Freitas & Torres [2002]; Veiga *et al.* [2009-3]].

Elimination of the causes (source of water type B, C and D described in table 4):

- Repair of the roof, of the drainage systems and of the rainwater collectors
- Construction of drainage ditches along the exterior walls to prevent the accumulation of rain water
- Construction of ventilation ditches at the base of exterior walls, in order to facilitate the evaporation of water rising from the ground
- Ventilation tunnels under the floor of the ground-floor, with perforated tubes connected to the exterior to avoid capillary rise.

Minimization of the effects (source of water type A described in table 4):

- Removal of impermeable external paints and replace them by permeable renders and plasters.
- Allow the drying of the renders before the application of the final paint.
- Promotion of ventilation during the works by opening the windows.
- Removal of the impermeable plasters from the walls and ceilings and substitute them by traditional plasters to improve the evaporation of the water retained inside the ceilings, vaults and walls.
- Execution of a gap between the floor footers and the floor to allow the ventilation of the interior walls and the continuous drying of masonry over time.

5 SUBSTITUTION RENDERS

Mortars to use in old buildings must be compatible with the background and the pre-existing mortars. The compatibility is a concept dependent on the characteristics of the old masonry and on the specific conditions of the building. In each case, an evaluation must be carried out concerning the strength,

deformability and water permeability of masonry and of the old mortars in contact. In parallel, an assessment of the main physical conditions must be performed, considering specifically: the water transport situation (capillary rising water and exposure to rain), the climatic conditions (humidity and temperature ranges, wind and rain intensity) and the environmental issues, such as air pollution and salt environment [Freitas & Torres [2002]; Veiga *et al.* [2009-3]; Veiga *et al.* [2009-4]].

Case studies 1 to 10 present sources of water from type A to D (Table 4). When the anomalies due to water are localized and not severe, (cases 1 and 4) they can be solved by washing and/or substituting the degradated zones by new compatible renders or paintings. When the anomalies are more severe, the choice of the renders solution should be done case by case. In those cases when the presence of water inside the walls is extended in time due to difficulty of evaporation because of the use of less permeable renders than the old ones, they should be removed and substituted by lime based ones (pure or with small contents of hydraulic additions), more porous and permeable [Otossen *et al.* [2008]; Veiga *et al.* [2009-4]]. The impermeable renders and paintings (synthetic finishings, polymeric paints and other polymeric products) should be replaced by materials more compatible with wet walls, such as lime based mortars and silicate based paints [Veiga & Tavares 2002]. In the interior the plasters should be replaced by lime or lime and gypsum plasters and ventilation should be promoted in the interior spaces. The use of sands free of salts is always required, to reduce risks due to salt crystallization [Veiga *et al.* [2009-3]].

Case studies 11 and 12 [Veiga *et al.* [2009-1]; Tavares *et al.* [2008]] present a source of water type E (Table 4). These kind of old buildings (fortresses) placed in coastal areas are subjected to particularly severe actions. They require the use of substitution renders with special properties to assure durability to the referred actions [Veiga *et al.* [2009-4]]. The mortars must have high mechanical strength to resist erosion of sea wind and salt crystallization pressure, moderate elasticity modulus to accommodate deformations due to sudden thermic variations, moderate capillary coefficient and high water vapour permeability to retard the entrance of water and allow for quick drying [Veiga *et al.* [2009-4]]. Samples collected from several constructions located in Lisbon and coastal surroundings show clearly that very resistant and durable materials were used [Santos Silva [2002]], usually based in air lime and additions or aggregates that promoted pozzolanic reactions. The use of mortars composed by air lime and lower content in cement can be adequate, although there are some risks of introducing salts into masonry. Mortars formulated with air lime and pozzolans can be adequate to those buildings depending on the type and proportion of pozzolan and curing conditions of the mortar [Veiga *et al.* [2009-4]]. It is particularly important to check if there is rising capillary water. If this is the case and it is not possible to eliminate the water source, problems with salt crystallization inside the wall are likely to appear and it is usually safer to adopt, for renders and plasters, water permeable mortars, classified as salt transport solutions [Hees & Naldini [2007]].

6 CONCLUSIONS

In interventions in old buildings the mortars and paintings must be carefully studied case by case, considering the state of conservation of the renders, plasters and paintings, the extension of anomalies present and, as most important in this study, the source and quantity of moisture present as well as its distribution and localization.

The elimination of the causes of anomalies whenever possible or the minimization of their effects are the first goal in an intervention.

The capillary rising water from the ground, present in the walls, is the most difficult cause to eliminate. To promote drying of the walls' bases and mitigate the effects of capillary rising, ventilation should be performed as well as removal of the impermeable renders.

The state of conservation and the methodology of diagnosis allowed the definition of the causes of anomalies. The main repair recommendations were defined: increase water drying rate to the exterior, turning it as close as possible to the capillary rising rate, and limiting the water volume that reaches the walls. The choice of repair or substitution solutions for renders, plasters and paintings of old

buildings are of the utmost relevance to promote the functionality and durability of the masonry walls, especially when they are affected by high water content due to capillary rising or to previous infiltrations by the roof.

ACKNOWLEDGEMENTS

FRADICAL Lda. Company and FCT (Portuguese Foundation for Science and Technology) for their support under the scholarship SFRH / BDE / 33800 / 2009.

REFERENCES

Borrelli, E. 1999, *Conservation of Architectural Heritage, historic structures and materials salts*, ICCROM, Rome.

Charola, E.A., 2000 'Salts in the deterioration of porous materials: an overview', *Journal of the American Institute for Conservation*, **39**[3], pp. 327-343.

Freitas, V.P., Torres, M.I., Ascensão, A. And & Gonçalves, P.F. Tratamento da humidade ascensional na Igreja de Vilar de Frades (Treatment of capillary rising water in Vilar de Frades Church.. Património Estudos, nº 3, 2002, pp. 54-62.12].

Gonçalves, T. 2007, *Salt crystallization in plastered or rendered walls*, PhD Thesis, IST, Lisbon.

Henriques, F.M. 2001, *Humidades em paredes*, LNEC, Lisbon.

Lubelli, B., van Hees, R.P.J. & Groot, C.J.W.P. 2006, 'Sodium chloride crystallization in a "salt transporting" restoration plaster', *Cement and concrete Research* **36**, pp. 1467-1474.

Magalhães, A.C., Veiga, M.R. & Cartaxo F. 2006, 'Characterization of lime mortars with water repellent for use on ancient building's walls', Proc. 7th International Masonry Conference (7IBMAC), London, United Kingdom, British Masonry Society.

Magalhães, A.C. & Veiga, M.R. 2009, 'Physical and mechanical characterisation of ancient mortars. Application to the evaluation of the state of conservation', *Materiales de Construcción*, **59**[295], pp. 61-67.

Massari, G. & Ippolito 1993, *Damp Buildings, Old and new*, ICCROM, Rome.

Otossen, L.M., Rorig-Dalgaard, I., & Villumsen, A., 'Electrochemical removal of salts from masonry: Experiences from pilot scale', Proc. International Conference on Salt Weathering on Buildings and Stone Sculptures, Copenhagen, Denmark, October, 2008.

Santos Silva, A., 2002 'Caracterização de argamassas antigas – casos paradigmáticos', eds Cadernos de Edifícios, Lisboa, **2**, pp. 87-101.

Tavares, M., Magalhães, A.C., Veiga, M.R., Velosa, A.L. & Aguiar, J. 2008, 'Repair mortars for a maritime fortress of the XVII century'. Proc. Construction heritage in coastal and marine environments: Damage, diagnostics, maintenance and rehabilitation, Lisbon, Portugal.

Van Hees, R.P.J. & Naldini, S. 2007, eds. Compass - 'Compatibility of plasters and renders with salt loaded substrates in historic buildings'. Community research—Final report.

Veiga, M.R., Velosa, A.L. & Magalhães, A.C. 2009-1, 'Experimental applications of mortars with pozzolanic additions: Characterization and performance evaluation', *Construction & Building Materials*, **23**[1], pp. 318-327.

Veiga, M.R., Fragata, A., Tavares, M.L. 2009-2, Estudo dos revestimentos interiores da igreja do Santíssimo Sacramento, em Alcântara, LNEC, Julho de 2009. Relatório 232/2009 – NRI. Confidencial. Lisboa.

Veiga, M.R., Fragata, A., Tavares, M.L., Magalhães, A.C. & Ferreira, N. 2009-3, 'Inglesinhos Convent: Compatible renders and other measures to mitigate water capillary rising problems', *Journal of Building Appraisal* **5**, pp. 171-185.

Veiga, M.R., Fragata, A., Velosa, A.L., Magalhães, A.C. & Margalha, G. 2009-4 'Lime based mortars: discussion of their viability to be used as substitution renders in historical buildings'. *International Journal of Architectural Heritage*, **4**, pp. 177-195.

Veiga, M.R. & Tavares, M. 2002, 'Características das paredes antigas. Requisitos dos revestimentos por pintura', eds APTETI, Lisboa.

XII DBMC
International Conference on Durability of Building Materials and Components
PORTO - PORTUGAL, April 12th-15th, 2011

Jeruzalem Frankendaal Amsterdam Temporary Duplex Can Stay Forever

Hielkje Zijlstra[1]
Herdis Heinemann[2]

ABSTRACT

Past, present and future are all relevant to the buildings. Three levels of analysis have been used to cover these phases. The objective of my research was to identify the qualities of buildings which are relevant when trying to shift from decay to preservation. The influence of construction engineering, the way we can learn from it now, and the way in which a building is able to accommodate change determine the chances of a building's long term survival – the outcome of the interaction of continuity and change: Continuity + Changeability = Durability. This has been worked mine research method: Analysing Buildings from Context to Detail in time (ABCD research method).

An application of the ABCD research method has been used at the residential district of Jeruzalem, Frankendaal, Amsterdam. This research created new opportunities for Frankendaal. After the second World War in Holland housing shortage led to flexible options for new dwellings. Duplex was one of those. First the house was separated in two dwellings, later it could be joined. The urban settlement Jeruzalem was built in 1952 by Merkelbach & Elling and included 792 duplex dwellings. The building system of concrete prefabricated elements determined the design and provided opportunities for future changes. In 1987 the wooden window frames on the rear elevation were replaced, loggias were closed up, the concrete was painted and the end elevations were fitted with cladding. When refurbishment is an option firstly, these changes made would be undone. The original architectural design could be regained by fitting internal thermal insulation. The duplex houses have not been combined. In 2002 the site became the victim of the new approach of the housing association, rather like that of a commercial project developer. It was decided to save some blocks of houses especially the Jeruzalem blocks. In 2005 the plans were postponed for financial reasons. In 2009 a new plan has been made and finally in 2010 part of the site became a state listed monument. In the end of 2010 the firm of Hooyschuur Architects started to take apart one of the houses and started to develop a restoration plan on the basis of those results for all the dwellings listed as monuments.

KEYWORDS

Post war, refurbishment, prefabrication, exposed concrete, monument, durability, research method

[1] Faculty of Architecture, dep. ®MIT of the Delft University of Technology, Delft, NETHERLANDS, h.zijlstra@tudelft.nl
[2] Faculty of Architecture, dep. ®MIT of the Delft University of Technology, Delft, NETHERLANDS, a.h.heinemann@tudelft.nl

1 INTRODUCTION

The built environment is continuously changing and such changes are particularly important when regenerating buildings. These changes add something to existing buildings and make new programmes possible. The existing buildings - history - determine continuity and form a clear additional, time-dependent layer. In general, the large number of buildings built between 1940 and 1970 cannot be listed (in the Netherlands) as national monuments and are therefore essentially unprotected especially the residential post-war areas. Furthermore, buildings from this period in particular are currently being considered for regeneration or threatened with demolition. Apart from studying relevant literature and other sources I studied seven buildings to develop a method for analysing buildings to be able to understand them. The research resulted in the Analysing Buildings form Context till Detail in time research method (ABCD⊕) that was guided by the next three research themes [Zijlstra 2009]. Those will be explained first. Secondly, the research of Jerualem Frankendaal in Amsterdam will be worked out more in detail and finally some conclusions and future aspects will be discussed. Unique in this case is that after a period of more than ten years of theoretical planning the restoration will be based on the practice of taking apart one house carefully and make a total plan for all the dwelling on basis of these results.

2 RESEARCH THEMES

The ABCD⊕ research method was guided by the following themes:

2.1 Observation - with an engineer's eye

I considered engineering and technology and the views of both architectural critics and practising architects about technology by studying the relevant literature and sources. Technology evolved after the Second World War as a result of the use of new materials, changes in legislation and standards, and the industrialisation of the construction process. This last aspect was primarily relevant to residential construction projects. Building practices changed after 1940, however, the role of technology in the process did not change materially. Comments about the contribution, or lack thereof, of technical progress to a higher architectural quality were always personal visions primarily shaped by personal taste and habits. Architects developed from supervisors to architect-managers of the entire construction process. Time schedules became an important instrument and working together with structural engineering and building services consultants became steadily more important. The cooperation between these parties affected the overall result, and all needed each other. Consequently, regular teams of architects and consultants developed, e.g. Peter Rice and Renzo Piano. The best results were developed based on synergy between the two disciplines [Rice 1994].

2.2 Research analysis

When designing completely either new objects or objects to be incorporated into an existing structure it is important to learn from the past. Not to copy it, but to analyse it and apply the lessons learned while respecting the present context. We have to evaluate knowledge and methods and develop our own design method. This applies to architecture students as much as to practising architects.
This learning aspect is emphasised when a design commission concerns an existing building, but even a new build project always has a context. When dealing with an existing building that building provides the primary context and immediately becomes an element of the key points of the architect's brief. In my view, studying criticism, experiences and interviews, and thoroughly analysing the work of others is not adequately included in the education and training of architects as designers. It would appear that architecture (the study of the requirements for constructing buildings) education should teach students and practicing architects the skills to do this, and appreciate the rewards.

2.3 Regenerative conclusions

This theme defines the approach I took when developing the conclusions of my thesis. Regeneration concerns changes which add a new period, a new generation, to the lifecycle of buildings.
Life means change and the past means that we progress in a spirit of tradition and memory. Furthermore, change cannot happen without continuity. Changes to buildings are affected by both financial and technical considerations. As a student, the examples set by Gunnar Asplund and Carlo Scarpa showed me that although designing new buildings (even when embedded in the existing context) is an exciting challenge, making changes within the context of an existing building is actually a far greater challenge (Fig.1). The existing adds a layer of history which can never be created in a true new build project. That's when refurbishment truly becomes durable: Continuity + Changeability = Durability.



Figure 1. Castel Vechio in Verona refurbished by Carlo Scarpa.

3 RESEARCH METHOD

The work for my PhD research didn't only result in the relevant conclusion Continuity + Changeability = Durability, but also in the ABCD research method which will be applied to the subjects covered by ®MIT at the Faculty of Architecture of Delft University of Technology and could be used on international scale. It is a method to analyse the existing before changing it. That is the only way to regenerate buildings, residential urban areas, parts of cities and urban landscapes with conscience.

Analysing Buildings from Context till Detail in time aims to discover the qualities of a building, rather than its value. Observation, the first stage of the research, aims to obtain information from the literature, the building itself, archives and interviews with stakeholders. The second stage, analysis, includes structuring, analysing and interpreting the information. In the third stage, conclusions can then be drawn on the basis of the research themes discussed above. The information is structured in accordance with the research brief. In the long term, it will be possible to identify connections (concerning both buildings and building construction) between the results of Analysing Buildings from Context till Detail in time, using the research themes as defined before.

The information obtained in the observation stage is reduced to the contextual information which affected the design, creation, existence and preservation/decay of the building. As far as the typology is concerned, we should not only consider the functional or chronological classification of buildings based on building type. Instead, we should analyse the buildings on the basis of a spatial typology, as the spatial conditions will either remain the same or change when the function of the building changes.

4 ABCD RESEARCH MATRIX

Context is the title of the first section in which the contextual aspects are discussed: commission; location; architect; typology and design process. The later sections, which consider the building itself

in greater detail, are initially ordered by time: arising, continuing and expiring. Within these, the elements of the building are analysed at three levels: space (interior and exterior); structure (load-bearing elements and elements which determine the structure); material (shaping the space through materials which affect light, colour, texture, surface, sound, impression, smell, size and weight); building services (climate control, comfort, maintenance and communications). By combining this the actual ABCD Research Matrix was created (Fig. 2).

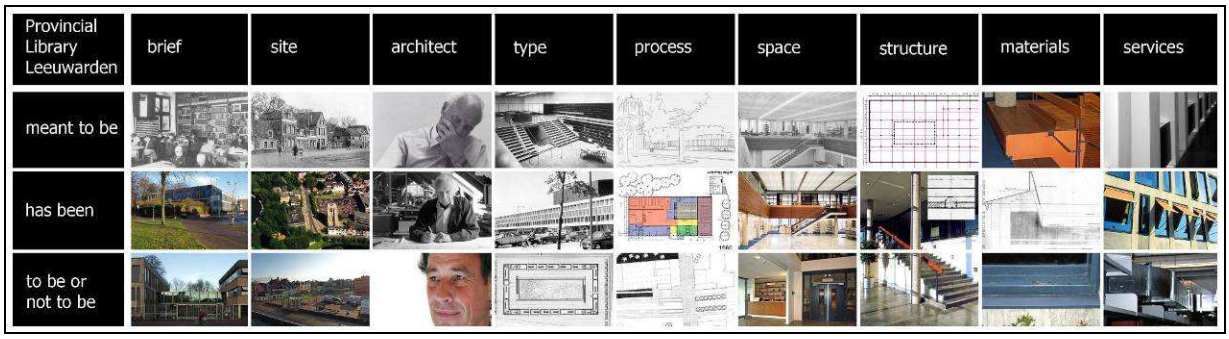

Figure 2. ABCD℗ research matrix applied on the Provincial Library in Leeuwarden.

5 JERUZALEM FRANKENDAAL AMSTERDAM

Learning from existing buildings by investigating them should be a regular element in architects' education. A course on Restoration and Renewing, my working field at ®MIT at the Delft Technical University, should not be limited to preservation, but especially address new designs, like refurbishments, in existing contexts where internal changes will always be necessary. Such changes can provide the impetus to ensure the survival of buildings. The method has been applied as well for urban residential area as well for solitaire buildings. In the field of this conference I will present the research I worked out for Jeruzalem Frankendaal in Amsterdam.

5.1 Context

The architects were B. Merkelbach (1901-1961), Ch.J.F. Karsten (1904-1979) and P.J. Elling (1897-1962). The commission in 1947 included the construction of 792 dwellings designed as duplex apartments (upstairs and downstairs) which could later be combined into larger houses. The urban design was developed by J. Mulder (1900-1988) within the Algemene Uitbreidingsplan (General Expansion Plan) for Amsterdam, under the supervision of Cornelis van Eesteren (1897-1988) [Mulder 1952]. Interesting urban planning features include the first use of an open cluster structure around courtyards within a strip layout; the greenery designed by M. Ruys (1904-1999) and the playgrounds designed by A.E. van Eyck (1918-1999) [Van Eesteren 1952]. The project was built from 1949 till 1952 [Schilt & Van Rossem 2002] (Fig. 3 and 4).

5.2 Buildings

The houses were designed on a grid of 6.30 metres. The use of pre-fabricated concrete meant that this could be realised in a single span, allowing freedom in the use of the space. The facades were built with 50 x 116 cm concrete panels. On the side facing the garden, the facade was divided by the vertical chimneys in fair faced brickwork, balconies and loggias. At the front, the flat facades were divided by the vertical rainwater pipes, and only the front doors which would continue to be used after the apartments had been joined into one house had concrete canopies. All elements were designed to suit the dimensions of the Dotremont-Ten Bosch building system. This was the only project built in the Netherlands using this system. It has similarities with the Airey system that was more often used in the Netherlands but the used system was based on concrete elements [Priemus 1970] (Figs. 7 and 8). This makes it more suitable for later refurbishment because no structural damage occurred by oxidation of the load bearing structure. The roof had a slight pitch to the front of the house, hence

rainwater fittings were only needed on this side. All window frames were made of wood. This included a large window frame at the backside and smaller frames at the front side (see Figs. 9 and 10).

5.3 Future plans

From 2000 till 2010 different plans came up to restructure the whole neighbourhood of Jeruzalem Frankendaal. The plans varied from complete demolishing to partly refurbishment. In between 2000 and 2006 plans were made but financially impossible. The National Heritage Committee wasn't able to list post war buildings at that moment. For instance in 2003 there was a shortage of 23 million Euro's. Finally in the beginning of 2010 six blocks became national listed monuments and in the end of 2010 Hooyschuur Architects started to dismantle the façade of one of the dwellings to investigate the possibilities of a durable refurbishment and a financially sound restoration plan (see Fig. 13).

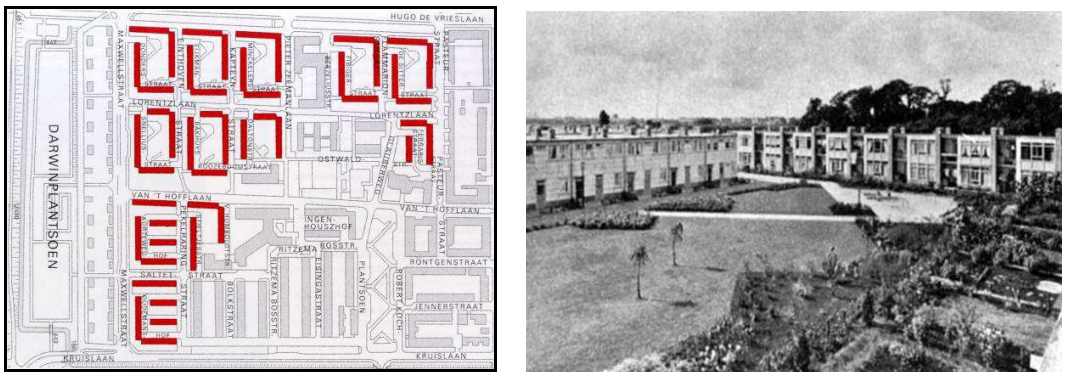

Figures 3 and 4. Site plan and original appearance of one of the courtyards.

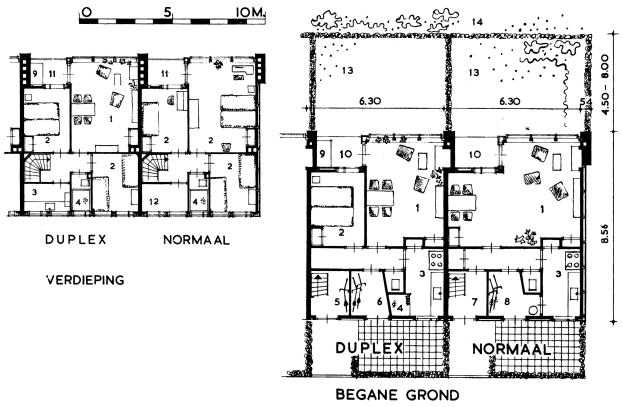

Figures 5. Floor plans of the houses.

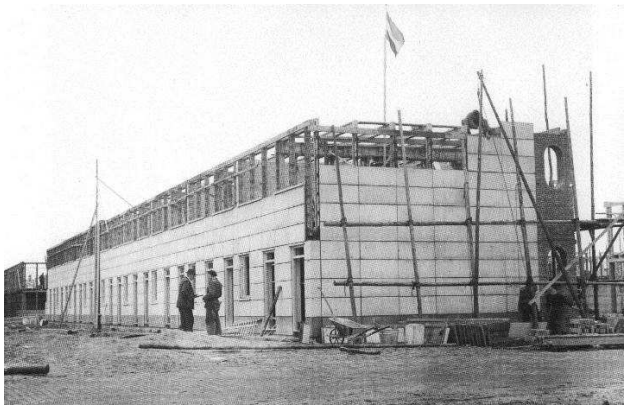

Figures 6. The houses under construction.

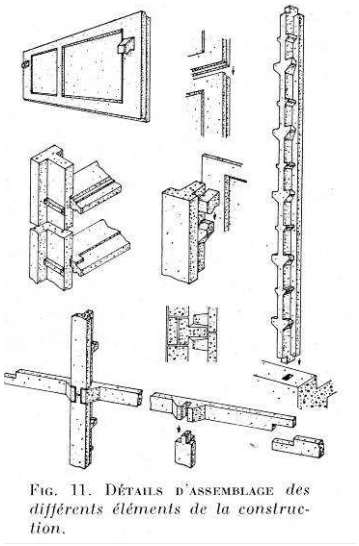

FIG. 11. DÉTAILS D'ASSEMBLAGE *des différents éléments de la construction.*

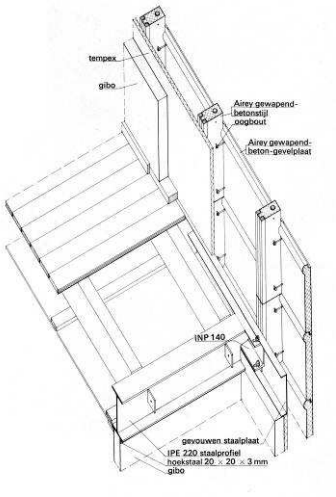

Figures 7 and 8. On the left the Dotremont-Ten Bosch building system and on the right the Airy system, based on the system of Sir Edward Airey from Leeds UK. The Airy system used steel and concrete. The Dotremont-Ten Bosch system used concrete only.



Figure 9 and 10. Left the original presentation of the façades and right the façade covered with wood and brick around 1987.



Figures 11 and 12. Ronald Plasterk, minister of culture, listed six blocks of Jeruzalem Frankendaal as national monument in 2010 [RCE 2010].



Figure 13 The façade ready for inspection in February 2010.





Figures 14 and 15. The façade taken apart and investigated and new concrete panels are tested for the new in December 2010.

6 CONCLUSIONS

Reasons to work out this case study were:

- the duplex design, based on the assumption of change
- a building system using small prefabricated concrete elements
- the location in a garden village near the centre of Amsterdam in the general expansion plan
- the first courtyard layout and the integration of environment and architecture
- the question why only a few houses had been combined by 2002
- the inappropriate renovation (devaluation) in 1987
- plans for demolition and refurbishment on-going from 2000
- the first post war residential neighbourhood listed as a national monument in 2010
- plans to refurbish these houses by taking apart one carefully and develop a plan on basis of those results in 2011.

The building system determined the design and provided opportunities for future changes. So in 1987 the three housing associations replaced the wooden window frames on the rear elevation by plastic frames, the loggias were closed up, the concrete was painted and the end elevations were fitted with

cladding (Fig. 10). In 2000 they decided to demolish the houses and get them replaced by new ones. After a lot of protest, debate and struggle the residents succeeded in 'Saving Jeruzalem'. So in 2003 Bertus Mulder of the Werkplaats voor Architectuur was commissioned to make a plan for the regeneration of the houses. I got the chance to practice my ABCD research method at this project. The research was finished before Bertus Mulder started his refurbishment project. Conclusions of my report where adopted by Mulder and made proposals possible for mature solutions. Firstly, the changes made in 1987 would be undone. The support structure, determined by the building system, made it possible to join dwellings either horizontally or vertically. The original architectural design could be regained by fitting internal thermal insulation. The originally designed window frames could be reproduced because the drawings of it still existed.

The residents did not feel the need for refurbishment. They were happy with the low rent and the unique location. The target group of the duplex houses moved from families to single people, the elderly and students. The site became the victim of the new approach of the housing association, rather like that of a commercial project developer, to make money from the site through new building projects. However, under pressure it was decided to regenerate the houses. In 2005 the plans were postponed for an indeterminate period for financial reasons. Nothing has been done since, only the proposal to nominate the project as a listed monument continued and succeeded in February 2010 [RCE 2010] (see Figs. 11 and 12). In 2010 Jos Kroon of Hooyschuur Architects started to find out what the possibilities are for a sustainable and durable refurbishment using the outcomes of the ABCD research. He at first dismantled one façade and secondly investigates in consideration with the present-day possibilities He deals with different contractors how things can be worked out and tests have been done (see Figs. 14 and 15). He works out a restoration plan for the whole project on a sound and durable basis. The housing associations and the local government are responsible for funding.

The ABCD research made clear that this project has possibilities to survive in a durable way by refurbishment. It is used twice during the process once in 2002 to result in a plan based on the original façade design and secondly in 2010 to find out how the dwellings were constructed originally so a new generation at the life time cycle of Jeruzalem Frankendaal will be added.

ACKNOWLEDGMENTS

Bertus Mulder, Werkplaats voor Architectuur, Utrecht, Jeroen Schilt, Bureau Monumentenzorg Amsterdam and Jos Kroon from Hooyschuur Architects Wormerveer.

REFERENCES

Kroon, J. 2010, *Bouwkundig Rapport 090302gev.100927jk*, Hooyschuur Architecten bna Wormerveer.

Mulder, J. 1952, 'Frankendaal, *Polytechnisch Tijdschrift*, [45/46], 789b-793b.

Rice, P. 1994, *An Engineer Imagines*, Artemis London.

RCE 2010, 'Jeruzalem als eerste wijk naoorlogsmonument', www.rce.nl, 5 February.

Schilt, J and V. van Rossem 2002, *Tuindorp Frankendaal*, Bureau Mounentenzorg Amsterdam.

Van Eesteren, C. 1952, 'Frankendaal: een woonbuurt in de Watergraafsmeer te Amsterdam', *Forum*, [6/7], 187-193.

Zijlstra, H. 2003, 'Jeruzalem blijft!', in: *Vijfennegentigste Jaarboek van het genootschap Amstelodamum anno MMII*, M. Vrolijk (ed.), Genootschap Amstelodamum Amsterdam, pp. 215-237.

Zijlstra, H. 2009, *ABCD research method*, IOS Press/DUP Amsterdam.

XII DBMC
International Conference on Durability of Building Materials and Components
PORTO - PORTUGAL, April 12th-15th, 2011

Roof Durability in National Monuments: San Esteban´s Romanesque Church of Pineda de la Sierra, Burgos, Spain

Javier Garabito [1]
Jose Carlos Garabito [2]
Victor Echarri [3]
Jesus Gadea [4]
Angel Rodriguez [5]

ABSTRACT

We prioritize the interventions in the historic buildings´s roof in order to prevent subsequent deterioration of the monument. To set the intervention criteria is necessary to take into account the durability of both the material and the construction system to be employed.

San Esteban´s church of Pineda de la Sierra was listed as National Monument the year 1983. Its construction started in the first third of the twelfth century and belongs to the Romanesque style. It has a unique nave with a semicircular apse at its eastern end. The tower and the sacristy are located at its northern flank while in the Southern one there is an atrium. An intervention was carried out in the roofs, the year 1992, restoring the timber structure and replacing the ceramic tile coverage. Ten years later it was necessary a new intervention. The roof tiles had suffered movements and breakages that allowed water infiltrations. This tile was not the most appropriate for Pineda's harsh climate. The lack of coverage waterproofing had caused the rot of the roof´s structural elements. In the new intervention, these roof tiles were completely replaced by pressed clay tiles while the building system was changed, since the roof tiles were placed with no humidity, nailed on a framework composed by three levels of battens, completely breathable.

We analyzed the characteristics of both roof tiles, in order to verify the adequacy of the new roof tile.

KEYWORDS

Heritage, clay roof tile, permeability, frost resistance, restoration.

[1] Architect of the Cathedral of Burgos, Department of Building Construction, University of Burgos, Spain, jgarabito@ubu.es
[2] G.L. Architects, Burgos , Spain, jcgarabito@glarquitectura.es
[3] Department of Building Construction, University of Alicante, Spain, victor.echarri@ua.es
[4] Department of Building Construction, University of Burgos, Spain, jgadeamc@ubu.es
[5] Department of Building Construction, University of Burgos, Spain, arsaizmc@ubu.es

1 INTRODUCTION

We have to prioritize the interventions in the historic buildings´s roof in order to prevent subsequent deterioration of the monument. To set the intervention criteria is necessary to take into account the durability of the coverage material and the construction system as well. In this paper we carry out a study of the roof durability in a historic monument, the San Esteban´s church of Pineda de la Sierra, which was restored in 1992 and needed new works in 2007.

2 HISTORICAL BACKGROUND OF SAN ESTEBAN´S CHURCH OF PINEDA DE LA SIERRA

Pineda de la Sierra is a town located 50 km east from Burgos. The church of San Esteban is one of the most interesting and best preserved monument of all the Romanesque in Castilla and Leon.
Pineda is listed as a historic site by the Spanish Ministry of Culture since 1982, while the church was declared as a National Monument next year. Its construction began the first third of the twelfth century. It belongs to the Romanesque of the "school of the sierra," more sober and collected than the Romanesque of the monasteries of Silos, Ardanza and Oña. Despite the stylistic purity and unity throughout the whole, this temple suffered alterations and renovations, which changed its original structure over the centuries (Figs. 1 and 2).



Figure 1. South elevation.



Figure 2. Northeast elevation.

This temple is located on the highest part of the town, occupying a land gently sloping to the south. The main material is stone, using a local reddish sandstone of Buntsandstein [Moreno 1993]. It presents a nave, crowned at its eastern end with a semicircular apse, and accompanied in his northern flank with the tower and the vestry, while in the southern there is a large portico.

2.1 Historical Summary of Construction

2.1.1 Romanesque period

The construction began with the semicircular header. Externally the apse is divided into five sections separated by single columns, each one raised on a high podium, and surmounted by capitals. In the three central panels there are open windows formed by loopholes framed by archs. The construction of the nave and the tower was undertaken in a second phase. These elements have suffered major alterations in subsequent interventions than in the apse. This is a great prism reinforced with buttresses in the back. The original layout of the church´s plan was respected in subsequent interventions. However his elevation has increased its height, as shown by the line of corbels preserved on its southern wall. The same thing happens to the tower, replaced by another in the sixteenth century. The third phase covers the construction of the façade´s doorway attached to the south wall. It consists of five levels of semicircular archivolts on columns. It is one of the latest and most brilliant works of the Romanesque architecture of the mountains. This phase ends with the

addition of the portico, which was built on the south facade. It consists of a eleven arches gallery, that are arranged around a central door.

2.1.2 XVI century

The old roof of the nave was replaced by a stone vaulted roof. Thus it was increased the height of the walls and large windows were opened as well. The roof is composed of three sections of starry vaults. The second major work is the reconstruction of the tower. It consists of a simple square-based prismatic structure, showing completely smooth walls.

2.1.3 XVII century

The new sacristy was built in 1617, under the auspices of licenciado Proszola [AGDBU, LP, Pineda de la Sierra, L.F. (1620 – 1671)]. It is located in the northern façade of the temple. It consists of a small rectangular structure, covered with quadripartite ribbed vault.

3 ANALYSIS OF THE SITUATION AND PATHOLOGICAL STUDY

In 1991 works were carried out to replace the roofs of the nave, apse, sacristy and porch.

The roof structure is raised on a new line of dogs, supported by a concrete perimeter ring beam, visible from the outside. During the intervention some Romanesque corbels emerged on the north wall, which were hidden by the sacristy roof. In order to display these items it was raised a gable roof, which in the encounter with the wall was almost flat, and had produced serious leaks in the sacristy (Fig. 3). At the same time, it was replaced most of the existing roof tile by a roof tile that had not certified its resistance to frost.

Ten years later, the roof tiles had suffered partial displacements and cracks that allowed water intrusion. The positioned roof tile is not appropiate to continental climate, so it exfoliates and breaks. The construction system is not the most successful, because the mortar, with too much of sand, is completely degraded (Fig. 4). This lack of waterproofing of the roof coverage brings rot to the roof board and the structural elements as well.



Figure 3. Sacristy roof. The roof is almast flat to show the Romanesque corbels.



Figure 4. Conservation status of the roof tile

4 INTERVENTION CRITERIA: ROOFS´S RESTORATION.

The wood structure is treated in situ, except in the atrium and the tower that have to be replaced. The structure of the roof of the nave was in better condition with specific damages. The roof board and the roof tile coverage have to be replaced. It is also necessary to reinforce the structure and replace the damaged items. All wood needs to be treated with an anti-xilophagus. The new elements are made of pine wood.

The roof of the apse was made up of a lime mortar with battens embedded in it, and roof tile nailed on them. It is neccessary a restoration of this mortar in order to regularize the slopes with lime mortar, placing new battens embebed perpendiculars to the eaves. Later there is the execution of a framework composed by two levels of battens to nail the roof tiles (Fig. 5).

The roof structure of the atrium was rather spoiled by the humidity, so it was substituted by a new structure with braces, rafters, struts and ground beam, all done in pine. The formation of the roof board is made by pine wood from Soria of 3.00 x 12.00 centimeters, nailed to purlin.

The vestry roof retained its minimal slope to allow observing the corbels of the original construction. To prevent infiltration of water runoff is disposed a lead sheet of 3 milimeters over the wood sheathing. Above the lead sheet is set the ceramic roof tile with the double wooden battens system.

The roof tile was replaced by another one with similar appearance, but with best technical conditions and therefore better durability. The roof tile chosen is a pressed clay spanish tile, nailed on a framework composed by three levels of battens. The valleys are resolved with copper plate 0.6 mm thick (Fig 6).

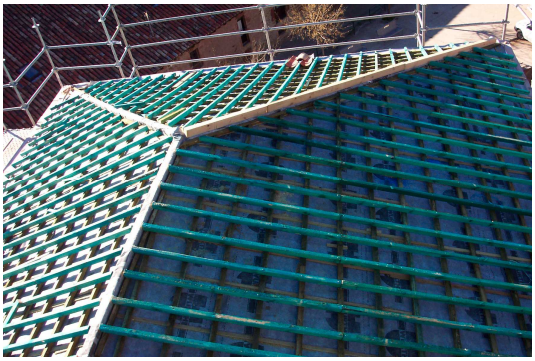

Figure 5. View of the framework composed by three levels of battens to nail the roof tiles.



Figure 6. Final state of the nave´s roof, with copper valleys and life-line to easy maintenance.

5 TESTS. BACKGROUND

We choose two specimens of roof tiles from the church. The roof tiles that we have chosen are one of the hand-made old roof tile which remained in the restoration of the year 1992, and another new one used in 2005. Then we carry out the following tests:

- Determination of the cereamic roof tiles permeability according to UNE EN 539-1/2007 (clay tile for discontinuous laying. Determination of physical characteristics. Part 1: Permeability Test)
- Determination of frost resistance of clay tile UNE EN 539-2/2007 (clay tile for discontinuous laying. Determination of physical characteristics. Part 2: Frost resistance Test)

6 PERMEABILITY TEST

6.1 Specimen Preparation

The pieces have been subjected to preliminary processing before being tested, as the reference standard. They were submerged in tap water at room temperature for 48 ± 8 hours. Subsequently they have been dried at 110 ± 5 ° C, until the difference between two weighings is less than 0.5% of the previous reading, at an interval of 24 hours. Finally we allowed them to cool at room temperature for 4 hours.

6.2 Test Execution and Results

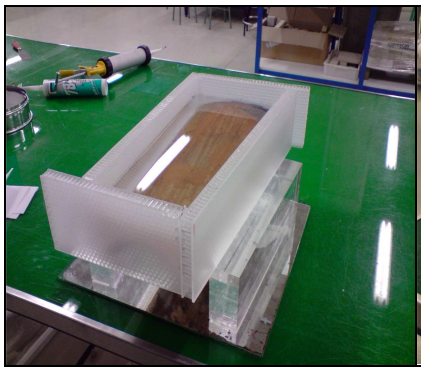

Figure 7. Old roof tile in permeability tester.

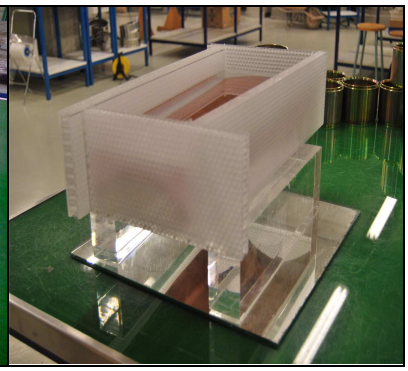

Figure 8. New roof tile in permeability tester.

We carried out the method 2 of the standard to execute the test (Figs. 7 and 8). We determined the time to fall the first drop of water, after applying water on its surface usually into the air. After 20 hours we considered completed the test, obteining the following results [Table 1]:

Table 1. Permeability results of the roof tiles

	Elapsed time for first drop (hours)	*Permeability coefficient (ICi)*	*Permeability classification (according to UNE 1304)*
Old roof tile	7 Hours	0,5	CATEGORY 1
New roof tile	After 20 hours no drop falls	0	CATEGORY 1

6.3 Comments

6.3.1 Calculation of permeability coefficient

$$ICXi = \frac{20 - Xi}{20} \qquad ICX = \frac{20 - X}{20}$$

where Xi is the elapsed time in hours aproximated to 0.25 h, until the fall of the first water drop in a piece of the sample. X is the average time in hours aproximated to 0.25 h, until the fall of the first water drop in the whole of the sample.

6.3.2 Classification criteria according to UNE-EN 1304/2006

Category 1: The average permeability coefficient of the specimens after the test must be less than or equal to 0.8, and all the individual results should be less than or equal to 0.85.

7 FROST RESISTANCE TEST

7.1 Specimen Preparation

We only check it the old roof tile with this test, because the new roof tile, model languedocienne manufactured by Terreal, had certified its resistance to frost, according to french rules NF EN 1304.

Before being tested the piece is divided, by cutting disk, in 6 samples and subjected them to preliminary treatment, as the reference standard (Figs. 9 and 10).



Figure 9. Roof tile before the test. We can see the cut marks to get the 6 specimens tested.



Figure 10. Roof tile before the test . Interior view.

We examined the samples indicating the existing defects, then they are dried at 110 ± 5 º C, until the difference between two weighings is less than 0.5% of the previous reading, at an interval of 24 hours. Then we weigh them, after cooling the air, scoring their initial dry mass. Subsequently they have to be saturated by gradual immersion in tap water at room temperature. They must remain in the water container for 24 hours.

7.2 Test Execution and Results

We have followed the alternative test method C, according to norm in point 7.5.3 for the assay. Is performed by freeze / thaw using a freezer at -15 degrees C and a refrigerator at 12 º C. Water-saturated specimens are introduced in the freezer at least for 3 hours, bagged in plastic to prevent water evaporation during freezing. Subsequently the specimens are introduced into a container of water, remaining in the refrigerator at 12 º C. There are two daily cycles, remaining specimens in water between cycles. The test ends when 50 cycles are performed.

Once all cycles are performed, the specimens are air dried for 24 hours in an oven at 110 ± 5 º C for another 24 hours. Then the specimens were allowed to cool in air. They were brushed lightly to remove the damaged parts and they dried to constant mass. We take its final dry weight M ' (Figs. 11 and 12).

We calculate the mass loss due to damage to each specimen:

$$(M\text{-}M´) \times 100/M$$

where M is the initial dry mass and M' is the final dry mass, once the cycles are completed. The results are as follows [table 2]:

Table 2. Permeability results of the roof tiles

Specimen	*M (g)*	*M´(g)*	*Mass loss (%)*
1	362,2	359,0	0,9
2	383,7	379,4	1,1
3	400,8	397,5	0,8
4	413,4	411,5	0,5
5	328,8	325,2	1,1
6	304,8	298,3	2,1



Figure 11. Specimens after the test. Exterior view.



Figure 12. Specimens after the test. Interior view.

As a result of the test we observed a chipping in the samples 2, 5 and 6. Samples 5 and 6 show stones of 14 mm in diameter, around which there has been much loss of material. No more changes are observed (Figs. 13 and 14).



Figure 13. Siliceous aggregate included in the roof tile.



Figure 14. We can see debris particulate of ceramic recycling.

7.3 Comments

The criteria for evaluation of the results obtained are given in paragraph 7.6 of the standard. The criteria are:
It is considered that the specimens subjected to freeze-thaw cycles have passed the test if none of the specimens shows some of the defects listed below:

- Delamination.
- Breakage.

- Loss of nerve (s).
- Structural crack.
- Exfoliation.
- Surface crack.
- None presents a mass loss greater than 1% of the original mass due to frost damage, particularly by chipping.

8 CONCLUSIONS

Regarding the roof tile, we can conclude that the old tile is close to the limit permitted to be considered frost damaged in terms of loss of mass. The cutting of the tile has facilitated the mass loss by increasing the exposed surface.

In the cutting process of the old roof tile we can see affected surfaces as well as the the presence of contaminants in the clay (siliceous aggregate and recycled ceramic particles) due to the traditional process used in its moulding, with a clay barely selected.

The behavior of the old roof tile is very different depending on its inner or outer face, because the exterior face has been treated properly. Their placement as a cover tile or pan tile may bear different pathological processes.

With all the above, we believe that the roof damages are due mainly to the choice of the laying system for the roof tile, employing a very poor mortar with too much sand, and replacing most of the old roof tiles, that had some resistance to frost, with low quality ones, that had not certified its resistance to frost.

ACKNOWLEDGMENTS

The authors would like to thank the Dirección General de Patrimonio [General Directorate of Heritage] of the Junta of Castile-Leon for its financial contribution towards the restoration of the Church of San Esteban and their involvement in the restoration and conservation of architectonic heritage.

REFERENCES

Palomero, F. & Ilardia, M. 1995, "*El arte románico burgalés, Un lenguaje medieval actual*", Lancia, Madrid.

Palomero, F. 2000 "*Rutas para descubrir el arte de la Sierra de la Demanda*", Ambito Ediciones, Valladolid.

Moreno, J. L. 1993 "*Burgos. La configuración física del espacio provincial*", in *Historia de Burgos, desde sus orígenes hasta nuestros días. Tomo 1. Desde los orígenes al año 1000*, Diario 16 de Burgos, Burgos.

Lafora, C. R. 1988 "*Por los caminos del románico porticado. Una fórmula arquitectónica para albergar el derecho a la libertad"*, Ediciones Encuentro, Madrid.

Archivo General Diócesis de Burgos, Libro de la Parroquia, (AGDBU, LP) Pineda de la Sierra, parroquia de San Esteban, L.F. (1620 – 1671), L-F. (1671 – 1694), L.F. (1695 – 1750), L.F. (1750 – 1825), L.F. (1883 – 1955).

XII DBMC
International Conference on Durability of Building Materials and Components
PORTO - PORTUGAL, April 12th-15th, 2011

Salt Crystallization Tests on Brick Masonry Reinforced by CFRP Textiles

Luigia Binda [1]
Cristina Tedeschi [2]
Maria Rosa Valluzzi [3]
Enrico Garbin [4]
Matteo Panizza [5]

ABSTRACT

Repair of historic masonry by Fiber Reinforced Polymers (FRP) systems is being more and more used especially in seismic areas. A rather great deal of experimental research on the mechanical behaviour of the repaired masonry has been carried out but very small experimental work has been done on the durability of FRP repairs when masonry is exposed to aggressive environments.

Carbon FRP (CFRP) have been applied on the surface of both soldier course and running bond specimens respectively as bonds in thin vaults and in solid walls. A total number of 20 specimens have been prepared and tested. A RILEM pre-standard procedure was followed for the evaluation of resistance to sulphates of the specimens. The damage evolution has been monitored by visual observation and by quantification of material loss in the vertical section at each 4 week cycle and the first results are here reported which show the importance of a carefulr application of FRPs.

KEYWORDS:

Brick masonry, FRP repair, durability to salt solutions

[1] Department of Structural Engineering, Politecnico di Milano, Milano, ITALY, tedeschi@stru.polimi.it
[2] Department of Structural Engineering, Politecnico di Milano, Milano, ITALY, binda@stru.polimi.it
[3] DAUR, University of Padova, ITALY, valluzzi@dic.unipd.it
[4] DCT, University of Padova, ITALY, garbin@dic.unipd.it
[5] DAUR, University of Padova, ITALY, panizza@dic.unipd.it

1 INTRODUCTION

FRP systems application to historic masonry repair is being more and more used in Italy, especially in seismic areas. FRPs are now preferred to other systems as r.c. and steel due to their light weight and adaptability to complicated shapes [Ajello, 2003]. Even if a rather great deal of experimental research on the mechanical behaviour of the repaired masonry has been carried out [Briccoli Bati, 2001], and a standard exists in Italy for their application [CNR DT 200, 2004] still some doubt remain on the impact of this technique on the authenticity of the historic buildings. Furthermore very small experimental work has been done on the durability of these repairs when exposed to aggressive environments (thermal cycles, high humidity, etc.).

It is well known that salt crystallization is one of the most frequent causes of surface damage of masonry in aggressive environments. Therefore once the repair by FRP is carried out the presence of salts should not reduce the lifetime of the masonry [Binda, 1985].

In order to check the durability of FRP systems applied to masonry structures to these phenomena, salt crystallization tests on brick masonry assemblages have been performed [Cardani, 2001].

Carbon FRP have been applied on the surface of both soldier course and running bond specimens respectively as bonds in thin vaults and in solid walls. Considering two tests for each condition plus a reference non strengthened specimen, four different strengthening patterns for each of the two textures have been chosen. A total number of 20 specimens have been prepared and tested.

A RILEM 127MS [RILEM MS-A1, 1998] pre-standard procedure is followed for the evaluation of resistance to sulphates of tested materials. The wallettes were submitted to the salt crystallisation test by immerging them in a sodium sulphate solution and exposing one surface to 20°C and 50% relative humidity (R.H.) in a climatic chamber, then adding water every 4 weeks, in order to create a sort of cycle.

Damage evolution has been monitored by visual observation and by quantification at each 4 week cycle, of material loss by a profilometer. The results show the rising of salt from the uncovered surface since the first week of observation, and also perhaps a concentration of stresses underneath the fibres. Thermographic images of the bonded strips were taken before the test and after 8 cycles in order to compare the eventual evolution of the bond. The specimens have now reached the 8th cycles and the tests will continue for other four cycles. Eventually pull off tests will be carried out on the surviving specimens at the end of the tests. The results obtained after the first 8 cycles are reported in the following with some critical remarks.

2 EXPERIMENTAL

The experimental program aimed at investigating the durability of masonry repaired by FRP to salt crystallisation was proposed within the RILEM TC 243 MSC. and within a the European Contract NIKER (FP7-ENV-2009.1-N.244123).

FRP strips were applied on masonry elements (small assemblages with mortar joints) and tested in the presence of a sodium sulphate solution. The test is simulating an aggressive environment in which salts can arrive into the masonry by capillary rise.

The experimental campaign included the following tests:

1. Crystallisation tests on masonry assemblages
2. Damage measurement with a laser profilometer
3. Bond investigation by a non destructive technique (thermography) which allows to check the connection between the FRP and the substrate.
4. Pull-off tests will be eventually carried out after the end of the cycles on the surviving specimens.

2.1 Test Description and Aims

The aim of the research was the analysis of damage induced by salt crystallisation to the support and to the bond between CFRPs and the masonry in order to predict the effectiveness of the bond adhesion in time, as well as in "real" environmental conditions. Some hypotheses had to be checked: (i)the presence of the stiff and waterproof strips could induce higher damages into the surrounding masonry, (ii) crypto-efflorescence could be formed underneath the strips and bring to the delamination of the strip itself.

2.1.1 Materials choice and preparation of the specimens

Solid units are 56x122x255 mm soft mud facing bricks were provided by Sant'Anselmo (Padova), having a mass of 1400 kg/m^3 and a water absorption of 26% [UNI EN 771-1]. Laboratory tests performed at the University of Padua allowed estimating a mean strength of 16.51 MPa in compression, 4.75 MPa in flexure, 3.39 MPa in splitting tension and 1.27 MPa after direct pull-off. The mortar is a premixed product based on natural hydraulic lime provided by Tassullo (Trento), having (after 28 days) a declared compression and a flexural strength of 3.7 and 1.3 MPa respectively, and Elastic Modulus of 6130 MPa.

Mercury porosimetry tests have been carried out on brick and joint samples. The results are the following: a) total porosity 48 - 28% respectively for brick and mortar, b) median pore radium 0.6822 - 0.3476 μm respectively for bricks and mortar.

Finally, textile MBrace Carbon C5-3 has been applied with Wet Lay Up system, as provided by BASF Italia (Treviso). Carbon fibers are unidirectional and have high modulus (390000 MPa), a tensile strength of 3000 MPa, an ultimate strain of 0.8% and a coefficient of thermal dilation of 10^{-7} K^{-1}. Bicomponent epoxy resins used at the interface compose both the primer and the saturant. Porperties declared by the provider are as follows (obtained after 7 days of curing, at T=20°C and RH=90%). The primer has a compression and tensile strength >40 and >20 MPa, respectively, whereas Elastic Modulus on the same stress conditions are 1900 and 1200 MPa, respectively. The saturant has a corresponding values of >80 and >25 MPa for compression and tensile strength, and 3100 and 3300 MPa for the Elastic Modulus.

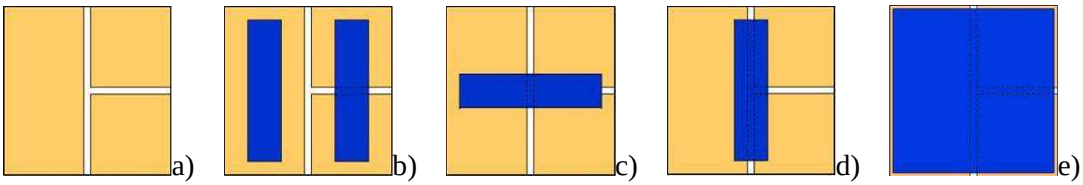

Figure 1. Soldier course specimens for crystallisation tests:a) S1; S1a, plain sample (only brickwork); b) S2,S2a, configuration 1, c) S3,S3a; configuration 2, d) S4, S4a; configuration 3, 4) S5, S5a, configuration 4, FRP covering the whole surface of the specimen.

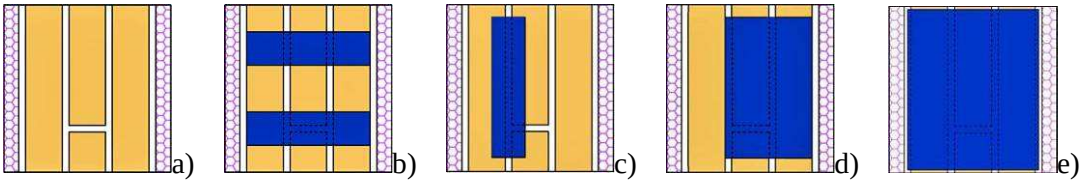

Figure 2. Running bond specimens for crystallisation tests:a) T1; T1a, plain sample, (only brickwork); b) T2,T2a, configuration 1, c) T3,T3a; configuration 2, d) T4, T4a; configuration 3, 4) T5, T5a, configuration 4, FRP covering the whole surface of the specimen.

Two series of specimens have been subjected to the crystallisation tests. Pilot unstrengthened specimens have been considered too, as reference condition. The specimens simulated different bond configuration, as showed in Figure 1 and 2. The specimens were small assemblages simulating diffused masonry textures as:

a) soldier course specimens, with courses of bricks laid with the long sides upright (as in thin vaults),
b) running bond specimens simulating common textures of masonry walls .
For each type of specimens the strips were applied according to four configurations (Fig. 1 and 2). The specimens were called S in the case of soldier course, and T in the case of running bond. For each configuration two specimens a,b were tested.

2.2 Test Procedure

The test was carried out according to the Recommendation RILEM MS A.1 [RILEM MS A1, 1998]. The wallettes (approx. 250x200x120 mm), were put in contact with their bottom side with a 10% (w%) Na_2SO_4 solution (anhydrous Na_2SO_4 reagent grade, Fluka)(Fig. 3a) and then stored over a layer of dry gravel in a plastic container (Fig 3b) open at the top, sealed along the borders (Fig.3c) with the upper face exposed to the environment (controlled laboratory environment of 20°C and 50% R.H.).

After four weeks the first crystallization "cycle" or step was concluded.The wallettes were subjected to a) visual inspection, b) photographic survey, c) cleaning from efflorescence and detached materials with a soft brush and a vacuum cleaner, d) photographic survey, e) description of the observed damage, f) reading of the surface profiles by means of a laser profilometer which allowed to quantify the damage, d) thermographic tests before crystallisation and after 7 cycles. De-mineralised water was then added and a new 4-weeks cycles began.

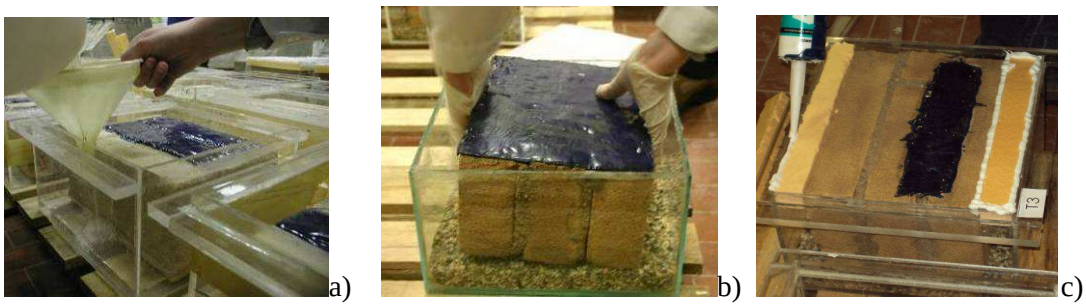
a) b) c)

Figure 3. Details of the test: a) salt solution addition b) positioning of the specimen on sand, c)sealing of the box,

2.3 Damage Measurement by Laser Profilometer

A laser profilometer was used to monitor the damage (Fig. 4a) [Cardani, 2002]. The use of the laser profilometer allows to measure, with a very good resolution, the loss of material from the exposed surface, calculated at subsequent times.

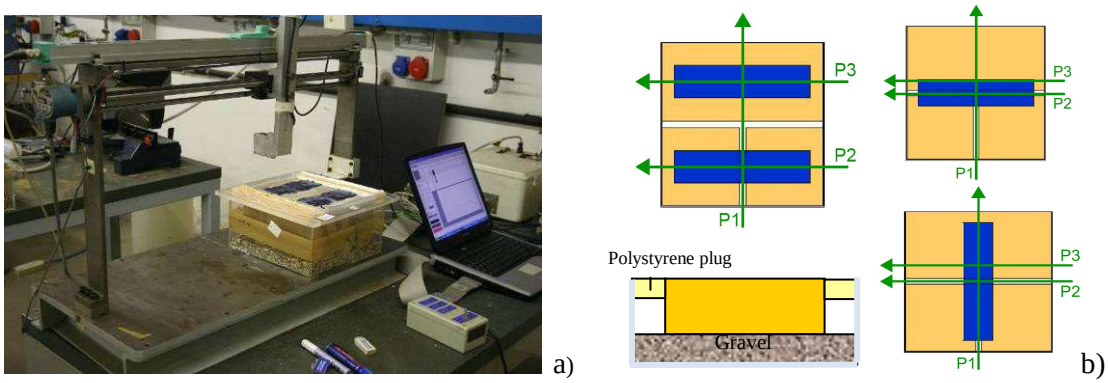

a) b)

Figure 4. Damage measuring device: a) lasers profilometer, b) scheme of the measurement.

Profiles recorded at the end of each 4-weeks cycle show how the surface is changing during time due to the progress of the decay and the loss of material can be measured by calculating the area loss% between profiles after each cycle [Cardani, 2002].

3 RESULTS AND DISCUSSION

As said above the damage was checked at every four weeks the wallettes were subjected to i) visual inspection and photographic survey, ii) reading of the surface profiles by means of a laser profilometer which allowed to quantify the damage.Subsequrntly the area loss % at each cycle were calculated and the results were copmpared with the blank specimens ones. Furthermore IR thermographic tests were carried out before crystallisation and after 7 cycles in order to detect in a non destructive way possible detachment of the FRP strips after the crystallisation tests.These results were checked by cutting specimen S5. Due to lack of space only the results obtained for the soldier course specimens will be presented and discussed in this work.

3.1 Visual Inspection and Description of Damage

Visual inspection and photographic survey were carried out on each specimen at every four week cycle and pictures were taken before and after brushing the damaged specimen. Due to lack of space here the pictures taken after 7 cycles of the blank specimen and of specimen in configuration 1, S2a are presented in Figure 5 a),b),c),d).

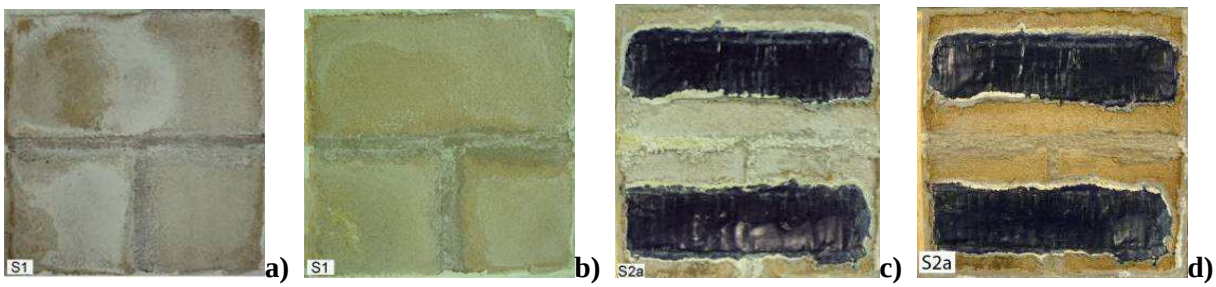

Figure 5. a), b) blank specimen S1 before and after brushing; c), d) specimen S2a before and after brushing.

Some general comments can be made at the end of the 7th cycle. The blank specimens and the repaired ones behaved in different ways even if the types of damage were similar. In Fig.5a),b) the specimen $S_1$is presented before and after brushing. The specimen was covered with salt encrustations on top of the bricks and of the mortar joints. After brushing some delamination of the brick surface was visible. In Fig.5c) and d), the specimen S_2a before and after brushing is presented. Also this specimen was covered of salt encrustations. Outside the FRP strips, the materials were highly humid and apparently a deeper damage was intersting the bricks. Even after brushing salt accumulation around the strips was evident, with some signs of detachment of the trips at the borders.

3.2 Profile Measurements

The profiles measured by the profilometer at cycles 2,3,5,6 and 7 are reported in Figure 6, for the specimens S1 and S2a for profiles P1 In the diagrams, apparent increase in vertical coordinate correspond to bulging of the surface at the starting of delamination and spalling.

The damage by the salt crystallisation is due to the fatigue caused to the material by the repeated cycles This measurement is possible because the decay due to salt crystallisation in these porous materials is proceeding from the external surface inward [Cardani, 2001]. The decay mechanisms induced by the salts crystallising into the pores are influenced not only by the porosity characteristics, but also by the pore distribution which varies from material to material. Furthermore; in these cases it seems that a different damage is induced by the presence of FRP which are partially covering the specimen upper surface.

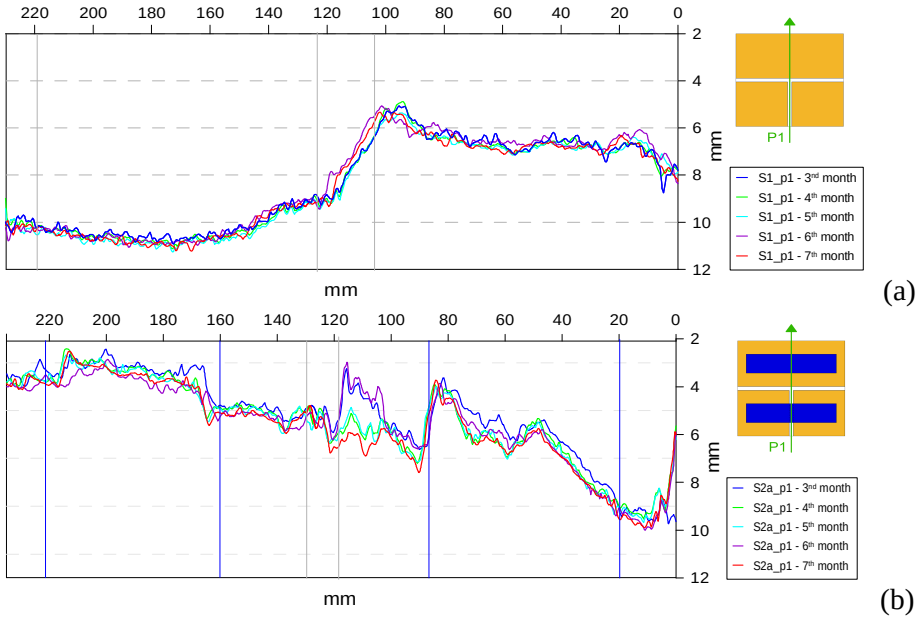

Figure 6. Diagrams of the profiles for specimens S1 (a), and S2a (b) measured at cycles 3, 4, 5, 6 and 7

3.3 Damage Progression under the Crystallisation Cycles

Each profile represents the border of the vertical section of the specimen. The difference between two subsequent profiles at each cycle can be considered as material loss (or apparent increment in the case of bulging) and the calculated area as % of the specimen vertical section can be assumed as damage parameter (loss (%)) and even be used for the implementation of deterministic or probabilistic mathematical models to predict the material behaviour under salt crystallisation damage [Binda et al. 1985].
In Figure 7a the damage diagrams (area lost at each measurement in mm^2) are given. The values were obtained by elaborating the data read by the profilometer for the brick-mortar profile and for the mortar joint. Cleaning of the temporary bulging due to detaching of layers was also carried out The curves show that the specimen MA was the most damaged.

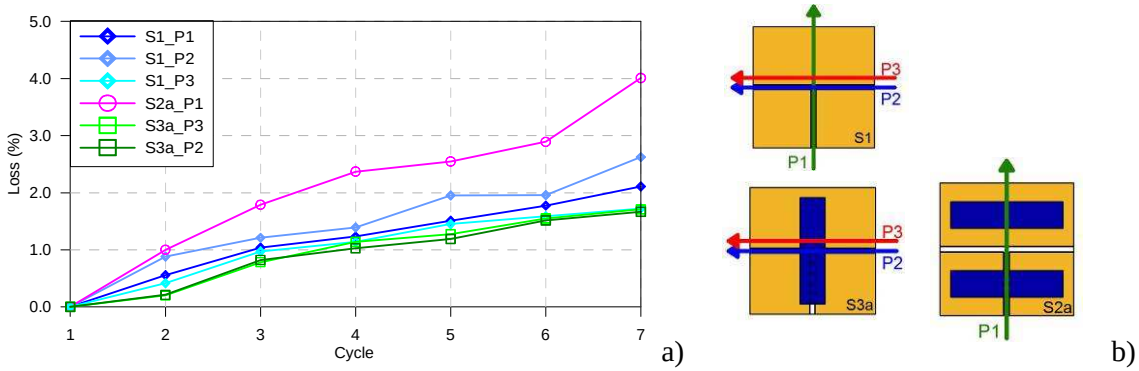

Figure 7. a) Area loss % against number of cycles for some of the obtained profiles, b) specimens and profiles.

3.4 IR Thermography Application

IR Thermography reveals the infrared radiations emitted from a heated surface of an object in a certain time. As a result, a thermal image of the object is obtained, by a color scale or a gray scale. Working in the infrared radiations range, this technique is able to detect the energy emitted by any material in the form of electromagnetic radiations. This property of the materials is strictly connected to their thermal conductivity and their heating capacity: the first parameter determines the capability of a material to transmit heath, while the second one defines the attitude of a material to hold heath.

The thermographic test is based on the acquisition of thermal images by an infrared camera: observing with this device the temporal changes of the surface temperature distribution, near surface characteristics of the material can be detected. To obtain measurable temperature differences on the surface of the observed element, a previous heating of the material is necessary. It can be done by solar radiation (passive method) or using heating systems (active method). Recording images during the cooling down phase, when the solar radiation is no more present or after removing the heating source, the results are detectable. Differences in the distribution of the temperature on an area that has been previously heated in uniform way can be connected with significant information concerning the composition and the presence of defects in the structures of traditional buildings.

All the specimens were submitted to IR thermography before and after testing and the images were restituted by an infrared camera Nec-AVIO TVS 500E model equipped with a photographic camera, based on a detector formed by a matrix 320 (H) x 240 (V), Vanadium Oxide microbolometer type. The spectral field of this device is 8 – 14 μm.

The first thermography was carried out on specimens dried into the oven at constant mass and gives a rather uniform deistribution of temperatures. It is possible to to see that some bond original defects were present before the tests on S3a and S5a in coincidence with the joints.The second one was madeafter 7 cycles; the specimens were heated with a IR lamp. Of course they were wet due to the presence of sodim sulphate. So a direct comparison was not possible. Nevertheless Figure 8 shows the presence of humidity at the external perimeter of the FRP strips and it can be hypothised that detachments are taking place around (Fig.8a,b,c) and even under the FRP (Fig.8 d)

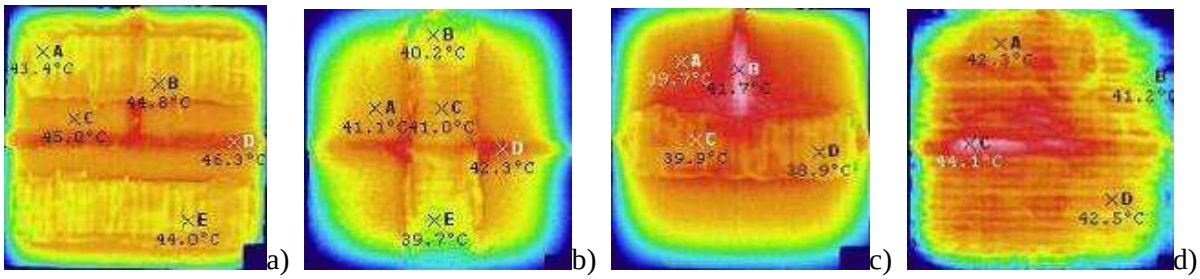

Figure 8. Thermographic restitution of S2a, S3a, S4a, S5a upper face, dried in oven before the cycles

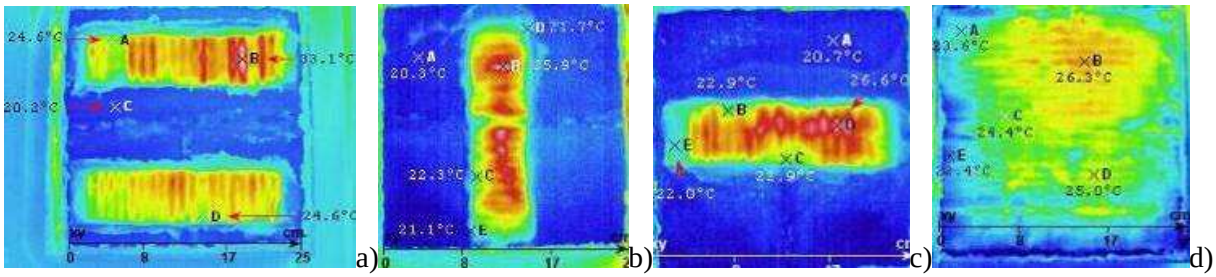

Figure 9. Thermographic restitution of S2a, S3a, S4a, S5a upper face after 7 cycles

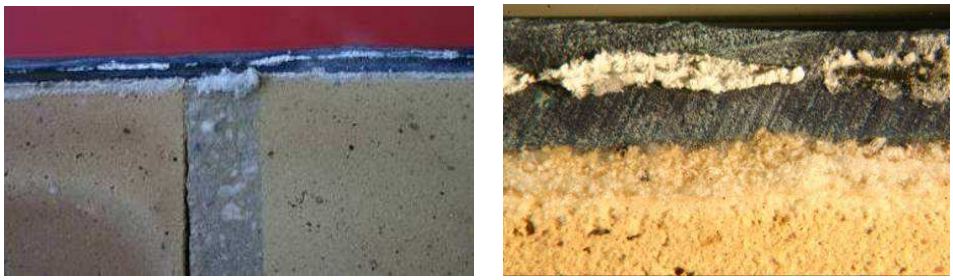

Figure 10. A vertical section of the specimen upper surfaces. Subefflorecence at the depth of penetration of the primal into the brick and within the FRP strip

Specimen S5a was cut in order to check the results of thermography (Fig.9) It is possible to see that the salts crystaòllise underneath the external surface causing a double damage: a) at the penetration depth of the primal and b) within the FRP itself with its delamination and detachment from the masonry specimen.

4 CONCLUSIONS

Masonry specimens repaired with CFRP strips were subjected to sodium sulphate crystallisation tests according to a RILEM Recommendation. After seven steps (cycles) of the test lasting each four weeks the effect of the salts damage were surveyed and measured by the use of a laser profilometer. The damages caused by the salts on the bond between FRPs and the masonry and under the FRPs were also detected by using IR thermography as NDT. Some comments can be drawn even if the tests will still continue:

- The damage caused by the salts seem to be higher on the masonry when repaired with this technique than on the blank specimens, due to higher accumulation of humidity and salts around the strips and withing them.
- The salts crystallise as cryptoflorescence underneath the depth of penetration of the primal and within the strip itself causing delamination and detachment of the strip.
- Further tests are needed in order to check whether the type of application of the strip can influence the results.

ACKNOWLEDGMENTS

The experimental work is included in the activities of the Rilem 223MSC TC "Masonry Strenghtening with Composite Materials" www.rilem.net and is also supported by the EC Contract NIKER (FP7). Authors wish to thank Basf (Treviso) for supporting composite materials, S.Anselmo Laterizi (Padova) and Tassullo (Trento) for providing bricks and mortar, respectively; M. Beggiato, A. B. Silva, S. Perego, M. Taccia, M. Cucchi e M. Iscandri, are kindly aknowledged for their contribution in the laboratory phases and analyses.

REFERENCES

Aiello, M.A., Sciolti, M.S., Pecce, M. 2003, 'Experimental investigation on bond between FRP sheets and natural masonry blocks', *10th Int. Conf. SF&R-2003*, London, UK.

Basilio, I., Oliveira, D., Lourenço, P. 2005, 'Experimental Characterization of FRP Masonry interface Behaviour', *5th Int. Conf. on Analytical Models and New Concepts in Concrete and Masonry Structures AMCM-2005*, Gliwice-Ustron, Poland.

Briccoli Bati, S., Rovero, L. 2001, 'Experimental validation of a proposed numerical model for the FRP consolidation of masonry arches', *3rd Int. Conf. Structural Analysis of historical construction - SAHC 2001*, Guimaraes, Portugal.

CNR DT200 2004, *Guide for the design and construction of an externally bonded FRP system for strengthening existing structures*, Italian National Research Council CNR, Rome, Italy.

RILEM MS-A1, Determination of the resistance of wallettes against sulphates and chlorides, 1998.

Panizza M., Garbin E., Valluzzi M. R., Modena C. 2009, 'Experimental study of the FRP-clay interface subject to normal stresses', Proc. MuriCo3, 22-24 April 2009 Venice, Italy.

Valluzzi, M.R. 2008, 'Strengthening of masonry structures with Fibre Reinforced Plastics: from modern conception to historical building preservation', *Structural Analysis of Historic Construction – SAHC08*, Bath, UK, vol. 1, p. 33–45.

UNI EN 771-1 Specification for masonry units - Part 1: Clay masonry units, 2005

Binda L, Charola A E, Baronio G 1985 'Deterioration of porous materials due to salt crystallization under different thermohygrometric conditions', *5th Int. Conf. on Deterioration and Conservation of Stone*, Losanna, 279-288, 1985.

Cardani G, Tedeschi C, Binda L, Baronio G., 2001 'Laboratory Crystallisation Tests for Damage Evaluation' *Maintenance of Pointing in Historic Building: Decay and Replacement*, N. Contract EV-CT98-0706, Final Report to EC.

Cardani G., Tedeschi, C., Binda L., Baronio G., 2002, Crystallisation Test on Treated Brick/Stone Masonry Specimens for Damage Evaluation, *Int. Conf. 9th Durability of Building Materials*, 17-20/03/2002, Brisbane, (Australia), CD-ROM, paper 039, 2002.

XII DBMC
International Conference on Durability of Building Materials and Components
PORTO - PORTUGAL, April 12th-15th, 2011

Moisture and Temperature Influence on FRP Masonry Bonding

Maria Rosa Valluzzi [1]
Enrico Garbin [2]
Matteo Panizza [3]
Luigia Binda [4]
Cristina Tedeschi [5]

ABSTRACT

Durability and bonding of FRP system on masonry is crucial, especially for possible application in historical context, where moisture in the support can influence the application phases, and thermal cycles occurring in the environment can cause de-bonding.

Durability tests as humidity variation and thermal cycles were programmed. The pull-off test was chosen as reference test in order to check the loss of bond. Solid brick samples, and small assemblages including mortar joints have been strengthened with CFRP strips in three different configurations. The bond was firstly checked on reference unreiforced specimens. Two types of damage were studied: the effects of three different humidity conditions of the support, and of ageing due to thermal cycles. Both the phenomena can happen in nature.

As for thermal ageing tests, in a preliminary set of specimens, subjected to a temperature variation ranging between -10°C and +70°C, applied without stopping for 40 cycles, it was not possible to perform pull-off tests since most of the strips lost their bond. Then, for a second series of specimens, their conditions were controlled at low number of cycles, so that it was possible to identify the debonding cycle and to perform some pull-off tests. Although these tests are still in progress, some significant preliminary results are commented in the paper.

KEYWORDS

Brick masonry, durability, FRP repair, humidity, temperature variation.

[1] DAUR, University of Padova, ITALY, valluzzi@dic.unipd.it
[2] DCT, University of Padova, ITALY, garbin@dic.unipd.it
[3] DAUR, University of Padova, ITALY, panizza@dic.unipd.it
[4] DIS, Politecnico di Milano, ITALY, binda@stru.polimi.it
[5] DIS, Politecnico di Milano, ITALY, tedeschi@stru.polimi.it

1 INTRODUCTION

Effectivenes of composite materials as FRP (Fiber Reinforced Polymer) used in architectual and engineering works is strongly dependent on bond at the interface with the support [De Lorenzis *et al.* 2001] [Aiello *et al.* 2003] [Basilio *et al.* 2005] [Valluzzi 2008]. Nevertheless, the characterization of bond itself, especially for masonry structures, is still problematic, due to lacking in standardization [CNR DT200 2004] [ACI 440M 2004], both on experimental procedures and definition of parameters essential for analyses. At current, a simple method used for a preliminary assessment of bond between support and FRP textiles is the pull-off test [ASTM C1583 2004]. It allows evaluating the strength at the interface for loads perpendicular to the layer of application, as well as the failure mode (in the weakest cases involving the interface layer or even the fibers) [Panizza *et al.* 2009]. If compared with the whole aspects of the bond phenomenon, only limited information can be provided; nevertheless, this method is easily applied onsite too, and therefore taken in this study as reference for the evaluation of the preliminary strength in reinforced conditions.

On the other hand, the intervention effectiveness can be easily affected by the environment, as humidity and thermal cycles. Moisture in the support can influence the application phases, as well as low and high temperatures deteriorate the materials and their interaction [Binda *et al*, 1993] [Briccoli Bati & Rotunno 2001] [Camata *et al.* 2007]. Nevertheless, in this context, standards or reccomendations on procedures applicable on building materials, especially concerning masonry, are not available yet, therefore further studies are still in need.

A research program on the effect of humidity and of thermal cycles on the delamination of the FRP strips from the masonry support was started and it is still ongoing, based on laboratory tests carried out on bricks (basically a porous, soft mud type) and masonry specimens strengthened by FRP. For the humidity in the support before fibers application, three moisture conditions have been considered: (i) environmental, (ii) saturated, (iii) intermediate state. Results showed the reduction of bonding for increasing humidity rates, as well as the rupture at the interface of FRP-masonry.

For the thermal cycles, both on bricks and on masonry specimens, a program described in the following was applied. A first test was carried out submitting the masonry specimens to 40 cycles; the temperature ranged between -10°C and +70°C, taking into account that to check durability the most significant values can be the peaks in a façade exposed to the sun (easily reaching, during summer, up to 60-70°C in some regions), rather than the maximum and minimum temperatures of the environment. At the end of this first series, debonding was taking place in all the specimens. Therefore, it was decided to control the specimens every two or three cycles, in order to follow step by step their behaviour, and define at which cycle debonding appears. The test was then repeated using also a different type of brick (extruded instead of soft mud).

The first results are reported in the following Sections; the study is anyway still continuing on further masonry specimens. This research is performed in the ambit of a comprehensive experimental work aimed at checking the durability of FRP systems applied on masonry structures, promoted by the Rilem 223-MSC TC, and is included also within the EU Contract NIKER.

2 LABORATORY TESTING

2.1 Experimental Program

Two series of specimens (both single brick and small masonry assemblages) have been subjected to: (a) different moisture content before fibers application, and (b) to thermal cycles after strengthening. Pilot unstrengthened samples have been considered too, as reference condition. The influence of mortar joints has been also investigated, both on soldier course and running bond configuration, as showed in Fig. 1. They simulate thin components (as vaults) and more solid walls, respectively. Pull-off area is about 5 cm on diameter, including the mortar joint in the masonry specimens (Fig. 2).

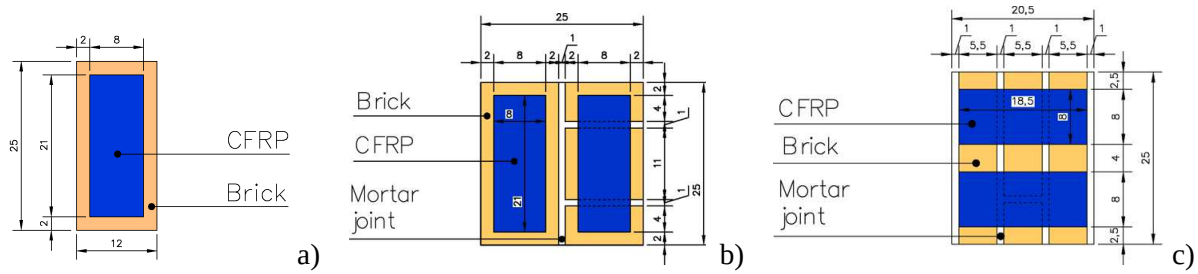

Figure 1. Specimens for absorption-adhesion tests and thermal ageing tests: a) single brick, b) soldier course specimen, c) running bond specimen.

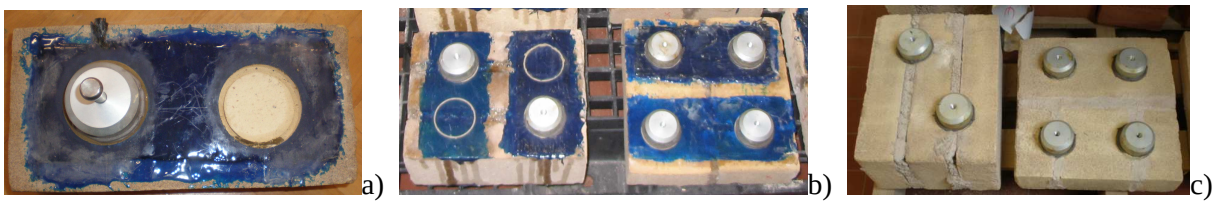

Figure 2. Positioning of pull-off area on samples: a) single brick, b) soldier course and running bond reinforced masonry, c) pilot unreinforced masonry. Cut pull-off area, as well as glued metal element to be pulled during test are visible.

For the effect of humidity in the support before fibers application, three moisture conditions have been considered: (i) environment (20°C and 50% RH, about 5-6% of water content for the chosen bricks, (ii) in saturated conditions (about 24% of water content), (iii) in intermediate degree of water absorption between saturation and environment condition (about 14% of water content), for a total of 12 pull-off tests on 6 single bricks specimens, 56 pull-off tests on 8 soldier course small assemblage specimens and 56 pull-off tests on 8 running course ones. In the paper the result of 48 pull-off tests on 6 soldier course small assemblages reinforced with CFRP sheets are presented. Similar results are obtained for brick and running course assemblage specimens, which are currently under elaboration.

Thermal ageing tests are still in progress and foreseen a range of temperature between -10°C and +70°C, applied ciclically with a gradient of 0.8 or 1.0°C/min (see specification in the following), on samples realized with the same three strengthening patterns. Then pull-off tests can be performed at laboratory environmental conditions.

2.2 Material Properties

Solid units are 56x122x255 mm soft mud bricks, having a mass of 1400 kg/m^3 and a water absorption of 26% [UNI EN 771-1]. This brick simulates the properties of a unit in a “historic” masonry. Laboratory tests performed at the University of Padova allowed estimating a mean strength of 16.51 MPa in compression, 4.75 MPa in flexure, 3.39 MPa in splitting tension and 1.50 MPa after direct pull-off. A second type of brick (54x118x245 mm) was also considered, but only for the thermal cycles; it is a extruded brick, thus having properties of a “modern” material. The mass is 1710 kg/m^3 (from datasheet), whereas laboratory tests estimated a mean strength of 43.03 MPa in compression, 6.40 MPa in flexure, 4.94 MPa in splitting tension and 3.11 MPa for pull-off. In the absence of direct measurements, this last value for pull-off strength was derived from elaboration of several tests performed at University of Padova and compared with the compressive strength of bricks, as explained in [Panizza *et al.* 2010].

The mortar is a premixed product based on natural hydraulic lime, having a compression and a flexural strength (after 28 days) of 3.7 and 1.3 MPa respectively, and Elastic Modulus of 6130 MPa (all values are from datasheet).

Textile MBrace Carbon C5-30 has been applied with Wet Lay Up system. Carbon fibers are unidiretional and have high modulus (390000 MPa), a tensile strength of 3000 MPa, an ultimate strain of 0.8% and a coefficient of thermal dilation of 10^{-7} K^{-1}. Bicomponent epoxy resins used at the interface compose both the primer and the saturant. Porperties declared by the provider are as follows (obtained after 7 days of curing, at T=20°C and RH=90%). The primer has a compression and tensile strength >40 and >20 MPa, respectively, whereas Elastic Modulus on the same stress conditions are 1900 and 1200 MPa, respectively. The saturant has a corresponding values of >80 and >25 MPa for compression and tensile strength, and 3100 and 3300 MPa for the Elastic Modulus. The thermal coefficient is 6.21 10^{-5} C^{-1} for the primer and 6.01 10^{-5} C^{-1} for the saturant, much higher than the one of the masonry, that should be around 5.0 10^{-6} °C.

Mercury porosimeter tests were carried out at Politecnico of Milano on the two types of bricks and on a mortar joint. The following results were found: the total porosity was 48.48%, 30.26% and 28.14%, whereas the median pore radius was 0.682, 0.205, 0.35μm, for soft mud, extruded brick and mortar, respectively. The mortar seems be more compact but it probably has lower permeability than bricks, as confirmed by the results discussed in the next Section.

3 INFLUENCE OF HUMIDITY ON BOND

Both imbibition phase and pull-off tests have been performed at the Experimental Laboratory of DCT, University of Padova. Following the ASTM C1583 the most tipical failure mode is type “A” (failure within the substrate), thus confirming the good adhesion of the reinforcement to the support. Failure type “B” involves the interface between reinforcement and support, thus revealing anomalies in bonding (Fig. 3). Finally, ruptures type “C” or “D” concern the fibers themselves or the interface between the pulling element and the reinforcement surface; they are ascribable to an improper impregnation of the fibres and gluing of metal elements, respectively. Consequently, ruptures type “C” or “D” are not considered in the data elaboration.

In the following, only results on soldier course specimens (Fig. 1.b) are presented. As shown in Fig. 4 (left), as expected, the higher is the content of water in the support, the lower is the pull-off strength: values of pull-off strength considering the whole masonry specimen (i.e. including both portions with and without mortar) are 1.43 MPa, 1.28 MPa and 1.19 MPa for environmental, intermediate and saturated conditions, respectively, showing a reduction of 16.8% moving from environment to saturated conditions. Highest values of pull-off strenght (1.49 MPa, 1.45 MPa and 1.35 MPa for the three humidity conditions, respectively) are registered when the support does not include mortar (only brick substrate, Fig. 4, centre), ranging from a decreasing of 2.6% and 9.4% in in the case of intermediate and satured conditions, respectively. On the contrary, a reduction of 21% was recorded moving from environmental to saturated conditions for brick & mortar substrate (values are 1.33 MPa, 1.13 MPa and 1.05 MPa for for the three humidity conditions, respectively; Fig. 4, centre). The trend has a decrising slow rate of about -0.52% per 1% of of water content for brick substrate and of about -1.26% per 1% of of water content for brick & mortar substrate, respectively (Fig. 4, centre and right).


a)
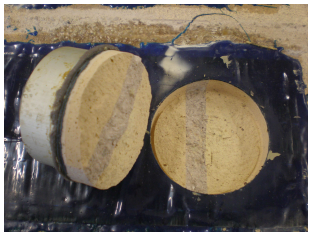
b)

c)

Figure 3. Rupture type “A” (substrate) at: (a) brick, and (b) brick-mortar position; rupture type “B” at bond interface (c).

Noteworthy, the occurrence of failure mode (Fig. 5), shows that when the support is interested by an increasing content of water, the rupture shifts from “A” (the strongest, within the substrate), to “B” (at

the interface between masonry and reinforcement). Therefore, bonding is reduced and the effectivenes the intervention is consequently compromised.

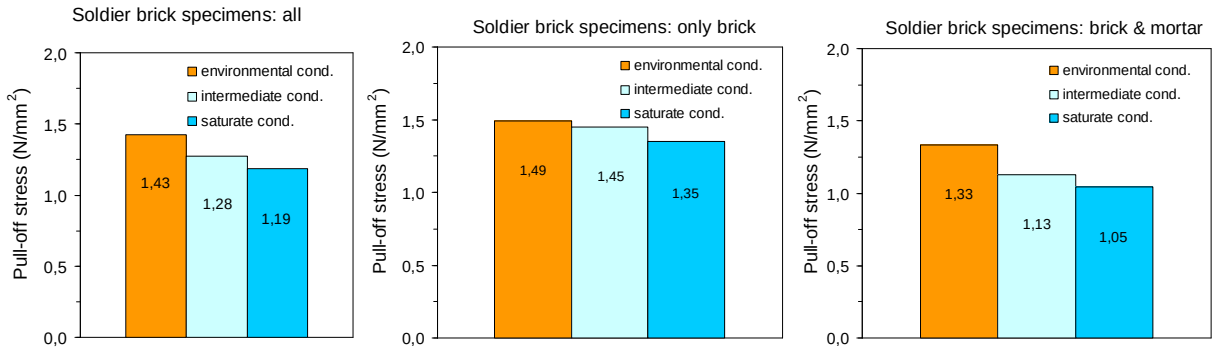

Figure 4. Pull-off strength on single brick and masonry assemblages in different humidity conditions.

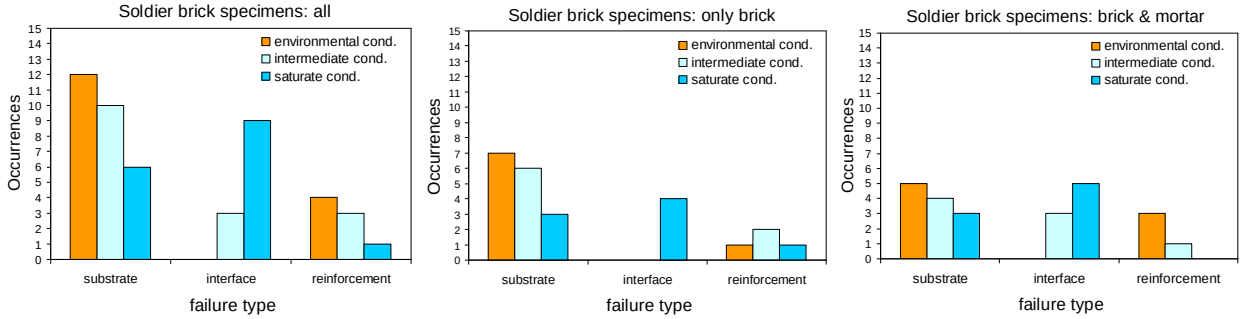

Figure 5. Occurrence of failure type due to pull-off tests in different humidity conditions.

4 BOND UNDER THERMAL CYCLES

In the absence of standardized method, both test program and procedure were proposed according to other previous experiences, basically thermal cycles carried out in the presence of epoxy resin injections [Binda *et al*, 1993], and taking into account that the temperatures measured on the surface of façades during summer can even reach 70°C.

The specimens have been prepared at University of Padova and tests have been performed at the Laboratory of DIS, Politecnico di Milano. Before applying the thermal cycles, the specimens should have a moisture lower of 12% and cured in control environment (20°C and 50% RH) for 24 hours.

The proposed artificial ageing shall be carried out as follows (at 60% RH):

a. +20 to +70°C in 1 h (0.8°C/min)
b. 3 hours at 70°C
c. +70°C to -10°C in 1:30 h (1.0°C/min)
d. 3 hours at -10°C
e. -10°C to +70°C in 1:30 h (1.0°C/min)

The initial idea was to repeat the procedure from (b.) with an automatic control for at least 40 cycles. In this phase one specimen for each type of configuration (single brick, soldier course, runnig bond) was considered. Soft mud bricks were used.

The results obtained at the end of the 40 cycles were rather shocking. All the three specimens had a deep delamination (Fig 6.a,b,c) and being the test authomatically carried out it was impossible to

detect when the delamination started. Furthermore, all the delamination occurred in the brick, at a certain depth in its thickness.

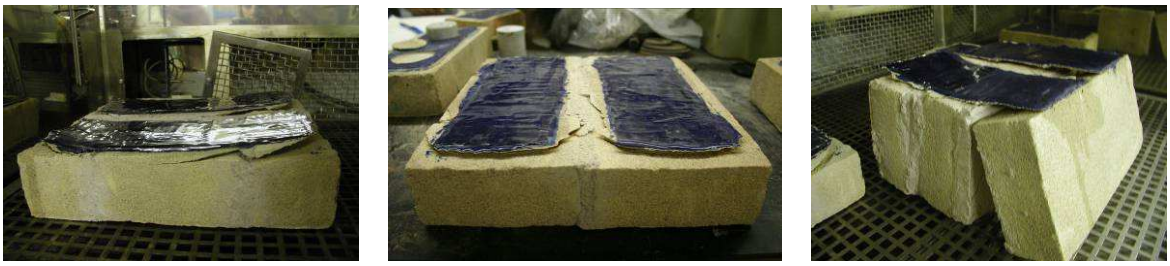

Figure 6. Damage observed in the three type of specimens after 40 thermal cycles.

The delaminated layer was cut and the section observed at the stereomicroscope. In Figure 7.a the different layers of FRP, as well as the zone in the brick impregnated by the primer and the resin are visible. There was a clear penetration of the primer into the brick (1-2 mm), as it is clear that the brick impregnated is more compact and probably stronger. On the contrary, the deeper part not impregnated remained porous and weak, where actually the delamination occurred. Figue 7.b shows the delaminated layer with a clear horizontal crack 1 or 2 cm under the fibers. The reason why this phenomenon happened is still unclear: it can be connected to the "fusion temperature" of the epoxy resin or to the differential deformation of the epoxy penetrated into the brick. Nevertheless, it is worth to remind that on a façade exposed to South or West in the Southern part of Italy the temperature can easily reach 70°C.

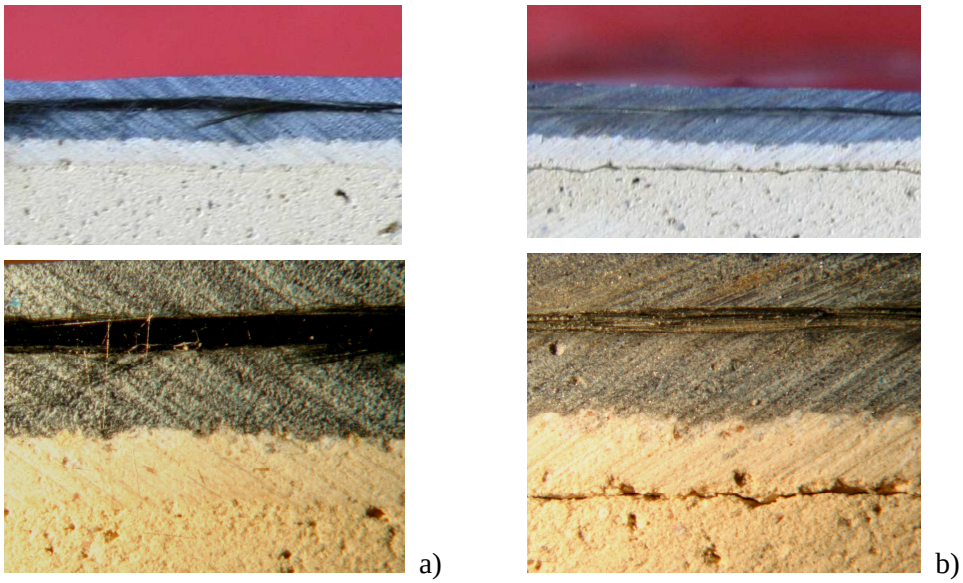

Figure 7. Analysis at stereomicroscope showing two types of rupture: a) presence of a border below the fiber at the limit of the impregnated layer; b) detachment of the border and failure in the brick.

It was then decided to repeat the experience on new specimens in order to stop every two cycles and check the possible debonding of the FRPs. Therefore, six single brick specimens were used (as in Fig.1.a), one belonging to the same type of bricks used for the masonry specimens (soft mud ones, chracterized by high porosity), the other five belonging to the extruded type, characterized by a low porosity (Fig. 8.a). The porous brick suffered delamination after only one cycle (Fig. 8.b), while the five extruded bricks did not have any delamination after all the 40 cycles.

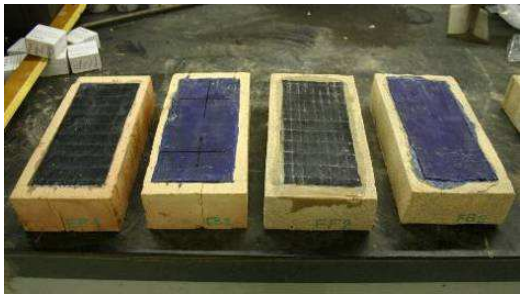
a)

b)

Figure 8. Additional series of specimens: a) general view, b) delamination on the porous brick.

Finally, on the delaminated brick and on the non damaged five ones, some preliminary pull-out tests after the thermal cycles were performed (at present limited only on the single brick samples) (Figure 9.a,b). Results showed a very low strength in the soft mud brick (0.21 MPa), and a high strength in the extruded ones (2.96 MPa as mean value). The failure always occurred in the brick. The values found for the soft mud brick show a clear reduction if compared to the initial strength (1.50 MPa, without considering the moisture influence), due to the damage already present, while the values found for the extruded bricks denote actually no damage (3.11 MPa as reference, by following the formulation detected on empirical basis as in Panizza *et al.* 2010).


a)

b)

Figure 9. Pull-off tests after thermal cycles: a) soft mud brick, b) extruded brick.

5 CONCLUSIONS

Thanks to a fruitful collaboration between the Politecnico of Milano and the University of Padova, a preliminary study on the effects of humidity and thermal cicles on bond, as the most critical aspect related to the effectiveness of application of FRPs on masonry, has been presented. At this stage, only pull-off tests have been performed.

Results showed the reduction of bond strenght for increasing humidity rates, as well as the rupture at the interface of FRP-masonry, rather than within the support. The presence of mortar also influence bonding negatively, both at intermediate and saturated conditions.

The experimental research under thermal cycles showed that some irreversible damage can occur due to the different behaviour of the resin connecting the FRP to the masonry, in case of weak highly porous bricks, as findable in the historical context. In case of less porous bricks the damage does not apparently occur.

It is clear that further investigation is needed on this topic. Anyway, it can be suggested at least to protect the masonry against high temperatures on its surface exposed to sun, e.g. by using proper rendering.

Further studies will be focussed on the use of different resins and different kind of bricks, to clarify the influence of physical and mechanical properties on the investigated phenomenon. In particular,

new tests on masonry specimens are now in progress, during which the damage will be checked at low number of temperature cycles, in order to clarify some aspects still under discussion.

ACKNOWLEDGMENTS

The experimental work is included in the activities of the Rilem 223MSC TC "Masonry Strenghtening with Composite Materials" www.rilem.net. Authors wish to thank Basf (Treviso) for supporting composite materials, S.Anselmo Laterizi (Padova) and Danesi Laterizi (Cremona) for providing bricks, and Tassullo (Trento) for the mortar. Matteo Beggiato, Ana Beatriz Silva, Sara Perego and Massimo Iscandri are kindly aknowledged for their contribution in the laboratory phases and analyses. Part of this work was also supported by NIKER EU Project.

REFERENCES

ACI 440M Guide Draft-1 2004, *Guide for the Design and Construction of Externally Bonded FRP System for Strengthening Unreinforced Masonry Structures*, ACI Committee 440, USA.

ASTM C1583 2004, *Standard Test Method for Tensile Strength of Concrete Surfaces and the Bond Strength or Tensile Strength of Concrete Repair and Overlay Materials by Direct Tension (Pull-off Method)*, American Society for Testing and Materials, USA.

Aiello, M.A., Sciolti, M.S., Pecce, M. 2003, 'Experimental investigation on bond between FRP sheets and natural masonry blocks', Proc. of SF&R-2003, London, UK.

Basilio, I., Oliveira, D., Lourenço, P. 2005, 'Experimental Characterization of FRP Masonry interface Behaviour', Proc. of the 5th Int. Conf. on Analytical Models and New Concepts in Concrete and Masonry Structures AMCM-2005, Gliwice-Ustron, Poland.

Binda, L., Baronio, G., Tiraboschi, C. 1993, 'Repair of brick-masonries by injection of grouts: experimental research', *Journal of Structural Engineering*, Madras, India, **20**[1], 29-44.

Briccoli Bati, S., & Rotunno, T. 2001, 'Environmental durability of the bond between the CFRP composite material and masonry structures', Proc. of SAHC 2001, Guimaraes, Portugal.

Camata, G., Pasquini, F., Spacone, E. 2007, 'High temperature flexural strengthening with externally bonded FRP reinforcement', Proc. of FRPCS-8, 16-18 July 2007, Patras, Greece.

CNR DT200 2004, *Guide for the design and construction of an externally bonded FRP system for strengthening existing structures*, Italian National Research Council CNR, Rome, Italy.

De Lorenzis, L., Miller, B., Nanni, A. 2001, 'Bond of FRP laminates to concrete', *ACI Materials Journal*, **98**[3], 256-264.

Panizza M., Garbin E., Valluzzi M. R., Modena C. 2009, 'Experimental study of the FRP-clay interface subject to normal stresses', Proc. of MuriCo3, 22-24 April 2009 Venice, Italy.

Panizza M., Garbin E., Valluzzi M. R., Modena C. 2010, 'Experimental investigation on local aspects of the FRP strengthening of masonry arches', Proc. of 8th MONUBASIN Symposium *on* Monuments in the Mediterranean Basin, Patras, Greece.

Valluzzi, M.R. 2008, 'Strengthening of masonry structures with Fibre Reinforced Plastics: from modern conception to historical building preservation', Proc. of SAHC08, Bath, UK, vol. 1, p. 33–45.

XII DBMC
International Conference on Durability of Building Materials and Components
PORTO - PORTUGAL, April 12th-15th, 2011

Investigation of Retrofit Solutions of Window-Wall Assembly Based on FMEA, Energy Performance and Indoor Environment

Martin Morelli [1]
Diana Lauritsen [2]
Svend Svendsen [3]

ABSTRACT

Multi-storey buildings built before the 1960s have a large energy saving potential. The windows and facades are the two components with largest saving potentials. Many buildings from the period before the 1960s have windows and facades worth preserving from an architectural point of view and therefore outside insulation is not possible. Development of new retrofit solutions should be long-lasting and not cause collateral damage to the existing structures. This paper describes a rational optimisation approach for analysing retrofit solutions based on durability, energy savings and indoor environment. The failure mode and effect analysis is used for assessing the durability. The energy saving is calculated as the heat loss through the structure. Daylight simulations are performed to evaluate the indoor environment. In the paper a window with a secondary glazing and a box window, both with internal insulated walls, are investigated. The thermal result shows that a box window has the lowest heat loss and heat loss transmittance. The daylight for the two window-wall assemblies performs equally, but worse than the existing window-wall assembly. The durability of the assemblies is most critical to moisture from the inside. The box window has the lowest temperatures on the cavity surface and is therefore more vulnerable toward condensation. The basis of the rational optimisation approach is the total economy considering the initial, operational and maintenance costs over the lifetime of the building. The maintenance costs can be found from the durability assessment as the indoor environment and energy calculations cover the operational costs. These investigations are needed to analysis the retrofit solution.

KEYWORDS

Window-wall assembly, FMEA, Energy savings, Retrofit optimisation

[1] Department of Civil Engineering of the Technical University of Denmark, Kgs. Lyngby, DENMARK, marmo@byg.dtu.dk
[2] Department of Civil Engineering of the Technical University of Denmark, Kgs. Lyngby, DENMARK, dila@byg.dtu.dk
[3] Department of Civil Engineering of the Technical University of Denmark, Kgs. Lyngby, DENMARK, ss@byg.dtu.dk

1 INTRODUCTION

Retrofitting old multi-storey buildings built before the 1960s have a large energy saving potential and can contribute to meet the demand in EUs energy and greenhouse gas emission target for 2020 [EU 2008]. Windows and facades are the two components with the largest saving potential [Wittchen 2009]. Many of the buildings are with facades worth preserving hence only inside insulation is possible. In Denmark the 4-light "Dannebrog" windows have to be kept from an architectural point of view. Applying inside insulation increases the thermal bridge in the window-wall assembly. Inside insulation also takes up room space and herby reduces the daylight into the room. Retrofitting the windows combined with internal insulations on the walls leaves a thermal bridge in the window-wall assembly. This thermal bridge can be difficult to minimize without also reducing the window size. For low-energy buildings the thermal bridges greatly influence the total heat loss. The assembly between the window and wall will be analysed using Failure Mode and Effect Analysis (FMEA) with regard to durability, and will furthermore be analysed considering energy saving and indoor environment.

When retrofitting old buildings, it is important that no collateral damage to the existing structures occurs. It is therefore necessary to develop new long-lasting retrofit solutions that have been thoroughly tested for failures. The use of quality improvement tools, such as FMEA, can be very valuable when analysing the solutions. This paper presents a rational optimisation approach for analysing retrofit solutions based on durability, energy savings and indoor environment, as retrofit solutions often only consider energy savings. In this paper, a window with a secondary glazing and a box window are investigated.

1.1 FMEA and Window-Wall Assembly

Layzell and Ledbetter [1998] applied FMEA to cladding systems. The causes of failures were found from test failures and from experiences on site. The knowledge of causes helped determine a more precise risk priority number (RPN). In IEA-SHC Task 27 [Köhl 2007] solar collectors and windows were investigated using FMEA. The RPN was based on knowledge-based data for occurrence. Zhang et al. [2010] studied a knowledge RPN based on method integrating weighted least square method. The fuzzy RPN was determined on a multidimensional scale spanning occurrence, severity and detection along with their different interaction under a fuzzy environment. The focus is on component level and not interaction between components. The determination of the RPN can be done in several ways and can influence the durability of the structure greatly. Another approach could be Monte Carlo simulations. Salzano et al. [2009] has identified the interaction between window and wall as a significant source to water intrusion trough the building envelope in high-humidity, hurricane-prone areas. The same problem occurs with high loads of driving rain.

FMEA has been applied on a component level with many approaches to determine the RPN. The FMEA will be applied on the interaction between two components, where the RPN will not be determined. Unlike the previous work, the FMEA will be used on an assembly instead of a component, because the challenge is to maintain the original window and wall without making any changes to the architecture. The window-wall assembly is interesting because the appearance of the window and wall should be preserved. Previous work has shown that a lot of moisture problems occur in this assembly and large energy savings can be achieved.

2 WINDOW-WALL ASSEMBLY

Figure 1 shows the principle structures in the window-wall assembly for the existing structure, a window with secondary glazing and a box window.

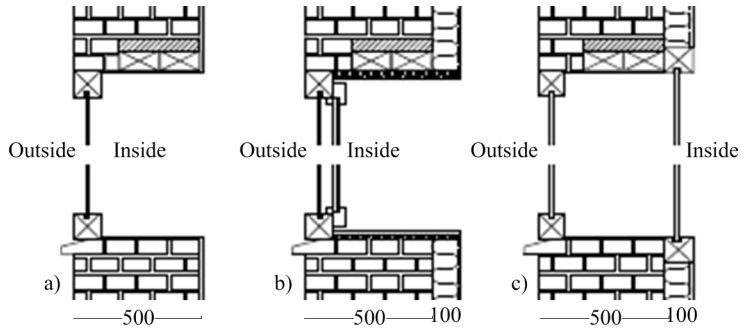

Figure 1. a) The existing structure with single glazed window. b) Solution 1, existing window with new secondary energy window. c) Solution 2, existing window with new energy window in the inside insulation.

The existing structure consists of a 0.5 m wide brick wall where the window with one layer of glass is placed outside in the wall. Above the window, wooden beams support the brick wall. In both renovation solutions, the outer wall is insulated with 100 mm internal insulation. In solution 1, a double glazed energy window is added as a secondary glazing on the inside of the existing window. To minimize the heat loss, the thermal bridge in the window panel is insulated with 20 mm mineral wool. The frame for the second glazing is made of wood. In solution 2, a double glazed energy window is added on the inside of the wall without any connection to the original window. The frame, which is made of glass-reinforced plastic (GRP), is placed in the insulation layer.

3 FAILURE MODE AND EFFECT ANALYSIS (FMEA)

FMEA was developed in the aerospace industry and has been adapted in many other lines of business. The FMEA method is a systematic and analytic quality planning tool for identifying effects of potential failures. In Fig. 2, the three general steps of the FMEA process are shown which is also described by Stamatis [2003] and McDermott *et al.* [2008].

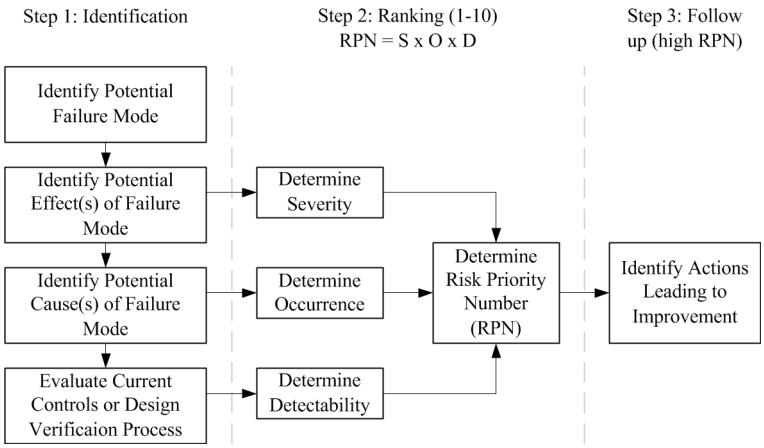

Figure 2. The process of Failure Mode and effect Analysis

In Talon *et al.* [2006] the practical use of FMEA is described in several different papers. A example of a double glazing unit case study using FMEA is described by Lair [2003].

3.1 FMEA on Window-Wall Assembly

The FMEA focuses on identifying potential failures which affects the durability of the retrofitted window-wall assembly. In Table 1, the failures for both retrofit solutions are shown combined with

potential effects and causes. The effects of the potential failure are described in Table 2, based on rational assessments and referred to with numbers in Table 1.

Table 1. Potential failure mode, effects and causes for the two retrofit solutions.

Failure mode	*Effects* (Table 2)	*Causes*
1. The caulking joint is leaking. Water accumulates under the window panel.	6	The existing joint is old and cracked or the joint is missing.
2. The weatherstrip between the existing casement and pane is leaking. Drying to the inside is reduced due to the new window.	4	The weatherstrip has lost the attachment because of aging or workmanship.
3. The weatherstrip between existing and new casement is leaking. – This is only important if failure mode 2 also occurs (only valid for solution with second glazing).	1, 2, 4, 5	The weatherstrip has lost the attachment or is missing.
4. Draughty assembly in the vapour barrier, which cause condensation in the structure.	6, 8	There have been penetrations of the vapour barrier while carrying out or afterwards.
5. The weatherstrip between casement and frame in the existing window is leaking. Drying to the inside is reduced due to the new window.	3, 4, 5	The weatherstrip is old and must be replaced or is missing. The weatherstrip is pushed instead of pressed when the window is closing.
6. Deformation of window hole, as a consequence of the inside insulation which affects the temperature profile in the wall.	7	Subsidence in the building because of the changed temperature in the wall by internal insulation.
7. The bearing construction (the wooden beam over the window) decomposes as a consequence of moisture accumulation.	9	The wall gets cold because of the internal insulation and reduced drying potential.
8. Moisture accumulation in the wall.	8	The drying potential is reduced because of the internal insulation.
9. Condensation in the cavity on the inside of the outer window and wall (only valid for the box window).	3, 6	The temperature in the cavity is below dew-point when warm humid air entered the cavity through draughty weatherstrip.

Table 2. Potential effects by retrofitting window and wall.

Potential effects	
1. Condensation on the inner side of the outer pane	6. Decomposition of panel in the window (rot)
2. Increasing the heat loss	7. Failure in the tightening
3. Moisture in the cavity	8. Mould between wall and inside insulation
4. Decomposition of the casement (rot)	9. The wall is collapsing
5. Decomposition of the frame (rot)	

In the FMEA analysis most of the failures are the same if the solution with secondary glazing or a box window is chosen. It is clear that most of the failures are related to the weatherstrips different places in the structure; hence moisture is the most critical issue.

4 METHODS FOR SIMULATIONS

4.1 Geometry

In Fig. 1 the three window-wall assemblies are shown. In the thermal calculations the masonry wall was 0.5 m thick and 1 m high. On the inside of the wall 100 mm insulation with wooden skeleton was applied. The existing window frame was 83 x 128 mm (H x W) and the box window frame was 57 x 119 mm. The window height was 0.2 m and applied as 1 layer glazing, 1+2 with small (30 mm) and large air cavity (452 mm). As cold bridge insulation 20 mm mineral wool was applied in solution 1.

4.2 Boundary Conditions and Materials

The interior and exterior environment was described by boundary conditions for temperature and relative humidity. The inside air temperature was constant 20°C and the relative humidity 50%. The exterior climate was described by a constant outside air temperature of 0°C and a relative humidity of 80%. The surface heat transfer resistance was 0.13 ($m^2 \cdot K$)/W for internal surfaces with horizontal heat flow and for outside surfaces 0.04 ($m^2 \cdot K$)/W according to [EN ISO 6946:2007]. For the box window the resistance of the air cavity was calculated and distributed to the cavity surfaces with half (0.10 ($m^2 \cdot K$)/W) of the total cavity resistance (0.20 ($m^2 \cdot K$)/W).

The thermal calculations were performed with the material properties listed in Table 3, taken from [DS 418:2002].

Table 3. Material properties for thermal calculations.

Material	*Thermal conductivity, λ* [W/m·K]	*U-value* [W/m^2·K]
Mineral wool (7% wood skeleton)	0.044	
Mineral wool	0.037	
Brick (1800 kg/m^3)	0.75	
Glazing, 1 layer, (4 mm)	1.66[1]	5.8
Glazing, 2 layer energy, (4-16-4)	0.033[1]	1.1
Glazing, 1+2, (4-30-4-16-4)	0.068[1]	0.9
Wood frame	0.13	
GRP frame (119 mm)	0.207[1]	1.42

[1] The thermal conductivity is calculated based on the total U-value and thickness excluding the surface heat transfer coefficients.

4.3 Thermal calculations

The thermal performance of the window-wall assembly was analysed as a 2D steady state problem investigated in HEAT2 ver. 7.1 [Blomberg 1996]. The heat loss through the assembly and frame was calculated as the 2D coupling coefficient (L_{2D}) subtracting the 1D heat loss through the wall (Φ_{wall}) and window pane (Φ_{pane}) divided with the temperature difference (ΔT); $\Psi = (L_{2D} - (\Phi_{wall} + \Phi_{pane}))/\Delta T$. For the box window the coupling coefficient was calculated as described in [EN ISO 10211:2007] for cases with more than two boundary temperatures. For all three window-wall assemblies, the grid was analysed changing the numbers of cells from n to 2n allowing a deviation of 1%.

4.4 Dew-Point Method

To evaluate the risk of moisture problems in the structures, the dew-point method was applied. From the thermal calculations, the surface temperatures were determined in critical points of the structure. These temperatures were compared to the dew-point temperature for the surrounding environment.

4.5 Daylight

The indoor environment was evaluated based on the amount of accessible daylight for the three windows. Velux Daylight Visualizer ver. 2.5.7 [Labayade *et al.* 2009, Velux 2010] was used for evaluating the daylight factor on a horizontal plane 0.85 m above the floor in a room of 3.8 x 5 m with two windows. A standard CIE overcast sky was used at the location for Denmark (latitude 55.4 and longitude 12.34). The internal surface reflectance was set to 0.9 for the walls, ceiling 0.9 and floor 0.35. The reference window was 1.6 x 1.1 m as the window with secondary glazing and box window. The windows were placed with a distance to each other of 0.8 m, 0.4 m away from the inner wall and 0.8 m above the floor. The light-transmittance for the reference window was 0.87 and 0.70 for the windows used for retrofitting.

5 RESULTS

5.1 Thermal

The thermal performance of the window-wall assembly is evaluated based on the total heat loss and the linear heat loss transmittance through the assembly and window frame. The existing window has a total heat loss of 55.3 W/m and the cold bridge is 0.41 W/(m·K). Adding a secondary energy glazing, 20 mm insulation in the cold bridge and 100 mm internal insulation, the heat loss through the assembly is 0.37 W/(m·K) and the total heat loss is reduced to 17.4 W/m. The total heat loss for the box window is 12.8 W/m, and the heat loss through the frame and assembly is 0.14 W/(m·K). Insulating the wall in the cavity between the panes of the box window has only minor influence on the heat loss transmittance.

5.2 Dew-Point

The critical dew-point temperature is about 8°C regarding the internal environment and about 12°C concerning mould growth. The reference window-wall assembly has condensation problems at the inside of the window pane. For the reference structure the inside surface temperature on the casement is critical to mould growth, which is not the case for the retrofit solutions. For the two retrofit solutions, condensation can occur in the wall-insulation interface and on the inside of the outside window. Generally the air cavity is a critical point if warm humid room air enters the cavity. In solution 1, the joint between the frame, wall and insulation panel has a critical temperature about 7.5°C. Solution 2 has lower temperatures at the surfaces and in the structure because the new window is placed at the inside of the wall. The cavity surface temperatures are 3-5°C on the inside of the outer frame and outside of the inner frame.

5.3 Daylight

The amount of daylight entering the room for the reference structure and the two retrofit solutions are shown in Fig. 3.

In the reference window the daylight factor is around 3.3% about 1.2 m in the room. At the same place the daylight factor is around 2.4% for the retrofitted solutions. Choosing a box window, the amount of daylight entering the room is insignificantly higher than using secondary glazing, which will decrease compared to the existing structure.

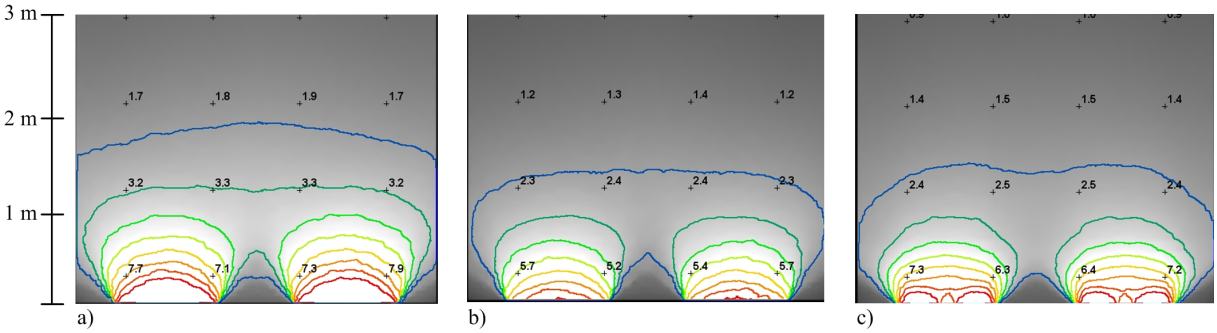

Figure 3. The daylight factor for the three windows with a CIE overcast sky. a) the existing window, b) the window with secondary glazing and c) the box window.

6 DISCUSSION AND CONCLUSION

Selection of new retrofit solutions is often chosen based on cost-efficiency according to energy savings. The choice of solution should instead be based on several different parameters e.g. durability, energy saving and indoor environment. Also non rational parameters should be considered as architecture and view out. An alternative approach to the cost-efficiency is the total economy considering the initial, operational and maintenance costs over the building lifetime. As the lifetime and economy is not included in the study, the rational optimisation approach is attempted illustrated.

From the FMEA, there are no larger differences in failure modes, consequences and causes between the box window and window with secondary glazing. The existing structure in the box window will be colder than for a window with secondary glazing as an effect of moving the "warm" building envelope to the inside of the room. As an effect of colder surface temperatures, the cavity in the box window is more critical towards mould growth than for the window with secondary glazing. On the other hand, the box window allows slightly more daylight to enter the room. It has also a lower heat loss compared with the secondary glazing window. Hence the heating and electricity consumption is decreased compared to the window with secondary glazing. In the total economy, the maintenance costs are based on the founding in the FMEA, and the operational costs are determined from the simulation of the energy saving and indoor environment. The retrofit solution is then chosen based on the total economy over the buildings lifetime.

From the study of two window-wall assemblies, a rational optimisation approach is illustrated about the total economy. The FMEA is used to investigate the durability of the component. Further the energy consumption and indoor environment is calculated as the heat loss, linear thermal transmittance and daylight for the two assemblies. In the total economy approach, the initial costs, operational and maintenance costs need to be included over the lifetime of the building. The performance of the indoor environment influences the total energy consumption as overheating leads to cooling, reduced daylight increases electricity consumption, and energy savings leads to less energy use for heating. In the rational approach, every parameter needs to be included in the total economy over the buildings lifetime.

The future work is to quantify the durability found in the FMEA using e.g. stochastic simulations. Further, the determination of the operational and maintenance costs and the lifetime of the building are needed.

ACKNOWLEDGEMENT

The research is supported by the Landowners' Investment Association, LavEByg, an innovation network for low-energy solutions in buildings and ZEB (Zero Energy Buildings). This financial support is gratefully acknowledged.

REFERENCES

Blomberg, T. 1996, *HEAT CONDUCTION IN TWO AND THREE DIMENSIONS Computer Modelling of Building Physics Applications*, Report TVBH-1008, Department of Building Physics, Lund University, Sweden.

DS418:2002, *Beregning af bygningers varmetab. Calculation of heat loss from buildings,* (in Danish).

EN ISO 6946:2007, *Building components and building elements – Thermal resistance and thermal transmittance – Calculation method*.

EN ISO 10211: 007, *Thermal bridges in building construction – Heat flows and surface temperatures – detailed calculations*.

EU. 2008, Communication from the Commission to the European Parliament, the Council, the European Economic and Social Committee of the Regions, 2008, 20 20 by 2020, Europe's climate change opportunity.

Köhl, M. 2007, *Performance, durability and sustainability – of advance windows and solar components for building envelopes*, IEA Task 27, project B3, IEA-SHC, Germany.

Labayrade, R., Jensen, H.W. & Jensen, C. 2009, 'VALIDATION OF VELUX DAYLIGHT VISUALIZER 2 AGAINST CIE 171: 2006 TEST CASES', Eleventh International IBPSA Conference, Glasgow, Scotland, July 27-30 2009, pp. 1506-1513.

Lair, J., 2003, *Failure Mode Effects and Criticality Analysis (FMEA) – a tool for risk analysis and maintenance planning*, Report submitted to the CIB W80/RILEM 175-SLM Service Life Methodologies, February, CSTB France.

Layzell, J. & Ledbetter, S. 1998, 'FMEA applied to cladding systems-reducing the risk of failure', *Building Research & Information,* vol. 26, no. 6, pp. 351-357.

McDermott, R.E., Mikulak, R.J. & Beauregard, M.R. 2009, *The basics of FMEA,* 2nd edn, Productivity Press, New York.

Stamatis, D.H. 2003, *Failure mode and effect analysis: FMEA from theory to execution*, 2nd edn, ASQ Press, Milwaukee, US.

Talon, A., Chevallier, J-L. & Hans, J. (Eds.), 2006, *Failure Modes, Effects and Criticality Analysis – Research for and Application to the Building Domain,* CIB Publication No. 310, Rotterdam, (ISBN Number 90-6363-052-2).

Velux. 2010, Velux visualizer 2: Simulation program for daylight. http://viz.velux.com/ viewed on 27-10-2010.

Wittchen, K.B. 2009, *Potentielle energibesparelser i det eksisterende byggeri*, SBi 2009:05, Statens Byggeforskningsinstitut, SBI, Hørsholm, Denmark, (in Danish).

XII DBMC
International Conference on Durability of Building Materials and Components
PORTO - PORTUGAL, April 12th-15th, 2011

Limestone Porosity Determines the Protective Effect of a Biogenic Carbonate Surface Treatment

Willem De Muynck [1]
Stijn Leuridan [2]
Nele De Belie [3]
Willy Verstraete[4]

ABSTRACT

Microbially induced carbonate precipitation has been explored by several researchers for the protection and consolidation of ornamental limestone, a process known as biodeposition. The influences of microbial aspects and chemical parameters on the efficiency of this kind of treatment have been widely documented. This is the first paper in which the influence of the type of stone on the treatment efficiency is reported. In this study, an ureolytic biodeposition treatment was applied on four different limestones. Durability of treated stones was assessed by means of transport and degradation processes. A higher weight increase due to carbonate precipitation was observed for stones with higher porosity. The presence of a layer of biogenic carbonate crystals resulted in a decreased rate of water absorption, the effect being more pronounced for the more porous stones. For the most porous stone, i.e. Savonnières, the biodepostion treatment resulted in a decrease of the sorptivity by a factor 17. The biogenic carbonate exerted a consolidating effect on all type of stones. For prisms of 40 mm × 20 mm × 10 mm, the biodeposition treatment resulted in a 50 % lower weight loss upon sonication compared to untreated samples. From this research, it is clear that the porosity, and more specific, pore size distribution has a major influence on the effectiveness of a biodeposition treatment. Pore size governs bacterial adsorption, and hence, the amount of carbonate that can be precipitated. From this study, it follows that biodepostion is less effective on microporous stones such as Massangis.

KEYWORDS

Biomineralization, conservation, MICP, ageing tests, bacteria, stone

[1] Magnel laboratory for concrete research and LabMET, Ghent University, Ghent, Belgium, willem.demuynck@ugent.be
[2] Magnel laboratory for concrete research, Ghent University, Ghent, Belgium, stijn.leuridan@ugent.be
[3] Magnel laboratory for concrete research, Ghent University, Ghent, Belgium, nele.debelie@ugent.be
[4] Laboratory for microbial ecology and technology (LabMET), Ghent University, Ghent, Belgium, willy.verstraete@ugent.be

1 INTRODUCTION

Since the discovery that microbiologically induced carbonate production (MICP) can be applied for the protection of stone [Adolphe *et al.* 1990], several researchers have tried to optimize its performance (an overview of the different approaches can be found in the review paper by De Muynck *et al.* [2010a]).

In a first attempt to improve the effectiveness of the biodeposition treatment, previous studies of our research group were focused on the ureolytic pathway [De Muynck *et al.* 2008a; De Muynck *et al.* 2008b; Dick *et al.* 2006; Hammes *et al.* 2003]. Contrary to other metabolic pathways (see Castanier *et al.* [1999]), the hydrolysis of urea can be easily controlled and allows for the production of high concentrations of carbonate within a short amount of time. The hydrolysis of urea is catalyzed by means of urease. Urea is hydrolyzed to carbonate and ammonium, resulting in an increase of the pH and carbonate concentration in the bacterial environment [Stocks-Fischer *et al.* 1999]. In the presence of calcium ions, this will result in calcium carbonate precipitation, once a certain level of supersaturation is reached. The fast production of carbonate and the fact that no additional nutrients are required, make the hydrolysis of urea a very feasible pathway for biodeposition applications in practice (for a more detailed discussion, see De Muynck *et al.* [2010a]). In an effort to further improve the effectiveness of the ureolytic biodeposition treatment, we have recently investigated the influence of the chemical aspects of the biogenic calcium carbonate precipitation, i.e. the dosage of urea and calcium [De Muynck *et al.* 2010b]. From that study, it appears that there exists an optimum dosage of urea and calcium above which the beneficial effect of an additional amount of urea and calcium (i.e. additional precipitation of carbonate, and hence, an increased protective effect) will be much smaller compared to the detrimental effects (i.e. accumulation of salts and discoloration of the stone). For Euville limestone, the optimal calcium dosage could be tentatively estimated to be about 13.4 mg $Ca^{2+}cm^{-2}$.

So far, most efforts to improve the effectiveness of the biodeposition treatment were mainly related to the microbiological and chemical factors of the biogenic carbonate surface treatment. One of the most important parameters affecting the performance of a surface treatment, i.e. its ability to penetrate a stone, remained, however, largely overlooked. Torraca [1975] indicated that a consolidant should be able to penetrate a stone to such a depth that all loose material is consolidated and attached to the intact core of the stone. The latter should result in a gradual transition of thermal and mechanical properties from the treated outer surface towards the inner volume of the stone. Up to now, however, only limited penetration depths have been reported for the different types of biodeposition treatments, ranging from few micrometers to several millimeters. Furthermore, large variations exist in the thickness of the layer of biogenic crystals between the different types of treatments. Reported values of layer thickness range between a few to hundred micrometers. To a large extent, the variability in penetration depth and layer thickness can be attributed to the microbiological and chemical parameters that govern the biogenic carbonate precipitation (for a more detailed discussion, we refer the reader to the review by De Muynck *et al.* [2010a]).

For all types of surface treatments, the depth of penetration depends on a variety of parameters. In addition to climatologic conditions (temperature and relative humidity), it is influenced by viscosity, surface tension, rate of deposition, application procedure and rate of solvent evaporation. Moreover, since liquid transport also depends on the pore structure of a stone (more specific, porosity, pore shape and pore connectivity [Cnudde *et al.* 2004]), the latter will also affect the penetration depth of a surface treatment. Maravelaki-Kalaitzaki *et al.* [2008] demonstrated that the performance of silicon based consolidants was greatly dependent on the pore size of the stone. In addition, the consolidative action of alkoxysilanes depends on the intergranular space of the stone, alkoxysilanes being unable to consolidate granularly decayed stone [Wheeler 2005]. For the biodeposition treatments, the depth of penetration not only depends on liquid transport through stone, but also that of bacteria. Transport of bacteria through a porous material depends both on the pore structure of the stone and the adsorption of the bacteria on the mineral matrix. Transport of bacteria occurs in pores of which the diameter is at

least two times that of bacteria [Vance 1995]. Adsorption of bacteria, on the other hand, is governed by a variety of physical, chemical and microbiological factors [Stevik *et al.* 2004]. Physical factors relate to the porous medium (specific surface, surface roughness and electrostatic charges), temperature and rate of water transport. Ionic strength and pH are examples of chemical factors. Microbiological factors, finally, relate to hydrophobicity, chemotaxis and cell surface charges.

The aim of this research was to investigate how pore structure affects the protective effect of a biodeposition treatment. To our knowledge, this has not been reported before. For the purpose of this research, the ureolytic biodeposition treatment was applied on four types of limestone, with pore sizes ranging from micro- to macropores. The biodeposition layer was characterized by means of microscopic investigations. The protective and consolidating effect of the treatment was evaluated by means of a water absorption test and a sonication test, respectively.

2 MATERIALS AND METHODS

2.1 Materials

Experiments were performed on four types of French limestone (Fig. 1). Stones were provided by a Belgian restoration company. Selection of stones was directed by availability and (historical) use in Belgian cultural heritage. Massangis (Roche Jaune) and Savonnières are oolitic limestones. Euville is a crinoidal limestone, cemented together by crystalline calcium carbonate. Avesnes stone is a sandy limestone characterized by laminations and bioturbations.
For the biodeposition experiments, stone blocks were cut into specimens with different dimensions: (1) prisms of 40 mm x 20 mm x 10 mm and (2) cubes of 45 mm side. Prior to the experiments, all specimens were stored in an oven at 80°C until a constant weight (a weight change of less than 0.1% between two measurements at 24 h intervals) was achieved.

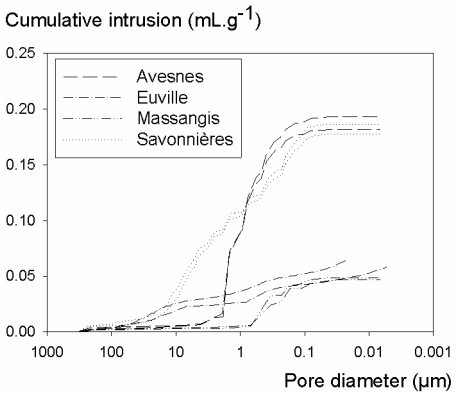

Figure 1. Pore size distributions of the different types of limestone used in this study as determined by means of mercury intrusion porosimetry.

2.2 Microorganisms

Bacillus sphaericus LMG 22557 (Belgian coordinated collections of microorganisms, Ghent) was used for this study. Selection of this spore-forming strain was based upon earlier work [Dick *et al.* 2006]. Liquid culture media consisted of 20 $g.L^{-1}$ yeast extract and 20 $g.L^{-1}$ urea (VWR International, Belgium). Liquid media were sterilized by autoclaving for 20 min at 120°C. Urea was added after autoclaving by means of filtration through a sterile 0.33 µm Millipore filter (Millipore, USA). For all experiments, *B. sphaericus* cultures were obtained after subsequent culturing (two times and 1% inoculum) from a -80°C stock culture. Cultures were incubated for 24 h at 28°C on a shaker at 100 rpm. Culturing was performed under sterile conditions.

2.3 Biodeposition Treatment Procedure

The biodeposition procedure was performed in two steps, similar to the procedure described in [De Muynck *et al.* 2010b]. In the first step, stone specimens were immersed for 24 hours in a one day old culture of *B. sphaericus*. After this incubation period, specimens were removed from the culture solution and gently wiped with a paper towel to remove excess liquid from the surface. In the second step, specimens were immersed for four days in a biodeposition medium containing 20 $g.L^{-1}$ urea and 50 $g.L^{-1}$ calcium chloride. Among different concentrations of urea and calcium tested, this composition appeared to be most suited for biodeposition purposes [De Muynck *et al.* 2010b]. Cubes (n=4) were immersed to a depth of about 1 cm, while prisms (n=6) where fully immersed in aluminum vessels containing 200 and 300 mL of biodeposition medium, respectively. The treatment was performed in an incubation room at 28°C under static and non-sterile (open to the air) conditions.Next, the specimens were left to dry for three days at 28°C before they were stored in an oven at 80°C until a constant weight was obtained.

2.4 SEM and Thin Section Analyses

The influence of the lithotype on the thickness, morphology and composition of the crystal layer was determined by means of thin section and SEM analyses. Fluorescent epoxy impregnated thin sections were prepared following the procedures described by [Jakobsen and Brown 2006]. For the treatments under investigation, two thin sections were prepared from one specimen. Thin sections were analysed by means of a Leica DMLP microscope (Leica Microsystems, Germany) connected to a Canon S50 camera. Limestone samples for SEM analysis were coated with gold with a SCD005 Sputter Coater (Bal-Tec AG, Principality of Liechtenstein). The samples were subsequently studied by means of a FEI XL30 scanning electron microscope (FEI, The Netherlands) equipped with a LaB6 filament and with an energy dispersive X-ray spectroscopy (EDX) detector (EDAX, The Netherlands).

2.5 Weight Increase Due to Biodeposition

The amount of carbonate precipitation on the specimens could be estimated from the weight increase of the specimens. The weight gain was calculated from the difference in weight before and after treatment, after drying in an oven at 80°C until constant weight (precision of balance: 0.1 mg).

2.6 Capillary Water Absorption

The waterproofing effect of the biodeposition treatment was investigated by means of a sorptivity test. After drying in an oven at 80°C, until a constant weight was obtained, the four sides of the specimen adjacent to the treated side were coated with butyl tape, in order to prevent evaporation of water through the sides during the water absorption experiments. Determination of the water absorption by capillarity was performed on four specimens per treatment according to EN 1925:1999.

2.7 Resistance Towards Sonication

The adhesion of the newly formed carbonates to the limestone specimens and the consolidating effect of the biodeposition treatment was determined by means of sonication, as proposed by Rodriguez-Navarro *et al.* [2003]. Sonication is an effective means of disrupting materials adhered to a surface. The weight loss upon sonication gives an indirect estimate of the adhesion of materials to a substrate. For biodeposition treated stones, sonication can give an estimate of the adhesion of the biogenic crystals to the surface and the efficiency of the consolidation.The prisms were subjected to six cycles of sonication (i.e. application of ultrasound energy). During each cycle, the specimens were immersed for five minutes in demineralized water in a 35 kHz ultrasonic bath (Haver VSC 200-76; 120-240W; Haver & Backer, Germany). After each cycle, samples were dried for 48 hours in an 80°C oven and subsequently weighed.

3 RESULTS AND DISCUSSION

3.1 SEM and Thin Section Analyses

The biodeposition treatment resulted in the presence of a layer of biogenic calcium carbonate crystals on the surface of the different types of stone (Fig. 2). In general, large differences in morphology and crystal size could be observed between the layers deposited on different types of stone (Fig. 2). The largest crystals were observed on the surface of Savonnières limestone (Fig. 2 E and F). Furthermore, different types of stone exhibited different degrees of coverage with biogenic crystals. The smallest amount of carbonate crystals could be observed on the surface of Massangis limestone (Fig. 2B). The differences in coverage can be attributed to differences in the pore structure (see further). EDX analyses confirmed that these newly formed crystals (Fig. 2 C and F) consisted of calcium carbonate. The differences in pore structure between the different types of stone can be clearly observed from the thin sections (Fig. 2 A and D). The biggest amount of macropores could be clearly observed for Savonnières (Fig. 2D).

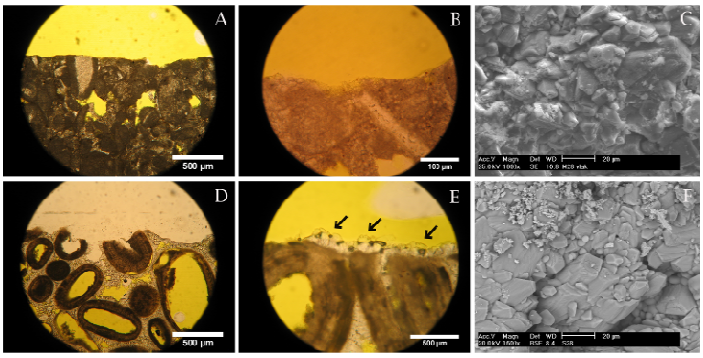

Figure 2. Thin section and SEM analyses of untreated (A and D) and biodeposition treated (B, C, E and F) Massangis (A-C) and Savonnières (D-F) limestone. Notice the large crystals precipitated on Savonnières, as indicated by means of arrows (E). SEM pictures (C and F) show the presence of the biodeposition layer on the surface of the treated stone.

3.2 Weight Increase Due to Biodeposition

The biodeposition treatment resulted in a weight gain of all stones, the effect being more pronounced for the more porous stones (Table 1). For the least (Massangis) and most (Avesnes) porous stones, an absolute weight gain of about 0.27 g and 0.61 g could be observed, respectively. The highest weight gain, however, was observed for Savonnières, i.e. 0.65 g. The weight gain can be mainly attributed to the presence of biogenic calcium carbonate on the surface (Fig. 2) and inside the pores (data not shown). Since the amount of calcium carbonate that can be produced, depends on the number of bacteria present, it can be expected that stones that can retain more bacteria will also gain more weight from calcium carbonate precipitation. Samonin and Elikova [2004] reported that for a maximum absorption of microbial cells, the absorbent pores must be two to five times larger than the cells. Since cells of *B. sphaericus* have dimensions of about 1-4 µm, bacteria will be mainly absorbed in macropores (i.e. pores with diameter larger than 7.5 µm). These macropores are nearly absent in Massangis (Fig. 1), which accounts for its low weight gain. For this type of stone, calcium carbonate precipitation is the result of the activity of bacteria attached to the surface. Savonnières, on the other hand, exhibits the highest amount of macropores (Fig. 1). The latter might explain for the highest weight gain observed. For this type of stone, carbonate production is not limited to the outer surface of the stone. The absorption of bacteria in (macro-)pores and an improved penetration depth may be beneficial for applications in practice. This absorption may protect them from dessication or washing out from rainfall, and hence, failure of the biodeposition treatment. As such, it seems that biodeposition will be more feasible on macroporous stone compared to microporous stone.

Table 1. Weight gain of stone prisms due to microbial carbonate precipitation. Notice the higher weight gain for the more porous stones.

	Stone	*Porosity(%)*	*Absolute weight increase (g)*	*Relative weight increase (%)*
Less porous:	Massangis	9.98 ± 0.66	0.27 ± 0.01	1.49 ± 0.04
	Euville	14.12 ± 0.34	0.55 ± 0.02	3.02 ± 0.13
More porous:	Savonnières	30.92 ± 0.14	0.65 ± 0.01	4.51 ± 0.05
	Avesnes	32.10 ± 0.05	0.61 ± 0.01	4.34 ± 0.05

3.3 Capillary Water Absorption

The biodeposition treatment resulted in a decreased rate of water uptake for all stones under investigation (Fig. 3). The largest decrease was observed for Savonnières. For this type of stone, a 17 times decreased sorptivity could be observed for biodeposition treated stone. For the other types of stone, decrease in sorptivity was about 2 (Euville) to 4 (Avesnes) times. For all lithotypes under investigation, no significant differences could be observed between the final water absorption values of treated and untreated stones. As indicated in our previous study, decrease in water uptake could be attributed to the presence of biogenic carbonate crystals, since no decrease in water absorption could be observed for control series without bacteria and/or a calcium source [De Muynck *et al.* 2010b]. Furthermore, it was observed that treatments which resulted in a higher amount of carbonate precipitation gave rise to a more pronounced decrease in water absorption. The presence of biogenic crystals resulted in blocking of the pores and/or decreased pore diameters. The fact that Savonnières exhibited the highest decrease in water uptake, might be attributed to the higher amount of biogenic carbonate deposited in the pores and on the surface (Table 1 and Fig. 3).

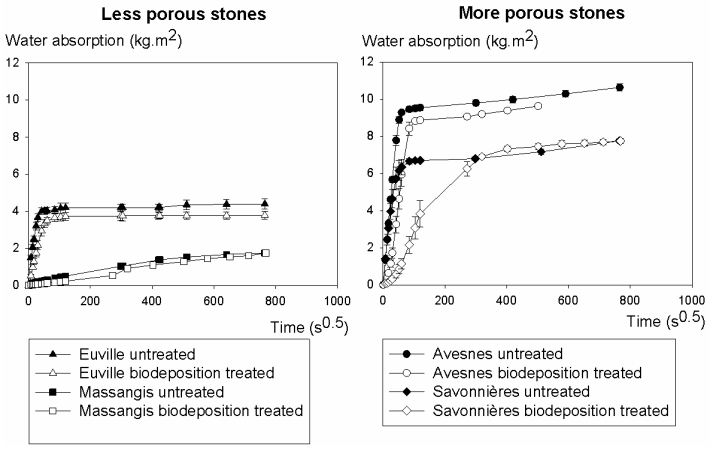

Figure 3. Influence of the biodeposition treatment on the water absorption of stones with different porosity.

3.4 Resistance Towards Sonication

Biodeposition treated stones showed about 50% less weight loss upon sonication compared to untreated stones (Fig. 4). Furthermore, the weight loss was much smaller compared to the weight gain due to the biodeposition treatment (Table 1). These findings indicate that the biogenic carbonate crystals were firmly attached to the surface and that they exerted a consolidating effect. Furthermore, this indicates that the newly formed carbonates were more resistant to mechanical stress (i.e. sonication) than the carbonate crystals of the stone.This is in agreement with observations made by Rodriguez-Navarro *et al.* [2003] and previous work [De Muynck *et al.* 2010b]. According to the former authors, the consolidating effect can be attributed to the formation or an extension of the cementing layer between two grains. With an increased contact area between two grains, there is a

decreased chance of detachment upon sonication. From Fig. 4., the differences in cohesion between the different types of stone can be clearly observed. For untreated stones, it could be observed that, in general, more porous stone exhibited a higher weight loss upon sonication. For the most porous stone, i.e. Avesnes, a weight loss of about 1.4% (0.19g) could be observed. For the least porous stone, i.e. Massangis, the weight loss amounted to about 0.4% (0.10g).

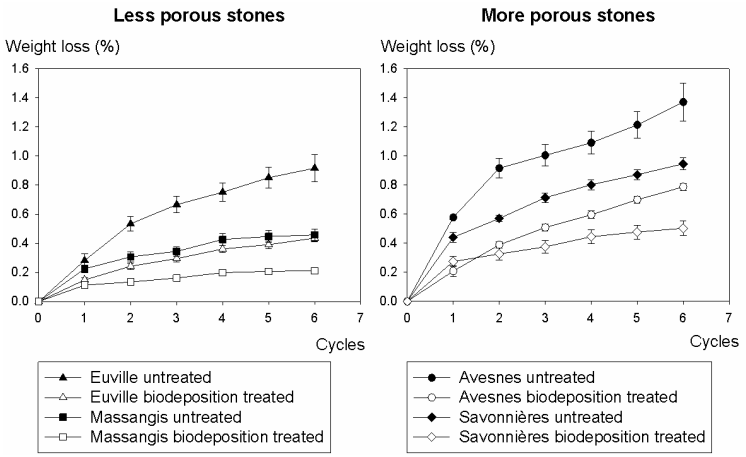

Figure 4. Influence of the biodeposition treatment on the resistance of stone towards sonication. The lower the weight loss, the greater the consolidating effect of the treatment.

4 CONCLUSIONS

From this study, it is clear that lithotype, and more specific, pore structure has an important influence on the protective effect of a biogenic carbonate surface treatment. For the same type of biodeposition treatment (i.e. similar dosage of bacteria and nutrients), the highest protective effect was observed for the most macroporous stones. Pore structure not only affects the penetration depth of the bacteria, but also the amount of bacteria adsorbed. Since biogenic carbonate production depends on the number of cells present, the latter has an important influence on the amount of calcium carbonate that can be deposited in a stone. In this study, the largest biogenic carbonate production occurred in stones with a high amount of macropores (Savonnières and Avesnes). This can be attributed to the fact that adsorption of cells (1-4 µm) is known to occur in pores with dimensions between 4-10 µm. This higher carbonate production accounts for the larger protective effect observed for more macroporous stones. From this study, it is clear that biodeposition is less effective on microporous stones. For that type of stones, bacteria are only adsorbed on the outer surface. As such, they will be more prone to dessication or wash-out due to rainfall. Biodeposition, on the other hand, is very feasible for macroporous stone, on which more biogenic carbonate can be produced. For these types of stones even higher dosages of bacteria and nutrients may be applied.

ACKNOWLEDGMENTS

Willem De Muynck works as a Postdoctoral Fellow of the Flemish agency for Innovation by Science and Technology (IWT Vlaanderen, Belgium).

REFERENCES

Adolphe, J.P., Loubière, J.F., Paradas, J. and Soleilhavoup, F. 1990, 'Procédé de traitement biologique d'une surface artificielle', European patent 90400G97.0 (after French patent 8903517, 1989).

Castanier, S., Le Metayer-Levrel, G. and Perthuisot, J.-P. 1999, 'Ca-carbonates precipitation and limestone genesis -- the microbiogeologist point of view', *Sedimentary Geology*, **126**[1-4], 9-23.

Cnudde, V., Cnudde, J. P., Dupuis, C. and Jacobs, P. J. S. 2004, 'X-ray micro-CT used for the localization of water repellents and consolidants inside natural building stones', *Materials Characterization*, **53**[2-4], 259-271.

De Muynck, W., Cox, K., De Belle, N. and Verstraete, W. 2008a, 'Bacterial carbonate precipitation as an alternative surface treatment for concrete', *Construction and Building Materials*, **22**[5], 875-885.

De Muynck, W., De Belie, N. and Verstraete, W. 2010a, 'Microbial carbonate precipitation in construction materials: A review', *Ecological Engineering*, **36**[2], 118-136.

De Muynck, W., Debrouwer, D., De Belie, N. and Verstraete, W. 2008b, 'Bacterial carbonate precipitation improves the durability of cementitious materials', *Cement and Concrete Research*, **38**[7], 1005-1014.

De Muynck, W., Verbeken, K., De Belie, N. and Verstraete, W. 2010b, 'Influence of urea and calcium dosage on the effectiveness of bacterially induced carbonate precipitation on limestone', *Ecological Engineering*, **36**[2], 99-111.

Dick, J., De Windt, W., De Graef, B., Saveyn, H., Van der Meeren, P., De Belie, N. and Verstraete, W. 2006, 'Bio-deposition of a calcium carbonate layer on degraded limestone by Bacillus species', *Biodegradation*, **17**[4], 357-367.

Hammes, F., Seka, A., de Knijf, S. and Verstraete, W. 2003, 'A novel approach to calcium removal from calcium-rich industrial wastewater', *Water Research*, **37**[3], 699-704.

Jakobsen, U.H. and Brown, D. R. 2006, 'Reproducibility of w/c ratio determination from fluorescent impregnated thin sections', *Cement and Concrete Research*, **36**[8], 1567-1573.

Maravelaki-Kalaitzaki, P., Kallithrakas-Kontos, N., Agioutantis, Z., Maurigiannakis, S. and Korakaki, D. 2008, 'A comparative study of porous limestones treated with silicon-based strengthening agents', *Progress in Organic Coatings*, **62**[1], 49-60.

Rodriguez-Navarro, C., Rodriguez-Gallego, M., Ben Chekroun, K. and Gonzalez-Munoz, M. T. 2003, 'Conservation of Ornamental Stone by Myxococcus xanthus-Induced Carbonate Biomineralization', *Applied and Environmental Microbiology*, **69**[4], 2182-2193.

Samonin, V. V. and Elikova, E. E. 2004, 'A study on the absorption of bacterial cells on porous materials', *Microbiology*, **73**[6], 696-701.

Stevik, K., Kari, A., Ausland, G. and Hanssen, F. 2004, 'Retention and removal of pathogenic bacteria in wastewater percolating through porous media: a review', *Water Research*, **38**[6], 1355-1367.

Stocks-Fischer, S., Galinat, J. K. and Bang, S. S. 1999, 'Microbiological precipitation of CaCO3', *Soil Biology and Biochemistry*, **31**[11], 1563-1571.

Torraca, G. 1975, 'Treatment of stone in monuments. A review of principles and processes', Proc. International Symposium on Conservation of Stone I, Bologna, Italy, 1975, pp. 297-315.

Vance, D. B. 1995, 'Particulate transport in groundwater part II - bacteria', *National environmental journal*, **5**[1], 25-26.

Wheeler, G. 2005, *Alkoxysilanes and the consolidation of stone*, Getty Publications, Los Angeles, California.

XII DBMC
International Conference on Durability of Building Materials and Components
PORTO - PORTUGAL, April 12th-15th, 2011

The Importance of Design in Porto's Ancient Buildings Interventions. Characterization of the Pathological Context through a Constructive Model

Joaquim Teixeira [1]
Rui Fernandes Póvoas [2]

ABSTRACT

This article stems from an ongoing research that aims primarily at designing a methodology for intervention in old buildings (in particular, in the bourgeois houses of Porto), targeted for the rehabilitation of traditional construction systems and based on "best practice" procedures in heritage conservation.

A brief essay describing the usefulness of drawing in defining a constructive model that characterizes the existing buildings is presented, in particular in the context of its most frequent pathologies, emphasizing its importance in conceiving a methodology for intervention.

The ongoing research that the authors has been developed on traditional construction in northern Portugal has contributed to the definition of this model, namely through studies on the ordinary housing in the city of Porto, also called bourgeois houses, and the recent research into the collection of CRUARB, the municipal office responsible between 1974 and 2002 for the urban heritage conservation of the Historical Centre.

The investigation in progress has been confirmed the belief that the drawing is essential for the establishment of a methodology for intervention in old buildings, supporting the entire process, from the survey analysis of the existing built environment, through the stages of conception and construction, to the maintenance of buildings during their lifetime. The universal language of drawing also adds to the ability of bringing together the interests of the various disciplines involved in the actions of heritage conservation.

KEYWORDS

Heritage, Architectural conservation, Inspection and diagnosis.

[1] Faculty of Architecture of the University of Porto (FAUP), Porto, PORTUGAL, jteixeira@arq.up.pt
[2] Faculty of Architecture of the University of Porto (FAUP), Porto, PORTUGAL, rpovoas@arq.up.pt

1 INTRODUCTION

The city of Porto has an historical centre classified as World Heritage by UNESCO in 1996, covering an area of about 50 hectares and a population of about 13.000 inhabitants spread over 1.796 buildings. Although subject to heritage conservation actions since 1974, when CRUARB (Commissariat for the Urban Renewal of the Ribeira and Barredo Areas) was founded, very little was accomplished. Currently, it is evident that the vast majority of buildings requires urgent intervention works, ranging from simple maintenance to extensive works of rehabilitation. According to the last Management Plan for the Historic Centre [Loza *et al*. 2008] the state of conservation of buildings was as follows: 25% Good, 36% Average, 32% Poor and 4% Ruin, being the remaining 4% was undergoing works.

Also, the various incentives created by central government were not able to stop this dereliction process, partly driven by the freezing of rents the law from 1950, only abolished in 2005. It is crucial to overturn this situation, calling for the cooperation of the whole society, from politicians, through the universities and interested companies, to the citizens.

The solution for the urban rehabilitation problem, when happening naturally in an integrated manner, and particularly the rehabilitation of its historic built environment, necessarily entails the establishment of rules of engagement, the rationalisation of procedures and the definition of objectives and strategies, appropriate to the existing context, without disregarding the uniqueness of each building. Therefore, it is equally important to define general and specific rules, delineating procedures for action, with the ability to understand and accept the uniqueness and specificity of each intervention, when concerning the pre-existence and the intervention program.

"Best practice" in heritage conservation is understood to be the set of procedures that inform the actions of intervention, resulting from a consensus based on the practical and intellectual experience of civilizations, of which the international documents (charters, conventions and recommendations) are its maximum expression.

In fact, "best practice" recommends that in the process of intervention in an old building special attention should be paid to the initial survey and characterization of the existence, as the deepening of this knowledge is crucial to the development of the project and the success of the intervention. The attention given to this stage is also important so that the intervention meets two important criteria, namely to ensure compatibility of materials (traditional and new) and the conservation of the authenticity of the intervened object.

Unfortunately, it appears that the characterization of the existence stage involves a lot of resources, including surveys (topographic, photographic and geometric), various inspections, registration and fault diagnostics, historical research, archaeological survey, etc.., thus being often overlooked or taken lightly.

Accordingly, it is of utmost importance to look for ways of streamlining the tasks necessary to perform the steps of characterization of buildings in intervention action. The rationalisation of constructive solutions through idealized models, the characterization of changes or phenomena associated with major pathologies, will be undoubtedly important contributions, whose success is dependent on the degree of experience of the professionals involved. We should nonetheless highlight that each case is unique, and that this information does not replace more rigorous inspections or examinations whenever appropriate.

2 THE CONSTRUCTIVE MODEL

The constructive system of the bourgeois houses of Porto, as of the old buildings in general, is the result of an empirical know-how, by using a very narrow set of readily available materials, without being subject to any prior conception of the project (in Porto, the street elevation is only required in planning applications from 1889). These buildings are characterized by a diversity of technical solutions, languages and forms of functional organization, which constitute an heritage deemed of systematization, as indeed has happened to the housing typologies in the study by [Fernandes 1999].

Indeed, a careful analysis shows that, despite the uniqueness of each building, it is possible to identify many intransience and a high degree of systematization and standardization of constructive methods. This is very notorious for the period of the nineteenth century, which also corresponds to the most consistent season of this historical legacy, and is linked to the great expansion of the city, which began in the late eighteenth century, and certainly was also influenced by the reconstruction of Baixa Pombalina destroyed by the earthquake of 1755.

2.1 The Importance of Implementation and Dissemination of Research about Old Buildings

The study on the constructive system of bourgeois houses of Porto has started with the academic research that led to a first systematization [Teixeira 2004] and is being further addressed through consulting the information available in the collection of CRUARB. However, at this stage of the research and against our best expectations, there appears to be few documents relating to surveys (geometric, photographic, records of anomalies, diagnoses, etc.). The explanation for this, not yet evaluated, may relate to various reasons: loss of documentation, lack of capability or simply the option of not proceeding (due to the advanced state of disrepair of the buildings).

The lack of published studies on the materials and construction techniques used on the old buildings in Portugal, developed within academia or resulting from the municipal offices practice, probably indicates that the scenario of Porto is not unique in the country, as the same happens with the other cities, with the exception of the Baixa Pombalina. This status contradicts the recommendations of international documents since the Venice Charter (1964).

Despite these setbacks, it is based on the existing systematization that we currently undertake the development of a constructive model designed to be part of a methodology for intervention in old buildings in general and, in particular, in the bourgeois houses of Porto.

2.2 The definition of the Constructive Model

The constructive model is composed of one or more building (s) representing the main features of the constructive system of the houses. Its idealization results from the classification methods and techniques of the various elements that compose the building, based on the observation frequency of their occurrence. The result is a building which iconography identifies with the existing ones, representing their common characteristics.

In the case of Porto, the number of occurrences that characterize the still existing houses exceeds its materialization in a single consistent building, and it is therefore necessary to increase their number. In this case, it is essential to find a logic for the other buildings still to create, being its classification by eras one hypothesis.

When analyzing the systematization of the types of housing developed by [Fernandes 1999], which classifies the old buildings into three main types, corresponding to the merchants (seventeenth century), enlightenment (eighteenth century) and liberal periods (nineteenth century), the adaptability to the occurrences recorded was noted, so these types were adopted for the definition of the buildings that will compose the constructive model.

2.2.1 The Merchant House, XVI / XVII century

The merchant's house is located inside the overcrowded wall, in compact blocks, fully occupying the small plots. It usually has only one facade facing the street, and has several floors, four to six, many of them in sway.

Only the ground-floor walls are in granite masonry (stone abundant in northern Portugal), the remainder being on wood as well as the floors and roofs. These walls of wood or 'of frontage', are composed of a square grid structure, filled with mortared small stones or filled brick. The floors or 'sobrados' are made of wooden logs simply peeled, coated with pine planking on the floors and ceilings, if any. The structure of the roofs, usually hip type, also consists of wooden logs like the previous ones, being its coating initially with straw, which was progressively replaced by ceramic tiles.

Corresponding to a time when the housing space had not yet been specialized, these houses are predominantly multifunctional and the ground-floor is designed for retail or workshops and the other floors would often house the for property owners and employees.

2.2.2 The Enlightenment House, XVIII century

The Enlightenment house began to develop in depth, usually featuring two facades both facing streets or one facing the inner courtyard, depending on the type of plot.

The construction of the Enlightenment house becomes more robust, because the front walls are being replaced by granite masonry. Several houses belonging to wealthy property owners, have remarkable facades with monumental works, trying to imitate the exuberance of the Baroque style. The structure of the houses still uses wood logs, as well as the roofs, which remain hip type. Inside, the highlights are the ceilings in wood, in the shape of a "skirt-shirt" or more elaborate, in the form of panels. At the end of this century, the first coating in stucco develop and on the outside, the first frames with glass panels.

In regards to its internal spaces, the house retains the same multifunctional organization although there was however a specialization and hierarchy of the housing spaces due to society changes.

2.2.3 The Liberal House, XIX century

The major innovation that the liberal house (Fig. 1) introduces, in terms of functional organization relates to changing the type of usage, from multifunctional to single use as it is designed exclusively for residential purposes. Consequently, the ground-floor where the social spaces are located, moves away from the street, whereas the kitchen and services move to the basement, whilst the bedrooms are kept on the upper floors. The setback top floor, which is much used, and the attic of the roof are intended primarily as storage rooms and to support spaces or dormitories for employees.

The plots slightly increase in width (6.5 m average) and significantly in depth, as a consequence of the spatial evolution of housing, where the introduction of a central skylight allows for the existence of interior compartments. Health concerns determine an increase of the ceiling height and the introduction of toilets that are located on the facades of masonry.

Constructively, the systematization of the elements and construction processes is noted. The exterior walls are entirely in brick, with the exception of the facades of recessed floors, supported on the logs. The facades acquire a more austere design, starting to use the tile as a preferential coating choice. In the structure of the floors, as well as on the roof, the application of wooden log coexists with the squared beams. The finish of the floor continues to use pine planks and the ceilings are already coated with stucco work more or less elaborate depending on the economic capabilities of the owners. The hip type roof remains and the gable type emerges, all with more slope, allowed for by the use of the

Marseille tile. The skylights, raised or low-flying, square or circular, are new elements to emerge in the rooftops worthy of highlighting.

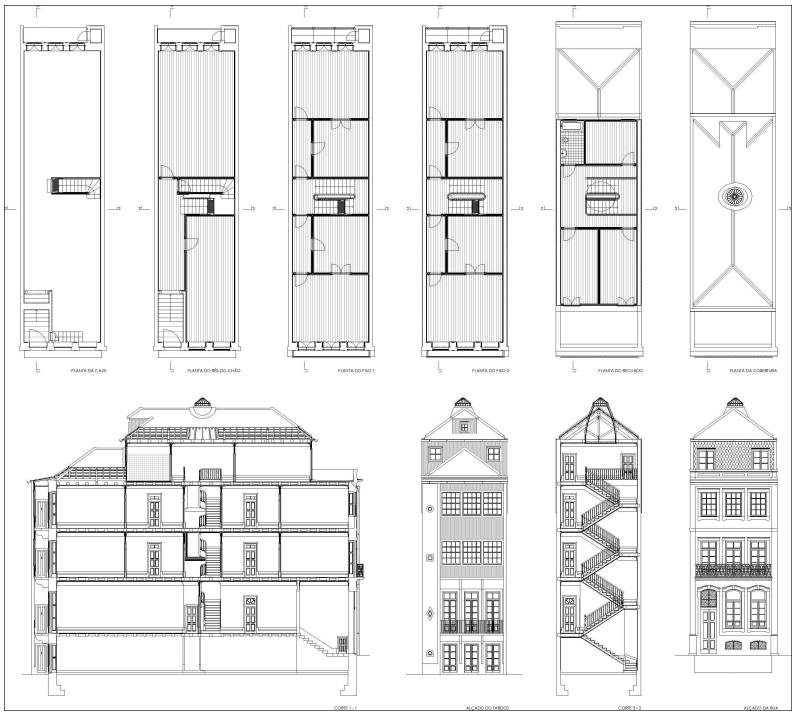

Figure 1. Plans, sections and elevations of the buildings that constitute the constructive model, namely a liberal house, corresponding to the nineteenth century.

The constructive model is represented in the drawings of plans, sections, elevations and typical-details, in scales never less than 1:50, representing the general, and up to 1:1, for detail.

The model representing the constructive system of the houses in detail, as well as other information characterizing the buildings, for example: the most frequent anomalies or commonly introduced changes [Teixeira & Póvoas 2009] should be a supporting tool for the preliminary design assessment and diagnosis, but also for the design and construction, helping to streamline the complexity of interventions. In this sequence, by analogy, it is possible for the technicians to regulate inspection of the existing, making it more assertive, thus reducing the time spent in the preliminary diagnosis. Moreover, this procedure will prevent or minimize the inconvenience that these operations are having on users, where it is necessary to keep the buildings open.

3 FROM THE CONSTRUCTIVE MODEL TO THE CHARACTERIZATION OF THE PATHOLOGICAL CONTEXT

The characterization of the anomalies most important and most frequent, to apply to the constructive model refers mainly to the phenomena noticeable by simple observation, which does not require more complex testing, involving varying degrees of intrusiveness. This systematization stems from the authors personal experience, from consulting existing documentation in the offices of the local authority responsible for the historic centre urban conservation, the old CRUARB, currently under the Society for Urban Renewal (SRU), Porto Vivo, and the establishment of similarities with other published studies such as [Cóias 2006]: [Feiffer 1995], [Cabrita 1993], [Appleton 2003], [Aguiar *et al*. 2005], etc.

Research done to the collection of CRUARB has revealed the existence of too brief or insufficient information regarding the characterization of buildings worked on, particularly with regard to surveys

(geometric and photographic) and records of inspection and diagnosis of abnormalities. If at the start of this government agency activity this lack of records can be justified by the unstable post-revolutionary period of April 25, nevertheless the responsibility for the heritage conservation of the historic centre that is granted later should have imposed more rigorous performances. As for the existing documentation in the current SRU relating to the buildings recently intervened upon, there are only short surveys, virtually brief descriptions based on simple observations, unrelated to the geometric survey, as well as a generalized absence of more detailed inspections.

3.1 The Form of Representation

The organization of the pathological context through the graphic elements is done from the general to the particular, following the scales normally used in the projects: plans, sections and elevations to scale 1:50; internal spaces or relevant areas to the scales 1:25 or 1:20; unique elements such as exterior and interior joinery, to scale 1:10 and typical details to scales 1:5, 1:2 and 1:1.

The 1:50 scale encompasses drawings of plans, sections and elevations, representing an overview of the building and the integration of different parts in the development. This scale can cover a lot of information about the various anomalies, indicating for example its exact location, some quantitative and qualitative data or reference to other drawings where there is a detailed approach (Fig. 2).



Figure 2. Elevations, of street and courtyard, to scale 1:50, of a bourgeois house in Porto. Model, corresponding to the Liberal period, indicating the most frequent anomalies.

The 1:20 or 1:25 scales consist mainly of drawings of plans, sections and elevations, representing partial areas of the building or specific elements which are considered worthy of mention. Examples: excerpts from the walls, the main interior spaces, unique elements such as skylights or dormers, etc.. The ability of these scales to contain more detailed information allows for the inclusion in the drawing of more data about the anomalies and the elements in the analysis (Fig. 3).



Figure 3. Plans, of floor and ceiling, and elevations of a main interior space of a bourgeois house in Porto, to scale 1:20, indicating the most frequent anomalies.

The 1:10 scale, which may still consist of plans, sections and elevations, often represents the elements whose specificity is worthy of emphasis, such as interior and exterior joinery (Fig. 4), skylights, windowpanes, dormers, etc. Finally, the scales 1:5, 1:2 and 1:1, typically consist of drawings of sections, used to represent the typical details, of transition or closing situations, examples of which include: gutters (of parapet or division wall), eaves, transitions existing on roofs, transitions between floors and between exterior or interior walls, etc.

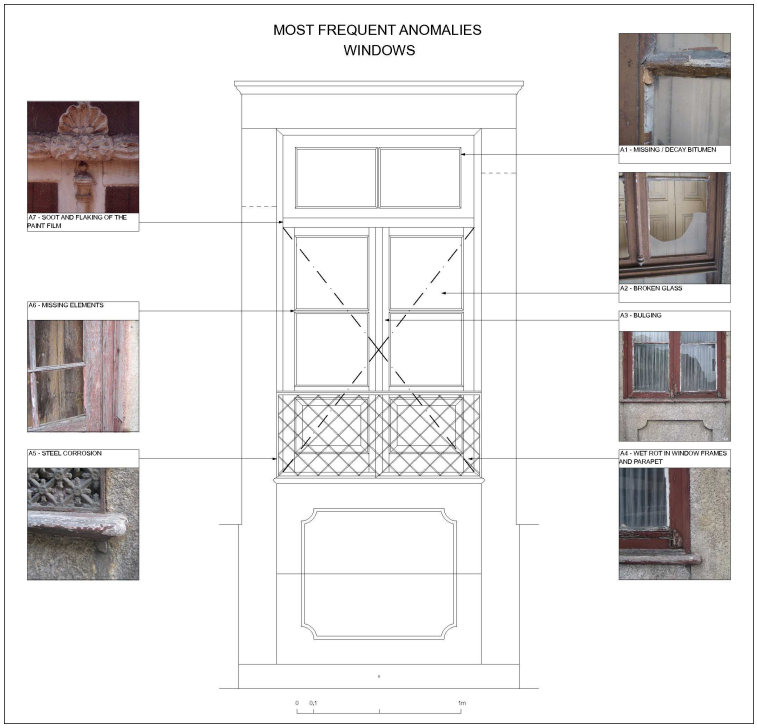

Figure 4. Elevation of a window to scale 1:10, indicating the most frequent anomalies.

Since the various scales which constitute the most frequent characterization of the pathologies of bourgeois houses of Porto are interdependent and complementing each other, it is essential to ensure the good connection between the drawings in order to enable their easy reading and coherence.

The graphic elements described will be accompanied by inspection and diagnosis summary reports with other complementary data, such as: causes and consequences of deficiencies, repair solutions and prevention methods, considered essential to a better definition of the pathological context of the buildings.

We hope that this proposed constructive model with an indication of the pathological context of bourgeois houses in Porto will form a valuable contribution to the development of a methodology for intervention in these and other ancient buildings, helping to streamline the complex process that characterizes this type of actions, thus fulfilling the objectives of increasing its number and quality, of preserving the authenticity of an heritage property, as well as of a sustainable activity.

ACKNOWLEDGMENTS

The authors thank the Portuguese Foundation for Science and Technology (FCT) the financial support of the R&D Unit where they are integrated – Centro de Estudos em Arquitectura e Urbanismo (CEAU) da Faculdade de Arquitectura da Universidade do Porto. JT hereby acknowledges the FCT for the scholarship with the reference SFRH/BD/61158/2009.

REFERENCES

Aguiar, J. *et al*. 2005, *Guião de apoio à reabilitação de edifícios habitacionais*, LNEC, Lisboa.

Appleton, J. 2003, *Reabilitação de edifícios antigos: Patologias e tecnologias de intervenção*, Edições Orion, Amadora.

Cabrita, A. *et al*. 1993, *Manual de Apoio à Reabilitação de Edifícios do Bairro Alto*, CML, LNEC, Lisboa

Cóias, V. 2006, *Inspecções e Ensaios na Reabilitação de Edifícios*, IST Press, Lisboa.

Feiffer, C. 1995, *Il progetto di conservazione*, Franco Angeli, Milano.

Fernandes, F. 1999, *Transformação e permanência na habitação portuense. As formas da casa na forma da cidade*, Publicações FAUP, Porto.

Loza, R. *et al*. 2008, *Centro Histórico do Porto Património Mundial: Plano de Gestão – Volume I*, Porto Vivo - SRU, CMP, Porto.

Teixeira, J. 2004, *Descrição do sistema construtivo das Casas Burguesas do Porto entre os Séculos XVII e XIX. Contributo para uma história da construção arquitectónica em Portugal*, FAUP, Porto.

Teixeira, J. & Póvoas, R. 2010, 'Proposta de Metodologia de Intervenção para a Reabilitação do Património Urbano Edificado. As Casas Burguesas do Porto – Coberturas', Proc. Reabilitar 2010 – Encontro Nacional Conservação e Reabilitação de Estruturas, Lisboa, Portugal, 23 25 June, pp. 94-95.

Teixeira, J. & Póvoas, R. 2009, 'Tipificação das alterações correntemente introduzidas no sistema construtivo das casas antigas do Porto', Proc. Patorreb 2009 - 3.º Encontro Sobre Patologia e Reabilitação de Edifícios, Porto, Portugal, 18 20 March, pp. 697-702.

XII DBMC
International Conference on Durability of Building Materials and Components
PORTO - PORTUGAL, April 12th-15th, 2011

Evaluation of Salt Removal from Azulejo Tiles and Mortars Using Electrodesalination

Célia M.D. Ferreira [1]
Lisbeth M. Ottosen [2]
Iben V. Christensen [3]
Sabina H. Brammer [4]
Daniela A. F. Sveegaard [5]

ABSTRACT

Azulejo tiles are part of the Portuguese cultural heritage and are worldwide appreciated. The durability of this building material is affected by the accumulation of salts, causing fractures and peeling of the glazing and ultimately leading to the degradation of the tile panels and the irremediable loss of historic value. In this work preliminary studies with single tiles presenting an underlying layer of mortar have been conducted to assess the amount of salts that can be removed from the building material using a new technique called "electrodesalination", in which the salt's ions are transported out from the tiles by applying an electric current on the backside.

Results shown here include an assessment of how much of the salts did come out in comparison to what was originally there, and additionally if the electrodesalination succeeded in removing salts down to a point where the tile and underlying mortar are no longer at risk of salt induced decay.

The main conclusions are that the technique is successful in extracting salts from mortars (removals efficiencies between 88% and 92%) but not as good for the tile (removals between 10% and 80%). The risk of salt damage to the mortar and tile was either considerably reduced or disappeared, except for one situation with nitrates, thus showing that even though some optimisation is needed, electrodesalination stands as a promising in-situ technique to improve durability of the historic valuable Portuguese Azulejo tile.

KEYWORDS

Azulejo, Salt removal, Electrokinetic

[1] CERNAS-Centro de Estudos de Recursos Naturais, Ambiente e Sociedade, Coimbra, PORTUGAL, celia@esac.pt
[2] Technical University of Denmark (DTU), DENMARK, lo@byg.dtu.dk
[3] Technical University of Denmark (DTU), DENMARK, ivch@byg.dtu.dk
[4] Technical University of Denmark (DTU), DENMARK
[5] Technical University of Denmark (DTU), DENMARK

1 INTRODUCTION

Azulejo tiles are part of the Portuguese cultural heritage and are worldwide. The durability of this building material is affected both by the original materials used and by the environmental conditions. The appearance of salts at the surface damages the tile (fractures, peeling, granular disintegration, etc.) and ultimately leads to the degradation of the tile panels, with the loss of historic value. Electrodesalination, also called electrokinetic extraction of salts, is a method under development which is based on well-established electrochemical principles: under the electric field positive ions move towards negative electrodes and negative ions move towards positive electrodes. As time passes ions will be depleted from the tile and concentrate in the vicinity of the electrodes (more detailed information about the technique can be found in Ottosen *et al.* 2010). One important advantage of electrodesalination compared to traditional poulticing (next to offering a faster transport of salts out from the material) is that the poultice with electrodes does not have to cover the whole surface to be desalinated. The electric field will be strongest where the conductivity is highest and that is where the ionic concentration is highest. Thus the electric field will be strongest exactly where the salts are concentrated even though the electrodes are not placed directly in this place.

Electrodesalination has been applied with success to single bricks (99% removal of NaCl; Ottosen & Rorig-Dalgaard 2009) and in a pilot scale experiment of a salt contaminated masonry from an old house (Ottosen *et al.* 2008). In a preliminary study on the desalination of Portuguese Azulejo tiles (Ottosen *et al.* 2010) significant decreases in salt content (>81% Cl^-, 59% NO_3^-, 22% SO_4^{2-}) were reported for single tiles without an underlying layer of mortar. However, in real situations the tile is usually applied to a wall with a layer of mortar, and this can affect the success of the desalination process. In the work presented in this paper the investigation was taken a step further by performing desalination on tiles which have an original underlying layer of mortar.

2 EXPERIMENTAL

2.1 Tiles

Azulejo tiles from 3 different epochs were used in the current work (see Fig. 1). A piece of tile (8x 6 x1,5 cm) from the **XVII-century** was collected from the Alentejo region (south and central Portugal) and presents a yellow biscuit with white and blue glazing on the surface. On the backside there is a layer of mortar approximately 1.5-2 cm thick. A reference sample was obtained by cutting off a small piece from the corner.

The tile from the **XVIII-century** was removed from Palacio Centeno (in Lisbon) during renovation works due to severe salt damage. The biscuit is yellow, and measures 14 cm by 14 cm and is 0.9 cm thick. On the backside there is a layer of mortar between 0 and 1.5 cm thick. The mortar easily disintegrated and felt like coarse-grained sand. A reference sample was taken by cutting off a small piece from the corner.

The tile from the **XX-century** presents a red biscuit with dimensions 14cm x 14 cm x 1.5 cm. On the backside there is a 1 cm thick layer of mortar. Approximately one third of the surface is covered by a yellow and white glazing. One of the 2 tiles available was used as reference and the other was used in the electrodesalination experiments. The tile used as reference was segmented into 8 pieces: 4 used as reference for the mortar and 4 as reference for the biscuit.

2.2 Electrokinetic Desalination Experiments

The tiles had been stored in a box at room temperature and were almost dry, so before the experiments they were wetted by spraying distilled water on the back (mortar side) until the tile would not absorb any more water. For the experiment the tiles were wrapped in plastic film (to

prevent evaporation) and placed with the glazing facing down. Two square holes (3x3 cm, each) were cut in the upper surface of the plastic film, as far apart as possible. A plastic frame (approximately 4 cm high) was placed over each hole and filled with a poultice (mixture of kaolin and $CaCO_3$). An inert electrode mesh was placed over the poultice and covered with another thin layer of poultice. Plastic film was wrapped around these and the electrode mesh was connected to a power supply.

At the beginning of the desalination experiments the current was set to 5 mA and the voltage was around 20V. During the experiments the voltage was read once or twice a day (except for weekends) and the current was kept constant as long as the voltage did not increase more than 137 V. If the voltage was too low and remained unchanged for the following days then the current would be increased manually to a maximum of 20 - 25 mA (depending on the voltage).



Figure 1. Photographs of Azulejo tiles used in the electrodesalination experiments (left: front of tile; middle: back of tile, with mortar; right: side view)

The poultice consistency was checked regularly to prevent drying. For the XX-century tile small amounts of distilled water were added to the poultice whenever it was too dry. However, fearing that this might flush salts that had been previously removed, it was decided to instead change the poultice (which occurred around day 23 of the experiment). Poultice for the XVIII-century experiment was initially changed once a week. After increasing the current, first to 10 mA and then to 20 mA, it was decided to change the poultice twice a week since at these higher currents acid production increases. The XVII-century experience lasted for seven days, so poultice was collected only at the end. Table 1 summarises the experimental conditions.

Table 1. Current, voltage and duration in the tile electrodesalination experiments.

	XVII	*XVIII*	*XX*
Current [mA]	1,51 →0,47	4,99→10→20	4,99 →0,99 →0,54
Voltage [V]	20,7 - 75,0	2,4 - 31,8	13,7 – 91,7
Duration [days]	7	24	34

After the experiments the tiles were unwrapped and segmented into pieces (mortar and biscuit) with a hammer and a chisel, as depicted in Figs. 2 to 4. Segments were numbered from 1 to 3/4, with an anode placed over segment 1.

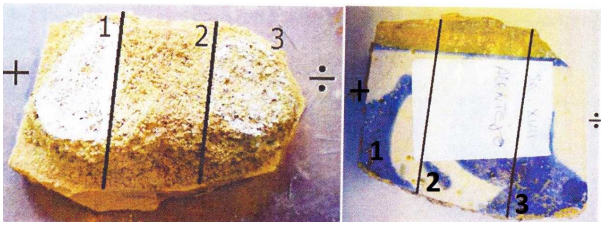

Figure 2. XVII-century. Left: segmentation of mortar; right: segmentation of biscuit.

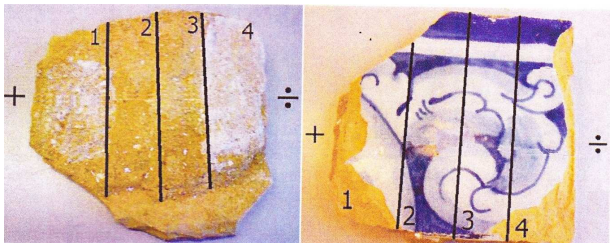

Figure 3. XVIII-century. Left: segmentation of mortar; right: segmentation of biscuit.

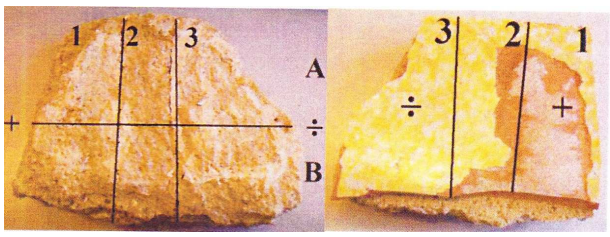

Figure 4. XX-century. Left: segmentation of mortar; right: segmentation of biscuit.

2.3 Analytical

Each segment (including references taken before the desalination experiments) was weighed, dried at 105ºC for 24h and weighed again to determine water content. The dried pieces were then powdered by hand using a mortar and pestle. Extractions in distilled water (10g powdered tile suspended in 25 mL) were made and after 24-h agitation the pH was measured with a pH electrode and conductivity with a conductivity electrode directly in the suspension; the suspension was subsequently filtered and the concentrations of Cl^-, NO_3^-, SO_4^{2-} measured by ion chromatography and Na^+ by atomic absorption.

3 RESULTS AND DISCUSSION

This investigation includes 3 electro-desalination experiments, each conducted with a tile from a different epoch: XVII-century, XVIII-century and XX-century.

3.1 Biscuit and Mortar Characterization

Values for conductivity, pH and ion concentrations measured in the different biscuits and mortars are shown in Table 2. These values were measured on references samples taken before the electrodesalination experiments. For the XX-century tile 4 fragments were used, whereas for the other epochs only one sample was analysed, which consisted in a small piece taken from the corner of the tile. Standard deviation in the XX-century reference shows a high variability for salt concentrations, indicating that biscuit and mortar are not homogeneous. This variation is more generally related to the salinization process than to the composition of the original base materials. When water evaporates at the surface of the tile leaving the salts behind (one of the possible salinization processes) it draws more water and salts from the surrounding materials (wall and ground) by capillary forces. The tile surface is covered with an impermeable glazing and water either evaporates at the joints (between the

tiles) or through cracks in the glazing. This means that water channels are formed within the biscuit and that the spatial distribution of salt is highly variable: i.e., a sample taken from a particular spot might not have salts at all, whereas another taken 2 or 3 mm away might have singular amounts. As a consequence, it is important to note that reference values for XVII and XVIII century tiles, which are based on a single, small sample taken from the corner of the tile before electrodesalination might not in any case be representative of the entire specimen.

To evaluate the initial anion concentrations in the tiles and mortars (shown in Table 2) comparison is made with the Austrian Önorm B3355-1 "Dehumidification of masonry – Building diagnostics and planning principles". This standard gives two thresholds (see Table 2): If the concentration is below the lowest threshold there is no risk; if the concentration exceeds the highest threshold, active salt removal is advised; in between the two thresholds values an individual, specific evaluation must be performed. Additionally to this standard classification the authors use the expression "severe problem" whenever the salt concentration is at least 4 times higher than the upper threshold value.

Table 2. Reference values for tiles and mortars (before experiments).

Century		*No. of samples*	*pH*	*Conductivity* [mS/cm]	Cl^- [mg/kg]	NO_3^- [mg/kg]	SO_4^{2-} [mg/kg]	Na^+ [mg/kg]
XVII	mortar	1	9,0	0,31	93	126	32	41
	biscuit	1	9,1	0,26	53	42	53	53
XVIII	mortar	1	8,9	15,07	6656	13921	64	3480
	biscuit	1	8,2	17,61	7927	17036	350	4680
XX	mortar	4	9,5±0,1	1,28±0,89	222±111	133±62	1542±1493	47±18
	biscuit	4	9,6±0,2	0,59±0,39	78±18	39±24	653±585	38±7
Önorm B3355-1	Low:	-	-		300	500	1000	-
(Thresholds)	High:	-	-		1000	1500	2500	-

The concentrations of Cl^-, NO_3^- and Na^+ in the XVIII-century tile are very high, largely exceeding Cl^- and NO_3^- upper threshold values, thus indicating a severe salt problem. The panel from where this tile was collected showed visible signs of salt damage, and high salt concentrations were expected.
For the XX-century tile concentrations of SO_4^{2-} lays between the two thresholds of values given in the B3355-1 standard, indicating that this ion might cause problems. Concentrations of other anions are below the lower threshold and therefore do not constitute a problem.

The XVII-century tile had comparatively small amounts of salts, all lying well below the lowest threshold of the B3355-1 standard. According to these results, summarised in Table 3, there are 3 situations where desalination is required or advisable, namely: removal of Cl^- and NO_3^- from the XVIII-century tile and removal of SO_4^{2-} from the XX-century tile.

3.2 Desalination Results

Discussion of electrodesalination results of the 3 tiles will focus on the situations where salts are a problem, namely Cl^- and NO_3^- from the XVIII-century tile and SO_4^{2-} from the XX-century tile. The sections under this heading include (1) concentration profiles of salt in mortar and biscuit after desalination; (2) removal efficiencies; and (3) evaluation of final salt concentrations.

3.2.1 Profiles after the desalination

The reference analysis of the **XVIII-century** tile indicated that it had a severe salt problem, with concentrations of Cl^-, NO_3^- and Na^+ reaching several thousand mg/kg, After being submitted to electrodesalination for 24 days the concentrations in the mortar were considerably reduced (Fig. 5) for all ions but SO_4^{2-}, whose initial concentrations were already low (<100mg/kg). The concentrations were also decreased in the biscuit. Ion concentration varies in the 4 segments, forming a typical

profile: as the ions move towards the target electrodes through the segments they become depleted in the segment from which they migrated and accumulate in the next segment. The results shown in Fig.5 are consistent with ion's charge: negative ions (Cl^- and NO_3^-) move under the electric field towards the anode (target electrode) placed over segment 1, resulting in lower concentrations in segment 4, while the positive ion (Na^+) moves towards the cathode placed over segment 4, with concentrations being minimum in segment 1. Accumulation of ions near the target electrode means that the desalination is not yet completed, and that ions are still moving from the segment into the poultice. As opposed to the differentiated profiles obtained for Cl^-, NO_3^- and Na^+, it can be seen that SO_4^{2-} concentrations are approximately even in the 4 segments, probably meaning that all mobile molecules under the electric field were removed, and only a residual, non-mobile fraction remains.
The **XX-century** tile has high initial concentrations of SO_4^{2-}, which decreases considerably after the 34-day electrodesalination experiment (for both tile and mortar). Residual values are similar in the three slices, indicating that all mobile SO_4^{2-} has been removed (Fig.6).

Table 3. Recommendations for the different materials according to their ion-concentrations

Tile/Mortar	*Cl^-*	*NO_3^-*	*SO_4^{2-}*	*Recommendation*
XVII-century	No problem	No problem	No problem	No action required
XVIII-century	Severe problem	Severe problem	No problem	Desalinization is required to remove Cl^- and NO_3^-
XX-century	No problem	No problem	Might be a problem	Desalinization might be advisable to remove SO_4^{2-}

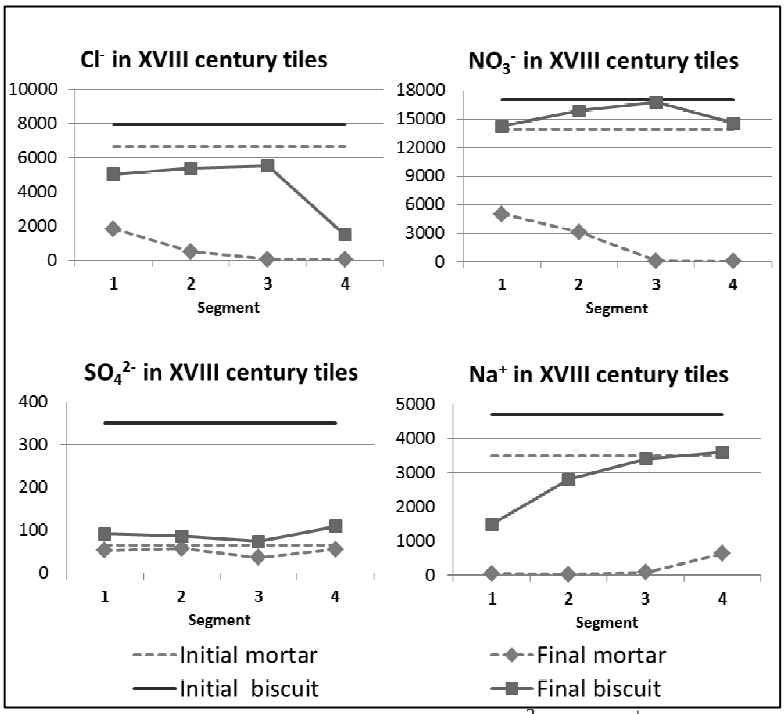

Figure 5. Concentration profiles (mg/kg) of Cl^-, NO_3^-, SO_4^{2-} and Na^+ in mortar and biscuit of XVIII-century tiles after electrodesalination

3.2.2 Removal efficiency

This section estimates how many ions the electrodesalination process was able to remove from the building materials as a percentage of what was originally there. Removal efficiencies are shown in Fig. 7 for the previously identified situations. When looking at these results one must keep in mind that they are based on an assessment of the initial concentrations which might not be representative of the tile, as was previously discussed (section 3.1).

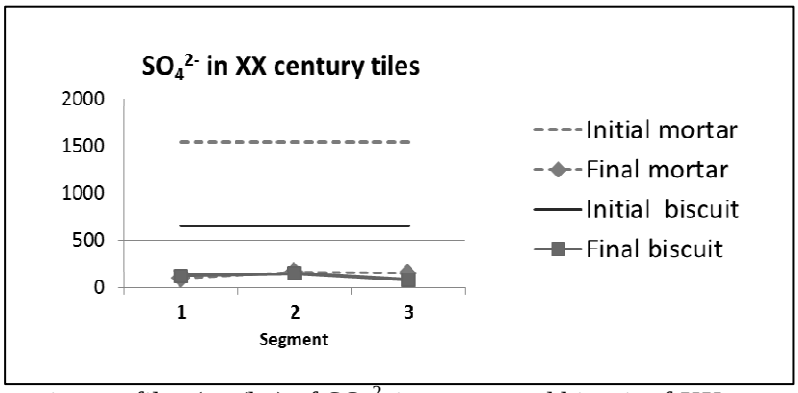

Figure 6. Concentration profiles (mg/kg) of SO_4^{2-} in mortar and biscuit of XX-century tiles after electrodesalination

Figure 7 shows that removal of ions from the mortar was very successful, with efficiencies between 88% and 92%. Biscuit desalination was not as good, with efficiencies ranging from 10% to 84%.
Why the biscuit seems to be more difficult to desalinate then the mortar can only be hypothesized at this point, but possible explanations range from the lay-out selected (electrodes are placed on mortar side, to physical characteristics (porosity, water content, chemical form of salts) all of which influence the solubility and mobility of the ions.

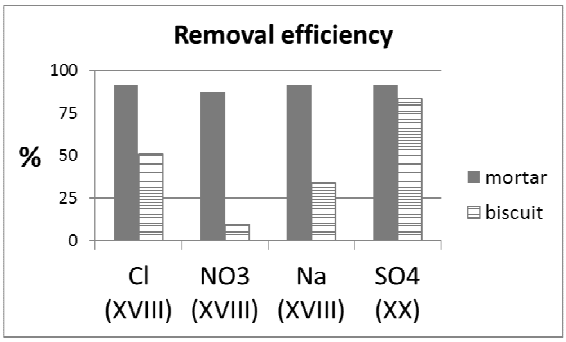

Figure 7. Removal efficiencies for different building materials (mortar and biscuit)

By analysing the results so far it has been possible to establish the amount of salts removed from the building materials into the poultice, and to show how much that is compared to what was originally there. But is it enough? Did the electrodesalination succeed in removing salts down to a point where the tile and underlying mortar are no longer at risk of being damaged due to high salt content? In the following section the success of the desalination experiments is further evaluated by comparing final concentrations in the building materials with the absolute values given in the B3355-1 standard.

3.2.3 Final concentrations in the biscuit/mortar against standard *B3355-1*
In this section the electrodesalination is further evaluated by comparing final concentrations in the building material against the values given in the B3355-1 standard. The concentrations given in the standard can be discussed as they are developed for single salts, which we do not have in the experimental tiles, but these are the only limiting values which are given and thus they are used for the evaluation.

On the basis of the initial assessment of salt levels in the building materials, three situations have been previously identified as requiring some type of action. Salt levels after the electrodesalination are now represented together with the upper and lower thresholds given in standard `B3355-1(Fig. 8) and an update of the salt problem after desalination is presented in Table 4.

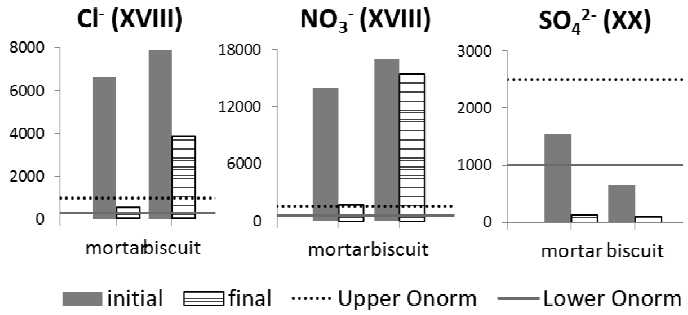

Figure 8. Comparison of initial and final levels of Cl^-, NO_3^-, SO_4^{2-} (mg/Kg) in mortar and biscuit with the thresholds of Austrian standard B3355-1.

From Fig. 8 and Table 4 it can be seen that mortar concentration were successfully lowered to either "no problem" or "possible problem". Results for the biscuit were not as good: NO_3^- continued to pose a severe problem (even though considerable amounts of NO_3^- were removed) and Cl^- concentrations are still several times higher than the upper threshold of the norm.

Table 4. Update of salt problems after electrodesalination

		Cl^- Before → after	*NO_3^- Before → after*	*SO_4^{2-} Before → after*	*Problem solved?*
XVIII	Mortar	Severe → possible problem	Severe → possible problem	-	MAYBE
	Biscuit	Severe → Problem	Severe → Severe	-	NO
XX	Mortar	-	-	possible → no problem	YES

4 CONCLUSION

Salts removal from the mortar adjacent to single tiles was very successful, with efficiencies ranging from 88% to 92%. Results were not as good for the biscuit, since salts were only slightly removed (efficiencies between 10% and 84%). This work shows that electrodesalination is a promising technique to desalinate mortar (and eventually the wall behind), but it still needs to be optimised to desalinate the tile. Further work will be conducted to solve the issues raised so that the technique can be applied in future restoration of the historically valuable Portuguese tile.

ACKNOWLEDGMENTS

The authors would like to thank Ivo Férin and colleagues (Loubet and Isabel) for providing the tiles used in this work.

REFERENCES

Ottosen, Lisbeth M., Ferreira, Célia M.D., Christensen, Iben. 2010, "Electrokinetic desalination of glazed ceramic tiles", *Journal of Applied Electrochemistry*, 40, 1161-1171.

Ottosen, L.M. & Rorig-Dalgaard, I. 2009, "Desalination of a brick by application of an electric DC field", *Materials and Structures*, 42[7], 961-971.

Ottosen, L.M., Rorig-Dalgaard, I., Villumsen, A 2008, "Electrochemical removal of salts from masonry – experiences from pilot scale", Proc. International Conference on Salt Weathering on Building and Stone Sculptures, Copenhagen, Denmark, 22-24 October 2008, pp. 341-359.

XII DBMC
International Conference on Durability of Building Materials and Components
PORTO - PORTUGAL, April 12th-15th, 2011

Improving the Durability of Portuguese Historical Gypsum Plasters Using Compatible Restoration Products

Teresa Freire [1]
Maria do Rosário Veiga [2]
António Santos Silva [3]
Jorge de Brito [4]

ABSTRACT

The study of the composition of mortars used in the protection of walls and ceilings in the past is extremely important to define sustainable strategies of intervention, concerning the preservation of these construction elements. These strategies should follow the modern theories of conservation and restoration, where authenticity and chemical, physical and aesthetic compatibility can only be achieved if based on the knowledge of the original materials and techniques of application.

In Portugal, the presence of gypsum plasters was particularly significant between the second half of the XVIII century and the first half of the XX, representing two centuries of important heritage never studied before.

This paper describes and discusses a methodology to establish compatibility criteria for the development of gypsum plaster restoration products and presents some requirements they should comply with based on the results of characterization of the old samples collected, from several case studies.

KEYWORDS

Portuguese gypsum plasters, restoration products, compatibility, cultural heritage

[1] National Laboratory of Civil Engineering (LNEC), Lisbon, PORTUGAL, mtfreire@gmail.com
[2] National Laboratory of Civil Engineering (LNEC), Lisbon, PORTUGAL, rveiga@lnec.pt
[3] National Laboratory of Civil Engineering (LNEC), Lisbon, PORTUGAL
[4] Instituto Superior Técnico, Technical University of Lisbon (IST-UTL), Lisbon, PORTUGAL, jb@civil.ist.utl.pt

1 INTRODUCTION

The use of gypsum-based materials for interior plastering of walls and ceilings was particularly significant in the Portuguese monumental and domestic architecture in the period between the 18th century and the first half of the 20th century. However, studies on this subject are rare and not focused on the materials science's point of view.

Insufficient information on the composition of the historic mortars is one of the main difficulties in the restoration and conservation of these materials and of the buildings in which they were applied. Portuguese gypsum plasters are not an exception. This lack of information on traditional materials and techniques of construction is leading to a significant loss of important heritage.

The study presented in this paper occurs in this context and is part of an extensive work developed in the National Laboratory of Civil Engineering (LNEC), a public institution of the Portuguese Ministry for Public Works, Transports and Housing, where the physico-chemical characterization of the Portuguese historical gypsum plasters from the 18th to the 20th century was the first step to reach the main purpose: the development of new compatible gypsum plasters for repair of these old materials.

2 EXPERIMENTAL PROGRAMME

2.1 Case Studies

The results presented in this work belong to eleven case studies located in four different regions: North, Centre, Centre-South (Lisbon area) and South of Portugal. Some are constructions of high patrimonial and architectonic value (e.g. palaces and churches) and others are more common buildings, used for dwelling purposes, but of architectural interest. They were all built between the second half of the 18th century and the first half of the 20th century (Table 1).

Table 1. Case studies: identification and main information.

Region	*Case study*	*Period*	*Location*	*No. of samples analysed*
North	Porto cathedral: *Santíssimo's* chapel (SP)	19th century	Porto	3
	Bolsa palace (PB)			5
	Cine-Theatre building (CTF)	20th century	Fafe	2
Center	*Barão Salgueiro* palace (PBS)	19th century	Leiria	3
	Garage building (EG)	20th century		5
	Beira-Rio building (EBR)			3
Centre-South (Lisbon region)	*Casa de Pesca* from the Marquis of Pombal property (CP)	18th century	Oeiras	3
	Monserrate palace (PM)	19th century	Sintra	5
	Liberty avenue building (EAL)	20th century	Lisbon	1
South	Church of the old *S. Francisco's* convent (ISF)	19th century	Tavira	3
	Estoi Palace (PE)	19th-20th century	Estoi, Faro	4

2.2 Samples

A total of 37 samples were collected by the authors in two different ways: indirectly, i.e. they had been previously detached due to some reason; directly on site. They all belonged to buildings needing an intervention or with an intervention occurring.

As the aim of this research work is to characterize the original gypsum plasters and the techniques of application used to apply them, special care was taken on the collection of the samples, namely by avoiding areas in the buildings where anomalies had occurred. This procedure was adopted to prevent

affecting the results by any kind of adulteration suffered by the materials.

In the samples where the presence of a finishing product was detected, its removal was carefully performed in order to avoid contamination of the plasters. Whenever a sample was composed by more than one layer (something that in some cases could only be detected by the observation of its polished surface at the stereo-zoom microscope), special care was taken in order to collect them separately and consider it as individual samples, making a total of 49 samples analysed.

2.3 Analytical Techniques

The mineralogical and chemical properties of the samples were determined using the analytical methodology developed by Santos Silva *et al.* [2005]. After a detailed visual observation of the samples and photographic register, they were dried at 40 ºC for about 12 hours. To enable the detection of hygroscopic compounds or soluble salts that could lose their crystallinity the samples were not dried to mass constancy. Each specimen was split into several fractions to be used for different techniques.

Polished surfaces of the gypsum samples were prepared by impregnation under vacuum with an epoxy resin. They were observed with an Olympus stereo-zoom microscope and images were recorded digitally. The stereo-zoom microscope was used to study the textural properties of the existent layers in the samples (stratigraphy) and to also identify the mineralogy and morphology of the aggregates and possible pigments.

X-ray diffraction (XRD) was performed to allow a further insight on the mineralogy of the binder and other constituents such as the aggregates. A Philips X'Pert diffractometer with cobalt Kα radiation, step of 0.05º/s, between 2θ 3º and 74º, was used. The thermogravimetry and differential thermal analysis (TGA/DTA) provided additional data on the quantitative composition of the samples, namely the relationship between the gypsum and calcite content. A Setaram TG-DTA analyser was operated in an argon atmosphere with a uniform heating rate of 10 ºC/min from room temperature to 1000 ºC.

Observations were made using a scanning electron microscope (SEM) JEOL JSM-6400 coupled with an OXFORD energy dispersive spectrometer x-ray detector (EDX), both on polished surfaces (with backscattered electrons - BSE images) and freshly fractured surfaces (using secondary electrons - SEI images) that were sputtered with carbon in a JEOL JEE-4X vacuum evaporator or with gold-palladium film in a BALTEC sputter coater.

Some physical and mechanical properties were also determined using in some cases techniques specially developed for irregular, often friable samples [Veiga *et al* 2004, Válek & Veiga 2005]. The samples collected were irregular and they were cleaned of any powder and biological colonisation before being subjected to a controlled environment (23 ºC and 50% RH).

Water absorption tests were made by the capillary absorption by contact technique [Veiga *et al.* 2004].

In the compressive strength test, the regular shape necessary for adaptation to the compressive machine and for the calculations was achieved through the use of a confinement mortar, designed to be stronger than the analysed samples and composed by cement and siliceous sand, with volumetric proportions of 1:3 [Válek & Veiga 2005, Magalhães & Veiga 2009].

The dynamic modulus of elasticity was determined using ultrasounds, based on the emission of high frequency sound waves and the measurement of their velocity through building materials, allowing the calculation of elastic parameters (BS 1881-203 1986).

The water vapour permeability was determined through the method described in EN 1015-19, adapted

to the dimensions of the sample. The method is based on the measurement of the water vapour flux through the sample by evaporation due to a pressure differential, determined by the weight variations.

The method used to evaluate hygroscopicity [Magalhães & Veiga 2007] consisted on measuring the weight variations of samples previously dried and then placed at constant temperature (23 ± 0.5 ºC) and subjected to increasing moisture conditions (30%, 50%, 70%, 90% - adsorption conditions). The same samples were then subjected to the same relative humidity levels in inversed order (dessorption conditions). The porosimetric structure was evaluated by the Mercury Intrusion Porosimetry (MIP) technique, based on the relationship between the pores' diameter and the pressure needed to fill them with mercury [ASTM D4404-84 1998].

3 RESULTS AND DISCUSSION

3.1 Chemical and Mineralogical Characterization of the Samples

The mineralogical characterization by XRD indicated that all samples are mainly composed of gypsum and calcite with traces of quartz, as already detailed in previous works [Freire *et al.* 2008, 2010a, 2010b]. The only exceptions were PE4/2, where the presence of hematite (pigment used to colour the plaster) and anhydrite was also detected and PM1, composed by gypsum and anhydrite. The latter compound was probably used as a binder that did not rehydrate completely, as SEM observations of PE4/2 seem to indicate [Freire 2009]. SEM observations and EDS analysis can also confirm that the aggregates, perceptible in most of the cases, are fine and of calcitic origin [Freire *et al.* 2010a].

Thermal variations associated with the chemical and physical transformations, such as dehydration of calcium sulphate dihydrate ($CaSO_4.2H_2O$) in the range 85-250 ºC and decomposition of carbonates ($CaMg(CO_3)_2$, $CaCO_3$) in the range 600-850ºC, were obtained by TGA-DTA analysis. From these data, the amount of gypsum and calcite were calculated and the results of XRD could be confirmed [Freire *et al.* 2008, 2010a, 2010b]. They show that in precast decorations gypsum is practically the only constituent. The small amounts of calcite detected in some samples (1-6%) are probably an impurity of the raw material, very common in gypsum quarries. In the samples where application has been made directly on site, the addition of calcitic lime was common, in order to improve the workability of the fresh materials. This is even more noticeable in the samples of smooth surfaces, especially those with a lower thickness, whose application needed a longer time (Table 2).

Table 2. Chemical and mineralogical results obtained by XRD and DTA-TGA analyses.

Type of sample	*Number of samples analysed*	*Calculated average content (%)*	
		Gypsum ($CaSO_4.2H_2O$)	*Calcite ($CaCO_3$)*
Smooth surface	19	38	53
Regularization layer	3	67	28
Moulded on site	5	57	40
Moulded on a bench	5	39-94*	2-57*
Plaster bonding layer	2	48	50
Precast	15	90	7

*Due to the great variability of results obtained, the minimum and maximum values are presented.

Samples of the same type coming from distant regions have similar compositions, suggesting that the working techniques did not vary inside the country.

Additional information was obtained from TGA-DTA analyses as weight loss (3-4%) in the range 250-600 ºC was observed in some samples, suggesting the presence of organic compounds. FT-IR analyses were performed in these samples and traces of grease-like additions were detected [Candeias & Valadas 2010], which was not a surprise as the use of these materials was a common practice in the old gypsum plasters recipes [Turco 1990, Arcolao 2001].

3.2 Physical Properties

The determination of some physical properties was carried out in those samples where sufficient quantity was available for the execution of the corresponding experimental techniques (Table 3). In the samples of smooth surfaces the dynamic modulus of elasticity (DME*)*, the compressive strength, the hygroscopicity and the water vapour permeability (WVP) tests were performed in the gypsum plaster layers together with the underlying mortars, which undoubtedly influenced and introduced a greater variability in the results obtained. This was taken into account in the discussion of these results.

Four samples showed values of the dynamic modulus of elasticity within a moderate range (2500-4000 MPa); three samples were lower (two from smooth surfaces and one from a regularization layer, PE2/1; all of them thin and tested with the underlying mortars) and one higher (PE4/2).

Similarly, most samples with compressive strength lower than the medium range 1.5-2.5 N/mm^2 belong to the smooth surfaces group and again PE2/1 from the regularization layer group. It was not possible to test PE4/2 separately, but the value obtained for the set PE4/1+PE4/2 (PE4) points to high strength for PE4/2, consistent with its dynamic modulus of elasticity (9735 MPa).

Table 3. Results of the physical properties determined.

Test	*Smooth surface*	*Moulded on site*	*Moulded on a bench*	*Precast*
DME (MPa)	**1123-3908**[(1)] (6)	**1885, 2875** (PE2/1, EG5/2)	**2572-9735** (PE4)[(2)]	**2590-4312** (5)
Compressive strength (N/mm^2)	**0.88-1.43** (3)	**1.10, 2.52** (PE2/1, EG5/2)	**2.66** (PE4)	**1.41-2.63** (3)
Ccc-5min ($kg/m^2h^{1/2}$)	**0.39-10.44** (7)	**16.62** (EG5/2)	**13.03** (PE4/1) **1.80** (PE4)	**0.82-11.28** (3)
Hygroscopicity at 90% RH (%)	**0.18-0.40** (4)	**0.58, 0.25** (PE2/1, EG5/2)	**0.98** (PE4/1) **0.98** (PE4/2)	**0.19-0.66** (5)
WVP (ng/m.s.Pa)	**20.07-30.70**	**21.88** (PE1/1)	**13.61 (**PE4)	-
Total porosity (%)	**42.75-52.45** (4)	**59.70, 53.05** (PE2/1, EG5/2)	**12.30** (PE4/2)	**45.95-53.05** (3)

Note: In brackets is the number (or the name) of samples in which the test was performed.
[(1)]In the thinner samples it was measured on the surface ("indirect method"). [(2)]Sample PE4 was tested in three different ways: altogether; PE4/1 - interior layer; PE4/2 - decorated layer simulating a marmorino [Freire, 2009].

The capillary coefficients were found to be scattered: typically high in half the tested samples and low or very low in the other half. No direct relationship between these results and total porosity was found, which suggests a probable interference of organic compounds of hydrophobic behaviour [Turco 1990, Arcolao 2001] and is consistent with the grease-like additions identified by Candeias & Valadas [2010].

In fact, the usual relationship between compressive strength and modulus of elasticity directly related, and capillary coefficient and total porosity inversely related to both of them, is not clear in most of the cases. One thing that is certainly responsible for this is the fact that it was not possible to test the very thin plaster layers separately from the regularization mortar; a second thing is the presence of the referred organic compounds, typically used for plasticity and decorative purposes. For example, PE1/2 and PE2/2, two samples that were expected to have similar values (they are both precast gypsum plaster decorations, with very close gypsum/calcite content) have rather different compressive strength values (2.63 and 1.41 N/mm^2) and capillarity coefficients (respectively 0.82 and 4.13 $kg/m^2h^{1/2}$). The irregular shape of the samples tested is also an extra variable. The same could be said of PE4/2, although in this particular case the density of the sample (twice that of PE4/1) has to be considered and

is in accordance with the respective DME and Ccc-5min [?] results, indicating a very stiff and compact material.

Another important feature was the MIP curves obtained. These results show that the samples where gypsum is the only constituent (or almost) the amount of pores under 0.1 micron is negligible, and the maximum is around 1 micron. On the contrary, the gypsum-lime plasters have always a significant amount of pores with radiuses under 0.1 micron and the maximum is usually located in the range 0.3-0.7 micron. To illustrate that, the MIP curves of four samples belonging to the *Estoi* Palace case study (Fig. 1) and the corresponding chemical content (Table 4) are presented.

The hygroscopic behaviour of these samples was studied and the results were in agreement with the MIP curves: the samples with a significant amount of pores under 0.1 micron showed, in general, higher hygroscopicity than those where the porosity was almost 100% above this value (Fig. 2).

The morphological study of samples PE2/2 and PE5 by SEM showed very distinct structures (Fig. 3): PE2/2 has long prismatic crystals, resulting from the hydration of calcium sulphate hemihydrate and PE5 is mainly composed of small hexagonal, laminar and sometimes almost round shaped crystals, with much less empty space between them. These observations are also in agreement with the corresponding MIP curves (Fig. 1) discussed in the previous paragraphs.

Finally the water vapour permeability values obtained are high and in the same range in all the samples, except for sample PE4, which also shows a very low porosity and high modulus of elasticity. When compared to the results usually obtained for lime mortars [Margalha, 2009; Veiga et al., 2010], the values of most of the samples are similar, again with the exception of PE4, which is much lower.

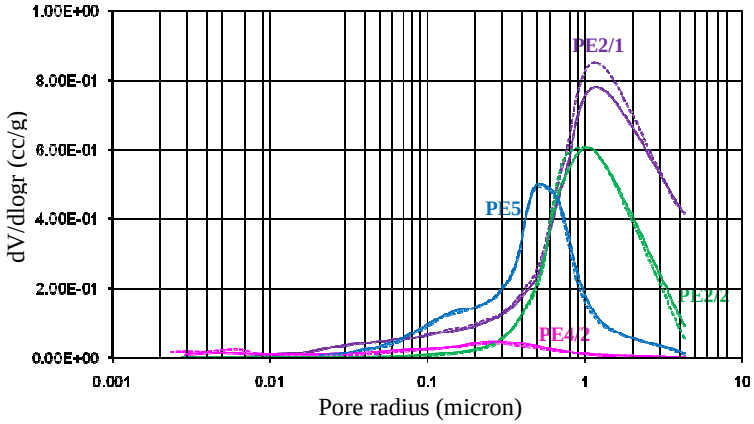

Figure 1. Porosimetric distribution of four samples from *Estoi* Palace.

Table 4. Gypsum and calcite contents in *Estoi* Palace samples.

Sample	*Calculated content (%)*	
	Gypsum	*Calcite*
PE2/1	48	48
PE2/2	82	16
PE4/2	85	2
PE5	30	65

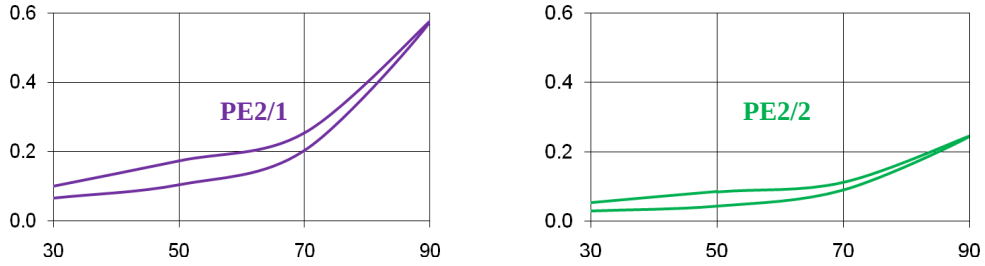

Figure 2. Hygroscopic behaviour of PE2/1 and PE2/2 samples from *Estoi* Palace.

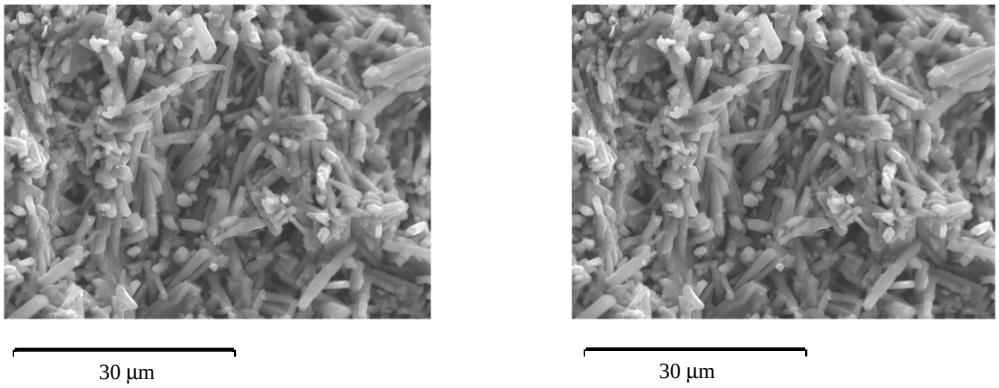

Figure 3. SEM microphotographs of samples PE2/2 (left) and PE5 (right) (2000 X).

4 RESTORATION PRODUCTS

The restoration products for gypsum plasters should be compatible with the existing materials and should not contribute to accelerate their degradation. Thus it is paramount that they have similar chemical and physical characteristics.

Based in the present results, three restoration products will be designed using industrially produced calcium sulphate hemihydrate (HH) and hydrated lime (HL), both in powder form. It is advised that the physical characteristics of these products follow the compatibility ranges proposed in Table 5. The mix proportions are presented in weight. However, these ranges should be adjusted in a more advanced phase of the research, when more results become available.

Table 5. Compatibility ranges for the restoration products.

Restoration product	Smooth surfaces (R1) 20% HH + 80% HL	Moulded on site (R2) 50% HH + 50% HL	Precast elements (R3) 90% HH + 10% HL
DME (MPa)	800-1500	1500-2500	2500-3500
Compressive strength (N/mm^2)	0.7-1	1-1.5	1.5-2.5
Ccc-5min ($kg/m^2h^{1/2}$)	5-10	10-15	5-10
Porosity (%)	40-55	50-60	40-55
WVP (ng/m.s.Pa)	> 20	> 20	> 20

5 CONCLUSIONS

The characterization of old Portuguese gypsum plasters (XVIII to middle XX centuries), from different kinds of buildings and regions of the country, showed different compositions according to their function in the building and the application technique: smooth surface plasters are made of similar proportions of lime and gypsum, while precast decorations' only binder is usually gypsum, sometimes with organic additions.

The physical and mechanical characteristics also vary, in accordance with the lime-gypsum proportions and are affected by the organic additions, sometimes with hydrophobic behaviour.

The shape and size of the samples are an important restriction to the number and type of tests that is possible to perform. However, some trends are identified and a comparison with old lime mortars (with more results available) is possible.

The total porosity obtained through MIP test is between 40-55%, a range much higher than the 20-45% for old lime mortars [Magalhães *et al.* 2004]. The compressive strength is another important feature, within the range 1.0-2.5 N/mm^2. This range is also common for old mortars, although rather higher values are also found [Magalhães & Veiga 2009]. The water vapour permeability of gypsum-based plasters seems to be similar to lime mortars', except when organic additions or superficial treatments are present, reducing significantly this property. Capillarity is the most variable characteristic in the tested samples, making it impossible to establish consistent ranges.

The determination of the physical properties in the samples of the old gypsum plasters collected is still in progress. However, based in the results obtained until now, it is possible to identify three classes of restoration products for Portuguese old gypsum based plasters, and to define, in a first approach, the respective compatibility ranges for some parameters. These ranges will, if necessary, be adjusted later, considering all the results obtained.

The conclusion of the characterization work of the samples collected will now proceed parallel to the development of the restoration products, contributing to complement and improve them until final formulations are achieved.

ACKNOWLEDGMENTS

Teresa Freire's PhD research is being supported by the scholarship SFRH/BD/40128/2007 from Fundação para a Ciência e Tecnologia (FCT). The authors would like to thank technicians Susana Couto and Paula Menezes from the Materials Department and Ana Maria Francisco and Luís Carmo from the Buildings Department of LNEC, for their support in the execution of the experimental work.

REFERENCES

Arcolao, C. 2001, *Le ricette del restauro - Malte, intonaci, stucchi dal XV al XIX secolo*, 2nd edition, Marsilio Editori, Venice (in Italian).

Candeias, A. & Valadas, S. 2010, *Analysis of IR spectra of gypsum samples*, report HERC/02/010, Hercules Centre, Uni. of Évora, Portugal, May (in Portuguese).

Freire, T., Santos Silva, A., Veiga, M. R. & Brito, J de 2008, 'Characterization of Portuguese historical gypsum mortars', Proc. 1st Historical Mortars Conf., HMC08, Lisbon, Portugal, 24 26 September 2008, T_I_54_HMC008 (available in CD).

Freire, T., Santos Silva, A., Veiga, M. R. & Brito, J de 2010a, 'Characterization of Portuguese historical gypsum mortars: a comparison between two case studies', *Materials Science Forum*, **636-637**, 1258-1265, online since 2010/Jan/12 http://www.scientific.net

Freire, T., Santos Silva, A., Veiga, M. R. & Brito, J de 2010b, 'Characterization of decorative Portuguese gypsum plasters from the XIX-XX centuries: the case of the *Bolsa Palace* in Oporto', Proc. 2nd Historical Mortars Conf. and Final Workshop of RILEM TC 203-RHM , HMC2010, Prague, Czech Republic, 22 24 September 2010, pp. 165-174.

Freire, T., Santos Silva, A., Veiga, M. R. & Brito, J de 2009, 'Characterization of a 19th century gypsum plaster piece: the role of microscopy', Proc. 12th Euroseminar on Microscopy Applied to Building Materials, Dortmund, Germany, 15 19 September 2009, pp. 416–427.

Magalhães, A. C., Moragues, A. & Veiga, M. R. 2004, 'Application of some methods on evaluation of porous systems of wall renderings', Proc. VII Congreso Internacional de Rehabilitación del Patrimonio y Edificación, Lanzarote, Spain, July.

Magalhães A. C. & Veiga M. R. 2007, *Hygroscopicity characterization of lime based mortars*, Report No. 201/2007 - NRI, National Laboratory of Civil Engineering (L.N.E.C.), Lisbon, Portugal, June (in Portuguese).

Magalhães, A. C. & Veiga, M. R. 2009, 'Physical and mechanical characterisation of ancient mortars. Application to the evaluation of the state of conservation', *Materiales de Construcción*, **59** (295): 61-77 doi: 10.3989/mc.2009.41907.

Margalha, M. G. 2010, *Mineral air lime binders. The influence of slaking processes and curing time on their quality*, PhD Thesis, Technical University of Lisbon, Lisbon (in Portuguese).

Turco, T. 1990, *Il gesso, lavorazione, transformazione, impieghi*, 2nd edition, edited by Hoepli, Milan (in Italian).

Santos Silva, A., Paiva, M., Ricardo, J., Salta, M., Monteiro, A. M. & Candeias, A. E. 2005, 'Characterization of roman mortars from the archaeological site of Tróia (Portugal)', *Materials Science Forum* **516**, 1643-1647.

Válek, J., Veiga, R. 2005, 'Characterisation of mechanical properties of historic mortars - Testing of irregular samples', Advances in Architecture Series **20**, 365-374.

Veiga, M. R., Magalhães, A. & Bosilijkov, V. 2004, 'Capillarity tests on historic mortar samples extracted from site. Methodology and compared results', Proc. 13th International Brick and Block Masonry Conf., Amsterdam, The Netherlands, July 2004.

Veiga, M. R., Fragata, A., Velosa, A. L., Magalhães, A. C. & Margalha, M. G. 2010, 'Lime-based mortars: viability for use as substitution renders in historical buildings', *International Journal of Architectural Heritage* **4** (2), 177-195, Paulo B. Lourenço and Pere Roca eds. Special Issue: Selected papers from HMC 2008 - The first Historical Mortars Conference. ISSN 1558-3058.

XII DBMC
International Conference on Durability of Building Materials and Components
PORTO - PORTUGAL, April 12th-15th, 2011

Performance and Durability of External Post-Insulation and Added Roof Constructions

Eva B. Møller [1]
Ernst Jan de Place Hansen [2]
Erik Brandt [3]

ABSTRACT

Additional insulation of the building envelope has been used in Denmark for more than 40 years and the use is increasing due to energy saving requirements. Today when the building envelope is renovated, the heat insulation must always be improved if it is cost-efficient.

The development of energy requirements for new and existing buildings in the Danish Building Regulations is presented and it is shown that the main effort on post-insulation of buildings for housing should be put into those built before 1979. Other reasons for renovation than energy savings are highlighted.

The performance and durability of external façade insulation and roof constructions added to 17 Danish housing estates from the 1950s, 1960s and 1970s are examined. A majority of the estates are to be renovated a 2nd time in the upcoming years, implying that the 1st renovation made in the 1980s and 1990s was neither cost-efficient nor sufficient.

It is discussed whether a 40-year service life for post-insulation is realistic and how it is possible to avoid that mistakes made in the past are repeated when buildings are renovated. It is concluded that renovation has to be thorough and that care in choice of material, planning and execution is just as important in renovation projects as in new buildings. In 2011, building inspections will be implemented in renovation projects of publicly funded housing to reduce the number of defects and damages.

KEYWORDS

External insulation, roof constructions, renovation, cost-efficiency, service life.

[1] Danish Building Research Institute / Aalborg University, Hørsholm, DENMARK, evm@sbi.dk
[2] Danish Building Research Institute / Aalborg University, Hørsholm, DENMARK, ejp@sbi.dk
[3] Danish Building Research Institute / Aalborg University, Hørsholm, DENMARK, ebr@sbi.dk

1 INTRODUCTION

Approximately 40 % of the energy consumption in Denmark is due to heating of buildings [StatBank Denmark 2010]. To reduce this energy consumption building regulations for new buildings have been tightened during the last decades. However, new buildings per year constitute only 1 % of the total building stock, making it relevant to look at existing buildings. One way to reduce energy consumption in existing buildings is to apply additional insulation to façades and roofs.

Post-insulation has been used in Denmark for more than 40 years. Although energy consumption might have been one of the reasons for applying additional insulation; comfort, reduced repair costs and architectural reasons probably were the main arguments for post-insulation in the early examples. Nowadays energy consumption is more important and the society asks for U-values in walls and roofs of existing buildings similar to the U-values in new buildings and therefore the challenge is to create solutions that are durable even when the insulation thickness is high. But before that is possible, we have to analyse how post-insulations carried out 15-30 years ago have performed so far.

To analyse the type and age of buildings where the main effort to post-insulate should be made, the first part of the paper describes the development of the energy requirements in the Danish Building Regulations. Selected cases of 15-30 years' old renovation projects are presented in the second part focusing on the post-insulation. In the last part the cases are discussed in relation to durability, sufficiency and cost-efficiency.

2 ENERGY REQUIREMENTS IN THE DANISH BUILDING REGULATIONS

To be able to determine how much additional insulation is needed, the U-value of the existing elements of the building envelope must be known. In Denmark the U-value of façades, roofs and other parts of the building envelope did not change significantly within the different types of houses from 1850 to 1961, when the first set of Danish Building Regulations were introduced [Wittchen 2009].

2.1 Building Regulations Over Time

The U-values in the first Danish Building Regulations were merely a reflection of what was normal in the better part of new buildings, but with the energy crisis in the 1970s the U-value requirements were tightened significantly to reduce energy consumption. Since then the U-values required by the Building Regulations have been a driver for the market, not only a reflection of what was already used. Figure 1 shows how the requirements for multi-storey buildings have been tightened over time in the Danish Building Regulations (BR). Requirements have been slightly tighter for detached and row houses.

Since 1979, according to BR 1977, it has been possible to calculate the overall heat loss instead of using U-values and in 1995 calculation of the energy consumption was introduced as another alternative. Since 2006 calculation of the energy consumption has been mandatory for new buildings with some maximum U-values less restrictive than the U-value requirements exemplified in Figure 1 which nowadays are used for extensions and conversion projects in existing buildings.

The main part of the building stock in Denmark was built before 1979; only 19 % of the registered housing square meters were built later, as shown in Figure 2. According to Figure 1 and Figure 2, the main effort to post-insulate buildings for housing should be made on detached and row houses built before 1979. A majority of these houses are privately owned houses and post-insulation projects based on a preceding performance analysis in order to identify the necessary performance properties for the post-insulation are rare. Such analyses have often been made when multi-storey buildings were post insulated, and these types of buildings are therefore the main subject of this paper.

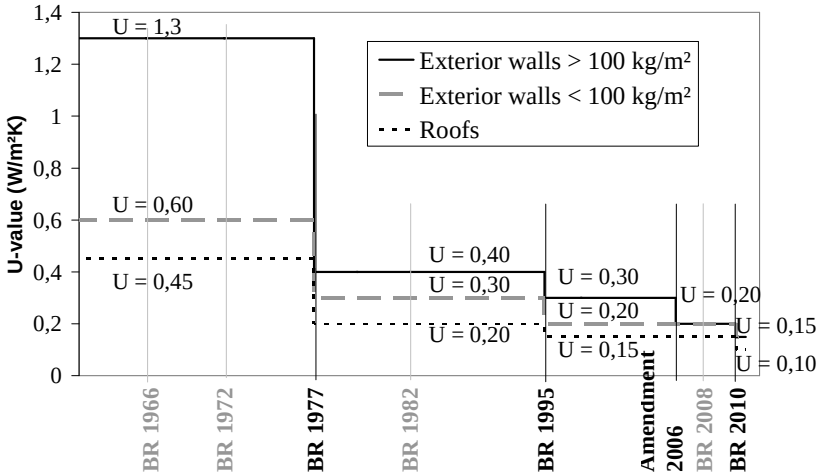

Figure 1. Requirements for U-values for multi-storey buildings in the Danish Building Regulations (BR) since 1961. The potential for energy savings is highest in buildings built before 1979, when BR 1977 became effective.

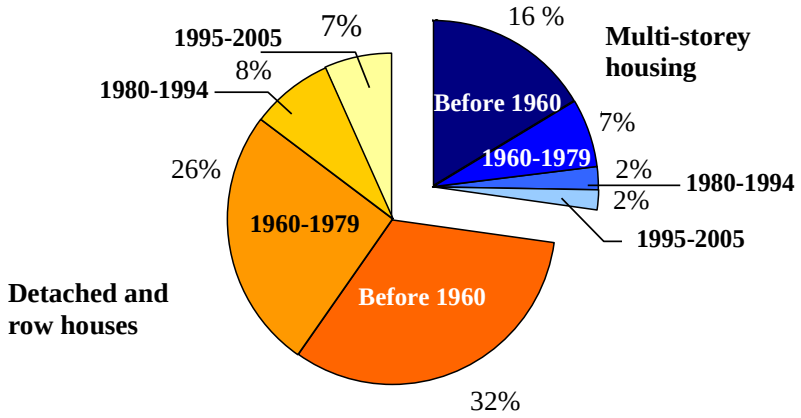

Figure 2. Distribution of housing (m²) built before 2006 according to age of the building. 48 % of the housing stock was built before heat loss was regulated in any way (before 1960), 33 % was built with very moderate requirements to U-values (1960-1979).

2.2 Building Regulations Requirements for Renovation of the Building Envelope

Many older houses have been renovated within the last 25 years. However, this does not mean, that the insulation standard corresponds to the insulation standard at the time of the renovation. The Building Regulations (BR) have changed on this point too:

- Until 2006 renovated buildings had to fulfil the requirements of the BR valid at the time the building was erected, i.e. reduction of energy consumption was only an issue if the building owner had a special interest.
- From 2006 renovated buildings had to comply with the energy requirements for extensions at the time of the conversion, if the conversion affected more than 25 % of the building envelope or did cost more than 25 % of the public property valuation. The energy requirements also had to be fulfilled for individual measures. The requirements had only to be fulfilled if the measures were cost-efficient, expressed by the ratio between the savings per year multiplied by the service life of the renovation, and the investment. Since 2006 BR have stipulated that the service life of post-insulation should be 40 years.
- From 2010 the given U-values for individual measures must be met regardless of its cost-efficiency if floors, façades, doors, windows or roofs are renewed (not just renovated, but replaced).

2.3 Post-insulation for other Reasons than Energy Consumption

Post-insulation is often just a side effect of a renovation project undertaken for a number of reasons; energy consumption is seldom the main motivator, but when a renovation project starts, the extra costs for additional insulation are often small compared with the total costs. The following reasons can also be found in the examples in section 4 Examples.

2.3.1 Durability of the existing construction

Many renovation projects are initiated owing to lack of durability of the existing construction, either because the construction is old and has exceeded its expected life time or because it has defects that can be fatal. The massive use of flat roofs and concrete sandwich elements as exterior walls in the 1960s and 1970s are typical examples of structures that proved to be susceptible to defects.

In the 1960s concrete technology was in its infancy. As a result the concrete structures deteriorated, and after 25 years many façades, balconies, etc. had to be renovated. To avoid a spotted façade the surface could be painted or covered by a new structure. In many cases this could be exterior insulation. The advantages would be reduced expenses for concrete renovation, reduced heat loss and a new visual appearance; useful if there is architectonic need for a change, cf. 2.3.3 Social problems.

For a short period in the 1960s and 1970s completely flat roofs (i.e. horizontal) were popular in Denmark. Unfortunately the roofing materials were not durable for completely flat roofs, and many roofs were leaky. One way to rectify the situation was to apply additional insulation on the existing roof. The advantages would be a roof without leakage, a slope of the roof of minimum 1:40, reducing the risk of a new leakage and reduced heat loss.

2.3.2 Comfort

Cold and draughty houses mean thermal discomfort, risk of mould growth and restrictions on how to use the house, e.g. furniture cannot be placed against the external walls. To reduce these nuisances post-insulation and tightening of the building envelope are often used. Comfort is the aim, but reduced energy consumption is a beneficial side effect. Some renovation projects have lessened the thermal discomfort, but increased the moisture problems, especially when internal façade insulation has been used or the building envelope has been tightened without installing openings for controlled ventilation.

2.3.3 Social problems

Some residential areas seem prone to social problems and formation of ghettos. Their architecture is often blamed for monotony - large estates are not appealing - and economically advantaged people avoid those areas [Ministry of Refugee, Immigration and Integration Affairs, 2004]. To change the demography, the monotony of the area must be broken. In several cases this has been done by changing the façades, roofs and/or surroundings, and often in a way so that buildings that used to be alike now have different appearances either in colour, shape or architectural expression. External post-insulation is a powerful tool for this. New top storeys will also change the architectural expression, and if the flats are attractive, they might attract economically advantaged people.

3 METHODS

Figure 2 showed that the main effort on post-insulation of buildings for housing should be made on detached and row houses built before 1979, but available information on post-insulation of buildings mainly exists for multi-storey buildings. This of course is a major limitation since it is not necessarily the same problems that initiate renovation of detached and row houses and multi-storey buildings. On the other hand, it can give some relevant information about how an external post-insulation act 15-30 years after it was implemented.

The selection of buildings examined in this study was based on a report from the Danish Construction and Housing Agency [1997] in which renovation of 22 different publicly funded housing estates are described before and after renovation. The estates represent housing construction from the 1950s, 1960s and 1970s where the requirements for U-values were non-existing or very moderate, cf. Section 2.1. In most cases the buildings experienced lack of durability of the façade elements made of concrete and/or the roofs, for some estates just 14-16 years after construction. This resulted in concrete damages, leaking façade elements or leaking roofs.

The caretakers were interviewed by telephone about the conditions of the buildings at present (2010) and asked whether the renovation that took place in the 1980s and 1990s did solve the problems that motivated the renovation. 17 of the 22 caretakers responded. The corresponding 17 cases are summarised in the following section. The interviews focused on the condition of the renovation described in [Construction and Housing Agency 1997]. Only in some cases it was possible to get statements on whether the post-insulation did reduce the energy consumption in the long term, whether the residents used glass-covered balconies as a balcony and not as an extension of the living room, or whether mould problems were eliminated. This type of feedback is not treated further.

4 EXAMPLES

17 examples of estates from [Construction and Housing Agency 1997] are summarised in Table 1 in relation to year of construction and renovation, the age at renovation and the type of renovation. The size of the estates varies from 90 to 1921 flats (9,200 to 164,000 m^2).

Table 1. Estates from [Construction and Housing Agency 1997] identified by B (blocks of flats), H (high-rise buildings) or R (row houses) and a number. The numbering includes all 22 estates. Year of construction and renovation, age at renovation, and type of renovation. *B1, B2, H1: Windows were replaced in a minor renovation in the beginning of the 1980s. *B10: Glass-covering of the balcony was an option. *B12: Windows and balconies were protected by a window hood.

ID	*Year of*		*Age at renovation*	*Roof*			*Facades*			*Other*	
	construction	*renovation*		*Post-insulation*	*Sloped roof*	*Roof flats*	*Concrete repair*	*Post-insulation*	*Balconies (glass covered)*	*Windows (replaced)*	*Ventilation system*
B1	1948-50	1991-93	43			X		X	X	*	
B2	1949-59	1994-96	41	X			X	X		*	
B5	1967-72	1994-96	26		X		X		X		
B6	1968-70	1993	24				X		X		
B8	1968-72	1992-96	24		X	X	X		X		
B10	1969	1992-94	24			X	X	X	*	X	
B11	1969-72	1993-97	24.5		X		X	X	X		X
B12	1971-73	1985-88	14.5		X			X		*	
B13	1971-75	1992-96	21	X			X	X	X		
H1	1950-52	1993-95	43	X				X		*	
H2	1961-63	1992-94	31					X	X		
H3	1962-67	1989-93	26.5				X		X		X
H4	1968-71	1991-92	22				X	X			
H6	1974	1994-95	20.5		X			X	X		
H7	1974-77	1988	12.5				X		X		
R1	1963-66	1979-82	16		X			X		X	
R2	1970-71	1991-94	22.5		X	X		X			X

In almost every example presented in Table 1 the renovation included external façade insulation. This consisted of 50-125 mm thermal insulation, a wind barrier and a ventilated cladding made of 2-8 mm boards typically made of cement-based materials, aluminium or polymers. In some cases a compact solution was chosen with a façade plaster applied directly to the insulation.

Often the renovation included a replacement of the existing flat roof with a sloped roof; in some cases combined with non-luxurious penthouse flats on top of the building. The slope of the new roof was double- or single-sided, with marked eaves and a 1:40 slope as minimum. In some cases the roof was made with a curved shape. Roofing felt, profiled boards of fibre-cement, profiled plates of steel, plates of zinc, or cement roof tile was used as roof material.

5 REVISITING THE ESTATES - PROBLEMS TODAY

Table 2 summarises the outcome of the interviews with caretakers carried out in 2010.

Table 2. Condition today of 17 estates from [Construction and Housing Agency, 1997] including a description of a possible 2nd renovation. Blocks of flats (B), high-rise buildings (H), row houses (R). Numbers in '( )' describe service life of plastic windows, which were not replaced in the 1st renovation.

ID	*2nd renovation*	*No. of years since 1st renovation*	*Part of 1st renovation*	*Comments*
B1	Ongoing	10	Yes	Partial replacement of fibre-cement boards
	Upcoming	18 (25) 18	No and yes	Plastic windows from the 1980s are replaced Windows in roof flats are replaced
B2	Upcoming	15 (27)	No	Plastic windows from the 1980s are replaced The wall adjacent to the balcony is cold
B5	Planned	15	Yes	Renovation to reduce social problems
B6	No			
B8	Planned	15	No	Post-insulation of facades at entrance side
		15	Yes	Partial replacement of roof fibre-cement boards
B10	No			
B11	2007	10	No	Post-insulation of facades at entrance side
B12	Planned	23	Yes	Replacement of fibre-cement boards at roof and facades
B13	No			Façade is washed every 6th year
H1	Upcoming	15 (25)	No	Plastic windows from the 1980s are replaced The wall adjacent to the balcony is cold
H2	2008	15	Yes	Windows and aluminium cladding replaced
H3	2005	22	No	Post-insulation of gables
H4	2004	12	No	Replacement of original windows
H6	No			
H7	2009	22	No	Renovation of the roof Post-insulation of gables
R1	Planned	32	Yes	Major renovation
R2	Planned	15	Yes	Major renovation (mainly caused by damaged fibre-cement boards)

Figure 3 shows the outcome in a schematic form.

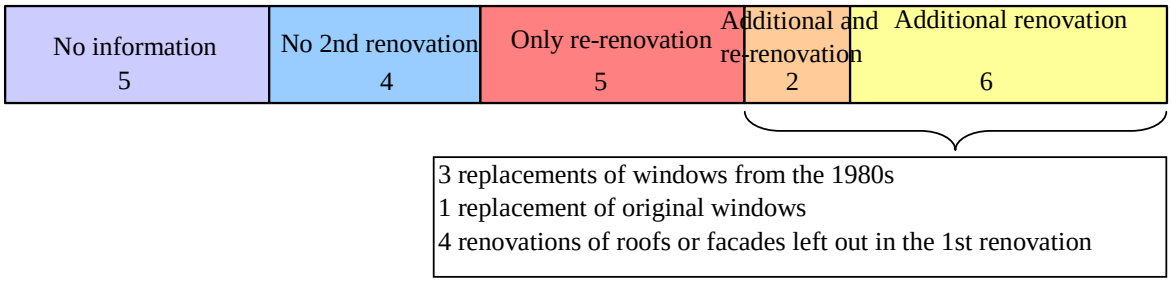

Figure 3. The original study included 22 estates, 17 of which were investigated in 2010. Re-renovation describes cases where the same parts of the building are renovated in the 1st and the 2nd renovation, while additional renovation describes cases where other parts are renovated.

As seen in Table 2 and Figure 3, a 2nd renovation is planned or already carried out in 13 of the 17 estates, implying that the 1st renovation did not solve all the identified problems. In 8 of these 13 cases the 2nd renovation covers other parts of the building envelope than the 1st renovation, 4 of these were window replacements. In the 3 oldest estates constructed in the 1950s (B1, B2 and H1), the original windows were already replaced with plastic windows in a previous minor renovation in the 1980s. In 4 of the 7 cases with re-renovation, the main cause is defective fibre-cement boards.

6 DISCUSSION

About 15-20 years after the 1st renovation, 13 of the 17 investigated estates are or will be renovated a 2nd time, no matter how old the buildings were when the 1st renovation took place. This questions whether the chosen solutions were durable, in relation to the cases where the 1st and the 2nd renovation covers the same parts of the building envelope (re-renovation), or sufficient, in relation to the cases where the 2nd renovation covers parts of the building envelope, that were not included in the 1st renovation (additional renovation).

Re-renovation shows lack of durability, e.g. in the 4 cases where fibre-cement boards will be replaced. These boards were 1st generation of asbestos-free fibre-cement boards which exhibited very poor durability and much shorter service life than expected. If all fibre-cement boards have to be replaced, the renovated roof or façade must comply with the current Danish Building Regulations if the renovation is cost-efficient, e.g. the post-insulation of the 1st renovation has to be supplemented.

Additional renovation is a sign of insufficient renovation; in 8 cases the 2nd renovation covered parts of the building envelope that were not included in the 1st renovation. Economic reasons, technical complexity, or an assessment of some parts to be in a good condition, are the most obvious reasons for not letting the 1st renovation include the whole area of the facades and roofs. It was not possible to uncover which of these explanations was the dominant one.

Regardless of whether the chosen solution showed lack of durability or was insufficient, a 2nd renovation was necessary. How does this affect the cost-efficiency? In 4 cases, the 1st renovation only lasted about 15 years and was therefore hardly cost-efficient. One could question whether 40 years as stipulated in the current BR, is a realistic service life for post-insulation. Based on the studied renovation projects it is too early to conclude, since none of the renovations are older than 30 years. The 4 cases where the 1st renovation only lasted about 15 years indicate that the answer should be 'no', or at least that the scatter of service life is high. On the other hand these renovations were made at a time when no service life was stipulated, i.e. there was no guide for how long post-insulation was expected to last.

To avoid the use of solutions with a short service life, focus should be on ensuring that the solutions used in renovation projects are well-known and tested, if necessary by performing test renovations where the solutions are monitored closely or accelerated tests comparing the new solutions with well-

known solutions. This would also limit the possibility of repeating mistakes made in the past, as the massive use of asbestos-free cement-fibre boards in the 1990s seems to be a repetition of the way concrete was used in the 1960s.

Since 1986 the Danish Building Defects Fund (BSF) has carried out building inspections in new publicly funded housing projects as part of the Danish Quality-Assurance and Liability Reform, which has greatly reduced defects and damages; from building defects in 36 % of the projects built from 1987 to 1992 to 4 % in the projects built from 1999 to 2009 [The Danish Building Defects Fund, 2010]. To accomplish a similar improvement in renovation projects and react to the many examples of unsuccessful renovation projects as exemplified in this study, such building inspections will be extended also to cover renovation projects; a new bill has been introduced that is expected to become law and effective from July 2011.

7 CONCLUSIONS

Seventeen large Danish housing estates that were renovated in the 1980s and 1990s are the core of this paper. The renovation included external post-insulation and/or changed roofs (external post-insulation or new top storey). Telephone interviews in 2010 with caretakers of these estates showed:

- In 4 cases no 2nd renovation is planned, apparently the 1st one solved the problems and was durable.
- In 5 cases a 2nd renovation of already renovated parts has been performed or is in planning.
- In 6 cases the 1st major renovation was not sufficient and additional renovation of parts that were not covered in the 1st renovation was necessary.
- In 2 cases the 2nd renovation includes both already renovated and previously not covered parts.

The studied renovation projects leads to the following conclusions concerning performance and durability:

- Renovations involving external post-insulation have to be thorough; if parts are left out additional renovations are likely to be necessary within the expected service life of the 1st renovation.
- Care in choice of material, planning and execution is just as important in post-insulation renovation projects as in new buildings.
- To expect a 40-year service life of external post-insulation, as stipulated in the current Building Regulations, might be too optimistic; in almost 25 % of the cases it was approximately 15 years.

REFERENCES

Construction and Housing Agency, 1997, *22 overfrakker: Facadeinddækninger – en eksempelsamling* (author's translation from Danish: 22 over coats: Facade covering – a collection of examples), Project Renovation, Ministry of Housing, Copenhagen, Denmark.

The Danish Building Defects Fund, 2010, *Årsberetning* (author's translation from Danish: Annual report), The Danish Building Defects Fund, Copenhagen, Denmark.

Ministry of Refugee, Immigration and Integration Affairs, 2004, *Regeringens strategi mod ghettoisering* (author's translation from Danish: the Government's strategy against ghettoisation), Copenhagen, http://www.inm.dk

StatBank Denmark, 2010, *Statistical information on the Danish society*, www.statdank.dk.

Wittchen, K., 2009, *Potentielle energibesparelser i det eksisterende byggeri* (author's translation from Danish: Potential energy savings in the existing building stock), SBi report 2009:05, Danish Building Research Institute, Hørsholm, Denmark.

XII DBMC
International Conference on Durability of Building Materials and Components
PORTO - PORTUGAL, April 12th-15th, 2011

Controlled Ventilation of Historic Churches – Assessment of Impact on the Indoor Environment Via Hygrothermal Building Simulation

Andreas Hagen Holm [1]
Florian Antretter [2]
Ralf Kilian [3]
Fabian Ritter [4]
Barbara Wehle [5]

ABSTRACT

Historic churches, when they are unheated, often face problems of summer condensation. After the cold season warm, humid air enters the building and condenses on the walls, a problem that can occur during the entire warm season. This leads to moisture related problems such as mould or algae growth on building surfaces. High humidity can also damage works of art inside these churches. One possibility to lower the level of relative humidity is by bringing dryer air inside the church whenever this is suitable to lower relative humidity On the other hand, too many fluctuations may also cause damages on works of art and bringing in cold air will further lower the temperatures of the whole building and its walls thus being conter productive to the drying process. An automatic system for ventilating historic, unheated churches is assessed using building simulation software (WUFI Plus) on a case study of the St. Margaretha church in Roggersdorf, near Holzkirchen, Germany.

KEYWORDS

Historic Building, Controlled Ventilation, Whole Building Simulation, Summer Condensation

[1] Fraunhofer-Institut für Bauphysik, Holzkirchen, GERMANY, andreas.holm@ibp.fraunhofer.de
[2] Fraunhofer-Institut für Bauphysik, Holzkirchen, GERMANY
[3] Fraunhofer-Institut für Bauphysik, Holzkirchen, GERMANY
[4] Fraunhofer-Institut für Bauphysik, Holzkirchen, GERMANY
[5] Fraunhofer-Institut für Bauphysik, Holzkirchen, GERMANY

1 INTRODUCTION

1.1 The Chapel of Ease St. Margaretha in Roggersdorf

After a complete renovation of the chapel of ease St. Margaretha (Fig. 2) in September 2004, the churchwarden again noticed moisture damage on the walls. A subsequent climate measurement showed that the damage was a matter of condensation that occurs mainly in the transitional period during spring-time. At that time of the year the building is still cold because of the winter. If warm, humid air enters the building due to natural air flow or uncontrolled ventilation inside, it condenses on the cold wall surfaces. But even in the summer and fall warm humid weather conditions can cause problems due to condensation.

From December 2004 to August 2006 the temperature and relative humidity were measured inside and outside the church. To asses condensation events the wall surface temperature was also measured on the Western wall at the joint to the floor. Weather data was available from the Fraunhofer IBP outdoor testing facility at Holzkirchen, only 5 km away from Roggersdorf. During the period when measurements were taken the climate inside the church showed a high average humidity with values over 75% rh for more than half of the time of the year (Fig. 1). During winter time the church also freezes with temperatures below 0° C for more than six weeks in a row [Kilian 2007]. Subsequently, the church starts with very low wall temperatures into spring time and the warm season.

Another problem that became evident was the uncontrolled opening of windows and doors over the warming period of spring, , that was supposed might reduce the moisture levels in the space by ventillating. In the summer 2005 “vetilation traffic lights” showing the times when the water content of the outdoor air was lower than indoors were used to give advice to the guardian of the church. This significantly increased the daily fluctuations of rh; in the spring and summer 2005 the fluctuations were above 15% rh for more than 30 days. Daily changes above 15% rh are thought to be critical to works of art [Holmberg 2001], as the risk of structural damages due to swelling and shrinking of materials increases with the range of rh change per day. Also the newly restored altarpiece from the 19th century started showing additional damages at the gilding.

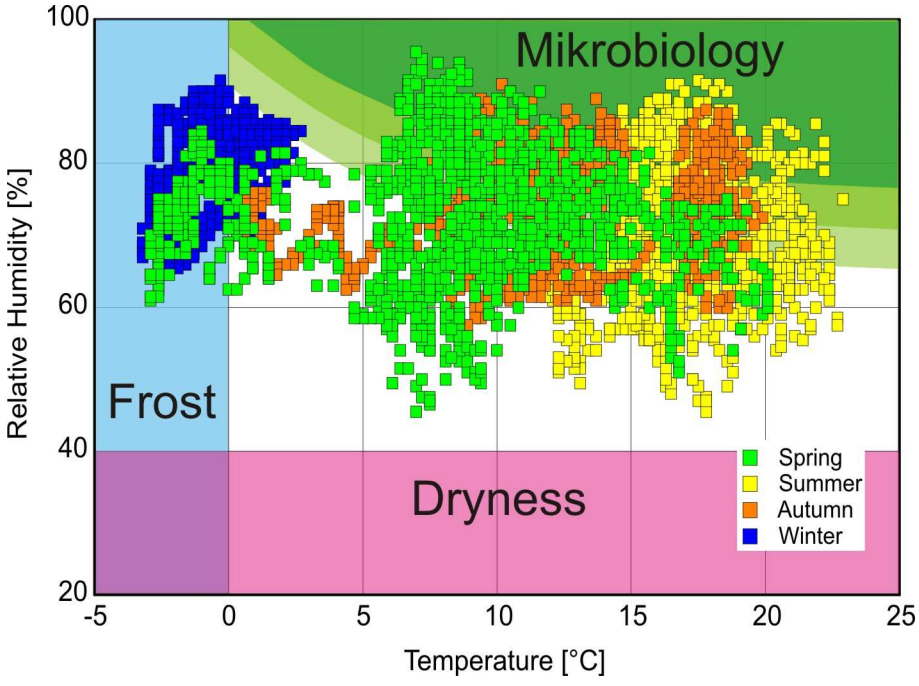

Figure 1. Temperature and humidity during 2005. Half of the time rh lies above 75 %, during winter the church freezes for 6 weeks.

As a consequence, the installation of a controlled ventillation system was discussed with the church authorities. Such systems permit comparing the absolute humidity inside and outside the building. Whenever the outer humidity is lower, a ventilator starts bringing dryer air into the building. Also, boundary conditions for the lower temperature can be given, as well as a maximum allowed range of RH change in the last 24 hours. Practical experience has shown that this type of ventilation system can help reduce the RH range and reduce the overall moisture in a room over the year, as was done for the church located in Urschalling, Bavaria [Künzel 2003]. However, the open questions are: how good is the system for the respective location; what can it achieve; how much energy does it use; and, what is the overall impact when bringing colder air into the building during winter and in summer nights? To assess the possibilities and limitations of these systems, whole building simulation was used to predict the indoor environment in the church using weather data from Holzkirchen.

2 METHODS

For the simulation of the hygrothermal building behaviour the software tool WUFI Plus was used [Holm et al. 2003]. In the following the general conditions, the assumed building geometry and materials as well as the heating, ventilation and air conditioning are described.

2.1 Boundary Conditions

The time of calculation lasted from January, 1st to December, 31st of the year 2005. The simulation was carried out in time steps of 5 minutes to reproduce a realistic ventilation control. Given that the location of the church was in Roggersdorf, which is located near Holzkirchen, the meteorological data of Holzkirchen for the year 2005 was used for the simulation. A weather file was created which consisted of 5-minutes values of exterior temperature, relative humidity (both in Fig. 3), global and diffuse radiation, rain, wind and barometric pressure. Additionally a file with ground temperatures at a depth of 0.5 m in the soil was generated to take into account conditions below the foundation of the church. Inner loads were not taken into account for the base case, assuming that there is no church service.

2.2 Building Geometry and Material Data

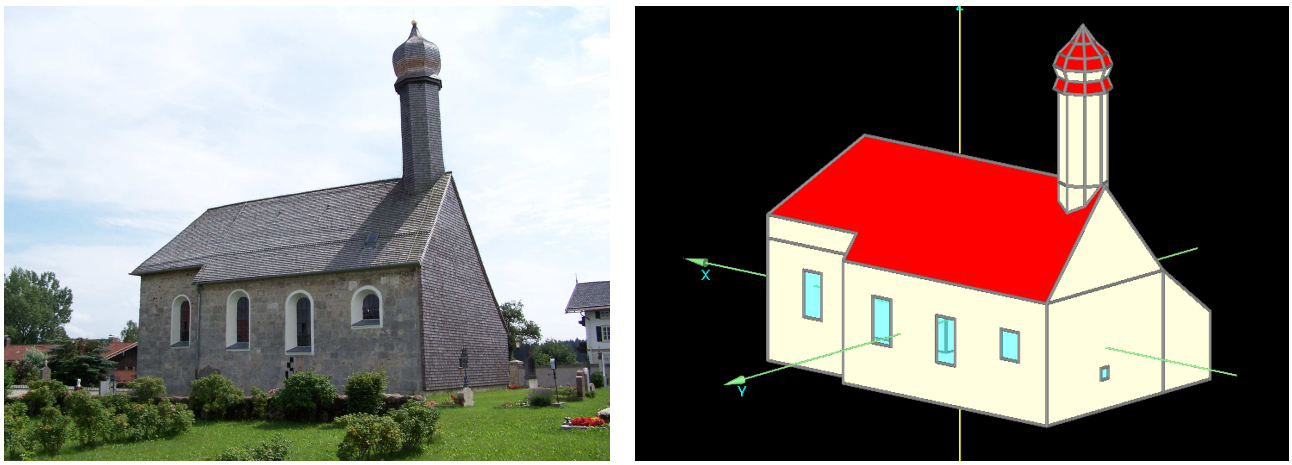

Figure 2. Picture and screenshot of the computer model of the exemplary church.

A detailed model of the chapel's geometry was created in WUFI Plus (Fig. 2). The main building is about 12 m long and 9 m wide. The height from the ground to the top of the roof is about 6m and to the top of the tower about 9 m. For the simulation the main body was divided into three zones where the climate was modelled: the nave, sacristy and the attic. In the nave a ventilation system was

assumed with a control to ventilate this zone with outside air with an air exchange rate of 5 1/h, in that instance when the outside absolute humidity was lower than the absolute humidity inside the church with the limitation that the exterior temperature had to be above 0°C. The infiltration ventilation air was taken from outside, with an infiltration air exchange rate of 0.4 1/h for the nave. The tower as well as the entrance area was treated as an attached unheated zone with assumed exterior temperature and relative humidity in the zones.

The outer walls of the chapel are built from sandstone with a thickness of 0.52 to 0.77 m. At the inner surfaces there is a layer of lime plaster which is 2 cm thick. The base plate exists of a layer with loose material (0.15 m) which is mainly covered by natural stone plates with a thickness of 5 cm. Under the benches at the north and south side of the church there are panels of hard wood instead. The ceiling to the attic has an overall thickness of 0.3 m consisting of 2.5 cm softwood, a 15 cm thick air layer, 10 cm mineral wool and again 2.5 cm softwood. The chapel's roof and its covering with a thickness of 3 cm is mainly built with softwood and shingles on the outside. The windows have a single glazing with an overall thermal transmission value of 3.7 W/m²K.

2.3 Parameter Variations

The simulations were run with different parameter variations. The base case is a simulation as that described in the previous section. The simulation results of this variant are always compared to a variant without any ventilation control, i.e. only natural ventilation mainly by infiltration. Further simulations were run with air change rates of 1 1/h and 10 1/h to show the influence of the capability of the ventilation system. A further simulation was run where only the energy transport was modelled whereas the coupled equations for heat and moisture transport in the building envelope were not modelled. This simulation allowed assessing the necessity of a simulation model capable of modelling the coupled transport eqution s.

3 RESULTS

Figure 3 shows the modelled temperature and relative humidity inside the nave without additional ventilation and with an assumed air change rate of 5 ACH for ventilation during all periods with lower exterior absolute humidity than inside and while exterior temperatures are above 0 °C. The inner climate conditions are compared to outer climate conditions.

Expectedly lower fluctuations for temperature as well as for relative humidity are found for the interior conditions compared to the outside climate. Not only the peaks are damped, but also in longer periods with very low exterior temperatures the inner temperatures do not reach the mean low temperature. The fluctuations are lowest in the model without additional mechanical ventilation. Especially in spring, the relative humidity is reduced in the controlled ventilation case, but also the temperature inside the church. No effect is found in the cold month due to the temperature limitation at 0° C of the ventilation control.

The modelled ventilation control acts on abolute humidity. A comparison in Fig. 4 for absolute humidity inside and outside shows also a dampening of the fluctuations from outside to inside for the case without ventilation. The general trend is followed pretty close. The above mentioned effectiveless of the ventilation control in the cold month is reflected by the related ventilation status. Almost no ventilation actions are performed from mid November until end of March. In warm month the peaks in exterior absolute humidity appear reduced inside, but the minima can be followed by ventilation control which shows the lowering of absolute humidity in the ventilation case.

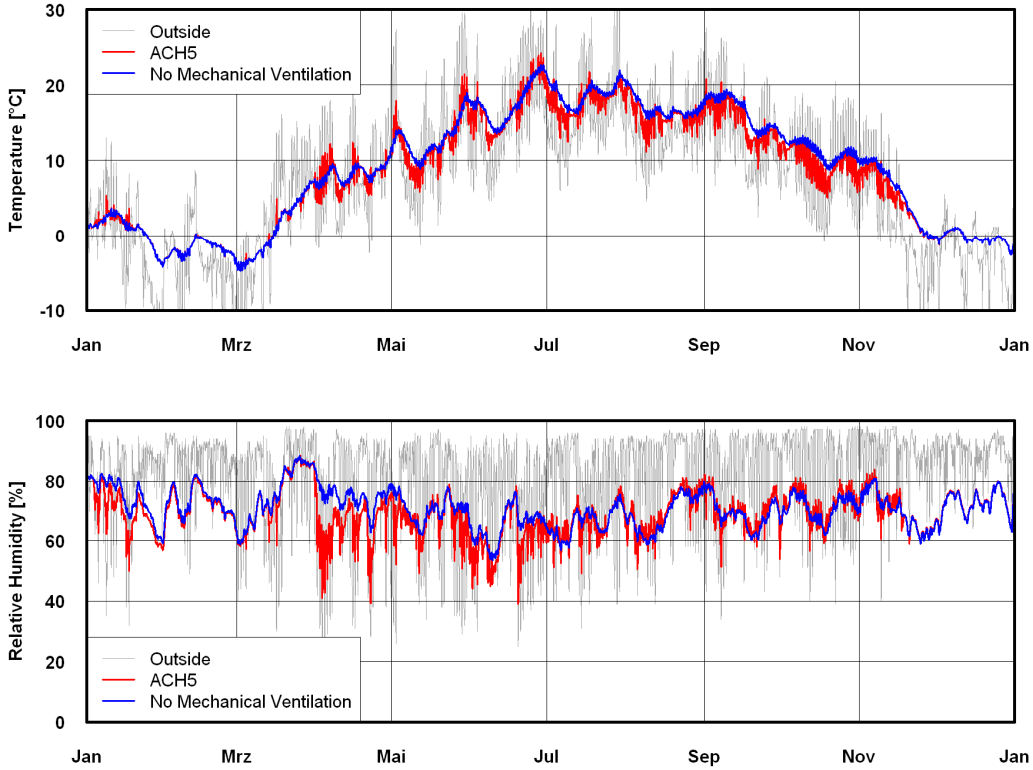

Figure 3. Temperature and relative humidity outside and modelled conditions inside the church during the whole simulation period with (Air Exchange 5 1/h) and without mechanical ventilation

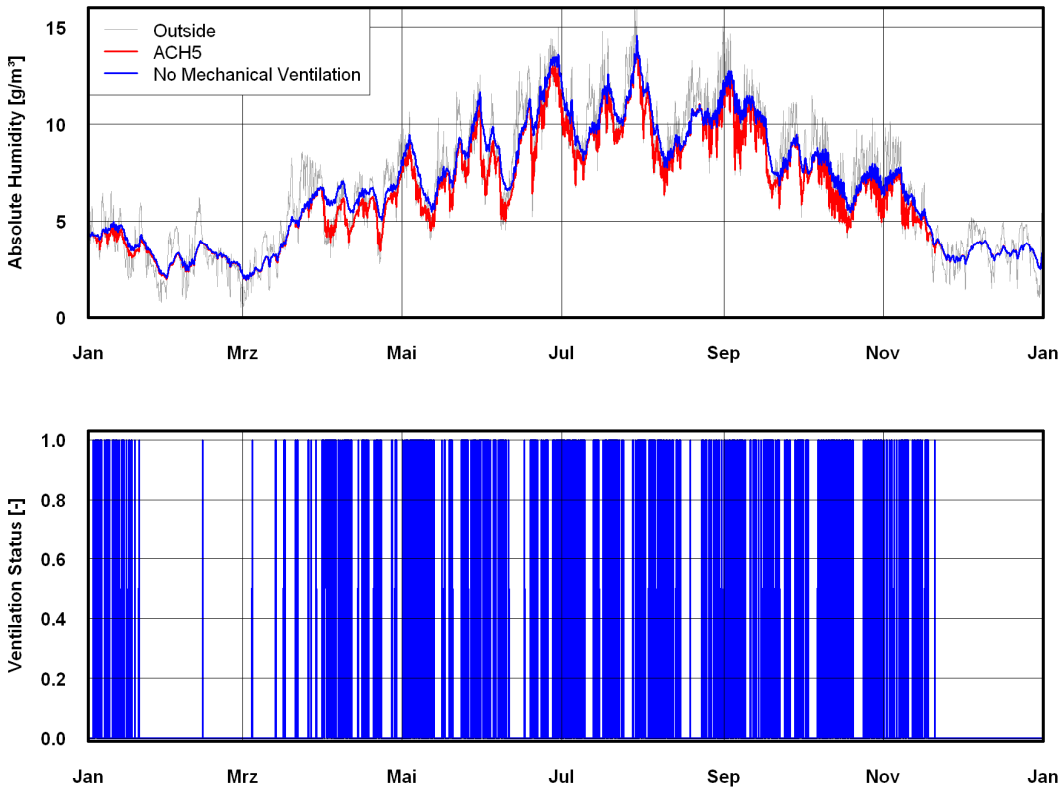

Figure 4. Absolute humidity outside and inside the church as well as ventilation status during the whole simulation period

A closer look on the absolute humidity conditions only in October are given in Fig. 5; details are provided of the resulting higher fluctuations of absolute humidity – and with it relative humidity – inside the building because of active ventilation control. But it also clearly shows that lower interior absolute humidities are achievable with effective ventilation during periods with lower exterior humidity.

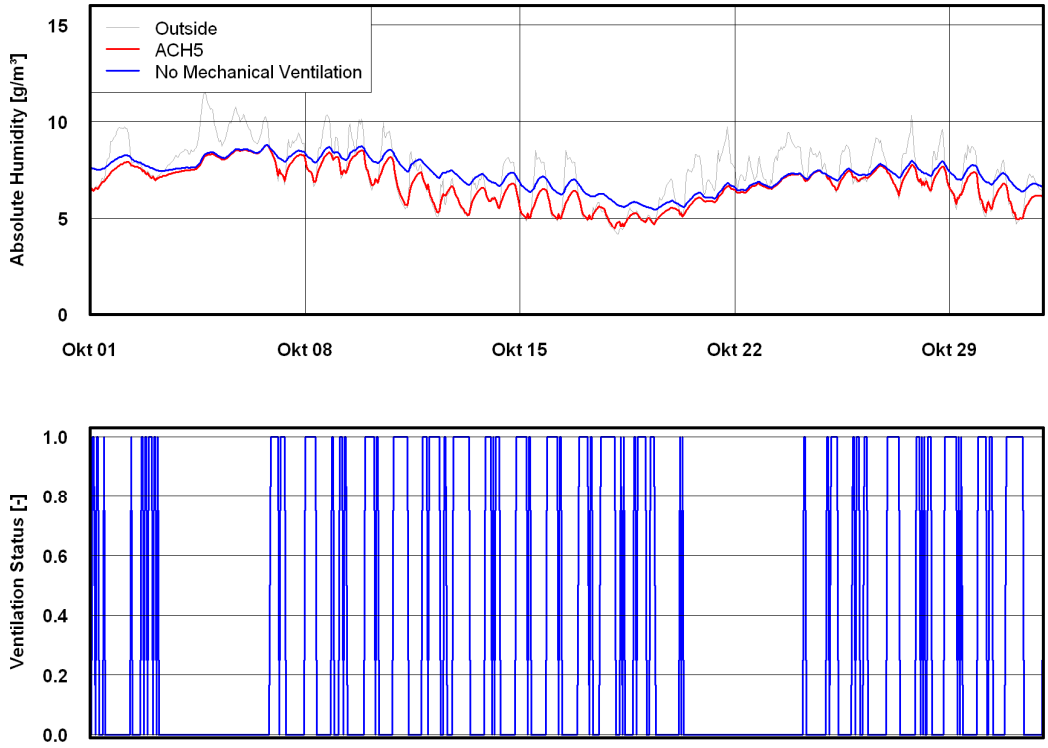

Figure 5. Absolute humidity outside and inside the church and ventilation status for simulation in October

A variation of different air change rates as well as a simulation without moisture buffering – therefore only a building energy simulation – was performed and the results for October are shown in Fig. 6. An improvement in efficiency is achievable by increasing the air change rate during control action from 1 ACH to 5 ACH. In the modelled case, a further increase up to 10 ACH does not further reduce the absolute humidityindoors , as the exterior minimum absolute humidity is also reached with 5 ACH. In the case of a simulation without modelling the coupled heat and mass transfer in the building envelope but using only a mass balance for interior humidity, the interior absolute humidity follows very closely the exterior absolute humitidy.

4 DISCUSSION

It was found, that daily fluctuations of temperature and relative humidity are much higher with mechanical ventilation control compared to the climatically free floating church. Especially in cases with valueable interior artifacts that are sensitive to high RH fluctuations, this potentially can cause problems. The daily fluctuations are compared in Fig. 8 for the case without mechanical ventilation and the ventilation control case with 5 ACH during operation of the mechanical ventilation. The average daily variation is 3 % RH without and 7 % RH with ventilation with maximum daily fluctuations of 15 % and 39 % respectively.

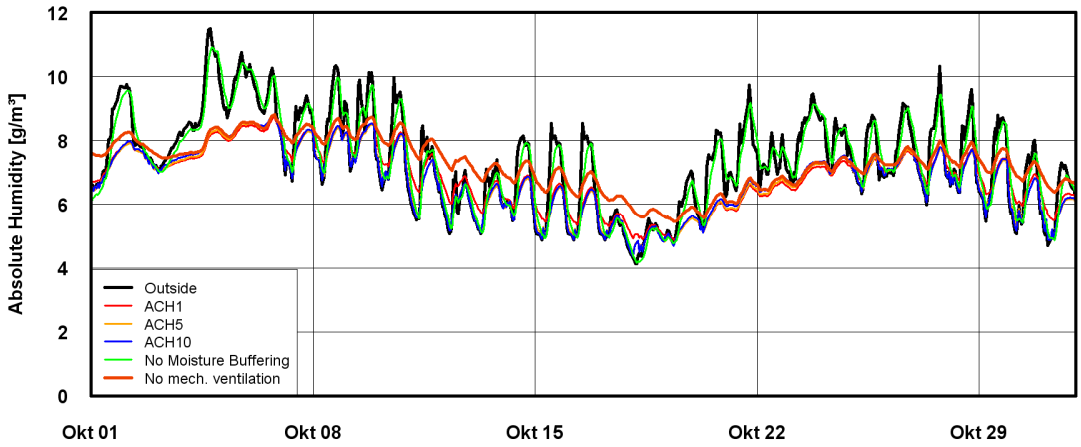

Figure 6. Absolute humidity outside and inside the church with different parameters for simulation during representative month October

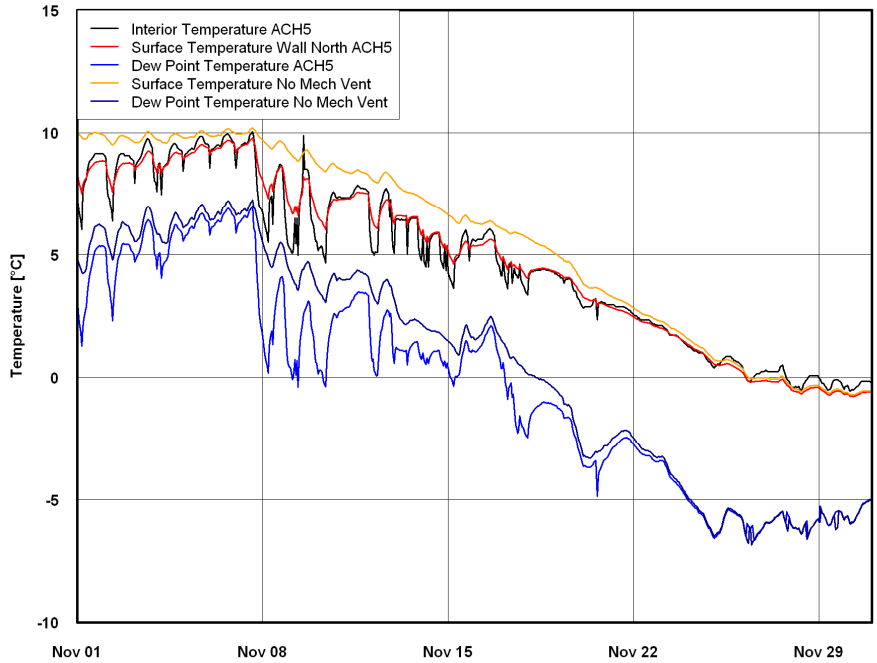

Figure 7. Surface temperature and dew-point temperature for North wall without mechanical ventilation and with ventilation control and ACH 5 1/h

5 SUMMARY AND CONCLUSIONS

A simulation model of a church was implemented. Parameter variations were undertaken, to assess the effectiveness of a controlled ventilation to lower humidity conditions inside the church. A model of the free floating building without mechanical ventilation was compared to the same building with a mechanical ventilation system. This ventilation system was controlled to be active while inner absolute humidity was higher than exterior absolute humidity with the limitation that exterior temperature had to be above 0°C.

The results of the simulation permited determing that it is possible to lower the inner absolute humidity during some times of the year with the ventilation control system assesed in this study. The main limitation of the system is that moisture removal can never reduce the inner absolute humidity to

a level below exterior conditions. This limits its effectiveness in cases of a free floating building with low inner moisture loads.

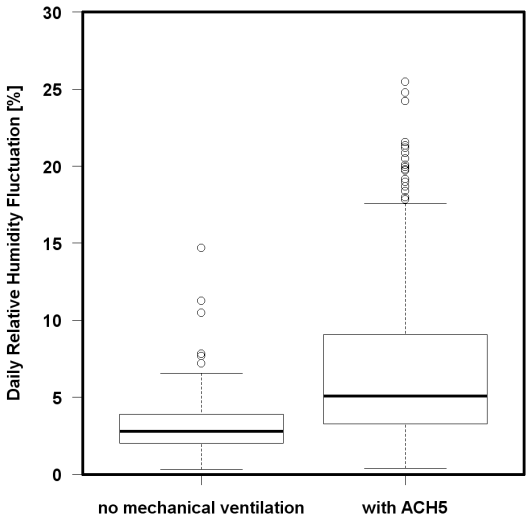

Figure 8. Boxplots of simulation results for all daily fluctuations of relative humidity in the space without ventilation and the space with ACH 1/h

Critical conditions due to moisture vented or infiltrated into the building leading to high relative humidity or even fluid water on the envelope surface can not always be avoided. The daily cycle and other fluctuations in exterior absolute humidity are low. Potential for active ventilation is not always available. Therefore also ventilation systems that create low air change rates allow the full removal of excess moisture. A further increase in air change rate is not necessary. In compareable free floating cases with no inner loads humidity condtions can still be critical. Improvement in the indoor humidity level is bought at the expense of stabile humidity conditions. Fluctuations of temperature and humidity are much higher with controlled ventilation than without. This effect has to be balanced with the small improvements in moisture level. To undertake a similar assessment, it was shown that it is critical to model coupled heat and moisture transport processes in the envelope and its interaction with the room. Relative humidity level and fluctuations can only be represented if moisture buffering effects are taken into account in the simulation.

ACKNOWLEDGMENTS

This work is part of the European research project “Climate for Culture” on the impacts of Global Climate Change on Cultural Heritage that is funded by the European Comission.

REFERENCES

Holm A. H., Künzel H. M., Sedlbauer K. 2003, *The hygrothermal behaviour of rooms: combining thermal building simulation and hygrothermal envelope calculation*, Eight International IBPSA Conference, Eindhoven, The Netherlands, 11-14 August 2003, 499-505

Holmberg, J. G. 2001, *Environment Control in historical buildings*, Royal Institute of technology builiding services engeneering, Bulletin No. 53, Stockholm, 2001

Künzel, H. 2010, *Bauphysik und Denkmalpflege*, Fraunhofer IRB Verlag, Stuttgart

Kilian, R. 2007, *Statistische Untersuchungen der Klimaschwankungsbreite in unterschiedlich genutzten Kirchenbauten*, in *WTA Almanach 2007*, WTA-Publications, München

XII DBMC
International Conference on Durability of Building Materials and Components
PORTO - PORTUGAL, April 12th-15th, 2011

Residential Building Stock Survey in São Miguel Island, Azores: Pathologies and State of Degradation

Maria Margarida Machado Pires [1]
Maria João Barros [2]

ABSTRACT

Although concerns about the preservation of the existing building stock have been growing in our society, cases of inadequate indoor conditions, lack of durability and safety are still too common. Remedial measures are needed. However, up to date information on the characteristics of the building stock and its most common pathologies is not available in a form that makes it easily accessible.

This paper presents the results of a survey of residential buildings typology, materials and pathologies in the island of São Miguel, Azores, in order to gather the data necessary to evaluate the degradation state of the housing stock and to assess a preliminary diagnosis. The identification of the main pathologies which appear in residential buildings can further help researchers in establishing sound methodologies for an improved quality and durability of the Azorean building stock.

When the pathologies develop prematurely, a considerable additional financial effort is necessary to rehabilitate buildings. We have to keep in mind that a well preserved building stock is a key issue to the economic sustainability of a Region.

KEYWORDS

Residential buildings, survey, building materials, pathologies, degradation state.

[1] Universidade dos Açores, Ponta Delgada, PORTUGAL, margaridap@uac.pt
[2] Universidade dos Açores, Ponta Delgada, PORTUGAL, mbarros@uac.pt

1 INTRODUCTION

Building deterioration is a process that usually occurs in a progressive manner under the effect of climate, lack of maintenance or quality of the construction. When the pathologies develop prematurely, a considerable additional financial effort is necessary to rehabilitate buildings.

Although concerns about the preservation of the existing building stock and the reduction of their energy consumption having been growing in our society, rehabilitation is still an underexploited subject but, nevertheless, a necessary activity.

To assess the degradation state of the building stock of a region and correlate it with energy consumption patterns, it is necessary to have up to date information on the main characteristics of the building stock, their most common pathologies and their energy consumption by end-uses in that region. It is also desirable to do it in a way that makes it easily available. This knowledge can further help researchers in establishing benchmark strategies for an improved quality and durability of the building stock. Nevertheless its importance, the correlation between the degradation state of the building stock and the energy consumption patterns will be not object of analysis in this paper.

The use of surveys as a tool for the gathering of this kind of relevant information has already been successfully implemented in several regions. Since in the Azores case inadequate indoor conditions, lack of energy efficiency and durability are still too frequent, a Residential Building Stock Survey (RBSS) was developed [Fortuna *et al.* 2010].

The Azores are a nine island Portuguese archipelago of volcanic origin located in the North Atlantic Ocean. The islands vary considerably in size and population, from the largest and most populated island of São Miguel (133 816 inhabitants of a total of 244 780 inhabitants in the Azores -values of 2008- [SREA 2010]) to the smallest and least populated island of Corvo, also the most northern. The RBSS was applied in São Miguel during the months of July and August 2010. Its methodology involved inhabitant interviews and external and internal visual survey of the buildings.

Section 2 of this paper explains the methodology used for applying the survey. In section 3 some of the survey results are presented, correlated and discussed, namely those concerning building typologies, materials and construction technologies and pathologies patterns. Next, in section 4, a novel method for the evaluation of residential buildings degradation state is introduced. The method was implemented on São Miguel and permitted the assessment of a preliminary evaluation of its residential building stock degradation state (section 5). Finally, section 6 sets out some concluding remarks and suggestions for further study of buildings.

2 RESIDENTIAL BUILDING STOCK SURVEY

The RBSS was developed by the University of the Azores, in the framework of the Green Islands Project, a project which associates the Massachusetts Institute of Technology and several Universities in Portugal. The RBSS intends to characterize in a detailed manner the building stock of the Azores regarding the building envelope and surroundings, equipments and appliances and behavioural issues, nevertheless, it can easily be adapted to be applied in any other part of the world. The survey is organized in seven main sections [Fortuna *et al.* 2010]:

- General Data;
- Characterization of the Building;
- Characterization of the Household Unit (HU);
- Characterization of the equipments;
- Characterization of the occupants;
- Characterization of the occupants behaviour;
- Historical energy consumption.

This paper focuses on the characteristics of the buildings and the characteristics of the Household Unit (which may be the same as the building or just a part of the building, as in the case of apartments), namely the typology, materials and existing external pathologies. The selection of the variables to be gathered in the survey is consistent with previous studies [Gaspar & Brito 2005], [Rodrigues & Teixeira 2006], [Vaz *et al.* 2003], [Pina dos Santos & Rodrigues 2009] and national and regional thermal legislation on this subject. The relevant characteristics can be grouped as shown on Table 1.

Table 1. Main collected building and household unit characteristics.

Item	*Characteristics*	*Variable*
General data		Type of property (owner occupied, rented or lent space)
Surroundings	Nearby construction and obstructions	Relative height of nearby obstructions, relative height of the adjacent buildings
	Climate	Nearest Meteorological Station
Building	Location and exposure	Latitude, longitude, altitude, distance to the ocean, wind exposure
	Building typology and general characteristics	Type of building (house/apartments building), dominant orientation of the building, number of floors in the building (including ground floor), year of construction
	External Pathologies	Moisture staining and/or fungi, location and type of superficial (minor) cracking and of deep cracking, efflorescence, spalling of coating or wall surface
Household Unit	HU typology and general characteristics	Type of HU (house/apartment), typology (T0, T1, …)
	HU and envelope characteristics (dimensions, orientation, materials and construction technologies)	External walls: areas; orientation; type (materials and technology); thickness; location, type and thickness of thermal insulation; external coating, main internal coating
	HU changes (works and improvements)	Time since last roof exterior maintenance works, type of maintenance works (painting of exterior/interior walls/doors/windows, …) done during the last 6 years, time since last expansion and type of last expansion, time since last rehabilitation/retrofit and type of last rehabilitation/retrofit, time since last reconstruction

The RBSS as a whole was applied to a representative sample of 500 households in São Miguel, distributed by municipalities according to population concentration.

The methodology involved three stages: preliminary data collection and field work consisting of building external and internal visual survey upon arrival to the location of the building and inhabitant interviews. The preliminary data collection concerns the gathering of information prior to field data collection itself. This includes all the information that can be retrieved starting from the knowledge of the building's address, such as, for example: latitude, longitude, altitude, distance to the sea, nearest Meteorological Station.The external visual survey included the external pathologies of the building façade and, as much as possible, building dimensions and physical (envelope) characteristics. The objective of the internal visual survey was to gather information about the characteristics of the interior of the household unit (floor covering and ceiling covering, ceiling height, amongst others) and its interior pathologies (type and location). In the interviews, the data that could not be obtained by visual survey was retrieved from the interviewed resident. Up to 500 household respondents were personally interviewed in their homes (one interview per household unit).

2.1 Identification of Main External Pathologies and Characterization of the Building Stock

An empirical method based on field work was used, as described in section 4, through which the existing (detectable) defects were gathered. The pathologies and defects considered respected both the exterior and interior of the buildings, in order to gather the data necessary to evaluate the degradation state of the housing stock and to assess a preliminary diagnosis. In this paper only the external problems are considered. The empirical method combines the information concerning the defects on a single numerical index, the External degradation Level (EDL).

The first task was to identify the main external pathologies that can affect the residential buildings (only the façades) and the affected location on the building façade. The approach was based on a ranking of importance concerning the affected area (extension) and depth of the problem. To complete the characterization of the pathologies, it is also necessary to characterize the existing residential building stock. This not only helps to understand the causes and consequences of the pathologies, and their relationship with building envelope characteristics, but also can contribute to make the definition of remedial measures much easier.

3 SURVEY RESULTS

As it was pointed out, the survey included extensive information about residential buildings surroundings, envelope, equipments, and also about its occupants.

3.1 Typology

From the survey results it is possible to define the most common residential household unit typology in São Miguel island: single family buildings are the dominant type of housing. These residential buildings are most commonly connected to other buildings on one side or two sides (row house). There are also detached houses and apartment buildings exist but in a smaller number (Table 2).

The household units were classified in accordance with their number of rooms T_n, in this case n being an index whose value equals the number of rooms minus 1. As such, a T2 residential building has three rooms (one of which is usually considered to be a living room). This can be considered a dimension characteristic, as the bigger the number of rooms usually the larger the area of the household unit, even though this is not necessarily always true. The most common typology is T3, followed by T2 (less than half the frequency) and T4. Surprisingly, the results found some T7 and in a larger number than the T0 households. The most common number of floors in residential buildings is 3 (including ground floor), 57.6%, followed by 2 floors, 29.0%, and 11.2% of the buildings have 4 floors.

Table 2. Identification of the typology of the household unit.

Typology	*Percent*
Single-family isolated dwelling house	12.4
Single-family row house	29.4
Single-family connected house	55.6
Single-family apartment in a building with six or fewer units	2.4
Single-family apartment in a building with more than 6 units	0.2

Of the 500 inquiries that were made, 33.2% did not know the approximate year of construction of the building. Of the remaining, the majority mentioned that the building was originally constructed before 1940. A high concentration of frequencies occured between 1980 and 1999 with a continued concentration in 2000 to 2005 (Table 3). This is consistent with a construction boom that occurred after the 1980's and lasted until 2007.

Table 3. Year range of construction of the building.

Range	*Before 1940*	*1940-1949*	*1950-1959*	*1960-1969*	*1970-1979*	*1980-1989*	*1990-1999*	*2000-2005*	*2006-2008*	*2009-2010*
Percent	14.6	2.0	5.2	6.6	5.2	11.8	10.2	8.6	2.2	0.4

Most of the surveyed buildings (90%) are situated at an altitude below 150 m. Almost one third of the residential buildings are located at an altitude of less than 30 meters. As to what respects the distance to the ocean, a considerable portion of the residential buildings (one fifth) is located within 250 meters to the ocean and more than half is located within 750 m.

About 37% of the questionnaires picked up rural settings, 20% suburban and the remaining urban settings. Looking at the surroundings, 67.8% of buildings were surrounded by buildings of the same relative height, 13.8% with taller buildings, 11.2% with smaller buildings and the remaining were set in open spaces. About 23.6% of the buildings were highly exposed to wind. Looking at ownership, the vast majority of residential units is owner occupied, 86.4%, with only 8.4% rented and the remaining 5.2% classified as lent space.

3.2 Materials

The most common types of external walls are stone walls, with or without masonry mortar (45.8%), and aggregate concrete masonry units walls (35.4%). There are only a few cases of double aggregate concrete masonry unit walls (0.8%). As to the external rendering of the external walls, the most commonly used material is cement mortar (63.2%). Lime mortar is also referred in the case of external stone walls. Ceramic wall tiles, wood or natural stone are not very common.

In the majority of cases the walls are 25 cm thick or 35 cm thick. For about four decades, 25 cm walls have dominated. Before 1950, walls are typically thick. After a progressive transition period, thinner walls (35 cm and 25 cm) become more common. However, it is expected that 35 cm thick walls (including rendering) will become dominant in the future, as opposed to thinner walls, due to thermal legislation. It is worth noting that in 22.4% of the cases the walls are 55 cm thick or more, most of them pertaining to buildings built before 1960, probably stone walls.

3.3 External Pathologies

The survey results showed that, considering all possible locations (see Table 1), the most common external pathology is fungi (38%), followed by painting degradation (33%). As for superficial cracking on façades, 31.8% of the buildings showed it on the exterior of the household unit at some location: 21% showed superficial cracking on the continuous walls and the rest (10.8%) is localized at edges, corners and around openings.

Deep cracking problems were detected on 8.8% of the survey sample. Considering the severe nature of this problem, this is a high value. As for the location, deep cracking was detected on continuous walls (3.8%) and, on 5% of the surveyed cases, it was detected only on locations which are not continuous walls (2.8% on the copings and/or below the eaves, 1.2% on edges and 1.0% around the openings and/or in junction of walls with roofs and/or under balconies and/or corners). The number of buildings on which it was detected deep cracking in various locations of the façade is, however, small, meaning that deep cracking occurs mainly as a localized phenomenon. Efflorescence was found on 16.4% of the cases, more remarkably on the walls near the ground level (11% of the cases) than on the copings. Only on a few cases was it found simultaneously near the ground level and on the copings (2.2%).

Excluding painting degradation, spalling of coating of wall surface on the exterior of the household unit was detected on 10.6% of the households. Once again, continuous walls are the most degraded

parts of the façade, with spalling problems on 7.4% of the surveyed cases, while localized parts were affected on only 4.8% of the cases.

4 METHODOLOGY OF ASSESSMENT OF THE EXTERNAL DEGRADATION LEVEL

The established method aimed at providing a quantitative value capable of defining the façade's level of degradation and which could be used for the assessment of the existing residential buildings external degradation state.

The degradation state of the residential building stock was established using an objective and simplefied method, based on a compact index named the External Degradation Level (EDL), which was applied to each surveyed building's façade. During the visual survey the pathologies in the surveyed façade were registered and rated according to a scale which takes into account the location, extension and depth of the detected pathology. As such, the EDL expresses the overall degradation level of the façade at the moment of the survey by weighting the pathologies into a single value, the EDL_{value}. The index EDL has six possible discrete values, from 0 to 5, the lowest value being a façade without anomalies (Table 4).

Table 4. External degradation level (EDL)**.**

External degradation level (EDL)	*Value*
0 (No visually detectable degradation)	$EDL_{value} = 0$
1 (Good)	$0 < EDL_{value} \leq 0.5$
2 (Light degradation)	$0.5 < EDL_{value} \leq 1$
3 (Medium degradation)	$1 < EDL_{value} \leq 2$
4 (Broad degradation)	$2 < EDL_{value} \leq 3$
5 (Extensive degradation)	$3 < EDL_{value} \leq 4$

The EDL_{value} was computed as a weighted value, according to the following:

$$EDL_{value} = a_1C_1 + a_2C_2 + a_3C_3 + a_4C_4 + a_5C_5$$

Each of the coefficients a_1, a_2, a_3, a_4 and a_5 expresses the extension and depth of the detected pathologies and its value is obtained directly from the answers to the survey. The value follows a hierarchy such that when the corresponding pathology is not detected on the façade the value is zero; its maximum value is unity and corresponds to the maximum extension and depth defined in the survey for that pathology. The coefficients C_1, C_2, C_3, C4 and C5 define the ranking of importance of pathologies, according to their relative depth (Tables 5 and 6).

Table 5. Values of the coefficients a and C.

Survey question	*Coefficient a*	*External pathologies*	*Coefficient C*	
Problems with fungi and/or humidity staining	a_1 = answer/7	Fungi and/or humidity staining	0.25	C_1
Location of superficial cracking	a_2 = answer/6	Superficial cracking	0.75	C_2
Location of deep cracking	a_3 = answer/6	Deep cracking	1.05	C_3
Efflorescence	a_4 = answer/3	Efflorescence	0.75	C_4
Spalling of coating on wall surface	answers 00 or 01: a_5 = answer/1 answers 02 to 07: a_5 = answer/9	Degradation of painting	0.15	C_5
		Detachment of coating	1.05	

Table 6. Answer values.

Is there Efflorescence in the exterior of the HU?	
0	No
1	In the copings
2	On the walls near the ground level
3	In the copings and on the walls near the ground level

Are there problems with fungi and/or humidity staining?		*Is there spalling of coating on wall surface?*	
0	No	0	Not applicable
1	On walls	1	Only degradation of painting
2	In the copings	2	On walls
3	Near ground level	3	In the corners and/or edges
4	In the corners or at the junction of walls with roofs or around the openings/ underneath porches or under the eaves	4	Around the openings/under balconies
5	On the walls and near the ground level	5	On walls and corners and/or edges
6	On walls and corners or junction of walls with roofs or around openings / beneath porches or under the eaves	6	On the walls and around the openings/under balconies
7	In the copings and near the ground level	7	With steel rods in sight in the corners and walls

Location of superficial cracking?		*Location of deep cracking?*	
0	Not applicable	0	Not applicable
1	Copings and/or below the eaves	1	Copings and/or below the eaves
2	On walls	2	On walls
3	On edges	3	On edges
4	Around the openings and/or in junction of walls with roofs and/or under balconies and/or corners	4	Around the openings and/or in junction of walls with roofs and/or under balconies and/or corners
5	On walls and edges	5	On walls and edges
6	On walls and around the openings and/or junction of walls with roofs and/or under balconies and/or corners	6	On walls and around the openings and/or junction of walls with roofs and/or under balconies and/or corners

5 EVALUATION OF THE DEGRADATION STATE

The methodology presented in the previous section was applied to each of the 500 surveyed household units, resulting on an EDL for each of them. The results are shown on Fig. 1.

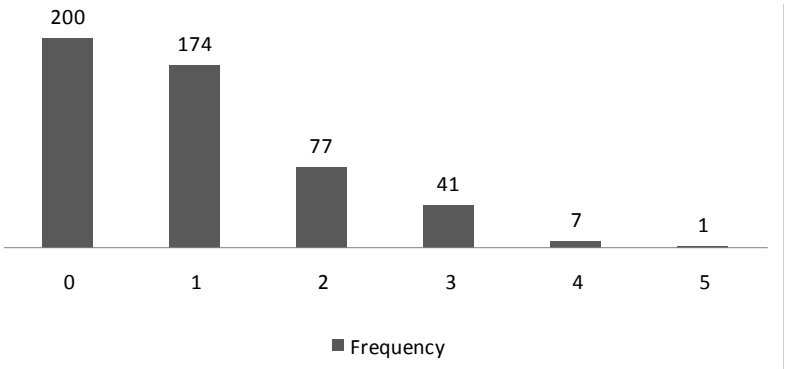

Figure 1. EDL results.

From these results, 40% of the surveyed residential building stock shows no visually detectable degradation. However, 25% of the surveyed residential buildings need average to extensive repair works (EDL=2, 3, 4 or 5).

Considering the degradation state of the buildings over the decades, it can be noted that buildings built in the 1950´s, 1970´s and 1990´s are the ones which show more problems, in spite of maintenance and repair works having been done. In fact, around 70% of the buildings from these decades had painted the exterior walls in the last six years but only 30% have EDL =0. Buildings from the 1950´s and 1970´s show superficial cracking (about 45% of the surveyed buildings). In the 1990´s, many of the surveyed household units had fungi and mould problems. So, it seems that buildings from these periods have lesser quality.

Deep cracking problems affect almost uniformly buildings with different ages. Globally, 9% of the buildings are affected. Nonetheless, 23% of the buildings from the seventies have deep cracking problems but only 4% of the buildings the nineties show these problems.

Nevertheless, maintenance works, namely, high values of wall painting (61.8% in the last six years), play an important role in the conservation of the building stock and achieving a low EDL value. Considering the surveyed residential building stock, it is noticeable that almost 90% show no signs of detachment or painting degradation.

The most populated municipality in the archipelago, Ponta Delgada, also shows the lowest proportion of buildings with a high conservation state (lowest degradation level): only 38% of the surveyed buildings have ELD=0. Another neighbouring municipality, Lagoa, also shows a similar but even worse pattern: only 33% of the surveyed buildings have EDL=0. Together these two municipalities represent about 59% of the sample and can be considered to be, in the fact, the most important concentration of residential building stock in the Azores.

6 CONCLUSION

From the results of the Residential Building Stock Survey in the São Miguel island, it was found that a considerable number of buildings are affected by pathologies. Signs of external degradation were visually detected in 60% of the surveyed buildings (EDL=1, 2, 3, 4, or 5). Since 25% of the surveyed residential buildings need medium to large repair works, the state of conservation of the residential building stock is far from good and could and should be improved.

In the most problematic decades (1950´s, 1970´s and 1990´s) a considerable number of maintenance works were done. Nevertheless, problems of superficial cracking, deep cracking and spalling were found. The percentage of the residential building stock with the lowest degradation level (ELD=0) is small, about 30%.

Maintenance is important, we dare say essential, for a well preserved building stock. However, it is not enough to solve all the problems, additional measures are needed, like rehabilitation works and improving contruction quality. Although the global economic crisis has also had its effects in this region, the construction business plays an important role in the local economy, so maintenance as well as rehabilitation works can be both a good opportunity window for best exploration business of all those involved in the Construction practices.

We have to keep in mind that a well preserved building stock is a key issue to the economic sustainability of a Region.

REFERENCES

Fortuna, M., Estrela Rego, I., Rosa Nunes, J., Machado Pires, M., Barros, M. J., Cunha, R., Inquérito ao Consumo de Energia em Edifícios de Habitação, 2010, Green Islands Project, UAc - MIT Portugal.

Gaspar P.L. & Brito, J. 2005, "Assessment of the overall degradation level of an element, based on field data", 10DBMC Int. Conf. on Durability Materials and Components, Lyon, France, 17-20 April.

HOPE: Health Optimisation Protocol for Energy-efficient Buildings, Pre-normative and socio-economic research to create healthy and energy efficient buildings, http://hope.epfl.ch/, 24-09-2010.

Machado Pires, M., Barros, M. J. & Fortuna, M., 2010, "Characterization of the envelope and surroundings of the residential building stock through a Survey: the Azorean case", 15 CCIA, V Seminário International de Ingenieria Civil, Hidráulica y Geociencias**,** Cuba , 29 November-3 December.

Gaspar, P. L. & Brito, J. 2008, "Quantifying environmental effects on cement-rendered façades: A comparison between different degradation indicators", *Building and Environment* **43,** 1818 – 1828.

Pina dos Santos, C. A. & Rodrigues, R. 2009, *Coeficientes de transmissão térmica de elementos opacos da envolvente dos edificios, soluções construtivas de edifícios antigos, soluções construtivas das Regiões Autónomas, ITE 54*, LNEC, 3ª Edição.

U. S. Energy Information Administration, Residential Energy Consumption Survey, http://www.eia.doe.gov/emeu/recs/contents.html, 24-09-2010.

Rodrigues, M. F. S., Teixeira, J. M. C. 2006, "Building Pathologies in social Housing: The Portuguese State of Art", JOINT 2006 CIB W065/W055/W086 SYMPOSIUM, Construction in the XXI century: local and global challenges, Rome, Italy.

SREA, Serviço Regional de Estatística dos Açores – http://estatistica.azores.gov.pt, 24-09-2010.

Vaz, V., Neto, J., Reis, V. 2003, "Conservação e Reabilitação de Edifícios. Anomalias não estruturais [Breves notas]", *Construção magazine* nº5, 2º trimestre 2003.

XII DBMC
International Conference on Durability of Building Materials and Components
PORTO - PORTUGAL, April 12th-15th, 2011

Ventilated Stone Veneer: Mechanical Behaviour, Calculation Methodologies, Major Pathologies and Existing Tests

Carlos Pérez Carramiñana [1]
Mónica Mateo García [2]
Beatriz Piedecausa García [3]
Cesar Daniel Sirvent Pérez [4]
Antonio Maciá Mateu [5]

ABSTRACT

The increase of building pathologies related to the use of stone materials and the use of ventilated stone veneers, requires the reformulation of design concepts in building façades and also the reformulation of the architectural project.

The aim of this paper is to identify, analyze and evaluate synthetically building pathologies in stone ventilated façades in order to obtain the main technical conditions to be considered in the architectural design, by interpreting its mechanical behavior and capabilities to prevent such pathologies and to ensure the proper features during the building lifetime.

The methodology is based on both laboratory stone tests and in situ tests about construction systems, by analyzing physical and mechanical behavior of the outer layer in relation to other building requirements.

The results imply the need of proper sizing, specific quality control and practical application of calculation methods, to control high concentration pressures in ventilated façades by reaching appropriate project solutions.

In conclusion, the research about different pathologies of stone ventilated façades, the study of their mechanical behavior, their anchorage and their connection with their constructive aspects, will help to improve the construction quality of the stone ventilated façade in buildings and to enhance the use of natural stone in modern architecture.

KEYWORDS

Ventilated stone veneer, mechanical behavior, measurement, stone pathology, testing.

[1] Architectural Construction Department. University of Alicante. SPAIN, c.perez@ua.es
[2] Architectural Construction Department. University of Alicante. SPAIN, monica.mateo@ua.es
[3] Architectural Construction Department. University of Alicante. SPAIN, piedecausa@ua.es
[4] Architectural Construction Department. University of Alicante. SPAIN, sirvent@ua.es
[5] Department of Construction Engineering, Public Works and Urban Infrastructure. University of Alicante. SPAIN, antonio.macia@ua.es

1 INTRODUCTION

The traditional use of stone in architecture (with a massive character as a building element independent from the façade and the structure), has turned into a use as a coating material and in the case of ventilated façades is designed as a floating sheet in a constructive sub-system.

This evolution in the use of stone materials and ventilated façade systems in buildings involves a radical transformation of the concept of stone façade. Design and constructive implementation of building façades should be considered from the project to avoid preconceived architectural ideas, to prevent sizing errors in the project or in the material execution and to provide complex technical solutions without generating construction deficiencies.

The aim of this paper is to identify, analyze and evaluate synthetically the main technical factors considered in the construction process that influence the design of ventilated stone façades, by interpreting their specific characteristics and their particular mechanical behaviour.
It should be considered that the ventilated stone cladding differs from the traditional stone wall cladding or from the adhered veneer due to its capability to bear higher efforts with the minimum material and important mechanical requirements due to its geometric features and its constructive configuration in a separate and independent sheet.

These intrinsic characteristics of the stone ventilated veneer involves new formal and constructive conditions to analyze and evaluate:

- The resistant element should be a substructure capable of transmitting the building loads that affect the coating to the structure, by concrete walls, massive or perforated brick walls, concrete block walls or auxiliary metal substructures. Hollow brick wall does not provide a sufficiently homogeneous and strong resistant element for the high stresses transmitted by the anchorages and that´s why it is unacceptable to use it as a resistant element for ventilated façades.
- Anchorage must be able to combine differential deformations and dimensional tolerances between the stone cladding and the resistant element. They must allow some adjustment of distance and the differential movements between the resistant element and the plate, absorbing the rheological and thermal deformation (contraction-expansion) but also resist to electrochemical corrosion, being stable against gravitational actions as the weight of the plates, the wind, impacts, earthquakes and fires. The size and choice of anchorages must take into account not only the loads to be transmitted, but also the characteristic strength of the resistant element.
- An air gap does not prevent direct sunlight (the stone does) it doest reduce heat transmission (with a quite low efficiency) and enhance moisture diffusion, but reducing condensation risk.For this, it is very important to ensure an adequate ventilation by avoiding bottlenecks and by sizing some chamber holes to let the air in and out, especially at the base and at the coronation of the façade to facilitate the flow ascension of hot air and to reduce the vapor pressure inside the chamber.

  Also, it is essential to ensure a proper drainage at the bottom of the camera by providing evacuation to the outside of the condensed water, coming from rain or humidity absorbed by capillary action by any of the component materials of the building system.
- The stone veneer joints must be designed not only based on formal criteria but also on a distribution respecting the structural and expansion joints of the building structure, allowing the movement of expansion and contraction of the stone cladding due to the significant temperature changes experienced.

The lack of consideration of the issues outlined above provoques most of the damages detected in ventilated stone facades. Injuries can be summarized mainly in the following list:

- Broken stone plates by bending efforts due to the pressures and suctions produced by wind action, impacts or thermal movements of the cladding or the resistant element.
- Broken stone plates by pulling out between the anchorage and the veneer in the attachment points due to wind, impact, thermal based efforts or seismic action.

- Stone element collapse by pulling out between anchorage and the resistant element due to overloading because of the existance of an insufficient number and distribution of anchorages (over-dimensioning of the plates or the distance between anchorages) or poor resistance to transmit loads by the anchorage.

Moreover, the low thickness of the stone cladding in a ventilated façade increases the importance of the factors affecting the durability of the veneer, both intrinsic factors (physical and chemical properties of the stone) and environmental factors (temperature changes, wind erosion or ocean spray action) that generate problems that can be summarized mainly in the following list:

- Anchorage breaking due to resistant section decreasing by the presence of voids or internal cracks which reduce the resistance of the stone plate.
- Stone breaking due to cutting force or flexion effort by the lack of homogeneity or insufficient molecular cohesion.
- Aesthetic and resistant transformations by the presence of ferrous salts in aggresive environments.
- Stone cracking by freezing action due to excessive porosity and lack of resistance in aggressive environments.

Due to the obvious increase in the optimization of the stone building solutions because of the ventilated façade, it is pertinent to consider the need to incorporate methods for calculating the correct sizing of the plates and anchoring systems.
In order to increase accuracy in the sizing of stone cladding in the project and its execution control, we propose the practical application of computational methods and quality control for the stone materials and the construction system.

The methodology is based on both laboratory tests of selected stone and tests of the construction system executed on site, analyzing the physical and mechanical behavior of the façade related to the actions and building demands. These calculation methods applied to ventilated facades are substantially simpler than those used for the dimensioning of steel structures or concrete but also they have new characteristics and specific conditions which we proceed to determine by the experimental work described below.

2 MATERIALS AND METHODS

2.1 General

For the correct sizing of a ventilated stone façade is necessary the use of an experimental design and modeling allowing both the verification of the resistance of natural stone plates to bending and pulling testing between the stone and the anchorage, and the calculation of pullout resistance between the anchorage and the anchorage and the resistant element.

Trying to find this aim, we have conducted laboratory tests using natural stone and also in situ testing of the construction system executed on site, by analyzing both physical and mechanical behavior of the cladding related to the most important requirements suffered once the building's façade is constructed. Therefore, on the one hand we first made bending tests to stone plates in laboratory and we found breaking patterns of the stone anchorage used. On the other hand, we also made in situ pullout tests in existing buildings between the anchorage and the resistant element.

2.2 Materials and Methods

To be able to compare both results, in the laboratory tests we used natural stone slabs with the same dimensions and weight as those analyzed in the existent façade.

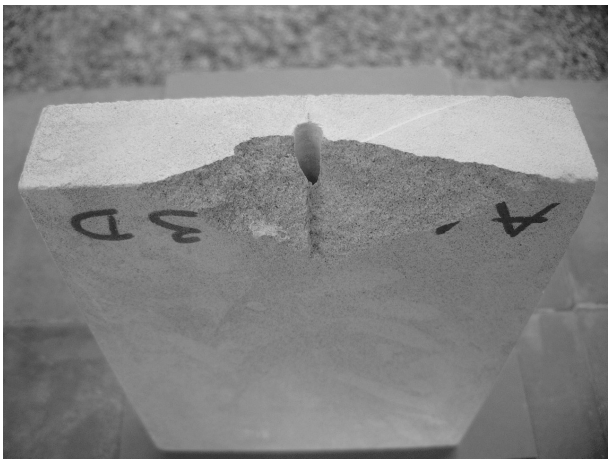

Figure 1. Test pullout (anchorage-plate).

In situ tests were carried out by pullout tests anchorage-resistant element, using a pressure plunger and an hydraulic pump (Enerpac) applied to the anchorage tested.



Figure 2. Test pullout (anchorage-resistant element).

Actions referred to the stone cladding are based on the height of the façade crowning on the building, related to the wind zone of the building location and the type of exposure depending of the legislation, as well as the degree of seismic intensity and the seismic coefficient for the location, according to DB SE-AE, the NTE-CVD and the seismic legislation PDS-1/1974 because of being more restrictive than the current legislation.

3 RESULTS

Results show high tensions and stresses in natural stone plates and anchorages considering usual actions in these constructive elements as part of a ventilated façade, exceeding the breaking strength and causing a cladding falling.

Table 1. Results of tests and calculations.

Breaking study	**Testing results**	**Calculated loads and stresses**	
Cladding breaking	(laboratory) pullout stone-anchorage *Qadm1=42,78 Kp (average)* *Qadm2=31,94 Kp (minimum)*	Fh wind *Fh's =30,38 Kp <Qadm2<Qadm1*	Suitable
		Fh seismic *Fh's =3,50 Kp <Qadm2<Qadm1*	Suitable
	(laboratory) flexion and traction test *σ adm=1,31 Mpa*	Wind flexion *σ max = 0,25 Mpa < σ adm*	Suitable
		Seismic flexion *σ max = 0,058 Mpa < σ adm*	Suitable
Anchorage-resistant element breaking	(in situ test) Pullout anchorage-resistant element *Qadm1=44,83 Kp (average)* *Qadm2=26,89 Kp (minimum)*	Fh wind *Fh's =30,38Kp <Qadm1 >Qadm2*	NO Suitable
		Fh seismic *Fh's =3,50 Kp <Qadm2<Qadm1*	Suitable

It´s important to consider the high tensions caused by the suction wind effect on the areas near the corners of the façade perpendicular to the faces more exposed to wind. Data show that the falling of the veneer in many cases is due to insufficient resistance to pullout from the anchorage and the resistant element, andnot due to stone breaking. Calculations also show that wind action on a ventilated stone cladding is much more damaging than seismic action because of being a large area exposed to horizontal wind action.

Moreover, it should be noted that the results of the tests reflect the wide variation in the values of breaking according to the nature of the stone, the resistant element and the type of anchorage and it´s necessary to establish higher safety factors than those used in the structural design of reinforced concrete or steel. In the same sense, we can find regulations as the ASTM C 1242-96 b or the probabilistic methods of calculation of the UNI 32045130 proposing two hypotheses of safety factors depending on the degree of knowledge about the veneer by previous tests.

Also, modeling allows the calculation of the anchorage resistance on a ventilated stone facade and presents significant problems to establish rigorous behavior hypothesis due to the wide variety of sizes of plates used in a façade design, the distance between anchorages, the different thicknesses of stone used and the size of the holes drilled in situ.

The cost and difficulty of making a high number of breaking or pullout tests in stones used buildings, and the high variability of the results obtained due to the nature of a natural stone material make necessary to increase the safety factor for absorbing the risk of incidents such as variations of loads

and stresses or changes in the strength of the material because of its heterogeneity, alterations of resistant sections for cladding, physical or chemical changes over time or other material weaknesses in the implementation of the work.

From the characteristics of the mechanical behavior of the ventilated stone façade, its modeling, testing and the results obtained, it can be deduced:

- The need to choose the adequate type of stone to be used not only in terms of aesthetic factors but also because of its mechanical resistance to pulling, bending and impact, and therefore also because of its homogeneity and lack of cracks or voids, its resistance to humidity and frost changes, its risk of exfoliation or its content on ferrous salts.
- The suitability of evaluating the mechanical behavior of the union resistant element-anchorage and anchorage-cladding based on the expected solicitations, to make a correct dimensioning of the thickness of the cladding, the distances between anchorages and the anchorage type.
- The need to reduce potential weaknesses in material construction through the resolution and definition on design by distributing the adequate anchorage for the plates and the resistant elements and also by carrying out the holes in the edges of the plates in the workshop or using drilling templates on site.
- The need to increase quality control of the work by laboratory testing of physical and chemical characteristics of the stone used and by pullout testing of the anchorage system in situ.

4 CONCLUSION

Nowadays, the traditional massive character of the use of natural stone in the stone ventilated façade in architecture has been transformed into a thin skin exposed to high features within a set of functionally specialized layers. Differences between ventilated façade and adhered veneer are relevant, essentially those related to mechanical behavior and to anchorage, making necessary the domain of their major design features, the calculation methodologies and the appropiate testing to ensure the construction quality and durability.

REFERENCES

ASTM C1242 – 10. 2010, *Standard Guide for Selection, Design, and Installation of Dimension Stone Attachment Systems*, American Society for Testing and Material, United States.

Código Técnico de la Edificación. 2006, *DB-SE-AE*, Boletín Oficial del Estado, Ministerio de la Vivienda, Madrid,España.

NCSE-02. 2002, *Norma de Construcción Sismorresistente*, Parte General y de Edificación, Comisión Permanente de Normas Sismorresistente, Real Decreto 997/2002 del 27 de septiembre de 2002, Boletín Oficial del Estado.

NTE-ECV, 1988, *Estructuras. Cargas de Viento*, Boletín Oficial del Estado, Ministerio de Fomento, Madrid, España.

PDS-1/1974. 1974, *Norma Sismorresistente P.D.S.-1*, Comisión Interministerial del la Presidencia del Gobierno, Decreto de 30 de agosto de 1974, Boletín Oficial del Estado, 279, 21 de noviembre de 1974, Ministerio de Obras Públicas, Transporte y Medio Ambiente, España, pp. 3723-3740.

UNI 11018:2003. 2003, *Rivestimenti e sistemi di ancoraggio per facciate ventilate a montaggio meccanico - Istruzioni per la progettazione, l'esecuzione e la manutenzione - Rivestimenti lapidei e ceramici*, Ente Nazionale Italiano di Unificazione.

Vera, R. 2003, *Temas de construcción 2. Fachadas de edificios con aplacado de piedra transventilado*, Imprenta Gamma, España, pp.85-90.

XII DBMC
International Conference on Durability of Building Materials and Components
PORTO - PORTUGAL, April 12th-15th, 2011

Timber in Buildings: Estimation of Some Properties using *Pilodyn*® and *Resistograph*®

Dulce Franco Henriques [1]
Lina Nunes [2]
José Saporiti Machado [3]
Jorge de Brito [4]

ABSTRACT

At the conservation and/or rehabilitation stage of a building the condition state of the timber structural elements strongly limits the actions to be adopted. A non-destructive survey of their state is therefore a frequent need. Due to their handling facility and the direct results obtained two inspection and diagnosis less-destructive or non-destructive tests (NDT) [Machado & Cruz, 1997] gain relevance in the *in situ* characterization of timber properties: the *Pilodyn*® and the *Resistograph*® methods.

This paper presents the experimental procedures and the results obtained to find a possible correlation between the results obtained with these test readings and some properties of timber. The results were correlated with the density and the compression strength of two different species of pine timber with different ages, frequently used in buildings in the Lisbon area in the two last centuries. Thus, the following test campaigns were performed in *Pinus sylvestris* samples with approximately 80 and 150 years and recent *Pinus pinaster* samples: i- density; ii - compressive strength; iii - *Pilodyn*® and *Resistograph*® readings.

Though further work is envisaged, a correlation was found between the timber properties and the values obtained with the non-destructive equipments used.

KEYWORDS

Pine timber, NDT, density, compression strength

[1] Department of Civil Engineering, Instituto Superior de Engenharia de Lisboa, PORTUGAL, mfhenriques@dec.isel.ipl.pt
[2] Structures Department, Laboratório Nacional de Engenharia Civil, Lisbon, PORTUGAL, linanunes@lnec.pt
[3] Structures Department, Laboratório Nacional de Engenharia Civil, Lisbon, PORTUGAL, saporiti@lnec.pt
[4] Department of Civil Engineering and Architecture, Instituto Superior Técnico, Lisbon, PORTUGAL, jb@civil.utl.pt

1 INTRODUCTION

The problem of evaluating wood decay and related residual strength capacity in existing wooden structures in both recent and historical buildings is particularly important when deciding on the possibility of restoration and the kind of strengthening intervention needed [Ronca & Gubana, 1998]. A non-destructive survey of their state is therefore a frequent need. But in order to interpret the results obtained it is necessary to establish laboratory correlations for the various timber species [Uzielli 1992, Caselli & Mannucci 2005, Lourenço *et al.* 2007].

The evaluation of the physico-chemical characteristics of timber applied in buildings using non-destructive tests (NDT) has been for over three decades the object of important studies involving laboratorial research [Uzzieli 1992, Ronca & Gubana 1998, Machado 2000, Feio 2006, Lladró *et al.* 2006, among others]. While thermography, ultra-sounds, spectrography, tomography and other image-related methods have provided promising results, the *Resistograph* and the *Pilodyn* deserve to be in the limelight for their simplicity of use and the relative adequacy of the response to the objectives. There have been several authors that elected the resistographic technique as the one that better allies' ease of execution *in situ* with type of data it provides [Teles & Valle 2001, Caselli & Mannucci 2005, Ceraldi *et al.* 2001, Feio *et al.* 2007, Bamonte *et al.* 2001].

The *Resistograph* device has been seen as a reasonable tool to evaluate mechanical characteristics of timber, even though that was not its original objective [Rinn, 1994], nor its most usual application field. Evaluating the density of various species with the *Resistograph* has been done in laboratory conditions to estimate this characteristic in timber applied on site [Machado & Cruz, 1997]. The mechanical strength and modulus of elasticity have also been correlated with the *Resistograph* results [Feio 2006, Lladró *et al.* 2006, Palaia *et al.* 2008, Branco *et al.*, 2010]. The *Pilodyn* is also applied to calibrate the surface physico-mechanical characteristics of timber [Palaia *et al.* 2008, Teles & Valle 2001].

2 MATERIALS AND METHODS

2.1 Timber Specimens

Test specimens with 30 x 60 x 180 mm were obtained from different pine timbers (*Pinus pinaster* and *Pinus sylvestris*) free of defects. Both sapwood and heartwood were present, the fibres were parallel to the piece axis and the tops were plane and perfectly perpendicular to the faces. A sample was put together with the widest spectrum possible of densities in order to scope the maximum possible prospective situations within the group of pine timbers commonly used in the Lisbon area. The *P. pinaster* (recent timber) specimens were obtained from three different providers of structural timber. The *P. sylvestris* specimens were cut from structural elements, apparently without any durability problems, collected in two buildings that were 80 and 150 years old.

The complete sample consisted of 174 specimens with densities ranging approximately from 400 to 800 kg/m^3. 82 of these were from recent *P. pinaster*, 64 from 150-year old *P. sylvestris* and 28 from 80-year old *P. sylvestris*. To obtain fungal degraded material, 30 specimens were selected to be submitted to decay. The degradation by fungi of the 30 specimens was made in a natural environment adapting standard DD CEN/TS 15083-2 for a 6-month period. Losses of masses between 3% and 12% were obtained, i.e. a low decay level. The remaining specimens were paired according to density. In each pair one of the specimens was tested in axial compression and the other subjected to non-destructive tests

2.2 Non-Destructive Tests

2.2.1 Resistograph

This device drives a 1.5 mm diameter drill inside the timber at a speed of 8000 rpm. The resistance to

drilling is concentrated at the tip twice as large as the needle, thus eliminating lateral friction [Rinn, 1994]. The relative measurements allow evaluating the hardness of timber and detected the softest zones of the material, giving out an on-line graph in real size that represents the drill resistance path through the section [Breda 2003, Figure 1 a.].
In this study two holes were made in each specimen, using the IML Resi-B equipment regulated to a penetration speed of the needle of 7 cm/min. The resistance to drilling values are registered every 0.04 mm of depth thus providing the density profile in each perforation (Figure 1 a. and b.). The average value of the measurements in each specimen was used

a. 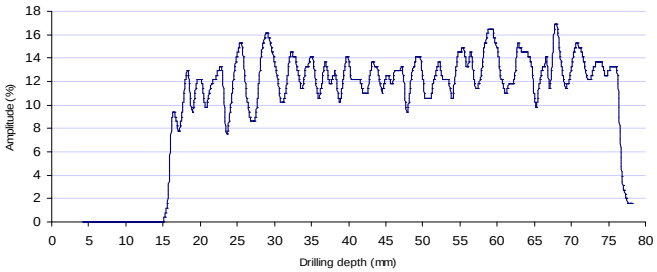

b. 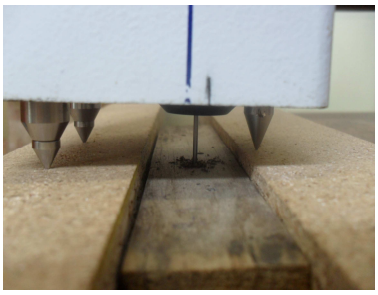

Figure 1. a. *Resistograph* density profile; b. Performing the *Resistograph* test.

The resistographic measurement, RM, valid for sound and defects-free timber, is given by the ratio between the area integral and the drilling depth, *h* (Eq. 1) [Lourenço *et al*, 2007]. It depends on the device type, the speed of drilling and the timber moisture content, and that is why it must be interpreted by comparison with values established in identical conditions [Machado & Cruz, 1997].

$$RM = \frac{\int_0^h Area}{h} \quad (1)$$

2.2.2 Pilodyn

The dynamic impact method consists of introducing a metal pin in the timber with a given energy, the penetration depth being inversely proportional to the timber hardness in the cross-section (Figure 2 a). The penetration depth can be used as a measure of the timber's density and also of the intensity and depth of fungal decay [Cruz *et al.* 1999, Teles & Valle 2001]. A real disadvantage of the method is the fact that it only measures the surface properties [Zombori, 2001]. Results depend on the test location in the element, the anisotropy and density of timber, the percentage of late wood, defects or decay, and the operator [Bonamini, 1995]. As with the *Resistograph* the values variation range in timber defects-free must be known and conclusions have to be drawn by comparison.
In this study the non-destructive test device *Pilodyn* 6J was used in order to obtain correlations between surface hardness of each specimen, its density and its mechanical strength. The dynamic impact exerted by the device is responsible for the penetration of the piston in the timber's surface, whose depth is read on a dial and varied from 0 to 40 mm (Figure 2 a).

2.3 Compression Test

The axial compression test (parallel to fibres) was performed in accordance with NP618:1973 until rupture of each specimen, and the corresponding value was presented in N/mm^2 (Figure 2 b.).

3 RESULTS AND DISCUSSION

The sensitivity of this NDT test in terms of density and compression strength of the sound and decayed timber is now analyzed. A further analysis is made of the relationship obtained between density and mechanical strength, by comparing it with similar tests by other authors.

a.  b. 

Figure 2. a. Performing the *Pilodyn* test; b. Performing the axial compression test.

3.1 Sound Timber Tests

3.1.1 Relationship between density and compressive strength

Density was measured according to NP 616 (1973) for a moisture content of 12% given by the Equation 2, where $m_{12\%}$ is the mass and $V_{12\%}$ is the volume of the specimen

$$\rho_{12\%} = \frac{m_{12\%}}{V_{12\%}} \quad (2)$$

Density is one of the most important parameters to determine the compressive strength of timber. Figure 3 a. shows the scatter of values and the regression line obtained in this study. A reasonable linear regression was found, according to equation $f_{c,0}$ = 0.068ρ + 3.68 (N/mm^2), where 75% of the specimens' compressive strength $f_{c,0}$ is explained by their density ρ.

Mateus [1961] tested pre-selected *P. pinaster* and obtained a variation law given in present units by equation $f_{c,0}$ = 0.115ρ - 18 (N/mm^2), as shown in Figure 1b. The mechanical strength values obtained by Mateus are generally higher than the ones from this study. This can be explained by the deliberate present choice of a much wider spectrum of origins, species and ages. Green *et al.* [1999] present the following exponential relationship between softwood's *G* (dry weight by unit of volume at 12%) and compressive strength parallel to the fibres: $f_{c,0}$ = 93.7 $G^{0,97}$ (N/mm^2). These authors refer that the relationship tends to be linear recommending that linear lines are used to study individual species as in the present study.

Figure 3 b. shows the regression lines that portray the relationships obtained by Green *et al.* [1999], Mateus [1961] and the present study.

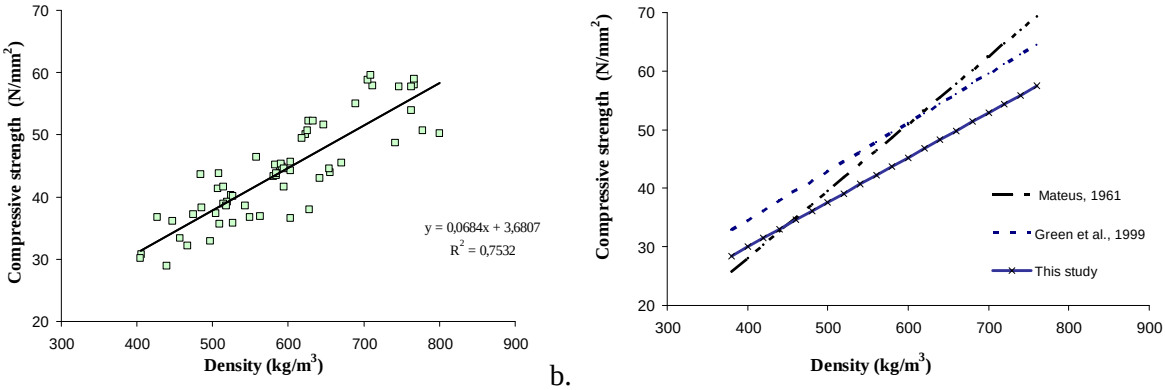

a. b.

Figure 3. Density *versus* compressive strength: a. Individual values from the present study (*P. pinaster* and *P. sylvestris*); b. Comparison with the regression lines proposed by other authors.

Even though the results of Green *et al.* [1999] were obtained from a diverse range of softwoods woods from the USA and the present study only includes *P. pinaster* and *P. sylvestris*, the lines obtained are

very similar.

3.1.2 Relationship between NDT results and density

Figure 4 a. and b. show the scatter graphs between density and the resistographic measurements, RM, as well as the values from the *Pilodyn* test.

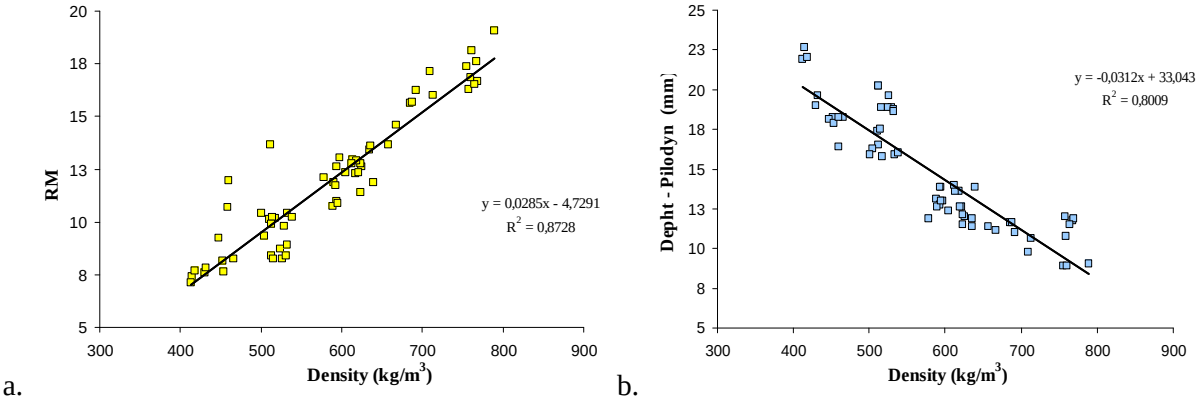

a. b.

Figure 4. Density *versus*: a. Resistographic measurement; b. Penetration depth using *Pilodyn*.

A good correlation, with r^2=0.87 (Figure 4 a.), was obtained for the relationship between the average perforation resistance values obtained using the *Resistograph* and density. The test made by Machado & Cruz in 1997 with defects-free *Pinus pinaster* in similar circumstances to those of this study led to a correlation factor equal to r^2 = 0.76, lower but also significant. Lladró *et al.* [2006], after testing 100 beams of Spanish *Pinus radiata* with the *Resistograph*, observed that it is possible to use the device to evaluate *in situ* and reliably the density. Testing old and recently cut chestnut wood (*Castanea sativa, Mill.*), Feio *et al* [2007] obtained a correlation factor equal to r^2 = 0.81 between density and RM. Machado & Cruz [1997] argue that the device, even though not allowing a strict determination of the average density of a timber structural element, can provided in some cases (12% water content and penetration speed of 7 cm/min) a significant approximation.

A good correlation (r^2 = 0.80) (Figure 4 b.) was also obtained for the relationship between *Pilodyn* and density, with a reminder that the test is made in defects-free timber specimens. Feio *et al* [2007] obtained a stronger correlation (r^2 = 0.91) in specimens of oak timber, old and new. Gorlacher [1978], cited by Branco *et al.* [2010], having tested several timber species, obtained determination coefficients from the linear regression analysis between *Pilodyn* results and density from 0.74 and 0.92, depending on the number of measurements and the species.

3.1.3 Relationship between NDT results and compressive strength

The correlations between the ultimate compression strength parallel to the fibres and the results from the NDT tests made on the corresponding specimen pair are shown in Figure 5 a. and b. There is a satisfactory correlation between the compressive strength of the set of specimens tested and the corresponding resistographic measurement, in which 70% of the results of one of the parameters are explained by the other. The correlation between the *Pilodyn* results and the mechanical strength was moderate (r^2 = 0.61).

Since all specimens were defects-free, these values must be looked with caution and should not be extrapolated directly for structural elements. Lladró *et al.* [2006] also found it imprudent to evaluate the average compressive strength directly from non-destructive tests for real structures. Nevertheless, the NDT approach has proven to be extremely useful when used together with other inspection tools (Machado & Palma, 2010).

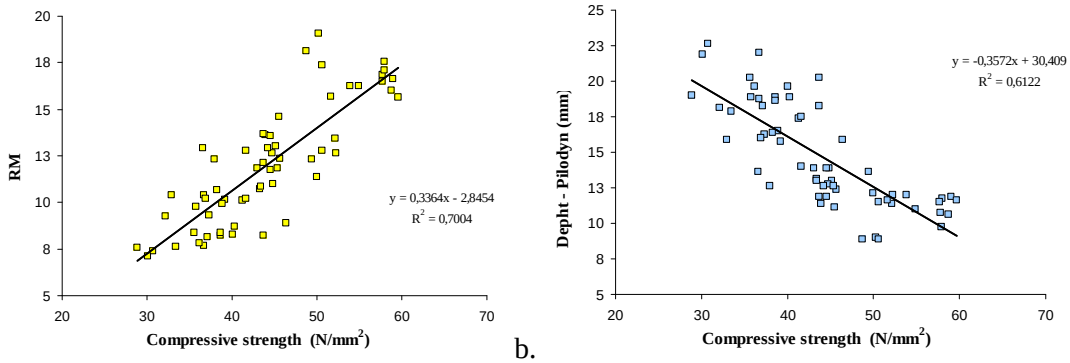

a. b.

Figure 5. Compressive strength *vsersus*: a. Resistographic measurement; b. Penetration depth using *Pilodyn*.

3.2 Decayed Timber Tests

3.2.1 Relationship between mass loss and compressive strength

A very common way of measuring the level of fungi decay undergone by timber is through its mass loss. Mass loss (percentage) was obtained using Equation (3), where *fdm* is the theoretical dry mass of the specimen at the end of the test and *idm* is the theoretical dry mass at the beginning of the test determined using the timber average initial moisture content.

$$massloss = \frac{idm - fdm}{idm} x100 \qquad (3)$$

Studies by Henriques *et al.* [2010] and Nunes *et al.* [2005] have determined the relationship between compressive strength and mass loss for *Pinus pinaster*. Figure 6 also contains the values obtained by Reinprecht [2010] in *Picea abies* specimens decayed by fungi. From these values it is concluded that there is a significant loss in the mechanical strength of timber even for small decay levels. With only 15% of mass loss the average value of compressive strength decreases around 50%.

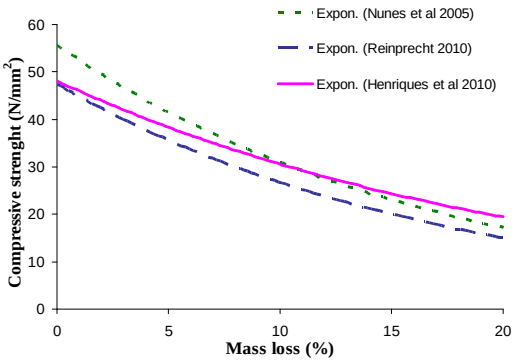

Figure 6. Mass loss *versus* compressive strength of decayed wood.

Nunes *et al.* [2005] in their experimental work also observed that even a small mass loss (e.g. 10%) can result in a severe reduction (of almost 50%) of compressive strength parallel to fibres. Curling *et al*. [2002] demonstrated that incipient decay of timber by brown-rot fungi causes measurable strength loss in a ratio of strength to weight loss of approximately 4:1.

3.2.2 Relationship between mass loss and Resistograph results

Resistograph results (RM) were obtained from decayed specimens after stabilization of the moisture content. In Figure 7 the comparison between the RM values and density is presented for sound and decayed specimens, with mass loss between 3% and 12%. These levels of mass loss led to decreases in mechanical strength between 20% and 45%. The linear regression line relating density of decayed timber with the corresponding RM value is below the one for sound timber. However since the mechanical strength fell by 20% to 45% lower RM values and greater dispersion of the results were expected.

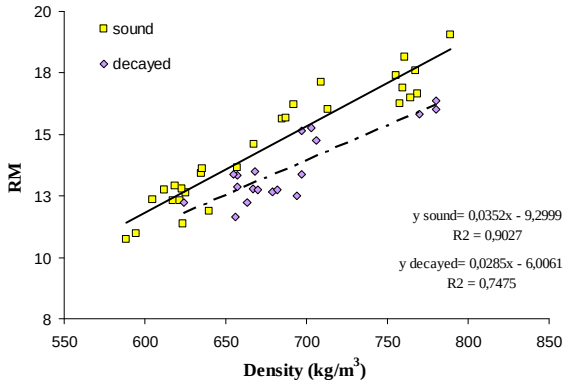

Figure 7. Density *versus* resistographic measurement for sound and decayed timber.

3 CONCLUSIONS

The *Resistograph* test method can be applied to estimate the average density of timber as long as its water content and the device's characteristics are known. The *Pilodyn* test method also provides good correlation with density.

The estimation of the mechanical strength, for defects-free timber, can be made with the *Resistograph* as a satisfactory correlation was found between the compressive strength of the set of specimens tested and the corresponding resistographic measurement. The correlation between the *Pilodyn* results and the mechanical strength was not so high but still significant.

Though the extrapolation of these correlations to structural elements must be done with care, the NDT approach, particularly using the *Resistograph* has proven to be extremely useful when used together with other inspection tools.

ACKNOWLEDGMENTS

The authors would like to thank Fundação para a Ciência e Tecnologia (FCT) for the PhD scholarship awarded to Dulce Henriques (ref. SFRH/BD/44216/2008) and the project "Safety evaluation of timber structures through non-destructive methods and stochastic analysis" under contract PTDC/ECM/66527 / 2006. The collaboration of the ICIST - IST research centre is also acknowledged.

REFERENCES

Bonamini, G., 1995 'Restoring timber structures – Inspection and evaluation' in *Timber Engineering STEP 2. Design – Details and structural systems,* Edit. Centrum Hout, pp. D3/1-D3/9

Branco, J.M., Piazza, M., Cruz, P.J.S. 2010, 'Structural analysis of two King-post timber trusses: Non-destructive evaluation and load-carrying tests', *Constr. Building Materials,* **24** (2010), pp. 371–383.

Breda, K., 2003 'Restoration of historical trusses' (in portuguese), in *3º ENCORE – Encontro sobre Conservação e Reabilitação de Edifícios*, LNEC: Lisbon, pp. 261-270.

Caselli, G. & Mannucci, M. 2005 'La copretura monumentale della gipsoteca dell´istituto d´arte do Firenze', in *Int. Conf. Conservation of Historic Wooden Structures*, Florence, vol II, pp. 242-254.

Ceraldi, C., Mormone, V., Ermolli, E.R.; 2001 'Resistographic inspection of ancient timber structures for the evaluation of mechanical characteristics' in *Materials and Structures*, vol. 34, nº 1, pp. 59-64.

Cruz, H., Machado, J.S., Nunes, L., 1999 'Inspecção e Avaliação de estruturas de Madeira', in *Estruturas de Madeira: Reabilitação e Inovação*, GECoRPA: Lisboa, pp 13-28.

Curling SF., Clausen CA., Winandy JE. 2002, 'Relationships between mechanical properties, weight loss and chem. comp. of wood during incipient brown-rot decay', in *F. Prod Journ.*, **52[7-8]**, pp. 34-39.

Feio, A.O. 2006, *Inspection and Diagnosis of Historical Timber Structures: NDT Correlations and Structural Bahavior*, PhD Thesis in Civil Engineering, presented to University of Minho, Portugal.

Feio, A., Lourenço, P., Machado, J. 2007, 'Non-destructive evaluation of the mechanical behaviour of chestnut wood in tension and compression parallel to grain', *Int. J. Arch. Heritage*, **1[3],** pp. 272–292.

Green D.W., Winandy J.E., Kretschmann D.E. 1999. 'Chapter 4 – Mechanical properties of wood' *Wood handbook—Wood as an engineering material.* Gen. Tech. Rep. FPL–GTR–113. Madison, WI: U.S. Department of Agriculture, Forest Service, Forest Products Laboratory. 45 p.

Henriques D.F., Nunes L., Brito J. de, 2010, "Performance of Paraloid B72® combined with the application of biocides on wood degraded by fungi", in *4th Int. Conf. on Wooden Cultural Heritage: Inter. Between Wood Sc. and Conserv. of C. H.*, COST Action IE0601: 20-22 October, Izmir, Turquey.

Lladró, R.C., Barra R.D., Botelho, J., Faria, J.A., 2006, 'Assessment of timber structures with in situ tests', (in portuguese), in PATORREB 2006, 20-21 March, Oporto, Portugal, pp. 139-148.

Lourenço, P.B., Feio, A.O., Machado, J.S. 2007, 'Chestnut wood in compression perpend. to the grain: Non-destr. correl. for test results in new and old wood', *Const. Build. Mater.* **21** (2007), pp. 1617–27.

Machado, J.S., 2000, *Avaliação da variação das propriedades mecânicas de pinho bravo (Pinus pinaster Ait.) por meio de ultra-sons*. PhD thesis presented to Technical University of Lisbon, 265 pp.

Machado, J.S. & Cruz H. 1997, 'Assessment of timber structures. Determination of density profile by non-destructive methods' (in portuguese), in *Revista Por. de Engenharia de Estruturas*, 42, pp. 15-18.

Machado, J.S. & Palma, P. 2010, 'Non-destructive evaluation of the bending behaviour of in-service pine timber structural elements. *Materials and Structures*. DOI 10.1617/s11527-010-9674-9.

Mateus, T.H.E. (1961): *Basis for the design of timber structures* (in portuguese). National Laboratory for Civil Engineering, Lisbon, Portugal. 306 pp.

Nunes, L., Cruz, H., Duarte, A.P., Bordado, J.C., Nero, J.M.G. 2005 'Wood consolidation by impregnation with reactive polymers' in *International Conference Conservation of Historic Wooden Structures*, Collegio degli Ingenieri della Toscana, Florence, vol II, pp. 323-327.

Palaia, L., Monfort, J., Sánchez, R., Gil, L., Álvarez, A., López, V., Tormo, S., Pérez, C., Navarro, P., 2008, 'Assessment of timber structures in service by using combined methods of non-destructive testing together with traditional ones', in *9th Inter. Conf. on NDT of art*, Jerusalem, Israel, May 2008.

Reinprecht, L. 2010, 'Effect of natural conservation substances on some moisture and mechanical properties of decayed spruce wood' in *4th Int. Conf. on Wooden Cultural Heritage: Interaction Between Wood Science and Conserv. of C. H.*, COST Action IE0601: 20-22 October, Izmir, Turquey

Rinn, F. 1994, 'One minute polé inspection with RESISTOGRAPH micro drillings', in Intern. Conf. on wood poles and piles, March 21-23, Fort Collins, Colorado, USA.

Ronca, P. & Gubana 1998, 'Mechanical characterisation of wooden structures by means of an in situ penetration test' *Construction and Building Materials*, **12** (1998), pp. 233–243.

Teles, C. & Valle, A., 2001, 'Wood structures: Acting before deterioration', in *3th International Seminar on Historical Constructions 2001*, Guimarães, Portugal, pp. 857-866

Uzielli, L. 1992, 'Evaluation of timber elements bearing capacity'. *L'Edilizia*. 12, pp. 753-762.

Zombori, B., 2001 'In situ Nondestrutive Testing of Built in Wooden Members', in *NDT.net*, **6[3]**.

XII DBMC
International Conference on Durability of Building Materials and Components
PORTO - PORTUGAL, April 12th-15th, 2011

Effect of the Inspection Conditions on the In-Situ Infrared Thermographic Examination of Facades with Adhered Ceramic Cladding

Ecem Edis [1]
Inês Flores-Colen [2]
Jorge de Brito [3]

ABSTRACT

Ceramic based facade materials are widely used in Portugal. Some of the durability problems of ceramic facades are joint failures, delamination and efflorescence, and one of the reasons of this kind of problems is water/moisture caused by condensation, rising damp or precipitation.

Infrared (IR) thermography is a well developed non-destructive examination technique in terms of detecting thermal and air infiltration problems, and the environmental inspection conditions are well studied. Inspection of moisture problems using IR thermography is a comparatively new field, and most of the studies either focus on applications on historical buildings or investigate the applicability on different materials in laboratory conditions. Environmental factors affecting in-situ thermographic inspection of moisture problems of different building technologies are not well studied yet. In-situ inspection of adhered ceramic facades to detect presence of moisture before the occurrence of any visible signs is a possible accomplishment of IR thermography.

In relation with these facts, suitable inspection conditions in terms of solar heat gain for in-situ examination of adhered ceramic facade claddings by IR thermography are discussed in the paper. Parameters like characteristics of ceramic tiles or inspection time and their effects on the inspection of moisture problems present in the facade system are studied theoretically, and case studies are presented as well.

KEYWORDS

Infrared thermography, adhered ceramic facade cladding, in-situ inspection, environmental inspection conditions, moisture.

[1] Istanbul Technical University, Faculty of Architecture, Istanbul, TURKEY, ecem@itu.edu.tr
[2] DECivil-IST, Technical University of Lisbon, Lisbon, PORTUGAL, ines@civil.ist.utl.pt
[3] DECivil-IST, Technical University of Lisbon, Lisbon, PORTUGAL, jb@civil.ist.utl.pt

1 INTRODUCTION

Ceramic based facade claddings are widely used in Portugal as one of the traditional materials. However durability problems such as cracking, efflorescence or detachment are also noted [LNEC, 2006; APICER, 2003]. Water/moisture caused by precipitation, condensation or rising damp is one of the reasons of this kind of durability problems.

In building/construction sector, infrared (IR) thermography is one of the non-destructive examination (NDE) techniques that is used to detect thermal irregularities and air infiltration problems of building envelope, moisture and delamination problems and defective areas of mechanical and electrical systems [Balaras & Argiriou, 2002]. In the application of IR thermography, providing certain (environmental) conditions depending on the type of problem is required and important to perform the inspection. In the detection of thermal irregularities and air infiltration problems, these conditions are defined in standards such as in ASTM C 1060-90 [2003] or ISO 6781 [1983]. However, this kind of standardized procedures and conditions does not exist for detection of moisture problems.

Either in adhered ceramic claddings or in other cladding technologies, detection of moisture within a system before the occurrence of visible signs such as efflorescence is important to take the necessary preventive measures. Due to its non-destructive nature, using IR thermography to detect the presence of excessive moisture can be beneficial. Considering this a research study based on in-situ inspections in Lisbon, Portugal, was conducted to adapt general IR thermographic procedures to its particular application in adhered ceramic claddings to detect moisture and also delamination problems [Edis et al., 2010]. As part of this research the effect of parameters such as ceramic type, amount of solar heat gain or inspection timing on in-situ IR thermographic inspection was studied and is presented here.

2 CERAMIC BASED FACADE MATERIALS

European standard EN 14411 [CEN, 2006] classifies ceramic tiles into three main groups according to their water absorption characteristics as: (i) group I - water absorption lower than or equal to 3%, (ii) group II - water absorption between 3% and 10%, and (iii) group III - water absorption higher than 10%. Tiles with a high rate of water absorption (i.e. within group III) can either be glazed to prevent water absorption from the surface like the traditional tiles of Portugal (i.e. azulejo) or left unglazed like some veneering bricks. Tiles with lower absorption rate can also be glazed or polished for decorative purposes. Glazing increases water vapour diffusion resistance, as well as improving the water absorption from the surface.

3 DETECTION OF MOISTURE BY IR THERMOGRAPHY

3.1 Driving Forces Helping to Detect Moisture Problems by IR Thermography

In IR thermography, objects whose temperature varies from the environmental temperature, in other words, objects which are not in thermal balance with the surroundings or readily absorbing moisture from the air, can be observed with an IR sensing system [Barreira & de Freitas, 2007]. The same applies to observing surface temperature variations of an object.

In the detection of moisture within a system, there are generally two different driving forces that create observable surface temperature differences, which are: (i) evaporative cooling, and (ii) higher thermal inertia of water *versus* building materials' thermal behaviour [Rosina & Ludwig, 1999], in other words increased heat capacity of moist material.

In evaporation, depending on the relative humidity and temperature of air near the object surface, water content and physical characteristics of the object, and soluble salt content, surface cooling occurs in moist areas due to endothermic nature of evaporation [Rosina & Ludwig, 1999; Barreira & de Freitas, 2007]. When soluble salts are present in the material, evaporation rate decreases and therefore the decrease in surface temperature and temperature difference between moist and dry zones becomes less significant [Matias et al., 2008; Rosina & Ludwig, 1999]. High relative humidity of air,

e.g. more than 80%, also prevents evaporation and temperature difference between moist and dry areas due to surface cooling becomes less significant [Rosina et al., 1998].

Specific heat capacity of water is higher than that of most construction materials [Rosina & Ludwig, 1999]. Therefore, the presence of moist increases the heat capacity of construction materials, which is the quantity of heat required to raise the temperature of a body of material by 1 ºK [Bolton, 2006]. In unsteady thermal conditions, different thermal capacities of the moist areas cause colder or warmer surface temperatures depending on being in the heating or cooling period, and these zones can be identified by thermography. The observation location in respect to the heating location affects the observed surface temperature distribution as well.

Apart from these two driving forces that generate observable surface temperature differences, another physical fact is the increased thermal conductivity of moist material generating surface temperature differences under steady heat flux. The presence of moist thermal insulation in the case of stud walls can be detected with this approach as mentioned in ASTM C 1060-90 [2003]. However, in order to generate observable temperature differences, the thickness of the damp area should be large. Therefore, it is less favorable in detection of moisture within components that have smaller thicknesses, such as plaster or ceramic claddings.

3.2 Detection of Moisture by IR Thermography In Facades with Adhered Ceramic Cladding

In facades with adhered ceramic cladding, the type of ceramic tile in terms of water absorption and surface treatment (i.e. glazed or unglazed) determines the driving force that can be used while detecting moisture problems by IR thermography. In most of the research studies on detection of moisture by IR thermography, porous materials such as render, aerated concrete or stone, which allow evaporation, were considered [Matias et al., 2008; Barreira & de Freitas, 2007; Rosina & Ludwig, 1999]. However, in adhered ceramic claddings, tiles that are unglazed and that have high water absorption rate (e.g. unglazed veneering bricks with high water absorption) can only be detected by using the evaporative cooling as the driving force. In the case of tiles that are glazed and/or that have low water absorption, the driving force that can generate observable surface temperature differences is the higher thermal inertia of moist material because of the high water vapour diffusion resistance and low water absorption of tiles, and it requires unsteady thermal conditions as mentioned in the previous section, either provided by an active or a passive approach.

In the passive approach, the heat flux is generated by natural boundary conditions [Grinzato et al., 2002]. In the active approach, artificial heating is used and thermograms are taken during or after heating [Rosina & Robison, 2002]. The use of solar radiation, which is sometimes considered in the passive approach and sometimes in the active approach, is one of the feasible heating methods in the case of in-situ inspection of facades, especially of middle or high-rise buildings. However, apart from the other limitations related to inspected building such as uneven solar heat gain due to projections, one of the major drawbacks of using solar radiation is that the intensity of solar radiation is orientation dependant, influencing the amount of solar heat gain and inspection timing.

4 CASE STUDIES TO DETECT MOISTURE IN ADHERED CERAMIC CLADDINGS

In the in-situ inspection of the case buildings presented here, a FLIR ThermaCAM B2 type IR camera with a spectral range of 7.5 to 13 μm, thermal sensitivity of 0.1 ^{o}C and field of view of 33.8^{o} was used. Air temperature and relative humidity was measured with Rotronic HydroLog-D and HydroClip SC05. Moisture content measurements were also made with Tramex's Survey Encounter, which is a surface moisture meter using electrical impedance to determine relative moisture content.

While evaluating the condition of the facade and surface temperature variations during both in-situ IR thermographic inspection and assessment of thermograms, the 'reference' method was used. In the reference method, surface temperature distribution at a particular location can be evaluated considering the general temperature distribution at that building. In addition, reference thermograms

that were taken from other buildings with similar characteristics during inspections with similar environmental conditions can be used [ISO, 1983; Rosina & Ludwig, 1999].

4.1 Moisture Detection in Facades with Unglazed Adhered Ceramics (Veneering Brick Application)

The east facing facade of a building clad with veneering bricks and with reinforced concrete frame structure with brick/block infill walls was inspected during the rainy season, in April 2010. The 1st inspection was performed in the morning hours of a cloudy day, before any solar heat gain. The 2nd inspection was performed on the same day close to the sunset hours without direct sunlight on the facade. The exterior air temperature (°C) and relative humidity (%) measured during the inspections and the weather forecast of the Meteorology Institute of Portugal (IM-IP) are given in Table 1.

Table 1. In-situ inspection of veneering brick application - measured environmental conditions and weather forecast of IM-IP.

	Exterior air temperature - °C	*Exterior relative humidity - %*	*Sky*
Inspection 1- *morning*	22.8	57.4	Cloudy
Inspection 2 - *evening*	21.6	51.7	Light clouds
Weather forecast of IM-IP	Minimum: 14 Maximum: 20	-	a.m.: periods with heavy clouds p.m.: sky with light clouds

In the first inspection, surface temperature variations indicating a possible problem was observed as shown in Fig. 1-(a) and a surface moisture meter measurement was made at the location marked as Ar1 in the same figure. A general analysis of the temperature profiles[4] (Li1, Li2 and Li3 in Fig. 1-(b)) and surface moisture meter readings (Fig.2-(a)) revealed that there were moisture content changes at that location and lower moisture content generally showed up in the thermogram as areas with colder surface temperature due to evaporative cooling. However, an exact correlation between temperature profiles and moisture meter readings cannot be found with a high probability due to efflorescence, i.e. white stains observed on the surface. The reliability of both methods decreases in the presence of efflorescence, since soluble salts decrease the amount of evaporation as aforementioned, and increase the measured moisture content in moisture meters using electrical impedance [Burkinshaw, 2002].

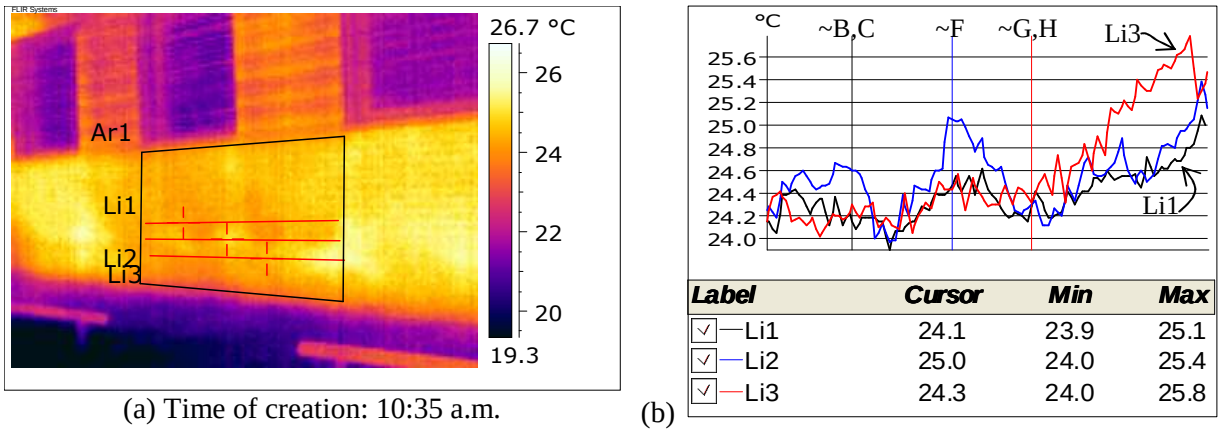

Figure 1. In-situ IR thermographic inspection of a veneering brick application: (a) thermogram of the facade taken during morning hours; (b) temperature profile of the thermogram in (a).

In the second inspection performed after heat gain through solar radiation and exterior air temperature, surface temperature variations observed in the first inspection cannot be seen, rather the material difference at the substrate, i.e. the location of reinforced concrete structural members and

[4] In the thermograms the name label marks the beginning of the temperature profile line and its direction in the temperature profile graph is from left to right. The cursor to mark a specific location on a line is presented with a '+' sign, and the place of the cursor is presented with a vertical line on temperature profile graph.

infill walls, can be identified as given in Fig. 3-(a). Only at the location marked with the cursor on the temperature profile line Li2, a similar surface temperature drop of about 0.2-0.4 °C was observed. In the thermogram taken before heat gain, the temperature drop at this location was about 0.8 °C. This probably indicates that heat loss after solar heat gain masks the effect of evaporative cooling.

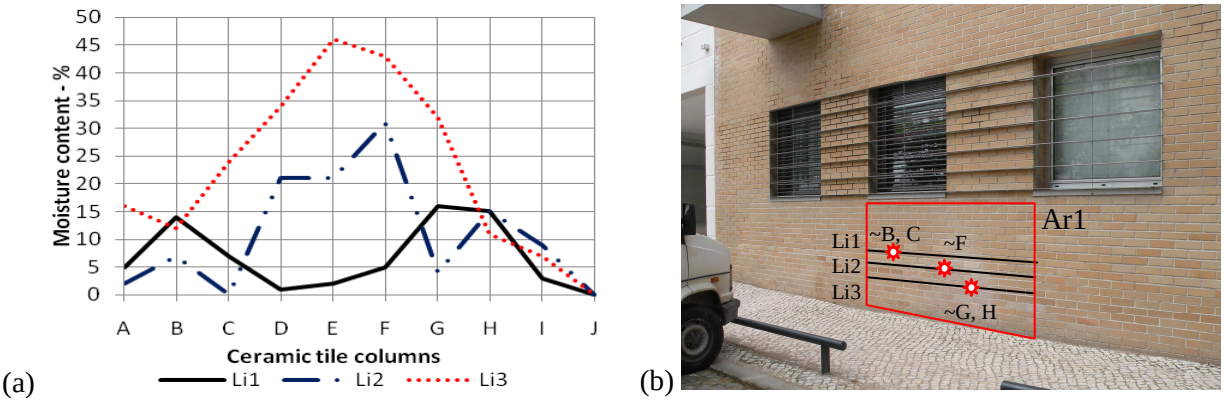

Figure 2. In-situ IR thermographic inspection of a veneering brick application: (a) surface moisture meter readings with 'brick' option; (b) photograph of the facade, location of analysis lines and approximate locations of cursors in relation with ceramic tile columns.

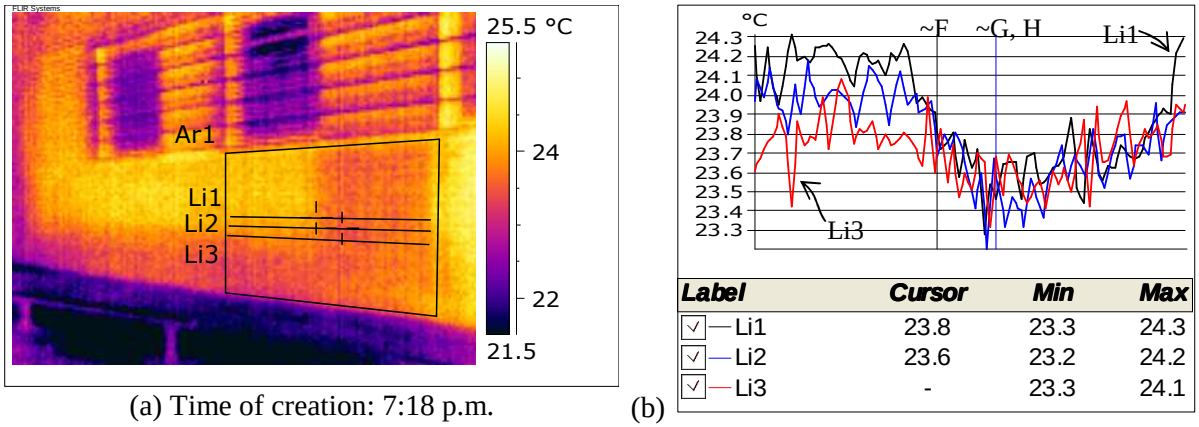

Figure 3. In-situ IR thermographic inspection of a veneering brick application: (a) thermogram of the facade taken during the late afternoon hours; (b) temperature profile of the thermogram in (a).

Rosina & Ludwig [1999] reported that, while monitoring the walls of Santa Maria delle Grazie at Milano during the interior space heating period, the surface temperature difference between dry and damp zones increased as the interior air temperature increased. Rosina et al. [1998] also suggested that active direct heating of the wall either with radiation or convection should be avoided for a proper inspection. Considering this information and in-situ inspection data it can be said that, in the case of unglazed adhered ceramics, it is possible to distinguish damp and dry zones during the beginning of the heating period, before the heat gain of the substrate. However, after heat gain of the substrate, it is hard to observe and distinguish damp and dry zones of ceramic cladding with IR thermography.

4.2 Moisture Detection in Facades with Glazed Adhered Ceramics

West facing facade of a building clad with glazed ceramic tiles and with infill walls within reinforced concrete structural frame, was detected in the rainy season, in May 2010. The first inspection was performed in the evening hours. The second inspection was performed in the morning of the following day before solar heat gain, when the sky was cloudy. The exterior air temperature (°C) and relative humidity (%) measured during inspections and the weather forecast of IM-IP are given in Table 2.

In the first inspection performed after heat gain, surface temperature increases were observed in zones close to the ground level. As seen in the thermogram and its temperature profile in Fig. 4-(a) and (b)

respectively, the surface temperature difference ranged between 2.3 and 3.2 °C. A general moisture content control made with 'brick' option of the surface moisture meter at each row showed that the moisture content increased when it got closer to the ground level as seen in Fig. 4-(c). Areas with higher moisture content showed up in the thermogram as areas with higher surface temperature since glazing prevented evaporation and increased thermal capacity caused by increased moisture content was the driving force generating observable surface temperature difference.

Table 2. In-situ inspection of glazed ceramic application - measured environmental conditions and weather forecast of IM-IP.

	Exterior air temperature - °C	*Exterior relative humidity - %*	*Sky*
Inspection 1- *day 1, evening*	21.4	55.0	-
Inspection 2 - *day 2, morning*	19.4	66.5	Cloudy
Weather forecast of IM-IP	Day 1 - Min.: 14, Max.: 22 Day 2 - Min.: 15, Max.: 22	-	Day 1 - a.m. & p.m.: periods with heavy clouds Day 2 - a.m.: periods with heavy clouds

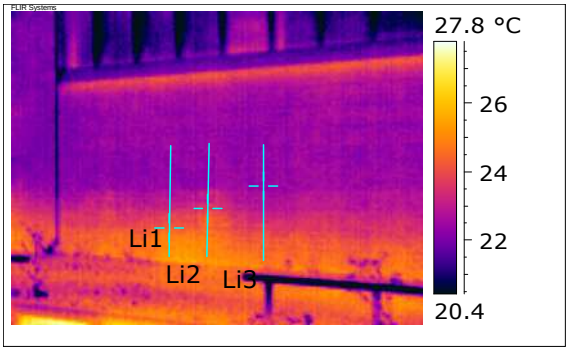

(a) Time of creation: 8:30 p.m.

(b)

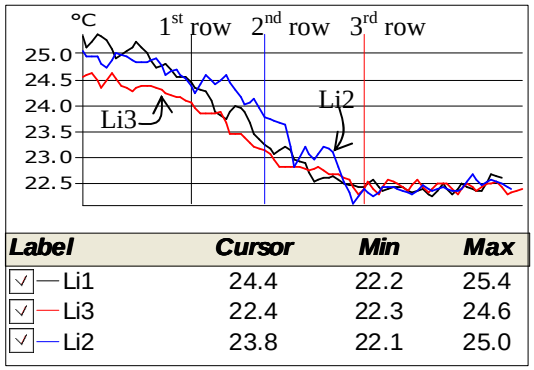

(c)

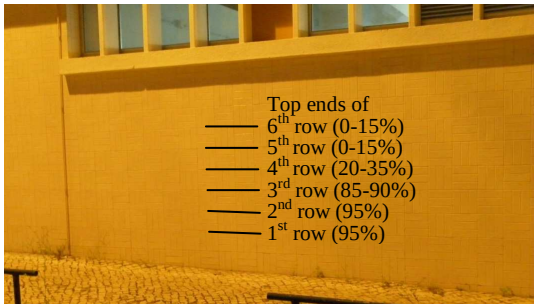

Figure 4. In-situ IR thermographic inspection of a glazed ceramic application: (a) thermogram of the facade taken in the evening after heat gain; (b) temperature profile of the thermogram in (a); (c) photograph of the facade, location of the tile rows and approximate moisture contents.

In the second inspection performed before solar heat gain, a similar surface temperature increase was observed at the same location but with a smaller temperature difference which ranged between 1.2 and 1.4 °C as seen in Fig.5. When assessed together with the thermogram taken in the evening after heat gain, it can be said that solar heat gain increases the observed surface temperature differences when there is a moisture content change, and thus identification of damp zones becomes easier.

5 DISCUSSION AND CONCLUSION

In-situ IR thermographic inspection of different ceramic types at different hours of the day to detect moisture problems confirmed the theoretical discussion made in section 3.2. that, in the case of reinforced concrete structural frame with brick/block infill walls clad with adhered ceramic tiles and when solar radiation is used for providing unsteady thermal conditions:

- Driving forces that generate observable surface temperature differences during IR thermographic inspection change according to the surface treatment and water absorption characteristics of the ceramic tiles;
- The effect of solar heat gain changes according to the characteristics of ceramic tiles and the driving force to generate temperature differences.

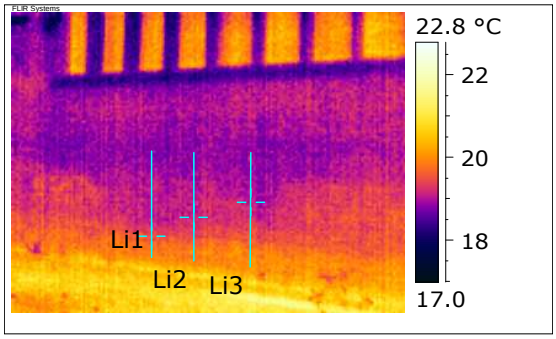

(a) Time of creation: 9:00 a.m.

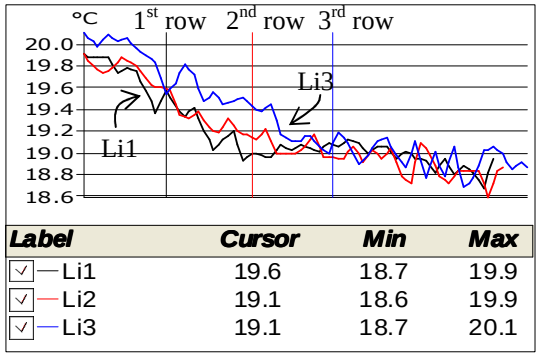

(b)

Figure 5. In-situ IR thermographic inspection of a glazed ceramic application: (a) thermogram of the facade taken in the morning before solar heat gain; (b) temperature profile of the thermogram in (a).

In unglazed ceramics with high water absorption rate like veneering bricks:

- The driving force that generates surface temperature differences is evaporative cooling in damp zones and damp areas are observed as colder areas in the thermograms;
- Heat gain either by solar radiation or convection initially increases the observability of damp zones. However heat gain of the substrate masks the effect of evaporative cooling especially when different materials, e.g. reinforced concrete and brick, are used as the substrate, and thus prevents performing an appropriate IR thermographic survey.

Considering this, it can be said that in the case of unglazed ceramics it is better to perform an IR thermographic inspection in the morning hours, at the initial periods of heat gain. Depending on the orientation of the facade, cloudy sky conditions may be required to prevent direct sunlight on the surface which may cause false indications when using thermography. In addition, it should be kept in mind that the presence of efflorescence decreases the rate of evaporation and thus the observed surface temperature differences by IR thermography, and on the contrary it increases moisture content readings made with impedence type surface moisture meters.

In glazed ceramics and in ceramics with low water absorption:

- The driving force that generate surface temperature differences is the increased thermal inertia, in other words increased heat capacity of moist material and damp areas are observed as warmer areas in the IR thermographic inspection since evaporation is not possible;
- Heat gain either by solar radiation or convection increases the observed temperature difference between moist and drier areas. Therefore performing an in-situ inspection becomes easier, although heat gain of the substrate has the same effect like in the veneering brick application as observed in in-situ inspection of other buildings which are not mentioned here.

Considering this, it can be said that in the case of glazed ceramics and ceramics with low water absorption, it is better to perform the IR thermographic survey after solar heat gain. However it should be considered that the amount of solar heat gain is orientation dependant and feasible inspections may not be performed for every orientation.

In conclusion it can be said that IR thermography is a possible NDE technique that can be used in the detection of moisture problems of adhered ceramic claddings, although reliability of this technique is affected by many different factors such as those mentioned here (efflorescence or orientation of facade), or by factors such as reflection or surface stains which are not mentioned here. In order to increase the reliability of this NDE technique, further field and laboratory research studies, which also cover destructive examinations, are required.

ACKNOWLEDGMENTS

The first author of this paper was financially supported by the Scientific and Technological Research Council of Turkey (TÜBİTAK) during this research. The authors thank Building Physics group and Maria da Glória Gomes from IST, DE-Civil for the technical support and use of IR equipment.

REFERENCES

APICER, 2003, *Manual of application of ceramic claddings* (In Portuguese), Ed.s: Sousa, A. V., de Freitas, V. P., & da Silva, J. R., Associação Portuguesa da Indústria de Cerâmica, Coimbra, Portugal.

ASTM, 2003, *Standard practice for thermographic inspection of insulation installations in envelope cavities of frame buildings, ASTM - C 1060-90,* American Society for Testing and Materials (ASTM) International, USA.

Balaras, C. A., & Argiriou, A. A, 2002, Infrared thermography for building diagnostics, *Energy and Buildings,* 34[2] 171-183.

Barreira, E., & de Freitas, V., 2007, Evaluation of building materials using infrared thermography, *Construction and Building Materials*, 21[1] 218-224.

Bolton, W., 2006, *Engineering science* (Fifth edition), Elsevier Newnes, Oxford, UK.

Burkinshaw, R., 2002, What is the moisture meter trying to tell us, *Structural Survey,* 20[5] 162-172.

CEN, 2006, *Ceramic tiles - Definitions, classification, characteristics and marking*, *EN 14411,* European Committee for Standardization, Brussels, Belgium.

Edis, E., de Brito, J., Flores-Colen, I., 2010, *Diagnosis of exterior wall failures by in-situ inspection techniques - Inspection of facades with adhered ceramic cladding (Preliminary report),* Universidade Tecnica de Lisboa - Instituto de Engenharia de Estruturas, Território e Construção (UTL - ICIST) DTC No. 06/2010, July.

Grinzato, E., Bison, P. G., & Marinetti, S., 2002, Monitoring of ancient buildings by the thermal method, *Journal of Cultural Heritage*, 3(1) 21-29.

ISO, 1983, *Thermal Insulation - Qualitative detection of thermal irregularities in building envelopes - Infrared Method, ISO 6781,* International Organization for Standardization, Switzerland.

LNEC, 2006, *Technical guide of rehabilitation of housing (Vol. 2)* (in Portuguese), Instituto Nacional de Habitação - Laboratório Nacional de Engenharia Civil, Lisbon, Portugal.

Matias, L., Vilhena, A., Magalhães, A., Santos, C. P., & Veiga, R., 2008, Performance of masonry specimens in contact with salt water - Absorption by capillary rise and evaportaion phenomena, *Proceedings of 1st International Conference on Construction Heritage in Coastal and Marine Environments,* Laboratório Nacional de Engenharia Civil (LNEC), Lisbon, Portugal.

Rosina, E., Ludwig, N., & Rosi, L., 1998, Optimal Environmental Conditions to Detect Moisture In Ancient Buildings: Case Studies in Northern Italy, *Proceedings of Thermosense XX*, pp.188-199, SPIE, Orlando,USA.

Rosina, E. & Ludwig, N., 1999, Optimal thermographic procedures for moisture analysis in building materials, *Diagnostic Imaging Technologies and Industrial Applications,* SPIE, Vol. 3827, Germany.

Rosina, E. & Robison, E. D., 2002, Applying infrared thermography to historic wood-framed buildings in North America, *APT Bulletin*, 33[4] 37-44.

XII DBMC
International Conference on Durability of Building Materials and Components
PORTO - PORTUGAL, April 12th-15th, 2011

Statistical Study of Pathologies in Post-Delivery of Real Estate Ventures

Eduardo Linhares Qualharini [1]
Elaine Garrido Vazquez [2]
Lais Amaral Alves [3]
Victor A. Libonati dos Santos [4]

ABSTRACT

This paper intends to present legal, regulatory and legislative aspects to attest the efficiency and product quality in the construction industry. It describes the methodology to approach pathological problems that present outward characteristic manifestation, from the definition of the nature, origin and mechanisms of the phenomena involved. From the database of the pathological manifestation, the paper develops a statistical analysis aiming to point a qualitative of the pathologies encountered in caring for post-occupation. The period of collection of information is from January 2005 to May 2008, in the city of Rio de Janeiro. The article is structured in four parts: description and justification of the issue in question; basic concepts of pathology and its methodology for diagnosis and intervention; approach to the organizing the sector of technical assistance, with its dynamic service, processing of requests and approval of data to create a database and closing remarks. It is hoped from this work, to show cause, origin and frequency of requests. It serves as feedback data to the company sectors, such as acquisition, design and construction, enabling preventive action of relapse in new projects or constructions in progress. Besides emphasizing the importance of databases, which generate the necessary tools for the process of continuous improvement of the quality management system.

KEYWORDS

Pathology, Technical Assistance, Post-delivery

[1] Universidade Federal do Rio de Janeiro (UFRJ), Rio de Janeiro, BRASIL, qualharini@poli.ufrj.br
[2] Universidade Federal do Rio de Janeiro (UFRJ), Rio de Janeiro, BRASIL, elaine@poli.ufrj.br
[3] Universidade Federal do Rio de Janeiro (UFRJ), Rio de Janeiro, BRASIL, laisamaral@poli.ufrj.br
[4] Universidade Federal do Rio de Janeiro (UFRJ), Rio de Janeiro, BRASIL, v.libonati@ig.com.br

1 INTRODUCTION

To adapt to changes in Brazilian legislation (Code of Consumer Protection (*CDC – Código de Defesa do Consumidor*) through the Law nº 8078 of 1990, the new Civil Code in force since January 2008) and the new consumer facing this scenario more informative, the construction sector had to readjust processes. To minimize the additional costs in the stage of post-occupation, the companies began to write owner's manuals and invest in quality programs and staff training. According to Picchi (1993), the focus of the quality management of building construction sub-sector has evolved from a correction view, based on inspection, aproaching even the most modern views, based on preventive measures and systemic approach.

The implementation of quality systems, high competition in the housing market and increasing consumer demand made companies constantly seek to develop policies focused on product quality, differentiated customer service, satisfaction not only at the time of sale, enterprise development geared to the needs and expectations of customers, always seeking differentiation to conquer them.
So in the construction industry, among the main services added to products, technical assistance is of great importance. It's main functions are attending to customer complaints, feedback from the system to produce buildings and ownership costs of pathological problems (Resende, Melhado and Medreiros, 2002).

2 OBJECTIVE

This paper aims to present legal, regulatory and normative aspects to attest to the efficiency and product quality in the construction industry. It describes the methodology to deal with pathological problems that present outward manifestation characteristic, from the definition of the nature, origin and mechanisms of the phenomena involved. From the database of the pathological manifestation, the paper develops a statistical analysis aiming to point in a qualitative way the pathologies encountered in caring for post-occupation, pointing out its causes. Thus it serves as feedback data to the company's sectors, such as acquisition, design and works, enabling a preventive action of relapse in new projects or works in progress. Besides emphasizing the importance of databases, which generate the necessary tools for the process of continuous improvement of the quality management system. The results of this study will assist in the verification of building systems that are experiencing higher costs for treating their constructive addictions in the analysis of the requests providing an assessment of the quality of designs, of the performance of constructive systems used in buildings delivered.

3 METHODOLOGY

Initially, a literature research was accomplished from already published material, consisting of standards, technical articles, reports, books and material available on the internet, having as the primary source of information studies about pathologies.

Gil (2002) mentions that "literature research is developed based on existing material that consists primarily of books and scientific papers." Thus, the theoretical foundation aims to build a substruction that subsidizes the proposition of guidelines for the work.

Besides the bibliographic research, the work was leaned on a case study, based on a data bank that stores pathological problems by their type, frequency and costs incurred, consisting of information on attending of requests for technical assistance of a company, in the years 2005, 2006, 2007 and 2008. To preserve the identity, the company will be named as builder A.

4 LEGAL AND REGULATORY ASPECTS

Users are increasingly demanding, and supported by laws that assume the role of regulatory efficiency and quality of products purchased by them. As regulatory laws, can be refered the new Civil Code, with the following items listed on Table 1.

Table 1. Adapted from Articles 618, 445 e 937 – Civil Code.

Transcript of Articles 618, 445 e 937 – Civil Code
Art. 618 : The contractor is responsible for safety and soundness of the construction for five years.
Art. 445, parágrafo 10: The deadline for claiming latent defects are one year from the delivery.
Art. 937: The owner of the building or construction is liable for damages resulting from its ruins, if it comes from lack of repairs that expressed necessity.

In addition, some other factors encouraged the motivation for the evolution of the sector, such as: the development of the consumers code (*CDC - Código de Defesa do Consumidor*), in effect since March 1991, which brought the legal support and agility to the processes of reporting flaws or defects in construction of buildings, reduction of State investment, hinder the survival of businesses in the market and leading to a restructuring of these, in search of greater competitiveness, and the creation of the Brazilian Program of Quality and Productivity (*Programa Brasileiro de Qualidade e Produtividade - PBQP)* and its deployment in ways of a sub-program sector to build buildings (MELHADO, 1994).

To prevent these legal implications, the builders have been trying to shield, taking some care since the estimates of clauses in contracts of sale, manual guarantees, until the term of inspection and collection of keys, which should specify very well what and how the property is being delivered, all with very transparent and monitored by the consumer. Delivery of the owner's manual, with specifications regarding the required maintenance is also very important. Therefore, the more detailed these procedures and the creation of legal artifices on the guarantee validation of some security services, the better to prevent problems with the law.

5 NORMATIVE ASPECTS

When the enterprise that results in a building implies a relation of consumption, it is governed by the *CDC*, whose Article No. 39 (Section IV: "*Das Práticas Abusivas*" - Of Abusive Practices) recognizes the *CONMETRO* as an entity with legal authority to prepare and issue technical regulations (*Regulamentos Técnicos - RT's*) in the absence of regulations issued by the official competent body (these ones effectively with the force of law, such as those issued by government regulatory agencies). Thus, in its absence, apply the standards approved and registered by *CONMETRO*, whose Resolution No. 6 / 92 recognizes and legitimizes as Brazilian rules those approved by the National Forum for Standardization, which, when registered in, are given the designation "*NBR"* (*Norma Brasileira Registrada*- Brazilian Standard Registered in the *CONMETRO*).

Resolution No. 7 / 92 from *CONMETRO* appointed the Brazilian Technical Standards Association (*ABNT – Associação Brasileira de Normas Técnicas* - a private non-profit organization recognized as Public Utility) the Forum of the National Standardization System, with attribution, on its behalf, to develop technical standards.

So, by delegation of authority, compliance with *ABNT* standards on engineering projects whose product results in the consumption process, until then optional, representing only a technical reference, at least since 1992 became compulsory, supported by Article No. 39 of the *CDC*.
Since then, any nonconformities regulations found in buildings, on technical standards related to *ABNT*, either on their projects, or as it is actually installed, are pathologies, manifested or potential.

The issue of delivery of buildings are addressed in the rules of *ABNT*, butwithout any discrimination of technical methodology. These standards indicate, about the subject, only as described in Table 2 below:

Table 2. Delivery of buildings – as *NBR5675/80* and *NBR5671/90*

Delivery of buildings – as *NBR5675/80* and *NBR5671/90*
NBR 5675/80 (Standard for Receving Services and Engenniring and Architecture works) Commission of receiving services and / or work of engineering and architecture is the group of experts designated by the owner or administration in order to proceed to formal receipt, (partial or final services and works).
NBR 5671/90 (Stakeholder participation in services and engineering and architecture) It is responsibility of the owner to inspect the venture with technical inspection assistance, if it is convenient, pointing out formally, in writing, any irregularities; receive the enterprise, with technical inspection assistance, if it is convenient, confirmed the absence of visible defects, before taking possession, providing the respective term of receipt.

However, note that these recommendations do not address technical and legal aspects. Moreover, taking into account, according to Souza and Ripper (1988) quoted in Thomas (1989), that the pathology in construction can be understood as the end of the satisfactory performance of buildings and their components, with regard to stability, aesthetics, serviceability, and especially its durability relating to the conditions that are submitted.

The lack of benchmarks to determine the performance of a structure, was solved largely by the new Performance Standard. The Technical Standard for Performance of Buildings Housing up to Five Floors (*Norma Técnica de Desempenho de Edifícios - NBR15575-1 to NBR15575-6*) published on 05/12/2008 establishes requirements and criteria for measuring the performance of building systems.

Among the main innovations is the clear definition of parameters to evaluate the performance of systems: structures, floors, walls and sealing, roofing and hydrosanitary. From these indexes, it will be possible to determine parameters to evaluate the performance of building systems for each building, which will be required to meet minimum criteria, or differentiate, with ratings of intermediate and upper levels.

Another important clarification for the sector is the difference between the warranty period and the concept of life cycle, the latter understood as the estimated period of time during which the system can be used under satisfactory conditions of safety, health and hygiene, and in accordance with the expected performance. According to the standard, the life cycle tries to express, in an objective way, the time predicted for the systems covered by the draft standard. This means that if consumers meet the planned maintenance program in the operating manual, use and maintenance delivered by the builder, his property should last according to the period expressed in the contract.

In addition to meeting the care to use, the confirmation of life cycle, which must be defined at the stage of incorporation, also depends on good execution, the use of elements and components without a manufacturing defect by the builder and the use of building as provided in the project. According to the text of the standard, the concept has the purpose of demarcating the designers in the specification of systems, elements and components that are have durability compatible with the life cycle established for each of them.

According to standard, the period for guarantee should start as soon as the certificate of occupancy (CO) is obtained, including: foundations, the main structure, peripheral structures, retaining walls have, in the Standard, a warranty period of five years; electrical facilities, three years, but are not included equipments which include sockets, switches, circuit breakers, wires, cables, conduits, boxes and frames. Table 3 follows with all the parts that make up this standard.

Table 3. Building Delivery – according to *NBR5675/80* and *NBR5671/90.*

Performance standards – *NBR15575 – Edifícios habitacionais de até cinco pavimentos/Desempenho* (Residencial Buildings up to five floors/Performance)
i) ABNT NBR15575-1 - Parte 1: Requisitos gerais (General Requirements)
ii) ABNT NBR15575-2 - Parte 2: Requisitos para os sistemas estruturais (Requirements for structural systems)
iii) ABNT NBR15575-3 - Parte 3: Requisitos para os sistemas de pisos internos (Requirements for the internal floors systems)
iv) ABNT NBR15575-4 - Parte 4: Sistemas de vedações verticais externas e internas (Systems of external and internal partition walls)
v) ABNT NBR15575-5 - Parte 5: Requisitos para sistemas de coberturas (Requirements for roofing systems)
vi) ABNT NBR15575- - Parte 6: Sistemas hidrossanitários (Hydrosanitary systems)

6 PATHOLOGIES IN BUILDINGS

According to Souza and Ripper (1998) The pathology of the structures involve a new field of Constructions Engineering that deals with the study of the origins, forms of manifestation, consequences and mechanisms of occurrence of failures and degradation systems of the structures.
Except for the cases corresponding to the occurrence of natural disasters, in which the violence of requests, coupled with the remarkably unpredictable nature of these, is the predominant factor, the pathological problems have their origins motivated by failures that occur during the execution of one or more activities inherent to the generic process which is called civil construction, a process that can be divided into three basic steps: conceiving (planning / design / materials), implementation and use.

6.1 Methodology for Addressing the Pahological Problem

The problem generally is identified based on their action or pathological symptoms which are reflected by functional or structural changes in the building or affected party, representing the warning signs of a defect. The demonstrations, once known and correctly interpreted, can lead to understanding of the problem, allowing its resolution from an intervention whose level is linked mainly to the relationship between performance established for the product and performance verified.
In this context, note that the structure of the generic method consists basically of three parts: i) gathering of subsidies (obtaining the necessary information so that we can understand the problem occurred. Information can be obtained from four basic sources: site inspection, historical survey of the problem and the building (case history), exams and research (literature, technological, scientific and normative)), ii) diagnosis of the situation (definition of the pathological problem associated with a particular cause to create hypoteses for evaluation), iii) procedure definition (preparation step of alternative interventions and among the possible actions choose the one that is best suited to reduce or eliminate the perceived deviation).

7 PRESENTATION AND ANALYSIS OF RESULTS

7.1 Introduction

It is intended, in this case study, to point out the procedures in the technical assistance sector relating to requests and bad statistical analysis of pathologies and defects of construction work, causing the increase of the costs post-delivery. Was analyzed a large national company, active in construction market. Whose respective database used is comprehended between the period of January 2005 through May 2008. This database refers to residential and commercial medium and high standard, located in *Barra da Tijuca* and the South Zone of Rio de Janeiro, with diverse ages, 0-5 years from the inhabitant.

Using the software (PeopleSoft) a database was built from the year 2004, when it began operation in Company A. This database belongs to this area of technical assistance from the contractor, responsible for customer service in the post-delivery of enterprises, until the final term of the warranty, 5 years. Information obtained in the company's database received treatment according to how they were collected, ie, the data area of technical assistance were analyzed quantitatively.

7.2 Technical Assistance Sector

After the CO, the work remains for three months in a delivery period of autonomous units and common areas in the venture. In the same period a team has already began to meet the owners who have received their property. This is when the database of this new venture is born, being fed by new demands and possible flaws in construction that are identified. After two months of the assembly or one month before delivery to the Area of Technical Assistance, the engineer responsible for the work should start on the process of moving their work to the Area of Technical Assistance, which will cater to owners within the assurances given in the owner's manual and / or assignee's manual.
Both provided counseling to clients immediately upon receipt of the unit and already with the technical assistance area, are included in the company's operating system as a flowchart as showed in figure 1 below.

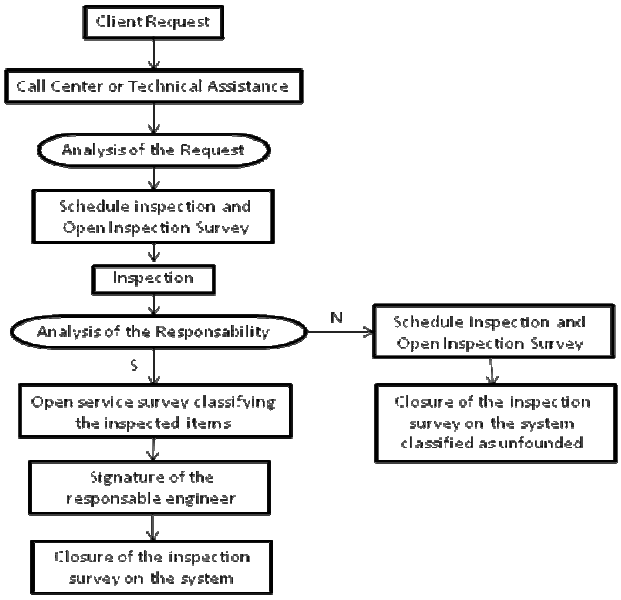

Figure 1. Flowchart of attendance in the Area of Technical Assistance

Customers come in contact with the Service Center, stating their request and registering the contact in an occurrence in the operating system. At this moment, is scheduled a visit to inspect the unit in accordance with the days and times provided by the buildings technic or intern engineering responsible for the undertaking in question, generating a *FV* (*ficha de vistoria* - survey form) and recording the number of the case.

The event generated by the Call Center is referred to the analyst of the Technical Assistance who visualizes it by the worklist in the operating system. Once generated the *FV*, the one responsible for the inspection should check the file system and the Area of Technical documentation for the venture / unit under review.

Based on reference documents, the technicians perform the inspection of the requesting enterprise or unit registering the relevant items with a digital camera, verifing if the attendance of the request is or not the responsibility of the builder (founded or not), analyzing the terms and conditions of the guarantees established in owner's and the assignee's manuals.

After the inspection, the technician complements the data sheet with the conditions and verifications of the technical diagnosis verified as the items inspected.On the founded cases, the construction problems inspected will be classified according to cause and sub-cause as existing classifications within the operating system. After grading and filling of the FV on the system, the service is performed by guarantee of the contractor that performed it initially or by a new contractor.Recalling that all the costs generated by the solution of the pathology, are computed to their respective request.

7.3 Static Analysis

Hereafter are described and analyzed the data in the form of tables and charts of 53 real estate. The data obtained are compiled by the request type of the pathology, ie, counting and grouped one by one according to their cause. Then the statistics generated from the data used are presented, followed by considerations, comments and results.

7.3.1 Solicitation x Cause

The statistic to be displayed is characterized by the relationship between pathologies occurred in these enterprises and their respective cause. The studies are grouped in time scale and not by ventures.
Figure 2 consists in a graph that was constructed compiling data on the number of founded requests, during the period of January 2005 to May 2008, showing what are the causes of the most recurring pathologies. It presents the general scenario of the founded requests that occurred during the 40 months and the amount of requests grouped by pathological manifestation, in order to provide a less specific order of magnitude.
Analyzing the graph below, the hydralic sub-system is configured as the most significant of all causes of pathologiess, reaching the total of 25.79% of all claims in these three years. Followed by water tightness and painting with 15.95% and 7.88% respectively.

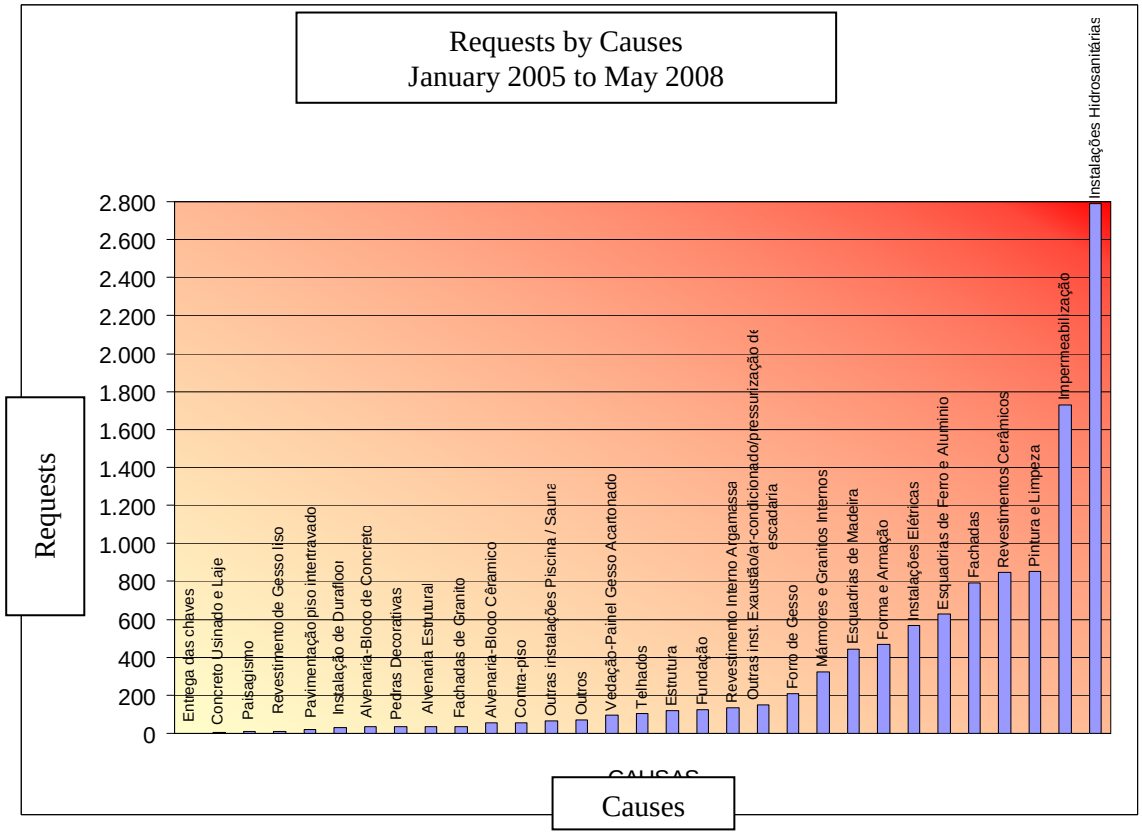

Figure 2. Requests by cause – jan 2005 / mai 2008

8 FINAL CONSIDERATIONS

The lack of disclosure and notes about pathological problems in buildings hinders the development of techniques for designing and building, a fact which limits training of new professionals, once they are not given information on how to avoid mistakes that have been committed in the past. This reality is found in the concern of the companies in hiding the pathologies from users and competitors, because reporting is admiting flaws in the production process.

Therefore, the choice of theme was determined by the availability of access to a database of the technical assistance area, allowing to expose valuable information that can provide continuous improvement in final product quality and the much desired reduction in maintenance costs for a company.

In this context, companies should, in addition to pursuing higher-quality products, also adopt mechanisms that describe these products while regulating their relations with users and identifying the responsibilities of both parties. These actions will serve to enable them to keep a competitive market, always exceeding the expectations of their users, and not limited solely to satisfying them.

REFERENCES

Conselho Regional de Engenharia, Arquitetura e Agronomia do Estado de São Paulo (CREA/SP). Código de Defesa do Consumidor. São Paulo. 80p.

Brasil. *Novo Código civil, de 10 de janeiro de 2002*. Available in: http://wwwt.senado.gov.br. Acess in August 15, 2008.

Melhado, S.B. *Qualidade do projeto na construção de edifícios: aplicação ao caso das empresas de incorporação e construção. São Paulo*, 1994. 294 p. Thesis (Doutors Degree) – *Escola Politécnica, Universidade de São Paulo*.

Picchi, F.A. *Sistemas de qualidade: uso em empresas de construção de edifícios*. 1993. 462p. Thesis (doutor degree) – *Escola Politécnica, Universidade de São Paulo. São Paulo.*

Associação Brasileira de Normas Técnicas (ABNT). NBR-5674: Manutenção de edificações – Procedimento. Rio de Janeiro, 1999.

Associação Brasileira de Normas Técnicas (ABNT). NBR-14037: Manual de operação, uso e manutenção das edificações. Rio de Janeiro, 1998.

Desempenho de edifícios habitacionais de até 5 pavimentos. Parte 1: Requisitos gerais. Procedimento - CE 02.136.01. Rio de Janeiro, 2006.

Meier, R.L. & Shen, Q. 1987, Efficient, Ecologically Balanced Settlement on Estuaries, Centre for Environmental Design, Research Working Paper No. 2, Uni. of California, Berkely, February.

Construção de Edifícios. M.M. Resende; S.B. Melhado; J.S. Medeiros. In: *Congresso de Engenharia Civil*, 5, 2002, *Juiz de Fora (MG*).

Gil, Antonio Carlos. *Como elaborar projetos de pesquisa*. 4. ed. *São Paulo*: Atlas, 2002.

De Souza, Vicente Custódio Moreira e RIPPER, Thomaz, *Patologia, Recuperação e Reforço de Estruturas de Concreto, Editora Pini*, ed #1, *São Paulo*, 1998

XII DBMC
International Conference on Durability of Building Materials and Components
PORTO - PORTUGAL, April 12th-15th, 2011

Technical Condition of Prefabricated Concrete Large Panel Apartment Buildings in Estonia

Targo Kalamees [1]
Karl Õiger [2], Teet-Andrus Kõiv [3], Roode Liias [4]
Urve Kallavus [5], Lauri Mikli [6], Andres Lehtla [7], Georg Kodi [8], Endrik Arumägi [9]

ABSTRACT

The majority of apartment buildings built with prefabricated concrete elements (PCLPAB) were constructed primarily between 1961-1990. Today the first dwellings from this "constructional wave" are approaching the end of the service life intended by the designer. Commonly, the mechanical resistance and stability is fulfilled in most cases and the main problems relate to building physics, indoor climate, and energy efficiency. Despite the overall acceptable condition of external surface of external walls, serious problems with joints between panels (lack of wind- and water-tightness) exist. Status with the frost resistance of the concrete of the facade and balcony elements is of high concern. Facades need to be repaired, reinforced and/or protected. Serious thermal bridges are a major problem in old PCLPAB, resulting in mould growth, surface condensation, soiling of surfaces, larger energy loss etc. Mould growth and surface condensation on the internal surfaces of thermal bridges are unavoidable without additional external insulation and/or lowering internal humidity loads. The performance of ventilation in the studied apartments was very low and concentration of CO_2 was high. The buildings under study need extensive renovation. As large investments are needed to improve and maintain the quality of dwellings, renovations should be conducted in a cost-effective way. The largest saving here is to make the investment once and in a correct way.

KEYWORDS

Technical condition of dwellings, service life, energy efficiency, prefabricated concrete large panel.

[1] Chair of Building Physics and Architecture of Tallinn University of Technology, ESTONIA, targo.kalamees@ttu.ee
[2] Chair of Building Physics and Architecture of Tallinn University of Technology, ESTONIA, karl.oiger@ttu.ee
[3] Chair of Heating and Ventilation of Tallinn University of Technology, ESTONIA, teet.koiv@ttu.ee
[4] Chair of Construction Economics and Management of Tallinn University of Technology, ESTONIA, roode@staff.ttu.ee
[5] Centre for Materials Research of Tallinn University of Technology, ESTONIA, urka@staff.ttu.ee
[6] Chair of Building Physics and Architecture of Tallinn University of Technology, ESTONIA, lauri.mikli@mail.ee
[7] Chair of Structural Engineering of Tallinn University of Technology, ESTONIA, andres.lehtla@ttu.ee
[8] Chair of Structural Engineering of Tallinn University of Technology, ESTONIA, georg.kodi@ttu.ee
[9] Chair of Building Physics and Architecture of Tallinn University of Technology, ESTONIA, endrik.arumagi@ttu.ee

1 INTRODUCTION

In Estonia multi-storey apartnment buildings constitute about 60% of the whole dwelling stock. The majority (75%) of apartment buildings were built primarily between 1961-1990. Today the first buildings of that "construction wave" are approaching the end of their design life (service life intended by the designer - 50 years).

Service life is the period of time after installation during which a building or its parts meet or exceed the performance requirements. In most cases we may use six essential requirements set in the Construction Products Directive [CPD 1988] for the performance requirements: mechanical resistance and stability; safety in case of fire; hygiene, health and the environment; safety in use; protection against noise; energy economy; and heat retention. The service life of a building and its components is a function of: the quality of the component, design level, work execution level, indoor environment, outdoor environment, in-use conditions, and maintenance level [ISO 15686-2].

The overall living standards in the older part of the housing stock need to be improved to meet today's requirements in the functional, urban design, architecture and constructional-technical terms. The extent and selection of renovation works depend strongly on the technical condition of buildings and on the renovation works done. As thoroughgoing investigations and surveys are a good basis for the renovation design, different investigations should be done. During the 1990s many investigations [EKK 1994, EstKonsult 1996, Õiger et. al. 2000, Õiger 2006] were conducted in Estonia to find out primary renovation needs. Today, after 15 years, the possible decay has progressed, energy prices have increased, understanding about the quality of indoor climate and living condituons has changed. Therefore technical investications should be revised and up-to-date renovation solutions should be worked out. This paper presents the current technical condition of prefabricated concrete large panel apartment buildings in Estonia, but the overall results of the study about Estonian old multi-storey apartment buildings composed of prefabricated concrete elements are reported in [Kalamees et al. 2009].

2 METHODS

2.1 Types of Buildings Studied

Field investigations and measurements were conducted in prefabricated concrete panel apartment buildings (PCLPAB). Load bearing structures under study were: alongside and transverse, internal and external concrete walls and reinforced concrete ceiling (floor) panels. The external walls were insulated (by ~10 cm of fibrolite, mineral wool, phenoplast or expanded polystyrene) sandwich panels (U≈0.8…1.2 W/(m^2·K)) or 300…350 mm thick single-layer expanded-clay lightweight concrete walls (U≈1.2…1.5 W/(m^2·K)). PCLPAB represent one of the most common construction types for apartment buildings in the former Soviet Union. The main type-series of PCLPAB were: 1-464, 121, 111-133, 111-66, and 84. These types of PCLPAB were constructed in Estonia from the 1960s up to 1990. Today's Estonian housing stock is constituted of 96 % of privately owned and 4% of social (municipal) housing. As most of the buildings are privately owned (each apartment has an independent owner), it would be controversial and complicated to demolish these buildings.

Databases of the Union of Co-operative Housing Associations and local administration were used to select the buildings. Detailed research and long-term measurements were conducted in 20 buildings. In addition, visual investigation and expertise was done in a number of buildings. Building types, ages (min. 19, average 32, max. 48 years) and heights (5-9 storeys) all differed. The typical ventilation system was passive stack ventilation with window airing (referred to as natural ventilation in this study) and a one-pipe (less pipe material) system (typically without room thermostats on radiators) was the typical heat distribution system.

2.2 Research Methods

This research is composed of the following studies and measurements:

- preliminary work: collection of initial information about the drawings of the building, information about main damages, results of previous research and investigations in similar buildings, risk assessment, analysis of research alternatives, and drafting of the research plan;
- survey of conditions of facades (frost resistance (EVS 814), compressive strength (EN 12390, EN 12504), carbonization of concrete, quality of finishing joints between the panels, corrosion of reinforcement, salt depositions etc.);
- investigation of technical systems (heating, ventilation, water, sewerage, electricity, and gas);
- thermography investigation (EN 13187) and numerical simulation (EN ISO 10211) of thermal bridges;
- measurement of air tightness of building envelope (EN 13829);
- long-term (1 year at 1-hour interval) measurement of indoor climate (temperature, relative humidity, CO_2, performance of ventilation and heating) and internal humidity loads (moisture excess and moisture production);
- measurements (EN ISO 140) and calculations (EN 12354) of sound insulation;
- to analyze active mould content in air, the air sampler RCS was used; to determine inhabiting fungi on the surface of structural elements and the interior, the tape lift sampling was used;
- analysis of hygrothermal performance of external walls (EN ISO 13788);
- calculations of load bearing structures for possible extensions;
- financial viability of renovation and energy-saving concepts;
- questionnaire for the survey of occupant habits, typical complaints, and symptoms related to indoor air quality, etc.

3 RESULTS

Commonly, the first essential requirement of mechanical resistance and stability is fulfilled in most cases and the main problems relate to building physics, indoor climate, and energy efficiency. Mechanical resistance and stability may emerge as topical when the fulfilment of other requirements shows improvement. In the following some main technical problems of PCLPAB are described.

Despite the overall acceptable condition of external surface of external walls, serious problems with joints between panels (lack of wind- and water-tightness) exist. This was somewhat surprising because earlier studies have already highlighted this problem and proposed solutions for renovations. Unmade renovations indicate passivity of occupants to deal with renovation works that will directly repair dangerous defects or that are not directly cost-effective (some energy saving renovation works). Carbonization depth was 2…3 cm from the external surface (Figure 1, left). The small corrosion depth could be the reason because of corrosion of the reinforcement existing only when the reinforcement was very close (<1 cm) to the surface of the panel (Figure 1, right). As carbonization depth depends strongly on the age of the building, it is a question of time when the neutralization of the concrete takes place and the alkaline protection for the reinforcement finishes. Therefore, facades need to be protected.

The frost resistance of facade concrete was studied based on the loss of mass after 56 cycles of freezing and thawing. For the facade (frost resistance class KK1), the loss of mass should be ≤ 0.5 kg/m^2. Both the laboratory tests (Figure 2, left) and visual inspection of buildings (Figure 2, right) indicated to a small remainder frost resistance of the facade concrete and balcony elements (Figure 3). Only half of the specimens fulfilled the criteria for the frost resistance: loss of mass ≤ 0.5 kg/m^2. None of the buildings fulfilled the criterion for the frost resistance. Status with the frost resistance of the concrete of the facade and balcony elements is of high concern. Facades need to be repaired, reinforced and/or protected.

In all the specimens, compressive strength was over the value, $f_{c,cube}$>15 N/mm^2 that characterizes the compressive strength of the concrete mark 150.

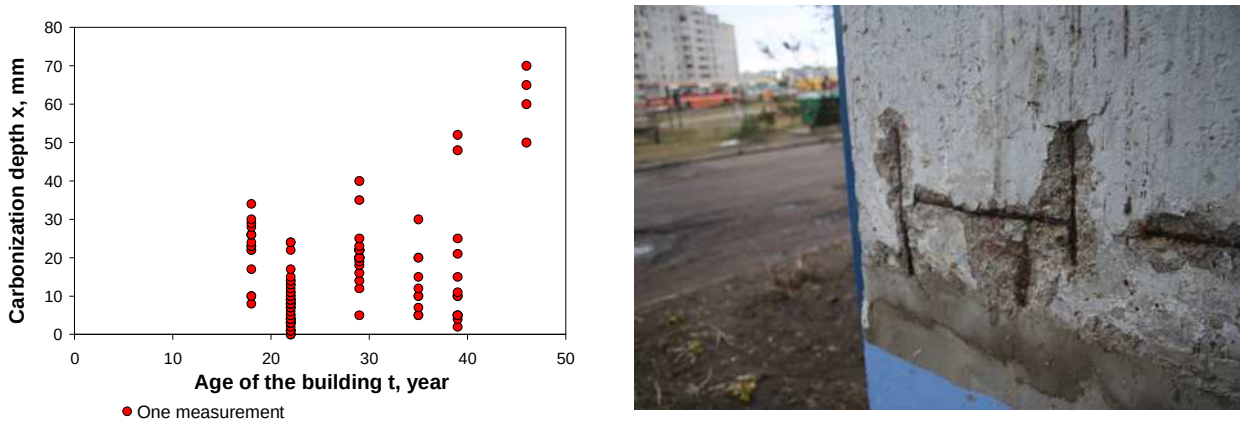

Figure 1. Carbonization (left) and corrosion of the reinforcement of the concrete facade (right).

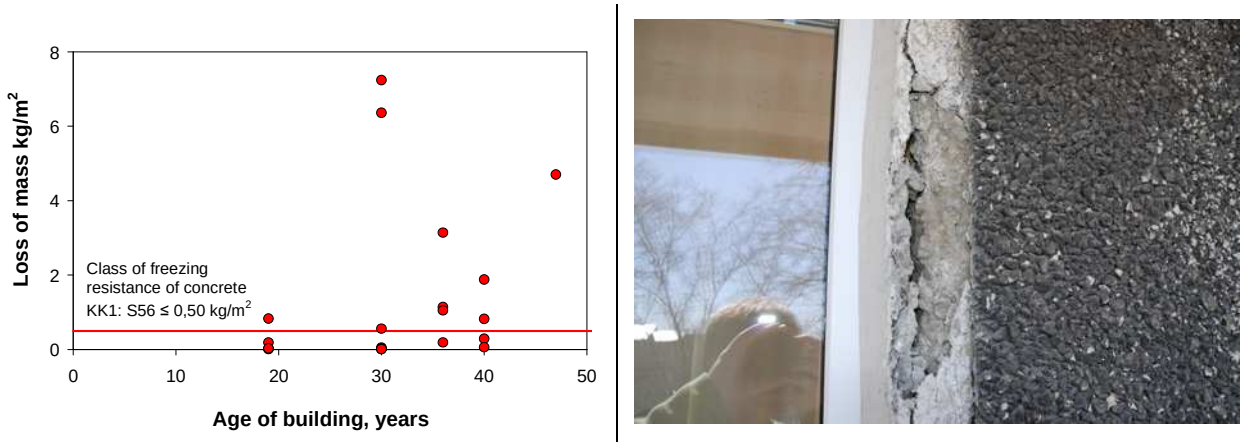

Figure 2. Loss of concrete mass of the facade panel during frost resistance tests (left) and decay of the facade due to low frost resistance (right).



Figure 3. Damages of balcony elements.

Serious thermal bridges are a major problem in old PCLPAB, resulting in mould growth, surface condensation, soiling of surfaces, larger energy loss etc. Field measurement showed that the main locations of thermal bridges in PCLPAB are: horizontal and vertical joints between external wall panels, junction of the external wall and the balcony slab, junctions of the external wall (especially end sides) and the roof, bonds between panels' inner and outer layers of the external walls, socket panels. The problem of thermal bridges is emphasized due to high indoor humidity loads (low

ventilation rate and high moisture production) that are typical of PCLPAB. An average temperature factor $f_{Rsi} = \frac{R_T - R_{si}}{R_T} = \frac{t_{si} - t_e}{t_i - t_e}$ was between 0.56 and 0.73. The limit value of the temperature factor is between 0.65 and 0.8 depending on indoor humidity loads [Kalamees 2006]. Mould growth and surface condensation on the internal surfaces of thermal bridges are unavoidable without additional external insulation and/or lowering internal humidity loads.

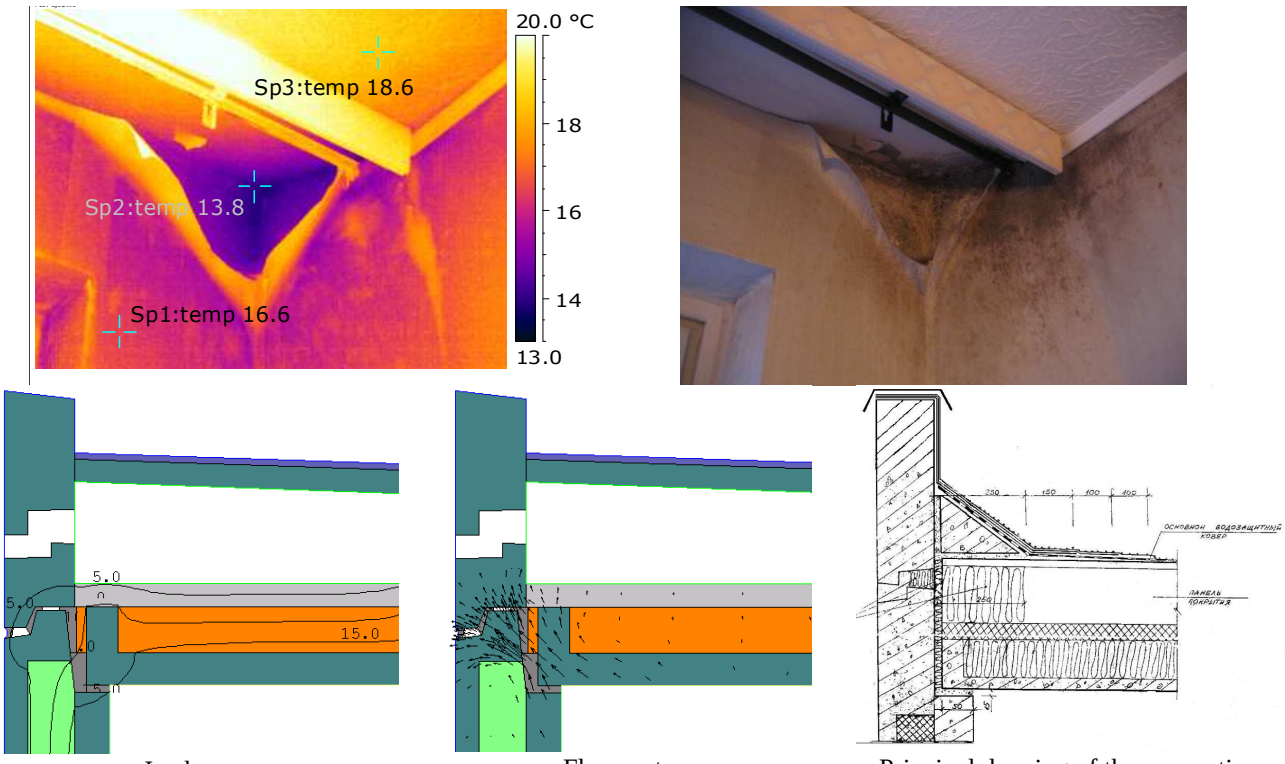

Isotherms | Flux vectors | Principal drawing of the connection

Figure 4. An example of the thermal bridge in the external wall and roof connection: thermographic investigation (above, t_i=3°C, t_e=19°C), numerical simulation (below).

The average value of the air leakage rate at the pressure difference of 50 Pa in the entire database was q_{50}=4.3 m^3/(h·m^2) (min. 1.1 m^3/(h·m^2) and max. 15.1 m^3/(h·m^2)). The average value of the air change rate at the pressure difference of 50 Pa from the entire database was n_{50}=4.9 h^{-1}. Newer buildings proved more airtight than older ones. The declared value to be used for energy calculations (50 % fractile with a confidence level of 95 %) of air tightness of old (built 1) was $q_{50,decl}$= 4.7 m^3/(h·m^2) and $n_{50,decl}$ = 6.8 h^{-1}.

According to the current standard (EVS 842), the sound insulation requirements in buildings are R'w ≥ 55 dB for air noise and for impact noise L'n,w ≤ 53 dB. Measurements and calculations showed deviations from the target values. Sound insulation of separating walls was between R'w 47…53dB and that of floors was between R'w 48…53dB. The sound insulation index of the impact sound was between L'n,w 54…67 dB.

Indoor temperature and RH were continuously measured in 39 apartments in 20 buildings at 1-h intervals over a 1-year period. Figure 5 shows the overall view of the indoor temperature (left) and relative humidity (right) dependence on the outdoor temperature. The one-pipe (less pipe material) heat distribution system is typical of old apartment buildings. Typically there are no room thermostats on radiators and the system is typically fitted from standpipe valves. Room temperature was regulated in the boiler room based on the outdoor temperature. This results in large variations of indoor temperature and low correspondence of the indoor thermal conditions to the target values of the indoor climate standard. In 41% of the apartments the room temperature did not correspond to the

lowest indoor climate category. Other problems concerning the heating system are: incorrect water flow rate of the heating system or risers, lack of direct room temperature control, difficulties to balance the one-pipe heat distribution system, lack of maintenance and improper modifications.

The performance of ventilation in the studied apartments was very low: average air change rate in bedrooms was 0.13 h^{-1} (cased on tracer gas (CO_2) measurement with closed windows). The performance of ventilation has worsened dramatically after the replacement of old windows. The replacement of windows without the renovation of ventilation results in lower air leakage and ventilation airflows. The concentration of CO_2 in bedrooms stayed between 370 and 3900 ppm. CO_2 concentration was below 1500 ppm only in three apartments. CO_2 concentration was above 1500 ppm during 26% of the measured time length (included also periods when the apartment was not used). It is practically impossible to increase airflows, if necessary, in apartments with natural ventilation. A possibility is to use window airing, but this may worsen the thermal comfort during winter. Because of worsened thermal comfort due to outdoor air inflow from stack (caused by wind), the occupants have sealed the stack and ventilation outlets.

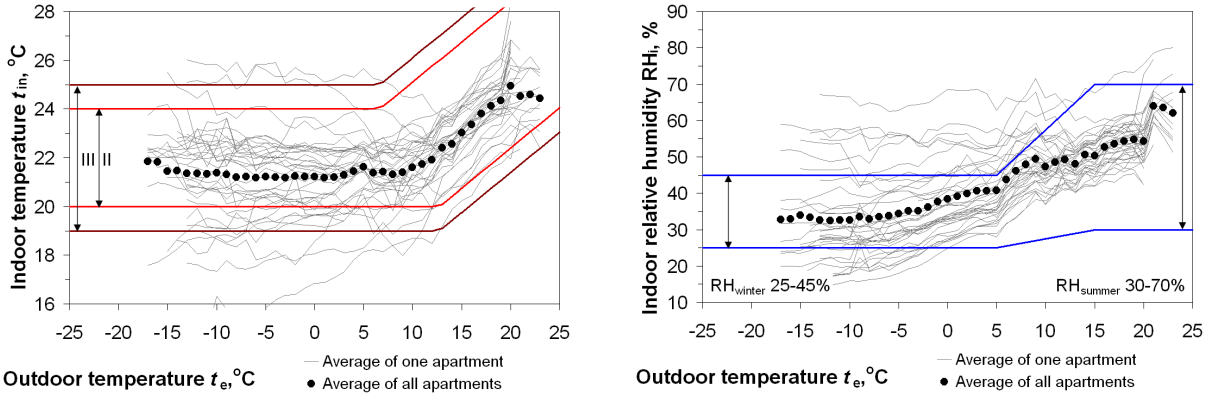

Figure 5. Dependence of the indoor temperature (left) and relative humidity (right) on the outdoor temperature in all rooms.

Indoor humidity load in the studied apartments was high: the moisture excess (the difference between indoor and outdoor air humidity by volume) at the 10% critical level was close to +7 g/m^3 during the cold period. This causes potentially serious moisture problems for the building envelope and health problems due to mould growth on the surfaces of the building envelope. The high indoor humidity loads were caused mainly due to the lack of ventilation and high occupancy.

The average annual specific heat energy consumption of old-type apartment buildings is 200…230 kWh/(m^2·a) (for space heating 170…220 kWh/(m^2·a) + for domestic hot water heating 15…50 kWh/(m^2·a).

Based on the questionnaire survey, the majority of occupants' complaints pointed out stuffy air (97% from answers), bad sound insulation (90%), condensation on windows (67%), mould growth (43%), high temperatures during summer (43%), and low temperatures during winter (27%).

4 NEEDS FOR RENOVATION

The condition of buildings is inadequate due to low requirements for energy performance in old building standards, historical lack of attention to the quality of construction materials and practices, poor record of operation, maintenance, and regular renovation.

The needs for renovation can be viewed from the following aspects:

- urgent repairs to guarantee safety of buildings (mechanical resistance and stability, safety in use, safety in case of fire);

- improvement of indoor climate (hygiene and health aspects, fulfilment of requirements to ventilation air rates and room temperatures);
- improvement of energy performance of buildings and HVAC systems;
- improvement of architectural planning, visual quality, overall living quality, and additional comfort.

The condition of main load bearing structures was found to be sufficient, allowing planning of renovation works instead of demolition. Similar results have also been obtained by other researchers [Roitman 1985, Ignatavičius 2000&2007]. The main renovation areas to guarantee mechanical resistance and stability include balconies, canopies, and facades. Balconies as the most badly damaged structures may need also rebuilding solutions. Because of low frost resistance and carbonization of facades, it is necessary to protect them. Improving thermal insulation of the building envelope (roof and walls), additional thermal insulation is unavoidable to remove serious thermal bridges. Therefore, additional thermal insulation is needed first of all to protect facades and to liquidate thermal bridges. As additional thermal insulation improves also the energy efficiency, the renovation work is double advantageous.

In the process of renovation the indoor climate and energy performance of buildings in cold climate the following three components must be keep:

- performance of ventilation;
- hygrothermal performance of building envelope;
- performance of heating systems.

To improve the air change in old apartment buildings, it is necessary to use either central or more flexible individual mechanical ventilation. Typically mechanical exhaust ventilation is the easiest solution to implement. Challenges here are how to guarantee the thermal comfort during winter (one possibility is to combine fresh air inlets with radiators). Energy performance can be improved by help of the heat recovery system with heat pumps (heat from exhaust air to heat up the domestic hot water of the heating system). The mechanical exhaust ventilation solution is not suitable for all types of buildings (especially for buildings with combined stack). Balanced ventilation with room units is another possible solution to renovation of the ventilation in old apartment buildings. During the design process the following questions have to be solved: where to place room units (a little space); how to solve problems with sound pressure levels; where to place air channels (rooms height 2.5m); how to solve air flow in the apartment through existing doors.

To allow for the temperature regulation in the room level, radiators should be equipped with thermostats. Other aspects that should be kept in mind in the renovation of heating systems are: correct control curve of the temperature of the supply water of the heating system, correct water flow rate of the heating system or risers, balanced heat distribution system, and correct maintenance and proper modifications of the HVAC systems.

In addition to technical problems, also social/human questions need to be solved: possibilities and motivation of occupants to cover the cost of renovation vary.

The buildings under study need extensive renovation. As large investments are needed to improve and maintain the quality of dwellings, renovations should be conducted in a cost-effective way. Current economical calculations show that depending on the extent of required indoor climate- and energy-renovation works, the price of the renovation is between 100…300€/m^2 (plus renovations to guarantee structural safety of buildings). Under a standard condition, a bank can give a loan of up to 160€/m^2. Although complex renovation may be needed, but all renovations do not decrease energy consumption (structural renovation, improvement on ventilation air rates). Therefore, without external support and improved living quality and longer service life of building taken into account, renovations may not be rational in terms of cost-efficiency. During the design process it is possible to

compare and analyze different renovation alternatives. This allows for dwelling renovation works to be realized in a cost-effective way. The largest saving here is to make the investment once and in a correct way.

ACKNOWLEDGMENTS

Data used were derived from the national research project "Technical condition and service life of Estonian apartment buildings composed of prefabricated concrete elements" conducted at Tallinn University of Technology. The financial support of the Credit and Export Guarantee Fund KredEx and Tallinn University of Technology is gratefully acknowledged.

REFERENCES

CPD 1988. Council Directive 89/106/CE on the Construction Products.

EKK. 1994. 'Survey and renovation proposals of prefabricated concrete large panel apartment buildings in Mustamäe', (in Estonain).
EN 12354 'Building acoustics – Estimation of acoustic performance of buildings from the performance of elements', The European Committee for Standardization.

EN 13187 'Thermal performance of buildings - Qualitative detection of thermal irregularities in building envelopes - Infrared method', The European Committee for Standardization.

EN 13829 'Thermal performance of buildings - Determination of air permeability of buildings - Fan pressurization method', The European Committee for Standardization.

EN ISO 13788 'Hygrothermal performance of building components and building elements -- Internal surface temperature to avoid critical surface humidity and interstitial condensation -- Calculation methods', The European Committee for Standardization.

EstKONSULT. 1996. 'Renovation of dwellings in Mustamäe district in Talllinn', (in Estonain).
EVS 814 'Frost resistance of normal-weight concrete. Definitions, specifications and test method', Estonian Centre for Standardisation.

EVS 842 'Sound insulation requirements in buildings Protection against noise', Estonian Centre for Standardisation.

Ignatavičius Č. 2000. 'Aspects of rehabilitation and modernization of dwelling buildings in Lithuania', Bautenschutz Bausanierung, 23 [1], 16-18 p. (in German).

Ignatavičius, Č., Zavadskas, E. K., Ustinovičius, L. 2007. 'Modernization of large-panel houses in Vilnius', Proc. The 9th international conference "Modern building materials, structures and techniques, Vilnius, Lithuania, 16-18 May 2007, vol. 1. p. 258-264.

ISO 10211-1. 'Thermal bridges in building construction -- Heat flows and surface temperatures -- Part 1: General calculation methods', International Standardization Organization.

ISO 140 'Acoustics -- Measurement of sound insulation in buildings and of building elements', International Standardization Organization.

ISO 15686-2 'Buildings and constructed assets - Service life planning - Part 2: Service life prediction procedures', International Standardization Organization.

Kalamees T; Õiger K; Kõiv T-A, et al. 2009. 'Technical condition and service life of Estonian apartment buildings, built with prefabricated concrete elements'. Tallinn University of Technology (in Estonian).

Kalamees, T. 2006. 'Critical values for the temperature factor to assess thermal bridges'. Proceedings of the Estonian Academy of Sciences. Engineering, 12(3-1), 218 – 229.

Õiger, K. 2006. 'Examenation of Service Life and Serviceability of Concrete Element Houses'. Proc. European Symposium on Service Life and Serviceability of Concrete Structures ESCS-2006, Espoo, Finland, 12-14 June 2006, pp. 57 - 61.

Õiger, K., Hääl, K., Sasi, L. 2000. 'Renovation and energy saving in multi-storey apartment buildings in Estonia', Proc. Baltic Symposium on Indoor Air Quality and Building Physics: a satellite conference of Healthy Buildings 2000, Tallinn University of Technology, Estonia, 11-12 August, 2000, p. 36-49.

Roitman A. G. 1985. 'Reliability of building structures in service'. Moscow: Stroyizdat., 176 p. (in Russian).

XII DBMC
International Conference on Durability of Building Materials and Components
PORTO - PORTUGAL, April 12th-15th, 2011

Toward a Protocol for Active IR Thermography to Assess the Durability of Building Components

Claudia Amatulli [1]
Mariella De Fino [2]
Giambattista De Tommasi [3]
Fabio Fatiguso [4]
Pietro Stefanizzi [5]

ABSTRACT

Active IR thermography is an effective investigation technique for construction components under stimulated emission. It allows at detecting characteristics of materials and structures, surface decay and detachments, cracking and dampness patterns, heat dispersion and energy performances. It is speedy, simple and low intrusive, so that it can easily address the periodical durability assessment of building components throughout their service life. The paper is going to propose some recommendations for an operation protocol, on the basis of simulation models and laboratory measurements, in order to set up the optimal parameters for active IR thermography. Specifically, the protocol will focus on the characteristics of the surfaces (geometry, stratigraphy, thermal properties); environmental conditions (air temperature); and technical features of the equipment (power and relative position to the surface). Since standards and regulations (e.g. UNI EN 13187, ASTM Standard D4788-88, ISO 18434-1) are numerous, but more industry oriented, the protocol can be an useful tool, in terms of technical optimization of procedures, time and costs as well as methodological guide for analysis and interpretation of results in the building sector.

KEYWORDS

Active IR Thermography, Building Components, Investigation Protocol, Durability Assessment

[1] Faculty of Engineering of the Technical University of Bari (PoliBa), Bari, ITALY, claudia_amatulli@libero.it
[2] Faculty of Engineering of the Technical University of Bari (PoliBa), Bari, ITALY, m.defino@poliba.it
[3] Faculty of Engineering of the Technical University of Bari (PoliBa), Bari, ITALY, g.detommasi@poliba.it
[4] Faculty of Engineering of the Technical University of Bari (PoliBa), Bari, ITALY, f.fatiguso@poliba.it
[5] Faculty of Engineering of the Technical University of Bari (PoliBa), Bari, ITALY, p.stefanizzi@poliba.it

1 INTRODUCTION

IR thermography is a non destructive investigation technique to detect the temperature distribution on a surface based on the emitted infrared radiation, according to the well known equation:

$$q = \sigma \varepsilon T^4 \quad (1)$$

where q is the hemispherical total emissive power (radiated energy per unit area, W/ m^2), σ the Stefan-Boltzmann constant (5.67051 x 10^{-8} W/m^2K^4), ε the total hemispherical emissivity of the surface ($0 < \varepsilon < 1$) and T the surface absolute temperature (K). It follows that the emispherical total emissive power q is directly related to the temperature T, once the emissivity ε is known.

The emitted infrared radiation, as well as the temperature, varies according to the materials, in terms of their properties and structural and environmental conditions. As a result, infrared thermography is an effective tool to detect characteristics of materials and structures, surface decay and detachments, cracking and dampness patterns, heat dispersion and energy performances. It is speedy, simple and non-intrusive, so that it can easily address the durability assessment of building components that may be undertaken periodically throughout their service life [Chenga *et al.* 2008; Meoloa *et al.* 2005; Avedelis & Moropoulou 2004; Clark *et al.* 2003; Balaras & Argiriou 2002; Titman 2001].

Particularly, active IR thermography relies on the artificial heating of the surface to be investigated in order to enhance the emission. In fact, all the bodies with a temperature other than absolute zero (−273.15°C or 0 K) emit in the IR part of the electromagnetic spectrum. However, the absolute temperature should be high enough to activate a significant emission and, thus, to let the devices detect different thermal responses among similar materials. Nevertheless, active IR thermography allows reducing the influence of surrounding conditions and collecting more accurate and reliable data [Hung *et al.* 2009; Wiggenhauser 2002].

Within the research activities at the Department of Architecture and Town Planning (Technical University of Bari, Italy) on non-destructive diagnostics of building materials and components, a proposal in made in this paper for recommendations on an operation protocol for active IR thermography. These recommendations are made on the basis of simulation models and laboratory measurements form which the optimal operational parameters were determined. Specifically, the protocol will focus on the characteristics of the surfaces (geometry, stratigraphy, thermal properties), the environmental conditions (air temperature) and the technical features of the equipment (power and relative position to the surface).

There are numerous standards and regulations on the topic, including UNI EN 13187 "*Qualitative assessment of building thermal envelope through infrared thermography"*, ASTM D4788-88 "*Test method for detecting delaminations in bridge decks using infrared thermography*" and ISO 18434-1 "*Condition monitoring and diagnostics of machines. Thermography. General procedures*". However, they are more industry oriented and not yet comprehensive. For these reasons, the protocol can be a useful tool, in terms of technical optimization of procedures, time and costs, as well as methodological guide for analysis and interpretation of results derived from the active IR thermography for use in the building sector.

2 RESEARCH METHODOLOGY

Active IR thermography through emission stimulated by IR heaters on materials and components involve some of the following critical issues concerning:

- Optimal power and position of the heaters for suitable heat transfer; they depend on geometrical and technical characteristics of the heaters.
- Optimal heat flux and duration for suitable thermal exchange among several materials, including the surrounding environment, so that significant surface temperature differences can be detected;

they depend on geometrical, stratigraphical and physical characteristics of the building components and air temperature.

Within the operation protocol are defined the above critical parameters before the actual investigation is carried out, in order to eliminate any onsite "trial by error" procedures and, thus, reduce any uncertainty in data acquisition and elaboration. Specifically:

- In order to assess the optimal power and position of heaters used in an investigation, a performance graph is prepared for each device being used. Such a graph relates the surface heat flux to the heater power, as well as to the view factor between heater and surface. Specifically, the view factor varies according to the distance d and the angle θ between radiating device and irradiated surface. It should be underlined that the graph can be applied in the investigation of any surface, as it does not depend on the morphological characteristics of the building component.
- In order to assess the optimal heat flux and duration, a finite element model is formulated on the basis of the geometrical and dimensional characteristics and physical properties of the construction component. Such a model simulates the temperature distribution on the surface, given the heat flux and duration.

3 VIEW FACTOR

First, a graph was determined for the specific IR heaters that are available at the Laboratory of Building Technologies (Technical University of Bari, Italy), in order to evaluate the relationships among heat flux Q on a surface, the power W of the heater and the heater/surface view factor F, where:

$$F = \Phi / W \tag{2}$$

In detail, the graph was formulated based on some laboratory measurements on a plastered brick wall, heated by an IR TERM 2000 (Burda) device. The power was set by a dimmer BHC3600 at 1650 W, from measuring the electric current by an ammeter and the electric potential difference by a voltmeter. On the wall surface, a 3x3, 50 cm spaced, grid was traced (Fig.1). Then, some specific positions of the heaters were selected, combining three distances d from the surface (1m, 2m and 3m) with four angles θ (18°, 36°, 54° e 72°) on the surface perpendicular passing through the grid centre. For all the resulting 12 combinations, the heater was turned on for 5 minutes and the heat flux was measured by a fluxmeter BSR240 (LSI-Lastem) every minute. The procedure was repeated for all the 9 points of the grid and the flux was calculated as the difference between Φ_{max} while testing and Φ_{min} before testing, assuming a constant heat regime after 5 minutes. Given the device power and the average heat flux on the grid, the view factor was calculated for all the combinations, according to [2]. Then, a graph was determined by interpolating the values (Fig.2). Specifically, the graph allows determining the view factor, given d and θ, and, thus, at calculating the heat flux, given the power ($\Phi = F\ W$). It should be observed that such a graph is referred to the grid area (1 m^2).

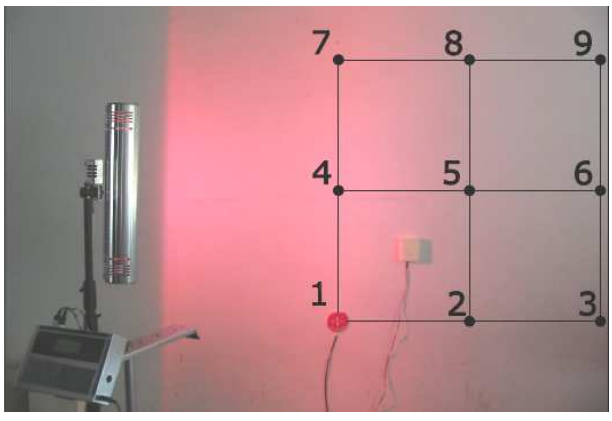

Figure 1. Experimental set up

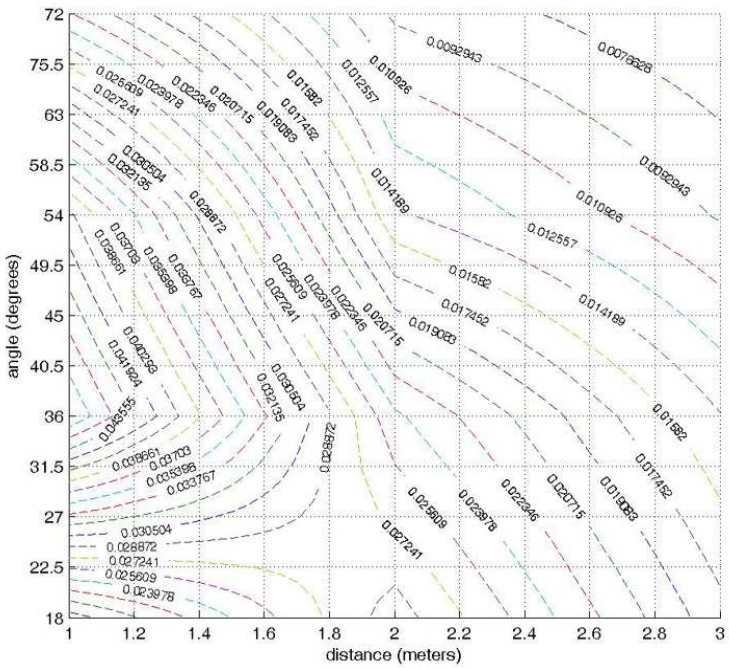

Figure 2. View factor graph

4 FINITE ELEMENT MODELS

A numerical simulation was run to assess the surface temperatures of some building components, under artificial heating by electrical infrared devices. Specifically, two finite elements models were formulated for brick and tuff walls, lately investigated by active IR thermography. The brick wall, 12 cm thick, is composed of hollow bricks, 25x25x10 cm, with 1 cm cement mortar joints. It is covered by lime plaster, 1 cm on each side. The tuff wall, 22 cm thick, is composed of structural tuff blocks, 35x25x20 cm, with 1cm cement mortar joints. It is covered by lime plaster, 1 cm on each side, as well. Specifically, two 2D blocks for each wall were modelled using the computational program Strauss7 (Finite Element Analysis System, Strand7 Pty Ltd, Rel. 2.3.7.), with known geometry and the physical properties of the materials. As far as the physical properties (Tab.1) are concerned, references were found in UNI 10351 "*Building Materials - Conductivity and Permeability*" and UNI EN 1745 "*Masonry and masonry products - Methods to assess design thermal values*".

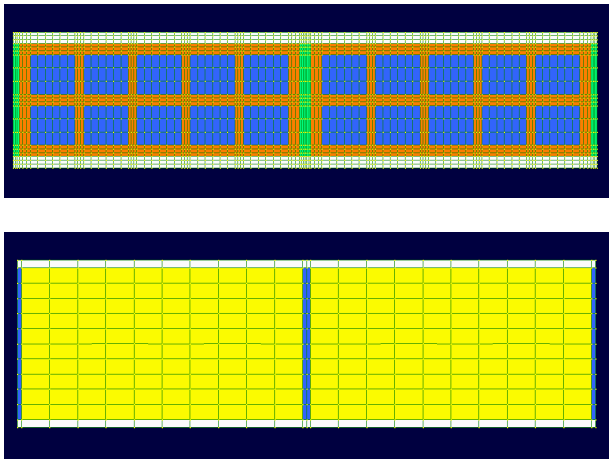

Figure 3. FE models of brick (top) and tuff (bottom) walls

Table 1. Physical properties of materials

Brick Wall				Tuff Wall			
Materials	**C_p (J/kgK)**	**λ (W/mK)**	**ρ (kg/m^3)**	**Materials**	**C_p (J/kgK)**	**λ (W/mK)**	**ρ (kg/m^3)**
Mortar	840	1,4	2000	Mortar	840	1,4	2000
Plaster	840	0,7	1400	Plaster	840	0,7	1400
Brick	840	0,9	1800	Tuff	840	1,5	2000
Air	1000	0,267	1,2				

The air temperature was also required as input data. In fact, a low environmental temperature implies a long exposure to a specific heat flux in order to get a certain surface temperature. This is due to the heat exchange between air and surface. At this stage, an expected air temperature was set up. The models are able to simulate the surface temperature distribution, given the heat flux (Φ) and duration (t).

Two different heat fluxes were selected for the models, also in order to verify the reliability of the view factor graph. Specifically, for the brick wall, the heat flux corresponded to the heater at d = 2 m and θ = 36°, whereas for the tuff wall this corresponded to the heater at d = 1,2 m and θ = 45° (the latter values were calculated by interpolation). Both the configurations were chosen, after checking the onsite conditions where the experimental investigation was supposed to be later carried out (presence of obstacles and barriers). From the view factors in the graph, the heat flux was calculated, as follows:

$$\Phi_1 = 2 \cdot 1000 \text{ W} \cdot 0{,}023978 = 48 \text{ W} \quad \text{and} \quad \Phi_2 = 2 \cdot 1000 \text{ W} \cdot 0{,}04 = 78{,}8 \text{ W}$$

where 1000 W is the power of each of the 2 heaters, symmetrically placed in front of the surface. It was decided not to set the maximum power, because of the limited onsite electricity supply. Figure 4a shows the surface temperature distributions on the models at the last minute of heating.

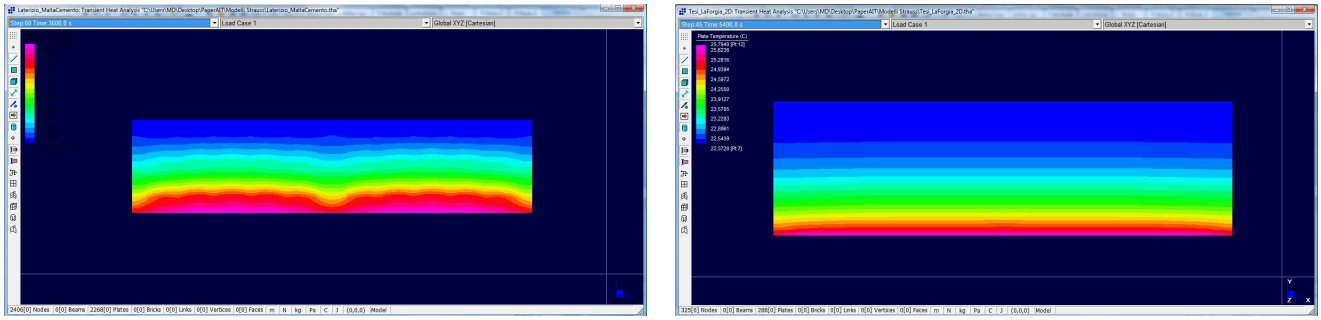

Figure 4. Temperature in the model of brick (t= 60', right) and tuff (t=90', left) walls

Particularly, as far as the brick wall is concerned, it can be noticed that a temperature difference between blocks and mortar joints (about 0,4° C) occurs after 60 minutes. Such a difference is detectable by the thermo-camera Neothermo TVS-700 (Avio) to be used in the experimental investigation. As a consequence, a period of 60 minutes of heating can be considered as suitable to detect the different response of the materials in the component. Whereas in the case of the tuff wall, the physical properties of blocks and mortar joints are very similar. As a consequence, the temperature is almost constant throughout the surface even if the heating lasts several hours. Moreover, several simulations were run, by setting different values of heat flux and air temperature; however, the output did not change. Consequently, for this type of component, the thermographic investigation would not enable the detection of the wall layout.

5 EXPERIMENTAL ASSESSMENT

An experimental assessment was carried out by onsite active thermography on building components, which corresponded to the models. Specifically, the heaters were placed in order to transmit a suitable heat flux, according to the reference view factor graph. The brick and tuff walls were heated for 60 and 90 minutes respectively.

The thermograms were acquired with a Neothermo TVS-700 (Avio) IR camera. A Pt100 probe, controlled by a multi-acquisition monitoring system BABUC/A (LSI-Lastem), was used to measure the air temperature. The total hemispherical emissivity of the surface (ε) was set at 0,95, by comparing the actual surface temperature measured by a Pt100 probe and the surface temperature detected by the thermocamera. While heating, a thermogram was collected every minute; Fig. 5 and Fig. 6 show the average temperature trend on the surfaces.

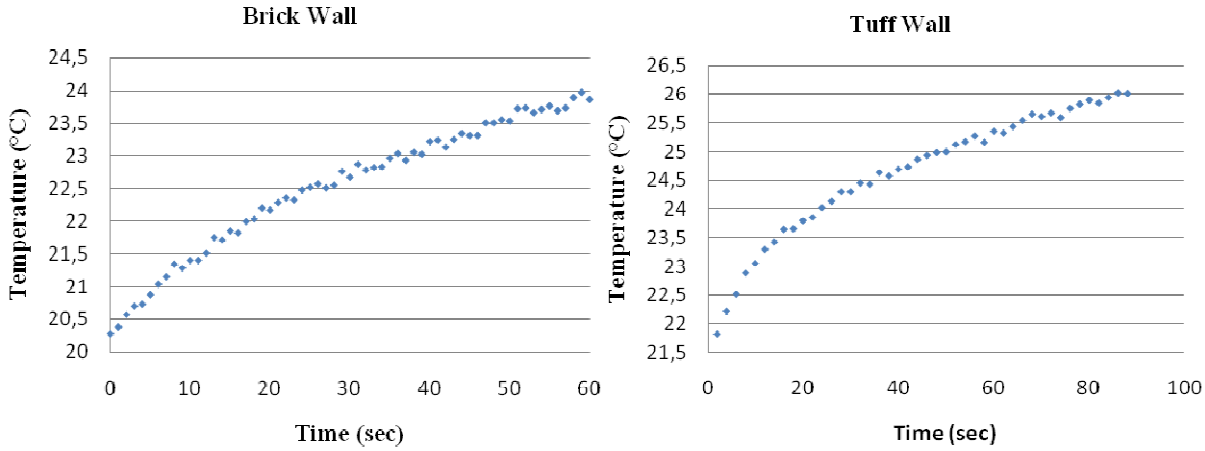

Figure 5. Surface temperature trends on brick (left) and tuff (right) walls

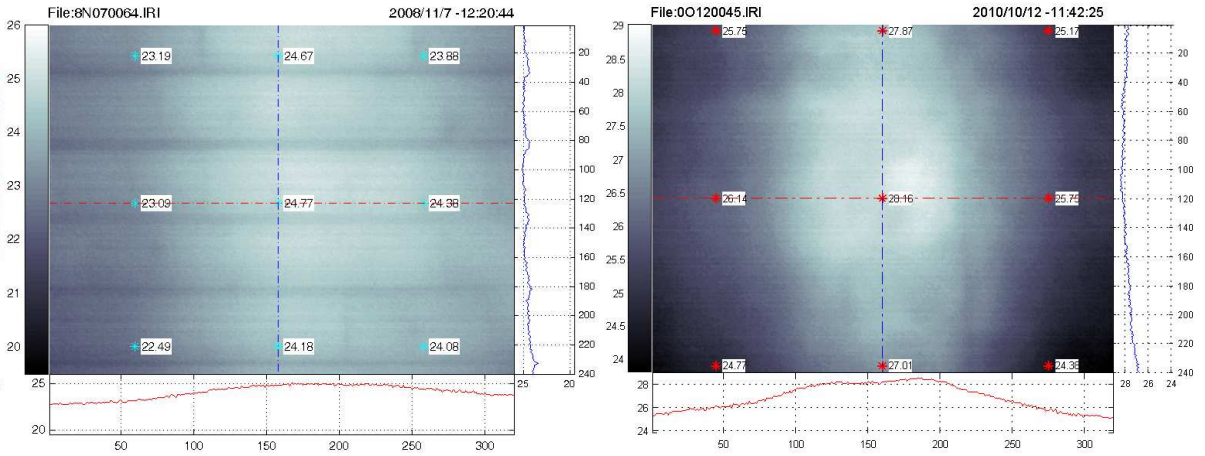

Figure 6. Last thermogram on brick (t= 60', left) and tuff (t=90', right) walls

The thermograms confirmed the results from the models. After 60 minutes, the brick wall configuration was detectable, whereas after 90 minutes the thermal image of the tuff wall was still meaningless. Nevertheless, for both cases, the experimental surface temperatures were compared against the values in the simulation. For that purpose, the actual initial air temperatures were set up in the models, at 20.34°C and 22.3°C respectively. In both cases, the results show a good consistency (Table 2). Particularly, for the brick wall, the measurements confirmed the temperature difference between blocks and mortar (23,39°C and 23,03°C after 60 minutes).

Table 2. Theoretical and experimental average temperatures of the last thermograms.

	$Temp_{model}$	**$Temp_{wall}$**
Brick Wall	23,86°C	23,21°C
Tuff Wall	26,11°C	25,80°C

6 TOWARD A PROTOCOL

Based on the validation of the view factor graph and the finite element models, some recommendations for a protocol are proposed that might help define the optimal conditions for data acquisition before an onsite investigation is carried out:

1) Survey of geometrical and dimensional characteristics for all the materials in the building component. This phase is based on technical reports and drawings, as well as on direct investigation.
2) Definition of physical properties (specific heat, conductivity, density) for all the materials of the building component. This phase is based on measurements, technical data and regulations.
3) Determination of a view factor graph for all the heaters that are going to be used in the investigation. The graph should relate the heat flux on a surface to the power of the heater, as well as to the view factor (distance d and angle θ) between heater and surface. This phase is carried out only once, as the graph does not depend on the characteristics of the building component.
4) Formulation of a finite element model of the building component, setting all the information gathered throughout the previous phases as input data. Within this phase, an expected air temperature can be set up.
5) Assessment of the optimal heat flux and duration to detect different thermal responses from the materials in the model. This phase should be carried out by iterative simulations, in order to consider some specific onsite limitations:
   - Accessibility to limited areas for the heaters, due to the presence of obstacles and barriers and/or vulnerability of the surroundings to the heating exposure.
   - Limited availability of power supply, especially when portable generators are employed.
   - Need to prevent the surface from exceeding some critical temperatures, particularly when some decorations and/or artworks are present.
   - Need to save time in order to interfere as little as possible with the ongoing ordinary activities and/or to extend the investigation to several building components on the same site.

If the results from the model are satisfactory, the protocol should include:

6) Experimental set up, according to the parameters (heat flux and duration) from the model and the layout (distance and angle of the heaters) from the reference view factor graph.
7) Thermography survey of the surface and collection of thermographs at suitable frequency.
   It should be pointed out that the protocol is meaningful, only if the thermography survey is carried out properly, particularly by avoiding reflection from the surroundings. Such a reflection might occur when the thermocamera is symmetrical to the heaters (reflection of devices), as well as when there are heat sources (light lamps, radiators) and transparent surfaces (mirrors, windows) nearby.

Then, a final cross-check can be performed by:

8) Comparison of theoretical and experimental surface temperatures, after setting up the actual initial air temperature in the model.

Finally, it should be observed that the model, along with the graph, can be used for the same components, as well as for similar components, for further investigation, in order to assess any changes, and, thus, any durability issues. Nonetheless, whenever some different elements show up in the thermograms, the local surface temperatures can be used to calibrate *ad hoc* FE models, where input data are iteratively changed until theoretical and experimental responses match.

7 CONCLUSIONS

Active IR thermography on building components requires a preliminary program, in order to consider, on the one hand, some relevant parameters (characteristics of surfaces, environmental conditions, technical and operation requirements of devices), on the other hand, some onsite limitations (presence of obstacles and barriers, availability of power supply, vulnerability of surfaces and their surroundings, time saving). Herein, the paper has proposed some tools, namely view factor graphs of the heaters and finite element models of the components that help assess the distribution of surface temperature, given the heat flux and duration. Those tools, which have been validated on some construction components, can address an operation protocol in order to plan and control the investigation. Specifically, the protocol should be followed before the actual testing is carried out, in order to eliminate any onsite "trial by error" procedure and, thus, to reduce any uncertainty in data acquisition and elaboration.

Finally, within a plan for durability assessment, the protocol can support the selection of building components where the investigation is meaningful and feasible, making thermography even more speedy and less intrusive. Nevertheless, the models can be used to interpret some anomalies (surface decay and detachments, cracking and dampness patterns) in limited areas and/or in following periodical surveys, as well as to predict and compare the response of different components to specific environmental scenarios (potential heat dispersions and energy performances).

ACKNOWLEDGEMENTS

We would like to acknowledge Mr. Rocco Rubino, Technical Manager of the Laboratory of Building Technologies, Department of Architecture and Town Planning, Technical University of Bari. His contribution to carry out the experimental investigation is greatly appreciated.

REFERENCES

Cheng, C.C., Cheng, T.M. & Chiang, C.H., 2008, 'Defect detection of concrete structures using both infrared thermography and elastic waves', *Automation in Construction* **18**, 87-92.

Meoloa, C., Di Maio, R., Roberti, N. & Carlomagno, G.M., 2005, Application of infrared thermography and geophisical methods for defect detection in architectural structures, *Engineering Failure Analysis* **12**, 875-892.

Avedelis, N.P. & Moropoulou, A., 2004, Application of infrared thermography for the investigation of historic structures, *Journal of Cultural Heritage* **5**, 119-127.

Clark, M.R., McCann, D.M. & Forde, M.C., 2003, Application of infrared thermography to the non-destructive testing of concrete and masonry bridges, *NDT&E* **36**, 265-275.

Balaras, C.A. & Argiriou, A.A., 2002, Infrared thermography for building diagnostics, *Energy and Buildings* **34**, 171-183.

Titman, D.J., 2001, Application of thermography in non-destructive testing of structures, *NDT&E* **34**, 149-154.

Hung, Y.Y., Chen, Y.S, Ng, S.P., Liu, L., Huang, Y.H., Luk, B.L., Ip, R.W.L., Wu, C.M.L. & Chung P.S., 2009, Review and comparison of shearography and active thermography for nondestructive evaluation, *Materials Science and Engineering* **64**, 73–112.

Wiggenhauser H., 2002, Active IR-applications in civil engineering, *Infrared Physics & Technology* **43**, 233–238.

XII DBMC
International Conference on Durability of Building Materials and Components
PORTO - PORTUGAL, April 12th-15th, 2011

In Situ Testing to evaluate the mechanical performance of Rendered Facades - Rebound Hammer and Ultrasound Techniques

Jorge Galvão [1]
Inês Flores-Colen [2]
Jorge de Brito [3]

ABSTRACT

Facades are directly affected by the performance of external renders because these elements are the first barrier against degradation agents. In service there is a progressive reduction of their performance until they are no longer able to fulfil their required functions during the life cycle, such as of water-proofing, protection and finishing of walls.

The evaluation to understand how a render performs over time is a complex activity, not only due to the multiple factors concerning its exposition, but also to the difficulty to assess the in-service behaviour. According to this, the use of in situ tests is very important because it gives the possibility to obtain the information about in-service performance of renders in real conditions.

The present paper summarizes a MSc thesis that studied the application of the ultrasonic method and the pendulum rebound hammer on the evaluation of mechanical performance of facade rendering. In this study, two experimental campaigns were made in renders applied on several walls located in places of natural ageing. First, the sensitivity of *in situ* tests was analyzed, which allowed identifying some of the main factors that influence the results of these techniques, related both to the rendering system and to the inspection procedure.

Furthermore, rendering mechanical behaviour was analyzed based on the campaigns' results. This study has confirmed the usefulness of these *in situ* tests to evaluate the mechanical performance of the facades rendering, allowing the establishment of a methodology to perform that evaluation over time.

KEYWORDS

Rendering façade, mechanical performance, *in situ* testing, rebound hammer, ultrasound

[1] VIROC PORTUGAL, S.A, Est. Nacional 10, km 44.7 Vale da Rosa, 2914-519, Setúbal, Portugal, jgalvao@viroc.pt
[2] DECivil-IST, Technical University of Lisbon, Av. Rovisco Pais, 1049-001, Lisboa, Portugal, ines@civil.ist.utl.pt
[3] DECivil-IST, Technical University of Lisbon, Av. Rovisco Pais, 1049-001, Lisboa, Portugal, jb@civil.ist.utl.pt

1 INTRODUCTION

1.1 The Performance of Rendering Mortars

Rendering using a mineral binder is the most widely-used rendering solution in Portugal. Essentially, this is due to its initial low cost and lack of complexity in application [Gaspar 2002]. Of all the existing types of rendering, traditional rendering prepared on-site using traditional technologies has become the solution most commonly adopted for the majority of construction projects in Portugal. Nowadays, however, the use of non-traditional products is becoming more widespread, as their availability and rapid application are better suited to the current available space o a construction site.

The concept of performance is directly related to the way in which buildings and their components achieve the goals demanded from them. In order to meet requirements rendering must ensure waterproofing and protection for walls, finishing for surfaces, and durability in terms of external actions and adequate use [Veiga 2005].

The performance of rendering mortars during their service life depends on their performance in relation to mechanical, thermal and dynamical actions. During its service life, the exposure of external rendering to destructive actions leads to the emergence of anomalies (including cracking, loss of adherence and loss of cohesion) which reduce its performance to the minimum acceptable level (in terms of physical or functional failure), if no corrective measures are taken.

The shape and microstructure of renders influence their in-service degradation and the fulfilment of the main protective function of this coating system. Nero [2001] emphasises that the flat shape of renders, with its greatly reduced thickness (5 mm to 40 mm) in comparison with the other dimensions results in large surfaces being exposed to the environment in relation to the small volume of material involved. On the other hand, Magalhães [2002] emphasises the porous structure of rendering, which allows the entrance of water, thus making it more susceptible to the action of this degradation agent.

Due to the reduction over time in the performance of external rendering, it is vital to carry out service evaluations by assessing the most important performance characteristics. With regard to the mechanical performance of rendering, this essentially involves adherence, internal mechanical resistance, surface resistance and deformation [Flores-Colen 2009]. However, it is only possible to carry out an in-service evaluation of these features by using *in situ* testing techniques, which provide information on the characteristics of the mortars that have been applied.

1.2 *In Situ* Testing Techniques to Evaluate Rendering Performance

The in-service evaluation of performance can be carried out in several ways. In most cases, a visual inspection is enough to detect pathological phenomena affecting the rendering because of the evident and visible symptoms [Tavares *et al*. 2005]. However, this can produce data that is dubious or difficult to interpret. It is also affected by the education and experience of the technician carrying out the inspection, as well as the accessibility of the area being inspected. Furthermore, most problems affecting performance are often not visible, which means that they need to be measured [Tavares *et al*. 2005; Flores-Colen *et al.* 2006].

From this perspective, the use of auxiliary diagnosis techniques reduces the subjectivity of visual inspections, making it easier to obtain a more reliable evaluation. For these reasons, the use of those auxiliary techniques, in particular in situ techniques, has proved increasingly beneficial in characterising in-service performance, as a complement to visual inspection [Flores-Colen *et al.* 2006].

Nowadays there is a great variety of *in situ* testing techniques that can be used in in-service evaluations of the performance of external rendering. An *in situ* technique is more suitable if it is easy/quick to perform and if the resulting information proves useful to the in-service evaluation of performance.

1.2.1 Ultrasound testing

Ultrasound testing works by finding out how fast an ultrasonic impulse travels between two points, with a view to obtaining information about the characteristics of the elements being tested. It is a test with low destruction level and that also has the advantage of being quick and easy to perform.
The classic use of ultrasound testing is to evaluate the characteristics and properties of concrete. In the particular case of wall rendering, it shows the state of degradation of the elements tested, since the existence of discontinuities in the form of cavities and cracks affects the speed at which the waves are transmitted [Magalhães *et al.* 2003].

Materials in poor condition or with weaker cohesion register lower speeds than compact or less degraded materials. Because of this, ultrasound testing is used to diagnose anomalies, allowing potentially deteriorating areas (cracks, detachments, cohesion loss) to be located [Santos *et al.*, 2003]. More recently, Flores-Colen [2009] has confirmed the usefulness of ultrasound testing in improving identification of deterioration and performance in façade rendering made from cement-based mortars.

1.2.2 Pendulum rebound hammer testing

Testing with a pendulum sclerometer hammer is based on the rebound method, in which the reflection of an elastic mass launched against a surface depends on the surface hardness of the material under analysis [Gomes 1995]. The result is shown on the sclerometric index as the rebound number, which is arbitrary as it depends on the mass and the energy stored by the device's spring. The softer the material, the greater the energy absorbed and the smaller the rebound [Magalhães *et al.* 2003].

The sclerometer is a device used in conjunction with other destructive or non-destructive tests mainly to calculate the resistance of a material from its surface hardness or to compare the quality of materials. It is quick to use and has been employed to test concrete and, more recently, in the *in-situ* characterisation of wall rendering (Magalhães *et al.*, 2003). In the latter case, it was used to evaluate the quality of the adherence of the rendering, as well as its homogeneity and uniformity [Gomes 1995].

Sclerometer testing is useful in characterising degradation and in determining the mechanical performance of rendering. Flores-Colen [2009] has concluded that the pendulum sclerometer allows mapping areas of poor performance (associated to the presence of moisture or lack of adherence).

2 EXPERIMENT PROGRAM

2.1 Case Studies

Two series of experiments were carried out at natural aging stations, one at the National Laboratory of Civil Engineering (LNEC), in Lisbon, and another at a manufacturer's building yard, at Carregado.
The LNEC station was built at the end of the 1970s and since then has been used in several studies on rendering mortar, thus allowing service performance to be studied. The station has a huge variety of applied renderings, ranging from thirty-year old traditional rendering to pre-mixed renderings using recent formulations. The prototype walls are mostly built from brick masonry to a thickness of 20 cm and the upper sections are protected by ceramic tiles (Figure 1).
The rendering is applied to this support, and whilst traditional renderings are usually applied in 2 layers, with a total thickness of 2.5 cm, pre-mixed renderings are normally applied using a single-layer system 2 cm thick. These products are usually applied by technicians who have experience in application, so they can reproduce the methods used on-site as faithfully as possible.
The manufacturer's ageing station was built at the beginning of 2004 with the aim of monitoring the performance of pre-mixed products over time. The prototype walls consist of a masonry support made from 7 cm thick bricks protected on top by ceramic roof tiles, onto which the rendering was applied to a thickness of around 2 cm (Figure 2). The rendering was done by a builder's team who were specialists in the application of this kind of product. The current rendering was applied in July, 2004 and the same pre-mixed product was used on all the prototype walls.

During the series of experiments, the following types of rendering were analyzed:

- TC - traditional rendering made of cement; two kinds of rendering were analyzed: TC1, with a volumetric ratio of 1:5, and TC2, with a volumetric ratio of 1:4:
- TC (I) - traditional rendering made of cement, separate from the support, reinforced with welded wire mesh;
- TCH - traditional hydraulic lime rendering, volumetric ratio 1:4;
- TC (FV) - traditional cement rendering, volumetric ratio 1:4, with fibreglass incorporated into the mixture (0.3%);
- TC (FPP) - traditional cement rendering, volumetric ratio 1:4, with polypropylene fibre incorporated into the mixture (1%);
- TBC-CA - traditional ordinary rendering, made of cement and aerated lime, volumetric ratio 1:1:6;
- PD - pre-mixed rendering made of cement; ten different types of pre-mixed rendering were analyzed, PD1 to PD10; when possible, several formulations of the same product were also analyzed.
-



Figure 1. Prototype walls at the LNEC station



Figure 2. Prototype walls at the manufacturer's station

2.2 Methodology

2.2.1 Ultrasound testing

Ultrasound testing was carried out in accordance with Standard EN 12504-4 [CEN 2004] for concrete, with due adaptations. PUNDIT equipment directly measuring transition time was used, employing transducers with a frequency of 54 kHz and a diameter of 5 cm.

The testing procedure began with the calibration of the measuring device, using the device's calibration bar, to a known transition time (26.2 µs). Measurements were taken using the indirect method (Figure 3), concentrating on areas with no apparent degradation. Vaseline or toothpaste were used to ensure contact between the transducers and the rendering.

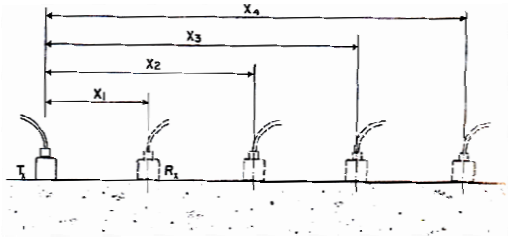

Figure 3. Diagram showing measurement of ultrasound pulse velocity [CEN 2004]

The adopted method was to analyse 400 mm paths divided into 100 mm distances, although in some cases 350 mm paths were analyzed, divided into 70 mm distances, in order to obtain the results.

The apparent pulse velocity was calculated using equation 1:

$$V_{ap} = \frac{d}{t} \quad \text{(Eq. 1)}$$

In which:

V_{ap} - apparent ultrasound pulse velocity (km/s);
d - distance between the transducers along the path (mm);
t - transition time (µs).

2.2.2 Testing with the pendulum rebound hammer

Pendular sclerometer testing was carried out in accordance with Standard NP EN 12504-2 [IPQ 2001] for concrete, with due adaptations. The testing directly measured rebound values, with 6 to 9 measurements taken per wall. Contrary to established procedures for concrete, surfaces were not polished, as this has a significant aesthetic effect on the rendering (changing the colour and texture of the product), and therefore the roughness of the render surface was also analyzed.

3. DISCUSSION OF RESULTS

3.1 Precision of Techniques

Due to the large number of situations analyzed, it was possible to carry out an analysis of the precision of the techniques used, given the various parameters. The results are summarized in Table 1 for ultrasound testing and Table 2 for pendulum rebound hammer testing.

Table 1. Results for analysis of ultrasound testing precision

Factors analyzed	ULTRASOUND TESTING			
	Influences the results	Does not influence the results	Not conclusive	Maximum difference (%)
Type of rendering	✓			38
Type of masonry support		✓		-
Roughness of finishing		✓		-
Cracks	✓			33
Paint finishing	✓			46
Application conditions			✓	-
Inspection conditions	✓			11
Distance between measurements	✓			12
Contact material used	✓			23
Replacement of contact material	✓			29

Table 2. Results for analysis of pendulum rebound hammer testing precision

Factors analyzed	PENDULUM SCLEROMETER TESTING			
	Influences the results	Does not influence the results	Not conclusive	Maximum difference (%)
Type of rendering	✓			46
Type of masonry support	✓			25
Roughness of surface	✓			29
Paint finishing	✓			58
Application conditions			✓	-
Inspection conditions		✓		-
Position of the measurements	✓			25

Ultrasound testing appears to be the most precise test, since it involves more complex procedures than pendulum sclerometer testing. On the basis of all the factors analyzed, it can be concluded that the type of rendering, the existence of paint finishing layer and the inspection conditions influence the results. In addition, factors inherent to the technique itself also exert an influence, as well as the distance between measurements, the contact material used and its replacement.

Out of all the factors mentioned, the type of rendering, the existence of a paint finishing and the presence of cracks in the rendering were identified as the factors which had the greatest influence.

The maximum differences analyzed were between 30% and 50%. However, other parameters also had an important influence, such as the contact material and its replacement, which registered differences between 20% and 30%. Finally, factors such as the inspection conditions and the distance between measurements had a lesser influence, of about 10%.

According to the cases analyzed, certain factors such as the support material and the roughness of the surface do not have any significant influence on the results of ultrasound testing. In conclusion, it is worth mentioning that the analysis of application conditions, especially the time of the year when the rendering was applied, is not conclusive, particularly given the number of cases available for analysis. Pendulum rebound hammer testing appears to be less precise in terms of the number of factors involved, given that their influence is greater than the corresponding influences in ultrasound testing. The results showed that most of the parameters tested affect the results, including the type of rendering, support, roughness of finishing, painting and the number of measurements by position.

The type of rendering and the existence of a painted finishing were the factors with the greatest influence on the results of pendulum sclerometer testing, registering values of 45% to 60%, whereas the maximum differences for the remainder were between 25% and 30%. According to this analysis, inspection conditions do not significantly influence the results of the testing and, as with ultrasound testing, it was not possible to reach any conclusions on inspection conditions.

Based on the precision analysis, it can be concluded that the techniques used in *in situ* testing are sensitive to the influence of several factors. These must be controlled as far as possible during testing and must be taken into account in the analyses of the results. In the case of pendulum rebound hammer testing, it is useful to bear in mind in which factors exert the greatest influence and the extent to which they are felt. Figure 4 provides a summary of the results obtained.

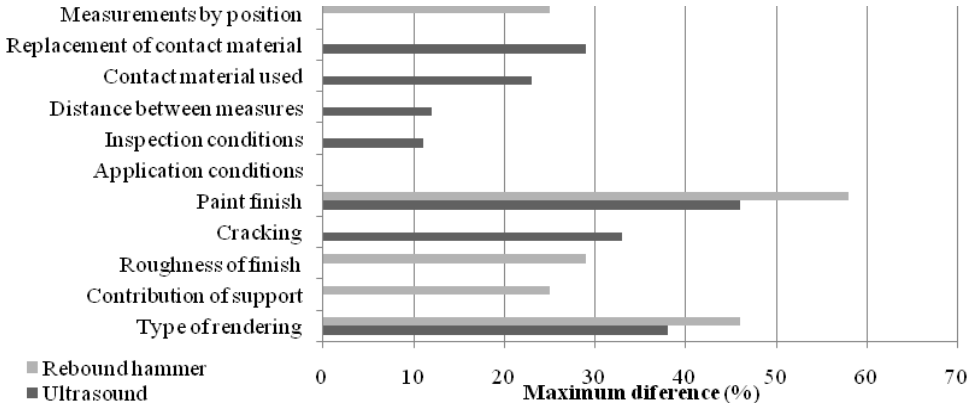

Figure 4. Summary of results for precision analysis for both techniques

Despite these difficulties, the techniques used are acceptable for evaluating performance, as they allow for distinctions to be made between different materials and situations since they are particularly sensitive to different mechanical characteristics and can identify variations between them. The following examples show the results obtained for several parameters, according to rendering type. Figure 5 shows ultrasound testing and Figure 6 pendulum sclerometer testing.

The examples show that the *in situ* testing techniques used enabled the various parameters to be distinguished in terms of rendering type and also allowed variations in characteristics between parameters with the same rendering to be detected.

Figures 5 and 6 also illustrate the possibility of cross-referencing the results of both techniques, since there is a trend towards a greater rebound value and vice-versa, depending on the propagation velocity. However, exceptions may occur due to internal heterogeneity or variations in the actual techniques used that make it impossible for a quantitative relationship to be defined for the series of tests.

Another possible use for *in situ* testing is monitoring over time of the mechanical performance of rendering. Figures 7 and 8 show the evolution over time of the parameters analyzed, by comparing results from this study with those of previous studies of the same parameters, in the walls of manufacturer's natural station [Flores-Colen 2009].The comparison of results over approximately one year shows that apparently there was no significant variation in the rendering's mechanical characteristics during this

period. Only small differences were noted and fall within the variations associated with this type of technique (coefficient variation ±13%).

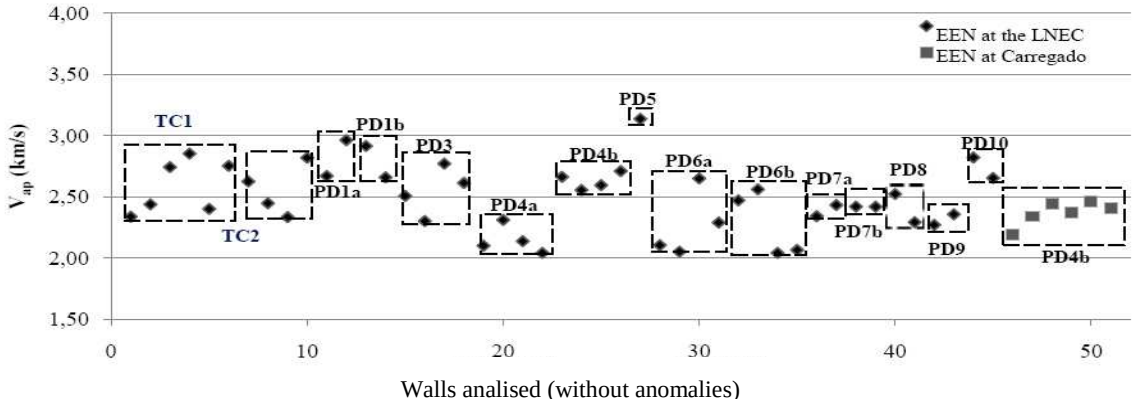

Figure 5. Ultrasound test results (apparent pulse velocity) for the various tested walls

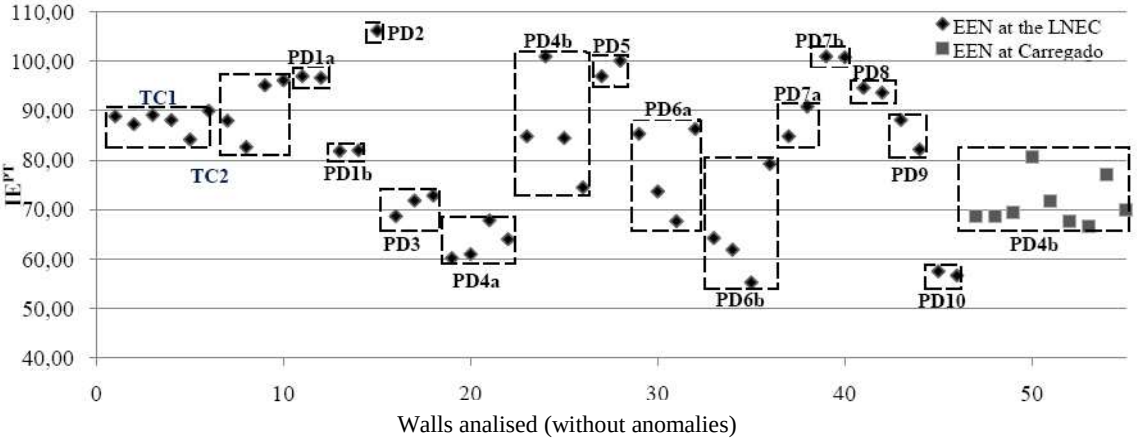

Figure 6. Pendulum rebound hammer results (sclerometer index) for the various tested walls

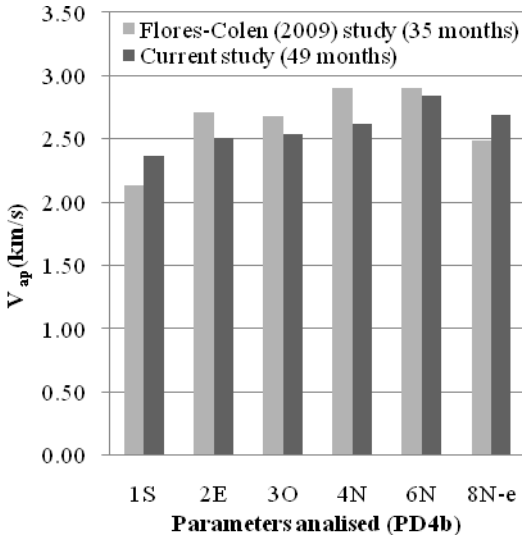

Figure 7. Evolution of ultrasound pulse velocity

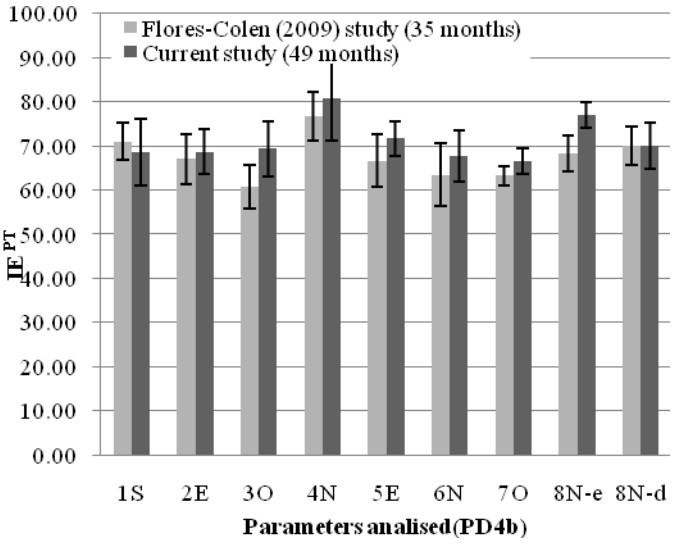

Figure 8. Evolution of pendulum sclerometer index

4 CONCLUSIONS

This study has extended existing knowledge of the use of ultrasound and pendulum rebound hammer testing to evaluate the mechanical performance of wall rendering. As these techniques are still not widely used in wall rendering in in-service diagnosis, it is a contribution towards creating a basis for their implementation in practice.

The precision of the techniques in relation to several parameters was studied, with the aim of identifying which parameters are influential and how this influence is shown in the results, so that they can be taken into consideration in future analyses. Of all the parameters analyzed, it was concluded that the composition of the rendering and the existence of paint finishing layer were the parameters which had the strongest influence in both techniques tests. Other factors, such as presence of cracking or material used in ultrasound testing, and roughness of the finishing surface and contribution of the support in the pendulum hammer testing, also have a significant influence on the results.

In addition, results were studied in order to evaluate the influence on mechanical performance of the parameters analyzed, in order to assess the potential of the techniques used in this evaluation. The results showed that both ultrasound and pendulum hammer can be used in the in-service evaluation of mechanical performance, as the results reflect the mechanical characteristics of the mortar and enable variations to be identified. However, the study also proved that this analysis is not always easy, and that it is advantageous to cross-reference the results of both techniques in order to clarify the more ambiguous situations. These techniques can be considered complementary and their combined use is thus advisable. On the other hand, the techniques used seem to be very helpful in monitoring performance over time, enabling significant variations in the characteristics evaluated to be detected.

In the light of the above, this work attests to the usefulness of ultrasound and pendulum hammer testing in evaluating the mechanical performance of rendering, by demonstrating the potential of this evaluation and identifying the main factors that need to be taken into account in the analysis. It can therefore be considered that the more widespread use of these techniques would be relevant.

ACKNOWLEDGEMENTS

Thanks are due to the Rosário Veiga from LNEC and to Luís Silva from Weber for the chance to study the walls renderings at natural ageing stations respectively; and to the ICIST - IST research centre.

REFERENCES

CEN 2004 - EN 12504 - *Testing concrete - Part 4: Determination of ultrasonic pulse velocity*. CEN: European Committee for Standardization.

Flores-Colen, I.; Brito, J. de; Freitas, V. 2006 - *In-situ test techniques to support predictive maintenance of façade rendering (in Portuguese)*. In: PATORREB 2006 - 2nd Meeting on Pathology and Rehabilitation of Buildings, Porto: FEUP, pp. 701-710.

Flores-Colen, I. 2009 - *Methodology of in-service performance evaluation of rendered facades from a predictive maintenance viewpoint (in Portuguese).* Civil Engineering PhD thesis, Lisbon: Instituto Superior Técnico, 487 p.

Gaspar, P. 2002 - *Methodology to determine durability of external current renders (in Portuguese).* Dissertation for Masters in Construction, Lisbon: Instituto Superior Técnico, 209 p.

Gomes, A. 1995 - *Characterization of traditional mortars used in external coatings of buildings (in Portuguese)*. Civil Engineering PhD thesis, Lisbon: Instituto Superior Técnico, 269 p.

IPQ 2001 - NP EN 12504 - *Testing of concrete in structures - Part 2: Non-destructive test. Determination of the sclerometric index (in Portuguese)*. Lisbon: Instituto Português da Qualidade.

Magalhães, A. 2002 - *Pathology of old renders (in Portuguese)*. Buildings Cahiers, No. 2, Lisbon: LNEC, pp. 69-84.

Magalhães, A.; Veiga, M. do R.; Costa, D. 2003 - *Diagnosis of anomalies in wall coatings using in situ test techniques. Evaluation of mechanical resistance (in Portuguese).* In: 3º ENCORE - Meeting on Conservation and Rehabilitation of Buildings, Lisbon, pp. 419-427.

Nero, J. 2001 - *Renders - Part II (in Portuguese).* Arquitectura e Vida, No. 21, pp. 90-95.

Santos, C.; Matias, L.; Magalhães, A.; Veiga, M. 2003 - *Application of thermography and ultrasounds for wall anomalies diagnosis. A laboratory research study*. In: International Symposium on Non-Destructive Testing in Civil Engineering, Berlin: DGZIP, CD-Rom.

Tavares, M.; Magalhães, A.; Veiga, M.; Aguiar, J. 2005 - *Diagnosis methods for coatings of ancient buildings. Importance and applicability of in situ tests (in Spanish).* In: Revista Boletín del Instituto Andaluz del Patrimonio Histórico, available at http://conservarcal.lnec.pt (access May 2009).

Veiga, M. 2005 - *Performance of façade mineral-based coatings. Functional requirements and performance evaluation (in Portuguese).* In: 1st National Congress, APFAC, Lisbon, CD-Rom.

XII DBMC
International Conference on Durability of Building Materials and Components
PORTO - PORTUGAL, April 12th-15th, 2011

Application of Numerical Analysis to Study the Adherence of Renders on Walls

Sara Gaspar [1]
Cristina Matos Silva [2]
Inês Flores-Colen [3]

ABSTRACT

Renders should guarantee an adequate adherence to the substrate throughout their service life. The loss of adherence of these coatings leads to detachments that may be increased by the action of various degradation agents and originate hazardous situations to users and passers-by. Several factors influence adherence such as nature of the substrate (surface roughness, initial moisture content and capillary suction) and type of coating material (materials composition, thickness, age, and weather conditions during application).

Finite element analysis in which an interface is modelled between the wall and the render can play an important role in the study of the mechanism of adherence of the render on its substrate. The constitutive behaviour of the interface model simulates the mechanism of the render adhesion loss.

This paper presents the numerical analysis used on a Master Thesis to study the interface between render and its substrate, using commercial software. In this context, a state of the art about the study of adherence (definition, methods of evaluation, and criteria) is presented, following a discussion of the software ANSYS application to the study of adherence (including several simulations in which render and/or interface properties and/or characteristics were modified in order to model factors that might influence the render adhesion, such as render thickness or rendering mortar application process).

Additionally, the pull-off test is modelled and the maximum force and fracture pattern obtain with the numerical analysis is compared with experimental results.

This paper contributes to a better understanding of the factors that influence adherence of renders and also of the results of pull-off test (technique commonly used to evaluate in situ the adherence of coatings).

KEYWORDS

Adhesion; renders; interface; ANSYS; numerical analysis; pull-off test.

[1] 5th year student of Civil Engineering Integrated Master - IST, Technical University of Lisbon, saraggaspar@live.com.pt
[2] Assistant professor at the Department of Civil Engineering and Architecture - IST, Technical University of Lisbon, Av. Rovisco Pais, 1049-001, Lisboa, Portugal, Phone +351 21 8418356, Fax +351 21 8497650, cmsilva@civil.ist.utl.pt
[3] Assistant professor at the Department of Civil Engineering and Architecture - IST, Technical University of Lisbon, Av. Rovisco Pais, 1049-001, Lisboa, Portugal, Phone +351 21 8418372, Fax +351 21 8497650, ines@civil.ist.utl.pt

1 INTRODUCTION

Adhesion strength is one of the mandatory properties of renders, so that construction works in which they are applied can meet the requirements of in-use safety and durability, established in the Construction Products Directive (Council Directive 89/106/EEC). The European standard EN 998-1 [CEN, 2003] lists the requirements and properties for hardened mortar, including its adhesion to the substrate. According to this standard, the value of the adhesion strength of mortars can be determined with pull-off tests described in the EN 1015-12 [CEN, 2000]. There have been several experimental studies to extend the knowledge of the adhesion mechanism between a mortar and its substrate and determine which factors can influence that render property. In these studies, researchers often perform microscopic analysis of the interface of the system substrate/mortar and measure the strength of the interfacial bond, with pull-off tests.

Adhesion loss is a frequent defect of external renders and cannot be neglected as the render detachments can cause hazardous situations to passersby. Therefore, in situ evaluation of the renders adhesion strength, in-service conditions, must be performed periodically. For instance, the American standard ASTM E2270 [2005] in a frequent detailed building facade inspection recommends to conduct at least three pull-off tests per facade elevation.

Performing a pull-off test in a rendered facade causes a certain degree of damage which must be repaired after the test. That is an important disadvantage of this technique and is the main cause for the reduced number of field experimental campaigns in which this technique is used. However, the assessment of the adherence of renders in-service conditions can be useful in order to understand the problems that are not visible on the surface and also when a quantitative evaluation is needed to support the decision of repair. For instance, Flores-Colen *et al*. [2009] performed pull-off tests in building facades with render adhesion loss in some areas to evaluate the adhesion capacity of the remaining renders to the wall. Freitas *et al.* [2008] also performed lab and in situ evaluation of mortar adhesion to study the evolution of this property through (accelerated and natural) weathering cycles.

Finite element analysis in which the interface between the wall and the mortar is modeled can play an important role in the identification of factors that might influence the mortar's adhesion. The commercial software ANSYS has been used in numerical analysis in several areas of engineering (civil, mechanics, aerospace). In this software the constitutive behavior model of the interface can simulate the mechanism of the render adhesion loss.

This paper intends to discuss the application of a numerical analysis to study first, the factors that influence the effective adherence of applied renders on walls (simulation of real conditions), and second the results of pull-off test (this technique gives values of stress in rupture conditions, however the interface render/substrate behaviour before rupture is not well studied, therefore it is important to model this common technique and compare the theoretical with experimental results).

2 SUBSTRATE/MORTAR ADHESION

2.1 Bond Mechanism of a Mortar to a Substrate

The mechanical bond of a mortar to its substrate is due to the penetration of mortar fluids and fines into the pores and cavities of the substrate follow by the crystallization of binder hydration products such as ettringite and C-S-H gel; the solid crystals provide the mechanical connection between mortar and substrate (Figure 1). The substrate capillary suction is responsible for the movement of the mortar fluids and fines to the substrate/mortar interface and into the pores of the substrate (when the mortar contacts with the substrate, its pores are bigger than the substrate pores, which are unsaturated). The substrate suction of mortar fluids decreases the mortar water/solids ratio which leads to its plastic shrinkage, and as a consequence the mortar pores size decreases and eventually become smaller then the substrate pores; that is when the occurring suction stops. Chemical bonding, namely, covalent and Van der Waals bonding, contributes also to mortar's adhesion but with a minor share.

2.2 Factors that Influence the Rendering Mortar Adhesion to the Substrate

Several studies have been performed by different authors with the aim to identify factors that influence the adhesion bond between a mortar and its substrate. In these studies several factors are modified in a substrate/render model and pull-off tests are performed to evaluate the normal strength of the bond between them. The factors that influence a mortar adhesion have different nature; some are related with the mortar characteristics (cement proportion, consistency), others are related with the substrate type (surface roughness, initial rate absorption) and others are external to the substrate/render system (weather conditions during the mortar application, mortar application process). Regarding the factors related to mortar characteristics, it is known that the increase of cement proportion in a mortar also increases the strength of its normal and shear bond to the substrate; also mortars with higher compressive and tensile strength have more adherence capacity. Mortars less viscous and easy to apply or with a higher capacity to retain water perform better in terms of adhesion.

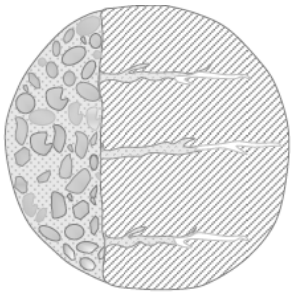

Figure 1. Mechanical bond between a mortar and its substrate [Quintela, 2006].

The substrate nature is also significant in the development of the adhesive bond with the substrate. A rough surface texture helps the penetration of mortar fluids into the substrate pores. The initial rate absorption can also influence the substrate/render bond strength; there is an optimal range of values for this substrate property for which the strength of the mentioned bond is maximum.
The presence of dust and oil in the surface of the substrate prevents the penetration of mortar fluids into its pores and cavities and the substrate/mortar bond is unable to develop. Moist-curing and the application of render through mechanical projection are external factors that have proven to improve the mortar adherence capacity. The factors mentioned in this sub-chapter 2.2 have been identified after literature review and are systemized in the ongoing Master Thesis of the first author (Table 1).

Table 1. List of factors that according to the literature can influence the substrate/mortar bond

Factors related to the rendering mortar	Factors related to the substrate	External factors
• composition (includes cement and aggregates characteristics and proportion); • characteristics such as: compressive and tensile strength, consistency, water retention; • thickness; • number of rendering system layers; • age.	• surface texture; • initial rate absorption; • porosity; • initial moisture content; • cleaning; • surface treatments.	• render application process; • moist-curing; • weather conditions during application.

2.3 Methods to Evaluate the Adhesion of Mortars

The pull-off test (Figure 2, left) is the most used method to measure the adherence capacity of a mortar to the substrate. This test, described in the European standard EN 1015-12 [CEN, 2000], consists of extracting with a pull-off device in the disc previously adhered to the coating; to make sure the pulling off occurs only under the disc, a groove 2 mm deeper than the render's thickness must be cut in the perimeter where the disc is to be glued. The pull-off device measures the force necessary to extract the disc. The ratio between this force and the disc transverse section is the maximum normal tension that can be applied to the coating. This standard defines three failure types that can occur in the pull-off test that are related to the location of the rupture: type *a* - adhesive rupture of the interface between the render and substrate (Figure 2, right); type *b* - cohesive rupture of the render (Figure 2, centre); type *c* - cohesive rupture of the substrate. When the rupture is of type *a* then the result of the test is the adherence stress; if the rupture is of type *b* and *c* the value obtained is a minimum limit of the adherence stress.

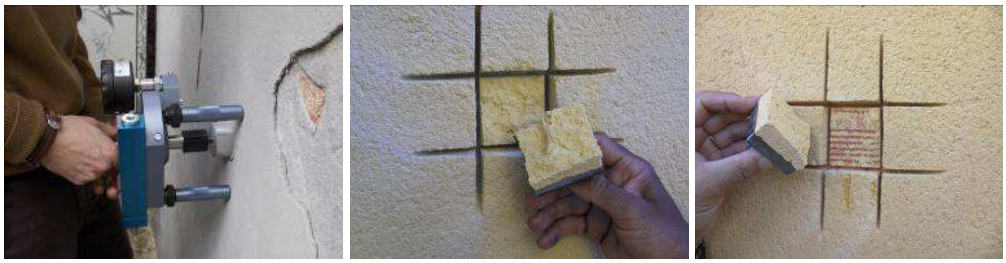

Figure 2. Pull-off test (right); cohesive rupture of the render (centre); adhesive rupture of the interface (left) [Flores-Colen, 2009]

3 MODELING A SUBSTRATE/RENDER SYSTEM IN ANSYS SOFTWARE

3.1 Overview of the ANSYS Software

ANSYS is a general finite element-based models package for numerically solving a wide variety of engineering problems. These problems include: static/dynamic structural analysis (both linear and non-linear), heat transfer and fluid problems, as well as acoustic and electromagnetic problems. ANSYS is often used by mechanical engineers to determine in-use stress distributions of vehicle components. In the civil engineer area, ANSYS can be a helpful tool in modeling the most complex structures if combined with the CivilFEM package software that runs within ANSYS Multiphysics.

3.2 Modeling an Interface with ANSYS Multiphysics 11.0

ANSYS Multiphysics 11.0 provides, in its finite element library (called "interface elements") for modeling interfaces between structural elements. The several interface elements available differ in their node number. The 2D models of a rendered facade (Figure 3) and of the pull-off mechanism that were built in ANSYS, to study the influence of the interface between a render and its background wall, have a plane geometry. Therefore the finite interface element type INTER202, which is a plane element with four nodes, was used to model the interface in this case (Figure 4).

In the beginning of the solution the interface element doesn't have thickness, which means some of its nodes are initially coincident; with the application of forces in the model, the displacement between nodes within the interface element increases, simulating an interfacial displacement between the wall and the render surfaces. The interface elements behave according to the exponential cohesive zone model introduced by Xu and Needleman [1993]. The cohesive zone model consists of a constitutive relation between the traction (T) acting on the interface and the corresponding interfacial separation (Δ). The interface traction and separation are defined in the normal (n) and tangential (t) interface direction; these directions are based in the element coordinate system which is shown in Figure 4. The

exponential form of the cohesive zone model uses a surface potential (Φ) to define the interface normal and tangential traction, according to Eq. (1) and Eq. (2):

$$T_n = \frac{\partial \phi(\Delta)}{\partial \Delta_n} \qquad (1) \qquad T_t = \frac{\partial \phi(\Delta)}{\partial \Delta_t} \qquad (2)$$

If the work associated with the separation process in the normal and tangential direction is assumed to be the same, then the surface potential is given by Eq. (3):

$$\phi(\delta) = \exp(1)\,\sigma_{max}\,\delta_n \left[1 - \left(1 + \frac{\Delta_n}{\delta_n}\right) \exp\left(-\frac{\Delta_n}{\delta_n}\right) \exp\left(-\frac{\Delta_t^2}{\delta_t^2}\right)\right] \qquad (3)$$

where σ_{max} represents the maximum normal traction at the interface, δ_n is the normal interfacial separation where σ_{max} is attained in a particular case in which there is no tangential separation (Figure 5, right) and δ_t is the shear interface separation for which $(\sqrt{2}/2)\delta_t$ is the shear separation corresponding to the maximum shear stress at the interface (τ_{max}), again for a particular case, but this time in which there is no normal interfacial separation (Figure 5, left). From Eq. (1), (2), accordingly, and (3), the normal and shear interface traction of the interface are obtained and expressed in Eq. (4) and (5). A graphical representation of these two equations for the particular cases mentioned above is shown in Figure 5.

$$T_n = \exp(1)\,\sigma_{max}\,\frac{\Delta_n}{\delta_n} \exp\left(-\frac{\Delta_n}{\delta_n}\right) \exp\left(-\frac{\Delta_t^2}{\delta_t^2}\right) \qquad (4)$$

$$T_t = 2\,\exp(1)\,\sigma_{max}\,\frac{\delta_n}{\delta_t}\,\Delta_t\,(1 + \Delta_n) \exp\left(-\frac{\Delta_n}{\delta_n}\right) \exp\left(-\frac{\Delta_t^2}{\delta_t^2}\right) \qquad (5)$$

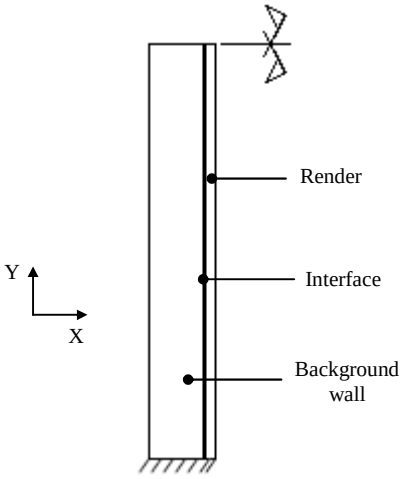

Figure 3. Building facade geometry.

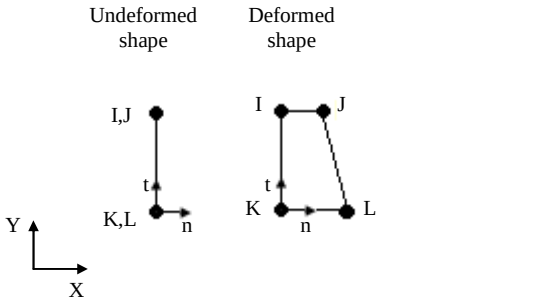

Caption:
I,J,K,L - element nodes
X,Y - global coordinate system
n,t - element coordinate system

Figure 4. Finite element INTER202 geometry.

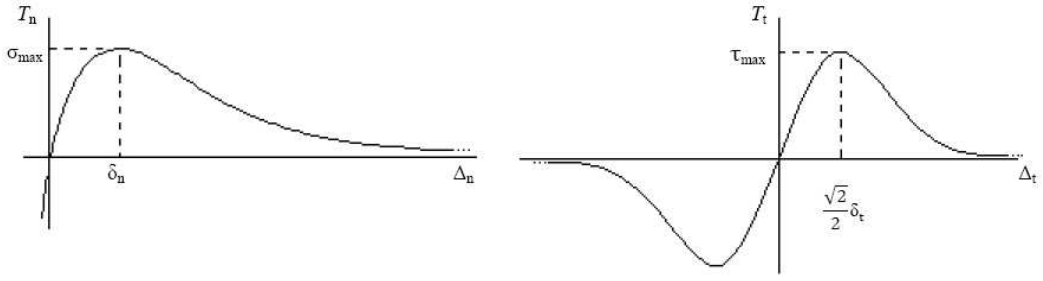

Figure 4. Left, graphical representation of Eq. 5, for $\Delta_n = 0$; Right, graphical representation of Eq. 4, for $\Delta_t = 0$.

The value of the parameters σ_{max}, δ_n, and δ_t must be specified in ANSYS Multiphysics 11.0 so that the interface can be modeled, they represent the interface element inputs. As for the interface element outputs, they consist in the normal and shear interface traction and separation. When the interface traction in the normal or tangential direction is almost as high as the correspondent maximum traction, the interface element stiffness in that direction is almost zero. This fact causes a numerical instability and the solution cannot converge. At the point where the solution doesn't converge it is known that the interface stress is too high, which in reality means the render detachment can occur.

3.3 Modeling a Substrate and a Render with ANSYS Multiphysics 11.0

In the model of the substrate and the render of the facade with the geometry presented in Figure 3, the structural, plane element with four nodes, PLANE182 was used. The render and the substrate material behave according to a linear constitutive model (Figure 6) with a maximum Von Mises stress (σ_1) that the material can resist and after this stress the rupture is reached.

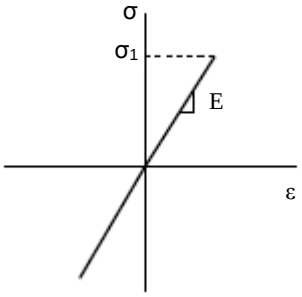

Figure 5. Render and substrate behavior constitutive model.

The outputs of the PLANE182 element are material properties such as Poisson ration, Young's modulus (E), density and maximum Von Mises stress (σ_1). The element's outputs are mainly stresses and strains.

4 NUMERICAL ANALYSYS OF THE INTERFACE OF A WALL/RENDER SYSTEM

4.1 Parametric Analysis

Of the three interface parameters (σ_{max}, δ_n and δ_t) only the value of σ_{max} can be determine through experimental tests, namely, pull-off tests; as the value of δ_n and δ_t are not known it is important to perform an analysis of their influence in the interface behavior. In these analyses the wall/render models were subject to a uniform traction applied on the render surface besides the action of their weight; the value of the three interface parameters were altered and the resulting interface tractions and separation were compared. The first mentioned action intends to simulate the wind suction that affects external render in-use conditions, which is an action that can be directly inputted in the models. The results analysis shows that the values of δ_n and δ_t can have an influence in the shear traction that can be installed in the interface as a result of the normal traction applied. If the analysis takes into account only the normal behavior of the interface in a model were wind suction and the gravity acceleration are the only actions, the value of δ_n and δ_t will serve only as a scale for the interface separation. Therefore no matter the value of these two parameters it is possible to compare interfaces with different properties or characteristics and conclude which can influence adhesion loss.

4.2 Modeling of Factors that Influence Substrate/Render Adhesion

In section 2.2 a list of factors that can influence the render's adhesion to its background was presented. Factors such as render compressive strength, render thickness or the number of layers of the rendering system can be directly modeled in ANSYS. The rest of the factors listed in Table 1 can only be inputted indirectly. For instance, a rough substrate provides a stronger render adhesion; this means that increasing the value of σ_{max} in an interface can simulate surface roughness; however in this case it is

necessary to know *a priori* the effect of surface texture in the mortar's adhesion. So, if the effect that a certain factor has on the adhesion property of the mortar is known, than the factor can be modeled by a change of the values of σ_{max}, δ_n and δ_t.

Some of the listed factors can have an effect in the mortar or the interface characteristics which can be inputted in the numerical model. The lack of cleaning of the background wall, manual application of the mortar, high viscosity of the rendering mortar are all factors that can generate macro-defects in the wall/render interface, which are areas in the interface where there's no bond between the two elements. In this study, an interface for the model presented in Figure 7 was modeled with 10% of macro-defects; the macro-defects were modeled through the elimination of interface elements. The values of the wall/render system properties in this analysis are listed in Table 2; the uniform traction, simulating wind suction, that was applied, has the value of 1000 Pa. The normal traction and separation of the interface with macro-defects were than compared to the ones obtained in a perfect interface, i.e., without macro-defects.

Table 2. Facade wall/render system properties.

Property		Wall		Interface		Render	
E (MPa)		2000		N/A		7420	
υ		0,2		N/A		0,2	
Bulk density (kg/m^3)		900		N/A		1350	
σ_1 (MPa)		0,2		N/A		3,98	
σ_{max} (MPa)		N/A		0.34		N/A	
δ_n (m)	δ_t (m)	N/A	N/A	0,01	0,01	N/A	N/A

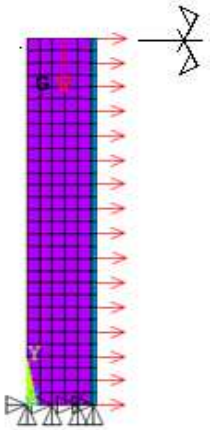

Figure 6. Facade finite element model.

As it can be seen in Figure 8 the presence of macro-defects translates in the increase of stress and separation in the interface, thus adhesion loss is more likely to occur when macro-defects are present.

T_n in the interface without macro-defects	T_n in the interface with macro-defects	Scale	Δ_n in the interface without macro-defects	Δ_n in the interface with macro-defects	Scale
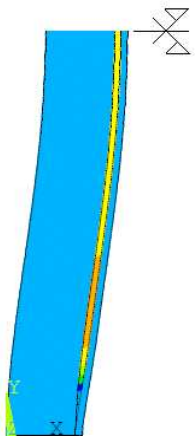	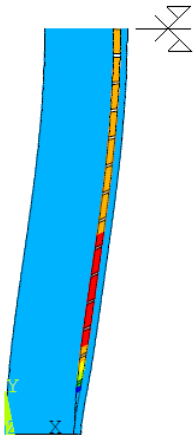	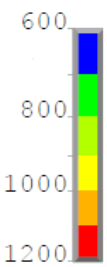	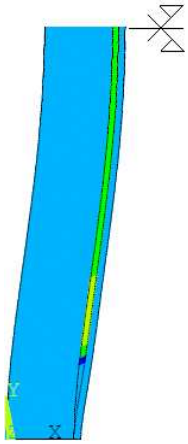	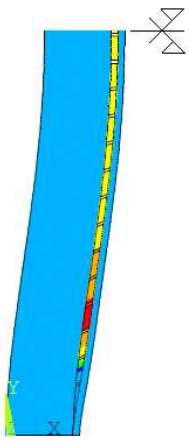	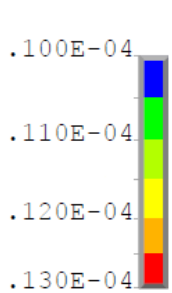

Figure 7. Normal traction and separation in an interface without macro-defects and an interface with macro-defects, when the model has the properties listed in Table 2.

In a similar analysis, cracks were modeled in the render, and the results have shown that the presence of these cracks will increase interfacial separation, therefore will affect adhesion loss.

5 MODELING OF THE PULL-OFF TEST

The model of the pull-off test was based in the principles explained in section 3. The objective of modeling the pull-off test is to determine the value of the render, substrate and interface properties that need to be introduced in the numerical model so that the numerical results can match the experimental ones. For instance, given the set of experimental results (Exp) which is the pull-off force identified according to the facture pattern (P.) (*a*, *b* or *c*), obtained in another on-going Master Thesis, it is possible to reproduce numerically a result (last point of the F-d/δ_n curve) that is consistent with the experimental ones (for the same facture pattern, the numerical value of F_{ANSYS} is between two experimental ones) if σ_{max} = 0,54 MPa, render σ_1 = 1,26 MPa and substrate σ_1 = 0,75 MPa; as shown in Figure 9; *d* represents the displacement of the superior surface of the render during the pull-off test.

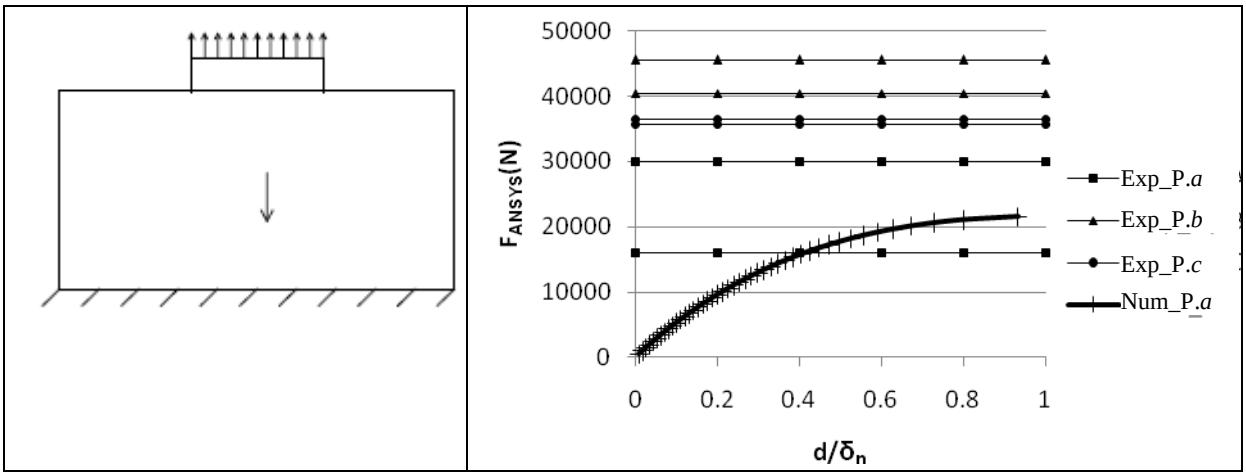

Figure 8. Left, Model of the pull-off test; Right, comparison between experimental results and numerical analysis, when σ_{max} = 0,54 MPa, render σ_1 = 1,26 MPa and substrate σ_1 = 0,75 MPa.

6 CONCLUSIONS

Using ANSYS Multiphysics is possible to model interfaces between a given background substrate and a render. This software provides several finite element types with that purpose; these interface elements behave according with the exponential cohesive zone model simulate the adhesion loss mechanism; this behavior model is defined by three interface parameters σ_{max} (interface resistance), δ_n e δ_t. Several factors have an influence in the mechanism of adhesion loss. All factors can be numerically modeled through value change of the interface parameters; even though their effect on the render adhesion is known. However, some factors like render thickness can be directly modeled and factors like moist-curing or render consistency can be modeled with the introduction of render cracks and interface macro-defects, accordingly.

The results of the pull-off technique model have shown that numerical analysis can complement experimental results in terms of the displacements of the render before its fracture (this information can be used in further research in order to understand the correlation between the mechanism of adherence in in-service walls and the results that are obtained in pull-off technique).

REFERENCES

ASTM 2005 - *Standard practice for periodic inspection of building facades for unsafe conditions*.

ASTM E 2270. Philadelphia: American Society for Testing Materials.

CEN (2003) - *Specification for mortar for masonry - Part 1: Rendering and plastering mortar*. EN 998-1. Brussels: Comité Européen de Normalisation.

CEN 2000 - *Methods of test for mortar for masonry - Part 12: Determination of the adhesive strength of hardened rendering and plastering mortars on substrates.* EN 1015-12. Brussels: Comité Européen de Normalisation.

CPD 1989 - *The Construction Products Directive*. OJ L 40, 11.2.1989, 12p.

Flores-Colen, I.; Brito, J. de; Branco, F. A. 2009 - *In situ adherence evaluation of coating materials*. *In*: Experimental Techniques. 33(3): pp. 51-60.

Flores-Colen, I. 2009 - *Methodology of the performance evaluation in service of façades for predictive maintenance* (in Portuguese). Civil Engineering PhD thesis, IST, Lisboa, 487p.

Freitas, V. P.; Corvacho, H.; Sá, A. V.; Quintela, M. A. 2008 - *Discussing the durability assessment of cement mortars - a contribution for a prediction model*, 11 DBMC, Istanbul, Turkey, May 11-14, CD.

Quintela, M. 2006 - *Durability of external one-coat renders of walls* (in Portuguese). Ms Sc Thesis, FEUP, Porto, 117p.

Xu, X. P.; Needleman, A. 1993 - *Numerical simulation of fast crack growth in brittle solids*. Journal of the Mechanics and Physics of Solids, vol 42: pp. 1397-1434.

XII DBMC
International Conference on Durability of Building Materials and Components
PORTO - PORTUGAL, April 12th-15th, 2011

Applicability of the Pull-Off Test: Teachings from a Large Sample of I*n Situ* Tests

Nuno M.M. Ramos [1]
M. Lurdes Simões [2]
João M.P.Q. Delgado [3]
Vasco Peixoto de Freitas [4]

ABSTRACT

The Pull-off test is a very popular way of evaluating the adhesion strength of renderings or ceramic revetments. Several standards frame the application of this test and its results interpretation. The Laboratory of Building Physics (LFC-FEUP) has used the pull-off test results in several cases to support the diagnosis of causes for building anomalies.

In this article, 56 case studies based on in situ tests are analysed. The sample was retrieved from 16 test reports conducted by LFC-FEUP. In each of these reports different situations were analysed in terms of wall components, expected hygrothermal loads, and in testing procedures followed. This large number of tests support a discussion on two subjects: the applicability of the pull-off test and the parameters that can influence the results observed in this sample.

The first subject, the applicability of the pull-off test, was observed for different systems, including ceramic tiles applied with cement based adhesives, cement based renderings and ETICS. Difficulties and opportunities of the test are analysed for each material.

In the second subject, the variability observed in each case study was used in different correlations revealing patterns that can be expected when applying this test. These results support a discussion on uncertainty appraisal of the pull-off test.

KEYWORDS

Pull-off test; Adhesion strength; Finishing materials.

[1] Faculty of Engineering of the University of Porto (FEUP), Porto, PORTUGAL, nuno.ramos@fe.up.pt
[2] Faculty of Engineering of the University of Porto (FEUP), Porto, PORTUGAL, maires@fe.up.pt
[3] Faculty of Engineering of the University of Porto (FEUP), Porto, PORTUGAL, jdelgado@fe.up.pt
[4] Faculty of Engineering of the University of Porto (FEUP), Porto, PORTUGAL, vpfreita@fe.up.pt

1 INTRODUCTION

The adhesive bonding of exterior revetments applied on façades is an important factor to ensure the safety and durability of the building. The failure of adhesive bonding has imediate consequences and therefore is a common concern for the building industry and building owners. The Pull-off test, classified as a near-to-surface, partially destructive method, is a classic way of evaluating the adhesion strength of renderings or ceramic revetments. Several standards frame the application of this test and its results interpretation. The Laboratory of Building Physics (LFC-FEUP) has used the pull-off test results in several cases to support the diagnosis of causes for building anomalies. In this article, 56 case studies are analysed. The sample was retrieved from 16 reports of in situ inspections conducted by LFC-FEUP.

The objective of this article is to sinthetize the information that resulted from the large number of pull-off test results available at LFC. The average bonding strength and variability for each situation were statistically analysed, allowing for the definition of patterns and correlations of involved parameters, namely substrate, revetment, test procedure and façade exposure.

2 APPLICATION OF THE PULL-OFF TEST

The LFC-FEUP test reports revealed that the pull-off test can be usefully applied for the test of different finishing systems. The test method and its specificities for each application are described in this chapter.

2.1 Test method

The adhesive strength is determined as the maximum tensile strength applied by a direct load perpendicular to the surface being tested. The tensile load is applied by means of a defined pull-head plate glued to the test area. The adhesive strength is the quocient between the failure load and the test area.

On all the tests described in this paper, the test area was pre-cut in situ, fitting the size of the pull-head plates. These could be square metallic plates of 50 mm x 50 mm or circular metallic plates with diameter of 50 mm.

The test machine for direct direct pull tensile force test is in accordance with standard requirements, with the additional feature of automatic control of the applied force provided by an attached electrical engine, as presented in Fig. 1.

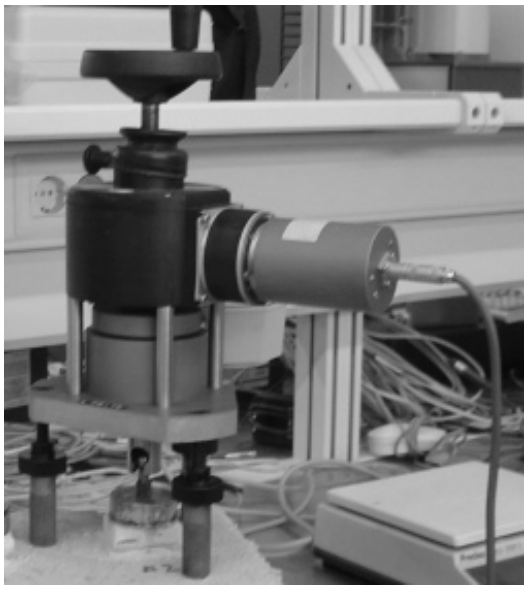

Figure 1. Pull-off test machine.

2.2 Studied systems

Façade cladding systems in Portuguese buildings are frequently composed of ceramic tiles bonded to substrates by means of adhesive. Adhesive bonding strength, both in tension and in shear, plays an important role on the tile bonding strength. Several standard testing methods have been established to measure and evaluate tile bonding strength (see EN 1348 [2007]). One of the difficulties of the implementation of this test in situ is to perform a low disturbance pre-cut of each specimen. Usually, square specimens are preferred, as they are easier to produce. Another aspect is where to take the pre-

cut. If it is performed deep in a render that's acting as subtrate for the adhesive mortar, the failure will probably occur in the substrate, resulting in a false low result. It can however be interpreted as a performance indicator of the substrate and not of the adhesive.

Cement based renderings are also very common in Portuguese façades. The application of the pull-off test in this case is described in several standards (see EN 1015-12 [2000]). A specific analysis must be performed after the test, since a rendering can be produced in one or several layers and, therefore, interpretatiorn is done based on the failure mode which can be cohesive inside a layer or adhesive in an interface between two layers.

Another popular application of the pull-off test is the evaluation of ETICS (External Thermal Insulation Systems) components proposed, for instance, in ETAG 004 [2000]. Again, an adequate pre-cut is essential for the test success. Since insulation is often not fixed continuously to the substrate, testing the thin rendering behaviour implies that the pre-cut must not go too deep into the insulation core.

Although standards exist, supporting the application of the pull-off test to the refered finishing systems, they are meant for laboratory tests and not in situ and therefore chareful adptation has to be made of the proposed methodologies. The RILEM [2004] recomendation is meant for in situ tests of renderings.

The pre-cut on the the three different systems application of the pull-off test is presented in Fig. 2.



Figure 2. Pre-cut a) ceramic tiles, b) rendering, c) ETICS

3 EXPERIMENTAL STUDY

This experimental study is based on data retrieved from inspections of buildings on operation phase. This implies that several factors conditioned the behaviour of the tested components such as the initial quality of the materials, their actual application conditions, substrate, façade exposure, age of the buildings and maintenance operations. The results of these tests cannot be directly compared since the conditions that lead to each set of results are unique.

The available data, however, presented an interesting opportunity to develop a statistical portrait of the adhesive strength that can actually be measured in revetments of building façades. The focus of the study is not only on the average values found but, more importantly, the spread of those values and the factors that influence it. The sample originated by the available data is random as it resulted from the study of buildings whose owners asked for inspections due to façade anomalies.
The results from 16 different in-situ inpections were analysed. In each inspection, different zones in the building were tested, characterized by different components and/or different exposure. The data was therefore grouped by zones of identical conditions, allowing isolating more accurately the

variables that contributed to the measured adhesion strength. The selected studies focused on claddings and cement based renderings as they were the ones with more data available.
Hence, the studied sample includes 213 valid measurements grouped in 56 case studies. All the invalid measurements were discarded from this analysis resulting, for some case studies, in a rather low number of measuremets. Table 1 presents the relation between the different tests and the original inspection report. Table 2 presents the variables that were isolated in this study.

Table 1. Inspection reports and connected case studies.

Inspection report	*Case studies*	*Measurements*
1	5+4+4	13
2	2+3+3+3	11
3	10+10	20
4	5+3	8
5	4+4+5	13
6	2+5+2+7	16
7	3+3	6
8	3+3+3+3+3+2	17
9	5+5	10
10	2+3+3	8
11	3+3+3+3	12
12	3+3+3+6+3+3	21
13	5+5+4	14
14	2+1	3
15	5+5+5+5+5+5	30
16	3+6+2	11

Table 2. Variables considered in this study.

Variable	*Cathegories*	*Frequency*	*%*
Tested Material	Cement based adhesive	97	45.5
	Rendering	116	54.5
Substrate	Concrete	15	7.0
	Stone masonry	35	16.4
	Brick masonry	160	75.1
	Wood-cement panels	3	1.4
Pre-cut	Circular	75	35.2
	Square	138	64.8
Failure mode	Adhesive	81	38.0
	Cohesive	70	32.9
	Plate detachement	21	29.1

The sample is apparently in line with the typicall Portuguse buildings characteristics. A study by Paes Afonso [2003], based on Censos 2001, revealed that rendering has the highest incidence in Portuguese buildings and the sample includes 54.4% of cases where rendering was the tested material. Regarding substrates, concrete and brick masonry are typical solutions for buildings of the last decades while stone masonery is common for older buildings. The only example of a non traditional solution included in this study was the application of ceramic tiles on wood-cement panels. Regarding substrate, there's a clear predominance in these tests of brick masonry, which corresponds to the Portuguese reality.

4 RESULTS

An overview of the results retrieved from the 56 case studies is presented in Figs. 3 and 4, divided between rendering and cement based adhesives. Each case study is represented by the mean value and standard deviation. The graphs also include a reference values for each material, namely 0.3 MPa for renderings and 0.5 MPa for cement based adhesives. The latter value is adopted as reference although an adequate and safe result would be above 1.0 MPa. It can be observed that the mean values for adhesive strength of renderings were typycally low and frequently below the recommended value of 0.3 MPa. The tested cement based adhesives exhibited higher strength and were frequently above the reference value of 0.5 MPa and even above 1.0 MPa. On both types of tested materials, significant variations of the standard deviations could be found. The low values observed, especially for renderings, could be related to the fact that these inspections were done in façades where anomalies could be observed.

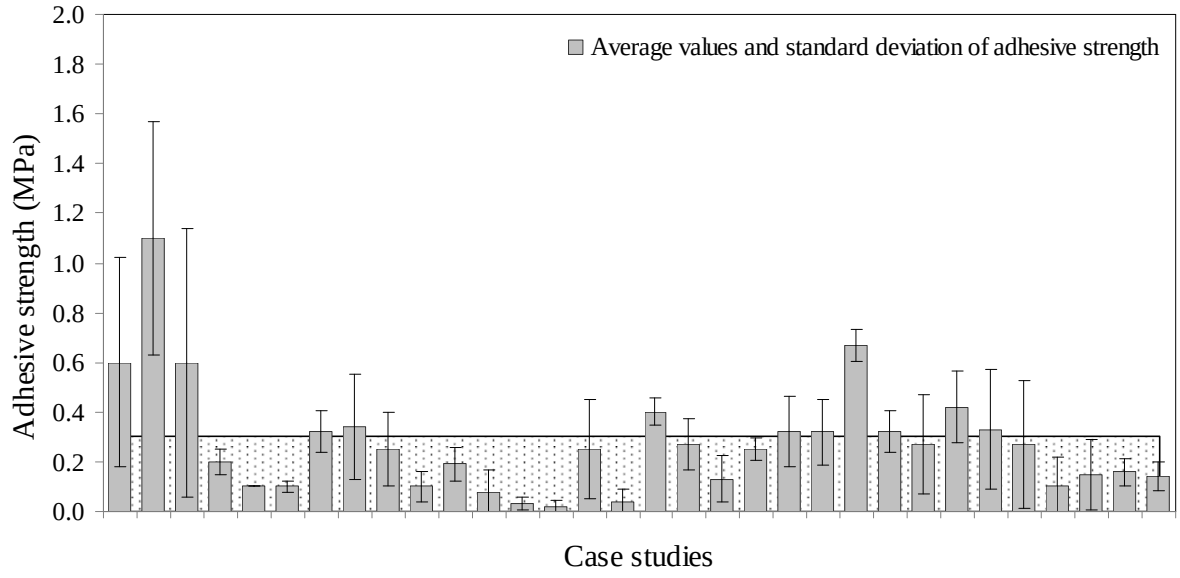

Figure 3. Average values and standard deviation for rendering case studies

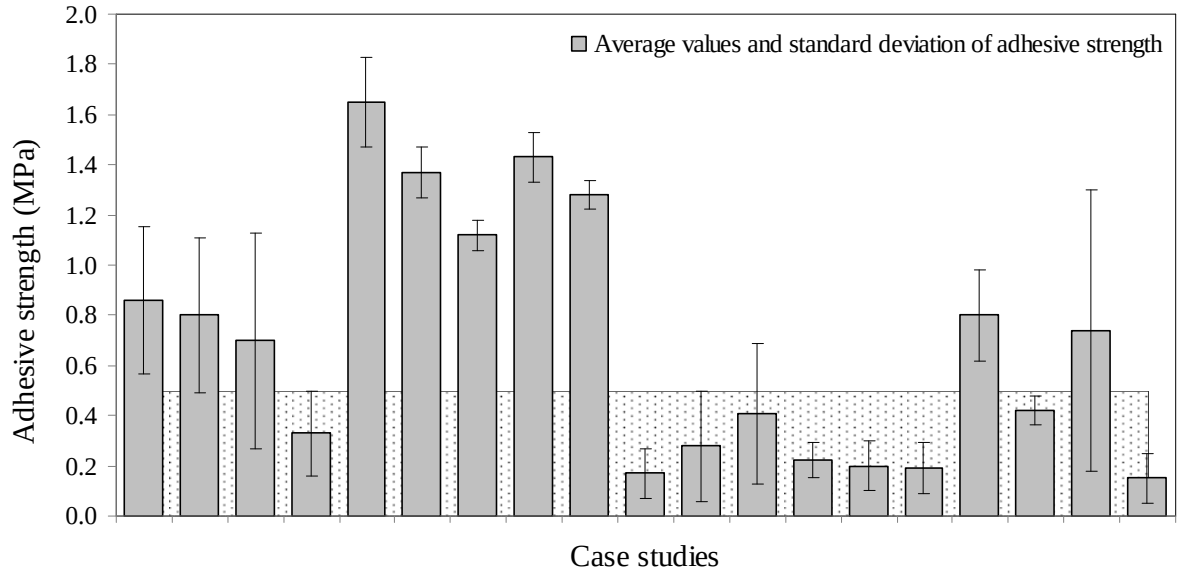

Figure 4. Average values and standard deviation for cement based adhesives case studies

5 ANALISYS

A deeper analysis of the adhesive strength found for renderings and cement based adhesives is presented in Figs. 5 and 6. The distributions found for each tested material were significantly different. While renderings presented a log-type distribution with predominant results below 0.3 MPa, cement based adhesives no theoretical model could be easily assigned. The mean was found above the reference value of 0.5 MPa. The box-plots for each material confirm this observation since, for cement based adhesives, no outliers were defined while for renderings, several values were defined as outliers, all corresponding to high resistance values.

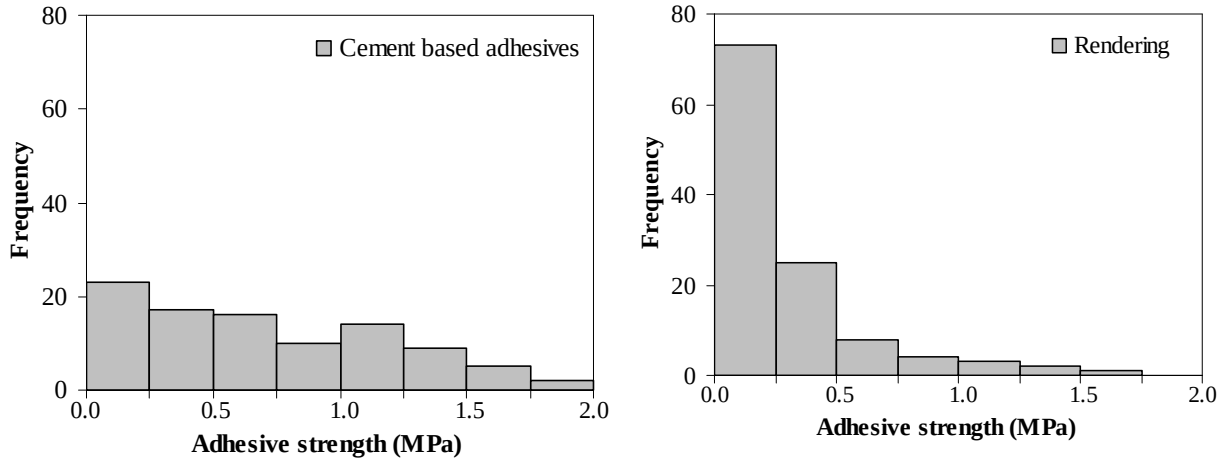

Figure 5. Adhesion strength distribution for the tested materials

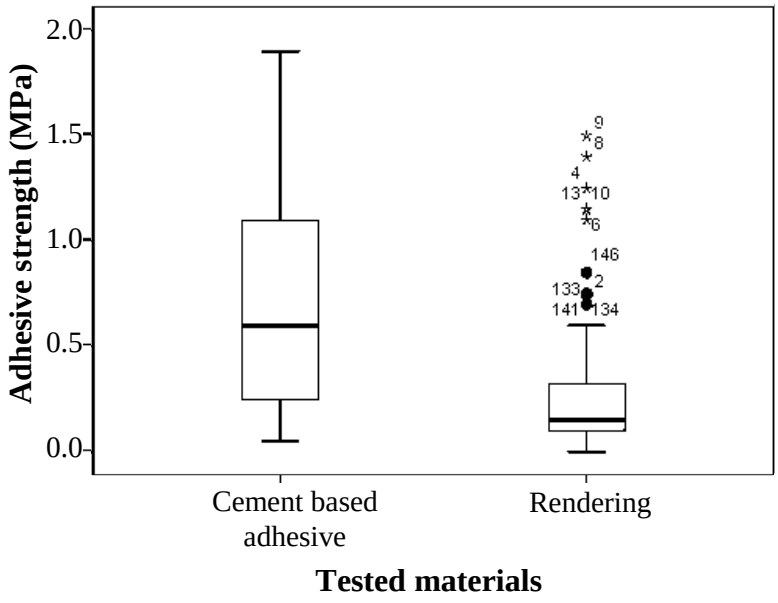

Figure 6. Adhesive strength box-plots for tested materials.

The correlation between solar exposure and mean adhesive strength was tested for renderings. The results are presented in Fig. 7. The results weren't totally conclusive but still it could be observed that the values found on the East oriented façades were higher than the ones found on South and West oriented façades. Surprisingly, the North oriented façades had the lowest values. Except for this orientation, a correlation between surface temperature in summer could almost be derived from these tests. The behaviour of the North façade may implie that other factors, such as wind driven rain or moisture accumulation would have to be taken into consideration. But for the exposure variable the

sample is quite reduced for each cathegory implying that no actual correlations can be strongly supported.

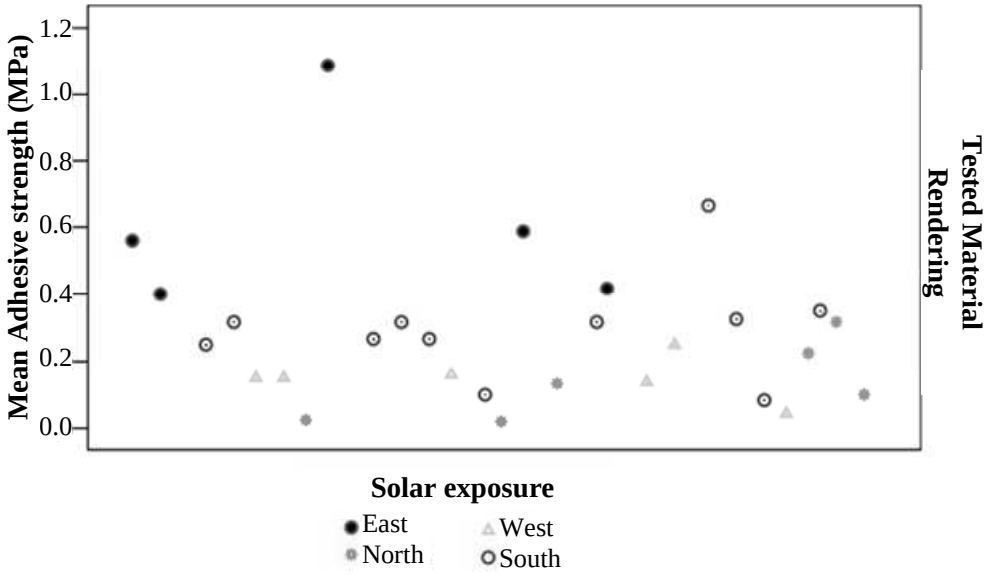

Figure 7. Mean adhesive strength for renderings correlated to solar exposure.

The analysis of the number of measurements influence on the variability of results is presented in Fig. 8. It can be observed that the average variation coefficient is very high and the actual variation can, in a specific test, range from almost 0 to 100%. It can also be observed that the cases where the variation coefficient was very low correspond to tests where a low number of valid pull-offs was performed. The correlation with the number of valid measurements, therefore, seems to indicate that the greater the number of valid pull-offs the greater the probability of not missing the actual variability of adhesive strength under evaluation. The eventual lack of trust in a method that results in such high variability is controlled by standards as minimum values are imposed for single valid tests and not only to the mean value. The problem of in situ tests is that often the adequate number of valid tests is not achieved due to the obvious difficulties in repeating the tests.

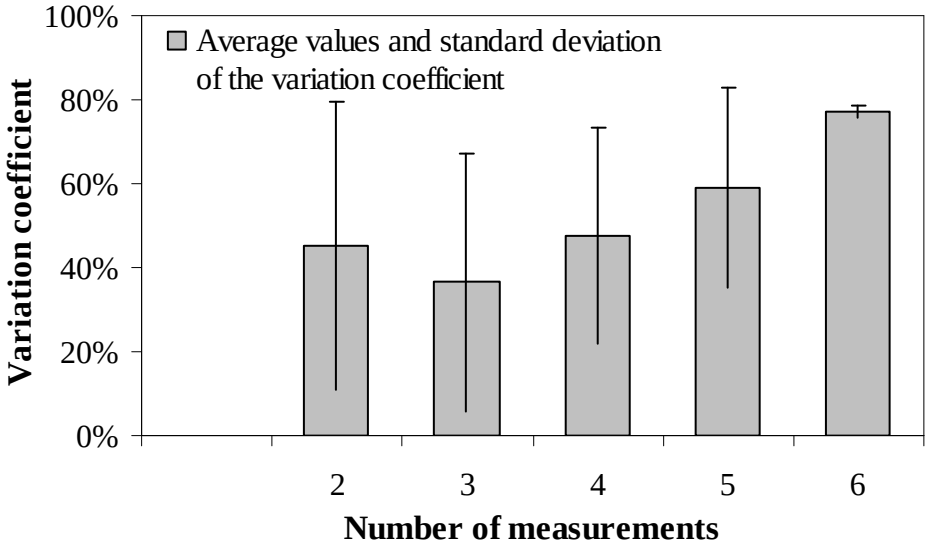

Figure 8. Variation coefficient correlation with the number of measurements per case study.

6 CONCLUSIONS

The analysis of case studies of in situ pull-off test applications to adhesion strength evaluation retrieved from inspections to Portuguese buildings resulted on the following conclusions:

- Pull-off test is used frequently as a decision support tool for building pathology studies;
- Adhesion strength can be measured for different systems and components according to international standards. These standards are however focused on laboratory tests. Documents for in situ measurements are scarse and not adapted to the entire range of components applied on façades;
- Although pull-off tests were applied by LFC-FEUP to different types of components, including ETICS, cement based renderings and cement adhesives used on ceramic tiles, only the tests related to the latter two were explored in a statistical study;
- The adhesion strength distribution found for renderings was logarithmic, presenting many values below recommended resistance while for cement based adhesives no theoretical distribution could be assigned and the mean value corresponded to an acceptable resistance;
- Regarding the influence of façade exposure on renderings adhesive strength, a tendency was found. But the number of cases per orientation is too low to retrieve a definitive conclusion on this subject;
- The variability found in these tests was usually very high, corresponding to variation coefficients ranging from 40% to 100%.

Although a large statistical sample was studied, the number of cases correlated to certain variables weren't sufficiently high to support definitive conclusions. Nevertheless, certain patterns were identified and the variabillity found for adhesive strength in situ tests inspires a cautious interpretation of results and a need for standards adapted to this specific subject.

REFERENCES

EN 1015-12, 2000, *Methods of test for mortar for masonry. Determination of adhesive strength of hardened rendering and plastering mortars on substrates*, Brussels: European Committee for Standardization.

EN 1348, 2007, *Adhesives for tiles. Determination of tensile adhesion strength for cementitious adhesives*, Brussels: European Committee for Standardization.

ETAG 004, 2000, *Guideline for european technical approval of External thermal insulation composite systems with rendering*, European Organisation for Technical Approvals (EOTA), Brussels, Belgium.

Paes Afonso, F., 2003, *Potencialidade do mercado de reparação e manutenção face às características do parque edificado*, Instituto Nacional de Estatística (in Portuguese).

RILEM, 2004, 'Recommendation MDT D. 3. Determination in situ of the adhesive strength of rendering and plastering mortars to their substrate', *Materials and Structures*, **37**, 488–490.

XII DBMC
International Conference on Durability of Building Materials and Components
PORTO - PORTUGAL, April 12th-15th, 2011

Characterization of Wood Mould Fungi by FTIR – A Valuable Step for Prediction of Initiation of Decay

Barun Shankar Gupta [1]
Bjørn Petter Jelle [2]
Per Jostein Hovde [3]
Jonas Holme [4]

ABSTRACT

Wood is widely used as a building and construction material in many countries. Durability and service life are key criteria for a material or component in its optimum operating condition. However, the durability and service life are decreased by decay, and predicting decay initiation and consequently the service life prediction of wood materials are important tasks. Deterioration may initiate either by solar radiation, biological or mechanical attacks. Wood fungi are aggressive biological agents at certain climatic conditions. In many cases, the signs of mould fungi are the predictor of onset of attack by decay fungi. The objective of this work is to characterize wood mould fungi through attenuated total reflectance - Fourier transform infrared (ATR-FTIR) spectroscopy. Four common fungi were selected, namely, *Aureobasidium pullulan*, *Alternaria alternate*, *Cladiosporium cladosporides* and *Ulocladium atrum*. The four fungi were inoculated and grown on fresh randomly selected pine wood specimens. Preliminary data reveal that ATR-FTIR spectroscopy may be used to differentiate various fungi. Specifically, the regions showing the transmittance bands of fatty acids, amide and polysaccharides were clearly distinguished. Further research will involve detailed spectral analysis and chemical interpretation of representative spectra.

KEYWORDS

Climate, Degradation, Service life, Durability, ATR-FTIR.

[1] Norwegian University of Science and Technology, Department of Civil and Transport Engineering, Trondheim, Norway, barun.gupta@ntnu.no
[2] Norwegian University of Science and Technology, Department of Civil and Transport Engineering, SINTEF Building and Infrastructure, Department of Materials and Structures, Trondheim, Norway, bjorn.petter.jelle@sintef.no
[3] Norwegian University of Science and Technology, Department of Civil and Transport Engineering, Trondheim, Norway, per.hovde@ntnu.no
[4] SINTEF Building and Infrastructure, Department of Materials and Structures, Trondheim, Norway, jonas.holme@sintef.no

1 INTRODUCTION

Wooden components are usually used as outer envelopes for building façades as well as for structural load bearing members. Wooden façades may have painted or unpainted surfaces. The unpainted surfaces are a tradition for carved walls and log houses in Scandinavian countries since many centuries (Cestari et al. 2002). Within a built environment, façade components endure above ground exposure and control large parts of the building heat, air and moisture (HAM) balance. Biodeterioration of wood is a critical factor for wood industries and end users. Humidity, temperature, material properties and time of wetness (TOW) may generate a favorable condition for mould, stain or rot fungi to grow on wood. Dampness, moist air, moisture accumulation and mould are potential creators of complicated problems to the inhabitants. Stains are getting importance because along with aesthetic damage they may conceal incipient decay.

Any leakage of moisture through façades would evidently lead to serious attacks by mould fungi inside the building. Mould fungi have serious effects on breathing air quality in cold areas where the buildings are made air tight to preserve indoor heat. Depending on the availability of nutrient sources, temperature, carbon / nitrogen ratio, pH, oxygen and water, mould fungi act as a quick invader of wood. Fungi are filamentous eukaryotes that are principal decomposers of organic materials and are food sources for a range of microfauna and insects. Signs of stain or mould fungi are indicators that the internal moisture content of the wood substrate has reached the optimum moisture concentrations for faster attacks by other wood attacking microorganisms and insects.

Mould and stain growth on wood are more common than decay or rot. Problems caused by mould fungi are aesthetic damage, odour and occupational illness like bronchitis, fever, asthma, mucous irritation and chronic pulmonary diseases. Common mould fungi for buildings are *Chaetomium* spp., *Ophiostoma* spp., *Ceratocystis* spp., *Ascomycetes* spp., *Leptographium* spp., *Cephaloascus* spp., *Phialophora* spp., *Alternaria* spp., *Acremonium* spp., *Aspergillus* spp., *Aureobasidium* spp., *Fusarium* spp., *Oidiodendron* spp., *Cladiosporium* spp., *Penicillium* spp., *Stachybotrus* spp., *Trichoderma* spp., *Coprinus* spp. and *Peziza* spp. (Singh, 1994 ; Strong, 2005 ; Zabel, 1992) . The risk of mould growth and consequent fungal decay can be prevented / eliminated by wiser design and careful control of moisture content of wood. Ideally, the moisture content of wood should be below 20 % to avert the colonization of any type of fungi. Typical moisture content for rapid growth of mould fungi at wood surface is 80-85 % even at temperatures as low as 10 ^{o}C. Onset of attack at limit state is facilitated by the water in wood which in turn facilitates germination, hyphal penetration and survival of spores. Hyphae penetrate into wood cells by the process of enzymatic degradation of cellulose and other wood components. Refractoriness of wood species and the presence of natural extractives and phenolic substances prevent enzymatic breakdown of cellulose and hemicelluloses, and thereby hindering rapid growth of decay. Spraying of fungicide and / or sodium hypochlorite solution at the freshly cut moist wood surface prevents mould and decay fungi attack. For old houses and components, paint and preservative chemicals act as water repellants to improve the durability and prevent decay hazard.

The difference between a mould and decay attack is that a mould attack does not cause any structural damage. Decay fungi on the other hand, change the elastic modulus (MOE), flexural properties and mass of wood. However, apart from other standardized durability levels, wood quality is judged by the mould index (Gobakken et al. 2010; Viitanen 1997). According to this index a surface is graded on appearance by a mould rating scale and can be categorised as rejected / damaged due to the inability to satisfy aesthetic requirements. Aesthetic distortion of wood surfaces may occur due to human abuse and also by deposition of foreign matters. Aesthetic losses are difficult to quantify and may be negligible over the service life for short term uses, but could become significant for long term use. Repair and maintenance costs for damaged components add to the original costs of the building construction and changes the lifetime distribution curve for the components. As detailed in the CIB W080 / RILEM TC 140 guidelines (Jernberg et al. 2004), the degradation factors critical for predicting service life are mechanical, electromagnetic, thermal, chemical and biological agents. These factors are applicable both for sheltered and unsheltered conditions as per UN-ECE-ICP draft (Haagenrud 1996). The microclimate / microenvironment or meteorological factors that are at the closest

proximities to the material surfaces are crucial for predicting material degradation. Though many investigations have been performed on degradation measurement and mapping, the problem of complexities involved in climatic load at different geographical locations for the same building system shows clear lack of data. The objective of this study is to define a quantification process to characterize and make distinction in common mould fungi that may occur on wooden façades. Fourier transform infrared (FTIR) spectroscopy is a powerful tool to characterize a material up to several micron depths (Ehrlich et al. 2007; Erukhimovitch et al. 2005; Genestar and Palou 2006; Gupta et al. 2010; Jelle et al. 2008; Mohan 2004; Naumann et al. 2005; Novák et al. 2010). The broader objective is to generate a FTIR database for mould and decay fungi that would lead to a procedure to prevent wood damage and help wood pathologists to formulate a roadmap for sustainable use of natural resources.

2 EXPERIMENTAL

Materials: Pine woods (*Pinus* sp) obtained from commercial sources were cut to 70 mm x 70 mm x 25 mm square pieces. Four fungi, namely, *Aureobasidium pullulan* (DSM 2404), *Alternaria alternate* (DSM 62010), *Cladiosporium cladosporides* (DSM 62121) and *Ulocladium atrum* (DSM 63068) were supplied by the Norwegian Forest and Landscape Institute (UMB), Ås, Norway. The fungal strains were originally procured from the Deutsche Sammlung von Mikroorganismen und Zellkulturen GmbH (DSM, Germany).

Inocculation: Four types of fungi were cultivated separately in an agar medium containing 0.5 l of ionized water, 6.25 g Bacto malt and 10 g NMD agar (NMD = Norsk Medisinal depot AS). Approximately 50 ml of sterilized water having 0.02 % Tween 80 (1.073-1.083 density at 20 ^{o}C / 4 ^{o}C, 65-80 hydroxyl value, MERCK, Germany) was poured on the top of the agar containing grown up fungi and stirred with a spatula. Immediately, the resulting aqueous blends containing fungal spores were filtered through cotton in a 100 ml Erlenmeyer flask. One drop of the fungal spore suspension was poured on a counting glass (0.0025 mm^2 / 0.04 mm^2, Bürker CE, Germany) to count spores under microscope (Olympus BX 51). The spore concentration was determined by the following formula:

$$Spore\,Concentration = \left[\frac{No.of\ spores\ in\ a\ 0.25\,mm \times 0.25\,mm\ square}{0.0000125\,ml} \right] \quad (1)$$

For all four types of fungi, the spore concentration was maintained at 2 x 10^6 spores/ml. More water was added to increase the volume of the spore suspensions to 200 ml in a 250 ml glass bottle. Approximately 50 ml of each fungal spore suspension was poured into an Erlenmeyer flask fitted with a glass nozzle and air pump. Wooden specimens were completely immersed in water for 2 days before inoculation. Each specimen was numbered and randomized to generate 5 sets of 5 wooden specimens. Each set containing five pieces of wood (70 mm x 70 mm) were spray-coated homogeneously by each type of fungal spore suspensions by the pump. Figure 1 shows the set-up box for fungal growth on wood surfaces. Inoculated wood pieces were stored in separate glass covered plastic trays at a saturated humidity condition and ambient laboratory temperature (21 ^{o}C - 23 ^{o}C). Wooden specimens in boxes were monitored for 2 months. Each plastic box contained water to maintain the atmospheric humidity at saturation level.

FTIR spectroscopy: The wooden surface grown fungi were harvested by tweezers and qualitative analysis of functional groups was performed by an attenuated total reflection (ATR) Fourier transform infrared (FTIR) spectrometer (Thermo Nicolet 8700). Fungi specimens were pressed against a diamond crystal in the Smart Orbit accessory of the FTIR. The spectrometer was purged (60 psi) continuously by a gas generator (Parker Balston, USA) to remove CO_2 and H_2O from the spectrometer. An average of 32 scans at a resolution of 4 cm^{-1} was recorded for each spectrum by the OMNIC software. A minimum of three random replicate spectra were recorded for each type of fungi. No further spectral correction was performed. In order to accommodate the variation in spectral baseline, we proposed the cell amide index by normalizing the absorbance of amide peaks at 1650 cm^{-1} (amide I) and 1546 cm^{-1} (amide II) by the fatty acid at 2921 cm^{-1} :

$$Cell\ amide\ index = A.I. = \frac{Absorbance\ at\ 1650\,cm^{-1}\ or\ 1546\,cm^{-1}}{Absorbance\ at\ 2921\,cm^{-1}} \quad (2)$$

Where absorbance (A´) of a pure specimen is governed by Beer-Lambert's law as $A' = \log_{10}(1/T)$, T being the transmittance.

SEM: A piece of carbon tape was touched on the top of fungal colony to collect spores and hyphae on tape. The tape was used for scanning electron microscopy (SEM) images from S-3400N Hitachi SEM at an accelerating voltage of 15 kV. Back scatter images (BSE) were captured for better representation.

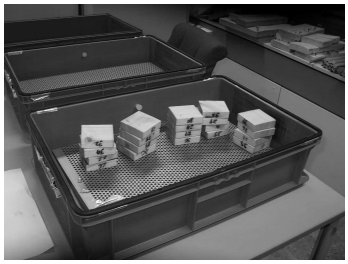

Figure 1. Wood mould fungi culture boxes covered by glass plates.

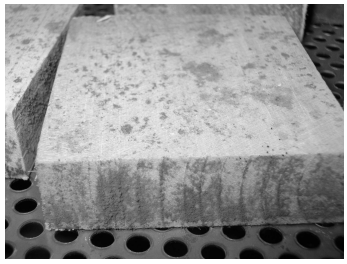

Figure 2. Mould growth (*Aureobasidium* sp.) on pine wood substrate.

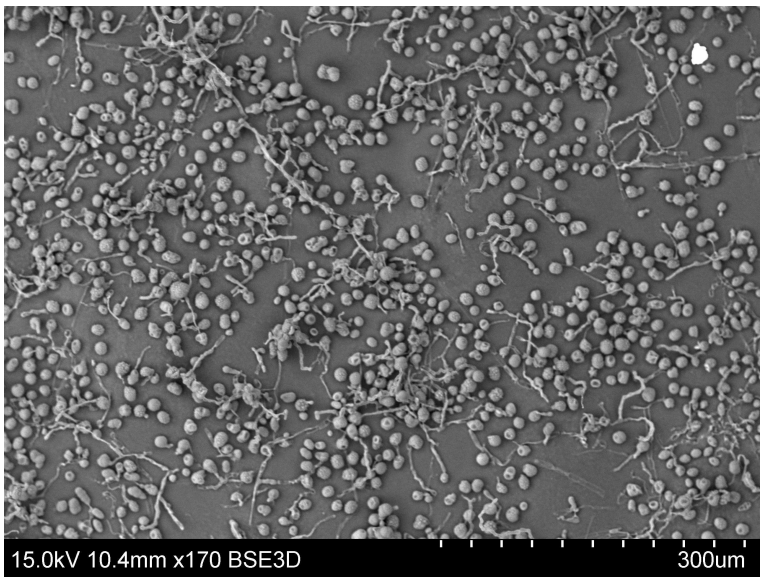

Figure 3. SEM image of mould fungi spores and hyphae (background material is a carbon tape).

3 RESULTS AND DISCUSSION

In home environment, sources of *Cladiosporium*, *Alternaria* and *Aureobasidium* are carpet, wool materials, humidifiers, HVAC systems and indoor plants especially if they are moistened. Fungi reproduce by spores that serve as a mean of dissemination, surviving in unfavorable condition and as gametes. Spores are formed from hyphal cells. A single filament of fungi is called hypha.

3.1 Image study

Figure 2 shows the images of fungal growth on a wood surface after 8 weeks of inocculation. Mould fungi were formed in patches on the surface of the wood. As observed in Figure 2, the growth of fungi has a negative effect on the aesthetic property of the wood. Susceptibility of the sapwood against fungi is evident. The SEM microscopic image in Figure 3 shows the spores and hyphae of mould fungi cultivated on agar plates. The tiny, round shaped spores are invisible by human eyes and have a dimension of 5 µm - 40 µm in diameter. The ribbon shaped hyphae are ~ 2 µm in width. Colony of the

fungal spores and hyphae in collection is known as mycelium that gives discoloration to the surface as seen in Figure 2. Colonization / conglomeration of the hyphae varied distinctively from species to species. Compared to other studied species, the growth of *Aureobasidium pullulan* was faster on wood.

3.2 Qualitative FTIR Spectroscopy

Figure 4 shows the best survey spectra for all types of fungi in mid-IR region. There is a general similarity in the spectral pattern at higher wavenumbers. The spectral regions correspond to the following structures: broad 3300-2500 cm^{-1} for bonded O-H stretching vibration, shoulders at 2800-2500 cm^{-1} for overtones and coupling between O-H in-plane bending and C-O stretching vibration region of fatty acid, 1700-1600 cm^{-1} for carbonyl and C=O stretching vibration of amide I, 1620-1500 cm^{-1} for N-H in-plane bending vibration of amide II, 1400-1250 cm^{-1} for C-N stretching and N-H in-plane bending of amide III, 770-620 cm^{-1} for OCN bending deformation of amide IV band, 700 cm^{-1} for N-H out-of-plane bending of amide V, 630-530 cm^{-1} for OCN bending vibrations of amide VI band and 1200-900 cm^{-1} for polysaccharides in cell structure. Amide bands appeared from proteins or from cell wall chitins.

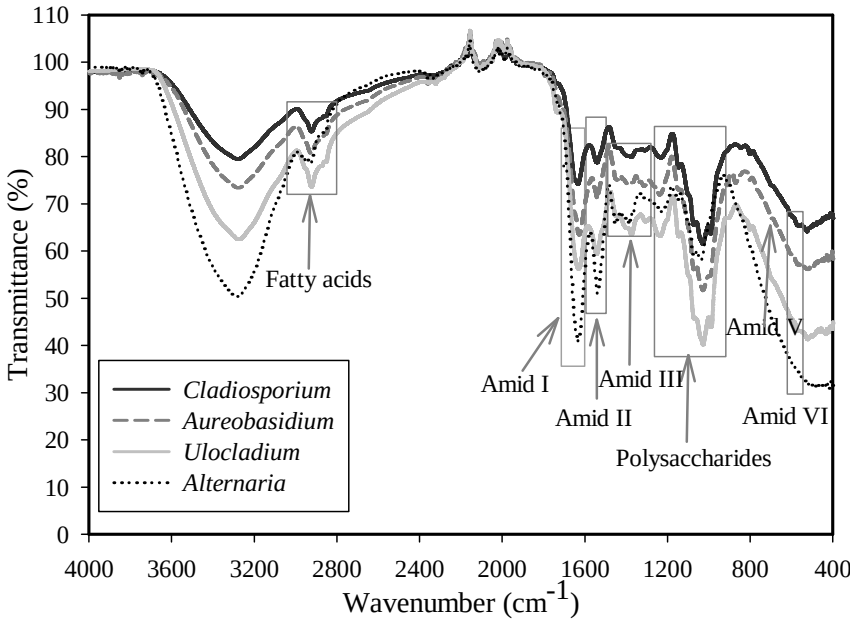

Figure 4. Transmittance FTIR spectra of four wood mould fungi.

Figure 5 shows spectral region of 1800-700 cm^{-1}. The 'finger print' region shows dominant band at ~1650 cm^{-1} for C=O stretching vibrations of protein amide I, 1546 cm^{-1} for N-H in-plane bending of protein amide II and the band at 1460 cm^{-1} for asymmetric CH_3 bending modes of the protein ethyl groups. Cell lipids show band at 1465 cm^{-1} for CH_2 bending mode, band at 1402 cm^{-1} for C=O symmetric stretching of COO groups and the band at 1377 cm^{-1} for C-H bending mode of CH_2. Phospholipids and PO_2 show bands at 1237 cm^{-1} and 1082 cm^{-1} for asymmetric stretching and symmetric stretching vibrations, respectively.

The cell carbohydrates show bands due to vibration modes at 1064 cm^{-1} of CH_2OH and C-O stretching vibration coupled with the C-O bending mode, 1773 cm^{-1} for C=O carboxyl stretching vibration, 1713-1711 cm^{-1} for carboxyl C=O, 1662-1659 cm^{-1} for amide C=O, 1592 cm^{-1} and 1615 cm^{-1} for asymmetric COO^-, 1546 cm^{-1} and 1552 cm^{-1} for NH bending deformation, 1502 cm^{-1} and 1516 cm^{-1} for C=C aromatic, 1454 cm^{-1} and 1466 cm^{-1} for CH_2 bending deformation of lipid and polysaccharide, 883-892 cm^{-1} for β-chitin, γ-CHx vibration at 962 cm^{-1} of α-chitin and 750-700 cm^{-1} for C-H out-of-plane bending vibration. In general, from Figure 5 it might be said that there are four regions, namely, RI, RII, RIII and RIV that show qualitative variation in cell contents for different fungal species.

Specifically, the peak at 802 cm^{-1} is absent for *Alternaria* sp, 877 cm^{-1} is absent for *Alternaria* sp and *Ulocladium* sp, 1200 cm^{-1} is absent for *Aureobasidium* sp, 1276 cm^{-1} absent for *Alternaria* sp, shoulder at 1523 cm^{-1} is absent for *Alternaria* sp and 1654 cm^{-1} is absent for *Ulocladium* sp.

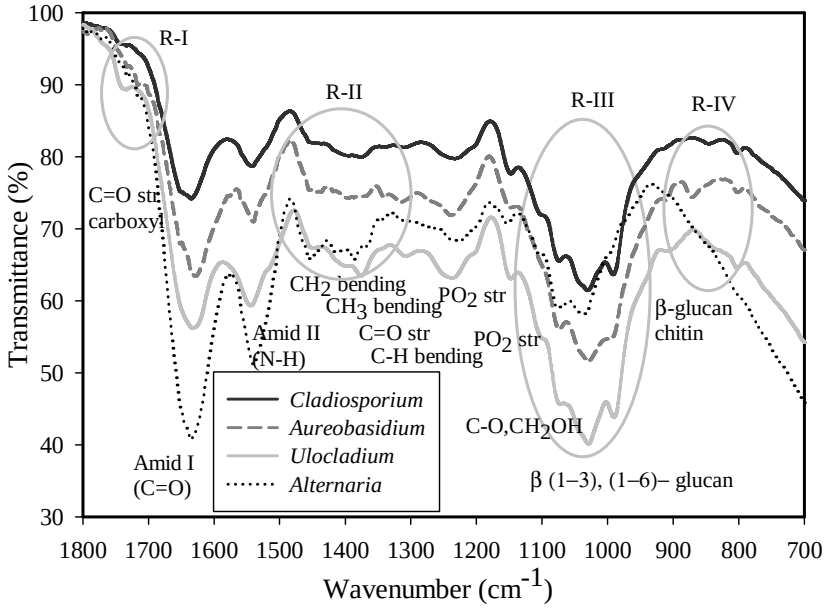

Figure 5. Spectra showing infrared bands for four wood mould fungi.

For example, Figure 6 shows the pattern of the spectral region 1750-1700 cm^{-1} (80-100 %T) for three replicates of four types of wood mould fungi. *Alternaria* sp and *Aureobasidium* sp shows two distinct peaks at 1733 cm^{-1} and 1717 cm^{-1}, *Ulocladium* shows a broad peak at higher wavenumber 1740-1733 cm^{-1} and *Cladiosporium* shows a relatively flattened appearance. If the same process of magnification of IR band is followed for all the regions, similar evidence of difference in spectral pattern between fungi is expected. However, increase in number of replicates will add confidence to the observations.

3.3 Quantitative FTIR Spectroscopy

Figure 7 shows the arithmetic mean of the amide indexes (A.I.) for the four fungal types as calculated from Equation 2. Each error bars denotes one standard deviation of the mean value. The A.I. calculated for Amid I for *Alternaria* sp. is maximum (3.03 ± 0.35) as compared to the other studied fungi species. On the other hand, the Amid II is minimum for *Cladiosporium* sp. (1.54 ± 0.03). Contrarily, the A.I.s for both Amid I and Amid II for *Ulocladium* sp. are nearly same. Absorbance is the amount of energy that is used for vibration of a chemical bond. Higher absorbance indicates greater density. Therefore, the fatty acid content for the fungi *Cladiosporium* sp., *Aureobasidium* sp. and *Ulocladium* sp. are less than the amount of fatty acid found in the cells of *Alternaria* sp. making their A.I . nearly 1.0. However, the disparity in the amount of spores present in each inspected specimen could be the other important factors for A.I. variation. Moreover, there are indeed quantitative differences between the four types of fungi.

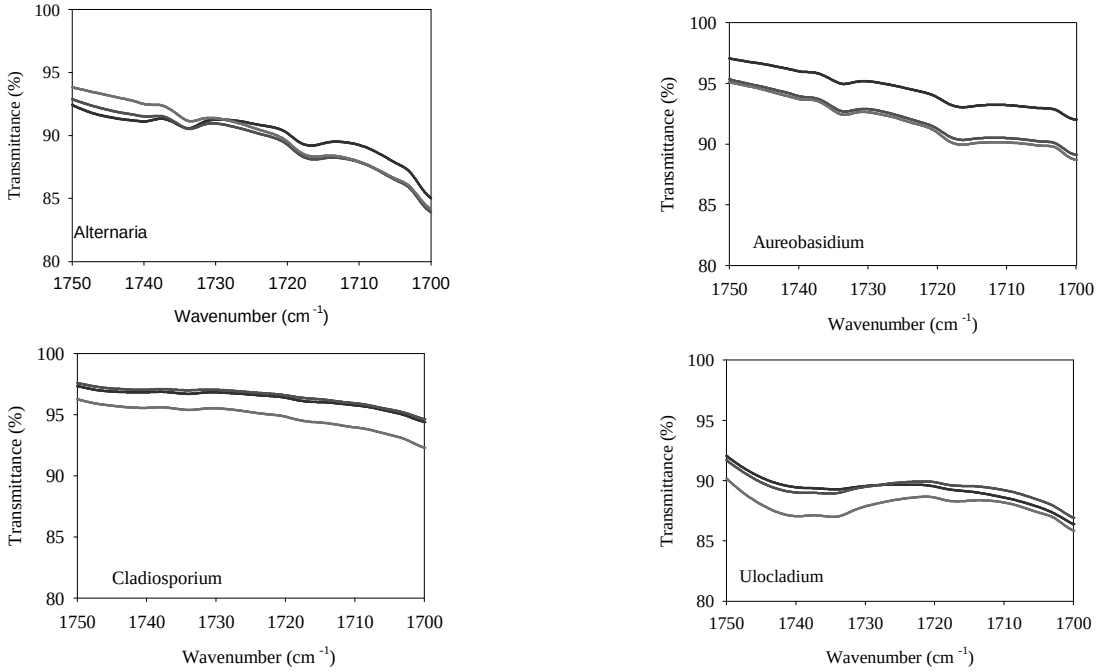

Figure 6. IR band for carboxyl group of *Alternaria, Cladiosporium, Aureobasidium, Ulocladium* spp respectively.

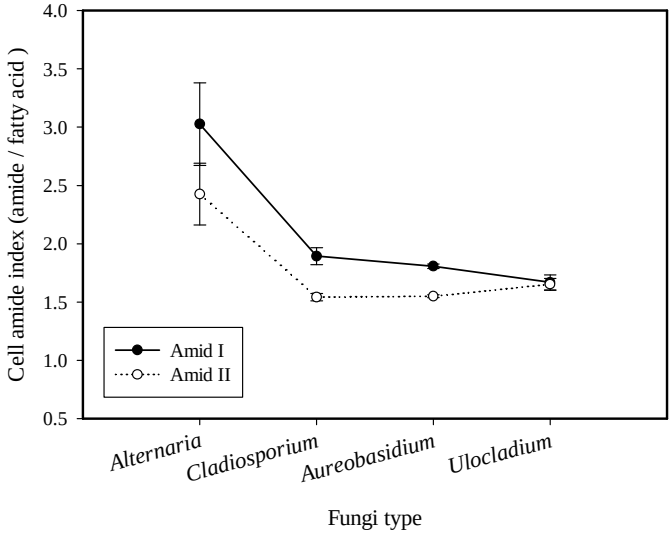

Figure 7. Amide index (absorbance) of cellular materials from 4 wood mould fungi (Eq. 2).

4 CONCLUSIONS

Four types of mould fungi have been successfully cultivated on Norwegian pine (*Pinus* sp.) wood surfaces in laboratory conditions. It was observed that the *Aureobasidium* sp. is a much more rapid invader than the other species. Fungal cellular contents were characterized by the FTIR spectroscopy. Amides, fatty acids and carbohydrates show characteristic bands at the mid-IR region. Four separate spectral regions comprising carboxyl, carbohydrates and cell-glucans show qualitative differences between the types of fungi studied. The amide index formulated with the fatty acid peak as reference, show considerable quantitative differences between *Alternaria* sp. and other fungal species. The same procedure may be followed in future for quantitative determinations of the cell-glucan complexes without performing complex cellular protein extraction procedures. The present study can also be used to initiate microbial burden based research to create a data bank of wood fungi and help improve the currently used ISO standard by including indoor air quality guidelines (ISO 15686-1 2000). Furthermore, quantitative FTIR characterization of fungi at the onset of visible fungal attack on wood

can be used (a) to determine whether the fungi is a mould or a decay fungi, (b) to modelgrowth of wood mould and decay fungi.

ACKNOWLEDGMENTS

The authors would like to thank the Research Council of Norway, Viken Skog BA, Treindustrien, the Wood Technology Research Fund at the Norwegian Institute of Wood Technology, Jotun AS and Kebony ASA for the financial support of the research project. Further, we would like to thank the research partners of the project for the research cooperation – the Norwegian University of Life Sciences (UMB), the Norwegian Forest and Landscape Institute (Skog og Landskap) and the Norwegian Institute of Wood Technology (Treteknisk). Additionally, the first author would like to acknowledge personal communication with Dr. Lone Ross Gobakken from UMB-Ås.

REFERENCES

Cestari, C.B., Faria, J.A., & Soikkeli, A. 2002. *European timber buildings as an expression of technological and technical cultures- Proceedings of Culture 2000 project: Finnish and Portuguese actions* Paris, Elsevier.

Ehrlich, H., Maldonado, M., Spindler, K.D., Eckert, C., Hanke, T., Born, R., Goebel, C., Simon, P., Heinemann, S., & Worch, H. 2007. First evidence of chitin as a component of the skeletal fibers of marine sponges. Part I. Verongidae (Demospongia : porifera). *Journal of Experimental Zoology Part B-Molecular and Developmental Evolution*, 308B, (4) 347-356.

Erukhimovitch, V., Pavlov, V., Talyshinsky, M., Souprun, Y., & Huleihel, M. 2005. FTIR microscopy as a method for identification of bacterial and fungal infections. *Journal of Pharmaceutical and Biomedical Analysis*, 37, (5) 1105-1108.

Genestar, C. & Palou, J. 2006. SEM-FTIR spectroscopic evaluation of deterioration in an historic coffered ceiling. *Analytical and Bioanalytical Chemistry*, 384, (4) 987-993.

Gobakken, L.R., Høibø, O.A., & Solheim, H. 2010. Mould growth on paints with different surface structures when applied on wooden claddings exposed outdoors. *International Biodeterioration & Biodegradation*, 64, (5) 339-345.

Gupta, B.S., Jelle, B.P., Hovde, P.J., & Rüther, P. 2010. FTIR spectroscopy as a tool to predict service life of wooden cladding. *Proceedings from CIB World Congress 2010, Salford, U.K., May 10-13*.

Haagenrud, S.E. 1996. Guide and bibliography to service life and durability research for buildings and components, Part 2: Factors causing degradation. *Joint CIB W080 / RILEM TC 140 - Prediction of Service Life of Building Materials and Components* 1-104.

ISO 15686-1 2000. *Building and constructed assets - Service life planning.* International Organization for Standardization, Geneva, Switzerland.

Jelle, B.P., Myklebost, I., Holme, J., Hovde, P.J., & Nilsen, T.N. 2008. Attenuated total reflectance (ATR) Fourier transform infrared (FTIR) radiation studies of wood rot decay and fungus growth on building materials. *Proceedings of the 11 DBMC International Conference on Durability of Building Materials and Components, Istanbul, Turkey, May 11-14*, 2, 665-672.

Jernberg, P., Sjöström, C., Lacasse, M., Brandt, E., & Siemes, T. 2004. Guide and bibliography to service life and durability research for buildings and components, Part 1: Service life and durability research. *Joint CIB W080 / RILEM TC 140 - Prediction of Service Life of Building Materials and Components* 1-59.

Mohan, J. 2004. *Organic Spectroscopy- Principles and Applications*, Second ed. Alpha Science International Ltd., Harrow, U.K.

Naumann, A., Navarro-Gonzalez, M., Peddireddi, S., Kues, U., & Polle, A. 2005. Fourier transform infrared microscopy and imaging: Detection of fungi in wood. *Fungal Genetics and Biology*, 42, (10) 829-835.

Novák, M., Synytsya, A., Veselá, A., Gomba, G.K., & C´opíková, J. 2010. Structural investigation of glucan complexes isolated from *Phellinus* and *Inonotus* wood fungi. *Chem.Listy* (104) 236-242.
Singh, J. 1994. *Building mycology, management of decay and health in buildings*, E & FN Spon, London, U.K..

Strong,N., Webber,J., & Eaton,R. 2005. Factors affecting the fungal colonization of pine lumber. *Forest Pathology*, 35, (3) 195-203.

Viitanen, H.A. 1997. Modelling the time factor in the development of mould fungi - The effect of critical humidity and temperature conditions on pine and spruce sapwood. *Holzforschung*, 51, (1) 6-14.

Zabel, R.A. & Morrell, J.J. 1992. *Wood microbiology- Decay and its prevention*, Academic Press, Inc., U.S.A.

XII DBMC
International Conference on Durability of Building Materials and Components
PORTO - PORTUGAL, April 12th-15th, 2011

Durability of the Facades from the Perspective of Architectural Decisions

Osmar João Consoli [1]
Wellington Longüini Repette [2]
Maria Alba Cincotto [3]

ABSTRACT

The aging of buildings is a natural process but it can be accelerated by deficiencies and omissions on construction specifications, resulting in premature need for maintenance and restoration. The objective of this study is to, within a selection of buildings in Brazil, diagnose the diseases found on façades and originated due to bad design practices. The methodology used was to confront the results of post occupancy evaluations, the specifications that were part of the architectural building projects and the maintenance records. The information gathered supported the understanding of the most incident pathological phenomena. The data were mapped accordingly with the type of occurrence, frequency and severity of the problem, making possible the identification of problems related with errors or omissions in the façades design. The results show that there are several problems derived from omission of construction details, specifications, and lack of a schedule for maintenance actions that could be easily improved in order to result more durable and less costly building façades in Brazil.

KEYWORDS

Building façades, durability , building problems, design specifications.

[1] Universidade Tecnológica Federal do Paraná (UTFPR), Pato Branco, BRASIL, oconsoli@gmail.com
[2] Universidade Federal de Santa Catarina (UFSC), Florianópolis, BRASIL, wellington@ecv.ufsc.br
[3] Universidade Federal de São Paulo (USP), São Paulo, BRASIL, maria.cincotto@poli.usp.br

1 INTRODUCTION

Since the beginning, humankind has been seeking shelter, and modern buildings are but an expression of that protection. Buildings must provide protection against natural phenomena such as rain, solar radiation, changes of temperature, winds, humidity, atmospherical pollution, among others, in order to offer enough conditions to answer the needs of users, as described in the 1984's ISO-DP 6241.

The façades durability depends on several interdependent factors and how these factors are delt with along the many phases of construction, especially during design. Many different tools for service life prediction are available to help designers to estimate buildings and components durability, altough most archtects in Brazil do not make use of them to specify materials and construction solutions for construction of building façades. This article presents
discussing the project variability for architecture within the context of 5-floor-buildings, in the reinforced concrete and joint gasket ceramic masonry, main type of construction in Brazil.

The research took place in the city of Pato Branco, Paraná southwest, (26 ° 13 '44 "S 52 ° 40' 15"), with an average altitude of 760 meters and sub-tropical climate history by applying the method of APO Ornestein [1992]. Thus, we sought to identify, classify and categorize the existing anomalies in the façades originated in the design phase, whether by errors or omissions in specifications and descriptive graphics, maintenance procedures that occurred, their frequencies, so that they would fit within the context described by ISO 15686-7 [2006].

In the investigation of façades diseases we pointed to a phenomenon of similar behavior between the buildings where the highest frequencies and intensities lie on top of buildings and façades in the south, as well as the procedures of premature building maintenance actions triggered by the psychological discomfort users. As we interpreted the façade projects it was identified that the graphics are insufficient to power the production process, so the recommendations point to the need of expanding the variables in the elementary act of project development, and maximize the economic and environmental resources employed in the façades.

2 DURABILITY OF FACADES OF BUILDINGS AND THEIRS INTERFACE WITH ARCHUCTETURE DESIGN

Despite being negligible the contents of scientific production concerning to approaches of projects in the efficiency of durability [Kumar et all, 2010], an alternative is the applience of the principle of quality in the project design because it allows that graphic elements to be made concisely with control over the flow of information with required quantification and qualification [CASTELLS e HEINECK, 2001]. The lack of details in design that considers the degradation agents - atmospheric, biological, load, incompatibility and use. [ASTM E632-82,1996], is an influential factor in life reduction of façades materials and components. [Gaspar e Brito, 2005; Pavitt e Gitt, 2003; Romero e Vianna, 2003]. Especially by phatological manifestations originated from the downward flow of rainwater, which penetrate into the shrinkage cracks in the mortar [Gaspar e Brito, 2005]. In this phase should also be considered the agents of degradation on the materials, as the temperature gradient [CHEW 1998], the maintenance actions [Flores-Colen, 2003], among others.

According to [Chew et al 2007], the decisons of facades design interfere in service life as they propose solutions that are resistant to natural aging, it is important to identify materials with improved durability gradient, identified by previously tested methods. However, it is difficult to accurately predict the service life and meet the overall durability of the façade to be composed of several layers and with different thickness [Mendes Silva and Falorca, 2009]. As regards the project of brick nogging walls can be prepared by production method [Pena and Franco, 2004], guidelines, and facades coating [Manechi e Melhado, 2008]. For mortar coating there should be a set of measures in the design phase in order to promote a specific coating as ideal, thus, for (Baía and Sabbatini, 2000;

Ceotto et al 2005) the design of facades coating shall be prepared and be a guiding factor during the production process of this coating.

3 BUILDING FACADES CHARACTERIZATION AND ITS CONSTRUCTION SYSTEM

The objective was to select buildings with characteristics of modern architecture, 5 floors and about 10 years old, and significant amount of pathology on the facades, and from this, diagnose what are the interference that the architectural design cause in them durability. The building system of these buildings is traditional from Brazil, made of concrete structure, seals usually with masonry of hollow ceramic blocks of red clay, setting with the holes in the horizontal with physical characteristics governed by [ABNT 15270-1, 2005]. The seals also are built less frequently by concrete blocks, governed by [ABNT 7173, 1982], and limestone-block [ABNT, 14974-1, 2005]. All set with cement mortar, lime and sand, and additives. The set of layers below are regularization – roughcast, and mortar of plaster, of connection or settement - plaster and finishing - usually through acrylic paints, acrylic texture, and textured finish (grafiato), and less frequently, by finishing in ceramic and glass tiles, granite, marble and composed aluminum, as shown in Figure 1.

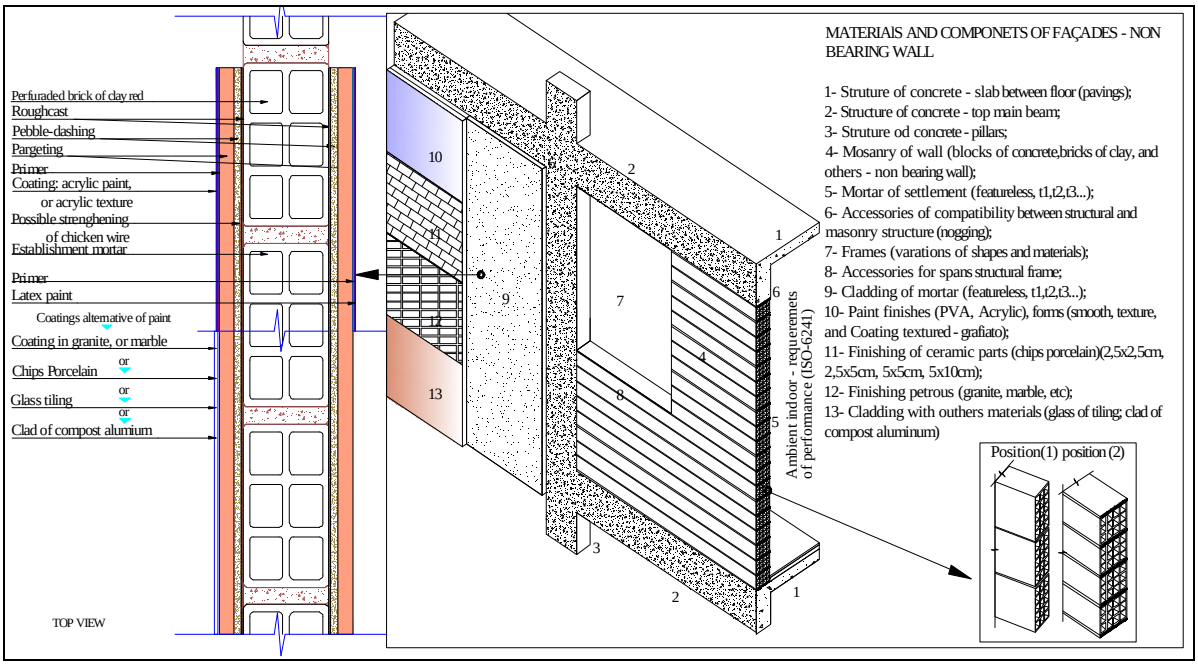

Figure 1. Process constructive of façade of building traditinal in the Brazil

Name	Building-1	Building-2	Building-3	Building-4	Building-5	Building-6	Building-7	Building-8
Geometric shape of the floor plan. Each floor with a height of 3 meters	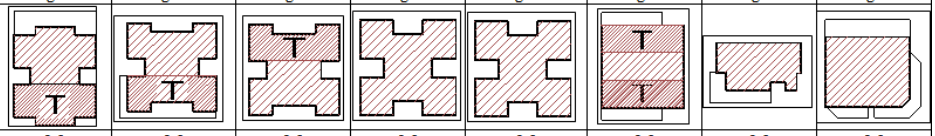							
Tipe of roof [1], [2]	[1]	[1]	[1]	[2]	[2]	[1]	[2]	[2]
Type of facade finishing: [3], [4], [5]	[3]	[3]	[3]	[3]	[3]	[3]	[3]	[3]
Presence of balcony [*], [6], [7]	[6]	[6]	[6]	[*]	[*]	[6]	[7]	[7]
Openings of aluminum [8], [9]	[8]	[8]	[8]	[8]	[8]	[9]	[8]	[9]
Maintenance affectionate [10], [11], [12], [13]	[11],[12],[13]	[11],[12],[13]	[11],[12],[13]	[10],[11],[12], [13]	[10],[11],[12], [13]	[10]	[11]	[10]

[1] Coverage built on platband	[2] Penthouse with terrace and exposed slab - T	[3] Painting with acrylic latex loam
[4] Coating with ceramic insert	[5] Coating with other materials	[*] There is no presence of balcony
[6] Balcony railing with brick	[7] With metal balcony railing	[8] Without the presence of canting strip
[9] With the presence of canting strip (granite), with errors constructive	[10] Only Refinishing	[11] Corrections in the plaster and repainting
[12] Corrections in the structure of concrete, plaster and repainting	[13] The pathologies were recurring in the same locations	

Figure 2. Characterization of the facades of buildings surveyed

3 INVESTIGATION, RESULTS AND DISCUSSIONS.

The investigation was based on constructive pathologies was appropriate for each plan (Table 1), pre-established in order to qualify and classify the identified anomalies.

Table 1. Roadmap for data collection in buildings

| | | |

3.1 Behavior Painting Coverings

The finishing touches on the facades of buildings were mostly of acrylic texture and acrylic paint, on plaster smoothing, without the existence of joint work of the mortar substrate. The paints were the most affected by the pathological manifestations. The severity and intensity of these problems were classified and characterized by Cincotto [1988] and real estate firms specialized in paint, by pointing pathologies of: spots, blisters, craters; separation; detachment; efflorescence; wrinkles; spots due to air pollution; saponification ; crack and differences of tone.

When analyzing the severity and location of the pathological manifestations of the paintings, it was made for solar orientation and heights - floors, so when apply to analysis of variance with 95% confidence, it was found that there is no significant influence between the floor and the orientation of the facade, however, allowed to extract some considerations:

a.1) The influence of the facades is not significant, however, the south facades have the greatest numbers of diseases, indicating the presence of increased moisture by the absence of sunlight and decrease in the durability of the material, being dirt from the atmosphere, cracking and stains for fungi, the most significant.

a.2) Only the influence of the storeys is significant. It allows us to make some observations on the downside of the facades. The points described below are those of figure 1.

a.2.1) In Section A1,B and B1 - platband - the most frequent pathologies are the spots of fungi mold and dirt from the atmosphere, with aspects of bleeding in the downward direction on the walls, especially in buildings 1, 2 and 3. This is because of the constant presence of moisture from dew and rainfall retained in the absence of materials protected by eaves (metal or stone) to ward off the flow of water from the walls, and that the thermal cycles develop microorganisms. See photo 1.

a.2.2) In Section D - Body of walls - the diseases largely result from the fissures and cracks in paints caused in the mortar, which eventually result in the reaching of the paints, thus allowing water infiltration.

a.2.3) In Section E - where walls meet the ground - the diseases in the presence of moisture, caused by the splashing of rain and cleaning water, can reach a height of 1 (one) meter with impregnated dirt, but also by moisture from the soil which, by capillary materials, reach up to 2 meters high, fading and creating bubbles in the paints also being able to detach the plaster.

a.2.4) In Section G - areas of the masonry below the position of windows - areas of flat and sloped sills susceptible to deposition of dust from the atmosphere, causing bleeding in the facades with the flow of rainwater in the position of the drip pan, by construction errors or lack of them in many buildings, which did not allow adequate drainage of the flow of water circulating through the facades.

Table 2. Equation linear of pathologies in paints

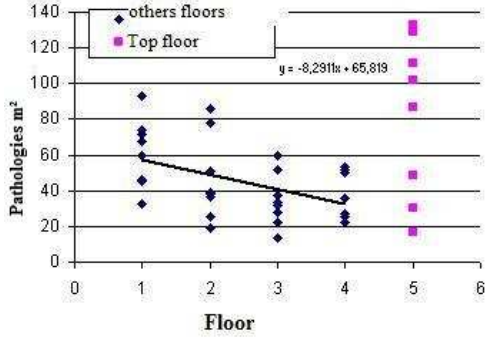

Photo 1. Treatment of top of building



The conditions explained from the viewpoint of a linear equation estate that the loss of durability the facades suffer is significant at the height. The linearity of the pathological phenomenon (Table 2) is possible up to the fourth floor through the line "y =- 8.2911 +65.819 x", however, the last values are significantly larger in numbers and severity of diseases, indicating that these sites are more sensitive to degradation agents.

3.2 Behavior of Mortar Coatings

The pathological manifestations of this coating is structured by the severity and intensity, depending on the classification and characterization of Cincotti [1988], which identifies the most frequent manifestations, while Santos Filho [2004] classifies them as to severity by the size of the openings as reference in Table 1, along with steamed zone, crack, mapped fissures, with dustiness detachment, detachment with blistering and detachment on boards.

The comments seek to establish a relationship between solar orientation and height of the facades for the emergence of diseases, thus when applying the analysis of variance with 95% confidence, was obtained:
• The influence of solar orientation of the facades is significant, and the south facade is most affected with 29% of the total, while the north facade is less affected with 21% of outbreaks.
In this context, the points with highest incidences were pathological: D with 18%, 13% B, B1 and C with 12% each.
• The influence of the storeys is significant, in that tall buildings gain pathologies increased with an exponential scale on the last floor.
• The pathological implications in mortars by "intensity" were observed respectively due to cracks in several directions, horizontal fissures, cracks and horizontal cracks. Since the horizontal planes were unprotected sites with higher incidence of infiltration of moisture, and greater presence of these pathologies.
• The pathological incidences in mortar coatings with the severity criterion showed the highest incidences were in the top floor: horizontal cracks in the zones of wedging, cracks, holes and cracks on the pavement terraces, areas of deployment, especially at the ends of parapets.
• Areas with a high incidence of cracks at 45 degrees were observed in the vicinity of openings in casings, both in the position of wicker, rattan and counterinsurgency.

3.3 Procedures Relating to Maintenance of the Facades were Observed

The collection of data from apartment manager showed that there is not structured format (planned actions, preventive maintenance) maintenance actions, the lack of spaces destined to archive projects and managing the building when it is in use and operation, beyond:
• All maintenance actions that occurred were triggered by visual discomfort owners. In 64% of the time without professional technical guidance, 24% of the interventions were repeated diseases, 8% of the time the liquidators were able to identify the period of early manifestation. The conditions with higher recurrence were on the last floor (ledge) in particular to the extremities, where even the structure of reinforced concrete (slabs and pillars) had fissures and cracks.
• Diagnoses of therapy do not appear as corrections were performed, since there is no documentary record, not even the basic designs and projects or as built.
• In 50% of cases of pathological reincidence, there were broken parts, cracks and moisture, being higher in those buildings where there is the presence of roof terrace.

3.4 Analysis of Architectural Design of these Buildings Facades

The set of graphic elements of the facades and specifications provided by the architects for the other designers of the subsystems, and for the production stage of the handiwork show some similar characteristics with each other, in other words:

• The facades graphics in all basic architectural designs were abstract figures with geometric configurations of the desired form, and with some general specifications, as well as in the description techniques for the building. They had more the function of comply with legal formalities than properly to guide the activities of the execution phase of handiwork. In a few cases were observed construction details indicating the selection of material to be used, like bricks and finishings.
• When crossing the diagnosed point in the facades with high rates of disease due to lack of drainage of rainwater flow and surface condensation, few solutions are presented in the graphics. Related to graphics solutions, where the diseases were more severe, there was also lack of detailing.
• In the approach with archtects, designers of these buildings in question about the importance given by them in the graphics solutions for their projects related to durability of the facades. May observe that professionals does not hold a domain of the basic concepts of the topic, as well as service life, obsolescence, as well as a further and domain of degradation agents. However, all agree with the importance and nobility that have the facades.

4 FINAL REMARKS

Regarding the finishing touches on paint, it is known that the most significant pathologies were respectively the dirt from the atmosphere, cracking, staining fungi and bacteria, more difference in tone (fade), which together accounted for 88% of the diseases. The most affected points are A1, G, H, I, L, which have horizontal planes as the top of walls and slabs. The architectural solutions adopted by designers for these points shown as disabled did not allow efficient drainage of the facades. This can be verified through research with these designers and graphic material specifications evaluated for these points. However, it would be possible, during the project design, provide much more detailed decisions for constructive solutions that incorporated storm water drainage of the facades. Apply drip pan and casings, included on horizontal planes, drip pan facade on each floor independently of the existence of frames, take actions such as specification, detail chart due to repeated standardized solutions for facades (structures, fences and window frames) for new buildings, and monitoring the implementation phase, because many cases were designed drip pan, but lack this element in the facade, or had faulty construction in the "grooves" of the lower parts without creating a discontinuity in order to place the drip of water off the facade.

The specifications for paint project are insufficient, with a focus on material cost, however, should opt for more durable types of paint, or replace it with more durable finishes such as ceramic inserts, stony coating. They have extremely low levels of water absorption, and when constructed in accordance with the regulatory rigor to show infinitely more life and lower maintenance procedures, although apparently it shows the highest costs in the production phase. Conclusively, it is essential for the compression of the architects of the phenomena of degradation and lifetime of materials for facades, to review the design procedures.

REFERENCES

ASTM – E632-82 – Standart practice for developing accelerated tests to aid prediction of the service of building components and materials, 1996.

Brazilian Association of Techincal Standards. Ceramic components – NBR 15270 Part 1: Hollow ceramic blocks for non load-bearing masonry – Terminology and requirements, 2005.

Brazilian Association of Techincal Standards ceramic blocks for non load-bearing masonry - Terminology and requirements. NBR 14974-1 - Calcium silicate brick for masonry - Part 1: Requirement dimensions and methods of test. 2005.

Brazilian Association of Techincal Standards. Ceramic components – NBR 7173 Plain concrete hollow blocks masonry without structural function. 1982.

Castells, E., Heineck, L.F.M. The application of quality concepts in the design process of architectural design - a critical review. [in Portuguese]. São Carlos - Brazil. 2001.

Ceotto, L. H., Banduk, R. C., Nakakura, E. H. Mortar of coatings - good practices in designing, implementing and evaluating . Habitare. Porto Alegre. 2005.

Chew, M.Y.L. Assessing building façades using infra-red thermography. Structural Survey. V16. n.2 p.81-86. 1998.

Chew, M. Y. L., Silva, N., Tan, P.P., Das, S. Grading of risk parameters for facade maintainability. International Juornal on Architecture Science. 2007.
Cincotto, M. A. Pathologies of mortar coatings: analysis and recommendations [in Portuguese]. Florianópolis. 1988.

Flores-Colen. I. Plants of proactive maintenance in recent buildings. Proc. 3rd ENCORE- Conf. on Conservation and Rehabilitation of Buildings, LNEC, Lisbon, Portugal, [In Portuguese]. 2003.
Gaspar, P. L., Brito, J. Mapping defect sensitivy in external mortar renders. construction and building materials. v.19 p. 571-578. 2005.

ISO – National Organization for Standartization. Performance Standards in Buildings: principles for their preparation and factors for inclusion – ISO 6421. London. 1984.

ISO 15686 - 7. Buildings and construced assets – Service Life Planning – 7: Performance evalution for feedback of service life data form practice. 2006.

kumar, d., Setunge, s., Patnaikuni, i., Prediction of Life-Cycle Expenditure for Different Categories of Cuoncil Buildings. Journal of Performance of Constructed Facilities, ASCE, 2010.

Maneschi, K., Melhado, S. B. Scope of design for production of partition walls and facade coatings. [In Portuguese]. 2008.

Mendes Silva, J.A. ., Falorca, J. A model plan for buildings maintenance with application in the performance analysis of a composite facade cover. Const.& Building materials, 23 p. 3248-3257. 2009.

Ornstein, Sheila. Post- Occupancy evaluation [in Portuguese]. São Paulo: Studio Nobel. 1992.
Pavitt T. C., Gibb G. F. Interface Management within Construtions: In Particular Building Façade. Journal Construction and Management. Vol. 129, Issue 1, pp. 8-15. 2003.

Peña, M.D., Franco, L. S., Project preparation methods for the production of vertical seals in masonry [in portuguease]. BT/PCC/363. 2004.

Roméro, M. A.; Vianna, N. S. Methodological procedures for application of post-occupancy evaluation in housing for low-income population: the urban design of the housing unit. [in Portuguese]. São Paulo, 2003.

Santos Filho, M. L. Pathology of buildings [in Portuguese]. UTPR. 2004.

XII DBMC
International Conference on Durability of Building Materials and Components
PORTO - PORTUGAL, April 12th-15th, 2011

The Perception of Damage on Rendered Façades

Pedro Lima Gaspar [1]
Jorge de Brito [2]

ABSTRACT

In this paper, a methodology to quantify the global degradation level of rendered façades is presented. The results are discussed and compared with the responses of the perceived damage according to different building actors (designers, researchers and owners), based on queries and interviews, for a sample of cases studied.

These data demonstrates that different building actors tend to perceive damage on rendered façades differently: while specialists and researchers generally focus on degradation mechanisms and their effects on the durability of the material, non-specialists tend to intuitively perceive the holistic sum of defects and how it affects the general image of the façade.

KEYWORDS

Severity, damage perception, degradation mechanisms, render, façade.

[1] Technical University of Lisbon, Faculty of Architecture, Lisboa, PORTUGAL, pmgaspar@fa.utl.pt
[2] Technical University of Lisbon, Instituto Superior Técnico, Lisboa, PORTUGAL, jb@decivil.ist.utl.pt

1 INTRODUCTION

For most buildings and their parts under current maintenance conditions [Flores-Colen *et al.* 2006], service life tends to be shorter than design life [Horst *et al*. 2005], either because of changing performance requirements (from owners and users) or because of critical loss of performance (due to defects and in-use conditions) [Burati *et al*. 1992]. In these situations, repair work has to be scheduled to renew, replace or mend damaged or degraded parts. More often than expected, such decisions are based on the overall perception of the façade's degradation, rather than from strict rational criteria (that is, according to a cause-effect rationale such as global cost reduction or of technical durability of parts) [Aikivuori 1999; Balaras *et al*. 2005].

In this paper, a methodology to quantify the global degradation level of rendered façades is briefly presented, based on fieldwork data relative to the condition of cement-rendered facades of residential buildings. This methodology provides a numeric indicator ("overall degradation level") that expresses loss of performance over time due to physical deterioration of renders. The overall indicator of degradation allows benchmarking of different façades and provides a useful tool for service life estimation and maintenance planning. In order to validate the model proposed, the results obtained are compared with the responses of the perceived damage according to different building actors (designers, researchers and owners), based on queries and interviews, for a sample of cases studied.

2 BACKGROUND

Building facades are particularly sensitive to the effects of environmental agents for they present a large exposed surface (under the direct influence of rain, wind, sunlight and atmospheric pollutants) but a relatively thin width. Cement renders account for about 62% of façade claddings in Europe and show a high prevalence of defects which are generally expensive to put right, as it has been demonstrated time and again [Parnham 1997; Watt 1999; Chew & Ping 2003; Balaras *et al*. 2004].

During their life cycle, rendered façades work their way along a relatively clear path of degradation: starting off with the early occurrence of light soot and dirt stains, water runoff stains and often hairline cracking - all of which may evolve in terms of condition and extent of damage - until loss of bond within the rendering and/or loss of adhesion to the façade finally occurs. Loss of adhesion, cracking, visual degradation and disfigurement of the facade are often pointed out as a problem, which has a strong impact on the aesthetic performance of a building envelope and on the quality of the urban environment [Parnham 1997, Flores and de Brito 2003].

3 OVERALL DEGRADATION LEVEL (ODL) OF THE FAÇADE

To establish a model for the ODL of cement-rendered façades, data on the condition level of this building element were collected in the Lisbon region, Portugal. A sample of 100 buildings was thus randomly chosen and filtered in order to select case studies matching the following criteria: a) buildings with cement-rendered façade, b) no known records of deterioration as a result of accidental actions, and c) with known records of past maintenance actions or the age of construction. The last condition is regarded as indispensable so that the pattern of variation of the ODL in time can be identified.

The buildings surveyed correspond to current construction practice in Portugal: slab and beam concrete structure, infill fired clay brick walls, provided with surface roughness to promote the adhesion of external renders. Renders are generally applied in several layers. Typical render mixes vary from 1:2 (cement, sand), in the first layer, to 1:1:5 and 1:1:6 (cement, hydraulic lime, sand) in the following layers.

During the field survey, data were gathered based on a discrete level classification system of the defects detected – from "0" (no degradation) to "4" (immediate action required) – for each of the three

main defect categories: “staining”, “cracking” and “detachment” of render.

The overall degradation level of each façade was obtained according to the “severity of degradation” indicator expressing the performance loss of the façade [Gaspar 2009; Gaspar and de Brito 2008a]. This indicator combines the affected area of the façade, as obtained through direct measurement of the façades assessed, with the depth of registered defects, according to the corresponding condition level. The result is then compared with a set reference degradation area that corresponds to the total exposed rendered area of the façade, affected by the worst condition for all possible defects, see equation (1).

$$ODL = \sum (A_n \,.\, k_n \,.\, k_{a,\,n}) \,/\, (A_r \,.\, k) \qquad (1)$$

Where,

ODL	overall degradation level, as a percentage;
A_n	area of a façade affected by defect n, in square meters;
k_n	condition level for defect n, where $k_n \in \{0, 1, 2, 3, 4\}$;
k	constant, equivalent to the value of the worst condition level;
$k_{a,\,n}$	relative importance of the defects detected, where $k_{a,\,n} \in]0, +\infty[$;
A_r	exposed rendered surface area of a façade, in square meters.

In the present work k is equal to 4, corresponding to the worst condition level of the ranking system proposed {0, 1, 2, 3, 4}. To obtain the ODL for the cases studied, defects are weighted ($k_{a,\,n}$ in expression 1) according to their hazard level and cost of repair. The cost of repair is obtained through an index that compares average market prices of different repair work with the average market price of applying new renders (Table 1).

Table 1. Relative weight of defects ($k_{a,\,n}$) for each condition level, according to repair costs of renders (Portuguese market).

Condition	*Staining*	*Cracking*	*Detachment*
1	$k_{a,\,n} = 0.12$	$k_{a,\,n} = 0.95$	$k_{a,\,n} = 1.53$
2	$k_{a,\,n} = 0.53$	$k_{a,\,n} = 0.95$	$k_{a,\,n} = 1.53$
3	$k_{a,\,n} = 0.53$	$k_{a,\,n} = 1.12$	$k_{a,\,n} = 1.53$
4	$k_{a,\,n} = 0.53$	$k_{a,\,n} = 1.53$	$k_{a,\,n} = 1.53$

The distinction between the hazard levels of defects is based on empirical evidence that suggests that for normal ageing processes, minor degradation - associated with staining, soot and dust deposition - occurs before cracking and detachment of render [Parnham 1997]. As deterioration progresses there is more simultaneous action of different degradation agents. The combined effects of different types of degradation, such as cracking and water penetration, also lead to increasingly hazardous defects, such as salt attack or thaw/freezing cycles deeper into the render layer [Henriques 1992].

3.1 Modelling Loss of Performance Over Time

The ODL indicator obtained for the 100 cases surveyed is plotted in a scatter diagram, expressing Condition (as the dependent variable) *versus* Time (as the independent variable), as shown in Figure 1. A degradation path is hence obtained through linear regression, well suited to express continuous degradation mechanisms such as environmental actions. The results obtained suggest a good statistical relevance of the model ($R^2 = 0{,}86$), especially given the wide range of variations associated to real-life service conditions.

In Figure 1 the best fitting regression curve represents the average degradation path for the sample studied. Once different minimum reference levels of performance are established [Gaspar and de Brito 2008b], scatter diagrams can provide a straightforward methodology for service life estimation [Moubray 1991] and later incorporation of results in methodologies such as the factorial method [Gaspar and de Brito 2008c].

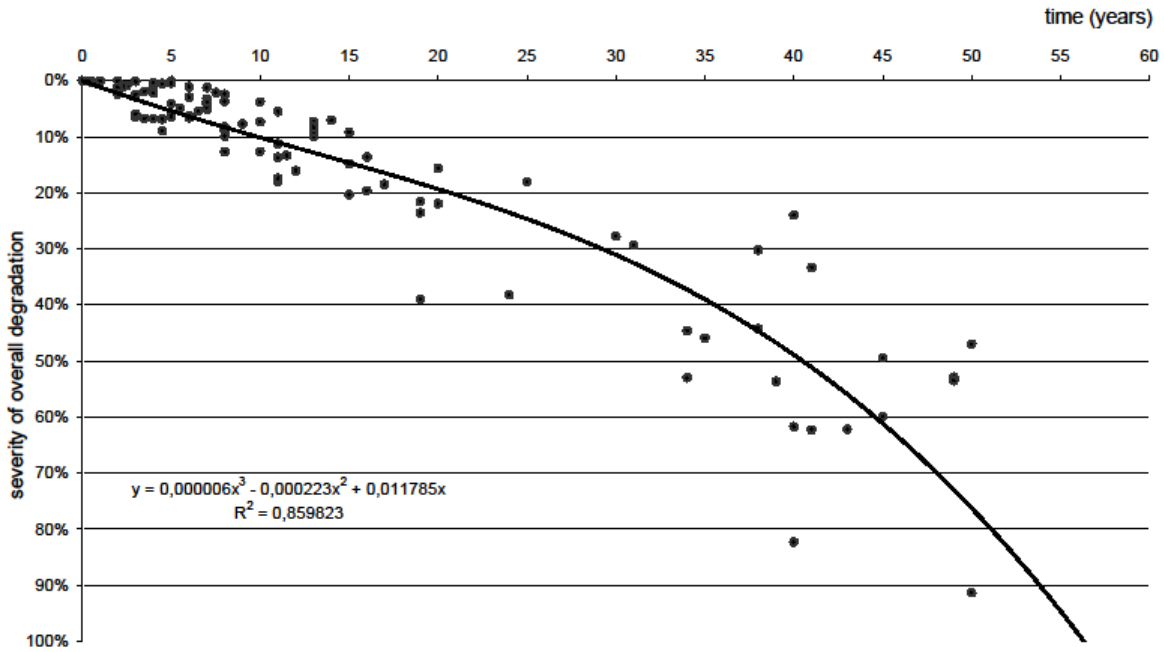

Figure 1. Scatter diagram and average degradation curve of 100 fieldwork results, expressing severity of overall degradation over time.

Although it may be possible to establish independent development patterns for each of the studied failure modes – staining, cracking and detachment – until a critical level is reached, ODL is a holistic degradation indicator. In fact, ODL takes into account the overlapping effects of all failure modes, according to the respective condition level, in spite of the part of the façade affected, and allows benchmarking of different case studies in terms of location, area and geometry of the façade, exposure conditions, among other aspects. As such, the validation of the model was done based interviews and expert opinion, as opposed to laboratorial or ageing testing methodologies.

4 VALIDATION OF THE MODEL

Experimental validation of results in construction is not always possible. All buildings, especially if under service conditions, are prototypes - unique in the combination of exposure, use, construction and maintenance conditions [Bordass 2000; Bordass *et al*. 2001] – that seldom allow direct comparisons amongst them. Validation of studies in the field of service life is even more difficult to do, because for most situations, in is not feasible or socially acceptable to wait for the outcome of results. A number of authors have proposed alternative methods to validate results and methodologies:

a) Expert and users' opinion, collected through surveys, interviews and questionnaires [Chew and Tan 2004; Chew 2005; Bordass & Leaman 1997];
b) Adaptation of statistical and chain decision techniques such as risk analysis or decision trees [Millet 1999; Balaras *et al*. 2004; Humphreys 2005];
c) Model analysis with complex mathematical tools such as neural network models or Markov chain algorithms [Moselhi *et al*. 1991; Kirkham and Boussabaine 2005; Maged *et al*. 2005].

In the present research, a questionnaire followed by an interview was made to twelve different stakeholders in the theme of rendered façades: a) researchers (3 valid answers), b) professionals in the fields of renders and façade repair (2 valid answers), c) designers (4 valid answers) and d) other peo-

ple, with no affiliation to the construction cluster (3 valid answers).

4.1 Questionnaire Elaboration and Application

A questionnaire was developed with a strong graphic component in order to obtain a simple and rapid tool – 5 to 10 minutes – to collect answers and lay the ground for a following interview. Through the questionnaire the correspondence between the degradation indicator ODL and the individual perception of damage of the respondents was evaluated. The interview was used to gather informal feedback and understanding about the criteria for the decisions of the respondents.

In the first part of the survey, a personal evaluation of the degradation level of the façades studied was requested. In order to reach this aim, several general and detailed photographs of different cases were shown as well as the vector drawn representation of the façades and their defects. Soon a pattern emerged in which respondents first consulted the drawn representations (where cracking is easier to identify) and later conferred with the photographs. It was also noted that just small scale variations of the drawings tend to greatly influence the answers obtained. Therefore, all representations were presented at just one and the same scale for the different cases.

In order to be able to compare answers, a four step questionnaire was implemented, in which growing levels of decision-making were demanded of the respondents as each of them got more acquainted with the notion of overall degradation level:

a) step 1 – general evaluation of the model: 5 sample cases were presented, which represented all condition levels in even degradation intervals; respondents were asked to sort them from the least to the most deteriorated; the given answers were classified according to a 5 point scale (from 1, no matches, to 5, all cases sorted according to the output of the model proposed);
b) steps 2 and 3 – evaluation of the capability of the model to express extreme situations of degradation: for each step, 5 sample cases were presented, which represented condition levels associated to high degradation (step 2) and low degradation (step 3); respondents were asked to sort them from the least to the most deteriorated; the given answers were classified according to a 5 point scale (from 1, no matches, to 5, all cases sorted according to the output of the model proposed).
   After the first rounds of the questionnaire, it was considered that respondents were more familiar with the decision process associated to the classification of overall degradation of façades. They could therefore be given broader levels of freedom of judgement in random sample cases, even though in no time they were informed of the agreement between their answers and the output of the model:
c) step 4 – independent evaluation of the degradation level of façades: respondents were asked to chose randomly 5 sample cases and to sort them from the least to the most deteriorated; it was also requested that they expressed the decision process associated to their choices, as if in a situation of visual assessment of the degradation level of rendered façades; the answers obtained were classified according to a 5 point scale (from 1, no matches, to 5, all cases sorted according to the output of the model proposed).

In the second part of the survey, an open interview was conducted aimed at understanding the principles associated with the choices in the process of evaluation of damage of façades. Emphasis was given to the decision process: whether photographs or drawings had been used, which had been used first and which had been used as benchmark or confirmation of the decisions made.

4.2 Discussion of the Results

The results from the questionnaire were classified according to a five point scale that expressed the accordance between the respondents' perception of damage and the output results of the model: from 1 (very low agreement), 2 (poor agreement), 3 (moderate agreement), 4 (good agreement) e 5 (very good agreement).

The results obtained were homogeneous. The average score for all the answers corresponds to 4.15 (good agreement). The detailed results of all steps of the questionnaire were: a) step 1: 4.8; b) step 2: 3.1; c) step 3: 4.9 and d) step 4: 3.8.

According to these results it is possible to conclude that the proposed model to quantify the ODL of rendered façades produces outputs similar to the perception of damage of the respondents, especially for the situations in which there are clear intervals of degradation between sample cases (step 1) or for low levels of deterioration of the façade (step 3). For the situations of very high levels of deterioration (step 2), there is not such a good accordance of results between the model and the perception of damage of the respondents. During the interview the latter consider it very difficult to distinguish between levels of deterioration unanimously evaluated as "high" or "very high", though. Finally, step 4 scores almost 4, which is considered a good result given the high levels of freedom and complexity associated with the decision process of evaluating damage in randomly chosen cases.

5 PERCEPTION OF DAMAGE

From an early stage of the questionnaire, it became clear that respondents were somewhat uncomfortable to validate an absolute classification of damage (in other words, a numerical indicator of overall degradation) without further indications to sustain their judgement. It was found that visual evaluation of damage is made mostly (if not fully) from a qualitative point of view, by comparison with previous experience or with other sample cases. Often respondents would focus on a sample case (for instance, the highest or lowest deteriorated cases presented) and would proceed with their choices referred to the elected "reference point". In the end, the questionnaire was especially directed to compare qualitative perception of damage (from the respondents) with the quantitative sorting of the sample, as obtained by expression 1.

Through the interview it was possible to identify different patterns as far as the given data were used by the respondents:

a) respondents with little or no relationship with the building cluster (that stand as representative of most users and owners of building assets) made their choices solely based on photographs – probably because such group may not be so used to interpret vectorial drawings or because their evaluation may be based mostly on comparisons to previous experience of an empirical and qualitative nature;
b) through the answers to the interviews it was possible to conclude that researchers and industry professionals distinguish between "visual deterioration" and "loss of performance" due to cracking and loss of adhesion; as such, if a façade were stained or defaced, they would classify it as deteriorated as, say, the previous group; researchers and industry professionals therefore often began their evaluation by analysing vectorial drawings of the façades, especially looking for the occurrence of damage mechanism of cracking and detachment, both of which were reported to be "very hard to detect in pictures";
c) design professionals (architects and engineers) consulted photographs first; however, before finishing their decision process, they would check vectorial drawings; thus, the latter were actually used as a decision-making tool; in some way, this group can be said to stand between researchers and owners both as far as sources of information are used and in terms of the holistic appreciation of the damage on the façade.

6 CONCLUSION

This paper presents the validation process of the model for overall quantification of damage on rendered façades. The model collects data on the condition level of loss of adhesion, cracking and staining defects and combines them into a numeric indicator of degradation, in percentage. The results of the application of the model to 100 field case studies of residential buildings in the area of Lisbon, Portugal, demonstrate statistical relevance in agreement with other field studies.

After the preliminary results, a survey was made in order to compare the results of the model with the perception of damage of different actors of the building cluster (owners, designers and researchers). The results obtained showed that the model can quantitatively express the qualitative opinions of the respondents, regarding both a general evaluation of different sample cases and detailed evaluation of extreme situations.

These findings also suggest that distinct actors tend to analyse and evaluate information differently. Owners and, up to a certain point, designers perceive damage on façades in a holistic manner, that is, considering the simultaneous occurrence of defects and their contribution to the overall defacement of the façade. Researchers and industry professionals tend to focus on degradation mechanisms and evaluate their implications on the loss of performance of the render and wall.

Although these views complement each other, for the purpose of maintenance planning and service life estimation, the results obtained recommend that overall damage quantification of façades should be done using holistic tools and models, as opposed to mechanism focused analysis and testing isolated from the context and from the synergetic effects of other mechanisms.

REFERENCES

Aikivuori, A. 1999, 'Critical loss of performance - what fails before durability', Proc. 8th Int. Conf. on Durability of Building Materials & Components, Vancouver, Canada, 30 May 3 June 1999, pp. 1369-1376.

Balaras, C., Droutsa, K., Daskali, E., Kontoyiannidis, S., 2004, *Building Deterioration Assessment Guidelines*, in Investimmo Report 62-098, March 2004, National Observatory of Athens, Greece.

Balaras, C., Droutsa, K., Dascalaki, E., Kontoyiannidis, S. 2005, 'Deterioration of European apartment buildings', *Energy and Buildings*, **37**[5], 515-527.

Bordass, W. 2000, 'Cost and value: fact and fiction', *Building Research & Information*, **28**[5-6], 338-352.

Bordass, W., Leaman, A., Ruyssevelt, P. 2001, 'Assessing building performance in use 5: conclusions and implications', *Building Research & Information*, **29**[2], 144-157.

Bordass, W., Leaman, A. 1997, 'Future buildings and their services', *Building Research & Information*, **25**[4], 190-195.

Burati, J., Farrington, J., Ledbetter, W. 1992, 'Causes of quality deviations in design and construction', *Construction Engineering and Management*, **118**[1], 34-49.

Chew M. & Ping T. 2003, *Staining of facades*, World Scientific Publishing, Singapore.

Chew, M., Tan, S. 2004, 'A multivariate approach to maintenance prediction of wet areas', *Construction Management and Economics*, **22**[4], 395-407.

Chew, M. 2005, 'Defect analysis in wet areas of buildings', *Construction and Building Materials*, **19**[3], 165-173.

Flores-Colen I. & de Brito J. 2003, 'Premature stains in façades of recent buildings', Proc. CIB/W87 2nd International Symposium. Lisbon, Portugal, 6 8 November 2003, pp. 311-320.

Flores-Colen, I., de Brito, J., Freitas, V.P. 2006, 'Expedient *in situ* test techniques for predictive maintenance of rendered façades', *Journal of Building Appraisal*, **2**[2], 142-156.

Gaspar, P. 2009, *Service life of buildings: methodology for service life prediction of building components. Application to external cement-renders*, PhD Thesis (*in Portuguese*), Technical University of Lisbon, Lisbon.

Gaspar, P., de Brito, J. 2008a, 'Quantifying environmental effects on cement-rendered facades: a comparison between different degradation indicators', *Building and Environment*, **43**[11], 1818-1828.

Gaspar, P., de Brito, J. 2008b, 'Minimum required performance level for rendered facades', Proc. 11th Int. Conf. on Durability of Building Materials & Components, Istambul, Turkey, 11 14 May 2008, vol. 3, pp. 1177-1184.

Gaspar, P., de Brito, J. 2008c, 'Service life estimation of cement-rendered facades', *Building Research and information*, **36**[1], 44-55.

Henriques, F. 1992, *Humidity on walls*, PhD thesis (in Portuguese), Technical University of Lisbon, Lisbon.

Horst, S., O'Connor, J., Argeles, C. 2005, 'Survey on actual service lives of north American buildings', Proc. 11th Int. Conf. on Durability of Building Materials & Components, Lyon, France, 17 20 April 2005, pp. 851-858.

Humphreys, M. 2005, 'Quantifying occupant comfort: are combined indices of the indoor environment practicable?', *Building Research & Information*, **33**[4], 317-325.

Kirkham, R.J., Boussabaine, H. 2005, 'Forecasting the residual service life of NHS hospital buildings: a stochastic approach', *Construction Management and Economics*, **23**[5], 521-529.

Maged, E.G., Chang, L., Zhang, L. 2005, «Prediction of engineering performance: a neurofuzzy approach', *Construction Engineering and Management*, **131**[5], 548-557.

Millet, R. 1999, 'Failures: How to avoid them', *Management in Engineering*, **15**[5], 32-36.

Moselhi, O., Hegazy, T., Fazio, P. 1991, 'Neural networks as tools in construction', *Construction Engineering and Management*, **117**[4], 606-625.

Moubray, J. 1991, *Reliability-centred Maintenance*, Butterworth-Heinemann, Oxford.

Parnham P. 1997, *Prevention of premature staining of new buildings*, E & FN Spon, London.

Watt D. 1999, *Building pathology: principles and practice*, Blackwell Science, Oxford.

XII DBMC
International Conference on Durability of Building Materials and Components
PORTO - PORTUGAL, April 12th-15th, 2011

The Application of Thermal Imaging as a Nondestructive Test in Historic Buildings

Samira Nikzad [1]
Behrouz M. Kari [2]
Farhang Tahmasebi [3]

ABSTRACT

Thermal imaging -or infrared thermography- is the use of infrared imaging camera to show and determine the surface temperature via measuring the thermal energy emitted from an object. Thermal imaging is a nondestructive test. The structures of historic buildings commonly exhibit performance problems that are basically appeared during different construction and maintenance phases in numerous years of their existence. These problems can impact comfort conditions, building energy performance and structural integrity.
Regardless of building type, thermal imaging can provide remarkable information about the historic buildings including;

- Validation of structural details,
- Location of thermal bridges and insulation failures,
- Location of air leakage,
- Location of moisture intrusion,
- Location of condensation in the building envelope,
- Identification of structural, mechanical and electrical degradation and aging infrastructure.

In this article, numerous useful applications of thermal imaging technology for inspection of the historic building envelopes have been studied. Also considerations, requirements and related inspection methods for historic buildings are being surveyed.

KEYWORDS

Thermal imaging, Infrared, Emissivity, Historic Buildings, Thermal Bridge, Moisture, Air leakage.

[1] Faculty of Architectural Conservation- Isfahan University of Art, Isfahan, Iran, samira_nikzad@yahoo.com
[2] Scientific board member of BHRC-Iran also Faculty of Architecture- Tehran University, Tehran, Iran, kari@bhrc.ac.ir
[3] Faculty of Architecture- Tehran University, Tehran, Iran, farhang.tahmasebi@gmail.com

1 INTRODUCTION

Building structures commonly exhibit quality and performance problems caused during construction and maintenance that can impact energy performance and, in some cases, render them dangerous. Regardless of the building type involved, infrared imaging has been shown to provide details in building performance.

The application of infrared thermography is to assess building envelope anomalies[4] in historic buildings. However, infrared thermography alone will not identify the cause and source of any given anomaly nor does it quantify the depth and intensity of the cause or damage. In fact, proper interpretation based on a thorough assessment of the building is necessary for the inspectors to understand the nature of anomalies and suggest the sequence of resolving them. Normally, in historic buildings, the cause or source of the problem must be unwound first to result in resolved anomalies.

According to Sharon C. Park [1996], 'hidden construction problems that significantly reduce energy efficiency and the integrity and performance of the building envelope include condensation and mold growth inside building envelope elements, insulation damage, rot and corrosion in structure, frozen pipes in mechanical systems and failure of critical electrical components.'[5]

The scope of this study is to provide an increased level of knowledge to the historic building experts for an improved awareness of the benefits and limitations of using infrared thermography for inspecting serious anomalies of a historic building.

1.1 History of Thermal Imaging

According to Chris Linville [2002], 'Sir William Herschel discovered infrared radiation in 1800. His son, Sir John Herschel, more interested in photography, managed to record the heating rays on the infrared side of the spectrum. He termed this image a thermogram.'[6] This laid the foundation for the sophisticated thermal imaging devices.

Today, heat sensed by an infrared camera can be very precisely quantified, or measured, allowing us to not only monitor thermal performance, but also identify and evaluate the relative severity of heat-related problems. Recent innovations, particularly detector technology, the incorporation of built-in visual imaging, automatic functionality and infrared software development deliver more cost-effective thermal analysis solutions than ever before.

1.2 Basics of Thermal Imaging

As a physics law, heat flows from a higher temperature zone (or body) to a lower temperature one. Such heat flow can take place in three forms of conduction, convection and radiation.According to S. V. Szokolay [2008], 'Radiation transpires from a body with a warmer surface to another, which is cooler. Thermal radiation is a wavelength band of electromagnetic radiation, normally taken as 700–10000 nm (10μm). 'Short infrared' is between 700–2300 nm (2.3 μm) while 'Long infrared' represents the wavelength between 2.3–10 μm (some suggest up to 70 μm). The temperature of the emitting body determines the wavelength. '[7] According to energy efficiency fact sheet, 'Emissivity is a material property**,** an efficiency factor that varies between 0-1.0, correction factor. For different materials, emissivity amount defines Blackbody (ε =1.0), Real body (ε <0.1) and Perfect reflector

[4] John R. Kominsky et al., "A *thermal anomaly* is defined as a thermal pattern of a surface that varies from a uniform color or tone when viewed with an infrared imaging system."
[5] Sharon C. Park, AIA, 'Controlling Unwanted Moisture in Historic Buildings', Washington, 1996.
[6] Chris Linville, Thermography has become an invaluable asset for insulation energy audit, 2002.
[7] S. V. Szokolay, ' Introduction to architectural science: the basis of sustainable design', 2008.

(ε=0.0).'[8] High emissivity include non-shiny surfaces, while low emissivity surfaces pertians to high thermal reflection in materials. Emissivity can change according to material, surface, wavelength and temperature while emittance changes with Angle of view.

2 THERMAL IMAGING

Thermography is the use of an infrared imaging and measurement camera to show and measure thermal energy emitted from an object. According to John R. Kominsky et all [1998]; 'In thermography, infrared imaging system (an infrared camera) converts the spatial variations in infrared radiance from a surface into a two-dimensional image, in which variations in radiance are displayed as a range of colors or tones. As a general rule, objects in the image that are lighter in color are warmer and darker objects are cooler. Pertaining to the thermal imagery of building envelopes, the atmosphere (in most cases) is considered transparent in the spectral bands of interest where absorption is limited to 3 to 5 μm (short waves) or in the 8 to 12 μm (long waves). The image is viewed through the eyepiece of a video scanner and can be recorded on videotape.'[9]

Maximizing the difference between the inside air temperature and the outside air temperature provides the greatest contrast between the hot and cold areas on the video image. Therefore, process equipment should be heated or cooled for testing if their normal operation does not provide an adequate temperature difference.

2.1 Infrared Thermal Imager

Infrared cameras for building applications are available in a wide variety of models and price ranges. Apart from using the proper camera and lens for a given application, the qualifications of the person operating the camera and performing the inspection is the most determining factor in obtaining an accurate assessment of the performance of the building envelope. Skilled interpretation can diagnose problems that affect the surface temperature. Most materials are opaque to infrared so items behind covers or doors are only detectable if they are so hot and so close as to transmit heat onto a clearly defined part of the cover. An excellent camera used with the wrong settings and under inappropriate environmental conditions will ultimately yield misleading and inaccurate results. Reporting results based on an inaccurate assessment will have an important impact on the subsequent decision making process. As a consequence, the wrong decision making may end in needless recommendations concerning building anomalies or it might result in important problems being overlooked.

2.2Thermal Imaging Regulations and Conditions

In most cases, sample thermal images must be taken to demonstrate the majority of areas with anomalies or defects as well as the parts of the building with no anomalies, which demonstrate the correct functioning of building components.

Thermal images should be taken as close to perpendicular to the investigating surfaces as possible. Area and location of surfaces obscured by mirrors, metal, reflective tile or other low emissivity coverings might affect interpretation. Therefore, it is recommended that the images being taken in different angles.

Precipitation in the form of rain or snow will create an obstacle between the infrared camera and the exterior surfaces being inspected and this includes mist and fog. 'According to The minimum temperature criterion for satisfactory thermal conditions for an inside to outside temperature

[8] Energy Efficiency Fact Sheet, ' Principles of Heat Transfer', Washington University, 2008.

[9] John R. Kominsky et al., "A *thermal anomaly* is defined as a thermal pattern of a surface that varies from a uniform color or tone when viewed with an infrared imaging system."

difference of the wall surfaces is at least 10°C for a period of 24 hours. (Ref: ISO 6781, 5.1, a. recommends 10°C for a period of 24 hours.[10]

Investigation of any anomalies is done through physical examination of the building details, moisture meters, surface temperature devices, air exhaust devices and experience of the investigator. Exterior surfaces should be dry and surfaces should not be heated by direct solar radiation for a period of approximately 3 hours for frame construction and for approximately 8 hours for masonry veneer construction. Also exterior investigations should be planed for an appropriate time after sunset, before sunrise, or on an overcast day when the influence of solar radiation can be determined to be minimal. Standards suggest that wind speed should be less than 3.6 m/s.[11] It is necessary to mention that interior investigations can also be influenced by wind, sun, sky condition and moist exterior surfaces. These influences typically lag the more direct exterior influence depending on conditions and structure type.

As a case study, David house[12] has been chosen for structural and thermal investigations through infrared thermal imaging. The building envelope in David house consists of adobe structure and clay façade. In some parts, the clay façade has been replaced by brick. There are several openings in building envelope.

In thermography in David historic house the environmental conditions have been considered before thermal imaging. The best time for thermal imaging in order to detect airleakage, thermal bridges and insulation degradation is the coldest hours of the day and night that is before dusk. Thermography of David historic building was done on 10th december 2009. while the astronomical dusk was 5:18[13], taking thermal images finished at 6:45 (Before sunrise). The wind speed on different hours of 10th december is presented in Figure 1.
The temperatures inside and outside the building were 18°C and 7ºC respectively. Figure 2 indicates the temperature of the outside of the building on 10th december 2009. also Meteorological reports indicate that the sky was partly cloudy on 10th december 2009. but no perticipation or mist was reported on the specific day.

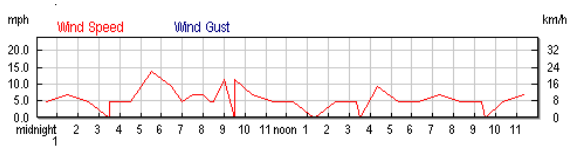

Figure 1. Wind direction and speed on December10th 2009- Isfahan, Iran. (Source: Iran Meteorological Organization).

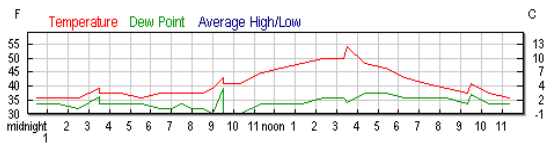

Figure 2. Hourly temperature on December 10th 2009- Isfahan, Iran. (Source: Iran Meteorological Organization)

3 THERMAL IMAGING IN BUILDINGS

Regardless of building type, thermal imaging can provide remarkable, nondestructive information about the historic buildings that facilitate the inspection and further maintainance phases.

3.1 Validation of Structural Details

In a well-insulated wall, the framing may not be as obvious; However, darker lines stemed from thermal bridges may exist where two or more surfaces, such as wall-ceiling, wall-wall and at corners,

[10] Resnet Interim Guidelines for Thermographic Inspections of Buildings [2010] state: *"a minimum of 3/U degrees"*; for example, 6 K for a U value of 0.5 W/m^{2}K.
11 Resnet Interim Guidelines for Thermographic Inspections of Buildings, 2010.
[12] David house is a historic residential building that is built in Isfahan, Iran more than 150 years ago. Today, this building is being used by Isfahan University of Art, Faculty of architectural conservation.
[13] Iran Meteorological Organization, http://www.irimo.ir/english/index.asp.

meet. The success of a survey depends on understanding the construction under inspection. Also Construction drawings should be reviewed as part of the survey procedure. The construction details of specific areas can help to explain any identified weaknesses. Where no drawings are available, the operators must familiarize themselves with the building type and construction.

While construction drawings help in determining the nature of the problems highlighted by a survey, it is always best to undertake a visual inspection of the areas affected, as variation from design is not uncommon. Some examples of structural validation include grouted cells with re-bar in block walls, structural elements in poured wall, subsurface details in historic buildings.

3.2 Location of thermal bridges and insulation failures

Moisture in the insulation substantially reduces its R-value and increases heating and cooling costs. Wet insulation absorbs more solar gain during the day and it releases more stored solar heat during the night. Heat flux sensing equipment or calorimetry using a 'hot box' can be used to monitor heat flow across a building element over a period of time.

In David house, as case study, the building envelope has been checked for thermal bridges and insulation failure. By the date of David house development, thermal insulation was not conventional. Therfore, the building envelope does not consist thermal insulation. The thicknes of adobe walls in David house vary from 60cm to 150cm and provide time lag in heat flow through building envelope. Figure 3 represents thermal time lag difference in concrete, clay brick and adobe walls. In Figure 4 attenuation of exterior/interior temperature variation, for different thickness of concrete, clay brick and adobe walls is represented. Considering these results, the thermal time lag becomes meaningless when the thickness is more than 50 cm, because temperature variation decreases more than 95 %.

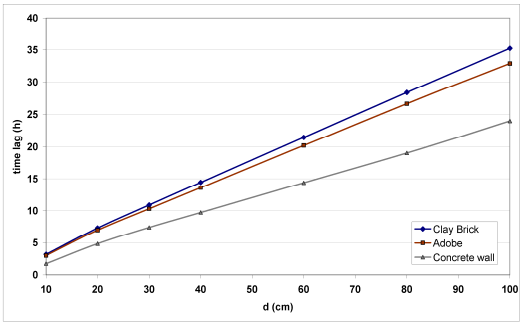

Figure 3. Time lag for clay brick, adobe and concrete walls.

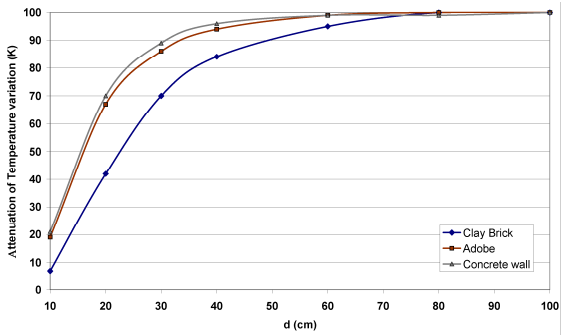

Figure 4. Relative temperature attenuation of clay brick, adobe and concrete walls.

3.3 Inspection of building insulation and envelope for thermal bridging

Anomalies in building envelope usually pertain to problems with insulation system or defects in envelope that cause thermal bypasses to occur. Incomplete or discontinuous insulation in walls cause large amounts of thermal loss in the buildings and decrease thermal comfort for the occupants. Thermography can assist building inspectors to identify insulation failures and thermal bypasses. Before any application regarding thermography, the insulation type and construction details of the buildings should be detected and documented. Also the best inspection is done from both inside and outside.

As mentioned before, thermal imaging for inspection of defects in insulation and building envelope is a qualitative method. Quantifying the results in technical reports, include thermal lag of the envelope that is measured through thermometers installed on the sides of the wall to quantify the thermal resistance, transmittance and inertia of the building envelope components.

In the case study, the building envelope in David house includes adobe walls with brick facades in some parts. Also there are several opening in the building envelope. These openings are mostly woodframed windows with a dingle glased glass or wooden doors with loose conjunctions with the rest of the envelope.

Thermography of David house indicates that the most important thermal bridges of the envelope were single glazed windows. Figure 5 and Figure 6 Show thermal bridges in David house. The red parts in the windows represent thermal loss through single glazed windows, which are considered as thermal bridges. In order to resolve thermal defects through windows, their glasses should be double glazed or another frame should be added in front of the old window from inside or outside the envelope. The decision making on double glazing the existing window or adding another frame depends on the structure of window in terms of bearing the laod of a new material and historic preservation theories.

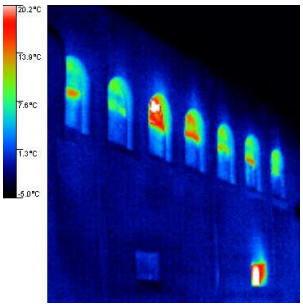

Figure 5. Thermal bridges in thermal images of David house, Isfahan, Iran.

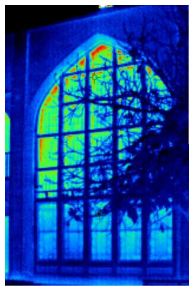

Figure 6. Thermal bridges in thermal images of David house, Isfahan, Iran.

3.4 Location of Air Leakage

Apart form thermal discomfort for occupants and thermal loss form the building, air leakage is usually rainwater ingress pathways too. Therefore, it is nessecary to spot the thermal bypasses in the building envelope to stop rainwater ingress along with unwanted ventilation.

IR is an important tool for quickly finding the highest impact air leakage locations in existing buildings. Because air leakage sites may be difficult to locate under natural conditions, air must be artificially forced across the building enclosure by use of a fan such as a blower door or by using the mechanical and/or ventilation system(s) in the building. Building depressurization and inside inspection are preferred because of less interference of solar radiation and wind. The outside air is at a different temperature than the inside air and will therefore leave a thermal signature for the infrared imaging system to capture. The thermal image for air leakage will appear as “fingers” or “streaking” showing as dark when cold air is observed and lighter colors when warm air is viewed.

The thermal images will produce irregular shapes with uneven boundaries and large temperature variations. These air leakage sites are often at joints, junctions or penetrations in the enclosure. There is often a temperature gradient within a finger or streaking area. A scan of all interior surfaces may reveal indications of significant air leakage in locations not imagined as connected to the exterior. Discrimination between thermal bridging sites and thermal bypass or air leakage sites should be done by sufficient accuracy. Thermal bridging sites will not change size or shape during the inspection. Also the inspection should be done from both sides to make sure that all the points of infiltration and exfiltration have been detected. Infiltrating cold air itself cannot be seen; however, infiltration can be located because the materials and surfaces that are washed by the cold air flowing through or past them are cooler. Moving air patterns are normally not well defined and are irregular in shape. Fan shaped patterns or semicircular dark areas originating along seams or penetrations reveal the location of holes or linear cracks.

Quantifying the results of thermography need de/pressurization of the building that is done by Blower door fans, Household exhaust fans and HVAC systems. The extent or a gradation in the contrast typically indicates the direction of flow to the thermographer. Endoscopes (or borescopes) allow visual inspection, through a small hole, of gaps in insulation and air leakage pathways.

In David house, locations of air leakage in building envelope are mostly loos conjunctions between openings and the rest fo envelope. Figure 7 shows the heat loss from top of the wooden doors through their conjunction. In most cases, in historic buildings, the loos conjunction occurs when the framing materials have lost their initial shape. In most cases, airleakage problems are solved through repairing the framing parts for giving them their initial shape and injection of some materials such as polystyrene foams in their gaps.

3.5 Location of Moisture

Moisture in building materials can destroy structural integrity and nurture mold. The first step in moisture problem remediation is to locate and remove all sources of moisture quickly and accurately. On the other hand, as liquids evaporate, they draw heat energy from their surroundings. Therefore, damp surfaces will typically be cooler. Thermography can identify surface temperature variations of the building envelope, which can indicate problems in a building's moisture content.

Water leakage is the number one cause of damaged insulation and substrate, corrosion and weakening of metal decks and building structure, even structural collapse and the growth of mold. Infrared thermography locates moisture anomalies in building envelopes by exploiting the thermal properties of water. The greater the specific heat[14], the more energy is required to heat or cool a particular material. Consequently, water looses or gains heat much slower than wood or brick under similar conditions[15]. Because the heat capacity of a water-damaged material is greater than that of a dry material and air, areas of high-moisture content appear either warmer or colder than the surrounding infrastructure. The difference in temperature can be imaged and measured using an infrared camera.

In David house the ditected moisture problems mostly stemed from rain water ingress inside the material of the building envelope near the roof. The moisture intrusion was because of defect in draiange system on the roof. Figure 8 Represents the moisture problems in David house.

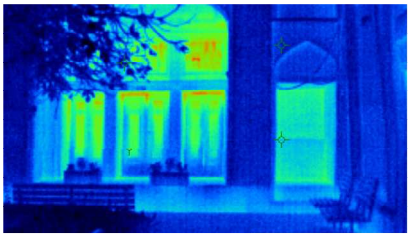

Figure 7. Heat loss from wooden doors through their conjunction, David house, Isfahan, Iran.

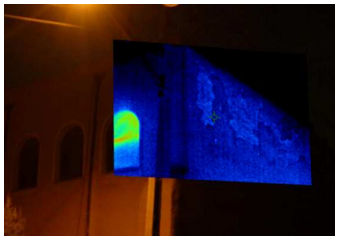

Figure 8. Moisture problems in David house, Isfahan, Iran.

A hand-held moisture meter can be very useful in diagnosing thermal anomalies. Masonry walls are often found to have variable moisture contents leading to thermal patterns not directly related to insulation placement. According to Resnet Interim Guidelines for Thermographic Inspections of Buildings [2010] 'Wet thermal insulation will also give thermal anomalies and can be confirmed with a moisture meter. It is worthy to remind that prior to the moisture inspection in structures, no precipitation should be occurred for at least 24 hours'.[16] The location of condensation in the building envelope appears to be the same method for moisture inspection.

[14] Specific heat is the amount of heat required to raise the unit mass of material one unit of temperature

[15] For example, water has a higher specific heat (4,180 J kg^{-1} $^{o}C^{-1}$) than pine (2,800 J kg^{-1} $^{o}C^{-1}$) used as framing lumber or common building brick (840 J kg-1 ^{o}C-1).

[16] Resnet Interim Guidelines for Thermographic Inspections of Buildings, 2010.

3.6 Identification of Structural, Electrical and Mechanical Degradation

Structural degradation
Aging in buildings may cause the occurrence of wood rot, metal corrosion, staining of bricks and concrete. Any of the mentioned anomalies are traceable through thermal imaging. The rotten parts of wooden structure may seem lost or party absent in thermal imaging. Also the biological activities of bacteria and fungus cause the rotten parts of wood to present different thermal patterns in structure. Corroded metal have different surface properties, such as emittance and reflectance, comparing to normal parts of the structure. Chemically stained concrete parts and bricks also exhibit different behavior in thermal imaging that stems from the change in their surface properties. Consequently, their patterns differ in thermal imaging. Detection of cracks in concrete structures is possible through thermal imaging since the cracks appear as thermal bypasses in structure and stand out.

Electrical degradation
IR inspections of electrical installations can be used to locate both loose and corroded connections before they cause a catastrophic failure or serious damage, with a possible serious impact on the connected equipment or even become a fire hazard and endanger the life of occupants and technical personnel.

Mechanical inspection
IR inspections of mechanical equipment can be used to identify sediment in boilers and tanks. In other cases boilers with missing and damaged insulation resulting to increased heat losses and energy costs may be inspected in building mechanical system. Overhanging motors have a shorter life span and a lower efficiency since it takes a lot of extra energy to produce that much heat. Thermography can also be used on mechanical plant such as pumps, compressors, fans, motors and coils.

Difficult to access HVAC installations can be inspected. For example, IR imaging can be used to distinguish air supply and exhaust outlets from hard to reach ceiling diffusers and determine their operational status. It is also possible to locate and trace hot and cold pipes inside building elements (i.e. floor piping in water heating systems), to identify the loops and minimize the guesswork when there is a need to replace them, to check for heat losses as a result of poorly insulated pipes and ducts, etc.

Finding boiler refractory or insulation breakdown, blocked cast iron sections, scale buildup, hot gas leaks and furnace tube blockages also can pay dividends in energy conservation, save countless maintenance hours and prevent boiler failure. Accurately detecting refrigeration and air conditioning air leaks, energy loss, heat exchanger, refrigerator and air conditioning efficiency and clogged condenser/heat exchanger tubes, will prevent inefficient operation and wasted energy.

4 THERMOGRAPHY RESULTS

The results of the scan can be subtle and customarily require the interpretation of the experienced thermographer. After reviewing the scan, a visual site inspection of problem areas, and a review of photos and detail drawings may be necessary to understand how the building envelope is constructed and to completely understand the causes of its problems. In some cases, other types of testing will be used to corroborate or pinpoint air leakage sites in remote locations. This may include the necessity of opening critical parts of the building envelope so that they can be visually inspected.

5 INFRARED MEASUREMENT PROBLEMS

Infrared thermography alone will not identify the cause and source of any given anomaly, nor does it quantify the depth and intensity of the cause or damage. Also thermal images can be difficult to interpret accurately when based upon certain objects, specifically objects with erratic temperatures; However, this problem is reduced in active thermal imaging. Accurate temperature measurements are

hindered by differing emissivities and reflections from other surfaces. Most of thermal imaging cameras are not as accurate as contact methods also they are only able to directly detect surface temperatures.

6 CONCLUSION

Thermography of David house indicates anomalies in building envelope that are mostly because of the age of building and lack of maintainance during recent years. The most intense problems are considered as heat loss through thermal bridges and thermal bypasses. Since building anomalies may show up in a building from time to time, it is better to check the building by thermal imaging more frequently. Therefore, building anomalies are detected while it is not too late for further actions.

Thermography of David house revealed thermal and moisture problems, however; building investigation could be more accurate if it could be accompanied by quatitative methods such as heat flux sensing, moistur meter and blower door. Furthermore, more resolution of thermal imager could yeild in sharper images and consiquently more accurate inspection and interpritation.

The investigation about the existing condition of David house has put into evidence few problems related to thermal bridges and moisture infiltration. It is obvious that in any rehabilitation action, the existings problems of the envelope must be took into consideration, and the monitoring of the building after rehabilitation must be performed, for documentation and controling the effectiveness of improvement actions.

The investigations demonstrate that qualitative infrared thermography coupled with an informed visual inspection and quantitative substantiation is an effective protocol to detect building anomalies. Infrared thermography provides a means of seeing the invisible thermal signatures that are related to many building enclosure problems and conditions.

Infrared thermography is a useful and effective tool for the detection of thermal and moisture anomalies in building envelope systems. Aslo structural, electrical and ,mechanical degradation are detected through this method in buildings. Although different complexities of building during construction and performance can be detected by thermal imaging, considerable care must be exercised in both collection and interpretation of thermographic data.

REFERENCES

Kominsky, J. R., Luckino, J. S. & Marin, T. F. 1998, *Passive Infrared Thermography- A Qaulitative Method for Detecting Moisture Anomalies in Building Envelopes.*

Park, S.C. 1996, *Controlling Unwanted Moisture in Historic Buildings*, Washington.

Linville, C. 2002, *Thermography has become an invaluable asset for insulation energy audits.*

Szokolay, S.V. 2008, *Introduction to architectural science: the basis of sustainable design.*

Roos, C. 2008, *Principles of Heat Transfer*, Energy Efficiency Fact Sheet, Washington University.

RESNET Standards 2010, *Resnet Interim Guidelines for Thermographic Inspections of Buildings*.

Iran Meteorological Organization, http://www.irimo.ir/english/index.asp.

XII DBMC
International Conference on Durability of Building Materials and Components
PORTO - PORTUGAL, April 12th-15th, 2011

Strengthening of the Terminal B of the Leixões Harbour Oil Complex. Petrographic Study of Concrete

Madalena Teles [1]

ABSTRACT

Recently, in order to decide the eventual strengthening of a concrete structure it has been required not only the physical and mechanical characterization of the concrete, but also a petrographic study to evaluate the state of hydration of the cement paste and to identify the chemical reactions that originate new products.

A case study that allowed deciding for the strengthening of the structure is presented: the diagnosis of the concrete of the Terminal B of the Leixões Harbour Oil Complex , based on the petrographic analysis. Terminal B is a mass concrete berthing structure, about 40 years old.

The cement paste was well hydrated, showing hydrated calcium silicates and portlandite crystals. The hydrated calcium silicates are the main responsible for the resistance and binding properties of the cement paste and the portlandite, for long-term stability of the silicates.

The concrete showed essentially three main products of neoformation, corresponding to four chemical reactions: the reaction between the chlorine ion and the cement aluminates, the sulphate attack, the carbonation and a precipitation of calcite from seawater.

The first reaction is not damaging to the concrete, delaying the chloride-induced corrosion of any embedded metal. The sulphate attack though it did not cause any damage to the concrete yet, can become destructive in the long term. The formation of calcite, despite contributing to corrosion of the reinforcement does not cause any damage to the mass concrete.

KEYWORDS

Concrete pathology, concrete petrography, strengthening of structures.

[1] Faculty of Engineering of the University of Porto (FEUP), Porto, PORTUGAL, mteles@fe.up.pt

1 INTRODUCTION

The importance of petrographic techniques in the study of concrete is now widely recognized, allowing the retrieval of information that cannot be achieved by other means. When combined with other techniques and physical tests, these combined methods provide a very efficient means of characterizing concrete and mortar and are also highly useful in providing insights into the mechanisms for their deterioration [Teles et al. 2004].

The focus of this paper is a case study on the diagnosis of concrete used to construct Terminal B of the Leixões Harbour Oil Complex. Terminal B is a mass concrete berthing structure of about 40 years old ('Fig. 1').

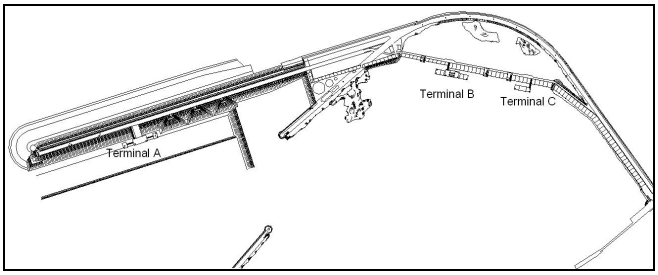

Figure 1. Aerial schematic of Terminal B, Leixões Harbour Oil Complex (adapted from Mota-Miranda, 2006).

Recently, the port authority had had interest in allowing berthing of larger tankers at Terminal B and as a consequence it was determined that the structure required strengthening. The physical and mechanical characterization of the concrete shows values compatible with the reinforcement. The petrographic study presented in this work showed [Teles 2010] that the cement paste was well hydrated, as evidenced by the formation of hydrated calcium silicates, which are the primary hydrates responsible for the resistance and binding properties of cement paste, and portlandite crystals, that are responsible for long-term stability of the silicates. The concrete showed essentially three main products of neoformation, corresponding to four chemical reactions; specifically, reactions: (i) between chlorine ions and cement aluminates; (ii) sulphate attack; (iii) carbonation, and (iv) precipitation of calcite from seawater. The first reaction is not damaging to the concrete, since this process delays the chloride-induced corrosion of any embedded metal. Whereas sulphate attack, though it did not yet cause any evident damage to the concrete, can become destructive in the long term. The formation of calcite, despite contributing to corrosion of the reinforcement does not cause any damage to the mass of concrete.

2 SAMPLING AND METHODOLOGY

Ten fractions of a set of six cores were extracted from the concrete throughout the depth of the structure at two different locations, close to the cores extracted for physical and mechanical tests [Teles 2010]. To avoid possible dissolution of soluble salts, samples were extracted dry. To observe and analyse the concrete by scanning electron microscopy (SEM) and energy dispersive spectrometry (EDS), a set of 30 samples were prepared. To achieve good global analysis, sample surfaces were prepared to ensure that they were, to their extent, as smooth as possible. Thus, samples for these analyses were obtained by sawing the concrete cores to appropriate size. Two other samples were prepared for X-ray diffraction analysis.

Macroscopic analysis of the cores showed a compact mass concrete without cracks. The coarse aggregates consisted of different types of granite, each type having varying degrees of weathering.

3 RESULTS AND DISCUSSION

3.1 Semi-quantitative chemical analysis of concrete

For each core extracted from a given location three semi-quantitative global analyses were completed using SEM/EDS [Teles 2010] for which their respective spectra are given in Figure 2. Since concrete is a heterogeneous material, the analysis are different, as is evident in 'Fig. 2' and the values of elemental oxides are considered as relative values and only for elements that occur in greater quantity.

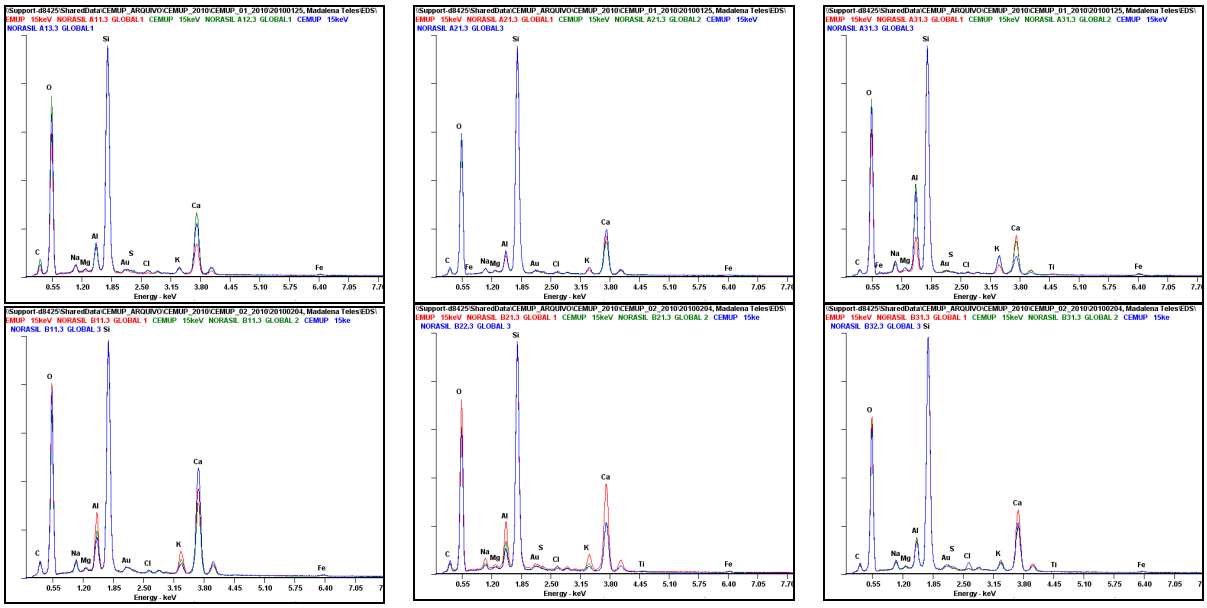

Figure 2. Spectra of the three global analysis of each core.

The semi-quantitative analyses are consistent with those of a well hydrated concrete. However, the peaks of some spectra suggest the possible presence of alkali-rich products that could be an issue in respect to deterioration. Also, in some spectra, there is the occurrence of chlorine and sulphur "spectrum noise", indicating the presence of compounds of these elements.

3.2 Observation and analysis of concrete

The SEM/EDS observations and analysis showed that the composition of the concretes in the samples of the two different locations are similar and are therefore treated together.

The observations and analysis also showed that the sand is the same for all samples, essentially composed of quartz and alkali feldspars, generally rich in potassium, sometimes showing cleavage planes ('Fig. 3'). The presence of small amounts of biotite and shell fragments were also evident. Some particles of calcite from the cement filler were identified in all samples.The presence of feldspars may provide an explanation for the more pronounced alkalis peaks in the spectra obtained from the global analysis. Another possible explanation is the probable use of alkali-rich cement.The cement paste is mainly composed of hydrated silicates, containing smaller amounts of hydrated aluminates. That is why the spectra generally show silicon and aluminum "noise". The cement paste, in all samples, often showed, either needles or balls of needles of hydrated calcium silicates ('Fig. 4') and portlandite, calcium hydroxide, ($Ca(OH)_2$). The concrete was rich in portlandite often showing a foliate aspect, occurring sometimes in large crystals or showing dissolution forms ('Fig. 5'). The aluminates were isolated in just one sample, because they are poorly crystalline and its most common form is a rosette of very small dimensions, which is very difficult to analyse.

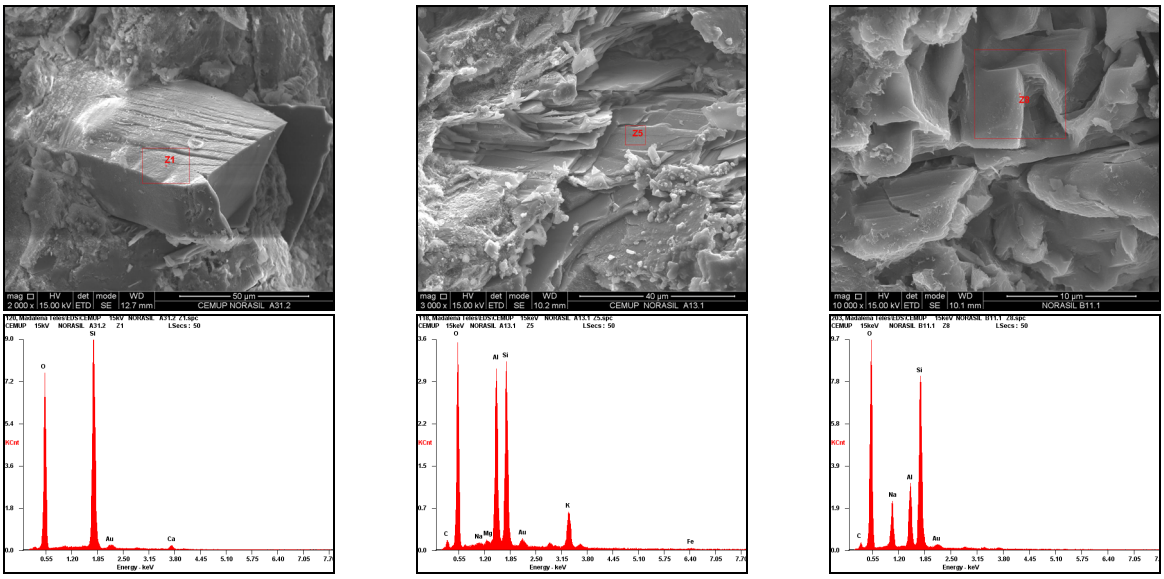

Figure 3. Images and spectra of quartz, potassium feldspar and sodium feldspar.

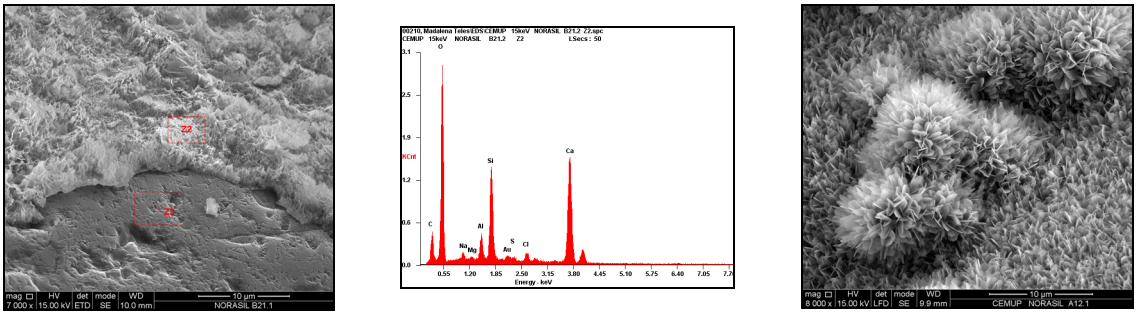

Z3 - Quartz

Figure 4. Images and spectrum of hydrated calcium silicates.

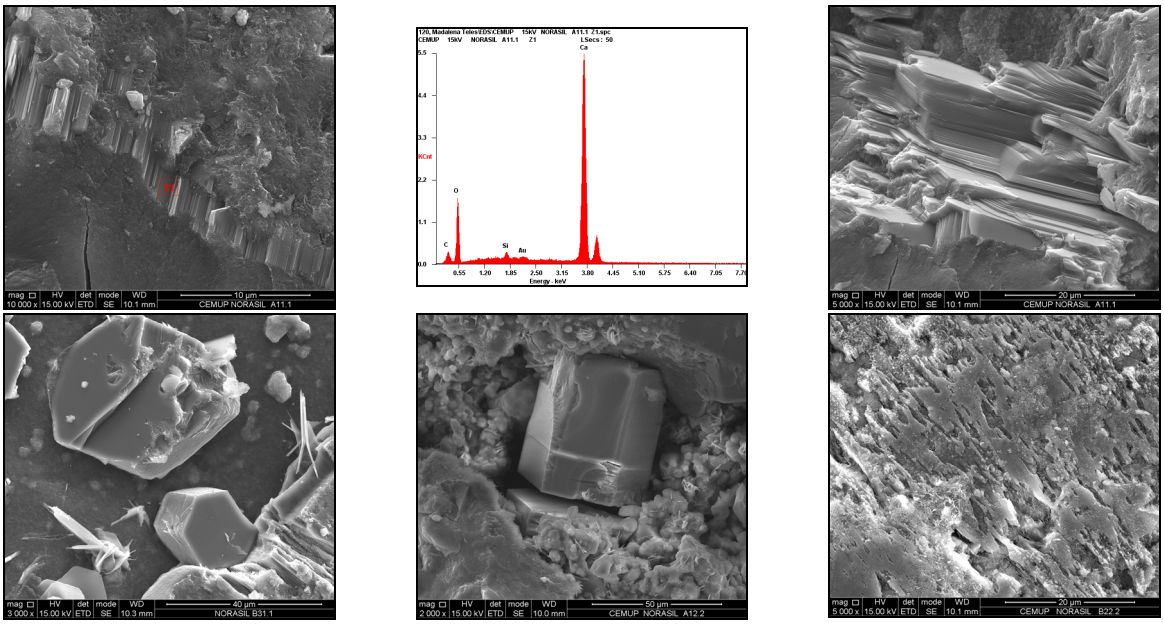

Figure 5. Images and spectrum of portlandite.

The silicates are only stable when in contact with supersaturated solutions of calcium hydroxide and portlandite is a reserve and it can be dissolved when the concentration in calcium hydroxide is reduced. The concrete is rich in portlandite, showing the use of a cement rich in tricalcium silicate.

As the new compounds are preferentially located in the pores, the observation of their concentration within the pores gives an overview of the concrete in the samples. All samples often exhibited empty or poorly filled pores. Filled pores were found only exceptionally (‘Fig.6’). The products identified in the pores were calcium chloro-aluminate hydrate ($3CaO.Al_2O_3.CaCl_2.10H_2O$), sometimes referred to as Friedel’s salt, ettringite, calcium sulpho-aluminate hydrate ($3CaO.Al_2O_3.3CaSO_4.32H_2O$), calcite, calcium carbonate (CO_3Ca) and portlandite.

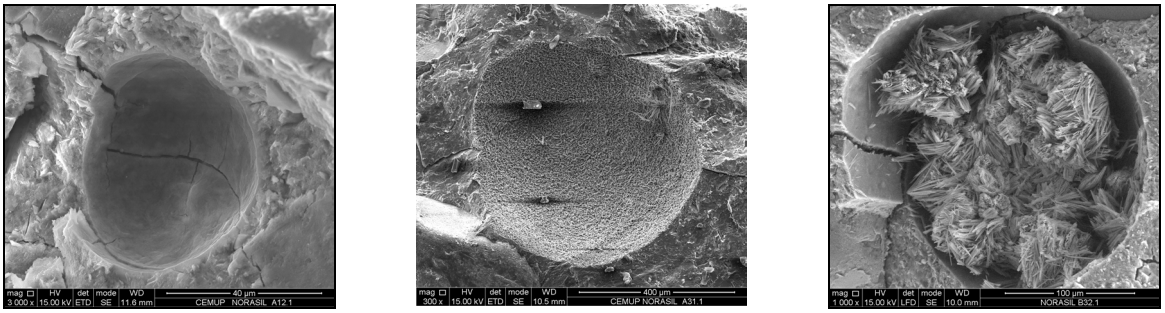

Figure 6. Empty, poorly filled and filled pores.

All the cracks of all samples were investigated to clarify if some cracks could be attributed to expansive reactions. Only one crack was found that related to the development of ettringite (‘Fig.7’).

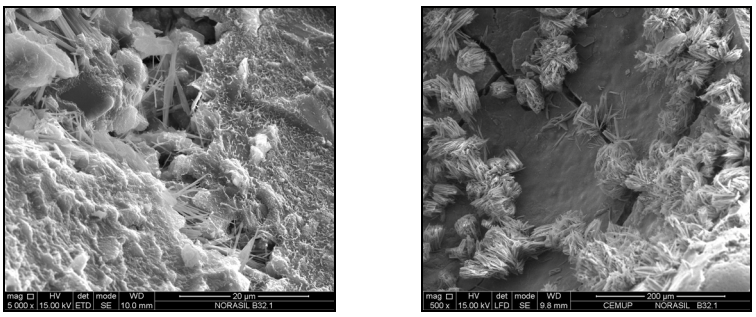

Figure 7. The crack on the left side is caused by the formation of ettringite. The cracks on the right are subsequent to its formation.

The neoformation products founded were, in essence, calcium chloro-aluminate hydrate, ettringite, and calcium carbonate. All samples, except one, showed hydrated calcium chloroaluminate, although in very small amounts (‘Fig.8’). In general, the ettringite occurred in very small amounts. In one of the samples, it was not identified, and in another, it appeared in larger quantities (‘Fig. 9’). The calcium carbonate was identified in small quantities and only in four samples (‘Fig.10’).

The reaction of chloride ion with the cement aluminates yields calcium chloro-aluminate. This reaction delays corrosion by the action of the chloride ions since only free ions, not those already combined, in fact contribute to the destruction of the passive film that covers the reinforcement, or any embedded metal in the concrete. The presence of ettringite revealed that the concrete was subjected to sulphate attack . This attack, though it did not yet cause any damage can become destructive in the long term. Sulphates have different origins, either internal or external to the concrete. Although the location of the structure points to an attack by external sulphates contained in seawater, the concrete showed no other salts, such as halite, brucite and gypsum, that might usually be present when seawater attack on concrete begins to develop. These circumstances, together with the

fact that a mass concrete structure during concreting can reach very high temperatures, particularly if the concreting is done in hot weather, leads to the possibility of an attack by internal sulphates. The calcium carbonate results from carbonation of the concrete in the superficial samples, and in the other samples could be attributed to the precipitation of calcium carbonate from seawater that had penetrated the concrete. The formation of calcite, despite contributing to corrosion of the reinforcement does not cause any damage to the mass concrete. [Teles 2009] [Teles 2010].

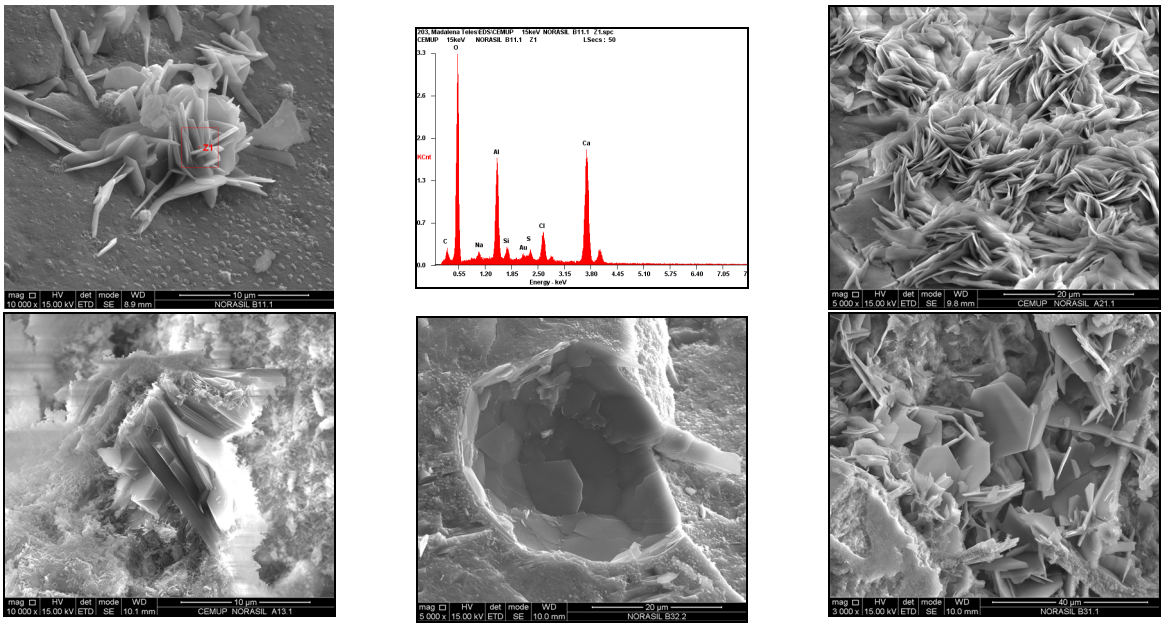

Figure 8. Images and spectrum of calcium chloroaluminate hydrated.

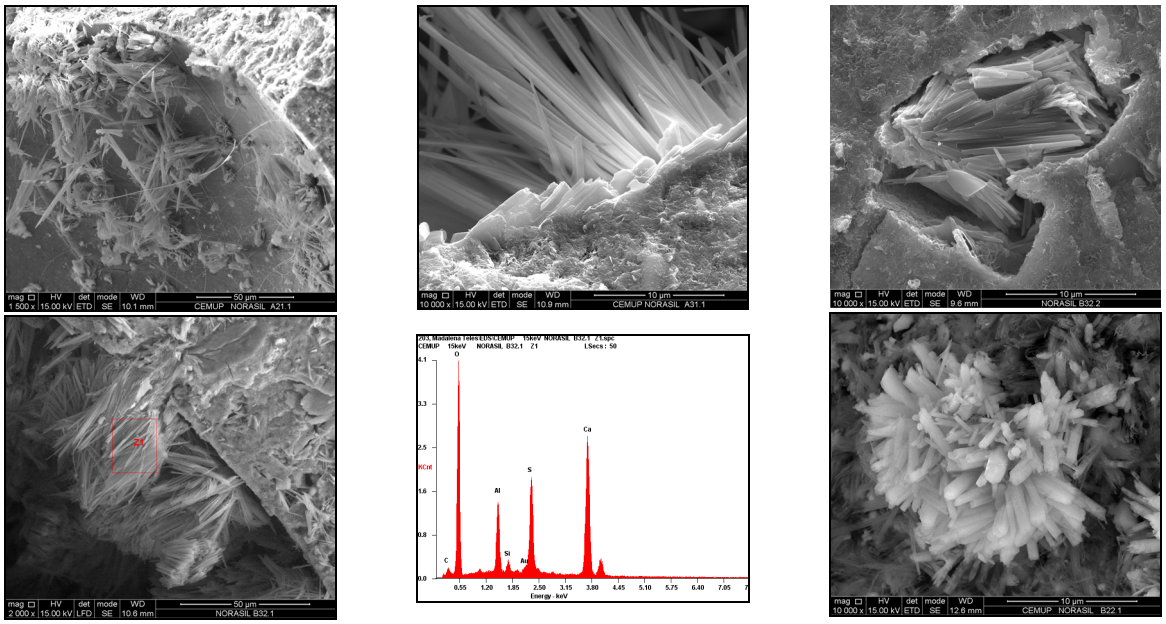

Figure 9. Images and spectrum of ettringite.

Other neoformation products were identified very occasionally in two samples. Therefore, these products are less important than the others referred to above. These products were, alkali silicates, trona and calcium hydroxide. The sodium-rich alkali silicate had a smooth and cracked aspect and, the calcium-rich alkali silicate showed like balls of needles. In one sample, a set of needles of trona ($Na_3H(CO_3)_2.2H_2O$) (‘Fig. 11’) was identified. All these products were on quartz grains (‘Fig. 11’).

Figure 12 shows some crystals and one spectrum of a neoformation product. Despite that there was a strong suggestion for portlandite precipitation, an X-ray diffraction was carried out to ensure that no calcium oxide was present (‘Fig. 13’). This analysis confirmed that the product was portlandite.

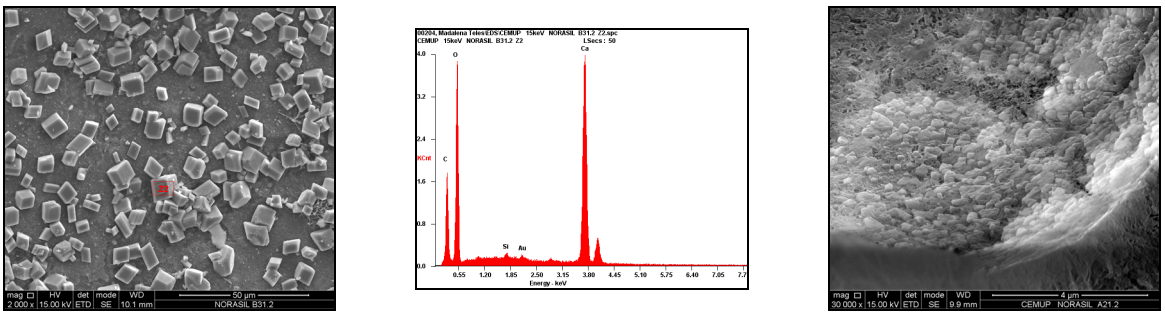

Figure 10. Images and spectrum of calcite.

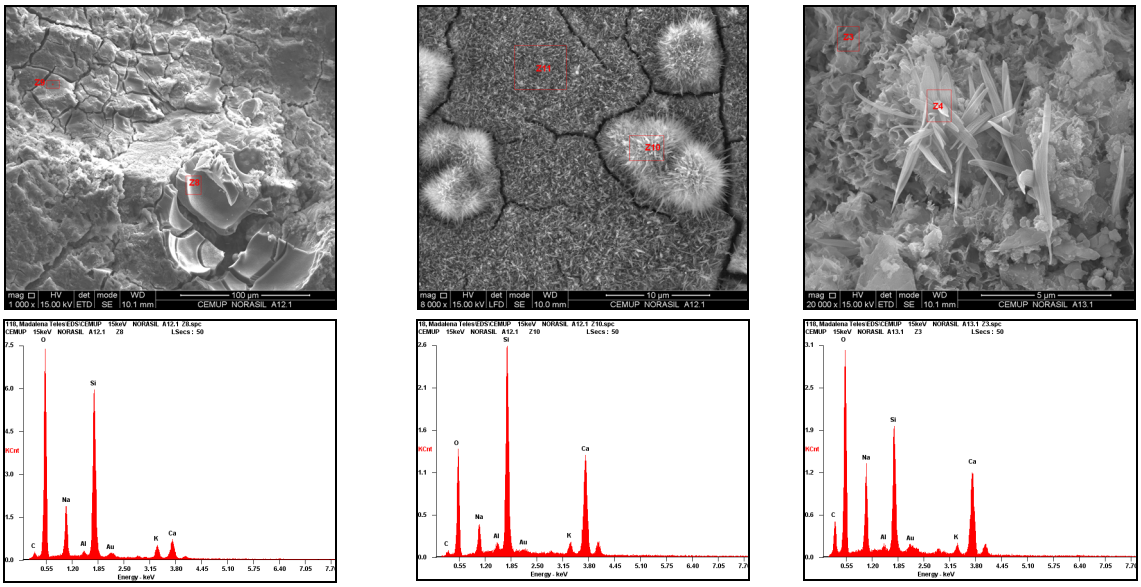

Figure 11. Images and spectra of sodium-rich alkali silicate (Z8 and Z9 are similar) and calcium-rich alkali silicate (Z10 and Z11 are similar) and needles of trona (Z3 and Z4 are similar).

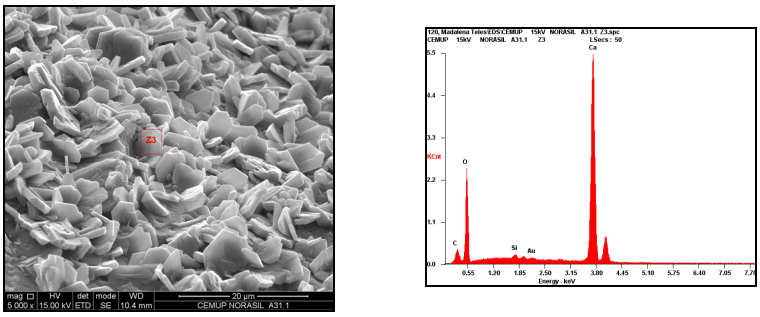

Figure 12. Images and spectrum of neoformation calcium hydroxide.

The alkali silicates result from alkali-silica reactions [Teles 2009]. The trona, a soluble salt, is often associated to these reactions. The alkali-silica gel can cause damage in the structure. The fact that none of the manifestations associated with the occurrence of these reactions had been observed in the structure (map cracking, pop-outs, exudations, efflorescence, discoloration of the borders of the

cracks), associated to the age of the concrete (about 40 years old), to the concrete composition (rich in alkalis and in calcium hydroxide) and to a wet environment, points to some occasional reactions between grains of quartz sand and the alkalis, not having any global significance. The neoformation calcium hydroxide is not adverse to the concrete. Its formation results from a dissolution of portlandite, followed by precipitation, when there is a change in environmental conditions.

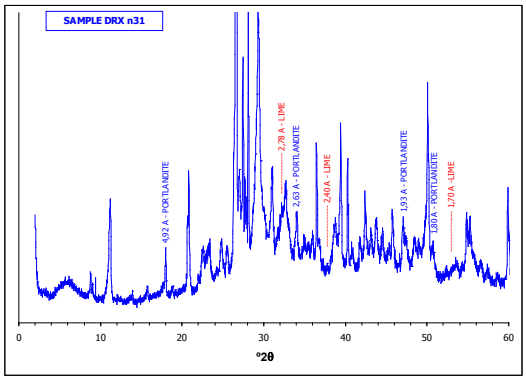

Figure 13. Diffractogram. Portlandite is identified by their main peaks. (CaO − lime), (CaO_2),(CaO_4) and (Ca O_2.8H_2O) were not identified. The three main peaks of lime are marked.

4 CONCLUSIONS

This study provided evidence that the cement paste was well hydrated, showing hydrated calcium silicates, which are the main components responsible for the resistance and binding properties of the cement paste, and portlandite, responsible for long-term stability of the silicates. The concrete showed essentially three main products of neoformation, corresponding to four chemical reactions: the reaction between the chlorine ion and the cement aluminates, the sulphate attack, the carbonation and a precipitation of calcite from seawater. The first reaction is not damaging to the concrete, delaying the chloride-induced corrosion of any embedded metal. The sulphate attack though it did not cause any damage to the concrete yet, can become destructive in the long term. The formation of calcite, despite contributing to corrosion of the reinforcement does not cause any damage to mass concrete.

Today, in Portugal, almost all of the Technical Specifications for the rehabilitation of special structures (dams, bridges, viaducts, berthing structures, high buildings and so on) imposed the petrographic study of the concrete. However, results of investigations from different authors are sometimes of uneven quality and reliability. To avoid these unconformities, it is essential that the technician who undertakes the petrographic study of the concrete have a deep knowledge of concrete and its pathologies, and obviously know how to utilize petrography techniques.

REFERENCES

Mota-Miranda, A. 2006, *Influência da proximidade do mar em estruturas de betão,* Tese de Mestrado da Faculdade de Engenharia da Universidade do Porto, Porto, pp.204.

Teles, M., 2009, *Patologia do Betão*, Mestrado em Reabilitação do Património Edificado 2009/2010, http://www.fe.up.pt, pp.242.

Teles, M. 2010, *Análise Petrográfica de um Betão do Terminal B do Complexo Petrolífero do Porto de Leixões.Parecer sobre o Estado do Betão,* Laboratório de Ensaio de Matérias de Construção, Relatório, Porto, Portugal, pp.30.

Teles, M., Begonha, A. Fernandes, I. 2004, 'Estudo petrográfico de betões e argamassas', *Revista Internacional Construlink – Estruturas e Construções*, nº5 Fev. 2004 vol.2, pp.4–20.

XII DBMC
International Conference on Durability of Building Materials and Components
PORTO - PORTUGAL, April 12th-15th, 2011

Access Viaducts to the Drawbridge of Leixões Harbour - Diagnosis of Concrete Deteriorations

Andreia Mota-Miranda [1]
Madalena Teles [2]

ABSTRACT

The two access viaducts to the drawbridge of Leixões harbour are connected with the metallic structure of the drawbridge and allow the passage between the two towns, Leça da Palmeira and Matosinhos. The viaducts are concrete structures, composed of wall-columns and abutments, in reinforced concrete, supporting longitudinal beams placed side by side and braced by transversal beams, all of prestressed concrete. The slab is also in reinforced concrete.

The viaducts built between 1957 and 1960, were repaired between 1991 and 1993. As the drawbridge was inadequate for both the road and the harbour traffic, it was replaced and some of the spans of the viaducts were demolished and all the concrete was repaired between 2006 and 2008.

The aim of this work was, before this last rehabilitation, to make a diagnosis of the deterioration of the concrete viaducts. After collecting and analyzing all the information about the characteristics of the different materials used in concrete and its composition and properties, a visual inspection of the structure was made, and all relevant evidence of deterioration was recorded and photographed. Some samples of apparently non-deteriorated concrete and visually deteriorated concrete were extracted for analysis. The carbonation and the chloride ingress were determined in samples of apparently non-deteriorated concrete. All samples were observed and analyzed by scanning electronic microscopy (SEM) and energy dispersive spectrometry (EDS).

KEYWORDS

Concrete, durability, petrography, pathology.

[1] Novopca, Contrutores Associados, S.A., Porto, PORTUGAL, andreiamotamiranda@gmail.com
[2] Faculty of Engineering of the University of Porto (FEUP), Porto, PORTUGAL, mteles@fe.up.pt

1 INTRODUCTION

The two access viaducts are located 500m from the sea at Leixões harbour, the biggest port infrastructure in the north of Portugal (‘Fig.1’). The viaducts are concrete structures, composed of wall-columns and abutments, in reinforced concrete, supporting longitudinal beams placed side by side and braced by transversal beams, all of prestressed concrete. The slab is in reinforced concrete.



Figure 1. Aerial view of Leixões harbour.

The viaducts, built between 1957 and 1960, were repaired between 1991 and 1993. The repair work in the concrete consisted of a reconstruction of the concrete in the support zone, filling cracks in the beams and the application of grout repair and painting of beams, wall-columns and abutments. As the drawbridge was inadequate for both the road and the harbour traffic, it was replaced and some of the spans of the viaducts were demolished and all the concrete was repaired between 2006 and 2008 (‘Fig.2’).



Figure 2. Access viaducts and drawbridge before and after the repair work in 2006.

In this work, a diagnosis of the deterioration of the concrete viaducts, before this last rehabilitation, was done [Mota-Miranda 2006].

The engineering design, the construction and any subsequent repairs on the viaducts were studied by collecting and analyzing the information kept in the archives of the Leixões harbour. The composition of the concretes of all structural elements was identified (‘Fig. 3’), as well as the origin and properties of the materials used. A visual inspection of the structures was made and the most relevant deteriorations were recorded and photographed. Some samples of apparently non-deteriorated concrete and visually deteriorated concrete, as well as some stains and efflorescence were extracted for analysis. The carbonation and chloride ingress were determined in samples of concrete apparently non-deteriorated. All samples were observed and analyzed by scanning electronic microscopy (SEM) and energy dispersive spectrometry (EDS) to study their mineralogy and chemical composition.

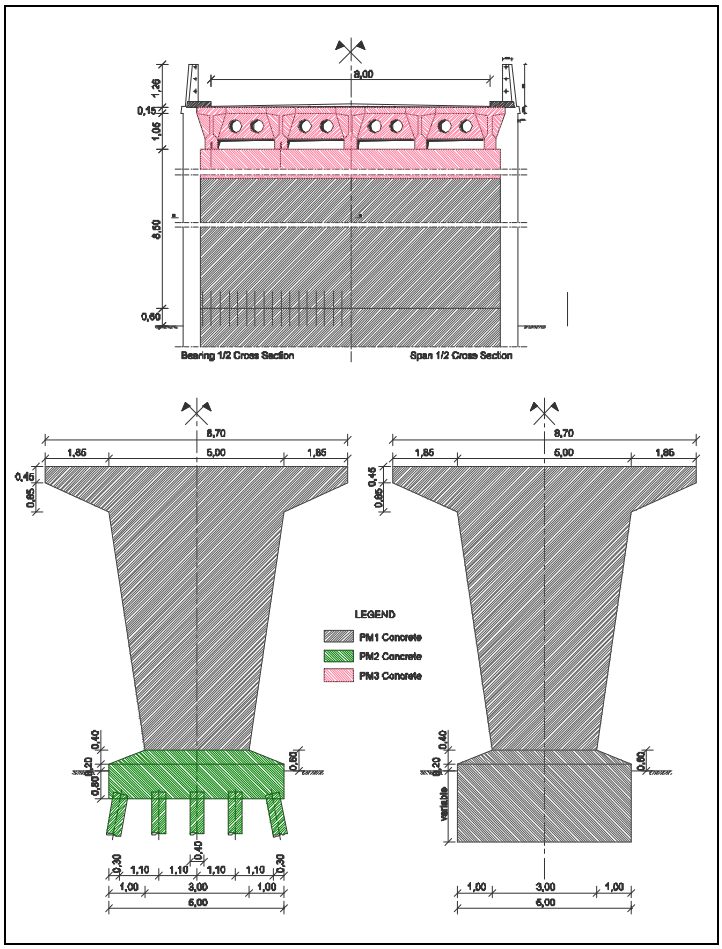

Figure 3. Concrete identification.

2 EXPERIMENTAL STUDY AND DISCUSSION

2.1 Tests

Several tests to characterize the concrete of the viaducts physically, mechanically and chemically were performed [Mota-Miranda 2006]. Only the results of the progression of carbonation and chloride ingress tests, closely associated with the deterioration process of the concrete are shown. The two tests had been carried out in two cores extracted at the same location.

The carbonation depth was determined from the cores from a wall-column of the viaduct with an alcoholic solution of phenolphthalein of 1% [RILEM 1988]. The carbonation depth was 5mm.

Measurements of chloride ingress were made according to specification E 253 [LNEC 1971]. Initially, the chloride content in the concrete was determined at a depth of 5 mm. The determination of the actual chloride content in the cement was done by taking into consideration the concrete composition. The chloride content was 0.02% in the concrete and 0.16% in the cement. Carbonation depth and chloride content were very small.

2.2 The Petrographic Study of the Concrete

Samples of non-deteriorated concrete and visibly deteriorated concrete, as well as samples of all the relevant deterioration (brownish stains and white and dark efflorescence) were observed and analyzed by SEM/EDS [St John et al. 1998].

The visibly deteriorated concrete was obtained from locations near non-structural cracking at the base of one wall-column, at beams (along the reinforcement) and under stains and efflorescence (‘Fig. 4’).



Figure 4. Visually deteriorated concrete, stains and efflorescence.

The observations and analysis of apparently non-deteriorated concrete of the two access viaducts showed good quality concrete, compact and with a well hydrated cement paste, showing hydrated calcium silicates and portlandite, calcium hydroxide, ($Ca(OH)_2$) (‘Fig. 5’). The neoformation products found were calcite, calcium carbonate (CO_3Ca), sylvite, potassium chloride (KCl), ettringite, calcium sulfo-aluminate hydrated ($3CaO.Al_2O_3.3CaSO_4.32H_2O$) and gypsum, calcium sulphate bi-hydrated ($CaSO_4.\ 2H_2O$) (‘Fig. 6’). Large quantities of calcite were found even at 5mm depth, very small quantities at 8mm and at 100mm depth no neoformation calcite was identified. This concrete also showed potassium chloride crystals next to the surface. Beyond 5mm the concrete showed an incipient sulphate attack with the development of ettringite and gypsum.

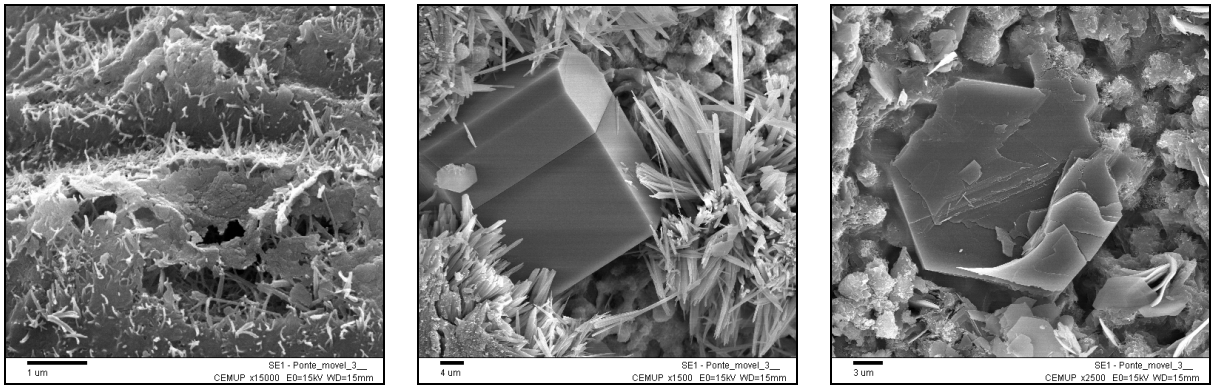

Calcium silicates | Portlandite Crystal | Portlandite Crystal

Figure 5. Calcium silicates and crystals of portlandite.

The cement paste showed hydrated calcium silicates, which are mainly responsible for the resistance and binding properties of cement paste, and portlandite crystals, responsible for long-term stability of the silicates. The observations of calcite are coherent with the carbonation test. The sylvite crystals next to the surface are probably due to the contamination of the repair mortar that had chloride in its’ composition [Mota-Miranda 2006]. The sulphate attack with formation of gypsum and ettringite is an

external attack due to the water from the "Leça" river. Analysis of this water showed a very high sulphate content [Mota-Miranda 2006].

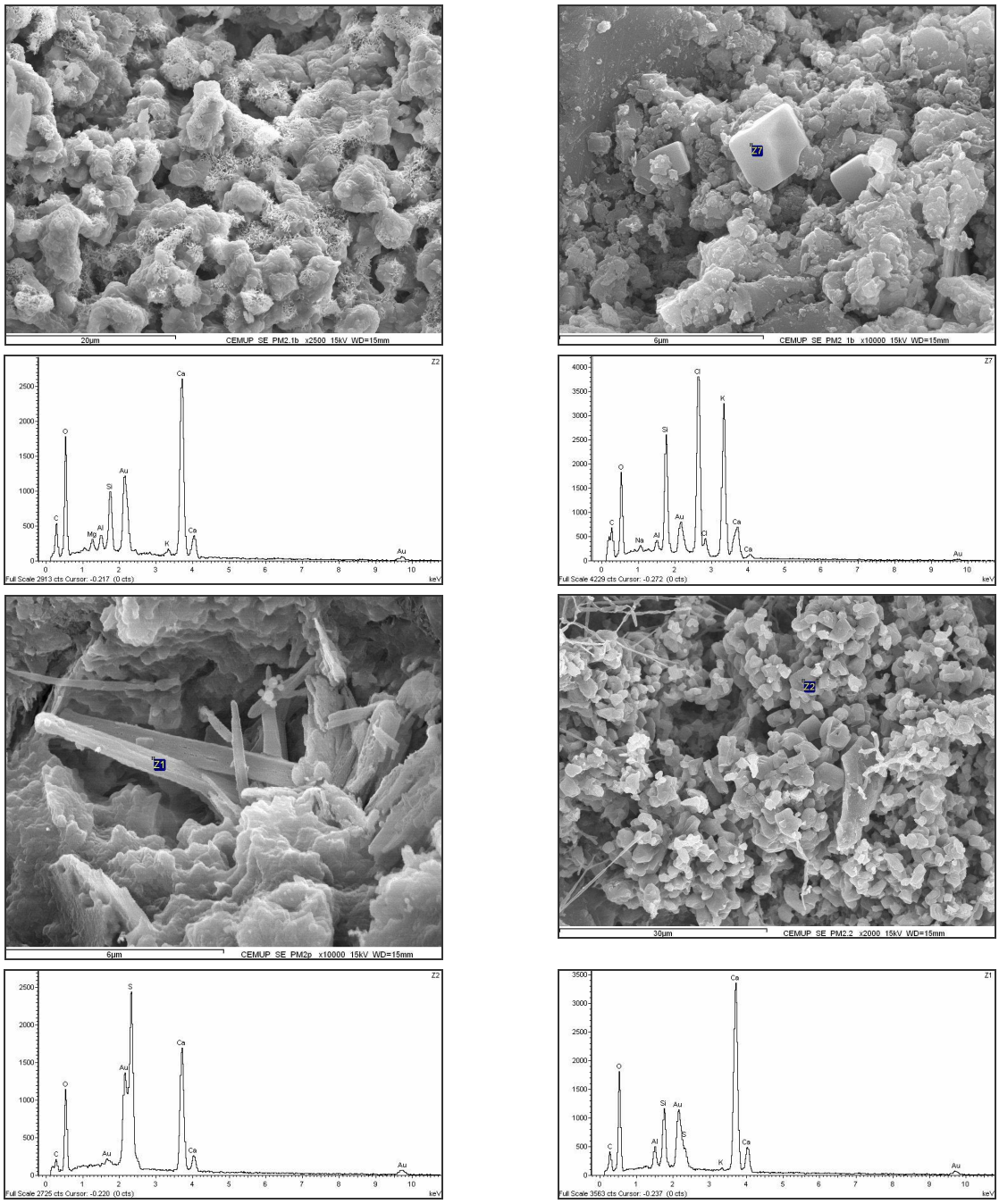

Figure 6. Calcite (dissolution forms), sylvite, ettringite and gypsum images and spectra.

The concrete of the base of one wall-column with a non-structural crack, showed calcium silicates and aluminates, along with large quantities of calcium carbonate and halite, sodium chloride, (NaCl) ('Fig.7').

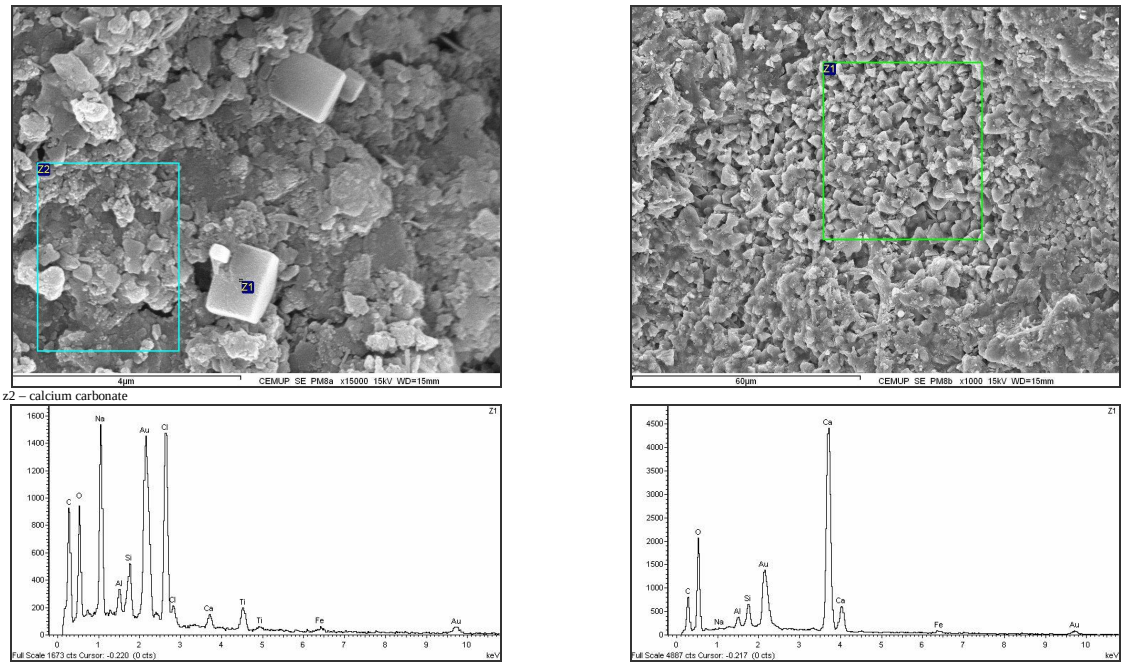

Figure 7. Images and spectra of sodium chloride and calcium carbonate.

The concrete facing south showed many crystals of calcium carbonate and of sodium chloride. This is the original concrete, without treatment, so, the origin of chloride is associated with environmental contamination; it rapidly develops in areas exposed to rainwater. Calcite is due to the penetration of carbonation which is easier when you have crack openings.

The observations and analysis of the concretes that are partially detached from the structures, near non-structural cracking along the reinforcement, showed that these concretes are very rich in calcite. The brownish stains found, on these concretes, were all of iron oxides (‘Fig.8’).

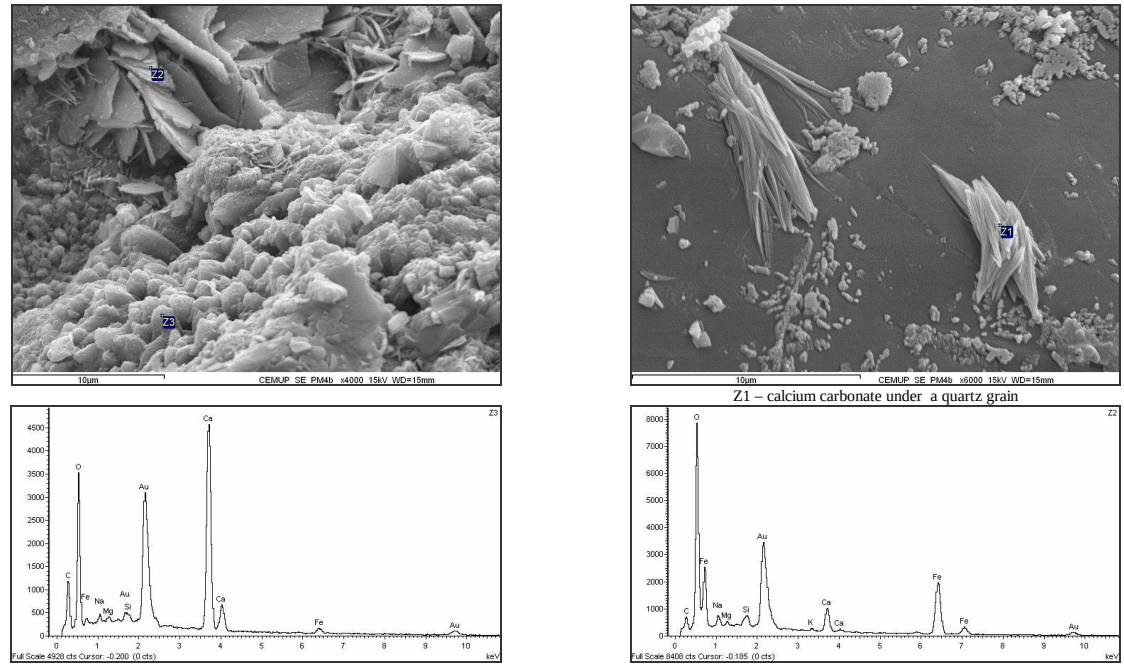

Figure 8. Calcite and iron oxides images and spectra.

These concretes show corrosion due to carbonation. The results of the chloride content analysis show that the corrosion of the reinforcement are caused by carbonation and not by high chloride content. The stains on these concretes consisted totally of iron oxides, and are caused by steel corrosion. The non-structural cracking along the reinforcement and the concrete spalling or delamination are due to the formation of expansive products of steel corrosion.

White and dark efflorescence were also analyzed. The white efflorescence consisted essentially of calcium carbonate (‘Fig. 9’). The black efflorescence was organic substances (‘Fig. 10’).

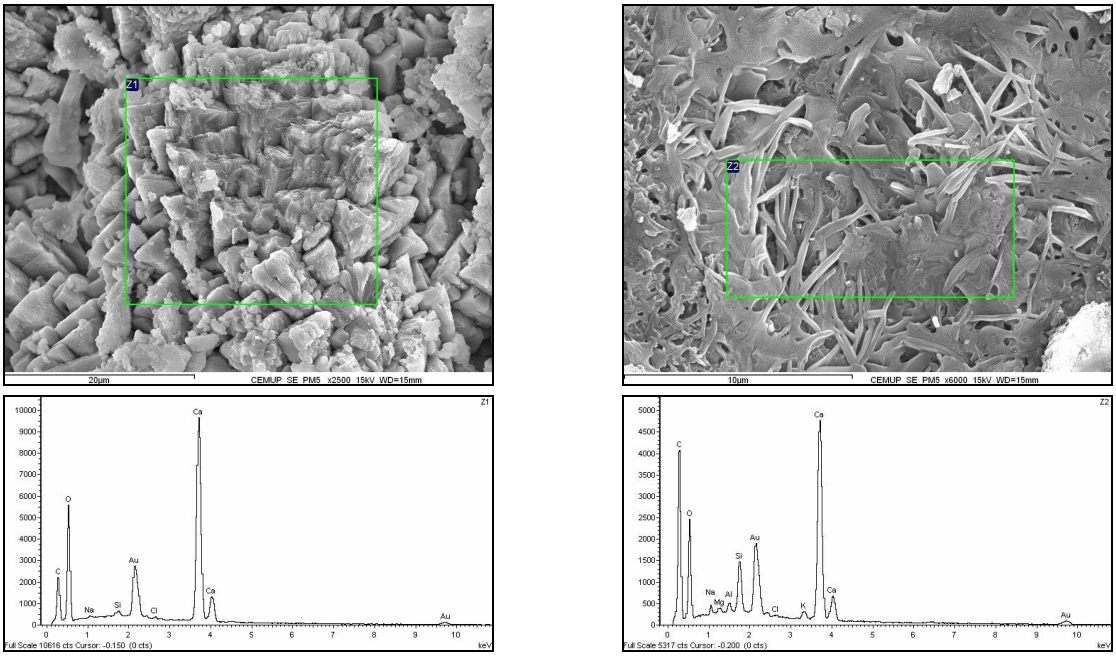

Figure 9. White efflorescence images and spectrum.

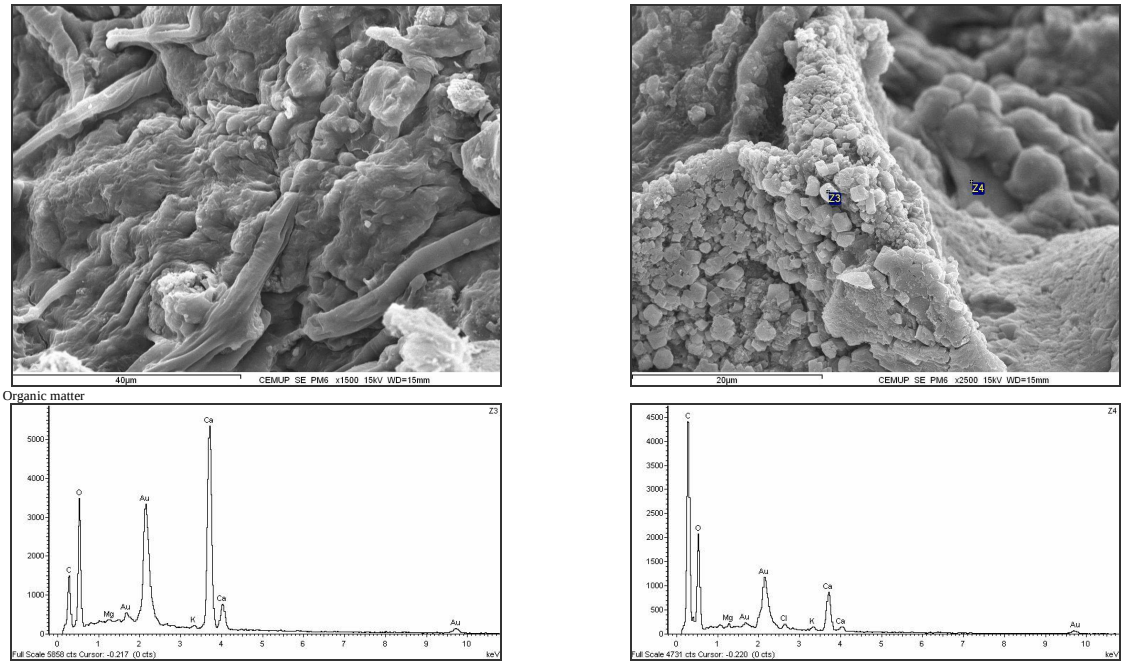

Figure 10. Black efflorescence images and spectra.

The white efflorescence has its genesis in the leaching of lime compounds in the concrete and its carbonation at the surface. The dark efflorescence is an organic substance caused by moisture.

3 CONCLUSIONS

From the evaluation of the results, we can conclude that:
The carbonation depth in concrete was very small, much less than the coating thickness, which in the worst case was 20 mm.

The chloride content results at a depth of 5 mm showed that the risk of corrosion is negligible or low. For this reason it was not necessary to take measurements at greater depths. The chloride content, showed smaller values than those allowed by the European legislation for chlorides in concrete mix of construction located in proximity to marine environment, (total chlorides for each concrete component).

Given these results, it may seem strange that the structures essentially show corrosion by carbonation. However, problems occurred during the repair work done between 1991 and 1993 [Mota-Miranda 2006] that resulted in a repair which did not eliminate all sources of corrosion.

The SEM/EDS observations and analysis of apparently non-deteriorated concrete showed well hydrated cement paste with hydrated calcium silicates, which are mainly responsible for the resistance and binding properties of the cement paste, and portlandite, is responsible for long-term stability of the silicates. This concrete showed four main products of neoformation: calcite, sylvite, ettringite and gypsum. The calcite is due to carbonation and the observations are coherent with the results obtained from the carbonation test. The sylvite is probably due to the contamination of the repair mortar that had chloride in its composition. This shows the importance of controlling the repair mortar composition, since this mortar was rich in chlorine, an element clearly aggressive for corrosion of reinforced and pre-stressed concrete. The ettringite and gypsum result from a sulphate attack due to external sulphates from the water of the Leça river. This attack is until now incipient with no visible manifestations.

The SEM/EDS observations and analysis of visibly deteriorated concrete and of brownish stains confirm that the concrete detachments spalling or delamination has their origin in corrosion of the concrete reinforcement.

The SEM/EDS observations and analysis of white and dark efflorescence prove that the white efflorescence are due to the leaching of lime compounds and the dark efflorescence are caused by moisture.

REFERENCES

Mota-Miranda, A. 2006, *Influência da proximidade do mar em estruturas de betão*, Tese de Mestrado da Faculdade de Engenharia da Universidade do Porto, Porto.

RILEM, 1988, *Measurement of Hardened Concrete Carbonation Depth*, Recommendation CPC-18, Materials and structures. 21, nº.126, pp. 453-455.

LNEC, 1971, *Inertes para Argamassas e Betões – Determinação do Teor em Halogenetos*, Laboratório Nacional de Engenharia Civil, Especificação E-253, Lisboa.

St John, D.A. Poole A.W. and Sims I.,1998, *Concrete Petrography. a Handbook of Invesgative Techniques*, Ed. Arnold, London.

XII DBMC
International Conference on Durability of Building Materials and Components
PORTO - PORTUGAL, April 12th-15th, 2011

Aging Effect on the Integrity of Traditional Portuguese Timber Roof Structures

António Murta [1]
Humberto Varum [2]
Jorge Pinto [3]
Luís Ramos [4]
Vítor Cunha [5]
Rui Cardoso [6]
Lina Nunes [7]

ABSTRACT

Traditional buildings basically include natural and autochthonous construction materials and are built with sustainable construction techniques. The knowledge of these materials's state and construction techniques is required for a proper conservation/renovation work. It is well known that the lack of maintenance is one of the main causes that contribute to the high degree of degradation that the Portuguese traditional buildings unfortunately have. That degradation may even compromise the overall structural integrity of the building thus reducing its lifetime`s expectation. Meanwhile, a partial or even full demolition of a building is still an often occurrence in the Portuguese context. From a sustainable and building heritage perspectives that practise may be inadequate. Taking into account that generally the degradation problems are linked with roof`s leaking anomalies and that the structural components of the roof tend to be the first ones to be affected, this timber structural roof components of Portuguese dwellings were the object of the research work here presented.

KEYWORDS

Aging effect, Used timber, Rehabilitation, Sustainability, Roof structures.

[1] Department of Engineering of Trás-os-Montes e Alto Douro University (UTAD), Vila Real, PORTUGAL, amurta@utad.pt
[2] Department of Civil Engineering of Aveiro University (UA), Aveiro, PORTUGAL, hvarum@ua.pt
[3] Department of Engineering of Trás-os-Montes e Alto Douro University (UTAD), Vila Real, PORTUGAL, tiago@utad.pt
[4] Department of Engineering of Trás-os-Montes e Alto Douro University (UTAD), Vila Real, PORTUGAL, lramos@utad.pt
[5] Department of Engineering of Trás-os-Montes e Alto Douro University (UTAD), Vila Real, PORTUGAL, vcunha@utad.pt
[6] Instituto Politécnico de Coimbra (IPC), Escola Superior de Tecnologia e Gestão de Oliveira do Hospital (ESTGOH), Oliveira do Hospital, Portugal, rui.cardoso@estgoh.ipc.pt
[7] Structures Department. Laboratório Nacional de Engenharia Civil (LNEC), Lisboa, Portugal, linanunes@lnec.pt

1 INTRODUCTION

In general, traditional Portuguese dwellings have stone or earth-based masonry materials, timber beams and as the main roof's structural components, timber trusses. The majority of the building materials are both local and natural [Carvalho *et al.* 2008].

These types of buildings have however shown signs of deterioration related to the natural aging of the materials but also as a result of a lack of conservation [Murta *et al.* 2010]. When rehabilitation processes take place it is typically a requirement to identify and to characterise existing materials, to determine their strength capacity such that the aging effect can be taken into account.

Wood is one of the most complex building materials and old or aged wood is even more difficult to analyse because to complete a useful analysis requires the consideration of both the effects of the direct aging of the material and as well, the risk of degradation by external factors. In respect to the risk to degradation by external factors, one must consider that during its lifetime, structural timber elements may be subjected to a variety of biological agents, e.g. fungi, bacteria and insects, which may also modify its material and thus mechanical properties.

Of current interest to the building industry, is a concern for the rehabilitation of building processes and as well consideration for sustainable building practices in which the intent is the reuse of wood. It is in this context that this research work was developed. The intent of the study described in this paper is to examine aging effects on the most relevant traditional timber roof systems used in Portuguese dwellings. For this purpose a real beamed timber roof system was used as a reference point.

This paper is structured as follows: (i) the most common traditional Portuguese roof timber structural system types are identified and briefly described; (ii) one of these systems, namely, the beam solution of a real dwelling is designed according to the current applied regulations; (iii) Considerations relating to the aging effect of timber are delivered; (iv) Some practical design procedures proposed by different authors for dealing with the complexity of aged wood in structural applications are presented. Some additional alternative procedures related to this issue are also proposed; (v) the primary conclusions derived from this study are drawn.

2 TRADITIONAL PORTUGUESE ROOF STRUCTURES

The most common traditional Portuguese roof structures of dwellings are trussed timber systems as shown in Fig. 1-a, or beamed system as depicted in Fig. 1-b. In both cases, the trusses or the beams support the purlins; in turn, the purlins support the boards, which themselves support the roof covering. The traditional type of roof covering may change along the national territory but ceramic tiles are the most widely used in the Portuguese context.



a) Trussed



b) Beamed

Figure 1. The most common traditional Portuguese roof timber structural systems.

3 TRADITIONAL PORTUGUESE ROOF STRUCTURE ANALYSIS

The ancient traditional Portuguese roof structures were built based on empirical knowledge in which the experience of the constructors was fundamental. At those times, there were no codes or computer programs that guided the building design processes for these heritage structures. This fact inspired us to verify if an existing traditional roof timber structure was in fact in accordance with the actual applied regulations, in particular that given in ENV 1995-1 [EC5 1998]. For this purpose, the analysis of an existing beamed roof timber system was completed as a "real example" of a solution prior to the implementation of design codes. A timber system consisting of maritime pine (*Pinus pinaster*) of wood E class [EC5 1998] , and part of a dwelling located in the central region of the Portuguese coast was used; its dimensions are given in Fig. 2. The cross sectional area of the existing beams, dimensions of which were collected during an inspection of the structure, is 0.07×0.14 m^2; the beams are placed 0.50 m apart. The permanent and the variable loads acting on the roof (i.e. dead load, wind, snow and seismic) and their respective combinations were defined according to RSA [1985]. An elastic analysis was performed.

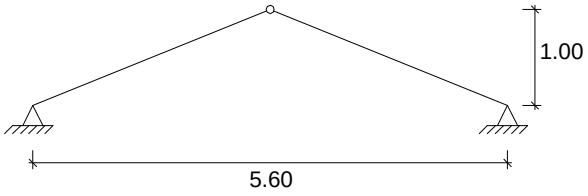

Figure 2. Beamed roof timber structural system model (m).

The most severe combination of loads for this structure was the one related to the dead load. The respective results of both the deformed and forces diagrams are depicted in Fig. 3.

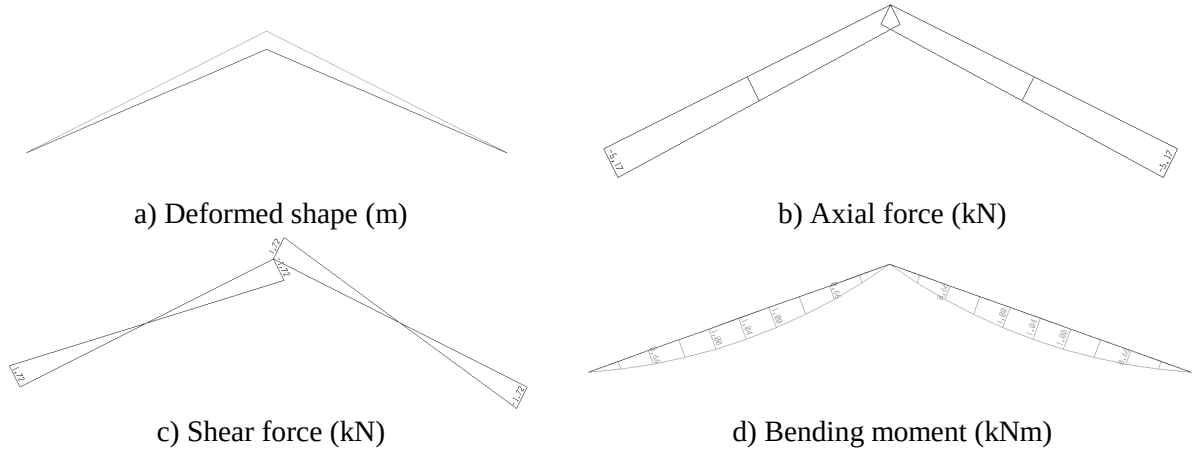

a) Deformed shape (m) b) Axial force (kN)

c) Shear force (kN) d) Bending moment (kNm)

Figure 3. Diagrams.

Using the results derived from the structural analysis and the recommendations given in ENV 1995-1 EC5 [1998], the designed cross section for the beams, if fixing the beam's width to $b = 0.07$ m, corresponds to a section of 0.07×0.05 m^2. Note that this cross section is obtained purely from an academic point of view since in a general sense the element's largest cross sectional area moment of inertia should be mobilized to resist the greatest bending moment. Comparing this result with the existing cross section we concluded that the analysed roof structure is indeed in conformance with the recommendations given in ENV 1995-1 EC5 [1998]. In fact, it is oversized. as well, the aforementioned cross section design resulted from the verification of the ultimate limit state condition when considering bending with compression, or as expressed in ENV 1995-1:

$$\left(\frac{\sigma_{c,0,d}}{f_{c,0,d}}\right)^2 + \frac{\sigma_{m,d}}{f_{m,d}} \leq 1 \tag{1}$$

where, $\sigma_{c,0,d}$ is the compressive stress due to the axial compression force applied parallel to the grain; $f_{c,0,d}$ is the compressive strength due to the axial compression force applied parallel to the grain; $\sigma_{m,d}$ is the flexural stress due to the bending moments and $f_{m,d}$ is the bending stress due to imposed moment on the bean.

4 AGING EFFECT OF TIMBER STRUCTURES

Hoffmeyer stated in Timber Engineering [1995] that wood is a natural, organic cellular solid. It is a composite made of a chemical complex of cellulose, hemicellulose, lignin and extractives. It is highly anisotropic. These are some of the reasons why wood is perhaps considered one of the most complexes building materials with which to design. The analysis of the wood's aging effect, in particular for timber structures, becomes even more complex because it is a time dependent and a process difficult to predict. A timber beam is shown in Fig. 4a that is the remaining element of what was once the timber floor of a traditional Portuguese dwelling. The advanced level of deterioration of this beam is clearly evident in Fig. 4; this level of deterioration was a result of the unprotected conditions in which the beam was to perform and the nonexistence of conservation measures to the beam over time. In this case, the aging effect has been materialized by a progressive process of material degradation complemented by a reduction of cross section as illustrated in Fig. 5.



a) Simple supported beam b) Detail of the support

Figure 4. Aged timber beam.



Figure 5. Detail of the degradation stage of the left edged of the beam.

We consider that the material degradation corresponds to the material changing due to fungal attack. Its physical properties, such as density ρ, and the stiffness properties, such as the modulus of elasticity *E* and the shear modulus *G*, are all affected. Since this change progresses through time the above material properties become time (t) dependent (i.e. ρ(t), *E*(t) and *G*(t)). This process of progressive material degradation is schematically represented, in a simplified way, in Fig. 6. As illustrated in Fig. 6 the aging effect manifest itself as different layers of material each at specific degradation levels that are formed over time. This scenario suggests that there is an increasing of anisotropy through time and, consequently, an increase in the complexity of modelling aged timber structures.

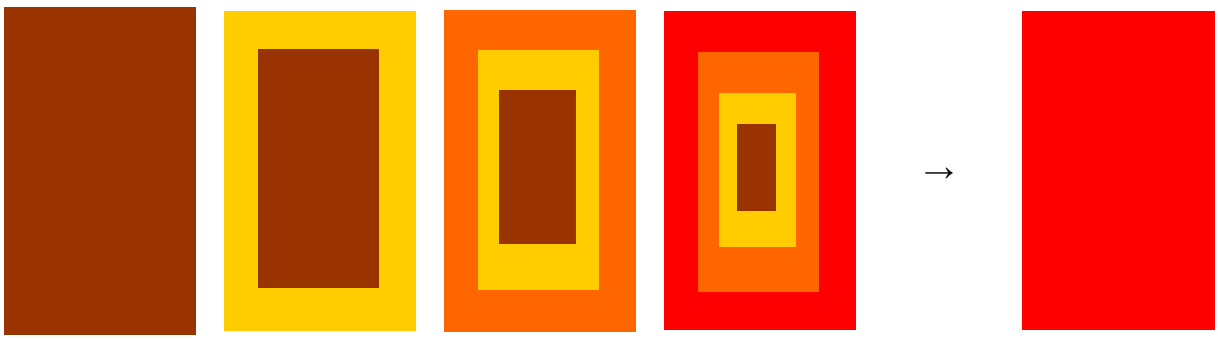

Figure 6. Material properties evolving through time.

Meanwhile, the reduction of the cross section can be due to the attack of insects such as beetles and termites if no treatment measures are taken. Fig. 7 shows, schematically and in a simplified manner, a progressive reduction of a cross section of a timber structural element process through time until no remaining material remains. The area of cross section A and the second moment of inertia I are affected and thus these properties "deteriorate" through this degradation process which develops through time (i.e. $A(t)$ and $I(t)$). The density is of course also affected in this case.

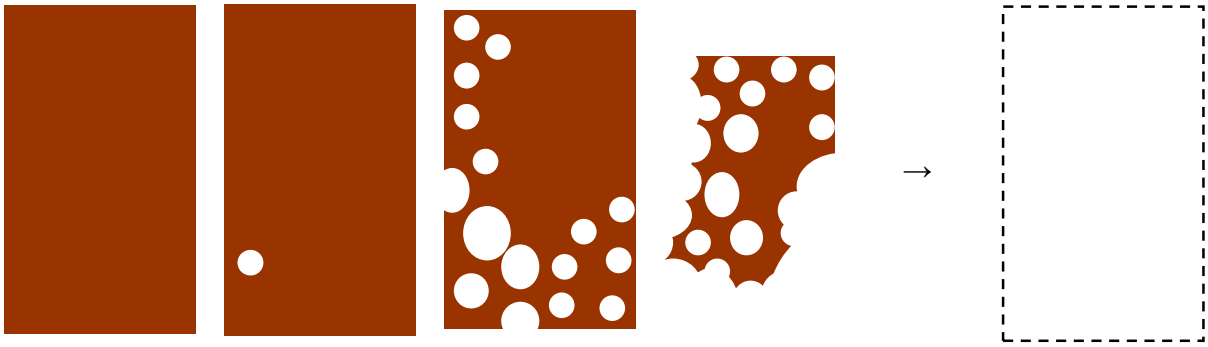

Figure 7. Reduction of cross section through time.

On the other hand, the two degradations processes can take place simultaneously as shown in Fig. 8. In this case, all the above identified properties change through time. Furthermore, it is very likely that there are different levels of degradation among of the different cross sections of a timber structural element. All these aspects drastically increase the complexity of obtaining an accurate numerical model of an aged timber structural element such as the beamed roof timber structural system used as an example in this paper.

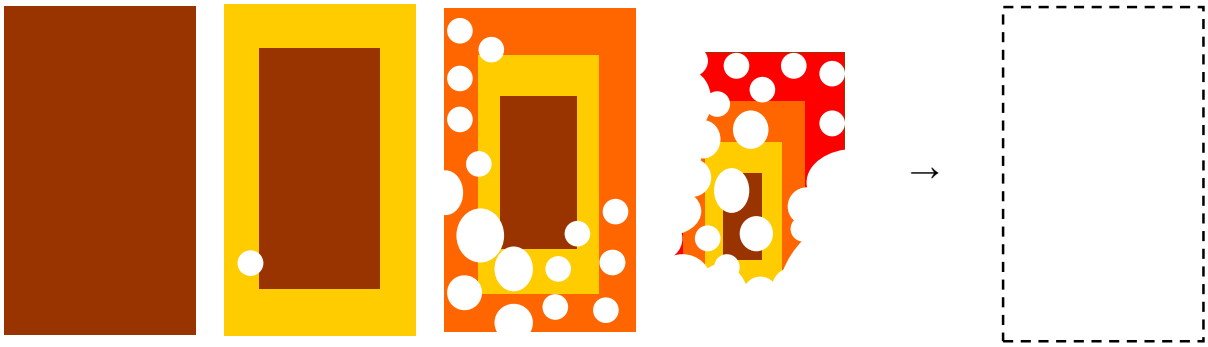

Figure 8. Material changing and reduction of cross section through time.

Taking into account that the variables given in Equation 1 are dependent on the above properties, the design of timber structural elements using aged wood or the structural study of existing old timber elements requires additional care. A future experimental research programme is being prepared, in order to ascertain the effect aging on the structural response of aged timber structures.

5 DISCUSSION AND PRACTICAL SUGGESTIONS

Within the application of ancient timber context, Ross and Wang [2005] suggest that the material properties of old timber require adjustments in order to take into account the aging effect. They stated that the timber elements such as beams removed from old demolished buildings can show deterioration that occurs in over 50% unrecoverable material. However, they also indicated that, in

many cases, the amount of waste material is smaller than 10% (i.e. 90% reusable) and that the deterioration was mainly caused by decay (surface and internal), splits, and mechanical damage. Pine wood is of course a species that has been extensively analysed following several years of direct exposure to weathering. In the same context, Marzo [2006] concluded that ancient timber elements may have their original modulus of elasticity decreased by approximately 25% and as a result of several factors, such as: material aging, poor construction labour, weak connections, among others. Meanwhile, Pilt *et al.* [2009] concluded that the ancient timber may have its strength capacity decreased by approximately 15%. In general, these authors propose practical analytical procedures to simplify the previously described complexity related to the aging effect of timber concerning the application of old timber in the building industry. In particular, in a sustainable and economical perspective, this may give guidance for cases like the one shown in Fig. 9.



Figure 9. Coexistent old and new timber structural elements.

For instance, considering the strength classes of *poplar* and *conifer* species which are C14, C16, C18, C22, C24, C27, C30, C35 and C40, the average reduction of bending strength between two subsequent classes is approximately 12%. On the other hand, for three subsequent classes (e.g. C14 and C18) this is about 24%. Note that this value (24 %) is quite similar to the strength reduction proposed by Pilt et *al.* [2009]. Meanwhile, in the example adopted, when performing the design according the legal standards, and not taking into account the aging effect, it was ascertained that the ancient timber structural elements were oversized (see section 3). Within the scope of maintaining or reusing timber and based on the abovementioned facts, an experimental research work is being prepared to access a correspondent smaller strength class for the design purposes in the existence of oversized cross section scenario in order to take into account the aging effect. The reduction strength class decision has to be supported on procedures able to access the extension of the material damaging. In the context of maintaining, these procedures usually have to be performed *"in situ"*. In some cases, the visual inspection might not be accurate enough as it will be unable to predict the internal damaging extension. Furthermore, the density is affected in both material changing and reduction of cross section degradation processes, thus this physical properties may be an adequate parameter for predicting the aging effect in timber structural elements.

6 CONCLUSIONS

A constructed beamed roof timber structural system solution of a traditional Portuguese dwelling was briefly described. This is one of the most common roof structural solutions applied in the context of construction of Portuguese dwelling. The main structural element of this system, a three hinged arch, was designed according to the current applied regulations and it was determined that the existing cross section of the beam was oversized. The aging effect of the timber was not taken into account in this analysis.

Some considerations related to the description of aging effect in timber were offered. It was highlighted that biological phenomena may attack and deteriorate the structural timber elements

progressively through time. If no treatment measures are taken to conserve the timber elements, these may degrade and could eventually collapse. Since the physical and mechanical properties, the stiffness and the strength properties are affected during aging and since they are also an analytical function on time. These aspects increase significantly the complexity of this problem.

It was presented some practical measures proposed by different authors to deal with this complexity. In this paper, other practical measures were suggested which intend to contribute to bringing some clarity to this issue.

REFERENCES

Carvalho J., Pinto J., Varum H., Jesus A., Lousada J., Morais J.; 2008; "Construção em tabique na região de Trás-os-Montes e Alto Douro". CINPAR 2008 – 4th International Conference on Structural Defects and Repair. Civil Engineering Department, University of Aveiro, Portugal.

CEN; 1998; *Eurocode 5 – Design of timber structures – ENV 1995-1*. Brussels.

Hoffmeyer P. 1995, Timber Engineering STEP 1. *Basis of design, material properties, structural components and joints*. First Edition, Centrum Hout, The Netherlands. ISBN 90-5645-001-8.

Marzo, A; 2006; " Methodology for the analysis of complex historical wooden structures"; *Pollack periodica*, Poland.

Murta A.; Pinto J.; Varum H.; Guedes J.; Lousada J.; Tavares P. 2010, Survey on the main defects in ancient buildings constructed mainly with natural raw materials - Portugal SB10, Sustainable Building, Affordable to All, Low Cost Sustainable Solutions. Edited by: Bragança L.; Baird G., Alcorn A., Haslam P.; 1997; "The energy embodied in building materials". IPENZ Transactions, New Zealand.

Pilt K.., Pallav V., Miljan M., Miljan J.; 2009; *Diagnosis of Timber Structures and Archaeological Wood of Cultural Heritage*; www.woodculther.com.

RSA; 1985; D.L. 235/85, *Regulamento de Segurança e Acções para Estruturas de Edifícios e Pontes*. Portugal.

Roos, R, J; Wang, X, 2005; "Condition Assesment of timbers". *STRUCTURE magazine*, September.

XII DBMC
International Conference on Durability of Building Materials and Components
PORTO - PORTUGAL, April 12th-15th, 2011

Pathologies of the Contemporary Constructions. The Case Study of a Residential Building With 36 Flats at Pignola (Potenza, Italy), Realized in Mixed-Traditional Technique

Francesco Paolo R. Marino [1]

ABSTRACT

The research concerns one residential building of a public housing programme, made by means of a call for bids of Potenza's IACP - Autonomous Institute for Popular Houses – held in 1984. The work, started in that year and continued until 1999, following the bankrupcy of the first firm, and the death of the owner of the second one. Because of the very irregular shape of the building that results in acute a angles to projections and many recesses, the analysis of pathologies (made by stregthened methods, stated by W086 *State-of-the Art Report*) identified unusual defects as well as typical phenomenons: such us spalling of concrete, cracks in many parts of non structural components made in reinforced concrete, bulges, spalling, staining and discolouration of the plasters and of the internal and external paints, caused by capillarity and by internal and/or surface condensation, especially next to thermal bridges.

A very exhaustive environmental analysis on the building was made which recorded the typical exposure to wind, rain, dampness and the sun throughout the year. It was possible to evaluate performances of the building and of the dwellings, both from typological, and technical point of view, identifying that about 70% of defects were caused by design errors, about 10% were caused by constructional errors, and about 20% by maintenance errors. A range of solutions for every problem found was identified.

KEYWORDS

Durability & environmental exposition, Pathologies, Envelope.

[1] Faculty of Engineering of the University of Basilicata (Department DAPIT), Potenza, ITALY, francesco.marino@unibas.it

1 INTRODUCTION

The research, made in 2005 thanks to the Thesis work of Eng. Gianna Cirillo coordinated by the author, concerns one residential block of a public housing programme, made by means of a call for bids of Potenza's Autonomous Institute for Popular Houses (IACP) in 1984. The work, started in that year, was going on until 1999, following the bankrupcy of the first firm and the death of the owner of the second one.

The project was draw up by the firm that was awarded the contract, the direction of the work was carried out, in succession, first by an engineer, then by an architect and a surveyor, all of them employees of the IACP; who exercised a direct and continuous control on the quality of the project and of the works during the course of their implementation.

2 DESCRIPTION OF THE BUILDING

This is a single block, consisting of a basement and four floors, with three staircases, with distribution "in line", which has 3 dwellings of 45 m^2, 12 of 65 m^2, 12 of 70 m^2 and 9 of 95 m^2. Some dwellings on the third floor are duplex-type, connected to the attic (see Fig.1). The building is located across a hillside that slopes to the North, and is aligned in a West-East direction. The block has a very irregular plan.

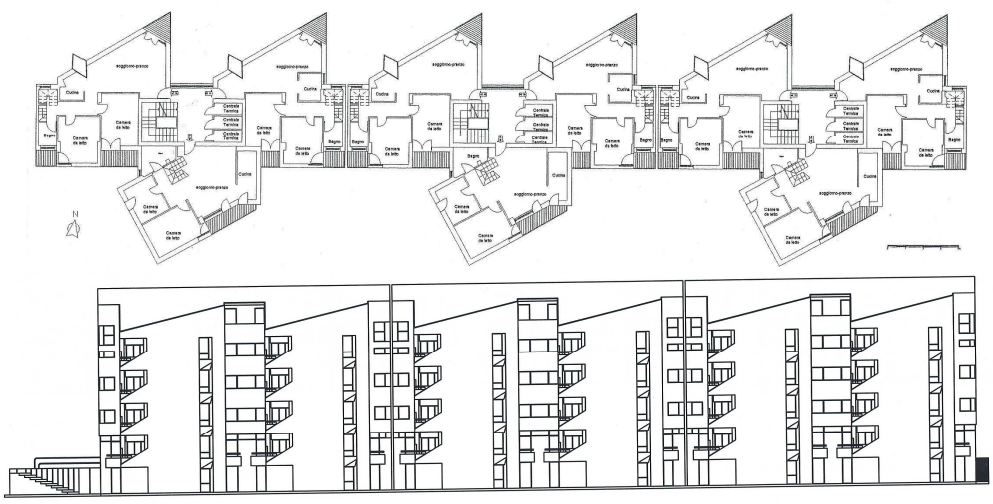

Figure 1. Plan of the third floor and elevation facing North-East.

The construction system is "traditional" anti-seismic structure with reinforced concrete column and beam cast in situ. The perimeter walls are made as follows (from inside to outside):
- plasterboard 0.5 cm internal
- block pre-coated plaster and expanded clay 8 cm
- 4 cm air cavity
- cement render 1 cm
- 20 cm block of expanded clay
- cement plaster 2 cm
- quartz painting (very not durable paint surface to the cement plaster)

and have a transmittance U = 0.76 W/m^2K.

3 DURABILITY PROBLEMS - EMERGING PATHOLOGIES

3.1 Generalities

The building has a number of problems of durability, which are the result of many pathologies related

to the building envelope. Most of them are typical and it is easy to determine the cause. It is interesting, in this case study, that they are directly related to the exposure condition of the building.

3.1.1 Geographical and climatic data, exposition conditions of the building

The City of Pignola is located at 40°34'26"76 Lat. North and 15°47'2"40 Long. East, at an altitude of 927 m o.s.l. and falls within the climate zone 4F (i.e. in the year there are 4 comfortable months and the total number of cold months is greater than 6). Winter temperatures are low, the summers are relatively warm, and large temperature changes occur. The relative humidity is high, especially in winter (see Table 1).

Table 1. Temperature and Relative Humidity - year 2005.

Month	*T max* [°*C*]	*T min* [°*C*]	*T average* [°*C*]	*RH* [*%*]
January	6	-1	3.6	77
Febraury	7	1	4.3	75
March	9	2	6.8	72
April	13	5	10.6	69
May	18	9	14.7	69
June	22	13	19.1	67
July	26	15	21.9	62
August	28	18	23.1	64
Semptember	21	13	18.9	66
October	16	9	13.7	72
November	11	5	9.3	76
December	8	0	5.2	78

The prevailing winds are from the West in the spring, and from the South-West in the winter (see Table 2):

Table 2. Direction of the winds and quantity of rain - year 2005.

Month	*Monthly average wind direction* [degree]	*Average monthly rainfall* [mm]
January	236.26	63
Febraury	244.74	54
March	256.37	53
April	275.82	60
May	258.49	46
June	260.98	42
July	263.55	29
August	267.78	36
Semptember	259.61	45
October	253.83	70
November	246.65	80
December	243.08	74

As a result different parts of the building are exposed to different amounts of rain/snow (see Fig.2), because of the configuration of the projections and recesses:

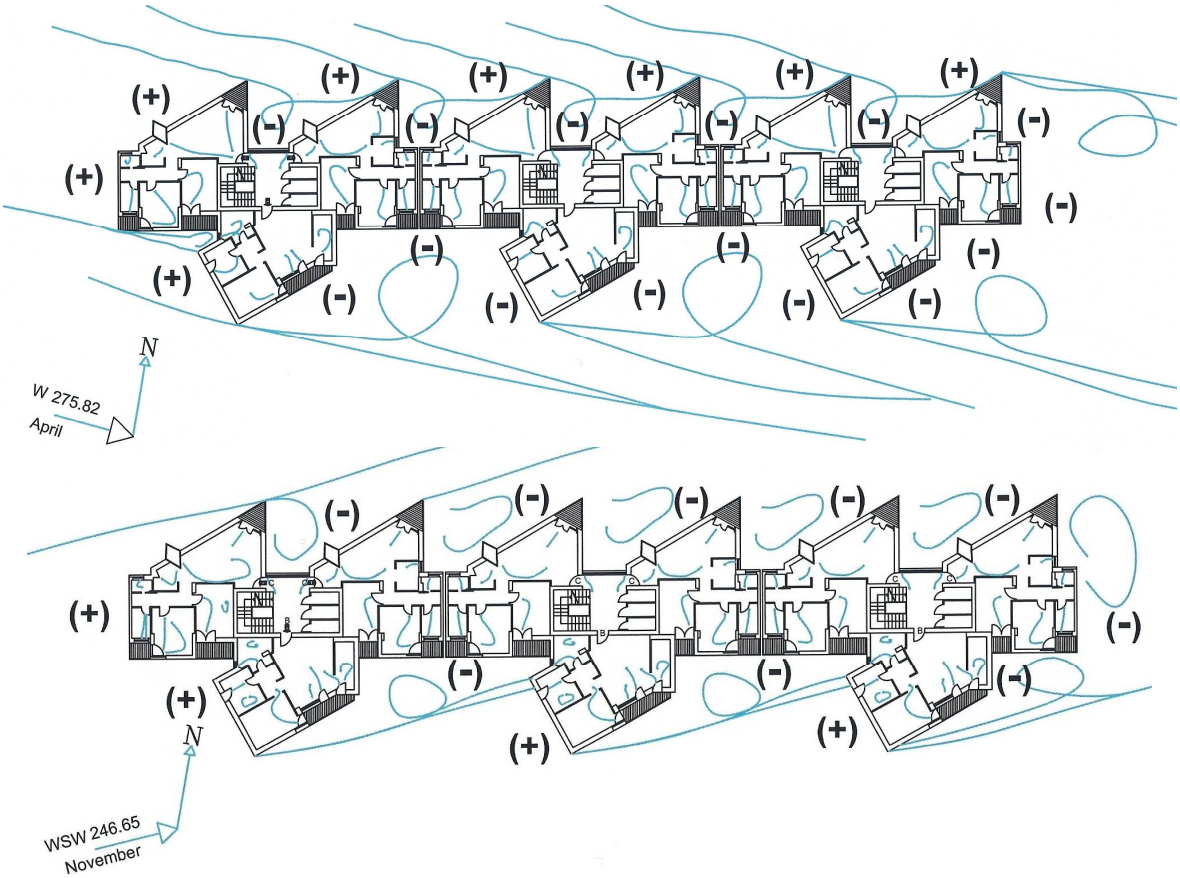

Figure 2. Exposure of building to the wind and rain in April and November.

There are also upslope winds, which have an alternating pattern during the day and the night. The other buildings on the slope affect the extent of exposure of the block to certain wind direction. In general the block is exposed to its South face (upstream) and sheltered to its North face from the descendings winds (nocturnal). Obviously, in this regard, the building projections and recesses make the behaviour of the flow of moist air around the building more complex and variable.

Obviously, the disposition in the West-East direction of the building leads to a marked difference in the solar radiation to which the different façades are exposed. In particular, the North face has many areas that never receive any sunlight, even in summer, partly because of shading caused by the projections (see Fig.3).



Figure 3. Solar radiation in January.

Finally, the building acts as a dam to block the slope, as a result of which all the rain run off and the ground water contained in the soil hit the building and increase the dampnes on the ground floor and the basement, with obvious consequences on the durability of parts of the same building, and creates the circumstances for specific pathologies.

3.2 Classic design faults, but pathologies emerging in worse exposition conditions.

3.2.1 Lack or incorrect execution of flashing is causing the detachment of paint and plasters

The lack of or incorrect execution of flashings (see Figs 4 and 5) have resulted in the separation of the external plaster in the most exposed positions (the upper floors, the lateral edges, eaves spouts).

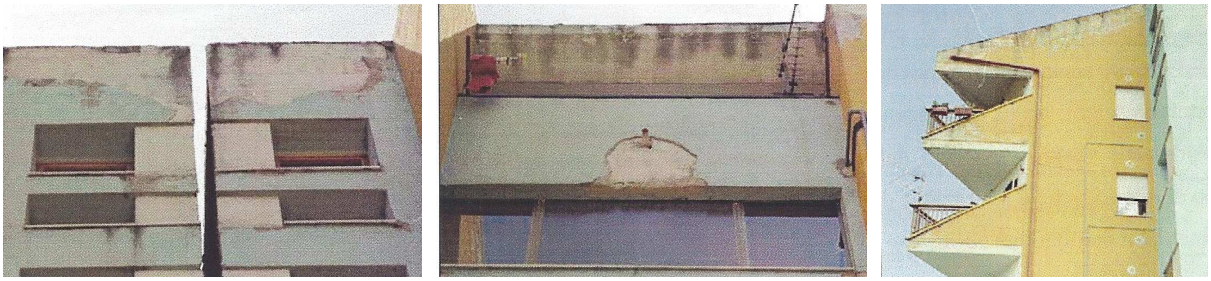

Figure 4. The lack of flashings is causing the detachment of paint and cement plasters – to the North-West and North elevations.

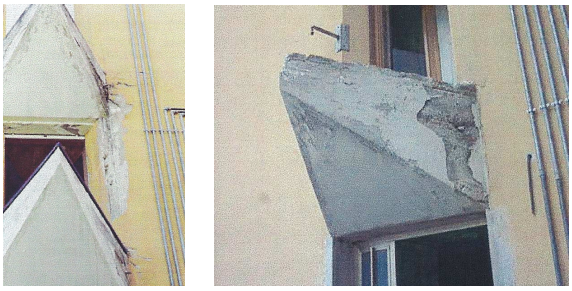

Figure 5. The lack of or incorrect execution of flashing is causing the detachment of paint and cement plasters – to the North-West and North elevations.

3.2.2 Too high vapour resistance of plaster and paint causes the detachment of paint and plaster

The paint coating and cement plaster has delaminated in those points that are highly stressed by wind/rain/ice (top of the building, vertical edges, see Fig.6). This is because the paint coating and cement plaster trap moisture within the wall, because they are too resistant to the passage of vapour compared to the expanded clay block below, and therefore the moistrure is unable to escape.



Figure 6. The erosive action of wind, rain and ice, together with the too high vapour resistance of paint and cement plaster, has caused the separation of paint and plaster in the most stressed areas.

3.2.3 Spalling of concrete

This phenomenon affects all the projections in North-West and North exposed façade and, in particular, the triangular balconies. It is caused by the inadequate concrete cover to the reinforcement and the carbonation of the concrete, and it is particularly evident in those parts most exposed to heavy

rain (see Figs 7 and 8).

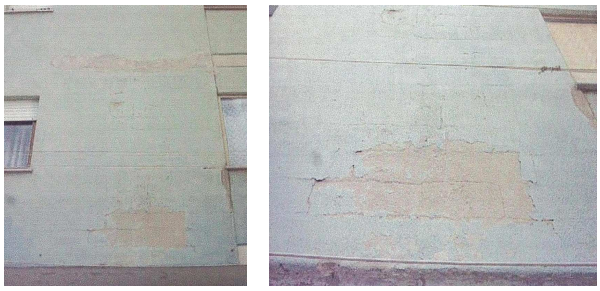

Figure 7. The strong sunlight on the South and the West facade is the factor that triggers the detachment of paint and the bulging of the plaster, due to their excessive vapour resistance.

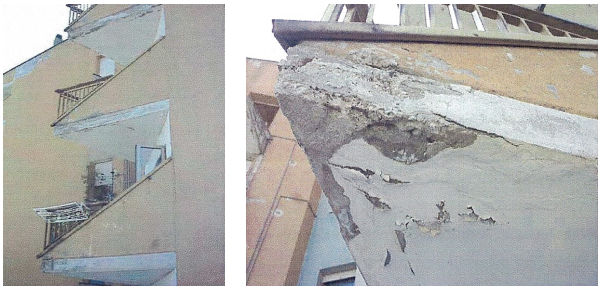

Figure 8. Spalling of concrete at balconies facing North.

3.2.4 Cracks to the junction between the reinforced concrete structure and the expanded clay walls

These occurred at the walls, facing East, West (see Fig.9) and South-West. This suggests that this phenomenon is due to the difference in coefficient of thermal expansion between the two materials, but the motivating factor is the strong solar radiation, just in these areas, which increases the value of the terms of the formula $\Delta L = (\alpha 1 - \alpha 2) \times L \times \Delta T$. There is a sharp reduction in the phenomenon from top to bottom.



Figure 9. Cracks between r.c. structure and external wall - facing West (left) and facing East (right).

3.2.5 Cracks to the junction between reinforced concrete parapets and expanded clay walls

Similarly, and for the same reasons, there were cracks at the junction between the balcony parapets and façades walls (see Fig.10).

3.2.6 Mould caused by condensation resulting from cold bridges

The distribution of condensation pathologies caused by thermal bridges exactly matches the distribution of the coldest parts of the buildings. Pathologies are manifested by surface condensation at all walls exposed to the East, North, and also in the recesses of the South front, over all floors. Two typical examples are shown below (see Figs 11 and 12).

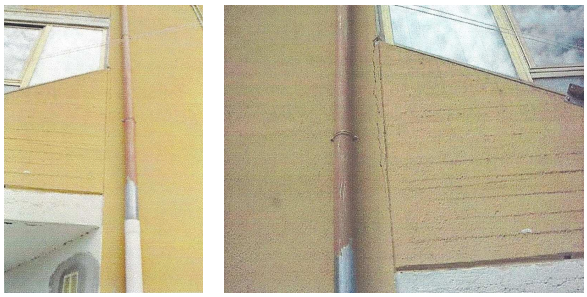

Figure 10. Cracks between reinforced concrete parapet and external wall – facing West (left) and facing East (right).

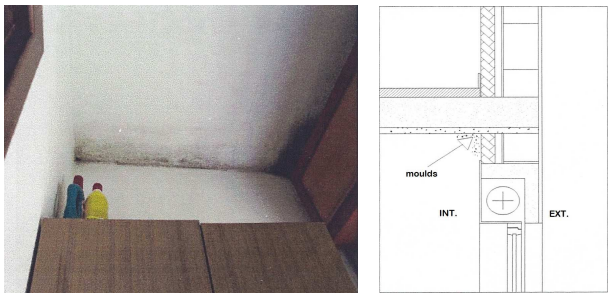

Figure 11. Moulds caused by thermal bridges in a dwelling of 2nd floor, wall facing North-West.

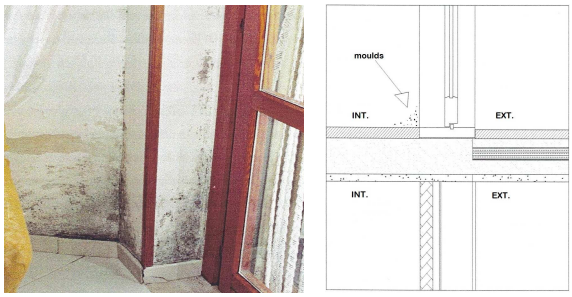

Figure 12. Humidity from ground attacks walls of the basement.

3.2.7 Pathologies due to insufficient waterproofing

The retaining walls to the basement level (see Fig.13) on the South, elevation were improperly sealed and separated from the ground and have been affected by groundwater. The walls on the ground floor, facing North-West and North are the most exposed to the rain, driven by the winds throughout the year (see Fig.14). The construction and maintenance provisions are insufficient.

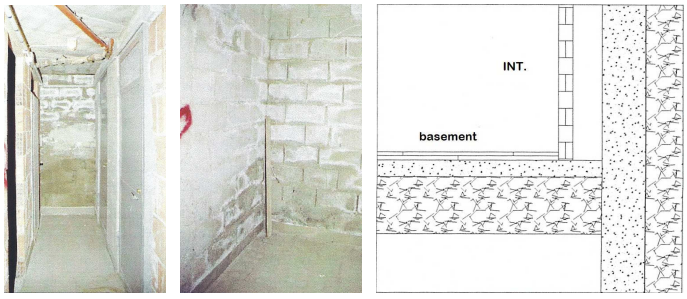

Figure 13. Moulds caused by thermal bridges in a dwelling at the basement level, wall facing North-West.



Figure 14. Water stains caused by rain to North-West and North facing walls.

4 RESPONSIBILITY FOR MISTAKES

Research highlighted that about 70% of defects were caused by design errors, about 10% were caused by constructional errors, and about 20% by maintenance errors, confirming that the design of the durability and prevention of pathologies are directly related (Lembo & Marino, 2002, pag. 18).

In particular the design seriously underestimated the severity of the climatic conditions and exposure, which needed very different design solutions (ventilated exterior wall at least of the type III according to the DTU 20.1, and no type IIb; with the elimination of thermal bridges, sheltering of the external building envelope from direct sunshine and rain) and a very different focus on solving particular defects (junction of the reinforced concrete and bricks, insulation, and water resistance of the elements of basement).

5 CONCLUSIONS

It was identified a catalogue of solutions for every problem found. The building can be taken as a "textbook example" of how design solutions must be devised according to the climatic conditions and exposure which characterise the specific building construction. There is no solution that will work in all locations. What may work in one place may not resolve the problems in another.

This is the task of the "*engineering design*" (Lembo, 2010), that is to link science to architecture, to achieve improved quality levels and greater achievements in building durability, *for a long-lasting beauty.*

ACKNOWLEDGMENTS

Many thanks to Eng. Gianna Cirillo, for his thorough research on the topic, and to ATER, now EPER of Province of Potenza, represented by its CEO, Eng. Raffaele Vita, and its Director, Arch. Michele Bilancia, for the great willingness to make available the original design documentation.

REFERENCES

Lembo, F. & Marino F.P.R. 2002, *Il comportamento nel tempo degli edifici. Cause di degrado e soluzioni progettuali dei sistemi edilizi "tradizionali" ed "industrializzati". Casi di studio* , EPC libri, Roma, ISBN 88-8184-241-6.

Lembo F. 2010, 'Pathologies of the Contemporary Constructions. The Case Study of a School Building Realized in Mixed-Traditional Technique', P. Barrett, D. Amaratunga, R. Haigh, K. Keraminiyage & C. Pathirage (edited by), Building a Better World CIB World Congress 2010, Full Paper Proceedings - CIB 2010 World Congress, Salford (UK), May, ISBN 978-1-905732-91-3.

XII DBMC
International Conference on Durability of Building Materials and Components
PORTO - PORTUGAL, April 12th-15th, 2011

Identification and Quantification of Failure Modes of New Buildings Façades in Brasília

Elton Bauer [1]
Eliane Kraus de Castro [2]
Giselle Reis Antunes [3]
Franz Eduardo Leal [4]

ABSTRACT

The occurrence of pathologies in buildings façades has shown up as a problem more and more frequent in Brasilia. The façades are frequently constituted of masonries, which are covered by rendering mortars and ceramic tiles. Several failure mode were observed, from stain, cracks, until the detachment of the façade covering.

The present study approaches the case of four buildings with different architecture, and from which, the analysis of the failure mode was developed. The methodology used consisted of: initial inspection, detailed inspection of the façade elements and, damages mapping, tests and diagnosis. From the observed results the most frequent degradation pattern recognized on the observed façades was: the detachment of ceramic tiles, following by the cracks. It was observed that the areas of larger incidence of pathologies are the sorounding of the openings, following by the continuous façades (large regions without openings).

As a contribution to the theme, the present study talks about the methodologies for identification and quantification of pathologies, as well as, it focuses on the results observed as a feedback for prevention of future pathologies.

KEYWORDS

Quantification of failure, Façade, Rendering mortars, Ceramic tile, Detachment, Cracks.

[1] Universidade de Brasília, Laboratório de Ensaio de Materiais, Brasília, BRASIL, elbauerlem@gmail.com
[2] Universidade de Brasília, Laboratório de Ensaio de Materiais, Brasília, BRASIL, kraus@unb.br
[3] NORIE-UFRGS, Porto Alegre, BRASIL, giselle_ra@hotmail.com.br
[4] Universidade de Brasília, Laboratório de Ensaio de Materiais, Brasília, BRASIL, fzleal@gmail.com

1 INTRODUCTION

Brasilia, capital of Brazil, is the first urban center of the twentieth century considered as a World Heritage Site by UNESCO. Inaugurated in 1961, the young capital completed 50 years with its buildings showing several detoriation symptoms. This study has its focus on the approach on building façades. Typically, the façades are made of masonry of ceramic and concrete bricks, covered mostly by ceramic tiles and stone cladding.

The deterioration of the façades is identified by both the incidence degree, and the severity of defects, among which, were could observe: detachment and lost of adhesion of ceramic tiles, cracks, stainings, ceramic tiles deterioration and desintegration.

The survey on the incidence of failures ia a systemic study which involves a sequency of operations aimed at identifying the active failure mode, as well as, at mapping the deteriorations. The end of all analysis sticks to the formulation of a mechanism, capable of clearly describe the formation and development of failure. To find a adequate failure mechanism is obviously necessery to go beyond a simple assessment of incidenced, requiring detailed inspections, as well as, tests of the respective material.

The Laboratório de Ensaio de Materiais – LEM (Laboratory of Material Test), Universidade de Brasília - UnB (University of Brasilia) , has a team of researchers on the subject, and has developed a methodoly already applied for several years, in which one seeks to study the main failure and degradation pattern of building façades in Brasilia . In summary, the methodology LEM-UnB is devided in the following steps, like descripted according Bauer *et al*. [2010] :

- **Preliminary information:** Which attempts to identify the history of interventions, the building´s architectural desposal, the exposure to weather and, to document the main deteriorated areas. It is common, at this stage, a vaste photografic record of the building´s entire façades.

- **Inspection:** This step has already made a detailed evaluation of the critical areas or, of all façades. It seeks both to document the composition and constructive details (materials and components details, thickness) of facing materials (mortars, ceramics, masonry), and also to identify the failure mode and its occurance extension. To implementof the inspection is necessary the use of rapel or the access by cranes. The final result is the mapping of failure modes in different façades of the building.

- **Tests:** The execution of tests on the spot, such as the tensile adhesion (pull-out), is one of the elements necessary for the identification of the mechanical stability of the façade. Tests on the material characteristics, such as the water absorption and surface cracking of ceraminc tiles helps in understanding the mechanism of occurancy of failure. Oftentimes, are developed experiments specific to investigate a certain occurance mechanism. In this sense, Pereira [2007] reports the use of thermal panels for the stydy of the detachment by shrinkage of the facing mortar, held out by inspection in LEM-UnB.

- **Diagnosis**: The diagnosis stage uses all information obtained in previous steps in the formulation of the mechanisms specific for the development of the degradation pattern. Were identified the causes, the intensity of deterioration fhenomena and, also were defined the mechanical stability and the façades security.

Other tools were developed for the study of the deterioration in façades, as described by Gaspar and Brito [2005], where was defined the sensibility of the occurrence of pathologies in certain façades from a probabilistic analysis. In order to better establish the diagnosis, Silvestre and Brito [2009] proposes the use of matrices of correlation between anomalies and probable causes. Antunes [2010] applied this concept and obtained matrices of correlation for the study of buildings in Brasilia.

2. METHODOLOGY

The present study preliminarily sought for identifying and quantifying which façade pathologies occurs in the studied buildings.In this metter, were evaluated the different buildings through the defects index, in which, it quantifies the number of defects per square meter of the façade. Antunes [2010] held a vast survey study of the defect index, in order to characterize the extension of the pathologic manifestations in Brasilia´s buildings. This study also sought to quantify the relative percentages of failures in relation to the total observed failures. The defect index is descrited in equation (1).

(1)

$$FI = \frac{NF}{FA}$$

Where:
FI– defects index
NF – number of defects (quantity)
FA – façade area (m^2)

The index of defects was determinated for each façade and for the total of every building. Subsequently, were identified which are the most vunerable regions of the façades, using the mapping of failure incidences. For that, was held a graphic sistematization in which, are expressed the façades areas and the level of occurance incidence obtained.

The study sample consisted of 4 buildings, with total façade area of aproximatly 12.000m^2. All buildings have reinforced concrete structure and masonry walls, which are coated with ceramic tiles. The number of floors are defined by Brasilia´s building code, according to the region and destination of the building. Table 1 presents details of the studied buildings. Buildings A, B and C located in Brasilia´s central area has 6 floors. Building D has 12 floors. The entire sample is formed by residential buildings.

Table 1. General Characteristics of studied buildings.

Buildings	*Number of floors*	*Age (years)*	*Façade area (m^2)*
A	6	11	3350
B	6	40	1200
C	6	40	3400
D	12	10	3840

During the determination of the preliminary evaluations the folowing main failure modes were identified:
- loss of adhesion : the ceramic tile has lost the continuity with the supporting wall given by the mortar but did not detach from the facade;
- detachment of ceramic tile: the detached ceramic tile has fallen out of the facade;
- grout failure: the grout between ceramic pieces cracked and/or fell off, allowing the access of rainwater ;
- cracking: there was cracking in the facade surface;
- efflorescence: white spots formed by the deposition of salts from the masonry or the façade materials;
- seal failure (joints between walls and windows): joints damage, especially in the neighborhood of windows and openings, from which occures the penetration on rainwater.

Due to different façade regions they were distinguished in order to give each one its own defects. So were analyzed and quantified the defects in the following areas:
- top: involves the last floor façade area, surrounding to coverage or roof;
- joints: corresponds to the region near the movement and dilatation joints;

- balconies: facade areas in where the facade elements are externally projected;
- corners and edges: neighboring area of the façades;
- transition between floors: area that includes the interferences of both floors;
- continuos walls: areas where the façade is a continous plane, without gaps (windows or balcony) ;
- openings: area surrounding windows and doors; - ground level: junction of the façade and the building base.

3. RESULTS AND DISCUSSIONS

Figure 1 presents the results observed by façade and by building for the defect index. We can observe that building B presents the higher global values, followed by building C. In these 2 cases we have buildings with higher age (40 years), what leads to a conclusion of a higher deterioration of the elements that compounds the façades. It´s important to emphazise that these buildings do not have a maintanance plan, and the pontual interventions are always done when the deterioration level is extremely high. Buildings A and D, eventhough with lower ages (11 and 10 years) presented a significant value of defect index. Building D presented the lower index observed.

In relation to the façade defect index, concerning the cardeal orientation, was observed that the same is higher when: in Building A is the northeast façade, in building B is the northeast façade, in building C is the north façade and, in building D is the northeast façade. Data shows that northeast, north and northwest façades are the ones that presented higher deterioration. One of the aspects that may influence the deterioration machanisms is the solar incidence. Excectly during the months of higher solar exposure (winter, from May to September) there is a diary solar movimentation that incides for longer period in North façade and its neighborhood (from east to west). This climatic incidence may be one of the main factors of façades deterioration.

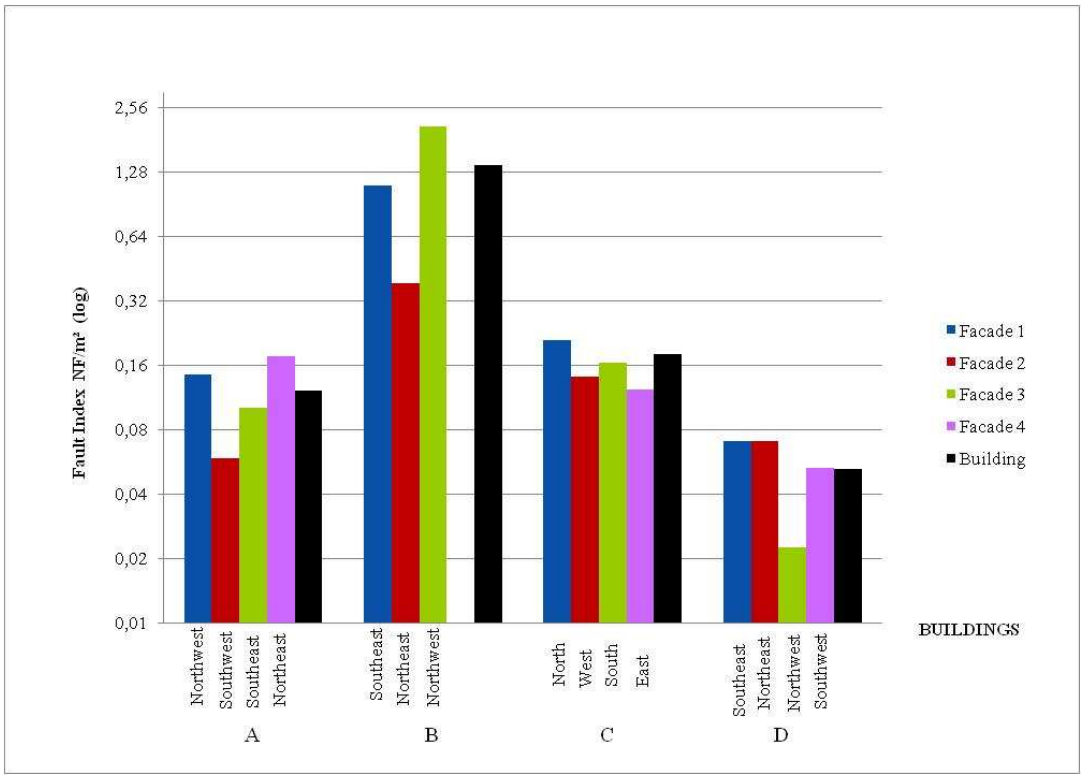

Figure 1. Defects index (FI) for façade and building (log scale).

Regarding the percentage of defects observed, Table 2 shows the values for the four buildings. It is observed that the defect with the highest incidence (over 55% in all cases) is the loss of adhesion of the ceramic tiles. Interestingly, the highest incidences occur for buildings A and D, just those of minor

age and with lower failure rates (Figure 1). One deduces from this fact that the predominant failure of newer buildings (A and D) is the loss of adhesion of the ceramic tiles.

The second defect with the highest occurrence is the failure of grout which occures mainly for buildings A and B. Interestingly, this type of defect is usually associated either with façades with large thermal effect (great efforts in the facades submited to sun action) or in situations of deteriorating of old grout. That last situation seems to be the case of building B, in which the grout has deteriorated compared to degradation over time.

Cracking appears in building B at higher percentage, mostly related to efforts in the neighborhood (corners) of the windows. Another region of crack incidences is the continuos walls ont the top of the building.

Sealing failure (defects) were significantly observed in buildings B and C. Typically, this defect is associated with lack of maintenance, since its effects, such as infiltration of rainwater, are strongly detected by the building user and require immediate repair. Buildings B and C, the oldest, presented higher degree of general deterioration (Figure 1) what can explain the greatest number of sealing defects.

Table 2. Incidence of defects observed in buildings.

Buildings	*A*	*B*	*C*	*D*
Ceramic- loss of adhesion	169 (82%)	926 (55%)	514 (83%)	183 (91%)
Ceramic detachment	6 (3%)	113 (7%)	0 (0%)	18 (9%)
Grout failure	23 (11%)	410 (24%)	39 (6%)	0 (0%)
Cracking	6 (3%)	201 (12%)	54 (9%)	0 (0%)
Efflorescence	2 (1%)	0 (0%)	0 (0%)	0 (0%)
Sealing failure (joints)	0 (0%)	25 (1%)	11 (2%)	0 (0%)
Total cases	206	1675	618	201

The mapping of defects is shown in Figure 2 for the buildings under study. Was held for such an adaptation of the methodology of Gaspar and Brito [2005] and of the aplications of Flores-Collen [2009]. The percentage of defects measured was associated to each façade area, trying to identify areas most susceptible to degradation.

The defects observed in the building top area ranged from 2 to 7%. Basically, they are ceramic detachment and grout defects.

In the joints surrounding area were observed 73% for building A and 10% for building B. Obviously the situation for building A is associated with a lack of maintenance of the moving joints, or to defects in materials and workmanship. Basically, these defects observed at the joints area consisted of detachments of the ceramic tiles, as with the failures of the joints associated with infiltration of water into the facade system, leading to a loss of adhesion in the surrounding region.

The balconies areas showed a low level of defects incidence. In situations as these (building A), problems observed were of detachment, grout faults and efflorescence. Because these regions suffer from high incidence of rainfall, the failure due to water are the most frequent.

Corners and edges presented rates of occurrence of 10 to 17%, consisting primarily of ceramic detachment and efflorescence. In these regions, because of the changing directions of the facade plans, often constructive failers are in greater number, what exacerbates the flaws in general.

The transition area between floors is critical in buildings B and D. In building B were loss of adhesion, grout failure and cracking. In Building D was the higher extension of loss of adhesion.

The region of continuous walls appears to be the most critical for the occurrence of faults, together with the openings. It was observed in buildings B, C and D high failure rates, reaching 44% for building D. It was observed that the loss of adhesion has the highest incidence, followed by grout failure and cracking.

Regarding the openings, it was observed that the older buildings (B and C) have much higher rates, compared to newer buildings (A and D). As the occurrence of defects is observed that cracking, detachment and sealing defects are the first.

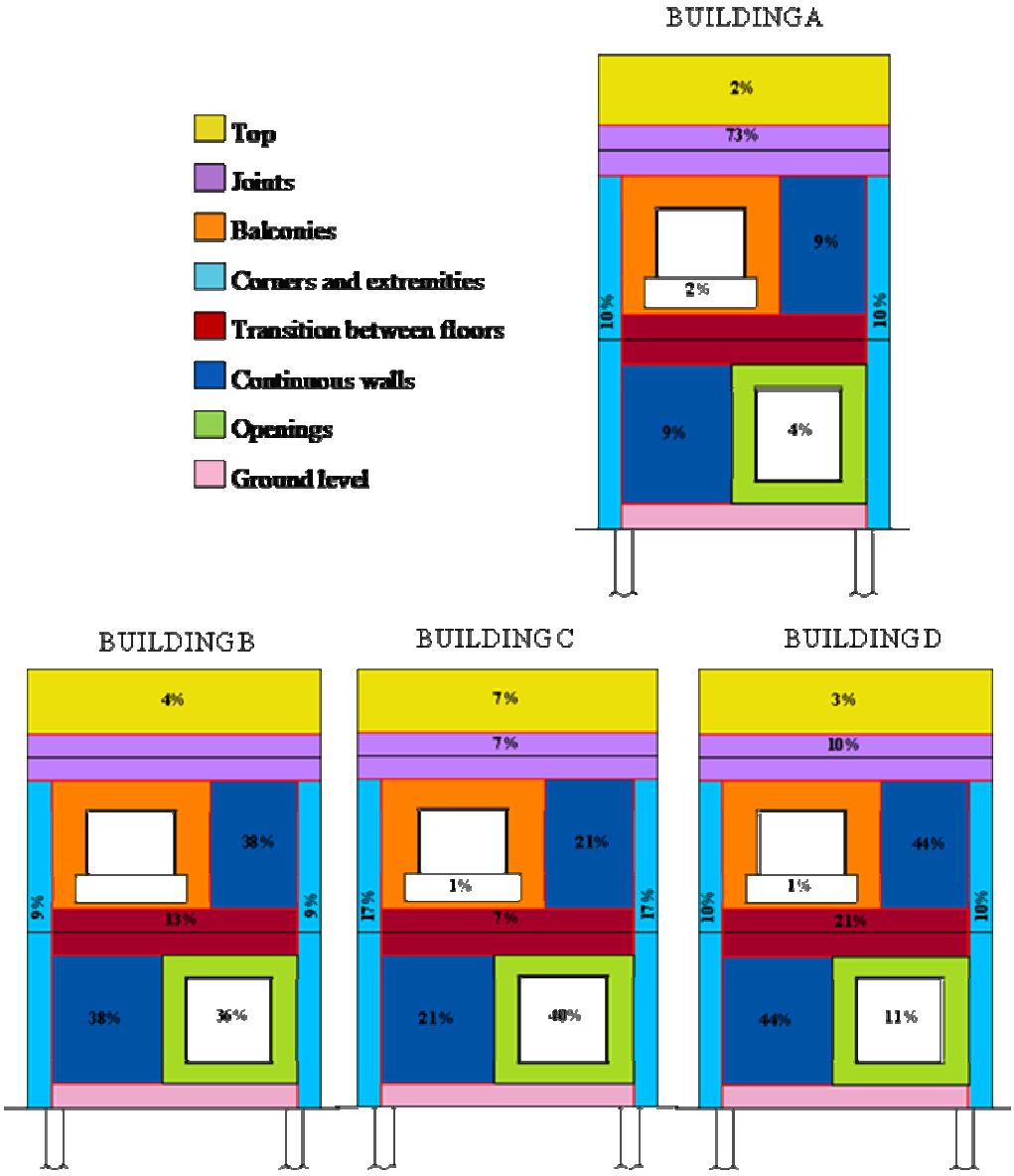

Figure 2. Mapping of the failure percentage allocated to each façade area.

4. CONCLUSIONS

From the presented study we can enumerate the following main conclusions:
- The defect index is a parameter that can be used to identify areas of further deterioration in buildings. The same was seen in the analysis of more older buildings, as well as in the identification of more aggressive façades regarding sun incidence. Another application is the simple comparison of

buildings with different typology (height, façade details), being compared to deterioration levels in different buildings.
- the great incidence of defects in ceramic loss of adhesion and detachment shows that this is one of the main problems in buildings. It is observed that both new buildings and older ones have a high incidence of detachment in almost all façade areas . It can be inferred that for buildings B and C (40 years) the detachment faults may have occurred by the very gradual deterioration of materials, infiltration and other actions. For new buildings (A and D), however, the high degree of detachment incidence may have as likely causes the constructive and material failings.
- the mappingof failures incidence in façades showed differences for each studied case. It was observed that for older buildings (B and D) the region of greatest problems is the region of solid walls and the region surrounding the windows. This leads us to interpret these failures as a result of the building structure aging, which present deformations in the structure causing cracks and ceramkic detachment.
- the absence of planned and appropriate maintenance procedures, seems to be a critical factor in the severity and incidence of observed defects. Even in newer buildings, one can infer that earlier intervention could increase the durability of the façade components.

ACKNOLEDGMENTS

The authors wish to acknowledge the support of the Laboratório de Ensaio de Materiais (LEM) and of the Centro de Apoio ao Desenvolvimento Tecnológico (CDT) of the University of Brasília (UnB).

REFERENCES

Bauer, E., Kraus, E., Antunes, G.R 2010, 'Patologias mais correntes nas fachadas de edifícios em Brasília'. Proc. 3º. Congresso Português de Argamassas de Construção - APFAC, Lisboa, Portugal.

Pereira, C.H., 2007, Contribuição ao estudo da fissuração, da retração e do mecanismo de descolamento de revestimentos à base de argamassa'. Tese (Doutorado em Estruturas e Construção Civil) – Departamento de Engenharia Civil e Ambiental, Universidade de Brasília, Brasília, Brasil.

Gaspar, P., Brito, J., 2005, 'Mapping defect sensitivity in external mortar renders'. Journal of Construction and Building Materials, 19[8], 571-578.

Silvestre, J., Brito, J., 2008, 'Inspeção e diagnóstico de revestimentos cerâmicos aderentes'. Revista Engenharia Civil, Universidade do Minho, Portugal.

Antunes, G.R., 2010, 'Estudo de manifestações patológicas em revestimento de fachada em Brasília – Sistematização da incidênica de casos'. Dissertação (Mestrado em Estruturas e Construção Civil) – Departamento de Engenharia Civil e Ambiental, Universidade de Brasília, Brasília, Brasil.

Flores-Colen, I., 2009 'Metodologia de avaliação do desempenho em serviço de fachadas rebocadas na óptica da manutenção predictiva', tese de Doutoramento em Engenharia Civil, instituto Superior Técnico de Lisboa, Lisboa, Portugal.

XII DBMC
International Conference on Durability of Building Materials and Components
PORTO - PORTUGAL, April 12th-15th, 2011

Corrosion Assessment in the Off-Shore Cooling water Outlet Channel RC Structure of Thermal Power Plant Placed in Caspian Sea: a Case Study

Mohammad Shekarchi [1]
Mehdi Khanzadeh-Moradllo [2]
Seyyed Rahman Taheri [3]
Sara Javidmehr[4]

ABSTRACT

One of the most aggressive environments for reinforced concrete is a marine environment. In this condition, corrosion of reinforcements due to diffusion of chloride is the main deteriorative mechanism. This paper presents the results of a study of 33 years old cooling water outlet channel RC structure of thermal power plant in Mazandaran, in Caspian Sea region. In 2009, the observations revealed signs of concrete deterioration. Moreover, Concrete durability factors were investigated using conventional and non-destructive tests to obtain the intensity of deterioration. The result showed that chloride induced corrosion was the main reason of concrete degradation in this structure. In other words, most points of structures, at least 3-5 cm in depth were affected by chloride and chloride concentration reached chloride threshold value.

KEYWORDS

Reinforcement corrosion; Durability; Concrete structure; Chloride; Uutlet channel.

[1] Construction Materials Institute (CMI), University of Tehran, Tehran, IRAN, shekarch@ut.ac.ir
[2] Construction Materials Institute (CMI), University of Tehran, Tehran, IRAN, khanzadeh11@gmail.com
[3] Construction Materials Institute (CMI), University of Tehran, Tehran, IRAN, srtaheri@ut.ac.ir
[4] Construction Materials Institute (CMI), University of Tehran, Tehran, IRAN, sara.javidmehr@gmail.com

1 INTRODUCTION

Concrete is the most commonly used construction material throughout the world and there is a staggering demand for its utilization in infrastructures of ports and oil exploration plants [Moradi-Marani *et al.* 2009]. Despite the fact that concrete is a reliable structural material with good durability performance, exposure to severe environments makes it vulnerable [Guettala & Abibsi 2006]. Corrosion of reinforcing bars induced by chloride ion ingress is a major cause of damage in marine environments. Reinforcement corrosion causes reduction in the service life of reinforced concrete structures so that service life reduction is one of the main challenges during last decades; therefore a regular schedule for maintenance and repair protocol is fundamentally important in controlling safe and efficient operation of a structure [Shekarchi *et al.* 2009]. Accordingly, special precautions are needed to be instituted in order to enhance the design life and durability of concrete infrastructures in saline environments [ACI Committee 305 1999].

Chloride penetration into the concrete has several mechanisms. These consist of absorption, diffusion, chloride binding, permeation, wicking, and dispersion. Absorption due to the capillary action and diffusion under influence of concentration gradient are the main mechanisms [Hong & Hooton 1999].

Once a detailed investigation to determine the extent and cause of degradation has been conducted, corrosion damage assessment can lead to selection of effective repair schemes. field investigations of repaired concrete structures are necessary to develop guidelines for adequate selection of concrete repair systems, improved repair procedures, extended durability of rehabilitated structures, and evaluation of discrepancies between laboratory results and field performance [Al-Bahar *et al.* 1998, Cusson *et al.* 2006].

This paper presents a case study where a cooling water outlet channel RC structure of thermal power plant is exposed to the marine environment of Caspian Sea. In this case study, Concrete durability factors were investigated using conventional and non-destructive tests to obtain the intensity of deterioration. The principal causes of this deterioration are highlighted and analyzed.

2 CASE STUDY

2.1 Description of Outlet Channel Structure

In the current study, a RC structure of cooling water outlet channels of a thermal power plant has been evaluated. The structure is located in southern coast of Caspian Sea in Mazandaran, Iran. The outlet channel of the RC structure is consisted of two eastern and western conveying channels which were in service since 1977. Approximately, each channel has the capacity to discharge 208000 liter water per hour. Figure 1 illustrates a layout of the channel structure.

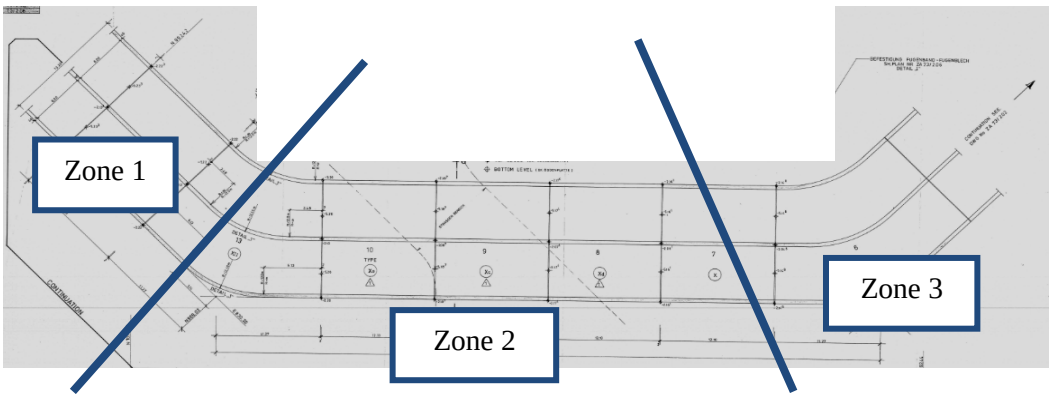

Figure 1. A layout of the conveying channels and zoning

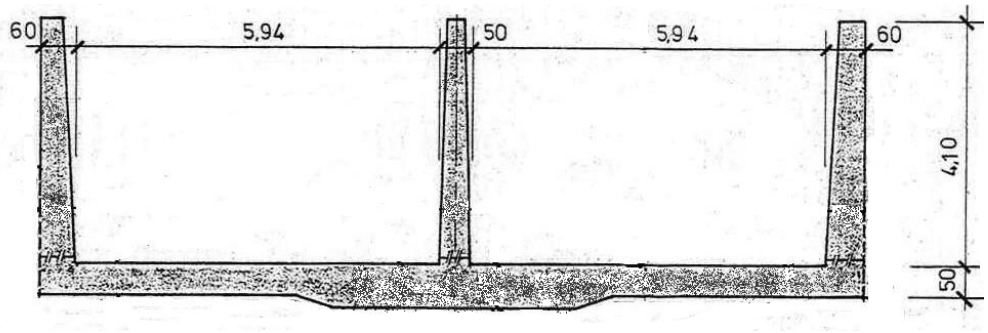

Figure 2. A cross section of conveying system (all of the values are addressed in cm)

Length of each channel is 756 m which is constructed by 36 concrete blocks. The Cross section of channel and concrete blocks are shown in Fig. 2. In addition, concrete blocks are separated by expansion gaps. Depth of water in these channels reaches 3 meters and some regions of conduit walls are exposed to seawater splash and spray as water discharge changes.

2.2 Environmental Condition

According to the literature, humidity and temperature of region that structure located there and salinity of sea water are significant parameters in deterioration of reinforced concrete structures in marine environment [Pargar *et al.* 2007]. The climate in Mazandaran is temperate in most of the seasons, with high relative humidity. The average of maximum temperature ranges from 13.2 to 32.2 □C, the former being recorded in January and the latter in August. The average of relative humidity ranges from 88.3% in July to 94% in November. Figure 3 compares monthly variations in average maximum temperature and average relative humidity in this region. The measurement of the chloride concentration as a main aggressive element of seawater and pH of seawater are illustrated in Table 1.

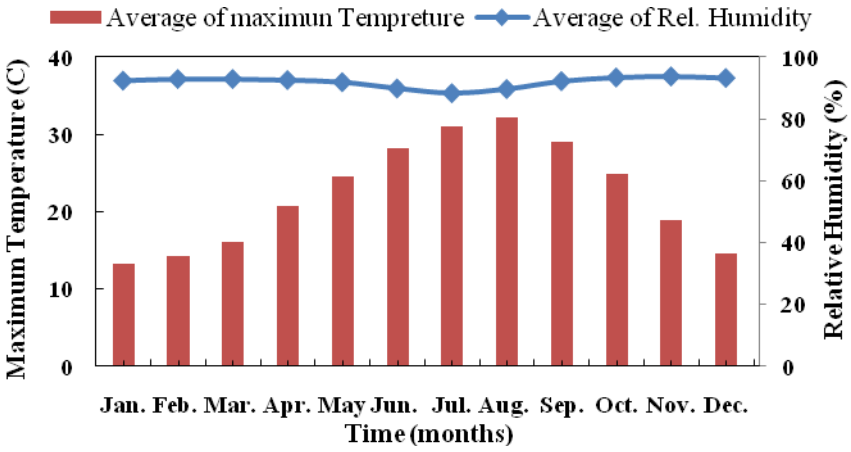

Figure 3. Climatic chart of Mazandaran

Table 1. Chemical analysis of water surrounding the structure

Water sample	*Caspian seawater*	*Eastern channel*	*Western channel*
Cl^- concentration (ppm)	*4800*	*5000*	*4900*
pH	*7.75*	*7.86*	*7.92*

3 STUDY OF STRUCTURE

3.1 Visual Inspection

Sampling, visual inspections and required tests are all undertaken on accessible parts of channel. Based on visual investigations and damage rates, channel can be divided to three zones. Figure 1 shows the division of structure to three zones. First zone includes first blocks and continues to the base parts of passing channel. In this parts, plastic shrinkage cracks pattern are detected on the surface of structure with width of less than 1 mm which could be caused by shrinkage of concrete within early ages. These cracks are also detectable by unequipped eyes; however, microscopic inspection evaluated these cracks to be approximately 400 µm width. In this zone, no sign of corrosion is detectable.

The middle part includes the most parts of channel and is addressed as zone 2. This part of the structure appeared to be better casted and placed than last zone concrete elements as no plastic shrinkage cracks pattern are detectable on the concrete surface. The most recognizable cracks are some horizontal cracks along the reinforcements. These cracks are much more detectable in the connection parts of concrete blocks to the galvanized plates attached to the concrete walls. Microscopic investigation as illustrated in Fig. 4 shows these cracks which are approximately 300 µm width.

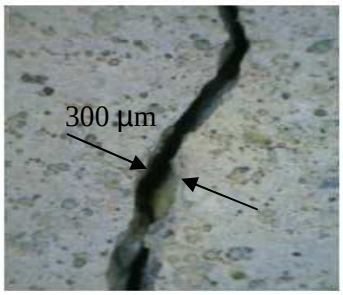

Figure 4. Cracks as depicted in microscopic photographometry in the second zone of channel.

The third zone consists of the last blocks in vicinity of sea (blocks have been counted from the Sea to the Power plant). These blocks are much more damaged and stain is detectable on the surface of the concrete. Some parts are also spalled (Fig. 5).



Figure 5. Cracks and deteriorated areas in the third zone.

In general, the structure is only slightly damaged in the second zone in comparison to the other two zones. In contrast, the first zone is then slightly more damaged which might be due to fluctuations caused by pumping at the inlet structure or poor quality of blocks as caused by inappropriate casting and construction. According to the visual inspection, the third zone of channel is the most deteriorated zone, which could be due to vicinity to seawater and hydraulic pressure of waves.

3.2 In-Situ and Laboratory Tests

3.2.1 Compressive Resistance

Compressive strength of concrete has been evaluated by test method undertaken on cores obtained from several parts of the structure as described in ASTM C39. According to the test results, the variation of compressive strength in different zones of structure is low and an average compressive strength of concrete is obtained 39 MPa.

3.2.2 Water Absorption and Specific Gravity

Water absorption test have been undertaken on number of cores obtained from different zones of the structure according to two test methods. One of these test methods is a 30-minute water absorption test of the concrete based on BS-1881. Another test method was saturated absorption test according to ASTM C642. Average of test results for different zones of channel are shown in Table 2.

It can be seen from Table 2 that water absorption and porosity of concrete are large in zone 3 in contrast to other zones. Moreover, concrete in the zone 2 exhibits good performances from absorption and porosity point of view.

Table 2. Results of water absorption and specific gravity.

Type of the tested element	*Zone*	*30 minutes absorption (%)*	*24 hour absorption (%)*	*Porosity (%)*	*Specific gravity (kg/m^3)*
Concrete cores	*1*	*1.71*	*4.4*	*11.5*	*2348*
	2	*1.56*	*4.1*	*10.2*	*2326*
	3	*1.89*	*4.3*	*12.4*	*1830*

3.2.3 Electrical Resistivity

Electrical resistivity can be used as an assessment of durability for concrete. The test is undertaken in this study according to four probe in-situ system according to ACI 222R-01. The electrical resistivity varied from 14.0 to 45.0 kΩ.cm for concrete that located in zone 1, 33.0 to 75.0 kΩ.cm for concrete located in zone 2 and 3.0 to 10.0 kΩ.cm for concrete in zone 3. Referring to ACI 222R-01, concrete in zone 3 showed higher corrosion rates in comparison with other zones. Also, visual inspection confirmed the measured values.

3.2.4 Carbonation

One of the in-situ tests is carbonation depth evaluation. The carbonation depths are measured at different locations by drilling a hole on the surface. Tests are performed along the concrete with a solution of 1% phenolphthalein and then observing color changes. Results showed that the carbonation is much lower than the concrete cover and ranged from 4 to 10 mm after 33 years. It can be concluded that carbonation cannot have a significant role in corrosion of the reinforcements.

3.2.5 Chloride Profiles

Chloride ions can cause corrosion of reinforced concrete structures when it reaches an amount known as chloride threshold value on surface of rebar. Sampling from the structure is carried out according to the NT BUILD 433, in which each grinned sample is analyzed separately for acid-soluble chloride content according to ASTM C 1152, and ASTM C 114, part 19. In the current study, it has been assumed that the diffusion mechanism mainly contribute to chloride penetration into concrete. Accordingly, the apparent diffusion coefficients and equilibrium surface chloride contents of concrete specimens are determined by curve fitting of the chloride profiles to Fick's second law of diffusion. Average of chloride profiles, diffusion coefficient and surface chloride content are shown in Figs 6, 7, and 8 for different zone of channel structure. Moreover, in this study the chloride threshold value is supposed to be 0.06% weight of concrete, based on the studies performed by Construction Materials Institute (CMI) in Caspian Sea region.

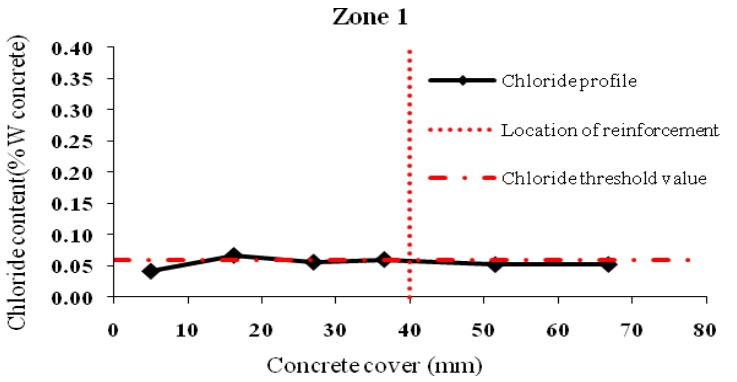

Dc: No fitting was made due to low regression coefficient,
Cs= 0.05 % W concrete

Figure 6. Average of chloride profiles, diffusion coefficient and surface chloride content in zone 1.

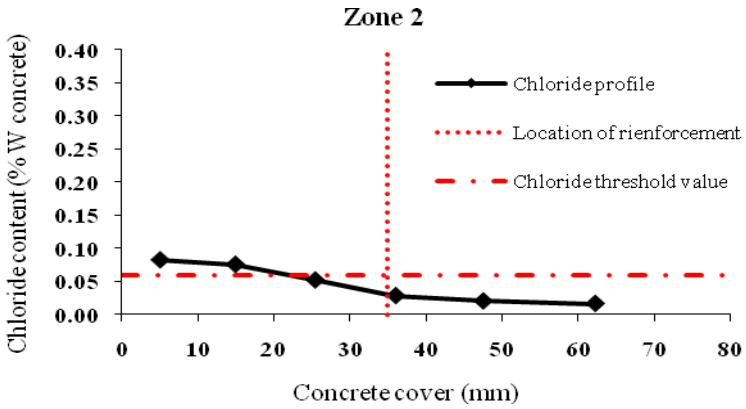

Dc= 7.58E-13 (m^2/s),
Cs= 0.1 % W concrete

Figure 7. Average of chloride profiles, diffusion coefficient and surface chloride content in zone 2.

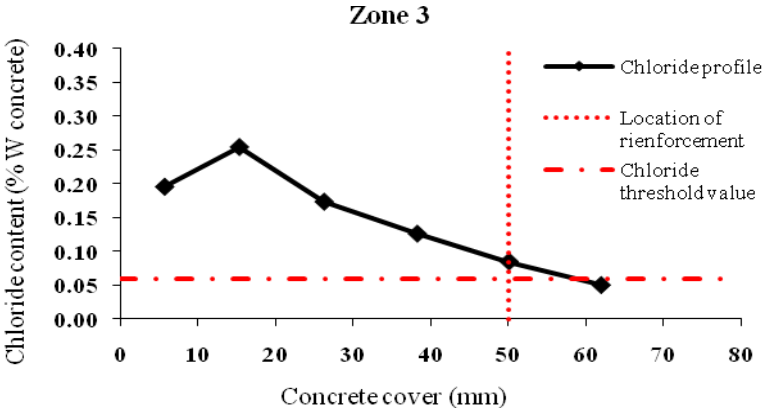

Dc= 8.35E-13 (m^2/s),
Cs= 0.35 % W concrete

Figure 8. Average of chloride profiles, diffusion coefficient and surface chloride content in zone 3.

It can be seen from Fig. 6 that chloride concentration reaches threshold value on level of rebar in zone 1. Also, it seems that initial chloride content is higher in this zone, which could be due to poor initial

casting and curing of concrete. Detected plastic shrinkage cracks in visual inspection confirm this result. Chloride profile in zone 2 indicates that chloride content on surface of rebar is lower than chloride threshold value. It can be concluded from Fig. 8 that chloride content on level of reinforced steel exceeds chloride threshold value. According to the calculated results for diffusion coefficient and surface chloride content, concrete in zone 3 exhibits the highest diffusion coefficient and surface chloride values. Visual investigations also affirmed the result.

3.2.6 Half Cell Potential Mapping

Many electrochemical methods have been used to evaluate the corrosion activity of the steel reinforcement. Among the techniques for monitoring corrosion, half-cell potential mapping is the common technique, which can be used in the laboratory and in-situ. Half-cell potential mapping is a non-destructive mean of locating areas of corrosion for monitoring and condition assessment. In this study, half-cell potentials are measured versus silver/silver chloride electrode (SCE), which is more stable, easily prepared and has long been used in electrochemistry. The ASTM C876-91 standard guide for interpretation of the half-cell potential measurements is given according to a standard copper/copper sulphate electrode (CSE). The values given by this standard guide are converted to the silver chloride reference electrode [Leelalerkiet *et al.* 2004] to enable the interpretation of the measured half-cell potentials (Table 3). The results of half-cell mapping are shown in Fig. 9 for all zones of channel.

Table 3. Evaluation of corrosion activity versus an Ag/Ag chloride electrode.

Interpretation	*Potential (Ag/Ag chloride electrode)*
Greater than 90% probability that no corrosion is occurring	$E_{Ag} > -83$ *mV*
Corrosion activity is uncertain	*-83 mV*$< E_{Ag} <$ *–233 mV*
Greater than 90% probability that corrosion is occurring	$E_{Ag} < -233$ *mV*

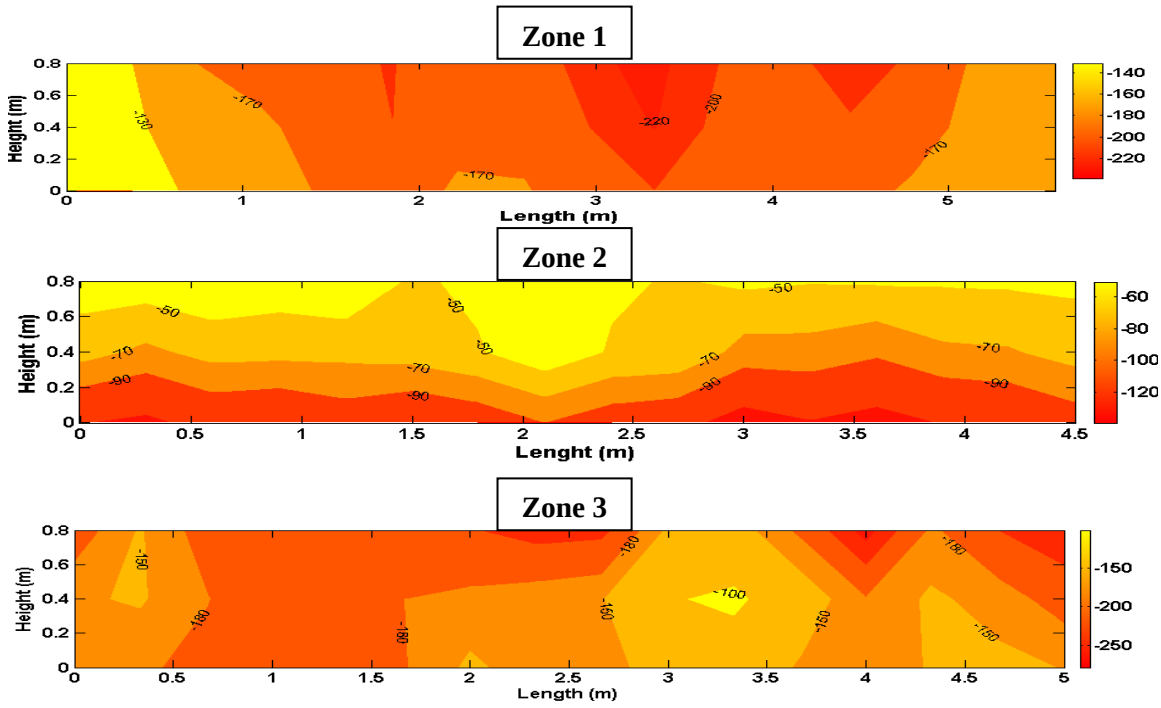

Figure 9. Half-cell potential mapping in all zones of channel versus an Ag/Ag chloride electrode.

According to results of half-cell test in zone 1, corrosion is quite probable in this zone and in most areas of this zone corrosion activity is uncertain. As it is depicted in Fig. 9, the results of corrosion potential mapping for zone 2 illustrate that the structure will not be corroded in this zone and there is a probability of greater than 90% that no corrosion is occurring. On the other hand, the results of corrosion potential mapping for zone 3 shows a high corrosion potential of concrete and there is a probability of greater than 90% that corrosion is taking placing. The results are even approved by other test results and visual investigations.

4 CONCLUSION

The purpose of this study was to determine principal mechanisms responsible for deterioration. The investigations proved the concrete of channel structure have acceptable mechanical properties. However, durability parameters of the concrete are not satisfactory. Corrosion of the reinforcing steel can be characterized as a complex process initiated by chlorides and accelerated by synergistic effects of initial cracks due to poor casting and curing of concrete.
As a result of these investigations, estimated repair thickness was 3-5 cm in most of the parts of the structure but reached 7 cm in some highly affected parts.

ACKNOWLEDGMENTS

The authors would like to acknowledge the technical support of the Construction Materials Institute (CMI) at the University of Tehran.

REFERENCES

ACI Committee 305, 1999, Hot weather concreting, Committee Report, ACI 305 R-91.

Al-Bahar, S. Attiogbe, E.M. & Kamal, H. 1998, 'Investigation of corrosion damage in reinforced concrete structure in Kuwait', *ACI Materials Journal*, 95[3], 226-231.

Cusson, D. Qian, S. & Hoogeveen, T. 2006, 'Field performance of concrete repair systems on Highway Bridge', *ACI Materials Journal*, 103[5], 366-373.

Guettala, A. & Abibsi, A. 2006, 'Corrosion degradation and repair of a concrete bridge', *Materials & Structures*, 39[4], 471–478.

Hong, K. & Hooton, R.D. 1999, 'Effect of cyclic chloride exposure on penetration of concrete cover'. *Cement and Concrete Research*, 29, 1379-1386.

Leelalerkiet, V. Kyung, J, Ohtsu, M. & Yokotab, M. 2004, 'Analysis of half-cell potential measurement for corrosion of reinforced concrete', *Construction and Building Materials*, 18[3], 155–162.

Moradi-Marani, F. Shekarchi, M. Dousti, A. & Mobasher, B. 2009, 'Investigation of corrosion damage and repair system in a concrete jetty structure', *Journal of Performance of Constructed Facilities (ASCE)*, doi: 10.1061/(ASCE)CF.1943-5509.0000112.

Pargar, F. Layssi, H. & Shekarchi, M. 2007, 'Investigation the effect of temperature and silica fume on the rate steel corrosion in concrete', Proc. 5th int. conf. on concrete under severe conditions: environment and loading (CONSEC'07), Tours, France, 4 6 June 2007, pp. 361–366.

Shekarchi, M. Moradi-Marani, & F. Pargar, F. 2009, 'Corrosion damage of a reinforced concrete jetty structure in the Persian Gulf: a case study', Structure and Infrastructure Engineering, iFirst article, 1-13.

XII DBMC
International Conference on Durability of Building Materials and Components
PORTO - PORTUGAL, April 12th-15th, 2011

Main Functional Elements Having Defects of Illegal Residential Buildings: The Case of Cova da Moura District

António Vilhena [1]
João Branco Pedro [2]
António Baptista Coelho [3]
José Vasconcelos Paiva [4]

ABSTRACT

The purpose of the paper is to describe the main functional elements with defects in illegal residential buildings. Three research questions are addressed: What are the main functional elements with defects in buildings and in dwellings? What are the main defects found? In which way these defects affect the use of buildings?

The defects were identified during a survey to the building stock of the Cova da Moura District (Amadora, Portugal), carried out in 2008. This district is made of illegal constructions, occupies an area of 16.5 ha and has approximately 5,000 inhabitants. During the survey 833 buildings and 1884 units were inspected.

The main results are: a) only 13% of these building presented defects in the building structure; b) about 60% of the buildings have defects in the roofing systems (e.g., damp and mould, infiltrations); c) more than 84% of the dwellings have defects in the technical installation such as gas or electrical installations most of them classified as severe defects.

The main conclusion is that most of the defects detected configure serious risk scenarios, particularly in terms of the minimum habitability conditions and fire safety. However, defects related to structural stability were not as serious as expected for this kind of construction.

KEYWORDS

Illegal buildings, Functional elements, Defects, Building pathology, Portugal.

[1] National Laboratory for Civil Engineering (LNEC), Lisbon, PORTUGAL, avilhena@lnec.pt
[2] National Laboratory for Civil Engineering (LNEC), Lisbon, PORTUGAL and Delft University of Technology (OTB-TUDelft), Delft, THE NETHERLANDS, jpedro@lnec.pt
[3] National Laboratory for Civil Engineering (LNEC) and Grupo Habitar (Habitat Group), LNEC, http://infohabitar.blogspot.com/, Lisbon, PORTUGAL, abc@lnec.pt
[4] National Laboratory for Civil Engineering (LNEC), Lisbon, PORTUGAL, jvpaiva@lnec.pt

1 INTRODUCTION

In the beginning of 2007, within the Portuguese governmental initiative *Critical Neighbourhoods*, a plan for qualification and rehabilitation of urban areas, the Portuguese Institute for Housing and Urban Rehabilitation (IHRU) requested the cooperation of the National Laboratory for Civil Engineering (LNEC) in the analysis of the condition of housing for those buildings located in the BACM neighbourhood (Bairro do Alto da Cova da Moura) to assess the feasibility of future urban rehabilitation. The BACM neighbourhood is a district located within Amadora, a city within the metropolitan area of Lisbon. The district is, in fact, an illegal urban development that started in the 1960s, with strong growth from the mid-1970s.

In response to this request a study entitled *Analysis of housing conditions of the existing buildings in the Bairro do Alto da Cova da Moura* was developed under the coordination of A. Baptista Coelho (Arch.). This study had three different phases [Coelho 2008; Vilhena & Coelho 2008]:

- (i) First phase: a local analysis was conducted to update and provide details of the existing cartographic support, and an assessment method to determine the buildings rehabilitation needs was also developed;
- (ii) During the second phase an experimental application of the assessment method was carried out, training was provided to inspectors involved in the survey and the fieldwork was conducted;
- (iii) In the third and final phase the results obtained in field work were interpreted and conclusions were drawn.

Over the last few years the LNEC has gained extensive experience in building condition assessment methods and the work published by Pedro *et al.* [2006a; 2006b; 2008] and Vilhena *et al.* [2007] attest to these ongoing developments in this domain... However, the specific type of buildings to be surveyed (*i.e.*, illegal construction) and the type of results required a new approach and methods.

The assessment method developed in the first phase, *Assessment Method for Building's Rehabilitation Needs* (MANR), is a multi-criteria method that pretends to establish a set of procedures to determine with accuracy, objectivity and transparency the rehabilitation needs for the building as a whole, regardless the number of units that compose it or the type of activity developed in them [Vilhena *et al.* 2010].

To achieve those objectives, it is considered that there are rehabilitation needs when the living conditions are compromised. This occurs whenever the functional requirements applicable to that type of buildings are not satisfied, in particular due to the existence of building defects, whether they are constructive defects or spatial defects (spatial defects are defects resulting from defective design of the building spaces).

The assessment was based on a visual inspection of the buildings, including all units and shared parts (where such existed). The survey was carried out by technicians of the IHRU with support of the LNEC. Initially 14 technicians of IHRU were involved in the survey, but during the work it was required to increase this number. All technicians that carried out inspections had specific training on the use of the MANR. Since the method helps verify both constructive and spatial defects, inspections were done by teams of two technicians, a civil engineer and an architect. Some inspections were done by teams of two architects, due to lack of civil engineers.

When assessing the constructive aspects, each functional element in which the building was disaggregated was assessed on the basis of three different factors, recorded sequentially: *severity* of the defect, *extent* and *complexity* of the intervention. For each functional element the assessment begins by determining the existence of defects, classified according to their severity from four categories of scale: *very slight, minor, medium* or *severe*. If the defects found were minor, medium or

severe, the extent and complexity of the intervention needed to complete the repair work were determined. The extent of the repair work took into account the amount of work required, and was assessed in four categories of scale: *localised*, *medium*, *extensive* or *total*. The complexity of the repair work took into account the usual difficulties for carrying out the work, and was assessed on three categories of scale: *simple*, *medium*, *difficult*. The assessment method was presented in more detail in a previous paper [Vilhena *et al.* 2010].

In this paper the BACM is described, as are the primary building defects detected from the survey, and finally, some conclusions are drawn from the overall effort. Lightning

2 MAIN CONSTRUCTIVE DEFECTS

2.1 BACM district

MANR was used to determine the rehabilitation needs of buildings located within the BACM. The BACM was divided into 61 blocks, according to the 2003 geographical map provided by the city council. The survey lasted six months and MANR was applied to 833 buildings and 1884 units. Of the total number of units, 1617 units had residential use (i.e. dwellings) and the remaining 267 had other uses (e.g., shop, warehouse, industry, indoor parking) [Vilhena & Coelho 2008].

The large sample size allowed characterizing BACM's buildings at construction and use levels and identifying the main functional elements with defects. The BACM is characterized by small blocks of buildings with varied compositions generally with few units. There is a similar distribution of buildings with 33% of buildings being single units, 32% with 2 units or 34% with 3 to 6 units; a few buildings were also found with more than 6 units (1%). The verification and analysis of defects were carried out considering for each building different building elements, coverings and equipments either in its existing common parts, or in each of its units.

Being of illegal origin, the buildings in BACM have been built without any design project or observation of rules or applicable legislation; their construction was simply based on the knowledge that the owners themselves had of building construction. This fact, along with the lack of maintenance and repair works has led to a large spectrum of defects to various functional elements, with different degrees and extent of severity that in some instances has led to situations of serious health and safety risk to their users.

2.2 Defects in buildings' common parts

The overall assessment of the buildings and of their respective common parts was carried out considering the following division in functional elements:

- E.1 | Structure
- E.2 | Roof
- E.3 | Salient elements
- E.4 | Walls
- E.5 | Floor coverings
- E.6 | Ceilings
- E.7 | Stairs
- E.8 | Doors and windows
- E.9 | Fall protection devices
- E.10 | Water distribution installation
- E.11 | Sewer installation
- E.12 | Electrical and lighting installation
- E.13 | Telecommunications and intrusion safety
- E.14 | Fire safety installation

Some functional elements presented defects in more than 50% of the buildings, namely: Roof (*e.g.*, lack of water tightness, lack of thermal insulation layer); External walls (*e.g.*, walls without any covering); Stairs (*e.g.*, severely degraded structure and steps unfinished or uncovered showing major deformation); Fall protection devices (*e.g.*, lack of any device). In the majority of the functional

elements the gravity of the defects observed was classified as 'Medium' or 'Severe' (Fig. 1), setting up situations where the use of spaces as well as comfort, safety and health of users are affected.

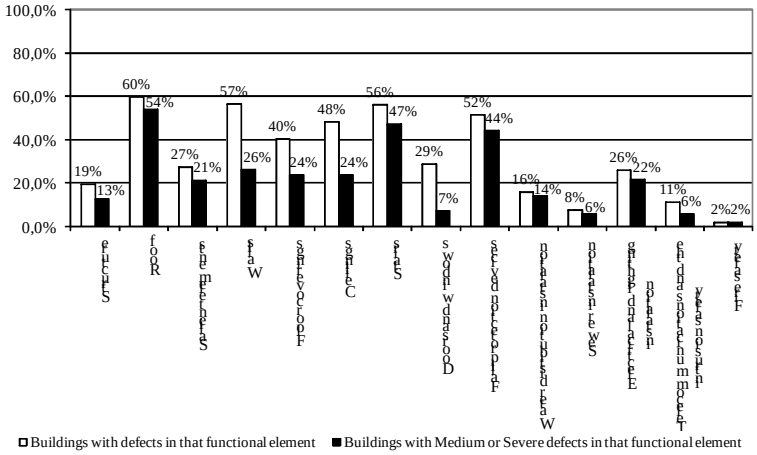

Figure 1. Distribution of defects in the functional elements by gravity.

It should also be noted in a large percentage of cases where the defects occur most elements need extensive or total repairs (Fig. 2). This fact, along with the complexity (Fig. 3) and cost of the rehabilitation intervention, shows that even in functional elements that have low defects rates, such as *Structure* (19%), the extension and the complexity of the intervention must be taken into account.

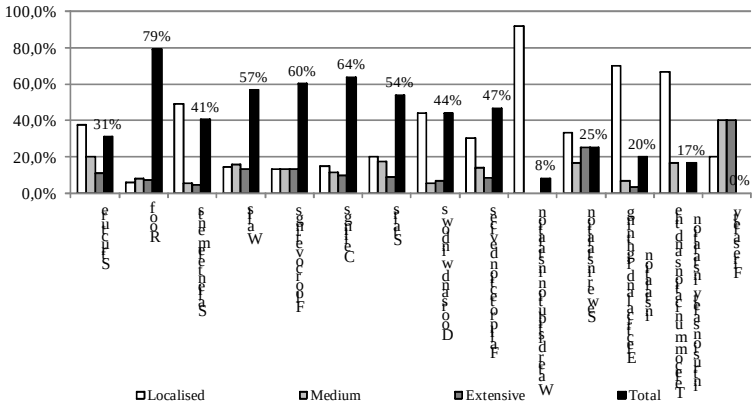

Figure 2. Distribution of defects in the functional elements by extension of the intervention.

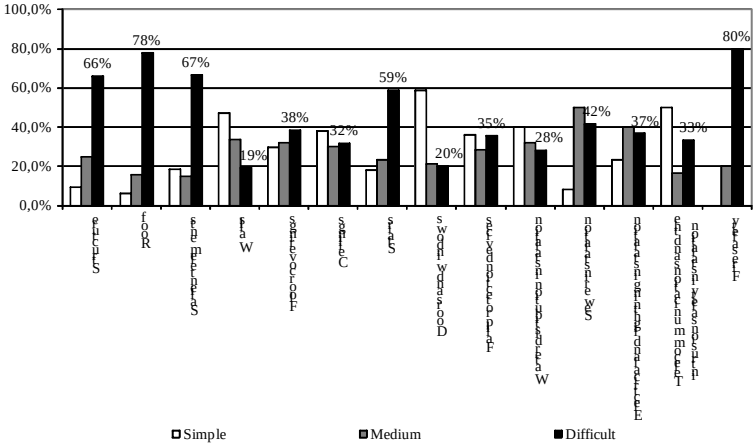

Figure 3. Distribution of defects in the functional elements by complexity of the intervention.

In the case of the functional element *Structure*, although the results of occurrence of defects show a reasonable maintenance condition of structures, building structures with damaged elements (Fig. 4) or lack of mechanical resistance were found. It is recalled that the survey was done by means of visual inspections, registering only the visible defects through evidences either in structural elements or other elements that could be affected by the structure, like walls.

Roof is the functional element that contains defects in a larger number of buildings. This fact is associated with a high rate of cases requiring total assistance, or complete replacement of the existing system. Being an element of the building envelope it is a constructive element with great impact in the living conditions, contributing to the occurrence of many defects in other functional elements (*e.g.*, walls, ceilings, electrical installation). Many of the observed defects are often due to lack of completion in case of flat roofs (Fig. 5), poor construction quality, particularly in pitched roofs, and lack of maintenance and repair works. In the functional element *Stairs*, it was observed stairs are frequently built in places with very small areas, and are often unfinished (Fig. 6); many of them present serious defects both at constructive and dimensional level.



Figure 4. Column with detached concrete covering and insufficient transverse reinforcement.



Figure 5. General appearance of a flat roof, without thermal insulation, waterproofing or any coating.



Figure 6. Stairs of poor construction quality.

The occurrence of defects in the functional element *Fall protection devices* presents very high values (52%). Most of these defects are related to lack of railings to ensure this function in areas where they would be compulsory due to the risk of a fall hazard to users.

2.3 Defects in building units

As performed in the buildings' common parts, the units' survey was done by inspecting the following 20 different functional elements.

- U.1 | External walls
- U.2 | Internal walls
- U.3 | External floor coverings
- U.4 | Internal floor coverings
- U.5 | Ceilings
- U.6 | Stairs
- U.7 | External joinery
- U.8 | Internal joinery
- U.9 | Shutters and blinds
- U.10 | Fall protection devices
- U.11 | Sanitary ware
- U.12 | Kitchen equipment
- U.13 | Water distribution installation
- U.14 | Sewerage installation
- U.15 | Gas installation
- U.16 | Electrical and lighting installation
- U.17 | Telecommunications and intrusion safety
- U.18 | Ventilation system
- U.19 | HVAC system
- U.20 | Fire safety installation

A large number of defects were found in the different functional elements. In more than 50% of the units it was possible to find defects in the following functional elements (Fig. 7): External walls; Internal walls; Ceilings; Gas installation; Electrical and lighting installation; and Ventilation system. In some of these elements (e.g., Stairs, fall protection devices, kitchen equipment, gas installation, electrical and lightning installation, ventilation system), most defects are of 'Medium' or 'Severe' gravity (Fig. 7), with serious consequences to users' comfort or health and safety.

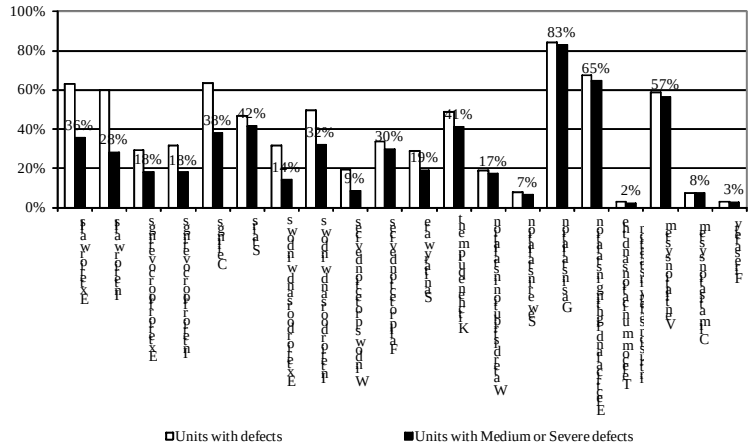

Figure 7. Distribution of defects in functional elements by gravity (units).

Taking into account the extent (Fig. 8) and complexity (Fig. 9) of the rehabilitation works needed, that there are more functional elements requiring attention than those mentioned, like the water distribution installations or the sewer installations, that present serious need for rehabilitation. A good portion of the dwellings had no kitchen equipment or a defined space for preparing meals, the usual being to use a makeshift space for this purpose.

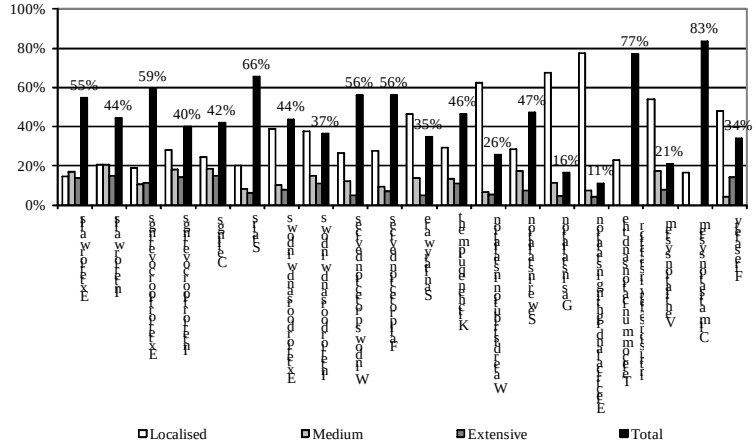

Figure 8. Distribution of defects in functional elements by extent (units).

It was also frequent to find severe defects in the electrical and lightning installation. The main defects found in this functional element included: dwellings without any installation; elements under tension installed in wet areas or in direct contact with water; electric cables under tension accessible to people.

There were serious situations detected in relation to gas installations. In fact, about 83% of the units presented defects classified as 'Medium' or 'Severe'. The most common defects detected, and that stand out for being a hazard for the use of space, are the existence of out of date rubber gas hoses or hoses with very long lengths; gas cylinders installed in unventilated cupboards; absent flue pipes connecting to combustion appliances or pipes with negative slope.

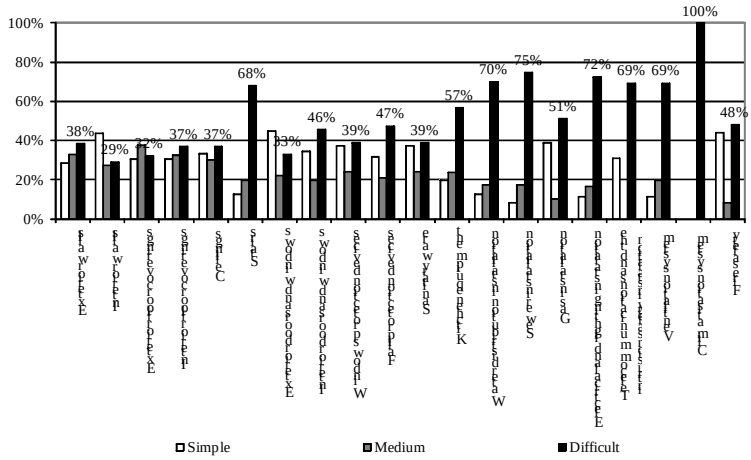

Figure 9. Distribution of defects in functional elements by complexity (units).

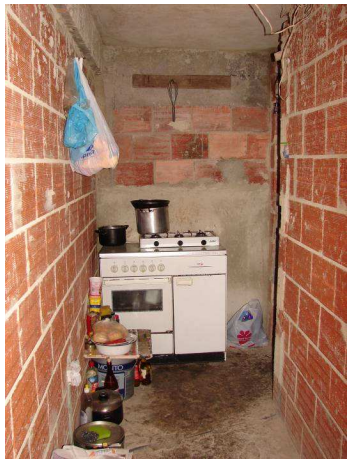

Figure 10. Improvised kitchen.

Many units presented serious health risks due to defects in external walls, ventilation system and/or roof. Most external walls are single brick masonry walls of 0.11 to 0.15 m of thickness, and that does not ensure appropriate water tightness or thermal insulation. Such construction practices allowed condensation problems to appear and the subsequent and rapid development of mould in interior finishes. In addition, it was common to find poor ventilation systems (natural or mechanical) and lack of roof watertightness, which gave rise to high relative humidity environments in the enclosed spaces. Regarding the "ventilation system" it was often found the absence of smoke gathering over the stove or even any extraction system of the products of combustion of the stove to the exterior.

3. FINAL REMARKS

The survey of the maintenance condition of the buildings in the Bairro Alto da Cova da Moura (BACM) was performed using an assessment methodology developed specifically for this purpose (MANR); this methodology intended to define the rehabilitation needs of the buildings in an objective, rigorous and independent way. The methodology implementation was carried out by teams of experts with experience in construction and with specific training in the assessment method. Along with these factors, the survey covered all buildings of BACM, allowing a very reliable picture of the maintenance condition of the buildings and units.

It was found that buildings, though built in a self-construction regimen without any design, do not present serious structural defects, in contradiction with what would be expected. In the external

envelope of buildings, the most affected functional element was the roof that showed defects in 60% of buildings. In many units the functional elements had defects with particular relevance to the electrical and gas installations that in most cases made up a hazard to the safety and health of users.

It should be remembered that this survey was based on visual inspections and it is possible that not all existing anomalies were detected.

The level of regulatory building performance is set in the context of the prevailing cultural, social, climatic, economic and technological conditions in a particular society. The general Portuguese building legislation is geared to construction of new housing. However these buildings fail to fulfil even the basic requirements set out in specific regulations for the regularization of illegal buildings. Therefore, the units that did not meet these basic requirements must be either demolished or made fit to live in.

ACKNOWLEDGMENTS

Thanks are extended to dwellers of the BACM, the IHRU technicians that participated in the inspections, Municipality of Amadora and colleagues from the LNEC involved in the study.

REFERENCES

Coelho, A. B. 2008, *Análise das Condições de Habitabilidade do Edificado Existente no Bairro do Alto da Cova da Moura – Organização geral do estudo e pré-análise*, LNEC, Report no. 247/2008 – NAU, Lisboa .

Pedro, J. B., Aguiar, J. & Paiva, J. V. 2006a, *Proposta de uma metodologia de certificação das condições mínimas de habitabilidade*, LNEC, Report no. 397/2006 – DED/NAU, Lisboa.

Pedro, J. B., Paiva, J. V., Raposo, S. & Vilhena, A. 2006b, *Proposta de um método de avaliação do estado de conservação de edifícios: Discussão e aplicação experimental*, LNEC, Report no. 185/2006 – DED/NAU, Lisboa.

Pedro, J. B., Paiva, J. V. & Vilhena, A. 2008, Portuguese method for building condition assessment, *Structural Survey*, 26[4], 322-335.

Vilhena, A., Pedro, J. B. & Paiva, J. V. 2007, *Apoio do LNEC na reavaliação do estado de conservação dos imóveis da fundação D. Pedro IV*, LNEC, Report no. 251/2007 – DED/NAU, Lisboa.

Vilhena, A. & Coelho, A. B. 2008, *Colaboração do LNEC na análise das condições de habitabilidade do edificado no Bairro do Alto da Cova da Moura. Avaliação das necessidades de reabilitação do edificado. Relatório de síntese*, LNEC, Relatório n.º 266/2008-DED/NAU, Lisboa, Novembro.

Vilhena, A., Pedro, J. B. & Paiva, J. V. 2010, 'Assessment method for buildings' rehabilitation needs. Development and application', Proc. '*CIB World Congress 2010 – Building a Better World*', The Lowry, Salford Quays, United Kingdom, 10-13 May 2010, pp. 99.

XII DBMC
International Conference on Durability of Building Materials and Components
PORTO - PORTUGAL, April 12th-15th, 2011

Reduced Service Life of Bathrooms Due to Leaks Around Floor Gullies and Pipe Penetrations

Erik Brandt[1]
Eva B. Møller[2]
Ernst Jan de Place Hansen[3]

ABSTRACT

Failures in bathrooms are generally related to ingress of water or condensation of moisture in the construction. Failures will normally lead to drastically reduced service life and quite often renovation is comprehensive and associated with excessive costs.

One of the most frequent causes to failures is leaks around the floor gully either because the gully is mounted incorrect or because illegal changes have been made to an existing floor gully – normally made in connection with renovation of the floor where the existing floor gully is extended to a new floor surface. Many problems are seen due to ingress of water through the extensions. Similar problems are seen around pipe penetrations in the floor.

The paper presents the Danish national rules for how floor gullies are mounted in order to achieve watertightness and gives examples on the problems experienced with illegal solutions. Further the paper presents the possibilities for approval of innovative system solutions (for so called "designer floor gullies"). For example approval of the mounting of a floor gully up against a wall. Approvals are always based on full scale testing with the purpose to simulate long term behaviour of the floor/gully by exposure to a harsh cyclic regime of water, temperatures and mechanical forces individually adjusted to the floor gully under test.

KEYWORDS

Bathroom, Wet room, Floor gullies, Service life, Watertightness.

[1] Danish Building Research Institute / Aalborg University, Hørsholm, DENMARK, evm@sbi.dk
[2] Danish Building Research Institute / Aalborg University, Hørsholm, DENMARK, evm@sbi.dk
[3] Danish Building Research Institute / Aalborg University, Hørsholm, DENMARK, evm@sbi.dk

1 INTRODUCTION

Leaks around floor gullies and pipe penetrations can lead to expensive damages in new buildings as well as at renovation. Damages may range from discolouration of the ceiling below to deterioration of the entire floor construction.

It is customary in Denmark that the floor and the walls in bathrooms are directly exposed to the water from the shower as no shower cabins or shower trays are used. It is therefore required in the building code that all bathrooms must have at least one floor gully (all water on the floor shall be led to a floor gully), and that bathroom constructions including penetrations for pipes and floor gullies are watertight as it is expected that they are exposed to water, high relative humidity etc.

Traditionally constructions have been made from heavy inorganic materials e.g. floors of concrete with iron beams and walls made from masonry or concrete. These types of constructions were considered to be watertight provided that they had a water repellent surface, e.g. ceramic tiles.

Different solutions have been invented to install bathrooms in older houses which originally did not have bathrooms. Traditionally old houses have floor constructions with wooden beams which were used to support a concrete slab used as floor in the new bathroom. In recent years also lighter construction materials have been used, e.g. plywood or particle boards. The advantage is that light weight materials are cheap, easy to install and without excess water. The drawback is a higher rate of damages resulting in reduced service life and excessive repair costs.

The type and use of floor gullies vary according to the construction. Originally floor gullies were made from cast iron embedded in the concrete floor. Later stainless steel and plastic floor gullies were introduced. All sorts of gullies are now also used in light weight constructions but they are mounted quite differently dependent on the material used for substrate and the actual floor covering.

Experience gathered from a large number of defects found during surveys of bathrooms shows quite a few problems with watertightness of floor gullies or pipe penetrations (or rather the mounting of the pipe or gully in the floor). The problems can have different reasons but are often related to the use of a wrong type of floor gully or simply bad design or bad workmanship of details around the floor gullies and pipe penetrations.

2 TYPES OF FLOOR GULLIES AND PIPE PENETRATIONS

To ensure a satisfying service life for the entire construction the requirements to penetrations in the floor are generally high due to the exposure to water and the consequences of failures which are most often very severe.

2.1 Types of floor gullies

The main types of floor gullies used are gullies for embedding in concrete and gullies for mounting in board materials. Further there are different types depending on the type of floor covering and whether a watertight membrane is required or not.

The traditional floor gully is embedded in concrete and in Denmark experience shows that a 100 mm concrete layer is sufficient to achieve watertightness (provided that the concrete is of a sufficient quality). In recent years the requirements to watertightness of the entire construction have been tightened as regards apartment houses where a supplementary watertight membrane on the floor is required. The membrane is normally attached to the gully either by applying it directly to a flange – at least 40 mm wide – on the gully or by means of a prefabricated collar either glued to the flange or attached with a clamping ring.

For constructions with board materials the flange is normally recessed into the board and mounted with screws. For board materials a watertight layer is always required; they are applied as described above.
Resilient floor coverings – especially PVC – are often used as floor covering in bathrooms. They are always connected to the gully with a clamping ring.

2.2 Pipe penetrations

Traditionally pipe penetrations were made by embedding the pipes in concrete. This is still a much used method but it is today supplemented with a skirting around the pipe to ensure the watertightness. For floors with board materials other types of watertightening methods are used normally including either a skirting in combination with a watertight membrane and/or a mechanical solution with O-rings of rubber ensuring the tightness, cf. Figure 1.

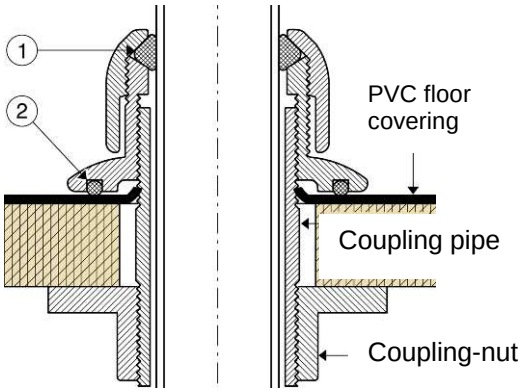

Figure 1. Pipe penetration in a bathroom floor made from chip-board. The bushing is tightened by screwing the upper part to the bushing pipe which is held in place by means of a coupling-nut underneath the floor. The watertightness to the pipe and the floor respectively is achieved by rubber O-rings (1 and 2).

3 COMMON FAILURES

Failures around penetrations of pipes and floor gullies are related to ingress of water in the construction. Failures will normally lead to reduced service life and quite often renovation is comprehensive and associated with excessive costs. Failures are seen in all bathrooms including the traditional ones made with floor constructions in concrete etc. However, the traditional/inorganic constructions are often more “tolerant” against small failures i.e. the consequences of small leaks are less severe and renovation not as comprehensive as for light weight constructions.

3.1 Wrong mounting of floor gully

Very often floor gullies are mounted incorrectly, e.g. not embedding the gully in concrete as required, mounting the gully to low in relation to the floor surface or mounting the gully so the lower and upper part of the floor gully is not in line vertically. In all cases the result is that a watertight connection between floor and floor gully is not ensured as the main watertight barrier is destroyed. Examples are shown in Figure 2 and Figure 3.



Figure 2. A) Floor gully removed from a fitness centre (in a shopping mall) with harsh exposure. It is seen that the floor gully was not entirely embedded in concrete as required. Instead it was attempted to make a watertight connection only with a collar and a membrane. This was not sufficient - especially not in a harsh environment with exposure of water throughout the day.
B) The gully seen from the underside before it was removed. Water was leaking through the joint between gully and floor resulting in expensive damages to goods and furniture below as well as expensive repair works.



Figure 3. Floor gully mounted before the plywood floor resulting in a weak connection between gully and floor (not possible to make a sufficient mechanical connection). Besides it is not possible to make a suitable and safe connection with a watertight membrane/collar between plywood and floor gully. The result was cracks in the tiles due to dimensional changes in the plywood which became wet due to water penetrating through the connection between gully and plywood.

3.2 Unsuited/wrong floor gully used

In some instances it is seen that unsuited floor gullies are used, e.g. a gully intended for embedding in concrete is used in a board floor or a gully intended for tiles is used for PVC floor covering. If the floor gully is not intended for the actual use it is hard or even impossible to make a safe and watertight connection, e.g. it is a prerequisite for using PVC floor covering that the gully is circular in order to bend the PVC down in the gully (and ensure the connection with a clamping ring). For floor constructions made from plywood or chipboard it is similarly necessary to make a good mechanical connection between the board and the gully; this is achieved by using a floor gully with a flange which is recessed in the board and attached with screws.



Figure 4. Floor gully intended for ceramic tiles used for PVC floor covering. The PVC cannot be bend down into a quadratic gully and in this case the PVC has further been cut around the frame i.e. no watertight connection.

3.3 Gullies at renovation

By far most problems are seen in renovation projects e.g. where new bathrooms are installed in old buildings, old bathrooms or toilet rooms are expanded or simply new floor coverings are installed. At the same time the old buildings are in general more vulnerable to damages caused by ingressed water as they more often than not are made with a large amount of organic materials e.g. wooden beams.

In connection with renovations it is often tried to maintain the old floor gully in order to reduce the costs. This is no problem if only the floor covering is changed with a new of the same type but might be a problem e.g. if the floor construction is changed or if a PVC floor is changed to a tile floor. It should be born in mind that often the floor to be renovated is no longer watertight (or the watertight layer e.g. terrazzo is removed during the renovation).

By renovation the floor construction is quite often raised by application of a screed on top of the existing floor or it is applied simply to level out an old substrate e.g. for a terrazzo floor. If the original floor gully is maintained and extended upwards there is a considerable risk that water will penetrate into and through the construction, cf. Figure 5. In the case with terrazzo it is common to remove the terrazzo before applying the screed and the construction underneath is rarely watertight.



Figure 5. An old floor has been renovated with a screed and the original floor gully has been maintained (seen 100 mm below the floor surface). The floor gully is close to the wall and a horizontal pipe on the wall making the execution of the work difficult and further a pipe is introduced in the screed (see lower right corner). On the picture to the right is seen water penetrating to the underlying flat due to lack of watertightness around the gully (easily achieved by testing where the gully is blocked and water is poured out on the floor for a period in order to establish a small head of water).

For PVC floors that are changed to tile floors the circular floor gully is not suited to receive a floor tile and consequently screed or extra frame(s) are placed over the original gully to make it suitable for the tiles, cf. Figure 6.





Figure 6. Left) Floor gully of cast iron originally modified (but not made for it) to be used with a PVC floor covering later further changed to be used with ceramic tiles. Note the nail (arrow) between PVC and tiles. Water penetrated to the flat underneath (tested same way as described in Figure 5). **Right)** Original gully for PVC flooring modified to floor tiles by adding supplementary frames. It is easily seen that the joint between gully and frames are not watertight – neither are the joints between the individual frames.

Also in renovation projects it is quite normal that restrictions apply as regards the position of the gully e.g. due to a stack pipe or pipes under the floor in the underlying flat that cannot be moved. This might result in mounting of floor gullies very close to adjoining walls which makes it difficult to make good and safe connection between floor and floor gully, e.g. it is very difficult to pour concrete satisfactory around a floor gully placed up against a wall.

3.4 Pipe penetrations

Most often problems with pipe penetrations are due to the fact that no attention is paid to make the penetration watertight, cf. Figure 7. Another common problem is that pipes, e.g. pipe stacks are exchanged and the floor is not closed sufficiently afterwards where for example watertight membranes are destroyed during the repair work.





Figure 7. Pipe penetrations in bathroom floors where obviously no attempt have been made to make the penetrations watertight. **Left)** Pipe in pipe system where the outer pipe is normally used to report any leaks in the inner pipe. Here it is of no use as it is guaranteed to be filled with water. **Right)** Penetrations in a bathroom floor made from chipboard which makes the construction very vulnerable to exposure of water as ingressed water will deteriorate the chipboard.

4 MEASURES TO IMPROVE SERVICE LIFE

As the number of problems is great and the damages resulting from leaks are normally very expensive different measures to improve the situation have been taken during the years.

The requirements to floor gullies are stated in the Danish Standard "Code of Practice for Sanitary Drainage - Wastewater Installations". The main requirements as regards the mounting are:

- the floor gully is an integrated unit and might include a trap (to avoid smell from the wastewater system)
- no water must be able to penetrate from the gully to the surrounding floor construction
- the top of the floor gully must be at the level of the floor surface
- the floor gully shall be easy to clean

As it can be seen from the standard it is not allowed to modify/change floor gullies i.e. very often it is a prerequisite that the floor gully must be changed in connection with renovation projects. Also the standard requires that the gully shall be easy to clean i.e. the risk for flooding of water and thereby also for water penetration is minimised.

In SBi direction 200 “Wetrooms” further requirements are given to the position of the floor gullies. The rules are now that the edge of the gully shall be at least 150 mm from neighbouring walls etc. This requirement is intended to ensure good working conditions, e.g. making it possible to pour concrete around the gully or making it practically possible to bend a PVC floor covering down in the gully. Similarly the direction has requirements to the position of pipes from walls etc.

During recent years a new type of floor gullies – so called “designer gullies” have been introduced on the market. These gullies are meant to be placed directly against walls or in corners, cf. Figur 8. These gullies have been rather popular. In order to ensure the watertightness a good design and good workmanship are crucial. In Denmark these gullies are normally approved. So far approvals have been national and issued by ETA-Denmark (national approvals are in Denmark designated MK-approval i.e. approval of materials (M) and constructions (K)).



Figur 8. A socalled “designer gully” intended for use against walls (or for other models corners). They have the advantage that the floor might be plane (but with a slope) but the disadvantage that the position set requirements to the design and workmanship to ensure a good performance i.e. watertightness.

Approvals are issued on basis of a full scale testing. The method used is a modified version of the method used for testing of watertightening kits. The method was originally developed as a Nordtest method (Nordtest Method 230, "Bathroom floors - watertightness", 1994). It is an accelerated test

with exposure to mechanical loads, humidity changes and cycles of hot and cold water. The exposure was chosen to simulate exposure under use conditions but with tougher extremes i.e. the testing is intended to show whether the mounting and the floor gully itself is able to resist in-use conditions under a long period of use. It can not be said how much the testing accelerates the real life exposure as this very much depend on the actual use i.e. whether the gully is used in private home or in a fitness centre.

During the past years an EOTA (European Organisation for Technical Approval) working group has been working on a European Technical Guideline (ETAG 022) for waterproofing of wet rooms. The work is currently under finalisation [EOTA, 2007]. In the guideline the above mentioned method has been further developed and in the future ETAs are expected to be issued under similar conditions as the Danish national approvals.

Other efforts to improve the situation is education of architects, engineers and craftsmen including post education courses and issuing of easy to read material about problems with gullies and how they can be avoided.

7 DISCUSSION

The workmanship is crucial for a good result. Even a good product/system is worth nothing if not installed properly. In Denmark the most common problem as concerns penetrations is probably that the importance of the watertightness is not taken seriously enough. Consequently the work is not always done with sufficient care. This calls for a quality control of the work best performed by the contractor himself and followed up by an independent body.

In Denmark a voluntary control scheme has so far only been used for works with PVC floor and wall coverings used as watertight membrane. For PVC works the contractor – actually the individual craftsman – controls his own work. This is followed up by independent surveys of randomly chosen bathrooms. The control scheme has led to a significant improvement of the quality of the work.

The increased requirements introduced over the past years have proved to have a good effect as the number of problems has been reduced significantly. Contributing to the reduced number of problems is also that a huge effort to teach consultants and contractors about the importance of good design and workmanship has been fruitful. Today most architects, engineers and craftsmen are very much aware that bathrooms constructions and especially gullies and other penetrations are complicated and require special attention.

It is believed that extended service lives can be achieved if

- the details around floor gullies and pipe penetrations are (better) described and – if necessary – tested for watertightness after completion,
- design as well as execution are brought under quality control with focus on watertightness and workability,
- the contractor is trained in being more aware of the importance of good workmanship.

REFERENCES

Danish Standard, DS 432, "Code of Practice for Sanitary Drainage - Wastewater Installations", 2009
SBi direction 200 “Wetrooms”, Brandt, E., Danish Building Research Institute, 2000.

Nordtest Method 230, "Bathroom floors - watertightness", 1994.

EOTA, ETAG 022, "Guideline for European Technical Approval: Watertight covering kits for wetroom flors and/or walls", Part 1 "Liquid applied membranes", 2007.

XII DBMC
International Conference on Durability of Building Materials and Components
PORTO - PORTUGAL, April 12th-15th, 2011

Deterioration of Foundation Elements of Buildings, Due to Sulfates Attack

Fuad Carlos Zarzar Júnior [1]
Romilde Almeida de Oliveira[2]

ABSTRACT

The external attack of sulfate is not completely understood. It is defined as an action of sulfate ions involving deterioration owing to chemical reactions with cement hydrated mortar. When this occurs, a physical manifestation will tend to produce an expansive reaction, resulting in cracks or fissures easy to identify at site, generating damage or deterioration. Systematic study of chemical reactions produced by sulfate attack on concrete is being developed to provide support to the civil engineer whenever confronting this kind of problem, so, they can recognize it immediately at work. In this article, a case study of building foundation is presented and the attack by elements of sulfates in its foundations is confirmed.

KEYWORDS

Attack by sulfate ions, Concrete, Pathology, Identification of attack, Repairing.

[1] Programa de Pós-Graduação em Engenharia Civil, Universidade Federal de Pernambuco (UFPE), Recife-PE, BRAZIL, fczj@yahoo.com
[2] Programa de Pós-Graduação em Engenharia Civil, Universidade Federal de Pernambuco (UFPE), Recife-PE, BRAZIL, romildealmeida@gmail.com
[3] Universidade Federal de Pernambuco (UFPE), Recife-PE, BRAZIL, andrea_negromonte@yahoo.com.br

1 INTRODUCTION

The objective of this article is to provide an understanding of the deterioration of the foundation of a structure and identify a set of techniques that facilitate the professionals who work with concrete pathologies in order to recognize the sulfate attack through the manifestation of the damage observed. A case study was carried out as a contribution to understanding the collapse of the structure of the Building Éricka, which was situated in Olinda - Recife Metropolitan Region (Brazil), in November 1999.

2 SULFATE AND SULFATE ATTACK

Sulfates are salts in which the negatively charged ion SO_4^{2-} forms a compound with a metal (positively charged ion), such as Ca^{2+}. On the ground, the sulfates soluble in water are of particular concern and can therefore be readily transported to react with the concrete. Such sulfates include gypsum (calcium sulfate, $CaSO_4$), epsomite (magnesium sulfate, $MgSO_4$), and sodium sulfate decahydrate, $Na_2SO_4.10H_2O$. For the sulfate attack to occur the sulfates must be carried to the interior of the concrete by interstitial water. Four sulfate compounds are soluble in water and common geological materials: calcium sulfate, magnesium sulfate, sodium sulfate and potassium sulfate. Calcium sulfate is the most predominant, but less soluble (giving a maximum dissolved concentration of about 1400mg SO4 per liter of water) and for this reason is less deleterious to concrete, [Communities and Local Government, 2008]. Of all these, the most damaging one is magnesium sulfate, since the cations of magnesium may on its own contributing to the destruction of the concrete. A feature of the magnesium ion attack on Portland cement paste is that the attack is eventually extended to the calcium silicate hydrate (C-H-S) which is the main cementitious component. Under prolonged contact with a solution of magnesium, the (C-H-S) in the cement paste hydrated gradually lose calcium ions, which are partially or sometimes completely replaced by magnesium ions. The final product of this substitution reaction is a magnesium silicate hydrate ($Mg3H_2Si_4O_{12}$). The formation of this salt is associated with loss of cementitious characteristics (loss of strength and disintegration of concrete), Neville [2004]. The amount of soluble sulfates present in the material is a significant factor in determining the potential of sulfate attack. Unfortunately, it can be difficult to obtain representative values of soluble sulfates in some materials because of their inherent variability.

2.1 Portland cement.

This type of cement is most vulnerable to sulfates attack, since it transfers to the concrete cement considerable doses of calcium aluminate hydrates and calcium silicate hydrates. Portland cement is a hydraulic binder obtained from clinker to which is added gypsum ($CaSO_4$). The clinker is the product of heating to high temperatures from a mixture of clay and calcium. Thus, Portland cement is composed primarily of calcium and silica in its composition. Besides the type of cement, the vulnerability of concrete to be attacked by sulfates depends on the easiness of sulfates to migrate to the interior. What controls this is the permeability of concrete to water, a property that depends on the size and interconnectivity of pores in the concrete. The concrete, thoroughly mixed and compacted, and cured, has a content ranging from moderate to high of cement and a low mixing ratio of water to cement is less permeable, and therefore has the greatest resistance to attack by sulfates. The concrete that has become partially or totally "carbonated" is more resistant to sulfate attack. Carbonation of concrete results from the reaction with airborne carbon dioxide (CO_2). The main reaction is with calcium hydroxide $Ca(OH)_2$ in the matrix of concrete, the final products are calcite ($CaCO_3$) and water. The reaction results in a loss of alkalinity that is associated with the presence of calcium hydroxide (pH can fall from 12 to less than 9) and as a result, the formation of expansive minerals, ettringite and thaumasite, that need a higher pH, is prevented. The carbonation of concrete proceeds more easily in permeable concrete that is exposed to the atmosphere with relative humidity, between 50-70 percent [BRE Digest 263, 1982], and is progressive with time, starting at the concrete surface. Humid conditions below 20% or above 95% delays or prevents carbonation to take place. Some cases of sulfate attack have been reported, in which the concrete has been contaminated with excess of sulfates as a result of impure cement production, or where there is contamination at the site with

gypsum plaster.

3 SULFATE MIGRATION

Sulfates in the hardcore or soil will not be damaging the concrete if they remain dry. Water is necessary to dissolve the sulfates and carry their anions into the concrete. The amount of water needed is not great. The surrounding soil needs not to be saturated, just be humid. In some cases the moisture content in the soil is just between 12-14 percent. A common source is water from the sub-soil that is carried up through the finer fraction of the hardcore due to capillary action. Once in contact with concrete, water is drawn by capillary action due to evaporation at the surface.

4 TYPES OF MECHANISMS OF ATTACK BY SULFATE

4.1 Conventional sulfate attack or in form of ettringite

In the conventional sulphate attack, sulfates and water react with the tricalcium aluminate-found in Portland cement to form a hydrate sulfoaluminate calcium ($3CaO.Al_2O_3.3CaSO_4.31H_2O$) known as ettringite. In the manufacture of portland cement 5% of sulfate in the form of gypsum to inhibit the instant setting time of clinker is added. This type of reaction, long known due to numerous publications on attack by sulfates, has been attributed to this modality. The formation of ettringite can be destructively expansive due to the fact that it has a solid volume larger than the original constituents and typically grows as acicular crystals which collectively can generate high internal stress in the concrete.

To produce deleterious amounts of ettringite, the reaction requires the presence of:

a) a significant concentration of sulfate soluble in water;
b) concrete containing a substantial content of calcium aluminate hydrates, such as the concrete produced with most Portland cement;
c) presence of humidity.

Sulfate SO_4^{2-} ions, which enter the cementitious component may react with calcium hydroxide $Ca(OH)_2$ in the matrix of cement of the concrete forming gypsum (calcium sulfate dihydrate, $CaSO_4.2H_2O$).

$$Ca(OH)_2 + C\text{-}S\text{-}H + SO_4^{2-} + H_20 \rightarrow CSH2 \text{ (gypsum)}$$

This reaction product also has a solid volume larger than the original constituents and in some cases may contribute to the degradation of concrete. The ions sulfate may also bond with other ions to form the various reactants that result in sulfate attack as, sodium sulfate ($NaSO_4$), and magnesium sulfate ($MgSO_4$). If the magnesium ions accompany the sulfates, they may also react with calcium hydroxide, producing brucite (magnesium hydroxide, $Mg(OH)_2$) that due to its low solubility precipitates out of solution, leading to a increase in solid volume. The magnesium ions can also attack calcium silicate hydrates, the primary bonding material in concrete [Communities & Local Goverment, 2008]. By-products caused by these reactions can create expansion that disrupts paste cohesion and leads to loss of strength in the concrete. Laboratory tests demonstrate that the first effect of the conventional form of sulfate attack is the increased strength and density of concrete as the reaction products fill the pores. When the pores are filled, future formations of ettringite induce expansive internal tensions that, if greater than the tensile strength of concrete, will produce the rupture of the affected region. These cracks with crystalline accumulations are characteristic signs of the conventional form of sulfate attack. According to Neville [2004],"When the analysis of the concrete demonstrate a high content of sulfate it does not necessarily mean a deterioration, although, inversely, the loss of strength or visual deterioration accompanied by a high content of sulfate would be evidence of attack by sulfate. He further emphasizes that "the presence of ettringite by itself is not a sign of sulfate attack."

4.2 Sulfate attack with formation of thaumasite

This form of sulfate attack was recognized initially in the UK in the 80s and early 90s and has been found in several cases of deterioration of buried concrete in which the cementitious matrix had been completely replaced by thaumasite transforming the concrete material in a soft material without cohesion. The reaction product is the mineral thaumasite which is a mixture of carbonate, sulfate and calcium silicate hydrate ($CaSiO_3.CaCO_3.CaSO_4.15H_2O$), [Communities & Local Government, 2008].

$$\text{Sulfates} + CSH \rightarrow \text{thaumasite}$$

Deleterious levels require:

a. significant concentration of sulfates soluble in water;
b. concrete containing calcium silicate hydrate, C-S-H (which looks like fibrous structures, is the component responsible for the mechanical strength of cement used in construction. C-S-H presents a partially crystalline phase resulting from hydration of silica-alumina with pozzolanic activity such as volcanic ash, silica, etc ...), as in most phases of cementitious calcium silicate in Portland cement;
c. a source of carbonate, usually from a limestone aggregate;
d. a pH of 10 or higher, as is found in non-carbonated concrete;
e. continuous wetting;
f. low temperature (generally below 15° C).

Since the hydrated calcium silicates provide the main bonding agents in Portland cement, this form of attack weakens the concrete, as well, causing some expansions and in advanced cases, the matrix of cement paste is reduced to a friable mass without cohesion. Therefore, due to tropical temperatures existing in the metropolitan area of Recife, it is unlikely that the thaumasite turns into a threat. According to the durable concrete guide ACI [1992], there are two mechanisms which may be sulfate attack: formation of gypsum and ettringite formation. It is believed that both products of these reactions deteriorate the concrete by the increase in solid volume in general. From the point of view of the engineers, what matters is what happened to the concrete: an action that does not result in deterioration or loss of durability is not considered an attack, [Neville 2004].

As Neville [2004] argues, the forms of external or internal attack are major causes of deterioration of concrete structures, [Skalny et al, 2002]. Overall, the deterioration related to sulfates are usually insignificant compared to the damage by corrosion of reinforcement or freezing and thawing.

5 TYPICAL DAMAGE OF THE SULFATE ATTACK

5.1 Mechanisms of damage

The reaction of sulfates in the concrete tends to produce expansion in the surrounding where the concrete is contained in the case of slabs in contact with sulfate soil, the concrete will tend to produce a horizontal expansion in the slab or in the concrete oversite. Generally, these concrete slabs are restrained by external and internal walls. As a result the slab or the concrete oversite is uplifted into a dome shape that over time can cause a deflection of several centimeters. The dome will produce traction on the top of the concrete, leading to a map pattern of cracking, see 'Fig 1'. In the case of magnesium sulfate, a low content of calcium hydroxide in hydrated cement is undesirable because it encourages the reaction of sulfates with calcium silicate hydrate C-S-H, leading to strength reduction of the cement matrix and mass loss, Neville [2004].

5.2 Visual appearance

The first visible sign of sulfate attack on a concrete slab is usually an unevenness surface in which can be accompanied by the appearance of cracks in the concrete oversite on the slab, initially narrow, but widens over time. Similarly the reaction of sulfates in blocks or concrete foundations, where there is any resistance to the expansion causes cracks in the form of map allowing more water to penetrate. This increases the degradation of concrete and consequent depassivation of the reinforcement, see

'Fig. 2'. The cracking frame is similar to that produced by alkali-aggregate reaction. The formation of ettringite in the concrete causes an increase in volume. This action requires moisture, sulfate in the environment or in the cement, pre-existing cracks in the structure and high porosity.



Figure 1. Sulfate attack on concrete oversite [Communities & Local Government, 2008].



Figure 2. Cracking in reinforced concrete base of a power grid tower [Thomaz 2008].

5.3 Influence of pH

The pH of the attacking solution also influences the formation of deleterious compounds to the cementitious structure, since the ettringite is stable at pH between 10.5 and 13.0 - Souza [2006].

5.4 Influence of the compressive strength

If there are registry values of the compressive strength of the concrete early in the beginning of construction, one can compare the results of tests performed at one moment with those of the beginning of construction and make a diagnosis of the deterioration. If the compressive strength at this moment is smaller than that of the structural design, this may be an indication of sulfate attack.

5.5 Sulfate-resistant Portland cement (SR-PC) – type V

According to the ABCP (Brazilian Association of Portland cement), Portland cement SR offers resistance to aggressive sulfated environment, as sewage or industrial wastewater, seawater and some types of soils.
The **SR-PC** can be used in concrete mixing plans, high performance concrete, structural rehabilitation works, shotcrete, reinforced and prestressed, precast elements of concrete, industrial floors, pavements, reinforced mortar, mortar as well as in concrete subjected to attack of aggressive environment, such as water and sewage treatment plants, works in coastal regions, groundwater and sea. According to NBR 5737, five basic types of cement - CP I, CP II, CP III, CP IV and CP V-ARI - may be resistant to sulfates, since it suits in one of the following conditions:

a) tricalcium aluminate content (C_3A) of clinker and additions of carbonate content with a maximum of 8% and 5% by mass, respectively;
b) furnace cement that contains between 60% and 70% of granulated slag by mass;
c) pozzolanic cements that contain between 25% and 40% of pozzolanic material, by mass;
d) cements with long term test results or work that confirm resistance to sulfates.

6 REPAIR

Corrective Adequacy depends on the severity of the damage, the perceived risk of future damage and the degree of security required. It is for professionals involved in a specific property, to decide which techniques to use. If the property has a slight damage attributed to sulfate attack, then it is not necessary to perform immediate correcting work, due to the fact that the process of sulfate attack is generally slow. Periodic inspections of the property including the existence of cracks may be carried out to monitor the progress of damage, and make a report of findings. Ensure complete removal and a

new concrete only when there is expansion and risk of sulfate attack by others components of the building.

Sulfates, water and cracks should be avoided, Thomaz [2008]. For this, one must:

a) avoid the use of cement with excess of sulfates. The cement type CPII-E (with the addition of granulated blast furnace), the CPII - (with slag-NBR5735) and SR-PC, are the best alternative to eliminate sulfates;

b) avoid access of sulfates from environment to the concrete, as occurs in silos of coal with high content of sulfates;

c) avoid contact of concrete with water in which the content of sulfate SO_4^{2-} is greater than 3.000 mg/liter, BS EN 196-2 [2005]. If unavoidable, one solution is to waterproof the concrete;

d) If the sulfate content in water is between 600 mg/lt < SO_4^{2-} <3.000 mg/lt, then use concrete with fck > 38MPa and concentration of sulfate-resistant Portland cement (SR_PC) > 340 kg/m^3 of concrete, microsilica content = 17kg/m^3 and super-plasticizer. Use water/(cement + micro-silica) less than 0.38, Thomaz [2008];

e) have a concrete cover of reinforcement not below 5cm;

f) avoid exposure to rain and moisture in industrial environments with high concentrations of sulfates, as the area of oil refineries;

g) use sealing.

Avoid also cracks caused by:

a) thermal shrinkage;
b) shrinkage due to cure defective;
c) steam curing temperature above 65 degrees centigrade.

7 CASE STUDY

7.1 Building Ericka

The collapse of the building Ericka happened by smashing of the masonry foundation, starting in the area bounded by walls corresponding to the two-bedroom of the ground floor apartment situated in the back of the building. Inspections were carried out after the collapse and the following aspects observed:

a) the building was located between two canals: Matadouro and the Rio Morto;
b) due to the influence of the local hydrographic grid the water level is high and it is common the presence of wetlands, especially in periods of intense rainfall;
c) the area has been occupied for over thirty years and has received aggregate for the construction of access roads and housing.

The smashing happened due to the loss of strength of concrete blocks from the external foundation that have deteriorated over time due to the attack of sulfates present in groundwater, the adoption of an inadequate constructive system and the use of the following bad points:

a) external walls built in a single layer of concrete blocks with a thickness of 14cm functioning as retaining walls of a high hardcore that accelerated the deterioration of these blocks;
b) the permanent contact of the hardcore with the concrete blocks of high porosity used in external foundation, where one side was subjected to moisture and having the other side free to evaporation, can help the chemical process resulting in leaching, Neville [2004];
c) the use of various types of concrete blocks and ceramic blocks with inadequate assembly;
d) It was also confirmed the phenomenon of moisture expansion, with loss of strength of the ceramic blocks present in small proportion in the foundations.

8 ACCOMPLISHED TESTS

8.1 Groundwater analysis

Aiming to identify the aggressiveness of the water found in the foundation quota, three water samples for chemical analysis were collected, and two samples collected in the foundation pit and collected in a borehole. The methodology for the determination of chemical parameters was recommended by "Standard Methods for Examination of Water and Wastewater, 1st Edition".

8.2 Analysis of ground water

Some results of the ground water were accomplished in three samples showed on Table 1.

Table 1. Results of ground water.

Determination	*Sample 01*	*Sample 02*	*Sample 03*
Ph	8,7	8,3	7,7
Free carbon dioxide (CO_2) - mg/L	0,0	0,0	7,7
Chloride (Cl) – mg/L	92,2	193,2	65,6
Sulfates (SO_4) – mg/L	460,5	815,0	758,5
Bicarbonate alkalinity ($CaCO_3$) - mg/L	74,1	51,5	121,9
Magnesium - mg/L	9,51	2,16	21,94
Calcium (Ca) – mg/L	92,47	63,4	282,2

According to the results presented in Table 1, we can make the following observations:

a. the water has a high concentration of calcium;
b. the results were analyzed according to Standard L1007 CETESB, revised in 1988 indicating that this is a water with high pH, average of 8.3, and by this aspect classified as a saline-alkaline water of low to medium aggressiveness in which the leading phenomenon of aggressiveness is the carbonation accompanied by leaching. According to the sulfate content (average 678mg/lt), and in accordance with the same standard, it was a brackish water with high degree of aggressiveness, where the leading phenomenon of aggressiveness is the expansion by the formation of gypsum and/or ettringite accompanied by leaching. In this particular case, it was found the presence of ettringite accompanied by leaching in the mineralogical characterization test by X-ray diffraction carried out by the Brazilian Association of Portland Cement - SP.

8.2 X-ray diffraction, mix proportion determination and compressive strength tests.

The mix-proportion determination tests indicated a sand and cement ratio of about 1:20, when it would be expected at most 1:10, according to local practice. X-ray diffraction tests revealed the mineral ettringite, resulting from the chemical reaction between sulfates and hydrated cement components found in whitish fragments of concrete blocks during visual inspections. This reaction has deleterious features causing the disintegration of the concrete. 6 concrete blocks were tested with dimensions 14cm x 19cm x 19cm taken from the base foundation of the building provided a mean compressive strength of 1.7Mpa.

9 CONCLUSIONS

It was proved the action of sulfate in the building Ericka, but the repairs were not made on time. Several chemical tests of water/soil were carried out, as well as X-ray diffraction, compressive strength, etc.. Soil drainage near the foundations is important, due to the fact that the dry salt does not attack concrete. The effectiveness of cement type SR-PC, as well as low w/c content, favors the

reduction of sulfate attack in concrete. The argument that only the test of compressive strength is sufficient is unfounded. Moreover, evaluating the extent of the damage by determining the change in compressive strength seems to be reliable, since one becomes aware of the values of the compressive strength at the beginning of construction project. Furthermore, the damage caused by sulfates can be easily avoided (or at least limited) with simple measures as those recommended in this article.

ACKNOWLEDGMENT

The authors would like to thank Karina Moraes Zarzar, PhD and Professor at the Delft Technology University, The Nederlands, for her important participation in the translation and understanding of this article.

REFERENCES

Communities and Local Government. 2008, *Sulfate damage to concrete floors on sulfate-bearing hardcore- identification and remediation*, February.

BS EN 196-2. 2005, *Methods of testing. Chemical analysis of cement*, publication date: 31/03/05.

British Research Establishment (BRE). 1982, *The durability of steel in concrete: Part 1, Mechanism of protection and corrosion*. BRE Digest 263

J.P. Skalny, I. Odler, J. Marchand. 2002, *Sulfate Attack on Concrete*, (Modern Concrete Technology Series, Volume 10), London.

Mehta P.K.; Monteiro, P.J.M. 2008, *Concreto - Microestrutura, Propriedades e Materiais*. Editora IBRACON. São Paulo

Neville, A. 2004, Review article, *The confused world of sulfate attack on concrete*, 8 April.

P.K. Mehta. 1993, *Sulfate attack on concrete: a critical review*, Materials Science of Concrete, vol. III, Amer. Ceramic Society, Ohio, 105– 130.

Souza, R. B. 2006, *Suscetibilidade de pastas de cimento ao ataque por sulfatos – método de ensaio acelerado*. 139p. Dissertação (mestrado) – Escola Politécnica da Universidade de São Paulo. São Paulo.

Thomaz, E. C. S. 2008, *Etringita, Exemplo Nº116*; site: (consultado em: setembro) http://www.ime.eb.br/~webde2/prof/ethomaz/fissuracao/exemplo116.pdf – IME

XII DBMC
International Conference on Durability of Building Materials and Components
PORTO - PORTUGAL, April 12th-15th, 2011

Long-Term Expectations and Experiences of ETFE-Membrane Constructions

Peter Flüeler [1]
Doerte Aller [2]

ABSTRACT

ETFE membrane constructions, ether as single-ply or as pneumatically inflated cushions having two or more membranes, have become the favoured building envelope material for architects. Stadiums, sport arenas, courts, exposition halls, zoo buildings, museums and other public buildings have been erected and their creators were awarded already at the design stage by juries and media. Little is known about real service life, long-term behaviour and maintenance costs of such constructions. In this paper the performance of 3 large buildings will be discussed (Masoala Rain Forest building Zoo Zurich, a pyramid building in Germany and Bush Hall of Burger's Zoo Arnhem NL). The latter, more the 23 years old, has been re-roofed in 2009 because of damages caused by a severe hail storm. Performance, special properties and experiences as well as their life-time assessment of the 3 buildings aforementioned are treated in this publication. In order to assess the Hail Impact Resistance (HIR) of such building materials, a new classification system connected to public register has been introduced by public building insurance companies in Switzerland (see www: hagelregister.ch). It serves primarily as designing tool for roofing & facade architects and engineers.

KEYWORDS

ETFE-membrane, Long-term behaviour, Hail impact, Resistance, Classification.

[1] Flüeler Polymer Consulting GmbH (FPC), Aathal ZH / EMPA Dübendorf ZH, Switzerland, peter.flueler@empa.ch
[2] Public Building Insurance of Canton of Zurich, Zurich, Switzerland, doerte.aller@gvz.ch

1 INTRODUCTION

Since 1980, foils made of the polymer type Ethylen-Tetra-Flour-Ethylen (ETFE) – a thermoplastic polymer copolymer – have been applied as elements of building envelopes more often. All types of customized cushions and shapes can be manufactured of relatively thin foils jointed by a thermo-fusion and thermo-forming process. Inflated cushions may form complete façades, roofs or their segments. Popular applications are stadiums, parking and exhibition roofs, spa halls, museums, atriums, zoo and other buildings mainly for public use. In addition, illumination techniques allow special visual effects in architecture. Therefore, architects are captivated by this material because of its nearly unlimited means of applications [LeCuver 2008]. However, little is known concerning aging behaviour of these constructions. Manufacturers are currently estimating the life-time of ETFE foils to be 50 years or more.

2 MATERIALS AND CONSTRUCTION

2.1 Material and foils

ETFE is a thermoplastic polymer consisting of polyethylene and poly-tetrafluorethlylene, a compound of tetrafluorethylene (4 parts) and of ethylene (one part) with a final density around 1.72 g/cm^3. As a thermoplastic, its melting point ranges at a temperature above 275° C. It can be processed by extrusion technology using fully mixed ETFE granules as raw material. The semi-crystalline polymer structure of foils thicker than 50 microns shows a slightly bluish appearance. The presence of the 4 flour atoms in the chemical structure provides excellent chemical resistance against most physical-chemical influences and fire.

ETFE-foils 1.5 to 2.0 m of width and 50 to 250 microns of thickness can be fused together by a thermo-fusion process to any size of cushion. In the jointed zone, the overlapped surfaces fully melt. With the help of pressure rolls, a solid jointing is created. This zone of 25 mm width is visible because of doubled thickness and surface imprints. CNC-controlled machinery is needed for precise cutting and jointing.





Figure 1 and 2. Jointing of ETFE-foils by hot fusion and inlay of keder in foil boundary loop.

2.2 ETFE-constructions

The construction of a pneumatically supported building consists of multiple elements bridging a stiff engineering structure made of wood, steel, concrete or a combination if all. The gaps between the engineering structures are filled by membrane cushions consisting of 2 or more ETFE layers. The connection to the engineering structure is realised by a linear fixation system called keder. At the boundary, membrane layers are formed to pockets containing plastic rods. The keders fit in EPDM gaskets and slotted aluminium profiles to provide water tightness. The cushions are inflated with dry air where it builds up an internal pressure in the range of 200 – 400 Pa. In order to maintain cushion shape and its adaptation to high wind forces, a detailed air duct system connects all cushions and

serves as a mandatory air pressure pump. In case of a membrane leakage, only few elements are connected and an auxiliary air pump provides sufficient air pressure. In case of inflation, the cushion height can exceed 1m or more. If the outside layer is separated from the inside layers by a special spacer profile, the air chambers provide excellent thermal insulation.

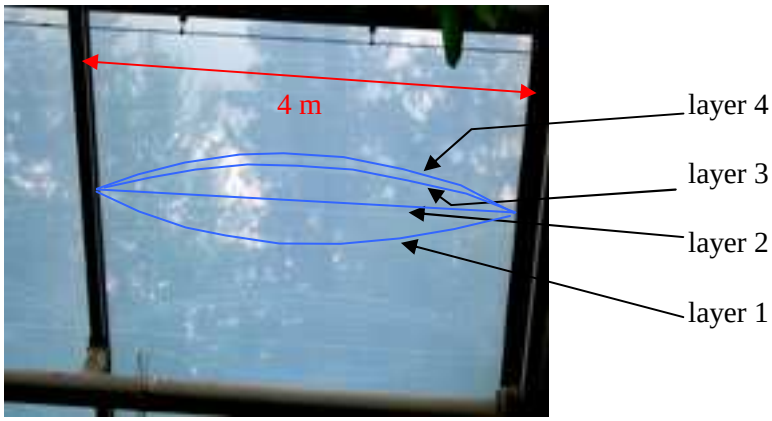

Figure 3. ETFE-cushions with 4 layers of MAS building at Zoo Zurich span 4 m. The 4th layer acts as protection against hail stones.

3 LIFE TIMES OF ETFE-MEMBRANES

3.1 General

Fluor polymers are known as being highly resistant against a large number of chemicals and environmental influences including UV radiation. As thin foils, this polymer was first applied in building envelopes around 1980 and was soon applied also on solar panels. Currently, many successful architectural applications around the world are equipped by ETFE-foils. On the other hand, non-UV-stabilized polyethylene foils for temporary use are known to decay only after a short period of use [Eyerer et al. 2005]. Crack initiation of the polymer chains starts soon after a few months of exposure. Records from outdoor applications of ETFE-membranes over extended time periods, promise a reasonable life-time [Lehnert, Schween 2005]. Therefore they seem to be apt for permanent buildings as well.

3.2 Investigated buildings

ETFE-foils from three buildings in the Netherlands, in Germany and in Switzerland were available for this investigation. The longest exposure time was 22 years at the Bush Hall of Burger's Zoo in Arnhem (BZA) [Fig. 4 an 5]. Whereas, the pyramid spa-hall (PSH) in western Germany was installed 13 years ago and the roof of the Masoala Rain Forest building (MAS) of Zoo Zurich 7 years ago [Fig. 6]. In table 1 the relevant building data are listed. From the MAS and PSH building, new membranes were also available where the results of the installation were taken from as reference data.

Table 1. Data from investigated buildings and thickness of installed ETFE-membranes.

Source of foils	*Year of installation*	*Age* [years]	*Raw material*	*Number of membranes layers*	*Thickness form outside to inside* [microns]
MAS* aged	2002	7	A	4	200/100/180
MAS new	2002	0	A	1	200
PSH**	1987	13	A	2	200/200
PSH new	2002	0	A	1	200
BZA***	1986	22	B	3	150/80/100

* With hail protection foil after hail damage ** damaged by hail storm in 2000
** damaged by hail storm in June 2008



Figure 4, 5 and 6. The roof of bush hall of Burger's Zoo Arnhem NL (left), inside view (centre) and the Masoala Rain Forest building at Zoo of Zurich (right).

3.3 Test methods applied

In order to assess the long-term performance of EFTE membranes, only a limited number of typical tests for polymers were selected in the first test series because of a given cost limit. Therefore, extended testing with sophisticated equipment has been postponed for the second investigatory level. The investigated properties were as follows:

- Surface analysis
- Tension test: E-modulus, extension and stress at yield and at break
- Impact tension test, to sense the loading rate influence
- Tear resistance: to check the reaction to micro-cracking sensibility
- Coefficient of thermal expansion
- Fourier-Transformation-Infra-red FTIR-analysis: to check for material base and physical changes
- Differential-Scanning-Caloriymetry DSC, for melting temperature and enthalpy

4 RESULTS

4.1 Surface analysis

Before analysis, the membrane from the BZA-building was intensely washed with common soap with water in order to remove dirt and bio-residuals stemming from the out-door deposit. All surfaces were visually inspected for defects, cracking and possible chemical attack. Critical spots were investigated by a regular magnifying glass of 6 xs.

Table 2. Results of the visual inspection of the membrane surfaces.

Aspect	*MAS, Zurich*		*BZA, Arnhem**		*PSH, Germany*	
	2002 new	*7y*	*22 y*	*22 y*	*2002 new*	*13 y*
Exposition	outside	outside	outside	inside	new	inside
Thickness	200	200	150	100	200	200
Appearance	new	as new	slightly mat	As new	new	as new
Colour	light bluish	light bluish	light bluish	clear	light bluish	light bluish
Light transparency	transparent	transparent	transparent	transparent	transparent	transparent
Gloss	very high	very high	high, dirt spots	high	very high	high
Contact with water	f. repellent	f. repellent	f. repellent	f. repellent	f. repellent	f. repellent
Defects	none	none	multiple	multiple	none	indents, slits
Deposits	none	none	bio-film, dirty	bio-film both sides	none	dust sticks
Faults /scratches	none	some	multiple	multiple	none	multiple

In general, all membranes were fully water repellent. All were transparent and of a light bluish colour. No signs of oxidation or deterioration were found on any of the membranes [Table 2]. With increasing age, more scratches and defects were located -especially on the BZA-membranes. Due to its application and high humidity on this membrane, a well-developed bio film on both sides of the interior foil was found.

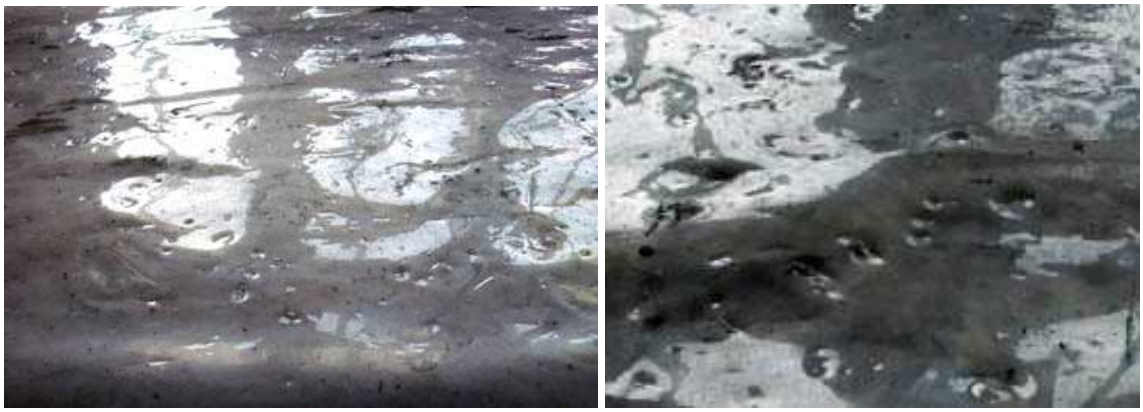

Figure 7 a and 7 b. Appearance of the BZA membrane with various indents, small perforations and surface contaminations.

4.2 Mechanical properties

All membranes were subjected to tension, impact tension and tear resistance. The tests revealed the values were nearly unchanged compared to new membranes. A higher scatter of the standard deviation was observed at the BZA-membrane due to little mechanical defects which were neglected during the test sample extraction. The tension test results of the PSH building showed a certain difference compared to the MAS and BZA building membranes [Figure 8 and 9].

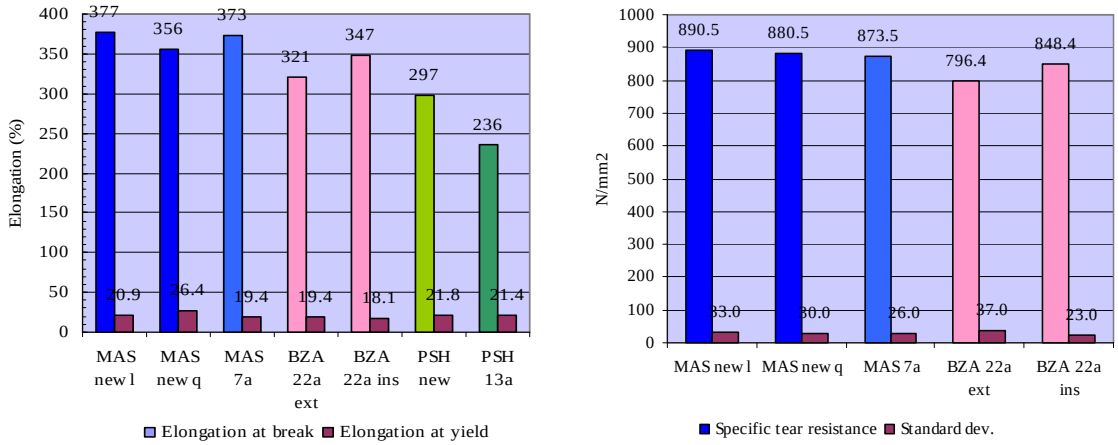

Figure 8 and 9. Elongation at break and at yield from tension tests (left) of all three buildings. Specific tear resistance in N/mm^2 of MAS and BZA buildings.

4.3 Physical properties

The FTIR investigations confirmed the nature of the polymer as Ethylene-Tetraflourethylene ETFE. Only minor differences of the wave number 754 cm^{-1} of BZA and PSH foils lead to the conclusion, that different raw materials were used. It didn't show any sign of aging or oxidative degradation at all.

DSC investigations pointed to the possibility that changes may have been influenced by the stored heat due to longer sun exposure of the BZA-building. However, these changes were minimal but detectable (Fig. 10 and 11).

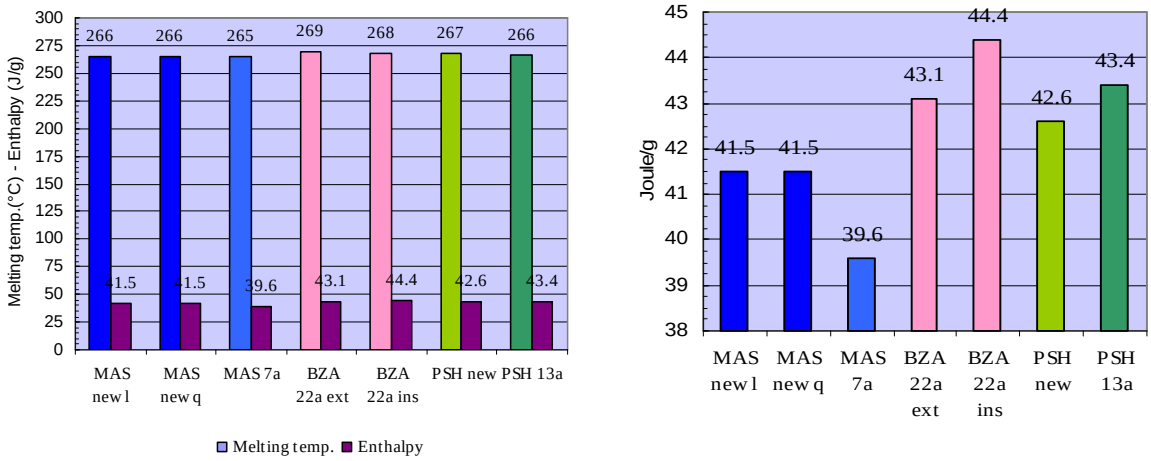

Figure 10 and 11. Melting temperature (° C) and enthalpy (J/g) for new and aged ETFE membranes (left). Enthalpy peaks blown up for better discrimination (right).

5 ASSESSMENTS

All mechanical properties exhibited nearly unchanged values compared to new conditions. Minor deviations could be associated to surface scratches, indentations and perforations. Degradation by physical-chemical influences could not be noticed. However, the surface was heavily contaminated with sticky dirt and fungi. Cleaning with soap water and action pressure was minimally successful. A certain contamination remained on the surface of BZA building. Figure 12 shows an overall assessment of the aging status after the exposed years with an intensity level. The intensity levels are connected to times and priority of measures to be taken. A special view was taken to the feasibility and to remark the early aging indication of the applied test method.

Property	**Aging status**			**Feasability of method**	**Remarques**
	MAS	**BZA**	**SPH**		
Exposure time (years)	7	22	13		
Tension at break				yes	
Tension at yield				yes	
Elongation at break				yes, good	early indicator
Elongation at yield				yes	
E-Modulus				yes	
Impact tension				excellent	early indicator
Tear resistance			n.t.	excellent	early indicator
Surface analysis			n.t.	yes	
Coeffician of thermal expansion		n.t.	n.t.	yes	
FTIR-analysis				excellent	early indicator
Melting temperature				yes, good	difference of run 1 to run 2
Enthalpy			n.t.	yes, good	difference of run 1 to run 2

	Aging level	**Measures to be taken**
Remarques:	none	none
	very little	none
n.t. = not tested	little	prepare
	detectable	begin
	strong	absolutly necessary

Figure 12. Overview of aging status and feasibility of test methods for early detection, MAS: Masoala Rain forest Building, BZA: Burger's Zoo Arnhem, PSH: Pyramid Spa-Hall.

6 What are life-time terminators of ETFE-membrane structures?

6.1 General

The mechanical properties depend strongly of the material thickness, the temperature, the specific failure mode and the rate of loading. Since the applied material thickness of the ETFE membrane cushions do not exceed more than 250 microns (older buildings only 150 microns) such constructions are highly vulnerable against sharp tools, knifes and sticks, flying foreign objects and animal/human attacks. Damages and vandalisms were already observed during the construction phase and in use. Some buildings required instant repairs or replacements.

6.2 Life-time terminators

Construction using cushions made of ETFE seem to last 3 decades or more. The membranes of the oldest buildings show only minor physical-chemical deterioration, if they are still in use like the Mangrove building of Burger's Zoo. Baring responsibility for this fact, are the strong chemical bonds of Fluor atoms in the molecular chain. The applied proportion of 29 % ethylene and 71 % tetra-Fluor-ethylene seem to function in the exposed environments. Despite that fact that several buildings had to be repaired or re-covered because of mechanical defects caused by snow overload, by impact of wind born debris or by hailstorms. The BZA-building was completely re-roofed in 2009 after a major hailstorm in June 22, 2008. Hail stones of irregular shape of 4 - 5 cm diameter perforated the outer foil. Also, the newly erected Masoala Rain Forest building was re-roofed after a sever hailstorm in June 2002, 14 days after installation was completed. For further protection the insurances required a protection against hail impact damage [Flüeler & Makarova 2002]. This was realised by a fourth, separately inflated ETFE-membrane to be replaced when perforated. In another hailstorm in 2004 only the protection foil was damaged. In 2006, a heavy snow fall deflated 90 % of the membrane cushions and forced an improvement of the air duct inlets.

7 Conclusions

Experience from this work demonstrated that ETFE-membranes exhibit an excellent physical-chemical long-term performance exceeding 30 years. It has also taught the building owners that all three buildings were exposed and damaged by hail impact during the 22 years' period of use. The MAS building suffered from severe damage caused by irregularly shaped hail stones 14 days after installation only and two years later for a second time. Therefore, such constructions need to be protected against hail and impact of sharp objects as well as against vandalism. For designers, owners and insurers the newly established register of hail impact resistant (HIR) building materials of the Swiss association of public building could serve as a know-how tank. In the testing protocol, all materials/systems of a building envelope are tested with -20° C cold ice balls of 1 – 5 cm in diameter. It forms the 5 HIR class systems and represents hail impact resistance of the declared size in centimetres at which no damage occurs. Details can be found in the register [VKF 2008]. For higher safety, thin and soft materials like ETFE-cushions and protection foils have to be evaluated also in regard to impact of irregularly shaped hails stones. Due to changing climate, hail storms will occur more frequently and intensely. They will also strike regions where up to date hail has been unknown.

ACKNOWLEDGMENTS

This investigation was supported by the public building insurance of the canton Zurich (www.gvz.ch). Testing materials were provided by Zoo Zurich (www.zoo.ch) and Burger's Zoo Arnhem and supported with labour hours by Flüeler Polymer Consulting. All supports are greatly appreciated.

REFERENCES

P. Eyerer, P. Elsner & T. Hirth 2005, *'Dominghaus*; *Die Kunststoffe und ihre Eigenschaften'*, book ed. by Springer, 6th edition, page 878-848

Lehnert S, Schween T. 2006,*'Bauen mit Folienkissen'*, journal Bauingenieur, volume 81

Flüeler, P.H. & Makarova I. 2002, *'Development and evaluation of a hail protection for Masoala Rain Forest Building Zoo Zurich'***,** r-d report no 425'873 (not public), EMPA Dubendorf, Nov. 14

Sia 261/1, *'Einwirkungen auf Tragwerke, Hagel'*, Swiss Society of engineers and architects (sia), 2001

Flüeler P.H 2007, *'ETFE-membrane structures – and what's about hail impact resistance?'* Proc. International Convention and Trade Show, RCI-Symposium, Orlando Fl. USA, pp. 31-37

LeCuyer A. 2008, ***'E****TFE – Technologie und Entwurf'*, book Birkhäuser Verlag AG, Basel, 160 pages

VKF, 2008, *'Hail protection register for building materials'*, on-line register of Swiss public building insurance companies, Bern Switzerland, www.hagelregister.ch

Flüeler P.H. et al., 2008 *'Hail impact resistance of building materials, testing, evaluation and classification'* Proc. International conference on durability of building materials and components 11th dbmc, Istanbul, vol. 3, pp. 1351-1359

Flüeler, P.H. 2010, ***'****Alterungsverhalten von ETFE-Folien in pneumatisch gestützten Membrankonstruktionen****'***, investigation report no 169-09/2 (not public), Dubendorf, 68 pages

Flüeler P.H, Lateltin O., Jordi M. 2010, '*Switzerland: public register for hail impact resistant building materials created'*. Proc. International Conference on Building Envelope Systems and Technology ICBEST 2010, Vancouver Canada 27-30 June, vol. 2, pp. 101-108

XII DBMC
International Conference on Durability of Building Materials and Components
PORTO - PORTUGAL, April 12th-15th, 2011

Diagnosis of Pathological Manifestations and Service Life Estimation of Reinforced Concrete Structures of Water Reservoirs with Different Ages: Case Study

Fuad Carlos Zarzar Júnior [1]
Elaine Cristina da Rocha Silva [2]
Mauro José Araújo Campelo de Melo [3]
Rafaella Larissa Santos Ribeiro [4]
Arnaldo Manoel Pereira Carneiro [5]

ABSTRACT

The lack of preventive maintenance is one of the major factors contributing to the deterioration of concrete structures in the metropolitan area of Recife (RMR). It was not different from what happened to the three reservoirs of the Pernambuco Sanitation Company (Compesa), located on Rua da Mata, Dois Unidos, Recife (PE), Brazil. The lack of preventive maintenance and the high content of chloride ions added to drinking water treatment that acts as a catalyst for the deterioration of these structures contribute to the emergence of different pathologies. It was proposed by the authors based on the pathological manifestations to compare the diagnoses of each of these reservoirs of different ages estimating the service life using the Factor Method [ISO 15681:1] and an alternative equation, as well as indicate the best way to repair these structures.

KEYWORDS

Reservoirs, Concrete, Pathologies, Diagnoses, Service life.

[1] Programa de Pós-Graduação em Engenharia Civil, Universidade Federal de Pernambuco (UFPE), Recife-PE, BRAZIL, fczj@yahoo.com
[2] Programa de Pós-Graduação em Engenharia Civil, Universidade Federal de Pernambuco (UFPE), Recife-PE, BRAZIL, elaine.rochas@hotmail.com
[3] Programa de Pós-Graduação em Engenharia Civil, Universidade Federal de Pernambuco (UFPE), Recife-PE, BRAZIL, maurocmelo@yahoo.com.br
[4] Programa de Pós-Graduação em Engenharia Civil, Universidade Federal de Pernambuco (UFPE), Recife-PE, BRAZIL, rafaelarisa@yahoo.com.br
[5] Programa de Pós-Graduação em Engenharia Civil, Universidade Federal de Pernambuco (UFPE), Recife-PE, BRAZIL, ampc@ufpe.br
[6.] Universidade Federal de Pernambuco (UFPE), Recife-PE, BRAZIL, andrea_negromonte@yahoo.com.br

1 INTRODUCTION

Climates changes are critical for the good performance of structures. It is understood that compatible materials and specialized personnel together with the climatic conditions of exposure of these structures lead to the planned durability and service life design. However, pathologies in reinforced concrete structures still remain a topic of relevant discussions. Sitter [1983] shows the importance of paying attention to quality in the stages of design, construction and preventive maintenance during the corrosion initiation period in relation to corrective maintenance taken during the propagation period.

In this context, several studies have been developed in order to improve the durability and service life of concrete structures. Saffarini and Samra [2001] used the calcium nitrite as an inhibitor and retarder of corrosion rate after initiation, as well as the hydrophobic pore blocker in the repair of concrete structures in marine environment in Jordan. Castro et al [2007] contributed to the improvement of the estimation of service life of concrete structures from C_s values (concentration of chloride ions on the surface) in the marine environment. In Brazil, studies of Medeiros [2008], Hoppe and Son [2008] refer to the control of the stages of planning/execution of structures, with investigative methods for identification and maintenance of pathology. Cascudo [2001] focuses on the materials and their interaction in concrete and environment of exposure. In the city of Recife some relevant studies involving pathologies theme in concrete structures were developed, particularly:
1. Andrade [1997] in his dissertation, researched the most common manifestations encountered in reinforced concrete structures, as well as practiced forms of repairs. This study found that the columns, followed by beams and slabs were the most affected due to reinforcement corrosion, associated with the effects of structural applications. The occurrences of the manifestations were interrelated with inadequate procedures during the phases of the constructive process: planning/design and implementation;
2. Carneiro [2004] has contributed to a further intervention and restoration of bridges presenting a map of deterioration and improvements necessary to compensate degradation effects);
3. Oliveira et al [2008] presented a methodology to quantify damages, check-list and the use of tests to verify the state of deterioration of reinforced concrete and estimate service life of three residential building;
4. Mota et al [2009] performed an investigation on reinforced concrete elements on the seafront using the analysis of the deterioration level established by the CEB Bulletin 162 [1983], suggesting the need for immediate intervention. A feature of the mentioned studies was the disposal of the structures in environments near the sea with aggressive agents, specifically chloride ions, interfering on durability and service life.

Unlike conventional structures that tend to deteriorate due to environmental exposure, and the action of agents from external to internal area. The water reservoirs were designed to be continuously in contact with aggressive materials, because its stored water has a significant concentration of chloride used for water treatment. In this case, the aggressive action tends to occur in the opposite direction.
Thus, this paper presents a diagnosis pertaining to the manifestations and analysis of service life in water reservoirs located in a distribution unit of the Pernambuco Sanitation Company (Compesa), in Recife (Brazil).

2 EXPERIMENTAL PROCEDURES

For the diagnosis of pathologies in the reservoirs some procedures were established, namely: 1. survey in the outer area (mainly in direct contact with the sun, rain and wind) and internal structures (mostly protected from the sun, rain and wind); 2. physical characterization of the elements from visual inspection by means of photographic records and follow-up form indicating the level of concrete deterioration, the latter based on the CEB Bulletin 162 [1983]; 3. characterization of mechanical and chemical properties from the following tests: sclerometric examination, depth of carbonation, crack mapping, location of the reinforcement and testing of electrochemical potential; 4. estimated service life calculated by the Factor Method [ISO 15686-1] and an alternative equation, taking as parameters

design life according to BS 7543 [1992]. At this stage, the effects of aggressive agents begin to manifest, as cracking of concrete, by chemical attack or stains due to corrosion of reinforcement.

For this study two types of tests were conducted, namely:

a) destructive tests: carbonation [RILEM CPC 18] and corrosion potential [ASTM C87/87];
b) non-destructive testing: checking the position and density of the rebars with pacometer [NBR 6124/80], [ACI 228 2R-98]; sclerometry [NBR 7584/95], [ASTM C 805], [ACI 228.1R- 98] and measurement of CO_2.

2.1 Characterization of environmental exposure of the researched structures

The region where the three reservoirs of this study is found has a rugged topography, altitude of 69 m, of difficult access, with narrow streets and closed vegetation in their surroundings. According to NBR 6118 [2003] the aggressive environment is Class IV due to the purpose of the building. The structures of the reinforced concrete reservoir are located in the community of Alto do Céu, located at Rua da Mata, in the neighborhood of Dois Unidos, Recife (PE), see 'Figs. 1 and 2 '. The location coordinates of the area are $7{,}9958^0$S e $34{,}9156^0$O.



Figure 1. Location of the reservoirs. Source: Google Earth [2010].



Figure 2. Location of the reservoirs (dashed area). Source: Google Earth [2010].

2.2 Description of the inspected reservoirs

Three reinforced concrete reservoirs were analyzed, aged 10, 20 and 40 years. The purpose of the reservoirs 10 and 20 years is the accumulation of water with subsequent distribution to the community around, while the 40 years reservoir is responsible for chlorination and supplying the other two. The 10 years old reservoir is composed by a reinforced concrete tank supported by six columns and both having a protective paint applied on them. The 20 years old reservoir is composed by reinforced concrete and has its tank also supported by six columns, however, visually more deteriorated than the previous one. Its surface has cement rendering layer and a much worn painting. The 40 years old buried water reservoir is composed by a reinforced concrete tank, presents painted mortar coating facades. Both inside and outside the reservoir the covering and lime paint are similar. There is no record of repair or any kind of intervention in the concrete structures inspected. Also, there was nor neither information regarding the construction process adopted at the time that it was built nor information of its structural design.

3 INSPECTIONS AND REPORT

3.1 Ten year old reservoir

3.1.1 Visual Inspection

The pathological manifestations present in this reservoir were minimal, some points of stains, mud and water infiltration were identified. Columns were in perfect conditions of exposure

3.1.2 Sclerometric test
The compressive strength test was estimated at three columns of this reservoir, respectively: 39.7 MPa, 35.1 MPa and 38.2 MPa, with a mean value of 37.7 MPa.

3.1.3 Concentration of CO_2.
Two concentration measurements of carbon dioxide (CO_2) were performed near the reservoirs, with the following results: 287 ppm and 237 ppm.

3.1.4 Level of concrete deterioration
During the investigation of the columns, it was observed that the level of deterioration in the scale of the CEB [1983] was "A".

3.2 Twenty years old reservoir

3.2.1 Visual Inspection
It was observed in the columns, cross-section reduction of the reinforcement bars, stains and sludge on the surrounding of the reservoir, see 'Figs. 3 a, b and c'.



(a) (b) (c)

Figure 3.Visualization of pathologies from the 20 years old reservoir structure.

3.2.2 Sclerometric test
The rebound hammer had an index below 20, presenting a separated concrete layer near the surface with fissures.

3.2.3 Concentration of CO_2
Four concentration measurements of carbon dioxide (CO_2) were performed near the reservoirs, with the following results: 355 ppm, 361 ppm, 337 ppm and 322 ppm, with an average of 343.75 ppm.

3.2.4 Carbonation test
The tests were performed with phenolphthalein in columns P1, P2 and P3 showing carbonation depth, 4.46 cm, 4.74 cm and 2.20 cm, respectively. All bars have started the process of corrosion due to carbonation.

3.2.5 Electrochemical Potential
The test was carried out at the columns P1 (- 236 mV), P2 (- 275 mV) and P3 (- 271 mV), and according to standard [ASTM C 876 / 87] the probability of corrosion was uncertain. It is important to note that the visual analysis showed that the corrosion process had already started.

3.2.6 Level of concrete deterioration
The classification levels of the concrete deterioration of the columns P1, P2 and P3 were D, C and D, respectively, requiring immediate intervention [CEB 1983].

3.3 Forty years old reservoir

3.3.1 Visual Inspection

It was observed small cracks in the coating, stains, sludge and mould on painting outside the reservoir. In the inner area mould stains, detachment of the plaster coating, exposing the masonry covering, and the arch beam with loss of section of the ties, and probably of the main reinforcement bars were visible, 'Figs. 4 a and b '.


(a)


(b)

Figure 4. deteriorated components.

3.3.2 Sclerometric test
The columns P1 and P2 on the outer surfaces showed average compressive strength 45.5 MPa and 36 MPa, respectively.

3.3.3 Carbonation test
Column 1 showed an almost imperceptible level of carbonation. However, the P2 had average carbonation depth of 8.5 mm, average cover thickness of 1.9 cm and average reinforcement cover of 3.2 cm 'Fig 5 '.

3.3.4 Electrochemical Potential
The average electrochemical potential of the external columns P1 and P2 were -271 mV and -332 mV, respectively. Again, the visual analysis showed that the corrosion process had already started, as shown in 'Figure 6 '.


Figure 5. The color shows the carbonation of concrete in column P2.


Figure 6. Application of the positive electrode on the face of wet concrete and connected to negative reinforcement in the column P1.

3.3.5 Level of concrete deterioration
According to the CEB [1983], the levels of deterioration of the concrete columns P1 and P2 were evaluated as A. The interior of the reservoir has also been investigated and classified as D.

4. SERVICE LIFE ESTIMATES OF THE RESERVOIRS

The service life estimations (VUE) of the respective reservoirs were calculated using the Factor Method equation [ISO 15.686-1:2000] and the alternative service life equation developed by Zarzar [2007] using multiple linear regression, taking as parameters a reference service life (VUR) = 60 years

according to BS 7543 [1992], and using values of minimum and maximum factors of 0.8 to 1.2 a range of [ISO 15.686-1:2000].

Service life equation of Factors Method: **VUE= VUR×A×B×C×D×E×F×G**

Alternative service life equation:

$\hat{Y}$(VUG) = VUR×(- 5,72 + 0,358×A + 0,797×B + 1,40×C + 1,23×D + 0,976×E + 0,777×F + 1,59×G)

Substituting the factors values in both equations the desired estimate is obtained [Table 1, Table 2].

Table 1. Factor values to estimate the service life of the 10, 20 and 40 years old reservoirs.

Reservoir of tem years		
Factor Classes	*Factors features*	*Factor values*
A	Quality of the component: reinforced concrete, fck estimated at 37.7 MPa.	1,1
B	Design level: good.	1,1
C	Work execution level.	1,0
D	Indoor environment: very moist, subjected to the action of chlorides.	0,8
E	Outdoor environment: wet, subjected to the action of chlorides and carbonation. No protection against wind, sun and rain.	0,9
F	In-use conditions: normal (for the reservoir).	1,0
G	Maintenance leve: bad.	0,8
Reservoir of 20 years		
Factor Classes	*Factors features*	*Factor values*
A	Quality of the component: reinforced concrete, fck estimated at 15 MPa; (This was the average value thirty years ago according to NB-1[1978]).	0,8
B	Design level: inadequate reinforcement cover.	0,8
C	Work execution level.	0,9
D	Indoor environment: very moist, subjected to the action of chlorides.	0,8
E	Outdoor environment: wet, subjected to the action of chlorides and carbonation. No protection against wind, sun and rain.	0,9
F	In-use conditions: normal (for the reservoir).	1,0
G	Maintenance leve: bad.	0,8
Reservoir of 40 years		
Factor Classes	*Factors features*	*Factor values*
A	The columns P1 and P2 have average compressive strength of 45.5 MPa and 36 MPa in the external sides, respectively.	1,1
B	Design level: inadequate reinforcement cover.	0,8
C	Work execution level.	0,9
D	Ambiente interno: muito úmido, sujeito a ação dos cloretos.	0,8
E	Outdoor environment: wet, subjected to the action of chlorides and carbonation. No protection against wind, sun and rain.	0,9
F	In-use conditions: normal (for the reservoir).	1,0
G	Maintenance leve: bad.	0,8

Table 2. Results of the service lives analyses, using both equations.

	10 years reservoir	20 years reservoir	40 years reservoir
Service life (FM)	41.8	19.9	27.4
Service life (**$\hat{Y}$(VUG)**)	51	21.8	28.3

5. REPAIR RECOMMENDATIONS

From the structural components analyzed and considering the data studied herein, the following major restoration work for each structure is suggested:

5.1 Reservoir of 10 years

The structure shows no significant damage, visually detecting stains. It is worth mentioning the need for developing and implementing a regular maintenance plan, since the reinforcement cover does not meet the specifications of ISO 6118. For the slab, the implementation of sealing is recommended.

5.2 Reservoir of 20 years

The deteriorated structured presented rust stains, loss of cross-sections bars around 25% and longitudinal cracks in beams and columns. According to Ripper [1998] strengthening of the reinforcement bars is recommended when loss of steel reinforcing bars is greater than 15%. However, this value is arguable for more serious cases. The recommendation is to structurally reinforce the steel bars that showed loss of cross-section in the columns and beams and follow the procedures in the literature, in particular Ripper [1998] and Helene [1992]. For the slab, which is less deteriorated, it is recommended an application of sealing and an appropriate maintenance plan, see 'Figs. 3b and c'.

5.3 Reservoir of 40 years

The external investigated columns showed no need for intervention. However, visual inspection of the inner area showed the need for further investigation, and likely, prompt intervention followed by structural strengthening. Because of the chlorination of water, the reservoir has high levels of chloride which leads to reinforcement corrosion. For the arched beams in the inner side, structural strengthening of the deteriorated structured with materials resistant to chloride ions is recommended. The implementation of sealing and an appropriate maintenance plan are also necessary.

6 FINAL CONSIDERATIONS

Some considerations about the investigation:

1. The design of structures should foresee the aggressive environment, since the reservoirs are kept constantly in contact with water and chlorine;
2. Until now maintenance plans were not known or implemented, which shows the vulnerability of the structures along the lifetime;
3. The maintenance plan becomes necessary in all reservoirs in view of the aggressive agents to which the structures are exposed. A consistent plan would provide appropriate designs to the in-use characteristics of the structures;
4. The concrete structures were not suitable to the aggressive environment. Other materials with better compatibility to the deteriorative environment could provide greater durability and performance;
5. The diagnosis results were divergent in the reservoir of 20 years. While the test showed electrochemical potential uncertainty of the corrosion process, the table of the CEB [1983] identified the need for immediate intervention. However, it did not invalidate the study, since the worst case was adopted;
6. The real service lives were consistent with the calculated ones using both methods (Factor Method and the alternative equation). The elements of the reservoirs of 20 and 40 years should have been repaired in the estimated ages of 19.9 and 27.4 years respectively. The estimated service life calculated for the elements of the reservoir of 10 years presented a service life of 41.8 years due to the present conditions of exposure. In summary, it was shown that service life was less than the design service life, given the conditions of planning, quality of materials, performance and exposure to aggressive environment; In summary, it was shown that service life was less than the design service life, given the conditions of planning, quality of materials,

performance and exposure to aggressive environment. The study was considered relevant, proposing further analysis with other types of tests (considering the microstructure and macrostructure of materials) and larger number of samples including other structural elements. However, the actual recovery of these structures will depend on their costs in comparison with the cost of a new structure.

ACKNOWLEDGMENT

The authors would like to thank Karina Moraes Zarzar, PhD and Professor at the Delft Technology University, The Netherlands, for her important participation in the translation and understanding of this article.

REFERENCES

ACI 228-1R-03, *In-Place Methods to Estimate Concrete Strength*. Reported by ACI Committee 228.
ASTM C 805/C 805M – 08, Standard Test Method for Rebound Number of Hardened Concrete.
ASTM C 805. 2008, *Standard Test Method for Rebound Number of Hardened Concrete*. West Conshocken.

American Society for Testing and Materials. 1991, *Standard test method for half-cell potencials of uncoated reinforcing steel in concrete*. In: *Anual Book of ASTM Standards*. V.04.02, p. 429-4333.ASTM C 876-87. Philadelphia.

Andrade, J.J. 1997, *Durabilidade das estruturas de concreto armado: análises das manifestações patológicas nas estruturas no Estado de Pernambuco*. Porto Alegre: UFRGS. Dissertação (Mestrado em Engenharia Civil), 148p.

Carneiro, A. 2004, *Inspeção nas pontes da cidade do Recife. Relatório Técnico – Prefeitura da Cidade do Recife*. Recife- PE. 228p.

Helene, P. R. L. 1992, *Manual de Reparo, Reforço e Proteção de Estruturas de Concreto*. São Paulo: PINI.

Hoppe Filho, J. 2008, *Sistemas cimento, cinza volante e cal hidratada mecanismo de hidratação, microestrutura e carbonatação de concreto*. São Paulo: EPUSP.

International Standard 2000, *Building and constructed assets – Service life planning – Part 1: General Principles.* ISO 15686-1: 2000.

Mota, J. M. F. , Pontes, R. B., J. A. Candeias Neto, M. F. Oliveira, H. T. Almeida, A. M. P. Carneiro 2009, *Análise das patologias em estruturas de concreto na zona litorânea da cidade do Recife*-PE.

Medeiros, M. H. F., Helene, P. 2008, *Estimativa da elevação da vida útil do concreto armado através do coeficiente de difusão de cloretos*. São Paulo: EPUSP.

NBR 6118/2003 - *Projeto de Estruturas de Concreto*.

NBR 6124/1980 – *Determinação de Elasticidade, Carga de Ruptura, Absorção de Água e da Espessura do Cobrimento em Postes e Cruzetas de Concreto Armado – Método de Ensaio*.

NBR 7584/1995 - *Concreto endurecido - Avaliação da dureza superficial pelo esclerômetro de reflexão*.

Oliveira, J. A. L. S.; Zarzar, F. C. J.; Oliveira, R. A.; Monteiro, E. C. B. 2008, *Avaliação de estruturas de concreto armado com vistas à reabilitação*. Universidade de Aveiro, Portugal.

RILEM - CPC 18. 1988, *Measurement of hardened concrete carbonation depth*, 1988.

Ripper, T. & Souza, V. C. M. 1998, *Patologia, Recuperação e reforço de estruturas de concreto*. Ed. PINI, São Paulo.

Sitter, W. R. 1983, *Costs for Service Life Optmization the "Law of Fives"*. Comite Euro International du Beton – CEB. Boletim Técnico. Copenhagen, Denmark, n. 152, p. 131 - 134.

Standard Test Method for Half Cell. 1987, *Potential of Uncoated Reinforcing Steel in Concrete* ASTM Designation C 876.

Zarzar, Fuad C. J. 2007, *Metodologia para estimar a vida útil de elementos construtivos, baseada no método dos fatores*, Recife (PE): UFPE. Dissertação de Mestrado em Engenharia Civil.

XII DBMC
International Conference on Durability of Building Materials and Components
PORTO - PORTUGAL, April 12th-15th, 2011

Pathologies of Industrialized Buildings Made by Bearing Precast Concrete Panels. The Case Study of Intervention with the Same Building System at Chiaromonte (27 dwellings), Francavilla in Sinni (27 dwellings) and Lagonegro (36 dwellings)

Filiberto Lembo [1]

ABSTRACT

The research concerns some residential buildings, realized by Potenza's IACP - Autonomous Institute for Popular Houses, by means of a call for bids made in 1984. Work begun the same year but, following the bankrupcy of the firm, occurred in 1986, it was necessary to re-assign it, and by doing so the work has been going on until 1991 for dwellings at Chiaromonte, 1995 for those at Francavilla and 1996 for those at Lagonegro.

Since the oneness of the system building in the three different locations, the interest of the research lies in the comparison between environmental features on one side, and on the other the state of preservation and pathologies who are there in the three interventions, with the aim of specifying how much these are connected with local environmental conditions, and how much on the contrary they follow on from defects of building systems of their's one, or from their use.

Since to date in many parts buidings are before made subjected to further retrofitting operations, with not completely satisfacting results, it is possible also to express some good practice criteria and workmanlike assessment in order to maintenance and thermal upgrade of this kind of buildings.

KEYWORDS

Durability & environmental exposition, Pathologies of envelope, Management mistakes, Design mistakes.

[1] Faculty of Engineering of the University of Basilicata (Department DAPIT), Potenza, ITALY, filiberto.lembo@unibas.it

1 INTRODUCTION

The research, made in 2005-2006 thanks to the Master Thesis work of Eng. Adele Oliveto, coordinated by the writer, concerns some residential building of a public housing program, made by means of a *call for bids* of Potenza's IACP – Autonomous Institute for Popular Houses - in 1984, originally designed to achieve 180 housing, but reduced to 90 due to problems of availability of land. The work begun the same year but, following the bankruptcy of the firm, occurred in 1986, it was necessary to re-assign it, and by doing so the work has been going on until 1991 for dwellings at Chiaromonte, 1995 for those at Francavilla and 1996 for those at Lagonegro.

The project was drawn up by the Firm successful undertaking of contract, the direction of the work was carried out by technical staff of IACP; for this reason it was possible a direct and continuous control on the quality of the project and works, in the course of their implementation. But such monitoring was not able to ensure good durability and the absence of diseases.

2 DESCRIPTION OF THE BUILDINGS

2.1 Typological characteristics

The 90 homes of three interventions in terms of types relate to a single model, which has three apartments to "windmill-type", around the staircase, repeated for a number of floors three to six. The coupling of two mirror image of the model determines unit buildings apparently different. The different size of housing, which are repeated across the column equal, does the rest (see Fig.1).

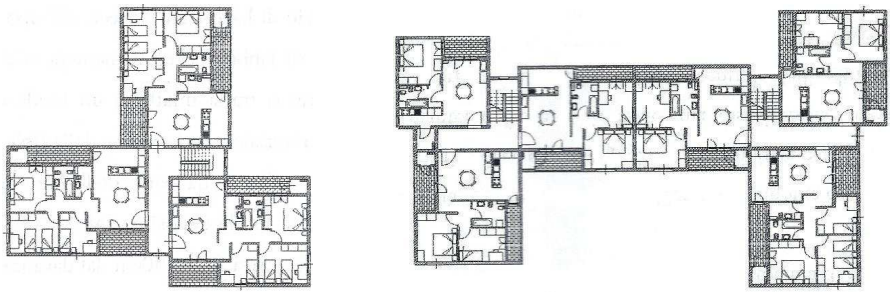

Figure 1. Plan of the basic model "windmill"(left) and specular double (right).

The orientation of housing is random, and the same blade mill basic model makes the housing environment (living rooms, bedrooms, kitchens and bathrooms) are pointing in all directions.

2.2 System Building

The building system, patented by successful undertaking of contract, the SACEP S.p.A., is called "S.B.S. System" and is characterized by large multitubular bearing precast panels, modular 120 cm, with the possibility of sub 30 cm, and this, for both floors, and walls, that are built on foundations made on site, with piles and continuous beams connection (see Fig.2a-b). The multitubular panels consist of two reinforced concrete walls R 30 with a thickness of 6.5 cm, connected to each other, each 60 cm, by 3.5 cm thick ribs to the panels of the facade, and 9 cm for those of floors. The cavities can be empty or (for facade panels) filled with high density polyurethane foam, thus achieving an average transmittance (according to the manufacturer) U = 0.64 W/m^2 K. Of course, on the two vertical edges, the need to connect the adjacent panels from the static point of view, they have each one vertical cavity of about 30 cm in length for the entire height of the panel, which is completely filled with concrete and reinforcement. It thus forms a thermal bridge 60 cm wide, all over the height of the panels, each time there are joints in line, in the corners to L, and T-junctions with internal bearing walls. A similar thermal bridge occurs horizontally, at the junction between the external chaining between bearing wall and floors. The joints between the panels forming the exterior walls

are butt joint type, with silicone jointing compound (see Fig.2c).

Prefabricated structural components for the flights of stairs, cantilevering from the side panels, balcony railings and crown, complete the system. The roofs are sloping with fake cold ventilated roof with two slopes, with a slope of 8-10%, bitumen sheet coated, in Chiaromonte and Francavilla (see Fig.3), and of 30% in Lagonegro, covered with concrete tiles.

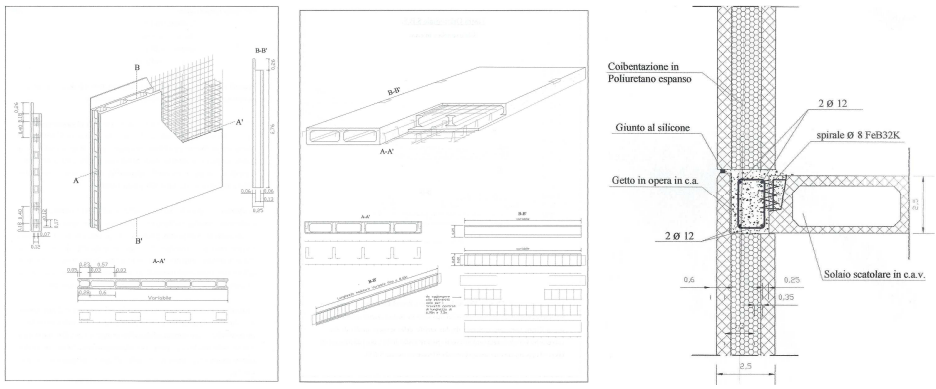

Figure 2. Precast panels for bearing walls and floors (a, b) and vertical joint between precast bearing panels for walls and floors (c).

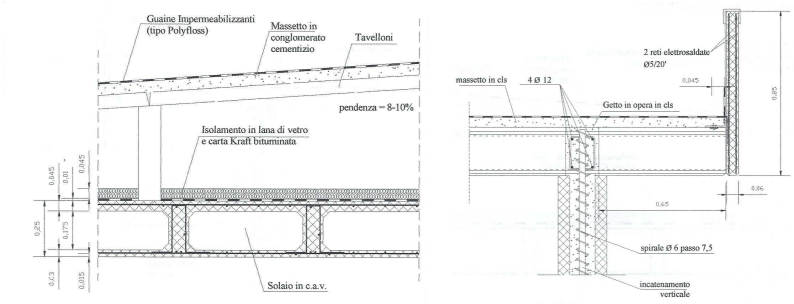

Figure 3. Roof sections, Chiaromonte and Francavilla; typical (left), edge (right).

3 GEOGRAPHICAL AND CLIMATIC DATA OF THE THREE LOCATIONS

3.1 Geographical data

The municipalities of Lagonegro, Chiaromonte and Francavilla in Sinni are located in the inner part of the mountain of Basilicata, at a latitude between 40°7'29" and 40°4'56" and a longitude 15°46'6 " and 16°12'51". The heights above sea level of municipalities and of places of work are very different between them: they are in Lagonegro 772 m, in Chiaromonte 645 m and in Francavilla 355 m a.s.l.

The configuration of the planimetric and altimetric sites where there are the buildings is quite different: at Lagonegro the building is located at the top of the country, along the contours of a slope of 13%, and is oriented with the axis in the sense North-South (see Fig.5); in Chiaromonte buildings are located on the southeast side of the mountain, along the contours of a slope of 25%, and oriented in the direction southwest-northeast (see Fig.6); in Francavilla they are placed at the foot of the hill on which stands the town, north of it, on a slope of 12%, and oriented in the west-east direction (see Fig.7).The insolation of the rooms - as a physical fact of departure - is similar for the three locations, but is strongly influenced by the layout plans of the buildings, which have random orientations, and rooms facing all sides, with therefore strong differences of insolation in the various seasons, for different exposures, and no bioclimatic attention. It should be noted that all the balconies are actually

internal loggias, surrounded on three sides by walls and railings bordered by two small vertical slots filled with 12 cm wide side, and then they determine strong shadows and stop the passage of air, while (including the absence of suitable eaves sprout) are suitable for accumulating rain water blown by the wind, resulting in stagnant water, water penetration, and therefore internal and external stains.

Surface/Volume ratio is 3:1 for basic "*windmill model*", 2.3:1 for two mirror image e 2.6:1 for the same in Lagonegro (six floors high).

3.2 Climatical data

The research, which examined the years 1988 to 1999, showed that, despite being located close together, the three sites have very different climatic conditions, but all with cold winters. *Lagonegro* is characterized by long, harsh winters with frequent snowfalls and long rainy seasons, and summers are short and cool; *Chiaromonte* has a humid climate, mild, hot summer's, but quite hard winter' s, with significant rainfall and also (albeit brief) of snow, with large daily temperature ranges, even in summer; *Francavilla in Sinni* has similar climatic characteristics to the nearby Chiaromonte, but with less rainfall (see Fig.4).

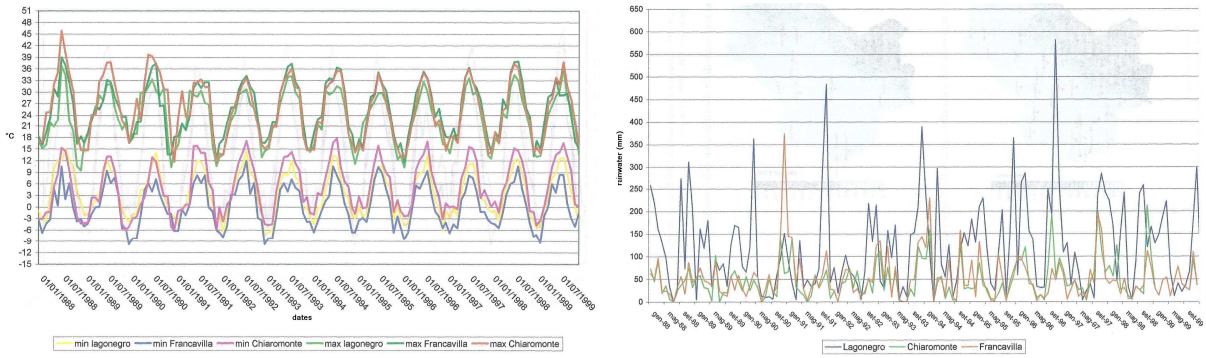

Figure 4. Maximum and minimum temperatures in the three sites, 1988-1999 (a), and Quantity of rain in the three sites, 1988-1999 (b).

The presence of a meteorological station in Lagonegro allowed to conduct a complete analysis of the wind direction and strength between January 1996 and April 2005. The results can be applied in two other locations, with details that say, plano-altimetric configurations on the sites, which influence their exposure to wind and wet clouds, or rain and snow. The remainder of the climatological data of *Chiaromonte* was derived from weather stations and Valsinni and Noepoli, and those of the weather station of *Francavilla* from Agromonte.

It appears that in winter the winds are predominantly from West and South-West (between 200° and 240°), with seasonal average intensities ranging between 1.4 m/s and 3 m/s, unless isolated on a weekly basis (especially during the months of January-February), in which the wind speed reached and even exceeded, the 5 m/s, posing a real threat to the proper maintenance of the functionality of the building envelopes. These periods appear to be also the wettest, so the danger of environmental conditions becomes greater. It's no accident that Basilicata is home to some major wind parks.

It should be noted that while the situation in relation to the orographic Lagonegro building is located in a *quiet area* at the foot of the slope, those of Chiaromonte found along the slope, in an area prone to *depression with the formation of vortices*, and those of Francavilla in areas with intermediate situation between *depression and the formation of eddies and zones of peace*. Have been studied the relationship between the configurations of the buildings and the flows of wind caress them, as previously defined, including in relation to the presence of obstructions such as other buildings, with reference to the form and all height of one and the other, as well as to the direction of the flow of air [Grosso 1997, De Pascalis 2005] (see Figs 5, 6 and 7).

4 CONSEQUENCIES IN TERMS OF PATHOLOGIES

In *Lagonegro*, West and South sides, and corners on exposed, affected by strong winds, heavy rain and snow, which caused illness by infiltration of meteoric water in the opaque parts of the facades and in that window, determining the need to ensure, after the construction of buildings, to placing of an insulating coating from outside. In contrast, the leeward side, there is little ventilation.

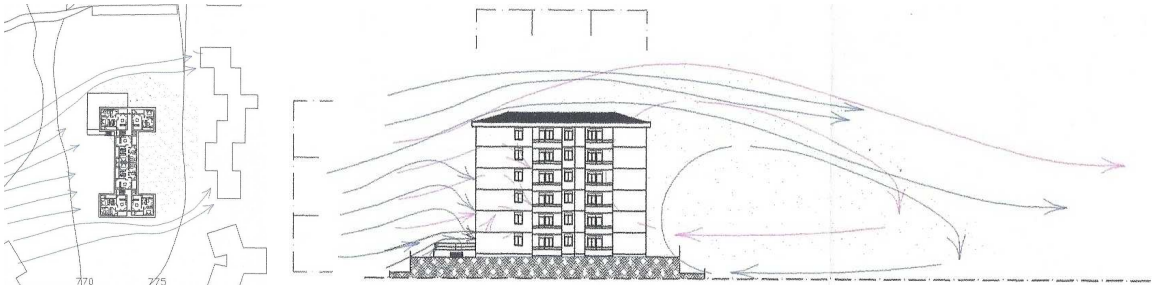

Figure 5. Wind exposition,, Lagonegro, in most raining period (27-31 January 2004).

In *Chiaromonte*, buildings are invested by the wind in parallel and a building is partially protected. From technical reports to file, that just the immediate damage and disease have arisen on the facades facing South-West led to the decision to intervene on these fronts with an insulation from the outside, which was then extended to other fronts. Again, the presence of protrusions and recesses resulting in the formation of vortical motion, and the concentration and storage of water in particular points (especially the loggias).

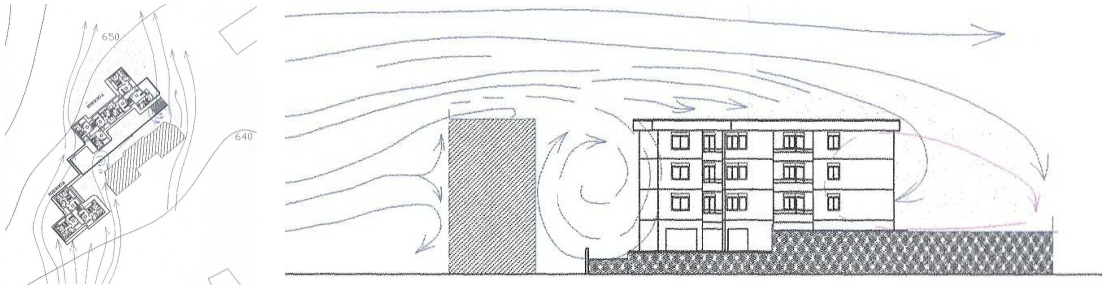

Figure 6. Wind exposition, Chiaromonte, in winter time (seasonal average direction, 225°).

In *Francavilla* buildings are protected from the prevailing winds from the nearby steep slope. In this case, there are no problems of infiltration water through the walls and windows, but on the contrary, problems, common to almost all housing, resulting from very poor ventilation and lack of internal evaporation of meteoric water, which collects in the recesses and the flat roof, although with lower intensity rainfall than the other two sites (see here above). The spread of diseases from condensing on the walls of housing has been such, that in this case it was necessary to resort to affix isolation from the outside, everywhere, even before the construction works were declared over. But without what turned out to be exhaustive.

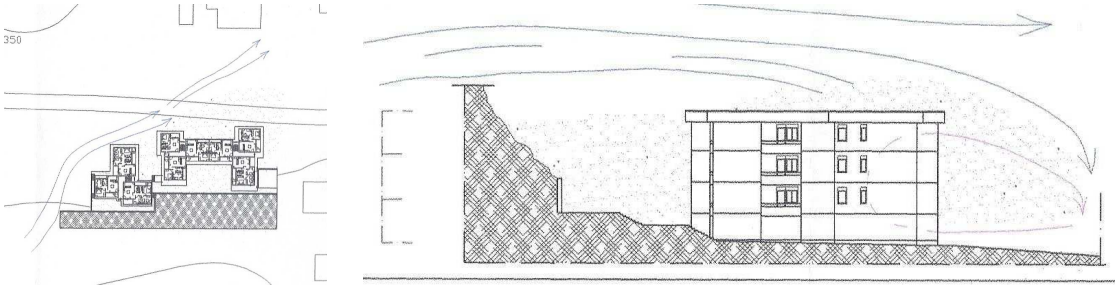

Figure 7. Wind exposition, Francavilla in Sinni, in winter time (seasonal average direction, 225°).

The analysis was carried out on time, building by building, for each apartment and room by room, the three sites, with reference to the Building Rules of the era of design and to feel more hours regulations in force, having the very outset, the *ab origine* overall failure rate for renewal of the air, particularly serious problem in buildings with walls almost impervious to air and steam, except that the boundary of the frames. It should be noted, moreover, the high humidity 's outdoor air, which in winter is often equal to 72-78%, and therefore makes it ineffective the ventilation made opening windows.

5 MANAGEMENT MISTAKES, PLANNING MISTAKES, CONSTRUCTIVE MISTAKES, REFURBISHMENT MISTAKES, AND THEIR INFLUENCE ON DURABILITY OF BUILDINGS

The analysis, the hygrothermal calculations, reconciliations and regulatory subsequent in-depth reflections, led to highlight the whole chain of errors that led to the serious problems of durability of the buildings in question, which will be listed below, which have compromised their habitability, and still cause serious problems for the occupants.

The form of contract, a call for bids, has allowed them to be bridged the traditional general conditions, referred to the "traditional" system building (in situ concrete pillar-beam system, with infill in double masonry wall, and insulation in between); in this contract, the rules have been suggested by the same manufacturer-designer, and the Commission for the award has not been able to understand that the proposed prefabricated system could not function in the harsh and rainy weather of the sites in question. Or if they have noticed the construction management, which has had to run buildings whose bad behavior was perfectly predictable, where he was referred to the *International Recommendations for Computing and Making of Structures in Large Panels* C.E.B.-C.I.B.-U.E.A.tc, edited in Italy by Associazione Italiana Tecnico Economica del Cemento, Roma, 1969 [Lugez, 1978], that's the only specific European legislation, existing at' era of 'contract; but a voluntary contract law, which applies only when invoked in the general conditions. In the notice, even if it allowed the participation of the licensees of prefabricated building systems, reference was made to the laws in force in Italy on the stability and safety of buildings in steel and r.c. and prefabricated (Law No. 1086 of 05/11/1971, Law No. 64, 2/2/1974, 3/10/1978 M.D., Circ. Min. No. 6090 of the Public Works' 11/ 8/1969) (where "prefabricated" means the individual structural elements such as floor joists or beams, and non-whole "system buildings"), and then with the notable absence of reference to the *Technical Standards* C.E.B.-C.I.B.-U.E.A.tc. But what does it say "*prefabricated buildings*" in the field of housing, but "*large panel building*"?

And the clear unpreparedness to manage the contracting system buildings that do not know. And, again, in Italy, the technical innovation, and in particular the industrialization 's construction and prefabrication, far from promoting the elevation of the quality of building products, have become the *Trojan horse* through which bypass the rules, and to ensure a market for products that are obsolescent elsewhere [see Lembo 2010]. Obviously, in this case, the final general conditions, which are attached to the contract, and that have been suggested by the manufacturer, make no reference to the Rules of C.E.B.-C.I.B.-U.E.A.tc. The reason is obvious: if you were referring to this rule, the S.B.S. system could not be taken into consideration. Just one example: the European Regulation prohibits the use of butt joints in the positions they are not easily serviceable, that they only allow planes to land or inside the lodges, here we have a building six floors above ground, and the other three or four floors. All this, in places hilly or mountainous areas, with high temperature amplitudes (and hence a strong potential differential movements of the panels), and intense rainfall. And moreover, a *management mistake*, or a *design mistake* take place in such a building system based on sandwich panels rigidly connected by ribs boundary at every 60 cm, abandoned the system, first in France and then throughout Europe after the first oil shock of 1973, for reasons of energy conservation, and the inability to solve the generalized problem of thermal bridges, and the resulting diseases from condensation? [Lembo 1977]? The writer believes that it is a *management mistake*.

For an expert in large prefabricated bearing panels would have been impossible to make good-value of the average transmittance of the facade panels indicated by the company proposing: the analytical tests performed show that a front panel S.B.S. with windows, given the thermal bridges, has an average transmittance of non-U = 0.64 W/m^{2}K, but W/m^{2}K of 1.49, with the risk of generalized condensation in all units of all three sites, because (see Rules C.E.B.-C.I.B.-U.E.A.tc) *f* is always greater than amply 0.25 [Lugez, 1978, cit., pagg. 64-65]. It's also, of course, a *management mistake*, for buildings in different geographical, topographical and climatological which are seen, and that the administration surely knew, and not to seek to impose through the general conditions that the walls of the buildings had such a typology, to allow them a high degree of impermeability to rain. In Italy there is not existing legislation such as that of the French DTU 20.11 or 20.01, but nothing prevents you (and prohibits) in Italy that could (and can) be prescribed, for example, with reference to that legislation, which offers the Company should (should) provide for the external walls of the third type ("walls drained" or directly "curtain walls and drained"). The outer wall of the System S.B.S. is classified as a wall of the first type ("*hydrophilic material in contact with insulating wool*") (corresponding to the ribs there is only one material, from internal to external) entirely unsuitable to the conditions of exposure there. So much so that even the application of an external insulation system thin render-on-insulator (which led to become the walls of IIa type to "*cut capillary vertically in wall thickness, consisting of an-hydrophilic insulating* ") was able to solve, under certain conditions, the problems of waterproofing the walls.

It's still a *management mistake* not to realize that in a building system with walls and floors made of two slabs r.c. prefab class R 30, each constituent vapor barrier, and which are horizontal and vertical tubular channels, you need precise control of the design solution not only structural and technological, but also plants, and careful monitoring on construction methods to ensure that ventilation of the rooms comply with the provisions of the Standards in order to keep low the relative humidity to internal environments, and that meteoric water cannot enter from the shell or facade, as happens in the buildings concerned, then that liquid water is conveyed in the most disparate from the tubular blank panels. If this happens, have a direct impact on the disease by condensation and the quality of indoor air, so be it (at least for building these systems), also in southern Italy, the centralized control of the change of air, heat recovery, as in *passive houses* in Germany, but with de-humidification too. Never mind, if you miss the traditional manual control of opening the windows, which is seen *per tabulas* they are usually held closed for too long, as naive defense against the errors and shortcomings in the design, construction that is part of that plant.

It's still quite a *mistake in the management control of the proposed solution* rather than a *design mistake* to take the good (in the race [call for bids], and then to construction management, and then Test) solution for the roofs which provides, on the multitubular slabs: 1.) in all three sites, a sheet of kraft paper bitumen (which the proposed project poses as vapor barrier); 4.5 cm of glass wool; a ventilated cavity with openings to the external, high ranging from 0 to 50 cm in Chiaromonte and Francavilla, from 0 to 150 cm in Lagonegro; clay tiles and then resting on brick walls every meter; a slab of concrete and the coating and waterproofing bitumen sheet in Chiaromonte and Francavilla, cement tiles in Lagonegro; 2.) on the edge of roofs of all three sites, a channel of internal collection of rain water, four feet wide, and consists of a simple slab of concrete with a slope no insulation, followed by a bitumen sheet turned up to 20 cm high, without flashing fixing higher, and no insulation over the surface of the raceway.

Obviously, the verification of Glaser shows that interstitial condensation occurs over the entire surface of the roofs. Obviously, the thermal bridge at the raceway has devastating consequences. Obviously, if the sheath of the channel has some gaps, the water falls vertically along the channels of the panels, and appear where it happens. But even more surprising to note that in the speeches of thermal retro-fitting completed by the owner of the body housing, the insulation from outside the jetties have been stopped under the crown, leaving intact the thermal bridges, as they stopped at the bottom connection between the first floors and the cellar, leaving intact the lower thermal bridges.

And yet, who is at fault if there are widespread phenomena of capillary at basement and ground floors? Who has not provided the planned cuts of capillary action, or who he has not alleged in the general conditions, and imposed in the Executive? Who is responsible if the basement or semi-basement panels are directly matched to the ground, without protection from cavities' ground water, and then soaked with water, making it unsuitable environments, even for only deposit? Who did not enforce, in the design and execution, the requirement to be met, or who, designing, it has not taken into account? And, with regard to durability, to accept a construction system that had such thin slabs and ribs connecting just 3.5 cm, mean time to accept a very risky bet in terms of durability, if you think that the carbonation depth reaches usually 25 mm in 25 years, and if it is true that the *Directives Communes pour l' Agrément des Procedés de construction par grands panneaux lourds préfabriqués* (Cahiers du C.S.T.B. n. 696, June 1966) showed even then that "*... all the materials, components, works, etc., with non-replaceable maintenance, must be such that we can estimate that they will retain for a period of at least 50 years, if the subject of regular maintenance treatments, the characteristics that allow them to remain consistent with the rules previously stated. ..* "

5 CONCLUSIONS

The analysis of environmental characterization has allowed to understand that most of the diseases and the consequent problems of durability of these buildings has its origin in errors in evaluation reports. The management would have to scrap a construction system that is patently unfit to perform well in a difficult environment. The geo-climatic characteristics have been the detonator of defects in design and meta-design that would have been recognized already in the tender process. Once again, the main responsible for the lack of rules that ensure the quality and durability of the buildings is the bidding process – *call for bids*. Retrofitting interventions have had only heat content and were not even aimed at substantially improving the meteoric water proofing of roofs and façades. They were also partial, and not sufficiently corrected by the technical point of view. It should have taken more complete solutions (façades ventilated and drained to the sides most vulnerable, isolated and well-designed covers, complete isolation from the outside, perimeter insulation of buildings from the ground, pieces of capillary action, automatic ventilators, dehumidifiers). It requires that Contracting Authorities must achieve the know-how suitable to the challenges posed by technological progress.

ACKNOWLEDGMENTS

Many thanks to Eng. Adele Oliveto, for his thorough research on the topic, and to ATER, now EPER of Province of Potenza, represented by its CEO, Eng. Raffaele Vita, and its Director, Arch. Michele Bilancia, for the great willingness to make available the original design documentation.

REFERENCES

Lembo F. 1977, *Le tecnologie di industrializzazione ed i sistemi di prefabbricazione utilizzati nell'edilizia civile*, Special Issue n. 7-8, July-August 1977 "*Industrializzazione dell' edilizia e prefabbricazione – Parte 2^*" of "*L' Industria Italiana del Cemento"*.

Lugez, J. 1978, *La prefabbricazione a pannelli nell' edilizia residenziale*, edited by F. Lembo, Edizioni C.E.L.I., Bologna.

Grosso, M. 1997, *Il raffrescamento passivo degli edifici*, Maggioli Editore, Milano.

Lembo, F. & Marino F.P.R. 2002, *Il comportamento nel tempo degli edifici. Cause di degrado e soluzioni progettuali dei sistemi edilizi "tradizionali" ed "industrializzati". Casi di studio*, EPC libri, Roma, ISBN 88-8184-241-6.

De Pascalis, S., 2005, *Progettazione Bioclimatica*, Dario Flaccovio Editore, Palermo.

Lembo, F. 2010, *Causes: Processes in which there is lack of Quality Control, Errors in Planning or Executing*, CIB W 86 *State-of-The Art Report*, CIB W 86 Annual Meeting, Santander 29 October 2010.

XII DBMC
International Conference on Durability of Building Materials and Components
PORTO - PORTUGAL, April 12th-15th, 2011

Corrosion of Reinforcement in Existing Conrete Facades

Jukka Lahdensivu [1]
Hanna Tietäväinen [2]
Pentti Pirinen [3]

ABSTRACT

The most common degradation mechanism causing the need to repair concrete facades in Finland, is corrosion of reinforcement due to carbonation and small cover depths of reinforcement. During last almost 20 years repair of concrete facades and balconies has been very active and this work has produced a lot of information of actual condition of those repaired buildings. This active condition assessment and repair work have produced extensive, growing information base, which can be used, for example, for anticipating the upcoming repair need of concrete structures. For this purpose the data is gathered from 946 buildings, which includes distribution of different kind of states of damage and interdependence of the damage and other factors.

According to this database 59.2 % of Finnish concrete facades was seen visual corrosion damages. 53.5 % of those were local, and 5.7 % were wide spread. The corrosion of reinforcement was induced by carbonation of concrete and small cover depths of reinforcement. In four cases only contamination of chlorides was enough for corrosion. Corrosion appears first in the facades where cover depths are the smallest and which gets more rainfall. In practice this intends corrosion damages on southern and western facades because prevailing wind directions during rain. In the same time corrosion is very rare on northern and eastern facades, because the amount of rainfall to those facades is very small compared to others.

KEYWORDS

Corrosion of reinforcement, Carbonation, Concrete facade, Annual rainfall, Condition assessment.

[1]Department of Civil Engineering of the Tampere University of Technology (TUT), Tampere, FINLAND, jukka.lahdensivu@tut.fi
[2] Finnish Meteorological Institute (FMI), Helsinki, FINLAND, hanna.tietavainen@fmi.fi
[3] Finnish Meteorological Institute (FMI), Helsinki, FINLAND, pentti.pirinen@fmi.fi

1 INTRODUCTION

Since the 1960's a total of about 44 million square meters of concrete-panel facades have been built in Finland [Vainio et al. 2005]. In fact, more than 60 % of the Finnish building stock has been built in the 1960's or later. Compared with the rest of Europe, the Finnish building stock is rather young.

Despite of the quite young age of the Finnish concrete building stock, several problems have been encountered in their maintenance and repair. The structures have deteriorated due to several different deterioration mechanisms whose progress depends on many structural, exposure and material factors. Thus, the service lives of structures vary widely. In some cases the structures have required remarkable and often unexpected, technically significant and costly repairs less than 10 years after their completion. For this reason many new methods have been developed in Finland for maintaining and repairing these concrete structures during the last 20 years. The methods include a condition investigation practice and its extensive utilization, rational repair methods and their selection, as well as first-rate repair products and appropriate instructions for managing repair projects.

Concrete structures have been repaired extensively in Finland since the early 1990's. During the almost 20-year period, approximately 10 percent of the stock built in 1960 to 1980 has been repaired once. It is estimated that the total annual value of building repair work in Finland is approximately 5500 million euros, of which approximately 30 % involves external structures (walls, balconies, roofs, windows, etc.). The total annual volume of facade renovation is approximately 15 million m^2. In addition, 40,000 balconies are repaired annually and 4500 new balconies are added to old buildings. It is estimated that the volume of facade renovation will grow 2 % annually [Vainio et al. 2005 and 2002].

Because of the great amount of these existing concrete structures, it is very important to solve their incident repair need economically and in a technically durable way. This means that the most suitable repair methods have to be used for each case and it is also important to be able to determine the optimal time of the repairs.

1.1 Structures of Concrete Facade Panel

Prefabricated concrete facades have been the most common facade type in residential buildings in Finland since the late 1960's, at least in blocks of flats. A typical concrete element consists of an outer layer, thermal insulation and an inner layer. The outer and inner layers are connected together by trusses. The outer layer is typically between 40 and 85 mm thick, and the strength of concrete is typically near C20. The thermal insulation is usually mineral wool with a design thickness of 70 to 140 mm. Due to the compaction of thermal insulation, the actual thickness is usually between 40 and 100 mm. The thickness of the inner layer is normally from 150 to 160 mm (load bearing element) or 70 mm (non-load bearing elements).

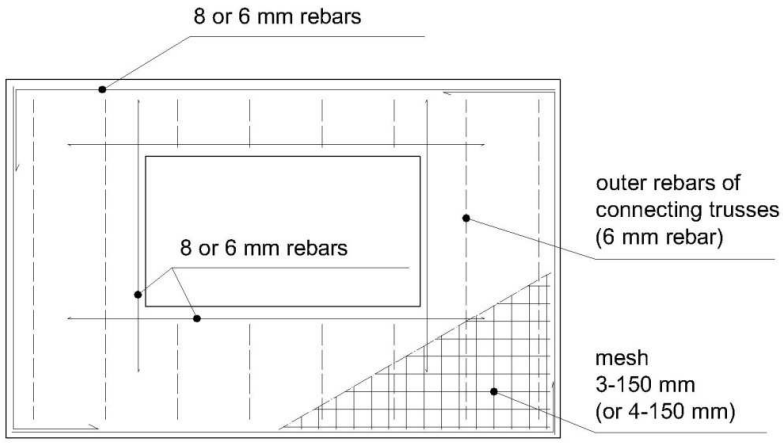

Figure1. Typical outer layer of a prefabricated Finnish concrete façade panel.

1.2 Objective

The objective of this paper was to study the factors that have actually had an impact to the existence and progress of corrosion of reinforcement in existing Finnish concrete facades.

2 CORROSION OF REINFORCEMENT

The most common deterioration mechanisms causing the need to repair concrete facades in Finland, and concrete structures in general, are corrosion of reinforcement due to carbonation or chlorides as well as insufficient frost resistance of concrete which leads to, for instance, frost damage [Pentti et al. 1998]. Reinforcing bars within concrete are normally well protected from corrosion due to the high alkalinity of concrete pore water. Corrosion may start when the passivity is destroyed, either by chloride penetration or due to the lowering of the pH in the carbonated concrete [Page 1988].

2.1 Carbonation of Concrete

Carbonation is a chemical reaction where atmospheric carbon dioxide diffuses into the pore system of concrete and reacts with the alkaline hydroxides of concrete. Due to carbonation, the pH of the concrete decreases from the level of 13 to the level of 8.5 and the passivity of reinforcing steel loses its passivity. Carbonation begins at the surface of a newly constructed member and propagates slowly as a front at a decelerating rate deeper into the structure. The speed of propagation is influenced mainly by the quality of concrete (amount of cement and porosity of concrete) as well as moisture exposure. Heavy moisture exposure, for example due to rainfall, slows down carbonation because water blocks the pores from CO_2 [Parrott 1987, Tuutti 1982 and Richardsson 1988].

2.2 Chloride Contamination

The passivity of steel may be destroyed also by the presence of chlorine ions derived either from the environment or from the use of contaminated constituents of concrete. Chlorides act as catalysts to corrosion and, therefore, the corrosion process may proceed rather quickly. The threshold value of chloride contamination for corrosion to start in non-carbonated concrete is extremely low, i.e. around 0.03 - 0.07 weight percent [Anon. 2002]. Whereas carbonation-induced corrosion leads to more or less uniform corrosion, chloride attack usually causes localised corrosion, which can result in severe reduction in steel diameter. Chloride-induced corrosion becomes highly accelerated when carbonation reaches reinforcement depth. This means that the extent of visible corrosion damage may increase strongly in a short time. Steel corrosion in chloride migrated concrete has been widely studied by Parrott [1987], Richardson [1988], Schiessl [1994], Broomfield [1997] etc.

2.3 Active Corrosion

Once the passivity is destroyed either by carbonation or by chloride contamination, active corrosion may start in the presence of moisture and oxygen [Parrott 1987]. Corrosion may run for a long time before it can be noticed on the surface of the structure. Because corrosion products are not water soluble, they accumulate on the surface of steel nearby the anodic area [Mattila 1995]. This generates an internal pressure, because the volume of the corrosion products induced by carbonation is four to six times bigger than original steel bars [Parrot 1987 and Tuutti 1982].

Internal pressure caused by corrosion products leads to cracking or spalling of the concrete cover. Visible damage appears first on the spots where the concrete cover is smallest and the moisture content of concrete is highest. According to Tuutti [1982] relative humidity of concrete has a strong influence on corrosion speed. The rate of corrosion proceeds significantly only if the relative humidity of concrete exceeds 80 %. In typical Finnish outdoor climate during September to April,

relative humidity in concrete facades is between 90 and 95 %. This intend corrosion rate of 0.1 to 1 $\mu A/cm^2$ respectively.

3 RESEARCH MATERIAL

The research material consist of the database of deterioration and material properties of existing Finnish concrete facade panels built up during 1961 to 1996, and weather observations since 1961 made by Finnish Meteorological Institute (FMI)

3.1 Database

Condition assessment systematic for concrete facades and balconies has been developed in Finland since the mid-1980's. A large body of data on implemented repair projects has been accumulated in the form of documents prepared in connection with condition assessments. About a thousand five hundred precast concrete apartment blocks have been subjected to a condition assessment, and painstakingly documented material on each one exists, including the buildings' structures and accurate reports on observed damage and need for repairs based on accurate field surveys and laboratory analyses.

The condition assessment data from 946 buildings has been gathered to a database. Those condition assessment reports have been collected from companies which have conducted such investigations as well as from property companies owned by cities.

3.2 Weather Data

Weather data consists of annual liquid precipitation i.e. rain and wet snow. Both of them can be capillary adsorbed to pore structure of concrete. Wind directions and wind speed during rain and in all times (including also snowfall and dry weather) during September to April was gathered, too. All weather data was gathered from Jyväskylä (inland), Vantaa (south costal area) and Turku (coast line) since 1961.

4 RESULTS AND DISCUSSION

Most of the blocks of flats stock in Finland is situated southern part of Finland. In the database the building stock has been divided in three different group based on their geographical position: coastal area, inland and North Finland. About third of those buildings are situated on coastal area and two-thirds on inland. Only few of the buildings in the database is situated North Finland.

Basically all prefabricated concrete panels have been made in the same way, but there are a lot of differences in their surface finishing and manufacturing. Those have a strong influence, for instance, on the situation of rebars and the quality of concrete. In the database the most common surface finishing is brushed painted concrete, exposed aggregate concrete and painted plain concrete. The distribution of surface finishing on the database is shown in Fig. 2.

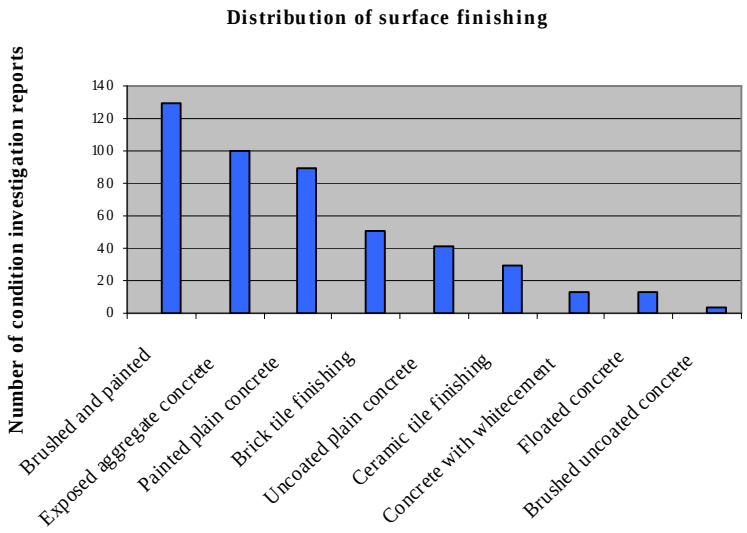

Figure 2. Distribution of surface finishing in the database (n= 946 single buildings).

4.1 Carbonation Depth of Concrete Compared with Cover Depths of Reinforcement

Carbonation cannot be seen visually on facades. The determination of the carbonation depth of concrete always requires sampling and laboratory testing. The most typical carbonation depths of concrete facades constructed in the 1970's or earlier, is nowadays around 10 and 20 mm if the concrete quality is normal. Concrete facades covered with ceramic or brick tiles can be carbonated only thorough the cement based pointing of tiles. Also paintings used on concrete facades have resistance against the diffusion of carbon dioxide. The average carbonation speed of different concrete facades is shown in Fig. 3.

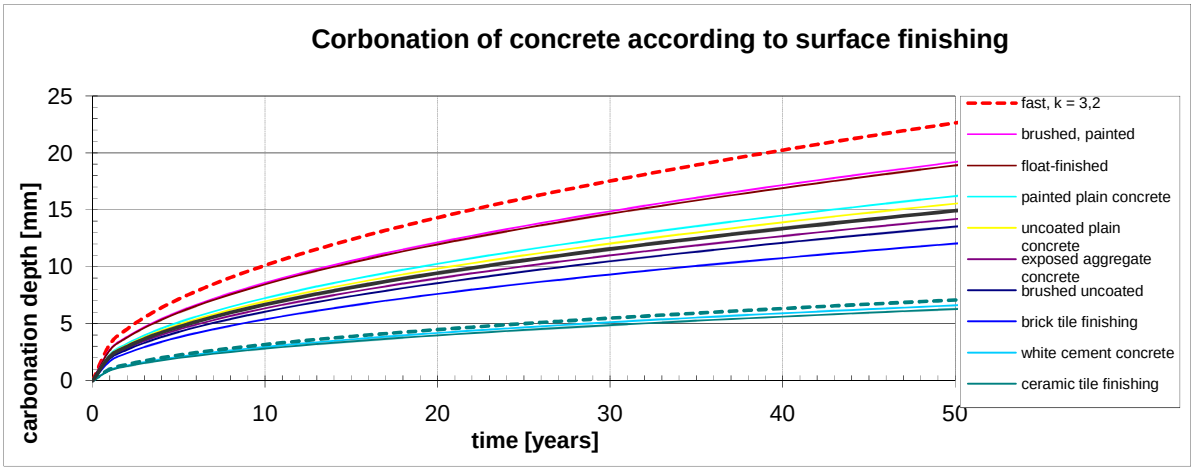

Figure 3. Average carbonation speed of concrete has a lot of variation according to surface finishing.

According to Fig 3 average carbonation depth is in the concrete facade made in the year 1970 now between 6 and 17 mm depending on the surface finishing of concrete. However, there is a lot of scattering in carbonation rate also in each group of surface finishing.

The depth of the concrete cover on reinforcement varies a lot, depending on the manufacturing of concrete panels and quality of labour work. Cover depth of reinforcement varies between 0 and over 50 mm. Determining the suitable repair method for concrete facade, the amount of cover depths under 10 mm is critical in most of the cases. Typical amount of small cover depths is 5 to 10 per cent of all

reinforcement in facades. In most cases the smallest cover depths are in ceramic tile finished facades, where reinforcement is situated just behind the tiles.

Carbonation of concrete has widely achieved the reinforcement of all concrete facades made during 1960's and 1970's. And corrosion has been possible for 20 to 30 years for now.

4.2 Visual Corrosion Damage

According to the database 59.2 % of Finnish concrete facades was seen visual corrosion damages during condition assessment. 53.5 % of those were local, and 5.7 % were wide spread. The corrosion of reinforcement was induced by carbonation of concrete and small cover depths of reinforcement. Much more visual corrosion damage was seen in coastal area than inland. Despite small cover depths of reinforcement in carbonated concrete, 40.8 per cent of facades could not seen any visual corrosion damage.

The corrosion rate has strong dependence on moisture content in carbonated concrete. According to Mattila and Pentti [2004] dencity of corrosion current is high in uncovered concrete if the annual rainfall is 480 mm or higher. In Fig 4 the annual liquid prcipitation, i.e. rain or wet snow, in Finland is shown.

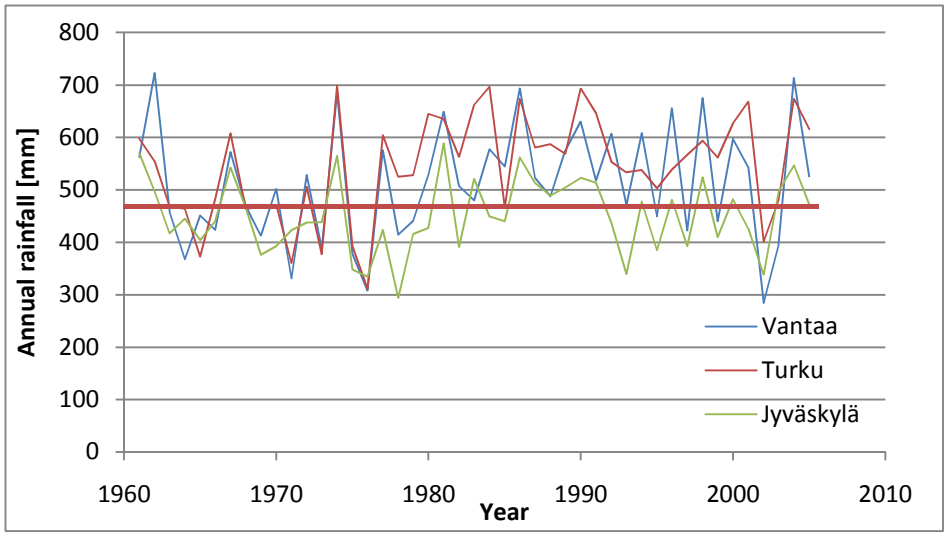

Figure 4. Annual liquid precipitation in Jyväskylä (inland), Vantaa (south costal area) and Turku (coast line) during 1961 to 2005. The horizontal line expresses the annual rainfall that leads to faster corrosion rate.

In coastal area (Turku) and southern Finland (Vantaa) the amount of annual rainfall is compared to inland (Jyväskylä). In coastal area and southern Finland the annual rainfall also exceeds the critical amount of 480 mm per year most of the years, especially after 1980's. In 1980's also the carbonation of concrete has achived the near surface stayed reinforcement. Thus the higher rainfall amounts would be a reasonable explanation for more corrosion damage in coastal area than inland.

4.3 Influence of Prevailing Wind Direction

The amount of annual rainfall is not uniformly distributed to facades. The distribution of rainfall depends on the height of the building and also prevailing wind directions during rain. The upper parts and corners of facades get more rainfall than lower and central parts as seen in Fig. 5.



Figure 5. Head of the concrete building in the beginning of a rain event. Upper parts get more rain than the lower ones.

Prevailing wind directions and wind speeds have a strong influence on the distribution of rainfall on a building. Most of the liquid precipitation in wintertime comes with southerly to westerly winds. Rain events with wind from other directions have been rare, see Fig. 6. The effect of the wind direction to the distribution of the rainfall on the facade can be seen in practice in Fig. 5. No rain is falling on the window facade in this case.

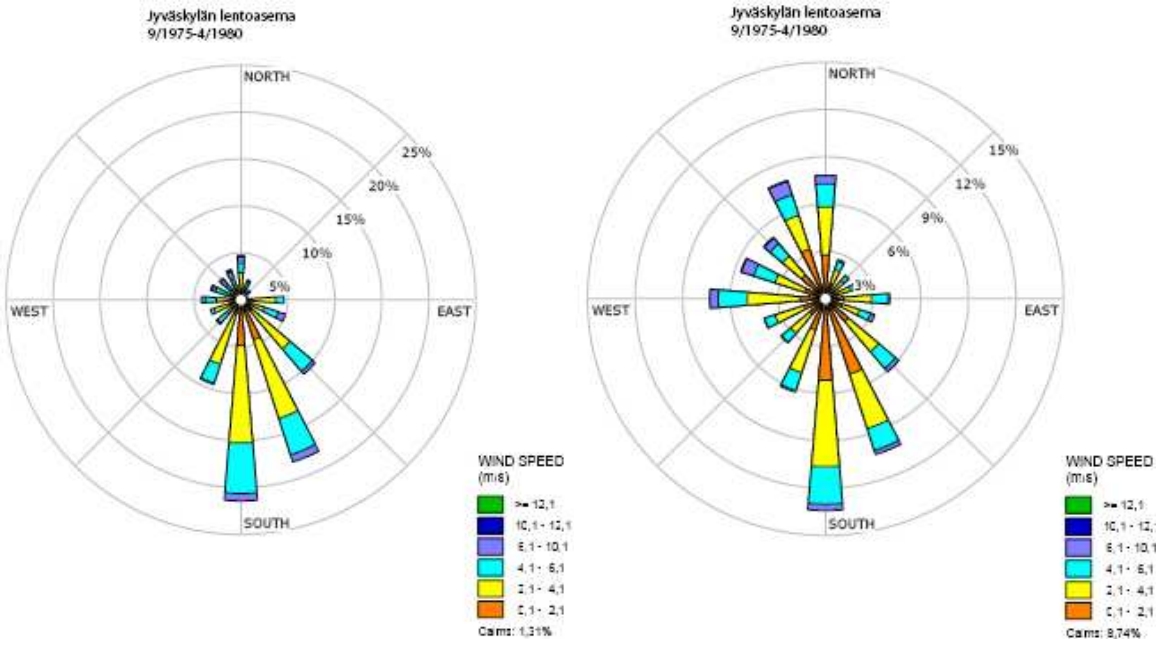

Figure 6. Prevailing wind directions in wintertime during liquid precipitation on the left and in all times including snowfall and dry weather on the right. Weather data is measured at Jyväskylä airport during Sept. 1975 to Apr. 1980.

Hardly any corrosion damage can be seen on the north or east facades despite of reinforcement is situated in carbonated concrete as well as on the south and west facades. The high outdoor relative humidity in Finland during winter time is not sufficient to upraise the humidity of carbonated concrete high enough for corrosion. Thus, the high corrosion rate needs also rainfall. In Finland, prevailing wind direction during rainfall in winter are southerly to westerly. Snowfall can not be adsorbed in the pore structure of concrete. This is a reasonable explanation for more corrosion damage on southern and western facades than northern and eastern.

4.4 Corrosion Induced by Chlorides

Chloride-indused corrosion is very common in bridges and marine structures, but not in Finnish concrete facades. Only four cases out of 946 buildings chloride content was high enough for corrosion. In those cases chlorides were used as an accelerator in fresh concrete and manufacturing of those concrete facade panels was taken place at winter time on construction site.

5 CONCLUSIONS

The corrosion of reinforcement in Finnish concrete facades was induced by carbonation of concrete and small cover depths of reinforcement. In four cases only out of 946 contamination of chlorides was enough for corrosion.

The carbonation of concrete has widely advanced in the facades made in 1970's or earlier. The corrosion of reinforcement has been possible approximately last 20 to 30 years in those facades. Despite insufficient cover depths of concrete and far advanced carbonation of concrete, visually seen corrosion damages are relative rare. Corrosion damages appear mostly on facades, which get more rain. In Finland those are upper parts of southern and western facades.

REFERENCES

Anon. 2002. *Condition Investigation Manual for Concrete Facade Panels*. Helsinki. Concrete Association of Finland BY 42, 178 p. (In Finnish).

Broomfield J. 1997: Corrosion of steel in concrete – understanding, investigation and repair. London. E & FN Spon. 240 p.

Mattila J. 1995: Realkalisation of concrete by cement-based coatings. Tampere, Tampere University of Technology, Structural Engineering. Licentiate´s Thesis. 161 p. (In Finnish).

Mattila J., Pentti M. 2004: Performance of protective measures in Finnish concrete facades and balconies. Tampere, Tampere University of Technology, Publication 450. 111 p.

Page C. L. 1988. *Basic Principles of Corrosion*, In: Schiessl, P. (ed.), Corrosion of Steel in Concrete, London, Chapman and Hall, pp. 3-21.

Parrott L.J. 1987: Review of carbonation in reinforced concrete. Cement and Concrete Association. Wexham Springs. 42 p.

Pentti, M., Mattila, J., Wahlman, J. 1998. Repair of concrete facades and balconies. Part 1: Structures, degradation and condition investigation. Tampere. Tampere University of Technology, Structural Engineering. Publication 87. 156 p. (In Finnish).

Richardson M. 1988: Carbonation of reinforced concrete. Dublin, CITIS. 203 p.

Schiessl P, Breit W, Raupach M. 1994: Durability of local repair measures on concrete structures damaged by reinforcement corrosion. Mathora, V.M- (editor). Durability of concrete. Detroit. American Concrete Institute. Pp. 1195-1215.

Tuutti K. 1982: *Corrosion of Steel in Concrete*. Stockholm. Swedish Cement and Concrete Research Institute. CBI Research 4:82. 304 p.

Vainio, T. et al. 2002: Repair, maintenance and improvement work in Finland 2000-2010. Espoo 2002. VTT Research Notes 2154. 60 p. + app. 25 p. (In Finnish).

Vainio, T., Lehtinen, E., Nuuttila, H. 2005. Building and renovation of facades. Tampere. VTT 26 p. + app. 13 (In Finnish).

XII DBMC
International Conference on Durability of Building Materials and Components
PORTO - PORTUGAL, April 12th-15th, 2011

Guidelines for Ornamental Stone Use in Building Facades

Antônio Gilberto Costa [1]
Antônio Neves de Carvalho Júnior [2]
Luiz Antônio Melgaço Nunes Branco [3]

ABSTRACT

This work shows the importance of the designs for ventures in the field of construction of buildings, with a focus on the stone coatings. The text is divided into four main parts describing the context of design development; basic recommendations for the development of facade coating designs, the positive impacts of the development of these projects for the construction and other sectors involved, and finally, draws some conclusions about the subject.

Much has been said about building pathologies (an allusion to the terminology adequate of biological areas) as visible defects and / or invisible that can cause damages in the enterprise, and that its origins can be found out in the stage of design, because the correct specification of materials has vital importance in the performance of the system for coating the facades. Faults in the specifications of the various materials that make up the system of coating can be capital in the emergence of "defects" such as debonding of coatings, efflorescences, etc.. Some cases of pathologies are presented as well as discussion of how they could have been avoided.

KEYWORDS

Ornamental stones; Pathologies; Facades; Mortars.

[1]Instituto de Geociências da Universidade Federal de Minas Gerais (IGC/UFMG), Belo Horizonte, BRAZIL, agcosta@uol.com.br
[2]Escola de Engenharia da Universidade Federal de Minas Gerais (IGC/UFMG), Belo Horizonte, BRAZIL, ancjunior@demc.ufmg.br
[3]Instituto de Geociências da Universidade Federal de Minas Gerais (IGC/UFMG), Belo Horizonte, BRAZIL, luizmelg@gmail.com.br

1 INTRODUCTION

Much has been said about pathologies of buildings (in a reference to the terminology itself of biological areas) as visible and /or invisible defects that may affect the enterprise, as can be found in Ripper [1984].

During the process of design development, the designer must address some basic requirements such as: parameters for the functioning and overall quality of the work, the interactions between different parts of the building, and constructability. Thus, it is often the emergence of so-called congenital defects, i.e. construction defects generated at the design stage, by failure to comply with the established rules or accepted practice of building design (NBR 13531/95 and 13532/95)[4],defect. Grunau [1981] presented statistics showing that in European countries, over 40% of all defects presented in constructions originate in deficiencies related to the design of buildings. An example can be seen in Figure 1.



Figure 1 – Stained marble.

In Brazil, often, defects attributed to errors of execution actually originate in the design stage.

Furthermore, the supply chain for the civil construction sector has a wide range of actors and agents of partial products, created during the production process. The various players have incorporated different quality standards and that will affect the quality of the final product. Some of the actors involved are:
-- Users, the regions of the country and the specifics of the work;
-- The agents responsible for the planning of the venture;
-- Those responsible for the preliminary studies;
-- The designers of each specialty;
-- Manufacturers of construction materials at all stages;
-- Those involved in the stage of implementation of the works; and
-- Those responsible for the in-use operation and maintenance of the buildings.

2 THE VARIOUS DESIGNS IN CIVIL CONSTRUCTION

It is common practice in building construction that architectural design is the starting point for the development of several others that are needed for an enterprise, and after receiving the approval from the municipality, it becomes an important factor of technical decisions.

According to Melhado [1992] "the design should have its development led to aggregate maximum efficiency and construction technological rationalization, given the performance and functionality requirements of the building."

Meanwhile, activities that relate to the quality of a product range from the initial contractor's needs

[4] NBR is Norma Brasileira Registrada (Brazilian Standards)

identification to the satisfaction of the end user. In the construction continuum that is the activity of construction, is another customer (known as intermediary), which should also have their needs addressed. But if the quality depends on several projects, materials and professionals, we recommend, as pointed out by Juran [1992], that a series of qualities can be understood as "a conceptual model of the interaction of the activities that affect the quality of the product or service in various stages, covering the identification of needs through to the assessment of whether those activities are being met."

There are already mechanisms for ensuring the quality of materials and designs, where the application of the ISO 9000 series of standards has become routine. But there are new products coming to market daily that consumers often the pressure designers to specify. When a particular product is identified in specifications or construction documents there is often an additional "or similar", leaving the buyer to decide on the best option. What must be transfered, from a strictly technical perspective, are the performance characteristics and properties of the product. The product selections should not be done in isolation, but must take into account the global knowledge of the performance parameters as well as the requirements of the building as a whole.

Specifically on the art of designing, Thomaz [2001] says that, amongstother questions, it is necessary to "know the most frequent defects of the item under study, seeking to avoid those problems in details and construction specifications." So when the designer ceases to observe basic requirements relating to function, overall quality of the work, and interactions between the phases of construction and constructability, there is and increased frequency of so-called congenital defects, that is, constructive pathologies are more likely to be generated even at the design.

As to the planning system, the most difficult and arduous task requires recognition that integrated design and construction planning be done by various professionals from different positions within the organization and in various stages of the design. This high planning must focus on the overall goals and limitations throughout the design. These goals drive the lowest level of the planning process.

The primary benefit of improved performance of the planning system will be to enhance the production unit's quality of outputs of data, or the quality of the final design produced.

In order to improve performance of the planning system, it is essential to analyze non-conformities leading to the identification of root cause(s) and then recommendations to make improvements in future performance.

The root cause of poor quality or failures in the implementation of the planned work can be found at any organizational level, process or function.

3 THE FACADE COATING DESIGN

The failure to comply with existing technical norms and recommendations relating to material specifications and construction techniques, too often, leads to defects in the buildings, which in addition to becoming a great inconvenience to the parties involved (and condominium construction) become matters of easy challenge by experts in lawsuits (since the basic documents in the case, technical standards, were not followed).

On several occasions the Department of Materials and Civil Construction of EE.UFMG, through its group of teaching, research and extension in the area of finishing the construction, has been called to intervene with construction and condominiums to develop laboratory tests and designs, and the restoration of facade coatings. In a significant number of cases, design deficiencies have been identified as the main factor in the occurrence of defects.

According to Silva [2003], several measures should be taken for facade coatings to have satisfactory in service performance. Among them there is a need for preparation of a design for implementation of the

facade on which is a series of detailed information relating to the specification of materials and execution techniques, as well as the positioning and sizing of the movement and control joints. Moreover, you should exercise strict control over the quality of the substrate material, mortar settlement, as well as the very material used in the coating. Construction companies in Belo Horizonte (third largest city of Brazil), especially those engaged in medium and high quality residential building construction, are constantly faced with the need to construct ceramic coated facades (coating noble and high acceptance by the consumer market, usually used in conjunction with other coatings, high standard, such as granite and aluminum).

The remaining text of this section outlines the recommended procedures and considerationsfor preparation of the executive design, specification of materials, and the installation of the facade coatings using ceramic and/or ornamental stone material.

A - Stage of elaborating the executive design
In constructing facades coated with ceramic tile and/or ornamental stone, it is of paramount importance that the executive design provide adequate detailling of the dilatation, movement and control joints [Carvalho Júnior 1999]. The absence or incorrectly sizing these joints are design flaws that can cause the detachment of the ceramic tile or ornamental stones facades.

The joints should have sufficient width to be absorptive and remain resilient (i.e., in the elastic regime) during thermal and hygroscopic events. The movement joints should be positioned in a staggered pattern over the coating (preferably located in regions of transition structure / masonry) and should be full-depth, from the outer surface to the back of the assembly, filled with resilient materials, able to release the tensions generated by movements of the structure and ceramic/ornamental stones ranges they delimit. Figure 2 illustrates this kind of joints.

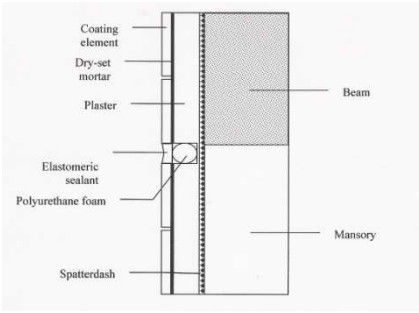

Figure 2 – Example of movement joint.

Control joints are used on the changes of direction (such as corners and protrusions), as well as at the transition between different coatings, also with the task of absorbing the tensions that arise in these places. Figure 3 illustrates this type of joint.

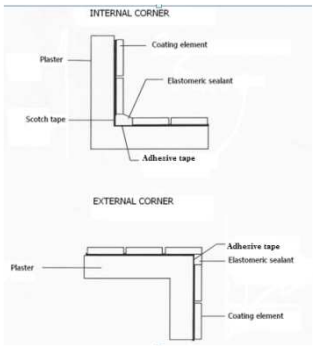

Figure 3 – Examples of control joints.

B - Stage of specification of materials
The correct specification of materials is vital in the performance of the coating system used on the facade. Failure to properly specify the various materials that make up the coating system can be capital in the emergence of defects such as tile debondings.

The spatterdash is a layer of mortar to ensure greater plaster anchor of the masonry / structure [Carvalho Júnior 1999]. The spatterdash used on masonry is usually composed of cement and sand (materials proportions 1:3) with fluid consistency. The surface of concrete should typically be treated with an industrialized spatterdash or the addition of a resin (preferably acrylic-based) to conventional spatterdash mentioned earlier for use on masonry.

The plaster is a layer of regularization, applied directly over the base, with the task of defining the vertical plane and giving support to the next layer, the ceramic and/or ornamental stone coating itself. The plaster must meet the recommendations for resistance and bond strength in accordance with standard ABNT NBR 13749 (Coating of walls and roofs with inorganic mortars- Specification (1996)). This document stipulates that in the trial, to determine the bond strength by pull-off tests, the least 04 values of 06 cps tested should be greater than or equal to 0.30 MPa.

The dry-set mortar (used to set the tiles) must be at least of the type AC-II (also known as flexible polymeric dry-set mortars). For tiles and / or ornamental stones of low water absorption (such as porcelain stone-ware tile and / or granites) it is recommended to use dry-set mortar type AC-III. The resistance and bond strength requirements in the standard ABNT NBR 13755 (Coating of external walls and facades with tiles and the use of dry-set mortar - Procedure (1996)) for tiles set in facades, using dry-set mortar, state that in the trial to determine the bond by pull-off tests at least 04 values of 06 cps tested should be greater than or equal to 0.30 MPa.

The tiles to be used as facade coating must also fulfill specific characteristics [Neto 1999]. The ANFACER (National Association of Manufacturers of Ceramics) recommends that ceramics pieces to be used in facades present water absorption less than or equal to 6.0%. For pressed tiles, with water absorption of between 3 and 6%, standard ABNT NBR 13818 (Ceramic plates for coating - Specification and methods of testing (1997)) recommends that the plates have an hygroscopic dilation less than or equal to 0.6 mm / m. There is still, as positive features, the use of clear colors, small dimensions (e.g. 10cm x 10cm) and poly-oriented claws in back.

Concerning grouting of mortars, the standard ABNT NBR 14992 (Mortar the basis of Portland cement to grouting of tiles - requirements and methods of testing (2003)) recommends, for use in facades, the grout type II, which can be applied to tiles with absorption of water less than 3% and in areas whose extensions should use movement joints.

C - Implementation stage
The setting of the coating system itself must also be done with care because, flaws in this step will probably lead to a premature detachment of the plates.

The dry-set mortar used in to place tiles or ornamental stones requires a minimum time from the mixing of the product with water (usually of the order of 15 minutes). Open time, corresponds to the time that the dry-set mortar can be applied to the plaster without any loss of adhesion. For dry-set mortar type-II open time should be no more than 20 minutes (reference value, taken in the laboratory), and this should be verified on site for the setting ceramic tile and/or ornamental stone coating. The presence of any of the following conditions indicates that the open time has been exceeded: i) bright whitish film on the surface of the dry-set mortar; ii) lack of tackiness or no transfer of dry-set mortar when touched with the fingertips; and iii) inadequate adhesion to the mortar bed, as verified by a pull-off inspection of a newly set ceramic or ornamental stone.

It is also important that the mortar mixture be used in a period less than 2 ½ hours after first contact with water. When setting ceramic or ornamental stone pieces larger than 20 cm x 20 cm, it is

recommended to also apply mortar to the back of the work piece (beyond that already applied on the plaster with the use of appropriate tool).

Thus, there are three distinct and important steps toward the development of any specific facade coating design: executive design, material specification and implementation. Of course designers, responsible for the first two steps, should also contribute significantly to the stage of implementing the so-called generating design for production, which, according to Aquino and Melhado [2002] should provide enough detail to direct the execution activities.

4 POSITIVE IMPACT ON DEVELOPMENT PROJECT IN FACADES COATINGS

Observe that the development of specific design for implementation of the facade coatings contributes enormously to the reduction of possible defects from the non-observation of details exposed in the previous item.

Furthermore, in the current scenario businesses also have a social role in ecological and should become more in step with society, the general population and the workforce. As is happening with companies in other product sectors, the building industry needs to change the aims, focusing actions toward workers and the surrounding environment.

The construction industry must invest in improvements to human resource potential, recognizing itself as part of society and its problems. As well, the sector should focus on the environmental interactions and loadings when considering putting a building in-place; impact of time of implementation, addressing the issue of waste (such as consumption of materials and time beyond what is necessary) and generation of pollution.

The experience of the Department of Materials and Civil Construction of EE.UFMG, through its group of teaching, research and extension in the area of construction finishing, has clearly shown that, since 1996, works that were implemented with the use of an executive design have provided satisfactory performance relative to loads that facades routinely encounter (wind, sun, rain, humidity, among others).

Some of the benefits for construction and users that comes from this procedure are:
• Significant reduction in defects such as infiltration of moisture and water from rain, debonding and falling of the coatings;
• Identification of well performing designs and construction techniques that require less repair later in the facade service life; (This is in contrast to the frequently occurring situation since 1996, where the Department of Materials and Civil Construction of EE.UFMG has investigated, proposed improvements to, and reported on several poorly performing buildings that had not had executive facade design and installation plans.)
• The absence of rework (come from the need to repair facades with infiltration or collapse of coatings) means the absence of the nuisance to users of buildings (natural when performing repairs to the building occupied), maintaining the good image of the construction in the market, in addition to lower costs of maintenance of buildings; and
• Reduction in material waste in the form of rubble generated by the corrective actions during construction and subsequently because, in most cases, several layers of the coating system are not re-usable, generating a significant amount of rubble and various types of pollution and costs (noise, dust generation, obstruction of flow of water courses, proliferation of vectors of disease, destruction of layers of soil nutrients, in addition to the cost of materials, transmission and deposition).

To be sure that pathologies can be avoided by correct techniques; some pathologies are shown in sequence. In the Figure 4, mortar is not appropriate because of low plasticity; Figure 5 shows improper use of granite in a facade; Figure 6 shows an inadequate sealant in a joint. To avoid these and many other cases, the technological characterization of the ornamental stones is highly recommended before use.



Figure 4 – Lack of adherence.



Figure 5 – High capillarity of granite.



Figure 6 – Lack of sealant.

5 CONCLUSION

As observed, there is a significant influence of the executive design (involving specification of materials and techniques) upon the performance of facade coatings. This, therefore, denotes a fundamental importance of carrying it out.

The preparation of a detailed, consistent and feasible design will be possible provided that it is consistent in adequacy of transferring theory to practice, as well as in its recommendations, taking the significance of quality of workmanship (direct and indirect), as found in civil construction, into account.

ACKNOWLEDGMENTS

The authors wish to thank UFMG - Universidade Federal de Minas Gerais (Instituto de Geociências e Escola de Engenharia) and FAPEMIG – Fundação de Amparo do Estado de Minas Gerais.

REFERENCES

Aquino, J. Q. R. A. & Melhado, S. B.; The importance of the design for production in the design process management in building construction. *10 th Annual Conference Proceedings International Group for Lean Construction.* Gramado, Brazil, 2002.

Associação Brasileira de Normas Técnicas. NBR 13531 Elaboração de projetos de edificações - Atividades técnicas. Rio de Janeiro: ABNT, 1995.

___NBR ISO 9000 Quality management systems -- Fundamentals and vocabulary. Rio de Janeiro: ABNT, 2005.

___NBR 13532 Elaboração de projetos de edificações – Arquitetura. Rio de Janeiro: ABNT, 1995.

___NBR 13749 Revestimento de paredes e tetos de argamassas inorgânicas – Especificação. Rio de Janeiro: ABNT, 1996.

___NBR 13755 Revestimento de parades externas e fachadas com placas cerâmicas e com utilização de argamassa colante – Procedimento. Rio de Janeiro: ABNT, 1997.

___NBR 13818 Revestimento de parades externas e fachadas com placas cerâmicas e com utilização de argamassa colante – Procedimento. Rio de Janeiro: ABNT, 1997.

___NBR 14992 A.R. - Argamassa à base de cimento Portland para rejuntamento de placas cerâmicas - Requisitos e métodos de ensaios. Rio de Janeiro: ABNT, 2003.

Carvalho Júnior., A. N. Techniques of coating. Apostila expertise in the Course of Construction, Department of Materials Engineering and Construction of EE.UFMG. Belo Horizonte, 1999.

Grunau, E. B. Et Alli *Aus Bauschaden Lernen, injuries in the buildings,* Barcelona: Institut d'Etudes de Materiales de Construcción of Erfstadt, Ediciones ECAC, 1981.

Juran, J. M. *The quality from the project: new steps for the planning of the quality of products and services.* Sao Paulo: First, 1992.

Melhado, S. B. & Violani, M. A. F. The quality in the construction and design of buildings. Sao Paulo: EPUSP, 1992.

Neto, F. M., Silva, A. P. & Carvalho Júnior., A. N. Expertise in Conditions of Coatings in Facades. *Proceedings of the X Brazilian Congress of Engineering and Expertise Ratings.* Porto Alegre, 1999.

Ripper, E. *How to avoid errors in construction.* São Paulo: Pini, 1984.

Silva, A. P. & Carvalho jùnior., A. N. Conditions of coatings - Case Study: The relationship between the expansion of moisture and detachment of the tiles, curved, *Anais XII of the Brazilian Congress of Engineering Evaluations and Expertises - COBREAP*. Belo Horizonte, 2003.

Thomaz, E. *Technology, management and quality in construction.* Sao Paulo: PINI, 2001.

XII DBMC
International Conference on Durability of Building Materials and Components
PORTO - PORTUGAL, April 12th-15th, 2011

Durability of Concrete and Brick Facades of Apartment Buildings Built Between 1960-90 in Estonia

Simo Ilomets [1]
Targo Kalamees [2]
Tõnis Agasild [3]
Karl Õiger [4]
Lembi-Merike Raado [5]

ABSTRACT

This paper analyzes durability issues related to brick and concrete facades of apartment buildings built between 1960-90 in Estonia. Frost resistance, compressive strength and problems of efflorescence, salt deterioration, carbonation, and corrosion were investigated among other topics in two large-scale research projects during 2008-2010. The apartment buildings studied were built with walls of prefabricated concrete elements and ceramic or calcium silicate bricks. The condition of 50-30 year old concrete or brick facades is of high concern in terms of residual frost resistance according to the common assessment standard. Nevertheless, this study shows that the current methodology used for the evaluation of the frost resistance of ceramic bricks needs to be improved for brick behaviour studies in real climatic conditions. Carbonation depth of a concrete facade varies from 0 to 70 mm (generally 10-40 mm) with faster carbonation of paint coated facades as compared to rubble bulk. Corrosion appeared mainly on the lower side of awning panels of both building types. It was also observed on concrete elements with thin (<10 mm) concrete covering layer and brick facades without zinc coating siding bonds. The condition of steel or brick bonds has to be carefully investigated before installing external insulation. Results of this research show that the situation is worrisome and that concrete and brick facades of apartment buildings built between 1960-90 need renovation.

KEYWORDS

Durability, Frost resistance, Carbonation, Corrosion.

[1] Chair of Building Physics and Architecture of Tallinn University of Technology, ESTONIA, simo.ilomets@ttu.ee
[2] Chair of Building Physics and Architecture of Tallinn University of Technology, ESTONIA, targo.kalamees@ttu.ee
[3] Chair of Building Physics and Architecture of Tallinn University of Technology, ESTONIA, tonis.agasild@gmail.com
[4] Chair of Building Physics and Architecture of Tallinn University of Technology, ESTONIA, karl.oiger@ttu.ee
[5] Chair of Building Materials of Tallinn University of Technology, ESTONIA, lemera@staff.ttu.ee

1 INTRODUCTION

According to statistics, more than 80 % of dwellings in Estonia have been built after World War II, mainly between 1961-1990. The majority of apartment buildings are composed of prefabricated concrete large-panels and bricks. First concrete panel buildings were erected at the beginning of the 1960s when the production technology was imported from France and the design was provided by a central designing institute in Moscow. Use of calcium silicate and ceramic bricks started even earlier. Concrete of facades is typically covered with rubble bulk or paint. Calcium silicate or ceramic hollow core facades are uncovered.

Estonian climate is strongly influenced by to the adjacent Baltic Sea and it is between maritime and continental. There are four seasons of near-equal length with average temperatures from 1961 to 1990 +16°C in July and -6°C in February, and with annual average of +5°C. The average precipitation range is from 535 to 727 mm and an annual number of rainy days is between 102 and 127. Average speed of wind is 4.3 m/s and time of the sunshine 1726 hours. Heating period lasts for about 7-8 months, at an average air temperature of about 0ºC.

Outdoor climate influences the durability of building`s facades in several ways. Outdoor temperature around 0ºC combined with driven rain influences the durability of building facades. When the water in the facade freezes, it expands and may decay the material of the facade. Corrosion of reinforcement is another factor that influences the durability of concrete facades due to surface cracking and subsequent spalling of the cover concrete due to the expansion of the corroding steel [Ahmad 2002]. The corrosion of fasteners influences the connection of the external layer of the external facade (both brick and concrete). Collapse of the fasteners is an important safety question. Carbonation of concrete or penetration of acidic gases into concrete are the main causes of the possibility of reinforcement corrosion. As concrete provides protection to reinforcing against corrosion due to its high alkalinity, during carbonation of concrete it is neutralized and the protection properties of steel are lost. Secondary ettringite mechanism formation has been suggested also as one of the critical mechanisms causing concrete deterioration. Damage of concrete results from ettringite swelling or crystal growth. Today the designed service life of older apartment buildings (50 years) is close to elapsing and to work out renovation solutions it is necessary to establish the current condition of the facade. The future of old apartment buildings is under discussion in Estonia, as well as internationally [Hagentoft 2010]. Even external walls need to be additionally insulated due to serious thermal bridges in them, high thermal transmittance of original external walls (0.7-1.0 W/(m^2·K)) and rising energy prices, the condition of original walls must be investigated to design fasteners for insulation and durability renovation measures.

In this study, the condition of concrete and brick facades of apartment buildings built between 1960-90 in Estonia was investigated using data from the primary source and laboratory measurements. As many factors affect the processes and the speed of deterioration, one of the most reliable ways to determine the current condition is to analyze different types of buildings. However, the extent of pilot research may appear insufficient to represent the whole building stock. Nevertheless, it may give useful information for future thoroughgoing research. The results presented in this paper are part of a larger national research project of the technical condition and service life of old multi-storey apartment buildings in Estonia [Kalamees *et al.* 2009] and [Kalamees *et al.* 2010].

2 METHODS

2.1 Buildings studied

The buildings studied were typical apartment buildings with 5, 9 or 16 floors, built mainly between 1961-90. As apartment buildings composed with prefabricated concrete large-panels and bricks were most widely used for structural solutions during this period, these building types were investigated. Prefabricated concrete large-panel external walls are composed of two layers of reinforced concrete

(75…130 mm thick loadbearing inner layer and 50…60 mm thick external core) and insulation material between them (50…125 mm thick of fibrolite (chip-cement plate), mineral wool, expanded polystyrene, or phenolic foam). Concrete of the facade is typically covered with rubble bulk or paint.

Brick walls have a similar principal solution: 250…630 mm thick loadbearing inner layer (typically calcium silicate brick), 60…120 mm thick mineral wool and 120 mm external core layer (calcium silicate or ceramic brick). In this study plastered brick walls were not investigated.

2.2 Field study

Overall technical conditions of facades were investigated to predict their durability as part of a large-scale research project. Field study comprised large-scale visual inspection (based on experience) of the facades, opening representative envelopes locally, and taking specimens of facades for future laboratory tests. Specimens of facades were taken by drilling Ø 110 mm holes to the concrete facade or removing bricks from the brick facade. Specimens for laboratory tests were taken only from visually undamaged areas.

2.3 Laboratory tests

2.3.1 Frost resistance

Concrete samples drilled from seven buildings were tested according to the Estonian standard for frost resistance of concrete [EVS 814]. A test piece of 50 mm thickness was sawn out from the cylinder and the parallel surface with the facade was tested. Mass loss from the surface (kg/m^2) was measured after 7, 14, 28, 42 and 56 freeze-thaw cycles. Careful visual survey and rapping of the facade were done and a representative spot was chosen before action.

Calcium silicate and ceramic brick samples were taken from the facades of twelve building (6 calcium silicate and 6 ceramic) and to find out residual frost resistance, three different methods were used:

- To compare the concrete and the brick facade both calcium silicate and ceramic bricks were tested according to the standard for the frost resistance of concrete [EVS 814].
- In addition, calcium silicate bricks from two buildings were tested according to [EVS-EN 772-18]. Test specimens were sawn out and put into water step by step during 24 hours at the temperature +20 ± 5 °C. After taking out from water, specimens were frozen and later thawed in water. Damages were estimated visually after 50 freeze-thaw cycles and damaged pieces were tested for compressive strength.
- Ceramic bricks were also tested after [GOST 7025] because no modern standardized methods are available to evaluate the frost resistance of ceramic bricks. Test specimens with ~50 mm thickness were sawn out and the previous surface of the facade was tested in the refrigerating device with air circulation at the temperature -18 ± 2 °C for 4 to 16 hours. Thawing in regular water lasted from 6 to 18 hours. Visual inspection and weighting of mass was conducted after 25, 50, 75 and 100 freezing-thawing cycles. The result is considered to be satisfactory if no visual damages or changes of mass appear.

To assess the test results the lowest environmental class for the impact of freezing/melting XF1 was used, i.e. moderately saturated with water and without anti-icing agent (example: vertical concrete surfaces unprotected from rain and cold). Target values of frost resistance class KK1 were used, which allows 0.5 kg/m^2 seceded amount of material after 56 freeze-thaw cycles.

2.3.2 Compressive strength

To study the compressive strength, samples were taken from the walls of seven buildings according to [EVS-EN 12504-1] and were tested according to two methods:

- Destructive method where pieces were sawn into cubes and cylinders, then pressed according to EVS-EN 12390.
- Non-destructive test with the Schmidt hammer was carried out according to EVS-EN 12504-2.

Bricks were taken from facades of twelve buildings (6 calcium silicate and 6 ceramic), cut into half and compressed according to EVS-EN 772-1. Since compressive strength of a wall depends on the properties of bricks and mortar, also status of mortar was estimated during the extraction process of bricks.

2.3.3 Corrosion of steel

Corrosion of reinforcement of concrete large-panels and brick walls was studied via visual survey. Also, elements of balconies and awning panels connected to brick walls were inspected. In some places, constructions were locally exposed, depending on the purpose. In addition, a few chosen samples of concrete were investigated with a light microscope.

2.3.4 Carbonation of concrete

Two methods were used to detect carbonation depth of the concrete of the facade:

- First, phenolphthalein was used to visualize the depth of carbonation of 112 test pieces. Measurements were taken both from the inside and outside of the test piece and rubble bulk layer was excluded from the readout.
- Secondly, X-Ray diffractometry (XRD) was used to analyze the content of $Ca(OH)_2$ and $CaCO_3$ in the powder made of the sample.

3 RESULTS

3.1 Frost resistance

Both visual inspection of buildings (Figure 1) and laboratory tests (Figure 2) indicated to problems with the residual frost resistance of concrete and brick facades. Only half of the specimens fulfilled the criteria for the frost resistance of concrete in the XF1 environmental class: loss of mass ≤ 0.5 kg/m^2. Frost resistance of older buildings were in the worst condition. To compare concrete and brick according to the same conditions, brick specimens were tested according to the standard for the frost resistance of concrete [EVS 814] (Figure 2 right). It was found that brick showed much worse performance than concrete, independent of the building age. Nevertheless, frost resistance tests of two buildings based on calcium silicate brick [EVS-EN 772-18] showed no loss of compressive strength after freeze-thaw cycles. Frost resistance tests of ceramic bricks (three buildings) according to the old GOST 7025 test method did not show large mass loss in most of the specimens. Furthermore, the mass of some test specimens grew due to filling cracks of brick with water.

In addition to differences in test procedures, also the place where the test specimens were taken influences the results. South and southwest facades were found to be in the worst conditions in terms of frost resistance. In the building with brick facade the residual frost resistance was satisfactory up to three storeys. Bricks from higher storeys, below windows, around the balcony and loggia, and around the downpipe were in a worse condition.



Figure 1. Frost damages of concrete (left), ceramic (centre) and calcium silicate brick (right) facades.

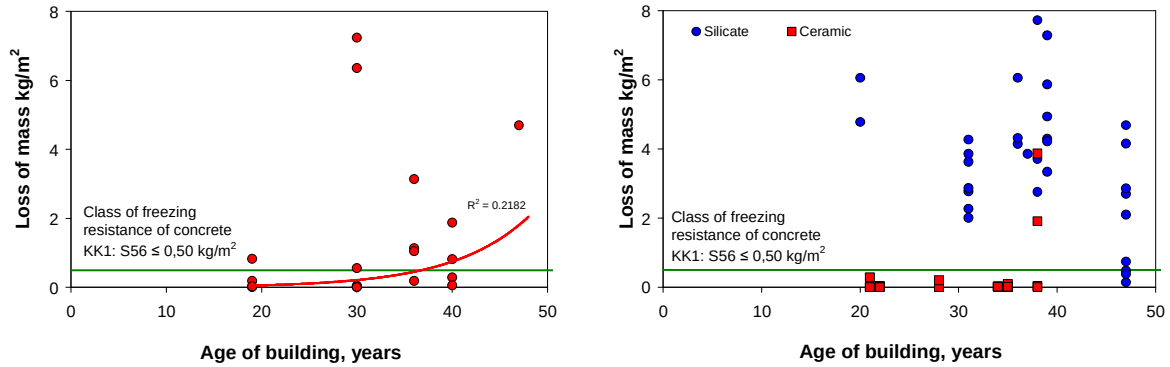

Figure 2. Mass loss of concrete (left) and brick (right). Green line refers to maximum allowed mass loss for a concrete facade 0.5 kg/m^2.

3.2 Compressive strength

As a result of the comparison of compressive strength of all concrete and brick test specimens (Figure 3) for the reference designed value 15 N/mm^2, it is possible to conclude that the compressive strength of concrete or brick is not the limiting factor for loadbearing capacity or stability that were set to it at the time of erection. In all the specimens, compressive strength exceeded the value, $f_{c,cube}$>15 N/mm^2 that characterizes the compressive strength of the concrete mark 150 (corresponds to 15 N/mm^2). Strength of mortar between bricks was variable: in some cases mortar was removed quite simply by handtools and striking drill had to be used in other cases.

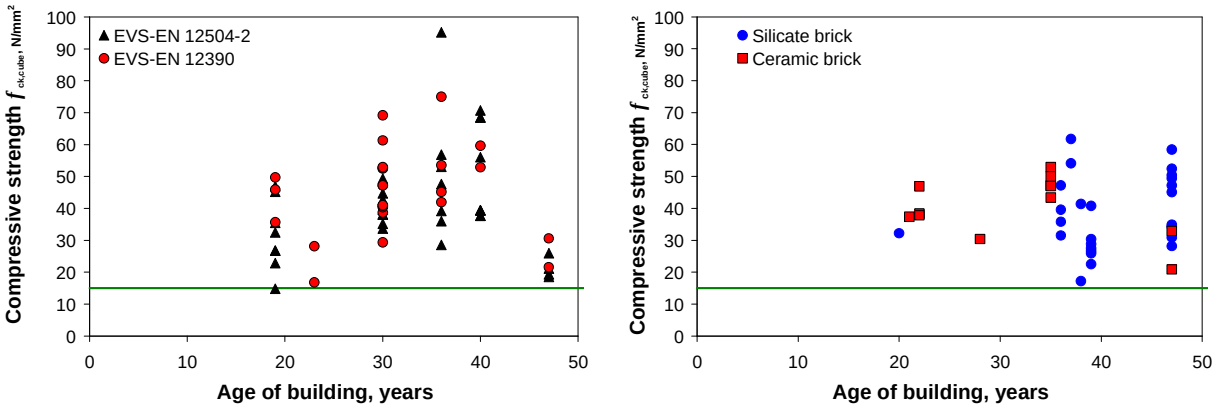

Figure 3. Compressive strength of concrete (left), calcium silicate and bricks ceramic bricks (right).

3.3 Corrosion of steel

Corrosion of concrete large-panels and brick walls was studied via visual survey and with a light microscope (Figure 4). Corrosion of reinforcements of external wall layers of panel concrete in apartment buildings was generally minor. Reinforcement was corroded only when it was very close (≈<2 cm) to the external surface (Figure 4 left). Serious corrosion of reinforcement existed at awning panels and balconies and also in places of concrete wall panels. These structural elements have more severe water loads, therefore small frost resistance has made cracks into concrete and corrosion may develop more easily.

3.4 Carbonation of concrete facades

Carbonation depth of concrete facades was between 0-70 mm, typically 10-40 mm, see Figure 5. left. Comparison of paint finish and rubble bulk finish showed that facades with paint layer had

significantly larger carbonation. The speed of carbonation can be calculated also with the square root function [Pentti *et al*. 1998]:

$x = k \cdot \sqrt{t}$,

where x is carbonation depth, mm; k is carbonation constant (normally 1.5…3.5 mm/$\sqrt{\text{year}}$; t is the age of concrete in years. The distribution of the carbonation constant is presented in Figure 5. right.

Based on the comparison of XRD measurement and phenolphthalein measurement results, it can be concluded that the result of phenolphthalein measurements is not adequate.. It means that though with phenolphthalein no possible carbonation was detected, there existed $CaCO_3$ crystals in concrete.



Figure 4. Corrosion of reinforcement via visual survey (left) and microscope: non-corroded (2nd from left), partly corroded (2nd from right) and fully corroded (right) reinforcement.

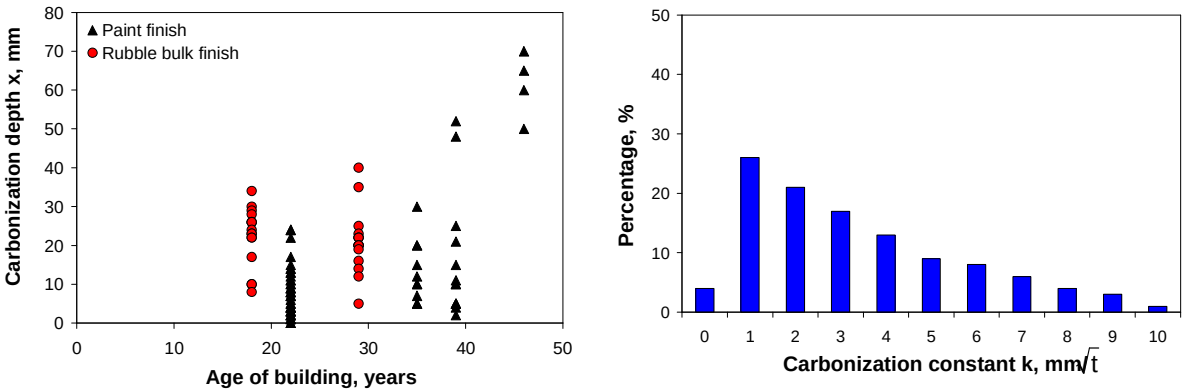

Figure 5. Carbonation depth of concrete of the apartment buildings composed with concrete large panels (left). Carbonation constant to calculate the theoretical carbonation depth (right).

4 DISCUSSION

The main target of the study was to find the condition and durability of concrete and brick facades of apartment buildings built between 1960-90 in Estonia and to collect information for further research.

According to the tests of the frost resistance of concrete and brick facades, the condition of the facades is serious. The results of the evaluations also depend on the criteria and methods of evaluation. In this study different methods were used to evaluate the frost resistance of bricks. Results of the laboratory tests showed the result opposite to that observed in the field survey. According to the tests, ceramic tiles perform much better than concrete or calcium silicate bricks. Visual inspection of buildings can provide the opposite result: facades with old ceramic bricks are in the worst condition in Estonia. There can be many reasons for this difference:

- The horizontal surface of ceramic bricks has much higher capillarity properties as compared to vertical surfaces. In standard test conditions there are no suction possibilities from horizontal surface, but these exist in real facades. Therefore, if ceramic bricks are tested according to the concrete frost resistance standard, test conditions should be modified to be closer to the real condition of bricks in the facade.

- The bricks tested were visually undamaged and it may be assumed that visually undamaged bricks have also better residual frost resistance. Thus, in future studies both visually damaged and undamaged bricks should be tested.
- The capillarity speed and suction properties of brick and concrete are different. Therefore the amount of water sucked during the wetting period in the frost resistance test is different. Larger amounts of water influence the result of the loss of mass. If bricks are tested according to the concrete frost resistance standard, the period of wetting should be shorter for testing the bricks.

Our research has proved that problems exist in choosing the proper method for testing the frost resistance of ceramic bricks in Estonia. In a comparative research, they [Mačiulaitis *et al.* 2004] conclude that the frost resistance of ceramics and concrete depends mostly on density, reserve of porous volume and effective porosity - the higher the density, the reserve of porous volume and the smaller the effective porosity of the porous material, the higher is the exploitation of the frost resistance of ceramic and concrete products. At the same time in common engineering practice it is also necessary to develop quick methods for the estimation of residual frost resistance and the compressive strength of the facade, because thorough tests are not always possible due to high time consumption and expenses.

Since none of the apartment buildings composed with large concrete panels were found to fulfil the criterion for the frost resistance and the tested specimens were visually undamaged, a question was raised if the limit value for the loss of the mass (0.5 kg/m^2) is relevant for testing the facades. Further studies and the comparison of different methods are needed when producing new test standards.

Comparison of compressive strength of all concrete and brick test specimens fulfilled the reference designed value 15 N/mm^2. The compressive strength of mortar influences also the compressive strength of the brick wall. The condition of mortar was evaluated only visually. The compressive strength of mortar should be studied more thoroughly in the future.

There is also a question about measuring accurary of carbonation depth. Theoretically, there is a partly carbonated zone [Thiery *et al.* 2007] which is not detected by phenolphthalein. Light microscope detected elements of $CaCO_3$ were also found in the area not detected by phenolphthalein.

5 CONCLUSION

Overall condition of concrete facades is satisfactory, except the low frost resistance and corrosion of reinforcement when the reinforcement was situated close to the facade. Carbonation depth has reached reinforcement in some cases, but corrosion of reinforcement of the outer core is still minor.

Condition of brick facades is variable. Main problems are related to the low frost resistance of ceramic bricks and bonding of the facade, which tend to be broken in some cases (that occurs more often where inner and outer layers are composed of different types of bricks – silicate and ceramic).

Nevertheless, though the test methods and interpretation of results are somewhat problematic, based on this preliminary study it may be concluded that low frost resistance is the critical property of the facades of apartment buildings built between 1960-90 in Estonia. Depending on the extent of the damage, two basic options for renovation should be considered:

- Facades which have not yet been significantly damaged should be covered. It is economically reasonable to apply additional insulation, as because of high thermal transmittance (U_{walls} ~0.7-1.0 W/m^2K) and rising energy prices it is presently expedient.
- Facades with more severe damages should be renovated first. Loose particles can be removed by blasting sand or water and gaps could be filled up. Several technologies for concrete covering have been worked out - with mineral or organic protective layers and impregnation. Secondly, additional insulation could be installed.

Covering the concrete facade is effective in terms of corrosion – temperature in a previous facade is higher and RH lower, which means a slower corrosion process. Furthermore, carbonation process could slow in covered concrete. For both concrete and brick walls, lower temperature gradient means smaller temperature based deformations. Constant temperature over 0°C avoids freeze-thaw cycles.

ACKNOWLEDGMENTS

The financial support of the Credit and Export Guarantee Fund KredEx and Tallinn University of Technology are gratefully acknowledged.

REFERENCES

Ahmad, S. 2002. Reinforcement corrosion in concrete structures, its monitoring and service life prediction—a review. Cement and Concrete Composites, Volume 25, Issues 4-5, May-July 2003, Pages 459-471.

EVS 814:2003. Frost resistance of normal-weight concrete. Definitions, specifications and test method. Estonian Centre for Standardisation.

EVS-EN 12504-1:2003. Testing concrete in structures - Part 1: Cored specimens - Taking, examining and testing in compression. Estonian Centre for Standardisation.

EVS-EN 772-18:2005 Methods of test for masonry units - Part 18: Determination of freeze-thaw resistance of calcium silicate masonry units. Estonian Centre for Standardisation.

GOST 7025-91. Silica brick and silicate and ceramic stones. Methods of determination of water absorption, density and frost-resistance.

Hagentoft, C.-E. 2010. Importance of a correct overall performance assessment – Probability assessment of performance and cost. “Large scale national implementation plans for building airtightness assessment : a must for 2020! “We should start now to be ready in 2020”. June 14-15 2010 Brussels, Belgium.

Kalamees T; Õiger K; Kõiv T-A, et al. 2009. Technical condition and service life of Estonian apartment buildings, built with prefabricated concrete elements. Tallinn University of Technology (in Estonian).

Kalamees T; Õiger K; Kõiv T-A, et al. 2010. Technical condition and service life of Estonian brick apartment buildings. Tallinn University of Technology (in Estonian).

Mačiulaitis R., Nagrockienė D., Malaiškienė J. Comparative research on exploitation of frost resistance of ceramics and concrete. Journal of Civil Materials Science (Medžiagotyra), Vol. 10, No. 4. 2004, p. 353 – 358.

Pentti, M., Mattila, J., Wahlman, J. Betonijulkisivujen ja parvekkeiden korjaus. Osa 1. Rakenteet, vauriot ja kunnon tutkiminen. Tampereen teknillinen korkeakoulu, talonrakennustekniikka. Julkaisu 87. 1998.

Thiery M., Villain G., Dangla P., Platret G. Investigation of the carbonation front shape on cementitious materials: Effects of the chemical kinetics. Cement and Concrete Research, 2007;37:1047-1058.

XII DBMC
International Conference on Durability of Building Materials and Components
PORTO - PORTUGAL, April 12th-15th, 2011

State of Repair of Marquees on Buildings in Recife, Brazil: Case Study and Quantitative Analysis

João Ribeiro de Carvalho [1]
Thiago de Oliveira Chaves [1]
Eudes de Arimatea Rocha [1]
Antonio Carlos de Albuquerque Melo [2]
Kalline Almeida [2]
Eliana Cristina Barreto Monteiro [3]

ABSTRACT

In Brazil, the practice of undertaking periodical repairs to buildings still unfortunately seems tenuous for owners and the technical sector proper. Since no building was designed or built to last forever, each day more buildings appear with a shorter service life due to lack of maintenance. In this sense, the marquees, isostatic structures in balance, which have little connection with the rest of the structure, become slabs quite vulnerable to the action of pathological expressions, such as corrosion, efflorescence, mildew and damp. To assess the state of repair of the marquees of the buildings in downtown Recife, a visual inspection with photographic report follow-up and later quantitative analysis of the pathological expressions found were proposed. The qualitative conservation of marquees was analyzed in three case studies that were chosen in earlier inspections because of their poor state of repair, their peculiar or representative interventions, and pathologies that would primarily allow easy access for their inspection. This paper is even more relevant when the collected data herein give a general idea of the state of repair of marquees of buildings in downtown Recife, and could be used to repair the degraded marquees, thus preventing accidents.

KEYWORDS

Marquee, Inspection, Pathologies, Repair.

[1] Undergraduate in Civil Engineering – University of Pernambuco, Pernambuco, Brasil, eng.jribeiro@gmail.com; tiago.tc@ig.com.br; eudesdearimatea@gmail.com.
[2] Currently undertaking Master's course in Civil Construction – University of Pernambuco, Pernambuco, Brazil, mouramelo.antonio@gmail.com; kallinealmeida@yahoo.com.br.
[3] PhD Professor in Civil Construction – Department of Civil Engineering at the Catholic University of Pernambuco, Pernambuco, Brazil, nana.monteiro@uol.com.br

1 INTRODUCTION

Reinforced concrete structures not only undergo mechanical but also biological, chemical and physical actions that contribute to the deterioration of concrete and reinforcement over time. It is essential to consider in the design stage all those degradative actions involved during the structure's service life and plan strategies for their preventive maintenance.

One of the methods for analysing the quality of buildings was to undertake qualitative and quantitative studies on the group of degraded marqueemarquees. According to Castro (1994), studies on damage to buildings have been performed in several countries through public or private agencies.

Among the existing structural elements, it was decided to study the state of repair and durability of the marquee, bearing in mind that this structural element is a common feature of buildings in the centre of Recife. Its role is to protect and shelter the population but because of the typical lack of care with maintenance it has a high rate of accidents.

2. INSPECTION METHODOLOGY

There are many techniques involved in the inspection of concrete structures, namely detecting, identifying, assessing, characterising and monitoring the pathologies. These techniques are very valuable for control of the phenomenon, whether in preventive operations or in solving the problem.

According to the parameters mentioned by Clímaco; Nepomuceno (1994), who indicate that the methods recommended for a structural appraisal must be adopted in stages in order that no problem or pathological expression goes unnoticed. The flowchart in 'Fig. 1' shows the routine of an inspection on the concrete structure.

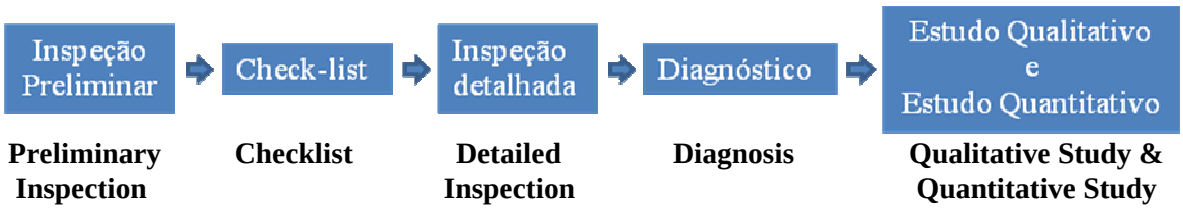

Figure 1. – Activities involved in the inspection routine.

Qualitative studies of the state of repair of the marquees were performed on three (3) different locations, each being a separate case study (investigation); these were chosen from a set of previously maintained marquees because they were in a poor state of repair, and with pathological expressions of interest to the overall study, or peculiar or representative interventions that had been put in place following previously prescribed maintenance actions. The case study of the marquee on Marquês de Olinda Avenue was also performed; this structure had partially collapsed in February, 2009 and this accident had repercussion in the media since it occurred close to the city's carnival centre (Marco Zero do Recife) , and only two days following the end of the yearly festivities.

By adopting a predefined inspection methodology, a survey was carried out along the main streets in the centre of Recife and 121 marquees were inspected to comprise the sample of the quantitative study, and on which was based the state of repair of marquees in Recife. The marquees chosen from the sample space are located in the busiest pedestrian streets, since in those streets there is greater risk to causing an accident of great proportions given the possibility of a structural collapse.

In this research study, the inspection methods were based on those studies carried out by Jordy (2006), given the success achieved from results of inspection of marquees in the city of Rio de

Janeiro. The work of Jordy (2006) offered a inspection methodology typically focusing on the inspection of marquees. Accordingly, some of the main points described in this methodology were adopted, and in which the essential elements for defining the state of repair of the structure were given,, such as: location and description of marquee, geometrical survey, general waterproofing status, status of the drainage system, hazards and, the reinforcement layout.

3 PROGNOSIS AND SOLUTION OF CASE STUDIES

The aim of the study that is described in this paper was to quantify the recurrence of pathological expressions, maintenance and repair interventions completed and acquire any other relevant data in regard to the condition state of the marquees. Such information provided a general idea of their state of repair that was in fact referenced by quite a representative sample size.

The criterion for choosing the structures for analysis was based on: (i) the potential risk that the marquees represented for the population in case of collapse; (ii) accessibility to parts of the marquee; (iii) its environmental zone, and; (iv) the level of pathological expressions that were evident. Four case studies have been carried out where they had construction failures, concrete pathologies and faults referring to earlier repairs.

3.1 Case Study 1 (M1)

The first case study performed was on a marquee located on Bom Jesus Street in the neighbourhood of Recife Antigo, Recife. The marquee, forming part of the first floor slab, is 100 metres long, 1.5 metres wide, with an average thickness of 12.5 cm and is located at a height of 2.80 metres above ground level. This marquee was built about forty-three years earlier and is included in the concrete environmental aggressivity class III (standard NBR 6118 (2007)) and had had no routine maintenance. Consequently various different pathological expressions were evident. For example, these included: dampness (moisture uptake); crumbling of concrete and of the protective coating; longitudinal and transversal cracking; exposed and corroded reinforcement.

For the marquee in question (M1), the side view of which is shown in ‘Fig. 2’, the reinforcement of the support beam can been seen exposed at several points. Shown in ‘Fig 3’ an area of the marquee where exposed reinforcement is evident.



Figure 2. – Side view of M1



Figure 3. – Measuring M1’s rated cover

It is apparent, therefore, that it is advisable to repair marquee M1 as an emergency corrective action, in which the defects evident in respect to waterproofing, drainage and structural repair will be corrected.

3.2 Case Study 2 (M2)

The second marquee investigated (M2) located in the Boa Vista neighbourhood, was supported by beams and was located in a zone of environmental aggressivity of class II. This marquee showed

signs of repair intervention to its' structure but had not undergone any routine preventive maintenance.

On the date of inspection of marquee M2 the following pathologies were evident: dampness; vegetation growth in the top part of the marquee; a break in a portion of the marquee due to the presence of a lamp post; an opening in the slab through which rainwater drainage pipes ran from the roof; and transversal cracking in the slab.

The stains from the dampness of the slab were caused by blocked drainpipes in the marquee, the pipes being used to drain rainwater from the roof. Dampness was also likely caused and by flaws in the waterproofing, mainly in the areas close to the drainage pipe 'Fig. 4'. It was also found that an intervention to place a public lamp post in M2, part of which was demolished with no planning, suppressed existing reinforcement bars and was not reinforced. This caused structural damages to the marquee, giving rise to cracks around the affected area, with crosswise and radial clefts around the demolished area 'Fig. 5'.



Figure 4. – M2 pipes and damp stains



Figure 5. – Cut made in M2 for a lamp post



Figure 6. – Vegetation growing out of M2

Another pathology found when inspecting the marquee was the proliferation of vegetation growth and the growth of fungi; lack of maintenance aggravates such situations. This problem is quite common among marquees in Recife and cities with high rates of relative humidity. As well, the presence of a large number of birds also exacerbates the situation and. Birds, namely pigeons, for example, are responsible for carrying seeds that are dropped onto the slab surfaces, where plants and fungi begin to grow, as shown in 'Fig. 6'.

Proposed recovery of the M2 marquee recommends restoring the structure of the damaged areas, cleaning using a hydrochloric acid (HC1) and water solution to eliminate the microorganisms that feed on the concrete and thereafter coating of the slab, checking the need to reinforce or complement the reinforcement bars that were cut, and repairing the waterproofing and drainage.

3.3 Case study of the partial collapse of the structure of the marquee on Marquês de Olinda Avenue (M4)

The structural stability of a marquee is directly linked to the state of reinforcement corrosion in the stressed regions. Many people believe that the marquee is only designed to protect access to buildings and does not require maintenance. Accordingly, even some engineering professionals do not give due importance to this structural element, not to mention that even within the standard NBR 6118 (2007) the marquee is not give due importance, permitting it to be dimensioned in Stage II, where cracks of 0.02-0.04 mm may occur. If the primary cause of an accident involving marquees is reinforcement corrosion, followed by overload on the structure, design error, incorrect use of the building, failures in execution and water seepage, it is necessary to look not only at one pathology directly affecting the marquee, deteriorating it, but rather the set of those degrading agents that cause it to reach its ultimate service limit state more easily through the presence of cracks. This demonstrates how important it is

to prevent cracking in marquees right from the design stage, dimensioning them in Stage I, where the concrete must not crack, to the execution stage and thereafter, undertaking preventive maintenance.

Two days after the 2009 Carnival celebrations, part of the M4 marquee collapsed, in the Old Recife neighbourhood of the city, an area with large concentration of people at that time. According to the information retrieved following an investigation of the collapse, it was found that the building was derelict and had had no routine maintenance whatsoever. Although there was no physical damage, the collapse of this marquee represented an extremely dangerous situation for the local shopkeepers and passersby who work in this region, and also demonstrates the neglect of the owner and relevant authorities with regard to the state of repair of the city's historic buildings. From historical and architectural data collected from the Institute of National Historic and Artistic Heritage (IPHAN) it was found that the building had been built in the 1930s, and its architecture modified long after its construction to include the existing marquee. See 'Figs. 7 and 8'.



Figure 7. – Total collapse of part of the M4 marquee.



Figure 8. – Part of the M4 marquee that collapsed.

Also in the preliminary assessment stage several pathological expressions were discovered, some of which are worth mentioning, for example: longitudinal cracks in the slabs and consoles with corrosion of the reinforcement; loss of a section of reinforcement due to corrosion and later bending of the steel; broken reinforcement bars; generalised seepage along the entire marquee slab; presence of sludge and vegetation in the slabs and consoles.

A console with a missing section in the lower reinforcement, including the stirrups, is shown in 'Fig 9'. The slabs show signs of dampness and fungi growth that resulted from no waterproofing in these areas. It was found that the rainwater from the roof of the adjacent building falls onto the marquee from a height of around nine metres. The impact caused by this falling water was sufficient to break up the mechanical protective layer of the waterproofing and damaged it. Thus seepage onto the marquee occurred through the deteriorated waterproofing causing water to reach the consoles that also eventually collapsed with part of the structure 'Fig 10'.



Figure 9. – Rusty reinforcement, cracked slabs & seepage.

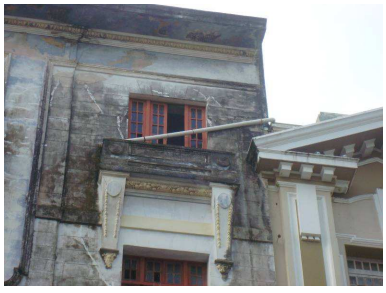

Figure 10. – Rainwater drainpipes over M4.

4. DISCUSSION OF RESULTS

4.1 Quantitative analysis of pathologies

With a sample of 121 marquees for the study, it was possible from graphs to quantify the primary pathological expressions found through the investigation. The information provided in Table 1 shows the incidence of the pathologies in the marquees, namely, it provides the percentage of marquees that have a certain pathology. It was found that only 7% of the marquees studied did not have pathological expressions.

It can be seen from [Table 1] that the most active pathology in the marquees is dampness, followed by peeling of the coating and paintwork (69%) and mould, mildew and slime (64%). It is found that these pathologies are related to each other and caused by the presence of dampness, therefore showing that from a single pathological expression several other pathologies can develop.

Another quite common pathological problem found in 56% of the marquees analysed is the growth of plants that, due to the accumulation of water in their roots, causes further dampness and brings about other pathologies. The breakdown in the concrete (spalling) was found in 41% of the marquees studied. This pathology is the result of the expansion of oxidised steel, and it is quite common in old buildings, since there used to be a practice of using clay materials and others such as agglomerates in the production of concrete, a fact that reduces the concrete's strength, increases the number of voids to make the concrete more porous, with a higher degree of absorption and with low adhesion to the reinforcement. Such concrete is therefore prone to corrosion of the reinforcement and the subsequent loosening of the concrete cover.

Table 1. - Percentage of pathological manifestations.

Pathological Expressions	Percentage
Dampness	77%
Peeling of coating	69%
Mould, mildew and slime	64%
Vegetation growth	56%
Broken (spalled) concrete	41%
Cracks	33%
Corrosion	17%
Efflorescence	11%
Leaching	9%
Chinks	2%

There were also a large number of cracks, approximately 33%. There are cracks accepted by standards, due to deformation, heat dilation, execution and others from various pathologies, thus causing such a high percentage. However, what is unusual is the lack of technical monitoring and no maintenance, so that these cracks now become agents for other pathologies. It should be stressed that a large number of these cracks were caused by undue interventions to the structure by the owners, a sign of poor use of the marquee. Many cracks were found next to the shop signs, regions of contact between marquee, cuts and openings made in the slab, and other interventions that were responsible for the formation of cracks.

[Table 1] also shows that corrosion of reinforcement was found in only 17% of the inspected marquees, but it is important to emphasise that the statistical figure of this type of pathological expression refers to exposed corrosion. Only visual inspections were undertaken to determine the

pathologies and in some cases the diagnosis was based on evidence such as, for example, reddish stains and cracks in the direction of the reinforcement, as has been discussed by Helene (1992).

Efflorescence and leaching were found in 11% and 9% respectively of the marquees in downtown Recife. These pathologies appear together, since both occur by the dissolving of calcium hydroxide in the cement paste due to water penetrating the concrete pores. It is believed that the percentages of these pathologies must be higher than those indicated by the study, since even a slight change to the coating of the marquee would conceal the symptoms of the pathology and hinder its identification.

Chinks are broader cracks that are indicative of a high degree of deterioration of the structure. These pathological expressions were the lowest rate of observance of marquees (2% of the structures studied). Although they represent a small percentage compared to the other pathologies the presence of these chinks are a clear sign that the marquee may collapse should no immediate intervention occur.

4.2 Quantitative analysis of exposed reinforcement and existing routine maintenance

A survey was made of the quantity of marquees found with exposed reinforcement that contributes therefore to accelerating the reinforcement corrosion process and consequent structural instability.

For these marquees it was possible to measure the actual coating of these reinforced concrete parts, and it was therefore possible to compare the actual coating with the coating determined by standard NBR 6118 (2007). The rated coating of 2.5 cm and 3.5 cm was taken into account for the marquees located in the Environmental Aggressivity II and III classes, respectively. Therefore, the coating of 73% of the marquees with exposed reinforcement is less than the prevailing standard's requirement, which was to be expected, considering that they were dimensioned under past regulations.

Since one of the objectives of the study was to analyse the conservation of the marquee structures in downtown Recife, those with routine maintenance were also quantified, since the preventive maintenance is an essential step towards conservation and prolonging the durability of the structures.

It was found that 76% of the marquees analysed did not have routine preventive maintenance, which was corroborated by the need to take steps to undertake inspections to check that periodical maintenance services are being done, in order therefore to reduce further occurrences of collapse.

4.3 Quantitative analysis of the interventions in marquee structures

Very often the pathologies are caused by the aggressivity of the environment, but many pathologies appear or are intensified because of interventions made without the guidance of a skilled professional, very often aggravating the existing pathologies. According to this research, it was found that 80% of the sample marquees in this study underwent some form of unsuitable intervention.

When looking at [Table 2], the data worth pointing out are the overload percentages: caused by shop signs (50%); air conditioners (14%); and garbage (11%). These overloads can cause marquees to crack, considering the overload that they carry. In addition to cracks, presence of air conditioners or garbage on the marquees, there is the aggravation of water constantly dripping onto the structure and its retention due to blocked drains or no drainage at all.

[Table 2] shows that 14% of the marquees under study had their slab perforated close to the fitting, after completion, to place pipes for draining the rainwater from the roof, and in 11% of the marquees their slab was cut to install a lamp post for the electricity network. It was found that 5% of the sample marquees in this study are coated with PVC lining and facings. This was the most economic solution found by some owners to improve the aesthetics of their shops, and thus hiding the flaws in the state

of repair of the marquees. This is a very dangerous solution, since it not only hinders visual inspection of the structure but also very often prevents the inspector's access and may induce some less experienced inspectors to give a wrong diagnosis.

Table 2. - Percentage of interventions on marquees.

Most common interventions	Percentage
Overload caused by a shop sign	50%
Overloads caused by air conditioners	14%
Hole in the slab close to the fitting for placing drainage pipes	14%
Overload caused by ceramic tile border	11%
Overload caused by garbage	11%
Cut into the slab to install a lamp post	11%
Structure supported on adjacent marquee	5%
Structure supported on neighbouring marquee	5%
PVC coating	5%

5 FINAL CONSIDERATIONS

It is found that it is necessary to be aware of the importance of preventive maintenance on marquee structures, principally in historic buildings, due to the quality of the materials used, mainly those found in the regions where the environmental aggressivity is greater than II since, in addition to the quality of the material deployed and aggressivity of the environment, there is a lack of necessary coating for the reinforcement, and having a maintenance plan would increase its service life.

It is imperative to increase inspection for this type of structure, to warn the owners of the buildings of their liability, and make it mandatory to have periodical maintenance and compliance with the regulations on the use and conservation of the buildings.

REFERENCES

ABNT – Associação Brasileira de Normas Técnicas. NBR 6118/2003: Projeto de Estruturas de Concreto. Rio de Janeiro, 2003.

E. K. Castro, Desenvolvimento de metodologia para manutenção de estruturas de concreto armado. Master's dissertation, University of Brasilia, Brasilia, 185p, December 1994.

J.C.T.S. Clímaco, A.A., Nepomuceno, Parâmetros para uma metodologia de manutenção de estruturas de concreto. 36th Annual Meeting of IBRACON – Instituto Brasileiro do Concreto, Vol. 1, pp 109-119, Porto Alegre, September 1994.

Jordy, J.C. & Mendes, L.C. Análise e procedimentos construtivos de estruturas de marquises com propostas de recuperação estrutural. PhD dissertation, Federal Fluminense University, Rio de Janeiro. 2006.

Helene, Paulo R. L. Manual para reparo, reforço e proteção de estruturas de concreto. 2nd edition. São Paulo: Pini, 1992.

XII DBMC
International Conference on Durability of Building Materials and Components
PORTO - PORTUGAL, April 12th-15th, 2011

Service Life Estimation of Facades - Use of the Factor Method in Practice

Christian André Listerud [1]
Svein Bjørberg [2]
Per Jostein Hovde [3]

ABSTRACT

In the past years there has been an increasing focus on service life and sustainability in the building sector. This has led to the publication of a range of new international standards and guidelines. ISO 15686 is a standard which purpose is to describe a uniform method for service life planning. One of the key inputs of the method described is the estimated service life. Part 8 of the standard suggests a method for estimation of service life using the factor method. The purpose of this paper is to show examples on how to use the factor method in practice.

The method is tested through a case study comprising service life estimation of a building element. The tools presented here are mainly based on ISO 15686 Part 8 and other standards that deal with service life and degradation environment. The work has shown that there is a need for well documented reference service life data for use in the factor method. Such data is scarcely available today. In order to estimate the value of factors such as outdoor environment, there is need for methods for classification of degradation environment for various materials. Through the research communities various tools have been suggested to carry out calculations by using the factor method. Common for many of the tools presented is that they are regarded as complicated for practical use. In order to use the factor method in practical matters there is need for an uncomplicated usability of tools that also takes the uncertainty of the calculation into consideration.

KEYWORDS

ISO 15686, Factor method, Service life planning, Service life estimation.

[1]MULTICONSULT, Oslo, NORWAY, cl@multiconsult.no
[2] MULTICONSULT, Oslo, NORWAY, sb@multiconsult.no
[3] Norwegian University of Science and Technology, Trondheim, NORWAY, per.hovde@ntnu.no

1 INTRODUCTION

In the last decade, there has been an increasing focus on sustainable development, both economically, socially and environmentally. It has been stated that the building and construction sector is of outmost importance for such a development [CIB, 1999]. Service life of buildings and components is an important issue in evaluation of sustainability, and there is a need for service life planning. Such a planning process aims to ensure that the actual service life is equal to or greater than the design life, while the total economy is taken into account. Methods and procedures for sustainability and service life have been developed, and ISO 15686 Service life planning is such a standard. The standard now comprises 9 parts, and two alternative procedures for determination of service life are presented in Part 2 (service life prediction) and Part 8 (service life estimation), respectively. However, there is still a great lack of practical experience and case studies from application of the standard, and of input data for calculation of service life of different materials and components.

2 METHOD

The method for service life estimation was first presented in ISO 15686 Part 1 [ISO, 2000], and is later described in Part 8 [ISO, 2008]. The method is called the factor method, and the estimated service life (t_{ESL}) is calculated by an equation comprising a reference service life (t_{RSL}) and 7 factors representing various conditions that influence on the service life. The equation is written as

$$t_{ESL} = t_{RSL} \times \Phi_A \times \Phi_B \times \Phi_C \times \Phi_D \times \Phi_E \times \Phi_F \times \Phi_G \qquad (1)$$

and the factors are: Φ_A: inherent performance level; Φ_B: design level; Φ_C: work execution level; Φ_D: indoor environment; Φ_E: outdoor environment; Φ_F: usage conditions; Φ_G: maintenance level. This paper aims to demonstrate use of the factor method through a practical example.

3 PREVIOUS STUDIES

The factor method is based on a Japanese method that was developed at the beginning of 1990s [Architectural Institute of Japan, 1993]. There are currently very few examples of using the factor method in actual construction projects. After the Japanese work was published in 1993 there have been a number of studies where the method has been discussed [Hovde, 2004], [Moser, 2004], [Marteinsson, 2005]. The main issues that have been discussed are: The method is too simple and unreliable; the factors are difficult to determine and the result therefore will be uncertain; and the method is deterministic. The reason that deterministic methods have been criticized is that there is a general agreement that degradation is a stochastic process. The factor method is basically a deterministic method, but both part 1 and 8 of the standard emphasize that the factors may consist of a single number or a distribution. [Marteinsson, 2005] criticized the method because it assumes that factors are independent variables. Results from condition surveys showed that the factors are not always independent. In that case, the maintenance level depended on the degradation environment.

4 CASE STUDY

4.1 Building and degradation environment

This paper is based on a Master thesis from the Norwegian University of Science and Technology in 2009 [Listerud, 2009]. The case selected for this study was the new theatre and concert house located on an island just outside the city of Kristiansand, Norway. The building will, when finished, have a gross area of about 15 000 square meters and will have room for almost 2200 visitors. The project is planned due in late 2011.

The building is located near the sea and will therefore be exposed to high humidity. Weather data are available from two official weather stations that are located within a radius of 10 km from the building site. The climate can be classified as maritime with high concentration of chlorides in lashing rain, windy and a relatively high temperature. The amount of lashing rain towards the actual wall is very high. The wall facing the sea will have stained oak heartwood as cladding. The other facades will be covered with enamelled aluminium sheets.

Table 1 shows the levels of a range of different climate and environmental factors. The factors selected are considered to have an effect on the degradation of wooden materials and surface finishing. Each of the factors is classified with a value between 1 and 5 as suggested in Part 7 of the ISO 15686 standard. The value 1 means that the conditions are better than the reference conditions and 5 means that the conditions are worse. The reference conditions are the conditions that are related to the reference service life.

Table 1: Climate and environmental factors in the area. [Listerud, 2009]

	Concentration	*Classification*
SO_2	<5 µg/m³	3 Normal
NO_2	>50 µg/m³	4 High
PM_{10}	20-40 µg/m³	4 High
O_3	60-80 µg/m³	4 High
Salt content in rain water	5,71 mg/l 22 mg/m²/day	5 Very high
pH-rain water	<4,8	5 Very low
Rh	76 %	3 Normal
Average temperature	7,0 °C	4 Above normal
Precipitation	1380mm	4 Above normal
Lashing rain	500mm	5 Very high
Sun radiation (horizontal surface)	108 W/m²*hour (3,4 GJ/m²*year)	3 Normal
Scheffer's Climatic Risk Index	50	3 Normal
Frost decay index	650	4 High

The effects of SO_2, NO_2 and O_3 are mainly related to degradation of the surface finishing. High levels of these are usually found in areas with heavy traffic.

Particles (PM_{10}) may have an effect on both the surface finishing as well as the material beneath. Particles often contain substances that accelerate degradation of the surface finishing. Further, the particles have a tendency of being very hygroscopic and absorb water at a relative humidity as low as 50 to 65 %. This leads to extended time of wetness (TOW) of the material surface and a reduction of the service life. Salts possess many of the same characteristics as particles. In addition they have a strong corrosive effect on metals.

Frost decay index is a measure of the relative potential of frost decay of porous materials. Degradation as a consequence of frost depends on the amount of water absorbed by the material. The index is set by summing the accumulated 4-day precipitation in advance of days with temperature below the freezing point of water.

4.2 Identifying degradation factors

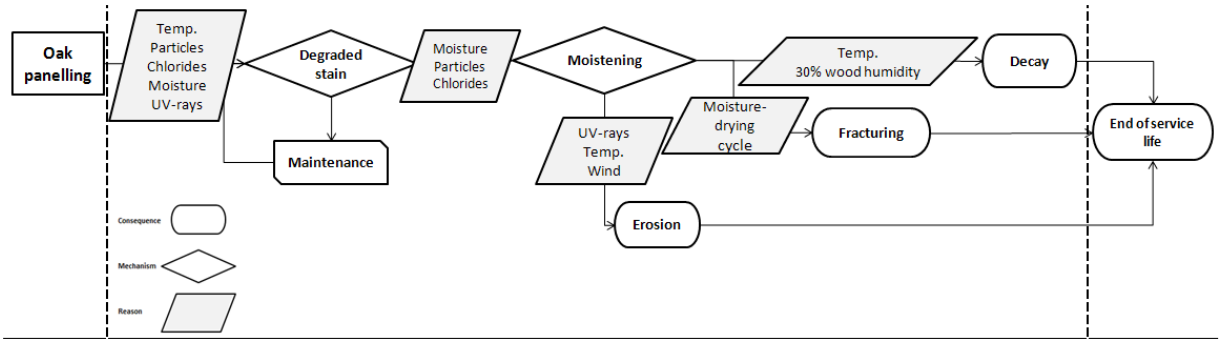

Figure 1: Relevant degradation factors and their effect. [Listerud, 2009]

Figure 1 shows the relevant degradation factors and the effects of these. It is assumed that the degradation of the surface finishing will have to be considerable before further degradation will occur. The degradation of the stain depends on the temperature, moisture, UV-radiation, chlorides and particles. Maintenance of the wall is planned to be carried out all at the same time, and once every four years. Experience shows that stain has a service life between 1 and 6 years, with an average of 4 years, in Norwegian climate. In the areas of the wall that will be most heavily exposed to the environment the service life of the stain will be shorter than the maintenance intervals. These parts will probably be left raw years before maintenance is carried out. The most exposed areas are expected to be located along the edges, and in the upper parts of the wall. The three main potential degradation mechanisms are decay, fracturing and erosion. Erosion is normally a very slow process in wood, only 6mm every hundred years. For harder types of wood, such as oak, the erosion will be even slower. If the temperature and wood humidity is sufficient there will be a risk of wood decay evolving. Studies has shown that the wood humidity in heartwood of pine rarely exceeds 20 percent and never exceeds 30 percent. Heartwood of oak is classified as more durable than heartwood of pine according to EN 460. For wood decay to evolve the wood humidity must be at least 28 percent over a long period of time and the temperature must stay between 5°C and 40°C. Scheffer's climatic risk index has a value of about 50 in the area where the building will be located. This is considered as medium risk of decay for wood materials.

A consequence of frequent wet / dry cycles is fracturing or warping of the wood. Studies have shown that high density wood have a tendency to shrink and swell more than low density wood. Oak is a high density wood and therefore fracturing and warping is more likely to occur than with other types of wood used for cladding. Taking the available information into account the most important degradation mechanisms are considered to be fracturing/warping and probably wood decay in some areas.

4.3 Reference service life

In ISO 15686 Part 1 the reference service life is defined as the service life that a building or parts of a building is predicted to have in a certain set of in-use conditions. Service life data are rarely presented with information about in- use conditions. Today the available records of service life are often based on unstructured data records taken from experience.

Oak heartwood is rarely used for building materials, both today and in the past. Therefore there are few sources for reference service life available. Three old sources have been found (1949) (1951) (1963). The three sources state that raw heartwood from oak has an average expected service life of about 80 years. The first two also state that the expected service life has a variation between 50 and 120 years. These sources do not contain any information about the in-use conditions. Thus, it has been necessary to make an assumption about the in- use conditions corresponding to the reference service life. Further it has been assumed that the in-use conditions reflect the normal/average climate in Norway and the low and high factors respectively reflect better or worse climate.

4.4 Determining the factor values

ISO 15686 Part 8 does not contain guidance on how to determine the factor values. The basis for determining the factor values here is the span in reference service life given in section 4.3.

Table 2: The factor values corresponding to the span in reference service life. [Listerud, 2009]

Factor	*Low*	*Average*	*High*
Reference service life	50	80	120
A- Inherent performance level	0,9	1,0	1,1
B- Design level	0,9	1,0	1,1
C- Work execution level			
D- Indoor environment	-	-	-
E- Outdoor environment	0,77	1,0	1,24
F- Usage conditions	-	-	-
Product of factors	**0,624**	**1,0**	**1,5**
G- Maintenance level	1,0	-	1,5
Total product of factors	**0,624**	-	**2,25**

Table 2 shows information divided into low, average and high factor values corresponding to the span in the given reference service life. If assumed that the service life rarely exceeds 120 years, or is less than 50 years, the low service life has a total factor value of 0,62 (50/80) and the high has a total factor value of 1,5 (120/80). The reference service life applies to raw heartwood of oak. In this case the oak boards will be protected by surface finishing and maintenance will be conducted every four years. It is assumed that the longest service life (120 years) represents the expected service life in a climate with low humidity, and with good design and work execution. The purpose of the surface finishing is to prevent water from being absorbed into the material beneath. Therefore it is reasonable to assume that the surface finishing will have much of the same effects as placing raw wood in a dry climate if maintained sufficiently. On that basis, it is assumed that the average service life can be extended up to 120 years at the most, which corresponds to a factor of 1.5

4.5 Estimate service life using the factor method

Three methods for calculation of estimated service life are considered in this paper. These are multiplication level, Monte Carlo simulation and a simplification using the beta distribution.

4.5.1 Multiplication level

As a quality assurance of both detailing and material a model of the wooden facade has been built in Kristiansand. Such quality assurance will most likely result in a design level that is better than the reference conditions. The factor value has been set to 1.05 to take this into account. The inherent performance level will vary, but because of the quality assurance the factor value is not likely to be below the reference performance level. Therefore the factor value is set to 1.00 in this case. The quality of execution is a factor that is difficult to assess, since the wall not yet has been built. In this case it is assumed that possible building/component failure will be corrected before the building is handed over to the building owner. Therefore the factor value for work execution is set to 1.00.

In section 4.1 the relevant degradation mechanisms in this case are discussed. Moisture is the factor that influences the degradation the most. The amount of driving rain is usually high, up to 500mm per year. Particles and chlorides will also bind moisture to the surface. Acid rain will increase the decomposition rate. Because of the structure's inward sloping design, not all parts of the facade achieve the same high moisture levels. The classification of the main degradation factors from Table 1 indicates that the overall conditions are poor and the factor value is therefore set to 0.85.

Maintenance will have a positive effect on service life. As mentioned in section 4.4, it is assumed that the effect of maintenance can increase the service life with a factor of 1.5. In this case maintenance is planned to be done every four years. The service life of stain varies between 1 and 6 years, with an average of 4 years, as mentioned in section 4.2. The dominant degradation factors for stains are

temperature, moisture, UV radiation, chlorides and particulates in the air. The levels of these substances in the area indicate that the service life of the paint will be lower than the average service life. Depending on the area of the facade, it is reasonable to assume that the surface treatments service life will be between 2 and 4 years. This indicates that parts of the facade will not be optimally protected by the surface treatment between the maintenance intervals. The factor value is set to 1.30.

Table 3: The factor values used for calculation of estimated service life. [Listerud, 2009]

Factor	*Description*	*Factor value used*
A- Inherent performance level	Normal	1,00
B- Design level	Better than the reference conditions due to planning and quality assurance	1,05
C- Work execution level	Normal	1,00
E- Outdoor environment	Worse than the reference conditions. Large amounts of driving rain, high salt content in the air, particles in the air and acid rain.	0,85
G- Maintenance level	Better than the reference conditions. Surface treatment every four years.	1,30

The estimated service life is calculated to about 93 years when using the factor values from table 3.

4.5.2 Monte Carlo simulation

Estimation of service life by means of probability distributions is often done by simulation methods. In both Annex D in Part 8 of the standard [ISO, 2008] and in the examples from, among others [Moser, 1999] and [Moser, et al., 2002] Monte Carlo simulation is used to estimate service life. By using probability distributions to describe the different factors it may be possible to get a better picture of the overall uncertainty in the calculations. Material properties are often assumed to follow a normal distribution. The inherent performance level in this case is therefore described by a normal distribution, with a mean value of 1.00 and standard deviation of 0.025. The other factors in this case are described by the Pert distribution. The Pert distribution is similar to a triangle distribution where the extremes are taken less into account. The Pert distribution is today often used in context with risk analysis where the actual form of the distribution is unknown. Table 4 shows the data that is used in further calculations. The span expresses the uncertainty of the factor values chosen in section 4.5.1.

Table 4: The distributions and factor values used for calculation of estimated service life.

Factor	*Distribution*	*Min*	*Mean*	*Max*
A	Normal	0.93	1.00	1.06
B	Pert	0.98	1.00	1.05
E	Pert	0.80	0.85	1.00
G	Pert	1.10	1.30	1.40

Figure 2 shows part of the results of the service life estimation using a Monte Carlo simulation doing 30 000 iterations. The average service life is estimated to 89 years with a standard deviation of 6 years.

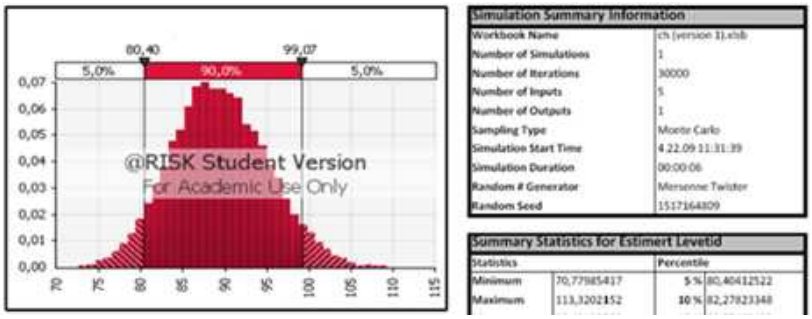

Figure 2: Result from a Monte Carlo simulation doing 30 000 iterations. [Listerud, 2009]

4.5.3 Other methods for calculation

In this case an alternative calculation method has been developed. The method is based on the beta distribution. The beta distribution can be described as a very flexible distribution, and is therefore often able to describe the appropriate probability density. The problem with the beta distribution is its complex functions describing the shape. Therefore a simplification of the original functions has been performed by using parts of the functions used in the Pert distribution. In addition there has been introduced a factor γ to control the standard deviation. A low value of the γ factor will make the shape of the distribution almost like a uniform distribution.

$$E(x) = \frac{A + (\gamma \times B) + C}{\gamma + 2} \qquad (2) \qquad\qquad \sigma = \frac{C - A}{\gamma + 2} \qquad (3)$$

The letters A, B and C in formula 2 and 3 correspond to the lowest, most likely and highest factor value assumed. This is a simple way of describing the uncertainty considering the factor values. Figure 3 shows an example of the workbook used in this case. The results of the service life estimation when using the same values as the Monte Carlo simulation is 89 years, with a standard deviation of 6 years. This result is equivalent to the result of the Monte Carlo simulation, and shows that the simplified method can be of value in calculations using the factor method.

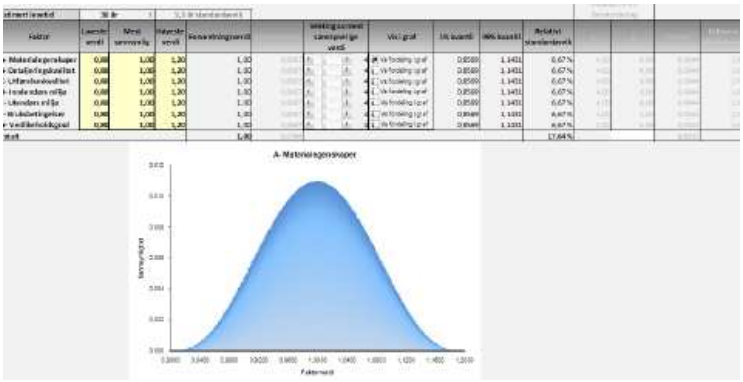

Figure 3: Screenshot from the excel sheet developed here. [Listerud, 2009]

5 DISCUSSION

Several parts of ISO 15686 are based on the estimated service life. Practical use of the standard as a whole therefore requires available reference service life data and calculation methods that are simple and reliable.

Today, well-documented service life data is difficult to obtain. In Norway it is primarily SINTEF who has registered and published service life data from practice. These data are not documented well enough for use as an input to the factor method. Many manufacturers possess much information about their own products. Some even carry out field exposure tests. Information from such tests can be of great help when estimating service life using the factor method. One problem is that the manufacturers rarely make results of such tests available to the public.
Climate and environmental factors can often be quantified, and based on that the factor value can be estimated. Factors such as the in use conditions, maintenance, the extent and quality of execution can be specified qualitatively. It is necessary to define what might be described as good or poor quality of these factors. The work execution level should be separated between poor quality and building faults. Building faults will often shorten the life considerably. Factors that in most cases only can be indicated qualitatively represent severe uncertainty. To take the uncertainty into account it may be advantageous to set these factors by using probability distributions.

Today information on how factor values can be estimated in practice is scarcely available. If one has quantitative data on experienced service life it will be possible to estimate the factors from the relative

difference between them. This requires that one has an idea of how much each factor affects the degradation of the material.

Three methods for calculation of estimated service life are considered in this paper, multiplication level, Monte Carlo simulation and a simplification using the beta distribution. Important aspects considering calculation methods are that the method should be reliable, easy and quick in use. The multiplication level is both easy and quick in use, but is not considered to be reliable because the factors are set using deterministic values. Monte Carlo simulation and the simplified method presented here are using probability distribution describing the factor values. The uncertainty is therefore taken into account. The entry level using Monte Carlo simulation is high. One needs both knowledge of statistics and a dedicated computer program. The simplified method presented in section 4.5.3 has a simpler approach than Monte Carlo simulation but is still taking uncertainty into account.

6 CONCLUSIONS

- Without well documented service life data the standard cannot be used with the result as intended originally. Today well documented service life data is scarcely available.
- In order to estimate the value of factors such as outdoor environment, there is need for methods for classification of degradation environment for various materials.
- There is a need for simple methods of using the factor method from ISO 15686-8 in a manner that brings the uncertainty into the calculations. In this paper, there has been shown that analytical approaches can be a good alternative to more advanced simulation methods.

7 REFERENCES

Hovde, 2004. Hovde, P. J.: Performance based methods for service life prediction. Part A Factor methods for service life prediction. CIB Report: Publication 294. CIB, Rotterdam, The Netherlands, 2004. ISBN: 90-6363-040-9.

Moser, 2004. Moser, K.: Performance based methods for service life prediction. Part B Engineering design methods for service life prediction. CIB Report: Publication 294. CIB, Rotterdam, The Netherlands, 2004. ISBN: 90-6363-040-9.

Marteinsson, 2005. Marteinsson, B.: Service life estimation in the design of buildings. A development of the factor method. Doctoral thesis in Building Materials Technology, KTH Research School – HiG, Gävle, Sweden, 2005.

CIB. 1999. Agenda 21 on sustainable construction. Rotterdam : CIB, 1999. ISBN 90-6363-015-8.

Architectural Institute of Japan. 1993. The English edition of Principal Guide for service life planning of buildings. s.l. : Architectural Institute of Japan, 1993.

ISO. 2000. ISO 15686-1. Buildings and constructed assets- Service life planning- Part 1: General principles. Geneve : s.n., 2000.

ISO. 2008. ISO 15686-8. Buildings and constructed assets- Service life planning- Part 8: Reference service life and service-life estimation. Geneve : s.n., 2008.

Listerud, 2009. Listerud, Christian André: Service life and life cycle costs for buildings. Master thesis, Norwegian University of Science and Technology, Trondheim, Norway, 2009.

XII DBMC
International Conference on Durability of Building Materials and Components
PORTO - PORTUGAL, April 12th-15th, 2011

Epistemic Uncertainty Propagation in Service Life Prediction Using the Factor Method

Fulvio Re Cecconi [1]

ABSTRACT

Factor method is probably the best known method for service life prediction of building components and since its introduction in ISO standard there has being disputes over its accuracy, i.e. over the error in the estimated service life due to uncertainty in the way mechanisms of degradation are taken into account by the modification factors. In fact, under the surface of its usability, factor method hides a great sensitivity to errors in input factors that can lead unaware users to large errors in the estimated service life. Many authors have proposed methods that deal with this sensitivity in different ways, for example using probability distribution function instead of numeric value for the seven factors or using grid that, driving the user thru a specific path for assessing each factor, minimize the probability of error by the user. The first approach, so far one of the few "engineering methods" for service life prediction known, may lead to unexpected results if used without attention to the assumption made when selecting distribution functions. This paper shows how to deal with uncertainty propagation in the factor method especially when the uncertainty is "epistemic", i.e. due to a lack of knowledge, and not aleatory, i.e. arising due to randomness, and it does so using a method based on the possibility theory, first introduced by prof. L. Zadehin 1978 as an extension of his theory of fuzzy sets and fuzzy logic. A case study shows a comparison between results obtained using the evolved factor method and the ones obtained using the evidence theory to highlight how much an estimated service life computed with the engineering method could be wrong.

KEYWORDS

Factor method, Service life prediction, Epistemic error, Uncertanity propagation.

[1] Department of Building Environment Science and Technology (BEST) of Politecnico di Milano , Milano, Italy, fulvio.rececconi@polimi.it

1 INTRODUCTION

"The objective of service-life planning is to ensure that the actual service life of a building or other constructed asset will equal or exceed its design life" [ISO 15686-9] and this is done ensuring that each building components either has a service life longer then the design life of the building or it is possible to maintain (or replace) it. Given this need for service life values, the best known method for estimating the service life of building components (and the only one presented in a standard) is most probably the Factor Method (FM), based on a similar method published in Japan some decades ago [Architectural Institute 1993].
Since the introduction of the method in ISO standard back in 2001 there has being disputes over its accuracy, i.e. over the error in the estimated service life due to uncertainty in the way mechanisms of degradation are taken into account by the modification factors. In fact, under the surface of its usability, FM hides a great sensitivity to errors in input factors that can lead unaware users to large errors in the estimated service life (ESL), an example of how big this sensitivity is can be found in Table 1, where changhing by 10% every factor lead to a prediction that differs from -52% up to almost 95%.

Table 1. An example of the sensitivity of FM to errors in input. An amount of ±10% variation in input lead to a -52% + 94% variation in the ESL.

ESL		RSL	A	B	C	D	E	F	G
11.95	-52.17%	25	0.9	0.9	0.9	0.9	0.9	0.9	0.9
25	0.00%	25	1	1	1	1	1	1	1
48.71	94.87%	25	1.1	1.1	1.1	1.1	1.1	1.1	1.1

Many authors have proposed methods that deal with the problem of accuracy in different ways, for example using probability distribution function instead of numeric value for the seven factors [Moser 1999 or Re Cecconi 2004] or using guidelines in form of tables [Hovde 2005] or grids [Re Cecconi 2005] that, driving the user thru a specific path for assessing each factor, minimize the probability of error by the user. The first approach, so far one of the few "engineering methods" for service life prediction known, may lead to unexpected results if used without attention to the assumption (maybe unconsciously) made when selecting distribution functions. In these evolved FM a distribution function is used to rappresent the uncertanity about the way to describe the influence of the indoor/outdoor climate, of the quality of materials/work etc. In risk analisys uncertainty is typically considered of two different types: randomness due to inherent variability in the system behavior and imprecision due to lack of knowledge and information on the system. The former type of uncertainty is often referred to as objective, aleatory, stochastic whereas the latter is often referred to as subjective, epistemic state of knowledge [Apostolakis, 1990] often referred as partial ignorance. In current service life estimation practice [Moser 1999] both types of uncertainties are represented by means of probability distributions and and the uncertainty propagation is often carried out by a Monte Carlo simulation. In case of partial ignorance, the use of a single probability measure introduces information that is in fact not available. This may seriously bias the outcome of service life estimation in a non-conservative manner. In fact, while it is commonly accepted that the aleatory uncertainty is appropriately represented by probability distributions, there has been some scientific disputes about the potential limitations associated to a probabilistic representation of epistemic uncertainty under limited information. In this respect, a number of alternative representation frameworks have emerged, e.g. fuzzy set theory [Klir 1995], evidence theory [Shafer 1976], possibility theory [Dubois, 1988], and others.

This paper shows how to deal with uncertainty propagation in the Factor Method especially when the uncertainty is "epistemic", i.e. due to a lack of knowledge, and not aleatory, i.e. arising due to randomness, and it does so using a method based on the possibility theory, first introduced by prof. L. Zadehin 1978 as an extension of his theory of fuzzy sets and fuzzy logic. Possibility theory is similar to probability theory in that it is based on set functions but differs in that it relies on two cumulative functions, called possibility and necessity measures 'Fig. 1 (d)', instead of only one 'Fig. 1 (b)', to

represent the uncertainty. It is possible to see the possibilistic triangle distribution ('Fig 1(c)') as the rappresentation of all the probabilistic distribution that have a cumulative distribution function lay between the two measures ('Fig. 1 (d)') of the possibilistic function and not only of the somehow similar probabilistic triangle distribution ('Fig 1(a)').

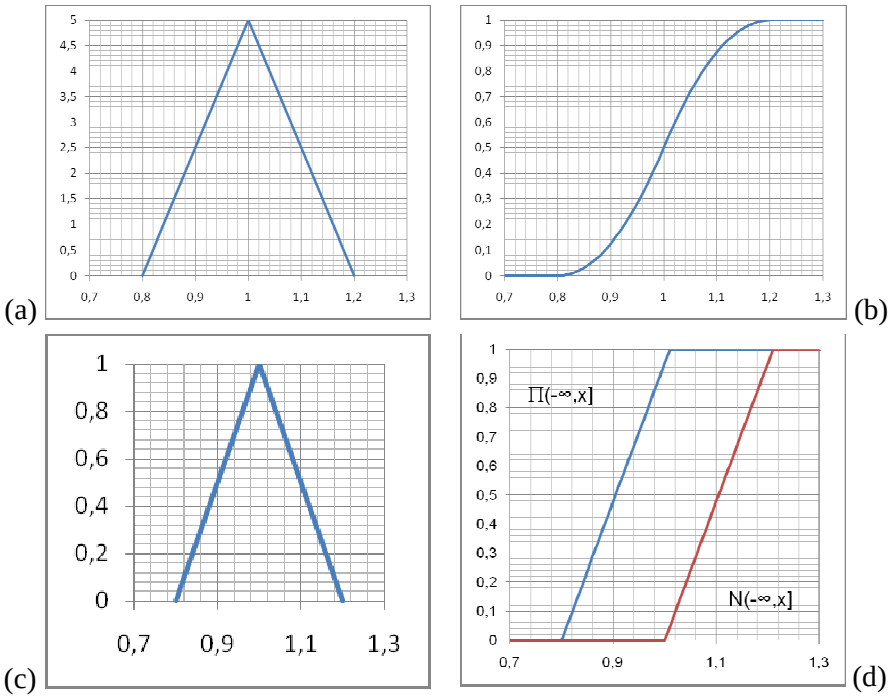

Figure 1. Comparison between (a) a triangular probabilistic distribution and its associated cumulative function (b) and (c) a triangular possibilistic distribution and its corresponding possibility Π and necessity N measures of the set A=(-∞,x].

2 EPISTEMIC UNCERTANINTIES AND POSSIBILITY THEORY

The first, and most important, reason for keeping epistemic and aleatory uncertainties separate is that it is mathematically more correct [Vose D. 2000]. Mixing both the uncertainties means that one cannot see how much of the total uncertainty comes from epistemic and aleatory uncertainties. If one knows that a large part of the total uncertainty is due to epistemic uncertainty then by collecting further information and thereby reducing total uncertainty one would be able to improve the estimate of the future. On the other hand, if the total uncertainty was nearly all due to variability, it is a waste of time to collect more information and the only way to reduce the total uncertainty would be to change the factor method, i.e. avoid the simple multiplication of the seven factors.

In this work, it is assumed that some of the seven factor used to estimate service life from a reference one are aleatory variables and are represented by probability distributions while other are epistemic variable represented by possibility distributions. To compute the ESL Monte Carlo sampling of the random variables is repeatedly performed to process the aleatory behaviour of some factors while possibilistic distribution analysis is carried out at each sampling to process the epistemic uncertainty in the remaining factors. This method leads to the computation of a possibilistic random distribution representing the ESL for each considered realization of the aleatory variables. Finally, the obtained possibilistic random distributions are combined into a set of limiting cumulative distributions characterized by different degrees of confidence [Cooper 1996 e Baraldi 2008]. Results will be compared to ones obtained by a pure probabilistic approach, based on the transformation of the possibilistic distributions into probabilistic distributions and the successive propagation of the uncertainty via MC sampling. The transformation from probabilistic distribution to possibilistic one

has been discussed by many authors [Dubois 2004, for probability to fuzzy] and the investigation of this problem is out of the scope of this paper.

The FM equation can be generalized in a model whose output is a function $f(\cdot)$ of n input variables Y_j, $j = 1, \ldots, n$; the uncertainty in the first k input variables (called "probabilistic" variables) is characterized by probability distributions $p_{Yj}(y)$ whereas the uncertainty in the last $n - k$ input variables (called "possibilistic" variables) is represented in terms of possibility distributions $\pi_{Yj}(y)$ measuring the degree of possibility that the linguistic variables Y_j be equal to y. For the propagation of such mixed uncertainty information, the Monte Carlo technique can be combined with the extension principle of fuzzy set theory by means of the following two main steps [Baudrit 2006]:

1. repeated Monte Carlo sampling of the probabilistic variables to process their uncertainty;
2. Fuzzy interval analysis to process the uncertainty connected with the possibilistic variables.

For the generic i_a-*th* k − tuple of random values, $i = 1, 2, \ldots, m$, sampled by Monte Carlo from the probabilistic distributions, a fuzzy set π_i^f estimate of $f(Y)$ is constructed by fuzzy interval analysis. After m repeated samplings of the probabilistic variables, the fuzzy set estimates π_i^f, $i = 1, \ldots, m$, are combined to give an estimate of $f(Y)$ as a fuzzy random variable (or random possibility distribution) according to the rules of evidence theory.
The operative steps of the procedure are [Baraldi 2008]:

1. sample the i_a-th realization $(y_1^{i_a}, \ldots, y_k^{i_a})$ of the probabilistic variable vector $(Y_1,\ldots,Y_k)$;
2. select a possibility value $\alpha \in [0, 1]$ and the corresponding α-cuts $A_\alpha^{Y_{k+1}}, \ldots, A_\alpha^{Y_n}$ of the possibility distributions $(\pi_{Y_{k+1}}, \ldots, \pi_{Y_n})$ as intervals of possible values of the possibilistic variables $(Y_{k+1},\ldots,Y_n)$;
3. compute the smallest and largest values of $f(y_1^{i_a}, \ldots, y_k^{i_a}, Y_{k+1}, \ldots, Y_n)$, denoted by $\underline{f}_\alpha^{i_a}$ and $\overline{f}_\alpha^{i_a}$ respectively, considering the fixed values $(y_1^{i_a}, \ldots, y_k^{i_a})$ sampled for the random variables $(Y_1,\ldots,Y_k)$ and all values of the possibilistic variables $(Y_{k+1},\ldots,Y_n)$ in the α-cuts $A_\alpha^{Y_{k+1}}, \ldots, A_\alpha^{Y_n}$ of their possibility distributions $(\pi_{Y_{k+1}}, \ldots, \pi_{Y_n})$. Then, take the extreme values $\underline{f}_\alpha^{i_a}$ and $\overline{f}_\alpha^{i_a}$ as the lower and upper limits of the α-cut of $f(y_1^{i_a}, \ldots, y_k^{i_a}, Y_{k+1}, \ldots, Y_n)$;
4. return to step 2 and repeat for another α-cut; after having repeated steps 2-3 for all the m_α α-cuts of interest, the fuzzy random realization (fuzzy interval) $\pi_{i_a}^f$ of $f(Y)$ is obtained as the collection of the values $\overline{f}_\alpha^{i_a}$ and $\underline{f}_\alpha^{i_a}$; in other words, $\pi_{i_a}^f$ is defined by all its α-cut intervals $\left[\overline{f}_\alpha^{i_a}, \underline{f}_\alpha^{i_a}\right]$;
5. return to step 1 to generate a new realization of the random variables. After having repeated steps 1-4 for ma times, exit.

At the end of the procedure an ensemble of realizations of random possibility distributions is obtained, i.e. $(\pi_1^f, \ldots, \pi_{m_a}^f)$. In this work, the information contained in the obtained random possibility distributions $(\pi_1^f, \ldots, \pi_{m_a}^f)$ is aggregated according to the Ferson method [Cooper 1996].
The procedure follows the next steps:

1. Select a possibility value α and consider the corresponding α-cut $A_\alpha^{i_a} = \left[\underline{f}_\alpha^{i_a}, \overline{f}_\alpha^{i_a}\right]$ of the possibility distribution $\pi_{i_a}^f(u)$;
2. Define a new possibility distribution $\pi_{i_a}^\alpha(u)$:

$$\begin{cases}\pi_{i_a}^{\alpha}(u) = 1\ if\ u\ \in A_{\alpha}^{i_a} \\ \pi_{i_a}^{\alpha}(u) = 0\ otherwise\end{cases}$$

3. Compute the possibility and the necessity measures associated to $\pi_{i_a}^{\alpha}(u)$, $\prod_{i_a}^{\alpha}(A)$ and $N_{i_a}^{\alpha}(A)$ respectively, for any set $A=(-\infty,u]$. This is equivalent to computing the possibility and necessity measures as:

$$\Pi_{i_a}^{\alpha}((-\infty,u]) = \begin{cases}1\ if\ u \geq \underline{f}_{\alpha}^{i_a} \\ 0\ otherwise\end{cases}$$

$$N_{i_a}^{\alpha}((-\infty,u]) = \begin{cases}1\ if\ u \geq \overline{f}_{\alpha}^{i_a} \\ 0\ otherwise\end{cases}$$

4. Repeat steps 1-3 for all a and finally compute an upper ($\overline{F}_{\alpha}$) and a lower ($\underline{F}_{\alpha}$) cumulative distributions for the α-cut chosen at step 1:

$$\overline{F_{\alpha}}(u) = \sum_{i_a} p_i \Pi_{i_a}^{\alpha}((-\infty,u])$$

$$\underline{F_{\alpha}}(u) = \sum_{i_a} p_i N_{i_a}^{\alpha}((-\infty,u])$$

This kind of representation captures the aleatory variability and epistemic imprecision of a random fuzzy interval in a parameterized way through the α-cuts and displays extreme pairs of cumulative distributions $\overline{F}_{\alpha}$ and $\underline{F}_{\alpha}$. The gap between $\overline{F}_{\alpha}$ and $\underline{F}_{\alpha}$ represents the imprecision due to epistemic variables; the slopes of $\overline{F}_{\alpha}$ and $\underline{F}_{\alpha}$ characterize the variability of the results caused by the aleatory uncertainty. A confident user who assumes high precision would work with the cores of the fuzzy intervals (α-cut=1), whereas a cautious one may choose α-cut=0 to work with their supports.

3 CASE STUDY

Two examples of joint of probabilistic and possibilistic uncertainty are showed here, in the first only one of the seven factor is treated as aleatory and all the others are treated as epistemic, in the second one three factors are described by probability distributions and four by possibility distributions. In both case reference service life is considered as a deterministic value. The first of these two cases may be considered as an example of a building component coming from an industrialized and quality controlled production process (factor A aleatory) where the reference service life is considered a deterministic value and the other factors are characterized by epistemic uncertainty. In this case a triangle probability distribution is used for the aleatory factor A and the values used for the computation are shown in Table 2.

Table 2. Input values for the first case study with only one aleatory factor

RSL	A	B	C	D	E	F	G
Deterministic	Probabilistic	Possibilistic	Possibilistic	Possibilistic	Possibilistic	Possibilistic	Possibilistic
25 years	Min. value 0,8	Min. value 0,8	Min. value 0,8	Min. value 0,8	Min. value 0,8	Min. value 0,8	Min. value 0,8
	Most prob. value 1	Most prob. value 1	Most prob. value 1	Most prob. value 1	Most prob. value 1	Most prob. value 1	Most prob. value 1
	Max value 1,2	Max value 1,2	Max value 1,2	Max value 1,2	Max value 1,2	Max value 1,2	Max value 1,2

Table 3. Input values for the second case study with three aleatory factor

RSL	A	B	C	D	E	F	G
Deterministic	Probabilistic	Possibilistic	Possibilistic	Probabilistic	Probabilistic	Possibilistic	Possibilistic
25 years	Min. value 0,8	Min. value 0,8	Min. value 0,8	Min. value 0,8	Min. value 0,8	Min. value 0,8	Min. value 0,8
	Most prob. value 1	Most prob. value 1	Most prob. value 1	Most prob. value 1	Most prob. value 1	Most prob. value 1	Most prob. value 1
	Max value 1,2	Max value 1,2	Max value 1,2	Max value 1,2	Max value 1,2	Max value 1,2	Max value 1,2

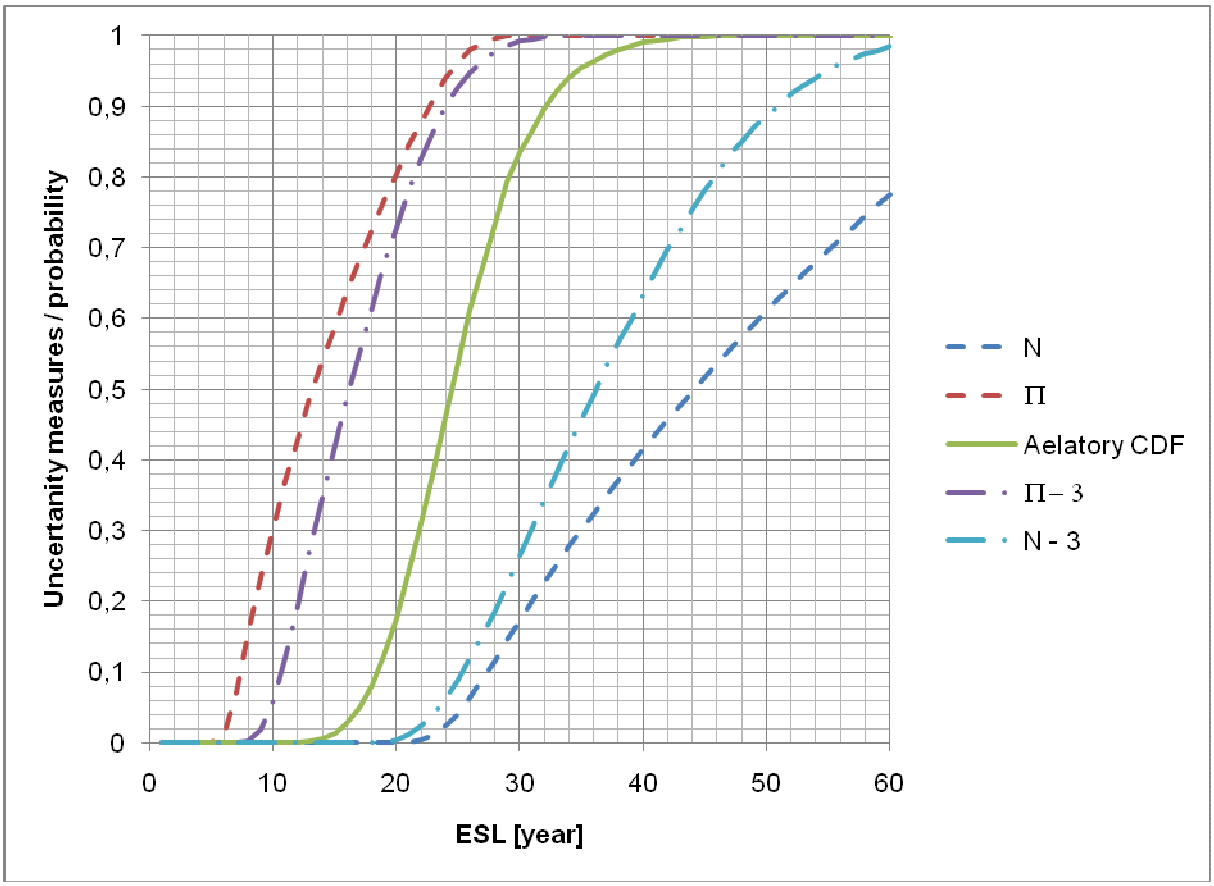

Figure 2. Comparison of the cumulative distribution functions of the probability of ESL obtained by a pure probabilistic approach for uncertainty propagation (centre) and by a hybrid approach for uncertainty propagation approach with the necessity (lower curve) and possibility (upper curve) functions.

The second example has three factors described by probabilistic distributions, let's say factor A, D and E, and four by possibility distributions, where uncertainty is due to lack of knowledge. As in the previous example RSL is considered as deterministic. Values used for the computation are shown in Table 3. The last casse study is the one with all triangular probabilistic distributions and where the uncertainty propagation is made by a Monte Carlo simulation like in [Moser 1999].

The results of uncertainty propagation in the three different examples are shown in Figure 2 where the case of pure probabilistic uncertainty propagation is the central solid line representing the cumulative distribution function (CDF) of the estimated service life when errors in the input factors are all due to inherent variability of the component behaviour. In the same figure the two dash-dot lines represent the necessity and possibility measure of the set $A=(-\infty,x]$ when only four of the seven factor are described by possibility distributions. At least, the two dashed lines show necessity and possibility measure of the set $A=(-\infty,x]$ when in six of the seven factors error is due to the lack of knowledge (epistemic uncertainty).

Table 4. Measures values of possibility distribution of estimated service life for three different *a*-cuts and comparison with percentile values of estimated service life in case of pure probabilistic uncertainty propagation.

ESL [years]	**Pure probabilistic**	**Four possibility distribution functions**		**Six possibility distribution functions**	
α	%tile	Possibility	Necessity	Possibility	Necessity
0.3	≅ 22	≅ 13	≅ 31	≅ 10	≅ 35
0.5	≅ 25	≅ 16	≅ 36	≅ 13	≅ 44
0.8	≅ 29	≅ 21	≅ 46	≅ 20	> 60

It may be useful to compare possibility and necessity measures associated to $\pi_{i_a}^{\alpha}(u)$ for three different α-cut to the corresponding percentile values of ESL when uncertainty is propagated in a pure probabilistic way. Table 4 shows that in case of six factors described by possibility distributions if $\alpha =$ 0.5 then the measure associated to the ESL possibility distribution are: possibility $\prod_{i_a}^{0.5}(A) \cong 13$ years and necessity $N_{i_a}^{0.5}(A) \cong 44$ years. This is quite a large range if compared to the 50% quantile of ESL computed by a pure probabilistic approach: $p_{50\%}(ESL) \cong 25$ years, it means a range from -48% to +76% of the probabilistic value. The range decreases but remains wide if only four factor are represented by possibility distributions, in this case ESL measures are $\prod_{i_a}^{0.5}(A) \cong 16$ and $N_{i_a}^{0.5}(A) \cong 36$, i.e. the ESL may vary from -36% to +44% of the $p_{50\%}(ESL)$ computed using only probabilistic distribution for the seven factors.

4 CONCLUSIONS

Uncertainty about the value of input factors when using the factor method for service life estimation may be of two different kinds: one related to the randomness of elements described by the factor and the other due to a lack of knowledge. It often happens, in the current practice, that information that are somehow linguistic, i.e. deriving from common sense or expert judgement, are used to build probabilistic distribution functions for the input factors. Unfortunately resorting to a probabilistic representation of epistemic uncertainty may not be possible when sufficiently informative data are not available for statistical analysis, even if one adopts expert elicitation procedures to incorporate diffuse information into the corresponding probability distributions, within a subjective view of probability. Indeed, an expert may not have sufficiently refined knowledge or opinion to characterize the relevant epistemic uncertainty in terms of probability distributions.
Results of the case study show that the consequence of a probabilistic representation of epistemic uncertainty in input factor, even if made unconsciously, may lead to big errors in service life prediction. To avoid these errors there are two ways: a) spend more time in investigating the problem and thus reduce the uncertainty of the seven factors; b) change the equation of the factor method, for example uncertainty on ESL decrease a lot if the RSL is multiplied by the mean value of the seven factors instead of by the multiplication of them.

REFERENCES

ISO 15686 – 9:2008, *Buildings and constructed assets -- Service-life planning -- Part 9: Guidance on assessment of service-life data*.

Architectural Institute 1993, *The English edition of Principal Guide for service life planning of buildings. Architectural Institute of Japan*, Japan.

Moser K. 1999, 'Towards: the practical evaluation of service life – Illustrative application of the probabilistic approach', Proc. 8th Durability of Building Materials and Components. Vancouver, Canada, June 1999, pp. 1319-1329.

Re Cecconi F. 2004, 'Engineering method for service life planning: the evolved factor method', Proc. of CIB World Building Congress 2004, Toronto, Canada, 2-7 maggio 2004.

Hovde P.J. 2005, 'The Factor Method – a simple tool to service life estimation'. Proc. of 10th Durability of Building Materials and Components, Lyon 17-20 aprile 2005.

Re Cecconi F., Iacono P. 2005, 'Enhancing the Factor Method – Suggestions to Avoid Subjectivity' Proc. of 10th Durability of Building Materials and Components, Lyon 17-20 aprile 2005.

Apostolakis, G. E. 1990. 'The concept of probability in safety assessments of technological systems'. *Science*, 250 (4986), 1359– 1364.

Klir G.J., Yuan B., 1995, '*Fuzzy Sets and Fuzzy Logic: Theory and Applications*', Upper Saddle River, NJ, Prentice-Hall.

Shafer G., 1976, '*A Mathematical Theory of Evidence*', Princeton, NJ: Princeton University Press.

Dubois D., Prade H., 1988, '*Possibility Theory: An Approach toComputerized Processing of Uncertainty*', New York, Plenum Press.

Vose D. 2000, *Risk analysis—a quantitative guide*. New York: Wiley.

Cooper J.A., Ferson S., Ginzburg L., 1996, 'Hybrid processing of stochastic and subjective uncertainty data', in *Risk Analysis*, Vol. 16, No. 5, pp. 785-791.

Baraldi P., Zio E., 2008, 'A Combined Monte Carlo and Possibilistic Approach to Uncertainty Propagation in Event Tree Analysis', in *Risk Analysis*, Vol 28, No. 5, pp 1309-1325

Dubois D., Foulloy L., Mauris G., Prade H., 2004, 'Probability-possibility transformations, triangular fuzzy sets, and probabilistic inequalities'. In *Reliable Computing*, 10, pp. 273–297.

Baudrit C., Dubois D., Guyonnet D., 2006, Joint propagation of probabilistic and possibilistic information in risk assessment. *IEEE Transactions on Fuzzy Systems*, 14, pp. 593–608.

XII DBMC
International Conference on Durability of Building Materials and Components
PORTO - PORTUGAL, April 12th-15th, 2011

The Value of Cultural Assets. Maintenance Costs and Economic Sustainability of Heritage

Gema Maria Ramirez Pacheco [1]
Federico Garcia Erviti [2]

ABSTRACT

This paper deals with the management and maintenance of the assets that constitute the Spanish Cultural Heritage. Conservation and maintenance has become a social demand necessary for the preservation of public values, requiring the investment of the necessary resources.

The preservation of cultural assets constitutes a way to generate social identities and plays an important role in the development of the Spanish economy. The legal framework involves a number of obligations and rights to ensure the conservation and protection of heritage. This legal duty of maintenance is necessary to preserve capacity to transmit the protected values.

This obligation implies a substantial financial effort to the owner of the property, either a public or a private entity, addressing a problem of economic sustainability. Economic exploitation, with the aim of contributing to effective maintenance, is sometimes the best way to acquire resources. The research work described in this paper has the following objectives: - establishment of processes for assessing total life cycle costs (LCC) during the planning stages with consideration of maintenance budgets to determine the most advantageous operating system selections; and determination of the relationship between the value of property and maintenance costs, and establishing a sensitivity analysis methodology.

KEYWORDS

Culture economy, Contingent valuation, Non-market asset evaluation, Maintenance cost.

[1] Faculty of Arquitecture of the University of Alicante (EPSA UA), Alicante, SPAIN, Gema.Ramirez@ua.es
[2] Faculty of Arquitecture of the Polytechnic University of Madrid (ETSA UPM), Madrid, SPAIN, fdgerv@arquired.es

1 ECONOMIC DIMENSION OF CULTURAL HERITAGE

Cultural Heritage is made up by a collection of assets which share a common legal governance regime and an artistic, historical or cultural interest. Cultural assets constitute a way to generate social identities and play an important role in the development of the Spanish economy. The reflection on the necessity of intervention on this heritage, in addition to establishing what should be done, brings up the need to define the reasons for taking action, the why and the what-for. Determining how to integrate these assets into the contemporary context and how to deal with our cultural legacy are essential decisions to establish if its maintenance is economically sustainable.

We face a discussion around culture, economy and the meaning of the value of cultural heritage for society. The main problem that arises when carrying out its economic valuation is that these assets are not directly reflected by market conditions, be it because of being public property or because the benefits associated to their use are intangible and non-marketable, even though a latent willingness to pay for their enjoyment exists. How can the investment in heritage conservation be justified in economic terms value can't be quantified?

The cultural heritage is a resource at the service of human development and cultural diversity, whose management should be based on an economic development model which respects the principles of a sustainable use of the resources. The importance of the cultural heritage lies in the benefits and values it generates. All the factors related to the life cycle cost of the building, which constitute a very important part of the property cost and therefore of the asset value, should be taken into account for the analysis of its economic sustainability. Among expenses, those linked to the legal duty of maintenance and conservation* stand out, and are necessary to prevent deterioration of heritage, therefore preserving its capacity to transmit the protected values. This maintenance obligation implies a very important economic effort, requiring an appropriate investment policy. It is patently clear that the conservation of the Cultural Heritage is a very complex matter, where economic management gains great relevance.

Therefore, the valuation of the cultural asset implies determining the break-even point between the borne costs and the obtained benefits. The actual value of the asset does not only depend on the initial investments but on the costs that occur during its service life and the social appreciation of the protected value. It is therefore essential to present new evaluation and assessment systems which use quality models throughout the life of the property and which incorporate intangible benefits in market scenarios.

2 MANAGEMENT OF THE CULTURAL CAPITAL: THE INVESTMENT IN HERITAGE

2.1 Management of the Historical Heritage and public investment

The present study focuses its analysis on immovable cultural assets which are, as reflected in article 334 of the Spanish Civil Code, properties inherent with the buildings or part of their environment. This type of asset is governed by Law 16/1985, of the Spanish Historical Heritage which implies a series of limitations, obligations and rights, whose fundamental aim is to guarantee the conservation and maintenance of the asset.

For the management of historical heritage, Spanish law has opted for a decentralized model of distribution of competences, where the action of the Autonomous Regions and Local Entities attains a considerable political and budgetary weight. The central government coordinates the actions through the Ministry of Culture and the Historical Heritage Council, and is responsible of applying the legal regime. It develops its activity through a series of lines of action that identifies investment in heritage by funding conservation works and the acquisition of cultural assets.

In article 46 of the Spanish Constitution it is established that public powers are bound to guarantee conservation and to promote the enrichment of the Historical, Cultural and Artistic Heritage of Spain. The Spanish Historical Heritage Law 16/85 implements this obligation through the "cultural one percent". This promotion measure establishes the obligation to assign an item in the public works contracts of at least 1% to finance the conservation works of the Spanish Historical Heritage or to promote the artistic creativity. This program is an effective instrument for the conservation viability of our built heritage which has made possible the rehabilitation and conservation of very valuable assets, generating new ways of conceiving the interventions on a joint and interrelated way. The investment of these resources is carried out by means of Plans and Programs which group the buildings with common typology and problems. These share a philosophy that can be summarized in the participation and co-responsibility of all the agents.

The data presented next is an estimate of the 2001 public sector expenses related to the conservation, restoration and regeneration of the properties that make up the Historical Heritage of Spain (the last period for which complete numbers and consolidated expenses exist for the whole Public Administration in the Historical Heritage). For this annual period, the total of the public expenditure in the Administration of the Historical Heritage of Spain amounted to 1526.01 million Euros. This expense is distributed among the different regional levels as follows: 36,74% from Central Administration (642.020.000 €); 27,60% of Autonomous Regions (482.240.000 €); 22,99% by Municipal Councils (401.720.000 €); 6,65% from Provincial Councils (116.150.000 €); and a 16,34% share by City Councils (285.570.000 €).

The main role within the public sector is played by the Central Administration, with the financial contribution of the Autonomous Administrations and Municipal entities being lesser. There has been a consolidation of the investment, fixing the financial efforts made by the Spanish public sector in the range of the expenses of the historical heritage at 0,23% of the GDP and at 0,59% of the total public expenditure. The investment made by the city councils in 2001 (expenses estimated as 285.570.000 €), was 1,37% of the total budget, an increase from the investment of 0,91% in 1998. As for the Provincial Councils, Town Councils and Island Councils, the estimated expenses in the preservation of the Historical Heritage in 2001 amounted to 116.150.000 €.

2.2 The private participation, patronage and sponsoring

The necessities required by the cultural heritage in Spain, regardless of the increase of budgets of the public administrations, need private contributions for their conservation. The concept of cultural patronage introduces the idea of social participation in the conservation and the enrichment of heritage through the incentives so-called "promotion measures" reflected in the Spanish Historical Heritage Law 16/1985. These measures were regulated by Law 49/2002 of the fiscal regime of non-profit entities and the fiscal incentives for patronage.

Private participation comes from three principle groups, the Catholic Church, various foundations and from individuals. The contribution from the private sector is approximately 221.330.000 € (2001), which represents 12,67% of the total expense. The Catholic Church, with its own resources, contributes to the conservation and restoration of its properties which are part of the Spanish Historical Heritage. The estimated total expense by the Catholic Church to preserve Historical Heritage is 119770000 € (2001), 54% of the total private expense and 6,85% of the total expenses.

As for the foundations, they participate essentially with their own funds for the preservation of the Historical Heritage. Their estimated 2001 contribution was 87.270.000 €, which represents 39,4% of the private expense and 4,99% of the total. It is worth noting though that 94% of these amounts come from the resources assigned by the "Social Work" of the Spanish Savings Banks Confederation in its program "historical, artistic and natural heritage". Finally, the contribution from individuals (determined by indirect estimates) amounts approximately to 14.290.000 €, which represents 6,5% of

the private expense and 0,82% of the total expense assigned to the conservation of the Historical Heritage in Spain.

It is worth noting the promotion measures established by Law 49/2002 (fiscal regime and incentives) for sponsoring with the aim of promoting, private sector collaboration for objects of public interest. Different types of tax deductions and exemptions are available (Property Tax, Wealth Tax, Construction and Installation Tax and imposition of added values in urban lands). As for fiscal incentives, reductions are established in relation to the Income Tax and the Corporate Income Tax for the acquisition of Spanish Historical Heritage assets, the conservation, diffusion and exhibition of the assets shown for their cultural interest, as well as the improvement of the infrastructures located in properties classed as World Heritage by UNESCO.

2.3 Examination of opportunities: the cultural tourism as a way of financing

The Exterior Promotion Plans of the Spanish Tourist Office established that the promotion of cultural tourism and the improvement of our historical heritage are ways to attract quality tourism based on sustainability. The Touristic Movements survey from the Tourist Study Institute indicates that in 2006, 10% of the tourists that visited Spain did so for cultural reasons, a product which is becoming consolidated year after year and still has a long way to go. Nationwide, the Autonomous Regions identified with a tourism offer of sun and sand are the ones with a lower rate of cultural tourism, whereas the regions farthest from the Mediterranean coast have a proportion of cultural tourism markedly over the national average.

Finally, it is worth noting that there are some factors that suggest a significant increase in the demand for cultural tourism short-term. On one hand, a demographic growth worldwide will cause the gradual aging of the population with an increase of European tourism. On the other hand, a substantial improvement in the accessibility to the destinations will make possible that a higher number of destinations of cultural interest develop tourist initiatives. The development of cultural tourism in Spain and its surrounding countries will be decided by the capacity to improve the destination administration processes and the coordination of the different resources which make up the cultural offer. Managing to transmit a differential value of the Spanish cultural destinations in the markets where the image is strongly associated to the sun and sand tourism implies new opportunities where we can find a clear way of financing through the economic exploitation of heritage.

3 ECONOMIC VALUE OF THE CULTURAL ASSET

3.1 Valuation techniques of the cultural asset. Value of non-market assets and cost-benefit analysis

The economic value of the cultural heritage lies in the benefits and values it can generate, both tangible and intangible. For their determination it is necessary to carry out a cost-benefit and cash-flow analysis for the purposes of financial, economic and social sustainability [Directorate General for General Policy, European Commission, 2003], determining the break-even point between the protected value, the costs linked to its lifecycle and the degree of satisfaction of the user with its preservation. The investment viability in cultural heritage will happen when the income created by investment in maintenance surpasses the ones created by other economic activities [Nypan, 2003].

In economic terms, this series of benefits are positive externalities which should be used to argue for the necessity and viability of asset maintenance. The benefits are divided into two, depending on if they derive from the direct or indirect use of the asset. Within the direct use values we could integrate the fiscal benefits, the increase of public facilities in the area derived from the existence of the asset, the exploitation opportunity of the asset and its power as an instrument for the renovation of other

uses such as residential, commercial, tourist, recreational or social. These concepts will be quantifiable with market techniques.

On the other hand, there is a series of intangible benefits associated with the preservation of heritage that are not linked to use. Included in this group are: the assessment of the asset's existence; the value of option or possibility to be able to enjoy the asset in the future; and the value of legacy to future generations. But how do we quantify economically intangible benefits? Is there a willingness to pay for their existence? The intangible character of these benefits implies that they can't be used by the market and consequently they can't be valued with market techniques. Therefore, the difficulty of the valuation lies in the quantification of that part of the asset that does not represent a marketable characteristic. The economy counts with different techniques classified into revealed preferences and declared preferences techniques [Abelson, 2000]. The former are indirect, estimating asset value from observation of other markets through the quantification of the implicit values that contribute to its formation. Within this group we find the hedonic price models and the displacement or trip costs models.

The hedonic price models, according to Rosen's formalization in Journal of Political Economy [1974], suggest that the value of a market asset can be determined by the addition of the implicit prices of their characteristics, be it intrinsic or derived from their specific location. In the case of assets of cultural interest, the object of valuation would not be the asset itself but that series of externalities that its existence generates and that determines the value of another property for which a well defined market does exist. By means of the hedonic price models we could define how the proximity to a certain asset or the possibility of enjoying its façade influences the market value of the residential or commercial use, quantifying the value of the aforementioned externality or benefit as an implicit price of the market value of the analysed use.

On the other hand, the travel cost method uses the cost of the trip to access the asset to develop an indicator of demand. It consists of establishing, through econometric procedures, the demand function between the number of visitors and cost of the trip, with the possibility of introducing other socio-economic variables. The complication when applying this type of method in the valuation of an asset of cultural interest lies in the fact that usually the value of the trip is not justified by just one place of interest but several, so it's difficult to estimate which part of the cost corresponds to the place being assessed [Riera, 1994].

Finally, preference or direct valuation techniques are used to estimate the value of assets which don't have a direct reflection on the market [Sanz & Herrero, 2006], but rather whose value answers to the appreciation of the future consumer. Among them is contingent valuation, which consists of creating a hypothetical market and obtaining, through a survey of public interest, the maximum disposition to pay for its enjoyment. From said quantification, established by the interviewed, values are assigned to the asset and to the different cultural elements (implied public interest in direct use). In the case of assets that don't imply direct monetary cost for the consumer, the disposition to pay equals the benefit that said consumer gains.

According to Riera [1994], this type of "ex ante" techniques are very important for rationally prioritizing public expenditures. The liability of the valuation depends on correct survey design, where different functions of demand and willingness to pay should be presented. For said functions of demand to not be punctual but extendable in time, heritage must become a justification for ex novo cultural creation, since the variation of the cultural offerings is essential to suggest credible estimates of the function of demand of non-marketable objects. Individuals are not going to judge their changes of wellbeing based on modifications in the prices, but on real or potential changes in the availability of enjoyable assets. We find therefore a heritage either inherited or a cultural product in itself, that we must turn into a flexible and variable cultural offering.

The measurements of benefit to consumers detected by the contingent valuation method are theoretically different to those obtained by indirect methods. This is because, in addition to the values that the user perceives when consuming the asset, the contingent valuation method determines other values that cause wellbeing or satisfaction. These are the "non-use" or passive use values, such as the option value or existence value. This difference between what contingent valuation measures and what indirect methods measure makes difficult to check the accuracy of the measurements obtained in hypothetical markets.

Nonetheless, the contingent value provides an economic approximation of the asset value, but not to a quantification of the intangible benefits derived from its existence and, if applicable, its exploitation. When faced with an economic sustainability analysis, a valuation scenario merging market and non-market valuation techniques must be established. But what should be the relationship between costs, non-market value and the benefits which would balance the generation of income account? A sensitivity analysis [Directorate General for General Policy, European Commission, 2003] will allow us to establish the link between variables, to determine the operation internal performance index and estimates about the economic sustainability of investing in heritage.

3.2 Buildings and Life-cycle Costing. Maintenance and operational cost

The valuation of the cultural asset implies the determination of an actual value that depends on the costs that occur during its useful lifecycle. According to different studies carried out, in the case of immovable properties with a service life of about 50 years, the initial or production costs represent an average proportion of 20-25% of the total costs and the remaining 75-80% corresponds to maintenance and operational expenses. In the case of cultural assets, the property's service life must carry on for the necessary preservation of the cultural value. As we increase property life, the exploitation expenses, both operations and maintenance, are quite more pronounced, putting more emphasis upon successful economic management.

An appropriate management of the building should only assume expenses relative to the property's generation of income and therefore the advantages that can be gained carrying out a life cycle costing (LCC) analysis by including the expenses of production, operation and maintenance in the course of the asset's service life are very clear [Davis Langdon, 2007]. The requirement for a global analysis of costs in the management of cultural heritage is justified in order to achieve the following objectives:

- Transparency and planning capacity by means of sinking funds of total future costs;
- Capacity of modifying and optimizing future costs during the design phases of the rehabilitation or reparation projects by evaluating alternatives;
- Capacity to fix exploitation programs through the complete cycle;
- Evaluation of environmental sustainability allowing the assessment of the benefits of incorporating systems of lesser environmental impact or higher energy efficiency; and
- Identification of opportunities with better efficiency of costs

The lack of conservation will cause the gradual degradation of heritage assets and subsequent economic prejudice, making essential an appropriate maintenance policy that prevents the devaluation of the cultural heritage and defines security, sustainability and profitability parameters. Therefore, the public policies and private initiatives for conservation and maintenance must become premises that permit cost reduction by increasing the value of assets, finding the break-even point between the evaluation of the protected value and cost, incorporating the degree of satisfaction reached by the user through the preservation of the heritage legacy to the first of these factors.

Within this context we could distinguish –as it has usually been done in the scope of industrial and machinery installations- between corrective maintenance and preventive maintenance [Pons, 1995]. Corrective or non-planned maintenance includes punctual actions carried out to reduce specific deficiencies that entail a functionality loss of the element or the building. This type of action does not

allow us to obtain a global view of the necessary management of maintenance since it answers to a cause-effect situation, and it does not facilitate the planning of expenses and tends to cause an economic increase in its emergency character. Therefore, it is obvious that the prevention and rationalization of the actions to carry out, proposing a process throughout time not limited to a series of occasional interventions, is more coherent at a level of heritage management.

Maintenance planning suggests that organized inspection and maintenance works, guaranteeing for the property an appropriate provision level and a correct protection of its value in the course of its service life. The economic management of these actions implies a comprehensive analysis of the evolution of the maintenance costs, necessary to carry out the different predictions of action, combining the financial, organizational and technical requirements. This financial prediction program is essential to determine the viability of preservation based on an analysis of costs and benefits.

There is many advantages that justify the application of and appropriate maintenance to the built heritage. We are suggesting concepts linked directly to the durability that can be assigned to the building and the service life periods that can be assigned to its different elements. By carrying out of these actions it is possible to obtain a continuous revaluation of the property, increasing the exploitation periods and, in short, turning the expense into an investment. In the case of a cultural asset, it is essential to guarantee the continuous, and controlled, preservation of value and the unlimited extension of service life. To this end, a strategy that takes as a reference point the economic viability of materializing said planning must be designed, establishing conservation and maintenance expenses acceptable to the owners', particularly those of reparation in the last phase, since otherwise we will tend towards an unavoidable deterioration of the built heritage. Life-cycle costing (LCC) analysis techniques can also allow us to identify the interactions between the maintenance costs and the repair costs derived from damages, making it possible to assess if a maintenance strategy is optimal form the costs point of view. But, what is the cost of a correct maintenance?

The real cost of the building maintenance is difficult to anticipate, since there are uncontrolled circumstances that in many occasions depend on its users attitude. A reference to determine the conservation and maintenance costs are the maintenance costs during the first ten years of the building which are limited to the mere conservation, not taking into account significant renovations of elements. According to our own estimates carried out for different typologies destined to residential use, the decennial maintenance costs vary within a 25-30% band of its material execution cost. These costs constitute a reference that can be extrapolated to the rest of the cycle. After this initial ten year period certain elements will reach the end of their expected service lives, requiring their replacement or repair. Therefore, the concept of maintenance will have to include both the conservation costs as well as the reparation costs.

To determine the amount of the reparation expenses it is necessary to establish the service life period of each element. From the estimated service lives, the frequency of renovations may be calculated (paving replacement every 30 years, woodwork and metalwork every 45 years, paint every 10 years,...), the possible degree of recovery and the percentage that each unit represents with regard to the global building costs. The remaining service life of each component will have to be established. This will permit the establishment of the planned number of complete renovations for each element, as well as their timing and the cost involved. According to Candel [1995], a part of these costs correspond to the actions of mere conservation (0,7 per cent a year over construction cost) and another part to the punctual investments depending on the renovation needs of systems or elements (1,3 per cent a year over construction cost), variable throughout the building's service life. The choice of preventive maintenance or only corrective maintenance through punctual reparation actions must answer an economic approach. Considering that maintenance is a global concept and that the product between mere conservation costs and repair costs remains constant [Candel, 1995], a minor investment in maintenance does not necessarily imply a lesser expense, since the cost of repairs and replacements will be very superior, while the remaining service life of the building will be reduced.

4 CONCLUSIONS

The economic management of the cultural Heritage requires new assessment and valuation system which use tools sufficiently integrated with quality models throughout the service life of the property/building. To this end, the global lifecycle must be optimized, intervening in the maintenance and the exploitation phase. Maintenance must be interpreted from an economic point of view, integrating it in a financial plan with important medium-term profitability, being essential to incorporate it as a design premise, with the objective of reducing costs and increasing the value of the assets. On the other hand, the lack of maintenance or inadequate maintenance causes the gradual devaluation of the cultural heritage and damages of increasing complexity and reparation costs. It is therefore patently obvious that the conservation of cultural heritage constitutes a complicated subject, for which economic management is very relevant. Presently the investment in heritage comes mainly from the public sector; none-the-less private contributions are needed to guarantee the conservation and maintenance of our built legacy.

REFERENCES

Abelson, P. *"Valuing the Public Benefits of Heritage listing of Commercial Buildings"*. Sydney: Applied Economics, 2000.

Candel Comas, R. "*Manual de mantenimiento de edificios. El libro del técnico mantenedor"*. Madrid: Consejo Superior de los Colegios de Arquitectos de España, 1995.

Davis Langdon Management Consulting . *"Life Cycle Costing (LCC) as a contribution to sustainable construction: a common methodology"*. 2007. Directorate General for General Policy, European Commission, "*Guía del análisis costes-beneficios de los proyectos de inversión"*. 2003

Lichfield, N; Hendon, W; Nijkamp, P; Ost, C; Realfonzo, A; Rostirolla, P. "*Conservation Economics*". Sri Lanka: ICOMOS, 1993.

Malkii, M; Mantisalo, R; Schmidt Tomé, K (eds.). "*Economics and built heritage. Toward new european initiatives.* Helsinki University of Technology, 2008.

Ost, C; Van der Droogenbroek, N. "*Report on economics of conservation. An appraisal of Theories, principles and methods"*. Center for economic research. Brussels business school. 1998.

Pons Pujol, A. "*Mantenimiento de los edificios. Desde el inicio del proyecto al final de su vidaútil"*. Barcelona: Col-legi d´Arquitectes de Catalunya, 1999.

Riera Micalo, P. *"Manual de valoración contingente"*. Madrid: Instituto de Estudios Fiscales, 1994.

Rosen, S**.** *"Hedonic Prices and Implicit Markets: Product Differentiation in Pure Competition."* The Journal of Political Economy, Vol. 82, No. 1, 1974

Sanz Lara, J; Herrero Prieto, L."*Valoración de bienes públicos relativos al patrimonio cultural. Aplicación comparada de métodos de estimación y análisis de segmentación de demanda"* Valladolid: Revista de Economia Pública, 2006.

Nypan, T.*"Cultural Heritage Monuments and Historic Buildings as value generators in a post-industrial economy"* Norway: Directorate for Cultural, Heritage, 2003.

XII DBMC
International Conference on Durability of Building Materials and Components
PORTO - PORTUGAL, April 12th-15th, 2011

Main Spatial Defects of Illegal Residential Buildings: The Case of Alto da Cova da Moura District

João Branco Pedro [1]
António Vilhena [2]
António Baptista Coelho [3]
José Vasconcelos Paiva [4]
Cláudio Cruz [5]

ABSTRACT

The purpose of the paper is to describe the main spatial defects in illegal residential buildings. Three research questions are addressed: What are the main spatial defects of the dwellings? What are the main spatial defects in the relation between buildings? What is the impact of spatial defects to the minimum habitability conditions of dwellings?

The defects were identified during a survey of the buildings of the Alto da Cova da Moura District (Amadora, Portugal), carried out in 2008. This district is made-up of illegal constructions, covers an area of 16.5 ha and has approximately 5,000 inhabitants. During the survey 833 buildings and 1,884 units were inspected. The main results are: a) 65% of buildings have problems with windows; b) about 20% of buildings have spatial defects in common stairways; and c) more than 50% of dwellings have spatial defects.

The main conclusion is that the lack of urban planning, the confinement of the terrain and the continuous arrival of new residents have led to an overcrowded and disordered urban fabric. Furthermore, buildings are mainly self-built by residents without design and do not comply with recognized technical good practices. As a result, there is a general lack of habitability and a quick decay of buildings' condition.

KEYWORDS

Illegal buildings, Building pathology, Spatial defects, Portugal, Bairro do alto da cova da moura.

[1] National Laboratory for Civil Engineering (LNEC), Lisboa, PORTUGAL and Delft University of Technology (OTB-TUDelft), Delft, THE NETHERLANDS, jpedro@lnec.pt
[2] National Laboratory for Civil Engineering (LNEC), Lisboa, PORTUGAL, avilhena@lnec.pt
[3] National Laboratory for Civil Engineering (LNEC) and Grupo Habitar (Habitat Group), LNEC, http://infohabitar.blogspot.com/, Lisboa, PORTUGAL, abc@lnec.pt
[4] National Laboratory for Civil Engineering (LNEC), Lisboa, PORTUGAL, jvpaiva@lnec.pt
[5] National Laboratory for Civil Engineering (LNEC), Lisboa, PORTUGAL, ccruz@lnec.pt

1 INTRODUCTION

In January 2006 the Portuguese Government created a national program for qualification and rehabilitation of problematic urban areas called *Initiative Critical Neighbourhoods*. Within this framework, the Institute for Housing and Urban Rehabilitation (IHRU) requested, in the beginning of 2007, the assistance of the National Laboratory for Civil Engineering (LNEC) in the analysis of the housing conditions of a district called *Bairro do Alto da Cova Moura* (BACM). This district is located within Amadora, a municipality within the metropolitan area of Lisbon. The district has an illegal development that started in the 1960s and had a strong growth from the mid-1970s.

In response to this request a study entitled *Analysis of housing conditions of the existing buildings in the Bairro do Alto da Cova da Moura* was developed, under the coordination of A. Baptista Coelho. This study had three different phases [Coelho 2008, Vilhena & Coelho 2008]:

- in the first phase, a local analysis was conducted to update and detail the existing cartographic support, and an assessment method to determine the buildings rehabilitation needs was developed;
- during the second phase, an experimental application of the assessment method was carried out, training was provided to technicians involved in the survey and the fieldwork was conducted;
- in the third and final phase, the results obtained in the field work were interpreted and the conclusions of the study were drawn.

The assessment method developed in the first phase, *Assessment Method for Building's Rehabilitation Needs* (MANR), is a multi-criteria model and a set of procedures to determine the building's rehabilitation needs [Pedro *et al.* 2008b]. A building requires rehabilitation whenever it does not ensure the satisfaction of functional requirements at a level stated in applicable Portuguese legislation for that type of building or determined by good practices of design and construction. Functional requirements may be compromised by constructive defects or spatial defects. Constructive defects may result from inadequate initial construction solution, poor execution of construction work or degradation of building elements. Spatial defects may result from inadequate conditions of the lot, a deficient initial partitioning solution or modification on the unit partitioning.

This paper describes the main spatial defects found in BACM. Three research questions are addressed: What are the main spatial defects of the dwellings? What are the main spatial defects in the relation between buildings? What is the impact of spatial defects to the minimum habitability conditions of dwellings? The main constructive defects found in BACM are presented in another paper.

In the following sections the research methodology is explained, the assessment method is presented, the main spatial defects are described and, finally, some conclusions are drawn.

2 RESEARCH METHODOLOGY

During the last years LNEC gained extensive experience in building condition assessment methods [Pedro *et al.* 2006a, Pedro *et al.* 2006b, Vilhena *et al.* 2007, Pedro *et al.* 2008a]. However, the specific type of building (*i.e.*, illegal construction) and the type of results required demanded a new method. To establish this new method, the following tasks were carried out: analysis of Portuguese and foreign assessment methods for building condition, definition of assessment criteria, selection of functional elements of dwelling and building, set weighting coefficients for the functional elements, definition of results' calculation formula and development of a computer tool. A first proposal of the method was discussed with several building and planning experts and a pilot test on different building types and units was carried out. The final version incorporated contributions from both experts and the experience acquired during the pilot test [Pedro et al 2008b].

For the survey, the BACM was divided into 61 blocks (Fig. 1), according to the 2003 geographical map provided by the city council. During the survey, 833 buildings and 1884 units were inspected. 1617 units had residential use (*i.e.* dwellings) and the remaining 267 had other uses (*e.g.*, shop, warehouse, industry, indoor parking) [Vilhena & Coelho 2008].

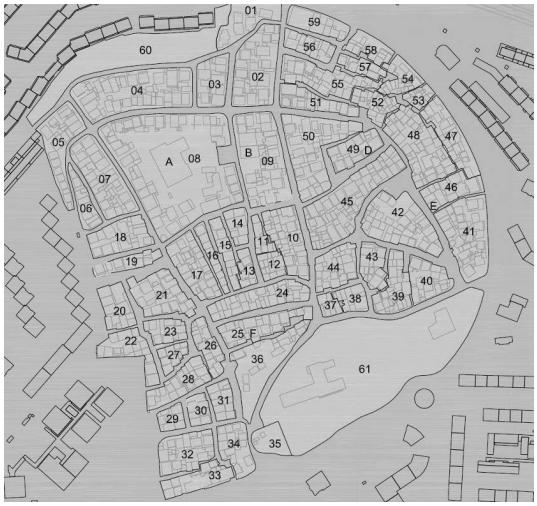

Figure 1. Blocks division of BACM.

The assessment was based on a visual inspection of the buildings, including all units and shared parts (where such exist). The survey lasted six months, from January to July 2008, and it was carried out by IHRU technicians with support of LNEC. Initially 14 technicians were involved in the survey, but during the work it was required to increase this number. All technicians that carried out inspections had specific training on the MANR. Since the method verifies both constructive and spatial defects, inspections were performed by teams of two technicians, a civil engineer and an architect. Some inspections were done by teams of two architects, due to lack of civil engineers.

3 ASSESSMENT METHOD

For each building, constructive defects, spatial defects and defects in the relation to other buildings were assessed.

To assess constructive defects the building was disaggregated into functional elements, such as, structure, roof, walls. Each functional element was assessed relative to three factors: *severity* of the defect, *extent* of the repair work and *complexity* of the repair work. First the *severity* of the construction defect was analysed and classified in a four categories scale: *very slight*, *minor*, *medium* or *severe*. Then, if there are *minor*, *medium* or *severe* constructive defects, the *extent* and the *complexity* of the repair work was determined. The *extent* of the repair work takes into account the amount of the work required and was assessed in a four categories scale: *localised*, *medium*, *extensive* or *total*. The complexity of the repair work takes into account the difficulties of carrying out the work and was assessed in a three categories scale: *simple*, *medium*, *difficult*.

The assessment of spatial defects was divided into two factors: *severity* of the defect and *feasibility* of the intervention. First, the *severity* was assessed on the same four categories scale used for the constructive defects, but according to the rules defined in applicable legislation (Table 1).

For spatial defects classified as *medium* or *severe*, the functional elements that had to be intervened to repair the defect were specified, indicating for each one the *extent* and the *complexity* of the intervention. These interventions are additional to those needed to repair constructive defects. The

feasibility of the intervention was also assessed, using the following scale: *in the building*, *in the lot*, *in other buildings*, *in contiguous lots* and *in the public space*.

Table 1. Rules for assessing the severity of the spatial defects.

Very slight	*Minor*	*Medium*	*Severe*
Fulfils the general legislation in force	Does not fulfil the general legislation in force	Does not fulfil the requirements of specific regulations for illegal buildings	Does not fulfil an absolute minimum, compromising the health and safety of persons

Defects in the relation to other buildings were assessed by five factors: *parts of contiguous buildings above or under the assessed building*; *distance between windows of the assessed building and windows of other nearby buildings*; *distance between the buildings' roof* (when it does not comply with fire resistance requirements) *and windows of nearby buildings*; *windows of the assessed building on the edge of a bordering lot*; and *obstacle-free distance of habitable room windows*. The assessment of each of these factors was carried out using the four level scale adopted for the *severity* of the defects. These factors aim to assess defects that could not be verified with the existing mapping.

A more detailed presentation of the assessment method was done in a previous paper [Vilhena & Pedro 2010].

4 MAIN SPATIAL DEFECTS

4.1 Relation between buildings

Regarding defects in the relation between buildings, the results were the following:

1) few buildings had parts overlapping other buildings;
2) almost half of the buildings had windows near windows of nearby buildings (*i.e.*, less than 6.0 meters) (Fig. 2);
3) few buildings had windows over roofs of nearby buildings (only roofs that do not comply with fire resistance requirements at a distance less than 3.0 meters);
4) almost one third of the buildings had windows over the edge of a bordering lot;
5) almost half of the buildings had windows near to obstacles that reduced natural light (Fig. 3).



Figure 2. Small distance between windows of neighbouring buildings.



Figure 3. Windows opened to an alley with about 1 meter width.

The prevalence of defects in the relation between buildings is presented in Table 2. If we combine the buildings that have medium or severe defects of number 2), 4) and 5), we find that 65% of the buildings have problems with windows. Furthermore, 12.5% of the buildings have the three types of problems simultaneously.

Table 2. Gravity of defects in the relation between buildings.

Type of defect	*Severity of defect (%)*			
	very light	*minor*	*medium*	*severe*
Parts overlapping other buildings	95.8	–	4.2	–
Windows near to windows of nearby buildings	54.8	1,7	13.3	30.2
Windows over roofs of nearby buildings	91.5	1.4	2.8	4.3
Windows over the edge of a bordering lot	70.8	–	29,2	–
Windows nearby obstacles that reduced natural light	51.2	2.5	10.1	36.2

4.2 Common use spaces

In about 60% of the lots there were no common use spaces (*i.e.* spaces whose use is shared by more than one unit). The evaluation of spatial defects in common use spaces included horizontal circulation (atria, corridors and landings) and vertical circulation (stairs and ramps).

Vertical circulation spaces have more defects than horizontal circulation spaces. In 19% of the lots there was vertical circulation spaces with severe and medium defects, while in only 10% of lots there were horizontal circulation spaces with some type of defect (Table 3).

Table 3. Gravity of defects in common circulation spaces of lots.

	Type of defect (%)				
	not applicable	*very light*	*minor*	*medium*	*severe*
Horizontal circulation	61	27	2	2	8
Vertical circulation	63	16	2	5	14

The most common defect in horizontal circulation spaces was an insufficient width of rest zones in front of the main doors of units or even the total absence of this zone. The most frequent defects in vertical circulation spaces were: low ceiling height, high rise and small tread of steps (Fig. 4) and narrow stairs (Fig. 5).



Figure 4. Stairs with high rise steps.



Figure 5. Narrow stairs with uneven development.

The main problem was the poor accessibility conditions in the buildings to access to units. This, in addition to affecting the safety and comfort in normal use, represents a special risk in emergency situations (*e.g.*, in case of fire).

The correction of spatial defects can be done within the boundaries of the building or on the lot in 84% of horizontal circulation spaces and in 88% of vertical circulation spaces. In the remaining cases, spatial defects can only be solved by using the adjacent lot, the adjacent building or the public space (Table 4). Therefore, it is feasible to solve the majority of spatial defects of the common spaces.

Table 4. Feasibility of the interventions to correct spatial defects.

	In the building (%)	*In the free space of the lot (%)*	*In the free space of adjacent lots (%)*	*In bordering buildings (%)*	*In the public space (%)*
Horizontal circulation	63	21	2	6	8
Vertical circulation	66	22	2	4	6

4.3 Units

The assessment of spatial anomalies in residential units was divided into habitable rooms (*i.e.*, kitchen, living room and bedrooms) and non-habitable rooms (*i.e.*, toilets, bathrooms, corridors, stairs, halls, marquees and pantries). When assessing the non-residential units no distinction was made between types of spaces. Due to the wide diversity of uses that non-residential units have, the specific requirements for the operation of each type of unit were not assessed. These requirements are verified by the municipal authority when the use permit is granted.

50% of the units had spatial defects (Fig. 6). This percentage increases to 54% for residential units. The main space defects in habitable rooms of residential units were: insufficient daylighting and ventilation, low ceiling height and cramped areas.

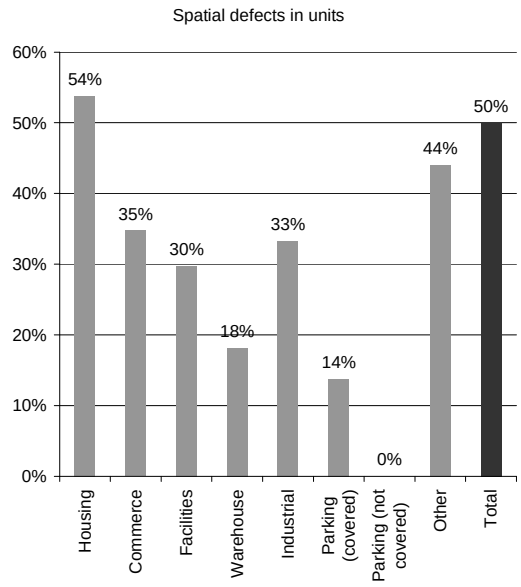

Figure 6. Spatial defects by type of use of units.

The insufficient daylighting and ventilation of rooms was found in about 70% of the units with spatial defects. This defect is due to rooms having small windows or no windows at all. Since many buildings only have one façade, many rooms inside the building only receive daylight through openings to other rooms.

Low ceiling height of rooms was found in about 30% of the units with spatial defects (Fig. 7). This defect is more common in units located in attics. Solving this defect requires extensive and complex interventions on the structure, roof, walls and installations.

Rooms with floor area below the regulatory provisions were found in about 15% of the units with spatial defects. The rooms used as kitchens or bedrooms are particularly undersized (Fig. 8). In some cases, storage spaces were converted into bedrooms, and have an area less than 3 square meters. In most cases, bedrooms with very small floor area had no daylighting or ventilation. Undersized rooms had also more constructive defects.



Figure 7. Bedroom with low ceiling height.



Figure 8. Undersized kitchen.

The main space defects in non-habitable rooms of residential units were: undersized toilets and bathrooms, low ceiling height, narrow corridors, high risers and small treads of steps. There were rooms with non-regulatory path of access, such as toilets with access through a kitchen, a common space or an outdoor space.

In non-residential units, the most frequent spatial defect was the low ceiling height of rooms, particularly in toilets. This defect was identified in 18% of the non-residential units.

5. FINAL REMARKS

The main conclusion is that the lack of urban planning, the confinement of the terrain and the continuous arrival of new residents have led to an overcrowded and disordered urban fabric. Buildings are built on any free space, decreasing public circulation spaces, escape routes and access to daylight and solar exposure. Furthermore, buildings are mainly self-built by residents without design and do not comply with recognized technical good practices. As a result there is a general lack of habitability and a quick decay of buildings' condition.

The overcrowding of the district, the urgent need to provide accommodation, the limited resources of the population, the lack of local authorities building control and the limited institutional support, led to the construction of a district where half the buildings do not meet the requirements set by the Portuguese building regulations. Building regulations set minimum quality requirements to ensure that

buildings are safe, healthy, energy-efficient and accessible to everyone who lives and works in and around them. Therefore, failure to comply with the building regulations means that habitability conditions are jeopardized.

The requirements of the building regulations are set in the context of the prevailing cultural, social, climatic, economic and technological conditions in a particular society. The general Portuguese building legislation is geared to construction of new housing. Thus, it can be argued that the performance level defined by these regulations is too demanding for a situation of acute urgency and need of lodging. However, these buildings fail to fulfil even the requirements set in specific regulations for the regularization of illegal buildings. Therefore, units that did not meet these requirements must be either demolished or made fit to live in.

ACKNOWLEDGMENTS

Thanks are extended to dwellers of BACM, IHRU technicians that participated in the inspections, Amadora Municipality and colleagues from LNEC involved in the study.

REFERENCES

Coelho, A. B. 2008, *Análise das Condições de Habitabilidade do Edificado Existente no Bairro do Alto da Cova da Moura – Organização geral do estudo e pré-análise*, LNEC, Report no. 247/2008 – NAU, Lisboa.

Pedro, J. B., Aguiar, J. & Paiva, J. V. 2006a, *Proposta de uma metodologia de certificação das condições mínimas de habitabilidade*, LNEC, Report no. 397/2006 – DED/NAU, Lisboa.

Pedro, J. B., Paiva, J. V., Raposo, S. & Vilhena, A. 2006b, *Proposta de um método de avaliação do estado de conservação de edifícios: Discussão e aplicação experimental*, LNEC, Report no. 185/2006 – DED/NAU, Lisboa.

Pedro, J. B., Paiva, J. V., Vilhena, A. 2008a, Portuguese method for building condition assessment, *Structural Survey*, **26**[4], 322-335.

Pedro, J. B., Vilhena, A., Bento, J., Paiva, J. V. & Coelho, A. B. 2008b, *Colaboração do LNEC na análise das condições de habitabilidade do edificado no Bairro do Alto da Cova da Moura: Método de avaliação das necessidades de reabilitação: Concepção, aplicação experimental e formação de técnicos avaliadores*, Report no. 267/2008 – DED/NAU, Lisboa, LNEC.

Vilhena, A., Pedro, J. B. & Paiva, J. V. 2007, *Apoio do LNEC na reavaliação do estado de conservação dos imóveis da fundação D. Pedro IV*, LNEC, Report no. 251/2007 – DED/NAU, Lisboa.

Vilhena, A. & Coelho, A. B. 2008, *Colaboração do LNEC na análise das condições de habitabilidade do edificado no Bairro do Alto da Cova da Moura. Avaliação das necessidades de reabilitação do edificado. Relatório de síntese*, LNEC, Report no. 266/2008 – DED/NAU, Lisboa.

Vilhena, A. & Pedro, J. B. 2010, 'Assessment method for buildings' rehabilitation needs: Development and application', Proc. *2010 CIB World Congress – Building a better world*, The Lowry, Salford Quays, United Kingdom, 10 13 May 2010.

XII DBMC
International Conference on Durability of Building Materials and Components
PORTO - PORTUGAL, April 12th-15th, 2011

Dependencies Between Laboratory Simulated and Real Degradations of Cooling Towers Surface

Zdeněk Šnirch [1]

ABSTRACT

The article is based on the results of the long term research made on such a real cooling tower, by which the regular technical structural researches were executed in the longest time-interval and the results of which were available. The results were processed into the form of "the degradation curves" describing the real time dependence of the degradation. Subsequently, the comparison of the coating composition degradation curves with the results of the long-term stressing of similar materials in strongly aggressive environments was done. Based on the experiments and the facts resulting from the long term technical structural researches, the new methodical procedures of the diagnostics and rehabilitation of reinforced concrete structures of cooling towers were formulated.

KEYWORDS

Cooling tower, Concrete, Surface, Degradation, Coat.

[1] Institute of Technology of Building Materials and Components, Faculty of Civil Engineering of the Brno University of Technology (BUT), Brno, Czech Republic, snirch.z@fce.vutbr.cz

1 INTRODUCTION

Cooling towers with natural gravity flow are designed in principle, in all countries, as reinforced concrete structures acting in a flexible state. The cooling tower of type ITTERSON and of height 30 – 120 m (Figure 1) is founded on circular reinforced concrete foundations in which the inclined props are fixed in such a way that each two create a "V" shape and support the shell structure of the tower. The tower is topped by a "U" shaped gallery. The monolithic shell in the form of a hyperboloid of revolution is made by the use of a flying concrete form. The top gallery has either stiffing or walking on function and there is an access steel ladder fixed into the shell. There is a built in pre-cast reinforced concrete cooling system (structure made of columns, beams and troughs) which is completely separated from the shell. There is also a water tank of to contain cooling water located at the bottom part on the bed at which are located the foundation pads for the columns of the built in cooling system. The entrance to the tower is made through a door in the shell.

2 SERVICE LIFE INFLUENCES

The durability of cooling tower casings is influenced not only by operational loading, but also by manufacturing defects. The most important defects are an insufficient concrete layer covering the steel reinforcement, poor workmanship or insufficiently treated construction joints and low quality concrete [Emmons, Drochytka and Jeřábek 1999].

Cooling towers are further repeatedly loaded by wind and temperature fluctuations. Temperature effects on concrete structures and their components become evident by changes in volume. As the results of these effects, stress gradients are formed and lead to damage of the structure. This stress can cause crack formation, separation of the surface layer, or excessive deflection. The temperature cycle causes continuous damage to cooling towers. The most serious damage occurs during interrupted operation of towers in the winter season, when the water cyclically freezes in the shell and the result is the destruction of the concrete. The consequence of repeated freezing and thawing is the disintegration or crumbling of the concrete. The freezing water in capillaries of the structure increases in volume during transformation into ice. The dilatation causes local stress, which tears the surrounding concrete.

The next significant influence, that is known to decrease the service life of cooling tower casings, is degradation caused by aggressive chemicals. Some chemical substances in solution can attack individual components of the concrete. Aggressive chemicals can be divided into: inorganic acids, organic acids, alkaline solutions, solutions of salts and different mixtures in solution. Concrete damage caused by acids is the result of the reaction between acid and alkaline calcium hydroxide of hydrated Portland cement. Soluble calcium compounds are formed in water during the reaction and they are eventually leached out. However, acids can dissolve even limestone and dolomite aggregates.

Among the important aggressive factors belong aggressive gases such as CO_2 and SO_2, which cause carbonation and sulphatation of concrete. Concrete carbonation is the reaction between carbon dioxide (CO_2) in the atmosphere, which has acidic characteristics, and the products of cement hydration. Normal air contains carbon dioxide in relatively low concentrations (0.03 %). The level of CO_2 in industrial atmospheres is generally higher. Carbon dioxide penetrates concrete pores by diffusion and reacts primarily with calcium hydroxide, which is dissolved in water. The result of this reaction is the decrease of concrete alkalinity, to a value of about pH 9.6, which causes the loss of reinforcement steel protection and which was initially secured by the concrete cover. Thus the layer of passive reinforcement protection is disturbed and the corrosion of reinforcement takes place [Matoušek and Drochytka 1998].

It is known that one of the main consequences of degradation is the decrease of concrete pH value, which leads to corrosion of reinforcement. The corrosion of reinforcement is mostly an electrochemical process which needs anode, cathode and electrolyte. The presence of moisture in the

concrete mass of the cooling tower is an appropriate electrolyte and the steel reinforcement forms the anode and the cathode. Electric current flows between cathode and anode and the reaction results in an increase of metal volume because (Fe) iron oxidizes to $Fe(OH)_3$ and $Fe(OH)_2$ and it is present as FeO(OH), i.e. rust. For this reaction to progress, the presence of water and oxygen are necessary. In concrete of good quality the corrosion process is slow. Accelerated corrosion takes place when the pH value (alkalinity) of the concrete decreases for instance by carbonation, sulphatation or when aggressive chemicals are added into cement and/or when the reinforcement is made from different metals. Further reasons can be vagabond currents and local concentration cells given by irregular chemical medium.

Without executing rehabilitation measures it is impossible to maintain the reliability of a degraded structure. Every delay of rehabilitation lowers its effectiveness and increases the costs for the realization of rehabilitation. In instances where measures for rehabilitation have not been realized, the ageing of concrete will accelerate and the result, owing to concrete degradation, will be the end of the structure's service life.

3 METHODS FOR DETERMINING THE STATE OF CONSTRUCTION

For successful and permanent rehabilitation of cooling tower casings, it is necessary to execute a detailed technical diagnosis of the state of concrete and reinforcement. On the one hand, from the physio-mechanical point of view, (chiefly compression strength, tensile strength of surface layers etc.) and on the other hand from the point of view of physio-chemical parameters (mainly e.g. degree of carbonation, contamination grade). By performing diagnostic tests it is possible to determine the actual state of the structure to record the total extent and severity of defects and failures, and define the main reasons for failure.

The normal method used for diagnosing these problems is the completion of a detailed building-technical survey. By building-technical survey one means carrying out activities that are capable of providing, by means of completing different field and laboratory methods, useful information concerning the condition state of the selected structure; this assumes that there is sufficient funding to ensure an in-depth survey.

The extent of the building-technical survey is given primarily by the intent of the survey, by the condition state of building to be examined and by other conditions. The extent of the survey should be defined by person responsible for the reconstruction or rehabilitation design who is also the most competent to evaluate the extent of information required [Drochytka *et al.* 2003].

Degradation curves for the concrete elements will be compiled pursuant to the long-term monitoring of the structure and retrieval of building technical inquiry records. . The overall cooling tower condition state would be calculated on the basis of the primary degradation curves, as shown in Figure 2, and from this a very exact estimate of the service life of the cooling tower can be obtained.

Degradation curves will be created separately for the outer and inner surface of the shell; to ensure proper processing of information from which the degradation curves will be developed, the shell has been divided in the manner shown in Figure 1.

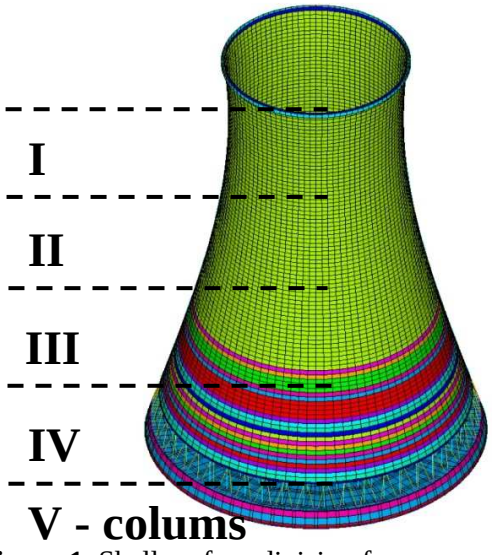

Figure 1. Shell surface division for curves creation.

Methods of processing degradation curves for the Itterson cooling tower; the degradation curves were created for these parameters:

- Concrete surface failures
- Carbonation depth
- Concrete compression strength
- steel reinforcement corrosion
- Modulus of elasticity of concrete

Records obtained from technical inquiries on buildings over several time periods were used as a basis for processing the degradation curves. The degradation curves were processed for every level the tower shell (Figure 1). From results of building technical inquiries obtained each year a set containing the values from each parameter will be created for every tower level (i.e. levels I to V) and on this basis, average values will be determined from data retrieved over several periods.

Conditions of degradation curves for each parameter are determined separately or each parameter as follows:

- Concrete surface failures
  Degradation curves will be process for each category of failure depth defined below:
  Category of failure depth for shell and diagonal columns
  - from 0 to 5 mm
  - from 6 to 25 mm
  - from 26 to 40 mm
  - from 41 to 60 mm
  - other categories by 20 mm concrete depth, depending on degradation level

- Carbonation depth
  Degradation curves which represent concrete carbonation depths will be processed from average values for each tower level and for the entire structure (shell, diagonal columns). One curve will be processed from each period.

- Concrete compression strength and modulus of elasticity
  Degradation curves which represent compression strength will be processed from average values for each tower level and for the entire structure (shell, diagonal columns).

One curve will be processed from each period.

The modulus of elasticity values will be calculated from compression strength tests undertaken according to ČSN 73 0038.

- Steel reinforcement corrosion
  Category of corrosion for Shell and diagonal columns
  - 0 - 5 % profile decrease
  - 6 - 15 % profile decrease
  - 16 - 30 % profile decrease
  - 31 – 50 % profile decrease
  - more than 50 % profile decrease.

4 LABORATORY TESTS METHODS

Changes of the behaviour and characteristics of the protective coatings used for the surfaces of the cooling tower were subjected to an aggressive atmosphere and monitored in the laboratory for 90, 180, 270 and 360 days. The protective coating product used to cover the surfaces of the cooling tower was Sikagard 680S. . To simulate the corrosion induced by the action of different aggressive media, as might be found in a real atmosphere within the cooling tower, the surface of specimens samples were exposed to the media provided in Table 1..

Table 1 Categories and properties of aggressive media.

	Concentration of substance	*Relative humidity of air*
Gaseous SO_2	100%	75%
Gaseous CO_2	100%	75%
Sulphate solutions	36 000 mg / l	---
Periodical frost influence	---	---

5 LONG-TERM MONITORING OF COOLING TOWER DEGRADATION

Figure 2 provides an example of a degradation curves for concrete failures of the tower shell. These curves include a line for each category and a line for the general degradation of the structure which is a sum of all categories. From Figure 2 it can be seen that the cooling tower was built in 1971. The results from the technical structural survey of the cooling tower are shown for the years 1993 to 2006. There were 5 surveys completed in this time period and the tower was completely rehabilitated in 1994. Thus given the rebuilding of the tower in 1994, this allowed monitoring of the degradation process of materials applied to the external surface of the tower and indeed from the very beginning of the process when the environmental factors causing degradation were first initiated.

5.1 Real stressing of the tower

To determine the nature of stressing the tower in-situ, the data from the daily operational hours were used and the average temperature of the environment was retrieved for the years 2002 to 2006. Based on this data it was possible to say, that one year consisted of 120 – 150 temperature cycles, which are equivalent the cycles of simulated freezing and thawing undertaken in the corrosion laboratory.

5.2 Shell surface degradation curves

The degradation curves created from the results of the technical structural survey do not only represent a particular environmental or corrosion effect, but the interaction of many influences acting on the structure's surface. Given the specific use of the cooling tower and the presence of aggressive gasses such as CO_2 and SO_2 as well as the effects of freeze-thaw cycles caused by temperature

fluctuations of the local environment within the tower and the ambient temperature conditions the tower is subjected to persistent and aggressive agents causing deterioration of the structure; indeed these are considered to be the primary deteriorating agents acting on the external surface of the tower structure. Hence the laboratory durability testing work that was carried out on the Sikagard 680S coating provided a comparison of the degradation curves and thus these results could be useful in determining any interacting effects among the different aggressive agents. The curves, which represent the laboratory testing of the Sikagard 6802S coating, were also created by summarising the losses of individual properties after long-term exposure to the aggressive action of the CO_2 and SO_2 gasses and the freeze-thaw cycles. Therefore they are values that in principle simulate the response of these three laboratory simulated deteriorating agents for 360, 540 and 720 days. The resulting degradation curves of selected surface properties of the cooling tower and the laboratory values are given in Figure 2 and Figure 3.

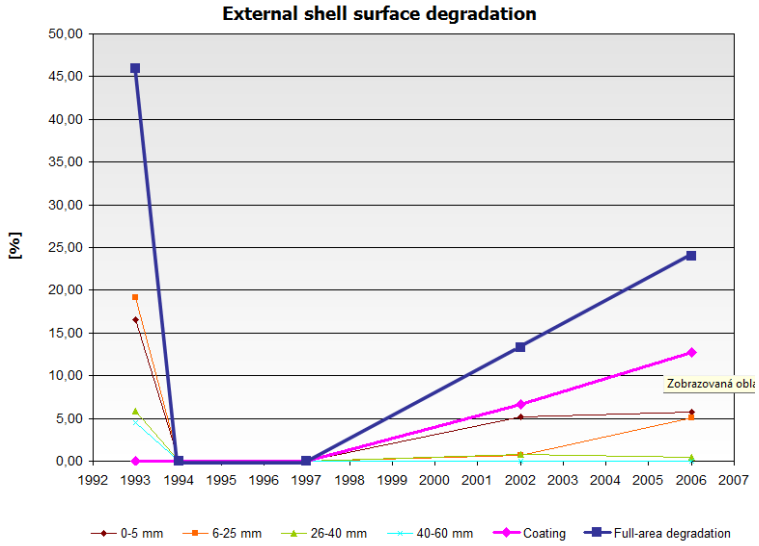

Figure 2. The degradation curves of the concrete and the paint of the entire tower.

The complete reconstruction of the tower in 1994 is clearly obvious from the chart. The extreme degradation before the reconstruction is also very noticeable. The external concrete surface of the tower was not protected by the coating, which is considered to be one of the main causes of degradation evident in 1993. The surface degradation itself started during the period between 1997 and 2002.

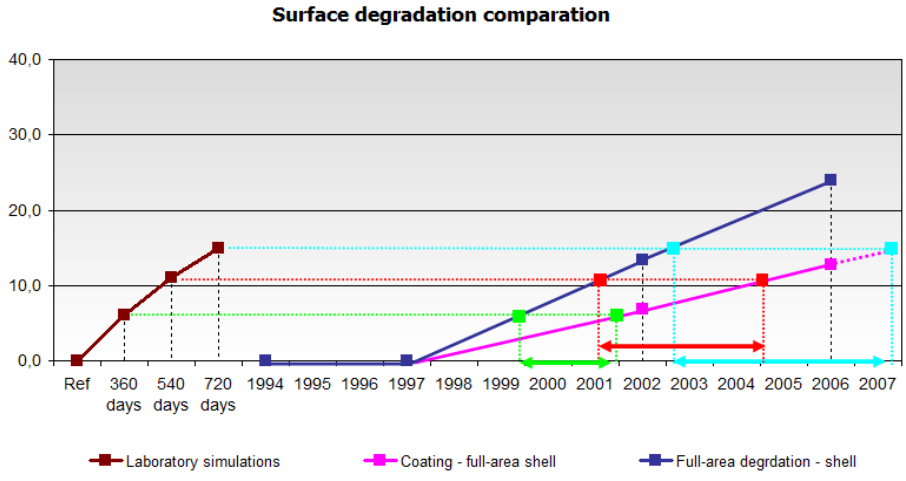

Figure 3. The comparison of the technical structural research results and the laboratory testing of the paint Sikagard 6802S durability.

It is not possible to say that the failure of the cooling tower surface is primarily caused only by the degradation of the coating. The corrosion of the reinforcing steel, which is caused by the carbonation or humidity under an otherwise good coating, is another one of the factors affecting surface degradation. Due to the pressures brought about by an increase in volume of corrosion products, spalling of the entire covering concrete layer may nonetheless occur even with good coating is applied to protect the concrete surface. These failures are thus not caused by the degradation of the coating. So the real degradation of the coating composition is by the given time period always in the interval between the real proven paint degradation and the real proven total degradation of the surface concrete layers.

Based on this principle real time periods are marked in the upper chart, which corresponds to a degree of degradation to times of observation of sample deposits in the aggressive environments, whereas the beginning of degradation is always set to the year of the rehabilitation 1994.

For example, the 360 day deposit of Sikagard 6802S paint in the environment of aggressive gasses CO_2 and SO_2 and the freezing cycles thus corresponds with the real degradation of the structure with the beginning in 1994 and end between years 1999 and 2001; so the real time in atmosphere of ca. 5 to 7 years.

The dependencies gained from the experiments and the degradation curves can be summarized into the following table:

Table 2. The dependencies between in a lab simulated and real environment.

Parameter	*Time of deposit in a lab [days]*	*Corresponding time on real structure [years]*
The surface degradation of the coating composite.	360	5-7
	540	7-10
	720	10-13
Cohesion with under layer	360	10-11
	540	11-12
	720	12-13
The depth of carbonation	360	0
	540	4
	720	8

The cyclic action of the frost is, no doubt, one of the biggest effects. The following formulated dependence is based on the number of cycles acting for one year on the cooling tower and on the fact that 90 days in cyclic testing apparatus is ca. 375 days in reality; Thus 360 days represents ca. 1500 cycles. When stating 120-150 cycles a year acting on the cooling tower envelope it is ca. 10-12.5 years of real exposure of the tower. With regards to this formulation it is possible to consider that the values given in the previous table as realistic.

5 CONCLUSIONS

The rehabilitation of cooling towers is technically and economically a very difficult task. Therefore it is necessary to carefully review the condition state of such towers. Long-term monitoring of the condition state of cooling towers is definitely the right way to obtain an reliable estimate of its service life. By optimization of results from these curves select one should be able to propose an appropriate rehabilitation method from both the technological point of view and from the point of view of the

rehabilitation of concrete materials. Values for the already completed degradation curves will be used as basis for the subsequent research.

The exact determination of the dependencies of concrete to in-lab simulated aggressive environments to that occurring in-situ is of course possible, however, as a very difficult one or almost impracticable and its general formulation is conditional on the long-term monitoring of the materials and under layers of totally identical properties and technologies used for their application. It was not possible to satisfy these requirements in this work and results of this part represent the initial steps needed to determine the expected long-term response of protected and coated concrete.

ACKNOWLEDGMENTS

The research work presented in this paper has been supported by the VVZ MSM 0021630511 "Progresivní stavební materiály s využitím druhotných surovin a jejich vliv na životnost konstrukcí" and GACR P104/10/P279" (i.e. "The development of Ecologicaly and Economicaly convenient coat systems primary for the protection of concrete against atmospheric corrosion)

REFERENCES

Bradáč, A.: Teorie oceňování nemovitostí. 2. vydání.Akademické nakladatelství CERM, Brno, 1994, 482 s.ISBN 80-85867-36-2.

Bydžovský, J.; Dufka, A.; Šnirch, Z. *Využití fyzikálně-chemických postupů pro stanovení stáří trhlin*. *Zpravodaj WTA CZ.* 2006. 2006(1-2). p. 9 - 11. ISSN 1213-7308.

Drochytka, R., Bydžovský, J., Brožovský, J. a kolektiv *Stavební vady od A do Z.* 1. vydání. Praha: Verlag Dashöfer, nakladatelství, spol. s r.o. 2004, ISSN 1214-7060.

Drochytka, R., Dohnálek, J., Bydžovský, J., Pumpr, V. Technické podmínky pro sanace betonových konstrukcí TP SSBK II. 1. vydání. (Technical conditions for rehabilitation of concrete structures) Sdružení pro sanace betonových konstrukcí, Brno 2003, 210 stran, ISBN 80-239-0516-3

Emmons, P., H., Drochytka, R., Jeřábek, Z. Sanace a údržba betonu v ilustracích. (Rehabilitation and maintenance of concrete in pictures) 1.vydání. Brno: Akademické nak-ladatelství CERM, 1999, 334 stran, ISBN 0-87629-286-4.

Matoušek, M., Drochytka, R. Atmosférická koroze betonů. (Atmospheric corrosion of concrete) 1. vydání. Praha: IKAS, 1998, 171 stran, IBSN 80-902558-0-9.

Šnirch, Z. *Možnost stanovení stáří trhlin v ŽB konstrukcích*. Silnice a železnice. 2007. 2(2). p. 20 - 23. ISSN 1801-822X.

XII DBMC
International Conference on Durability of Building Materials and Components
PORTO - PORTUGAL, April 12th-15th, 2011

Condition-Based Service Life Prediction and Planning in Practice

Johann McDuling [1]

ABSTRACT

This paper looks at service life prediction and planning based on a combination of condition assessments and the application of a service life prediction methodology using the stochastic Markov Chain with Neuro-Fuzzy Artificial Intelligence (Service Life Prediction Beyond the 'Factor Method' - 11DBMC Best Paper Award) to quantify changes in condition over time.

The model, which considers the seven modifying factors of the 'Factor Method' for service life prediction as well as the age and current condition of the building or component to calculate changes in condition over time, enables the calculation of typical degradation curves for a variety of building and component types in various physical and operational environments. These curves are used to predict the remaining service life, assess the effectiveness or appropriateness of the current maintenance regime or level, do life cycle planning and develop pro-active strategies to prevent premature failure or reduced service life.

The application of the service life prediction methodology in combination with condition assessments is illustrated with four case studies on an active learning environment building, a university campus and four multi level office buildings.

KEYWORDS

Condition assessment, Service life prediction curves.

[1] Asset Management Strategist, Melbourne, AUSTRALIA, johannmcduling@gmail.com

1 INTRODUCTION

The objective of this paper is to illustrate the use of a condition-based service life prediction methodology to provide asset managers with better-informed options and strategies.

A Service Life Prediction model [McDuling et al 2008] is used to predict changes in condition over time and produce Service Life curves for a building or component. By plotting the assessed current condition of the building or component on these curves, the remaining service life can be predicted and better informed asset management options and strategies can be developed.

The Service Life Prediction model is based on a combination of the Markov Chain and Neuro-Fuzzy Artificial Intelligence, and the seven modifying factors of the 'Factor Method' [ISO 15686-2:2001] for service life prediction, as well as the age and current condition of the building or component to quantify changes in condition over time.

This application of condition assessments in combination with service life prediction is illustrated with three case studies.

2 CONDITION ASSESSMENTS

A five-point colour-coded rating system is used to assess the percentage of the asset in each condition category as illustrated in Table 1 below.

Table 1. Condition assessment criteria.

Rating	*Condition*	*Action Required*	*Assessment* ***(Total = 100%)***	*Maintenance Type*
5	Excellent	Preventative Maintenance	% of asset in Condition 5	Normal Maintenance
4	Good	Condition-based Maintenance	% of asset in Condition 4	
3	Fair	Repairs	% of asset in Condition 3	Backlog Maintenance
2	Poor	Rehabilitation	% of asset in Condition 2	
1	Very Poor	Replacement	% of asset in Condition 1	

Assessing the percentage of the asset in each condition category enables the quantification of the extent of maintenance backlog and development of condition profiles as illustrated in Fig. 1 below.

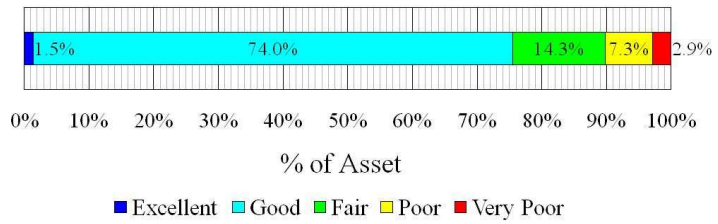

Figure 1. A typical condition profile, showing the percentage of the building in each condition category. The extent of maintenance backlog amounts to 24.5%.

The average assessed condition of the profile in Fig. 1 is 3.64 ('Fair'). If a single rating was applied the building's condition would be assessed as 4 ('Good') and the small percentages in Condition 1 ('Very Poor': 2.9%) and 2 ('Poor': 7.3%), with higher levels of associated risk, would not be visible to decision-makers and consequently overlooked.

3 SERVICE LIFE CURVES

A Service Life Prediction model [McDuling et al 2008] is used to quantify changes in condition over time and produce Service Life curves for a building or component. The model is based on a combination of the Markov Chain and Neuro-Fuzzy Artificial Intelligence, the seven modifying factors of the 'Factor Method' [ISO 15686-2:2001] for service life prediction, as well as the age and current condition of the building or component to quantify changes in condition over time [McDuling 2006].

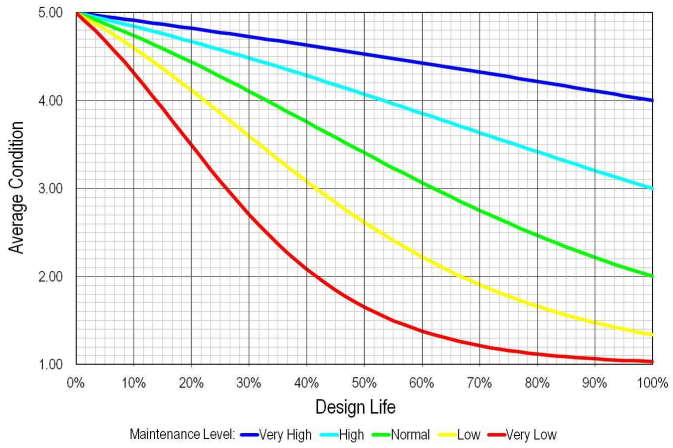

Figure 2. Generic service life curves showing the predicted change in average condition over the design life of the asset for various levels of maintenance, assuming high quality (4) of material/fabric and work execution, a high level (4) of design, slightly aggressive (3) external and internal climates and a less favourable (4) to slightly aggressive (3) operational climate using a rating scale similar to the condition rating scale in Tab. 1.

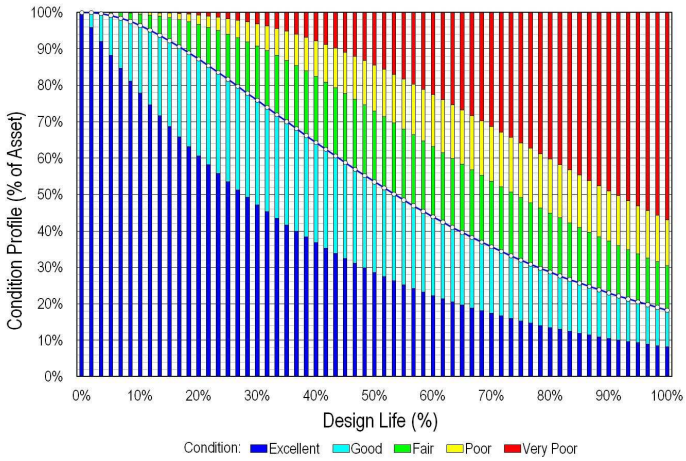

Figure 3. Predicted changes in the condition profile over the design life of an asset. The area below the blue curve represents the percentage of the asset in 'Excellent' and 'Good' condition.

According to De Sitter's Law of Fives [Vanier 2000], backlog maintenance (repairs, rehabilitation and replacement/renewal) can cost 5 to 25 times more than normal maintenance. The objective of strategic asset management is therefore to maximise the area below the blue curve (i.e. the percentage in 'Excellent' and 'Good' condition requiring normal maintenance) within limitations. The area above the curve represents the percentage of the asset requiring backlog maintenance.

The generic service life curves in Fig. 3 are used to develop asset management strategies by changing the horizontal axis to a time scale and selecting the appropriate design life of the building or component, condition threshold and rehabilitation or renewal strategy as illustrated in Fig. 5 below.

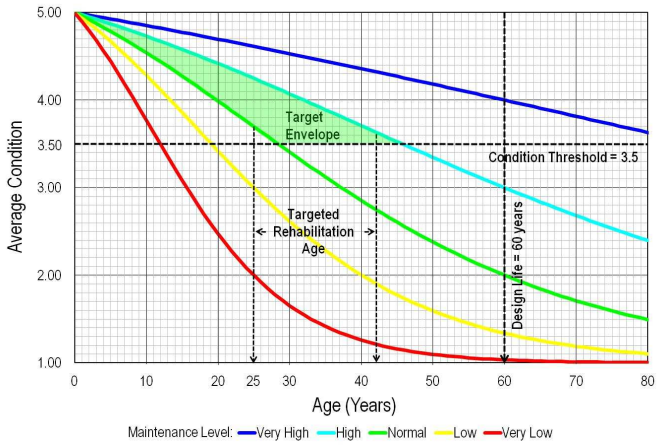

Figure 4. Service life curves illustrating condition threshold, target envelope and targeted rehabilitation age assuming a design life of 60 years.

The condition threshold is the minimum acceptable condition, while the target envelope is defined by the area between two maintenance level curves and the selected condition threshold, as illustrated by the shaded area in Fig. 5 above.

The appropriate maintenance strategy is determined by the decision to rehabilitate or renew the building during its design life or not (investment strategy) and the selected condition threshold. The objective of a strategy not to rehabilitate or renew the building during design life is to achieve a service life that exceeds the design life. The type of asset, design life, degradation and preservation factors [ISO 15686-2:2001] and obsolescence need also to be considered.

Depending on the condition threshold selected, a strategy not to rehabilitate or renew the building during its design life will require a higher maintenance level at a higher maintenance cost compared to a rehabilitation strategy. A higher condition threshold requires a higher level of maintenance at a higher cost during the asset's service life.

In the event of a rehabilitation strategy, a higher condition threshold means a shorter service life and requires an earlier or possibility more than one refurbishment during the asset's design life, but at a lower cost per refurbishment. This could be a good strategy for investment portfolios where retaining high profile tenants prepared to pay for premium accommodation is an objective, or where technical, functional or financial obsolescence could be a consideration.

A lower condition threshold means a longer service life and will require later or no refurbishment, but at a higher refurbishment cost. If the building condition is allowed to deteriorate below the threshold, the risk of losing existing or failure to attract new tenants increases.

To prevent that the average condition of the building deteriorate beyond the condition threshold, planning for the rehabilitation should ideally start two to three years before the condition reaches the threshold level. By doing regular and consistent condition assessments and plotting the assessed condition on the service life curves, maintenance planners can get early warning and start their planning in time before the condition has a negative impact on the performance of the building.

4 CASE STUDIES

4.1 Active learning environment building (Australia)

The first case study looks at a 26-year-old active learning environment building with an aggressive operational environment where students are trained in building trades such as bricklaying, plastering, tiling and stone masonry. The building has a large industrial/factory area as well as offices, lecturing rooms and ablution facilities. It has a gross floor area of 8,375 m^2 and an estimated replacement cost of Au$ 11,900,000. The assessed average condition of the building is 3.64

The required maintenance budget, as shown in Table 4 below, is based on the assessed condition of the building and a maintenance cost model, which is aligned with De Sitter's Law of Fives [Vanier 2000] and based on the estimated replacement cost of the building or component. This methodology is similar to the parametric approach of NASA to estimate deferred maintenance [NASA 2003].

Table 2. Condition-based maintenance budget (Au$) required.

	Normal Maintenance			
	Preventative Maintenance (Condition 5)	Condition-based Maintenance (Condition 4)	Allowance for Unplanned Maintenance	**Total for Normal Maintenance**
Assessed Condition*	1.45%	74.04%		75.49%
Budget Required	$ 148,773	$ 176,240	$ 89,264	$ 414,277
% of Budget Required	9.51%	11.26%	5.70%	26.47%
	Backlog/Deferred Maintenance			
	Repairs (Condition 3)	Rehabilitation (Condition 2)	Replacement (Condition 1)	**Total for Backlog Maintenance**
Assessed Condition*	14.34%	7.31%	2.86%	24.51%
Budget Required	$ 341,306	$ 435,102	$ 374,145	$ 1,150,553
% of Budget Required	21.81%	27.81%	23.91%	73.53%
	Estimated Total Maintenance Budget Required			**$ 1,564,830**

* % of building in each condition category weighted based on estimated replacement cost.

Table 4 illustrates the consequences of backlog maintenance and De Sitter's Law of Fives: 24.51% of the total building requires backlog maintenance, which amounts to 73.53% of the total budget required.

4.1.1 Maintenance Options

Option 1 provides for the allocation of available funds to the maintenance categories based on the ratio of budget required per category to total budget required (as shown in Table 4 above), i.e. 9.51% of the available budget is allocated to preventative maintenance. This method, the 'Balanced Approach', ensures that funds are also allocated to Preventative Maintenance and not just Backlog Maintenance. If an amount of $650,000 is allocated based on the 'balanced approach' the average condition will improve to 4.20, which is on the top end of the target envelope in Figure 6 below, i.e. it will take $650,000 allocated based on the 'balanced approach' to change the condition from the bottom to the top of the target envelope. This will increase the current estimated remaining service life from two years to 12 years.

Option 2 provides for the eradication of all Condition 1 ('Very Poor') and Condition 2 ('Poor') and requires $809,247. This will improve the average condition to 3.97 and the estimated remaining service life of nine years.

Option 3 provides for the eradication of all maintenance backlog and will require $1,150,553 to improve the condition to 4.26, and will add 12 additional years to the estimated remaining service life.

Option 4 provides for total refurbishment, which will require $1,277,245 to improve the average condition to 4.79 and extend the estimated remaining service life to 24 years.

4.1.2 Option comparison

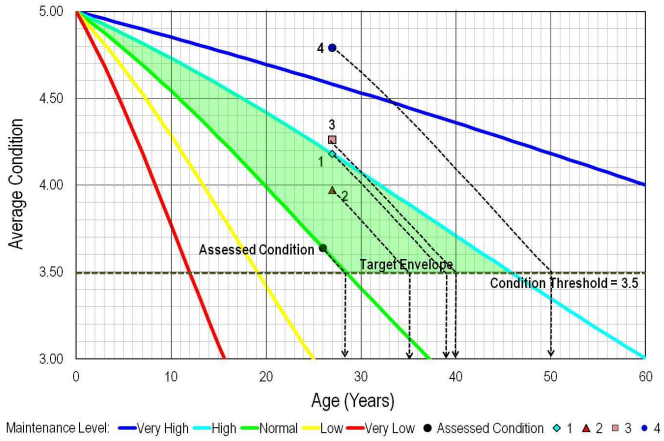

Figure 5. Average assessed condition of an Active Learning Environment Building with predicted changes in condition for four maintenance options assuming continuation of the current maintenance regime.

Table 3. Option Comparison.

Option and Strategy	Budget required (Au$)	Additional Service Life (years)	Cost per additional Service Life year	Condition	% Improve-ment in condition	Cost per 1% improve-ment in condition
1. Balanced budget allocation	$ 650,000	10	$ 65,000	4.20	15.38%	$ 42,250
2. Eradication of 'Poor' & 'Very Poor"	$ 809,247	7	$ 115,607	3.97	9.07%	$ 89,262
3. Backlog eradication	$ 1,150,553	12	$ 95,879	4.26	17.03%	$ 67,549
4. Total refurbishment	$ 1,277,245	22	$ 58,057	**4.79**	31.59%	$ 40,428

Graph 1. Predicted change in condition profile for various options.

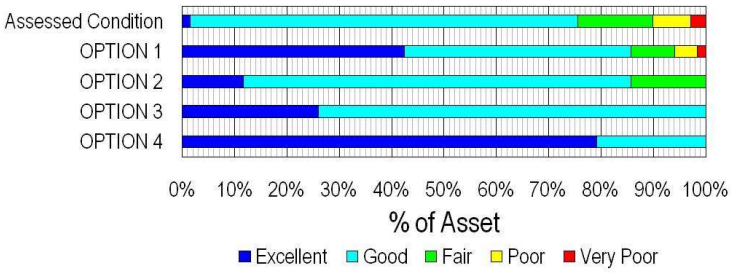

From Fig. 6 the estimated Remaining Service Life is two years.

4.2 Six academic hospitals (South Africa)

This case study of six academic hospitals in South Africa illustrates the value of regular and consistent condition assessments. The condition assessments were undertaken between 1996 and 2005.

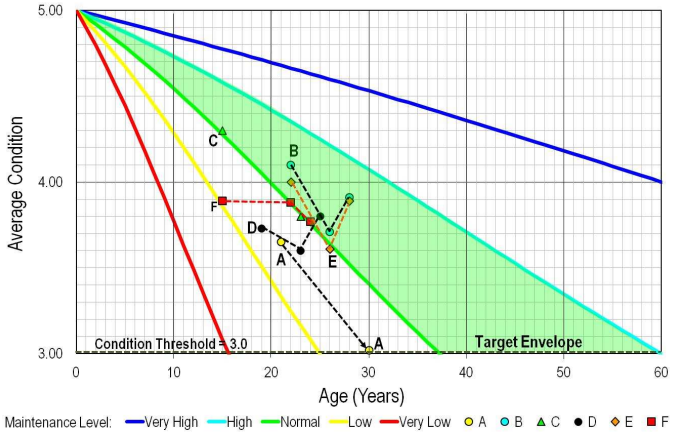

Figure 6. Six Academic Hospitals.

Hospital A illustrates the consequences of too long intervals between condition assessments and has reached the end of its service life only 30 years after it has been commissioned. The maintenance level of this hospital was clearly too low and there was no change in the maintenance regime after the first assessment. In contrast, Hospitals B, D, E and F clearly showed a positive reaction to the condition assessments by the improvement in their condition to fall within the target envelope. In view of the growing demands created by changes in medical and nursing technology and the risk of obsolescence, Hospital C and F may have better maintenance strategies.

4.3 University campus (Australia)

The average condition and age of two sets of university buildings are shown in Fig 1 below. The first set of buildings, numbered from 1 to 26, is academic buildings with a condition threshold of 3.5 and a target condition envelope between Normal and High Maintenance Levels. The second set of buildings, numbered from 27 to 51, is student accommodation with a condition threshold of 4.0 and a target condition envelope between High and Very High Maintenance Levels.

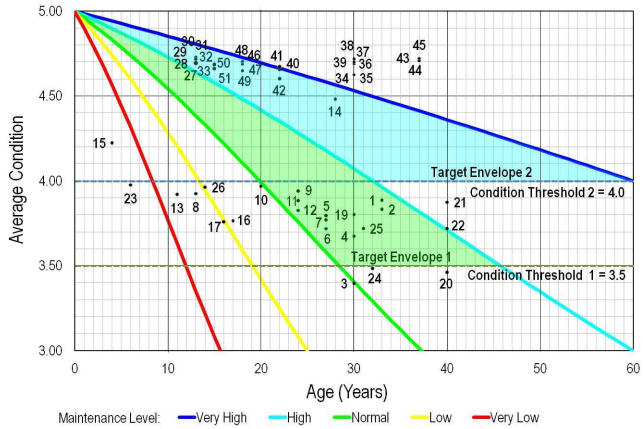

Figure 7. Average condition and age of buildings on a university campus.

4.3.1 Building Set Number 1 – Academic buildings

Although building numbers 1, 2, 4, 5, 6, 7, 9, 10, 11, 12, 19, and 22 and 25 all comply with the condition and maintenance targets, their remaining service life varies between three and eight years, and a strategic review of these buildings should be undertaken as soon as possible. The average condition of building numbers 3, 20 and 24 are below the condition threshold of 3.5 and should have been already rehabilitated or replaced. Building 21, which falls above the target envelope, was refurbished some time ago and has an estimated remaining service life of ten years. Building 14 has just been refurbished and based on the assumption that the current maintenance regime will be continued, has an estimated remaining service life of 30 years.

Building numbers 8, 10, 13, 15, 16, 17, 23 and 26 are all below the target envelope, which can be attributed to a number of factors, such as a too low level or quality of maintenance, quality of work execution, materials and design, and operational environment. These buildings are storage and workshop buildings and it is to be expected that the level of maintenance would be lower compared to the academic buildings. Of concern is however building numbers 15 and 23 that both showed a relatively fast rate of deterioration and although their condition is still well above the applicable condition threshold of 3.5, a detailed 'crawl-through' assessment by experts should be undertaken as soon as possible to establish the cause for the accelerated degradation. Building 15, which is four years old, has an estimated remaining service life of six years or a total service life of only ten years.

4.3.2 Building Set Number 2 – Student accommodation

An important source of income for Australian Universities is international students and in order to attract these students Universities need to provide good accommodation. Buildings providing accommodation for students are therefore refurbished on an annual basis and a higher condition threshold and target envelope apply to these buildings. The condition assessment was done just after these buildings have been refurbished at the beginning of the academic year before the students took occupation, which explains why the condition of building numbers 34 to 39 and 43 to 45 are above the target envelope.

REFERENCES

International Organization for Standardization, ISO 15686-1:2000, *Building and Construction Assets - Service Life Planning - Part 1: General Principles*, Geneva, Switzerland.

National Aeronautics and Space Administration, 2003, *NASA Deferred Maintenance Parametric Estimating Guide Version 2*, Facilities Engineering Division, [web page] http://www.hq.nasa.gov/office/codej/codejx/Assets/Docs/DMParametricEstimatingGuideApr03.pdf Date accessed: 07 November 2010.

McDuling, J.J., Horak, E. & Cloete, C. 2008, *Service Life Prediction Beyond the 'Factor Method'*, Proc. of the eleventh Int. Conf. on Durability of Building Materials and Components, 11dbmc, Istanbul, Turkey, 11-14 May 2008, vol. 4, pp. 1515-1522.

Mc Duling, J.J., 2006, *Towards the Development of Transition Probability Matrices in the Markovian Model for the Predicted Service Life of Buildings*, PhD Thesis, Department of Civil and Biosystems Engineering, University of Pretoria, South Africa.

Vanier, D.J., 2000, *Advanced Asset Management: Tools and Techniques*, Innovations in Urban Infrastructure Seminar of the APWA International Public Works Congress, Louisville, U.S.A, pp. 39-56.

XII DBMC
International Conference on Durability of Building Materials and Components
PORTO - PORTUGAL, April 12th-15th, 2011

Establishing Specific Criteria for the Application of ISO15686 Factor Method for Service Life Estimation

Helena Corvacho [1]
Marisa Antunes Quintela [2]

ABSTRACT

One of the main obstacles for the application of the well-known Factor Method for service life estimation proposed by ISO 15686-1 Standard is the unavailability of treated and systematic information on the real influence of Modifying Factors on the service life. The information is often scattered and presented in a way that hinders its use for the purposes of estimating service life.

The Reference Service Life of a construction material, component or assembly, the starting point for the application of the Factor Method, has been the object of numerous studies and databases have been constructed within a more specific or wider scope. However, the reliability of those figures is still a matter of discussion.

Furthermore, the methodology itself has recently seen interesting developments including non-deterministic approaches, so a focused research and a definition of criteria are needed.
In the last years, several studies have been carried out at the Building Physics Laboratory of FEUP, with the aim of establishing criteria for the determination of factors' values, including the collection and analysis of a great amount of relevant data for different construction materials, components or assemblies, in what concerns their intrinsic properties, their performance in time and their degradation.

In this paper, several worked examples of the construction of frameworks for the determination of factors' values are presented. The main difficulties of this task are identified and further developments are pointed out.

KEYWORDS

Service life estimation; Factor method; Evaluation criteria.

[1] University of Porto, Faculty of Engineering, Building Physics Laboratory (FEUP), Porto, PORTUGAL, corvacho@fe.up.pt
[2] University of Porto, Faculty of Engineering, Building Physics Laboratory (FEUP), Porto, PORTUGAL, marisa@fe.up.pt

1 INTRODUCTION

In the past few decades there has been a growing attention being paid to durability issues and the estimation of the service life of constructions became essential for two main reasons:

- Environmental concerns – on one hand, the scarcity of resources (materials and energy), being the construction sector one of the biggest consumers of those resources; on the other hand, the environmental impact of the construction throughout all its life cycle (including demolishing and reuse);
- Economical concerns – all life cycle costs, including those of use and maintenance must be considered and economical viability must be proved.

The frequent introduction of new products and new technological solutions have also determined the need to evaluate the durability of those choices since for them there is no application experience validated through time. Furthermore, studies are needed to fully characterise the performance of new solutions. The lack of an adequate knowledge of the in-use performance and the best execution practices often leads to precocious construction pathologies, jeopardizing an eventually longer expected service life.

2 ISO 15686 FACTOR METHOD

2.1 Short description of the method

Since its publication, in 2000, there have been numerous studies, applications and developments based on the Factor Method described in the ISO 15686-1 Standard [Hovde, 2004, 2005]. This method allows an estimate of the service life to be made for a particular component or assembly in specific conditions. It is a very simple method and it can be described as follows.

This method is based on a Reference Service Life that is an expected service life obtained for a set of standard in-use conditions and a series of modifying factors that take into account the deviation from the reference in each specific case. The formula to be used is as follows:

$$ESL = RSL \times factor\ A \times factor\ B \times factor\ C \times factor\ D \times factor\ E \times factor\ F \times factor\ G$$

Where:
ESL is the Estimated Service Life of a component or assembly;
RSL is the Reference Service Life of a component or assembly;
Factors A to G are modifying factors related to:

A – the quality of components;
B – the design level;
C – the work execution level;
D – the indoor environment;
E – the outdoor environment;
F – the usage conditions;
G – the maintenance level.

2.2 Reference service life

The value of the Reference Service Life (RSL) is a critical element for estimating service life. The standard ISO 15686 – Part 1 states that RSL can be based on the following:

a) Data provided by a manufacture, a test house or an assessment regime (for innovative components it will normally be based on the manufacturer's or supplier's exposure results); this may be a single figure or a distribution of typical performance;
b) Previous experience or observation of similar construction or materials in similar conditions;

c) Boards of Agreement in the EC state assessments of durability in their certificates or reports of national evaluation services;
d) Some books which are available and which include typical service lives;
e) Building codes which give typical service lives for components.

ISO 15686 – Part 2 describes in detail the principles for service life predictions of building components, considering various service environments. It provides a tool to determine a Reference Service Life (RSL) to be used in the Factor Method.

ISO 15686 – Part 8 gives guidance on the provision of the RSL and on RSL data which are the data describing the validity of the RSL, reported in a data record. The RSL data must include the reference in-use conditions in terms of the factor classes in order to enable estimations of the factors values for a specific project.

2.3 Modifying factors

As said before, the modifying factors express the deviation from the reference in-use conditions in each specific situation. Factors less than 1 reduce the estimated service life and factors greater than 1 increase it. Assessing the overall contribution of individual factors is not an easy task. The choice of values to use as modifying factors may be based on previous experience when available. "If the conditions prevailing in a specific case have led to early failure or to an extended service life, similar conditions elsewhere may be used as the basis for applying a modifying factor" [ISO 15686 – 1, 2000]. Factors values must be considered individually and also in combination with the other factors. As the standard point out, a combination of small modifying factors can have a significant effect overall. Therefore great care must be taken not to underestimate nor overestimate the effect of any factor and of the combination of them.

3 CONSTRUCTION OF FRAMEWORKS FOR THE EVALUATION OF FACTORS' VALUES

3.1 Aim

The aim of the studies carried out at FEUP in this field is the iterative construction of a working basis for the application of the Factor Method.

In a similar way as the work by Daniotti *et al* [2008], a development of the Factor Method based on the construction of evaluation frameworks has been undertaken at FEUP for more than 10 years now. A database collecting RSL values and evaluation criteria for factors' values is under construction.

First, for each studied construction material, component or assembly, the search for a large amount of information on RSL and on all aspects related with the modifying factors is needed. Then, that information must be treated in a systematic way in order to create a framework for further developments. This framework includes all the criteria identified as relevant for the determination of factors values. Simultaneously, laboratory ageing tests to support service life predictions have been performed [Freitas *et al.* 2008] and are still going on.

3.2 Methodology

For each construction material, component or assembly, the work was developed through the following steps:

- Full characterisation of the studied object, including its physical proprieties and expected in-use performances;
- Definition of performance requirements;

- Collection of standards and other regulatory documents concerning the item under analysis;
- Study of the possible degradation mechanisms in order to identify the most relevant degradation agents. Whenever possible building inspection data were collected. For some products, laboratory tests were performed [Freitas *et al*., 2008];
- Search for the available RSL values (simultaneously some studies on RSL prediction were carried out [Quintela, 2006]);
- Identification of the relevant factors affecting service life estimation;
- Proposal of sub-factors and evaluation criteria to be considered in a specific framework;
- Theoretical application of the Factor Method using conventional factors' values in order to allow the comparison of different situations, testing the suitability of the defined criteria.

3.3 Studied Examples

3.3.1 *Introduction*

A great number of materials, components and assemblies were studied during the last 10 years. With the exception of concrete structural elements, the great part of construction elements was covered. The main focus was on walls, roofs, and floors' coverings since these layers are the most exposed and the most vulnerable to ageing. Some examples of studied items can be given among many others:

- Walls:
  - Cladding (including natural stone, artificial stone, ceramic, wood, aluminium, etc);
  - Adherent ceramic coverings;
  - One-coat mortar render;
  - Painting on external render;
  - Brick masonry;
- Roofs:
  - Flat roof systems (waterproofing membranes, thermal insulation, mechanical protection);
  - Clay roof tiles;
  - Water drainage system;
- Floors:
  - Synthetic floor coverings;
  - Ceramic tiles for pavements;
  - Wooden floors;
- Other:
  - Glazed facades;
  - Suspended ceilings;
  - Window frames (aluminium, timber, PVC);
  - Etc.

In the following paragraphs examples of evaluation frameworks will be presented. They must be looked at as a work in progress. They were defined following the steps presented in section 3.2 and are now being inserted in a database. The established criteria may need further adjustments during the process of quantification of factors' values which will be the next step in our work.

For each example presented only a partial view of the framework is provided, given the limitation of this paper extension. The idea is just to illustrate the procedure for different factors and different construction items.

The factors values and the criteria for their determination are of course strongly dependent on RSL values and on the conditions for which RSL has been made available. The tables shown in this paper are just examples of a wider data base where all these scenarios are clearly defined.

3.3.2 Factor A, quality of components

Table 1 shows a proposal of a framework for the evaluation of factors' values related to the service life of painting on external renders [Fontes, 2010]; a partial view focused on Factor A is given. In the column "Factor Value" only three possibilities are considered: '>1' (extending service life); '=1' (similar to reference conditions); '<1' (reducing service life). Some of the choices are naturally discussable and care must be taken in the detailed description of the conditions of a specific situation. Sometimes a certain feature can be favourable or harmful depending, for instance, on the interfaces with other components.

Table 1. Factor A – Quality of components – Painting on external renders.

	Sub-factor	*Evaluation Criteria*	*Factor Value*
Factor A	A1 Supply to site	With CE marking and a quality certificate	> 1
		With CE marking issued by the producer or a quality certificate	= 1
	A2 Moisture permeability	High permeability – Class V1	> 1
		Medium permeability – Class V2	= 1
		Low permeability – Class V3	< 1
	A3 Liquid water permeability	Low permeability – Class W3	> 1
		Medium permeability – Class W2	= 1
		High permeability – Class W1	< 1
	A4 Resistance to cracking	High resistance – Classes A4 and A5	> 1
		Medium resistance – Classes A2 and A3	= 1
		Low resistance – Classes A0 and A1	< 1

3.3.3 Factor B, design level

Table 2 presents the set of criteria that was established for the evaluation of Factor B for a flat roof, in what concerns the waterproofing membrane [Raposo, 2009]. The type of membrane considered in this example was a self-protected one, installed as the upper layer of a non-accessible traditional flat roof system.

Table 2. Factor B – Design level - Self-protected flat roof waterproofing membrane

	Sub-factor	*Evaluation Criteria*	*Factor Value*
Factor B	B1 Design quality and level of detail	Complete specification and careful detailing	> 1
		Complete specification and general detailing	= 1
		Deficient specification and lack of details	< 1
	B2 Definition of circulation paths	Circulation paths allowing the access at every area of the roof	> 1
		Circulation paths allowing the access at the main areas of the roof	= 1
		Circulation paths not defined	< 1

Table 2. Factor B – Design level - Self-protected flat roof waterproofing membrane (continuation).

	Sub-factor	*Evaluation Criteria*	*Factor Value*
Factor B	B3 Lap joints between membrane sheets	Joints width greater than the recommended minimum	> 1
		Joints width complying with the minimum	= 1
		Joints width less than the minimum	< 1
	B4 Mechanical fixation to the substrate	Continuous fixation	> 1
		Fixation by points	= 1
	B5 Expansion joints	At a higher level than the roof surface	> 1
		At the same level of the roof surface	= 1
		Insufficient number of expansion joints or the membrane is laid over the joint without a discontinuity	< 1

3.3.4 Factor C, work execution level

Table 3 shows the set of criteria for the evaluation of Factor C for a wall adherent ceramic covering [Lopes, 2009]. In this case the sub-factors are quite generic and can be applied to a great part of exterior works on walls.

Table 3. Factor C – Work Execution Level – Wall Adherent Ceramic Covering.

	Sub-factor	*Evaluation Criteria*	*Factor Value*
Factor C	C1 Workmanship	Specialized and experienced workers	> 1
		Experienced workers	= 1
		Unqualified and inexperienced workers	< 1
	C2 Technical supervision and surveillance	Regular technical supervision by the contractor and regular independent surveillance	> 1
		Random technical supervision and external surveillance	= 1
		Lack of technical supervision and external surveillance	< 1
	C3 Weather conditions during the execution	Mild weather. Protection of the wall with a canvas	> 1
		Temperature above 5ºC and below 30ºC. The protection is used only when it rains or in Summer (intense solar radiation)	= 1
		Temperatures less than 5ºC or greater than 30ºC. Wall without protection.	< 1

Factors D and E concern indoor and outdoor environment. The relevant conditions for the ageing of the constructions were identified and frameworks were created. Due to their extension (especially the one of Factor E) they will not be presented in this paper.

3.3.5 Factor F, usage conditions

The Factor F reflects the effect of use of the building. In Table 4, a criterion is defined for the evaluation of Factor F for a wall external cladding [Ribeiro, 2010]. The location of the wall and the type of use of the building and its surroundings are important to define a grade of likelihood of occurrence of mechanical impacts, wear and tear or vandalism. The criterion is based on the required minimum classes of resistance to mechanical impacts defined in [CSTB, 2008] in function of the level of exposure of the walls.

Table 4. Factor F – Usage Conditions – Wall External Cladding.

Factor	*Evaluation Criteria*	*Factor Value*
F	Higher class of resistance	> 1
	Complies with the recommended minimum class of resistance	= 1
	Lower class of resistance	< 1

3.3.6 Factor G, maintenance level

Table 5 shows the framework created for the evaluation of Factor G for a wall adherent ceramic covering [Lopes, 2009].

Table 5. Factor G – Maintenance Level – Wall Adherent Ceramic Covering.

	Sub-factor	*Evaluation Criteria*	*Factor Value*
Factor G	G1 Maintenance frequency	Regular operations of preventive maintenance, repairs and general cleaning every 5 years	> 1
		Reactive or corrective maintenance with repairs every 10 years	= 1
		Lack of maintenance	< 1
	G2 Accessibility for maintenance	Building with no more than 2 storeys	> 1
		Building easily inspected from the outside	= 1
		Building with more than 2 storeys with a configuration that hinders a visual inspection	< 1

4. FINAL REMARKS

As mentioned before, a great amount of information for service life estimation of construction components has already been collected and treated and some proposals were made. However there is still an important task to perform which is the quantification of factors' values. In order to overcome one of the main weaknesses of the Factor Method, its deterministic principle, for the quantification of the factors' values the next step will be the collection of statistically significant data in order to obtain a probability distribution function of the influence of each factor and be able to deal with the related uncertainty.

The search for reliable values of the Reference Service Life is also a major concern that is followed by the best efforts in terms of developing suitable laboratory tests to produce reliable data.

REFERENCES

CSTB, 2008, 'Résistance aux chocs des bardages rapportés, vêtures et vêtages', Note d'information 11, Cahiers du CSTB, 7 pp., France.

Daniotti, B., Spagnolo, S. L. & Paolini, R. 2008, 'Factor Method Application Using Factors' Grids', Proc. 11dbmc International Conference on Durability of Building Materials and Components, Istanbul, Turkey, 11-14 May 2008, Vol. 4, pp. 1449-1457.

Fontes, A. R. 2010, ' Durabilidade de Pinturas Exteriores sobre Reboco. Estimativa da Vida Útil." (*Durability of Paintings on External Renderings. Service Life Estimation*), Ms. Sc. Thesis, 127 pp, Faculty of Engineering of the University of Porto, Portugal.

Freitas, V. P., Corvacho, H., Sá, A. V. & Quintela, M. A. 2008, 'Discussing the Durability Assessment of Cement Mortars – A Contribution for a Prediction Model', Proc. 11dbmc International Conference on Durability of Building Materials and Components, Istanbul, Turkey, 11-14 May 2008, Vol. 1, pp. 151-158.

Hovde, P. J., Moser, K. 2004, Performance Based Methods for Service Life Prediction: State of the Art Report, CIB Report, Publication 294.

Hovde, P. J. 2005, The Factor Method – a Simple Tool to Service Life Estimation, Proc. 10dbmc International Conference on Durability of Building Materials and Components, 17-20 April, Lyon, France, TT4-115.

International Organization for Standardization (ISO), 2000, 'Buildings and constructed assets – Service Life Planning — Part 1: General principles. ISO 15686-1'.

Lopes, C. A. S.. 2009, 'Durabilidade da Construção. Estimativa da Vida Útil de Revestimentos Cerâmicos de Fachadas' (*Durability of Construction. Service Life Estimation for Facade Ceramic Coating*), Ms. Sc. Thesis, 93 pp, Faculty of Engineering of the University of Porto, Portugal.

Quintela, M. A. 2006, 'Durabilidade de Revestimentos Exteriores de Parede em Reboco Monocamada' (*Durability of One-coat Rendering Mortar for External Use*), Ms. Sc. Thesis, 177p, Faculty of Engineering of the University of Porto, Portugal.

Raposo, T. F. 2009, 'Durabilidade da Construção. Estimativa da Vida Útil de Revestimentos de Coberturas Planas' (*Durability of Construction. Service Life Estimation for Flat Roofs Coverings)*, Ms. Sc. Thesis, 96 pp, Faculty of Engineering of the University of Porto, Portugal.

Ribeiro, M. S. 2010, 'Durabilidade da Construção. Estimativa da Vida Útil de Fachadas Ventiladas' (*Durability of Construction. Service Life Estimation for Facade Cladding*), Ms. Sc. Thesis, 68 pp, Faculty of Engineering of the University of Porto, Portugal.

Santos, M. R. P. 2010, 'Metodologias de Previsão da Vida útil de Materiais, Sistemas ou Componentes da Construção. Revisão Bibliográfica' (*Methodologies for the Estimation of the Service Life of Materials, Components or Assemblies in Construction. Bibliography Review*), Ms. Sc. Thesis, 129 pp, Faculty of Engineering of the University of Porto, Portugal.

XII DBMC
International Conference on Durability of Building Materials and Components
PORTO - PORTUGAL, April 12th-15th, 2011

Experimental Evaluation of Plasters Durability Aimed at Maintenance Planning and Scheduling

Giuseppe Alaimo [1]
Daniele Enea [2]

ABSTRACT

The phase of building management has a strategic importance because of the necessary scheduling of maintenance during executive planning. Moreover, in order to obtain the greatest sustainability of the intervention, a reasonable duration of service life must be balanced with global quality-cost ratio. A contribution towards this objective is given by the reduction in the achievable resources and raw materials consumption through the improvement of the durability requirement of building and its parts. This is true even for the interventions on the existing public building stock, especially if there is lacking of maintenance planning and scheduling. This work, taking cues from a maintenance intervention "at happened breakdown" on an Engineering school building in Palermo, deals with the introduction of process innovations in the management phase, directed towards preventive intervention strategies. Beyond the collection of the informative data, the time behaviour of envelope surfaces is monitored through a viewpoint system. Particular attention has been given to the surfaces colour and the physical decay of the finishing plaster (rasante) layer, to be evaluated depending on the different technical solutions and exposure to weather conditions. The study, following the methodology of ISO 15686, also foresees accelerated ageing tests on samples of different materials, in order to formulate hypothesis and correlations on the degradation evolution, from a maintenance planning and scheduling viewpoint. The paper reports the monitoring results of the first five years of the colours (white and gray) of the buildings facades, after the recovery interventions, related to those of the laboratory tests, showing a different changing of the two colours (more for gray), depending on different exposures.

KEYWORDS

Sustainability, Maintenance, Durability, Finishing plasters (rasanti), Colour.

[1] Faculty of Engineering of the University of Palermo (DPCE), Palermo, ITALY, alaimo@unipa.it
[2] Faculty of Engineering of the University of Palermo (DPCE), Palermo, ITALY, daenea@unipa.it

1 INTRODUCTION

A specific attention to the issue of maintenance programming was codified in Italy with a 1994 law, which requires, for the new government intervention, the establishment of a proper maintenance plan work, in the stage of final design. The UNI 11257:2007 specifies further the ideas expressed by law and provides guidance to the real estate management. This programming is becoming increasingly necessary because of the complexity in managing existing buildings, in a balanced global cost-performance ratio. With the established regulatory framework and increased sensitivity towards the sustainability of the whole building process, it is necessary to change management strategies of constructions, from a still widespread condition at happened breakdown into a preventive policy. For this reason, it is important to have knowledge of the durability of materials and building components, their ability to maintain acceptable performance characteristics over time. This paper reports the first results of a study inspired by a classic intervention at happened breakdown on a building of the Faculty of Engineering of the University of Palermo. The study aims to introduce elements of innovation in the methodology of management process (design, planning, execution) and the maintenance activities, and on the other hand to monitor the time behaviour of the building envelope, subject to intervention. Here we refer the studies, according to the methodology of ISO 15686, as implemented by the UNI 11156:2006, regarding the assessment of the durability of the plaster coatings' colour. The colour, by the class of requirements for appearance, not only contributes to the definition of the technological quality of the building, but also the involved environment (relevant architectures, planning the colour of the facades in the old towns, etc.). Therefore the assessment of the durability of the envelope surfaces' colour is relevant for the implications related to the definition of reliability and durability, especially when related to microclimatic parameters, from a maintenance planning and scheduling point of view.

2 CASE STUDY: THE FACULTY OF ENGINEERING OF PALERMO

The Building 8 under study is located within the university campus, Orleans' Park, and is part of the Faculty of Engineering of Palermo. Its construction dates back to the years 1953-'63, by professors of Architecture and Building Science: S. Benfratello, S. Caronia and E. Castiglia [La Mantia 2006]. The building in 'Fig. 1' has two main bodies: the body of Classrooms that are spread over four floors, over a terrace almost completely open, and the body of the departments that is shaped like a comb that is spread over three floors and is characterized by a long porch on the ground floor, five amphitheatre classrooms, protruding from the edge of the building, and the various academic departments.

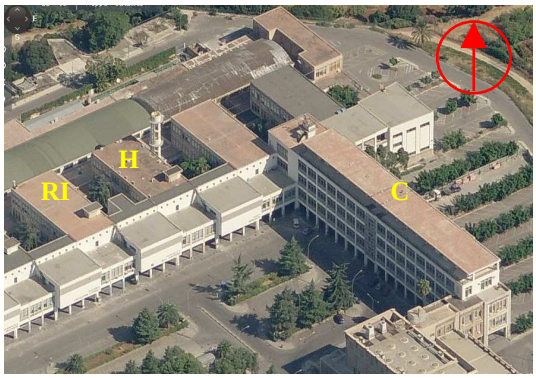

Figure 1. Isometric view of Building 8 (www.bing.com).

The three bodies are oriented in the north-west/south-east direction. The building as a whole, was built with a load-bearing reinforced concrete frame, divided into independent blocks, joined together, characterized by the presence on the facades of two or three levels of modular openings. The body of classrooms is characterized by the presence of a cantilevered reinforced concrete brise-soleil with

geometric designs, as in 'Fig. 2'. The external walls are made of yellow limestone square blocks. The maintenance intervention of the complex (the first since its construction), prepared by the Technical Department of the University, took place over the last five years and is the starting point of this study. Particularly, the surfaces of the body of Classrooms (C) and those of the Department of Hydraulics (H), as in 'Fig. 3', and the Department of Road Infrastructures (RI) were investigated.



Figure 2. The brise-soleil of the body of Classrooms.



Figure 3. The Department of Hydraulics.

2.1 Surfaces and pathology survey

The knowledge of the Building 8 and particularly the stratigraphy of the technical elements, object of the study, was based on a careful survey of the status quo, especially during the demolition of the degraded surface layers. The preliminary survey phase was, in fact, important to identify relationships between the different parts of the building, the boundary conditions (microclimate, exposure, etc.) and the used materials. As mentioned above, after more than fifty years from original, no maintenance had been applied on surfaces until May 2005. The evaluation of the degradation, according to the UNI 11182:2006, showed:

- Dripping stains below the drips of the window modules;
- Lack of plaster and concrete cover, due to the degradation of reinforced concrete of the window modules, as in 'Fig. 4';
- Superficial deposits, characterized by yellowing of the plaster surface, due to loose material, as in 'Fig. 5'.



Figure 4. Lack of plaster.



Figure 5. Superficial yellow patina.

The causes of degradation were attributed to:

- The weathering, in particular the action of wind, which is crucial for the transport of marine aerosol and loose material on the surface;
- The quality of raw materials making up the plaster and the concrete;

- The thick plaster (even more than 8 cm), misplacement of the window sills and consequent lack of appropriate slope.

2.2 The intervention and used materials

The intervention on the facades, after the consolidation of degraded reinforced concrete elements, provided for the restoration of the plaster base and the finishing with a plastic coating applied to continuous (RPAC), made of inorganic binder potassium silicate based, inorganic pigments and selected aggregates, at medium particle size, according to the classification of the UNI 8682:1984. The coating that has the nature of a smoothing product, which makes it akin to the class of plasters, was applied by stainless steel trowel, on plastered surfaces treated with an appropriate primer to enhance adhesion to the substrate. The nature of the RPAC provides thickness between 1 and 15 mm, depending on the size of the aggregates, that is between 1 and 7 mm, resulting in three classes of RPAC, known by the letters from G1 to G3, in ascending order of applied thickness. The product used in the case study has been classified as G3 and has a pasty consistency. In particular, the feature of silicate RPAC is to react with carbon dioxide present in the atmosphere, giving rise to colloidal silica fixing the coating components together and with the support, resulting in a structure similar to the plaster support. This ensures excellent breathability of the treated surface, as a consequence of the porosity to water vapour of the microcrystalline structure of thickness applied, arising from the crystallization of silica, while the treated surface is impermeable to weathering. In the application studied two different colours were used: white in the reinforced concrete structure and gray in the window modules.

3 METHODOLOGY, TESTS AND SPECIMENS

The research, conducted as part of national and international studies to evaluate the durability of construction products and elements, following the methods of ISO 15686 and UNI 11156, was based on the evaluation of the Reference Service Life and the Estimated Service Life, through the correlation between accelerated laboratory ageing tests and field exposure. Starting from the identification of potential agents that might affect the duration of components, the effects of degradation which might cause changing in the considered characteristic properties, especially the surface colour, were determined. On the basis of tests carried out, it was possible to proceed to the rescaling by comparison with the results of monitoring the field exposure. However, linking natural and laboratory ageing was not easy, especially because of the difficulty to reproduce in laboratory all the stresses that occur in reality (action of dust, hail, wind, vibration, etc.). The parameter that the research investigated and monitored was the colour of the surface where measurements were made in accordance with the recommendations from Normal 43/93. Observations were taken with a spectrophotometer (CM-2600 Konica-Minolta) with control number of gloss that provides simultaneous data for each measurement with the specular component included (SCI) and excluded (SCE). The observations were made with the standard illuminant D_{65}, as defined by the CIE, with an inclination angle of 10°. The colour space chosen to represent the colour is CIELAB, as defined by CIE in 1976, based on lightness, L*, and two chromaticity coordinates a* and b*. The lightness L* indicates the achromatic stimulus from black (0%) to white (100%), used to determine whether a colour is lighter or darker[3]. The coordinates a* and b* are referred to colour schemes in opposition to one another: red-green for a* and yellow-blue for b*. Starting from the coordinate values measured at zero time, the colour difference, ΔE*ab, over time, was observed through the formula:

$$\Delta E^*_{ab} = \sqrt{\left(\Delta L^*\right)^2 + \left(\Delta a^*\right)^2 + \left(\Delta b^*\right)^2}$$

[3] L* represents the lightness that is a feature associated with the visual perception of surface color, relating to the white reference and represents the fraction of light widely reflected.

The measurements[4], carried out on the samples and on the external surfaces of buildings, provided for each point the average of five measures, on an area representing approximately one square meter.

4 NATURAL AGEING

The monitoring of the effects of natural ageing applied on the exterior coating of the investigated buildings was applied on a representative set of points on the facades in the four different exposures, as in 'Fig. 6'. Interventions were made at different times relative to periods of natural ageing. In particular:

- February 2005 (T_3): North-East façade, body of the Classrooms;
- April 2006 (T_2): South-West facade, body of the Classrooms;
- November 2008 (T_1): North-East and South-West facades, Department of Hydraulics;
- December 2009 (T_0): North-East and South-West facades, Department of Road Infrastructures.

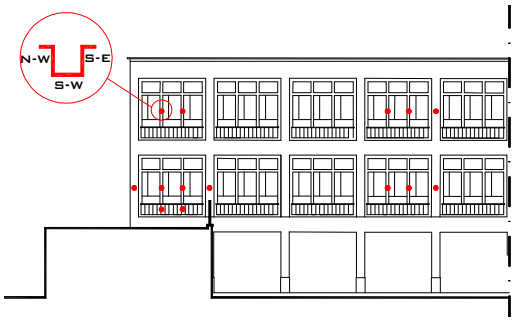

Figure 6. Department of Hydraulics South-West façade, with monitored points in red and the cross-section of a pillar, with different exposures.

Therefore data covered the period between 2005 and 2010. The configuration of the buildings allowed a favourable comparative investigation, because of the presence of morphologically identical facades in different exposures, treated with the same materials and colours. On each facade, the representative elements to be monitored have been identified, particularly in the framed structure, covered with the white coating, the fronts and the perpendicular surfaces to the facade were measured. The same was applied to reinforced concrete elements, part of prefabricated blocks, coated in gray. For each façade, measurements were derived from three different exposures. The results of the investigation on the N-E and S-W facades of the three bodies, showed that the measurements with the spectrometer, under conditions specular component included (SCI) and excluded (SCE) never differed by more than $\Delta E^*ab = 0.4$ (since opaque surfaces had a modest contribution of reflected specular light). Therefore, graphs and tables below refer to measures in specular component excluded, closest to that perceived by the eye. The colorimetric measures carried out on the fronts of the buildings showed for the white colour, a variation of the coordinate L* between 86.79 and 91.40 points; a variation between -0.06 and 1.09, for the coordinate a* and a range of values between 4.54 and 7.52, for b*. The gray ranges of values measured for the three colorimetric coordinates were as follows: L*= 60.15÷76.12, a*=0.12÷1.41 and b*=7.40÷12.75.

5 ARTIFICIAL AGEING

The samples reproduced the solution applied on the buildings surfaces, on a base of brick, and final

[4] Experimental activity was carried out in the Laboratory of Construction of the Department of Project and Building Constructions, University of Palermo.

dimensions were 250x250x70 mm, with the RPAC applied according to a thickness of about 15 mm, on a suitable primer of about 10 mm thickness. The edges of the samples were protected by applying a layer of waterproof cement mortar to prevent water absorption. For the tests of artificial ageing in the climatic chamber, an ageing cycle was developed and calibrated [Alaimo 2006], from weather data of the climatic context of Palermo[5], as showed in Table 1.

Table 1. The final artificial ageing cycle.

Phase	Hour	T (C°)	RH (%)
Rain (autumn season)	3.0	-	-
Cold (winter season)	1.5	2	-
Hot-humid (spring season)	5.0	60	87
Hot-dry (summer season)	2.5	50	56
TOTAL	**12.0**		

Three steps of artificial ageing were set both for the white samples and the gray ones, repeating the cycle 28, 56 and 84 times, corresponding to 336, 672 and 1008 hours of stressing action in the climatic chamber. The samples were placed in the climatic chamber inclined at 60° as in 'Fig. 7'. Measures were taken at zero time (S_0 corresponds to T_0 of the natural ageing), and after every step (S_1, S_2 and S_3). For each step, the colour measurement was taken on a couple of samples. The recorded values for the colorimetric coordinates were variable: for the white samples, the colour coordinate L* showed values between 89.21 and 90.64 points, the coordinate a* a variation between 0.14 and 0.37 and the coordinate b*, a range of values between 5.18 and 7.25. For the gray samples, ranges of values measured for the three colorimetric coordinates were: L*=65.92÷72.23, a*=0.43÷0.73, b*=11.75÷12.47.



Figure 7. The samples inside the climatic chamber.

6 RESULTS AND CONCLUSIONS

The collected data on colour changing, related to laboratory samples, were compared with colorimetric measures taken on the buildings' surfaces in terms of colour difference ΔE*ab, as in 'Figs 8 and 9'.

[5] Data processed by Tiziana Basiricò related to the research "Collecting and processing data related the framework of climatic agents of Palermo for the development of accelerated ageing cycles", funded by the PRIN 2003



Figure 8. Colour changing on the North-East facades (natural ageing).

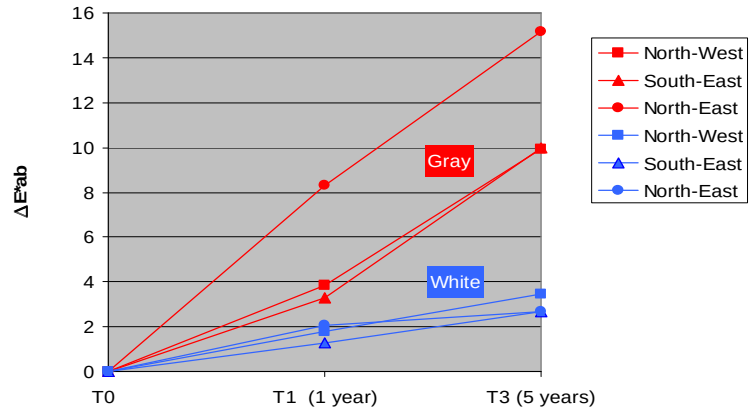

Figure 9. Colour changing on the South-West facades (natural ageing).

On the base of these comparisons, it was possible to make the following conclusions, for natural ageing:

- After one year of natural ageing, white colour showed a medium colour change of almost 2 points, becoming lighter, for all facades; after three years, on the South-West facade, the trend was increasing and the medium value is 3,5 points, with a maximum recorded of 4,5 points in the S-E front.
- After five years of natural ageing, North-East facades showed a medium white colour change equal to 2,5 points, with a maximum on the N-W front of over 3 points.
- For the gray colour, after one year of natural ageing, colour change was between 5 and 6 points in the South-West facades; the North-East facades showed higher colour difference equal to 3,5 points in the S-E e N-W exposures, while the difference was more evident on the N-E fronts, over 8 points.
- After three years, South-West facades had a medium gray colour change equal to 11 points and after five years, the North-East ones showed a strong difference between the main N-E front, over 15 points, and the other two orthogonal, 10 points, remaining the trend to become lighter gray.
- The environmental conditions and microclimate produced after three years, on the South-West oriented facades, a greater degradation than the North-East ones after five years, for both colours, white and gray, with the exception of the N-E, for gray, that was more faded after five years.
- On all the facades, the front surfaces did not show the greatest colour change, but those orthogonal to them.

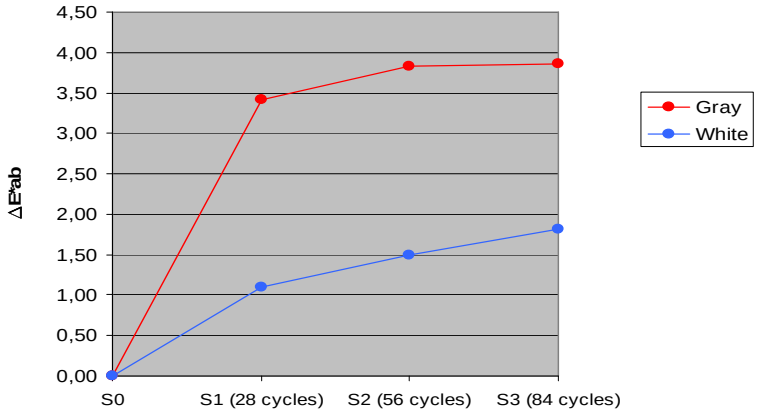

Figure 10. Colour changing on the laboratory samples (artificial ageing).

And for artificial ageing:

- The first attempt at rescaling, for white colour, showed that the degradation produced artificially in laboratory, after application of 84 cycles of ageing (S_3), was equal to the natural degradation measured on surfaces naturally aged after a year, so it is appropriate to proceed with further steps to reach ΔE*ab values comparable to natural ageing after a year. Regarding the gray colour, the application of three cycles of ageing involved a colour difference measured comparable to the North-East one after a year of natural ageing.

In conclusion, after about five years, the colour difference of the white plaster in different exposures, even if in different ways, remained below 5 points[6], with a progressive trend of surfaces to become lighter and yellow, even if the just noticeable difference, perceptible by human eye, around the value of 2.3, was exceeded [Sharma 2003]. The gray-coloured surfaces showed a greater tendency to degradation over a short period of time, in both natural and artificial ageing conditions. The stability of colour, compared to the original, was an often neglected aspect, despite contributes to characterize the quality of the envelope. We believe this issue deserves a healthy weight among the parameters to be monitored and a specific legislation would certainly give further important contribution to the maintenance of service quality of building structures, being necessary to establish functional limits of the colour of building surfaces.

REFERENCES

Alaimo, G. & Accurso, F. 2008, 'La durabilità del colore in edilizia: le vernici poliestere su supporto metallico', in *L'Edilizia*, [154], pp. 32-37.

La Mantia, F.P. 2006, *Contributi per una storia della Facoltà di Ingegneria di Palermo*, Edizioni Fotograf, Palermo.

Alaimo, G. & Basiricò, T. 2003, 'La manutenzione dell'edilizia economica-popolare a Palermo', Proc. "Involucri quali messaggi di architettura – Building envelopes as architecture's messages", Napoli.

Alaimo, G. & Accurso, F. 2006, 'The assessment of sandwich panel durability. Thermo-phisycal and colour characteristics', in Pietroforte, R. & De Angelis, E. & Polverino, F. Proc. Joint International Symposium of CIB "Construction in the XXI Century: Local and global challenges", Rome.

Alaimo, G. 2006, *Valutazione sperimentale della durabilità delle coperture discontinue. Un'applicazione al pannello sandwich*, EdiTecnica, Palermo.

[6] The ASTM D-2244 imposes for pre-painted coils, after 5 years of external exposure, ΔE*ab less than 5 units CIELAB

Sharma, G. 2003, *Digital Color Imaging Handbook*, CRC Press.

Maggi, P.N. 2002, *La qualità tecnologica dei componenti edilizi. La valutazione della durabilità. Risultati della prima fase sperimentale*, Epitesto, Milano.

XII DBMC
International Conference on Durability of Building Materials and Components
PORTO - PORTUGAL, April 12th-15th, 2011

Planned Preventive Maintenance Activities: Analysis of Guidance Documents

Sónia Raposo [1]
Manuel Fonseca [2]
Jorge de Brito [3]

ABSTRACT

In Portugal there is, traditionally, a greater concern with the design and construction development phases than with the operating and maintenance phases. The lack of preventive and planned activities throughout the years and the systematic postponement in the execution of works due to financial constraints has led to a profound and widespread degradation of Lisbon elementary public schools.

A research study is being carried out aiming at the definition and implementation of sustainable maintenance practices by the Lisbon Municipal County. Based on a comprehensive survey of published literature and reports on international case studies, a performance maintenance management model was developed on the basis of this study, which allows for an evaluation and a sustainable intervention in the Lisbon elementary public schools built park.

The planned preventive maintenance activities and the statutory planned preventive activities in five school facilities were established through international references and consultation of national regulations and the opinion of Portuguese construction product manufacturers.

This paper presents a critical analysis of four guidance documents, intended to provide facility managers with planned preventive activities and related costs. The analysis revealed that these documents do not equally address all the construction elements, systems and equipments and outer spaces. The discrepancies between documents are discussed, and also the need to modify and adapt these guidance documents to better address the requirements of Portuguese facility managers.

KEYWORDS

Planned maintenance, Guidance documents, Maintenance management, Elementary public schools.

[1] National Laboratory of Civil Engineering (LNEC), Buildings Department, PORTUGAL, sraposo@lnec.pt
[2] National Laboratory of Civil Engineering (LNEC), Buildings Department, PORTUGAL, mfonseca@lnec.pt
[3] Instituto Superior Técnico (IST), Civil Engineering and Architecture Department, PORTUGAL, jb@civil.ist.utl.pt

1 INTRODUCTION

Today the management of public built assets gains a significant importance owing to their size, social relevance and the corresponding working, operational and maintenance costs. Since it is economically relevant to the total cost of a building, the activity of maintenance management cannot be done in an improvised and casual way. Currently, initiatives undertaken in this field aim at a sustainable development, or seek to rationalize and optimize the available resources through the implementation of integrated and cost-effective solutions, allowing an acceptable performance of buildings along its life cycle as well as its services [OGC 2003, Cooper 2008].

Based on a comprehensive survey of published literature and international case studies reports, an objective and flexible methodology for measuring and evaluating the performance of the building stock a Maintenance Management Systems (MMS) was developed and tested in a sample of five primary schools in Lisbon. The study presents an analysis tool that integrates key performance indicators on technical, economic and organizational aspects (Figure 1).

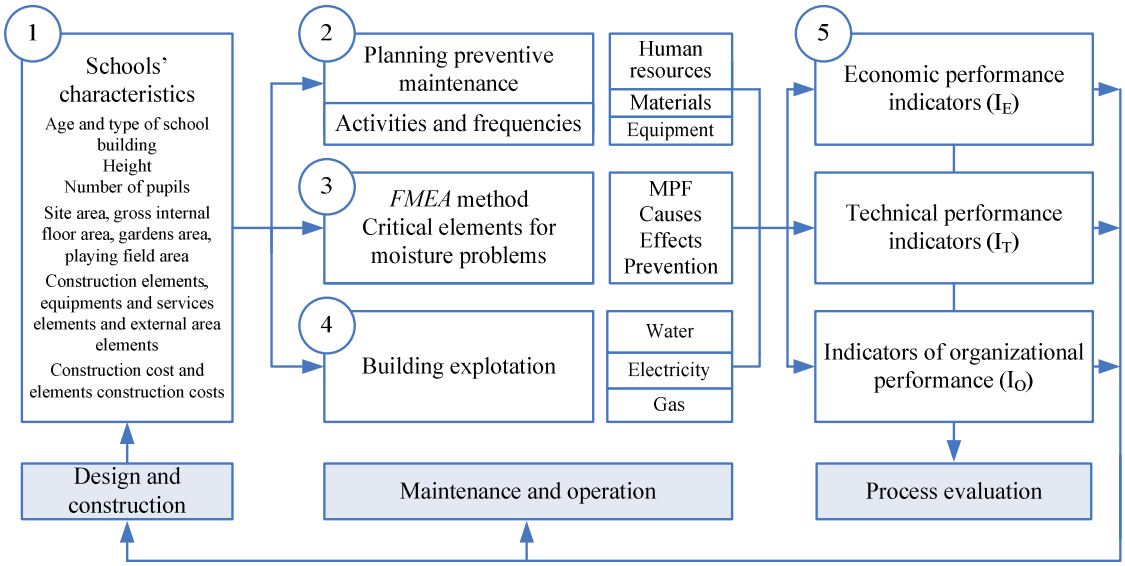

Figure 1. Methodology for measuring and evaluating the performance of the building stock Maintenance Management Systems. [Raposo 2010]

The planned preventive maintenance activities and the statutory planned preventive activities were established through international references and national regulations consultation and national manufacturers' opinion. Four databases, containing information about maintenance activities were consulted: a French source "*La maintenance des bâtiments en 250 fiches pratiques*" [Albano 2005], a Spanish source "*Fitxes rehabilitació of ITeC*" [ITeC 1991], an English source "*Housing component life manual*" [HAPM 2003] and a North American source "*The Whitestone facility maintenance and repair cost reference 2009-2010*" [Abate *et al.* 2009].

2 GUIDANCE DOCUMENTS INFORMATION

The French book "*La maintenance des bâtiments en 250 fiches pratiques*" [Albano 2005] presents maintenance activities for 9 major groups of building elements: structure, exterior envelope, roofing and waterproofing, interior construction, plumbing, HVAC, electrical equipments components, other electrical installations, basements and other services and external works and landscaping. Each sheet presents the maintenance activities, frequencies and maintenance ratios, broken down in five levels: inspection, cleaning and preventive maintenance, light intervention, heavy intervention and replacement. Lastly, the maintenance activities covered by specific legislation, such as fire protection or electrical installations are presented, allowing a comparison of the French and Portuguese

legislation in these areas. This source was chosen as a basis for the study, as it presents recent information (i.e. published in 2005) from a country with a significant number of similarities in terms of building construction techniques.

The document "*Fitxes rehabilitació of IteC*" is made available online by the Institut de Tecnologia de la Construcció de Catalunya website [ITeC 1991] and is divided into three volumes: building maintenance, services maintenance and urban spaces maintenance. Even though it is an old document, its geographical proximity to Portugal and the use of similar building technologies led to the data available being also analysed.

The building is divided into exterior elements, roof covering elements and exterior finishes, windows and doors, and interior elements, covering the finishes, the interior doors and the sanitary and kitchen equipments. The volume related to facilities includes: smoke evacuation installations, ventilation and waste disposal facilities, HVAC, kitchen facilities, water supply and sewer facilities, valves, pumps and pressure groups, electric and lighting systems, transportation facilities, fire protection facilities and installations of audio and video. The volume of urban areas includes: fences and gates, paving elements, equipments, services and landscaping.

For each element, the sheets contain a list of the most common anomalies, the maintenance activities and frequencies and their service life (except for services installations). The Spanish document presents three maintenance levels, high (A), medium (M) and low (B), according to specific environmental exposure or use factors.

In the "*Housing component life manual.*" [HAPM 2003], the information is structured into the seven following groups of components: floor components, wall and cladding components, roof components, doors, windows and ironmongery, mechanical equipment components, electrical equipment components and external works. In general, each group is divided into types and sub-types that are assigned a score corresponding to one of the following classes: A = 35+ years, B = 35 years, C = 30 years, D = 25 years, E = 20 years, F = 15 years, G = 10 years, and H up to 5 years.

The "*Whitestone Facility Maintenance and Repair Cost Reference 2009-2010*" reference [Abate *et al.* 2009] provides maintenance and repair costs from various sources of information and various types of North American establishments. This reference represents the result of 14 years of continual work from the Whitestone Research Company with several US government agencies and consulting firms that work in this area. This collaboration yielded the information needed to calculate the cost of maintaining a building over its service life, the amount and type of resources associated with this maintenance and the lifespan of the various constituents of the building.

The document uses the North American classification system UNIFORMAT II (classification of asset elements), published by *ASTM - American Society of Testing and Materials* [ASTM E1557 2009], which includes the following items: substructure (foundation and basement construction), shell (super structure, exterior envelope and roofing), interiors (interior construction, stairs and interior finishes), services (lift, plumbing, HVAC, fire protection and electrical) and equipment and furnishings.

The data presented refer to maintenance and repair activities (M&R) and are divided into: preventive maintenance (PM), unscheduled maintenance (UM) and replacement (R). PM and minor repair consists on scheduled tasks that sustain a component's level of service during a prescribed service life. The UM consists of service calls, emergency response, and other tasks that cannot be individually anticipated and replacement consists of component overhaul or major replacement tasks. These tasks extend a component's service life, and reset the schedule of PM and minor repair tasks. Activities related to facilities operation, such as landscape maintenance, are not included in this book.

The book features 72 maintenance profiles for various types of facilities and equipment, for a study period of 50 years, with the costs of maintenance and repair, per m^2 of building area and as a percentage of replacement value. An example of a maintenance profile of a North American primary school is given in Figure 2; the school, of 3.7 m height, has a gross internal floor area of 4360 m^2, built of reinforced concrete, screed, carpet and vinyl floor tiles and ceilings with plaster finish. The building has a replacement cost of 7251764 € [Abate *et al*. 2009].

Distribution of M & R costs

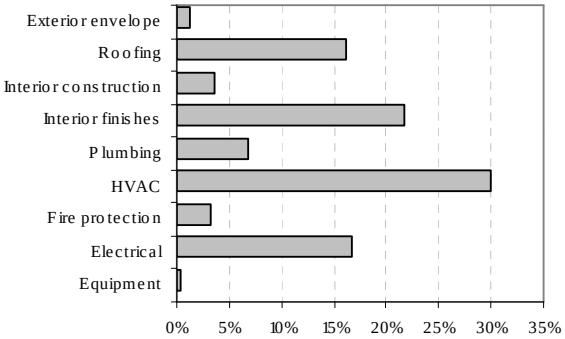

50-year M & R cost summary

Task type	50 year total cost	Annual cost per gross internal floor area	Annual cost as % of replacement
PM & minor repair	1044770 €	0.44 €	0.29%
Unscheduled maintenance	805085 €	0.35 €	0.22%
Renewal & replacement	4114134 €	1.75 €	1.13%
Total	**5963990 €**	**2.53 €**	**1.63%**

Figure 2. Maintenance and replacement cost profile for an elementary school. [Abate *et al.* 2009]

In the current study, information on preventive maintenance activities was collected, including routine inspections (I), maintenance and cleaning routine (M), and component replacement (S). In Table 1 a summary of the collected data and the main application fields of the model to measure and evaluate the performance of the building stock Maintenance Management Systems (MMS) are presented.

Table 1. Type of data available in the references listed and application fields in the research study.

Type of information available	*Whitestone 2009*	*Albano 2005*	*HAPM 2003*	*ITeC 1999*	*Scope*
Service life	Yes	Yes	Yes	Yes	I_T
Factors influencing the service life	No	No	Yes	Yes	Sensitivity analysis
Description of maintenance activities and their periodicity	Yes	Yes	Yes	Yes	I_T
Factors that influence the maintenance activity	Yes	Yes	No	No	Sensitivity analysis
Human resources and labour hours per maintenance activity	Yes	No	No	No	I_O
Data to calculate the maintenance activity cost	Yes	No	No	No	I_E
Most frequent anomalies in components and building system	No	No	No	Yes	Failure modes *FMEA* (I_T)

3 RESULTS AND DISCUSSION

In the five schools studied the exterior envelope is made of double walls with hollow ceramic brick masonry and thermal insulation and exterior openings with anodized aluminium frame and colourless single-pane glass (colourless double-paned glass in Alto da Faia school) (Figure 3). The walls should be subject to regular inspections every three years and the windows and doors every six months. The condition state of the finishing of the frame, operation and state-setting mechanisms for openings and fittings, condition of gaskets and mastics and verification of clearance at outlets for water flow should be followed [Albano 2005].



Figure 3. View of school São Bartolomeu (left); Posterior view of Alto da Faia school (centre); South view of Alto da Faia (right).

Preventive maintenance of the exterior walls consists in their cleaning and eventual closing of cracks and joints, whenever the conservation status of the walls requires or once every 10 years [Abate *et al.* 2009]. The exterior walls service life exceeds 50 years of the research study, and according to Abate *et al.* [2009] it exceeds 75 years, whereas Albano [2005] does not mention any period. The outer openings require a yearly maintenance of hardware replacement, lubrication of door locks and joint replacement. The replacement of windows and doors is indicated every 25 years in Albano [2005], with replacement of mastics to occur between 10 and 15 and the fittings around 15 years. The HAPM reference [2003] and Abate *et al.* [2009] differ in terms of the service life of window elements, offering 35 and 75 years respectively, and the service life of exterior doors, 30 and 50 years respectively.

Roofs are predominantly of sheet steel and reversed flat roof types. The former must be annually inspected, performing at the same time preventive maintenance activities, such as cleaning the surface and checking the tightness of fasteners; unclogging the rainwater plumbing and checking the proximity of tree branches. For the latter, inspections should be carried out every six months with maintenance activities to be held annually. The metal roof's service life is 25 years [Albano 2005], whereas ITeC [1991] makes a distinction between the roof metal covering's service life (30 years) and the support structure repair (50 years). The service life of flat roofs depends primarily on the conservation status of the layers of support, thermal insulation and waterproofing; Albano [2005] suggests every 20 years.

Skylights should be inspected annually by verifying the conservation status of the window frames, glass, gaskets condition and mechanisms for opening and closing the windows. Maintenance activities, to be held twice a year, consist of cleaning, lubrication and adjustment of all moving parts. The rain water drainage system should be inspected and cleaned every six months, checking the condition of connections and pipes and all system performance, namely the water flow. Albano [2005] refers the entire system replacement after 15 years, whereas Abate *et al.* [2009] mentions the need to replace up to 20% of pipe after 30 years and total replacement after 40 years.

The interior walls are in general made of single pane perforated ceramic brick masonry (in thicknesses ranging 0.20 m to 0.35 m) and should be subjected to regular inspections every three years verifying the opening of cracks, deformations or moisture stains presence. The replacement of these elements occurs every 30 years [Albano, 2005]. Ceilings in gypsum board are an uncommon solution in school buildings, appearing occasionally in recent schools in circulation areas or in the lobbies of entrances to the classrooms. Annually one should proceed to a visual inspection/maintenance, to check the aspect and its attachment to the support structure. Replacement occurs after 20 years, during which one should be aware of its possible deformation or the existence of water originating from the underlying services.

The interior openings are mostly in wood finish, with sliding doors in the separation between the classrooms and areas of artistic expression. Control inspections should be performed annually, in

general verifying all moving elements. Maintenance should be held biannually with the lubrication and adjustment of the moving parts and hardware. The service life of the doors was considered to be in general 20 years and that of sliding doors 15 years.

The exterior cladding of the facades' schools is predominantly painted plaster. The control inspections should take place every three years, checking the general appearance of walls, in particular the aspect of painting and the existence of cracks and spots [Albano 2005]. The current maintenance activities include cleaning stains and dirt in localized areas. ITeC [1991] refers a periodicity of 15 years for repainting walls and ceilings and at 40 years a more in depth intervention on the plaster must be performed before repainting.

In external walls, ceramic tiles, varnished concrete and wood panels are used less frequently. In ceramic tiles the superficial appearance of walls, joints and the flatness of the surfaces should be checked. The main maintenance activity consists on cleaning surface dirt and efflorescence stains. The replacement of this type of coating is usually not considered. Walls in exposed varnished concrete require regular monitoring at 10 years intervals, to determine the need for surface treatment with waterproofing products, and cleaning maintenance every 20 years. Normally their replacement is not considered [ITeC 1999]. Wood panelling demands an annual monitoring inspection to check the surface of condition the panels, the performance of the support elements and the integrity of joints. It should be cleaned periodically [ITeC 1999]. Replacement of the support elements occurs around 40 years.

The flooring currently adopted for the classrooms is linoleum (in the older schools ceramic or wood can be found). The inspection of the linoleum flooring is to be done annually (every three years according to ITeC) focusing on the verification of the pavement condition in current areas (flatness) and localized areas (fixation and mechanical performance). Flooring requires periodic cleaning and its service life varies from 10 [Albano 2005], 18 [2009 Whitestone] to 20 years [ITeC 1999].

Wood flooring is a solution currently adopted for administrative areas and the monitoring inspection should be held annually, noting the state of conservation of surfaces and signs of moisture. The application of suitable surface products such as varnishes or wax is part of cleaning and routine maintenance. The referred service life of this pavement is 40 years [Albano 2005, Abate *et al.* 2009]. The floor finishing used in wet areas is ceramic tiles that have a service life of 50 years [ITeC 1999, Whitestone 2009]. It is a type of floor finishing that does not require great frequency of inspection but must be subjected to a weekly cleaning with products suited to its surface.

The most common coating for walls and ceilings is painted plaster. There should be an inspection every year to verify the existence of cracks or other damage and the adherence condition to the support. For paint coating, the surface appearance must be verified and as well, the presence of moisture, dirt stains or detachment of material verified. Washing the surfaces is the appropriate maintenance procedure to be carried out once every 3 years. Repainting should occur every 15 years, including the repair of the support. In wet areas and in circulation areas, ceramic wall coating is used requiring an annual inspection control of the surface aspect of the wall and cleaning of surface dirt and efflorescence stains, where necessary.

In Table 2 a summary (extract) is presented of the information collected on different elements preventive maintenance activities and frequencies and their impact in the number of intervention in building (technical performance indicator). The Albano [2005] source was chosen as a basis for the study and the Whitestone-W [2009], ITeC-I [1999] and HAPM-H [2003] sources were used to assess the former information.

4 CONCLUSIONS

The work presented resulted from the need to investigate the content of information sources in the area of preventive maintenance planning activities and the potential for its practical implementation. Currently the information on maintenance activities in Portugal is still scattered in different study areas that relate to building elements and components and in the various government agencies that manage building parks.

Table 2. Summary of information on preventive maintenance (extract). [Raposo 2010]

Element	*I*	*M*	*S (years)*	*Number of intervention (50 years)*
Exterior envelope				
Exterior walls	3 y	10 y (W)	NC	I=16; M=5; S=0
Windows	6 m	1 y	25; 35 (H); 75 (W)	I=100; M=50; S=2; 1(H); 0(W)
	1-4 y (I)	1 y (I)	50 (I)	I=50/12; M=50; S=1 (I)
Doors	6 m	1 y	25; 30 (H); 50 (W)	I=100; M=50; S=1(H); 1 (W)
	1-4 y (I)	1 y (I)	50 (I)	I=50/12; M=50; S=1 (I)
Mastics	-	-	10/15	S=5/3
Joinery	-	-	15	S=3
Joint	-	-	10	S=5
Roofing				
Metal roofing	1 y	1 y (I;H)	25; 30 (I); 40 (W)	I=50; M=50; S=2; 1(I;W)
Flat roof	6 m	1 y (A;I)	20	I=100; M=50; S=2
	5 y (W)	1 y (W)	35 (W)	I=10; M=100; S=1 (W)
Skylights	1 y	6 m	20/30; 40(W)	I=100; M=100; S=2/1; 1 (W)
Rain water drainage	6 m	6 m	15; 40(W)	I=100; M=100; S=3; 1 (W)
Interior construction				
Walls	3 y	10 y (W)	30	I=16; M=5; S=1
Gypsum board	1 y	2 y	20	I=50; M=25; S=2
Interior doors	1 y	2 y	20; 50 (I); 40 (W)	I=50; M=100; S=2; 1 (I;W)
Ironmongery	-	5 y	10 (W)	M=10; S=10 (W)
Sliding interior doors	1 y	2 y	15; 40 (W)	I=50; M=25; S=3; 1 (W)
Finishes				
Painted wall render	3 y	3 y	15 (A,I); 10 (W)	I=16; M=16; S=3; 5 (W)
Ceramic wall cladding	1 y; 5 (I)	20 y (I)	NC	I=50; 10(I); M=2; S=0
Concrete	10 y (I)	20 y (I)	NC (I); 75 (W)	I=5; M=2; S=0 (I,W)
Wood panelling	1 y	-	30 (I)	I=16; M= -; S=1 (I)
Linoleum flooring	1 y	-	10; 18 (w)	I=50; M= -; S=5; 2 (W)
	3 y (I)	-	20 (I)	I=16; M= -; S=2
Wood parquet flooring	1 y	2-5 y	40 (A; W)	I=50; M=25/10; S=1 (A;W)
Electrical				
Fluorescent lighting fixture	1 y	1 y	8-10; 20 (W)	I=50; M=50; S=6/5; 2 (W)
Fire protection	1 y (A;I)	2 y; 6m	20	I=50; M=25/100 (I); S=1
Fire doors	-	1y (W)	40 (W)	I= -; M=50; S=1 (W)
	1 y (*)	1 y (*)	20/30 (*)	I=50; M=50; S=2/1
Fire extinguisher	-	5y (W)	12 (W)	I= -; M=10; S=4 (W)

(*)Portuguese legislation

In this study it was found that the major maintenance costs that are incurred over the 50 years of a building's service life results from the renewal and replacement of components and elements at the end of their service life. This information is not always coincident in the different consulted sources and can considerably change the results of a life cycle cost analysis. The use of a standardized reference data for the presentation of maintenance costs (e.g. UNOFORMAT II or others) is important step to enable carrying out benchmarking actions. For instance, in *Whitestone*, the North American reference, [Abate *et al.* 2009] the item on wall external finishes is included in the exterior envelope, whereas in Portugal this item would be classified in coatings and finishes (both internal and

external).

In some regulated areas, such as the electrical equipment components or gas installations, Portuguese legislation is unclear on the type of maintenance activities nor their frequency of application. Lifts, fire protection and HVAC systems are subject to specific regulations, recently published, which require the existence of user manuals and maintenance plans.

REFERENCES

Abate, D., Towers, M., Dotz, R. & Romani, L. 2009, *The Whitestone facility maintenance and repair cost reference 2009-2010.* 14th Ed. Whitestone Research, California, USA.

Albano, Jean-René 2005, *La maintenance des bâtiments en 250 fiches pratiques*, Editions Le Moniteur, Paris.

ASTM E1557 - 09, "Standard classification for building elements and related sitework - UNIFORMAT II". American Standard of Testing Materials, Philadelphia, USA.

HAPM 2003, *Component life manual*, E&FN SPON, CD.

Institut de Tecnologia de la Construcció de Catalunya 1991[a], *Manteniment de l'edifici. Manteniment installacions. Manteniment urbanització Fitxes*, Barcelona. http://www.itec.es. Last accessed: 29.10.2010.

Cooper, J. & Jones, K. 2008, *Routine maintenance and sustainability of existing social housing*, CIB W070 Conference in Facilities Management, Edinburgh. pp. 361-368.

Office of Government Commerce (OGC) 2003, *Achieving excellence in construction. Guide 7: Whole-life costing* *http://www.ogc.gov.uk/ppm_documents_construction.asp*. Last accessed: 29.10.2010.

Raposo, S., Fonseca, M. & de Brito, J. 2008, *Survey of the state of degradation of the school buildings of the Lisbon region*, 11 DBMC International Conference on Durability of Building Materials and Components, Istanbul, Turkey, pp. 1081-1088.

Raposo, S. 2011, *The management of maintenance activity in public buildings. Model and strategies for a sustainable intervention.* PhD thesis, Instituto Superior Técnico (IST), Technical University of Lisbon, Portugal.

XII DBMC
International Conference on Durability of Building Materials and Components
PORTO - PORTUGAL, April 12th-15th, 2011

Comparison of Methods Used in European Countries to Assess Buildings' Condition

António Vilhena [1]
João Branco Pedro [2]
Jorge de Brito [3]

ABSTRACT

This paper presents a comparative analysis of methods used in European countries to assess buildings' condition. The following methods were compared: a Portuguese method to assess buildings condition, an English housing health and safety rating system, a French method to assess buildings that may be declared inhabitable, a Dutch standard about buildings condition assessment and the assessment methods developed within the European projects EPIQR & TOBUS. The comparative analysis included three tasks. First, each of the methods was described separately. Then, the main features of the methods were compared. Finally, some guidelines to improve the Portuguese method were drawn.

The main differences of the methods are the objectives and scope of the assessment, the disaggregation level of the global assessment, the calculation formula used to aggregate partial assessments, the type final results obtained and the tools developed for their implementation. The main similarities are that the assessment is carried out mainly by visual inspection, the condition of the building is assessed by a systematic analysis of the entire building divided into functional elements, the severity of defects is the assessment criterion used, weighting coefficients are used to determine the importance of each partial assessment in the final result and surveyors need specific training.

The recommendations about the Portuguese method are to maintain the present assessment model, to carry out the training courses of surveyors, to create a complementary tool for the diagnosis of the causes of defects and to develop a computer program to support surveyors during inspections.

KEYWORDS

Building pathology, Condition assessment, Buildings condition, European methods.

[1] National Laboratory for Civil Engineering (LNEC), Lisboa, PORTUGAL, avilhena@lnec.pt
[2] National Laboratory for Civil Engineering (LNEC), Lisboa, PORTUGAL and Delft University of Technology (OTB-TUDelft), Delft, THE NETHERLANDS, jpedro@lnec.pt
[3] Instituto Superior Técnico from the Technical University of Lisbon (IST/UTL), Lisboa, PORTUGAL, jb@civil.ist.utl.pt

1 INTRODUCTION

The assessment of a building's condition is a technically complex task, requiring expertise, time and equipment. This assessment is usually done with methods that require a systematic registration of defects that occur in the various functional elements of the building. The diagnosis of the causes of the defects is not done, but based on the information gathered during the surveys it is possible to lay down intervention strategies and/or conservation and maintenance policies.

In several European countries, including Portugal, different buildings condition assessment methods have been developed, many of which within institutional or legislative initiatives. In these methods the assessment of buildings condition may be used to: determine the value of the property; set taxes, charges or rents; verify habitability conditions; or support decision on rehabilitation, repair or maintenance works.

The purpose of this paper is to compare methods used in European countries to assess the buildings condition. The methods compared were chosen due to their institutional character. Two main research questions are addressed: What are the main differences and similarities of the methods analysed? What recommendations can be drawn to improve the Portuguese method?

The following section briefly describes the assessment methods studied. Section 3 presents the comparative analysis of the methods and in Section 4 some conclusions are drawn.

2 METHODS TO ACCESS BUILDING'S CONDITION

2.1 Portuguese method for building condition assessment

A Portuguese method to assess the condition of buildings (MAEC) was developed within the framework of the Urban Tenancy Regime (Law No. 6/2006) [Portugal 2006a]. This method was approved by Ministerial Decree 1192-B/2006 [Portugal 2006b] and is beng applied since January 2007.

This method sets a maintenance coefficient that is used to calculate the maximum value of the rent of a dwelling unit. Assessment using MAEC is based on the verification of the gravity of the defects that occur in the building elements and equipments and on the condition of the whole dwelling and of the common parts of the building [Pedro *et al.* 2008].

2.2 Housing Health and Safety Rating System

The English method Housing Health and Safety Rating System (HHSRS) [United Kingdom 2004] was created to replace the previous Housing Fitness Standard of the United Kingdom. The HHSRS is being applied since 2000.

The purpose of this system is to evaluate the potential risks to health and safety from the deficiencies identified in dwellings. HHSRS is based on the evaluation of both the likelihood of an occurrence that could cause harm and the probable severity of the outcomes of such an occurrence. The assessment using HHSRS is made based on the condition of the whole dwelling.

2.3 Method for assessment of the condition of buildings that may be declared inhabitable

The French method to assess the condition of buildings that may be declared inhabitable was set by the Health Ministry in the Circular No. 293 (2003-06-23) [France 2003], for renewing the procedure for declaration of unhealthy buildings established in 1971, conducted by the law on solidarity and urban rehabilitation of 13 December 2000 [France 2000].

The purpose of this method is to do a technical assessment of a dwelling habitability conditions and to

gather information about physical degradation of the building. The results support the declaration of inhabitability by the French Hygiene Departmental Council and provide information to guide the works necessary to mitigate the detected defects. The assessment is based on the verification of the gravity of the defects that occur in the building elements and equipments.

2.4 Dutch standard NEN 2767

The Dutch standard for assessment of buildings' condition was published in 2006 (NEN 2767). This standard has three parts: presentation of the method [NEN 2006], list of common defects by gravity [NEN 2008]; calculation formula [NEN 2009].

This assessment method intends to guide the implementation of rigorous and independent technical buildings assessments. The information collected is used to support an objective definition of the condition of each building as well as to plan maintenance interventions, prioritize investments, monitor the progress of building elements degradation and compare the condition of different buildings. The assessment is based on the detection of defects in functional elements, and on the definition of their importance, extent and intensity [Straub 2009].

2.5 EPIQR and TOBUS methods

The EPIQR (Energy Performance Indoor Environmental Quality Retrofit) and TOBUS (Tool for Selecting Office Building Upgrading Solutions) were developed within European research projects. The EPIQR project was completed in 1998 and the TOBUS project was completed in 2000. Specialists from seven European countries worked in the development of these methods (Germany, Denmark, France, Greece, Netherlands, United Kingdom and Switzerland).

The EPIQR project applies to residential buildings and its main objective is to improve energy efficiency and air quality issues, taking into account not only energy consumption and air quality but also the degradation of building elements [Balaras 2000]. The TOBUS project applies to office buildings and was developed to support the refurbishment of buildings to meet the new requirements of energy efficiency, accessibility and facilities [Caccavelli & Gugerlib 2002]. This method used much of the experience acquired with EPIQR but adds new situations and factors applicable to office buildings. These two methods were developed to be applied in the early stages of the rehabilitation/refurbishment design projects. The condition assessment is based on the identification of defects, the definition of the degradation and the extent of the works needed.

3 COMPARATIVE ANALYSIS OF METHODS

The main characteristics of the methods studied are summarized in Table 1. The following paragraphs analyse the results of each feature compared.

3.1 Objective

The methods studied have a wide variety of objectives, such as determine the maintenance condition of dwellings, verify minimum housing conditions and define maintenance plans and repair works.

3.2 Scope

Three of the methods studied apply only to dwellings (HHSRS, French method and EPIQR). The remaining methods may be applied to different types of buildings and their units. The scope of the Dutch method is not an individual unit of the building but the whole building or a building stock.

Table 1. Summary of the assessment methods main characteristics.

	MAEC	*HHSRS*	*INHABITABLE BUILDINGS*	*NEN 2767*	*EPIQR/TOBUS*
Objectives	Determine the condition of the dwelling	Verify minimum housing conditions	Verify minimum habitability conditions	Define maintenance plans and repair works	Define scenarios for rehabilitation and refurbishment
Scope	Rented dwellings and non-residential units	Dwellings	Dwellings	Dwellings and non-residential units	Dwellings (EPIQR) and non-residential units (TOBUS)
Inspection method	Visual inspection	Visual inspection and simple tests	Visual inspection and simple tests	Visual inspection	Visual inspection and simple tests
Attributes assessed	Functional elements and equipments	Functional elements and equipments	Functional elements, equipments and salubrity conditions	Functional elements and equipments	Functional elements and equipments
Disaggregation level	3 main parts; 37 elements	29 hazard categories	3 main parts; 52 elements	4 main parts; 52 elements	50 elements (housing); 72 elements (non-residential)
Weighting coefficients	Based on elements significance	Based on probability of an occurrence that could cause harm	Based on elements significance	Based on repair costs	Based on construction costs
Assessment criteria	Defect gravity (1-5)	Class of harm (I-IV) Likelihood (1-1/5600)	Defect gravity (0-3)	Importance (1-3), intensity (1-3) and extent (1-3) of defects	Degradation level (a-d); Degradation extent (a-d)
Calculation formula	Weighted average	Calculation algorithm	Weighted average	Weighted average	Cost calculation
Results	Defect index and condition rate	Hazard class (A-J)	Unhealthy level	Conservation index	Cost
Surveryors	Civil Engineers, architects and civil technical engineers	Trained technicians	Trained technicians	Civil Engineers and architects	–
Implementation tools	Checklist; Application instructions illustrated; Internet site	Checklist; PDA software; PC software; Application guidance	Checklist, Application guidance	List of items and defects	Computer software

3.3 Inspection method

In the methods studied, information to assess the buildings and their units is obtained by visual inspection. If the surveyor has to point out the works to repair the defects, some simple tests to look for non visible defects are also planned. These complementary tests usually demand longer surveys.

3.4 Attributes assessed

The attributes assessed are similar in the methods studied. In all methods the construction elements and equipments condition are assessed. The French method also includes the assessment of some safety, health and comfort requirements, as well as the analysis of dimensional design factors. HHSRS also includes the building location or its surroundings.

3.5 Disaggregation level

The disaggregation level of the global assessment is different in the methods studied. The methods that are mandatory and have an extensive application use 30 to 40 attributes (*e.g.*, MAEC, HHSRS). The methods that intend to depict a more accurate analysis and are optional use 50 or more attributes (*e.g.*, Dutch method, EPIQR & TOBUS methods). The French method, although for extensive application, also uses 50 attributes but it also assesses salubrity conditions.

3.6 Weighting coefficients

All methods studied have weighting coefficients that set the importance of each functional element in the final result, but the criteria to set these coefficients is different. The weight coefficients of the MAEC and the French method are based in the contribution of element for the global assessment of the buildings condition. In MAEC structural and building's envelope elements (*e.g.*, external walls, windows and doors) have higher weights and in the French method non-constructive elements (*e.g.*, light, moisture) have higher weights. In the Dutch method and the EPIQR &TOBUS methods the weight coefficients are based on construction costs. In HHSRS the weighting coefficients are based on the probability of an occurrence that could cause harm.

3.7 Assessment criteria

The methods studied use different assessment criteria, but in all of them, except HHSRS, buildings' condition is measured by the defects recorded. In MAEC and the French method the *gravity* of defects is the criteria used. Gravity includes the effects of defects on the functional requirements, the type and extent of the repairs required the relevance of the affected space or facilities to the unit's use, and the existence of alternatives to the affected space or facilities. In the EPIQR &TOBUS methods the *level* and *extent* of defects are used. In the Dutch method *importance*, *intensity* and *extent* of defect are used. In HHSRS the *class of harm* and the *likelihood of accidents* due to defects are used.

3.8 Calculation formula

MAEC, the French and the Dutch methods use calculation formulas based on weighted averages. MAEC also has rules to prevent the attenuation of extreme values. The calculation formula used in HHSRS is different from the others and more complex. This method uses a formula based on the risk of accidents due to existing housing hazards in the dwellings, affecting the most vulnerable age groups of all the users of the space. The definition of values for all the variables involved is a difficult process that requires surveyors with adequate training. The EPIQR &TOBUS methods calculate the cost of rehabilitation.

3.9 Results

The methods studied present different results:

- The French method provides an index calculated independently for each part of the building assessed (common shares and dwelling units);
- MAEC sets a condition index that integrates the assessment of the unit and the common parts;
- HHSRS indicates the degree of risk of accidents due to a certain danger;
- The EPIQR & TOBUS methods determine the rehabilitation cost.

3.10 Surveyors

In the methods studied, the technicians who can conduct surveys need specific training. Only the EPIQR & TOBUS methods do not have this requirement, but these methods are mainly used for academic purposes. The demand for specific training of the surveyors is understood as a key factor in all the methods. The importance of this factor was demonstrated in a previous study carried out in the United Kingdom [Hollis & Bright 1999].

3.10 Implementation tools

Implementation tools were developed for all the methods studied, but the amount and nature of the tools differs. The main tools are the following:

- *Checklist* – All methods studied have a checklist to guide surveyors and record information;
- *Instructions* – All methods have general instructions with examples of common defects, but with different levels of development. The instructions of MAEC and HHSRS have, for each functional element, examples of defects, many of them illustrated. The instructions of the French method also include illustrations of common defects for some functional elements. The Dutch standard presents a list of the most common defects for all functional elements, coded and prioritized, but illustrations have not been included yet, although it acknowledges their importance to help the surveyor;
- *Computer program* – the EPIQR & TOBUS methods and HHSRS, which are particularly complex, have computer programs to support surveyors. These programs record information and calculate results;
- *Website* – MAEC has a website to manage the entire assessment procedure (http://www.portaldahabitacao.pt/).

4 FINAL REMARKS

What are the main differences and similarities of the methods analysed?
The analysis showed that the methods studied have different objectives and scopes. Consequently, they also vary regarding the disaggregation level of the global assessment, the calculation formula used to aggregate partial assessments, the type of the final results obtained and the tools developed for their implementation. However, some similarities among the methods studied were found. In almost all methods the assessment is carried out mainly by visual inspection, the condition of the building is assessed by systematic analysis of the entire building divided into functional elements, the severity of defects is the assessment criterion used, weighting coefficients are used to determine the importance of each partial assessment in the final result and surveyors need specific training.

What recommendation that can be drawn to improve the Portuguese method?
Based upon the results of the comparative analysis, the following recommendations are made for MAEC:

- No changes are required on the inspection method, attributes assessed, disaggregation level, weighting coefficients or calculation formula. The increase in the number of attributes would

increase the time taken for the survey without substantial benefits to the accuracy of the result. Training courses of surveyors are essential to assure a correct application of MAEC.

- In Portugal the owner of a rented unit that has been assessed with MAEC may ask the municipality to define the repair works needed to improve the defect index obtained previously. The information gathered with MAEC is insufficient for this purpose. A second survey would be required using a checklist that identifies the *level* and the *extent* of defects, and conducting simple tests to look for non visible defects. With this information a correct diagnosis of the causes of defects would be possible.
- A computer program to support surveyors during inspections should be developed. This tool should run on a PDA and be able to present the instructions, register answers, record photos and make calculations. Once connected to the Internet, the surveyor could then submit the filled in checklist to the central website.

REFERENCES

Balaras, C. A. 2000, A special issue devoted to EPIQR, *Energy and Buildings*, Vol. 31, No. 2

Caccavelli, D.; Gugerlib, H. 2002, TOBUS – a European diagnosis and decision-making tool for office building upgrading, *Energy and Buildings*, Vol. 34, No. 2, pp. 113-119.

France 2000, *Loi n° 2000-1208 du 13 décembre 2000* [in French].

France 2003, *Circulaire DGS/DGUHC/SD7C/IU H4 n° 293 du 23 juin 2003* [in French], Ministère de la Santé, de la Famille et des Personnes Handicapées.

Hollis, M. & Bright, K. 1999, Surveying the surveyors, *Structural Survey*, Vol. 17, No. 2, pp. 65-73.

NEN 2006, *NEN 2767–1:2006 – Conditiemeting van bouw- en installatiedelen – Deel 1: Methodiek* [in Dutch], Delft, NEN.

NEN 2008, *NEN 2767–2:2008 – Conditiemeting van bouw- en installatiedelen – Deel 2: Gebrekenlijsten* [in Dutch], Delft, NEN.

NEN 2009, *NEN 2767–3:2009 (Publicatie uitsluitend voor commentaar) – Conditiemeting van bouw- en installatiedelen – Deel 3: Aggregatie conditiescores tot Technische Index* [in Dutch], Delft, NEN.

Pedro, J. Branco; Vilhena, A. & Paiva, J. A. Vasconcelos 2008, Portuguese method for building condition assessment, *Structural Survey*, Vol. 26, No. 4, pp. 322-335.

Portugal 2006a, Lei n.º 6/2006 [in Portuguese], *Diário da República*, Série I, no. 41 (2006-02-27), pp. 1558-2187.

Portugal 2006b, Portaria n.º 1192-B/2006 [in Portuguese], *Diário da República*, Série I, No. 212, Suplemento, (2006-11-03), pp. 7708(9)-7708(15).

Straub, Ad. 2009, Dutch standard for condition assessment of buildings, *Structural Survey*, 1, Vol. 27, No. 1, pp. 23-35.

United Kingdom 2004, *Housing health and safety rating system guidance (version 2)*, London, Office of the Deputy Prime Minister.

XII DBMC
International Conference on Durability of Building Materials and Components
PORTO - PORTUGAL, April 12th-15th, 2011

Calculation Example for Anticipating the Repair Need of Concrete Facade and Balcony Structures

Arto Köliö [1]
Jukka Lahdensivu [2]

ABSTRACT

At the moment finding new strategies for the repairing of concrete facades is of great importance concerning finnish residential buildings. In the Finnish building stock relatively young buildings have required often unexpected and extensive repair. Condition assessments of these buildings' facade structures have been conducted actively for 20 years supplementing a large pool of data on degradation and the material properties of these facades. A model has been developed from the basis of this data to describe the degradation of existing concrete facades in Finnish climate.

The repair need of Finnish precast concrete facades of 1965 – 1995 is being calculated using the degradation model. A sample of 496 concrete buildings was gathered as input data for the model. The sample was distributed to five localities covering the majority of Finland. As the complete calculation is still under process, this paper evaluates and compares the repair need of facades in two localities, Helsinki and Tampere. The results show that repair needs exist in two-thirds of the facades. Mostly the needed repairs at the moment are light coatings and patch repairs, but the continuing degradation increases the share of more expensive repairs. The repair measures have to be prioritised for all of the repairs can not be done with present resources. The average increase of repair need is 10 % every five years. This share has to be covered in order to maintain the present level of condition.

KEYWORDS

Service life, property management, condition assessment, degradation, concrete facade structures.

[1] Faculty of Civil Engineering, Tampere University of Technology (TUT), Tampere, FINLAND, arto.kolio@tut.fi
[2] Faculty of Civil Engineering, Tampere University of Technology (TUT), Tampere, FINLAND, jukka.lahdensivu@tut.fi

1 INTRODUCTION

This paper discusses a study where a new estimation was calculated for the repair need of existing concrete facades in Finland. The finnish building stock consists of a total of 56 000 apartment houses that involves 44 million m2 of concrete facade and 975 000 concrete balconies. Of these apartment houses 46 % have been built in the 1960s and 1970s due to increasing demand of urban apartments. This is the time when the use of prefabricated units in construction was being actively developed. Condition assessment systematics for concrete facades and balconies has been developed in Finland since the mid-1980s. Information on the degradation of concrete facades has been gathered and documented constantly in connection with every condition assessment. The condition assessment data of nearly a thousand facades has been gathered to a database for analysis.

This estimate is the first one that relies on a database of real measured data. The study includes prefabricated concrete facades and balconies of residential multi-storey buildings in Finland from 1965 – 1995. The repair need discussed here is induced by degradation of the structures and it does not include aesthetical, scheduled or other non-degradation related reasons to initiate facade repairs. In absence of reliable statistics on facade renovation, the effect of annual repair activity is not included in the calculation. The increment of repair need is assessed in a situation where the facades degrade freely. This viewpoint gives us information on the annual volume of repairs that is required to maintain current condition of the building stock and how the repairs should be distributed over time. It is arguable to believe that many facades are repaired needlessly with too heavy repair measures "just in case". This study is meant to prove, that the annual costs of facade renovation can be reduced significantly with a predictive strategy to facade renovation.

2 DEGRADATION OF CONCRETE FACADES

2.1 Prefabricated Concrete Facades

The facades of buildings from 1965 – 1995 have been constructed using mainly similar prefabricated units consisting of outer and inner layer of concrete and an insulation layer of mineral wool in between. The importance of frost durability of concrete was not truly recognized until 1980. However, concrete has occasionally been air-entrained to improve workability. The strength of concrete used has been approximately C20 and the thickness of the outer layer 40 – 85 mm. The outer layer is reinforced with a mesh and anchored to the inner layer with diagonal trusses travelling through the insulation layer. The most common type of Finnish balcony after late 1960s consists of prefabricated frame, slab and parapet units that are assembled as a balcony tower. The parapet elements of balconies have rather heavy reinforcement. [Concrete Association of Finland, 2002].

2.2 Degradation Mechanisms

The degradation of concrete structures is caused by simultaneous influence of environmental, structural and material factors. Degradation eventually results in cracking or spalling of concrete that reduces bearing capacity or bonding reliability of the structures. Harsh climate increases the requirements for durable materials. The major mechanisms in Finnish climate are corrosion of facade reinforcement due to carbonation and weathering of concrete [Pentti et al. 1998]. The presence of chlorides in facade structures is very rare.

Concrete reinforcement is protected from corrosion by high alkalinity of concrete pore water. This alkalinity is over time neutralized by carbon dioxide in the surrounding air resulting in corrosion which, especially with shallow cover depths, leads to cracking or spalling of surrounding concrete. [Broomfield. 1997]. Structures are protected against corrosion by placing the reinforcement inside the structure using sufficient depths of concrete cover. In this matter, cover depths of under 15 mm are critical. The design values for concrete cover have been sufficient to withstand carbonation and tensile stresses caused by corrosion, but the deviation in construction has resulted in also very shallow concrete covers, even less than 5 mm.

Frost weathering is caused by the combined effect of temperature alterations and moisture. The freezing of water in fully saturated pores of concrete causes cracks if the tensile strength of concrete is exceeded by stresses from the freezing. [Pigeon & Pleau, 1995]. The importance of frost durability of concrete was not aknowledged in the 1960s and the 1970s construction. Therefore many of presently existing facades have proneness to frost damage. The most effective way to protect concrete structures is to prohibit the entry of water to the structure, which, however, is impossible concerning facade structures. Increase in the compressive strength makes concrete more dense decreasing the amount of water the pore structure is able to hold thereby improving frost durability. The requirement for compressive strength is less crucial, when sufficient air entraining is used. Air entraining of concrete creates protective pores in concrete where the pressure caused by freezing can escape. According to Finnish guidelines the coefficient for frost resistant concrete is ≥ 0.20. That is 20 % of the pores in concrete are of the correct size to remain air filled in all conditions [Concrete Association of Finland. 2002].

2.3 Condition Assessment and Repair

The goal of condition assessments of facades is to find out the current state, rate and extent of damaging and the tendency of damage propagation in the future. The assessment is composed of the inspection of building designs and related documents, field investigation and laboratory analyses. The concrete association of Finland has published a manual for these assessments, which is used by practically every assessor. [Concrete Association of Finland, 2002]. The produced information is then used in planning of the facade repair work. Concrete facades and balconies can be repaired by methods of mainly three different magnitude. Protective methods e.g. coatings are used for slowing down the advancing of degradation where patch repair is a traditional method widely used for repairing local damages caused by both weathering and corrosion. Properly made patch repairs together with protective coating can extend the service life of concrete structures remarkably [Mattila, 2003]. If the damaging is widespread the patch repair method is substituted by different cladding methods that usually include an added thermal insulation layer. Total renewal of the existing structure is arguable when large areas of the facade are extensively deteriorated.

3 THE DEGRADATION MODEL

3.1 The Main Principles and the Condition Assessment Database

According to earlier studies, the factors contributing to the degradation of Finnish buildings constructed using prefabricated units in 1965 – 1995 can be simplified and narrowed down to but a few major ones. This is mainly because of the tradition of using similar techniques in the fabrication of building elements. [Lahdensivu et al., 2010]. The systematics of condition assessments has made it possible to gather and analyze data for same comparable information is available from each investigated building. The collected database consists of building identification information, geographical location, data from measurements and specific laboratory tests and repair measure recommendations given on the basis of the assessment. Data includes 947 buildings from 1960 to 1995 of nine different surface types of concrete facades: brushed concrete (uncoated or painted), floated concrete, form surfaced concrete (uncoated or painted), exposed aggregate concrete, clinker surfaced, tile surfaced and white concrete.

A degradation model for concrete facades and balconies has been developed from the basis of the assembled database including frost weathering of concrete and carbonation induced corrosion of reinforcement. These degradation mechanisms lead, depending on material properties and the extent of damage, to repair method proposals that include coating, patch repair, cladding, renewal or no repair need. Determining the correct repair measures is systematised with decision paths, fig 1.

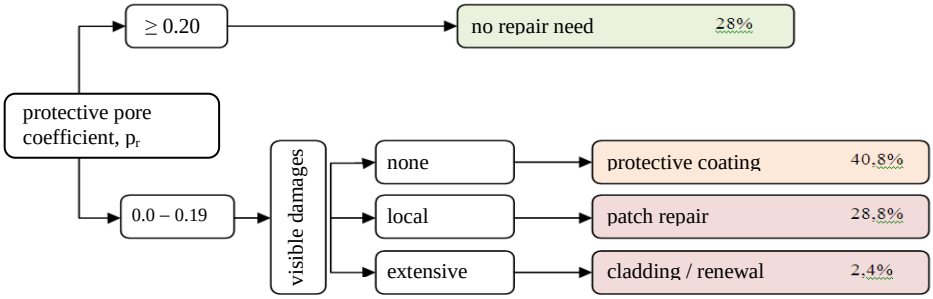

Figure 1. A decision path for determining correct repair measures for frost damages according to the rate of damages.

The repair need caused by weathering or corrosion are first assessed as separate and then combined using an algorithm that weighes the heavier repair method over the lighter one. Because the model uses real measured properties of the facade materials it is arguable to claim that it represents the existing building stock accurately including e.g. errors made in construction. Because the values stored in the database represent the date of the condition investigation, it was essential to be able to advance the degradation to a desired date of examination. The damage propagation was modelled by setting different propagation times for different ranges of damaging related material properties.

3.2 Corrosion of Reinforcement

Carbonation induced corrosion of reinforcement developes first through an initiation stage involving the carbonation process after which the actual corrosion starts in the propagation stage. In this study the end of service life of reinforcement is set to the end of initiation stage i.e. the moment when carbonation has reached the reinforcement. This is a rather rough estimate because the service life of concrete structures is not yet compromised at that moment. In a lack of reliable propagation stage model for reinforcement corrosion, the calculation at this point has to be acknowledged as an estimate on a safe side.

The model uses cover depths and carbonation depths derived from the condition assessment database according to building year. Different fabrication methods and deviation in the fabrication of elements create variation to the cover depth. Also the ingress of carbon dioxide to concrete varies. The amount of reinforcement in carbonated concrete, illustrated in fig. 2, is calculated by the publication *Condition investigation manual for concrete facade panels* [Concrete Association of Finland, 2002] first multiplying the total amount of reinforcement at a certain point (5 mm range) inside the structure with the percentage of carbonation depths that exceed the examination point for we can be certain that this amount of reinforcement is located in carbonated concrete. To this value is then added the same amount of reinforcement multiplied with the percentage of carbonation depths at the examination point divided by two. The division by two is done for the values used are averages of each 5 mm range.

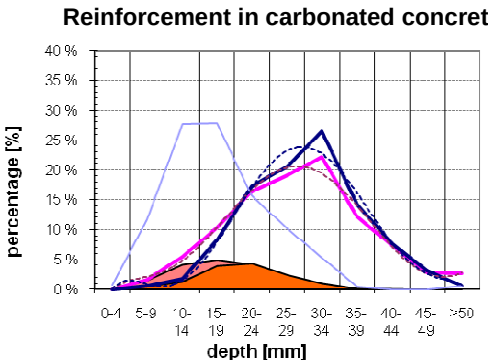

Figure 2. Tthe amount of reinforcement in carbonated concrete (red area) and the distribution of cover depths (dark blue) and carbonation depths (light blue).

Carbonation advances in concrete first rapidly and then with decreasing speed. For the modelling of the concrete carbonation the model uses the square root equation (1) introduced by Tuutti [1982].

$$x = k \cdot \sqrt{t} \qquad (1)$$

When the examination year is set to the model, it extends every measured value of carbonation depth using the equation. The intensity of carbonation is in the equation characterized with carbonation factor *k*. The values of *k* are in this case derived from the condition assessment database. The result *x* is the carbonation depth in concrete and *t* is time in years, which in this case is the time from the building dates in the database to the examination year. After the advancement of carbonation the amount of reinforcement in carbonated concrete is recalculated.

3.3 Frost Weathering of Concrete

The pore structure of concrete is essential for the frost durability of concrete structures. Both the strength of concrete and air entraining alter the pore structure for better frost resistance. The condition assessment database however does not include information on the compressive strength forcing the use of pore structure measurement data. Frost weathering is assessed through the amount of non-capillary pores of concrete and observed frost damage in the structures. Facades with protective pore coefficient, $p_{r,}$ values above 0.20 are considered intact and undamaged whereas values lower than 0.20 result in repair measures. The extent of repairs is then determined using the amount of visible frost damage. Extensive visual frost damage leads to cladding repairs or renewal of the old structure while local frost damage results in patch repairs and no visual damage leads to protective methods.

The progression of frost damages is modelled as the increment of visible damage over time. The value of p_r and the geographical location determines the progression speed. Damaging does not advance in concrete with p_r value of over 0.20. The lower the value gets the faster the progression is. Value of p_r is assumed constant over time although over time there may occur reactions that fill pores e.g. the formation of ettringite. In Finnish climate the number of harmful freeze-thaw cycles is 30 – 60 per winter season depending on the geographical location. Buildings located in coastal climate deteriorate remarkably faster than the ones located inland. The impact of material properties and location to the progression of frost damage is illustrated in fig. 3.

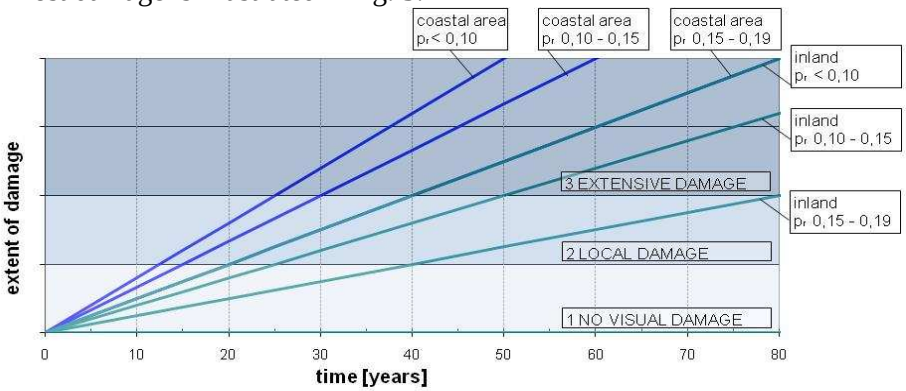

Figure 3. Progression model for the weathering of concrete facades and balconies.

3.4 Utilization of the model

The model has been formed into a computer application to automatise the calculation process. Because of the statistical nature of the examination, it can only be applied on a group of buildings, a certain area or a suburb. The case-specific properties of single buildings can not be estimated, but in a larger group the properties even out. A preliminary survey for gathering input data has to be conducted on the area. The model writes out the information for a certain year and surface type after which the

information has to be adjusted to the surface type and age distribution of buildings on the area. This principle is illustrated in fig. 4.

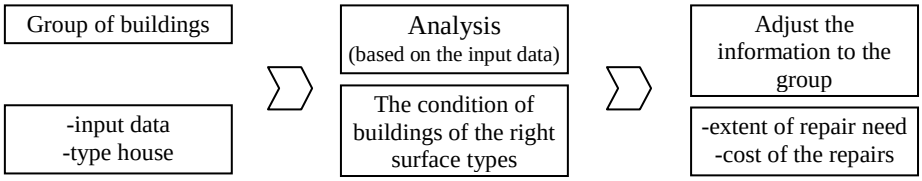

Figure 4. The principle of the calculation

The model operates with input data that consists of the surface type and the age and geographical location of buildings. The age and quantity of balconies is needed for the evaluation of balcony structures. This information may be acquired by investigating the documents and drawings on the building group or by surveying the area. The analysis of repair needs is then carried out using this collected input data. These percentages of different repair alternatives are then converted to quantities and costs by multiplying them to the surveyed building group. An average type house is used in the converting calculations.

4 CALCULATION EXAMPLE

4.1 Initial conditions

To acquire the input data for the degradation model a sample of 496 concrete buildings was gathered in a survey. The sample was distributed to the localities of Helsinki, Turku, Tampere, Jyväskylä and Oulu covering the majority of Finland. Information was gathered studying building design archives, surveying areas by foot and using internet searches. This paper discusses the repair need calculations from the samples of Tampere, located inland with approximately 200 000 inhabitants, and Helsinki,located at the south coast of Finland with about 500 000 inhabitants. The geographical location is different in these localities causing different degradation progress. The building stock itself is very much similar in both cities. Only the distribution amongst surface types is a little more diverse in Helsinki. The average height of residential buildings in Tampere is 5.0 storeys and in Helsinki 4.6 storeys. The average facade area of one building is in Tampere 1230 m^2 and in Helsinki 1130 m^2.

For determining repair expenses, average cost estimates from the year 2009 were input to the model: facade repairs 40 – 195 €/m^2 and balconies 5000 – 9000 €/balcony depending on the repair method. The same repair costs were used in calculation in every locality regardless of the changes in local price levels. This will bring forth the differences caused by the technical repair need over the local price level. This evaluation includes the costs of only the repair of the concrete facade. The calculation does not include e.g. the changing of windows that is typically done in connection with facade renovation.

4.2 Inventory of the building stock

This input data includes the surface type and age distribution of buildings shown in tables 1 and 2.

Table 1. Surface types of facades in Tampere (n=191)

surface type	building year					
	65 – 69	70 – 74	75 – 79	80 – 84	85 – 89	90 – 94
exposed aggregate	1	2	8	16	6	2
form surfaced, painted	0	1	0	1	0	0
brushed, painted	41	32	20	7	2	3
clinker surfaced	8	3	0	0	0	0
tile surfaced	0	0	0	5	15	13
white concrete	0	0	0	0	0	5

Table 2. Surface types of facades in Helsinki (n=117)

surface type	building year					
	65 – 69	70 – 74	75 – 79	80 – 84	85 – 89	90 – 94
exposed aggregate	6	16	3	1	3	0
form surfaced, painted	1	0	1	0	5	10
form surfaced, not painted	1	0	2	2	0	0
brushed, painted	14	6	2	3	1	3
floated	1	1	0	0	0	0
clinker surfaced	0	0	0	0	0	5
tile surfaced	0	0	5	15	8	2

4.3 Results

The repair need of concrete facades in Tampere and Helsinki was calculated using the above initial conditions. The results are shown in figure 5. This distribution represents the actions required to be taken on the building stock at the moment 2010. The total present cost of repairs is in Helsinki 275 M€ and in Tampere 84 M€.

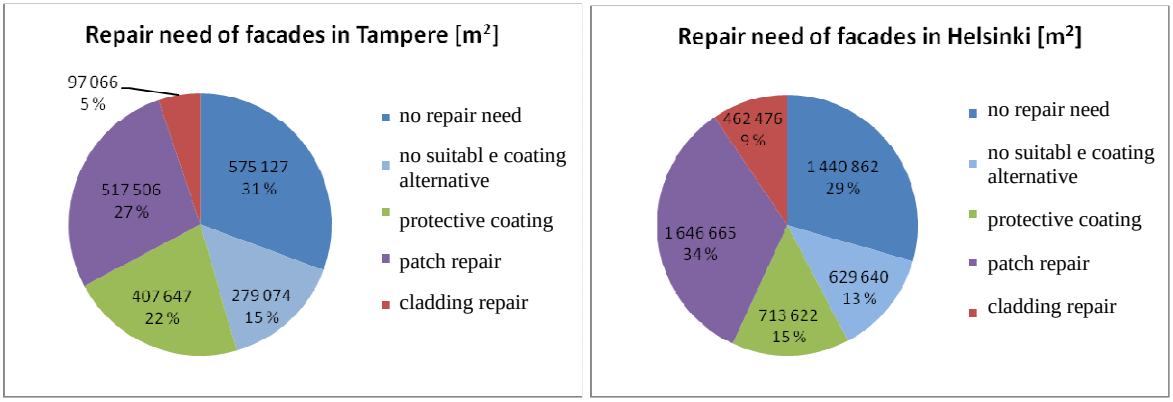

Figure 5. Repair need of prefabricated concrete facades in Tampere and in Helsinki.

The costs of the repairs accumulate from the repair measures. Over time the lighter and inexpensive repair measures are substituted by more expensive cladding repairs. The formation of repair costs was calculated at eight time intervals. The repair cost progression of facades in Tampere is shown in fig. 6. Fig. 7 illustrates the differences of repair costs in Tampere and Helsinki.

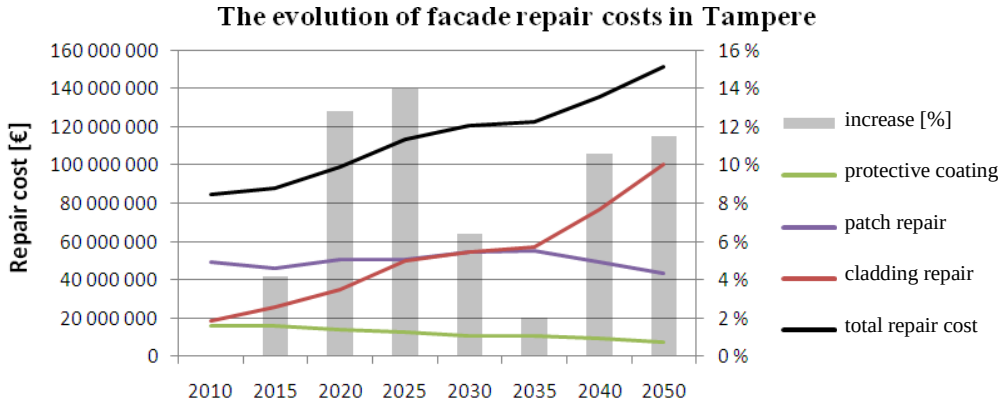

Figure 6. The repair cost is composed of repairs of three types.

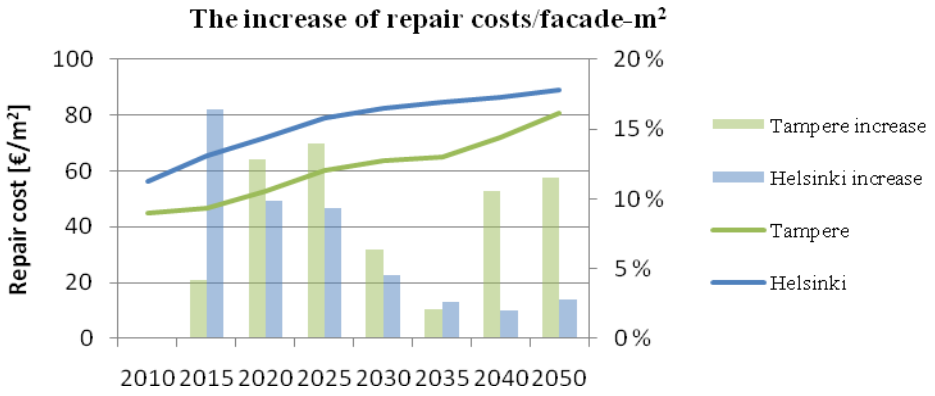

Figure 7. The differences between degradation of facades in Tampere and Helsinki

5. CONCLUDING REMARKS

The model and the example calculation introduced in this paper are a step towards anticipatory property management where problems relating to different surfaced concrete facades can be prepared for. This predictive tool, being based on extensive real measured data, can be argued to represent the Finnish building stock rather accurately including, for instance, deviation in building quality showing as insufficient protective pore coefficient values or very little cover depths of reinforcement. The model works well for the precast concrete facades from 1965 – 1995. Buildings of that age have been constructed very much using the same techniques and same kinds of building units fabricated the same way.

According to the calculation the most needed repairs at the moment are light coatings and patch repairs. If no repair measures are taken, the share of heavier cladding repairs will increase rapidly and outstrip patch repairs by the end of 2025. As a whole the present repair needs accumulate costs of 84 M€ in Tampere and 275 M€ in Helsinki. The average increase of repair costs is 10 % every five years over the 40-year period. This share has to be accounted for to maintain the present condition of the building stock. By investing now to the protective repair of concrete facades, the progression of degradation could be remarkably slowed down.

REFERENCES

Broomfield, J. 1997. *Corrosion of Steel in Concrete*, E & F Spon, London.

Concrete Association of Finland. 2002, *Condition investigation manual for concrete facade panels*, Concrete Association of Finland, Helsinki. (In Finnish)

Lahdensivu, J., Varjonen, S. & Köliö, A. 2010, *Repair strategies of concrete facades and balconies*, Tampere University of Technology, Structural Engineering. Research report 148, Tampere (In Finnish)

Mattila, J. 2003, *On the durability of cement-based patch repairs on Finnish concrete facades and balconies*, Tampere University of Technology, Structural Engineering. Publication 123, Tampere (In Finnish)

Pigeon M., Pleau R. 1995. *Durability of concrete in cold climates*. London. E & FN Spon. 244 s.

Tuutti, K. 1982, *Corrosion of Steel in Concrete*, Swedish Cement and Concrete Research Institute CBI Research 4:82, Stockholm.

XII DBMC
International Conference on Durability of Building Materials and Components
PORTO - PORTUGAL, April 12th-15th, 2011

A Study on an Improved Construction Inspection System in Taiwan

Ko-Ming Huang [1]
Chun-Ta Tzeng [2]

ABSTRACT

The quality of construction is quite often denounced in Taiwan. Contractors are using lower bid prices to win job contracts and using cheap materials and poor labor at the construction sites. There are currently not enough personnel to enforce the abundance of rules and regulations set forth by the government. Additionally, the present statutes in place do not clearly state where the responsibility of safe and well-made construction lies, with the architect or the government inspectors. The study will show a mock up of an improved inspection system of construction which could replace the present one and its obvious inefficiencies. The study helps determine if we implement this improved inspection system of construction, it will be risen that the quality of construction, as well as, the safety of buildings in Taiwan.

KEYWORDS

Building construction, Supervision, Inspection system, Quality control.

[1] Ph D. candidate, Department of Architecture, National Cheng-Kung University, Taiwan.
[2] Associate Professor, Department of Architecture, National Cheng-Kung University, Taiwan

1 INTRODUCTION

The production process of a building can be broadly divided into ‘eight stages of site survey, planning, schematic drawing license application, contracting, construction, inspection, completion, usage management [Su 2001]’, in which construction and inspection are the most two important stages that affect the quality of construction. Currently, the inspection system on the building construction in Taiwan is enforced by the personnel who are in charge of constructions, as well as by government authorities. The current Taiwan construction law does not explicitly define the substantive contents of words between the “inspection” and “supervision”. Therefore, whenever an event of inferior quality or disaster of construction occurs, there has been always a controversy over the attribution of the responsibility to constructor or inspector. In his book of "Engineering Construction Specification", Joseph Goldbloom wrote out very clear definitions to the words of Inspection and Supervision as follows: The Engineer "inspects" the work to ensure that it conforms to and is in accordance with the requirements of the contract. He does not "observe" it, he "inspects" it. ‘The Contractor "supervises", because he controls and directs the various construction operations [Robert D. Young et al. 1979]’. Thus, inspection means examination between different systems; ‘Supervision refers to the same body, the superior (supervisor) to the lower level [Chang 1994]’. In fact, owing to the lack of manpower in the government agencies, most of its inspection tasks can only be carried out in sampling method. Similarly, the gate keeping job of construction quality inspection by inspector has been also loosen, mostly only focuses on the written examination and supervision. For this phenomenon, it is necessary to explore the inspection system as well as to develop countermeasures to improve.

2. THE COMPARISON OF CURRENT SUPERVISION SYSTEM AMONG TAIWAN, THE UNITED STATES, AND JAPAN

Similar to Japan, the Taiwan current inspection system has assigned the architect to inspect the construction works. Under the existing U.S. system, the designer does not do the work of inspection; instead, the government will authorize an inspector to implement the inspection for the construction of architecture body. This approach is what Taiwan's current inspection system lacking and is worthy of us to reflect and learn. This research, based on the study of current construction inspection models of the United States and Japan, aimed to seek measures for improvement of current Taiwan inspection system.

2.1 The U.S. construction inspection system

The relationship among owner, contractor, architect, inspectors and the City Construction Management Office in the U.S. is illustrated as Figure 1. (e.g. the construction inspection system of Los Angeles) [Fu 2000].

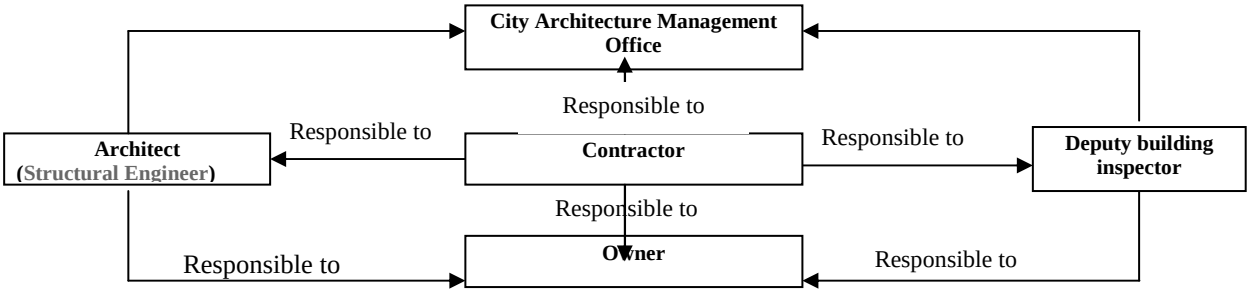

Figure 1. The relationship among owner, contractor, architect, inspectors and the City Architecture Management Office in the U.S.

Take the Los Angeles, California in the US for example, architects generally are only responsible for the designs and the supervision and management of construction is enforced by "Building Inspectors" of local government. The construction proprietor may increase the task of supervision to architect on the design contract if necessary; if not, the architects do not perform the supervision duty. This is different from "Taiwan existing systems of combining the design and inspection tasks together for an architect, or separating both tasks and assigning each one to different architect" [Liu 2000]. The United States allows architects to design and construct the same building, as for the inspection of building construction; it is enforced by an inspector of Inspection Company commissioned by the proprietor. The inspector is on behalf of city government for the inspection of constructions, who is so called as "Deputy Building Inspector". Employees in the U.S. inspection company must be licensed professional personnel. While in contracting out of project, the proprietor must look for inspector from the inspection company for construction inspection and bear the inspection fees, instead of paying by construction companies so as to avoid jerry-building. The inspector should work in coordination with the time schedule of the construction company. In the case of special circumstances that the inspector has to leave the site, he/she must inform the site leader of the construction company and the City Architecture Management Office, and ask the inspection company to send another inspector to take over the inspection job. If no one takes in charge of the inspection task, the construction must not be done. Inspector's validation reports include reports of the confirmation for each single item structure construction. According to IBC Building Code [International Building Code 2000] 1704 - special examination provisions any structural safety related project shall require a licensed special inspector to monitor the whole constructional process and to complete a detail report of the required inspections to the government agencies. As the structural safety has been entirely monitored by professional inspector(s), "the government's construction inquest regulated in the IBC building codes is mainly to check equipments outside the structure, fire protection, and relevant provisions of urban planning" [Fu 2000].

2.2 The intermediate inspection system in Japan

Intermediate inspection system is set up owing to the lesson of Great Hanshin-Awaji earthquake in Japan which led to the amendment of 'Building Standard Law' as a countermeasure to solve the problem of inferior constructions. That is, to set a third party assigned by the validation project administration and inspection authority (the so-called civil professional unit), to have a right and opportunity to inspect during the construction process in order to compensable the impossible inspections after the completion of the construction structure. The system of Japan inspection institutes: "the relation diagram of separation pattern of design and construction among construction owner, designer, supervisor, constructor, and the intermediate inspection agency" [Ochi Takaharu 1989] is illustrated in Figure 2.

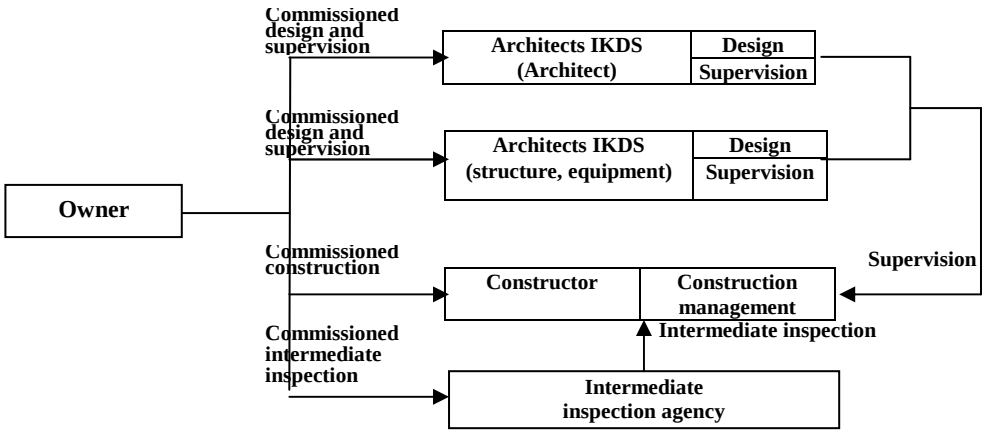

Figure 2. The separation pattern of design and construction.

2.3 The current inspection system in Taiwan

Situations of the manpower shortage, unclear responsibility, and inefficient public power of construction management under the current inspection system in Taiwan are mainly owing to the following reasons:
(1) The architects bear the responsibility of statutory inspection, but the inspection will become formalized once the construction developers to be the same persons of proprietors and constructors or the conglomerate [Xiao & Du 2000].
(2) The current legal responsibilities for the architect's inspection are very complex and vague. "During the constructing process, the constructors frequently ask architects to instruct and explain, but never stand on its own to solve the technical problem they have faced" [Tsai 1992].
(3) For major projects, "the government office usually entrust project Construction Management (CM) constructors to provide technical services. However, the services provided on behalf of Construction Management mostly are the contents of inspection" [Yeh & Chang 2000].
(4) The sponsor agencies fail to implement the construction inspection system. According to the spirit of this article, construction inspectors must take responsibility for inspection, and the architecture administration agencies are not necessarily to do the inspection which naturally without having to bear the heavy responsibility of inspection.
(5) In the current economic downturn, based on the cost savings, the construction inspectors and contractors have reduced manpower in the supervision dispatching, winning bids with competitive low price, and employed low-paid, junior or no experienced, insufficient educated staffs in order to reduce the cost.
(6) There is a considerable gap existing between the low quality and high expectation in terms of construction.

Under the organization of current supervision system in Taiwan, the relation of duties among the designer, supervisor, constructor, owner, and architecture administration agency are illustrated in Figure 3.

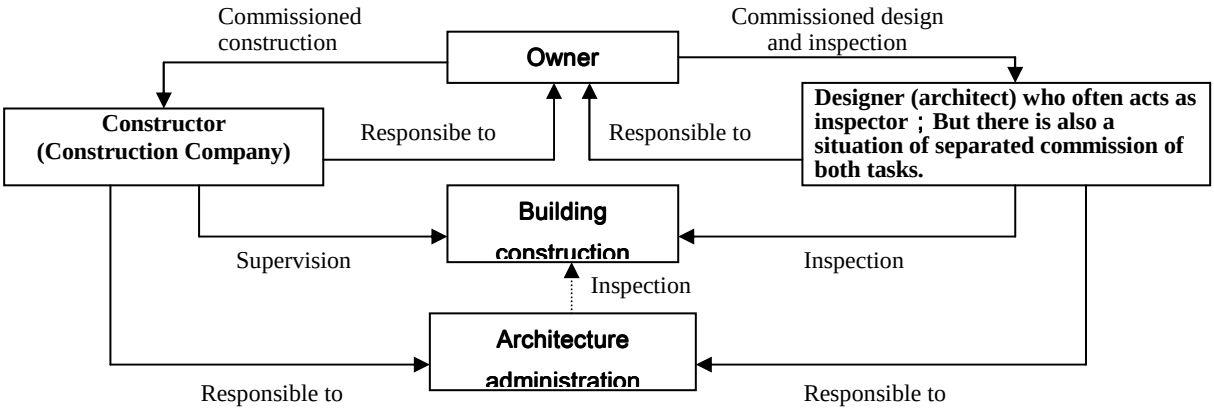

Figure 3. The relation of duties among the proprietor, designer, inspector, constructor, and construction competent authority.

3. THE DEVELOPMENT OF A IMPROVED CONSTRUCTION INSPECTION SYSTEM

The proposed construction inspection system of this study was organized and illustrated in Figure 4. In this system, the designer simply works on building design as well as provides consultation and necessary assistance for owner's design modifications or engineering bidding and tender events, but without involving the inspection of the construction process. Such system with independent design, construction and inspection approaches should be able to improve the bid rigging phenomenon generated by current inspection system combining with functions of design and inspection.

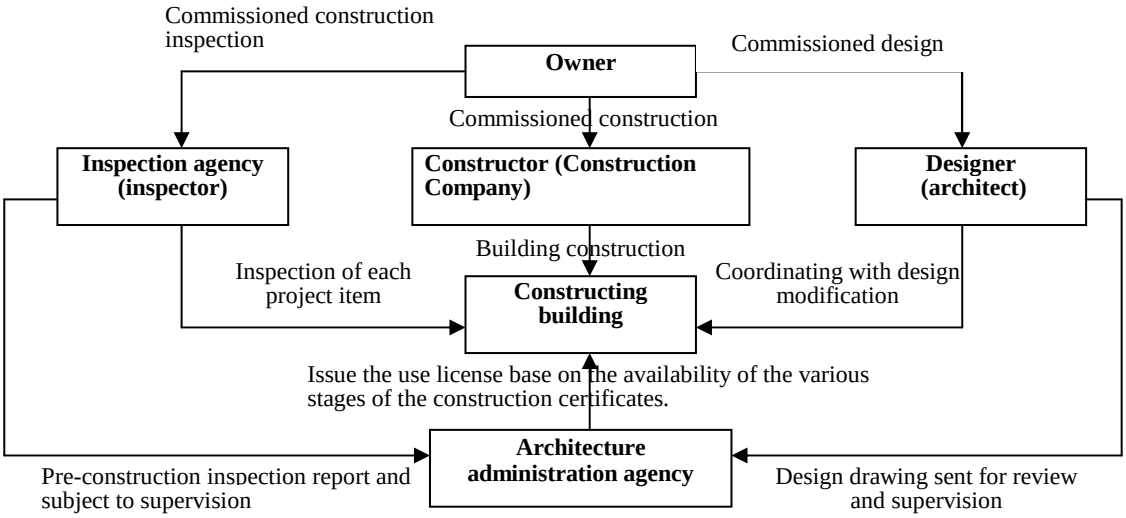

Figure 4. The organization structure of construction inspection system.

Under such construction inspection system, government agencies can switch the irregular site inspection owing to limited construction and management manpower to the supervising personnel who conduct the inspection of the building construction, going over the inspection results as well as reports, and issue certificate of each construction phase to those which are in line with the requirements of provisions. When the building construction is completed, only those which have obtained the various stages of the construction certificates are allowed to apply to the architecture administration agency to issue the use license. The inspection company must recruit professionally trained, tests qualified as well as licensed people, and the inspection body must be a legal institution which satisfies the conditions required by the government. In accordance with various phases of construction process and target items assigned by the Architecture Administration Agency to be inspected, the inspect company dispatches expertise person in line with the project to inspect. In the inspecting process, the inspector must report to the Architecture Administration Agency and accept their supervisions. Without the inspector's signature for the approval and confirmation of each construction phase, the next phase of construction is not allowed to proceed. This research suggested improving part of the existing inspection system to replace the construction management staffs and building inspector with the inspector in implementing the inspection and supervision for the building. Such professional inspection manpower provided by civil organization not only can make up the man-power shortage of official construction and management, but also can be regarded as official and private cooperation models in improving the construction quality and ensuring the building safety. The inspection company and the inspector should bear the main civil and criminal liability of the whole project. Thus, the inspection organizations must first cover the inspection liability to insurance company for the compensation of inaccurate inspection which results the building damage or the loss of life and property. The system modification has to be through the amendment of existing laws, and by law the government must authorize the public power and inspection, which used to be enforced by the original construction management personnel, to civil authorities and the inspection agencies to implement. The provisions of the Civil Code can be the legal basis for the construction inspection system proposed by this study in obtaining the government public power and act as agency in implementation for building supervision and inspection. All inspectors must pass through the government-organized professional examinations and obtain certification of professionals. For example, the architects, civil engineers, structural engineers who want to obtain the qualification to perform the task of building construction inspection must receive a certain number of hours of advanced training and pass the examination. In addition, those qualified person also have to join legally established inspection company with sizable number of employees. After being paid and commissioned by the proprietor, the inspection company dispatches and schedules various types of

expertise to carry out the inspection task for each construction phase and takes the full responsibility to the proprietor. The responsibility is also accompanied by a civil and criminal liability, and should be insured by liability insurance for any reasonable compensation owing to inspector's negligence which causes the losses of life or property.

4. CONCLUSIONS

The construction inspection system proposed by this research was to unify the inspection and supervision tasks of architecture administration agency and inspection unit into one, and have the inspector coordinate the tasks of inspection for building construction to avoid responsibility confusion. The advantages of implementing the construction inspection system proposed by this research were as follows:

(1) To resolve the manpower shortage of government construction and management agencies that results in poor performance of supervision and inspection.
(2) If authorized by the legislation, construction inspector may obtain the legal status on behalf of the government to implement the inspection which will improve the situation of unclear rights and responsibilities under current system.
(3) To improve existing overlapping system of inspection and supervision to avoid the situation of responsibility hedging, and oblige the inspector to take the responsibility for the supervision of building construction.
(4) In line with the promotion of constructional insurance system to add the inspection liability insurance premium in inspection cost items, for the compensation of personnel or property loss damaged by the inspector's negligence.
(5) To improve the current situation of serving concurrently a designer and a building inspector which prone to the bid rigging phenomenon.
(6) The improved inspection and supervision on construction process will reduce the extent of heavy casualties caused by natural disasters.
(7) To complement and cooperate each other between government and civil professional manpower, enable the whole construction system to be more integrated, and upgrade construction levels as well as international competitiveness.

REFERENCES

Chang Hwang (1994), "Inspection or Supervision?", Chinese Technology, Article 24: 87-90.

Fu Wen-Chang (2000), 'The structure construction inspection system in Los Angeles, California, Architecture and Building Foundation, Taiwan.

International Building Code, 2000, International Building Code, Inc., USA

Liu Fuxun (2000), "The status of American professional engineers system", Construction Management Quarterly, 43, summer: 2 p.

Ochi Takaharu (1989), "The responsibility of construction defect and disputes responsibility", p. 38, Japan.

Young, R. D., Dunham, C. W. and Bockrath, J. T. (1979), Contracts, Specifications and Law for Engineers, McGraw-Hill, USA.

Su Yu-De (2001), "The research of the services and responsibility architect should be responsible for in the construction", Collection of the 13th Architectural Research Results Presentation Institute, Taiwan

Tsai Yi-Hong (1992), "The study of the powers and responsibilities of inspection of the architect", Master Thesis, Architecture Department of Tamkang University, Taiwan

Xiao Jiang-Bi, Du Chen-Sheng (2000), "The Study of Establishment of Compulsory Liability Insurance System on Architecture", Research Project Report, Architecture and Building Research Institute", Ministry of the Interior, Taiwan.

Ye Hong-An, Chang Jun-Zhe (2000), 'The mechanism of construction management and quality control of construction engineering", in: "The topic compilation of construction system review and prospect after the 921 earthquake": Republic of China National Association of Architects, pp. 153-165.

XII DBMC
International Conference on Durability of Building Materials and Components
PORTO - PORTUGAL, April 12th-15th, 2011

Development of a Safe and Environmentally Friendly Method for Sealant Renewal. Part 2: Examination of Viscosity and Softening Effect of the Remover

Takeshi Ihara [1]
Satoru Ohsawa [2]
Shingo Yoshida [3]
Takumi Itaya [4]
Kenji Motohashi [5]

ABSTRACT

The proposed remover, which is made from Limonene and used in TSR method, is a transparent liquid and flows out or volatilizes easily if applied directly to sealed joints. Therefore, its effects, like swelling and softening, cannot be expected neither on vertical, horizontal nor oblique sealed joints within panels, sashes or glass.In order to overcome such shortcomings and engender required properties of removers, such as sagging resistance, wettability, dry rate, workability and removing task, the viscosity of the remover is improved trough composition and mixing ratios, and swelling and softening of sealants are confirmed after being soaked in the improved remover. TSR method has taken shape through trials carried out on real buildings where the remover's viscosity has been confirmed. These trials also allowed the evaluation of the cost for sealant renewal based on the used amount of the remover, the work efficiency and the selected procedure, and indicated that TSR method can decrease the life cycle cost and making it lower than the cost relative to the conventional method.This paper reports the procedure for improving the remover and the studies on its properties of swelling and softening in actual structures. The paper reports also the removal performance of sealants during the trials, as well as the calculation related to life cycle cost.

KEYWORDS

Sealant, Renewal, Sealant residuals, Gel, Remover, Life cycle cost.

[1] TAKENAKA Research and Development, Chiba, JAPAN, ihara.takeshi@takenaka.co.jp
[2] TAKENAKA Research and Development, Chiba, JAPAN, ohsawa.satoru@takenaka.co.jp
[3] TAKENAKA Research and Development, Chiba, JAPAN, yoshida.shingoa@takenaka.co.jp
[4] TAKENAKA Corporation Hokkaido Office, Hokkaido, JAPAN, itaya.takumi@takenaka.co.jp
[5] SHIBAURA INSTITUTE OF TECHNOLOGY, Tokyo, JAPAN, Dr.Eng., motoken@shibaura-it.ac.jp

1 INTRODUCTION

An innovative sealing renewal method, named Thin Sealant Removeal method (TSR method) have been developed. Contrary to conventional methods which cannot remove completely remaining thin layers of previous sealants that affect the water tightness reliability, this method can completely remove them. The companion paper (Part 1) concluded that Limonene made from oranges owns essential performance and is appropriate as a remover. However, because Limonene is a transparent liquid and flows out if applied directly to seal joints, its effet, like swelling and softening, can not be expected in a construction site. The purpose of this study is to improve the form of Limonene and provide it with required properties of a remover. This paper reports the improvement made on the composition and mixing ratio of Limonene in order to adapt a suitable viscosity. While the evaluation of softening effect of the improved remover by pulling test are reported in the companion paper (Part:1), herein life cycle cost of the TSR method based on trial installations is presented.

2 SUMMARY OF EXPERIMENT

2.1 Tested Materials

Some additives were mixed to Limonene to create gel-type and sol-type(paset-type) Limonene. The viscosity of gel-type and sol-type were intended to be applied to seal joints with a brush. The arranged Limonene was used in tests as a remover. Popular sealants were used for the test after curring them according to Japanese Industrial Standard (JIS) A5758 and A1439. The tested sealants are listed below.

1.Two-component silicone sealant (named SR-2)
2.Two-component poly isobutylene sealant (named IB-2)
3.Two-component poly modified silicone sealant (named MS-2)
4.Two-component poly polysulfide sealant (named PS-2)
5.Two-component poly urethane sealant (named PU-2)
6.One component silicone sealant (named SR-1)

2.2 Workability of Applying and Removing Test

In order to evaluate the workability of the remover containing Limonene by brush, and its effect on residuals of the previous sealant, the following procedure was applied.
1. Six removers which were arranged for gel-type and sol-type were produced by way of trials.
2. For test pieces, H shaped test pieces were prepared according to JIS A1439 as shown in Fig 1. After curring the test pieces according to the specified process in JIS A1439, the sealants were cut off leaving a thickness of 1 millimeter on the Aluminum alloy plate. SR-2 silicone sealant was chosen for the test because it showed the largest weight increase ratio after soaking it in Limonene (refer to the tests in Part:1). Fig 1 shows the sealant setup used in the test where the plane of the sealant was set vertically.
3. The trial remover was applied on the vertical plane of the sealant by a brush. An abundant weight of the remover was applied. Three grades were assigned to the applied weight and removing evaluated as good, not enough and bad.
4. After 3 hours, the remover was wiped off and the sealant was removed with a scraper as done in the tests in Part:1. When removing the sealant, a regular worker evaluated the workability according to the three-grades (good or not enough or bad) set in Part:1. The weight of the treated sealant was measured at five stages (A,B,C,D,E). Stage A was before applying the remover, stage B was just after applying the remover, stage C was after three-hour treatment, D was after wiping off the remover, and E was after removing residuals with a scraper. The maximum weight of the applied remover is evaluated as (B-A), the volatilized weight of the remover is evaluated as (C-B), the absorbed weight is evaluated as (D-A), Limonene content of SR-2 is evaluated as (D-A)/(E-A), the volatilized ratio is evaluated as (C-B)/(B-A), and the absorbed ratio is evaluated as (D-A)/(E-A).

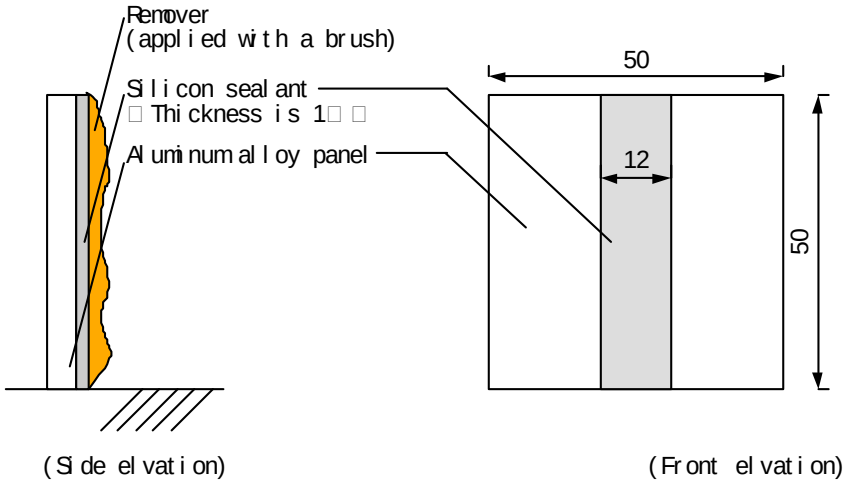

Figure 1. Sealant specimen used in applying and removing test.

2.3 Pulling Test

Fig 2 shows the form of the sealant test piece. Sealants with 2 millimeter thickness were cut into the form shaped as the No.3-dumbbell defined by JIS K 6251. The middle of the dumbbell shape was soaked in improved gel-type remover for a few hours and then pulled at the speed of 200mm/min. The maximum pulling strength was measured.

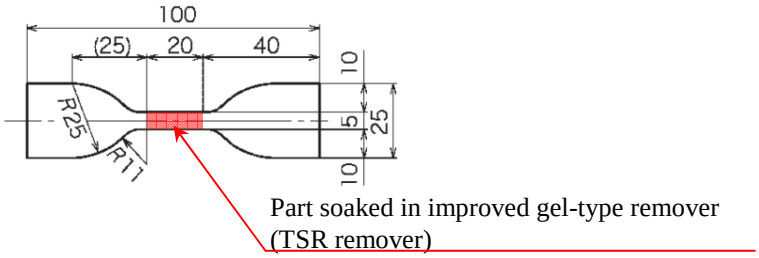

Figure 2. The form of the tested sealant for pulling test.

3 RESULTS AND DISCUSSION

3.1 Result of Workability of Applying and Removing Test

Table 1 shows the Result of the workability of the applying and removing test. Fig 3 shows the maximum weight of applied remover, volatilized ratio and absorbed ratio. For the conditions of Type A, the workability of applying the remover was very good, applied weight was large and slump was small. However, the workability of removing residuals was not enough because the volatilized ratio of the remover was large and the remover did not remain in the sealant for three hours. Moreover, Type A resulted in a dirty applying area as it dried due to a solid additive in type A. For Type B and Type C, it was difficult to apply them on the sealant with a brush and the applied weight was small. Therefore, the workability of applying the remover was bad. The workability of removing residuals was not enough. For Type D, workability of applying was good. However the slump was large, and it was easy to flow. Therefore, the workability of removing residuals was not sufficient. For Type E, it was hard to apply large weight onto the sealant. Therefore, the workability of applying remover was not sufficient. For Type F, it was easier to apply the remover onto the sealant with a brush compared to Type B and Type C, but still the workability of applying the remover was not satisfactory. However, the applied weight was appropriate. Slump and workability of removing residuals were good. As a general observation, it was easier to remove the sealant when the absorbed ratio (Limonene content of SR-2) increased. Our experimental results show that the optimum

conditions which can achieve required workability of applying the remover and removing residuals are obtained when the gel viscosity is appropriately arranged to control slump. Based on the knowledge aquired in this test, the production and evaluation of the remover was done by way of trials. As a result, the appropriate composition and mixing ratios for the remover which is named TSR remover has been reached.

Table 1. Form of remover and Result of workability of applying and removing.

Type	Form	Explanation	Workability Of Applying	Slump	Workability Of Removing
A	Sol	This sample was similar to tooth paste.	○	○※1	△
B	Gel	This sample was gelatinous and tough (hard gel form).	×	—※2	△
C	Gel	This sample was gelatinous and very tough (hard gel form)..	×	—※2	△
D	Gel	This sample was gelatinous grain whose diameter was about 1～3 millimeter (soft gel form).	○	△	△
E	Gel	This sample was similar to liquid (soft gel form).	△	○	○
F	Gel	This sample was gelatinous and soft (soft gel form).	△	○	○

very good:○ > not enough:△ > bad:×

※1 Slump was appropriate. But, it dried due to a solid additive in type A.

※2 It was impossible to evaluate slump because applying volume was small.

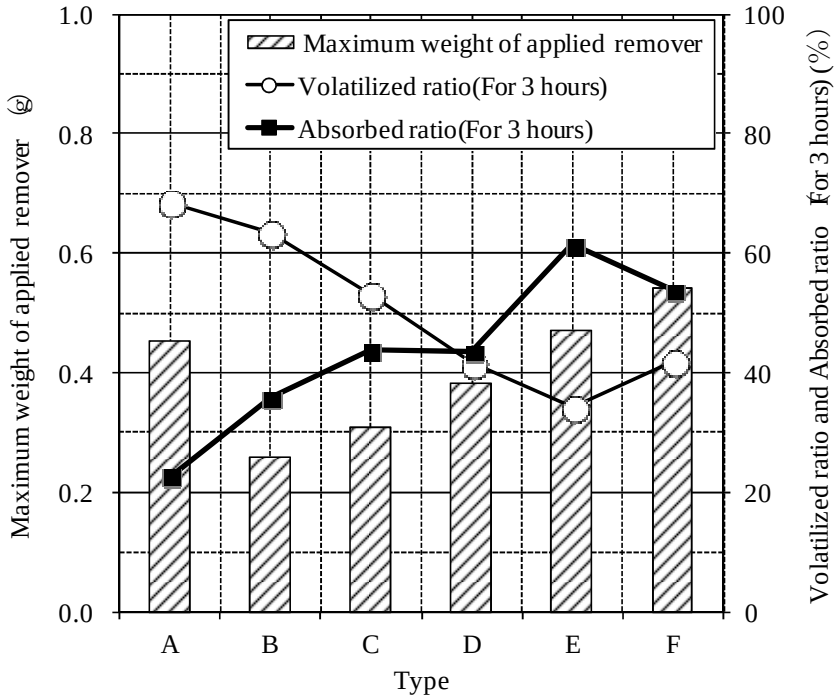

Figure 3. Maximum weight of applied remover, volatilized ratio and absorbed ratio

3.2 Result of Pulling Test

Fig 4 shows the relationship between the soaking time for TSR Remover and the maximum pulling strength which is measured by pulling a dumbbell test piece. The maximum pulling strength of major sealants decreases greatly after soaking for half an hour and continue decreasing gradually over another half an hour. Similar results were obtained when major sealants were soaked in Limonene (Part:1). Our experimental results showed that major sealants are softened by soaking them in the TSR remover.

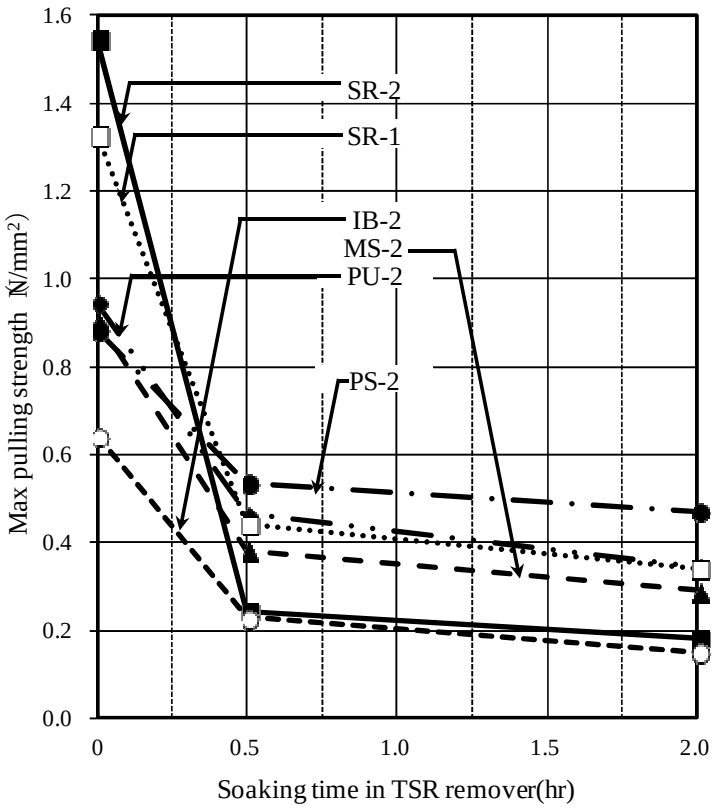

Figure 4. Results of pulling test**.**

4 TRIAL OF TSR METHOD

Pic 1 shows a trial process of the TSR method. Many trials were carried out on real buildings. The following results have obtained. TSR method can engender the required properties of swelling, softening and removing for major sealants except for PS-2 which contains lead as a hardening agent. Negative effects such as discoloring, swelling, or softening of the finishing materials around the joints are prevented by an appropriate cure. Given the work efficiency , the process of the TSR method have been defined (Fig 4). The Process of applying the Limonene remover is added to the conventional methods.



Picture 1. Trial of TSR method

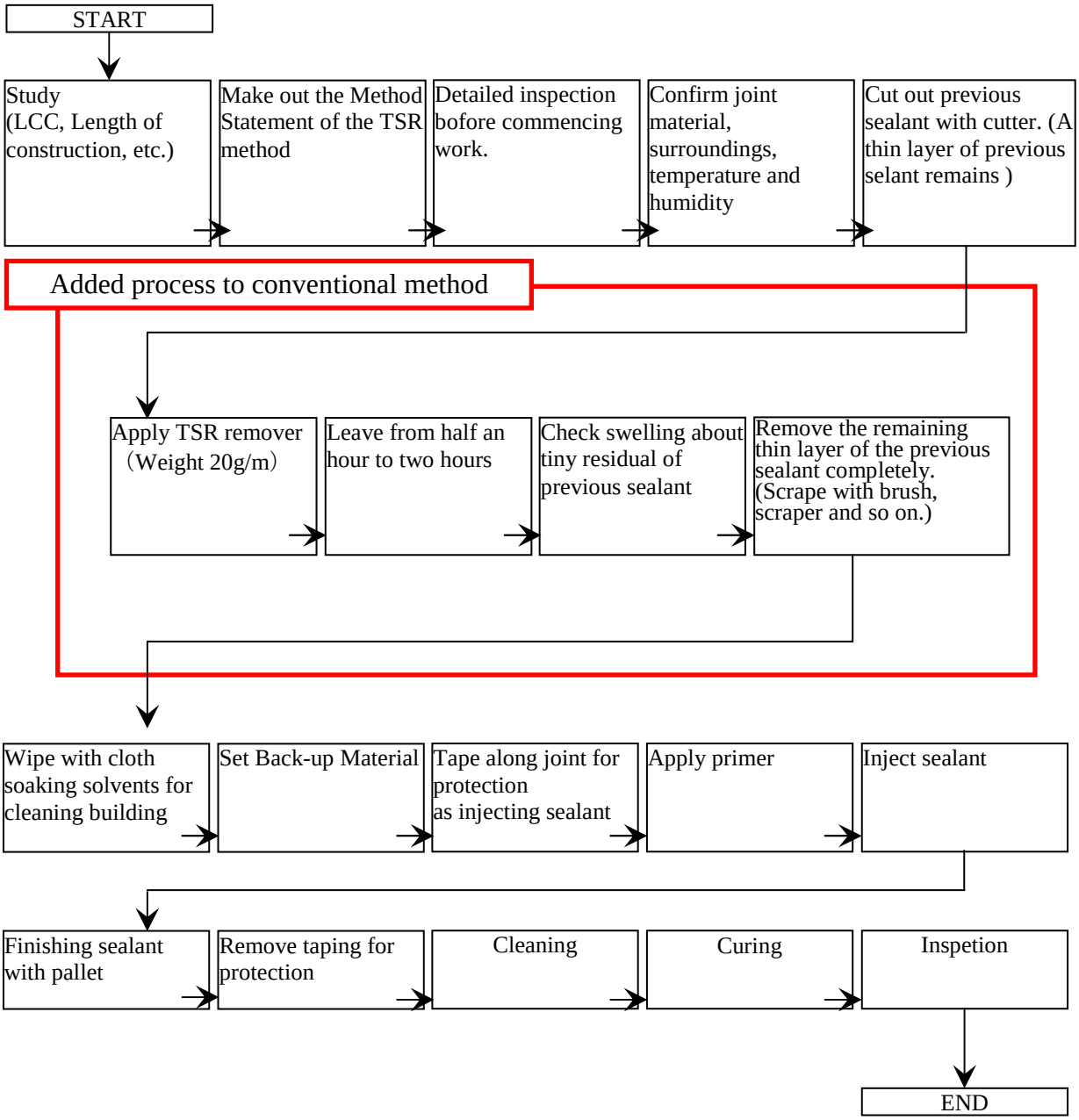

Figure 5. Process of TSR method

5 CALCULATION OF LIFE CYCLE COST (LCC)

Durability of sealants is worse in renewed buildings than it in new buildings because of the remaining layer of the previous sealant that interfers between the adhering new sealant and the joint surfaces at renewal. In Japan, sealants maximum longevity on preventing water leaking is guaranteed for ten years in new buildings and seven years in renewed buildings. Because TSR method can remove all remaining thin layers and render joint surfaces conditions as those in new buildings, the maximum longevity on preventing water leaking for renewed sealants can be prolonged from seven years to ten years. Fig 5 shows the life cycle cost comparison between the TSR method and conventional method. The life cycle cost is calculated based on the used amount of the remover, the work efficiency and the selected procedure. The calculation is based on the following:

1. a ten-story appartment building.
2. a total floor area of 5,700 square meters.

3. a floor height of 3.5 meters.
4. a total length of joints in the external wall of 15,000 meters.
5. a width of joints of 15 millimeters.
6. a depth of joints of 10 millimeters.
7. The Sealant used for Renewal is MS-2.
8. For the conventional method, the guaranteed maximum longevity on preveting water leaking is seven years.
9. For the TSR method, the guaranteed maximum longevity on preventing water leaking is ten years.

Because the number of stages of the TSR method are more than the conventional method, in the beginning, the cost of renewal is higher. However, when looking at LCC over 20 years, the cost using the TSR method falls below the conventional method. This is because the TSR method can ensure performances equal to those of a sealant of a new builing by removing the previous sealant completely. The LCC using the TSR method is less than conventional method which use grinder to remove previous sealant completely because the task to remove sealant and the work to cure are less in the TSR method.

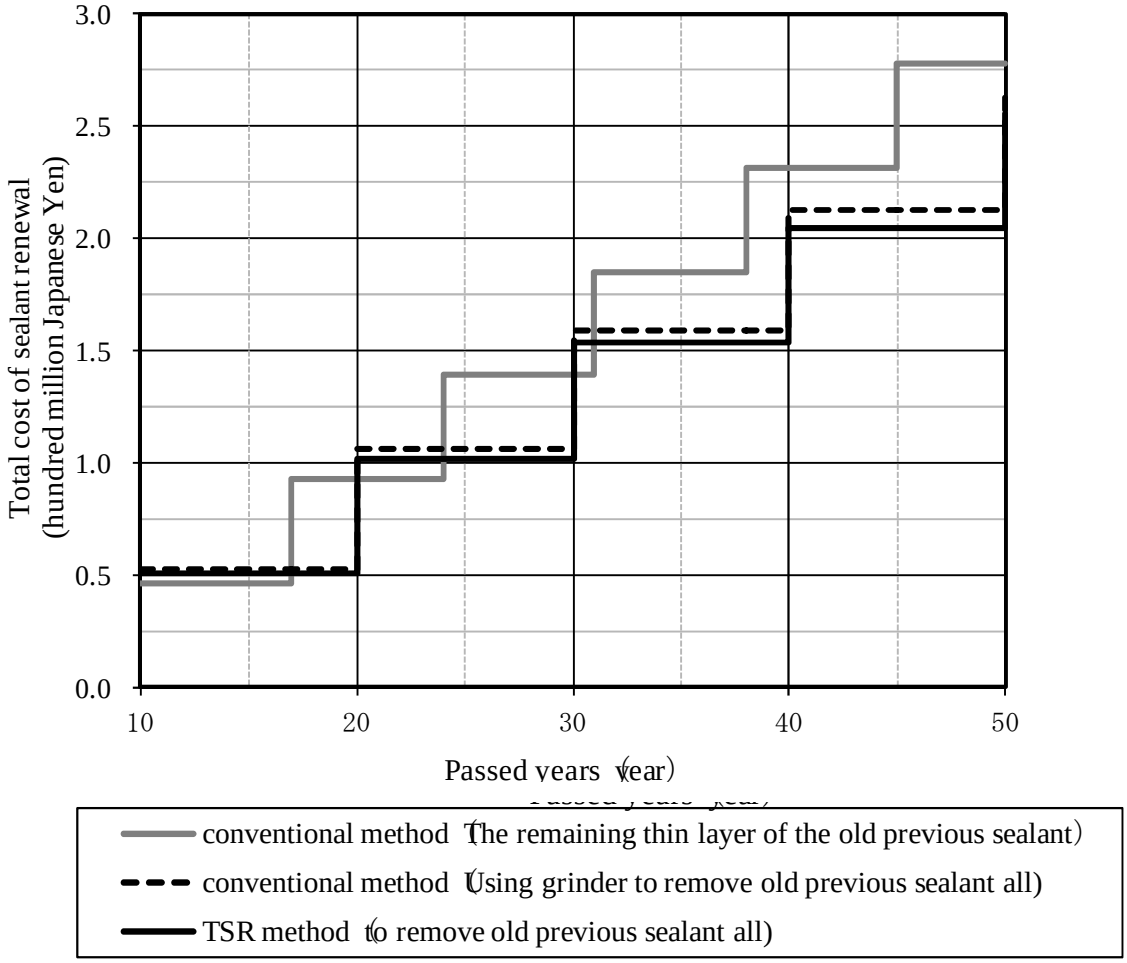

Figure 6. Life cycle cost of TSR method and conventional method (a ten-story appartment building)

6 CONCLUSION

In order to solve problems in conventional sealant removal methods, the TSR remover have been developed and evaluated through experiments. The TSR remover was applied for trial and the effectiveness of the TSR method was evaluated. The LCC of the TSR method has fallen below the one of the conventional method because of the longevity of the implemented sealant and the higher water-tight reliability of TSR method. To the best of the authors' knowledge, at the time being this method is unsurpassed.

ACKNOWLEDGMENTS

The technical assistance of Sunstar Engineering Inc., Riken Industry.co.,Ltd and NIHON Building Engineering Inc. is acknowleged.

REFERENECES

JIS A 5758(2010) Sealants for sealing and glazing in buildings

JIS A 1439(2010) Testing methods of sealants for sealing and glazing in buildings

JIS K 6251(2004) Rubber,vulcanized or thermoplastic - Determination of tensile stress - strain properties

Singo Yosida et al. 2009, 'Development of a Safe and Secure Construction Technique for Sealant Renewal Part2 : Examination of Viscosity and Softening Effect of the Remover' SUMMARIES OF TECHNICAL PAPERS OF ANNUAL MEETING ARCHITECTURAL INSTITUTE OF JAPAN 2009 A-1, pp65-66

Singo Yosida et al. 2009, 'Development of a Safe and Secure Construction Technique for Sealant Renewal' JAPAN SOCIETY FOR FINISHINGS TECHNOLOGY 2009, pp75-78

XII DBMC
International Conference on Durability of Building Materials and Components
PORTO - PORTUGAL, April 12th-15th, 2011

Maintenance Management in Basic Health Units

Priscila Souza Pereira [1]
Maria Aparecida Steinherz Hippert [2]
José Gustavo Francis Abdalla [3]

ABSTRACT

Basic Health Units are buildings designed to serve the population with regard to health issues. Interventions in these areas for carrying out repairs, of whatever nature, can reduce or even prevent access to them. Some of these units in Juiz de Fora (Brazil) have a number of problems, due either to flaws that were not dealt with when they started operating, or due to the lack of regular inspections and maintenance. The aim of this paper is to present a Maintenance Plan developed for these buildings.

Preliminary assessments by the personnel responsible for the maintenance indicate that this plan can contribute to a better organization of maintenance activities, and thus to an improvement in the quality of these facilities. Moreover, this plan outlines the conditions in which interventions can be undertaken in a planned manner, with minimum interference with the access to the units, or with their functioning.

KEYWORDS

Maintenance management, Quality management, Inspection.

[1]Faculty of Engineering of the Federal University of Juiz de Fora (UFJF), Juiz de Fora, BRASIL, priscila.pereira@engenharia.ufjf.br
[2]Faculty of Engineering of the Federal University of Juiz de Fora (UFJF), Juiz de Fora, BRASIL, aparecida.hippert@ufjf.edu.br
[3] Faculty of Engineering of the Federal University of Juiz de Fora (UFJF), Juiz de Fora, BRASIL, gustavofrancis@ig.com.br

1 INTRODUCTION

1.1 Public Healthcare System in Brazil

Implemented by Federal Law 8.080, September 19, 1990, SUS (*Sistema Único de Saúde*, or Single Healthcare System) is responsible for providing healthcare services and actions to the Brazilian population. This system consists of federal, state, and local public agencies and institutions, with private institutions also being allowed to participate complementarily.

Amongst the various SUS attributions are: healthcare promotion, recovery, and protection; sanitation, epidemics and food inspection; therapeutic and pharmaceutical worker assistance; healthcare-related aid for human resources; basic sanitation actions; healthcare-related product, service and substance inspection and control [Lei Federal 8.080, 1990].

The SUS system is single-managed by different agencies as a result of the government sphere, with the Ministry of Health acting as a nation-wide manager. In the state and local spheres, management is under the responsibility of the State Healthcare Department and the Municipal Healthcare Department, respectively [Ministério da Saúde, 2002].

1.2 Basic Healthcare Units and the city of Juiz de Fora

Basic Healthcare Units (UAPS's) are part of the SUS basic care units which, according to the Ministry of Health, must be a municipal priority in managing the system because when the system operates appropriately this is where the population will have most of their healthcare-related issues solved. This may even lead to improvements in intermediate to high complexity service organization and performance [Ministério da Saúde, 2009].

UAPS's normally consist of: a waiting room, a reception desk, a meeting room, rest rooms, a drug storage room, a wound dressing room, a vaccination room, a gynaecology office, clinical and dental offices, a sterilization room, a cleaning supplies storage room, a kitchen, a stock-room, and laundry.

According to IBGE (2010), the city of Juiz de Fora lies in the Southeastern part of the state of Minas Gerais, covering a surface of 1,436.85 km² with an approximate population of 526,706 inhabitants. There are 58 UAPS's throughout its area, all of them built or adapted to the prevalent sanitation model. Despite that, history tells us that most healthcare centers operate in adapted buildings with inadequate infrastructure [Minas Gerais, 2008].

Within this context, buildings used as UAPS's in the city present a number of pathological occurrences, warranting the need for corrective maintenance. It is important to create a Maintenance Plan to help carry out these interventions, and this is the main focus of this investigation.

2 BUILDING MAINTENANCE vs. FACILITIES MANAGEMENT

Building maintenance is defined by ABNT NBR 5674 [1999] as a "set of activities to preserve and recover the functional capability of a building and its parts to meet user needs and security." Thus, during the maintenance stage, predicting and planning potential interventions throughout a building's life cycle is critical to reduce anomalies.

In a building, anomalies can be rated in four types: endogenous, exogenous, natural, and functional. The endogenous anomalies originate when planning for a building, whether in the design, material or construction stage. The exogenous anomalies, in turn, are due to external factors, i.e., interventions by third parties. Natural anomalies can be predictable or not and, as the name suggests, they are produced by natural phenomena. On the other hand, functional anomalies originate from the use and the end of a life cycle of systems and elements that are part of a building [IBAPE-SP, 2009].

Facilities management can be understood as a strategic management of people, spaces, work processes and investments within an organization. Thus, in the building maintenance area, it seeks to establish administrative and operational guidelines that may ensure perfect building operation [Ferreira, 2005].

According to Ma and Liu [2010], *facilities* management significantly impacts the performance of a building and workers, as well as a company or organization. By potentializing a building's life cycle, such management is able to interfere with an organization's value chain as well as promote a more sustainable future. Nevertheless, a successful *facilities* management is determined by quality services and client satisfaction.

In this same context, Kamaruzzaman and Zawawi [2010] state that the main goal in *facilities* management should not only be optimizing costs to make a building operate but also to increase its efficacy and suitability in managing people, processes, and spaces, so as to reach the organization's goals with the best quality/cost/efficiency combination.

Although the literature shows several definitions with different emphasis on this type of management, some characteristics repeat such as a focus on the workplace, for example. This scenario is defined as the place where work is done, regardless of its nature. Thus, it is implicit that *facilities* management is applicable to several types of buildings with various purposes such as educational, industrial, commercial, healthcare-related, amongst others [Tai and Ooi, 2001].

We can therefore conclude that creating a Maintenance Plan can be seen as an extremely important auxiliary tool for a successful healthcare *facilities* management.

3 RESEARCH METHODOLOGY

The methodology used for this research started with the initial bibliographical review including book, article, and newspaper analyses. Based on this study, the data collection instrument was designed and the first UAPS to be inspected was chosen in order to validate the instrument.

After collecting the data some changes were made in the worksheet. These changes were all discussed in groups and the final version was then created. The so defined worksheet consists of two parts: one general part consisting of data such as inspection date, inspectors in charge, and surveillance direction on each site; and a second part including specific building data.

- Site – Room or area investigated. e.g.: Wound Dressing Room, Aisles, Kitchen, etc.
- Material – Description of material used for: external paving, sidewalks, stairways, ramps, floors, door sills, baseboards, interior walls, fencing walls, doors, gates, windows, ceilings, roofs, counters, drains, sinks, toilet bowls, water tanks, and other as seen on site that are relevant for maintenance.
- Structural System. e.g.: Reinforced Concrete, Structural Masonry, among others.
- Electrical System – Sockets, switches and light bulbs (including type of bulb: fluorescent, incandescent, double, single, etc.)
- Anomalies – Pathologies and other irregularities such as: soil-related upward humidity, cracks due to no window headers or sills, sheathing/coating detachment, roof seepage, stairways with no handrails.

After creating and validating the data collection instrument, and with the UAPS architectural designs as provided by the local Healthcare Department, other buildings were chosen for inspection. Selection criteria were based on priorities as defined by the Healthcare Department. These inspections involved detailed visual examination, including iconographic instruments (photographs).

4 RESULT ANALYSIS

Since corrective maintenance knowingly acts directly on building anomalies, Table 1 shows results for irregularities that were diagnosed at 3 inspected UAPS's serving as the basis for the proposed preliminary plan.

Table 1. Anomalies as diagnosed at the Basic Health Units of Juiz de For a.

ANOMALIES		*UAPS*		
		1	***2***	***3***
Fissures and Cracks	No window headers or sills	**x**	**x**	**x**
	Coating mortar retraction		**x**	**x**
	Humidity	**x**	**x**	
	Wall junction	**x**	**x**	**x**
	Brick/Structure junction	**x**		**x**
	Structural problems		**x**	**x**
	Other (e.g.: Object mounting, openings)	**x**	**x**	
Humidity	Soil-related, upward	**x**	**x**	**x**
	Accidental (from sinks, leaks, etc)	**x**	**x**	
	Wall building defects		**x**	
Sheathing/Coating/paint deterioration	Furniture friction	**x**	**x**	**x**
	Humidity present	**x**	**x**	**x**
	Inappropriate service	**x**		**x**
	Life cycle exceeded	**x**	**x**	**x**
	Deteriorated paint	**x**	**x**	**x**
Doors and Windows	Poorly mounted parts (e.g.: doorknobs)	**x**	**x**	
	Broken parts (e.g.: glass)	**x**	**x**	**x**
	Insect-related deterioration (e.g.: termites)	**x**		
	Oxidation (Rust)	**x**	**x**	**x**
Baseboard deterioration		**x**		**x**
Wrong floor slope			**x**	
Floor wear/deterioration due to inappropriate abrasion strength		**x**		
Ceramic tile detachment (e.g.: floor and wall tiles)		**x**		
Ceiling seepage		**x**	**x**	**x**
Microorganisms due to humidity (e.g.: mould)		**x**	**x**	**x**
Efflorescence				**x**
Exposed wiring		**x**	**x**	**x**
Physically disabled safety grab bars damaged				**x**
No hand-rail in stairways		**x**		
Electrical system parts damaged (e.g.: switches)		**x**		**x**
Water and sewage system parts damaged (e.g.: flush system)		**x**		**x**

Data analysis shows that several anomalies started with a *design vs use* incompatibility (functional reason) and with disregarding building maintenance, although endogenous pathologies were also detected. Thus, the need for corrective intervention is clear and of utmost importance for a functional building so as not to interfere with the services rendered to people.

A definitive maintenance plan for such healthcare units is created at the end of this investigation, when all or most units have been inspected. However, since this study requires more time and the need for corrective intervention is great, a preliminary corrective maintenance plan was created to help maintenance personnel based on surveillance results from these three units.

5 PRELIMINARY CORRECTIVE MAINTENANCE PLAN

In a maintenance plan, knowing the criticality level of anomalies is extremely important so as to define an action strategy, from the most critical to the least critical level as shown in Figure 1. Thus, according to the Brazilian Institute of Engineering Assessments and Inspections [IBAPE-SP, 2009], the following criticality levels were defined as: critical, regular, and minimal.

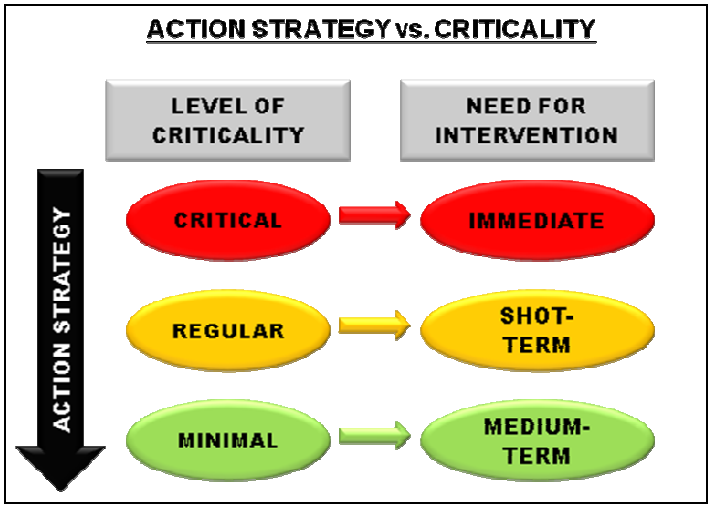

Figure 1. Action strategy for maintenance interventions vs. Anomalies criticality level.

At the most severe (critical) level, the need for intervention is immediate because anomalies can cause unrecoverable damage to users' health and safety or to the environment. This condition can also cause excessive performance decline. For this investigation, anomalies classified for this level could significantly interfere with serving the population at those UAPS.

Regular anomalies are those where interventions can take place in the short term, since building functionality and performance as well as its systems are partially recoverable. Anomalies that could partially interfere with a unit's good performance were also classified as regular.

Finally, the least severe anomalies are those with a minimal criticality. Their impact can be recovered and thus interventions can take place in the medium term. Therefore, anomalies with little or no interference with the normal operation of a UAPS fall in this level.

Once anomaly criticality levels were set for each UAPS, corrective measures were determined to produce corrective intervention guidelines as shown in Table 2, which shows part of the final chart.

Table 2. Corrective Measures and Instructions for detected anomalies (partial example).

ANOMALIES	*CRITICALITY/UAPS*			*CORRECTIVE MEASURES AND INSTRUCTIONS*
	1	*2*	*3*	
Floor wear/deterioration due to inadequate abrasion strength	**C**			Floor replacement with another whose abrasion strength matches building use.
Ceiling seepage	**R**	**R**	**C**	Waterproof ceiling or correct existing waterproof faults.
Microorganisms on coating/sheathing due to humidity (e.g.: mould)	**M**	**M**	**M**	Identify and eliminate root cause for humidity for future affected coating/sheathing recovery.

The table was completed according to the following criticality level terminology:

- CRITICAL – letter "C" in red;
- REGULAR – letter “R” in yellow;
- MINIMAL – letter “M” in green

The level of criticality selected is not based on the anomaly only but also on its degree of risk. For example, in reviewing Table 2 for ceiling seepage, UAPS’s 1 and 2 were rated in the criticality degree of "R", since both showed seepage-related deteriorated coating and needed short-term intervention. However, such anomaly in these units did not pose a threat to user health and safety. On the other hand, at UAPS 3, the same anomaly is causing ceiling coating to detach inside the building with a high risk of user accident. Therefore, in Unit 3, this anomaly was rated with a degree of criticality of “C”.

After completing the table, we have an overview of the anomalies found for all buildings, the level of criticality for each anomaly in each Unit, and the corrective measures that need to be taken. This way information can be more easily obtained for healthcare unit facilities, such as:

- Most critical elements in a building;
- Buildings requiring emergency corrective interventions;
- More frequent anomalies
- Complexity of the necessary corrective measures;

From these elements, priority units and services as well as the sequence of interventions can be determined, producing a UAPS corrective maintenance plan. It is suggested that maintenance work start with the most critical units, ideally with the most critical jobs [Table 3] as diagnosed for each, and then on to those with a lower level of criticality as shown in Figure 2.

Table 3. Quantitative Diagnosed Pathologies vs. Level of Criticality.

UAPS	***Quantitative Pathologies against Level of Criticality***		
	C	***R***	***M***
1	3	8	14
2	1	4	15
3	2	6	15

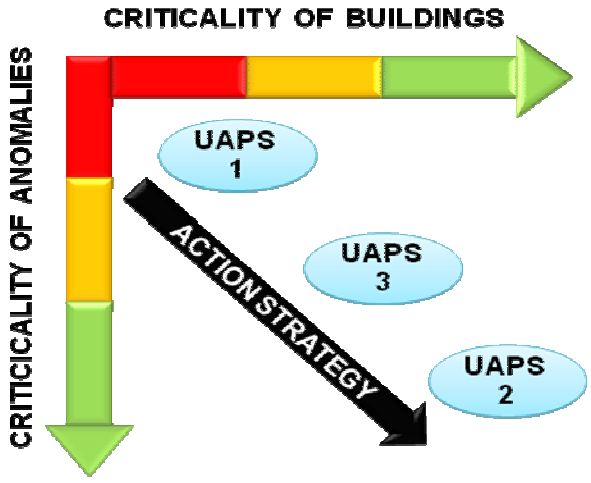

Figure 2. Action Strategy Overview for UAPS maintenance jobs.

6 DISCUSSION

For public facilities management, challenges go far beyond determining action plans since economic, social, and political factors directly influence strategic issues. On the other hand, the lack of such plans affects management system efficiency by making it more difficult for management professionals to work and by decreasing interest in these activities.

Within the *facilities* management context, the corrective maintenance plan proposed for UAPS tries to set technical and strategic guidelines to help managers work and a perfect building operation, partially meeting user needs.

However, for a better building performance and therefore increased user satisfaction, the ultimate goal of the investigations in progress is to create a maintenance plan involving not only corrective interventions but also preventive and predictive actions. This way a more satisfactory combination may be achieved for building quality, maintenance costs and work and management efficiency.

Nevertheless, the main objective of this article is to call the attention to building maintenance in the *facilities* management universe and make people aware of its importance for and interference with other workplace activities, especially those in which interventions can affect the basic service needs of the population.

ACKNOWLEDGMENTS

FAPEMIG - Fundação de Amparo à Pesquisa do Estado de Minas Gerais.

REFERENCES

ABNT, Associação Brasileira de Normas Técnicas. *NBR 5674:1999 – Manutenção de Edificações - Procedimento*. Rio de Janeiro, 1999.

Ferreira, Flávia Poestch. *Gestão de facilities: Estudo exploratório da prática em empresas instaladas na região metropolitana de Porto Alegre*. UFRGS, Porto Alegre, 2005.

IBAPE-SP. *Inspeção predial: check-up predial: guia da boa manutenção*. Instituto Brasileiro de Avaliações e Perícias de Engenharia de São Paulo, 2ª Ed., São Paulo, 2009.

IBGE. Cidades. Site da Internet. Disponível em:
<http://www.ibge.gov.br/cidadesat/topwindow.htm?1>. Acesso em: 29/09/2010.

Kamaruzzaman, Syahrul Nizam & Zawawi, Emma Marinie Ahmad. *Development of facilities management in Malaysia*. Journal of Facilities Management, vol. 8, n. 1, Emerald Group Publishing Limited, 2010.

Lei Federal Nº 8.080. Setembro, 1990.

Ma, Yu & Liu, Kecheng. *Impact Analysis of Facilities Management Outsourcing – through a Case Study of Cisco HQ Building*. World Congress of Intelligent Control and Automation, Jinan, China, 2010.

Minas Gerais, Secretaria de Estado de Saúde. *Construindo ou reformando unidades básicas de saúde e unidades básicas de saúde rural*. Maria Rizoneide Negreiros de Araújo *et al*, Belo Horizonte, 2008.

Ministério da Saúde. *O Sistema Público de Saúde Brasileira. Seminário Internacional: Tendências e Desafios dos Sistemas de Saúde nas Américas*, São Paulo, 2002.

Ministério da Saúde. *O SUS de A a Z Garantindo Saúde nos Municípios*. 3ª ed., Brasília, 2009.

Tai, Linda& Ooi, Joseph T. L. *Facilities Management: a "Jack of all trades"?*. Facilities, vol. 19, n. 10, MCB University Press, 2001.

XII DBMC
International Conference on Durability of Building Materials and Components
PORTO - PORTUGAL, April 12th-15th, 2011

In Situ Testing Techniques for Evaluation of Water Penetration in Rendered Facades - the Portable Moisture Meter and Karsten Tube

Ruben Duarte [1]
Inês Flores-Colen [2]
Jorge de Brito [3]

ABSTRACT

Several reasons can explain the urgency of proactive maintenance implementation and of in-service performance knowledge of buildings' facades, in order to guarantee adequate levels of users' satisfaction. In this context, periodic inspections practice (predictive maintenance) depends on the reliability of in-service diagnosis and on the existence of parameters that can be measured and monitored during the life cycle.

The water resistance of external renders is a relevant property, because it can significantly affect the durability and hygrothermal behaviour of facades. Water is the main in-service degradation agent which has several origins and mechanisms of transport (ground moisture, driving-rain, wetting/drying of surfaces, among others), leading to different pathological phenomena (physical and/or chemical).

This paper summarizes a MSc thesis about the study of water resistance of rendering facades in in-service conditions, through expedient techniques for field diagnosis, such as moisture meter and Karsten tube. In-service parameters (surface moisture and water absorption under low pressure) are measured and the sensitivity of these techniques to in-service factors is analysed (roughness, exposure and inspection conditions, existing anomalies, coating and finishing types). Testing was conducted on a set of walls with traditional and non-traditional renders. These experimental campaigns also allow the analysis of the capacity of each technique to assess and monitor in-service performance. Finally, several issues are proposed in order evaluate criteria for in-service performance assessment of rendering facades.

KEYWORDS

Rendering facade, Physical performance, In situ testing, Moisture meter, Karsten tube.

1 Integrated Master in Civil Engineering, DECivil-IST, Lisboa, Portugal, rubenmduarte@hotmail.pt
2 DECivil-IST, Technical University of Lisbon, Av. Rovisco Pais, 1049-001, Lisboa, Portugal, ines@civil.ist.utl.pt
3 DECivil-IST, Technical University of Lisbon, Av. Rovisco Pais, 1049-001, Lisboa, Portugal, jb@civil.ist.utl.pt

1 INTRODUCTION

1.1 Physical performance of rendering mortars (water resistance)

According to Sousa et al. [2005], external rendering has a decorative function, since it represents the image of the building. It also has a protective function, as it protects walls from several degradation agents. The choice of a suitable external rendering reflects its ability to fulfil the functions over a particular period of time under in-used conditions. It is therefore necessary to translate functional demands into quantifiable in-service performance characteristics.

Several laboratory studies have been carried out on the performance of rendering. However, there is a lack of in situ diagnosis showing the effective degradation to rendered surfaces during their service life, which may (or may not) corroborate laboratory findings. One of the most relevant factors in the use of the various types of façade cladding is the way they react to moisture. According to Verçoza [1991] is considered a key agent in the appearance of efflorescence, rust, mould and splintering/blisters in paintwork. Rilem [1993] states that permeability is the characteristic that determines the (major or minor) possibility of water flow in mortar. Water penetration may occur due to infiltration, pressure, capillarity or the diffusion of water vapour. In addition, Coutinho [1988] states that permeability is the property of mortars to be penetrated by gases or fluids acting on the surface under pressure.

In order to minimize the degradation, regular inspections are required to evaluate the performance of every element during its service life. One of the problems with evaluation is the impossibility of defining certain development parameters for cladding using in situ testing only. The required water performance indicators are water absorption under low pressure, the water absorption coefficient under low pressure, surface moisture levels and cracking.

1.2 In situ testing techniques to evaluate rendering water resistance

In-service evaluation of performance can be carried out in several ways. In most cases, a visual inspection is enough to detect pathological phenomena affecting the rendering because of evident and visible symptoms [Tavares et al. 2005]. However, this can produce data that is dubious or difficult to interpret. It is also affected by the education and experience of the technician carrying out the inspection, as well as the accessibility of the area being inspected. Furthermore, most problems affecting performance are often not visible, and need to be measured [Flores-Colen *et al.* 2006]. From this perspective, the use of auxiliary diagnosis techniques reduces the subjectivity of visual inspections, making it easier to obtain more reliable evaluations. An in situ technique is more suitable if it is easy/quick to perform and directly provides useful data to in-service performance evaluation.

1.2.1 Karsten tube or pipe method

This test method allows resistance to liquid water penetration on vertical surfaces to be determined by measuring water absorption under pressure, either in the laboratory or in situ. The Karsten tube is a pipe-shaped graduated device, made of glass (Figure 1, left). It must be glued with silicone to the cladding and filled with water until a zero reading is obtained, corresponding to a wind dynamic pressure of 39.6 m/s [LNEC, 2002]. Following this, the drop in the water level over time (cm^3/h) is measured and subsequently may be processed graphically. This technique can also contribute to a better understanding of renders water resistance in terms of open porosity, hydrophobic agent influence, and existence of micro-cracking, surface protection influence [Flores-Colen et al. 2006].

1.2.2 Portable moisture meter

The portable moisture meter is a device that allows the surface moisture level of several materials to be measured. It is a non-destructive method. The equipment has two electrodes on its base that are placed in contact with the surface of the testing material (Figure 1, right). These electrodes transmit a low-frequency signal, according to the type of pre-selected material [Massari & Massari, 1993]. This in situ testing method is based on the theory that the electrical impedance of a porous zone varies according to the quantity of water present in its pores [Flores-Colen, 2009] and it therefore establishes a connection between these values, which are inversely proportional.



Figure 1. Karsten tube (left) and portable moisture meter (right).

2 EXPERIMENTAL PROGRAM

Two experimental programs were conducted at natural aging stations, at the National Laboratory of Civil Engineering (LNEC) - EENRevPa, in Lisbon, and at a manufacturer's building yard - EEN-RevPb, in Carregado. At EENRevPa, coatings have been applied externally to areas exposed to natural agents. The support material is brick masonry (20 cm thick), with the exception of expanded clay wall (prototype 21). The upper areas of the walls are protected by ceramic roof tiles. At this natural aging station (Figure 2), 24 wall prototypes were tested, covering various cladding types, reflecting both traditional coatings (lime-based, cement-based and waterproof render/paint) and technological advances (insulation, one-coat coloured renders and waterproof membranes). These claddings were applied to the walls from 1979 to the present day with the dimensions of 2 m x 2 m. North- and south-facing surfaces were analysed. The inspections (using Karsten tube and moisture meter) took place between March and May 2009, under different weather conditions.



Figure 2. General view of the EENRevPa prototype walls at LNEC.

At EENRevPb, the renders had been applied by the manufacturer in July 2004, taking all 4 points of the compass into consideration. Nine wall prototypes were tested with the portable moisture meter; only 4 walls were fitted with the Karsten tube. At this natural aging station two types of one-coat pre-mixed red-brick colour render were analysed and two types of finish (smooth-sand and scraped).

3. DISCUSSION OF RESULTS

3.1 Sensitivity of Karsten tube technique

Traditional renders (RT) (Figure 3):

i) Traditional lime-based renders have more water absorption (RTA - hydraulic lime based render; RTCA - cement, aerated lime) than cement-based renders;

ii) Traditional renders with pigmented waterproof finishing (RIP) and cement render with a ceramic finishing (RTP ceram.) were highly waterproof, presenting reduced permeability;

Non-traditional renders (Figure 4):

i) Water absorption is less than 2 cm^3 in ready-mixed single-layer renders, i.e. about half the water absorption rate of traditional coatings with finishes. These results are explained by several factors, namely: 1) on average, the traditional coatings are older; 2) most non-traditional coatings include an hydrophobic agent; 3) traditional coatings have a greater level of degradation, which increases the probability of the test occurring in an area of internal micro-cracking;

ii) In RMPCO(P) - cement render with stone finishing, both north and south facing wall prototype surfaces, showed abnormally high values for water absorption in comparison with other non-traditional coatings; during in situ testing a circular stain appeared around each Karsten tube. The appearance of surface water was not the result of any failure in the technique as: 1) the silicone around the tube was dry at the end of testing; 2) the water stain was circular and not oval, indicating flow.

This is explained by communication between the pores and the absorption of water into the area in contact with the tube through capillarity, emerging afterwards on the surface;

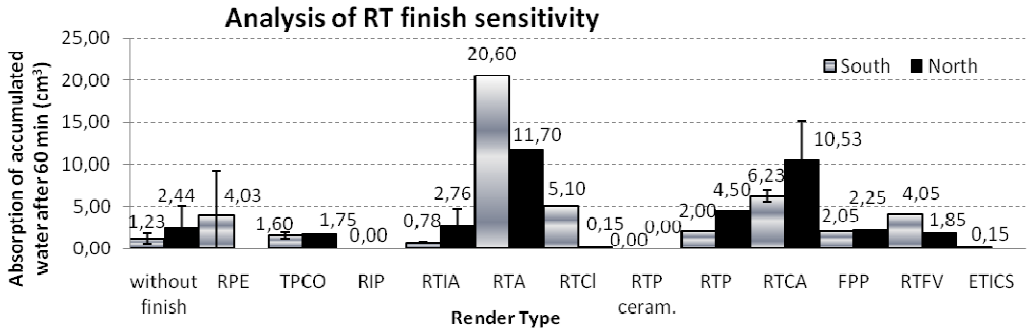

Figure 3. Average values and standard deviation of water absorption under low pressure in traditional renders (RT)

Masonry material:

A non-traditional cement-based mortar was the only render applied to the different support materials at the LNEC EENRevPa. The support material was not relevant to the results in this case; the renders that were applied to expanded clay block masonry and to brick masonry presented similar rates of water absorption (4.82 cm^3 and 5.25 cm^3 after 60 min, respectively). Other authors, such as Crescêncio and Barros [2005] concluded that the Karsten tube technique only allows for a superficial evaluation, at mortar level. However, a recent study [Gonçalves, 2010] concluded that the suction of the suport and the effective adherence of the mortar to the support can afect the results of this technique.

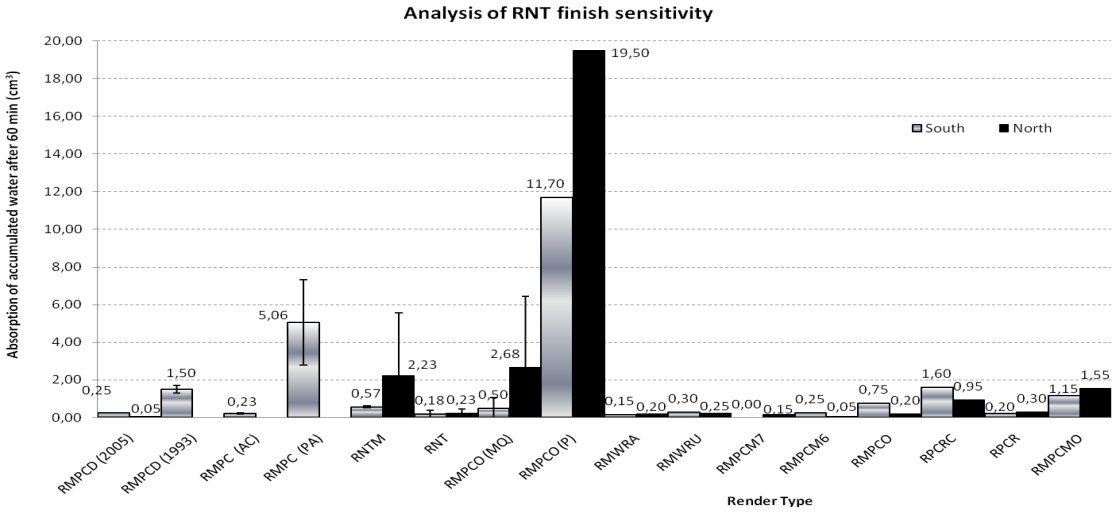

Figure 4. Average values and standard deviation of water absorption under low pressure in non-traditional renders (RNT).

3.2 Sensitivity of moisture meter technique

At LNEC EENRevPa 838 measurements were made in 24 walls. In all inspections, weather conditions (relative humidity and temperature) were measured with a thermo-hygrometer and the anomalies were registered in an inspection sheet. The experiments took place between March and July, 2009.

Sensitivity to temperature and relative humidity

i) In order to analyse the sensitivity of this technique to changes in relative humidity and temperature, certain tests were carried out under different inspection conditions and on different facades (Table 1). Test 2 and 3 were performed on a traditional wall render without a finishing. Test 4 was carried out on a façade with a traditional render and an ochre paint finishing.

ii) On average, the temperature variation (6º C) and relative humidity (30%) implied an increase in surface moisture of 13%. Thus, it was proved that the technique is rather sensitive to inspection conditions (Figure 5) and therefore at least two inspections were proposed for this technique, with significant variations in inspection conditions.

Table 1. Summary of inspection conditions

Measurements	*Test 1*	*Test 2*	*Test 3*	*Test 4*
First meausurement	H.R.-33.3% / T.-19.7ºC	H.R.-51.9% / T.-18.3ºC	H.R.-80.5% / T.-15.5ºC	H.R.-80.5% / T.-15.5ºC
Second meausurement	H.R.-59.7% / T.-16.5ºC	H.R.-42.0% / T.-22.9ºC	H.R.-42.0% / T.-22.9ºC	H.R.-42.0% / T.-22.9ºC

Sensitivity to the presence of degradation

i) Walls mappings proved to be a very effective way of evaluating the surface moisture level. The top of the façade showed 10% to 15% moisture on the surface (Figure 6), in spite of flows. In the lower zone of the façade it was possible to detect the existence of biological colonisation, which implied that the surface moisture in this area was around 40%. The presence of biological colonisation was tested using the technique described in ASTM D 1610:1998 (technique for identification of fungus or algae using sodium hypochlorite at 5% through the change of colour in the affected area).

ii) Figure 7 clearly shows the presence of a crack, around which some measurements were taken, registering approximately 50% of surface moisture. It is therefore possible to infer that the existence of cracks visible to the naked eye, with openings of more than 0.1 mm, implies increased surface moisture. This crack was measured using a 30x optical microscope and it was found out that it had a width of 0.5 mm.

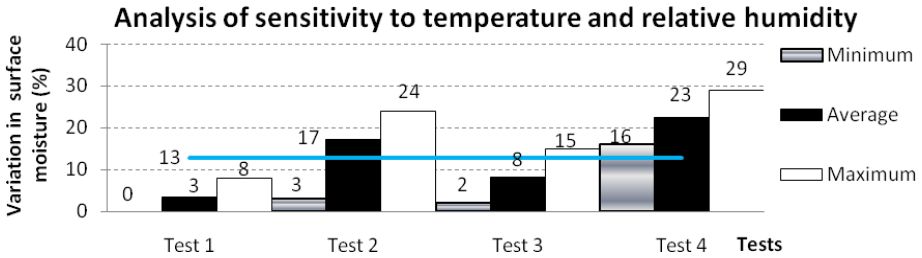

Figure 5. Analysis of sensitivity of moisture meter to temperature and relative humidity

3.3 Performance analysis with Karsten tube technique

In Table 2 it is possible to observe the average Karsten tube accumulated water absorption rate over 60 minutes and the absorption coefficient (determined from the angle of the mass variation and time root graph over a contact area of 5.7 cm^2 and assuming 1 g/cm^3 for the water) of each type of cladding. According to Flores-Colen [2009], the relationship between this parameter and the capillarity coefficient is valid only during the first 60 minutes (it is confirmed that capillary pores contribute to both results, although these parameters represent different absorption/water intrusion mechanisms).

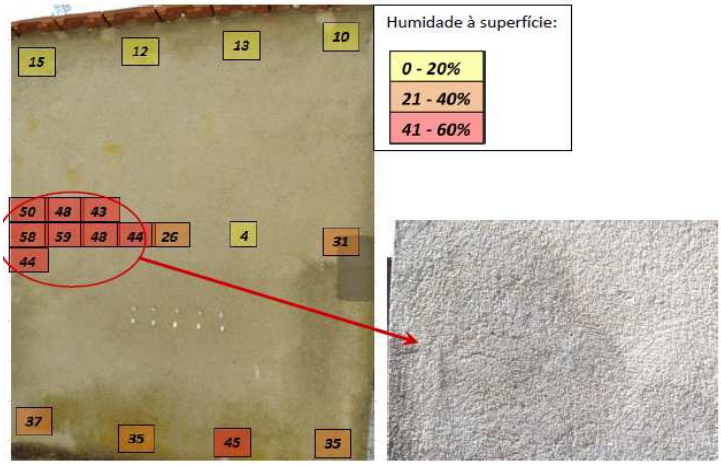

Figure 6. Mapping of façade 5 north **Figure 7.** Cracking of the walls

Following the previous author's criteria, in the evaluation of the performance of external renders using the Karsten tube technique, traditional cement-based renders show a water absorption coefficient of between 0.2 and 1.5 kg/m^2.min$^{0.5}$ after 60 min. All the facades with traditional renders that were analysed in the experimental campaigns registered lower water absorption coefficient values than the proposed upper limit, with the exception of RTCA and RTA walls (that are lime-based renders). With regard to evaluating the performance of non-traditional renders, Flores-Colen [2009] suggests that the water absorption coefficient under low pressure after 60 min given by the Karsten tube should be less than 0.2 kg/m^2.min$^{0.5}$. Among the non-traditional coatings analysed, only half had a water absorption rate less than the proposed upper limit. The water performance resistance of these renders is lower, but it is important to distinguish the age of each render (between 4 and 16 years), which can explain different product formulations and also the probable low effectiveness of the hydrophobic agent over time.

Table 2. Karsten tube results obtained in LNEC EENRevPa station.

Type of coating	*Average absorption of accumulated water (cm^3)*					*Slope between Abp and √t*	$C_{ab(60\ min)}^{tk}$	*Rlinear^2*
	5	*10*	*15*	*30*	*60*			
RT without finish	0.33	0.45	0.55	0.96	1.53	0.225	0.39	0.986
RPE	0.89	1.43	1.89	2.93	4.03	0.576	1.01	0.996
TPCO	0.60	0.75	0.83	1.13	1.65	0.191	0.33	0.990
RIP	0.00	0.00	0.00	0.00	0.00	0.000	0.00	(n.d.)
RTA	2.30	3.60	4.85	9.40	16.15	2.584	4.53	0.985
RTCl	0.35	0.55	0.78	1.48	2.63	0.423	0.74	0.984
RTP ceramical	0.00	0.00	0.00	0.00	0.00	0.000	0.00	(n.d.)
RTP	0.45	0.73	1.05	2.05	3.25	0.527	0.93	0.992
RTFV	0.65	0.95	1.15	1.73	2.95	0.415	0.73	0.982
FPP	0.3	0.48	0.68	1.18	2.15	0.340	0.60	0.982
RTCA	1.46	2.29	2.90	4.8	8.38	1.261	2.21	0.985
RMPCD	0.22	0.30	0.39	0.65	0.96	0.139	0.24	0.994
RMPC (PA)	1.00	1.51	1.91	3.25	5.06	0.753	1.32	0.994
RNTM	0.24	0.41	0.54	0.85	1.40	0.210	0.37	0.995
RMPCO (MQ)	0.18	0.25	0.36	0.85	1.59	0.268	0.47	0.970
RMPCO (P)	2.45	3.55	5.55	10.40	15.60	2.504	4.39	0.991
RMPCWRA	0.05	0.05	0.08	0.13	0.18	0.025	0.04	0.973
RMPCWRU	0.08	0.08	0.13	0.18	0.28	0.038	0.07	0.974
RMPCM6	0.08	0.08	0.10	0.13	0.15	0.015	0.03	0.959
RMPCO	0.08	0.13	0.15	0.28	0.48	0.073	0.13	0.985
RPCR	0.08	0.10	0.10	0.23	0.25	0.035	0.06	0.899
RPCRC	0.25	0.35	0.48	0.73	1.28	0.187	0.33	0.982
RMPCMO	0.20	0.38	0.45	0.90	1.35	0.214	0.38	0.992

Key: RPE - thick plastic cladding; TPCO - pigmented ochre paint; RIP - pigmented waterproof cladding; RTA - Traditional A11 coating (hydraulic lime, river sand); RTCl - Traditional Cl coating (cement, river sand + Corroios sand); RTP ceramic - Ceramics with traditional P coating (cement, river sand) 1:4; RTCA - Traditional CA coating (cement, aerated lime, river sand) 1:1:6; FFP - Polypropylene fibre; RTFV - Traditional fibreglass coating; RMPCD - Single-layer, premixed D cement cladding applied in 1993 and 2005; RMPC (PA) - Single layer premixed PA cement cladding; RNTM - Non-traditional M coating; RMPCO (MQ) - Single-layer premixed O cement cladding with rubbed finish; RMPCO (P) - Single-layer premixed O cement cladding with stone finish; RMPCWRA - Single-layer premixed W cement cladding (rubbed); RMPCWRU - Single-layer premixed W cement cladding (rough); RMPCM6 - Single-layer premixed M6 cement cladding; RMPCO - Single-layer premixed O cement cladding; RPCRC - Single-layer premixed RC cement cladding; RPCR - Single-layer premixed R cement cladding; RMPCMO - Single-layer premixed MO cement cladding.

3.4 Performance analysis with moisture meter technique

Table 3 summarizes the results obtained in experiment testing A using the portable moisture meter, separately comparing measurements taken in areas with and without visible anomalies and in mixed areas. It confirms the need for the separate analysis of measurements taken with a portable moisture meter in areas with or without clear anomalies.

Flores-Colen [2009] proposed that the upper limit for the surface moisture level should be 11%, for both traditional and non-traditional renders, as one of the evaluation criteria for the degradation of external renders. This criterion has proved appropriate for analysing areas without anomalies for the three types of cladding analysed. Nevertheless, areas with clearly visible anomalies in the traditional renders needed a more specific criterion. Such areas with non-traditional renders did not show a sig-

nificant increase in their surface moisture level and even registered values less than 11%.

In spite of the comparative nature of the testing, it is extremely important to quantify the surface moisture level. Therefore with this study it can be concluded for traditional renders that: below 10% - without anomalies; cracking - 25% to 40%; dirt deposits - 10% to 20%; biological colonisation - 35% to 50%. For ready-mixed renders: 5% - without anomalies; above 10% - loss of effectiveness of the hydrophobic agent (values related with dry inspections conditions).

Table 3. Average level of surface moisture measured in LNEC EENRevPa station.

Walls	*Orientation*	*Number of walls tested*	*Moisture level on the surface in mixed areas (%)*	*Moisture level on the surface in areas without anomalies (%)*	*Moisture level on the surface in areas with anomalies (%)*	*Main anomalies detected*
RT without finish	South	3	17.3	7.7	29.1	Fissuration; flows; biological colonisation
	North	5	17.0	5.7	33.9	
RT with finish	South	17	10.2	3.3	23.9	Fissuration; flows; biological colonisation
	North	10	16.5	6.1	27.1	
RNT	South	21	0.5	0.4	5.8	Fissuration
	North	17	2.3	2.2	8.0	

4 CONCLUSIONS

The Karsten tube technique was shown to require some experience and precision from the inspector. One of the main observations drawn from these experiments is that water is likely to appear on the surface of the wall prototype even if the tube wall is well-sealed, given that there is migration between pores and water may be absorbed through capillarity into the area in contact with the tube, emerging later on the surface of the wall prototype. As far as the sensitivity of the Karsten tube technique is concerned, it is possible to infer that the masonry material is not relevant to water absorption. Surface roughness is one factor that may create more difficulties or even prevent the tests from being carried out. The tested traditional lime-based renders showed high levels of water absorption (they are not waterproof, are older and more degraded). Non-traditional renders as tested have a lower permeability to liquid water than the tested traditional coatings, but their water resistance can reduce over time due to the presence of micro-cracking and also to the loss of effectiveness of the hydrophobic agent.

For the portable moisture meter, it was concluded from the experiments that this analysis must be carried out separately on areas with and without anomalies. This is because the technique is highly sensitive to the presence of anomalies, namely cracks, flows and biological colonisation. The technique used to determine growth of fungus or algae using sodium hypochlorite at 5% proved useful and expeditious. Through the change of colour in the affected area, from yellow to red, it was possible to confirm the presence of biological colonisation. Conditions at time of inspection affected the observed measurements and it is suggested that two inspections are needed, particularly for cases evaluating surface moisture levels. The portable moisture meter does not evaluate performance quantitatively, since results are comparative.

These results show that the selected techniques are viable, since they enable the comparison of performance of different renders. The methods studied may be used as the basis of further testing to enhance the accuracy of the “in situ” evaluations carried out to analyze the condition of rendering facades.

ACKNOWLEDGEMENTS

Thanks are due to Rosário Veiga from LNEC and to Luís Silva from Weber for the chance to study the walls renderings at natural ageing stations and to the ICIST - IST research centre.

REFERENCES

Coutinho, S.A. *Production and properties of concrete* (in Portuguese), V I. LNEC, Lisbon, 1988.

Crescêncio, R.M.; Barros, M. - *Single-layer's evaluation of the waterproof to the rain water* (in Portuguese). VI SBTA - VI Simpósio Brasileiro de Tecnologia de Argamassas. Florianópolis, 2005, pp. 540-550.

Flores-Colen, I. - *Methodology of the performance evaluation in service of facades towed in the optics of the predictive maintenance* (in Portuguese). Civil Engineering PhD thesis, Instituto Superior Técnico, Lisboa, July 2009.

Flores-Colen, I.; Brito, J. De; Freitas, V. P. Expedient in situ test techniques for predictive maintenance of rendered facades, *Journal of Building Appraisal*. 2(2), 2006: pp. 142-156

Gonçalves, A. E. Study of the influence of the application factors in the in-service performance of renders through in situ testing (in Portuguese), MSc Thesis in Integrated Civil Engineering, Instituto Superior Técnico, Lisboa, October 2010.

LNEC - *Covering of walls. Water absorption test under low pressure (in Portuguese*). Laboratório Nacional de Engenharia Civil, Lisbon, 2002.

Massari, G.; Massari, I. - *Damp buildings. Old and new*. Roma: International Centre for the Study of the Preservation and the Restoration of Cultural Property (ICCROM), 1993.

RILEM - *Draft recommendation for in-situ concrete strength determination by combined non-destructive methods*, RILEM, 1993, RILEM draft recommendation, Materials and structures, 26, 1993, pp. 43-49.

Sousa, V.; Pereira, F. D.; Brito, J. De - Main causes of deterioration in traditional cladding (in Portuguese), Universidade do Minho, *Engenharia Civil*, 23, 2005, pp. 5-18.

Tavares, M.; Magalhães, A.; Veiga, M.; Aguiar, J. 2005 - *Diagnosis methods for coatings of ancient buildings. Importance and applicability of in situ tests* (in Spanish). In: Revista Boletín del Instituto Andaluz del Patrimonio Histórico, available at http://conservarcal.lnec.pt (access May 2009).

Verçoza, E. J. - *Constructions anomalies* (in Portuguese). Porto Alegre, Editora Sagra, 1991. 172 p.

XII DBMC
International Conference on Durability of Building Materials and Components
PORTO - PORTUGAL, April 12th-15th, 2011

Inspections and Maintenance Programmes for the Conservation of Historic Architecture - Some Critical Issues Related to Degradation and Durability

Paolo Gasparoli [1]
Matteo Scaltritti [2]

ABSTRACT

The durability of architectural technical solutions and materials, especially regarding historical buildings and monuments, is directly dependent on the frequency and mode of maintenance.

The contribution covers the definition of an operational methodology that is based on preventive activities aimed at a programmed maintenance, developed on an outstanding case study: the central archaeological area in Rome.

The reasons that suggest facilitating inspection and maintenance-type processes have long been known but have not yet been found the availability of effective contributions of an applicative nature.

Ensuring the extension of the life cycle of materials and components, in fact, is a specific objective of the conservation of historic remains and is considered a priority to structure maintenance processes aimed at control and "cure" rather than entrust the outcome to a more invasive restoration, sometimes carried out with products and techniques that are deemed to be effective, but which are often unreliable.

A further and equally important objective is to promote the opportunity of limiting the use of individual actions unrelated in time and to promote an idea of maintenance as a process. This is a radically new way of thinking and acting, which promotes strategies (prevention and treatment) rather than tactics (restoration as a solution to all problems), and the pursuit of long-term effectiveness rather than the pursuit of pure efficiency and immediate benefit.

KEYWORDS

Planned conservation, Cultural heritage, Inspection, Durability, Archaeological sites.

[1] Politecnico di Milano, Dept. BEST, paolo@gasparoli.it.
[2] Politecnico di Milano, Dept. BEST, matteo.scaltritti@polimi.it

1 INTRODUCTION

The durability of technical solutions and materials in architecture, especially regarding historical buildings and monuments, is directly dependent on the frequency and mode of maintenance. Addressing the issue of prevention and maintenance of historic buildings, however, requires careful rethinking of some questions related to the concepts of the *life cycle*, *durability*, *degradation*, *pathology* and *obsolescence* of materials and components, starting from the fact that these words take on significantly different meanings when applied to historic architecture rather than to newer residential buildings.

The statement that frequent maintenance is able to contain the progress of deterioration in historic buildings is quite obvious yet rarely followed.

If the adage that "prevention is better than cure" is commonly agreed due to common sense, in the area of construction activities - including Cultural Heritage work - the ideal of regular care with a very low technological content most of the time remains merely a ritual enunciation that is hardly every put into practice. Indeed, the topic of scheduled maintenance, evoked for decades in conferences and seminars, has not yet found the availability of effective contributions in terms of application to define its contents and delimit it areas of intervention.

It is believed that the cultural and practical difficulties inherent in this type of procedure cannot be overcome except by deploying an effective organization that is able to control the entire process, including the management of feedback arising from the outcomes of the activities, thereby building up knowledge.

The reflections produced here were made following the important experience gained by the working group from Politecnico di Milano (scientific manager Prof. Paolo Gasparoli) which was appointed by the Commissioner Delegated by the Italian prime minister[3], defined an operational methodology for implementing prevention and maintenance processes starting from the case study of the archaeological area in Rome [Cecchi 2009, Cecchi 2010, Cecchi & Gasparoli, 2010].

Enforcement procedures, work instructions and registration forms were chosen for this work with the intention of giving substance and structure to the "good intentions" and made the preventative action operational by means of a defined methodology. An equally important purpose of this study was also to promote a change of perspective proposed in order to limit recourse to individual actions that are disconnected over time, such as those tending to favour extraordinary restoration events, in order to promote the idea of maintenance as a *process*.

It is therefore useful, within the framework that has been briefly outlined, to reiterate the different theoretical and operational meanings that the "maintenance" project and process assumes in the cultural and methodological areas proper to Cultural Heritage conservation, as compared to those of industrial maintenance, which, as is known, primarily involve maintenance strategies, procedures and methods aimed at more recently constructed property assets.

The themes of prevention, and therefore loving, attentive and thorough "care", assume particular importance in the context of Cultural Heritage buildings, starting from Ruskin's (now hackneyed) heartfelt appeal [1981] for maintenance consisting of simple and repetitive activity.

Moreover, the "culture of maintenance", which would require, at least conceptually, the use of traditional practices established over centuries, involves the realization that past maintenance activities were consistent and frequent, aimed at carrying out repairs as soon as possible in order to save on materials, which were notoriously expensive compared to labour costs.

[3] L'architetto Roberto Cecchi è Commissario delegato per la realizzazione degli interventi urgenti nelle aree archeologiche di Roma e Ostia Antica (OPCM 28 maggio 2009, n. 3774)

The research work on the central area in Rome was therefore started from the development of structured inspections that subsequently led to the definition of Scheduled Maintenance Plans. Methodological ideas were gained from these experiences that were applicable to different types of Cultural Heritage buildings.

2 INSPECTION ACTIVITY

The Inspections consist of structured monitoring activities on the construction heritage.

Monitoring activities are mainly characterised by inspections, which are necessary for the periodic assessment of the buildings' state of conservation, for the identification of more evident critical aspects and for accessibility, inspection and maintenance checks.

These may already be scheduled as part of a maintenance plan or they can be organised independently, but to ensure their effectiveness, they must always be planned and carried out with pre-established timeframes. Minor maintenance activities can also be performed together with the inspections, if necessary.

All information pertaining to the buildings, their components and respective state of conservation is collected and recorded during the inspections.

The results of the inspections are described and articulated in the Final Report, which gives information in regard to:
- defects/degradation observed on the building;
- problems relating to critical points and individual technological elements;
- expected degradation and areas at risk;
- interactions between individual elements and the structure;
- reviews on the accessibility of the building system and the possibility of inspecting the elements that constitute it.

3 PLANNED MAINTENANCE ACTIVITIES

The objective of the Maintenance Plan[4] is to monitor and re-establish a satisfactory relationship between the state of operation of a system and its functional units and the quality standard used as a reference. With specific regard to Cultural Heritage, this consists firstly in the provision of all the maintenance activities required for the preservation of the building, through maximization of the permanence of its materials and components, for which the frequency, cost indications and medium and long-term implementation strategies are estimated in relation to the state of conservation and functional efficiency of the building itself.

Within the maintenance plan can be found different levels of maintenance activities, operating at different intensities, which contribute to the preservation of the building:
- Prevention activities: these are indirect activities.This category includes both management activities (such as regulations of use) and maintenance activities aimed to controlling or containing situations of risk to which the asset is subject due to the surrounding conditions (such as the cutting of surrounding vegetation, the correction of counterslopes, etc.)
- Preventively effective activities carried out on the building: these are activities that, while directly involving the building, in view of minimal invasiveness on the asset and conservation objectives, can be considered as preventive activities due to their remarkable effectiveness in controlling

[4] UNI 10874:2000.

degrading actions (they include, for example, cleaning gutters, dusting decorative displays, eliminating biodeteriogens, temporary surveillance and safety provision measures, etc.)

- Protection activities: these are direct activities aimed at providing additional resources for the building and its components, such as structural reinforcements, protective surface layers, or that include the addition of new technological elements. Such activities may include: applying protective top layers (provisional coverings, casing, metal covers, covering plaster), application of protective fluids (reaggregates, waterproofing, etc.) maintenance activities : these are activities that directly involve the material of the building and are considered essential in order to slow or contain the progression of damage. They are designed and implemented with the aim of redressing situations of damage, by removing the causes wherever possible.

The maintenance activities included in the plan and scheduled in the maintenance program are normally simple, repetitive activities, often preventive in nature (such as cleaning gutters, dusting decorative displays, using covers, eliminating biodeteriogens and temporary surveillance and safety provision measures, etc.) In any case, the decisions made once the Plan's documents and schedules have been drawn up can be continually adjusted to deal with unforeseen events, which often occur with historic buildings and archaeological structures.

The executive works, scheduled in the programme, are guided by operational instructions.

They define, in a logical sequence of actions, the methods, criteria and recommendations for implementing and controlling all specific executive activities.

The problems that emerged in the development of the above-mentioned research led to reflection on the special features of maintenance activities regarding Cultural Heritage and to the gaining of some awareness that allowed essential principles to be established regarding criteria for choosing maintenance strategies and executive interventions. As already mentioned, these concern the concepts of life cycle, degradation, disease, durability and reliability.

4 MAINTENANCE AND "LIFE-CYCLE"

All the maintenance definitions contained in the voluntary regulations refer to a "life cycle" of buildings and argue that the task of maintenance is to restore the service system to how it was when the building was completed. This implies that without adequate maintenance the "life cycle" of a building can be less than that which is expected. In the area of Cultural Heritage it must first be understood that the term "life cycle" cannot be used with the same criteria applicable to newly constructed plants or buildings. It is therefore necessary to distinguish between Cultural Heritage buildings that are in use and those that are defunctionalised or collapsed. For buildings in use the topic of the service response must be commensurate with:

- the system of requirements and with the compatibility of the functions installed or to be installed in relation to any functional obsolescence phenomena that may have occurred;
- the system of technological requirements related to the events of degradation or damage.

For buildings not in use or that have collapsed, the problem may be limited to the need to ensure at least the minimum technological requirements connected with the decline in performance due to events of degradation or damage. It should be repeated, however, that the "no-use" does not mean no-*usefulness*: in fact, without doubt Cultural Heritage has an irreplaceable cultural, documentary and informational function as well as providing a material witness.

In any event, the purpose of the maintenance work on the monuments cannot be that of restoring the subsystem or component to its initial level of service (which is, in any case, only theoretically possible), but to control the effects of deterioration agents through interventions of different intensity and frequency that allow the life of the asset to be prolonged and ensure the conservation of its authenticity and identity through the permanence of original materials and components.

It is possible, however, that within the maintenance process it may be necessary to "realign" some levels of performance, at least partially, before implementing a maintenance plan: as in the case of the plaster becoming partially detached, which need re-bonding to the support; of structural elements that require work to reinforce their static function; or of roofs that require a significant review of their water- and wind-proofing performance. In all of these and other similar cases, the works to realignment performance are designed to bring the level of functional quality not necessarily to the building's original levels, but to one which is consistent with its specific function.

In the area of building maintenance (individual buildings or real estate assets) the "life cycle", "useful life" or "life duration" is essentially connected to building's recognised capacity to still provide services, and is therefore calculated in assessments related to the possibilities and modes of use. At the end of the "life cycle", i.e. when there no more apparent possibility of use at affordable costs, the building would be decommissioned.

The "life cycle" of buildings, however, is never either linear or predictable, since it depends on widely different factors of a technical, social and economic nature that involve varying rates of deterioration and obsolescence.

The concept of "life cycle" in the above mentioned terms is therefore inapplicable to Cultural Heritage, bearing in mind the fact that, in general, the usefulness of a cultural asset cannot decay over time and the issue of decommissioning does not arise.

With regard to component parts, the "life cycle" is connected to possibilities of repairing them based on economic criteria. With industrial components, replacement is envisaged at the end of the "life cycle".

The replacement of component parts of historical buildings and monuments (plaster, stone elements, structural elements, etc...) is only permissible when their conditions of degradation or damage may jeopardize the existence of the asset itself. As already noted, punctual, diligent and constant maintenance are specifically intended to keep these components in operation, regardless of their chronic state of disrepair.

It is completely normal, however, that in certain cases, even in the area of Cultural Heritage, once the permanence of the object's identity and authenticity data has been safeguarded, *new added elements* with a protective function, as a "sacrificial layer", or one of enhancement (implants), can be maintained and periodically replaced. In all cases, as can be seen, the topic of the "life cycle" of materials and components is not foreign to the field of Cultural Heritage: one can, in fact, also speak in terms of a "life cycle" for new structures and protective elements (roofs, top covers over collapsed walls, etc..), safety measure systems and new technological systems implemented during preventive or maintenance activities.

5 MAINTENANCE "DETERIORATION AND BUILDING PATHOLOGY"

The concept of deterioration and the criteria for interpreting the events connected with its cause and progress do not differ substantially in the field of Cultural Heritage from that of recent building work. Deterioration is therefore an expected event, which can be viewed as the response of the materials and components of a building to the actions of weather and the anthropic aggression connected with its uses. There is natural deterioration when it occurs at a rate that corresponds to the expected life span of the technical solution. Pathological degradation occurs when there are situations of disturbance, normally caused by design or process errors, that accelerate the natural deterioration phenomena causing degenerative events in times that are greatly anticipated compared to normal natural aging dynamics ("lifetime" or "life cycle") [Croce 1994].

In the case of Cultural Heritage buildings, it could also be added that deterioration, which is physiological in a building that is already old, should not to be understood in a negative sense and does not always require corrective interventions; it should be recognised, in any case, that it will never be entirely eliminated. Secondly, the deterioration which becomes evident with aging as time passes, leaves "signs" and "patinas" on the building that, rather than being removed, should be preserved in as much as they give to object the value of antiquity and characteristics of authenticity that makes it unique and unrepeatable. Maintenance work will therefore be aimed at managing the "chronicity" of the deterioration through "treatment" [Treccani 1996] that will be most effective when performed in a continuous and constant manner.

Assessments of the gravity of the damage and urgency of intervention are relevant from the operational point of view. Gravity involves an assessment of the phenomenon of deterioration observed, expressed in relation to its consistency, extent and impact on the state of conservation of the asset as a whole. Urgency, however, refers to an assessment of the greater or lesser need for rapid intervention, in relation to a greater or lesser propensity of the object to deteriorate at varying rates of acceleration (connected with the intensity of the agents, their interactions, the state of preservation, etc.) and depending on the risk of further loss of material. This means that a high degree of seriousness in ongoing deterioration does not automatically correspond to a high degree of urgency. Building pathology [Croce 1994] is the discipline that studies factors of disturbance (whether human, environmental, technical, technological, physical or chemical) and the mechanisms that lead, at an early date, to deterioration or damage related to physical alterations that may undermine the natural aging process. Since, as stated above, the deterioration of Cultural Heritage buildings in general can only be natural, i.e. due to continuous and long-term exposure to the elements, one of the most common causes of possible pathological damage to these buildings is incorrect maintenance. This may be due to an insufficiently detailed diagnostic analysis of the causes of deterioration, the use of incompatible materials or techniques, or the use of insufficiently trained personnel. Knowledge of the range of phenomena that have led to the unexpected deterioration of materials and components (which is also acquired through the development of inspection and monitoring activities, recording the results in an information system), or of maintenance activities that have had little long-term effect, enables the causes of the defects and process errors to be traced and more appropriate maintenance work to be developed.

To ensure efficient repair work, therefore, it is essential to preventively remedy any signs of trouble by correcting defects (faulty design, implementation or use) and designing interventions (e.g. "sacrificial" protection or layers, stabilising unsound elements) that are able to slow down or reduce the likely actions of agents of deterioration and situations of risk.

Within certain limits, and according to a certain point of view, even lack of maintenance may be a cause of "pathological" deterioration, in that failure to provide necessary repairs in a timely manner in cases of predictable, well-known or overt phenomena can greatly accelerate degenerative processes, partly due to the combination of the effects of various agents that progressively speed up the progress of the degenerative phenomena.

6 MAINTENANCE, "DURABILITY AND RELIABILITY"

The issue of durability in the field of Cultural Heritage buildings becomes critical when you start to think of the "limit state" beyond which the component or subsystem should be replaced. The argument once again involves the topic of the "useful lifetime." Granted that, for obvious reasons, the a priori substitution of elements, even in situations of degradation, is excluded, the need for intervention can be assessed in various ways, according to the development of the diagnostic phase.

It is evident, however, that the issue of durability is justified, even in the field of Cultural Heritage:

- firstly as an assessment of the reliability of the techniques or materials used in previous maintenance;

- secondarily, as an assessment of the "limit state", beyond which the component must necessarily be replaced. This evaluation requires consideration of the specific features of the element, its function and the relationship it has with the adjacent components; its actual state of deterioration in relation to the minimum functional requirements; and the level of residual performance in relation to that which is expected;
- lastly, as a criterion for choosing the most appropriate measures, which may be preventive or maintenance.

The topic of greater or lesser durability, therefore, together with that of reliability, will be a criterion for the choice of intervention techniques and will also determine the most appropriate criterion for the predicting and sequencing of the subsequent intervention.

7 MAINTENANCE AND "OBSOLESCENCE"

Obsolescence is a phenomenon inherent to the passage of time, which necessarily refers the theme of the life cycle.

Even in the field of Cultural Heritage, the concept of obsolescence is connected, for buildings that are in use, to the loss of benefits that is evidenced by the loss of functional efficiency of an object, a plant or an environmental unit as a result of a change in the framework of needs, regulatory modifications, or in the case of plants, due of the implementation of technological improvements.

The services are constituted by behaviours that the various building components and objects (either individually or in relation to each other) are able to implement in response to the requirements connected with needs of use. In the case of the project on an existing building, unlike one for a new construction, it is necessary to consider that every existing building object is always able to deliver performance. Perhaps minimum performance, due to age, functional obsolescence or a precarious state of conservation, but these should be evaluated and, where possible, measured through the tool of performance analysis. This will tell us the quality and consistency of existing performances. The comparison between existing performance and design requirements will tell us, instead, what can be preserved and what needs to be transformed. Another key aspect of the concept of performance is given by variability over time. It is known that over time, some items may lose benefits due to obsolescence, wear and aging, to the point of no longer being suitable to perform the function for which they are intended, leading back the to the issue of life cycle.

It is clear that performance analysis is mainly applicable to buildings in use. But also for abandoned buildings, especially for Cultural Heritage, new possibilities of use can and must be found, to give rise to a new "life cycle", starting precisely from an analysis of existing (or residual) benefits. This however requires the capacity of studying, with good sense and refined planning, which utilities we see that these buildings still capable of offering, to provide answers to our diversified needs. Furthermore, if they are carefully re-used and maintained, with the passage of time adds they are enhanced by new and hitherto unknown information, data and experiences.

8 MAINTENANCE PLANNING

One can therefore say in summary:

- outside of a maintenance plan (or where, within a maintenance plan, unforeseen events occur), maintenance activities are generally aimed at partially re-aligning existing performance, or parts thereof, in relation to the condition of walls, surfaces, components and systems, avoiding, as far as possible, invasive procedures or replacement. They nevertheless must always be properly managed by a project phase that defines their characteristics and limitations, each time re-evaluating their objectives more precisely. To coherently address the maintenance project on a historical building, certain levels of performance need to be more adequately considered, or

reconsidered, such as those of "durability" or "functional efficiency" and, more generally, those associated with issues of needs and performance, in respect to the assessment criteria for more recent buildings which, in this area, cannot be taken as absolute.

It will be necessary therefore to consider that different criteria may exist, for example, on historic surfaces with varied degrees of disintegration - which bear the marks of the passage of time and that, because of this, are able to convey essential documentary information - compared to the demands of "functional efficiency" for the facade of a new building: in other words ... if it is logical to think of the new because you are slowly growing older, it is absurd to think that aging is a priority issue for a building that is old " [Della Torre 1999], especially if is defunctionalised, as is the case, for example, with Archaeological Heritage.

– If provided for as part of a maintenance plan, it will be a question of repetitive, normally low-tech activities, but always performed in a controlled manner, that are defined and programmed according to predetermined intervals and performance criteria laid down in codes of practice (Operational Instructions). Maintenance activities performed as part of a scheduled maintenance plan, moreover, should never affect the stratigraphic reading of the buildings, nor be conceptually identified as new phases of the long process of transformation of the asset over time. It can be reasonably argued, in fact, that the operations related to activities of caring for building structures (such as removing dust and small ruderal vegetation, cleaning gutters and downspouts, maintaining roofs, integrating small faults, restoring sacrificial layers, implementing temporary static safeguards for the securing of unsound parts etc..) can be procedured and defined a priori in their scale, intensity and extent. These works, therefore, structured as part of a more complex maintenance "service", would not require specific planning, but would be performed by maintenance experts, properly trained and supervised by specialised technicians. It is an observation shared by operators and maintenance technicians, in fact, that in practice, given the universe of possibilities, of the mutability and often amazing uniqueness of sites, significant similarities reappear in practice with a considerable frequency.

They provide a good approximation, based on experience, or even on the basis of a focused analytical assessment, to re-use techniques and methods of intervention that have already been used in previous similar experiences and, therefore allow in fact, by totally reusing procedures already in place (or some variant), to validate previous choices wherever positive result are observed.

9 CONCLUSIONS

An experience of planned maintenance process, guided by this pricipals, is, just now, being applied to some buildings of the central archaeological area of Rome where a few case studies have been selected. The planned maintenance strategy has to face the specificity of the archaeological heritage, made of ruined building with a particular behaviour. The first output of this process is surely a growing knowledge of the buildings and a increase of the operators consciousness. Planned maintenance indeed involves managing authority, conservation operator and also users in a partecipate process of conservation and enhancement of the cultural heritage.

REFERENCES

Cecchi, R. 2009, *Roma Archaelogia. Interventi per la tutela e la fruizione del patrimonio archeologico, primo rapporto*, Electa, Milano.

Cecchi, R. 2010, *Roma Archaelogia. Interventi per la tutela e la fruizione del patrimonio archeologico, secondo rapporto*, Electa, Milano.

Cecchi, R. & Gasparoli, P. 2010, *Prevenzione e manutenzione per i beni culturali edificati. Procedimenti scientifici per lo sviluppo delle attività ispettive. Il caso studio delle aree archeologiche di Roma e Ostia Antica*, Alinea, Firenze.

Croce, S. 1994, "Patologia edilizia: prevenzione e recupero"**,** in AA.VV., *Manuale di Progettazione Edilizia*, Vol III, Progetto tecnico e qualità, Hoepli, Milano.

Della Torre, S. 1999, 'Manutenzione o Conservazione? La sfida del passaggio dall'equilibrio al divenire', in *Atti del Convegno Scienza e Beni Culturali* "*Ripensare alla Manutenzione*", Arcadia Ricerche, Venezia.

Della Torre, S. (ed.) 2003, *La conservazione programmata del patrimonio storico- architettonico: linee guida per il piano di manutenzione e il consuntivo scientifico*, Guerini, Milano.

Ruskin, J. 1981., *The Seven Lamps of Architecture*, 1849, nella traduzione di M. Pivetti per Jaca Book, Milano.

Treccani, G.P. 1996, 'In principio era la cura. Medico e restauratore: un paragone da rivisitare', *Tema*, 3.

XII DBMC
International Conference on Durability of Building Materials and Components
PORTO - PORTUGAL, April 12th-15th, 2011

A Comparative Assessment of Bond Strengths in Mortar Coatings Applied by Mechanical and Manual Projection

Antonio Carlos de Albuquerque Melo [1]
João Ribeiro de Carvalho [2]
Angelo Just da Costa e Silva [3]
Eliana Cristina Barreto Monteiro [4]

ABSTRACT

This article aims to show the importance of facing mortar in the context of Construction, going to search for higher levels of rationalization and modernization of its production process. Motivated by the absence of a more orderly management and production planning, we seek to provide a comparative assessment of the adherence of coatings applied by mortar projection manual and mechanical projection. Indices will be presented concerning the bond strength to tension between the two methods with the use of more than one type of mortar, and produced in industrialized construction site. For this study experiments were performed with the use of machine gunning of mortar, the type "*Canequinha*" with four outputs, and also the same mortar applied manually, "chapada". The results of this study indicated that the use of mortar launched by projection provides greater mechanical bonding strength to strength, lower standard deviation and greater uniformity in comparing yourself with mortars launched manually. Also observed that, in the same conditions of application and environment, the mortar industrialized showed increased resistance produced in the mortar bed. Finally, it was also diagnosed increased levels of resistance in the presence of coarse mortar on the bases.

KEYWORDS

Coating, Mortar, Manual projection, Mechanical projection.

[1] Currently undertaking Master's course in Civil Construction – University of Pernambuco, Pernambuco, Brazil, mouramelo.antonio@gmail.com
[2] Undergraduate in Civil Engineering – University of Pernambuco, Pernambuco, Brasil, eng.jribeiro@gmail.com
[3] PhD Professor in Civil Construction – Department of Civil Engineering at the Catholic University of Pernambuco, Pernambuco, Brazil, angelo@tecomat.com.br
[4] PhD Professor in Civil Construction – Department of Civil Engineering at the University of Pernambuco, Pernambuco, Brazil, nana.monteiro@uol.com.br

1 INTRODUCTION

It is a known fact that mortar coating is almost entirely responsible for protecting the constructive elements of a building, regardless of its dimensions and finishing standards. The mortared coating serves to protect the main structure of the building, whether of reinforced concrete or metal, and serves in this latter case, as protection against fire, as well as providing comfort, attractiveness, waterproofing and a greater resistance to the parts that have been coated.

Mortared coating is also responsible for a substantial part of the construction costs, especially in buildings, and is also responsible for many of the problems, which often emerge on buildings throughout our region. These problems range from poor quality to a lack or loss of adhesion, and may bring about serious problems for the occupants of the building, and may even directly interfere in their daily lives.

Given the international tendency towards the use of applying mechanically projected mortar, and in view of the lack of regional technical research regarding this subject, the present study was developed to undertake a comparative assessment of the bond strengths of mortar coating applied by mechanical and manual projection.

The greatest difficulty encountered locally in managing the process of applying mortar coating is the lack of skilled manpower, which has forced most enterprises to maintain manual application of mortar coating. Gonçalves and Bauer (2005) have demonstrated that the manual application of mortar coating is responsible for many variables in bond strength. Therefore, the encountered solution has been the use of mechanical application.

According to Duailibe ; Cavani; Oliveira (2005), the mechanical application of mortar coating has the potential of not only improving this stage of the process, but also the quality of the final product. The authors studied the influence of mortar application on tensile bond strength, and were able to achieve an increase of 55% in relation to manual application.

It is evident, even with the results already obtained, that very few studies are currently available that assess its global efficiency, and it is precisely this which has led us to analyze the results obtained from the form of mortar application suggested.

The main aim of this study has been to present a set of results that may compare the bond strength of mortar coatings applied by mechanical and manual projection. Furthermore, two types of mortar coatings were employed, industrialized mortar mix and that made at the construction site, thus extending the comparison to the use of different types of mortar.

2 FORMS OF APPLYING MORTAR COATINGS – DISCUSSING THE POTENTIAL ADVANTAGES

2.1 Manual application

In his study, Fernandes et al. [2006] states that : “Replacing the manual application of mortar coating with mechanical application has become an international trend. This has been due to factors such as increased productivity through mechanized production. Fernandes et all. [2006] stated that in manual projection there is a considerable variation of energy, since the speed employed by the bricklayer varied from 2.5 to 15 m/s, and that this energy level may affect the occurrence of defects at the mortar-base interface”.

Since the strength of the coating is one of its most important properties and given that this depends on the energy with which the mortar coating is applied, problems therefore occur both in the short and long term.

Fernandes et al. [2006] go on to state that "while the mortar is being applied, it receives a certain quantity of kinetic energy, which dissipates when it reaches the base, whether during its plastic deformation (spreading), or in the form of elastic deformation (reflection) or in the form of heat. In order to guarantee a satisfactory bond strength, the mortar must be applied with the correct energy, permitting it to be adequately spread, and thus eliminating most of the possible defects at the mortar-base interface (air bubbles between the layers), as well as guaranteeing a large extension of adhesion [Carasek 1996].

3 EXPERIMENTAL PLANNING

3.1 Employed materials

In order to conduct the present study, the following materials were employed:

a) Industrialized mortar mix: External rendering mortar;
b) Mortar made on the construction site for plastering, for external rendering, used in the experiment in the following proportions:
– Intermediate mortar (kg:kg) – 1:10 (hydrated lime CHI – supplied by Carbomil: medium sifted sand);
– Final mortar (kg:liter) – 1 : 5.2 (Portland cement CPIIF32 – supplied by Nassau: intermediate mortar).
c) Roughcast: Industrialized mortar for external rendering, the same for plastering;

In all cases the quantity of water was used in accordance with manufacturer's recommendations or in accordance with the necessities of the application as required by the laborer, simulating normal conditions of use.

3.2 Preparation of samples

In order to conduct the practical experiments for the present study, an experiment was undertaken by a large incorporated company based in the metropolitan region of the Recife, in the northeast of Brazil. On one of the floors in one of their buildings under construction, located in the district of Casa Forte, experimental applications of mortar were performed with both the traditional method and mechanical projection onto bases of masonry, using both industrialized mortar mix and mortar made at the construction site. Furthermore, samples were also prepared with and without roughcast, in order to carry out a comparison.

With the use of a mortar projection machine, industrialized mortar mix was projected onto masonry with and without roughcast, and then using the same machine with mortar made at the construction site, with the same water/cement ratios as the industrialized mortar, onto walls with and without roughcast. Using the same team of workers, mortar made at the construction site was manually applied to a panel without roughcast.

After a period of 28 days, with the panels classified as samples, 5x5cm cuts were made. For this, it was necessary to use a cutting machine and then small plates of the same dimensions were inserted with Epóxi adhesive. The samples were then subdivided into points, and after a waiting period of 72 hours, tests for Tensile Bond Strength were applied.

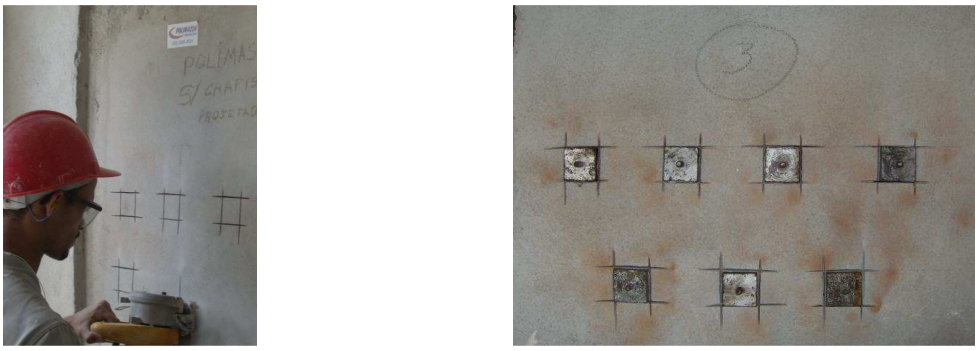

Figure 1. – Executing the cuts, application of metal plates and traction.

After 72 hours, the tensile bond strength test began. Equipment and engineering supervision were provided by the TECOMAT, a specialized company in performing this type of test in this region, with the use of an ALFA 3105C Test Indicator (fig. 2), coupled to traction device. Once the adhesion tester had been fixed to the wall (fig. 1) and the traction device screwed to the plate, force is applied in order to remove the plate. This force, expressed in kgf is registered on the test indicator. This process was repeated on all points of all samples (Fig.3).



Figure 2. – ALFA 3105C Test Indicator and the same machine coupled to a traction device



Figure 3. – Conducting the test – the wheel of the traction device is turned until the test pieces rupture and Comparing the ruptured piece with the site where it had been applied

Throughout the test, the exact rupture site on the substrate surface is observed (Fig. 3), verifying if it was between the base and the roughcast, the base and the mortar, the roughcast and the mortar or between the plate and the mortar (Fig.3). These results were then recorded.

Once all data had been obtained, a set of tables was drawn up to present the bond strengths at each point of each sample and the rupture site in the substrate, as below table 1 until the table 6.

Table 1. Results of the Bond Strength test from Sample 1 (base without roughcast).

Point	Bond (Kgf)	Strength (MPa)	Rupture Site
1	28.80	0.12	Coating/Base
2	35.40	0.14	Coating/Base
3	14.50	0.06	Coating /Base
4	79.00	0.32	Coating /Base
5	29.70	0.12	Coating /Base
6	95.90	0.38	Coating /Base

Table 2. Results of the Bond Strength test from Sample 2 (base with roughcast).

Point	Bond (Kgf)	Strength (MPa)	Rupture Site
1	106.00	0.42	Coating/roughcast
2	82.0	0.33	Coating/roughcast
3	58.20	0.23	Coating/roughcast
4	90.80	0.36	Coating/roughcast
5	63.50	0.25	Coating/roughcast
6	41.30	0.17	Coating/roughcast
7	63.70	0.25	Coating/roughcast

Table 3. Results of the Bond Strength test from Sample 3 (base without roughcast).

Point	Bond (Kgf)	Strength (MPa)	Rupture Site
1	45.50	0.18	Base/Coating
2	18.20	0.07	Base/Coating
3	79.50	0.32	Base/Coating
4	37.50	0.15	Base/Coating
5	31.30	0.13	Base/Coating
6	58.50	0.23	Base/Coating
7	96.20	0.38	Base/Coating

Table 4. Results of the Bond Strength test from Sample 4 (base without roughcast).

Point	Bond (Kgf)	Strength (MPa)	Rupture Site
1	86.70	0.35	Base/Coating
2	99.10	0.40	Base/Coating
3	79.10	0.32	Base/Coating
4	110.40	0.44	Base/Coating
5	6.62	0.03	Base/Coating

Table 5. Results of Bond Strength test from sample 5 (base with roughcast).

Point	**Bond (Kgf)**	**Strength (MPa)**	**Rupture Site**
1	61.90	0.25	Coating
2	66.30	0.27	Coating
3	63.50	0.25	Base/Coating
4	87.10	0.35	Coating
5	43.60	0.17	Base/Coating
6	36.50	0.15	Base/Coating

4 RESULTS AND DISCUSSION

This section will analyze the results obtained during the tests, seeking to compare the types of application employed (manual and mechanical), types of mortar used (industrialized and made at the construction site) and the type of base on which these mortar coatings were applied. For this, it will be necessary to observe Table 6, below, in which the points were classified in ascending order of tensile bond strength. Finally, the arithmetic mean values of the four highest bond strengths and the standard deviations are described.

Table 6. Classification of the Sample in ascending order of Tensile Bond Strength.

Points in Order	Tensile Bond Strengths of the Samples				
	1	2	3	4	5
1	0.06	0.17	0.07	0.03	0.15
2	0.12	0.23	0.13	0.32	0.17
3	0.12	0.25	0.15	0.35	0.25
4	0.14	0.25	0.18	0.40	0.25
5	0.32	0.33	0.23	0.44	0.27
6	0.38	0.36	0.32		0.35
7		0.42	0.38		
Average	0.24	0.34	0.28	0.38	0.28
Standard Deviation	0.112	0.061	0.078	0.046	0.041

It may be concluded from this comparison that the mechanically projected mortar (Sample 4/table 4), achieved higher bond strengths than the manually projected mortar. Sample 3 presented a higher standard deviation than Sample 4, which was certainly due to the lack of uniformity in the projection of the mortar. In this case, there would also be a tendency for this to become even higher, since manually projected mortar depends on the force of the bricklayer who is applying it. Thus, if in such a small sample the standard deviation is able to illustrate the lack of uniformity, it is not difficult to imagine how this lack of uniformity would be represented by the end of the day, when tiredness has set in and the consequent loss of physical strength.

In this case, industrialized mortar mix (Sample 1/table 1) and mortar made at the construction site (Sample 4), were both mechanically projected on to a base without roughcast, where Sample 1 was exposed to the outside elements and Sample 4 was protected inside the building.

It may observed that the outside elements have a considerable influence over tensile bond strength, since although the two samples ruptured at the same site, between the base and the mortar coating, sample 1 (industrialized mortar mix) presented a lower mean bond strength and a higher standard deviation, thus illustrating the influence caused by the lack of roughcast.

The following discussion is based on mortar coating made at the construction site and projected mechanically onto brick surfaces without roughcast (Sample 4/table 4) and without roughcast (Sample 5/table 5).

In the analysis of these samples, the following conclusion was reached: Sample 4, projected onto masonry without roughcast has a bond strength much higher than the same mortar coating applied to masonry with roughcast. How may this be explained?

The fact is that Sample 4 was applied to an inside wall, and Sample 5 was applied to an external base, exposed to the outside elements, and even though it had been applied to a roughcast base, it still presented a lower performance.

It may also be observed that, despite the considerable difference between the mean values of bond strength, the two samples presented a similar standard deviation. Therefore, confirming the expected effects of a coating which is exposed to external weather conditions.

Based on what has been discussed throughout the present study, it is possible to make the following considerations:

– Industrialized mortar mix mechanically projected onto a base exposed to the outside elements, presents higher bond strength and lower standard deviation when compared to manually projected mortar coating.

– The environmental conditions to which the base is exposed has a negative effect on bond strength.

– The external base without roughcast, not only presented lower mean bond strength, but also a higher standard deviation.

– The mortar coating mechanically projected onto a base with roughcast, exposed to the outside elements, presented a bond strength lower than the same mortar coating applied to a base without roughcast and no external elements.

– The same type of mortar applied to bases exposed to different exposure conditions, presented different mean strengths, while presenting similar standard deviations.
Mortar made at the construction site and projected mechanically presented higher bond strength and a lower standard deviation than the manually projected mortar.

5 FINAL CONSIDERATIONS

Thus, it can be observed that very favorable results have been obtained for the use of mechanically projected mortar, a fact which therefore calls for further research in this area, to explore new relationships between the forms of application and the types of mortar coatings.

We strongly recommend that this type of study should be conducted for other types of bases, such as concrete, pre-fabricated blocks and steel structures, amongst others.

As discussed throughout this article, the present study should serve as one more instrument for the development of new construction technologies within the region, with a view to reducing costs while increasing productivity and, especially, higher performance standards on construction sites.

REFERENCES

Gonçalves, S. R. de C.; Bauer, E. Estudo de caso da variação de resistência de aderência à tração em uma parede. In: VI Simpósio Brasileiro de Tecnologia de Argamassas, Florianópolis, 2005. Anais... Florianópolis, 2005, p. 562-567.

Duailibe, R. P.; Cavani, G. R.; Oliveira, M. C. B. Influência do tipo de projeção da argamassa na resistência de aderência à tração e permeabilidade à água. In: VI Simpósio Brasileiro de Tecnologia das Argamassas. Anais. Florianópolis, 2005. p 508-517.

Fernandes, H. C.; Antunes, R. P. N.; Barros, M. M. S. B; John, V. M. Energia de lançamento da argamassa na projeção por spray a ar comprimido. In: XI Encontro Nacional de Tecnologia do Ambiente Construído. Anais. Florianópolis, 2006. p 4093-4108.

Carasek, H. Aderência de argamassa à base de cimento Portland a substratos porosos – avaliação dos fatores intervenientes e contribuição ao estudo do mecanismo da ligação. São Paulo, 1996. Tese (Doutorado) – EPUSP – Universidade de São Paulo.

XII DBMC
International Conference on Durability of Building Materials and Components
PORTO - PORTUGAL, April 12th-15th, 2011

Risk Management in Rehabilitation of Structures

João Parreira [1]
Vítor Cóias [2]

ABSTRACT

The problems related to the durability of materials and constructed assets have deserved special attention due to the evident consequences both in terms of safety and costs arising from inadequate performance over time. Given the high frequency of unfortunate premature failures there is an increased interest to assess the risk of undertaking extended rehabilitation interventions and preventive actions to maintain the integrity of structures over the long-term.

In the rehabilitation of structures this problem is perhaps more acute given the difficulty in resolving problems that normally involve many causes, as well as, the uncertainty in the long-term performance.

The present study is intended to provide evidence on the current performance of structural interventions. A database was developed integrating all pertinent information allowing a diagnosis of the interventions and from which a risk management plan for the implementation of the interventions can be made. The database provides information about the verification of failures and anomalies, the degree of success of the corrective action and the durability of the structural systems under repair.

KEYWORDS

Risks, Rehabilitation of civil infrastructures, Inspections.

[1] Stap, sa, Lisboa, PORTUGAL, jcparreira@stap.pt
[2] Stap, sa, Lisboa, PORTUGAL, vitorcoias@gestip.pt

1 INTRODUCTION

Recent events made it clear that effective risk management is a critical element for success, and indeed, for long term survival, not only for industrial firms, but also for construction firms. The world is filled with all manner of risks, and so risk management must be extended far beyond the use of standard directive instruments in routine edging applications.

Construction companies take big risks associated to project mistakes, incorrect execution, wrong utilization, lack of maintenance and the inexistence of monitoring and controlling risk plans. Due to this, an information system that allows collecting information needed to manage risk and assess the performance of construction rehabilitation projects was developed.

The main objective consists of evaluating the present state of the rehabilitated infrastructures by the company since 1980 (during thirty years of activity). Another objective is to analyze the performance of the techniques used along with the structural behaviour, and also to detect the recurrence of anomalies of structural nature.

2 STATE OF THE ART

According to the Project Management Institute in the guide PMBOK [page 273], risk management involves six processes:

1. Plan Risk Management [P1] - The process of defining how to conduct risk management activities for a project;
2. Identity Risks [P2] - The process of determining which risks may affect the project and documenting their characteristics;
3. Perform Qualitative Risk Analysis [P3] - The process of prioritizing risks for further analysis or action by assessing and combining their probability of occurrence and impact;
4. Perform Quantitative Risk Analysis [P4] - The process of numerically analyzing the effect of identified risks on overall project objectives;
5. Plan Risk Responses [P5] - The process of developing options and actions to enhance opportunities and to reduce threats to project objectives;
6. Monitor and Control Risks [P6] - The process of implementing risk response plans, tracking identified risks, monitoring residual risks, identifying new risks, and evaluating risk process effectiveness throughout the project.

Each process occurs at least once in every project and occurs in one or more of the project phases.
Risk is an uncertain event or condition that, if it occurs, has an effect on at least one project objective. This can include scope, schedule, cost, and quality. A risk may have one or more causes and, if it occurs, it may have one or more impacts. A cause may be a requirement, assumption, constraint, or condition that creates the possibility of negative or positive outcomes.

Project risk has its origins in the uncertainty present in all projects. Known risks are those that have been identified and analyzed, making it possible to plan responses for those risks. Specific unknown risks cannot be managed proactively. Organizations perceive risk as the effect of uncertainty on their project and organizational objectives. Organizations and stakeholders are willing to accept varying degrees of risk. This is called risk tolerance. Risks that are threats to the project may be accepted if the risks are within tolerances and are in balance with the rewards that may be gained by taking the risks. Individuals and groups adopt attitudes towards risk that influence the way they respond. These risk attitudes are driven by perception and tolerances which should be made explicit wherever possible.

A consistent approach to risk should be developed for each project, and communication about risk and its handling should be open and honest. Risk responses reflect an organization's perceived balance between risk taking and risk avoidance.

To be successful, the organization should be committed to address risk management proactively and consistently throughout the project. A conscious choice must be made at all levels of the organization to actively identify and pursue effective risk management during the life of the project. Moving forward on a project without a proactive focus on risk management increases the impact that a realized risk can have on the project and can potentially lead to project failure.

3 RISK MANAGEMENT PLAN

1. **Enterprise environmental factors** both internal and external that0 influence the project's success. These factors come from all of the enterprises involved. Includes:
   - Organizational culture, structure, and processes;
   - Government or industry standards;
   - Stakeholder risk tolerances;
   - Organization's established communications channels;
2. **Design and implement system information** to contain all the information necessary;
3. **Discussion with stakeholders** to select the projects based on factors like probability, monetary value, patrimonial value and structural safety impacts.
4. **Field inspections** and status report of the infrastructure rehabilitation projects.
5. **Perform qualitative risk analysis;**
6. **Plan risk responses**.

4 INFORMATION SYSTEM (IS)

The design of the IS allows the collection of technical and administrative data. To achieve this objective Windows MS Office/ Access was used. In Figure 1 one of the interfaces to input the data into the system is illustrated.

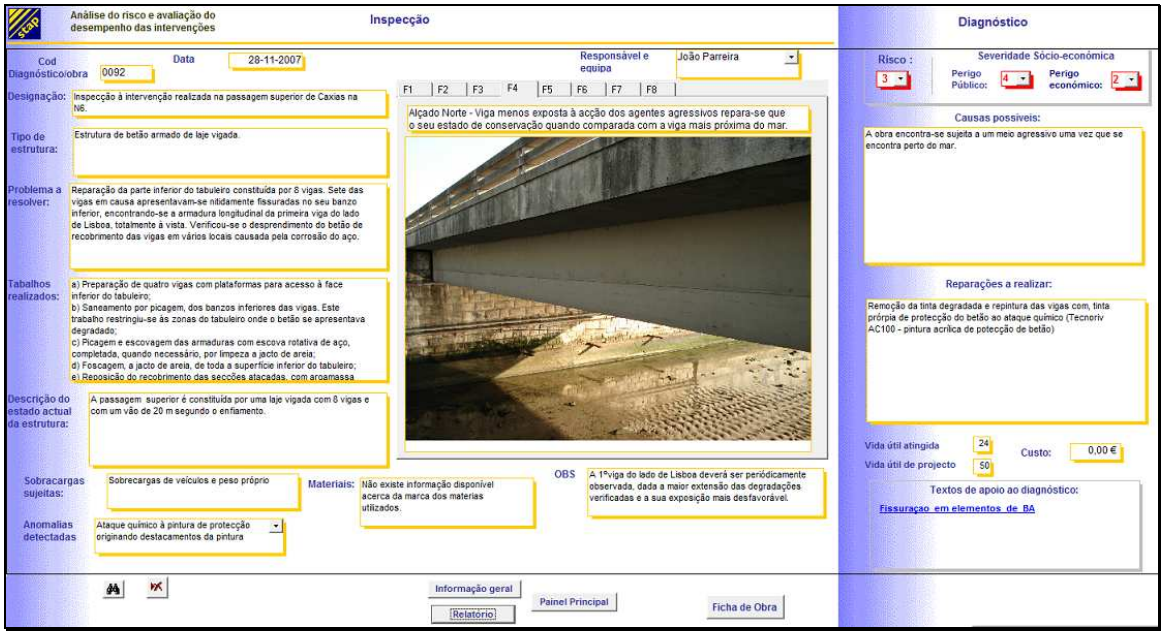

Figure 1. System Form - Field inspections and risk assessment.

As a result, this system allows several reports to be obtained by the management, by assessing the performance of the enterprise's project risks and planning strategies.

5 METHODOLOGY

Identifying Risks [P2] is an iterative process because new risks may evolve or become known as the project/product progresses through its lifecycle. Stakeholders outside the project, also provide additional objective information.

According to the *"Guide to the Maintenance, Repair and Monitoring of Reinforced Concrete Structures"* [page 691] published by the American Concrete Institute (ACI), a structured approach to identifying risk exposures will produce the best results. Having identified the risk exposures and, if possible, quantified their potential impact, it is useful to prioritise them [P3]. Risk exposures are ranked by order of impact, being determined by:

Risk = Probability (P) x Impact (I)

Risk solutions are identified with the aim of either eliminating or reducing the impact of risk exposure. The inspection and maintenance appear as solutions for high risks with the objective to eliminate or reduce their probability of occurrence, even for any risks that do not directly involve the company. In Table 1 is an example of specific risks for a structural reinforcement solution.

Table 1. Example of risk solution exercise for a reinforced concrete structures using steel plate bonding.

Risk	Success criteria	Solutions/risk reduction
Debonding of steel plates and loss of transmission of tensions to the element of reinforcement.	Full bonding action and polymerisation of epoxy resin	Routine inspection and maintenance repair
Diminishing resistance.	Lack of steel plates and fasteners.	Routine inspection and maintenance repair
Corrosion, concrete delamination.	Non-existence of concrete cracking	Routine inspection and maintenance repair

Evaluating the consequence and cost of a given risk will be determined on a case-by-case basis. Each infrastructure presents its own unique characteristics, for this reason the guidance notes do not seek to provide calculations for given risk exposures and each structure must be considered separately.

In this study a method based on the following criteria, was adopted:
- infrastructure degradation;
- present utilization conditions;
- frequency of maintenance and inspection.

In Table 2 and 3 are the criteria impact and probability.

Table 2. Utilization conditions and impact scale.

Category	Description
Demolish	Demolition of the infrastructure represents a very low/null impact.
Inactive	The infrastructure is inactive and represents a low impact. If reactivated requires a new risk evaluation.
Modify	The system presents different functions from those for which it was designed. Impact varies according to a higher or lower exigency level (case by case evaluation).
Active	The system preserves the same functions for which it was designed. Impact varies from high to very high (case by case evaluation).

1 - Very low	2 - Low	3 - Moderate	4 - High	5 - Very high

Table 3. Probability classification.

Probability	Description
1 – Rare	Remains unaltered after the intervention. Anomalies are non-existent.
2 – Unlikely	The infrastructure presents symptoms to the occurrence of anomalies, but without compromising the structural performance or cause serious lesions.
3 – Possible	The infrastructure presents anomalies that do not represent a structural risk in the short term meanwhile at long term it can compromise its structural function.
4 - Likely	The infrastructure presents substantial anomalies and damages. Recurrence of the problems that originated the intervention.
5 – Certain	Eminent collapse resulting in infrastructure total loss.

Perform Qualitative Risk Analysis [P3]. In order to do this, a short list of previously identified risks was created. The shortlisted risks could be further analyzed in the quantitative risks analysis, but in this case we move directly to plan risk responses process.

The risk-rating rules are specified by the organization in advance of the project and included in organizational process assets. Risk-rating rules can be tailored to the specific project in the plan risk management process. Evaluation of each risk's importance and, consequently, priority for attention, was conducted using a probability and impact matrix (see Table 4). This type of matrix specifies combinations of probability and impact that lead to rating the risks as low, moderate, or high priority. The red area represents high risk, the gray area represents low risk, and the yellow/orange area represents moderate risk.

Table 4. Probability and impact matrix.

		Probability (P)				
		Rare	Unlikely	Possible	Likely	Certain
Impact (I)	Very high	5	10	15	20	25
	High	4	8	12	16	20
	Moderate	3	6	9	12	15
	Low	2	4	6	8	10
	Very low	1	2	3	4	5

This matrix is used to sort or rate risks to determine which ones deserve an immediate response and which should be put on the "watchlist". This analysis is usually a rapid and cost-effective means of establishing priorities for plan risk responses.

Plan Risk Response [P5]. Depending on the case, responses include doing one or all of the following for each risk:

- do something to eliminate the threats before they happen;
- Decrease the probability and/or impact of threats.

The following three strategies applied to risks that have a negative impact:
Avoid - Eliminate the threat by eliminating the cause;
Mitigate - Reduce the probability or the impact of the threat;
Transfer - Make another party responsible for the risk.

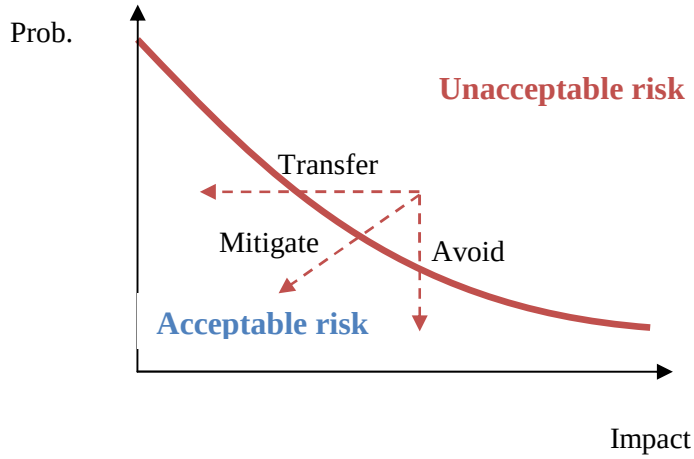

Figure 2. Risk response strategies.

6 CASE ESTUDY [CE]

More than forty jobs were selected, below are some examples:

Work 301 - The work on a school building involved using micro-piles and slope stabilization with sprayed concrete (1991). The performance appraisal conducted in 02-07-2008 found the structure presents anomalies that do not represent a structural risk in the short term. Meanwhile, in the long term it can compromise its structural function



Figure 3. Sprayed concrete - 1991.



Figure 4. Micro-piles head block - 2008.

After inputting data in the IS and according to the tables described in this paper, the final result was:
P = 3
I = 5
Risk (P x I) = 15 (see Table 5)

Work 451 - The work on the Central Post Office building involved metallic reinforcement of beams and pillars and surface repair of damaged structural elements (1994). The performance appraisal conducted in 05-05-2008 found the structure to be generally well-preserved, exhibiting a very low degree of degradation and maintaining the function for which it was originally conceived.



Figure 5. Metallic reinforcement beams and pillars - 1991.



Figure 6. Reinforcement beams and pillars - 2008.

After inputting data in the IS and according to the tables described in this paper, the final result was:
P = 1
I = 5
Risk (P x I) = 5 (see Table 5)

Work 727 - Rehabilitation of the access viaduct to the oil terminal (1997 to 1999). This contract job was the first practical case of desalination treatment successfully applied to a road viaduct made of reinforced prestressed concrete. The performance appraisal conducted in 30-06-2008 found that the structure is generally well-preserved and exhibits a low degree of degradation. The electrochemical desalination of the viaduct seems to have been successful, having met the expectations in terms of the results obtained, the safety of its implementation and the elimination of the cause of deterioration of the concrete structure.



Figure 7. Norcure desalination system in operation - 1998.



Figure 8. Viaduct - 2008.

After inputting data in the IS and according to the tables described in this paper, the final result was:
P = 1
I = 5
Risk (P x I) = 5 (see Table 5)

7 CONCLUSION

In this CE, the evaluations of the risk focus on interventions that represent higher costs for the society and the patrimony. This system adopted by the company, allowed monitoring principal risks, alerting any anomalies. The consequences of the risks were determined case by case including its costs to avoid, mitigate and transfer.

The risk management is a determinant factor on the project's performance. All interventions have specific expositions, deserving a specific diagnosis in accordance with the criteria described in chapter 5.

Table 5. Risk classification and response in all evaluated jobs.

Risk [R]	R = P x I	Case Study Occurrence (%)	Response
Unacceptable	17 - 25	(0%)	Develop a rehabilitation project.
Significant	13 - 16	(35%)	Implement a maintenance plan.
Substantial	9 - 12	(24%)	Special attention - Plan fields inspection and reports.
Acceptable	5 - 8	(16%)	Attention - Plan fields inspection and reports.
Insignificant	1 - 4	(25%)	Monitor

The results demonstrate (Table 5) that none of the structures were classified as unacceptable, and, approximately 35 % of the structures present a significant risk. However, this result is classified as unacceptable and preventive and corrective actions were required. In 24% of the cases (substantial) no serious structural risk was detected, although, the anomalies detected could influence the structural function in the long term. Finally, acceptable and insignificant risks were detected in 41% of the cases, which simply require monitoring.

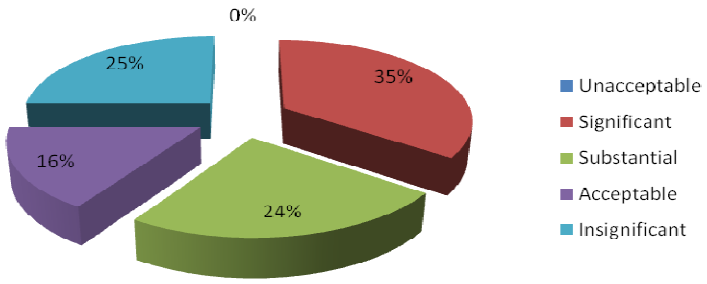

Figure 9. Risk classification

Based on the response plan defined to each of the risk groups, technical reports and diagnosis were elaborated in order to minimize associated risk in each intervention. In summary, inspections contribute to guarantee a good future performance, by alerting to the resolution of problems.

Infrastructure rehabilitation projects are even more sensitive to these questions and risk management allows response to risks and avoids their consequences. This CE had the aim of alerting all the stakeholders to the importance of risk management, especially in projects involving repair, strengthening, stiffening, protection, modification and demolition of structures.

REFERENCES

BRE DME D53 – Guide to the Maintenance, Repair and Monitoring of Reinforced Concrete Structures, in ACI, BRE, Concr. Society, ICRI - Concrete Repair Manual, 2.ª Edição, 2003, p. 691.

Cóias, Vítor – Inspecções e ensaios na reabilitação de edifícios;

Miguel, A. 2009. Gestão Moderna de Projectos: Melhores técnicas e práticas. FCA - Editora de Informática.

NP ISO 100006. 2006. Sistemas de Gestão da Qualidade. Linhas de orientação para a gestão da qualidade em projectos.

Project Management Institute. 2008. A Guide to Project Management Body of Knowledge (Fourth Edition).

XII DBMC
International Conference on Durability of Building Materials and Components
PORTO - PORTUGAL, April 12th-15th, 2011

Dirt Collection Extension in Buildings Façades

Pedro Vaz Paulo [1]
F. A. Branco [2]
Jorge de Brito [3]
Mário Garrido [4]

ABSTRACT

In building management there is a need for selective and updated information regarding the condition of building components, in order for the decision processes to take place adequately. This assessment is essential in planning maintenance or repair actions that may be required, either in a curative form or in a preventive attitude. The aim of this paper is to present a new methodology for the visual analysis and condition assessment of building façades. This methodology is based on the chromatic analysis of digital imaging, and provides quantitative outputs that can be used to monitor the condition of building stocks and establish laws to model the degradation processes. This methodology, placed in practice via the Photo Color application of the BuildingsLife platform, was used to quantify the extension of staining in building façades due to dirt accumulation. The Photo Color analysis requires having a digital image of the whole building façade. This implies a photographic registry of the façade, which can be performed during a building inspection. Generally it is very difficult to capture such a broad area in a single camera shot. For this reason, partial images of the façade should be taken, which can later be mounted together to produce a single image of the whole building façade. This methodology was applied over 300 façade's buildings in Lisbon - Portugal considering the dirt collection severity.

KEYWORDS

Pathology, Building façades, Dirt collection, Maintenance management, Monitoring.

[1] Instituto Superior Técnico (IST), Lisboa, PORTUGAL, ppaulo@civil.ist.utl.pt
[2] Instituto Superior Técnico (IST), Lisboa, PORTUGAL, fbranco@civil.ist.utl.pt
[3] Instituto Superior Técnico (IST), Lisboa, PORTUGAL, jb@civil.ist.utl.pt
[4] Instituto Superior Técnico (IST), Lisboa, PORTUGAL, majgarrido@gmail.com

1. INTRODUCTION

In building management there is a need to access selective and updated information regarding the condition of building components to ensure that adequate decisions are made in respect to building maintenance processes. This is an essential element in the planning of maintenance or repair actions, whether undertaking remedial activities or indeed, preventive actions. The aim of this paper is to present a new methodology for the condition assessment of building façades on the basis of visual analysis of the façade component. This methodology is based on digital imaging of façade surfaces and the subsequent chromatic analysis of the image, that provides quantitative output. Such outputs s can be used to monitor the condition of the facades of building stocks and help establish relationships that can be used to model the degradation processes. This methodology was used in practice within the Photo Color software application that forms part of the BuildingsLife platform [Paulo 2009], and was used to quantify the ee deg of staining on building façades due to the accumulation of dirt and soot on the façade surface over time.

The concept of using digital images and colorimetric properties to study the degradation processes and quantify defects in construction materials is not new. Work has been done in this area, especially in the field of stone soiling and general stone decay (Maurício et al., 2000; Grossi et al., 2003; Thornbush et al., 2004; Thornbush et al., 2008). This concept has also been used to assess the performance of stone maintenance techniques (Fort et al., 2000). One of the most interesting and elaborate uses of this concept was that presented by Lemaire et al. (2005); these authors suggested a technique to evaluate the quality of concrete surfaces using an image analysis process. In this technique, concrete surfaces were photographed and the chromatic properties of the digital image were used to quantify and grade defects or surface characteristics. The authors worked with the RGB, CIEXYZ and CIELab colour systems. This technique includes a photo correction step to account for different lighting conditions and camera characteristics, which was achieved by normalizing L* (lightness coordinate in the CIELab colour system) to correspond to that of the D65 light source; this light source is defined as "standard daylight", according to the International Commission of Lighting (CIE) (1986). The corrected images were then analyzed and measurements were made concerning lightness and defect density.

2. BUILDINGSLIFE AND THE PHOTOCOLOR TOOL

2.1 The BuildingsLife platform

BuildingsLife is a web-based platform designed to provide assistance in the management of building stocks and for research concerning the service life of building components [Paulo 2009]. The Photo Color tool is one of the platform's integrated applications, and it allows for an analysis of building façades based on their chromatic properties and corresponding evolution of chromatic properties with time.

2.2 The Photo Color method

2.2.1 Building inspection and construction of a façade image

The Photo Color analysis requires having a digital image of the entire building façade. This implies a photographic registry of the façade which can be performed during a building inspection. Generally it was very difficult to capture such a broad area of the different façades in a single camera shot. For this reason, partial images of the façade were taken, which could later be "stitched together" to produce a single image of the entire building façade. Because relative areas were to be measured during the analysis process, as explained further on, it was required that the façade image be free of perspective related distortions; otherwise, the measurements would be incorrect. To do so, an orthogonalisation of each of the images was performed. Both these procedures (photo stitching and orthogonalisation) were easily performed using available commercial image handling software. The façade image obtained was then uploaded onto the BuildingsLife platform for further analysis.

2.2.2. Lightness correction

Colour is a relative property of materials, and the way it is perceived is highly dependent on the characteristics of the observer and of the light source. The influence of the observer in the perception of colour is usually translated by a set of colour matching functions (CMF). These consist of numerical descriptions of the observer's chromatic response to a certain stimulus, and are usually known and tabled for an average human observer for the most common colour spaces. Influence of the light source is translated by a spectral power function (SPF) in which is described a distribution of the radiometric quantity per wavelength (Fairchild, 2005). These functions are also tabled and easily available for the most common light sources. For example, the International Commission of Lighting (CIE) provides, among others, the SPF for illuminant D65 which is defined by this commission as standard daylight at roughly mid-day in Western Europe and Northern Europe.

When taking pictures of building façades, it is not always easy to have exactly the same lighting conditions. For different buildings the photos may be taken at different times of day, seasons, orientations or meteorological conditions. Thus, even though the actual light source is always the sun, its light reaches the façade in many different conditions. To account for this factor, it is necessary to perform colour corrections on the digital image that, as much as possible, permit balancing the degree of illumination of the different images.

2.2.3 Photo Color analysis

2.2.3.1 Quantification methodology

The chromatic analysis of building façades with the Photo Color method is useful to quantify defects such as staining (e.g. caused by soot or dirt deposition), loss of colour of the paint coating (fading), paint chalking or contamination by fungal or algal growth. The focus in this paper will be on describing the quantification of the area of staining due to dirt accumulation. The method is based on the detection of the primary colours of which are comprised an area of the façade selected by the user. These colours are quantified in terms of their relative extension inside those areas and in terms of their coordinates in the RGB, CIEXYZ and CIELab colour spaces. This makes it possible to measure defects by selecting the colours that are associated with defects and analyzing their relative area over which they are apparent, that is their degree of "extension".

2.2.3.2 Stain quantification - Dirt collection

To illustrate the ability of using this method to analyze stains on building façades, the instance of staining caused by dirt deposition will first be considered. Dirt collection on a façade can be analyzed with respect to its degree of "extension" and the intensity of the defect with the extension "zone". Extension concerns the relative area of the façade that is affected, whereas intensity is related to the maximum concentration of dirt particles in a given part of the façade, or the degree of "blackness" that the dirt imprints on the given façade part. With these distinctions in mind, two different measurements of the dirt collection can be made using the Photo Color method - stained area and stain colour; the latter is not further explored in the present paper.



Figure 1. ID 645's original façade image and the indication of the area which will be used to illustrate the effect of introducing colour detail reductions.

The Photo Color tool then identifies the main colours that are included in the selected areas and presents them in terms of their relative area with the corresponding coordinates in the RGB, CIEXYZ and CIELab colour systems. By identifying those colours corresponding to the dirt covered zones of the façade it is possible to estimate the percentage of the façade affected by this defect. The use of such a large detail reduction (ΔRGB) for this analysis is explained by the fact that when the objective is to estimate a relative façade area, having too many colours occupying small areas identified in the analysis makes that estimation a difficult task. In Figures 1 and 2 a façade from one of the buildings under study (ID 645) is shown; the various colour detail reductions are presented to illustrate the effect of imposing this ΔRGB.



Figure 2. Illustration of the effect of introducing colour detail reductions by means of minimum ΔRGB values (ID 645).

For the first two reduction values (6.375 and 12.75) detail there are little visible changes in the image's colours. At ΔRGB=25.5 the reduction in the number of colours begins to be clearly visible, and it is even more noticeable from ΔRGB=51 onward.

The polygon drawn over the several images of Figure 2 delimitates the area that shows dirt accumulation. The image with the ΔRGB=51 detail reduction presents five different colours inside that area, which means that the quantification of the stained area could be made by calculating the relative area of each of these five colours in the façade image and adding them up. For ΔRGB values higher than 51 and up to 102 the number of colours to include in the quantification is only reduced to four. Associated with this small reduction in the number of colours is a great loss of detail in the image, and for this reason it was considered that the value of ΔRGB=51 was the most indicated for colour area measurements. In fact, this detail reduction level is high enough to visibly and sufficiently reduce the number of colours in the image to an easy to handle value, while not taking away too much of the image's detail.

2.3 Application to a building population - sample characterization

The presented methodology was used to quantify the façade area affected by dirt accumulation in 627 buildings extracted from the BuildingsLife platform's database. The platforms ability to sort the buildings according to information filters was also used, namely to breakdown the buildings studied according to whether or not they had "outstanding elements" in the façade, and according type of paint coating applied to the façade surface.

The "Outstanding Elements" information filter accounts for the presence of façade components that create sheltered zones where dirt accumulation is favoured (e.g., balconies), in contrast with façades that are fully exposed to the washing effect of driving rain. The "Paint Surface" information filter accounts for different textures in a façade's coating that may influence its degradation rate in terms of soot deposition. It is normally expected that a textured coating would accumulate dirt faster than a smooth coating. Performing this analysis while sorting the buildings studied according to their paint surface gave an indication whether this assumption was correct or was not. The breakdown of the buildings studied for each of these categories is shown in Table 1.

Table 1. Distribution of buildings studied in the performed analyses.

Study buildings (total sample)	Outstanding elements		Paint surface					
	Yes	No	Smooth, oil	Smooth, plastic	Smooth, membrane	Smooth, silicate	Textured	Undetermined
627	216	411	31	127	8	28	116	317

3. RESULTS AND DISCUSSION

3.1 Degradation graphs and degradation levels

By plotting the results from defect quantifications with data from the maintenance history for each building, one could obtain a graph that represented the evolution of the degradation process. To do so, the buildings were divided by degradation levels (DL). For each DL an average time that had elapsed since the previous maintenance action was performed was calculated based on the data from buildings that were at the same degradation level. In this manner, degradation graphs were obtained in which the vertical axis represents the degradation level and the horizontal axis contains the average time it takes for buildings to reach a specified degradation level. The line connecting the points in the graph can be defined as the degradation curve.

Six degradation levels were considered (i.e. DL0, DL1, DL2, DL3, DL4 and DL5), which represent the extension of staining by dirt accumulation in terms of the relative area of affected façade. Each DL is defined by an interval of percentages of affected area, with DL0 corresponding to the most favourable condition and DL5 to the least favourable condition. Defining the delimitation between DL's, that is selecting the range of values for affected areas at a given DL level, was achieved with the

objective of guaranteeing a balanced distribution between the DL of buildings studied and attempting to assure that the average time elapsed since the application of the render was always larger for a given DL than it was for the previous DL.

Depending on the information filter used (i.e., outstanding elements and paint surface) different DL settings were found to better adjust to the degradation curves generated in each case. This can be explained by the fact that by segregating the data according to key characteristics, different behaviours can be isolated and distinct degradation paths can be observed. In this situation it is possible that the DL setting that better adjusts to a specific dataset is not the most adequate for a different dataset; this was exactly the scenario encountered in the present study.

Taking into account the previous considerations, two sets of DL's were used. Their range of values are as presented in Table 2. Using the combinations shown in Table 2 the results obtained in an analysis of the entire sample (no information filters applied) are as presented in Table 3.

Table 2. Border values of the two DL combinations used.

	Combination I *(Outstanding elements)*	**Combination II** *(Paint surface)*
DL0	0.0% - 4.9%	0.0% - 4.9%
DL1	5.0% - 9.9%	5.0% - 14.9%
DL2	10.0% - 19.9%	15.0% - 29.9%
DL3	20.0% - 29.9%	30.0% - 59.9%
DL4	30.0% - 49.9%	60.0% - 89.9%
DL5	50.0% - 100%	90.0% - 100%

Table 3. Results without information filters using the two combinations.

Combination I								**Combination II**						
DL_i	**N_i**	**n_i**	**t_i**	**s_i**	**CV_i**	**R_i**	**R**	**N_i**	**n_i**	**t_i**	**s_i**	**CV_i**	**R_i**	**R**
0	125	20%	16.42	14.52	0.88	57		125	20%	16.42	14.52	0.88	57	
1	56	9%	17.61	13.48	0.77	52		108	17%	18.19	12.27	0.67	52	
2	104	17%	20.62	11.64	0.56	52	54.83	123	20%	22.95	13.94	0.61	55	49.67
3	71	11%	23.35	15.10	0.65	55		179	29%	27.41	15.41	0.56	59	
4	127	20%	26.26	14.99	0.57	56		85	14%	30.75	14.49	0.47	56	
5	144	23%	30.29	14.86	0.49	57		7	1%	25.14	6.96	0.28	19	
Total	627	100%						627	100%					

Where the following terminology is used: DLi - degradation level i; Ni - number of buildings that are at DLi; ni - percentage of buildings studied that are at DLi; ti - average time since last maintenance for the buildings at DLi; si - standard deviation of the results at DLi; CVi - coefficient of variation associated with DLi (ratio between si and ti); Ri - full range of the results in DLi, expressed in years since last maintenance; R - average range associated with a given combination of degradation levels.

The degradation graphs obtained in this case are shown in Figure 3. By observing the degradation graph given by Combination II it is clear that its t5 value is not adequate in relation to the other t values, since it does not fulfil the requirement of being higher than t4.

Nonetheless, given the small number of buildings found at DL5 for Combination II (only 7 buildings or 1% of the sample) it is legitimate to disregard the t5 value, since it was calculated from a subsample that is not statistically representative.

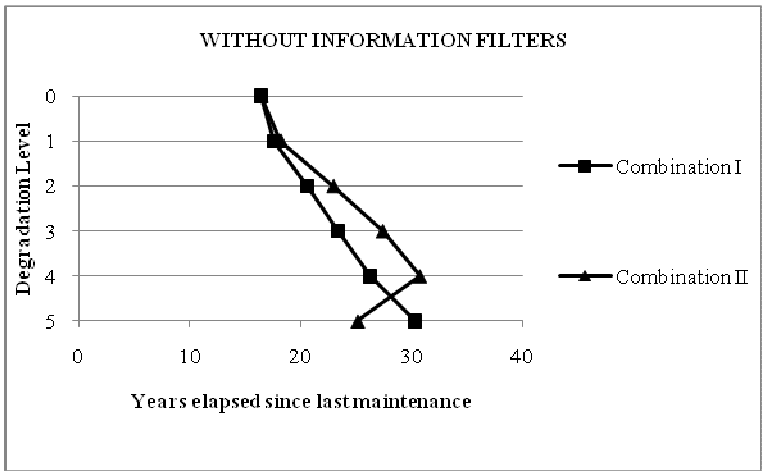

Figure 3. Degradation graphs from the two DL combinations without using information filters.

Outstanding elements

To analyze the influence of outstanding façade elements on the degradation rate associated with dirt accumulation defects, a degradation graph was produced using Combination I. The results obtained are as shown in Table 4 and Figure 4. They are divided according to whether or not the buildings have significant outstanding elements in the façade. The degradation graphs suggest the onset of degradation earlier for buildings with outstanding façade elements. This was expected since the presence of these elements creates sheltered areas that are more prone to dirt accumulation. Yet, for DL2 and forth (affected areas higher than 10%) one can observe that the degradation of buildings without outstanding elements is, on average, faster than for those with these elements. This is due to a steep descent in the degradation curve of buildings without outstanding elements, and to a reduction in the degradation rate of buildings that incorporate outstanding elements after an initial period of higher dirt accumulation localized in the sheltered façade areas.

The steep descent of the degradation curve of buildings without outstanding elements is somewhat odd. It may be due to the existence of other important factors that influence the rate with which the dirt deposition occurs. This affects the results causing a high dispersion, which is visible across the data shown here.

Table 4. Results using the Outstanding Elements information filter and the Combination I of DL's.

Outstanding elements: Yes								**Outstanding elements: No**						
DL_i	**N_i**	**n_i**	**t_i**	**s_i**	**CV_i**	**R_i**	**R**	**N_i**	**n_i**	**t_i**	**s_i**	**CV_i**	**R_i**	**R**
0	45	21%	13.18	13.14	1.00	56		80	19%	18.25	14.93	0.82	54	
1	25	12%	15.68	12.96	0.83	52		31	8%	19.16	13.68	0.71	45	
2	42	19%	21.88	11.45	0.52	39	48.50	62	15%	19.76	11.68	0.59	52	53.17
3	32	15%	27.06	15.87	0.59	53		39	9%	20.31	13.70	0.67	55	
4	51	24%	28.06	13.53	0.48	48		76	18%	25.05	15.78	0.63	56	
5	21	10%	30.95	12.78	0.41	43		123	30%	30.18	15.18	0.50	57	
Total	216	100%						411	100%					

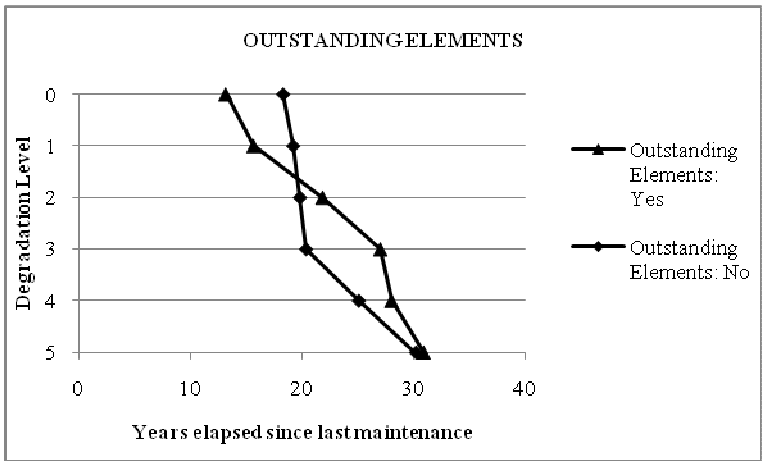

Figure 4. Degradation graphs obtained using the Outstanding Elements information filter and the Combination I of DL's.

Paint surface

To further understand the possible influence of the paint surface in respect to the accumulation of dirt on its surface and the evolution of defects with time, two degradation graphs were constructed using Combination II of the DL's. These graphs correspond to the analysis of buildings with textured coatings and to buildings with smooth plastic coatings, these being the most common types of coatings applied to buildings sampled in this study.

The results as presented in Table 5 and Figure 5.

Table 5. Results using the Paint Surface information filter and the Combination II of DL's.

PAINT SURFACE (Combination II)

Smooth, Plastic								**Textured**						
DL_i	**N_i**	**n_i**	**t_i**	**s_i**	**CV_i**	**R_i**	**R**	**N_i**	**n_i**	**t_i**	**s_i**	**CV_i**	**R_i**	**R**
0	28	22%	8.39	5.22	0.62	20		18	16%	14.33	6.73	0.47	27	
1	35	28%	17.23	10.78	0.63	45		22	19%	17.82	7.13	0.40	25	
2	27	21%	21.81	13.92	0.64	47	33.00	30	26%	19.57	7.54	0.39	27	25.6
3	25	20%	31.52	14.81	0.47	53		34	29%	18.74	6.58	0.35	26	
4	11	9%	32.64	11.07	0.34	33		12	10%	22.83	7.70	0.34	23	
5	1	1%	17.00	0.00	0.00	0		0	0%	-	-	-	-	
Total	127	100%						116	100%					

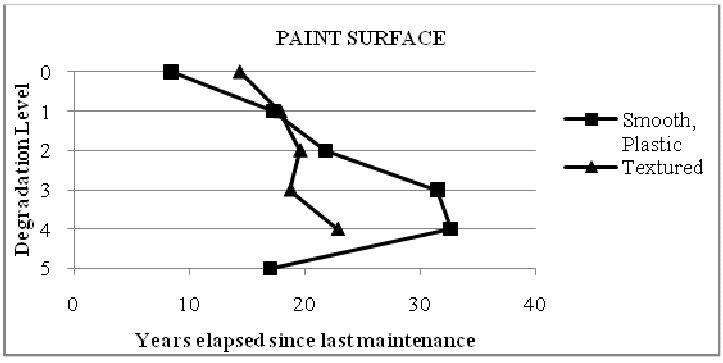

Figure 5. Degradation graphs obtained using the Paint Surface information filter and the Combination II of DL's.

4. CONCLUSIONS

The existence of salient elements (Figure 4) on the facade (e.g…..) does not allow rainwater to wash the facade leading levels of degradation (DL2, 3, 4 and 5) earlier than in buildings that do not have

salient elements on the facade. The levels of degradation DL0 and DL1 have a lack of representativeness contain levels of dirt collection zero percentage or approximately zero percentage.

Another very important factor to consider in facade dirt collection degradation is the paint surface. Looking at Figure 5, textured paints (higher roughness than smooth paint) shows accelerated degradation when compared with the smooth paint. The roughness is presented as a feature that will contribute to the retention of dirt and offer a limited washing action of rain water.

The results demonstrate that colour degradation through dirt collection is related to surface roughness and the existence of projecting elements. The deterioration of a façade related to dirt collection - colour is darker for high surface roughness and for buildings with projecting elements such as balconies (because they do not allow rainwater to circulate below the element). The best performance is shown by façades with low roughness and without projecting elements.

REFERENCES

Fairchild, M. (2005), Color Appearance Models, John Wiley and Sons, 2nd ed., pp. 55-59.

Flores-Colen, I., de Brito, J., de Freitas, V. (2008), Stains in facades' rendering - Diagnosis and maintenance techniques' classification, Construction and Building Materials, Vol. 22, No. 3, pp. 211-221.

Fort, R., Mingarro, F., López de Azcona, M.C., Rodriguez Blanco, J. (2000), Chromatic parameters as performance indicators for stone cleaning techniques, Color Research and Application, Vol. 25, No. 6, pp. 442-446.

Grossi, C. M., Esbert R. M., Díaz-Pache, F., Alonso, F. J. (2003), Soiling of building stones in urban environments, Building and Environment, Vol. 38, No. 1, pp. 147-159.

International Commission of Lighting (CIE) (1986), Colorimetry, 2nd ed., Vienna, Austria, CIE Publication.

International Standards Organization (ISO) (2007), Paints and varnishes - Evaluation of degradation of coatings - Designation of quantity and size of defects, and of intensity of uniform changes in appearance - Part 6: Assessment of degree of chalking by tape method, ISO 4628-6:2007, ISO, Geneva.

Lemaire, G., Escadeillas, G., Ringot, E. (2005), Evaluating concrete surfaces using an image analysis process, Construction and Building Materials, Vol. 19, No. 8, pp. 604-611.

Maurício, A., Figueiredo, C. (2000), Texture analysis of grey-tone images by mathematical morphology: a non-destructive tool for the quantitative assessment of stone decay, Mathematical Geology, Vol. 32, No. 5, pp. 619-642.

Paulo, Pedro Vaz (2009), A Buildings management system (Buildingslife) - application of deterministic and stochastic models with genetic algorithms to building façades, Instituto Superior Técnico, Lisbon.

Thornbush, M. J., Viles, H. A. (2004), Integrated digital photography and image processing for the quantification of colouration on soiled limestone surfaces in Oxford, England, Journal of Cultural Heritage, Vol. 5, No. 3, pp. 285-290.

Thornbush, M. J., Viles, H. A. (2008), Photographic monitoring of soiling and decay of roadside walls in central Oxford, England, Environmental Geology, Vol. 56, No. 3-4, pp. 777-787.

XII DBMC
International Conference on Durability of Building Materials and Components
PORTO - PORTUGAL, April 12th-15th, 2011

Methodology of a New Building Diagnostic System

Attila Koppány [1]

ABSTRACT

The diagnostic system described in this paper is primarily based on in-situ visual examination, its method is suitable for the examination of almost all important structures and structural changes of buildings. While using the diagnostic system a large amount of data – valuable for the professional practice – was collected and will be collected in the future, the analysis of this dataset is especially suitable for revaluing construction and the practical application of the experiences later during building maintenance and reconstruction work. A so-called "morphological box" has been created, that contains the hierarchical system of constructions, linking with the construction components' thesaurus appointed by the correct structure codes of these constructions' place in the hierarchy. The thesaurus was not only necessary because of the easy surveillance of the system, but in the interest of unified data handling, to exclude the usage of structure-name synonyms. Our system uses a hexagonal morphological box as a tool for the quick review of the results of the visual examination; showing the actual checked constructions or all constructions of the building. The various conditions of the building constructions can be marked with corresponding colours in the box-field. The analysis of which dataset is suitable for revaluing previously built constructions and can help to create knowledge-based new constructions for the future.

KEYWORDS

Building diagnostic, Morphological box, Thesaurus of components.

[1] Széchenyi István University (SZE), Győr, HUNGARY, koppany@sze.hu

1. INTRODUCTION

It is important, that people in architectural science provide a useful guide – especially concerning questions raised by new trends of the changing, transforming building activities and construction development – to the profession practice. The appearance of new constructions and building materials always raises new problems to be solved, and the experts in practice, busy with the daily tasks of the profession according to Möller [1945], 'cannot always pay enough attention to them'. An efficient diagnostic activity plays a very important part in the formation of maintenance costs and elimination of damage. It has a just as important part in the preparation of a decision, as having a clear picture of the technological conditions of buildings or group of buildings can be of service at the preparation before making financial decisions of great significance.

2. DIAGNOSTIC SYSTEM

A faulty diagnosis can lead to incorrect decisions causing financial loss. The research group of the Széchenyi István University (Győr) worked out a comprehensive diagnostic system (see Fig. 1.) which contains a common inspection method according to Molnárka [2000] for the vast majority of construction components (for traditional and currently used constructions in Hungary), and can be used for computer data registration and analysis.

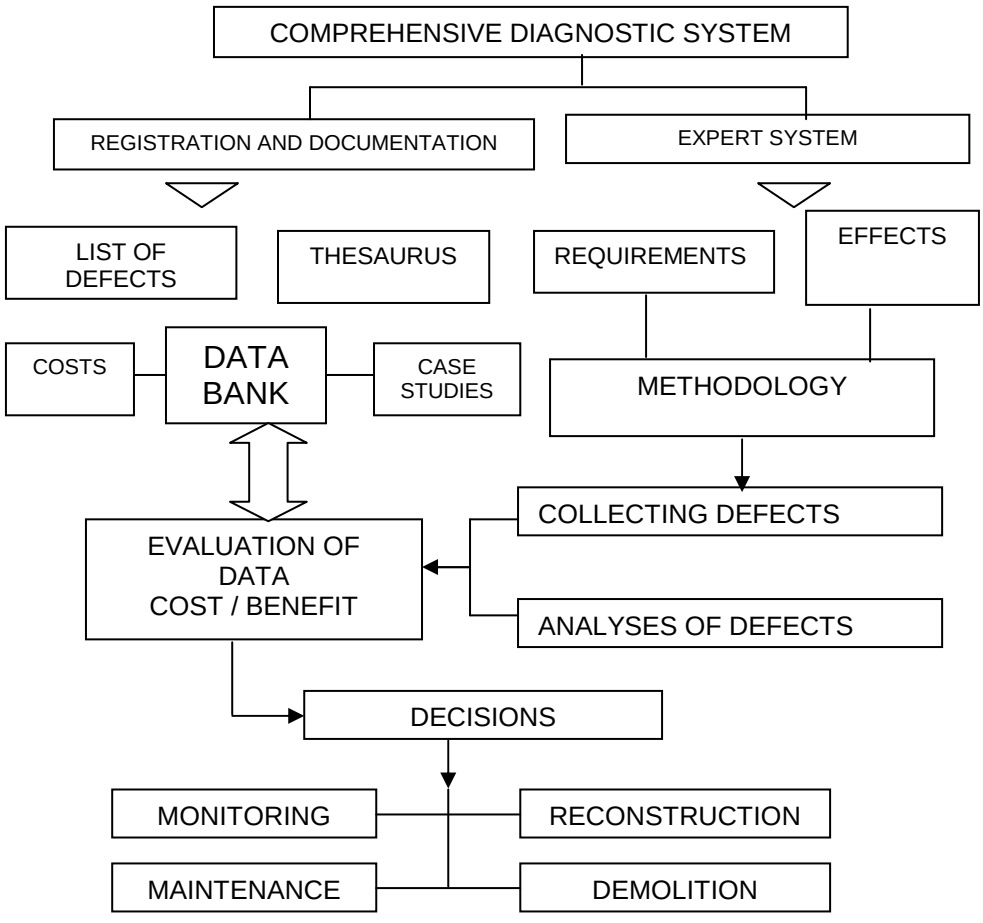

Figure 1. Main algorithm of the diagnostic system

The morphological box [Zwicky 1966] is connected with the construction components' thesaurus denoted by the correct structure codes of these constructions' place in the hierarchy. The theory of using morphological box for data registration in the process of building diagnostic was published in

Hungary [Koppány 1977]. The "matrix" construction of our morphological box fits to the methodology of the visual examination and to the hierarchy of the common building constructions in Hungary [Koppány 2002] (see Table 1).

Table 1. The construction-hierarchy in the morphological box (Koppány 2002).

MAIN CONSTRUCTIONS	CONSTRUCTIONS AND THEIR SUPPLEMENTARY CONSTRUCTIONS			
CODE ⇒ A.	A.X	A.0X	A.00X	A.00X
1. FOUNDATIONS	1.1 Shallow foundations 1.2 Deep foundations		1.001 Insulations against ground-water	
2. VERTICAL LOAD BEARING CONSTRUCTIONS, NON LOAD BEARING CONSTRUCTIONS AND THEIR SUPPLEMENTARY STRUCTURES	2.1 Load bearing walls 2.2 Frames	2.01 Non load bearing walls 2.02 Partition walls 2.03 Doors and windows in internal walls	2.001 Wall-insulations 2.002 Plasters on facades 2.003 Plasters inside 2.004 Claddings inside	2.0001 Grates, balustrades, parapets
3. HORIZONTAL LOAD BEARING CONSTRUCTIONS, NON LOAD BEARING CONSTRUCTIONS AND THEIR SUPPLEMENTARY STRUCTURES	3.1 Ring beams 3.2 Arches, lintels 3.3 Floors, vaults	3.01 Suspended ceilings	3.001 Water-proofings to floors 3.002 Floorings	
4. STAIRCASES, BALCONIES, OPEN CORRIDORS, LOFTS AND THEIR SUPPLEMENTARY STRUCTURES	4.1 Staircases 4.2 Balconies, open corridors,lofts		4.001 Stair-tread covering 4.002 Balconies flooring 4.003 Open corridors flooring 4.004 Lofts flooring	4.0001 Balustrades, parapets, handrails to stairs 4.0002 Balustrades, parapets, handrails to balconies 4.0003 Balustrades, parapets, handrails to open corridors 4.0004 Balustrades, parapets, handrails to lofts
5. ROOFS, ROOF ACCESSORIES, CHIMNEIS, VENTILATION	5.1 Pitched roofs 5.2 Flat roofs 5.3 Roof superstructures 5.4 Chimneis 5.5 Air shafts 5.6 Vent pipes	5.01 Roofings	5.001 Water-proofing 5.002 Thermal insulation 5.003 Vapour-proofing 5.004 Flat roofs tiles and other functional layers 5.005 Roof edges and joining accessories	5.0001 Roof accessories
6. FACADES		6.01 Skirting board	6.001 Surfacings	6.0001 Grates, balustrades, parapets on the facades

The main strength of our thesaurus (graphic-version) is to help the visual survey. It can be very useful to understand the hierarchy and the connections in the field of building constructions (see Fig. 2.). The thesaurus is not only necessary to facilitate surveillance of the system, but to exclude the usage of structure-name synonyms in the interest of unified handling. We have another tool for the quick survey of the results of the visual examination; it is the hexagonal morphological box. The box shows the actual checked constructions or all constructions of the building. The various conditions of the building constructions can be marked with corresponding colours in the box-fields.

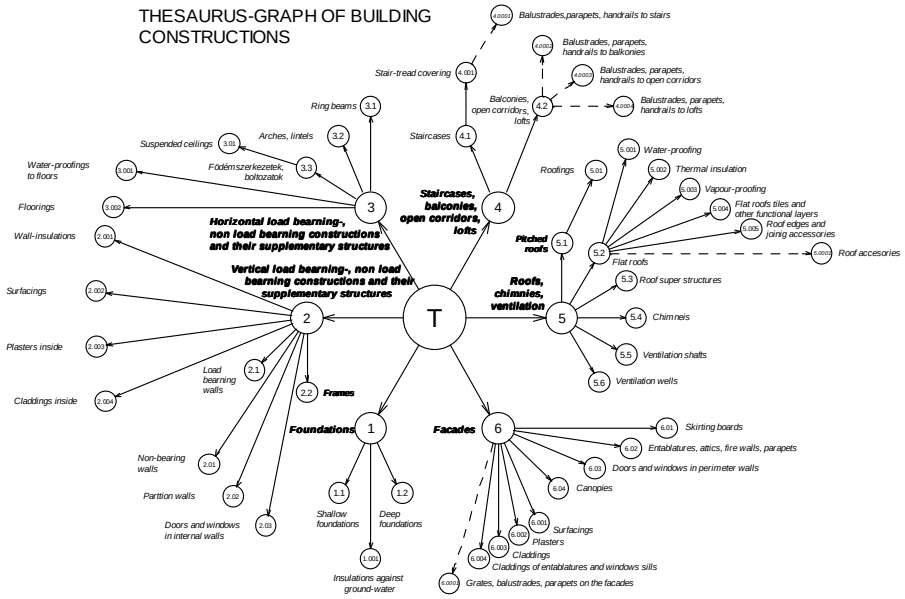

Figure 2. The thesaurus-graph with the main groups of building constructions.



Figure 3. The hexagonal morphological box shows the hierarchy of building constructions.

The results of an examination are shown in Figs. 4 through 7. The diagnostic system has been successfully checked in the course of an examination involving 60 buildings.

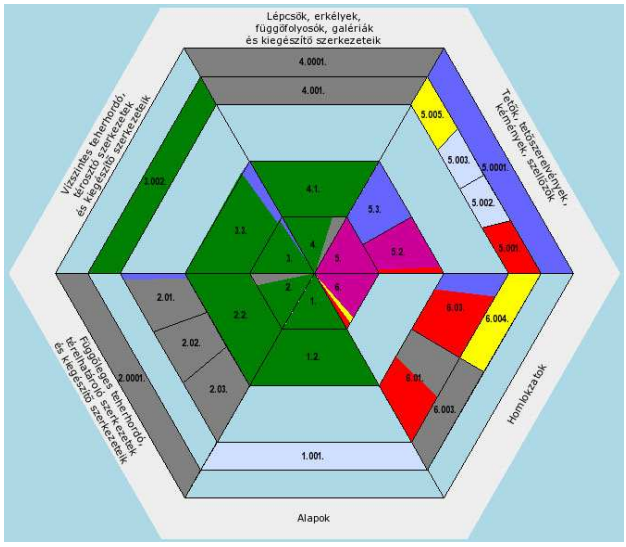

Figure 4. Conditions of constructions can be marked with corresponding colours.

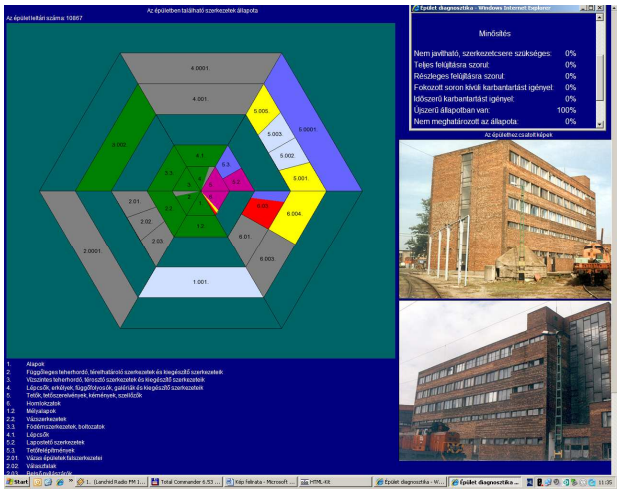

Figure 5. Conditions of constructions can be marked with corresponding colours.

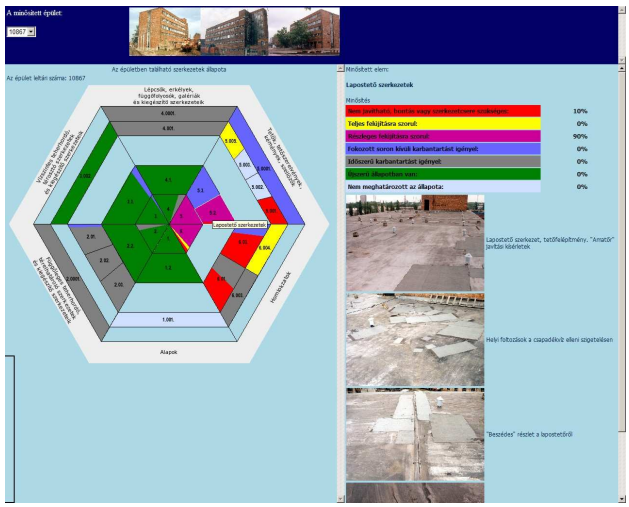

Figure 6. Condition of flat roof detals.

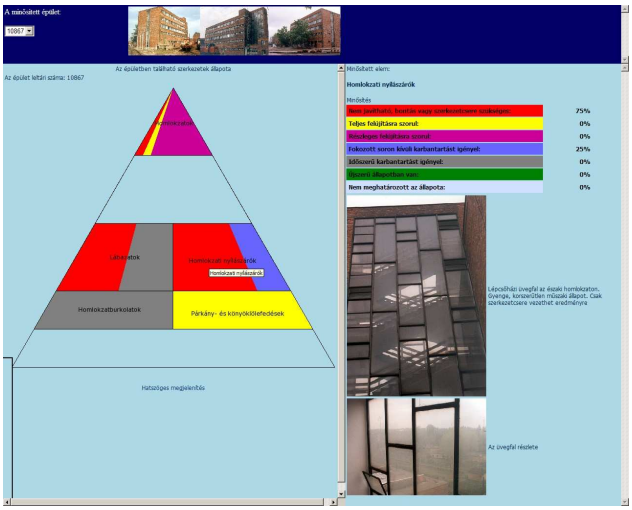

Figure 7. Qualification of the façade-details with a part of the hexagonal morphological box.

3. EXPERIENCES OF FLAT ROOFS EXAMINATION

The majority of the defects forming on *the flat roof water-proofing and heat insulation* can be observed on the conventional insulated roof. From the point of view of the protection of substance and providing of the proper application of the building it is very important to explore and professionally repair the failures as soon as possible. In order to keep costs relatively low, it is very important to explore and repair failures in the early stages as considerably more repair expenditure can be expected as damage becomes more extensive. It should be noted for example, that the waterproofing should be checked by experts at least yearly to prevent several extended and expensive damages. The typical failures of the roof can be systematised according to various points of view. The analysis can be performed by the layers of the roof construction (insulation and water-proofing) or according to the contribution to the creation of the roof insulation (e.g. material manufacturing, planning, execution, operation), but it can also be carried out according the so called weak points, details of the structural nodes.

Before introducing the diagnostic procedures and testing methods applied for the flat roof construction it is reasonable to determine some principles in connection with the examinations as follows:

- the examination must not inhibit the proper use of the building;
- the examination should be quickly performable with easily used tools;
- during the whole process of the examination, the least possible damage should occur to the waterproofing; and
- if destructive examination is unavoidable, it should cover the least possible area and the sampling location should be immediately repaired and made waterproof.

The diagnostic work can consist of several phases - which are important from the end point of view. At first before the on-site examination, it is reasonable to gather basic data on the structures and conditions of the building to be examined. In case of an old roof, this step is not always possible since the plans and other documents could be lost and/or cannot be reconstructed. In a significant number of the cases, the structural character, layer construction, the materials and technologies used will be identified during the on-site examination.

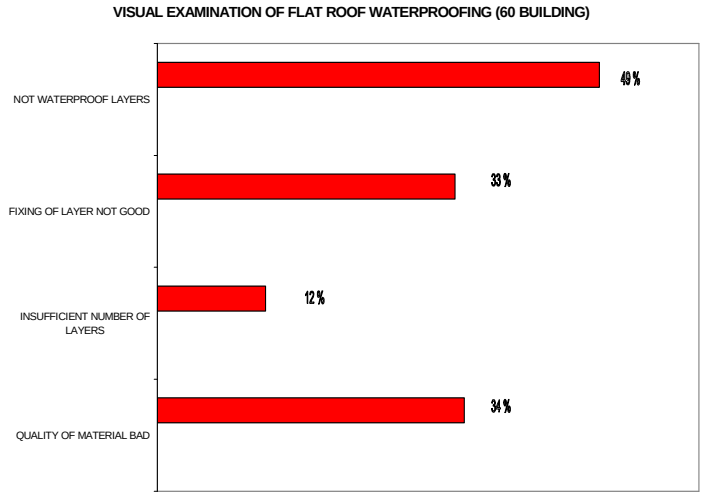

Figure 8. Results of a visual examination of flat roofs.

During the visual examination, failures should be documented and analyzed. During the visual examination, the identification of the place of leak for large discontinuities (damages) on the waterproofing layer is generally of no difficulty. In case of quick examination, the condition of the roof waterproofing is determined with visual examination, completed with a non-destructive instrumental measurement if necessary (see Fig. 8).

Comprehensive examinations procedures cover all structural and complementary elements of the roof. The condition, load capacity, deformation of the roof deck should be examined, and the physical properties of the deck structure, etc. should be evaluated.

There is a lot of interesting data from the examination of 60 flat roof constructions. Figure 9. shows the frequency of typical defects on the examined flat roofs. The greatest number of defects were in the expansion joints area, nearly fifty percentage. The average age of the examined roofs was 20 years. The roofs of the older industrial buildings had the worst condition, most being in bad repair.

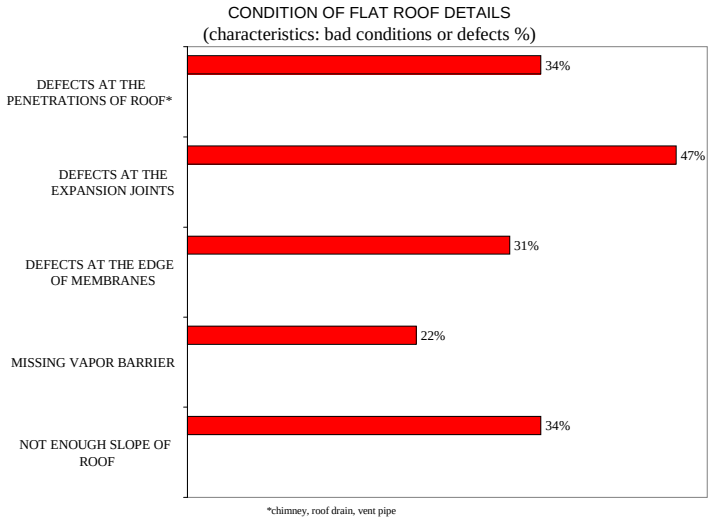

Figure 9. Results of the examination of flat roof details.

So in order to determine the condition, and eventually assure the maintenance of the safety and durability of the flat roof (waterproofing and insulation) all significant factors should be examined even with a destructive examination if necessary. It can happen that the diagnostics are started within the framework of a quick visual examination but develops into a complex examination to determine exactly the causes of the abnormalities and observed defects.

4. CONCLUSION

This paper reports on the development and structure of a field based survey methodology by the research group at the Széchenyi István University. The system, providing a set of practical diagnostic decision support tools, was developed for one of the biggest building holder-operator organisations in Hungary. The diagnostic system is primarily based on in-situ visual examination.

An important basic requirement for this system was the visual display of the results of the examinations. The tools of system were expected to be able to show the general conditions of the buildings as well as the condition of selected constructions. In the process of visual examination, experts acquire a large amount of data. To effectively handle and use the data, the research group of the university created a registration subsystem with the following tools:

- a morphological box for building constructions; and
- a thesaurus of building construction (providing linkages to the morphological box).

The morphological box was not previously used as a diagnostic tool in Hungary. The first testing this tool was successfull and our client, the building holder-operator, has installed this tool in their data registration subsystem.

Using these tools, experts can survey the connections of the examined constructions and can also use a clear visual survey of the different durability of the existing constructions. Some details from the results of the visual examination of 60 different flat roofs can illustrate the efficiency the new subsystem.

The overall objective was that the results of the construction diagnostics and the experiences of the pathologic analyses would facilitate the work of experts using our registration subsystem. The practical diagnostic decision support tool can help with the selection of appropriate corrective maintenance procedures, to remedy, the real causes of the failure.

REFERENCES

Möller, K.1945, *Építési hibák és elkerülésük. (Building defects and prevention of defects)*, Egyetemi Nyomda, Budapest, pp.32.

Molnárka, G.2000, *The methodology in visual examination in building pathology*. Hungarian Electronic Journal of Science, 2000. (www.sze.hu) pp. 10.

Zwicky, F. 1966, Entdecken, *Erfinden, Forschen im Morphologischen Weltbild*, Droemer/Knaur, München/Zürich pp. 174.

Koppány, A. 1997, *Épületszerkezetek morfológiai rendszere.(Morphological System of Building Constructions)*, Research Working Paper, p.40, SZIF, Győr.

Koppány, A. 2002, Building Diagnostics. *Construction and City Related Sustainability Indicators (CRISP). EU 5. Framework.* CRISP Working Committee Conference, Budapest. ÉMI. p. 8 (summary on: http://crisp.cstb.fr /Database-Hungary).

XII DBMC
International Conference on Durability of Building Materials and Components
PORTO - PORTUGAL, April 12th-15th, 2011

Plastering and Rendering Mortars Incorporating Regranulated of Expanded Cork to Improve Durability

Miguel Martins [1]
Lina Nunes [2]
Fernando Branco [3]

ABSTRACT

Plastering and rendering mortars anomalies are frequently associated to cracks, leakages, fungi colonization, etc. Frequently, these anomalies are related to the presence of moisture or lack of ventilation and thermal insulation from these materials. To try to reduce these problems and to improve the properties of the plastering and rendering mortars, a new material was tested that is mortars incorporating regranulated of expanded cork (REC), a sub-product of the cork industry. The objective of this work was to obtain mortars with better thermal insulation, reducing the condensation problems in walls. Results of the experimental tests conducted are presented for the evaluation of properties of the new material. The material proved to be a promising solution in relation to the classical cement mortar and can be applied to rehabilitate similar types of plastering mortars.

KEYWORDS

Plastering mortars; Rendering mortars; Regranulated of expanded cork; Durability; Thermal conductivity.

[1] Univ Tecn Lisbon, Inst Super Tecn, DECivil, P-1049-001 Lisbon, PORTUGAL, miguel.fsm@gmail.com
[2] LNEC, Structures Department, P-1700-066 Lisbon, PORTUGAL, linanunes@lnec.pt
[3] Univ Tecn Lisbon, Inst Super Tecn, DECivil, P-1049-001 Lisbon, PORTUGAL, fbranco@civil.ist.utl.pt

1 INTRODUCTION

Plasters must provide, in general, the wall surface regularity, while at the same time there is security against risks of fire, resistance to actions of shock and water tightness. In exterior walls can still be other requirements, due to greater exposure that these plasters are exposed to [LNEC 2000].

The problems in rendering and plastering mortars are increasingly common. These problems can be caused by poor ventilation, poor maintenance and inadequate thermal behavior of used materials. Thus, anomalies like humidity stains, cracks and fungi develoment may restrict the performance of mortars.

This situation requires solutions that can be achieved by reducing the thermal conductivity improving the durability of plastering mortars thus increasing their service life. To reduce the thermal conductivity of mortars, sand can be replaced by other kind of aggregates, such as in the present case, regranulated of expanded cork (REC). This renewable material, 100% natural, has been used regularly as a thermal, accoustic and anti-vibratic insulation material.

The replacement of traditional rock aggregates for other types of aggregates is common in mortars/concrete filling, although it does not happen for plastering mortars [Marques, 2008; Hernández-Olivares et al., 1999]. Thus, this study aims to determine the actual impact of such substitution, analyzing the advantages in thermal conductivity and other properties that determine the durability of plasters. To achieve these objectives, the mortars were tested for flexural and compressive strength, for water absorption by capillary action, for water absorption under low pressure, for water absorption by immersion, for drying after immersion, for adhesion of painted mortars, for fungal resistance and finally, the thermal performance. In the fresh mortar, with the purpose of determining the amount of water to be added to each mortar, tests of consistency were also conducted.

In this study, mortars were produced (50% hydraulic lime + 50% cement) using various replacement rates (0, 20, 40, 60, 80 and 100%) of sand by REC, at three different particle sizes.

2 EXPERIMENTAL PROGRAM

2.1 Materials

For the laboratory work fine river sand and REC, provided by Unibetão, S.A. and Sofalca, Lda. Respectively, were used. Three different sizes of REC were used, in particular, cork powder (R3), with very small particles (<0.250 mm), and two particle sizes (R1 and R2). Cement CEM II / BL 32,5 N and hydraulic lime NHL5, were both supplied by SECIL.

Analysis of the minimum dimensions (Dmin) and maximum dimensions (Dmax) of all aggregates revealed that the aggregate sizes of REC used are quite distinct from the sand (Table 1).

Table 1 – Minimum and maximum dimensions of the aggregates.

	Aggregates			
	Sand	**R1**	**R2**	**R3**
D_{min} [mm]	0,125	1,0	0,500	-
D_{max} [mm]	1,0	4,0	8,0	0,250

Therefore, with the exception of cork powder (R3), REC has a bigger particle size than the sand. There are also some important differences between the regranulated R1 and R2, because the R1 has a particle size variation less extensive than the R2.

2.2 Mortars

In total, eight different mortars were produced. The mortars have all the same binder-aggregate volumetric ratio, B/Ag, (0,5:0,5:3, hydraulic and cement mortars), as well as an equal consistency. Several mixtures of aggregates were used to produce the mortars for the proposed objectives. The relative volume of each aggregate, for each mortar, in the set of aggregates is indicated in Table 2.

Table 2 - Relative volume of each aggregate in hydraulic lime and cement mortars.

Mortar	**% of each aggregate in the set of aggregates**			
	Sand	**R1**	**R2**	**R3**
100A	100%	-	-	-
60A+R1	60%	40%	-	-
60A+R2	60%	-	40%	-
40A+R1	40%	60%	-	-
40A+R2	40%	-	60%	-
20A+40R1+40R3	20%	40%	-	40%
20A+40R2+40R3	20%	-	40%	40%
30R1+70R3	-	30%	-	70%

In order to produce mortars with equal consistence, tests were performed according to EN 1015-3 (1999). The results of this test are presented in Table 3.

Table 3 – Consistence and W/B adopted for each hydraulic lime and cement mortar.

	100A	**60A+R1**	**60A+R2**	**40A+R1**	**40A+R2**	**20A+40R1+40R3**	**20A+40R2+40R3**	**30A+70R3**
W/B	0,79	0,65	0,65	0,62	0,63	0,85	0,94	1,16
Consistence	65,7%	62,4%	63,5%	67,8%	64,8%	63,2%	66,2%	67,1%

With the presented results, it can be noted that in relation to the reference mortar, with the introduction of regranulated R1 and R2 the water required is lower. However, this situation does not occur when using R3 together with R1 or R2. This is due to high water absorption which characterizes the cork powder (R3) or others REC with a small grain size.

3 EXPERIMENTAL RESULTS

3.1 Compressive and flexural strength

The compressive and flexural strength tests were performed using the procedure described in EN 1015-11 (1999). These tests aimed to check whether the mortars produced have minimum values of mechanical strength. For this reason, it was considered sufficient to analyze the samples for 14 days instead of the usual 28 days. Figure 1 presents the test results of compressive strength of mortars produced.

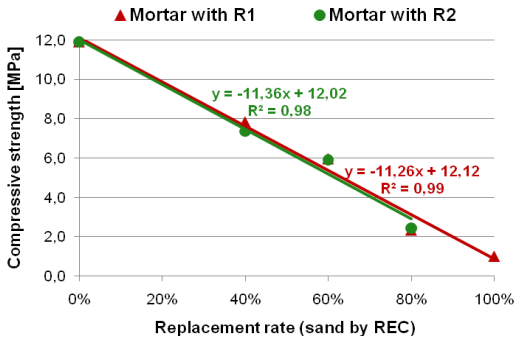

Figure 1. – Compressive strength of mortars with REC.

With these data, it is observed that with the introduction of REC the compressive strength decrease is approximately linear. It is also clear that in the compressive strength, the performance of mortars with R1 and R2 is similar. It should also be noted that the value considered as the minimum limit (0.4 MPa, according to EN 998-1: 2003), though almost reached at the maximum replacement rate, was never crossed. Figure 2 presents the values of flexural strength of the mortars with REC.

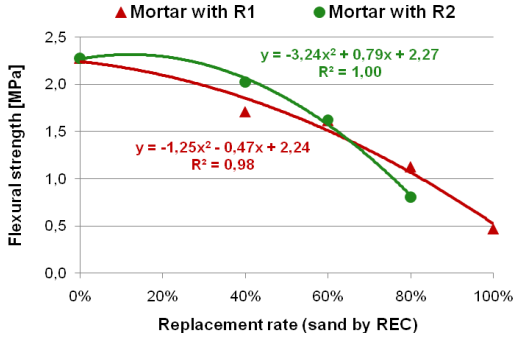

Figure 2. – Flexural strength of mortars with REC.

On flexural strength, mortars with REC don't have a loss of performance as pronounced as in compression. Some important differences between the mortars with R1 and R2 were also identified. This may be attributed to the microstructure that is created between the binder and aggregates.

3.2 Water absorption by capillary action

The test of water absorption by capillary action was performed according to specification LNEC E 393 (1993). Figure 3 present the results of water absorption by capillary action in mortars.

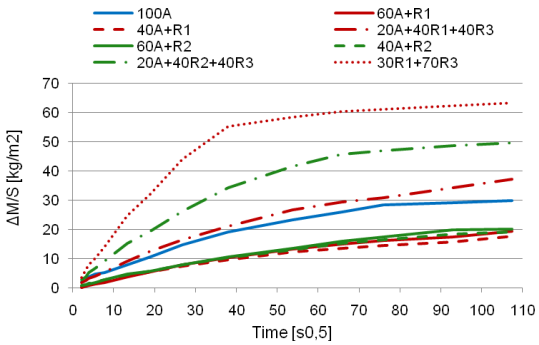

Figure 3. - Water absorption by capillary action in mortars.

These results show that the initial rate of water absorption by capillarity decreases when replacing sand by (only) R1 or R2. However, when the mortars has also R3 (cork powder) this effect is opposite and the water absorption increases.

3.3 Water absorption under low pressure

The results of water absorption under low pressure tests are shown in Figure 4.

In these mortars, the REC causes significant changes in the rate of absorption. And, as happened in the absorption test by capillary action, with the use of R3 absorption increases, while with (only) R1 or R2 absorption decreased significantly.

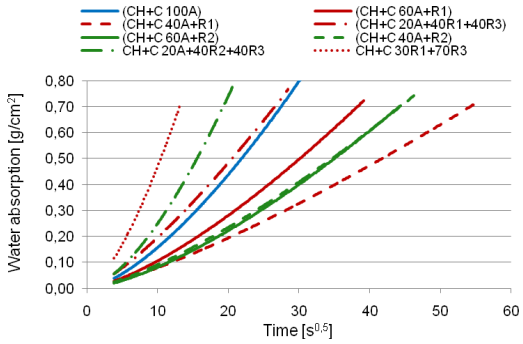

Figure 4. – Water absorption under low pressure in mortars.

3.4 Water absorption by immersion

The test of water absorption by immersion was performed according to specification LNEC E 394 (1993). Figure 5 has the results for the tests of mortars.

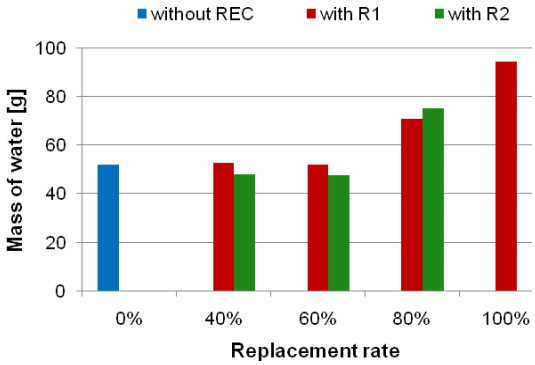

Figure 5. – Water absorption by immersion in mortars.

The hydraulic lime and cement mortars, there are only significant changes in the absorption of water by immersion if the mortar has R3 (cork powder).

3.5 Drying after immersion

The results of drying after immersion tests are shown in Figure 6.

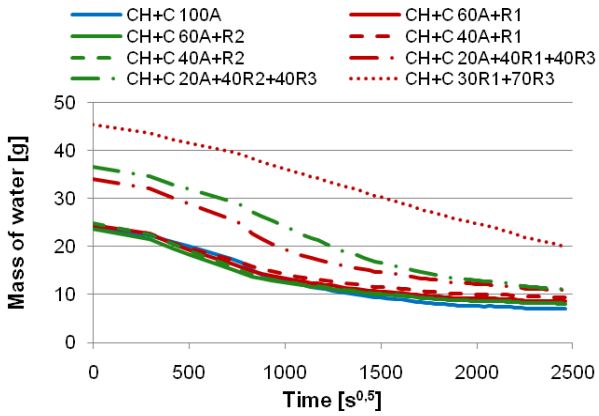

Figure 6. - Results of drying tests.

These data indicate that the mortars with REC, at the end of the test, present a greater quantity of water than the control mortars, though with one exception, they will all reach similar water contents after drying for 2500h.

3.6 Adhesion of painted mortars

The pull-off test in painted mortars was performed according to specification ISO 4624 (2002). Figure 7 shows the results of the adhesion in painted hydraulic lime and cement mortars.

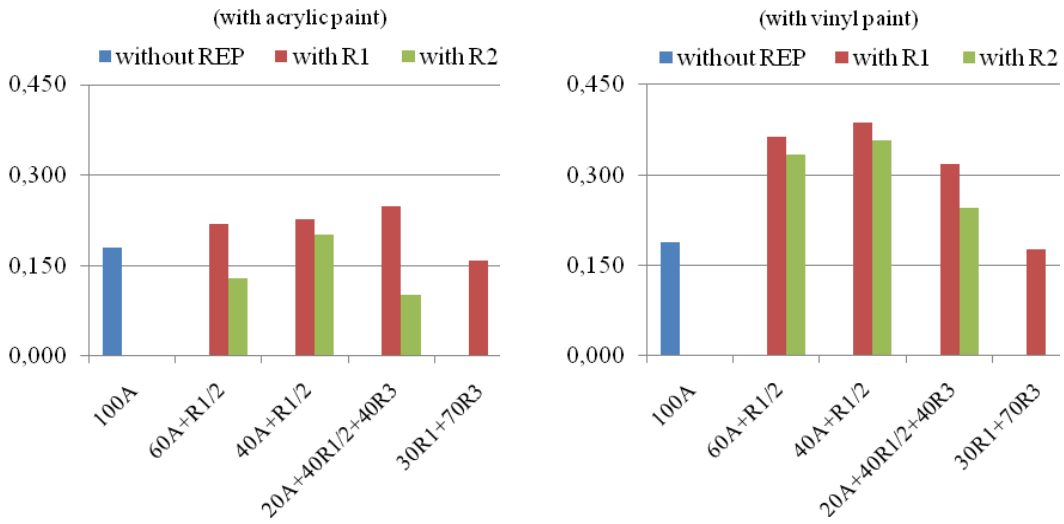

Figure 7. - Pull-off strength of mortars [MPa].

The adhesion of the coating of paint at mortar is lower when using R2 (compared to R1). We can also see that the pullout strength of hydraulic lime and cement mortars not decreases strongly. In some samples (with lower replacement rates) there was even an increase in pullout strength.

3.7 Fungal resistance

The fungal resistance test was performed according to an adaptation of ASTM D 5590-00. The average results of this test are shown in Figure 8.

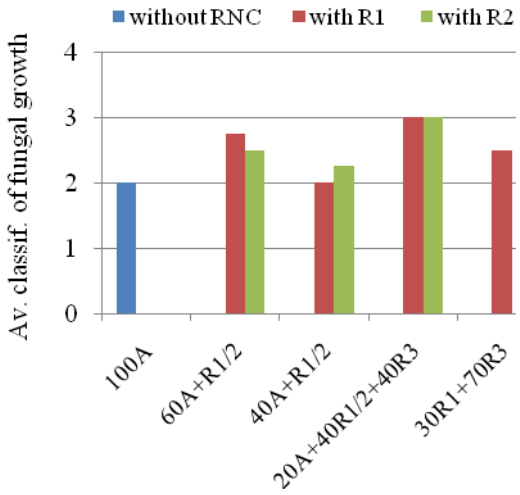

Figure 8. – Average classification of fungal growth.

In the test mortars, the level of fungal growth at the end of four weeks remains close to that of the control mortar, even at replacement rates of 40%, 60% and 100%. For the replacement rate of 80%, the mortars have higher fungal growth than the control mortar.

3.8 Thermal conductivity

The thermal conductivity test was performed according to EN 12664 (2001) and the summary results are presented in Table 4.

Table 4 – Thermal conductivity of mortars with REC and other construction materials.

Materials	Specific Weight [kg/m3]	λ [W/m.ºC]
Hydraulic lime mortars (*)	1600	0,800
Mortar "40A+R1"	1238	0,444
Mortar "40A+R2"	1199	0,357
Mortar "20A+40R1+40R3"	919	0,221
Mortar "20A+40R2+40R3"	846	0,198
Mortar "30R1+70R3"	581	0,108
Agglomerate of expanded cork (*)	90 - 140	0,045

(*) – reference values [Santos e Matias, 2006]

These results show that mortars with REC have a thermal conductivity with low values. It is also concluded that the use of R2 compared with R1, enables better thermal performance.

Finally, the analysis of the values of thermal conductivity shows that the mortars have produced a behavior much more satisfactory than conventional mortars.

4 CONCLUSIONS

This study aimed to examine the potential benefits of the use of mortars with REC, a highly sustainable material, when compared to traditional mortars, also studying the potential problems of using this type of material along its service life. Thus, the following conclusions can be highlighted:

- The mortars with REC have lower strength, although the minimum requirements are met;

- The layer of plaster with REC is a good support for finishing with paint;
- The use of REC in mortar facilitates the long term absorption of water. However, the mortars with thicker REC particles absorbs water at a rate lower than the sand, while with the thin REC particles absorbs water at a higher speed;
- The existence of REC in the mortars did not cause (necessarily) a worse behavior of these mortars in a situation of colonization by fungi;
- The mortars with REC have a very satisfactory thermal performance. This characteristic can enhance the durability of these materials, as the occurrence of surface condensation can be reduced;
- The use of mortars with REC can bring more problems in plastering than rendering, given the tendency of these materials to retain more water than control mortars.

REFERENCES

ASTM 5590-00 (2000) Determining the Resistance of Paint Films and Related Coatings to Fungal Defacement by Accelerated Four-Week Agar Plate Assay. ASTM International, Pennsylvania, USA.

Hernández-Olivares, F., Bollati, M. R., Rio, M. e Parga-Landa, B. (1999) Development of cork gypsum composites for building applications. *Const. and Building Materials*, 13 (1999), pp. 179-186.

EN 1015-3-11 (1999) Methods of test for mortar for masonry. Part 3: Determination of consistence of fresh mortar (by flow table). Part 11: Determination of flexural and compressive strength of hardened mortar.Instituto Português da Qualidade, Lisboa.

EN 12664 (2001) Thermal performance of building materials and products. Determination of thermal resistance by means of guarded hot plate and heat flow meter methods. Dry and moist products of medium and low thermal resistance. Instituto Português da Qualidade, Lisboa.

IPQ (1999) – NP EN 933-2:1999 – Ensaios para determinação das características geométricas dos agregados. Parte 2: Determinação da distribuição granulométrica. Peneiros de ensaio, dimensão nominal das aberturas. Instituto Português da Qualidade, Lisboa.

ISO 4624 (2002) Paints and varnishes – Pull-off test for adhesion. ISO – International Organization for Standardization, Geneva.

LNEC (1993) E 393 - Determinação da absorção de água por capilaridade. E – 394 - Determinação da absorção de água por imersão. Ensaio à pressão atmosférica. LNEC, Lisboa.

LNEC (2000) Curso de especialização sobre revestimentos de paredes – 1º Módulo. 4ª Edição. Laboratório Nacional de Engenharia Civil, Lisboa.

Marques, J. (2008) *Caracterização de Betões Leves de Regranulado de Cortiça*. Tese de Mestrado em Engenharia Civil, Instituto Superior Técnico, pp. 5-63.

RILEM (1980) Water Absorption Under Low Pressure. Pipe Method. Test Nº 4 II.4., Recommendations Provisoires. Réunion Internationale des Laboratoires et Experts des Matériaux, Paris.

Santos, C. e Matias, L. (2006) Coeficientes de Transmissão Térmica de Elementos da Envolvente dos Edifícios, Versão Actualizada 2006. ITE 50. LNEC, Lisboa.

XII DBMC
International Conference on Durability of Building Materials and Components
PORTO - PORTUGAL, April 12th-15th, 2011

Impact of Sulphate Exposure on Blended Cements

David William Law [1]
Emilie La Rosa [2]

ABSTRACT

While concrete structures will normally provide long service life, certain problems are associated with these types of materials. One area of major concern is degradation of concrete structures due to sulphate attack. This form of degradation of the concrete occurs due to selective attack of specific constituents within the cement structure. In determining the life expectancy of these structures, developing laboratory investigations simulating the deterioration process can be quite challenging. First, the determination of the level of sulphate concentration requires careful analysis. Secondly, the development and calibration of an accelerated testing method is required to measure deterioration in the laboratory within a reasonable time period. The research work presented here covers the development of a method for accelerated testing of concrete exposed to sulphate attack. Specimens were immersed in three solutions, 500, 5000 and 50000 ppm Sodium and Magnesium Suphate. Investigations have been conducted over approximately a 18 month period to date. Susceptibility to sulphate attack was monitored using weight change (discontinuous gravimetric) measurements as a function of time, as well as elongation m,easurements, on the immersed samples. In addition the strength of the concrete was monitored at fixed intervals.

KEYWORDS

Sulphate, Concrete, Durability.

[1] School of the Built Environment, Heriot Watt University, Edinburgh, EH14 2LF, UK, d.w.law@hw.ac.uk
[2] Faculty of Engineering, University of Lyon 2,69007 Lyon FRANCE, emilie.la-rosa@wanadoo.fr

1 INTRODUCTION

Deterioration of concrete due to sulphate attack is a major durability problem for structures exposed to sulphate ions, either from soil and groundwater or in sewage systems, such as septic tanks, sewage pipes and water treatment plants. Under continuous exposure to a sulphate-rich environment, concrete loses its strength and durability resulting in a reduction of the specified service life. Sulphate attack is the term used to describe a series of chemical reactions between sulphate ions and the components of hardened concrete, principally the cement paste, caused by exposure of concrete to sulphates, oxygen and moisture [Skalny, 2002].

The sulphates react with the tricalcium aluminate ($3CaO.Al_2O_3$, also known as C_3A) in the hardened concrete cement paste and forms calcium sulfoaluminate; expansion occurs, disrupting the paste [Neville, 1996]. The primary products of the chemical sulphate attack in concrete are ettringite and gypsum due to the chemical reaction between sulphate solutions and the cement hydration products. Sodium sulphate reacts with calcium hydroxide to form calcium sulphate known better as gypsum according to the equation 1.1. Depending on the surrounding environmental conditions these reactions proceed to a greater or lesser extent. In flowing water conditions with constant supply of sulphate ions which also ensures removal of calcium hydroxide, the reactions may continue until leaching of all calcium hydroxides. On the other hand in a steady environment with the presence of a fixed amount of sulphate the reaction may reach an equilibrium position. According to Tian and Cohen gypsum formation is expansive in nature and the tensile stresses during gypsum formation may be the cause of expansion and the subsequent cracking [Tian and Cohen, 2000].

Calcium sulphate or gypsum can subsequently react with hydrated calcium aluminates ($4CaO\ Al_2O_3\ 13H_2O$), hydrated calcium sulfoaluminates ($4CaO\ Al_2O_3\ SO_3\ 12\text{-}18H_2O$) or unhydrated tricalcium aluminate (C_3A) to produce ettringite ($3CaO.Al_2O.3CaSO_4.32H_2O$) according to the equation 1.2. According to the published literature ettringite is said to be expansive in nature, though the expansion mechanism is not fully understood yet [Mehta, 1983].

$$Ca(OH)_2 + Na_2SO_4 + 2H_2O \longrightarrow CaSO_4.2H_2O + 2NaOH \quad (1.1)$$

$$4CaO.Al_2O_3.13H_2O + 3CaSO_4.2H_2O + 14H_2O \longrightarrow 3CaO.Al_2O_3.3Ca_2SO_4.32NaOH \quad (1.2)$$

The secondary effect of chemical sulphate attack is the decalcification of C-S-H gel and loss of cementitious structures of concrete which begins in low pH (<10). This secondary effect of decalcification of C-S-H gel is found only when Mg is present as a cation in the solution [Skalny, 2002]. Thaumasite is also formed during sulphate attack at low temperatures (0 to 5 ^{0}C). Thaumasite formation occurs as a result of the reaction between C-S-H gel and SO_4^{2-} , CO_2 or CO_3^{2-} and water. Thaumasite has also been reported to form as a result of the interaction of ettringite with the C-S-H gel in the presence of CO_2.

The current ASTM test methods for assessing the sulphate attack of cement mortars ASTM C1012 [2004] and ASTM C 452 [2006] assesses the expansion rate of mortar prisms by measuring the length change in a sulphate solution of 0.176 mol/L. However, these standards are for testing mortar prisms, rather than concrete specimens. While there is no specific ASTM for assessing the expansion rate of concrete specimens due to sulphate attack ASTM C 157M is a specified test for concrete specimens for length change. The standard states that where all of the aggregate passes a 50mm sieve, the specimen shall be a prism of 100 mm square cross-section and approximately 285 mm long. However, a prism of 75 mm square cross section shall be used if all of the aggregate passes a 25 mm.

In ASTM C1012 provision is kept for the researchers to change the concentration of solution to suit the exposed environment. Deterioration of concrete in a sulphate environment takes several years to

reach the ultimate failure state. With the use of more severe conditions, a generalized model can be developed and then the actual field behavior of samples can be extrapolated using field data. For assessing sulphate attack on concrete most researchers have used higher concentrations of sulphates than that available in the groundwater or in soil [Khatri et al., 1997]. In the experimental program presented here, higher concentrations of sulphate solution are considered with heating cycles at monthly intervals where samples are kept for 24 hours in an oven in 105°C.

The ASTM C1012 standard also enables researchers to use blended cement in concrete to examine the resistance to sulphate attack by replacing certain percentage of OPC. While ordinary Portland cement (OPC) is one of the common mix designs as specified for use in Australia, growing interest surrounds the use of an alternative mix design, namely pulverised fly ash (PFA) mix. When fully hardened, PFA has the capacity for decreased porosity relative to OPC making it less susceptible to water absorption with an elevated strength. These properties combined with its high alkalinity, has the potential to make it extremely resistant to sulphate corrosion [Neville, 1996]. Consequently, research indicates that a pulverized fly ash (PFA) mix is potentially resistant to sulphate attack.

It has been reported 20% PFA blended cement showed no signs of surface deterioration when exposed to 1%, 2%, 2.5% and 4% Na_2SO_4 and performed better than OPC concrete [Al-Dulaijan et al., 2003]. Similar findings were observed by Torii et al. [1995]; except that 30% PFA blended concrete (300kg/m^3 binder) was observed to have small visible cracks after two years of exposure to 10% Na_2SO_4. Twenty per cent PFA blended samples (with OPC) exposed to 2% Na_2SO_4 experienced a 3% decrease in compressive strength after 4 months and a 7% reduction at the end of 24 months (Al-Dulaijan et al., 2003). Sahmaran et al. [2005] investigated blended cement mortars with varying amounts of natural pozzolan and/or Class-F fly ash exposed to 5% sodium sulphate (Na_2SO_4) solution. This report showed that cements blended with Class-F fly ash had improved performance compared to OP cement. The results of the experimental investigation by Sahmaran et al. [2007] showed that the blended cement was more resistant to sulphate attack and had better performance when the w/c was increased compared to the low resistant cements (OP cement) with higher C_3A amounts. The OP cements showed a more pronounced effect from sulphate attack in response to increasing the w/c ratio.

2 EXPERIMENTAL

Given the reported improved performance of PFA mixes when subjected to sulphate exposure a 30% PFA mix was selected for the investigation. The mix design is given in Table 1 and corresponds to a standard mix design as specified in Australia complying with AS 3600. Specimens were cast were in accordance with Australian Standard AS 1012.8.1-2000. Following casting the specimens were demoulded after 24 hours and placed in a curing tank at 23°C for 28 days. The mix had a 28 day strength of 43.9 MPa as determined from compression tests on 3 x 100 mm cubes. The specimen dimensions were selected in accordance with ASTM C 157M, 285 x 75 x 75 mm as the aggregate size was below 25 mm. A total of 40 specimens were cast.

A total of 6 exposure regimes were selected to represent the range of concentrations that concrete could be exposed to in the environment. Ranging from low to high concentrations. These corresponded to 500, 5000 and 50000 ppm. Specimens were exposed to both sodium and magnesium sulphate as research has shown that the anion associated with the sulphate can hace a significant impact on the deterioration observed. Dewah, [2007] reported that several researchers found $MgSO_4$ to be more severe on concrete than Na_2SO_4. Magnesium sulphate attacks the hydrated silica phases to form gypsum, brucite and hydrated silica, and when the pH is below 10.6, also attacks ettringite. A total of 6 specimens were placed in each sulphate solution and 4 specimens were kept as control specimens.

Table 1. Mix design for PFA concrete.

Material	Quantity (kg/m^3)
20 mm aggregate	550
14 mm aggregate	350
10 mm aggregate	280
Course Sand	370
Fine Sand	264
Superplasticizer	1.200
Mortar Plasticizer	0.560
Water (potable tap water)	159
GP Cement	280
PFA	120

The specimens were placed in sealed containers and submerged in the sulphate solution. The containers were stored in the laboratory. The temperature in the laboratory was monitored at 20 ^{o}C +/- 3 ^{o}C, over the annual cycle. At monthly intervals the specimens were removed from the sulphate solutions, surface dried and placed in an oven at 105 ^{o}C for 24 hours, to dry to constant weight. After 24 hours the specimens were removed, weighed and the length measured along all 4 axes and the average recorded. A visual inspection of the specimens was also undertaken and any cracks noted. The specimens were then returned to the sulphate solutions. The control specimens were subjected to the same monitoring, to account for the effects of the handling of the specimens. The high temperature both allows the specimens to be weighed to constant mass for consistancy and accuracy and will act as an accelerated wetahering process. A complimentary set of testing not reported in this paper is investigating effects of natural exposure to compare the accelerated regime to standard conditions.

3 RESULTS

To date the specimens have been exposed for a total of 600 days. Initial cracks were observed in two specimens exposed in the 50,000 ppm Sodium Sulphate solution after 222 days, with these specimens losing integrity after 245 days, Figure 1. All six specimens exposed to 50,000 ppm sulphate displayed cracks after 288 days and all had lost integrity by 433 days. The first specimen exposed to 50,000 ppm Magnesium Sulphate showed cracking after 288 days with three now having cracks evident, though none have yet completely lost integrirty. Specimens exposed to the 5,000 ppm Sodium Sulphate solutions displayed initial cracks after 321 days with all six specimens having cracks present after 495 days. The 5,000 ppm Magnesium Sulphate solution also showed initial cracks after 321, though this is the only specimen of this type showing any cracks after 600 days. One of the 500 ppm Sodium Sulphate specimens had displayed cracking, after 433 days, with all displaying cracking by 560 days. To date none of the 500 ppm Magnesium Sulphate specimens have any visible cracks. The craking data is summerised in Table 2.

The change in mass for the specimens is presented in Figure 2. The data is presented as the average of the six specimens in each sulphate solution. The data has also been compensated for the control. Such that the data points for each solutions are given by;

$$M_t = [[M_1 + M_2 + M_3 + M_4 + M_5 + M_6]/6 – [C_1 + C_2 + C_3 + C_4]/4] - M_i \quad (1)$$

Where M_t is the initial mass at time t, M_i is the initial mass (average of six specimens), $M_{1\text{-}6}$ are the mass of the specimens at time t and $C_{1\text{-}4}$ are the mass of the control specimens at time t. When a specimen undergoes structural failure it is removed from the testing regime and the avaerage of the remaining specimens presented.

Table 2. Time to Cracking.

Exposure Regime	Time to Crack (1st Specimen) (Days)	Time to Crack (All Specimens) (Days)	Time to Failure (1st Specimen) (Days)	Time to Failure (All Specimens) (Days)
500 ppm Na_2SO_4	433	560		
5000ppm Na_2SO_4	321	495		
50000ppm Na_2SO_4	222	288	245	433
500 ppm $MgSO_4$	-			
5000ppm $MgSO_4$	321			
50000ppm $MgSO_4$	288			



Figure 1. Failure 50,000 ppm Na_2SO_4.

The data show an initial mass gain for most specimens of approximately 1.5-2.5%. The specimens then all follow a similar trend with a steady rise followed by sharp fall, with the pattern repeated a number of times. It is hypothesised that the initial rapid rise is due to reaction of the sulphate with the surface layers which are rich in cement paste. Once this initial layer of cement has reacted the sulphates must diffuse into the bulk concrete to react with the cement, thus the rate of reaction is slowed and the rate of increase in mass is also reduced.

As the reaction progresses the level of damage in the specimens increases, eventually resulting in small pieces of the specimen being lost. Thus a rapid fall in mass followed by the continued diffusion and reaction of the sulphate ions. This process is repeated until the level of expansive ettringite in the specimen causes an internal stress sufficient to cause cracking. As cracks widen sulphate is able to enter the cracks, such that diffusion is no longer the only meacnism by which sulphates can progress through the concrete, thus the the level of deterioration increases until structural integrity is lost.

The data shows that initially the 50,000 Sodium , 50,000 ppm Magnesium Sulphate specimens have the highest level of mass gain, as would be expected, while the 5,000 Sodium Sulphate specimens also show a similar % mass gain. The 5,000 ppm Magnesium Sulphate specimens show a lower mass gain with the 500 ppm Sodium Sulphate and 500 ppm Magnesium Sulphate specimens following a similar trend, displaying the lowest mass increase. It is interesting to note that the 5,000 ppm Sodium sulphate specimens profile closely resemble the 50,000 ppm specimens, both Sodium and Magnesium, rather tha the 5,000 ppm Magnesium specimens. This also reflects the visual observations were the 5,000

ppm Sodium Sulphate specimens display considerably more deterioration than the same concentration of Magnesium Sulphate specimens. While they showed an initial crack at a later point in time than the first Magnesium Sulpahte specimen, all six are now showing deterioration while still only one of the Magnesium specimens shows any evidence of deterioration.

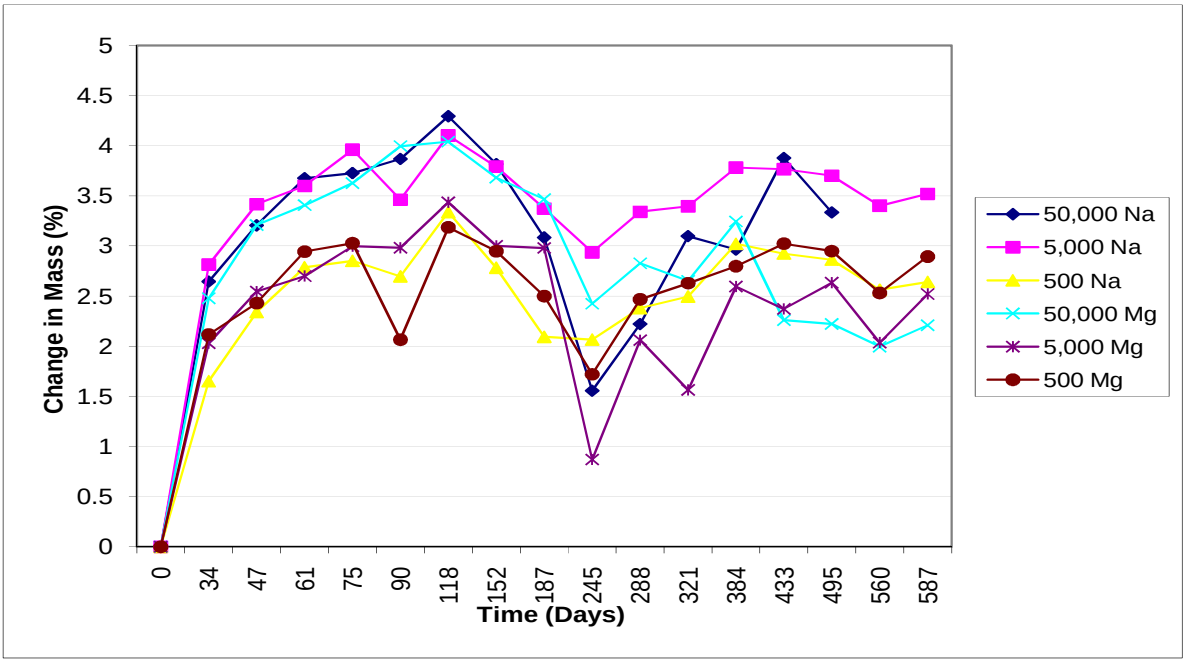

Figure 2. Mass change (%) vs Time for Magnesium and Sodium Sulphate specimens

Once the specimens start to exhibit cracking and failure, around the 200-250 day period the order of the specimens changes significantly. This is attributed to the level of deterioration on the individual specimens, with some starting to lose significant amounts of concrete. This is particularly evident in the 50,000 ppm Sodium and Magnesium Sulphate specimens. These changes correlate directly with the visual observation of cracks and spalls from the specimens.

The data indicates that for a similar concentration of sulphate a larger increase in mass is observed for the sodium specimens than the Magnesium specimens. This correlates with the visual observations where a higher level of deterioration is observed for the Sodium specimens.

The expansion data is shown in Figure 3, again the data shown is the mean of the six specimens compensated for the expansion of the control specimens. The data for the % length change shows a number of variations to the mass change. Initially only the 50,000 ppm Magnesium Sulphate specimens show any clear expansion, though all specimens displayed a distinct mass increase in this initial period. Overall it takes in excess of 200 days until all the specimens have a net increase in length, though all have gained over 2% mass by this point and indeed are starting to display a fall in mass at this point, irrespective if cracks have been observed.

The 50,000 ppm Magnesium Sulphate specimens dispay the highest level of expansion for most of the time period, until cracking is observed on the 50,000 ppm Sodium suplahte specimens. At this point the cracks become the primary factor in the expansion of the specimens until ultimate failure. The 5,000 ppm Sodium Sulphate specimens display the highest mass increase, yet the second lowest increase in length.

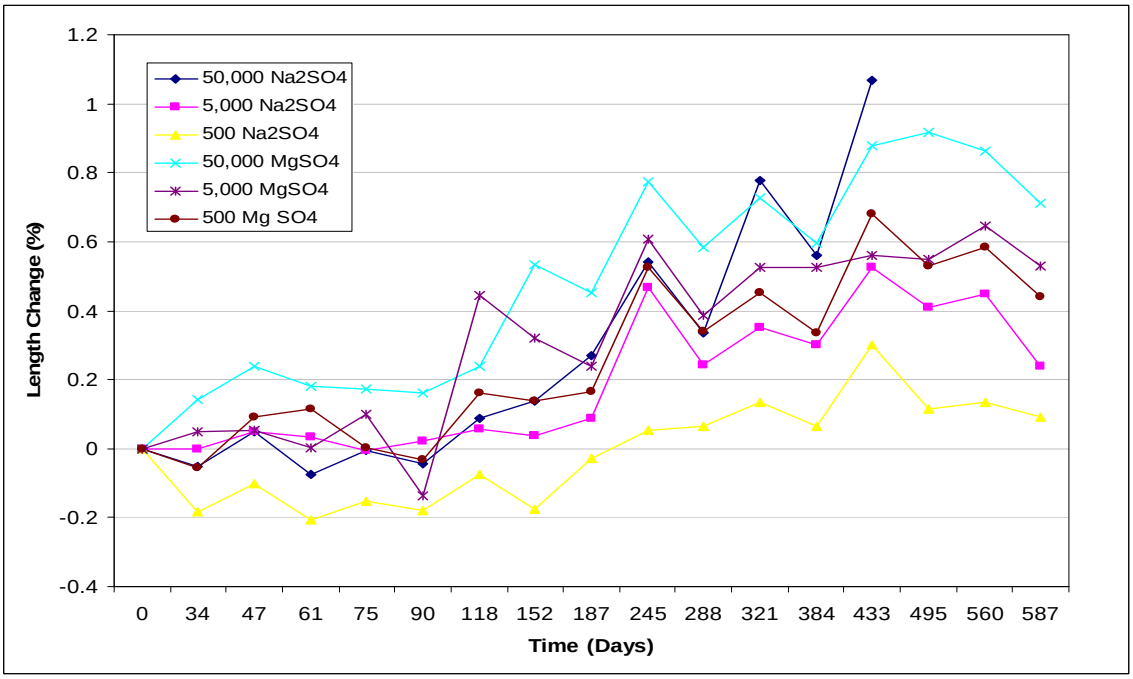

Figure 3. Change in length (%) vs Time for Magnesium and Sodium Sulphate specimens.

In both the mass change and length change graphs, the 50,000 ppm give the largest increase followed by the 5,000 ppm and then the 500 ppm for both the Sodium and Magnesium sulphate specimens, as would be expected.

The data would indicate that mass gain idoes not immediately result in elongation. It also indicates that an equivalent mass gain causes a higher level of expansion in the Magnesium specimens than the Sodium specimens and that the level of expansion measured does not directly correlate to observed deterioration. This evidence suggests that a different mechansim exists for the Sodium and Magnesium anions, as has been observed by other authors.

Table 3. Compressive Strength Data.

Exposure Regime	**Compressive Strength (MPa)**		
	56 days	**90 days**	**365 days**
Control	43.9 (28 days)	59.5	73.5
500 ppm Na_2SO_4	54.0	59.0	64.3
5000ppm Na_2SO_4	57.6	61.0	70.4
50000ppm Na_2SO_4	59.0	60.4	68.4
500 ppm $MgSO_4$	55.8	58.5	64.4
5000ppm $MgSO_4$	55.7	54.3	65.8
50000ppm $MgSO_4$	52.5	53.1	55.3

Strength tests were undertaken after 56, 90 and 365 days exposure, other than the initial control which was at 28 days. The results are given in Table 3. The data shows a increase with time for all specimens. However, the Sodium specimens show a greater increase than the Magnesium specimens for the 5000 ppm and 50000 ppm solutions. This increase is 5 MPa at 5000 ppm and 13 MPa at 50000 ppm. For the 500 ppm specimens there is no identifiable difference. These results would indicate that the Magnesium is having a more deleterious effect than the Sodium, in agreement with other authors [Dehwah, 2007:Prasad, 2006]. This contrasts with the visual observations were more severe deterioration has been observed on the Sodium specimens.

4. CONCLUSIONS

A standard 30% PFA concrete as used on site in Australia was exposed to three Sodium Sulphate and three Magnesium Sulphate solutions at 500 ppm, 5,000 ppm and 50,000 ppm. After 600 days exposure the data showed;

- All specimens had an initial mass gain for most specimens of approximately 1.5-2.5%. The specimens then all follow a similar trend with a steady rise followed by sharp fall, with the pattern repeated a number of times
- The 50,000 ppm Sodium and Magnesium Sulphate specimens and the 5,000 Sodium Sulphate specimens showed a similar mass gain untill initial cracking was observed.
- Initial cracking was observed first on the 50,000 pp Sodium Sulphate specimens after 222 days and all specimens had failed after 433 days. The 50,000 ppm Magnesium Sulphate specimens and the 5,000 ppm Sodium Sulphate specimens displayed initial cracking after 288 days and 321 days, though all Sodium Sulphate specimens have now cracked but still only three Magnesium Sulphate specimen.
- Cracking was observed on the 5,000 ppm one Magnesium specimen after 321 days and one 500 ppm Sodium Sulphate specimen after 433 days.
- Initially only the 50,000 ppm Magnesium Sulphate specimens showed any expansion. Overall it took in excess of 200 days until all the specimens have a net increase in length
- The specimens exposed in the Sodium solutions displayed a greater increase in compressive strength, for the 5000 and 50000 ppm, than those exposed to the Magnesium.

REFERENCES

Al-Dulaijan, S.U. Masledhuddin, M. Al-Zahrani, M.M. Sharif, A.M. Shameem, M. & Ibrahim, M. 2003, Sulphate resistance of plain and blended cements exposed to varying concentrations of sodium sulphate, *Cement & Concrete Composites*, **25**[4], 429-437.

Dehwah, H. 2007. Effect of sulfate concentration and associated cation type on concrete deterioration and morphological changes in cement hydrates. *Construction and Building Materials*,**21**, 29–39.

Mehta, P.K. 2000, Sulfate attack on concrete: Separating the myth from reality. *Concrete International*, **22**[8], 5-12.

Neville, A.M. 1996, Properties of Concrete, 4th Ed, Wiley, New York.

Prasad, J. A. 2006. Factors influencing the sulphate resistance of cement concrete and mortar. *Asian journal of civil engineering (building and housing)*, **7**[3], 259-268.

Sahmaran, M. 2005. Sulfate resistance of plain and blended cements exposed to wetting–drying and heating–cooling environments. *Construction and Building Materials*, **21**,1771–1778

Sahmaran, M. Kasap, O. Duru, K. & Yaman, I.O. 2007, Effects of mix composition and water-cement ratio on the sulphate resistance of blended cements, **29**[3], 159-167.

Skalny, J.M. & Odler, I. 2002, *Sulfate Attack on Concrete.*

Torii, K, Taniguchi, K & Kawamura, M. 1995, Sulphate resistance of high fly ash content concrete, *Cement and Concrete Research*, **25**[4], 759-768.

XII DBMC
International Conference on Durability of Building Materials and Components
PORTO - PORTUGAL, April 12th-15th, 2011

Rice Husk Ash - Importance of Fineness for its Use as a Pozzolanic and Chloride-Resistant Material

Joana Sousa Coutinho[1]
Vagelis G. Papadakis[2]

ABSTRACT

The cement industry contributes over 6% to global CO_2 emissions, thus making cement production an important sector for CO_2 emission mitigation strategies, such as increasing use of pozzolanic additions. The work presented herein involves two laboratory studies on mortar where cement was partially replaced by rice husk ash (RHA), a waste material made available from the rice industry.

In the first study, the cement replacement considered was 10 and 15% with two different types of RHA, with regular grinding. Mortars with 10% and 15% cement replacement with RHA were produced with the same workability as control mortar (0% RHA) and also as silica fume mortar with 10% cement replacement by commercial silica fume. Specimens were tested for strength, absorption by capillarity, chloride ion penetration, accelerated carbonation and resistivity. Both types of RHA mortar with 10% and 15% cement replacement performed worse than the control mortar regarding strength, resistance to chloride penetration and carbonation resistance. Perfomance in terms of resistivity was similar to control and in terms of sorptivity, performance increased with replacement percentage. Unsatisfactory results were explained by insufficient fineness evaluated by laser particle distribution on the RHA samples.

A second study involving cement replacement in mortar with 10 and 20% of RHA ground very finely (mean particle size of 6μm) led to equivalent or better results to control mortar, in terms of strength, but, principally, the chloride resistance was dramatically increased thus leading to the conclusion that fineness is a key issue in terms of RHA use as a cement replacement material.

KEYWORDS

Chrorides, Additions, Mortar, Durability, RHA, Rice husk ash, Fineness.

[1] Faculty of Engineering of the University of Porto (FEUP), Porto, PORTUGAL, jcouti@fe.up.pt

[2] Department of Environmental and Natural Resources Management, University of Ioannina, Agrinio, GREECE, vgp@psp.org.gr

1 INTRODUCTION

Cement production growth is estimated to range between 120 and 180% in 2020 [Middendorf et al. 2005]. It is known that for every ton of portland cement produced, cement plants generate about the same amount of green house gases (GHG), primarily carbon dioxide – one of the main GHG, besides being an energy- intensive industry [Samarin 1999]. The cement industry contributes over 6% to global CO_2 emissions making this industry an important sector for CO_2 emission mitigation strategies such as the increase use of pozzolanic additions [Worrell et al. 2001; Naik 2005]. In fact, efforts have been made to promote the use of pozzolans. It has been shown that if just 30% of cement used globally was replaced with supplementary cementing materials (SCM), the rise in CO_2 emissions from cement production could be reversed [Ecosmart Concrete 2010]. Measures to decrease the rate of CO_2 emissions during cement manufacture can be classified into two main approaches:

a) attaining a higher efficiency in the production process, by decreasing fuel consumption;
b) reducing the rate of clinker production by using mineral replacements (additions or SCMs, added during manufacture or directly through cement replacement at the building site.

Experience from all over the world, both historically and during the last several decades, shows that the portland cement – pozzolanic/cementitious materials composite system will always be inherently superior to the portland cement system in its microstructural and durability properties. This implies that there are strong technical and economic arguments and evidence to modify the fineness of the industrial (or agricultural) byproducts rather than that of portland cement, and thus ensure that they are manufactured for durability rather than for strength [Swamy 2007; Papadakis 2000, Papadakis & Tsimas 2003]. The most commonly-used pozzollanic materials are fly ash, granulated slag, silica fume and various natural and calcined pozzolans such as rice husk ash and metakaolin, most of which are waste materials.

It is well known that rice husk ash (RHA), an agricultural waste material, can be a highly reactive pozzolanic material, produced by controlled burning of rice husk and providing several advantages, such as improved strength and durability properties, reduced materials cost due to cement savings and, environmental benefits. Reactivity of RHA is attributed to its high content of non-crystalline silica, and to its very large surface area governed by the cellular structure of the particles [Mehta 1994; Zhang & Malhorta 1996; Chandra 1997; Sousa-Coutinho 2003; Saraswathy 2007]. When pozzolanic materials are added to cement, the silica (SiO_2) present in these materials reacts with free lime released during the hydration of cement and forms additional calcium silicate hydrates as new hydration products which improve the mechanical properties of concrete formulation [Ganesan & Thangavel 2007].

Generally, reactivity of a pozzolanic material can be favored by increasing fineness [Mehta,1994; Saraswathy 2007]. When burning temperature exceeds 600ºC partially changing silica to cristobalite, quartz and trydimite (a crystalline material), grinding is especially important. The burning of rice husk generates a significant volume of RHA that commonly ends up being dumped, blemishing the environmental footprint of the rice industry. Given that rice husk comprises approximately 20% of the unrefined rice and that RHA is 18% of rice husk, it is estimated that the total quantity of RHA generated globally is close to 21 million tons per year. It has been demonstrated that RHA exhibits significant pozzolanic potential; however the way in which the material develops its potential is largely influenced by inherent factors, principally fineness and reactive silica [Mehta 1978; Mehta, 1992; Malhotra and Mehta 1996; Agarwal 2006].

The study presented herein, examines the potential of an European RHA where two types were considered differing in reactive silica content and then fineness, in order to better understand the nature of this waste stream. Fineness levels were kept, for one RHA type, first at a regular level and then at a significantly lower level than those reported in the literature, in an effort to assess the reactivity of the material as a function of grinding. RHA was added in mortar systems and then in concrete and factors like strength and durability characteristics were determined to conclude on the potential of the local by-product.

2 RESEARCH PROGRAM

In a first study, the cement replacement considered was 10% and 15% with two different types of RHA obtained from an European industry, named A and Θ. Mortars with 10% and 15% cement (CEM I) replacement with each RHA were produced, as well as a silica fume mortar with 10% cement replacement by commercial silica fume. All mortars with the same water/binder ratio were dosed with superplasticizer in order to present equivalent workability. Specimens were tested for strength, absorption by capillarity, chloride ion penetration, accelerated carbonation and resistivity. In the first study, the fineness of RHA presented a mean particle diameter much greater than cement (65-70 μm for RHA in comparison to cement of 20 μm). In a second study, RHA (type A) was ground very finely (with mean particle size of 6μm) and the cement replacement was 10 and 20%.

2.1 Materials

Materials used to produce mortar were tap water, CEM I 42,5 R type of cement, commercially available silica fume and the two experimental types of rice husk ash A and Θ, superplasticizer and standard CEN sand. Particle size distribution curves of RHA and cement and SEM photos of RHA are shown in Fig 1. Chemical analyses are shown in Table 1 and compaired to results by other authors.

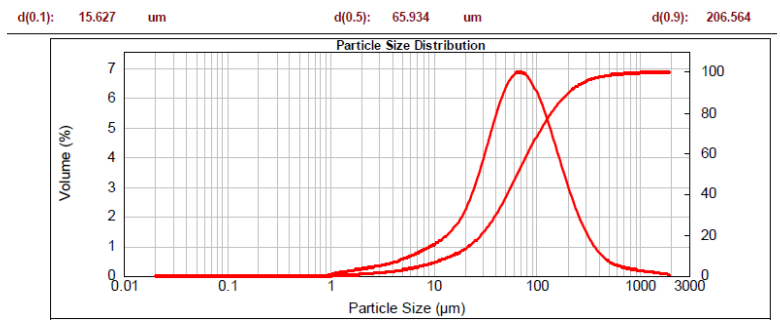

RHA A

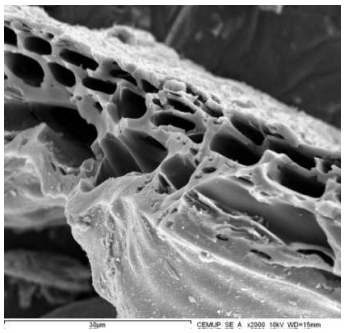

RHA A ×2000

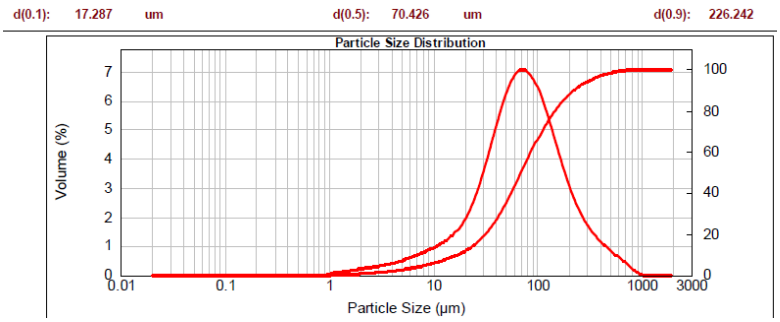

RHA Θ

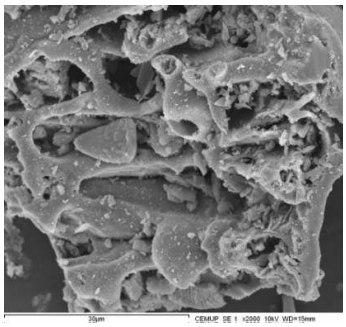

RHA Θ ×2000

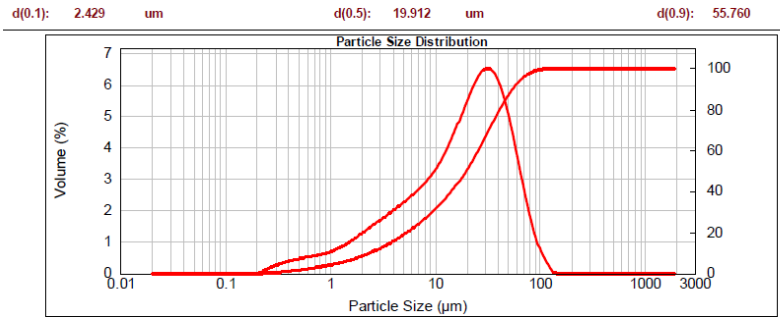

Cement CEMI 42,5R

	A	Θ	CEM
		μm	
d(0,1)	15,63	17,29	2,43
d(0,5)	65,93	70,46	19,91
d(0,9)	206,56	19,91	55,76

Figure 1. Particle size distribution curves of RHA (non-ground) and cement and SEM photos of RHA.

Table 1. Chemical analysis for cement and RHA A and RHA Θ and results for RHA by other authors. [Umamaheswaran & Batra 2008; Mehta 1994]

	cement	*RHA A*	*RHA A*	*RHA Θ*	*RHA Θ*	*RHA*	*RHA*
		IETCC	supplier	IETCC	supplier	Umamaheswaran & Batra 2008	Mehta 1994
LOI [%]	2,85	6,34	-	6,30		0,80	3-18
total SiO_2 [%]	20,41	89,05	88 - 98	86,50	88 - 98	93,52	80-95
reactive SiO_2 [%]	-	81,43	-	78,64	-	-	-
Al_2O_3 [%]	4,74	1,73	< 1	2,70	< 1	0,01	-
Fe_2O_3 [%]	3,08	1,31	-	0,00	-	0,51	-
CaO [%]	62,28	3,05	< 1	4,40	< 1	0,68	-
MgO [%]	1,90	2,15	-	1,97	-	-	-
free CaO [%]	1,01	0,46	-	0,0	-	-	-
K_2O [%]	-	-	< 1	-	< 1	-	1-2

Reactive SiO_2 determined by EN -197-1

2.2 Mixture proportions and workability

Mortar specimens according to mixture proportions shown in Table 2 were produced according to NP EN 196-1 [1996] after assessing workability. Workability was measured following the procedure described in ASTM C230 [2003] and ASTM 1437 [2001]. Control mortar (CTL) workability was set as target workability and superplasticizer added so as to obtain equivalent workability (±10mm) for all types of mortar. Average flow diameters for all batches are shown in Table 3.

Table 2. Mixture proportions and workability.

	CTL	$SF_{10\%}$	$A_{10\%}$	$A_{15\%}$	$\Theta_{10\%}$	$\Theta_{15\%}$
sand (g)	1350	1350	1350	1350	1350	1350
Cement (g)	450	405	405	382,5	405	382,5
ash (g)	0	45	45	67,5	45	67,5
water (g)	225	225	225	225	225	225
Superplasticizer (g)	0	3.4	1.2	2.2	1.2	2.2
workability	210.2	210.1	204.4	209.6	203.3	206.1

2.3 Strength

Mortar strength was determined at 7, 28 and 90 days, following the standard procedure described in NP EN 196-1 [1996].

2.4 Absorption by Capillarity

Transport properties of the concrete surface, which play a major role in durability of reinforced concrete, are controlled by three mechanisms; namely, capillary absorption, permeability, and diffusion [Neville 1998]. Usually, concrete that is more resistant to the ingress of aggressive agents (water or carried ions, oxygen, and carbon dioxide) will be more durable. In the present study water absorption by capillarity, chloride ion migration, resistivity, and accelerated carbonation tests were carried out to assess durability. To consider the ability of the concrete surface to absorb water by capillary suction, the RILEM TC116-PCD [1999] recommendation was adopted as a basis. The molded side faces of 100 mm diameter and 50 mm height cylindrical specimens were tested, instead of the molded bottom face of 150 mm cube specimens used in the RILEM recommendation. The 56 (instead of 28) days old standard-cured (water at 20ºC) specimens were allowed to dry in a ventilated heater at 40ºC until constant mass was achieved. After cooling to 20ºC, the specimens were put on rods in a shallow bath of water at 20ºC, approximately 3 mm deep. The uptake of water by capillary absorption was measured through the weight gain of each specimen at time intervals until 4-1/2 h of contact with water. The absorption of water into concrete under capillary action is dependent on the square-root of time and may be modeled as [Hall 1989]:

$$A = a_0 + St^{0.5} \quad (1)$$

where, A (mg/mm^2) is the water absorption by unit area since the time the specimen was dipped in the shallow bath; S (mg/(mm^2×min.^{0,5})) is the "sorptivity" of the material; t is the elapsed time in minutes, and a_0 (mg/mm^2) is the water initially absorbed by pores in contact with water. Testing each specimen led to average (of 3) sorptivity results with correlation coefficients (R) over 0.978.

2.5 Chloride ion penetration

Chloride ion penetration was assessed by the Luping method, which is a non-steady state migration method based on a theoretical relation between diffusion and migration. The method enables the calculation of the apparent chloride diffusion coefficient (Dns) from an accelerated test [NT BUILD 492 1999]. It is based on measuring the depth of color change of a silver nitrate solution sprayed on the specimens previously submitted to a migration test. Specimens (100 mm diameter by 50 mm height) were submitted to an electrical current corresponding to a potential difference, in this case, of 30 V, during 24 h. Chloride ions are forced to migrate out of a NaCl solution subjected to a negative charge at the surface of the specimen, through the concrete into a NaOH solution maintained at a positive potential at the opposite surface of the specimen. The specimens are then split open, sprayed with nitrate solution and the chloride penetration depth (x_d) is measured in order to enable calculation of the apparent diffusion coefficient (D_{ns}) (Equation 2).

$$D_{ns} = \frac{0.0239(273+T)L}{(U-2)t}\left(x_d - 0.0238\sqrt{\frac{(273+T)Lx_d}{U-2}}\right) \quad (2)$$

where D_{ns} is the non-steady-state migration coefficient (×10^{-12} m^2/s), U is the absolute value of the applied voltage (V), T is the average value of the initial and final temperatures in the anodic solution (ºC), L is the thickness of the specimen, usually 50 mm, x_d is the average value of measured chloride penetration depth (mm), and t is the testing period (h).

2.6 Resistivity

Concrete resistivity is another parameter that contributes to durability assessment. When pores are saturated, electric current flows more easily depending on the pore structure. Prior to the chloride migration test described above, specimens are pre-saturated. Therefore, when current is imposed during the test it is possible to evaluate resistivity (Equation 3) in saturated conditions to compare different types of concrete, in this case, mortar.

$$\rho \equiv R \cdot \frac{A}{L} \equiv \frac{V \cdot A}{L \cdot I} \quad (3)$$

where R is the electric resistance, (Ω - Ohm), I, current (A), V, voltage (V), ρ, electric resistivity (Ω.m), L, length (m), and A (m^2), the area of the test specimen across which current passes.

2.7 Carbonation

Accelerated carbonation tests were carried out following the procedure described in LNEC E391 [1993], using a chamber with 5% carbon dioxide and relative humidity (RH) of approximately 65%. 40×40×160 mm test specimens of each mortar type were kept in the chamber for two months, after 28 day curing in water at 20ºC. A slice from each test specimen was sawed off and sprayed with phenolphthalein solution, enabling the measurement of the carbonation depths.

3. TEST RESULTS AND DISCUSSION

Strength resutls at 7, 28 and 90 days, sorptivity results, resistance to chloride penetration, resistivity results at 56 days and carbonation results of each mortar type, are shown in Table 3. All these results refer to the regular ground form of RHA. Both types of RHA mortar with 10% and 15% cement replacement performed worse than the control mortar regarding strength, resistance to chloride penetration and carbonation resistance. Although a similar reduction, on average, in compressive strength was noticed at 28 and 90 days (10 % and 9% respectivelly) for all the RHA mortar samples, samples incorporating 15% RHA produced much higher carbonation depths (89% increase) than those incorporating 10% (17 % to 33 % increase).

Table 3. Mechanical and durability test results and enhancement by the use of RHA (regular ground).

Results and Enhancement		*CTL*	$A_{10\%}$	$A_{15\%}$	$\Theta_{10\%}$	$\Theta_{15\%}$	$SF_{10\%}$
$\sigma_{7\ dias}$ [Mpa]	*Rslt.*	38,7	37,1	37,5	38,6	37,1	48,7
	Enh.		-4%	-3%	0%	-4%	26%
$\sigma_{28\ dias}$ [Mpa]	*Rslt.*	48,0	42,5	42,9	44,6	42,6	58,8
	Enh.		-11%	-11%	-7%	-11%	22%
$\sigma_{90\ dias}$ [Mpa]	*Rslt.*	53,3	48,4	49,0	49,1	47,7	58,0
	Enh.		-9%	-8%	-8%	-11%	9%
S [mg/(mm^2.min$^{1/2}$)]	*Rslt.*	0,1510	0,1233	0,0653	0,1023	0,0533	0,0883
	Enh.		18%	57%	32%	65%	42%
D_{ns} [×10^{-12} m^2/s]	*Rslt.*	15,31	16,32	17,62	17,24	16,59	2,44
	Enh.		-7%	-15%	-13%	-8%	84%
Carbonation [mm]	*Rslt.*	3,0	3,5	5,7	4,0	5,7	4,8
	Enh.		-17%	-89%	-33%	-89%	-61%
Resistivity [Ω.m]	*Rslt.*	53,7	48,6	58,4	44,9	61,8	279,5
	Enh.		-9%	9%	-16%	15%	420%

Enhancement (Enh.)=(Rslt.$_{RHA}$-Rslt.$_{CTL}$)/Rslt.$_{CTL}$

In terms of resistivity, samples incorporating 15% RHA produced an increase compared to control (9% and 15% for RHA type A and Θ respectively), while on samples with 10% RHA the resistivity was decreased (16% maximum decrease for RHA type Θ). In terms of sorptivity, performance increased with replacement percentage (a 65% increase was noticed on samples incorporating 15% RHA type Θ).

In Table 4, strength and accelerated chloride test results on concrete are given for the second study, where RHA (type A) was ground very finely to obtain SRHA (Fig. 2) and used as 10 and 20%cement replacement in concrete.

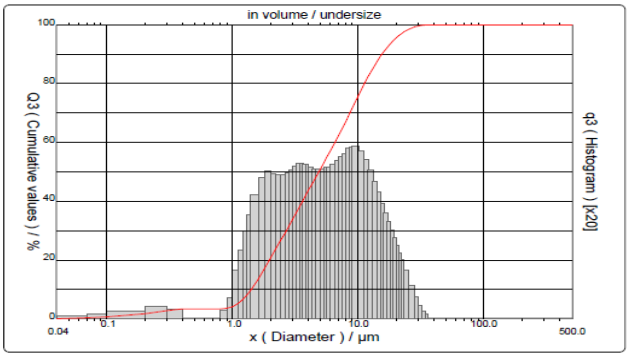

d(0,1): 1,41µm
d(0,5): 4,85µm
d(0,9): 15,43µm

Figure 2. Particle size distribution curve of SRHA.

At 7 days the compressive strength proved to be similar to control samples (1% increase for both 10% and 20% levels of RHA), while at 28 days strength was slightly increased up to 7% for samples incorporating 10% RHA. Superfine RHA performs better than cement, even for 20% replacement. In this second study the chloride resistance of mortar incorporating SRHA was also evaluated, using the ASTM accelerated penetration test method. The samples before testing, were immersed for a period of 55 days in saturated $Ca(OH)_2$ solution. This period of time is more than adequate for a sufficient level of cement hydration and pozzolanic reactions of the ash used, as previously shown. The overall excellent behaviour of the samples tested (in comparison to control) is given in Table 4, right, where the electric charge passed through the samples is given for both levels of SRHA used.

Table 4. Mechanical test results, left and electric charge, right, in concrete with superfine RHA.

	Control	*10% SRHA*	*20% SRHA*
7 d	38.7	39.2	38.9
28 d	48.0	51.2	50.2

	Charge passed [Coulombs]	*Permeability Class* [ASTM]
Control	2719	Moderate
10% SRHA	2569	Moderate
20% SRHA	864	Very Low

It is obvious that the mechanical grinding led to the development of smaller grain sizes than those of cement. It is generally acceptable that, at concrete level, the small grain sizes of ash strengthen (through the filler effect) packing among aggregates (specially in the case of fine aggregates) and cement grains. This is further enhanced with pozzolanic ash, reducing in this way the overall porosity (hence the permeability) of the final product. This is confirmed by results obtained according to the official classification by ASTM C1202 (see Table 4, right), where mortar incorporating SRHA exhibits low permeability to chloride ingress, in contrast to conventional mortar where permeability observed is of medium level.

CONCLUSIONS

The work presented in this study, examines the potential use of an European RHA where two types were considered differing in reactive silica and then fineness so as to better understand the nature of this waste stream. Fineness levels were kept, for one RHA type, first at a regular level and then at a significantly lower level than those reported in literature, in an effort to assess the reactivity of the material as a function of grinding. RHA was added in mortar systems and factors like strength and durability characteristics were determined to conclude on the potential of the local by-product. In the first study, cement replacement considered was 10 and 15% with the two different types of RHA, with regular grinding. Both types of RHA mortar with 10 and 15% cement replacement performed worse than control mortar in regard to strength, resistance to chloride penetration and carbonation resistance. Perfomance in terms of resistivity was similar to control and in terms of sorptivity, performance increased with replacement percentage. Unsatisfactory results were explained by insufficient fineness evaluated by laser particle distribution on the RHA samples. A second study involving cement replacement with 10 and 20% of RHA ground very finely, led to equivalent or better results compared to control concrete in terms of strength but, principally, chloride resistance was dramatically increased thus leading to the conclusion that fineness is a key issue in terms of RHA use as a cement replacement material.

As cement industry contributes significantly to global CO_2 emissions, making cement production greener is currently a very urgent challenge. Reducing the rate of clinker production by using mineral replacements, i.e., additions or supplementary cementing materials such as RHA with enhanced reactivity, contributes to greener concrete and thus sustainable construction.

ACKNOWLEDGMENTS

Authors wish to thank the Greek General Secretariat for Research & Technology for financial support under PYRICE project, Inês Grijó Pereira for collaboration, and Dr Rafael Tallero Morales (IETCC) for help with chemical analyses under the CYTED project "VALORES".

REFERENCES

Agarwal S.K. 2006, 'Pozzolanic activity of various siliceous materials', *Cement and Concrete Research*, **36**[9], 1735-1739.

ASTM 1202, 1994, *Standard test method for electrical indication of concrete's ability to resist chloride ion penetration*, American Society for Testing Materials.

ASTM C1437-01, 2001, *Standard Test Method for Flow of Hydraulic Cement Mortar*, American Society for Testing and Materials, January

ASTM C230M-03, 2003, *Standard Specification for Flow Table for Use in Tests of Hydraulic Cement*, American Society for Testing and Materials, January

Chandra, S. 1997, 'The use of rice husks in concrete', in *Waste Materials Used in Concrete Manufacturing*, William Andrew Publishing/Noyes.

Ecosmart Concrete, 2008, 'ENVIRONMENTAL IMPACT - Cement production and the CO2 challenge', Retrieved October 2010, *http://www.ecosmartconcrete.com/enviro_cement.cfm*

Ganesan, K. R. & Thangavel, K. 2007, 'Evaluation of bagasse ash as supplementary cementitious material', *Cement and Concrete Composites*, **29**.

Hall, C. 1989, 'Water sorptivity of mortars and concretes. A review', *Magazine of Concrete Research*, **41**[147].

LNEC E-391, 1993, *Betões. Determinação da resistências à carbonatação*, Laboratório Nacional de Engenharia Civil, Lisbon

Malhotra V.M. & Mehta P.K. 1996, 'Pozzolanic and cementitious materials', in *Advanced Concrete Technology vol. 1*, Gordon and Breach Publications, Canada.

Mehta P.K., 1992, 'Rice husk ash - a unique supplementary cementing material', In: *Advances in Concrete Technology*, ed V.M. Malhotra, pp. 407-413.

Mehta, P.K. 1978, *Siliceous ashes and hydraulic cements prepared there from*, United States Patent 4105459

Mehta, P.K. 1994, 'Mineral admixtures for concrete - an overview of recent developments', Proc of Engineering Foundation Conference: Advances in Cement and Concrete, Durham, ASCE.

Middendorf, B., Martirena, J.F., Gehrke, M. & Day, R.L. 2005, 'LimePozzolan binders: an alternative to OPC?', Proc International Building Lime Symposium, Orlando, Florida, USA.

Naik, T. R. 2005, 'Sustainability of Cement and Concrete Industries', Proc of Global Construction Ultimate Concrete Opportunities, Dundee, Scotland, UK.

Neville, A. 1998, *Properties of Concrete*, Longman Publishers.

NP EN 196-1, 1996, *Métodos de ensaio de cimentos. Parte 1: Determinação das resistências mecânicas*, IPQ, Portugal.

NT BUILD 492, 1999, *Concrete, mortar and cement-based materials: Chloride migration coefficient from non-steady-state migration experiments*, NORDTEST Method

Papadakis, V.G. & Tsimas, S. 2003, 'Supplementary Cementing Materials in Construction for Economic and Environmental Benefits', *International Association of Concrete Technology Journal*, **1**[1], 51-60.

Papadakis, V.G. 2000, 'Effect of Supplementary Cementing Materials on Concrete Resistance against Carbonation and Chloride Ingress', *Cement and Concrete Research*, **30**[2], 291-299.

RILEM, 1999, 'RILEM TC 116-PCD - Permeability of concrete as a criterion of its durability, C: Determination of the capillary absorption of water of hardened concrete', *Materials and Structures* **32**[2].

Samarin, A. 1999, 'Wastes in concrete: converting liabilities into assets', Proc of Exploiting Wastes in concrete, Dundee, Scotland, UK, Thomas Telford.

Worrell, E., Price, L., Martin, N., Hendriks, C. & Meida, L.O. 2001, 'Carbon dioxide Emissions from the Global Cement Industry', *Annual Review of Energy and the Environment*, **26**, 303-329.

Zhang, M.H. & Malhotra, V.H. 1996, 'High Perfomance Concrete Incorporating Rice husk Ash as a Supplementary Cementing Material', *ACI Materials Journal*, **8**.

Saraswathy, V. 2007, 'Corrosion Perfomance of Rice Husk Ash blended concrete', *Construction and Building Materials*, **21**[6].

Sousa-Coutinho, J. 2003, 'The combined benefits of CPF and RHA in improving the durability of concrete structures', *Cement & Concrete Composites*, **25**[9].

Swamy, R. N. 2007, 'Sustainable Concrete for the 21st Century. Concept of Strength through Durability', *The Indian Concrete Journal*, **81**[9].

Umamaheswaran, K. & Batra, V.S. 2007, 'Physicochemical characterization of Indian biomass ashes', *Fuel*, **87,** 628-638.

XII DBMC
International Conference on Durability of Building Materials and Components
PORTO - PORTUGAL, April 12th-15th, 2011

Durability Performance of SCC Mortars Including Different Types of Metakaolin

Helena Figueiras [1]
Sandra Nunes [2]
Joana Sousa Coutinho [3]
Joaquim Figueiras[4]

ABSTRACT

The design of high performance and high durability concrete materials demands an adequate selection and combination of constituent materials. The present paper intends to study and compare the performance of two different types of metakaolin included in a ternary cement blend and to provide a comprehensive procedure for the design of mortar mixtures which are adequate for self-compacting concrete (SCC), with defined performance requirements in terms of durability. The methodology used holds firstly, an experimental phase conducted according to a central composite design; second, a statistical analysis and model fitting of data collected during the experimental phase and; third, a numerical optimization of mixture parameters using the derived models. Two different types of metakaolin were assessed in combination with cement, limestone filler and superplasticizer. Each type of metakaolin interacts in a different way with other constituents resulting in different fresh and hardened properties. Mortar characterization tests included the flow cone and V-funnel tests for mortar fresh state and the electrical resistivity test for the hardened material state. This study clearly shows the improvement in durability given by the incorporation of metakaolin in mortars. Nevertheless, it was found that both types of metakaolin perform differently. After building the regression models that establish the relationships between mix design variables and the responses (mortar tests results), numerical optimization was used to determine the mixture parameters which exhibit best overall performance (including economic), while maintaining self-compactability.

KEYWORDS

Metakaolin, Limestone filler, SCC mortars, Durability performance.

[1] LABEST/FEUP Faculty of Engineering of the University of Porto (FEUP), Porto, PORTUGAL, hfig@fe.up.pt
[2] LABEST/FEUP Faculty of Engineering of the University of Porto (FEUP), Porto, PORTUGAL, snunes@fe.up.pt
[3] LABEST/FEUP Faculty of Engineering of the University of Porto (FEUP), Porto, PORTUGAL, jcouti@fe.up.pt
[4] LABEST/FEUP Faculty of Engineering of the University of Porto (FEUP), Porto, PORTUGAL, jafig@fe.up.pt

1 INTRODUCTION

Currently, durability, and especially prevention of reinforcement corrosion, has become a critical aspect of reinforced concrete structures. The design of durable structures should focus on one hand, on the possibility of using additional protective measures, like the use of controlled permeability formwork (CPF) or self-compacting concrete (SCC), that could delay the corrosion process and the deterioration of concrete, on the other hand, the composition design should be appropriate for the exposure class. Sustainable design of highly durable concrete requires an adequate selection and combination of constituent materials, exploiting synergies between different cements and additions.

Supplementary cementing materials have become an integral part of high strength and high performance concrete mix design. Pozzolanic materials including silica fume, fly ash, slag and metakaolin have been used in recent decades for developing high performance concrete with improved workability, strength and durability. Pozzolanic reactions change the microstructure of concrete and chemistry of the hydration products by consuming the released calcium hydroxide (CH) and production of additional calcium silicate hydrates (C-S-H), resulting in an increased strength and reduced porosity and therefore improving durability [Bentz & Garboczi 1991]. In recent years, there has been a growing interest in the use of metakaolin as a high reactive natural pozzolan. Metakaolin is a manufactured material produced by calcining kaolin clay at high temperature that essentially contains SiO_2 (50-55%) and Al_2O_3 (40-45%). Metakaolin pozzolanic reactivity depends on the crystallinity, particle size and the amorphization degree. These aspects are interrelated and modifiable through the production technology. The efficiency of a metakaolin in a composition also depends on the type of cement used, in particular the fine particle size complementarity and the differential electrostatic forces between particles [Sampaio *et al.* 2001]. It has been reported that the use of metakaolin helps in enhancing the early age mechanical properties as well as long-term strength properties of concrete. The partial replacement of cement with metakaolin reduces the water penetration into concrete by capillary action. Metakaolin modifies the pore structure of the cement matrix and significantly reduces permeability, resulting in higher resistance to transportation of water and diffusion of harmful ions which lead to the deterioration of the matrix. Although total porosity may be increased by metakaolin blending, the process also causes a refinement of pore structure [Siddique & Klaus 2009].

This paper discusses the durability properties of self-compacting mortars with mineral admixtures. Portland cement, limestone filler and two different types of metakaolin were used in binary (two-component) and ternary (three-component) cementitious blends. A methodology was developed for the design of mortar mixtures which are adequate for SCC [Nunes *et al.* 2009]. This methodology was developed in three phases: first, the experimental phase conducted according to a central composite design; second, the statistical analysis and model fitting of data collected during the experimental phase and, third, the numerical optimization of mixture parameters using the models derived in the previous phase. The numerical models obtained were used to find optimal solutions that satisfy performance requirements, including: fresh state (deformability and viscosity), hardened state (durability properties) and economic requirements.

2 EXPERIMENTAL PROGRAMME

2.1 Materials characterization

Mortars investigated in this study were prepared with binary mixtures, of Portland cement (CEM I 42.5R) and limestone filler, and ternary mixtures, including cement, limestone filler and metakaolin 1 (MTK1) or metakaolin 2 (MTK2). The specific gravity of cement, limestone filler, MTK1 and MTK2 was 3.11, 2.68, 2.20 and 2.55, respectively. Figure 1 shows the particle size distribution curves, in terms of volume, of each fine material used in this study. The mean particle size dimension was 14.61μm, 6.53μm, 7.12μm and 15.38μm for cement, limestone filler, MTK1 and MTK2, respectively.

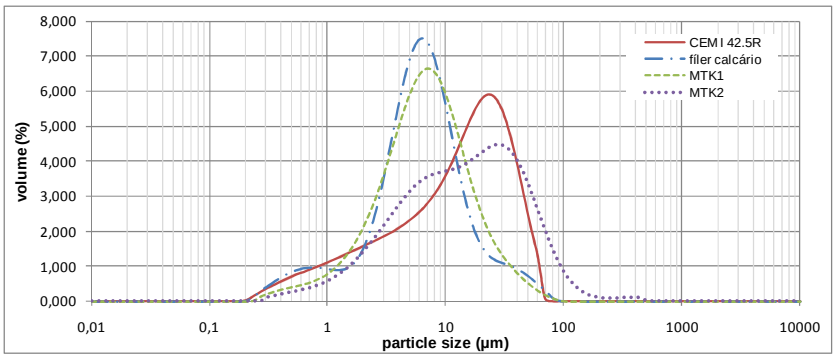

Figure 1. Particle size distribution curves in terms of volume.

The main differences in particles shape of the two types of addition used in this study can be observed in Fig. 2. Metakaolin particles have a very irregular shape with a flaky structure (Figure 2right), while limestone filler particles are more angular (Figure 2 left). MTK1 metakaolin is produced in USA and is white in colour, making it particularly attractive for architectural applications, while MTK2 is produced in Portugal and has a pinkish tone. MTK1 is currently marketed in Portugal at a price about 3.3 times MTK2.

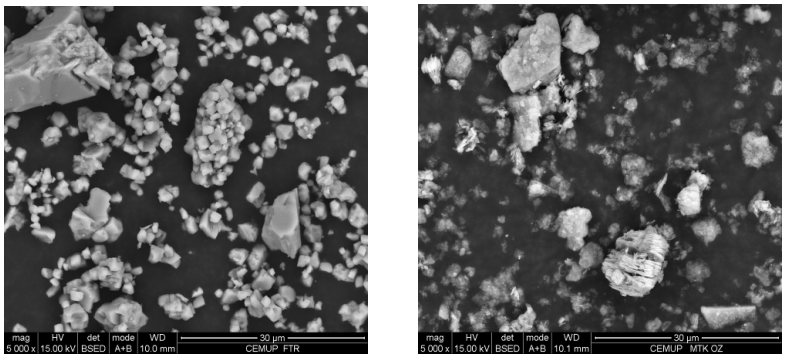

Figure 2. Backscattered electron images with a magnification of 5000x: limestone filler (left); metakaolin MTK1 (right).

Siliceous round natural sand (0.08–2 mm) was used with a specific gravity of 2.63 and an absorption value of 0.3 %, which is a reference sand conforming to CEN EN 196-1. A polycarboxylate type superplasticizer with a specific gravity of 1.05 and 25.5% solid content was employed for binary mixtures and a polycarboxylate type superplasticizer with a specific gravity of 1.07 and 26.5% solid content was employed for ternary mixtures.

2.2 Experimental design

To define the mortar composition three independent variables were selected, namely, water to powder volume ratio (Vw/Vp); water to cement weight ratio (w/c) and superplasticizer to powder weight ratio (Sp/p). For ternary mixtures it was necessary to include an additional variable to completely define the composition, which was metakaolin to cement weight ratio (mtk/c). In this study sand to mortar volume (Vs/Vm) was kept constant. The selection of these parameters, used widespread in the design of self-compacting concrete compositions, was based on the method developed by Okamura *et al.* [2000].

For binary mixes a 2^3 factorial statistical design [Montgomery 2001] corresponding to three parameters at two levels was carried out to establish models that describe key SCC properties and for the ternary mixes study a 2^4 factorial statistical design was adopted. To both experimental designs axial points and center points were added (Central Composite Design), allowing thereby a second-order model fitting. The effect of each factor was evaluated at five different levels $-\alpha$, -1, 0, $+1$, $+\alpha$. In order to make the design rotatable (i.e. the standard deviation of the predicted response is constant in all points at the same distance from the center of the design) the α value should be taken equal to

$n_f^{1/4}$, where n_f is the number of points in the factorial part of the design [Montgomery 2001]. Experimental programs also included central point repetition in order to evaluate the experimental error associated to conditions and test procedures variability. Table 1 presents the experimental plans characterization for binary and ternary mixtures.

Table 1. Experimental plans characterization.

Designation	Fine materials	Experimental design	Independent variables	[-α; +α]
Experimental design A (ED0)	Cem I 42.5R limestone filler	$\mathbf{2^3}$ α =1.692 n_c=4 n_f=8 n_a=6	Vw/Vp w/c Sp/p	[0.650; 0.900] [0.320; 0.510] [0.550%; 0,650%]
Experimental design B (ED1)	Cem I 42.5R limestone filler MTK1	$\mathbf{2^4}$ α =2.000 n_c=6 n_f=16 n_a=8	Vw/Vp w/c Sp/p mtk/c	[0.700; 1.000] [0.370; 0.490] [0.985%; 1.030%] [0.50; 0.20]
Experimental design C (ED2)	Cem I 42.5R Limestone filler MTK2			[0.650; 0.950] [0.360; 0.480] [0.978%; 1.023%] [0.05; 0.20]

n_c: nº of central points; n_f: nº of factorial points; n_a: nº of axial points

2.3 Response variables

Given the main objectives of this study, the selected response variables were: flow diameter (Dflow); V-funnel test (Tfunnel) and resistivity at 28 days ($Resistiv_{28d}$). The mortar flow test (Dflow) was used to assess deformability by calculating the flow diameter as the mean of two diameters in the spread area and the V-funnel test (Tfunnel) was used to assess the viscosity and passing ability of the mortar. These mortar tests using the flow cone and the V-funnel, with the same internal dimensions as the Japanese equipment were carried out to characterize fresh state (see [Okamura *et al.* 2000] for details on equipments and test procedures).

The resistivity test was selected to evaluate the durability of mixtures because it is a very simple and rapid, nondestructive test which enables the microstructure characterization. The electrical resistivity provides indications on the pore connectivity and therefore, on the concrete resistance to penetration of liquid or gas substances, and so resistivity is a parameter which accounts for the main key properties related to concrete durability [Andrade 2004]. Resistivity is an intrinsic property of the material that relates to the ability of concrete to carry electric charge and it depends mainly on the nature and topography structure, moisture condition, temperature and on the ion concentration in the interstitial solution. Regarding the influence of the chemical composition of pore solution, Andrade [2004] stated that its impact in the total resistivity is small providing the concrete remains alkaline. At high pH values the pore solution resistivity varies from 0.3 e 1.0 Ω.m, which is comparatively very small taking into account that concrete resistivity after several days of hardening is in the range of several hundreds Ω.m. Mortar resistivity was assessed by imposing a current passing through a mortar prism, in saturated conditions, and measuring the electric resistance which can be used to compute resistivity as follows,

$$R = V / I = \rho \cdot (L / A) \Rightarrow \rho = V \cdot A/(L \cdot I) \quad (1)$$

where R is the electric resistance, (Ω - Ohm); I, current (Amp.); V, voltage (Volts); ρ, electric resistivity (Ω·m); L, length (m); and A (m^2) the cross area of the test specimen through which current passes. Resistivity measurements were performed on prismatic specimens (4×4×16cm), in which stainless steel networks were embedded to work as electrodes. Mortar prisms were demoulded one day after casting and kept under water in a chamber under controlled environmental conditions (Temp.=20ºC and HR=95-98%) until testing. Since all the specimens were at the same moisture

(saturated) and temperature conditions, the resistivity measure can be used to evaluate the porous structure, and therefore constitute a measure of the amount and interconnectivity of the cementitious matrix pores.

2.4 Response models

For each response variable a quadratic model can be estimated from the central composite design data. The model parameters are estimated by means of a multilinear regression analysis. The generic form of a second order model is presented in Eq. 2, where y is the response of the material; x_i are the independent variables; β_0 is the independent term; β_i, β_{ii} and β_{ij} are the coefficients of independent variables and interactions, representing their contribution to the response; ε is the random residual error term representing the effects of variables or higher order terms not considered in the model [Montgomery 2001].

$$y = \beta_0 + \sum_{i=1}^{k} \beta_i x_{ij} + \sum_{i=1}^{k} \beta_{ii} x_{ij}^2 + \sum\sum_{i<j} \beta_{ij} x_i x_j + \varepsilon \quad (2)$$

3 FITTED MODEL ANALYSES

A commercial software (Design-Expert) was used to analyse the results for each response variable by examining summary plots of the data, fitting a model using regression analysis and ANOVA, validating the model by examining the residuals for trends, autocorrelation and outliers and interpreting the model graphically [Nunes *et al.* 2009]. Fitted models presented relatively high correlation coefficients (> 0.95) which indicates their good adjustment. The derived models also have good accuracy because the residual standard deviation and the standard deviation calculated from the central points (experimental error) were very close. The assumptions that the residuals are independent and normally distributed with zero mean and constant variance were also validated for all fitted models. Due to limitations of space, fitted models obtained for the fresh state (Dflow and Tfunnel models) will not be presented in the current paper. The results of the estimated models for the resistivity at 28 days ($Resistiv_{28d}$), including the residual error term, along with the correlation coefficients, are given in Table 2.

Table 2. Resistivity fitted numerical models (coded values of parameters) and relative influence of each parameter on the variation of response.

Response variable	*ED0 - R28d*		*ED1 - $R28d^{0.5}$*		*ED2 - $R28d^{-0.5}$*	
	(ohm.m)	*(%)*	*(ohm.m)*	*(%)*	*(ohm.m)*	*(%)*
Model terms: estimate						
independent	48,89		16.73		0.094	
Vw/Vp	-3.010	-20.6	-0.510	-9.8	0.003	11.8
w/c	-8.518	-58.3	-0.903	-17.4	0.004	17.6
Sp/p	-0.785	-5.4	NS	-	NS	-
mtk/c	NS	-	2.335	44.9	-0.015	-57.7
(Vw/Vp)×(w/c)	0.762	5.2	NS	-	NS	-
(Vw/Vp)×(Sp/p)	NS	-	NS	-	NS	-
(Vw/Vp)×(mtk/c)	NS	-	-0.513	-9.9	NS	-
(w/c)×(Sp/p)	NS	-	NS	-	NS	-
(w/c)×(mtk/c)	NS	-	NS	-	0.001	4.5
(Sp/p)×(mtk/c)	NS	-	NS	-	NS	-
$(Vw/Vp)^2$	NS	-	0.170	3.3	NS	-
$(w/c)^2$	1.525	10.4	NS	-	NS	-
$(Sp/p)^2$	NS	-	NS	-	NS	-
$(mtk/c)^2$	NS	-	-0.764	14.7	0.002	8.4
Residual error* std. deviation	1.189		0.039		0.002	
R^2 / R^2_{Adj}	0.986/0.980		0.977/0.971		0.991/0.989	

(NS) non-significant terms; (*) error term is a random and normally distributed variable with mean zero

The model coefficients presented in Table 2 give an indication of the relative influence of each mixture parameter on the Resistiv28d response variable. Naturally, higher values indicate greater influence of this parameter in the response and on the other hand, a negative value reflects a response decrease to an increase in this parameter. Observation of the table shows that, in the case of the experimental design without metakaolin (ED0), the water/cement ratio (w/c) is the variable that has a greater influence on the resistivity, while in experimental designs including metakaolin (ED1 and ED2) the metakaolin/cement ration (mtk/c) is the most influential variable. It is noted, however, that these two variables have opposite effects on the response. In the experimental plan ED0, beyond the great influence of the w/c variable, Vw/Vp and Sp/p parameters have some influence on $Resistiv_{28d}$, 20% and 5%, respectively. In the experimental plans including metakaolin as mineral admixture (ED1 and ED2) the influence of most relevant variables was quite similar.

The range of resistivity results of the mortars obtained with the three experimental plans was significantly different, varying between 39.1 e 67.2 ohm.m in ED0, between 87.4 e 437.3 3 ohm.m in ED1 and between 55.7 e 200.7 ohm.m in ED2. In order to highlight the differences between compositions including MTK1(ED1), including MTK2 (ED2) and without MTK (ED0), the chart shown in Fig. 3 presents the values obtained in the mortars for the three experimental plans (measured values) and the predicted values based on the $Resistiv_{28d}$ model derived for the ED2 plan (predicted values).

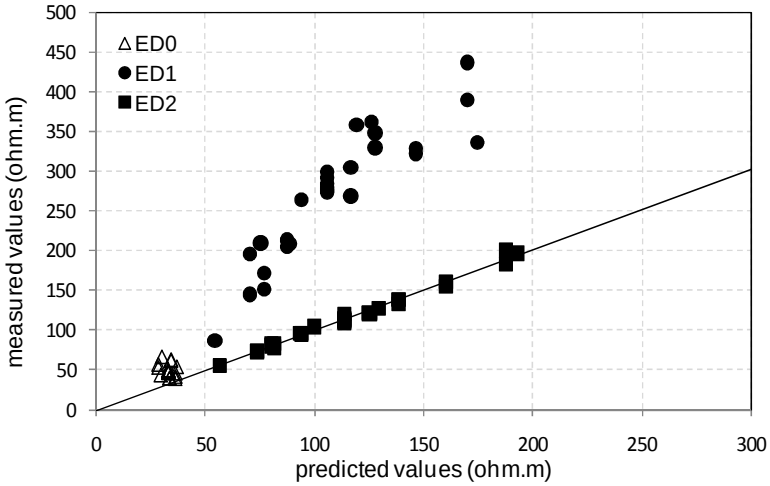

Figure 3. $Resistiv_{28d}$ predicted values based on the model derived for the ED2 plan versus measured values for plans ED0, ED1 and ED2.

From the analysis of this figure it can be concluded that the behavior of the three mixtures, binary mixture (CEM + filler), ternary mixture 1 (CEM + filler + MTK1) and ternary mixture 2 (CEM + filler + MTK2), with respect to the resistivity is fairly different. The adjusted model for the compositions including limestone filler and MTK2 (ED2) is not adequate to predict the behaviour of the compositions including MTK1 (ED1) and, although not as evident, the same seems to happen in the compositions including only limestone filler (ED0). The resistivity behaviour of mixtures including only cement and limestone filler (binary mixtures) is different from the behaviour of mixtures including metakaolin (ternary mixtures). Besides, the two metakaolins analysed performed differently), achieving higher values of resistivity, therefore better durability, in compositions including MTK1. According to Siddique and Klaus [2009] the partial replacement of cement by a pozzolanic material, like metakaolin, causes substantial changes on the pore structure of the mortar and on the chemistry of the hydration products. The metakaolin contributes to the microstructure improvement by the filler effect (like limestone filler) and by the pozzolanic reaction of metakaolin with calcium hydroxide. The different performances achieved with MTK1 and MTK2 may be due to the different particle size distribution and different origins and production systems of these metakaolins (different chemistry).

4 MIXTURE OPTIMIZATION

After building the regression models that establish relationships between mix design variables (Vw/Vp, w/c, Sp/p e mtk/c) and the responses (Dflow, Tfunnel and $Resistiv_{28d}$) the numerical optimization technique was used to determine a mortar composition that meets certain performance requirements defined in advance. These requirements may be set in terms of fresh and/or hardened state properties. With regard to the fresh state, it was defined that the optimal mortars from the standpoint of self-compactability should exhibit a Dflow between 260 e 280 mm and a Tfunnel between 8 e 12 sec, simultaneously. If a requirement related to resistivity is also imposed, say greater than 120 ohm.m, then self-compactable mortars based on cement and limestone filler (ED0) never fulfil this requirement (Fig.3). The set of optimized solutions based on the defined performance requirements: 260 mm ≤Dflow≤280 mm; 8 s ≤Tfunnel≤12 s and $Resistiv_{28d}$>120 ohm.m, for mixtures including metakaolin (ED2 and ED3), is presented in the graphs below (Fig. 4).

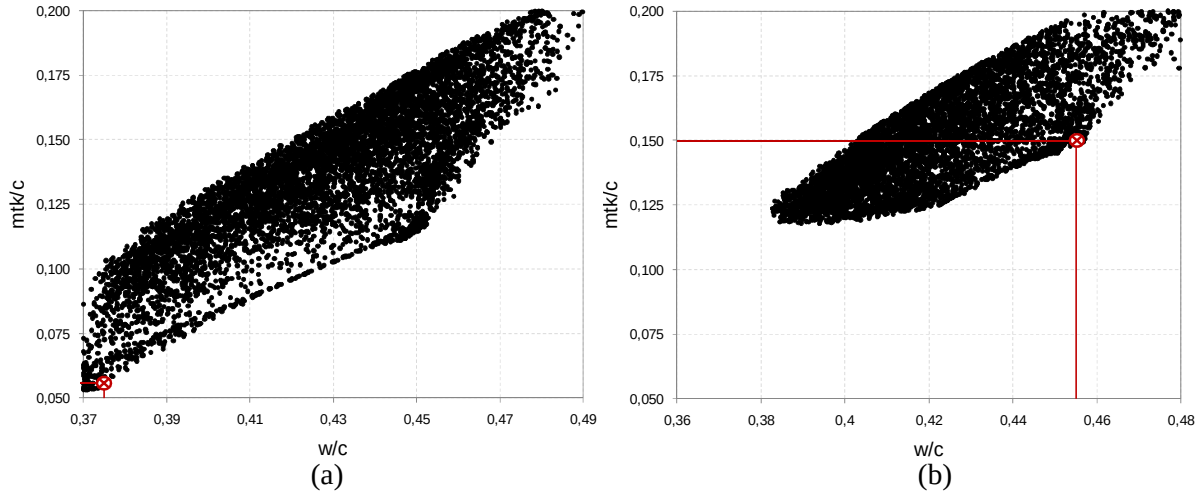

Figure 4. Range of values of the variables w/c and mtk/c for optimized mixtures: (a) ED1; (b) ED2.

By adding an economic constraint (minimizing cost) to the optimization criteria mentioned above, one single solution is obtained for each metakaolin type, identified in Figure 4. Table 3 shows the final optimized composition for each case, the respective fresh and hardened properties and the relative cost. Although both solutions have quite different w/c ratios, their performance in terms of fresh state properties and resistivity (durability) is very similar (see table 3). Nevertheless, the mixture including MTK2 exhibits lower cost.

Table 3. Mixture composition, fresh and hardened properties and the relative cost of optimized compositions

	Composition 1 (with MTK1)		**Composition 2** (with MTK2)	
	kg/m^3	**relative cost**	**kg/m^3**	**relative cost**
CEM I 42.5R	587	48.8%	487	40.5%
limestone filler	274	7.3%	316	8.4%
MTK1	32	21.9%	-	-
MTK2	-	-	73	15.5%
superplasticizer	8.8	22.0%	8.6	21.3%
Relative total cost		**100%**		**85.7%**
Dflow	279.7 mm		279.9 mm	
Tfunnel	12.0 sec		12.0 sec	
$Resistiv_{28d}$	120.2 ohm.m		123.0 ohm.m	

5 CONCLUSIONS

An experimental plan conducted according to a factorial design is useful to evaluate the effects of constituent materials and their interactions on SCC-mortar properties. Data collected during the experimental plan can be used to establish numerical models relating mixture parameters with the SCC properties of interest. Mortars including binary mixes (cement + limestone filler) and ternary mixes (cement + limestone filler + metakaolin) were study. Two different types of metakaolin were used in order to compare their performance. In this research, besides fresh state properties, deformability and viscosity, a durability related parameter (resistivity) was also analysed and mathematically modelled. The beneficial effect of metakaolin on durability indicators is clearly showed in this study. The variable mtk/c exhibited the greatest effect on resistivity. For mortars including only cement and limestone filler as fine materials, w/c was the mixture parameter that most influenced resistivity (durability). Furthermore, Vw/Vp also had a significant influence on resistivity. The superplasticizer to powder weight ratio (Sp/p) exhibited a reduce influence on resistivity. Other interaction and quadratic effects were found to be significant to explain SCC mortar durability property. The two types of metakaolin performed differently, which may be due to the different particle size distribution and different origins and production systems (different chemistry).

Numerical models established for the mortar mixtures can simplify the test protocol required to optimize a given SCC mixture, namely, to select the combination of powder materials with admixtures and to design a SCC mixture with defined performance requirements, in terms of fresh properties, hardened properties and economic constraints. For the optimization example presented in this paper it can be concluded that including MTK2 in the composition it is possible to satisfy all the requirements of fresh and hardened state (durability) with a lower cost than using MTK1. Compositions where only limestone filler was included were unable to meet the durability requirement (resistivity greater than 120 ohm.m).

ACKNOWLEDGMENTS

This research was financed by FCT – Portuguese Foundation for Science and Technology Research Project PTDC/ECM/70693/2006 and supported by PhD Research Grant SFRH/BD/25123/2005. Collaboration and materials supplying by SECIL, SIKA, COMITAL and Cerâmica Condestável is also gratefully acknowledge.

REFERENCES

ANDRADE, C. 2004, Calculation of initiation and propagation periods of service life of reinforcement by using the electrical resistivity, International symposium on Advances in Concrete through Science and Engineering, RILEM.

Bentz D, Garboczi E., 1991, Simulation studies of the effects of mineral admixtures on the cement paste-aggregate interfacial zone, *ACI Materials Journal* 88(5):518-529.

Montgomery, D. 2001, Design and analysis of experiments. 5ª ed. Wiley, New York.

Nunes S, Milheiro Oliveira P, Sousa Coutinho J & Figueiras J. 2009, Interaction diagrams to assess SCC mortars for different cement types, *Construction and Building Materials*, 23:1401–12.

Okamura H, Ozawa K & Ouchi M. 2000, Self-compacting concrete. *Structural Concrete*, 1:3–17.

Sampaio J, Coutinho J S, Sampaio N, 2001, Melhoria do desempenho de betões pelo metacaulino, 43º Congresso Brasileiro do Concreto, Instituto Brasileiro do Concreto, Brasil.

Siddique R & Klaus J, 2009, Influence of metakaolin on the properties of mortar and concrete: A review, Applied Clay Science, vol. 43, n. 3-4, p. 392.

XII DBMC
International Conference on Durability of Building Materials and Components
PORTO - PORTUGAL, April 12th-15th, 2011

Durability of Concrete Blended with Micronized Sands

Ying Wang [1]
Guang Ye[2]
Klaas van Breugel [3]
Michiel Haas [4]

ABSTRACT

In this study, micronized sand (MS) is selected as replacement of Portland cement to reduce the amount of cement used in concrete. This filler is considered as chemecally inert to water and hydration products. However, this material can influence the microstructure, affect the transport property and eventually change the service life of concrete structures significantly. In this paper, rapid chloride migration (RCM) tests are carried out. Chloride migration coefficients of concrete samples with and without MS are measured. The results, obtained from a wide range of finenesses (between 2400 and 13000 cm^2/g) and replacement levels (10% to 30%), show that migration coefficients of concrete samples with and without MS are different. The DuraCrete model is applied to predict the service life of structures made with this blended material. Migration coefficient of samples with 30% replacement increased and the required cover thickness of the structure to be increased in order to have 100 years' service life.

KEYWORDS

Micronized sands, Migration coefficient, Cement paste, Service life.

[1] Faculty of Civil Engineering & Geosciences of Delft University of Technology, Delft, NETHERLANDS, ying.wang@tudelft.nl
[2] Faculty of Civil Engineering & Geosciences of Delft University of Technology, Delft, NETHERLANDS; Faculty of Structure Engineering of Ghent University, Gent, Belgium. g.ye@tudelft.nl;
[3] Faculty of Civil Engineering & Geosciences of Delft University of Technology, Delft, NETHERLANDS, k.vanbreugel@tudelft.nl
[4] Faculty of Civil Engineering & Geosciences of Delft University of Technology, Delft, NETHERLANDS, E.M.Haas@tudelft.nl

1 INTRODUCTION

The production of Portland cement contributes to about 5-8% of global total CO_2 emission. This environmental problem is taken seriously by the concrete industry. In order to reduce the amount of cement used in the concrete industry, many pozzolanic and chemically inert mineral materials have been studied and used over last few decades, such as silica fume, fly ash, limestone powder and blast furnace slag. However, some of them are not always economical, like silica fume. Fly ash contains trace concentrations of heavy metals and other substances that are known to be detrimental to health. Quartz sand, on the other hand, is easy to get and has plenty of resource. It is obvious that the substitution of portland cement by sand can reduce not only the cost but also the emission of CO_2 (Lawrence 2003; Lawrence 2005). In this study, micronized sand (MS) is used, which is made by selected quartz sand and is purified both mechanically and chemically after extraction. The particle size distribution of quartz sand can be well controlled by adjusting the grinding treatment. Three types of MS are used here, with difference in fineness from 2400 to 13000 cm^2/g. This material is considered as an inert filler. However, the long term performance of this type of concrete is not clear. Since the chloride diffusivity is one of the important properties of concrete affecting the durability of a reinforced concrete structure, the rapid chloride migration (RCM) tests (Tang 1992; Tang 2006) were carried out to measure the chloride (Cl^-) migration coefficient of concrete made with MS. The DuraCrete model (DuraCrete 2000) is applied to evaluate the service life using the results from RCM test in which the different replacement levels are considered.

2 METERIALS AND METHODS

2.1 Meterials

Portland cement CEM I, 42.5N (OPC) and micronized sand (MS) produced by a Belgian company are used. Three types of MS of high purity are used, named M6 (coarse), M300 and M600 (fine), categorized by fineness. The chemical composition and physical properties of cement and MS are stated in table 1 and 2. The particle size distribuitons (PSD) of the materials are plotted in figure 1. It can be found that the particle size distribution of M300 is very similar to that of OPC. The mixture proportions for the RCM specimens are given in table 3. No superplasticizer or other additives are used.

Table 1. Chemical Composition of cement material (%).

Component	*Percentage* (%)
C_3S	65.83
C_2S	14.76
C_3A	8.31
C_4AF	11.11
CaO	0.6

Table 2. Material information of micronized sands (MS).

Type	*Density* (g/cm^3)	*Fineness* (cm^2/g)	*Mean Size* (μm)	*SiO_2* (%)
M6	2.65	2400	30	99.5
M300	2.65	4000	17	99.5
M600	2.65	13000	4	99.2

Table 3. Mixture composition (kg/m^3). w/b=0.40.

Sample	*OPC*	*MS*	*Water*	*Sand (0-4)*	*Grind (4-16)*	*Metselzand (0-2)*
Ref	390	0	156	498	1103	178
M6_10%	351	39 (M6)				
M6_20%	312	78 (M6)				
M6_30%	273	117 (M6)				
M300_20%	312	78 (M300)				
M600_20%	312	78 (M600)				

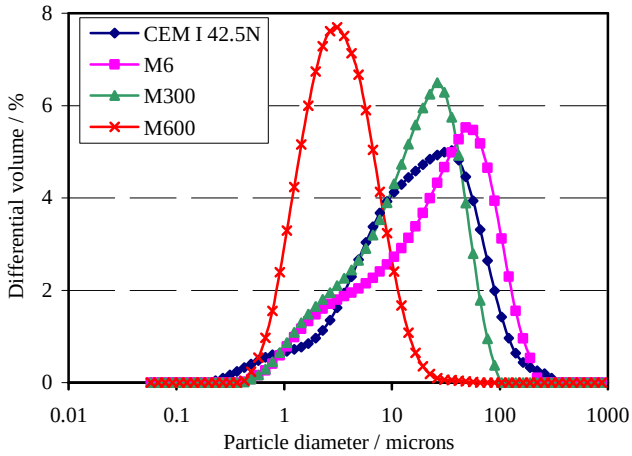

Figure 1. Differential volume of particle in different material (De Vries 2008).

2.2 Method

Rapid chloride migration (RCM) test (NT BUILD 492 1999) is used for evaluating the resistance of concrete to chloride ingress. Results are obtained quickly and with relatively good precision. The migration coefficient obtained from this method can be used as an input for service life prediction. The experimental set-up is shown in figure. 2. This method requires cylindrical specimens with a diameter of 100 mm and a thickness of 50 mm. Specimens with the mixture composition mentioned in table 3 are prepared in the laboratory using plastic moulds with Φ100mm. 5 liters of concrete is casted for each mixture. After 28 days, 3 samples with thickness of 50 ± 2 mm are cut from the cylinders. Under an external electrical potential, the cathode forces the chloride ions in the catholyte to migrate into the specimen. After a certain test duration (typically 24 hours), the specimen is axially split and a silver nitrate solution is sprayed on the freshly split sections. The chloride penetration depth can then be measured from the visible white silver chloride precipitation, after which the chloride migration coefficient can be calculated from this penetration depth (Tang 2006). The details of the procedure can be found in NT BUILD 492.

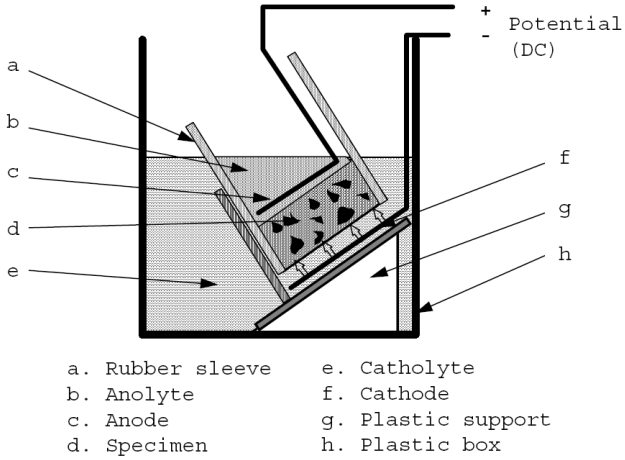

Figure 2. Rapid chloride migration test set-up (NT BUILD 492 1999).

3 RESULTS AND DISCUSSIONS

3.1 Results and Discussions

The non-steady-state migration coefficient can be calculated according to:

$$D_{nssm} = \frac{0.0239(273+T)L}{(U-2)t}(x_d - 0.0238\sqrt{\frac{(273+T)Lx_d}{U-2}}) \quad (1)$$

where:

D_{nssm}: non-steady-state migration coefficient, $\times 10^{-12}$ m^2/s;
U: absolute value of the applied voltage, V;
T: average value of the initial and final temperatures in the anolyte solution, °C;
L: thickness of the specimen, mm;
x_d: average value of the penetration depths, mm;
t: test duration, hour.

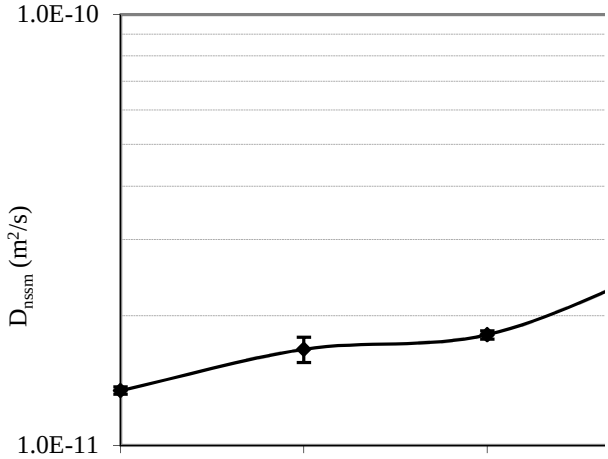

Figure 3. The non-steady-state migration coefficients (D_{nssm} m^2/s) as the function of replacement percentage of M6 (coars).

The results of concrete specimens with and without MS are shown in figure. 3 and 4. In these figures, it shown that the scatter of the results is very small. Therefore, the reproducibility of this method and results are considered reliable.

In figure. 3, coefficients of concrete specimens with coarse MS (M6) are plotted as function of the replacement percentage. When the replacement level of MS increases, the migration coefficient increases as well. The reason is that the amount of cement in the concrete is reduced, so that less hydration products are present in the system, resulting in a more porous microstructure (Wang 2010). The porosity of M6_30% is 28.51%, compared with 22.89% in OPC paste sample. This porous microstructure makes that Cl^- ion can easily penetrate into the material, especially in the specimens with 30% replacement by MS.

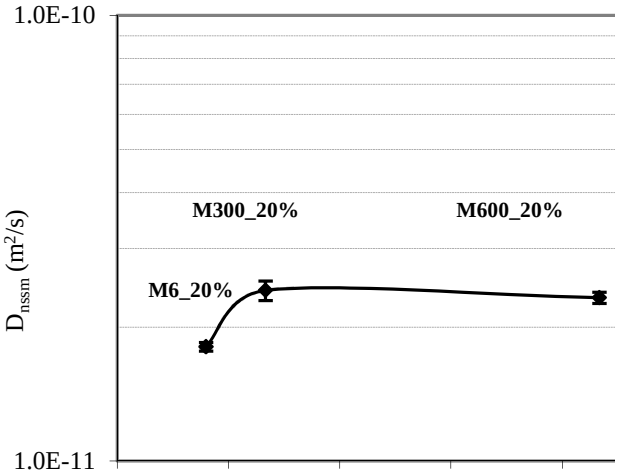

Figure 4. The non-steady-state migration coefficients (D_{nssm} m^2/s) as the function of fineness of MS.

In figure. 4, migration coefficients of concrete specimens with 20% replacement are plotted as function of the fineness of the MS. The influence of the particle size of MS on the migration coefficient indicates that concrete specimens with 20% coarse MS, i.e. M6, has the lowest value. This is attributed to the packing density of the blended system. The packing density of blended material is improved if the width of PSD is wider and the possibility of filling the voids is increased (De Vries 2008). In the present experiments, the particle size distribution of M6 is different from OPC and is wider than that of other fillers (figure. 1) which leads to a denser microstructure and thus, lower migration coefficient.

3.2 Service life prediction according Duracrete

DuraCrete model has been developed to predict the service life for a number of different concrete structures (Lindvall 1998; DuraCrete 2000). Following the DuraCrete model, chloride ingress can be calculated using equation 2.

$$C(x,t) = C_s - (C_s - C_i)erf\left[\frac{x}{\sqrt{\left\{4kD_0\left(\frac{t_0}{t}\right)^n t\right\}}}\right] \quad (2)$$

where:

- C(x,t): the chloride content at depth x at time t;
- C_s: the surface chloride content;
- C_i: the initial chloride content;
- k: a correction factor;
- n: the ageing coefficient;
- D_0: the D_{RCM}-value at the reference time t_0 (28 days).

Therefore, the time to initiation corrosion is defined as:

$$\Rightarrow t = \left\{ \left[\frac{x}{erf^{-1}(\frac{C_s - C}{C_s - C_i})} \right]^2 / 4kD_0 t_0^{\,n} \right\}^{\frac{1}{1-n}} \quad (3)$$

There are several parameter values that have to be set. The atmospheric condition is chosen in this study. The surface chloride content was assumed to be independent of the mix composition for reasons of simplicity: 1.5% for land based structures (DuraCrete 2000; Polder 2001). The initial chloride content of the concrete was taken equal to 0.1%. The correction factor depends on the binder type, the environment and the curing. The k-values were taken from report DuraCrete 2000 (DuraCrete 2000). The critical chloride content is taken as 0.6% by mass of cement (DuraCrete 2000). The information is summarized in table 4.

Table 4. Values of parameters using in equation 2.

Critical chloride content for rebar	C(x,t)	0.6%
Surface chloride content	C_s	1.5%
Initial chloride content	C_i	0.1%
Correction factor	k	1.53
Result from RCM test (m^2/s)	D_0	D_{nssm}
Reference time (sec)	t_0	28*24*3600
OPC atmospheric condition	n	0.65
Cover thickness (m)	x	0.03

After inserting the above parameters in equation 3, the time to initiation of corrosion can be obtained. Even though the coefficients (figure. 3 and 4) are in the same order of magnitude, the time to initiation of corrosion in concrete structures with and without MS shows a big difference. Therefore, the cover thickness of structure need to be adjusted in order to meet the requirement of 100 years' service life (table 5). Compared to a cover thickness 32.5 mm in the ordinary concrete structure, the increased cover thickness is calculated for the structure made with blended materials. For concrete made with M6_30%, the cover thickness of material should be increased 13mm in order to serve 100 years' in practice. Compared with the dimension of the structure, this increase is very little. For instance, if M6_30% cement paste is applied in a structure of 1m in width, the increase of the cover thickness compared to the dimension of the structure is less than 2%. However, this material can reduce almost 30% CO_2 emission. On the other hand, for many application of the concrete material, like many indoor structures, Cl^- migration evaluation is of little relevance. The advantage of this material on the environment and ecology is very obvious. This is a promising material which can be used in the cement industry.

Table 5. Cover thickness of structure under consideration of 100 years' service life.

Specimens	*Modified cover thickness (mm)*	*Increased thickness (mm)*
OPC	32.5	0
M6_**10**%	36	3.5
M6_**20**%	37.5	5
M6_**30**%	45.5	13
M300_**20**%	43.5	11
M600_**20**%	42.5	10

4 CONCLUSIONS

In this paper, the the non-steady-state migration coefficients of concrete with and without MS is studied using RCM test. Parameters, like replacement level and fineness of MS, are taken into account. Service life is predicted based on the migration coefficients using Duracrete model. The following conclusions are achieved:

- When the replacement level of MS is increasing, the Cl^- migration coefficient increases. The values of the coefficients are in the same order of magnitude, but the present of MS does influence the service life.
- Particle size distribution of M6 gives contributions to the packing density, which also improves the microstructure in comparison to the other blended materials and lead to a lower migration coefficient.
- For many indoor application, Cl^- migration evaluation is not the dominant problem. MS blended material could be a promissing material in this field.
- Even in case Cl^- migration to be considered, the cover thickness of structure needed to be increased 3.5-13mm to meet the engineering requirement of 100 years' service time. The increase of the cover thickness compared to the dimension of the structure is very little. However, this material can reduce big amount of CO_2 emission. The advantage of this material on the environment and ecology is very obvious.

ACKNOWLEDGMENT

The appreciations will be given to the China Scholarship Council (CSC) for the financial support.

REFERENCE

De Vries, W. 2008. *The use of micronized sand as cement replacement*. Delft, Delft University of Technology. Master.

DuraCrete 2000. *DuraCrete Final Technical Report R17*. Gouda, The European Union – Brite EuRam III, DuraCrete – Probabilistic Performance based Durability Design of Concrete Structures, CUR.

Lawrence, P., Cyr, M. & Ringot, E.. 2003. 'Mineral admixtures in mortars: Effect of inert materials on short-term hydration'. *Cement and Concrete Research* **33**[12], 1939-1947.

Lawrence, P., Cyr, M. & Ringot, E.. 2005. 'Mineral admixtures in mortars effect of type, amount and fineness of fine constituents on compressive strength'. *Cement and Concrete Research* **35**[6], 1092-1105.

Lindvall, A. 1998. 'DuraCrete-Probabilistic Performance Based Durability Design of Concrete Structures'. 2nd Int. PhD Symposium in Civil Engineering Budapest.

NT BUILD 492, 1999. *Concrete Migration Coefficient from Non-Steady-State Migration Experiments*.

Polder, R. B. 2001. 'Test methods for on site measurement of resistivity of concrete - a RILEM TC-154 technical recommendation.' *Construction and Building Materials* **15**[2-3], 125-131.

Tang, L. P. 2006. 'Chloride Induced Corrosion in Concrete Structures Testing and Modelling'. Bridge and Infrastructure Research in Ireland: Symposium. Ireland.

Tang, L. P. & Nilsson, L. O.. 1992. 'Rapid determination of the chloride diffusivity in concrete by applying an electrical field.' *ACI Materials Journal* **89**[1], 40-53.

Wang, Y., Ye, G. & van Breugel, K.. 2010. 'Performance of Cement Paste Partially Replaced by Micronized Sand'. 6th International Conference on Concrete under Severe Conditions Environment and Loading. Merida, Mexico, 7-9 June 2010, vol. 2, pp. 1551-1558.

XII DBMC
International Conference on Durability of Building Materials and Components
PORTO - PORTUGAL, April 12th-15th, 2011

Probabilistic Evaluation of the Durability of Ready Mix Mortars on the Maintenance of Historic Masonry

Cristina Tedeschi [1]
Luigia Binda [2]
Elsa Garavaglia [3]

ABSTRACT

One of the main causes of deterioration of masonry surfaces in aggressive environment is the salt decay; the phenomenon is emphasized by the presence of the mortar joint, faster vehicle of the salts. In case of surface damages re-pointing mortar mix is frequently used and the durability of the intervention depends on the quality of the new mortar.

To investigate the durability of different mix mortars for the maintenance of historic masonry, according to RILEM Recommendations MS-A1 crystallization tests were carried out on masonry specimens built with the same type of bricks and different types of mortar mix.

The parameter assumed as significant measure of material deterioration process is the loss of surface materials. The measure has been made with a laser profilometer over time.

The great randomness connected with the environment critical attacks, suggests studying the deterioration under a probabilistic point of view, Following this way, the deterioration process of the masonry samples was approached as a stochastic process of the random variables ℓ (where ℓ is the loss of surface material at each laboratory test cycle). The modelling adopted is the fragility curves modelling developed by the authors to analyze this kind of problems.

KEYWORDS

Masonry durability, Accelerated crystallization tests, Probabilistic model, Fragility curves approach.

[1] Department of Structural Engineering, Politecnico di Milano, Milano, ITALY, binda@stru.polimi.it
[2] Department of Structural Engineering, Politecnico di Milano, Milano, ITALY, tedeschi@stru.polimi.it
[3] Department of Structural Engineering, Politecnico di Milano, Milano, ITALY, garava@stru.polimi.it

1 INTRODUCTION

One of the highest causes of building materials damage especially in Mediterranean countries, is the crystallisation of soluble salts (sulphates, nitrates, clorides, etc.) present in the pores of the material itself. The decay due to salts can seriously compromise the conservation of the exposed surfaces of the cultural heritage. The related decay mechanisms have been discussed in several studies, as well as the influence of many factors affecting salt movement, crystallization location and degradation rate [Binda et al. 1985, Cardani et al. 2001]. The research has pointed out the great importance of the compositional and microstructural features of porous materials on their salt-decay attitude and the need for experimental work taking into account the masonry substrate.

The paper reports on evaluation and modelling of the data obtained from an experimental study carried out on natural hydraulic binders (NHL) and on commercial ready-mixed mortars proposed by the producers as materials for the conservation of the Cultural Heritage (C.H.). Several products are currently available on the market and their use is increasing, as they may represent a convenient alternative to the preparation of traditional hydrated lime-based mortars. Nonetheless, a thorough knowledge of their durability is still missing. It is therefore rather difficult to predict their behaviour at work, especially when these new materials are introduced in a heterogeneous system, as masonries of the built heritage almost always are. A complete characterization of the compositional, mineralogical, physical and mechanical properties has been performed on the mortars by means of a wide range of techniques, including optical microscopy, XRD, FTIR, SEM and reported in [Gulotta et al. 2009, 2010].

Salt crystallisation tests have been carried out on masonry specimens built with one type of soft mud bricks and 6 types of NHL mortars following the RILEM pre-standard procedure [RILEM MS-A1, 1998] for the evaluation of salt resistance to sulphates. Damage evolution of wallettes has been monitored by visual observation and by quantification of material loss from the surfaces after several crystallisation cycles. Remarkable differences in the damage extent and in the decay patterns have been observed, depending on the characteristic features of the different mortars.
The results of the crystallisation tests are reported in the following sections referring to the durability of the studied mortars when used as joints of a brick masonry.

On the basis of recorded experimental data, a suitable damage parameter describing the material deterioration process has been chosen. The parameter assumed is the loss of surface material at each measurement. The measurements have been made through a laser device along a chosen profile on the surface of the mortar joint and the loss is quantified as the variation of the profile depth over time.
The randomness present in the mortar conglomerate suggests to deal with the deterioration process as a stochastic process of the random variable ℓ (where ℓ is the loss of surface material). Therefore, the deterioration process would be interpreted with a process, $L(c,\ell)$, function of the time (or cycles) c and the damage ℓ. The modelling has been made following a Log Normal distribution. Considering some significant damage thresholds $\bar{\ell}$ and following the procedure developed by Garavaglia et al. (2002, and 2008) the building of the *fragility curve* describing the probability to reach or exceed $\bar{\ell}$, over time (number of cycles), will be approached. By using this approach, the magnitude of the expected damage over time and the occurrence time of it can be predicted.

2. EXPERIMENTAL PROGRAM

2.1 Mortar characterisation

Four ready-mixed commercial mortars and two commercial binders were selected. All products are proposed by the producers as materials for restoration purposes, and classified as cement-free, with a

minimum content of soluble salts and are based on NHL binders. The products here called MA, MB, MC, MD refer to the ready-mixed mortars, while the ones called LA and LB refer to the commercial binders. Materials characterisation of each product was performed both on anhydrous raw materials and on hardened mortars samples by means of: stereomicroscopy; X-ray diffraction; FT-IR spectroscopy; ionic chromatography; optical microscopy of thin sections observed under visible light and UV light; SEM+EDX analysis. The related results have been thoroughly reported in previous works [Gulotta et al. 2009, Gulotta et al. 2010] and are here only summarized.

Concerning the powdered raw materials, the main binder phase in most of the analyzed samples is Larnite. It is a di-calcium silicate (Ca_2SiO_4) analogous to C_2S, which is typical of NHL compositions and responsible for the hydraulic behaviour of the binders. Larnite is associated to portlandite ($Ca(OH)_2$) in the composition of all samples, expect for MD. Sample MA, differently from all others, only shows the presence of portlandite while no Larnite is traced. Aggregates of the ready-mixed products are quite heterogeneous: quartz and calcite are the most diffused mineral phases, which are present together with plagioclase, mica and dolomite. Analysis of samples from the hardened mortars provide further compositional and micro-structural information.

Mortar MA has residual non hydrated C_2S grains uniformly dispersed within the matrix and a high amount of fine grained calcite is present as carbonatic filler. The hardened matrix of MB is very compact and very rich in partially reacted slag fragments which contribute to the hydraulic behavior. C_2S is the main hydraulic phase traceable in the binding matrix of mortar MC, but few C_3S grains are present as well. The presence of an air-entraining additive in this mix leads to a peculiar microstructure with small and regular rounded shape pores. MD has a compact binder with only few residual not hydrated C_2S grains dispersed in the matrix. Samples LA and LB, which are prepared mixing together commercial binders and standard quartz-siliceous aggregate, show predominant C_2S and few C_3S grains in the hardened mortars. Moreover, in LB binder composition a carbonatic filler is present.
On the hardened mortar specimens porosimetry analyses were carried out by mercury porosimeter. In Table 1 the total porosity and the average pore radius in volume are reported.

Table 1. Porosity and Median Pore Radius (Volume).

Type of mortar	*Porosity* [%]	*Median Pore Radius* Volume [μm]
MA	30.37	0.05
MB	26.48	0.16
MC	27.08	0.43
MD	34.26	0.66
LA	22.59	0.27
LB	21.42	0.20

2.2 Test procedure

The test was carried out according to the Recommendation RILEM MS A.1 of RILEM TC 127-MS. [RILEM MS-A1, 1998]. Each wallette consisted of three courses of bricks with two horizontal bed joints and a vertical one (Fig. 1). A red soft-mud brick of high porosity, used for restoration was selected.

Anhydrous ready-mixed products were just added with the correct amount of pure water according to the indication of technical data sheets. Commercial NHL binders LA, LB were mixed with clean standard aggregate with a 1:3 B/A ratio (w/w) and then added with pure water. All mixing operations were conducted under controlled conditions with the aid of a mortar mixer. The masonry specimens were called MA, MB, MC, MD, LA and LB, as the mortars used for joints.

The wallettes (approx. 250x200x120 mm) were put in contact with their back side with a 10% (w%) Na_2SO_4 solution (anhydrous Na_2SO_4 reagent grade, Fluka) and then stored over a layer of dry gravel in a plastic container open at the top, sealed along the borders (Fig.2a) with the upper face exposed to a laboratory controlled environment (20°C and 50% R.H.).

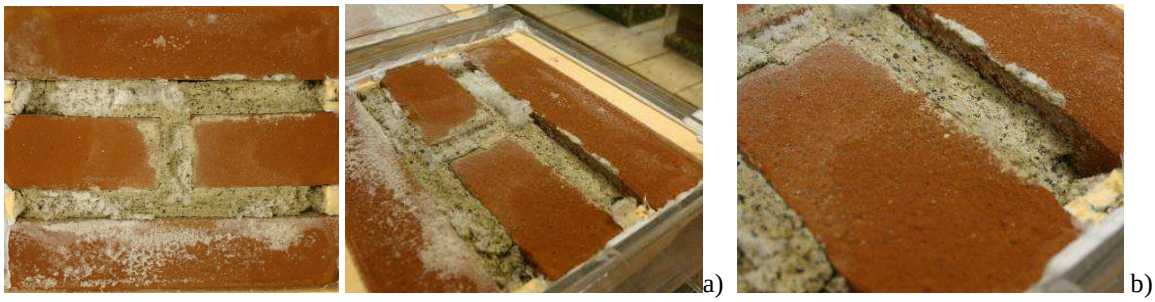

a) b)

Figure 1. Surface of MA wallette after 7 four week cycles: (a) after brushing (b) detail of MA specimen after 7 weekly cycles: severe scaling of the mortar can be observed.

After four weeks the first crystallization cycle (or step) was concluded, wallettes were subjected to a) visual inspection, b) cleaning from efflorescence and detached materials with a soft brush and a vacuum cleaner, c) photographic survey, d) description of the observed damage, e) reading of the surface profiles by means of a laser profilometer which allowed to quantify the damage. In Fig.1 a), b), c) picture of steps from a) to d) are shown, referred to the specimens made with mortar MA and also called MA. De-mineralised water was then added and a new 4-weeks cycle began.

2.2.2 Damage measurement by a laser profilometer

A laser profilometer was used to monitor the damage (Fig. 2 a,b,c) [Tedeschi et al., 2010]. The use of the laser profilometer allows to measure, with a very good resolution, the loss of material from the exposed surface calculated at subsequent times.



a) b) c)

Figure 2. a) wallettes in the boxes, b) laser profilometer, c) scheme of the measurement.

Profiles recorded at the end of each 4-weeks cycle show how the surface is changing during time due to the progress of the decay and the loss of material can be measured [Garavaglia et al., 2002]. The results can be used for probabilistic modelling of the progressing damage and the life cycle assessment of the material [Garavaglia et al., 2008].

Visual inspection continuously made during the tests revealed some common behaviour of the mortar joints. Since the first days soft efflorecences in the shape of needles appeared on the surface of MA (Fig.1a). In other cases efflorescence appeared at the interface brick-mortar joint. Later on, one month after the test beginning some bricks suffered delamination.

During the first and the second cycle of the test the highest loss of material as powdering or crumbling occurred. At the end of the second cycle the damage seemed to stabilise; in fact a phenomenon of local spalling and delamination takes place.

The most critical situation is represented by the MA specimen, on which the spalling appears to be the most evident even at visual inspection (Fig. 1). This behaviour could also be measured monthly by the laser profilometer as shown graphically in Fig. 3. Here only the results concerning the profiles taken in direction B-B (Fig. 2b) are elaborated and discussed. They only report the damages measured along the horizontal mortar joint in Figure 2c). A total number of 7 cycles has been carried out up to now, but the test will continue for at least other two months. In Figure 3, the profiles in direction B-B from the first to the last cycle are reported for the specimen MA.

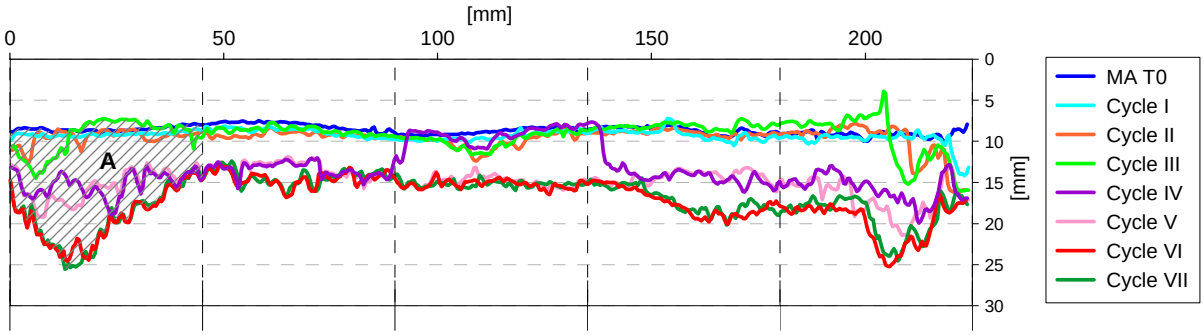

Figure 3. Damage evolution of the wallette MA during the test: progressive loss of material recorded by laser profilometer at the end of each 8-weeks cycle.

2.2.3 A significant paramenter to quantify the damage.

The loss of material, measured as the area between two contiguous profiles recorded cycle by cycle, will be here assumed as the significant parameter to quantify the damage due to salt crystallisation on the mortar joint. Therefore, for each profile *i* and at every cycle, the loss ℓ_i is assumed to quantify the damage for the decay due to salt crystallisation. To best compare the results obtained, the damage has been plotted in percentage:

$$\ell = \frac{\text{area, } \mathbf{A}\text{, lost}}{\text{area tranversal section}} * 100 \qquad (1)$$

The profile was divided into 5 parts and for each part the lost area **A** (Fig. 3, shadowed area) and its percentage ℓ_i were calculated at each cycle in order to collect the variation of the damage along the joint. A simple linear interpolation of the experimental point permits to better read the behaviour of the loss ℓ_i over time (linear splices). In Figure 4 the loss (in %) against the number of cycles is plotted for specimen MB, as an example.

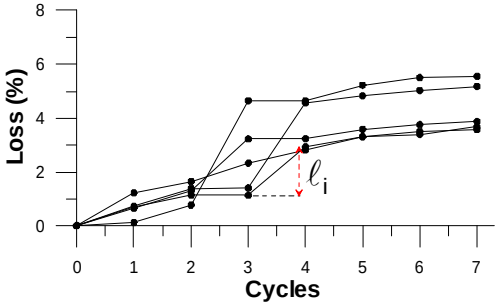

Figure 4. Mortar type MB-deterioration vs. cycles: example of behaviour.

3. EVALUATION AND DISCUSSION OF THE RESULTS

In Figure 5, the average loss (in %) over the 5 points of measurement along the horizontal mortar joint for all the mortars is plotted, showing that mortar MA has the maximum damage followed by mortar MB, LB, LA, MC and MD respectively. In order to explain and better understand the reason for these different behaviour a tentative was made to correlate the loss with the median pore radius of the

original mortars (see Table 1). It seems that the pore median parameter can be a good one to explain the behaviour of the specimens to the crystallisation test (Fig. 6). As it was said before in fact the salt damage highly depends from the porosity of the materials, or better from the pore size distribution: the lowest is the radius, the highest is the damage.
Figure 7 is a 3D representation of the damage as a function of median pore radius and of the number of cycles, better confirming what is shown by Figure 6 and Table 1 (five damage levels).

4 THE DETERIORATION PROCESS AS A STOCHASTIC PROCESS IN THE RANDOM VARIABLE ℓ

The deterioration process will be here interpreted as a stochastic process function of cycle c and damage ℓ, where ℓ is considered a r.v. because of experimental evidence. During the laboratory test the measurement are made at each cycle c*; by experience, the measurements made at the same cycle but on different samples show dispersion around an average value. Therefore, at each cycle c* the deterioration process can be viewed as function of the r.v. ℓ only**.** To modelling this behaviour, an opportune distribution must be chosen. This choice is not simple; it must be based on physical knowledge of the phenomenon modelled and on the knowledge of the mathematical frame governing the distribution's tails behaviour. In [Garavaglia et al. 2002] this subject is largely explained and the conclusion is that a plausible probability density function (PDF) able to interpret the dispersion in the material loss, cycle by cycle, is the Log-Normal distribution (Fig. 8).

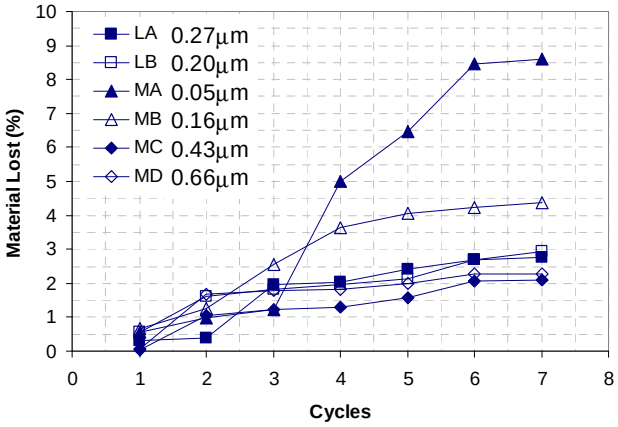

Figure 5. Deterioration (mean values) vs. cycles for the six mortar types.

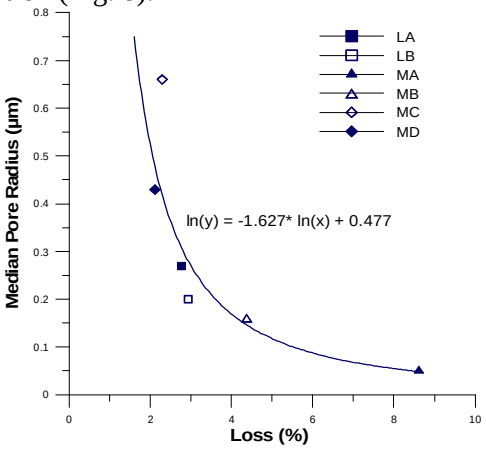

Figure 6. Pores dimension vs maximum percentage of material area loss

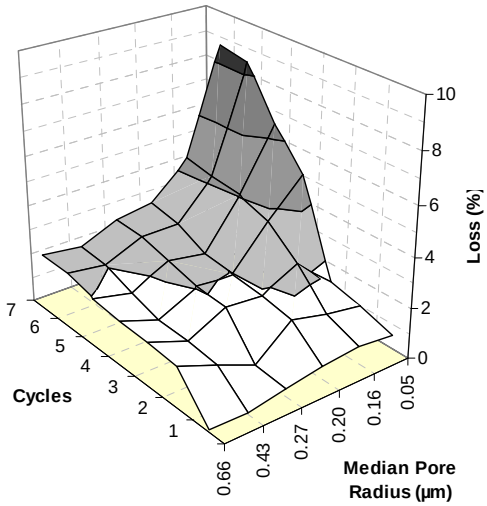

Figure 7. Damage behaviour as function of median pore radious and number of cycles.

If some significant damage thresholds $\bar{\ell}$ are considered and the variable time needed to exceed it must be predict; then the deterioration process must be treated as a reliability problem.

Indeed reliability $R(t)$ is concerned with the performance of a system over time and it is defined as the probability that the system does not fail by time t. Here is extended this definition by denoting by $\bar{R}(c)$ the probability that a system exceeds a given significant damage threshold $\bar{\ell}$ by the cycle c. The random variable that is used to quantify reliability is $\bar{C}$. $\bar{C}$ is the cycle in which the exceeding of the damage $\bar{\ell}$ can happen with a given level of probability. Thus, from this point of view, the reliability function is given by [Garavaglia et al. 2008]:

$$\bar{R}(c) = \Pr(\bar{C} > c) = 1 - F_{\bar{C}}(c) \qquad (2)$$

where $F_{\bar{C}}(c)$ is the distribution function for $\bar{C}$.

Computing $F_{\bar{C}}(t)$ for different damage levels $\bar{\ell}$ allows for building the *fragility curve* for each $\bar{\ell}$.

A fragility curve describes the probability of reaching or exceeding a given damage $\bar{\ell}$ over time (or cycles). For a chosen damage level $\bar{\ell}$ at a given cycle c^*, the probability to reach $\bar{\ell}$ can be seen as the area under the threshold $\bar{\ell}$ and the probability of exceeding it can be seen as the area over the threshold $\bar{\ell}$ (Fig. 9 - hatched area).

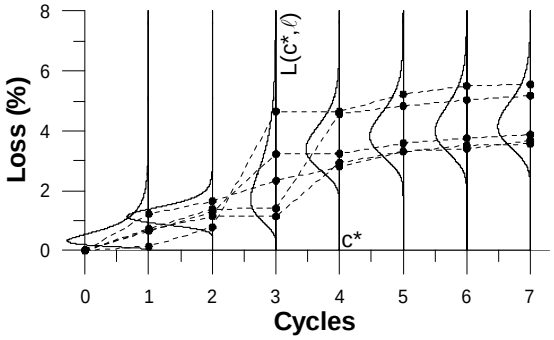

Figure 8. Mortar type MB-deterioration vs. cycles: modelling of dispersion.

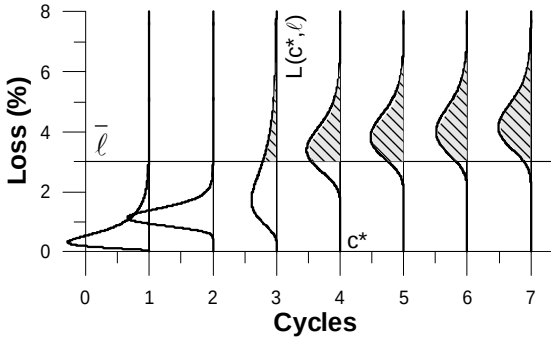

Figure 9. Mortar type MB-Exceeding probability to cross the threshold $\bar{\ell}$.

Indeed, the computed areas over different thresholds $\bar{\ell}$ provide the experimental exceeding probability used to fit the fragility curves. Therefore, the exceeding probabilities evaluated for each damage level $\bar{\ell}$ at every cycle c^*, lead to the building of the experimental fragility curves for each chosen $\bar{\ell}$ and their theoretical modelling $F_{\bar{C}}(c)$ with a Weibull distribution [Garavaglia et al 2002].

The evolution of the damage connected with the six mortars investigated is compared in Figure 10 through the theoretical fragility curves $F_{\bar{C}}(c)$. It is evident that mortars characterized by higher median pore radius (MC and MD) present significant exceeding probability of high damage thresholds only for high numbers of cycles. Vice versa mortars characterized by small median pore radius (MA and MD) present high probability of damage already from the first cycles.

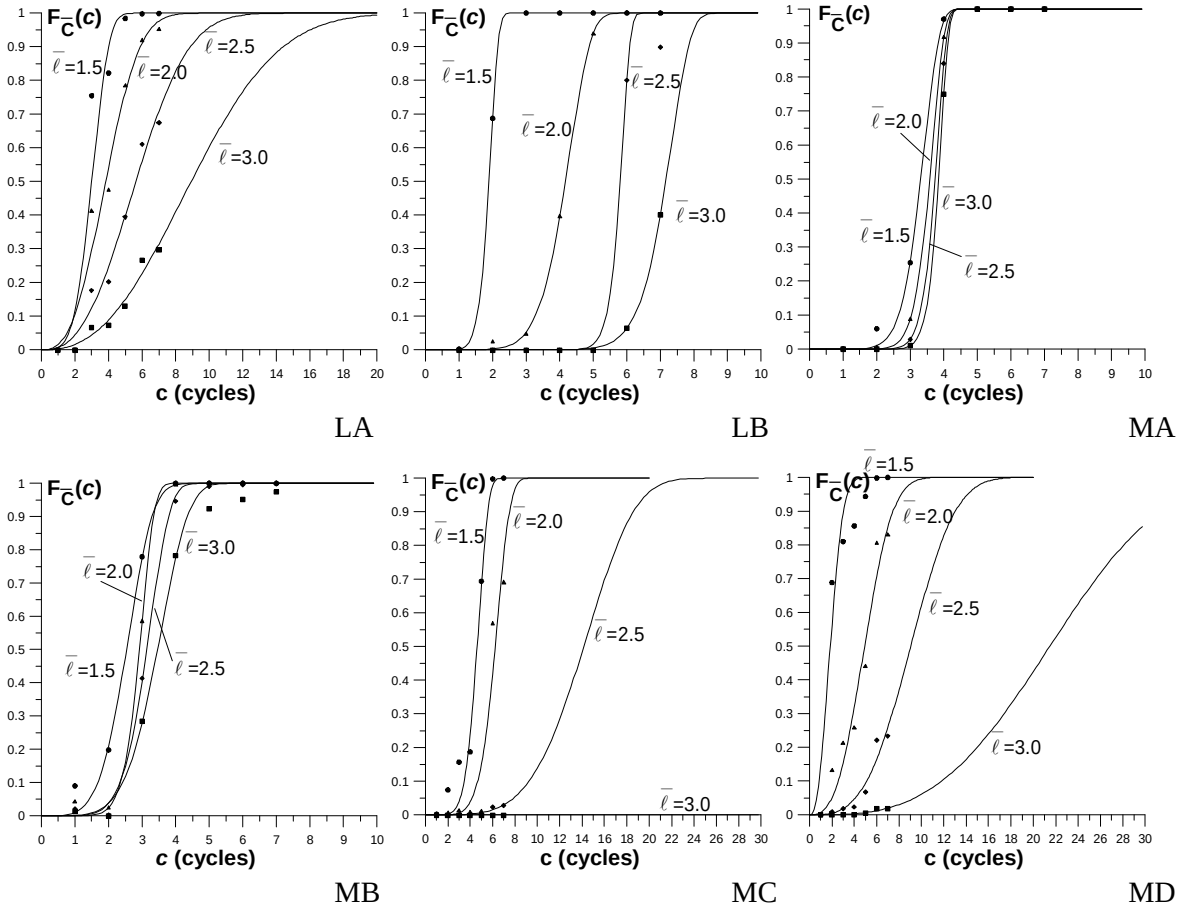

Figure 10. Fragility curves for different treshoulds $\bar{\ell}$**.**

5 CONCLUSIONS

The cristallysation tests have put in evidence some different behaviour of the tested ready mix mortar. The different behaviour seems to be connected with the size and dimension of the material pores. An important emerged evidence is the relationship between the median pore radious and the damage: smaller is the median pore radious faster is the damge. Therefore, it is possible to underline that the crystallisation test is an important test able to give information on the evolution time of the damage, and the median pore radious is one of the most suitable parameters in the description of the damage behaviour.

The results obtained by the relationship between median pore radious and damage (% of material lost) are confirmed by the behaviour of the theoretical fragility curves. In fact the fragility curves put in evidence a fast deterioration in the samples is MA and MB characterized by a small median pore radious, and a slow deterioration for MC e MD where the value of the median pore radius is higher; they can be used to predict the damage. As consequence, as shown in Figure 10, the exceeding of a high damage threshold happens in advanced time for materials chacterized by small median pore radius, and after a long time if the value of the median pore radius is high.

AKNOWLEDGEMENTS

The autors wish to thank Prof. L. Toniolo for work on the mortar characterisation, Dr. D. Gulotta, Mr. M. Cucchi for their collaboration on the profile measurement and Mr. M. Iscandri for the specimen preparation.

REFERENCES

Binda L, Charola A E, Baronio G 1985 'Deterioration of porous materials due to salt crystallization under different thermohygrometric conditions', *5th Int. Conf. on Deterioration and Conservation of Stone*, Losanna, 279-288, 1985.

Cardani G, Tedeschi C, Binda L, Baronio G., 2001 'Laboratory Crystallisation Tests for Damage Evaluation' *Maintenance of Pointing in Historic Building: Decay and Replacement*, Contract EV-CT98-0706, Final Report.

Garavaglia E, Lubelli B, Binda L. 2002, 'Two Different Stochastic Approaches Modelling the Deterioration Process of Masonry Wall over Time'. *Materials and Structures*, Spring Ed., **35**(248), 246-256.

Garavaglia E., Anzani A., Binda L., Cardani G. 2008, 'Fragility curve probabilistic model applied to durability and long term mechanical damages of masonry' *Materials and Structures*, Springer Ed., **41**(4), 733-749.

Gulotta D, Toniolo L, Binda L. Tedeschi C., 2009 'Investigation of commercial ready-mixed mortars for architectural heritage'. *Proc. of the 11th Conference on Structural Repairs and Maintenance of Heritage Architecture*, 22 - 24 July 2009, Tallinn, Estonia, WIT Press, 231-241.

Gulotta D, Toniolo L, Tedeschi C., Binda L., 2010 'Commercial ready-mixed mortars for the conservation of cultural heritage: characterization and preliminary durability test'. *7th International Conference on Structural Analysis of Historical Constructions*, 6-8 October 2010, Shanghai, China, 259-264.

RILEM MS-A1, 1998 'Determination of the resistance of wallettes against sulphates and chlorides'.

Tedeschi C., Binda L., Gulotta D., Toniolo L., 2010 'Durability to salt decay of commercial ready-mixed mortars for the conservation of cultural heritage, *2nd Historic Mortars Conf. & Rilem TC 203-RHM Repair Mortars for Historic Masonry*, IV.19, Prague, 22-24 September 2010, RILEM-PRO 78, Ed. J. Valek, C. Groot, J.J. Hughes, Rilem Publication, S.A.R.L., 1015-1022.

XII DBMC
International Conference on Durability of Building Materials and Components
PORTO - PORTUGAL, April 12th-15th, 2011

Durability of HPCs Containing Ternary and Binary Cementitious Materials

Mohammad Shekarchi[1]
Farnam Ghassemzadeh[2]
Babak Mohammadi[3]
Siavash Sajedi[4]
Mohammad Javad Mohebbi[5]

ABSTRACT

Concrete durability in different environment conditions especially in marine climate is always one of the important characteristic in choosing a specific mixture for it. Every year, deterioration of the concrete structures-which is mainly due to chloride induced corrosion of embedded steel bars- imposes hundreds of million dollars cost for these structures. So it is essential to select the suitable concrete materials to match the exposure severity and to adopt proper construction practices to obtain a high quality durable concrete. In this paper four different concrete mixtures are designed for investigation of efficiency of silica fume (SF) and ground granulated blast furnace slag (GGBS). These mixtures were assessed in four parts: Water absorption, Chloride diffusion, Oxygen permeability and Chloride diffusion which are the most important features of durability. The results of this study indicate that the durability performance of concrete with pozzolanic materials is higher than control concrete meanwhile Using combination of SF and GGBS shows better results than other concrete mixtures.

KEYWORDS

Durability, Concrete, Ground granulated of blast furnace slag, Silica fume.

[1]Associated Professor, Director of CMI, Department of Civil Engineering, University of Tehran, Tehran, Iran, shekarch@ut.ac.ir
[2]Research Assistance of Construction Material Institute (CMI), Dept. of Civil Engineering, University of Tehran, Tehran, Iran, ghassemyadeh@ut.ac.ir
[3]Bachelor Student, Construction Material Institute (CMI), Dept. of Civil Engineering, University of Tehran, Tehran, Iran, babak_mohammadi@ut.ac.ir
[4]Master Student, Construction Material Institute (CMI), Dept. of Civil Engineering, University of Tehran, Tehran, Iran, ssajedi64@ut.ac.ir
[5]Bachelor Student, Construction Material Institute (CMI), Dept. of Civil Engineering, University of Tehran, Tehran, Iran, Mjmohebbi@hotmail.com

1 INTRODUCTION

Supplementary cementitious materials (SCM) improve the engineering and performance properties of concrete when they used as partial cement replacement. So, during the last decades the application of super pozzolanic materials such as silica fume (SF) and ground granulated blast furnace slag (GGBS) is common and development of high performance concrete (HPC) has greatly increased in many parts of the world (Gupta et al. 2006).With the rapid development of HPCs and increasing the application of SF and GGBS to produce HPCs, there is a need to study the durability of cement concrete that includes these additives such that the understanding gained can be applied to provisions for durability of concrete incorporating these new products.

Unlike a prescriptive specification that defines a concrete mixture in terms of its constituents and their proportions, a performance specification defines a concrete mixture in terms of measurable plastic and hardened properties that show the mixture will satisfy certain performance criteria. The difference between these two approaches can be illustrated by looking at durability. In prescriptive specifications, durability is intended to be achieved by requiring particular ingredients, proportions, or construction operations. Each of these requirements is actually a means to an end, and durable concrete is likely to be the result of following these means [Bickley *et al*. 2006]. Durability is known by a group of features which denote the concrete performance against the problems that, for example, occur in a marine environment.

The HPCs are more resistant against corrosive conditions due to their supplementary cementitious materials which change concrete's characteristic to make it a durable product. To improve these features GGBS and SF are the most effective SCMs nowadays among the most widely used pozzolans. Several researchers have focused their attention on determining the permeability of concrete to chloride ions. For example, a study by Wee *et al.* [2000] shows that the addition of mineral admixtures such as GGBFS and SF to concrete enhanced the resistance of the mixture to chloride penetration compared with the control concrete. Maslehuddin's study on silica fume replacement dosage shows its beneficial effect on chloride permeability up to 15% replacement of cement [Maslehuddin. 1992]. Research on gas permeability also shows the advantages of HPC as compared to ordinary concretes. According to Austin *et al.* [1992] mixture design containing 50% slag replacement of cement shows better resistance to gas permeability in comparison to ordinary Portland cement (OPC) in three different curing methods. SF has also a sensible effect on electrical resistivity. Sharfuddin Ahmed *et al.* [2009] showed that SF concrete exhibits higher electrical resistivity than plain cement concrete.

The present research investigates the effects of GGBS and SF as supplementary cementitious materials on concrete durability. Four important characteristics of concrete were considered in the study: water absorption, chloride diffusion, oxygen permeability, and electrical resistivity. – These characteristics were considered as concrete durability "indicators"; the compressive strength being perhaps the most important feature must always must be considered. The experiments were completed on four mixtures: OPC, GGBS, SF and combination of GGBS and SF to compare their performance and denote the influence of using pozzolanic concrete in marine environments.

2 MIX PROPORTIONING OF HPCs

The chemical composition of the Portland cement, GGBS and SF that was used in this study are given in Table 1. The coarse aggregate was gravel having a maximum particle size of 16mm; the fine aggregate was graded silica sand with a fineness modulus of 3.2. The water to binder ratio and total binder content for all mixtures were 0.38 and 420kg/m^3 respectively.

Table 1. Chemical compositions (%) and properties of binding materials.

Binder	SiO_2	Al_2O_3	CaO	MgO	Fe_2O_3	SO_3	Na_2O	K_2O	Specific gravity
Cement	21.00	5.00	63.00	1.800	3.50	1.60	0.50	0.60	3.15
GGBS	35.50	10.00	36.50	9.500	0.70	1.86	0.50	0.53	2.86
SF	93.16	1.13	-	1.60	0.72	0.05	-	-	2.11

Four groups of HPRC mixtures were designed: R, R-SF, R-S, R-SFS as experimental samples, their mix proportioning is listed in Table 2. These four concrete mixtures are made of the same mix proportioning except the type of pozzolanic materials. Mixture R is plain concrete; In the R-SF Concrete, SF is replaced cement by 7.5% of cement weight; In Concrete R-S, GGBS replaced cement by 25% of cement weight while in Concrete R-SFS, 32.5% of cement was substituted by GGBS (25% of cement weight) and SF (7.5% of cement weight).

Table 2. Mix proportioning of HPRCs.

Concrete	Mix proportioning							Slump
	C	GGBS	SF	SP	Coarse Aggregate	Fine Aggregate	W/b	
	kg	kg	Kg	%	kg	Kg		mm
R	420.0	-	-	0.5	793	1000	0.38	145
R-SF	390.5	-	29.5	0.6	793	988	0.38	155
R-S	315.0	105	-	0.5	793	992	0.38	160
R-SFS	285.5	105	29.5	0.5	793	980	0.38	150

3 INDEX TESTS

3.1 Mechanical Strength

The compressive strength of specimens was determined for each concrete mixture in accordance with ASTM C196 and was then tested according to ASTM C39. The compressive strength tests were done on 15×15 cm cubes. The specimens were removed from the moulds 24 h after casting and were then cured in the water until the age of testing.

3.2 Water absorption

Water absorption testing was conducted in accordance with BS 1881-part: 122. To do this, three concrete cores, 75mm in diameter and 130mm in height, were obtained from three 200mm cubes for each concrete mixture after the concretes were cured for 28 days. The water absorption test was performed after the cores were oven-dried for 72 h. The absorption of each specimen was measured by calculating the increased mass resulting from immersion in water for 30 minutes as a percentage of the mass of the dry specimen.

3.3 Electrical Resistivity

Electrical resistivity testing was conducted on three 100mm cubes prepared for every concrete mixture during a period of 180 days after the casting of concretes. The specimens were submerged in water until the testing age. The electrical resistivity of the cubes was measured based on AC Impedance Spectrometry (ACIS) method using a concrete resistance meter [Shekarchi *et al.* 2008 & Ping *et al.* 1992]. The resistivity then was calculated by:

$$\rho = \frac{AR}{L} \tag{1}$$

Where ρ is the resistivity (kΩ.cm), A the area (cm^2), R the resistance (kΩ), L the length of the specimen (cm).

3.4 Oxygen permeability

The oxygen permeability test was carried out following the Cembureau-method according to ‘‘Rilem TC 116- PCD: Recommendations’’ [Kollek 1989]. The preconditioning regime which is used for testing is recommended by Cembureau and is recognized as regime B. Based on this method, oxygen under pressure was applied on one end of the specimen while providing a tightly fitting seal to the curved surface. The rate of gas flow from the other flat side was then measured using a soap bubble flow meter, when the flow rate had stabilized. The relationship proposed by Hagen-Poiseuille (Eq. (2)) was used to determine the intrinsic gas permeability coefficient. The flow was assumed to be laminar and unidirectional.

$$K_o = \frac{2.Q.P_a.L.\eta}{A(P^2 - P_a^2)} \tag{2}$$

Where K_o is the permeability coefficient (m^2), Q the volume flow rate of the fluid (m^3s^{-1}), A the cross-sectional area of the specimen (m^2), L the thickness of the specimen in the direction of flow (m), η the dynamic viscosity of the fluid at the test temperature ($2.02*10^{-5}$ $N.s.m^{-2}$ for oxygen at 22°C), P the inlet pressure ($N.m^{-2}$), P_a the outlet pressure ($N.m^{-2}$).

3.5 Chloride diffusion

Bulk chloride diffusion samples were prepared according to ASTM C 1565. Cylindrical specimens (150mm diameter × 300 mm thick) were cast, followed by 28 days curing, for each concrete mixture. Afterwards, the cylindrical specimens were sawn to provide a 100 mm thick slice from the top of the specimen. The slices were sealed with epoxy polyurethane coating on all sides expect the sawn surface to simulate one-dimensional diffusion. These specimens were then immersed in a sodium chloride solution with a concentration of 165 g/l and a temperature of 23°C. After an exposure period of one year, the specimens were removed from the salt solution. An opening having a diameter of 45 mm was drilled to produce pulverized material samples at incremental depths from the uncoated face. The resulting powder samples from each layer were collected separately to analyze the acid-soluble chloride content according to ASTM C 1152 and ASTM C 114. The resulting output of the test is a plot of acid-soluble chloride concentration versus the depth of the exposed surface. The apparent diffusion coefficient, D_a, and the surface concentration, C_s, were calculated from the established chloride concentration profile based on Fick’s Second Law of Diffusion and Crank’s solution (Eqs. (3) and (4)).

$$\frac{\partial C}{\partial t} = D_C \frac{\partial^2 C}{\partial x^2} \tag{3}$$

$$C_{(x,\,t)} = C_s\left[1 - erf\left(\frac{x}{2\sqrt{D_C t}}\right)\right] \quad (4)$$

Where x is the distance from the concrete surface (cm); t is the time (years); D_c is the diffusion coefficient (cm^2/year); C_s is the equilibrium chloride concentration on the concrete surface; C(x, t) is chloride concentration at the depth of x from the surface after the time t; and erf is the error function.

4 RESULTS AND DISCUSSION

4.1 Mechanical Strength

The experimental results for compressive strengths are listed in Fig. 1. The results show that the maximum and minimum compressive strength for the 3rd and 7th day belong to R-SF and R-S specimens, respectively. From the results, the maximum increase in the compressive strength until 28 and 90 days is for R-SFS and R-S specimens while the maximum compressive strength at 90-days is for GGBS mixes. In the specimens for which SF and GGBS mixes are used, the compressive strength increase starts at early age and continue over time in later ages. Jianyong & Yan [2001] reported similar results. The rate of increase of the compressive strength for R-SFS design is better with respect to other designs.

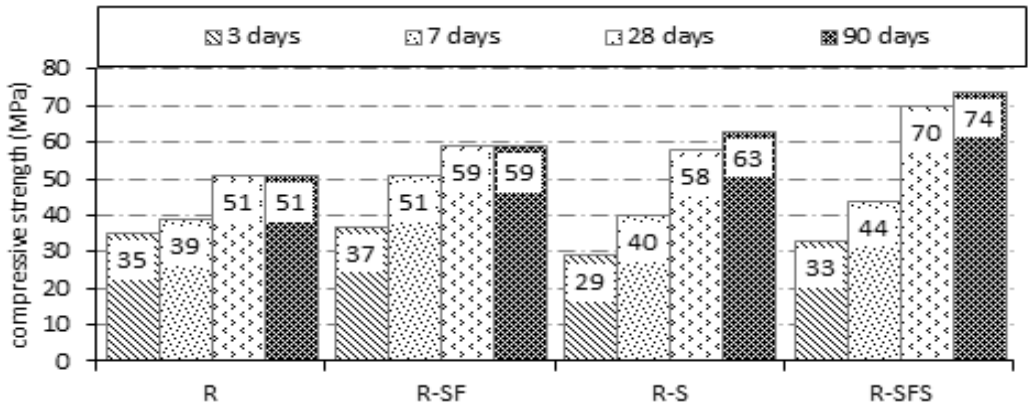

Figure 1. Different ages compressive strengths.

4.2 Water Absorption

The water absorption results of concrete specimens are presented in Fig.2. It can be seen that both the SF and GGBS concrete mixtures displayed lower water absorption than the R concrete which has not any pozzolanic materials. It can be found SF was more effective than GGBS in reducing the water absorption. For R-SFS concrete, using the combination of SF and GGBS, a greater effect in reducing water absorption was observed. This is due to the pozzolanic action of SF, GGBS and the filler effect, provided by SF.

4.3 Electrical Resistivity

Electrical Resistivity (ER) is a convenient factor for studying the durability of concrete especially the rate of corrosion of embedded steel after breakdown of the passivity layer. Figure 3 presents the ER of HPRCs

with the time (up to 180 days). As seen, R-SFS and R-SF mixtures (for which SF is used as pozzolanic materials) exhibited higher ER in both of early and later ages with respect to other concretes. Lowest ER is related to the Concrete R which is without pozzolanic materials. From the results, it's evident that the effect of SF on increasing of ER is more than GGBS. However, using the simultaneous of SF and GGBS as a pozzolanic material in concretes, increase the ER in early ages due to the existence of SF and in later ages due to the GGBS. Thus, for assess the HPCs with high ER; it seems that the use of SF is necessary. The same results about the SF efficiency on electrical resistivity observed by Sharfuddin Ahmed *et al.* [2009]. It was reported that the corrosion rate of reinforcing steel is low when the resistivity of concrete exceeds 20 kΩ.cm [Broomfield 1997].

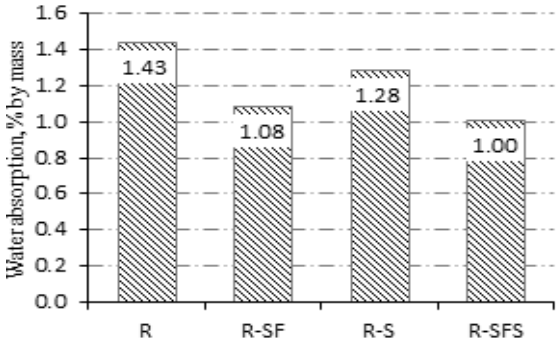

Figure 2. Water absorption of HPCs (28-day curing).

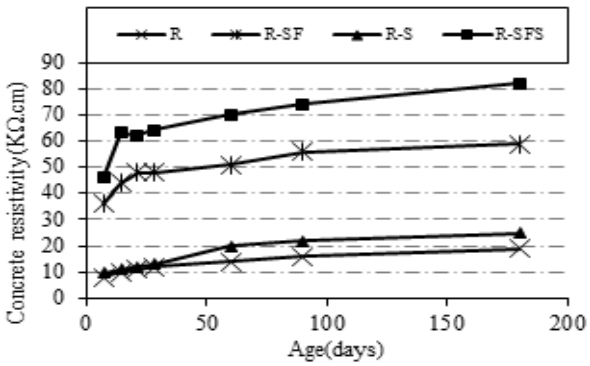

Figure 3. Electrical Resistivity of HPCs.

4.5 Gas Permeability

Figure 4 demonstrates the effect of SF or GGBS replacement on the oxygen permeability coefficient K_O of concrete mixtures. From the results, it can be seen that specific permeability coefficient decreases when pozzolanic materials was used. The effects of SF in decreasing of K_o is more significant than the effects of GGBS. The Lowest K_o belongs to R-SFS concrete which shows that the positive synergistic effect of GGBS and SF when used simultaneously in HPCs.

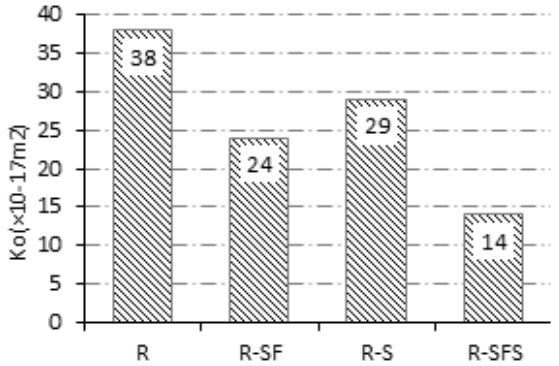

Figure 4. Oxygen permeability (Ko) of HPCs.

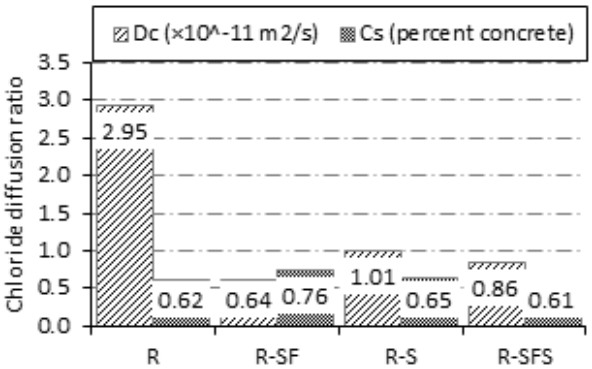

Figure 5. Chloride diffusion coefficient (D_c) and chloride concentration (C_s) of HPCs.

4.6 Chloride Diffusion

The values of apparent diffusion coefficient (D_c) and surface chloride concentration (C_s), determined for HPCs from Eq. (4), are shown in Fig. 5. These results show that pozzolanic concretes had a better effect on improving diffusion characteristics of concrete especially SF concretes with respect to other concretes. As a result, it was found that SF was more effective than GGBS in term of chloride diffusion of concrete. Seleem *et al*. [2010] observed similar results from their research on durability of high performance concretes. It can be concluded from these results that R-SFS concrete has a better general performance against chloride penetration. Other research on the durability of ternary concretes shows this as well [Bleszynski *et al.* 2002].

Figure 6 shows all the tests results on concrete mixtures. All data are scaled with R concrete result in each test. As it can be seen the R-SF concrete has the best result in chloride diffusion among other mixtures. But in a general view the R-SFS concrete which has both SF and GGBS as pozzolanic admixtures achieves the best results in different tests. As so it can be concluded that the combination of SF and GGBS is an ideal mixture for durable concrete. This conclusion also has done with other researchers that ternary blend concrete containing SF and slag has the best durability features between other concrete mixtures [Bleszynski *et al.* 2002].

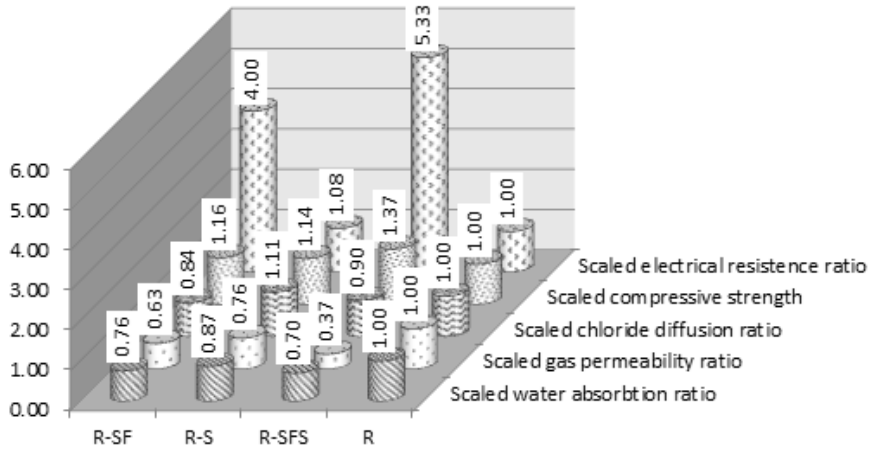

Figure 6. Scaled tests results for HPCs.

5 CONCLUSIONS

The following conclusions can be made from the tests results:

1. Using the combination of SF and GGBS shows the better compressive strength results than alone usage of SF or GGBS in concrete mixture.
2. Both SF and GGBS have great effect on reducing water absorption rate of concrete. But the combination of these pozzolans shows the best results on water absorption rate as a primary feature of durable concrete.
3. SF has a better effect on increasing electrical resistivity than GGBS, but using both SF and GGBS simultaneously improve the results much more than other mixtures.
4. Gas permeability can be reduced by using either SF or GGBS but the best result achieves when the combination of both of them use as concrete admixtures.

5. Results show that SF and GGBS both are effective on reducing chloride diffusion, but SF shows better results among other admixtures.
6. At all the ternary blend offers superior performance compared to other mixtures in term of durability features.

REFERENCES

Gupta, S.M., Aggarwal, P. & Aggarwal, Y. 2006, 'Shrinkage of high strength concrete', *Asian journal of civil engineering (building and housing), Vol. 7, NO. 2.*

Seleem, H., Rashad, M. & El-Sabbagh, A. 2010, 'Durability and strength evaluation of high-performance concrete in marine structures', *Construction and Building Materials 24, 878–884.*

Wee, H., Suryavanshi, K. & Tin S. 2000, 'Evaluation of rapid chloride permeability test (RCPT) results for concrete containing mineral admixtures', *ACI Materials Journal , V. 97, No. 2.*

Bickley, A., Doug Hooton, R. & C. Hover, K. 2006,'Performance specifications for durable concrete', *Concrete international.*

Maslehuddin, M. 1992, 'Concrete durability – The Arabian gulf experience', *Research institute of King Fahad university of petroleum and minerals, Dhahran, Saudi Arabia.*

Austin, S.A., Robins, P.J. & Issaad, A. 1992, 'Influence of curing methods on the strength and permeability of GGBFS concrete in a simulated arid climate', *Cement & concrete composites 0958-9465/93, Elsevier Science Publishers Ltd, England.*

Sharfuddin Ahmed, M., Kayali, O. & Anderson, W. 2009 'Evaluation of binary and ternary blends of pozzolanic materials usinig the rapid chloride permeability test', *Journal of materials in civil engineering © ASCE, 10.1061/(ASCE)0899-1561.*

Bleszynski, R., D. Hooton, R., D. A. Thomas, M. & A. Rogers, C. 2002, 'Durability of ternary blend concrete with silica fume and blast-furnace slag: laboratory and outdoor exposure site studies', *ACI Materials Journal, 99-M51.*

Broomfield, Jp. 1997, 'Corrosion of steel in concrete', *New York: E&FN Spon.*

Jianyong, L. & Yan, Y. 2001, 'A study on creep and drying shrinkage of high performance concrete', *Cement and Concrete Research 31, pp: 1203–1206.*

Kollek, JJ. 1989, 'The determination of the permeability of concrete to oxygen by the Cembureau method – a recommendation', *Mater Structural; 22(129), pp: 225–30.*

Ping, G., Xie, P., Beaudoin, JJ. & Brousseau, R. 1992, 'AC impedance spectroscopy (II): microstructural characterization of hydrating cement–silica fume systems, *Cement and Concrete Research; 23(1), pp:157–68.*

Shekarchi, M., Tahersima, M., Hajibabaee, A. &Laysi, H. 2008, 'Concrete mix proportions with ultra-high electrical resistivity',*In: 11th international conference on durability of building materials and components; Istanbul, Turkey.*

XII DBMC
International Conference on Durability of Building Materials and Components
PORTO - PORTUGAL, April 12th-15th, 2011

Chemical Resistance of Novel Waste Stabilization Cementitious Matrices

Francesco Colangelo[1]
Raffaele Cioffi [2]

ABSTRACT

A binding matrix containing calcium silicate β-$2CaO \cdot SiO_2$ and sulphoaluminate $4CaO \cdot 3Al_2O_3 \cdot SO_3$, and $CaSO_4$ that gives calcium silicate and trisulphoaluminate hydrates upon hydration has been used to stabilize solid waste from a galvanic treatment process.

The waste is destined for disposal in a hazardous wastes landfill to prevent the risk of cadmium, chromium and nickel release.

The binder's anhydrous calcium silicate and sulphoaluminate have been synthesized using a mixture containing powdered tuff in addition to bauxite and calcium carbonate and sulphate. Powdered tuff is quarry dust and, as such, is a true residue.

Experiments have been carried out with mixtures containing up to 60% waste in order to perform an environmental and technological assessment of the effectiveness of the stabilization process. Specifically, the study has been carried out with three different requirements in mind: the influence of the waste on the hydration process and on the technological properties of the stabilized products, the leaching behavior under selected conditions and the effect of the leaching medium on the chemical stability of the binding matrix in the stabilized system. The latter aspect has been considered with a view to evaluating the service life of waste–containing solidified materials in order to guarantee a safer disposal of wastes.

KEYWORDS

Calcium silicate, Trisulphoaluminate, Galvanic sludge, Stabilization, Chemical stability.

[1] Department of Technology, Faculty of Engineering of the University Parthenope of Naples, Naples, Italy, colangelo@uniparthenope.it
[2] Department of Technology, Faculty of Engineering of the University Parthenope of Naples, Naples, Italy, raffaele.cioffi@uniparthenope.it

1 INTRODUCTION

The European Union's most recent directives in matters of solid waste management assign high priority to the development of technologies addressed towards recycling and reuse as well as to the recovery of raw materials and energy from wastes. However, it is not always possible to meet these requirements as a suitable technology may be too expensive or even unavailable, leaving treatment processes as the only option for reducing the environmental impact of wastes. In the case of solid wastes, stabilization/solidification (S/S) processes are the most suitable.

S/S processes are already in widespread use for the treatment of hazardous industrial solid wastes, cement-based processes being the best suited for wastes containing heavy metals. Although they are mainly employed for safer waste disposal, they also have the intrinsic ability to yield products that may have high potential for use in the field of pre-formed building materials. This is due to the fact that these processes often lead to the formation of monolithic products.

In the stabilization of a specific waste by means of a specific binding matrix, a fundamental study is required to assess the actual potential of the S/S process with regard to the manufacture of building materials rather than safer disposal.

Current cement-based S/S technologies rely on the formation of a calcium silicate hydrate stabilizing matrix. A number of systems such as ordinary portland cement, blast furnace slag and mixtures of lime and coal fly-ash (or other pozzolanic materials) can be used [Conner 1990; Spence and Shi 2005].

In the present paper, a solid waste from galvanic treatment containing heavy metals has been stabilized by means of a novel cementitious matrix based on calcium silicate (β-$2CaO{\cdot}SiO_2$) and sulphoaluminate ($4CaO{\cdot}3Al_2O_3{\cdot}SO_3$). This matrix hydrates to calcium silicate hydrate and calcium trisulphoaluminate hydrate (ettringite) and offers several advantages in stabilization processes as heavy metals can be chemically entrapped by diodochy and isomorphic substitution. These pheomena may preferentially take place when ettringite is among the hydration products. This is demonstrated by the occurrence of ettringite-like minerals (sturmanite $Ca_6(Fe,Al)_2(SO_4)2(B(OH)_4)(OH)_{12}{\cdot}26H_2O$ and bentorite $Ca_6(Cr, Al)_2(SO4)_3(OH)_{12}{\cdot}26H_2O$) and also by the synthesis of ettringite derivatives reported by many authors [Pöllmann and Kuzel 1990; Csetenyi Laszlo and Glasser 1993].

Systems with the ability to generate ettringite and calcium silicate hydrate upon hydration have been tested in previous work for both physico-mechanical and stabilizing properties, proving to be suitable for the proposed application [Beretka *et al.* 1993; Beretka *et al.* 1994; Berardi *et al.* 1997, Luz *et al.* 2006 and 2009].

In our study, the behaviour of these solid matrices in contact with leaching media, that simulate the chemical environment in landill, has also been examined. The results of these experimentals have been provide further information on service life of these systems in different disposal scenarios.

2 EXPERIMENTAL PROGRAM

Previous works have synthesized clinkers containing β-$2CaO{\cdot}SiO_2$ and $4CaO{\cdot}3Al_2O_3{\cdot}SO_3$ starting from different sources of CaO, SiO_2, Al_2O_3, and $CaSO_4$. In particular, reagent grade chemicals, commercial materials (limestone, bauxite, etc.) and industrial by-products and wastes (phosphogypsum, coal fly-ash, etc.) were used [Berardi *et al.* 1997]. The choice of the raw materials required for synthesis may depend on the local availability of materials containing the above oxides. There is wide availability of zeolitic tuff quarries throughout southern Italy, as well as in the United States, Japan and other eastern European countries. Tuff dust is produced during the cutting of shaped stones for the manufacture of building elements and, as it is a true solid waste, it must be disposed of,

unless some other way of reusing it is found. As zeolitic tuff contains mainly SiO_2 and Al_2O_3, it has been judged that its quarry dust can be profitably employed for clinker synthesis. The tuff dust used in this work contained SiO_2 (52.93%), Al_2O_3 (17.21%), K_2O (7.27%), Fe_2O_3 (3.71%), CaO (3.54%), Na_2O (2.97%) and MgO (1.44%).

The composition of the clinker was to have β-$2CaO{\cdot}SiO_2$ and $4CaO{\cdot}3Al_2O_3{\cdot}SO_3$ in the theoretical weight ratio 1:1.5. According to previous findings, binders of good mechanical properties can be produced starting from a clinker of such a composition [Beretka *et al.* 1994]. The composition of the raw mixture for the synthesis was calculated to achieve the above theoretical composition. Then, mixtures of zeolitic tuff dust (13.27%), bauxite fines (31.09%), reagent grade $CaCO_3$ (45.37%) and $CaSO_4{\cdot}2H_2O$ (10.24%) were fired at 1200°C for times ranging from 15 to 360 min. The addition of bauxite fines was required to increase the Al_2O_3/SiO_2 ratio. Alumina content was 51.50% in this material. Figure 1 shows the results of the clinker synthesis in terms of X-ray diffraction (XRD) counts of the strongest peaks for the fired product's main components. It is seen that $2CaO{\cdot}Al_2O_3{\cdot}SiO_2$ and $3CaO{\cdot}Al_2O_3$ are formed together with β-$2CaO{\cdot}SiO_2$ and $4CaO{\cdot}3Al_2O_3{\cdot}SO_3$. Furthermore, the concentrations of $4CaO{\cdot}3Al_2O_3{\cdot}SO_3$, $2CaO{\cdot}Al_2O_3{\cdot}SiO_2$ and$3CaO{\cdot}Al_2O_3$ increase with firing time, while that of β-$2CaO{\cdot}SiO_2$ passes through a maximum. Based on these results, a 90 minute firing time was used for the clinker synthesis.

The binder was obtained by mixing the clinker and anhydrous $CaSO_4$ in the weight ratio 2.5:1. Anhydrous $CaSO_4$ was obtained by firing reagent grade $CaSO_4{\cdot}2H_2O$ at 850◦C for 2 h [Beretka *et al.* 1994]. The presence of anhydrous $CaSO_4$ in the binder is necessary for the formation of non-expansive ettringite [Pellettier *et al.* 2010].

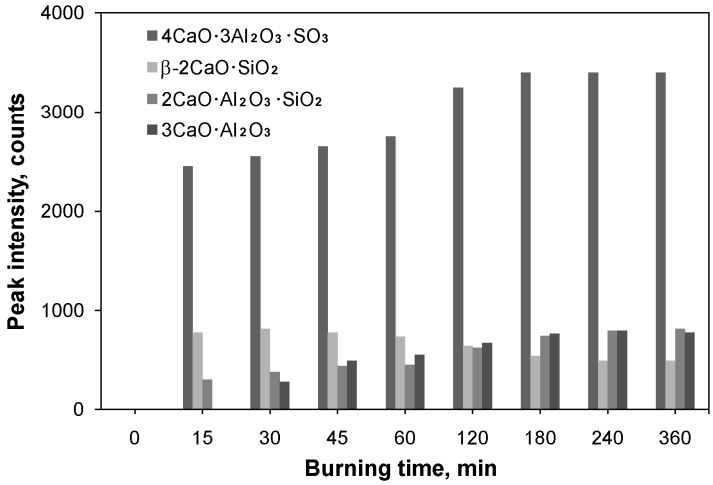

Figure 1. Clinker synthesis from XRD.

This study employed waste from the treatment of spent galvanic liquor. It contains the heavy metal oxides Cr_2O_3 (10.05%), NiO (1.50%) and CdO (0.06%). The main component is Al_2O_3 (73.58%), due to the use of aluminium salts as flocculants in the spent liquor treatment process. Although the European Waste Catalogue (EWC) classifies this waste as non-hazardous, it must neverthless be disposed of in a hazardous waste landfill because the release of heavy metals exceeds established limits in the compliance leaching test. The waste is classified with the EWC code: 06.05.01 [Commission Decision 2000/532/EC].

Binder–waste mixtures were prepared containing 0 (pure binder), 20, 40 and 60% of waste and hydrated at 25°C, 100% RH, and water/solid ratio equal to 0.40, 0.46, 0.50 and 0.56 for the systems containing 0, 20, 40 and 60% waste, respectively. These values were chosen in order to ensure constant workability. The hydration time ranged between 1 h and 28 days (672 h). Small samples (about 3 g) of each system were used to study the kinetics of hydration. This part of the study was

carried out by determining the amount of chemically combined water by ignition at 1000◦C for the time required to reach constant weight. In addition, the formation of hydrated products was monitored by XRD analysis. Cubic specimens 4x4x4 cm^3 of all the systems were tested for Unconfined Compressive Strength (UCS) measurements.

Samples from the mixtures containing 20, 40 and 60% of waste were subjected to the following three leaching tests: (a) a dynamic test with pH 4.94 acetic acid/sodium acetate buffer, liquid/solid ratio equal to 20 ml/g and leachant renewals at 1, 3, 8, 14, 24, 48, 96, 168, 376, 672 and 1344 h on monolithic cylindrical samples dxh = 2 cm x 3 cm; (b) the same test as (a) but with pH 3.86 CO_2 saturated solution instead of acetic buffer and renewals up to 672 h and (c) the availability test carried out on 3 g of pulverized sample (size < 180 µm) with 150 ml of pH 7 nitric acid solution for 3 h plus additional 150 ml of pH 4 HNO_3 solution for 3 h. In test (b) the initial pH in each step was 3.86 and the solution was kept constantly saturated by continuous feeding of gaseous CO_2. In spite of this, the pH increased during each step due to interactions with the solid. In test (c) the pH was maintained at 7 for 3 h and at 4 for an additional 3 h by adding, when necessary, the proper amount of HNO_3 1M solution. The choice of leaching tests was made not for the sake of compliance to some regulation, but to achieve a better understanding of the process effectiveness, the stabilization mechanisms and the chemical stability of the stabilizing matrix. The leaching solutions were analyzed by means of atomic absorption spectroscopy and the solids before and after leaching were characterized by means of XRD analysis.

3 RESULTS AND DISCUSSION

3.1 Syntesis of binder

The amount of normalized chemically combined water is reported in Figure 2. It can be seen that only the mixture containing 20% of waste behaves like the pure binder, while in the cases of the 40 and 60% mixtures the waste does not simply dilute the binder but its components inhibit binder hydration.

The results of XRD carried out on the samples of all the systems aged 28 days are reported in Figure 3. This figure shows the presence of the main 4CaO·3Al2O3·SO3 hydration product, namely $6CaO·Al_2O_3·3SO_3·32H_2O$ (ettringite). The presence of $2CaO·Al_2O_3·SiO_2$, β-$2CaO·SiO_2$, $3CaO·Al_2O_3$ and $CaSO_4$ is well documented by the numerous peaks linked to the above components. The absence of 4CaO·3Al2O3·SO3 peaks indicates that in all the systems this reactant is converted to such a degree that the residual quantities are below the detection limit of the XRD. Comparing the three XRD patterns with each other clearly points out that the presence of galvanic sludge in the systems does not alter binder hydration from the qualitative point of view.

The UCS values determined for the pure binder and mixtures with 20 and 40% waste are 25, 21 and 16 MPa, respectively. These are high enough to envisage the possible utilization of sulphoaluminate cement-waste mixtures as a binder for the manufacture of concrete blocks. As UCS is usually lower for the binder than for concrete blocks, there is a good potential to ensure at least medium-high mechanical properties. According to the Italian classification, pre-formed blocks manufactured as above could well comply with the specifications of the C20/25 class [UNI EN Standar 2009]. The value of 2MPa observed for the mixture containing 60% waste exceeds the value of 0.44 MPa recommended by Stegemann and Coté for segregated landfill disposal [Stegemann and Coté 1996].

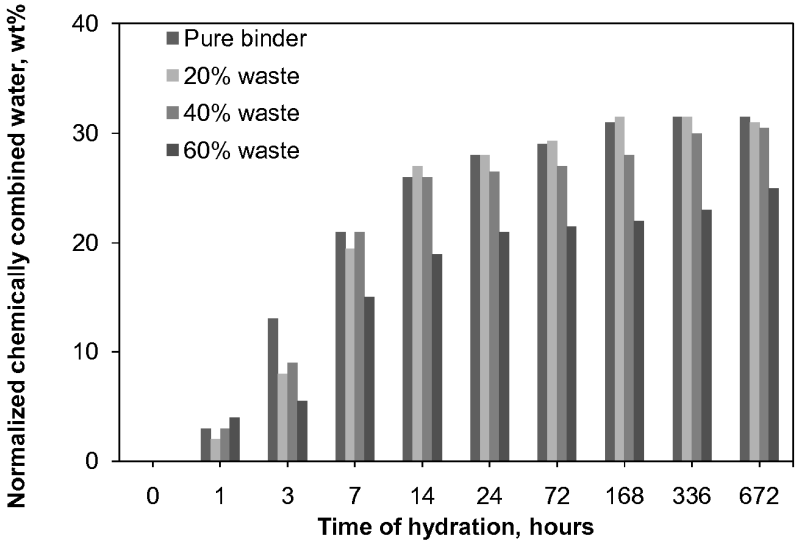

Figure 2. Kinetics of hydration for pure binder and binder-waste mixtures.

3.2 Leaching behaviour

The results of the three leaching tests carried out on the stabilized samples are reported in Figure 4. Specifically, for the two dynamic tests, the final cumulative values are reported. All the results are in terms of percentages of metal released in relation to the amount originally present in the samples. This helps to understand the effectiveness of the stabilization process. First of all, it is seen that in each test metals are released in the order Cd > Ni > Cr. Furthermore, an important observation is that in both the dynamic tests the amount released slightly increases with the amount of waste in the mixture, showing that metal release is not limited by metal solubility in the liquid phase, but by the intrinsic stabilizing properties of the matrix. In a previous work [Albino *et al.* 1994], it was found that this is not always the case, as copper was found to be leached in an amount limited by solubility in the leaching medium from stabilized model systems.

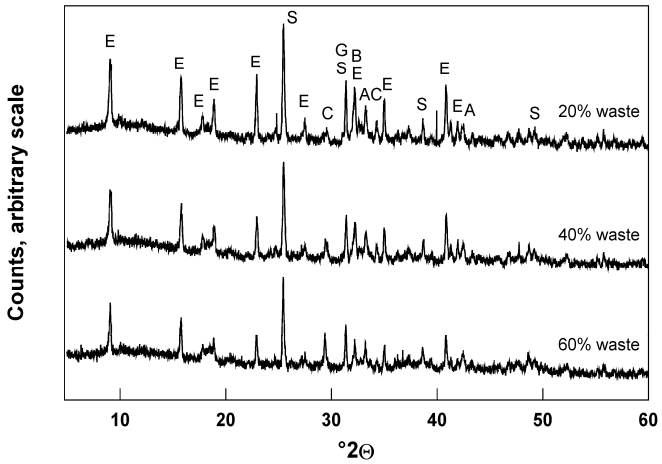

Figure 3. Results of XRD analyses carried out on binder-waste mixtures aged 28 days (A: Al_2O_3; AC: $3CaO{\cdot}Al_2O_3$; B: $-2CaO{\cdot}SiO_2$; C: $CaCO_3$; E: ettringite; G: $2CaO{\cdot}Al_2O_3.SiO_2$; S: $CaSO_4$). X-Ray intensity is reported as a function of 2-theta angle degree.

The two dynamic tests give differing results, as the cumulative amounts released in the acetate buffer test are invariably higher than those released in the CO_2-saturated solution test. The pH-values observed at the end of each leaching test range between 4.63 to 6.22 for both the dynamic tests. It has been seen that pH is always lower in the case of the acetate buffer test and this could explain the

difference observed. However, the effect of the leaching medium on the stabilizing matrix may also have a significant influence on the leaching results, as will be shown later.

Another important observation from Figure 4 is that release ranges between about 0.05 and 18% of the initial quantity in both the dynamic tests. This, in conjunction with the slight increase of metal released with increasing waste content, clearly shows that the matrix retains a good stabilization capacity even when the waste content is as high as 60%.

The overall effectiveness of the stabilization process, as argued from the results of the dynamic tests, does not clearly identify the roles of the physical and chemical stabilization mechanisms. To this end, the results of the availability test should be examined and discussed while bearing in mind that this test makes use of powdered samples in which the matrix is physically destroyed.

As far as cadmium is concerned, it is seen that the amount released increases from low values of about 3–5% (CO_2-saturated leaching test) and about 12–18% (acetate buffer test) to quite high values of about 56–59%. This makes it clear that this metal is stabilized by a prevailing physical mechanism, meaning that no respeciation leading to incorporation or micro-encapsulation within the neo-formed hydrated phases takes place after cadmium precipitation in the alkaline environment of cement [Conner 1990; Spencer 2005; Cocke 1990; Yousuf *at al.* 1992]. Specifically, Yousuf *et. al.* 1992 found evidence that cadmium is present in cementitious S/S systems in the form of calcium hydroxocadmiate $CaCd(OH)_4$ which results from the reaction of $Cd(OH)_4$ with calcium ions on the surface of cement grains.

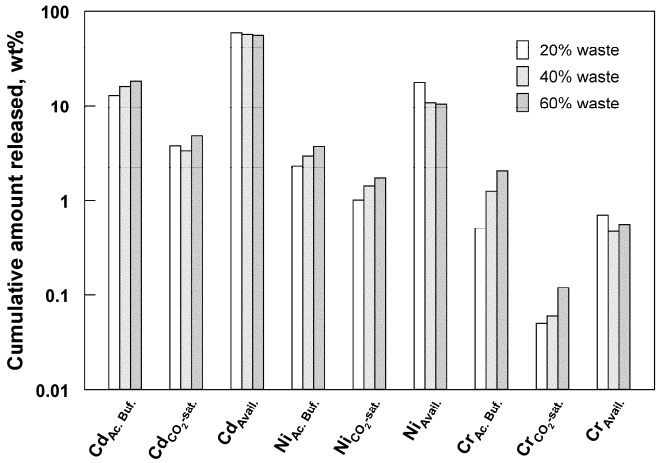

Figure 4. Results of the three leaching tests carried out on binder-waste mixtures aged 28 days.

In cement-based S/S systems, cadmium release can be almost complete due to the lack of chemical stabilization mechanisms for this metal [Conner 1990; Spence 2005]. In this work, however, the release of cadmium in the availability test, although high, is still far from total release, and this may be due to some form of cadmium entrapment by mechanisms like diadochy or isomorphic substitution in the presence of ettringite.

As regards nickel, the availability test results are greater than those found in the two dynamic tests, but in the order of 10%. It can therefore be concluded that chemical mechanisms strongly prevail over physical ones, but the latter occur to some extent. A comparison with literature data for nickel leaching [Conner 1990] confirms that there is no difficulty in fixing nickel by means of effective S/S systems.

Finally, in the case of chromium, the results of the availability test are of the same order of magnitude as those for the acetate buffer test and higher than those for the CO_2-saturated solution test. This means that the stabilization mechanism is exclusively chemical. This result is in agreement with those

reported by other authors [Conner 1990; Spence 2005] in the case of portland cement-based stabilization processes of this metal. Evidence was found that chromium is incorporated in the calcium silicate hydrate matrix. In this work, chemical stabilization can benefit from the substitution of aluminum with chromium in ettringite. The particularly low values observed for chromium release in the CO_2-saturated solution test may be due to a higher pH-value.

3.3 Matrices service life

It is well known that acidic leaching media can have significant effects on stabilizing matrices. Some authors have found that acid attack on calcium silicate hydrate matrix leads to an increased polymerization of calcium silicate hydrate with increased porosity and loss of mechanical properties [Ortego *et al.* 1991, Luz *et al.* 2007]. Previous studies on stabilizing matrices based on calcium sulphoaluminate alone also showed significant decomposition following an acid attack [Berardi *et al.* 1997; Cioffi and Santoro 2000]. The leaching media used in this work are certainly much more acidic and aggressive than those which are being proposed and used for compliance purposes both in the European Union and in Italy. For this reason they are much more useful for understanding the stability of the hydrated phases during the entire service life when they will be in contact with leaching media, and hence their long-term stabilization capacity.

When the cylindrical solidified samples were submitted to the attack of the acetic buffer and CO_2-saturated solution, a strong structural modification could be observed. The external part of the sample became more porous and friable, while the internal core was left unchanged. The boundary between these two parts moved inwards and the thickness of the external layer was equal to 2, 3 and 7mm after 28 days for the systems containing 20, 40 and 60% waste, respectively. This was independent of the type of leaching medium.

Samples from both the internal core and the external layer were submitted to specific analysis to verify the chemical modifications induced by the attack.

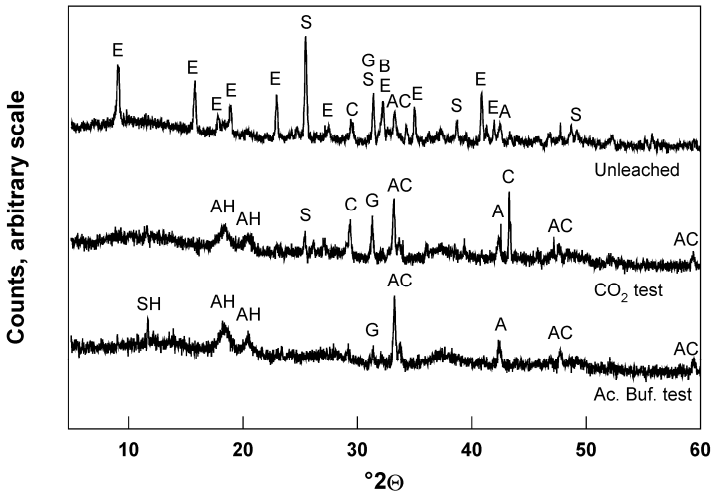

Figure 5. Effect of leaching solutions on stabilized products (A: Al_2O_3; AC: $3CaO{\cdot}Al_2O_3$; AH: $Al(OH)_3$; B: β-$2CaO{\cdot}SiO_2$; C: $CaCO_3$; E: ettringite; G: $2CaO{\cdot}Al_2O_3.SiO_2$; S: $CaSO_4$; SH: $CaSO_4{\cdot}2H_2O$). X-Ray intensity is reported as a function of 2-theta angle degree.

The results of XRD carried out on samples of the system containing 40% waste are reported in Figure 5. It can be seen that the peaks relative to ettringite disappear in the external layer, giving decomposition products which are somehow different from one medium to the other. Specifically, in the case of acetic buffer, calcium sulphate dihydrate and aluminium hydroxide are the observed

decomposition products, while in the case of CO_2-saturated solution, calcium carbonate appears together with calcim sulphate and aluminium hydroxide.

The study of the chemical stability of these systems was based on the assumption that the leaching behaviour of these matrix components is controlled by minerals such as: calcite, gibbsite ($Al(OH)_3$), ettringite, gypsum and portlandite as previously proposed by others [Cornelis *at al.* 2006].

Starting with a 1:1.5 ratio between β-$2CaO{\cdot}SiO_2$ and $4CaO{\cdot}3Al_2O_3{\cdot}SO_3$ in the clinker, a 1:4 ratio between calcium silicate hydrate and calcium trisulphoaluminate hydrate is obtained. Hence, the latter hydration product is present in 80% of all the hydrated phases. Therefore, its contribution to chemical stabilization must be significant.

In fact, in presence of carfonation reaction, although ettringite dissolves and transforms into gypsum and calcite, the contribution of calcium silicate hydrate to diadochy and isomorphic substitution remains active. In other words, carbonation at very high concentrations of CO_2 favours the polymerization of the calcium silicate hydrate, which affects the leaching processes and the concentration of heavy metals and other pollutants in the leachate solutions [De Windt *et al.* 2011].

4 CONCLUSIONS

The results of the experiments can be summarized as follows with respect to the three aspects of the study emphasized in the introduction.

As far as hydration chemistry is concerned, it has been shown that the addition of waste up to 60% does not alter the nature of the hydration products. However, the extent to which hydration takes place is reduced when the waste content is greater than 20%.

The Unconfined Compressive Strength value starts from 25MPa for the pure binder and falls to 21 and 16MPa when the waste content is 20 and 40%, respectively. It decreases to only 2MPa when the waste content is further increased to 60%. Consequently, the use of binder–waste mixtures for the manufacture of pre-formed building blocks can be taken into consideration for waste content up to 40%.

The leaching behavior under the conditions of the three tests employed has proved that cadmium is stabilized by the prevailing physical mechanism and that chemical entrapment plays a secondary role. Chemical mechanisms prevail in the case of nickel and are almost exclusively active in that of chromium. From the qualitative point of view, the leaching results agree with those for cement-based stabilization processes.

Finally, it has been found that the attack of different solutions on stabilized systems causes severe structural modification of the binder during its service life. In spite of the scarce durability of the matrices, chemical stabilization is retained in those cases in which the transformations occur and it is inferred that metals are chemically entrapped even in the decomposition products. This has been considered an important finding in view of long-term safer disposal of wastes.

REFERENCES

Albino, V., Cioffi, R., de Vito, B., Marroccoli, M. & Santoro L. 1994, 'Release of heavy metals from municipal solid waste incineration residue stabilized in non traditional matrices' in: *Environmental*

Aspects of Construction with Waste Materials, eds. J.J.J.M. Goumans, H.A. van der Sloot & Th.G. Aalbers, Elsevier, Amsterdam, pp. 789-800.

Berardi, R., Cioffi, R. & Santoro L. 1997, 'Matrix stability and leaching behaviour in ettringite-based stabilization systems doped with heavy metals', *Waste Management*, **17**, 535-540.

Beretka, J., Cioffi, R., Santoro, L. & Valenti, G.L. 1994, 'Cementitious mixtures containing industrial process wastes suitable for the manufacture of preformed building elements', *Journal of Chemical Technology & Biotechnology*, **59**, 243-247.

Beretka, J., de Vito, B., Santoro, L., Sherman, N. & Valenti, G.L. 1993, 'Hydraulic behaviour of calcium sulphoaluminate-based cements derived from industrial process wastes', *Cement and Concrete Research*, **23**, 1205-1214.

Cioffi, R. & Santoro, L. 2000, 'Effect of an acetic acid/sodium acetate buffered leachant on ettringite-based stabilizing matrices', *Environmental Technology*, **21**, 815-818.

Cocke, D.L. 1990, 'The binding chemistry and leaching mechanisms of hazardous substances in solidification/stabilization systems' *Journal of Hazardous Materials*, **24**, 231-237.

Conner, J.R. 1990, *Chemical Fixation and Solidification of Hazardous Wastes*, Van Nostrand Reinhold, New York.

Cornelis G., Van Gerven T. & Vandecasteele C. 2006, 'Antimony leaching from uncarbonated and carbonated MSWI bottom ash', *Journal of Hazardous Materials*, **A137**, 1284–1292.

Csetenyi Laszlo, J. & Glasser, F.P. 1993, 'Borate substituted ettringites', *Materials Research Society Symposium*, **294**, 273-278.

De Windt. L., Dabo D., Lidelöw S., Badreddine R. & Lagerkvist A. 2011, 'MSWI bottom ash used as basement at two pilot-scale roads: Comparison of leachate chemistry and reactive transport modeling', *Waste Management*, **31**, 267–280.

Luz, C.A., Pera J., Cheriaf, M. & Rocha, J. C. 2007, 'Behaviour of calcium sulfoaluminate cement in presence of high concentrations of chromium salts', *Cement and Concrete Research*, **37**, 624–629.

Luz, C.A., Rocha, J.C., Cheriaf, M. & Pera J. 2006, 'Use of sulfoaluminate cement and bottom ash in the solidification/stabilization of galvanic sludge', *Journal of Hazardous Materials*, **B136**, 837–845.

Luz, C.A., Rocha, J.C., Cheriaf, M. & Pera J. 2009, 'Valorisation of galvanic sludge in sulfoaluminate cement', *Construction and Building Materials*, **23**, 595–601.

Ortego, J.D. Barroeta, Y. Cartledge, F.K. Akhter, H. 1991, 'Leaching effects on silica polymerization. An FTIR and 29Si NMR study of lead and zinc in portland cement', *Environmental Science and Technology*, **25**, 1171-1174.

Pelletier, L., Winnefeld, F. & Lothenbach, B. 2010, 'The ternary system Portland cement–calcium sulphoaluminate clinker–anhydrite: Hydration mechanism and mortar properties', *Cement & Concrete Composites*, **32**, 497–507.

Pöllmann, H. & Kuzel, H.J. 1990, 'Solid solution of ettringites. Part II: Incorporation of $B(OH)^{4-}$ and $CrO4^{2-}$ in $3CaO\cdot Al_2O_3\cdot 3CaSO_4\cdot 32H_2O$', *Cement and Concrete Research*, **20**, 941-947.

Spence, R.D. & Shi C. 2005, *Stabilization and solidification of hazardous radioactive and mixed wastes*, CRC Press, Boca Raton, FL, USA.

Stegemann, J.A. & Coté, P.L. 1996, 'A proposed protocol for evaluation of solidified wastes', Science of Total Environment, **178**, 103-110.

UNI EN 12390-3:2009 *Standard. Testing hardened concrete*; issued on 15 May 2009.

Yousuf, M., Mollah, A., Tsai, Y.N. & Cocke, D.L., 1992, 'An FTIR investigation of cement based solidification/stabilization systems doped with cadmium', *Journal of Environmental Science Health* **A27**, 1213-1219.

XII DBMC
International Conference on Durability of Building Materials and Components
PORTO - PORTUGAL, April 12th-15th, 2011

Effect of Carbonation on the Microstructure and Moisture Properties of Cement - Based Materials

Mickaël Thiéry[1]
Paméla Faure[2]
Antoine Morandeau[1,2]
Gérard Platret[1]
Jean-François Bouteloup[1]
Patrick Dangla[2]
Véronique Baroghel-Bouny[1]

ABSTRACT

We provide a comprehensive understanding of the effects of carbonation on the microstructure, and the moisture properties of cement-based materials made of ordinary Portland cement (OPC) and fly ash (FA). The bulk porosity is measured on a large panel of non-carbonated or fully carbonated cement pastes and concrete specimens by hydrostatic weighing and by mercury intrusion porosimetry (MIP). The *carbonatable* amount of CH and C-S-H (corresponding to the maximum degree of carbonation that is reached for these hydration compounds) is assessed when the carbonation mechanism is considered stabilised. The induced reduction in porosity is correlated with the calcium carbonate (CC) content quantified by thermogravimetric analysis (TGA) and associated both with CH and C-S-H carbonation. The identified variation of molar volume occurring during the C-S-H carbonation is dependent on the CO_2 concentration and is different if pozzolanic C-S-H are considered since for this latter a negative difference of solid volume can be observed. The effect exerted by carbonation on the pore size distribution (PSD) is also elucidated by means of MIP and by analysing the diagrams of the spin-lattice relaxation time (T_1) determined by Nuclear Magnetic Resonance of proton H (NMR). The proportion of coarse capillary pores (radius>100 nm) increases with the degree of carbonation for materials of a high water/cement (w/c) ratio although a systematic reduction in total porosity for OPC systems is still measured. Moreover, this paper discusses the influence of carbonation on the water vapor desorption isotherms (WVDIs). An analysis of the T_1-diagrams and the WVDIs of carbonated and non-carbonated materials made of OPC shows that the same fine-textured morphology of the C-S-H seems remains in spite of a partial decalcification and polymerisation.

KEYWORDS

Carbonation, C-S-H , Mercury intrusion porosimetry, NMR, Water vapor sorption isotherm.

[1] Paris-Est University, LCPC, Materials Department, Paris, FRANCE, thiery@lcpc.fr
[2] Paris-Est University, Navier, Champs-sur-Marne, FRANCE

1 INTRODUCTION

Carbonation of cement-based materials is based on a complex reactive-transport mechanism governed by CO_2-diffusion within the porous network and the chemical reactions between CO_2 and the hydration compounds (generally CH and C-S-H). It is well established that carbonation is generally responsible for significant microstructural changes [Ngala & Page 1997]. For ordinary Portland cement (OPC) systems, carbonation leads to a reduction in porosity which is generally ascribed to the positive difference of molar volume between CH and the precipitated C$\underline{C}$ (4 $cm^3.mol^{-1}$ if calcite is forming). But it is obvious that the observed decrease in porosity cannot only be related to CH carbonation and consequently that the carbonation of C-S-H may also significantly contribute to this evolution. It is for this reason that a determination of the variation of molar volume of the solid phase occurring during the C-S-H carbonation should be investigated. Furthermore, it is also known that the carbonation of materials made of fly ash (FA) can lead to a coarser microstructure and a possible increase in porosity. Nevertheless, since the reasons for such behaviour are still not well understood, a comprehensive analysis of the evolution of the pore size distribution (PSD) caused by carbonation is necessary.

2 MATERIALS AND EXPERIMENTAL PROCEDURES

An grey OPC (C_3S 59%, C_2S 19%, C_3A 2%, C_4AF 14%, gypsum 5%), a white OPC (C_3S 54%, C_2S 28%, C_3A 11%, C_4AF 1%, gypsum 5%) and a class F fly ash (S 50%, A 23%, F 9%) were used in this study. Cement pastes were fabricated with a water-to-cement ratio (w/c) ranging from 0.25 to 0.60. Cement pastes of w/b=0.3/0.4/0.5 with two levels of cement replacement by FA (20% and 40%) were also fabricated. Cement paste specimens were prepared in plastic bottles tightly sealed to avoid water evaporation and rotated to keep an homogeneous material. The cement pastes were removed from their mould at 18 months. A concrete (M25) was also prepared with the same grey OPC cement (w/c=0.84, s/(s+g)=0.47) and was water-cured during 90 days. The cement paste specimens were crushed in small pieces (1 mm^3) which were dried in a desiccator where a NH_4NO_3 salt solution controls a relative humidity (RH) of 53% until mass loss stabilisation (i.e. at least 14 days). Cylindrical concrete specimens (2 geometries: diameter=11 cm and height=5 cm or 0.2 cm) were dried at 45°C during 28 days. After this pre-treatment, the crushed samples of cement paste and the concrete specimens were then exposed in a carbonation chamber where the CO_2 concentration is maintained constant (10% or 50%) and the RH is controlled by a NH_4NO_3 salt solution. The samples were held in this CO_2-incubator until the mass increase due to the CO_2 fixation onto the cementitious matrix is stabilised. This criterion is considered to represent a full carbonation state. Obviously, the carbonation duration depends of the CO_2 concentration and the size of the samples: a few days for the crushed cement paste samples, a few weeks for the 0.5-diameter concrete specimens and at least two months for the 5-cm diameter concrete specimens. Moreover, some cement paste samples were exposed to natural carbonation (CO_2=0.04%) in a laboratory room where the RH is maintained around 50%. Examples of mass increase kinetics during the exposure period to CO_2 are shown in Fig. 1 in the case of the cement paste samples made of OPC. It is worthwhile noting that the slight decrease in the sample mass towards the end of the test illustrates that the carbonation mechanism becomes stabilised and indicates that the free water released from the hydration products (CH and C-S-H) due to carbonation is starting to dissipate from the samples upon drying.

In order to investigate the influence of carbonation on the properties of the materials (chemical composition, microstructure changes and moisture properties), different techniques were performed on non- and fully-carbonated materials: thermogravimetric analysis (TGA), mercury intrusion porosimetry (MIP), assessment of the accessible-to-water porosity (P_w), spin-lattice relaxation (T_1) Nuclear Magnetic Resonance (NMR) measurements [Faure *et al.* 2005] and assessment of the water vapour desorption isotherms (WVDIs) [Baroghel-Bouny 2007].

3 INVESTIGATION OF THE POROSITY CHANGES DUE TO CARBONATION

3.1 Evaluation of the amount of *carbonatable* amount of CH and C-S-H

In order to correlate the evolution of the porosity with the amount of C$\underline{C}$ related to CH and C-S-H carbonation, it is first necessary to dispose of an accurate assessment of the maximum carbonation degree of CH and C-S-H when the carbonation mechanism is stabilised, *i.e.* when the material is considered as fully carbonated. The initial amount of CH and C$\underline{C}$ are measured by TGA during the heating, respectively in the temperature range 450°C-550°C and 550°C-950°C (see two examples of TGA results in Fig. 2 for carbonated and non-carbonated cement pastes made of or without FA). Of interest is the fact that the temperature range corresponding to the decomposition of C$\underline{C}$ during the heating is very broad which makes the determination of the C$\underline{C}$ content formed by carbonation difficult if a limestone aggregate is used (in mortar or concrete). Figure 3 illustrates the initial CH content n^0_{CH} for the studied cement pastes only made with OPC (determined by TGA on non-carbonated materials), as well as the initial C-S-H content assessed by means of a semi-analytical model [Bernard *et al.* 2003] (the chosen stoichiometry for the C-S-H is $C_3S_{1.7}H_z$). Figure 3 also shows the amounts of C$\underline{C}$ produced by the carbonation reactions of CH ($n_{C\underline{C}}^{CH}$) and C-S-H ($n_{C\underline{C}}^{CSH}$). These values are determined according to the characteristics of the non-carbonated specimens (n^0_{CH} and initial amount of C$\underline{C}$ $n^0_{C\underline{C}}$ indicating a possible slight air-carbonation during the fabrication or the pre-treatment of the samples) and to the total amount of C$\underline{C}$ ($n_{C\underline{C}}$) within the carbonated samples, i.e. $n_{C\underline{C}}^{CH}=n^0_{CH}-n_{CH}$ and $n_{C\underline{C}}^{CSH}=n_{C\underline{C}}-n_{C\underline{C}}^{CH}-n^0_{C\underline{C}}$.

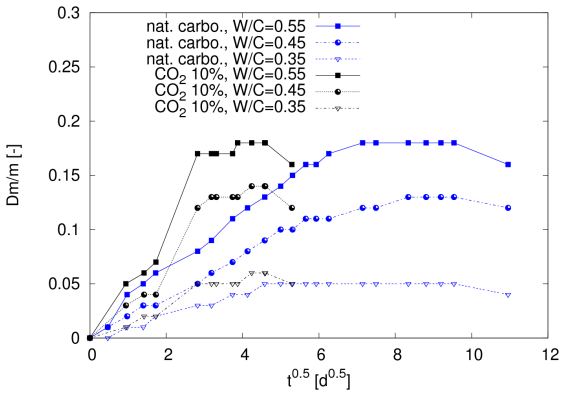

Figure 1. Kinetics of mass increase during the carbonation of cement paste samples (crushed) of w/c=0.35/0.45/0.55.

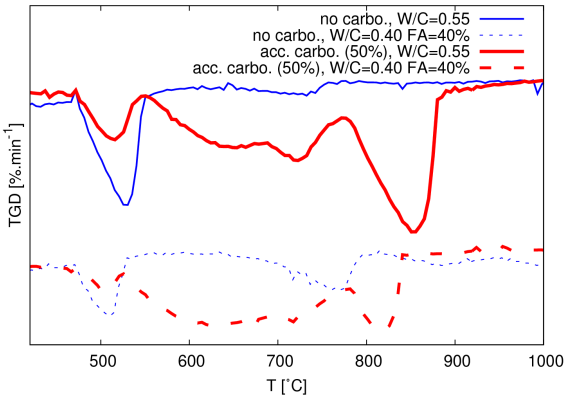

Figure 2. Examples of thermoanalytical curves (first derivative of the relative mass loss, TGD) for cement pastes (non-carbonated and fully-carbonated with CO_2=50%).

Figure 4 illustrates the degree of carbonation of CH ($n_{C\underline{C}}^{CH}/n^0_{CH}$) and C-S-H ($n_{C\underline{C}}^{CSH}/[3n^0_{CSH}]$) of the materials under study. It seems that CH cannot be fully carbonated and that a maximum carbonation level of 0.8 (for w/c=0.45 and accelerated conditions CO_2=50%) is observed. This behaviour is classically related to the formation of a C$\underline{C}$ coating around the CH hexagonal crystals that drastically hinders ion transfers and the carbonation kinetics of CH. Moreover, an optimum carbonation for CH can be noticed for w/c=0.45. Actually, when the w/c is high, massive clusters of CH crystals are observed [Gallucci & Scrivener 2007] and thus the reduction in accessibility and passivation effects are enhanced. On the other hand, when the w/c is low, CH crystals are certainly smaller but they are surrounded by a denser matrix of C-S-H that also makes them less accessible. Note that the maximum degree of CH carbonation depends on the CO_2 concentration. It is observed that the amount of *carbonatable* CH is higher when the CO_2 concentration is above 10%. Figure 4 also illustrates the equivalent behaviour between results at CO_2=10% and natural carbonation as regards the *carbonatable* amount of CH. Concerning C-S-H, the influence of reduction in accessibility occurring during the formation of C$\underline{C}$ is less pronounced thanks to a much higher exposed surface area to CO_2

than CH crystals. Consequently, for C-S-H a maximum degree of carbonation (close to 1) can be reached if the CO_2 concentration is high (50%) leading to an almost total decalcification.

3.2 Evaluation of the changes in porosity related to the carbonation level of CH and C-S-H

The amount of C$\underline{C}$ produced by CH carbonation makes possible the calculation of the drop in porosity due to the only carbonation of CH given that carbonation of CH is mainly responsible for the formation of calcite (polymorph of C$\underline{C}$) [Groves et al. 1991] and that the corresponding variation in molar volume is well known (Dv_{CH}=3.8 $cm^3.mol^{-1}$). The accessible-to-mercury porosity (applied Hg pressure from 0.01 kPa to 400 MPa) has been determined on the non-carbonated and fully-carbonated samples. Figures 5 and 6 illustrate the variation in porosity which is only related to the other hydration compounds than CH, in fact mainly C-S-H (i.e., $\Delta\varphi_{CSH}=\Delta\varphi-n_{C\underline{C}}^{CH}xDv_{CH}$). $\Delta\varphi_{CSH}$ is plotted as a function of the C$\underline{C}$ amount produced by the carbonation of the other hydration compounds than CH ($n_{C\underline{C}}- n_{C\underline{C}}^{CH}- n^0_{C\underline{C}}$) and measured by TGA. Since the cement used in this study to prepare the cement pastes has a very low C_3A content (in order to ensure a high resistance to the sulphate attack), the predominant hydrated compounds other than CH are mainly composed ,in this instance, of C-S-H.

In the case of pastes made of OPC, Fig. 5 shows, for each CO_2 concentration, a satisfactory linear relation between the C$\underline{C}$ content (per unit volume of porous material) thus related to the C-S-H carbonation and the corresponding variation in porosity. The slope reflects the change in volume Dv_{CSH} if a mole of C$\underline{C}$ is formed from C-S-H. It is found that Dv_{CSH}=17.5 $cm^3.mol^{-1}$ for CO_2=50%, Dv_{CSH}=21.6 $cm^3.mol^{-1}$ for CO_2=10% and Dv_{CSH}=28.5 $cm^3.mol^{-1}$ for natural conditions of exposure. It is possible to demonstrate that $Dv_{CSH}=v_{C\underline{C}}^{CSH}+(y/x)v_S-(1/x)v_{CSH}$ where x and y are the stoichiometric parameters defining the chemical composition of the C-S-H ($C_xS_yH_z$) and v_{CSH} and v_S are the molar volumes of the C-S-H and the formed amorphous silica gel, respectively. Whether the value of Dv_{CSH} is positive or negative is governed by the molar volume of silica gel (SH_t) which depends on the amount of chemically-bound water molecules silica gel contains. Actually, a great variability of v_S is reported in the literature: from 12 to 34 $cm^3.mol^{-1}$ according to Wolery [1992]. The positive value for Dv_{CSH} observed for the OPC systems under study shows that the formed silica gel has certainly a high degree of hydration (t close to 2). The lower observed values for Dv_{CSH} when the CO_2 concentration is higher may be understood if one considers that high CO_2 concentration preferentially leads the production of aragonite of lower molar volume than vaterite and calcite.

Figure 6 illustrates the evolution of porosity as a function of the content of C$\underline{C}$ produced by the C-S-H carbonation in the case of cementitious systems containing FA. Therefore, the amount of C$\underline{C}$ assessed by TGA also includes the C$\underline{C}$ formed by carbonation of the pozzolanic C-S-H. For a moderate degree of the C-S-H conversion ($n_{C\underline{C}}^{CSH}$<3000 $mol.m^{-3}$) and in the case of the cement pastes containing FA with a replacement ratio of 20%, the change in porosity as a function $n_{C\underline{C}}^{CSH}$ evolves similarly (with the same upward trend) than the OPC pastes without FA. For a higher carbonation degree of the C-S-H ($n_{C\underline{C}}^{CSH}$>3000 $mol.m^{-3}$), Fig. 6 reveals that a decrease in porosity as a function of $n_{C\underline{C}}^{CSH}$ is observed giving evidence that the C-S-H carbonation causes a drop of the volume of the solid phase. Undeniably, this effect is due to the carbonation of the pozzolanic C-S-H which may produce a poorly-hydrated silica gel of a low molar volume (v_S) due certainly to a release during carbonation of a great amount of free water initially chemically-bound within the C-S-H. Note that this peculiar behaviour observed for the pozzolanic C-S-H is more evident with a higher FA replacement ratio of 40% since given that it is observed in Fig. 6 that carbonation can then significantly contribute to an increase in porosity. This phenomenon is in agreement with other results taken from literature which show an increased porosity and a loss of strength for concrete made with a high FA (or slag) content (see for instance Thaulow et al., 2000). It is generally proposed to interpret this deleterious consequence of carbonation on the global porosity as an effect of the decalcification of the C-S-H which is more pronounced if pozzolanic C-S-H of lower initial C/S ratio (1.2-1.4) than ordinary C-S-H are concerned and if the CH content in the system is limited because for instance of the pozzolanic activity of FA [Thomas *et al.* 2003].

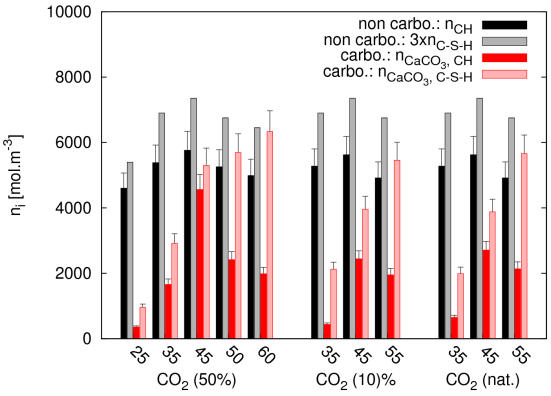

Figure 3. Initial CH and C-S-H contents for different cement pastes (w/c=0.25 to 0.55). CC produced by reaction of CH and C-S-H.

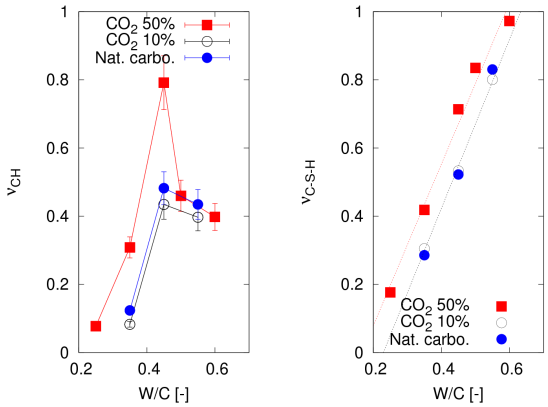

Figure 4. Carbonation levels of CH and C-S-H *vs.* W/C of different cement pastes and carbonation conditions.

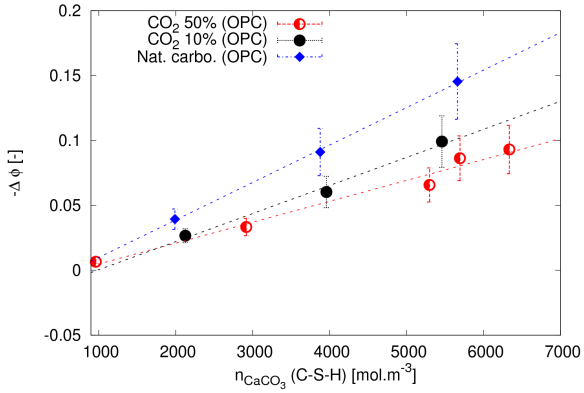

Figure 5. Variation in porosity related to the CC produced by C-S-H carbonation (case of OPC pastes).

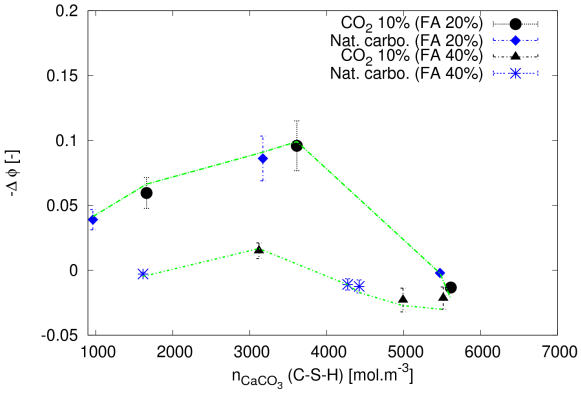

Figure 6. Variation in porosity related to the CC produced by C-S-H carbonation (case of pastes prepared with OPC and FA).

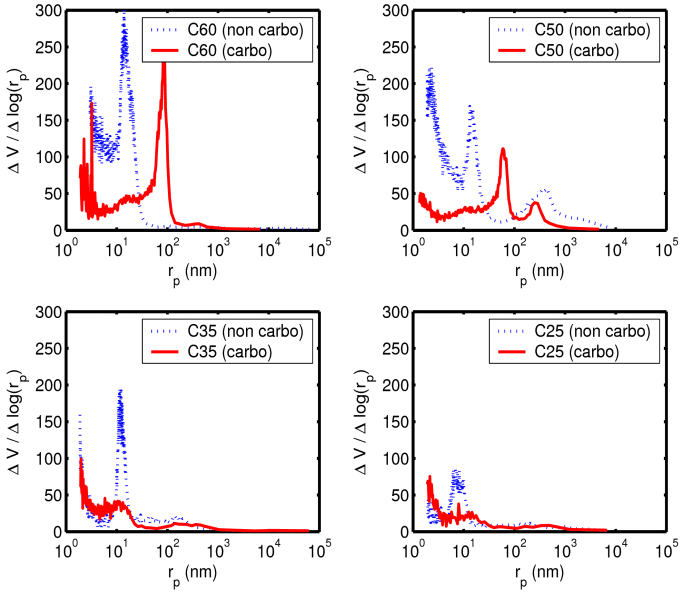

Figure 7. PSD of hardened OPC pastes (non-carbonated and carbonated with CO_2=50%) of different w/c (0.60, 0.50, 0.35 and 0.25). Determination by mercury intrusion porosimetry (MIP).

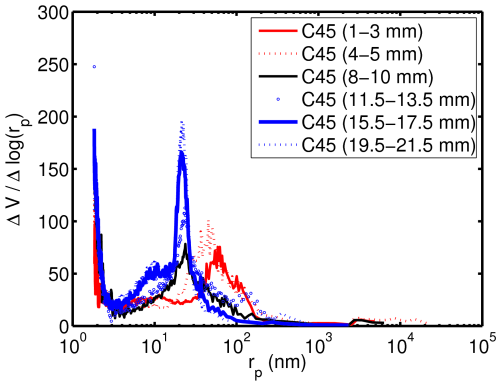

Figure 8. PSD determined by MIP of different slices sawn from the surface to the core of a specimen of OPC paste (w/c=0.45) exposed to CO_2 (50%) during 14 days.

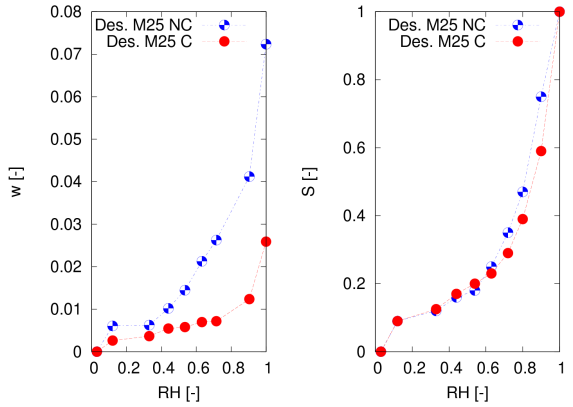

Figure 9. WVSIs of concrete M25 (non-carbonated and carbonated with CO_2=50%). Water content (w) and liquid water saturation (S) *vs.* RH.

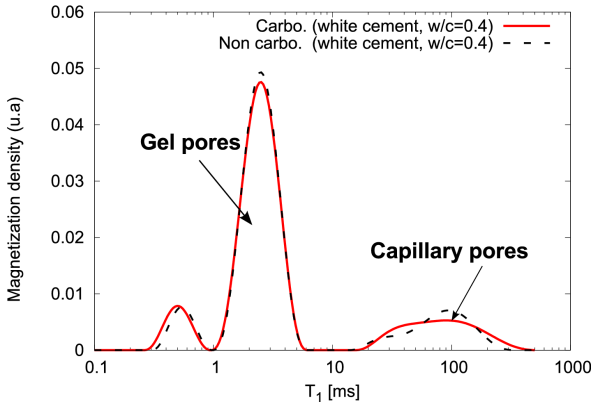

Figure 10. Distribution of T_1 relaxation time in the case of non-carbonated and carbonated (CO_2=50%) white cement pastes.

4 MICROSTRUCTURE CHANGES (INFLUENCE ON PORE-SIZE DISTRIBUTION)

Figure 7 illustrates the PSDs for non-carbonated and carbonated OPC pastes of w/c ranging from 0.6 to 0.25. These PSDs are determined by MIP performed on freeze-dried samples (lyophilisation). The analysis of the PSDs shows that, although carbonation is responsible for an apparent clogging of the microstructure between 10-100 nm (corresponding to capillary mesopores attributed to the voids among outer C-S-H clusters according to the general classification proposed by Mindess, 2002), carbonation is also capable of producing larger capillary macropores of 100-200 nm size if w/c is high enough (*i.e.* >0.45). To understand this feature a descriptive model can be used, such as the one proposed to interpret the evolution of the microstructure which takes place during the carbonation of non-hydraulic lime mortars [Lawrence *et al.* 2002]. Although the porosity in the range 10-100 nm is filled by C$\underline{\text{C}}$ of higher volume than the parent hydrated compounds CH and C-S-H, a new porosity may also appear between C$\underline{\text{C}}$ microcrystals which are packed within the pore space previously occupied by CH macrocrystals. This size of the created pores is of the same order of magnitude as the size of the C$\underline{\text{C}}$ crystals (calcite), i.e. around 100 nm. The creation of these macrocapillary pores seem reinforced if carbonation is occurring with a high CO_2 concentration and if the water content within the material is low given that these carbonation conditions prevent the diffusion of ions through the pore solution and thus contribute to a localised formation of C$\underline{\text{C}}$ crystals around the CH clusters. On one hand, the carbonation at high CO_2 (at least 50%) is so accelerated that the formation of C$\underline{\text{C}}$ crystals takes place directly at the surface of CH crystals where Ca^{2+} and CO_3^{2-} ions meet and form calcite. On the other hand, if the cement-based material is too dry, the water film covering the pore surface is too thin to facilitate the diffusion of ions. Note that for the studied cement pastes of high

w/c (0.5 and 0.6), the appearance of a coarser microstructure when the material is carbonated is more pronounced. This might be attributed to the formation of larger CH crystals embedded in a highly porous matrix which enables the expansion of calcite crystals and makes the cluster of C$\underline{C}$ crystals less dense.

Figure 9 represents the WVDIs (at 20°C) of concrete M25 (carbonated and non-carbonated) determined by the desiccator method. Concrete disks (2 mm-thickness) were submitted to decreasing RH steps from 100% (deionised water) to 3% (dry silica gel) by using saturated salt solutions for intermediate RH values and by waiting for weight loss equilibrium for each step (at least 2 months). The water content (w) and liquid water saturation (S) are plotted *vs.* RH. The significant reduction in porosity due to carbonation of this concrete made of OPC thus allows an explanation for the water content of the carbonated disks being clearly lower than the water content of the healthy samples. By choosing S instead of w to plot the WVSIs, the impact of the clogging effect of the porosity is side-stepped. It is thus possible to isolate the sole influence of the changes affecting the PSD caused by carbonation. Therefore, since carbonation does not significantly affect the WVSI if S is chosen to quantify liquid water inside the porous material, it seems that carbonation does not change the PSD in the range of the pore size accessible by this technique, i.e. mainly the intrinsic porosity of the C-S-H. This feature is observed even if carbonation results in a decalcification/polymerisation of the C-S-H which is thus likely to stay moderate in the case of OPC systems. A higher degree of decalcification (drop of C/S) may be observed if pozzolanic C-S-H with low C/S ratio are carbonated leading therefore to a serious modification of the microstructure of the C-S-H and a creation of a microporosity not observed in raw materials. The highly cross-linked formed silica gel has actually an open nature compared to non-carbonated C-S-H slits.

In Figure 9, the fact that the WVDIs of the carbonated and non-carbonated OPC concrete have relatively the same shape, illustrating thus the slight modifications of the microstructure of the C-S-H, is in agreement with the experimental observations dealing on the weak difference about the porosity variations, assessed either by MIP and by the determination of the accessible-to-water porosity, between carbonated and non carbonated samples. It confirms that the whole modifications of the microstructure caused by carbonation of OPC systems are entirely detectable by MIP.

Inverse Laplace processing of the spin-lattice relaxation data enables the determination of the T_1 distribution (distribution of the longitudinal relaxation time) which is known method to characterise the mobility of water molecules within cement-based materials. Since this mobility depends on the size of the pores, the analysis of T_1-diagrams gives information on the pore size distribution of hardened cement pastes by probing their water mobility. The T_1 distribution of hardened cement-based materials exhibits at least three modes as illustrated in Fig. 10 for a non-carbonated and a carbonated paste fabricated with a white cement (w/c=0.4). These materials are tested after saturation by liquid water. The diagrams are normalised by the water content of the tested specimens to get rid of the influence of the clogging effect on the porosity by the formation of C$\underline{C}$ and to highlight the changes in PSD. In Fig. 10, the three observed T_1 peaks are attributed to the chemically-bound water (very short T_1 values: 0.1-1 ms), to the gel pores (T_1>10 ms) and to capillary pores (T_1=1-10 ms). The gel and capillary porosities correspond to two distinct pore sizes: <10 nm and >10 nm, respectively [Faure et *al.* 2005]. The fact that the T_1 peak characterising the intrinsic porosity of the C-S-H remains unchanged proves that carbonation poorly affects the microstructure of the C-S-H confirming the previously observed WVSIs results. Nevertheless, carbonation seems to modify the capillary microstructure by filling one part of the capillary pores and by creating a new porosity as has been shown by MIP.

CONCLUSION

A comprehensive study of the consequences of carbonation on the microstructure of cement-based materials has been performed. Firstly, the changes of porosity have been quantified and correlated to the amount of C$\underline{C}$ formed due to the carbonation of CH and C-S-H. In this manner, the variation of

molar volume Dv_{CSH} related to the C-S-H carbonation has been determined. Hence it has been shown that Dv_{CSH} depends on the CO_2 concentration and if the C-S-H are pozzolanic or not given that decalcification of pozzolanic C-S-H by carbonation can lead to a significant reduction in the volume of the solid phase. These results help confirm the practical experience obtained from feedback about in field data showing that carbonation of concrete made of fly ash can provoke an increase in porosity. The impact of carbonation on the microstructure of cement-based materials has also been studied by complementary techniques (MIP, NMR, WVSI) making possible a thorough investigation of the changes of the PSD. Resulting from a rearrangement of the microstructure, it seems can the carbonation of OPC systems mainly affects the capillary pores, both by the reduction of the porosity among the outer C-S-H and the increase of macro capillaries corresponding to the disappearance of the clusters of CH crystals replaced by a packing of CC crystals leaving new voids. Furthermore, it has been shown that the intrinsic PSD of C-S-H is not really affected by carbonation.

ACKNOWLEDGMENTS

This research has been carried out in the framework of the French project *Carbonated Recycled Aggregates for Concrete* (CRAC) supported by the *Agence Nationale de la Recherche* and in the framework of the LCPC project on the service life prediction of Reinforced Concrete Structures (*11R062*).

REFERENCES

Lawrence, R., Mays, T., Rigby, S., Walker, P., D'Ayala, D., 2007, 'Effects of carbonation on the pore structure of non-hydraulic lime mortars', Cement and Concrete Research, **37**[7], 1059-1069.

Baroghel-Bouny V., 2007, 'Water vapour sorption experiments on hardened cementitious materials. Part1. Essential tool for analysis of hygral behaviour and it relation to pore structure', Cement and Concrete Research, **37**, 414-437.

Bernard, O., Ulm, F-J, Lemarchand, E., 2003, 'A multiscale micromechanics-hydration model for the early-age elastic properties of cement-based materials', Cement Concrete Research, **33**[9], 1293-1309.

Gallucci, E., Scrivener, K., 2007, 'Crystallisation of calcium hydroxide in early age model and ordinary cementitious systems', *Cement and Concrete Research*, **37**[4], 492-501.

Groves, G., Brough, A., Richardson, I., Dobson, C., 1991, 'Progressive Changes in the Structure of Hardened C_3S Cement Pastes due to Carbonation', *J. Am. Ceram. Soc.*, **74**[11], 1991, 2891-2896.

Thomas, J.J., Chen J.J., Allen, A.J., Jennings H.M., 2004, Effects of decalcification on the microstructure and surface area of cement and tricalcium silicate pastes, Cement and Concrete Research, **34**[12], 2297-2307.

Ngala, V.T., Page, C.L., 1997, 'Effects of carbonation on pore structure and diffusional properties of hydrated cement pastes', Cement and Concrete Research, **27**[7], 995-1007.

Faure, P., Caré, S., Po, C., Rodts S., 2005, 'An MRI-SPI and NMR relaxation study of drying-hydration coupling effect on microstructure of cement-based materials at early age', Magnetic Resonance Imaging, **23**, 311-314.

Mindess, S., Young J.F., Darwin, D., 2002, Concrete, 2nd ed., Prentice Hall, Englewood Cliffs, NJ.

Thaulow, N., Lee, R., Wagner, K., Sadananda, S., 2000, 'Effect of calcium hydroxide content on the form, extent, and significance of carbonation' in *Calcium hydroxide in concrete*, American Ceramic Society, 191-202.

Wolery, T., 1992, *Computer Program for Geochemical Aqueous Speciation-Solubility Calculation : Theoretical Manual, User's Guide, and Related Documentation* (Version 7.0), Technical report, Lawrence Livermore National Laboratory Report UCRL-MA- 110662 PT III.

XII DBMC
International Conference on Durability of Building Materials and Components
PORTO - PORTUGAL, April 12th-15th, 2011

Durability of Mortars with Expanded Polystyrene

Verónica Ferrándiz Mas [1]
Jose Antonio Huesca Tortosa [2]
Eva García Alcocel [3]

ABSTRACT

This work studies the influence of the addition of expanded polystyrene in the durability of Portland cement mortars. Its behaviour has been analyzed in terms of workability, mechanical strength, resistance to heat and freezing and capillarity. The mortars were produced with air-entraining agent, superplasticizer and water retainer additive to increase the workability and the final properties. The results show that with increasing proportions of expanded polystyrene the workability and mechanical strength decreases. The mortars subjected to heat cycles show small increase in compressive strength. The expanded polystyrene improves on freezing behaviour of the mortars because it works absorbing the crystallization pressure. The results show that the presence of expanded polystyrene in mortars causes a positive effect on their durability.

KEYWORDS

Expanded polystyrene (EPS), Mortar properties, Additives, Durability.

[1] Architectural Constructions Department of the University of Alicante, Alicante, ESPAÑA, v.ferrandiz@ua.es
[2] Architectural Constructions Department of the University of Alicante, Alicante, ESPAÑA, ja.huesca@ua.es
[3] Architectural Constructions Department of the University of Alicante, Alicante, ESPAÑA, eva.garcia@ua.es

1 INTRODUCTION

Expanded polystyrene foam (EPS) is a thermoplastic polymer closed cell structure. It is a biologically inert and nontoxic. EPS has interesting properties such as low density, thermal insulation, hydrophobicity and chemical resistance when exposed to acids and alkalis. EPS is granulated into small particles that can be considered as non-absorbent and lightweight polymeric aggregate.

Historically, lightweight concrete is used for both non-structural and structural uses [1]. Lightweight concretes manufactured with EPS have been used as covering panelling, curtain walls, coating systems for composite flooring and concrete blocks [2], as a sub-basis material in road pavement and railways; in sea floating structures, marine beds and barriers; as energy absorbing material for military buried structures protection and as screens in petrol platforms [3-5]. Concretes made with lightweight aggregates have shown an equal if not better durability, even when submitted to severe conditions [6]. EPS as a lightweight aggregate has been widely used in the concrete production. However, no bibliographic references have been located to prove the existence of scientific studies regarding its use in brickwork and special mortars production. On the other hand, there are commercialized mortars with more than 3 mm pearls EPS additions for some specific uses.

The main aim of this study is to evaluate the influence of the addition of EPS in the durability of Portland cement mortars. Physical, chemical, mechanical and microstructural properties of mortars made with different types and percentage of EPS were studied. Mortar properties were evaluated by comparison with mortars containing no EPS (control mortar).

2 EXPERIMENTAL

2.1 Materials

The following materials were used for this study: distilled water, Portland cement type CEM I 52,5R which was provided by Holcim Morteros S.A. and CEN UNE-EN 196-1compliant silica sand [7]. The following types of EPS were used: EPS_b (big size), EPS_s (small size), EPS_g (grinding). The main properties of EPS are given in table 1.

Table 1. Properties of EPS aggregate.

EPS type	*Recycled*	*Particle diameter (mm)*	*Particle geometry*	*Colour*	*Density (g/cm^3)*
EPS_b	No	>3	Spherical	White	0,0076
EPS_s	No	<3	Spherical	White	0,052
EPS_g	Yes	1-5	Irregular	Colour	0,017

AEA: Air-entraining agent additive (BASF RHEOMIX 934), WRA: a water retainer additive (Hidroxipropil metil cellulose) and SPA: superplasticizer additive (BASF RHEOMIX GT 205 MA) were used to increase the EPS quantity and to improve the mortar properties.

2.2. Preparation of the samples and operating procedure

Mortars with a cement/sand/water ratio (by weight) of 1:3:0.5 were prepared with 0 (control mortar), 10, 30, 50 and 70% EPS percentages replacement by volume of sand. The test of mortar workability was used to determine the amount of EPS to be dosed. The tests were carried out under laboratory conditions according to the UNE-EN 1015-3:2007 standard by the flow table method [8]. Mortars with 70% EPS were made with different additives. AEA additive was added to mortars in the following dosages: 0 and 0.8% w/w cement for all EPS types'. WRA additive was added to mortars in the following dosages: 0 and 0.3% w/w cement for all EPS types'. SPA additive was added to mortars in the following dosages: 0 and 0.1% w/w cement for EPS_b, 0.9% w/w cement for EPS_s and 0.5% w/w

cement for EPS_g mortar. Mortars were mixed under laboratory conditions according to the UNE-EN 196-1:2005 standard [7]. Prismatic 40 x 40 x 160 mm specimens were prepared through mechanical compaction of fresh mixtures into two layers. The specimens were demoulded after 24 h and cured under water at 20 ± 2ºC with curing times variable according to the test.

2.2.1 Mortar's physical properties

For the fresh paste, consistency was determined according to the UNE-EN 1015-3:2007 standard by the flow table method [8].The tests were carried out under laboratory conditions. Three measurements were made per sample.

In hardened state for capillary absorption test, three 40x40x160mm specimen were made per sample. After the curing period were cut into 4 cm cubes. After drying the samples, the lateral sides of each cube were sealed with an adhesive plastic film to restrict the water flow to the longitudinal cube axis. The capillary absorption (C_{90}) was determined according to the UNE-EN 1015-18:2003 standard [9].

2.2.2 Mortar's mechanical properties

Mortars were mechanically tested after 7, 28, and 120 days of curing. The mechanical tests were performed under laboratory conditions according to the UNE-EN 196-1:2005 standard [7]. For each mortar and curing age, three 40x40x160mm specimens were tested. Mortar samples were tested in bending, and the two resulting pieces were tested under compression.

To assess the durability against temperature the mortars were subjected to heat and freeze-thaw cycles. Six 40x40x160 mm specimen per sample were made and curing for 28 days. After the curing time were carried out the following process for the heat cycles with three specimens for each mortar: The samples were put into the oven at 60ºC± 5ºC for 18 hours, then removed from the oven and kept at room temperature for 6 hours and after 25 times were tested under compression. The other three specimens for each mortar were subjected to freeze-thaw cycles. In this case were made an adaptation to the UNE 67028 EX:1997 standard for ceramic bricks [10]. After the curing time, the samples were completely immersed in water at 15ºC± 5ºC for 48 hours. Next, the freeze-thaw cycles were carried out with the following process: The samples were removed from the water and drained, then put into the freezer at -15ºC ± 5ºC for 18 hours, then completely immersed in water at 15ºC± 5ºC for 6 hours and after 25 times were tested under compression. To complete the characterization a morphologic study were made by SEM.

3 RESULTS AND DISCUSSION

Table 2 summarizes the results of the workability studies for all studied mortars. A negative correlation between the increasing in the EPS' dosage and the mortar's consistency exists. Quantities from 50% EPS in the mortar without additives provide dry mortars with the spread in the flow table lower than 140 mm. These results agree with the fact that all mortars were made with standard dosage: 1:3:0,5 (by weight). The quantity of mixing water was constant. This means that for the same EPS percentage there are less particles when working with EPS_b. In this case, less water is required and are obtained mortars more workable.

The additives improve the workability of the mortars with EPS to allowing higher % EPS. It is possible to obtain workable mortars with 90% EPS_b. The air-entraining agent increases the workability between 15 and 40%, depending on the EPS' type. The water retainer additive causes an increase of the mix viscosity which leads to a drastic decreasing of the mix's workability when adding EPS. With EPS_b, the workability does not diminish excessively compared to the same mortar without additives. Mortars with EPS_s and EPS_g show consistency values below 120 mm. This complicates a proper placing. To obtain adequate workability should be mixed with other additives. The superplasticizer additive improves significantly the workability versus mortars made without additives. Regarding to

EPS_b, the workability improves around 35% versus the same mortar without additives, whereas for EPS_s improves 68% and for EPS_g improves 50%.

Table 2. Results of the workability tests.
(AEA: Air-Entraining Agent; WRA: Water Retainer Additive; SPA: Superplasticizer Additive)

EPS (%)	*Additive (%)*	*Flow table spread (mm)*		
		EPS_b	*EPS_s*	*EPS_g*
0	0	199	199	199
10	0	179	168	174
30	0	165	143	143
50	0	150	120	127
70	0	140	<120	<120
70	0,8% AEA	156,7	145,2	152,5
70	0,3% WRA	138,3	117,7	120
70	0,1%/0,9%/0,5% SPA	178	147,7	157

Figure 1 shows the 120 days compressive strength for mortars made with different types and percentages of EPS, expressed as a fraction of the compressive strength value found for the control Sci/Sco, where Sci is the strength of mortars with %EPS and Sco is the strength for the control mortar (0%EPS). The Sci values decreased with increasing EPS percentage in mortars, and these values were always lower than Sco. This is because increasing the amount of EPS in the mortar, the density decreases in the hardened state causing loss of compressive strength.

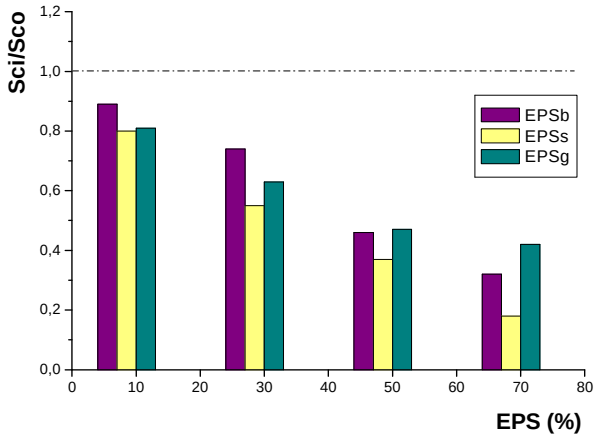

Figure 1. 120 days compressive strength for mortars made with different types and % of EPS expressed as a fraction of the value found for the control Sci/Sco. (Sci: compressive strength for a given EPS mortar; Sco: compressive strength for control mortar)

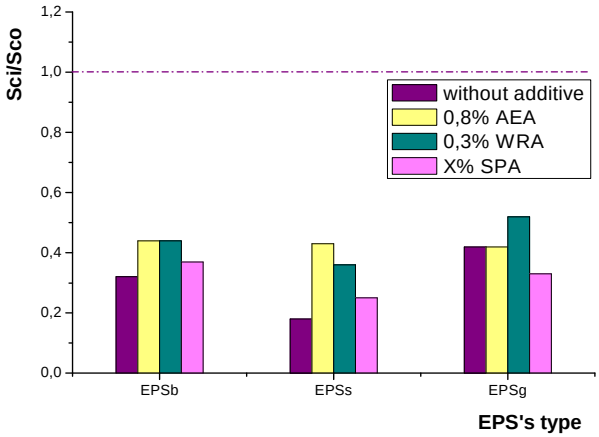

Figure 2. The Sci/Sco ratio for mortar cured for 120 days and fabricated with differents EPS types and additives. In all cases were used 70% EPS dosage. (Sci: compressive strength for a given EPS mortar; Sco: compressive strength for control mortar)

Regarding the influence of the type of EPS in Sc shows that the biggest loss in compressive strength are for mortars made with EPSs. This is due to its greater density. So for the same % replacement volume contains more of EPS. This produces lower mortar density and strength. The smallest differences were observed for mortars with 50% of EPS. They maintain a sufficient workability and strength with average values near to 25 N/mm^2. The mortars with 50% EPS meets the requirements of the UNE-EN 998:1 [11] and the UNE-EN 998:2 [12], for masonry, rendering and plaster mortars, in terms of nominal compressive strength, where 28-day compressive strength requirements are below 20 N/mm^2.

In order to evaluate the contribution of the different additives to long-term strength of 70% EPS mortars the Sci/Sco ratio are shown in Figure 2. It can be observed that the loss in resistence decreases compared to the mortar with 70% EPS without additives. Mortars with EPS_b show an improvement between 5 to 12 %, mortars with EPS_s decrease the loss of resistance between 5 to 26%. Mortars with EPS_g show similar behavior except those made with SPA that increased by a 10% the strength loss.

The results presented show that it is beneficial to use additives in mortars made with high % of EPS. In this way the amount of EPS in the mortar can be increased. It also improves the workability of the same and reduce the loss of compressive strength between 10 and 25% compared to those obtained with mortars without additives.

To assess the durability against temperature the mortars were subjected to heat and freeze-thaw cycles and after that were tested under compression. The mortars were made without additives and with EPS_b, EPS_s and EPS_g in the following dosage:0, 10, 30, 50 y 70%. Figure 3 shows the influence of heat and freeze-thaw cycles on the compressive strength for mortars made with EPS_b and EPS_s. For EPS_g mortars the trend is similar.

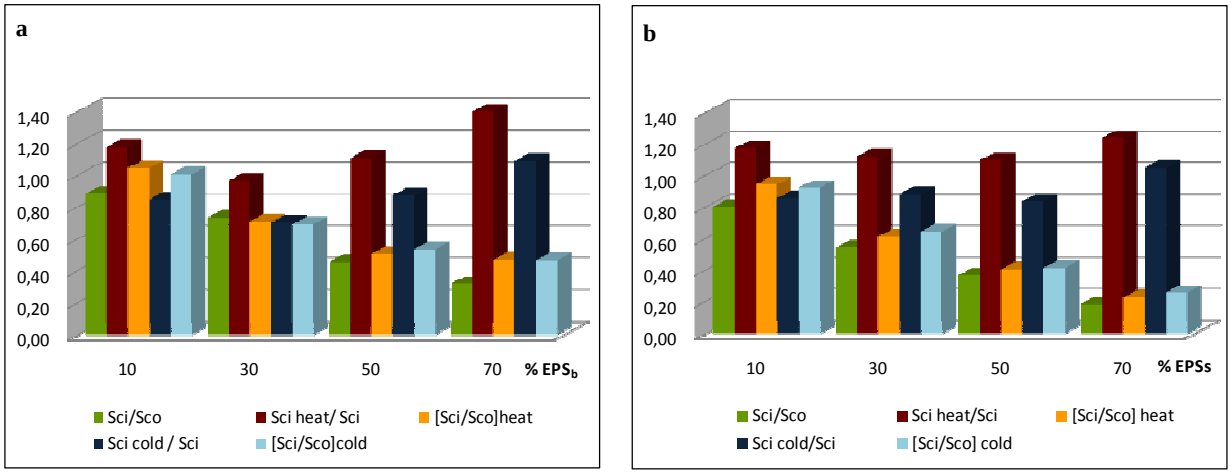

Figure 3. Compressive strength after the heat and freeze-thaw cycles for mortars made with 0, 10, 30, 50 y 70% EPS_b (a) and the same dosage of EPS_s (b), expressed as a fraction of the compressive strength value found for the control. (Sci: compressive strength for a given EPS mortar; Sco: compressive strength for control mortar (0%EPS); Sci heat: compressive strength of mortar after being subjected to heat cycles; Sci cold: compressive strength of mortar after being subjected to freezing-thaw cycles; Sco heat: compressive strength for control mortar (0%EPS) after being subjected to heat cycles; Sco cold: compressive strength for control mortar (0%EPS) after being subjected to freeze-thaw cycles).

First, the effect of the temperature over the control mortar must be indicated. The temperature used for the heat cycles was 60ºC due to the thermoplastic nature of the EPS. This temperature has practically no influence on the compressive behavior of the control mortar. The value of Sc_o heat/Sc_o ratio is 0.997. By contrast the effect of cold represents 25% resistance loss in the control mortar.

The Sc_i heat/Sc_i ratio shows the behaviour of mortar submitted to heat cycles versus the same mortar did not submitted to cycles. This ratio informs of the effect of heat on mortars made with EPS. It can be seen that, generally, heat improves the compressive strength for the mortar made with EPS. The same behaviour, to a lesser extent, can be observed if comparing the Sci/Sco heat versus the Sci/Sco ratio. The increase observed in compressive strength and therefore durability, could be explained for two possible causes. On the one hand, improvements in the microstructure of the hydrated cement paste due to fact that temperature allows a more extended hydratation reaction. On the other hand, improvements in the hydrated cement paste-EPS interface which allows more adherence between both. It can be seen in figure 4 that the mortars subjected to heat cycles show adequate adherence between EPS and hydrated cement paste.

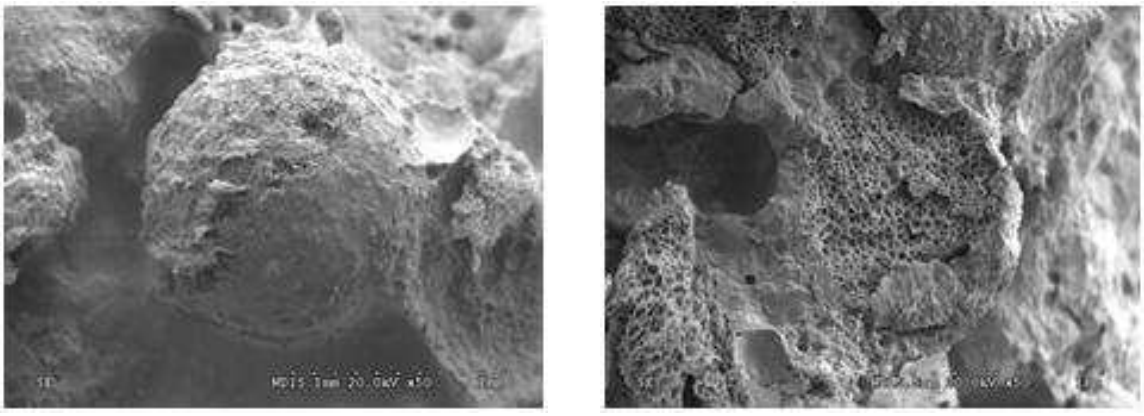

Figure 4. SEM images of mortar made with 70% of EPSs subjected to heat cycles.

Regarding the behavior of mortars against cold cycles, Sc_i cold/Sc_i ratio shows that this cycles causes losses around 25% in the compressive strength. This behavior is in good agreement with the mortars' porosity that facilitates the entry of water and the subsequent deterioration by the ice.

The Sci/Sco cold ratio shows influence of EPS in mortars submitted to cold cycles. It can be seen the strength losses against control mortar subjected to cold. Losses increases with EPS amount. The worst cases are the losses greater than 50% in mortars with a bigger amount of EPS. This behavior could be attributed to the porosity of the paste that facilitates the formation of microcracks by the expansive effect of ice. By comparing this behavior with the same mortars not subjected to cold, to see Sci/Sco ratio, it can be seen that the presence of EPS in mortars improve their durability to freeze-thaw cycles. Compressive strength values are kept because the EPS absorb part of the crystallization pressure and the deterioration is decreased. This could also be the reason for the decreasing in strength losses observed when studying the effect of cold on mortars made with EPS, to see Sci cold/Sci ratio. This behaviour improves with EPS amount.

Figure 5 shows the influence of heat and freeze-thaw cycles on the compressive strength for mortars made with 70% of each EPS type and 0,3% water retainer additive (WRA). The exclusive presence of the additive does not improve the behaviour against heat or cold as can be seen in Sc_{oa}heat/Sc_{oa} or Sc_{oa}cold/Sc_{oa} ratios.

The Sc_{ia} heat/Sc_{ia} ratio informs of the effect of heat on mortars made with EPS and additive. In these mortars the heat allows a keeping and even to improve of the mechanical properties. Nevertheless, from the point of view of mortars durability against to heat it can be seen that the combinated effect of EPS, additive and heat produce substantial losses in compressive strength The positive effect of heat is not enough for compensating the EPS negative effect in the mechanical properties (to see Scia/Scoa, Sc_{ia}/Sc_{oa}heat, and Sc_{ia}heat/Sc_{oa} ratio).

The freeze-thaw cycles in mortars with EPS and additives significantly decrease its durability. It affects around 70% resistance. The EPS presence in mortars with additives does not achieve any improvement to cold behaviour. (to see Scia/Scoa, Sc_{ia}/Sc_{oa}cold, and Sc_{ia}cold/Sc_{oa} ratio).

Figure 6 shows the influence of type and EPS percentage on the capillary absorption (C_{90}) expressed as a fraction of the C_{90} value found for the control mortar (C90i/C90o). As was expected, the water flux depended on the EPS dosage. In general, C_{90} decreases with EPS amount due to the EPS particles cut off the capillary net. This fact improves the mortar durability.

Figure 7 shows the influence of different additives in mortar made with 70% EPS on the capillary absorption (C_{90}) expressed as a fraction of the C_{90} value found for the control mortar (C90i/C90o). As

was expected, the presence of the additive has a marked positive effect on capillary absorption and therefore the durability of mortars. Air entraining agent (AEA) is the best additive for this parameter.

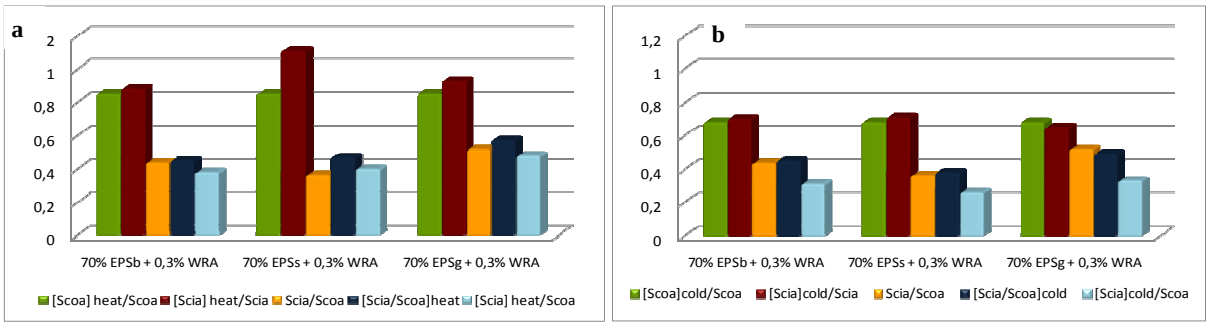

Figure 5. Compressive strength after the heat cycles (a) and freeze-thaw cycles (b) for mortars made with 70% EPS_b, EPS_s and EPS_g, with 0,3% water retainer additive (WRA), expressed as a fraction of the compressive strength value found for the control. (Scia: compressive strength for a given EPS mortar with additive; Scoa: compressive strength for control mortar (0%EPS and additive); Scia heat: compressive strength of mortar with EPS and additive after being subjected to heat cycles; Sci cold: compressive strength of mortar with EPS and additive after being subjected to freezing-thaw cycles; Scoa heat: compressive strength for control mortar (0%EPS and additive) after being subjected to heat cycles; Scoa cold: compressive strength for control mortar (0%EPS and additive) after being subjected to freezing-thaw cycles).

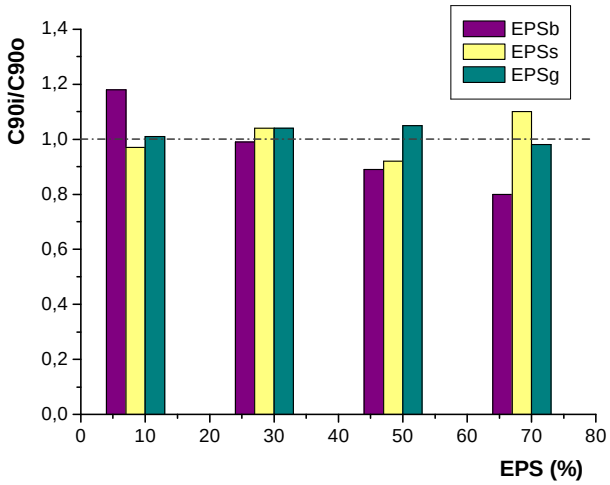

Figure 6. Capillary absorption (C_{90}) for mortars made with different types and % of EPS expressed as a fraction of the value found for the control (C90i/C90o). (C90i: Capillary absorption for a given EPS mortar; C90o: Capillary absorption for control mortar)

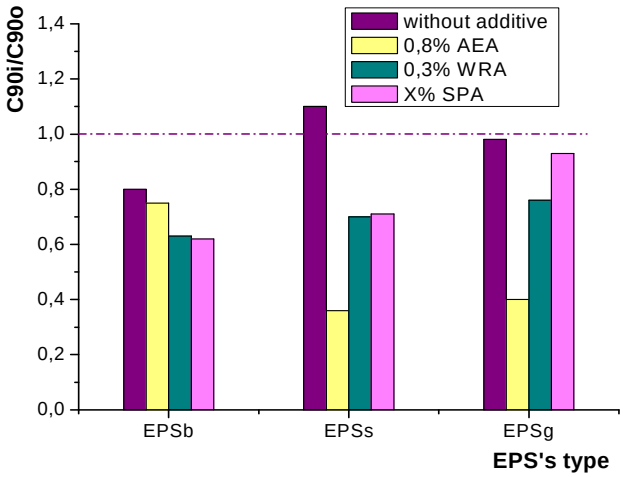

Figure 7. The C90i/C90o ratio for mortar fabricated with differents EPS types and aditives. In all cases were used 70% EPS dosage. (C90i: Capillary absorption for a given EPS mortar; C90o: Capillary absorption for control mortar)

4 CONCLUSIONS

The workability of the mortar and compressive strength decreases with increasing the amount of EPS. Nevertheless, mortars with 50% EPS meets the requirements of the UNE-EN 998:1 [11] and the UNE-EN 998:2 [12], for masonry, rendering and plaster mortars, in terms of nominal compressive strength. The EPS presence in mortars contribute to maintain the durability to heat and frost. Capillary absorption is enhanced by the presence of EPS in the mortar. If additives are included in the EPS mortar, it is posible to obtain mortars with higer EPS dosage that show adecuate workability, better compressive strength and lower capillary absorption. Therefore, better durability.

ACKNOWLEDGMENTS

The authors thank the Spanish Ministry of Science and Innovation of the Spanish Government for its financial support to this investigation (BIA 2007-61170 project).

REFERENCES

Sussman V., Baumann G.H., Expanded polystyrene beads lighten the load, Soc. Plastic Eng. J., 28, 18-21, 1972.

D.J. Cook, Expanded polystyrene concrete, en R.N. Swamy (Ed.), Concrete Technology and Design, New Concrete Materials, vol. 1, Surrey University Press, London, 41-69, 1983.

C. Bagon, S. Frondistou-Yannas, Marine floating concrete made with polystyrene expanded beads, Mag. Concr. Res., 28, 225-229, 1976.

S. H. Perry, P.H. Bischoff, K. Yamura, Mix details and material behaviour of polystyrene aggregate concrete, Mag. Concr. Res., 43, 71-76, 1991.

P.H. Bischoff, K. Yamura, S.H. Perry, Polystyrene aggregate concrete subjected to hard impact, Proc.-Inst. Civ. Eng. 2. Res. Theory 89, 225-239, 1990.

Zhang M-H, Gjorv OE, Permeability of high strength lightweight concrete, ACI Mater J., 463-469, 1991.

UNE-EN 196-1:2005: Métodos de ensayo de cementos. Parte1: Determinación de las resistencias mecánicas (Methods of cement testing. Part 1: Determination of Mechanical strengths).

UNE-EN 1015-3:2007: Método de ensayo de los morteros de albañilería. Parte 3: Determinación de la consistencia del mortero fresco (por la mesa de sacudidas). (Methods of test for mortars for masonry. Part 3. Determination of consistence of fresh mortar (by flow table)

UNE-EN 1015-18:2003: Métodos de ensayo de los morteros de albañilería. Parte 18: Determinación del coeficiente de absorción de agua por capilaridad de los morteros endurecidos.(Methods of test for mortars for masonry. Part 18. Determination of water absorption coefficient due to capillary action of hardened mortar).

UNE 67028 EX Norma experimental. Ladrillos cerámicos de arcilla cocida. Ensayo de heladicidad.

XII DBMC
International Conference on Durability of Building Materials and Components
PORTO - PORTUGAL, April 12th-15th, 2011

Characterization of Different Types of Ceramic Waste and its Incorporation to the Cement Paste to Evaluate Pozzolanic Reactivity

Valéria de Castro Almeida [1]
Ana Catarina Evangelista [2]

ABSTRACT

Porcelain tile is a product resulting from the technological development of ceramic plating industry. Its large acceptation in the market is probably associated to properties such as low porosity, high mechanical resistance, and easy maintenance, besides being a material of modern and versatile characteristics. The aim of this study was to investigate different ceramic wastes (glazed ceramic and porcelain tile) and evaluate its influence on the mechanical behavior in cement pastes and whether the ceramic waste presents pozzolanic activity. The wastes were characterized through chemical composition and size particle distribution. Cement pastes + wastes were prepared in 25% and 50% proportions and setting time, water absorption and compressive strength were determined. The results indicate that although the wastes do not show any significant variation in the elementary chemical composition, changes in the values of compressive strength were observed in the pure cement paste.

KEYWORDS

Mechanical properties, Chemical analyses, Cement.

[1] Federal University of Rio de Janeiro (UFRJ), Chemistry School Rio de Janeiro, BRAZIL, valeria@eq.ufrj.br
[2] Federal University of Rio de Janeiro (UFRJ), Polytechnic School,Rio de Janeiro, BRAZIL, anacatarina@poli.ufrj.br

1 INTRODUCTION

In recent decades the ceramic industry has undergone profound technological changes of manufacturing process as well as the characteristics of the final product. Porcelain, a ceramic coating, which has earned a growing role in the consumer market due to technical and aesthetic properties such as water absorption of less than 0.5% and high mechanical strength, came along with those innovations. Porcelain is characterized by a dense microstructure consisting of crystalline phases, mullite and quartz in less amount minority, mostly majority immersed in a glassy phase [Rosso *et al* 2005, Bernardin *et al* 2006].

Researchers from several countries have investigated industrial waste to reduce environmental impacts [Santos and Morelli 2002, Puertas *et al* 2008, Menezes *et al*, 2009]. In the civil construction industry is a great generation of rubbish that is landfilled in inadequate area. It is estimated that over 30% of this debris is ceramic waste (bricks, tiles, tile, and porcelain). It has been reported that fired clay may present pozzolanic activity which improves the performance of mortars and concrete. In addition, it has been cited the feasibility of ceramic tile in the replacement of part of portland cement and/or aggregates in mortars and concrete [Ay and Ünal, 2000, Torkittikul and Chaipanich, 2010]. Calcined clays have been used as pozzolans since distant times [Mehta 1987]. Clays in the raw form do not show pozzolanic activity, but when calcined and ground to an appropriate fineness clays can be used as pozzolanic admixtures for cement [Lavat *et al*, 2009].

The objective of this study was to characterize different ceramic wastes and evaluate their influence on the behavior of cement pastes.

2 EXPERIMENTAL PROGRAM

Porcelain and enamel ceramic wastes were collected randomly from debris from a house construction and separated in fragments of different sizes. The wastes were crushed in a jaw crusher and ground in a ball mill, then a spray disc was also used. The milling process began with manual breaking with the aid of a hammer in order to adjust the opening of the waste feed roll crusher and then the fragments were comminuted in a spray disk. After that, these fragments were classified using a rot up equipment according to Brazilian Standards meshes: 30, 50, 60, 70, 80.100, 120, 200, 230 and 270.

2.1 Materials

The following materials were used for tests:
• glazed ceramic (GC) waste
• porcelain (P) waste
•CPII - 32 F Portland Cement
• water

2.2 Mixtures proportions and casting

In order to verify the possibility of using this waste as partial replacement of Portland cement (pure cement paste), nine specimens (50mmx100mm) were prepared with the proportions of cement and waste indicated in Table 1. The samples were cast according to Brazilian Standard NBR 7215 [1997]. The specimens were cast in three layers of approximately equal thickness by applying 20 strokes per layer using a metal socket.
After casting, the specimens were kept in their moulds during the first 24 hours. After 24 hours, the specimens were cured in water until the day of the test. Three samples were used for each compression test aged at the age of 7, 14 and 28 days, and three samples were cast for the determination of water absorption, according to Brazilian Standards [NBR 5739 2007].

Table 1. Cement + ceramic waste compositions.

	Mixtures	*Compositions(g)*		
		cement	waste	water
C-100	100% cement	4880		1200
R25-GC	75% cement + 25% glazed ceramic	3660	1220	1150
R50-GC	50% cement + 50% glazed ceramic	2440	2440	1000
R25-P	75% cement + 25% porcelain	3660	1160	1375
R50-P	50% cement + 50% porcelain	2440	2320	1300

The setting time of the mixtures was determined using the Vicat apparatus according to Brazilian Standards, NBR NM 65 [2003]. The setting time of cement pastes is a physicochemical phenomenon which results in modification of their physical and mechanical properties. It is defined as the time when the cement paste reaches a consistency which turns it inadequate to be worked [Bauer 1994].

The physical and mechanical characterization of the specimens was made after 7 days, 14 days and 28 days. Also, the technique of X-ray fluorescence was used for mineralogical characterization of these wastes.

3 RESULTS AND DISCUSSION

After passing through the spray disk the wastes of Glazed Ceramic (GC) and Porcelain (P) presented the size distribution shown in Table 2. It is observed that 20.11% of glazed ceramic waste is composed of particles with a diameter greater than 0.59 mm, while 55.68% particles have diameter smaller than 0.30 mm and larger than 0.14 mm. The residue still has 23.89% of particles with diameter under 0.074. The porcelain waste is composed by 48.67% articles with diameter greater than 0.25 mm, while 35.39% particles are in the range from 0.074 mm to 0.21 mm and 15.64% particles still have diameter under 0.074 mm. The residue presented a larger size than cement, so it was classified as a fine aggregate. In terms of fineness, to increase to the pozzolanic reaction the waste should attain a minimum of 30% retained at sieve mesh 325 [NBR 12653, 1992].

The data obtained in determining the setting time and heat hydration of pure cement and cement plus ceramic waste are shown in Fig 1.

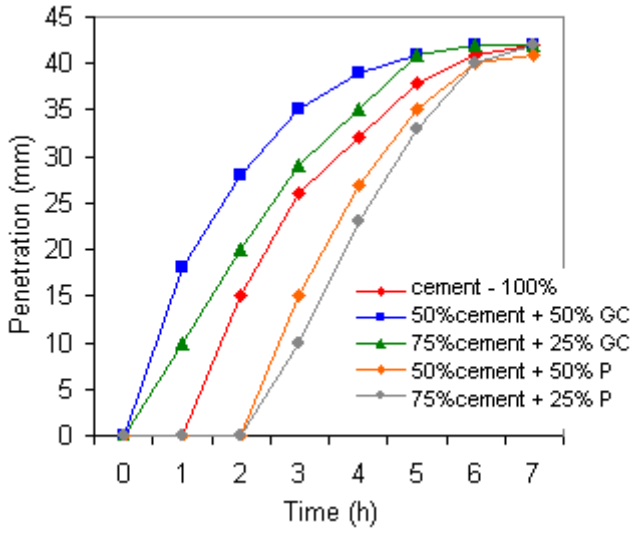

Figure 1. Setting time of cement paste and cement + ceramic waste pastes.

Table 2. Grain size distribution.

Mesh	Diameter (mm)	Passing% (GC)*	Passing% (P)*
30	0.59	79.89	100
50	0.30	46.4	100
60	0.25	46.4	51.33
70	0.21	33.8	51.33
80	0.177	33.8	43.27
100	0.149	24.21	36.16
120	0.125	24.21	27.63
200	0.074	14.32	15.94
230	0.062	14.32	7.08
270	0.053	4.15	7.08
bottom	<0.053	0.40	0.30

***GC – glazed ceramic and P – porcelain**

In the setting time graph (Fig.1), it is possible to observe that the introduction of glazed ceramic (GC) to the cement paste causes an acceleration of the reaction of cement hydration, whereas there is a decrease of setting time as the amount of waste increases in the mixture. This behavior can be attributed to the percentage of Fe2O3 (ferrous) present in the glazed ceramic residue (Table 3) that induces an acceleration of the cement hydration [Taylor, 1997]. The residue of porcelain (P) added to the cement paste slows these reactions. Probably this phenomenon is due to the presence of calcium sulphate which retards the hydration reactions.

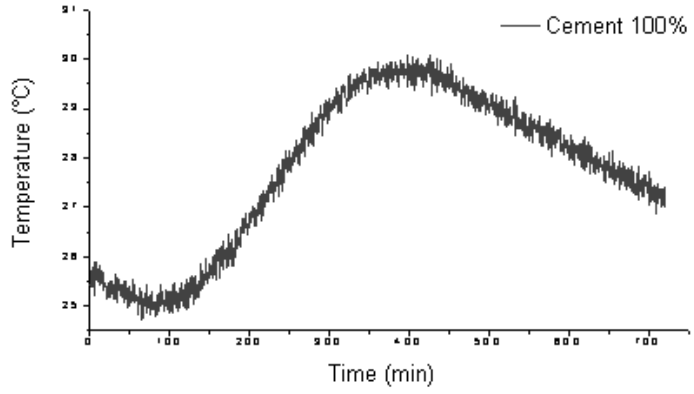

Figure 2. Heat of hydration of paste with 100% cement.

The development of the heat of hydration of cement paste and ceramic wastes pastes is presented in Fig. 2, 3a, Fig. 3b, Fig 4a, and Fig 4b. The cement paste (Fig. 2) presents the maximum temperature at 30°C in 300 minutes, and shows two characteristic zones: area 2 (area of induction) and area 3 (growth of CSH and Ca $(OH)_2$). The addition of glazed ceramic and porcelain wastes leads to a different hydration mechanism, whereas the induction period is not observed. From the beginning of hydration time an increase of heat release is observed as a consequence of rapidly forming CSH (from

C_3S) and calcium hydroxide In addition, the heat released decreases with the increase of waste added to the pure cement paste (Fig. 3a to Fig. 4b).

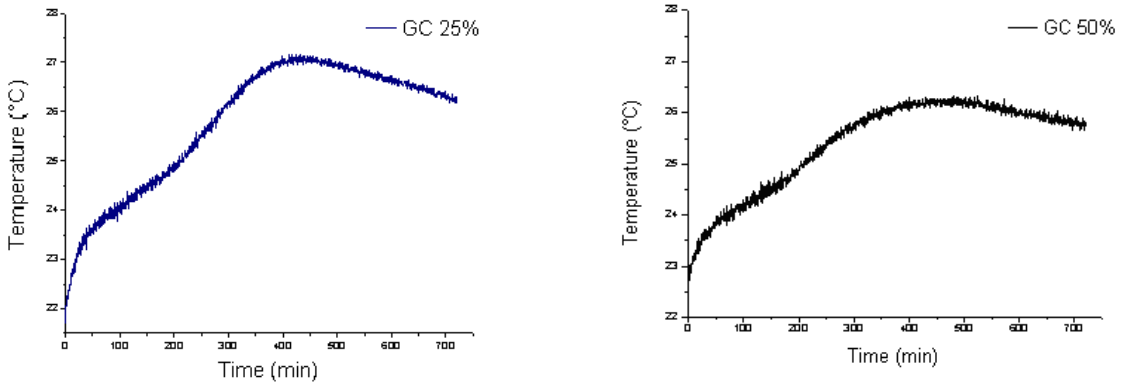

Figure 3. Hydration reaction with addition of 25% (a) and 50% (b) glazed ceramic

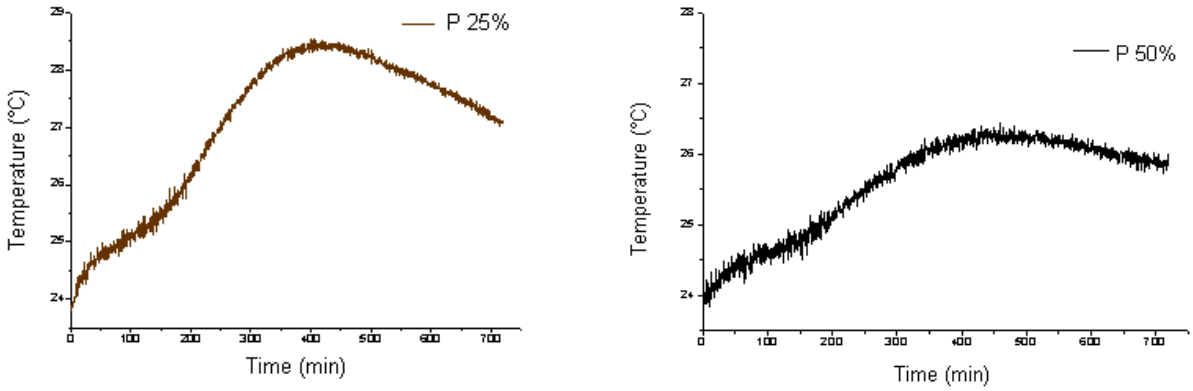

Figure 4. Hydration reaction with addition of 25% (a) and 50% (b) porcelain.

Table 3 presents the chemical analysis of residues obtained through the technique of X-ray fluorescence. High concentrations of silica, alumina, iron, calcium, magnesium, potassium and sodium can be observed in both residues. The other elements appear in concentrations below 1%. The content of silica (SiO_2) in both wastes is higher than 60% which is desirable to mineral admixtures. Also, the sum of the major components, SiO_2 + Al_2O_3 +Fe_2O_3, is around 80%, which is the minimum amount required for the chemical composition of pozzolans [Lavat *et al* 2009]. The pozzolanic reaction provides a higher content of hydrated silicates and hydrated calcium aluminates (Fig. 5), which are responsible for the mechanical strength developed and the enhancement of the durability of mortars and concrete [Metha 1987].

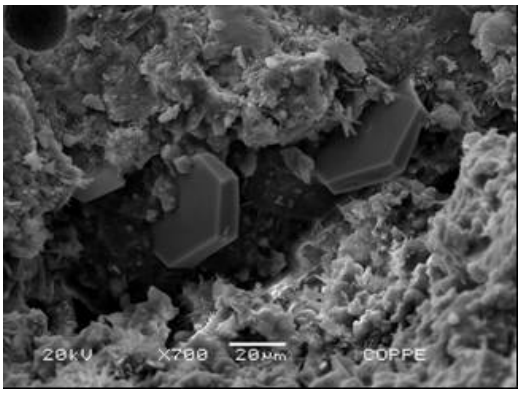

Figure 5. MEV of paste with 50% cement +50% P.

Table 3. Chemical composition of the glazed ceramic (GC) and porcelain (P).

Components	% (mass) GC	% (mass) P	Components	% (mass) GC	% (mass) P
SiO_2	62.525	62.013	Na_2O	1.239	1.350
Al_2O_3	20.064	23.212	P_2O_5	0.089	0.078
CaO	4.717	7.467	ZrO_2	0.786	0.423
Fe_2O_3	3.383	1.901	MnO	0.045	-
K_2O	2.651	1.909	SrO	0.023	0.037
TiO_2	0.659	0.568	ZnO	0.246	0.318
SO_3	0.061	0.093	Rb_2O	0.015	0.011
MgO	3.491	0.620	CuO	0.006	-

The water absorption test (Fig.8) was performed according to NBR 9778 [2009] at 7 days, 14 days and 28 days. The graph presented in Fig. 8 shows that at the age of 7 days the percentage of water absorption is similar for all mixtures studied. At the other test times there is an increase in the percentage of water absorption of the mixtures with ceramic waste which is proportional to the decrease of cement content in the studied mixtures. The same specimens were used in all aging times. They presented loss of mass because the residue on the specimen surface was leachated when immersed in water, producing pores that led to an increase of water absorption.

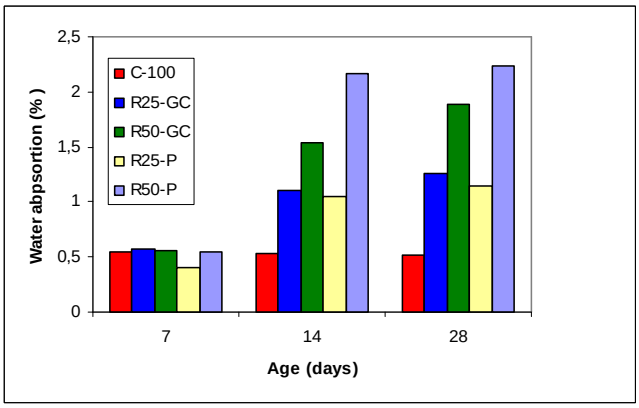

Figure8. Water absorption (%) *versus* Age (days).

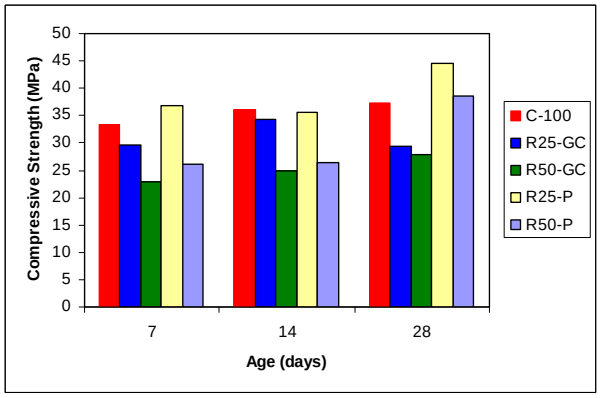

Figure 9. Compressive Strength (%) *versus* Age (days).

The compressive strength test (Fig.9) was performed according to NBR 5739 [2007] after 7days, 14 days and 28 days. The cement paste (C-100) was used as reference mixture to analyze the compressive strength data. The values obtained for the cement paste are in agreement with the mechanical requirements of Brazilian Standard [NBR 11578, 1997] for this type of cement CPII-32F (compressive strength $\geq$ 10MPa for 3 days, 7 days and 20MPa $\geq$ 28 days $\geq$ 32 MPa). The compressive strength of the pastes with glazed ceramic waste (R25-GC) and (R50-GC) decreased as the amount of waste increased. The replacement of part of cement in mixtures with the porcelain waste (R25-P and R50-P) is viable when the values of compressive strength are similar to or greater than those of pure cement paste. In general, the results of compressive strength of these blends (cement + ceramic) indicate their possible use as building materials with improved mechanical properties and durability performance.

4 CONCLUSIONS

An analysis of the results reveals that the residues investigated present mineralogical characteristics that classify them as siliceous-aluminous, according to their chemical composition, and when hydrated, they are responsible for increasing mechanical resistance and durability. The mixtures with porcelain residue present values of compressive strength equal to or greater than the cement paste indicating a possible mineral admixture, however the grain size reached was higher than the usual to cement admixtures. In addition, the mixtures with glazed ceramic waste, although they present compressive strength lower than the reference mixture, still have satisfactory mechanical performance and can be used to produce constructive elements. However, they are very susceptible to erosion caused by water. Whichever the origin of the ceramic waste, the pastes analyzed showed different mechanical characteristics. Considering that the strength values are fundamental to building materials, it is essential that the residue to be used can be characterized chemically and physically to ensure the quality of alternative construction materials.

REFERENCES

Associação Brasileira de Normas Técnicas. NBR 7215,1997, Cimento Portland – Determinação da resistência à compressão, Brasil.

Associação Brasileira de Normas Técnicas NBR 5739, 2007, Concreto - Ensaios de compressão de corpos-de-prova cilíndricos, Brasil.

Associação Brasileira de Normas Técnicas NBR NM 65, 2003, Cimento Portland - Determinação do tempo de pega, Brasil.

Associação Brasileira de Normas Técnicas NBR 9778, 2009, Argamassa e concreto endurecidos - Determinação da absorção de água, índice de vazios e massa específica, Brasil.

Associação Brasileira de Normas Técnicas NBR 12673, 1992, Materias Pozolânicos - Especificação Brasil.

Associação Brasileira de Normas Técnicas NBR 11578, 1997, Cimento Portland composto – Especificação, Brasil.

Ay, N., Ünal, M., 2000. 'The use of waste ceramic tile in cement production', *Cement and Concrete Research* , 30 , 497–499.

Bauer,L.A. F. ,1994, *Materiais de Construção*, LTC, Livros Técnico e Científicos, Rio de Janeiro.

Bermardin, A. *et al*, 2006, 'Characterization of cellular ceramics made by porcelain tile residues', *Materials Science & Engineering* , v.437, 222-225.

Lavat A. *et al*, 2009, 'Characterization of ceramic roof tile wastes as pozzolanic admixture', *Waste Management*, Volume 29, Issue 5,1666-1674

Mehta, P.K., 1987. 'Supplementary cementing materials for concrete', *CANMET* (sp. 86-8E), Ottawa, Canada.

Menezes, R., *et al*, 2009, 'Atividade pozolânica dos resíduos do beneficiamento do caulim para uso em argamassas para alvenaria', *Revista Brasileira de Engenharia Agrícola e Ambiental* v.13, n.6, 795–801.

Puertas, I. *et al*, 2008, 'Ceramic wastes as alternative raw materials for Portland cement clinker production', *Cement and Concrete Composites*, 30, Issue 9, 798-805.

Rosso,J.; Cunha.E.S.; Rojas-Ramirez,R.A., 2005, 'Características técnicas e polimento de porcelanatos', *Cerâmica Industrial*, v.10, n 4, 11-14.

Taylor, H.F.W. ,1997, *Cement Chemistry*, Thomas Telford 2ed, London.

Torkittikul P., Chaipanich A. 2010, 'Utilization of ceramic waste as fine aggregate within Portland cement and fly ash concretes', *Cement & Concrete Composites* 32, 440–449.

XII DBMC
International Conference on Durability of Building Materials and Components
PORTO - PORTUGAL, April 12th-15th, 2011

Properties of Mortars with Algerian Metakaolin

Mohamed Said-Mansour [1]
Said Kenai [2]
Mohamed Ghrici [3]
El-Hadj Kadri [4]

ABSTRACT

In this study, Algerian kaolin was treated thermally at 850 °C during 3 hours to produce Metakaolin. Binders in which Portland cement was replaced by up to 30% of metakaolin were tested for (i) hydration heat, (ii) compressive strength up to 365 days and (iii) Durability tests by resistance to two acid solutions. The results show that under the chosen conditions, the tested Kaolin was transformed to an amorphous phase and the use of blended cements made with heat treated metakaolin enhances the hydration heat of mortars and improves the early age and the long-term compressive strength. Durability was also enhanced as better acidic resistance was observed.

KEYWORDS

Algerian kaolin, Calcinations, Hydration heat, Compressive strength, Acidic attack.

[1] Civil Engineering Department, University of Tiaret, ALGERIA, msaidmansour@gmail.com
[2] Geomaterials Laboratory, University of Blida, ALGERIA, sdkenai@yahoo.com
[3] Civil Engineering Department, University of Chlef, ALGERIA, m_ghrici@yahoo.fr
[4] L2MGC Laboratory, University of Cergy Pontoise, FRANCE, El-hadj.kadri@u-cergy.fr

1 INTRODUCTION

Metakaolin (MK) is produced from a natural and accessible resource through the calcinations of kaolinite within the temperature range of 650–900°C. Calcination transforms a crystallized, organized phase (kaolinite) into a disorganized phase (MK) through crystal lattice failure. The dehydroxylation and disorganization of the kaolinite generate a reactive material with high pozzolanic properties at ambient temperatures.

Pozzolanic materials with high pozzolanic activity, such as MK, react with calcium hydroxide released in the hydration of ordinary Portland cement (OPC), increasing the hydration heat due to exothermic effect of the pozzolanic reaction, compared to 100% OPC [Frías et al. 2000, Ambroise et al. 1994]. The acceleration in OPC hydration is also apparent in the observed increased rates of heat evolution temperature in OPC-MK system.

In the past, it was common to coat concrete vulnerable to deterioration by acid attack with an anticorrosion coating of a resin in order to prevent corrosion. However, in several cases where the coating is not sufficient, the problem of deterioration would surface just a few years after the coating. Therefore, there is an increasing trend to make the concrete itself resistant to acid attack.

Among the methods to improving the resistance to acid attacks is to use supplementary cement materials (SCMs) such as natural pozzolan [Ghrici et al. 2007], fly ash [Goyal et al. 2009], silica fume [Rahmani & Ramazanianpour 2008] and MK [Hewayde et al. 2007]. The improvement reported by the authors may be due to the denser and improved microstructure of concrete resulting from SCMs incorporation. Hewayde et al. [2007] reported that MK reduced the mass loss of concrete specimens due to immersion for eight weeks in H_2SO_4. This is due to the formation of calcium aluminate hydrates (C_2ASH_8, C_4AH_{13}, C_3AH_6) in the MK-modified concrete. It is believed that calcium aluminate hydrates may be more chemically stable in highly acidic environments than calcium silicate hydrates.

In the light of the facts mentioned above, the main objective of this paper is to investigate the effects of Algerian metakaolin on the compressive strength, hydration heat and acidic attack resistance of mortars.

2 EXPERIMENTAL PROCEDURES

2.1 Materials used

The mixes constituents were ordinary Portland cement (OPC) CEM I 52.5, Algerian MK (obtained by heat treated of Algerian kaolin, from quarry of El-Milia in the East of Algeria, at 850 °C for 3 hours), water and standard sand (CEN EN 196-1). The superplasticizer (SP) used was polycarboxylate modified based liquid with 80% water and density of 1.07 g/cm^3. Composition and properties of OPC and MK are given in Table 1.

2.2 Mixes used

The mortar mixes had proportions of 1binder: 3 Sand. The binder consisted of cement and MK. The cement was formulated varying the replacement of MK from 0% to 30%. All replacements were made by mass. The water:binder (w/b) ratio was kept constant at 0.5. SP was added to obtain a flow time of mortar of about 10 ± 1 secondes. Table 2 shows the combination of blended cements studied in the determination of strength of mortars.

Table 1. Chemical composition and properties of OPC and MK.

	OPC	MK
SiO_2 (%)	20.23	55.50
Al_2O_3 (%)	4.29	40.00
Fe_2O_3 (%)	2.35	1.40
CaO (%)	63.67	0.08
MgO (%)	3.88	0.22
SO_3 (%)	2.80	--
Na_2O (%)	0.14	0.09
K_2O (%)	0.69	0.71
TiO_2 (%)	0.25	0.24
I. R (%)	0.39	--
L.O.I. (%)	1.63	1.00
$CaCO_3$		
$MgCO_3$		
Surface specific area (m^2/kg)	359.00	
Surface specific BET (m^2/g)		16.0
Initial time of set:	2h 45 min	
Final time of set:	4h 55 min	
Bogue composition of cement:		
C_3S: 66.90		
C_2S: 10.70		
C_3A: 8.40		
C_4AF: 7.60		

2.3 Specimen preparation, curing and testing

2.3.1 Compressive strength

Prismatic mortar specimens having 40x40x160 mm dimensions were used for the study of compressive strength. Specimens were cast in steel moulds and kept in a moist room at 20 °C for 24 h. Demoulding took place after that and specimens were placed in water at 20 °C for a total curing period of 365 days. Compressive strength was determined at 1, 7, 28, 90 and 365 days according to EN 196-1. The compressive strengths presented represent the average values obtained on three specimens.

Table 2. Mortar Mix proportions.

	Cement [g]	MK [g]	Sand [g]	W/B [%]	SP [%]
OPC	450	0	1350	0.5	0.0
10% MK	405	45	1350	0.5	0.3
20% MK	360	90	1350	0.5	0.5
30% MK	215	135	1350	0.5	0.9

2.3.2 Hydration heat

Hydration heat tests were applied according to NF EN 196-9 standard. The method is based on the Langavant Calorimeter. This semi-adiabatic method consists of quantifying the heat generated during cement hydration using a Dewar flask, or more exactly, a thermally isolated bottle. Since the exterior conditions are very influential, the test is carried out in a climatized room at 20 ± 2 °C.

The measurements were made over 6 days, since the heat increase is observed to be very low at later times, and also since the relative error of the measurement increases beyond that time. Using quasi-adiabatic calorimeter, the variation of the temperature of mortar with time was measured immediately after mixing. For each mixture, the heat flow was determined along with the temperature evolution of mortar. The hydration heat of mortar was the combination of the accumulated heat in the calorimeter and the heat dispersed in the environment. At time *t*, the hydration heat *q* by gram of binder (cement or cement + addition) is obtained by the formula:

$$q = \frac{C}{m_c}.\Delta\theta + \frac{1}{m_c}\int_0^t \alpha.\Delta\theta.dt \qquad (1)$$

where *C* is the total thermal capacity of the apparatus (J/°C), m_c is the cement or binder mass (g), $\Delta\theta$ is the mortar heating difference to the ambient temperature (°C), and α is the total calorimeter thermal loss coefficient (J/h °C).

2.3.3 Acidic attack

Resistance to acid attacks was conducted on mortar specimens by immersing in two solutions: 1%HCl and 2.5%H_2SO_4 and weight loss measured during a period of 225 days. The relative acid attack was determined in accordance with ASTM C-267. The mortars specimens were cured in water at 20 ± 2°C for 30 days before being subjected to acid attack. Three specimen of each mortar mix were immersed in 2.5% sulfuric acid (H_2SO_4) or 1% hydrochloric acid (HCl). The attacked portions of the mortar specimens were cleaned with de-ionised water and the acid attack then was evaluated through measurement of the weight loss (*WL*) of the specimens and determined as follows:

$$WL(\%) = \frac{W_1 - W_2}{W_1} \times 100 \qquad (1)$$

Where W_1 is the weight of the specimen before immersion and W_2 is the weight of the cleaned specimen after immersion. The solution was renewed every 15 days and the weight loss of the specimens measured.

3 RESULTS AND DISCUSSIONS

3.1 Heat of hydration

Figures 1 and 2 shows the temperature and the cumulative heat hydration cumulative heat hydration for 6 days respectively. According to Fig. 1, the OPC mortar gives the maximum temperature at about 18 hours, after that, a 10% substitution of Portland cement by MK gives a greater temperature released as compared with the concrete without MK. On the contrary a 30% substitution of cement gives a lower temperature. Fig. 2 shows the total hydration heat (J/g of binder) for the four mortars. In this case, the 10% MK mortar produces the highest hydration heat, followed by OPC and 20% MK mortars. 30% MK mortar gives a lower total hydration heat.

The reaction of MK with CH and H_2O (H) contributes to the cumulative heat development by the hydrating systems, to the extent that with increasing MK content (up to a specific limit) the total heat evolved is greater than that from 100% OPC. However the MK-CH-H reaction is controlled by the availability of CH which itself is provided by the hydrating OPC. Thus, as the proportion of MK increases and that of OPC decreases, the supply of CH from the hydrating OPC will decrease but the demand for CH, from the increasing proportion of MK, will increase. Hence there will be a limiting MK-OPC ratio above which the reaction of MK with CH will be deficient due to insufficient supply

of CH. This will decrease the rate of heat output and thus the maximum hydration heat reached by the PC-MK mortar.

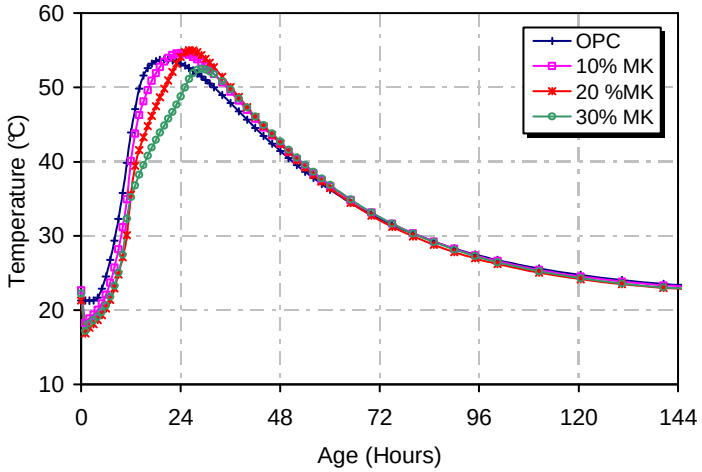

Figure 1. Effect of replacing cement with MK on the temperature profile.

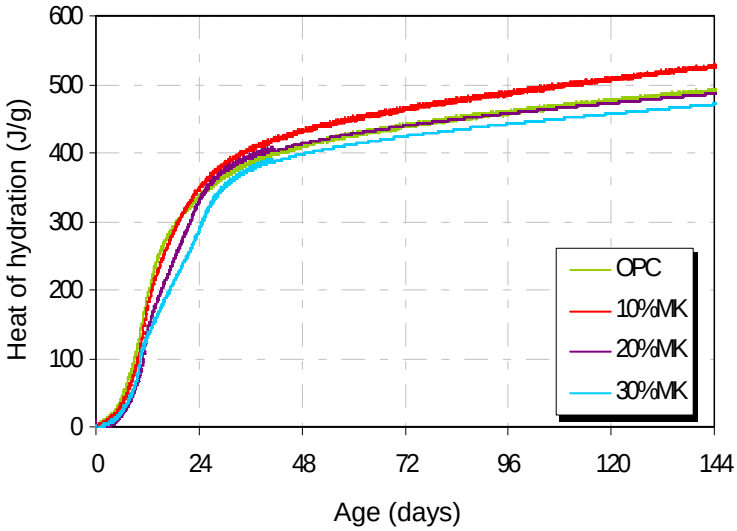

Figure 2. Cumulative heat hydration vs. time for mortar samples.

3.2 Compressive strength

The compressive strengths vs. curing time are reported in Fig. 3. The spread of the data at earlier ages (7 days) can be readily seen. The substitution of cement by 10% MK in mortar specimen gave a faster strength development than OPC mortar. After 365 days of curing, the mortar specimens with 10 and 20% MK presented a higher compressive strength than that of OPC mortar.

Figure 4 presents the relative strength versus curing time. The relative strength is the ratio of the strength of the MK mortar to the strength of OPC mortar at each particular curing time. The incorporation of 10 and 20% MK is particularly useful during the first 28 days, where the rate of strength development is considerably higher than the control. After 28 days of curing, the incorporation of MK does not cause an increase in the rate of strength development.

According to Wild et al. [1996], there are three elementary factors influencing the contribution that MK makes to compressive strength when it partially replaces cement in concrete. These are (i) the filler effect, which results in more efficient paste packing, is immediate, (ii) the acceleration of OPC hydration which has maximum impact within the first 24 hours and (iii) the pozzolanic reaction of MK with CH which makes the greatest contribution to strength somewhere between 7 and 14 days of age.

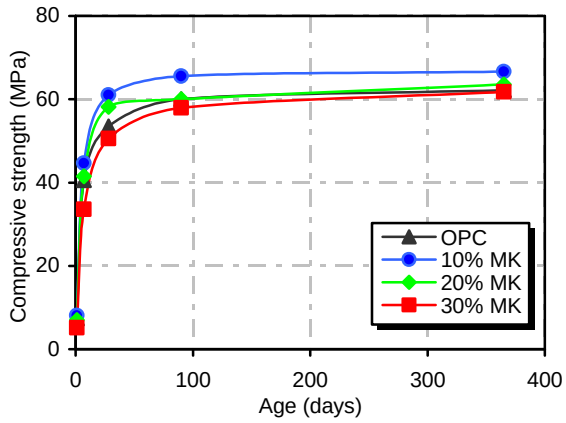

Figure 3. Compressive strength vs. time for mortar sapmles.

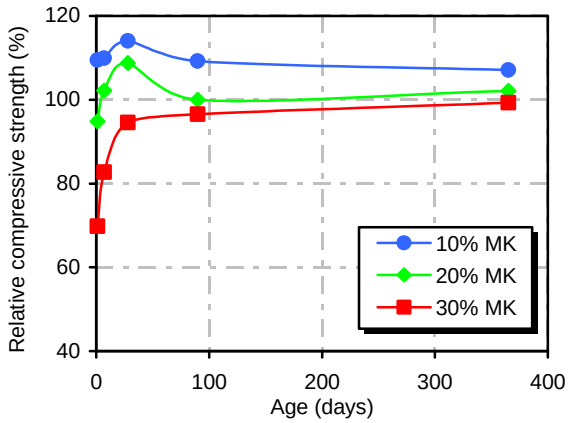

Figure 4. Relative compressive strength vs. time of mortars samples.

3.3 Durability

Figures 5 shows the test results of weight change versus time for mortar specimens exposed to 1% HCl and 2.5% H_2SO_4 solutions for 225 days, respectively. After 225 days exposure to 1% HCl solutions, the total loss in weight of OPC mortar was 25%. When the replacement level of cement is 10, 20 and 30% of MK, the loss in weight of mortar specimens was 17, 16 and 12% respectively.

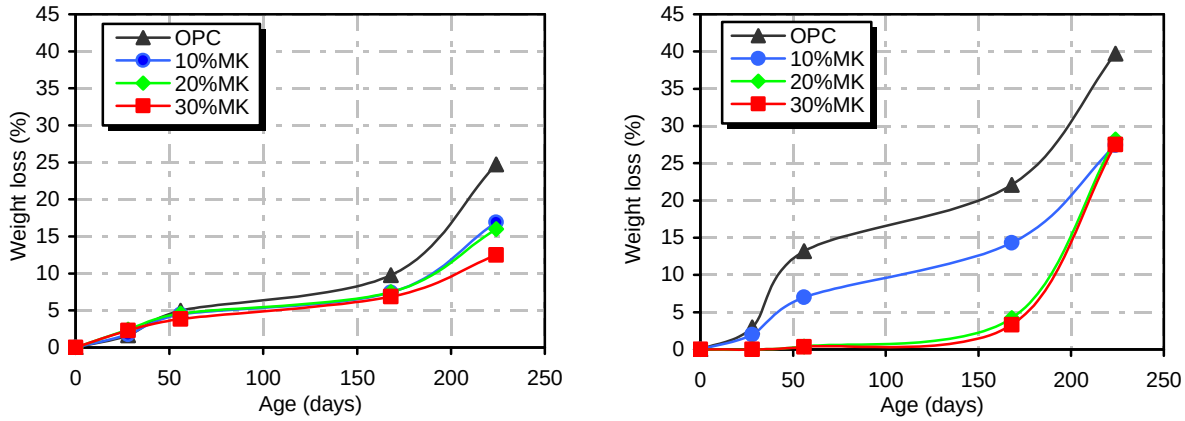

Figure 5. Weigth loss for mortar specimens immersed in (a) 1% HCl and (b) 2.5% H_2SO_4.

After 225 days exposure to 2.5% H_2SO_4 solutions, the total loss in weight of OPC mortar was about 40%. When the replacement level of cement is 10, 20 and 30% of MK the loss in weight of the three mortar specimens was 28%.

As a result, it can be concluded that MK can be used to improve the acid resistance of OPC mortar. According to Hewadey et al. [2007] this is due to the creation of calcium aluminate hydrates

(C_2ASH_8, C_4AH_{13}, C_3AH_6) in the MK-modified mortar. These hydrates are chemically stable in highly acidic environments than calcium silicate hydrates (C-S-H).

Goyal et al. [Goyal et al. 2009] studied the effect of an aggressive chemical environment on concrete prepared with ordinary Portland cement and silica fume. The adverse environmental conditions are simulated by using either 1% sulphuric acid, 1% hydrochloric acid or 1% nitric acid. The authors measured the mass loss and compressive strength for a period of one year. They found that the course of action of acid attack is dependent on the type of acid and solubility of the calcium salt formed. The presence of mineral admixtures was found to lower the detrimental effect of all types of acids on concrete.

4 CONCLUSIONS

Local kaolin has been thermally activated and used as a pozzolan in blended cement. This study leads to the following conclusions:

- Algerian MK is an active mineral admixture that could be used in cement concrete products. It has a good effect on the mechanical properties of cement mortars.
- The blended mortar with 10% MK can reach higher hydration heat with respect to OPC mortar. it would be preferable not to use MK concrete where hydration heat may be a problem, e.g. in mass elements where cracking is probable.
- Resistance to acid attack is higher for metakaolin cement mixes as compared to control ones.

REFERENCES

Ambroise, J., Maximilien S. & Peara, J. 1994, 'Properties of Metakaolin Blended Cements', *Advanced Cement Based Materials*, 1, 161-168.

Frías, M., de Rojas M.I.S & Cabrera, J. 2000, 'The Effect that the Pozzolanic Reaction of Metakaolin has on the Heat Evolution in Metakaolin-Cement Mortars', *Cement and Concrete Research*, 30[2], 209-216.

Ghrici, M., Kenai, S. & Said-Mansour, M. 2007, 'Mechanical Properties and Durability of Mortar and Concrete Containing Natural Pozzolana and Limestone blended cements', *Cement and Concrete Composites*, 29[7], 542-549.

Goyal, S., Kumar, M., Singh Sidhu, D., & Bhattacharjee, B. 2009, 'Resistance of Mineral Admixture Concrete to Acid Attack', *Journal of Advanced Concrete Technology*, 7[2], 273-283.

Hewayde E., Nehdi M. L., Allouche E., & Nakhla G. 2007, 'Using concrete admixture for sulfuric acid resistance', *Proceeding of Institution of Civil Engineering, Construction Materials* 160, Issue CMI, 25-35.

Rahmani, H. &. Ramazanianpour, A. A. 2008, 'Effect of Binary Cement Replacement Materials on Sulfuric Acid Resistance of Dense Concretes', *Magazine of Concrete Research*, 60[2], 145-155.

Wild, S., Khatib J.M & Jones, A. 1996, 'Relative Strength, Pozzolanic Activity and Cement Hydration in Superplasticizer Metakaolin Concrete', *Cement and Concrete Research*, 26[10], 1537-1544.

XII DBMC
International Conference on Durability of Building Materials and Components
PORTO - PORTUGAL, April 12th-15th, 2011

An Experimental Study on How Treated Bases Influence the Adhesion of Mortar Coatings

Angelo Just da Costa e Silva [1]
Helena Carasek [2]
João Manoel de Freitas Mota [3]
Fred Rodrigues Barbosa [4]

ABSTRACT

Over the years, a growing number of problems have been observed related to adhesion failure between mortar coatings and concrete bases. This problem has been aggravated by the use of concrete with increasingly high levels of resistance, and by the elevated number of mold reuses, motivated by the construction of multi-story buildings and the use of release agents with a lower degree of water dilution, which, evidently, provides greater insulation of the base. One alternative encountered to alleviate this problem is the use of rough textured molds, providing a greater contact surface in order to provide the system with a greater area of adhesion between the components. This experimental study presents a comparative evaluation of the adhesion between mortar coatings on concrete bases made with two different levels of mold roughness. The study confirms the hypothesis that surface roughness provides greater efficiency, and also considers the need of further study in order to demonstrate its economic viability.

KEYWORDS

Adhesion, Coating, Substrate, Surface roughness, Mold release agent.

[1] Faculty of Engineering of the University Catholic of Pernambuco (Unicap), Recife, BRASIL, angelo@tecomat.com.br
[2] Faculty of Engineering of the Federal University of Goiás (UFG), Goiânia, BRASIL, hcarasek@gmail.com
[3] Faculty of Engineering of the Vale do Ipojuca (FAVIP), Caruaru, BRASIL, joao@vieiramota.com.br
[4] Faculty of Engineering of the Vale do Ipojuca (FAVIP), Caruaru, BRASIL, fredbarbosa@compesa.com.br

1 INTRODUCTION

Throughout the world, improved techniques for constructing multi-storey buildings are continually under development, in the constant search for higher productivity, solutions to prevent problems, and yet with a focus on questions related to the environment and sustainability.

In the case of buildings executed in reinforced concrete, one of the issues under constant discussion is related to the durability of structural elements, where every effort is made to relate the expected service life with exposure conditions and aggressiveness of the environment. Accordingly, the most commonly used instruments are the increased thickness of concrete coating over the armature, as well as the adoption of lower cement/water ratios, which normally result in increased mechanical strength.

Although such actions help to provide greater protection to the reinforced concrete structure, they also generate great concern regarding the fixation of mortar coatings on the bases, which present a significant decrease in porosity, thus rendering the mortar fixation difficult by physico-chemical adhesion. Over time, this loss of adherence compromises the durability of the coating, which can cause detachments, as described by Mansur et al. [2006].

Therefore, the proposal of this article is to study the benefits obtained in the adhesion of mortar coatings by increasing the contact area of mortar with the concrete base, obtained by using rough textured molds.

2 THEORETICAL REVIEW

The study of the fixation between mortar coatings and bases with differing characteristics has been the object of discussion amongst several groups in Brazil over the last few years. This phenomenon, of an essentially mechanical nature, arises when the mortar paste penetrates the pores of the substrate, forming rigid support structures after cement hydration.

One theoretical model, known as the “theory of active pores”, helps to gain a better understanding of this behavior [Carasek, 2007]. According to the model, the paste flows from the pores with the largest diameter, as in the case of fresh mortar, to the pores with the smallest diameter, as in the case of the substrate. However, certain factors may interfere with this flow, such as hydration of the mortar cement (which tends gradually to reduce its porosity), aggregate gradation, and substrate roughness, amongst others [Scartezini, 2001].

In the case of executing buildings with a reinforced concrete structure with masonry walls, it may be noted that there are substrates which present different characteristics, especially concerning water absorption and surface roughness, and that have a strong influence on the anchorage of mortar coatings.

Another complicating factor is that, due to land scarcity in urban centers, urban growth has occurred with the construction of increasingly taller and slender buildings [Fonte et al. 2005], provoking high levels of lateral displacement, which has had an immediate reflection in the adhered outer coatings fixed to the buildings.

In multi-storey buildings where reinforced concrete is molded on-site, all efforts are made to use the same mold during the entire execution of the structure. This has forced construction companies to increase the number of times they reuse molds, and so have introduced more durable parts, with greater protection against water infiltration and the use of more efficient mold release agents [Costa e Silva, 2008]. In both situations, at the end of the process the concrete surface is much smoother, which also hinders the adhesion of mortar coatings. It decreases the penetration flow of the mortar paste into the pores of the concrete, reducing the physical adhesion, which is the base of the theoretical model known as “theory of active pores”. Therefore, the influence of substrate roughness

(the reinforced concrete structure) has been the target of researchers, such as Dancygier et al. [2009], who managed to obtain a good performance from mortar coatings applied to mechanically treated bases with a chipping hammer and brushing immediately after the molds are removed, one day after casting.

3 EXPERIMENT

3.1 Experimental planning

In order to conduct the experimental study, a sample of concrete was prepared with two different types of molds, with the aim of providing potential contact areas[5] of the separate substrates, in order to receive the mortar coating.

Thus, the adopted study variables were the potential contact area of the substrate with mortar coating, obtained from using two different types of molds (open texture and closed texture[6]), and the use and non-use of a mold release agent before placing the concrete.

In order to reduce the possible appearance of any other variables, a base measuring 0,80 x 0,80m was used, divided into 4 squares of 40cm each side, executed with the same mixture of concrete with an average compression strength of 25 MPa, commonly used on the local construction sites in the region (Fig. 1).



Figure 1. Image of the substrate divided into the 4 main squares**.**

After the base was prepared, a waiting period of 14 days (in laboratory conditions of environment – temperature 23ºC and relative humidity of 90%) was observed before applying a coat of roughcast, (proportion 1:3, Portland cement: sifted coarse sand), followed by an application of grout (25mm thick) to stabilize. This final coat was applied approximately 48 hours after applying the roughcast coating. After the grout had cured for a period of 28 days, tensile tests were conducted to determine adhesion strength.

3.2 Materials used

3.2.1 Molds

The molds used in the study were composed of smooth panels, made of recycled material (75% plastic and 25% aluminum), commercially known as “ecological panels”, measuring 40x40cm, with an average thickness of 12mm (Fig. 2).

[5] effective contact area between the base and mortar.

[6] open texture – bass-relief measuring 15x5cm, and closed texture – bass-relief measuring 1x1cm, both with depth of 4mm.

To provide different potential contact areas, when the material was being pressed, the manufacturer was requested to create bas-relief textures (Fig. 3) with an average depth of 4mm, measuring 15x5cm, referred to as open texture, and 1x1cm, referred to as closed texture.



Figure 2. View from above of the two forms of mold used in the study.



Figure 3. Geometric detail of the textured mold with closed grooves.

From the geometrical description, a simple calculation may be made to compare the potential contact areas of the two molds, which when compared to a smooth surface, resulted in increased areas of 22.5% with the open texture and 84% with the closed texture.

3.2.2 Concrete substrate

The concrete base used in the experiment was made in the laboratory, with a unit mass ratio of 1:2:3 (CPIIF32 Portland cement: medium sifted sand: maximum size gravel 25mm), and a water/cement ratio of 0.50 (Fig. 5). The results of compressive strength obtained in cylindrical test specimens of 10x20cm demonstrated values of 25 MPa, after 28 days. During the execution, half the surfaces received an application of mineral oil release agents, as per manufacturer's instructions.



Figure 4. Condition of the mold surface (a) and of the concrete surface after demolding (b).

3.2.3 Mortar coatings

After making the base, a coat of roughcast mortar was applied in the proportion of 1:3 (CPIIF32 Portland cement: sifted coarse sand), preceded by mechanical brushing, often currently used on constructions in this region. This coating was undertaken employing the traditional system, by applying it vigorously with a trowel, preceded by a light sprinkling of water.

After 48 hours applying the coat of roughcast mortar, in order to level the surface, a coat of industrialized grout was applied, composed of cement, sand and stone dust (Fig. 6), to ensure the regularity of the surface for the assay of adherence. The quantity of water used followed the manufacturer's instructions, as described on the package, which after 28 days, recommends values according to a compression strength of 45 MPa, very important for ensuring that rupture takes place near the surface of the substrate, the object of the present study.



Figure 5. Side view of the grout used during the study**.**

3.3 Test methods

After a 28-day curing period of grout coating, tests were carried out to determine the direct tensile adhesion strength. These tests followed the general methods of standard EN 1015-12 (2000), although with sections of the square test units measuring 5 cm. 6 test units were tested per situation, with a total of twenty four tests, as demonstrated in Fig. 7. The calculation of bond strength was made from the real area of mortar that was cutted, sometimes larger than the area of the metal plate used for the pullout.



Figure 6. Samples prepared for the test to determine adhesion strength.

4 RESULTS AND DISCUSSIONS

The results obtained are described below in Table 1, highlighting the values of adhesion strength calculated from the charges obtained in the tests, divided by the area encountered in each sample.

Table 1. Table indicating the general results of the tensile strength tests.

	Texture			
	Open		Closed	
	with agent	without agent	with agent	without agent
Mean tension (MPa)	0,45	0,94	0,59	1,01

In order to obtain a better assessment of the results, a variance analysis was conducted to evaluate the influence of both the surface area, and the use of release agents on the adhesion strength encountered in the samples (Table 2). In both cases, it was proven that the variables had a significant influence on the adhesion strength, to a significance level of 95% (the calculated F value greater than the critical F value). However, the interaction analysis indicated that there was no significant evidence that the combined effects provoked by the two factors, simultaneously, influenced the adhesion strength, for the quantity of tested samples.

Table 2. Results of the variance analysis.

Source of variance	SS	df	MS	F	P-	Critical F
Open texture	0.065104	1	0.065104	4.919401	0.038298	4.351243
Treatment of base	1.246704	1	1.246704	94.20345	5.21E-09	4.351243
Interactions	0.005104	1	0.005104	0.385681	0.541592	4.351243
Inside	0.264683	20	0.013234			
Total	1.581596	23				

With regard to the absolute values, the graph presented in Fig. 8 clearly illustrates the encountered mean values.

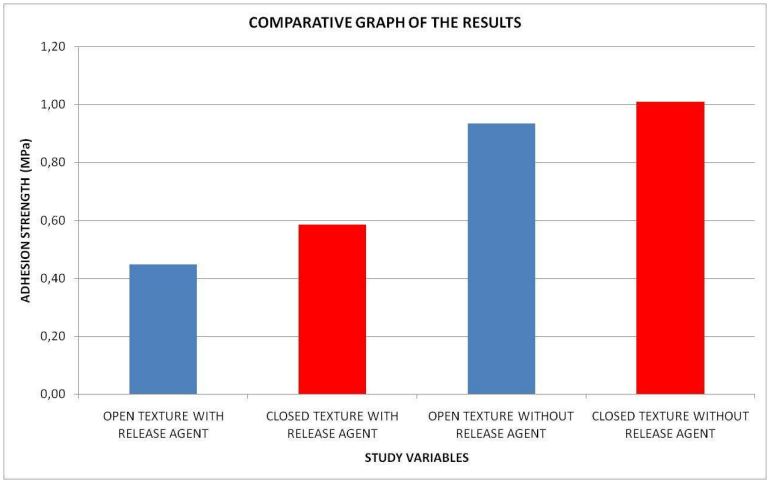

Figure 7. Comparative graph of the results obtained in the tensile adhesion strength test.

In the assessment of the use of release agents, an absolute percentage difference was recorded of 52%, with open texture and 42% with closed texture, increment values considered very significant.

With regard to the increase in the potential contact areas, the obtained increments were 30% and 8%, for the cases with and without release agents, respectively. It is important to emphasize that these

gains may also be considered relevant for the performance of the coating throughout time, especially concerning the conservation of the adhesion between the coatings submitted to repetitive shear fatigue tests, for example.



Figure 8. Condition of the main rupture occurring on the interface between the roughcast and the concrete substrate.

In addition to the absolute results, it is also important to assess the form of rupture encountered in the samples, which represents the most fragile link in the system (Fig. 9). From amongst the tested samples, the rupture was mostly encountered on the interface between the roughcast mortar and the substrate. It is noteworthy that the gain in tensile adhesion strength was not in the same relative proportion as the increment in the calculated area. It is believed however, that the greatest benefit achieved with the growth of the area should be what is referred to as shear strength, a particular property that has been under discussion by several research groups [Naderi, 2005], although not directly assessed in the present study.

5. CONCLUSIONS

Based on the discussions presented throughout this article, and on the obtained test results, it is possible to highlight a number of considerations, judged as being relevant for analysis:

- An increase of the potential contact area between the mortar coating and the substrate resulted in an absolute increase in the direct tensile adhesion strength, indicating that it would be appropriate to conduct further studies to encounter alternatives for molds with rough textured surfaces to produce concrete elements for buildings.
- The prospect exists of an even greater influence of the potential contact area of the mortar on the behavior of the shear strength, which was not assessed during this study. As an additional activity, it is recommended that new studies address the assessment of this increase in the area of mortar coating adhesion.
- The use of release agents in the mold proved to be very influential in the tensile adhesion strength, consequently, further complementary studies should be conducted in order to help develop molds that may be used in a more efficient manner (durability, stability) but without the need of this particular product.
- Because the mold used in this study is composed of polymers and aluminum, it presents a lower absorption of water, which reduces the necessity of using release agents. Another major aspect of its manufacture is that, contrary to what occurs in wooden molds, the pressure only causes an impression on the surface, without causing any tearing on the surface layer of wood, which may allow water to enter and thus lower the durability of the product.
- Data on the economic viability presented in the study must be confirmed for each case, especially with regard to durability (number of reuses) as presented by the supplier.

It is important to highlight that the results and discussions presented herein refer to the conditions and materials used in the experimental study, and should not be taken as definitive without the confirmation of further studies conducted with other variables not addressed by the present study.

REFERENCES

Carasek, H. 2007, *Argamassas,* Materiais de Construção Civil, 1ed. São Paulo, IBRACON.

Costa e Silva, A.J. 2008, *Método para gestão das atividades de manutenção em revestimentos de fachada,* Tese (doutorado), Universidade de São Paulo. São Paulo.

Dancygier, A.N., Baumb, N. & Turgeman, H. 2009, 'Adhesion of plaster coatings to RC walls subjected to bending'. *Construction and Building Materials,* **23**, 1815–1827

European Comittee for Standardization. EN 1015-12 2000. Methods of test for mortar for mansory – Part 12: Determination of adhesive strength of hardened rendering and plastering mortars on substrates. London.

Fonte, A.O.C.; Fonte, F.L.F.; Castillo, A.A.H.E.; Pedrosa, A.V.A.C. 'Características e parâmetros estruturais de edifícios de múltiplos andares em concreto armado construídos na cidade do Recife'. In: *47º Congresso Brasileiro do Concreto*. IBRACON. Recife, 2005. pXII274-XII284.

Mansur, A.A.P.; Nascimento, O.L.; Mansur, H.S. 'Data collections of Five years of exterior facade pathologies in Brazil'. In: *Qualicer 2006. IX World Congress on Ceramic Tile Quality. Vol. 2; Castellon; Spain; 12-15 Feb. 2006.*

Naderi, M. 2005, 'Friction-transfer test for the assessment of in situ strength and adhesion of cementitious materials', *Construction and Buildings Materials,* **19**, 454–459.

Scartezini, L.M.B. 2001, *Estudo do mecanismo de aderência entre argamassa e substratos porosos,* Dissertação (Mestrado), Universidade Federal de Goiás. Goiânia.

XII DBMC
International Conference on Durability of Building Materials and Components
PORTO - PORTUGAL, April 12th-15th, 2011

Performance of Blended and Modified Cements Exposed to Aggressive Environments

Asad-ur-Rehman Khan [1]
Najmus Sahar Zafar [2]

ABSTRACT

High quality and durable concrete is required to reduce the rapid deterioration of concrete in severe conditions. Among the factors related to declining concrete durability penetration of chloride-ions into concrete has been regarded as the major deterioration problem. This paper reports the results of a study conducted to evaluate the performance of different types of local cements (blended and modified) exposed to various aggressive sulphate and chloride environments. Four types of cements, namely Type I (OPC), Type V (SRC), Type I plus Fly Ash (FAC) and Type I plus polymer modified admixture (HPMC), were exposed to three magnesium sulphate solutions with sulphate concentrations of 1%, 2%, and 4%, magnesium sulphate solutions, seawater and sodium chloride solution to study the deterioration. Initiation of corrosion activity of embedded reinforcing steel bars was studied in presence of 5% NaCl solution. Maximum deterioration, due to sulphate attack, was noted in Fly Ash blended Type I cement followed by Type I cement, polymer modified Type I cement and Type V cement. Performance of Type I and Type I plus polymer modified admixture was not significantly different from each other. Corrosion probability of embedded steel bars was noted to be higher in OPC followed by FAC, SRC and HPMC concretes. The sulphate and corrosion resistance noted in blended and modified blended cement are indicative of the fact that percentage replacement of OPC used in the study was not sufficient to enhcance the performance of these cements in aggressive sulphate environments.

KEYWORDS

Performance, Sulphate attack, Corrosion, Strength reduction, Visual inspection.

[1] NED University of Engineering & Technology, Karachi, PAKISTAN, asadkhan@neduet.edu.pk
[2] NED University of Engineering & Technology, Karachi, PAKISTAN, najmsahar@neduet.edu.pk

1 INTRODUCTION

Strength and durability properties are usually used to judge the performance of concrete. Surrounding environmental and exposure conditions play a major role in durability of reinforced concrete. One of the main causes of deterioration in concrete structures is corrosion which is initiated due to the exposure of concrete to harmful chemicals that may be found in nature such as in some ground waters, industrial effluents and sea waters. Chlorides and sulphates are the most aggressive chemicals that affect the long term durability of concrete structures. The chloride dissolved in waters increase the rate of leaching of portlandite and thus increases the porosity of concrete, and leads to loss of stiffness and strength [Wee *et al*., 2000]. Calcium, sodium, magnesium, and ammonium sulphates are, in increasing order of hazard, harmful to concrete as they react with hydrated cement paste leading to expansion, cracking, spalling and loss of strength [Wee *et al*., 2000].

Cement manufacturing technology has undergone modifications recently and the extensive use of mineral admixtures has changed the chemical and mineralogical composition of the present day cements. Durability of concrete has been affected significantly particularly against the sulphate attack. Demands of construction industry, mainly due to considerations of cost saving, energy saving, environmental protection and conservation of resources, has led to the development and use of blended cements and the trend is growing rapidly [Ha *et al*., 2005]. Previous studies [Irassar et al. 2000, Hossain and Lachemi 2004] have shown that use of cement replacement materials such as blast-furnace slag, fly ash, silica fume, etc. may reduce greatly the probability of steel corrosion as well as the permeability of concrete.

Concrete durability problems are a major cause of concern all over the country especially in the coastal areas and marine structures where the structures have undergone deterioration well before their expected life and need proper attention and care. Realizing the aggressive nature of the environmental conditions and the local construction materials of the country, research was initiated at the Department of Civil Engineering, NED University of Engineering and Technology, to assess performance of concrete made with locally available cements under aggressive environmental conditions [Khan & Zafar 2009]. This paper reports the results of a study conducted to evaluate the performance of different types of cements namely Type I (OPC), Type V (SRC), Type I plus Fly Ash (FAC (10% fly ash and 90% OPC)) and Type I plus polymer modified (HPMC (10% Hi bond polymer and 90% OPC)), exposed to various aggressive sulphate and chloride environments. The performance was evaluated by evaluating the reduction in compressive strength and assessing the resistance to salt attack by visual inspection and gravimetric weight loss measurements.

2 EXPERIMENTAL PROGRAM

Mortar specimens were cast using four types of cements i.e., OPC, SRC, FAC and HPMC. Compositions of OPC and SRC used in the study were approximately 57% of C_3S, 16% of C_2S, 8.5% of C_3A, 12% of C_4AF and 55% of C_3S, 22% of C_2S, 3.5% of C_3A, 13% of C_4AF respectively. Fly ash used was of Class F. These specimens were exposed to three magnesium sulphate solutions with sulphate concentrations of 1%, 2%, and 4% to study the deterioration due to sulphate attack. They were also exposed to sea water having a pH of 8.4, Total Dissolved Solids (TDS) were 4760 mg/l and Electrical conductivity (EC) was found out to be 9725 micro-g/cm. The chloride content of water was 2316 mg/l. Reinforced mortar specimens of each type of cements were exposed to wetting and drying cycles in 5% NaCl solution to determine the corrosion resistance of embedded rebars using gravimetric weight loss measurements.

2.1 Mortar Specimens

Cement mortar specimens measuring 50 × 50 × 50 mm [Al-Dulaijan 2007] were prepared by mixing the selected cements with sand. The sand to cement ratio in the mortar mixes was 2.5 with water to

cement ratio of 0.45. Specimens were demoulded after 24 hours and were cured under water for further 27 days.

After 28 days of curing, the mortar specimens were divided into two groups. One group of specimens was continuously cured under water while the second group was placed in four tanks with 1%, 2%, and 4% magnesium sulphate solutions and seawater. These concentrations of magnesium sulphate and seawater were used to simulate the severe environments to which concrete can be exposed in real life especially in coastal areas as reported by Rasheeduzzafar *et al*. [1990]. The exposure solutions were prepared by mixing reagent grade magnesium sulphate with distilled water. Specimens representing similar composition were placed in each solution for up to 180 days. Three mortar specimens representing similar composition were retrieved from the test solutions after 90 and 180 days of exposure. The effect of sulphate concentration and seawater on the performance of selected cements was evaluated by visual examination and measuring the reduction in compressive strength. The mortar specimens were inspected after the designated exposure period and the deterioration was classified on a six point scale ranging from 0 to 5 [Al-Amoudi 1992]. A rating of 0 would indicate no deterioration while a rating of 5 indicates complete failure. The degree of deterioration was also evaluated by measuring the reduction in compressive strength. The reduction in compressive strength was calculated as follows:

$$\text{Reduction in compressive strength (\%)} = \frac{A-B}{A}\times 100$$

where A is the average compressive strength of three specimens cured under water, MPa or ksi; and B is the average compressive strength of three specimens exposed to the test solution.

2.2 Reinforced Mortar Specimens

The reinforced mortar specimens for the corrosion resistance of embedded bars were 50 × 50 × 50 mm cubes in which a 16mm diameter steel bar was centrally embedded. The steel bar was embedded into the cube such that its end was at least 20mm from the bottom of the cylinder. The initial weight of the rebar sample was taken before casting for gravimetric weight loss measurements. Specimens were demoulded after 24 hours and were cured under water for further 27 days. All the specimens were then completely immersed in 5% NaCl solution. The specimens was maintained in the same condition for 15 days and then subjected to drying in open air at room temperature for another 15 days. Each wetting and drying cycle thus consisted of 30 days. All the specimens were subjected to six (6) complete cycles (180 days) of test period.

3 RESULTS AND DISCUSSION

3.1 Visual Inspection

Deterioration rating for cement specimens exposed to 1%, 2% and 4% $MgSO_4$ solution and Sea water are shown in Table 1. Marginal wear and tear was observed in OPC and SRC specimens in all sulphate concentrations during first 90 days, while higher deterioration in comparison to OPC and SRC was noted in FAC and HPMC specimens with maximum deterioration noted in FAC specimens subjected to 4% $MgSO_4$ solution. A deterioration rating of 1 was assigned to all the specimens exposed to 4% $MgSO_4$ solution for 90 days except for FAC specimens which were asigned a rating of 2. Sea water had a little affect on each type of cement during the first 90 days. A deterioration rating of 1 was assigned to all the specimens exposed to seawater for 90 days.

Figures 1 - 4 show cement mortar specimens exposed to 1%, 2%, 4% $MgSO_4$ solutions and seawater for 180 days. Extent of deterioration was higher in all the specimens with the increase in exposure to

the above mentioned environments. FAC specimens were observed to be most affected in $MgSO_4$ solutions while OPC and SRC showed maximum deterioration in seawater. Disintegration of the edges and cracking of the surface skin, localized at the edges, was noted in almost all the specimens to 1% $MgSO_4$ solution (Fig. 1). In the specimens exposed to 2% $MgSO_4$ solution, the deterioration was more severe in FAC specimens as compared to other specimens. Deterioration represented by disintegration and cracking of edges, was noted in all other specimens, as shown in Fig. 2. A similar behavior was noted in all specimens exposed to 4% sulphate solution with FAC specimens being the worst affected, as can be seen in Fig. 3. The severity of deterioration in all specimens exposed to 4% sulphate solution was, however, more than that in similar specimens exposed to solutions with lower sulphate concentration. This type of deterioration is typical of the magnesium sulphate attack in moderate to high C_3A cements [Cohen & Bentur 1988, Lawrence 1990]. Magnesium sulphate significantly reduces the integrity of the cement thereby leading to a reduction in the compressive strength. This type of deterioration is related to eating away of the hydrated cement paste and progressive reduction into non-cohesive granular mass as can be seen in the case of FAC specimens (Figs. 2 and 3)

Table 1. Deterioration rating of specimens exposed to % $MgSO_4$ Solution and Sea Water.

Cement	Deterioration rating (days)							
	90 Days				180 Days			
	1%	2%	4%	Sea Water	1%	2%	4%	Sea Water
OPC	0	0	1	1	1	2	3	3
SRC	0	0	1	1	1	2	2	3
Flyash Modified	0	1	2	1	1	3	4	2
Hi bond Modifeid	0	1	1	1	2	2	2	2

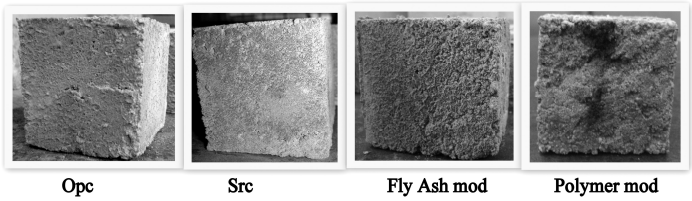

Figure 1. Cement mortar specimen exposed to 1% $MgSO_4$ solution for 180 days.

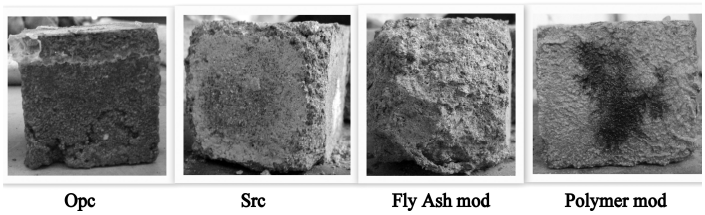

Figure 2. Cement mortar specimens exposed to 2% $MgSO_4$ solution for 180 days.

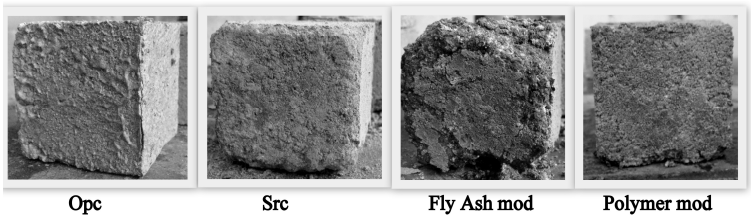

Figure 3. Cement mortar specimens exposed to 4% $MgSO_4$ solution for 180 days.

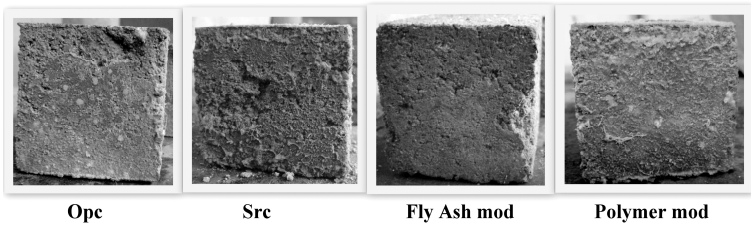

Figure 4. Cement mortar specimens exposed to Sea water for 180 days.

3.2. Reduction in Compressive Strength

The reduction in compressive strength of cement mortar specimens exposed to 1%, 2%, 4% $MgSO_4$ solutions and seawater is shown in Figs. 5 - 9. Strength reduction ranging from 17% to 26% was noted in OPC specimens exposed to 1%, 2%, and 4% $MgSO_4$ solutions respectively, while it was noted to be 22% in the case of exposure to seawater. Strength reduction in SRC specimens varied from 2% to 3% in exposure to 1%, 2% and 4% $MgSO_4$ solutions respectively, while it was found to be 49% when exposed to seawater. In FAC specimens, strength reduction varied from 17% to 40% in the case of exposure to 1%, 2% and 4% $MgSO_4$ solutions respectively while it was 32% when exposed to seawater. In the case of HPMC specimens, exposure to 1%, 2% and 4% $MgSO_4$ solutions causes strength reduction of 13% to 26% whereas 23% reduction in strength was noted when exposed to seawater.

After 180 days of exposure to the 1% $MgSO_4$ solution, the reduction in strength due to sulphate attack was the highest (17%) in OPC and FAC specimens followed by HPMC (13%) and SRC (2%) specimens (Fig. 5). Lowest reduction in strength, as expected, was noted to be in SRC specimen. In the case of exposure to 2% $MgSO_4$ solution maximum strength reduction (28%) was in FAC specimens followed by HPMC (23%), OPC (22%) and SRC (3%) specimens (Fig. 6). Similar trend was observed in the case of 4% $MgSO_4$ solution with FAC specimens showing maximum strength reduction (40%) followed by OPC (26%), HPMC (26%) and SRC (3%) specimens (Fig. 7). After 180 days of exposure to the seawater, the reduction in strength (49%) was highest in SRC specimens followed by FAC (32%), HPMC (23%) and OPC (22%) specimens (Fig. 8). Almost similar strength reduction was noted to be in OPC and HPMC specimen. Maximum strength reduction in SRC specimens may be attributed to low C_3A content of SRC and high chloride contents in the seawater. It can also be noted that performance of OPC specimens and HPMC specimens is more or less similar in all the environments indicating that 10% replacement of ordinary Portland cement by Hi bond polymer was not enough to enhance the performance of the modified cement. Results of FAC specimens are also indicative of the fact that 10% replacement of ordinary Portland cement by Fly Ash is not appropriate and it in fact resulted in deterioration of the performance of the modified cement.

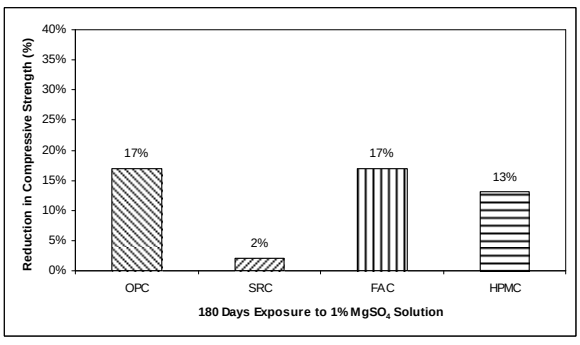

Figure 5. Reduction in Compressive Strength of OPC, SRC, FAC and HPMC specimens after exposure to 1% $MgSO_4$ environment for 180 days.

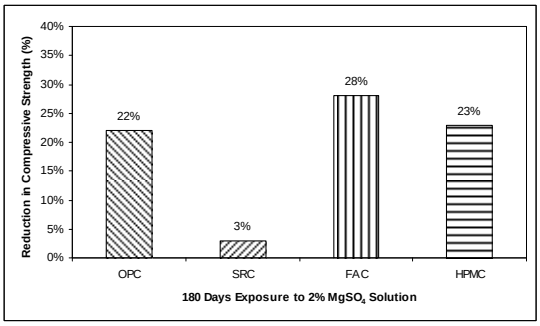

Figure 6. Reduction in Compressive Strength of OPC, SRC, FAC and HPMC specimens after exposure to 2% $MgSO_4$ environment for 180 days.

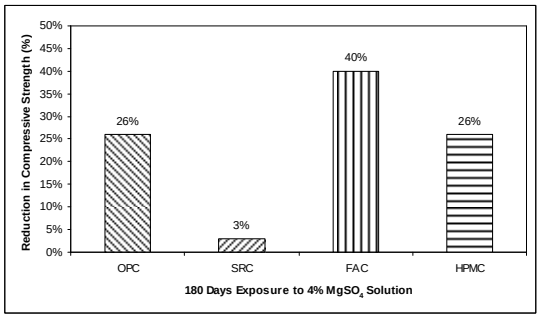

Figure 7. Reduction in Compressive Strength of OPC, SRC, FAC and HPMC specimens after exposure to 4% $MgSO_4$ environment for 180 days.

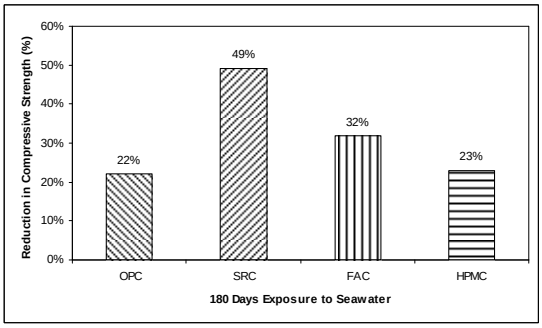

Figure 8. Reduction in Compressive Strength of OPC, SRC, FAC and HPMC specimens after exposure to seawater for 180 days.

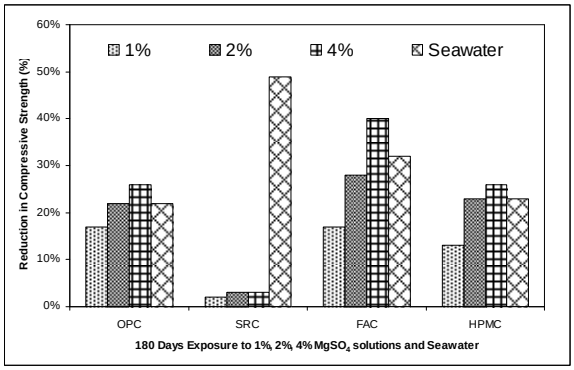

Figure 9. Comparison of reduction in compressive strength in the mortar specimens exposed to 1%, 2%, 4% MgSO4 solutions and seawater for 180 days.

3.3 Weight Loss Measurements

The corrosion resistance of OPC, SRC, FAC and HPMC reinforced specimens was related to weight loss in embedded rebars and is shown in Figure 10. From the figure it can be observed that the weight loss was minimum (1.6% per 180 days) in HPMC specimens followed by SRC, FAC and OPC specimens (2.2%, 4.2% and 6.0% per 180 days respectively). It can be noticed that in aggressive chloride environment performance of HPMC is superior than OPC indicating the effectiveness of Hi bond polymer in such environments. As chemical composition of the polymer used is not available readily from the manufacturer further comments seems to be unjustified until the polymer is thoroughly anlysed chemically.

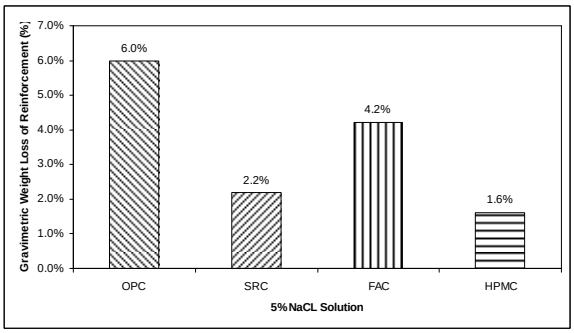

Figure 10. Gravimetric weight loss of reinforcement placed in OPC, SRC, FAC and HPMC specimens.

4. CONCLUSIONS

1) For the cement mortar specimens exposed to 1%, 2% and 4% $MgSO_4$ solutions, maximum strength reduction, due to sulphate attack, was noted in FAC specimens followed by OPC, HPMC and SRC specimens. Performance of OPC and HPMC specimens exposed to 1%, 2% and 4% $MgSO_4$ solutions was almost similar. The deterioration in all specimens increased with the increase in sulphate concentration in the exposure solution.

2) For the cement mortar specimens exposed to seawater, maximum strength reduction was observed in SRC specimens followed by FAC, OPC and HPMC specimens. Performance of OPC and HPMC was almost similar following the same trend as in the case of exposure to $MgSO_4$ solutions.

3) The gravimetric weight loss method for determining the corrosion resistance indicated that the HPMC reinforced mortar specimens exposed to 5% NaCl environment had superior performance as compared to the OPC, SRC and FAC specimens. After HPMC, SRC specimens performed better than FAC and OPC specimens with OPC being the worst affected. Superior performance of HPMC identifies the need of chemical analysis of the Hi bond polymer used.

4) HPMC performed better than FAC in all the environments but when compared with OPC performance of HPMC specimens was almost similar in sulphate environments indicating that 10% replacement of OPC with Hi bond polymer was not sufficient to enhance the performance of the cement in such environments whereas it performed remarkably well in chloride environment. It is recommended that in future studies higher percentage replacements of Hi bond polymer be used to define an optimum percentage of Hi bond polymer replacement.

5) Poor performance of FAC plain and reinforced mortar specimens can be attributed towards the fact that the amount of Fly Ash blended with OPC was not sufficient to produce the expected improved

performance of the blended cement. Results of FAC specimens in sulphate environments are similar to the findings of the authors [Khan & Zafar 2009] when granulated blast furnace slag cement was used in similar environments. It is recommended that in future studies higher percentage replacements of Fly Ash be used to define an optimum percentage of Fly Ash replacement.

6) The results in this study are in close agreement with the view regarding the influence of cement type in sulphate environments, in that the performance of SRC was better than that of OPC, FAC and HPMC. Therefore, realizing the role of C_3A on sulphate attack, cements with low C_3A are recommended in situations where the sub-structural components are exposed to severe and very severe sulphate as recommended by ACI 318 also.

ACKNOWLEDGMENTS

The authors are indebted to the Department of Civil Engineering at NED University of Engineering & Technology, Karachi, Pakistan and the University itself, in the pursuit of this work.

REFERENCES

Al-Amoudi, O.S.B. 1992, *Studies on soil foundation interaction in the sabkah environment in eastern province of Saudi Arabia*, PhD dissertation, Department of Civil Engineering, King Fahd University of Petroleum and Minerals, Dhahran, Saudi Arabia.

Al-Dulaijan, S. U. 2007, 'Sulphate resistance of plain and blended cements exposed to magnesium sulphate solutions', *Construction and Building Materials*, **21**, 1792-1802.

Cohen, M.D. & Bentur, A. 1988, 'Durability of Portland cement-silica fume pastes in magnesium sulphate and sodium sulphate solutions', *ACI Materials Journal*, **85**[3], 148 - 157.

Ha, T., Muralidharan, S., Bae, J., Ha, Y., Lee, H., Park, K. & Kim, D. 2007, 'Accelerated short-term techniques to evaluate the corrosion performance of steel in fly ash blended concrete', *Building and Environment*, **42**, 78-85.

Hossain, K.M.A. & Lachemi, M. 2004, 'Corrosion resistance and chloride diffusivity of volcanic ash blended cement mortar', *Cement and Concrete Research*, **34**[4], 695-702.

Irassar, E.F., Gonzalez, M. & Rahhal, V. 2000, 'Sulphate resistance of SRC cements with limestone filler and natural pozzolana', *Cement and Concrete Composites*, **22**, 361- 368.

Khan, A. R. & Zafar N. S. 2009, 'Performance of Different Types of Pakistani Cements Exposed to Aggressive Environments', Proc. 1st International Conference on Sustainable Built Environment Infrastructure in Developing Countries (1st SBEIDCO), Oran, Algeria, 12-14 October, 2009.

Lawernce, D. 1990, 'Sulphate attack on concrete', *Magazine of Concrete Research*, **42**[153], 249-264.

Rasheeduzzafar, Dakhil, F.H., Al-Gahtani, A.S., Al-Saadoun, S.S. & Bader, M.A. 1990, 'Influence of cement composition on the corrosion of reinforcement and sulphate resistance of concrete', *ACI Materials Journal*, **87**[2], 114-122.

Wee, T.H., Suryavanshi, A.K., Wong, S.F. & Rahman A.K. 2000, 'Sulphate resistance of concrete containing mineral admixtures', *ACI Materials Journal*, **97**, 536-549.

XII DBMC
International Conference on Durability of Building Materials and Components
PORTO - PORTUGAL, April 12th-15th, 2011

Evaluation of Pozzolanic Activity of Banana Leaf Ash

Rodrigo Cézar Kanning [1]
Kleber Franke Portella [2]
Marienne R. M. da Costa [3]
Rogério F. K. Puppi [4]

ABSTRACT

The present work is aimed at verifying the presence of pozzolanic activity in the deriving ash of the banana tree leaf. In this case, the samples have been collected after combustion in an oven and worn out in mill of balls in the times of (0.5; 1; 2 and 3) . The index of pozzolanic activity of the banana tree leaf ash was determined by means of the established whitewash as in norm NBR 5751/92 and by means of the cement, as norm NBR 5752/92. The results have shown that the ash of the banana tree leaf presented pozzolanic activity, insuring the prescribed minimum requirements, being these superiors 40% for whitewash and 17% for the cement.

KEYWORDS

Banana leaf ash, Pozzolan, Pozzolanic activity**.**

[1] Technological Federal University of Paraná (UTFPR), Curitiba, BRAZIL, rckanning@yahoo.com.br
[2] Federal University of Parana (UFPR), Curitiba, BRAZIL, portella@lactec.ogr.br
[3] Federal University of Parana (UFPR), Curitiba, BRAZIL, mariennecosta@uol.com.br
[4] Technological Federal University of Paraná (UTFPR), Curitiba, BRAZIL, rfkpuppi@gmail.com

1 INTRODUCTION

The use of alternative materials in construction has been increasingly intense. MARGON and ROCK (2003) describe that it is due to the large volume of materials consumed and the enhancement of its use in the construction industry and in environmental protection area. JOHN (2000) in their study indicate that the construction supply chain is already the largest recycler of the economy, since it has great potential to increase the volume of materials to recycle, consider the amount and characteristics of waste that consumes. Among the various types of construction waste that can employ highlights are the pozzolanic materials, which are characterized by possessing reactive activity when in contact with compounds of cement.

The use of pozzolanic materials combined with cement and lime to obtain mortar and concrete are durable and economical parts of the new technologies that ensure improvement in their characteristics. The implementation and use of mineral admixtures in mortars and concretes have been widely studied in recent decades in order to promote the improvement of the mechanical and durability of composites. Among them that stand out are the ash of rice husk ash and calcinated clay (NEVILLE, 1997; SOUZA, 2003; Santos, 1992).

Similar to this, buildings have shown a great potential to use waste from other industrial processes. Their use of alternative materials favours not only the correct composition, but also provides technically feasible solutions to technical analysis. The use of these materials is intended to obtain quality, properties, and satisfactory characteristics to be employed while seeking new sources of raw material (MARGON and ROCHA 2003).

The possibility of developing a new material with raw materials reused were studied and add improvements in the technical aspects for the mortar and concrete. In this context the need for the use of banana leaf ash as additive in the production of mortar and concrete is seen that the cement is the most consumed material in the world except water is concrete. However, the increase in the usage of these residues promotes the study of their applications and is a necessity, which not only contributes to the emergence of a new technology, but also a material focused on promoting sustainable practice.

2 MATERIAL AND METHODS

2.1 Materials

To make the mortar for the testing of pozzolanic activity index with lime and cement, we used the following inputs: lime, cement (type CPII - F 32), banana leaf ash, sand and water normalized.

2.2 Methods

The experimental program was based on a sequence of steps, aimed at clarifying the objectives, being:

- Characterization of the banana leaf ash by Diffraction and X-ray fluorescence, to identify the chemical nature present in the material;
- Strength of mortars with and without mineral admixtures;
- Trials to assess mechanical and rheological properties of mortars in the fresh and hardened state.
- Developing a database with statistical evaluation of results and performance of the product.

The experimental steps are described in Figure 1.

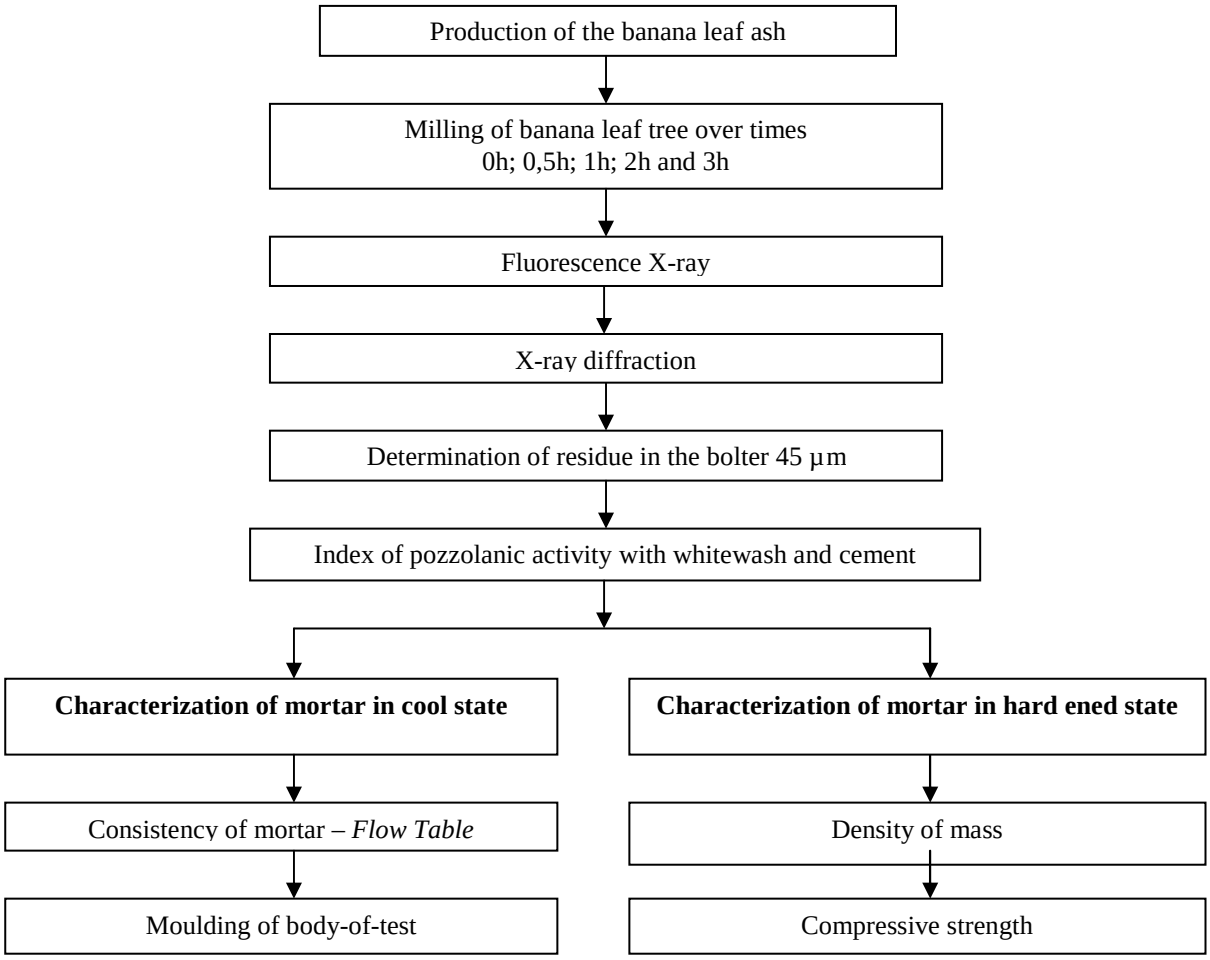

Figure 1. Stages of assay of the Experimental Program.

3 RESULTS

3.1 Production of banana leaf ash

Banana leaves of different lengths and weights were burned in a furnace at different temperatures. The first thermocouple was placed inside the furnace at a distance of 120 cm from the base showing a temperature of 290 ^{o}C. The second thermocouple positioned at a distance of 90 cm from the base showing a temperature of 850 ^{o}C. The third thermocouple was positioned at 60 cm from the base and had a temperature of 350 ^{o}C, and the fourth thermocouple positioned in the oven had a temperature of 85 ^{o}C.

The variation in firing temperature for the four thermocouples was due to a ventilation system injecting air to the furnace; this consisted of a 100 mm diameter pipe with a mini fan (Cooler RPM/12 3500 V) . As air was injected 60 cm above the bottom layer of gray that lies at the bottom has to be cooled slowly to be collected later.

Correlating the data on the percentage of ash of banana leaf with percentages of ash described by Mehta (1992) and Cincotta and Kaupatez (1988) has the results as shown in Figure 2. Note in Figure 2 that the percentage of banana leaf ash (10.57%) generated during the burning of dried material was equivalent to the same amount of gray leaf of wheat (10%) and leaf stalk of sunflower (11%), matching the class E as shown in NBR 12653/92 and class C according to ASTM 618-95. Along with that, on average, the feet of banana produced approximately 1343.3 grams of dried leaves, which represented a potential national annual average generation of 895 309 500 tons of dried leaves and

94634210 tons ash, corresponding to a plantation of 500,000 hectares and an average production of 1333 plants per hectare.

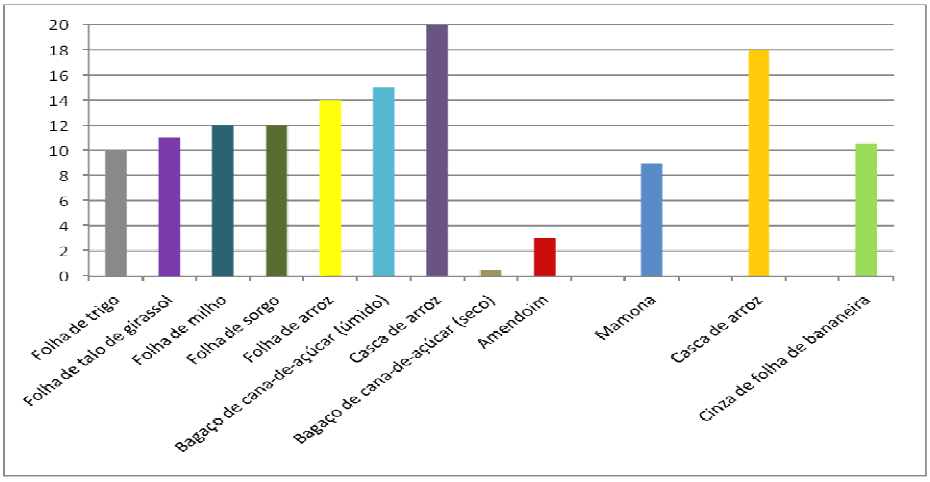

Figure 2. Generated gray amount during the burning for the diverse materials.

3.2 - X-ray Diffraction

The results of chemical analysis by X-ray diffraction can be found in Figure 3. Calcite and quartz were found in the resulting ash, which reduces the pozzolanic activity of the material in question because they are materials of little or no reactivity. Probably the calcite was obtained due to burning and the slow cooling of the ashes of banana leaf inside the oven at temperatures of 80 º C until its withdrawal. The diffractogram also showed small peaks with 2:03 Å and 2.34 Å which refer to the port samples.

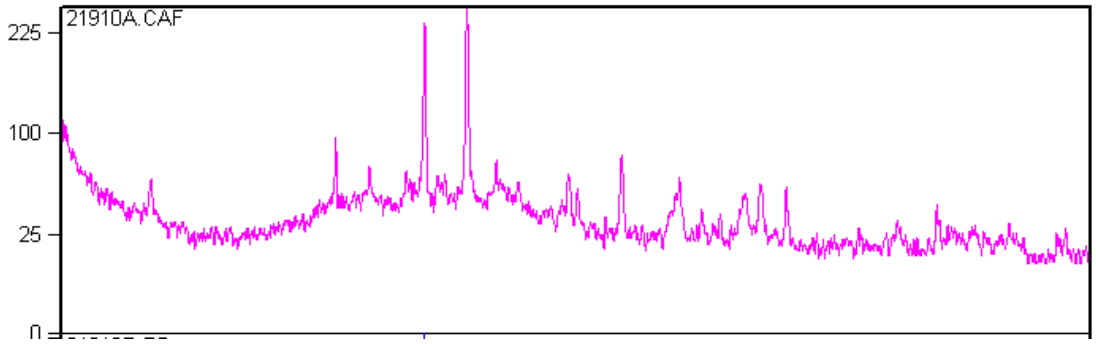

Figure 3. Diffraction of rays X of the banana tree leaf ash.

3.3 Determination of the residue in bolter 45 µm - NBR 9202/85

The determination of the residue in bolter 45 µm was stablished according to parameters of NBR 9202/85 and results presented as Figure 4.

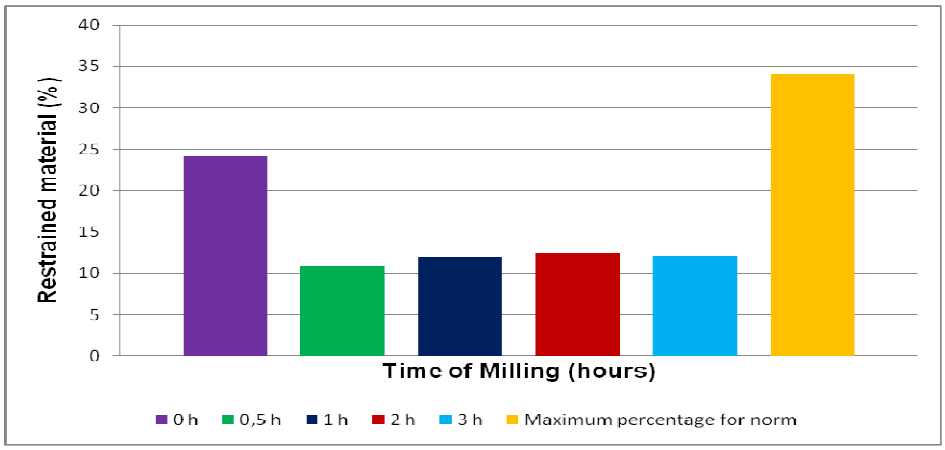

Figure 4. Percentage of restrained material in the bolter 45µm for each time of milling.

The results showed variations in the order of 24.1%, 10.9%, 11.9%, 12.4% and 12.0% for (0, 0.5, 1, 2 and 3 h) in the percentage of material retained on the sieve 45 micrometres with values below the permitted maximum of 34% by NBR 12653/92.

This factor may have been due to the particles after burning furnace already having a small footprint. Analyzing the results of the quantity of material retained on the sieve 45 micrometres before and after grinding times by the statistical method ANOVA, it was noted that the p-value = 0.838618 was greater than the significance level of 0.05, well as F <Fcrítical, demonstrating that the results do not present statistical differences, as shown in Table 1.

Table 1. Analysis of Variance (ANOVA) for the restrained material in bolter 45 µm.

Source of the variation	SQ	gl	MQ	F	value-P	F critical
Between groups	1,87E-05	2	9,33E-06	0,179487	0,838618	4,256495
Inside of the groups	0,000468	9	0,000052			
Total	0,000487	11				

Notes: SQ – it adds square shaped; gl – degree of freedom; MQ = SQ/GL – average square shaped; F – calculated value de F; Fcrítical – priced value of F for level of significance 0,05.

3.4 Specific mass of the ash of banana leaf - NBR NM 23/01

The results of density for milling times of 0, 0.5, 1, 2 and 3h are shown in Figure 5.

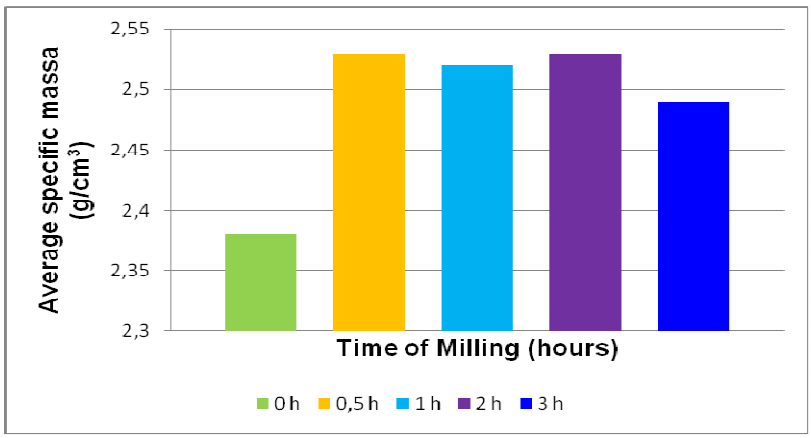

Figure 5. Specific mass of banana leaf leached ashes.

It was observed that the difference between the values of density when compared with the ash without grinding stood at 6.3%, 5.9%, 6.3% and 4.6% for milling times of 0.5; 1; 2 and 3 h, respectively. The values of the density of the samples showed high peaks and its variance resulted in 0.00333. It can thus be considered equal. Based on the data obtained an analysis was carried out of the variance in order to verify whether the values of density for different milling times were, on average, different; their data are presented in Table 2.

Table 2. Analysis of the variance for the specific mass of leached ashes.

Source of the variation	SQ	gl	MQ	F	value-P	F critical
Between groups	0,000117	2	5,83E-05	0,132075	0,877942	4,256495
Inside of the groups	0,003975	9	0,000442			
Total	0,004092	11				

Notes: SQ – it adds square shaped; gl – degree of freedom; MQ = SQ/GL – average square shaped; F – calculated value de F; Fcrítical – priced value of F for level of significance 0,05.

With a reliability level of 95% it was concluded that significant differences of specific mass had not existed statistical enter the different times of milling, a time that the value-p = 0.878 was greater that the level of significance of 0.05. Observing the values of F and Fcrítical, F was < Fcrítical, thereby accepting the hypothesis of the equality and concluding that there had not existed differences in the average between groups.

3.5 Method of air permeability - method Blaine - NBR NM 76/98

The data obtained from the results of air permeability in Figure 6.

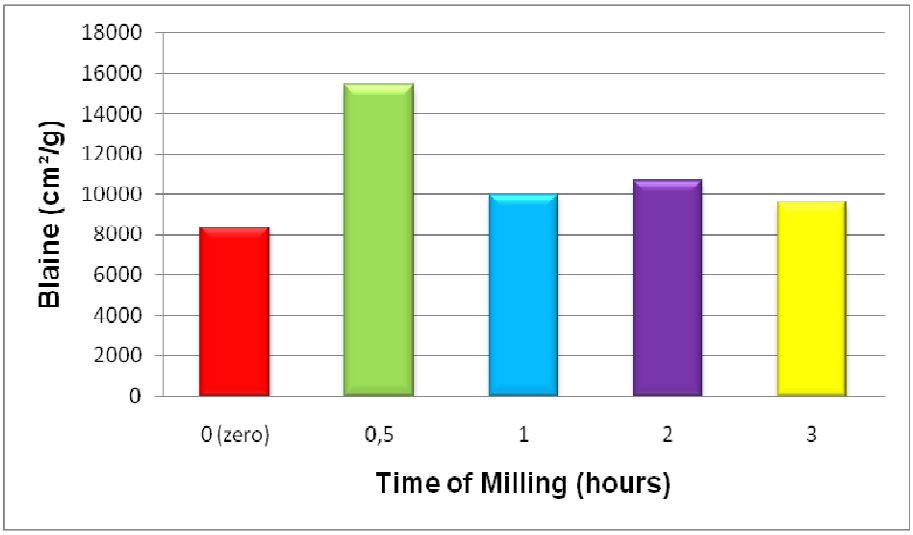

Figure 6. Variation of the Blaine fineness index for milling time.

It was observed that the values of Blaine for the various mills were situated close to the values of silica (13,000 cm^2/g) described by Holland (2005). The decreased levels of Blaine may have been due to fragmentation and better packing of particles of ash.

3.6 Pozzolanic activity index with lime - NBR 5751/92

The results obtained from tests for pozzolanic activity index with lime are shown in Figure 7.

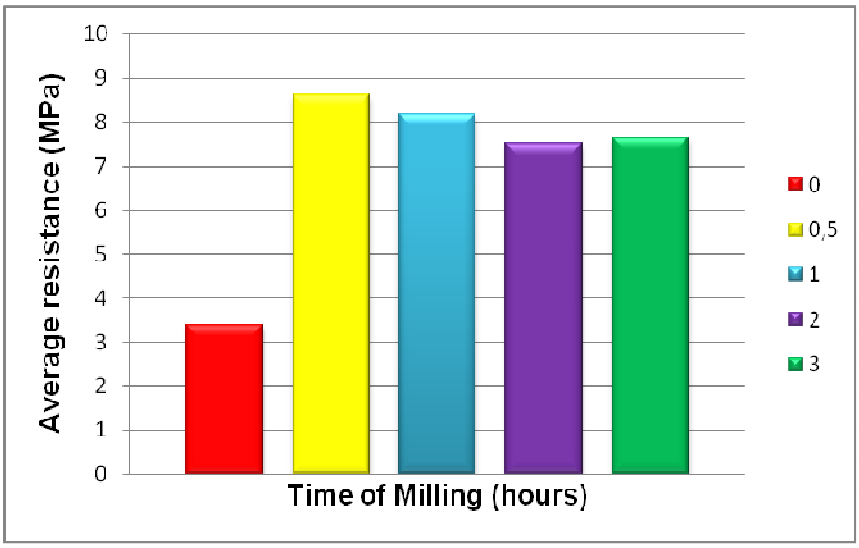

Figure 7. Index of individual pozzolanic activity for the different millings.

The increase in strength of body-of-proof banana leaf ash in 153.98% 141.88% 121.53% and 125.07% after passing through the process of grinding in ball mill by periods 0.5, 1, 2 and 3 h, may have been due to a possible reduction of particle size as shown in the test of air permeability (Blaine method).

Although the ash without grinding has not reached the minimum strength of 6 MPa at 7 days as prescribed by standard grinding NBR5751/92 caused reduction of the particles and increased its reactivity.

3.7 Pozzolanic activity index with cement - NBR 5752 / 92

The test results of pozzolanic activity index with cement are presented in Figure 8.

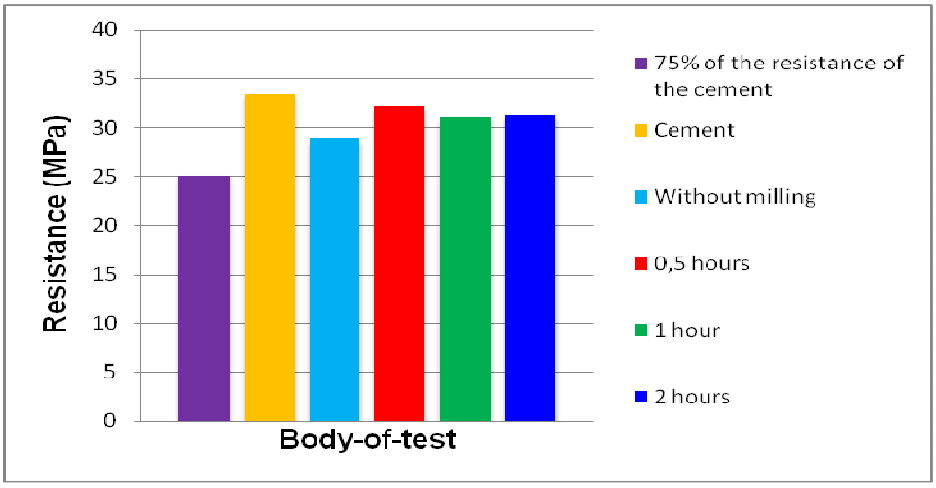

Figure 8. Pozzolanic activity of the leaf ash of banana tree with cement.

The values of pozzolanic activity of banana leaf ash with cement were higher than 10.46%; 21.41%; 17.81%; 18.41% and 10,46%, respectively for the times 0; 0 5; 1; 2 and 3 h. The NBR 5752/92 recommended a minimum of 75% of the reference mortar for 28 days of age. It was noted also that despite the grinding times values were found to be very close to mechanical compression of the reference mortar which showed a considerable ash pozzolanic activity of banana leaf. Based on data obtained an analysis of variance (ANOVA) was performed to investigate the statistical differences in the results of pozzolanic activity index with cement for different times of grinding of banana leaf ash, according to Table 3.

Table 3. Analysis of Variance (ANOVA) for the IAP with cement.

Source of the variation	SQ	gl	MQ	F	value-P	F critic
Between groups	96,2696667	5	19,25393333	23,96755187	1,3141E-08	2,620654
Inside of the groups	19,28	24	0,803333333			
Total	115,549667	29				

Notes: SQ – it adds square shaped; gl – degree of freedom; MQ = SQ/GL – average square shaped; F – calculated value de F; Fcríticcal – priced value of F for level of significance 0,05.

As seen in Figure 8 and the results of analysis of variance, the mechanical strength to mortars dosed with ashes in the ground times (0,5; 1; 2 and 3) h did not differ significantly from the values obtained by cement mortar since the p-value = 1.3141 E-08 was lower than the significance level of 0,05.

4 CONCLUSIONS

The banana leaf ash when burned at temperatures of 850 °C and subsequently milled in a ball mill showed pozzolanic activity above 40%the minimum stipulated by the NBR 5751/92 and 17% for the NBR 5752/92 standards. The optimum time for grinding banana leaf ash is 30 minutes. The banana leaf ash without grinding presented no activity with lime pozzolanic established by the NBR 5751/92. Also, as a result brought the appearance of crystals of calcite and silica in their composition. For relatively short times of milling, the reduction of the crystals sizes generates pozzolanic activity. It has been proved statistically that the pozzolanic activity of banana leaf ash with cement for various times of milling did not differ. It was concluded so that the ash originated from the burning of the banana leaf shows pozzolanic activity and can be used with addition in the cement, concrete and mortar.

REFERENCES

John, W.M. Reciclagem de Resíduos na Construção Civil - Contribuição à Metodologia de Pesquisa e Desenvolvimento. Tese de Livre Docência. Escola Politécnica da Universidade de São Paulo. 102p. São Paulo, 2000.

Margon, P.; Rocha, J. Argamassas com cinzas de carvão mineral dosadas por curva granulométrica. V SBTA – Simpósio Brasileiro de Tecnologia em Argamassas. São Paulo, 11 à 13 de junho de 2003.

Margon, P; Rocha, J. Argamassas dosadas com cinzas de carvão mineral de termelétrica. V SBTA – Simpósio Brasileiro de Tecnologia em Argamassas. São Paulo, 11 à 13 de junho de 2003.

Neville, A.M. Propriedades do Concreto, 2ª. edição, Editora PINI Ltda., São Paulo (1997).

Souza, P. S. L. Verificação da influência do uso do metacaulim de alta reatividade nas propriedades mecânicas do concreto de alta resistência. Porto Alegre. Tese de doutorado. Programa de Pós-Graduação em Engenharia Civil da UFRGS, 2003. 203p.

Santos, P.S. Ciência e tecnologia de argilas. 2ª ed. São Paulo: Edgard Blücher, 3v, 1992.

XII DBMC
International Conference on Durability of Building Materials and Components
PORTO - PORTUGAL, April 12th-15th, 2011

Influence of Sample Preparation and the Addition of BFS on Water Vapour Sorption Isotherms

Elke Gruyaert [1]
Céline Dieleman [1]
Nele De Belie [1]

ABSTRACT

Blast-furnace slag (BFS), a by-product of the steel production, can be added to a concrete mix as cement replacing material. However, the presence of BFS has a significant influence on the microstructure of the matrix. To study the pore structure of pastes in the micro- and mesopore range, dynamic water vapour sorption experiments were performed. This method allows to determine the water vapour adsorption/desorption isotherms by continuously monitoring the weight change of a sample placed in an environment with controlled temperature (20°C) and relative humidity. To obtain complete adsorption/desorption cycles, the relative humidity was increased/decreased in steps by mixing dry and humid nitrogen gas. The tests were performed on pastes with water-to-binder ratios of 0.5 and BFS-to-binder ratios of 0 (CP0), 0.5 (CP50) and 0.85 (CP85).

First of all, the effect of the predrying method on the sorption isotherms was investigated. The test results indicate that the water removed by vacuum drying can probably re-enter at high relative humidity. At low relative humidities, specific interactions possibly occur by formation of hydrogen bonds. This topic will be investigated in more detail in the near future. Furthermore, the mass water content at 100% RH after a step-by-step desorption/adsorption cycle never reaches the mass water content of saturated test specimens. A step-by-step adsorption to 100% RH cannot fill all of the large meso and macro pores. Moreover, a decrease of the RH to 0% induces no irreversible changes to the pore structure.

Secondly, the sorption isotherms of CP0 were compared with those of CP50 and CP85. Although differences are noticed between BFS and OPC pastes, additional tests are necessary to draw conclusions.

KEYWORDS

Water vapour sorption, Isotherm, Predrying, Microstructure, Blast furnace slag.

[1] Magnel Laboratory for Concrete Research, University of Ghent, Department of Structural Engineering, Ghent, BELGIUM, elke.gruyaert@UGent.be, nele.debelie@UGent.be

1 INTRODUCTION

Sorption experiments allow to characterize the pore structure of cement-based materials in the micro and meso porous range. The most common used gases are water vapour and nitrogen [Odler 2003] but it seems from literature review that the type of sorbate strongly influences the test results.

- Water penetrates the vacated interlayer spaces, which are inaccessible for nitrogen molecules but which should be excluded from surface area measurements [Garci Juenger & Jennings 2001]. However, not all researchers share this opinion. In Mikhail [1963], it is stated that the layer structure of tobermorite gel is not the cause of the difference between water and nitrogen adsorption.
- The 'bottle-neck' effect obstructs nitrogen to enter large pores with a small opening. Influencing parameters are the size of the nitrogen molecules, which are larger than water molecules, and the test temperature. Since water vapour sorption tests are performed at a higher temperature (ambient temperature in comparison to 77K for nitrogen adsorption [Odler 2003]), the permeability of water molecules is artificially increased by activated diffusion.
- Furthermore, the water molecules have a strong dipole moment, enabling the molecules to penetrate into the pore space [Mikhail *et al.* 1963].

Moreover, the drying process, preparatory to the gas adsorption tests, has a significant influence on the test results and complicates comparison between different research projects. Theoretically, the free and adsorbed water must be removed, while the interlayer water must remain behind. However, different drying techniques, as e.g. D-drying, P-drying, oven-drying, freeze drying remove different amounts of water and cause collapse of the CSH structure on nanometer scale to different extents [Odler 2003]. Therefore, water vapour sorption experiments sometimes start with a desorption instead of an adsorption process [Ahs 2008], [Rouquerol *et al.* 1999].

All the above-mentioned arguments clearly show that the sorption experiments are influenced by a lot of parameters. In this article, the difficulties associated with the technique of water vapour adsorption on cement based materials are discussed more in detail. Experiments were performed with water vapour since this is a natural adsorbate for building materials exposed to environments with changing relative humidities.

2 MATERIALS

Cement pastes with a water-to-binder ratio (w/b) of 0.5 and slag-to-binder ratios (s/b) of 0 (CP0), 0.5 (CP50) and 0.85 (CP85) were cast in cylindrical moulds, which rotated for 24 hours at a speed of 15 rotations per minute. Afterwards, the specimens were cured under water at a temperature of (20 ± 2)°C until the time of testing. The chemical composition of the used cement (CEM I 52.5N) and blast-furnace slag is tabulated in Table 1.

Table 1. Chemical composition of ordinary Portland cement (OPC) and blast-furnace slag (BFS). (IR = insoluble residue; LOI = loss on ignition).

	CaO [%]	*SiO_2* [%]	*Al_2O_3* [%]	*Fe_2O_3* [%]	*MgO* [%]	*K_2O* [%]	*Na_2O* [%]	*SO_3* [%]	*S^{2-}* [%]	*CO_2* [%]	*IR* [%]	*LOI* [%]	*Blaine* [m²/kg]
OPC	63.4	18.9	5.74	4.31	0.89	0.73	0.47	3.34	/	0.50	0.41	1.51	353
BFS	41.2	36.4	9.83	0.26	7.41	0.41	0.28	1.62	0.79	0.90	0.43	1.3(*)	394

(*) Correction for oxidation of sulfides has been taken into account

3 DYNAMIC WATER VAPOUR SORPTION (DVS)

3.1 DVS-apparatus

The test setup to perform dynamic vapour sorption (DVS) experiments is shown in Fig. 1 (DVS – SMS: Surface Measurement Systems, UK). This method allows to determine the water vapour

adsorption/desorption isotherms by continuously monitoring the mass change of a sample placed in an environment with controlled temperature and relative humidity. In this research, the temperature was maintained at 20°C and the RH was controlled by mixing dry and humid nitrogen gas. The RH varied between 100% and 0% and changed in steps of 10%. During each step the mass change was continuously recorded. When the software detected a change in mass lower than 0.002% per minute, the RH was changed automatically by 10%.



Figure 1. Dynamic water vapour sorption apparatus (http://surfaceenergyanalyzer.com).

3.2 Influence of the sample preparation on the sorption isotherms

Since sample preparation seems to have a considerable effect on the sorption isotherms (see introduction), some preliminary tests were performed on cement pastes, which were differently treated before the sorption experiments started. Part of these results were published in [De Belie *et al.* 2010].

3.2.1 DVS experiment starting from an adsorption process on vacuum-dried test specimens

In a first phase of the research, vacuum dried test specimens (at 80°C) were subjected to a dynamic water vapour sorption experiment, starting with an adsorption process [De Belie *et al.* 2010] (Fig. 2 (a)). As can be seen, the first adsorption isotherm deviates from the subsequent ones, and, from the second cycle onwards, the adsorption – desorption curves overlay each other. The dry masses, obtained by both techniques, diverge from each other and indicate that more water is evacuated by vacuum drying than by a step-by-step desorption. Since CSH in hydrated cement pastes contains different types of water (chemically bound water, interlayer water, adsorbed surface water), it is not surprising that different drying techniques can remove different amounts of water. De Belie et al. [2010] refer to [Jennings 2008] and [Feldman 1973] to interpret the chemical formula of CSH. When no surface adsorbed water is included, the chemical formula of the CSH is $C_{1.7}SH_{1.8}$, containing 1.3 mol chemically bound water and 0.5 mol interlayer water. When adsorbed surface water is included, the formula is $C_{1.7}SH_{2.1}$. The 0.3 mol extra water is formed as an outer monolayer at a relative humidity higher than 11%. From literature review, it seems that a step-by-step desorption to 0% RH only removes the monolayer water and part of the interlayer water [De Belie *et al.* 2010], while severe drying techniques as e.g freeze-drying, D-drying and oven drying at 105°C, can completely remove interlayer water [Baroghel-Bouny 2007]. Moreover, extraction of interlayer water induces collapse of the CSH structure. Due to the compression of the cement gel, the open meso gel pores diminish and the volume of capillary pores increases [Espinosa & Franke 2006]. However, no consensus exist concerning the re-entry of water molecules into this collapsed structure [Korpa & Trettin 2006]. According to Feldman (cited by [Espinosa & Franke 2006]) interlayer water is taken up in the CSH phases at low relative humidities. However, in our experiments the first and second adsorption isotherms are parallel for a relative humidity below 50%, indicating that no more water enters the paste in this RH range after vacuum-drying than after a step-by-step desorption. Since the slopes of both adsorption curves deviate from each other at relative humidities between 50% and 80% and the mass water content at 90% RH remains the same, De Belie et al. [2010] assumed that interlayer water will re-enter at higher RH, and will not (completely) be extracted again in the step-by-step desorption. Although this statement is in contradiction with that of Feldman, the theory of Lodewyckx [2008], who assumed that specific interactions occur at low relative humidities (interaction between the active sites on the surface and H_2O (hydrogen bonds) and formation of water clusters (again by hydrogen

bonding)) while micro and meso pore filling takes place at higher relative humidities, can give a suitable explanation. This implicates that the suitability of the BJH theory, to calculate pore size distributions, the t-curves as obtained by Hagymassy [1969] and the BET theory, to determine the specific surface area, on this kind of curves is questioned. This subject will be investigated more in detail in the near future. Additionally, it is not sure that equilibrium is attained during the step-by-step desorption. If equilibrium is not attained, the adsorption curve also alters and deviates from the first one. From her literature review, Baroghel-Bouny [2007] concluded that moisture transport is slow and consequently establishment of equilibrium is retarded, especially in the mid-range RH. In our research, the measurements automatically changed to the next RH step when the mass change was lower than 0.002% per minute. Nevertheless, after the relatively fast initial adsorption, a subsequent significantly slower uptake of water can take place [Odler 2003]. Lodewyckx [2010] also noticed a second increase in water uptake at later ages and ascribed this phenomenon to the transformation of the cluster structure of H_2O into a more ordered chain-like structure so that water nanochains are able to enter a small opening (ultramicropores with a diameter < 0.7 nm) if sufficient time is given.

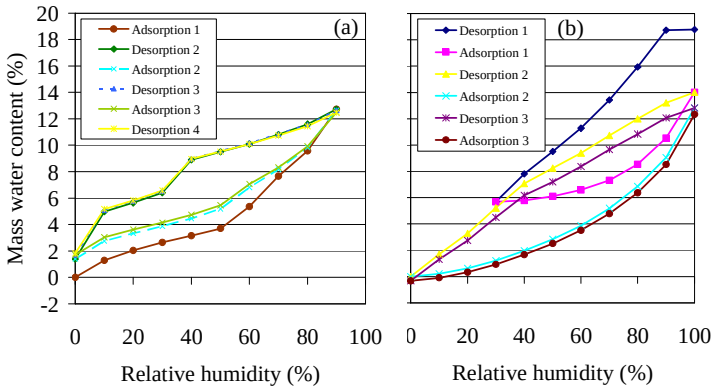

Figure 2. Dynamic water vapour sorption experiments: (a) starting from an adsorption process on vacuum dried cement paste (CP0) (age ~ 4M) [De Belie *et al.* 2010] and (b) starting from a desorption process on saturated test specimens (CP0) (age ~ 2M).

3.2.2 DVS experiment starting from a desorption process on saturated test specimens

In a second stage of this research, the experiments started with a desorption process of saturated test specimens. After all, in real building materials subjected to climate changes, the drying process is milder than freeze-drying, D-drying, vacuum-drying or oven drying and interlayer water, which is no pore water according to the definition of Feldman (cited by Espinosa [Espinosa & Franke 2006]), will not be (completely) extracted from the material in real circumstances. Moreover, this approach allows to preclude the complications associated with the different drying methods. An example of an isotherm, obtained in that way, is presented in Fig. 2 (b). Now, the first desorption isotherm deviates from the subsequent ones. To investigate whether this deviation would be caused by an irreversible process, test specimens were twice subjected to the same adsorption – desorption cycles. In between the two measurements, the sample was re-immersed in water. Since similar desorption isotherms are obtained in both dynamic sorption experiments as can be seen in Fig. 3 (a) and (b), the differences in mass water content between first and second desorption are probably due to a transition of hygroscopic water content into over-hygroscopic water content and filling of the macropores at RH above 90 - 95%. At these high RH, water layers can be formed on the pore walls of the larger meso and macro pores, however, no complete filling will be obtained by water vapour sorption. The saturation degree of these large pores after immersing in water will always be higher than after a step-by-step adsorption process.

Furthermore, literature review reveals that desorption processes below 10% RH would damage the pore structure [Ahs 2008], while other researchers claim that drying below 40% RH already induces collapse of low density CSH [Jennings 2000, Thomas & Jennings 2006]. Therefore, during the

preliminary experiments, the first desorption isotherm was limited to 30%, while the relative humidity was lowered to 0% RH during the second desorption. From Fig. 3, it seems that no remarkable influence could be detected between (i) the second and subsequent desorption isotherms and (ii) the mass water content at 100% RH obtained after drying to 30% and 0% RH. Based on these test results, it was decided to vary the relative humidity immediately between 0% and 100% in later experiments.

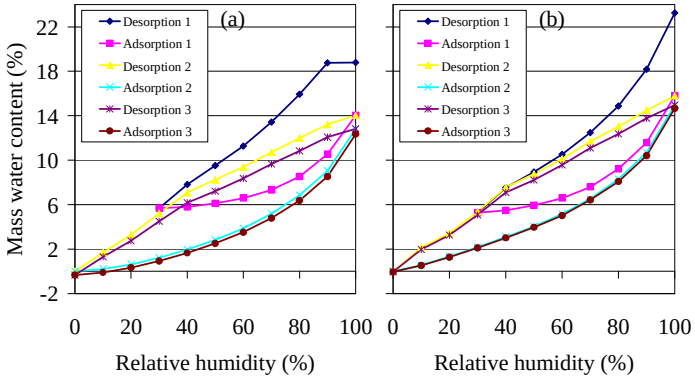

Figure 3. (a) Sorption experiment starting from saturated test specimens (CP0 – 2M) and a desorption process. (b) Repetition of experiment (a) on the same test specimens (CP0 – in the meantime 3M old), which was immersed in water between the two experiments.

Moreover, it is worth mentioning that the shape of the isotherms of Fig. 2 (b) and Fig. 3 corresponds more with that of a hydrophobic material. However, this is unexpected. A possible reason can be that not all pore water was extracted from the test sample during desorption (due to a too short equilibration time – see section 3.2.1) probably especially at low RH. As a consequence, the pores were still (partly) covered. Furthermore, a more detailed study of the test results reveals that the mass and size of the samples subjected to dynamic water vapour sorption tests also plays an important role within this story. The shape of the sorption isotherms of specimens with a dry mass (mass at 0% RH) lower than ~ 50 – 60 mg (Fig. 4) slightly differs from those obtained for samples with a higher dry mass (up to 130 mg for CP0 – 2M as presented in Fig. 2 (b)). Since the dimensions of heavier test specimens are larger, diffusion of water is delayed and the time necessary to achieve equilibrium is prolonged. Taking into account these considerations, it is advised to perform dynamic water vapour sorption tests on very small test specimens (mass < 50 mg) to obtain reliable test results within a relatively short time period and to reduce experimental errors caused by equilibration.

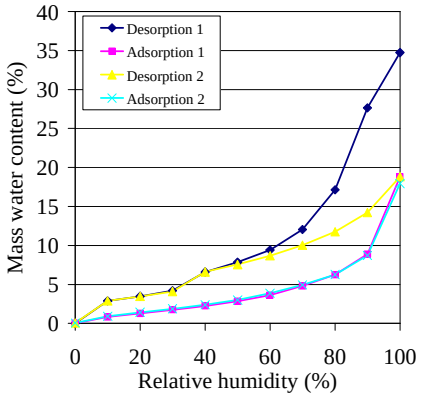

Figure 4. Sorption isotherms of CP85 – 7 days (dry mass at 0% RH = 21 mg).

3.3 Sorption isotherms of pastes containing different amounts of BFS

In Fig. 4, the sorption isotherms of CP0 (4M), CP50 (18M) and CP85 (18M) obtained by DVS measurements after vacuum drying are presented. As can be seen, the first adsorption isotherms

overlay each other between 0 and 10% RH. Between 10% and 50% there is a slight difference, while at RH above 50% the difference is more pronounced. Since the measurements above 90% are not reliable (see above), these will not considered in the further discussion. Moreover, the dry masses of CP50 and CP85 at 0% RH after a step-by-step desorption do not deviate considerably from those obtained after vacuum drying (~ 0.16% for CP50 and CP85 ↔ 1.99% for CP0). According to De Belie et al. [2010], this is due to the firm binding of interlayer water in the CSH structure which is more polymerized and becomes stronger and denser at later ages. Therefore this interlayer water will be removed by vacuum drying for young samples, but not for older ones. The lower increase in mass water content for pastes containing slag will then not necessarily mean that less micropores are present, but it is also possible that both drying techniques do not allow to extract all of the micropore or interlayer water. Above a RH of 80% the increase in mass water content of BFS paste is higher than for the reference paste. In the near future, these preliminary test results will be verified by extra measurements. Moreover, other techniques like IR spectroscopy, XRD and nitrogen sorption will be applied to clarify the observations from dynamic vapour sorption experiments.

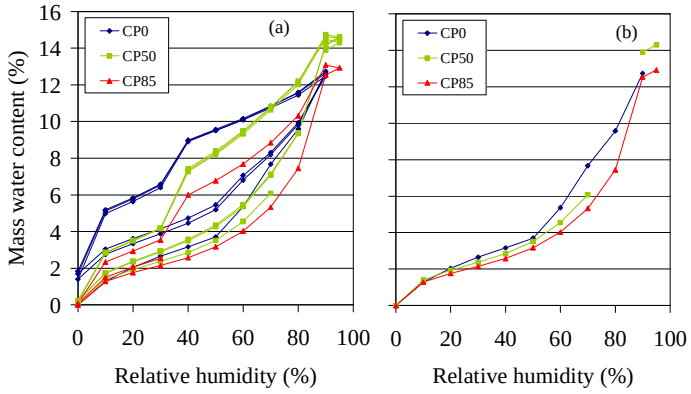

Figure 4. (a) Water vapour sorption isotherms of CP0, CP50 and CP85. (b) First adsorption isotherm of the vacuum dried test specimens [De Belie *et al.* 2010].

4 CONCLUSION

During this research, dynamic water vapour sorption experiments were performed on cement pastes to investigate the influence of sample preparation and measuring procedure on the isotherms. Although further research will be necessary, the first conclusions/recommendations can already be drawn.

- After a relatively fast initial adsorption, a subsequent significantly slower uptake of water can take place. Therefore, it is advised to verify if the specimens are in equilibrium at each RH step (also for the dynamic tests, which yield results much faster than the semi-equilibrium method, where samples are placed above saturated salt solutions). In some cases and depending on the settings (e.g. mass change < 0.002% per minute), the DVS equipment decides too fast to change the relative humidity.
- Use small specimens (mass < 50 mg) to avoid extra equilibration problems due to slow diffusion processes.
- A step-by-step desorption (to 0% RH) is less severe than vacuum drying (dry masses are different). However, it seems that interlayer water (micro pore range) can re-enter the pore structure at higher RH (between 50% and 80%) and therefore this removal of interlayer water cannot be considered to be irreversible. With ageing of the CSH, this interlayer water becomes more firmly bound. At low RH, specific interactions (hydrogen bonds) probably occur. This subject will be investigated more in detail in the near future.
- In situ, the drying processes are less strong. Therefore, we opted to start the experiments from saturated test specimens and subject them first to a desorption process. The test results demonstrate that no complete filling of the large meso and macro pores can be obtained by water vapour sorption. By lowering the relative humidity to 0%, pores probably do not empty completely and the pore structure does not change irreversibly. After resaturation (by immersing in water) the same isotherms could be obtained.

- The sorption isotherms of CP0, CP50 and CP85 slightly differ from each other. However, additional tests must be performed to draw conclusions.

ACKNOWLEDGMENTS

The author Elke Gruyaert is research assistant of the Research Foundation-Flanders (FWO-Vlaanderen) and would like to thank the foundation for their generous financial support. Moreover, we thank P. Van der Voort, M. Thommes and P. Lodewyckx for the helpful discussions and invaluable suggestions.

REFERENCES

Ahs, M. S. 2008, 'Sorption scanning curves for hardened cementitious materials', *Construction and Building Materials*, 22, 2228-2234.

Baroghel-Bouny, V. 2007, 'Water vapour sorption experiments on hardened cementitious materials. Part I: Essential tool for analysis of hygral behaviour and its relation to pore structure', *Cement and Concrete Research*, 37, 414-437.

De Belie, N., Kratky, J. & Van Vlierberghe, S. 2010, 'Influence of pozzolans and slag on the microstructure of concrete by means of water vapour and nitrogen sorption experiments and BET calculations', *Cement and Concrete Research*, 40, 1723-1733.

Espinosa, R. M. & Franke, L. 2006, 'Influence of the age and drying process on pore structure and sorption isotherms of hardened cement paste', *Cement and Concrete Research*, 36, 1969-1984.

Feldman, R. F. 1973, 'Helium flow characteristics of rewetted specimens of dried hydrated Portland cement paste', *Cement and Concrete Research*, 3, 777-790.

Garci Juenger, M. C. & Jennings, H. M. 2001, 'The use of nitrogen adsorption to assess the microstructure of cement paste', *Cement and Concrete Research*, 31, 883-892.

Hagymassy, J. J. R., Brunauer, S. & Mikhail, R. S. 1969, 'Pore structure analysis by water vapour adsorption - t-curves for water vapour', *Journal Colloid Interface Science*, 29[3], 485-491.

Jennings, H. M. 2000, 'A model for the microstructure of calcium silicate hydrate in cement paste', *Cement and Concrete Research*, 30[1], 101-116.

Jennings, H. M. 2008, 'Refinements to colloid model of C-S-H in cement: CM-II', *Cement and Concrete Research*, 38, 275-289.

Korpa, A. & Trettin, R. 2006, 'The influence of different drying methods on cement paste microstructures as reflected by gas adsorption: Comparison between freeeze-drying (F-drying), D-drying, P-drying and oven-drying methods', *Cement and Concrete Research*, 36, 634-649.

Lodewyckx, P. 2010, 'The effect of water uptake in ultramicropores on the adsorption of water vapour in activated carbon', *Carbon*, 48, 2549-2553.

Lodewyckx, P., Raymundo-Pinero, E., Wullens, H., Vaclavikova, M. & Béguin, F. 2008, 'Water isotherms of structurally identical carbons with different amounts of surface oxygen groups', Proc. International Carbon Conference, Nagano, Japan, 2008, CD.

Mikhail, R. S., Copeland, L. E. & Brunauer, S. 1963, 'Pore structures and surface areas of hardened Portland cement pastes by nitrogen adsorption', *Canadian Journal of Chemistry*, 42, 426-438.
Odler, I. 2003, 'The BET-specific surface area of hydrated Portland cement and related materials', *Cement and Concrete Research*, 33, 2049-2056.

Rouquerol, F., Rouquerol, J. & Sing, K. 1999, *Adsorption by powders and porous solids - Principles, methodology and applications*, Academic press, London.

Thomas, J. J. & Jennings, H. M. 2006, 'A colloidal interpretation of chemical ageing of the CSH gel and its effects on the properties of cement paste', *Cement and Concrete Research*, 36[1], 30-38.

XII DBMC
International Conference on Durability of Building Materials and Components
PORTO - PORTUGAL, April 12th-15th, 2011

Effect of Internal Hydrophobation, Silica Fume and W/C on Water Sorption of Hardened Cement Pastes

Mohammad Hajmohammadian Baghban [1]
Per Jostein Hovde [2]
Stefan Jacobsen [3]

ABSTRACT

Water sorption of hardened cement pastes (hcp) is an influential factor on durability, thermal conductivity and other physical properties of cement based materials. In this paper the results of an experimental study on water suction of different hcps with main variables water cement ratio (w/c), silica fume and hydrophobic agents are presented. Rapeseed oil and alkyl alkoxysilane were selected as hydrophobic agents. Alkyl alkoxysilane had a minor effect on reducing water suction of hcps, whereas Rapeseed oil was found more effective and a large fraction of the pore space not filled by atmospheric suction but needed 5 MPa water pressure to fill. The performance of Rapeseed oil was higher for lower w/c which is in contrast to previous observations for concrete samples. The reason can be pore-coarsening, absence of Interfatial Transition Zone (ITZ) and formation of micro cracks in hcps during drying. Moreover, reducing w/c reduces the total porosity and thus results in less water suction. Silica fume, when used as addition (i.e. reducing w/b) increased resistance to water transport due to forming a denser and more segmented pore structure, but it was not effective in reducing total capillary suction of hcps.

KEYWORDS

Hydrophobic agent, Silane, Silica fume, Oil, Water suction.

[1] Civil Engineering Department, Norwegian University of Science and Technology (NTNU), Trondheim, NORWAY, mh.baghban@ntnu.no
[2] Civil Engineering Department, Norwegian University of Science and Technology (NTNU), Trondheim, NORWAY, per.hovde@ntnu.no
[3] Structural Engineering Department, Norwegian University of Science and Technology (NTNU), Trondheim, NORWAY,, stefan.jacobsen@ntnu.no

1 INTRODUCTION

Water sorption is one of the main factors that can cause durability problems such as frost deterioration, sulphate and chloride ingress in concrete. Furthermore, thermal resistivity and thus energy efficiency of the material, as well as aesthetic appearance can be improved by reducing water transport. Water is mainly transported through the capillary pores in concrete, and increasing w/c increases capillary porosity. Thus, reducing w/c is usually the first solution to reduce water permeability [NS-EN 206-1 2001].

Moreover, silica fume as a pozzolanic material can react with the cement hydration products and produce more C-S-H gel with nano porosity which reduces the average pore size. Thus using pozzolanic materials in concrete mix can increase the resistance to water sorption. On the other hand, hydrophobic agents can be used to make concrete surface water repellent. Hydrophobation can either be done by surface treatment or internal hydrophobation [Årskog, et al 2004 and Justnes 2008]. However, water repellence property may be affected by UV light of the sun in case of surface treatment but internal hydrophobation does not have this disadvantage.

There are some researches conducted on the effect of internal hydrophobation on water sorption of the concrete [Justnes 2008], but there are still many unknown issues to be studied in this area. In this paper water sorption of different hcps as the important factor in concrete permeability is studied. A silane product with small molecular size and rapeseed oil as a natural replacement of silane products which is of interest concerning environmental issues were considered as hydrophobic agents. Further more, since low w/c and addition of silica fume results in a less porous material as well as smaller pore sizes and thus less water sorption, the effects of these variables were also studied to see the importance of each variable in water sorption of hcps.

2 MATERIALS AND METHODS

2.1 Materials

Three w/c of 0.58, 0.44 and 0.36 were investigated in four mix series. Portland cement (CEM I 45.5 R) with specific area of 550 (m^2/kg) and specific density of 3120 (kg/m^3) were used. The first series are the reference (Ref) series with three different w/c. Further more, two types of hydrophobic agents were used in the experiment. 1% of cement mass (m_c) of a silane based product (100% alkyl alkoxysilane) which has small molecular size of 5-10 angstrom was used in the 'Si' series in order to see the effect of hydrophobicity, presumably acting in the gel-pore size range and smallest capillaries of the cement based material [Jacobsen et al 1997]. In addition food quality rapeseed oil with 8% saturated, 62% mono-unsaturated and 30% poly-unsaturated fatty acids, was used as the other hydrophobic admixture in the 'Oil' series with dosage of 1% by mass of cement (m_c). The oil was selected as an environmental friendly substitute for existing chemical hydrophobic agents. The type and dosage of the oil in this study were considered according to recommendation of Justnes et al. [2004]. Chandra and Xu [1995] also used vegetable oils as an admixture in mortars. Moreover, densified silica fume with specific density of 2200 (kg/m^3) was used in 'SF' series with dosage of 20% m_c. This high dosage was considered to see the effect of finer pore structure in water suction of hcps.

In order to reduce undesirable macro air pores, an air-detraining admixture based on modified polysiloxanes with 0.5% dry matter was used in all of the mixes. In addition a plasticizer based on ligno-sulphonates with 40% dry matter and a super plasticizer (SP) base on modified acrylic polymers with 30% dry matter, were used in the cement paste mixes. The composition of the mixes is listed in Table 1. The water to binder ratio (w/b) is also given for the SF series in this table.

Table 1. Mix proportions for reference(Ref) samples and the sample containing 1% m_c rapeseed oil (Oil), 1% alkyl alkoxysilane(Si) and 20% Silica fume(SF).

Mix Type	*w/c*	*Alkyl alkoxysilane* [% m_c]	*Rapeseed oil* [% m_c]	*Silica fume* [% m_c]	*Plasticizer* [% m_c]	*Air detraining admixture* [gr/l]
Ref	0.58	0	0	0	0.6	8
	0.44	0	0	0	0.6	8
	0.36	0	0	0	0.6	8
Si	0.58	1	0	0	0.6	8
	0.44	1	0	0	0.6	8
	0.36	1	0	0	0.6	8
Oil	0.58	0	1	0	0.6	8
	0.44	0	1	0	0.6	8
	0.36	0	1	0	0.6	8
SF w/b=0.48	0.58	0	0	20	0.72	8
SF w/b=0.37	0.44	0	0	20	0.72	8
SF w/b=0.30	0.36	0	0	20	1.44 *(SP)*	8

2.2 Methods

2.2.1 Sample Preparation

A Kenwood Major kitchen blender was used to make one liter of cement paste for each mix. The following order was carried out for mixing: 1 minute medium rate mixing; cleaning the mixer wall with flexible plastic spatula; 4 minutes fast rate mixing; cleaning the mixer wall with spatula and finally 1 minute slow rate mixing. More over, the hydrophobic admixtures were mixed with water, plasticizer and air-detraining admixture for 1 minute, before adding to cement. The mixed fresh pastes were cast in plastic tubes with 200mm length and 25mm diameter and the ends were closed with plastic plugs.

The plastic plugs were removed after 1 day and the tubes were stored in water for 12 weeks. The specimens with w/c of 0.58 were cured on a slow rate rolling machine in the first day to avoid separation. Four 25mm slices were wet sawed from the mid section of the tubes with a Struers Minitom saw after two weeks, for the water suction test.

2.2.2 Capillary Suction Test

Smeplass and Skjølsvold [1996] improved the test for capillary suction by including information about the pore structure of hardened concrete [Sellevold 1986]. A similar method has been used here and is described in this section. In order to perform the capillary suction test, the specimens were placed in a ventilated incubator at 50°C for 2 weeks. Drying is usually done at 105 °C for this test, but a lower temperature with a long drying interval was chosen to reduce the effect of drying on pore structure and composition of hydrophobic agents. A similar procedure was used by Punkki and Sellevold [1994] and Justnes et al. [2004]. After drying, four parallel specimens from each mix were placed on a grating 1-2 mm below the water surface. The test was performed in the following order:

1. Drying at 50 °C for two weeks
2. Capillary suction for 4 days
3. Submersion in water for 3 days at 1 atm
4. Submersion in water for 1 day at 50 atm

5. The specimen volume (V) was recorded by suspending the specimen with a thin wire in water and considering the differential mass as volume change in water, according to the principle of Archimedes
6. Drying the specimen for one week at 105 ºC

3 RESULTS AND DISCUSSION

Parameters obtained from capillary suction test are given in Table 2. Capillary suction porosity (ε_{csuc}), capillary submersion porosity (ε_{csub}) and pressure saturated porosity (ε_{ps}) are calculated from the mass gain after capillary suction, submersion in water at 1 (atm) and submersion in water at 50 (atm) respectively. Furthermore Figs 1-3 show the pore distribution of different mixes with the same w/c. The results show that the total capillary porosities ($\varepsilon_{csuc}+\varepsilon_{csub}$) are decreased for the hydrophobed samples due to reduction in water absorption by using hydrophobic agents. Unlike impregnating agent emulsion that was used by Haugan [2010], alkyl alkoxysilane had a minor effect on internal hydrophobic treatment for all the three selected mixes with different w/c. The same results were obtained for some specimens that were cut after 12 weeks instead of two weeks, indicating that time of cutting has not made a significant effect on the results.

Furthermore, using silica fume has decreased ε_{csuc} and increased ε_{csub} and it is more obvious in lower w/c. In fact, there is a minor reduction in the total capillary porosity of SF samples, but the reason and amount of this reduction is different from the Oil samples. Moreover, considering Ref and SF samples with w/b in the same range we can see that although the total porosity has slightly increased for SF samples, ε_{csuc} has decreased, indicating more resistance to water transport in SF samples due to reduction in pore size and connectivity between the pores.

The oil shows the best effect on reducing absorption, with a large amount of pore space that can only be accessed by high water pressure. The performance of oil is probably due to some water repellency effect, whereas the performance of silica fume is due to reduction in pore size and connectivity between the pores.

Table 2. Initial moisture, capillary suction porosity (ε_{csuc}), capillary submersion porosity (ε_{csub}), pressure saturated porosity (ε_{ps}), total porosity (ε_{tot}), average density of solids (ρ_s) and dry sample density (ρ_d), derived from capillary suction test.

Mix Type		*w/c*	ε_{csuc} *[vol%]*	ε_{csub} *[vol%]*	ε_{ps} *[vol%]*	ε_{tot} *[vol%]*	ρ_s *[kg/m^3]*	ρ_d *[kg/m^3]*
		0.58	49.2±0.5	1.1±0.6	0.4±0.1	50.7±0.2	2696±2	1329±4
	Ref	0.44	42.3±0.1	0.4±0.0	0.4±0.0	43.1±0.1	2712±3	1543±3
		0.36	35.8±1.4	1.5±1.4	0.6±0.1	38.0±1.4	2737±10	1698±6
		0.58	46.6±0.7	2.7±0.5	1.7±0.3	51.1±0.1	2686±2	1315±3
	Si	0.44	39.9±0.4	1.7±0.6	1.3±0.5	43.0±0.3	2675±7	1526±14
		0.36	33.4±3.3	4.0±3.2	1.0±0.1	38.4±0.1	2724±3	1677±2
		0.58	29.8±1.9	12.0±1.4	7.4±0.8	49.2±0.1	2631±5	1335±2
	Oil	0.44	22.7±1.8	6.5±1.5	12.2±1.0	41.1±0.4	2642±6	1548±14
		0.36	19.6±0.6	3.8±1.6	13.3±1.1	36.7±0.1	2679±2	1695±4
	w/b=0.48	0.58	43.1±0.8	2.3±0.9	2.0±0.3	47.4±0.1	2687±2	1413±2
SF	w/b=0.37	0.44	33.1±2.4	4.8±2.2	2.9±0.1	40.8±0.1	2716±6	1607±1
	w/b=0.30	0.36	25.2±0.8	7.9±0.7	2.5±0.3	35.6±1.2	2719±31	1751±12

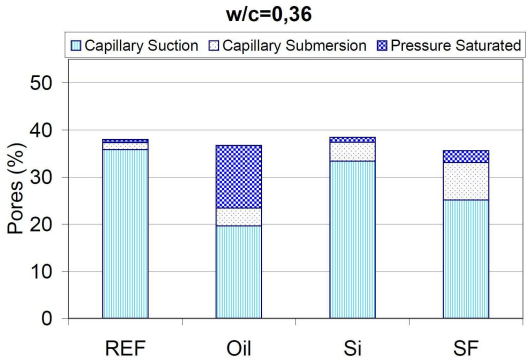

Figure 1. Pore distribution of different mixes with the w/c of 0.36 for reference (Ref) sample and the samples containing 1% rapeseed oil (Oil), 1% alkyl alkoxysilane (Si) and 20% Silica fume (SF).

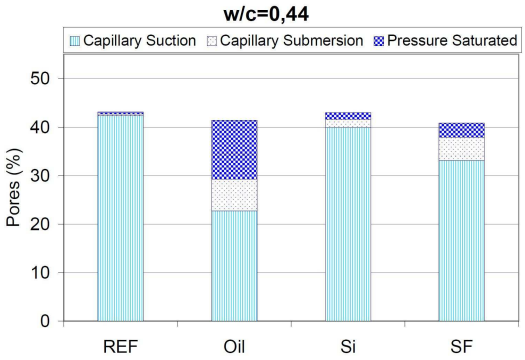

Figure 2. Pore distribution of different mixes with the w/c of 0.44 for reference (Ref) sample and the samples containing 1% rapeseed oil (Oil), 1% alkyl alkoxysilane (Si) and 20% Silica fume (SF).

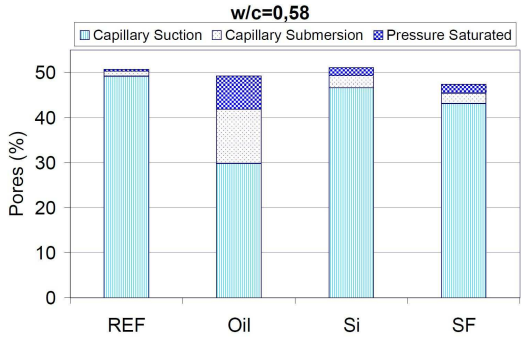

Figure 3. Pore distribution of different mixes with the w/c of 0.58 for reference (Ref) samples and the samples containing 1% rapeseed oil (Oil), 1% alkyl alkoxysilane (Si) and 20% Silica fume (SF).

In addition to the results shown in Table 2, degree of hydration was calculated from w/c and ε_{tot} shown in this table to calculate the dry sample density (ρ_d) according to Power's model [Sellevold 1986] which agreed very well with measured ρ_d (mainly less than 2% difference). Thus our hcps behaves as it should in terms of Powers model.

"Pore Protection Factor" (PF) is a criterion for assessing frost resistance of concrete in Finnish Standard SFS 4475 [1988]. It is defined as the air content as a percentage of the total porosity (PF = $\varepsilon_{air}/\varepsilon_{tot}$). It is note worthy that ε_{ps} is usually considered as ε_{air} for normal concrete, but our hcps contain a low amount of air pores as judged from Table 2 for the reference materials. On the other hand, in case of internal hydrophobation of our hcps a considerable amount of the capillary pores are not filled after 3 days submersion in water at 1 atm but they fill at 5 MPa pressure. The apparent air voids may

thus be a part of ε_{ps}. Figure 4 shows PF values for different mixes by considering ε_{ps} as ε_{air}. According to this figure, it is concluded that although silica fume gives a denser pore structure, it has a minor effect on blocking the pores from suction of water at atmospheric pressure. On the contrary, oil has been effective in increasing the PF value indicating water repellency effect in the pores. This effect has been increased by reduction in w/c.

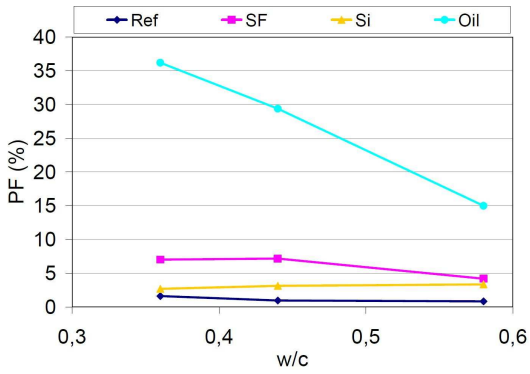

Figure 4. Pore protection factor (PF) for reference (Ref) sample and the samples containing 1% rapeseed oil (Oil), 1% alkyl alkoxysilane (Si) and 20% Silica fume (SF).

Equation 1, La Places- or Washburn's equation, shows the pressure that forces water with surface tension between air and water (σ) into a pore of radius (r). Since the contact angle for the hydrophobed surface is more than 90º, the pressure sign will be positive, thus the smaller the pore radius, the bigger the repellency effect if these small pores are hydrophobed. The pore structure of hcp is more complicated than a capillary tube with connections between the pores. In addition, the hydrophobic agents may not cover all the pore surface areas. One may generally assume that the pore structure of hcps with lower w/c is finer than the higher w/c, simply by comparing the volumetric fraction of gel pores. Consequently it is expected that water repellant admixtures will be more effective in lower w/c if these smaller pores are the main part of the pore system that is impregnated. The latter has however not yet been verified to our knowledge. This effect is observed in this study as an increase in ε_{ps} by using hydrophobic agents, but Aldred et al. [2001] and Haugan [2010] found hydrophobic agents more effective in higher w/c for concrete samples.

$$P = \frac{(-2\sigma \cos\theta)}{r} \tag{1}$$

A difference that can be mentioned between hcp and concrete specimens is that hardened cement paste gets some micro cracks during drying period. Visual observations of micro cracks on these pastes indicate that they cause faster water suction when placed on the water surface. These micro cracks will, however, close after water absorption and are not expected to highly change the total porosity, but they may open some of the pores that were not accessible to capillary water and reduce pressure saturated porosity. Since the effect of cracking can be more in higher w/c due to higher amount of capillary water, the PF value may be less for higher w/c compared to lower w/c for Oil samples. On the other hand the interfacial transition zone (ITZ) between the cement paste and aggregates in concrete that is the week part of the concrete matrix can be the reason for different behavior of hydrophobic agents in hcp and concrete.

In addition pore blocking by oil droplets and denser pore structure are the other possible reasons that have been mentioned by Justnes [2008] for less PF values in some concrete samples. The effect of denser pore structure can be seen in Fig. 4 by comparing the PF value for Ref samples with w/c=0.36 and SF samples with w/c=0.44 which have a w/b of 0.37. The PF values for SF samples are higher

than Ref samples due to denser and more discontinues pore structure, but this effect is not comparable to the water repellency effect of rapeseed oil.

4 CONCLUSIONS

The effect of internal hydrophobtion, silica fume and w/c on water sorption of hcps was studied in this paper. The hcps with lower w/c have less total porosity which results in less water sorption. In fact, capillary suction porosity (ε_{csuc}) was near to total porosity (ε_{tot}) for reference samples. In addition, silica fume increases resistance to water transport in hcps due to reduction in pore size and connectivity between the pores, but it is not effective in reducing the total water porosity of hcps.

A minor effect on water sorption was observed using alkyl alkoxysilane. However, rapeseed oil resulted in an obvious reduction in water suction of hcps. Although a higher performance of hydrophobic agents was observed for concrete with higher w/c in previous studies, they were more effective in lower w/c for hcps in this research. The reason can be effect of ITZ in concrete materials and formation of micro cracks in hcps during drying. In addition, pore blocking by oil droplets and denser pore structure can be the other possible reasons for less PF values in some concrete samples. However, effect of denser pore structure is not comparable to the water repellency effect of the oil.

ACKNOWLEDGMENTS

The authors gratefully appreciate the help given by engineer Ove Edvard Lorass and adjunct professor Roar Myrdal at NTNU.

REFERENCES

Aldred, J. M., Swaddiwudhipong, S., Lee, S. L. & Wee, T. H. 2001 'The effect of initial moisture content on water transport in concrete containing a hydrophobic admixture', *Magazine of Concrete Research (MCR)*, 55[2], 127-134.

Chandra, S. & Xu, A. 'Influence of Vegetable Oils Addition on Portland Cement Mortars', Proc. 7th International Congress on Polymers in Concrete (ICPIC), Oostende, Belgium, 3 5 July 1995, pp. 187-192.

Haugan, L. 2010, *Internal hydrophobation of concrete - short and long term effects*, SINTEF Building and Infrastructure, Project No. 3D006051, Trondheim.

Justnes, H. Østnor, T.A. & Barnils Vila, N. 'Vegetable Oils as Water Repellents for Mortars',Proc. 1st International Conference of Asian Concrete Federation, Chiang Mai, Thailand, 28 29 October 2004, Vol. 2, pp. 689-698.

Justnes, H. 2008, *Low water permeability through hydrophobicity*, SINTEF Building and Infrastructure, COIN Project report 1, Oslo.

Jacobsen, S., Gran, H. & Cornejo, G.M. 1997, 'Generic properties, functions and requirements of concrete coatings - an overview', Proceedings Int. conference on repair of concrete structures in Marine environment, Svolvær, Norway, 28 30 May 1997, Norw Publ Roads, ISBN 82-7207-453-4 pp. 465-474

NS-EN 206-1. 2001, *Concrete. Part 1: Specification, performance, production and conformity (Amendment prA1:2003 incorporated)*, Norwegian Standardization Board, Oslo.

Punkki, J. & Sellevold, E. J. 1994 *Capillary Suction in Concrete: Effect of Drying Procedure*, Nordic Concrete Research, Publication No. 15, Oslo.

SFS 4475. 1988, *Concrete. Frost Resistance. Protective Pore Ratio*, Soumen Standardoimisliitto SFS, Finland.

Smeplass, S. & Skjølsvold, O. 1996 *Concrete testing. Capillary suction and porosity*, SINTEF Internal Procedure KS 70 110(in Norwegian), Trondheim.

Årskog, V., Guofei, L., Ferreira, M. & Gjørv, O. 'Effect of Surface Hydrophobation on Chloride Ingress into Concrete Harbour Structures', 4th International Conference on Concrete under Severe Conditions (CONSEC'04), Seoul, Korea, 27 June 1 July 2004.

XII DBMC
International Conference on Durability of Building Materials and Components
PORTO - PORTUGAL, April 12th-15th, 2011

Durability of Impressed Current Realkalization Treatment Applied on Reinforced Concrete Slabsafter 5 Years

Mohamed Sahal [1]
Yun Yun Tong [2]
Beatriz Sanz Merino [3]
Véronique Bouteiller [4]
Elisabeth Marie-Victoire [5]
Suzanne Joiret [6]

ABSTRACT

The aim of this study was to explore the durability of a realkalization treatment using impressed current. Therefore, reinforced concrete slabs were cast and artificially carbonated. Carbonated slabs were then realkalized using an impressed current of 1A/m² of steel following the CEN/TS 14038-1 specification [CEN/TS 14038-1 2005]. The durability of the treatment was determined by several electrochemical measurements and analytical characterizations, at different times after its application, up to 5 years. Rapidly after the treatment, its efficiency was demonstrated both by a realkalization of the concrete matrix revealed by phenolphthalein tests and by a lowering of the corrosion current density values [Tong 2008]. But 5 years after realkalization, including 3.5 years of natural aging, although an alkaline concrete zone was still surrounding the rebars, both the rest potentials and corrosion rate were almost back to their initial values. SEM observations corroborated those results revealing the presence of large corrosion spots on the steel rebars.

KEYWORDS

Carbonation, Concrete rehabilitation, Realkalization, Impressed current, Durability.

[1] Université Paris Est, IFSTTAR, 58 Boulevard Lefebvre 75732 Paris cedex 15, France, mohamed.sahal@ifsttar.fr
[2] Université Paris Est, LCPC, 58 Boulevard Lefebvre 75732 Paris cedex 15, France, nuagestong@yahoo.com
[3] Dep. Ciencia de Materiales E.T.S.I. Caminos, Canales y Puertos, Universidad Politecnica de Madrid, Spain, bsanz@mater.upm.es
[4] Université Paris Est, LCPC, 58 Boulevard Lefebvre 75732 Paris cedex 15, France, veronique.bouteiller@ifsttar.fr
[5] Laboratoire de Recherche des Monuments Historiques, 29 rue de Paris 77420 Champs sur Marne, France, elisabeth.marie-victoire@culture.gouv.fr
[6] Université Pierre et Marie Curie, LISE, UPR 15, CNRS, 4 place Jussieu, 75252 Paris Cedex 05, France suzanne.joiret@upmc.fr

1 INTRODUCTION

High quality concrete supplies a good protection to steel reinforcement. Chemical protection is provided by the alkalinity of the concrete and physical protection by the concrete cover acting as a barrier blocking the access to aggressive species. Nevertheless, the corrosion of steel rebars is considered as the most common cause of failure in reinforced concrete structures. Two main mechanisms are responsible of the rebars corrosion: chlorides ingress and concrete carbonation. The carbonation process mainly consists in a consumption of Portlandite, due to a reaction with the atmospheric carbon dioxide, which induces a decrease of the concrete pH. The concrete cover is then no longer protective, and an active corrosion can take place on the depassivated metal [Broomfield 1997]. Since the volume of the corrosion products can be 2 to 4 times higher than that of steel, their expansion develops tensile stresses, which ultimately result in cracking and spalling of the concrete cover [Andrade *et al.* 1993]. Before spalling, reinforced concrete structures affected by carbonation could be cured by realkalization techniques [Mietz 1998], which are supposed to both generate hydroxyl ions around the rebars by hydrolysis, and induce a migration of alkaline ions from the electrolyte into the concrete. Several studies [Odden 1994, Sergi *et al*. 1996, Banfill 1997, Elsener *et al.* 1998, Gonzalez *et al.* 2000] dealed with the efficiency of the realkalization treatment, but very few explored its durability [Mattila *et al.* 1996, Hondel & Nebest 1998, Cailleux *et al.* 2006]. Therefore, the aim of this study was to evaluate the durability of a realkalization treatment using impressed current, up to five years after its application to reinforced carbonated concrete slabs. Its efficiency until 12 months after treatment had been demonstrated in a previous work [Tong 2008]. The durability issue was studied by electrochemical determination of open circuit potential, linear polarization resistance and corrosion rate, together with analytical characterizations such as pH measurements and SEM observations.

2 EXPERIMENTAL

2.1 Specimens

Reinforced concrete slabs (dimensions 300x300x50 mm) were cast using Ordinary Portland Cement (CEM I, 275 kg/m^3) and a 0.7 water to cement ratio according to the EN 1766 Standard. The reinforcement consisted in three parallel steel rebars (6mm in diameter) embedded in a 22mm concrete cover. In the middle of these rebars, a 200mm active zone was delimited using epoxy resin. After curing, one slab (1-S) was kept as a sound reference specimen and the others were preconditioned for one month (45°C, 60%RH) and then artificially carbonated for two months (22°C, 50%CO_2, 60%RH). Prior to the study, all the slabs were stored into water in order to prevent the carbonation of the sound concrete slab. After carbonation, one slab was kept as the carbonated concrete reference (2-C).

2.2 Realkalization Treatment Using Impressed Current

The realkalization treatment using impressed current was applied on 4 slabs referenced 4-R, 5-R, 6-R and 7-R. The rebars of each slab were connected together and used as a cathode. An anode (steel, 5x5 mm grid) was placed on the top surface of the slab, in sandwich position between two layers of a cellulose pad. The slabs were connected in series, and both anode and cathode were connected to an electrical supplier. The electrolyte was potassium carbonate (40g of K_2CO_3 per liter of solution). The pad was kept wet by electrolyte spraying during the treatment on a daily basis. In order to reach the 200A.h/m² efficiency threshold given in the European Specification [CEN/TS 14038-1 2005], a current density of 1A/m² of steel was imposed for 8.5 days.

2.3 Characterizations

Characterizations were performed before and after realkalization at different times (15 days, 3, 6, 12, 24, 30 and 60 months). During the first 18 months, the slabs were stored in controlled conditions of temperature (20°±2°C) and humidity (60 % ±10%). Then they were exposed outdoors until 60 months.

Non-destructive electrochemical measurements were used to estimate the corrosion state of the rebars on 3 slabs: 4-R, 5-R and 6-R. As such measurements strongly depend on temperature and relative humidity, the slabs were immersed in water for 24 hours the day before the tests. The electrochemical system was composed of a working electrode (rebar), a counter electrode (titanium/platinum-based grid, cylinder shape) and a saturated calomel reference electrode (E(NHE)=242 mV). The electrolyte was tap water. The electrochemical characterizations were conducted with a PARSTAT PAR2263, on 9 cells as illustrated on 'fig. 1a' [Martinez *et al.* 2008], using the following procedures. First, open circuit potential was followed-up for 10 minutes. Then, Linear Polarization Resistance (± 10 mV around E_{corr} at a sweep rate of 2.5 mV/min) was measured to determinate the slope (1/(Re+Rp) from E_{corr} to E_{corr}+10 mV). Then, the impedance technique (± 10 mV around E_{corr}, 39 MHz<frequency<100 kHz) was used to assess the concrete cover and electrolyte resistance (Re). Finally, corrosion current density (taking into account the ohmic drop) was calculated according to the Stearn and Geary formula [Stern & Geary, 1957]:

$$i_{corr}=B/(Rp.S) \qquad \text{(Eq. 1)}$$

with B a constant equal to 26 mV, Rp the polarization resistance and S the considered steel surface below each cell.

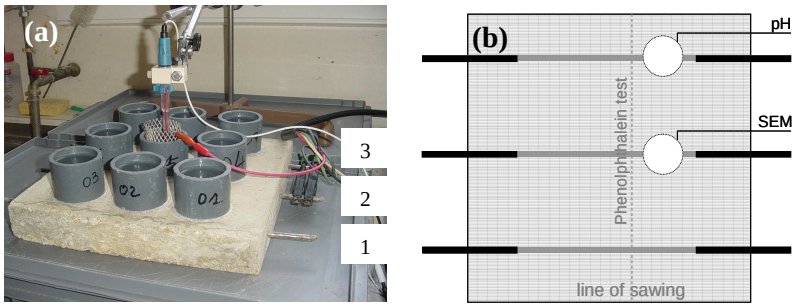

Figure 1. (a) Electrochemical system and cells positions. (b) Sampling positions for the analytical characterizations.

Destructive analytical characterizations were performed on slab 7-R. Sampling location on the slab is illustrated in 'fig. 1b'. For pH determination, both phenolphthalein tests on freshly sawed surfaces and pH-meter measurements were used. For the latest method, first, a core was sampled and cut in 10mm-thick slices. Then, the slices were dried at 45°C during 7 days. Then, they were crushed to 315 µm in diameter grains, and finally, pH was measured on a suspension made of 15g of this powder and 15g of distilled water, shaken 15 minutes [Räsänen 2004]. In order to highlight any cement matrix transformation, and to examine the steel/concrete interface, fractured and polished samples were observed using a Scanning Electron Microscope combined with an Energy Dispersive Spectrometer (JEOL JSM-5600 + Oxford Link-Pentafet-6587 EDS).

3 RESULTS AND DISCUSSION

3.1 Electrochemical Measurements

3.1.1 Rest potential

The corrosion potential values were statistically treated, so that for each slab the results obtained on the 9 electrochemical cells, at different times after treatment, were compiled into a graph of

cumulative probability versus E_{corr} 'fig. 2a'. In this graph, three populations of E_{corr} can be distinguished: the sound concrete reference, with the less negative values; the carbonated reference, with the most negative values; and the realkalized slabs in between. So the realkalization treatment clearly shifted the corrosion potential towards values less negative than those of the carbonated reference, without reaching those of the sound concrete. The drawback of this statistical exploitation, as cited by the RILEM TC 154-EMC [Elsener, 2003] is that the information on the position of measure is lost. Here, the information on the period of measurement is also lost.

Therefore, the evolution of the rest potential (average of the 9 cells per slab) versus time was also plotted 'fig. 2b'. For both the sound concrete slab (1-S), and the carbonated reference (2-C), E_{corr} was almost stable, with a light decrease after 6 months and then a stabilization ; values ranging respectively between -100 and -200 mV for slab 1-S, and –350 and –450 mV for slab 2-C. After 30 months, electrochemical measurements were stopped, these 2 slabs being cut for analytical characterizations.

For the realkalized slabs, two steps were observed. During the first 6 months E_{corr} clearly increased towards less negative values, with after 6 months a 130 mV shift between the carbonated concrete reference and the realkalized slabs. This evolution can be considered as an indicator of efficiency, as reported by Bertolini [Bertolini *et al.* 2003]. But gradually after 6 months, E_{corr} of the realkalized slabs decreased towards more negative values, comparable to that of the carbonated reference after 24 months and finally stabilized around -400 mV up to 60 months after treatment.

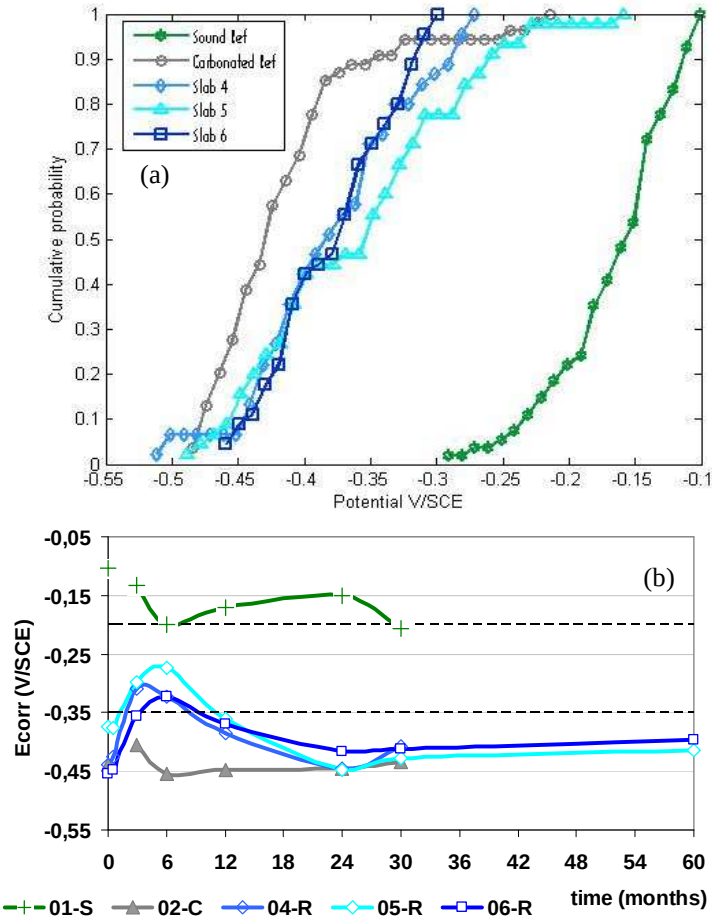

Figure 2. Cumulative probability distribution of corrosion potential measured on the 9 cells of each slab (a) during 60 months, and evolution of E_{corr} *vs.* time before and after realkalization (b).

3.1.2 Corrosion current density

The evolution of the corrosion current density (I_{corr}) versus time is illustrated in 'fig. 3'. According to the RILEM TC 154-EMC recommendation [Andrade *et al.* 2004], 4 ranges of corrosion activity can be distinguished from negligible, to weak, to moderate, up to high, the corresponding thresholds being 0.1, 0.5 and 1 µA/cm².

For the sound concrete (1-S), a very low corrosion current density (negligible to weak corrosion), stable with time, was observed, indicating a passive state. For the carbonated slab (2-C), I_{corr} was systematically higher than 1.5 µA/cm², indicating that without treatment, the corrosion activity can be quite high.

Concerning the treated slabs (4-R, 5-R and 6-R), before realkalization, I_{corr} was ranging between 1.1 and 2.0 µA/cm², indicating a high corrosion activity. During the first year after treatment, an 0.4 to 0.8 µA/cm² decrease of I_{corr} was observed, indicating a slow down of the corrosion activity and therefore an efficiency of the treatment. Nevertheless, the corresponding corrosion rates for all the treated slabs only decreased from high to moderate 'fig. 3', except for slab 4-R (which corrosion activity remained high). So the corrosion process was probably slowed down and may be stabilized but not stopped. Nevertheless, 24 months after treatment, for the 3 treated slabs, corrosion rates were back to a high level (comparable to that observed before realkalization), and finally stabilized around the 1µA/cm² threshold after 60 months.

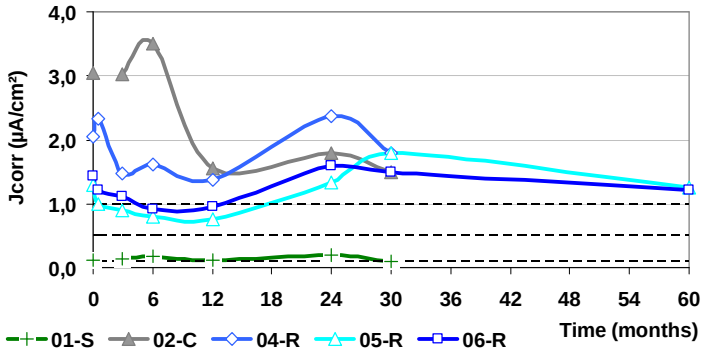

Figure 3. Corrosion current density vs. time before and after realkalization.

3.2 Analytical Characterizations

3.2.1 Concrete pH determinations

Pictures of the sawed slabs after phenolphthalein tests, respectively 15 days, 30 and 60 months after treatment are gathered on 'fig. 4'. Fifteen days after treatment, a realkalized zone around the rebars was evidenced by a pink color 'fig. 4a'. The realkalized concrete zone was about 10 mm-thick, which is in agreement with published results on mortars treated with the same conditions of current density and duration [Bertolini *et al.* 2003], [Mietz 1995] and with the performance criteria of the specification [CEN/TS 14038-1 2005]. Moreover, similar results were also reported for realkalized on-site structures [Cailleux *et al.* 2003, Bertolini *et al.* 2008]. Although the pink color tended to fade with time, it was still observable 30 and even 60 months after treatment 'figs. 4b and c', indicating that concrete realkalization around the rebars can be durable long time after treatment.



Figure 4. Phenolphthalein tests: a) 15 days, b) 30 months and c) 60 months after realkalization.

However phenolphthalein only indicates if the pH is higher or lower than 9-10. Therefore, quantitative pH determinations were performed 'fig. 5'. The results are in agreement with the phenolphthalein tests. The pH measured for the sound and the carbonated concrete references were respectively 12.5 and 9. On the realkalized slab, in the vicinity of the rebars, the pH remained almost constant, up to 60 months after treatment. But only an 11 value of pH was reached, clearly lower than the 12.5 of the sound concrete reference.

So may be the pH values reached after treatment are not sufficient to protect the steel from corrosion, which could explain the high corrosion rates and the cathodic free potentials. This hypothesis is in accordance with Yeih's results [Yeih & Chang 2005], which suggest that a pH of 9 is not enough to ensure a re-passivation, and that a pH value higher than 11 should be recommended. But this pH threshold of 11 might not be enough neither.

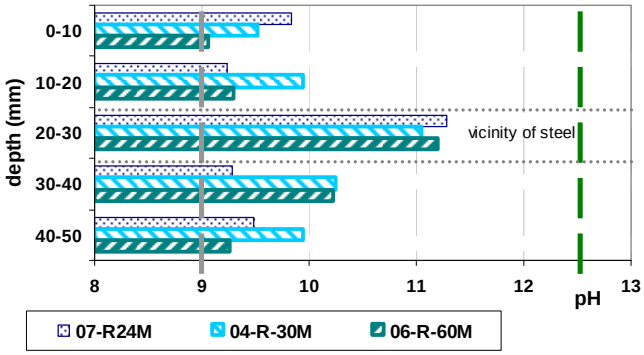

Figure 5. Quantitative pH measurements performed 24, 30 and 60 months after treatment. Vertical dashed lines are for carbonated concrete (left) and sound concrete (right).

3.2.3 SEM & EDS characterization of the steel / concrete interface

Both cross-sections perpendicular to the rebars (to visualize the steel/concrete interface), and fractures mostly parallel to the steel rebars (to investigate morphologies of corrosion products), were observed up to 60 months after treatment.

The examination of the carbonated concrete reference (slab 2-C), first confirmed the carbonation of the cement matrix, Portlandite being replaced by Calcite 'fig. 6a'. In addition, a large presence of crystallized corrosion products was observed on the concrete near the rebars 'fig. 6b', and a 15 µm-thick oxides layer was identified at the metal/cement matrix interface 'fig. 6c'.

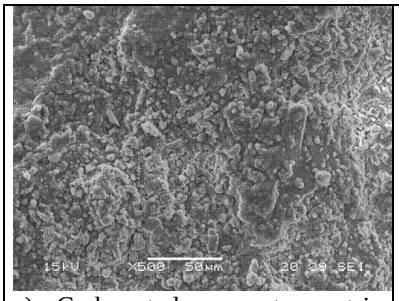

a) Carbonated concrete matrix (calcite mat).

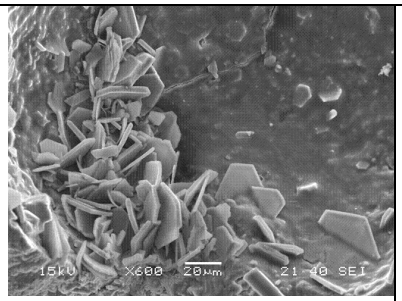

b) Corrosion products on the concrete around the rebar.

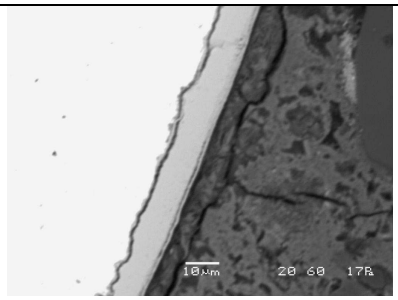

c) Compact 15µm-thick rust layer on the rebar, 12 months after carbonation.

Figure 6. SEM observations of the carbonated concrete control slab (fracture from a. to b and polished cross-section for c.). [Tong 2008].

The observation of cross sections of the realkalized concrete (slab 7-R) revealed a great heterogeneity of the corrosion development around the rebars. Thus in some areas, the metal/concrete interface showed no corrosion evidence 'fig. 7b'. In other places, the 15 µm-thick corrosion layer visible 12

months after carbonation had almost not evolved after 60 months, which seems to indicate that the corrosion was stabilized ‘figs. 6c, fig. 7a and c’. But is some areas, the corrosion had clearly spread after 60 months, a new 15µm-thick corrosion layer being visible adjacent to the initial 15µm-thick compact rust layer ‘fig. 7d’. The same informations were drawn from the fractures examinations along the rebars. Thus sound steel/concrete interfaces were observed ‘fig. 7e’, as well as corrosion products of various morphologies and sizes ‘fig. 7f’, such as laminar corrosion products containing sulfur (encircled zone on fig. 9f). These observations confirmed that in some areas the corrosion process was re-activated after 60 months.

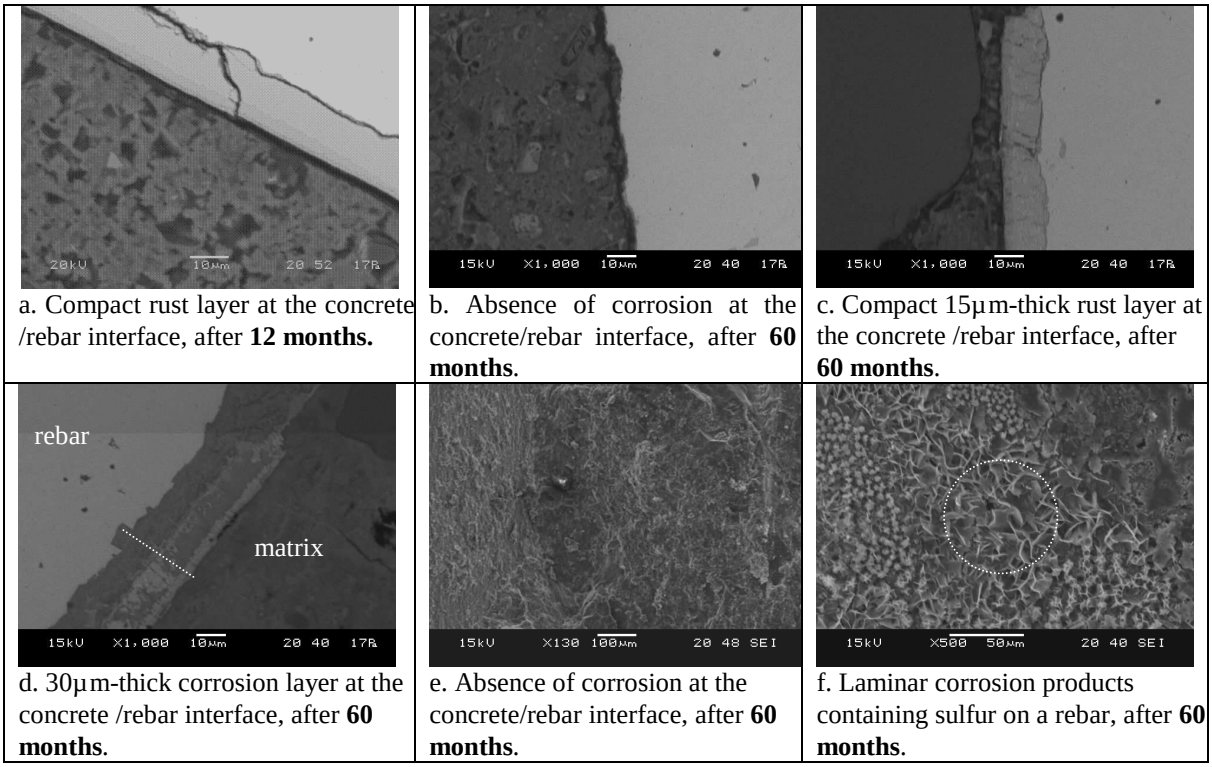

a. Compact rust layer at the concrete /rebar interface, after **12 months.**

b. Absence of corrosion at the concrete/rebar interface, after **60 months**.

c. Compact 15µm-thick rust layer at the concrete /rebar interface, after **60 months**.

d. 30µm-thick corrosion layer at the concrete /rebar interface, after **60 months**.

e. Absence of corrosion at the concrete/rebar interface, after **60 months**.

f. Laminar corrosion products containing sulfur on a rebar, after **60 months**.

Figure 7. SEM observations of the realkalized concrete (polished cross-section from a. to d. and fracture from e. to f.).

4 CONCLUSIONS

The purpose of this study was to evaluate the long-term durability (5 years) of a realkalization treatment using impressed current applied to reinforced carbonated concrete slabs, with treatment parameters fixed according to the CEN/TS 14038-1 specification. The results of phenolphthalein tests and pH measurements showed that such treatment was clearly able to increase the pH of the carbonated concrete in a long term basis. But, both electrochemical measurements and SEM observations evidenced that if the corrosion process was never stopped, it was slowed down during a period of 12 months, and reactivated after 12 months. One hypothesis could be that the realkalization treatment tested allowed an increase of the concrete pH around 11 or slightly below, which might not be sufficient to lead to the metal re-passivation. New experiments are ongoing in order to check if some changes in the impressed current or in the treatment duration, could lead to a better efficiency and/or durability.

ACKNOWLEDGMENTS

The authors wish to thank the Renofors Company for their technical contribution to this study, supported by the French Ministries of Culture, Research and Transport.

REFERENCES

Andrade, C., Alonso, M.C. & Molina, F.J. 1993, 'Cover cracking as a function of bar corrosion: Part I - Experimental test', *Materials and Structures*, Vol. 26, pp. 453-464.

Andrade, C. & Alonso, A. 2004, 'Test method for on-site corrosion rate measurement of steel reinforcement in concrete by means of the polarization resistance method', RILEM TC 154-EMC, *Materials and Structures*, Vol. 37, pp. 623-643.

Banfill, P.F.G. 1997, 'Re-alkalisation of carbonated concrete-effect on concrete properties', *Construction and Building Materials*, Vol. 11, pp. 255-258.

Bertolini, L., Carsana, M. & Redaelli, E. 2008, 'Conservation of historical reinforced structures damaged by carbonation induced corrosion by means of electrochemical realkalisation', *Journal of Cultural Heritage*, Vol. 9, pp. 376-385.

Bertolini, L., Pedeferri, P., Redaelli, E. & Pastore, T. 2003, 'Repassivation of steel in carbonated concrete induced by cathodic protection', *Materials and Corrosion*, Vol. 54, pp. 163-175.

Broomfield, J.P. 1997, '*Corrosion of steel in concrete, understanding, investigation and repair'*, E&FN SPON, ISBN 0-419-19630-7.

Cailleux, E. & Marie-Victoire, E. 2006, 'Influence of the concrete composition on the efficiency and the durability of realkalisation treatment', Proc. 2nd inter. Conf. on concrete repair, Saint-Malo, France, pp. 271-279.

Cailleux, E., Marie-Victoire, E., Texier, A.& Al. 2003, Experimental investigation of realkalisation treatments used for restoration of historical monuments made of reinforced concrete, Proc. 1st inter. conference on concrete repair, Saint-Malo, France, pp. 527-534.

Elsener, B., Zimmermann, L., Bürchler D., & Böhni, H. 1997, 'Repair of reinforced concrete structures by electrochemical techniques – field experience', Eurocorr'97, Trondheim, Norway, eds Mietz, J., Elsener, B. & Polder, R., European federation of corrosion publications, n° 25, pp. 125-140.

Elsener, B., 2003, Rilem TC 154-EMC: Electrochemical Techniques for Measuring Metallic Corrosion. Recommendations, *Half-cell potential measurements-Potential mapping on reinforced concrete structures*, Materials and Structures, Vol. 36, pp. 461-471.

FD CEN/TS 14038-1 2005, *Electrochemical realkalisation and chloride extraction treatments for reinforced concrete – Part I Realkalisation*.

Gonzalez, J.A., Cobo, A., Gonzalez, M.N. & al. 2000, 'On the effectiveness of realkalisation as a rehabilitation method for corroded reinforced concrete structures', *Materials and corrosion*, Vol. 51, pp. 97-103.

Mattila, J.S., Pentti, M.J. & Raiski, T.A. 1996, 'Durability of electrochemically realkalised concrete structures', Proc. 4th inter. Symp. Corrosion of reinforcement in concrete construction, Robinson college, Cambridge, United Kingdom, pp. 481-490.

Martinez, I., Andrade, C., Rebolledo, N., Bouteiller, V., Marie-Victoire E. and Olivier, G. 2008, 'Corrosion characterization of reinforced concrete slabs with different devices' The Journal of Science and Engineering Corrosion, Vol. 64 n°2, pp. 107-123

Mietz, J. 1995, 'Electrochemical realkalisation for rehabilitation of reinforced concrete structures', *Materials and corrosion*, Vol.46, pp. 527-533.

Mietz, J. 1998, 'Electrochemical rehabilitation methods for reinforced concrete structures – a state of the art report', European Federation of Corrosion Publication, number 24, IOM Communications Ltd, London, pp. 1-57.

Odden, L. 1994, 'The repassivating effect of electro-chemical realkalisation and chloride extraction', in Corrosion and corrosion protection of steel in concrete, eds R. Naryan Swamy, Sheffield Academic Press, Vol. II, pp. 1473-1488.

Pollet, V., Guerin, R., Tourneur, C., Mahouche, H.& Raharinaivo, A. 1997, 'Concrete realkalisation using sacrificial anodes', Proc. Eurocorr'97, Trondheim, Norway, pp. 523-528.

Räsänen, V., Penttala, V. 2004, 'The pH measurment of concrete and smoothing mortar using a concrete powder suspension', Cem. Conc. Res., 34, pp. 813-820

Sergi, G., Walker, R.J. & Page, C.L. 1996, 'Mechanisms and criteria for the realkalisation of concrete', Proc. 4th inter. Symp. on corrosion of reinforcement in concrete constructions, Cambridge, United Kingdom, pp. 491-500.

Stern, M. & Geary, A.L. 1957, 'Electrochemical polarisation, a theoretical analysis of the shape of polarization curves', *J. Electrochem. Soc.* 104, pp. 56–63.

Tong, Y.Y., Bouteiller, V., Marie-Victoire, E. & Joiret, S. 2008, 'Durability of a realkalisation treatment using impressed current', Proc. 11th Intern. Conf. on Durability of Buildings Materials and Components, Istanbul, Turkey, pp. 1751-1762.

Van den Hondel, A.W.M. & Nebest, B.V. 1998, Laboratory investigation of electrochemical realkalisation of reinforcement concrete, Proc. Eurocorr'98, Utrecht, The Netherlands.

Yeih, W., Chang, J.J. 2005, 'A study on the efficiency of electrochemical realkalisation of carbonated concrete', *Construction and Building Materials*, Vol. 19, pp. 516-524.

XII DBMC
International Conference on Durability of Building Materials and Components
PORTO - PORTUGAL, April 12th-15th, 2011

A Residual Service Life Assessment Tool for New Zealand

Nick Marston [1]
Shashi Vohora [2]
Mark Jones [3]

ABSTRACT

Practitioners (especially Building Officials, Builders and their trainers) require reliable information on in-service materials, and methods by which their remaining lives can be determined. Similarly, building research organisations require a consistent framework to assess materials in-service. Hence, the primary objective of this research is the creation of a broadly-applicable tool to guide the day-to-day decisions of building industry practitioners concerning the residual service life of buildings and building elements. This envisioned assessment tool will involve a simple deterministic estimate involving visual correlation of the condition of a component, or its defects, with an atlas of case study photographs. Although there are only a limited number of cases where degradation correlates with differentiated visual signs of distress in a predictable time sequence, the tool will provide useful and specific information to the end-user for a number of key building components. Ultimately the tool may be offered in a downloadable format from the internet or be accessible on handheld devices such as smart phones.

KEYWORDS

Residual Service Life, Assessment methods, Assessment tool.

[1] BRANZ Ltd, Judgeford, Porirua City, Wellington, New Zealand, Nick.Marston@branz.co.nz
[2] BRANZ Ltd, Judgeford, Porirua City, Wellington, New Zealand, Shashi.Vohora@branz.co.nz
[3] BRANZ Ltd, Judgeford, Porirua City, Wellington, New Zealand, Mark.Jones@branz.co.nz

1 INTRODUCTION

ISO 15686 defines "Service Life" as the "period of time after installation during which a building or its parts meets or exceeds the performance requirements" and "Residual Service Life" has been defined as the "service life remaining at certain period of consideration".
Hence, a residual service life (RSL) prediction for a building is an estimation of the remaining period of time during which the building or its parts will meet or exceed the performance requirements at any given point in time.

Examination of the literature suggests that models for estimating Residual Service Life fall into two broad approaches:

- Models based on assessing the degradation of building elements (e.g. EPIQR & Medic);
- Models based on assessing loss of functional capability (particularly the ISO 15686 suite of standards;

The ISO 15686 'factor method' is widely-accepted and has considerable momentum in Europe. This provides a deterministic approach to service life prediction, based on declaration of a reference life for a particular building component under a carefully prescribed set of conditions, plus a series of 'factors' (simple multiplicative modifiers) that permit estimation of service lives for the same component under other conditions. The factors account for variations in indoor and outdoor climate, workmanship, maintenance, design execution and in-service loading.

However, accurate quantification of the factors requires considerable expertise and experience and, despite the simple approach, considerable thought and work is necessary to derive conclusions from this approach. It is not well-suited to application by end-users.

The EPIQR/MEDIC type models answer typical questions on how to improve specific buildings, necessitating knowledge of past and future building states. These are typically expressed as probabilities of building elements transitioning from one condition to another in a given environment. Often a Markovian model is adopted to provide a sound mathematical basis for the manipulation of transition matrices describing these probabilities. This approach implies reasonably extensive and sophisticated databases and periodic re- inspection; most of the existing tools have been outside New Zealand and would require adaption to local conditions and associated verification.

A Centre Scientifique et Technique du Batiment initiative called EVA -DDVie, the 'Reference Service Life Evaluation Platform', aims to provide a central database of the service life of building materials and components. This appears to be garnering European support, particularly amongst CIBW080 members.

EVA-DDVie is an online implementation of the 'factor method' from ISO 15686 Part 8 'Reference Service Life and Service-Life Estimation'. The database, with an interim English version is intended to serve as a bridge between users, who need the estimated service life data, and the durability specialists providing the reference service life declarations. The creators expect the database will be voluntarily populated by interested participants, bringing together the experience of designers, observations from condition assessments, manufacturers' performance declarations and data from auxiliary research. A French PREBAT (Research and Experimentation on Energy in the Building) sponsored programme with multiple service providers also aims to develop data for 10 different building components within the next two years.

To practically make an estimate of the residual service life of building components in the field; photographs of degradation condition scales, in a predictable time sequence for commonly encountered components could be established and expanded as and when new components were encountered. This approach could also facilitate the identification of common defects or material degradation mechanisms by less experienced practitioners.

2 BRANZ RESIDUAL SERVICE LIFE TOOL

In light of the above, the Residual Service Life tool is an initiative to develop a broadly-applicable tool guiding the day-to-day decisions of building industry practitioners concerning residual service life of buildings and building elements. In essence, it involves the compilation of a database of authoritative and independent component condition information that covers the building components and materials commonly used in New Zealand residential construction. Ultimately it is anticipated that this will be delivered as an interactive web-based tool.

The delivered tool is intended to be helpful to people with a wide range of knowledge and experience. Envisaged users include designers, statutory bodies, manufacturers and wholesalers, in addition to building science researchers, building officials, builders and their trainers.

2.1 Expected Outcomes

The Residual Service Life Tool is expected to provide the following benefits:

- Documentation of methods for assessing residual service life. It is anticipated that information will be collected and stored using a wiki-like knowledge management system;
- A web-accessible tool for determining residual service life comprising assessment methodologies and photographic illustrations, which may also be downloaded or accessed on handheld devices ('smart phones', tablet PCs etc);
- A catalogue of existing residual service life information, including précis of, and references to, current New Zealand Building Code Acceptable Solutions;
- Condition assessments to be carried out on site allowing Auditors to use photographs from the site to compare with condition scales in the office;
- Condition scales for commonly encountered components established and expanded as and when new components were encountered. Differing components constructed of the same material should follow similar patterns for given conditions;
- An explicit mapping of gaps in residual service life knowledge for current building materials and environments of use, serving to focus the direction of future research.

On a broader theme, the hope is to provide the industry with the appropriate knowledge, tools and confidence to reliably identify defects and make sensible decisions on the retention or replacement of building components and materials.

3 METHOD

Buildings deteriorate with age and old designs may not match well with modern functional requirements. Consequently, cost-effective practices need to be developed for considering maintenance and refurbishment strategies. Understanding the Residual Service Life of existing building elements & components is an essential facet of evaluating said strategies.

The aim of the first stage of the Residual Service Life database project was the development of a detailed project brief through stakeholder meetings. The project brief needed to include agreement on

- Scope
- Knowledge transfer requirements
- Alignment of methodology with needs of house condition surveying

Contact was established with a panel of contributors made up of practitioners and other stakeholders. The panel encompassed the diversity of needs and interests in the New Zealand building industry.

The selected stakeholders were informed of the approach BRANZ considered appropriate to adopt in the development of the Residual Service Life database and input was invited and encouraged. Responses received from stakeholders are tabulated in Table 1.

Table 1. Responses received from contributors made up of practitioners and other stakeholders encompassing the diversity of needs and interests in the New Zealand building industry.

Stakeholder	**Key responses received**
Researchers	creation of better understanding and reliable knowledge
Academics	transmission of knowledge to the work place
Professionals	application of established knowledge
Tradesmen	definitive guidelines for their everyday practice
Policy makers	acceptability and enforcement of regulations
Regulators	more definitive standards and protocols
Recyclers	wanted information of feasibility of recycling

3.1 Analysis of Comments

From analysis of the comments and input received it was concluded that there was strong support for the establishment of a Residual Service Life database. Many stakeholders volunteered their active participation in progressing the project.

The "buy –in" demonstrated by the stakeholders indicated that it was appropriate to progress to the next stage of the project, the development of an interactive web-based tool for residual service life.

3.2 Design

Various web-site design options were investigated and trialed. The current developmental framework of the tool for presentation of reference images utilises the Wordpress publishing platform. Example pages are shown in Figures 1 and 2.

Figure 1 shows the entry level of the tool. This level is intended to prompt the user to first select the material of interest from the list in the left hand column.

Once a material of interest has been selected the images displayed to exemplify defect types and degree can be further refined by the selection of multiple material types (as shown in Figure 2). This returns items that comprise both materials, for example defects related to painted timber.

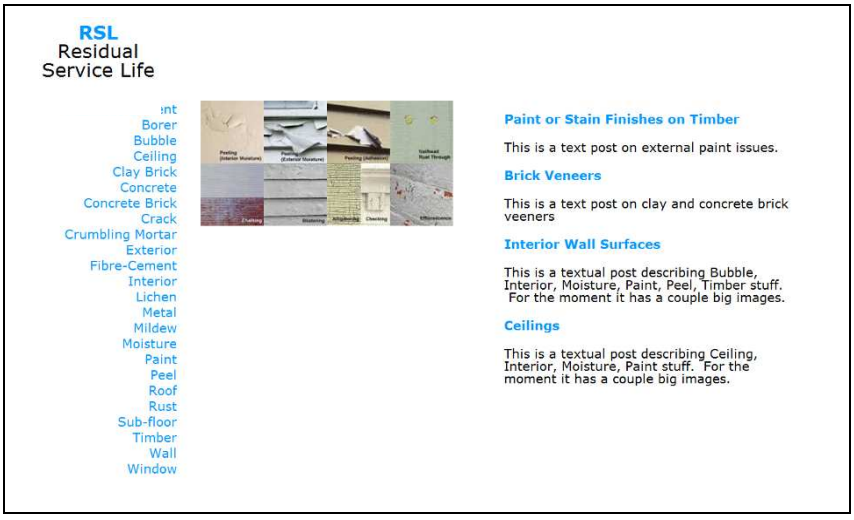

Figure 1. The current concept for the first level of the RSL tool prompts the user to select the material of interest.

Figure 3 shows the content manager interface of the tool. This 'dashboard' allows images to be tagged with applicable material types and this, in turn, controls which material categories they will be displayed under.

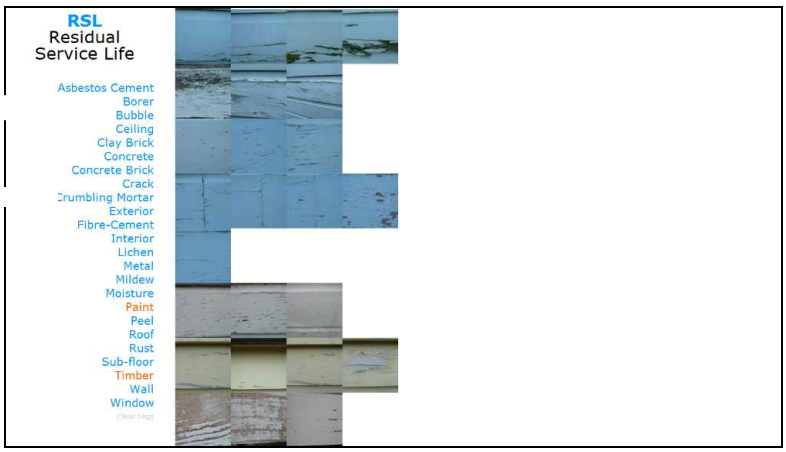

Figure 2. The current configuration of the RSL tool also allows the user to choose multiple material types. This returns items that comprise both materials, for example painted timber.

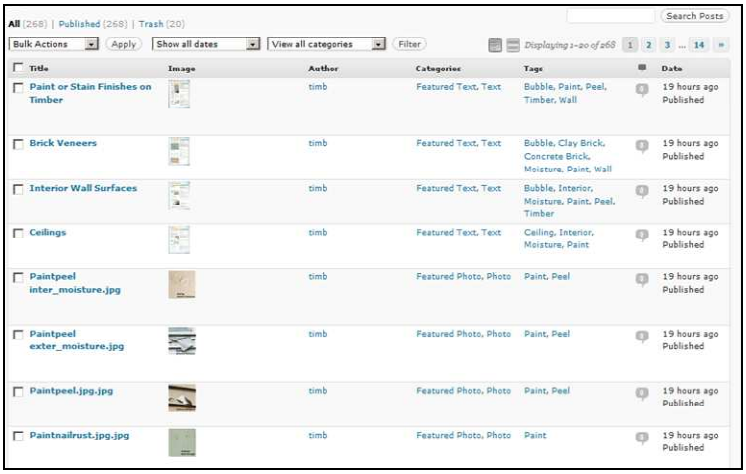

Figure 3. The image management system underpinning the current Residual Service Life development tool allows images to be tagged with applicable material types.

3.3 Project Status

With the preliminary design concept developed, current effort at BRANZ is focussed on populating the database with sufficient information to allow the most pressing gaps in current residual service life knowledge to be identified and prioritised. A working prototype of the interactive web tool is currently in development for distribution to interested parties to solicit the feedback necessary to evolve improvements in the interface and functionality.

4 CONCLUSIONS

The proposed assessment of Residual Service Life of a building element / component is a simple deterministic estimate, based upon visual recognition of correlation with an atlas of case study photographs. A number of technical risks have been identified in adopting this approach:

- Visual appearance may not be diagnostic of the cause of component / element distress;
- Only a limited number of cases exist where degradation correlates with differentiated visual signs of distress in a predictable time sequence;

- The history of a component (environmental exposure, workmanship, maintenance, design execution, and in-service loading) cannot be accounted for in estimation of remaining life despite their critical nature;
- Calibration of probability / time for transition of component from one condition state to the next (i.e. the residual life) is uncertain and component dependent;
- Approach has the potential to focus attention on individual components at the expense of a holistic approach that considers durability of assemblages;
- Misplaced confidence in guidance provided by the tool may discourage more thorough investigation and testing.

However, the positive feedback, offers of participation from stakeholders in this research and the work completed to date suggest that:

- It is practical to document the progress of some material failures to allow both early identification of defects and to offer insight into material degradation with time;
- Practitioners sometimes need assistance in identifying building materials, particularly when looking at older or discontinued products;
- The tool offers a route to access experts knowledge of material failures;
- The tool answers a genuine end-user need;
- With care and end user engagement the guidance provided will be both useful and robust.

ACKNOWLEDGMENTS

This work was supported by New Zealand Building Research Levy.

REFERENCES

http://blpinsurance.com/cdd/component-list.asp

A Durability Assessment Tool for the New Zealand Building Code, Lee *et al.,* 11DBMC International Conference on Durability of Building Materials and Components, ISTANBUL - TURKEY May 11-14th, 2008.

Building Industry Authority. 1992. *The New Zealand Building Code Handbook and Approved Documents*. Standards New Zealand, Wellington, New Zealand.

http://www.cstb.fr/actualites/webzine/editions/edition-de-juin-2009/evaluer-la-performance-des-produits-au-fil-du-temps.html

J-L Genre, F. Flourentzou, A. Faist, EPIQR a new refurbishment concept, Second European Conference: Energy Performance and Indoor Climate in Buildings (EPIC), Lyon November, 19-21 1998.

Flourentzou F., Genre J-L, Faist A., MEDIC: prediction method of probable deterioration scenarios and refurbishment investment budgets, EPIC conference, Lyon 1998.

International Organisation for Standards. 2000. *ISO 15686-1 Buildings and constructed assets – Service life planning – Part 1: General principles*. ISO Geneva, Switzerland.

http://www.prebat.net/

http://www.prres.net/Papers/Shah_Challenges_In_Residual_Service_Life.Pdf

XII DBMC
International Conference on Durability of Building Materials and Components
PORTO - PORTUGAL, April 12th-15th, 2011

Electrical Resistivity as a Means of Quality Control of Concrete – Influence of Test Procedure

Paula Cristina Silva [1]
Rui Miguel Ferreira [2]
Helena Figueiras [3]

ABSTRACT

The quality control of concrete, normally associated with the verification of the conformity of the mechanical and durability characteristics, usually requires lengthily procedures for the conditioning and preparation of the specimens, after which the specimen is typically destroyed while being tested.

In this paper, a part of the results of an ongoing research on the relationship between electrical resistivity measurements of concrete and other characteristics, such as the compressive strength.

The influence of several parameters on the relationship is taken into consideration, such as, different curing conditions of the concrete specimens, i.e., temperature, relative humidity, reading temperature, and the maturity of concrete. Another goal of the research is to establish a laboratorial procedure for the quality control of concrete enabling the NDT of several concrete characteristics based on electrical resistivity measurements.

Preliminary results demonstrate a good correlation between electrical resistivity and other characteristics of concrete. Different techniques on measurements on electrical resistivity are presented.

KEYWORDS

Electrical resistivity, Compressive strength, Quality control, Durability, NDT.

[1] Faculty of Engineering of the University of Porto (FEUP), Porto, PORTUGAL, pcsilva@fe.up.pt
[2] Territory, Environment and Construction Centre (C-TAC) of the University of Minho, Guimarães, PORTUGAL, rmf@civil.uminho.pt
[3] Faculty of Engineering of the University of Porto (FEUP), Porto, PORTUGAL, hfig@fe.up.pt

1 INTRODUCTION

The quality control of concrete, normally associated with the verification of the conformity of the mechanical and durability characteristics, usually requires lengthily procedures for the conditioning and preparation of the specimens, after which the specimen is typically destroyed while being tested. As in the case of compressive strength, testing is typically performed on standardized specimens at the age of 28 days. To keep up with the fast pace of construction, early age specimens are tested to obtain some insight as to what the 28-day compressive strength of concrete might be. Often there is no precise knowledge of the quality of the concrete, i.e. strength and durability performance. The influence of the environment on curing and concrete maturity is usually not considered.

In an attempt to ensure better construction quality and durability, there has been an increasing focus in recent years on the development of a better basis for performance-based quality control for concrete quality during concrete construction [[Gjørv 2004]; [Silva *et al.* 2006]; [Andrade 2004]]. One of the NDT commonly suggested in performance-based quality control programs is that of electrical resistivity (ER) [Ferreira & Jalali 2010].

The ER of concrete can be measured by several means [Polder *et al.* 2000]. Typically, electrodes are placed on the surface and the resistance is measured. From the cell geometry, the resistivity can be calculated. The resistivity is often related to corrosion and protection of steel reinforcement and to durability performance of concrete [[Sengul & Gjørv 2008]; [Ferreira & Jalali 2010]].

In concrete, the current flows through the pore liquid in the cement paste. Aggregate can be considered essentially inert. As a result, concrete is not a homogeneous conductor and the flow of measuring current will be heterogeneous. Concrete ER is a geometry-independent material property that describes the electrical resistance, i.e., the ratio between applied voltage and resulting current in unit cell geometry.

2 ELECTRICAL RESISTIVITY

The ER of concrete is related to the microstructure of the cement matrix, its pore structure, porosity, and pore size distribution. These characteristics are controlled by the degree of hydration of cement paste in concrete. As a result, ER of concrete will increase with time. One of the factors that control these features is the hydratation degree of the cement paste of concrete, thus resulting in an increase of ER with time. Others influential factors are the relative humidity, the concrete temperature, and the ions concentration and their mobility in the pore solution [Polder 2001]. Cement chemistry, cement content, water-cement ratio, and use of admixtures and supplementary cementations materials are factors which influence the microstructure of concrete as well as the pore solution chemistry, and therefore influence its ER [Ferreira & Jalali 2010].

ER can gauge the quality and durability performance of concrete. The ER of concrete may vary over a wide range, from 10^1 Ωm to 10^5 Ωm, influenced by the moisture content of the concrete (direct relation to the environment), the temperature and concrete quality (composition, cement type, etc.) [[Silva *et al.* 2006]; [Andrade 2004]; [Polder *et al.* 2000]].

In practice, the ER measurement of concrete is used mainly as an indicator of reinforcement corrosion activity. It plays a significant role in controlling the reinforcement corrosion rate. The higher the resistivity, the lower is corrosion current passing between anodic and cathodic areas of the reinforcing steel [[Gowers & Millard 1999]; [Broomfield 1997].

However, ER is directly related to durability performance parameters based on the theoretical background of the phenomena. For example, with regards to the diffusion coefficient of concrete, the Nernst-Einstein equation can be used [[Pruckner 2001]; [Andrade *et al.* 2007]]. In addition, research has shown correlations between the electrical resistivity and the durability performance parameters of a given concrete [[Silva *et al.* 2006]; [Ferreira 2000]; [Sengul & Gjørv 2008]].

There are several test methods to measure the ER of concrete that can differ in the type of applied current (alternating current (AC) and direct current (DC)) and electrode configuration used. According to Polder [2001], the measurement of ER in the concrete must be carried out using AC. The use of a DC equipment is not advisable because of the effect of inducing the electrodes polarization, resulting in significant errors [Polder et al 2001]. In this research two test method where used: the two plate electrode method applying AC and DC and the four-point electrode (Wenner) applying AC. A brief description follows of the test procedures used are described in the following paragraphs.

2.1 Two-Plate Electrode Method

The test procedure was performed at the LABEST-FEUP, and is based in the procedure propose by Polder [2001]. During testing, a low frequency electrical current passes between the two electrodes (passing through the entire specimen) while the voltage drop is measured. For AC measurements it was used a wave generate of brand mark Tektronic (model CFG253), and the power source for DC measurements is an Univolt equipment (model DT305TD). For both types of measuring AC and DC, was used a multimeter with high accuracy KEITHLEY (model 2000).

Specimens were removed from the curing conditions only a few moments before the test start. Each specimen was wiped with a damp cloth to remove excess surface water. To ensure good electrical contact between the specimen and electrodes (stainless steel plate with 1.95 mm thick) a wet sponge were placed and a force was applied to maintain a constant and uniform stress distribution over the entire face of the specimen. First measurements is performed on AC and then on DC current. **Figure 1** show, the test set-up used to ER measurements using the two-plate electrode method (AC and DC) on standard cubic and cylindric specimens.



Figure 1. Test layout of the two-plate electrode method for ER measurements the ER on cubes (left) and cylinders (right).

A preliminary study was undertaken to evaluate what type of wave frequency should be used in AC measurements. In this case, results showed that the sinusoidal current wave with a frequency of 10 kHz, had the best performance with good reproducibility to characterized the concrete. The electrical resistivity measurements using the technique of two-plate electrode method is obtained from the average of two measurements.

2.2 Four-point Electrode Method

The four-point electrode method is currently the most widely used technique for field concrete resistivity measurements. During testing, a low frequency AC current is applied between the two outer electrodes while the voltage drop is measured in the two inner electrodes. In this research, the ER measurements were performed with a commercially available four-point resistivity meter (Canin, Proceq).
The resistivity meter, with fixed electrode spacing of 50 mm, uses an AC with a frequency of 72 Hz, an impedance of 10 MΩ, a measuring range from 0 to 99±1 kΩ.cm. The apparent ER determined by the equipment is obtained from Eq. **(1)** considered valid for a homogeneous semi-finite volume of the material.

$$\rho = 2\pi aU/I \quad (1)$$

where ρ is the electrical resistivity (Ω.m), a is electrode spacing (m), U is voltage drop (V), and I is the current (A).

ER measurements on cubic specimens (150 mm) are performed on opposing surfaces, and in perpendicular directions on each surface. The average resistivity is obtained from six measurements taken on each side. The measurement of ER in cylindrical specimens (ϕ150 mm x 300 mm) are made in groups of two (performed in opposing directions), 120º apart on the surface of the specimen. The ER value represents an average of 6 readings. In **Figure 2**, the measurement procedure can be observed for both cubic and cylindrical specimens.

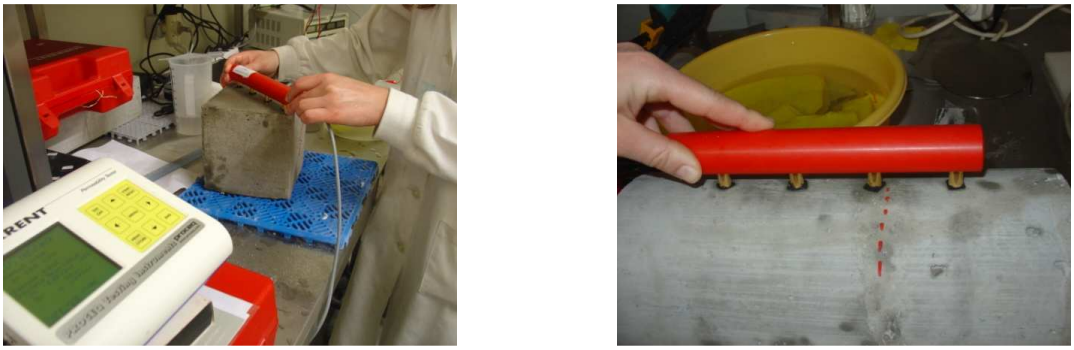

Figure 2. Performing four-point electrode method ER measurments on cubic (left) and cylindrical (right) specimens.

There are several factors that influence the resistivity measurement when the four-probe technique is used. These factors include 1) geometrical constraints, 2) surface contact, 3) concrete inhomogeneity, 4) presence of steel reinforcing bars, and 5) surface layers having different resistivity than the bulk of the concrete. These factors have been thoroughly investigated [[Gowers and Millard 1999]; [Whiting and Nagi 2003]; [Polder *et al.* 2001]; [Sengul and Gjørv, 2008]].

3 EXPERIMENTAL WORKS

The main goal of this research is to establish a laboratorial procedure for the quality control of concrete enabling the NDT of several concrete characteristics based on the ER measurements. To fulfill this goal, a comprehension of the relationship between ER and the mechanical and durability performance concrete characteristics, and the influence of external factors, is required. In this paper, only the influence of the external factors, namely temperature, relative humidity, test procedure and specimen type, on the relationship between ER and compressive strength is presented.

Several self-compacting concrete (SCC) specimens (150 mm cubes and ϕ150 mm x 300 mm cylinders) where concreted and cured in different conditions: in water at 30 °C, 20 ºC and 5 ºC, and in a climate chamber with 20 °C and 50 % RH. Three different measurements where performed on the specimens: two-plate electrode measurement with AC and DC, and four-point electrode measurements. Measurements have been performed on the concrete specimens at regular intervals starting with 24 hours up to 90/180 days.

3.1 Materials, Mix Design and Curing

In this study, a SCC mix was prepared with Portland cement (CEM I 42.5R) and limestone filler with a specific gravity of 3.11 and 2.68, respectively. The mean particle size of cement and limestone filler was 14.61 and 6.53 μm, respectively. A polycarboxylate type superplasticizer (Sika Viscocrete 3006) was used with a specific gravity of 1.05 and 18% solid content. Crushed granitic aggregate (2.36-12.5

mm), a siliceous natural fine sand (sand 1) with a fineness modulus of 2.47 and natural coarse sand (sand 2) with a fineness modulus of 2.87 were used (see Table 1). The specific gravity of the coarse aggregate, sand 1 and sand 2 were 2.64**,** 2.62 and 2.63, and absorption values were 1.15%, 0.40% and 0.20%, respectively. The composition of self- compacting concrete mix is given in Table 1**.**

The mixes were prepared in the laboratory in an open pan mixer in 50 liters batches. The mixing sequence consisted of mixing the sands and coarse aggregate with ¼ of water content during 2.5 minutes, waiting 2.5 minutes for absorption, addition of powder materials, addition of the rest of the water with superplasticizer and finally mixing concrete during 8 minutes.

After mixing, the fresh state of the concrete mixes was characterized with the following tests: Slump flow test (pr EN 12350-8), the V-funnel test (pr EN 12350-9), the L-Box test (pr EN 12350-10), and the segregation test (pr EN 12350-11). The average results obtained in each of the mixtures are presented in Table 2.

Table 1. Constituent materials.

Concrete mixture	(kg/m^3)
Cement (CEM I 42,5R)	407
Limestone filler	186
Sand 1	422
Sand 2	327
Course aggregate	823
Water	159
Superplasticizer (liquid)	7.7
water/cement	0.41
water/binder	0.28

Table 2. Fresh concrete test results.

D flow (mm, s)	735 (class SF2)
T50 (sec.)	2.6 (class SF2)
Tfunnel (sec.)	10.4 (class VF2)
L-Box	0.8 (class PA1)
Segregation resistance (%)	5.3 (class SR1)

After fresh concrete tests a series of 150 mm cubes as well as 150 mm x 300 mm cylinders were molded. All test specimens were demoulded one day after casting and immediately placed in the respective curing conditions: immersed in water at 30 °C, 20 ºC and 5 ºC; and in a climate chamber with 20 °C and 50 % RH.

4 RESULTS AND DISCUSSION

4.1 Influence of Specimen Type, Curing and Test Procedure on ER Measurements

Figure 3 presents the evolution of ER measurements with time performed on cylindrical (1, 3, 8, 15, 22, 29 and 91 days) and cubes (1, 3, 8, 29, 91 days) specimens, with the 4-point electrode method, for the different curing conditions. As expected the resistivity will increase (with time) because as the hydration reactions are occurring the concrete microstructure becomes more dense. Until 28 days the resistivity evolution is similar for all types of envoirements. After 28 days of age, cylinders placed in the environment of 20º C and 50% humidity, unlike the cylinders placed in other environments, have a great evolution of the resistivity, which may be related to some loss of moisture from the speciments.

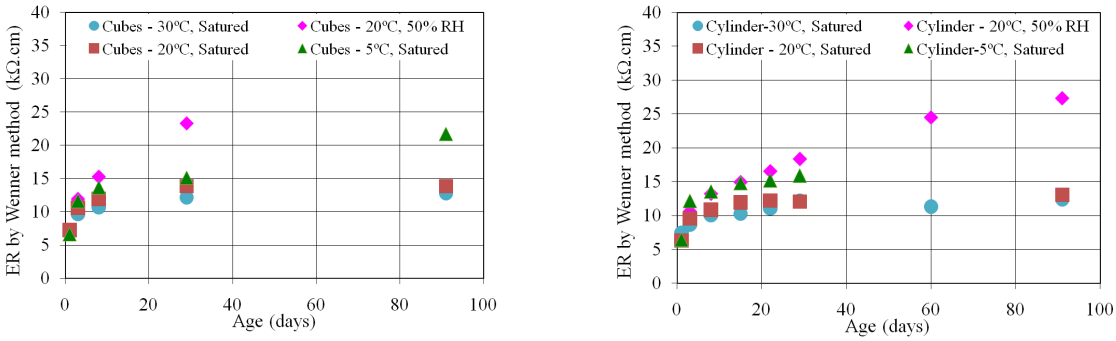

Figure 3. 4-point electrode ER measurements on cubic (left) and cylindrical specimens (rigth).

From **Figure 3** it is observed that the specimen geometry plays important role in the measurement of the ER. In this experimental program, and for the SCC used, it was observed that in the cubic specimens have higher ER compared with cylindrical specimens. A few exceptions exist such as the measurement of ER at 24 hours (not yet subject to different curing conditions). This is in agreement with research by Ferreira and Jalali [2010] and Sengul and Gjørv [2008]. These results can be justified by the boundary conditions of the specimens examined, for example, the spacing between the electrodes (e = 50 mm) and the geometrical particularities of the test method setup.

In the Figure 4, the relationship between ER obtained by four-point electrode method measurements and the technique by two-point electrode method (AC / DC), is presented.
Independently of the curing performed, there seems to be a consistent relationship between different ER measurement methods (lowest $R^2 > 0.9$). This is expected as the ER methods are influenced by the same factors (microstructure, etc.), the difference being arising from the different geometrical particularities of teach test method. Analyzing the results obtained using different techniques, by Wenner method and the measurement of two-plate electrode method (AC/DC), we conclude that the measurement of electrical resistivity using the technique of four-point (Wenner method) is highest around 45.7% (AC) and 36.1% (DC) measured in cubic specimens. The same trend is observed in cylindrical specimens, the measurement with the Wenner method is higher about 67% (AC) and 55% (DC).

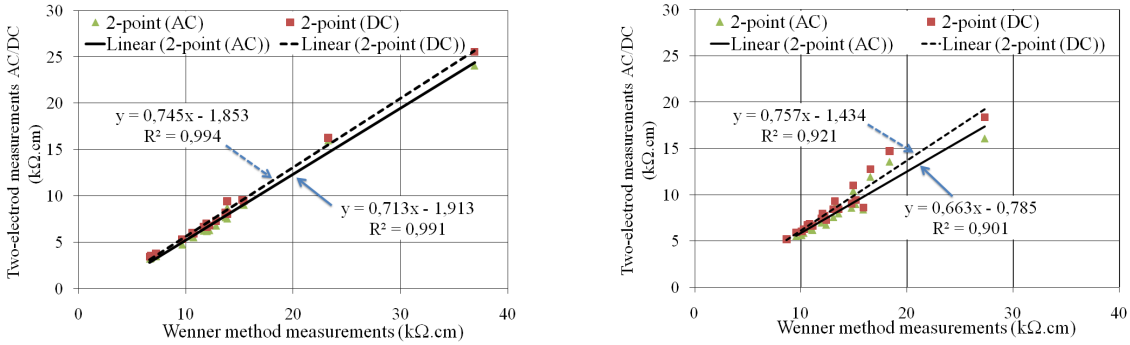

Figure 4. Relationship between ER obtained by Wenner method and two-plate electrode method (AC/DC), on cubic (left) and cylindrical (right).

The correlations on ER between the two point measurements and technique of the 4-point (Wenner method), obtained from cubic specimens of 150 mm edge were as follows: AC measurements (R^2= 0991), on DC (R^2 = 0994). In cylindrical specimens of 150 x 300 mm, the correlations obtained were as follows: measurements in AC (R^2 = 0.901) and DC (R^2 = 0.921).
With these results, it can be concluded that the correlations obtained by different assay techniques are satisfactory. It is observed that the ER measurements obtained by four-point electrode method are higher than those of the of two-plate electrode method (AC and DC).

In addition, in this work concludes that there a good relationship between ER measurements with AC and DC, for cubic (R^2=0.999) and cylindrical specimens was obtained (R^2=0.994), but measuring alternating current (AC) is lower than the measurement of electrical resistivity in DC. The ER (two-plate electrode method) measurement performed on cubic and cylindric specimens with alternating current (AC) is lower comparatively with DC measurements, about 7.17% on cubes and 6.71% on cylindric specimens.

4.2 Influence of curing on the correlation between ER and compressive strength

The average compressive strength was obtained from three 150 mm cubes tested in a Load Frame – MTS. The results of compressive strength test and ER measurements (4-point electrode), for different curing conditions, are presented in Table 3.

The correlation between compression strength and ER measurements are: 0.901 for speciments cured at 30ºC and saturated envoirement, 0.871 for speciments cured at 20ºC and saturated envoirement, 0.871 for speciments cured in climate chamber at 30ºC and 50% humidity and for speciments cured at 5ºC in a saturated envoirement the correlation coeficient was 0.932.

Table 3. Development of compressive strength and electrical resistivity (4-point electrode) with time.

	Curing conditions (cubes)							
	30ºC, Saturated		20ºC, 50 % RH		20ºC, Saturated		5ºC, Saturated	
t (days)	f_{cm}(MPa)	ρ_W(kΩ.cm)	f_{cm}(MPa)	ρ_W(kΩ.cm)	f_{cm}(MPa)	ρ_W(kΩ.cm)	f_{cm}(MPa)	ρ_W(kΩ.cm)
1	48.757	7.207	46.399	6.750	45.097	7.242	44.595	6.648
3	60.879	9.667	63.771	11.917	59.319	10.602	52.425	11.667
8	73.185	10.722	63.608	15.250	62.868	11.972	62.883	13.700
29	72.028	12.194	72.604	23.278	64.930	13.859	68.376	15.414
91	75.143	12.821	76.951	36.917	76.122	13.854	73.360	21.755
	(R^2 = 0.901)		(R^2 = 0.788)		(R^2 = 0. 871)		(R^2 = 0.932)	

The correlations between the compressive strength and electrical resistivity are very satisfactory, except for samples placed in a climatic chamber, 20 °C, 50% RH (R^2=0.788). As the humidity decreases, decreases the amount of water present in pores that carries the current, thus increasing the resistivity. Although the cement matrix still contains enough water for this relative humidity, the one that ends up trapped in the pores have a non-conducting behaviour.

The temperature plays an important role in the electrical resistivity, since the mobility of ions in the pores solution is largely affected by this parameter. In the Table 3 you can see that, for the same age, as the temperature increased (for a constant relative humidity) decreases the electrical resistivity.

5 CONCLUSIONS

Comparing the ER measurement performed with the Wenner method and the two-plate electrode method (AC/DC), it is observed that using the 4-point technique is obtained higher values than using 2 points technique. The technique of two-plate electrode method (AC/DC) show a good correlation. The evolution of electrical resistivity (NDT) presents an evolution identical to the mechanical strength, results demonstrate a good correlation.

The 4-point (Wenner method) is an simple and excellent technique for quality control the measurements of electrical resistivity on concrete.

The electrical resistivity may be an additional element of models for performance and durability of concrete structures, as defined in the project. This parameter can be measured during the construction and operation phase, thus contributing to sustainable development structures, minimizing repairs and maximizing the service life of concrete structures.

ACKNOWLEDGMENTS

The first author would like to thank the LABEST for all the support and contribution for this work.

REFERENCES

Andrade, C., et al, ‘A NDT performance based method based on electrical resistivity for specification of concrete durability’. ECCOMAS Thematic Conference on Computational Methods in Tunnelling (EURO:TUN 2007) J. Eberhardsteiner et.al. (eds.) Vienna, Austria, August 27-29, 2007.

Andrade, C., The limit of service life of concrete structures. (in Spanish) Encontro Nacional Betão Estrutural 2004, FEUP, Porto, 2004, p.1-25.

Broomfield, J.B., Corrosion of Steel in Concrete, FN Spon, an Imprint of Chapman & Hall, London, UK, 1997, 238 pages.

Ferreira, R.M, Jalali, S. 'NDT measurements for the prediction of 28 days compressive strength' in NDT&E International 43, 2010. pp. 55-61.

Ferreira, R.M. 2000: 'Avaliação dos ensaios de durabilidade do betão' Dissertação de Mestrado em Engenharia Civil, Universidade do Minho, Guimarães.

Figueiras, H., Maia L., Nunes, S., Coutinho, J.S., Figueiras, J. 'Optmização de uma argamasada destinada a BAC de elevada durabilidade' bac 2010 - 2.º Congresso Ibérico sobre betão auto-compactável, pp1-10.

Figueiras, H.I.S. 2006: 'Estudo e desenvolvimento experimental de composições de betão auto-compactável: aferição das suas características mecânicas e durabilidade' Dissertação de Mestrado em Estruturas de Engenharia Civil, Faculdade de Engenharia da Universidade do Porto, Porto.

Gjørv , O. E., "Durability Design and Construction Quality of Concrete Structures," Proceedings of 4th International Conference on Concrete Under Severe Conditions-Environment and Loading, B. H. Oh, K. Sakai, O. E. Gj?rv, and N. Banthia, eds., V. 1, Seoul National University and Korea Concrete Institute, Seoul, Korea, 2004, pp. 44-55.

Gowers, K. R., and Millard, S. G., 'Measurement of Concrete Resistivity for Assessment of Corrosion Severity of Steel Using Wenner Technique,' ACI Materials Journal, V. 96, No. 5, Sept.-Oct. 1999, pp. 536-541.

Nokken, M. R., Hooton, R. D.; Using pore parameters to estimate permeability or conductivity of concrete. Materials and Structures (2008) 41:1–16. DOI 10.1617/s11527-006-9212-y

Nunes, S.C.B. 2001:'Betão-auto-compactável: Tecnologia e Propriedades 'Dissertação de Mestrado em Estruturas de Engenharia Civil, Faculdade de Engenharia da Universidade do Porto, Porto.

P.J. Tumidajski, AS. Schumacher, S. Perron, P. Gu and J.J. Beaudoin. On the relationship between porosity and electrical resistivity in cementitous systems. Cement and Concrete Research, Vol. 26, No. 4, pp. 539-544, 1996.

Polder, R. Test methods on site measurement of resistivity of concrete – A RILEM TC-154 technical recommendation. Construction and Building Materials 2001. V(15): 125-131.

Polder, R.; Andrade, C.; Elsener, B.; Vennesland, O.; Gulikers. J.; Weidert, R.; and Raupach, M., 'RILEM TC 154-EMC: Electrochemical Techniques for Measuring Metallic Corrosion,' Materials and Structures, V. 33, 2000, pp. 603-611.

Pruckner, F., 'Corrosion and protection of reinforcement in concrete measurements and interpretation.' Doctoral Thesis, University of Vienna. 2001. 224 p.

Sengul, O., and Gjørv, O. E., 'Electrical Resistivity Measurements for Quality Control During Concrete Construction,' ACI Materials Journal, V. 106, No. 6, Nov-Dec. 2008.

Silva, B.J., Jalali, S., Ferreira, R.M., 'Estimating electrical resistivity based on early age measurements', Pro. Int. RILEM Workshop Performance based evaluation and indicators for concrete durability, Madrid, 2006.
Whiting, D.A., Nagi, M.A.; 'Electrical resistivity of Concrete – Literature review', PCA R&D Serial Nº. 2457, pg.57, 2003.

XII DBMC
International Conference on Durability of Building Materials and Components
PORTO - PORTUGAL, April 12th-15th, 2011

Durability Characteristics of Concrete Containing Supplementary Cementing Materials

Eva Vejmelková[1]
Martin Keppert[2]
Michal Ondráček[3]
Pavla Rovnaníková[4]
Robert Černý[5]

ABSTRACT

Durability characteristics of concrete containing supplementary cementing materials, namely metakaolin, fly ash, ground granulated blast furnace slag and ground brick, in higher amounts are studied. Reference concrete of a corresponding composition is analyzed as well. Basic characterization of the studied materials is performed by the measurement of bulk density, matrix density, open porosity, compressive strength and bending strength. Frost resistance, resistance against de-icing salts and chemical resistance in various environments are determined as the principal parameters characterizing durability of concrete. Experimental results show that the replacement of Portland cement by higher amounts of all applied supplementary cementing materials has a positive effect on their frost resistance and chemical resistance. Metakaolin and ground granulated blast furnace slag are found to increase resistance against de-icing salts but the use of fly ash and ground brick leads to its decrease.

KEYWORDS

Durability properties, Metakaolin, Slag, Fly ash, Ground brick.

[1] Department of Materials Engineering and Chemistry, Faculty of Civil Engineering, Czech Technical University in Prague, Thákurova 7, 166 29 Prague 6, CZECH REPUBLIC, eva.vejmelkova@fsv.cvut.cz
[2] Department of Materials Engineering and Chemistry, Faculty of Civil Engineering, Czech Technical University in Prague, Thákurova 7, 166 29 Prague 6, CZECH REPUBLIC, martin.keppert@fsv.cvut.cz
[3] Institute of Technology of Building Materials and Components, Faculty of Civil Engineering, Brno University of Technology, Veveří 95, 602 00 Brno, CZECH REPUBLIC, ondracek.m@fce.vutbr.cz
[4] Institute of Chemistry, Faculty of Civil Engineering, Brno University of Technology, Veveří 95, 602 00 Brno CZECH REPUBLIC, rovnanikova.p@fce.vutbr.cz
[5] Department of Materials Engineering and Chemistry, Faculty of Civil Engineering, Czech Technical University in Prague, Thákurova 7, 166 29 Prague 6, CZECH REPUBLIC, cernyr@fsv.cvut.cz

1 INTRODUCTION

During the last several decades the environmental aspects of construction began to gain in importance, and the necessity to decrease the amount of carbon dioxide in atmosphere led to considerable efforts aimed at the replacement of at least a part of Portland cement in concrete with environmental more friendly supplementary binders. Waste materials as silica fume [Chung 2002], fly ash [Lammertijn and De Belie 2008], ground granulated blast furnace slag [Chidiac and Panesar 2008] or ground ceramics [Pacheco-Torgal and Jalali 2010] became prospective options in that respect, as well as metakaolin [Kim et al. 2007] which is produced by thermal decomposition of kaolin without production of CO_2. The environmental regulations as for CO_2 production in EU and some other countries, together with their pozzolanic properties made them attractive for producers active in building industry.

In this paper, properties of four different cement based composites containing supplementary cementing materials as partial replacement of Portland cement, the first with ground granulated blast furnace slag, the second with metakaolin, the third with fly ash and the fourth with fine-ground ceramics are investigated in wider extent than it is usual in concrete research. The results are also compared with those obtained for reference material containing only Portland cement as binder.

The main original contribution of the paper consists in providing a complex set of basic physical properties and durability properties of several types of concrete which are more friendly to the environment than common cementitious composites containing just Portland cement as binder. The set of properties including open porosity, bulk density, matrix density, pore distribution, compressive and bending strength, frost-, de-icing-salt- and chemical resistance makes possible to assess the overall qualities of the analyzed types of concrete from the durability point of view which is important for their practical applications in building industry.

2 MATERIALS

The concrete mixes studied in the paper were prepared with Portland cement CEM I 42.5 R (its specific surface area was 341 m^2/kg) as the main binder. A part of cement (20-40% by mass) was replaced by ground granulated blast furnace slag, metakaolin, fly ash produced by burning bituminous coal and fine-ground ceramics. The chemical composition of fine-ground ceramics and slag is shown in Table 1. The specific surface area of fine-ground ceramics was 582 m^2kg^{-1}, for slag it was 380 m^2kg^{-1}. The chemical composition fly ash and of metakaolin is shown in Table 2, the specific surface of metakaolin was 13.06 m^2/g.

Table 1. Chemical composition of fine-ground ceramics and ground granulated blast furnace slag.

Fine-ground ceramics		*Ground granulated blast furnace slag*	
Component	*Amount* [%]	*Component*	*Amount* [%]
SiO_2	63.45	SiO_2	34.74
Al_2O_3	13.98	Al_2O_3	5.91
Fe_2O_3	5.39	Fe_2O_3	0.39
CaO	8.18	CaO	40.27
TiO_2	0.77	MgO	0.405
K_2O	2.43	K_2O	2.43
Na_2O	0.90	Na_2O	0.288
SO_3	0.10	SO_4^{2-}	0.39

The composition of the studied concrete mixes (denoted CM20, CF40, CS40, CB40), which was used in experimental work in this paper is shown in Table 3. For the sake of comparison, also a reference mix CR with only Portland cement as the binder but all other components the same was studied. The total mass of binder in the reference mix was the same as in the other concretes. The amount of water

in the mixes was chosen in such a way that the consistence of fresh mixes would be the same. The consistence was analyzed by the slump test according to [ČSN EN 12350-2 2000], using a conical mould (upper diameter 100 mm, lower diameter 200 mm, height 300 mm). The result of the slump test (in mm) was the difference between the height of the mould and the uppermost point of the specimen after the test. For the amounts of water in Table 3, the slump was for all mixes 130 mm.

Table 2. Chemical composition of metakaolin and fly ash.

Metakaolin		*Fly ash*	
Component	*Amount* [%]	*Component*	*Amount* [%]
SiO_2	21.89	SiO_2	49.82
Al_2O_3	5.60	Al_2O_3	24.67
Fe_2O_3	3.75	Fe_2O_3	7.05
CaO	62.33	CaO	3.91
MgO	1.04	MgO	2.68
K_2O	0.92	K_2O	2.78
Na_2O	0.11	Na_2O	0.70
TiO_2	0.30	SO_3	0.91
P_2O_5	0.17		
SO_3	2.88		

Table 3. Composition of studied concretes [kg m^{-3}].

Component	*CR*	*CM20*	*CS40*	*CF40*	*CB40*
CEM I 42.5 R	484.0	387.0	290	290	290
ground ceramics	-	-		-	194
slag	-	-	194	-	-
metakaolin	-	97	-	-	-
fly ash	-	-	-	194	-
aggregates 0-4 mm	812	812	812	812	812
aggregates 8-16 mm	910	910	910	910	910
plasticizer Mapei Dynamon SX	5.3	5.3	5.3	5.3	5.3
water	160	188	160	182	160

3 EXPERIMENTAL METHODS

3.1 Basic Material Characteristics

As fundamental physical material characteristics, bulk density, open porosity and matrix density were determined using the water vacuum saturation method [Roels et al 2004]. Each sample was dried in a drier to remove majority of the physically bound water. After that the samples were placed into the desiccator with deaired water. During three hours air was evacuated with vacuum pump from the desiccator. The sample was then kept under water not less than 24 hours.

Characterization of pore structure was performed by mercury intrusion porosimetry. The experiments were carried out using the instruments PASCAL 140 and 440 (Thermo Scientific). The range of applied pressure corresponds to pore radius from 2 nm to 2000 μm. Since the size of the specimens is restricted to the volume of approximately 1 cm^3 and the studied materials contained some aggregates about the same size, the porosimetry measurements were performed on samples without coarse aggregates.

The measurement of compressive strength was done by the hydraulic testing device VEB WPM Leipzig having a stiff loading frame with the capacity of 3000 kN. The tests were performed according to [ČSN EN 12390-3 2002] after 28 days of standard curing.

The bending strength was determined using the procedure described in [ČSN EN 12390-5 2007], after 28 days of standard curing as well.

3.2 Durability Tests

Frost resistance tests were carried out according to [ČSN 73 1322/Z1:1968 2003]. The samples were tested after 28 days of standard curing. The total test required 100 freezing and thawing cycles. One cycle consisted of 4 hours freezing at -20°C and 2 hours thawing in 20°C warm water. Frost resistance coefficient *K* was determined as the ratio of bending or compressive strength of specimens subjected to 100 freezing and thawing cycles to the strength of reference specimens which did not undergo the frost resistance test.

The resistance of studied concrete against de-icing salts was measured according to [ČSN 731326/Z1:1984 2003]. The tested specimens were saturated by water and put into a bath with 3% NaCl solution. Then, freeze/thaw cycles were applied. The test was finished after 100 cycles.

The chemical resistance in various environments was tested according to the procedure developed at the Brno University of Technology. The specimens were prepared in 100 × 100 × 400 mm molds and placed into a climatic chamber with 100% relative humidity environment. After 24 hours they were de-molded and stored in the same environment for another 27 days. Then, the specimens were cut to 100 × 100 × 50 mm blocks and put in groups of three into the chemical environments ($MgCl_2$ 17.76 g/L, NH_4Cl 2.97 g/L, Na_2SO_4 14.79 g/L, HCl 10^{-3} mol/L).

One set of specimens was just after the 28-days curing subjected to the compressive-strength test to obtain reference strength value. Test of concrete carbonation was performed in a desiccator where the CO_2 concentration was kept at 65 ± 5 vol.-% (the concentration was measured by an IR probe). The carbonation took place in an environment above saturated KNO_3 solution (85 ± 5% relative humidity). The specimens denoted as “air” were stored in common laboratory conditions at 21 ± 2°C and 45 ± 5% relative humidity; those marked “distilled water” were in distilled-water bath which was replaced every 10 days.

The duration of the chemical resistance test was 60 days. Then, the specimens were subjected to the compressive-strength test. The coefficient of chemical resistance K_{cr} was then determined as the ratio of the compressive strength after 60 days in a specific environment and compressive strength after 60 days in laboratory conditions. All the specimens were water-leached after the compressive-strength test and the pH value was determined by potentiometry.

4 EXPERIMENTAL RESULTS AND DISCUSSION

4.1 Basic Material Characteristics

Table 4 shows that both the open porosity measured by water vacuum saturation method and pore volume determined by mercury intrusion porosimetry of the reference concrete was lowest among the studied mixes. The highest pore volume characteristics exhibited the mix with fly ash.

The pore size distribution curves in Figure 1 revealed for all mixes one major peak at about 50 nm and a second at 300 nm which was most distinguished for CF40. This indicated possible durability problems for the mix containing fly ash.

Table 4. Basic material properties.

Material	*Bulk density* [kg m^{-3}]	*Matrix density* [kg m^{-3}]	*Open porosity* [% m^3 m^{-3}]	*Pore volume* [cm^3g^{-1}]	*Pore surface* [m^2g^{-1}]
CR	2430	2740	11.2	0.042	3.6
CM20	2372	2729	13.3	0.072	10.0
CS40	2351	2711	12.8	0.066	5.2
CF40	2211	2634	16.0	0.087	7.6
CB40	2330	2700	13.9	0.068	8.0

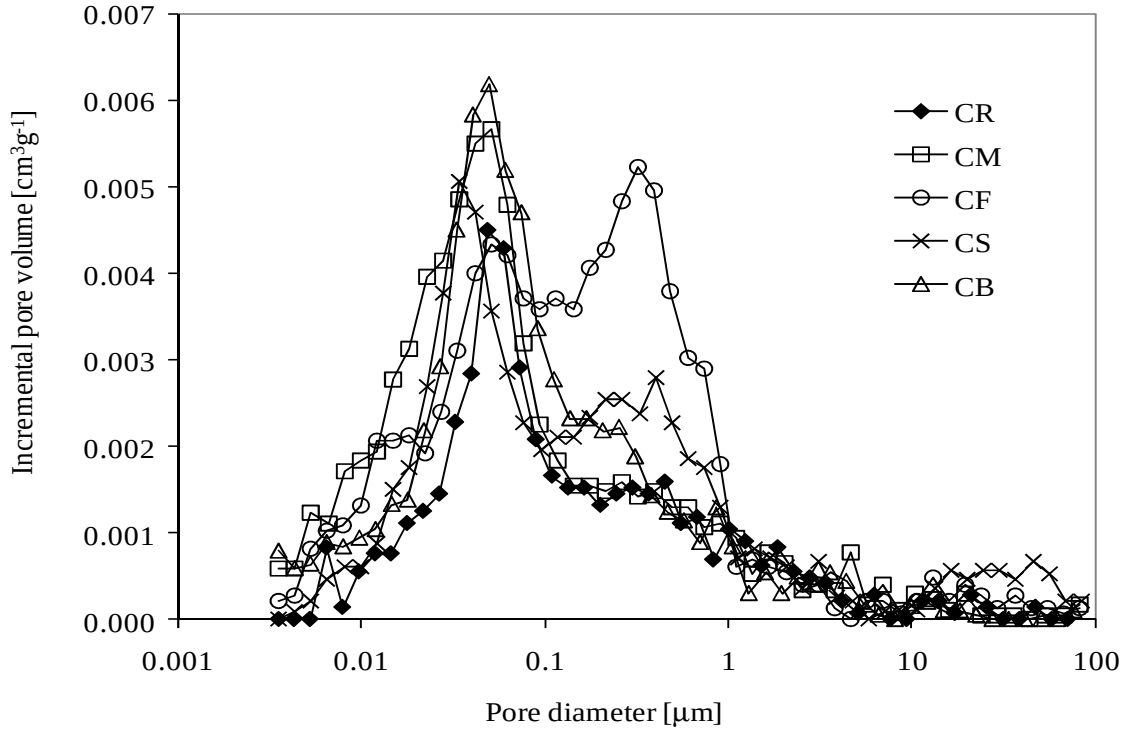

Figure 1. Pore size distribution.

The compressive strength of concrete with metakaolin was almost the same as of the reference mix (Table 4), the concrete with ground granulated blast furnace slag exceeded both of them by more than 10%. All of them met the common high performance limit of 60 MPa. On the other hand, the mixes with fly ash and ceramics performed much worse and did not meet the high performance limit. The data obtained for bending strength followed the same trend as compressive strength (Table 5). In a combination with the porosity data (Table 4 and Figure 1), the mechanical properties indicated that also the mix with fine-ground ceramics could meet certain durability problems.

Table 5. Mechanical properties.

Material	*Compressive strength* [MPa]	*Bending strength* [MPa]
CR	62.0	8.44
CM20	61.5	8.50
CS40	71.5	11.7
CF40	54.0	8.60
CB40	42.6	6.55

4.2 Durability Tests

The frost resistance of all mixes (Table 6) met the standard criterion of K > 0.75 which guaranteed sufficient performance. The best results were achieved for compressive strength with CM20 and CS40, for bending strength with CF40 and CB40. So, in the case of frost resistance the negative indications following from the measurements of pore volume and mechanical properties after 28 days of curing were not confirmed.

Table 6. Frost resistance.

Material	*Frost resistance coefficient K*	
	as the ratio of compressive strengths	*as the ratio of bending strengths*
CR	0.96	0.87
CM20	1.10	0.80
CS40	1.07	0.78
CF40	0.94	0.93
CB40	1.00	1.00

The results of the measurement of the loss of mass due to the de-icing salt action (Figure 2) provided quite different view on durability properties. The mixes with metakaolin and ground granulated blast furnace slag, together with the reference mix met quite safely the standard requirement of 1000 g/m^2 after 100 cycles. CS40 was far best among the studied mixes, CM20 was also better than CR. However, both CF40 and CB40 exhibited the mass loss several times higher than was the standard limit. Apparently, the lower compressive strength of both these mixes (Table 4) and the relatively high pore volume (Table 3) was responsible for the unsatisfactory results of this test.

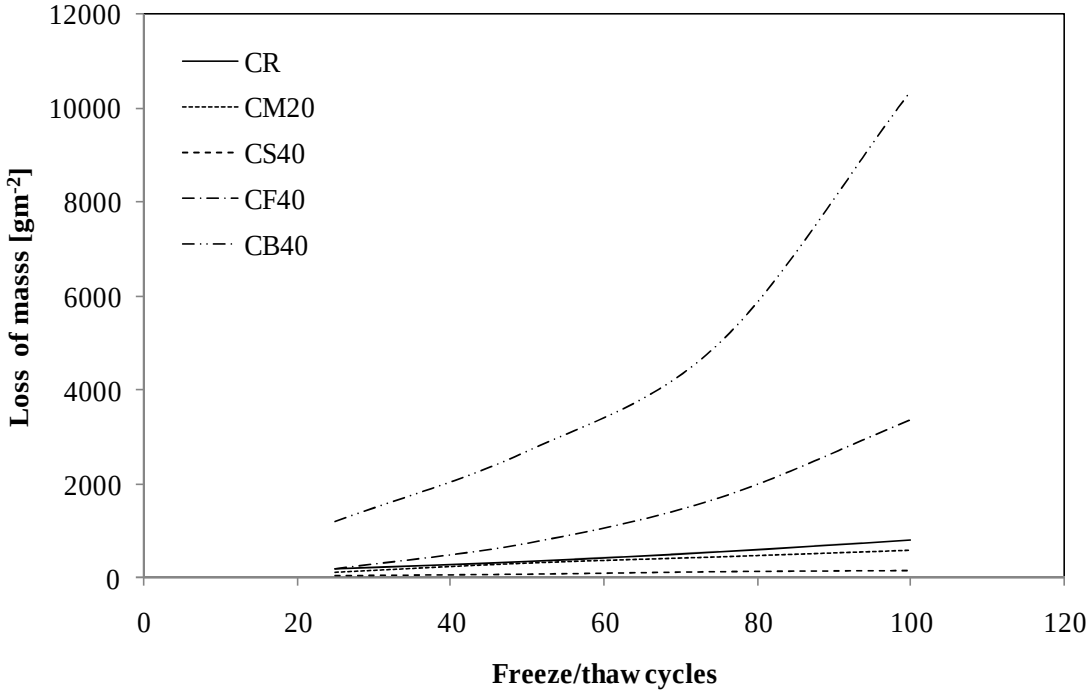

Figure 2. Loss of mass due to the de-icing salts action.

Table 7 shows that the chemical resistance of all studied mixes in all chosen environments (except for CR in Na_2SO_4) met the requirement of K_{cr} > 0.75 which guaranteed satisfactory performance. All mixes containing supplementary cementing materials (except for CS40 and CF40 in CO_2) achieved higher K_{cr} than the reference mix. So, similarly as with the frost resistance the lower compressive strength and higher porosity of CF40 and CB40 did not play as important role as in the case of de-icing salt action.

Table 7. Coefficient of chemical resistance K_{cr} in various environments.

Environment	*CR*	*CM20*	*CS40*	*CF40*	*CB40*
Air	1.00	1.00	1.0	1.00	1.00
Distilled water	0.76	1.00	1.07	1.11	0.85
$MgCl_2$	0.85	0.93	0.95	0.87	0.98
NH_4Cl	0.77	1.05	1.03	1.24	0.9
Na_2SO_4	0.66	1.00	0.96	1.26	0.9
HCl	0.76	1.02	0.97	1.01	0.91
CO_2	1.07	1.19	0.98	0.95	1.02

Table 8. Measured pH values of water leaches of specimens submerged for 60 days in various environments.

Environment	*CR*	*CM20*	*CS40*	*CF40*	*CB40*
Air	11.96	11.99	12.24	12.04	11.80
Distilled water	12.08	11.90	12.21	11.89	11.70
$MgCl_2$	11.61	11.88	11.96	11.82	11.63
NH_4Cl	11.72	11.93	12.00	11.96	11.64
Na_2SO_4	11.9	11.95	12.27	12.00	11.68
HCl	11.71	11.96	11.95	11.90	11.57
CO_2	11.91	11.23	11.61	11.33	9.85

The measured pH values of water leaches (Table 8) were for most mixes with complementary cementing materials (except for CB40) slightly higher than for the reference mix but the differences were low, 0.2-0.3 in maximum. In most cases, the pH values were higher than 11 which guaranteed the effective protection of steel reinforcement. The only exception was CB40 in CO_2 where pH decreased under 10 which was, for the first view, a surprising result; such substantial decrease in pH might indicate a higher carbonation extent which was not expected in materials where relatively high amount of Portland cement was substituted by fine-ground ceramics having much lower content of CaO (Table 1). The possible reason was the higher porosity of CB40 which could make the contact of CO_2 with the interior of the tested specimens easier.

5 CONCLUSIONS

The experimental investigations of durability characteristics of concrete mixes containing metakaolin, fly ash, ground granulated blast furnace slag or ground brick in higher amounts as supplementary cementing materials in Portland cement concrete showed that basically all these materials have a potential for future use. The replacement of Portland cement in the amount of 20-40% had a positive effect on the frost resistance and chemical resistance of all mixes containing the supplementary cementing materials. The only durability test where the results were not unambiguous was the resistance against de-icing salts. If metakaolin and ground granulated blast furnace slag were used the de-icing salts resistance increased but the application of fly ash and ground brick led to its decrease. Therefore, the last two supplementary cementing materials could probably not be recommended for applications in the areas where increased contact with de-icing salts was likely.

ACKNOWLEDGEMENT

This research has been supported by the Czech Science Foundation, under project No P104/10/0355.

REFERENCES

Chidiac S.E., Panesar D.K. 2008. Evolution of mechanical properties of concrete containing ground granulated blast furnace slag and effects on the scaling resistance test at 28 days. Cement & Concrete Composites 30, pp. 63–71.

Chung D.D.L. 2002. Review: Improving cement-based materials by using silica fume. Journal of Materials Science 37, pp. 673-682.

ČSN EN 12350-2 2000. Testing of fresh concrete – Part 2: Slump test. Czech Standardization Institute, Prague.

ČSN EN 12390-3 2002. Testing of hardened concrete – Part 3: Compressive strength. Czech Standardization Institute, Prague.

ČSN EN 12390-5 2007. Testing of hardened concrete – Part 5: Bending strength. Czech Standardization Institute, Prague.

ČSN 731326/Z1:1984 2003. Determination of the resistance of the surface of concrete against water and de-icing salts. Czech Standardization Institute, Prague.

Kim H.S., Lee S.H., Moon H.Y. 2007. Strength properties and durability aspects of high strength concrete using Korean metakaolin. Construction and Building Materials 21, pp. 1229–1237.

Lammertijn S., De Belie N. 2008. Porosity, gas permeability, carbonation and their interaction in high-volume fly ash concrete. Magazine of Concrete Research 60, pp. 535-545.

Pacheco-Torgal F, Jalali S. 2010. Reusing ceramic wastes in concrete. Construction and Building Materials 24, pp. 832–838.

Roels S., Carmeliet J., Hens H., Adan O., Brocken H., Černý R., Pavlík Z., Hall C., Kumaran K., Pel L., Plagge R. 2004. Interlaboratory Comparison of Hygric Properties of Porous Building Materials. Journal of Thermal Envelope and Building Science 27, pp. 307-325.

XII DBMC
International Conference on Durability of Building Materials and Components
PORTO - PORTUGAL, April 12th-15th, 2011

Properties of Corrosion Production Used in Concrete Cover Cracking Model

Yuxi Zhao [1]
Haiyang Ren [2]
Hong Dai [3]
Weiliang Jin [4]

ABSTRACT

After steel corrosion initiates, the volume of rust is larger than the original steel, inducing an internal pressure on the surrounding confining concrete to crack the cover. Therefore, the expansion coefficient of rust is one of the most influential factors during the concrete cracking process due to corrosion. In this paper, 8 types of rust samples collected from the different environments were investigated by X-ray diffraction (XRD), Thermogravimetry (TG) and Differential Thermal Analysis (DTA). The results showed that Fe_2O_3, Fe_3O_4, α—FeOOH, β—FeOOH and γ—FeOOH were identified in all rust samples; however, the peak intensities of these compositions for each sample are different due to their different servicing environments. Consequently, the samples formed in different environments have different expansion coefficients. The rust expansion coefficients corresponding to the different environments were proposed, which enables a rational prediction of concrete cover cracking.

KEYWORDS

Concrete structures, Rust, Chemical composition, Expansion coefficient, Cracking model.

[1] Institute of Structural Engineering of Zhejiang university ,Hangzhou ,CHINA,yxzhao@zju.edu.cn
[2] Institute of Structural Engineering of Zhejiang university ,Hangzhou ,CHINA, ren_hy@ecidi.com
[3] Institute of Structural Engineering of Zhejiang university ,Hangzhou ,CHINA, 20912117@zju.edu.cn
[4] Institute of Structural Engineering of Zhejiang university ,Hangzhou ,CHINA, jinwl@zju.edu.cn

1 INTRODUCTION

Reinforcing steel corrosion is one of the major deterioration mechanisms for reinforced concrete structures. It is known that the volume of the corrosion product is higher than that of the original metal[C. Anstice *et al*. 1993]. The ratio between the volume of expansive corrosion product and the volume of iron consumed in the corrosion process is called "rust expansion coefficient"[S. Caré *et al*. 2008]. The resulting increase in volume associated with the formation of corrosion products gradually induces tensile stresses within the surrounding concrete. Once the tensile stresses exceed the tensile strength of the concrete, cracks are initiated at the steel-concrete interface and propagate outwards of the surface of the concrete. These cracks provide a path for the more rapid ingress of aggressive agents into the reinforcement and accelerate the corrosion process. Therefore, the cracking of the concrete cover is an important state, usually defined as the serviceability limit state, and has received much attention from both scientists and practical engineers [K. Tuutti. 1982, F.J. Molina, C. Alonso, C. 1993, K. Noghabai. 1998, K. Lundgren. 2002,H.L Wang *et al*. 2008,C.H. Lu *et al*. 2010, Y.X. Zhao, W.L. Jin. 2006, K. Bhargava *et al*. 2006, D.V. Val1 *et al*. 2009, Liu and Weyers. 1998, S. Caré *et al*. 2008, C.Q. Li *et al*. 2006, J.J. Zheng *et al*. 2004, Y.G. Du *et al*. 2006].

To analyse the concrete cracking process due to reinforcing steel corrosion and predict the cracking time of the concrete surface accurately, the rust expansion coefficient is one of the key parameters in the cracking model. Its value directly affects the predicted cracking time. The expansion coefficient for the corrosion product varies from 2.2 to 6.4 [K. Tuutti. 1982]. In previous research on the model of concrete cracking due to corrosion, the values of the rust expansion coefficient varied between 2 and 4[F.J. Molina, C. Alonso, C. 1993, K. Noghabai. 1998, K. Lundgren. 2002,H.L Wang *et al*. 2008,C.H. Lu *et al*. 2010, Y.X. Zhao, W.L. Jin. 2006, K. Bhargava *et al*. 2006, D.V. Val1 *et al*. 2009, Liu and Weyers. 1998]. It has to be pointed out here that all of the values mentioned above were assumed by the authors and did not consider the compositions of the corrosion products and the influence of the environments, which in turn may affect the compositions. Syed[S. Syed. 2008] used X-ray diffraction (XRD) to characterise the corrosion products formed on steel after exposure to the open atmosphere for three years at 20 stations in the Kingdom of Saudi Arabia. His research showed that the different service environments caused various compositions of rust. However, he did not study the expansion coefficients of the corrosion products produced in different environments.

The objective of this work is to study the values of the expansion coefficient of rust obtained in different environments. These values can be utilised in the analytical and numerical analyses of the concrete cracking model due to corrosion. For this purpose, an experimental program was carried out on eight types of rust samples collected from different environments. X-ray diffraction (XRD) was used to characterise eight corrosion products. The thermal analysis, including thermogravimetric (TG) and differential thermal analysis (DTA), were used to differentiate hydroxy-oxides and oxygen oxides.

2 EXPERIMENTAL PROGRAM

2.1 Rust Samples

There were eight types of rust tested in this study. The details of these samples are listed in Table 1.

2.2 X-ray Diffraction

Eight types of the rust samples were characterised by means of X-ray diffraction (Rigaku D/max- ra XRD device) with the incident angle from 10° to 80°.

2.3 Thermal Analysis

All rust samples were investigated with a TG device (WRT-3P). The samples were heated in air at a heating rate of 10°C/min[Jinghong Chen, Chuanru Li 1985]. TG curves were recorded simultaneously from room temperature to 1000°C.

Table 1. Details of the rust samples.

Sample	*Source*	*Classical environment*[(a)]
A	An open-air ironwork in Ningbo (a coastal city in eastern China)	XD1
B	A facility from a factory for treatment of urban sewage in Shanghai, China	XD3
C	An ironwork at a waste yard in Gansu province (western China)	XD2
D	An iron rack in the durability laboratory of Zhejiang University, Hangzhou, China	XD1
E	A steel plate near the sea, Ningbo, China	XS1
F	The rebar in RC port, Yokosuka, Japan	XS3
G	The rebar in RC specimens, being treated by electroosmosis	XD2
H	The rebar being electrochemically treated in NaCl solution	XS2

[(a)] As Eurocode 2: Design of concrete structures —Part 1-1: General rules and rules for buildings (EN1992-1-1:2004)

3 RESULTS

3.1 X-Ray Diffraction (XRD)

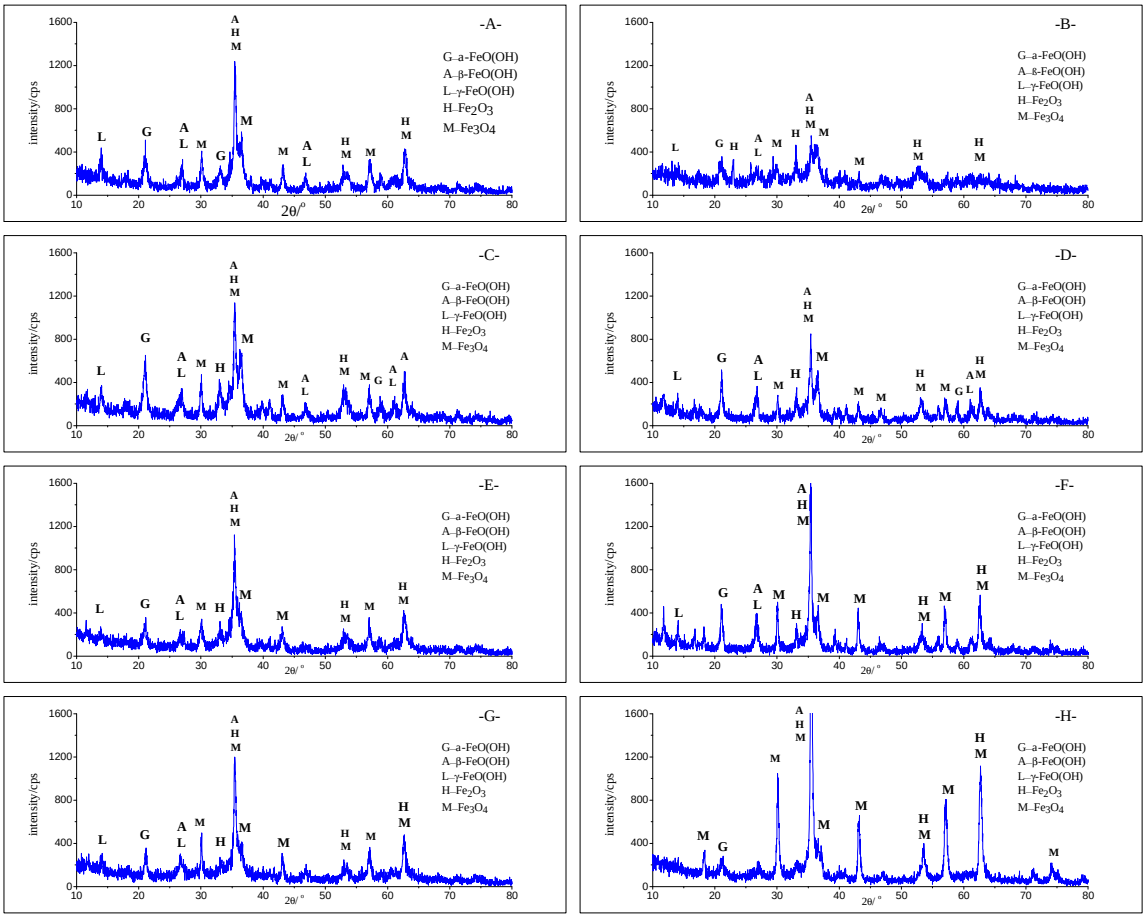

Figure 1. XRD pattern of eight different rust samples.

Figure 1 shows the XRD patterns for eight rust samples. A peak marked with a variety of compositions means that at least one of these products existed at this position. Figure 1 shows that qualitatively the compositions of Fe_2O_3, Fe_3O_4, α—FeOOH, β—FeOOH and γ—FeOOH were identified in all rust samples. However, the peak intensities of these compositions for each sample were different, showing that the percentage of every composition was different in each rust sample because the rust samples were generated in different environments.

3.2 Thermogravimetric (TG) Analysis

TG curves of all samples are given in Figure 2. Two distinct steps, 20-200°C and 200-400°C, are observed in every single TG curve. Step I, the decline stage from 20°C to 200°C in Figure 2, indicates the dehydration of the rust sample, resulting from the evaporation of physically adsorbed water in the rust. Step II, the steep decline stage from 200°C to 400°C, shows that the hydroxyl in the hydroxy-oxide is destroyed [R. M. Cornell, U. Schwertmann. 1996] as

$$2FeO(OH) \rightarrow Fe_2O_3 + H_2O \quad (1)$$

Recording the loss of mass during 200~400°C for each rust sample, the content of the hydroxy-oxide FeO(OH) in the rust sample can be estimated by the ratio of molar mass between FeO(OH) and H_2O in Equation (1), which is discussed in Section 4.2.

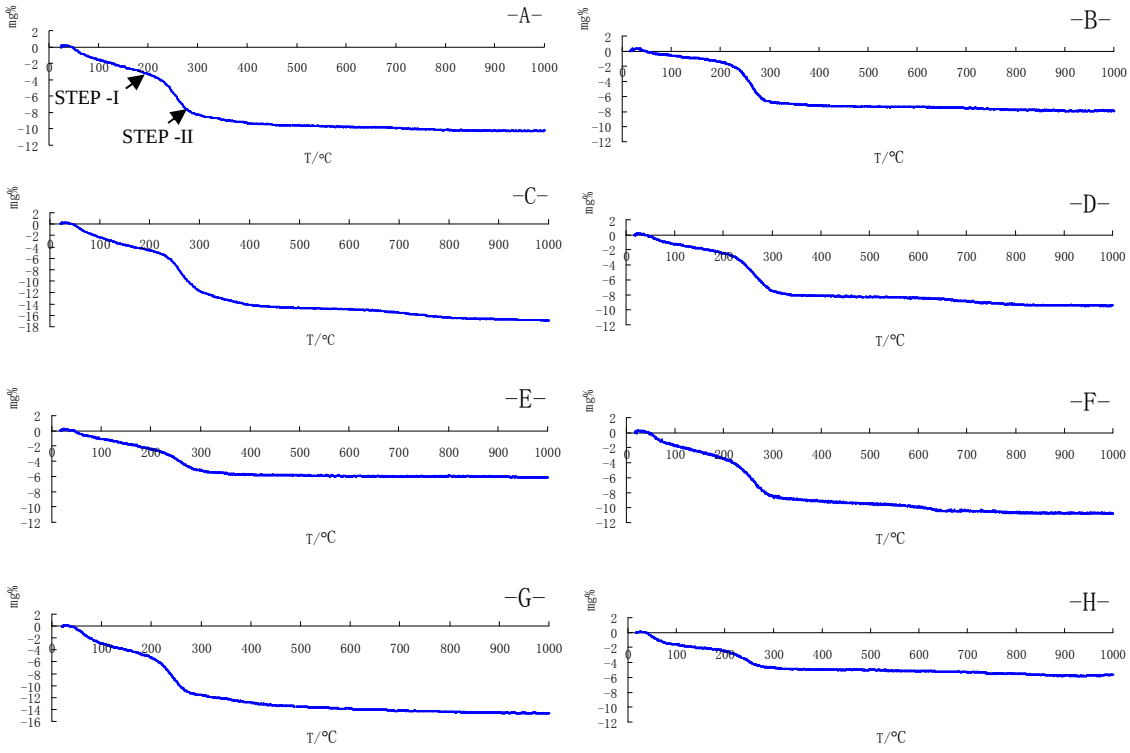

Figure 2. TG curves of all rust samples.

4 DISCUSSION

4.1 Composition of Rust Samples

The formation of corrosion products is affected by environmental factors[R. M. Cornell, U. Schwertmann. 1996, Q.X. Li *et al*. 2008, M. Yamashita *et al*. 2005, T. Ishikawa *et al*. 2005], such as humidity, temperature, oxygen supplementation and harmful ions (i.e., Cl^-, SO_4^{2-}). As shown in Figure 1, although all rust samples had similar compositions, the peak intensities of the compounds for each sample were different due to their different servicing environments. It needs to be pointed out that,

although Fe_2O_3 was detected in all the rust samples, it can not be a composition of corrosion products as the formation of Fe_2O_3 required a very high temperature[R. M. Cornell, U. Schwertmann. 1996]. Fe_2O_3 was considered to be the composition of the mill scale which formed before corrosion initiation but not generated during the rust expansion process. Therefore, Fe_2O_3 does not contribute to the volume expansion acting on the surrounding concrete cover, the subsequent calculations on the expansion coefficients of rust does not consider Fe_2O_3.

4.2 Expansion Coefficient of Rust Samples

All samples can be divided into two categories according to the water reduction in the range of 200~400°C of the TG curves: the oxygen oxides and the hydroxy-oxides. The contents of both categories of products can be calculated by the ratio of the molar mass between FeO(OH) and H_2O given in Equation (1). Table 2 lists the results.

Table 2. The content of two categories of products for eight samples.

Sample	*Total mass* [mg]	*Mass loss during 0-200°C* [mg]	*Mass loss during 200-400°C* [mg]	*Mass of hydroxy-oxides* [mg]	*Mass of oxides* [mg]
A	9.41	0.38	0.49 (5.26%)	5.69	3.34
B	9.66	0.17	0.56 (5.77%)	6.23	3.26
C	9.38	0.42	0.89 (9.53%)	8.83	0.13
D	8.75	0.22	0.51 (5.78%)	5.69	2.84
E	9.34	0.23	0.31 (3.32%)	4.17	4.94
F	10.01	0.38	0.56 (5.62%)	6.30	3.33
G	10.00	0.55	0.71 (7.09%)	7.47	1.98
H	9.39	0.26	0.23 (2.41%)	3.63	5.50

The expansion coefficient of the main hydroxy-oxides and oxides are listed in Table 3. Because Fe_2O_3 does not contribute to the volume expansion acting on the surrounding concrete cover as stated before, the table does not include Fe_2O_3.

Table 3. The expansion coefficient of the main hydroxy-oxides and oxides.

Corrosion product	*Rust expansion coefficient*
Fe_3O_4	2.10
α-FeO(OH)	2.95
β-FeO(OH)	3.53
γ—FeOOH	3.07

The rust expansion coefficients of eight samples could then be calculated, given in Table 4.

Table 4. The expansion coefficients for all rust samples.

Sample	*Rust expansion coefficient*
A	2.94
B	2.96
C	3.24
D	2.98
E	2.85
F	3.02
G	3.14
H	2.64

It is clear that the rust samples have different expansion coefficients, varying from 2.64 to 3.24, due to their different environments. This result enables us to establish the relationship between the environments and the expansion coefficients of rust.

4.3 Rust Expansion Coefficients in Different Environments

Three levels classified by the specific environmental conditions are proposed in Table 5 with regards to these two factors. The environmental conditions for all samples can be described and classified as shown in Table 6.

Table 5. Exposure classes related to environmental conditions.

Factor	*Level*	*Environmental condition*
Humidity	High	Subjected to long-term water contact or submerged in water
	Middle	Subjected to direct water contact occasionally (tidal zone and splash zone)
	Low	Normal atmosphere
Oxygen Availability	High	Exposed directly to air
	Middle	Not sufficient oxygen (at the rebar surface after cover cracking)
	Low	Oxygen deficiency (parts of the element including the rebar surface, immersed in water before cover cracking)

Table 6. Environmental classification for all rust samples.

Sample	*Oxygen Availability*	*Humidity*	*Presence of Cl^-*	*Description*
A	High	Low	Yes	Formed freely in a coastal city environment
B	High	Middle	Yes	Formed freely in an environment affected by the waste water
C	High	High	Yes	Formed freely in an environment affected by the waste water
D	High	Low	Yes	Formed freely in an environment with saline mist
E	High	Low	Yes	Formed freely in an environment beside the sea
F	Middle	Middle	Yes	Formed in concrete element beside the sea
G	Low	High	Yes	Formed in a concrete element being treated by electro-osmosis
H	Low	Low	Yes	Formed from a steel bar being electrochemically treated in a saline solution, heated at 60°C to dry

Table 7. Rust expansion coefficients corresponding to different environments(a).

Environment factors		*Humidity(water)*		
		High	*Middle*	*Low*
Oxygen Availability	*High*	3.3	3.1	2.9
	Middle	3.2	3.0	2.8
	Low	3.1	2.9	2.6

(a) Subtracting 0.5 for the environment without chloride ions ingress.

Based on the above discussion, the rust expansion coefficients corresponding to various environments are proposed, as given in Table 7. These values can be used in the analysis of the concrete cover cracking due to reinforcement corrosion.

5. CONCLUSIONS

(1) Fe_2O_3, Fe_3O_4, α—FeOOH, β—FeOOH and γ—FeOOH were identified by XRD in all rust samples; however, the peak intensities of the compositions of each sample were different due to their different in service environments. However, Fe_2O_3 was not generated in corrosion process but from the mill scale which exists before the corrosion process, and it did not contribute to the volume expansion acting on the surrounding concrete cover.
(2)The thermal technique can be utilised to classify the corrosion products into oxygen oxides and hydroxy-oxides, which can be further used to conduct the quantitative analysis of the compositions and the expansion coefficients for rust samples.
(3) The expansion coefficients of rust samples from different environments were estimated by the weighted-average method based on the percentage of the compositions in each sample and their expansion coefficients.
(4) The rust expansion coefficients corresponding to the different environments were proposed, taking humidity and oxygen supplementation as the most influential factors. This result can be applied for analysis of concrete cover cracking due to reinforcement corrosion.

ACKNOWLEDGEMENTS

Financial support from the National Natural Science Foundation of China with Grant No. 50808157 and No. 50920105806 is gratefully acknowledged. The authors also appreciate financial support from Science and Technology Department of Zhejiang Province with Grant No. 2010R10099. The authors are grateful to Dr. Ema Kato from Port and Airport Research Institute Japan for providing the rust sample collected from the rebar in the RC port, Yokosuka, Japan. We would also like to acknowledge Mr. Nianping Jiang and Mr. Linghang Shi in Zhejiang University for their help with the XRD and thermal analysis.

REFERENCES

C. Anstice, C. Alonso, F.J. Molina. 1993, Cover cracking as a function of bar corrosion: part I-experimental test. *Materials and structures* 26 .pp. 453-464.

S. Caré , Q.T. Nguyen, V. L'Hostis, Y. Berthaud. 2008, Mechanical properties of the rust layer induced by impressed current method in reinforced mortar.*Cement and Concrete Research* 38,1079–1091.

K. Tuutti. 1982, *Corrosion of steel in concrete*. Report 4, Swedish Cement and Concrete Research Institute, Stockholm, Sweden, April.pp.82.

F.J. Molina, C. Alonso, C. 1993, Andrade. Cover cracking as a function of rebar corrosion: Part 2 - Numerberical model. *Materials and Strutures*, 26.pp.532-548.

K. Noghabai. 1998, Effect of tension softening on the performance of concrete structures. PhD thesis 1998:21, *Division of Structural Engineering*, Lulea University of Technology, Lulea.

K. Lundgren. 2002,Modeling the effect of corrosion on bond in reinforced concrete. *Magazine of Concrete Research*, Vol.54,No.3,June, pp.165-173.

H.L Wang, W.L Jin, X.Y. Sun. 2008,Fracture m odel for protective layer cracking of reinforced concrete structure due to rebar corrosion. *Journal of Hydraulic Engineering*, Vol. 39 No. 4, pp. 863-869.

C.H. Lu, Y.X. Zhao, W.L. Jin. 2010, Modeling of time to corrosion-induced cover cracking in reinforced concrete structures. *Journal of Building Structures*. Vol.31,No.2,pp. 85-92.

Y.X. Zhao, W.L. Jin. 2006, Modeling the Amount of Steel Corrosion at the Cracking of Concrete Cover. *Advances in Structural Engineering*, Vol. 9 No. 5 .pp.687-696.

K. Bhargava, A.K. Ghoshb, Y. Mori, S. Ramanujama. 2006, Analytical model for time to cover cracking in RC structures due to rebar corrosion. *Nuclear Engineering and Design* 236 pp. 1123–1139.

D.V. Val1; L. Chernin; M.G. Stewart. 2009, Experimental and Numerical Investigation of Corrosion-Induced Cover Cracking in Reinforced Concrete Structures. *Journal of Structural Engineering. ASCE*, Apirl, pp. 376-38.

Liu and Weyers. 1998, Modeling the time to corrosion cracking in chloride contaminated reinforced concrete structures .*ACI Materials Journal*. 95(6),pp.675-681.

S. Caré,Q.T. Nguyen, V.L'Hostis, Y. Berhaud. 2008, Mechanical propertities of the rust layer induced by impressed current method in reinforced mortar. *Cement and Concrete Research*, 38, pp.1079-1091.

C.Q. Li, R. E. Melchers, J.J. Zheng. 2006, Analytical model for corrosion-induced crack width in reinforced concrete structures. *ACI Structural Journal*, Vol. 103, No. 4, July-August pp.479-487.

J.J. Zheng, X.Z. Zhou，C.Q. Li. 2004, Analytical solution for corrosion damage of reinforced concrete structure. *Journal of Hydraulic Engineering*, 12.pp.62-68.

Y.G. Du, A.H.C. Chan, L.A. Clark. 2006, Finite element analysis of the effects of radial expansion of corroded reinforcement. *Computers and Structures* 84 .pp. 917–929.

S. Syed. 2008, Atmospheric corrosion of hot and cold rolled carbon steel under field exposure in Saudi Arabia. *Corrosion Science* 50 .pp.1779–1784.

Jinghong Chen, Chuanru Li 1985, *Thermal analysis and application* .Science Press, Beijing, (Chinese).

R. M. Cornell, U. Schwertmann. 1996, *The iron oxides* . VHC Verlagsgesellschaft, Weinhaim, Germany.

Q.X. Li, Z.Y. Wang, W. Han, E.H. Han. 2008, Characterization of the rust formed on weathering steel exposed to Qinghai salt lake atmosphere . *Corrosion Science*. 50 .pp.365–371.

M. Yamashita, H. Konishi, T. Kozakura, J. Mizuki, H. Uchida. 2005, In situ observation of initial rust formation process on carbon steel under Na_2SO_4 and NaCl solution films with wet/dry cycles using synchrotron radiation X-rays . *Corrosion Science*. 47.pp.2492–2498.

T. Ishikawa, K. Takeuchi, K. Kandori, T. Nakayama. 2005 ,Transformation of γ-FeOOH to α-FeOOH in acidic solutions containing metal ions. *Colloids and Surfaces A: Physicochem. Eng. Aspects* 266.pp.155–159.

XII DBMC
International Conference on Durability of Building Materials and Components
PORTO - PORTUGAL, April 12th-15th, 2011

Chloride Aging Factor of Concrete Measured by Means of Resistivity

C. Andrade [1]
Marta Castellote [2]
R. d'Andrea [3]

ABSTRACT

One of the important parameters of the chloride models used for prediction of reinforcement corrosion is the fact of the decrease with time of the chloride diffusion coefficient which is attributed to the refinement of the pore structure and is named as "concrete aging". In a previous study this aging factor has been proposed to be calculated from the evolution of the electrical resistvity over time as the resistivity increases with time, the representation of its inverse value with time enables the calculation of the decrease of the D_{ap} due the relation of the resistivity with the diffusion mechanism. In present paper, the aging factors are calculated in a set of concretes fabricated with three cement families and cured in wet conditions. The aging factors obtained are in the same order of magnitude to those measured from the change of the diffusion coefficient with the advantage that the resistivity is a non destructive technique and enables the monitoring in the same specimen.

KEYWORDS

Concrete aging, resistivity, service life.

[1] Institute of Construction Science Eduardo Torroja, IETcc, CSIC, Madrid, SPAIN, andrede@ietcc.csic.es
[2] Institute of Construction Science Eduardo Torroja, IETcc, CSIC, Madrid, SPAIN, martaca@ietcc.csic.es
[3] Spanish Institute of Cement and its Application, IECA, Madrid, SPAIN, rdandrea@ieca.es

1 INTRODUCTION

Service life of concrete structures depends on the environmental aggressivity towards its reinforcement. The time to corrosion initiation is usually modeled by a diffusion process characterized by a rate parameter named non steady diffusion coefficient, D_{ns}, or Apparent Diffusion Coefficient, D_{ap} because it encounters not only the transport process but also the binding of chloride with cement phases. This D_{ap} is usually determined in short term tests after a certain curing period, usually 28 days. Several test types are available for this determination [Tuutti 1982]; [Whiting 1981]; [Page *et al.* 1981]; [Buenfeld *et al.* 1987]; [Andrade 1993]. With independence of the method of determination of the D_{ap}, it has been noticed that this parameters does not remain constant but varies with: a) time, b) external chloride concentration andc) temperature, among other influences [Mangat & Molloy 1994]; [Bamforth & Chapman-Andrews 1994]; [Andrade *et al.* 2000]; [Maage *et al.* 1996]. The variation with time supposes a decrease of the D_{ap} which can be very significant and has been named the "aging factor".

The degree of decrease of this aging factor has been identified to depend mainly of cement type. The decrease from early ages to 50-100 years, can be small (usual behavior in concretes made with pure OPC) or higher than one order of magnitude (reported in concretes with blended cements) which means a great impact on the prediction of the service life if it is not taken into account. There have been proposed several manners of approaching the consideration of aging in transport parameters. One of the first proposals was due to Mangat and Molloy [1994]. At present, the dependence of D_{ap} with time is modeled by means of equation (1) where the time is divided by a t_0 in order to make coherent the units [Maage *et al.* 1996]; [Gulikers 2006].

$$D_t = D_0 \left(\frac{t}{t_0}\right)^{-n} \quad (1)$$

Where D_t is the value at further ages, t, D_0 is the value at the testing time t_0 (usually 28 days of curing plus the testing time of 35 or 90 days) and *n* is an exponent indicating the slope of decreasing of D_{ns} with time. This equation is starting to be used also for practice and being adopted in pre-standards with the inherent risk of miss-prediction that it implies.

Several limitations have been identified in the use of this expression, being the most important one the impact that have the dates selected for fitting it [Gulikers 2006]. As the evolution is not exactly following a potential decay at early ages, the dates able to represent long term performance is significant for the selection of the best *n* factor value. This limitation also means that the second age may be too long time after mixing which makes the determination time consuming.

In order to overcome the limitations of the chloride testing, the use of the electrical resistivity for the prediction of service life of concrete structures has been postulated in previous works [Andrade 2004]. This parameter is a non destructive technique, NDT, and therefore its values can be monitored over time in a relatively easy and inexpensive manner which will facilitate the extrapolation of the prediction and the enables the embedding of sensors or the determination in the real structure. The model proposed is based in the measurement of the electrical resistivity at 28 days of wet curing.. Regarding the aging effects, the model takes into account the evolution of the resistivity with time in a parallel manner than is made when using the Diffusion Coefficient.

In a previous paper [Castellote *et al.* 2009] it has been proposed to measure the aging factor of the diffusion coefficient and of the model based in the resistivity, by monitoring this parameter over time in concrete specimen cured in wet conditions. The evolution of the resistivity over time can be made with the same mathematical expression as equation (1) but using and aging factor named *q*:

$$\rho(t) = \rho_0 (t / t_0)^{+q} \quad (2)$$

Where : $$q = 0.798\, n - 0.0072 \approx 0.8\, n \quad (3)$$

The aging factor of resistivity *q* has resulted different of that of the Diffusion Coefficient *n* because both, ρ and D_{ap} evolve differently with time [Castellote *et al.* 2009] due to the resistivity ρ represents the evolution of the pore network and its connectivity and D_{ap} variation reflects additionally to that of the pore structure, the binding ability and the variation of chloride surface concentration with time. In present paper is presented the *q* values calculated for concretes fabricated with three families of cements and their relation to the typical values published for the aging factors of the diffusion coefficient.

2 EXPERIMENTAL

Several concretes were fabricated with different types of cements according to Spanish standard [EHE-08]. The compositions and types of cements are given in Table 1.

Table 1. Composition of the Concrete used.

label	I-01	I-02	I-03	I-12	IIA-02	IIA-03	IIA-12	IIA-17	IIA-21	IIA-16	IIA-23	IIB-33	IIB-34
CEM I	x	x	x	x									
CEM II/A-P					x	x	x	x	x				
CEM II/A-V										x	x		
CEM II/B-V												x	x
cement (Kg/m^3)	300	275	275	400	275	275	344	340	350	320	281	300	325
w/c	0.65	0.6	0.55	0.45	0.6	0.55	0.59	0.55	0.52	0.55	0.49	0.55	0.52
sand (Kg/m^3)	820	643	850	811	643	880	704	810	770	859	904	839	727
Gravel (Kg/m^3)	582	893	722	404	893	692	578	522	552	735	690	641	686

All the specimens were cylindrical of 150 mm in diameter and 300 mm in high. They were demoulded after 24 hours of being cast and were cured during in a humid chamber (95% HR) and temperature of 25±3 ºC. The electrical resistivity was measured from the mixing for every specimen. The resistivity was measured by means of the four points or Wenner method by using a shape factor of 1.65 [AENOR-UNE 83988-2].

3 RESULTS

The results of the resistivity with time are given in figures 1, 2 and 3 in which the fitting to equation 2 is also shown. Figure 1 shows the *q* values for concrete made with cements type I, figure 2 for those made with cement type II-A-P and figure 3 for types IIA-V y IIB-V. The mean values and standard deviations of the *q* values is presented in figure 4.

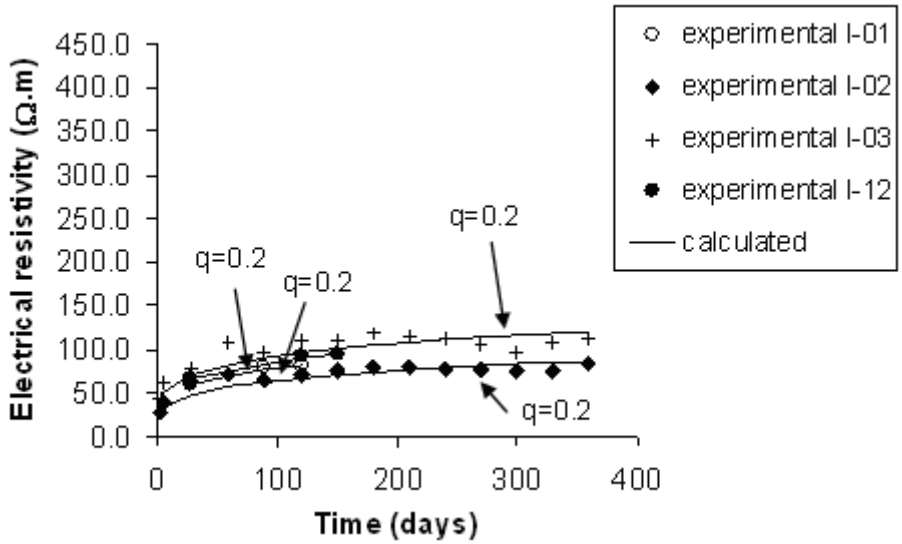

Figure 1. Experimental values of the resistivity and values of aging factor "q" obtained by fitting equation (2) in concretes made with cement type I.

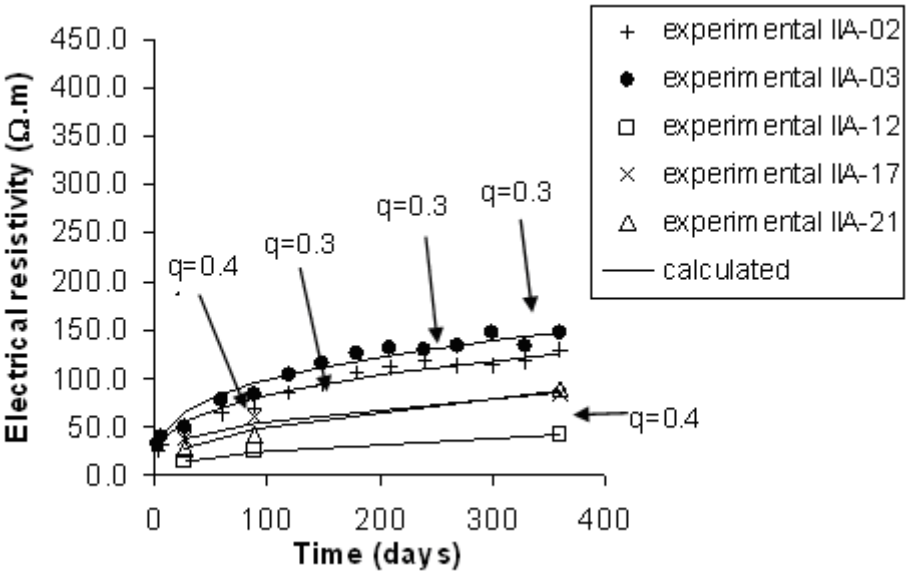

Figure 2. Experimental values of the resistivity and values of aging factor "q" obtained by fitting equation (2) in concretes made with cement type IIA-P.

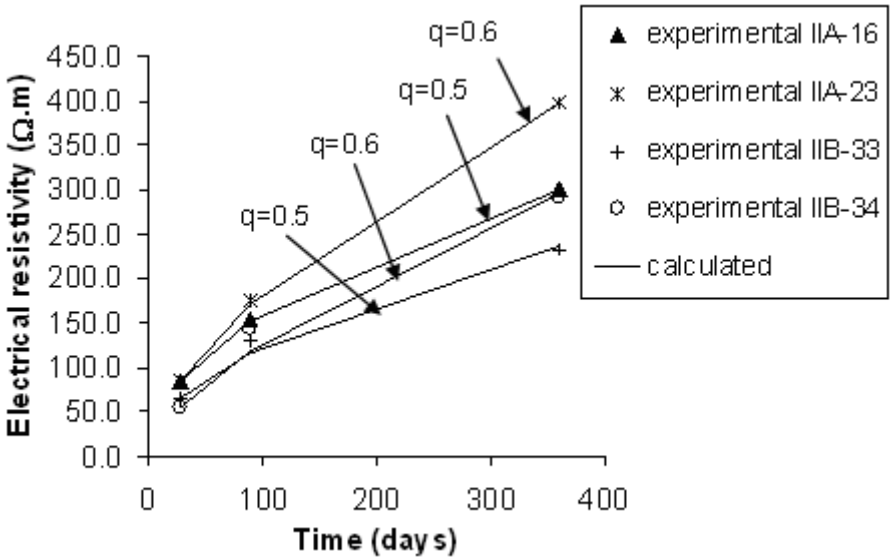

Figure 3. Experimental values of the resistivity and values of aging factor "q" obtained by fitting equation (2) in concretes made with cement type IIA-V y IIB-V.

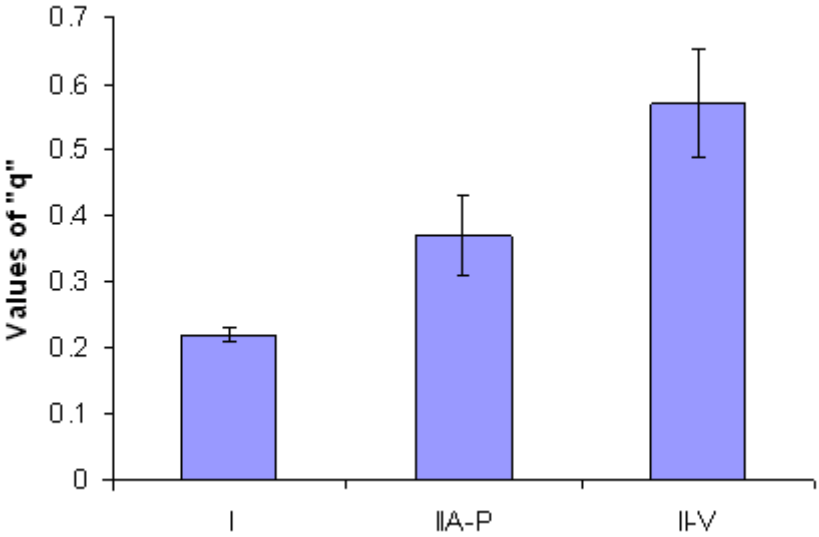

Figure 4. Mean values and standard deviation of aging factor "q" obtained in concretes made with cement types I, IIA-P, II-V (IIA-V y IIB-V)**.**

4 DISCUSSION

As was mentioned the decrease of D_{ap} with time has a tremendous impact in the prediction of the long term service life as shown in figure 5 where it is plotted for the hypothetical case of an initial D_{ap} value of $1x10^{-8}$ cm^2/s. In function of the exponent n, the initial D_{ns} value would decrease one or one and a half orders of magnitude after 100 years. With the change from 0.5 to 0.43 there is around 20 years difference in the prediction example shown in the figure. Therefore the most possible exact determination of exponent n is a crucial aspect for the whole reliability of a prediction.

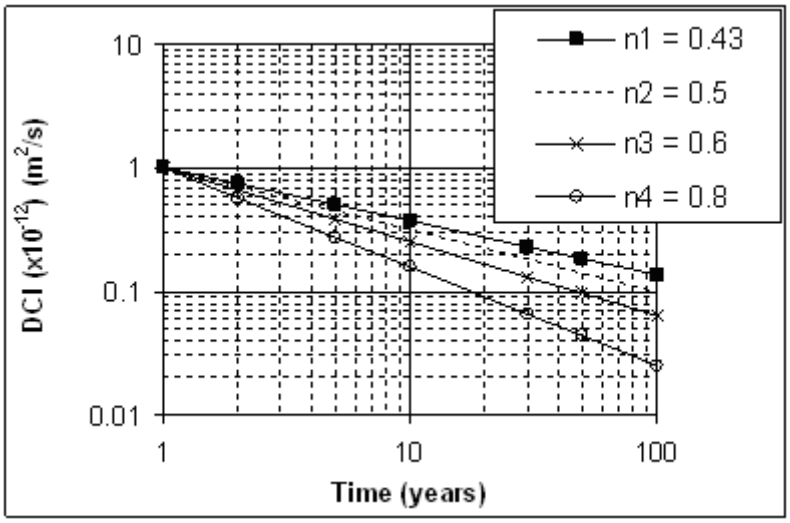

Figure 5. Effect of exponent *n* on the decrease of D_{ap} with time calculated by means of equation (1) assuming t_0= 1 year.

The refinement of the pore structure is one of the main reasons for the decrease of D_{app} with time. Its decrease with age is considered to be a consequence of: a) the progressive hydration due to the production of higher amounts of the smaller (gel) pores that aims into the decrease of the pore space for the access of the external aggressive substances, b) also decreases the pore space due to the formation of chloroaluminates, and finally c) there is an decrease in porosity in the concrete surface due to the leaching out of hydroxides and calcium as a consequence of the contact with the sodium chloride solution that has a neutral pH value. In the case that the concrete is not submerged another possibility of changing the microstructure is due to the carbonation which precipitates Calcium Carbonate. Then, the pore microstructure of concrete evolves with time and this evolution depends not only on the progression of the hydration but also of the particular effect of the environment where the concrete is placed.

The resistivity also evolves with time due to the pore refinement but it does not notice the chloride binding or the change in the chloride surface concentration and then, the aging factor should differ from that of the D_{ap}. The presence of mineral additions makes the aging factor to be higher as was detected by other authors [3,6]. These higher aging factors of cements with mineral additions are a consequence of their more tortuous pore network and the higher binding ability due the larger proportions of aluminate phases of the additions. Then, their presence not only decreases the D_{ap} at short ages of testing in comparison to ordinary Portland cement, but also induces a more pronounced decrease over time of the D_{ap}.

In the case of the resistivity, the presence of additions is noticed by higher values at short and long ages with respect to ordinary Portland cement, that is, the resistivity detects the additions effect in a parallel manner than done by the D_{ap}, although responding to different mechanism (resistivity detects binding by the decrease in the pore empty space due to the precipitation of chloroaluminates and not by the binding reaction mechanism itself).

Table 2. Values of q and n obtained in present work and from the literature.

		CEMENT YPE			
CEMENT TYPE		CEM I (portland cement)	CEM II/A-P (puzzolan <20%)	CEM II /A-V or CEM II/B-V (silicious fly ash:between 6 and 35%)	BFSC (70% slag)
Present results	measured	q=0.22 ±0.01	q = 0.37±0.06	q = 0.57±0.08	
	calculated	n = 0.275	n = 0.462	n = 0.712	
Bamforth [7]		n = 0.264		n = 0.699	n = 0.621

For the sake of comparison in table 2 are given values of the aging factor q measured in present work and the calculated from them n values, and the aging factors suggested by Bamforth [1994]. The orders of magnitude are very similar which means that the aging factor can be calculated from the evolution of resistivity with time with a very good approximation to the diffusion process.

Assuming this possibility, the resistivity due it can be repeated in the same specimen at the same age and over time, it facilitates the application to series of specimens in order to calculate mean or characteristic values by families of cement types and of concretes. Regarding whether the mean or the characteristic lower value would be more adequate, it seems that the lower 95% value would be more conservative and following the example of other concrete properties, as the mechanical strength or the K factor, this value might be used for the service life prediction.

4 CONCLUSIONS

In present paper the aging factors of the electrical resistivity of concretes fabricated with several cements types currently used, have been calculated in order to obtain their mean values and standard deviations. The main conclusion obtained is that the aging factors n calculated from the resistivity values measured over time are in the order of magnitude to those published by other authors, confirming that the resistivity aging factor q can be used for calculating the aging factor n of the diffusion of chlorides.

ACKNOWLEDGMENTS

The authors thank the Ministry of Science and Innovation and the CSIC of Spain for the funds provided through the CONSOLIDER-SEDUREC project which had enabled present work. They also thank the funds received from the Project CALIDUR supported by the Building Technical Code of Spain and to their members for the preparation of the specimens and measurements made.

REFERENCES

AENOR Pr UNE 83988-2 (Spanish standard). *Métodos de Ensayo. Durabilidad del hormigón. Determinación de la Resistividad Eléctrica. Parte 2: Método de las cuatro puntas o de Wenner.*(Test Methods. Concrete Durability. Determination of electrical resistivity. Four point or Wenner method).

Andrade, C. 1993, "Calculation of chloride diffusion coefficients in concrete from ionic migration measurements".*Cement and Concrete Research*, 23, (3), pp. 724-742.

Bamforth, P., Chapman-Andrews, J. 1994, "Long term performance of RC elements under U.K. coastal exposure conditions", International Conference on Corrosion and Corrosion Protection of Steel in Concrete, Sheffield Academic Press, Ed. N. Swamy Ed., pp. 139-156.

Buenfeld, N. R. and Newman, J. B. 1987, 'Examination of the three methods for studying ion diffusion in cement pastes, mortars and concrete',*Mater. Struct* **20**, pp. 3–10.

C. Andrade, J.L. Sagrera and M.A. Sanjuán. 2000, "Several years study on chloride ion penetration into concrete exposed to Atlantic Ocean water". Proceedings of the second international RILEM workshop on testing and modelling chloride ingress into concrete, RILEM, Paris, pp. 121 – 134.

C. Andrade. 2004, Calculation of initiation and propagation periods of service-life of reinforcements by using the electrical resistivity. International Symposium on Advances in Concrete through Science and Eng., RILEM Symposium, March 22-24, Evanston (Illinois, USA).

Castellote, M., Andrade C., d'Andréa, R. 2009, "The use of resistivity for measuring aging of chloride diffusion coefficient". Proceedings RILEM TC 211-PAE International Conference - Concrete in Aggressive Aqueous Environments, Toulose.

EHE-08. *Instrucción de Hormigon estructural* (Spanish Code for Strucural Concrete) . Ministry of Pablic Works. Spain (*Ministerio de Fomento*).

J. Gulikers. 2006, A Critical review of mathematical modelling of chloride ingress into concrete and the derivation of input data. Proceedings of the RILEM International Workshop on "Performance based evaluation and indicators for concrete durability" Madrid-Spain, pp 165-176.

Maage, M., Helland, S., Poulsen, E., Vennesland, Ø., Carlsen, J.E. 1996, "Service Life Prediction of Existing Concrete Structures Exposed to Marine Environment" in: ACI Materials Journal, vol. 93, no. 6 (November-December), pp. 602-608.

P.S. Mangat, B.T. Molloy. 1994, "Predicting of long term chloride concentration in concrete", Mat. Struct. 27, pp. 338–346.

Page, C.L. Short, N.R. and Tarras, A. 1981, "Diffusion of chloride ions in hardened cement pastes". *Cement and Concrete Research*, 11, (3), pp. 395-406.

Tuutti, K. 1982, Corrosion of steel in concrete, Swedish Cement and Concrete Research Institute (CBI), Report Fo 4.82. Stockholm.

Whiting, D. 1981, "Rapid determination of the chloride permeability of concrete". Federal Highway Administration. Report nª FHWA/RD-81/119.

XII DBMC
International Conference on Durability of Building Materials and Components
PORTO - PORTUGAL, April 12th-15th, 2011

Experimental and Theoretical Analysis of Effect of Mortar Composition on Chloride Binding

Hannah Benešová [1]
Milena Pavlíková [2]
Zbyšek Pavlík [3]

ABSTRACT

Portland cement concrete is considered as durable construction material over the world. However, concrete structures show degradation of structural and material performance in severe climatic and environmental conditions. Among the most aggressive environmental factors that negatively affect the durability and service life of concrete structures belongs chloride attack. Chloride action in inner structure of concrete leads to expansion, cracking, spalling, and deterioration of many civil engineering structures. On that account, detailed explanation of chlorides' ingress into the concrete is necessary for achievement of enhanced durability and service life of concrete structures. Within the chloride transport, not only diffusion and advection take place, but also significant effect of chlorides' binding must be considered. In this paper, chloride binding isotherms of several types of cement based mortars having different water/binder ratio, amount and size of aggregates, and cement weight, are measured. For the measurement, method utilizing the adsorption of chloride ions from solution of specific concentration is used. Within the experimental part of the paper, measurement of bulk density, matrix density, total open porosity and specific surface are done as well. The measured binding isotherms are theoretically analysed, and related to total mass of used binder, sample mass and specific surface. Finally, the mechanisms of chlorides' binding are identified and described.

KEYWORDS

Cement based mortar, Chlorides' binding, Binding isotherms, Specific surface.

[1]Czech Technical University, Prague, CZECH REPUBLIC, pavlikz@fsv.cvut.cz
[2]Czech Technical University, Prague, CZECH REPUBLIC, pavlikz@fsv.cvut.cz
[3]Czech Technical University, Prague, CZECH REPUBLIC, pavlikz@fsv.cvut.cz

1 INTRODUCTION

Probably the most often used construction material over the world is concrete. This material is exposed during its service life to unfavourable climatic and environmental conditions that critically affect its durability. Especially sulphates attack, thaumasite form of sulphate attack, sea water action, chloride crystallization and induced corrosion of concrete steel reinforcement are the most harmful mechanisms of salt induced damage of concrete structures [Pavlík 2009]. Since the complex study of salt induced damage of concrete would be to abroad, we focused in this work on chloride action only.

Nearly all structural concrete contains steel, and on this account there is necessary to study the problem of chloride induced steel corrosion. Crucially, the corrosion products of steel occupy considerably greater volume than the original steel. Rusting in the concrete and other steel reinforced materials causes cracking, and spalling of the concrete cover layer, leading to more rapid corrosion of the exposed steel and eventual loss of structural integrity. In the absence of carbonation and chloride ions, the alkaline conditions of concrete provide a protective environment for the steel reinforcement. The high pH of concrete (typically 12.5 – 13) is due to the $Ca(OH)_2$ from the cement hydration and the small amounts of Na_2O and K_2O in the cement. It is widely accepted that this pH halts steel corrosion due to the formation of a microscopically thin adherent layer of iron oxide (Fe_3O_4) at the steel surface. This layer itself represents corrosion product but the rate of corrosion becomes significantly small, and the steel becomes passivated (e.g. [Schiessel 1993]). When chloride ions are present in sufficient concentration at the steel surface, the protective film is destroyed, and the steel is depassivated even at high pH. While it is generally agreed upon that chlorides act as a catalyst to the corrosion reaction, the process of depassivation and activation is not fully understood [Zibara & Yamada, 2002]. Calcium chloride, or any chloride-containing admixture, is normally no longer permitted in concrete containing steel, but is generally accepted that small amounts of chlorides from any of other sources can be tolerated and that a threshold level is required to depassivate the steel allowing the corrosion start. A review of the literature shows that there is no unique value of the chloride threshold applicable to all mix ingredients, and under all exposure conditions. Instead, the published results show large variations in the chloride threshold levels.

Crystallization of salts is widely recognized as a cause of deterioration of porous building materials. Salt crystallization is physico-chemical degradation process characterised by salt crystals growth and exerted stresses on the pore system of materials that can lead to serious damage [Lewin 1982]. The degradation can be caused also by salt recrystallization, whereas the substances with higher number of molecules originate. In literature, different values of crystallization pressures can be found, depending on the temperature, material saturation and ratio of supersaturation of salt solution. In Table 1, orientation values of salt crystallization pressures are presented according to Rovnaníková [2007]. Looking at this table, one can see high crystallization pressures that can in relation to composition of materials' inner structure damage their structural stability and other related physical properties.

Table 1. Salt crystallization pressures.

Compound	*Crystallization pressure [MPa]*
$CaSO_4 \cdot 2H_2O$	28.2
$MgSO_4 \cdot 2H_2O$	10.5
$Na_2SO_4 \cdot 10H_2O$	7.2
$Na_2CO_3 \cdot 10H_2O$	7.8
NaCl	55.4

Except chloride crystallization and induced reinforcement corrosion, also the different thermal expansion of salts and solid materials of matrix play an important role within the process of concrete weathering and degradation. Typical example is NaCl that expands by approximately 9% between 0°C and 100°C, whereas the volumetric expansion of granites and calcite is only about 0.3% in this temperature range [Rijniers, 2004]. This mechanism was observed in many buildings, especially in structures that experience a day/night cycle.

Also the chemical action of chloride ions must be considered within the damage assessment of concrete structures. When cement reacts with water in the presence of chloride ions, the C_3A ($3CaO \cdot Al2O_3$) and C_4AF ($4CaO \cdot Al_2O_3 \cdot Fe_2O_3$) phases react with chloride to form Friedel's salt what is accompanied by volume changes as well.

As the chloride induced weathering and degradation of concrete structures represent serious problem from the point of view of their durability and service life, detailed investigation of chloride transport into the inner porous structure of concrete is necessary. Within the description of salt ions transport, one must take into account also the fact that part of the salt ions is immobilized in the material and bounded on its surface or into its structure. This process is realized either on physical principle, where the salt ions are held to the surface of material inner structure due to the van der Waals forces between salt ions and material constituents. In addition to the adsorption of ions on the pore walls, there is also another effect that could play a significant role in ion binding to the pore walls. This is a possible reaction of ions with active phases of material that may be considered as the most important potential chemical mechanism of ion binding in porous materials. However, it should be noted that these reactions are not yet explored in all detail at the moment, and there are even not any conclusions concerning their products that would be generally accepted by the investigators' community [Jiřičková & Černý 2006]. On that account, chloride binding isotherms of several types of cement based mortars having different water/binder ratio, amount and size of aggregates, and cement weight, are measured in this paper. The measured binding isotherms are theoretically analysed, and related to total mass of used binder, sample mass and specific surface. Finally, the mechanisms of chlorides' binding are identified and described.

2 EXPERIMENTAL

In the experimental part of the paper, measurement of chloride binding isotherms of different types of cement based mortars were done usign modified absorption method. These measurement were done in order to get information on the effect of sand size gradation on binding capacity of studied materials.

2.1 Studied Materials

In this paper we studied five mortars (denoted QI – QV) modified with different sand particle distribution. The filler granulometry was chosen in respect to sample size for the performed experiments. The composition of studied concretes is given in Table 1. Portland cement CEM 52.5 R is product of cement factory Českomoravský cement Radotín, Czech Republic, whereas the silicious sand is coming from sand-pit Bratčice, Czech Republic. The specific surface area of used cement was 384 m^2/kg. The tested mixtures were prepared from the different sand fractions, as showed in Table 2. The water/dry substances (w/d) ratio was then slightly modified in order to keep the workability of fresh mixtures on the same level.

Table 2. Composition of studied mortars.

Concrete	*Portland cement CEM I 52.5 R* [kg]	*Sand (0 – 4 mm)* [kg]	*w/d ratio* [-]
QI	0.5	-	0.45
QII	0.1	0.3 (0-1)	0.45
QIII	0.1	0.3 (0-1;1-2)	0.45
QIV	0.1	0.3 (0-1;1-2;2-4)	1.20
QV	0.1	0.3 (0-1;1-2;2-4)	1.00

The test specimens (prisms 160 x 40 x 40 mm) were prepared according to standard "ČSN EN 196-1 – Methods of cement testing". After the curing period of 28 days in wet conditions, the samples were stored at the laboratory temperature of 22 ± 2°C to remove moisture. The samples for the measurements of chloride binding isotherms were cut from the standard prisms. Final size of samples for chloride binding isotherms measurement was 40x40x10 mm.

For basic characterisation of studied materials and explanation of results, measurement of basic material properties was done. Bulk density was determined by gravimetric method with accuracy ± 3% according to the standard "ČSN EN 1936". Matrix density was measured with helium pycnometer Pycnomatic ATC. Porosity was calculated by help of density and bulk density with accuracy ± 3%. The basic properties of studied fine grained concretes are given in Table 3. Spesific surface was measured with Sorptomatic 1990 (ThermoFinnigen, Italy) using nitrogen adsorption. We can observe that absent 2-4 mm sand fraction in materials lead to lower bulk and matrix density, which corresponds to higher open porosity. Values of specific surface depend not only on the pore size and content, but also to particles size and distribution.

Table 3. Basic properties of mortars.

Concrete	*Bulk density* [kg/m^3]	*Matrix density* [kg/m^3]	*Total open porosity* [-]	*Specific surface* [m^2/g]
QI	1 893	2 199	14	8.8
QII	1 543	2 507	38	5.2
QIII	1 665	2 514	34	10.9
QIV	1 944	2 522	23	12.2
QV	2 036	2 529	19	12.3

2.2 Experimental Methods

Water movement is the most significant factor in the process of transporting salt ions from the surface into the porous matrix. However, the matrix is not inert to the ions and only a part of them penetrating into the porous system can be freely transported in the solution, another part of ions can be bound on the pore walls due to either physical or chemical mechanisms [Černý & Rovnaníková 2002]. Therefore, two basic ion phases are generally presented in material, namely free ions that are dissolved in pore water, and bound ions that are fixed on the pore walls.

It is very difficult to distinguish between the physical and chemical bonding mechanisms on the macroscopic level, so, for practical reasons both these effects are usually unified into one phenomenological ion storage parameter. This is the dependence of the amount of bound ions C_b [kg/m$^3_{(sample)}$] in the material on the free ion concentration C_f [kg/m$^3_{(solution)}$] in the pore solution in

equilibrium conditions that is called the ion binding isotherm. From that definition is clear, for its determination it is necessary to measure both the content of free ions and the content of bound ions in the same specimen under equilibrium isothermal conditions. In this work, the chloride binding isotherms of studied materials were measured using modified adsorption method [Jiřičková & Černý 2006]. Firstly, the samples were put into water salt solution of specific known concentration until the equilibrium is reached. Then, the salt concentration in particular sample was measured and point wise function $C_b=C_b(C_f)$ determined. In this paper, the salt concentration in the analyzed solutions was measured using ion chromatography.

Liquid-solid adsorption chromatography (LSC) is one of the forms of liquid chromatography in which the stationary phase is a solid adsorbent. In our case glass column is filled with hydroxyethylmethacrylate sorbent which is stable for pH 2-12. For anion concentration measurement as a mobile phase 5mM KHP, 5% CAN is used. Firstly, measuring device should be calibrated with no less than two different concentrated solutions. Tested solution has to be filtered into the syringe to remove solid particles. Then filtered solution is diluted and with Hamilton syringe injects into Rheodyne Injection Kit. This simple manual device for accurate and reproducible sample injecting consists of Rheodyne 7725i injecting valve, 20 µl sample loop, and holder for mounting of the valve to a pump or to a detector. MIK 010 enables injection of 1 µl to 5 ml of a sample according to used sample. Conductivity detector is designed to continuously determine electrical conductivity of liquids that pass through its detector cell (capacity 2.5 µl) which is connected to an ion chromatograph. As the solution conductivity is highly affected by its temperature, temperature around the detector cell is kept at a constant level by temperature control system using a heater. The last part of measuring device is intelligent instrument interface box designed to collect analogue data, and input and output digital signals. Special scientific software enables to control measuring process, to calibrate device, and to collect and evaluate results. Fig. 1 represents output of ion concentration measurement.

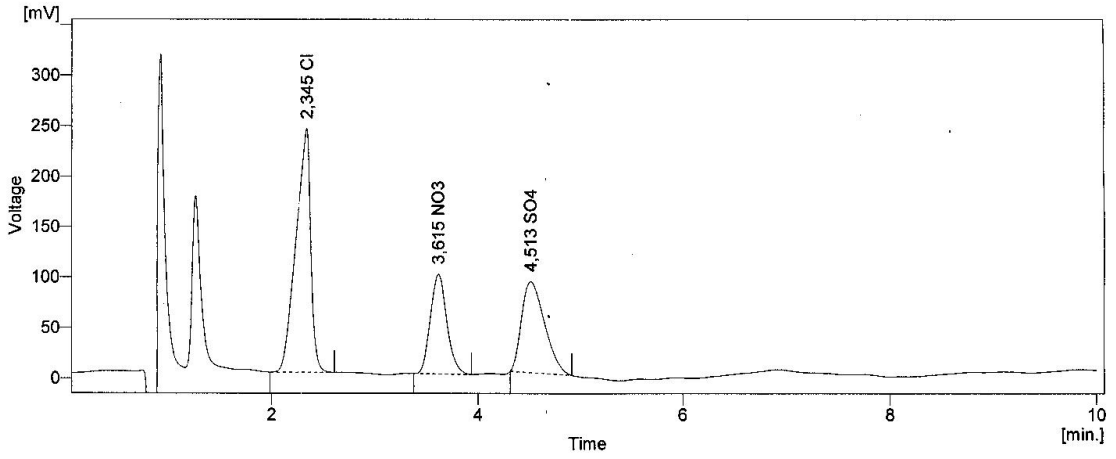

Figure 1. Output of ion chromatography measurement.

The ion chromatography is the most precise analytical method for very low ions concentrations determination. However, it should be noted that liquid chromatography is high sensitive device and it is important to use ultra-pure water with conductivity below 0.1 µS/cm.

3 RESULTS AND DISCUSSION

In the experimental work, the adsorption method investigated by Tang and Nilsson [Tang & Nilsson 1993] was followed with some modifications. The dry samples were placed into the cups with 200 ml chloride solution. Then they were stored in laboratory at the temperature of 22±2°C to reach equilibrium. The inside solutions were analyzed after 4 months and the concentration of chlorides was determined by liquid ion chromatography desribed above. From the obtained data the bound chloride

content was calculated and chloride binding isotherms were plotted. The ion binding isotherms measured for NaCl water solution by modified adsorption method are presented in Figs. 2-4.

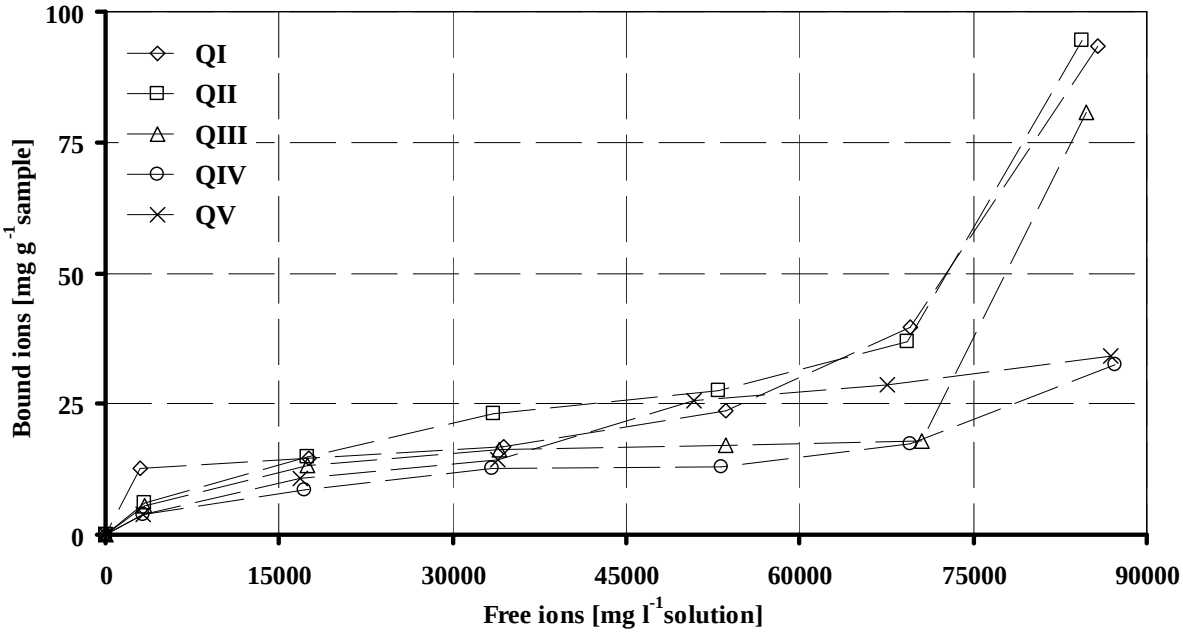

Figure 2. Chloride binding isotherms of studied mortars relative to the samples' weight.

Fig. 2 gives information on binding capacity of studied fine grained concretes relative to the samples' weight. This data represents the highest possible value of steady state bound salt concentration at specific concentrations of NaCl water solution. Looking at this data one can see that the measured binding isotherms are for all studied materials almost similar at lower free ions concentrations. On the other hand, at higher NaCl water solution concentrations, the remarkable differences between the binding capacities of particular materials can be observed. Typically, the highest values of bound chlorides were measured for materials QI, QII, QIII. The lowest values were obtained for materials QIV, QV.

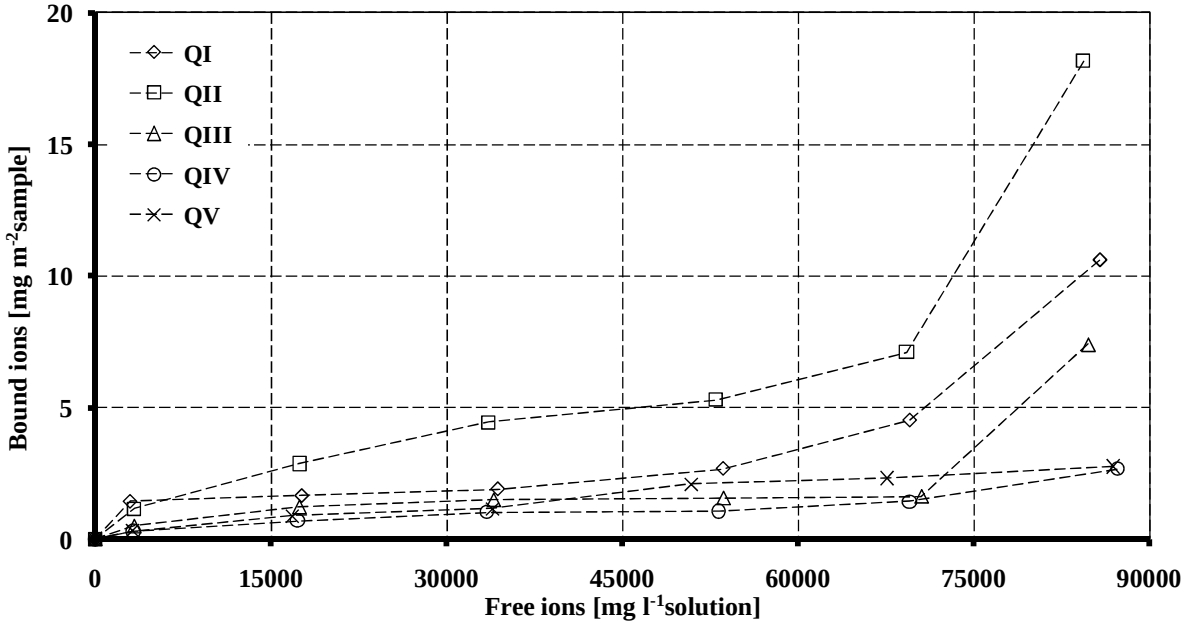

Figure 3. Chloride binding isotherms of studied mortars relative to the specific surface.

If the chloride binding isotherms are recalculated to the specific surface of each material, we obtain slightly different results as showed in Fig. 3. The highest binding capacity clearly presents sample QII (18 mg bonding Cl^- to m^2 of sample), lower capacity has cement paste QI (11 mg bonding Cl^- to m^2 of sample), and concrete QIII (7 mg bonding Cl^- to m^2 of sample). The lowest binding ability can be observed in samples QIV and QV (3 mg bonding Cl^- to m^2 of sample).

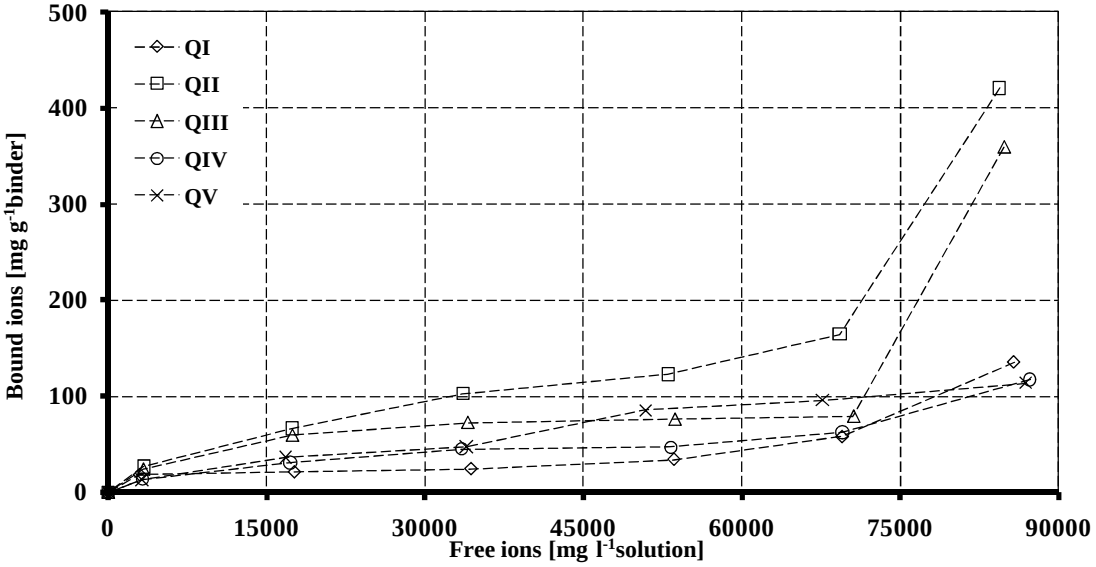

Figure 4. Chloride binding isotherms of studied mortars relative to the samples´binder content.

Finally, the amount of bound ions can be relative to the samples´ binder content as represents in Fig. 4. We can see quite different curves of binding isotherms. The highest binding capacity has again sample QII, with maximum of 420 mg bonding Cl^- to g of cement, the binding isotherm of QIII comes after, with maximum of 360 mg bonding Cl^- to g of cement. Consistent curves can be observed in sample QI and concretes QIV, QV, with maximum of 120 mg bonding Cl^- to g of cement.

4 CONCLUSIONS

In this work, chloride binding isotherms of several types of cement based mortars having different granularity of sand were measured. The obtained data represent significant information on studied materials' performance in contact with chloride water solution and can be used for damage assessment of investigated concretes. Looking at the obtained data, in all studied cases the measured chloride binding isotherms exhibited linear behavior characterized by to different slopes of the measured linear dependence of bound chloride concentration in material on free chloride concentration at solution.

The obtained results clearly demonstrates important role of the way of presentation of experimental results that can be relative to sample mass, specific surface or binder content. If materials having similar base, structure and specific surface are tested, the amount of bound salt ions can be attributed to the material sample's weight. In case of comparison of binding capacity of materials having different porosity, composition, etc., there is necessary to introduce another comparative parameter, for example specific surface for porous building materials of binder weight for materials on cement or lime hydrate basis. This finding reveals the mechanisms of chloride binding that are based either on physical principles relative to specific surface of materials or chemical principles relative to chemical and structural composition. However, for detailed explanation of binding process and its mechanisms, other analysis will be necessary. This research will be focused especially on chemical analysis of materials containing bound chloride ions and investigation of new chemical substances formed within the binding process.

ACKNOWLEDGMENTS

This work has been financially supported by the Ministry of Education, Youth and Sports of Czech Republic, under project No MSM: 6840770031.

REFERENCES

Černý, R. & Rovnaníková, P. 2002, 'Transport Processes in Concrete'. Spon Press, London.

Lewin, S. Z. 1982, 'The mechanism of masonry decay through crystallization', Conservation of Historic Stone Buildings and Monuments, National Acad. Press, Washington, DC, 120-144.

Navi, L., Saari-Nordhaus, R. & Anderson, J. M. 1993, 'Chromatographia', Journal of Chromatographia, **640**, 41-48.

Jiřičková, M. & Černý, R. 2006, 'Chloride Binding in Building Materials', *Journal of Building Physics*, **29**, 189-200.

Pavlík, Z. 2009, *Identification of parameters describing the coupled moisture and salt transport in porous building materials*, Habilitation thesis, CTU Press, Prague.

Rijniers, L. A. 2004, *Salt crystallization in porous materials: an NMR study*, Ph.D. thesis, Technische Universiteit Eindhoven, Eindhoven.

Rovnaníková, P. 2007, *Environmental deterioration of materials*, Chapter No. 7 - pollution effects on other building materials, WIT Press, Southampton.

Schiessel, P. 1993, 'Concrete as a Medium for Protecting Steel Reinforcement Against Corrosion', Durability of Reinforced Concrete in Aggressive Media, Balkema, Rotterdam.

Tang, L. & Nilsson, L. O. 1993, 'Chloride binding capacity and binding isotherms of OPC pasted and mortars', Cement and Concrete Research, **23**, 247-253.

Zibara, H. &Yamada, K. 2002, 'Chloride Penetration into Concrete – A Review of Mechanisms and Models', Journal of Research of the Taieheiyo Cement Corporation, **142**, 123-138.

XII DBMC
International Conference on Durability of Building Materials and Components
PORTO - PORTUGAL, April 12th-15th, 2011

The Effect of Moisture Environment on Lightness of Concrete

Lingzhi Liu [1]
Kyoji Tanaka [2]

ABSTRACT

When the exterior surfaces of concrete buildings become wet during rainfall, the gray color of the structures turns considerably dark. This is because concrete is a porous material, and the reflection of light by concrete is affected by the moisture entering into the fine pores. So the concrete surface are expected to change in color according to change of moisture of environment.

The effect of moisture on color of concrete, particularly lightness of cement paste surface and the mechanism of the change were studied. First, in absorption and desorption of moisture process, the lightness of cement paste of various water cement ratios, which were kept at nine stages moisture environments for more 3 months, were measured. It was found out that they have hysteresis loops in lightness as well as in weight in absorption and desorption of moisture process. Then the pore structures of them were furthermore studied through observation by the AFM and measurement by the mercury intrusion technique. The scattered granular clusters of hydrates were observed, and it was extremely similar to shape of the cement hydrates. And it indicated the existence of pores from which mercury draining is difficult even after decompression.

Therefore, the mechanism of the hysteresis in lightness of cement paste surface is explained using a model composed of pores of cone shapes and ink-bottled ones.

KEYWORDS

Cement paste, Moisture environment, Hysteresis in lightness change, Pore structure, Ink-bottle effect.

[1] Structural Engineering Research Center of Tokyo Institute of Technology, Tokyo, JAPAN, tanaka@serc.titech.ac.jp
[2] Structural Engineering Research Center of Tokyo Institute of Technology, Tokyo, JAPAN, liu.l.ab@m.titech.ac.jp

1 INTRODUCTION

When the exterior surfaces of concrete buildings become wet during rainfall, the gray color of the structures turns considerably dark. This is because concrete is a porous material, and the reflection of light by concrete is affected by the moisture entering into the fine pores. Further, the color of concrete changes when the environmental humidity is high because concrete has numerous gaps, and as a result, moisture is adsorbed on the concrete surface. The exterior vision assessment with building is not done in consideration of the change in the outdoor weather now. However, in the climate where the hydric environment changes greatly by the season like Japan, it seems that knowing whether the surface of concrete has caused the change in what lightness becomes a useful finding as basic information on the architectural exterior design.

In this study, we aim to examine how the lightness of the concrete surfaces changes when the environmental humidity changes or when they are exposed to moisture. Further, we wish to clarify the mechanism of change in lightness and the pore structure of concrete.

2 CHANGES IN THE WEIGHT AND LIGHTNESS OF CEMENT PASTE WITH ENVIROMENTAL HUMIDITY

2.1 Materials

Test pieces of portland cement paste (water content: 22%, 30%, or 40%) were used in this study. The cement-paste samples were then poured into a mold with a diameter of 50 mm and length of 100 mm from which they were removed on the same day and subsequently cured in water for 90 days. The obtained samples were then cut using a concrete cutter to obtain final discoid test pieces with a thickness of about 5 mm and a diameter of 50 mm.

2.2 Control of Environmental Humidity During the Experiment

In the humidity adsorption process, first, the test pieces were dried at a temperature of 105 °C for 24 h using a drying apparatus, and at the end of the drying process, the test pieces were assumed to be completely dry. Next, the test pieces were placed in a constant-temperature room (20℃±2℃). The test pieces were allowed to remain in this room until their weights became constant; the desiccator method was employed to obtain test pieces with constant weights. Table 1 lists the humidity control material (nine stages) used in the experiment, and Figure 1 shows the equipment used for humidity control (in the desiccator method).

Table 1. The humidity control material used in the experiment

Relative humidity (RH)	*Humidity control material*
0%	105℃, 24H
8%	SiO_2・nH_2O (drying agent)
33%	$Mgcl_2$・$6H_20$ saturated aqueous solution
53%	$Mg(NO_3)_2$・$6H_20$ saturated aqueous solution
75%	NaCl saturated aqueous solution
85%	KCl saturated aqueous solution
93%	KNO_3 saturated aqueous solution
98%	K_2SO_4 saturated aqueous solution
100%	removal of surface water after water pickup of 48 hours



Figure1. Photo of the Equipment.

In the humidity desorption process, the test pieces were first soaked in water for 48 h, at the end of which the pieces were taken out and their surfaces were thoroughly wiped with a dry cloth. Next, the

desiccator method was employed to obtain test pieces with constant weights; in this method, the samples were allowed to remain in the constant-temperature room until the weights of the test pieces became constant, as in the case of the humidity adsorption process. The change in the weight during the experiment was periodically measured, and it checked that it would be in an equilibrium situation about weight. In addition, in this experiment, the left period at given a given relative humidity (R.H.) was of three months.

2.3 Gravimetric Measurement and Measurement of Lightness

2.3.1 Gravimetric Measurement

The test pieces placed in the desiccator were weighed on an electronic balance. The electronic balance was placed immediately next to the desiccator so as to suppress the effect of environmental humidity on the measurement results to the maximum possible extent. In this case, the test pieces could be weighed as soon as they are removed from the desiccator (The minute weight change in the measurement was disregarded, and it was assumed the condition of equilibrium).

Moreover, the gravimetry when underwater soaking it was measured by two states that the test piece was taken out of water and the state that the dripping drop of water is lost and the surface are wiped off with the cloth.

2.3.2 Measurement of Lightness

In the humidity adsorption and humidity desorption processes, after the weight had been balanced, the lightness of the test pieces were determined by using the L*a*b* system. The L*a* b* uniform color space defined in JIS Z8729 was used in this study. The L*a*b* system is currently the most popular color specification system; it is a numerical scale that enables the user to visualize and match colors and is well suited for determining the color of concrete.

The measurement equipment used the spectrophotometric color difference meter (NF333 of NIPPON DENSHOKU INDUSTRIES CO., LTD).The range of light of the measurement receiving of this device was 8mmφ, and five points of each test piece were measured.

2.4 Experimental Results

2.4.1 Weight Change

The equilibrium moisture content of the test pieces were calculated from the R.H. using Eq. (1).

$$\text{Equilibrium moisture content (\%)} = \frac{W - W_{dry}}{W_{dry}} \times 100$$

Where W : the equilibrium weight of a test piece at a given R.H. (g)
W_{dry} : the bone-dry weight of the test piece (g)

Figure 2 shows the relationship between the R.H. and the change in the weight of the test pieces by the equilibrium moisture content. The equilibrium moisture content of each test piece tends to increase with the R.H. As shown by the results of numerous previous studies[1)], the weights of the test pieces do not change in the same manner during the adsorption and desorption processes; hysteresis is observed in the adsorption and desorption processes. That is, the equilibrium moisture content changed to the humidity desorption high overall compared with the moisture uptake process.

2.4.2 Change in Lightness

Figure 3 shows the lightness L* of each test piece at the equilibrium humidity and weight. It is expected that during rainfall, water films are formed over the exterior surfaces of buildings.

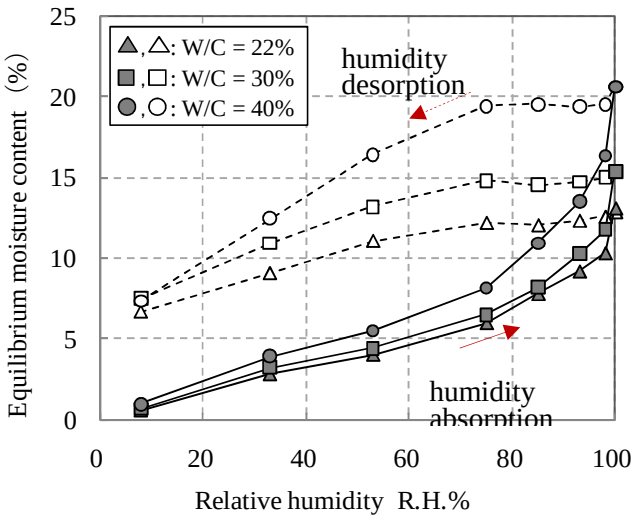

Figure 2. Equilibrium humidity content.

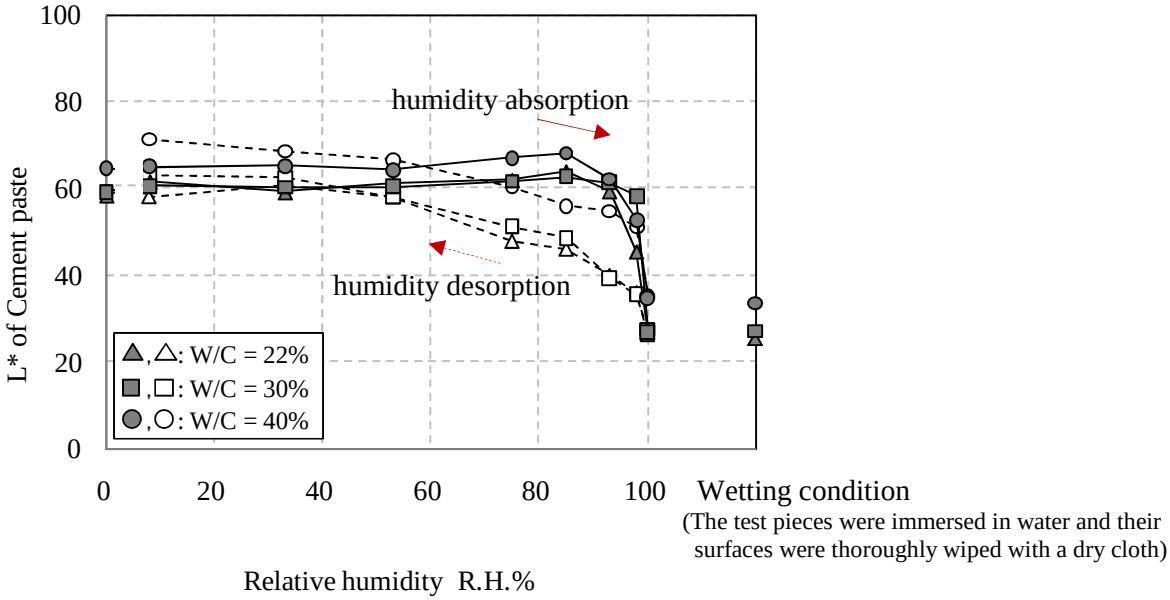

Figure 3. Chang in L* by relative humidity.

To determine the change in the lightness of the concrete as in the case of building surfaces during rainfall, the test pieces were immersed in water (Wetting condition) and the change in the lightness was measured. The influence of environmental humidity was evaluated on the basis of the change in L*, and the L* value of each test piece tends to decrease with R.H. However, the change in the lightness is comparatively higher in the case of high humidity. Further, the change in the equilibrium moisture content with the R.H. was as described in the preceding paragraph; in the case of low humidity, no changes were observed. Moreover, rapid changes in the lightness were observed under high-humidity conditions up to R.H. of 100%. This is exceeded, and the change in color observed in the case of the “Wetting condition” with excessive water is small.

In addition, the L* value of the test pieces do not change in the same manner during the adsorption and desorption processes; hysteresis is observed in the adsorption and desorption processes. During the humidity adsorption process, the change in the L* value is remarkable for a narrow R.H. range of 85% to 100%. On the other hand, during humidity process, the changes in the L* value is in a wide R.H. range of 55% to 100%.

3 PORE STRUCTURES OF CEMENT PASTE

3.1 Surface Structure

The fine surface structure of test piece of cement paste was studied by carrying out atomic force microscope (AFM) measurements. A nanoscale Hybrid N8000 (KEYENCE) with a probe of diameter 40 nmφ was used to carry out the AFM measurements. Since the observation area had to be less than 200 μm × 200 μm, measurements were performed at several points on the surface of the test piece.
Figure 4 shows the AFM observation results. The cross section of the part indicated by the broken lines in the photograph is also shown below Photograph 2. Since the surface of the test piece was scanned using a cantilever with the attached probe, a broad image was obtained to some extent. Scattered granular clusters of hydrates were observed, and regions where hydrated are absent with width of several micrometers are observed at some regions on the surface. This observed shape of the hydrates was extremely similar to "Type III C-S-H," which is the shape of the cement hydrates described in Literature [2)]. However, the surface was not very smooth, and projections and depressions with a height and depth of several micrometers, respectively, were observed over the surface; this was because the test piece was cut using a concrete cutter, and no grinding was carried out.

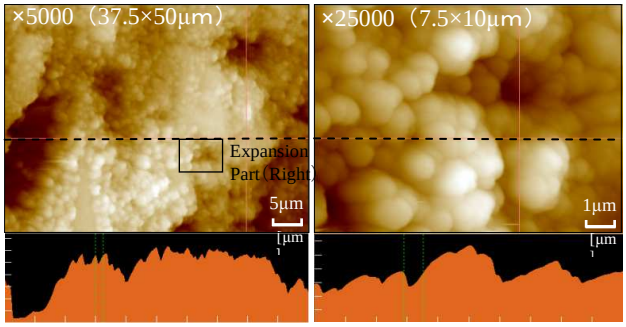

Figure 4. Photo of surface figure of cement paste by AFM measurement.

3.2 Internal Structure

The distribution of pore structures within the cement-paste test piece was studied using the mercury intrusion technique. Specimens with areas of several square millimeters were cut from the previously described test pieces (water–cement ratios: 22%, 30%, and 40%). They were dried in a dryer at 105 °C for 24 h, and then, analyzed using a mercury intrusion porosimeter (Autopore IV 9500, measured pore area: 5 nm–500 μm). The measurements were performed by carrying out the mercury intrusion process in which the specimens were compressed by applying a pressure of 228 MPa and the mercury drain processing in which the pressure was released.

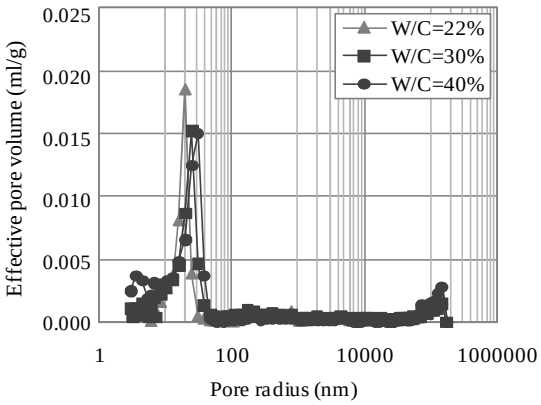

Figure 5. Distribution of pore radius.

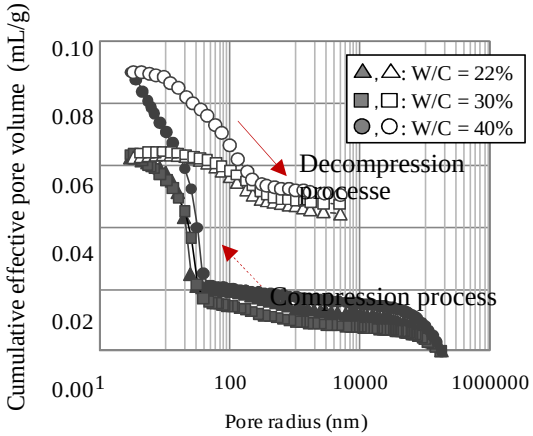

Figure 6. Accumulated effective pore volume.

Figure 5 shows the distribution of the radii of pores, determined by the mercury intrusion technique. It is observed that pores with radii of 20 to 30 nm are the most common, while pores with radii of 5 nm to 30 nm contribute to more than 70% of the total pore volume. These results are similar to those mentioned in the literature [3] for normal hardened cement.

Figure 6 shows the cumulative effective pore volume as a function of pore radius for the specimens subjected to compression and decompression. During the compression process, as the compression force increased, an increasing amount of mercury intruded into the cement paste and filled the supposedly cylindrical pores; as a result, the pore diameters decreased. In the decompression process, however, a considerable amount of mercury, which filled the pores during the compression process, did not drain out of the pores. The volume of mercury that did not drain out was about 50% of the total pore volume. This indicated the existence of pores from which mercury draining is difficult even after decompression. These pores are generally called ink bottle pores [4) – 6)].

4 DISCUSSION

4.1 Effects of Water on Color of the Specimens

In general, the surface of a solid substance is not completely smooth but has microscopic projections and depressions which cause the incident light to be diffusely reflected from the surface and as a result, the surface appears very bright and almost white in color. However, if a thin film of water is formed on the surface of the substance, a part of the incident light will be absorbed by the water film and the intensity of the reflected light will be low. In addition, water, which has a low rate of reflection, fills the small depressions and reduces the rate of diffuse reflection. As a result, the color of the surface appears to be darker.

It is considered that the lightness of cement paste reduces because of the water film to the surface. Thus, we assumed that with an increase in the environmental humidity, the number of pores that are filled with water increases, and therefore, the area over which diffuse reflection occurs decreases.

4.2 Hysteresis in Lightness

Hysteresis in the lightness of the surface is observed clearly during the adsorption and desorption processes. This indicates that the conditions for water adsorption into the pores are affected, and that the ink bottle model may be suitable for studying the hysteresis in lightness.

In general, the pores on the surface of hardened cement, which is a porous material, are considered to be cone shaped, i.e., with large openings and gradual reduction in size toward the deeper end, or reverse-cone shaped, i.e., with small openings and gradual increase in size toward the deeper end. In this study, we considered the former to be cylindrical pores with various diameters and volumes as shown in (a) on the right side in Figure 7 and the latter to be ink bottle pores with various opening diameters and volumes as shown in (b) on the right side in Figure 7. The pores of the hardened cement were considered to be a combination of many of these (however, in Figure 7, the illustration is simplified and only three examples of each type of pores are shown).

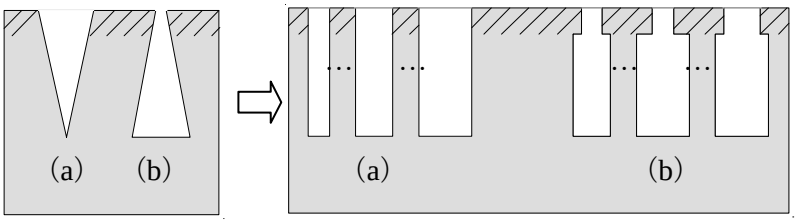

Figure 7. View showing a frame format of pore shapes.

According to the capillary condensation theory, in porous materials such as concrete, with an increase in the relative pressure during the water adsorption process, water from the pores with small diameters gradually fills the pores with large diameters (in the case of adsorption of a gas on a solid surface, first a monolayer and then a multilayer are formed as the relative pressure P/Po increases, and in addition to the adsorption of water, capillary condensation occurs if pores exist on the solid surface. This phenomenon can be explained on the basis of the relative humidity, which is calculated by using the Kelvin formula, which is given by equation (2). Figure 8 shows the condensation radius for the different relative humidities calculated by the Kelvin formula.

$$r_k = -\frac{2\gamma V_m}{\ln \frac{P}{P_0} RT}$$

Where, r_k : kelvin radius （m）
γ : surface tension of liquid （N/m）
Vm : molar volume of liquid （m^3/mol）
P: vapor pressure
P_0 : saturated vapor pressure
R: gas constant （J/mol・K）
T: absolute temperature （K）

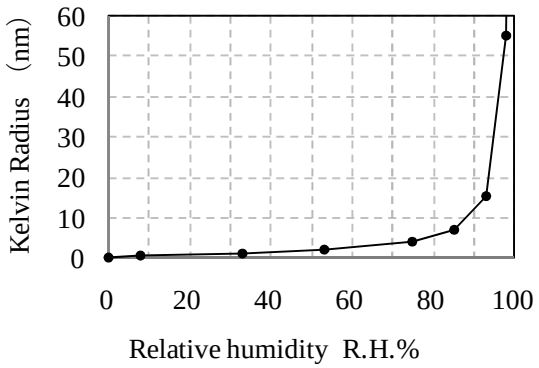

Figure 8. Kelvin radius with relative humidity （20℃).

During the desorption process, water from the pores with large opening diameters is drained first. Figure 9 shows a schematic illustration of the change in the lightness with the humidity observed when this pore model and the test piece in which water–cement ratio is 30% are used.

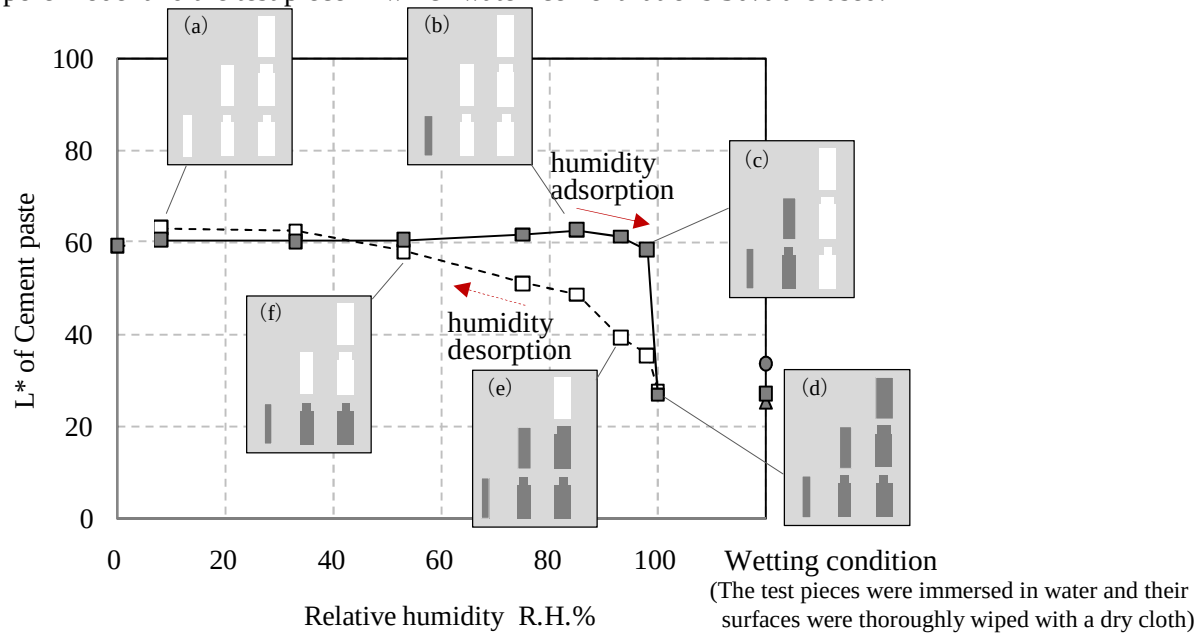

Figure 9. A schematic illustration of the change in the lightness with the humidity observed.

First, during adsorption process, nearly all gaps were empty in the low-humidity range (a), as shown in Figure 9. When R.H. was in the range of 85–90% R.H. (b), the water fills only the fine gaps, and the volume of water absorbed in the pores was small. At a higher R.H (c), water begins to fill the larger pores. For reference, water starts to condense in the pores with radii more than or equal to 10 nm when R.H. exceeds 90%, as shown in Figure 8. When humidity increases above 90%, the number of pores with radii of 20 nm increase, as shown in Figure 5, the number of empty gaps that cause diffuse reflection decreases, and the lightness decreases rapidly.
At relative humidity (R.H.) of 100% (d), all the pores except for those with significantly large diameters are filled with water. At this point, the lightness reaches the lowest value.

The lightness would decrease further if there is excess water that does not condense even at a relative humidity of 100% or if water fills even fairly large gaps (i.e., when water on the surface is excessive, e.g., in the case of heavy rainfall). However, this reduction in lightness would be small.

On the other hand, during desorption, water is first released from the pores with large opening diameters (e). However, water is not easily released from the ink bottle pores. Therefore, the increase in lightness occurs slowly during the desorption process. It begins to stabilize around the moderate humidity range of approximately 40–50% R.H. (f), and as the humidity continues to decrease, the change in the lightness are small. Then, the water is drained completely from all pores, and the conditions shown in (a) in Figure 9, i.e., conditions for absolute dry condition, are delivered by forcefully.

5 CONCLUSION

In this study, we analyzed the changes in the lightness of cement paste with changes in environmental humidity. The conclusions are summarized below:
(1) The lightness of the cement paste varies with the environmental humidity and decreases with an increase in the humidity.
(2) The changes in the lightness of cement paste during the adsorption process are different from those in the desorption process; hysteresis is observed.
(3) During the adsorption process, the lightness changes considerably within a relatively narrow R.H. range of 85 to 90%. On the other hand, during desorption, the lightness changes considerably for a relatively wide range of R.H. from 40 to 50%.
(4)We proposed a pore model that includes ink bottle pores and explained these phenomena qualitatively.

ACKNOWLEDGMENTS

The authors express sincere gratitude to Ph.D. Masayuki Tsukagoshi of Tokyo Metropolitan University, M.Eng. Taku Kano of Nomura Co., Ltd., Dr. Takashi Akatsu of Tokyo Institute of Technology and Dr. Naoya Miyajima of University of Yamanashi.

REFERENCES

Powers, T.C. and Brownyard, T.L.: Studies of the physical properties of hardened cement paste, J.ACI, Vol.18, No2, pp.101-132, 249-336, 469-504, 1946.

C&C Encyclopaedia [Basic explanation of cement concrete chemistry], Japan Cement Association, pp.22-26, pp.171-172, 1996.7.

Osamu Katsura, Kaname Urushizaki, Toshiyuki Yoshino and Eiji Kamada: The Relation between Moisture Desorption and Pore Structure Measured by Mercury Poresimetry, Concrete Researoh and Technoligy, Vol. 10, No. 1, Jan. 1999, pp. 65-77, 1999.

S. Lowell and Joan E. Shields: Hysteresis, Entrapment, and Wetting Angle in Mercury Porosimetry, Journal of Colloid and Interface Science, Vol. 83, Issue 1, September 1981, pp.273-278, 1981.

Koichi Maekawa, Rajesh Chaube and Toshiharu KishiE&FN SPON Press, 1999.

F. Moro and H. Böhni: Ink-Bottle Effect in Mercury Intrusion Porosimetry of Cement-Based Materials, Journal of Colloid and Interface Science, Volume 246, Issue 1, pp.135-149.

XII DBMC
International Conference on Durability of Building Materials and Components
PORTO - PORTUGAL, April 12th-15th, 2011

The Sulfate Attack in Concrete by Degradation of Iron Sulfides and the Effect of the Host Rock

Servando Chinchón-Payá [1]
Izelman Oliveira [2]
Antonio Aguado [3]
Servando Chinchón [4]

ABSTRACT

In this study we deal with the problems of durability of concrete made with reactive aggregates, and more particularly those containing oxidizable iron sulfides. These sulfides are oxidized in the presence of water, to generate sulfates. Those sulfates react with the cement aluminates to form ettringite and / or thaumasite, which are highly expansive nature.

We present an experience that demonstrates the differences in the amount of expansive compounds that are generated based on the type of iron sulfides (pyrite and pyrrhotite). The paper also makes clarifications on the role of host rock. In the case of limestone, the buffering effect of calcite minimizes the effects of degradation of sulfides in contrast to the shale type lithology.

KEY WORDS

Reactive aggregates, Iron sulfides, Ettringite, Thaumasite, Host rock.

[1] University of Alicante, Alicante, SPAIN, s.chinchonpaya@ua.es
[2] Polytechnic University of Catalunya (UPC), Barcelona, SPAIN, antonio.aguado@upc.es
[3] Polytechnic University of Catalunya (UPC), Barcelona, SPAIN, izelmanoliveira@yahoo.com.br
[4] University of Alicante, Alicante, SPAIN, s.chinchon@ua.es

1 REACTIVE AGGREGATES

The Durability problems in portland cement concrete due to reaction between cement alkalis with certain types of aggregates are well known. The most popular reactions are the alkali-aggregate AAR among which are the alkali-carbonate and alkali-silica. There is less documentation of the expansions produced in concrete as a result of the degradation of iron sulfides contained in aggregates, a phenomenon known as "internal sulfate attack".

The *alkali - carbonate* reaction occurs in some concretes with dolomitic rocks as aggregates. In an alkaline medium, portlandite reacts with dolomite (calcium-magnesium carbonate) to form brucite (magnesium hydroxide) and calcium carbonate in a reaction called dedolomitization. When brucite absorbs water, it increases in volume and causes expansions [Min and Mingshu 1993].

The alkali-silica reaction (ASR) is the most studied alkali-aggregate reaction, and it commonly occurs when the alkali present in the concrete pore solutions react with low crystallinity siliceous aggregates. After this reaction it is formed a gel that when imbibes water, increases in volume and expands [Hobbs 1988; Garcia-Diaz, *et al* 2006] (Fig. 1).

Fig. 2 shows the appearance of white gel, a symptom of alkali-silica reaction. The right part of the sample was stained with a selective staining to visually enhance and recognize these signs and the reaction products.

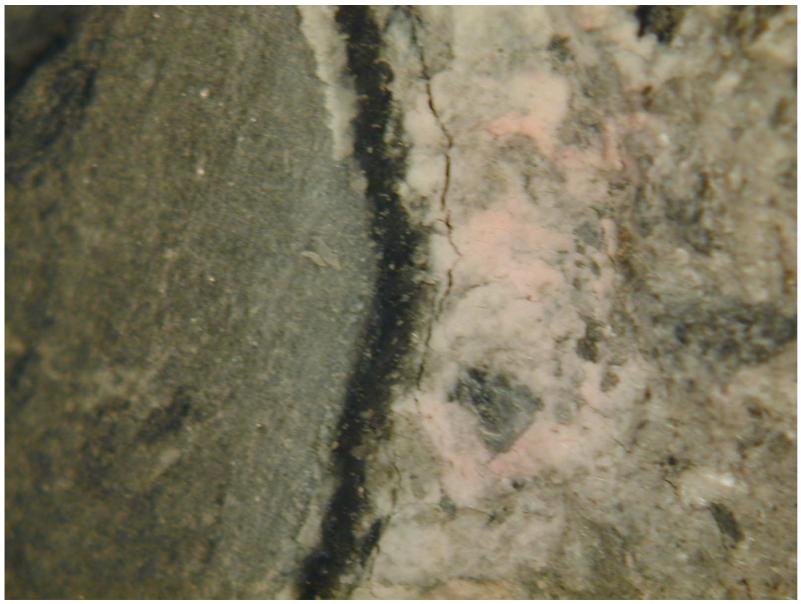

Figure 1. Characteristic features of the AAR. We can see the typical rims and the expansive gel. Photo of the authors.



Figure 2. Photograph that shows in the left side the typical (unstained) halos of AAR. In the right side, it has been applied a solution for staining the potassium. Photo of the authors.

The Internal sulfate reaction (ISR) is a phenomenon that occurs in some concrete made with aggregates with oxidizable iron sulfides. This type of reaction has been less studied and is less documented than the AAR but our Research Group has worked for years in the expansions of concrete dams with aggregates containing pyrite or pyrrhotite [Araújo *et al* 2008; Chinchón *et al*. 1990, 1993]. The identification of the type of iron sulfide is simple by SEM, by seeing its morphology and the S / Fe obtained from a precise EDX analysis by backscattered electrons, because the sample is conductive (Figs. 3 and 4).

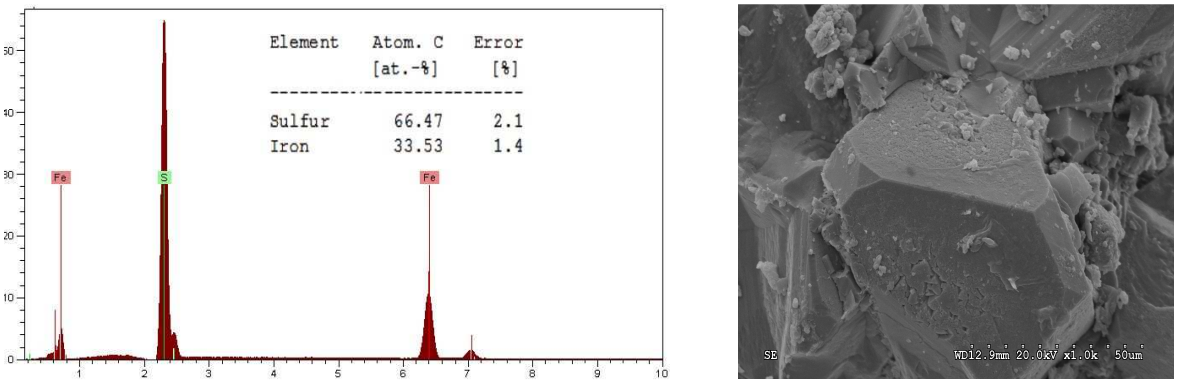

Figure 3. Morphology and EDX analysis of pyrite.

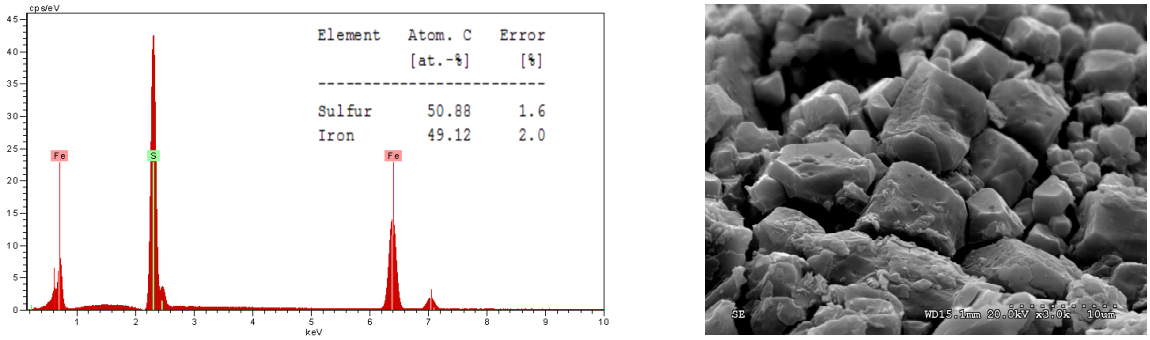

Figure 4. Morphology and EDX analysis of pyrrhotite.

When these sulfides are in an aqueous medium with dissolved oxygen they are oxidized to produce sulfates (equations 1 and 2) which can then form gypsum, secondary ettringite and in some cases thaumasite.

$$FeS_2 + 7/2O_2 + H_2O \rightarrow Fe^{2+} + 2SO_4^{2-} + 2H^+ \quad (1)$$

$$Fe_{1-x}S + (2-(1/2)x)O_2 + xH_2O \rightarrow (1-x)Fe^{2+} + SO_4^{2-} + 2xH^+ \quad (2)$$

In the literature there are references about the influence of the degradation of iron sulfides contained in aggregates on concrete durability, although nearly all the authors refer to the ettringite as the only neoformed expansive product [Ayora *et al* 1998; Tagnit-Hamou *et al* 2005], however under certain conditions thaumasite can be formed (Figs. 5 and 6).

The ettringite can form thaumasite if low temperatures and calcium carbonate are available. To form thaumasite there must be small ettringite crystals so that from them, epitaxially, the thaumasite crystals grow [Taylor 1997; Barnett *et al* 2003]. The thaumasite formation by sulfate attack is harmful to the durability of concrete because its formation causes expansion and because it consumes the CSH cement phase [Sahu *et al* 2002; Mehta 1993]. Although both ettringite and thaumasite have very similar acicular appearance when viewed by SEM, the presence of Si and the Al absence in thaumasite, and the presence of Al and no Si in the ettringite EDX analysis are decisive for its identification.



Figure 5. The SEM photograph shows an overall growth of ettringite crystals on the surface of concrete. Ettringite is filling the pores. A superficial crack in the cement paste can be appreciated.

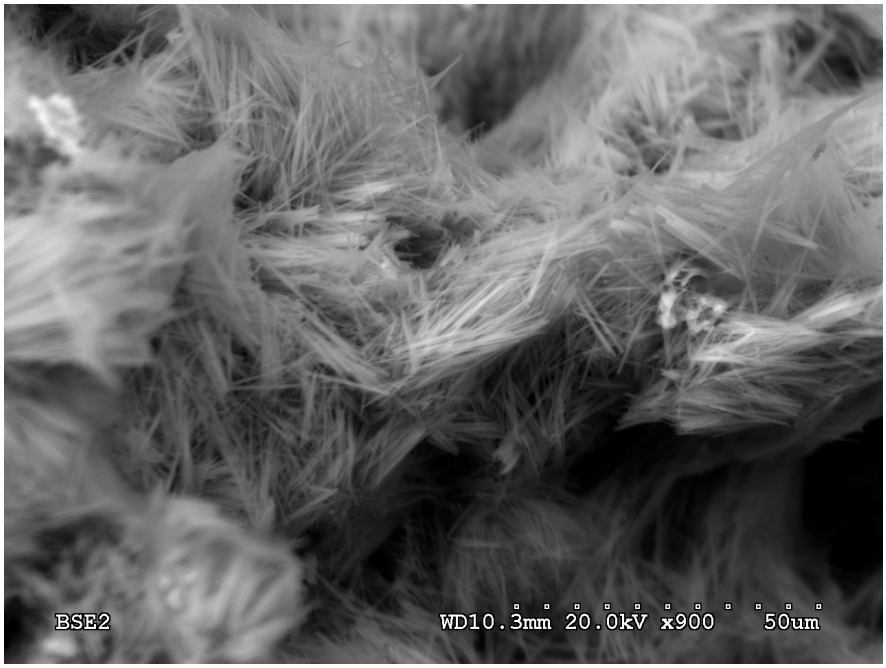

Figure 6. The SEM photograph shows an abundant acicular growth. EDX analysis confirmed that this is thaumasite crystals.

The Regulations governing the presence of iron sulfides in aggregates for concrete do not distinguish between pyrite and pyrrhotite, they neither refers to the importance of the host rock [EHE-08 2008; ASTM C294-05 2005]. These two aspects have been discussed in a recent paper that we sent, and is being evaluated, to the Engineering Geology magazine [Chinchón-Payá *et al* 2010].

2 DIFFERENCES BETWEEN DIFFERENT IRON SULFIDES

In the cited study [Chinchón-Payá *et al* 2010] we evaluated the oxidative degradation in aqueous of two iron sulfides, a sample of pyrite and another of pyrrhotite, in the same experimental conditions to differentiate the behavior they exhibit (Table 1).

Table 1. Analytical results of the dissolution of pyrite and pyrrhotite. It includes iron and sulfate concentrations solutions and the pH value when considered constant for both.

	Pyrite	Pyrrhotite
[Fe] (ppm)	270	455
[$SO4^{2-}$] (ppm)	1238,7	1517,8
pH	3.1	4.3

According to these results pyrrhotite provides over 20% more of sulfates to the water of dissolution. If these waters come into contact with a concrete could lead an aggressive attack to the concrete.

A fast decrease in pH is observed at the moment of putting them in contact with water, and a slight gradual decrease, until they reach constant values 50 days after beginning the experiment. According to the results, it seems clear that the pyrite dissolution leads to an environment with more protons than the pyrrhotite dissolution. This can be explained considering that the reactions that take place in the medium depend on the stechiometry of the sulfides (FeS_2 for pyrite and $Fe_{1-x}S$ to pyrrhotite). (See also equations 1 and 2).

3 THE ROLE OF THE HOST ROCK

Later to the aforementioned work [Chinchón-Payá *et al* 2010], an experience of dissolution of sulfides was designed similar to above but this time adding two different types of aggregates. The aggregate type A is a mixture of calcite, quartz and feldspar in proportions of 22%, 58% and 20% respectively, the aggregate type B is a silica sand used in Spain as a standard quartz that comes from the Institute of cement and construction Eduardo Torroja and having a SiO_2 content over 95%.

It were also evaluated, among other parameters, the change in pH and concentration of major ions Fe and SO_4^{2-} (see Table 2).

Table 2. Analytical results of the concentrations of sulfate and iron (ppm) and pH value of solutions when considered constant. Py and Po represent pyrite and pyrrhotite, respectively, while A is the aggregate with 22% calcite and B the silica aggregate.

Analyte	Sample Py +A	Sample Po +A	Sample Py + B	Sample Po + B
SO_4^{2-}	89,0	130,9	419,9	182,9
Fe	0	0	0	53,8
pH	8.1	8.2	6.1	5.3

When in the dissolution medium there are aggregates with carbonates, these will dissolve and mitigate the effect of the pure, and without influence, dissolution of iron sulfides.

In the dissolution of the iron sulfides with siliceous aggregates, this behaved as an inert component, since the solution from the very beginning presented pH values similar to those of the solution prepared with iron sulphurs but without any additions. That experience was considered complete after 10 days.

In the second one, the jointly dissolving of iron sulfides and carbonates, what we can see is the initial increase of pH due to the fast solution capacity of calcium carbonates:

$$CaCO_3 + H_2O \rightarrow Ca^{2+} + HCO_3^- + OH^-$$

As the system tends to equilibrium, pH will gradually fit the values typical of the carbonate buffer system.

As for the content of SO_4^{2-} in solution, approximately one third is generated in the solution containing the limestone coarse aggregate than in the solution which does not contain it (See Table 2), which should be understood as a shock-absorbing effect of carbonates.

4 DISCUSSION

There are certain types of aggregates that after its reaction with some components of the concrete will form expansive compounds that affect the concrete durability. The most studied process is known as alkali-aggregate reaction and affects dolomitic aggregates or those containing low crystallinity silica.

The internal sulfate reaction is a less documented expansion process that happens when oxidizable iron sulfides are as aggregates in the manufacture of concrete. The iron sulfides are oxidized in the presence of water to produce sulfate and then form gypsum, ettringite or thaumasite.

The Regulations governing the presence of iron sulfides in aggregates for concrete in some cases make no distinction between pyrite and pyrrhotite and others only the pyrrhotite is responsible. In this communication we refer to a study showing that both are bad but pyrrhotite is worse than pyrite.

Finally we show the results of an experiment in which we have evaluated the role of the host rock. The limestone rocks buffer the damaging effects of the dissolution of the sulfides (both pH and concentration of sulfate available for subsequent sulfate attack) while siliceous aggregates are more harmful.

ACKNOWLEDGEMENTS

This paper forms part of the studies carried out within the framework of the Horex Project. The authors want to express their gratitude to the firm IBERDROLA for its funding.

REFERENCES

Araújo, G.S. Chinchón, S. Aguado, A. 'Evaluation of the behaviour of concrete gravity dams suffering from internal sulfate attack', Ibracon Structures and Materials, Journal 1 (2008) 17-45.

ASTM C294-05 Standard Descriptive Nomenclature for Constituents of Concrete Aggregates (2005).

Ayora, C. Chinchón, S. Aguado, A. Guirado, F. 1998 'Weathering of iron sulfides and concrete alteration: thermodynamic model and observation in dams from Central Pyrenees, Spain', *Cement and Concrete Research* 28, 1223-1235.

Barnett, S.J. Macphee, D.E. Crammond N.J. 2003 'Extent of immiscibility in the ettringite–thaumasite system', *Cement & Concrete Composites*, 25, 851–855.

Chinchón, S. López-Soler A., Alastuey, A. Vázquez E. 1993 'X-ray diffraction (XRD) analysis of oxidables sulphurs in aggregates used in concrete', *Materials and Structures* 26, 24-29.

Chinchón, S. López-Soler, A. Querol, X. Vaquer R. 1990 'Determination of pyrrotite (Fe1-x S) occurring in aggregates by X ray fluorescence', *Cement and Concrete Research* 20, 394-397.

Chinchón-Payá, S. Aguado, A. Chinchón, S. 2010 'Degradation of Pyrite and Pyrrhotite Contained in Aggregates and the Effect of Host Rock' *Engineering Geology (submitted).*

EHE-08, Instrucción de Hormigón Estructural. Real Decreto 1247/*2008*, de 18 de julio (2008).

Garcia-Diaz, E., Riche, J., Bulteel, D. and Vernet, C. 2006, 'Mechanism of damage for the alkali-silica reaction', *Cement and Concrete Research*, 36 [2], 395–400.

Hobbs, D.W. 1988, *Alkali-silica reaction in concrete*, Thomas Telford, London.

Mehta, PK. *Concrete microstructure, properties and materials*, 2nd ed. McGraw-Hill, NewYork.

Min D., Mingshu T. 1993, 'Mechanism of dedolomitization and expansion of dolomitic rocks', *Cement and Concrete Research*, 23 [6], 1397-1408.

Sahu, S. Exline, D. L. Nelson, M. P. 2002 'Identification of thaumasite in concrete by Raman chemical imaging', *Cement & Concrete Composites*, 24, 347–350.

Tagnit-Hamou, A. Saric-Coric, M. Rivard, P. 2005 'Internal deterioration of concrete by the oxidation of pyrrhotitic aggregates', *Cement and Concrete Research*, 35, 99-107.

Taylor H.F.W., *Cement Chemistry*, 2nd ed., Thomas Telford Publishing, London.

XII DBMC
International Conference on Durability of Building Materials and Components
PORTO - PORTUGAL, April 12th-15th, 2011

Effect of Confinement upon Crack Behaviors Caused by Corrosion-Product Expansion around Corroding Bars

Yasuji Shinohara [1]

ABSTRACT

Finite element (FE) analysis is performed on reinforced concrete (RC) beams to investigate the effect of the confinement upon crack behaviors resulting from corrosion-product expansion of main reinforcement bars. Two-dimensional (2-D) plane stress elements having the same thickness (60 mm) as the spacing of the transverse reinforcements are chosen, and three main reinforcing bars are modeled by means of three holes (20 mm in diameter). The variation factors are the amount of transverse reinforcement of the three levels (0 mm^2, 28 mm^2, and 112 mm^2) in order to study the influence of the different confinement levels on crack behaviors. In addition to the effect of confinement by means of transverse reinforcement, the effects of the position of the reinforcing bars and the radial direction in expansion of corrosion-product are also discussed. Provided cracks appear separately for each main reinforcing bar, pressure-expansion relations are similar—despite the amount of transverse reinforcement, bar location, expanding direction and loading method controlled by internal pressure (load) or bar expansion (displacement). However, if cracks develop and connect to each other and propagate to the surface, pressure-expansion relations and crack behaviors depend greatly on the analytical conditions mentioned above. Furthermore, a relationship between the crack strain relating to a crack width and the corrosion penetration of main reinforcement, and a relationship between the stress in transverse reinforcement and the corrosion penetration of main reinforcement are shown to study the effect of the corrosion penetration upon the structural performance of RC structures. The analytical results are compared with the test results by other researchers for verification.

KEYWORDS

Crack behaviors, Corroding bars, Corrosion-product expansion, Confinement, Finite element analysis.

[1] Structural Engineering Research Center, Tokyo Institute of Technology, Tokyo, Japan, shinohara.y.ab@m.titech.ac.jp

1 INTRODUCTION

Corrosion of embedded reinforcing steel bars adversely affects serviceability and durability for continuous use of RC structures due to cracking of the cover concrete, caused by corrosion-product expansion, and to an increase in the stress of transverse reinforcement, and to a decrease in the bond between the concrete and the corroding reinforcement. However, there is still a question in regards to the extent to which a crack can propagate with increasing corrosion levels, taking into account the confinement from concrete and reinforcement.

The primary purpose of this paper is to investigate analytically the effect of the confinement upon crack behaviors induced by corrosion-product expansion of longitudinal reinforcement, and to clarify the relationship between a given corrosion level and the structural performance of RC structures. A corrosion level corresponding to the crack pattern obtained analytically is estimated based on volume increase and mechanical properties of the corrosion products (rust). The main parameters are the confinement provided by transverse reinforcement, reinforcing bar position, radial direction in expanding, and loading method controlled by pressure or expansion.

2 VOLUME INCREASE AND MECHANICAL PROPERTIES OF RUST

Corrosion-induced cracking occurs because corrosion products have a larger volume than the original steel of a corroding reinforcing bar. The volume increase of the corrosion products (rust) compared with the virgin steel was modeled in a corrosion layer by Lundgren [2002] and Berra *et al*. [2003]. In Lundgren's model, the rust accumulates around the corroded bar having the initial radius of r_b and does not penetrate into void and crack (Figure 1). On the other hand, Berra's model allows the rust to penetrate into the cracks and to reach the external surface of the cover concrete. Lundgren's model is adapted in this paper for simplicity. By giving the corrosion penetration, x, and assuming that the volume of the rust is v times the volume of the steel that has corroded, the distance of free increase, a, can be estimated, as shown in Figure 1. As different kinds of rust products have different densities and volume expansions, the value of v varies from 2.0 to 4.0 [Liu and Weyers 1998]. It is expected that crack initiation and propagation are directly proportional with the amount of corrosion products, that is, a value of v. A relatively small value of v=2.0 is used in this analysis because the diffusion of corrosion products into pores and cracks is not taken into account in Lundgren's model. a is the free increase of the radius when the normal stress is zero. The real increase of the radius, u_{cor}, is calculated from a strain, ε_{cor}, in the rust.

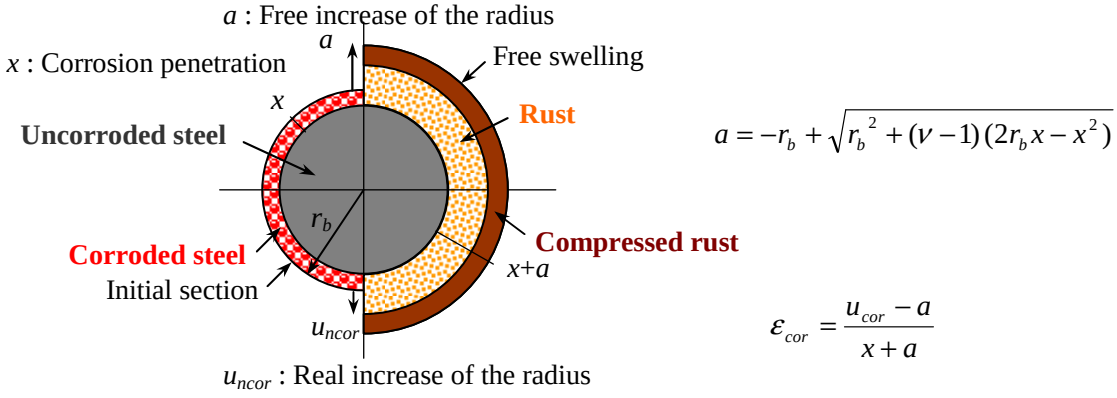

Figure 1. Corrosion penetration x and corrosion products expansion around bar.

Evaluating the deformability of the rust around the corroded bar, a non-linear relation has been proposed between the pressure, p, developing around the bar and the corresponding strain in the radial direction, ε_{cor}, in the rust [Lundgren 2002], as shown in Figure 2, where K_{cor} =7 GPa and m =7.0, which were chosen to give reasonable agreement with the results from the analyses of the tests.

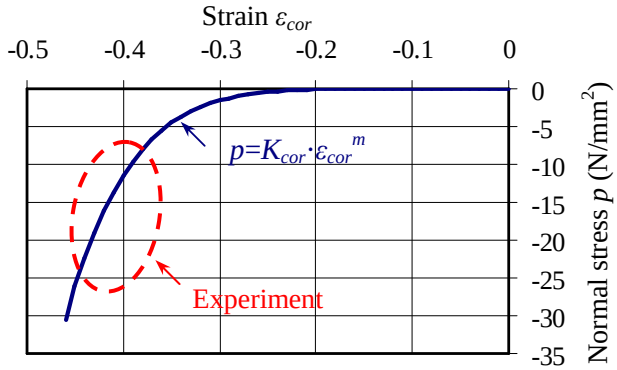

Figure 2. Normal stress versus strain in corrosion products.

3 IDEALIZATIONS AND PROCEDURES IN ANALYSIS

The model to be analyzed is shown in Figure 3. Although the corrosion of steel bars in concrete is three-dimensional (3-D) problem, 2-D model is used to study the effect of confinement on crack behaviors caused by a locally limited corrosion for the sake of simplicity. The model is a part cut out from an RC beam, and has a thickness of 60 mm—the same as the spacing of transverse reinforcement. Here, 2-D plane stress elements are used to model the concrete. Three longitudinal reinforcing bars spaced 60 mm apart are modeled by three holes that are 20 mm in diameter. All the degrees of freedom are restricted at the right edge of the section. A transverse reinforcement that has three different cross sections of 0 mm^2, 28 mm^2, and 112 mm^2 is modeled by embedded reinforcements to provide different confinements.

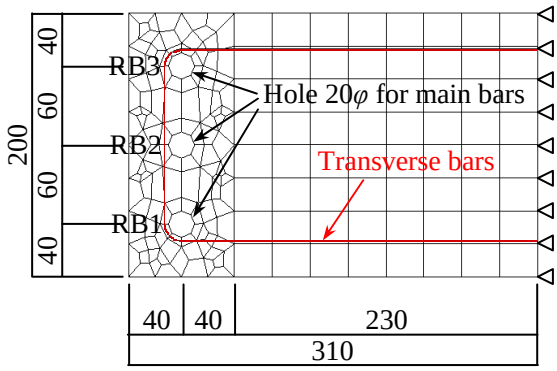

Figure 3. FE mesh and boundary conditions.

The mechanical properties of the concrete and the reinforcement are shown in Figure 4, together with the model used in the Finite element (FE) analysis. The concrete behavior in this analysis is dominated by tensile cracking at a low level of compressive stress, so that the concrete in the compressive zone can be assumed to behave in an elastic manner. The crack initiation is defined by the maximum tensile stress, or Rankine criterion. Thus, a crack forms in the direction normal to the maximum principle stress when this stress reaches the tensile strength of the concrete as found in a simple tension test, regardless of the normal or shearing stresses that occur on other planes. A multidirectional smeared-crack model that takes 60 degrees as the threshold value is used. The linear model having a fracture energy of 0.1 N/mm shown in Figure 4 is used for tension-softening behavior after the crack. The bilinear model shown in Figure 4 is used for transverse reinforcement.

The pressure buildup around the corroded bar is applied by two loading methods. One is pressure control by pressure in 0.1 N/mm^2 increments, and the other is displacement control by compulsive expansion in 0.0002 mm increments. Table 1 gives a description of the variables for all numerical calculations.

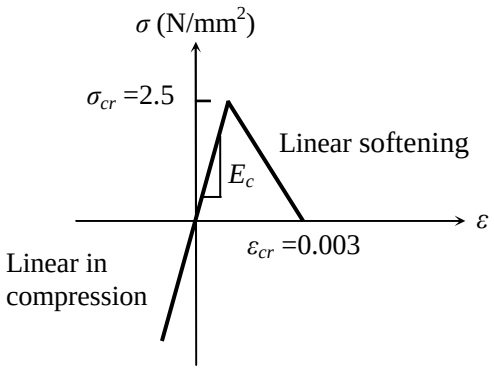

Stress-strain curve for concrete

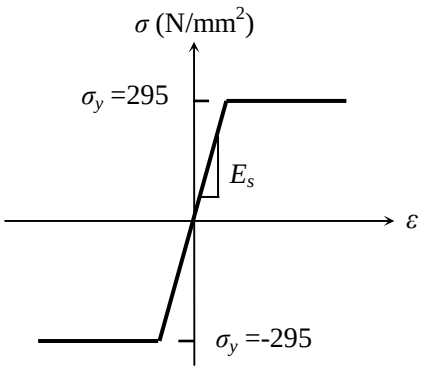

Stress-strain curve for reinforcement

Geometry and mechanical properties	
Thickness	200 mm
Elastic modulus E_c	30000 N/mm^2
Poisson's ratio v	0.2
Tensile strength σ_t	2.5 N/mm^2

(1) Concrete

Geometry and mechanical properties	
Sectional area	0, 28, 112 mm^2
Elastic modulus E_s	205000 N/mm^2
Yield strength σ_y	295 N/mm^2

(2) Transverse reinforcement

Figure 4. Mechanical properties and analytical model for concrete and reinforcement.

Table 1. List of analytical variables for specimens.

Designation	Loading method	Cross section of transverse
L-A0	Pressure control	0 mm^2
L-A1	Pressure control	28 mm^2
L-A4	Pressure control	112 mm^2
D-A0	Displacement control	0 mm^2
D-A1	Displacement control	28 mm^2
D-A4	Displacement control	112 mm^2

4 ANALYTICAL RESULTS AND DISCUSSTIONS

4.1 Crack Propagation Behaviors

Figures 5 and 6 show the crack strain behaviors and tenfold deformations obtained from the FE analysis at early stage of corrosion and when cracking reaches the concrete surface respectively. The pressure exerted by corrosion products on the surrounding concrete, p, increase in radius, e, maximum crack strain, $\varepsilon^{cr}_{\max}$, and stress of transverse, $\sigma_{s,\max}$ are also shown in these figures. Furthermore, the corrosion penetration, x, and the reduction of the cross sectional area of main bars, a_{Loss}, which are estimated by the method described in the previous section, are added to the corresponding loading steps.

The cracks appear first at the bar-concrete interface and then propagate radially until they reach the concrete surface. The analytical results indicate that only one micrometer of an increase in radius due to corrosion product is needed to initiate cracking around main bars. Provided the cracking caused by the corrosion of each main steel reinforcing bar propagates independently and does not make contact with other cracks, the expansion and the pressure increase in much the same way—despite the amount of transverse reinforcement, bar location, expanding direction and loading method controlled by pressure or expansion (see Figure 5). However, if cracks develop and connect with each other, and

reach the concrete surface, the pressure-expansion relations and crack behavior depend partly on the conditions mentioned above, particularly in the case of pressure control (see Figure 6).

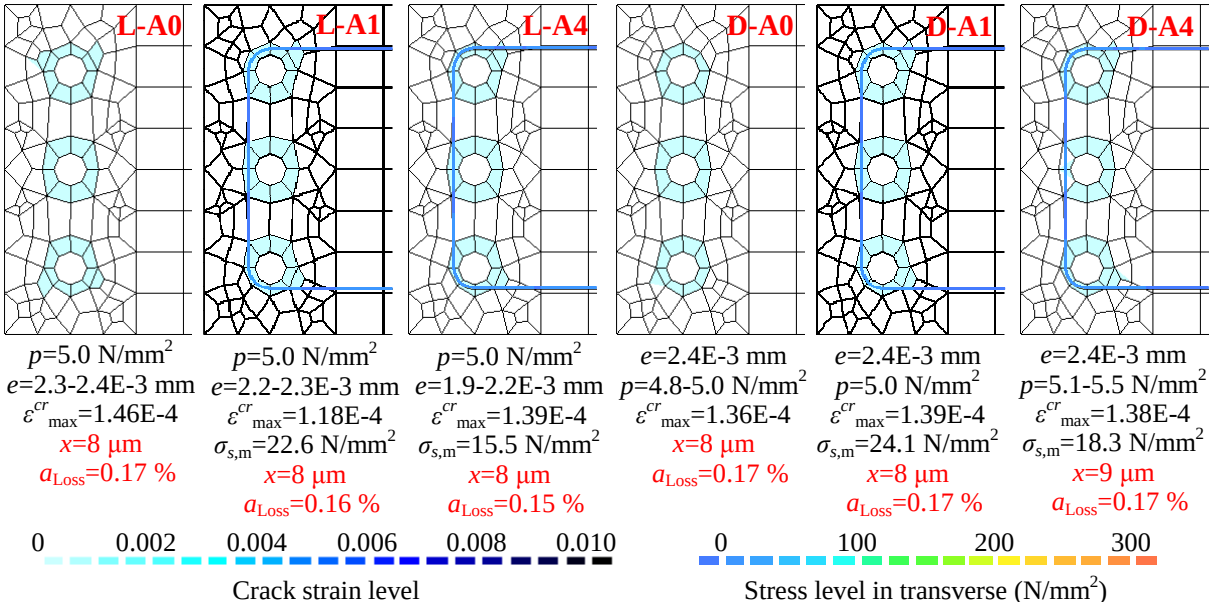

Figure 5. Comparisons of cracking at early stage of corrosion.

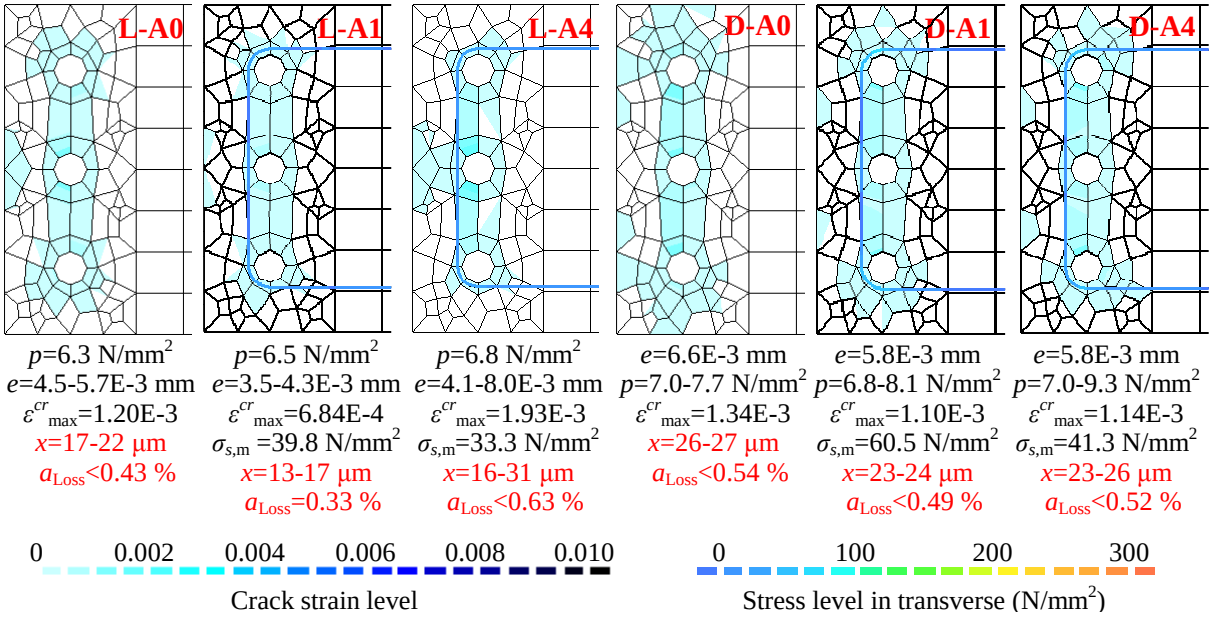

Figure 6. Comparisons of crack behavior when reaching the concrete surface.

Figure 7 shows the comparison of final cracking patterns and tenfold deformations for all analytical conditions. For the L-A0 specimen not having transverse reinforcement, the moment a crack reaches the surface of the cover concrete, the cover concrete spalls and cannot resist the increasing pressure. The spalling of the cover concrete is controlled for the L-A1 specimen immediately after the crack reaches the surface, but the deformation increases rapidly after the transverse reinforcement yields. Having four times the transverse reinforcement of the L-A1 specimen, the deformation decreases considerably up to the higher pressures due to the high confinement. The analytical results obtained by displacement-controlled methods are similar on the whole in crack behavior and pressure-expansion relations, despite the amount of transverse reinforcement, because transverse reinforcement only adds a little stiffness to the concrete. It seems that the behavior of corrosion-product expansion in

an actual RC structure is close to the results for pressure-controlled methods, as a round shape of corrosion-product expansion would be lost by cracking and spalling.

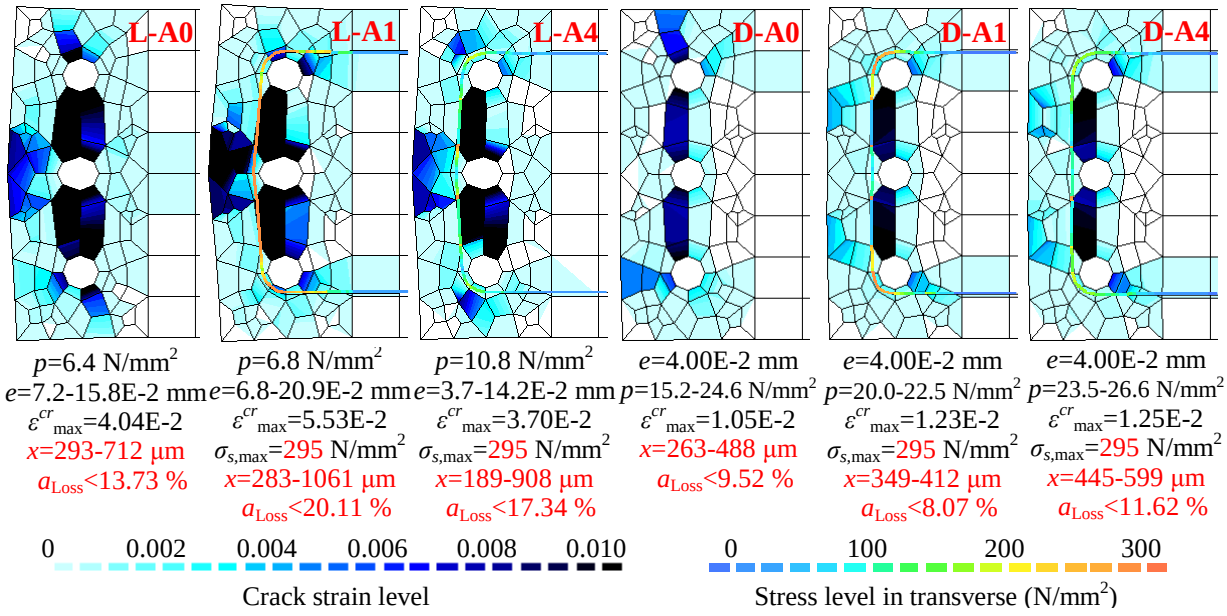

Figure 7. Comparisons of final cracking patterns and tenfold deformations.

4.2 Effect of Bar Locations and Expanding Directions on Pressure-Expansion Relations

Figure 8 shows the pressure-expansion (increase in radius) relations for eight directions of lower bar, RB1, middle bar, RB2, and upper bar, RB3 in the L-A4 and D-A4 specimens. They depend largely on the expanding directions, and represent the higher stiffness in the directions having the higher stiffness, such as the upper side of RB1, the upper and lower sides of RB2 and the lower side of RB3.

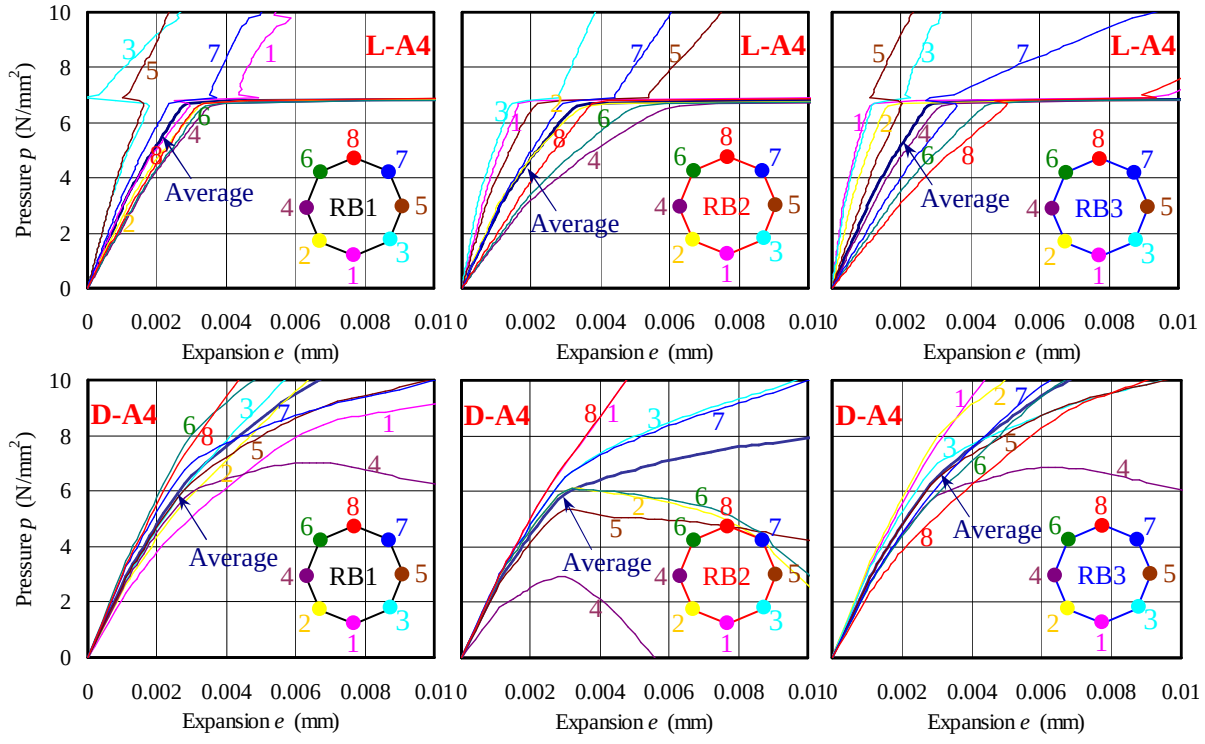

Figure 8. Pressure-Expansion relations for eight directions of each bar in L-A4 and D-A4.

4.3 Relations between Material Deteriorations and Corrosion Levels

Figure 9 shows the relationships between maximum crack strains and corrosion penetrations. The right figure is an enlarged drawing in a small corrosion level. The cracks appear at a few micrometers of corrosion penetration and reach the concrete surface by 20 to 30 micrometers. The reduction rate of bar cross section is less than 1 %, even if visible cracks spread in the concrete surface. This reduction has an insignificant influence on the bending strength of RC structures. In the end, the cover concrete of the L-A0 specimen spalls, but the crack strain of the L-A4 specimen is greatly controlled.

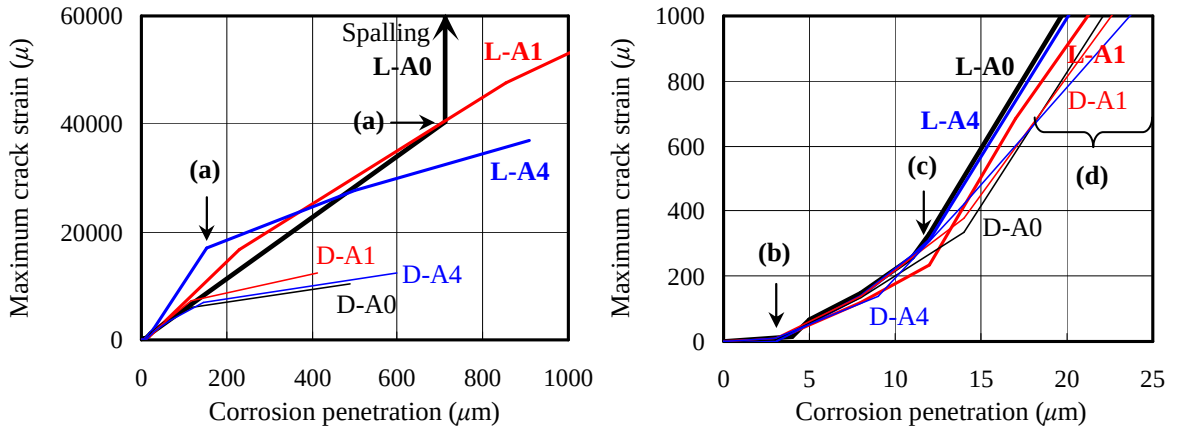

(a) : Cracking to all the surface **(b)** : Cracking initiated **(c)** : Cracking connected **(d)** : Cracking to the surface

Figure 9. Relationships between maximum crack strains and corrosion penetrations.

Figure 10 shows the relationships between maximum stresses in transverse rebar and corrosion penetrations. The stress in transverse rebar generates before cracking to resist pressure together with the concrete, and exceeds the allowable stress for sustained loading when the corrosion penetration increases 100 to 200 micrometers. This increasing stresses have a significant influence on the service life of RC structures , because the shear residual strength decreases greatly.

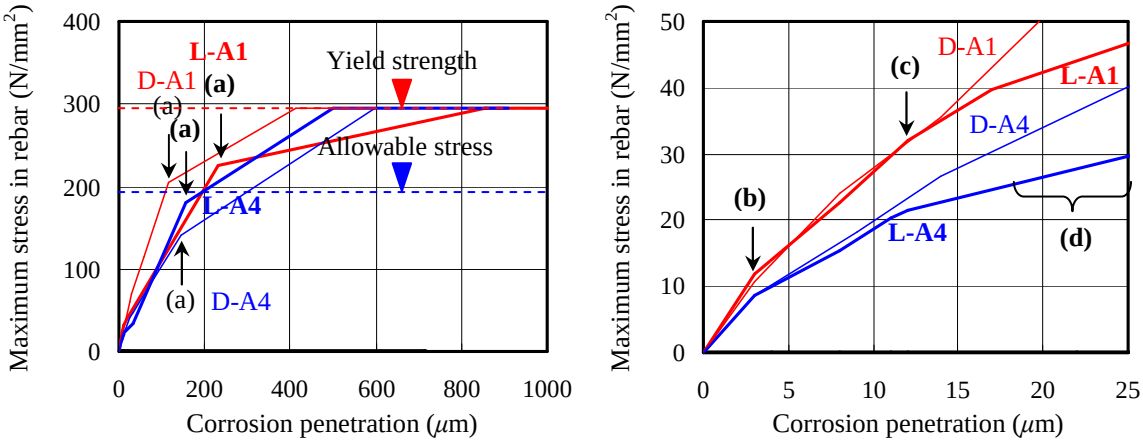

Figure 10. Relationships between maximum stresses in transverse rebar and corrosion penetrations.

4.4 Comparisons with Test Results by Other Researchers

Andrade *et al*. [1993] performed an accelerated corrosion test on small reinforced beams to study the amount of loss of bar cross-section needed to induce the crack at the surface (Figure 11). Their test results indicated that the corrosion penetration is 15 to 21 micrometers when visible cracks reach the concrete surface. This is consistent with the analytical results. And they showed that the corrosion penetration of 100 micrometers leads the maximum crack width of 0.4 mm. This crack width cannot

be directly compared with the crack strain from the analysis, but assuming crack spacing to be 30 mm which is the characteristic length, the crack width is estimated at 0.2 to 0.4 mm.

Vu *et al*. [2005] also carried out an accelerated corrosion test to simulate reinforcement corrosion of a typical RC bridge deck (Figure 12). They found that the corrosion penetration is 15 to 30 micrometers when cracks reach the concrete surface, and that the corrosion penetration of 100 micrometers causes the maximum crack width of 0.4 mm. These results are also consistent with the analytical results.

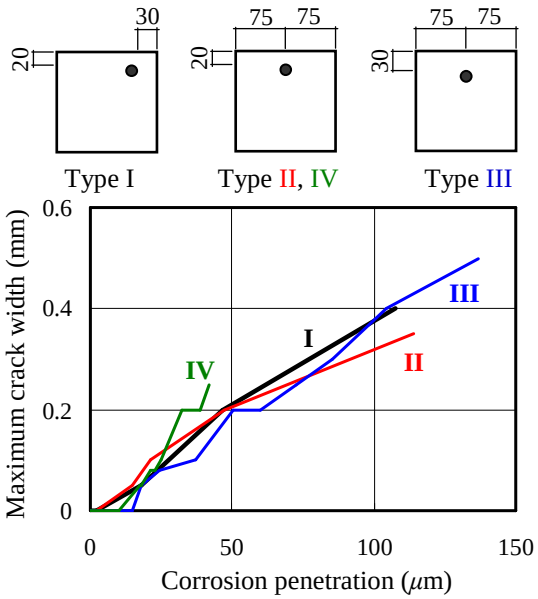

Figure 11. Relation between maximum crack width and corrosion penetration after Andrade.

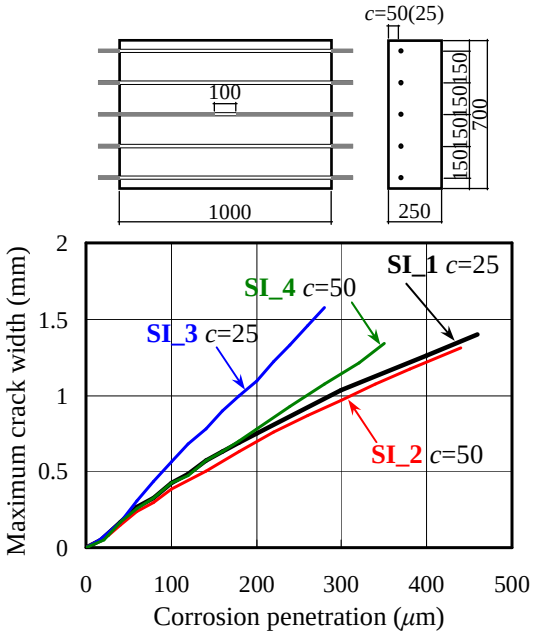

Figure 12. Relation between maximum crack width and corrosion penetration after Vu *et al*.

5 CONCLUSIONS

The cracking and spalling of cover concrete caused by the corrosion of rebars can be controlled by providing the confinement by means of transverse reinforcement. However, the shear strength may decrease resulting from an increase in the stress of transverse reinforcement. From the point of view of service life design, the corrosion penetration should be restricted to 50 micrometers or less.

REFERENCES

Karin Lundgre 2002, 'Modelling the effect of corrosion on bond in reinforced concrete', *Magazine of Concrete Research*, **54** (3), 165-173.

M. Berra, A. Castellani, D. Coronelli, S. Zanni and G. Zhang 2003, 'Steel-concrete bond deterioration due to corrosion: finite-element analysis for different confinement levels', *Magazine of Concrete Research*, **55** (3), 237-247.

Youping Liu and Richard E. Weyers 1998, 'Modeling the Time-to-Corrosion Cracking in Chloride Contaminated Reinforced Concrete Structures', *ACI Materials Journal*, **95** (6), 675-681.

C. Andrade, C. Alonso, and F. J. Molina 1993, 'Cover cracking as a function of bar corrosion: Part I – Experimental test and Part II – Numerical model', *Materials and Structures*, **26**, 453-464 and 532-548.

Kim Vu, Mark G. Stewart, and John Mullard, 'Corrosion-Induced Cracking: Experimental Data and Predictive Models', *ACI Structural Journal* **102** (5) (2005) 719-726.

XII DBMC
International Conference on Durability of Building Materials and Components
PORTO - PORTUGAL, April 12th-15th, 2011

Influence of Air Entraining Agents (AEAs) on Deicing Salt Scaling Resistance of High-Volume Fly Ash Concrete (HVFA Concrete)

Philip Van den Heede [1]
Jamie Furniere [2]
Nele De Belie [3]

ABSTRACT

It is usually concluded from laboratory tests that deicing salt scaling resistance of High-Volume Fly Ash concrete (HVFA concrete) is less than satisfactory. This is mainly attributed to the partial adsorption of the applied air entraining agent (AEA) by the unburnt carbon present in the fly ash. As a consequence, the presence of an adequate air void system in HVFA concrete can not always be garantueed. This explains why the use of HVFA concrete in pavements exposed to freezing and thawing with deicing salts, is still not generally accepted. Therefore, we carefully evaluated the air void system of this concrete type in the hardened state. This paper presents a full assessment of this air void system for two HVFA compositions with a total binder content of 450 kg/m³ (50 % cement, 50 % fly ash) and a water-to-binder ratio of 0.35. The two mixtures mutually differed in the type of fly ash used. For both of them, the minimum required air content in the fresh state was achieved with an AEA dosage of 5.0 ml/kg binder. The air void system was evaluated qualitatively using microscopic analysis on thin sections. The air content ($\geq$ 4 %) and spacing factor ($\leq$ 200 µm) were quantified with the Rapidair 457 apparatus. Although these two properties were similar for the two mixtures and they both met the applicable criteria, the air void system still seemed a bit less pronounced under the microscope for one of the mixtures. The salt scaling resistance of the latter mixture was also found to be significantly less after 28 days of curing and 28 severe freeze/thaw cycles. The mass loss due to salt scaling was found to be equal to more or less 1 kg/m², the maximum allowed value according to the applicable European standard, while the amount of scaled off material for the other mixture was much less (0.44 kg/m²).

KEYWORDS

Mix design, Fly ash, Deicing salt scaling resistance, Air void analysis, Thin sections.

[1] Magnel Laboratory for Concrete Research, Ghent University, Ghent, BELGIUM, philip.vandenheede@ugent.be
[2] Magnel Laboratory for Concrete research, Ghent University, Ghent, BELGIUM, jamie.furniere@ugent.be
[3] Magnel Laboratory for Concrete Research, Ghent University, Ghent, BELGIUM, nele.debelie@ugent.be

1 INTRODUCTION

Although the concept of High-Volume Fly Ash (HVFA) concrete has been proven successful in many, mostly less demanding concrete applications [Malhotra & Mehta 2005], its use in more critical environments is still not common practise. Indeed, many concrete manufacturers remain sceptical about replacing the larger part of the cement with pozzolanic fly ash from coal fired electrical power plants. This is mainly because the performance of these concrete compositions is unsatisfactory when subjected to accelerated test methods in the laboratory. With respect to salt scaling resistance, Malhotra & Mehta [2005] have reported a higher deterioration rate for HVFA concrete under laboratory conditions. However, the use of this concrete type in the field indicates otherwise. Concrete pavement in Wisconsin, and sidewalk sections in Halifax, Canada made with HVFA concrete and subjected to deicing salts, showed a good performance. Nevertheless, the applicable European standard does not specify the concrete's behavior under realistic conditions. Instead, a limiting value of 1 kg/m² is specified as the maximum mass loss per unit area after 28 severe freeze/thaw cycles with temperatures ranging from - 18 to 20 °C in 24 hours [NBN EN 1339 2003]. Within the scope of this paper, we developed a HVFA mix design that should meet the salt scaling criterion of 1 kg/m². In a first research phase, the air void system in hardened state (air content, spacing factor, ...) was characterized by means of microscopic analysis on thin sections and air void analysis conforming to ASTM C457 [2006]. In a second research phase, the salt scaling resistance itself was tested according to the procedure described in NBN EN 1339 [2003]. All tests were performed after 28 and 91 days of curing. Possible interaction between the applied air entraining agent (AEA) and the fly ash was investigated for fly ashes from two different sources.

2 MATERIALS AND METHODS

2.1 Concrete Mixtures

In total, six concrete mixtures were manufactured with the intention to be used in a XF4 environment with exposure to freeze/thaw attack in combination with deicing salts (Table 1). Two of these concrete compositions were considered as a reference concrete. Mix T(0.45) is a non air entrained concrete with the minimum cement content and the maximum water-to-cement ratio (W/C) conforming to the Belgian standard NBN B 15-001 for this XF4 environment. According to the European standard NBN EN 206-1, this concrete mix should have a minimum air content of at least 4 % in the fresh state. However, according to the Belgian standard NBN B 15-001 [2004] this air content should equal at least 5 % for a nominal maximum aggregate size of 16 mm. The American standard ACI 201.2R [2008] is even more strict. There, exposure conditions are considered to be severe when deicing salts are in play. Such an environment requires an air content of 6 to 7 %. Surely, air contents of this order of magnitude, normally require the use of an AEA. Therefore, an air entrained version of the reference concrete mix (T(0.45)A) was also manufactured. Since the initial air content equaled 6.6 %, this reference concrete is ought to be a suitable concrete for exposure to severe conditions. The minimum indicative strength class for both references T(0.45) and T(0.45)A is C30/37. However, Table 1 clearly shows that the strength class obtained for the references is significantly higher. Since a traditional concrete does not necessarily have to be air entrained for the environment under investigation, both non air entrained HVFA mixes (F(1)50 and F(2)50) and air entrained HVFA mixes (F(1)50A and F(1)50A) were evaluated in this research. The incorporation of the air entraining agent MICRO-AIR 103 con. 4% is indicated within the concrete mix name by means of the letter 'A'. Each HVFA composition was made twice: once with fly ash F(1) and once with fly ash F(2). Both of them meet the requirements to qualify for use in concrete: the loss on ignition (4.79% and 4.42%, respectively) was lower than 5% (Class A) and the 45 µm fineness was less than 40% (13.2 % versus 26.6%, respectively). As can be seen from Table 1, the incorporation of fly ash in concrete has its impact on the required AEA dosage. For the reference T(0.45)A, a dosage of 2.0 ml/ kg binder was sufficient to have an air content (6.6%) conforming to all standards. With respect to the HVFA mixtures F(1)50A and F(2)50A, a much higher AEA dosage (5.0 ml/kg binder)

resulted in an air content that was considerably lower than the 6.6 % of the reference. As a consequence, the criteria imposed by ACI 201.2R [2008] are not met. Nevertheless, values of 5.2% and 4.9% respectively, were still higher than the 4% minimum according to NBN EN 206-1 [2001]. Both air contents are more or less in correspondence with the 5 % minimum imposed by NBN B15-001 [2004].

Table 1. Mix proportions and properties of the tested concrete mixtures.

	T(0.45)	T(0.45)A	F(1)50	F(1)50A	F(2)50	F(2)50A
Sand 0/4 (kg/m³)	715	715	645	645	645	645
Aggregate 2/8 (kg/m³)	515	515	465	465	465	465
Aggregate 8/16 (kg/m³)	671	671	606	606	606	606
CEM I 52.5 N (kg/m³)	340	340	225	225	225	225
Fly ash (kg/m³)	-	-	225	225	225	225
Water (kg/m³)	153	153	158	158	158	158
W/B	0.45	0.45	0.35	0.35	0.35	0.35
AEA (ml/kg B)	-	2.0	-	5.0	-	5.0
SP (ml/kg B)	2.0	2.0	7.0	7.0	5.0	5.0
Air content (%)	2.8	6.6	2.6	5.2	2.8	4.9
Slump	S2	S3	S5	S5	S5	S5
Strength class	C55/67	C35/45	C45/55	C40/50	C40/50	C30/37

It should also be noted that all HVFA mixtures are characterized by a higher binder content (cement + fly ash) and a lower water-to-binder ratio (W/B) compared to the references T(0.45) and T(0.45)A. This was mainly done to ensure a strength class equal or higher than the the minimum required for a XF4 environnment. However, this approach resulted in a much higher compressive strength for the HVFA mixtures F(1)50, F(1)50 and F(2)50.

2.2 Curing and Sample Preparation

Two 400x400x100 mm concrete slabs were cast per mix. After casting the slabs were kept at a constant temperature and relative humidity of 20 °C and 95 %, respectively. Demoulding took place the next day whereupon the slabs were stored again under the same conditions until the age of testing. All tests were conducted after 28 and 91 days of curing.

2.3 Microscopic Analysis on Thin Sections

Per concrete mix and testing age, three 45 x 30 x 15 mm prisms (n = 3) were sawn from the concrete slabs in such a way that a 45 x 15 mm face was a casting surface. First, one 45x30 mm face was glued onto a piece of window glass. Then, the samples were cut and polished until the height of the concrete specimens and the glass equaled 10.1 mm. In a next step, the samples were impregnated under vacuum with a fluorescent epoxy. After impregnation, the excess epoxy, was grinded away and an object glass was glued onto the polished surface. In a final step, the window glasses were cut off and the concrete samples on the object glasses were polished until thin sections with a 25 µm thickness were obtained. A cover glass was glued onto them for protection. All thin sections were examined with a Leica DM LP polarizing microscope. A magnification of 5x10 was used. The luminous intensity of the polarized light equaled 5 on a scale of 10. The microscopic analysis on thin sections enabled a qualitative study of the air void system for all concrete mixtures under investigation.

2.4 Air Void Analysis

A more quantitative air void analysis is possible with the RapidAir 457 apparatus. In accordance with ASTM C457 [2006], the linear traverse method was used to determine the air content and air void

distribution of the hardened concrete. The test was performed on four cylindrical specimens (n = 4) with 80 mm diameter and a 20 mm height, all taken from the concrete slabs. The technique required a careful polishing of the sample surfaces since scratches are to be avoided and air voids must have sharp edges [Jacobsen et al. 2006]. Contrast enhancement was realized as follows: the polished surfaces were coloured with black ink and white $BaSO_4$ powder (maximum particle size ≤ 2 µm) was distributed on top to fill the air voids. After removing the excess of powder with a steel blade, the specimens were ready for testing. All samples were analyzed in two perpendicular directions using 10 probe lines per frame with a total traverse length 17733 mm and a scanned area of 50 x 50 mm.

2.5 Salt Scaling Resistance

Deicing salt scaling resistance was evaluated in accordance with NBN EN 1339 [2003]. Cores with a diameter of 100 mm were drilled out of the concrete slabs and sawn in half. Six cylinders (n = 6) of 50 mm height containing a casting surface were then glued into a piece of insulated PVC tube using epoxy. A 5 mm thick water layer was put on top of the cylindrical test surfaces for at least 72 hours to check for leakages. Then, the water layer was replaced with a 5 mm thick 3 % NaCl solution whereupon the specimens were subjected to 28 severe freeze/thaw cycles in a freezing chamber. Every 7 days, the scaled off material was collected, dried and weighed in order to determine the mass loss per unit area (Δm).

3 RESULTS AND DISCUSSION

3.1 Thin Sections

Per concrete mix and curing period, a series of photos was taken of the thin sections as observed under the microscope. Per thin section, 3 photos were taken near the casting surface and 3 photos near the saw cut surface. This resulted in 6 photos per thin section and thus 18 photos per concrete mix at a each age. Visual observation showed no obvious differences between them. Therefore, Fig. 1 shows only one representative photo of each concrete mix after both 28 and 91 days of curing. For all concrete compositions, the air void system obtained does not seem to depend so much on the curing age. For the non air entrained concretes, few air bubbles were present at both ages. For the air entrained concretes, a much higher number of air bubbles can be seen. Again, this observation is valid for the two curing ages. However, a comparison between the different mixtures with air entrainment, indicates that the use of a rather high dosage of AEA (5.0 ml/kg B, Table 1) did not result in a very pronounced system of artificial air bubbles inside the concrete matrix for mix F(1)50A. On the other hand, the incorporation of the same dosage of AEA in mix F(2)50A did result in an air void system similar to the reference T(0.45)A. However, with respect to the latter mix this was achieved by means of a much smaller AEA dosage (2.0 ml/kg B, Table 1). This clear difference between the mixes F(1)50A and F(2)50A is not in agreement with the more less similar air contents which were measured in fresh state (5.2% versus 4.9 %, Table 1). The strength class on the other hand, may indicate otherwise. It is known that the introduction of artificial air bubbles by means of an AEA results in a significant decrease in the compressive strength of the concrete. This decrease is obvious for the reference and the HVFA compositions investigated in this research. Nevertheless, the compressive strength class of mix F(2)50A (C30/37, Table 1) is two classes lower than the C40/50 specification of F(2)50, while there's only a difference of one strength class between F(1)50A and F(1)50 (C40/50 versus C45/55, Table 1). A more limited strength loss due to a denser concrete with fewer air voids supports the conclusions of the microscopic analysis. A correct characterization of the concrete's air void system cannot be done by just looking at thin sections. Conclusions drawn from these merely visual observations are qualitative and should be supported by a quantitative study of all relevant parameters with respect to this air void system. This can be done with air void analysis.

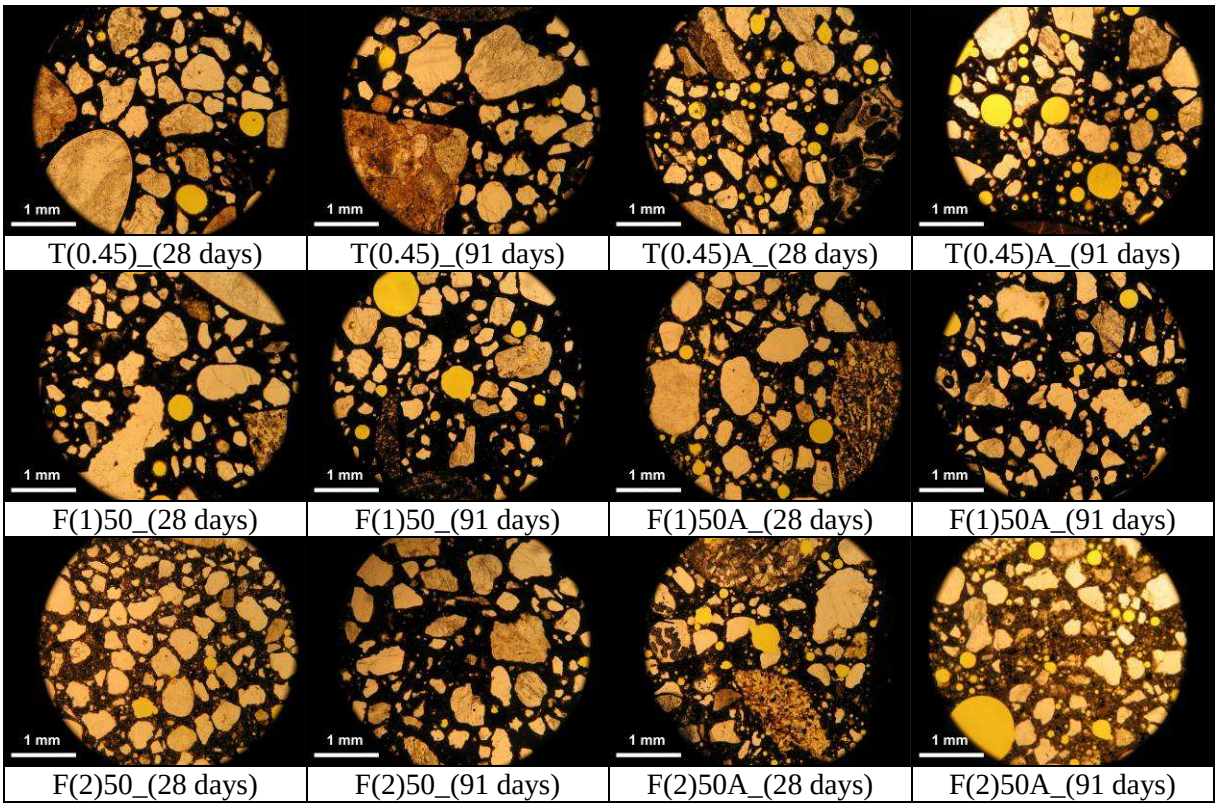

Figure 1. Microscopic analysis of the air void system (coloured yellow) clearly shows the effect of applying an AEA (A), though the difference between F(1)50 and F(1)50A seems less pronounced.

3.2 Air Void Analysis

Automated air void analysis enables the calculation of the air content and spacing factor of all concrete mixtures. The results obtained after both 28 and 91 days of curing are shown in Figs. 2 and 3. Error bars indicate the standard deviation on the individual values. An evenly distributed amount of air voids should be present throughout the paste portion of the concrete. Their spacing should be close enough to prevent the development of pressures from freezing to fracture the concrete. The total air content is the parameter generally specified since it is easily measurable in the field [ACI 201.2R 2008]. Although the minimum air contents mentioned in Section 2.1, normally apply to the air content in the fresh state, the values obtained for the hardened concrete were evaluated according to the same criteria (Fig. 2). Compared to T(0.45), the air entrained reference T(0.45)A was characterized by a much higher air content. The increase amounted to 6.5 % on average. As can be seen from the graph, this air content even tends to increase after prolonged curing. The higher value for the T(0.45)A reference mix is in correspondence with the rather high air content (6.6%, Table 1) in the fresh state. Regarding the HVFA compositions, air entrainment also resulted in an increase of this air void parameter, though the values obtained were lower than the criterion imposed by ACI 201.2R [2008]. Compared to F(1)50 and F(2)50, the air contents of F(1)50A and F(2)50A were increased with 1.3% and 2.6 %, respectively. Since the former value is about half of the latter, it can be concluded that the fly ash type seems to play a role in the effectiveness of the applied AEA. This is in accordance with the much less pronounced air void system observed on the thin sections of mix F(2)50A after both 28 and 91 days of curing (Section 3.1).

Not only a sufficient total air content is of importance, but also an adequate distribution of the artificial air bubbles. The fulfillment of the latter requirement is usually evaluated through the calculation of a spacing factor for the concrete. This is the maximum distance from any point within the concrete matrix to the edge of the nearest air bubble. 200 µm is seen as the maximum spacing factor for concrete exposed to freeze/ thaw attack [NBN B 15-001 2004; ACI 201.2R 2008]. Figure 3

clearly shows that the spacing factors of all air entrained concrete compositions (T(0.45)A, F(1)50A, F(2)50A) do not exceed this maximum value after both 28 and 91 days of curing. Without air entrainment, only the spacing factor of reference T(0.45) after 91 days meets the 200 µm criterion. All the other spacing factors range between 250 and 350 µm. The incorporation of an AEA resulted in a significant drop in spacing factor for the HVFA concrete. The type of fly ash used does not seem to have a significant impact.

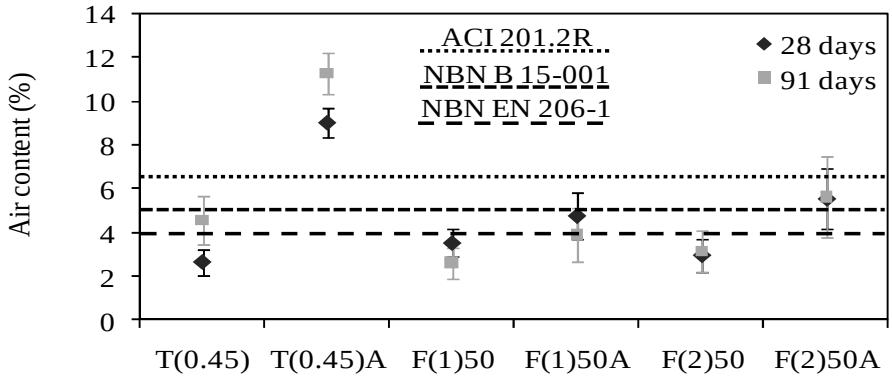

Figure 2. The use of an AEA (A) clearly results in an increased air content (%), although this increase is much less for HVFA concrete (n = 4).

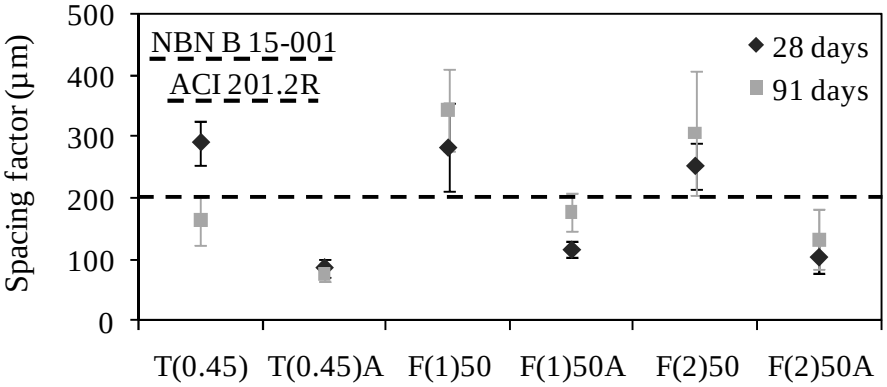

Figure 3. The incorporation of an AEA clearly results in a spacing factor (µm) lower than the maximum value of 200 µm for an adequate freeze/thaw resistance (n = 4).

3.3 Salt Scaling Resistance

Figure 4 presents the mass loss per unit area Δm (kg/m²), after 28 severe freeze/thaw cycles for all concrete mixtures after 28 and 91 days. Error bars again represent the standard deviation on the individual values. Each time, the results obtained are compared with the 1 kg/m² criterion imposed by the European standard NBN EN 1339 [2003]. With respect to the references T(0.45) and T(0.45)A, the following conclusions can be drawn. First, ordinary Portland cement concrete does not necessarily require air entrainment to ensure limited salt scaling. After 28 days of curing, the total amount of scaled off material at end of the test is lower than 1 kg/m². After 91 days, Δm is slightly higher than the maximum value, though a One Sample T test with a significance level of 5 % indicates that the difference between the measured Δm and the 1 kg/m² criterion is not significant. The acceptable mass loss per unit area for T(0.45) supports the choice of this concrete composition as a reference concrete type for a XF4 environment in NBN B 15-001 [2004]. Secondly, the addition of a limited amount of AEA (2.0 ml/kg B) to the same OPC concrete mix was found to be very effective, since Δm was neglectable after both 28 and 91 days of curing.

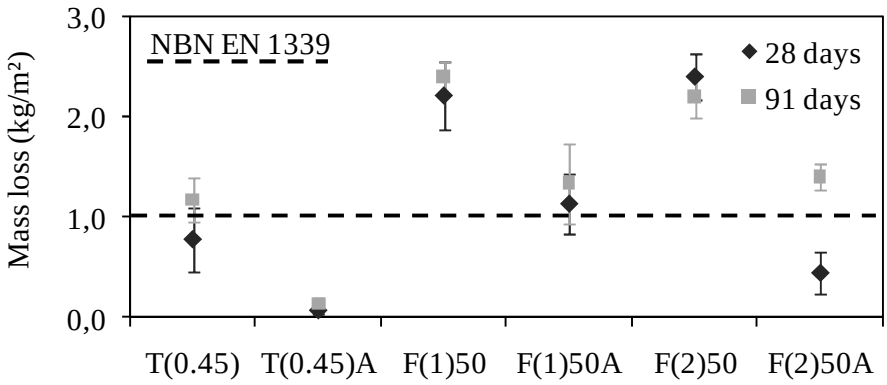

Figure 4. The use of an AEA clearly results in a significant reduction in mass loss due to salt scaling, though this reduction is significantly less for HVFA concrete (n = 6).

In contrast with reference mix T(0.45), the performance of the non air entrained HVFA mixtures subjected to the same experiment was far from acceptable. On average, Δm was more than twice the maximum mass loss allowed. Again, using an AEA significantly improves the salt scaling resistance. However, the effectiveness of the admixture was less than in reference T(0.45)A. Although the AEA dosage was more than doubled (5.0 ml/ kg B versus 2.0 ml/kg B), higher mass losses per unit area were recorded for the HVFA mixes F(1)50A and F(2)50A. The Δm value of HVFA mix F(1)50A slightly exceeds the 1 kg/m² criterion at ages of 28 and 91 days. Nevertheless, a One Sample T test with a significance level of 5 % shows that this exceeding is not significant. On the other hand, HVFA mix F(2)50A performed very well after 28 days since the mass loss per unit area is only 0.44 kg/m². After 91 days, this amount was increased significantly to 1.40 kg/m². For almost all tested concrete mixtures, a small reduction in salt scaling resistance was observed between 28 and 91 days. Statistical analysis showed that only for mix F(2)50A this difference was significant. This higher mass loss at later age was also not in correspondence with the conclusions drawn from the tests to characterize the concrete's air void system. An adequate air void system was observed under the polarizing microscope (Section 2.2). Moreover, the air content (5.6 %) was sufficient and the spacing factor (131 µm) was far below the maximum value according to the automated air void analysis (Section 2.3). Thus, based on the characterization of its air void system, a mass loss far below the 1 kg/m² criterion was also expected for mix F(2)50A after 91 days. Further research is imperative to find out why this was not the case.

3.4 Discussion

The overall results indicate that it is possible to design a HVFA composition with an adequate salt scaling resistance under laboratory conditions. To achieve this, a lot of attention must be paid to the applied AEA dosage. It is known that the unburnt carbon in the fly ash tends to adsorb the AEA. According to Pedersen et al. [2007], the following properties of the unburnt carbon are responsible for this adsorption: the amount, the specific surface area, the accessibility and the chemical properties of the carbon surface. The determination of the loss on ignition (LOI) of a fly ash is therefore unsufficient to evaluate its potential for adsorption. The results of this research confirm this statement. As mentioned in Section 2.1, the LOI values of the fly ashes F(1) and F(2) are quite similar (4.79 % and 4.42 %, respectively). However, the 28 days salt scaling resistance of the air entrained HVFA mixtures made with these two fly ashes is not. Although the fresh air contents, measured immediately after concrete mixing, were also similar (5.2 % and 4.9 %, respectively) the air void system in hardened state did not seem the same. Although the differences between F(1)50A and F(2)50A regarding the air content and the spacing factor were rather small, the microscopic analysis on thin sections clearly showed a much less pronounced air void system for mix F(1)50A. Apparently, partial adsorption of the AEA must still have taken place locally between the first measurement of the air content and the setting of the concrete. A time dependent monitoring of the air content in the first hours after mixing will therefore be considered in future research. This would give an idea on how

much the AEA dosage of 5.0 ml/kg B, must be increased to compensate for this adsorption and have an air void system similar to composition F(2)50A. For the latter mixture, both qualitative and quantitative proof of adequate air entrainment existed. The salt scaling resistance after 28 days of curing was more than acceptable although the minimum air content was not sufficient according to ACI 201.2R [2008].

4 CONCLUSIONS

HVFA concrete with a total binder content of 450 kg/m³ and a W/B ratio of 0.35 can have a an acceptable deicing salt scaling resistance (Δm: 0.44 kg/m² $\leq$ 1 kg/m²) when subjected to the more severe accelerated salt scaling test prescribed by the applicable European standard. To achieve this, the AEA dosage must be considerably higher than for OPC concrete (5.0 ml/kg binder versus 2.0 ml/kg binder). Even then, the entrained air void system was not always sufficient. This was observed more clearly on thin sections than from the parameters (air content, spacing factor) calculated with the automated air void analysis. An adequate artificially induced air void system is necessary to keep the mass loss due to salt scaling limited. Partial adsorption of the AEA by the unburnt carbon present in the fly ash was considered as the main cause for this phenomenon. A continuous monitoring of the fresh air content after mixing until the time of setting is therefore recommended. It is also advised to design HVFA concrete compositions in accordance with the more strict air content requirements (min. 6% to 7 %) imposed by ACI 201.2R [2008] instead of the 4 % and 5 % air contents proposed by NBN EN 206-1 [2001] and NBN B 15-001 [2004], respectively. This design approach would ensure more that the amount of air entrained with an AEA in the presence of fly ash is enough.

REFERENCES

ACI 201.2R. 2008, *Guide to durable concrete, Reported by ACI Committee 201*, American Concrete Institute, Farmington Hills.

ASTM C457. 2006, *Standard test method for microscopical determination of parameters of the air-system in hardened concrete*, ASTM, West Conshohocken.

Jakobsen, U. H., Pade, C., Thaulow, N., Brown, D., Sahu, S., Magnusson, O., De Buck, S., De Schutter, G. 2006, 'Automated air void analysis of hardened concrete – a round robin study', *Cement & Concrete Research*, **36**[8]: 1444–1452.

Malhorta, V.M. and Mehta, P.K. 2005, *High-Performance, High-Volume Fly Ash Concrete: Materials, Mixture Proportioning, Properties, Construction Practice, and Case Histories, 2nd Edn*, Supplementary Cementing Materials for Sustainable Development Inc., Ottawa.

NBN B 15-001. 2004, *Supplement to NBN EN 206-1 – Concrete – Specification, performance, production and conformity*, BIN, Brussels.

NBN EN 1339. 2003, *Concrete paving flags – Requirements and test methods*, CEN, Brussels.

NBN EN 206-1. 2001, *Concrete – Part 1: Specification, performance, production and conformity*, CEN, Brussels.

Pedersen, K.H., Jensen, A.D., Skjoth-Rasmussen, M.S., Dam-Johansen, K. 2007, 'A review of the interference of carbon containing fly ash with air entrainment in concrete', *Progress in Energy and Combustion Science*, **34**[2]: 135-154.

XII DBMC
International Conference on Durability of Building Materials and Components
PORTO - PORTUGAL, April 12th-15th, 2011

Belgian Implementation of the ECPC-Concept Following EN 206-1

Geert De Schutter [1]

ABSTRACT

The European Concrete Standard, EN 206-1, defines durability requirements for concrete exposed to different environmental conditions. These requirements are formulated for well-known cement types, like Portland cement and blast furnace slag cement, and taking into account partial cement replacement by puzzolanic additions like fly ash and silica fume. Going beyond well-known solutions, e.g. using new types of binder and/or new type of additions, the European Standard EN 206-1 generally defines the Equivalent Concrete Performance Concept (ECPC). By means of the ECPC-concept, the durability of non-traditional or alternative cementitious materials can be evaluated in comparison with well-known deemed-to-satisfy-solutions. However, the European Standard does not give a detailed method for the implementation of the ECPC concept. In Belgium, a new Standard has been developed for the practical implementation of the ECPC concept, enabling the evaluation and attestation of non-standard cement types and/or puzzolanic additions. The evaluation of the durability is based on comparative tests, comparing the non-traditional concrete composition with standard solutions accepted by EN 206-1. In this paper, this Belgian approach will be outlined, as implemented in the Belgian Standard NBN B15-100.

KEYWORDS

Concrete, Durability, Equivalent concrete performance concept, Standardization.

[1] Magnel Laboratory for Concrete Research, Faculty of Engineering, Ghent University, Ghent, BELGIUM, Geert.DeSchutter@ugent.be

1 INTRODUCTION

Although the knowledge is available to make durable concrete structures, it is sad to remark that in reality a lot of concrete structures clearly show durability problems. To a large extent, the durability of concete structures depends on the structural design, on the mix design, and on the execution (including aspects like concrete cover and casting, compacting, curing).

It is clear that the concrete should have the right composition for the right application. In the actual European concrete code EN 206-1 '*Concrete – Part 1: Specification, performance, production and conformity*', this is implemented by defining exposure classes and by requiring a minimum cement content and a maximum water/cement ratio in function of the considered exposure class. Strength calsses are also mentioned within the durability prescriptions, however as an indication only (It is not enough to just satisfy the strength prescription in order to guarantee a durable concrete for the considered exposure conditions). These 'deemed to satisfy' rules enable the concrete industry to easily design the right concrete composition for the considered application.

Clearly, the European concrte code EN 206-1 considers three important paramters in order to guarantee durable concrete structures: water/cement ratio, cement content, and strength. While this approach has the advantage of being practical, it is clear that each of the parameters is being criticized (Fig.1). It is clear that concrete strength is not a satisfying parameter to guarantee durable behaviour [Neville 1997]. A prescribed minimum cement content is also encountering criticisms in literature, as illustrated by Wasserman *et al.* [2008]. And on top of that, while it is commonly considered as the most important practical parameter when considering durability, even the water/cement ratio should be considered cautiously. Neville [1999] states that '*We should remember the limitations on its interpretation*'. Indeed, as long as the concrete binder is made of Portland cement and water, the definition of water/cement ratio is quite clear and not questioned. In this case, there is also a clear link between water/cement ratio and strength, as e.g. illustrated in Feret's law. Nevertheless, it has to be stated that even the historic evolution of cement properties has led to an increased durability risk when only looking at concrete strength and/or cement content, as clearly shown by Neville [1997] and De Schutter [2004].

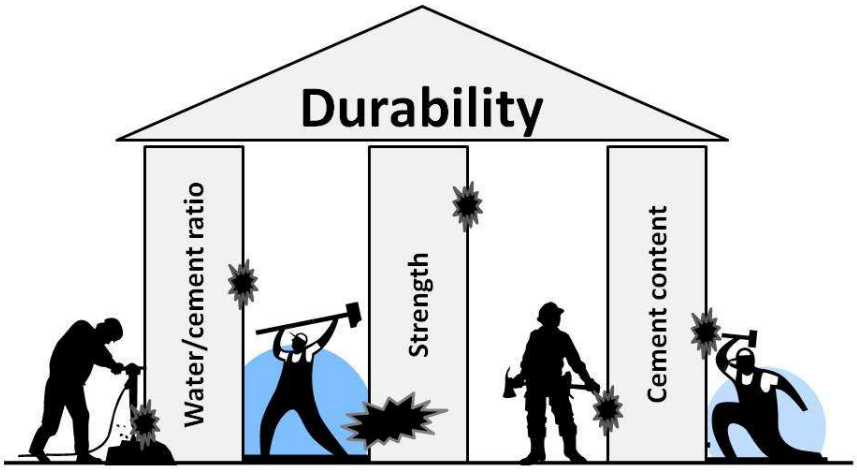

Figure 1. Water/cement ratio, cement content and compressive strength are being questioned as most important durability parameters.

Nowadays, considering the application of various types of supplementary cementitious materials, the definition of water/cement ratio is not straightforward. The European code EN 206-1 considers this problem by adopting the k-value concept, as e.g. explained by Neville [1999]. Although this k-value concept seems to be working for many cases, major discussions are going on about the level of the k-value and about the general validity of the k-value concept. As the k-value concept is principally based on concrete strength, the link with durability behaviour is not always straightforward. In Europe, the defined k-values differ from member state to members state, as listed in the various national application documents related to EN 206-1.

As an example of the European diversity within the application of the k-value concept, it can be mentioned that some countries define a k-value for the case of limestone filler, which in principle is a non-reactive filler (type I). While limestone filler is accelerating the hydration of Portland clincker due to improved nucleation possibilities, is is not chemically active (except for a minor percentage which could be chemically active in the formation of carbo aluminates) [Poppe & De Schutter 2005, Ye *et al.* 2007, Kadri *et al.* 2010]. In this way, limestone filler improves the strength development (hence the definition of a k-value within some countries), while the improvement by limestone filler of the pore structure and the long term durability performance is not always of the same degree [De Schutter & Audenaert 2008].

Considering the criticisms on water/cement ratio, cement content and concrete strength, attempts have been made to rely on other parameters, like water absorption by immersion. This is also implemented in the EN 206-1, as a potential additional requirement. Nevertheless, also the water absorption by immersion can be generally questioned as a governing durability parameter [De Schutter & Audenaert 2004].

In order to go around the discussion about the k-value concept, the European code EN 206-1 includes the possiblity to experimentally demonstrate the durability of a concrete containing an alternative binder system, by comparing the durability performance with a well accepted more traditional binder following the prescriptions based on the defined exposure classes. This approach is called the Equivalent Concrete Performance Concept (ECPC). An important practical problem however is that the European code does not give any detail on how the ECPC concept should be practically implemented. For this reason, a new code has been developed in Belgium for the practical implementation of the ECPC concept, enabling the evaluation and attestation of concrete with non-standard cement types and/or puzzolanic additions. The experimental durability evaluation is based on comparative tests, comparing the non-traditional concrete composition with standard solutions accepted by EN 206-1. In this paper, this Belgian approach will be outlined, as implemented in the Belgian code NBN B15-100.

2 EQUIVALENT CONCRETE PERFORMANCE CONCEPT

Paragraph 5.2.5.3 of EN 206-1 reads: "*the equivalent concrete performance concept permits amendments to the requirements in this standard for minimum cement content and maximum water/cement ratio when a combination of a specific addition and a specific cement is used, for which the manufacturing source and characteristics of each are clearly defined and documented*". Some further details on the ECPC-concept are given in the (informative) annexe E of EN 206-1: "*Testing should show that the performance of the concrete containing the addition should be at least equivalent to that of the reference concrete*." Annexe E furthermore provides some general guidance, on which a testing and acceptance procedure can be based.

The sequel of this paper presents the Belgian approach followed for the ECPC testing and acceptance procedure. The text is based on the Belgian code NBN B15-100, and on a previous publication on this topic [De Schutter 2009].

3 BELGIAN APPROACH: NBN B 15-100

The Belgian Standard NBN B15-100 determines a reference method for the attestation of the suitability of cements and type II additions (puzzolans), following the guidance of EN 206-1 and NBN B15-001. The suitability evaluation is based upon the comparison with reference concrete with known properties. NBN B15-100 is not questioning the rules given in EN 206-1 and NBN B15-001, neither can it be used to formulate alternative rules. NBN B15-100 only provides a framework to check the equivalence performance for a specific mix in a well-defined application environment.

The methodology of NBN B15-001 can be applied to the following cases:

- Cement normalised according to EN 197-1 and EN 197-1/A1, but normally not used in Belgium (The commonly used cement types in Belgium are listed in NBN B15-001, section 5.1.2)
- Cement normalised according to another standard than EN 197-1 and EN 197-1/A1.
- Non-normalised cement
- Blends of different cements
- Blends of cement and additions of type II

All constituent materials need to have an attestation (CE-mark or alternative).

While the Belgian code NBN B15-100 is intended to test new binder systems based on cement(s) and reactive powder materials, it is investigated at this moment whether the code could be extended to non-reactive powder materials which could be included into the binder system (fillers type I). As an example, the methodology described in NBN B15-100 could be applied without any problem to binder systems containing limestone filler. Showing the equivalent performance of limestone filler based systems would be a more coherent and safer way to show the beneficial effects of limestone filler, instead of applying the k-value concept without fundamental background in this case.

The standard NBN B15-100 considers two important terms: ‘general suitability’ and ‘specific suitability’. General suitability refers to the fact that a constituent material can be successfully used within concrete. Materials having a CE-mark (or alternative) are considered to be generally suitable. For non-certified materials, the general suitability first has to be evaluated experimentally (e.g. composition, alkali content, chloride content, mechanical properties, stability, heat of hydration, setting, loss on ignition, residue, sulphate content). The general suitability will not be focused upon in this paper, as it is quite comparable to other certification procedures for constituent materials.

The most important part of the standard NBN B15-100 is dealing with specific suitability. This refers to the suitability of a specific mix for a specific field of application and exposure conditions. The specific suitability has to be checked by means of Initial Type Testing (ITT) on real concrete mixes.

4 DETERMINATION OF THE SPECIFIC SUITABILITY

4.1 General Prescriptions

The specific suitability can only be evaluated after attestation of the general suitability. For each field of application, requirements have to be defined concerning the following items: cement and addition (identification, quantities, minimum contents), aggregates (type, grading curve), admixtures (type, dosage, restrictions in order to avoid side effects), water (content), mixing (guidelines for the mixing procedure of the concrete).

Within the procedure for the evaluation of specific suitability, several types of performance can be evaluated:

- mechanical properties: this part is optional. Information on mechanical properties is often already available from the evaluation of the general suitability.
- Durability: this part is compulsory. Durability performance has to be evaluated for an individual mix (level 1) or for the application within a certain exposure class as defined in EN 206-1 and NBN B15-001 (level 2). The methodology will be described in detail hereafter.
- properties related to casting and placement: all relevant properties have to be determined. This concerns properties related to workability, setting and hardening (consistency, density, setting, air content, strength development).

During the experimental investigation, all relevant guidelines concerning production, transport, casting and curing have to be determined and documented.

The evaluation of specific suitability consists of comparing the performance of the real mix with the performance of a reference mix which complies with the normalised prescriptions for the considered application. In case of level 1, the experimental investigation only concerns one composition for a given exposure condition. In case of level 2, the investigation can be performed for all exposure classes defined in EN 206-1 and NBN B15-001, except for classes EA1, EA2 and EA3 (aggressive environments) for which only a verification at level 1 is allowed.

4.2 Reference Concrete and Mortar

For a level 1 evaluation, the reference concrete should have a composition as normally prescribed for the considered application. The reference cement type is clearly indicated in some tables within NBN B15-100, depending on the exposure conditions. The mix to be evaluated has the same composition as the reference concrete, except for the binder system. If required, the workability of both mixes will be adjusted to the same level by means of plasticisers.

For level 2, limestone aggregates and quartzite sand have to be used. Also in this case, the reference cement type is listed in tables within NBN B15-100, depending on the exposure conditions. The reference concrete has to meet the requirements given in EN 206-1 and NBN B15-001 depending on the considered exposure classes. The mix to be evaluated has an identical composition, except for the binder. The binder composition has to be defined by the demander of the tests, in form of some tables similar to the F-tables within NBN B15-001, giving maximum water/cement ratio and minimum cement content for each exposure class considered. Also in this case, the workability of both mixes can be adjusted to the same level by means of plasticisers.

For some specific tests (see further), a reference mortar is also needed, made with high sulphate resisting cement. The water/cement ratio has to be defined in function of the considered application.

4.3 Curing

Two different during regimes have to be considered:

- ideal curing, consisting of 55 days storage under water at (20±2)°C. Storage under water can be replaced by storage at a relative humidity of 95% or higher.
- non-ideal curing, consisting of 55 days storage in a climate room at (20±2)°C and (60±5)% relative humidity.

The results obtained with the ideal curing conditions will be decisive for the evaluation of equivalent performance. The results obtained with non-ideal curing are informative only. In case non-equivalence would be obtained with the non-ideal curing, the user shall be informed in order to follow an accurate curing system in practice.

4.4 Durability Test Methods

The standard NBN B15-100 gives the test method to be followed, as well as the evaluation criteria to be applied. The test methods to be applied are listed in the standard, depending on the considered exposure conditions. As a general rule, alternative test methods can be used, however only after motivation.

The test methods are dealing with:

- **Carbonation**: in a carbonation chamber with 1% CO_2, at (20±2)°C and (60±10)% relative humidity. Higher concentrations of CO_2 can be considered if desired. The determination of the carbonation depth is performed after 28 days and 56 days, following the guidelines given by RILEM CPC-18. Taking into account the accuracy of the test method, the evaluation criterion at 56 days states that the carbonation depth of the concrete to be evaluated should not exceed 1.2 times the carbonation depth of the reference concrete.

- **Frost resistance**: 14 frost-thaw cycles following the European standard EN 1367-1. As an evaluation of the performance, the tensile splitting strength before and after frost testing is considered. The strength reduction of the concrete to be evaluated should not exceed 1.2 times the strength reduction obtained for the reference concrete.

- **Scaling resistance** (frost in combination with de-icing salts): 28 cycles according to EN 1339. The mass loss of the concrete to be evaluated should not exceed 1.2 times the mass loss of the reference concrete.

- **Chloride diffusion**: the non-stationary chloride diffusion coefficient is determined according to the standard NT Build 443. As an alternative method, NT Build 492 can be used. Considering the accuracy of the method, the evaluation criterion states that the chloride diffusion coefficient of the evaluated concrete should not exceed 1.4 times the diffusion coefficient of the reference concrete.

- **Resistance against sea water**: the test is performed on mortar specimens according to the French standard NF P18-837. The expansion of the evaluated mortar should not exceed 1.2 times the expansion of the reference mortar. The results are also accepted if the expansion of the tested mortar is below 0.05%.

- **Sulphate resistance**: the expansion of mortar specimens stored in sulphate solution is determined according to the prescriptions given in the Dutch document 'CUR Aanbeveling 48'. The evaluation criterion is identical as for resistance against sea water.

- **Acid attack**: 20 cycles of 1 day submerging in aggressive solution and 1 day drying at (20±2)°C and (60±10)% relative humidity. After drying, each exposed surface should be brushed twice (if the surface is exposed to erosion). The composition of the solution has to be defined in function of the considered application. The PH-value of the solution has to be maintained constant throughout testing. The mass loss of the evaluated concrete should not exceed 1.2 times the mass loss of the reference concrete.

- **Alkali Silica Reaction (ASR)**: In case the new binder approaches the composition of a known cement type, the alkali content of the binder has to be compared to limit values prescribed for the known cement type. Otherwise, testing according to the French Standard NF P18-594 is recommended. Testing of ASR is not compulsory according to NBN B15-100.

4.5 Equivalent Performance

For each test to be considered, the code NBN B15-100 defines acceptance criteria, as briefly indicated before, when explaining the test methods. Within these criteria, the experimental results obtained with the new binder type are compared with the experimental results obtained on the reference concrete.

As an example, when testing the carbonation performance of the new binder type, the following acceptance rule is defined, after 56 days of exposure in the carbonation chamber:

$d_{new} \leq 1.20\ d_{ref}$

with d_{new} the carbonation depth of the concrete with the new binder type, and d_{ref} the carbonation depth of the reference concrete.

The coefficient of 1.20 is introduced into the acceptance rule in order to consider the accuracy of the test method and the statistical variations on the test results.

When all relevant tests have been performed, in function of the considered exposure class(es), and when all criteria have been fulfilled, the evaluated concrete will be accepted as having 'equivalent concrete performance'. This concrete, with the evaluated binder system, will thus be accepted for applications within the considered exposure classes.

5 CONCLUSION

By means of the Equivalent Concrete Performance Concept (ECPC) as described in the European Standard EN 206-1, the durability of non-traditional or alternative cementitious materials can be evaluated in comparison with well-known deemed-to-satisfy-solutions. However, the European Standard does not give a detailed method for the implementation of the ECPC concept. In Belgium, a new Standard has been developed for the practical implementation of the ECPC concept, enabling the evaluation and attestation of non-standard cement types and/or puzzolanic additions. The evaluation of the durability is based on comparative tests, comparing the non-traditional concrete composition with standard solutions accepted by EN 206-1.

ACKNOWLEDGMENTS

The Belgian Code NBN B15-100 has been prepared within the Working Group EN 206-1 under supervision of the Belgian Normalisation Institute. The contribution of all members of this Working Group to the development of this code is greatly acknowledged.

REFERENCES

De Schutter, G. 2001, 'Evolution of cement properties in Belgium since 1950', *Magazine of Concrete Research*, **53**[5],291-299.

De Schutter,G. & Audenaert, K. 2004, 'Evaluation of water absorption of concrete as a measure for resistance against carbonation and chloride migration', *Materials and Structures*, **37**[273], 591-596.

De Schutter, G. & Audenaert, K. 2008, 'Final report of RILEM TC 205-DSC: durability of self-compacting concrete', *Materials and Structures*, **41**, 225-233.

De Schutter, G. 2009, 'How to evaluate equivalent concrete performance following EN 206-1 ? The Belgian Approach', Proc. 2nd International RILEM Workshop Concrete Durability and Service Life Planning - ConcreteLife '09, Haifa, Israel, 7 9 September 2009, ed. Konstantin Kovler, RILEM Publications (Bagneux, France), PRO 66, 1-7.

Kadri, E-H., Aggoun, S., De Schutter, G., & Ezziane, K. 2010, 'Combined effect of chemical nature and fineness of mineral powders on Portland cement hydration', *Materials and Structures*, **43**[5], 665-673.

Neville, A.M. 1997, 'Maintenance and durability of structures', *Concrete International*, November, 52-56.

Neville, A.M. 1999, 'How useful is the water-cement ratio', *Concrete International*, September, 69-70.

Poppe, A.-M. & De Schutter, G. 2005, 'Cement hydration in the presence of high filler contents', *Cement & Concrete Research*, **35**,2290-2299.

Wasserman, R., Katz, A., & Bentur, A. 2008, 'Minimum cement content requirements: a must or a myth', *Materials and Structures*, DOI 10.1617/s11527-008-9436-0.

Ye, G., Liu, X., De Schutter, G., Poppe, A.-M., and Taerwe, L. 2007; 'Influence of limestone powder used as filler in SCC on hydration and microstructure of cement pastes', *Cement & Concrete Composites*, **29**, 94-102.

XII DBMC
International Conference on Durability of Building Materials and Components
PORTO - PORTUGAL, April 12th-15th, 2011

Investigation of the Properties of Concrete Modified with Various Fibres

Ronald Nsubuga Mukalazi [1]
Chun Qing Li [2]

ABSTRACT

The use of concrete modified with fibres requires understanding of its mechanical properties and behaviour, in particular in long terms. Research on the degradation of the mechanical properties under long-term aggressive environment is limited. An experimental program is carried out to study key factors, such as dosage, fibre type, and water to cement ratio that affect the mechanical properties of concrete modified with fibres. Compressive strength, flexural strength, tensile strength and flexural toughness are determined for concrete modified with fibres. Tests, including direct uniaxial tension, three point bending, toughness and compressive strength, are carried out to produce results on important properties of concrete modified by steel and synthetic fibres. Test results presented in the paper are from short term tests which are part of a comprehensive long-term experimental program on steel fibre reinforced concrete exposed to marine environment. Empirical relationships between strengths and test variables are identified from short-term tests. Based on the test results models are developed for mechanical properties of concrete modified with fibres, which are expressed as a function of basic design variables. The developed models are verified with existing data. Modification and potential application of the developed models to prediction of deterioration of fibre concrete strength in long-term marine environment exposure is explored.

KEYWORDS

Fibres, Properties, Durability, Long-term, Empirical.

[1] School of Engineering, University of Greenwich, Kent, UNITED KINGDOM. r.n.mukalazi@gre.ac.uk
[2] School of Engineering, University of Greenwich, Kent, UNITED KINGDOM. c.q.li@gre.ac.up.uk

1 INTRODUCTION

The use of steel fibres for the reinforcement of concrete in civil engineering is becoming commonplace. Macro or "structural" steel fibres are of the order of diameter > 0.5 mm and length of 19 - 60 mm [BS EN 14889-1 [2006]]. At typical bulk fibre dosages, steel fibres added to concrete improve post-cracking tensile and flexural strengths, toughness and reduce cracking sensitivity [Romualdi and Mandel [1964]; Shah and Rangan [1971]; Concrete Society [2007a]]. To date various investigations on basic contributing factors on the effect of fibre reinforced concrete (FRC) strength have been performed in different engineering applications.

Kwak et al. [2002] have studied the effect of various steel fibre dosages and compressive strengths on shear strength of steel fibre reinforced concrete (SFRC) and reported a change from shear to flexural failure mode with increase in dosage. Krustulovic-Opara and Naaman [2000] have studied and reported the use of fibres in cementitious composites to self-develop prestress stresses. Plizzari et al. [2000] have found that steel and carbon FRC under cyclic tensile loads are more effective in improving fatigue life in high strength concrete (HSC) than in normal strength concrete (NSC). Banthia and Soleimani [2005] have studied and found synergy between fibres in some FRC hybrid composites in enhancement of their flexural toughness. Synthetic FRC has been studied under simulated elevated temperature settings to establish the durability and benefit of their use e.g. Sahmaran et al. [2010], Li et al. [2004]. Rodezno and Kaloush [2010] found that FRC round panel tests best captured the effect (toughness) of the addition of fibres to concrete; a value-added benefit was reported for polypropylene fibres. Bernard [2010] studied and concluded that post-cracked creep of SFRC was small in comparison with macro-synthetic FRC. Various advantages of using synthetic fibres in reducing shrinkage cracking have been investigated e.g. Najm and Balaguru [2002], Naaman et al. [2005], Voigt et al. [2004]. However, behaviour of steel fibre reinforced concrete (SFRC) in the long term is not altogether clear or certain.

For SFRC exposed to marine environment, various attempts have been made to study its long term behaviour affected by aggressive environment. Kosa and Naaman [1990] reported a decrease in tensile strength and toughness after 6 months of accelerated testing under corrosive environment. Lambrechts et al. [2003] performed long-term corrosive tests on cubes, performed the wedge-splitting test, and reported no loss in strength after 18 months exposure. Zhang et al. [2001] investigated the performance of SFRC panels after 10 years of exposure in Arctic marine environment and established the chloride ion-penetration in SFRC; but strengths of the SFRC structures were not investigated. From the review of research literature, it becomes clear that a systematic comprehensive test program under controlled environment is necessary to investigate important mechanical strengths of SFRC material and structures exposed to marine environment.

This paper aims to study and assess the effects of important design variables on mechanical strengths of fibre reinforced concrete (FRC), both steel and synthetic fibres, in particular the tensile strength and toughness. As part of a large ongoing long-term test program, this paper reports the cylinder compression, flexural strength and toughness for FRC under short-term conditions. Results for 28-day strengths are analysed and presented and will be compared with results from long-term marine environment exposure tests on SFRC. Based on the test results models are developed for mechanical strength of concrete modified with these fibres, which are expressed as a function of basic design variables.

2 EXPERIMENTAL PROGRAM

Details of the standard test specimens are given in Table 1. The respective number of specimens for each test under normal and aggressive environment conditions and using water cement ratios (w/c) = 0.47, 0.5 and 0.6 is shown. The weights of the constituent materials per m^3 (Table 2) were calculated according to the methods described by Teychennè et al. [1997]. Crimped steel fibres with a round cross-sectional area and length 60 mm were used.

Table 1. Specimens used in the test.

Strength property	Specimen	Dimensions (mm)	Number of specimens per mix for each test	
			Normal exposure	Marine environment
Cylinder compression	Cylinder	150 φ × 300	3	-
Flexural strength	Beams	150×150×525	3	6
Flexural Toughness	Round Panel	800 φ × 75	2	4
Direct uni-axial tension	Notched Cylinder	150 φ ×150	3	6

Table 2. Mixture proportions of steel fibre reinforced concrete in kg per m^3.
(add other proportions you used)

Water (kg)	Cement (kg)	Aggregate (kg)	Fibre Dosage (kg)
170	340	1841	40

Steel fibre dosages 35, 40 and 60 kg/m^3 were used. Macro/ mono-filamented polypropylene synthetic (HPP) fibres were added to the concrete at dosages of 2, 5, 6, 10 kg/m^3. Details of the fibres used are summarised in table 3. Dosages used are normal values recommended in the range of 20-80 kg/m^3 for steel fibres [Concrete Society [2007a]] and a range of 2-12 kg/m^3 for macro-synthetic fibres [Concrete Society [2007b]] for current bulk field applications to enhance post-cracking strength properties.

Table 3. Typical properties of fibres.

Fibre Type	Fibre Length *Lf* mm	Fibre Diameter *φf* mm	Specific gravity	*Lf/φf* Aspect Ratio	Reinforcing Index *RI = Vf*Lf/φf*	Elastic Modulus GPa	Tensile Strength GPa	Ultimate Elongation %
Steel URW 1050	60	1.0	7.84	50	45.92	210	0.5-2.6	0.5-3.5
Poly-propylene Synthetic HPP45	45	0.95	0.91	47.37	26.03	3.5-10	0.45-0.76	15-25

The cylinders were tested for compression. Beams were tested for flexure according to BS EN 14651 [2005] (Fig. 1) and round panels (rdp's) were tested for flexural toughness according to ASTM C 1550 [2005] (Fig.2). The notched cylinders were tested for maximum direct uniaxial tension at failure (without post-peak strain softening) according to RILEM TC 162-TDF [2003] (Fig.3). Ordinary sharp sand, 10 mm and 20 mm crushed aggregate were used. Ordinary Portland fly-ash cement was used.

The experiment rational is to establish the effect of different test variables in the short-term in normal strength concrete modified with various fibres. Strengths of identical samples modified with steel fibres only and exposed to marine environment will be determined. Due to time required for long-term exposure, this paper reports initial assessment and findings for short term testing. Key variables in the test program are concrete strength, fibre type, fibre dosage, and time of exposure for long term testing. Three average characteristic concrete strengths with w/c of 0.47, 0.5, and 0.6 were designed and tested. Two commercially available fibre types were used i.e. steel (URW1060) and synthetic (Enduro HPP-45) fibres.



Figure 1.



Figure 2.

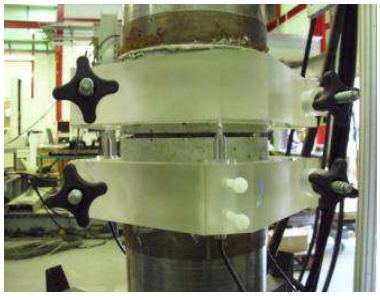

Figure 3.

Figures 1, 2, 3 Typical test set up for flexural toughness (Fig.1, Fig.2) and direct tension (Fig.3).

3 RESULTS AND ANALYSIS

3.1 Flexural Strength (f_{fl}) and Toughness (f_{flt})

Figure 4 and Figure 5 show plots of load verses crack mouth-opening displacement (CMOD) for fibre reinforced concrete for w/c=0.5 and 0.6. Maximum load for concrete reinforced with various fibres at various dosages is approximately the same. Plain concrete results in Fig. 4 appear to be higher than those for the same concrete mix modified with fibres. General trend of the plots of load verses displacement are similar. Area under load verses deflection curves (to 3 mm) is representative of flexural toughness of specimens tested.

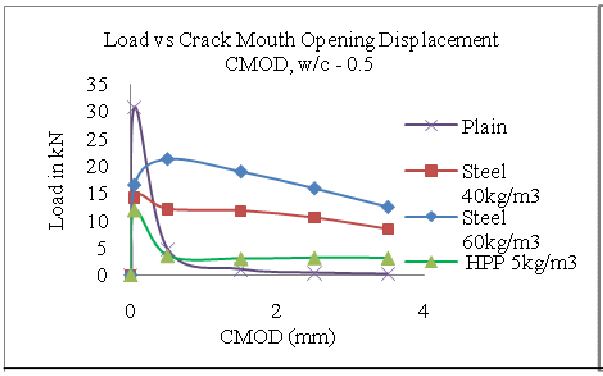

Figure 4.

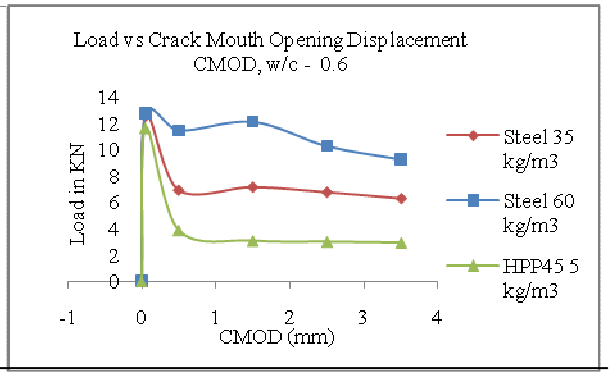

Figure 5.

Figures 4 and 5 Load verses crack mouth-opening displacement for FRC beams (CMOD).

At w/c=0.5, flexural toughness (f_{flt}) increased by 60.25 % for an increase in steel fibre volume fraction (V_f) from 0.5 to 0.77. A 202 % increase in f_{flt} for w/c=0.5 was observed for use of steel fibres at V_f=0.5 in comparison with macro-synthetic polypropylene fibres (PPF) at V_f=0.55. At w/c=0.6, f_{flt} increased by 122.81% for an increase in steel fibres from V_f= 0.45 to 0.77. A 47.33 % increase in f_{flt} for w/c=0.6 was observed for use of steel fibres at V_f=0.45 in comparison with PPF at V_f =0.55.

Flexural strength (f_{fl}) at w/c=0.5 increased by 45.05 % for an increase in steel fibre volume fraction V_f= 0.5 to 0.77. A 22.10 % increase in f_{flt} for w/c=0.5 was observed for use of steel fibres at V_f=0.5 in comparison with PPF at V_f - 0.55. At w/c 0.6, f_{flt} increased by 7.16 % for an increase in steel from V_f=0.45 to 0.77. An 8.06 % increase in f_{flt} for w/c=0.6 was observed for use of steel fibres at V_f=0.45 in comparison with PPF at V_f =0.55.

An increase of 3.362 % in f_{fl} was observed for use of HPP fibres at V_f=0.55 for concrete mixes of w/c=0.5 and w/c=0.6. A corresponding enhancement of 5.33 % in the flexural toughness was observed. An increase of 61.19 % in f_{fl} was observed between mix 7 with steel fibre V_f= 0.77 (w/c = 0.5) and mix 10 (w/c=0.6, V_f = 0.77). A corresponding enhancement of 61.17 % in the flexural toughness was observed.

3.2 Flexural Toughness (Tj)

Figures 6, 7 and 8 depict plots for load verses displacement (to 40 mm) for concrete reinforced with steel and PPF at various dosages. At a w/c =0.47 (Fig. 6) the use of a lower steel fibre V_f =0.5 in comparison with synthetic fibre V_f =1.1 increased the toughness marginally by 3.98 %. For w/c=0.47, increase in V_f for synthetic fibre from 0.22 to synthetic-fibre V_f=0.66 lead to 151.72% increase in flexural toughness. However, for w/c=0.47 increasing V_f of synthetic fibres from 0.22 to synthetic-fibre V_f =0.66 only lead to 63.98 % increase in flexural toughness. 312 % difference in flexural toughness was realised between synthetic fibres V_f=1.1 and 0.22.

At w/c =0.5 (Fig. 7) 356.65 % difference in flexural toughness between steel fibres at V_f=0.77 and synthetic-fibre V_f=0.55 was observed. 57.44 % increase in flexural toughness was noted for an increase in steel fibre V_f from 0.5 to 0.77 for w/c=0.5. Similarly, at w/c= 0.6 (Fig. 8) 236.95 % difference in flexural toughness between steel fibres at V_f=0.77 and synthetic-fibre V_f =0.55 was observed. 55.84 % increase in flexural toughness was noted for an increase in steel fibre volume fraction from V_f=0.45 to 0.77 for w/c=0.6. As a general observation, flexural toughness in concrete mix with w/c=0.5 was 36.74 % greater for steel fibre V_f=0.77 than steel fibre V_f=0.77 in concrete mix with w/c=0.6.

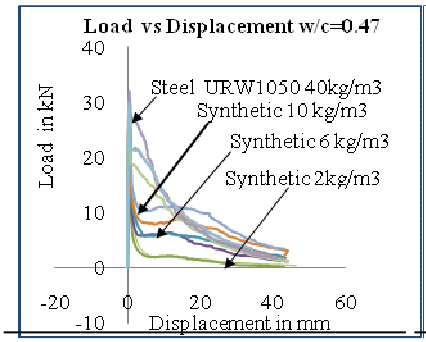

Figure 6.

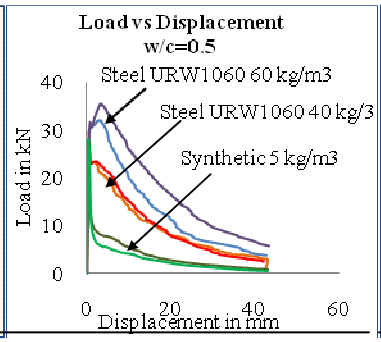

Figure 7.

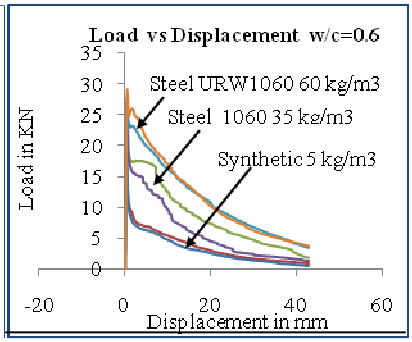

Figure 8.

Figures 6, 7 and 8 Flexural toughness in fibre reinforced concrete (FRC) round panels.

3.3 Tensile Strength

From the test data in this study (Table 4), plain concrete at w/c=0.5 appears to exhibit a superior ultimate tensile stress value in direct uniaxial tension in comparison with steel fibre reinforced concrete (SFRC). Difference in direct ultimate tensile stress (f_t) between plain concrete, w/c=0.5 and SFRC, w/c=0.5 with V_f=0.77 was substantial at 22.7 %. A similar loss in tensile strength of 24.62 % was observed between plain concrete w/c=0.5 and polypropylene fibre reinforced concrete (PPFRC), w/c=0.5 and V_f=0.55. However, a marginal 6.6 % increase in direct tensile strength was observed between steel fibre V_f=0.5 and steel V_f=0.77. For the mix w/c=0.5, SFRC mix (V_f=0.5) exhibited the lowest ultimate tensile strength value.

Table 4. Average values of ultimate tensile cylinder strength.

Mix	Fibre Dosage (kg/m3)	Average Ultimate Tensile Stress (MPa)
SFRC	40	1.9817
SFRC	60	2.1130
PPFRC	5	2.0618
Plain	-	2.7349

4 MODEL DEVELOPMENT AND DISCUSSIONS

Cylinder compressive strength (f_{cy}) for polypropylene fibre reinforced concrete (PPFRC) and steel fibre reinforced concrete (SFRC) increased marginally. f_{cy} in PPFRC and SFRC increased with V_f and reduced with increase in w/c. Multiple regression of the data for f_{cy}, w/c and V_f in this study gives equation 1 for SFRC and equation 2 for PPFRC.

$$f_{cy} = 103.67 - 129.9943w/c + 5.0V_f \quad (1)$$

$$f_{cy} = 54.65 - 47.53w/c + 2.2119V_f \quad (2)$$

BS EN 14651 [2005] computes flexural strength from equation 3 below which shows the dependence of flexural strength on maximum load sustained in the beam in flexure,

$$f_{fl} = FL/bh^2 \quad (3)$$

where f_{fl} is flexural strength, L is length of beam, b is width of beam, and h is beam depth. Maximum load the beam can carry is marginally increased by the modification of concrete with fibres. Dosages of fibres are not directly represented in equation 3 and therefore the advantage of modifying concrete with various fibres is not evident. Plain concrete in Fig. 4 appears to sustain a larger load in comparison to fibre reinforced concrete of identical mix design. JSCE-SF4 [1984] test was used to determine the flexural strength and toughness of plain concrete. Specimens are not notched therefore a more representative maximum load in flexure and flexural strength are realised However, the load is not related to the crack width. A crack width corresponding to a mid-span deflection of 3 mm will vary considerably depending on the position of the crack. Load deflection curves are therefore not completely defined by the toughness [Concrete Society [2007a]].

Concrete is notch sensitive and BS EN 14651 [2005] stipulates that beam specimens are notched at mid-span in testing for flexural strength and toughness of fibre reinforced concrete. While this ensures that fibre reinforced concrete beams crack at mid-span, it reduces the maximum load F and consequently reduces the flexural strength, equation 3. This test is recommended for testing fibre reinforced concrete. Attempts to test plain concrete for comparison with FRC specimens was impractical due to the instant failure of notched plain samples. Figures 9 and 10 show the relationship of flexural strength (f_{fl}) with w/c and V_f determined using SFRC beams. f_{fl} decreases with increase in w/c. f_{fl} increases significantly with V_f. Equation 4 for the multiple regression of data from this study relates f_{fl} to w/c and V_f for SFRC as,

$$f_{fl} = 7.4062 - 10.4098w/c + 2.6515V_f \quad (4)$$

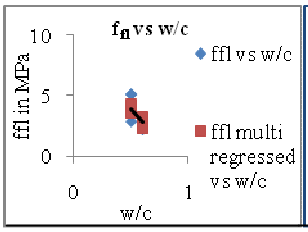

Figure 9.

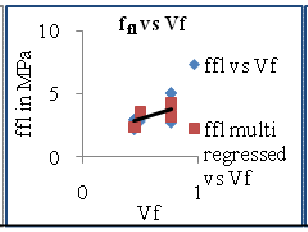

Figure 10.

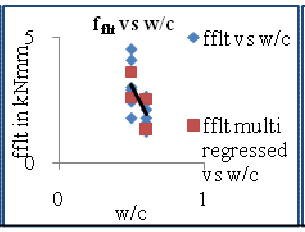

Figure 11.

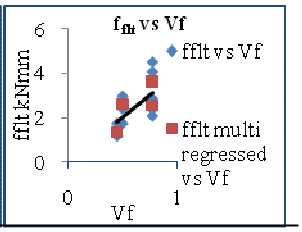

Figure 12.

Figures 9 and 10. Relationship of flexural strength (SFRC beams) with w/c and V_f.
Figures 11 and 12. Relationship of flexural toughness (SFRC beams) with w/c and flexural strength with V_f.

Flexural toughness of FRC using beam specimens is represnted by the area under the load deflection curves to a mid-span deflection of 3 mm. Enhancement of concrete toughness by addition of fibres increases with increase in fibre dosage. Toughness in steel fibres at lower dosages of 35 kg/m^3 is more significant in comparison to toughness in synthetic fibres at mid-range dosages of 5 kg/m^3 at the same w/c. Figures 11 and 12 show the relationship of flexural toughness (f_{flt}) determined using SFRC beams. f_{flt} decreases with increase in w/c. f_{flt} increases significantly with increase in V_f. Equation 5 for the multiple regression of data from this study relates f_{flt} to w/c and V_f for SFRC as,

$$f_{flt} = 5.6743 - 10.4027w/c + 4.1164V_f \quad (5)$$

Flexural toughness (Tj) as determined by FRC round panels indicate an increase in Tj with increase in V_f (Figs. 13 and 15) and decrease in Tj with increase in w/c (Figs. 14 and 16). Steel fibres tend to exhibit higher fexural toughness values in comparison with PPFRC. However from Fig. 3 above, at a central displacement between 15-40 mm, FRC at higher PPF dosages of 10 kg/m^3 exhibit superior flexural toughness qualities to those of SFRC at a dosage of 60 kg/m^3. This can be attribted to the high ultimate % elongation of PPF in comparison to steel fibres (Table 3). Equation 6 for the multiple regression of data from this study relates Tj to w/c and V_f for SFRC and equation 7 relates Tj to w/c andV_f for PPFRC as,

$$T_j = 2.94e2 - 6.3e2w/c + 7.88e2V_f \quad (6)$$

$$T_j = 1.16e2 - 2.27e2w/c + 2.84e2V_f \quad (7)$$

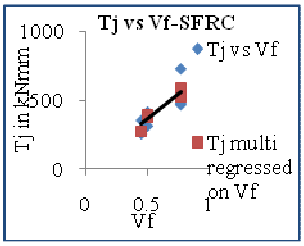

Figure 13.

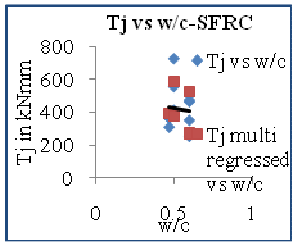

Figure 14.

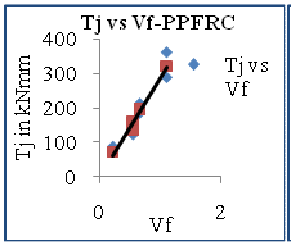

Figure 15.

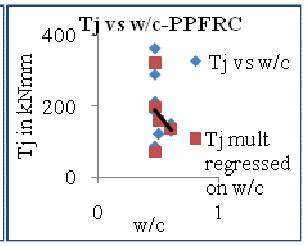

Figure 16.

Figures 13, 14, 15 and 16 Relationship of flexural toughness for FRC round panels with w/c and flexural toughness with V_f.

Tensile strength values are unclear. Bentur and Mindess [2007] reported situations in which the addition of fibres to concrete has lead to no enhancement in direct tensile strength of FRC. The importance of post cracking tensile strength as toughness in strain softening or strain hardening as area under the load deflection plot in accounting for the advantage of fibre addition is evident. Ideally tensile toughness plots should be assessed.

5 CONCLUSION

It has been found that addition of steel fibres at dosages ≥ 35 kg/m^3 to concrete marginally increases the cylinder compressive strength of normal strength concrete at water cement ratios 0.47 - 0.6. Loss in compressive strength of synthetic reinforced concrete compared to plain and steel fibre reinforced concrete is possible. Fibres at normal dosages do not significantly enhance the maximum load or flexural strength. However, at these dosages flexural toughness is considerably enhanced to values of the order of 200%. Flexural strength and toughness of plain concrete at normal strengths is low. A general trend is established showing an increase in area under the plots (toughness) with an increase in fibre dosage. Use of steel fibres instead of macro-synthetic polypropylene fibres enhances toughness more at most dosages. However, higher dosages of macro-synthetic polypropylene fibres (10 kg/m^3) significantly enhance flexural toughness in comparison with steel fibre reinforced concrete at a lower dosage (35-40 kg/m^3). Strength of FRC reduces with increase in w/c and strength increases with increase in dosage or fibre volume fraction (V_f). Relationships between strengths of FRC and key variables for short-term tests in this study are established.

REFERENCES

American Society for Testing and Materials, ASTM C1550. 2005 '*Standard Test Method for Flexural Toughness of Fibre Reinforced Concrete (Using Centally Loaded Round Panel))'*, West Conshohocken, Pennsylvania, USA: ASTM.

Banthia, N., & Soleimani, S. M. 2005 'Flexural response of hybrid fibre reinforced cementitious composites', *ACI, Materials Journal*, **102** [6] , 382-389.

Bentur, A., & Mindess, S. 2007, *Fibre Reinforced Cementitious Composites, Second Edition.* London: Taylor and Francis.

Bernard, E. S. 2010,' Influence of fibre type on creep deformation of cracked fibre-reinforced shortcrete panels', *ACI, Materials Journal*, **107**[5], 474-480.

BRITISH STANDARD INSTITUTION, BS EN 14651 2005, '*Test methods for metallic fibered concrete- Measuring the flexural strength (limit of propotionality(LOP), residual)*', London: BSI.

Concrete Society. 2007a, '*Guidance for the Design of Steel-Fibre-Reinforced Concrete, Technical Report No. 63'*, Camberley, UK: The Concrete Society.

Concrete Society. 2007b, '*Guidance on the use of macro-synthetic-fibre-reinforced concrete, Technical Report No. 65'*, Camberley, UK: The Concrete Society.

JSCE-SF4 1984, '*Methods of Tests for Flexural Strength and Flexural Toughness of Steel Fibre Reinforced Concrete. Concrete Library of Japanese Society of Civil Engineers, Japanese Society of Civil Engineers (JSCE),* **3**, Tokyo, Japan , pp. 58-61.

Kosa, K., & Namaan, A. E. 1990, 'Corrosion of Steel Fibre Reinforced Concrete, *ACI Materials Journal,* **87**[1], 27-37.

Kwak, Y. K., Eberhard, M. O., Kim, W. S., & Kim, J. 2002, 'Shear strength of steel fibre reinforced concrete beams without stirrups, *ACI, Structural Journal,* **99**[4], 530-538.

Lambrechts, A., Nemegeer, J., Vanbrabant, J., & Stang, H. 2003, 'Durability of Steel Fibre Reinforced Concrete', *ACI Special Publication,* **212** [42], 667-684.

Naaman, A. E., Wongtanakitcharoen, T., & Hauser, G. 2005, 'Influence of different fibres on plastic shrinkage cracking of concrete', *ACI, Materials Journal* , **102**[1], 49-58.

Plizzari, G. A., Cangiano, S., & Cere, N. 2000, 'Post-peak behaviour of fibre reinforced concrete under cyclic tensile loads', *ACI, Materials Journal,* **97**[2] , 1-11.

RILEM TECHNICAL COMMITTEES 2003, 'RILEM TC 162-TDF: Test and Design method for Steel Fibre Reinforced Concrete. Round-robin analysis of the RILEM TC 162-TDF uni-axial tensile test: Part 1', *Materials and Structures,* **36** , 265-274.

Rodezno, M. C., & Kaloush, K. E. 2010, 'Effect of different dosages of polypropylene fibres in thin whitetopping concrete pavements', *ACI, Material Journal,* **107**[1], 42-47.

Romualdi, J. P., & Mandel, J. A. 1964, 'Tensile Strength of Concrete Affected by Uniformly Distributed and Closely Spaced Short Lengths of Wire Reinforcement', *ACI Journal Proceedings,* **61**[6], 657-672.

Sahmaran, M., Lachemi, M., & Li, V. C. 2010, 'Assessing mechanical properties and microstruture of fire-damaged engineered cementitious composites', *ACI, Materials Journal,* **107** [3], 297-304.

Shah, S. P., & Rangan, V. 1971, 'Fibre Reinforced Concrete Properties', *ACI, Materials Journal,* **68**[2], 126-135.

Teychennè, D. C., Franklin, R. E., & Erntroy, H. C. 1997, 'Design of normal concrete mixes', *BRE Report 331*. Watford, UK: Building Research Establishment Ltd.

Zhang, M. H., Bilodeau, A., & Malhotra, V. M. 2001, 'Performance of Concrete after Ten Years of Exposure in the Arctic Marine Environment', *ACI Special Publication,* **200**[39], 621-646.

XII DBMC
International Conference on Durability of Building Materials and Components
PORTO - PORTUGAL, April 12th-15th, 2011

Effect of Ternary Cementitious System on Conductivity and Diffusion Coefficients Models

Pratanu Ghosh [1]
Paul J. Tikalsky [2]

ABSTRACT

Chloride ingress is one of the major contributing factors to the corrosion of reinforced concrete structures exposed to deicing salts. Electrical conductivity and diffusion coefficients are material properties that indicate the resistance to chloride ion transport to concrete. This paper presents an approach to determine the conductivity and diffusion coefficients using measurements from the chloride ion penetration test (CIPT) data. Equivalant steady state conditions were verified by comparing the numerical values of conductivity during 5 minute, 10 minute, 30 minute and 360 minute testing period. The Nernst-Einstein relationship was used to determine the diffusion coefficients from the conductivity measurements for different ternary cementitious systems including the control mixtures. This method of computing the diffusion coefficients includes the necessary adjustments due to the joule effect. Computed diffusion coefficients and conductivity measurements data showed that ternary cementitious materials can be designed to have low diffusion coefficients and high resistance to chloride ion transport compared to ordinary portland cement (OPC) and other permeable control mixtures.

KEYWORDS

Chloride diffusion, Ternary, Electrical Conductivity, Joule effect, Corrosion.

[1] Department of Civil and Environmental Engineering of University of Utah, Salt Lake City, USA, pratanug@gmail.com
[2] Department of Civil and Environmental Engineering of University of Utah, Salt Lake City, USA, tikalsky@civil.utah.edu

1 INTRODUCTION

One of the major premature deterioration processes in concrete structures is the reinforcement corrosion by chloride ingress. Diffusion is one of the properties that control the rate of chlorides and ions entering into concrete structures. The chloride salt ingression into concrete can take place in several ways, such as flow under a pressure differential, termed as "permeability", capillary movement into the pores termed as "adsorption" and transport due to the difference in concentrations, termed as "diffusion" [Ahmad *et al.* 2009]. Among these transport phenomena, diffusion is the most detrimental process related to the chloride ingress in concrete. As a consequence, the chloride diffusion coefficient is a necessary component in predicting the time of corrosion initiation and the rate of reinforcement corrosion [Azad *et al.*1987]. Typically the diffusion coefficients are determined by sampling concrete at different depths and fitting the profiles of acid soluble chloride concentrations versus sample depths using Crank's solution following Fick's second law [Nokken *et al.* 2006]. This was one of the possible methods a decade ago despite being highly variable. The problem of such a method is that a powdered concrete sample at any depth sample may represent a mortar or an aggregate material at a particular location, not the composite behavior of concrete material. The existing method is the chloride ion penetration test (CIPT) following ASTM C1202 specification. In this testing procedure, the transport of chloride ions is accelerated by applying an external electrical field. The current passed through an electrical cell containing the concrete specimen is measured at five minutes intervals for a 6 hour time period. The resistance to chloride ion penetration is assessed by the total charge passed during the 6 hours [Whiting 1981]. One major limitation of the CIPT results is that it does not account for the current exclusively carried by chloride ions as distinguished from the total ions in the migration process [Suryavanshi *et al.* 2002]. Another limitation of the CIPT is the high current flow in permeable concrete mixtures results in a "joule effect". The increase in temperature effectively decreases the electrical resistance and encourages the current to flow more rapidly and produce more heat which further accelerates the current flow [Betancourt *et al.* 2004]. Riding et al. developed a simplified method which is similar to the CIPT procedure except the specimen and gasket size to determine concrete resistivity as an index of concrete permeability. To eliminate gradual temperature rise problem only one current reading was taken (after 5 minutes) that could be applied to measure the concrete resistivity. An empirical correlation between the new method and the standard CIPT method established the validity and promise of the new simplified method. The disadvantage of this method is its application and suitability on core field samples as it has not yet been determined [Riding *et al.* 2008]. Snyder *et al*., 2000 has established that Ohmic heating during the 6 hour CIPT makes the raw data an unreliable measurement of any specimen transport property from the results [Snyder *et al.* 2000]. Despite of the limitations of the CIPT, it is still regarded as a repeatable experimental procedure for investigation of chloride ion ingress.

Electrical conductivity is a secondary parameter in durability modeling of concrete structures. The electrical properties of concrete correlated well with the durability of the concrete as an indirect measure of the capillary pore system and are a direct measure of the concrete's electrical conductivity which affects steel corrosion in concrete [Lane 2005]. Shi established that the CIPT is actually an indication of electrical conductivity of the concrete which depends upon the pore solution chemistry of the concrete. Results of this study showed that supplementary cementing materials such as silica fume, fly ash and ground blast furnace slag may have a significant effect on the chemistry or electrical conductivity of pore solution, depending on the alkali content of the supplementary cementing material, replacement level and age [Shi 2004]. Smith *et al.* 2004 has shown the significant advantage of using supplementary cementitious materials (SCM) in the development of high performance concrete. Their study revealed that use of SCM results in high values of concrete resistivity (inverse of electrical conductivity), thus causing a smaller likelihood of corrosion initiation [Smith *et al.* 2004]. According to Thomas *et al.* [1999], ternary based cementitious materials had high resistance to the penetration of chloride ions using diffusion experimentation method. They emphasized that ternary cementitious mixtures has low diffusivity at an early age and relatively large decay in diffusivity over time.

Most of the existing models for estimation of the corrosion initiation time and service life are not involved with significant number of ternary cementitious material's diffusion coefficients. The emphasis of this paper is on a reliable estimation of the diffusion coefficients of ternary based HPC system directly from electrical conductivity measurements using the CIPT data with incorporation of essential components of past research and adjustments due to the joule effect. This study demonstrates the influence of diffusion coefficients on several ternary cementitious mixtures of quality assurance specimens.

2 EXPERIMENTAL INVESTIGATION

Different types of binary and ternary cementitious mixtures along with control mixtures with a water/cementitious materials ratio of 0.44, typical of exposed bridge deck concrete, were designed to give a wide range of values for this experimental program. All mixtures contained 340 kg/m^3 of the cementitious material with a Coarse Aggregate Factor (CAF) of 0.67. Limestone coarse aggregate of size 19 mm meeting ASTM C33 No.67 gradation and ASTM C33 silica sand was used. Tests performed on mixtures using:

•ASTM Type I cement (TI)
•Portland-pozzolan blended cement(TIP (20))
•Limestone blended cement (E)
•Slag blended portland cement [TISM (25)]

Mineral additives used:

•Ground granulated blast furnace slag (G120S)
•Fly ash (Types C, F and F2)
•Silica fume (SF)
•Metakaolin (M)
•Volcanic tuft (S)

Medium range water reducing admixture and air entraining agent were also used to meet required slump flow and other durability performance specifications. Chloride ion penetration test (CIPT) was performed with different ternary cementitious mixtures including the control mixtures to use its data for computation of equivalent steady state diffusion coefficients. For each mixture, two 100 mm x 200 mm cylinders were cast and wet cured for 14 days and then they were air cured in lab conditions until the 98th day for testing. 98 days (i.e 14 weeks) was selected as sufficient time for pozzolanic reaction to develop. The concrete cylinders were cut to 50 mm slices and vacuum saturated with de-aerated water. In the testing process, each cell was filled with 3% NaCl solution on one side (cathode) and 0.3M NaOH solution on the other side (anode). This 3% NaCl is equivalent to 2.05 mole/l concentration in cathode cell. A potential difference of 60Vdc was applied across each cell during which the current and temperature were recorded every 5 minutes for 6 hours. A minimum of two specimens were tested and the average value of the specimens reading was reported to minimize the variation for each of the concrete mixture.

3 CONDUCTIVITY AND JOULE EFFECT

The electrical conductivity of concrete can be determined from the resistance of concrete and the geometry of the cylinder used in the CIPT and is expressed in Equation 1,

$$\sigma = \frac{l}{RA} \tag{1}$$

where σ is the conductivity in Siemens/m, l is the length of the specimen in m, R is the resistance in ohms and A is the cross-sectional area of the specimen in m^2. The CIPT is an electrical test operating under Ohm's law (Equation 2) in which the test result is a direct function of the resistance of the test specimen [Betancourt *et al.* 2004].

$$V = IR \tag{2}$$

where V is the applied voltage in the CIPT in volt and I is the current passing through the circuit. Substituting the value of resistance (R) from Equation 2 to Equation 1, the electrical conductivity can be expressed in Equation 3.

$$\sigma = \frac{lI}{VA} \tag{3}$$

3.1 Joule Effect

The application of the 60 Vdc in the chloride ion penetration test (CIPT) induces a large current flow from the begining of 6 hour test period. The resistor in this circuit consequently increases temperature and accelerates the current flow through permeable concrete mixtures during the test period resulting in a high value of charge passed. Betancourt *et al.* 2004, developed a temperature adjustment to reduce or eliminate this "joule effect" and improve the prediction of charge passed during 6 hour time period. The adjusted charge during the 6 hour test can be expressed in Equation 4.

$$Q_0 = e^{[\ln(Q_{c6hr}) + \beta(1/\delta T - 1/273)]} \tag{4}$$

In Equation 4, Q_0 is the joule effect adjusted charge passed through 6 hour CIPT and β is an experimental constant equal to 1245, Q_{c6hr} is the original charge passed through 6 hour CIPT, and δT is the difference in temperature increment in Kelvin during the 6 hour test. The adjusted average current is obtained by dividing the joule effect adjusted charge passed (Q_0) by time in seconds and it is expressed in Equation 5.

$$I_{adj} = \frac{Q_0}{t} \tag{5}$$

The adjusted average electrical current during 360 minutes can be substituted into Equation 2 to get adjusted resistance and then subsequently in Equation 1 to obtain the adjusted electrical conductivity during 360 minutes. Table 1 shows the conductivity of all cementitious mixtures. Electrical conductivity of concrete calculated from 5 minutes to 30 minutes data are nearly identical, because they contain minimal joule effect. The 360 minutes raw data produced a much higher electrical conductivity. When adjusted for the joule effect the electrical conductivity is within 10% of the 5 and 30 minutes results indicating that the joule effect is not only needed for coulomb readings but also for conductivity.

4 DIFFUSION COEFFICIENTS FROM ELECTRICAL CONDUCTIVITY

Electrical conductivity values adjusted for the joule effect during 360 minute emulates that equivalent steady state condition for the 6 hour of CIPT. Using Nernst-Einstein-relation, the diffusion coefficient D_{eff} can be derived from σ_{eff} and the salt concentration in the sample c_i and it is expressed in Equation 6, [Kudo and Fueki, 1990]

$$D_{eff} = \sigma_{eff} \frac{kT}{Z^2 Fec_i} \tag{6}$$

Where, k- Boltzmann constant (1.38E-23 J/K), T- Temperature in Kelvin, Z- Charge number, F- Faraday constant (96481 Coulomb/mole), and e- Electron charge (1.6E-19 Coulomb). The diffusion coefficients for ternary cementititous mixtures including the control mixtures are computed on 360 minutes by using Equation 6. Table1 depicts the diffusion coefficients for all the cementitious mixtures.

5 RESULTS

The values of electrical conductivity obtained from the CIPT data are in a similar range from 5 minutes to 30 minutes and it is shown in Table 1. However, high values are obtained where 360

minutes data is obtained. In-situ concrete is not exposed to sustained highly elevated temperatures. This phenomenon is evidenced by Figure 1 for two different mixtures one with 60Vdc for 6 hours and the other with 10Vdc for 36 hours of time. Figure 1 shows that temperature and current become nearly constant with the application of 10V dc over 36 hours time period in comparison with high temperature and current passed due to the application of 60Vdc over 6 hour time period. Considerations for the joule effect are necessary to adjust the current and therefore electrical conductivity. Figure 2 depicts this adjustment of electrical conductivity during 360 minutes and shows that it is nearly constant as compared to the 5 minutes electrical conductivity. This small difference in values of electrical conductivity (σ) implies further chloride ingress has been stopped and equivalent steady state condition has nearly been reached within the 6 hour of CIPT where adjustments due to the joule effect are incorporated.

Table 1. Electrical conductivity and diffusion coefficients for different cementitious mixtures.

Mix ID		Electrical conductivity (Siemens/m)				
	5 min	10 min	30 min	Raw 360 min	Adjusted 360 min	Diffusion coefficients (m^2/sec) x10^{-12}
100 TI	0.0188	0.0181	0.0196	0.0269	0.0148	2.10.E-12
80TI/20C	0.0215	0.0219	0.0237	0.0282	0.0164	2.35.E-12
60TI/20C/20F2	0.0220	0.0221	0.0251	0.0324	0.0171	2.49.E-12
60TI/30C/10F2	0.0210	0.0210	0.0233	0.0313	0.0162	2.34.E-12
60TI/30C/10F	0.0239	0.0245	0.0272	0.0320	0.0179	2.59.E-12
80TI/20F	0.0228	0.0227	0.0249	0.0358	0.0180	2.58.E-12
60TI/20F/20F2	0.0185	0.0196	0.0218	0.0288	0.0157	2.22.E-12
60TI/30F/10F2	0.0192	0.0195	0.0211	0.0262	0.0154	2.19.E-12
77TI/20F/3SF	0.0117	0.0114	0.0116	0.0149	0.0097	1.34.E-12
75TI/20F/5SF	0.0059	0.0058	0.0054	0.0071	0.0050	6.65.E-13
60TI/20F/20G120S	0.0077	0.0069	0.0069	0.0090	0.0055	7.34.E-13
75TI/20F/5M	0.0073	0.0073	0.0073	0.0100	0.0066	8.93.E-13
65TI/30F/5SF	0.0036	0.0036	0.0035	0.0044	0.0032	4.27.E-13
67TI/30F/3SF	0.0056	0.0056	0.0054	0.0071	0.0050	6.63.E-13
50TI/30F/20G120S	0.0049	0.0048	0.0049	0.0062	0.0045	5.92.E-13
65TI/30F/5M	0.0055	0.0054	0.0053	0.0072	0.0049	6.50.E-13
80TI/20F2	0.0096	0.0093	0.0094	0.0137	0.0085	1.15.E-12
60TI/30F2/10C	0.0213	0.0214	0.0243	0.0385	0.0172	2.49.E-12
75TI/20F2/5SF	0.0074	0.0075	0.0078	0.0103	0.0068	9.12.E-13
77TI/20F2/3SF	0.0101	0.0099	0.0100	0.0120	0.0083	1.13.E-12
60TI/20F2/20G120S	0.0101	0.0100	0.0100	0.0140	0.0087	1.20.E-12
75TI/20F2/5M	0.0109	0.0106	0.0106	0.0141	0.0084	1.15.E-12
65TI/30F2/5SF	0.0061	0.0060	0.0056	0.0066	0.0049	6.55.E-13
67TI/30F2/3SF	0.0090	0.0090	0.0088	0.0120	0.0078	1.07.E-12
65TI/30F2/5M	0.0127	0.0126	0.0130	0.0191	0.0111	1.53.E-12
65TI/35G120S	0.0067	0.0067	0.0063	0.0079	0.0056	7.49.E-13
50TI/35G120S/15F	0.0057	0.0056	0.0054	0.0064	0.0047	6.26.E-13
50TI/35G120S/15F2	0.0063	0.0062	0.0061	0.0073	0.0053	7.02.E-13
62TI/35G120S/3SF	0.0052	0.0052	0.0051	0.0059	0.0043	5.67.E-13
60TI/35G120S/5M	0.0045	0.0045	0.0045	0.0054	0.0039	5.21.E-13
100TIP	0.0134	0.0141	0.0156	0.0231	0.0118	1.64.E-12
85TIP/15C	0.0204	0.0207	0.0219	0.0309	0.0150	2.14.E-12
85TIP/15F	0.0155	0.0154	0.0158	0.0232	0.0129	1.80.E-12
85TIP/15F2	0.0085	0.0084	0.0080	0.0122	0.0073	9.82.E-13
65TIP/35G120S	0.0070	0.0070	0.0068	0.0093	0.0075	9.98.E-13
97TIP/3SF	0.0048	0.0048	0.0047	0.0057	0.0042	5.59.E-13
95TIP/5M	0.0037	0.0037	0.0037	0.0045	0.0033	4.35.E-13
75TIP/25C	0.0237	0.0242	0.0284	0.0401	0.0210	3.04.E-12
75TIP/25F	0.0177	0.0175	0.0192	0.0265	0.0149	2.09.E-12
75TIP/25F2	0.0210	0.0209	0.0233	0.0335	0.0169	2.43.E-12
50TIP/50G120S	0.0047	0.0047	0.0046	0.0056	0.0042	5.56.E-13
100TISM	0.0142	0.0153	0.0164	0.0255	0.0130	1.82.E-12
75TISM/25C	0.0151	0.0151	0.0164	0.0241	0.0132	1.84.E-12
75TISM/25F2	0.0122	0.0117	0.0124	0.0193	0.0105	1.45.E-12
65TISM/35G120S	0.0120	0.0118	0.0119	0.0162	0.0099	1.35.E-12
97TISM/3SF	0.0045	0.0045	0.0043	0.0057	0.0041	5.43.E-13
100E	0.0185	0.0187	0.0195	0.0312	0.0149	2.10.E-12
80E/20S	0.0163	0.0158	0.0167	0.0290	0.0144	2.03.E-12
80E/20F	0.0156	0.0155	0.0153	0.0250	0.0130	1.81.E-12
80E/20F2	0.0162	0.0164	0.0179	0.0251	0.0140	1.94.E-12
80E/20G120S	0.0122	0.0118	0.0116	0.0171	0.0099	1.35.E-12
80E/20C	0.0139	0.0137	0.0142	0.0208	0.0118	1.63.E-12
95E/5SF	0.0036	0.0036	0.0035	0.0049	0.0034	4.42.E-13
95E/5M	0.0060	0.0060	0.0060	0.0084	0.0055	7.33.E-13

Note: 75TI/20F/5M = 75% Type I cement, 20 % Class F Fly ash, 5% metakaolin

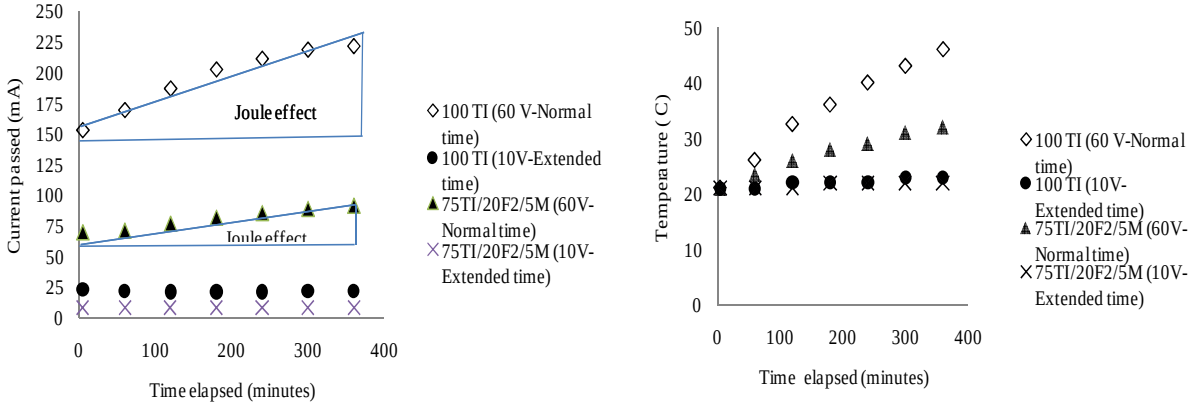

Figure 1. Joule effect on two concrete mixtures in terms of temperature and current passed.

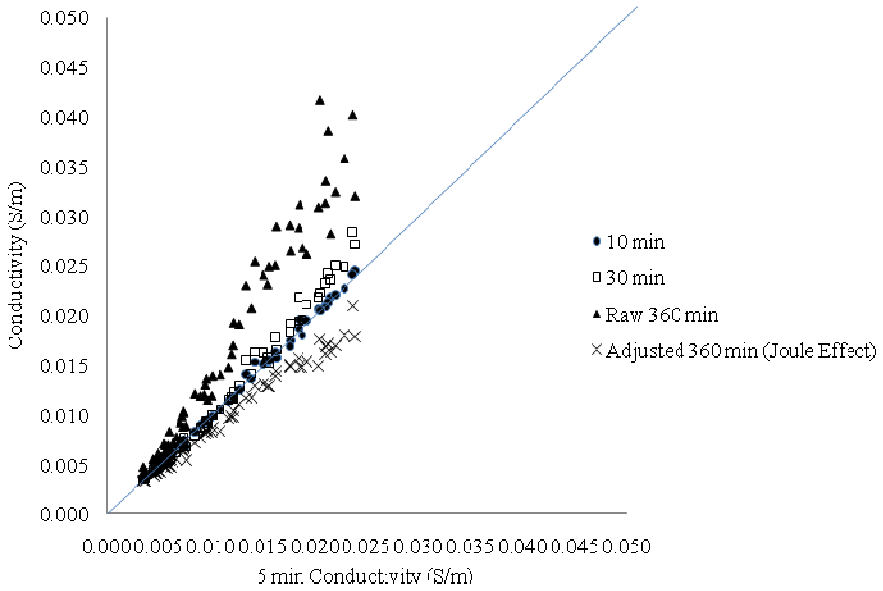

Figure 2. Comparison of chloride migration rate from 5minutes to 360 minutes.

Figure 3 shows group wise statistical distribution of diffusion coefficients of different cementitious mixtures except limestone blended cements. The whole rectangular box represents the range of diffusion coefficients those lay between the first quartile (Q1) and the third quartile numbers (Q3) for each group of mixture. Thus, the bottom most line of the box represents the first quartile number (Q1) and the topmost line represents the third quartile number (Q3). The horizontal line inside the box represents the median value of diffusion coefficient. The vertical line below and above the box represent the remaining values of diffusion coefficients excluding the outlier. It is evident from Figure 3 that all the Class C mixtures combined with other fly ashes have high value of diffusion coefficients (2.34E-12 - 2.59E-12 m^2/sec). Most of the Class F, F2, slag, TIP and TISM group of ternary mixtures performed remarkably well in the reduction of diffusion coefficients except some of the ternary mixtures namely Class F2 and TISM mixture combined with other pozzolans in the ternary blends. These mixtures are shown as outliers (*) in their respective group.

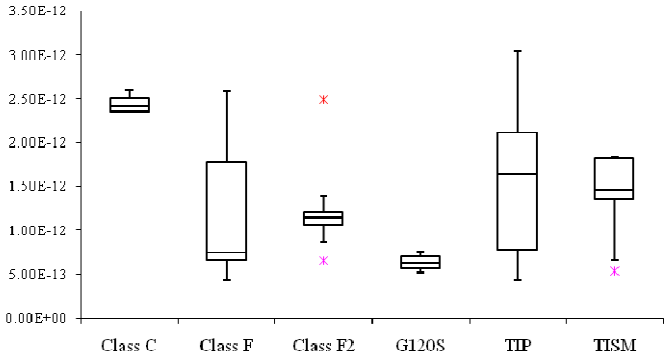

Figure 3. Group wise distribution of diffusion coefficients.

It has been observed from Figure 4 that the adjusted electrical conductivity correlated well with the diffusion coefficients as predicted by the Nernst-Einstein equation. It is also evident from Figure 4 that the joule effect is the prominent factor in computing the diffusion constants for permeable concrete mixtures and the joule effect does not have a predominant effect on impermeable/low permeable concrete mixtures. This observation has clear implication of significant beneficial effect of ternary mixtures on reduction of the diffusion coefficients and the electrical conductivity.

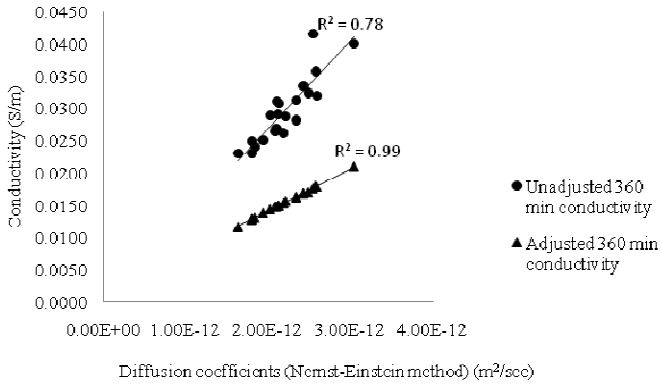

Figure 4. Correlation between diffusion coefficients and conductivity.

6 SUMMARY AND CONCLUSIONS

The work presented in this paper demonstrates the necessity of the temperature adjustment due to the joule effect in understanding the equivalent steady state condition of the diffusion process. As a result, this adjustment indicated a more accurate and reliable prediction of the electrical conductivity in hardened concrete within 6 hours of the CIPT. Thus, the Nernst-Einstein relationship is applicable to compute equivalent steady state diffusion coefficients for several ternary cementitious mixtures including the control mixtures from the CIPT data using electrical conductivity measurements.

Ternary cementitious mixtures have large effect for reduction of diffusion coefficients and electrical conductivity to increase long term resistance for chloride ion penetration. The key reason is the densification of the matrix brought about by the pozzolanic reactions of pozzolans tries to close the pores and results in reducing permeability.

Some of the pozzolans in combinations two fly ashes in the ternary blend did not produce desirable results in the computation of diffusion coefficients. Overall, the findings of these diffusion coefficients for ternary based HPC cementitious mixtures can provide reliable investigation of chloride ingress of new durable structures in harsh chloride environments.

REFERENCES

Ahmad, S., Al-Kutti, W.A., Al-Amoudi, B.S.O. & Maslehuddin, M. 2009, 'Correlations between depth of water penetration, chloride permeability, and coefficient of chloride diffusion in plain, silica fume, and fly ash cement concretes', *Journal of Testing and Evaluation,* **36**[2], 1-4.

Azad, A.K., Sharif, A.M., Navaz, M. & Loughlin, K.F. 1997, 'Chloride diffusion coefficient of concrete in the Arabian Gulf environment', *Arabian Journal Science Engineering,* Dhahran, Saudi Arabia, **22**[2B], 169-182.

Nokken, M., Boddy, A., Hooton, R.D. & Thomas, M.D.A 2006, 'Time dependent diffusion in concrete-three laboratory studies', *Cement and Concrete Research,* **36**[1], 200-207.

ASTM C1202-05, *Electrical Indication of Concrete's Ability to Resist Chloride Ion Penetration,* ASTM V04.02, ASTM, Philadelphia, PA, 2005.

Whiting, D. 1981, 'Rapid measurements of chloride permeability of concrete', *Public Roads,* **45**[3], 101-112.

Suryavanshi, A.K., Swami, R.N. & Cardew, G.E. 2002, 'Estimation of diffusion coefficients for chloride ion penetration into structural concrete', *ACI Materials Journal,* **99**[5], 441-449.

Betancourt, J.G.A. & Hooton, R.D. 2004, 'Study of the joule effect on rapid chloride permeability values and evaluation of related electrical properties of concrete', *Cement and Concrete Research*, **34**[6], 1007-1015.

Riding, A.K., Poole, J.L., Juenger, K.A. & Folliard, J.K. 2008, 'Simplified concrete resistivity and rapid chloride permeability test method', *ACI Materials Journal*, **105**[4], 390-394.

Snyder, K.A., Ferraris, C., Martys, N.S. & Garboczi, E.J. 2000, 'Using impedance spectroscopy to assess the viability of the rapid chloride test for determining concrete conductivity', *Journal of Research of the National Institute of Standards and Technology*, **105**[4], 497-509.

Lane, S. 2005, *Supplanting the rapid chloride permeability test with a quick measurement of concrete conductivity*, Final Report to Virginia Transportation Research Council, Charlottesville, Virginia, March.

Shi, C. 2004, 'Effect of mixing proportions of concrete on its electrical conductivity and the rapid chloride permeability test (ASTM C1202 or AASHTO T277) results', *Cement and Concrete Research*, **34**[2004], 537-545.

Smith, M.K., Andrea, J.S. & Tikalsky, P.J. 2004, 'Performance of supplementary cementitious materials in concrete resistivity and corrosion monitoring evaluation', *ACI Materials Journal*, **101**[5], 385-390.

Thomas, M.D.A, Shehata, M.H., Sashiprakash, S.G., Hopkins, D.S. & Cali, K. 1999, 'Use of ternary cementitious systems containing silica fume and fly ash in concrete', *Cement and Concrete Research*, **29**[1999], 1207-1214.

Kudo, T. & Fueki, K. 1990, *Solid State Ionics*, VCH, Tokyo.

XII DBMC
International Conference on Durability of Building Materials and Components
PORTO - PORTUGAL, April 12th-15th, 2011

Use of Tungsten Mine Sludge Waste in the Mitigation of Internal Expansive Reaction

S. Sousa [1]
A. Santos Silva [2]
A. Velosa [3]
F. Rocha[4]

ABSTRACT

The degradation of concrete structures by the internal expansive reactions (IER), which include the alkali-silica reaction (ASR) and the internal sulphate reaction (ISR) related with delayed ettringite formation (DEF), are two of the major problems that nowadays affect several concrete structures in the world. Therefore, it is essential to find preventive methods to inhibit the appearance of these reactions in new concrete structures.

This research work aims to investigate the effectiveness of tungsten sludge from a Portuguese mine in the inhibition of IER and is part of an extensive study to elucidate the role that the mineral additions have in the mechanism of inhibition of IER in concrete.

For this purpose several concrete mixes were produced by using tungsten sludge as a partial cement replacement.

The results of accelerated expansion tests and microestructural evolution of the concretes show that the incorporation of 30% of tungsten sludge as cement replacement appears to be effective in the mitigation of ASR and ISR.

KEYWORDS

Alkali-silica reaction, Internal sulphate reaction, Mineral additions, Mitigation, Tungsten mine sludge.

[1] Department of Geosciences, University of Aveiro (UA) , Aveiro, PORTUGAL
[2] Materials Department, National Laboratory of civil Engineering (LNEC), Lisboa, PORTUGAL
[3] Department of Civil Engineering, Geobiotec, University of Aveiro (UA), Aveiro, PORTUGAL
[4] Department of Geosciences, University of Aveiro (UA), Aveiro, PORTUGAL

1 INTRODUCTION

The degradation of concrete structures by alkali-silica reaction (ASR) and internal sulphate reaction (ISR) are a problem that affects an increasing number of concrete structures around the world.

The alkali-silica reaction (ASR) is the most frequent form of the alkali-aggregate reaction (AAR). It happens between the reactive silica present in some aggregates and the hydroxyl (OH^-) and alkaline (Na^+, K^+) ions in the cement paste. In the presence of enough water or high humidity, an alkali-silica gel is formed, and it can swell and cause cracking of the concrete [Cyr *et al* [2009].

The internal sulphate reaction (ISR) that occurs due to ettringite formation in a cementitious material after hardening is substantially complete and with only sulphate ions from inside the concrete constituents [Taylor *et al* 2001; Pavoine *et al* 2006]]. This form of sulphate attack is mainly observed in concretes that have experienced high curing temperatures, e.g. precast products made by elevated-temperatures or mass concretes in which the temperature has risen excessively due to the heat of hydration, in the presence of water.

The main issues in the cement industry are related to the environmental impact caused by the extraction of raw materials and the CO_2 emissions in the ordinary Portland cement (OPC) production.

Is well know that the use of by-products like fly ash, silica fume or blast-furnace slags in concrete, as pozzolanic materials, avoids the consumption of non-renewable resources and the environmental problems due to the disposal of these wastes. The use of these materials as a partial cement replacement in mass can prevent the ASR [Cyr, M. *et al* [*2009*] and ISR reactions [Ramlochan, T. *et al* [2003].

In Portugal, there is a large volume of mining wastes, which over the years have been dumped in landfills. These wastes can be reused and incorporated in the concrete industry as pozzolanic materials, bringing numerous benefits. They can contribute towards the reduction of CO_2 emissions from the OPC production, and can improve the durability of concrete structures, namely in the prevention of IER.

The mineral addition used in this study was tungsten sludge from a Portuguese mine. This material was previously subject to a heat treatment (950 ºC during 2 h), in order to increase its pozzolanic activity [Torgal, 2006].

This work presents the potential mitigation effect that mine sludge may have on the inhibition of ASR and ISR reactions in concrete.

2 EXPERIMENTAL METHODS

2.1 Materials

Tungsten mine sludge (TMS) of Portuguese origin was used. After being sieved, the TMS was subjected to a calcination process (2 h at 950ºC) in order to increase its pozzolanic reactivity [Torgal, 2006]. The chemical compositions, obtained by X-ray fluorescence spectroscopy, of the materials employed in this study are presented in Table1.

Table 1. Chemical composition of materials used in this study.

	TMS	**CEM I - A**	**CEM I - B**
Chemical Analysis (%)			
SiO_2	62,57	18,81	19,74
Al_2O_3	18,62	5,15	4,14
Fe_2O_3	9,99	3,18	2,69
CaO	0,63	63,70	63,54
MgO	2,15	1,50	2,42
MnO	0,13	--	--
SO_3	--	2,69	3,11
TiO_2	0,86	--	--
P_2O_5	0,24	--	--
K_2O	4,01	1,02	0,64
Na_2O	0,45	0,19	0,08
Na_2O_{eq}	3,09	0,86	0,50
LOI	0,34	3,18	3,13

2.2 Expansion Tests

To evaluate the effect of the TMS in the ASR inhibition, mortar and concrete prisms were cast using a reactive siliceous aggregate and a CEM I - A binder according to the requirements of ASTM C 1260, RILEM AAR-3 and AAR-4 test methods [ASTM C 1260[2001], [RILEM B-TC-106-3]. The mortar and concrete mixes studied are presented in Table 2.

In the ASTM C 1260 experiments, 3 mortars bars with 25 x25 x 285 mm were kept in a container with a 1N sodium hydroxide solution at 80º C during 28 days. In this test the efficiency of a certain pozzolanic material is positive in the ASR mitigation if the expansion at 14 days is less than 0.10%.

In RILEM AAR-3 and RILEM AAR-4 tests, concrete prisms (7,50 x 7,50 x 28,50 cm) were produced with a binder content of 440Kg/m^3, a water/binder of 0,45 and stored in a satured chamber for 24h.

After curing the concrete prisms in the RILEM AAR-3 test method were kept during 1 year in a chamber at 38ºC and HR>95%, while in the AAR-4 method the duration of the test is 20 weeks at 60ºC and HR>95%, and measurements are taken periodically.

Table 2. Mortar and concrete mixes used in the ASR expansion tests.

Test method	Aggregate type	w/b ratio	% of addition	
			Control	TMS
ASTM C1260	Alkali-reactive siliceous gravel	0,47	0	30
RILEM AAR-3		0,45		
RILEM AAR-4				

In the ISR study, concrete cylinders (11cm x 22cm) were produced with a CEM I - B binder and a non reactive siliceous aggregate. In the mixes (Table 3) it was used a binder content of 440 kg/m^3, with a water/binder of 0,45 and a fixed alkalis content of 5,50 kg/m^3 concrete. These mixes were tested

according to the accelerated MLPC No. 66 test method [Pavoine and Divet, [2007], being the expansion and mass measurements of the specimens taken periodically.

Table 3. Concrete mixes for the ISR expansion test.

Test	Aggregate type	W/b ratio	% of addition	
			Control	TMS
MLPC nº66	Non reactive siliceous gravel	0,45	0	30

2.3 SEM/EDS Examinations

Microestructural and X-ray microanalytical examination (SEM/EDS) of the mortars and concretes were performed on a scanning electron microscope JEOL JSM-4600 fitted with an OXFORD energy dispersive X-ray analyser. Polished specimens were prepared from mortar and concrete specimens at 28 and 90 days of storage after each expansion test method. The samples, after drying, were vacuum impregnated with a low viscosity epoxy resin, then polished and sputtered with a gold-palladium film.

3 RESULTS AND DISCUSSION

3.1 ASR Expansion Tests and SEM/EDS Observations

Figure 1 shows the expansion of the mortars with and without TMS tested according the ASTM C 1260 test method.

The results show that the control mortar (REF) exceeds the expansion limit criteria of 0,10% at 14 days of testing. At 28 days the REF mortar expanded by more than 0,50%. With 30% TMS no appreciable expansion (i.e., not greater than 0,07%) was obtained, which can be understood as effective in inhibition of ASR.

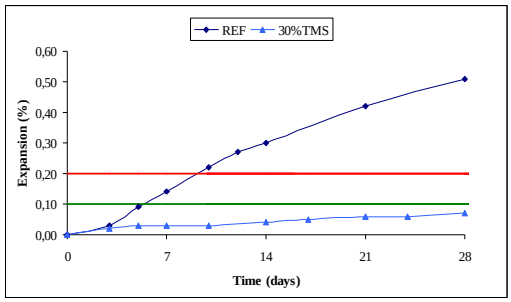

Figure 1. Expansion of mortars with cement (REF) and 30% TMS in ASTM C 1260 test method.

To confirm the mortar behaviour of the 30% TMS, concrete mixes were tested according to the RILEM AAR-3 and AAR-4 procedures [RILEM B TC-106-3]. According to the results obtained so far (Table 4) we can assume that the 30% TMS seems to be effective in the ASR mitigation.

Table 4. Results of the ASR expansion tests.

Test Methods	Expansion (%)	
	Limit	Results
ASTM C 1260	Exp< 0,1 at 14 days	0,04 at 14 days
RILEM AAR-3	Exp> 0,04 at 1 year	0 at 28 days
RILEM AAR-4	Exp> 0,02 at 3 months	0 at 28 days

Figure 2 shows the SEM/EDS observations on REF and 30% TMS mortars bars after 28 days of testing according ASTM C 1260.

The control mortar, REF, presents ASR gel in enough quantity, in aggregate/paste interfaces and filling the pores. These observations are in agreement with the results of expansion tests obtained.
The 30% TMS mortar also shows ASR gel but only inside voids. It's also visible that the TMS mortar is more microporous than the REF mortar, which can serve to accommodate the expansive products eventually formed.

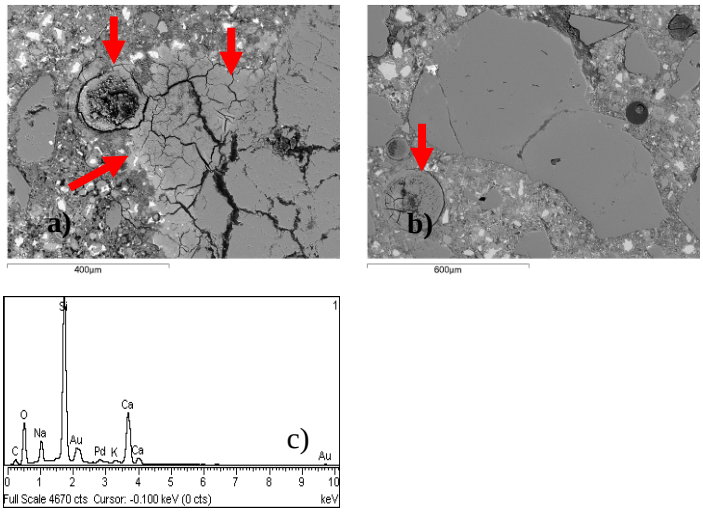

Figure 2. SEM/EDS images of ASR gel at 28 days in mortars tested according ASTM C 1260: a) Control; b) 30% TMS c) EDS spectrum of ASR gel.

To evaluate the modification of the CSH gel by the incorporation of 30% TMS, EDS microanalysis were taken at CSH locations on the mortars tested after 28 days in ASTM C 1260 test method. For statistical accuracy, approximately 10-15 EDS microanalysis were done in each mortar.

It is known that the pozzolanic mineral additions in concrete can change the Ca/Si ratio in the CSH gel, decreasing it. Also, in the last few years the matter of alkali fixation in CSH gel has been thoroughly studied [Hong and Glasser [1999, 2002];[Shehata and Thomas[2000,2002]; [Ke-rui *et al* [2004], and appears to be related with the Ca/Si ratio, increasing with the decrease of this ratio.
It is also known that pozzolanic additions rich in aluminium, such as fly ash and metakaolin, may cause a greater variation of the chemical composition of the CSH gel, due to the incorporation of a higher quantity of aluminium [Santos Silva [2005].

The evolution of the CSH atomic Ca/Si ratio (Figure 3) shows that the TMS mix presents compared to the REF mix, a decrease of this ratio. This may be due to ASR development, that predominates in the REF mix, which is related with the increased solubility of silica aggregates in the reaction, while in the TMS mix the decrease is main related to the consumption of $Ca(OH)_2$ due to the pozzolanic reaction.

The evolution of the Na_2Oeq content on the CSH (Figure 3) shows a higher value on TMS mix, which indicates a higher fixing capacity of the alkali ions by the CSH gels formed in this mix. This finding is in agreement with some papers, that showing this is one of the main inhibition mechanism of mineral admixtures in ASR [Hong and Glasser [1999, 2002];[Shehata and Thomas[2000,2002]; [Ke-rui *et al* [2004].

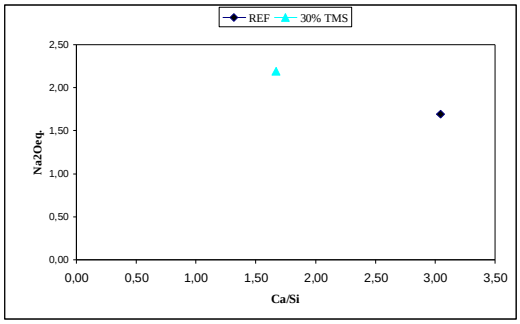

Figure 3. Existing Na_2Oeq vs. Ca/Si in the paste at mortar composition.

Figure 4 shows the obtained correlation between de expansion value at 28 days and the CSH Ca/Si ratio on ASTM C 1260 mortar test. This results confirms the good inhibition characteristics of 30% TMS on ASR.

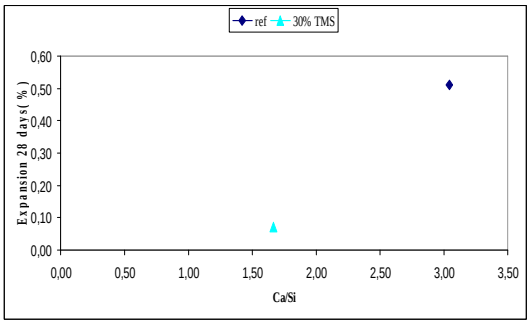

Figure 4. Expansion at 28 days vs. Ca/Si ratio of the CSH in the ASTM C 1260 test method.

3.2 ISR Expansion Tests and SEM/EDS Observations

The ISR expansion tests are still on going, but so far no expansion was verified (Table 5). This behaviour may be due to the pozzolanic effect of the TMS, accomplished by a reduction of the alkalinity in the pore solution, as happens with other mineral additions with known positive effects on ISR mitigation [Ramlochan, T., *et al* [2004].

Table 5. Results of the **MLPC No. 66 test method.**

Expansion (%)	
MLPC nº66 limit at 1 year	Result at 84 days
0,04	0,00

The SEM/EDS observations (Figure 5) didn't show ettringite formation on the 30% TMS, but rather calcium monosulfoaluminate. This finding could be due to a decrease in sulphate paste content as a result of its association to the CSH or also to an increase in reactive Al_2O_3 due to the addition replacement used.

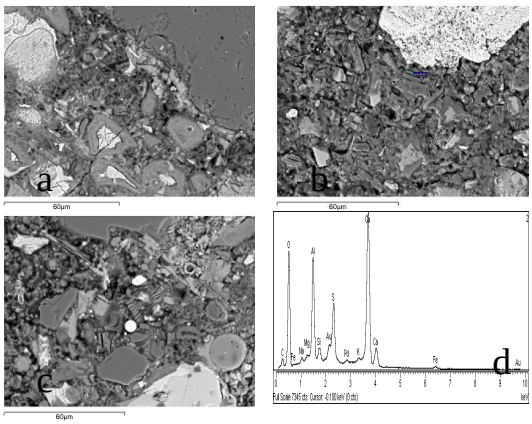

Figure 5. SEM/EDS images at 28 and 90 days of the concrete mixes tested on **MLPC No. 66 test method**: a) REF – 28d; b) 30% TMS – 28d; c) 30% TMS-90 d; d) Calcium monosulfoaluminate EDS spectra.

4 CONCLUSION

The tungsten sludge from a Portuguese mine seems to be effective as an addition in concrete in order to mitigate the ASR and ISR reactions.

It appears that 30% (by mass) of cement replacement with sludge may be efficient in the mitigation of such reactions.

The inhibition mechanism of the sludge seems to be related to its ability to reduce the alkalinity of the paste, as a result of the consumption of calcium hydroxide and alkali ions.

ACKNOWLEDGMENTS

The authors wish to acknowledge the Foundation for Science and Technology (FCT) for the financial support under project EXREACT (PTDC/CTM/65243/2006) and project DURATINET (Durable Transport Infrastructures in the Atlantic Area Network) for Transnational Programme Atlantic Area 2007-2003, co-financed by FEDER.

REFERENCES

ASTM C 2001, "Standard test method for potential alkali reactivity of aggregates (mortar-bar method)", ASTM International, West Conshohocken, United States, p. 5.

Cyr, M., Rivard, P., Labreque, F., 2009, "Reduction of ASR-expansion using powders ground from various sources of reactive aggregates", Cement and Concrete Composites, vol. 31, p. 438-446.

Hong, S.Y: and Glasser, F.P., 1999, "Alkali binding in cement pastes. Part I. the C-S-H phase"; Cement and Concrete Research, vol. 29, 12, p. 1893-1903.

Hong, S.Y: and Glasser, F.P.,2002, "Alkali sorption by C-S-H and C-S-A-H gels. Part II. Role of alumina"; Cement and Concrete Research, vol. 32, 7, p. 1101-1111.

Ke- rui, Y., Cai-Wen, Z., Zhi-gang, L., Cong, N., 2004, "A study on alkali-fixation ability of C-S-H gel", Proceedings of the 12th International Conference on Alkali-Aggregate Reaction in Concrete, Beijing, China, p. 221-225.

Pavoine, A., Divet, L., Réactivité des bétons vis-à-vis d'une réaction sulfatique interne. Essais de performance. Techniques et méthodes des LPC., Méthode d'essai des lpc, vol. 66, 2007 p. 19.

Ramlochan, T., Zacarias, P., Thomas, M. D. A., Hooton, R.D., 2003, "The effect of pozzolans and slag on the expansion of mortars cured at elevated temperature. Part I: Expansive behaviour", Cement and Concrete Research, vol. 33, p. 807-814.

RILEM Recommendations: B-TC-106-3-Detection of potential alkali-reactivity of aggregates- Method for aggregate combinations using concrete prisms, materials.

Santos Silva, A., Degradação do betão por reacções álcalis-sílica. Utilização de cinzas volantes e metacaulino para a sua prevenção., Tese de Doutoramento, LNEC/Universidade do Minho, (2005).

Shehata, M. H. and Thomas, M.D.A., 2000, "The effect of fly ash composition on the expansion of concrete due to alkali-silica reaction", Cement and Concrete Research, vol. 30, 7, p. 1063-1072.

Shehata, M. H. and Thomas, M.D.A., 2002, "Use of ternary blends containing silica fume and fly ash to suppress expansion due to alkali-silica reaction in concrete", Cement and Concrete Research, vol. 32, p. 341-349.

Torgal, F. Pacheco, Desenvolvimento de ligantes obtidos por activação alcalina de lamas residuais das minas da Panasqueira. Tese de Doutoramento, Engenharia Civil, Departamento de Engenharia Civil e Arquitectura da Universidade da Beira Interior, (2006).

XII DBMC
International Conference on Durability of Building Materials and Components
PORTO - PORTUGAL, April 12th-15th, 2011

Durability of Reinforced Concrete Structures in a Petrochemical Complex: a Case Study

Milad Hallaji [1]
Mohammad Shekarchi [2]
Rahman Taheri [3]
Masoud Moradian [4]
Mohammad Hosein Eftekhar[5]

ABSTRACT

Most structures in a petrochemical complex are fully or partially constructed by reinforced concrete and since in this environment various high corrosive materials exist, these structures must possess a durable behaviour during their service life in order to perform satisfactorily. In this study, some reinforced concrete structures of a petrochemical complex in Shiraz city of Iran have been evaluated. First of all, a thorough visual inspection (in order to observe different deterioration mechanisms) accompanied with a comprehensive set of conventional experiments in assessing durability of concrete (such as water absorption, carbonation depths, electrical resistivity, half-cell potential maps) were carried out. It was concluded that a petrochemical complex provides a harsh environment from durability of concrete point of view. Second of all, appropriate repair schemes according to the extent of damages to different units were discussed. At last, some useful recommendations about the maximum w/c ratio and concrete cover of reinforcement for designing structures in such environment were provided.

KEYWORDS

Carbonation depth, Chloride content, Durability, Petrochemical complex, Reinforced concrete.

[1] Construction Materials Institute (CMI) Of the University of Tehran, Tehran, IRAN, mhallaji@ut.ac.ir
[2] Construction Materials Institute (CMI) Of the University of Tehran, Tehran, IRAN, shekarch@ut.ac.ir
[3] Construction Materials Institute (CMI) Of the University of Tehran, Tehran, IRAN, srtaheri@ut.ac.ir
[4] Construction Materials Institute (CMI) Of the University of Tehran, Tehran, IRAN, mmoradian@ut.ac.ir
[5] Construction Materials Institute (CMI) Of the University of Tehran, Tehran, IRAN, h.eftekhar@ut.ac.ir

1 INTRODUCTION

Most of the structures in a petrochemical complex are fully or partially constructed by reinforced concrete. Therefore, the concrete should be specified with special measures to resist deterioration when placed in a harsh environment to help ensure the long-term performance of such structures. This becomes even more important knowing that in such an environment, in addition to carbonation (ordinary corrosion-induced phenomenon in offshore structures), the rate of concrete deterioration is greater than usual because of the presence of highly aggressive chemicals such as ammonium nitrate and chloride. Moreover, due to the short distances between different units of a petrochemical complex, each unit discharging gases may affect the durability of the concrete in adjacent units.

In the following sections of this paper, the present condition of concrete in three operational units of a petrochemical complex is first investigated, where it will be seen that the different units experienced a high level of deterioration; for this purpose after a complete visual inspection of the structures, common tests such as density, water absorption and electrical resistance were performed on several extracted concrete cores. Secondly, three repair methodologies for these three units will be proposed. Finally, some useful recommendations about the w/c ratio and concrete cover of structures in such environment will be presented. As well, the probable interaction between adjacent units that occurs in a petrochemical complex was also considered.

2 ANALYSES OF DAMAGED STRUCTURES

2.1 Ammonium Nitrate Unit

The ammonium nitrate unit is located at the centre of the petrochemical complex and consists of three main parts: (1) Prill tower and its upper structure (Figure 1); (2) Accessing concrete tower which is built to provide accessibility to the prill tower by means of an elevator and staircase; (3) Two steel structures.

Although a protective epoxy coating was applied to concrete surfaces, the prill tower nonetheless showed severe deterioration due to the long time exposure to ammonium nitrate. Damages were mainly softening of concrete (to the extent that even extracting cores from the tower's foundation was not possible) and removal of concrete cover (Figure 2). Therefore a thorough investigation was performed to assess the causes of these damages and also the level of deterioration.

One of the products of a petrochemical complex is chemical fertilizer which is often sold as small particles known as prills. These small particles are produced by converting liquid ammonium nitrate into solid granules. This conversion process is implemented in a tall tower called a prill tower (Figure 1).

Ammonium nitrate is very corrosive to concrete [Schneider & Chen 2004; Schneider & Chen 1999; Schneider & Chen 1998] and continuous exposure of concrete to this chemical leads to dissolution of cement-based materials. The simplified reaction equation is the following:

$$2NH_4NO_3 + Ca(OH)_2 \rightarrow Ca(NO_3)_2 + 2NH_3 + 2H_2O \quad (1)$$

The reaction products are ammonia and calcium nitrate, which are both easily soluble in water. As a result, in the presence of water or a damp environment and due to the removal of these products, concrete permeability will be increased. Besides, it is clear from the aforementioned chemical reaction that ammonium nitrate decalcifies hardened cement paste due to the removal of calcium hydroxide (Eq. (1)). This results in dissolution of other products of the hardened cement paste and leads to a reduction of the pH-value. Consequently, steel reinforcement corrosion may occur at an accelerated rate. As well, the deterioration of the cement-based material will be intensified and accelerated, when the material suffers under a corrosive attack accompanied by a mechanical load ([Schneider & Chen [2004]).



Figure 1. The ammonium nitrate prill tower.



Figure2. Destruction of concrete cover.

The results of density, compressive strength, water absorption and electrical resistance of concrete cores extracted from the tower are presented in Table 1. It is obvious that concrete of the foundation has a worse quality in comparison with concrete of the tower's body. This also justifies the higher level of deteriorations in the foundation (even sampling from the foundation was not feasible because of loose concrete).

Although, concrete has been decalcified up to about 30 mm from its surface, reinforcement corrosion was negligible along the ammonium nitrate prill tower.

Table 1. Results of different tests on extracted cores from the ammonium nitrate prill tower.

Cores location	*Density (Kg/m^3)*	*Half an hour water absorption (%)*	*Saturated water absorption (%)*	*Electrical resistance (kΩ-cm)*	*Compressive strength (MPa)*	*Carbonation depth (mm)*
Ammonium nitrate tower body	2318	1.9	5	4	18	30
Ammonium nitrate tower foundation	2055	4	10	1.5	19	-

2.2 Chloride Unit

The chloride unit is located at the northern part of the petrochemical complex. Most columns of this unit's structures are constructed by reinforced concrete. High concentration of chloride ions in the atmosphere of this unit was the most important finding obtained from the visual inspections; these results served to confirm the high degree of deterioration that was evident on the different concrete elements. Figure 3 presents a column of this unit. It is obvious that the concrete cover has been totally removed and reinforcement corrosion is observed.



Figure 3. A view of supporting columns of the structure of chlorine unit.

Results of different laboratory experiments on the extracted cores with in-situ measurements of carbonation depths are summarized in Table 2. Results confirm the poor condition of the concrete. The depth of carbonation is rather high and according to Figure 4, carbonation phenomenon has pushed the maximum peak of diffused chloride ion from surface of concrete to its depth. Moreover, the concentration of chloride ion at the location of the reinforcement bars (40 mm depth) is far beyond the chloride threshold value ([Pargar et al. [2007]). Therefore, reinforcement corrosion is highly probable. This was in complete agreement with the results of visual inspection and half-cell potential map (changing of absolute potentials along a short distance is an obvious indication of steel corrosion).

Furthermore, according to different measurements, the concrete cover of the columns in this unit was about 4 cm which is clearly not sufficient from a durability point of view given the extremely harsh environment to which the structure has been subjected.

Table 2. Results of different tests on extracted cores from the chloride unit.

Density (Kg/m^3)	*Half-hour water absorption (%)*	*Saturated water absorption (%)*	*Electrical resistance (kΩ-cm)*	*Compressive strength (MPa)*	*Carbonation depth (mm)*
2269	2.6	5.5	3.5	15	30

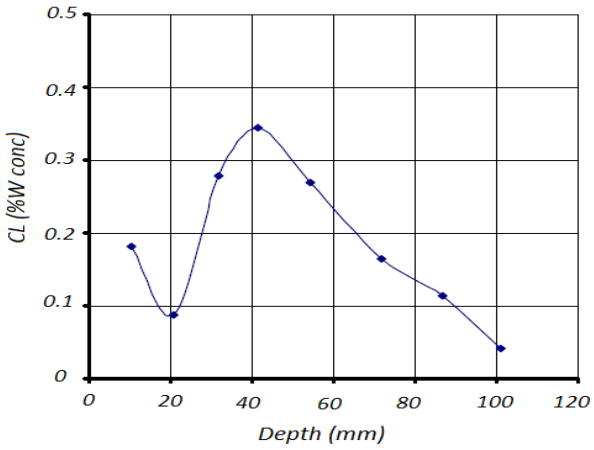

Figure 4. Chloride diffusion profile of a selected column.

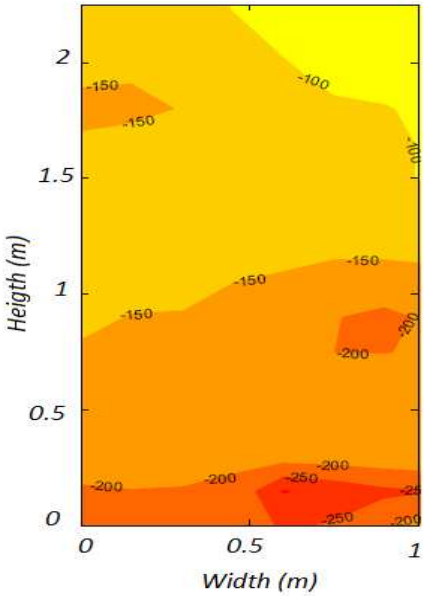

Figure 5. Half cell potential map of a selected column.

2.3 Cooling Tower Unit

This unit is located at the north western part of the petrochemical complex and next to the Chloride unit. The function of this unit is to reduce the temperature of water gathering from cooling systems of different units by spraying it from the top to the bottom of the cooling tower. As the drops of hot water fall, they evidently lose temperature. Therefore, high humidity conditions exist where water is sprayed and the concrete is thus almost near the saturation limit for large areas of this structure. Concrete elements of this unit consisting of peripheral frames such as columns, beams and walls are pre-fabricated and the columns rest on pedestals that are almost two meters in height (Figure 6).



Figure 6. A view of the cooling tower unit.

In some of the columns and walls of this unit, longitudinal cracks with almost 2 mm size were observed (Figure 7).

In Table 3 average test results of concrete cores extracted from the cooling tower unit and also carbonation depth measurement are presented. As shown, the water absorption factor is high and specific electrical resistance of concrete is low. These results together with those obtained for compressive strength and depth of carbonation indicate an inappropriate quality of concrete used in this complex.

Various studies have suggested that different half-cell potential ranges should be considered instead of absolute potential values in order to determine the locations of "high-probability" corrosion activity within a reinforced concrete structure [RILEM TC 154-EMC 2003]. Figure 8 displays half-cell potential contours of a wall which exhibited many longitudinal cracks that likely originated from reinforcement corrosion. In this figure, high fluctuations of potential values in both ends of the wall were observed which is indicative of a high likelihood of the presence of steel corrosion.



Figure 7. Longitudinal vertical cracks of almost 2 mm size in a selected column.

As it was mentioned earlier, this unit is located beside the chloride unit and because of the high concentration of chloride ions in the atmosphere of the latter unit; the chloride-induced corrosion also threatens the durability of concrete in the cooling towers unit. Figure 9 provides an overview about the penetrating chloride ion to the concrete on a western wall of the cooling tower unit. As was the case in Figure 4, the existence of carbonation phenomenon is apparent since the maximum peak of the curve is transferred from surface of the concrete to its depth. Chloride content is somehow high. At the location of bars (40 mm depth) chloride content of approximately 0.06% by weight of concrete which is very close to chloride threshold value is observed. Meanwhile, results of chloride profile of the farther units from the chloride unit showed a little amount of diffused Chloride. Therefore, the hypothesis of occurring interactions between adjacent units is highly presumable and should be considered in designing or at least allocating sufficient distances between different units.

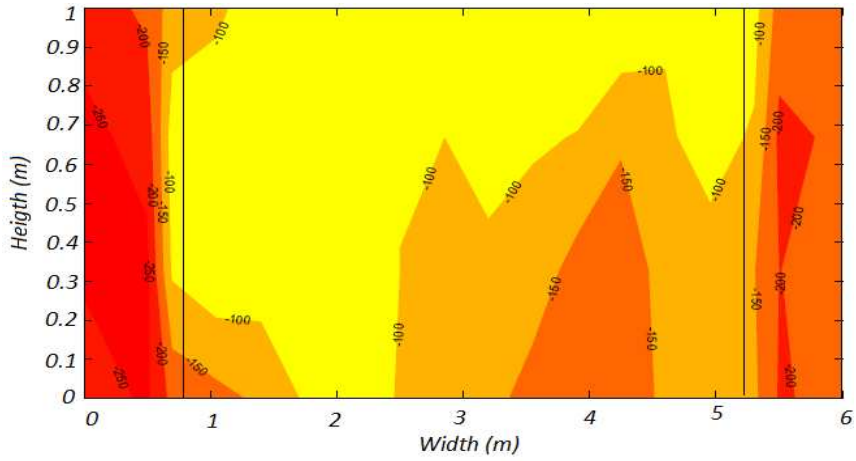

Figure 8. Half cell potential map of a the western wall of the cooling tower unit.

Table 3. Results of different tests on extracted cores from the cooling tower units.

Density (Kg/m^3)	*Half-hour water absorption (%)*	*Saturated water absorption (%)*	*Electrical resistance (kΩ-cm)*	*Compressive strength (MPa)*	*Carbonation depth (mm)*
2185	2.5	7.4	4	17	30

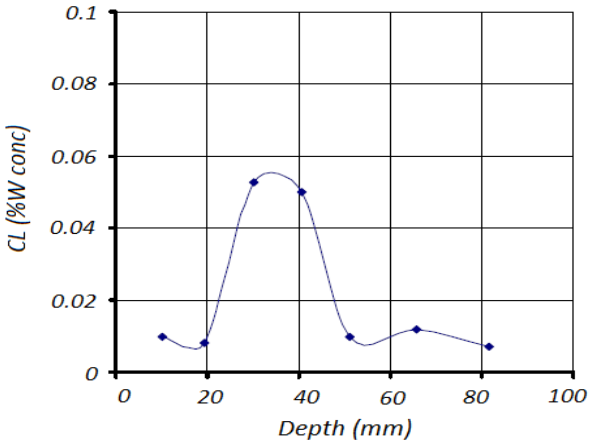

Figure 9. Chloride diffusion profile of a selected wall.

3 PROPOSED REPAIR METHODOLOGIES

1) For the ammonium nitrate unit in which the concrete was decalcified to a depth of 30 mm from its surface but for which reinforcement corrosion was not observed, the best repair scheme would be to remove concrete up to 30 mm depth and replacing with a high quality and compatible repair material [Vaysburd et al. 2004;Moragn 1996]. This should be followed by placing a protective and breathable coating on the exposed surfaces.

2) As was the case for the ammonium nitrate unit, for the cooling tower units the best repair method would be local patch repairs. But in some locations of these units, reinforcement corrosion was observed and in some regions the chloride content in proximity to the reinforcement was around the threshold value. Therefore, not only must the contaminated concrete be substituted by high quality and compatible concrete, but the corroded reinforcements must also be replaced by new rebars.

3) Most parts of the concrete structure of the chloride unit are contaminated by chloride ions far beyond the threshold value and up to 8 cm depth from its surface; reinforcement corrosion was observed to be well developed. Therefore it would be more cost-effective to build a new chloride unit than perform repair operations; in any case, durability parameters should be taken in to account.

4 CONCLUSIONS AND RECOMMENDATIONS

In this study the durability of some reinforced concrete structures forming part of a petrochemical complex and which showed early signs of deterioration since their construction were investigated. Results indicated various levels of deterioration due to different exposure conditions. The study was useful in that the results help further emphasize that environment conditions in which a structure is to perform should be thoroughly reviewed during design process to subsequently ensure satisfactory performance of such structures during its lifetime. Disregarding basic principles of durable structural design, may in fact lead to over expenditures for premature repairs during its utilization simply to ensure that it is maintained in an operational mode.

The investigations carried out in this study helped confirm that a concrete cover of 4 cm was not adequate for the aggressive environment in which this petrochemical complex operates. In addition, results of water absorption, electrical resistivity and compressive strength tests suggest that the w/c ratio used in the mix design was too high.

In conclusion, it is recommended that the petrochemical complex environment be considered as a harsh environment from durability of concrete point of view. Since there is no specific code and recommendations in this case, given value of nominal concrete cover (65 mm) provided in ACI 357R84 for a wall located in splash and atmospheric zone is highly recommended. It should be noted that concrete covers of reinforcement should not be significantly greater than the prescribed value to restrict the width of possible cracks. This would be more critical for those members in flexure. Moreover the concrete must be of low permeability therefore the w/c ratio must not be taken too high; a maximum w/c ratio of 0.4 is recommended (this is the value given in ACI 201.2R-01 for class 3 exposure to sulphate attack).

REFERENCES

American Concrete Institute (ACI) Committee 201. 2001, *Guide to Durable Concrete,* ACI 201.2R-01.

American Concrete Institute (ACI) Committee 357. 1984, *Guide for the Design and Construction of Fixed Offshore Concrete Structures,* ACI 357R84.

Mehta, P. & Monteiro, P. 2005, "Concrete: microstructure, properties and materials (3rd ed.)." McGraw Hill.

Moragn, D.R. 1996, "Compatibility of concrete repair materials and systems." *Construction and Building Materials,* 10[1], 57-67.

Pargar, F. Layssi, H. & Shekarchi, M. 2007, Investigation of chloride threshold value in an old concrete structure, Proc. 5th Concrete under Severe Conditions Environment and Loading (CONSEC'07) Conf, Int .Tours, France. pp. 175–182.

RILEM TC 154-EMC. 2003, "Electrochemical techniques for measuring metallic corrosion Half-cell potential measurements - Potential mapping on reinforced concrete structures." *Materials & Struct*ures, 36[261], 461-471.

Schneider, U. & Chen, S.W. 2004, "Deterioration of high-performance concrete subjected to attack by combination of ammonium nitrate solution and flexure stress." *Cement & Concrete Research.* 35[9], 1705-1713.

Schneider, U. & Chen, S.W. 1999, "Behavior of High-Performance Concrete under Ammonium Nitrate Solution and Sustained Load." *ACI Materials Journal* 96[1], 47-51.

Schneider, U. & Chen, S.W. 1998, "The chemomechanical effect and the mechanochemical effect on high-performance concrete subjected to stress corrosion." *Cement & Concrete Research* 28[4], 509-522.

Schneider, U. & Chen, S.W. 1998, "Modeling and empirical formulas for chemical corrosion and stress corrosion of cementitious materials." *RILEM: Materials & Structures* 31[10], 662-668.

Vaysburd, A.M., Emmons, P.H., Mailvaganam, N.P., McDonald, J.E. & Bissonnette, B. 2004, "Concrete Repair Technology—A Revised Approach is Needed." *Concrete International* 26(1), 58-65.

XII DBMC
International Conference on Durability of Building Materials and Components
PORTO - PORTUGAL, April 12th-15th, 2011

Concrete Rehydration after Heating to Temperatures of up to 1200 °C

Markéta Chromá [1]
Pavel Rovnaník [2]
Dita Vořechovská [3]
Patrik Bayer [4]
Pavla Rovnaníková [5]

ABSTRACT

The research presented in this paper involves the study of the possible regeneration of cement binder in concrete subjected to high temperatures. An ongoing experimental program is simulating the heating of a concrete structure by a fire during which the temperature in the structure gradually increases. The experimental program is designed to analyze concrete behaviour after heating to 200 – 1200 °C and is investigate investigating the consecutive reactions of phases (which originate after heating) with water. The laboratory specimens (40×40×160 mm) are manufactured from fine-grained concrete with a water to cement ratio of w/c = 0.45. After heating and cooling, the specimens are placed under the following conditions for a time period of 2 months: (i) laboratory conditions (t = 22 ± 2 °C, R.H. = 55 ± 5 %), (ii) water (t = 22 ± 2 °C) and (iii) laboratory conditions (t = 22 ± 2 °C, R.H. = 55 ± 5 %) with periodical immersion of the specimens in water. To investigate the mechanism of concrete regeneration mercury intrusion porosimetry and X-ray diffraction (XRD) analysis are performed. In order to quantify the changes in concrete properties, the specimens are tested in compression and three point bending. The results of the research could make an important contribution to decisions made concerning the reconstruction of concrete structures affected by fire. In suitable cases it would be possible to regenerate parts of a concrete structure instead of totally re-building it, which would significantly decrease repair costs.

KEYWORDS

Concrete, Temperature, Rehydration, XRD, Porosimetry.

[1] Brno University of Technology, Faculty of Civil Engineering, Brno, CZECH REPUBLIC, chroma.m@fce.vutbr.cz
[2] Brno University of Technology, Faculty of Civil Engineering, Brno, CZECH REPUBLIC, rovnanik.p@fce.vutbr.cz
[3] Brno University of Technology, Faculty of Civil Engineering, Brno, CZECH REPUBLIC, vorechovska.d@fce.vutbr.cz
[4] Brno University of Technology, Faculty of Civil Engineering, Brno, CZECH REPUBLIC, bayer.p@fce.vutbr.cz
[5] Brno University of Technology, Faculty of Civil Engineering, Brno, CZECH REPUBLIC, rovnanikova.p@fce.vutbr.cz

1 INTRODUCTION

The behaviour of concrete structures at extreme temperatures is presently the subject of research concerning the safe operation of various types of structures (fire safety in tunnels and at chemical factories, industrial and high-rise buildings, power plants, etc.).

Concrete exposed to high temperatures and its properties after heating is a subject under investigation by many authors. Arioz [2007] studied the effect of heating concrete up to temperatures of 200 to 1200 °C on its strength, bulk density and surface texture. Visible damage was present on the surface for specimens heated to 600 °C and higher. At a temperature of 1200 °C, the binder in the concrete completely disintegrated. Strength significantly decreased with increasing temperature. Matesová [2007] compared the strength of concrete tested immediately after heating and cooling with that of concrete tested several months after cooling. Significant strengthening occurred for concrete specimens exposed to a laboratory environment for several months after heating. It was found that concretes with higher w/c ratios are more affected than concretes with lower w/c ratios. Shui et al. [2009] analyzed the rehydration of cement paste heated to temperatures of 300 to 900 °C. Hydrated cement paste was ground to a grain size of < 75μm and heated to temperatures of 300 to 900 °C with 2.5 hours of exposure at the maximum temperature. The specimens were mixed with water after cooling and the obtained cement pastes were cast into a mould (20×20×20 mm). The initiation, time of hardening and compressive strength after 3, 7 and 28 days were further evaluated for the cement pastes. The initiation and time of hardening decreased with increasing temperature; compressive strength increased with time. The highest strengths were reached for specimens heated to a temperature of 800 °C after 28 days. They had 60 % of the strength of the hydrated paste that was not heated. Alonso & Fernandez [2004] studied the microstructural changes in an OPC cement paste subjected to temperatures of 100 to 750 °C using ^{29}Si MAS-NMR, thermogravimetry and XRD. The rehydration process in the specimens after placing them in a saturated chamber (100 % R.H.) at room temperature for 3.5 months was also studied.

The presented experiments show the ability of concrete to rehydrate significantly in a certain environment during a long time period after heating. To be more specific, it has been found that the rehydration of concrete placed into water for a time period of 2 months after heating up to temperatures of 200 to 1200 °C leads to a significant increase in compressive and flexural strength at temperatures ranging from 600 to 1000 °C. These experiments indicate that it makes sense to investigate this field in more detail and find an appropriate explanation regarding the mechanism of concrete strengthening and stiffening after heating.

2 EXPERIMENT

Laboratory specimens (40×40×160 mm) made of fine-grained concrete (in the next text only concrete) with a water to cement ratio of w/c = 0.45 were manufactured. The compounds in the mix, namely CEM I 42.5 R cement according to ČSN [1993] from the cement works at Mokrá and 3 fractions of quartz sand according to ČSN [1994], were mixed in weight ratios of 1:1:1:1. At the same time, specimens (20×20×100 mm) made of cement paste were prepared for use in the study of phase composition before and after heating using X-ray diffraction (XRD) analysis.

All of the manufactured specimens were unmoulded 24 hours after casting under laboratory conditions (t = 22 ± 2 °C, RH = 55 ± 5 %) and placed into water for another 27 days. Afterwards, the specimens were dried to a constant weight at 60 °C [Mendes *et al.* 2009] and heated in a muffle furnace to maximum temperatures of 200, 400, 600, 800, 1000 and 1200 °C with a heating rate of 5 °C/min and with 120 min of exposure to the maximum temperature.

After cooling, the specimens were placed under the following conditions for periods of 2 months: (i) laboratory conditions (t = 22 ± 2 °C, R.H. = 55 ± 5 %), (ii) water (t = 22 ± 2 °C) and (iii) laboratory conditions (t = 22 ± 2 °C, R.H. = 55 ± 5 %) with periodical immersion of the specimens in water (every Monday, Wednesday and Friday for 3 minutes). Each configuration (defined by the maximum temperature, time and conditions after heating) was tested on three specimens.

In order to quantify the changes in concrete properties, the specimens were tested in compression (compressive strength) and three point bending (modulus of rupture) immediately after cooling and after 2 months of being placed under all conditions (i)-(iii).

Undamaged specimens after cooling and after 2 months of being placed in water were subjected to pore structure analysis using mercury intrusion porosimetry. Powdered cement paste specimens were subjected to XRD analysis to detect the presence of crystalline phases also after cooling and after 2 months of being placed in water.

3 RESULTS AND DISCUSSION

3.1 Compressive Strength

The effect of placing concrete under various conditions after heating on its compressive strength is shown for individual maximum temperatures in Fig. 1 (left). It follows from the figure that both placement in water and the periodical immersion of specimens in water have a significant effect on the rehydration of concrete after heating primarily to 400, 800 and 1000 °C (specimens placed in water) and to 600 and 800 °C (specimens periodically immersed in water) compared to specimens tested immediately after cooling. The strength of specimens placed under laboratory conditions decreases compared to specimens tested immediately after cooling.

3.2 Modulus of Rupture

The effect of placing concrete under various conditions after heating on its modulus of rupture is shown for individual maximum temperatures in Fig. 1 (right). A significant increase in the modulus of rupture has been found for specimens heated to 600, 800 and 1000 °C for both specimens placed in water and specimens periodically immersed in water compared to specimens tested immediately after cooling.

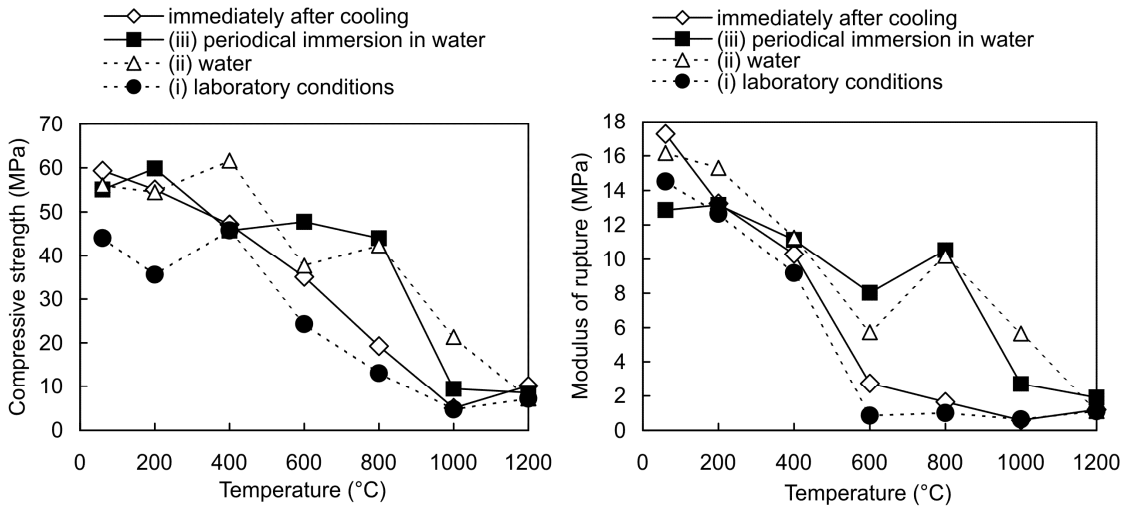

Figure 1. The effect of placing concrete under various conditions after heating on its compressive strength (left) and modulus of rupture (right) is shown for individual maximum temperatures.

3.3 Pore Structure

The distribution of pores and changes to it after exposure to elevated temperature are presented in Figure 2 (left). The specimens investigated mainly contained pores smaller than 1 μm in diameter. The smaller pores cause a rapid increase in vapour pressure due to the dehydration of CSH gel upon heating [ref], and for this reason, and consequently crack formation and spalling result in concrete heated to elevated temperatures. The differences in cumulative pore volumes for specimens heated up to 400 °C are not significant. However, data measured at above 400 °C indicate that the modification of heating temperature significantly affects pore characteristics. Above 400 °C, the cumulative pore volume and pore size gradually increased and at 1200 °C only pores larger than 10 μm can be found in the structure. The increased volume of pores with a higher radius results in a decrease in compressive strength.

The distributions of pores after exposure to elevated temperatures and placement in water for 2 months are presented in Figure 2 (right). Pore distributions are similar to those measured immediately after cooling except for specimens heated to temperatures of 600 and 800 °C. Pores at these temperatures are only slightly increased compared to those obtained for temperatures up to 400 °C. This results in a relative increase in compressive strengths and moduli of rupture compared to specimens measured immediately after heating and cooling.

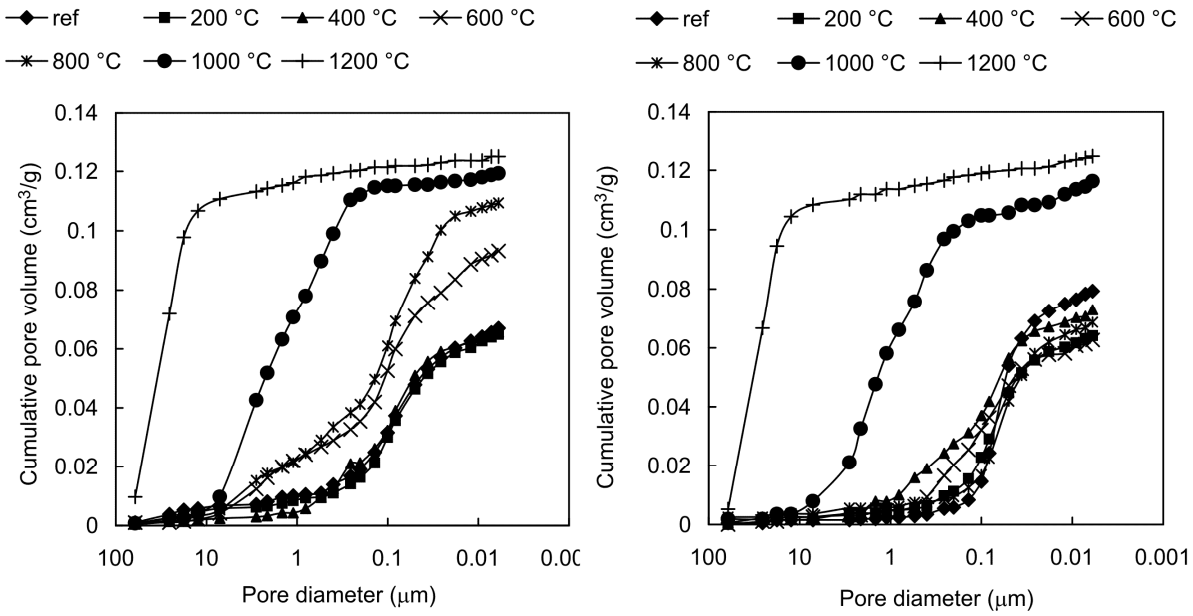

Figure 2. The cumulative intruded volume of pores immediately after heating and cooling (left) and after 2 months of placement in water (right).

The results for total porosity observed immediately after heating and cooling and after 2 months of placement in water for different exposure temperatures are presented in Figure 3. The differences in the total porosity after heating up to 400 °C and cooling are not significant; they are within the range of standard deviations. Above 400 °C, the total porosity gradually increases – the value at 1200 °C is 1.8 times higher compared to the value at 400 °C.

After rehydration the total porosity is similar in the specimens preheated up to 800 °C and increases further at higher temperatures. By comparison of the total porosity before and after hydration it can be seen that the values obtained are very close except in the case of specimens heated to 600 and 800 °C, in which instance the total porosity before rehydration is higher.

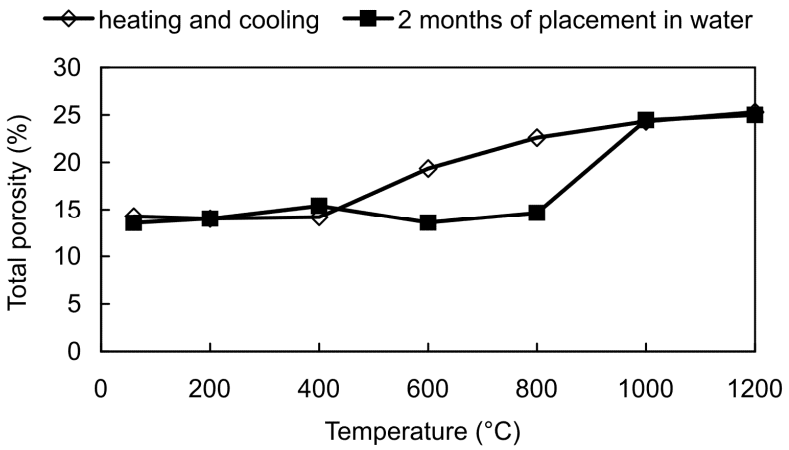

Figure 3. Total porosity.

3.4 XRD analysis

The qualitative composition of specimens and changes in the content of individual phases are summarized in Tables 1 and 2 for specimens measured immediately after heating and cooling and specimens tested after 2 months of placement in water, respectively. Only a comparison of the relative contents of individual phases in all specimens has been performed.

Table 1. Phase composition immediately after heating and cooling.

phase/ specimen	*ettringite*	*monosulphate*	*gypsum*	*anhydrite II*	*silicocarnotite*	*yeelimite*	*portlandite*	*calcite*	*vaterite*	*free lime*	C_3S	C_2S	C_3A	*mayenite*	C_4AF
Ref.	+	+	+	–	–	–	+++	++	–	–	+	+	?	–	+
200 °C	–	–	–	–	–	–	+++	++	+	–	+	+	?	–	+
400 °C	–	–	–	–	–	–	+++	++	++	–	+	+	?	–	+
600 °C	–	–	–	+	–	–	++	+++	–	–	+	+	?	–	+
800 °C	–	–	–	++	–	–	+	+	–	?	+	+	?	–	+
1000 °C	–	–	–	–	++	–	–	–	–	+	+	++	?	++	++
1200 °C	–	–	–	–	+	+	–	–	–	+	+	+++	?	+	+++
Legend: +++, ++, +…relative content of phase (regarding other specimens) –…phase is not present ?...presence of phase is uncertain															

X-ray diffractograms of the reference specimen and the heated specimens at various temperatures are shown in Fig. 4a. Typical reflections associated with ettringite ($C_3A\cdot 3C\hat{S}\cdot H_{32}$), monosulphate ($C_3A\cdot C\hat{S}\cdot H_{12}$), gypsum ($C\hat{S}H_2$), portlandite (CH), calcite ($CaCO_3$), alite (C_3S), larnite (C_2S) and brownmillerite (C_4AF) have been found in the reference sample. After heating, some reflections disappeared, such as those corresponding to ettringite, monosulphate and gypsum, which were identified in the initial specimen but not in the samples heated to 200 °C and higher. Gypsum is decomposed to anhydrite II at temperatures of 600 to 800 °C and anhydrite II is further partly transformed to CaO and SO_3. A reduction of diffraction peaks related to portlandite is also observed at temperatures above 400 °C, which proves the dehydroxylation of CH and the formation of CaO. For temperatures above 800 °C the diffraction peaks of CH are absent. The peaks of calcite increase

in intensity above 400 °C and gradually disappear at the higher temperatures due to the calcite decomposition to CaO and CO_2. The partial increase in the intensity above 400 °C is probably caused by the partial transformation of decomposed portlandite into calcite [Stepkowska et al 2004]. Free lime (CaO) is identified in the specimens heated to 800 °C and higher; it originates from the transformation of portlandite, calcite and anhydrite II. At temperatures of above 1000 °C the peaks of sulphate crystalline phases are observed – silicocarnotite ($Ca_5(SiO_4)_2SO_4$) and yeelimite ($Ca_4Al_6O_{12}SO_4$). Also, the presence of mayenite ($C_{12}A_7$) and peaks with increasing intensity related to larnite and brownmillerite are evident.

Table 2. Phase composition after 2 months of placement in water.

phase/ specimen	*ettringite*	*monosulphate*	*gypsum*	*anhydrite II*	*silicocarnotite*	*portlandite*	*calcite*	*free lime*	*C_3S*	*C_2S*	*C_3A*	*mayenite*	*C_4AF*	*gismondine?*	*katoite*	*CAH + CASH (except for gismondine)*
Ref.	+	+	+	–	–	+++	++	–	+	+	?	–	+	–	–	–
200 °C	+	–	–	–	–	+++	++	–	+	+	?	–	+	–	–	–
400 °C	+	–	–	–	–	+++	++	–	+	+	?	–	+	–	–	–
600 °C	+	–	–	–	–	+	+++	–	+	+	?	–	+	+	–	–
800 °C	?	–	–	–	–	+	+	–	+	+	?	–	+	++	–	–
1000 °C	–	–	–	–	++	+	+++	–	+	++	–	?	+		+	–
1200 °C	–	–	–	–	+	++	+	–	+	+++	–	?	++		–	+
Legend:	+++, ++, +…relative content of phase (regarding to other specimens) –…phase is not present ?...presence of phase is uncertain															

The XRD diffractograms corresponding to the rehydrated specimens are presented in Fig 4b. The specimens, after heating up to 800 °C and being rehydrated, contain reflections of ettringite, and peaks related to portlandite and calcite are observed in all specimens. After rehydration, peaks of free lime are not present in the specimens heated to 800 °C and higher due to the rehydration of lime into portlandite, which can carbonate to form calcite. After rehydration, katoite (C_3AH_6) has been identified in the specimen preheated to 1000 °C and CAH + CASH in the specimen preheated to 1200 °C. The occurrence of other crystalline phases in all specimens is similar to that before rehydration.

4 CONCLUSIONS

The experimental works presented in this paper involved the study of the possible regeneration of cement binder in concrete subjected to high temperatures. It is shown that water treatment of concrete specimens preheated to temperatures of 200 to 1200 °C leads to a significant increase in compressive strength and modulus of rupture. This has been found for both the constant placement of specimens in water and their periodical immersion in water. The results are supported by microstructural analyses – porosimetry and XRD analysis. The results show that it is possible to partly regenerate concrete that has been subjected to high temperatures, e.g. that are prevalent during a fire.

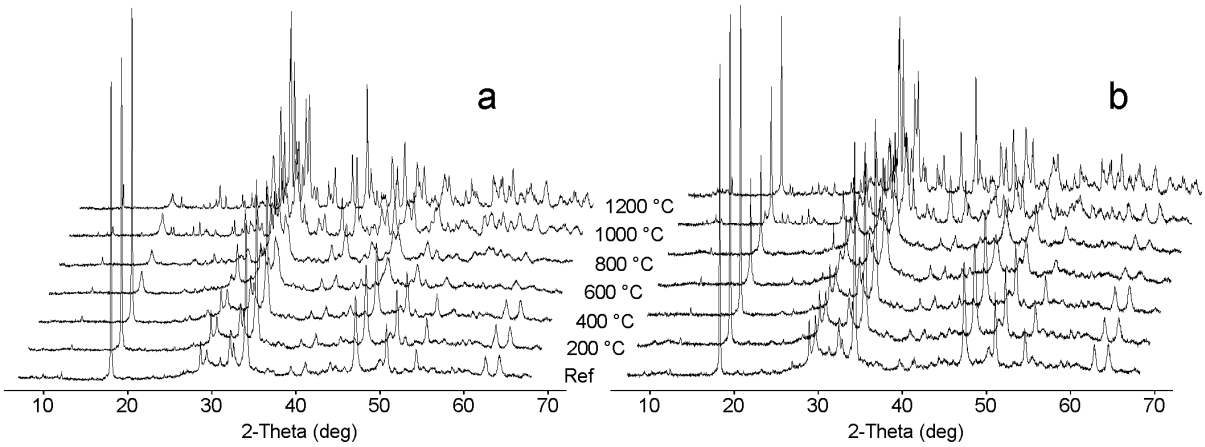

Figure 4. XRD immediately after heating and cooling (a) and after 2 months of placement in water (b).

ACKNOWLEDGMENTS

This outcome has been achieved with the financial support of the Czech Ministry of Education, project No. 1M0579, within the activities of the CIDEAS research centre.

REFERENCES

Alonso, C & Fernandez, L. 2004, 'Dehydration and rehydration processes of cement paste exposed to high temperature environments', *Journal of Materials Science* **39**, pp. 3015–3024.

Arioz, O. 2007, 'Effects of elevated temperatures on properties of concrete', *Fire Safety Journal* **42**, pp. 516–522.

ČSN EN 197-1 1993, 'Cement. Složení, jakostní požadavky a kritéria pro stanovení shody. Část 1: Cementy pro obecné použití (Cement. Composition, qualitative requirements and criteria for conformity assesment)'. In Czech.

ČSN 721200 1994 'Křemenné písky. Základní technické požadavky (Siliceous sands. Basic technical requirements)'. In Czech.

Matesová, D. 2007, 'Effect of exposure time after heating and w/c ratio on residual strength of concrete: pilot studies', in *XIth International Conference on Ecology and New Building Materials and Products*, Telč:VUSTAH, Czech Republic, pp. 345–348.

Mendes, A., Sanjayan, J.G. & Collins, F. 2009, 'Long-term progressive deterioration following fire exposure of OPC versus slag blended cement pastes', *Materials and Structures* **42**, pp. 95–101.

Shui, Z., Xuan, D., Chen, W., Yu, R. & Zhang, R. 2009, 'Cementitious characteristic of hydrated cement paste subjected to various dehydration temperatures', *Construction and Building Materials* **23**, pp. 531–537.

Stepkowska, E.T., Blanes, J.M., Franco, F., Real, C. & Pérez-Rodríguez, J.L. 2004, 'Phase transformation on heating of an aged cement paste', *Thermochimica Acta* **420**, pp. 79–87.

XII DBMC
International Conference on Durability of Building Materials and Components
PORTO - PORTUGAL, April 12th-15th, 2011

Bond between Reinforcement and Concrete – Influence of Steel Corrosion

Mohammed Sonebi [1]
Richard Davidson [2]
David Cleland [3]

ABSTRACT

The investigation into the deterioration of the bond between concrete and reinforcement was carried out using a series of beam-type pullout specimens. The specimens were designed to allow investigation into cover depths of 20 mm and 50 mm and bar diameters of 12 mm and 20 mm. The beam-type specimens also allowed the relative bond strength developed at top and bottom bars to be examined. The compressive strength of the concrete was kept constant throughout the study. Factors that cause the bond strength to be lower include; reduction in cover depth, increasing bar diameter and location near the top of a section. Comparisons were drawn between the design bond stress used for anchorage length in the Eurocodes and the results of this study.

Applied anodic current was used to accelerate the corrosion. This method resulted in uniform corrosion along the rebar. Three levels of corrosion were investigated and as the corrosion levels increased cracks developed and were measured in each sample. Based on the results of this study the bond strength decreased as corrosion level increased. At severe corrosion level, the improvement of bond strength with higher cover was less significant. The Eurocodes underestimate the bond strength where no corrosion is present by 20%, while samples with severely corroded reinforcement exhibited bond strength only 60% of the design bond strength. In general, the bond strength was lower for bars of larger diameter but this was less significant for severe corrosion.

KEYWORDS

Bond strength, Bar diameter, Corrosion, Cover level, Top-bar effect.

[1] School of Planning, Architecture and Civil Engineering, Queen's University, Belfast, BT7 1NN
[2] School of Planning, Architecture and Civil Engineering, Queen's University, Belfast, BT7 1NN
[3] School of Planning, Architecture and Civil Engineering, Queen's University, Belfast, BT7 1NN

1 INTRODUCTION

Among the pathological manifestations that accelerate the performance loss of reinforced structures, rebar corrosion is one the most important. Steel corrosion of reinforced bars leads to cracking, reduction of bond strength, reduction of steel cross section and loss of serviceability life of a concrete structure [Mangat and Elgarf 1999]. The factors which alter the rate of corrosion include; availability of oxygen, humidity level, permeability of the concrete, chloride content, temperature, and depth of carbonation [Vennesland *et al.* 2007]. These factors if controlled can limit the damage caused by corrosion. Regions such as the Arabian Gulf is one of the most aggressive environments where some of the structures need significant repairs in just 10 – 15 years [Almusallam *et al.* 1996]. Pullout of the reinforcing bars associated with bond characteristics is one of the main factors affecting the ultimate behaviour and failure of reinforced concrete members. It is known that bond strength between concrete and reinforced steel bars is usually much lower for reinforcement located near the top of a cast section than for those near the bottom, which is known as the "top-bar" effect (ACI 318). The top bar effect is assumed to be due to a weakened interfacial transition zone (ITZ) caused by bleeding and settlement in the fresh concrete mix.

The objective of this investigation is to study the effect of corrosion on the bond strength of reinforced bars. Three levels of corrosion have been used and the effect of the cover level was examined together with different bar diameters on the bond strength of reinforced steel bars. In this paper, a total of 24 specimens of concrete with reinforcing steel bars were cast with differing cover level and different bar diameters using a set-up suggested by Ghana [1996]. The specimens, measuring 300 mm deep by 200 mm wide by 300mm long were subjected to three levels of corrosion, severe, moderate and without corrosion. The specimens without corrosion were used as control specimens.

2 EXPERIMENTAL PROGRAM

2.1 Materials

All mixes were prepared using ordinary Portland cement (CEM II) with a water/cement ratio of 0.50. The total cement content was kept constant at 425 kg/m^3. The fine aggregate was natural siliceous sand with a fineness modulus of 2.9, a saturated surface dry specific gravity of 2.60 and water absorption of 1.5%. The total content of sand was 730 kg/m^3. Crushed basalt with a maximum nominal size of 10 and 20 mm, a saturated surface dry specific gravity of 2.65 and water absorption of 0.8%was also used. The dosages of 10 mm and 20 mm aggregates were 505 and 505 kg/m^3, respectively. The NaCl solution was used in mix at 10% of cement content (42.5 kg/m^3).

2.2 Method of Acceleration of Corrosion

The corrosion in the samples was accelerated by setting up a potential difference between the reinforced steel bars and a nearby cathode. The electrolyte in the cell is the concrete pore solution containing sodium chloride (NaCl), in this case added at the mixing stage. The Cl- ions from the sodium chloride are then attracted to the anode to accelerate the corrosion. The circuit setup can be seen in Fig. 1.

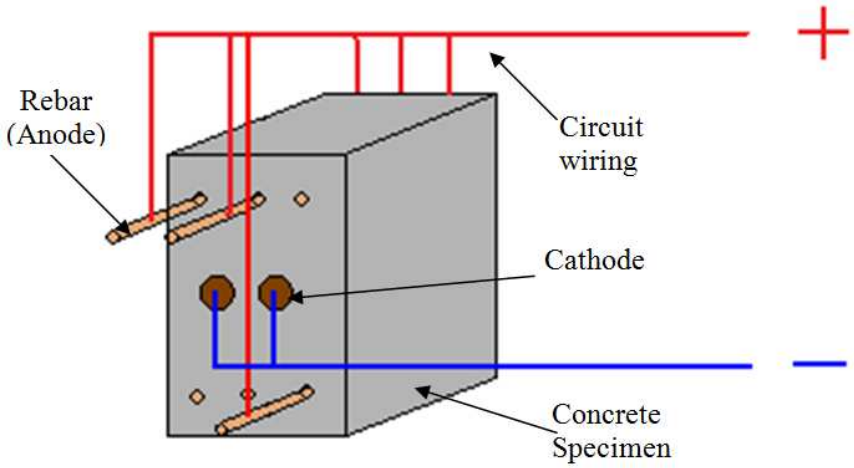

Figure 1. Circuit setup for accelerated corrosion.

The potential difference was applied first to the specimens which were to be moderately corroded. The level of corrosion was deemed to have been achieved when a longitudinal crack of width 1.5 mm developed. This took three weeks at one volt and a further four weeks at three volts. The other eight specimens were subjected to a potential difference of eight volts for a period of four weeks to achieve severe corrosion and this led to longitudinal cracks of 8 mm in width. The method used to measured corrosion was by weighting the loss of the bar after it had been removed from the sample.

2.3 Method of Pullout Test of Specimen

The pullout specimens were prepared with the horizontal reinforced bars protruding from the vertical surface on the side of the specimens. The bond properties between reinforced bar and concrete were studied by conducting direct pullout test of reinforced bars embedded in the specimens. During the experimental study, two different covers were used (20 and 50 mm). The positions of reinforced bars at the time of casting and the direction of concrete casting are shown in Fig. 2. There were eight moulds with the dimensions of 300 mm×200 mm×300 mm and six holes for each mould to insert the reinforced bars of which three holes at the top and three at the bottom. Four moulds were manufactured for the 12 mm diameter bars and another four for the 20 mm diameter bars; two of each set of four moulds had 20 mm and two had 50mm cover spacing. Deformed reinforcing steel bars having 15 mm nominal diameter and 400 MPa nominal yield strength were used for pullout tests. Steel bars were cleaned with a wire brush to remove any rust from the surface just before casting the concrete specimens. After casting specimens were sealed with wet burlap and stored in a temperature controlled environment. All specimens were demoulded after 24 h and transferred to a laboratory environment until they were tested.

The test method used in the study was similar to that proposed by Chana [1990] where more detailed information on the pullout test setup can be found. The direct pullout test setup is shown in Fig. 2 and single reinforced bar pullout tests were conducted. A load cell, a hydraulic jack, a mounting system, and a linear variable differential transducer (LVDT) were assembled as shown in Fig. 2. The hydraulic jacking system was adopted to apply a pullout force to the reinforcing bar. When bond slip occurs, the displacement of the reinforced bar can be obtained from the measurement of the LVDT attached to the reinforced bar. During testing, the pullout load and reinforced bar slip displacement were measured and recorded automatically. The rate of loading used was increased in increments of 2 kN/s for the specimens with moderate and no corrosion. It was considered more reliable to take results every 1 kN/s with the severely corroded specimens as their failure loads were considerably smaller.

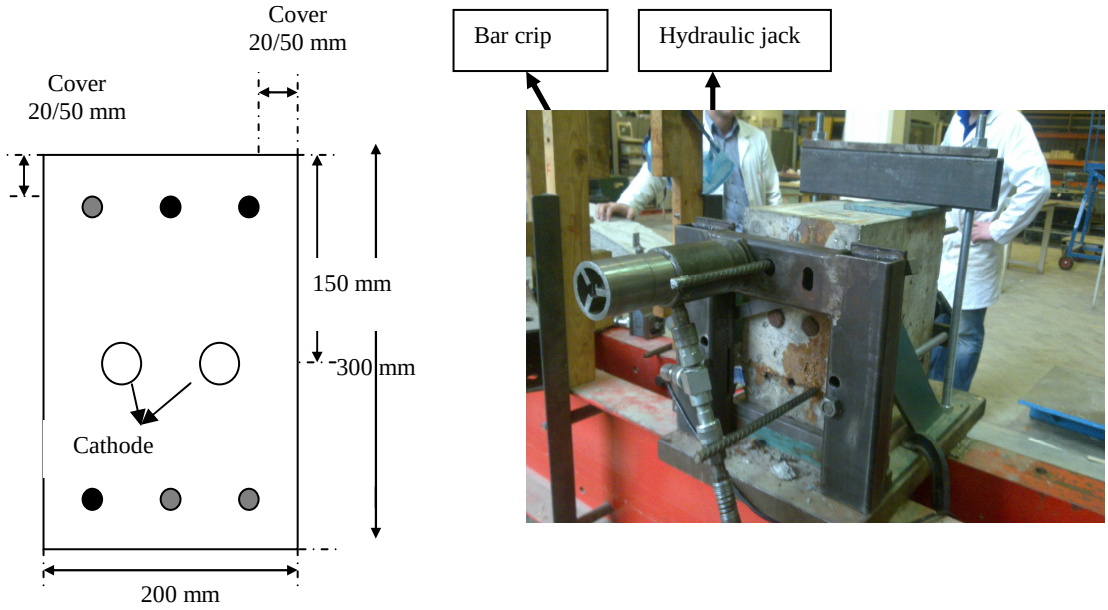

Figure 2. Experimental setup used for pullout test.

3 TEST RESULTS AND DISSCUSSION

3.1 Effect of Top-bar

Figure 3 presents the variation of the bond strength with the top-bar effect and level of corrosion. As expected, the bond strength reduced as the corrosion level increased. In concrete without accelerated corrosion, there was a 25% reduction in bond strength due to the top-bar effect [Soylev *et al.* 2003]. Chana [1990] compared the top and bottom cast bars using a similar setup of specimen and concluded a comparable reduction of the bond strength for concrete having the same compressive strength. The corrosion at moderate level (between 0.5 and 1.5% weight loss) did not show a significant difference in bond strength for different positions of the bars. Whilst the specimens undergone a severe corrosion levels (3 to 4% weight loss) a top bar bond strength 30% lower than the bottom bar. It can be concluded that the top-bar effect is highly influenced by the level of the corrosion of reinforced bars. The phenomenon of top bar effect facilitates the penetration of oxygen, water and chlorides to the interface between the concrete and steel reinforcement leading to an increase of the rate of corrosion.

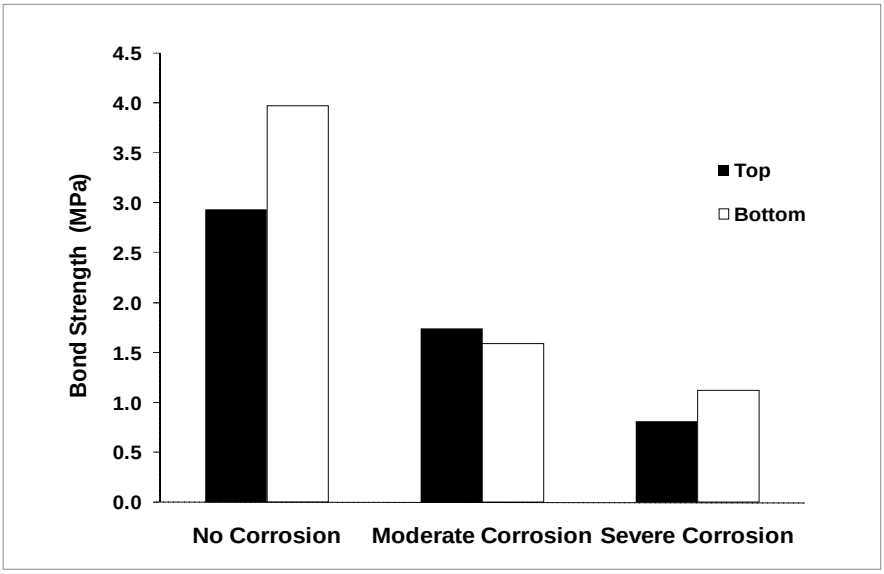

Figure 3. Variation of bond strength between top and bottom reinforcement.

3.2 Effect of Cover and Level of Corrosion on Bond Strength

The results illustrated in Fig. 4 show consistently that increasing the cover from 20 mm to 50 mm had a positive impact on the bond strength at all levels of corrosion. The 50 mm of cover exhibited an improvement of bond strength by 30% for no corrosion level, 66% for moderate corrosion, and 25% for severe corrosion level, respectively, compared to 20 mm cover. The failure mechanism remained split failure due to the longitudinal corrosion cracks, irrespective of the cover level. During testing the hoop tension forces in the concrete surrounding the reinforced bar was best resisted by the greater confining 50 mm cover. It was interested to note that the bond strength difference between cover levels was lower where the corrosion had reached severe level (3 – 4%). This is due to the corrosion cracks in the specimen which result in the loss of the confinement effect of the cover concrete.

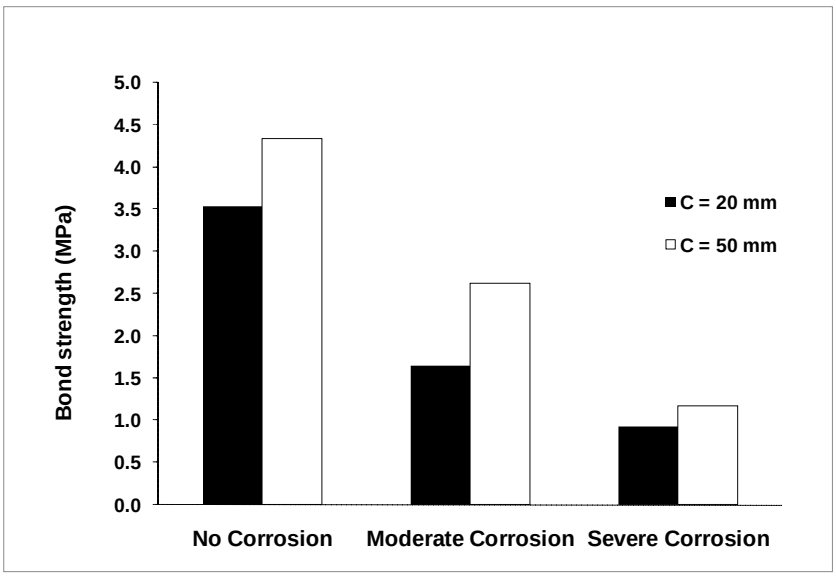

Figure 4. Effect of cover on bond strength of three levels of corrosion.

3.3 Effect of Diameter on Bond Strength with Different Levels of Corrosion

It is illustrated in Fig. 5 that as the corrosion level was increased, the bond stress decreased as expected but the difference of bond strength between the two bar diameters was reduced significantly. The increase in diameter of the reinforced bar has a significant impact on the bond strength. The specimens with no corrosion had strength for 20 mm bars 45% lower than the strength for 12 mm bars. These bond strength results can be compared with the guidelines given in Eurocode 2 which, for the set of conditions considered, recommend ultimate bond strength 1.79 MPa, and this value remains valid for bar diameters up to 32 mm. In the specimens containing 12 mm diameter bars with no corrosion, the Eurocode underestimated the experimental bond strength by a factor of almost three. Even when the samples of reinforced concrete were corroded to a moderate level (0.5 - 1.5% weight loss), the 12 mm diameter reinforced bars had a bond strength greater than the value calculated by the Eurocode [BSI Eurocode 2. 2002], while the bond strength with 20 mm diameter reinforced bar was below the design value recommended by the Eurocodes. Hence the results illustrate how the durability of structures can be influenced by the choice of diameter of reinforcing bar.

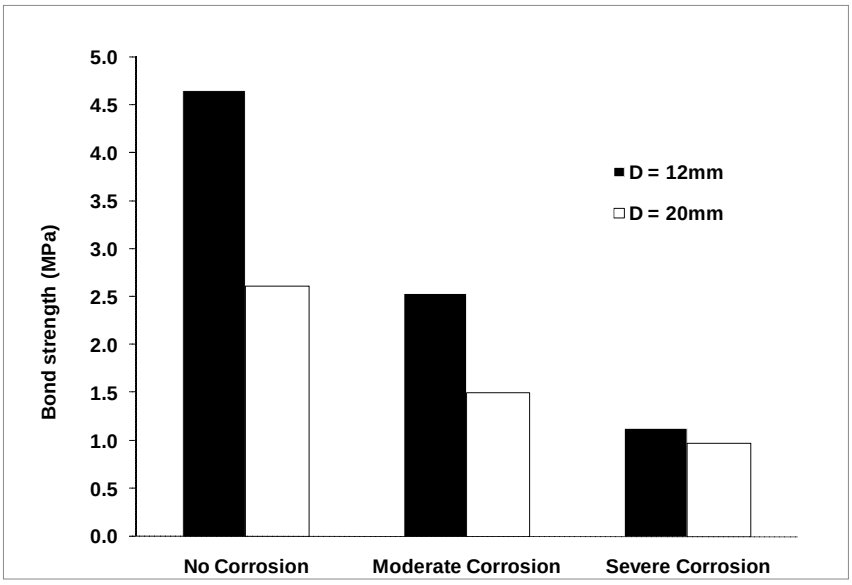

Figure 5. Effect of bar diameter on bond strength of three levels of corrosion.

3.4 Effect of Crack Width on Bond Strength with Different Levels of Corrosion

The results in Fig. 6 show the relationship between the actual corrosion level and crack width. The actual corrosion level was obtained using the mass loss method similar to the research reported by Ouglova *et al*. [2008]. The corrosion level was then calculated as a percentage of the weight of corroded material per unit length of bond [Fang *et al*. 2006]. Figure 6 demonstrates that as the corrosion level increased the crack width increased. This finding confirms some results reported in literature which suggest a linear correlation between the loss of cross section area and the corrosion level [Apostolopoulos *et al*. 2006]. This is due to corrosion products resulting in an increase in volume and thus causing a strain within the concrete [Cabrera 1996]. The most obvious cracks are the longitudinal cracks parallel to the reinforcement.

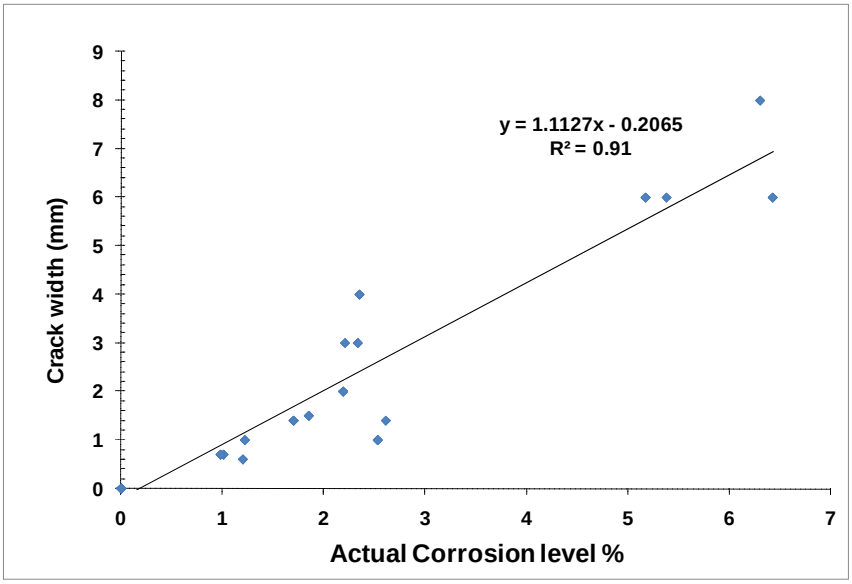

Figure 6. Relationship between crack width and increasing corrosion level.

4 CONCLUSIONS

This study discusses an experimental program of bond strength of reinforcing bars embedded in normal concrete and subjected to corrosion. The effects of corrosion, two cover depths and two bar diameters were studied. Based on the results of this paper the following conclusions can be drawn:

- As expected, the increase of level of corrosion led to a reduction in the bond strength of steel reinforcing bars.
- The bond strength of top bars was 25% lower than bottom bars for specimens without any corrosion, and 30% for bars with severe corrosion. However, in case of moderate corrosion, there was no signifcant difference of bond strength between top and bottom bars.
- The increase of the cover of concrete from 20 to 50 mm resulted in an improvement of the bond strength for the three levels of corrosion considered in this study. However the difference of bond strength between both cover was less pronounced for the severe corrosion level.
- The increase of the diameter of bars led to a reduction of the bond strength. This reduction was highly significant for specimens without corrosion, followed by specimen having moderate corrosion. However, in case of severe corrosion, the effect of diameter on bond strength was only marginal.
- Corrosion cracking is critical for the bond strength. Very little corrosion after cracking is required to lead to a reduction of bond strength to an unacceptable level.

REFERENCES

Almusallam, A., Al-Gahtani, A., Aziz, A. Rasheeduzzafart, 1996. 'Effect of reinforcement corrosion on bond strength', *Construction and Building Materials*, **10**, 123-129.

Apostolopoulos, CA., Papadopoulos, MP., Pantelakis, SG. 2006, 'Tensile behavior of corroded reinforcing steel bars BSt500s', *Construction and Building Materials*, **20**, 782-789.

ACI Committee 318, 2005. 'Building code requirements for structural concrete (ACI 318-05)', *American Concrete Institute,* Farmington Hills, Michigan, 151 p.

British Standards Institution. 2002, Eurocode 2, 'Bond stress'. *BSI: London*, BS EN 1992-1.

Cabrera, J.G., 1996, 'Deterioration of concrete due to reinforcement corrosion'. *Cement and Concrete Composites*, **18**, 47-59.

Chana, P.S., 1990, 'A test method to establish realistic bond stress', *Magazine of Concrete Research*, **42**, 83-90.

Fang, C., Lundgren, K., Plos, M., Gylltoft, K., 2006, 'Bond behaviour of corroded reinforcing steel bars in concrete', *Cement and Concrete Research*, **36**, 1931-1938.

Mangat, P.S., Elgarf, S.M., 1999, 'Bond characteristics of corroding reinforcement in concrete beams', *Materials and Structures*, **32**, 89-97.

Ouglova, A., Berthaud, Y., Foct, F., François, M., Ragueneau, F., Petre-Lazar, I., 2008, 'The influence of corrosion on bond properties between concrete and reinforcement in concrete structures', *Materials and Structures*, **4**1, 969-980.

Soylev, T.A., François, R., 2003, 'Quality of steel-concrete interface and corrosion of reinforcing steel', *Cement and Concrete Research*, **33**, 1407-1415.

Vennesland, Ø., Raupach, M., 2007. Recommendation of RILEM TC 154-EMC: 'Electrochemical techniques for measuring corrosion in concrete- measurements with embedded probes', *Materials and Structures*, **40**[8], 745-758.

XII DBMC
International Conference on Durability of Building Materials and Components
PORTO - PORTUGAL, April 12th-15th, 2011

Method for Evaluation of Concrete Permeability

Valdir Moraes Pereira [1]
Gladis Camarini [2]

ABSTRACT

Permeability of cement based-materials is the principal factor that provides their durability. This kind of test is an important parameter for estimate their service life. Several concrete permeability tests has been realized to try to measure and understand the movements of fluids in concrete porous and to associate it with its durability. In this context, Thenoz method has demonstrated satisfactory results when measuring air permeability of concrete. Thus, the aim of this work is to evaluate Thenoz methodology, measuring outflow velocity and Reynolds number during air permeability tests of concrete. In this way, concrete specimens were produced and submitted to two curing conditions (in water and at laboratory conditions). The specimens were tested at 14 days, 28 days and 350 days. Results obtained have shown that Thenoz methodology is efficient and an economical method for measuring air permeability of concrete. Concrete age and curing conditions influenced air permeability results. The method used shows that outflow regime can be considerate as laminar, in accordance Reynolds number obtained in this study.

KEYWORDS

Concrete, Air permeability, Thenoz method, Reynolds number.

[1] Faculty of Civil Engineering, Architecture and Urban Design, State University of Campinas (FEC-UNICAMP), Campinas, São Paulo, BRAZIL, valmop@gmail.com
[2] Faculty of Civil Engineering, Architecture and Urban Design, State University of Campinas (FEC-UNICAMP), Campinas, São Paulo, BRAZIL, camarini@fec.unicamp.br

1 INTRODUCTION

Permeability of cement-based materials has been seen as the main responsible for its durability because it controls the movement rate of aggressive ions inside concrete and may cause its physical/chemical degradation. So, several approaches have been proposed to evaluate this concrete property, having as main goal the search for an effective, viable and economic methodology to measure and describe air permeability of concrete [PERRATON, 1989; SONG & NWON, 2007].

Discrepancies found in concrete permeability results may occur due to many factors such as inadequate mathematical equations or methodology employed where results obtained cannot correspond to physicals phenomena really involved. Mathematic equation cannot take in account some physical phenomena and presents mathematical inadequacy to the type of flow mechanisms measured. Therefore, for permeability tests apparatus and proposed methodologies have been proven to be sought not only to evaluate the permeability of these materials, but the credibility and validation of the test apparatus employed [GARDNER *et al.* 2008]. Thus, some factors may be employed for measuring the validation of results for concrete air permeability: Reynolds number (Re) is one of them.

Permeability results can not be realistic due type of fluids movement into porous media, where fluids which flow in high velocities can entail pressure drop, causing flow turbulence and generate deviations in Darcy's law. These phenomena can generate results that cannot be real. One way of assessing the fluid turbulence in outflow can be achieved by Reynolds number measurement. Reynolds, analyzing the behavior of an ink filet inside water flow, observed that when flow velocity was low, the ink fillet disposed of in a macroscopically organized way and parallel to the tube. By the other hand, when the flow velocity was increased, fluid molecules movement was totally random [VENNARD, 1966; ROMA, 2006]. Thus, Reynolds characterized these types of outflow in accordance three numbers, that after, came to be called by his name: Reynolds number. The three types of outflow, at tubes, were classified, as follows.

- Laminar flow regime: characterized by Reynolds number lower than 2100 ($Re < 2100$);
- Transition flow regime: this flow type is characterized by a region of uncertainty where there is a transition from laminar to turbulent flow. This flow type can be characterized by Reynolds number between 2100 and 4000 ($2100 < Re < 4000$).
- Turbulent flow regime: this phase can be observed for Reynolds numbers above 4000 ($Re > 4000$).

Among methodologies employed to measure concrete air permeability there is the Thenoz method [THENOZ, 1989]. This method has shown good applicability in this kind of material. Initially, it has been developed to determine the rocks permeability and it was based in Darcy's law equation to calculate air permeability values. However, in order to prove the credibility of the Thenoz methodology used in concrete, some analysis must be conducted to assess the flow mechanisms provided by this method.

Thenoz method employs Darcy's law to describe physically and to measure concrete air permeability. However, some considerations may be realized when mathematics equations based in Darcy's law are employed, as follows [BANTHIA & MINDESS, 1989].

- Pressure inside of porous material caused by fluid movement must be disregarded;
- Fluid compressibility on triaxial stress may be ignored;
- Outflow regime must considered as laminar;
- Temperature effects also must be neglected.

The aim of this work was to determine outflow regime occurred during the test of concrete air permeability by Thenoz method. It was observed the results of air flow velocity into concrete porous, which is necessary to determine Reynolds number of outflow. Thus, it were possible to evaluate Thenoz method to measure concrete air permeability, and also to determine if air flow into concrete porous occurred in laminar or turbulent regime as observed by Banthia & Mindess [1989].

2 EXPERIMENTAL PROCEDURES

Materials used in this experimental work were: blastfurnace slag Portland cement named CPIII 40 according to Brazilian standards and Type IS according to ASTM, river sand and crushed stone. Their properties are shown in Table 1. Concrete specimens and mixtures used are shown in Table 2.

Concrete specimens were cast in cylindrical molds (100 mm diameter and 200 mm height). They remained in molds for 24 hours and after they were demolded and remained in laboratory conditions (LC – temperature of 23 ºC and 60% of relative humidity), and in water (IC – immersed curing) until the age of the tests. These specimens were cut and a slice of with 100 mm diameter and 50 mm height (Figure 1) was used for air permeability tests (Figure 2). Air permeability tests were carried out in concrete at the ages of 14, 28 and 350 days (Table 2).

Table 1. Materials properties.

Material	Properties
Cement CP III – 40 (Brazilian Standards)	Fineness (*%retained sieve # 200*)……...……..5,8 Blaine (cm^2/g).....682,63 Specific Gravity (g/cm^3)…….....……...2,99 Initial Setting Time (*h:min*)……....2:57 Final Setting time (*h:min*)…….....…4:37 Normal Consistency (w/c ratio)……..0,31
Fine aggregate	Fineness Modulus……...…2,53 Maximum Size (mm)……...…..2,40 Specific Gravity (g/cm^3)……...…..2,60 Bulk Weight (g/cm^3)……...……1,43
Coarse Aggregate	Fineness Modulus……...……3.38 Maximum Size (mm)……..19,0 Specific Gravity (g/cm^3)……...…..2,99 Bulk Weight (g/cm^3)……...……1,52

Table 2. Concrete specimens, mixtures and curing conditions.

Name	w/c ratio	Age	Mix proportion (c:s:cs)*	Curing process
LC1	0,50	7-28-350	1:2:3	Laboratory conditions (LC)
LC2	0,46	7-28-350	1:2:3	LC
LC3	0,42	7-28-350	1:2:3	LC
IC1	0,50	7-28-350	1:2:3	Immerse curing (IC)
IC2	0,46	7-28-350	1:2:3	IC
IC3	0,42	7-28-350	1:2:3	IC

**c=cement; s = sand; cs=crushed stone.*

Before the test, specimens were 24 hours oven dried at 80 ºC in order to eliminate the water inside the porous of concrete. After that, concrete specimens had their lateral surface sealed. This makes the air flow only uniaxial and perpendicular to cross sectional area of the specimens.

All the results presented in this paper were an average of four (4) specimens for each curing condition and age.

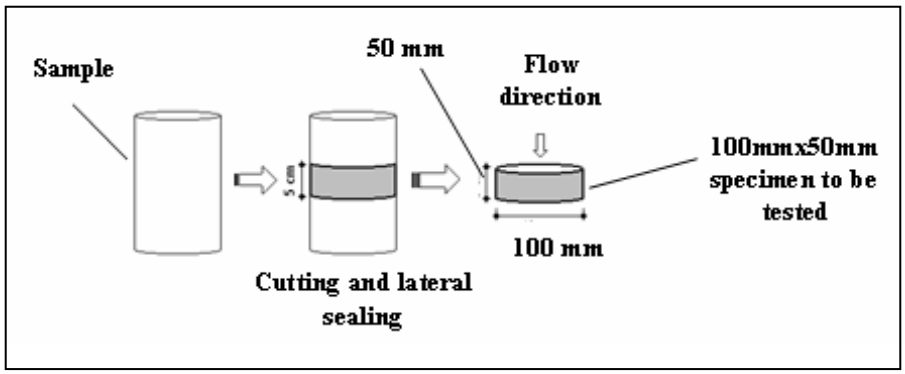

Figure 1. Preparation of concrete specimens to air permeability tests.

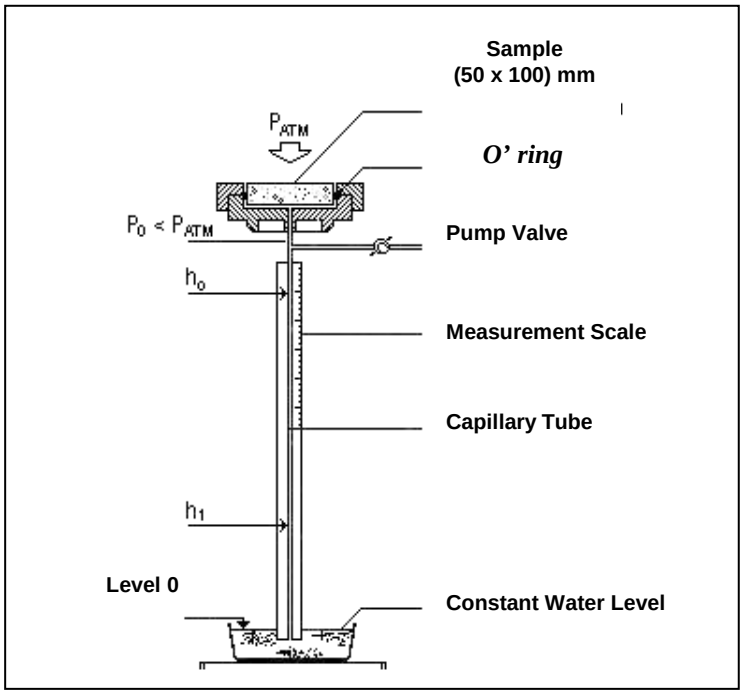

Figure 2. Scheme of air permeability apparatus.

3 RESULTS AND DISCUSSION

3.1 Air Permeability

Air permeability of concrete results was obtained according to Thenoz methodology. The calculus was made according to Equation 1.

$$k = \frac{\mu}{\rho . g} . \frac{s}{S} . \ln \frac{h_0}{h_1} . \frac{l}{t} \qquad \text{Equation 1.}$$

Where:
k = air permeability coefficient (m^2);
μ = air viscosity at room temperature (*Pa.s*);
s = across sectional area of the capillary tube (m^2);
l = specimens height (*m*);
ρ = fluid density used in capillary tube (g/cm^3);
S = across sectional area of the specimens (m^2);
h_0 = initial height (*m*);
h_1 = final height (*m*);
t = time to go to the net height h_0 to h_1 (*s*).
The relation $ln\ (h_0/h_1) = 1$ in Equation 1 were employed in order to have laminar flow [Ferreira Jr, 2003]. Heights h_0 and h_1 when determined by the relation $ln\ h_0/\ h_1 = 1$ is based on the same considerations to guarantee that the outflow occurs in laminar regime [YSSORCHE *et al*., 1995]. Thus, in this work h_0 = 30.8 *cm* height and h_1 = 83.93 *cm*.

The results have shown that all variables involved (curing method and age) in the test modify the air permeability of concrete (Figure 3). As expected, air permeability results for immerse curing are lower than concrete cured on laboratory conditions.

A global analysis of air permeability results report that air permeability of concrete diminished approximately 150 per cent (150%) when immerse curing were utilized (Figure 3). The age of concrete also modify air permeability results. For the same curing condition, as soon as time goes by permeability is lower. Higher values were obtained for curing in laboratory conditions, indicative that curing is important for improve this property. These results are in accordance with other works [PEREIRA *et al*., 2008; BODIN & ZAHARIEVA, 2002].

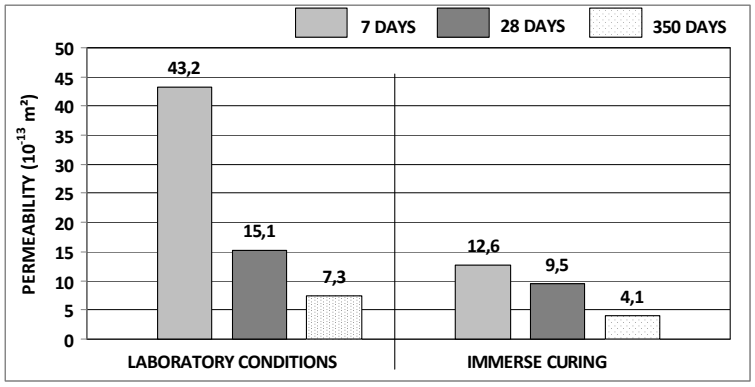

Figure 3. Air permeability of concrete.

Values of air permeability coefficients obtained were not far from the results obtained in other studies [FERREIRA Jr. 2003; BARDELLA 2005]. This comportment can be explained due to different types of seal of lateral surface specimens. However, results of air permeability obtained in this paper demonstrate similar others studies, as that report by Pereira *et al*., [2008] and; Camarini *et al.*, [2008].

3.2 Air Flow Velocity

Flow velocity results are shown in Figure 2. They were obtained from air permeability values, according to Equation 2.

$$V = -\frac{k}{\mu}\frac{\Delta P}{L} \qquad \text{Equation 2.}$$

Where:
V = outflow velocity (*m/s*);
k = air permeability constant (m^2);
μ = fluid viscosity (*Pa.s*);
ΔP = Pressure variation (N/m^3); and
L = specimen height (*m*).

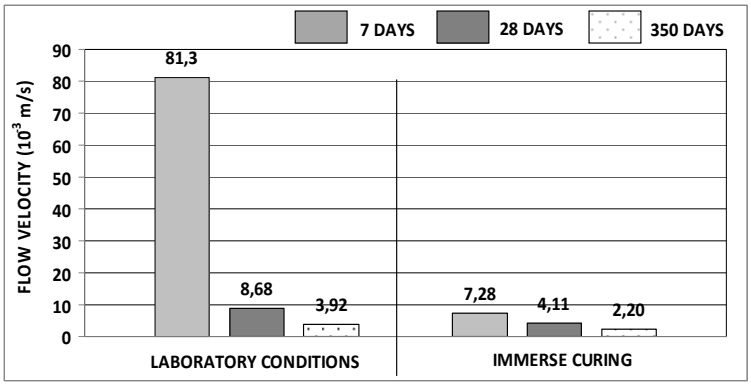

Figure 4. Air flow velocity.

Results of air flow velocity obtained had a profile similar to air permeability. At first ages the air flow velocity is high, and it diminishes with time. These results confirm that curing conditions and age of concrete (hydration degree) can be considered an important factor that controls the movements and entrance rate of fluids into concrete. This reports the importance that curing methods and age of concrete have to its durability.

3.3 Reynolds Number

Results of Reynolds number of outflow are presented at Figure 3 and were obtained according to Equation 3.

$$R = \frac{Vd\rho}{\mu} \qquad \text{Equation 6.}$$

Where:
V = average flow velocity (*m/s*);
d = diameter of the sample, which is responsible for flow (*m*);
ρ = fluid density (kg/m^3);
μ = fluid viscosity (*Pa.s*).

For Reynolds number evaluation, some considerations were realized, such as:

- Porous of concrete were considered as small capillary tubes;
- Thus, outflow regimes (laminar, transient and turbulent regimes) were considered for tubes.

Reynolds number results are presented in Figure 3 and indicated that outflow occur in laminar flow regime, i.e., Re < 2100, according to Vennard [1966] and Roma [2006]. Thus, considerations realized in Thenoz method can be ignored because mathematics equation does not need to consider this effect.

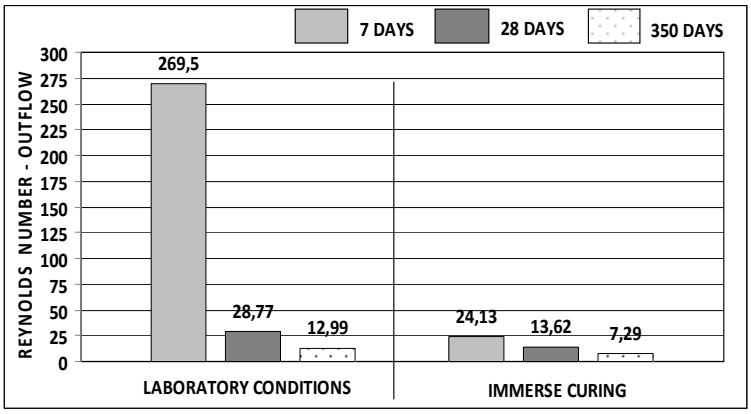

Figure 3. Reynolds number of outflow.

4 CONCLUSIONS

This paper studied air permeability of concrete obtained according to Thenoz method and evaluate flow mechanisms of air in this test. To do so, it was evaluated both: air flow velocity and Reynolds number of outflow.

Results obtained in this paper show some modifications of concrete air permeability when curing conditions and age of concrete were modified. The values of air permeability obtained allowed observing the decreasing of this concrete property with age. Results also have shown that immerse curing can decrease significantly the values of concrete air permeability.

Results of air flow velocity into concrete porous in air permeability tests shown that this concrete property decrease when immerse curing is employed and concrete age is more advanced. Reynolds number obtained, when Thenoz methodology is used to measure concrete air permeability, reported that, in this case, air outflow occur at laminar regime, i.e., $Re < 2100$.

The results show that this method is possible to measure the air permeability of concrete. Even though the results were very promising, more tests are necessary to prove that this method is a good way to determine transfer properties of concrete, which is related to its durability. It is also important to make tests with other cement based materials, which is still being done at our laboratory.

ACKNOWLEDGMENTS

The authors thank the technicians of the Laboratory of Materials Constructions (LMC-FEC/UNICAMP) and the Laboratory of Binders and Wastes (LARES-FEC/UNICAMP) for the support for this research. We also thank the National Council for Scientific and Technological Development (CNPq) for the financial support of this research (Process 133850/2006-4).

REFERENCES

BANTHIA, N.; MINDESS, S. Water permeability of cement paste. *Cement and Concrete Research*, 19, pp. 727-736, 1989.

BARDELLA, P. S. Valuation of phisycals and mechanicals properties of concretes produzed with HPC, with blast slag furnace and silica fume cements employng thermical curing. *Master degree tese*. State University of Campinas. Campinas-Brazil, 2005.

BODIN, F. B.; ZAHARIEVA, H. Influence of industrially produced recycled aggregates on flow properties of concrete. *Materials and Structures*, vol. 35, pp. 504-509, 2002.

CAMARINI, G., BARDELLA, P., PEREIRA, V. M. Evaluation of Thenoz method for measure concrete air permeability. *ACI-SP-253*, pp. 201-216, 2008.

FERREIRA Jr. E. L. Evaluation of blast slag furnace and HPC concretes properties submeted to diffences curing types properties. *Master degree tese*. State University of Campinas. Campinas-Brazil, 2005.

GARDNER, D. R.; JEFFERSON, A. D.; LARK, R. J. An experimental, numerical and analytical investigation of gas flow characteristics in concrete. *Cement and Concete* Research. vol. 38, nº 38, pp. 360-367, 2008.

PEREIRA**,** V. M.; CAMARINI, G.; CARVALHO, E.; BARDELLA, P. S. Fluid-dynamic analysis of the flow in air permeability measurement of mortars prepared with blast-slag furnace Portland cement. *Cerâmica*, Jun 2008, vol.54, nº 330, p.160-166. ISSN 0366-6913.

PERRATON, D. GIBERGUES, A., AITCIN, P. C.; THENOZ, B. Air Permeability measurement. *Materials Research Society*, vol. 137, pp. 191-201, 1989.

SONG, H. W. NWON, S. J. Permeability characteristics of carbonated concrete considering capillary pore structures. *Cement and Concrete Research*, vol..37, nº 6, pp. 909-9015, 2007.

ROMA, W. N. L. *Phenomena of transport to engeneering*. 2ª ed. Ed. RIMA, São Carlos-Brazil, 2006

THENOZ, B., Measure de la perméabilité et de la poorosité dês roches très compactes. *G.R.A.S*., 243, 1964, pp. 289-291.

VENNARD, J. K.; STRETT, R. L. *Fluid mechanics elements*. Ed. Guanabara Dois, Rio de Janeiro-Brazil, 1978.

YSSORCHE, M. P.; BIGAS, J. P.; OLLIVIER, J. P. Measure de la perméabilité à l'air des betons au moyen d'un perméamètre à charge variable. *Materials and Structures*, vol. 28, n° 181, pp. 401-405, 1995.

XII DBMC
International Conference on Durability of Building Materials and Components
PORTO - PORTUGAL, April 12th-15th, 2011

Durability Properties of Concrete with Recycled Waste Tyres

Dubravka Bjegović [1]
Ana Baričević [2]
Marijana Serdar [3]

ABSTRACT

Concrete industry is one of the major consumers of natural resources. The main aim of sustainable development is to find alternative resources, which could decrease negative effect of concrete industry on environment and contribute to preservation of natural resources. Huge amounts of waste tyres accumulated all over the world are recognized as good supplement for natural resources in concrete.

In this paper is given an overview on possible use of waste tyres in concrete as replacement of part of the aggregate. Research encompassed comparison between mixtures with different chemical and mineral admixtures with the main aim of achieving economically eligible, ecologically acceptable and more efficient concrete mixture. The investigation included examination of mechanical and durability properties such as: compressive strength, gas and water permeability, capillary absorption, chloride diffusion and resistance on spalling due to freezing and thawing of CRT (Concrete with Recycled waste Tyres). Results presented in the paper show that in specific applications CRT is interesting alternative to normal concrete.

KEYWORDS

Concrete with recycled waste tyres, Mechanical properties, Durability properties.

[1] Faculty of Civil Engineering of the University of Zagreb, Croatia, dubravka@grad.hr; Institut IGH d.d., Zagreb, Croatia, J, dubravka.bjegovic@igh.hr
[2] Faculty of Civil Engineering of the University of Zagreb, Croatia, abaricevic@grad.hr
[3] Faculty of Civil Engineering of the University of Zagreb, Croatia, mserdar@grad.hr

1 INTRODUCTION

Concrete industry spends annually 1.5 billion tons of cement, 900 million litres of water and 9 billion tons of sand and stone [Mehta, 2002]. Since concrete industry is one of the major consumers of natural resources, until today many efforts were made in order to replace non-renewable resources with renewable one without significant influence on concrete properties. In numerous research studies different waste materials were incorporated, depending on properties needed from composite.

One of today's major environmental problems are waste tyres; left in environment, they present great danger for earth and living creatures. That is why EU has adopted Directive 1999/31/EC [European Commission 1991] which clearly prohibits any kind of waste tyre disposal in environment. Taking into account that mechanical recycling of waste tyres is environmental friendly process, without any further gas emissions, by using obtained products significant contribution to natural resource conservation is achieved through reduction of new and existing waste amounts.

The aim of present study is to explore the influence of rubber particles obtained from mechanical recycling of waste tyres on concrete properties in fresh and hardened state, depending on the amount, size and shape of particles. The highlight is given to durability properties of concrete which could eventually be improved by substitution of part of the aggregate with rubber particles.

2 EXPERIMENTAL PROGRAM

In order to explore the effect of substitution of aggregate with rubber particles two sets of concrete mixtures with different chemical and mineral admixtures were prepared. First set of mixtures included reference mixture R1 and three mixtures (mixtures labelled M1 to M3) prepared with 10% of rubber by total volume of aggregate including different sized and shaped rubber particles. Polymer was added to improve bonding between rubber and cement matrix and to consequently achieve targeted mechanical properties of CRT. Second set included reference mixture R2 and six mixtures (mixtures labelled M4 to M9) prepared with substitution of 5, 10 and 15% of aggregate volume with different types (shredded and granulate) of rubber particles. These set of mixtures were prepared with addition of superplasticizer (based on a carboxylic ether polymer) and mineral admixtures (silica fume and fly ash). Silica fume was added to improve mechanical properties of concrete, whilst fly ash was added to fill pores between rubber particles and cement matrix, and consequently improve durability properties of CRT.

2.1 Materials

The cement used in this study was CEM I 42.5 R for reference mixture R1 and CRT mixtures M1 - M3 and CEM II/A-S 42.5 R for reference mixture R2 and CRT mixtures M4 - M9 both in accordance with EN 197-1. Preliminary tests showed that chemical admixtures are needed in CRT to improve workability, so 5% of polymer was used for first set of mixtures and 0.4% of superplasticizer for second set, both added by weight of cement.

Rubber particles used in research are obtained from mechanical recycling of waste tyres in three different shapes; granulate, shredded and small granulate. Particle size and shape is represented in Fig. 1.



a) 2 – 3.5 mm Granulate **b) 2 – 4 mm Shredded** **c) 0.5 – 2 mm Small granulate**

Figure 1. Distribution of particles size used in mixture preparation.

In order to increase reduced compressive strength by presence of rubber in second set of concrete mixtures 5% of silica fume by weight of cement was added. Fine particles of fly ash were used by 10% cement weight to improve durability properties and to reduce concrete permeability.

Cement, rubber and mineral admixtures were initially dry mixed in mixer. The volume ratio of rubber ranged from 5% to 15% by volume of the aggregate. Water and chemical admixture content was adjusted to achieve constant workability (i.e. consistence class S1; slump between 10 and 40 mm). Investigated mixtures with main differences in mixture design are shown in Table 1.

Table 1. Investigated concrete mixtures with addition of rubber particles.

Mixture	Rubber type	Rubber content % aggr. vol.	Chemical admix.	Mineral admix.
R1	-	-	superplasticizer	-
M1	granulate	10	latex	-
M2	shredded	10	latex	-
M3	small granulate	10	latex	-
R2	-	-	superplasticizer	silica fume and fly ash
M4	shredded	5	superplasticizer	silica fume and fly ash
M5	shredded	10	superplasticizer	silica fume and fly ash
M6	shredded	15	superplasticizer	silica fume and fly ash
M7	granulate	5	superplasticizer	silica fume and fly ash
M8	granulate	10	superplasticizer	silica fume and fly ash
M9	granulate	15	superplasticizer	silica fume and fly ash

2.2 Test Procedure

The properties of concrete incorporating rubber particles were tested in fresh and hardened state according to European standards for concrete testing, all listed in Table 2. All tests were performed on three specimens.

Table 2. Derived testing and belonging procedures.

Testing	Norm	Mixture
Properties of fresh concrete		
Slump	EN 12350-2	R1, M1-M3, R2, M4-M9
Properties of hardened concrete		
Compressive strength	EN 12390-3	R1, M1-M3, R2, M4-M9
Water absorption	EN 13057	R2, M4-M9
Water permeability	EN 12390-8	R2, M4-M9
Gas permeability	EN 993-4	R2, M4-M9
Chloride diffusion	NT BUILD 492	R2, M4-M9
Freezing and thawing	CEN/TS 12390-9	R2, M4-M9

Research was conducted in two phases; first phase encompassed investigation of mechanical properties of concrete with recycled waste tyres (CRT). Comparison between influence of different chemical and mineral admixtures were done in order to determine economically eligible, ecologically acceptable and more efficient concrete mixture. Second phase included investigation of durability properties of selected mixtures.

3 RESULTS AND DISCUSSION

3.1 Properties of Fresh Concrete

3.1.1 Slump

Increase in rubber content by total volume of aggregate usually causes decrease in slump values [Khallo et al. 2008, Bjegovic et al. 2009; Lakusic et al. 2010; Bjegovic et al. 2010]. The influence of rubber particle shape on the workability of concrete mixture is shown in Fig.2a. The decrease of concrete workability in comparison to reference mixture versus the increase in the amount of rubber particles is shown in Fig.2b.

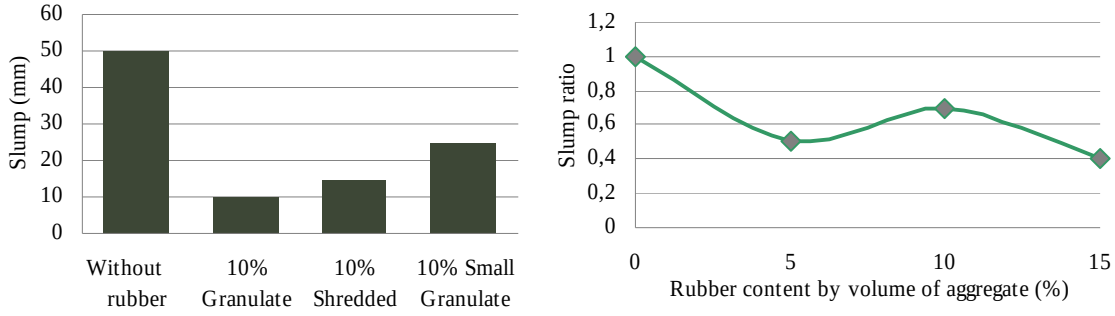

Figure 2. Properties of fresh concrete: (a) Influence of different particle size and shape on slump value (b) Reduction of slump value with increase in rubber content.

Results presented on Fig.2a show that larger rubber particles have somewhat higher influence on concrete workability than smaller ones and that improved workability can be achieved with use of fine particles instead of coarse ones. These results are in accordance with previous research focused on influence of particles size and shape on workability of concrete with recycled waste tyres (CRT); [Khallo et al. 2008]. Same research confirms that beside size, shape of rubber particles can also influence on slump value, although it cannot be said that this is determine factor. Figure 2b present reduction of slump value, averagely 50% is observed if 5% of rubber particles are added in concrete mixture.

3.2 Properties of Hardened Concrete Mixtures

3.2.1 Compressive strength

Rubber has significant influence on compressive strength of CRT. Its reduction is strongly dependent on the percentage of rubber by total volume of aggregate, rubber size as well as on surface roughness.

Due to the non polar nature of rubber particles, air entrapped around rubber surface causes higher air content in CRT [Nehdi & Khan 2001] accordingly causing, lower compressive strengths. Reduction is also dependent on size of the aggregate that is being replaced. If finer aggregate is replaced with smaller rubber particles, lower loses of compressive strength are expected [Benazzouk et al. 2003]. Stated is in accordance with observations made by optical microscopy; that the amount of pores formed around the larger rubber particles is higher than around smaller particles [Panzera et al. 2009]. Strength of the bond on rubber/cement matrix interface depends on rubber surface roughness. Namely, presence of zinc stearat on rubber surface as consequence has reduction of CRT properties [Serge, Monteiro & Sposito 2002] so different pre-treatments are used to remove it; from soaking and washing rubber particles with water to acid etching all in order to assure better cohesion of rubber particles with cement paste [Nehdi & Khan 2001].

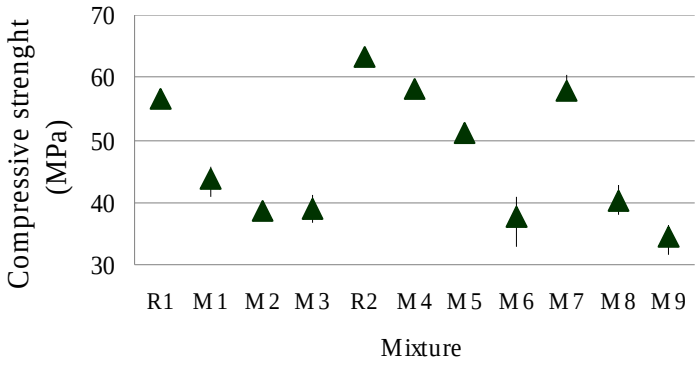

Figure 3. Influence of rubber content, size and shape on compressive strength.

The influence of rubber particle content, size and shape on compressive strength of CRT is shown in Fig.3. From results it can be seen that the addition of rubber particles by total volume of aggregate reduces compressive strength from 10 to 40% depending on the amount of rubber particles. It can also be observed that mixtures containing superplasticizer and mineral admixtures have higher strength if compared to the mixture without mineral admixtures, which is mostly due to the addition of silica fume.

Different properties of rubber particles if compared to natural aggregates are certainly reason for reduction of compressive strength. Cement paste containing rubber particles is much softer than hardened cement paste without rubber. Besides that, lack of proper bonding between rubber and the cement paste is certainly one of the major reasons for reduction of compressive strength. Large pore between rubber particle and cement matrix in hardened concrete taken by optical microscope is shown Fig.4.



Figure 4. Bonding between cement paste and rubber particle.

3.3 Permeability

According to the results obtained during the first phase it was decided that testing of durability properties of CRT will be performed on mixtures incorporating superplasticizer instead of polymer. Comparison of results indicated that use of polymer is economically non eligible since obtained results during testing have not showed significant improvement.

In order to explore the influence of rubber particles on concrete durability following penetrability tests were performed: water permeability, capillary absorption, gas permeability and chloride diffusion.

3.3.1 Water permeability and capillary absorption

Non polar nature of rubber particles is determining factor when capillary absorption is observed. Ability to entrap air in closed pores and repeal water at the same time causes reduction in capillary absorption. Since rubber does not absorb water, volume accessible to water and hence capillary porosity is reduced [Benazzouk et al. 2007]. Amount of absorbed water is closely related to the porosity of the concrete structure giving a picture of the internal microstructure [Segre & Joekes 2000]. From literature overview it is observed that mixtures containing pre-treated rubber absorb less water, indicating better adhesion of rubber particles to matrix.

Figure 5 presents comparison between water absorption of CRT and ordinary concrete.

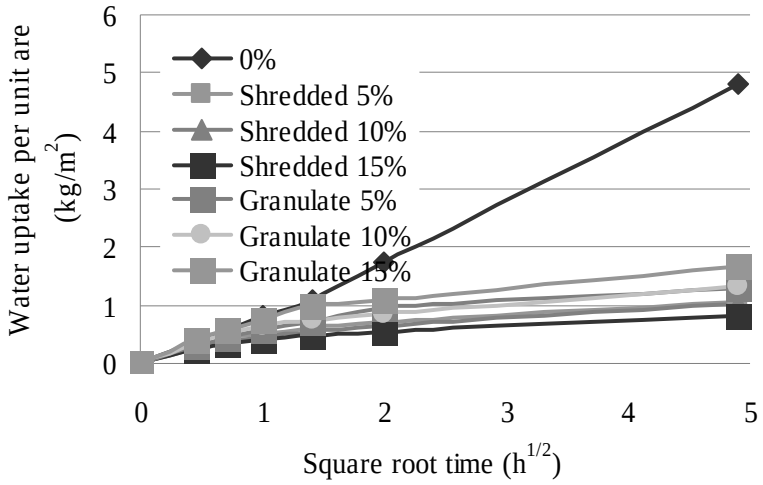

Figure 5. Capillary absorption of CRT (mixtures incorporating mineral admixtures).

From Fig.5 it can be seen that the increase in rubber content causes decrease in water absorption for averagely 78%, if rubber content is kept between 5% and 15% by total volume of the aggregate.

Replacement of natural aggregate by rubber particles increases water permeability depth in concrete mixtures [Ganjian et al. 2009]. During water permeability testing water penetrates into concrete under high pressure which neutralizes initial water repel by rubber. Lack of proper bonding between rubber particles and cement paste, acts as bedding for pressurised water to flow into concrete.

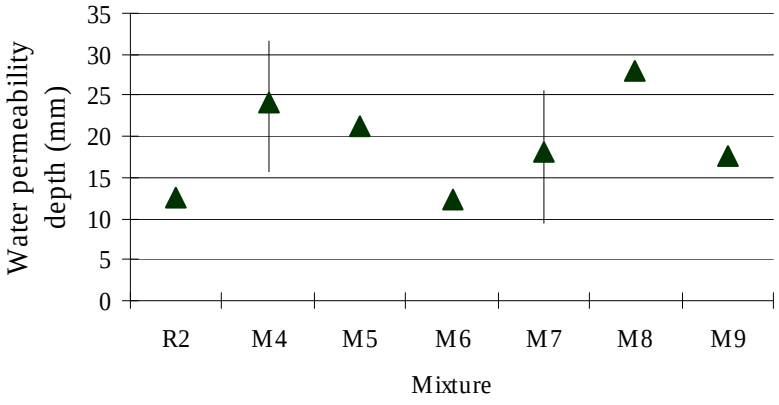

Figure 6. Influence of rubber content and shape on water permeability.

From results presented in Fig.6 it can be seen that if rubber content by total volume of the aggregate is increased; consequently water permeability depth is also increased. Addition of 10% of rubber

particles by total volume of aggregate causes average increase of almost 100% in water permeability depth.

Consequently, use of rubber particles as non-sorptive additives decreases capillary absorption at the same time increasing water permeability due to higher amount of air voids entrapped around rubber surface.

3.3.2 Gas permeability

Investigation of gas permeability with addition of rubber particles was conducted in order to determine dependencies between permeability properties of concrete and presence of rubber particles in concrete [Bjegovic et al. 2010].

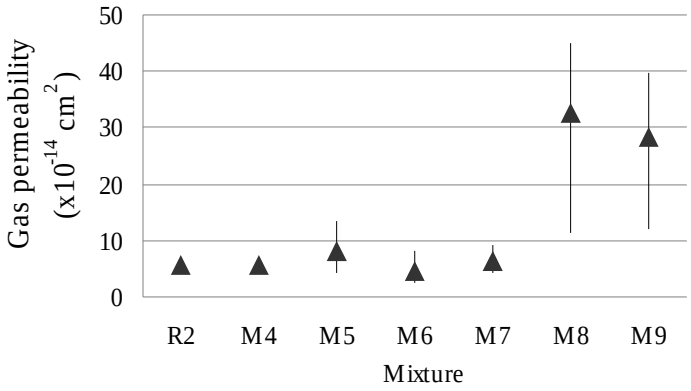

Figure 7. Effect of replacement of part of the aggregate with rubber particles on gas permeability coefficient.

During investigation no improvement in gas permeability was achieved, Fig.7. Presence of high amount of air voids on rubber/cement paste interface results in lack of proper bonding between rubber particles and surrounding matrix influencing on gas permeability results. Different results were obtained with use of different shaped rubber; four time higher values of gas permeability coefficient is obtained if granulate rubber is used instead of shredded one.

3.3.3 Chloride diffusion

Presence of rubber particles in concrete assures higher resistance to chloride ion penetration [Oikonomou & Mavridou 2009].

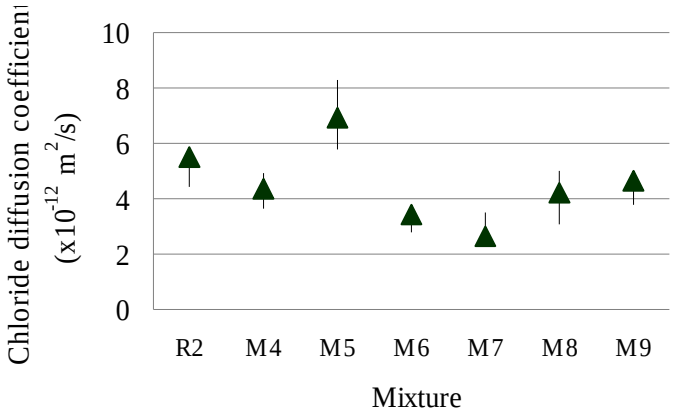

Figure 8. Effect of replacement of part of the aggregate with rubber particles on chloride diffusion coefficient.

Presented results represent effective diffusion coefficient obtained during non-steady state diffusion process where the gradient of the free chloride ions in the pore solution is the effective driving force. Figure 8 shows that if compared to the ordinary concrete reduction of chloride ion penetration can be achieved if part of the aggregate is replaced with rubber particles. Better fillment of voids present between rubber and natural aggregate, causing higher homogeneity and uniform distribution of ingredients in concrete microstructure and consequently lower permeability for chloride ions is assured with granulate rubber particles. Observed reduction of chloride diffusion coefficient can be explained with isolating properties of rubber, making CRT more electrically resistant, compared to ordinary concrete.

3.3.4 Freeze – thaw resistance

Rubber in concrete gives concrete performance similar to that of air-entrained concrete. Conducted research [Bjegovic et al. 2010] showed significant reduction of spalling due to freezing and thawing for CRT. Other researches [Siddique & Naik 2004] have also observed improvement of concrete resistance to freezing and thawing. Figure 9 presents effect of rubber particles on CRT resistance to freezing and thawing.

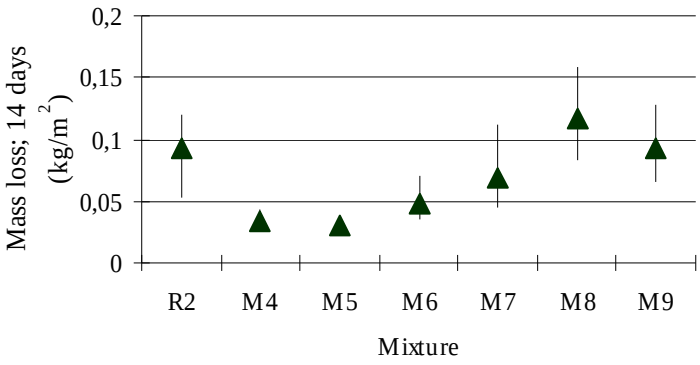

Figure 9. Effect of replacement of part of the aggregate with rubber particles on freezing and thawing resistance of CRT.

Through results review it is observed that with increase in rubber content higher resistance to spalling due to freezing and thawing is obtained if shredded rubber is used rather than granulate one. Presence of 10% shredded rubber particles on total volume of aggregate causes reduction of CRT mass loss for almost 70%, Fig.9. The reason for this is probably their fibre shape as well as elastic behaviour of rubber, which serve as accumulators of stresses caused by ice formation in concrete pores.

4 CONCLUSIONS

The use of rubber particles obtained during mechanical recycling process of waste tyres as replacement of part of the aggregate is justified for preparation of concrete for tailored use. Investigation confirmed that presence of rubber particles in concrete induces improvement of durability properties while at the same time mechanical properties such as compressive strength can be reduced. However, with optimisation of ingredients (incorporation of superplasticizer and mineral admixtures) it is possible to prepare CRT with satisfying both mechanical and durability properties. According to the reduced capillary absorption (averagely 78%) and improved resistance to freezing and thawing (almost 70%) use of CRT could be interesting alternative in aggressive environments, especially in environments exposed to freezing and thawing.

ACKNOWLEDGMENTS

Presented research was performed within the project “The Development of New Materials and Concrete Structure Protection Systems”, 082-0822161-2159, funded by Croatian Ministry of education, science and sport. Authors would like to thank GUMIIMPEX for their support and students Josip Beus, Martina Alibegic and Martina Pezer for their contribution during experimental work.

REFERENCES

Benazzouk, A., Douzane, O., Langlet, T., Mezreb, K., Roucoult, J., & Queneudec, M. 2007, „Physico-mechanical properties and water absorption of cement composites containing shredded rubber wastes“, Cement & Concrete Composites, 29, pp. 732-740.

Benazzouk, A., Mezreb, K., Doyen, G. G., & Queneudec, M. 2003, „Effect of rubber aggregates on the physio-mechanical behaviour of cement-rubber composites-influents of the alveolar texture of rubber aggregates“, Cement&Concrete Composites, 25, 711-720.

Bjegovic, D., Lakusic, S., Serdar, M., & Baricevic, A. 2010, „Properties of concrete with components from waste tyre recycling“, Proc. Concrete Structures for Challenging Times, Marianske Lazne: Czech Concrete Society (CCS) and CBS Servis, s.r.o., 29-01 September 2010, pp 134-140

Bjegovic, D., Lakusic, S., Serdar, M., & Opacak, K. 2009, „Properties of concrete made with recycled waste tires“, 11th national and 5th international scientific conference iNDiS 2009 Planning, design, construction and building renewal, Novi Sad, Serbia, 25-27 November 2009.

European Commission 1991, Council Directive 1999/31/EC of 26 April 1996 on the landfill of waste, Official Journal.

Ganjian, E., Khorami, M., & Maghsoudi, A. A. 2009; „Scrap-tyre-rubber replacement for aggregate and filler in concrete“, Construction and Building Materials, 23, pp. 1828-1836.

Khallo, A. R., Dehestani, M., & Rahmatabadi, P. 2008, „Mechanical properties of concrete containing a high volume of tire-rubber particles“, Waste Management, 28, pp. 2472-2482.

Lakusic, S., Bjegovic, D., & Serdar, M. 2010, „Use of recycled tires on the roads“, in Roads - new technologies and materials, ed. S. Lakusic, University of Zagreb, Faculty of Civil Engineering, Department of Transportation, pp. 7-47.

Mehta, P. (2002) “Greening of the Concrete Industry for Sustainable Development”, Concrete International, 24 (7), pp 23-28.

Nehdi, M., & Khan, A. 2001, „Cementitious composites containing recycled tire rubber: An overview of engineering properties and potential applications“, Cement, Concrete and Aggregates, 23, pp. 3-10.

Oikonomou, N., & Mavridou, S. 2009, "Improvement of chloride ion penetration resistance in cement mortars modified with rubber from worn automobile tires", Cement & Concrete Composites, 31, pp. 403-407.

Panzera, T., Strecker, K., Assis, M., Paine, K., & Walker, P. 2009, „Recycling of rubber waste into cementitious composites“, Proc. of the 11th International Conference on Non-conventional Materials and Technologies NOCMAT 2009, Bath, UK.

Serge, N., & Joekes, I. 2000, „Use of tire rubber particles as addition to cement paste“, Cement and Concrete Research, 30, pp. 1421-1425.

Serge, N., Monteiro, PJM & Sposito, G. 2002, „Surface characterization of recycled tire rubber to be used in cement paste matrix“, Journal of Colloid and Interface Science, 248(2), pp. 521-523.

Siddique, R., & Naik, T. R. 2004, "Properties of concrete containing scrap-tire rubber - an overview", Waste Management, 24, pp. 563-569.

XII DBMC
International Conference on Durability of Building Materials and Components
PORTO - PORTUGAL, April 12th-15th, 2011

Accelerated Carbonation of Concrete Specimens Employing High-Absorption Limestone Aggregate

Eric I. Moreno [1]
Romel Solís-Carcaño [2]
Jorge Varela-Rivera [3]

ABSTRACT

Besides chlorides, concrete carbonation may promote corrosion of the reinforcing steel in concrete. In urban tropical locations, away from the marine environment, carbonation may be the single cause of corrosion in reinforced concrete elements. Previous investigations in reinforced concrete buildings have showed significant concrete carbonation after only 20 years of service. As lower mechanical strength is required for concrete elements involved in housing construction than that required for concrete buildings, faster carbonation rates are expected in concrete houses than those observed in concrete buildings. This investigation is aimed at the impact of carbonation in concrete elements used for building and housing construction. Four different water/cement ratios were used employing high absorption limestone aggregate. Plain and reinforced concrete specimens were exposed in a 4% carbon dioxide chamber at 60% relative humidity. After full carbonation, reinforced concrete specimens were transferred to a 95% relative humidity chamber. The corrosion behavior was monitored using a linear polarization resistance technique. Results indicate that the lower the water/cement ratio the lower the carbonation rate despite the high concrete porosity observed in all concrete mixtures due to the use of high absorption limestone aggregate. Estimates of the length of the corrosion initiation period based on the measured carbonation coefficients are presented.

KEYWORDS

Accelerated tests, Carbonation, Corrosion, Limestone aggregate, Reinforced concrete.

[1] College of Engineering of the Autonomous University of Yucatán (FIUADY), Mérida, MEXICO, emoreno@uady.mx
[2] College of Engineering of the Autonomous University of Yucatán (FIUADY), Mérida, MEXICO, tulich@uady.mx
[3] College of Engineering of the Autonomous University of Yucatán (FIUADY), Mérida, MEXICO, vrivera@uady.mx

1 INTRODUCTION

Reinforcing steel is protected in concrete structures from the atmospheric environment due to the high alkaline environment provided by the pore solution (pH>12.5 units). However, it may corrode if this protection is lost. The protection may be lost due to the neutralization of the concrete pore solution surrounding the reinforcing steel. This neutralization of the pore solution is also called concrete carbonation. Concrete carbonation is the result of the reaction of hydrated cement compounds with atmospheric CO_2. Carbonation reduces the pH of the concrete pore solution (pH≈ 8 units), developing uniform corrosion in the reinforcing steel. This uniform carbonation-induced corrosion accelerates the crack formation if the right conditions of temperature and humidity are present. In places with tropical climate, atmospheric conditions may encourage the carbon dioxide aggressiveness due to high humidities and temperature [Veleva *et al*. 1998]. Carbonation rate depends on several factors [Bakker 1988], such as the type and amount of cement, porosity of the material, type and amount of pozzolanic additions, etc. [Moreno 1999, Moreno & Sagüés 1998].

Previous investigations in reinforced concrete buildings made with high absorption limestone aggregate have showed significant concrete carbonation after only 20 years of service [Castro *et al*. 1999, Moreno *et al*. 2002]. Those concrete buildings, with compressive strength values in the range of 20 to 30 MPa, had carbonation coefficients in the range 5 to 8 mm/year^{½}. According to the literature, more than 6 mm/ year^{½} indicates a bad quality concrete [Ho & Lewis 1987].

Another indication of concrete quality is the value of the porosity of concrete. The porosity results obtained in those concrete buildings ranged from 18.6% to 30.4% [Castro *et al*. 1999, Moreno *et al*. 2002]. According to the literature [Troconis-Rincón *et al*. 2000], values exceeding 15% of porosity are considered bad quality concrete. These high porosity values are attributed to the high absorption limestone aggregate employed.

The question remains whether good quality concrete can be obtained with the use of high absorption limestone aggregate. Therefore, this investigation is aimed at the impact of carbonation in reinfored concrete elements with high absorption limestone aggregates used for building and housing construction.

2 METHODOLOGY

2.1 Specimens and Materials

Four different concrete specimens were used. Instrumented concrete prisms 50 mm by 100 mm by 200 mm were used to monitor the corrosion process. They were reinforced with two corrugated steel bars (rebars #3), 9.5 mm in diameter, and an internal reference electrode made of activated titanium rod covered with mix-metal oxide (ATR) was placed in the middle of each specimen [Castro *et al*. 1996]. Specimens were prepared in triplicate (Fig. 1). In addition, plain concrete cylinders 150 mm by 75 mm diameter were used to monitor the carbonation progress. Plain concrete cylinders 50 mm by 100 mm diameter were used for porosity measurements and plain concrete cylinders 300 mm by 150 mm diameter were used for compressive strength determinations.

Four water/cement ratios were used (0.8, 0.7, 0.62, and 0.55, that correspond to 15, 20, 25, and 30 MPa). The cementitious material was Ordinary Portland Cement with no mineral additions. Crushed limestone was used as coarse and fine aggregate, with absorptions of 5.5 and 4.7 %, respectively [ASTM C 642 2004]. Mixture designs were prepared according to ACI specifications [ACI 211 1997] and the specimens were cast following ASTM standard procedures [ASTM C 192 2002]. Concrete specimens were cured by immersion in lime saturated water for 15 days.

As carbonation proceeds a slow rate, a carbonation chamber was set up to accelerate the process. To ensure enough maturity at the time of the accelerated test, the specimens were allowed to condition at the lab environment for 80 days as a pretreatment and then exposed to a 4% CO_2 environment (~60% RH) in the carbonation chamber for ~100 days, except for mixture 0.55 that was exposed for longer time (176 days) to ensure complete carbonation.

After carbonation, the instrumented specimens were placed in a moisturizing chamber (>90% RH) to increase the corrosion rates.

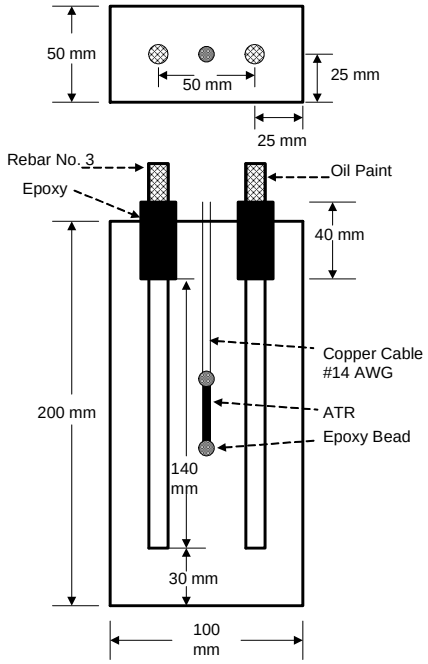

Figure 1. Sketch of the reinforced concrete specimens.

2.2 Porosity Measurements

Two concrete specimens were employed per mixture design to measure concrete porosity. Measurements were performed according to ASTM C 642 [2004]. Acceptance criteria are less than 10% is considered good quality concrete, more than 15% means bad quality concrete [Troconis-Rincón *et al*. 2000].

2.3 Compressive Strength Measurements

Three concrete specimens were employed per mixture design to measure compressive strength. Measurements were performed according to ASTM C 39 [2004].

2.4 Carbonation Depth Measurements

Two plain concrete specimens per mixture design were removed from the carbonation chamber at different times. A ~50 mm slice was split from each specimen and a 1% phenolphthalein solution was sprayed on top of the broken surfaces following the RILEM criteria [CPC-18 1988]. Non-carbonated concrete reacted with the phenolphthalein solution showing a dark pink color. Carbonated concrete remained colorless. Carbonation depth was measured at eight different points using a caliper. Each measurement was corrected from radial measurements in a cylinder into carbonation depth measurements that would be obtained in a semi-infinite plane [Moreno 1999]. Once corrected, the average was obtained for each cylinder, and the result was averaged with the result from the other concrete specimen, obtaining an average from each pair of specimens. After that, carbonation

coefficient was estimated using the time of accelerated exposure and corrected for the initial carbonation occurred during the conditioning period [Moreno *et al*. 2007]. Acceptance criteria are less than 3 mm/year^{½} is considered good quality concrete, more than 6 mm/year^{½} means bad quality concrete [Ho & Lewis 1987]. After taken the carbonation measurements, the remaining portion of the non-instrumented concrete cylinders were placed back in the carbonation chamber.

2.5 Half Cell Potentials

Half cell potentials were measured for each rebar against the internal reference electrode during the carbonation period after calibration against an external copper-copper sulfate electrode placed on the external concrete surface. Corrosion criteria used was that of the literature [Troconis-Rincón *et al*. 2000].

2.6 Concrete Electrical Resistance

Electrical resistance of the concrete was monitored using an AC electrical resistance meter with a Wenner probe. The electrical resistance was measured from one rebar to the other using a two point array.

2.7 Corrosion Rates

Linear polarization resistance tests using a potentiostat were performed during the carbonation and the moisturizing periods without removing the specimens from the chambers. The tests were conducted starting from the open circuit value in the negative direction (-10 mV), to minimize possible capacitive effects, at a scan rate of 0.01 $mV \cdot s^{-1}$ [Sagüés *et al*. 1997]. One rebar (X-bar) was always used as working electrode (WE), the other rebar (Y-bar) was used as counter electrode (CE). Corrosion rates were obtained multiplying 26 mV by the inverse of the polarization resistance from the test. Acceptance criteria are, less than 0.1 $\mu A/cm^2$ is considered meaningless corrosion, more than 0.5 $\mu A/cm^2$ means active corrosion [Troconis-Rincón *et al*. 2000].

3 RESULTS AND DISCUSSION

Table 1 shows the average results of compressive strength and porosity values obtained from the tests. Compressive strength values were above the design compressive strength. Density was in the range for normal concrete although close to the lower limit. Absorcion and porosity were high but as expected based on the absorption values of the aggregates employed. According to the mentioned criteria, these porosity values would qualify the concrete mixtures as of bad quality, even for the low water/cement ratio of 0.55.

Table 1. Average compressive strength, absorcion, porosity and density of concrete mixtures.

Mixture	Compressive strength (MPa)	Absorption (%)	Porosity (%)	Density
0.80	18.0	10.1	23.4	2.27
0.70	21.7	12.9	23.1	2.24
0.62	26.1	11.9	24.1	2.23
0.55	30.9	12.2	22.9	2.23

Table 2 shows the results from the carbonation depth measurements. Concrete specimens were fully carbonated when the carbonation depth was 37.5 mm. Due to the fact that mixture 0.55 was a better mixture than the others, carbonation depth was not determined at 51 days but at 112 days, instead. By day 51, mixtures 0.7 and 0.8 were fully carbonated.

Table 2. Carbonation depth measurements and standard deviations (mm).

Mixture	Days of exposure at 4% CO_2							
	15		37		51		112	
0.80	15.7	1.0	37.5	--	--		--	
0.70	13.7	1.6	24.2	1.4	37.5	--	--	
0.62	10.8	1.3	20.2	1.3	23.1	1.0	n.a.	
0.55	7.8	1.2	14.6	1.4	n.a.		22.3	1.3

Table 3 shows the carbonation coefficients at 4% CO_2 environment. Each coefficient was obtained from day 0. As the test is destructive in nature and different specimens were employed in each test, an average was calculated in order to minimize the experimental error. The higher the water/cement ratio of the mixture, the higher the carbonation coefficient. Therefore, there is a correlation between the water/cement ratio and the carbonation coefficient, despite the high porosity of all mixtures.

Table 3. Carbonation coefficients at 4% CO_2 exposure (mm/year^{½}).

Mixture	Days of exposure at 4% CO_2				Average
	15	37	51	112	
0.80	77.0	--	--	--	77.0
0.70	68.0	83.5	--	--	75.8
0.62	54.0	71.2	57.0	n.a.	61.7
0.55	39.1	51.7	n.a.	42.8	44.5

Table 4 shows the carbonation coefficients transformed to ambient CO_2 exposure (about 400ppm), following the procedure published elsewhere [Moreno *et al*. 2007]. According to the literature, concrete mixtures 0.80, 0.70, and 0.62 should be considered of low quality. Concrete mixture 0.55 should be considered medium quality concrete; also, it is consistent with previous results employing a 0.50 mixture made with river rock as aggregate (K equal to 4.2 mm/year^{½}) [Moreno 1999].

Table 4. Transformed carbonation coefficients at ambient CO_2 exposure (mm/year^{½}).

Mixture	$K_{4\%CO2}$	$K_{0.04\%CO2}$
0.80	77.0	8.4
0.70	75.8	8.2
0.62	61.7	6.7
0.55	44.5	4.8

Assuming a concrete cover of 25 mm and 19 mm diameter reinforcing steel, 30 mm could be considered as average carbonation depth for active corrosion. Thus, the end of initiation time for active corrosion may be reached after 14 years for mixtures 0.80 and 0.70, 20 years for mixture 0.62, and 39 years for mixture 0.55. The estimated 14 and 20 years for corrosion initiation are consistent with the previous results from concrete buildings [Castro *et al*. 1999, Moreno *et al*. 2002].

Figure 2 shows the average potentials as a function of time. Potentials from mixtures 0.8, 0.7, and 0.62 showed a transition of more than 300 mV toward more negative values after 20 days of exposure. Mixture 0.55 has a less pronounced potential change after 70 days of exposure.

After moving the specimens to the humidity chamber, the potentials dropped ~150 mV in the less positive direction. The potentials tended to stabilize in the range -500 to -600 mV, which is the expected range for steel in concrete under active corrosion.

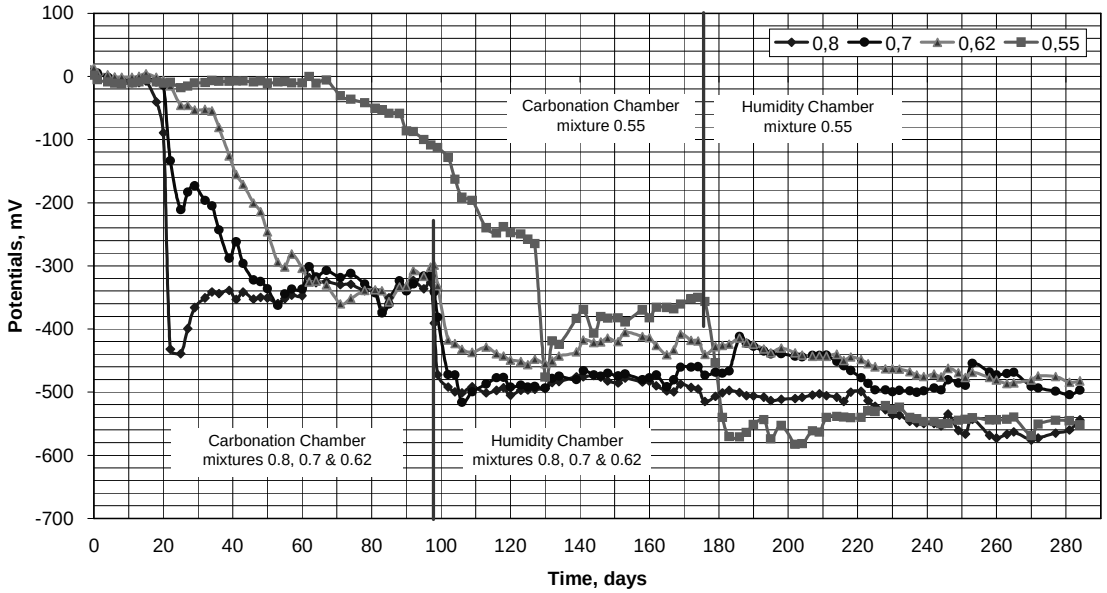

Figure 2. Average potentials as a function of exposure time.

Figure 3 shows the average concrete resistance with time. As the carbonation proceeded, the electrical resistance increased. However, once in the humidity chamber, the resistances dropped to very low values. It is noticeable that the final values were inversely correlated with the water/cement ratio; the higher the water/cement ratio, the lower the concrete resistance.

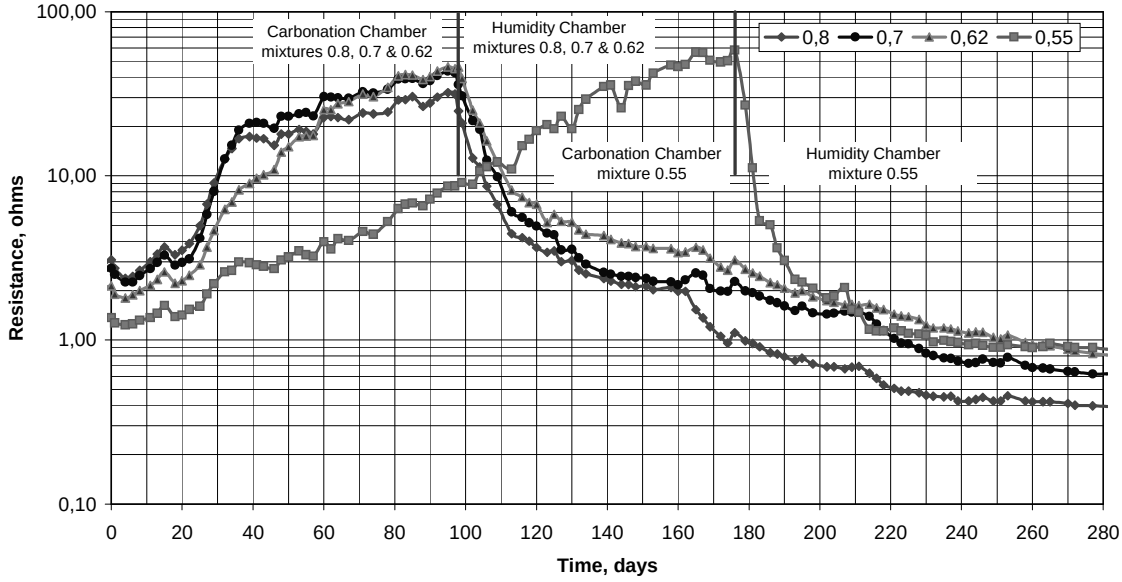

Figure 3. Average concrete resistance as a function of exposure time.

The apparent corrosion rates are presented in Fig. 4. As observed in previous investigations, corrosion rates during the accelerated carbonation period were very low. It is only after the specimens were moisturized than the onset of corrosion developed and active corrosion rates were achieved. As opposed to the electrical values, corrosion rates were directly correlated with the water/cement ratio; the higher the water/cement ratio, the higher the final corrosion rate. Extremely high corrosion rates above 1 $\mu A/cm^2$ were recorded only for the highest water/cement ratio of 0.8. According to the literature, if constant this value would be enough to crack the concrete cover after only 2 years; again, this estimate is consistent with the previous results from concrete buildings [Castro *et al*. 1999, Moreno *et al*. 2002].

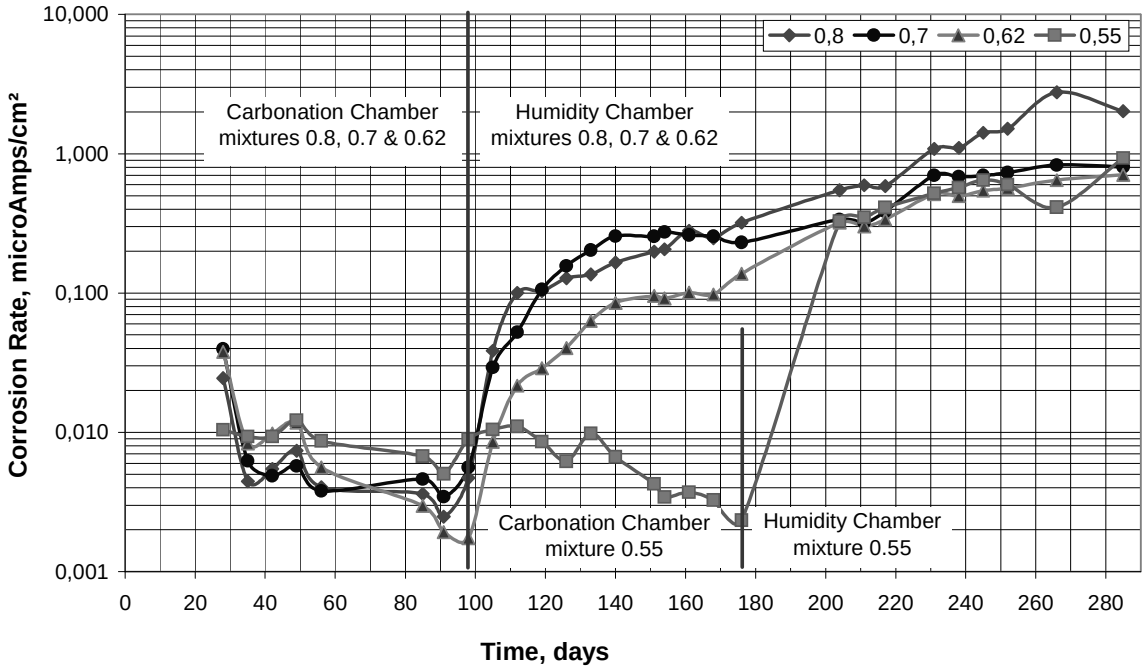

Figure 4. Average corrosion rates as a function of exposure time.

4 CONCLUSIONS

- The lower the water/cement ratio the lower the carbonation rate despite the high concrete porosity.
- Highest corrosion rates were observed at the highest water/cement ratio.
- Good quality concrete may be obtained even when using crushed limestone aggregate of high absorption.

ACKNOWLEDGMENTS

The authors would like to acknowledge the partial support from CONACyT (grant J34433-U), and Universidad Autónoma de Yucatán in several stages of this investigation. The opinions and findings of this investigation are those of the authors and not necessarily those of the supporting organizations. The authors are indebted with E. Cob, G. Domínguez, F. Duarte, and W. Castillo for performing some of the tests reported here.

REFERENCES

ACI 211.1-91 1997, *Standard Practice for Selecting Proportions for Normal Heavyweight, and Mass Concrete*, ACI International, Farmington Hills, MI.

ASTM C 39-03 2004, *Standard Test Method for Compressive Strength of Cylindrical Concrete Specimens*, ASTM International, West Conshohocken, PA.

ASTM C 192-98 2002, *Standard Practice for Making and Curing Concrete Test Specimens in the Laboratory*, ASTM International, West Conshohocken, PA.

ASTM C 642-97 2004, *Standard Test Method for Density, Absorption, and Voids in Hardened Concrete*, ASTM International, West Conshohocken, PA.

Baker, R. F. M. 1988, 'Initiation period', in *Corrosion of Steel in Concrete*, ed. P. Schiessl, Chapman and Hall, London, UK, p. 22.

Castro, P., Sagüés, A. A., Moreno, E. I., Maldonado, L., Genescá, J. 1996, 'Characterization of Activated Titanium Solid Reference Electrodes for Corrosion Testing of Steel in Concrete', *Corrosion*, **52**[8], 609-617.

Castro, P., Moreno, E. I., Genescá, J. 1999, 'Carbonation-induced corrosion of concrete coastal buildings in the north of Yucatan, Mexico', CORROSION/99, paper no. 565, NACE International, Houston, TX.

Ho, D.W., Lewis, R. K., 'The water sorptivity of concretes: The influence of constituents under curing', *Durability of Building Materials*, **4**, 241-252.

Moreno, E. I. 1999, *Carbonation of Blended Cement Concretes*, Ph.D. dissertation, University of South Florida.

Moreno, E. I., Sagüés, A. A. 1998, 'Carbonation-induced corrosion on blended-cement concrete mix designs for highway structures', CORROSION/98, paper no. 636, NACE International, Houston, TX.

Moreno, E. I., Castro, P., Leal-Murguia, J. 2002, 'Carbonation-induced corrosion of urban concrete buildings in Yucatan, Mexico', CORROSION/2002, paper no. 220, NACE International, Houston, TX.

Moreno, E.I., Solís-Carcaño, R. G., Serrano-Ixtepan, D., Arias-Palma, C. A. 2007, '*Performance of concrete coatings against carbonation-induced corrosion*', NACE Corrosion/2007, Paper 07297.

RILEM Recommendations CPC-18 1988, 'Measurement of hardened concrete carbonation depth', *Materials and Structures*, **21**, 453-455.

Sagüés, A. A., Kranc, S. C., Moreno, E. I. 1995, 'Time Domain Response of a Corroding System with Constant Phase Angle Interfacial Component: Application to Steel in Concrete', *Corrosion Science*, **37**[7], 1097-1113.

Trocónis-Rincón, O., Romero-Carruyo, A., Andrade, C., Helene, P., Díaz, I. 2000, *Manual for Inspecting, Evaluating and Diagnosing Corrosion in Reinforced Concrete Structures*, CYTED, Maracaibo, Venezuela.

Véleva, L., Castro, P., Hernández-Duque, G., Schorr, M. 1998, 'The corrosion performance of steel and reinforced concrete in a tropical humid climate. A review', *Corrosion Reviews*, **16**[3], 235-284.

XII DBMC
International Conference on Durability of Building Materials and Components
PORTO - PORTUGAL, April 12th-15th, 2011

Carbonation in Concrete with Recycled Concrete Aggregates

Ana Paula Werle [1]
Marlova Piva Kulakowski [2]
Claudio de Souza Kazmierczak [3]
Jeferson Alcântara Alves Sentena [4]

ABSTRACT

The use of recycled aggregates obtained from the processing of construction and demolition waste has been applied increasingly. The usual alternative for recycling crushed concrete from building demolition is as granular sub-base layers in road pavements and drainage, but more recently recycled aggregates have been used as aggregate in concrete. There are many researches and reports about the fresh and hardened properties of concrete made with recycled concrete aggregate, but there is insufficient knowledge about the durability of this concrete. This paper discusses the performance of concretes with recycled concrete aggregate submitted to carbonation. Concrete with different strengths (18, 37 and 50MPa) were produced, in laboratory, crushed and as recycled aggregates were used in different mixture proportions (25%, 50%, 75% and 100%) in a 32.5MPa concrete. After cure and humidity equalization, they were submitted to accelerated carbonation (chamber with 1% CO_2 and 70% RH). Results indicate that higher amounts of recycled concrete aggregates increase the carbonation depth, when using recycled concrete aggregates from concrete with lower strength than the new concrete, but recycled concrete aggregates from concretes with higher strength do not result in lower durability due to carbonation.

KEYWORDS

Carbonation, Recycled aggregates, Durability.

[1] Post-graduate Program in Civil Engineer of Unisinos (PPGEC), São Leopoldo, Brasil, anhapaula@gmail.com
[2] Post-graduate Program in Civil Engineer of Unisinos (PPGEC), São Leopoldo, Brasil, marlovak@unisinos.br
[3] Post-graduate Program in Civil Engineer of Unisinos (PPGEC), São Leopoldo, Brasil, claudiok@unisinos.br
[4] Undergraduate Program in Civil Engineer of Unisinos (PPGEC), São Leopoldo, Brasi, jefersonalcantara@yahoo.com.br

1 INTRODUÇÃO

Construction and demolition waste (CDW) in Brazil account for approximately 50% of all municipal solid waste [Ângulo et al. 2003]. This amount comes from civil construction work, such as new construction, renovations and demolitions. CDW consists of residues of materials used throughout the construction process. In Brazil, the recyclable CDW are denominated, according to The National Council on the Environment Resolution CONAMA 307 [Brasil 2003], 'Class A waste', that is composed of ceramic, mortar, concrete and soil. Among these, the present study opted for concrete waste, due to its mechanical properties, which provide a good utilization expectation, in the form of aggregate, in a new concrete matrix. Studies using concrete aggregates [Butler 2003, Bazuco 1999, Levy 2001] evidence their good mechanical characteristics. However, there is few data on the durability of this material. Durability is a very relevant issue when the intention is to design a structure with long lifecycle, low maintenance and therefore, more sustainable. In this study the durability of concrete with recycled concrete aggregate is evaluated from the perspective of carbonation.

The phenomenon of carbonation of concrete results from the combination of several factors, such as the concentration of carbon dioxide that the structure is subjected to, the type of binders used in the preparation of concrete and the pore distribution of the hardened concrete. Besides the pore network of the concrete, the internal moisture conditions exert a determining factor for reactions to occur, as the pore must be partially saturated to provide a suitable environment for both the dissociation of CO_2 from the atmosphere and the dissociation of the concrete hidroxides, forming calcium carbonate, which precipitates and alters the pH of the concrete. Other factors, such as the temperature of concrete and the presence of microcracks will also interfere in the speed of the phenomenon. The simplified carbonation reaction is shown in Equation 1.

$$Ca(OH)_{2(s)} + CO_{2(g)} \leftrightarrow CaCO_{3(s)} + H_2O_{(l)} \qquad \textbf{Equation 1}$$

The carbonation phenomenon affects the integrity of reinforced concrete structures due to a decrease in the pH of concrete, destabilizing the passivating layer that acts as a barrier to protect the steel bars against corrosion. The corrosion process results in the generation of oxides along the steel bar, which results in internal stresses that can overcome the concrete's tensile strength and lead the concrete cover to collapse.

Carbonation in concrete with natural aggregate is a widely studied phenomenon. However, when inserted aggregate with different characteristics, such as high porosity aggregates, the properties of the aggregate and the alterations that might occur in the mortar and in the paste-aggregate interface may result in substantial changes in the penetration speed of the carbonation front.

2 METHOD

This study performs a comparison in the behavior of compressive strength and carbonation depth in concretes made with recycled concrete aggregates (RCA) The RCA were obtained from the crushing of concrete that was made in laboratory, which compressive stregnth were 18 MPa, 37 MPa and 50 MPa. The replacements of natural aggregate to RCA were performed at different substitution percentages (25, 50, 75 and 100%), and because of the aggregate porosity was carried out a pre-wetting process in different percentages 0, 25, 50, 75 and 100%, related with RCA's total water absorption. The involved variables are part of a fractional factorial experimental project.

2.1 Materials

It was used Portland cement (high-early strength) in order to obtain a high hydration degree until the scheduled date for the recycling of the concrete (63 days). As fine aggregate was used a quartz sand with fineness modulus of 2.73; maximum dimension of 4.8 mm; specific gravity of 2.49 g/cm³ and bulk density of 1.61 g/cm³. Crushed basalt was used as natural aggregate, fineness modulus of 6.69; maximum

dimension of 19 mm; specific gravity of 2.75 g/cm³ and bulk gravity of 1.49 g/cm³. The particle size distribution is between 12.5 and 25 mm. Figure 1 presents an image of the recycled concrete aggregates.



Figure 1. Recycled concrete aggregates.

2.2 Production and Caracterization of Recycled Concrete Aggregate

The recycled concrete aggregate was obtained from the crushing of concretes that were produced in laboratory. The aim of concrete production in laboratory was to know all the characteristics of this by-product, the aggregate, and as consequence to reduce the possible unknown variables. Also it was a oppotunity to simulate the situation of prevailing in precast concrete plants.Three different concretes were produced and their characteristics are presented in Table 1. The concretes were molded into cylindrical specimens, 100 mm (diameter) x 200 mm (high) and maintained submerged during the cure period (63 days). The mortar content adopted for the concrete was α = 49% that generated a satisfatory level of workability of 100 ± 20 mm. The compositions of original concrete are presented in Table 1 and the physical characteristics of the aggregates obtained by them are presented in Table 2.

Table 1. Composition of original concretes.

w/c ratio	*Sand content (kg)*	*Natural Aggregate content (kg)*	*Cement Content (kg)*	*Compressive strength (28 days - MPa)*
0.85	21.75	28.36	5.50	18
0.56	18.40	28.21	8.70	37
0.43	16.54	30.75	13.00	50

* In order to nominate the different types of recycled concrete aggregates was decided to use the original concrete resistance as definition.

Table 2. Physical characteristics of recycled concrete aggregates.

RCA	*Maximum size (mm)*	*Fineness modulus*	*Specific gravity* (g/cm³)	*Total Absorption* (%)
18 MPa	25	7.68	2.50	8.49
37 MPa	25	7.61	2.47	6.07
50 MPa	25	7.70	2.49	5.24

After a cure period of 63 days (to obtain a high degree of hydration), the concrete specimens were crushed in a in a jaw crusher. With a sieving process, the aggregates were divided into fractions of the following sizes: coarse (between sieve # 25 mm and sieve # 4.8 mm) and fine (between sieve # 4.8 mm and sieve #0.15 mm), just the coarse fraction was used. The particle size distribution of the RCA is between 12.5 and 25 mm. The crushed concrete was kept dry before sieving to avoid any carbonation in the aggregates until use them in the new concrete mixtures. To maintain the dry condition, the aggregates were kept in shut plastic containers.

2.3 Production of Concrete with RCA

The materials used to produce the concretes with RCA were the same that were used to produce the original concrete of RCA. However, it was necessary to change the mortar content from $\alpha = 49\%$ to $\alpha = 53\%$.The trace obtained from the reference concrete , using such conditions, was 1:3,13:3,67 (cement : fine aggregate : natural coarse aggregate, respectively) and w/c ratio of 0.64. Past 28 days of submerged cure, the reference concrete obtained compressive strength of 32,5 MPa. The different RCA were introduced into the new concrete matrix in levels of 25, 50, 75 and 100% substitution of natural aggregate to RCA. The replacement was made considering the compensation of the RCA volume through the specific mass of RCA and natural aggregates, as shown in Equation 2.

$$M_{RCA} = \frac{M_{NA}}{\gamma_{NA}} \times \gamma_{RCA}$$

Equation 2

Where: M_{RCA}= mass of recycled concrete aggregate; M_{NA} = mass of natural aggregate; γ_{RCA} = specific mass of RCA; γ_{AN} = specific mass of natural aggregate.

The porosity of the RCA was compensated through the execution of pre-wetting, which was performed also with different levels (0, 25, 50, 75 and 100%) in a room with controlled temperature and humidity (T = 21°C ± 2°C; RH 90 ± 5%). To maintain the workability in 100 ± 20 mm, were performed adjustments, then the final water/cement ratios were modified. Such adjustments (initial water content - or + final water content) created a new independent variable in the project with random levels.

2.4 Production of Specimens of Concrete with RCA

Cylindrical specimens (100 x 200 mm) were molded in order to evaluate compressive strenght according to the Brazilian standard ABNT NBR 5739:2003. To evaluate the carbonation profile, were used prismatic specimens (60 x 60 x 180 mm), compacted in horizontal vibrating machine and kept in a submerged cure for 63 days. After the cure the specimen were submitted to drying and stabilization of the internal moisture content, in order to achieve an apparent internal moisture content of 70%, according to the modified RILEM TC 116 PCD procedure. The modification is related to the period of stabilization (RILEM – 14 days; the present work = 28 days) and the internal moisture estimate method. In this work the determination of apparent internal moisture was made using the difference of the mass between a saturated specimen and a dried specimen. The specimens were kept in oven (50°C) until the loss of 30% of the mass difference, reaching in a internal apparent moisture of 70%.

The phase of the redistribution of moisture aims to homogenize the internal moisture of the prisms. Afterwards, the prisms were kept in a chamber for the accelerated carbonation test, adopting exposure conditions of 1% CO_2 and relative humidity of 70%. The prisms were kept under these conditions for 147 days, and then the carbonation depth was determined, using phenolphthalein and an image analysis with the software *Image Tool 3.00*, as seen in Figs. 2 and 3.



Figure 2. Carbonated specimen.

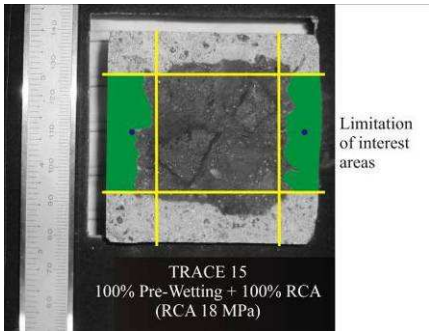

Figure 3. Identification of the carbonated area.

From the data obtained through the accelerated test, the behavior of the advance of the carbonation front over time was determined and the influence of the presence of recycled concrete aggregates in new concrete matrix was examined.

3 PRESENTATION AND DISCUSSION OF RESULTS

3.1 Compressive Strength

The results of compressive strength are presented in Table 3. Through analysis of variance (ANOVA) was possible identify the significant influence of the variable RCA content and type of aggregate.

Table 3. Average results of compressive strength from executed combinations (avarage of 3 specimen).

*RCA Type**	*Recycled concrete aggregate content*	*Pre-wetting rate*				
		0%	*25%*	*50%*	*75%*	*100%*
18 MPa (w/c 0.85)	*25%*		33.3		27.2	
	50%	29.9		30.4		28.5
	75%		27.9		26.6	
	100%	26.8		25.5		25.6
37 MPa (w/c 0.56)	*25%*	29.5		35.4		32.7
	50%		31.6		33.7	
	75%	30.8		29.3		27.1
	100%		26.7		30.7	
50 MPa (w/c 0.43)	*25%*		32.7		25.8	
	50%	33.5		34.3		33.8
	75%		28.2		25.7	
	100%	31.1		32.6		28.8

* The reference concrete has presented a compressive resistance of 32.5 MPa.

The data show that the concrete with recycled concrete aggregate, which presents porosity equal or lower than the new matriz, in general, obtained a similar resistance or presented some addition of resistance (+ 8%). In concrete with RCA porosity higher than the new matrix,it has presented a reduction of the compressive resistance, about less than 10%.

3.2 Carbonation Depth

The results obtained from the accelerated carbonation test are presented in Table 4 and were treated statistically. It was used the software StatGraphics Centurion Data Analysis, to check which variables have significant influence on its behavior.

Table 4. Average results of carbonation depth (mm) after 147 days to CO_2 exposure.

*RCA Type**	*Recycled concrete aggregate content*	*Pre-wetting rate*				
		0%	*25%*	*50%*	*75%*	*100%*
18 MPa (w/c 0.85)	*25%*		10.6		8.4	
	50%	8.3		9.3		11.0
	75%		11.6		11.9	
	100%	13.1		11.8		12.1
37 MPa (w/c 0.56)	*25%*	9.3		9.7		8.4
	50%		11.3		10.3	
	75%	11.4		10.2		9.8
	100%		10.5		11.4	
50 MPa (w/c 0.43)	*25%*		10.5		8.8	
	50%	10.5		8.7		8.8
	75%		9.7		8.8	
	100%	8.9		10.3		9.7

* The reference concrete presented a compressive resistance of 8.8 mm.

** Average of 4 specimen.

The regression equation obtained (presented in equation 3) had a coefficient of determination (r2) of 0.97, that is, the proposed model explains 97% of the data observed for the carbonation phenomenon over time. A significance level of 99% was adopted.

$$Cd = EXP \times (b0 + (b1/FC) + (b3/WCR) + (b12 \times ARC/FC) + (b23 \times ACF/ARC)) \times (T^{\wedge} b4) \quad \textbf{Equation 3}$$

Where: Cd = carbonation depth (mm); FC = resistance of original concrete of aggregates (MPa); WCR= final w/c ratio; ARC = aggregate replacement content (%); T: time; bn = equation constant.

From this regression, the behavior of different admixtures was estimated with theoretical w/c ratios of 0.45, 0.65 and 0.75, as a result of a independent variable with random levels, as seen in Figure 4.

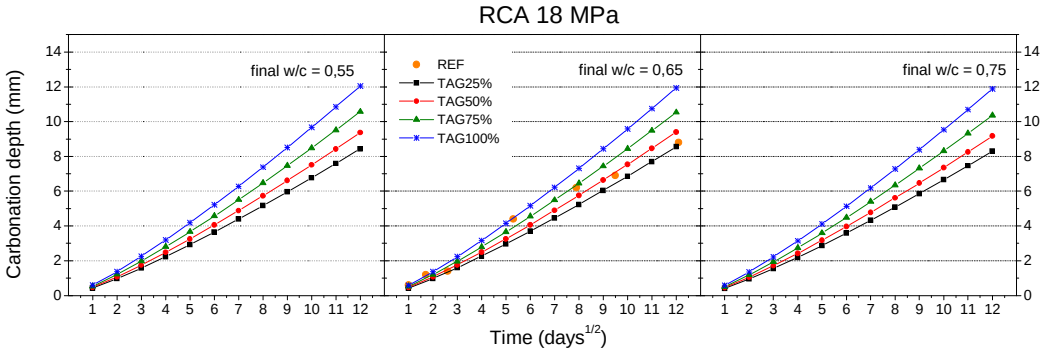

Figure 4. Behavior of concrete with RCA versus carbonation during 147 days.

The variables that most had influence on the carbonation behavior were *replacement content* and *type of aggregate*. *Replacement content* has generated an expected result. The more RCA content in the mixture, the higher will be the carbonation depth. The *type of aggregate* had a significant influence over carbonation behavior. Through the utilization of aggregates with known characteristics, it was possible to identify the influence of the type of the RCA in the phenomenon of carbonation.

As can be seen in Fig. 5, for every type of aggregates has occurred a high variation in the carbonation depth. However, when only the aggregate 'RCA 18 MPa' was analyzed, their variation wass meaningly higher than the other mixtures. This behavior would be assigned to original porosity of this material. Meanwhile the 'RCA 37 MPa' and 'RCA50 MPa' presented a smaller variation and a lower carbonation depth at the final test period (147 days).

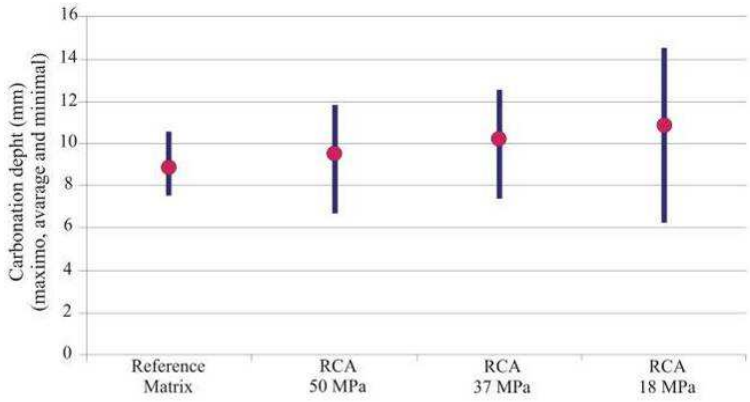

Figure 5. Behavior of carbonation depth related to the type of aggregate.

Considering the matrix where the aggregates are inserted, as presented in Fig. 6, it can be verified that in the concrete with 50 MPa aggregate there was no change behavior in the carbonation front, independently of the amount of aggregates in the mixture. As well as when it was used 37 MPa aggregates in all admixtures

studied, there was a small influence of the recycled aggregate content. The highest differences appeared with higher recycled aggregate content in the mixtures. However these mixtures preserved a similar behavior.

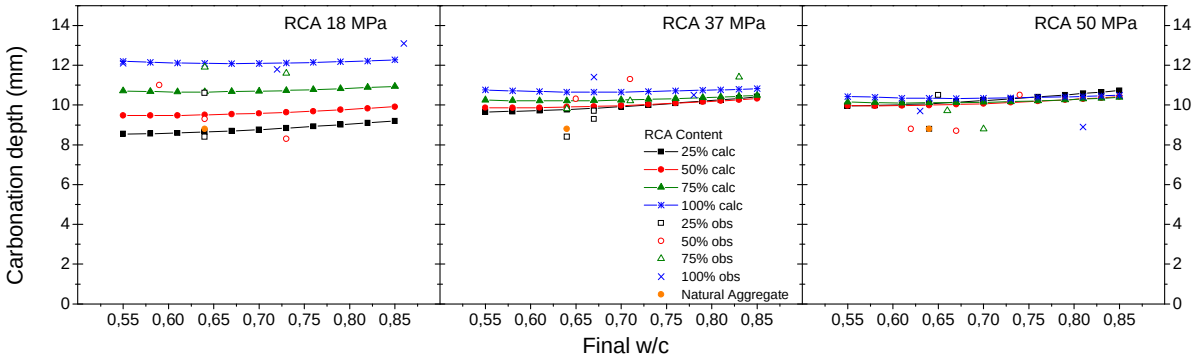

Figure 6. Carbonation depth considering different aggregates content in matrix with different w/c ratio.

The presence of 'RCA 18 MPa' leads to increase the carbonation depth and the differences of carbonation depth related with the RCA content are more expressive among the concretes. In this case the aggregate content becomes a significant factor that can turn unfeasible the use of the aggregates in a new concrete.

Apparently, there is no difference of carbonation depth in concretes with the same content of recycled aggregate, when using aggregates from original concretes of 37 and 50 MPa, as well as with different final water/cement ratios. In relation to the reference concrete, those ones made with RCA 37 MPa have carbonated a little more than the reference concrete. The results are similar to Levy [2001], who performed an accelerated carbonation test in samples of concrete with RCA 35.5 MPa in a matrix with fc= 32.5 MPa. Concretes with a RCA 50 Mpa carbonated even less than the reference concrete. In the latter situation, where RCA 18MPa was used, a material with significantly more porous than the matrix, a higher carbonation depth was found, it was also noticed a significant influence on the amount of substitution of natural aggregate by RCA 18 MPa. The result is consistent to Wu and Song's [2006] apud Li [2008], which concluded that, the higher the RCA content, the higher the carbonation depth. The authors found out that the carbonation depth is up to 62% higher than the reference concrete, for an aggregate substitution content of 60%, and have asserted that the high porosity of the aggregate is responsible for this outcome. Gomes and Brito [2009] claim that the carbonation depth for concretes with up to 50% RCA content, results in a small increase in carbonation depth, in the order of 10% higher than the reference concrete.

4 CONCLUSIONS

Independently of the type and content of RCA, the new concrete tends to be more porous than the reference one and consequently more susceptible to carbonation. Concretes with RCA 18 MPa presented a carbonation depth until 1.8 times greater than the reference concrete. With RCA 37 MPa the carbonation depth was 1.3 times greater than the carbonation depth of reference concrete and concrete with RCA 50 MPa the carbonation depth was 1.2 times greater. In this study, a concrete with RCA of equal or higher porosity (37 and 50 MPa) than the new matrix (32.5 MPa), the carbonation depth in 147 days is similar to the reference concrete. However, when using high porosity RCA (18 MPa), the carbonation depth shows higher dispersion of results and is substantially higher than the reference concrete (approximately 50%).

The increase in carbonation depth is directly proportional to the increase in RCA content. For concrete with RCA of 37 MPa or 50 MPa, the carbonation depths found out for each substitution content, were proportional one another. When using RCA from a more porous concrete (18 MPa), the differences in carbonation depth become more expressive. The studied carbonation depths were in the range of 9.5 mm, for 25% and 50% content of RCA, changing to 12.1 mm for 75 and 100% content of RCA, an increase of 27% in the carbonation depth related to the RCA content.

An important information about the method tested is relative to the exposure time. By using concrete with RCA until the first 28 days the results tend to be quite similar to the reference concrete but afterwards, between 63 and 91 days such a behavior tends to change.

ACKNOWLEDGMENTS

The authors thank FINEP and CNPq for research funding and the scholarship.

REFERENCES

Ângulo, S. C.; Kahn H.; John, V. M.; Ulsen, C. 2003. "Metodologia da caracterização de resíduos de construção e demolição". In: *Seminário Desenvolvimento Sustentável e a Reciclagem na Construção Civil – Materiais Reciclados e Suas Aplicações*, São Paulo. Anais IBRACON, v.6.

Bazuco, R. S. 1999. "*Utilização de agregados reciclados de concreto para a produção de novos concretos*"**.** 103p. Dissertação (Mestrado em Engenharia) – Pós-graduação em Engenharia Civil. Universidade Federal de Santa Catarina, Santa Catarina.

Buttler, A. M. 2003. "*Concreto com agregados graúdos reciclados de concreto- influência da idade de reciclagem nas propriedades dos agregados e concretos reciclados*". 187p. Dissertação (Mestrado em Engenharia) – Escola de Engenharia de São Carlos. Departamento de Engenharia de Estruturas. Universidade de São Paulo, São Paulo.

CONSELHO NACIONAL DO MEIO AMBIENTE**. Resolução CONAMA n° 307/ 2002**. At HTTP://www.mma.gov.br/port/conama/res/res02/res30702.html. Access 18/02/2009.

Gomes, M.; Brito, J. 2009. Structural concrete with incorporation of coarse recycled concrete and ceramic aggregates: durability performance. *Materials and Structures*, v. 42, p. 663 – 675.

Levy, S. M. 2001. "*Contribuição ao estudo da durabilidade de concretos, produzidos com resíduos de concreto e alvenaria*". 182p. Tese (Doutorado em Engenharia) – Escola Politécnica da Universidade de São Paulo, 2001.

Li, X. 2008. Recycling and reuse of waste concrete in China. Part I. Material behavior of recycled aggregate concrete. *Resources, Conservation and Recycling*, v. 53, p. 36 – 44, 2008.

RILEM TC 116 PCD. Permeability of concrete as a criterion of its durability. Concrete durability – an approach towards performance testing. *Materials and Structures*, v. 32, p. 163 – 173, 1999.

XII DBMC
International Conference on Durability of Building Materials and Components
PORTO - PORTUGAL, April 12th-15th, 2011

Embeddable Chloride Sensor for In Situ Monitoring the Durability of Concrete Structure

Xiaojian Gao [1]
Xiuli Lu [2]
Yingzi Yang [3]

ABSTRACT

One type of all-solid-state chloride sensor was fabricated using a MnO_2 electrode and a Ag/AgCl electrode. The electrochemical stability of sensor was examined in a synthetic concrete pore solution with different concentrations of chlorides. Sensors were also embedded into concrete specimens prepared with the mixing water containing chloride and the potential development was studied for about 3 months. The results show that there is a good uniformity of potential among the fabricated sensors for the same concentration chloride solutions. The sensor shows a good linear potentiometric response to a wide range of chloride concentrations from 0.005 M to 5.0 M as shown in Nernst equation. Other possible ions in concrete, such as sulfate, calcium and sodium, show inconsiderable influences on the potential reading of the sensor. The potential reading of sensor in concrete shows a decreasing tendency with time at early ages due to the reduction of free water, and an increasing tendency at later ages due to the more binding chloride in concrete. During the test period, the sensor was working stably and maintained a linear potential-chloride activity relationship as found in solution test. Therefore, it is recommended that this chloride sensor can be possiblly used for in situ monitoring the chloride-induced durability of concrete structures.

KEYWORDS

Concrete structure, Chloride-induced corrosion, In situ monitoring, Embeddable sensor.

[1] School of Civil Engineering, Harbin Institute of Technology, Harbin, CHINA, xjgao2002@yahoo.com.cn
[2] Harbin FRP Institute , Harbin, CHINA, xjgao-lian@163.com
[3] School of Civil Engineering, Harbin Institute of Technology, Harbin, CHINA, yzyang@hit.edu.cn

1 INTRODUCTION

Chloride-induced corrosion of the steel reinforcement has become the principal cause of premature deterioration of concretes under de-icing salts or marine environments all over the world [Kassir & Ghosn 2002], and it has been estimated that these failures can account for more than 35% of the total volume of construction work in Europe. It is well known that after reaching a threshold concentration, the soluble "free" chloride ions in concrete pore solution result in the passive film collapse and corrosion of steel [Rasheeduzzafar *et al*. 1991]. Therefore, monitoring of free chloride content is one of the most important methods to prevent and control premature deterioration of concretes under chloride environments. Two types of methods have been used for such purpose: leaching method [Cáseres *et al*. 2006] and the pore-pressing technique [Anstice *et al*. 2005]. These two procedures, although well-established, are destructive and time-consuming, and require periodical sampling from the concerned structure. The use of embeddable sensors for continuous and in situ monitoring chloride content is in its essence a much more straightforward procedure.

Ag/AgCl electrodes are stable, easily prepared, and have long been used in the electrochemistry field as chloride ion selective or reference electrodes [Valdés-Ramíreza *et al*. 2005]. Its equilibrium potential value depends on the chloride ion activity (concentration) of surrounding solution according to Nernst Law. The use of Ag/AgCl electrodes to determine chloride activity in simulated cement pore solution, in pressure-extracted cement pore water and even in mortar and concrete samples has been described in literatures [Miguel *et al*. 1996; Montemor *et al*. 2006]. The Ag/AgCl wire was even used as a sensor for determination of water soluble chloride in admixtures and aggregates for cement [Junsomboon *et al*. 2008]. At the same time, all the experiments in literatures were carried out by using saturated calomel or saturated Hg_2SO_4 electrodes as references. These reference electrodes are unsuitable for in-situ monitoring because the liquid electrolytes in them may occur any leakage or become invalid upon cold temperature. It was found that the MnO_2 electrode has a long-term stability in concrete environments and even the addition of chloride has little influence on its performance. One embeddable MnO_2 reference electrode has been developed for measuring the potential of the steel rebar to evaluate the corrosion status [Muralidharan *et al*. 2008].

This paper aims at fabricating one type of all-solid-state embeddable chloride sensor using a Ag/AgCl electrode as working electrode and a MnO_2 electrode as reference, which can indicate chloride activity through its potential reading without the need for any additional reference electrodes. The performances of such chloride sensor were extensively evaluated by using synthetic concrete pore solutions. At the same time, the workability of such sensors embedded in concrete were also studied.

2 EXPERIMENTAL

2.1 Raw Materials

For the fabricaiton of the sensor, the following materials were used: ordinary Portland cement (OPC) conforming to GB175-2007; poly-vinyl alcohol (PVA) fiber with a diameter of 39 μm and length of 3-5 mm; a MgO-based expansive agent for compensating the cement shrinkage; manganese dioxide and acetylene carbon black reagent grade ≥92% purity for making the reference electrode cell; Ag and AgCl powder reagent grade ≥99.9 % purity for making the working electrode. NaOH, KOH, CaO, Na_2SO_4, NaCl, $CaCl_2$ and KCl were selected with analytical-reagent grades to prepare different chloride sulitions. Distilled deionized water was used to prepare all aqueous solutions.

For the concrete test, besides the OPC cement, NaCl and distilled deionized water, crushed limestone gravel was used as coarse aggregate with a maximum nominal size of 25mm; a quartz sand was used as fine aggregate with a fineness modulus of 2.85 according to Chinese standard. To obtain a good

workability, a commercially available, naphthalene-based, high-range water-reducing agent Mighty 100 produced by Kao Chemical Corporation Shanghai, was also used.

2.2 Fabrication of Chloride Sensor

As shown in Fig.1(a), this chloride sensor is a PVC tube with a multilayer filling. The fabrication process of the sensor can be briefly described as follows:

1) A suitable PVC tube was chosen with a diameter of 10 mm and length of 15 mm. This tube should be strong enough to protect the sensor from any mechanical damage or chemical corrosion.

2) Cement, PVA fiber and MgO-based expansive agent were mixed with water to prepare a fiber-reinforced cement paste. Proper mix proportioning was performed to minimize the risk of shrinkage cracking. About 2~3 mm depth of such cement paste was applied in the tube with a 3~4 mm distance from the bottom. This cement paste layer had a very low permeability and improved cracking tendency, therefore, the leakage of the alkali from the top of this layer can be diminished markedly.

3) A special alkaline slurry composed of sodium, potassium and calcium hydroxides was placed on top of the cement paste after several days of wet curing. The pH of the slurry was equal to that of the cement paste.

4) MnO_2 powder was mixed with a known quantity of acetylene carbon black, which is used to improve the electrical contact among MnO_2 particles, and then compressed into a cylindrical shape with a specially designed steel mould. The MnO_2 cylinder was planted with a low resistance conducting wire during the preparation. It was finally placed into the tube from the top with a controlled pressure to ensure tight contact between the cement paste, alkaline gel and MnO_2 cylinder.

5) The top of the tube was sealed with epoxy to complete the MnO_2 reference electrode. After the hardening of the epoxy, the MnO_2 sensor electrode was activated with synthetic concrete pore solution (0.2 M NaOH + 0.6 M KOH + saturated $Ca(OH)_2$ solution) for a few days. The half-cell potential of MnO_2 electrode is determined by MnO_2/Mn_2O_3 equilibrium potential. In this study, the compressed MnO_2 was surrounded by the slurry with a stable alkalinity of pH 13.5. Therefore, the activated MnO_2 electrode kept a stable potential and was used as the reference electrode.

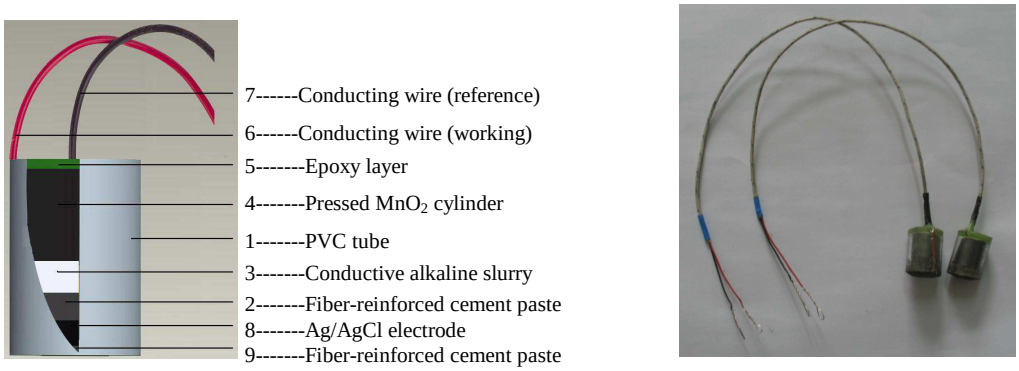

(a) Schematic layout **(b)** Photograph

Figure 1. the schematic layout and photograph of the chloride sensor.

6) A mixture of Ag and AgCl powder with an optimal proportion was compressed into a tablet shape with a height of about 1.5 mm and diameter of less than the PVC tube. The Ag/AgCl tablet, as the working electrode (chloride ion selective electrode), was placed at the bottom of the above mentioned tube assembled with MnO_2 electrode and then installed and encapsulated with a fiber-reinforced cement paste with a higher porosity than the one mentioned above.

Completed all-solid-state chloride sensors are shown in Fig.1(b). When exposed to chloride environment with temperature *T* and chloride ion activity of α_{Cl^-}, the potential of Ag/AgCl electrode $E_{Ag/AgCl}$ is given by the Nernst equation:

$$E_{Ag/AgCl} = E^0_{Ag/AgCl} - \frac{RT}{F}\log \alpha_{Cl^-} \quad (1)$$

where $E^0_{Ag/AgCl}$ stands for the standard electrode potential of the Ag/AgCl electrode, R for the universal perfect gas constant, T for absolute temperature (K), F for Faraday constant.

The MnO_2 electrode acts as the reference electrode (with the potential of E_{ref}) in this study, and the sensor potential can be expressed as:

$$E = E_{Ag/AgCl} - E_{ref} = (E^0_{Ag/AgCl} - E_{ref}) - \frac{RT}{F}\log \alpha_{Cl^-} \quad (2)$$

The potential *E* can be measured through two conducting wires of the sensor, and then the chloride activity can be determined according to the calibrated curve.

2.3 Solution Measurement

1) Potentiometric response to chloride: The potential of the sensor was tested in synthetic concrete pore solutions with different concentrations of NaCl ranging from 0.05 to 5.0 M. The working stability was assessed through measuring the potential development during 60 days of immersion in synthetic concrete pore solution. Two parallel sensors were measured in these tests.

2) Influences of other ions and pH on potentiometric response to chloride: Ions such as Ca^{2+}、K^+、Na^+、SO_4^{2-} may exist in concrete in different concentrations depending on raw materials and service environments. For the fully carbonated concretes, the pH value of the pore solution decreases to as low as 7.5. Therefore, four series solutions were prepared: distilled water (O), saturated $Ca(OH)_2$ solution (A), synthetic concrete pore solution (B) and synthetic concrete pore solution plus 0.1M concentration of SO_4^{2-} (C), and then 0.1 M and 1.0 M concentrations of chloride ions were added using NaCl, KCl and $CaCl_2$ respectively. Potential readings of the sensor in these solutions were tested.

2.4 Concrete Measurement

Three concrete mixtures were prepared with different water to cement ratio of 0.32, 0.4 and 0.5, as shown in Table 1. For every concrete, 4 % NaCl was added by weight of cement to supply free chloride ions in pore solution. Cubic specimens with size of 100×100×100-mm were cast according to the above mixture proportions, and the chloride sensor was embedded centrally in each specimen. Immediately after moulding, the specimens were cured in a moist cabinet for 24 h, removed from the mould, wrapped with the plastic sheet and cured at room temperature (20±2℃). Potential readings of the sensors in concrete samples were monitored over time after demoulding.
Three paste mixtures were prepared with the same ratios of water: cement: plasticizer: NaCl and the same curing conditons as the concrete mixtures. At 1, 3, 7, 10, 14, 21, 28 and 56 days, some paste samples were selected for measuring the free water and free chloride ion content, then the chloride concentration in cement paste at different ages can be calculated for representing the chloride concentration of pore solution in the concrete specimens. For the free water test, the paste were crashed into 1-mm size particles and the weight loss was measured before and after a vaccum drying treatment for 3 days at 60 ℃. The free chloride ion content in paste sample was determined according to the standard ASTM C 1218/C 1218M-99 (R2008) (Standard Test Method for Water-Soluble Chloride in Mortar and Concrete).

Table 1. Mixing proportion of concrete.

No.	*w/c*	*Concrete composition* [kg/m^3]					
		Water	*Cement*	*Sand*	*Gravel*	*Plasticizer*	*NaCl*
1	0.32	136	425	702	1053	6.4	17
2	0.4	170	425	702	1053	3.5	17
3	0.5	213	425	702	1053	0	17

3 RESULTS AND DISCUSSION

3.1 Potentiometric Response to Chloride Activity

The potentiometric responses of two parallel sensors (CSC1 and CSC2) to chloride ion activities in synthetic concrete pore solutions are presented in Fig. 2. The activity coefficient of Cl^- at different concentration solutions were determined according to Vera's work [Vera *et al*. 2000] on the basis of the Pitzer approach. For every chloride ion activity (concentration), a very limited difference in potential reading was observed between the two sensors: a maximum of 3.2 mV for 0.05 M concentration and 1.2 mV for 5.0 M concentration. For each sensor, the potential reading decreases with increasing chloride ion concentration ranging from 0.05 to 5.0 M, and a good linear relationship (with a correlation coefficient of higher than 0.98) is observed between the potential reading and the logarithm of chloride ion activity as described by the Nernst equation. However, a slight bigger deviation from linearity can be found at low Cl^- concentrations as reported by Miguel *et al*.[1996]. Therefore, such sensors showed a lower sensitivity at low chloride concentrations which are not very important in most cases for embeddable monitoring of steel-reinforced concrete. The Ag/AgCl electrode can maintain a stable potential (±2mV deviation) when exposed to simulated concrete pore solution for 40 days [Duffo *et al*. 2009]. It was reported that the potential vs. SCE of MnO_2 electrode was increased by 6 mV after 90 days exposure to synthetic concrete pore solution [Muralidharan *et al*. 2006]. For the chloride sensor assembled by an Ag/AgCl electrode and a MnO_2 electrode, a better potential stability was found in Fig. 2. After 60 days of exposure to synthetic concrete pore solution, the potential reading difference from the initial value is less than 2.2 mV for all the solutions. The improved potential stability of the sensor should be attributed to the better performance of the MnO_2 electrode which is encapsulated in the top part of sensor, indicating the possible application for long-term monitoring in concrete environment.

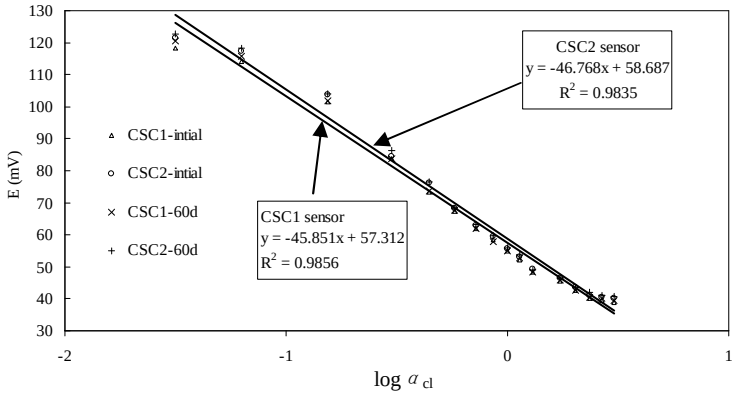

Figure 2. Potentiometric response of the sensor to chloride activity.

3.2 Influences of Other Ions on Potentiometric Response

Figure 3 presents potential readings of the sensor in chloride solutions containing other ions. Every solution sample was tested six times with the same sensor and the average value was obtained. The

potential values showed a very low standard deviation (less than±0.7mV) for each solution. Under the same chloride ion concentration of 0.1 M, the sensor potentials in solutions based on distilled water (O) and saturated $Ca(OH)_2$ solution (A) presented 5.0~6.3 mV higher than those in solutions based on synthetic concrete pore solution (B). This decreased potential values in synthetic concrete pore solution, which has a notably higher pH value (13.5) than distilled water (7.0) and saturated $Ca(OH)_2$ solution (12.0), is mainly due to the interference from hydroxide (OH^-) ions. This deviation at low chloride contents could be attributed to the formation of AgOH [Elsener *et al*. 2003]. No visible difference (less than 1.0 mV) in potentials were found before and after the addition of 0.1M SO_4^{2-} in solutions B. When the chloride ion concentration increased to 1.0 M, the potential of the sensor in saturated $Ca(OH)_2$ solutions was a little lower (1.4~1.7 mV) than those in distilled water solutions. However, the potentials in synthetic concrete pore solutions were (0.7~1.8 mV) higher than those in distilled water solutions. After the addition of sulfate, the potential was increased by 0.9~2.0mV. Therefore, the potential variation is less significant in 1.0 M chloride solution. For both 0.1 and 1.0 M chloride concentraitons, different cations (Ca^{2+}、K^+、Na^+) have very limited influence on potentiometric response to chloride (average less than 1.0 mV). The pH value of a fresh concrete may be as high as 13.5. As carbonation proceeds, the pH value of the concrete pore solution decreases to as low as 7.5 [Chang & Chen 2006]. According to the above results, the pH value should be simultaneously detected in order to precisely determine the chloride content in chloride-slightly contaminated concretes.

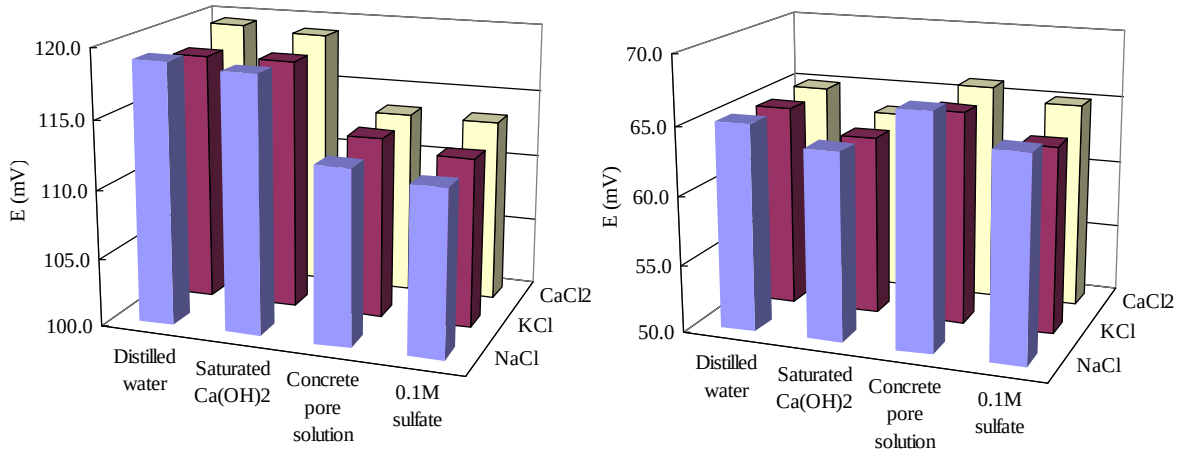

(a) 0.1M concentration of Cl^- (b) 1.0M concentration of Cl^-

Figure 3. Influences of other ions and pH value on potentiometric response of the sensor to chloride.

3.3 Potentiometric Response of the Sensor Embedded in Concrete

Figure 4 presents the potential of the sensor embedded in concrete specimen and the measured chloride ion concentrention of pore soluiton at different ages. It can be found that the potential value increased with the increasing water to cement ratio, indicating the decreased chloride ion concentration. This is consisitent with the chloride ion test results as shown in Fig. 4 (b)，being attributable to the same additon of NaCl for each concrete and the more free water existing in the higher w/c concrete. The potential of the sensor in every concrete decreased with time to one minumum value at 5-8 days, and then increased with the further increasing curing time. The same development tendency was found for the chloride concentration measurement as shown in Fig. 4 (b). This result was caused by simultaneously occurring free water consumption induced by the cement hydration and the binding of chlorides in cement matrice resulting from the formation of Friedel's salt [Dhir *et al*. 1996]. The free water consumption dominates at the beginning then decreases over time, the binding of chlorides decreases steadily with time. There is a good linear relationship between the potential value and the chloride activity for every concrete sample as show in Fig. 5. The sensors in concrete specimens revealed reasonable stability for the duration of the experiment. Nevertheless, the question of the lifetime of the sensor requires further testing.

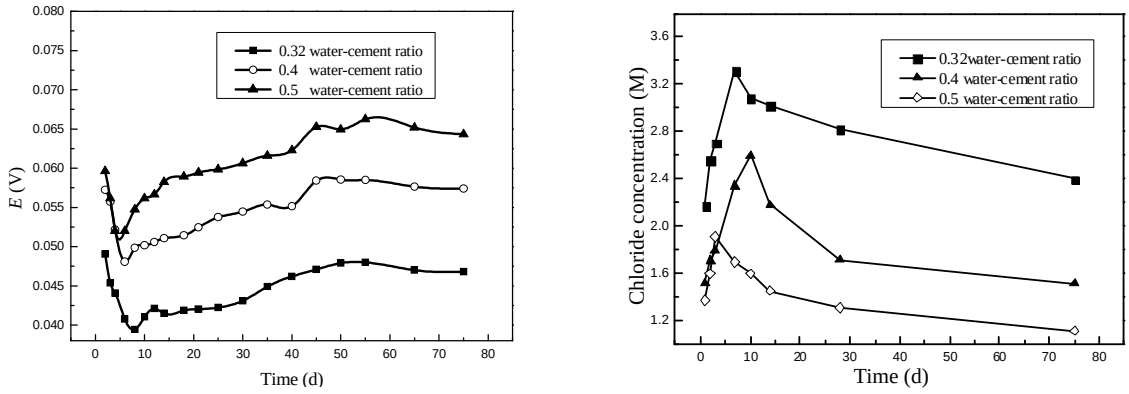

(a) Sensor potential reading (b) Chloride concentration

Figure 4. The sensor potential and chloride concentraiton development in concrete with time.

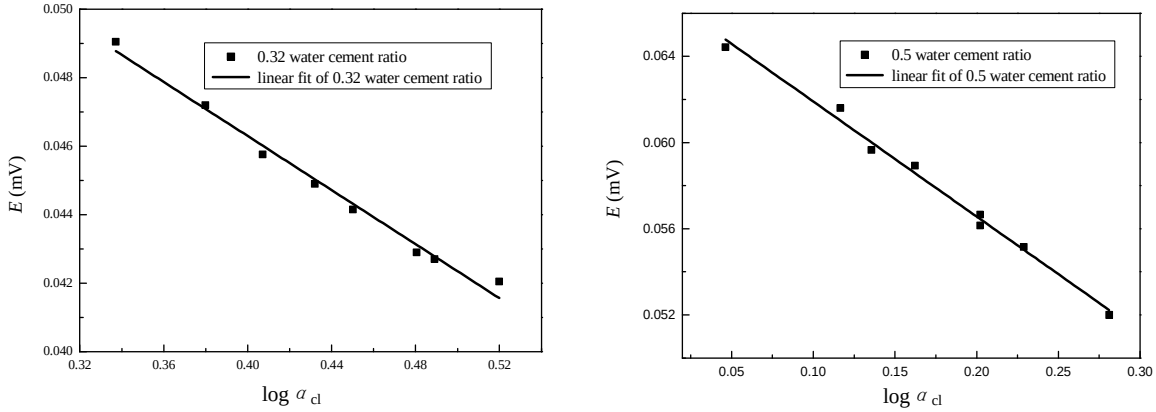

(a) w/c=0.32 (b) w/c=0.5

Figure 5. Relationship between the sensor potential and chloride activity in concrete.

4 CONCLUSIONS

1) One kind of all-solid-state chloride sensor was fabricated using a MnO_2 electrode and a Ag/AgCl electrode, and a good linear relationship exists between the potential reading of the sensor and the logarithm of chloride ion activity (0.05~5.0 M) in high-alkaline simulated concrete pore solutions.

2) The existence of K^+, Ca^{2+}, Na^+, SO_4^{2-} ions influences very little the potentiometric response of the sensor to chloride, indicating that such developed sensors have great potential to be applied in different concrete environments.

3) The sensor shows a very stable performance when being embedded in real concrete samples, showing a linear potential-chloride activity relationship as found in solution test. Therefore, it is recommended that this chloride sensor can be possiblly used for in situ monitoring the chloride-induced durability of concrete structures.

ACKNOWLEDGMENTS

This work is funded by the National Natural Science Foundation of China (No. 50878086).

REFERENCES

Kassir, M.K. & Ghosn, M. 2002, 'Chloride-induced corrosion of reinforced concrete bridge decks', *Cement and Concrete Research,* **32**[1], 139–143.

Rasheeduzzafar, Hussain, S.E. & Al-Saadoun, S.S. 1991, 'Effect of cement composition on chloride binding and corrosion of reinforcing steel in concrete', *Cement and Concrete Research,* **21**[5], 777–794.

Cáseres, L., Sagüés, A.A., Kranc, S.C. & Weyers, R.E. 2006, 'In situ leaching method for determination of chloride in concrete pore water', *Cement and Concrete Research,* **36**[3], 492–503.

Anstice, D.J., Page, C.L. & Page, M.M. 2005, 'The pore solution phase of carbonated cement pastes', *Cement and Concrete Research,* **35**[2], 377–383.

Valdés-Ramíreza, G., Álvarez-Romero, G.A., Galán-Vidal, C.A., Hernández-Rodríguez, P.R. & Ramírez-Silva, M.T. 2005, 'Composites: a novel alternative to construct solid state Ag/AgCl reference electrodes', *Sensors and Actuators B: Chemical,* **110**[2], 264–270.

Miguel, A.C., Estanislao, V.P. & Ma, L.A. 1996, 'Embeddable Ag/AgCl sensors for in-situ monitoring chloride contents in concrete', *Cement and Concrete Research,* **26**[8], 1157–1161.

Montemor, M.F., Alves, J.H., Simões, A.M., Fernandes, J.C.S., Lourenço, Z., Costa, A.J.S., Appleton, A.J. & Ferreira, M.G.S. 2006, 'Multiprobe chloride sensor for in situ monitoring of reinforced concrete structures', *Cement and Concrete Composites,* **28**[3], 233–236.

Junsomboon, J. & Jakmunee, J. 2008, 'Determination of chloride in admixtures and aggregates for cement by a simple flow injection potentiometric system', *Talanta,* **76**[2], 365–368.

Muralidharan, S., Ha, T.H., Bae, J.H., Ha Y.C., Lee, H.G., Park, K.W. & Kim, D.K. 2006, 'Electrochemical studies on the solid embeddable reference sensors for corrosion monitoring in concrete structure', *Materials Letters,* **60**[5], 651–655.

Muralidharan, S., Saraswathy, V., Thangavel, K. & Palaniswamy, N. 2008, 'Evaluation of embeddable potential sensor for corrosion monitoring in concrete structures', *Electrochimica Acta,* **53**[24], 7248–7254.

Vera, G., Hidalgo, A., Climent, M.A., Andrade, C. & Alonso, C. 2000, 'Chloride ion activities in synthetic concrete pore solutions: effect of the accompanying ions', *Journal of the American Ceramic Society,* **83**[3], 640–644.

Duffo, G.S., Farina, S.B. & Giordano, C.M. 2009, 'Characterization of solid embeddable reference electrodes for corrosion monitoring in reinforced concrete structures', *Electrochimica Acta,* **54**[3], 1010–1020.

Elsener, B., Zimmermann, L. & Bohni, H. 2003, 'Nondestructive determination of the free chloride content in cement based materials', *Materials and Corrosion*, **54**[6], 440–446.

Chang, C.F. & Chen, J.W. 2006, 'The experimental investigation of concrete carbonation depth', *Cement and Concrete Research,* **36**[9], 1760–1767.

Dhir, R.K., El-Mohr, M.A.K. & Dyer, T.D. 1996, ' Chloride binding in GGBS concrete', *Cement and Concrete Research,* **26**[2], 1767–1773.

XII DBMC
International Conference on Durability of Building Materials and Components
PORTO - PORTUGAL, April 12th-15th, 2011

Durability Assessment at Advanced Age of Public Rental Buildings in Hong Kong

H. W. Pang [1]
C. O. Chan [2]
W. B Chan [3]

ABSTRACT

The Hong Kong Housing Authority (HKHA) maintains some 700,000 public rental flats in over 1000 buildings and is keen to know whether some of the old buildings are becoming no more cost-effective to keep, or whether it would be more cost-effective to demolish these buildings and build new ones. Although various service life prediction models have been developed, it is proposed in this paper that direct knowledge of the degradation conditions and corrosion rate measurements can be employed to project the future performance of different categories of building components of the building, the time when the threshold will be reached, and the repair required. This paper outlines the 5-parameter probabilistic approach proposed for service life prediction and gives illustrative examples. The unique conditions in each and every flat will require a well-structured regular inspection and repair strategy to ensure that the buildings can be sustained for their residual service life.

KEYWORDS

Service life, Corrosion rate, Maintenance, Structural investigation.

[1] Estate Management Division, Hong Kong Housing Authority, Hong Kong, China, hw.pang@housingauthority.gov.hk
[2] Estate Management Division, Hong Kong Housing Authority ,Hong Kong, China, co.chan@housingauthority.gov.hk
[3] Estate Management Division, Hong Kong Housing Authority ,Hong Kong, China, *wb.chan@housingauthority.gov.hk*

1 INTRODUCTION

The Hong Kong Housing Authority (HKHA) maintains some 700,000 public rental flats in over 1000 buildings, a stock which has gradually built up over the past half a century. The HKHA is keen to know whether some of the old buildings are becoming no more cost-effective to keep, or whether it would be more cost-effective to demolish these buildings and build new ones. As redevelopment is a long process, such knowledge has to be acquired in good time. Service life prediction models which are based on a multitude of factors applied to a basic value or equation for the service life of the building, such as the factor method proposed in ISO 15686 Part1 [2000] and Part 2 [2001], and the Engineering Design Method as contained in CIB Report: Publication 294 by Moser [2004] throw light on what can be done to acquire such knowledge. However, it is proposed that direct knowledge of the degradation conditions and corrosion rate measurements can be employed to project the future performance of different categories of building components of the building, the time when the threshold will be reached, and the repair required. Such durability assessment involves the analysis of 5 sets of measured data – namely carbonation depth, chloride content, concrete cover, steel area loss and corrosion rate measurements. This paper outlines the method and gives illustrative examples. The method is developed primarily for HKHA's aged buildings only and appropriate modifications and adaptations are required for other applications.

2 DURABILITY ASSESSMENT OF HKHA AGED BUILDINGS - METHODOLOGY

Durability assessment of an existing building requires knowledge on the current conditions as well as the estimated rate of deterioration of it. As part of its maintenance strategy the HKHA carried out comprehensive structural investigation on all her public rental buildings of age around 40 years since 2005. The purpose is to ascertain their structural conditions and to provide necessary information to enable the HKHA to decide if these aged buildings can be sustained for another 15 years or if demolition would have to be considered. The investigations have generated large amount information relating to the existing structural conditions of the buildings, such as carbonation depth, chloride content and steel area loss. Inspection and testing are however mainly carried out in public area and limited number of vacant flats to minimize disturbance to tenants. Investigation is further affected by past repairs and presence of finishes and furniture. In recent years, corrosion rate measurements have been made in a number of these aged buildings. Based on these information, an attempt to conduct a durability assessment was made on HKHA's aged buildings in four estates, which was described in the following paragraphs.

The investigation methodology is tailored made to suit the specific conditions of HKHA's building stock as detailed in Pang et al. [2008]. The five-stage approach for the investigation adopted and the typical rates for some routine tests are shown in Fig. 1 and Table 1 below.

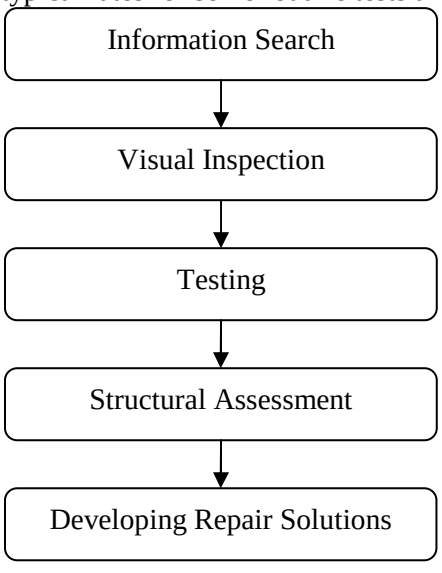

Figure 1. Flowchart for the methodology.

Table 1. Typical testing rates.

Type of Test	Items of test	Testing rate
Concrete Core Compression	Concrete strength Void inside concrete	1 per $50m^3$
Opening up, Reinforcement Survey and Carbonation Front	Concrete cover Screed thickness Size of steel bar Carbonation depth	1 per $25m^3$
Chloride Content	Chloride ion content as percentage of cement content	1 per $150m^3$

Tests were mainly conducted in common areas and vacant flats and include opening up and reinforcement survey, concrete core compression test, chloride content and profile tests, carbonation front measurement and moisture meter measurement. Presence of large number of structural elements and vast difference in usage in a building also make it nearly impossible to inspect and test all elements. Thus, a representative sampling approach has been used in the investigation. This is further supported by adopting method of grouping and categorization of elements of similar properties or deterioration performance.

As for the methodology for the durability assessment, the following 5-step approach is adopted:

- Categorization of elements of different performance based on the 5 sets of measured data on chloride content, carbonation depth, concrete cover, steel area loss and corrosion rates;
- Plotting the Cumulative Frequency Curves of the steel area loss for the vertical elements and estimating the reserved capacity of the elements;
- Predicting the residual life of building at 90% probability based on the measured corrosion rates and the allowable steel area loss;
- Plotting the Cumulative Frequency Curves of the steel area loss for the horizontal elements; and
- Estimating the amount of future repair required at 90% probability based on the measured corrosion rates and the allowable steel area loss.

3 RESULTS AND DISCUSSIONS

3.1 Conditions of HKHA Aged Buildings

The four estates are typical aged HKHA estates containing 5 to 12 reinforced concrete buildings of 7 to 25 storeys high basically of slabs and walls construction. Concrete grade 20 was used for all these buildings. Their ages ranges from 34 to 48 years and have all undergone the comprehensive structural investigation. The large volume of test data enables the current structural conditions of the buildings in these four estates be determined. Because of difference in performance between various elements in a building, the test data are grouped under different elements. A summary of the more important parameters reflecting the current conditions are list in Table 2 below. It shows the mean and standard deviation of the measured level of chloride content, carbonation depth, concrete cover and steel area loss of these four estates. Steel area loss is the maximum loss of sectional area of the steel bars exposed in concrete open-ups typically 300mm by 150mm in size.

A number of observations can be made from these information on the conditions of these four estates. Firstly, performance between these estates varies such as the mean chloride level at the toilet slabs can be as low as 0.2% in one estate but can be as high as 0.56% in the other. Variation of performance between elements within an estate is also significant, for example, steel area loss in Estate A ranges from 13% to 27 % amongst different elements. Even within the same element, the large standard deviation of measured results also indicates a significant variation of performance of the same type of elements in the same estate. Secondly, it is obvious that slabs and walls behaved remarkably differently. Slab bars have much smaller concrete covers, carbonation fronts have gone pass the steel bars, and steel area losses are much more significant. Walls, on the other hand, have larger designed cover and carbonation fronts in a large portion of them have not yet reached the steel bars. Thirdly, steel area loss in toilet and balcony slabs are generally larger than that for walls.

Table 2. Summary of mean and standard deviation (SD) of levels of chloride content, carbonation depth, concrete cover and steel area loss of four estates**.**

Estate	Weight of Chloride ions expressed as % of Cement Content							
	Toilet Slab		Balcony Slab		Living Room Slab		Wall	
	Mean	SD	Mean	SD	Mean	SD	Mean	SD
A	0.54	0.72	0.15	0.26	0.07	0.03	0.16	0.22
B	0.20	0.22	0.12	0.09	0.08	0.04	0.10	0.10
C	0.56	0.40	NA	NA	0.46	0.24	0.34	0.23
D	0.43	0.45	0.28	0.26	0.25	0.16	0.20	0.10
Estate	Carbonation (mm)							
	Toilet Slab		Balcony Slab		Living Room Slab		Wall	
	Mean	SD	Mean	SD	Mean	SD	Mean	SD
A	29	16.02	38	15.46	43	12.07	41	21.22
B	25	16.07	32	14.68	37	9.96	38	23.73
C	NA	NA	NA	NA	NA	NA	NA	NA
D	19	14.45	22	16.42	20	13.33	26	19.59
Estate	Cover (mm)							
	Toilet Slab		Balcony Slab		Living Room Slab		Wall	
	Mean	SD	Mean	SD	Mean	SD	Mean	SD
A	21	6.55	22	7.05	21	6.77	45	9.21
B	17	5.81	19	6.51	20	10.79	41	10.36
C	22	7.07	19	8.23	19	12.68	32	10.56
D	21	9.75	19	8.70	18	10.84	35	8.59
Estate	Steel Area Loss (%)							
	Toilet Slab		Balcony Slab		Living Room Slab		Wall	
	Mean	SD	Mean	SD	Mean	SD	Mean	SD
A	27	19.48	18	5.68	15	6.29	13	6.32
B	17	9.45	15	6.90	13	5.37	13	5.83
C	11	9.63	6	3.83	6	4.15	8	8.88
D	24	22.88	15	12.01	14	8.58	12	7.15

3.2 Corrosion Rate Measurements

Corrosion of reinforcing bars is an electro-chemical process, by which the iron atoms of the reinforcement are chemically combined with oxygen to form oxides (rust) and release out in the process free electrons into the surrounding concrete generating a local circuit. Making quantitative measurement of the electric current intensity so induced can theoretically tell the corrosion rate and hence, by Faraday's Law, the loss rate of the reinforcing bar diameter. A reliable measurement of the corrosion rate can therefore give a good projection of the building residual life. In this aspect, extensive corrosion rate measurements have been carried out in the existing buildings with the application of GECOR, a corrosion rate meter making use the relation between current and concrete resistivity along with linear polarization technique for corrosion rate measurements of reinforcing bars in concrete. The application of GECOR was studied under the US National Research Council Strategic Highway Research Program [1993] and the report was favourable.

It is widely believed that the rate of corrosion is significantly influenced by the level of moisture, chloride, carbonation in the concrete. And the development of these is to a considerable extent influenced by how the area is used and the locations of the relevant concrete members. For example, toilet floor slabs always have a comparatively higher level of moisture as well as chloride content probably originating from daily showering water and even from leakage of salt flushing water. To make the corrosion rate study comprehensive and representing, so far over 800 GECOR measurements have been carried out in six public rental estates, covering 36 buildings from which the corrosion rate measurements were sampled in different categorized areas including slabs and walls in toilets, balconies, living rooms and public areas of both lying indoor and exposing to weather. The relevant field measurement exercise is still undergoing to extend further the tested estates coverage. Line charts were plotted at Fig. 2 below illustrating the wide variation in the corrosion rate measured in different elements in the 4 estates.

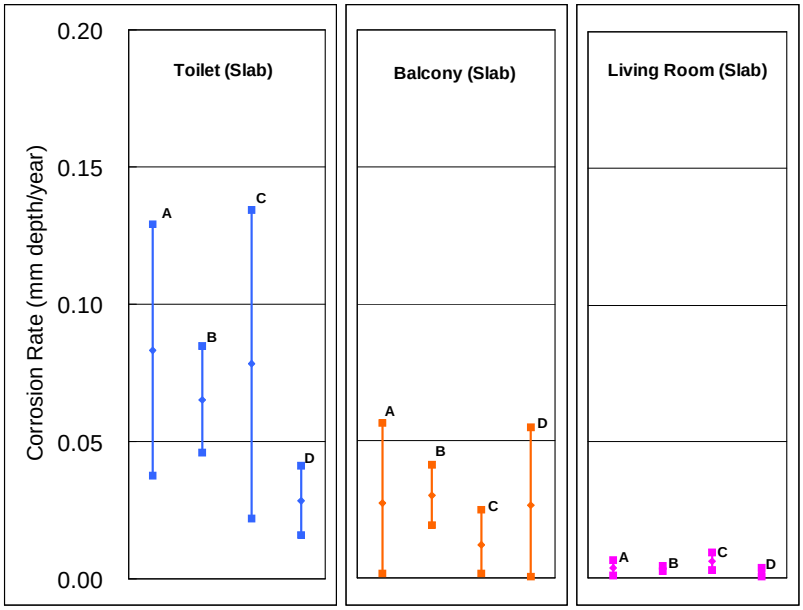

Figure 2. Corrosion rates based on corrosion current measurements.

3.3 Analysis of the Corrosion Rate Measurements

The cumulative frequency curves for the corrosion rate measured in the four estates were plotted. Fig. 3 below shows the results that were plotted on estate basis. It can be seen that the distribution of the corrosion rates in each estate differs. Take for example, at 80 percentile, the corrosion rate for the four estates ranges from 0.017 mm/year in Estate D to 0.053 mm/year in Estate B. Obviously, it can be predicted that Estate D would have a much better future performance than Estate B.

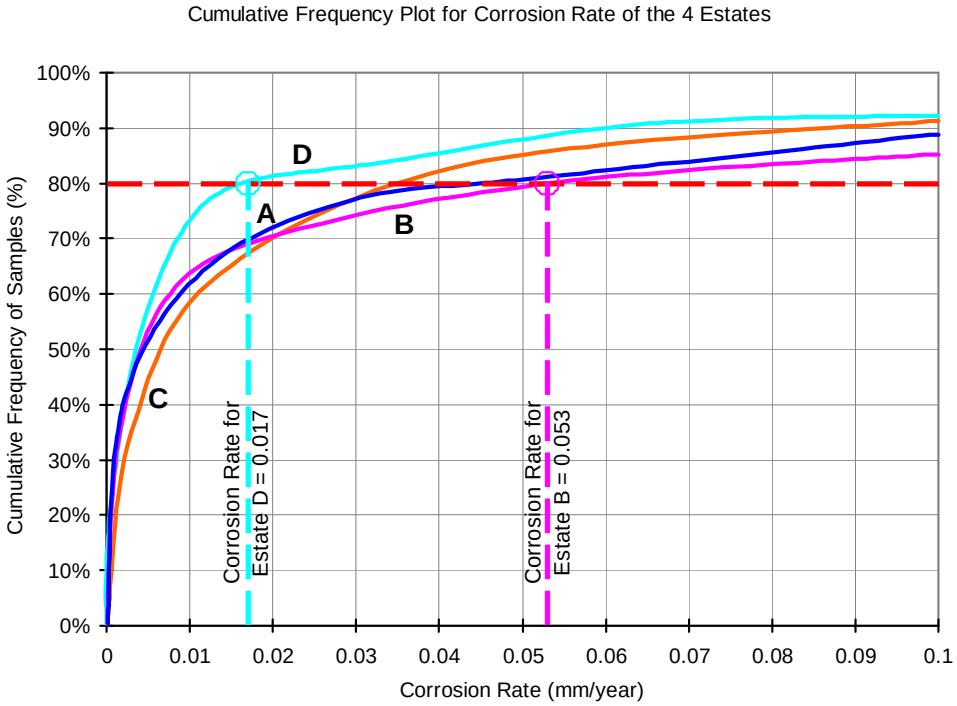

Figure 3. Cumulative frequency curves for the corrosion rate measured in the four estates.

The results were then grouped into elements of different performance. For this study, toilet slabs, balcony slabs, living room slabs and walls were selected and cumulative frequency curve for each of these elements were plotted and shown in Fig. 4 below. It can be seen that similar levels of variation

in performance are apparent. Being under relatively inferior design and environmental ambients as reported by Pang et al. [2008], the condition of the toilet slab is poorer than that of other elements. Take a corrosion rate of 0.075 mm/year as an example, only about 63% the toilet slabs would have corrosion rate less than this figure. Whereas, nearly all walls and living room slabs are with rates less than the same figure. It can therefore be predicted that the future performance of the toilet slabs will be the poorest whilst the wall is the best.

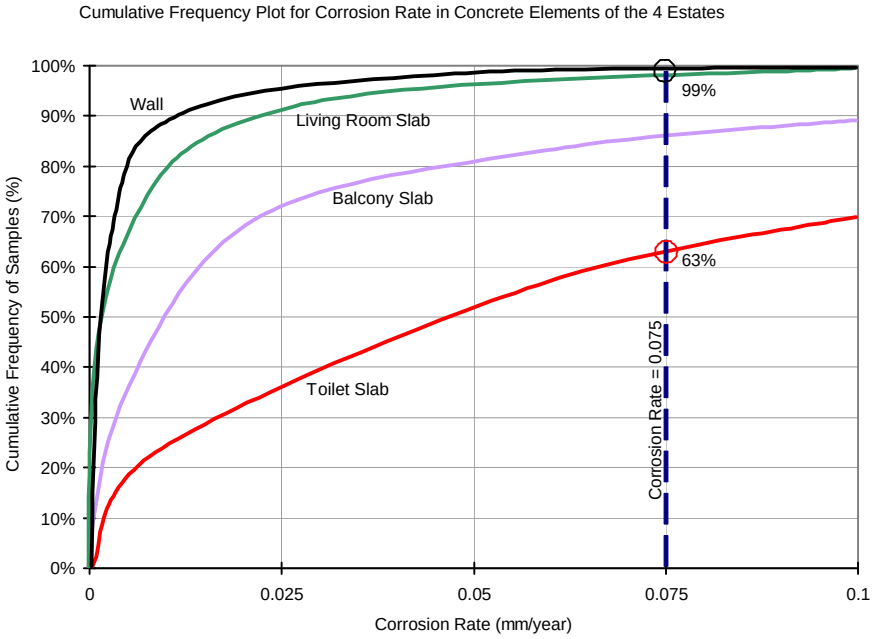

Figure 4. Cumulative frequency curves for the corrosion rate measured in concrete elements of the four estates.

4 DURABILITY ASSESSMENT

A durability assessment can provide good information to answer the question of when the owner would decide not to keep the building. For HKHA, the current strategy is not to demolish the aged buildings unless they are structurally unsafe or beyond economical repair. Whilst global structural safety of a building would hinge on the performance of its major load bearing elements, which are mainly load bearing shearwalls in HKHA's buildings, floor slabs, which are replaceable during their lifetime and do not affect the global safety, may attract the major portion of maintenance costs. Walls are usually covered by finishes and furniture and are difficult to inspect and repair. On the other hand, floor slab ceilings are normally exposed without any finishes and are easy to inspect and repair. Therefore in this study, separate assessments are made on walls, focusing on the safety aspect and on floor slabs, focusing on predicting the future maintenance costs.

4.1 Assessment of Walls

The cumulative frequency curves for the steel area loss in walls of the four estates were first plotted. From the comprehensive investigation results, the reserve in the walls capacity can be determined and based on the corrosion rate measured in walls of these estates, the likely residual period of time before the steel corrosion reach a state that inadequate reserve is available can then be predicted. Take for example of Estate D, cumulative frequency curves for the steel area loss at 10 years interval from now were plotted as shown in Figure 5 below by applying a corrosion rate at 90% taken from the cumulative frequency plot of corrosion rates as a prudent approach. Assuming an allowable steel area loss of about 30%, the period of time before steel corrosion will affect the global safety is found to be about 50 years at 90% probability as shown.

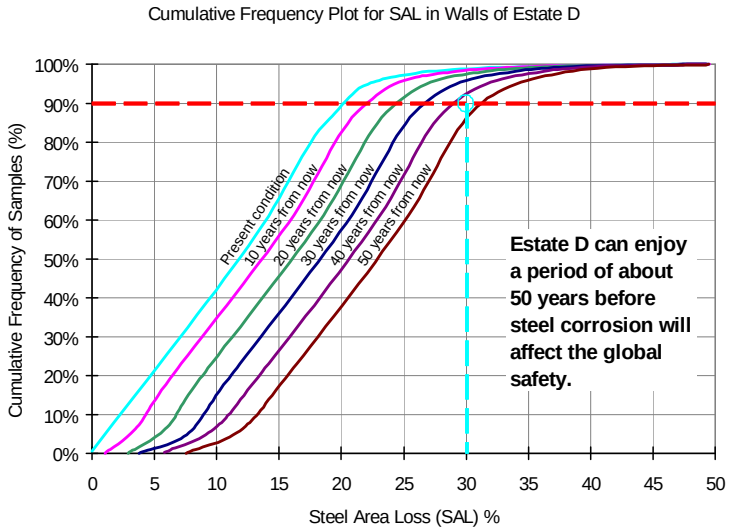

Figure 5. Cumulative frequency curves for the SAL in walls of the Estate D.

4.2 Assessment of Slabs

In assessment the floor slabs, one of the estates, Estate C, was selected for illustration. Cumulative frequency curves for each of the three types of slab elements, toilet, balcony and living room, were plotted and shown in Fig. 6 below. Different from walls, serviceability is more important for slabs. Concrete spalling and water seepage will cause unacceptable nuisance to the tenants who will demand for repair. Therefore based on the mean corrosion rate measured in slabs, cumulative frequency curves for the existing steel area loss, and assuming a maximum tolerable steel area loss, we can estimate the occurrence probability for the slabs to fail in serviceability in the coming certain period of time, say the next 15 years. The mean corrosion rate used as the serviceability threshold is fixed at 15% steel area loss, which normally trigger spalling repair. With this, the proportion of these elements that do not meet this condition at 90% probability can be estimated from these curves. This group of element will require repair to maintain their performance and hence the cost. The time period will depend on the owner's requirement in consideration of disturbance to tenants allowed and budget available.

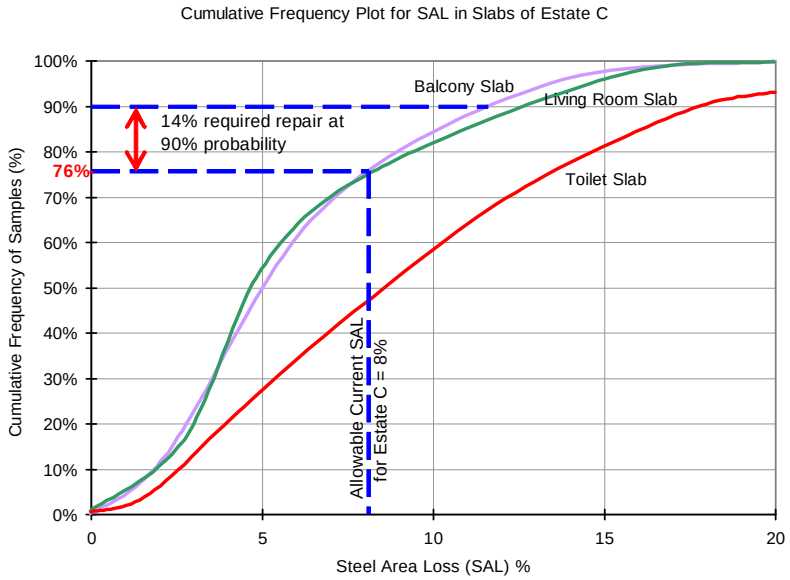

Figure 6. Cumulative frequency curves for the SAL in slabs of Estate C.

In this Estate C, taking balcony slabs as an example, current steel area loss is of 8% will give rise to serviceability failure at 15 years. From the curve, it can be found that 76% will meet the required serviceability requirement for the assumed period of time. To enable at least 90% of the slabs meet the serviceability requirements, the amount of slabs requiring repair is estimated to be 14% as shown on the curve. This figure forms a very good basis for estimating the repair costs required. This type of estimation requires the development of appropriate repair method and costing of various trades of works and is outside the scope of this paper, which will be discussed separately.

4.3 Discussions

The above analysis illustrates that the 5 sets of measured date provide a good basis for categorization of elements of different performance. Different behaviour between slabs and walls can be attributable to being subject to different concrete covers, finishes as well as environmental effects. These data also enable a prediction of the future performance of these elements. Depending on their future performance, the choice of repair solutions and easiness of repair, a cost-effective and appropriate repair and inspection strategy can be developed to suit different elements in the buildings.

5 CONCLUSION

A 5-parameter approach is proposed for service life prediction, which is a probabilistic approach involving categorization of elements to take care of their difference in performance. During the course of the work, significant difference in performance was observed between flats, probably due to flats being subject to difference in occupancy, usage and level of maintenance. Such unique conditions in each and every flat will require a well-structured and regular inspection and repair strategy to ensure that the buildings can be sustained for their residual service life.

REFERENCES

ISO 15686-1:2000, *Buildings and Constructed Assets- Service life planning- Part 1: General principles*, International Standards Organisation.

ISO 15686-2:2001, *Buildings and Constructed Assets- Service life planning- Part 2: Service life prediction procedures*, International Standards Organisation.

Moser, K., *Task Group Performance Based Methods for Service Life Prediction - State of the Art Reports - Part B: Engineering Design Methods for service life prediction*, CIB Report: Publication 294, 2004.

Pang H. W. and Chan C. O. 2008, 'Structural Investigation of Hong Kong's ageing public rental buildings', *Creating and Renewing Urban Structures, 17th Congress of IABSE,* Chicago 2008, pp. 168 – 169.

US National Research Council Strategic Highway Research Program Report: *Condition Evaluation of concrete bridges relative to reinforcement corrosion, Volume 2: method for measuring the corrosion rate of reinforcing steel*, Washington, DC, US 1993.

XII DBMC
International Conference on Durability of Building Materials and Components
PORTO - PORTUGAL, April 12th-15th, 2011

The Effect of Ground Limestone Addition on Carbonation and Chloride Resistance of Concrete

Luca Bertolini [1]
Federica Lollini [2]
Elena Redaelli [3]

ABSTRACT

In Italy, as in many other European countries, a growing diffusion of limestone cements has been observed in the recent years. Several studies were carried out since the late 1970s in order to evaluate the role of limestone in the hydration reactions of the clinker and the effect of limestone on concrete performance, in terms of mechanical properties and durability. Although the knowledge level has continuously extended, there is a partial disagreement on some topics, especially related to the durability issues. In particular the available information on the contribution of limestone to the resistance to chloride and carbonation penetration are limited and controversial. This paper presents a study aimed at the evaluation of the effects of the partial replacement of portland clinker with ground limestone, as a function of the water/cement ratio and the cement content. In particular hardened concrete was characterised by means of measurements of compressive strength, electrical resistivity and resistance to chloride and carbonation penetration. Results showed that both mechanical properties and resistance to penetration of aggressive agents, i.e. of carbonation and chloride, decreased by increasing the limestone content.

KEYWORDS

Ground limestone, Chloride, Carbonation, Reinforced concrete.

[1] Dipartimento di Chimica, Materiali e Ingegneria Chimica, Politecnico di Milano, Milano, ITALY, luca.bertolini@polimi.it
[2] Dipartimento di Chimica, Materiali e Ingegneria Chimica, Politecnico di Milano, Milano, ITALY, federica.lollini@polimi.it
[3] Dipartimento di Chimica, Materiali e Ingegneria Chimica, Politecnico di Milano, Milano, ITALY, elena.redaelli@polimi.it

1 INTRODUCTION

Recently an increase in the use of limestone cements has been observed in Italy as well as in many other European countries. Limestone cement is obtained by replacing portland clinker with ground limestone (up to 35% in accordance with the standard EN 197-1).
Due to the increment of limestone cement production and of its utilization, several studies were carried out since the late 1970s in order to evaluate the participation of limestone to the hydration reactions of the clinker and the effect of limestone on concrete performances, related to mechanical properties and resistance to penetration of aggressive agents [Dhir *et al.* 2007, Hornain *et al.* 1995, Liversey 1991, Matthews 1994, Tsivilis *et al.* 2002, Zelić *et al.* 2000]. Regarding the carbonation resistance, according to Tsivilis *et al.* [2002] after 1 year of exposure lower carbonation depths were measured in portland limestone concrete with limestone content up to 35% compared to portland cement, while for Dhir *et al.* [2007] for cement with up to 15% of limestone there was no significant influence on carbonation resistance, while higher limestone content showed a lower resistance to carbonation. As far as the resistance to chloride penetration is concerned, some authors reported that the addition of limestone filler reduces the diffusion coefficient of chloride ions, due to the filler effect of limestone [Hornain *et al.* 1995], whilst other authors reported that differences in diffusion coefficient, measured by means of an accelerated test, of concrete with up to 15% of limestone substitution, were relatively minor and they increased slightly with water/cement ratio compared to OPC concrete [Dhir *et al.* 2007]. Hence, although the knowledge level has continuously extended, the available information on limestone contribution to the resistance to chloride and carbonation penetration are limited and controversial.
This paper presents a study aimed at the evaluation of the effect of ground limestone, as a function of water/cement ratio, cement content and curing time, on various performances of the hardened concrete (e.g. compressive strength, carbonation rate and chloride diffusion coefficient evaluated by means of accelerated tests).

2 EXPERIMENTAL PROCEDURES

In order to investigate the effects of the partial replacement of portland cement with ground limestone on performances of hardened concrete, different types of concrete were cast. A portland cement CEM I 52.5R (OPC), according to EN 197-1 standard, was used for the reference concrete mix. Part of this cement was replaced with 15% (15%LI) and 30% (30%LI) of ground limestone, in order to simulate cements CEM II/A-L and CEM II/B-L. The particle size analysis of both OPC and limestone is given in Figure 1. Each type of binder (OPC, 15%LI and 30%LI) was used to produce concrete with three different water/binder ratios (*w/b*), equal to 0.42, 0.46 and 0.61, and different binder dosages (*b*), ranging from 250 kg/m^3 to 400 kg/m^3.

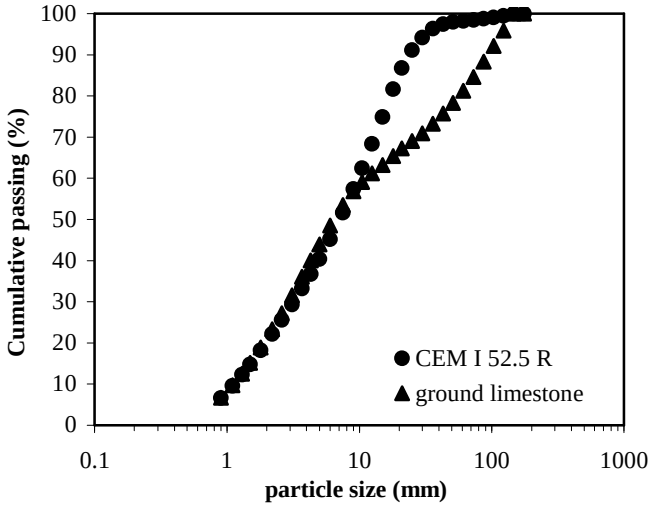

Figure 1. Grain size analysis of OPC and cement limestone.

Crushed limestone aggregates with maximum size of 16 mm were used, and an acrylic superplasticiser was added to the mixes in order to achieve a class of consistence *S4* according to EN 206-1 standard, i.e. a slump of 160-200 mm. Table 1 summarizes the concrete mixes.
After the mixing, concretes were cast into moulds with different shapes, covered with a plastic sheet and stored in laboratory at 20°C for 24 h, until demoulding. 100 mm cubes were cured at 20°C and 95% relative humidity for 7, 28, 90 and 180 days. At the end of the curing, as well as after demoulding, compressive tests were carried out, according to EN 12390-3 standard. Electrical resistivity was measured as a function of time on 50×50×100 mm specimens cured under water. In order to evaluate the resistance to the penetration of carbonation, 100 mm cube specimens were cast and cured 1, 7 and 28 days at T = 20°C and R.H. = 95%. After 28 days from casting specimens were masked with epoxy, so that carbonation was allowed only from two opposite faces, and exposed to an environment with 20°C, 65% R.H. and a constant flux of 2%CO_2 (accelerated carbonation). Carbonation depth was measured with the phenolphthalein test on 20 mm diameter cores, after different times of exposure (i.e. 28 days, approximately 3 and 6 months). Carbonation depths, *d*, measured after different time, *t*, were fitted through the relationship:

$$d = K_{acc} \cdot \sqrt{t} \qquad (1)$$

and the carbonation coefficient K_{acc} was evaluated according to the minimum square methods.
Resistance to penetration of chloride ions was tested on cylindrical specimens, cured 28 days at T = 20°C and R.H. = 95%, by means of the so-called Rapid Chloride Migration (RCM) test, according to NT-BUILT 492 standard [1999]. A plastic tube was mounted coaxially to a 50 mm thick concrete cylinder, and a chloride-free solution was poured inside. The specimen, laid on an inclined plastic support, was placed in a container with a 10% NaCl solution. A potential difference of 30 V was applied, the initial current was measured and, according to its value, the applied voltage was adjusted and the duration of the test determined (6-96 hours). At the end of the test, the specimen was split axially, and on its fracture surface a 0.1 M $AgNO_3$ solution was sprayed. The average chloride penetration depth x_m (m) was measured and the chloride diffusion coefficient D_{RCM} was calculated as:

$$D_{RCM} = \frac{RT}{zFE} \cdot \frac{x_m - \alpha\sqrt{x_m}}{t} \qquad (2)$$

where *R* is the gas constant (J/K mol), *T* the average temperature in the anodic solution (K), *z* the absolute value of charge number (=1), F Faraday's constant (96500 C/mol), *t* time (s); E =(U-2)/L (U is the applied voltage in V, L the thickness of the specimen in m) and α is defined as:

$$\alpha = 2\sqrt{\frac{RT}{zFE}} erf^{-1}\left(1 - \frac{2c_d}{c_0}\right) \qquad (3)$$

where c_d is the concentration at which the colour change is observed (assumed equal to 0.07 N) and c_0 the chloride concentration of the test solution (2 N) [NT-Built 492 1999]. Further details on experimental procedures, concrete compositions and results of other experimental tests are given elsewhere [Bertolini *et al.* 2007 and Bertolini *et al.* 2008].

3. RESULTS AND DISCUSSION

Mechanical properties of hardened concrete were evaluated after different curing times. Table 1 summarizes results of compressive test and electrical resistivity measurements, evaluated as the average value of two replicated specimens, after 28 and 180 days of curing.
Figure 2 shows the influence of partial replacement of portland cement with ground limestone, of water/binder ratio and binder content on compressive strength of specimens cured 28 and 180 days. Regardless of the days of curing, the replacement with 15 and 30% of limestone led to a decrease in the compressive strength. For instance specimens with *w*/*b* 0.61 and cement content of 300 kg/m^3, cured 28 days had a strength that decreased from about 60 MPa when portland cement was used to 45 and 37 MPa when 15% and 30% of cement was replaced with limestone 'Fig 2*a*'. The decrease in the compressive strength of concrete could indicate the inert behaviour of limestone, i.e. limestone does not react and, substantially, acts as a dilution of cement, increasing the effective water/cement ratio.

Table 1. Composition and mechanical properties of the tested concretes (average values of two samples): *w/b* = water/binder ratio; δ = density; R_c = compressive strength and ρ = electrical resistivity.

Series	*w/b*	binder (kg/m^3)	δ (kg/m^3)	R_c (MPa)		ρ (Ω·m)	
Curing[*]			28	28	180	28	180
OPC	0.61	300	2489	59.2	63.1	38	79
	0.46	300	2544	87	94.9	53	153
	0.46	350	2461	70.7	91.5	44	115
	0.42	350	2525	86.6	127.6	52	140
15%LI	0.61	250	2474	54.5	59.8	27	63
	0.61	300	2431	45.2	53.3	29	59
	0.46	300	2571	47.8	83.0	40	92
	0.46	350	2461	67.3	80.4	38	101
	0.42	350	2511	83.3	99.4	40	112
	0.42	400	2470	63.7	94.1	39	101
30%LI	0.61	300	2472	36.7	44.1	27	59
	0.46	300	2492	62	78.3	39	95
	0.46	350	2461	57.4	72.1	36	86
	0.42	350	2490	66.6	79.9	43	103

[*] Days of wet curing at 20°C and 95% R.H.

Moreover it was observed that both water/binder ratio and binder content influenced the compressive strength: not only the water/binder ratio led to the well known decrease in compressive strength, but also a strength decrease was observed when the binder content increased.

Figure 3 shows the effect of limestone on the electrical resistivity measured after 28 and 180 days of curing. The electrical resistivity is an important parameter used to measure the resistance of a material to ion penetration. It is strongly influenced by the moisture content of concrete; nevertheless in a saturated material the effect of the humidity can be avoided thus enabling the resistivity to be related mainly to the microstructure of the material (assuming that the composition of the pore solution does not significantly change in the different concrete).

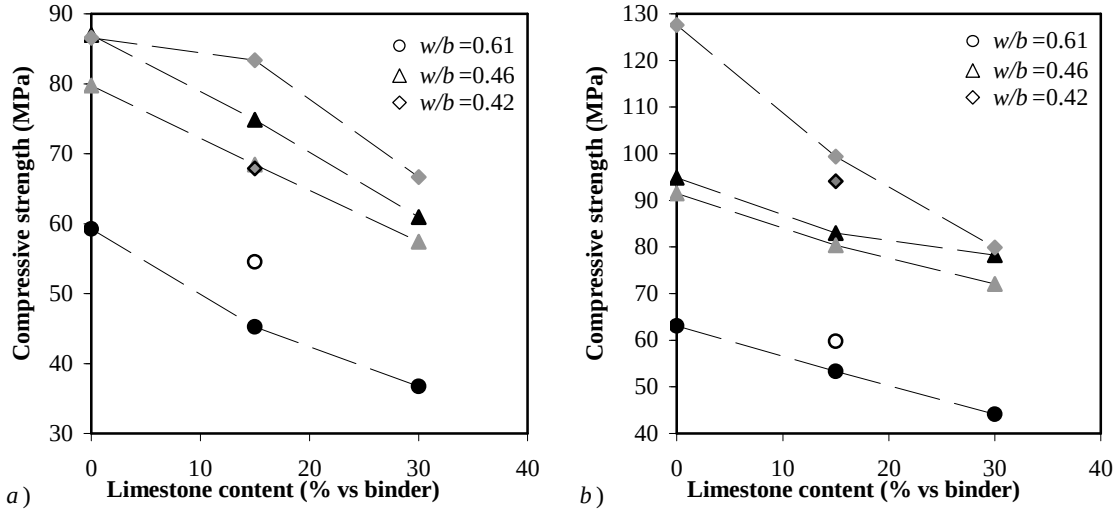

Figure 2. Effect of the partial replacement of portland cement with limestone, of water/binder ratio and binder dosage (white symbols = 250 kg/m^3, black symbols = 300 kg/m^3, grey symbols = 350 kg/m^3 and dark grey symbols = 400 kg/m^3) on compressive strength after 28 (*a*) and 180 (*b*) days of curing.

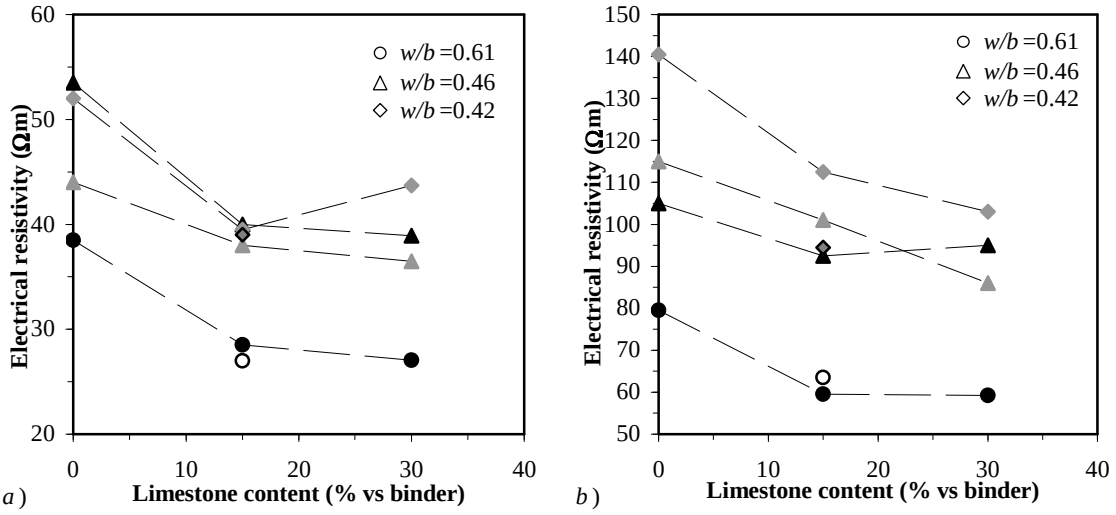

Figure 3. Effect of the partial replacement of portland cement with limestone, of water/binder ratio and binder dosage (white symbols = 250 kg/m^3, black symbols = 300 kg/m^3, grey symbols = 350 kg/m^3 and dark grey symbols = 400 kg/m^3) on electrical resistivity after 28 (*a*) and 180 (*b*) days of curing.

Therefore a concrete electrical resistivity, in a water saturated specimen, is an indirect measure of the concrete porosity and it can be used to follow the evolution in time of the hydration. For each water/binder ratio and curing, the replacement of ground limestone led to a decrease in electrical resistivity of hardened cement paste. For instance, on 28-day cured specimens with water/binder ratio of 0.46 and binder dosage of 350 kg/m^3 electrical resistivities of 53, 40 e 38 Ω·m were measured on portland, 15 and 30% of limestone concrete 'Fig. 3*a*'. The electrical resistivity decrease in saturated concrete with the increase of the limestone percentage shows that, for the same curing time and water/binder ratio, the replacement of portland cement with limestone leads to an increase of the capillary porosity of cement paste.

Table 2. Carbonation coefficient, K_{acc}, from accelerated test and diffusion coefficient, D_{RCM}, from rapid chloride migration test (average value of two replicate samples).

Series	*w/b*	binder (kg/m^3)	$K_{acc,1}$ (mm/year$^{0.5}$)	$K_{acc,7}$ (mm/year$^{0.5}$)	$K_{acc,28}$ (mm/year$^{0.5}$)	D_{RCM} (10^{-12} m^2/s)
Curing			1*	7*	28	28
OPC	0.61	300	30.6	21.2	18.4	12.55
	0.46	300	15.9	12.8	3.9	7.69
	0.46	350	19.2	12.9	4.6	7.75
	0.42	350	-	7.3	-	5.43
15%LI	0.61	250	36.9	29.5	20.5	18.92
	0.61	300	32.2	26.6	22.2	19.81
	0.46	300	17.9	11.8	8.4	15.08
	0.46	350	17.9	12.1	7.8	13.62
	0.42	350	-	11.2	-	11.30
	0.42	400	-	13.6	-	11.42
30%LI	0.61	300	40.4	34.6	27.4	38.27
	0.46	300	29.2	20.7	16.8	18.05
	0.46	350	22.5	23.2	16.1	23.51
	0.42	350	-	12.2	-	13.12

(*)Tests started 28 days after casting (after wet curing specimens were exposed in the laboratory at 20°C and about 65% R.H.).

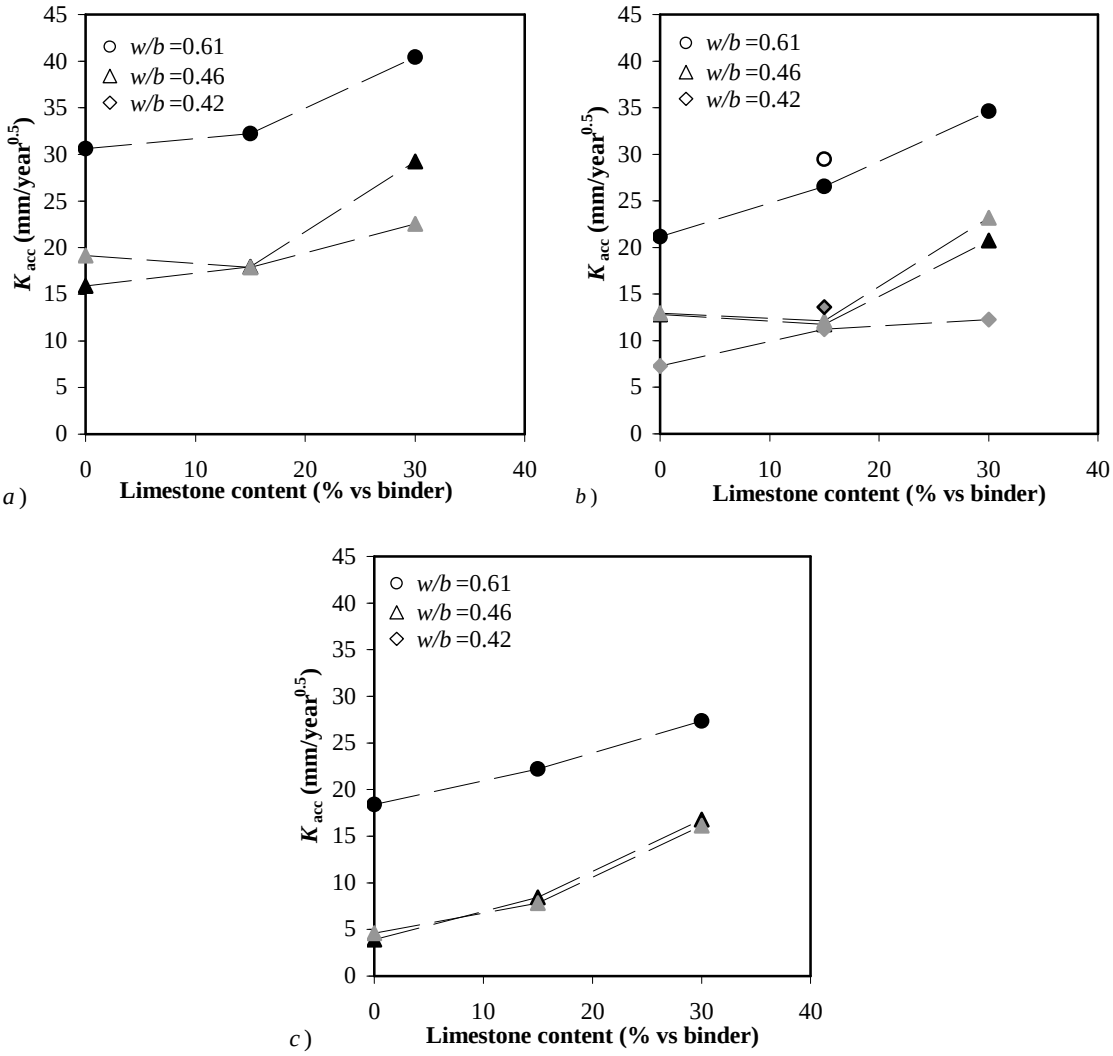

Figure 4. Effect of the partial replacement of portland cement with limestone, of water/binder ratio and binder dosage (white symbols = 250 kg/m^3, black symbols = 300 kg/m^3, grey symbols = 350 kg/m^3 and dark grey symbols = 400 kg/m^3) on accelerated carbonation coefficient, K_{acc}, on specimens cured 1 (*a*), 7 (*b*) and 28 (*c*) days.

The penetration of carbonation was evaluated on specimens exposed under accelerated conditions. After different exposure times the carbonation depth was measured and the carbonation coefficient, K_{acc}, was calculated through the relationship (1) [Table 2]. Figure 4 shows the influence of limestone replacement on carbonation coefficient, K_{acc}, measured on concrete cured 1, 7 and 28 days. When part of portland cement was replaced with 15% of limestone and specimens were cured 1 and 7 days, compared to a porland cement only slight differences in the carbonation coefficient were observed 'Figs 4*a* and 4*b*'. For instance, for 1-day cured concretes with *w/b* = 0.61 and *b* = 300 kg/m^3, the accelerated carbonation coefficient was 30.6 and 32.3 mm/year$^{0.5}$ respectively for OPC and 15% LI. However increasing the curing time up to 28 days OPC concretes performed better than 15% LI since they showed a lower carbonation coefficient, i.e. a higher resistance to the penetration of carbonation 'Fig. 4*c*'. For instance K_{acc} increased from 4 to 8.4 mm/year$^{0.5}$ for 28-day cured concrete with *w/b* = 0.46 and *b* = 300 kg/m^3, when 15% of cement was replaced with limestone. Regardless the curing time, the replacement of part of portland cement with 30% of limestone led to a higher carbonation coefficient, which was more than doubled for 28-day cured specimens. For instance, 7-day cured specimens with *w*/*b* ratio of 0.42 and binder content of 350 kg/m^3 had an accelerated carbonation coefficient that increased from about 7.3 mm/years$^{0.5}$ when portland cement was used to 12.2 mm/years$^{0.5}$ when 30% of cement was replaced with ground limestone.

At any time of curing, a significant influence of the water/binder ratio, whose decrease led to a reduction in the accelerated carbonation coefficient, can be observed, while the binder content did not strongly influence the accelerated carbonation coefficient. Comparing concretes with the same composition at different curing times, a strong decrease in the carbonation coefficient, which led to a more impervious material, can be observed when curing increased from 1 to 7 or 28 days. For instance in concrete with 15% limestone, 350 kg/m^3 of binder and *w*/*b* ratio of 0.46, values of accelerated carbonation coefficient of 17.9, 12.1 and 7.8 mm/year$^{0.5}$ were measured respectively on specimens cured 1, 7 and 28 days.

The resistance to chloride penetration was investigated by means of the Rapid Chloride Migration test on specimens cured 28 days [Table 2]. Figure 5 shows the diffusion coefficient D_{RCM}, calculated through equations 2 and 3, as a function of concrete composition (limestone content, water/binder ratio and binder content). A remarkable influence of the limestone content was observed; with the replacement of 15% of cement with limestone the diffusion coefficient was doubled. For instance specimens with *w/b* ratio of 0.46 and binder content of 300 kg/m^3 had a diffusion coefficient that increased from $7.69 \cdot 10^{-12}$ m^2/s when portland cement was used to $15.08 \cdot 10^{-12}$ m^2/s when 15% of cement was replaced with ground limestone. The D_{RCM} further increased with 30% of limestone and, in this case, a higher sensitivity to the water/binder ratio was observed, which led to a rather high value of D_{RCM} in concrete with *w/b* ratio of 0.61. For instance taking into account a water/binder ratio of 0.42 the diffusion coefficient was $5.43 \cdot 10^{-12}$ and $13.12 \cdot 10^{-12}$ m^2/s respectively for OPC cement and 30% limestone. For any binder the significant role of reducing the *w/b* ratio clearly appears in 'Fig. 5', while the binder content showed a negligible effect. For instance for OPC concrete the diffusion coefficient decreased from $12.55 \cdot 10^{-12}$ to $5.43 \cdot 10^{-12}$ m^2/s, when the water/binder ratio decreased from 0.61 to 0.42.

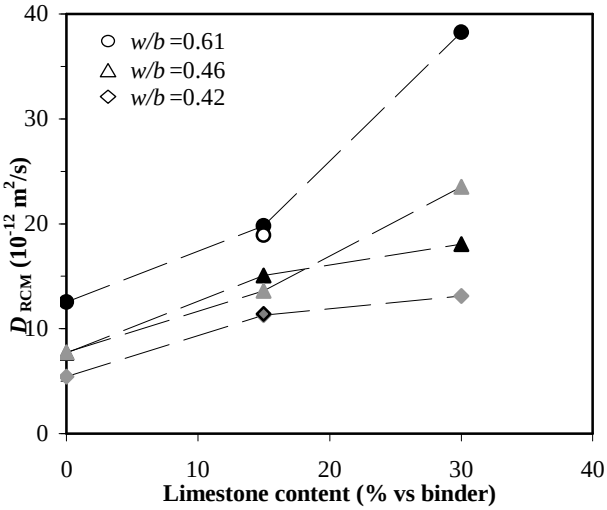

Figure 5. Effect of the partial replacement of portland cement with limestone, of water/binder ratio and binder dosage (white symbols = 250 kg/m^3, black symbols = 300 kg/m^3, grey symbols = 350 kg/m^3 and dark grey symbols = 400 kg/m^3) on the rapid chloride migration coefficient, D_{RCM}, on 28-day cured specimens.

4 CONCLUSIONS

The influence of limestone content as well as other parameters such as water/binder ratio, binder content and curing, on the properties of hardened concrete was studied with particular regard to the resistance to carbonation and chloride penetration, measured by means of accelerated tests. The effect of limestone content was studied by replacing part of the portland cement with 15 and 30% of ground limestone in concretes with different values of water/binder ratio and binder content. Results showed that both compressive strength and electrical resistivity decreased by increasing the limestone content.

The replacement of 15% of limestone only slightly influences the carbonation resistance compared to a portland cement, while increasing the substitution content the resistance to carbonation is drastically reduced.

A remarkable increase in the chloride diffusion coefficient was observed even replacing in concrete with 15% limestone, showing that limestone cements are not suitable in chloride bearing environments.

The beneficial effect related to the decrease in the water/binder ratio and the increase in curing time was estimated and some influence of the dosage of binder was observed in the compressive resistance.

ACKNOWLEDGMENTS

This research was financed by the Italian Ministry of University and Research (MIUR), Holcim Italia S.p.A. and Sismic.

REFERENCES

Bertolini, L., Lollini, F., Redaelli, E. 2007, 'Influence of concrete composition on parameters related to the durability of reinforced concrete structures', Proc. of the International RILEM Workshop: Integral Service Life Modelling of Concrete Structures, Guimarães, Portugal, 5 6 November 2007, pp. 71–78.

Bertolini, L., Lollini, F., Redaelli, E. 2008, 'Concrete composition and service life of reinforced concrete structures exposed to chloride bearing environments', Proc. 1st International Symposium on Life-Cycle civil Engineering, IALCCE'08, Varenna, Italy, pp. 113–118.

Dhir, R.K., Limbachiya, M.C., McCharthy, M.J., Chaipanich, A. 2007, 'Evaluation of Portland limestone cements for use in concrete construction', *Materials and Structures*, **40**[5], 459–473.

Heikal, M., El-Didamony, H., Morsy, M.S. 2000, 'Limestone-filled pozzolanic cement', *Cement and Concrete Research*, **30**[11], 1827–1834.

Hornain, H., Marchand, J., Duhot, V., Regourd, M. 1995, 'Diffusion of chloride ions in limestone filler', *Cement and Concrete Research*, **25**[8], pp. 1667–1678.

Livesey, P. 1991, 'Performances of limestone-filled cements', in: *Blended Cements in Construction*, ed R.N. Swamy, Elsevier, London, pp. 1–15.

Matthews, J.D. 1994, 'Performance of limestone filler cement concrete', in: *Euro-cements, impact of ENV 197 on concrete construction*', eds R.K. Dhir, M.R. Jones, E & FN Spon, London, pp. 113–147.

NT BUILD 492, 1999, 'Concrete, mortar and cement-based repair materials: chloride migration coefficient from non-steady state migration experiment', NORDTEST.

Sersale, K. 1999, 'Advances in portland and blended cement', Proc. 9th International Congress of the Chemistry of Cement, New Delhi, India, vol 1, pp. 109–115.

Tsivilis, S., Chanitakis, E., Kakali, G., Batis, G. 2002, 'An analysis of the properties of Portland limestone cements and concrete', *Cement and Concrete Composities*, **24**[3-4], pp. 371–378.

Zelić, J., Krstulović, R., Tkalčec, E., Krolo, P. 2000, 'The properties of Portland cement-limestone-silica fume mortars', *Cement and Concrete Research*, **30**[1], 145–152.

XII DBMC
International Conference on Durability of Building Materials and Components
PORTO - PORTUGAL, April 12th-15th, 2011

Influence of Mineral Additions on the Chloride Threshold for Rebar Corrosion in Concrete

Luca Bertolini [1]
Federica Lollini [2]
Elena Redaelli [3]

ABSTRACT

The service life of reinforced concrete (RC) structures exposed to chloride bearing environments, related to the exposure to seawater or de-icing salts, is limited by corrosion of steel bars. In order to predict the service life of a RC structure, and especially the initiation time, an accurate estimation of both the chloride penetration in time and the chloride threshold is required. Nevertheless, these parameters are strongly influenced by many factors related to the environment aggressiveness and concrete properties. Several studies were carried out on the penetration of chloride ions as a function of concrete composition, while there is lack of knowledge regarding the chloride threshold. The chloride threshold is not a well defined value, but it is normally indicated as a range of values of chloride content where corrosion initiation is likely to occur. An experimenal research was carried in order to evalute, by means of ponding tests the role of concrete composition and type of binder on the critical chloride threshold. Results showed the high variability of this parameter and the limits of the ponding test in the evaluation of the effect of design parameters on it.

KEYWORDS

Mineral additions, Chloride threshold, Reinforced concrete, Corrosion.

[1] Dipartimento di Chimica, Materiali e Ingegneria Chimica, Politecnico di Milano, Milano, ITALY, luca.bertolini@polimi.it
[2] Dipartimento di Chimica, Materiali e Ingegneria Chimica, Politecnico di Milano, Milano, ITALY, federica.lollini@polimi.it
[3] Dipartimento di Chimica, Materiali e Ingegneria Chimica, Politecnico di Milano, Milano, ITALY, elena.redaelli@polimi.it

1 INTRODUCTION

The service life of reinforced concrete (RC) structures exposed to chloride bearing environments, related to the exposure to seawater or de-icing salts, is limited by the corrosion of steel bars [Bertolini 2008]. Corrosion may have several consequences on the serviceability and safety of reinforced concrete structures, such as cracking, spalling in localized areas, or delamination of concrete. Reduction of bond of the reinforcement to the concrete may also occur. A proper design and execution of such structures allows preventing or delaying the damage of the structure. Nevertheless, for this purpose, reliable tools for the design of service life are needed.

Regarding corrosion of steel, service life is the sum of the initiation time and the propagation time [Tuutti 1982]. The initiation period can be defined as the time required for the chloride to reach a critical threshold at the depth of the outermost steel bars. Once the chloride content has reached the threshold value at the steel surface, the propagation period begins. The propagation period ends when a given limit state is reached beyond which consequences of corrosion cannot be further tolerated and a repair work is needed. This distinction between initiation and propagation periods is useful in the design of RC elements, since different processes and variables should be considered in modelling the two phases [Bertolini 2008].

In the initiation phase several factors, which are summarized in 'Fig 1', are involved. Initiation of corrosion takes place at time t_i when the chloride profile is such that, as shown by the black line in 'Fig 1', a chloride threshold value (Cl_{th}) is reached on the surface of the steel reinforcement, i.e. at a depth equal to the concrete cover thickness.

In order to predict the service life of a RC structure and in particular to model the initiation of corrosion, a reliable estimation of both chloride penetration and the chloride threshold is required. Nevertheless, both parameters are strongly influenced by many factors related to both the aggressive environment and the concrete. Several studies were carried out on the penetration of chloride ions as a function of concrete composition, while there is lack of knowledge regarding the chloride threshold. The main factors affecting the chloride threshold, such as the dependence on the corrosion potential, the pH of the pore solution, the temperature, microstructure and composition of the steel-concrete interface, composition and surface finishing of the steel bar, have been widely investigated and some of them are well known. However a quantification of chloride threshold values for steel in concrete is still rather difficult. First of all, pitting corrosion initiation is a stochastic phenomenon that is influenced by a great number of parameters. Hence the chloride threshold is not a well defined value, but it should be properly defined only through probability distributions that take into account the effect of all the parameters; however, such an approach requires a huge amount of experimental data which is not available in the scientific literature. Usually, for atmospherically exposed structures, the chloride threshold is simply indicated as the range of 0.4-1% by mass of cement, regardless of the composition of concrete.

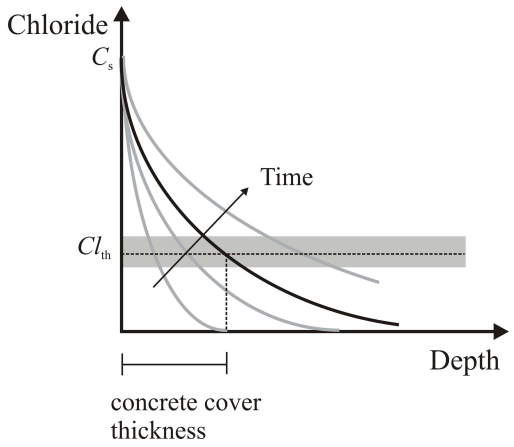

Figure 1. Parameters involved in the initiation of chloride induced corrosion.

However, the wide range of concrete compositions and binders nowadays available would require a more detailed description of the effect of concrete materials and composition on critical chloride threshold.

This paper presents the results of a research study aimed at the evaluation of the role of concrete composition on the chloride threshold. Laboratory tests were carried out to investigate the effect of different additions (fly ash, natural pozzolan, ground granulated blast furnace slag and ground limestone), water/binder ratio, binder content and curing time.

2 EXPERIMENTAL PROCEDURE

In order to investigate the influence of concrete composition (i.e. mineral additions, water/binder ratio, dosage of binder) and curing on the critical chloride threshold, 26 types of concrete were cast. Different types of binder were obtained by modifying, in a cement factory, a portland cement (OPC) with the replacement of different percentages of cement with ground limestone (15%LI and 30%LI), coal fly ash (30%FA), a natural pozzolan (30%PZ), and ground granulated blast furnace slag (70%BF). Water/binder ratios ranging from 0.42 to 0.61 and binder dosages ranging from 250 kg/m^3 to 400 kg/m^3 were considered. More details on concrete composition and characterization with regard to mechanical properties, drying shrinkage and chloride penetration resistance are given elsewhere [Bertolini *et al.* 2008, Bertolini *et al.* 2010]. Reinforced specimens were cast in order to simulate the behaviour of components exposed to the action of seawater and to collect data on the initiation and propagation of corrosion 'Fig 2'. Each specimen had three rebars at different cover depth (i.e. concrete cover thickness was 10, 25 and 40 mm respectively for the upper (*u*), medium (*m*) and lower (*l*) bar) and stainless steel wires were used as electrode for electrochemical measurements. A pond was mounted at the upper surface of the specimen and a 35 g/l chloride solution was poured inside, in order to simulate seawater. The corrosion behaviour of steel was monitored throughout the exposure period by means of electrochemical measurement of half-cell potential of steel (E_{corr}) versus a saturated calomel electrode (SCE) and corrosion current density, measured from linear polarisation resistance measurements (R_p) as: v_{corr} = B/(R_p), where *B* was assumed equal to 26 mV.
When corrosion initiation was detected on any of the three rebars, a sample was cored and the chloride profile was measured by analyzing the total chloride content (acid soluble) at intervals of 10 mm on, at least, 4 layers. The chloride profiles were fitted with the relationship:

$$C(x,t) = C_s\left[1-\mathrm{erf}\left(\frac{x}{2\sqrt{Dt}}\right)\right] \qquad (1)$$

and the apparent diffusion coefficient, *D*, and the surface content, C_s, were calculated. Additional coring for the determination of the chloride profile was carried out after one year of exposure regardless the occurrence of corrosion on bars.

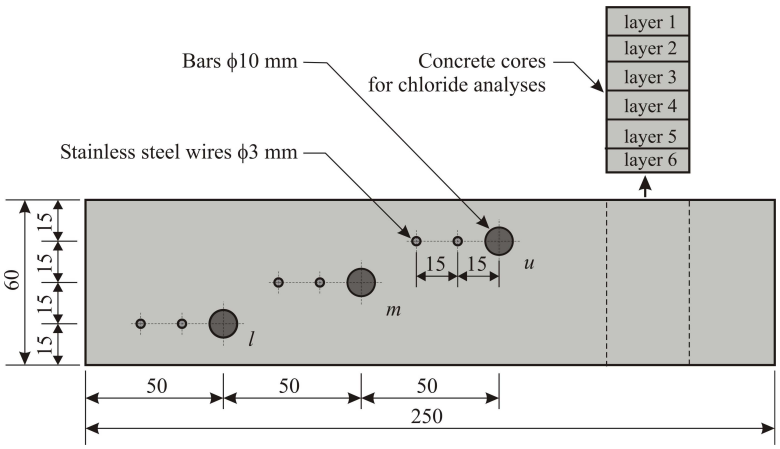

Figure 2. Reinforced concrete specimen (dimensions in mm).

3 RESULTS AND DISCUSSION

The chloride threshold for corrosion initiation, in principle, is defined as the amount of chlorides in the concrete measured (exactly) at the depth of the bar and (exactly) at the time of corrosion initiation. Unfortunately, there is no standardised or a generally accepted method for the evaluation of the chloride threshold on laboratory specimens [Bertolini *et al.* 2009, Page 2009, Alonso e*t al.* 2009, Glass 1997, Frederiksen 2009]. Several test methods proposed by different Authors differ regarding both the way concrete is contaminated by chlorides (e.g. mixed-in or penetrated in different ways), the way corrosion initiation is detected (e.g. by different electrochemical methods) and the way chloride at the depth of the bar and at the time of corrosion is measured.

In this paper, in order to detect the critical chloride threshold in specimens with concrete of different compositions, the corrosion conditions of steel bars at different depth has been monitored during chloride penetration by ponding.

Figure 3 shows, as an example, the time evolution of the corrosion potential and the corrosion rate of the three bars of the reinforced specimen with 15% limestone, *w/b* ratio of 0.61 and dosage of cement of 250 kg/m^3. In time, due to ponding with the NaCl solution, chloride penetration took place. When corrosion occurred on each of the three rebars, a sharp decrease in the corrosion potential and an increase in corrosion rate were observed. At the beginning of the exposure the corrosion potential of each bar was around -100 mV vs SCE, whilst the corrosion rate was lower than 1 μm/year. After only 10 days of ponding the potential of the upper bar dropped to about −400 mV vs SCE 'Fig 3a' and corrosion ratio increased up to about 4 mA/m^2 'Fig 3*b*', indicating that corrosion had initiated on this bar (initiation time is shown by × in 'Fig 3'). After about 300 and 320 days from the beginning of the exposure, corrosion initiated also on the second and third bars. Also for these bars, corrosion potential decreased from about -100 mV vs SCE to about -350 mV vs SCE and corrosion rate increased up to 8 μm/year. On specimens where corrosion occurred the corrosion potential before the initiation ranged between -50 and -150 mV vs SCE indicating conditions of aerated concrete.

In order to evaluate the critical chloride threshold, corrosion initiation should be detected as soon as it takes place and chloride content should be measured at the steel surface. Since corrosion initiation may be detected by sharp decrease in corrosion potential and increase in corrosion rate, a criterion for detection of corrosion initiation time was defined as the time when corrosion potential increased to values lower than -250 mV vs SCE and corrosion rate increased up to 2.5 μm/year. Each time this criterion was fulfilled on a bar, the chloride content was detected.

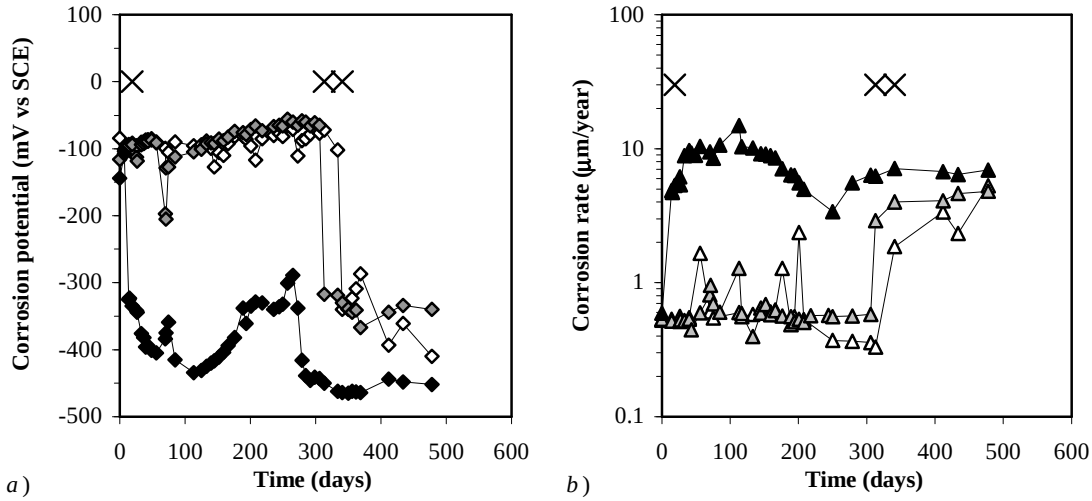

Figure 3. Corrosion potential (*a*) and corrosion rate (*b*) as a function of time in the specimen made of concrete with 15% limestone, *w/b* ratio of 0.61 and binder content of 250 kg/m^3 [symbols: black = upper bar (# = 3), grey = intermediate bar (# = 2), white = lower bar (# = 1)].

To assess the critical chloride threshold the knowledge of the chloride content near the surface where pit initiated would be needed. Such a measurement is unfeasible since, even if the rebar was removed from concrete, it would be impossible to detect a pit which has just initiated. Therefore, to estimate the chloride content at the depth of the bar where corrosion initiated, a sample was cored from the specimen and the chloride profile was measured and fitted with relationship (1) considering t equal to time of initiation (values of surface content C_s and an apparent diffusion coefficient D_{app} have been discussed elsewhere [Bertolini *et al.* 2010]). Figure 4 shows, as an example, the chloride content measured when corrosion initiated on the upper bar (after 10 days of exposure) on the specimen made with 30% limestone, *w/b* ratio of 0.61 and binder dosage of 300 kg/m^3 and the fitting line. From the fitting line, considering the bar depth (i.e. 10-20 mm for the upper bar), three values were determined: a maximum and a minimum value of the chloride content, Cl_{max} and Cl_{min}, and an average value, Cl_{ave}. After one year of exposure corrosion occurred only on a limited number of specimens and no data are available for concretes with fly ash, because corrosion had not initiated. Therefore after 1 year of ponding exposure chloride profiles were measured also on specimens where corrosion did not initiate. Table 1 shows the average value of chloride content, Cl_{ave}, when corrosion occurred on one of the three bars (grey cells), while white cells show Cl_{ave} after about one year of exposure at the depth of the upper rebar (*u*). Chloride content at the depth of the deepest bars (*m* and *l* bars) is not reported since it was lower than the chloride content at upper bar, due to the chloride profile decrease in depth.

Figure 5 shows the chloride content measured at the depth of the bars where corrosion had just initiated, as a function of the initiation time and concrete composition. Symbols show the average values (which can be assumed as an average value of the critical chloride threshold, $Cl_{th,ave}$), while the variation interval shows the range between Cl_{max} and $C_{,min}$. Even though the experimental data normally fall in the range of 0.4-1% by mass of binder, which is the usual threshold reported in the literature for structures exposed to the atmosphere, for OPC, 15%LI and 30%LI, several values below and above this range can be observed. For instance in the specimen with portland cement, *w/b* = 0.61 and *b* = 300 kg/m^3 a critical chloride threshold of 1.33% by mass of binder was evaluated, whilst in the specimen with 15% limestone, *w/b* = 0.61 and *b* = 300 kg/m^3 a critical chloride threshold of 0.19% by mass of binder was measured. A wide scatter of results can be observed, which reflects the great variability of this parameter. The few values of $Cl_{th,ave}$ and their variability make the evaluation of the role of concrete composition and curing on the critical chloride threshold rather difficult and uncertain. Moreover even on specimens with the same type of concrete rather variable critical chloride contents were measured. For instance in 7-day cured concretes with 30% LI, *w/b* = 0.46 and *b* = 350 kg/m^3 $Cl_{th,ave}$ varied between 0.55 and 0.94% mass of binder.

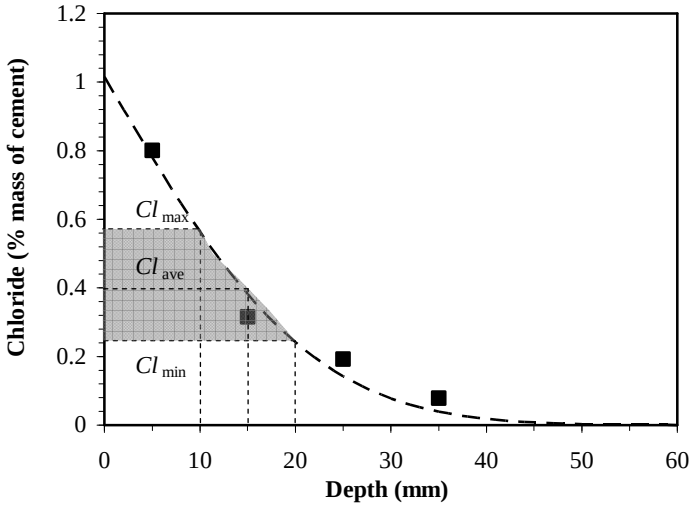

Figure 4. Chloride profile measured when corrosion occurred on the upper rebar in the specimen with 30% limestone, *w/b* ratio of 0.61 and binder content of 300 kg/m^3.

Table 1. Composition and mechanical properties of the tested concrete; Cl_{ave} = average value of chloride content at rebar depth. Grey and white cells refer to cores taken respectively when corrosion had initiated on a rebar and after approximately one year of exposure.

	w/b	*b*	R_c	*bar*	Cl_{ave}	*bar*	Cl_{ave}	*bar*	Cl_{ave}
	-	kg/m^3	MPa		(% mass)		(% mass)		(% mass)
Curing			28	7		7		28	
OPC	0.61	300	59.2	*u*	1.33				
				u	2.27				
	0.46	300	87	*u*	0.85		-	*u*	0.81
		350	70.7	*u*	0.54		0.43	*u*	0.50
	0.42	350	86.6	*u*	0.59	*u*	0.5	*u*	0.51
15%LI	0.61	250	54.5	*u*	0.53				
				m	1.072				
				l	0.33				
		300	45.2	*u*	0.19				
				m	0.31				
				l	3.07				
	0.46	300	47.8	*u*	0.98	*u*	0.99	*u*	1.21
		350	67.3	*u*	0.81	*u*	1.07	*u*	0.46
	0.42	350	83.3	*u*	0.46	*u*	0.58	*u*	0.46
		400	63.7	*u*	0.74	*u*	0.90	*u*	0.48
30%LI	0.61	300	36.7	*u*	0.38				
				m	0.99				
				l	0.59				
				u	2.21				
	0.46	300	62	*u*	1.51	*u*	0.55	*u*	0.91
				u	1.24	*u*	0.96	*u*	1.44
		350	57.4	*u*	0.55	*u*	0.94	*u*	0.97
				u	1.23	*u*	1.51	*u*	0.90
	0.42	350	66.6	*u*	0.99	*u*	1.06	*u*	0.68
								u	0.65
30%FA	0.61	300	43.9	*u*	0.76				
	0.46	300	76.2	*u*	0.38	*u*	0.66	*u*	0.61
		350	74.6	*u*	0.39	*u*	0.69	*u*	0.39
	0.42	350	80.5	*u*	1.22	*u*	0.43	*u*	1.04
30%PZ	0.61	300	42.7	*u*	0.64				
				m	0.2				
				u	1.86				
	0.46	300	69	*u*	1.46	*u*	1.54	*u*	1.08
		350	45	*u*	0.87	*u*	0.73	*u*	0.79
	0.42	350	72.6	*u*	0.72	*u*	0.67	*u*	0.67
70%BF	0.61	300	45.3	*u*	0.40				
				u	1.48				
	0.46	300	55.1	*u*	0.95	*u*	0.65	*u*	0.83
		350	54.7	*u*	0.57	*u*	0.51	*u*	0.44
	0.42	350	82.6	*u*	0.83	*u*	0.56	*u*	0.90

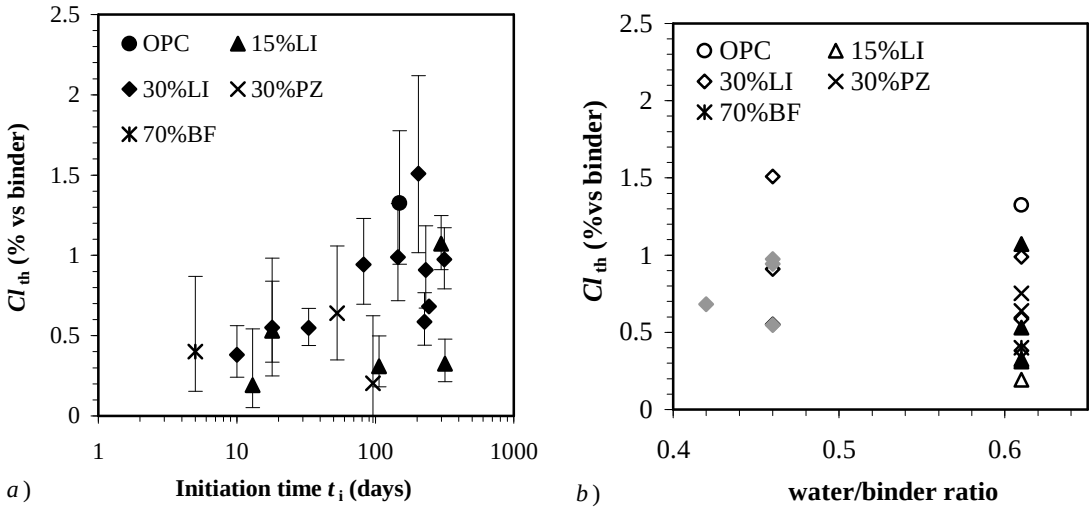

Figure 5. Chloride content measured at the depth of the bars just after corrosion initiation, as a function of initiation time (*a*) and the water/binder ratio (black symbols: b = 250 kg/m^3, white symbols: b = 300 kg/m^3; grey symbols: b = 350 kg/m^3) (*b*).

In order to investigate the influence of the type of binder on the critical chloride content, concretes with *w/b* ratio of 0.61 were compared 'Fig. 5*b*'. A higher critical chloride threshold was measured on portland cement concrete compared to limestone cement concrete. For instance $Cl_{th,ave}$ of 1.33, 0.53 and 0.38% by mass of binder were respectively measured at the depth of the upper rebar in specimens with OPC, 15%LI and 30%LI. In concretes with natural pozzolan and ground granulated blast furnace slag cement on the upper bar corrosion initiated for chloride contents of respectively 0.64 and 0.4% by mass of binder, which are lower than values measured on portland cement concrete. In 70%BF concrete with *w/b* 0.61, corrosion occurred after only few days of ponding.

For OPC, 30%PZ and 70%BF available data do not allow to clearly detect the critical chloride content. For these types of binder as well as for fly ash concrete, chloride content measured after one year of exposure can give an indication of the minimum chloride content which has to be reached at the bar depth to initiate corrosion ('Table 1'). After one year of exposure on 7-day cured concrete with 70%BF and 30%FA, although chloride content respectively between 0.51 and 0.95% and between 0.39 and 1.22% by mass of binder was reached, corrosion did not occur. Even higher values of chloride content were detected, after one year of exposure, on specimens with natural pozzolan. For instance values of about 1.5% by mass of binder were not enough high to initiate corrosion on specimens with *w/b* ratio of 0.46 and binder content of 300 kg/m^3.

The comparison among concretes with 30% LI allows to comment on the effect of water/binder ratio on chloride threshold. Although a clear trend does not appear, a slight increase of the critical chloride threshold seems to occur as the water/binder ratio decreases ('Fig. 5*b*'). For instance, on the upper bar corrosion occurred for chloride contents of 0.39% in specimen with *w/b* ratio of 0.61 and between 0.55 and 1.55% by mass of binder in specimens with *w/b* of 0.46. Data on 15%LI concretes seem to confirm this tendency. In fact although a chloride content between 0.19 and 0.53% by mass of binder led to corrosion initiation on the upper bars in concretes with *w/b* 0.61, in concretes with *w/b* of 0.46 and 0.42 corrosion had not initiated with the same and an even higher chloride content.

These results showed not only the high variability of the critical chloride content, which makes the estimation of the time of initiation rather difficult, but also the long duration required for the ingress of chloride in concrete. Although tests in concrete subjected to chloride penetration are representative of real conditions, there is the need to develop a more rapid test to detect the critical chloride content on a large number of specimens and thus evaluate also its variability.

5. CONCLUSIONS

Ponding tests on reinforced concrete specimens were carried out aimed at studying the influence of concrete composition (i.e. type of binder, water/binder ratio, binder content) and curing on the critical chloride threshold. These tests allowed the natural penetration of chlorides into concrete, simulating the exposure conditions of a real structures. A long period of time was required in order that the amount of chlorides at the bars depth reached the critical threshold. After more than one year of exposure, corrosion occurred only on the outmost bars of a limited number of specimens. On concretes with higher resistance to chloride penetration the critical chloride content, even at lower depth of 10 mm, was not reached. Although the greater part of experimental data fell in the well-known range of 0.4-1% by mass of binder, values below and above this range were detected. The high variability and the few values of critical chloride content which could be obtained did not allow a statistically-based assessment of the role of concrete composition and curing. Although this type of test takes into account the ingress of chloride into concrete, its long duration leads to the need of developing more rapid tests, in order to get a reliable and statistically-based estimation of the chloride threshold as a function of design parameters.

ACKNOWLEDGMENTS

This research was financed by the Italian Ministry of University and Research (MIUR).

REFERENCES

Alonso, M.C. & Sanchez, M. 2009, 'Analysis of the variability of chloride threshold values in the literature', *Materials and corrosion*, **60**[8], 631–637.

Bertolini, L., 2008, 'Steel corrosion and Service Life of Reinforced Concrete Structures', *Structure & Infrastructure Engineering*, **4**[2], 123–137.

Bertolini, L., Lollini, F., Redaelli, E. 2008, 'Concrete composition and service life of reinforced concrete structures exposed to chloride bearing environments', Proc. 1st International Symposium on Life-Cycle civil Engineering, IALCCE'08, Varenna, Italy, pp. 113–118.

Bertolini, L. & Redaelli, E. 2009, 'Depassivation of steel reinforement in case of pitting corrosion: detection techniques for laboratory studies', *Materials and corrosion*, **60**[8], 608–616.

Bertolini, L., Lollini, F., Redaelli, E. 2010, 'Comparison of resistance to chloride penetration of different types of concrete through migration and ponding tests', submitted to joint Fib-Rilem Workshop on modelling of corrosion concrete structures.

Frederiksen, J.M. 2009, 'On the need for more precise threshold values for chloride initiated corrosion', *Materials and corrosion*, **60**[8], 597–601.

Glass, G.K. & Buenfeld, N.R. 1997, 'Chloride threshold level for corrosion of steel in concrete', *Corrosion science*, **39**, 1001–1013.

Page, C.L. 2009, 'Initiation of chloride-induced corrosion of steel in concrete: role of the interfacial zone', *Materials and corrosion*, **60**[8], 586–592.

Tuutti, K. 1982, Corrosion of steel in concrete, Swedish foundation for concrete research, Stockholm.

XII DBMC
International Conference on Durability of Building Materials and Components
PORTO - PORTUGAL, April 12th-15th, 2011

Chloride Ions Penetration in Concrete with Recycled Concrete Aggregates

Aline Troian [1]
Ana Paula Werle [2]
Marlova Piva Kulakowski [3]
Claudio de Souza Kazmierczak[4]

ABSTRACT

The use of construction and demolition waste (CDW) aggregate is being a practice that starts to gain importance, both for the environment and the society in general. For use on structural concrete and on pre-cast concrete, the recycled concrete aggregate is mostly indicated. Some kinds of recycled concrete aggregate can be generated with the renovation and demolition of concrete structures. The difference among these aggregates is related to the compressive strength and porosity that they have, which can be variable. Both aggregate compressive strength and porosity will influence on the fresh or hardened concrete properties. The greater porosity of recycled concrete aggregate will influence on its absorption as well on the water demand for the maintenance of the concrete slump. A pre-wetting of recycled aggregate is generally adopted, for this case, as a proceeding to compensate its absorption, not existing nonetheless any consensus related to what amount of pre-wetting water must be utilized. The aim of this essay is evaluating the behavior of chloride penetration of concrete prepared with recycled concrete aggregate. The concrete production was effectuated with three different recycled concrete aggregate, from three concretes with different compressive strengths (18, 37 and 50 MPa), with five contents of recycled concrete aggregate in replacement to the natural aggregate, as well with five water amounts to pre-wetting of recycled concrete aggregate . The resistance to chloride ions penetration was conducted according ASTM C-1202 Method. The results were analyzed by statistical methods and indicate that the independent variables and their interaction have a significantly influence on resistance to chloride ions penetration.

KEYWORDS

Recycled concrete aggregate, Concrete waste, Chloride ion penetration, Durability, Recycling.

[1] Post-graduate Program in Civil Engineer of Unisinos (PPGEC), São Leopoldo, Brasil, aline.troian@gmail.com
[2] Post-graduate Program in Civil Engineer of Unisinos (PPGEC), São Leopoldo, Brasil, anhapaula@gmail.com
[3] Post-graduate Program in Civil Engineer of Unisinos (PPGEC), São Leopoldo, Brasil, marlovak@unisinos.br
[4] Post-graduate Program in Civil Engineer of Unisinos (PPGEC), São Leopoldo, Brasi, claudiok@unisinos.br

1 INTRODUCTION

The use of recycled aggregates from construction and demolition waste (CDW) is an increasingly important practice, as it can benefit both the environment and the society. In generaI it has been a consensus in many studies that concrete is the most indicated CDW for use as an aggregate be it in structural concrete or in the production of pre-cast concrete. By being the water absorption of recycled coarse aggregates greater than it is in conventional aggregates, there is a need to compensate for any eventual water absorption from the new concrete mixing water by the new recycled material. According to Vieira [2003] the high water absorption rate in recycled aggregates must be discussed. Concrete made with such a type of aggregate which is more porous, will demand a larger amount of water to achieve the same workability that the conventional aggregates do. Due to this, many authors have elaborated concrete mixtures using different amounts of water so that both the mortar slump and the workability can be satisfied. However the water-cement ratio is altered, influencing on the strength of these concrete, making impossible the comparison between the conventional concrete and the recycled aggregate concrete. In fact, what can be observed is that the performance of concrete with recycled aggregate, regarding to workability, is considered unsatisfactory due to loss of slump, especially with the increase in percentage of coarse aggregate in the mixture. For aggregates previously saturated before mixing, there will be water mobilization in the fresh mixture, once the water absorbed by the aggregate can be considered free water and, therefore, when mobilized to the fresh mixture it will cause an increase in the w/c ratio in the transition zone, a fact that augments voids, and results in reduction of strength [BUTTLER, 2003].

Villagrán-Ziccardi et al. [2008] analyzed the penetration of chloride ions plus chloride, combined in a concrete made with recycled aggregate from concrete. There have been levels of 50 and 75% of natural aggregate in recycled aggregate, with the ratio w/c varying from 0.35 to 0.60 plus two types of cement. The residual concrete employed to obtain the recycled aggregate had different strengths and was not segregated on basis of its resistance, since the absorption of the RCA was of 4.6% versus 0.3% of the granite aggregate. The slump test results varied from 120 a 60 mm. The authors, at that stage of the study, concluded that the w/c ratio has more influence on the penetration rate of chloride ions than on the porosity of the RCA.

According to Eguchi et al [2007], high levels of recycled coarse aggregates, in concrete mixture, reduce the compressive strength and the modulus of elasticity, increasing drying shrinkage. Concrete quality must be assured from the adjustments of an optimal substitution content of a natural aggregate for a recycled aggregate, turning the workability and the structural performance compatible with the conventional concrete performance. Poon and Kou [2006], studying compressive strength, pore distribution and chloride ions penetration in recycled concrete aggregate concluded that the increase in RCA content reduces its strength, however this reduction can be compensated by reducing the ratio w/c in the mixture. Total porosity and average pore diameter increase with the high content of RCA. However, high contents of RCA linked to the employment of low ratios of w/c plus 25% of fly ash reduces chloride ions penetration, also reducing pore diameter and total porosity.

Therefore, further studies are needed to indicate the influence of the resistance of recycled concrete behavior made of recycled aggregate concrete incorporated into the new matrices of concrete, as well the influence of the amount of aggregate replacement and the influence of a pre-wetting to compensate for the water absorption of RCA. This study evaluated the influence of type and content of RCA in the penetration of chloride ions in concrete made with RCA, as well as the influence of pre-wetting rate to compensate the water absorption of the waste.

2 METHODS

2.1 Analysed Variables

Given the target of the present essay the analyzed response variables have been “total charge passed”, which show the resistance of the concrete to chloride ion penetration, and “compressive strength”. The control factors have been: “recycled concrete aggregate content”, with levels of 0, 25, 50, 75 e 100%; “compressive strength

of recycled concrete aggregate", with fixed levels of 18, 37 e 50 MPa; "rate of pre-wetting"', with fixed levels of 0.25, 50, 75 and 100% of total absorption of RCA. The control variables have been tested through an experimental project of the fractionated factorial type.

2.2 Materials

A commercial Portland high early strength type CP V-ARI according to ABNT NBR 5733 [1991] was used, with density of 3.12 g/cm³. It was used as fine aggregate the quartz sand, with a fineness modulus of 2.73; characteristical maximum dimension of 4.8 mm, density of 2.49 g/cm3, and unit mass of 1.61 g/cm3. As coarse aggregate it was used crushed gravel of basalt, with granulometry comprehended between 12.5 and 25 mm, fineness modulus of 6.69, characteristical maximum dimension of 19 mm, specific mass of 2.75 g / cm ³, and unit mass of 1.49 g / cm ³. More characteristics of the materials can be found in Troian [2010].

2.3 Recycled Concrete Aggregates

The concrete recycled as RCA was produced in laboratory, in order to obtain three different compressive strength levels. The material used to produce this concrete was the same materials from the new matrix where the RCA were inserted. The physical characteristics of concrete and RCA are presented in Table 1, the water absorption was measured according to Werle et al. [2010].

Table 1. Physical characteristics of recycled concrete aggregates.

w/c ratio	*Compressive strength (28 days - MPa)*	*Maximum size (mm)*	*Fineness modulus*	*Specific gravity* (g/cm³)	*Total Absorption* (%)
0,85	18	25	7,68	2,50	8,49
0,56	37	25	7,61	2,47	6,07
0,43	50	25	7,70	2,49	5,24

2.4 Concrete Production with RCA

The concrete used as reference on which partial and total replacements of natural aggregate by RCA were performed, has pre-established workability of 100 ±20 mm, with a proportion of cement: fine aggregate: coarse aggregate 1:3, 13:3, 67; w/c ratio 0.64 and 28 days strength of 32.4 MPa. The slump test was defined in 100±20 mm and should be assured in all mixtures. When the RCA was introduced, with different pre-wetting rates, it was necessary to adjust the mixing water with reductions or augmentations, so that the slump was assured. Such an adjustment generated a concrete matrix with a modified w/c ratio, if compared to the reference concrete, obtaining different values of w/c ratio, for each combination of variables. The result was a new independent variable which was defined as final w/c, that is (initial w/c + adjustment w/c), with random levels.

2.5 Experimental Methods

The concrete here studied was characterized regarding to axial compression strength according to the Brazilian standard ABNT NBR 5739 [2003]. The ASTM C 1202-07 - Rapid Chloride Ions Penetration Test - RCPT was used to determine rapid chloride ions penetration.

3 RESULTS

3.1 Compressive Strength

The analysis of variance (ANOVA) has showed that only the RCA strength and the RCA content can affect significantly the concrete compressive strength. The influence of the type of aggregate on strength is shown in the box-plot chart in Figure 1.

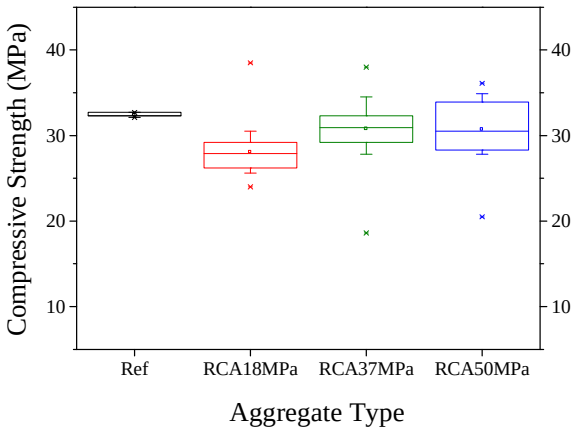

Figure 1. Effect of compressive strength of RCA on compressive strength of new concrete.

3.2 Chloride Ion Penetration

The resulting total charge for each combination of variables is presented in Table 2. The statistical analysis of the observed data for total charge passed in concrete was measured through multiple linear regression.

Table 2. Chloride ion penetration.

*RCA Type**	*Recycled concrete aggregate content*	*Pre-wetting rate*				
		0%	*25%*	*50%*	*75%*	*100%*
18 MPa (ABS 8,49%)	*25%*		4924		5110	
	50%	8607		5814		6222
	75%		7946		9542	
	100%	9430		9158		9963
37 MPa (ABS 6,07%)	*25%*	4795		5414		8388
	50%		5541		5846	
	75%	5405		6601		7380
	100%		8043		8680	
50 MPa (ABS 5,24%)	*25%*		4742		4806	
	50%	6237		5634		5749
	75%		6312		6820	
	100%	6847		6832		8142

* The total charge for plain concrete is 4077 Coumlombs.

The resulting total charge for each combination of variables is presented in Table 2. The statistical treatment analysis of the observed data for total charge passed in concrete was measured through multiple linear regression. The analysis of variance (ANOVA) of the calculated model is presented in Table 3 and the calculated parameters for the independent variables analyzed (factors) are presented in Table 4. In this analysis the variable called 'aggregate type' was represented by total water absorption (ABS) of the recycled aggregate and the levels of study were presented on Table 2. The value of 'p' inferior to 0.01 shown in Table 3 indicates that the relation between variables is statistically significant at a confidence level of 99%. The obtained coefficient of determination r^2 of 0.8834 shows that the model explains 88.34% of the values variability observed for total charge passed. It is emphasized that the variability of the test proposed by ASTM C-1202-07 is high.

Considering the variables analyzed in the models and their interactions, the results in Table 6 indicate that the aggregate substitution content (ASG) and the pre-wetting rate (PWR) are statistically significant at a confidence level of 99%, as they present "p" with value inferior to 0.01. The final w/c ratio (WCR) shows significant effect on the total charge passed, in form of a quadratic term, but at a confidence level of 90%, once

the "p" value for this factor is 0.08. Likewise, it was found that the interaction of the analyzed ABSxASG variable shows significant influence on the total charge passed. This result shows that such a type of aggregate, in this analysis represented by its absorption (ABS) only has significant effect on the variable when associated to the aggregate substitution content (ASG). The interactions between ASGxWCR plus PWRxWCR have been control factors which did influence significantly the behavior of the total charge passed, which evidences the resistance to chloride ion penetration at a level of 99%, resulting in "p" value lower than 0.01, i.e., it was proved that the interaction between this variables is statistically significant. Equation 1 shows the model used for total charge passed.

Table 3. ANOVA for chloride ion penetration model.

Source	*DF*[a]	*SQ*[b]	*MQ*[c]	F_{calc}	*Significance - p*
Regression model	9	7,1532	7948	17,68	0,0000
Residual	21	9,44282	2,50	1,21	
Corrected total	30	8,09748	2,49	1,21	

[a] Degrees of freedom; [b] Sum of squared.; [c] Squared mean.

Table 4. Regression parameters for the factors studied for total charge.

Factor	*Parameter*	*Estimate*	*Standard error*	*t-test*	*p*
Constant	b0	-1864,92	3514,57	-0,530626	0,6012
ASG	b1	291,143	92,0107	3,16423	0,0047
PWR	b2	-339,905	84,4363	-4,02558	0,0006
ASG^2	b3	0,602833	0,223394	2,69852	0,0135
PWR^2	b4	0,903205	0,213384	4,23277	0,0004
WCR^2	b5	14867,5	8232,41	1,80597	0,0853
ABS*ASG	b6	9,73207	1,46102	6,66117	0,0000
ASG*PWR	b7	0,837158	0,257582	-3,25007	0,0038
ASG*WCR	b8	-508,871	150,242	-3,38701	0,0028
PWR*WCR	b9	-460,893	110,221	4,18152	0,0004

$$Q = -1864{,}92 + 291{,}143\times ASG - 339{,}905\times PWR + 0{,}602833\times ASG^2 + 0{,}903205\times PWR^2 + 14867{,}5\times WCR^2 + 9{,}73207\times(ABS\times ASG) - 0{,}837158\times(ASG\times PWR) + 508{,}871\times(ASG\times WCR) + 460{,}893\times(PWR\times WCR) \quad \textbf{Equation 1}$$

Where: Q = Total Charge (Columbs); ASG = aggregate substitution content (%);PWR = pre-wetting rate (%); WCR = final w/c ratio; ABS = total water absorption of recycled aggregate (%).

The graphs in Figures 2, 3 and 4 show the behavior curves for total charge passed after 6 hours, for three fixed levels of final w/c ratio, ranked in lowest and highest values of final w/c ratio seen in the experimental program.

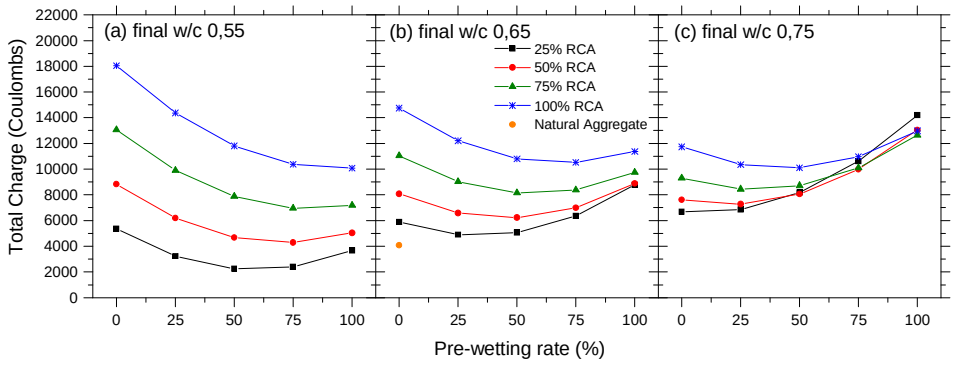

Figure 2. Total charge for concrete with RCA 18 MPa.

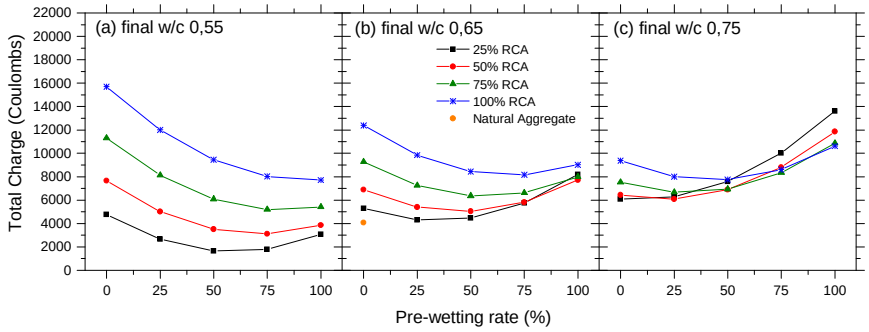

Figure 3. Total charge for concrete with RCA 37 MPa.

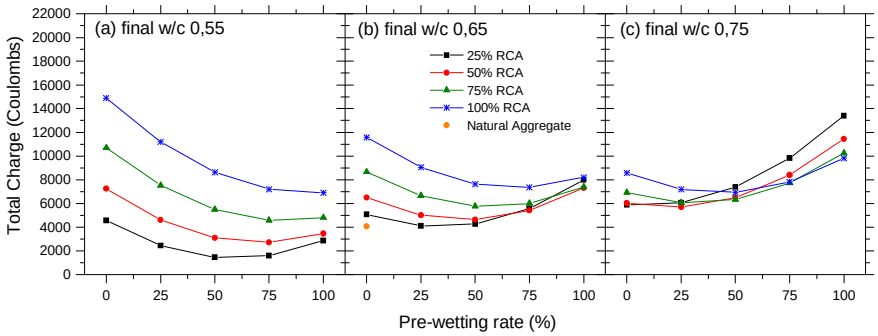

Figure 4. Total charge for concrete with RCA 50 MPa.

The concrete with RCA of 18 MPa, pre-wetting values up to 50% and substitution content (ASG) exceeding 50%, had higher total charge passed when w/c ratio was lower, as seen in the curves of the adjusted models, shown in the graphs in Figure 2 (a) and (b). However, for w/c ratio of 0.75, when pre-wetting rates exceed 50%, the lowest substitution contents show higher total charge passed (Figure 2(b)). The concrete with RCA of 37 MPa (Figure 3) and 50 MPa (Figure 4), had the same behavior trend once that the total charge passed does not show significantly differences when comparing concrete with these types of aggregate. However, regarding the concrete with 18 MPa RCA, both showed a significantly difference.

The results for total charge passed for concrete produced with 18 MPa RCA show an average increase of 90.15% when compared to the reference concrete. Similarly, the concrete with RCA of 37 and 50 MPa, respectively, showed an average increase of 62.11% and 52.37% compared to the reference concrete (Figure 3). It can also be stated that regardless of the aggregate's strength, the concrete with pre-wetting rate superior to 50%, substitution content of 50% and higher final w/c ratio, had higher values for total charge passed.

Another important aspect is that the higher the w/c ratio of the concrete matrix is, the higher is the charge passed, or, the lower is the resistance to chloride íons penetration; clearly evidenced when (each type of aggregate) is compared to the curves for concrete with w/c ratio of 0.55, 0.65 and 0.75. It is also emphasized that it is possible to analyze the results for the traces produced with final w/c ratio of 0.65, pointing out that this result is similar to the reference concrete's, which was 0.64. The reference concrete, which has the same matrix as the RCA concrete, already has high porosity, and this fact alone results in concrete with high penetration of chlorides, according to the classification ASTM C 1202-07. The averages of the results for total charge passed for concrete with RCA were high and superior to the reference concrete's. This means that the RCA concrete has high penetrability of chloride ions. Or be it, for all levels tested in the variables of the study which are 'type of aggregate', 'substitution content' and 'pre-wetting rate', by simulating a water/cement ratio of 0.65, the concrete showed low resistance to chloride ions penetration.

According to the ASTM C 1202-07 classification, the concrete with total charge of less than 2000 Coulombs have low penetrability of chloride ions, and the concrete with total charge passed between 2000 and 4000 Coulombs have moderate penetrability of chloride ions. Figures 3(a) and 4(a), correspond to the graphs of behavior curves for concrete with final w/c ratio of 0,55, for 37 and 50 MPa RCA concrete, respectively. The curves of substitution content at 25%, and between pre-wetting rate of 50 and 75% , show low penetrability of

chloride ions. Regarding to the concrete with 18 MPa RCA and final w/c ratio of 0.5, the concrete with RCA at 25%, show moderate penetrability of chloride ions. Observing the graphs of total charge passed, for the new concrete with final w/c ratio of 0.65, the behavior trend until 50% PWR is reversed. The interaction between the pre-wetting rate and the final w/c is observed in the change of inflection of the curves, that is, after a 50% amount it increases the total charge passed. However, it was found that the type of aggregate is not determinant when it is used in a matrix with a higher w/c ratio.

Gomes and Brito (2009) by conducting an experimental study similar to this, have evidenced that the concrete with RCA has shown a slightly higher penetration of chloride ions, with maximum differences around 6%, when compared to concrete with natural aggregate. This low reduction in compressive strength so observed by the referred authors may be attributed to the low w/c ratio of the concrete matrix where the RCA was incorporated (ratio of 0,43), while the present study has used 0.64; then this could explain the higher differences compared to the reference concrete. Poon and Kou (2006) showed in their research, that with a reduction of 0.55 to 0.45 in w/c, there was a significantly decrease in penetration of chloride ions, once the volume of pores decreases letting the concrete more impermeable and, in conformity with this, the resistance to penetration of chloride ions increases. The results showed a decreased resistance to penetration of chloride ions, with the increase of recycled aggregate. However, according to the authors this reduction could be compensated with the addition of 25 to 35% of pozzolanic material. Being so, it is evident that the final w/c ratio of the cement matrix strongly influences the behavior of the property in question, and if this experimental program had included other matrices of concrete then, possibly the results would have been more satisfactory.
In general, the statistical analysis indicates that, in average, the higher the RCA substitution content and the pre-wetting rate are, the higher is the total charge passed.

The porosity of the aggregate, evidenced by the RCA compressive strength, shows a critical limit for the penetration of chloride ions, which must be, for experimental conditions, between 18 and 37MPa, because in this interval it is possible to be observed an inflection in the behavior of the ARC concrete. In the concrete with higher RCA strength (37 and 50 MPa) there is no significant difference in total charge passed.

4 CONCLUSION

The resistance to penetration of chloride ions is influenced by the analysed variables. In general, it can be stated that the concrete produced has shown a decrease in resistance to penetration of chloride ions due to the porosity of the RCA, that is, the lower the resistance of the ARC is, in this case 18MPa, the higher is the total charge passed, and consequently lower is the resistance penetration of chloride ions. However, observing the aggregates with higher resistance, in this case above 37 MPa, the values were not significantly different from each other. Another aspect noticed was regarding to the final w/c ratio of the concrete matrix, since the higher the w/c ratio is, the higher is the charge passed, regardless of the RCA type, because when the aggregate is inserted in a matrix that already has high porosity, the resistance of the RCA does not seem to influence the results.

From the regression analysis of the results, it is possible to say that the aggregate substitution content has an important isolated effect on the concrete behavior. However, this variable in interaction with the pre-wetting rate also has an expressive effect, which is reflected by the fact that until 50% of pre-wetting, the higher the percentage of substitution can be (ASG) the greater can be the total charge passed, proving the influence of the substitution content. But when the pre-wetting rate exceeds 50% this behavior does not seem to have significancy, namely, the substitution content does not have a strong influence.

The ‘aggregate substitution content’ also has a significant effect when interacting with the final water/cement ratio of the matrix. It can also be inferred that the percentage of pre-wetting rate (PWR), when exceeding 50% and with higher final w/c, has demonstrated increase in total charge passed of the concrete. Another aspect that can be pointed out is the interaction of the variable PWR with the variable ASG. The traces have represented the lowest percentage of pre-wetting and higher RCA substitution content, consequently, have shown higher values in total charge passed.

ACKNOWLEDGMENTS

The authors thank FINEP and CAPES for research funding and the scholarship.

REFERENCES

American Society for Testing Materials. 2007. ASTM C1202-07: *Standard Test Method for Electrical Indication of concrete's Ability to Resist Chloride Ion Penetration*. Philadelphia, 2007.

Buttler, A. M. 2003. '*Concreto com agregados graúdos reciclados de concreto- influência da idade de reciclagem nas propriedades dos agregados e concretos reciclados*'. 187f. Dissertação (Mestrado em Engenharia) – Escola de Engenharia de São Carlos. Departamento de Engenharia de Estruturas. Universidade de São Paulo, São Paulo, SP, Brasil.

Eguchi, K.; Teranishi, K; Nakagome, A.; Kishimoto, H.; Shinozaki, K.; Narikawa, M. 2007. 'Application of recycled coarse aggregate by mixture to concrete construction'. *Constr. & Build. Mat*., 7 [21], p.1542-1551.

Gomes, M; Brito, J. 2009. 'Structural concrete with incorporation of coarse recycled concrete and ceramic aggregates: durability performance.' *Materials Structures*, [42], p.663-675.

Grub, M. 2010. '*Estudo das propriedades no estado fresco e mecânicas de concretos com agregado reciclado de concreto*.' 105p. Dissertação (Mestrado em Engenharia Civil) – Programa de Pós-graduação em Engenharia Civil: Gestão de Resíduos. Universidade do Vale do Rio dos Sinos, São Leopoldo, RS, Brasil – Em desenvolvimento.

Kulakowski, M. P. 1994. '*Argamassa com Adição de Microssílica para Reparos Estruturais: Estudo da Penetração de Cloretos.'* 106p. Dissertação (Mestrado em Engenharia Civil) Programa de Pós-Graduação em Engenharia Civil, UFRGS. Porto Alegre, RS, Brasil.

Poon, C. S.; Kou, S. C. 2006. 'Compressive strength, pore size distribution and chloride ion penetration of recycled aggregate concrete incorporating class-fly ash.' *Journal of Wuhan University of Tecnology*, 4[21], p130-136.

Siqueira, H.C. 2008. '*Penetração de cloretos em concretos compostos com cimento Portland branco e escória de alto forno, ativados quimicamente*.' 141p. Dissertação (Mestrado em Engenharia) – Pós-graduação em Engenharia Civil. Universidade Federal de Santa Maria, Santa Maria, RS Brasil.

Troian, A. 2010. '*Avaliação da durabilidade de concretos produzidos com agregado reciclado de concreto frenta à penetração de íons cloreto.*' 127f. Dissertação (Mestrado em Engenharia Civil) – Programa de Pós-graduação em Engenharia Civil: Gestão de Resíduos. Universidade do Vale do Rio dos Sinos, São Leopoldo, RS, Brasil.

Vieira, G. L. 2003. '*Estudo do processo de corrosão sob a ação de íons cloreto em concretos obtidos a partir de agregados reciclados de resíduos de construção e demolição.*' 151f. Dissertação (Mestrado). Programa de Pós-Graduação em Engenharia Civil da Universidade Federal do Rio Grande do Sul, Porto Alegre, RS, Brasil.

Villagrán–Ziccardi, Y.A; Zega, C.J ; Di Maio, A. A. 2008. 'Chloride penetration and binding in recycled concrete.' *Journal of Materials in Civil Enginnering*, 6[20], June, p. 449-455.

Werle, A.P. 2010. '*Determinação de propriedades de concretos com agregados reciclados de concreto com ênfase na carbonatação*.' 154f. Dissertação (Mestrado em Engenharia Civil) – Programa de Pós-graduação em Engenharia Civil: Gestão de Resíduos. Universidade do Vale do Rio dos Sinos, São Leopoldo, RS, Brasil.

Werle, A.P.; Troian, A.; Alcântara, J.; Kulakowski, M.P.;. Kazmierczak, C.S. 2010. 'Análise de metodologias utilizadas para a determinação da absorção de água de agregados reciclados', in XIII *Encontro Nacional de Tecnologia do Ambiente Construído*, Associação Nacional de Tecnologia do Ambiente Construído, Porto Alegre, RS, Brasil.

XII DBMC
International Conference on Durability of Building Materials and Components
PORTO - PORTUGAL, April 12th-15th, 2011

Behaviour of Chloride Content at the Surface of Concrete in Submerged Test Conditions

André Tavares da Cunha Guimarães [1]
Carlos Antón Gil [2]
Miguel Ángel Climent Llorca [3]
Guillem de Vera Almenar [4]

ABSTRACT

Several studies show a variation of chloride content on the surface of concrete structures (Cs) located in marine environment in the early years of use, especially in the mist area and splash zone. Crank [1975] presented, in several ways, solutions of Fick's Second Law considering constant Cs over time and variable Cs as a function of time. These equations show diffusion coefficient values significantly different when Cs is considered variable as a function of time, related to the constant Cs.

This study aims to investigate the behaviour of Cs over time on tests of concrete in the submerged condition and analyze the variation of the diffusion coefficient for concrete tested with different concentrations of NaCl solutions.

We conclude that the value of the chloride content in the concrete surface does not vary significantly over time and that the chloride diffusion coefficient was not significantly different when different NaCl solutions where used for the immersion test. Tests with a solution containing high concentrations of NaCl showed very close results at 7 days and 35 days. New tests should be performed in order to use this method as an accelerated test, obtaining data in short ages. Tests with higher content of NaCl in the solution could be performed, as the value of 165 g/dm^3 ± 1 g/dm^3 is still quite distant from the saturation value of the solution.

KEYWORDS

Chloride, Concrete, Dffusion, Marine environment, Coastal construction.

[1] Escola de Engenharia da Universidade Federal do Rio Grande, Rio Grande, Brasil, atcg@vetorial.net
[2] Departamento de Ingeniería de la Construcción, Obras Públicas e Infraestructura Urbana. Universidad de Alicante, Alicante, Spain, c.anton@ua.es
[3] Departamento de Ingeniería de la Construcción, Obras Públicas e Infraestructura Urbana. Universidad de Alicante, Alicante, Spain, ma.climent@ua.es
[4] Departamento de Ingeniería de la Construcción, Obras Públicas e Infraestructura Urbana. Universidad de Alicante, Alicante, Spain, guillem.vera@ua.es

1 INTRODUCTION

Several studies show a variation of chloride content on the surface of concrete structures (Cs) located in marine environment in the early years of use, especially in the mist area and splash zone [Castro et al. 1999; Meira et al. 2007; Silva and Guimarães 2010]. During this research, no work was found that studies the behaviour of Cs over the early ages of concrete in submerged structures.

Crank [1975] presented several solutions of Fick's Second Law considering constant Cs over time and variable Cs as a function of time. These equations show as solution, values for the diffusion coefficient significantly different when variable Cs as a function of time is compared to constant Cs.

This study aims to study the behaviour of Cs over time on tests of submerged concrete, because this type of test is widely used in research, with some standardized methods, such as that given in NT BUILD 443 [1995]. An analysis is also provided on the variation of the diffusion coefficient for concrete tested with different concentrations of NaCl solutions.

2 DIFFUSION COEFFICIENT WITH CONSTANT AND VARIABLE VALUES OF C_S

Equations 1 and 2 represent a solution of Fick's Second Law considering constant Cs [Crank 1975]

$$\frac{Cx-Co}{Csconst-Co} = erfc\frac{x}{2\sqrt{D_{Csconst}\,t}} \qquad (1)$$

Where: C_x = concentration of chloride at depth x; C_o = initial chloride concentration; C_{sconst} = concrete surface concentration, considered constant over time; x = depth; $D_{Csconst}$ = diffusion coefficient considering C_s constant over time.

$$M_t = 2Csconst\left(\frac{D_{Csconst}\,t}{\pi}\right)^{1/2} \qquad (2)$$

Where: M_t = total mass of chloride that diffuses at time t.

The variation in Cs when it varies linearly over time is represented in Equation 3 whereas equations 4 and 5 are the solution of Fick's second law considering this variation [Crank 1975].

$$C_{x=0} = Csvar = kt \qquad (3)$$

Where: C_{svar} = concrete surface concentration, considering its increase as time dependant; k = constant of proportionality.

$$C_x = kt\left\{\left(1+\frac{x^2}{2D_{Csvar}t}\right)erfc\frac{x}{2\sqrt{D_{Csvar}t}} - \frac{x}{\sqrt{\pi D_{Csvar}t}}exp\left(-\frac{x^2}{4D_{Csvar}t}\right)\right\}$$

$$= 4kt\,i^2erf\frac{x}{2\sqrt{D_{Csvar}t}} \qquad (4)$$

Where: D_{Csvar} = diffusion coefficient considering Cs variable over time.

$$Mt = \frac{4}{3}kt\left(\frac{D_{Cs\,var}t}{\pi}\right)^{1/2} \qquad (5)$$

Where: M_t = total mass of chloride that diffuses at time t.

Equation 6 represents the variation of Cs as a function of the square root of time and equations 7 and 8 are the solution of Fick's Second Law considering this condition [Crank 1975].

$$C_{x=0} = Csvar = kt^{1/2} \quad (6)$$

$$C_x = kt^{1/2}\left\{exp\left(-\frac{x^2}{4D_{Csvar}t}\right) - \frac{x\pi^{1/2}}{2\sqrt{D_{Csvar}t}}erfc\frac{x}{2\sqrt{D_{Csvar}t}}\right\}$$

$$= k(\pi t)^{1/2} ierf \frac{x}{2\sqrt{D_{Csvar}\, t}} \quad (7)$$

$$Mt = \frac{1}{2}kt(\pi D_{Csvar})^{1/2} \quad (8)$$

The correlation of equations (2) and (5) gives equation (9), which represents the relationship between the diffusion coefficient obtained when constant Cs is considered and when Cs varies linearly with time.

$$D_{Csvar} = 2.25\ D_{Csconst} \quad (9)$$

Correlating equations (2) and (8) we obtain equation (10), which represents the relationship between the diffusion coefficient considering constant Cs and variable Cs as a function of the square root of time.

$$D_{Csvar} = 1.62\ D_{Csconst} \quad (10)$$

Writing the equations 9 and 10 in the form:

$$Dcsvar = Y\ .\ Dcsconst \quad (11)$$

And taking into account that:

- For constant Cs we have n=0 and $Cs = k(t)^n$, where

Dcs var = 1. Dcs const.

- For Cs varying with the square root of time (n = 0.5)

Dcs var = 1.62 Dcsconst

- When Cs varies linearly with time (n= 1) we have:

Dcsvar = 2.25 Dcs const

Figure 1 shows Y value as a function of the exponent *n*.

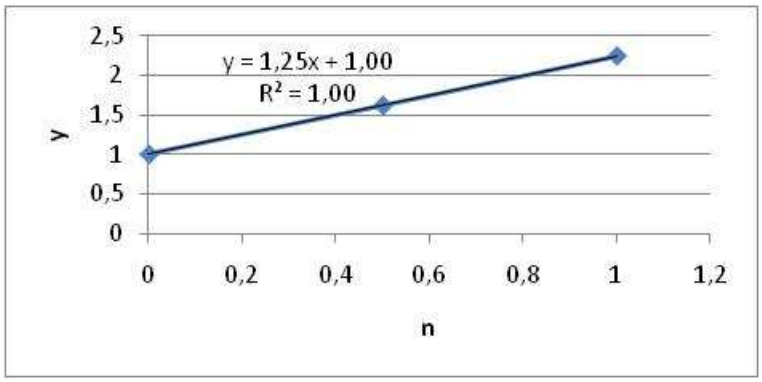

Figure 1. Y as a function of n.

It is observed in Figure 1 that Y varies linearly with n, i.e. the larger n, the greater the value of Y. Thus, the higher the value of the exponent n of time, the greater the difference in considering constant C_s and variable C_s.

Silva and Guimarães [2010] obtained profiles at ages of 4.5 years and 9.5 years researching reinforced concrete located in southern Brazil. They concluded that Cs varied approximately as a function of the square root of time, adjusting well to equations 6, 7 and 8.

3 EXPERIMENTAL

To verify the behaviour of C_s over time several tests were performed in concrete according to NT BUILD 443 [1995] with NaCl solution of 165 g/dm^3 ± 1 g/dm^3 for 7 days, 21 days and 35 days. Aiming to verify whether different NaCl solutions have different diffusion coefficients, as well as the behaviour of C_s over time, tests on specimens immersed in a solution of 0.5 M NaCl at 30 days and 90 days were also carried out. Physical properties of the concrete used are shown in Tables 1 and 2, and this concrete was about 3 years old when the tests were performed. Temperature was 26ºC ± 2ºC while tests were performed.

Table 1. Dosage.

Cement (Kg/m^3)	350 Cem I 42.5R
Sand (Kg/m^3)	662.8
Gravel 4/6 (Kg/m^3)	489.5
Gravel 6/12 (Kg/m^3)	714
Distilled water (Kg/m^3)	175
w/c ratio	0.5
Plastifier (% cem. ref.)	1.4 (Viscocrete 3500)

Table 2. Physical properties of concrete.

Compressive strength (MPa)	40.3
Absorption (%)	5.6
Voids (%)	12.6
Spec. mass (kg/m^3)	2230

3.1 Testing as NT BUILD 443 (1995) – NaCl 165 g/dm^3 ± 1 g/dm^3

For this test concrete cylinders were cast and samples of 100 mm diameter and 60 mm length sawn from thecentral parts of the cylinders, and then coated with epoxy resin on all sides except one of the tops. These specimens were subjected to chloride diffusion tests as per NT BUID 443 standard.

At ages 7 days, 21 days and 35 days powder samples were extracted in layers of zero to 1 mm, 1 mm to 3 mm, 3 mm to 5 mm, 5 mm to 8 mm, 8 mm to 12 mm, 12 mm to 16 mm, 16 mm to 20 mm and 20 mm to 25 mm. Three samples were tested at each age. The result of the first layer has been neglected in the regression of the profile as NT BUILD 443 [1995]. The profiles obtained are shown in Figure 2 and their regressions by the least squares method are shown in Figure 3.

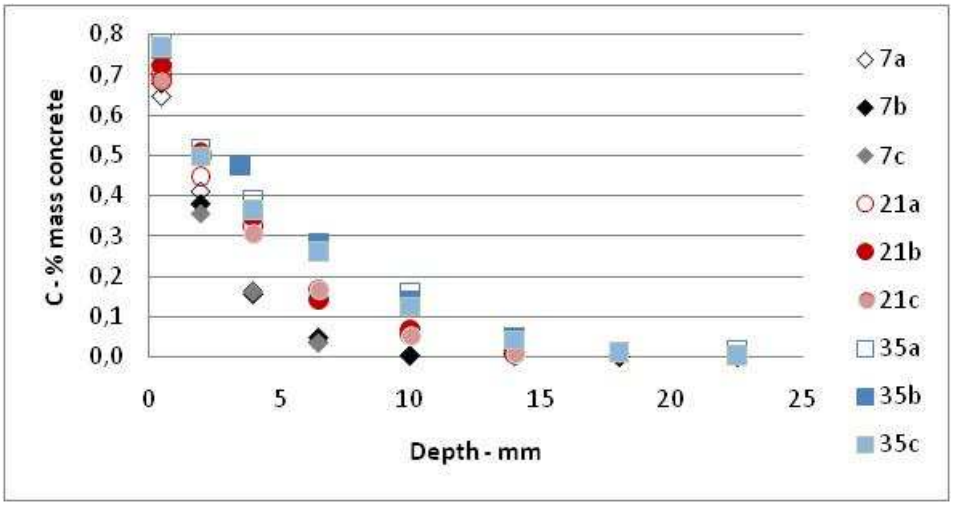

Figure 2. Chloride profiles for test duration of 7 days, 21 days and 35 days-tests submerged in a 165 g/dm^3 ± 1 g/dm^3 NaCl solution.

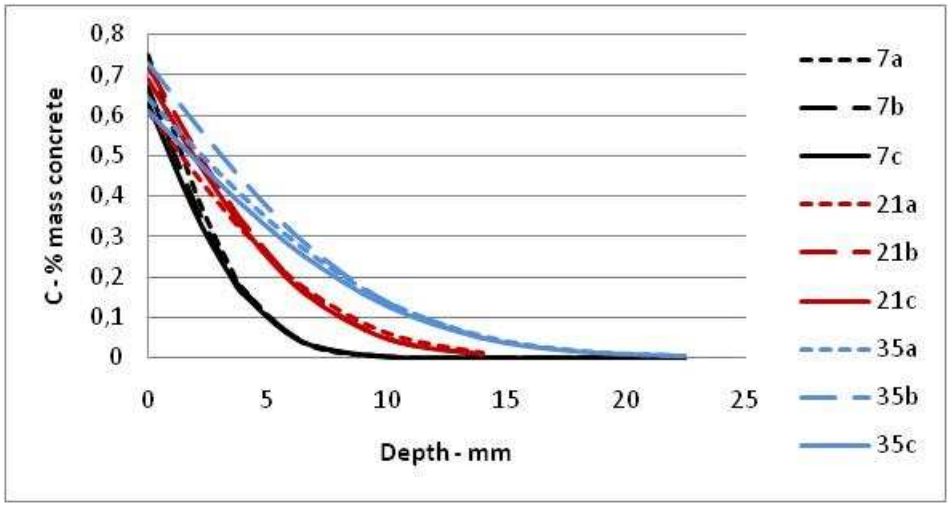

Figure 3. Profiles obtained by regression excluding the first point – tests submerged in a 165 g/dm^3 ± 1 g/dm^3 NaCl solution.

The mean values of Cs obtained in these tests were very close, with no significant difference (Fig. 4a). It was also found that even for early age, the mean diffusion coefficient values were very close, showing significant overlapping if we take into account their corresponding variation bars (Fig. 4b).

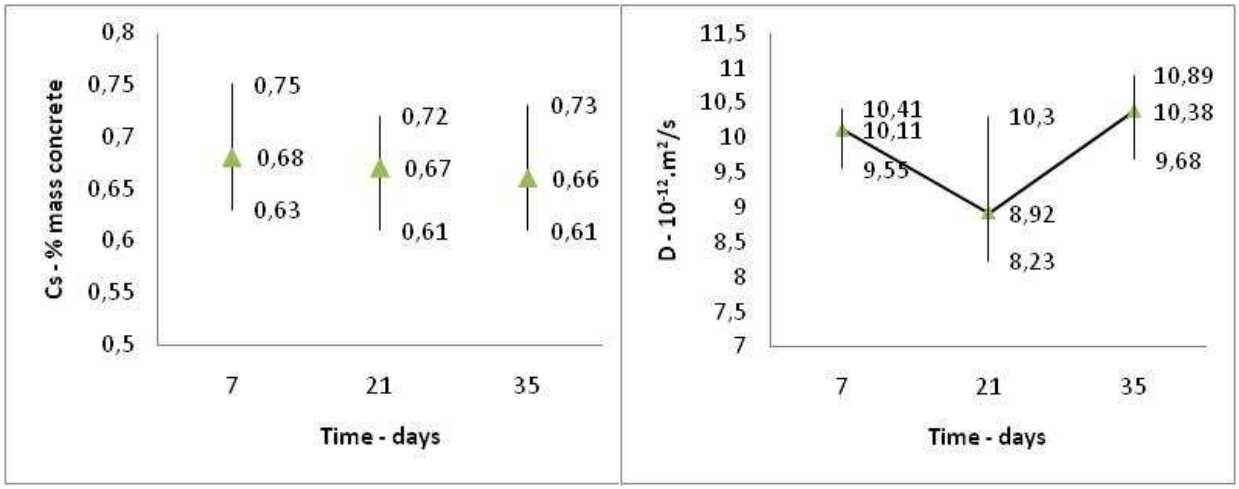

Figure 4. Maximum, minimum and mean values of **(a)** Cs and **(b)** Diffusion coefficient- tests submerged in a 165 g/dm^3 ± 1 g/dm^3 NaCl solution.

3.2 Tests with NaCl 0.5 M

Two cylindrical samples (100 mm diameter and 30 mm length) were sawn from the abovementioned concrete cylinders, and then coated with epoxy resin on all surfaces except the top. They were subjected to chloride diffusion tests similar to NT BUIL 443, but with a 0.5 M chloride concentration (29.2 g NaCl / dm^3). This concentration is equivalent to that of seawater.

At the ages of 30 days and 90 days powder samples were extracted, the first and second layers were of a depth of 1 mm in and the remaining layers each 2 mm. Only one test was performed by age. The result of the first layer has been neglected in the regression of the profile according to NT BUILD 443 [1995]. The profiles obtained in these tests are shown in Figure 5.

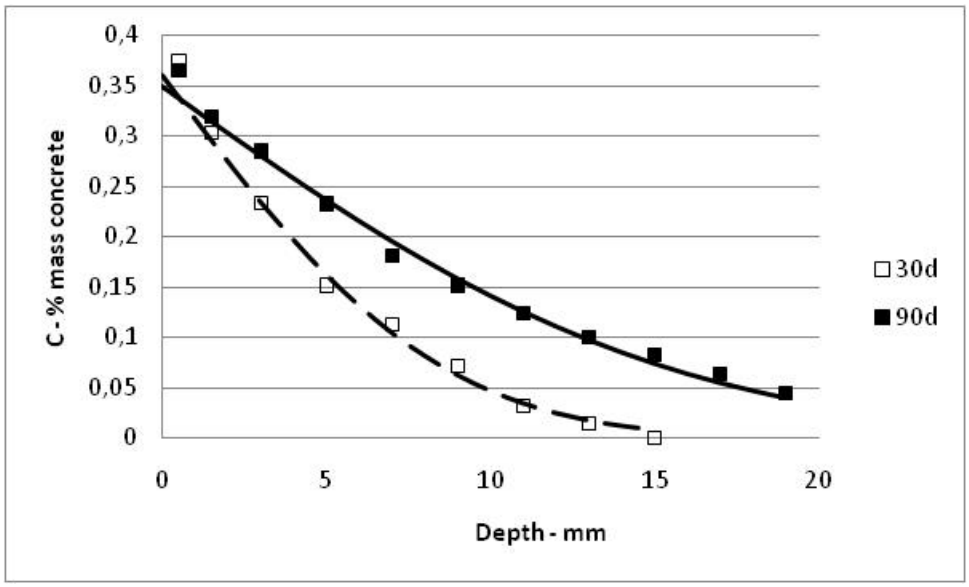

Figure 5. Values of chloride content and the regression curve excluding the first point – tests submerged in a 0.5 M solution.

Figure 5 shows that Cs has no significant difference for both ages (0.36% at 30 days and 0.35% at 90 days), being considered constant over time.

The values of the diffusion coefficient were 8.5 m^2/s and 9.3 m^2/s for 30 days and 90 days tests, respectively. These values were close to those found for the test with a NaCl solution of 165 g/dm^3 ± 1 g/dm^3, and the obtained values were in the range of deviation of this test.

Tang [1999] showed that the diffusion coefficient, obtained in natural diffusion tests and migration tests with different NaCl solutions, increases its values when the NaCl concentration is decreased.

However, when looking at Figure 6 presented by Tang [1999] using data from Arsenault et. al. [1995] and data from Zhang [1997], it is appreciable that the variation of the diffusion coefficient measured through natural diffusion tests shows small variations with different NaCl solutions ranging from approximately 0.04 M to 0.5 M. The magnitude of these differences is similar to the variation range of time for these tests performed under equal conditions.

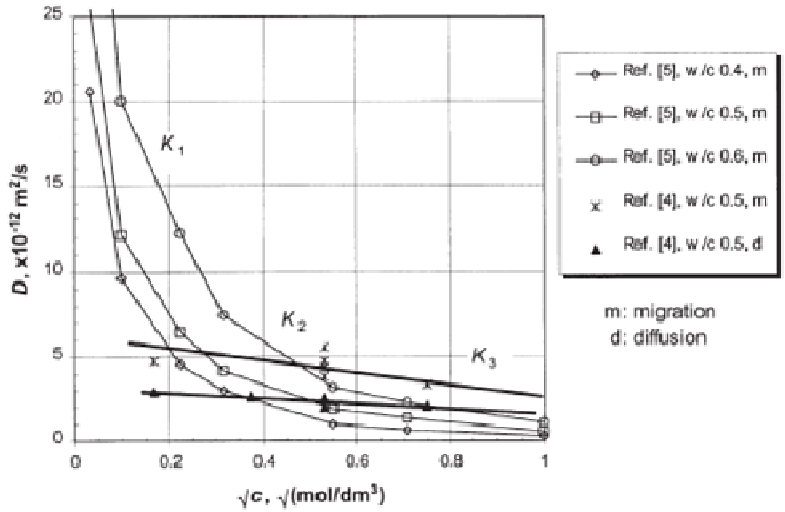

Figure 6. Influence of temperature on chloride penetration in natural diffusion tests and migration tests (Tang [1999]) - [4] data extracted from Arsenault et. al. [1995] and [5] data extracted from Zhang [1997].

Therefore, it can be seen that data collected from this research are consistent with the research of Arsenault et. al. [1995] as quoted by Tang [1999].

4 CONCLUSIONS

The value of the chloride content in the concrete surface does not vary significantly over time for natural diffusion tests in submerged conditions. Therefore, the profile analysis must be performed according to Equations 1 and 2.

The diffusion coefficient of chloride was not significantly different when different NaCl solutions were used for the immersion test, one containing a total amount of chloride ions similar to seawater and another with a content of approximately 5 times greater.

Tests with a high content of NaCl solution, as the accelerated test method NT BUILD 443 [1995], showed very similar values at ages of 7 days and 35 days. New researches should be performed with the purpose of using this method as an accelerated test, from which data can be obtained in a short time period of perhaps less than 35 days. Tests may be performed with a higher NaCl content in the solution, since the value of 165 g ± 1 g/dm^3 is still quite distant from the saturation value of the solution. These tests should verify if the diffusion coefficients obtained are similar to those corresponding to seawater.

ACKNOWLEDGMENTS

We thank the Coordenação de Aperfeiçoamento de Pessoal de Nível Superior – CAPES for scholarship Internship Senior Abroad granted André Tavares da Cunha Guimarães, allowing this research to be conducted with the University of Alicante - Alicante - Spain. We are also grateful to the Ministerio de Ciencia e Innovación of Spain and Fondo Europeo de Desarrollo Regional (FEDER) for the funding received for this research through project BIA2010-20548. Finally thanks are also given to Holcim Spain for kindly providing the cement and aggregates needed for this research.

REFERENCES

Arsenault, J., Bigas, J.P., Ollivier, J.P., 1995, 'Determination of chloride diffusion coefficient using two different steady state methods: Influence of concentration gradient', Proc. RILEM Intl. Workshop on Chloride Penetration into Concr., St Rémy-les-Chevreuse, France, p. 150-160.

Castro, P., De Rincón, O. T. & Pazini, E. 1999, 'Chloride penetration profiles in marine environments', Proc. II Internacional Conference on High-Performance Concrete, and Performance and Quality of Concrete Structures, Gramado, Brazil, pp. 371-389.

Crank, J. 1975, *The Mathematics of Diffusion*, second ed., Oxford Univ. Press,Oxford, UK.

Meira, G. R., Andrade, M. C. , Padaratz, I. J., Alonso, M. C. & Borba Junior, J. C. 2007, 'Chloride penetration into concrete structures in the marine atmosphere zone - relationship between deposition of chlorides on the wet candle and chlorides accumulated into concrete', *Cement & Concrete Composites*, **29**, p. 667-676.

NT BUILD 443, 'Accelerated chloride penetration', 1995.

Silva, C.A. & Guimarães, A.T.C. 2010, 'Comportamento dos perfis de cloreto em tetrápodes localizados nos molhes da Barra. (Rio Grande – RS – Brasil)', Proc. 4º Seminário e Workshop em Engenharia Oceânica, Rio Grande, Brazil, 3 5 November 2010, CD.

Tang, L., 1999, 'Concentration dependence of diffusion and migration of chloride ions. Part 1. Theoretical considerations, *Cement and Concrete Research*, **29**, p. 1463-1468

Tang, L., 1999, 'Concentration dependence of diffusion and migration of chloride ions. Part 2. Experimental evaluations', *Cement and Concrete Research*, **29**, p. 1469--1474

Zhang, T., 'Chloride diffusivity into concrete and its measurement from steady state migration testing', Doctoral Thesis, 1997:132, Trondheim , University of Sci. & Techn., Norway, 1997.

XII DBMC
International Conference on Durability of Building Materials and Components
PORTO - PORTUGAL, April 12th-15th, 2011

Mechanical Performance of Concrete Partially Exposed to Sulfate Solution under Hydrostatic Pressure

Zanqun Liu [1]
Geert De Schutter [2]
Dehua Deng [3]
Yunhua Liu [4]

ABSTRACT

In an extended experimental program, the development of mechanical performance of concrete cylinders partially exposed to sodium sulfate solution under hydrostatic pressure was investigated. The effects of relative humidity, concrete carbonation, fly ash and surface coating on concrete performance under sulfate attack were studied. The experimental results showed that (1) the concrete cylinders showed more severe damage in a humid environment than in a dry environment, (2) concrete carbonation could promote the failure of concrete, (3) fly ash concrete was more susceptible to damage than ordinary concrete, (4) the surface coating was an effective way to prevent sulfate attack on partially exposed concrete. Finally, the mechanism of sulfate attack on partially exposed concrete was explained.

KEYWORDS

Sulfate attack, Partially exposed, Hydrostatic pressure.

[1] School of Civil Engineering and Architecture, Central South University, Changsha, Hunan 410075, P.R China, Liuzanqun_2001@hotmail.com
[2] Magnel Laboratory for concrete Research, Department of Structural Engineering, Ghent University, Ghent, 9052 Belgium, Geert.Deschutter@ugent.be.
[3] School of Civil Engineering and Architecture, Central South University, Changsha, Hunan 410075, P.R China, dlx0216@163.com
[4] Magnel Laboratory for concrete Research, Department of Structural Engineering, Ghent University, Ghent, 9052 Belgium, Geert.Deschutter@ugent.be.

1 INTRODUCTION

Normally, there are two types of partially exposed concrete structures, column structures (piers) and platy structures (tunnels). In long term field tests [Irassar, E.F.*et.al* 1996]; [Mcmillan, F.R. 1949]; [Stark, D. 1989, 2002], the performance of column structures under sulfate attack has been extensively studied. The effects of W/C ratio, the chemical composition of cement, the mineral additions and the surface treatment on the concrete sulfate resistance were compared. The results showed several common appearances: (1) Upper parts of concrete beams in contact with air, regardless of cement content, cement composition, mineral additions, surface treatments and coarse aggregate, were deteriorated severely. The lower parts of concrete beams under ground, however, showed little or no deterioration; (2) Pozzolanic additions, such as fly ash, blast furnace slag or silica fume, played a negative role in the concrete damage in these conditions. (3) Surface coating could effectively improve the concrete sulfate resistance.

However, there are few reports about performance of platy structures partially exposed to sulfate environment. In this paper, the tests were designed to simulate the exposure conditions with hydrostatic pressure. The mechanical strenght development was studied to show the effects of relative humidity (RHC), accelerated carbonation (ACC), fly ash (FAC) and surface coating (SCC) on the concrete sulfate performance.

2 EXPERIMENTS AND RAW MATERIALS

2.1 Raw Materials

An ordinary Portland cement (CEM I 52.5 N), complying with EN 197-1 (2000), was used. Table 1 gives the chemical composition of cement and fly ash used in this study. A polymer named LDM 6119 from Celanese was used for the surface coating on concrete.

Table 1. Chemical composition of cement and fly ash (% by mass).

	CaO	SiO_2	Fe_2O_3	MgO	Al_2O_3	SO_3	CO_2	Na_2O	K_2O	Ignition loss
Cement	62.21	19.12	3.79	0.86	5.39	3.06	0.72	-	-	1.65
Fly ash	4.46	53.31	7.53	2.45	26.43	0.9	-	1.15	0.9	4.0

2.2 Specimens Preparation, Curing and Testing

The mixture proportions for tests are shown in table 2.

Table 2. Mixture proportions of concrete.

Mix	Water (Kg/m^3)	Cement (Kg/m^3)	Fly ash (Kg/m^3)	Sand (Kg/m^3)	Gravel (Kg/m^3)	W/(C+FA)	Slump (mm)
NC	131.6	375.9(I)	——	777	1165.5	0.35	11
FAC	180	262(I)	163.75	737.7	1106.55	0.55	16

The fresh concretes were cast in big moulds. After 14 days' curing, concrete cylinders (Ø100 ×250) mm were drilled. At the age of 29 days, specimens were moved into a climate room (20°C±2°C and 60%±5%). 6 cylinders of NC were dried in an oven at 60 ^oC for 48 h. After drying, cylinders were half covered with tape and moved into an accelerated carbonation chamber with 10% CO_2 concentration at 20 ± 2 ^oC and 60% ± 5% RH for 14 days. At the age of 29 days, 12 cylinders were placed in the climate room for one week and then half covered with tape. The polymer LDM 6119 was brushed every two days on the uncovered surface of cylinders for three times,. At the day when the carbonated cylinders were moved out from the accelerated carbonation chamber, the tapes were removed from the accelerated carbonated concrete (labeled as ACC specimen) and the surface coated cylinders (labeled as SCC specimen). Then 6 ACC specimens, 12 SCC specimens, 24 NC specimens, and 12 FAC specimens were were half sleeved by PVC tubes (120 × 400 mm) using epoxy (shown in

Fig.1) After another 7 days, the PVC tubes were filled with 5% sodium sulfate solution. One group of 12 NC speimens were placed in the curing room at 20±1°C and 98% RH (these NC specimens were labeled RHC). The other cylinders were placed in the climate room. 6 NC sepcimens were immersed in water at 20±1°C.

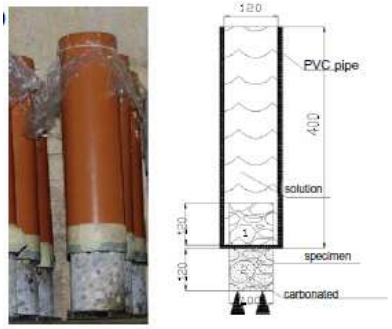

Figure 1. Setup of immersion tests.

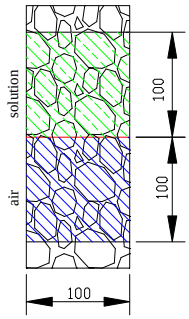

Figue 2. Vertical cross section of cylinder.

The sulfate solution was replaced each month. Each specimen was weighed ever month. After 3, 6, 9 and 12 months of exposure, the cylinders were moved out from the PVC sleeve and cut into two parts along the interface of air and solution, as schematically shown in Fig.2.

3 RESULTS

In order to evaluate the effect of different factors on the sulfate performance of concrete, two parameters were used, (1) the mass increase through unit volume of cylinders ΔM (Eq. 1), (2) the difference of compressive strength ΔP between two parts (Eq.2).

$$\Delta M = \frac{M_i - M_0}{D_0} \quad (1)$$

Where, M_i is mass of cylinder at i age (g). M_0 is initial mass of cylinder before immersion (g). D_0 is mass of unit volume concrete before immersion (g).

$$\Delta P = P_I - P_A \quad (2)$$

Where, P_I is the compressive strength of part of concrete cylinder in the solution; P_A is the compressive strength of part of concrete cylinders in the air.

Normally, researchers are used to choosing the whole mass of concrete as the reference to describe the mass development of specimens in the tests of sulfate attack on concrete. In this study, the concrete cylinders are just partially exposed to sulfate solution. There is no essential relationship between the whole mass of specimen and the mass increase of specimen. In this case, the solution will transfer from the concrete part in the solution to the part in the air. Obviously the density of concrete (mass of unit volume) has influence on the transfer of solution and the mass increase of concrete specimens. In Eq.1, the density of concrete is used as the reference.

Normally, the development of compressive strength of concrete attack by sulfate solution is shown in Fig.3 [D. Deng 2007].

So, when the immersion age is from 0 to t, (1) if the two parts of concrete cylinders are both attacked, they will show synchronous mechanical performance, ΔP should be small. (2) If the part in the air is attacked more severely than in the solution, the strength of this part will be higher than of the part in the solution, and ΔP will be negative. (3) If only the solution part is attacked, but the part in the air is not, ΔP should be large. So, larger ΔP means that the concrete has better sulfate resisting performance.

Figure 4 and Figure 5 show the mass increase and the difference of compressive strength of NC, SCC, RHC and ACC.

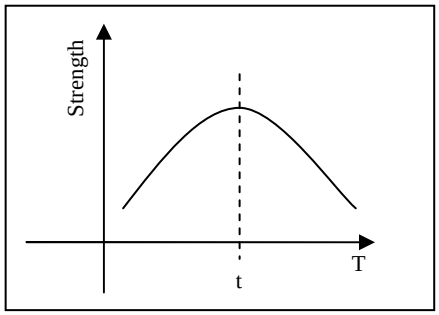

Figure 3. Development of strength of concrete immersed in sulfate solution.

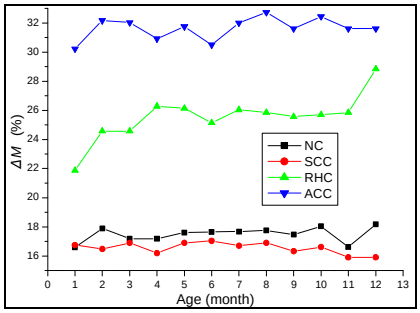

Figure 4. Mass increase (ΔM) of NC, SCC, RHC and ACC.

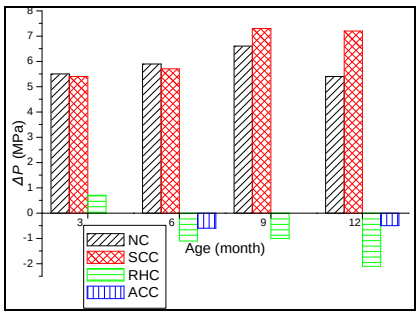

Figure 5. Difference of compressive strength (ΔP) of NC, SCC, RHC and ACC.

In Figure 4 and Figure 5, (1) the ACC shows the fastest mass increase. After 6 months exposure, the compressive strength of upper part was already higher than the lower part of concrete. (2) the SCC shows the best performance in this situation. (3) When the cylinders were exposed to the environment at 98% RH, the mass also increased faster than NC. After 6 months the strength of upper part in contact with air was already higher than the part in the solution.

In Figure 6, we can find that the compressive strength of SCC was still increasing. The strength of upper part of concrete was lower than in the solution. This means that in effect the upper part did not suffer from sulfate attack due to the preventing effect of surface coating.

In Figure 7, similar to Figure 6, the compressive strength of concrete was still increasing. However, the strength of upper part of concrete was higher than in the solution. This means that more expansive products were formed due to more severe sulfate attack and filled in the pore, resulting in higher strengths.

Figure 8 shows the case of FAC, impressively, after 3 months exposure the strength of concrete in contact with air already decreased and after 6 months the strength was lower than in the water. This

means that the FAC in contact with air was already severely deteriorated, showing the worst resistance against sulfate attack.

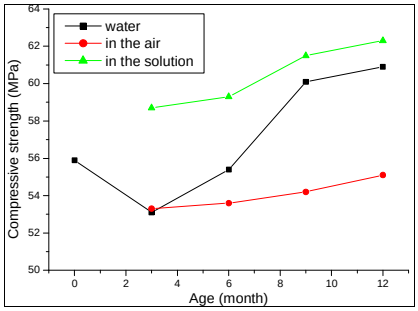

Figure 6. Development of compressive strength of SCC.

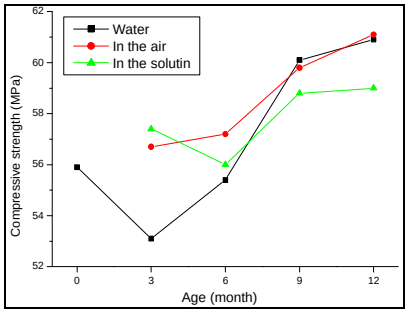

Figure 7. Development of compressive strength of RHC.

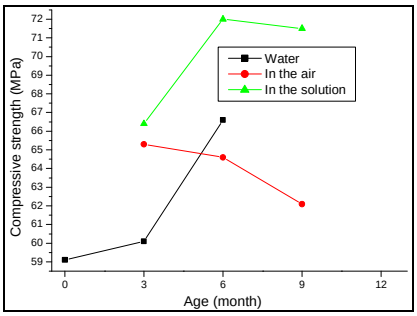

Figure 8. Development of compressive strength of FAC.

4 DISCUSSION

When the porous materials are partially exposed to sulfate environment, researchers attribute salt weathering, salt crystallization or physical attack to material damage. Wick action is the transport of water (and any species it may contain) through a porous material (concrete) face in contact with water to a drying face with less than 100% relative humidity of air [Buenfeld, N. R. et.al 1995], consisting of capillary suction and evaporation. Capillarity draws the salty water into the concrete. Evaporation occurs at a wet-dry interface located at a penetration depth near the dry face of the concrete in contact with air, and water vapor diffused out into the dry zone with less than 100% relative humidity. After some time, an equilibrium (wet-drying interface) will be established in a position where the rate of salt solution entering the concrete by capillary absorption matched by the rate of water leaving the opposite face of the concrete element by water vapour diffusion. Salts cannot be carried by the vapour and therefore built up at this position. This concentration effect causes back-diffusion of salt away from the wet-dry interface.

Nuclear magnetic resonance (NMR) is used to study the crystallization of sodium chloride due to wick action. Measuring the moisture and ion profile in porous material, an efflorescence pathway diagram is plotted [Pel et. Al. 2002, 2004]. In the slow drying or high relative humidity environment, the ion profile remains homogeneous and for some time no salt crystallization will occur. The average NaCl concentration slowly increases until the complete sample has reached saturation. In the fast drying or low relative humidity environment, ions are directly advected with the moisture to the part of sample near the solution surface, and a saturation peak will build up with a very small width. Sub-efflorescence will be formed, resulting in porous materials damage in the case.

However, in the test [Ferraris, C. F. et. al, 2006], two concrete specimens were partially immersed in the same Na_2SO_4, solution. One specimen was placed at 80%±5% RH and the other at 30% ±5%. After 75 days of exposure to a constant temperature of 25 ^oC, the specimens at 80% RH showed signs of deterioration first over a very large area, starting from above the solution level. On the contrary, at

30% RH, the zone of deterioration was narrower and was situated at a certain distance above the solution level. In this case, the first sign of deterioration was a crack, not spalling. This appearance indicates that high RH is favor of the concrete damage. In another paper [Haynes, H. et, al, 2008], the similar experimental result was also be observed. In this paper, the mechanical performance of concrete also supports that the concrete will be susceptive to being deteriorated in a moist environment. Obviously, this appearance is opposite to the classic principles of salt weathering on porous materials, and intends to support that the chemcial sulfate attack is still the main mechanism for concrete damage. Because as abovementioned, in the moist environment the ion profile remains homogeneous and for some time no salt crystallization will occur in the materials, and the average salt concentration slowly increases until the complete sample has reached saturation. I.e. in a moist environment a wider high salt concentration pore solution zone will generate in the sample. So, it is the chemical sulfate attack occurring in the high concentration sulfate pore solution responsibe for the appearance that concrete is susceptive to being deteriorated. In effect, according to the authors' previous researches [Liu, Z.Q. et al, 2010-1,3], in the cementitious materials partially exposed to Na_2SO_4 and $MgSO_4$ traces of sulfate crystals could not be detected by means of XRD, ESEM and EDS. As a comparison, sulfate crystals can be easily found in stone [Benavente, D. et, al, 2004, 2007]. On the contrary, a large amount of ettringite, gypsum and brucite crystals, the chemical sulfate attack products, were observed in the cement paste or concrete.

The negative effect of carbonation on corrosion of reinforcing steel in concrete is well known. As to the sulfate attack on concrete, as a result of carbonation, the total porosity would be reduced and the permeability of concrete could be improved [Ngala, V.T.& Page, C.L. 1997, Song, H.W. 2007]. So, Gao [GAO, R.D. et. al 2009] pointed out that the carbonation layer could mitigate diffusion of sulfate ions to some extent in the full immersion situation. However, in this paper the concrete specimens were partially exposed to Na_2SO_4 solution, the results show that concrete carbonation accelerate the concrete damage by sulfate attack. The reason for this appearance may be the effect of carbonation on the ratio of capillary to total porosity of concrete. V.T. Ngala [Ngala, V.T.& Page, C.L. 1997] studied the effect of carbonation on the ratio of capillary to total porosity of cement paste. The results showed that the capillary pore fraction greatly was improved after carbonation. Obviously, carbonation can help the capillary suction of concrete and draw more solution into the concrete. On the other hand, the pores will become smaller due to concrete carbonation. A height of solution can be raised by capillary rise in the concrete (Eq.4) [Francis Yong, J et. al 2006] .

$$h = \frac{2\gamma_{LV} \cdot \cos\theta}{rg\rho} \tag{3}$$

where h is the height of capillary rise, γ_{LV} is the liquid/vapor interfacial energy, θ is the contact angle, r is the pore radius, g is the gravitational acceleration, and ρ is the density of solution. So in the concrete a wider pore solution zone will be formed due to the concrete carbonation. As a result, a more severe chemical sulfate attack will occur, causing worse concrete damage.

Normally, in laboratory, 5% sulfate solutions are used and the storage temperature is controlled at 23.0 ± 2.0°C [ASTM C 1012 – 04]. Under this exposure condition, the tests always showed that the fly ash addition could improve the sulfate resistance of cementitious materials. However, when the concrete is partially exposed to 5% Na_2SO_4 solution, a higher than 5% sulfate pore solution (about 8%) could be formed in the upper part of cement paste in contact with air [Liu, Z,Q., 2010-2]. Fly ash contains a large amount of reactive aluminum as solid spheres of glass [Mehta, P. K. 2006] that is stable, but can be activated by some methods, such as thermal activation, mechanical activation and chemical activation [Wu, ZC & Naik, T. R.2003]. Na_2SO_4 is an effective activator and often used to activate the pozzolanic reaction of fly ash and cement paste [Shi, CJ, Day, R.L. 2000-1.2]. Moreover, more sulfates can be drawn into concrete due to the refinement of fly ash, forming a higher concentration sulfate pore solution [Liu, Z,Q., 2010-2]. So, in effect fly ash can be activated in the high concentration sulfate solution, more ettringite and gypsum formation [Liu, Z,Q., 2010-2]causing more severe concrete damage.

Wick action consists of capillary suction and evaporation. The layer of surface coating can block the capillaries, the capillary suction will be stopped. The high concentration sulfate pore solution can not be generated in the upper part of concrete, escaping the strong chemical sulfate attack.

5 CONCLUSIONS

In this paper, the development of mechanical performance of concrete cylinders partially exposed to sodium sulfate solution under hydrostatic pressure was investigated. The experimental results indicated that the cylinders under hydrostatic pressure showed a similar scaling performance to cylinders without hydrostatic pressure. On the other hand, concrete carbonation, moist ambient environment and fly ash addition could accelerate the concrete damage. Surface coating could effectively improve the concrete sulfate resistance. These findings support the idea that chemical sulfate is the mechanism responsible for the deterioration of concrete elements partially exposed to sulfate environment.

ACKNOWLEDGMENTS

This work was supported by the financial support from NSF P. R. China under contract #50378092, the scholarship from CSC and the co-funding from Ghent University of Belgium.

REFERENCES

ASTM C 1012 – 04, Standard Test Method for Length Change of Hydraulic-Cement Mortars Exposed to a Sulfate Solution.

Benavente, D., García Del Cura, M.A.,García-Guinea, J, Sánchez-Moral, S, Ordóñez, S 2004, Role of pore structure in salt crystallisation in unsaturated porous stone, J. Cryst. Growth 260 (3-4): 532-544.

Benavente, D. J. Martínez-Martínez, N. Cueto, M.A. García-del-Cura 2007, Salt weathering in dual-porosity building dolostones, Eng. Geol., 94(3-4): 215-226.

Buenfeld, N. R., Shurafa-Daoudi, M. T., Mloughlin, I. M. 1995, Chloride transport due to wick action in concrete, RILEM International Workshop on Chloride Penetration into Concrete, 315-324.

Dehua Deng 2007, Study of relationship between degradation mechanism and mode of sulfate attack on concrete, final report of item 50378092 supported by National natural foundation of China.

Ferraris, C. F., Stutzman, P. E., Snyder, K. A. 2006, Sulfate Resistance of Concrete: A New Approach, Research and Development Information PCA R&D, Serial No. 2486.

Francis Yong, J., Sidney Mindess, Robert J. Gray, Arnon Bentur 2006, The science and technology of civil Engineering materials, Chinese Architecture & Building Press.

Gao, R.D., ZHAO S.B., LI. Q.B. 2009, Deterioration Mechanisms of Sulfate Attack on Concrete under the Action of Compound Factors, Journal of building materials, 12(1): 41-46.

Haynes, H. O'Neill, R., Neff, M. P., Mehta, K. 2008, Salt Weathering Distress on Concrete Exposed to Sodium Sulfate Environment, ACI Mater. J., 105(1):35-43.

Irassar, E.F., Di Maio, A., Batic, O.R. 1996, Sulfate attack on concrete with mineral admixtures, Cem. Concr. Res. , 26(1):113-123.

Liu, ZQ. De Schutter, G., Deng, DH, Yu, ZW. 2010, Micro-analysis of the role of interfacial transition zone in ‘‘salt weathering” on concrete, Constr. Build. Mater., 24(11): 2052–2059.

Liu, Z,Q., 2010, study of the basic mechanism of sulfate attack on cementitious materials, Central South University China, Ghent University Belgium.

Liu, ZQ. De Schutter, G., Deng, DH, Yu, ZW., Micro-analysis of “salt weathering” on cement paste, submitted to Cem. Concr. Compos. 2011; 33(1):179-191.

Mehta, P. K. 2006, Concrete: structure, properties, and materials, 3nd Ed, Prentice Hall.

Mcmillan, F.R., Stantion, T.E., Tyler, I.L., Hansen., W. C. 1949, Long-Time Study of Cement Performance in Concrete, chapter 5. Concrete exposed of sulfate solis, Portland Cement Association.

Ngala, V.T., Page, C.L. 1997, Effect of carbonation on pore structure and diffusional properties of hydrated cement paste, Cem. Concr. Res. 27(7): 995-1007.

Pel, L., Huinink, H., Kopinga, K. 2002, Ion transport and crystallization in inorganic building materials as studied by nuclear magnetic resonance, Appl. Phys. Lett., 81(15): 2893-2895.

Pel, L., Huinink, H., Kopinga, K, Van Hees, R.P.J., Adan, O.C.G. 2004, Efflorescence pathway diagram: Understanding salt weathering, Constr. Build. Mater., 18(5): 309-313.

Shi, CJ, Day, R.L. ‘Pozzolanic reaction in the presence of chemical activators. Part I. Reaction kinetics’**,** Cem Concr Res. 2000, 30(1):51-58.

Shi, CaJ, Day, R.L., ‘Pozzolanic reaction in the presence of chemical activators: Part II. Reaction products and mechanism’, Cem Concr Res. 2000, 30(4): 607-613.

Song, H.W. 2007, Seung-Jun Kwon, Permeability characteristics of carbonated concrete considering capillary pore structure, Cem. Concr. Res., 909–915;

Stark, D. 1989, Durability of concrete in sulfate-rich soils, Research and Development Bulletin, vol. RD O97, Portland Cement Association,.

Stark, D. 2002, Performance of Concrete in Sulfate Environments, RD129, Portland Cement Association.

Wu, ZC, Naik, T. R. 2003, Chemically activated blended cement, ACI Mater. J., 100(5): 434-440.

XII DBMC
International Conference on Durability of Building Materials and Components
PORTO - PORTUGAL, April 12th-15th, 2011

Assessment of Residual Pull-Out Bond Strength Subjeted to Process of Accelerated Corrosion

Luciane Fonseca Caetano [1]
Roseane Shimomukay [2]
Vitor Cury Perrone [3]
Luiz Carlos Pinto da Silva Filho[4]

ABSTRACT

Corrosion is one of the most common pathologies and known as the main responsible for causing extensive damage in reinforced concrete structures. Besides the appearance of cracking, due to formation of corrosion products, there is also a considerable reduction of bond strength between reinforcement steel bar and the surrounding concrete, mainly caused by the loss of constrainment of the steel bar. Furthermore, the better understandment of the effects of loss of cross-sectional area is essential to comprehend the mechanisms of bond degradation. In order to estimate the residual pull-out bond strength of specimens subjected to a process of accelerated corrosion, an experimental program was carried out enabling the development of a representative mathematical model of bond behavior. The parameters analysed in this study were concrete compressive strength (25, 45 and 65 MPa), rebar diameter (8, 12.5, 16, 20 and 25 mm) and five levels of mass loss from 0 up to 16%.

KEYWORDS

Pull-out test, Bond degradation, Accelerated corrosion.

[1] Federal University of Rio Grande do Sul (UFRGS), Porto Alegre, Brazil, lucianefc@gmail.com
[2] Federal University of Rio Grande do Sul (UFRGS), Porto Alegre, Brazil, roshimomukay@gmail.com
[3] Federal University of Rio Grande do Sul (UFRGS), Porto Alegre, Brazil, vitor.perrone@gmail.com
[4] Federal University of Rio Grande do Sul (UFRGS), Porto Alegre, Brazil, lcarlos66@gmail.com

1 INTRODUCTION

Among the most important pathologies in civil structures, reinforcement corrosion is known as the most frequent, also responsible for the greater impact in terms of structural damage and economic costs. The rebar corrosion induces changes in the structural properties of the material, creating considerable deleterious effects as loss in cross-sectional area and rise of the tensile internal stress, leading to posterior cracking of the concrete cover, due to accumulation of corrosion products in the concrete pores, and decrease of the concrete-steel bond.

The relevance of this deleterious effects caused by reinforcement corrosion, in terms of durability and structural performance, justify the importance of this issue and the attention spent by the scientific community. However, there are still many points to elucidate regarding the way this pathology affects the concrete-steel bond behavior. According to the FIB Bulletin 10 [2000], the bond behavior is sorely affected by the global corrosion of the rebar while the local corrosion is the main responsible for the loss of cross-sectional area. Nevertheless, the research published by Auyeng [2001] points that a 2% reduction in rebar diameter can cause an 80% decrease in bond strength.

Other researchers [Almussallam *et al*. [1996]; Al-Sulaimani *et al.* [1990]; Coronelli *et al.* [2002]] assess the concrete-steel bond behavior associated with corrosion by analyzing exclusively the presence of cracking. According to these authors, as long as the corrosion does not induce cracking, there is an increase in the bond strength, due to the deposition of corrosion products in the concrete pores around the rebar. However, in the presence of cracks, the loss of confinement takes place, leading to a marked decrease of the bond strength performance.

As matter of fact, the bond behavior is rather complex, depending on a variety of factors, which refer to the confinement conditions of the surrounding concrete and the superficial conditions of the reinforcement bar. The disturbance in the physical interlocking characteristics of rebar surface can be caused by local corrosion, loss of cross-sectional area, changes in rib geometry and formation of an interfacial layer with lower hardness around the rebar.

Therefore, the good understanding of the effects of corrosion in bond strength behavior is essential, as well the correct determination of residual bond strength of corroded structures.

2 EXPERIMENTAL PROGRAM

The concrete-steel bond was analysed trough pull-out test according to RILEM [1973] and the parameters studied were the concrete compressive strength (25, 45 and 65 MPa), the rebar diameter (8, 12.5, 16, 20 and 25 mm) and the mass loss percentage from 0 up to 16%.

2.1 Materials and Mix Proportion

The specimens were casted in three different mix proportions, as shown in Table 1, in order to obtain the specified compressive strength. The specimens dimensions will be described in Section 2.3 of this chapter.

Table 1. Mix proportion used to cast speciments.

Compressive Strength (MPa)	Mix proportion (cement : sand: coarse aggregate)	w/c ratio
25	1 : 3,42 : 4.08	0.56
45	1 : 2.12 : 2.80	0.42
65	1 : 1.34 : 2.16	0.32

The materials used are commonly found in south of Brazil. These materials are detailed in Table 2.

Table 2. Materials used in the study.

Material	Specification
Cement	Portland cement High early strength, Sulfate resistant Type CP-V
Fine Aggregate	river sand quartz $\gamma = 2.62$ g/cm³ fineness module = 2.42
Coarse Aggregate	crushed stone basaltic $\gamma = 2.82$ g/cm³ Dmax = 19 mm fineness module = 6.82
Rebar	CA 50 (yield strength = 500 MPa)
Super plasticizer admixture	content = 0.5% by cement mass

2.2 Corrosion Acceleration Procedures

Considering the long period necessary to establish the corrosion process and the time limitations related to the development of the experimental program, it was shown necessary the adoption of a corrosion acceleration technique, in order to obtain higher percentages of mass loss (up to 16%) in a short period of time.

In this study, a corrosion acceleration method developed by the research group at LEME/UFRGS was used, known as CAIM - Modified Accelerated Corrosion by Immersion. The CAIM method was originally applied by Lima [1990], based on an initial design proposed by Varela *et al.* [1988]. Over time, Torres [2006] e Graeff [2007] have modified and improved the corrosion procedure.

The basic idea of the test is to place a steel bar embedded in concrete. The specimen is then placed in a saline solution with a NaCl concentration of 35 g/l. As shown in the Figure 1, the specimen is immersed up to the level of the bottom of the rebar, an experimental setup that allows both moisture and oxygen to easily diffuse to the vicinity of the steel. An electrical wire is positioned over the rebar, without direct contact, to act as a cathode and attract the chloride ions. Another wire is placed in the saline solution, behaving as anode.

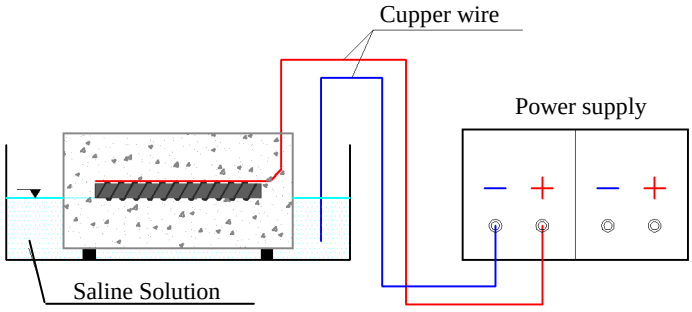

Figure 1. CAIM set up.

For the constant current, as used in this research, or constant voltage, chloride migration is stimulated by the application of a potential difference between the bar and the saline solution. The output results are obtained in terms of corrosion currents over time and mass loss. The last one is obtained by the splitting of specimen after the induced corrosion, allowing the recovery and weighing of the steel bar. Before weighing, the corrosion products are removed by the immersion of the bar in a cleaning solution containing hydrochloric acid and hexamethylenetetramine ($C_6H_{12}N_4$), according to ASTM A380 [1996].
In order to hasten the process of corrosion, in this research, the chloride was incorporated in the mixing water, eliminating the initiation period. Therefore, it was not necessary to wait for the chloride ions to migrate from the surface of the concrete to the surroundings of the bar for the depassivation to occur.

Concerning the chloride concentration, there is no consensus in the literature about the chloride threshold that triggers the corrosion. Glass and Buenfeld [1997] carried out an extensive literature review, leading to the conclusion that the proposed values are clustered between 0.17 and 2.5% of chloride by weight of cement. To assure the set off of the bar corrosion, it was chosen a chloride concetration highly above the limit indicated. Thus, a content os 5% of NaCl by mass of cement was used, in order to gurarantee a concentration of 3% of chloride by mass of cement in the moisture, same content used by Bolina *et al.* [2007], Glass *et al.* [1997], and others.

The electric current density of 500 μA/cm² used in the test was chosen according to the reccomendation of Graeff [2007], for considering that this density does not imply in significant distortions in the corrosion phenomenon. It is noteworthy that the recommendation of current densities show great variability in the literature, presenting values from 45 μA/cm² [Bonacci *et al.*, 1998] up to 10400 μA/cm² [Almusallam *et al.*, 1996].

2.3 Test Specimens / Pull-Out Test

The specimens used for the pull-out test were prepared and tested following the requirements of RILEM [1973]. It is important to mention that prior to casting, the bars were subjected to a mechanical cleaning procedure to remove the superficial rust and any other residue that might be attached to the bar surface. Afterwards, according to the RILEM recommendation, the length of the bar which was not to be bonded to the concrete was marked and isolated by the placement of a plastic tube.

The specimens consisted of a bar passing through a cubic concrete block, with edge size equivalent to 10 times the bar diameter. The Figure 2 shows the experimental set-up used for the pull-out tests.

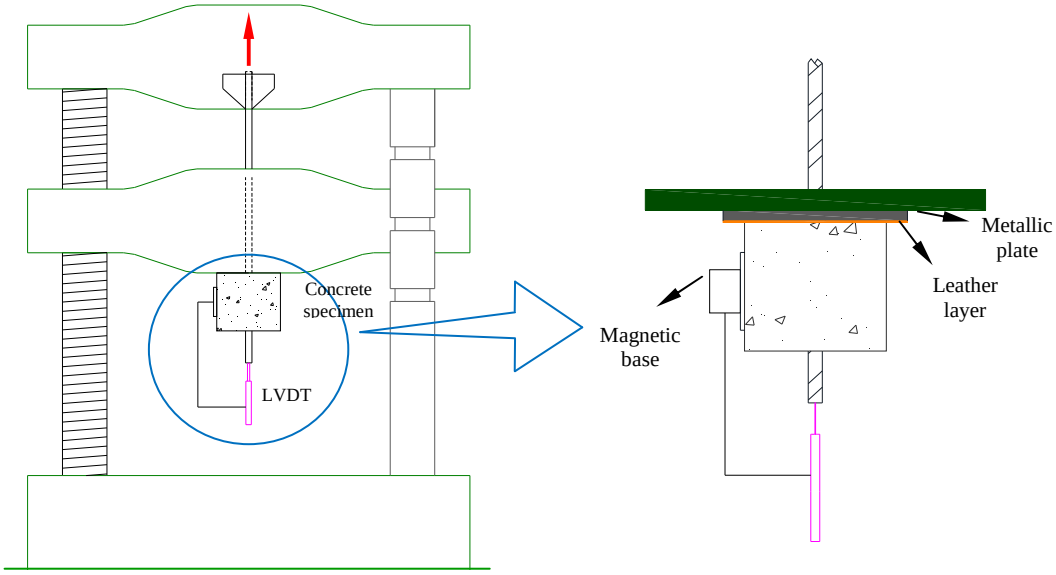

Figure 2. Experimental set-up.

As seen in Figure 2, the concrete prism is placed against the lower crosshead of the testing machine, while the bar was fixed on the upper crosshead. The free tip of the bar was instrumented with a displacement transducer (an LVDT) fixed on the concrete block to avoid any distortion of the slip measurements.

2.4 Experimental Methods / Statistical Planning

In order to reduce the number of specimens necessary to develop the experimental program, a statistical fractioning method was aplied. Futhermore, this method allowed the elaboration of a mathematical model to evaluate the phenomenom through the analysis of the obtained results.

3 RESULTS

For the construction of the mathematical model, the data was analysed in the software Statgraphics Plus 2.1 and modeled using an analysis of non-linear regression. First of all, in order to obtain a mathematical model capable of providing bond strength estimations according to the pull-out test, a survey was conducted regarding the influence of each variable in the concrete-steel bond behavior, allowing to elaborate a draft of the equation.

Concernig to the term referring to the rebar corrosion, a more meticulous analysis was necessary. First of all, it was necessary to determine the inflection point, ie, the point on a curve at which there is a change in behavior. For small values of mass loss, the bond stress increases and, from the point of inflection, there is a shift in behavior. In order to determine the mass loss value that causes this inversion, values between 1% up to 4% were simulated as the inflection point. The best fit and the higher value of the coefficient of determination (R^2) were obtained with the inflection point as 1% of mass loss.

As the inflection point of the corrosion behavior referring to the bond stress, it was sought to obtain an equation to represent the phenomena observed in the experimental tests. After several attempts and interactions, the Equation 1 was obtained and considered as being more appropriate:

$$\tau_u = 12{,}3 \times fc_c^{\,0{,}5} \times \frac{1}{\phi_c^{\,fc_c^{0{,}5}}} \times \left(\frac{0{,}3 + GC_c}{0{,}3 + GC_c^{\,1{,}4}} \right) \qquad (1)$$

where:

τ_u = bond stress [MPa];
fc_c = encoded compressive strength [MPa];
GC_c = encoded mass loss [%];
ϕ_c = bar diameter [mm].

It should be noted that, due to the wide variation of the variable values, it was needed to encode the experimental data for the insertion on the software. The encoding used are detailed in the expressions 2 to 4. In order to use the model, it is necessary to perform the data transformation according to them.

$$\phi_c = \frac{\phi}{16} \qquad (2)$$

$$fc_c = \frac{fc}{30} \qquad (3)$$

$$GC_c = \frac{GC}{2} \qquad (4)$$

where:

ϕ = bar diameter [mm];
F = compressive strength [MPa];
GC = mass loss [%].

3.1 Bond Stress versus Bar Diameter versus Mass Loss Percentage

In order to plot the curves and verify the bond stress values regarding the corrosion manifestation and the diameter variation, the compressive strength (30 MPa) was kept constant. The Figure 3 shows that smaller diameters leads to higher bond strength values, as expected. It is noticed that bars of diameter 8 mm presents much higher bond strength values when compared to the other analysed diameters. This behavior must be taken carefully, once there is only one combination of the variable levels to this diameter.

Initially, it is important to emphasize that the presence of corrosion showed no interaction with any of the other variables in this research. The inflexion observed in the bond strength behavior as increasing

mass loss was also noted by Auyeng *et al*. [2000] and Al-Sulaimani *et al.* [1990], differing of the behavior percieved by Graeff [2007] and Almussallam *et al.* [1996].

Analysing the results published by Al-Sulaimani *et al.* [1990], for bars 20 mm in diameter, it is observed that the bond strength values is 17% higher than the values obtained through the model developed in this research. Although the comparison between both research's results allow to verify the behavior tendency, the direct comparision of the bond strength values is difficult to be analysed, due to the divergence of the adopted procedures.

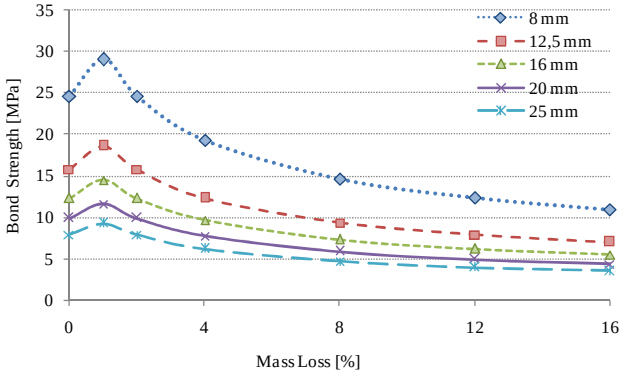

Figure 3. Bond strength performance – mass loss percentage versus bar diameter.

The bond strength increase, in comparision with bars not affected by corrosion, was of 17.8% for specimens with 1% of mass loss. Almusallam *et al.* [1996] obtained similar values, however this increase corresponds to 4% of mass loss. The improvement of the bond strength performance, as described in the literature, occurs due to the formation of oxides,which are deposited around the bar, providing better interlock between the bar and the concrete. The Table 3 describes the residual bond strength for each percentage of mass loss.

Table 3. Residual bond stress to mass loss percentage.

GC [%]	0	1	2	3	6	9	12
τ_R [%]	100	117.8	100	78.3	66.6	56.4	50.1

3.2 Bond Strength versus Diameter versus Compressive Strength

As observed in the Figure 4, the higher the compressive strength and the bar diameter, the lower the bond strength. Furthermore, higher compressive strength affects significantly the diameter effect. This fact can be related to the tendency to brittle fracture of specimens of higher compressive strength, due to the greater strength concrete wedges between the ribs, hindering the concrete crush and, consequently, breaking the rib slip that occurs in lower compressive strength concretes. The high bond stress developed results in a strong tendency to a blunt splitting failuire. This effect is aggraveted by the increase in the rib size, which is associated to the rebar diameter.

As observed in Figure 4, the bond strength values for 8 mm in diameter are greatly high, differing form values found by Graeff [2007].

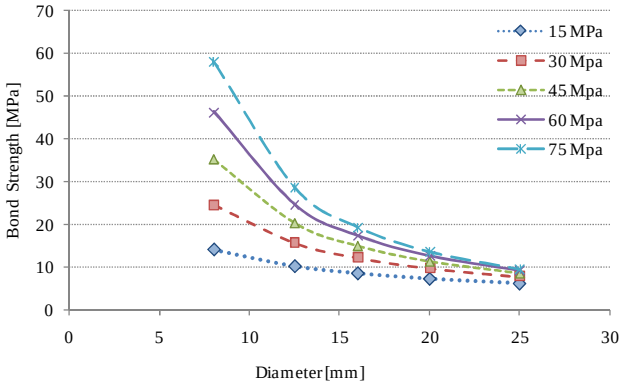

Figure 4. Bond strength performance – compressive strength versus bar diameter.

The results obtained by de Larrard *et al.* [1993], however, were more consistent with the results obtained in this research. For compressive strengh of 95 MPa and bar diameters of 10, 16 and 25 mm, the researchers obtained bond strength values of 64.9, 39.8 and 24.8 MPa, respectively. The decrease of the bond strength performance obtined by de Larrard *et al.* [1993] when the diameter ranged form 10 to 16 mm was of 39%, while the model presented in this research estimates this decrease in 53.7%. It is noteworthy that the test method used by the researchers was the beam test, and a bar slip of 100 μm was considered as the limit of the test for the analysis. This value is considered rather conservative, once it is known that beams usually reach their rupture at the magnitude of 1000 μm.

Soroushian e Choin [1989] registered values of 17.5 and 13 MPa for bar diameters of 16 and 25 mm, respectively, for compressive strength of 30 MPa. As shown in Figure 3, the bond strength values estimated by the model for this combinations (16.2 and 10,4 MPa, repectively) are very close to those obtained by the researchers, considering the differences between the test methods and the variability of measurements.

It is noticeable that, even though the model developed in this research presents consistency with the bond strength values found in the literature review, it must be taken carefully when analysing bars with diameters smaller than 12.5 mm.

4 CONCLUSIONS

It is verified that the final mathematical model obtained in this research was proved sensitive to experimental variations and presented a high potential for representation of the bond strength, reaching a coefficient of determination of 0.82.

The rebar diameter showed significant influence in the bond strength. There is a tendency to smaller diameters to generate higher bond stress values. It is worth noticing that the use of the mathematical model for diameters smaller than 12.5 mm must be cautious, since it was noticed that the model can slightly overestimate the bond strength values.

Concerning the strong interaction between the bar diameter and the concrete compressive strength in the structural failure, it was noticed that higher compressive strength, combined with larger diameters (over 12.5 mm), favors splitting failure, reducing the potential bond strength.

Therefore, in concretes with compressive strength higher than 50 MPa, it is recommended the use of high levels of confinement, in order to inhibit the splitting cracking and allow the mobilization of all the bond strength potential.

The model points that rebar corrosion causes an increase in bond strength due to deposition of corrosion products in concrete pores, increasing compacity of the matrix around the steel bar. Beyond 1% of mass loss, the oxides affects negatively the concrete-steel bond, favoring the rebar slipping.

ACKNOWLEDGMENTS

The authors would like to acknowledge the sponsorship of CNPq and the support of technicians and research assistants of the Laboratório de Ensaios e Modelos Estruturais (LEME/UFRGS), to Arcelor Mittal, for the donation of all the steel rebars, and to Votorantim Cimentos, for the donation of the cement.

REFERENCES

Al Sulaimani, G. J. *et al*. 1990, 'Influence of corrosion and cracking on bond behavior and strength of reinforced concrete members', in *ACI Structural Journals*. v.87, no2, p. 220-229.

Almusallam, A. A.; Al-Gahtani, A. S.; Rasheeduzzafar, A. R. A. 1996, 'Effect of reinforcement corrosion on bond strength', in *Construction and Building Materials*. Vol. 10, n.2, p. 123-129.

Auyeung, Y.B.; Balaguru, B.; Chung, L. 2000, 'Bond behavior of corroded reinforcement bars', in *ACI Materials Journal*. Vol. 97, n.23, pp. 214-221.

Bolina, C.C. *et al*. 2007, 'Estudo de corrosão das armaduras frente ao ataque por cloretos e carbonatação em estruturas de concreto armado no laboratório de materiais de construção da Universidade Federal de Goiás', in Trabalho Técnico. Goiás.

Coronelli, D. 2002, 'Corrosion cracking and bond strength modeling for corroded bars in reinforced concrete', in *ACI Structural Journal*. Vol. 99, no. 3, p. 267-276.

De Larrard, F.; Schaller, I.; Fuchs, J. 1993, 'Effect of bar diameter on the bond strength of passive reinforcement in high-performance concrete', in *ACI Materials Journals*, v.90, n.4, p.333-339.

Fang, C. *et al*. 2006, 'Bond behavior of corroded reinforcing steel bars in concrete', in *Cement and Concrete Research*. Vol. 36, n. 10, p. 1931-1938.

FIB BULLETIM 10, 2000. 'Fédération Internationale de Béton Bond of reinforcement in concrete, State-of-art report'10. Ed. by Fib Task Group 4/2 bond models, Convener Ralejs Tepfers, 427 pp.

Glass, G.K.; Buenfeld, N.R. 1997, 'The presentation of the chloride threshold level for corrosion of steel in concrete', in *Corrosion Science*, v.39, n.5, p.1001-1013.

Graeff, A. G. 2007, 'Avaliação Experimental e Modelagem dos Efeitos Estruturais da Propagação da Corrosão em Elementos de Concreto Armado'. Dissertação (Mestrado em Engenharia). Programa de Pós Graduação em Engenharia, UFRGS, Porto Alegre.

RILEM; FIP; CEB, 1978. 'Essai portant sur l'adherence des armatures du béton. 1. Essai per flexion (7-II-28D). 2. Essai par tracion (7-II-128) Recommendations Provisoires'. *Matériaux et Constructions*. Paris, v. 6, n. 32, p. 96-105, 1978.

Soroushian, P.; Choi, K.B. 1989, 'Local bond of deformed bars with different diameters in confined concrete', in *ACI Structural Journal*, v.86, n.2, p.915-922.

Torres, A. S. 2006 'Avaliação da sensibilidade do ensaio CAIM – corrosão acelerada por imersão modificada – frente ao processo de corrosão de armaduras de concreto armado'. Dissertação (Mestrado em Engenharia) – Programa de Pós-Graduação em Engenharia Civil, UFRGS, Porto Alegre.

Lima, M. G. 1990, 'Influência dos componentes do concreto na corrosão de armaduras'. Dissertação (Mestrado em Engenharia) – Programa de Pós-Graduação em Engenharia Civil, UFRGS, Porto Alegre.

XII DBMC
International Conference on Durability of Building Materials and Components
PORTO - PORTUGAL, April 12th-15th, 2011

Comparative Study of Nano-SiO_2 and Silica Fume on Gas Permeability of Concrete

Mahdi Valipour [1]
Alireza Mirdamadi [2]
Mohammad Shekarchi [3]

ABSTRACT

Permeability is a microstructure property of concrete which indicates the ability of concrete to bypass a fluid with specific viscosity under a pressure gradient. In this paper the influence of nano-SiO_2 (NS) addition on properties of concrete as compared with silica fume (SF) has been studied through measurement of compressive strength, electrical resistivity and gas permeability test. In the program the effect of NS was studied by replacing a part of SF with NS as a pozzolan in mix design and result were compared with control concrete. The results show that replacement of portion of SF with NS will improve the durability characteristic of concrete.

KEYWORDS

Compressive strength, Electrical resistivity, Gas Permeability, Nano-SiO_2, Silica fume.

[1] M.Sc student, School of Civil engineering, University of Tehran
[2] Research Assistant, Construction Materials Institute (CMI), Texas A&M University
[3] Director of Construction Materials Institute (CMI), University of Tehran

1 INTRODUCTION

Durability has been of the main concern at the stages of design and maintenance of concrete structures [Nishiwaki *et al*. 2004]. It is generally accepted that concrete durability to a large extent is governed by its resistance against the transport of aggressive elements into its pores [Nasir, Shafiq and Cabrera 2004]. The durability and mechanical properties of HPC are mainly dependent on the gradually refining structure of HPC and the gradually improving paste-aggregate interface incorporating additions and admixtures. Many researchers have applied silica fume (SF) to improve cement-based materials properties, and have achieved great successes. But the activity of SF at early ages is low according to the literature [Qing *et al*. 2004; Mitchell *et al.* 1998; Larbi *et al.* 1990; Papadakos, Vagelis 1999; Li *et al.* 1985].

Recently, nanotechnology has attracted considerable scientific interest due to the new potential uses of nm scale. A new pozzolanic material produced synthetically, in form of water emulsion of ultra-fine amorphous colloidal silica, is available on the market and it appears to be potentially better than silica fume for the higher content of amorphous silica (> 99%) and the reduced size of its spherical particles (1-50 nm) [Iliff and Dhanasekar 2003]. Therefore, it is supposed to the pozzolanic activity of nano-SiO_2 is more than that of silica fume. Scanning electron micrographs (SEM) of silica fume and nano-SiO_2 are shown in Fig. 1 [Byung-Wan Jo *et al.* 2007]. Permeability is a measure of the concrete's ability to resist penetration of water or other substance. It is important that the permeability of concrete should be kept low in order to protect the reinforcing steel bar contained within or if concrete is used for a water retaining structure. Controlling the permeability of concrete can be done different ways such as water or gas permeability [Calogovic 1995]. Permeability of concrete to oxygen is usually determined by a method developed by the Cembureau [Kollek 1989]. Although other test methods including non-destructive Torrent method and South African oxygen permeability index (OPI) have been developed to evaluate gas permeability, all permeability methods applied on concrete samples lead qualitatively to the same trend of permeability coefficient [Afrem 1996]. In this research gas permeability and compression strength tests were performed on specimens of concrete to investigate the durability and mechanical properties of concrete containing nano-SiO_2 combined with silica fume as compared with silica fume.

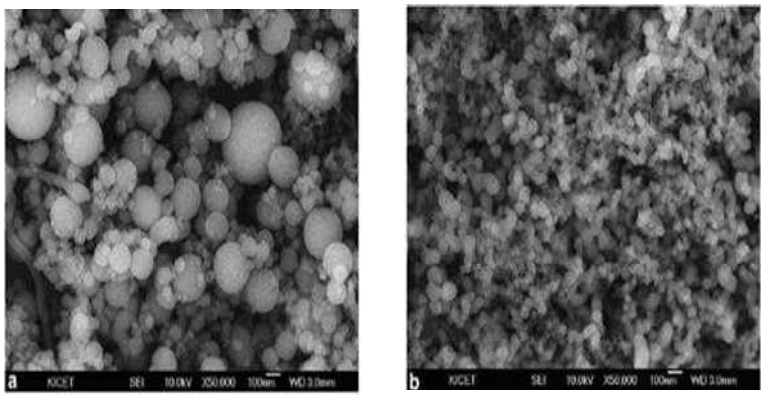

Figure 1. SEM photographs of materials: (a) silica fume (b) nano-SiO_2 [Byung-Wan Jo *et al.* 2007].

2 SPECIMEN MANUFACTURE AND TEST PROCEDURE

For each mixture proportion, 3 numbers of 150 mm cubes and a cylindrical specimen, 150 mm in diameter and 300mm in height which is cut in three discs after curing, prepared for the measurement of strength and gas permeability respectively. Compressive strengths of concrete specimens were measured after 28 days while gas permeability tests were carried out after 35 days. After the curing, specimens of permeability were dried in the oven (105±1°C) for 5 days. This preconditioning regime is recommended by Cembureau and is recognized as regime B [Parrot 1988]. Before permeability

testing, each cylinder is cut into three discs with the thickness of 50 mm suited for placing in the test cell. In the Cembureau method, the underlying principle is the Hagen-Poiseuille relationship for laminar flow of a compressible fluid through a porous body with small capillaries under steady-state condition. The relationship proposed by Hagen-Poiseuille for determining specific permeability coefficient can be written:

$$k = \frac{2.Q.P_a.L\eta}{A(P^2 - P_a^2)} \quad (m^2)$$

Where Q = volume flow rate of the fluid (m^3/s)
A = cross-sectional area of the specimen (m^2)
L= thickness of the specimen in the direction of flow (m)
η = dynamic viscosity of the fluid at test temperature ($N.s/m^2$)
P=inlet pressure (absolute)(N/m^2)
P_a=outlet pressure, assumed in this test to be equal to atmospheric pressure (N/m^2)

By using oxygen as a fluid and standard reference specimen of 150 mm diameter and 50 mm thickness, the relationship simplified to:

$$K_{oxygen} = \frac{1.14 \times 10^{-4} Q.P_a}{(P^2 - P_a^2)}$$

The essential elements and testing equipment consist of a gas supply, a pressure regulator with pressure gage, the testing cell, flow meter and a stop-watch. The detail of gas permeability device is shown in Fig. 2 [Bakhshi *et al.* 2006, Torrent 1999].

The oxygen permeability coefficient of the specimen K_{oxygen} would be obtained by evaluating the mean K from the five K_i values obtained for the five pressure stages.

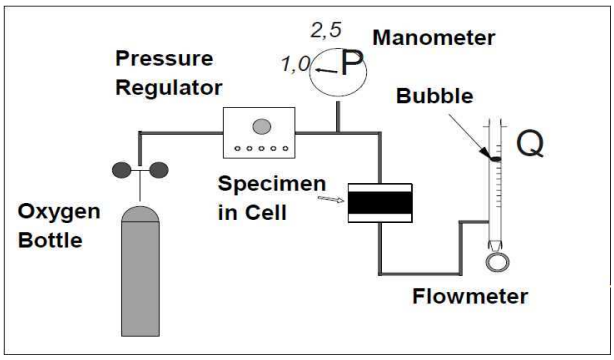

Figure 2. Details of gas permeability device [Torrent 1999].

3 MATERIALS

The cement used was commercially available ASTM Type II Portland cement with a specific gravity of 3.14 and a fineness of 290 m^2/kg. Table 1 shows the chemical analysis and the physical properties of the Portland cement. Crushed aggregates with maximum size of 19 mm were used. Polycarboxylate super- plasticizer was used in order to improve the workability of fresh material. Aggregate had specific gravity and absorption values of 2.59 and 3%, respectively. The fineness modulus of fine aggregates was 3.4. Silica fume (SF) obtained from Azna ferro-silicon alloy manufacture. The samples were prepared from a colloidal silica sol containing 15 wt% of solid material. The particle size was 5 nm with a specific surface area of 500 m^2/g.

Table 1. Chemical analysis and properties of cement.

Composition (%)	SiO_2	Al_2O_3	Fe_2O_3	CaO	MgO	K_2O	Na_2O	SO_3	CO_2	Blaine fineness (m^2/g)
Cement	22.1	4.6	3.34	62.68	3.68	0.62	0.14	1.49	0.56	0.34

Table 2 shows the mixture concrete properties. According to table 2, two concrete mixtures had been used that include: mix concrete containing Silica fume 7.5% (MSC) and mix concrete incorporating Silica fume 6% plus nano-SiO_2 1.5% (NSC).

Table 2. Mix Properties.

Mix Code	MSC	NSC
Cement (kg/m^3)	370	370
Silica Fume (kg/m^3)	30	24
Nano-SiO_2 (kg/m^3)	0	6
Corse aggregate (kg/m^3)	800	800
Fine aggregate (kg/m^3)	970	970
Water (kg/m^3)	180	180
Super plasticizer (% by mass of cement)	0.24	0.61
w/c	0.45	0.45
Slump (mm)	85	85

4 RESULTS AND DISCUSSION

4.1 Electrical Resistivity Results

In this investigation, the AC current method was applied on the saturated surface dried (SSD) specimens with 1.1 kHz frequency. Figure 3 shows the cell and system used to measure resistance of samples. After measuring the resistance, the resistivity of the concrete was derived from a simple equation:

$\rho = (R \times A) / H$

Which ρ is the resistivity (kΩ·cm), R is the electrical resistance (kΩ), A is the surface area (cm^2) and H is the height of the slice (cm).

The results of electrical resistance tests are shown in table 3. The reported electrical resistivity of the specimen is the average of three records obtained after 28 day curing. As it is shown the electrical resistance of the sample NSC is more than sample MSC. Addition of nano-SiO_2 to silica fume concrete, leads to more compacted structures.

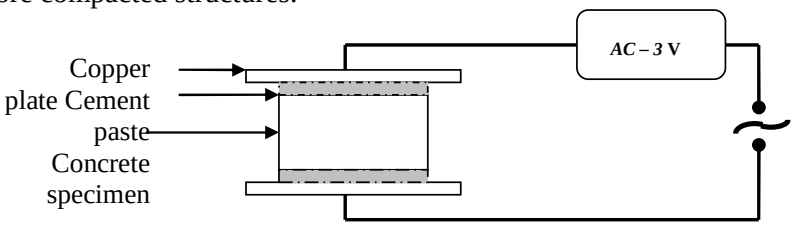

Figure 3. Electrical resistivity measuring instrument.

Table 3. Electrical resistivity of concrete samples

Code	Electrical resistivity (KOhm.cm)
MSC	18.5
NSC	20.5

4.2 Compressive Strength Results

Figure 4 presents the compressive strengths of the tested specimens. As it is shown the compressive strength is approximately the same for both samples in all ages.

4.3 Gas Permeability Results

The average results of gas permeability tests are summarized in Table 4. The NSC mixture showed higher resistance to gas permeability at 28-day age compare to the MSC mixture. Despite the result of compressive strength shows the same amount for the both pozzolans, the durability factor of concrete containing nano silica showed better performance.

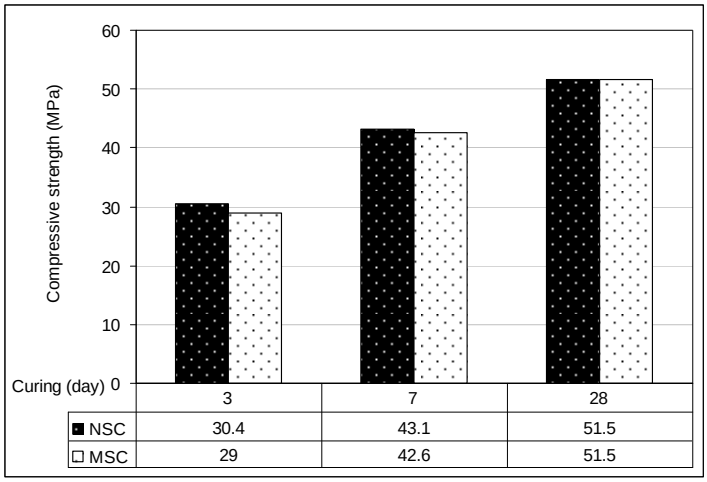

Figure 4. Compressive strength of samples.

Table 4. Coefficient of Gas Permeability of samples (m^2).

MSC	disc 1	2.37 E-16	average	2.9±0.5 E-16
	disc 2	2.96 E-16		
	disc 3	3.44 E-16		
NSC	disc 1	1.8 E-16	average	1.9±0.2 E-16
	disc 2	2.19 E-16		
	disc 3	1.78 E-16		

5 CONCLUSIONS

According to the results it can be concluded:
(1) Nano-SiO_2 pozzolan is more active in early age than silica fume due to the larger specific surface area and fineness.
(2) A durability characteristic in form of gas permeability is improved in concrete containing nano silica in comparison to concrete incorporating silica fume. Hence, it can be concluded that the microstructure of the nano-SiO_2 concrete is containing fewer porosity than that of the concrete incorporating Silica fume.
(3) The electrical resistivity of concrete increases by replacing nano-SiO_2 for cement. An electricity resistance test reveals that the microstructure of concrete with nano-SiO_2 is more uniform and compacted than that of concrete containing silica fume.

ACKNOWLEDGMENTS

This study has been funded by Iranian Nanotechnology Initiative and authors of this paper especially thank Dr. M. Tadayon, representative of the Iranian Nanotechnology Initiative. As well, the support of the Construction Materials Institute at the University of Tehran is highly appreciated.

REFERENCES

AFGC-AFREM, 1996, 'Essai de perméabilité aux gaz du béton durci : Mode opératoire recommandé', Durabilité des Bétons, AFGC-AFREM, Toulouse, France, 1996.

Byung-Wan Jo, Chang-Hyun Kim, Ghi-ho Tae, Jong- Bin Park. 2007.'Characteristics of cement mortar with nano- SiO2 particles', Construction and Building Materials, Vol. 21, pp. 1351–1355.

Bakhshi, M., Mahoutian, M., Shekarchi, M., 2006, 'The gas permeability of concrete and its relationship with strength', In: Proceedings of the fib, 2nd International Congress, June 5–8, 2006 – Naples, Italy.

Calogovic, V., 1995, 'Gas permeability measurement of porous materials (concrete) by time-variable pressure difference method', Cement and Concrete Research, Vol. 25 (5), pp. 1054-1062.

Iliff, L. and Dhanasekar, R. (2003), 'Investigating The Water Permeability of Concrete By Means of The Constant Flow Method, Central Queensland University, Rockhampton, Australia.

Kollek, J.J., 1989, 'Determination of the permeability of concrete to oxygen by the Cembureau method – a recommendation', RILEM Mater. Struct. 1989;22(129):225–30

Larbi JJ, Fraay ALA, Bijen JM. 1990. 'The chemistry of the pore fluid of silica fume – blended cement systems', Cement and Concrete Research; 20: 506.

Li, S., Roy, D. M., Kumar, A. 1985. 'Quantitative determination of pozzolans in hydrated systems of cement or Ca(OH)2 with fly ash or silica fume', Cement and Concrete Research; 15:1079.

Mitchell DRG, Hinczak I, Day, R. A., 1998, 'Interaction of silica fume with calcium hydroxide solutions and hydrated cement pastes', Cement and Concrete Research; 28: 1571– 84.

Nasir Shafiq, Cabrera, J. G., 2004. 'Effects of initial curing condition on the fluid transport properties in OPC and fly ash blended cement concrete', Cement and Concrete Composites Vol. 26(4), pp. 381-387.

Nishiwaki, T., Leite, J.P, de B. and Mihashi, H.. 2004. 'High performance fibre reinforced cementitious composites: a sustainable building material for controlling water permeability', RILEM International Symposium on Environment-Conscious Materials and Systems for Sustainable Development, Sept. 6-7, 2004, Koriyama, Japan, pp. 279-286.

Papadakis, V. G., 1999. 'Experimental investigation and theoretical modelling of silica fume activity in concrete', Cement and Concrete Research; 29:79–86.

Parrot, L. J., 1988, 'Moisture profiles in drying concrete', *Advances in Concrete Research*, Vol. 1, No.3j, pp. 164-170.

Qing, Y., Zenan, Z., Deyu, Chen K, Rongshen C, 2007. 'Influence of nano-SiO_2 addition on properties of hardened cement paste as compared with silica fume', Construction and Building Materials Vol. 21(3), pp. 539-545.

Torrent, R. 1999. 'The Gas-Permeability of High- Performance Concretes: Site and Laboratory Tests', High-Performance Concrete, *Performance & Quality of Concrete Structures*, ACI SP-186, Paper 17, pp. 291- 308.

XII DBMC
International Conference on Durability of Building Materials and Components
PORTO - PORTUGAL, April 12th-15th, 2011

Comparison of Chloride Diffusion in Nine Months Concrete Specimens Containing Metakaoline and Silica Fume Pozzolans

Mahdi Valipour [1]
Farhad Pargar [2]
Mohammad Shekarchi [3]

ABSTRACT

Corrosion induced by chloride is one of the major causes of deterioration of concrete structures in Persian Gulf. A large amount of research has been conducted to study the chloride diffusion of concrete, both theoretically and experimentally. In this paper, chloride diffusion of concretes contain metakaoline (5%, 10%, 15%) and silica fume (5%, 7.5%, 10%) as a replacement of cement compared with control specimen after nine months exposure in tidal and splash zones in Persian Gulf. The results show replacements of cement with silica fume and metakaoline reduce the chloride penetration into concrete, significantly.

KEYWORDS

Chloride diffusion, Metakaoline, Silica fume, Tidal zone, Splash zone.

[1] Graduate Research Assistant Construction Materials Institute (CMI), University of Tehran
[2] Graduate Research Assistant Construction Materials Institute (CMI), University of Tehran
[3] Director of Construction Materials Institute (CMI), University of Tehran

1 INTRODUCTION

The premature deterioration of reinforced concrete due to chloride-induced corrosion of reinforcement is a serious problem in Persian Gulf region. The most common form of deterioration is caused by chloride ingress through concrete, resulting in corrosion of the reinforcing steel. This situation is exacerbated for structures that are close to, or located in, a marine environment. When chlorides accumulate within the surface layer of concrete, a concentration gradient of chloride ions is established within the concrete cover with the result that chloride ions migrate toward the reinforcement in the concrete [Sreejith et al. 2008].

In this region, the use of silica fume as a supplementary cementitious material has increased substantially in concretes used for marine structures in the Persian Gulf. The reason for use of silica fume in these structures is claimed to be an increase in the durability of coastal structures. In recent years, there has been a growing interest in the use of MK as a mineral admixture for a similar purpose.

High reactive metakaoline, produced by controlled thermal treatment of kaolin, is the most recent mineral admixture to be commercially introduced to the concrete construction industry. Concrete incorporating of metakaoline has showed a faster strength development at early ages, but had similar strength after 28 days compared to concrete containing silica fume at the same amount of replacement of cement. It has been concluded that the resistance of concrete containing metakaoline to diffusion chloride was significantly higher than the ordinary concrete but similar to the concrete incorporating of silica fume [ACI 232.1R. 2000].

An important difference between MK and natural pozzolans or other types of artificial pozzolans is that MK is a primary product, while SF and FA are secondary products or by-products. Thus, MK can be produced with a controlled process to achieve the desired properties. When compared with SF concrete at the same level of replacement, MK concrete showed a faster strength development at early ages, but had similar strength after 28 days. With respect to the durability aspects, it has been reported that the resistance of MK concrete to chloride ion penetration was significantly higher than the control concrete but similar to the SF concrete [ACI 232.1R. 2000]. However, if very large percentages (greater than 20 percent) of the SF and MK be used, the levels of calcium hydroxide reduce significantly [ACI 544.1R, 2002].

Previous study by Pargar et al. at the laboratory condition showed that MK concretes had higher compressive strength increases at early ages than at SF and test results related to the resistance of concrete to salt attack, according to Nordtest NT Build 443, revealed that the performance of MK was similar to SF [Pargar *et al.* 2009].

In this study, chloride diffusion of concretes contain metakaoline (5%, 10%, 15%) and silica fume (5%, 7.5%, 10%) as a replacement of cement compared with control specimen after nine months exposure in tidal and splash zones in Persian Gulf.

2 EXPERIMENTAL PROGRAMS

2.1 Materials

In this study, the cementitious materials were Hormozgan Portland cement type II (Iran), silica fume (SF) obtained from Azna ferro-silicon alloy manufacture and metalaoline. The chemical and physical properties of these are outlined in Table 1. A poly carboxylate superplasticizer was used for the mixes to achieve desirable slump at a water-to-binder ratio of 0.4.

2.2 Mixture Proportions

Silica fume and metakaoline were incorporated to make concrete mixes. In addition to control type II cement mix, the replacement cement with 5%, 7.5% and 10% silica fume and 5%, 10% and 15% metakaoline were used.

Concrete mixes set on site with water-cement ratio of 0.4 and approximately coarse and fine aggregate of 710 and 1140 kg/m3, respectively. Water content in all mixtures is 160 kg/m3. The concrete were cast in 150×150×150 mm cubes for compressive strength test and 150×150×600 mm which used for chloride diffusion test. The compressive strength test specimens were removed from the moulds after 24 hours and moist cured up to 7 and 28 days. But 150×150×600mm cubes were moist cured in baths for 3 days and after sealing all sides except one, were placed in exposure conditions. Three specimens were used to determine the compressive strength at each age and one chloride profile were prepared for determination of surface chloride.

Table 1. Chemical composition of cement, metakaoline and silica fume.

Components	*Cement (%)*	*Silica Fume (%)*	*Metakaoline (%)*
SiO2	21	93.16	51.85
Al2O3	5	1.13	43.87
Fe2O3	3.5	0.72	0.99
CaO	63	---	0.2
MgO	1.8	1.6	0.18
SO3	1.6	0.05	---
Na2O	0.5	---	0.1
K2O	0.6	---	0.12
L.O.I	2	1.58	0.57
Total	99	98.24	97.79

Table 2. Concrete mix proportions.

Mix Code.	*w/b*	*Cement kg/m3*	*MK kg/m3*	*SF kg/ m3*
C	0.4	400	0	0
MK5	0.4	380	20	0
MK10	0.4	360	40	0
MK15	0.4	340	60	0
SF5	0.4	380	0	20
SF7.5	0.4	370	0	30
SF10	0.4	360	0	40

2.3 Exposure Condition

After 3 days of curing, the five sides of prism specimens were sealed with an epoxy coating to ensure that diffusion would occur in only one dimensional of the specimens. Then they were exposed to two different conditions in Persian Gulf region'Figs.1 and 2.

The area between minimum and maximum height of water tide defines tidal zone. The above of this zone has been named splash zone in which seawater particles wash out concrete surface.



Figure 1. CMI exposure site in Persian Gulf-Tidal zone specimens.

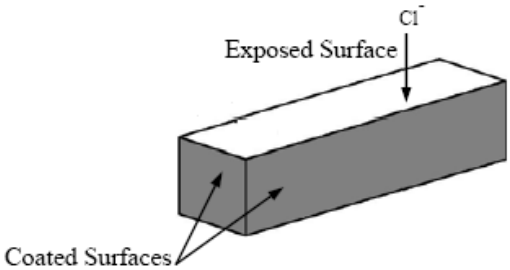

Figure 2. Typical concrete prism specimen and preparing the slice for powder sample.

2.4 Sampling

After nine months of exposure in seawater in Persian Gulf, powder samples for chloride analysis were ground off by Profile Grinder parallel to the exposed surface with the accuracy 0.1 mm at 9 different depths. The first three steps had 2mm depth, the next two steps were in 3 mm depth and the others had 4 mm depth. It should be noted that the 1 mm from concrete surface was removed from the surface before sampling. Also, the first step was not included in calculations as it might be affected by actions such as skin effect 'Fig.3'. 10g sample at each depth was collected and analyzed separately for acid-soluble chloride according to ASTM C 114, part 19 [Shekarchi *et al*. 2009, Ghods *et al*. 2007].

3 RESULT AND DISCUSSION

3.1 Hardened Concrete Properties

The compressive strength of hardened concrete specimens is given in Table 3, where each value is averaged from the results of three cubes. Specimens of 7 and 28 days old were cured in laboratory condition. As it was expected, the compressive strength increases with the use of silica fume and metakaoline compared with control mix. The compressive strength of cubes containing silica fume is more than metakaoline in 7 and 28 ages. Results of enhanced extent of compressive strength at 7 and 28 days show silica fume content of 7.5 to 10% and metakaoline content of 10 to 15% by weight of cement correspond to maximum enhanced extent of compressive strength. The results show that the rate of increase in strength between MK10 and MK15 is similar to MK5 and MK10 in all days. In other words, the most remarkable strengths were developed for replacement rates from 10% to 15% in both ages while in SF concretes the rate of increase in compressive strength at 28 days was more between 5 to 7.5% than 7.5 to 10%. At the 7 days we can see that the compressive strength decreases with the increase in SF content from 7.5 to 10%. The SF concretes of 7.5 and 10% have the maximum compressive strength at the ages of 7 and 28 days among all the concrete mixes.




Figure 3. Sampling of concrete specimens using the Profile Grinder in exposure site.

Table 3. Compressive strength of hardened concrete.

Code	*Compressive strength (MPa)*			
	7days	*Enhanced extent (%)*	*28days*	*Enhanced extent (%)*
C	27	100	38	100
SF5	34	126	45	118
SF7.5	41	152	50	132
SF10	38	141	52	137
MK5	32	119	43	113
MK10	36	133	45	118
MK15	39	144	47	124

3.2 Chloride Profiles

The chloride penetration rate as a function of depth from the concrete surface and time can reasonably be represented by Fick's second law of diffusion according to the following expression (Crank 1975):

$$\frac{\partial c}{\partial t} = D\frac{\partial^2 c}{\partial x^2}$$

The solution for this differential equation is:

$$C(x,t) = C_0\left(1 - erf\left(\frac{x}{2\sqrt{D \cdot t}}\right)\right)$$

where x is distance from concrete surface (m); t is time (s); Dc is diffusion coefficient (m^2/s); Cs is equilibrium chloride concentration on concrete surface; C(x,t) is chloride concentration at the depth of x from the surface at time; and erf is error function. Using a computer statistical analysis program, the regression was carried out on the experimental data and by curve fitting of Fick's second law of diffusion, the values of Dc and Cs were determined. Also, the chloride concentration of 0.07% by weight of concrete has been shown for comparing profiles and better understanding of chloride resistance of concretes (Pargar et al. 2007, Shekarchi et al. 2009).

The evolution of the diffusion coefficient for different silica fume and metakaoline mixes at sampling age of 9 month is represented in Figures 4 and 5, respectively. Table 4 presents depth corresponds to chloride value of 0.07% by weight of concrete. The chloride profile of control mix is transverse by chloride value of 0.07 at the depths of 29.5 mm and 33.5 mm in splash and tidal zones, respectively; While SF10 and MK15 have the lowest depths in both zones.

Table 4. Depth of corresponding to chloride of 0.07% by weight of concrete (mm).

Code	*Splash zone*	*Tidal zone*
C	29.5	33.5
MK5	23	20.2
MK10	16.3	15.5
MK15	14.3	13.6
SF5	22.7	21.8
SF7.5	20.4	17.4
SF10	17	14.4

The values of diffusion coefficient (D) and surface chloride concentration (Cs) are given in Table 5. It is clear that the diffusion coefficient of concrete incorporating 15% metakaoline decreases up to 86% in the splash zone and 90% in the tidal zone. While diffusion coefficient of concrete containing 10% silica fume decreases up to 77% in the splash zone and 87% in the tidal zone compared to the control mix. Also, it can be found that using higher percentage of metakaoline decrease the diffusion coefficient significantly in splash and tidal zones. On the other hand, silica fume and metakaoline concretes at the same replacement (5%, 10%) have similar diffusion coefficient in splash and tidal zones. The surface chloride content at the splash zone is higher than tidal zone. The wetting and drying cycles in both zones, especially in splash zone, caused the large amount of surface chloride content.

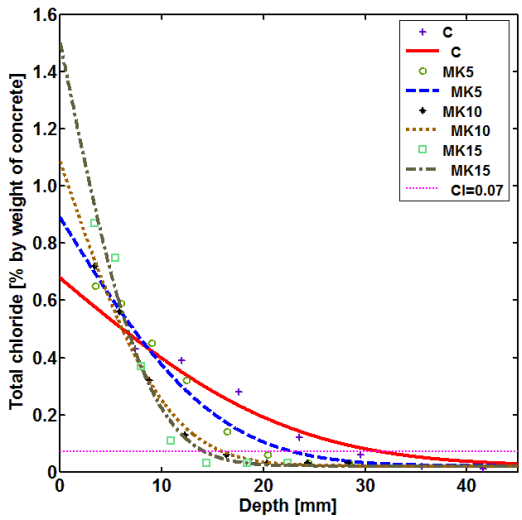

a) Chloride profiles of concretes contain metakaoline

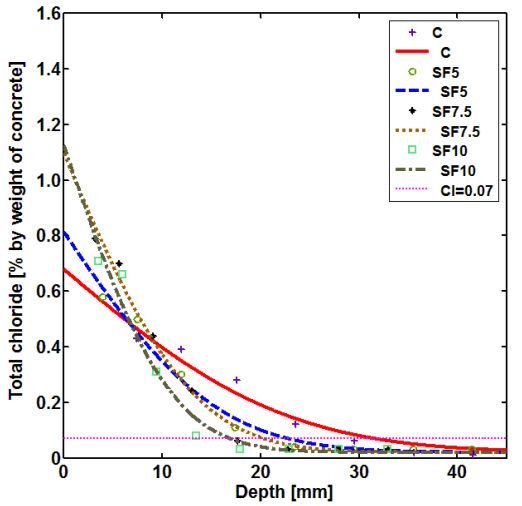

b) Chloride profiles of concretes contain Silica fume

Figure 4. Chloride concentration profiles in splash zone.

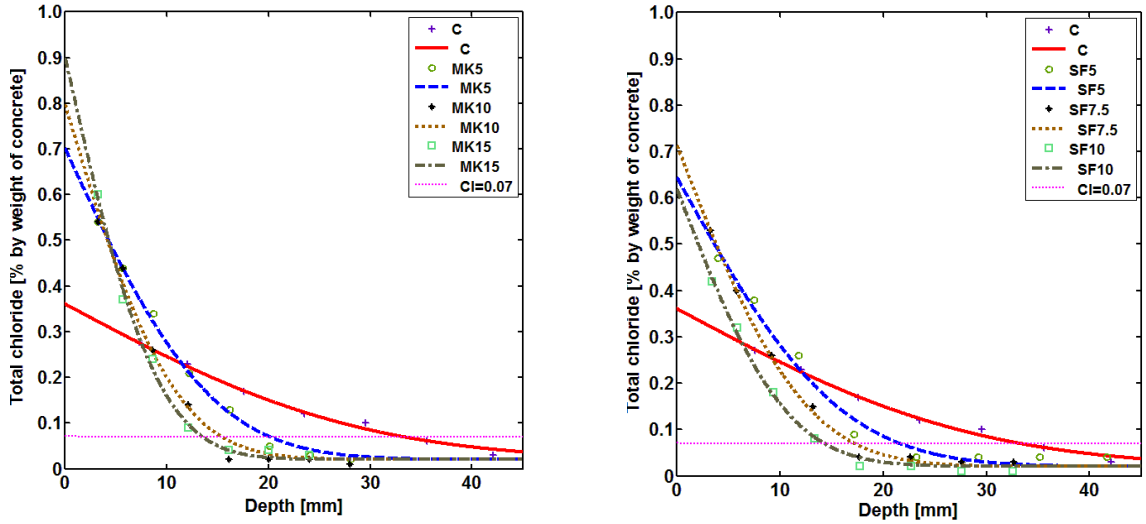

a) Chloride profiles of concretes contain metakaoline

b) Chloride profiles of concretes contain Silica fume

Figure 5. Chloride concentration profiles in tidal zone.

Table 5. Values of diffusion coefficient and surface chloride concentration after nine months of exposure.

Zone	*Code*	*Cs*	*Dc×1012*	*Reduction in Dc vs. control mix*
		% wt. of concrete	*m2/s*	*%*
Splash	C	0.66	6.66	0
	MK5	0.87	3.09	54
	MK10	1.1	1.38	79
	MK15	1.48	0.95	86
	SF5	0.79	3.2	52
	SF7.5	1.08	2.2	67
	SF10	1.1	1.5	77
Tidal	C	0.34	11.07	0
	MK5	0.69	2.68	76
	MK10	0.78	1.47	87
	MK15	0.88	1.06	90
	SF5	0.63	3.23	71
	SF7.5	0.69	1.94	82
	SF10	0.59	1.44	87

4 CONCLUSION

1- Results of compressive strength show an optimum silica fume content of 7.5% to 10 % and metakaoline content of 10% to 15% by weight of cement.

2- Depth of chloride penetration reduces as the replacement of admixture increases.

3- Cs value increases as the replacement of pozzolans increases. But the diffusion coefficient decrease with the increase in the replacements of pozzolans.

4- The surface chloride content of concrete in splash zone is more than tidal zone.

5- At the same replacement, concretes containing metakoaline have similar diffusion coefficient and chloride in depth to those of silica fume. But the surface chloride content of metakaoline is more than silica fume.

REFERENCES

ACI 232.1R. 2000.' Use of raw or processed natural pozzolans'. Reported by ACI committee 232. American concrete institute.

ACI 544.1R, 2002. State-of-the-art report on fiber reinforced concrete. Reported by ACI committee 544. American concrete institute.

Crank. J. 1975.' The Mathematics of Diffusion', 2nd ed., Oxford Press, London.

Ghods, P. Chini, M. Alizadeh, A. Hoseini, M. Shekarchi, M. Ramezanianpour, A.A. 2005. 'The Effect of Different Exposure Conditions on the Chloride Diffusion into Concrete in the Persian Gulf Region'. ConMat 05, Vancouver, Canada.

Pargar, F. Mirdamadi, A.Dosti, A. Shekarchizadeh, M. 2009. 'Durability Characteristics of Metakaolin in comparison with Silica Fume', ConMat'09, International Conference on Construction Materials, Performance, Innovations and Structural Implications, Nagoya, Japan, pp. 915-920.

Pargar, F. Layssi, H. Shekarchi, M. 2007.'Investigation of chloride threshold value in an old concrete structure', CONSEC'07 Tours, France, pp. 175–182.

Shekarchi, M, Moradi-Marani, F, Pargar, F. 2009. 'Corrosion damage of a reinforced concrete jetty structure in the Persian Gulf: a case study,Structure and Infrastructure Engineering', pp .1-13.

Shekarchi, M .Rafiee, A .Layssi, H .2009 .'Long-term chloride diffusion in silica fume concrete in harsh marine climates'. Cement and Concrete Composites, Vol 31, Issue 10, pp. 769-775.

Sreejith V. Nanukuttan, Lulu Basheer, W. John McCarter, Des J. Robinson, andP. A. Muhammed Basheer.. 2008. 'Full-Scale Marine Exposure Tests on Treated and Untreated Concretes'. Initial 7-Year Results. ACI Materials Journal, vol. 105, pp. 81-87.

XII DBMC
International Conference on Durability of Building Materials and Components
PORTO - PORTUGAL, April 12th-15th, 2011

Study of Variation in Surface Chloride of Concrete Containing Different Pozzolans When Exposed to a Tidal Climate in the Persian Gulf Region

Mahdi Valipour [1]
Farhad Pargar [2]
Mohammad Shekarchi [3]
Sara Khani [4]

ABSTRACT

The most common form of deterioration is caused by chloride ingress through concrete, resulting in corrosion of the reinforcing steel. One of the factors affecting the penetration of chloride ions is the amount of surface chloride (Cs). In this paper, the amount of chloride on the surface of concrete specimens made with different pozzolan in tidal and splash zones is considered. The results show that the amount of surface chloride in the specimens of concrete sited in splash zone is more than tidal zone.

KEYWORDS

Corrosion, Surface chloride, Splash zone, Tidal zone.

[1] Research Assistant Construction Materials Institute (CMI), University of Tehran
[2] Research Assistant Construction Materials Institute (CMI), University of Tehran
[3] Director of Construction Materials Institute (CMI), University of Tehran
[4] Research Assistant Construction Materials Institute (CMI), University of Tehran

1 INTRODUCTION

Chloride diffusion is known to be a major cause of deteriorating concrete structures exposed to marine environments such as the Persian Gulf which is characterized as one of the most aggressive environments for concrete in the world because of its high relative humidity and elevated temperature that can be as high as 50 degrees on some days and may lead the a rise in surface temperature of up to 75 degrees [Ramezanianpour *et al*., Shekarchi *et al.*]. Reinforcing steel can be greatly corroded due to attack of aggressive ions such as chloride and thus reduce the life span of steel reinforced concrete structures [Bader 2003, Sandberg *et al.*]. Therefore, the severity of this environment is of concern to those who maintain concrete structures located in this specific region.

However, to determine chloride ingress and estimate the time to corrosion, the amount of surface chloride (Cs) must be known. It is interesting to note that when solving Fick's second law, a constant value for surface chloride has been widely used whereas the accumulation of chloride on the surface of concrete can vary in accordance with different exposure conditions [Ann *et al.* 2009, Nokkena *et al.* 2006].

According to a study completed by Bruce [2001] on reinforced concrete structures located in the Eastern Province of Saudi Arabia, the values for Cs are greatest in areas subject to wetting and drying. When salty water evaporates, any chloride in the water will remain in a crystalline form on the surface of the concrete. In marine structures, the value of Cs will reach a maximum just above the sea water level in the splash zone. For reinforced concrete bridge and building structures, the value of Cs will attain a maximum just above ground level where water is drawn through the concrete and then evaporates from the surface. When estimating the time to corrosion of reinforced concrete structures, for which values of Cs are required, engineers should use actually measured values of Cs taken from samples collected from existing structures; ideally this should be done in those seasons when the daily temperatures attain the annual average temperature. He determined the surface chloride of 0.6-0.9% by weight of concrete to simulate the exposure condition of extreme. The majority of samples were taken from the cover zone which had cracked as a result of the expansion of rusting steel reinforcement. Concrete mix design may also influence the value of Cs as modern dense concretes typically have finer pore structures and reduced chlorides are absorbed. On the other hand, the use of pozzolans in the concrete mix may either increase or decrease the surface chloride content of the concrete depending on their ability to bind chloride ions.

In other words, the degree of exposure with chlorides in a marine environment is a key factor that determines each different level of surface chloride content. The values of Cs for a concrete exposed to seawater may not be changed over time due to chemical equilibrium, but at the tidal zone the chloride content on the concrete surface can increase in relation to the number of wet and dry cycles to which it is exposed. Also it is seen that the degree of contact with seawater greatly influences the value of Cs. For example, the value of Cs obtained from concrete placed in submerged conditions in seawater was higher than that for exposure to tidal or splash zones and specimens and structures exposed to airborne chloride ions produce the lowest values for Cs. However, the value of Cs from published data does not provide a clear relationship in respect to the time of exposure due to various factors that affect chloride ion transport including binder type, free water/binder ratio (W/B), curing conditions, location of sampling in the structure and weathering [Song *et al*. 2008].

For this purpose a study is conducted at Qeshm Island (Iran), in which four concrete specimens were made using different water to cement ratios of 0.35, 0.4, 0.45 and 0.5 respectively. Also, the performance of concrete specimens containing silica fume (5%, 7.5% and 10% of replacement level), metakaolin (5%, 10% and 15% of replacement level) and zeolite (10%, 20% and 30% of replacement level) with constant w/c ratio of 0.4 were also examined. The surface chloride of concretes were determined and compared for two exposure conditions, specifically the splash and tidal zones. The compressive strength of specimens was also determined for all exposed specimens.

2 EXPERIMENTAL PROGRAM

2.1 Materials

Type II Portland cement was used throughout the investigations. The chemical and physical properties of cement and pozzolanic materials used in preparing the concrete specimens are shown in Table 1.

Table 1. Composition of cement, silica fume, metakaolin and zeolite.

Oxide composition %by mass	*PC*	*Silica Fume*	*Metakaolin*	*Natural Zeolite*
SiO2	21	93.16	51.58	67.79
Al2O3	5	1.13	43.87	13.66
Fe2O3	3.5	0.72	0.99	1.44
CaO	63	-	0.2	1.68
MgO	1.8	1.6	0.18	1.2
SO3	1.6	0.05	-	0.5
Na2O	0.5	-	0.01	2.04
K2O	0.6	-	0.12	1.42
L.O.I	2	1.58	0.57	10.32

2.2 Mixture Proportions

The investigation was carried out on 13 concrete mixes, in which, as previously mentioned, there were four different water to cement ratio, and other mixtures incorporating different replacement levels of silica fume, metakaolin and natural zeolite. The mix proportion of concrete samples are presented in Table 2. Crushed limestone (largest size of 19 mm) was used as coarse aggregate and the fine aggregate was river sand. Also, to achieve the desired workability the use of poly carboxilate-based superplasticiser was necessary. All specimens were moist cured for 3 days and then placed at the respective tidal and splash zones located on the shores of Qeshm Island in the Persian Gulf's.

2.3 Test Procedure

Concrete prisms of 150×150×600 mm in size that had been prepared for determination of chloride penetration were placed at the tidal and splash zones for a 9 month period. Concrete cores of 70 mm diameter were then taken from each specimen and powder samples were obtained from these cores. The samples were examined to determine their compressive strength and the amount of chloride ion at a depth of 20 mm. Compressive strength tests were carried out on three cubes of 150×150×150 mm at 7and 28 days of moist curing.

After 3 days of curing, five sides of the concrete prism specimens were sealed with an epoxy coating to ensure that diffusion would occur only in the direction of the exposed side of the specimens. Then they were then exposed to two different conditions in the Persian Gulf region: the tidal zone and the spalsh zone. The tidal zone is that area between the minimum and maximum level reached by the tide water whereas above this zone resides the splash zone. In this zone seawater washes out the concrete surface.

Table 2. Mix Proportions for concrete samples.

Sample	*W/B Ratio*	*Cement (kg/m3)*	*Content of Cement replacement Material (kg/m3)*	*Water (kg/m3)*	*Super plasticizer (kg/m3)*	*Slump (cm)*
C1	0.35	400	_	140	0.35	8
C2	0.4	400	_	160	0.2	7
C3	0.45	400	_	180	0.1	15
C4	0.5	400	_	200	0	18
SF5	0.4	380	20	160	1.2	6
SF7.5	0.4	370	30	160	1.4	5
SF10	0.4	360	40	160	1.6	8
MK5	0.4	380	20	160	0.8	5
MK10	0.4	360	40	160	1.4	5.5
MK15	0.4	340	60	160	1.6	8
ZE10	0.4	360	40	160	4	6
ZE20	0.4	320	80	160	8	8
ZE30	0.4	280	120	160	14	6

After nine months of exposure in seawater of the Persian Gulf, powder samples were prepared for chloride analysis using a Profile Grinder to grind off a layer of concrete parallel to the exposed surface; samples were extracted with the grinder at 9 different depths to an accuracy 0.1 mm. It should be noted that 1 mm of the concrete surface was removed before sampling. Also, the initial samples were not included in calculations as it was considered that this might be affected by actions such as those of the skin effect, as shown in Figure 3. Using this technique, a sample of 10g at each depth was collected and analyzed separately for acid-soluble chloride according to the methods described in ASTM C 114 [Shekarchi et al. 2009].

A commercially available, curve-fitting software program was used to determine the value of Cs (surface chloride concentration) and Da (apparent diffusion coefficient) from the data using a non-linear, least-squares method, with Fick's Second Law of diffusion using Crank's solution. The best fit curve was determined by adjusting both the unknowns to achieve the highest coefficient of determination (r^2).

3 RESULTS AND DISCUSSION

3.1 Compressive Strength

Figure 1 illustrates the compressive strength of all specimens at ages of 7 and 28 days. As it can be seen, increasing the w/c ratio reduces the compressive strength for specimens cured for at both 7 and 28 days. Specimen C4 with the highest w/c ratio showed the lowest compressive strength whereas specimen C1 with the lowest w/c ratio obtained the highest compressive strength. Lowering the w/c ratio can bring about improvements in the microstructure of concrete leading to the development of higher compressive strengths.

Using pozzolan as a cement replacement resulted in an increase in compressive strength at ages of 7 and 28 days in comparison to the results obtained for the control concrete specimens. However, this was not true for specimens ZE20 and ZE30 at an age of 7 days or for specimen ZE30 at an age of 28 days. Based on the results, lower compressive strength was achieved when greater amounts of zeolite were used in the mix; given that the ZE30 specimens had the lowest compressive strength this likely can be attributed to the fact that at a high dosage of zeolite, the hydration process remains incomplete.

For concretes incorporating silica fume, the concrete mix having a replacement level of 7.5% of silica fume reached the highest compressive strength after 7 days whereas SF10 attained the highest 28 day compressive strength. For specimens containing metakaolin the compressive strength at both ages increased with an increase in replacement level noting that MK10 attained the highest compressive strength.

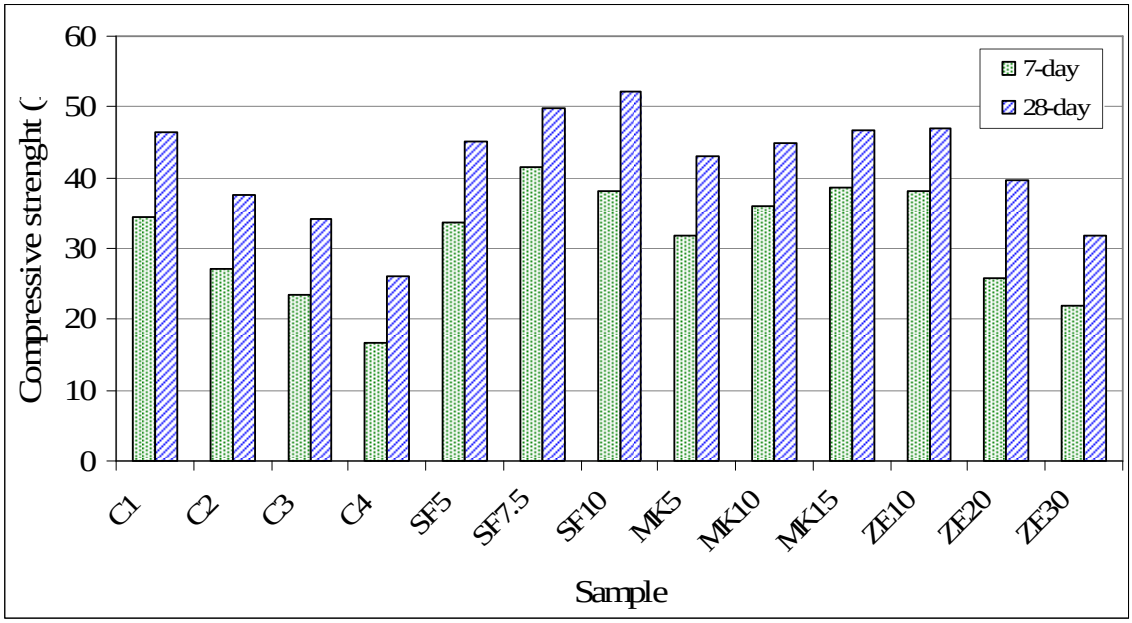

Figure 1. Compressive strength of specimens at ages of 7 and 28 days.

3.2 Surface Chloride

The surface chloride contents are given in Table 3 and Figure 2. The amount of surface chloride (by weight of concrete) in specimens not containing pozzolan did not follow any specific trends. The variation of surface chloride amount at tidal and splash zones show that the amount of surface chloride present in concretes exposed to the splash zone is greater than that of specimens exposed to the tidal zone. The highest percentage increase belongs to specimen C1 which has the lowest w/c ratio (0.35). It can be noted that although the surface chloride of specimens exposed to both the tidal and splash zones fluctuates, the amount of chloride in concrete specimens at a depth of 20 mm exposed to the tidal zone is almost constant with the exception of specimenC1 which has lower chloride content as compared to other specimens. Whereas concrete specimens exposed to the splash zone shows a tangible increase in chloride content with increasing w/c ratio.

Specimens containing silica fume (SF) exposed to both tidal and splash zones have higher surface chloride contents and lower chloride contents at a 20 mm depth than those concrete mixes not containing pozzolans. Therefore, it can be observed that among specimens containing silica fume, with additional dosage of pozzolan there is reduction in the amount of surface chloride content and in the amount of chloride at a depth of 20 mm. For those specimens incorporating with silica fume and exposed to the splash zone an increase in surface chloride content of 5 to 10% is evident whereas the amount of chloride at a depth of 20 mm decreases. A comparison of results obtained for concrete specimens exposed to these two exposure conditions shows that the amount of surface chloride content in all silica fume specimens is higher for specimens exposed to in the splash as compared to those in the tidal zone.

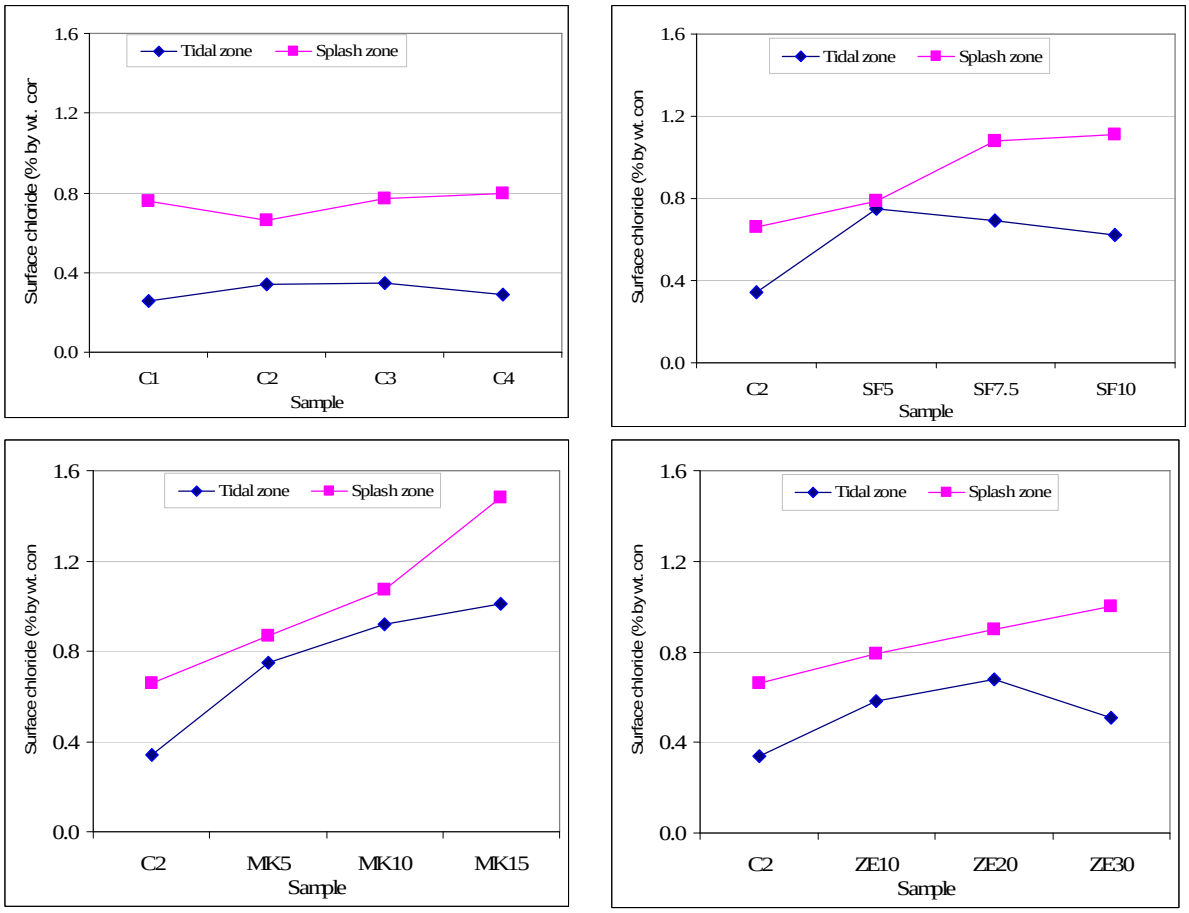

Figure 2. Surface chloride of concretes with different w/c and pozzolanic materials exposed to tidal and splash zone conditions.

For specimens containing metakaoline (MK), an increase of replacement level from 5 to 15% in specimens exposed to either zones results in increases in the amount of surface chloride content whereas the amount of chloride at a depth of 20 mm decreases. It is clear that the amount of surface chloride content in specimens exposed to the splash zone is greater than that of specimens exposed to the tidal zone. In contrast with specimens incorporating SF, an increase in the replacement level of MK, produces a sharp increase in the amount of surface chloride content, whereas the chloride content at a depth of 20 mm decreases with the proportional reduction similar to that observed for SF concrete at the same replacement level.

For specimens containing natural zeolite (ZE), the performance of specimens having a 10% replacement level of zeolite and exposed to the splash zone was found to be similar to that of concrete specimens SF5. By increasing the replacement level up to 30% of ZE the surface chloride content for specimens exposed to the tidal zone fluctuates whereas the degree of chloride penetration was somewhat reduced. The surface chloride content for specimens exposed to the splash zone increased whereas the reduction of chloride penetration was not noticeable. The results obtained for surface chloride content for specimens exposed to either marine zone confirms that for replacement levels of 10, 20 and 30%, the surface chloride content and chloride penetration were higher for specimens exposed to the splash zone as compared to those exposed to the tidal zone.

The comparison of natural zeolite (ZE) with MK and SF shows that higher replacements of ZE are less effective and do not noticeably change the chloride resistance of the concrete.

Table 3. Surface chloride and chloride content at a depth of 20 mm in different specimens.

Code	*Tidal zone*		*Splash zone*	
	Chloride content at the depth of 20 mm	*Surface chloride by weight of concrete*	*Chloride content at the depth of 20 mm*	*Surface chloride by weight of concrete*
C1	0.01	0.26	0.15	0.76
C2	0.15	0.34	0.19	0.66
C3	0.15	0.35	0.25	0.77
C4	0.16	0.29	0.33	0.8
SF5	0.06	0.75	0.10	0.79
SF7.5	0.05	0.69	0.07	1.08
SF10	0.03	0.62	0.04	1.11
MK5	0.06	0.75	0.10	0.87
MK10	0.03	0.92	0.03	1.07
MK15	0.02	1.01	0.02	1.48
ZE10	0.05	0.58	0.11	0.79
ZE20	0.05	0.68	0.10	0.90
ZE30	0.04	0.51	0.09	1.00

4 CONCLUSIONS

(1) In specimens without pozzolan, increasing the w/c ratio caused an increase in the amount of chloride penetration into the concrete with no perceptible trend in the amount of surface chloride content for specimens exposed to either the tidal or splash zones.

(2) Surface chloride content and the amount of chloride at a depth of concrete is found to have an inverse relation in specimens containing pozzolans; increasing the replacement level increases the amount of surface chloride content but decreases the amount of chloride at a depth of 20 mm.

(3) Increasing the replacement level of pozzolans in concrete specimens exposed to either the splash or tidal zones had a positive effect on reducing the degree of chloride ingress yet an increase in the amount of surface chloride content was evident.

(4) All specimens showed higher degree of chloride penetration and surface chloride content for specimens exposed to the splash zone as compared to those exposed to the tidal zone; this indicates that a greater concentration of surface chloride may induce a higher degree of chloride ion penetration into the concrete.

(5) Among the specimens investigated in this study that were cured for a short term (3days), the performance of natural zeolite in terms of chloride diffusivity was significant in comparison to the other well known pozzolans such as silica fume and metakaolin. The 10% replacement level for zeolite and for specimens exposed to the tidal zone showed a better result as compared to those having 5% replacement of silica fume and metakaolin. For specimens exposed to the splash zone the performance of these specimens was similar to that of specimens containing silica fume and metakaolin.

REFERENCES

Ann, K.Y., Ahn, J.H. &. Ryou, J.S. 2009. 'The importance of chloride content at the concrete surface in assessing the time to corrosion of steel in concrete structures', *Construction and Building Material,* pp. 239–245.

Bader, M.A. 2003, 'Performance of concrete in a coastal environment', *Cement & Concrete Composites*, pp. 539–548.

Nokkena, M., Boddy, A., Hootonc, R.D. & Thomas M.D.A. 2006. 'Time dependent diffusion in concrete—three laboratory studies', *Cement and Concrete Research*, pp. 200– 207.

Ramezanianpour, A.A., Ashrafi, H.R. & Ramezanianpour, A.M. 'Chloride diffusion models for persian gulf environment', Amirkabir University of Technology,Tehran, Iran.

Smith, B. G., 2001.'Durability of silica fume concrete exposed to chloride in hot climate', ASCE journal of materials in civil engineering.

Shekarchi, M., Ramezanianpour, A.A., Ghods, P., Chini, M., Alizadeh, R. & Hoseini, M. 'The effect of different exposure conditions on the chloride diffusion into concrete in the persian gulf region.

Sandberg, P., Tang, L. & Andersen, A. 'Recurrent studies of chloride ingress in uncracked marine concrete at various exposure times and elevations', *Cement and Concrete Research*, vol. 28, pp. 1489–1503.

Song H. W., LEE C. H., Ann, K. Y. 'Factors influencing chloride transport in concrete structures exposed to marine environments', Cement & Concrete Composites, vol. 30, pp. 113–121.

Shekarchi, M .Rafiee, A .Layssi, H .2009 .'Long-term chloride diffusion in silica fume concrete in harsh marine climates'. Cement and Concrete Composites, Vol 31, Issue 10, pp. 769-775.

XII DBMC
International Conference on Durability of Building Materials and Components
PORTO - PORTUGAL, April 12th-15th, 2011

Galvanostatic Pulse Corrosion Measurements on Onsite Reinforced Concrete Specimens in Persian Gulf

Mahdi Valipour [1]
Farhad Pargar [2]
Mohammad Shekarchi [3]
Sara Khani [4]

ABSTRACT

A majority of concrete structures in marine environment shows signs of degradation due to the corrosion of the reinforcement in the presence of chlorides. The galvanostatic pulse technique, which is one of the several NDT-techniques, has been developed for such measurements since last decade and has been utilized both in lab and in-situ for many years. In this paper, corrosion of reinforced concrete specimens made with different water to cement ratios using Galvanostatic pulse corrosion measurements have been evaluated. The results show the effect of harsh environment on corrosion of steel in concretes with different water to cement ratios.

KEYWORDS

Corrosion, Galvanostatic pulse technique, Water to cement ratio.

[1] Research Assistant Construction Materials Institute (CMI), University of Tehran
[2] Research Assistant Construction Materials Institute (CMI), University of Tehran
[3] Director of Construction Materials Institute (CMI), University of Tehran
[4] Research Assistant Construction Materials Institute (CMI), University of Tehran

1 INTRODUCTION

Corrosion of embedded steel rebars in concrete structures in chloride containing environments is the most common cause of premature deterioration and failure of concretes leading to the reduction of their life expectancy and tremendous economic losses. Rebars of reinforced concrete in aggressive environment, start to corrode by penetration of chloride ions into concrete pores, after a prolonged exposure [Fajardo *et al.* 2009, Gu¨neyisi *et al.* 2007, Shekarchi *et al.* 2009]. To characterize in a quantitative way the corrosion activity on reinforcing steel surface, it is essential to evaluate the corrosion rate. However, there have been different measuring techniques and test methods introduced to the field. Galvanostatic pulse method, which is the latest technique for assessing the risk of corrosion to the reinforcement in concrete structures, is found to be reliable for the evaluation of reinforcement corrosion in anaerobic concrete environment [Lue & Schutter 2006, Klinghoffer & Berge]. The corrosion rate of steel reinforcements as well as the electrical resistance of concrete and half cell potential can be measured using galvanostatic pulse technique. Galvanostatic pulse method is a rapid non-destructive polarisation technique, which has been used for evaluation of reinforcement corrosion both in laboratory and on site. A short time anodic current pulse is impressed to reinforcement galvanostatically from a counter electrode placed on concrete surface together with a reference electrode. The applied current is normally in the range of 5 to 400 mA and the typical pulse duration is up to 10 seconds. The small anodic current results in change of reinforcement potential, which is recorded as a function of polarisation time. Reinforcement is polarised in anodic direction compared to its free corrosion potential [Esmaeilpoursaee 2007].

In present investigation field studies are conducted in order to investigate the corrosion rate of concrete reinforcement using galvanostatic pulse technique. As w/c ratio plays an important role in improving the strength and durability of concrete, reinforced concrete specimens with different water to cement ratios of 0.35, 0.4, 0.45, and 0.5 were prepared and exposed to tidal zone in Qeshm island in Persian Gulf region where is highly contaminated by chloride ions and are known to provide the most sever conditions for concrete structures in marine environments [Ghods *et al.* 2005]. Then using the galvanostatic pulse technique, the corrosion rate and half cell potential measurements are obtained.

2 EXPERIMENTAL PROGRAMS

2.1 Materials

In this study, the cementitious materials were Hormozgan Portland cement type II (Iran). Two commonly used local coars and fine aggregates from different sources were employed. Total aggregate mass was about 1850 Kg/m^3 with a largest size of 19 mm. Chemical composition of materials used during the experiment is given in Table 1. To achieve desired workability superplasticizer was used in all mixes. The superplasticizer was based on modified polycarboxylic ether.

Table 1. Chemical composition of materials.

Components	**SiO_2 (%)**	**Al_2O_3 (%)**	**Fe_2O_3 (%)**	**CaO (%)**	**MgO (%)**	**SO_3 (%)**	**Na_2O (%)**	**K_2O (%)**	**L.O.I (%)**
Cement	21	5	3.5	63	1.8	1.6	0.5	0.6	2
Gravel	7.88	0.53	1.07	44.12	4.61	0.1	0.03	0.36	40.86
Sand	**50.73**	**5.91**	**7.45**	**15.16**	**7.33**	**0.003**	**1.46**	**0.65**	**10.21**

2.2 Mixture Proportions

Four mix proportions with different w/c ratios used for casting the concrete specimens. The details of mix proportion are shown in Table2.

Table 2. Mix Proportions.

Samples	W/CM	Cement (Kg/m^3)	Water (Kg/m^3)	Superplasticiser (kg/m^3)
C1	0.35	400	140	0.35
C2	0.4	400	160	0.2
C3	0.45	400	180	0.1
C4	0.5	400	200	0

2.3 Test Procedure

Concrete specimens of size 550X300X200 mm were prepared according to ASTM G109 [2003]. Each specimen were made in a way that three rebars at the top and six rebars at the bottom were embedded at the depth of 30mm, so that for every rebar at the top there was a three rebar at the bottom. The specimens were then moist cured in potable water for 3 days and then they were coated by epoxy resin on every side except for the top of specimens to be exposed to chloride ions. After the exposure in tidal zone for 9 months, the corrosion rate, electrical resistivity and half cell potential measurement were obtained using Galvanostatic pulse method. The method set-up is shown in Fig. 1. A short time anodic current is imposed galvanostatically on the reinforcement through a counter electrode. The applied current is usually set between 5μA and 400μA with the typical pulse duration is up to 10 seconds. The reinforcement is polarized in the anodic direction compared to its free corrosion potential. The typical potential transient curve is shown in Fig. 2.

When a constant current of I_{app} is applied to reinforcement, the polarised potential V_t at a given time t can be expressed as [Lue & Schutter 2006]:

$$V_t = I_{app} [R_p [1-\exp (-t / R_p C_{dl}))] R_\Omega] \quad (1)$$

where: R_p is the polarization resistance; C_{dl} is the double layer capacitance and R_Ω is the ohmic resistance.

By using the linear form of Equ. 1 R_p and C_{dl} can be determined separate from the ohmic resistance R_Ω:

$$\ln (V_{max} - V_t) = \ln (I_{app} R_p) – t / (R_p C_{dl}) \quad (2)$$

where V_{max} is the final steady state potential value.
After the polarization resistance R_p is determined, the corrosion current I_{corr} can be calculated from Stern-Geary formula:

$$I_{corr} = (26 A)/R_p \quad (3)$$

where A is the confined area (in cm^2) of the reinforcement below the central counter electrode.

The corrosion rate can therefore be estimated as:

$$\text{Corrosion Rate (μm/year)} = 11.6 I_{corr} /A \quad (4)$$

The factor 11.6 is for black steel.

Table 3 gives the threshold values for quick evaluation of corrosion rate measured by Galvapulse.

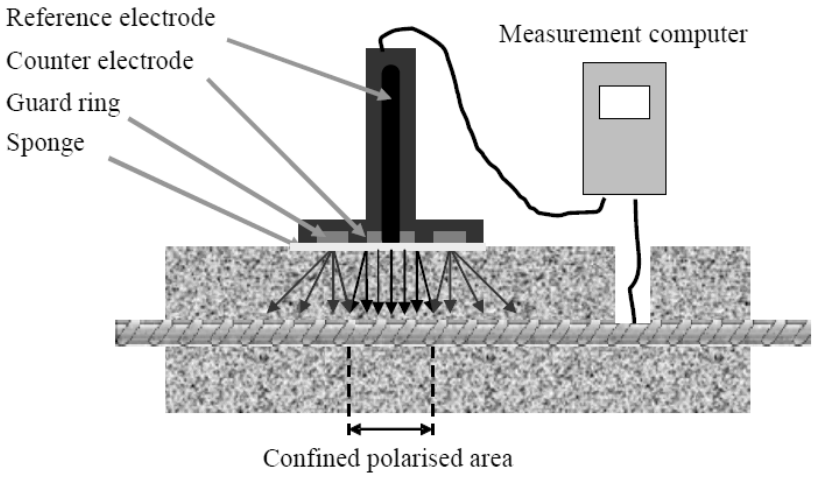

Figure 1. Schematic plan of Galvapulse [Esmaeilpoursaee 2007].

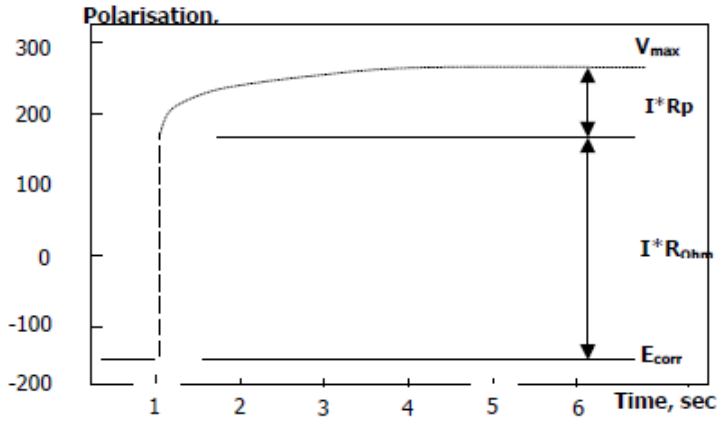

Figure 2. Typical polarization pattern [Klinghoffer & Berge].

Table 3. Quick evaluation of corrosion rate [Andrade & Alonso 1996].

Measurment (μA/cm^2)	Corrosion rate
<0.5	Negligible
0.5 - 5	Slow
5 - 15	Moderate
>15	High

3. RESULT AND DISCUSSION

3.1 Corrosion Rate

Figure 3 illustrates the corrosion rate of specimens at tidal zone. By increasing w/c ratio the corrosion rate increases as specimen C4 shows the highest corrosion rate and the lowest corrosion rate belongs to specimen C1. The variation rate indicates that the corrosion in specimen C4 was initiated after a few months, while in specimen C1 almost no corrosion activity was observed until 22 month of exposure. The performance of specimens C2 and C3 is quiet strange and in two cells of C3 the corrosion rate was lower than threshold value before month 11. So the corrosion rate of C3 was lower than C2. One of the possible reasons which can justify this situation is the micro cracks due to fortuitous poor curing condition in C2.

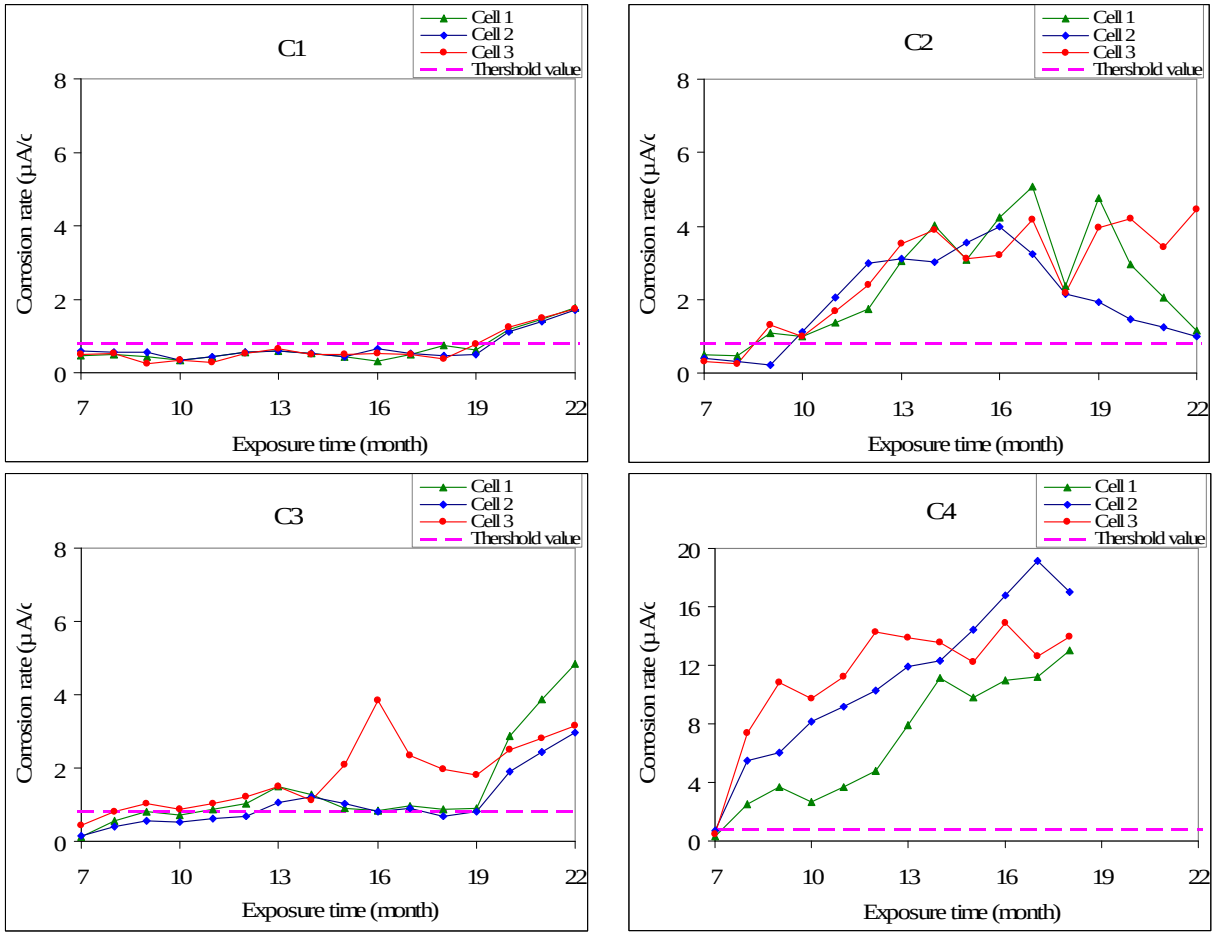

Figure 3. Corrosion rate measurements of each water to cement ratio.

3.2 Half-Cell

It can be observed from Fig. 4 that even after 22 months of exposure the specimen C1 has not reached the threshold value. This is due to the fact that lower w/c ratio leads to an improvement of concrete microstructure. The rebar embedded in specimen C2 shows active potential after about 9 months and it tends to become more negative with time. The potential value of specimen C3 varies slightly and yet no evidence of corrosion initiation is observed. Although specimen C2 has lower w/c ratio than specimen C3, both of them attain the threshold value at nearly the same time. The reason can be the formation of micro cracks on the surface of concrete due to the short term curing and environmental conditions. For specimen C4, it attained the potential value of more negative than -230 mV before the first reading which indicates the initiation of the corrosion process even before the first readings were recorded. Therefore it is clear that increasing w/c ratio causes the half cell potential to reach the threshold value in less time and thus the corrosion process initiates much earlier.

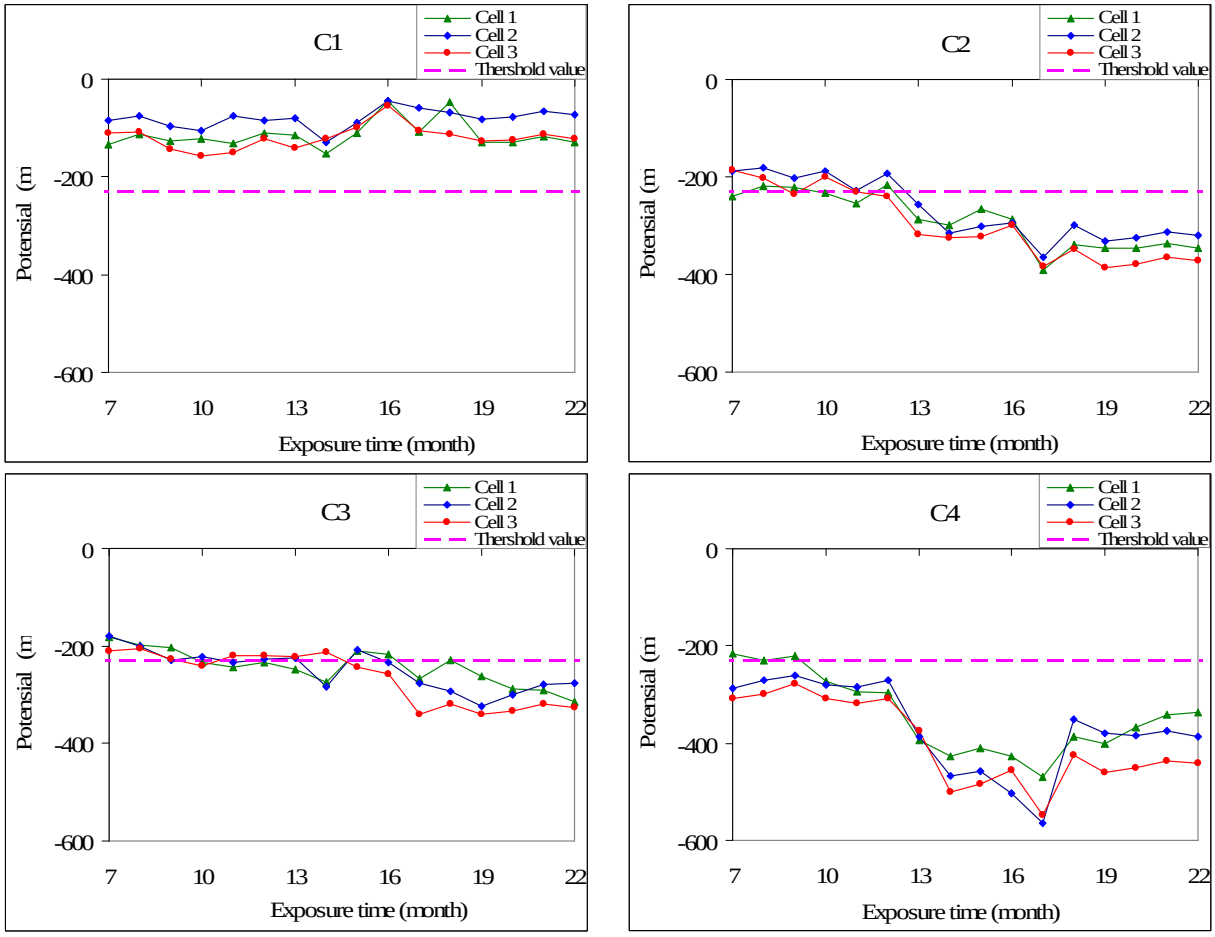

Figure 4. Half-Cell potential variation of each cell in different w/c ratios.

3.3 Electrical Resistivity

The results of electrical resistivity of each specimen are illustrated in Fig. 5. It is interesting to note that not much difference is observed among the results obtained by each specimen and all specimens have almost followed a same trend. However, according to the results obtained by corrosion rate and half cell potential, a decrease in electrical resistivity was expected by increasing w/c ratio. It seems that the resistivity of specimens is affected by continuous humidity of tidal zone. Therefore, it can be concluded for this period of time that the results of electrical resistivity are not reliable enough for durability evaluation and other evaluating methods must be considered.

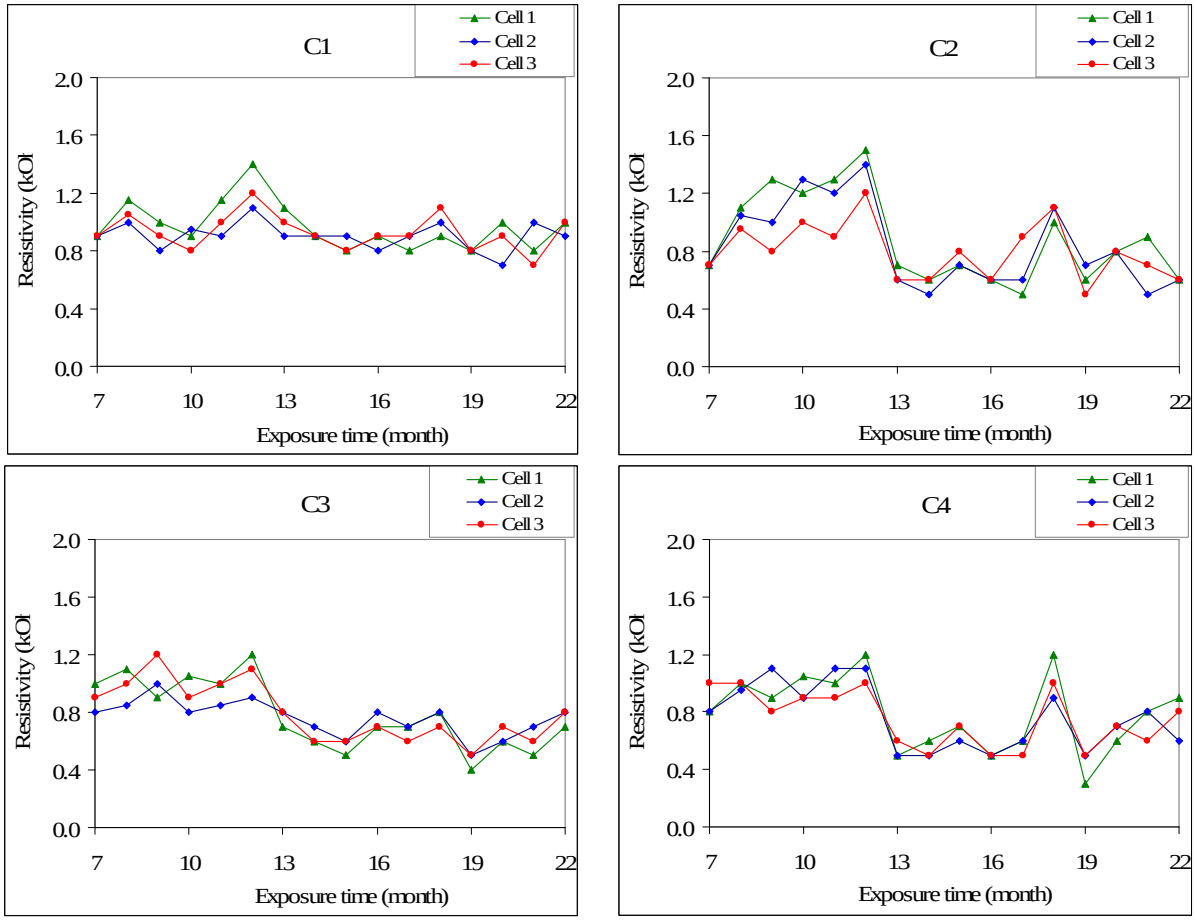

Figure 5. Resistivity of concrete specimens with different w/c ratio over time.

4 CONCLUSION

1- The galvanostatic pulse method is a rapid non destructive polarization technique for the evaluation of reinforcement corrosion on site.

2- Results of half cell potential test correlates well with those of galvanostatic pulse method.

3- The electrical resistivity at tidal zone is found to be unreliable for durability evaluation due to its sensitivity toward the tidal humidity.

4- Corrosion rate and half cell potential show no corrosion in concrete with water to cement ratio of 0.35 after 22 month exposure in harsh environment.

5- The results of present paper show that in chloride containing environments such as Persian Gulf with low concrete cover and short term curing, even concrete with w/c ratio of 0.4 does not satisfy the requirements and thus the modification of concrete structures by using pozzolans, additives and reduction of water to cement ratio are inevitable.

REFERENCES

Andrade, C. & Alonso, C. 1996, 'Corrosion rate monitoring in the laboratory and on-site', *Construction and Building Materials,* pp. 315-328.

ASTM G109, 2003, Standard Test Method for Determining Effects of Chemical Admixtures on Corrosion of Embedded Steel Reinforcement in Concrete Exposed to Chloride Environments.

Esmaeilpoursaee, A. 2007, 'An Analysis of the Factors Influencing Electrochemical Measurements of the Condition of Reinforcing Steel in Concrete Structures', *Thesis presented to the University of Waterloo.*

Fajardo, G., Valdez, P. & Pacheco, J. 2009, 'Corrosion of steel rebar embedded in natural pozzolan based mortars exposed to chlorides', *Construction and Building Materials* ,pp. 768–774.

Ghods, P., Chini, R., Alizadeh, R., Hosseini M, Shekarchi M. & Ramazanianpour, AA. 2005, 'The effect of different exposure conditions on the chloride diffusion into concrete in the Persian Gulf region', ConMat'05, Vancouver, Canada.

Gu¨neyisi, E., O¨zturan, T.& Gesoglu, M. 2007, 'Effect of initial curing on chloride ingress and corrosion resistance characteristics of concretes made with plain and blended cements', *Building and Environment* , pp. 2676–2685.

Klinghoffer, O. & Erik Berge, H. 'Methods for test reinforcement material properties based on mix of stainless steel and carbon steel', *NORDTEST Tekniikantie 12 FIN-02150 ESPOO Finland.*

Luo, L.& De Schutter, G. 2006, 'Galvanostatic pulse corrosion measurements on a recent thermal swimming pool containing seawater', *Concrete Repair, Rehabilitation and Retrofitting – Alexander.*

Shekarchi, M., Moradi-Marani, F. & Pargar, F. 2009,' Corrosion damage of a reinforced concrete jetty structure in the Persian Gulf: a case study', *Structure and Infrastructure Engineering* , pp. 1-13.

XII DBMC
International Conference on Durability of Building Materials and Components
PORTO - PORTUGAL, April 12th-15th, 2011

Effect of Different Pozzolanic Admixtures on Sulfuric Acid Resistance of Concrete

Masoud Moradian [1]
Milad Hallaji [2]
Behnam Kian i[3]
Mohammad Shekarchi [4]
Mehdi Nemati Chari [5]

ABSTRACT

Sulfuric acid environment is one of the most aggressive conditions which puts the durability of concrete in danger in many industrial structures. In this study, 10×10 concrete cube specimens containing silica fume, zeolite and metakaolin and also control specimens were made all with a w/c ratio of 0.45. After 28 days of water curing, specimens were placed in sulfuric acid solutions with pH=1 and pH=2. In order to keep the pH of solutions in a constant value, daily pH control was performed and required amount of acid added to solutions to reach the desired pH (the increase of pH value is result of reaction between concrete and acidic solution). During exposure period, weight changes of specimens as well as sulfate penetration depth were measured for comparing the performance of different mixtures. The results revealed that concrete specimens including pozzolanic admixtures performed considerably better than ordinary concrete without pozzolan.

Keywords

Blended cement, Durability, Pozzolan, Sulfuric acid, Weight change.

[1] Research assistant, Construction Materials Institute (CMI), School of Civil Engineering, University of Tehran, Tehran, Iran, Corresponding author. Tel.:+98-21-88969112; Fax: +98-21-88959740.
E-mail addresses: mmoradian@ut.ac.ir, URL: http://cmi.ut.ac.ir
[2] Research assistant, Construction Materials Institute (CMI), School of Civil Engineering, University of Tehran, Tehran, Iran, mhallaji@ut.ac.ir
[3] Research assistant, Construction Materials Institute (CMI), School of Civil Engineering, University of Tehran, Tehran, Iran, behnam_kiani@ut.ac.ir
[4] Associate Professor, Director of Construction Materials Institute (CMI), School of Civil Engineering, University of Tehran, Tehran, Iran, shekarch@ut.ac.ir
[5] Research assistant, Construction Materials Institute (CMI), School of Civil Engineering, University of Tehran, Tehran, Iran, chari@ut.ac.ir

1 INTRODUCTION

Concrete is the most widely used material in construction of structures. When concrete is exposed to environment containing sulfuric acid, it experiences severe deterioration due to neutralization reactions. Sulfuric acid reacts with the free lime [$Ca(OH)_2$] in the concrete forming gypsum ($CaSO_4 \cdot 2H_2O$). Another destructive action is the reaction between calcium aluminate and the gypsum crystals. These two products form the less soluble reaction product ettringite ($3CaO \cdot Al_2O_3 \cdot 3CaSO_4 \cdot 32H_2O$) [Moradian et al. 2010, Clifton and Ponnersheim 1994]. Both gypsum and ettringite cause expansion which results in cracking of concrete [Bonakdar and Mobasher 2010]. The corroded surface becomes soft and white. When the corrosion continues, the corroded concrete structure loses its mechanical strength [Monteny et al. 2001].

To extend the life of concrete in acidic environment, it is essential to find a way to control these processes. The rate of deterioration depends on the concentration of sulfuric acid, ambient temperature, cement type, water to cement ratio, porosity and presence of admixtures [Tumidajski 1995]. Generally, adding pozzolan results in a concrete with a denser structure, better able to withstand sulfate attack, but it also reduces or eliminates the free, leachable calcium hydroxide [Pavlík and Uncík 1997].

Among all mineral admixtures, silica fume (SF) has found to have the best performance in resistance of concrete in acidic environment [Dazko et al. 1997]. The effect of silica fume on concrete microstructure is well reported in the literature. Silica fume is an artificial pozzolan that increases the compressive strength of concrete as a result of making stronger transition zone as well as the increase in the rate of hydration at early ages [Ghods et al. 2007, Shekarchi et al. 2009]. Metakaolin is silica based and active pozzolan product that improves the mechanical properties of concrete in both short and long term [Nai-qian et al. 1990; Liguori et al. 2004; Perraki et al. 2003]. The prefix Meta refers to the calcination of kaolinite at certain temperature and the production of Metakaolin.

However, there is another admixture which has not got enough attention and its ability to improve performance of concrete in aggressive environments has almost left unknown. Natural zeolite (NZ) is a crystalline mineral that has siliceous and aluminum oxide in its chemical compound that like other mineral admixtures produces more C-S-H gel through pozzolanic activity [Ahmadi and Shekarchi 2010]. It is enunciated that 10% replacement of zeolite could lead to the production of high quality concrete with lower water absorption, chloride ion diffusivity coefficient and permeability. Although the usage of superplasticizer to reach the required workability is imperative [Ahmadi and Shekarchi 2010]. The porosity reduction can only obtained by limited amount of zeolite replacement which is claimed to be about 15% [Poon et al. 1999].

2 EXPERIMENT PROGRAM

2.1 Used Materials

Calcareous aggregate was chosen for the concrete mixes. Using calcareous aggregates instead of siliceous type provides additional alkalinity of concrete and increases durability of concrete in sulfuric acid environment [Barnard 1967; Thistlethwayte 1972]. The chemical analysis of aggregate is presented in table 1. Three types of pozzolan including silica fume, Metakaolin and zeolite were used in order to perform the tests. Table 2 includes the chemical analysis of cement as well as pozzolanic materials.

Table 1. Chemical analysis of aggregate.

Oxide	*Fine aggregate (%)*	*Coarse aggregate*

SiO_2	0.4	2.34
TiO_2	0.04	0.03
Al_2O_3	0.91	0.59
Fe_2O_3	0.21	0.12
CaO	46.98	47.58
MgO	0.68	0.59
Na_2O	0.05	0.04
K_2O	0.25	0.20
SO_3	0.4	0.11
L.O.I	41.03	42.69

Table 2. Chemical analysis of cement and pozzolanic materials.

Oxide	*Cement*	*Silica Fume*	*Metakaolin*	*Zeolite*
		(%)		
SiO_2	22.71	93.16	51.85	67.79
Al_2O_3	4.91	1.13	43.87	13.66
Fe_2O_3	2.93	0.72	0.99	1.44
CaO	59.55	-	0.2	1.68
MgO	2.81	1.6	0.18	1.6
Na_2O	0.32	-	0.01	2.04
K_2O	0.87	-	-	1.42
SO_3	2.99	0.05	-	0.5
L.O.I	2.31	1.58	0.57	10.23

2.2 Mix Design

The mix design is presented in Table 3. The water to binder ratio was kept 0.45 in all the batches and cubic 10×10×10 cm specimens were made for placing in the acid solution. Moreover, polycarboxylate superplasticizer was employed to reach the slump of near 20 cm.

Table 3. Concrete mix design.

Code	*Cement (Kg/m^3)*	*W/C*	*Silica fume (% replacement)*	*Zeolite (% of replacement)*	*Metakaolin (% of replacement)*	*Slump (cm)*
MC	400	0.45	-	-	-	22
MSF	370	0.45	7.5	-	-	20
MZE	360	0.45	-	10	-	22
MME	360	0.45	-	-	10	21

2.3 Performed Tests

Concrete specimens were put in sulfuric acid solution after 28 days of moist curing. The pH of solutions were kept 1 by adding additional sulfuric acid. Figure 1 shows the pH increase of solution during a period of 150 days. The weight change and also sulfate penetration in depth of concrete were measures in order to compare the performance of each specimen. For weighing of specimens, they were taken out of the tanks and let them be out for 4 hours for drying of their surfaces. Then weighting was performed using digital balance. For measuring the depth of sulfate penetration, concrete powder samples were taken from four different depths of specimens. The sulfate measurement was performed using gravimetric analysis.

In addition, some specimens were put in a solution of the pH=2 and the visual observation were assessed for this group.

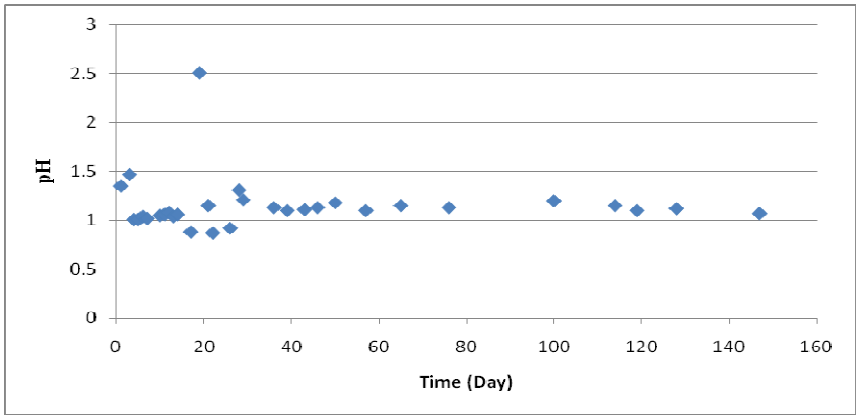

Figure 1. pH change of solution.

3 RESULTS AND DISCUSSION

As expected, the concrete surface was corroded uniformly because of the calcareous base of aggregate. Existence of gypsum is the sign of sulfuric acid attack occurrence. However, considerable amount of efflorescence dissolve in solution and disappear from the specimen surface because of strong sulfuric acid. But, gypsum is visible on the surface of specimens which were placed in solution with pH=2. Figure 2 shows the specimens appearance after 120 days of exposure in sulfuric acid solution with pH=1.

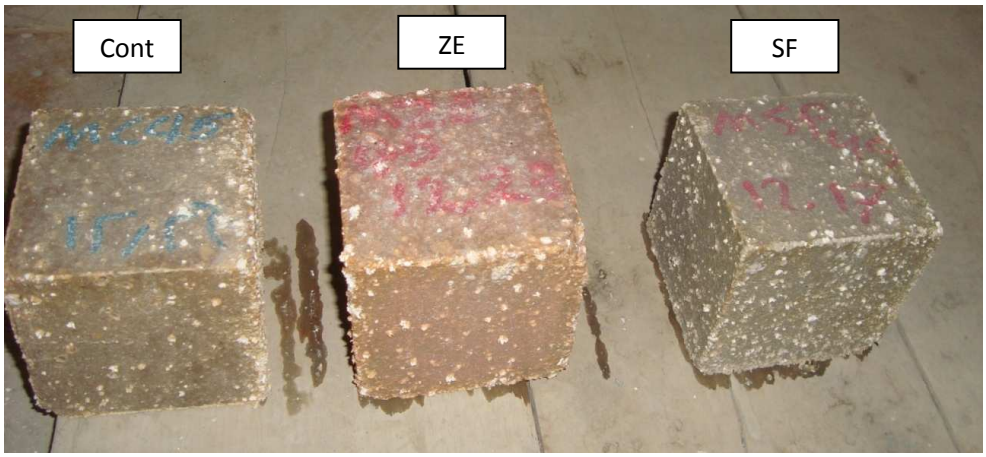

Figure 2. Specimens after 120 days exposure in sulfuric acid (pH=1).

The specimens are visually resemble and no definite conclusion could be drawn. However, the specimen containing zeolite seems to have more efflorescence on its surface. Figure 3 shows the weight change of specimens after 200 day (each data is the average of results of 3 specimens). After 200 days of exposure in sulfuric acid with pH of 1 no weight loss was observable in none of specimens. The weight gain could be the result of completion of hydration reaction and also filling of pores by expansive products like gypsum and ettringite. It is possible that they experience weight loss after an undetermined period.

The specimens made with metakaolin showed more weight gain compared to other pozzolanic material. Control specimens weight changed less than three other codes as well. It could be concluded that using pozzolans improves the resistance of concrete exposed to acidic environments.

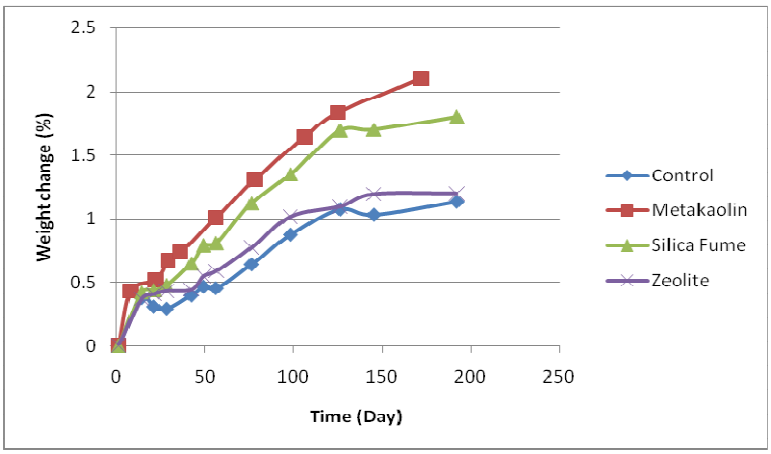

Figure 3. Weight change of specimens in acid sulfuric (pH=1).

Sulfate profiles in depth of concrete are presented in Fig. 4. This test could be more expressive than weight change of concrete. The surface sulfate in specimen congaing zeolite is more than others. However the amount of sulfate of this specimen in depth of concrete is less than three other specimens. This test could support the idea of confident using of zeolite for making resistant concrete in sulfuric acid environment. The control specimen showed the worst performance and this implies the necessity of using pozzolanic for controlling the rate of deterioration in acidic environment.

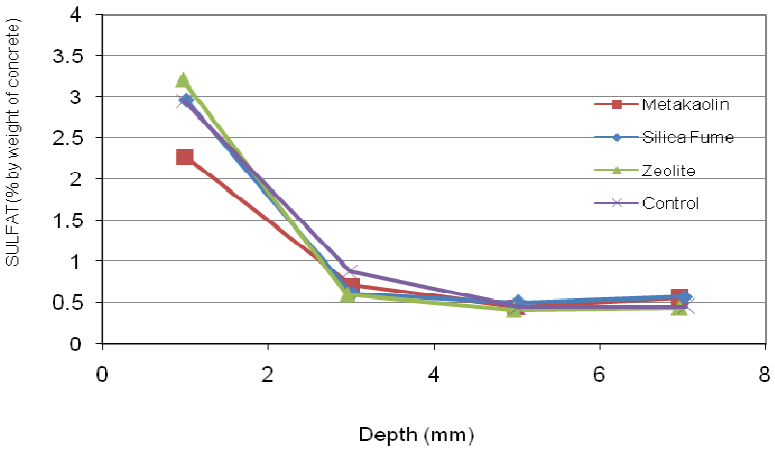

Figure 4. Sulfate profile in depth of concrete.

It is noted that formation of effloresce on the surface of concrete decrease the rate of deterioration and could be a protective layer against aggressive agents. Figure 5 shows the formation of this layer on the surface of concrete in sulfuric acid with pH of 2. In the case that aggregates are calcareous, this layer is thicker and more considerable. However, effloresce in stronger acid solution dissolves rapidly and has less important effect.

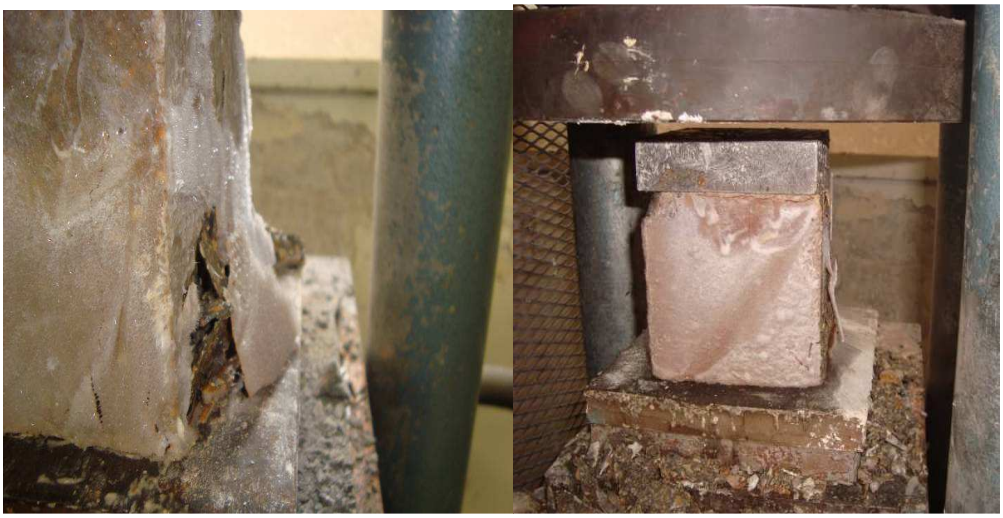

Figure 5. Formation of protective layer on the surface of concrete in sulfuric acid solution (pH=2).

4 CONCLUSIONS

Investigation of concrete in sulfuric acid is important for simulation of concrete in environments like sewage pipes or industrial plants. In this paper, three different pozzolans were tested for comparing the performance of them in sulfuric acid environment. Based on the results of tests, the following conclusions could be drawn:

- Calcareous aggregate improves the properties of concrete exposed to acidic environment, because calcareous aggregates provide more alkalinity for concrete.
- Pozzolans improves mechanical and durability properties of concrete. Using pozzolans is one of the easiest ways to increase the resistance of concrete in acid sulfuric environment.
- Efflorescence formation occurred on the surface of concrete. This suggests the sulfate attack existence in concrete.
- In spite of elapsing near 200 days of exposure, the specimens not only did not lose their weight, but also gain weight. This is attributed to completion of hydration reaction and also filling the pores with the products of sulfate attack. The specimens contained metakaolin showed more weight gain.
- The specimens contained zeolite had the greatest amount of surface sulfate. However, the sulfate in depth of specimen is least.

REFERENCES

Ahmadi, B., & Shekarchi M. 2010. “Use of natural zeolite as a supplementary cementitious material.” *Cement and Concrete Composites*, 32[2], pp. 134-141.

Bonakdar, A., & Mobasher, B. 2010. “Multi-parameter study of external sulfate attack in blended cement materials.” *Constr. Build. Mater*, 24[1], pp. 61–70.

Clifton, J. R., & Ponnersheim, J. M. 1994. “Sulfate attack of cementitious materials: volumetric relations and expansions.” *NIST IR 5390*, Gaithersburg, MD.

Daczko, A., Johnson, D., & Arney, S. 1997. "Decreasing concrete sewer pipe degradation using admixtures" *Materials and Performance Journal*., 10[1], pp. 51-56.

Ghods, P., Alizadeh, R., Hosseini, M,. Chini, M,. Ghalibafian, M,. & Shekarchi, M. 2007. "Durability-based design in the Persian Gulf." *Concrete International (CI)*, 29[12], pp. 50-55.

Liguori., B., Caputo, D., Marroccoli, M., & Colella, C. 2004. "Evaluation of zeolite-bearing tuffs as pozzolanic addition for blended cements" *Eighth CANMET/ACI International conference on fly Ash, silica fume, slag, and natural pozzolans in concrete.*

Monteny, J., De Belie, N., Vincke, E., Verstraete, W., & Taerwe, L. 2001. "Chemical and microbiological tests to simulate sulfuric acid corrosion of polymer-modified concrete" *Cem Concr Res*, 31[9], pp. 1359-1365.

Moradian, M., Shekarchi, M., Pargar, F., Bonakdar, A., & Valipour, M. in Press. "Deterioration of concrete caused by complex attack in sewage treatment environment", *Journal of Performance of Constructed Facilities.*

Nai-qian, F., Li G. Z., & Zang, X., W. 1990. "High-strength and flowing concrete zeolitic mineral admixtures." *Cement, Concrete and Aggregates*, 12[2], pp. 61-69.

Pavlík, V. & Uncík, U. 1997. "The rate of corrosion of hardened cement pastes and mortars with additive of Silica Fume in acids", *Cem Concr Res* **27**, pp. 1731–1745.

Perraki, T, H., Kakali, G., & Kontoleon, F. 2003. "The effect of natural zeolites on the early hydration of portland cement." *Microporous and Mesoporous Materials*, 61[1-3] pp. 205-212.

Poon, C. S., Lam, L., Kou, S.C, & Lin, Z.S. 1999. "A study on the hydration rate of natural zeolite blended cement pastes." *Constr Build Mater*, 13[8], pp. 427-432.

Shekarchi, M., Rafiee, A,. & Layssi H. "Long-term chloride diffusion in silica fume concrete in harsh marine climates." *Cem Concr Comp*, 31[10], pp. 769-775.

Thistlethwayte, D. K. B. 1972. "The control of sulphides in sewage systems." *Butterworths, Sydney.*

Tumidajski, P. J., Chan, G. W., & Philipose, K. E. 1995. "An effective diffusivity for sulfate transport into concrete." *Cem Concr Res*, 25[6], pp. 1159–1163.

XII DBMC
International Conference on Durability of Building Materials and Components
PORTO - PORTUGAL, April 12th-15th, 2011

Experiments for Determining the Corrosion Activity of Reinforced Concrete

Ali Osman Kuruşcu [1]
Meltem Vatan [2]

ABSTRACT

This study aims to assess the severity of corrosion of the steel elements in the reinforced concrete structures by investigating the NaCl effect in the experimental tests. The corrosion tests are based on the electrochemical techniques as half-cell and macro-cell potential measurements. These tests are the simplest way of assessing the severity of the steel corrosion in order to investigate the corrosion potential of the reinforced concrete specimens.

The main principle of the experiments done in this study is investigation of the NaCl effect on the corrosion of steel bars. In order to investigate the NaCl effect it is decided to make two different tests' set up that are producing of RC specimens by using NaCl in the concrete mixture and producing concrete RC specimens without NaCl by curing those specimens in the NaCl solution. The set up of the experiments includes eight samples with NaCl and eight samples without NaCl in the concrete mixture which shapes are prismatic and dimensions are set according to the ASTM C-876-91 standard. The experiments were based on measurements in dry and wet condition that were made weekly by electrochemical monitoring over a period of ten months. The aim of the experiments was measuring of the potential difference of half-cell and macro-cell by using multimeter devise in order to investigate the increase of the corrosion in the reinforced steel bars under NaCl effect.

The results of the study showed that the active corrosion period of samples with high water-to-cement (w/c) ratio is shorter than samples with low w/c ratio.

KEYWORDS

Corrosion, Durability, Electrochemical half-cell test, Reinforced concrete.

[1] Faculty of Architecture of the Yildiz Technical University (YTU), Istanbul, TURKEY, okuruscu@yildiz.edu.tr
[2] Faculty of Architecture of the Yildiz Technical University (YTU), Istanbul, TURKEY, vatan@yildiz.edu.tr

1 INTRODUCTION

The corrosion of the reinforcing steel is recognized as the most important threat to the structural concrete durability. It is widely accepted as the primary cause of degradation of reinforced concrete structures such as bridges, parking garages, transit system tunnels, piers and RC residential buildings. Corrosion causes decrease of steel strength capacity and material degradation. In turn, this corrosion damage is largely related to the use of de-icing salts and chlorides found in marine environments, as well as carbonation of the concrete from CO_2 in the atmosphere. The safety and the service life of the RC structures are dependent to the corrosion of reinforcing steel elements. For this reason, quantitatively assessment of the corrosion degree and prediction of its evolution need some measurements.

The high alkaline environment of good quality concrete forms a passive film on the surface of the embedded steel that normally prevents the steel from further corroding. However, under the influence of chloride and carbonation, the passive film disrupts or destroys and steel corrodes. The corrosion products occupy a large volume and these induce stresses in the cover concrete resulting in cracks, delamination and spalling [Revathy et al. 2009].

This study aims to assess the severity of corrosion of the steel elements in the reinforced concrete structures by investigating the NaCl effect in the experimental tests. The corrosion tests are based on the electrochemical techniques as the half-cell and macro-cell potential measurement. These tests are the simplest way of assessing the severity of the steel corrosion in order to investigate the corrosion potential of the reinforced concrete specimens.

2 EXPERIMENTAL STUDIES

The main principle of the experiments is investigation of the NaCl effect on the corrosion. In order to investigate the NaCl effect it is decided to make two different tests' set up that are producing of RC specimens by using NaCl in the concrete mixture and producing concrete RC specimens without NaCl by curing those specimens in the NaCl solution. The set up of the experiments includes eight samples with NaCl and eight samples without NaCl in the concrete mixture which shapes are prismatic and dimensions are according to the ASTM C-876-91 standard. The experiments were based on measurements in dry and wet condition that were made weekly by electrochemical monitoring over a period of ten months. The aim of the experiments was measuring the potential difference of half-cell and macro-cell by using multimeter devise in order to investigate the increase of the corrosion in the reinforced steel bars under NaCl effect. The results of the study showed that the active corrosion period of samples with high water-to-cement (w/c) ratio is shorter than samples with low w/c ratio.

2.1 Materials

Cement and binders: The specimens considered in this test program were produced by using CEM I (PÇ 42,5) type cement subjected to the TS-EN 196-1,2,3. All experiments such specific weight of the cement, physical and mechanical properties tests were made according to that standard. Table 1 shows mechanical properties of cement and Table 2 shows physical and chemical properties of cement used in the experimental tests.

Table 1. Mechanical properties of cement.

	Bending strength (MPa)		Compression strength (MPa)	
	7th day	28th day	7th day	28th day
Cement (PÇ 42,5)	6,3	9,3	33,9	50,1

Table 2. Physical and chemical properties of cement.

Chemical properties	Portland cement (PÇ 42,5)		
CaO	64,01	Ignition loss	2,27
SiO_2 (Soluble)	20,01	Unsoluble particle (max)	0,32
Al_2O_3	5,28	Specific weight (gr/cm^3)	3,14
Fe_2O_3	3,65	Specific surface (cm^2/g)	3570
MgO	1,21	Setting time Vicat sonde (hour)	Starting: 2 hours 25 minutes Ending: 3 hours
SO_3	2,47	3 CaO. SiO_2	71,51
Cl⁻	0,033	3 CaO. SiO_2	3,80
Na_2O/K_2O	0,25/0,81	3 CaO. Al_2O_3	7,82
Sulphur	-	3 CaO. Al_2O_3. Fe_2O_3	11,11

Aggregate: Properties of the aggregate and the granulometric tests are according to the TS 3529 and TS 706. Figure 1 shows aggregate mixture size distribution.

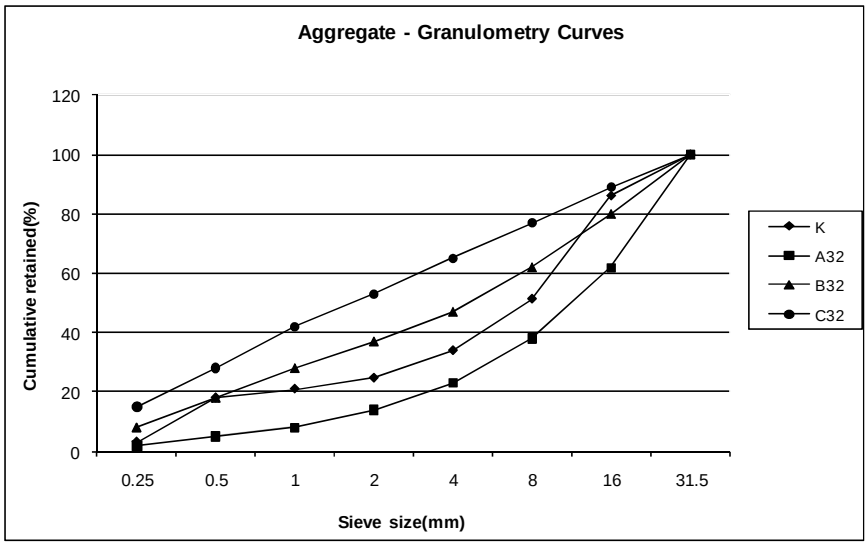

Figure 1. Aggregate mixture size distribution - Granulometric curves.

Water: Mixing water was provided according to the TS EN 206 and TS EN 1008.

Reinforcement: Diameter of used ribbed steel bars is 16mm. Steel bars are consistent to the DIN 17000 ST 37.2/ASTM A36 ASTM A529-GR 50.

Plasticizer: For using in the different water quantity and dosage of the concrete the plasticizer was used in the concrete mixture. The properties of the used plasticizer which is 3rd generation concrete plasticizer and high level water reducing agent are given below:

Standard:	EN 934-2 & SIA 162 (1989)	Origin:	Modified polycarboxylate
Appearance:	Light yellow	% solid material:	34
Density:	1.10±0.02 kg/l	Viscosity:	Low
pH:	7.3	Chloride:	None

Concrete mixture: In the experimental studies, specimens were produced with different dosage of cement and water. Four different type of concrete with the dosage of 260 kg/m^3 and 300 kg/m^3; and with water/cement ratio of 0,50 and 0,65 were produced. Twenty-four of those specimens were

cylindrical 100/200 mm dimensioned and twenty-four were cubic 150/150/150 mm dimensioned. Produced specimens were cured in the water and weather condition for 28 days. Group A specimens were cured in the water without NaCl, Group B specimens were cured in the weather condition with NaCl with 40000 mg/l Cl^- concentration in the mixing water. Mixture ingredients and specifications, which are based on previous experiments, are given in the Table 3. The first group of specimens (A) without sodium chloride (NaCl) in the mixture water of concrete and also, the second group of specimens (B) all steps were the same except sodium chloride (NaCl) which was added into the mixture water.

Table 3. Material quantities required for 1 m^3 fresh concrete.

Code	Cement Dosage (kg)	Water + Humidity (kg)	Plasticizer		No2 Coarse Agr. (kg)	No1 Coarse Agr. (kg)	Crushed Sand (kg)	Natural Sand (kg)	β (kg/m^3)
			(%)	(g)					
260/65/A	263	147+22	0,5	39	768	608	296	299	2381
260/65/B	262	147+22	0,5	39	795	630	307	309	2465
260/50/A	260	107+23	0,7	55	800	634	309	311	2421
260/50/B	261	107+23	0,7	55	753	597	291	293	2280
300/65/A	310	174+21	-	-	750	594	289	292	2420
300/65/B	309	174+21	-	-	778	616	300	303	2509
300/50/A	296	128+22	0,5	45	756	599	292	294	2372
300/50/B	298	128+22	-	-	767	608	296	298	2398

2.2 Experiments

2.2.1 Compression test

Compression tests on the concrete specimens were made in the beginning of the experiments and in the end of wet-dry condition cycle. Tests, were done on 100/200 mm cylindrical specimens with 3000 kN auto test compression devise which has 2,4 KN/h velocity. All tests were according to the TS EN 12390-3 (2002) so ultimate load (P_k, kN) and compression strength (f_c) were determined and presented at Table 4.

2.2.2 Split test

In order to determine the tensile strength of the concrete test set up was made according to the BS 1881: Part 117 (1983). Tests were done on 24 100/200 mm cylindrical specimens with the 3000 kN universal compression device. As results of the tests, ultimate load (P_k, kN), split strength (f_{cts}, N/mm^2) were determined (Table 4).

2.2.3 Ultra sound test

Ultrasonic concrete test is based on the pulse velocity method to provide information on the uniformity of concrete, cavities, cracks and defects. The pulse velocity in a material depends on its density and its elastic properties that in turn are related to the quality and the compressive strength of the concrete. Therefore, it is possible to obtain information about the properties of components by sonic investigations according to the ASTM C 597-02 (Table 4).

Table 4. Test results that made on concrete.

Code		Compression test, fc (Mpa)				Split test, fcts (Mpa)				Ultra sound test (km/sn)			
		A		B		A		B		A		B	
		Wet	Dry	Wet	Dry	Wet	Dry	Wet	Dry	Wet	Dry	Wet	Dry
260.65	1	-	27,58	-	22,50	3,08	-	1,83	-	4,71	4,70	4,60	4,40
	2	-	25,40	-	23,00	2,76	-	2,39	-	4,74	4,76	4,65	4,45
	3	-	27,37	-	21,50	2,92	-	2,67	-	4,74	4,75	4,55	4,65
Average		**26,78**		**22,33**		**2,92**		**2,30**		**4,73**		**4,55**	
260.50	1	-	34,40	-	26,18	4,15	-	2,36	-	4,84	4,67	4,65	4,65
	2	-	34,18	-	27,21	4,24	-	2,21	-	4,72	4,93	4,65	4,65
	3	-	33,96	-	32,82	3,94	-	2,29	-	4,84	4,82	4,60	4,70
Average		**34,18**		**28,74**		**4,11**		**2,29**		**4,81**		**4,65**	
300.65	1	-	30,56	-	26,00	2,89	-	2,24	-	4,58	4,72	4,55	4,50
	2	-	31,28	-	27,00	2,64	-	2,68	-	4,55	4,73	4,60	4,55
	3	-	29,22	-	26,40	2,39	-	2,46	-	4,60	4,85	4,55	4,50
Average		**30,35**		**26,47**		**2,64**		**2,46**		**4,67**		**4,54**	
300.50	1	-	35,80	-	22,82	4,00	-	3,00	-	4,78	4,66	4,60	4,65
	2	-	36,00	-	35,34	4,20	-	2,58	-	4,75	4,79	4,65	4,70
	3	-	36,72	-	37,39	4,06	-	2,16	-	4,88	5,05	4,65	4,70
Average		**36,17**		**31,85**		**4,09**		**2,58**		**4,82**		**4,66**	

2.2.4 Corrosion test

Reinforced concrete specimens whose size are 400/ 250/ 150 mm, were produced according to the ASTM G 109-92 (1992) and were cured up to 28th day for having 100% relative humidity. Before wet-dry condition cycle, the steel bars that were outside of the concrete were covered for protecting from the weather. In upper part of each specimen, pool from polystyrene was made with 76.2/76.2/152.4 mm dimensions for wet-dry cycle (Figure 2). Two steel bars positioned in the down part were considered as cathode and all steel bars were connected by the 100 Ω resistor and conductor wire for measuring the electro potential between anode and cathode (Smith J.L., 2000).

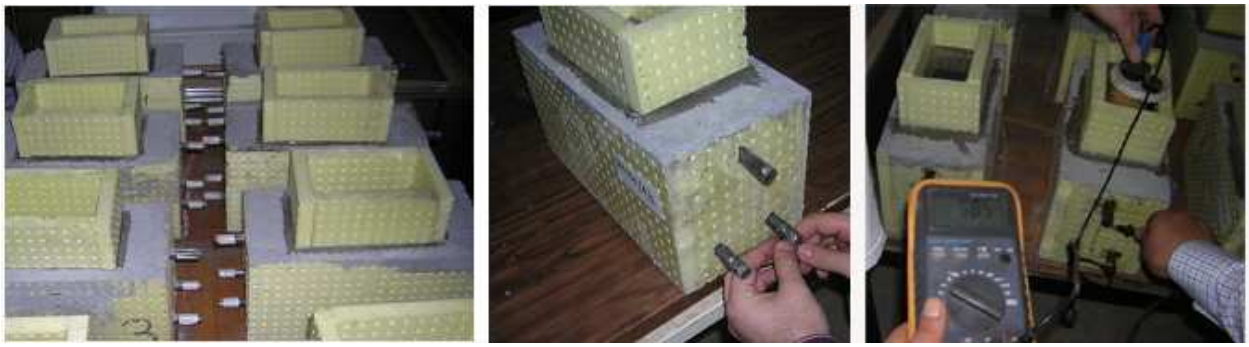

Figure 2. Corrosion test set up.

Aging was made by filling the liquid (water, solution) in the pools of upper part and taking off of the liquid during the drying. Pools were covered during the wetting for avoiding the evaporation.

2.2.4.1 Half cell potential measurements

The simplest assessment technique for steel corrosion damage in the reinforced concrete is the measurement of the corrosion potential (or rest potential, half-cell potential). A measurement procedure is described in the ASTM C876-80 standard, the basis of which is the corrosion potential of the steel bars will shift in the negative direction if the surface changes from the passive to the active state. The set up of the corrosion test and half-cell measurement are shown in Figure 2.
The criterion of the ASTM C 876 for corrosion potential is given in the Table 5.

Table 5. Criterion of the ASTM C 876 for corrosion potential (Keleştemur, O, 2009).

Half Cell Potential Value CSE (SCE)	**Corrosion condition**
E < -350mV (-270mV)	High corrosion risk (<90% risk of corrosion)
-350mV<E<-200mV(-120mV)	Intermediate corrosion risk
-200mV < E	Low corrosion risk (10% risk of corrosion)

2.2.4.2 Macro cell potential measurements

Another method for assessment of corrosion damage in steel bars is measuring the electro-potential difference between two steel bars that are connected with 100 Ω resistant and conductor wire. Electro potential difference was measured by the high sensitive and 0.01mV stepped multimeter device weekly in a period of 30 weeks. Table 6 shows the corrosion rates of steel bars in reinforced concrete specimens.

Table 6. Criterion of corrosion rates of steel bars in reinforced concrete specimens.

Rate of corrosion	**Corrosion current density (i_{corr}) A/cm^2**
High	10 - 100
Medium	1 - 10
Low	0,1 - 1
Passive	< 0,1

2.3 Results of the Experiments

Figure 3 and Figure 4 show the results of half cell potential measurements. Figure 5 and Figure 6 show the results of macro cell potential measurements

3 CONCLUSIONS

Corrosion is the most important threat to the reinforced concrete buildings. Even though this is well known all over the world in many countries that do not have well enough economic potential the most important cause of damage on RC buildings is still corrosion.

Turkey has been experienced 1999 earthquake (7,4 RS) and after that event Turkish Specification for Buildings to be Built in Seismic Zones has been changed significanlty. However the practice of building construction still has its problems and the control of construction period is not working well enough. Because of that reason this paper highlihgtes the importance of corrosion effect on RC buildings and techniques on its measurement. Sea sand is used widely in building constructions which includes salt that is the main reason of corrosion. Due to this fact this paper stresses on the well known topic that has researches and publications for many years in the world wide.

Many kinds of electrochemical rebar corrosion measurement techniques are available presently, each with certain advantages and limitations. The complexity of measurements and required specialists' know-how in applying these techniques also varies significantly. It is recommended to use a combination of different corrosion measurement techniques in order to evaluate the corrosion state of the structure. Furthermore, it is very important to make decision based on different corrosion measurements. Briefly:

- Dosage of cement is affective on compression strength and split strength, but also water/cement ratio is very important to determine strength of concrete.
- Dosage of cement is very important in occurrence of corrosion on steel bars.

- Corrosion can be increase in case of high water/cement ratio for producing concrete.
- If there is a sodium chloride salt that is added into concrete mixture, corrosion degree will be high and corrosion will occur more early than mixture with no salt
- Half-cell potential measurements are not enough to decide the corrosion quantity. Both macro cell measurements and half cell measurements have to be considered for having precise results
- Under these long term corrosion tests in terms of durability, 35 MPa concrete which has 0.50 w/c ratio with cement content of 300 kg/m^3 has better performance than the other specimens.

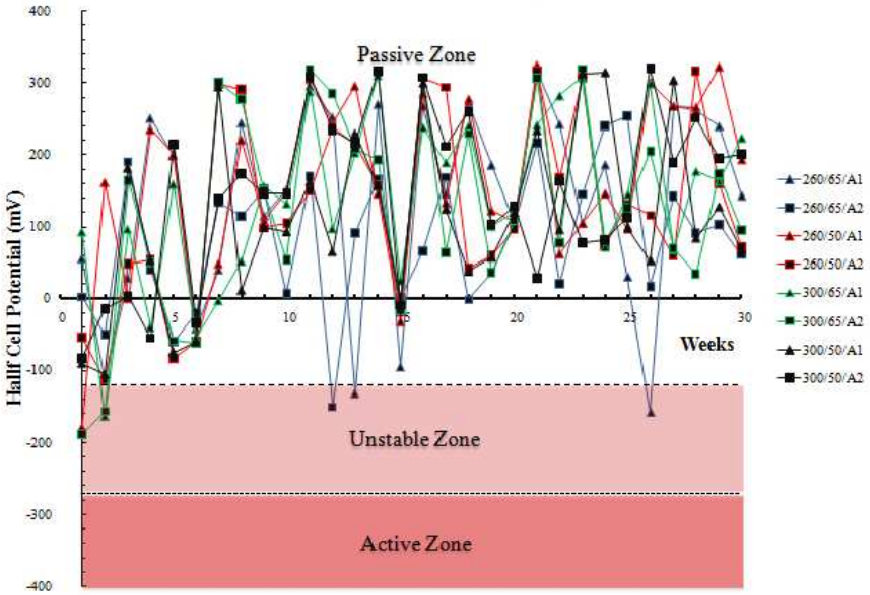

Figure 3. Half cell potential measurements of all A specimens.

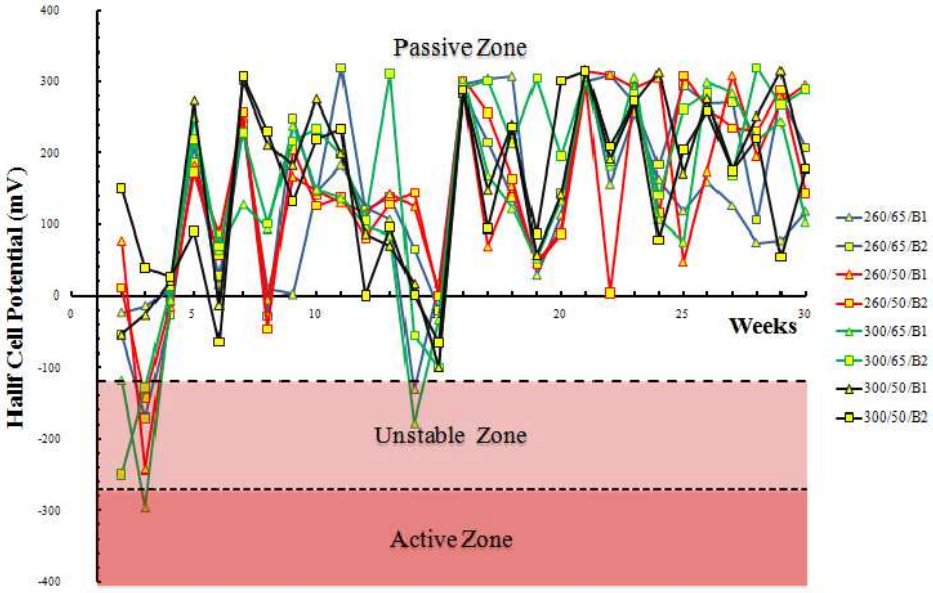

Figure 4. Half cell potential measurements of all B specimens.

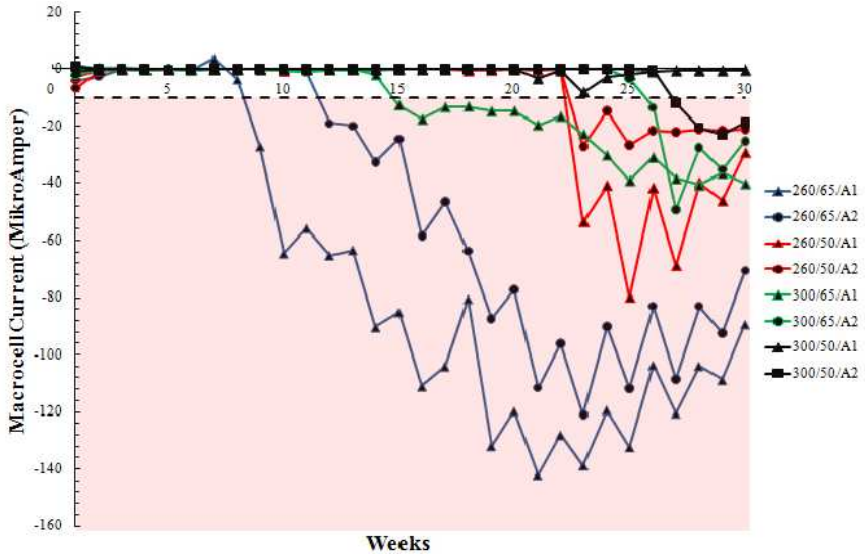

Figure 5. Macro cell measurements of all A specimens.

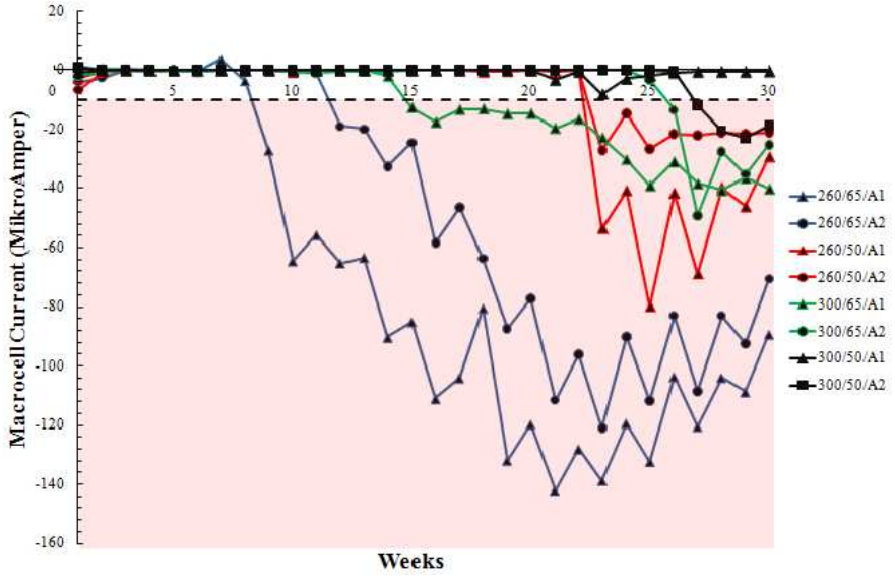

Figure 6. Macro cell measurements of all B specimens.

REFERENCES

ASTM C 597-02 Standard Test Method for Pulse Velocity through Concrete.

ASTM C 876-91, Test Method for Half-Cell Potentials of Uncoated Reinforcing Steel in Concrete.

ASTM C876 Standard Test Method for Half Cell Potentials of Reinforcing Steel in Concrete, Annual Book of ASTM Standards, 4 (2) 1983.

ASTM C-876-91, Standard Test Method for Half-Cell Potentials of Uncoated Reinforcing Steel in Concrete.

ASTM G 109-92, Standard Test Method for Determining the Effects of Chemical Admixtures on the Corrosion of Embedded Steel Reinforcement in Concrete Exposed to Chloride Environments.

Bertolini, L., Carsana, M., Pedeferri, P., "Corrosion behaviour of steel in concrete in the presence of stray current", Corrosion Science 49, 2007, Pages 1056–1068.

BS 1881-117:1983 Testing concrete. Method for Determination of Tensile Splitting Strength.

DIN 17000 ST 37.2/ ASTM A529 / A529M - 05(2009) Standard Specification for High-Strength Carbon-Manganese Steel of Structural Quality.

Keleştemur, O., Yıldız, S., "Effect of various dual-phase heat treatments on the corrosion behavior of reinforcing steel used in the reinforced concrete structures" , Construction and Building Materials, Volume 23, Issue 1, January 2009, Pages 78-84.

Revathy, J., Suguna, K. & Raghunath, P.N., "Effect of Corrosion Damage on the Ductility Performance of Concrete Columns", American J. of Engineering and Applied Sciences 2 (2), 2009 Pages 324-327.

Sagüés, A. A., Pech-Canul, M. A., Shahid Al-Mansur, A. K. M., "Corrosion macrocell behavior of reinforcing steel in partially submerged concrete columns" Corrosion Science, Volume 45, Issue 1, January 2003, Pages 7-32.

Smith, J.L., Virmani, Y.P., "Materials and Methods for Corrosion Control of Reinforced and Prestressed Structures In New Construction" Report No:FHWA-RD-00-081, Federal Highway Administration, DC, August 2000.

TS 3529 Beton Agregalarının Birim Ağırlıklarının Tayini.

TS 706 EN 12620 Beton Agregaları.

TS EN 1008 Beton Karma Suyu.

TS EN 12390-3. Beton – Sertleşmiş Beton Deneyleri – Bölüm 3: Deney Numunelerinde Basınç Dayanımının Tayini.

TS EN 196-1 Çimento Deney Yöntemleri-Bölüm 1: Dayanım.

TS EN 196-2 Çimento Deney Yöntemleri -Bölüm 2: Çimentonun Kimyasal Analizi.

TS EN 196-3 Çimento Deney Yöntemleri -Bölüm 3: Priz Süresi ve Hacim Genleşme Tayini.

TS EN 206-1 Beton- Bölüm 1: Özellik, Performans, İmalat ve Uygunluk.

TS EN 934-2 Kimyasal Katkılar-Beton, Harç ve Şerbet İçin-Bölüm 2:Beton Katkıları, Tarifler ve Özellikler, Uygunluk İşaretleme ve Etiketleme.

XII DBMC
International Conference on Durability of Building Materials and Components
PORTO - PORTUGAL, April 12th-15th, 2011

The Influence of Early Loading in a Study from Compressive Strength, Tensile Strength and Microcracking Formation

Geilma Lima Vieira [1]
Denise C. C. Dal Molin [2]

ABSTRACT

The companies aiming competitiveness in the market are in search of solutions to increase the speed of their constructions, like reduction of structure execution time, reduction of shoring time and anticipating masonry execution time. The process of removing the shoring in early ages submits the concrete structure to a premature load, that damages the cement hydration reaction and unleashes the microcracking process. This study evaluated the mechanical properties behavior of concretes produced with four different cements types (III, III MS, IP MS, I MP), when submitted to precoce compression loads. The analysis included evaluation of the results of compressive strength, split tensile strength and scanning electron microscopic. Were analyzed the effect from strengths in different levels, when submitted to a early loading, in different ages and in different percents of load. The results showed that the mechanical properties of compressive strength of all concretes tend to improve when the age of loading increases. The microscopy analysis makes possibly the visualization of microcracking caused by early loading, as well the recovering microcracking. In the other cements were observed a small decrease in tensile strength.

KEYWORDS

Concrete, Early loading, Compressive strength, Tensile strength, Microcracking formation.

[1] Department of Civil Engineer, Federal University of Espirito Santo (UFES), Vitoria, BRAZIL, geilma.vieira@gmail.com
[2] Department of Civil Engineer, Federal University of Rio Grande do Sul, Porto Alegre, BRAZIL, dmolin@ufrgs.br

1 INTRODUCTION

The rationalization and industrialization process for construction has brought changes in the way buildings are constructed and erected. The construction process is being modified as well as the structural design process and construction management techniques. There has occurred an evolution in concrete strength, hence the structures and typologies are more daring and masonry is more accurate. In consequence of this, there have arisen new types of structures never yet observed in construction nor observed by professionals. However as a consequence of such new construction there has arisen evidence that enclosed walls are breaking, cracking is visible on masonry and covering problems are more frequent. Cracking and compression of the masonry has originated from the inherent mechanism imposed on the materials since these have to release built up strains. External cracking in general occurs because of the incompatibility between reinforced concrete structures and masonry. This incompatibility has been observed as being a function of differential movements between the reinforced concrete elements of the structure and the walls. The inadequacy of the sequence of execution of the work as well as the rate of execution together with an absence of consideration of the interaction between those subsystems, leads to problems of cracking and premature deterioration. The lack of proper project details and execution techniques are the evident source of the fundamental problems associated with the "new" construction process.

To assure their competitiveness in the market place, many construction companies seek solutions that are capable of increasing the rate of construction; for example, reduction in time is sought for execution of the primary structure, reduction of shoring time and anticipating the time needed to execute masonry construction. As a result, the instantaneous deformation of the structure tends to increase and thus also intensify the pathologies evident in such buildings [Medeiros 2005].

In Figure 1, the execution cycle for concrete placement is 7 days and there are only two sets of shoring (Situation A). In this configuration, and to complete the execution of concreting of the third floor (Situation B) the shoring has been removed. In this situation the shoring of the first floor (Situation A) has to be withdrawn even though the concrete has only cured for 15 days, and nonetheless needs support, in addition to its self-weight, the loads occurring due to the upper floor elements.

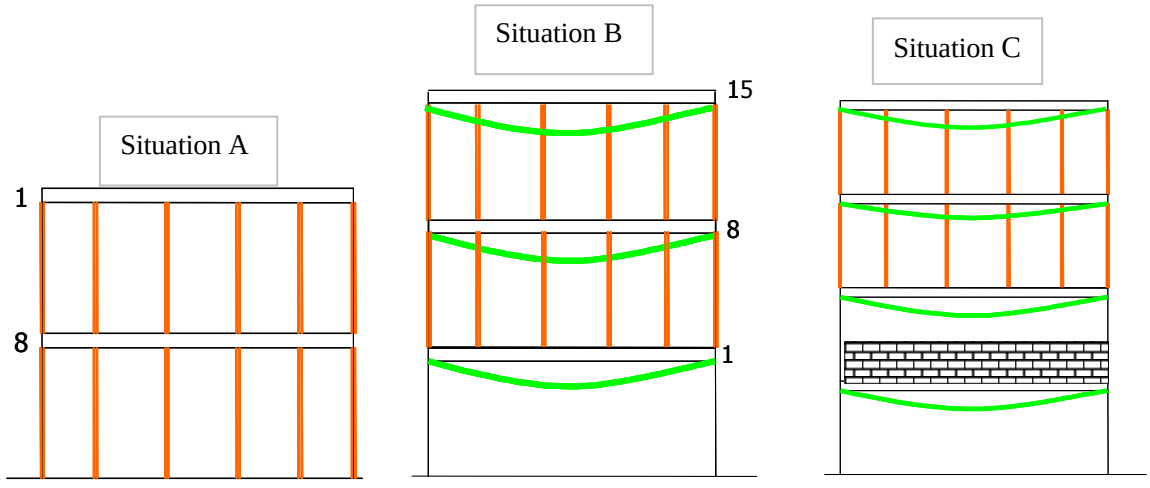

Figure 1. Execution scheme of concrete cycle, shoring, withdrawal of supports and masonry execution of a building.

Thus each recently concreted element is sustained by the other that in turn has not developed sufficient strength to support additional loads. In addition to this situation, there is also the need to anticipate the execution of masonry structures (Situation C) that can possibly add to the undesired effects acting on the structure as a whole, since in each construction step that is completed, a new

component of strain must be absorbed by the structural concrete elements, whether or not the concrete has adequately cured. Without enough resistance and permanent shoring that could help sustain the additional loads, deformations can occur that are not expected in projects in which the concrete execution cycle has insufficient support. The unforeseen deformations can bring about cracking in structures as a function of premature loading.

The Brazilian standard specifications (NBR 14931/2003) do not provide establish values for the withdrawal of support to concrete structures, but it does indicate that support can only be removed when there is sufficient concrete strength to resist loads acting above it. There is no information in the standard on structures having unacceptable deformations for concrete cured less than 28 days. As well, no information is provided on the expected higher deformation for concrete having lower modulus of elasticity when cured less than 28 days. The standard (NBR 14931/2003) does provide the recommendation to monitor the gradual evolution of concrete strength from an early age.

As part of the construction rationalization process, the development of new construction materials and the acknowledgement of the need for improved structural performance at a deeper level have arisen as issues of great importance in the search for improved structures. The evaluation of some singular properties such as the compressive strength of concrete became an insufficient parameter in the study of the performance of the whole structure submitted to early age loadings. In this context, it became relevant to study the other mechanical properties of concrete (i.e. tensile strength) when subjected to early loading, as well as the constituent material of concrete and the hydration phase. The results of such studies would not only help assure construction safety but also the long-term performance of the structure during its service life.

2 EXPERIMENTAL PROCEDURES

The concretes produced were tested at four preloading levels (0%, 25%, 50% and 75%, in relation rupture load), that were applied at 1, 3 and 7 days of curing, using different water/cement ratios (0.35; 0.50 and 0.70). The concretes submitted to a preload were tested at different ages, including at 28 days, which is the age at which tests are normally carried out and the parameter of reference for the majority of structural designs. The influence of microcracking was verified in compressive strength, tensile strength and on the formation of microcracking produced in the different types of concretes. Four (4) types of cement (III, III MS, IP MS and I MP) were used with the objective of verifying the influence of its different compositions and its performance under compressive loads in the early ages of cure and hydration. Table 1 provides water cement ratios, values for cement quantity in the mix, slump test values, as well as temperature and moisture values for the concrete at the casting stage.

Table 1. Experimental admixture.

Cement	*w/c ratios*	*Cement kg/m³*	*mix*	*Slump (cm)*	*Temperature (ºC)*	*Moisture (%)*
I (MP)	0,35	627	1 : 0,77 : 1,63	12,0	16,2	74
	0,50	357	1 : 1,68 : 2,47	20,0	16,0	74
	0,70	257	1 : 2,89 : 3,59	18,0	15,0	78
IP MS	0,35	604	1 : 0,68 : 1,49	4,6	20,0	89
	0,50	360	1 : 1,68 : 2,38	13,0	15,0	70
	0,70	255	1 : 3,00 : 3,55	12,5	16,4	80
III	0,35	627	1 : 0,98 : 1,75	7,0	20,0	68
	0,50	374	1 : 2,09 : 2,74	13,5	15,0	95
	0,70	261	1 : 3,56 : 4,05	5,5	22,0	52
III MS	0,35	624	1 : 0,95 : 1,79	5,0	24,0	60
	0,50	368	1 : 1,95 : 2,73	11,0	26,0	65
	0,70	266	1 : 3,29 : 3,96	12,0	26,0	70

After specimens were cast in molds, the concretes remained in a closed chamber to avoid loss of water by evaporation in the first 24 hours. Afterwards the molds were removed from the specimens, identified, and kept in a curing chamber having relative humidity conditions in excess of 95% and maintained at a temperature of 23 ± 2°C, until the test age was attained.

The rate of applied load during testing was maintained constant for all loads; this was 200 kN/min (0.50 MPa/s); after preloading, the specimens were returned to the curing chamber until the subsequent testing stage.

3 RESULTS AND DISCUSSION

3.1 Compressive Strength

Mathematical models were developed and adjusted for each cement type using linear multiple regression analyses on the respective compressive strength results. Table 2 shows regression models for each cement type, as well as the coefficient of determination (R^2). The regression models incorporate all the variables that influence the compressive strength including: water/cement ratio, test age, preload age and percent of applied preloading.

Table 2. Regression linear model for each cement type in compressive strength.

cement	*Model*	*(R^2)*
I (MP)	$fc = -19{,}08 + \frac{15{,}43}{wc} + 0{,}42 \times age - \frac{0{,}56}{\sqrt{load} \times ageload^2} - \frac{0{,}24 \times ageload}{wc^2}$	95,49
IP MS	$fc = -15{,}37 + \frac{15{,}98}{wc} + 0{,}43 \times age + \frac{0{,}027 \times load}{\sqrt{wc}} - 1{,}22 \times ageload \times wc^2 - \frac{0{,}061 \times load}{ageload}$	97,12
III	$fc = -13{,}27 + \frac{18{,}40}{wc} + 0{,}37 \times age + \frac{0{,}045 \times load}{\sqrt{wc}} - 1{,}66 \times ageload \times wc^2 - \frac{0{,}058 \times load}{ageload}$	98,00
III MS	$fc = -7{,}61 + \frac{13{,}28}{wc} + 0{,}61 \times age - 0{,}789 \times age \times wc^2 + \frac{0{,}006 \times load}{wc^2} + 0{,}695 \times ageload \times \sqrt{wc}$	91,15

Where: fc – compressive strength, (MPa); w/c – water/cement ratio; age – age of specimen, (days); load – preload percent (%); ageload – age of preload, (days).

Figure 2 shows the interrelation between the age at which the concrete was preloaded and the water/cement ratio. The graphics in Figure 2 indicate that in cements with slower hydration reactions, such as I MP for example (Figure 2a), the strength gain was higher at all water/cement ratios with increases in the preload age. This fact is probably due to the evolution in the hydration process. For concrete mixes incorporating high initial strength cements, the increase in preload age does not or little influences gain in compressive strength.

Each one of Portland cements shows a different hydration rate; the finer the cement, the faster the evolution of concrete strength. Comparing a concrete mix using high initial strength cement to one having ordinary cement, in early ages, the former mix will be less porous. Over time, the pores of ordinary cement mix are filled with hydration products and the final porosity can be the same as for concrete mixes having high initial strength cement. Therefore, the influence of cement type is more significant at early curing age. The initial high strength cement has finesse indices higher than other types of cement, and this helps explain the greater strength gain at early curing ages [Neville 1997].

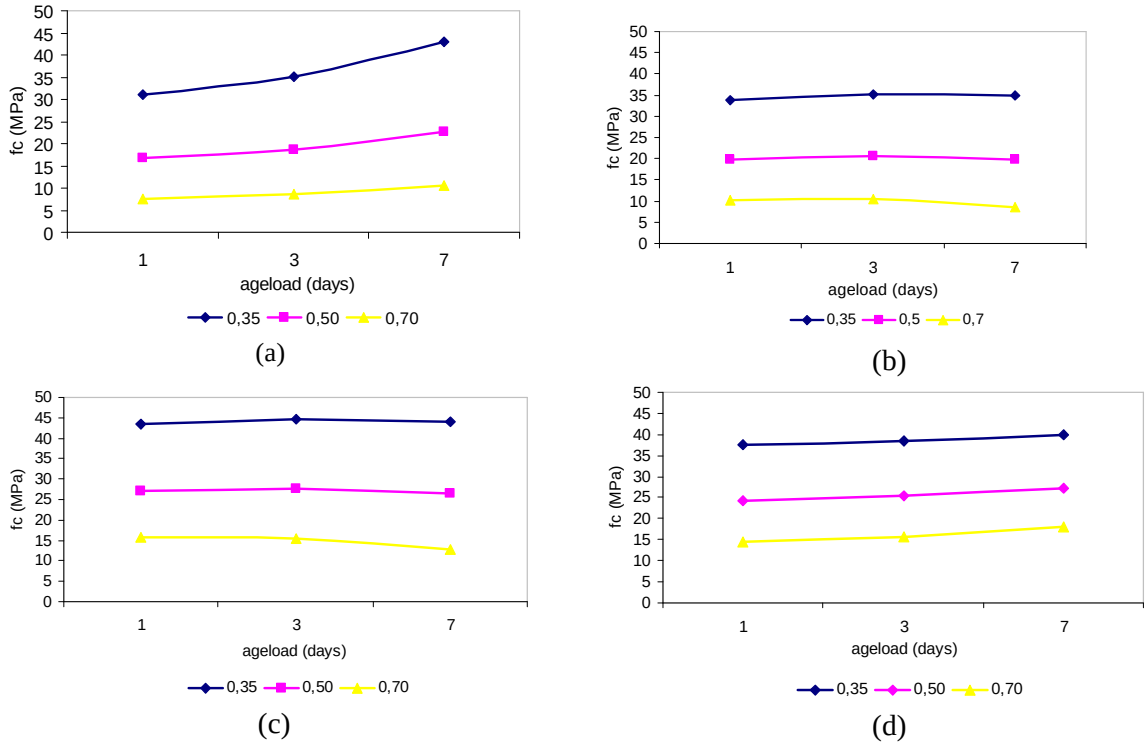

Figure 2. Interaction between preload age and water/cement ratio above compressive strength. (a) I MP. (b) IP MS. (c) III. (d) III MS.

3.2 Tensile Strength

For the tensile strength analysis, a mathematical model was developed on the basis of split tensile strength tests using multiple regression analyses and considering all relevant variables affecting the tensile strength of the concrete (water/cement ratio, test age, preload age and preload percentage). As was achieved for the evaluation of compression strength, the mathematical model for the evaluation of the tensile strength was developed for each cement type as provided in Table 3.

Table 3. Regression linear model for each cement type in tensile strength.

cement	*Model*	*(R^2)*
I (MP)	$f_{t'D} = -0{,}488 + \frac{1{,}00}{wc} - \frac{1{,}620}{age} + 0{,}012 \times age \times \sqrt{ageload} + \frac{5{,}11}{load} - 0{,}038 \times wc^2 \times ageload^2$	93,38
IP MS	$f_{t'D} = -1{,}314 + \frac{1{,}443}{wc} + 0{,}019 \times age + 0{,}107 \times ageload - \frac{0{,}004 \times ageload^2}{wc^2} - \frac{0{,}004}{wc^3 \times \sqrt{load}}$	87,07
III	$f_{t'D} = 2{,}416 + \frac{0{,}288}{wc} - \frac{7{,}580 \times wc^2}{age^2} - \frac{0{,}760}{ageload} + \frac{0{,}0788 \times \sqrt{load}}{ageload} - 0{,}4598 \times wc^3 \times \sqrt{load}$	92,48
III MS	$f_{t'D} = -0{,}728 + \frac{1{,}2111}{wc} + 0{,}1452 \times age + 0{,}1139 \times ageload - \frac{0{,}0803 \times age}{wc} + 0{,}0332 \times \sqrt{load}$	94,93

Where: ft'D – split tensile strength, (MPa); wc – water/cement ratio; age – age of specimen, (days); load – preload percent (%); ageload – age of preload, (days)

Differently to compressive strength, were not observe tensile strength increases as long as percentage load increases (fig. 2), which can induct to a possible microcracking state. The filling effect of microcracking was evident for compressive strength, but for tensile strength are signs that microcracking recovering doesn't occurs totally. This process will depend on the quantity remained anidro material disposal, quantity of microcracking formed and opened. Furthermore, when the

concrete is submitted to a compressive load, the direction and propagation of microcracking tends to orthogonal distribution towards the direction of load, what strongly damage the tensile strength. Although the compressive strength increase, probably due to residual strength, the preload doesn't implicates in tensile strength increase. The interaction effect between preload percentage and water/cement ratio is shown in Figure 3. The values were obtained from equations in Table 3.

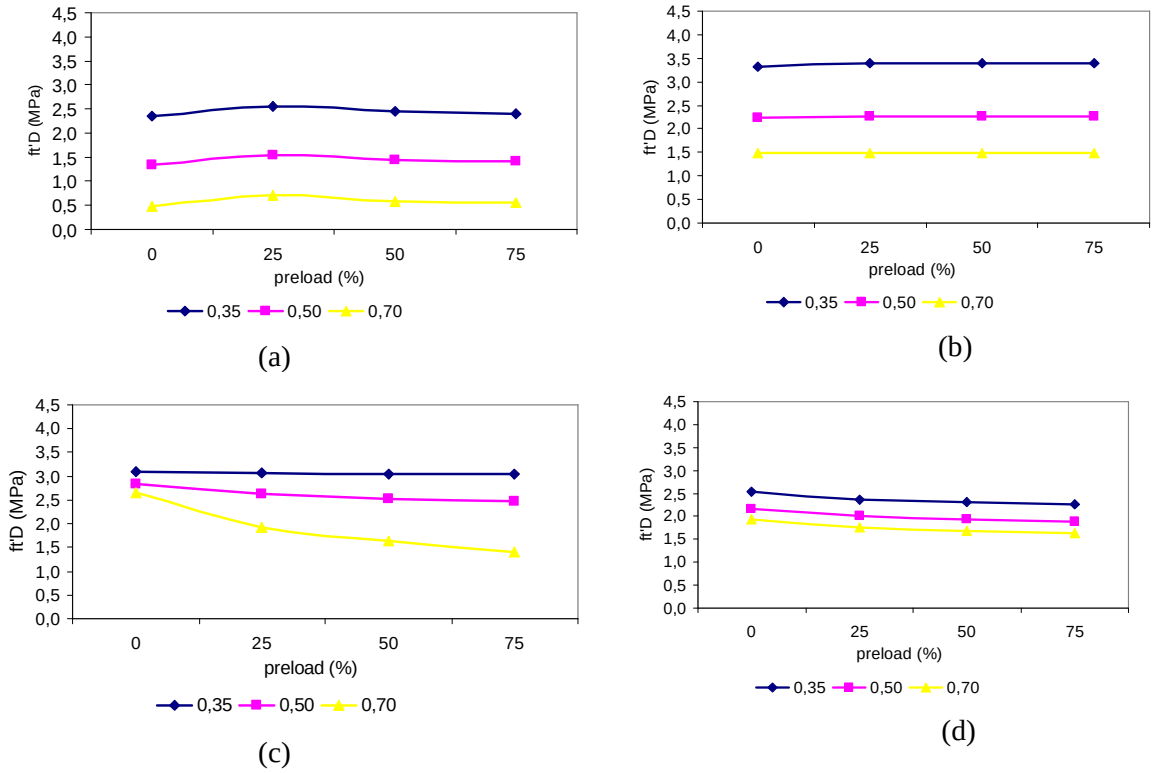

Figure 3. Interaction between preload percent and water/cement ratio above tensile strength. (a) I (MP). (b) IP MS. (c) III. (d) III MS.

Figure 3 indicates that the water/cement ratio has direct influence on the load percentage. With an increase of percentage load a decrease in tensile strength is evident, mainly for mixes having higher water/cement ratios and for mixes using type III cement. For mixes having smaller water/cement ratios, the tensile strength levels remain the same; this differs from the results obtained for compressive strength. In mixes having higher water/cements ratios the degree of cracking caused by preloading does not provoke improvements in tensile strength. Applying load, the possible fracture of calcium hydroxide crystals does not provoke improvements in tensile strength. The possible partial recovery of microcracking is not sufficient to retain the tensile strength; this is evident from a comparison to those specimens that had not been preloaded. Given that a considerable number of microcracks formed under preload, it is necessary for all microcracks to recover to ensure that the tensile strength is retained.

From Figure 4 it can be observed that preloaded concretes at higher ages had superior values of tensile strength. For all cement types analyzed, except IP MS, whose values remained stable, As long as the load percentage increased there was a reduction in tensile strength. At 75% load percentage the loss in tensile strength increases to ca. 15%, in all load ages when compared to reference values (without load). In this configuration it is possible observe the influence of preload on the tensile strength and the relation of tensile strength loss with the formation and propagation of microcracking, as a function of preload. Neville [1997] represented the microcracking criteria and concrete rupture by substituting many factors acting together (cure, cement type, stress acting) with only one strength parameter, the uniaxial tensile strength. This property is responsible for the progressive development of microcracking in the internal structure of concrete, especially at the interfacial transition zone.

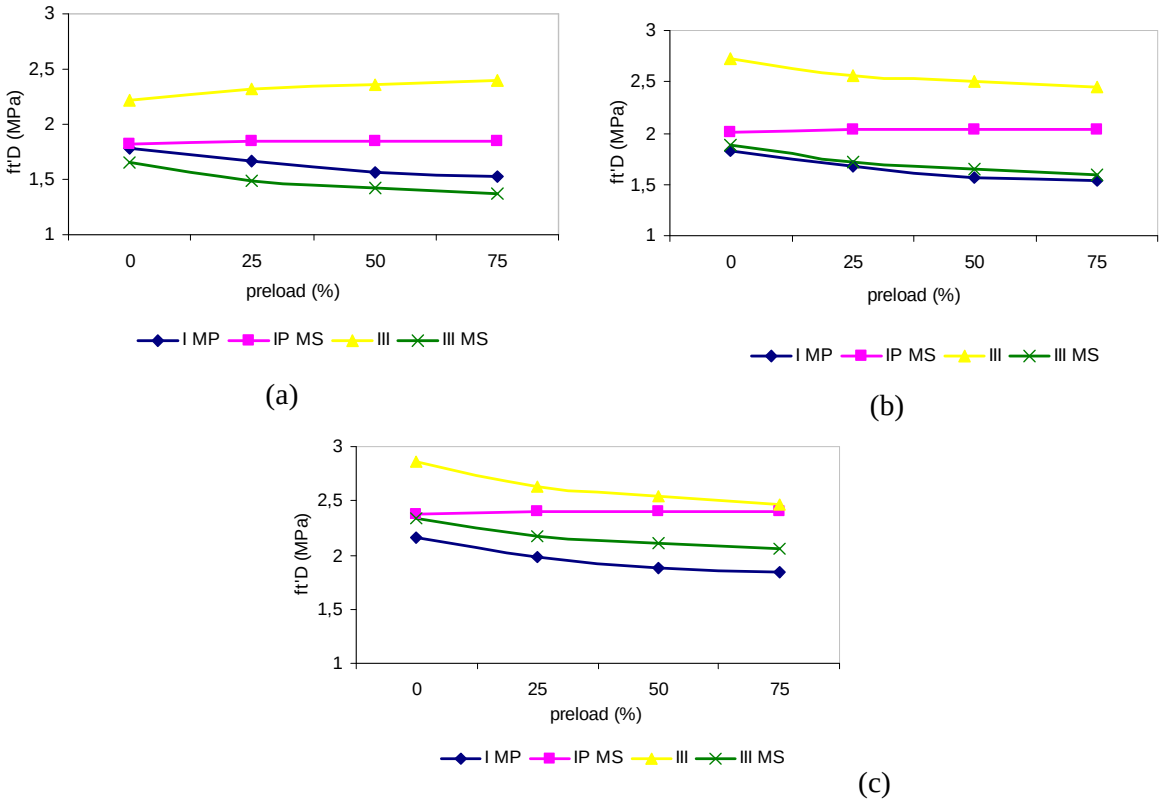

Figure 4. Interaction between preload percent and preload age above tensile strength. (a) age of preload of 1 day. (b) 3 days. (c) 7 days.

3.3 Microstructure of Concrete under Compressive Preload

One way to verify the microcracking process is by using microscopy and the scanning electron microscope (SEM). This technique permits a better understanding of the internal structure of concrete under different load percentages. It was thus possible to observe the development and propagation of microcracking formed with preload. The SEM were completed on concrete samples having 0.5 water/cement ratio, preload age of 7 days, 50% preload percentage, and for type III and IP MS cements. Figure 5 shows the microcracking condition of samples that received 50% of preload.

The information in Figure 5 helps confirm the presence of microcracking in the preloaded concretes at 50% rupture load. The microcracking seems to follow a random trajectory in the cement paste. In regions having voids present, the microcracking tends to follow to the inside of the pores (Figure 5c), since this is a region of high stress concentration [Barbirato 1999]. The voids present in the mortar favour the propagation of microcracking. Since voids represent areas where microcracks may originate, without connections to others compounds, the region between pores can favour the formation of microcracking. With the application of external loads the pores deform in all directions, and thus microcracking develops resulting in tensile stress concentrations in these zones.

When the load is no longer applied, microcracks that may have formed tend to recover because of the recent hydration process in early age concrete. In this study, the specimens returned to the moisture cure environment after having received the applied preload. This behaviour thus corroborates a possible recovery of connections between cement compounds that had not yet hydrated.

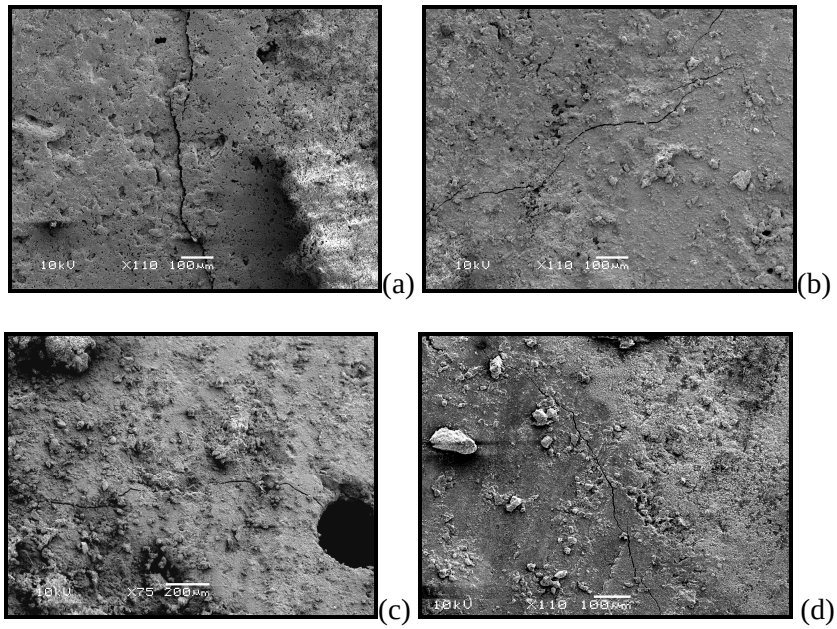

Figure 5. Microcracking caused by early loading.

Figure 6 shows a micrograph of concretes that received preloading at 7 days and after that, returned to the moisture chamber. It is possible to verify on the basis of these images the recovery of some microcracking caused by early loading. The concrete specimens when returned to the moisture chamber have access to water particles that originate from the cure environment and that permeate inside the specimen, in time reaching voids formed by the microcracking, and thereby favouring the hydration of compounds not yet hydrated and that remained exposed with the opening of microcracks. Thus the water that infiltrates inside the concrete brings about the colmating process and the ultimate recovery of microcracks.

This behaviour was observed in type III cement. Therefore, it can be verify that hydration of products not yet hydrated occurs with microcracking, a fact that contributes to recovering compressive strength after preload. However, in spite of a recovery in compressive strength it is observed that some microcracking remains. Figures 6b, 6c, 6d provide indications that some microcracking was not recovered. In these instances, microcracking bridges were not interrupted, or perhaps there was not sufficient water to hydrate cement compounds subjected to microcracking. This helps explain tensile strength performance, in which there were no improvements with the application of a preload.

4 CONCLUSION

Experimental results on concretes subjected to compressive and tensile preloads have been presented in this paper. Good performance was achieved for the compressive strength of concrete specimens, the tensile strength values were adversely affected with the application of load. Microscopy permitted visualising and detecting microcracks and the microcracking process in concretes under compressive loads. Furthermore, the recovery of the effects of microcracking was verified and helps confirm the hypothesis of autogeneous filling, fracture of brittle crystals and the subsequent hydration of the concrete that in turn increases the compressive strength as it cures. However, the recovery process is not complete since it was observed that not all microcracking is recovered, and this negatively influences tensile strength development of the concrete as it cures. In general, the results attest to the existence of the microcracking process caused by the action of loading of early aged concretes. This is an important outcome as it relates to the issues cited previously in the introduction: The effects on structures that arise from an accelerated building practice should be considered when the execution of work is being planned.

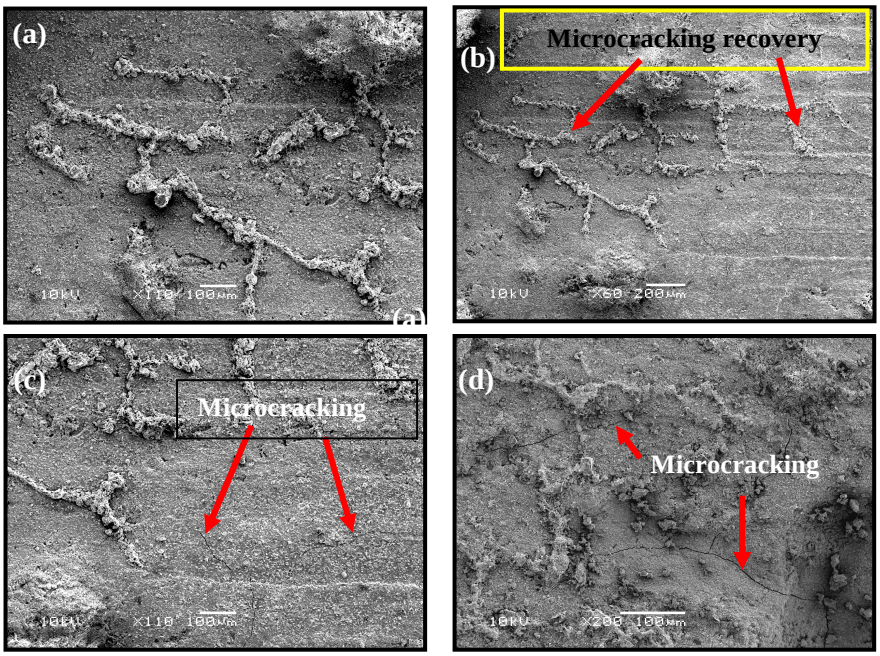

Figure 6. Microcracking recovery in concretes that received preload.

The adoption of simple measures to consider the curing time, degree of hydration and evolution of concrete strength would be useful; respecting the recommendations provided in the current normative standards would likely reduce the problems originating from early loading actions, thereby promoting improvements in construction techniques currently being used.

ACKNOWLEDGMENTS

The authors would like to thank CAPES, research agency of the Brazilian government, by granting of scholarships that enabled the realization this work.

REFERENCES

Barbirato, J. C. C. *Método dos elementos finitos de contorno com a reciprocidade dual para a análise transiente tridimensional da mecânica do fraturamento* (Finite element method boundary with dual reciprocity for the three-dimensional transient analysis of the mechanics of fracture). São Carlos, 1999. 270 p. Tese (Doutorado). Escola de Engenharia de São Carlos. Universidade de São Paulo.

Burlion, N.; Bourgeois, F.; Shao, J.F. Effects of desiccation on mechanical behavior of concrete. *Cement & concrete Composites*. n 27, p. 367-379. 2005.

Mazars, J.; Bazant, Z.P. Cracking and Damage: strain localization and size effect. *In: France-US Workshop on strain localization and size effect due to cracking and damage. Proceendings*. Londres: Elsevier Applied Science, 1989, 550 p.

Medeiros, H. (2005), *Alerta! Deformações excessivas - Edifícios expõem patologias de todo tipo, principalmente na alvenaria. Por que as estruturas estão deformando como nunca*? (Alert! Excessive deformations - Buildings expose pathologies of all kinds, especially in masonry. That structures deform as never before), Disponível em: <http://www .piniweb.com.br> Acesso em: 25 maio 2006.

Neville, A.M. (1997), *Propriedades do Concreto* (Properties of Concrete), Tradução Salvador E. Giammusso. 2 ed. São Paulo: PINI, 1997. 828 p.

XII DBMC
International Conference on Durability of Building Materials and Components
PORTO - PORTUGAL, April 12th-15th, 2011

The Influence of Glycerophosphates on the Transfer Properties of Concrete Cover

Oly Vololonirina [1]
Simone Julien [2]
Ginette Arliguie [3]
Alain Sellier [4]

ABSTRACT

This article deals with the effects of a sodium and lithium glycerophosphate based corrosion inhibitor, applied to the concrete surface, on the transfer properties of the concrete cover. Two configurations are considered: with or without previous carbonation of the concrete cover. The properties studied are the coefficient of capillary absorption in non-saturated media, the diffusion coefficient in saturated media and the intrinsic permeability. The tests were carried out after impregnation of the concrete by the inhibitor and were compared with tests performed on the same concrete without preliminary impregnation. The tests are interpreted using an additional analysis focused on chemical interactions between the corrosion inhibitor and the cement matrix.

KEYWORDS

Corrosion inhibitor, Concrete, Glycerophosphate, Impregnation, Transfer.

[1] Laboratoire Matériaux et Durabilité des Constructions (LMDC), Toulouse, FRANCE, oly.vololonirina@insa-toulouse.fr
[2] Laboratoire Matériaux et Durabilité des Constructions (LMDC), Toulouse, FRANCE, juliens@insa-toulouse.fr
[3] Laboratoire Matériaux et Durabilité des Constructions (LMDC), Toulouse, FRANCE, ginette.arliguie@insa-toulouse.fr
[4] Laboratoire Matériaux et Durabilité des Constructions (LMDC), Toulouse, FRANCE, alain.sellier@insa-toulouse.fr

1 INTRODUCTION

Several solutions are available for limiting corrosion damage to the reinforcement of concrete structures. Among them are corrosion inhibitors, which emerged in the construction field in the 1970s. The first requirement for a corrosion inhibitor is that it should lower the corrosion rate of steel without affecting the properties of the other constituents of the media. Pure sodium glycerophosphate was studied by Monticelli *et al.* [1993] [2002] for its inhibitory properties regarding the corrosion of concrete reinforcement but its effect on the cement matrix has not been investigated. The use of lithium glycerophosphate for such purposes is covered by a patent [Lutz 2004].

The impact of other corrosion inhibitors on concrete properties such as setting time, workability, permeability to gas or chlorides has also been studied, particularly with calcium nitrite, amine and ester or aminoalcohol based organic inhibitors, and other commercial inhibitors [Luo & De Schutter 2008; Tritthart 2003].

In the present article a study is described of the influence of a glycerophosphate-based corrosion inhibitor on the physical and chemical properties of cementitious materials (concrete and mortar) in the hardened state. As the inhibitor under study is intended to be applied to the concrete surface, its action on sound or altered (by carbonation) material was determined. The latter state is more representative of the cover zone of corroded reinforced concrete. To evaluate the mode of penetration of such products, the absorption coefficient in unsaturated media, the diffusion coefficient in saturated media and the gas permeability are investigated according to the degree of saturation of the concrete.

2 MATERIALS AND METHODS

2.1 Materials

2.1.1 Cement

The cement used was a CEM I 52.5 R, selected for its regularity and representativeness of its chemical composition, the chemical constituents of which are described in Table 1.

Table 1. Chemical composition of the cement used.

	SiO_2	Al_2O_3	Fe_2O_3	CaO	MgO	K_2O	Na_2O	SO_3	S^{--}	Cl^-	CO_2	free CaO
%	20,15	4,97	2,77	64,10	1,40	0,83	0,12	3,30	0,01	0,01	1,28	0,6

2.1.2 Mortar

The mortars were made according to EN 196-1 with a water/cement ratio of 0.5 and a cement/sand ratio of 1/3. They were made with standard Leucate sand.

2.1.3 Concrete

An ordinary C25 concrete was chosen as transfer phenomena occur fairly rapidly in this concrete. This type of material is representative of a concrete in use for current construction that potentially suffers from reinforcement corrosion. The amount of cement was 300 kg/m^3. The aggregates used were rolled siliceous aggregates from the Palvadeau sandpit, with 42% mass of sand ($0 \le \phi \le 4$mm) and 58% of aggregate (4mm $\le \phi \le 12$mm). After casting, the concrete and mortar specimens were kept in a curing room at 20 °C and 100% relative humidity until the beginning of each test.

2.1.4 Corrosion inhibitor

Chemical composition

The corrosion inhibitor studied here was a glycerophosphate-based additive with the proportions shown in Figure 1-a. It comes in the form of a yellowish brown liquid with a pH of about 8. Chemical analysis of cations of the active matter revealed the presence of large amounts of sodium and small quantities of lithium. Regarding the anions, the ion chromatography analysis showed the presence of glycerophosphate isomers α and β ($C_3H_7O_6P$), orthophosphates (PO_4) and by-products of incomplete synthesis of glycerophosphate: D1 and D2 on Figure 1-b [Grignard 1939; Vololonirina 2010].

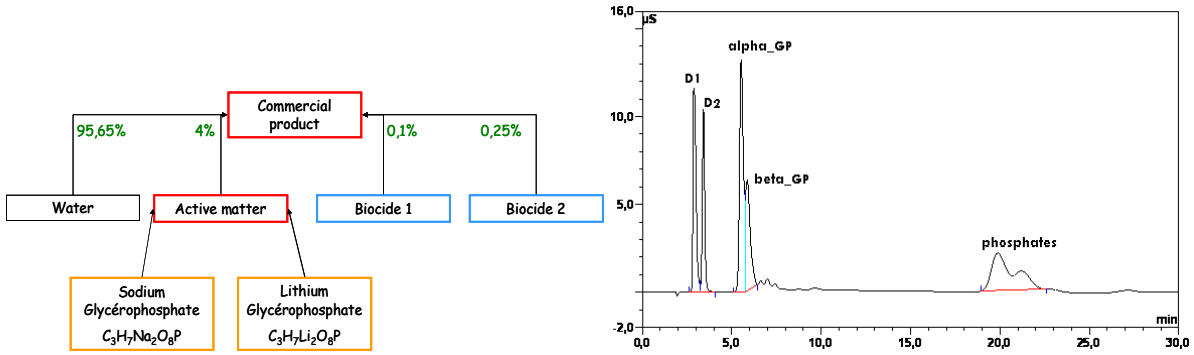

(a) (b)

Figure 1. Composition of the commercial product and the active matter of the corrosion inhibitor and anion analysis by ion chromatography.

Capillary properties

Measurements of surface tension, listed in Table *2*, showed that the values of surface tension of the active matter and the commercial product were lower than that of water. Viscosity values of the commercial product and water were respectively 1.1 and 1.0 mPas.

Table 2. Results of measurements of surface tension.

	Water	*Active matter*	*Commercial product*
Surface tension (mN/m)	71	59,7	53,3

2.2 Test Methods

The different tests are summarized in Table 3 with the number of specimens used for each of them. Detailed descriptions of the tests are given in a reference document [Vololonirina 2010].

Table 3. Summary of transfer tests performed and number of samples used.

Test	*Sound material*		*Carbonated material*	
	With product	*Without product*	*With product*	*Without product*
Total water porosity	2	2	2	2
Capillary absorption	3	3	3	3
Chloride migration	3	3	3	3
Gas permeability	3	3	3	3

2.2.1 Process to obtain a carbonated material

After the 28 days of curing, some of the mortar and concrete specimens underwent conditioning to favour the process of carbonation according to the procedure recommended by AFPC-AFREM [Grandubé 1997]. Characterization tests were then performed once the samples were fully carbonated.

2.2.2 Total water porosity

The purpose of this measurement was to evaluate the effect of corrosion inhibitor on the porosity of the mortar and concrete specimens. Water porosity was determined as recommended by AFPC-AFREM [Grandubé 1997].

2.2.3 *Capillary absorption test*

This test compared the speed and height of capillary rise through an unsaturated specimen of mortar or concrete, for the commercial product and for water. The tests were carried out following the AFPC-AFREM [Grandubé 1997] protocol.

2.2.4 Chloride ion migration test

The objective was to determine whether the corrosion inhibitor had an effect on the diffusion of chemical species, such as chloride ions, in saturated media. The method used was the LMDC-test that was developed in the laboratory [Truc *et al.* 2000]. This is a steady state test in the presence of an electrical field, which gives the effective diffusion coefficient.

2.2.5 Determination of gas permeability

The test consisted of subjecting a cylindrical specimen to a constant gas pressure gradient. The permeability was determined from flow measurements in the steady state using a CEMBUREAU permeameter [Kollek 1989] with oxygen at constant load. The tests were performed as recommended by AFPC-AFREM [Grandubé 1997].

Regarding the application method, the specimens with inhibitor are vacuum saturated with the active matter before testing, except for capillary absorption test [Vololonirina 2010].

3 RESULTS OF TRANSFER TESTS

3.1 Total Water Porosity

The results are presented in Figure 2.

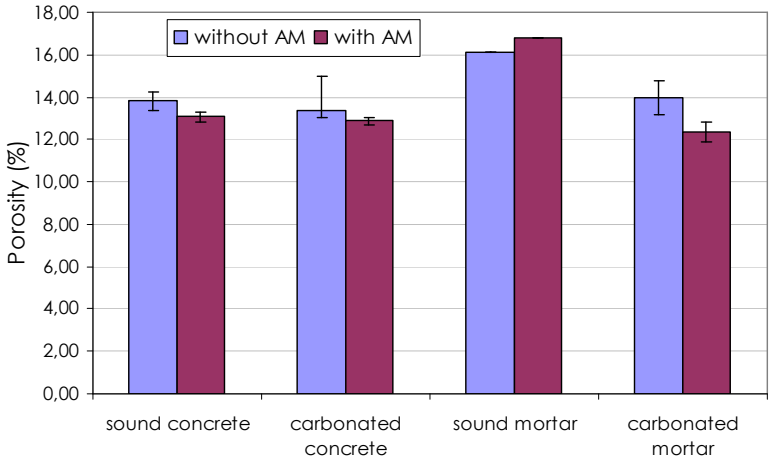

Figure 2. Values of water porosity for specimens of concrete and mortar (AM: Active Matter).

These values show that saturating the concrete or mortar specimens with the active matter at 4% before the test did not induce large changes in the values of total porosity accessible to water, on either sound or carbonated material.

3.2 Capillary Absorption Test

The results of the tests on concrete samples (Figure 3-a) show that the capillary rise of the commercial product varied practically at the same rate as for water, especially between 0 and 8 hours of immersion. From 8 hours of immersion, there was a slight difference in favour of water for both absorption coefficient and height of capillary rise.

The trend was the same for mortars (Figure 3-b), but it was more marked than for concrete because of the higher proportion of paste in the mix. We also observed that, for mortars, the values of the coefficient of capillary absorption and the height of capillary rise, with water and the commercial product, were significantly higher for sound specimens. This was due to the decrease in porosity (from 16% for sound mortar to 14% for carbonated mortar *cf.* Figure 2) by the formation of calcite within the carbonated mortar specimens.

These results show that when the material is completely dry, the commercial product tends to penetrate into the cementitious material by capillarity with a lower rate and intensity than those of water. We also note that the commercial product continues to penetrate into the material beyond 48 hours up to a height of 4.20 cm in the concrete and 2.08 cm in the mortar. This means that the commercial product does not block the concrete pores, for either sound or carbonated specimens.

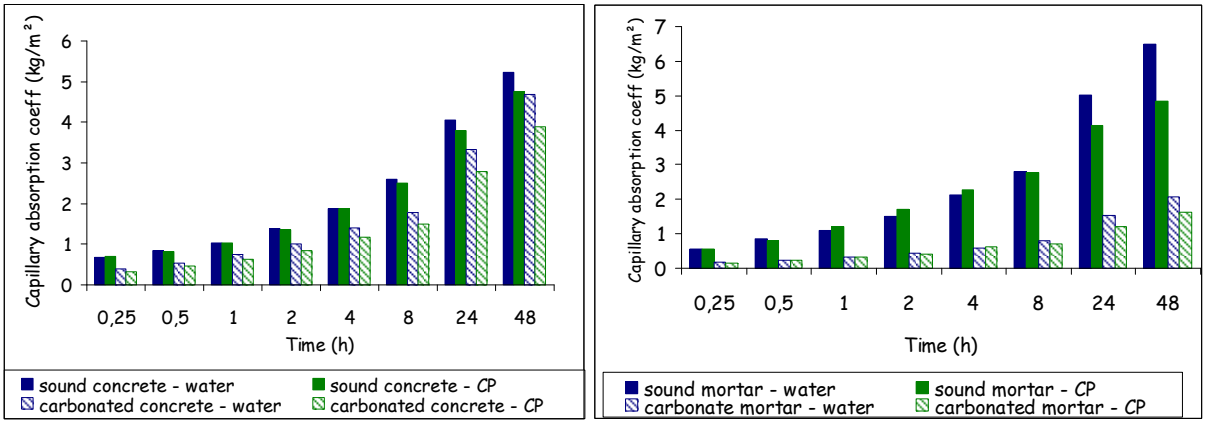

(a) (b)

Figure 3. Results of capillary absorption tests on sound and carbonated concrete and mortar samples (CP: Commercial Product).

3.3 Chloride Ion Migration Test

For this test, the commercial product was not used to avoid possible interactions of biocides with the alkaline solution used to saturate the specimens before testing [Vololonirina 2010]. Only the active matter in the same percentage was used and as can be seen in Figure 4, in all cases, the diffusion coefficient was lower when the material was carbonated. We can also see that impregnation with the active matter tended to increase the diffusion coefficient in sound materials. In the case of carbonated material, there was no significant difference between the diffusion coefficient of specimens with or without prior impregnation with the active matter. A determination of water porosity after completion of the test showed that a side effect due to leaching of the specimen during the preliminary saturation test did not permit explaining the variation in the diffusion coefficient on sound materials.

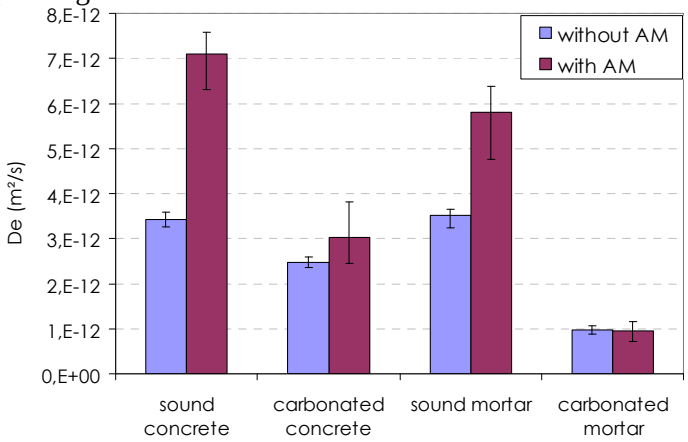

Figure 4. Results of chloride migration test on specimens of mortar and concrete. (AM : Active Matter)

3.4 Gas Permeability Test

The results of permeability tests on concrete or mortar specimens are shown in Figure 5a and Figure 5b.

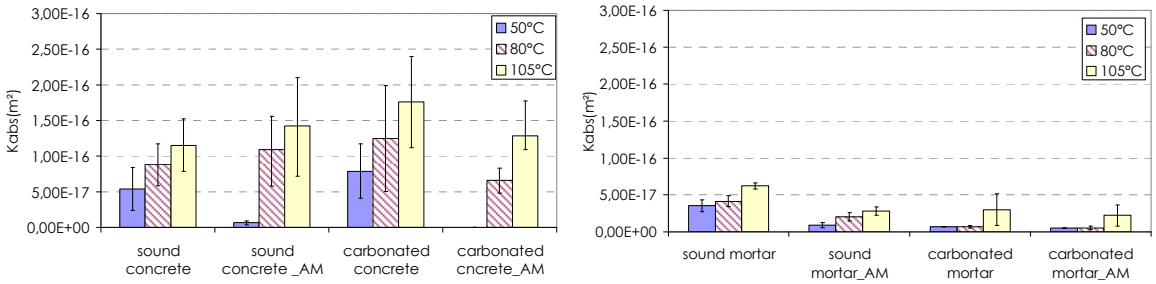

(a) (b)

Figure 5. Results of Gas permeability test on sound or carbonated specimens.

Despite the relatively large dispersion, the results show that there was no significant difference between the values of the permeability of sound or carbonated concrete samples, with or without additional active matter 4% (Figure 5-a). The same observation was made for mortar specimens (Figure 5-b) with just a slight decrease in permeability for sound mortar impregnated with the product.

3.5 Conclusion about Transfer Tests

The results of the transfer tests can be summarised as follows:

- When the material is dry, the commercial product penetrates the cementitious material by capillarity but with a rate and an intensity slightly lower than that of water;
- When the material is saturated, the active matter has an effect only on sound materials (not on carbonated materials) by increasing the value of the effective diffusion coefficient;
- The impregnation with the active matter has a smaller effect on the results of gas permeability, except for a slight decrease in the permeability of sound impregnated mortar.

Knowing that the diffusion and permeability do not involve the same range of pore sizes: the pores of the CSH gel (Φ <2 nm) influence the diffusion coefficient whereas the capillary pores (2nm <Φ <50 nm) rather influence permeability and porosity [Ranaivomanana 2010]. It is probable that the active matter interacts with the noncarbonated cement matrix thereby modifying the microporosity and hence the diffusion coefficient. On carbonated material the effect is smaller. This suggests that the addition of the compound would have no major impact on the structure of carbonated material, which consists mainly of calcium carbonate.

4 STUDY OF CHEMICAL INTERACTION BETWEEN CEMENT PASTE AND INHIBITOR

To corroborate these hypotheses, we performed 3 types of tests to determine the possible interactions of the active matter with the cement paste, the chemical stability of the inhibitor according to the pH and its reaction with lime. The details of how these tests were performed are given in the reference document [Vololonirina 2010]; only the main results are reported below.

4.1 Interaction Between Cement Paste And Active Matter

For this test, sound and completely carbonated cement pastes were crushed before being immersed separately in the active matter at 4%. After a few hours, a white precipitate had formed only in the vessel containing the sound cement paste. The diffractogram of the precipitate (Figure 6-a) showed an amorphous gel.

After the precipitate had been dissolved in nitric acid, chemical analysis showed a calcium / phosphate ratio (Ca/P) of about 1.94, which corresponds to that of a non-stoichiometric hydroxyapatite [Legeros *et al.* 1969; Cazalbou *et al.* 2004]. We then introduced 2g of powdered

cement either from sound or carbonated paste in 100 ml of the active matter dosed at 4%. After one week, the insoluble residue was analyzed with XRD (Figure 6-b and c).

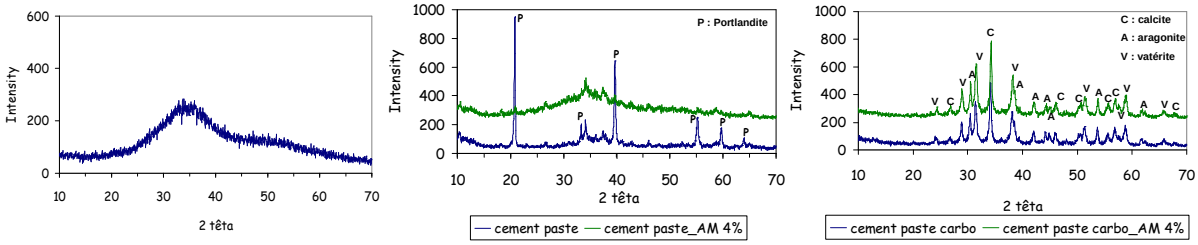

(a) (b) (c)

Figure 6. Diffractograms of the precipitate formed (a) - sound (b) and carbonated (c) cement paste before and after immersion in the active matter.

On the diffractogram of the sound cement paste (Figure 6-b), we find the characteristic peaks of portlandite, while on that of sound cement paste immersed in active matter, portlandite peaks have disappeared, giving way to a halo typical of the precipitate that we analyzed before. Figure 6-c) confirms that no precipitate forms when the carbonated cement paste is mixed with the active matter. So, we made the hypothesis that the components of the active matter evolve with high pH.

4.2 Stability of the Active Matter in Basic Medium

The stability in basic medium was studied in a pH range from 8 to 13, thus covering the pH of carbonated and sound concrete. The interpretation of tests shows that:

- When 8 <pH <12: active matter dosed at 4% is stable;
- When pH ≥ 12: the active matter undergoes transformations including a slight increase in the amount of glycerophosphates isomers α and β and a slight decrease in the amount of orthophosphate.

4.3 Interactions between Lime and the Inhibitor

After studying the stability in a basic medium, we investigated the conditions for the formation of calcium phosphate cement in the cementitious matrix. Increasing amounts of lime were added to 100ml of solution of active matter diluted to 4%. The comparison of the value of $\Delta[PO_4^{3-}]$ and $\Delta[Ca^{2+}]$ (Figure 7) shows the same shape of curve from pH = 12.26. This means that, from this pH value, a part of the calcium in solution was combined with the orthophosphate to form a precipitate with an average Ca / P of 1.99, almost the same as that obtained by placing the crushed sound cement paste with active matter dosed at 4%. These tests indicate that adding lime leads to the formation of the calcium phosphate precipitate when the pH is close to 12.

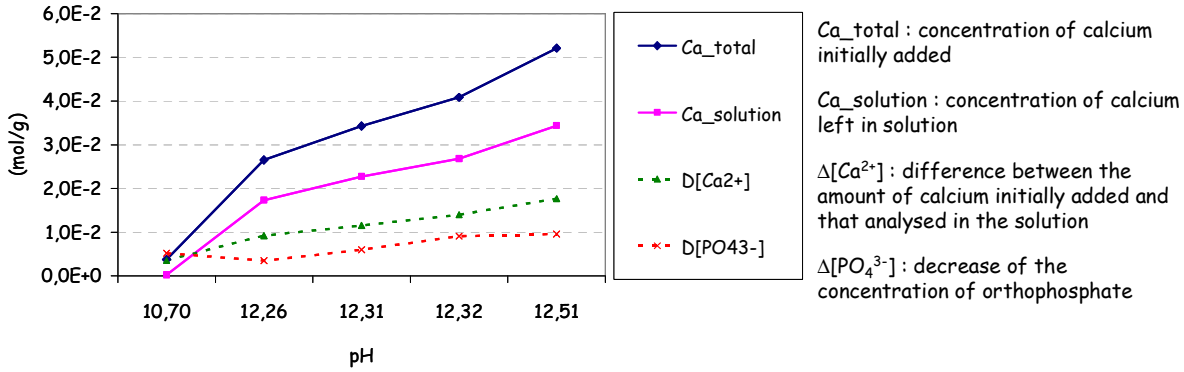

Figure 7. Interactions between active matter and lime: evolution of the concentration of calcium and orthophosphate for progressive addition of lime.

5 CONCLUSIONS

- When the material is completely dry, the glycerophosphate based inhibitor penetrates through the porosity by capillary action with a rate slightly lower than that of water. There is no short-term impact on the porosity of the sound or carbonated material probably because the kinetics of chemical reactions are too slow compared to those of capillary phenomena.
- When the pH is above 12, an imbalance occurs in the components of the active matter. We find the same instability with lime associated with formation of a non-stoichiometric hydroxyapatite with a Ca/P close to 1, 99. This same precipitate occurs in the presence of cement paste.
- In sound concrete or mortar, phosphates combine first with calcium from portlandite dissolved in the capillary pores, then with calcium of C-S-H to form a calcium phosphate. The formation of this precipitate causes a change in the pore structure of the hydrates, leading to an increase in the diffusion coefficient when the material is saturated. Prior saturation with the active matter has a limited influence on permeability and porosity showing both that the products formed have a volume close to those dissolved and that capillary porosity is only slightly affected.
- When the pH is about 9, as it is the case for the carbonated material, there is no precipitate formation. Transfer properties are therefore not significantly changed. It is encouraging for the use of the corrosion inhibitor by impregnation on an old carbonated concrete.

The continuation of this work is to study the effectiveness of the inhibitor on samples of concrete and reinforced mortar. Several types of preconditioning of the material will be tested.

ACKNOWLEDGMENTS

The authors would like to thank the PAREXLANKO Group for their support.

REFERENCES

Cazalbou, S., Eichert, D., Drouet, C., Combes, C. & Rey, C. 2004 ‘Minéralisations biologiques à base de phosphate de calcium’, *Comptes rendus Palevol*, 3, pp. 563–572.

Grandubé, ‘Méthodes recommandées pour la mesure des grandeurs associées à la durabilité’, décembre 1997, Presses de l’ENPC.

Grignard, V. 1939 *Traité de chimie organique*, Tome VI, Masson et Cie.

Kollek, J.J. 1989 ‘The determination of the permeability of concrete to oxygen by the Cembureau method—a recommendation’, *Materials and Structures*, 22, n°3, pp. 225-230.

Legeros, R.Z., Trautz, O.R., Klein, E. & Legeros, J.P. 1969 ‘Two types of carbonate substitutions in the apatite structure’, *Cellular and molecular life sciences*. 25, n°1, pp. 5-7.

Luo, L. & De Schutter, G. 2008 ‘Influence of corrosion inhibitors on concrete transport properties’, *Materials and Structures*, 41, pp.1571–1579.

Lutz, T. 2004 ‘Produit pour le traitement des structures en béton armé’, WO2004/089844.

Monticelli, C., Frignani, A. & Trabanelli, G. 1993 ‘A study on corrosion inhibitors for concrete application’, *Concrete Research* 30, pp. 635-642.

Monticelli, C., Frignani, A. & Trabanelli, G. 2002 ‘Corrosion inhibition of steel in chloride-containing alkaline solutions’, *Journal of Applied Electrochemistry* 32, pp. 527–535.

Ranaivomanana, F. 2010 ‘Transfert dans les milieux poreux réactifs non saturés’ Thèse de doctorat en Génie Civil, Université Paul Sabatier.

Tritthart, J. 2003 ‘Transport of a surface-applied corrosion inhibitor in cement paste and concrete’, *Cement and Concrete Research*, 33, pp. 829–834.

Truc, O., Ollivier, J.P. & Nilsson, L.O. 2000 ‘Numerical simulation of multi-species transport through saturated concrete during a migration test’. *Cement and Concrete Research*, 30, pp. 1581-1592.

Vololonirina, O. 2010 ‘Rapport d’avancement’, LMDC Toulouse - Octobre 2010.

XII DBMC
International Conference on Durability of Building Materials and Components
PORTO - PORTUGAL, April 12th-15th, 2011

Relationship between Fractal Dimension of Fine Aggregates and Chloride Resistance of Concrete

Wen Xue [1]
Lei Zhang [2]
Ju Chen [3]
Weiliang Jin [4]

ABSTRACT

The fractal dimension theory is used to study the effect of fine aggregates on the chloride resistance of concrete in this paper. Equations, which are describing the relationship between the volume fractal dimension and the void volume of fine aggregate piles and the the chloride resistance of both concrete and mortar specimens, are established. A test program containing 12 concrete specimens and 7 mortar specimens was conducted. The mortar and concrete specimens have same mix design parameters except for the coarse aggregates. The chloride resistances of concrete specimens were tested by using the rapid chloride migration method. In addition, wet and dry cycling method was also used for the chloride ingress in the mortar specimens and the chloride concentration profiles were measured by a potentiometric titration method. Both test results for concrete and mortar specimens indicate that the chloride resistance was significantly enhanced with the increasing in fractal volume dimension of the fine aggregates.

KEYWORDS

Chloride resistance, Fine aggregates, Fractal theory, Mass fractal dimensions, Volume fractal dimensions.

[1]Institution of Structural Engineering, Zhejiang University, Zhejiang, CHINA, xuewen@zju.edu.cn
[2]Hangzhou Urban Infrastructure Developing Center, 310006, Hangzhou, Zhejiang, PRC, jbdgzhb@126.com
[3]Institution of Structural Engineering, Zhejiang University, Zhejiang, CHINA, cecj@zju.edu.cn
[4]Institution of Structural Engineering, Zhejiang University, Zhejiang, CHINA, jinwl@zju.edu.cn

1 INTRODUCTION

Aggregate takes up 60%-90% of the total volume of concrete. Proper selection of aggregate particle size distribution affects the main properties of concrete: workability, strength, permeability, chloride resistance and even the total cost of hardened concrete. Therefore, aggregate design is an essential part of concrete mix design. The fineness module (M_x) is widely used to describe the aggregate characters. However it is rough in describing the characters of the fine aggregates. Fractal dimension of the aggregate is recently adopted in aggregates researches.

The fractal theory, which focused on the irregular geometric items, was established by Mandelbrot and so called 'fractal geometry' [Mandelbrot, [1984]]. It was then developed quickly and extended to use in the researches on the other irregular or unstable problems in nature, such as the studies of soil particles and geotechnical materials [Xie, [1997]; Lange,*et al*,[1993]; Saouma & Barton, [1994]]. Current researches reported that fractal value of a certain object actually describes its complexity quantitatively. It is potential to connect the macro performance with the micro structures by using this parameter.

Concrete material is well known for its anisotropy. It could be attributed to the complexity of its microstructures which is a kind of fractal system. The aggregates were composed of large numbers of particles in different sizes. The distribution of the particles is considered as a generalized fractal problem in mathematics [AASHTO,[1989]]. Current design standard only provide the size limitations on aggregates [ACI 318,[2005]]. In this study, the mass and volume fractal dimensions of the fine aggregates were calculated. By taking concrete and mortar durability experiments, the effects of fractal dimensions of fine aggregates on the chloride resistance of concrete were investigated. The fractal dimension is suggested to be a design index in concrete mixtures.

2 FRACTAL DIMENSIONS

The particle size (sieve size) generates a distribution which could be described using a fractal method. In addition, the mass distribution (sieving ratio) and the volume architectures can both also be described by using fractal method as presented below.

2.1 Mass Fractal Dimension

For the particles of size *x*, the distribution function could be written as Eq.(1):

$$F(x) = \frac{N(x)}{N} \tag{1}$$

where $N(x)$ is the number of fine aggregates whose size are less than or equal to *x*;

Since the size of fine aggregates could be classified as 'point problem', the fractal dimension *N(x)* could be calculated as Eq.(2), according to [Xie, [1997]]:

$$N(x) = N_0\left(\frac{x}{x_{\max}}\right)^{0-D} \tag{2}$$

where $x_{\max}$ represents the maximum size of the fine aggregate particles, N_0 is a constant, *D* is the size fractal dimension value.

By substituting Eq.(2) into (1), the size distribution function could be rewritten as Eq.(3) with the boundary conditions of $F(x_{\max})=1$ and $F(x_{\min})=0$:

$$F(x) = \left(\frac{x}{x_{\max}}\right)^{-D} \tag{3}$$

The mass distribution function could be obtained in the same way:

$$P(x) = \frac{M(x)}{M} \tag{4}$$

where M is the total mass of the aggregates, $M(x)$ is the mass of particles less than or equal to size x, $P(x)$ is the sieving ratio.

Mass is the product of particle density ρ and volume $U(x)$, and the particle density ρ is assumed to be constant, thus the could be written as Eq. (5). It should be noted that the ρ is the density of single particle, therefore it could be assumed to be constant.

$$dM(x) = \rho \cdot U(x) \cdot dN(x) \tag{5}$$

Assuming particles of fine aggregate are all spherical, the volume $U(x)$ could be expressed as:

$$U(x) = k_v \cdot x^3 \tag{6}$$

Thus Eq(4) could be rewritten as Eq(7), with the boundary conditions of $P(x_{max})$=1and $P(x_{min})$=0:

$$P(x) = \frac{x^{3-D} - x_{\min}^{3-D}}{x_{\max}^{3-D} - x_{\min}^{3-D}} \tag{7}$$

Thus the equation relating the sieving ratio $P(x)$ to the size fractal dimension D has been established. Provided sufficient test data of the sieving ratio $P(x)$, the mass fractal dimension value D could be obtained by regressing in double logarithmic axis.

2.2 Volume Fractal Dimension

When numerous particles with different sizes are piled together, there is void among them. The volume fractal character could be used to describe the void filling capacity of those particles [Xu,[1991]]. The volume of fine aggregates could be classified as 'volume problem', the fractal dimension $V(x)$ could be calculated as Eq.(8), according to [Xie, [1997]]:

$$V(x) = V_0\left(\frac{x}{x_{\max}}\right)^{3-D_v} \tag{8}$$

where $V(x)$ is the fractal volume, D_v is the volume fractal dimension.

$$dV(x) = dV_0\left(\frac{x}{x_{\max}}\right)^{3-D_v} \tag{9}$$

$$dV_0 = \frac{M \cdot dP(x)}{\rho} \tag{10}$$

Based on the simultaneous Eqs. (8-10), the fractal volume could be calculated using Eq.(11):

$$V(x) = \frac{3-D}{6-D-D_v} \cdot \frac{M}{\rho} \cdot \frac{x_{\min}^{6-D-D_v} - x_{\max}^{6-D-D_v}}{x_{\min}^{3-D} - x_{\max}^{3-D}} \cdot x_{\max}^{D_v-3} \tag{11}$$

In addition, the void volume of the particles pile could be calculated using Eq(12):

$$V_{void} = \frac{\frac{M}{\rho} - V}{\frac{M}{\rho}} = 1 - \frac{3-D}{6-D-D_v} \cdot \frac{x_{\min}^{6-D-D_v} - x_{\max}^{6-D-D_v}}{x_{\min}^{3-D} - x_{\max}^{3-D}} \cdot x_{\max}^{D_v-3} = 1 - \frac{\gamma}{\rho_0} \tag{12}$$

where γ is the compacted density and ρ_0 is the gross density of the particles pile.

Provided the measured value of V_{void}, x_{max} and x_{min} of a certain pile of fine aggregates, the volume fractal dimension D_v could be calculated using Eq.(12).

3 RELATIONSHIP BETWEEN FRACTAL DIMENSIONS AND MORTAR/CONCRETE DURABILITY PERFORMANCE

3.1 Fine Aggregates Gradation

Seven series of fine aggregate particle size distribution were designed in this study. All the fine aggregates were oven dried and sieved to different sizes (see in Table 1) using the automatic sieve shaker. Then the particles of different size were mixed following the design distribution in Table 1. The maximum size of fine aggregates is 4.75 mm. The void volumes of each aggregate set was tested according to the standard [JGJ/T 70-2009]. The mass and volume fractal dimensions were calculated using Eqs. (7) and (12) and presented in Table 2. Fig.1 shows a decreasing linear relationship between the volume fractal dimension values D_v and void volumes. An linear relationship between the percentage of voids and D_v could be obtained as Eq.(13):

$$V_{void}\%=-31.61\times D_v+113.58 \quad (13)$$

It may be explained that with the increasing of volume fractal dimension, the filling capacity of particles increasing which results in reduction of void.

Table 1. Fine aggregate particle size distribution.

Sieve size [mm]	*Accumulated sieve ratio* [%]						
	I	*II*	*III*	*IV*	*V*	*VI*	*VII*
4.75	4	3	3	2	2	1	1
2.36	45	41	38	34	31	26	22
1.18	69	65	61	57	53	46	41
0.60	83	80	77	73	70	63	58
0.30	92	83	87	85	83	77	73
0.15	97	96	95	93	92	89	87
<0.15	100	100	100	100	100	100	100

Table 2. Fractal dimensions of fine aggregates.

Groups	ρ_0 [g/cm^3]	γ [g/cm^3]	*Void* [%]	*D*	D_v
I	2.00	1.6393	18.03	2.23	2.6458
II	2.50	1.6667	33.33	2.32	2.5775
III	2.38	1.7544	26.32	2.43	2.7183
IV	2.33	1.7241	25.86	2.52	2.7429
V	2.70	1.8868	30.19	2.60	2.7040
VI	2.50	1.8519	25.93	2.75	2.7825
VII	2.33	1.7241	25.86	2.85	2.7980

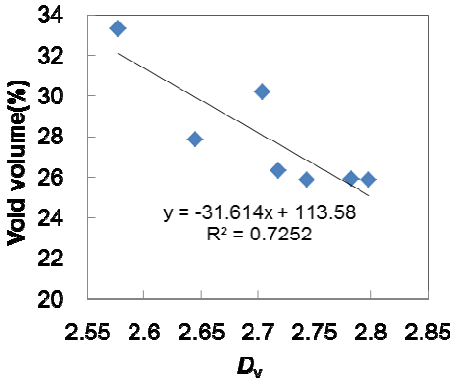

Figure 1. Relationship between D_v and void%.

3.2 Relationship between Fractal Dimensions and Chloride Resistance of Mortar Specimens

Seven series in total of 7 mortar specimens were tested for chloride resistant test. The mixture information of mortar specimens was presented in Table 3.

Table 3. Mixture design of the mortar specimens [kg/m^3].

Cement	*Fly ash*	*Slag*	*Fine aggregate*	*Water*	*Admixture*
313	102	137	629	176	12

All the specimens were kept in tap water under room temperature (average of 25°C) for 28 days. Then the specimens were put into an artificial accelerating testing chamber and subjected to wet-dry cycles for 60 days. Mangat and Gurusamy [1987] found a significant difference between the diffusion rates of chloride through the casting face and the bottom face (during casting) of the prism. To eliminate the casting effect, all the faces of the specimens for chloride resistant test were coated with epoxy except the top surface. The top surface is vertical to the casting direction. The specimens was under salt water spraying for 3 hours (wet cycle) out of 48 hours and, for the remaining 45 hours, they were left in the ambient laboratory conditions at a temperature of 45°C (dry cycle). After 60 days' cycling, the powder samples were drilled out from each specimen along the ingression direction. Three holes were drilled in dry condition using a 14-mm diameter rotary impact drill for each specimen. Powdered samples were taken at every 5 mm depth. The chloride concentration profile of each powder sample was measured by using the potentiometric titration method. Previous research [Gao, [2008]] indicate that diffusing dominate the chloride's moving inside concrete away from the surface more than 7 mm. In this study, the apparent chloride diffusion coefficient D_a(cm^2/s) was obtained by Fick's second law without the test data at the depth of 5mm:

$$C(x,t) = C_s \times \left(1 - erf\left(\frac{x}{2\sqrt{D_a \cdot t}}\right)\right) \tag{14}$$

where $C(x,t)$ is the chloride concentration at depth x and age t, C_s is the surface chloride concentration.

The results are presented in Table 4 and Fig.3:

Table 4. Apperant chloride diffusion coefficient [$\times 10^{-12}$cm^2/s].

I	*II*	*III*	*IV*	*V*	*VI*	*VII*
6.03	11.30	6.08	5.13	5.37	4.55	4.91

$$D_a = -21.6 \times D_v + 64.56 \tag{15}$$

It should be noticed that all the specimens were cast in same mixture design except for the fine aggregate gradation. Therefore, the difference of chloride resistant ability of the mortar specimens could be only attributed to the difference of the fine aggregate distribution. The results indicate mortar specimens with high D_v have high chloride resistance. The difference of fine aggregate causes approximately 250% difference in the chloride resistant ability of mortar specimens. It may be explained that higher volume fractal dimension leads to higher compacting ability of the particles. It might complicate the transfering pathes of the chloride ions. This might result in the reduction in the apparent chloride diffusion coefficients. It is also shown that small D_v may have extra benefits, because the second series of mortar specimen which D_v was 2.575 has much higher diffusion coefficient than other groups.

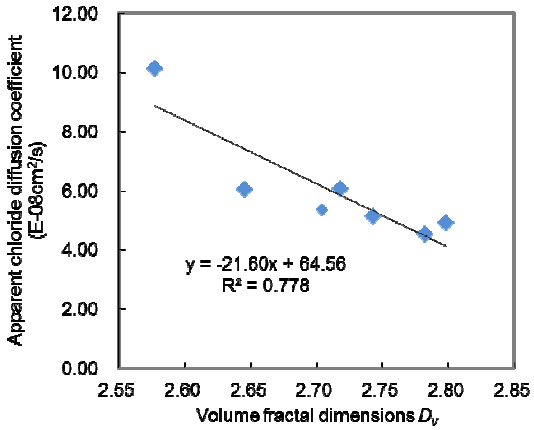

Figure 2. Relationship between D_v and apparent chloride diffusion coefficient.

3.3 Relationship between Fractal Dimensions and Chloride Resistance in Concrete Specimens

For concrete specimens, coarse aggregates take about half of the total volume. The chloride moving route in concrete is probably changed due to the existing of coarse aggregate. Therefore, the effect of fractal dimensions of fine aggregates on the chloride resistance of concrete is investigated in this study.

Four series in total of 12 concrete specimens were tested, and each series has three specimens. The fine aggregate distributions of each series are presented in Table 5 and the mixture is presented in Table 6. Only the fine aggregate distribution is the variable parameter for all specimens. The mass and volume fractal dimensions were calculated using Eqs. (7) and (12) and presented in Table 7. The specimens were prepared in the same way as the mortar specimens. After a 28-days curing period, the rapid chloride migration test method [CCES01-2004] was used to measure the chloride penetration depths of concrete specimens. The chloride diffusion coefficient D_{RCM} values were calculated based on the measured chloride ingress depth [CCES01-2004]:

$$D_{RCM}=2.872\times10^{-6}\frac{Th(x_d-\alpha\sqrt{x_d})}{t}$$
$$\alpha=3.338\times10^{-3}\sqrt{Th} \qquad (16)$$

where T is the average temperature of the anticathode cell (K); h is the height of the specimen (mm); t is the testing duration (s); x_d is the average ingress depth (mm).

Table 5. Fine aggregate particles distribution in concrete specimens.

Sieve size [mm]	*Accumulated sieve ratio* [%] I	II	III	IV
4.75	3	10	10	5
2.36	11	13	25	20
1.18	20	24	26	30
0.6	41	69	43	70
0.3	70	71	89	91
0.15	98	96	90	92
<0.15	100	100	100	100

Table 6. Mixture design of the mortar specimens [kg/m^3].

Cement	*Fly ash*	*Slag*	*Fine aggregate*	*Coarse aggregate*	*Water*	*Admixture*
313	102	137	629	1014	176	12

Table 7. Fractal dimensions of fine aggregates in concrete specimens.

Series	ρ_0 [g/cm^3]	γ [g/cm^3]	Void [%]	D	D_v
I	2.6667	1.6129	39.52	2.0490	2.3239
II	2.1137	1.7604	16.71	2.1831	2.8058
III	2.8840	1.8025	37.50	2.2948	2.4871
IV	2.6736	1.7856	33.21	2.1816	2.5316

The concrete testing results shows the same trend as the mortar testing results (see in Figs.(3) and (4)), but the effect of fine aggregate on the chloride resistance of concrete specimens is even significant. The difference of fine aggregate causes approximately 300% difference in chloride resistant ability of concrete specimens. This result indicates the importance of volume fractal dimensions of fine aggregates for the chloride resistance of concrete.

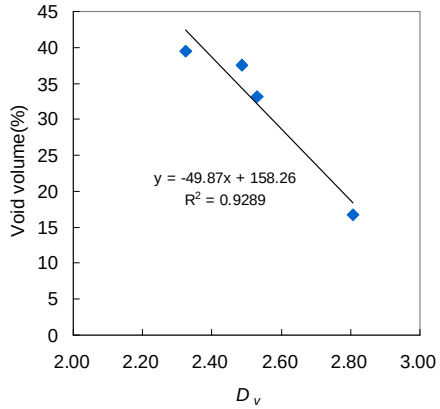

Figure 3. Relationship between D_v and void% in concrete.

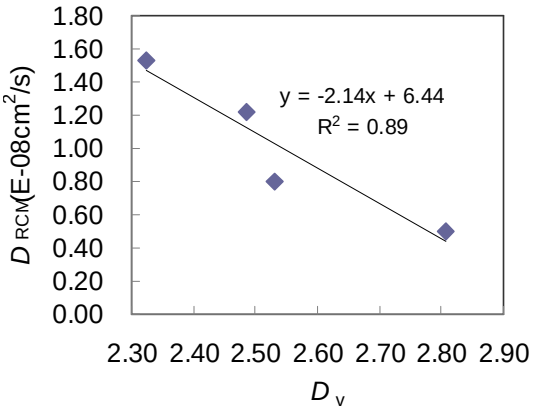

Figure 4. Relationship between D_v and $D_{RCM.}$

The relationship between V_{void}% or D_{RCM} and D_v in the case of concrete are written as Eqs. (17) and (18) based on the testing results:

$$V_{void}\%=-49.87\,D_v+158.26 \quad (17)$$

$$D_{RCM}=-2.14\,D_v+6.44 \quad (18)$$

4 CONCLUSIONS

In this study, the relationship between fractal dimension of fine aggregates and chloride resistance of concrete was investigated. The testing results indicated that with the increasing of D_v, the voids of the fine aggregates piles decrease, as well as the chloride moving ability in either the mortar specimens or the concrete specimens. The equations for the relationships between the void volume, chloride resistance and volume fractal dimension D_v in the case of mortar had been established by using fractal theory. In addition, equations for the relationship between void volume, chloride resistance and D_v were obtained in concrete.

ACKNOWLEDGMENTS

The research of this paper is supported by the National Natural Science Foundation of China (513000-N10901), Natural Science Foundation of Zhejiang Province of China (Y1100063).

REFERENCES

Mandelbrot, B.B.. 1984, 'Fractal character of fracture surfaces of metals of metals'. *Nature*,308,721-723.

Xie, H.P. 1997, 'Fractal- Geomechanics Introduction'. *Science Press*, Beijing, 168-257.

Lange, D.A. et al. 1993, 'Relationship between fracture surface roughness and fracture behavior of cement paste and mortar'. *Journal of American Ceramic Society*. 76[3], 589-597.

Saouma, V.C., Barton , C.C.. 1994, 'Fractals, fracture and size effect in concrete'. *Journal of Engineering and Mechanics*. 120[4], 835-854.

AASHTO. Report of the Joint Task Force on Rutting. Washington, D C: *AASHTO Publishers*, 1989.
ACI Committee 318 (ACI 318). Building code requirements for structural concrete and commentary. Detroit, USA: American Concrete Institute; 2005.

Xu, S.F.. 1991. 'Study of prediction,control, prevention and cure about highway Asphalt Pavement' s rutting'. Shanghai: Tongji University.

JGJ/T 70-2009, Standard for test method of basic properties of construction mortar.

Mangat, P.S., Gurusamy, K..1987, 'Chloride diffusion in steel fibre reinforced marine concrete'. *Cement and Concrete Research*, 17 [3], 385-396.

CCES01-2004, Guide to Durability Design and Construction of Concrete Structures. Beijing 2005:37-38.

Gao, X.J. 'Study on chloride penetration of in-situ harbor structures'. 2008. *Master thesis*. Zhejiang University, China.

XII DBMC
International Conference on Durability of Building Materials and Components
PORTO - PORTUGAL, April 12th-15th, 2011

The Nail Plate Method to Determine the Partially Restrained Shrinkage of Cement-Based Mortars and Concretes

Kari Saastamoinen [1]

ABSTRACT

Cement products shrink due to desiccation. The shrinkage can cause cracking and deformation even long time after casting. The amount and effects of the shrinkage of a particular mortar or concrete product are needed to be anticipated when considering the suitability of that product for repair applications.

A standard measuring method determines the relative strain of the prismatic test body and it requires a very accurate measurement apparatus. A standard method for restrained shrinkage determines only the loss of adhesion and the tendency to crack when the test specimen is applied to a reference concrete substrate.

The nail plate method is perfect for testing repair materials. It is developed in Tampere University of Technology. Its advantage over the standard measurement of free movement is that the nail plate method requires a less accurate measuring apparatus. It also takes into account the fact that when the shrinkage is partially restrained it differs from the free shrinkage. The testing arrangement approximates the true application.

With the nail plate method, the shrinkage is determined by measuring the deflection of about one meter long mortar nail plate -composite structure. The nail plate prevents the strain of the other side of the composite structure. This causes the structure to bend, and the deflection is bigger than the length change itself. From the measured deflection it is possible to calculate the shrinkage strain of tested material.

KEYWORDS

Shrinkage, Deformation, Measurement.

[1] Tampere University of Technology, Structural Engineering, Tampere, FINLAND, kari.saastamoinen@tut.fi

1 INTRODUCTION

The shrinkage of cement based products can cause cracking, bending and stress. It is necessary to control the amount of shrinkage of a particular cement product when developing a new product or monitoring its quality. Especially the product's usability to repairs can be very sensitive to the tendency to shrink, because the repair products are often exposed to fast desiccation and they often have no other attachment to the substrate than their own adhesion, which can be weakened due the shrinkage stresses. Also, if used as a large layer on a substrate that is non-shrinking or prevents the desiccation, and which has insufficient bending stiffness, the shrinkage can cause bending.

There are several methods to define the amount of shrinkage or its particular effects. Probably the most obvious is to determine the shrinkage by the change of length of a prismatic specimen. The loss of adhesion can be measured simply by applying tested material on a reference substrate and measuring the adhesion at different moisture conditions. For example, European standard EN 12617-4 describes standardised methods for these two types of test. Also the crack formation can be observed at the same test. Specifically, the tendency to crack can be determined by ring specimens with a steel core.

When measuring the length of a prismatic specimen in aim to determine the amount of the shrinkage, a very accurate measuring instrument should normally be used. With the nail plate method next to be introduced, it is possible to access more accuracy with a rough measuring instrument. The nail plate method also takes into account the fact that partially restrained shrinkage is different than the free shrinkage and therefore it supposedly represents the behaviour of a real structure, for example a concrete floor or a plastering, better.

2 SHRINKAGE OF CEMENT BASED PRODUCTS

The nail plate method can be used to determine the long term shrinkage of cement based products. The long term shrinkage is caused by desiccation. In addition to physical desiccation, also chemical hydration of the cement desiccates the product. Also stress can induce local desiccation, which is supposed to cause creep deformation.

In concrete (or any such cement based product) there are electrical forces between water molecules and molecules of rigid particles of concrete. These forces cause the capillarity, surface free energy and repulsive forces. These three phenomena are all represented as the cause of the desiccation shrinkage of concrete [Wittmann 1972, Bazant 1972, Ferraris 1987, according to Baroghel-Boundy et al. 1999]. Still, most commonly only capillarity is considered to cause the shrinkage.

In fresh concrete pores are water filled. As concrete desiccates capillary stresses are generated at local water surfaces. Intensity of capillary stress is inversely proportional to the size of the pore. Capillary stress pulls cement particles closer each other, which causes shrinkage. Total amount of shrinking stress is dependent on the size, the amount and the water content of the pores in concrete.

The grain and hardened cement restrains the shrinkage which leads to internal stresses. Also uneven desiccation, reinforcements or adjacent structures may restrain the shrinkage.

The water evaporates or soaks from the surface of the moister body. When the hydraulic flow in the concrete is slower than the evaporation rate, the concrete body desiccates more near the surface than inner. If desiccation is possible only from other side of concrete body, the uneven shrinkage can lead to bending or cracks.

When shrinkage is restrained, the stress leads to creep strain. For this reason restrained shrinkage is not equal to free shrinkage. On the other hand, desiccation shrinkage is always stronger near the surface because of the moisture gradient, so usually purely free desiccation shrinkage can not occur.

Because restrained shrinkage is less than free shrinkage, and uneven desiccation inevitably leads to restrainment of shrinkage, shrinkage strains defined with different methods are not comparable. Different sizes of test specimens, different drying conditions or different curing time may cause the test results to be non-equal. However, this applies also to other tests normally used for construction materials, for example compressive strength test, and for this reason standard methods are used. Also, shrinkage strain test results should not be considered as a material constant but only test results. They only give the magnitude of the shrinkage and arrange materials tested by only in the exactly same way.

3 THE NAIL PLATE METHOD

The nail plate method is developed in Tampere University of Technology. It is an alternative method of measuring the shrinkage of a cement-based product due to changes in the moisture content. The ideal test objects are products that are used in conditions where the shrinkage is partially restrained. Especially this method is suitable for controlling the shrinkage on site.

The nail plate method is already used in some cases to determine the shrinkage, but it should be developed further. Especially the calculation from the measured deflection to the value of shrinkage strain has been inexact. In this chapter the method of the test done this far is presented substantially, so that the principle of the test method and the magnitude of the measures become clear.

3.1 Principle

The shrinkage is determined by measuring the deflection of a mortar – nail plate -composite structure. The nail plate restrains the movement of the other side of the structure, which results the structure to bend. The structure is laid on two supports and the deflection of the middle point is measured. The deflection of the span is bigger than the length change itself, and can thereby be measured proportionally more accurate. The actual shrinkage is calculated from the measured deflection.

3.2 Apparatus

- **Nail plate,** which causes the restrain in the composite structure. The nails function as dowels in composite structures. The nail plate used is 1016 mm long, 102 mm wide and its nails are about 10 mm in height. The perforated area of the nail plate is 21 %. Near the other end of the nail plate where the other support is to be, is drilled a small hole that is used to adjust the test body to the measuring apparatus. A picture of a proper nail plate is presented in Fig. 1.

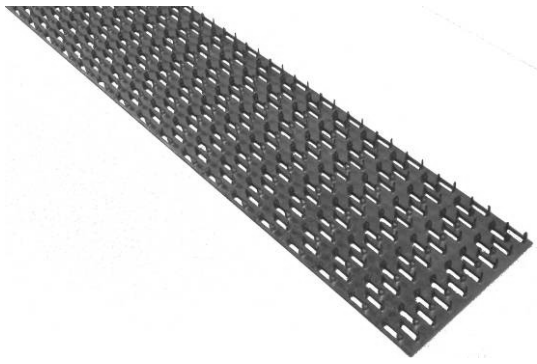

Figure 1. An example of a proper nail plate used in the test.

- **Mould,** where the specimen is applied on the nail plate.
- **Plastic film,** which is wrapped over the mould and the specimen for 24 hours after the application. The plastic film prevents the moisture from evaporating too early.
- **Application and compaction tools.** The compaction method is in accordance with the manufacturer's instructions.
- **Measuring apparatus.** The measuring apparatus consists of a rigid stand, two supports for the test specimen and a measuring device. One of the supports should be tapered so that it can be adjusted to the adjusting hole of the nail plate. The other support should be wide enough to keep the body upright. The span length between the supports has to be less than the length of the specimen, so that the bond between the nail plate and the concrete body can develop outside the span. The used span length is 965 mm. Measuring device should be fixed to suitable height for the supports in the middle of the span. The definition of the measuring device is not critical. For example, accuracy of ± 0.05 mm of deflection measurement means accuracy of about ± 0.017 ‰ of unit shrinkage. Usually, it is easy to achieve accuracy of ± 0.01 mm. The measuring apparatus is shown in Figure 2.

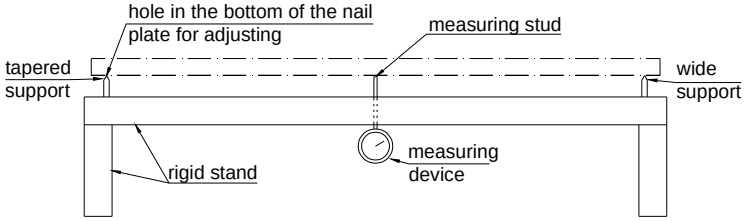

Figure 2. Measuring apparatus. The test specimen is presented with dot-and-dash line.

3.3 Test Specimen

After the adjust hole is drilled near the other end of the nail plate, the nail plate is placed on the bottom of the water-nonabsorbent mould with nails upwards. Then the mould is filled with the tested material by two layers so that the first layer covers the depth of the nails. Both layers are compacted with care and the excess grout is cut out.

The height of the test specimen should be at least four times the size of the maximum grain size or 25 mm. Low specimen is vulnerable.

The specimen is cured in the mould with plastic film around it for 24 hours. After that the mould can be removed and the height of the specimen and the initial deflection can be measured.

3.4 Measurement

The test specimen is laid on the supports of the measuring stand so that the tapered support meets the adjusting hole of the nail plate. It is important to ensure that the specimen is properly on the both supports and that the measuring stud is properly against the nail plate. The measure is read as soon as possible after the specimen is set on the measuring stand, so that no excessive creep bending occurs.

It can be worthwhile to measure the weight of the specimen every time the deflection is measured, to find out how much the specimen has lost water. Also, the specimen should be every time checked for any excessive deformations (i.e. not longitudinal bending) or injuries and the detections are documented.

3.5 Storage

The specimen has to be stored on its narrow side. The mount should be such that does not restrict the deformation of the specimen.

The storage conditions, like the drying climate, can vary according to the research plan. A different drying rate, however, leads to results which are not comparable.

3.6 Calculation

This far the equation to give the unit strain from the measured deflection is the following:

$$\varepsilon_{shrinkage} = \frac{8 \cdot h \cdot v}{L^2}, \quad (1)$$

where $\varepsilon_{shrinkage}$ is the shrinkage unit strain, h is the height of the specimen, v is the measured deflection and L is the span length. This equation gives the difference in length between free side and nail plate side. This is dealt more in Chapter 4.2.

4 IMPROVEMENTS TO THE NAIL PLATE METHOD

Equation (1) does not take into account the stiffness of tested material body in proportion to nail plate. If tested specimens of different heights or if the modulus of elasticity is different between tested materials, the results are not comparable. Also the magnitude of shrinkage of any tested material may be not relevant if the stiffness is not valid.

The nail plate method could, however, be used also to define the modulus of elasticity of the tested material. When the modulus of elasticity is known, it is possible to deduce stricter equation between the measured deflection and the shrinkage strain.

4.1 Definition of the Modulus of Elasticity

The modulus of elasticity can be studied by laying a known load on the specimen set on the measuring apparatus and defining the excess deflection at the middle point. The calculation of the deflection caused by a known load if the modulus of elasticity is known is a basic strength calculation. The modulus of elasticity can be calculated inversely when the load and the deflection are known.

4.2 More Exact Calculation

The following calculations are made with presumption that the bend line is circular. This is not the exactly true form of bend line of a uniform stiff structure when the bending moment is not uniformly distributed. Still, this presumption greatly simplifies the calculations and the difference between the presumed and the true bend line is insignificant.

From the geometry presented in Fig.3 and according to the Pythagorean theorem follows the Eq. 2:

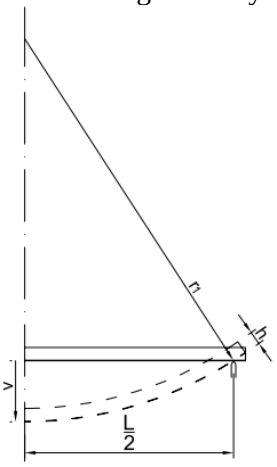

Figure 3. The geometry of the other half of the bended test specimen.

$$r_l^2 = \left(\frac{L}{2}\right)^2 + (r_1 - v)^2 , \tag{2}$$

where r_1 is the bending radius to the lower surface, L is the span length and v is the deflection. From the Eq. 2 it is possible to solve the bending radius r_1 as follows:

$$r_l = \frac{L^2 + 4v^2}{8v} . \tag{3}$$

Because the bending radius to the upper surface is $r_u = r_l - h$ and the term $4v^2 << L^2$, it is possible to write the rough Equation (1) as presented in following:

$$\frac{r_l - r_u}{r_l} = \frac{r_1 - (r_1 - h)}{r_1} = \frac{h}{r_1} \approx \frac{8 \cdot h \cdot v}{L^2} . \tag{4}$$

If the modulus of elasticity or the height of the tested material is high, the nail plate will be shortened elastic. The elastic strain of the nail plate, ε_s, will be the following:

$$\varepsilon_s = \varepsilon_{shrinkage} + \varepsilon_0 + \varepsilon_1 , \tag{5}$$

where $\varepsilon_{shrinkage}$ is the shrinkage strain of the tested material, ε_0 is the elastic strain caused by the normal force of the nail plate and ε_1 is the elastic bending strain at edge of the concrete body, caused by the bending moment from the nail plate. Using the approximation that the strain of the nail plate is constant in the cross-sectional area of the nail plate, the expressions are much clearer and the accuracy of the calculations will not deteriorate notable.

The edge strain ε_1 is defined as follows:

$$\varepsilon_1 = \frac{L_1 - L_0}{L_0} , \tag{6}$$

where L_1 is the length of the lower surface and L_0 is the length of the neutral axis of the concrete body (in the centre line). Because L_1 and L_0 are proportional only to the bending radius of their surfaces, the strain ε_1 can be written as follows:

$$\varepsilon_1 = \frac{r_1 - (r_1 - \frac{1}{2}h)}{(r_1 - \frac{1}{2}h)} . \tag{7}$$

By placing the Eq. (3) to the Eq. (7) the following result is obtained:

$$\varepsilon_1 = \frac{4\,h\,v}{L^2 + 4v^2 - 4\,h\,v} . \tag{8}$$

According to the Hooke's law the normal force of the nail plate is

$$F_s = \varepsilon_s E_s A_s \tag{9}$$

and, with the approximation that the thickness of the nail plate is insignificant, the bending moment is

$$M = \varepsilon_s E_s A_s \cdot \tfrac{1}{2}h . \tag{10}$$

The edge stress of the concrete body is

$$\sigma_1 = \frac{M}{W} = 3\frac{\varepsilon_s A_s E_s}{A_c} \ , \tag{11}$$

where W is the moment of resistance of the concrete body, A_s and A_c are the cross-section areas of the nail plate and the concrete body respectively, and E_s is the average modulus of elasticity of the nail plate. According to Hooke's law the edge strain ε_1 is the following:

$$\varepsilon_1 = 3\frac{\varepsilon_s A_s E_s}{E_c A_c}, \tag{12}$$

where E_c is the modulus of elasticity of tested material.

Because the normal force is even but opposing in the concrete body and in the nail plate, the strain ε_0 is proportional to the strain ε_s as following:

$$\varepsilon_0 = -\frac{\varepsilon_s A_s E_s}{E_c A_c} \tag{13}$$

By combining the Eqs (5), (8), (12) and (13) it is possible to solve the shrinkage strain:

$$\varepsilon_{shrinkage} = -\frac{4\,h\,v(A_c E_c + 4A_s E_s)}{3A_s E_s (L^2 + 4v^2 - 4\,h\,v)} \ . \tag{14}$$

If wanted to simplify expressions, the Eq. (14) can be expressed approximated as the following:

$$\varepsilon_{shrinkage} \approx -\frac{4\,h\,v\left(\frac{h}{1mm}\frac{E_c}{E_s} + 4\right)}{3L^2} \ , \tag{15}$$

when the thickness of the nail plate is 1 mm and the terms ($4v^2$) and ($4hv$) are insignificant in comparison with the term (L^2).

When defining the average modulus of elasticity of the nail plate, it is important to minus the perforated proportion from the material elasticity. For example, if the modulus of elasticity of steel is 210 GPa and the perforated area of the nail plate is 21 %, the $E_s = 0.79 \cdot 210\ \text{GPa} \approx 166\ \text{GPa}$.

SUMMARY

The nail plate method facilitates the defining of shrinkage strain, because the deflection of the nail plate composite, that is measured, is considerably bigger than the length change of a concrete body, and thus the test is not so sensitive to the inaccuracy of the measurement itself. With this testing arrangement it is also possible to define the modulus of elasticity of the tested material. If the modulus of elasticity is known, it is possible to use more exact calculation to determine the real shrinkage of the material.

The method has been used in special cases to determine the material's tendency to deflect when the shrinkage is eccentrically restrained. The value of shrinkage strain has been suitable for such survey. For this paper there has not been proper test data to compare the more exact calculated results of nail plate test to normally accepted standard test.

REFERENCES

Baroghel-Boundy, V., Mainguy, M., Lassabatere, T. & Coussy, O. 1999, 'Characterization and identification of equilibrium and transfer moisture properties for ordinary and high-performance cementitious materials', *Cement and Concrete research,* **29**, pp. 1225–1238.

Bazant Z.P. 1972, 'Thermodynamics of hindered adsorption and its implications for hardened cement paste and concrete', *Cement and Concrete Research,* **2[**1], pp. 1–16.

Ferraris, C.F. & Wittmann, F.H. 1987, 'Retrait de la pâte de ciment durcie', *Chantiers,* **4**, pp 289–292.

Wittmann, F.H. 'Interaction of hardened cement paste and water', *Journal of the American Ceramic Society,* **56**[8], pp. 409–415.

XII DBMC
International Conference on Durability of Building Materials and Components
PORTO - PORTUGAL, April 12th-15th, 2011

Chloride Penetration into Mortar-Concrete Systems – Analysis of the Additional Protection in Delaying Chloride Ingress

Raphaele de L. Meireles de C. Malheiro [1]
Munique Silva de Lima [2]
Gibson Rocha Meira [3]
Normando Perazzo[4]

ABSTRACT

Most reinforced concrete structures placed in marine environments have an external mortar rendering. This research analyses the effect of the possible additional protection role of mortar rendering layer and its influence on starting corrosion process. Cubic concrete specimens were cast with the dimensions 8 x 8 x 8 cm and water to cement ratio (w/c) ratio of 0.55. Three mortar mixtures were used to cover one of the cube sides, which were applied on a thin spatter dash layer. After air curing periods of 28 days for concrete, 3 days for the spatter dash layer and 28 days for rendering mortars, the remaining sides of the specimens were painted with epoxy resin to simulate one dimensional chloride transport. Then, the specimens were subjected to accelerated tests of natural diffusion and wetting and drying cycles in one molar sodium chloride solutions over a period of 49 weeks. After this period, chloride profiles were obtained from samples taken every 5 mm, from the surface inwards. Results indicate that, regardless the mortar mixture and the type of accelerated test, there is an accumulation of chloride ions in mortar-concrete interface followed by a significant decrease in chloride content in concrete side. This decrease shows that, although mortars have higher porosity than the concrete, they can represent an additional protection for reinforced concrete structures, delaying chloride penetration into bulk concrete. This contributes to increase the service life of reinforced concrete structures with regards to the phenomenon of reinforcement corrosion.

KEYWORDS

Chloride transport, Concrete, Durability, Mortar.

[1] University of Minho (UM), Guimarães, PORTUGAL, raphamalheiro@gmail.com
[2] Federal University of Campina Grande (UFPB), Campina Grande, BRAZIL, munique10@gmail.com
[3] Federal Institute of Education (IFE), João Pessoa, BRAZIL, gibsonmeira@yahoo.com
[4] Federal University of Paraíba (UFPB), João Pessoa, BRAZIL, nperazzo@yahoo.com.br

1 INTRODUCTION

International building codes demand that concrete structures might be designed for durability. Regarding Brazilian and Portuguese standards, for example, the designed service life for reinforced concrete structures can vary between 10 and 100 years, taking into account the importance level of the structure [LNEC E465 2007]. Despite these guides, several cases of early degradation of concrete structures are still seen around of the world.

There are many aspects that contribute for these cases of early degradation. The incompatible design of concrete structures for the environmental aggressiveness to which the structure will be subjected represent an aspect that plays an important role. Considering this scenario, the action of chloride ions is one important factor for concrete degradation due to reinforcement corrosion [AITCIN 2000]. Thise ions penetrate into concrete, mainly by diffusion and capillary sorption [KROPP *et al*. 1995, NILSON & TANG 1996]. This transport can take place either by a direct contact with sea water or, in many cases, due to the contact with marine aerosol [LINDVALL 2007, MEIRA *et al.* 2007]. When diffusion takes place, Fick´s second law has been widely used to represent chloride transport.

Aspects like the influence of material characteristics on chloride transport into concrete structures have been studied. These studies usually analyse concrete or mortar behaviour under accelerated laboratory tests taken individually [JENSEN 1999, MONTEIRO *et al.* 2003, TONG & GJøRV 2001]. Field exposure tests are less common [MEIRA 2004, Oh 2006, LINDVALL 2006]. Modelling of chloride transport into concrete structures represent another set of studies about this phenomenon [HETEK 53 1996, ANDRADE *et al.* 1997, GUIMARÃES & HELENE 2009].

Although there are several studies about concrete and mortar individually, the behaviour of these materials taken together, as a layered composite, has not been studied. Nevertheless, the rendering of concrete structures by a mortar layer is used in many countries. Although it is not the main purpose, this mortar rendering layer can contribute as an additional physical barreer for chloride penetration into concrete [MALHEIRO 2008].

Taking into account the skin effect, Andrade *et al.* [1997] proposed the Equations 1-3 to represent chloride transport by diffusion in materials with different characteristics between surface and bulk. However, experimental studies that consider chloride transport in layered composite materials are still scarce.

$$C_1 = C_s \sum_{n=0}^{\infty} \alpha^n \left(erfc\left[\frac{2ne + x}{2\sqrt{D_1 t}} \right] - \alpha erfc\left[\frac{(2n+2)e - x}{2\sqrt{D_1 t}} \right] \right) \quad \text{[Equation 1]}$$

$$C_2 = \frac{2kC_s R}{k+1} \sum_{n=0}^{\infty} \alpha^n erfc\left[\frac{(2n+1)e + k(x-e)}{2\sqrt{D_1 t}} \right] \quad \text{[Equation 2]}$$

$$C_1 = RC_2 \quad \text{[Equation 3]}$$

This work experimentally studied the influence of chloride transport in mortar rendering on chloride penetration into concrete, taking into account double layered systems.

2 EXPERIMENTAL WORK

The specimens used in this research were developed to simulate, in laboratory, the use of mortar rendering layer over concrete structures is Brazilian constructions. The specimens were made

following the stages practiced in field, as said in following paragraphs. Reference concrete specimens (without mortar layer) were also made with the objective of being used in comparisons with the first.

Prismatic concrete specimens (substrates) with 8 x 8 x 8 cm were made with a high early strength Brazilian Portland cement (ASTM type III), which chemical and physical characteristics are presented in Table 1. Concrete mixture characteristics are presented in Table 2. After being removed from the moulds, concrete specimens were cured in laboratory environment up to 120 days to simulate a delay that usually occurs in real building process between casting concrete elements and execution of rendering layer. This condition was also followed by reference concrete specimens. After this, the concrete substrates had one of their faces cleaned by manual brushing and received a thin layer of bonding spatter dash treatment. After three days, mortar rendering layer was executed with 2.5 centimetres thickness. For this purpose, three different mortar mixtures were used, which are represented by their proportions in volume as mortars 1:3, 1:1:6 and 1:2:9 (cement: sand and cement: lime: sand).

Table 1. Chemical composition and physical properties of cement and hidrated lime.

Composition/property		*Portland cement*	*Hidrated lime*
SiO_2 (%)		20.06	0.44
Al_2O_3 (%)		5.99	-
Fe_2O_3 (%)		2.18	0.08
CaO (%)		60.48	67.76
MgO (%)		3.82	2.82
Na_2O (%)		0.94	0.18
K_2O (%)		1.06	0.05
Insoluble Residue –IR (%)		0.46	0.12
Loss on Ignition – LI (%)		2.65	27.49
Potencial composition	C_2S(%)	19.49	-
(Bogue Equations)	C_3S(%)	50.40	-
	C_3A(%)	12.18	-
	C_4AF(%)	6.63	-
Blaine (cm^2/g)		4815	-
Specific density (g/cm^3)		3.09	2.42
Compressive strength – 28 days (MPa)		34.94	-

Table 2. Mixtures and properties of concrete and mortars.

Material	*Concrete*	*Mortar 1:3**	*Mortar 1:1:6**	*Mortar 1:2:9**
Relative proportions				
Cemente (kg)	1	1	1	1
Hydrated lime (kg)	-	-	0.3	0.59
Sand (kg)	932.4	3.53	7.05	10.58
Coarse aggregate (kg)	891.7	-	-	-
Water to bind ratio	0.55	0.6	0.83	1.11
Cement (kg/m^3)	370	437	250	173.5
Air content (%)	-	2	2	4
Slump/ Consistence level (mm)	7 +-1	262	264	262
Compressive strengh (MPa) – 28 days	30.43	23.59	11.82	5.65
Capillary sorption (g/cm2)	1.43	-	-	-
Water absorption after immersion (%)	4.86	8.24	10.40	11.33
Dry specific density (g/cm3)	2.25	2.21	2.13	2.09
Total porosity (%)	10.95	18.19	22.13	23.72

Three specimens were used for each experimental condition. All of them had five of their six faces painted with epoxy resin 28 days after the execution of the mortar rendering layer. A unique free face was used for the penetration of chlorides into concrete with the objective of simulating a unidirectional flux. It is important to point out that the choice of the used cement is related to its low level of additions. Mortars characteristics are related to the constructivists practice used in João Pessoa city, Brazil. [MALHEIRO et al, 2007]. The main preparations steps of specimens used in this work are presented in Fig. 1.



Figure 1. The main steps in preparing the combined specimens.

The specimens were then subjected to diffusion tests and wetting and drying tests. During diffusion tests, the specimens remained 49 days immersed in one molar sodium chloride solutions in laboratory environment. For wetting and drying tests, the specimens were subjected to weekly cycles with three immersion days and four days drying. This set of experiments was also carried out during 49 days. The choice of this exposure period happened with the objective of adjusting the differences on chloride transport velocity in mortar and concrete, as these materials have significant differences on their mass transport characteristics. This was a consequence of preliminary tests carried out with mortars and concrete specimens subjected to different exposure periods. The reference specimens were subjected to the same conditions imposed to the layered specimens.

When the exposure period was over, the specimens were marked and powdered at each five millimetres from surface to bulk. Close to the interface between mortar and concrete, the thickness was reduced to 2.5 millimetres, which had the objective of improving the accuracy of chloride measurements in this region. Fig. 2 schematically shows samples extraction from the specimens.

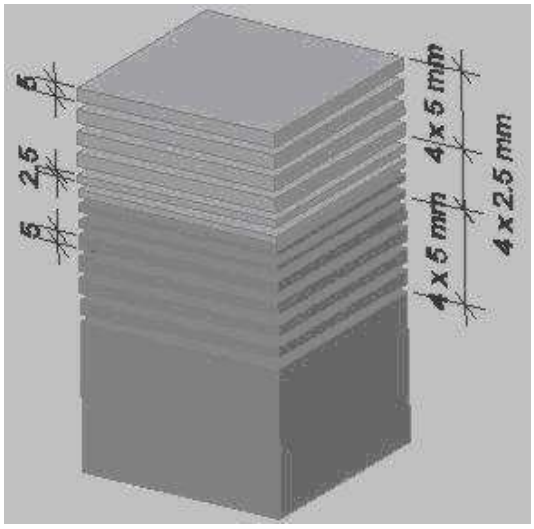

Figure 2. Schematic representation for obtaining samples from the specimens.

After this extraction, total chloride content in each powered sample was measured using the potentiometric titration method, according to ASTM C114 [ASTM 1994].

3 RESULTS

Fig. 3 shows chloride profiles obtained from diffusion tests (a) and wetting and drying tests (b) Each point depicted represents the average value from three samples for each depth.

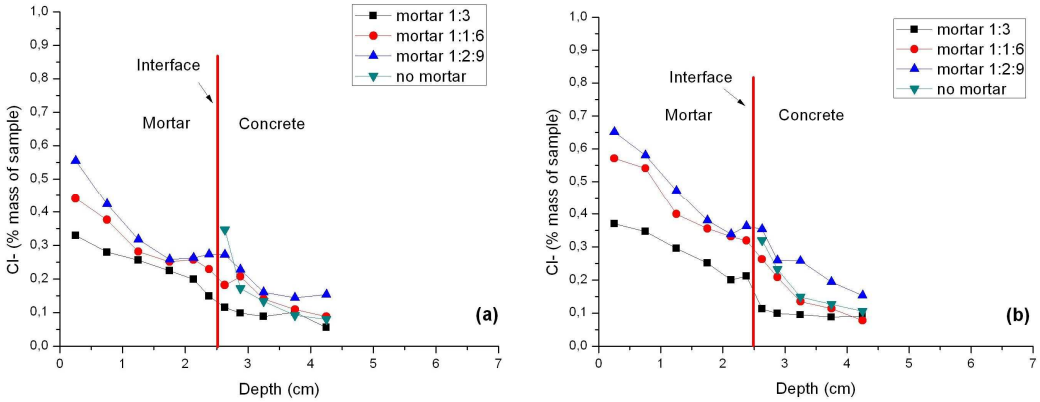

Figure 3. Chloride profiles for diffusion tests (a) and wetting and drying tests (b).

Based on Fig. 3 and Table 2, it can be seen that chloride content increases with mortar porosity. Taking into account the accelerated tests used in this work, it can be seen that chloride contents are slight higher for wetting and drying tests, which can be attributed to the additional contribution capillary sorption on chloride transport.

4 DISCUSSION

4.1 Influence of Mortar Characteristics on Chloride Penetration into Concrete

Equations 1 – 3 were fitted to chloride profiles presented in Fig. 3, considering different material layers according to Andrade *et al.* [1997], which resulted in curves presented in Fig. 4.

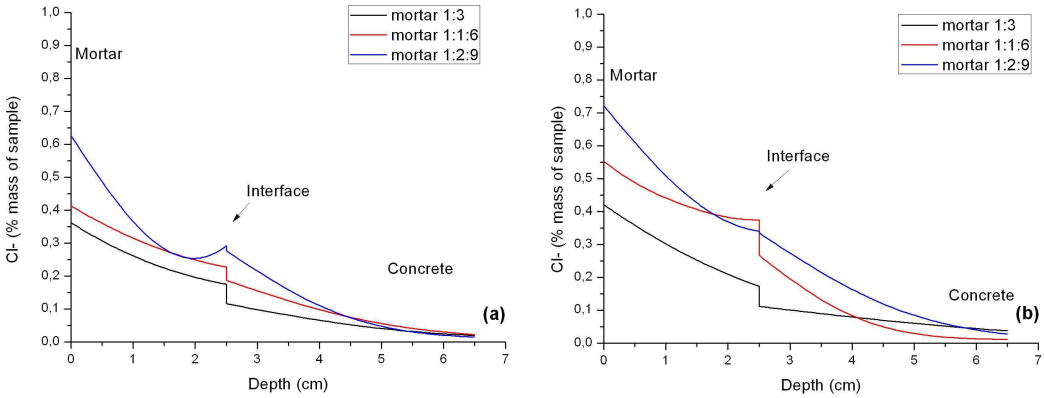

Figure 4. Fitted curves to data from diffusion tests (a) and wetting and drying tests (b).

By chloride profiles it can be seen that rendering mortars have different behaviours concerning chloride transport. There is a general tendency of decreasing chloride contents in concrete and mortar layers, as a consequence of mortar porosity decrease [Table 2]. The richer in cement is the mortar less porous is it and, consequently, lower chloride contents are observed in mortar and concrete layers. The chloride transport also is influenced by the water to cement ratio, which influences on materials porosity [Jensen *et al.* 1999, SILVA 2003, GJøRV and TONG 2001].

Furthermore, the higher chloride binding capacity of richer mortars contributes for lower chloride contents. Higher cement consumption means a higher content of C_3A available to help in binding chloride ions [OH and JANG, 2007]. This higher binding capacity reduces the amount of free chlorides, which are those that effectively take part in mass transport and, consequently, generates chloride profiles with lower contents.

Analysing chloride profiles shown in Fig. 3b, a tendency of soft peaks in the region close to the surface of the mortars can be seen. These peaks are typical formations of the cycles of gain and loss of moisture in the material surface [Coutinho, 1998]. Considering that this form is only a tendency, which is not clearly defined, and that the internal form of profiles resembles diffusion profiles, it was considered that transport by diffusion has prevailed in wetting and drying cycles too.

Regarding the influence of different mortar mixtures in chloride transport in concrete, Fig. 4 shows that there is a good harmony between chloride profiles in rendering layer and those in concrete layer. If less chloride ions arrive at the interface between the materials, even less will be transported into concrete. It means that the behavioural differences observed in mortar layer have a direct influence on results obtained for concrete layer.

It is also possible to observe the resistance effect in mortar-concrete interface for all studied mortars (Fig. 4), which is characterized by an accumulation of chloride ions in the region just before the interface between the two materials, followed by a reduction on chloride contents in the region just after the same interface. This effect occurs as a consequence of the different material abilities for mass transport.

For better understanding the effect of mortar rendering layer on chloride transport in concrete, chloride profiles obtained in concrete region for layered and reference specimens are extracted from Fig. 4 and presented in Fig. 5.

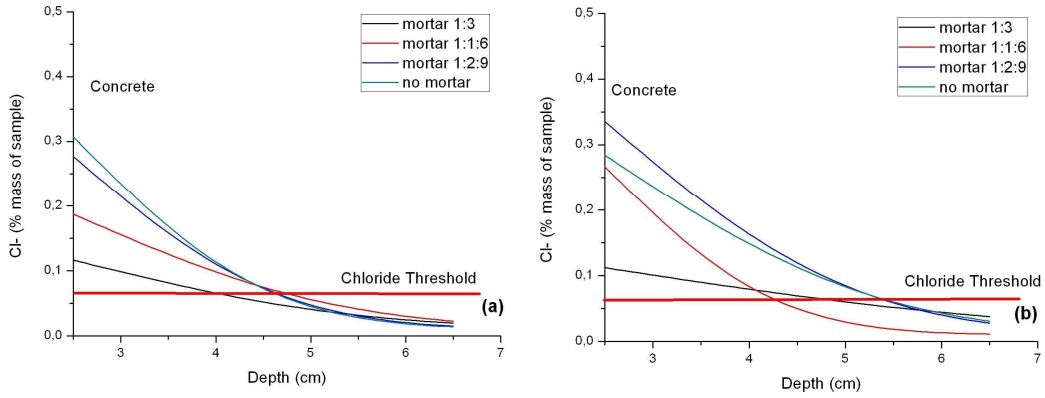

Figure 5. Fitted profiles for concrete region - diffusion tests (a) and wetting and drying tests (b).

By Fig. 5, it can be seen that mortar rendering layer plays a role in delaying chloride penetration into concrete. This is clearer for less porous mortars. Furthermore, by analyzing the critical chloride content (0.4 % cement mass - 0.065% sample mass) [GLASS 1995], it can also be seen that this value

is reached at deeper depths in reference specimens [Fig. 5]. However, as mortar porosity increases this effect becomes weaker.

4.2 Influence of Accelerated Test

Analysing chloride profiles shown in Fig. 3b, a tendency of soft peaks in the region close to the surface of the mortars can be seen. These peaks are typical formations of the cycles of gain and loss of moisture in the material surface [Coutinho, 1998]. Considering that this form is only a tendency, which is not clearly defined, and that the internal form of profiles resembles diffusion profiles, it was considered that transport by diffusion has prevailed in wetting and drying cycles too.

The short time for drying period, associated with high relative humidity in laboratory environment (typical of the region) contributed for a partial and superficial drying of specimens used in this work, leaving the bulk concrete with enough moisture to nurture the process of diffusion.

Although chloride concentrations obtained for wetting and drying tests are slightly higher than those obtained for diffusion tests, considerations made in the last one can be taken for both, without major deviations from reality.

5 CONCLUSIONS

Results indicate that, regardless of mixture used for mortars and the type of accelerated test, there is an accumulation of chloride ions in mortar-concrete interface, which characterises resistance effect. This behaviour is slightly higher for wetting and drying cycles test and for poorer mortar and is followed by a significant reduction in chloride content level in concrete.

This reduction shows that, although mortars have higher porosity than concrete, they represent an additional protection in delaying penetration of chloride ions into concrete, helping on increasing service life of concrete structure with regards to the phenomenon of reinforcement corrosion.

ACKNOWLEDGMENTS

The authors thank the team of Materials and Structures Laboratory of Federal University of Paraíba and the Federal Institute of Education, Science and Technology of Paraíba for helping on this research project activities. Authors also thank the Brazilian Council of Scientific and Technological Improvement (CNPq) and CAPES (Brazilian Government Agency for the Improvement of Graduated Professionals) for supporting this research.

REFERENCES

Aitcin, P. C. 2000, *Concreto de Alto Desempenho*. Pini, São Paulo.

American Society for Testing aAnd Materials 1994, *ASTM C-1152*.

Andrade, C., Diez, J. M. & Alonso, C. 1997, “Modelling of skin effects on diffusion process in concrete”, *Advn Cem Mat*, [6], 39-44.

Coutinho, J. S. 1998, *Melhoria da Durabilidade dos Betões por Tratamento da Cofragem.* Tese (Doutorado em Engenharia Civil), Universidade do Porto, Porto.

Hetek 53 1996, *Chloride penetration into concrete. State of the Art. Transport processes, corrosion initiation, test methods and prediction models*. Report No. 53.
Laboratório Nacional de Engenharia Civil 2007, *LNEC E 465*.

Glass, G. K. & Buenfeld, N. R. 1995 "Chloride threshold levels for corrosion induced deterioration of steel in concrete" in *International RILEM Workshop on Chloride Penetration into Concrete*, eds O. L. Nilsson & J. P. Ollivier, RILEM, Paris, pp. 429 – 440.

Guimarães, A.T.C. & Helene, P.R.L. 2009, "Modelo para estimar a penetração de cloretos em concreto com perfil formando pico: verificação da sua precisão", *Revista Matéria*, [14], 983-992.

Jensen, O. M., Hansen, P. F., Coats, A. M. & Glasser, F. P. 1999 "Chloride ingress in cement paste and mortar", *Cement and Concrete Research*, [29], 1497-1504.

Kröpp, J., Hilsdorf, H. K., Grube, H., Andrade, C. & Nilsson, L. O. 1995 "Transport mechanisms and definitions", in *Performance Criteria for Concrete Durability (report 12 – RILEM)*, eds J. Kröpp & H. K. Hilsdorf, E & FN Spon, London, pp. 4-14.

Lindvall, A. 2007, "Chloride ingress data from field and laboratory exposure – Influence of salinity and temperature", *Cement and Concrete Composites*, [29], 88-93.

Malheiro, R.L.C. 2008, *Influência do revestimento argamassado no transporte de cloretos em estruturas de concreto armado inseridas no meio urbano.* João Pessoa. 2008. 144 f. Dissertação (Mestrado em Engenharia Urbana) – Faculdade de Engenharia Civil, Universidade Federal da Paraíba, João Pessoa.

Meira, G. R. 2004, *Agressividade por cloretos em zona de atmosfera marinha frente ao problema da corrosão em estruturas de concreto armado.* 2004. 369 f. Tese (Doutorado em Engenharia Civil) – Universidade Federal de Santa Catarina, Santa Catarina.

Meira, G., Andrade, C., Alonso, C. & Borba, Jr. J. C. 2007 "Chloride penetration into concrete structures in marine atmosphere zone – influence of environmental characteristics", in *International RILEM Workshop on Integral Service Life Modelling of Concrete Structures*, eds R. M. Ferreira, J. Gulikers & C. Andrade, RILEM, Guimarães, pp. 47-54.

Monteiro, E.B. *et al*. 2003 "A técnica de extração eletroquímica de cloretos nova técnica de reabilitação de estruturas com problemas de corrosão", Proc. 45 Congresso Brasileiro do Concreto, Vitória, Brasil.

Nilsson, L. O. & Tang, L. 1996 "Transport mechanisms in porous materials - an introduction to their basic laws and correlations", in *International Congress on Modelling of Microstructure and its Potential for Studying Transport Properties and Durability*, eds J. Kröpp & K. Scrivener, Kluwer Academic Press, Saint-Rémy-lés-Chevreuse, pp. 289 – 311.

Oh, B. H. & Jang, S. Y. 2007, "Effects of material and environmental parameters on chloride penetration profiles in concrete structures", *Cement and Concrete Research*, [37], 47-53.

Silva, D. A. *et al*. 2003 "Argamassas intermediárias de cal e areia para revestimentos: efeitos das características da areia", Proc V Simpósio Brasileiro de Tecnologia das Argamassas, São Paulo, Brasil.

Tong, L. & Gjørv O. E. 2001, "Chloride diffusivity based on migration testing", *Cement and Concrete Research*, [31], 973-982.

XII DBMC
International Conference on Durability of Building Materials and Components
PORTO - PORTUGAL, April 12th-15th, 2011

Observations about the Corrosion of Reinforcement in Marine Environments

Robert E. Melchers [1]

ABSTRACT

The corrosion of reinforcement bars and prestressing strands in concrete structures such as bridges and coastal and harbour facilities is a significant maintenance and renewal issue. Mostly such structures are considered to have useful lives of 2-3 decades, but, surprisingly perhaps, there are a considerable number of structures still in existence with much longer useful lives, some showing little evidence of reinforcement corrosion despite being either exposed directly to hostile marine environments or very likely to have been made with seawater as mixing water. A small number of the latter, and a recent review of the performance of many (>300) of such structures is given. That review did not support the conventional thinking that modern cements were responsible for the poorer long-term durability of modern structures. Instead it was proposed, on the basis of electrochemical arguments and observed experience, that the properties of the aggregates is a key factor. To test this hypothesis a series of exposure tests were commenced several years ago in which seawater was used as mixing water and with different aggregates, including those rich in calcium-carbonate, which the conventional wisdom suggests lowers the concrete pore solution sufficiently to initiate reinforcement corrosion. Preliminary results from these tests are described and it is shown that calcium carbonate concretes, even with seawater, do not lead to early corrosion initiation. Results for the effect of higher cement content, water cement ratio and the presence or absence of salt water in the concrete mix also are presented.

KEYWORDS

Corrosion, Seawater, Reinforcement, Concrete, Structures.

[1] Centre for Infrastructure Performance and Reliability, The University of Newcastle. Australia, rob.melchers@newcastle.edu.au

1 INTRODUCTION

The long-term durability of reinforced concrete structures particularly in marine environments remains a matter of concern despite many years of practical experience with reinforced and prestressed concrete and very extensive research programs. The consensus of opinion favours very dense concretes with high cover to the reinforcement on the basis that this will reduce the diffusion of chlorides (or carbon dioxide or both) from the external environment to the reinforcing bars. Various additives also are known to further reduce the pore-spaces and hence the diffusion of water, oxygen and chlorides and/or carbon dioxide to the reinforcement. Most of the practices currently considered desirable are derived from short-term laboratory experiments and practical observations. Nevertheless, there are two broad aspects that should be of concern in the present state of understanding. One is that despite these practices, there are numerous examples of relatively modern apparently well-designed reinforced concrete structures that show signs of reinforcement corrosion giving, overall, likely shorter serviceable lives than might be expected. Particularly in coastal environments, evidence of corrosion initiation for reinforcement is observed already after a few years and for many modern structures serious cracking and spalling of the concrete occurs within 2-3 decades. Conversely, for a considerable number of reinforced concrete structures, including many that would today be considered of inferior quality, there is little or no evidence of reinforcement corrosion even after many decades of exposure in severe marine environments [Melchers & Li 2009a].

Most commonly the difference in long-term durability of reinforced concrete structures is attributed to changes in the making of cement and having had a negative impact on durability. Changes in cement-making originated in the USA during the 1930s and were aimed at producing higher strength concretes with higher earlier strengths. This was achieved with higher clinkering temperatures and finer clinker grind. The changes were adopted later in the UK and Australia - not until the 1960 - despite vocal opposition on the grounds that durability would be adversely affected. Certainly the composition of the cements changed somewhat [Nixon & Spooner 1993] but there is only anecdotal evidence that this affected durability. Using reports of the actual behaviour of reinforced concrete structures and reasonable estimates of durability, a recent study indicated only poor correlation between changes in cement making practice and reinforcement corrosion severity [Melchers and Li 2009a]. Since that study a number of other cases have become available - all examples of structures that have shown a high degree of durability despite aggressive environments and in many cases without the benefit of what is today considered to be good practice [Melchers 2010a,b]. This raises the question whether the current conventional wisdom is sufficient to explain long-term durability.

The next section summarizes observations of the actual durability of older reinforced concrete structures. This is followed by a brief review of some fundamental aspects of the corrosion of steel in marine environments and the effect of the concrete surrounding the steel. It will be argued that assumptions commonly made in the reinforcement corrosion literature are not always in accord with fundamental corrosion science principles. The final section describes, briefly, on-going long-term durability tests of reinforced concrete samples made with various combinations of materials, including seawater as mixing water and seawater with additional salt added, and various types of aggregates.

2 OBSERVATIONS FROM ACTUAL STRUCTURES

The present work was prompted by observations of the surprising long-term satisfactory behaviour of multiple, simple reinforced concrete elements (Fig. 1a), made without high level technology or modern quality control (Fig. 1b) and for more than 65 years subjected to North Sea exposure [Melchers & Li 2009b]. One surprising feature was that this concrete showed very high levels of chloride contamination and very high content of seashells (Fig. 1c). This raised the question whether high levels of carbonates in the concrete might be beneficial, even though at first sight this contradicts the notion of ‘carbonation’. In the event, an extensive literature survey was conducted and this found

many reports (300+) of cases (54 groups of data ranging from just one element to more than 1000) where reinforcement corrosion took many years to initiate and to become sufficiently active for remedial or other action to be taken.



Figure 1. (a) Reinforced concrete balustrade at Arbroath, Scotland (b) typical cover of balustrade railing and (c) evidence of seashells in the concrete [Melchers & Li 2009b].

Each case was assessed for two parameters, the time to initiation and the time to active corrosion, both judged from all information available. Laboratory based experimental observations, and in particular those from accelerated tests using impressed currents to stimulate the anodic corrosion reaction, were ignored. The corrosion science literature recognizes that such tests produce only relative observations, not results that can be related directly to the behaviour of actual structures, particularly when bacteria are involved [e.g. Cord-Ruwish 2000]. Because of lack of information, the influence of concrete mix and concrete cover, of average or range in temperature and local weather conditions was ignored and treated as variability in the data. Estimates for the degree of chloride contamination were considered but relative to the other influences this parameter turned out to be of only of secondary importance, particularly for the time to active corrosion [Melchers and Li 2009a]. Fig. 2 shows that despite scatter in the data, the trends for calcareous (alkaline) and normal aggregates are remarkably different.

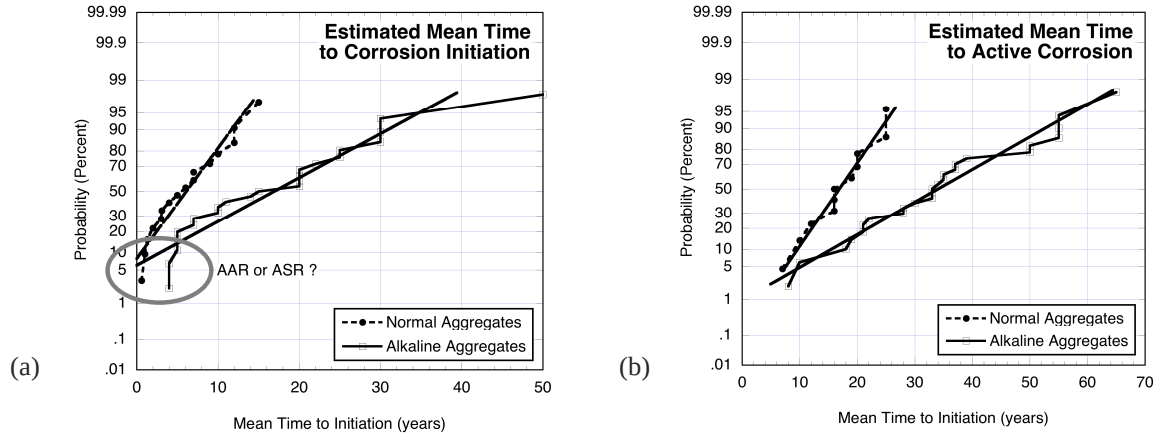

Figure 2. Normal cumulative probability plots for (a) time to initiation and (b) time to active corrosion showing normal aggregates and 'alkaline' aggregates.

Figure 2(a) also shows that some data may have been influenced by alkali-aggregate or alkali-silicate reactivity of the aggregate. Typically these reactions cause early concrete cracking and thus loss of adequate cover. Evidently, this is a different failure mode and does not belong to the same data cohort as failures resulting primarily from reinforcement corrosion [Melchers & Pape 2010].

3 SUBSEQUENT OBSERVATIONS

In parallel to the literature survey, several older existing concrete structures were examined, in some cases as a direct result of the author being alerted to their existence by practitioners who had become

aware of the thesis underlying the present and earlier papers. A number of these structures are summarized in Table 1. Overwhelming they were found to be consistent with the findings reflected in Fig. 2. Some of structures are heritage protected and it was not possible to obtain cores but, as indicated in Table 1 and in the references, in many cases there is sufficient circumstantial evidence to indicate they were, or are likely to have been, constructed using calcareous sands, limestone and/or unreactive dolomite aggregates or, in some cases, blast furnace slag as aggregate.

Table 1. Examples of older reinforced concrete structures.

21st Street Bridge, Tacoma, Washington, USA, 1909.
This early bridge has had minimal exposure to carbonation effects and chloride ions. The presence of seashells and acid soluble chloride contents around 0.2% by weight of cement indicates concrete was mixed with seawater. It was estimated that reinforcement corrosion did not commence until some 60 years after construction and most likely is the result of carbonation.

Portland Cement Works, exposed to southern Pacific, Maria Island, Tasmania, Australia, 1923
Maria Island consists of limestone that was used for early cement-making and also for construction of the works. It was abandoned in 1930 and has been without maintenance until recently. The four RC cement silos and clinker house largely are free from reinforcement corrosion. Akthough there are areas of spalling, there is little sign of heavy rusting or of rust staining on the concrete.



Beach-side Railing, Mordialloc, Australia, 1928
Directly on marine environment at Port Philip Bay and not maintained until recently. There were very limited signs of reinforcment corrosion. Highly likely to have been constructed using local beach sand known to be rich in seashells. Photograph taken prior to recent maintenance.



Tongue Sands Tower, Thames Estuary, UK, 1943
Two 7.3m diameter, 18.3m high RC cellular caissons on a RC foundation pontoon, several miles off the UK coast was investigated in detai. Reinforcement corrosion was confined mainly to areas where concrete cover was much less than specified (32mm) or where inferior local mortar mixes had been used. Overall in '... remarkably good condition.' Many cores showed the presence of seashells in the concrete and high chloride levels, suggesting the use of beach sands and seawater as mixing water. High levels of 'carbonation' also detected.

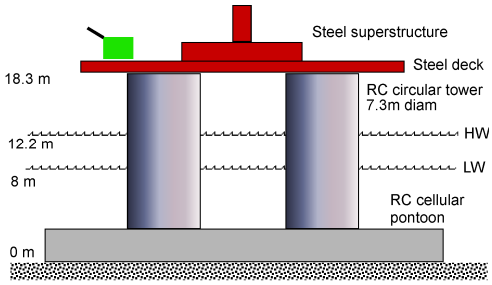

Two-storey Pill Box Forts, Thames Estuary, UK, 1943
Constructed in groups of 4-5 and connected together with structural steelwork walkways and surmounted with steel gun platforms, given extensive exterior rust staining. These have all disappeared - presumably corroded away. Remarkably little external evidence of reinforcement corrosion. It is reasonable to assume that the reinforced concrete for these structures also used beach sand for aggregate and seawater as mixing water.

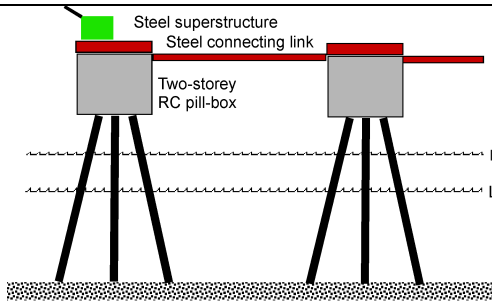

Pacific Ocean Harbor fortifications, Newcastle, Australia, 1943

Prior to its first ever maintenance in 2006 showed some loss of cover and little reinforcement corrosion. Coarse blast furnace slag (BFS) aggregate, present in concrete, was a common by-product of the iron and steel making and was widely used as an aggregate for concretes. Its a high alkali content maintains pH at around 9-10. Photograph taken just prior to recent maintenance.



1.6 km long RC Balustrade, Arbroath, Scotland, 1943

More than 90% of the 1000 original RC elements exposed to North Sea marine atmosphere and splashing show little external rust staining, spalling or cracking. The other 10% were replaced in 1968 and 1993 and nearly all of these show extensive and severe longitudinal cracking and damage. Clear evidence of seashells in 1943 concrete mix, suggesting also seawater was used as mixing water.



Mulberry Harbour Caisson, Langstone Harbour, UK, 1943-4

Few ofmore than 200 Phoenix units built still survive. Built very quickly with un-skilled labour, using available materials, withoutdurability considerations. The unit at Langstone Harbour broke during beaching. It has little obvious reinforcement corrosion. Use of beach sands and flint nodules (found in chalk i.e. limestone) likely.



Mulberry Harbour Caissons, Portland Harbour, UK, 1943-4

The two caissons in Portland Harbour are offshore and in completely exposed locations. They appear to be in generally good condition showing reinforcement corrosion around the mean-tide zone where cover appears low, but little reinforcement corrosion elsewhere. There is some concrete spalling.



Concrete lighters, Purton, Severn Estuary, UK, 1940's

Reinforced concrete lighters were used for bulk transport in fresh and tidal waterways but fell out of favour. Some are partly buried on the southern bank of the Severn Estuary to aid shore protection. They are exposed to high tidal ranges but show little reinforcement corrosion. Where there was physical damage to the concrete cover there is moderate reinforcement corrosion. The fine aggregates appear to be calcareous.



Concrete piles, Bar Beach, Newcastle, Australia, 1940's?

Concrete piles supporting a reinforced concrete slab located immediately adjacent to the Pacific Ocean. The underside of the slab shows reinforcement corrosion but the piles are essentially free from reinforcement corrosion, despite the bars being visible (at arrows) from the top and the concrete cover varying significantly. There is no rust staining. The concrete contains BFS aggregate.



Florida bridge piles (1000+) in tidal zone, Florida panhandle region, USA, 1960s?
Very low incidence of signs of reinforcement corrosion, despite approx 35 mm concrete cover. Steel showed no or very light rusting. Chloride penetration varied widely and poorly correlated to cracking and corrosion. Porewater pH measurements still 11-13. Some aggregates are limestone, others 'river rock', which US Geological Survey information indicates is predominantly limestone.

Concrete Ammunition Lighters (6 + others), Sydney Harbour, Australia, 1970s
Essentially RC boats of cast construction used in marine conditions. Except for one limited hairline crack, no evidence of any reinforcment corrosion. Igneous large aggregate but most likely calcareous sand from Kurnell Beach, Sydney's only sand supply at the time.



4 EXPRIMENTAL OBSERVATIONS

A long-term test program, commenced in 2003 is examining the effect of several factors on corrosion of reinforcement. Some 700 samples, 150mm x 50mm x 50 mm in size, with one centrally-placed 6 mm diam. mild steel round bar, were made in steel forms under high quality control, weight-batching of air-dried sand and aggregates and highly controlled, timed vibration. All bars were sourced from the same batch and, except as noted, the same cement, sand and aggregates were used throughout, and natural seawater was used as mixing water so as to accelerate the time to initiation of reinforcement corrosion. The specimens were cured for 4 weeks in the fog-room prior to being air-stored in the laboratory while the remaining specimens were made. The last specimens were made during June 2004. Six months later the specimens were placed in the fog room on open web plastic racks to ensure specimen were exposed on all sides. Six years later (2010) none of the specimens showed visible external evidence of reinforcement corrosion such as rust stains, cracking or spalling.

After 3 years exposure (2007) one of each type of specimen was broken open and the reinforcing bars visually examined. The surface condition of the bars ranged from apparently 'as new' condition to extensive but still quite thin rust coverage. Since mass loss differentials would be problematic, the relative visual surface corrosion condition was rated using the simple scale: 0 = no rust visible, 1 = small spots of rust, 2 = rust patches over 50% of surface, and 3 = most of the surface covered by rust. Herein attention is restricted mainly to the effect of (i) saline mixing water and (ii) the use of limestone as the main aggregate. Table 2 gives some of the rating results. Figure 3 shows the relative corrosion ratings as a function of aggregate/cement ratio. Analysis of the ratings showed almost no difference as a function of water/cement ratio. It shows that limestone aggregate appears to lower the relative corrosion, that low-heat cement may be beneficial, that there is an effect apparently due to aggregate/cement ratio and, perhaps surprising in the conventional wisdom in reinforcement corrosion, that chloride content does not necessarily increase corrosion severity [Melchers 2010b].

Table 2. Selected test program and reinforcement surface rating result after 3 years exposure.

Series	Mark	**a/c**	**w/c**	Rating	Series	Mark	**a/c**	**w/c**	Rating
Base case	B1	2	0.5	1.5	**+ 50%NaCl**	D2	4	0.8	0.5
	B2		0.65	1.5		D3		0.95	1.5
	B3		0.8	1.5		D5	6	0.8	1
	B5	4	0.8	2		D6		0.95	1
	B6		0.95	2	**Limestone**	E2	2	0.8	0.5
	B8	6	0.8	1	**aggregate**	E3		0.95	1
	B9		0.95	0.5		E5	4	0.8	2
						E6		0.95	1

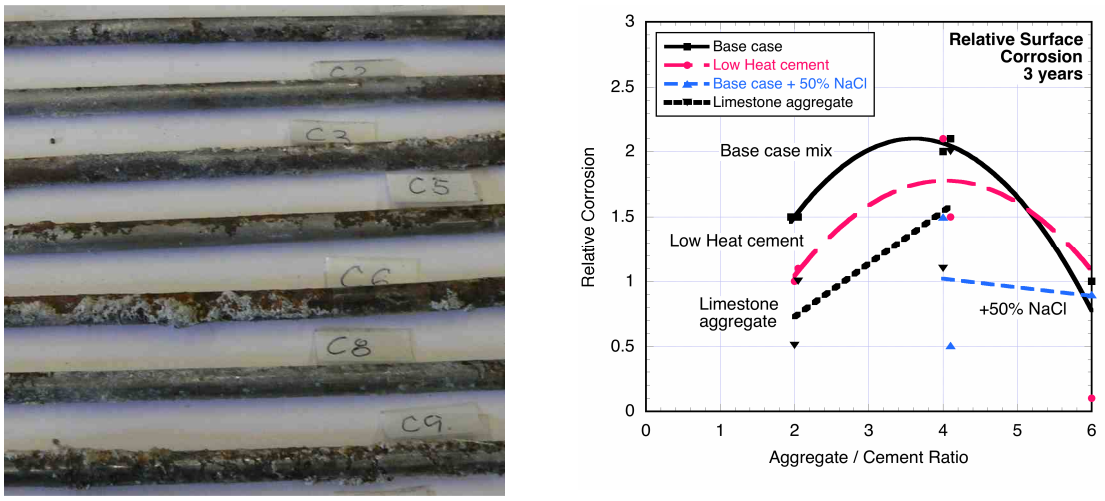

Figure 3. View of reinforcing bars (left) and relative corrosion rating (right) as a function of aggregate cement ratio showing effect of limestone aggregate, low heat cement and added salt [Melchers 2010b].

5 DISCUSSION

Chlorides in seawater (or in de-icing sprays) diffusing into the concrete conventionally are considered responsible for reinforcement corrosion. The use of seawater as mixing water for concrete has been prohibited since the 1960s. This was based, in part, on (short-term) laboratory findings [e.g. Shalon & Raphael 1959] that showed earlier corrosion initiation of steel bars in calcium hydroxide solutions when chlorides were present. Similar findings were obtained for realistic concrete samples made with seawater as mixing water (and for curing) when exposed to actual marine exposure conditions, at least within the first 3 years of exposure. But after 5 years this was not the case and after 10 years both the corrosion area and the average corrosion rates were about one third of those for concretes made with fresh waters [Boqi et al. 1983]. This is consistent with the field exposure observations at Arbroath.

The role of NaCl in the corrosion of steel has long been debated in the corrosion science literature [e.g. Schilling 2006]. Physical chemistry free energy considerations show that of all the possible reactions the conventional oxidation reaction of iron (Fe) with water (H_2O) and oxygen (O_2) is the most likely to occur. It does not involve NaCl - the chloride ions are 'spectators'. The primary rate-controlling step in the corrosion of steel in water is the rate at which the electron acceptor (usually oxygen) can reach the corroding surface. This does not depend, in a significant sense, on the salinity of the water, as shown both in laboratory and in field investigations [Mercer & Lumbard 1995, Melchers 2006]. To be sure, under low oxygen conditions $FeCl_2$ and other corrosion products involving chlorides may be produced, such as the chloride-bearing β-FeOOH [Waseda & Suzuki 2006]. Salt is hygroscopic and this may increase the 'time of wetness' for situations where the concrete cover is no longer effective.

The apparent positive influence of calcareous aggregates (shell fragments, calcium carbonate or non-reactive dolomite sand or aggregates, or blast furnace slag aggregates) has support in controlled corrosion science experiments [Davies & Burstein 1980]. Also, chemical thermodynamics show that increasing the alkali content delays corrosion initiation and reduces the rate of corrosion. The main issues can be summarized as [Melchers & Pape 2010]:

1. The alkalinity of the porewaters, that is, the buffering capacity of alkalis, determines when corrosion initiation will occur. Conventionally this has been associated only with the alkalinity derived from the reaction of the setting cement.
2. Laboratory studies show that (calcium) carbonate has a buffering effect and that higher concentrations of calcium carbonate inhibits the initiation of corrosion.

3. Under higher concentrations of (calcium) carbonate the presence of chloride ions does not have a strong influence on the initiation of corrosion.
4. Initiation of chemical reactions, including corrosion initiation, is determined by free energy considerations. When calcium carbonate can be involved in the chemical reaction there is the possibility to form protective $FeCO_3$ (siderite). It will tend to retain concrete pH at around 10.
5. Fundamental corrosion science, thermodynamics and field observations show that corrosion initiation cannot commence until the local pH has dropped below about 9.
6. The most likely mechanism for lowering of pH is leaching of the alkalis [Popovics, et al. 1983, Melchers & Li 2006]. Both KOH and NaOH are highly soluble. The low solubility of $Ca(OH)_2$ is increased by several orders of magnitude in saline conditions.
7. Outward alkali leaching is simultneous with inward diffusion of chlorides and governed by the same factors - concrete permeability and external surface washing. This may be the reason that most attention has been given only to the most obvious mechanism – chloride diffusion.
8. In marine environments the presence of calcium carbonate in concrete, usually attributed to 'carbonation' is much more likely to be the direct result of deposition since seawater is well-known to be (super-)saturated with carbonates. Evidently, this will inhibit oxygen diffusion.

It is considered that these points, taken together, go a long way towards explaining the various observations for long-term exposures of reinforced concrete structures in realistic environments, as opposed to results from short-term laboratory experiments. They also cast a new light on the role of chlorides and of carbonation in the corrosion of reinforcement steel.

6 CONCLUSION

Field and controlled laboratory observations show that alkali aggregates such calcium carbonate, non-reactive dolomite, or sands containing seashell fragments can add to the alkalinity of the concrete and delay the initiation and the rate of reinforcement corrosion, provided other deterioration mechanisms do not interfere. Moreover, calcium carbonate (cf. ‘carbonation’) does not lower the pH sufficiently immediately adjacent to the reinforcement to permit corrosion initiation. Additional mechanisms such as the leaching of alkalis must occur also. The chloride content immediately adjacent to the reinforcing bars has little effect on the time to active corosion since the progression of corrosion is governed by the rate at which oxidation can occur. In real seawaters this is inhibited by the build-up of carbonates.

ACKNOWLEDGMENTS

The support for this project provided by the Australian Research Council and by many people in industry and in various countries (acknowledged in detail elsewhere) is much appreciated.

REFERENCES

Boqi C, Dinghai H, Hengquan G. & Yinghao Z. 1983. Ten-Year field exposure tests on the endurance of reinforced concrete in harbor works, *Cement and Concrete Res.* 13: 603-610.

Cord-Ruwisch, R. 2000. Microbiologically Influenced Corrosion, *Environmental Microbe-Metal Interactions* D.R. Lovely (Ed.), Washington: ASM Press, 159-173.

Davies, D.H. & Burstein, G.T. 1980. The effects of bicarbonate on the corrosion and passivation of iron, *Corrosion* 36(8) 416-422.

Melchers R.E. 2006. Modelling immersion corrosion of structural steels in natural fresh and brackish waters, *Corrosion Science* 48(12) 4174-4201.

Melchers, R.E. 2010a. Observations about the time to commencement of reinforcement corrosion for concrete structures in marine environments, *Consec* 2010, Mexico, CRC Press, Boca Raton, 617-624.

Melchers R.E. 2010b. Observations about the performance of reinforcement in marine environments, *ASEC2010*, Sydney, CDROM.

Melchers, R.E. & Li, C.Q. 2006. Phenomenological modelling of corrosion loss of steel reinforcement in marine environments, *ACI Materials Journal*, 103(1) 25-32.

Melchers R.E. & Li C.Q. 2009a. Reinforcement corrosion initiation and activation times in concrete structures exposed to severe marine environments, *Cement and Concrete Research*, 39: 1068-1076.

Melchers, R.E. & Li, C.Q. 2009b. Reinforcement corrosion in concrete exposed to the North Sea for over 60 years, *Corrosion*, 65(8) 554-566.

Melchers R.E. & Pape T. 2010. Aspects of long-term durability of reinforced concrete structures in marine environments, *Medachs2010*, La Rochelle, 28-30 April 2010.

Mercer A.D. & Lumbard E.A. 1995. Corrosion of mild steel in water, *British Corrosion J*, 30(1) 43-55.
Nixon P.J. & Spooner D.C. 1993. Concrete proof for British cement, *Concrete* 27(5) 41-44.

Popovics, S., Simeonov, B. & Barovsky, N. 1983. Durability of reinforced concrete in seawater, *Corrosion of Reinforcement on Concrete Construction*, Ellis Horwood, Chichester, 19-38.

Shalom, R. & Raphael, M. 1959. Influence of sea water on corrosion of reinforcement, *Journal of the American Concrete Institute*, 30(12) 1251-1268.

Schilling M. 2006. Soluble salt frenzy - junk science, *Corrosion & Materials*, 31(5) 10-15.

Waseda Y. & Suzuki S. (Eds) 2006. *Characterization of Corrosion Products on Steel Surfaces*, Springer, Berlin.

XII DBMC
International Conference on Durability of Building Materials and Components
PORTO - PORTUGAL, April 12th-15th, 2011

Moisture Effects in Externally Strengthened Concrete

Antonio Bonati [1]
Vittorio Galimberti [2]

ABSTRACT

An investigation was recently carried out at the ITC-CNR[3], to study the influence of moisture on the mechanical performance of two externally strengthened systems applied on concrete: i.e. Carbon fibre reinforced polymers (C-FRP) and fibre reinforced cementitiuos mortars (FRCM). Several samples were prepared and subjected to long-term conditioning and thereafter bending and shear tests were completed at specific times. A new method for measuring relative humidity and temperature in small cavities located inside samples was also developed that allowed gaining useful data about the conditions at the zone. Results showed both the real risk of reduced performance in case of the presence of moisture at the interface for extended periods time and a comparison amongst the different performances of the strengthening systems analysed in the study.

KEYWORDS

Carbon fibre, Carbon fibre reinforced polymers, Fibre reinforced cementitious mortars, Moisture influence.

1 Engineer, researcher at ITC-CNR, S. Giuliano Milanese, (Milan) ITALY, antonio.bonati@itc.cnr.it
2 Architect, researcher at ITC-CNR, S. Giuliano Milanese, (Milan) ITALY, vittorio.galimberti@itc.cnr.it
3 Construction Technologies Institute of The Italian National Council of Research – S. Giuliano Milanese (Milan) ITALY, www.itc.cnr.it

1 INTRODUCTION

Carbon fibre reinforced polymer (C-FRP) systems have been used for several years in the field of structural repair of buildings and engineering works, whereas fibre reinforced cementitious mortar (FRCM) systems have been employed only more recently with the same purpose. Although it is well known that due to high-humidity environments and where such repair systems may be in contact with water for extended periods of time, the externally strengthened repair system for structural elements and made of C-FRP, may change chemical and physical characteristics and thereby also affecting the mechanical resistance of the overall structure. This in turn, may bring about a decrease in resistance should be bond between the repair system and structure deteriorate. In this regard there is only few data that are available for FRCM systems. To verify and quantify the extent of such degradation phenomena on externally strengthened repair systems a new research study was carried out at the ITC-CNR in 2010.

2 METHODS FOR HUMIDITY MEASUREMENT OF INTERFACE AREA IN EXTERNALLY STRENGTHENED CONCRETE

The common epoxy resins used for fibre reinforced polymer (FRP) plate applications in building restoration may absorb more or less 5% of water by weight: as a consequence, plastic deformation is generated and may lead to a loss of adhesion between strengthening element and support; this aspect has been widely investigated in recent years especially in the case of C-FRP, [Nguyen *et al.* 1998]. Before starting to evaluate water absorption influence on mechanical performance of C-FRP and FRCM systems, it was decided to develop methods for T and RH measurements at the interface zone, between strengthening element and support, to gain useful information on how humidity change over the time. Thus, after having evaluated different technical devices, the following two methods were adopted (Figure 1):

- Method “A” , developed at ITC-CNR, used to obtain temperature and relative humidity (T; RH) of the air at the interface zone of the externally strengthened concrete reference samples; this was achieved by inserting a pipe during the preparation of samples to create an air gap at the zone of interest (Figure 2).
- Method “B”, used to obtain T and RH of the air at the zone of debonded concrete, after having removed the external strengthening element from the concrete samples that had been subjected to mechanical resistance tests [Ouyang and Baolin 2006].

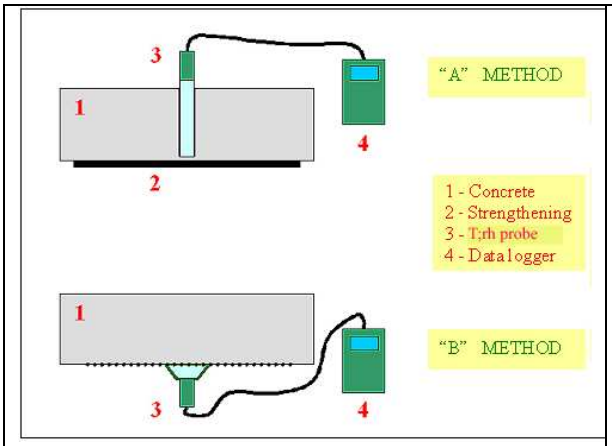

Figure 1. T and RH Air measurement methods at interface between concrete and strengthening system.



Figure 2. Sample with PVC tube inserted before pouring concrete in the mould.

2.1 Method "A": Air T and RH Measurements at Internal Interface of Sample

Reference samples, with the same characteristics of similar samples prepared for mechanical tests, were prepared inserting a PVC cylindrical pipe (20 mm internal diameter; 150 mm length), during the casting of concrete, a few mm away from the bottom: in such a way it was possible to connect the top of the tube of each reference samples with the "T and RH probe" of a data logger. The measurements were settable in continuous or discontinuous mode in relation with the expected speed of the phenomenon being monitored.

2.1.1 T and RH measurements

In Table 1 are included all types of samples monitored in different lab environments by continuous measurements of air in small cavities (Method "A") to find out the speed increase of T and RH and the minimum time needed to gain saturation condition at strengthening element-support interface.

Table 1. List of measurements using Method "A": continuous measurements of T and RH of air in small cavities of samples placed in different lab environments (°C; %RH).

A - Concrete sample in air (23°C; 100% rh)
B - Concrete sample + C-FRP in air (23°C; 100% rh)
C - Concrete sample + FRCM in air (23°C; 100%rh)
D - Concrete sample + C-FRP in air (40°C; 100% rh)
E - Concrete sample + FRCM in air (40°C; 100%rh)
F - Concrete sample in water (23°C)
G - Concrete sample + C-FRP in water (23°C)
H - Concrete sample + FRCM in water (23°C)
I - Concrete sample + C-FRP in water (40°C)
L - Concrete sample + FRCM in water (40°C)

2.2 Method "B": Air T and RH Measurements on External Surface of Samples

This method, developed to measure T and RH on the external concrete surface after delaminating caused by bend tests or shear tests, was usefully adopted in this experimentation even though it was slightly modified; the main reason to use the Method "B" was not only to have measurements after mechanical tests but also to verify the measurements taken on similar samples by the Method "A". The process has to be started with the complete removal of the external strengthening element, usually broken after mechanical test; then the sample has to be wrapped with polyethylene film and kept at room conditions with the same T and RH values as the test room; as soon as possible a little cut has to be made on the film to allow the entry of the probe; T and RH measurements have to be recorded right after sealing.

2.3 Results on Confined Air T and RH Measurements (Method "A")

A great number of data were collected from several measurements campaigns and this allowed outlining the hygrothermal behaviour over the time of samples in different ageing conditions (Figs. 3 and 4). From the data processed it was possible to compare T and RH air measurement at the interface zone in similar samples, one partially immersed in water and the other placed in a conditioned room: in the former case it was observed that the migration of humidity was much faster than in the latter.

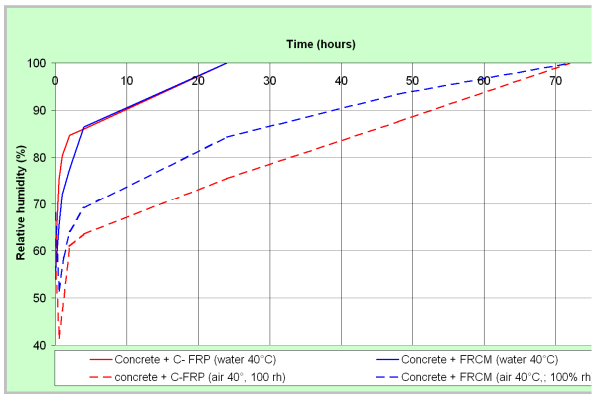

Figure 3. T and RH measurements of air at interface region (Method "A"): samples partially immersed in water (40°C) compared with samples in air (40°C and 100%RH).

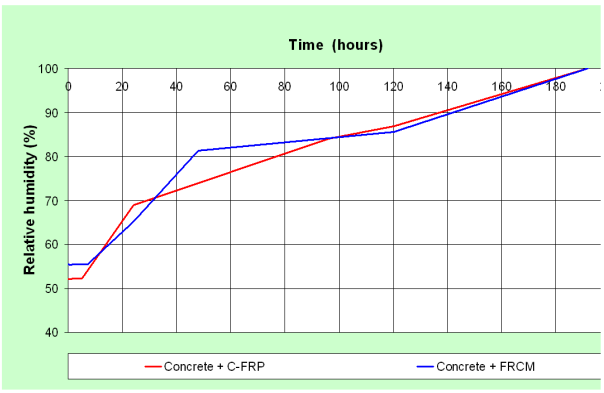

Figure 4. T and RH measurements of air at interface region (Method "A"): samples partially immersed in water (23°C).

3 METHODS AND TIME PERIODS FOR AGEING OF SAMPLES

As stated above, on the basis of T and RH measurements at interface region (Method "A") of reference samples, it was possible to choose both methods and ageing time periods, to establish the plan for ageing all the samples with C-FRP and FRCM. Precisely, concerning the speed variation of relative humidity observed at the interface, it was decided to draw attention to the time needed to have samples with saturation at interface region (air RH=100%).

The samples were put in the following accelerated ageing conditions before being subjected to mechanical tests:

- Partial immersion of samples in water at a given temperature (Figure 5);
- Positioning of samples inside a room at defined values of temperature and relative humidity.

After the curing periods (see §4) all the samples were positioned at different lab environments as specified in Table 2. The main condition adopted for ageing the sample was the partial immersion in water, that, even though a similar situation seems to be rather unusual on site, nevertheless it was a fast way to reach the same result obtainable by positioning samples in a room at defined values of temperature and relative humidity for a long time.

Table 2. Methods and time periods for ageing strengthened concrete samples.

Concrete samples + C-FRP		Concrete samples + FRCM	
Ageing conditions	Days	Ageing conditions	Days
Water (23°C)	5	Water (23°C)	5
Water (23°C)	9	Water (23°C)	9
Water (23°C)	40	Water (23°C)	40
Water (23°C)	74	Water (23°C)	74
Water (23°C)	74	Water (23°C)	74
+		+	
Air (23°C and 50% rh)	30	Air (23°C and 50% rh)	30
		+	
		Water (23°C)	5
Water (30°C)	5	Water (30°C)	5
Air (30°C and 100% rh)	9	Air (30°C and 100% rh)	9
Water (30°C)	74	Water (30°C)	74
Water (30°C)	74		
+			
Air (23°C and 50% rh)	30		
Water (40°C)	4	Water (40°C)	4
Air (40°C and 5% rh)	4		

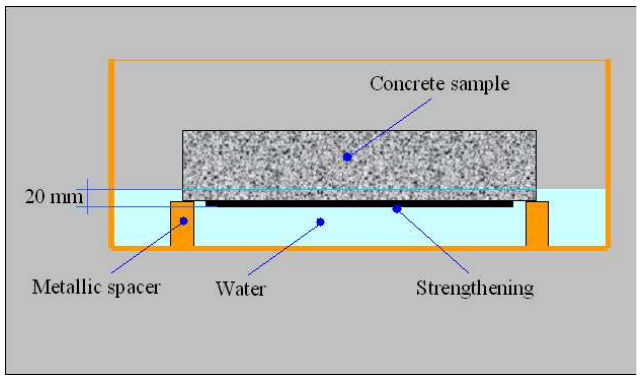

Figure 5. Outline of tank with water for partial immersion of samples.

4 CONCRETE SAMPLES

In relation with the high number of test deadlines and with a minimum number of 3 samples per test, the following samples were prepared:

- **48** concrete samples (60 x 15 x 8 cm) with C-FRP external strengthening for bend tests (primer, epoxy resin, carbon fibre fabric);
- **45** concrete samples (30 x 15 x 15 cm) with C-FRP external strengthening for shear tests (primer, epoxy resin, carbon fibre fabric);
- **48** concrete samples (60 x 15 x 8 cm) with FRCM external strengthening for bend tests (fibre reinforced cement mortar, PBO mesh;

After a 60-day curing period all the concrete samples were completed with strengthening applications and kept for a further 60 days in the same lab conditions (23°C and 50% RH).
Some samples of each type described above were also equipped with PVC pipes (see §2.1) to have confined air T and RH measurements at interface region by the Method "A" (see §2.3).



Figure 6. Example of concrete samples, for bend tests, with C-FRP (above) and with FRCM (below).



Figure 7. Example of concrete sample with C-FRP protruding plate for shear test.

5 MECHANICAL RESISTANCE TESTS

Both the undisturbed samples kept at room conditioning (23°C and 50% RH) and aged samples (see Table 2) were subjected to the following tests for each test deadline:

- Bend test;
- Shear test (only for C-FRP samples).

Just to avoid unwanted interference in collected data, all the tests were conducted inside a conditioned room with T and RH similar to the conditions used to age the test samples. Special care was taken during the handling of samples from ageing room to test room. The apparatus for mechanical tests (Figure 8), placed in the conditioned test room with the main aim to have the possibility to perform both bond and shear tests consecutively. Test management control unit and data acquisition unit were placed outside the test room while samples were visible from the room's window during the tests. The following elements were used to assemble the apparatus: high-stiffness metal frame, dual hydraulic piston with stroke up to 200 kN with load cell up to 300 kN commanded by appropriate controller, load cell up to 50 kN (placed directly in contact with the sample under test), displacement transducers, loads and displacements/deformation capture unit. In the case of shear test, the load, generated by the hydraulic piston, was transmitted horizontally to the sample by pulley and steel cable.

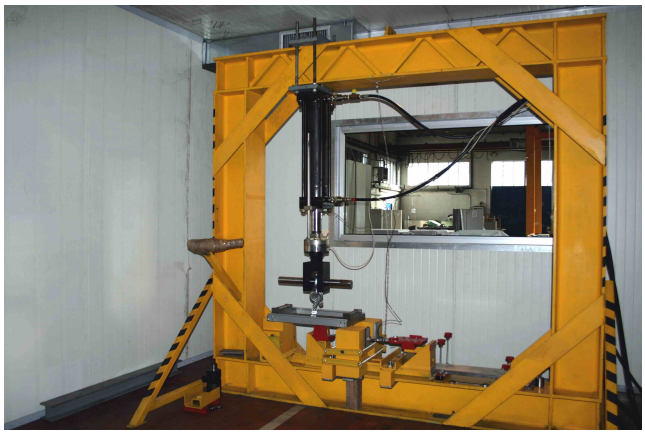

Figure 8. Apparatus for bend and shear tests.

5.1 Bend Test

The samples were subjected to 3 point flexural testing (Figs 9 and 10). At the end of the test, observations were made on how the sample had broken, pictures were also taken and, when necessary the air T and RH of the sample was measured using the Method "B", after all the strengthening elements had been removed.

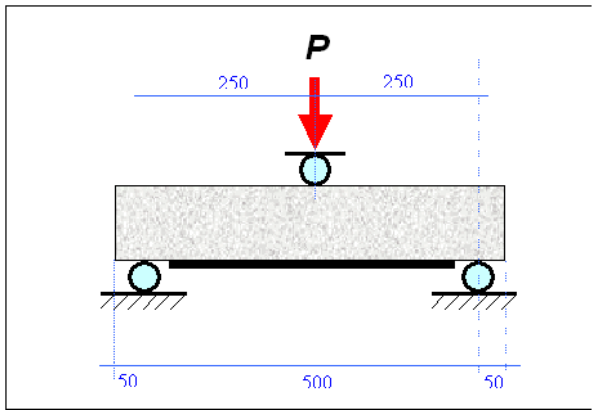

Figure 9. Outline of 3 point flexural test.



Figure 10. Bend test of a concrete sample externally strengthened by FRCM.

5.2 Shear Test

The test was developed at ITC-CNR and based on the principle of coplanar traction to the sample (Figs. 11 and 12) a concrete block with a partially protruding strengthening element. Once the sample was placed on the metallic adjustable support, the C-FRP had to be aligned with the line of load transmission by means of a laser levelling instrument; the rear of the sample had to be fixed with anti-tip lock device to avoid overturning, while the protruding C-FRP plate had to be locked by bolts in clamping metal plates; finally the torsional stability device had to be placed. After maximum load threshold and load gradient/displacement gradient were set, the data acquisition unit test was started and finally the application of load was also started. At the end of the test, observations had to be conducted on how the sample had broken and pictures were also taken; when necessary all the strengthening element was removed and sample surface was subjected to T and RH measurements on the externally air using Method "B".

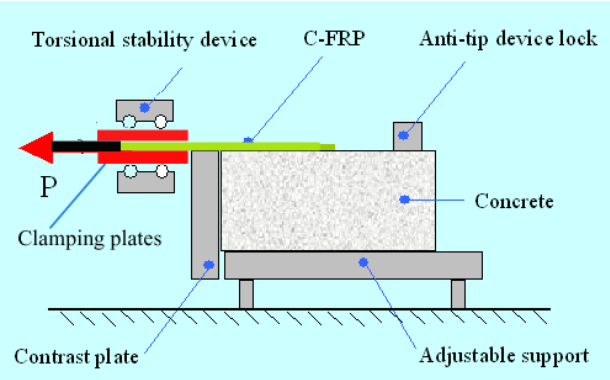

Figure 11. Outline of shear test.

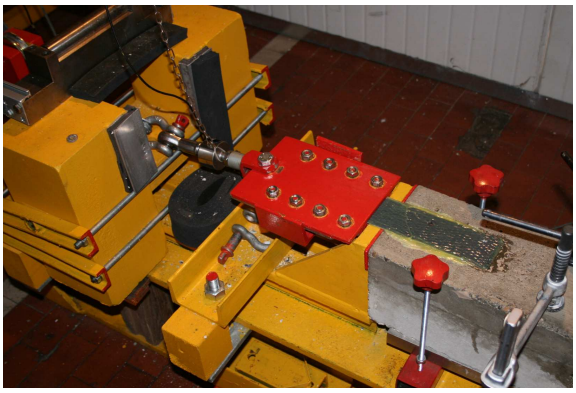

Figure 12. Concrete sample Shear test with C-FRP plate.

5.3 Bend and Shear Tests Results

As the research is ongoing and has still to be finished, is not possible at present to show all the processed data, thus in the following paragraphs the focus will be placed on the type of degradation observed in relation with the mechanical performance of the samples.

5.3.1 On bend tests - concrete samples with C-FRP plates

Obviously, the best bending performance was noted in undisturbed samples with breaking of "cohesive" type in strengthening elements: during the test C-FRP were separated from the concrete blocks and thin parts of concrete were embedded (Figure 13); instead, lower values of bending resistance were obtained in the case of "adhesive" detachment, that is when there was a clear separation at the support-strengthening element interface (Figure 14) both with samples maintained partially immersed in water for a long time period, and with samples aged inside the room with air at saturation conditions (T≥30°C and 100% RH).



Figure 13. Example of "cohesive" breaking of C-FRP due to bend test.



Figure 14. Example of "adhesive" breaking of C-FRP due to bend test.

5.3.2 On shear tests - concrete samples with C-FRP plates

The same phenomena described above for bend tests is valid for the evaluation of shear resistance results: it was noted that the reduction percentage of mechanical strength shear, due to the effect of prolonged saturation at the interface between strengthening element and support, was in line with the results of mechanical strength bending of wet samples.

5.3.3 On bend tests - concrete samples with FRCM plates

Conditioning in water caused a decrease in resistance at short exposure period time which retrieved gradually until it reached or exceed the initial values. Visually (Figs. 15 and 16) it was observed that the break had occurred nearly always in the same way, that is cohesive breaking in strengthening element (inside the mortar close to the mesh). By analysing data, still to be fully processed, it has emerged that the tested FRCM were insensitive to environmental parameters (T and RH) in the long run.



Figure 15. Undisturbed concrete-FRCM sample broken by bend test.



Figure 16. Concrete-FRCM sample broken by bend test after partial immersion in water for 74 days.

6 CONCLUSIONS

The processing of data is still in progress and at present, it is not feasible to show all details of the results. Nevertheless we can already anticipate that, in principle, the FRCMs that were tested were less sensitive to the imposed ageing conditions which led to saturation at the interface between the strengthening element and support as compared to the C-FRPs that were tested. It should also be mentioned that the first tests of reversibility showed that C-FRPs seem to resume at least some of their initial performance characteristics.

Experimentation is coming to an end and we are firmly convinced that this will lead to detailed analyses in support of what has already been observed in qualitative terms. A further phase of investigation will soon be started both on FRCM and concrete samples with FRCM in order to better define and limit of those variables affecting, weakening in the short term that were observed to occur after a short period of partial immersion in water.

REFERENCES

Ouyang, Z., Baolin, W. (2005), "*Bond Deterioration Between CFRP Plate and Concrete after Exposure to Moisture*", DCEE, Marquette University, Milwaukee, Wisconsin USA.

Nguyen, T., Byrd, .W E., Alsheh, D., et al. (1998), "*Water at the Polymer/Substrate Interface and its Role in the Durability of Polymer/Glass Fiber Composites/Durability of Fibre Reinforced Polymer (FRP) Compisites for Construction*" (CDCC'98) Proceedings of the 1st International Conference, Canada, 1998: 451-462.

XII DBMC
International Conference on Durability of Building Materials and Components
PORTO - PORTUGAL, April 12th-15th, 2011

Durability of Glass Fibre Reinforced Polymer (FRP) Materials in Concrete – Effect of Carbonation on Bond Strength

S. Demis [1]
V.G. Papadakis [2]

ABSTRACT

The research community agrees on that corrosion of reinforcing steel, due to the diffusion of carbon dioxide from the atmosphere and ingress of chloride ions (in combination with seismic loading) is the predominant factor responsible for premature concrete deterioration observed in a wide range of structures in the last decades. New technologies such as FRP increase the choice available to engineers for corrosion resistance solutions in aggressive environments. However, given the concerns expressed in some cases, on the effect of concrete alkalinity on certain types of FRP bars, the effects of environmental corrosion (through accelerated carbonation) on the bond properties of fibre reinforced polymer (FRP) bars with the surrounding concrete are presented in this paper, as part of an extensive project addressing the durability of FRP in concrete in environments of different initial alkalinity.

It was found out that, contrary to what is generally believed, concrete alkalinity does not have a major impact on the durability of FRP bar and its bond strength. Carbonation had a considerable effect on concrete strength, increasing the strength of carbonated concrete. Until the carbonation front reaches the FRP bar, no significant deterioration of bond took place. Soon after the carbonation front reaches the bar, a relative deterioration of bond was observed. However, the observed bond deterioration is more than compensated by the increase in strength due to time and carbonation, contrary to steel reinforcement, hence there is no need to take into account the carbonation effect on the stress reduction factors used for durability design.

KEYWORDS

FRP, Carbonation, Concrete, Durability, Bond strength.

[1] Civil & Structural Engineer (Ph.D., MSc.Eng) Durability Consultant, Patras Science Park, Patras, Greece, demis@psp.org.gr
[2] Associate Professor, Department of Environmental and Natural Resources Management, University of Ioannina, Agrinio, Greece, vgp@psp.org.gr

1 INTRODUCTION

It is a widely accepted fact that corrosion of the steel reinforcement, impairs not only the appearance of a structure, but also its strength and safety due to the reduction in the cross-sectional area and on the mechanical properties of the reinforcement and also due to the subsequent deterioration of bond with the surrounding concrete [Lundgren 2007; Fang et al. 2004]. Bond between reinforcement and concrete is of paramount importance to ensure the composite interaction of the two materials. A number of investigations have been undertaken to investigate the influence of corrosion on bond capacity [Lundgren 2007; Fang et al. 2004, 2006a, 2006b]. Conclusions on how a certain level of corrosion affects bond to a certain degree vary quite a lot, but the general trend observed is a small initial increase in bond strength with corrosion, due to an increased frictional component of bond caused by the radial stresses applied from the corroded bar to the surrounding concrete, , followed by a considerable decrease (caused in general by longitudinal cracking). Ways to overcome the above mentioned problem, by utilising traditional methods (of reducing the risk of reinforcement corrosion) do not always guarantee corrosion free steel for the service life of a structure [Demis 2007]. No system provides an ideal cost-effective solution to corrosion and the various techniques available might add further complications to the future maintenance requirements and expected service life of the structure. New technologies such as FRP increase the choice available to engineers for corrosion resistance solutions in aggressive environments.

FRP are composites comprising of at least two materials, fibres which act as reinforcement and polymer binders. The purpose of the polymer is to integrally bind the fibre reinforcement together so as to distribute external loads to the fibre via bond, whilst protecting it from adverse environmental effects [Demis 2007].

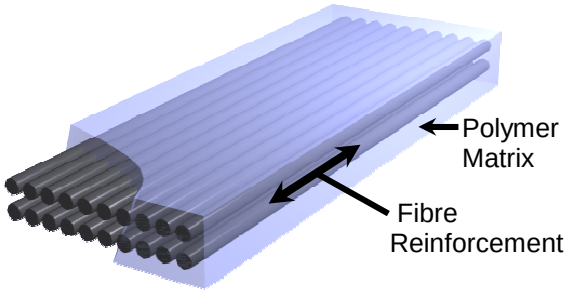

Figure 1. Schematic diagram of a Fibre Reinforced Polymer.

There are currently a number of FRP reinforcing bars commercially available, composed of carbon, glass or aramid fibres within polyester or vinylpolyester-epoxy resins, manufactured using a number of techniques, with pultrusion being the most common [Demis 2007]. FRP rods have different properties and mechanical characteristics from conventional steel. The mechanical properties vary from one product to another, depending mainly on the nature and volume of fibres, the shape of the cross section and the resin. Great electromagnetic neutrality, corrosion resistance and tailored design are some of the advantages compared to steel reinforcement. FRP rods develop greater tensile strength than the steel bars, depending on the nature of the fibres and have strength to weight ratio of up to 10 times that of steel. Bond of FRP to concrete is different to that of steel. In the case of steel reinforcement, mechanical interlocking due to the bar lugs against concrete provide the necessary interaction [Achillides & Pilakoutas, 2004; fib, 2000]. However, in the case of FRP, once chemical adhesion is overcome, bond with concrete is usually achieved mostly through friction [Demis 2007].

Concerns have been raised for the effect of concrete alkalinity on certain types of FRP bars. It is believed that particular types of FRP composites can be damaged by chemical attack of the alkaline environment of cement and by the growth of hydration products between fibre filaments [Karbhari et al. 2005; Yilmaz et al. 1992]. The implication of this is that whilst these materials may perform well structurally in the short term, they may well still degrade in alkaline concrete environments.

Considering that although significant steps have been taken on understanding and modeling the physiochemical processes and mechanisms which lead to the reduction of the service life of a reinforced (with conventional reinforcement) concrete structure, including the development, verification and utilization of proven predictive tools for the estimation of service life under harsh environments [Papadakis et al. 1991, 2007], in the case of FRP reinforcement, the effect of the above mentioned mechanisms have not been examined to such an extend. The key question that has not been answered until now is what is the rate at which this deterioration takes place and how this is affected by the pH level of the concrete.

On that note, an extensive project addressing the durability of FRP in concrete, under different conditions of initial alkalinity, aiming to develop test methods and predictive models was undertaken [Demis 2007]. A part of this work , the effect of low alkalinity (an important factor for the initiation of corrosion) through the use of cement replacement materials and accelerated environmental carbonation, on the bond strength of FRP bars, is briefly presented in this study.

2 EXPERIMENTAL METHODOLOGY

Pull-out concrete cubes (150 mm), made from Portland Cement (CEM I) and pozzolanic cement replacement materials (30% fly ash and 70 % blastfurnace slag), with a centrally embedded glass FRP bar, were immersed in an accelerated environmental carbonation facility for a period of 2 years. A large-scale computerised controlled carbonation tank was designed, manufactured and calibrated by the author, for the purpose of this study [Demis 2007] (CO_2 15%, RH 55%). The bond strength of the specimens was determined at different time intervals. The compressive strength of the tested concrete and its carbonation development were also monitored at each testing age. In addition to the use of phenolphthalein indicators on concrete prisms carbonation growth was also evaluated relative to the position of the embedded FRP bar using pull-out samples [Demis 2007].

3 RESULTS

An initial observation is that bond increased with exposure time for every environment (Figure 2a). The observed gain in bond, since the quality of the embedded FRP bar does not improve, can only be attributed to the effect of the environment surrounding the bar, hence to the obvious factor improving with time, the concrete compressive strength. Relationships that correlate bond strength to concrete tensile strength can be found in most European Codes [Demis 2007; Demis et al. 2007]. Tensile concrete strength is also related to the concrete compressive strength, through empirical equations. As a result, the relationship between the concrete compressive strength and bond strength, can be easily determined. Using the Eurocode 2 [2004] previously briefly mentioned relationships, the measured bond strength results were normalized to a common compressive strength, according to Equation 1:

$$f_{b,n} = f_b \cdot \left(\frac{f_{c,m28d}}{f_{c,m(t)}} \right)^{2/3} \quad (1)$$

where, $f_{b,n}$ is the normalized bond strength (MPa), f_b the measured bond strength (MPa), $f_{c,m28d}$ the mean 28 day concrete compressive strength (MPa) and $f_{c,m(t)}$ the mean concrete compressive strength on the day of testing.

It was seen (Fig. 2b) that although bond strength increased for all concrete environments used (carbonated or not), the non-carbonated (control) samples exhibited the biggest increase.

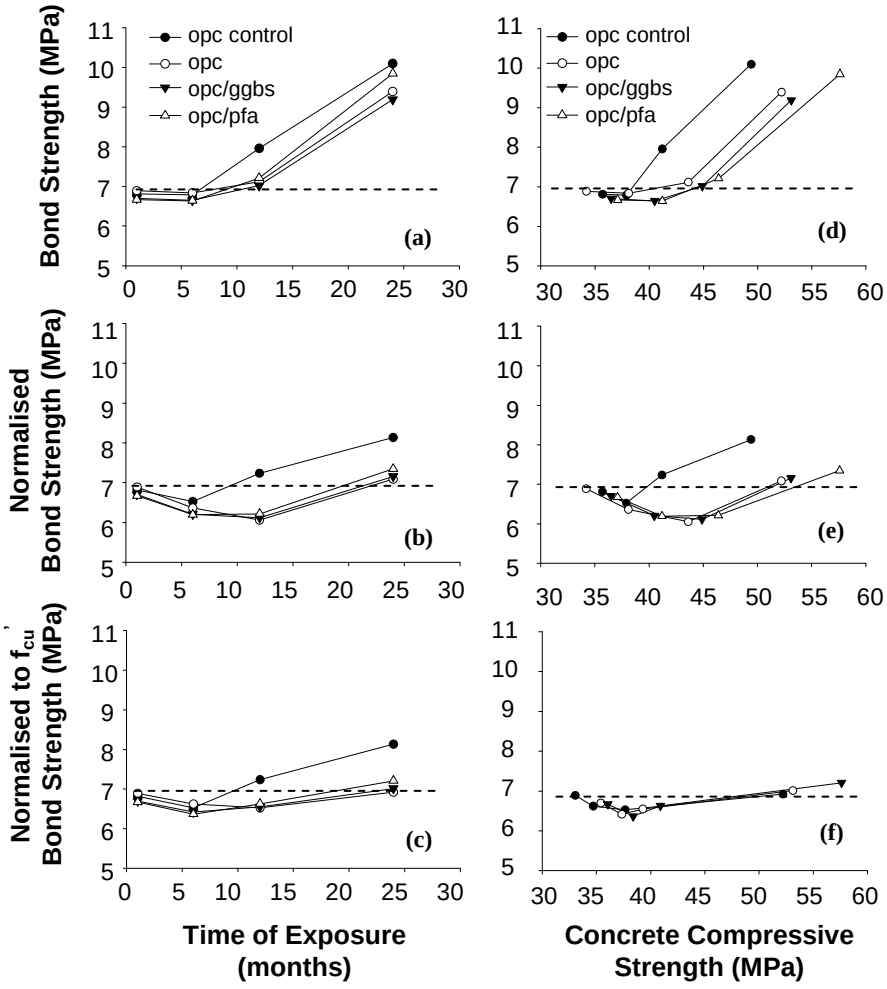

Figure 2. Bond Strength Development.

Investigating the effect of carbonation on the concrete compressive strength, it was found that carbonation increased the compressive strength of concrete by around 15 % (Fig. 3).

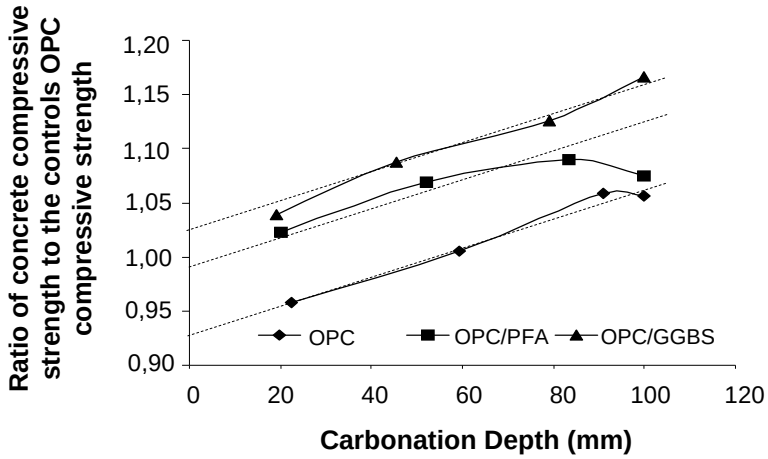

Figure 3. Cube compressive strength of carbonated cements vs carbonation growth.

However, this increase in strength is confined in the part of the concrete that is carbonated. Since the bond of the bar is influenced by concrete strength, then the effect of carbonation away from the bar should be taken out of the equation. A new concrete strength of the carbonated samples around the bar (f_{cu}') was calculated by subtracting the carbonation effect (until the carbonation front reaches the bar) as:

$$f_{cu}^{'} = f_{cu(t)} - \left(0.15 \cdot f_{cu(t)} \cdot \frac{d_{pr}}{100} \right) \quad (2)$$

Where, d_{pr} is the carbonation depth measured on a concrete prism, and $f_{cu(t)}$ is the compressive concrete strength at age (t).

To help decouple the effect of compressive strength, the mean values of bond strength versus the cube compressive strength are shown in Figs. 2d-f. It can be seen that the initial gain in compressive strength does not influence the bond strength, but the gain in strength after 12 months has a significant impact (Fig. 2d). By adopting the classical normalization of bond strength with respect to concrete strength (see Fig. 2e), a decrease in bond strength is noted following the initial gain in compressive strength. This is surprising since it goes against what is expected and may indicate a chemical deterioration mechanism. When bond strength is normalized with respect to the revised concrete compressive strength this reduction is almost eliminated (Fig. 2f). Bond increases marginally after 6 months, with respect to the concrete compressive strength. It can be concluded that the increase in bond strength obtained in the experiments can be attributed entirely to gain in compressive strength in the region of the bar. However, in comparison with the OPC (control) samples (Fig. 2c) there is a relative loss of bond strength. The reasons for this behavior and the relative differences in bond strength between the carbonated and the uncarbonated samples suggest a chemical mechanism of deterioration. Using ANOVA analysis (Table 1) to examine the statistical validity and significance of the key parameters in this investigation, crucial conclusions were made.

Table 1. ANOVA Statistical analysis of key parameters.

Source of Variation	Sum of Squares (SS)	df	Mean quare (MS)	P-value	F_A	$F_{critical}$	$F_A / F_{critical}$
Mean values of normalized bond strength							
Time of Exposure	1.49	3	0.49	0.011	6.69	3.86	1.73
Cement Type	0.66	3	0.22	0.089	2.98	3.86	0.77
Analysis of the mean values of the normalized bond strength							
Time of Exposure	4.58	3	1.53	0.004	5.19	2.90	1.79
Cement Type	2.03	3	0.68	0.096	2.30	2.90	0.79
Values up to 6 months of the control and normalized carbonation bond strength (carbonation has not yet reached the FRP bar)							
	0.07	3	0.02	0.665	0.57	6.59	0.09
Values after 6 months of the control and normalized carbonation bond strength (carbonation reached the FRP bar)							
	1.19	3	0.40	0.243	2.09	6.59	0.32
Values between and after carbonation of bond strength (comparison of bond strength values before CO_2 reached the FRP bar with the bond strength values after CO_2 reached the bar)							
	1.99	1	1.98	0.021	5.67	4.05	1.4

SS is a measurement of the variability of the dependent variable (bond strength in this study), *dF* is the degrees of freedom of the analysis, representing the number of observations of the variables in the analysis, *MS* is a measurement of the variance of the population of the analysis (of the total number of samples), F_A is a measurement of the contribution of the independent variables (time of exposure, cement type) in predicting the dependent variable (bond strength), *P* is the probability of being wrong in concluding that there is an association between the dependent and independent variables (the smaller the *P* value, the greater the probability that there is an association).

ANOVA aims to identify the effect of different parameters in a comparative manner. If the value of F_A (as described on the footnote of Table 1) is greater than a critical value $F_{critical}$, or P-value is less than 0.05, then that particular parameter is of significance and should be taken into account through a mathematical model.

As expected the time of exposure was found to have significant effect on bond (since the concrete strength increases with time), contrary to the effect of the cement type/initial alkalinity that was found to be marginally insignificant. Comparing the bond strength values between the control and the carbonated specimens, before and after carbonation, a significant statistical difference was found, indicating chemical deterioration once the carbonation front reaches the FRP bar. This is a key finding and two models are required to predict this behavior. One model for the prediction of the penetration of the carbonation front and another model for the estimation of the effect of carbonation on the bond strength.

Using equations that describe the growth of the carbonation front in the carbonation tank in the form of $d=K\cdot t^{1/2}$ (where "d" is the carbonation depth and "t" is the time of exposure), the time (months) of accelerated exposure that carbonation reached the FRP bar was estimated [Demis 2007]. Combining these equations with an effective time scale [Demis 2007], the time needed for carbonation to reach the position of the embedded FRP bar was calculated in real exposure time (years of natural exposure). Using the experimental data of bond strength, the relative bond strength retention (t_R) in time of exposure (years) after carbonation reaches the bar was estimated. The expected bond strength (t_{exp}) as increased with time due to the increase of concrete compressive strength was calculated according to Eurocode 2 [Demis 2007], by taking into account the gain in compressive strength due to both time and carbonation (15 % increase). In this way the expected bond strength due to the effect of carbonation was calculated as ($t_{exp}\cdot t_R$). Finally the total bond strength retention in time ($t_{R\ total}$) was estimated as the ratio of ($t_{exp}\cdot t_R$) after carbonation reached the bar to the ($t_{exp}\cdot t_R$) before carbonation reached the bar, and it is shown in Fig. 4, for different concrete cover depths.

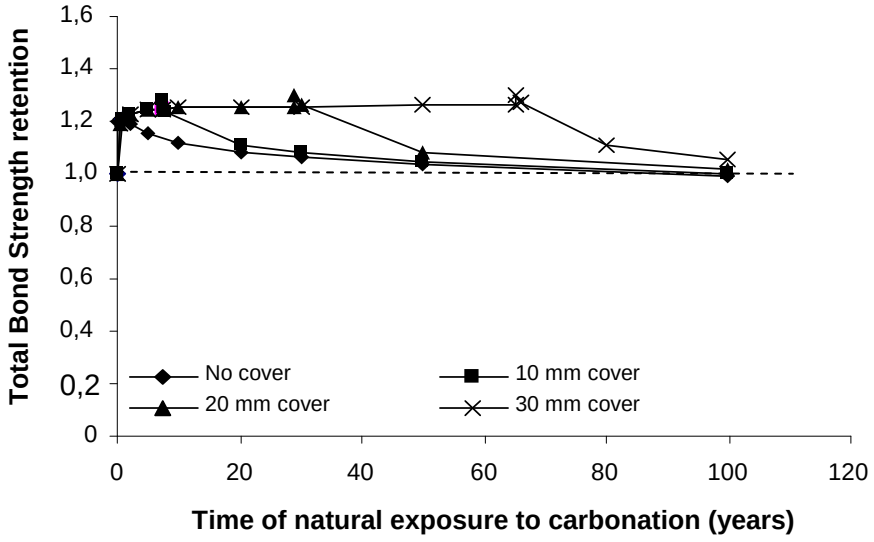

Figure 4. Total bond strength retention.

It is evident from the above figure that the negative effect of carbonation is counteracted by the gain in strength with time.

4 DISCUSSION

This work has shown that until the carbonation front reaches the FRP bar, despite differences in concrete alkalinity, no significant deterioration of bond takes place. Once the FRP is covered with

concrete, the free moisture reduces and its adverse effects are mitigated. For concrete kept at moisture, of around 55 %, the adverse effects of moisture on FRP bond to concrete outstripped the beneficial effects of increasing concrete strength only marginally during the first 6 months. This was true for all concretes used. Since the three concretes started with different pH values, but behaved similarly up to the point of carbonation means that the alkalinity did not play a major influence on the bar strength. In fact, the OPC which has the highest alkalinity exhibited less normalized bond reduction than the blended cements. Additional evidence that concrete alkalinity does not deteriorate the FRP by itself is given by the samples after carbonation reached the FRP bar. At this stage alkalinity drops from a pH value of 12.5 – 13.6 down to a pH of around 9. Despite the significance drop in alkalinity, the carbonated samples for all concretes showed a relative normalized bond deterioration. The carbonation process, is also responsible for reducing the permeability of concrete and that again should have reduced any alkali attack.

Since it has been established above that alkalinity does not have a major impact on FRP bond, the impact of carbonation has to be viewed with respect to the other processes that are taking place. The first major impact is on concrete strength. The gain in strength can be associated with the formation of $CaCO_3$ and to some extend to the release of moisture which can lead to further hydration. The strength gain has been attributed only to carbonated regions and has been eliminated from the bond strength through normalization with compressive strength, in the same way as the effect of time has been taken into account.

It was found out that soon after the carbonation front reaches the bar, a relative deterioration of bond takes place. This deterioration can be attributed to the detrimental effect of $CaCO_3$ crystals that penetrate into the FRP surface and can damage both the resin and the glass fibres. The incorporation of blended cements, that facilitate the formation of C-S-H gel, assists in the deterioration of the fibres. That is despite the fact that their carbonation proceeds at a slower rate than the carbonation of calcium hydroxide in OPC. It has been suggested that C-S-H is responsible for dissolution and thus degradation of the glass fibre [Demis 2007]. Their refined pore structure does not contribute as much as expected in lessening the carbonation attack. A relative decrease of 11.4 % in normalized bond was noticed on carbonated OPC/PFA samples, compared to 13.7 % and 14.8 % on OPC/GGBS and OPC carbonated samples, respectively. Hence the conclusion that carbonation operates as a switch on the deterioration of FRP can be made.

5 CONCLUSIONS

No significant difference in the relative bond behaviour of FRP bars was observed between the different concretes, neither in the pre- nor post-carbonated state. Hence, contrary to what is generally believed, it is concluded that alkalinity does not have a major impact on the FRP bar and its bond. Carbonation had a major impact on concrete strength, increasing the strength of carbonated concrete. Until the carbonation front reaches the FRP bar, no significant deterioration of bond takes place. Soon after the carbonation front reaches the bar, a relative deterioration of bond takes place. It was out found that the expected bond deterioration due to carbonation is more than compensated by the increase in strength due to time and carbonation, contrary to steel reinforcement. Hence there is no need to take into account the carbonation effect on the stress reduction factors used for durability design.

ACKNOWLEDGMENTS

A great amount of gratitude goes to Professor Kypros Pilakoutas and to the late Dr. Ewan Byars, for their extremely significant contribution, guidance and support provided throughout this project.

REFERENCES

Achillides, Z. & Pilakoutas, K. 2004, 'Bond Behaviour of Fiber Reinforced Polymer Bars under Direct Pullout Conditions', *Journal of Composites for Construction*, ASCE, 173-181.

Demis, S. 2007, *An Investigation of Durability of FRP in Concrete*, Ph.D. Thesis, University of Sheffield, UK.

Demis, S., Pilakoutas, K. & Byars, E. 2007, 'Durability of Fibre reinforced Polymers in Concrete - Procedures for reduced alkalinity Exposures' Proc. FRPRCS-8, University of Patras, Patras, Greece, July 16-18.

Fang, C., Lundgren, K., Chen, L. & Zhu, C. 2004, 'Corrosion influence on bond in reinforced concrete', *Cement and Concrete Research*, **34**, 2159-2167.

Fang, C., Lundgren, K., Plos, M. & Gylltoft, K. 2006a, 'Bond behaviour of corroded reinforcing steel bars in concrete', *Cement and Concrete Research*, **36**, 1931-1938.

Fang, C., Gylltoft, K., Lundgren, K. & Plos, M. 2006b, 'Effect of corrosion on bond in reinforced concrete under cyclic loading', *Cement and Concrete Research*, **36**, 548-555.

*f*ib 2000, *Bulletin 10 - Bond of Reinforcement in Concrete. State-of-Art Report prepared by Task Group Bond Models (former CEB Task Group 2.5)*, Federation Internationale du Beton, August, Eurocode 2, Design of Concrete Structures – Part 1.1: general Rules and Rules for Buildings, EN 1992-1-1 (2004).

Karbhari, V.M., & Chu, W. 2005, 'Degradation kinetics of pultruded E-glass/vinylester in alkaline media', *ACI Materials journal*, **102**, 34-41.

Lundgren, K. 2007, 'Effect of corrosion on bond between steel and concrete: an overview', *Magazine of Concrete Research*, **59**[6], 447-461.

Papadakis, V.G., Vayenas, C.G. & Fardis, M.N. 1991, 'Fundamental Modelling and Experimental Investigation of Concrete Carbonation', *ACI Materials Journal*, **88**, 363-373.

Papadakis, V.G., Efstathiou, M.P. & Apostolopoulos, C.A. 2007, 'Computer-Aided Approach of Parameters Influencing Concrete Service Life and Field Validation', *Computers & Concrete*, **4**, 1-18.

Yilmaz, V.T., & Glasser, F.P. 1992, 'Chemical attack on alkali-resistant fibres in a hydrates cement matrix: characterization of corrosion products', *Journal of Non-Crystalline Solids*, **151**, 236-244.

XII DBMC
International Conference on Durability of Building Materials and Components
PORTO - PORTUGAL, April 12th-15th, 2011

Influence that Ratio of Length to Diameter of High-Strength Concrete Core to Compressive Strength of Concrete

Sumie Suzuki [1]
Tadatsugu Kage [2]
Shigeki Seko [3]

ABSTRACT

It is necessary and very important to take concrete core from structures for researching the durability and strength of existing RC structures.

When taking core from concrete structures, sometimes the ratio of length to diameter [L/D] of cores for strength testing are shorter than 2.00.

If the L/D of the specimen is less than 2.00, the strength correction factor should be used to estimate the compressive strength of concrete cores.

The strength correction factor is provided for the concrete of normal compressive strength up to 40 N/mm^2 in JIS A 1107 or ASTM C42. Therefore, it is not applied to high-strength concrete.

As a result of the consideration for relationship between the L/D and the compressive strength of concrete cores that would be tested in accordance with JIS A 1107, it was confirmed that the strength correction factor listed on JIS A 1107 and ASTM C42 are valid for high-strength concrete up to 100 N/mm^2.

KEYWORDS

High-strength concrete, Concrete core, Ratio of length to daimeter, Strength correction factor.

[1] Japan Testing Center for Construction Materials (JTCCM), Soka, JAPAN, sumie-sk@jtccm.or.jp
[2] Building Research Institute (BRI), Tsukuba, JAPAN, kage@kenken.go.jp
[3] AICHI Institute of Technology (AIT), Toyota, JAPAN, seko@aitech.ac.jp

1 INTRODUCTION

It is necessary and very important to take concrete core from structures for researching the durability and strength of existing RC structures.

When the service life of RC structures are presumed, the durability of concrete, for example, carbonation depth or the corrosion level of reinforcement in the concrete are measured.

For the verification of the progress level of the carbonation depth, the strength presumption by the strength test or non-destructive tests.

In addition, for last 30 years recently, the high-strength concrete has increased to use for RC structures, especially for the high rise buildings in the world. It also needs to execute an accurate strength estimation for the durability of building materials, when the seismic retrofit or repairing of RC structures in the future.

This research shows very important technical intelligence to execute an accurate strength estimation, when durabirity of existing concrete structure would be presumed.

To determine compressive strength of structural concrete, concrete core specimens are taken from structural members. Generally, compressive strength tests are carried out on core specimens of 100mm diameter and 200mm length.

However, in some cases, high-strength concrete structure members are thinner than specimen's length. It was because that the bar arrangement is different or sometimes drilling core specimens are accidentally sawed short with small length-to-diameter ratios. It would be resulting in high values of core concrete strength that do not reflect actual strength of structural concrete.

Because of such inversely proportional relationship between the compressive strength of short cores and their length-to-diameter ratios, the strength correction factor is recommended in standards JIS A 1107-2002 and ASTM C42-2004.

These correction factors are valid for cores of concrete strength under 40MPa [N/mm^2], so it does not applied to cores of higher strength concrete.

When the compressive strength of cores above 70MPa [N/mm^2] would be measured, the strength correction factor may become larger than listed on JIS A 1107 and ASTM C42. According to the experiments of Bartlett and MacGregor [1994], Tomosawa *et al.* [1989] and Pertersons [1971], when the compressive strength increased to high-strength concrete, the strength correction factor become larger than normal strength concrete.

2 EXPERIMENTAL INVESTIGATIONS

2.1 Experimantal Program

Based on compressive strength tests, this study estimates the strength correction factor would be applied for high-strength concrete cores, compressive strength up to100 N/mm^2.

Target compressive strengths were two normal strength concrete [30 and 45 N/mm^2] and three high strength concrete [60, 80 and 100 N/mm^2].

Concrete core specimens of 100mm and 75mm diameters were cut into different lengths with respect to the following length-to-diameter [L/D] ratios 1.00, 1.25, 1.50, 1.75 and 2.00.

Core specimens of 75mm diameter are suitable when structure member are thinner than 200mm or bar arrangement interval narrow than core diameter of 100mm.

Parameter and level of the compressive strength test for cores in this experimental study are showed in Table 1.

Table 1. Parameter and level of the compressive strength test for cores.

Parameter	*Level*
Target Compressive Strength [N/mm^2]	30, 45, 60, 80, 100
Ratio of length to diameter [L／D]	1.00, 1.25, 1.50, 1.75, 2.00
Diameters of core [mm]	ϕ 100, ϕ 75
Types of mock-up [Direction of drilling core to placing concrete]	Wall shape [vertical], Slab shape [horizontal]
Testing age [day]	28 , 56

2.2 Materials and Mix Proportions

Concrete component materials and specifications are showed in Table 2.

Table 2. Concrete component materials and specifications.

Concrete component materials		*Specifications*
Cement	OPC	Conforming JIS R 5210, Specific gravity 3.16 g/cm^3
	MHPC	Conforming JIS R 5210, Specific gravity 3.21 g/cm^3
Fine aggregate	River sand	SSD specific gravity 2.61 g/cm^3 Absorption 1.16 %, F.M. 2.80
Coase aggregate	Crushed stone	SSD specific gravity 2.70 g/cm^3 Absorption 0.75 %, Solid content 60.0 %
Admixture	Water reducing agent	Sodium Lignosulfonate, Specific gravity 1.07 g/cm^3
	Super plasticizer	Polycarboxylate, Specific gravity 1.07 g/cm^3

Ordinary Portland Cement [OPC] were used for the strength levels of 30, 45, 60 and 80 N/mm^2. Moderate Heat Portland Cement [MHPC] was used for the strength level of 100 N/mm^2.

River sand and crushed stone were used for the aggregate of all concretes.

Water reducing agent was used for the strength level of 30 N/mm^2 and super-plasticizer were used for the other strength levels.

Mix proportions of concrete are showed in Table 3.

For the strength levels of 30 and 45 N/mm^2, water to cement ratio were decided aiming to reach the target strength at age of 28 days of core specimens. For the strength levels of 60, 80 and 100 N/mm^2, these water to cement ratio were decided aiming to reach the target strength at age of 56 days.

Table 3. Strength level and mix proportions of concrete.

Strength level [N/mm^2]	*Water to cement ratio [%]*	*Cement [kg/m^3]*	*Water [kg/m^3]*	*SSD fine aggregate [kg/m^3]*	*SSD coase aggregate [kg/m^3]*	*Admixture [kg/m^3]*	
						Water reducing agent	*Super plasticizer*
30	61.0	292	178	880	940	2.92	—
45	45.0	378	170	833	934	—	3.78
60	37.5	453	170	780	926	—	4.67
80	28.0	607	170	710	867	—	8.19
100	27.0	630	170	715	851	—	9.77

2.3 Wall and Slab Shape Mock-up

To prepare concrete core specimens of different length-to-diameter ratios, a wall shape mock-up was made for each strength level, and a slab shape mock-up was made for the strength levels of 30 and 60 N/mm^2.

Figure 1 shows the wall shape mock-up size and concrete core drilling locations.

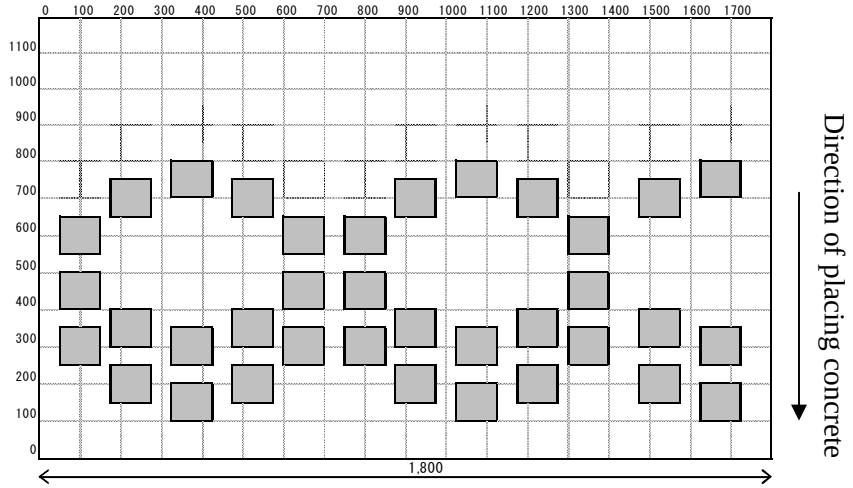

Figure 1. Wall shape mock-up size and core drilling locations [Dimensions in millimetres].

Two types of mock-up were made, which would be compared to compressive strength correction factor effecting of core drilling direction to placing concrete direction.

The wall shape mock-up was placing concrete into the plywood forms from the top of the mock-up. And then, when the drilling core from the mock-up, it was vertical angle to the wall shape mock-up. The other hands, the slab shape mock-up was placing concrete and drilling concrete, that would be same direction.

The mock up of wall shape was 1800mm width, 1200mm height and 325mm thickness and the mock up of slab shape was 1800mm×1200mm width and 325mm thickness.

After placing concrete into plywood forms, each mock-up were cured until the age of 14 days for the strength levels of 30, 45, 60 and 80 N/mm^2, and until 21days for the strength level of 100 N/mm^2.

For the strength levels of 30 and 45 N/mm^2, core specimens were drilled at the age of 21 days. For the strength levels of 60, 80 and 100 N/mm^2, core specimens were drilled at the age of 49 days.
After drilling, all core specimens were cured in water at job site until moving to the testing center.

2.4 Preparation of Core Specimens

Concrete cores were drilled from the mock-up 1week before the compressive strength test. After drilling, concrete cores were sawed into lengths each of the following ratios, L/D=1.00, 1.25, 1.50, 1.75 and 2.00 and grounded on both ends.

Figure 2 shows specimen's lengths from concrete cores before sawed and grounded on both ends. 7 core specimens for every parameter were tested.

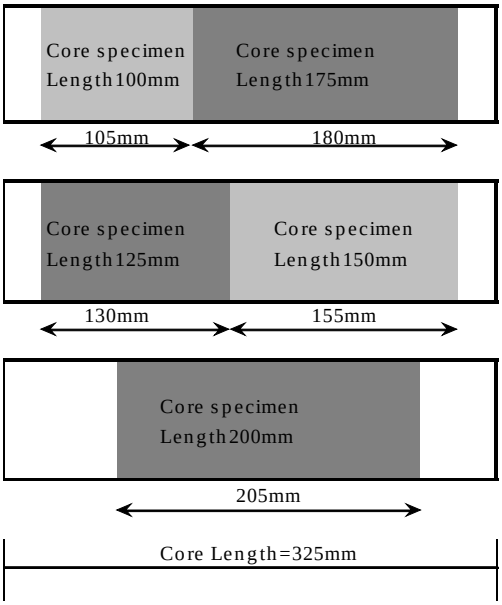

Figure 2. Specimen's length from concrete cores before sawed [e.g. Diameter of core：100mm].

2.5 Compressive Strength Test

The compressive strength test was carried out in accordance with JIS A 1108 at one testing center that conformed ISO17025 laboratory. At the testing centre, specimens were cured in water at 20±1℃ until the compressive strength test.

For the strength levels of 30 and 45 N/mm^2, core specimens were testing at the age of 28 days. For the strength levels of 60, 80 and 100 N/mm^2, core specimens were testing at the age of 56 days. Testing days were decided by the measure of the compressive strength of the specimens making by mould with mock-up. The loading rate was kept at around 0.6 N/mm^2/sec during the compressive strength test.

3 RESULTS AND DISCUSSION

3.1 Compressive Strength and Strength Correction Factor

The mean values of the compressive strength and the standard deviation of the core specimens which taking from wall shape mock-up are given in Table 4 and the core specimens taking from slab shape mock-up are given in Table 5. The standard deviation are denoted in parentheses.
The compressive strength increased as the length-to-diameter ratio decreased at any strength levels. The compressive strength ratio, which is the ratio of the compressive strength of each specimens to the compressive strength at L/D=2.00 of the same strength level, was estimated for each strength levels.

The compressive strength ratio of the core specimens taking from wall shape mock-up are given in Table 6 and the core specimens taking from slab shape mock-up are given in Table 7.

Table 4. Result of the mean values of the compressive strength and the standard deviation of core specimens taking from wall shape mock-up.

L/D	*30 N/mm²*		*45 N/mm²*		*60 N/mm²*		*80 N/mm²*		*100 N/mm²*	
	ϕ100	*ϕ75*	*ϕ100*	*ϕ75*	*ϕ100*	*ϕ75*	*ϕ100*	*ϕ75*	*ϕ100*	*ϕ75*
2.00	27.3 [1.66]	28.9 [1.51]	40.9 [3.89]	45.3 [1.08]	55.8 [1.25]	59.9 [2.71]	67.8 [1.84]	69.2 [1.84]	84.9 [2.74]	86.0 [2.82]
1.75	28.0 [1.15]	—	41.7 [2.80]	—	57.9 [1.76]	—	68.8 [3.06]	—	86.8 [2.54]	—
1.50	27.7 [1.36]	30.8 [2.10]	40.2 [5.05]	42.5 [2.97]	57.4 [2.24]	61.0 [6.53]	69.1 [2.79]	71.4 [2.74]	88.7 [1.78]	90.9 [2.70]
1.25	29.1 [1.93]	—	44.9 [3.34]	—	60.4 [5.20]	—	71.9 [3.00]	—	91.4 [3.80]	—
1.00	32.5 [1.27]	33.5 [3.18]	47.3 [2.74]	50.2 [3.64]	64.5 [3.52]	68.4 [4.32]	75.5 [3.08]	78.3 [1.98]	94.9 [4.11]	96.8 [5.73]

Table 5. Result of the mean values of the compressive strength and the standard deviation of core specimens taking from slab shape mock-up.

L/D	*30 N/mm²*	*60 N/mm²*
	ϕ100	*ϕ100*
2.00	30.6 [0.62]	54.5 [0.75]
1.50	30.8 [1.35]	54.2 [3.44]
1.00	33.9 [1.22]	59.8 [5.25]

Table 6. Result of compressive strength ratio of core specimens taking from wall shape mock-up.

L/D	*30 N/mm²*		*45 N/mm²*		*60 N/mm²*		*80 N/mm²*		*100 N/mm²*	
	ϕ100	*ϕ75*	*ϕ100*	*ϕ75*	*ϕ100*	*ϕ75*	*ϕ100*	*ϕ75*	*ϕ100*	*ϕ75*
2.00	1.00	1.00	1.00	1.00	1.00	1.00	1.00	1.00	1.00	1.00
1.75	1.03	—	1.02	—	1.04	—	1.01	—	1.02	—
1.50	1.01	1.06	0.98	0.94	1.03	1.02	1.02	1.03	1.04	1.06
1.25	1.07	—	1.10	—	1.08	—	1.06	—	1.08	—
1.00	1.19	1.16	1.16	1.11	1.16	1.14	1.11	1.13	1.12	1.13

Table 7. Result of compressive strength ratio of core specimens taking from slab shape mock-up.

L/D	*30 N/mm²*	*60 N/mm²*
	ϕ100	*ϕ100*
2.00	1.00	1.00
1.50	1.01	0.99
1.00	1.11	1.10

The compressive strength ratio respective to length-to-diameter ratio and compared to the coefficient from the strength correction factor listed on JIS A 1107 and ASTM C 42 are shown in Fig. 3. The strength correction factor listed on JIS A 1107 and ASTM C 42 are same.

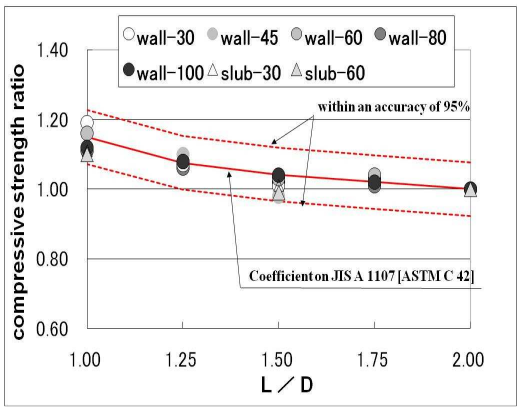

[Diameter of core：100mm]

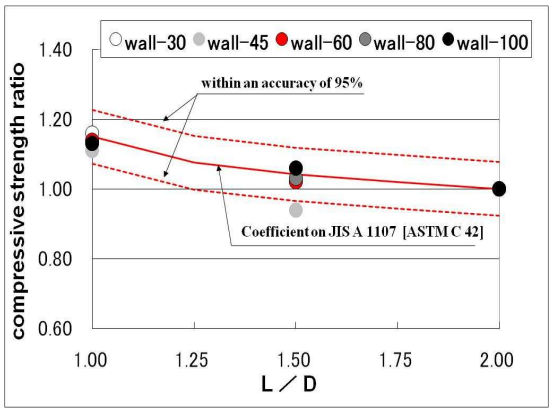

[Diameter of core：75mm]

Figure 3. Compressive strength ratio respective to length-to-diameter ratio.

The compressive strength ratio increases as length-to-diameter ratio decreases, and it would be similar to the correction factor on JIS A 1107 at almost strength levels, diameters of core and types of mock-up, except one data of 45N/mm^2 level.

Accorrding to the experiments of Akaogi *et al*. [2008] and Kesler [1959] , compressive stregth ratio below 1.00 at the length-to-diameter ratio 1.50.

The compressive strength ratio at L/D=1.50 would be below 1.00, it is guessed that the test outcome was caused by some different mechanism to other L/D of the core specimens.

From this experimental compressive strength test results, the compressive strength ratio of any strength levels up to 100 N/mm^2 were within an accuracy of 95%.

Some datas of high-strength concrete, which the compressive strength ratio at L/D=1.00 were above the correction factor on JIS A 1107 and ASTM C42. The datas above the correction factor at L/D=1.00 would become an evaluation of the safety side. That means the strength correction factor listed on JIS A 1107 [ASTM C42] are valid for high-strength concrete up to 100 N/mm^2.

4 CONCLUSIONS

Based on compressive strength tests, this study estimates the strength correction factor of high-strength concrete cores of compressive strength in the range of 30 N/mm^2 to 100 N/mm^2.

Concrete core specimens were cut into different lengths with respect to the length-to-diameter ratios 1.00, 1.25, 1.50, 1.75 and 2.00.

The following results are drawn. Compressive strength ratio increases as length-to-diameter ratio decreases, and it would be similar to the correction factor on JIS A 1107 from the strength levels 30 to 100 N/mm^2.

The strength correction factor listed on JIS A 1107 and ASTM C42 are valid for high-strength concrete up to 100 N/mm^2.

Some case of length-to-diameter ratio at 1.50, the compressive strength retio was below 1.00. It is guessed that the test outcome was caused by some different mechanism to other length-to-diameter ratio of the core specimens. It is planning to examine and research to clarify in the future.

ACKNOWLEDGMENTS

The authors wish to express sincere appriciation to Japan Concrete Institute for financing this research work. The authors also would like to thank commitee of JIS revision in JCI [chairman Dr. Michihiko Abe] for thier invaluable contributions to several aspects of the work for revison of JIS A 1107 reported in this paper.

REFERENCES

JIS A 1107-2002:Method of sampling and testing for compressive strength of drilled cores of concrete, JSA.

ASTM C 42-2004:Standard test method for obtaining and testing drilled cores and sawed beams of concrete, ASTM International.

Bartlett, F.M and MacGregor, J.G, 'Effect of Core Length-to-Diameter Ratio on Concrete Core Strength', *ACI Material Journal*, Vol.91, No.4, 1994, pp.339-348.

Tomosawa, F., Masuda, Y., Tanano, H., Uenish, T., Noguchi, T., & Onoyama, K., 1989, *Study on Standard test method for compressive strength of high strength concrete [Part.3: Effect of height/diameter of cylindrical test specimen]*, Summaries of Technical Paper of Annual Meeting, Architectural Institute of Japan, A, October 1989, pp.509-510.

Pertersons, N., 1971, 'Recommendations for Estimation of Quality of Concrete in Finished Structures ', *Materials and Structures*, Vol.4, No.24, 1971.

Akaogi, M., Abe, M., Kasami, H. & H., Tamai, T., 2008, *The effects of height-diameter ratio of cylindrical specimens on compressive strength*, Summaries of Technical Paper of Annual Meeting, Architectural Institute of Japan , A-1, September 2008, pp.769-770.

C.E. Kesler: 'Effect of Length to Diameter Ratio on Compressive Strength', *ASTM Proc.* Vol.59, 1959.

XII DBMC
International Conference on Durability of Building Materials and Components
PORTO - PORTUGAL, April 12th-15th, 2011

Evaluation on Drying Shrinkage of Concrete Using Shrinkage Reducing Admixtures

Tadatsugu Kage [1]
Yoshiaki Ohno [2]

ABSTRACT

The shrinkage prediction equation considering the influence of mix proportion and curing method of concrete was proposed in 'Recommendations for Practice of Crack Control in Reinforced Concrete Buildings (Design and Construction) (2006)' published by Architectural Institute of Japan (AIJ). On the other hand, recent research has been reported the effect of shrinkage reducing admixtures, for examples, expansive additives or shrinkage reducing agents, as a countermeasure for reducing the shrinkage of concrete. Also, the shrinkage prediction equations based on these studies was defined as a function with correction factor representing the effect of mix proportion, concrete materials, and shrinkage reducing agents. However, the effect of expansive additives has not yet been considered.

In this study, it was evaluated that the effects of shrinkage reducing admixtures, compared predicted value with measured values, which were obtained by some experiments results of drying shrinkage of concrete using expansive additives and shrinkage reducing agents.

As the results, the effects of shrinkage reducing admixtures could be estimated by using the existing prediction equations. However, it were evaluated that the expansive additives was slightly higher, but the shrinkage reducing agents was slightly lower, because the correction factor of shrinkage reducing admixtures was not prepared in the prediction equation of shrinkage.

KEYWORDS

Drying shrinkage, Expansive additive, Shrinkage reducing agent, Prediction equation.

[1] Building Research Institute, Tsukuba, JAPAN, kage@kenken.go.jp
[2] Center for Better Living, Tsukuba Building Research and Testing Laboratory, Tsukuba, JAPAN ohno@tbtl.org

1 INTRODUCTION

Harmful cracks occur in reinforced concrete structure and this causes the deterioration of the overall long-term performance of structures (durability), loss in watertightness, and strength. Such cracks often occur due to drying shrinkage of concrete which can occur early on as the concrete sets are over time as the concrete cures. It was therefore of interest to the joint research group (BRIC), that included members of the Building Research Institute, the Centre for Better Living of Japan and several Japanese construction companies, to necessarily examine beforehand countermeasure for reducing drying shrinkage in concrete that is a precursor to concrete cracking. Hence a study was conducted on the influence of the types of concrete materials and mix proportions on the drying shrinkage of concrete, and a summary of the findings of this study are reported in this paper.

On the other hand, the effects of admixtures, shrinkage reducing agents and expansive additives, have been extensively reported in literature as have the countermeasure to control the shrinkage of concrete. For example, the Architectural Institute of Japan (AIJ) has proposed a design control method for shrinkage cracks of reinforced concrete structures 'Recommendations for Practice of Crack Control in Reinforced Concrete Buildings (Design and Construction)' [AIJ 2006]. In the AIJ recommendation, the influence of mix proportions, curing methods and conditions for concrete was also considered within the shrinkage prediction equation for concrete.

In this study, the effect of shrinkage reducing admixtures, derived from a review of literature available in Japan and well from experiments conducted on concrete using both shrinkage reducing agents and expansive additives. The results were reported in relation to concrete shrinkage predictions made using an existing shrinkage equation. Also, it was also of interest to confirm the influence of the type and usage of shrinkage reducing admixtures on the drying shrinkage and mechanical properties (compressive strength, Young's modulus) of concrete.

2 EVALUATION OF EFFECT OF SHRINKAGE REDUCING ADMIXTURE - A LITERATURE REVIEW

2.1 Content of Literature Review

Concrete shrinkage, including drying shrinkage and autogeneous shrinkage, using shrinkage reducing agents or expansive additives were investigated from a review of literature provided in the Japan Concrete Institute proceedings which were published between 1980 and 2006 [JCI 1980-2006]. The review provided basic information on concrete strength (i.e. design strength, nominal strength, and blending name), on concrete mix proportions and materials (i.e. water-cement ratio, unit water content, unit weight of coarse aggregate, types of cement, aggregate, and admixture), and test results (slump, air content, compressive strength, shrinkage strain, test specimen size, curing conditions, and shrinkage of concrete).

2.2 Evaluation of Effect of Shrinkage Reducing by Shrinkage Prediction Equation

The predicted value of concrete shrinkage was calculated by the shrinkage prediction equation and experimental values were then compared with consideration to types of admixture present in the concrete. The predicted value of concrete shrinkage using an arbitrary age at which drying began was calculated by equation [1], and the predicted value of the ultimate shrinkage was calculated using equations [2] and [3].

$$\varepsilon_{sh}(t,t_0) = k \cdot t_0^{-0.08} \cdot \left\{1 - \left(\frac{h}{100}\right)^3\right\} \cdot \left(\frac{(t - t_0)}{0.16 \cdot (V/S)^{1.8} + (t - t_0)}\right)^{1.4 \cdot (V/S)^{-0.18}} \quad [1]$$

$$k = (11 \cdot W - 1.0 \cdot C - 0.82 \cdot G + 404) \cdot \gamma_1 \cdot \gamma_2 \cdot \gamma_3 \quad [2]$$

where: $\varepsilon_{sh}(t,t_0)$: Drying shrinkage at age t when drying initiated drying at age t_0 [$\times 10^{-6}$]
$\varepsilon_{sh\infty}$: Ultimate drying shrinkage [$\times 10^{-6}$]
W : Water content [kg/m^3], C : Cement content [kg/m^3]
G : Aggregate content [kg/m^3], h : Relative humidity [%] (40%≤h≤100%)
S : Surface area [mm^2], V/S : Volume/surface area ratio [mm] (V/S≤300mm)
γ_1 : Correction factor for Aggregate (Lime crushed stone0.7, Sand or Gravel1.0)
γ_2 : Correction factor for Cement (OPC, BB1.0, HPC0.9)
γ_3 : Correction factor for Admixture (SR0.7, SF0.8,FA0.9)

$$\varepsilon_{sh\infty} = \frac{\varepsilon_{sh}(t_s)}{\left(\frac{t_s}{0.16 \cdot (V/S)^{1.8} + t_s}\right)^{1.4 \cdot (V/S)^{-0.18}}} \quad [3]$$

where: $\varepsilon_{sh}(t_S)$: Drying shrinkage for age t_S [$\times 10^{-6}$]
t_S : age for drying

However, when if correction factors for the concrete constituent materials (i.e. aggregate, cement, or admixture) was not provided, then the correction factor was assumed to be 1.0.

2.3 Outline of Findings

There were a total of 346 research papers that were reviewed and from which information on the shrinkage of concrete were reported and useful information extracted. From this literature review, it was determined that Ordinary Portland Cement (OPC) was used in 77% of the concrete mixes, crushed stone as the coarse aggregate used in 39% of the mixes, river sand or crushed sand was used 78% or 8% as the fine aggregate. Moreover, shrinkage reducing agents were only used in 47% of the mixes and the expansive additives only used 12%. The use of both types of admixtures (shrinkage reducing agents and expansive additives) only occurred in 13% of the mixes, amongst all the different concrete mixes found through this review. The age at which concrete shrinkage was measured varied widely ranging between 14 days and even up to 356 days.

2.4 Comparison between Predicted Value and Experimental Value of Shrinkage

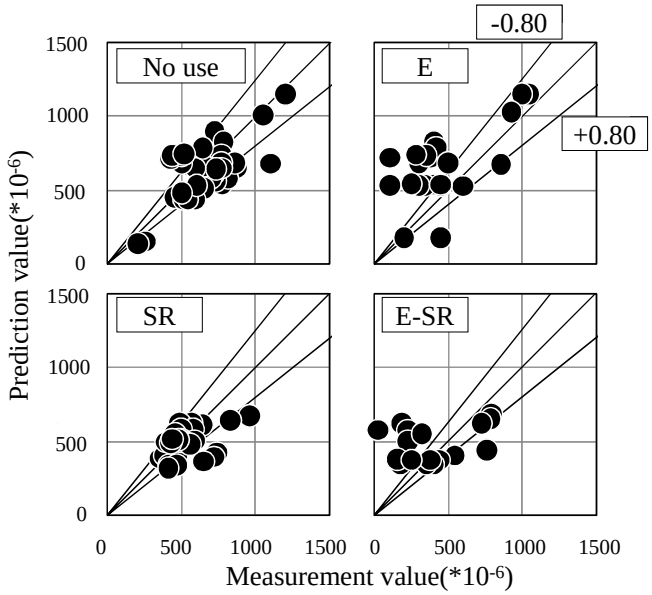

Figure 1. Comparison with experimental value and predicted value of shrinkage.

Figure 1 shows a comparison of the experimental values for shrinkage derived from literature and the predicted value, as calculated using Eqs. [1] and [2]. The different graphs show comparisons where no admixtures were used (No use), only expansive additives were used (E), only shrinkage reducing agents used (SR) and finally, where both E and SR (E-SR) admixtures were used in the concrete mixes respectively; in each of these predictions an arbitrary value was chosen for the initial age at which drying began. The predicted value and the experimental were roughly corresponded in those cases where only the shrinkage reducing agents were used (SR), or when admixtures were not used (No use). On the other hand, in case of using only the expansive additives (E), the experimental value of shrinkage ranged between 100 to 500×10^{-6}, and this small value as compared to the predicted value ($500\text{-}800\times10^{-6}$) widely varied.

2.5 Influence of Admixture on the Ultimate Shrinkage

Figure 2 shows the ultimate shrinkage of concrete using admixtures, which was calculated by Eq. [3]. When expansive additives and shrinkage reducing agents were used, both shrinkage reducing effects were confirmed. However, it was also evident that the differences were caused by the age chosen to obtain measurements to estimate the ultimate drying shrinkage of concrete. Moreover, it was confirmed that the effect of shrinkage reducing agents was larger than that of expansive additives. On the other hand, the effect of expansive additives used together the shrinkage reducing agents was not confirmed because the ultimate shrinkage prediction did not include the effect of the expansive additives in the prediction equation.

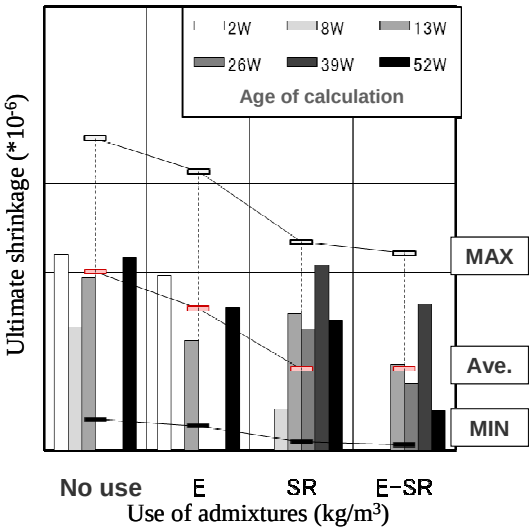

Figure 2. Ultimate shrinkage calculated by Eq. [3].

2.6 Relation between Usage of Admixture and the Ultimate Shrinkage

Figure 3 shows the relation between the usage of admixtures and the ultimate shrinkage ratio. It was used for calculating the ultimate shrinkage ratio of the test specimens used OPC and crushed stone, and not used other special admixture, as the concrete materials. Moreover, the test specimens were cured under of 20 degrees centigrade in temperature and 60% in relative humidity.

The usage of the shrinkage reducing agents in concrete ranged between 3 and 22 kg/m^3, but on average the usage was 10 kg/m^3. The shrinkage ratio for concrete using an average amount of shrinkage reducing agents (i.e. 10 kg/m^3) was estimated to be 0.68 for drying shrinkage, and 0.87 for autogeneous shrinkage. It was confirmed that the drying shrinkage using shrinkage reducing agents showed the same correction factor as was given in Eqs. [1] and [2].

Moreover, the usage of expansive additives in concrete ranged between 10 and 50 kg/m^3, and on average was 25 kg/m^3. The shrinkage ratio for average usage of expansive additives was estimated to be 0.67 for drying shrinkage and 0.37 for autogeneous shrinkage. It was also confirmed that the usage of admixtures and the effect of shrinkage reducing agents were almost in a proportional relation, specifically expansive additives were effective in reducing autogeneous shrinkage in concrete at early ages when autogeneous shrinkage is predominant, whereas shrinkage reducing agents were effective in reducing drying shrinkage at latter ages when drying shrinkage becomes predominant.

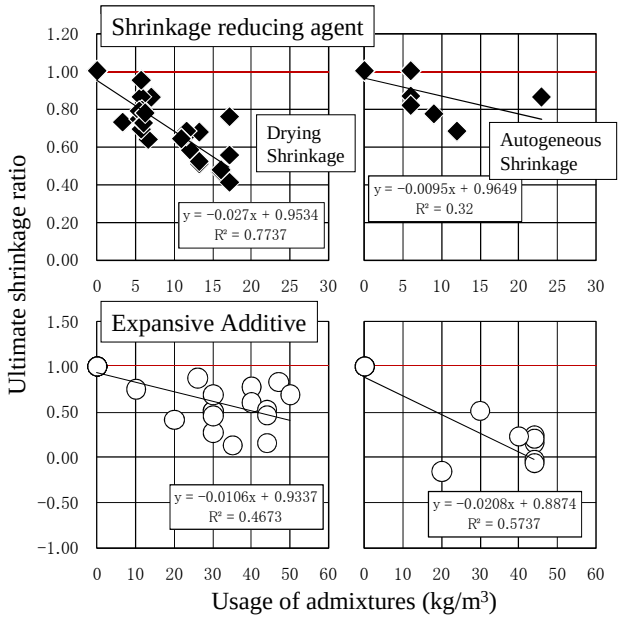

Figure 3. Relation between usage of admixture and ultimate shrinkage ratio.

2.7 Influence that Usage of Admixture on Compressive Strength of Concrete

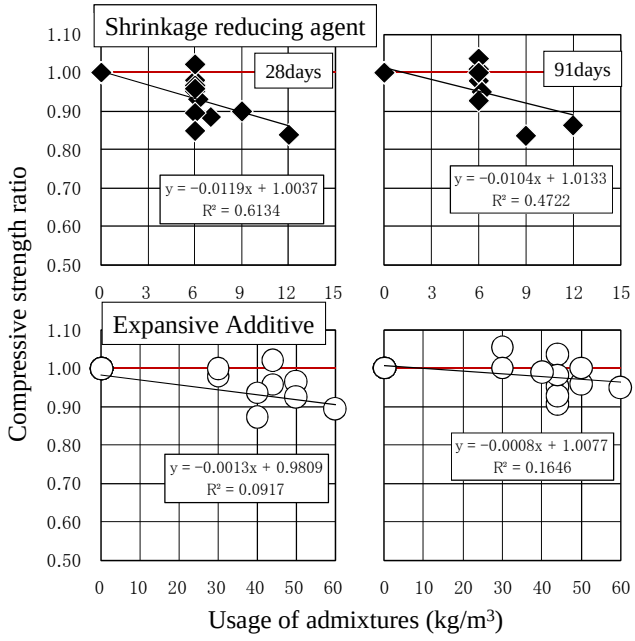

Figure 4. Relation between usage of admixture and compressive strength of concrete.

Figure 4 shows the relation between the usage of admixtures and the compressive strength of concrete. The compressive strength ratio when 10 kg/m^3 of shrinkage reducing agents were used was 0.88 at 28 days, and 0.91 at 91 days. It was confirmed that the decrease in compressive strength was roughly in proportion to the amount of shrinkage reducing agents used. On the other hand, the compressive strength ratio when 25 kg/m^3 of expansive additives were used was 0.95 at 28 days, and 0.99 at 91 days. The influence of expansive additives on the compressive strength was small compared to that obtained when the shrinkage reducing agents were used.

3 EXPERIMENTAL STUDIES ON SHRINKAGE REDUCING EFFECTS WITH ADMIXTURES

3.1 Concrete Materials and Mix Proportions

Information on the concrete materials, mix proportions are given in Table 1 and the test results on concrete in Table 2. The kind of cement and the aggregate used were those commonly used as concrete materials. The mix proportions were based on N5-18N (W/C 0.50, W 185kg/m^3), and changed according to the type and use admixture included in the mix. The target slump and air content were assumed to be 18.0±1.5 cm, and 4.5±1.0 % respectively. The bulk volume of coarse aggregate was constant at 0.56m^3/m^3.

Table 1. Concrete materials and specifications.

Concrete materials		*Specification*
Cement	C : OPC	Specific Gravity 3.16g/cm^3
Fine Aggregate	S : River Sand(Oigawa River)	Specific Gravity 2.57g/cm^3,Absorption 1.02%
Coarse Aggregate	G : Crushed Stone (Hard Sandstone, Iwase)	Specific Gravity 2.65g/cm^3,Absorption 0.71%
Admixture	Ad : AE water-reducing agent	Lignosulfonic Acid type
Shrinkage Reducing Admixture	EX : Expansive Additive	Lime based type (Low addition type)
	SR_1: Shrinkage Reducing Agent 1	Glycol Eether type
	SR_2: Shrinkage Reducing Agent 2	Lower Alcohol Alkylene Oxide type

Table 2. Concrete mix proportions and test results.

Symbol	*W/C (%)*	*s/a (%)*	*Unit Content(kg/m^3)*							*Ad (C× %)*	*SL*[*1] *(cm)*	*Air*[*1] *(%)*	*Comp. Strength*[*2] *(N/mm^2)*			*Young's modulus*[*2] *(kN/mm^2)*	
			W	*C*	*S*	*G*	*EX*	*SR_1*	*SR_2*				*7-7*	*7-28*	*28-28*	*7-28*	*28-28*
N5-18N	50	47.8	185	370	778	894	-	-	-	0.30	19.5	4.7	27.4	41.1	40.5	27.4	27.9
E5-18E	50	47.8	185	350	778	894	20	-	-	0.30	20.0	4.6	28.4	42.8	40.2	28.2	28.4
F5-18S_1	50	47.8	185	370	778	894	-	6.0	-	0.30	19.5	0.6	35.1	51.9	51.6	30.7	31.6
G5-18S_2	50	47.8	185	370	778	894	-	-	6.0	0.30	19.0	5.1	29.7	40.7	40.8	28.1	29.2
H5-18ES_2	50	47.8	185	350	778	894	20	-	6.0	0.30	19.0	3.7	29.0	42.8	40.5	29.2	29.8

3.2 Experimental Method

The drying shrinkage and the mass change of concrete were measured using each 3 test specimens (100×100×400 mm) prepared in accordance with JIS A 1129-2 (Method of test for length change of mortar and concrete -Part2 : Method with contact-type strain gauge). The stud gauge (base length 300 mm) was attached on both sides of the test specimen after the form removal, and the initial length was measured after standard curing for 7 days. Also, the drying shrinkage of concrete was measured for 182 days in laboratory conditions (20 degrees centigrade and 60% relative humidity).

The compressive strength and the Young's modulus of concrete were measured in accordance with JIS A 1108 (Method of test for compressive strength of concrete) and JIS A 1149 (Method of test for static modulus of elasticity of concrete). The 100×200 mm cylindrical specimens for compressive tests cured under standard curing conditions for 7, 28, and 91 days, and thereafter were tested. Also, the specimens cured under standard curing conditions for 7 days and further "air cured" for 21days, which were same curing conditions as JIS A 1129, were tested at 28 days. Three test specimens were prepared for each mix proportion and for each curing age.

3.3 Fresh Properties, Compressive Strength and Young's Modulus of Concrete

Table 2 also shows the fresh properties, compressive strength and Young's modulus of concrete. The slump was within almost 18.0±1.5 cm for all mixes, the air content was within 4.5±1.0 % excluding mix F5-18S_1. As the results show, the target values were almost all achieved. It was confirmed that compressive strength of concrete (W/C 0.50) corresponded roughly to the base mix (N5-18N) regardless of the test age. The result for F5-18S_1, in which a shrinkage reducing agent was used, shows about 27% higher strength as a consequence of the air content not kept consistent. Moreover, it was shown that the results for Young's modulus were similar to the tendency shown for compressive strength. However, the influence of the curing condition was not confirmed from these tests.

3.4 Test Result of Drying Shrinkage and Mass Change of Concrete

Figure 5 shows the test results of drying shrinkage and mass change of concrete. The ratio of shrinkage for mix N5-18N after 182 days of curing was 0.95 using the expansive additive (E5-18E), 0.79 using the shrinkage reducing agent (SR_1, F5-18S_1), 0.87 using the shrinkage reducing agent (SR_2, G5-18S_2), and was 0.67 using both the expansive additive and shrinkage reducing agent (SR_2, H5-18ES_2). The effect of the shrinkage reducing agent was greatest for H5-18ES_2, which indicated 230×10^{-6}, as the drying shrinkage, which was smaller than the base concrete (N5-18N).

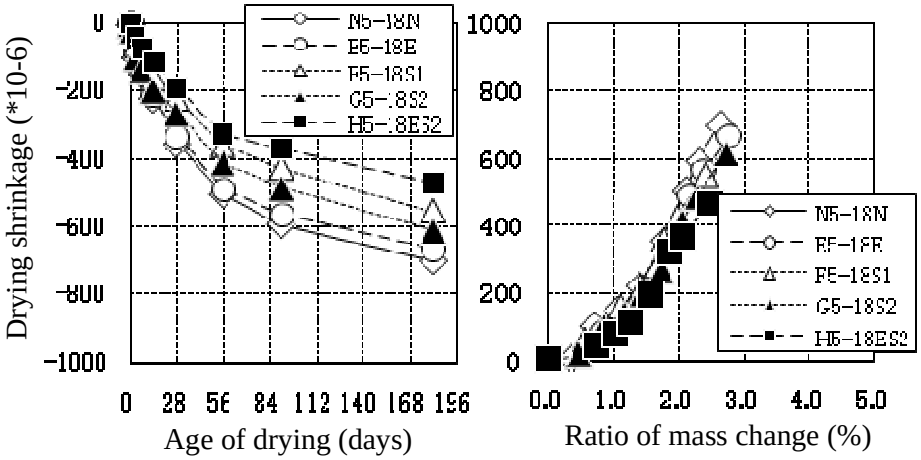

Figure 5. Test result of the drying shrinkage and the mass change of concrete.

3.5 Comparison between Predicted Value and the Experimental Value of Shrinkage

Figure 6 shows a comparison between the predicted value and the experimental value of shrinkage at 182 days of drying. The ratio of predicted value to experimental value when concrete included the shrinkage reducing admixture ranged between 0.87-1.17. The experimental value in which only expansive additive was used, and using both an expansive additive and shrinkage reducing agent, was determined to be higher than the predicted value. On the other hand, the experimental value obtained when using only shrinkage reducing agent was evaluated as lower than the predicted value. These

results were due to the predicted value calculated by Eqs. [1] and [2] and did not consider the effect of the expansive additive.

Based on these results, it could be stated that $60\sim70\times10^{-6}$ was obtained as a shrinkage value or that $\gamma_3=0.9$ should be suggested as a correction factor in order to consider the shrinkage reducing effects of expansive additives in the existing drying shrinkage prediction equation.

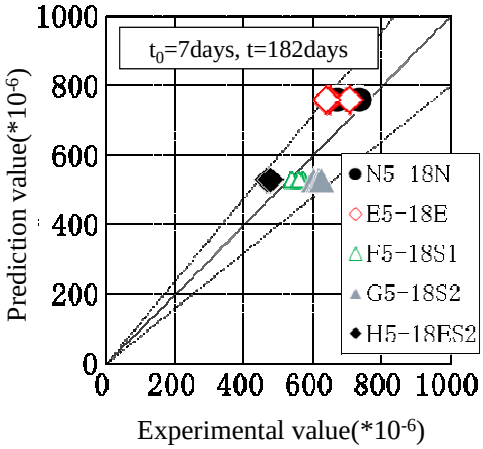

Figure 6. Comparison between predicted value and experimental value of shrinkage.

4 CONCLUSIONS

In this study, some results, obtained from a literature review were compared on the basis of experimental results of concrete shrinkage using shrinkage reducing agents or expansive additives, indicate the following:

1) The effect of shrinkage reducing admixtures estimated using the prediction equations, showed that slightly higher values of shrinkage were obtained for expansive additives whereas slightly lower were obtained for shrinkage reducing agents because the correction factor used in the shrinkage prediction equation was not prepared.
2) The effect of shrinkage reducing was confirmed to be proportional to the usage of shrinkage reducing agents or expansive additives, as the case may be.
3) It was confirmed that the influence of expansive additives on the compressive strength of concrete was somewhat small compared with that obtained for the shrinkage reducing agents, though the influence of each admixture was ultimately small.
4) When the drying shrinkage of concrete was estimated, it was necessary to examine the influences of the shrinkage reducing admixtures, especially the expansive additives, the age at which measurements are taken, and the curing conditions.

REFERENCES

Architectural Institute of Japan, 2006 'Recommendations for Practice of Crack Control in Reinforced Concrete Buildings (Design and Construction)', pp.53-60.

Japan Concrete Institute, 1980-2006, 'The proceedings of the JAPAN CONCRETE INSTITUE (1980-2006)'.

XII DBMC
International Conference on Durability of Building Materials and Components
PORTO - PORTUGAL, April 12th-15th, 2011

Experimental Study on Influence of Environmental Condition and Materials to Drying Shrinkage of Concrete

Yoshiaki Ohno [1]
Yoshihiro Masuda [2]
Tadatugu Kage [3]

ABSTRACT

Architectural Institute of Japan " Recommendations for Practice of Crack Control in Reinforced Concrete Buildings (Design and Construction) (2006)" shrinkage prediction equation defined to considering external factors such as volume surface-area ratio and relative humidity, in addition to internal factors of concrete such as materials and mix proportion. Prediction equations of shrinkage are experimental formula based on previous and a lot of studies, which are based on test results under some conditions, such as temperature of 20 degrees, humidity of 60%RH and specimen size (100*100*400mm). However, effects of test or environmental conditions are not examined a little. In addition, a recent study on drying shrinkage has been reported the effect of concrete materials, especially about coarse aggregate.

In this study, considered coarse aggregate and relative humidity affect the drying shrinkage of concrete, relative humidity and a sort of coarse aggregate, mix proportions of concrete was verified the effect of drying shrinkage. The drying shrinkage prediction equations, the coefficients for mix proportions of concrete (K_1), coefficient of started for drying age (K_2), coefficient of relative humidity (K_3) was considered, and this study K_3 was tried to quantify. The experimental results show significant influence of coarse aggregate and relative humidity on drying shrinkage, water content and water-cement ratio was less influenced on drying shrinkage.

KEYWORDS

Drying shrinkage, Relative humidity, Coarse aggregate, Young’s module, Prediction equation.

[1] Center for Better Living, Tsukuba Building Research and Testing Laboratory, Tsukuba, JAPAN ohno@tbtl.org
[2] Utsunomiya University, Graduate School of Engineering, Utsunomiya, JAPN, masuday@cc.utsunomiya-u.ac.jp
[3] Building Research Institute, Tsukuba, JAPAN, kage@kenken.go.jp

1 INTRODUCTION

In Previous studies about the drying shrinkage of concrete which is a cause the cracks, influence of water-content, materials, and coarse aggregate has been reported, and research on the affect of concrete with shrinkage-reducing admixtures and expansive admixtures. Architectural Institute of Japan " Recommendations for Practice of Crack Control in Reinforced Concrete Buildings (Design and Construction) (2006)" [Architectural Institute of Japan 2006] (It is shown with an Recommendations as follows)shrinkage prediction equation defined to considering external factors such as volume surface-area ratio and relative humidity, in addition to internal factors of concrete such as materials and mix proportion.
Influence of coefficient of relative humidity (K_3) of shrinkage prediction equation defined to become K_3=1.0 in environment at relative humidity 60% and temperature of 20 degrees, for experiment results and based on coefficient of relative humidity at CEB-FIP1990[Thomas Telford, 1990] equation, so previous studies of experiment result was performed in environment at relative humidity 60%. In previous studies[Sugiyama,*et al.* 1995][Sugiyama,*et al.* 1996]reported for evaporation of the waters changes by around relative humidity 55% greatly, and so relationship relative humidity and drying shrinkage was not always tilt of constant value.
In this study, considered coarse aggregate and relative humidity affect the drying shrinkage of concrete, relative humidity and a sort of coarse aggregate, mix proportions of concrete was verified the effect of drying shrinkage.

2 OUTLINE OF EXPERIMENTAL

In the study, this experiment was planned for considered coarse aggregate and relative humidity. The range of the relative humidity was planned in 40~80% of shrinkage prediction equation based on a Recommendations. Relative humidity of experimental planed 60%RH of basis, because based on falls to annual average 60%RH for urbanization reason. In addition, coarse aggregate pick out sandstone (2 localities), limestone, andesite as a typical.

2.1 Materials

Ordinary portland cement (density 3.16g/cm^3) was used mixture of equal amounts of three kind cements. Ordinary portland cement (density 3.16g/cm^3) was used mixture of equal amounts of three kind cements. Fine aggregate used sand (locality: Ooigawa, density in saturated surface-dry: 2.57g/cm^3, Density in over-dry:2.49g/cm^3, Water absorption: 1.02%, Finesse Modulus: 2.81), and coarse aggregate listed on **Table 1** used Iwase from sandstone,Ome frome sandstone, Sumita form limestone, Hokkaido from andesite.Chemical admixture used lignosulfonate water reducer, entraining air controlling agent.

Table 1. Properties of aggregate.

Sort	*Symbol*	*Density [g/cm^3]*		*Q*	*F.M.*	*Va*
		DS	*DD*	*[%]*		*[m^3/m^3]*
Coarse aggregate	I	2.65	2.63	0.71	6.59	0.56
	O	2.64	2.61	0.78	6.71	0.56
	S	2.69	2.69	0.50	6.53	0.56
	H	2.67	2.62	1.78	6.59	0.56

DS: Density in saturated surface-dry, DD: Density in over-dry, Q: Water absorption, F.M.: Finesse Modulus
Va: Volume fraction of coarse aggregate

2.2 Mix Proportion and Properties of Ready-Mixed Concrete

Table 2 is mix proportion and properties of ready-mixed concrete. Measurement method according to JIS A1101:2005(Method of test for slump of concrete), JIS A1128:2005(Method of test for air content

of fresh concrete by pressure method). The target slump 18±1.5cm, the target air volume 4.5±1.0%, and the volume of coarse aggregate in a planned unit 0.56m^3/m^3.

Table 2. Mix proportions of concrete.

Symbol	*W/C*	*s/a*	*Unit weight(kg/m^3)*				*Ad*	*Slump*	*Air*
	(%)	*(%)*	*W*	*C*	*S*	*G*	*C×%*	*(cm)*	*(%)*
I-50-185	50	47.8	185	370	778	894	0.30	19.5	4.7
I-40-185	40	45.4	185	463	705	894	0.30	17.0	4.4
I-60-185	60	49.4	185	308	826	894	0.30	19.5	5.0
I-50-170	50	49.7	170	340	839	894	0.50	19.5	3.8
I-50-200	50	45.8	200	400	717	894	0.00	19.0	4.4
O-50-185	50	47.4	185	370	771	896	0.30	19.5	4.8
S-50-185	50	46.3	185	370	753	940	0.10	19.0	4.8
H-50-185	50	47.7	185	370	775	895	0.30	19.0	5.1

W/C: Water-Cement ratio, s/a: Sand-aggregate ratio, W: Water, C: Cement, S: Fine-aggregate,
G: Coarse-aggregate, Ad: Chemical-admixture

2.3 Specimen Dimensions and Curing Method

Specimen dimension is 100*100*400mm and quantity is three. Concrete were molded faster after mixed, wet-curing at the test room by 20 degrees.
Removal of concrete forms after 24hr times, bond gage plugs to both sides of concrete surface, furthermore 24hr wet-curing for adhesives, after that water curing 7days.

2.4 Method of Test for Compressive Strength and Young's Modulus of Concrete

The measurement of compressive strength was carried out by the test method of JIS A1108:2006 (Method of test for compressive strength of concrete), the measurement of Young's modulus was carried out by the test method of JIS A1149:2001 (Method of test for static modulus of elasticity of concrete). Each of quantity is three, water curing age of temperatures 20 degrees is 7, 28, 91days.
The measurement of Young's modulus was longitudinal compressive strain by static strain instrument, a secant static modulus is compressive stress of corresponding amount one- third by the maximum load and $50*10^{-6}$ strains. As results of Compressive strength and static modulus is shown in **Table 3**.
In case of standardize age 91days of I-50-185, compressive strength and young's modulus is large so that water-cement ratio is large. However, compare compressive strength I-50-185 with I-50-170 (water content 170kg/m^3), in this case I-50-170 is +9.6N/mm^2 large.

Table 3. Result of concrete test.

Symbol	*Comp. Strength [N/mm^2]*			*Young's modulus [kN/mm^2]*		
	7d	*28d*	*91d*	*7d*	*28d*	*91d*
I-50-185	27.4	40.5	48.0	26.7	27.9	32.5
I-40-185	41.7	55.2	63.4	28.0	30.5	33.8
I-60-185	20.1	29.7	34.2	22.3	26.2	28.8
I-50-170	34.5	47.2	57.6	29.0	30.9	33.4
I-50-200	33.6	45.8	51.1	24.3	28.4	31.7
O-50-185	31.3	42.4	49.6	22.6	26.8	30.6
S-50-185	32.2	43.2	52.5	25.4	31.1	33.8
H-50-185	30.7	43.6	53.2	22.2	29.0	31.8

2.5 Method of Test for Drying Shrinkage and Environment Conditions

The measurement of drying shrinkage was carried out by the test method of JIS A1129 (Methods of measurement for length change of mortar and concrete - Part 2: Method with contact-type strain gauge). The measurement of drying shrinkage is the average of both side gauges on surfaced concrete. And measurement distance is 300mm; measurement of basis length is water-curing age of 7days. After this dry specimens in the test room. The measurement of drying age is 0, 1, 3, 7, 14, 28, 56, 91, 182 days. Term of drying age is environment condition that **Table4**, and specimen was stored under test room or test chamber. The test chamber is constant air circulation of velocity, relative humidity 80%, temperature 20 degrees.The test room is almost calm condition, relative humidity 40% or 60%, temperature 20 degrees. In this study, test room velocity condition is not need to consider such factors.

Table 4. Environmental conditions.

Symbol	*Relative humidity [%RH]*		
	40	*60*	*80*
I-50-185	○	○	○
I-40-185	-	○	-
I-60-185	-	○	-
I-50-170	-	○	-
I-50-200	-	○	-
O-50-185	○	○	○
S-50-185	○	○	○
H-50-185	○	○	○

3 EXPERIMENT RESULT AND CONSIDERATION

3.1 The Influence of Drying Shrinkage by Water Content

As results of drying shrinkage at effect of water content is shown in **Figure 1**. As results of relationship between drying shrinkage and weight loss ratio is shown in **Figure 2**.
By the comparison according to the water content, in this case of standardize age 182 days of I-50-185, the difference of drying shrinkage has that I-50-170 was $60*10^{-6}$ small, I-50-200 was $17*10^{-6}$ large, it is not considered to a little difference. However, water content was increase slightly same that drying shrinkage. Likewise, the difference of weight loss ratio has that I-50-170 was 0.20% small, I-50-200 was 0.07% large, water content was increase slightly same that drying shrinkage.

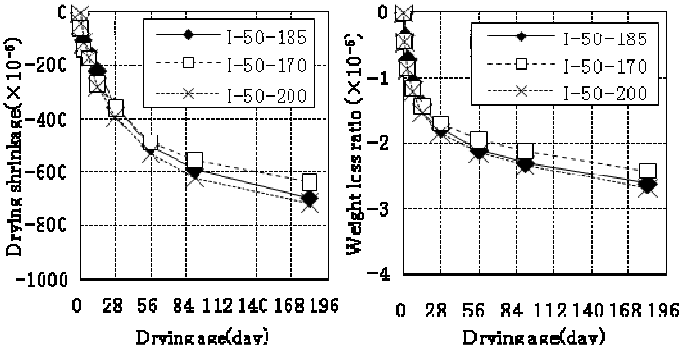

Figure 1. Result of drying shrinkage and weight loss ratio.

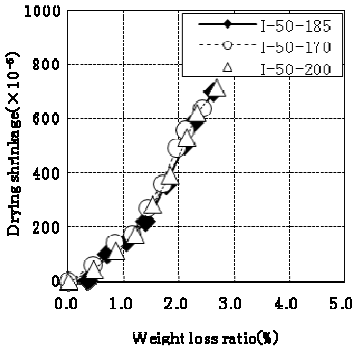

Figure 2. Relationship between drying shrinkage and weight loss ratio.

As the reason why these have little influence, and in the case of the same water cement ratio was the almost same as organization of the hydration product. The experiment result was a little influence of water content. In the case of same water-cement ratio, relationship between drying shrinkage and weight loss ratio was the ratio that weight loss ratio decreased by was the same as drying shrinkage regardless of water-content. In the case of constant water-cement ratio, when water content increases, some water non-reaction increases. When non-reaction of water evaporates from concrete, only the amount affects the dry shrinkage. However, in the range of water content 170~200 of the experiment, a difference is small for the dry shrinkage. Therefore, it is guessed that the absolutely needed quantity of non-reaction water in this range does not have many differences.

3.2 The Influence of Drying Shrinkage by Water-Cement Ratio

As results of drying shrinkage at effect of water-cement ratio is shown in **Figure 3**. As results of relationship between drying shrinkage and weight loss ratio is shown in **Figure 4**.
The difference of drying shrinkage is very small until drying age 182days. However, the weight loss ratio has a difference from the early days, and a difference becomes big until 28th, but the difference after 28th becomes almost constant. By the comparison according to the water-cement ratio, in this case of standardize age 182 days of I-50-185, the difference of drying shrinkage has that I-40-185 was $17*10^{-6}$ small, I-60-185 was $24*10^{-6}$ small, it is considered to almost same. However, the difference of weight loss ratio has that I-40-185 was 0.57% small, I-60-185 was 0.53% large, weight loss ratio decreased greatly so that the water-cement ratio was large.

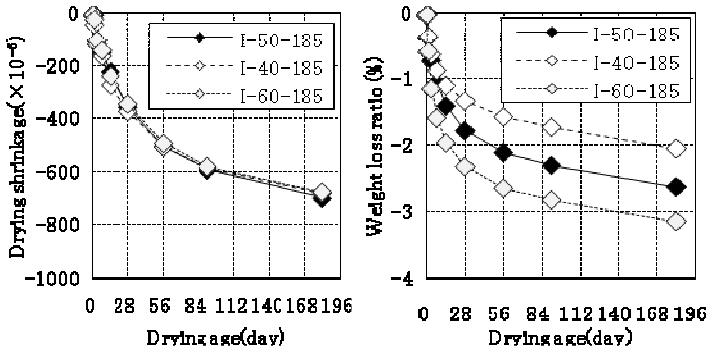

Figure 3. Result of drying shrinkage and weight loss ratio.

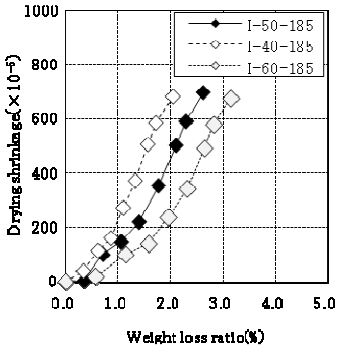

Figure 4. Relationship between drying shrinkage and weight loss ratio.

Because there is much non-reaction water so that the water cement ratio is large, it is guessed that water is easy to evaporate in the atmosphere from concrete. In addition, the capillary tube tension to occur by water evaporating is expressed in equation [1]. The capillary tube tension is influenced by surface tension and the pore diameter, and surface tension is small that pore diameter is large. Therefore in the case that water-cement ratio is large, a lot of water evaporation in the young age, it is guessed that comparatively large of diameters pore was easy evaporated the non-activity water. In addition, when the water-cement ratio was different, after 28 days of weight loss ratio is constant to difference. Therefore, the capillary tube tension based on shrinkage stress is thought for almost same, so it is guessed that pore diameter is almost same.

$$\Delta P = -2\gamma/r \qquad [1]$$

where: ΔP : The capillary tube tension [N]
γ : Water surface tension [N/m]
r : Radius of pore [m]

The influence of drying shrinkage by water-cement ratio and water content for constant of volume of coarse aggregate is small. However, influence of weight loss ratio by water-cement ratio is large.

3.3 The Influence of Drying Shrinkage for Coarse Aggregate and Relative Humidity

As results of drying shrinkage for coarse aggregate and relative humidity is shown in **Figure 5**. The influence of drying condition is little of drying shrinkage in case to higher of relative humidity by regardless of a coarse aggregate. In addition, the difference of the dry shrinkage is small with around $10\sim50*10^{-6}$ in the young age, however a difference becomes large with the progress to age after drying age 28 days. And progress of the dry shrinkage becomes slow after drying age 56 days of humidity condition 80%RH. By the comparison according to kind of coarse aggregate is shown in **Figure 6**, in this case of standardize age 182 days of I-50-185, the difference of drying shrinkage has that O-50-185 was $126*10^{-6}$ large, S-50-185 was $69*10^{-6}$ small, H-50-185 was $87*10^{-6}$ large, limestone of S-50-185 was small of drying shrinkage. In addition, results are different in the area where even the same rock was produced. This is so that the generation, depth, the weathering that a rock is the same, and stratum was produced is different. By the comparison according to kind of relative humidity is shown in **Figure 7**, in this case of standardize age 182 days of 60%RH. The difference of drying shrinkage to I-50-185 has that 40%RH was $111*10^{-6}$ large , 80%RH was $135*10^{-6}$ small, it was difference to almost large that relative humidity was low. In addition, the difference of drying shrinkage to O-50-15 has that 40%RH was $68*10^{-6}$ large, 80%RH $256*10^{-6}$ small, 40%RH~60%RH has slowly change, but 60%RH~80%RH has large change.

Because young's modules was higher as for S-50-185 to shown in **Figure 8**, resistance of mortar shrinkage. Therefore, it is smaller to drying shrinkage. In addition, I-50-185 was produced slightly unevenness by young drying age. I-50-185 compared to other mix proportions of concrete, and the difference of young's module was $1.3\sim4.5kN/mm^2$ at drying age 7 days. Therefore, under the environment that the drying shrinkage less than 60%RH produces, the dry shrinkage is large so that young's module of concrete was the small growth. However, under the environment of 80%RH, after drying age 56 days the stress shrinks so that the drying shrinkage converges. The fall of the shrinkage stress shows that there becomes little influence of young's module. Therefor, under the environment of the high humidity, influence on drying shrinkage by the kind of coarse aggregate relatively shrinks.

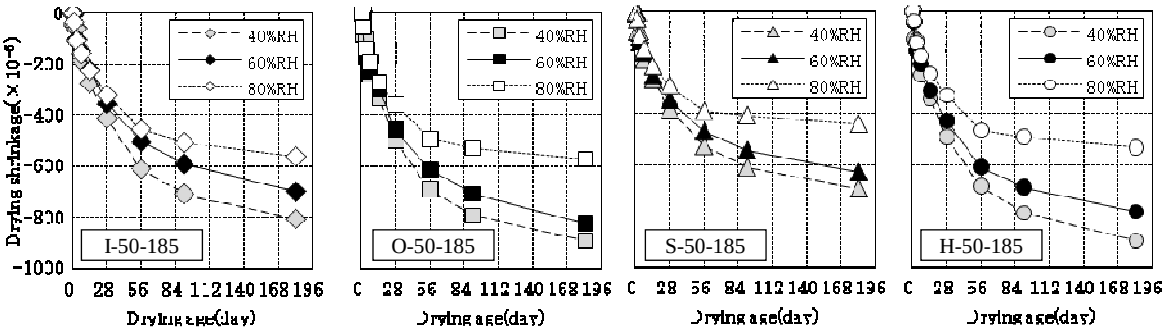

Figure 5. Result of drying shrinkage test.

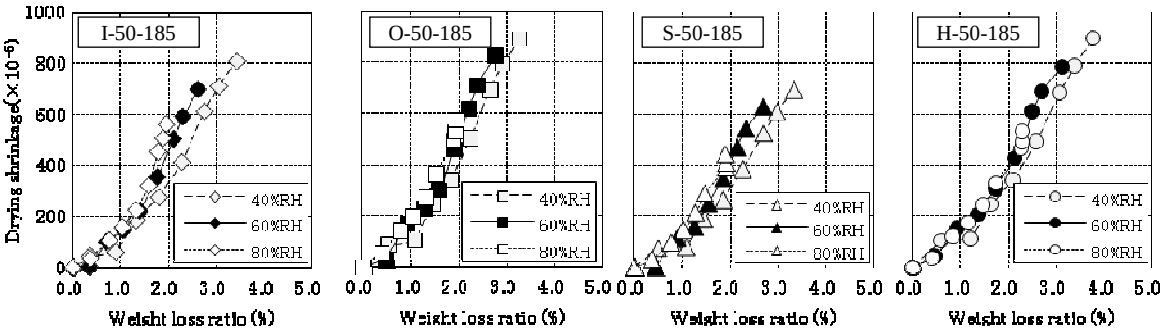

Figure 6. Relationship between drying shrinkage and weight loss ratio of coarse aggregate.

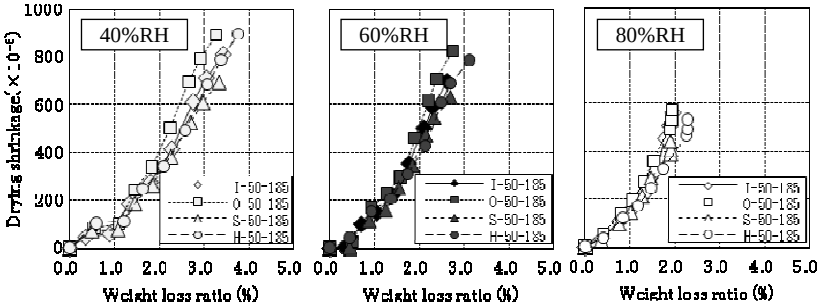

Figure 7. Relationship between drying shrinkage and weight loss ratio of relative humidity.

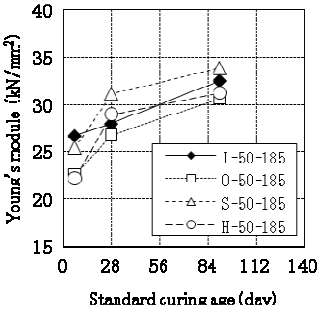

Figure 8. Relationship between young's module and standard curing age.

4 THE QUANTIFICATION ABOUT THE INFLUENCE ON DRYING SHRINKAGE OF THE RELATIVE HUMIDITY

Shrinkage prediction equation based on a recommendations defined by equation [2]. This equation considered to the influence of equation [3] ~ [6], it is expressed in the product of mix proportions and drying age for start and relative humidity. In this study, the quantification about the influence of the relative humidity is examined by coefficient of relative humidity [K_3].

$$\varepsilon_{sh}(t,t_0)=\varepsilon_{sh\infty}\cdot\left(\frac{(t-t_0)}{\alpha+(t-t_0)}\right)^{\beta} \quad [2]$$

$$\varepsilon_{sh\infty}=K_1*K_2*K_3 \quad [3]$$

$$K_1=(7.4W-0.7C-0.55G+270)*\gamma_1*\gamma_2*\gamma_3 \quad [4]$$

$$K_2=1.17t_0-0.08 \quad [5]$$

$$K_3=1.28*[1-(h/100)^3] \quad (40\%\leq h<99\%) \quad [6]$$

where: $\varepsilon_{sh}(t,t_0)$: Drying shrinkage of started for drying age t_0 [$*10^{-6}$]
$\varepsilon_{sh\infty}$: As for last time, drying shrinkage [$*10^{-6}$]
K_1 : The coefficients for mix proportions of concrete
K_2 : The coefficients for started for drying age
K_3 : The coefficients for relative humidity
α, β : The coefficient to express progress of drying shrinkage
W : Water content [kg/m^3]
C : Cement content [kg/m^3]
G : Aggregate content [kg/m^3]
$\gamma_1,\gamma_2,\gamma_3$: The amended coefficient of influence for aggregate, cement, admixture

Table 5. Result of coefficient a and exponent b.

Symbol	*a*	*b*	R^2
I-50-185	1.04	5.2	0.985
O-50-185	1.20	5.1	0.999
S-50-185	0.92	5.1	0.999
H-50-185	1.21	4.3	0.999

$$K_{3_exp}=a*[1-(h/100)^b] \quad (40\%\leq h<99\%) \quad [7]$$

$$K_{3_cul}=\varepsilon_{sh\infty}[K_1/K_2] \quad (40\%\leq h<99\%) \quad [8]$$

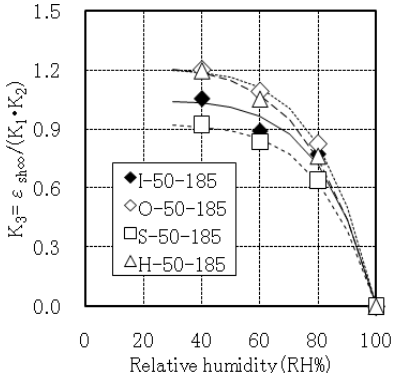

Figure 9. Relationship between Relative humidity and K_3.

The equation [7] assumed for amended relative humidity, K3_cul is calculated based on results by equation [8]. The least-squares method calculated to coefficient "a" and "b". However, the dry shrinkage assumed it 0 at relative humidity 100% (in other words, K_3=0), and the results was calculated asγ_1=1, γ_2=1, γ_3=1 by the amended coefficient of influence for aggregate, cement, admixture. In addition, it was assumed that the coverage of the expression was more than relative humidity 40%RH. As results of calculated is shown in **Table 5** and **Figure 9**.
Coefficient "a" was calculated in 0.92-1.21 ranges and showed the result that was lower than the coefficient of recommendations. Coefficient "a" is different by a kind of the coarse aggregate. In addition, coefficient "a" shows a tendency to become small so that Young's module of concrete is large. It is thinkable for influence of the kind of the coarse aggregate, and it is examined in future.
Index "b" was calculated in 4.3-5.2 ranges and showed the result that was slightly larger than recommendations. When index b was calculated for b=3 by recommendations, drying shrinkage in the high humidity environment of 80%RH is shown that predicted results is larger than experimental results. In previous study[Sugiyama,*et al.* 1996], it was reported to have a big width micro crack when environment of humidity was lower. So that shrinkage stress is relaxed in the low humidity area, index "b" is overestimate, and it is guessed in the high humidity environment when experimental results of drying shrinkage became larger than a predicted results.

5 CONCLUSIONS

On the basis of the results obtained from the experimental investigation, followings could be shown.
(1) Water-cement ratio and water conten in the mix proportion show rather slight effect to the drying shrinkage, however, water-cement ratio is an influential factor to the weight loss ratio.
(2) Diiferent relative humidity conditions and difference of coarse aggregate act as the significant effect to the factor in a way to predict drying shrinkage of concrete.
(3) The revision coefficient of the relative humidity in drying shrinkage predictive equation expresses relative humidity by exponential function of cubic, and it is corrected the clause with coefficient 1.28. In this study, coefficient and index in the revision equation of the relative humidity was calculated based on an experiment result. When revision equation of coefficient and index were compared with recommendations, coefficient a was small in 0.92-1.21 ranges, and index b showed result bigger than an recommendations in 4.3-5.2 ranges.

ACKNOWLEDGMENTS

This experimental project has been carried out in conjyunction with the activities of the joint resarch group ‘Reinforce Concrete’, members are from Building Resarch Institute, Center for Better Living and nine construction companies.

REFERENCES

Architectural Institute of Japan, 2006 ‘Recommendations for Practice of Crack Control in Reinforced Concrete Buildings (Design and Construction)’, pp.53-60.

Thomas Telford, 1990, COMITE EURO-INTERNATIONAL DU BETON: CEB-FIP Model Code 90.

Sugiyama, H *et al.* 1995, ‘Influence of humidity condition on drying shrinkage of concrete’, Cement Science and Concrete Technology, pp.594-599.

Sugiyama, H *et al.* 1996, ‘Fundamental study on length change of concrete caused by drying shrinkage’, Cement Science and Concrete Technology, pp.460-465.

XII DBMC
International Conference on Durability of Building Materials and Components
PORTO - PORTUGAL, April 12th-15th, 2011

Durability Evaluation of Highly Reflective Coating Materials for Roofing

Kenji Motohashi [1]
Masataka Tamura [2]

ABSTRACT

Highly reflective coating materials for roofing (cool roof paints) are becoming popular in Japanese market. It is expected that these coating materials can reduce the energy costs of buildings in the summer and also control the heat island phenomenon in urban regions.

In this context, various highly reflective coating materials obtained from the market were evaluated by an outdoor exposure test for up to three years and a sunshine carbon arc-type artificial aging test for up to 4000 hours. Reflectance of solar radiation, gloss retention, and the color difference of the painted specimens were monitored for 24 brands of highly reflective coating products (color: gray, N = 6.0) in the study.

Polymer binders can be classified as polyurethane resins, silicone resins, and fluoropolymer resins. In general, the gloss retention percentages of commercial reflective coating materials were higher in order of fluoropolymer resins, silicone resins, and polyurethane resins in the sunshine carbon arc irradiation test. The color difference of the specimens exposed to the outdoor condition increased after one year and did not change so much after two years. However, it changed to a large extent after three years again. The color differences of some products increased and those of other products decreased after three years.

The solar reflectance values did not show changes in both the outdoor exposure test and the accelerated aging test.

KEYWORDS

Accelerated aging, Coating material, Cool roof, Outdoor exposure, Solar reflectance.

[1] Faculty of Engineering, Shibaura Institute of Technology, Tokyo, JAPAN, motoken@shibaura-it.ac.jp
[2] R&D Department, Rock Paint Co. Ltd., Tokyo, JAPAN, masataka.tamura@rockpaint.co.jp

1 INTRODUCTION

The heat island phenomenon is becoming a serious problem in urban areas in Japan. Table 1 shows the estimated temperature rise in Japanese cities. For example, the annual average temperature in Tokyo is estimated to increase by 3.0 degrees Celsius after 100 years. On the other hand, the annual average temperature in small cities is estimated to increase by 1.0 degree Celsius. For this reason, the central government and local governments including large cities have adopted various countermeasures against the heat island phenomenon.

Table 1. Estimated temperature rise in Japanese cities. (Metrological Agency, Japan)

City	*Rise in average temperature per 100 years* [degree in Celsius]		
	Annual	*January*	*August*
Sapporo	+2.3	+3.0	+1.5
Sendai	+2.3	+3.5	+0.6
Tokyo	+3.0	+3.8	+2.6
Nagoya	+2.6	+3.6	+1.9
Kyoto	+2.5	+3.2	+2.3
Fukuoka	+2.5	+1.9	+2.1
Ave. in Large Cities	+2.5	+3.2	+1.8
Ave. in Small Cities	+1.0	+1.0	+1.0

The application of highly reflective coating materials for roofing is considered to be one of the effective countermeasures. Highly reflective coating materials, often called “cool roof paint,” are those coating materials that can form coated layers having high reflectance especially for the infrared ray region.

Figure 1 shows the solar reflectance distribution of a highly reflective coating layer and an ordinary coating layer. The color of both coating layers was gray (N = 6.0). As shown in Fig. 1, there was little difference in the reflectance percentage within the visible wavelength region; however, there was a large difference in reflectance percentage within the infrared wavelength region. Therefore, users can select reflective coating materials irrespective of the color of the coated layers. Highly reflective coating materials have a great potential in the market even though the color of roofing materials in Japan is mostly dark.

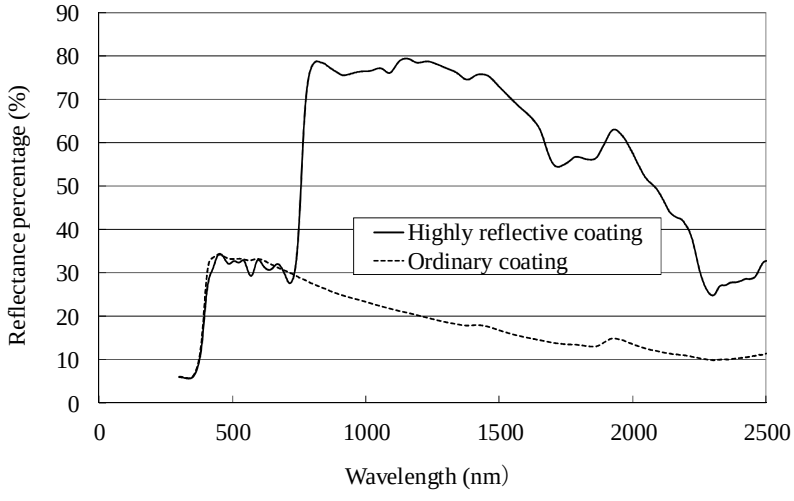

Figure 1. Solar reflectance spectra of a highly reflective coating and an ordinary coating.

There are various reflective coating materials in the Japanese market. To assist users in selecting appropriate coating products, standardization of such coating materials is in progress. As a part of such activities, JIS K 5602:2008 (Determination of reflectance of solar radiation by paint film) has been already standardized. The standardization of highly reflective coating products is also in progress. One important aspect for the standardization of reflective coating products is the durability of the materials and their solar reflectance performances over time. To investigate these points, their outdoor exposures for three years and accelerated aging for 4000 hours have been analyzed in this study.

2 EXPERIMENTAL

2.1 Objected Coating

The objected coating products are listed in Table 2. We evaluated 24 products of highly reflective coating materials in this study. The color of all the reflective coatings was gray (N = 5.9 ~ 6.1). Some tested coating products were applied on a metallic roof sheet, and such types of coating products were coated on an aluminum sheet (0.5-mm thick) standardized in JIS H 4000:2006 (Aluminum and aluminum alloy sheets and plates, strips and coiled sheets), according to the manufacturer's specifications.

The other coating systems of the objected coating projects were applied to cementitious roofing substrate; therefore, such coating products were coated on fiber-reinforced cement sheet (3.0-mm thick), standardized in JIS A 5430:2008 (Fiber reinforced cement boards), according to the manufacturer's specifications. The ordinary coating products listed in Table 1 have also been evaluated for comparison.

Table 2. Objected coating products.

Type	Binder	Color	Number of Products
Highly reflective coating	Solvent type polyurethane	Gray	4
	Solvent type silicone	Gray	7
	Solvent type fluoropolymer	Gray	1
	Water based silicone	Gray	11
	Water based fluoropolymer	Gray	1
Ordinary coating	Solvent type polyurethane	Gray	1
	Solvent type polyurethane	White	1
	Solvent type polyurethane	Black	1

2.2 Outdoor Exposure Test

The specimen size was 150 by 300 mm for both aluminum and fiber-reinforced cement sheets. The coated specimens were mounted on a rack at an angle of 45 degrees facing south at the outdoor exposure site of the Building Research Institute located in Tsukuba city, which is about 80 km north of Tokyo. The specimens were exposed for three years.

2.3 Accelerated Aging Test

The specimen size was 70 by 150 mm for both substrates. A sunshine carbon arc irradiation test standardized in ISO 4892-4:1994 was conducted for the coated specimens. Water spraying was applied for 18 minutes every 120 minutes. The ultraviolet irradiation intensity (wavelength range: 300-700 nm) was monitored at the position of the specimen surface by using an accumulated photometer. The test was conducted for 4000 hours.

2.4 Measurement of Color, Gloss, and Solar Reflectance

The color differences (delta E*ab), gloss values (reflection at 60 degrees), and solar reflectance were measured periodically in the outdoor exposure test and the accelerated aging test. The solar reflectance was measured on the basis of JIS K 5602:2008. According to JIS K 5602:2008, the solar reflectance is defined as follows;

$$\rho_e = \frac{\sum_{\lambda} [(E\lambda \times \Delta\lambda) \times \rho(\lambda)]}{\sum_{\lambda} (E\lambda \times \Delta\lambda)} \quad (1)$$

ρ_e : Solar reflectance
$\rho(\lambda)$: Specific reflection percentage (%)
$E\lambda \times \Delta\lambda$: Weighting coefficients based on ISO 9845-1:1992 (W/m^2)
λ : Wave length (nm)

3 RESULTS AND DISCUSSION

3.1 Changes in Color Difference

Figs 2 and 3 show the changes in the color difference values of typical reflective coating specimens for each type of polymer binder for the outdoor exposure test and the accelerated aging test, respectively. In the outdoor exposure test, there was little difference in the color difference values between after one year and after two years; however, the values of some products increased again, and the values of the other products decreased after three years. We speculated that soiling was the predominant deterioration within 2 years; however, chalking behavior or degradation of the surface polymers progressed in addition to soiling after three years.

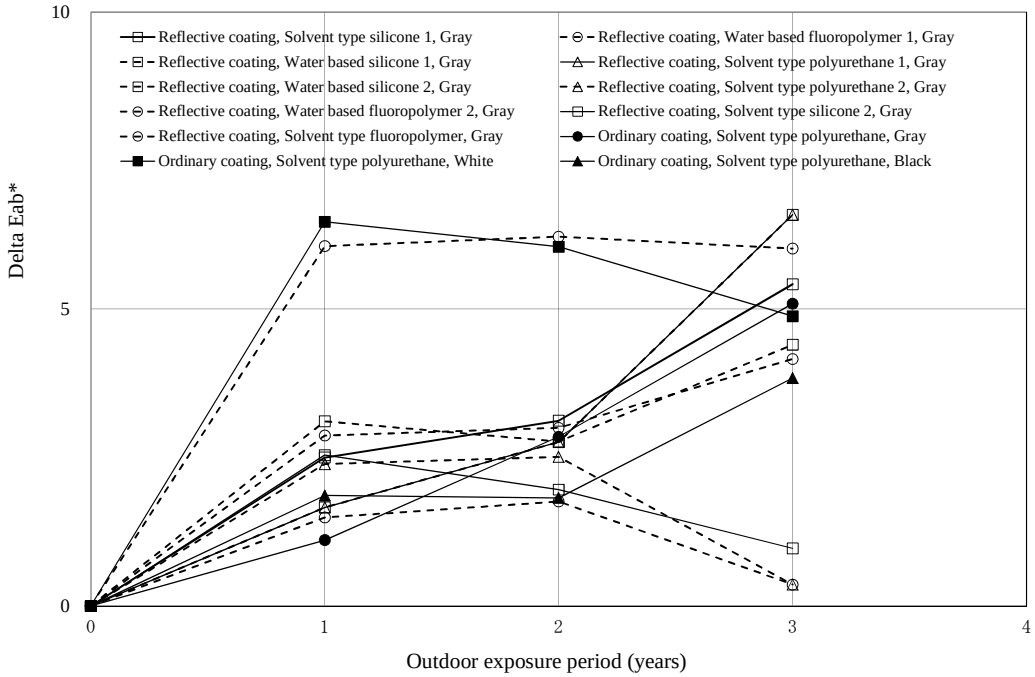

Figure 2. Changes in the color difference values of the specimens without washing in the outdoor exposure test.

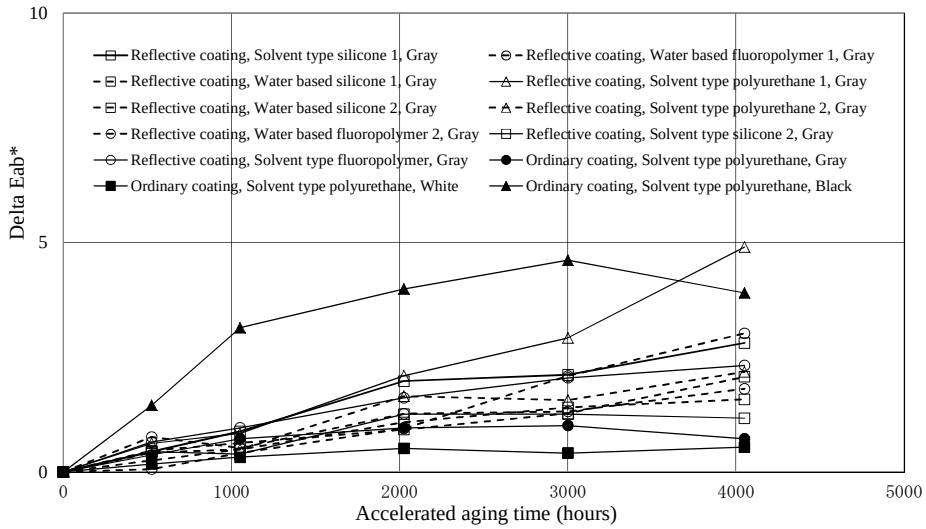

Figure 3. Changes in the color difference values of the specimens in the accelerated aging test.

In the accelerated aging test, the color difference values of most products seemed to increase gradually with the acceleration periods, and those of the other products seemed to reach almost constant values. The influence of the polymer binders on the color differences were different for the outdoor exposure test and the acceleration test. The deterioration of the polymer binders and the color changes of the pigments were the main factors for the color changes of the specimens in the acceleration test, and soiling was another factor in the outdoor exposure test.

3.2 Changes in Gloss Retention

Figure 4 plots the gloss retention percentages in the accelerated aging test. The gloss retention percentages decreased gradually with the acceleration time as shown in Figure 4. In general, gloss retention is related to the durability of the polymer binders of the coating products. The gloss retention values were higher in order of fluoropolymer resins, silicone resins, and polyurethane resins. This result was consistent with the past results reported by [Motohashi 1993] and [Motohashi *et al.* 1998].

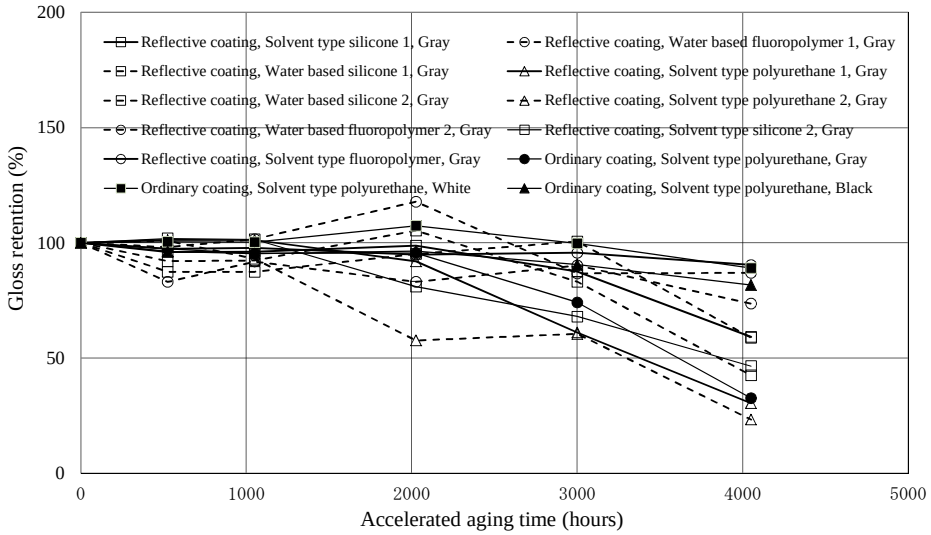

Figure 4. Changes in gloss retention of specimens in the accelerated aging test.

Although the data are not shown, we confirmed that the gloss retention percentages in the outdoor exposure test showed different tendencies from the results obtained in the acceleration test. The attachment of dirt affected the gloss retention values in the outdoor exposure test; however, the attachment of dirt could not be simulated in the accelerated aging test.

3.3 Changes in Solar Reflectance

Figure 5 shows the changes in the solar reflectance values of typical specimens without washing for each type of polymer binder for the outdoor exposure test. In general, there was little difference in the solar reflectance values for the outdoor exposure test and the accelerated aging test.

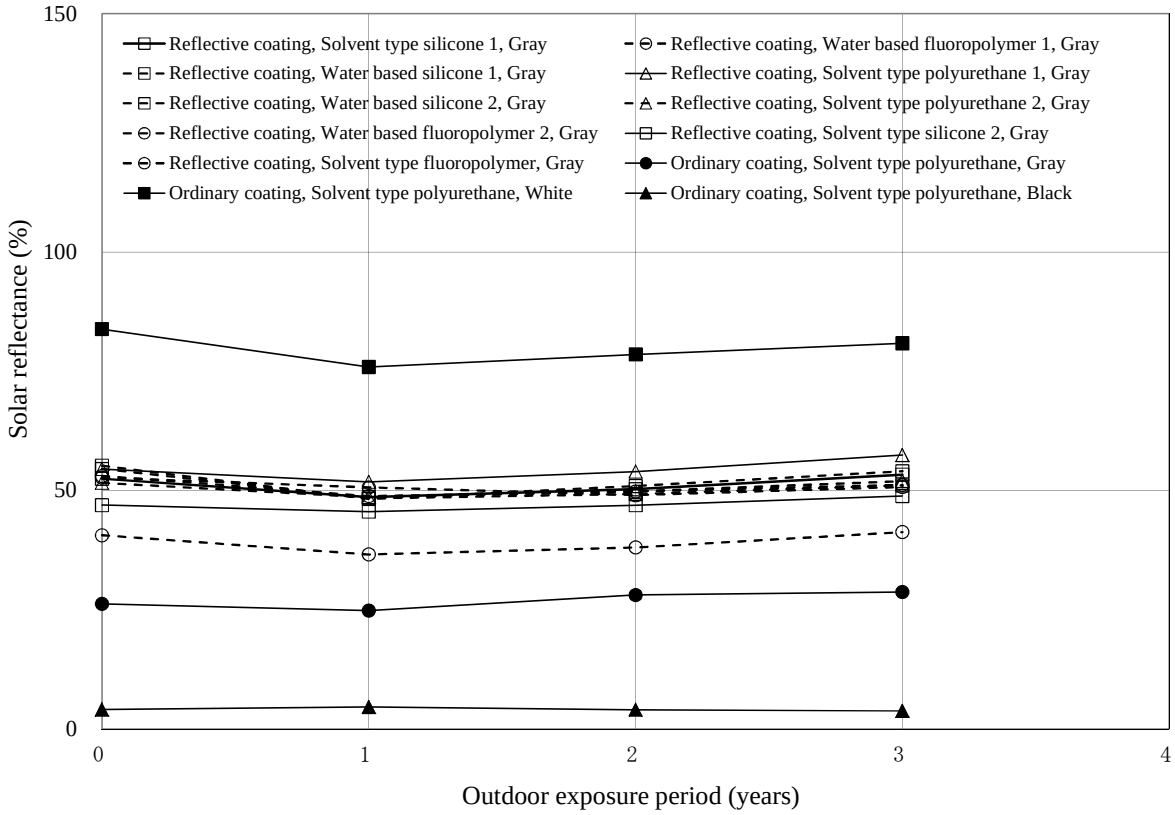

Figure 5. Changes in solar reflectance of specimens without washing in the outdoor exposure test.

Figure 6 shows the relationship between the color difference values and solar reflectance values before washing for all highly reflective coating specimens evaluated in the outdoor exposure test. As shown in Figure 6, a strong correlation exists between the delta E*ab values and the solar reflectance values for the specimens that had been exposed for one year and two years. However, there was no correlation between the two values for the specimens that had been exposed for three years.

It can be reasonably considered that the soiling phenomenon can affect the solar reflectance values. In other words, the solar reflectance values decreased because of soiling. The strong correlation between the delta E*ab and the solar reflectance for the specimens exposed for one or two years can be understood with this reason.

However, after three years, the specimens did not demonstrate the same tendency. Some of the specimens displayed chalking behavior after three years. As shown in Figure 2, the delta E*ab values after one year and after two years showed a uniform trend, i.e., they increased gradually. However, they did not show a uniform trend after three years. The delta E*ab values of some specimens

considerably increased after three years, and the values of the other specimens considerably decreased; this suggests that the occurrence of chalking or discoloration of the specimens exposed for three years in outdoor conditions was probably the reason for no correlation between the delta E*ab values and the solar reflectance after three years.

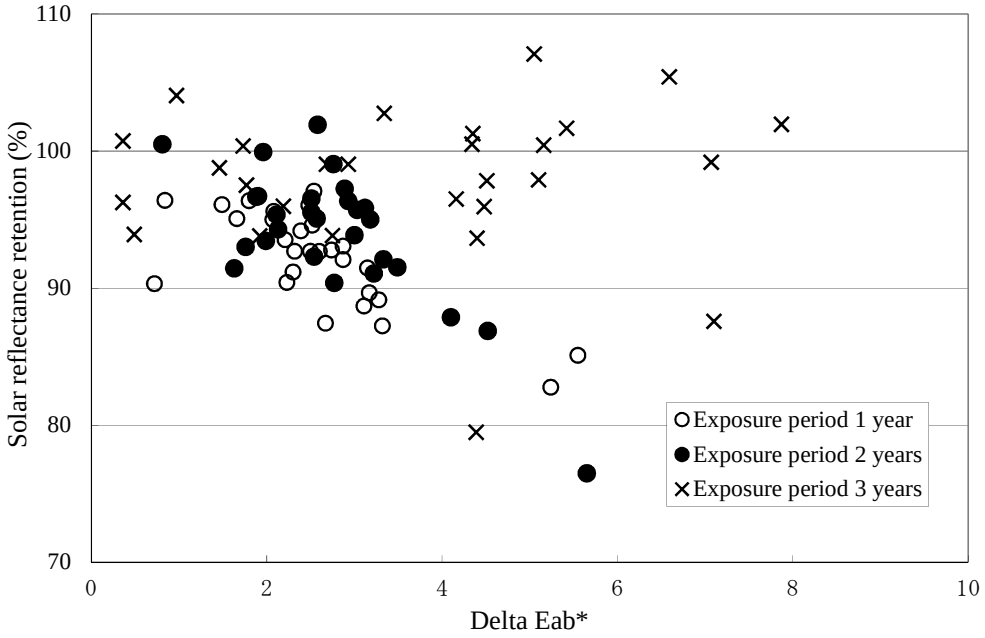

Figure 6. Relationship between color difference and solar reflectance for all the specimens that were coated with highly reflective coating products.

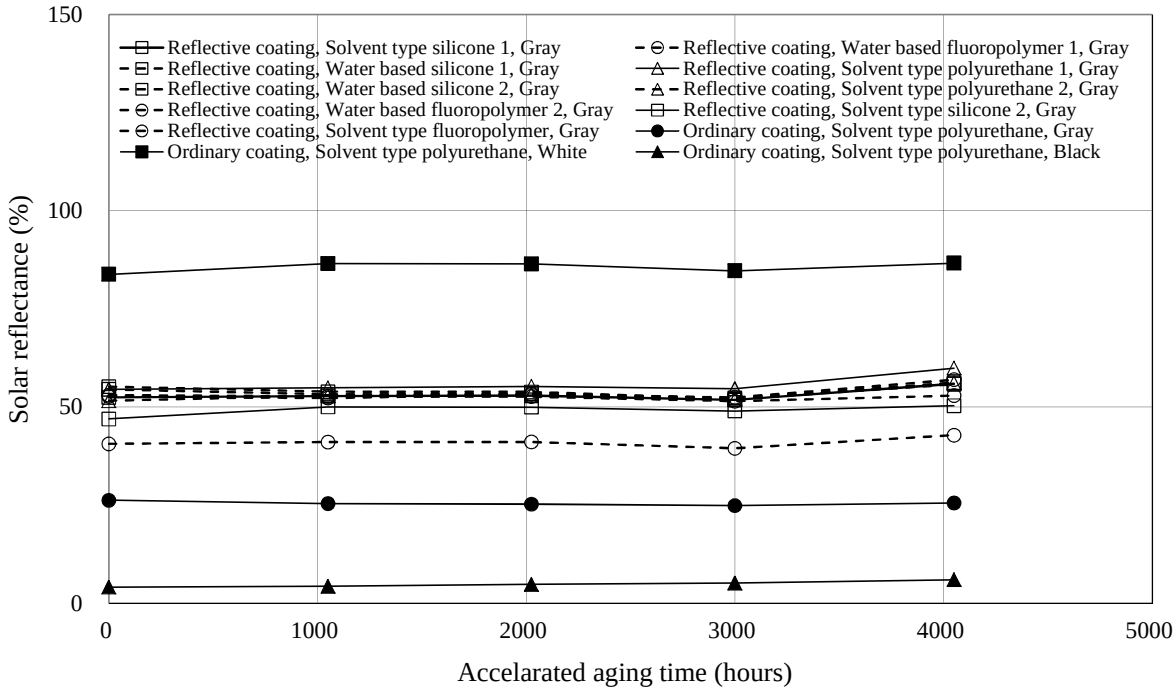

Figure 7. Changes in the solar reflectance of the specimens in the accelerated aging test.

Figure 7 the changes in the solar reflectance values of a typical specimen in the accelerated aging test. Compared to the outdoor exposure test, there were smaller changes in the solar reflectance values in the acceleration test because the soiling phenomenon (attachment of dirt) did not occur in the

sunshine carbon arc type irradiation test. We recognized that the solar reflectance values of some specimens slightly increased after 4000 hours and speculated that chalking or degradation of the surface polymer might have occurred in those specimens after 4000 hours of irradiation. It can be reasonably considered that the chalking behavior increase the solar reflectance values of the specimens.

4 CONCLUSIONS

We evaluated the highly reflective coating products obtained from the market by an outdoor exposure test and a sunshine carbon arc-type artificial aging test. Changes in the color difference, gloss retention, and solar reflectance were monitored in the study. The main results are summarized as follows:

1) The color difference increased within one year and did not change much. However, it changed considerably after three years. The color difference of some specimens increased, and color difference of other specimens decreased after three years.

2) The gloss retention values gradually decreased with the aging time in the accelerated aging test. The gloss retention percentages were dependent on the types of polymer binders.

3) In general, the solar reflectance values showed little change in the outdoor exposure test as well as the accelerated aging test. A high correlation was recognized between the color difference and the solar reflectance for the unwashed specimens exposed for one year and two years in the outdoor condition. However, such correlation was not confirmed for the specimens exposed for three years, which seems to be because of the occurrence of chalking or discoloration of the specimens after three years.

ACKNOWLEDGMENTS

The study was conducted in conjunction with the research activity of the Japan Building Coating Materials Association.

REFERENCES

Motohashi, K. 1993, ‘Performance Evaluation of Newly Developed and Highly Durable Coating Materials,’ Proc. 6th International Conference on Durability of Building Materials and Components, Omiya, Japan, vol. 2, pp. 724–733.

Motohashi, K., Hirano, T., Miyazaki, N., and Yamanouchi, M. 1998, ‘Durability Evaluation of Newly Developed Fluoropolymer Emulsion Paints,’ Proc. CIB World Building Congress on Materials and Technologies for Sustainable Construction, Gavle, Sweden, vol. 1, pp. 357–364.

XII DBMC
International Conference on Durability of Building Materials and Components
PORTO - PORTUGAL, April 12th-15th, 2011

Longterm Field Studies and Residual Service Life Prediction of FPO Roofing Membranes

Hans-Rudolf Beer [1]
Carine Kerber [1]
Günther Rieche [2]
Jean-Luc Schläpfer [1]
Hansrudolf Unold [3]
Stefan Wehrle [2]

ABSTRACT

The results of fields studies after 10, 15 and 20 years of roof exposure of FPO membranes from a European manufacturer will be presented as well as data from continuous monitoring of designated roofs. On-site roof inspections and laboratory testing of aged roof samples were used for the assessment of the durability of the polymer membranes.

The results of these studies are used as input for estimations of the residual service life of the membranes. The time dependant behaviour of the mechanical strength in comparison to standard design requirements is used for these estimations. The findings of these residual service life prediction procedures are discussed.

KEYWORDS

FPO, Roofing, Service life, Durability, Membranes.

[1] Sika Technology AG, Sarnen, Switzerland, beer.hans-rudolf@ch.sika.com
[2] Institut für Bautenschutz, Baustoffe und Bauphysik, Fellbach, Germany, info@rieche-schuerger.de
[3] Sika Services AG, Sarnen, Switzerland, unold.hansrudolf@ch.sika.com

1 INTRODUCTION

The use of flexible polyolefin membranes in roofing has only been possible after the introduction of powerful light stabilisers. Hindered amine light stabilisers are accessible to roofing since the mid 1980's. First FPO roofs have been installed in 1988 in Europe. Full market introduction of FPO roofing membranes was in February 1991 in Europe and somewhat later in North America. Since then these roofing membranes have gained wide acceptance in the European as well as in the North American market place (Baxter [1998], Beer [1995, 1997], Foley [1997], Paroli [1999]). The common designation for this type of roofing membranes is FPO (flexible polyolefins) in Europe and TPO (thermoplastic polyolefins) in North America.

Durability of building materials is a key topic in building construction. When innovative materials are introduced to the market, well based predictions of their service life are of prime importance. Lacking track records, the extrapolation of data from accelerated ageing tests is the only means for meaningful predictions on the durability of the new products. At the time of the first test installations only such predictions could be used for the estimation of the material's durability. Based on the manufacturer's experience, comprehensive testing programs and a series of field tests which had begun in 1988, the service life of the new kind of membranes was predicted at several decades. Now, more than twenty years later, these assumptions can be verified. On the occasion of 20 years of field experience with flexible polyolefin roofs the manufacturer Sika commissioned in 2008 a third party testing institute (Wehrle [2009]) with the task of an expert report on the durability of their FPO membranes.

This testing institute had already carried out expert studies after ten and fifteen years of field experience with FPO membranes (Rieche [1999, 2004]). The results were presented to the roof waterproofing community (Beer [2000, 2008]). The overall assessment of these studies was very positive regarding the durability of the manufacturer’s FPO roofing membranes. The fact that the observed deterioration of the material properties was only marginal supports the previous assumption of a service life of several decades.

2 METHODOLOGY

The investigation described here is based on a field study of roofing membranes on 139 roofs covered with Sarnafil T FPO membranes with fiber glass mat inner layer (referenced as G-type) for ballasted applications or with combined reinforcement of fiber glass mat and polyester scrim (referenced as S-type). The roofs inspected were exposed to Central European climate (no heat/desert or arctic extremes). It has to be noted that fire behaviour tests (external fire performance) are less severe in Central Europe than in other countries like USA or UK. Thus they contain a lower amount of flame retardents or even none (G-type), which may have a positive influence on their longevity. On behalf of the manufacturer the German Institute for Building Protection, Building Materials and Construction Physics (Wehrle [2009]) examined and evaluated four roofs of various age, taking into consideration the overall evaluation 139 roofs monitored by the manufacturer. A total of more than 200 samples of FPO roofing membranes with ages up to 20 years were collected and examined The data of samples aged 13-20 years were collected from generation 1 products (PE base). The other samples are PP based. The roof assessment and testing of material samples of the four roofs was done by the institute independently of the manufacturer’s surveys, according to the following criteria:

Roof assessments: General condition of roofing, roof assembly, flashings, welded seams, construction technology aspects were inspected and assessed on site.

Material samples: Laboratory testing included determination of thickness, tensile strength, elongation at break, low temperature flexibility, peel strength and shear strength of site-welded seams, and microscopic investigation of the membrane surface.

These properties are essential for predicting the durability of polymeric waterproofing membranes. By merging the data of the institute and the manufacturer the long-term stability and durability of FPO roofing membranes of types G and S can be predicted, supported by a broad base of data and using methods of accelerated artificial weathering. The longer the observation period and the larger the number of investigated roofs, the more reliable the data obtained through field investigation is for predicting service life. A more detailed discussion on providing a forecast in the product and system development phase has been presented by Beer [2000].

3 RESULTS

3.1 Roof Assessments

The on-site assessments of four roofs were performed by the testing institute. Roofs A and B were on industrial buildings in Germany. They were covered with mechanically attached S-type membranes. The membranes on roofs C and D were G-type with gravel ballast, located in Switzerland. Roof C was on a shredding and recycling company and roof D was on car parking garages.

All four examined roofs were found to be in good general condition (Figures 1-4). They were all fully functional and showed no signs of leakage or membrane deterioration. Soiled spots could easily be cleaned, even rust arising from metal parts (Figure 2). Edge securings, flashings at penetrations such as curbs (Figure 2) and skylights (Figure 3), corners and other details were intact. All seams probed with a screwdriver were tight. All sampling locations could easily be patched by hot air welding using the standard methods described in the manufacturer's installation guidelines (Figure 4).



Figure 1. Overview of roof A at Fellbach.



Figure 2. Curb flashing detail. Rust stains can can easyly cleaned.



Figure 3. Overview of roof C at Flawil.



Figure 4. Closing of sampling area on roof C.

3.2 Laboratory Testing of Samples

In order to pool the characteristics of various polymeric waterproofing membranes in uniform terms, one can express the change of properties over time in relation to the properties of new material (value of sample after ageing divided by value of new material. A value of 1.0 means no change after ageing. This method was used for presenting the data in this paper.
Mechanical properties of new materials show a certain distribution of values, due to various technical aspects of production and measurement. This distribution of values can be quantified using standard deviation methods. For the graphic display a confidence interval of 99% was chosen. 99 out of 100 measured values of new material lie within the range of the indicated scatter band. If values measured on a sample from an exposed roof are within this confidence interval, this means that the material properties have not changed significantly compared to their initial value. Testing was generally done according to EN 13956 [2005].

Figures 5 and 6 show that ageing of both type of membranes up to 20 years has virtually no influence on the thickness of the membranes.

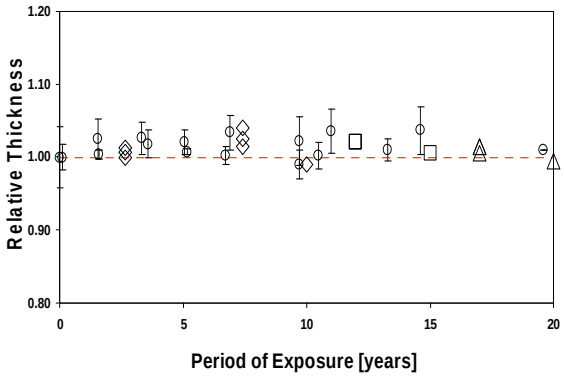

Figure 5. Thickness of aged G-type membranes.
◇ data from 1999 study by Rieche [1999]
□ data from 2004 study by Rieche [2004]
△ data from 2009 study by Wehrle[2009]
○ manufacturer's data from 139 roofs, with 99% confidence band.

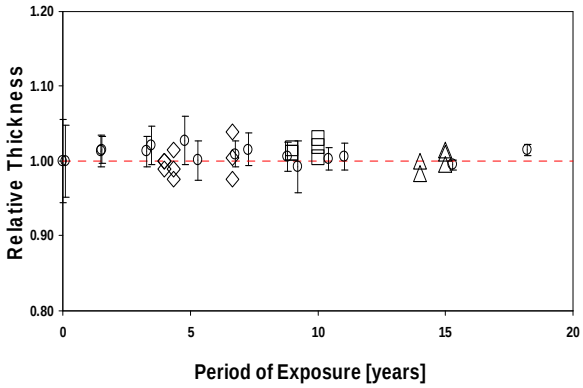

Figure 6. Thickness of aged S-type membranes. Legend as Figure 5.

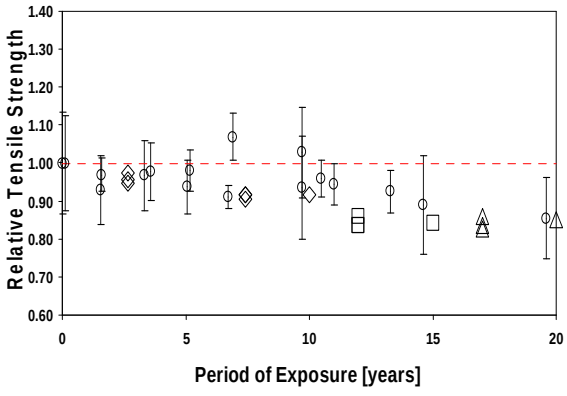

Figure 7. Tensile strength (longitudinal) of aged G-type membranes. Legend as Figure 5.

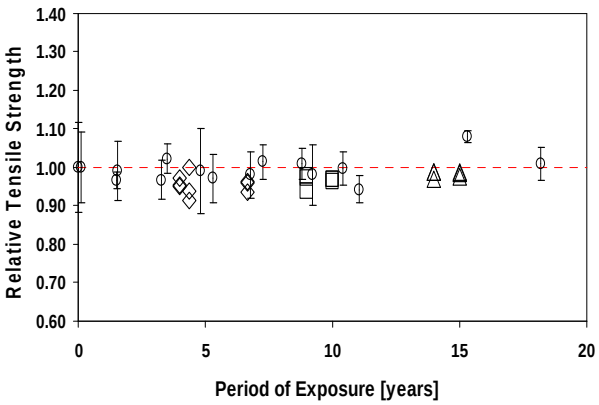

Figure 8. Tensile strength (longitudinal) of aged S-type membranes. Legend as Figure 5.

Figures 7-10 show the development of tensile strength and elongation at break of the membranes with increasing ageing duration. A slight decrease of the tensile strength over the period of 20 years can be

noticed in G-type membranes. No significant change was registered for the elongation at break. In G-type membranes the tensile strength and elongation at break are mainly determined by the properties of the polymer matrix. In S-type membranes these characteristics are governed by the properties of the embedded polyester scrim reinforcement.

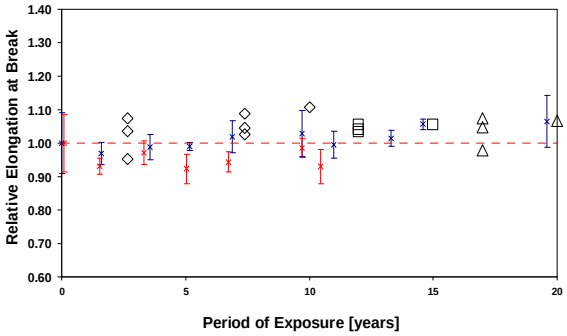

Figure 9. Elongation at break (longitudinal) of aged G-type membranes. Legend as Figure 5.

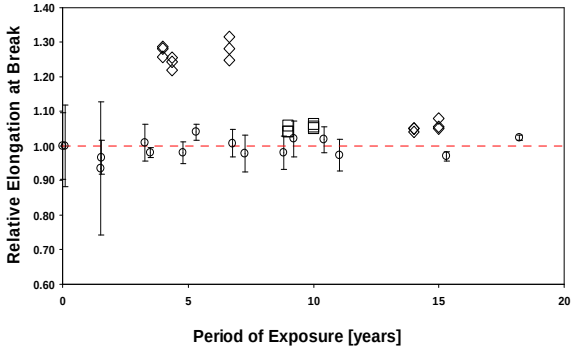

Figure 10. Elongation at break (longitudinal) of aged S-type membranes. Legend as Figure 5.

Elongation at break and tensile strength of S-type membranes did not exhibit any changes over the observation period of 18 years. The runaway values (◇) in Figure 10 were caused by a measurement mistake during the first expert study after 10 years (Rieche [1999]).

The shear and peel strength of seams were determined for both membrane types. The respective data did not exhibit any change from the original values..

All of the tested samples in the 20 year expert study (Wehrle [2009] passed the low temperature folding test EN 495-5 at -30 °C. Five out of seven passed at -35 °C.

Microscopical examination of 20 year old samples of G-type, applied under gravel ballast, revealed no significant changes in comparison to unaged material (Figures 11,12).

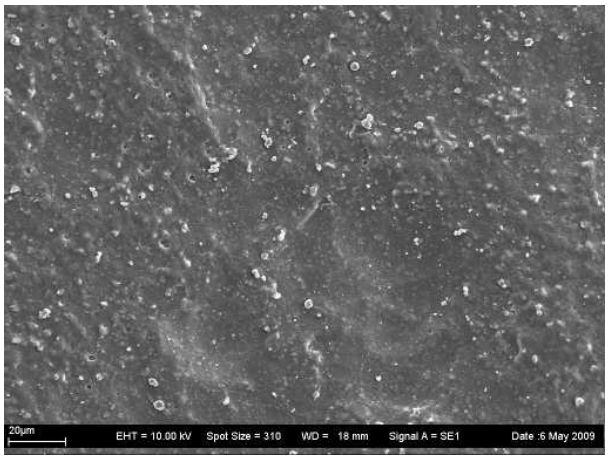

Figure 11. SEM photograph of surface of unaged G-type membrane.

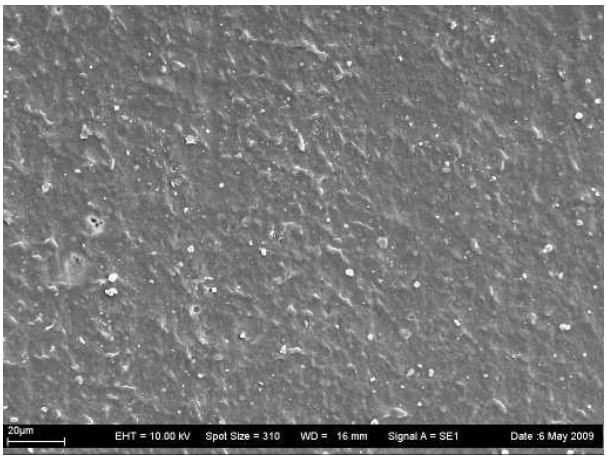

Figure 12. SEM photograph of surface of 20 year roof aged G-type membrane.

The surface of an S-type membrane aged for 15 years in sunlight exposed conditions shows some pollution particles but no degradation in optical microscopy (Figure 13). At higher magnification some faint and isolated crazing was detected (Figure 14). The length of the crazes was below 100 µm, the width 2 µm and the depth was estimated at 10-20 µm.

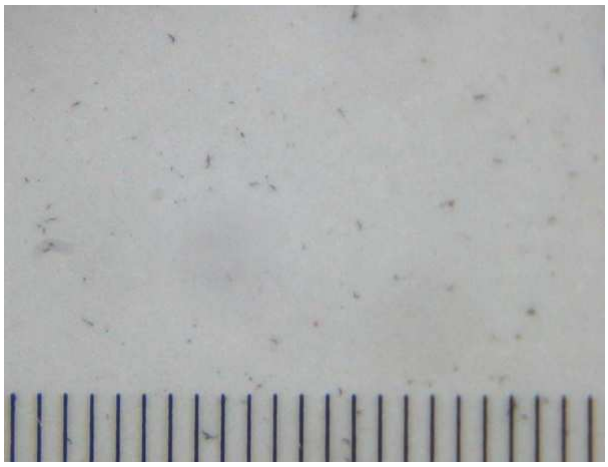

Figure 13. Surface photograph of 15 year roof aged of S-type membrane. Scale division is 1 mm.

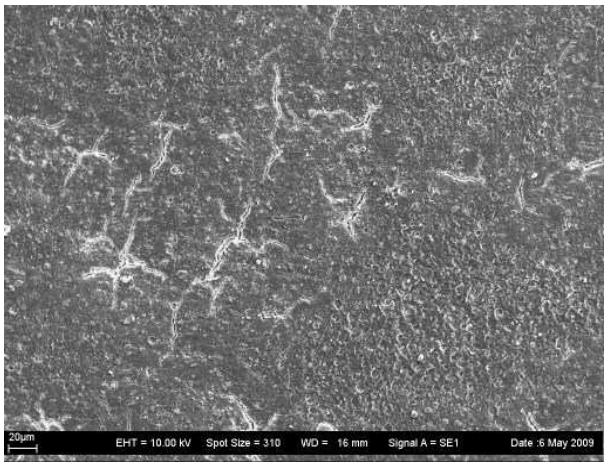

Figure 14. SEM photograph of surface of 15 year roof aged S-type membrane.

Only a small excerpt of all the collected data can be included in this paper. The data shown are a representative selection of all data. In most cases data of the oldest roof of each material type are depicted in this paper. Comparison of all mechanical data does not reveal differences between properties measured in longitudinal or cross direction of the membranes.

4. DISCUSSION

4.1 G-Type Membranes

The roofs investigated with G-type polymeric roofing membrane have been exposed for periods of 17 and 20 years. Thickness of the roof samples did not decrease over the observed period. The SEM inspection of the G-type sample showed no signs of surface changes after 20 years of roof exposure. Mechanical properties, such as elongation at break and flexibility at low temperatures, have not changed over the 20 years of service. All these facts are strong indicators that the material has not undergone significant degradation.

Aged welded seams had the same strength in shear and peel mode as new material. It is an important finding that properly welded seams are not affected by outdoor weathering and are still perfectly tight after 20 years. Another evidence of the non-degrading of the material is the fact that the sampling areas could easily be re-welded with fresh membrane pieces.

A slight reduction in the tensile strength of G-type membranes was observed. The decrease depends on duration of usage. Considering the results from the 15 year study (Rieche [2004], the last five years show a slower reduction of tensile strength in comparison to the reduction during the first decade.

Based on this time-dependent change of the tensile strength a rough estimation of the service life expectation of G-type membranes can be attempted. The membranes are subject to tensile forces arising from thermal expansion and contraction. With a thermal expansion coefficient of 35×10^{-6} 1/K and a temperature difference of 45 °C (+25 °C under application conditions, -20 °C in winter conditions) a length reduction of approximately 0.2% has to be taken into account. This dimensional change leads to a force of approximately 0.3 N/mm^2. The requirement of the standard DIN 18531-2 [2008] is an initial tensile strength value of 5 N/mm^2 for new roofing membranes. Model calculations based on data like in Figures 7 and 8 produce a period of 55 to 100 years before the tensile strength drops to 5 N/mm^2.

According to the manufacturer's long-time experience with mechanical attachments 1.5 N/mm^2 seem to be sufficient for dimensioning of the forces to be dealt with. Allowing for reduction of the above DIN requirement to 3 N/mm^2 after ageing this would still be a double safety margin with the regards to 1.5 N/mm^2 arising from experience and a six to ten fold safety margin with regard to the forces induced by thermal movement. The rough estimation with the 3 N/mm^2 produces a service expectation above 100 years. It needs to be clearly stated that such figures are based on experience data of maximum 20 years and represent theoretical extrapolations. They assume that no conditions during the extrapolated service life will change with regard to the practically experienced duration so far (e.g. no change of climatic conditions, no change in ageing mechanism, etc.). Additionnally it is worth mentioning that the absence of flame retardents is believed to have a positive influence on the long term durability.

4.2 S-Type Membranes

The findings of the S-type membranes are mostly identical with those of the G-type membranes. Due to the embedded polyester reinforcement scrim they show no hint of deterioration in mechanical properties. Faintest surface crazes were found after 15 year outdoor weathering with direct exposure to sunlight. Ultraviolet radiation might have caused the crazes. Crazing is very faint, it cannot be detected by optical microscopy at up to 40 times magnification. In two out of seven samples the low temperature folding value was decreased from -35 °C to -30 °C.

Service life estimations for S-type membranes cannot be done the same way as with G-type membranes due to the reinforcement scrim. However, simple linear extrapolations of the data collected during 18 years suggest further service life expectations of at least the length of the so far experienced service years. However, the testing institute's and the manufacturer's investigations of S-type membranes show that the results of samples from roofs 14 to 15 years old lie within the scatter range of results obtained by internal monitoring of new materials, in other words, within the normal scatter ranges encountered in production. All specimens passed the low temperature folding test at intensified test conditions of –30 °C. With the exception of two specimens (14 years old specimens), no test failures occurred even at testing conditions of –35 °C. Thus the results of the present investigation confirm the data collected by the manufacturer for roofs up to 18 years old. The 1999 and 2004 durability assessments of S-type membranes are confirmed after additional 5 years by the results of this investigation on 20 years old membranes.

There are now two decades of proven, positive experience for the durability of S-type membranes of this manufacturer. The results suggest that the polymeric roofing S-type membranes will fulfil their waterproofing function for further decades, provided they are used in compliance with the application and maintenance requirements and conditions.

5. CONCLUSIONS

The results of this long term study and two decades of proven, positive experience with the type of the investigated FPO membranes suggest that these membranes will be able to fulfill their waterproofing function for further decades. However, this conclusion is restricted to the moderate Central European climate and does not hold for dramatic climatic changes and it assumes the exclusion of exceptional weather events and environmental impacts. Another precondition is the use of the membranes in compliance with the application and maintenance requirements.

No comparative investigations were made with membranes from FPO or TPO manufacturers in other regions. Experience shows that the performance of these kinds of membranes is strongly dependant on their specific formulation (Beer [1997], Carlson [2006]). Improper combination of raw materials and additives can lead to premature failure. Taking these considerations into account the authors

claim that the findings of this investigation are specific to the European FPO membranes examined in this study. An application of these findings to other types of FPO or TPO membranes and other regions is not appropriate.

ACKNOWLEDGMENTS

The authors would like to express their sincere thanks to all building owners who have granted access to their roofs and have agreed to sample collection.

REFERENCES

Baxter D. 1998, "Observations from the field during 1997", Professional Roofing, 2, pp. 22-30.

Beer, H.R. 1995, "Flexible Polyolefin Roofing Membranes - Properties and Ecological Assessment", Proc. 6th Int. Waterproofing Assoc. Congress, Amsterdam, Netherlands, pp. 81-89.

Beer, H.R. 1997, "Longevity and Ecology of Polyolefin Roof Membranes", Proc. 4th. Intl. Symp. on Roofing Technology, Gaithersburg, USA.

Beer, H.R and Keiser, S. 2000, "Flexible Polyolefin Roofing Membranes: Ten Years of Field Experience", Proc. 6th Int. Waterproofing Assoc. Congress, Florence, Italy, pp. 154-172.

Beer, H.R. and Mayr, A, 2008, “Flexible Polyolefin Roofing Membranes: 15 Years Of Field Experience”, Proceedings of the 11th International Conference on Durability of Building Materials and Components, Istanbul, Turkey.

Carlson J., Delgado A.H., Rosenow E., Barnhardt K.C., Paroli R.M. 2006, "Performance Evaluation of Unexposed and Field-exposed Thermoplastic Polyolefin (TPO) Roof Membranes", Roofing Consultants Institute (RCI) 21st International Convention, Phoenix AZ, USA.

EN 13956:2005, "Plastic and rubber sheets for roof waterproofing", Beuth Verlag, Berlin, Germany.

EN 495-5:2000, "Determination of foldability at low temperature", Beuth Verlag, Berlin, Germany.

DIN 18531-2:2008, "Dachabdichtungen", Beuth Verlag, Berlin, Germany.

Foley, R.K. and Rubel, W. 1997, "Polyolefines – The New Roofing Technology", Interface, October, pp. 30-32.

Paroli, R.M., Liu K.Y., Simmons, T.R. 1999, "Thermoplastic Polyolefin Roofing Membranes", Construction Technology Update, NRCC, Ottawa, Ontario, Canada, 30 (Dec.).

Rieche, G. and Wehrle, S. 1999, "Expert report 3460 on the durability of flexible polyolefin roofing membranes of type Sarnafil TS and Sarnafil TG for roofs", Institut für Bautenschutz, Baustoffe und Bauphysik, Fellbach, Germany.

Rieche, G. 2004, "Expert report 4708 on Durability of Sarnafil T polymeric roofing membrane", Inst. für Bautenschutz, Baustoffe und Bauphysik, Fellbach, Germany.

Wehrle, S. and Rieche, G. 2009, "Summary report of Expertise No. 70006: Durability of Sarnafil T polymeric roofing membrane", Inst. für Bautenschutz, Baustoffe und Bauphysik, Fellbach, Germany.

XII DBMC
International Conference on Durability of Building Materials and Components
PORTO - PORTUGAL, April 12th-15th, 2011

Durability of Roof Insulation in Re-Roofing Applications

Steven P. Bentz, P.E., R.R.C. [1]
Ron Erdman, R.R.C., R.R.O. [2]

ABSTRACT

Designers expect that the components of a facility last for the life of that facility. Buildings are increasingly being expected to perform longer due to a shrinking availability of land, sustainability practices, and economic trends that force re-purposing of space. The roof system of a building may be expected to perform for 25-30 years. Re-covering or re-roofing may be needed, which may be predicated on the leak history reported or the deterioration of the roof membrane. When decisions are made about the next roof system, the condition of the original roof insulation should be considered. We will explain how various technologies including thermographic imaging, nuclear-moisture gauge readings, laboratory moisture testing, and visual assessment can be used to determine if the existing insulation is suitable for re-use in the new roof system. Consideration is also given to the long-term thermal resistance (LTTR) and what R-Value can be expected from wet insulation that remains in place after re-covery. This paper examines options associated with various types of insulation considering relative first-cost, potential for re-use, durability, assessment of remaining material, likelihood of damage, LTTR, R-Value of wet insulation, migration of water through the insulation, and eventual recycling. Both low-slope roofs and protected membrane roofs will be considered. The right insulation, if selected at the time of design, is more cost-effective over the life of the facility.

KEYWORDS

Durability, Wet insulation, Long-term thermal resistance (LTTR), R-value, Sustainability.

[1] Facility Engineering Associates, P.C., Senior Engineer, Fairfax, Virginia 22030, USA, Phone 703 5914855, Fax 703 5914857, bentz@feapc.com

[2] Facility Engineering Associates, P.C., Office Manager, Dallas, Texas 75248 USA, Phone 972 7594406, Fax 972 7594411, ron.erdman@feapc.com

1 INTRODUCTION

Key tenets of sustainability include keeping building products in-use as long as possible and avoiding contributions to landfills and waste production. Most agencies recognize that increasing the average R-Value of the roof system will lead to decreased heating and cooling costs. Additionally, it is widely accepted that increasing the reflectively of the roof system will aid in decreasing conditioning costs in most climates as well as in lessening the urban heat island effect. With all these aspects of sustainability in mind, the benefits of a complete tear-off and replacement of a roof system must be carefully weighed against the impact of the waste created when disposing of the existing material. When performing a complete roof replacement, the existing insulation that is removed is many times the bulkiest component and eventually ends up in a landfill.

It is not the intent of this paper to assess roof membrane options for initial construction or re-reroofing, but rather to look at the insulation as an independent component and determine what insulation type presents the most viable option for re-use at the time when the membrane deteriorates to the point of no longer being a viable weatherproof layer. If various insulation characteristics are considered at of initial construction, with the end goal of re-use in mind, the roof system will be more sustainable. The paper is a starting point for further research into insulation design and selection. It is not the intent of this paper to develop a methodology for insulation selection or define limits on insulation moisture content; such activities would be undertaken during the development of standards related to the re-use of insulation.

2 INSULATION TYPES

Insulation types have varied widely over the past 30-40 years. Prior to the energy crisis of the 1970's in the United States, insulation used in commercial roof systems was minimal to non-existent. Most roof systems were simple multi-layered built-up roofs on concrete or thin layers of rigid fibreglass which was installed more as a backing for the roof over a metal deck rather than as a thermal layer. As energy regulation became stricter and building energy consumption for heating and cooling came under the microscope, the need for more thermal insulation in the roof system increased. Over the past approximately 40-years, insulation types have varied as manufacturers have tried to create thinner materials with higher R-Values. Today, several insulation types may be combined in the roof system in order to achieve various design criteria. For example, an insulated roof system with sloped primary thermal insulation may incorporate polyisocyanurate (ISO), extruded polystyrene (XPS), or expanded polystyrene (EPS) as the thermal insulation with a coverboard of glass-faced gypsum board (GB), perlite board (PB), or wood fibreboard (WFB). These layers can be mechanically-fastened, ballasted, or adhered. Sloped lightweight concrete with insulating fill (LWIC) is also an option as the primary insulating material. The R-Values of the insulations just mentioned are shown in Table 1. LTTR is a method to calculate the 15-year, time-weighted average R-value of roof insulation. Over time, the R-value of polyisocyanurate insulation can drop as the low-conductivity gas escapes and air replaces it.

Table 1. Insulation R-Values. Values are for typical average based on dry insulation and Long-Term Thermal Resistance (LTTR) is used where designated by a double plus (++).

Insulation Type	*R-Value per inch* [ft^2*hr*^oF/BTU]	*Abbreviation*
Polyisocyanurate	6++	ISO
Extruded Polystyrene	4.8++	XPS
Expanded Polystyrene	3.7	EPS
Glass-Faced Gypsum Board	1.0	GB
Perlite Board	2.6	PB
Wood Fibreboard	2.6	WFB
Lightweight Insulating Concrete	5.0+	LWIC

+ Value varies with concrete density. Value includes EPS in conjunction with LWIC.

For the purposes of this paper, we are limiting our discussions to insulations in membrane roofing systems. Consequently, we have not considered sprayed-polyurethane foam (SPF).

3 WET R-VALUE

For many of the various insulation types listed in Table 1, the detrimental effects of moisture on R-Value have been documented through various studies [Tobiasson & Ricard 1979] [Tobiasson, *et.al* 1991]. The various insulations lose R-Value when exposed to moisture as shown in Table 2.

Table 2. Insulation R-Values. Wet R-Value based on Tobiasson, Greatorex, & Van Pelt 1991.

Insulation Type	*Dry R-Value per inch* [ft^2*hr*^oF/BTU]	*Wet R-Value per inch* [ft^2*hr*^oF/BTU]	*Percent Decrease* [%]	*Time Wetting at end of test* [Days]	*Moisture Content* [% mass water]
ISO	6.0++	3	50	300	150
XPS	4.8++	3.8	20	1000	150
EPS	3.7	1.7	50	1000	150
GB	1.0	0.4	60	50	150
PB	2.6	0.91	65	300	150
WFB	2.6	1	62	100	150
LWIC	5.0	2.5	50	50	150

As seen from Table 2, less than half of the insulations retain even half of their R-Value when wet. Furthermore, it can be seen that XPS retains its R-Value best when exposed to moisture, hence the reason for the wide-spread use of XPS in Protected Membrane Assembly (PMA) roof systems. Based on field observations and experience, XPS, EPS, and LWIC retain their many of their physical properties when wet; however the other materials, ISO, GB, PB, and WFB begin to degrade when exposed to high moisture levels. In the case of GB, PB, or WFB the remaining insulation breaks down to the form of a powder in a liquid suspension. In the case of ISO the material becomes saturated similar to a sponge.

The effect of leaving wet insulation in-place and performing a recovery roof application has been documented [Desjarlais, A. 0. *et. al*. Oak Ridge National Labs (ORNL) 1995]. Current industry standard remains much the same as discussed in the ORNL paper of 1995. The amount of wet insulation must be determined prior to the recovery roof application and the designer must decide to either remove and replace the wet insulation or cover over it and attempt to vent the trapped moisture. The effects of trapped moisture on built-up roofing were well documented by Cash [1985]. Moreover, our experience has shown that similar effects occur on other types of membrane roof systems such as blistering of the membrane due to evaporation of trapped moisture and loss of attachment due to

insulation and fastener degradation. In general, trapped moisture can lead to structural deck deterioration, compromised roof system attachment, internal pressures on the membrane (blistering), and a continued deterioration of insulation. All these factors must be considered when designing a recovery roof system. The insulation that remains will likely have a decreased R-Value which should be accounted for in the design.

4 INITIAL INSTALLATION CONSIDERATIONS

Relative to the cost of replacement, first cost of a new insulated membrane roof system meeting today's standards for attachment, R-Value, and fire-rating is low. The labor component of the roof replacement along with accessibility and material removal and disposal make re-roofing significantly more difficult and expensive than installation over an unoccupied, unfinished space at the time of initial construction. However, at the time of initial construction, often times the benefits of a longer lasting roof are over-looked in the interest of lesser-cost or faster installation. As indicated in Table 3 below there are various installation aspects of each insulation type that contribute to the first cost of the system.

Table 3. Insulation Initial Installation Considerations.

Insulation Type	*Installation Types* [Board or Fluid]	*Resistance to Construction Traffic*[Yes/No]	*Flexibility* [Yes/No]	*Attachment* [M, A, or B]	*PMA* [Yes/No]
ISO	Board	No	No	M or A	No
XPS	Board	No	No	M, A, or B	Yes
EPS	Board	No	Yes	M or B	Yes
GB	Board	No	No	M, A, or B	No
PB	Board	No	No	M, A, or B	No
WFB	Board	No	No	M, A, or B	No
LWIC	Fluid	Yes	Yes	None	Yes

For Flexibility, Yes=ease in accounting for in-field changes and variations, No=difficulty in accounting for field variations due to need for fabrication.
For Attachment, M=Mechanically-Attached, A=Fully-Adhered, B=Ballasted.

To meet code requirements for the R-Value of a roof system, different average thicknesses of the various insulations must be used. Therefore, for a given roof system, it can be seen that ISO would typically represent the least average thickness required because of the higher R-Value per inch. When costs are considered, ISO many times will prove to be the lesser first cost insulation, even though the cost per square foot may be more. ISO has variability in attachment methodologies and the ability to be fabricated in a given taper layout in advance. The lack of resistance to construction traffic and the decreases in R-Value over time due to moisture are not typically weighed against the first cost. However, if the cost of expensive re-fabrication of tapered sections and patchwork repairs due to damage from other trades during the construction process are considered, the ISO system starts to approach the cost of the LWIC system.

While LWIC seems to excel in many categories, the first cost of LWIC is usually the highest of the indicated insulations. The inherent constructability issue of dealing with the water from the placement process presents an added complication for the construction team. Once installed, the system is highly resistant to construction traffic and, can be left open during construction since typically an underlying waterproofing layer is used to contain the water from placement. This can delay the installation of the roof membrane, therefore not exposing it to construction traffic until the building is nearly complete.

5 POTENTIAL FOR RE-USE

In order to re-use insulation, the material must meet the hygrothermal, mechanical, and physical properties of the new roof assembly. In evaluating insulations, the properties shown in Table 4 are typically considered in initial design and in assessing the potential for re-use. These properties relate to the selection of the intended recovery roof system as well as the evaluation of the actual condition of the insulation. Aged-in-place insulation can have differing characteristics than new insulation and when planning to bury the insulation under a recovery roof the effects of further aging must be considered. Additionally, the aged-in-place material will respond differently to the construction process than would the new material, so consideration must be given to how much damage will be caused by the process of reroofing. Utilizing an insulation that exhibits the least change in properties over time will result in a more viable re-use situation. When selecting a suitable insulation type for either new construction of for re-use in a recovery roof, the compressive strength of the insulation is vital to the overall performance of the roofing system. Not only can the wetting and drying cycle of insulation reduce the R-value, but increased mechanical loads, such as heavy foot traffic, and impact damage, such as the effects of hailstorms, can also reduce the R-value of roofing insulation. Testing and research by various organizations has shown that mechanical and impact damage will reduce R-value within insulation. This research is still under development and the testing and limits for these reduced R-values have not yet been established. This is mentioned in this paper as an example of other ways R-value can decrease in a material over time and is not intended to serve as a references to such testing.

Table 4. Insulation Properties.

Property	*Description*
Hygrothermal	
Dry Density	The mass of one cubic meter of dry material.
Air Permeability	Rate of airflow across the material and the pressure differential.
Sorption & Desorption	The equilibrium moisture content as it relates to relative humidity.
Thermal Conductivity	Heat flow rate of the thermal gradient in the direction of flow.
Water Vapor Permeability	The ratio between density of the vapor flow rate and the vapor pressure in the direction of flow.
Water Absorption Coefficient	The amount of water diffusion from the surface of the material to the interior of the material.
Heat Capacity	The energy need to raise the temperature of the material
Mechanical & Physical	
Dimensional Stability	Material change in dimension from exposure over time.
Compressive Properties	The response of the material under axial loads.
Flexural Strength	Ability to resist deformation under loads that induce bending.

6 DURABILITY

As previously mentioned, LWIC has an inherent resistance to construction foot traffic which adds to what could be considered the initial or post-installation durability of the material. Durability of insulation is defined as resistance to compromised strength, R-Value, or attachment while subject to the loads imposed on the material during pre-construction, construction, service, and potential re-use. If designers understand the loads, and specify insulation materials that adequately support the intended loads, then the insulation will have the greatest potential for re-use and extended service life. Conversely, if some of the loads are not considered it can affect the life of the roof system. Table 5 on the following page summarizes the typical loads that may be imposed on insulation during the service life of the material.

7 ASSESSMENT OF WET INSULATION

The assessment of wet insulation can be performed in the form of several non-destructive techniques, nuclear hydrogen testing, electrical capacitance survey, and infrared thermography. Destructive testing through core sampling can also be performed; however, for this paper we look to non-destructive methods as a means of determining insulation re-use. Destructive tests may decrease the amount of insulation that is available for re-use and should only be performed to obtain comparative samples for analysis. If during the assessment of the insulation more than 40% of the roof plan area can be seen to have wet insulation, especially in sporadic areas, the cost to salvage the remaining insulation may outweigh the cost for full replacement. The specifics of these testing methodologies are beyond the scope of this paper. The means to assess the amount of wet insulation that is present in a roof system are available to assessors and should be utilized any time insulation re-use is considered. What is important to note is that, regardless of the type of testing that is selected, confirmation of the detected anomalies should be verified by either core samples that are oven-dried to determine the moisture content or by probing the suspected areas with an electrical resistivity probe. The electrical resistivity probe is designed to test moisture levels in building materials through qualitative comparative readings. The moisture content of the roof material is read through two electrical probes that are inserted into the roof insulation. The concept being dry insulations are poor conductors of electricity and wet insulations are good conductors, thus sending the reading to the probe.

The type of existing membrane and surfacing may affect the ability to utilize different methods of assessment and; therefore, may be cause for concern when considering insulation re-use. Re-use of insulation should only be considered when quantitative data can be obtained and a strategy for dealing with entrapped moisture can be developed and implemented.

Table 5. Loads on Insulation.

Load Type	*Description or Components of Each Load Type* *Loads Specific to LWIC Shown in Italics*
Pre-Construction	
Manufacturing	Internal stresses in the material created from the manufacturing process, blowing agents, chemical reactions, heating and cooling, *and/or curing*.
Storage	Sustained loading while in stacked storage, damage due to warehouse or other traffic, warehouse temperature and humidity concerns, compromised protective coverings *or torn bags*.
Shipping	Stacking of pallets, transport within the warehouse, forklift damage, transport on trucks to the site, damage due to road hazards, *or time on the road or in the mix truck.*
Delivery	Lifting by crane or hoist to the roof level. Man-handling into elevators, stairwells, or through hatches. On-site storage and exposure to the elements. *Hydraulic forces when pumping to the roof.*
Construction	
Insulation Installation	Impact of dropping tools on the material. Storage of other roofing materials on top of the insulation. Cutting material to fit. Stresses induced by the installation process including heat from asphalt cooling, adhesive curing, primer flash-off, screw penetration, *or heat of hydration and drying shrinkage.*
Construction Traffic	Movement of people or products across completed roof sections.
Wind Uplift *(also a Service Load)*	Force exerted due to suction on the roof from wind moving across the roof. The insulation may need to accommodate the wind uplift prior to membrane installation.
Ultra-Violet Radiation *(also a Service Load)*	Exposure to sunlight before membrane installation. Exposure due to wind scour in PMA systems.
Membrane Installation	Impact of dropped rolls on the roof, fastened installation, adhesive or primer application, or screwing of fasteners.
Service Loads	
Heat Transfer	Resistance to heat flow across the material, typically addressed by R-Value and thickness of the material.
Vapor Transmitance	Resistance to the flow of water vapor across the material, typically addressed by permeance or adding a vapor retarder at the deck level.
Leak Migration	Resistance to the movement of liquid water through the insulation.
Live Load	Support of code required live loads such as snow and ice on the roof, rain, ponding, or personnel.
Dead Load	Support of material self-weight.
Roof Traffic	Activity on the roof due to service personnel and other trades. Façade access equipment on the roof.
Reroofing Loads	
Membrane Removal	Potential for damage to the insulation during removal of the existing membrane, storage of trash on the roof,
Reroofing	Installation of the new roof membrane over the old insulation.

8 LEAK MIGRATION

Insulation type and installation methodologies can play a role in the way water from leaks and condensation move through the roof system. Material properties as indicated in Table 4 can be specified to provide a level of moisture storage within the insulation, as well as the incorporation of vapor retarders. Each of the indicated insulations has an inherent resistance, or lack thereof, to the

movement of moisture through the matrix. Furthermore, the method of installation can help prevent or become a detriment to the movement of water throughout the system.

Table 6. Attachment Effects on Resistance to Leaks.

Attachment	*Effects*
M	Fastener corrosion, potential compromised attachment, leaks and thermal breaks at fasteners, lateral movement beneath insulation and between layers highly likely.
A	Facer delamination, resistance to lateral movement of leaks, potential for adhesive to act as a vapor retarder, adhesive can dry out along with insulation.
B	No resistance to lateral movement of moisture, moisture storage within insulation only, but vapor retarder can be loose-laid and minimal installation loads result in less potential for damage to the insulation.

Attachment: M=Mechanically-Attached, A=Fully-Adhered, B=Ballasted as shown in Figure 1.

Water penetration through leaks into the roofing system can not only result in degradation of the insulation, but it can also shorten the life of an existing roofing system and a recovery system. Through solar loading the entrapped moisture turns to vapor and the vapor pressure exerts pressure on the roofing system that can delaminate the membrane from the insulation. The delaminations increase the vulnerability of the roofing system to physical and mechanical damage and decrease the ability of the system to shed water by creating non-uniform surface conditions.

9 RECYCLING AND SUSTAINABILITY

Re-use, reduce, and recycle are three key words when discussing sustainability. Recycling and re-use will ultimately reduce the consumption of goods needed as well reduce the amount of disposed materials sent the landfills. In the United States, there are several initiatives for recycling roofing products such as PVC, EPDM, and TPO membranes, asphaltic based material such as shingles, and insulations produced with plastics, such as EPS, XPS and ISO. The initiative so far is on a small scale and is slowly gaining momentum. For the most part, the recycling of roofing products is mainly on residential properties with selective commercial sites across the country adding to the mix. Recycling roofing insulation is in its infancy as an industry; re-using the existing insulation on a re-cover or roof replacement is a viable alternative to recycling when trying to achieve some degree of sustainability related to the roof system. Re-using the existing insulation can save the building owner the expense of disposal costs and also reduce the costs of purchasing and installing the new materials.

The U.S. Environmental Protection Agency (EPA) estimates that the construction industry generates approximately 320 billion pounds of solid waste each year. The total estimated solid waste generated from roofing waste accounts for 80 billion pounds each year. To put that into perspective; the average cost of disposal for 2,000 pounds of roofing debris is approximately fifty dollars that is equivalent to over two billion dollars a year in roofing generated waste, not to mention the environmental impact on the country's landfills. The U.S. Green Building Council's (USGBC) LEED program will issue one point under the heading of Solid Waste Management: Facility Alterations and Additions if the requirement of diverting 70% of the waste (by volume) generated by facility alterations and additions from disposal to landfills and incineration facilities is met. Regardless if the building owner is aspiring to gain a LEED certification, the practice of recycling construction debris is a good measure, and potentially re-using the existing insulation can play a large part in achieving this goal.

10 SUMMARY

Using the various aspects discussed in this paper, a basis for the selection of insulation with durability and eventual re-use in-mind can be developed. No one insulation will likely meet every need and roof

system maintenance will always play a vital role in the preservation of insulation integrity for use in re-roofing. If roofs are well-maintained, the likelihood of having viable, re-useable insulation will certainly increase. If re-use is not possible, recycling options should also be considered in more detail for the disposed insulation. As "cradle-to-grave" analysis becomes increasingly more prevalent and building designers and owners are aiming for achieving the least impact, the choice of a roof insulation that may eventually be re-useable could be an untapped resource for sustainability.

REFERENCES

Baxter, D. August 1986, '1001 Reasons Not to Roof Over Wet Insulation', *Roofing Spec*, pp. 27.

Hogan, Lyle D. June 2001, 'Using Two Layers Of Insulation In Single-Ply Roof Systems', *Interface*, pp. 11-14.

Cash, C.G. 1985, 'Moisture and Built-Up Roofing', Proc. Of the NRCA Second Internationsl Symposium on Roofing Technology, Paper Number 24, pp. 416–427.

Tobiasson, W. and Ricard, J. 1979, 'Moisture Gain and Its Thermal Consequences for Common Roof Insulations', Proc. Of the 5th Conference on Roofing Technology, NBS/NRCA, pp 4-16.

Cash, C.G. 1977, 'Optimization of the Thermal resistance of Roof Insulation in Reroofing', Proc. Of the Symposium on Roofing Technology, Paper Number 24, pp 208-214.

Desjarlais, A. 0. Petrie, T. W. Christian, J. E. McLain, H. A. C u d s, P. W., 'A Whole Building Demonstration of Re-Cover Over an Existing Wet Roof', 11th Conference on Roofing Technology, NIST/NRCA, Gaithersburg, Maryland, September 21-22, 1995, pp 1-24.

Roe, R. March 2007, 'Long-Term Thermal Resistance Five Years Later', *Interface*, pages 12-16.

Tobiasson, W. Greatorex, A. and Van Pelt, D. 1991, 'New Wetting Curves for Common Roof Insulations', Proc. Of the 1991 International Sysposium on Roofing Technology, NBS/NRCA, pp 383-391.

XII DBMC
International Conference on Durability of Building Materials and Components
PORTO - PORTUGAL, April 12th-15th, 2011

Dynamic Response of Mechanically Anchored Waterproofing Membrane Exposed during Typhoon and Evaluation of Its Wind Resistance

Hiroyuiki Miyauchi [1]
Nobuo Katou [2]
Kyoji Tanaka [3]

ABSTRACT

Damages of mechanically-anchored waterproofing membrane system from strong wind have been occurring. Thus, this study provides investigation on the behavior of waterproofing sheets and fasteners exposed during typhoon, and the difference between the static pressure test and typhoon test. The polyvinyl chloride waterproofing membrane reinforced with polyester fiber was constructed on a flat roof with dimensions of 6m by 6m on the island of Miyako in Japan. The billowing of the membrane was observed visually, and the wind speed, wind direction, wind pressure, billowing height of waterproofing membrane and the load of fastener were measured. At first, a pressure test was carried out by using a compressor. As a test result, the transmission rate of load to the fasteners from pressure caused in the waterproofing membrane was high in a static pressure test using a compressor. However, the billowing heights of the waterproofing membrane around fasteners were approximately the same. Afterwards, the response of mechanically-anchored waterproofing membrane system located atop a building when subjected to strong winds from a typhoon in 2009 was measured. Visual observation confirmed that the billowing height of the waterproofing membrane on the windward side was higher than that of leeward side. Therefore, the billowing height of the waterproofing membrane around the fasteners in the pressure test and the wind typhoon test was different. Both axial force and lateral force of mechanically-anchored waterproofing membrane system were measured under high speed wind, and lateral force was significantly large. It is presumed that such lateral force causes waterproof membrane damage that ripped the sheet in the lateral direction as if in a typhoon.

KEYWORDS

Waterproofing membrane, Typhoon, Field test, Fastener, Axial and lateral force.

[1] Chungnam National Universty, Dept. of Architectural Engineering, Daejeon, SOUTH KOREA, miyauchi@cnu.ac.kr
[2] Tokyu Construction, Institute of Technology, Kanagawa, JAPAN, katou.nobuo@tokyu-cnst.co.jp
[3] Tokyo Institute of Technology, Structural Engineering Research Center, Kanagawa, JAPAN, tanaka@serc.titech.ac.jp

1 INTRODUCTION

Mechanically anchored waterproofing membrane systems are directly fixed to the roof substrate with a series of fasteners. Comparing the performance of these systems to that of an adhered waterproofing membrane system, mechanically anchored waterproofing membrane systems do not depend on the conditions of the substrate to ensure adequate attachment to the roof and are also reasonably easy to replace, given the means of attachment. However, the wind resistance of these membrane systems depends on the reliability of the fasteners, and there is some apprehension as to the safety of these systems in respect to wind resistance, especially when they are subjected to high winds loads, such as those occurring during a typhoon. For example, the maximum instantaneous wind speeds exceeded 50 m/s (180 kph) for typhoons No.18 and No.22 that recently occurred in Japan, and this apprehensiveness may be well founded.

Recently, a method for testing the wind resistance of waterproofing membrane systems was proposed and tested in Canada by the Special Interest Group for Dynamic Evaluation of Roofing Systems (SIGDERS) [Baskaran et al. 2009a, 2008b, 2007c, 2005d, 1999e; Lei. W et al. 2001]. A cycle model of wind loads method was proposed by Uematsu [Uematsu et al. 2009; Furuichi et al. 2005] in Japan for buildings that incorporate a parapet. The present authors have tested the behavior of a mechanically anchored waterproofing membrane system in conjunction with an actual size test specimen by using a fatigue test apparatus [Bartko et al. 2006a, 2005] and wind tunnel tests [Ichikawa et al. 2004a, 2007]. However, the obtained wind load data are based on wind tunnel tests and laboratory tests, and the relationship between the data and the actual outdoor environment is not clear. Therefore, we constructed a test building on the island of Miyako, in Japan, and installed a mechanically anchored waterproofing membrane system on the roof.

In this study, the static pressure test and the typhoon test were carried out on a flat roof of test building in the outdoor. Afterwards, the lateral and vertical force-induced fasteners around the waterproofing membrane were measured by a 6-component force transducer during a typhoon in 2009, and both wind pressure and force were compared.

2. OUTLINE OF MEASUREMENT IN FIELD TEST

2.1 Test location and test building

The measurements in the field test were performed at the Miyako Island test site of the Japan Weathering Test Center, in the southern part of Miyako Island City in Okinawa Prefecture (Fig. 1). Sloping land is at the north face of the test building and is 6m lower than the ground where the test building is built. However, the area surrounding the building is generally flat and there are no obstructions to the flow of wind across the test building. The building constructed for the tests is shown in Fig. 2. The test building is a rectangular structure made of reinforced concrete with dimensions of 6m by 6m width and 3m height, and incorporates a waterproofing membrane on a flat roof without any parapets.

2.2 Waterproofing membrane system

The 1.5-mm thick waterproofing membrane is made of polyvinyl chloride (PVC) reinforced with polyester fiber. The polyester fibers, having a thickness of 556 dtex, are mixed at a density of 1.5filaments/cm in both directions of the sheet. The relationship between the elongation and the tensile stress of a dumbbell shaped PVC sheet is shown in Fig. 3.

The waterproofing membrane was fixed using a prefabricated technique, whereby the membrane is mechanically fastened using circular fixing plates. After drilling holes into the concrete substrate, as shown in the upper part of Fig. 4 plates (ext. diam.: 75 mm; thickness: 1.7 mm) were fixed by means

of anchors (stainless steel screws of diam. 6 mm and nylon plugs) inserted into the drilled holes and non-styrene epoxy acrylate resin adhesive. The waterproofing membrane was then adhered to the plates. Fasteners were spaced 0.6 m apart (a typical value), as shown in Fig. 4, resulting in a total of 81 points over the surface of the roof.

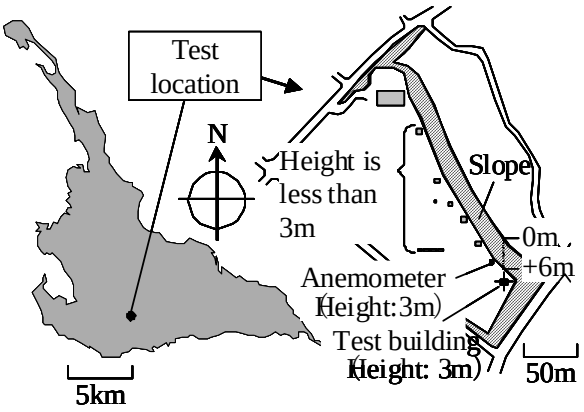

Figure 1. Test location in Miyako Island

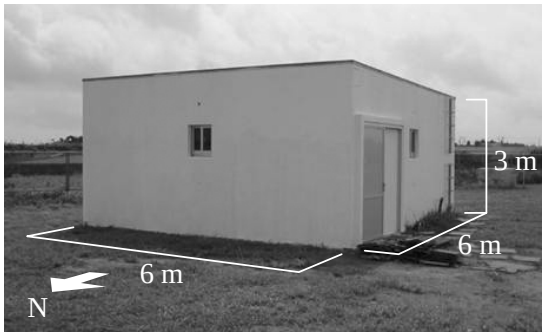

Figure 2. Test building

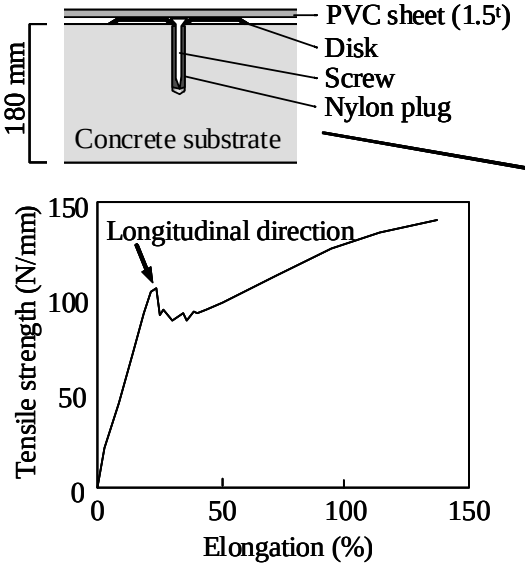

Figure 3. Mechanical property of PVC sheet

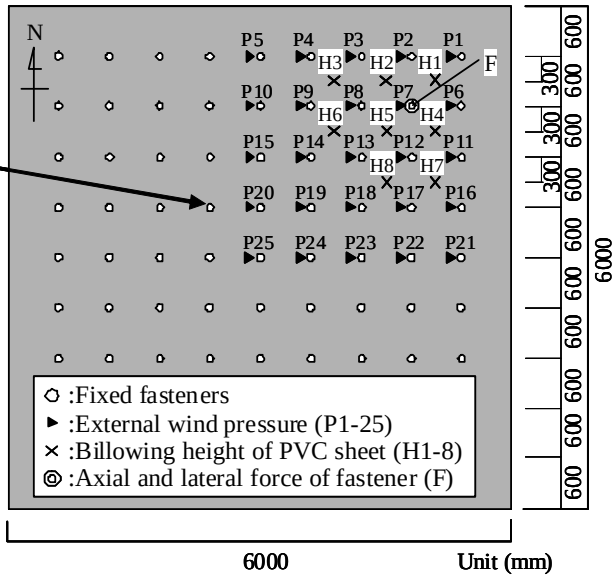

Figure 4. Waterproofing membrane system and outline of the measurement

3. STATIC PRESSURE TEST USED TEST BUILDING ROOF

3.1 Out line of pressure test method

The static pressure test method is shown in Fig. 5. 40-mm holes in the concrete substrate were drilled to apply pressurized air from the compressor to the space between the waterproofing membrane and the concrete substrate, and the pressure hole was connected with the pressure entrance of the compressor. Pressure was then applied from the back of the waterproof membrane, and the waterproof membrane was billowed artificially. The pressure between the waterproofing membrane and the concrete substrate were measured by using a pressure-tube anemometer through a vinyl tube pipe. The measurement parameters are the pressure between the waterproofing membrane and concrete substrate, the billowing height of the waterproofing membrane, and the force induced in the fasteners.

3.2 Test results

The billowing condition of the waterproofing membrane during the static pressure test is shown in Fig.6. The waterproofing membrane was sucked up by the pressure applied by the compressor, and it was assumed that the stress was concentrated in the waterproofing membrane around the fasteners.

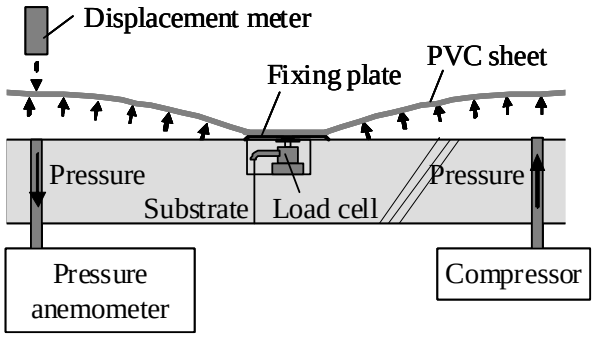

Figure 5. Static pressure test method.



Figure 6. Billowing condition of waterproofing membrane during the static pressure test.

The force induced in the fastener at point F in the pressure test is shown in Fig.7. A horizontal line shows the force induced in the fastener calculated from the area of the waterproofing membrane that shares the load of one fastener. Namely, this equivalent load is calculated by the following equation: the load of one fastener = Pressure × Area of waterproofing membrane ($0.36m^2$). The load measured by the load cell and the equivalent load calculated by the above equation have a linear relationship and the transmission rate from the pressure to the load cell was 94% at point F. Therefore, it was clarified that the transmission rate of the load from the pressure caused in the waterproofing membrane to the fastener is high.

Relationships between the pressure and the billowing condition of the waterproofing membrane in the pressure test are shown in Fig. 8. The billowing heights of the waterproofing membrane at points H1 and H2 were approximately the same.

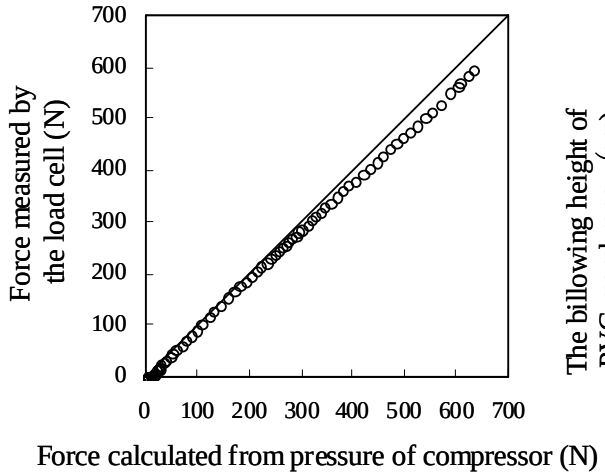

Figure 7. Load transferred from wind pressure to load cell by pressure test of compressor.

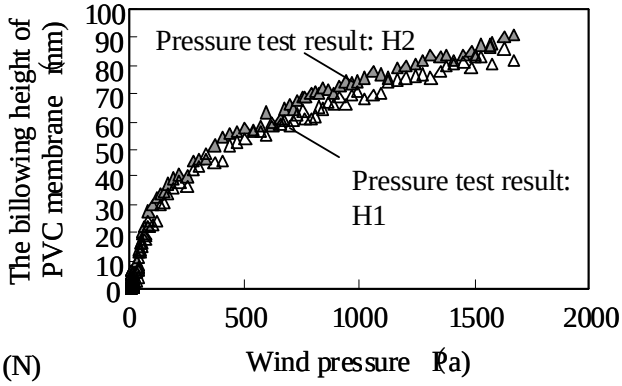

Figure 8. Relationship between pressure and the billowing height of PVC membrane.

4. TEST RESULTS DURING TYHPOON No.8 in 2009

4.1 Outline of measurements

The following parameters were measured directly: wind direction, wind speed, wind pressure, the billowing of the waterproofing membrane, and axial-lateral force at fastener.

The equipment utilized for taking these measurements is as follows. We set up an ultrasound wind direction and wind speed meter, FT702 (measurement range: 0.01 to 60 m/s), 25 m away from the test building in the NW direction, 3 m above the ground (the same height as the test building).

25 wind pressure measurement points were established on the surface of the roof waterproofing sheet, denoted by P1 to P25, as shown in Fig. 4, and the method used to measure wind pressure is outlined in Fig. 9. The external pressure on the roof surface is conducted to a pressure anemometer, via an external pressure measurement pipe (positioned at the fixing plate) and a PVC tube of internal diameter 8 mm, thereby enabling the difference between this external pressure and reference wind pressure to be determined. As a waterproofing measure, we positioned the ends of the pipes 25 mm above the roof surface. In order to isolate the external pressure from the effects of rainwater, we used a Y-shaped wind pressure branching tube (so that rain water could be collected in a water tank).

We located the measurement points for billowing at the midpoints between locations where the waterproofing membrane was fixed to the roof, where billowing is expected to be greatest. These eight points, H1 to H8, are shown in Fig. 4. To measure the billowing membrane, we drilled 40-mm holes in the concrete substrate, as shown in Fig. 9, and then measured the displacement relative to the bottom through these holes, using an ultrasound displacement meter.

The 6-component force transducer was set up to measure the axial force and lateral force at a fastener around waterproofing membrane. This 6-component force transducer enables simultaneous measurement of 3 forces (Fx, Fy, Fz) in 3 axial directions orthogonal to the transducer and 3 moment (Mx, My, Mz) around the axes.

Measurement data was recorded continuously, by observers who proceeded to the test locality as the typhoon approached Miyako Island, for the entire period during which the Miyako Island area was classified as being within the “strong wind zone.” The data for each measurement point were sampled at 25 Hz for wind pressure and at 100 Hz for sheet billowing and strain, with all data saved to the hard disk of a PC. In addition, video footage of the roof behavior during exposure to strong wind was also recorded.

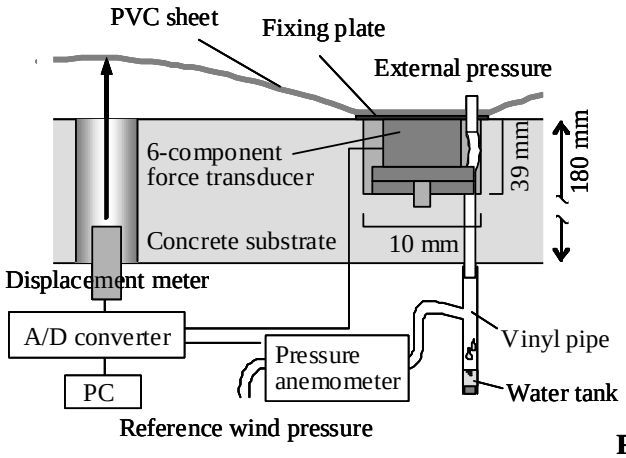

Figure 9. The cross section of measurement method for the field test during typhoon

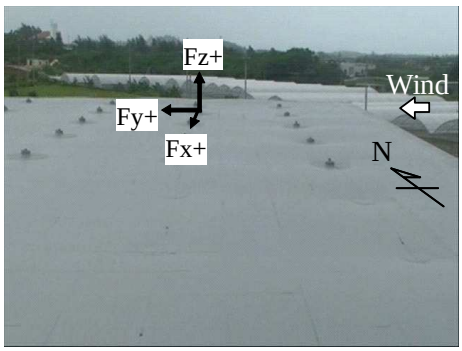

Figure 10. The direction of Fx, Fy, Fz at 6 compo nent transducer and the billowing condition of the PVC sheet during Typhoon No.8 in 2009

4.2 Wind characteristics of TYHPOON No.8 in 2009

Between August 6 and 7, 2009, Typhoon No. 8, which was accompanied by heavy wind and rain, came as close as southwest of Miyako Island. The wind direction changed from NE to SE. The highest mean wind speed over 10 min was 18.8 m/s. Also, the wind direction and wind speed values measured at the test building corresponded closely with the figures from the meteorological observatory.

4.3 Observation results

Wind direction was from the east. Fig.10 shows the billowing condition of the PVC sheet exposed during the 10-minute mean wind speed 15m/s, the direction of Fx, Fy, Fz at the 6-component transducer, and the position of the PVC sheet billowing height. As a result of observation of the PVC sheet during the typhoon, we found that waterproofing membranes were sucked up by wind pressure and that the billowing was high on the windward side but relatively low on the leeward side. Moreover, in response to the strong wind, the PVC sheet appeared to exhibit a combination of two behaviors: billowing condition during constant billowing and an intermittent flapping in the direction of the wind. Therefore, the billowing height of the waterproofing membrane around the fasteners in the pressure test and the wind typhoon test was different.

4.4 Measurement results and discussion

Fig.11 shows the relationship between wind pressure and the billowing height of the PVC sheet. The billowing height of the PVC sheet was highest at the H4 point and was 40mm at 15m/s-mean wind speed. The billowing of the PVC sheet at windward was higher than that of leeward, and its value was 15mm at H6 point. Then, the standard deviation means the fluttering condition of the PVC sheet, and the position of H4-H5-H6 was 5mm to 7mm.

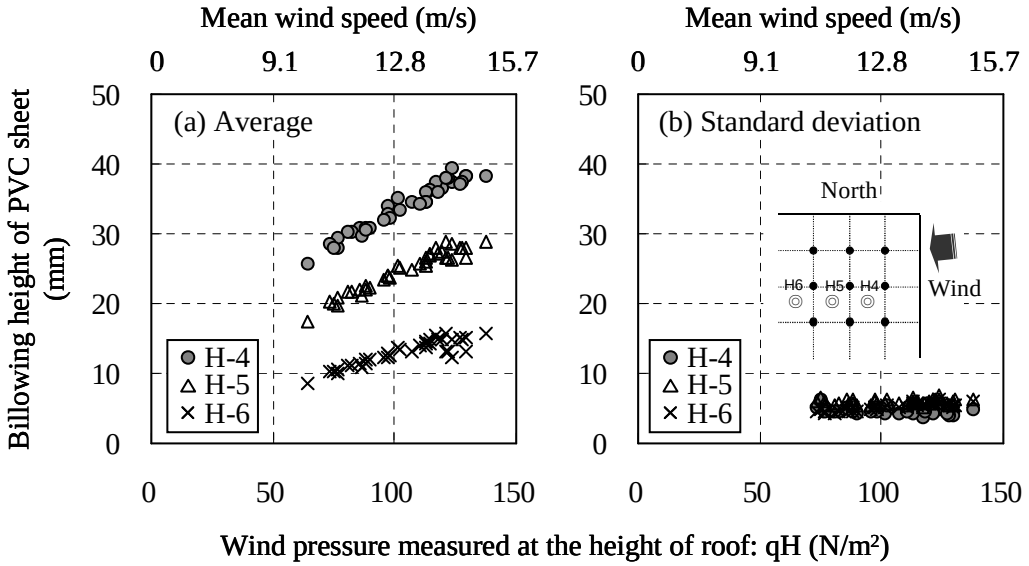

Figure 11. Billowing height of PVC sheet during Typhoon No.8 in 2009 (2009.8.7)

Fig.12 shows the comparison between the lateral force (Fy) and the axial force (Fz). The lateral force and the axial force were linearly proportional to wind pressure and they increased with increased wind pressure. The Fz at the wind speed of 14.6 m/s was 40 N; by contrast, at Fy, the lateral force was 30 N, namely, about 75% of the Fz, while the axial force was larger than the lateral force. However, the the standard deviation of the lateral force (Fy) was higher than that of the axial force (Fz). Therefore,

the fasteners were shaken back and forth or to the right and left by the strong winds. In case of the high wind pressure, it is necessary to consider not only the axial tension but also the lateral force for the design of the fastener.

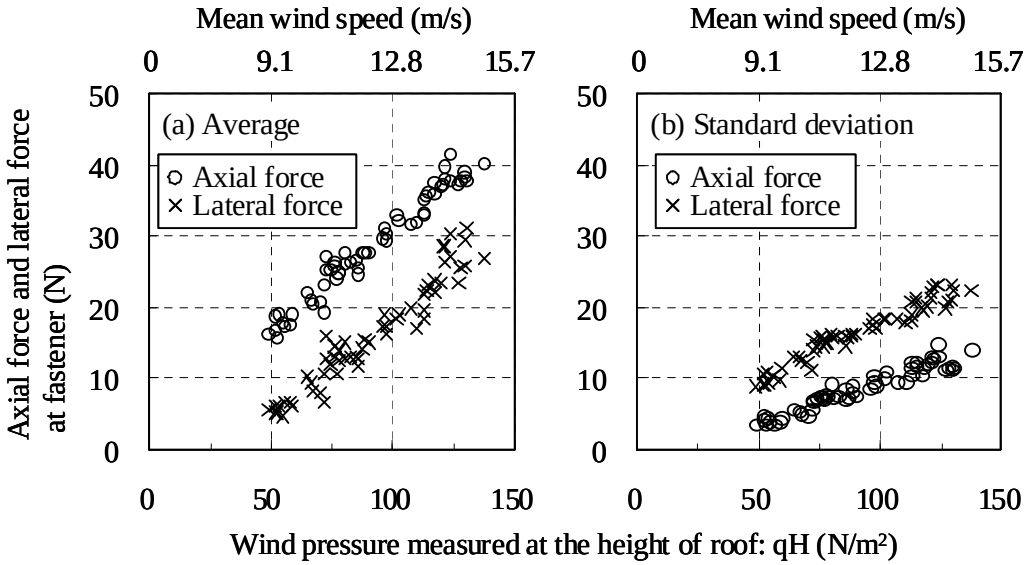

Figure 12. Axial force and lateral force at fastener during Typhoon No.8 in 2009 (2009.8.7)

5. CONCLUSION

The results of the tests conducted were as follows.

1) The transmission rate of load to the fasteners from pressure caused in the waterproofing membrane was 94% in a static pressure test using a compressor, and therefore it was clarified that the transmission rate of load was high.
2) The billowing of the PVC sheet at windward was higher than that of leeward during typhoon. Therefore, the billowing height of the waterproofing membrane around the fasteners in the pressure test and the wind typhoon test was different.
3) The Fz at the wind speed of 14.6 m/s was 40 N; by contrast, at Fy, the lateral force was 30 N, namely, about 75% of the Fz, while the axial force was larger than the lateral force. On the other hand, the the standard deviation of the lateral force (Fy) was higher than that of the axial force (Fz). The higher the axial force, the higher the lateral force and the ratio of lateral force/axial force is increasing.

ACKNOWLEDGMENTS

The authors wish to thank Mr. Chea Daravuth and Mr. Yousuke Furusawa for their help with this project. This work was conducted as part of research activities of a working group for Assessment of Wind Endurance of Mechanically Anchored Waterproofing Membranes of the Waterproofing Membrane System of the Architectural Institute of Japan with the financial support of the following committee members: the Synthetic Polymeric Roofing Sheet Manufacturers Association (KRK), the Asphalt Waterproofing Manufacturers Association (ARK), the Torch-Applied Roofing Manufacturers Association (TRK), and fastener manufacturers. This work was supported by KAKENHI (20360249, Grant-in-Aid for Scientific Research (B)) in Japan, and Basic Science Research Program through the National Research Foundation of Korea (NRF) funded by the Ministry of Education, Science and Technology (2009-0069919). Some researchers were supported by Brain Korea 2nd (BK21) funded by the Korean Government. We are grateful to all these parties for their support.

REFERENCES

Baskaran, B.A. Ko, S.K.P. Molleti, S., 2009a, A novel approach to estimate the wind uplift resistance of roofing systems. *Building and Environment*, 44, (4), pp.723-735, 2009.

Baskaran, B.A.; Ko, S.; Molleti, S., 2008b, RCI continues its support for SIGDERS. phase V research and development activities, *RC Items*, pp.4-5, 2008.

Baskaran, B.A.; Paroli, R.M.; Kalinger, P., 2007c, Advancements and changes in the North American commercial roofing industry. *International Conference on Building Envelope Systems and Technology 2007*, pp.275-286, 2007.

Baskaran, B. A., Ko. S.K.P., 2005d, A guide for the wind design of mechanically attached flexible membrane roofs. *Construction Innovation*, **Volume 10, Number 4**, NRC-IRC, 2005.

Lei. W and Baskaran, B.A., 2001, SIGDERS wind uplift resistance data on mechanically attached single ply roofing systems – effect of vapour/air barrier. *Research Report* **IRC-RR-823** National Research Council, Canada, 2001.

Baskaran, B.A., Chen, Y. and Vilaipornsawai, U., 1999e, A new dynamic wind load cycle to evaluate flexible membrane roofs, *ASTM Journal of Testing and Evaluation*, **27 (4)**, pp.249-265, 1999.

Uematsu, Y., Nakamura, S. and Sera, M., 2009, Wind pressure loading cycles for evaluating the wind resistance of mechanically attached waterproofing systems on flat roofs. *5th European & African Conference on Wind Engineering*, pp.375-378, 2009.

Furuichi, K., Uematsu, Y, Nakamura, S. and Sera, M., 2005, Evaluation of dynamic wind loads for mechanically-attached waterproofing membrane systems. Proc. *19th National Symposium on Wind Engineering*, pp.471-476, 2005.

Bartko, M., Miyauchi, H. and Tanaka, K., 2006a, Fatigue resistance of mechanical fastened waterproofing systems to ALC substrate by repetitive loadings. *Journal of Technology and Design, Architectural Institute of Japan*, **No.24**, pp.21-46, 2006.

Bartko, M., Miyauchi, H. and Tanaka, K., 2005b Development of wind resistance test method of mechanically anchored waterproofing system with ALC substrate. Journal of Structural and Construction Engineering, Architectural Institute of Japan, **No.598**, pp.7-12, 2005.

Ichikawa, H., Bartko, M., Kato, N., Miyauchi, H., Sasaki, T. and Tanaka K., 2004a, Behavior of mechanically anchored waterproofing membrane exposed to high wind speed of wind tunnel, *Journal of Structural and Construction Engineering*, Architectural Institute of Japan, **No.593**, pp.17-24, 2004.

Ichikawa, H., Katou, N., Miyauchi, H. and Tanaka, K., 2007b, Wind tunnel tests of various mechanically anchored waterproofing membrane, *Journal of Structural and Construction Engineering, Architectural Institute of Japan*, **No.615**, pp.47-52, 2007.

XII DBMC
International Conference on Durability of Building Materials and Components
PORTO - PORTUGAL, April 12th-15th, 2011

Development of Wind Resistance Test Methods for Mechanically Anchored Waterproofing Systems

Kyoji Tanaka [1]
Naoyuki Koshishi [2]
Hiroyuki Miyauchi [3]
Nobuo Kato [4]
Tao Lin [5]

ABSTRACT

New test apparatus and test procedure for evaluating wind resistance of mechanically anchored waterproofing systems was developed on the basis of new findings, which was obtained through the measurements of induced forces by strong winds in some typhoons, that the same level of lateral force is simultaneously induced as well as uplift force at fixing portions in waterproofing systems.

Two kinds of apparatuses with different mechanism to reproduce uplift and lateral forces were prototypically made. As for the first apparatus, a membrane was bloated by two air bags inserted between a membrane and a substrate and then inflated by high pressure gas. For the second one, uplift force was applied by pulling down at the fixing portion in the specimen that a membrane is fixed between the two steel rings, and lateral force was directly applied through lateral moving mechanism to the specimen.

Some tests of mechanically anchored waterproofing membranes were carried out using the two apparatuses, and advantages and disadvantages of those test methods were discussed.

KEYWORDS

Waterproofing membrane, Mechanical anchor, Wind resistance, Test apparatus, Strong wind.

1 INTRODUCTION

Mechanically anchored systems are used for fixing waterproofing membranes to the substrate at specific points via supporting plates using fasteners. The method offers many advantages: (1) it is unaffected by movement at the cracks and points of contact between the substrate and the membrane; (2) it is rapid in construction; (3) it can be used even for slightly moist substrates. Therefore, mechanically anchored systems are becoming immensely popular, especially for use in reroofing work. However, in this method, the waterproofing membrane is attached to the substrate only at certain points, and hence, sufficient measures must be taken to increase the wind resistance of the resulting structures.

The abovementioned importance has been recognized since the first development of the systems, and some wind tests have been proposed for estimation wind resistance for them. To the best of our knowledge, the wind resistance tester for flat roofs, which was developed upon investment by American Insurance Association and Underwriters' Laboratories [Benjamin & Bono 1967]], is the first full-fledged wind resistance test apparatus. Since then, similar test apparatus have been developed by many researchers to be used in the study or evaluation of the wind resistance of the systems. The largest test apparatus is that developed by Canadian research team [Baskaran et al. 2009]]; this apparatus has been identified by the Canadian Standard Association as a high-performance apparatus capable of evaluating waterproofing membranes employed in practical applications and is being used worldwide.

The need for evaluating the wind resistance of waterproofing membranes has been also identified in Japan, and the test method has been proposed by the Japanese Architectural Standard Specification JASS8 Waterproofing and Sealing. This test method is being employed in Japan for wind resistance evaluation.

However, evaluation tests reveal that wind pressure is generated in the vertically upward direction, thereby the membrane is ruptured around the disc, as shown in Fig. 1. This kind of damage is a little bit different from those of being observed in strong wind, as can be seen in Fig. 2. This difference in the damage patterns is thought to be due to the fact that conventional apparatus can only reproduce the behavior in which the waterproofing membrane is pulled in the upward direction.

Recently, a wind tunnel was used to measure the force generated at the point of attachment between the waterproofing membrane and a substrate [Nobuo Kato et al. 2010]]; further, measurements were performed on a waterproofing membrane during a typhoon on Miyako Island [Hiroyuki Miyauchi et al. 2010]]. The results revealed that a lateral force that is nearly equivalent to the vertical uplift force acts on the fixing device. This indicated that the effect of the lateral force must also be taken into consideration when reproducing the actual behavior.

The purpose of this study is to develop a test apparatus that can help carry out more reasonable wind resistance evaluation, based on the new findings.

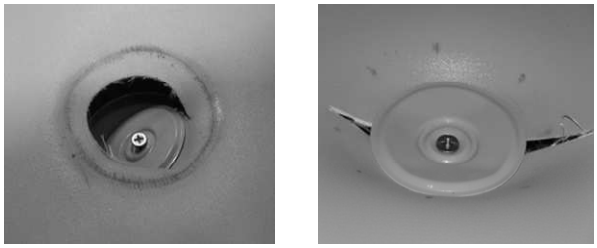

Fig. 1 Damages observed around fixing device by wind uplift test



Fig. 2 Damage observed in attached area of membrane after typhoon

2 CONDITIONS NEEDED FOR WIND RESISTANCE PERFORMANCE EVALUATION

2.1 Behavior to be reproduced

When the waterproofing membrane is exposed to strong wind, an uplifting force is generated, and the membrane is pulled upward by the stream of wind. A fixing device comprising various components such as an attached disc and a fastener is used to prevent a membrane from being uplifted. Since the waterproofing membrane is connected to the substrate only at the points where the fixing devices are attached, the membrane bloats under the influence of the uplifting force.

Conventionally, several test methods and systems have been developed to reproduce this bloating behavior. However, on the basis of the observations on the behavior of the waterproofing membrane during a typhoon, we state that the entire waterproofing membrane does not bloat all at once; rather, the membrane bloats from one end to the other in the windward direction. As a consequence, a lateral force is generated at the anchored parts of the waterproofing membrane, in addition to the uplift force that attempts to pull these parts in the upward direction. This behavior is schematically shown in Fig. 3. Thus, the behavior to be reproduced must include the uplift and lateral forces that act simultaneously on the fixing devices.

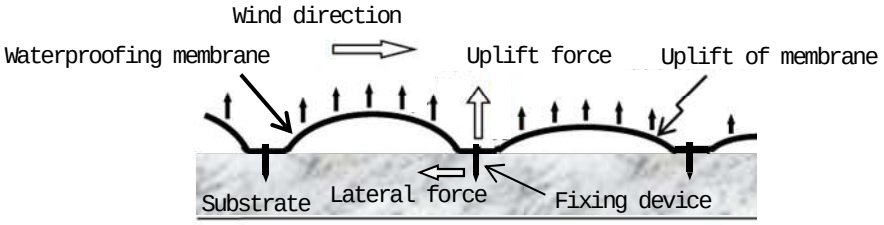

Fig. 3 Deformation of membrane of mechanically attached waterproofing system in strong wind

2.2 Conditions to be formulated using the test apparatus

2.2.1 Uplift force

The vertical uplifting force is related to the wind velocity. On the basis of Japan's recommended level in the book of Recommendations for Loads on Buildings, the design velocity pressure is expressed as follows:

$$q_H = \frac{1}{2}\rho U_H{}^2 \quad \cdots\cdots (1)$$

Where, q_H: Design velocity pressure (N/m^2)
ρ :Air density 1.22 (kg/m^3)
U_H : Design wind speed (m/s)

While U_H is determined from the height of the given building and the return period of the wind velocity, the wind load on the waterproofing membrane has not been elucidated accurately. Therefore, we use the basic wind velocity recommended by Japanese standards for the maximum uplifting force. Thus, the uplifting force is calculated by using the following equations:

$$W_C = q_H \hat{C}_C A_C \quad \cdots\cdots (2)$$

$$\hat{C}_C = \hat{C}_{pe} - C_{pi}^{*} \quad \cdots\cdots (3)$$

Where, W_C: Uplifting force (N)
A_C : Area of component under consideration (m^2)
$\hat{C}_C$: Peak pressure coefficient
$\hat{C}_{pe}$: Peak external pressure coefficient
C_{pi}^{*} : Effective internal pressure

The $\hat{C}_C$ value recommended for exterior materials that are used to construct flat roofs depends on the position on the roof surface. The recommended $\hat{C}_C$ value is -2.5 for the central area of a roof. The expected wind load is calculated to be 3813 N/m^2 (1525N/m^2 × 2.5) from the maximum basic wind velocity in Japan (50 m/s, internal pressure not considered).
Since the standard distance between the fixing device (interval distance) is approximately 600 mm (a smaller interval may be adopted depending on the circumstances), the area of the waterproofing membrane covered by each fixing device is 0.36 m^2, and a force of 1373 N acts on the fixing device. Therefore, the test apparatus must be capable of reproducing the uplifting conditions up to this level.

2.2.2 Maximum value of horizontal force
The results of force measurements carried out on the fixing device of the waterproofing membrane in a mechanically anchored system on Miyako Island when Typhoon No. 8 struck the island in 2009[6] show that a lateral force whose magnitude is about 0.7-1.0 of that of the uplift force acting on the fixing device is generated, as shown in Fig. 4. Hence, it is necessary for the apparatus to reproduce a lateral force that is nearly equivalent to the uplift force.

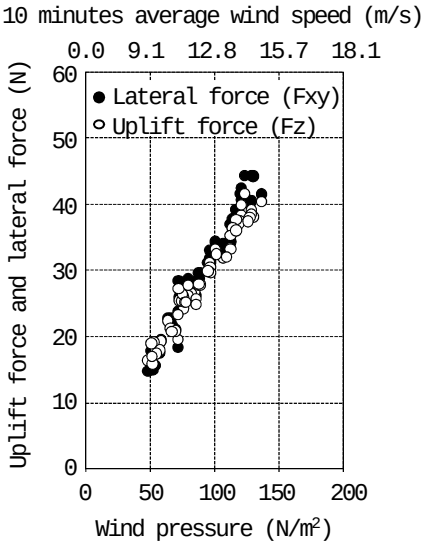

Fig.4 Lateral force (Fxy) and uplift force (Fz) observed during the typhoon at Miyako Island, August 7, 2009

3 LOADING METHOD ADOPTED TO GENERATE LATERAL FORCE ON THE FIXING DEVICE IN ADDITION TO UPLIFT FORCE

3.1 Method for uplifting waterproofing membrane using two air bags

3.1.1 Basic concept
Bloating of a roofing membrane is caused by the uplifting force is often reproduced by putting a suction box over a membrane and reducing the air pressure inside the box. This behavior can also be reproduced by pushing up the waterproofing sheet from below. When doing so, it is not necessary to cover the waterproofing sheet with a large suction box, and hence, the test apparatus is greatly simplified. In addition, the use of this method makes close-up observations possible because the specimen is exposed during a test. Therefore, in this study, we adopted a method in which the waterproofing sheet is pushed to the upward direction by compressed air supplied from beneath the membrane.

However, it is extremely risky to introduce compressed air from directly below the waterproofing membrane, as this may cause severe damage to the sheet instantaneously. Furthermore, excessive gas leakage (even from small ruptures) may cause the gas supply to become insufficient and thus render

the experiment unsuccessful. For this reason, we attempted to bloat the waterproofing membrane by inserting air bags below it.

As shown in Fig. 5, the system is designed to have a mechanism in which uplift and lateral forces are generated simultaneously; for this purpose, two air bags are positioned on both sides of the fixing device, and the volume of gas injected into each bag is adjusted appropriately. The force generated on the fixing device is measured by a six-component force transducer installed below it.

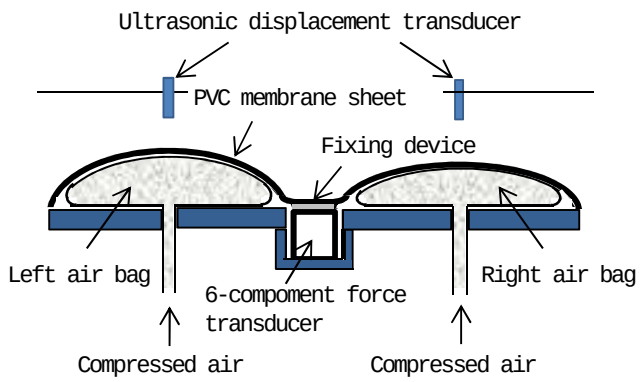

Fig. 5 Concept to produce uplift and lateral force at attached area

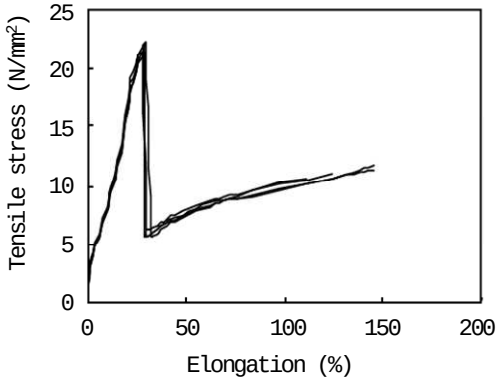

Fig. 6 Mechanical property of PVC membrane reinforced by polyester fiber fabrics

3.1.2 Test specimen and prototype test apparatus

The test specimen was 1 m × 1 m in size; at the center of the specimen a fixing device was attached to the waterproofing membrane. A commercially available PVC sheet reinforced with polyester fabrics with mechanical properties as shown in Fig. 6 was used as the waterproofing membrane.

The test apparatus is shown in Fig. 7; two right and left air bags with hemispherical notches on one side are installed on top of the steel substrate and covered by a PVC membrane sheet which in turn is fixed to a six-component force transducer installed below and connected via a disc. The air bags are connected to compressed air bombs for injecting high-pressure gas, and the flow rate is adjusted by a meter installed on the hose connecting the bag and the bomb.

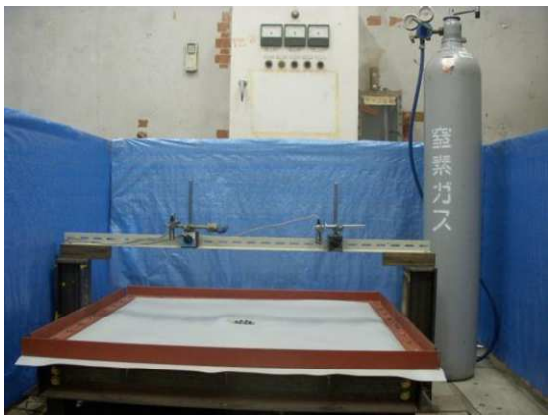

Fig. 7 Test apparatus using two air bags

3.2 Method for moving specimen

3.2.1 Basic concept

To develop mechanically anchored systems in practical level, tests must be needed for various combinations of materials and system parts. Hence, an easy test method is furthermore in demand. We

simulated the bloating of the waterproofing membrane and moved the bloated membrane so that the fixing device is subjected to both uplift and lateral forces.

3.2.2 Test specimen and prototype test apparatus

As shown in Figs 8, the test specimen is prepared by inserting a waterproofing sheet between two steel rings (inner diameter: 600 mmφ) and installing a fixing device at the center. The fixing device comprises a disc plate and a PVC sheet welded by high-frequency induction heating. A force transducer can be attached below the fixing device to measure the force generated during testing.

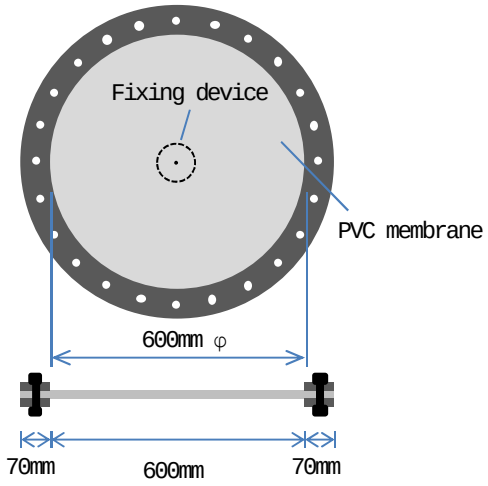

Fig. 8 Test specimen

The test apparatus is shown in Fig. 9. The uplift force is generated by moving the fixed section of the specimen downward. The apparatus is equipped with a mechanism for moving to the right or left, as shown in Fig. 10, so as to generate the lateral force. The lateral force is controlled by the transducer installed in the moving rod, and the load is controlled by the program controller so that the specified waveform is obtained.



Fig. 9 Test apparatus

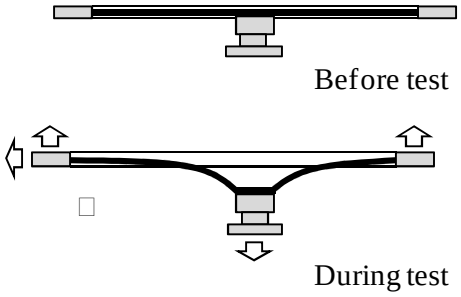

Fig. 10 Concept to produce uplift and lateral forces to attached area

4 TESTS AND TEST RESULTS

4.1 Method using air bags

4.1.1. Test procedure

Since a lateral force is generated on the fixing device, in addition to the uplift force, the rate of compressed gas injection into each air bag was controlled independently. The injection rate was also controlled manually by observing the uplift- and lateral-force monitors. In this case, the uplift and lateral forces were controlled such that the corresponding pressurization rates were nearly equivalent

(500 N/min), and pressurization was continued until both these forces reached the maximum value of 1300 N. The bloating heights of the right and left waterproofing sheets were also measured.

4.1.2 Test results

The result is shown in Fig. 11. In this case, a large volume of compressed gas was injected into the left air bag, and there was a large difference between the bloating heights of the waterproofing membrane (90 mm on the left and 13 mm on the right). This enabled the generation of a lateral force that was nearly equivalent to the uplift force, and hence, the performance of the test system was confirmed to be satisfactory.

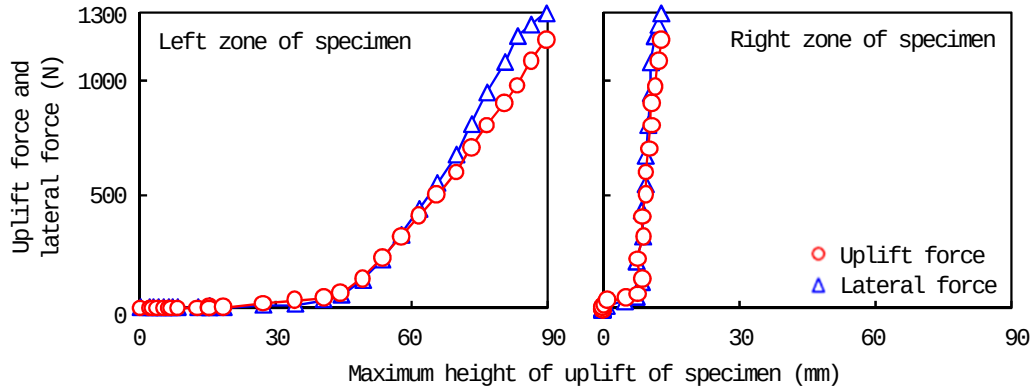

Fig. 11 Test result by filling compressed air into left bag

4.2 Test method for moving the specimen

4.2.1 Test procedure

First, the waterproofing sheet was attached to the test apparatus, with the center of the sheet fixed to the force transducer placed below the membrane. In the test, the bloating behavior was reproduced by manually lowering the fixed section while checking the load value for the transducer. Then, a lateral force was applied on the membrane via the crank rod. The applied force was controlled while observing the transducer output; the uplift and lateral forces were increased to a maximum of 1500 N. During the test, the load and displacement were measured.

4.2.2 Test results

The result is shown in Fig. 12. As the specimen was moved laterally while the fixed section was pulled downward, the figure is shown for each of vertical direction and lateral direction. The uplift force increased as the fixing device was pulled downward, and the lateral force increased as the specimen was moved sideways. However, the displacement in the vertical direction upon the application of the lateral force in addition to the uplift force was 110mm. The displacement in the lateral direction was very small, 11mm. Uplift and lateral forces could be generated to the fixing device and increased to the necessary level so that the desired performance seems to be achieved.

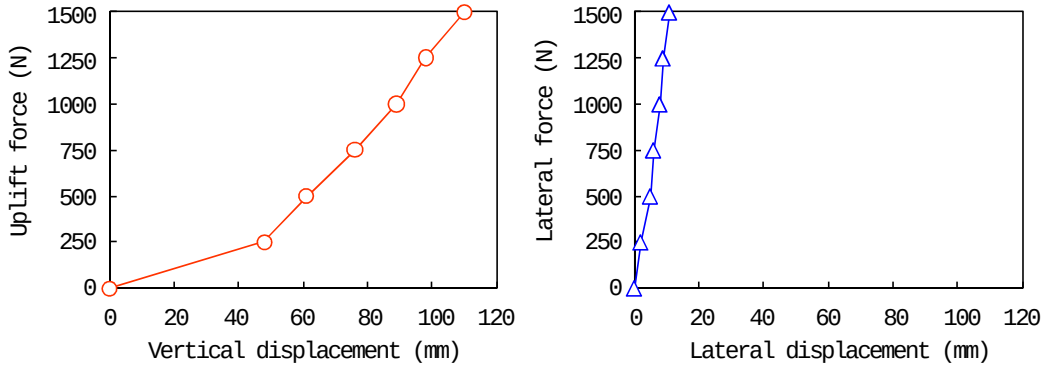

Fig. 12 Test result of moving specimen

5 DISCUSSION

It was revealed through the tests that each test method has certain advantages and disadvantages.
In principle, in the method used for bloating the waterproofing membrane, elaborate experimental setup is required; on the other hand, in the method used to move the test specimen, small test specimens are employed and the procedure is simple. Furthermore, it is suited when the moving process is repeated many times.

Thus, we state that the method for moving the test specimen can be employed to test a large number of specimens within a relatively short period and hence may be more suited for use in the initial stage of development of mechanically anchored systems. Meanwhile, the method for bloating waterproofing membranes by air bags may not be suitable for conducting tests consecutively on many specimens but may be suited for the examination of the overall behavior of mechanically anchored membrane systems.

6 CONCLUSION

The conclusions are as follows:
(1) We developed a test method to reproduce the uplift and lateral forces generated on the fixing devices of waterproofing membranes exposed to strong winds, by installing two air bags below the waterproofing membrane and bloating them.
(2) We also developed a simple test method to reproduce the uplift and lateral forces by using a mechanism for simultaneously pulling the fixing section of a specimen in the downward direction and moving in the lateral direction.
(3) We discussed the actual applications of the developed methods by considering their advantages and disadvantages.

ACKNOWLEDGMENTS

The authors express sincere gratitude to Mr. Hajime Ishi and Mr. Kimio Kawashima for fabricating the two apparatuses. This work was partially supported by the Grant-in-Aid for Scientific Research (B) in Japan.

REFERENCES

I.A. Benjamin and J.A. Bono, 1967, 'Wind-Resistance Tests of Roof Shingles and Roof Assemblies', *ASTM STP* 409, 110-137.

Baskaran, B.A., Ko, S.K.P. and Molleti, S., 2009, 'A novel approach to estimate the wind uplift resistance of roofing systems', *NRCC*-48177, 1-37.

Nobuo Kato, Hiroyuki Miyauchi and Kyoji Tanaka, 2010, 'Characteristic Difference of Mechanically Anchored Waterproofing Membrane System in Pressure Test and Wind Tunnel Test', *Proceedings of ICBEST 2010*, 63-64.

Hiroyuki Miyauchi, Nobuo Kato and Kyoji Tanaka, 2010, 'Behavior of Fastener Area under Dynamic Wind Load of Mechanically Anchored Waterproofing Membrane Exposed during Typhoon', *Proceedings of ICBEST*, 53-54.

XII DBMC
International Conference on Durability of Building Materials and Components
PORTO - PORTUGAL, April 12th-15th, 2011

Development of Test Method for Evaluating Root resistance of Waterproofing Membrane and Root Barrier Sheet for Roof Garden Study with Thickening Growth of Rhizome of Bamboo Grass

Saori Ishihara [1]
Kyoji Tanaka [2]

ABSTRACT

Waterproofing membrane and root barrier sheet for roof gardens should not damaged due to the growth of plant roots. Because roots act as the external force of the greening systems and causes damage and water leak. To avoid such defects, we must first assess the behavior of plant roots and evaluate next if they are safe or not against the force of plant roots. In particular, rhizome of bamboo grass used in the Japanese garden causes serious damages. The purpose of this study is to develop evaluating root resistance test method focus on the thickening growth of rhizome of bamboo grass.First we measured enlargement force of a rhizome caused by thickening growth. The force was measured in early summer when rhizomes are expected to grow up actively. It was found that the force reached to approximately 26.5N/cm during 12 days. Next the apparatus for similarly reproducing the thickening growth of the rhizome was developed on the basis of the actual enlargement force of the rhizome.Thickening growth of rhizome was simulated by inflated rubber tube which have similar diameter to rhizome and adding pressure using hydraulic jack at the same level of enlargement force which observed the actual plant. For evaluated objects are joint parts of waterproofing membrane with different adhesive strength. As a result, it was found that low adhesion strength caused damage with low pressurization force, and also evaluating of root resistance using this apparatus was available.

KEYWORDS

Roof garden, Root resistance, Waterproofing membrane, Root barrier sheet, Rhizome of bamboo grass.

[1] Tokyo Institute of Technology, Yokohama, JAPAN, saori@serc.titech.ac.jp
[2] Tokyo Institute of Technology, Yokohama, JAPAN, tanaka@serc.titech.ac.jp

1 INTRODUCTION

Resistance to damage by plant roots is a necessary quality for building components such as waterproofing membranes, root-resistant sheets, blocks, and bricks used in roof garden since plant roots exert external forces on these components and may exacerbate damage or cause water leaks by penetrating small gaps or weak parts and then growing in thickness. Figure 1 shows an example of damage caused by the entry and subsequent enlargement growth of roots under joint parts of root barrier sheet.

To prevent such damage, the suitability of components used in roof garden needs to be studied in terms of their resistance to root growth. One method is to study the root resistance of these components by using actual plants. However, given the requirement of large-scale tests and long test period when actual plants are used, it is necessary to establish a root resistance evaluation method that involves the use of simulated roots that is replacement of the enlargement root growth with a mechanical force. First of all to observe the enlargement root growth and the force it exetrs is necessary. There are some articles that observed the growth of the root [e.g. M.G.HICK *et al.* [1970], Michel Genard *et al.* [2001]], but there are not the articles that observed the enlargement force of the root.

Therefore, the purpose of this study is to observe the enlargement root growth and the force it exerts, and to develop a simulated root to be used in the evaluation of the root resistance of components used in roof garden.



Figure 1. Damage example due to root growth.

2 IDENTIFICATION OF PARTS SUITABLE FOR MEASUREMENT OF ENLARGEMENT FORCE DURING ROOT GROWTH IN BAMBOO GRASS RHIZOME

Enlargement force is generated by the growth of a root. It is thought that some root parts exhibit rapid growth while other parts do not. The parts that are suitable for measurement of the root enlargement force are those showing rapid enlargement growth and no extension growth. To identify these parts, we measured the enlargement growth and extension growth of roots.

2.1 Subject plant

The subject plant was bamboo grass (*Sasa veitchii* (Carr.)), and it is shown in Fig. 2. This is a rhizomatous plant with extremely high thriftiness. It is also one of the most popular plants for roof garden in Japanese gardens.



Figure 2. Bamboo grass.

2.2 Enlargement growth and extension growth measurement apparatus

To allow the rhizome to grow freely, we constructed the measurement apparatus shown in Fig. 3. The system comprised a planting area and a measuring area. A hole (10-mm diameter) was made on the side of the planting container, and guided the rhizome into the measuring area from the hole. The measuring area was made of a PVC pipe (diameter 18 mm, length 150 mm), which was attached to the hole on the side of the planting container. To maintain favorable growing conditions, we filled the measuring area with high water-absorption polymer and added liquid fertilizer (approximately 1% concentration).

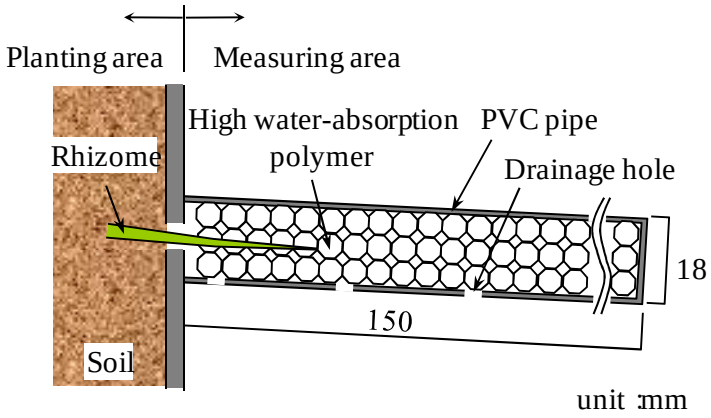

Figure 3. Enlargement growth and extension growth measurement apparatus.

2.3 Measurement of enlargement growth and extension growth

After sufficient curing in the planting area, the rhizome was guided into the measuring area. The rhizome measurement points are shown in Fig. 4. The rhizome diameter was measured at the 4 measurement points specified, at 10-mm intervals from the tip, and the distance between the measurement points was measured at 5-mm intervals from the tip.

The PVC pipe was removed at 8:00 a.m. daily, and the rhizome diameter in both the vertical and horizontal directions was measured using vernier calipers. The distance between measurement points was determined from the photograph.

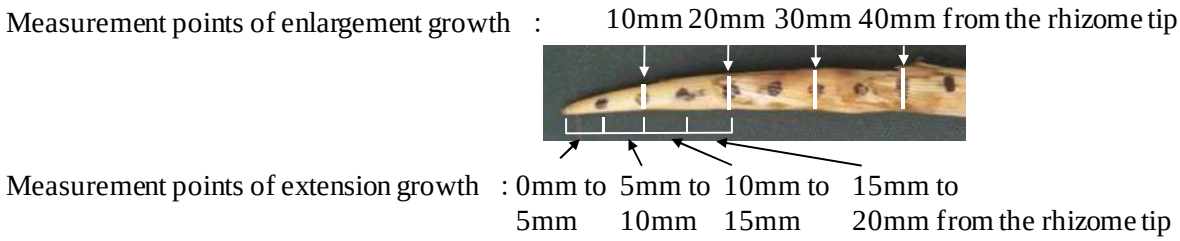

Figure 4. The rhizome measurement points.

2.4 Measurement results

An example of the daily changes in vertical and horizontal diameters at the measurement point 10 mm from the rhizome tip is shown in Fig. 5. Whereas the diameter increased on daily basis, the rhizome cross-section enlarged mostly in the circumferential direction, with little difference between the vertical and horizontal directions. The averages of the vertical and horizontal diameters of the daily changes at each measurement point are shown in Fig. 6. Naturally, the initial diameters are smaller for the points closer to the tip. These grew over time, but the enlargement growth at points farther from the tip was smaller, although the initial diameter was larger.

In addition, the extension growth of the rhizome at each measurement point is shown in Fig. 7. Considerable extension growth is observed for the section from the tip to 5 mm, but little extension growth is observed for the sections closer to the base at 5 mm to 10 mm in length.

On the basis of these measurement results, it is suggested that the most appropriate section for measurement of the enlargement force is that 10 mm from the tip.

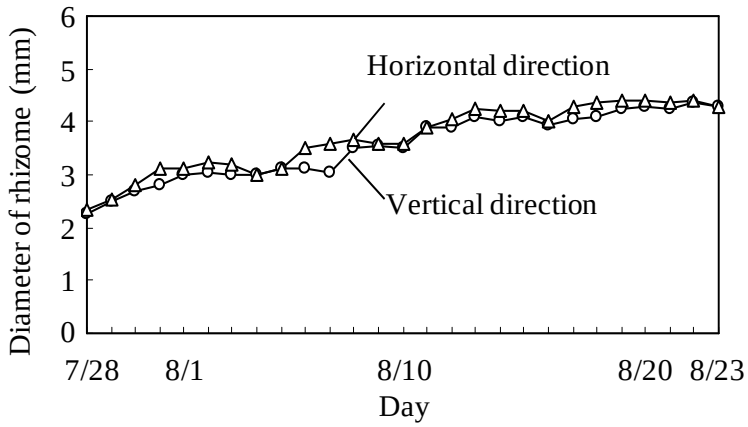

Figure 5. An example of the changes in vertical and horizontal diameters at the measurement point 10mm from tthe rhizome tip.

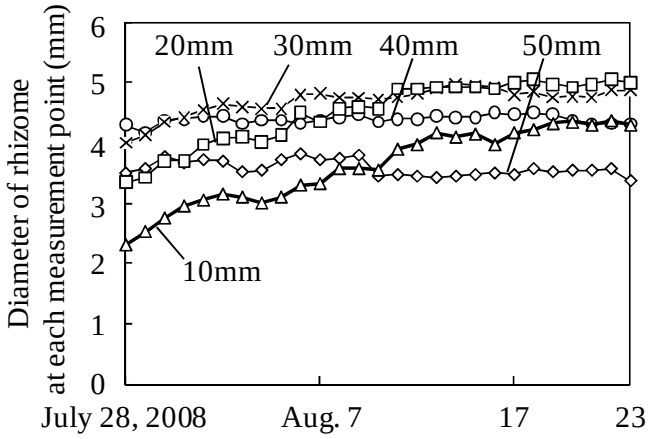

Figure 6. Daimeter of rhizome.

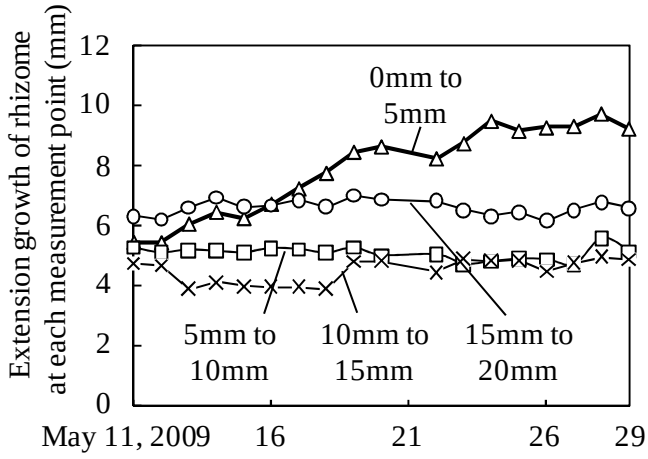

Figure 7. Extension growth of the rhizome.

3 MEASUREMENT OF ENLARGEMENT FORCE OF BAMBOO GRASS RHIZOME

3.1 Enlargement force measurement apparatus

The enlargement force measurement apparatus is shown in Fig. 9. The rhizome was pinched from above and below by the enlargement force catching plates attached to the load cell, and the force applied to the plates by the rhizome in enlargement growth was measured. The area around the force catching plates was filled with moist soil to allow rhizome growth.

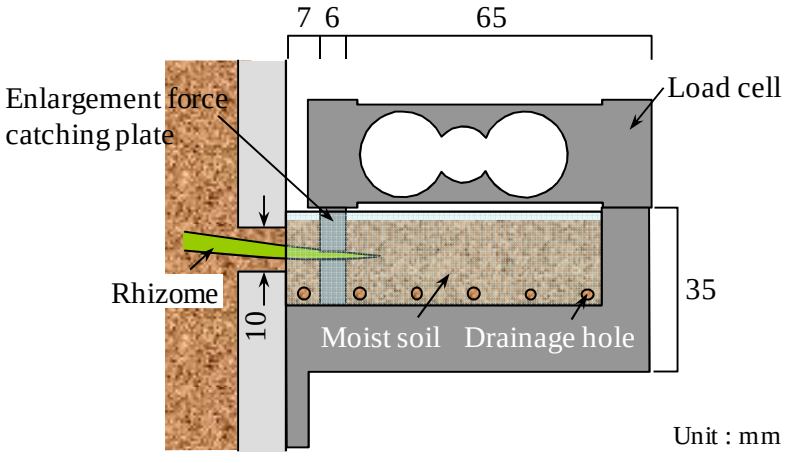

Figure 8. Enlargement force measurement apparatus.

3.2 Enlargement force measurement procedures

A hole (10-mm diameter) was made on the side of the planting container, and the enlargement force measurement apparatus was attached to fit the hole. A rhizome was guided into the force catching plate in May 27, 2009. The subject plant was bamboo grass, and the measurement point was 10 mm from the rhizome tip.

3.3 Measurement results

The measurement results are shown in Fig. 9. The enlargement force increased overall, while showing a repeating cycle: an increasing force from midday to night, and a decreasing force from dawn to midday, in conjunction with transpiration. However, it reached its peak value of 25.6 N/cm after 12 days, and showed no further increase.

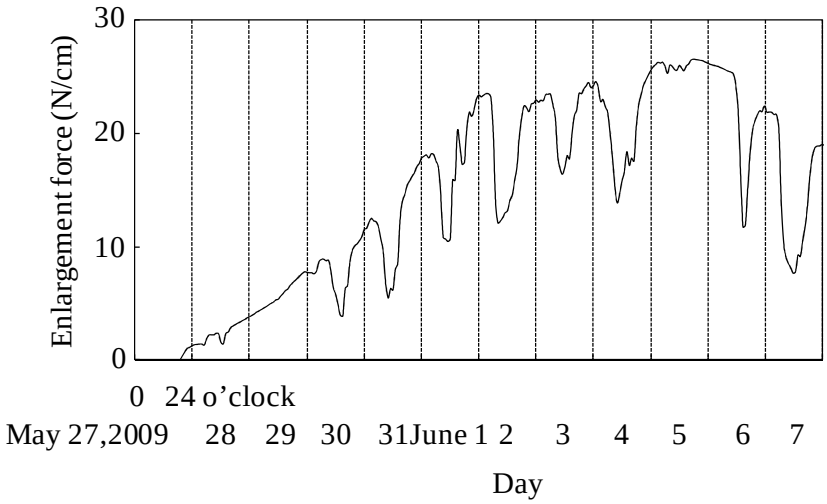

Figure 9. Measurement results of enlargement force.

4 DEVELOPMENT OF THE SIMULATED ROOT

4.1 Simulated root

The simulated root must be capable of applying a force of 26.5 N/cm or larger (26.5 N/cm is the force observed in "3. Measurement of enlargement force by bamboo grass rhizome"). Our simulated root was therefore constructed using the simulated root axis to apply the pressure, and a rubber tube to cover it, it was filled with oil, and pressure was applied internally to enlarge the rubber tube as a mechanism to reproduce the force.

The simulated root axis made from of brass is shown in Fig. 10. Nine 0.8-mm pores were made at 5-mm intervals on the simulated root axis (length 70 mm). The mechanism consisted of this simulated root axis connected to a hydraulic jack; this enabled the rubber tube to be pressurized by feeding oil from the pump to fill the rubber tube from the holes on the simulated root axis. The rubber tube length was set to 60 mm, and the end was bonded to the simulated root axis with epoxy resin to prevent the oil from leaking. The pressure inside the rubber tube could be measured using the pressure gauge attached to the hydraulic jack.

Depending on the material and wall thickness of the rubber tube covering the simulated root axis, it may become excessively deformed, or succumb to the pressure and break, failing to apply the force of 26.5 N/cm observed for the bamboo grass rhizome. Therefore, we used 4 types of rubber tubes with different materials and wall thicknesses as shown in Table 1, and measured the enlargement force of the simulated root when pressure was applied within the rubber tube.

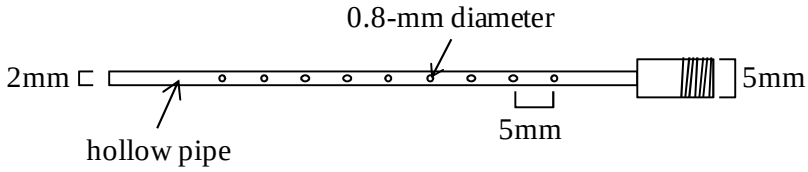

Figure 10. Simulated root axis.

Table 1. Rubber tube with diffenert materials and wall thickness.

Materials	Internal diameter (mm)	External diameter (mm)
Nitrile rubber (thick)	2	6
Nitrile rubber (thin)	4	6
Silicone rubber	2	6
Vinyl chloride high molecular polymer rubber	2	5

4.2 Measurement of enlargement force of the simulated root

The enlargement force of the simulated root was measured by inserting the simulated root into the measurement apparatus shown in Fig. 8. The enlargement force needs to exceed 26.5 N/cm, but because this is not necessarily always the maximum value, we increased the pressure in the rubber tube by 0.1 MPa until the enlargement force of the simulated root reached 50 N/cm. The measurement points were the center of the simulated root.

The relationship between the pressure inside the rubber tube and the enlargement force by the simulated root is shown in Fig. 11. The rubber tubes became damaged when the enlargement force of the simulated root reached 27N/cm, 30 N/cm and 36 N/cm, respectively, for nitrile rubber (thin), silicon rubber and vinyl chloride high molecular polymer rubber. However, no damage was caused to nitrile rubber (thick) for forces up to 50 N/cm.

Therefore, we decided to use nitrile rubber (thick) as the rubber tube for our simulated root. Figure 12 shows the simulated root.

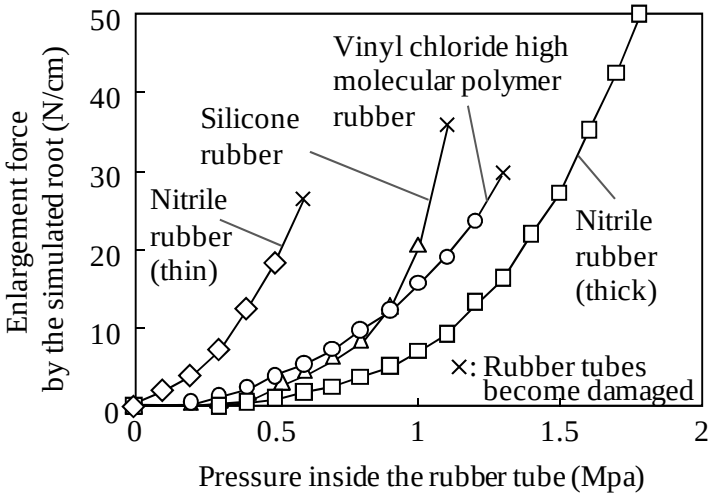

Fig.12 Relationship between internal pressure and enlargement force of simulated root

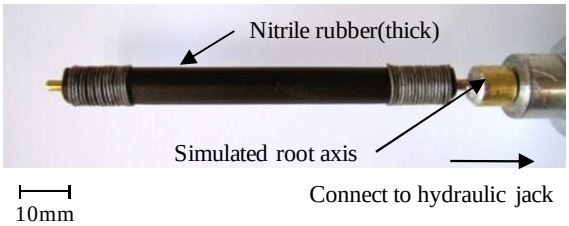

Fig.13 Simulated root

5 APPLICATION OF THE SIMULATED ROOT IN EVALUATION OF ROOT RESISTANCE OF WATERPROOFING MEMBRANE JOINTS

The usefulness of the prepared simulated root in the root resistance evaluation method was examined by using the waterproofing membrane joint as an example.

5.1 Test specimen

The adhesion strength is considered to affect the root resistance of waterproofing membrane joints. We therefore prepared different specimens with varying peel strengths at the joints, as shown in Table 2. To enable observation of the peeling conditions at the joints when the enlargement force of the simulated root was applied, the test specimen was attached on one side to a glass-cloth reinforced composite vinyl chloride resin sheet, which is generally used as waterproofing membrane, and on the other side to a clear vinyl chloride resin sheet. The specimen shape was 200 mm × 40 mm.

Table 2. Specimens with varying peel strengths at the joints.

Specimen	Peel strength* (N/cm)
Jointed by over lapping without adhesives	0
Jointed by double-coated adhesive sheet	3.5
Jointed by solvent welding solution	36.8

*Temperature:20℃, Tension rate;10mm/min, Number of specimens:5

5.2 Test method

The simulated root was placed at the center of the glass-cloth reinforced composite vinyl chloride resin sheet, and the clear vinyl chloride resin sheet was bonded from above. The test specimen was fixed on the fixing plate with double-coated adhesive sheet. A cut (9-mm width) was made at the center of the fixing plate to allow expansion when the simulated root was pressurized. The test conditions are shown in Fig. 13. The pressure inside the rubber tube was adjusted for 10-N/cm increments, so that the enlargement forces of the simulated root were 0, 10, 20, and 30 N/cm. The peeling length of the waterproofing membrane joint advanced under the application of each force was measured using vernier calipers. The numbers of specimen were three for each specimen.

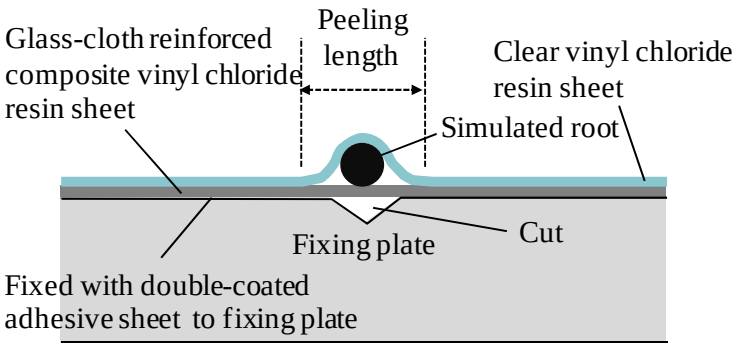

Figure 13. Cross section of test specimen for evaluating root resistance of waterproofing membrane joints.

5.3 Test results and discussion

The test results are shown in Fig. 15. Peeling was observed soon after pressurizing the simulated root in cases where jointed by over lapping without adhesive specimen but peeling was mitigated in cases where jointed by double-coated adhesive sheet. But both cases, Peeling was obserbved before enlargement force by simulated root reached 26.5N/cm, as observed in the enlargement force measurement of bamboo grass rhizome. On the other hand, peeling was not observed in cases where

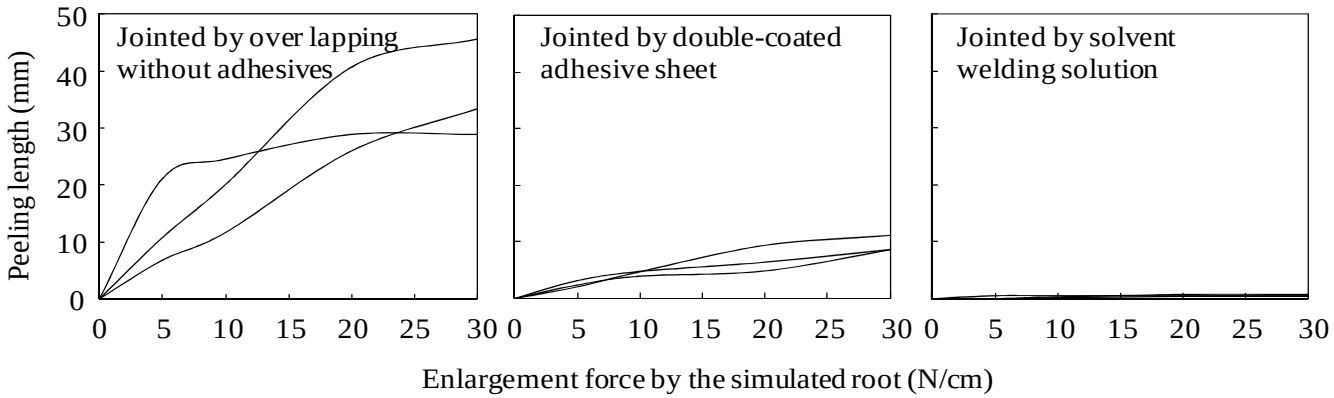

Figure 15. Peeling length of waterproofing membrane joint.

jointed by solventwelding solution specimen even if the enlargement force by sumulated root reached 26.5N/cm.

In the root resistance evaluation test using the simulated root, the specimen would be considered root-resistant with no peeling advance if it had a peeling strength of at least 26.5 N/cm, as observed in the enlargement force measurement of the bamboo grass rhizome.

6 CONCLUSION

1) We have established a method for the measurement of the enlargement force of the bamboo grass rhizome. This force, measured 10 mm from the tip, had shows a tendency to increase overall while exhibiting cyclic changes in concurrence with transpiration. The force peaked at 26.5 N/cm.
2) On the basis of the actual measurement of the enlargement force and the growth of the bamboo grass rhizome, we have developed a simulated root comprising a simulated root axis connected to a hydraulic pump.
3) Using this simulated root, we have conducted root resistance tests on waterproofing sheet joints. We have demonstrated the usefulness of the simulated root in root resistance evaluation tests.

REFERENCES

M.G.HUCK, BETTY KLEOOER, H. M. TAYLOR. 1970, Diurnal Variations in Root Diameter, Plant Physiology, Vol.45, pp.529-530.

Michel Genard, Svetlana Fishman, Gilles Vercambre, Jean-Gerard Huguet, Claude Bussi, Jacques Besset and Robert Habib. 2001, A Biophysical Analysis of Stem and Root Diameter Variations in Woody Plants, Plant Physiology, Vol.126, pp.188-202.

Kyoji TANAKA, Saori ISHIHARA, Soonju PYO, Hiroyuki MIYAUCHI. 2008, Development of Test Method for Evaluating Root Resistance of Waterproofing Membrane, Proceedings of the Eleventh International Conference on Durability of Building Materials and Components, 11dbmc, Vol.3, pp.1047-1056

XII DBMC
International Conference on Durability of Building Materials and Components
PORTO - PORTUGAL, April 12th-15th, 2011

Designing for 60 Year EPDM Roof System Service Lives

Thomas William Hutchinson [1]
AIA
CSI
FRCI
RRC

ABSTRACT

A common theme of many sustainable building discussions is the achievement of a service life of 60 years. Recent inspections of aged EPDM roof systems over 25 years of age found them to be in excellent condition. Samples of EPDM membrane from several of the oldest EPDM roofs in the United States were taken and tested to determine their current physical characteristics. Test results revealed that nearly all retained performance attributes above and beyond the minimal requirements of today's EPDM membranes. This author's empirical experience has shown that well designed and installed EPDM roof systems can attain service lives of 25 years and more. New innovations and improvements in EPDM membrane and associated components, in combination with superior design, suggest that EPDM roofs can attain supreme long-term service lives. Based on the author's extensive experience with EPDM roof systems over the last 25 years, this paper will demonstrate an approach to achieving 60 year service lives with EPDM roof system, through design, construction, planned assessment and interventions. This paper will review test results of aged in situ EPDM membranes and design considerations to achieve long-term performance. Examples of existing long-term performing EPDM roofs, their design elements, and how they were managed in an attempt to provide extended watertight protection will be reviewed. Examples of current day EPDM roof systems designed for service lives of 60 years will be reviewed as well.

KEYWORDS

Durability, Long-term service life, EPDM.

[1] Principal, Hutchinson Design Group, Ltd., Barrington, Illinois, U.S.A., hutch@hutchinsondesigngroup.com

1 EMPIRICAL EXPERIENCE

This author, an architect who has chosen to specialize in roof system design, has always been keen on detailing and holds two concepts sacred when roof system design is concerned: 1.) All building elements that impinge on the roof need to be designed into the roof system and detailed accordingly; and 2.) Quality, long-term roof systems, that in time will achieve sustainability, need to be designed as systems and detailed specifically for the project in question. EPDM roof systems designed, detailed and specified under these concepts, designed by the author, and installed over 24 years ago were inspected in the summer of 2009 and found to be in excellent condition and on their way to achieving long-term performance.

Inspection of aged EPDM roof systems over the years has resulted in a common denominator; no matter the design, construction and/or overall condition, the EPDM membrane was found to be in "almost as good as new condition". These observations were confirmed in research by Dr. Tim Trial [Hutchinson 2005] in which aged in situ EPDM samples were tested for there physical properties and almost without question the physical characteristics of the aged, in situ, climatically exposed EPDM meet or exceed the minimum requirements of new membrane being manufactured today. Another study being undertaken by the author, in which the oldest known EPDM roofs in place, over 30 years old, have had samples taken and the membranes' physical characteristics tested, which correlated with the Trial research, and confirmed that ageing EPDM membrane holds it physical characteristics.

The SKZ (Süddeutsche Kunststoff Zentrum) in Wuzburg, Germany recently issued a research report (Life Expectancy of EPDM Roofing Membrane Over 50 Years Scientific Approach) on the testing of exposed, in situ ballasted roofs up to 30 years old, all which are watertight and still performing, and concluded that EPDM roofs have a predicted life expectancy of over 50 years.

In the summer of 2009, the EPDM Roofing Association (ERA) embarked on a study of in situ long-term service roof systems; 29 years of age and older. The roofs were located in the Midwest and South Central portions of the United States. The membrane on all the roofs was 45 mil EPDM, the standard membrane at the time of installation. The roof systems were both ballasted and fully adhered. Samples were taken and sent to Momentum Technologies in Union Town, Ohio and their physical properties tested. Results for elongation and tensile reveal that even after 30 years of in field service that the EPDM roofing membrane holds its physical characteristics. These tests confirm empirical experience by this author, that aged in situ EDPM roof membranes continue to perform well into their forth decade.

Roof system designers, architects, building owners and property managers can be assured of EPDM's long-term, sustainable and environmentally complimentary performance. This author believes that building owners should demand long-term service roof systems and that designers have a fiduciary responsibility to design roofs to achieve this goal.

2 ACHIEVING LONG-TERM PERFORMANCE

Achieving roof system service lives in excess of warranty length involves several phases, the first of which is design.

As roofing professionals have applied the concept of sustainability to their construction and roofing replacement projects, they have come to learn that several key areas provided opportunities for improvement. These areas were identified by the CIB (International Council for Research and Innovation in Building Construction) Working Commission W.83 or RILEM (International Union of Testing and Research Laboratories for Materials and Structures) Technical Committee 166RMS (CIBW.83/RILEM166RMS); of which this author was a co-chairman of.

Three main areas for improvement were identified: 1.) Minimize the burden on the environment by responsible use of materials; 2.) Conserve energy by improving thermal efficiency of roofs; and 3.) Extend roof lifespan by improving long-term performance [Hutchinson 2004].

This paper will focus on the third key item, in particular, how roofing professionals and building owners can extend the lifespan of their roofing systems, specifically EPDM membrane, after installation.

Certainly much can be done to ensure long-term performance prior to bringing in the construction crew. Gaining a consensus among all parties as to the goals and performance expectations is an important step, as are factoring in the budget for the project, the specific characteristics of the building, and its geographic location.

2.1 Material Selection & Design

Choosing the appropriate materials is certainly a major factor in the procurement of a sustainable roofing system. While many products on the market advertise their ability to produce sustainability, only quality materials with proven historical records of long-term performance should be used. Materials and systems which offer the promise of performance without the historical data to support this claim should be avoided. EPDM has over a 40-year history of performance.

While roof system design is worthy of an entire article in itself, this paper will focus on general guidelines and concepts to achieve the intended goals.

The project's roof system designer, a project consultant equal in importance to other project consultants; structural, mechanical, plumbing, etc., should be part of the design process, providing information to the design team so that architecture detrimental to roof system performance can be avoided and/or the costs to protect the roof discussed. Discussion of building and roof use, as well as the anticipated construction process should be undertaken and understood so that the appropriate roof system can be designed and specified.

Roof Membrane: Historical evidence of long-term service life revolves around 45 mil EPDM membranes, as that was the standard 30 years ago. Current architectural standard dictates 60 mil EPDM. This author, who designs roof systems for 40 years or more of planned service life specifies 90 mil EPDM, due to its durability, ease of installation, and of course expected long-term service life performance.

Selecting system components that compliment the EPDM membrane and provide to potentially enhance the materials performance should be reviewed. Substrates of suitable material and compressive strength should be considered. Material attachment methods need to be considered. Protective cover boards often provide a tripartite of benefits: protection from the mechanical fasteners, protection of the insulation boards from compaction or crushing, and protection of the membrane from physical damage due to excessive foot traffic, especially during the construction process.

Incorporating a vapor barrier/temporary roof into the design has many benefits: dries in the building quickly and allows for interior mechanical and architectural work to proceed, provides a work surface for the various trades whose work either impinges upon the roof or requires using the roof as a work surface. The author finds this singular purpose to be an outstanding benefit to the quality of the roof system and to achieving optimal life service. Vapor retarders, depending on the building use (note how important early understanding of the building use can be), are critical in protecting roof systems from the deleterious effects of condensation. Buildings designed under the LEED parameters, with positive building pressure have been found to create damaging effects below mechanically fastened single ply membranes, resulting in their removal and replacement within years of their initial installation, costing millions of dollars.

Redundancies in a roof system are a valuable aspect of achieving long-term service life. EPDM roof systems, by virtue of their seam tape products and ease of adhesive use allow for the quick installation of redundancies. Examples include lap seam cover strips, protective layers of EPDM around roof curbs and areas with a high volume of roof top use, as well as double layers of flashing at penetrations.

A relatively new concept that designers need to come to grips with and design for is the concept of a "Roof as a Platform". The roof has evolved into an important real estate commodity and thus cannot be left abandoned. Roofs are now being asked to perform beyond their principal function of protecting the building from the effects of the climate, to being a platform for garden roof covers, wind powered electrical generation, solar panel support and a new generation of HVAC equipment.

While there are certainly a number of options to consider while compiling a list of materials and design options, focusing on long-term performance should be given priority, whenever possible, over initial costs. Life cycle analyses have been conducted validating the value of focusing on long-term performance, including one written by Jim Hoff [Hoff 2006], former Vice President of Quality, Technology and Product Development, Firestone Building Products. These reports support the proposition advanced by many roofing consultants, including this author, that the investment in enhanced system design can produce relevant economic return to the building owner.

As an example, Hoff, using the Equivalent Uniform Annual Cost (EUAC) calculations, 20-year roofing systems in the study offered long-term costs 10% to 15% lower than their 15-year counterparts. In addition, the EUAC of the single 30-year system studied offers an additional cost savings of 12% beyond a similar 20-year system. It appears that 60-year performance of EPDM roof systems would provide a building owner with substantial economic benefit.

A critical component in achieving roofs with long-term sustainable roof systems is comprehensive construction drawings that appropriately communicate to the bidding contractors both the design intent and scope of work. Simply put, specifications are not enough; the roofing system should be designed and drawn.

No amount of text can properly describe the detailing required in complex situations. Even simple details can become confusing when not properly drawn. Manufacturers' standard details and requests to have contractors basically design the roof with shop drawings are inappropriate for achieving long-term performance. Comprehensive drawings add greater clarity in understanding the project, eliminating many doubts and points of confusion that can lead to mistakes and, in some cases, legal action.

Effective communication has become more important in the past few years, if only because it has become more challenging. Much of today's workforce consists of people for whom English is not a first language, or a language they speak at all. Visual information overcomes any language barrier.

During the roof system process and commitment of the design to graphic representation, the roof system should be in continuous contact with others on the building team, such as the mechanical, plumbing, and structural engineers, as well as the design architect, so that all elements of the building that impinge upon the roof and/or whose installation process has the potential to impinge upon the roof can be discussed and designed for appropriately [Hutchinson 2002].

Prior to releasing the contract documents for bidding, this author recommends pre-qualification of contractors, to confirm their suitability and qualifications for the particular project. Be selective; eliminate the non-qualified early in the process. A poorly qualified contractor can result in less than expected results.

2.2 Construction Administration – An Integral Part of Commissioning

Following the bidding, the emphasis shifts to construction administration and observation. Roof construction and the impact of the construction process, differing trades who impact the roof, and the need to provide a dry interior are all drivers that potentially can derail a roof system's ability to achieve a long-term service life. Oversight in the office, as well as the field, needs to be provided. This activity should be considered an integral component in the roof system's commissioning, as observing the assemble is inherently of more value than a surface inspection.

The oversight commences in the office often months prior to the commencement of the roof construction in the form of shop drawing and submittal review. Shop drawings should be project specific and provide clear evidence of the contractors understanding of the project and impinging factors. Incorrect shop drawings should be rejected and returned for resubmittal. Another often-overlooked responsibility of both the roof contractor and design team is the understanding of and incorporation of equipment and materials that impact the roof, and the need for contractors to communicate amongst themselves so that their respective shop drawings can appropriately reflect the work required. The project design team should also be coordinating the various trade shop drawings and assuring that the various contractors that impact the roof understand the needs of the roofing contractors. Communication, the sharing of information and the submission of shop drawings that complement each other are required. This type of coordination requirement should be specified and followed through. An example of this type of requirement can be seen in the installation of roof top solar arrays, where multiple professional design and trade disciplines meet and interact.

In the field there is an acute need to diligently review the work being performed, to ensure installation complies with the contract documents and lives up to the terms of the contract. An important part of contract administration is answering questions and arriving at decisions when dealing with situations unforeseen at the start of the project.

Additionally, weather issues need to be considered. Installing roofing in inappropriate weather cannot be tolerated. If observed or discovered, it should be rejected. We all have horror stories of a project kept "on schedule" by working through bad weather. The ultimate punishment comes when the roofing system fails to perform as expected because of this push to meet a deadline.

Roofs of inappropriate, non-compliant and unacceptable workmanship, or portions thereof should be rejected and required to be removed and replaced. Empirical experience with attempts to placate contractors only seems to delay and often exacerbate the concern, only to be more costly to correct.

The bottom line is that the maintenance of the installed roofing system and the materials in it are the responsibility of the owner, not the manufacturers. They can only produce a product with the potential for outstanding performance. High quality design and installation are important parameters in the goal of long-term service life achievement, but it is the maintenance of these materials (roof system) that will ultimately determine their performance on a particular roof.

2.3 Roof System Maintenance – Managing the Durability of Your Asset

Most roof system warranties require regular performance of maintenance in order to keep the warranty provisions in place. However, even the specter of keeping your warranty viable doesn't encourage every building owner to implement a maintenance plan. In fact, most would not want to answer the question, "Do you spend as much time maintaining the roof as your other investments?" Building owners who desire attaining roof systems of long-term service lives must commit to a proactive and sustained roof

management program, one whose ultimate goal is to keep the roof in a condition where is can continue to perform, year after year.

This author believes the industry standard of a twice-a-year maintenance program is not good enough. While inspection of, and perhaps maintenance of roofs in spring, following winter's storms and then late fall, prior to the onset of winter, as well as following violent storms are good, additional inspections are recommended and required. Proactive building owners and managers are requiring monthly inspections, documentation of corrective action, causes for any concerns and managing who has access to the roof. In addition, particular roof concerns are being addressed accordingly. For instance, roofs with overhanging or adjacent trees, which have a sustained period of leaf loss in the fall, need weekly removal of the leaves from the roof and especially around the drains to prevent drain blockage and resultant ponding, interior moisture intrusion and roof structure overloading, and additional inspections are also required following all HVAC maintenance work.

Visual observation is mandatory; the roofing consultant and/or the owner should walk around the roof and pay careful attention. Has a screw fastener backed out? Did the insulation attached to asphalt or spray foam buckle up? The roof observation walk and subsequent follow-up work should be documented and placed in a historical file.

Roof curbs in particular should be closely observed, as the installation of the roof flashing involves a great deal of handwork. Roof curbs are also often used by crews such as window washers to secure ropes.

In addition to monitoring the roof, track those who access it. A building owner/manager should track activity on the roof by workers sent up to conduct repair or maintenance of HVAC and other equipment on the roof. Accidents may happen and won't be reported. To avoid this, require all appropriate parties to notify you when they access the roof and notify them that you will inspect the roof following their visit. This action commonly increases the level of responsibility of all parties accessing the roof.

This may seem ridiculously obvious, but fix conditions of concern right away. Contact the appropriate manufacturer in writing ASAP so they can document the report and contact a roofing contractor to make the appropriate repairs if warranted, or be held responsible if the repairs don't occur. If the particular item is not covered by the warranty, be sure the owner realizes that they are responsible for payment.

2.4 Planned Assessments and Interventions

There is no low slope roof system, even with excellence in design and construction that can attain a 60-year service life without interventions at some point in the roofs life. Every ten years for the first thirty and every five thereafter a full roof system, membrane and flashing assessment should be undertaken to determine current conditions and prognosis for continued service.

Additionally, there are known vulnerabilities within EPDM roof systems, whose intervention and updating can be anticipated and planned for. Following are some of the interventions that a building owner should consider be undertaken and a suggested year of intervention.

1. Lap Seams: If lap seams have not been overlaid with a cover strip, lap seam inspection, repair and installation of a self-adhering cover strip should be planned for (year 10).
2. Re-flashing of roof curbs and penetrations (year 15, 30 and 45).
3. Re-flashing of roof drains (year 15, 30 and 45).
4. Gravel Ballast: Removal of fractured gravel ballast and installation of new (year 20 and 40).
5. Concrete paver ballast: Removal of fractured concrete paver ballast and installation of new (years 20 and 40).

6. Removal of abandoned and/or obsolete roof top equipment and curbs (ongoing).
7. Removal and replacement of damaged and/or wet insulation (on occurrence).
8. Removal and replacement of backing out fasteners (on occurrence).
9. Application of acrylic roof coatings (every 10 years).

2.4.1 Historical and Modern Day Examples

Waukegan Public School District 60, Waukegan, IL: In 1986, this author designed new 45 mil (60 mil EPDM was not yet available at the time of design and installation) EPDM roof systems for the Waukegan School District No. 60 (Carmen-Buckner Elementary School, Glen Flora Elementary School, North Elementary School, Washington Elementary School, Lincoln Center and Waukegan High School – Washington Campus). Each roof system incorporated tapered thermal insulation to provide positive drainage and roof edges that were raised as required to accommodate the new enhanced insulation heights. Prefinished aluminum fascias and copings were also designed. Cudahy Roofing of Cudahy, Wisconsin was the installing roofing and sheet metal contractor.

The design and detailing were well above what the industry standard at the time. On site observation found excellent workmanship and overall the installation was excellent. 10 warranties were issued.

The roofs were inspected in the summer of 2009 as part of a roof system assessment project and found to range from good to very good, to almost excellent condition. The question often asked is what accounts for this longevity?

The owner, while performing less than desired maintenance inspections, did perform two outstanding roof care items: 1.) They virtually eliminated all but the absolute necessary roof foot traffic; and 2.) They immediately had Cudahy Roofing perform repairs on any noted deficiencies resulting in moisture intrusion.

The roofs, while in good condition, are at the age where the assessment determined minor vulnerabilities that if left unattended could result in the end of the roofs' services lives. Restorative work was completed in the summer of 2010. It is anticipated that following this restoration work another 10 to 15 years of service life can easily be achieved/procured.

Hawthorn School District 73 – Vernon Hills Elementary School, Vernon Hills, IL: In January 1983, this author spent 30 days of full time roof construction observation at the new Vernon Hills Elementary School in Vernon Hills, IL; 25 miles north of Chicago. The roof designed consisted of two layers of rigid insulation on a metal roof deck, structurally sloped to interior roof drains. A 45 mil ballasted EPDM roof system was installed. The perimeter roof edge metal was a gravel stop.

A roof assessment was performed in the spring of 2006, twenty years after installation, for the purpose of assessing the roof systems conditions and estimated remaining service life. While no moisture intrusion was reported, concerns with the uncured membrane over the gravel stop flange end, where splitting was observed and minor bridging at some of the base flashing conditions were noted. Prior to the assessment basic roof maintenance items were performed, but roof top access was closely guarded.

In the summer of 2006, Sullivan Roofing of Schaumburg, IL performed roof restoration services at the gravel stop, lap seam, roof curb, penetrations and lap seam conditions. This intervention cost $52,000.00, over $400,000.00 less than the estimated roof replacement cost. The district hopes for another 10 to 15 years more service life of the roof.

Community Consolidated School District 59 - John Jay Elementary School, Arlington Heights, IL: The school district desired a sustainable long-term solution for this reroofing project, which also came to

involve a great deal of HVAC work. Hutchinson Design Group, Ltd. worked with CS2 Design Group, LLC to design and coordinate a new roof system and HVAC roof top unit replacement. The roof system design, to be successful, needed to take into consideration the anticipated construction sequence of related trades such as carpentry, plumbing, sheet metal, pipe fitters, steel erectors, sheet metal duct work, and electricians. Very detailed construction documents coordinated roof and HVAC integration issues such as pre-flashing roof curb extensions, pipe curbs, pipe supports, stairs and walkways were prepared.

The new roof system employed a vapor retarder, temporary roof, which allowed for carpentry, plumbing, HVAC, pipe fitting, new roof hatch, pipe curbs and the raising of roof curbs, rtu curbs and plumbing vents without the potential of damage to the new roof system. A fully adhered EPDM roof system was designed with base and tapered thermal insulation layers, cover board, and fully adhered 90 mil EPDM. Additionally, sheet metal components included metal siding, expansion joint covers, fascias, copings, counter flashings, and metal siding to clad offset roof elevations walls. All roof drains were removed and replaced with the new, and plumbing vents raised. Protective 2" thick rubber walkways were placed, as well as roof top access stairs to provide safe access.

The new roof system was designed for 40+ years of service, and received a 30-year full roof system manufacturer's warranty.

3 CONCLUSION

The current trend toward increased focus on "green" construction should assist roof system designers in their efforts to promote long-term service sustainability and roof systems that live up to Gro Harlem Brundtland's words "meeting the needs of the present without compromising the ability of future generations to meet their own needs."

EPDM roof systems are already achieving 30-year plus service lives with membrane testing showing 'like new' characteristics. EPDM roof systems properly designed, installed and managed certainly have the potential of meeting the 'Holy Grail' of 60 years of service life.

REFERENCES

CIB (International Council for Research and Innovation in Building Construction) Working Commission W.83 or RILEM (International Union of Testing and Research Laboratories for Materials and Structures) Technical Committee 166RMS (CIBW.83/RILEM166RMS) 2001, 'Towards Sustainable Roofing', *CIB Publication No. 271*.

Hutchinson, T.W. 2002, 'Integrating Building Components in Roof System Design for Long-Term Roof System Performance', Proceedings of the 2002 9th International Conference on Durability of Building Materials and Components, Brisbane, Australia.

Hutchinson, T.W. 2004, 'Sustainable Low-Slope Roof Systems Designed for the Long-Term - Getting It Right the First Time', 2004 CIB World Congress, Toronto, Canada.

Hutchinson, T.W. 2005, 'EPDM Roofing Membranes and Long-term Performance', *The Construction Specifier*, pp. 24-34.

Hoff, James 2006, 'Equivalent Uniform Annual Cost (EUAC): A New Approach to Life Cycle Analysis', Proceedings of 2006 RCI 21st International Convention and Trade Show, Phoenix, Arizona.

XII DBMC
International Conference on Durability of Building Materials and Components
PORTO - PORTUGAL, April 12th-15th, 2011

Development of a Safe and Environmentally Friendly Method for Sealant Renewal. Part1: Development Background and Preliminary Investigation

Satoru Ohsawa [1]
Takeshi Ihara [2]
Shingo Yoshida [3]
Takumi Itaya [4]
Kenji Motohashi [5]

ABSTRACT

With the increase of environment protection issues and the shift toward a stock valued based society, reliable maintenance methods are required to ensure longer service life, safety and security of buildings.Water leaking on external walls or through sealed joints has been a critical issue proving the insufficiency of existing sealing techniques. Sealant renewal by conventional methods does not ensure a durable adhesion of the newly applied sealant due to the presence of tiny residuals of the previous sealant that cannot easily be removed. Therefore, there has been an urgent need for an innovative method with higher water-tight reliability.An innovative and eco-friendly method, named “Thin Sealant Remove” method (TSR method), has been developed using a material, which has as a major component Limonene. Limonene, extracted from Oranges was found to be an efficient agent that softens sealants and caused them to increase in volume. This paper reports the process of selecting Limonene as a remover as well as the preliminary examination results on the removal performance of various sealants by Limonene.

KEYWORDS

Sealant, Renewal, Sealant residuals, Limonene, Gel, Safety.

[1] TAKENAKA Research and Development, Chiba,JAPAN, ohsawa.satoru@takenaka.co.jp
[2] TAKENAKA Research and Development, Chiba,JAPAN, ihara.takeshi@takenaka.co.jp
[3] TAKENAKA Research and Development, Chiba,JAPAN, yoshida.shingoa@takenaka.co.jp
[4] TAKENAKA Corporation Hokkaido Office, Hokkaido,JAPAN, itaya.takumi@takenaka.co.jp
[5] SHIBAURA INSTITUTE OF TECHNOLOGY, Tokyo, JAPAN, Dr.Eng., motoken@shibaura-it.ac.jp

1 INTRODUCTION

The purpose of this study is to propose an innovative sealing renewal method with higher water-tight reliability.With the increase of environment protection issues and the shift toward a stock valued based society, reliable maintenance methods are required to ensure longer service life and safety of buildings. There are more and more cases where warranty on the water proof performance is required on renewal works for external sealants, and the establishment of a reliable method is an urgent issue. Water leaking on external walls or through sealed joints has been a critical issue proving the insufficiency of existing sealing techniques. Sealant renewal by conventional methods does not ensure a durable adhesion of the newly applied sealant due to the presence of tiny residuals of the previous sealant that cannot easily be removed. Therefore, there has been an urgent need for an innovative method with higher water-tight reliability. An innovative and eco-friendly method, named "Thin Sealant Remove" method (TSR method), has been developed using a material, which has as a major component Limonene. Limonene extracted from Oranges was found to be an efficient agent that softens sealants and caused them to increase in volume. This paper reports the process of selecting Limonene as a remover as well as the preliminary examination results on the removal performance of various sealants by Limonene. The companion paper (Part 2) reports results of a study about the viscosity of the remover and the removal performance.

2 QUESTIONS ON EXISTING SEALING MAINTENANCE TECHNIQUE

The following is the practiced process in existing sealant maintenance techniques.

1. The old deteriorated sealant is roughly cut out with a cutterknife.
2. Tiny residuals of the previous sealant are removed as much as possible, with a cutterknife and other tools.
3. Cleaning of the joint's surface where the renewed sealant is to be adhered.
4. Primer for new sealant is applied.
5. New sealant is installed.

Sealants are designed and worked to adhere strongly to the component of joints and be able to absorb joint movement caused by temperature and wind. Therefore, sealants should show a good performance and be with a long water-tight reliability. In the step 2 of the process, it is difficult to remove completely the deteriorated sealant, as it turns out that thin layers and tiny residuals of the previous sealant remains. As usual practice, a new sealant is installed after applying a primer that should adhere to the remaining layer of the previous sealant and to the joint's material. But in fact the remaining layer of the previous sealant interferes between the adhering new sealant and the joint surface, and therefore the reliability of the water tightness of the new sealant becomes lower. In order to remove the residuals of the previous sealant layer in the step 2, a disc grinder can be used. However using a disc grinder will make noize and dust, and it is not effective when the joint is of a complex shape. Beside this, the component of joint may be broken. Therefore, the method using a disk grinder can only be used in particular cases.

3 CONCEPT OF THE INNOVATIVE SEALING RENWEAL METHOD

An innovative sealing renewal method is proposed in order to solve the problems in existing sealing maintenance techniques. Fig.1 shows the concept of the new proposed method. First, the old deteriorated sealant is roughly cut out with a cutter knife. Second, a remover is applied which causes the sealants to swell and soften. Third, the swelled and softened sealants are scraped and removed using a handle-spatula and brush. Finally, a primer is applied and new sealant is injected. This innovative method can solve problems related to noise, vibration, dust and safety, compared to using a grinder.The primary consideration to set up the innovative method is the development of the remover which satisfies four conditions.

1. Safety of workers and the environment.

2. Ability to apply it on complex joints.
3. Easy removal of the previous sealant residuals with handle-spatula.
4. Durable adhesion.

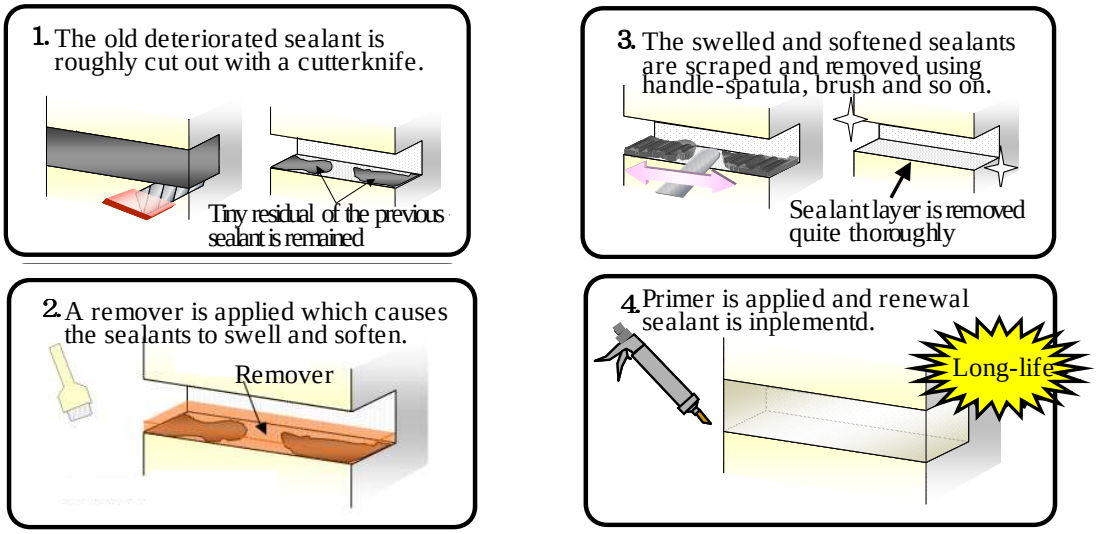

Figure 1. Concept of TSR(Thin Sealant Remove) method.

4 SELECTION OF THE MAJOR COMPONENT OF THE REMOVER

It is well known that Silicone sealant has the best performance among all sealants for building joint filling, and that is why it is difficult to remove such sealant in the first place. Therefore, our study focused on this type of sealant.

First, considering the safety of the human body, three organic solvents were choosed: Limonene, Dimethyl sulfoxide and N-Methylpyrrolidone. Second, the swelling and softening performance of sealants for three solvents was tested by a simple and easy experiment, using the following procedure. Silicone sealants with a size of 10 x 10 millimeters (thickness was 2 millimeter) were soaked in each of the 3 solvents. After a few hours, the sealant soaked in Limonene, which is made from oranges, was the easiest to tear off by hand and its weight increased. The sealant after soaking it in Limonene was three times heavier and became larger in volume than before soaking. Therefore, it was assumed that Limonene would be suitable as a major component of remover. Table 1 shows the safety properties of Limonene compared to some popular solvents for building cleaning. The flash point of Limonene is the highest among other popular solvents. The inhaled volume of Limonene when used by workers is the lowest because its boiling point is the highest among other popular solvents, which brings safety to workers and environment and makes it appropriate as a major component of the intended remover.

Table 1. Property of Limonene and other popular solvents for building cleaning.

Solvent	Raw material	Flash point	Boiling point
		℃	℃
Limonene(Orenge oil)	Orange	45	170
Toluene	Oil	5	110
Hecane	Oil	-22	69
Methylcyclohecane	Oil	-5	100

5 EXPLORATORY EXPERIMENT

5.1 Summary Of Experiment

In order to evaluate the performance of Limonene as a major component of the proposed remover for popular sealants, swelling, pulling and removing tests were conducted.

5.1.1 Tested Materials

The sealants used for the tests are those listed below. These sealants were installed and cured according to Japanese Industrial Standards (JIS) A5758 and A1439. Limonene available in the market was used for the tests.

1.Two-component silicone sealant (named SR-2)
2.Two-component poly isobutylene sealant (named IB-2)
3.Two-component poly modified silicone sealant (named MS-2)
4.Two-component poly polysulfide sealant (named PS-2)
5.Two-component poly urethane sealant (named PU-2)
6.One component silicone sealant (named SR-1)

5.1.2 SwellingTest

The size of a test piece of the sealant was 20 x 20 millimeters (thickness was 2 millimeter). The sealant test pieces were soaked in Limonene for different time lengths: three, six, twelve, and twenty four hours. After soaking, the weight was measured, and the ratio of the weight before soaking to the weight after soaking was calculated.

5.1.3 Pulling Test

Fig 2 shows the form of the tested sealants. Sealants are sliced to the thickness of 2 millimeters and were cut into a dumbbell-shape form, defined in JIS K 6251 as shape No.3. The middle of the dumbbell-shape was soaked in Limonene for the specified time and pulled at the speed of 200 millimeters/min. The maximum pulling strength was measured.

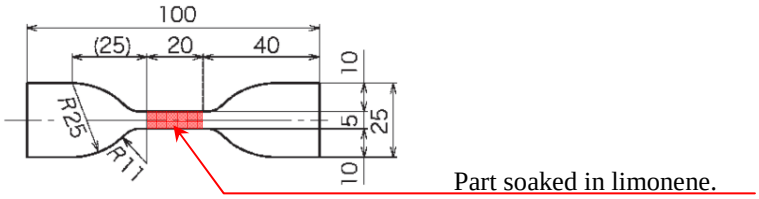

Figure 2. The form of the tested sealant for pulling test.

5.1.4 Removing Test

Fig 3 shows sealant test piece adhered on an aluminum alloy panel. The sealant test pieces are representatives of a case where there is a remaining previous sealant layer. Tested sealants were soaked in Limonene for a few hours. After soaking, sealant was removed by scraper equipped with a load cell. The maximum load of the load cell was measured.

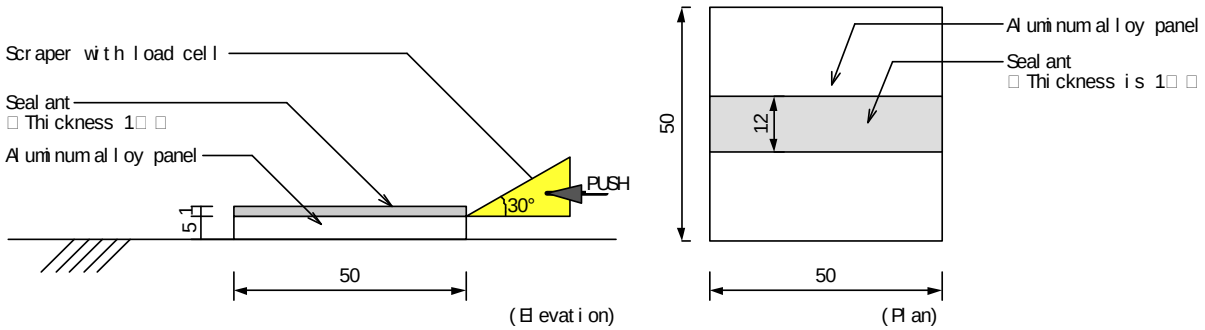

Figure 3. Sealant test piece adhered on an aluminum alloy panel.

6 RESULTS AND DISCUSSION

6.1 Swelling Test

Fig 4 shows the results of the swelling test and reveals that Limonene has the effect to swell major sealants and affected them differently. The increase of the weight ratio of all sealants stops after soaking for about three hours. The weight ratios relative to SR-2, SR-1 and PU-1 are the largest. The weight increases up to between three times to four times the original weight. The ascending weight ratio is in the order SR-2, SR-1, PU-1, followed by MS-2, IB-2, and PS-2.

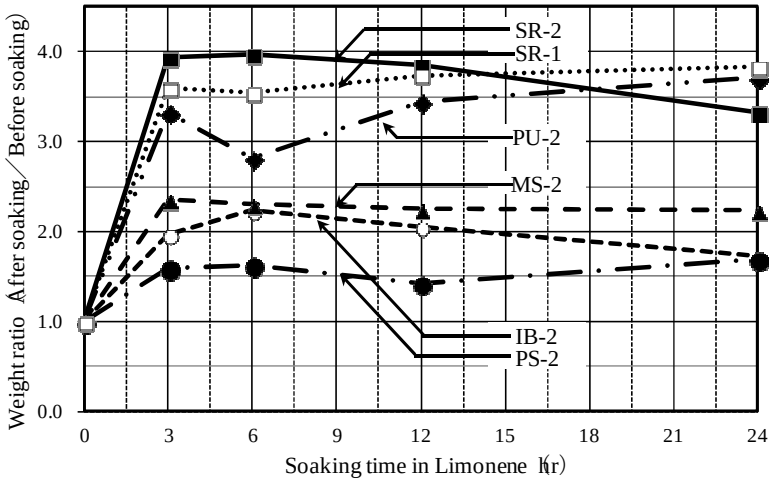

Figure 4. Results of swelling test.

6.2 Pulling Test

Fig 5 shows the relationship between the soaking time and the maximum pulling strength measured on pulling dumbbell specimens. The maximum pulling strength of major sealants decreases greatly after soaking for half an hour and continue decreasing gradually over another half an hour as well.

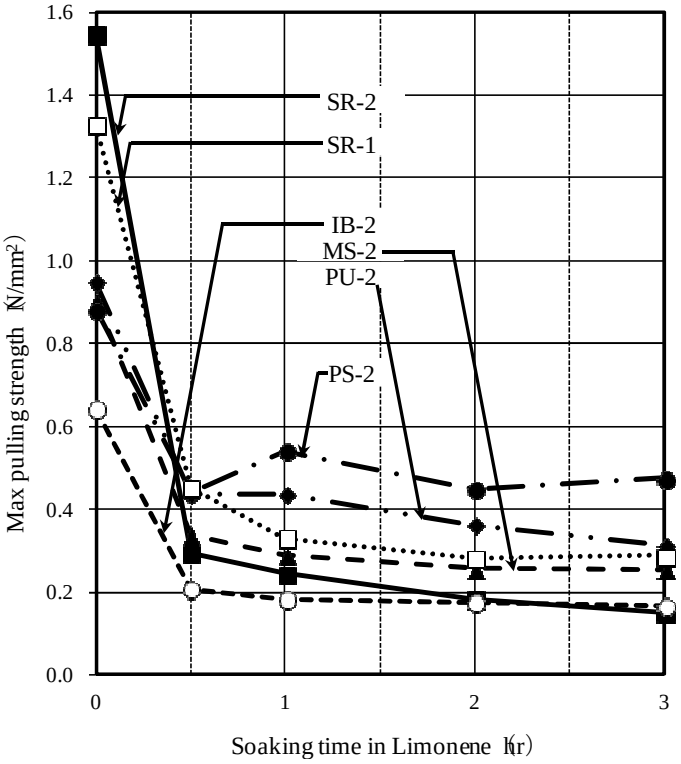

Figure 5. Results of pulling test.

6.3 Removing Test

Fig 6 shows the relationship between the soaking time and the maximum load when the remaining sealant layer is removed with a scraper. For SR-2 and PU-2 the maximum load decreases clearly as soaking time increases. But, for sealants other than SR-2 and PU-2, the maximum load is nearly constant. The effect of swelling and softening of sealants after soaking in Limonene causes the decline of adhesion and for all major sealants it is easier to remove them completely when the soaking time exceeds half an hour including valuation of handling effect.

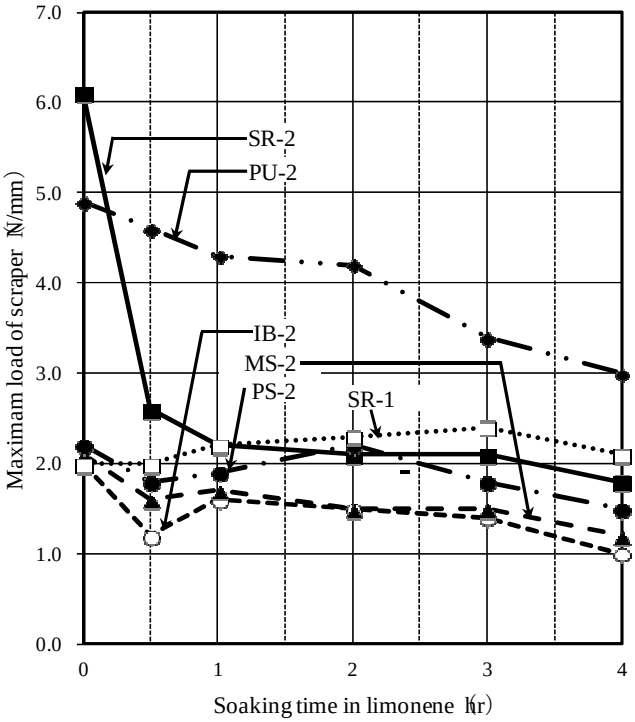

Figure 6. Result of removing test.

7 CONCLUSION

In order to solve the problem of existing sealing maintenance technique, an exploratory experiment has been conducted for the purpose of developing the TSR method which can remove the remaining sealant layer completely with a remover whose major component is Limonene. As a result, the experiments showed that Limonene can swell and soften major practiced sealants for buildings. The results show that Limonene a performable remover.

REFERENECES

JIS A 5758(2010) Sealants for sealing and glazing in buildings

JIS A 1439(2010) Testing methods of sealants for sealing and glazing in buildings

JIS K 6251(2004) Rubber,vulcanized or thermoplastic - Determination of tensile stress - strain properties

Satoru Ohsawa et al. 2009, 'Development of a Safe and Secure Construction Technique for Sealant Renewal Part1 : Background of the Development and the Preliminary Experimental Result' Summaries of Technical Papers of Annual Meeting Architectural Institute of Japan 2009 A-1, pp63-64

Singo yosida et al. 2009, 'Development of a Safe and Secure Construction Technique for Sealant Renewal' Japan Society For Finishings Technology 2009, pp75-78

XII DBMC
International Conference on Durability of Building Materials and Components
PORTO - PORTUGAL, April 12th-15th, 2011

Performance of External Thermal Insulation Composite Systems (ETICS) with Finishing Ceramic Tiles

Sofia Malanho [1]
Maria do Rosário Veiga [2]

ABSTRACT

External Thermal Insulation Composite Systems (ETICS) are innovative systems; their application improves the buildings' thermal insulation, reduces thermal bridges, protects the walls from temperature variations thus increasing the structure durability. They enable the application of a diversity of finishing materials.

Ceramic tiles finishing, which are very traditional in Portugal, can improve the impact resistance of those systems.

The assessment of ETICS performance and durability is carried out based on "ETAG 004 – Guideline for European Technical Approval of External Thermal Insulation Composite Systems with rendering", that establishes requirements and test methods.

However, systems with ceramic tiles finishing are not covered by ETAG 004. Therefore, it is necessary to adapt test methods and requirements for this type of systems.

This paper presents an assessing methodology for performance of External Thermal Insulation Composite Systems (ETICS) with ceramic tiles finishing and its application to a specific system. An experimental campaign is being carried out and tests of bond strength in ETICS after natural weathering were already performed and are presented. Those tests measure bond strength between base coat and insulation board and between tiles and base coat.

KEYWORDS

Assessment methodology, Thermal insulation systems, ETICS, Finishing ceramic tiles.

[1] National Laboratory of Civil Engineering (LNEC), Lisboa, PORTUGAL, smalanho@lnec.pt
[2] National Laboratory of Civil Engineering (LNEC), Lisboa, PORTUGAL, rveiga@lnec.pt

1 INTRODUCTION

External Thermal Insulation Composite System (ETICS) are applied in opaque areas of facades and contribute significantly to energy efficiency. These solutions contribute for the increase of thermal insulation, the correction of thermal bridges and the reduction of interior condensations. ETICS also have the function of protecting the structure and the masonry from thermal impact, thus increasing the durability of these elements.

The ETICS are considered multi-component systems [Collina & Lignola 2010] applied on external walls, composed by insulating boards fixed to the substrates by a bonding material or by mechanical elements, a mesh embedded in the base coat and a finishing coat with decorative functions and of complementary water and impact protection.

The compatibility between the different components is essential for the good performance of the global system, contributing for its durability [VEIGA & PINA SANTOS 2009 e COLLINA & LIGNOLA 2010].

In these systems a diversity of finishings can be applied: paintings, synthetic coverings, mineral binder finishings such as silicates or cement. It is also possible to use discontinuous coverings, like ceramic tiles, stone slabs or of another nature, although these kinds of finishing are not covered by ETAG 004 [EOTA 2000]. The use of ceramic elements on external walls has a large tradition in Portugal. On the other hand, this kind of finishing presents good impact resistance and improves the behavior to fire, contributing for the satisfaction of the requirements of fire safety.

ETICS can be fixed to substrate by bonding or by mechanical elements or by both methods. Bonding is the most used type of fixation, and usually the product used as base coat can also be used as adhesive; bonded systems can also be used with some supplementary mechanical fixings (for example anchors), that according to MORAIS [2007] enable the fixation of thermal insulation boards until the set of the adhesive product. In the mechanical fixation systems, the connection of the insulation boards to the substrate can be constituted by direct anchors or by profiles (for example metallic non-oxidable material). The mechanical fixed systems can include or not complementary adhesive [EOTA 2000]. Choosing the fixing process to the support through vertical profiles allows the existence of a blade of air, allowing the elimination of the risk of condensation in the thermal insulation. However, they are more sensible to the wind pressure due to the suction effect.

ETICS can be applied on masonry of clay units, cement blocks or stone, or on concrete substrates (either cast in situ or prefabricated) [EOTA 2000]; however, they should not be applied on thick and porous old walls, especially if they have high water content, as it would retard the water evaporation, leading to the appearance or acceleration of degradation processes [VEIGA & MALANHO 2010].

ETICS are considered innovative systems and their performance evaluation should be based on ETAG 004 - *Guideline for European Technical Approval of External Thermal Insulation Composite Systems with rendering* [EOTA 2000], which establishes requirements and test methods for assessment of the Essential Requirements defined in the Construction Products Directive.

Products or systems not covered by this or another ETAG, will require the preparation, by the approval Institute, of a simplified specific guideline (CUAP - Common Understanding of Assessment Procedure) which must be submitted to the members of EOTA.

2 PERFORMANCE EVALUATION OF EXTERNAL THERMAL INSULATION COMPOSITE SYSTEMS (ETICS) WITH FINISHING CERAMIC TILES

2.1 Characteristics of ETICS

To validate the assessment methodology an ETICS was analyzed, constituted by thermal insulating boards bonded to the substrate, a mesh embedded in the base coat and finishing of ceramic tiles. For the tests, two kinds of ceramic tiles finishings will be used with equal tile dimensions and water absorption, only differing in the joint width: one with 80 mm standard joints (the most common in the market) and the other one with 1 to 2 mm joint width, simulating a critical situation, to assess the sensibility of the method. The ETICS was applied on two rigs of brick masonry, one rig located inside LNEC´s Wall Renders Test Station and subjected to the hygrothermal test 28 days after its application (Fig. 1) and another with smaller dimensions, in LNEC´s Natural Test Station, subjected to natural exterior environment (Fig. 2). In each rig two areas with different joint widths were set (Fig. 2 – 1 and 2). For comparison, it was also analyzed a similar system with 80 mm standard joints after two years of natural weathering by exposition to exterior environment (Fig. 3).

The comparison between the results obtained permits the evaluation of the effect of the accelerated ageing test and its comparison with natural weathering.

The behaviour of the system with the two ceramic tiles finishing variants will be compared with the same system with a classic finishing of synthetic painting, which has been already fully tested and considered fit for use.



Figure 1. ETICS subjected **to** hygrothermal cyclic testing (with 80 mm and with 1 to 2 mm joint widths).

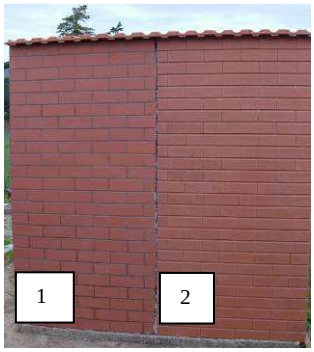

Figure 2. ETICS after 28 days of weathering (1- with 80 mm standard joints and 2 - with 1 to 2 mm joint width).



Figure 3. ETICS after 2 years of weathering (with 80 mm standard joints).

2.2 Methodology for assessment

The methodology for assessment of the fitness for use involves an experimental campaign according to the rules and test procedures specified in ETAG 004 [EOTA 2000] whenever applicable. In the situations not covered by ETAG 004 [EOTA 2000] specific test methods and requirements were developed or adapted based on existing specifications.

The experimental campaign was developed in order to answer to the most serious defects that can occur in ETICS with ceramic tiles finishing: detachment of tiles; condensation inside thermal insulation caused by the decrease of water vapour permeability; increase of the system mass per m^2 and influence on bond strength of the adhesive; cracking of the joints (causing infiltrations of water); differential dimensional variations of the tile finishing due to different coefficients of thermal expansion of materials and different thermal absorption coefficients of the various colours and also related with the thicknesses of the joints.

a) Detachment of tiles

Detachment of tiles of buildings' facades is one of the most serious problems, producing fall of tiles and thus reducing the safety level (Lucas & Abreu 2005), especially for tiles applied on high zones. To analyze the tendency of occurrence of this anomaly a bond strength test will be carried out between the basecoat plus finishing and the thermal insulation board, according to ETAG 004 [EOTA 2000]. The results will be analyzed taking into account the action of tiles' self weight.

b) Condensations

The ceramic tiles have a low water vapour permeability compared with current synthetic finishings, so the diffusion of water vapour will take place mainly through the joints between tiles. For the system with ceramic tiles and joints the test procedures for determining the water vapour permeability, according to NP EN 12086 [IPQ 1997] will be adapted, using a specimen simulating the system tile-joints-adhesive-insulation.

d) Cracking of joints

To analyze the problem of water infiltration by the joints, the Karsten tubes technique will be used. This technique is based on a methodology adopted by RILEM [RILEM 1980] and has been used in previous studies of LNEC [Magalhães 2002, Veiga et al. 2009]. It consists on placing Karsten tubes on the system, covering tiles joints, filling them with water and measure the amount of water lost to the substrate, by water permeability under low pressure, after certain periods of time (Fig. 6).

c) Increase of mass per m^2 of the system (due to the mass of tiles) and its influence on the adhesive bond strength

It will be checked if the mass of the tiles used contributes significantly to the increase of the total mass of the ETICS, by calculating the mass of the system before and after application of the tiles.
To simulate the mass increase and verify how it may affect the adhesive bond strength a weight will be placed on top of ETICS (insulation product + render) and its effect will be analysed on the deformations and on the bond strength between ETICS and substrate.

e) Thermal expansion

The coefficients of linear expansion of tiles and mortars will be determined according to EN ISO 10545-8 [IPQ 1996] and will be compared. Susceptibility of the system to the differential thermal dimensional variations will be checked.



Figure 5. Test of water vapour permeability.



Figure 6. Water permeability under low pressure test with Karsten tubes.

2.3 Experimental campaign

The bond strength tests were already accomplished, in order to analyze the problem of detachment of tiles with 80 mm joints applied on a ETICS. These tests were carried out after 28 days (Fig. 2 – 1) and after 2 years (Fig. 8) of natural weathering.

ETAG 004 [EOTA 2000] requires the test of bond strength between base coat and insulation board to accomplish safety in use requirements. As ceramic tiles finishing is not covered by ETAG 004, it was necessary to adapt this test to analyze the adhesion of the tile to the base coat.

For the bond strength between base-coat and insulation board the incisions were made until the insulation board (Fig. 7). In the case of the bond strength between tiles and base-coat the incisions were made until the tiles (Fig. 7). Results are presented in Tables 1 and 2.

Table 1. Bond strength test between base-coat and insulation board.

ETICS with analysed	*Bond strength*		*Standard deviation*	*Fracture pattern*
	Individuals values [N/mm^2]	*Average values* [N/mm^2]		
ETICS after 28 days of natural weathering	0.24	0.21	0.03	cohesion fracture in the insulation board
	0.20			
	0.20			
ETICS after 2 years of weathering	0.12	0.17	0.07	
	0.22			

Table 2. Bond strength test between tiles and base-coat.

ETICS analysed	*Bond strength*		*Standard deviation*	*Fracture pattern*
	Individuals values [N/mm^2]	*Average values* [N/mm^2]		
ETICS after 28 days of natural weathering	0.25	0.30	0.05	cohesion fracture in the base-coat
	0.32			
	0.34			
ETICS after 2 years of weathering	0.15	0.17	0.02	50% cohesion fracture in the insulation board and 50% cohesion fracture in the base-coat
	0.19			50% cohesion fracture in the insulation board and 50% cohesion fracture in the base-coat

For ETICS with paintings, synthetic coverings or mineral binder finishings such as silicates or cement, ETAG 004 (EOTA 2000) requires that, after hygrothermal cyclic testing, the minimum bond strength between base coat and insulation product should be at least equal to 0,08 N/mm^2 or failure occurs in the insulation product.

Values obtained in bond strength test between base-coat and insulation board are higher than 0,08 N/mm^2 and the failure occurred in the insulation board (Table 1 and Fig. 10 - 1), addressing the requirements. .

Values obtained in bond strength test between tiles and base-coat are also higher than 0,08 N/mm^2 (Table 2) addressing the requirements (Fig.10 - 2).

Results show that after two years of weathering the system suffers a small decrease in bond strength between base-coat and insulation board. A higher decrease seems to occur in the test between tiles and base-coat, however, the failure in the system weathered for two years was partly in the insulation board and may have been due to lack of precision of the incision, that may have exceeded the thickness of the tile and reached the insulation (Fig.11).

The complete set of tests described in 2.2 will be carried out in the next year, on the system after natural weathering and also on the system after accelerated ageing tests. Additionally, all the tests referred to ETAG 004 [EOTA 2000] which are applicable on ETICS with ceramic tiles finishing will also be performed, such as impact with hard body of 3 J; impact with hard body of 10 J; resistance to perforation (Perfotest).

The differences obtained for systems with normal and thin joints will give information about the influence of thickness of joints. The results will also be compared with those obtained for a similar system with a synthetic finishing.



Figure 7. Incisions on ETICS.



Figure 8. Bond strength test.

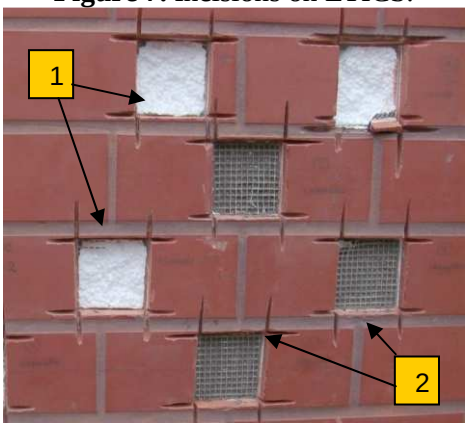

Figure 10. Results of bond strength test between base-coat and insulation board (1) and between tiles and base-coat (2).



Figure 11. Results of bond strength test between tiles and base-coat on ETICS after 2 years of weathering.

3 CONCLUSIONS

The application of ceramic tiles finishing on ETICS is expedted to provide an improvement of impact resistance and fire behaviour of systems.

However, ETICS can present several kinds of anomalies. Taking into account their degree of severity, some anomalies involve consequences which may endanger the users´ safety and other less serious anomalies, which nevertheless contribute to poor performance of the system. Thus, a methodology for evaluating performance to respond to the main problems which may occur in buildings with these kind of systems was developed to assess the fitness for use of ceramic tiles as ETICS finishing. As this type of finishing is not covered by ETAG 004, it was necessary to adapt test methods and requirements based on existing ones and develop specific test methods.

The methodology is being applied to a specific ETICS, with two different joint withes. Adhesion tests were already carried out on the system after 28 days weathering and after 2 years weathering to try to predict the behaviour of ETICS with tiles finishing over time and analyze the problem of detachment.

The bond strength values decreased with time, but after two years weathering they are still higher than the ETAG requirements.

The results of the system performance after accelerated and after natural weathering will be compared. A comparison between the specific system studied and a similar one with a synthetic painting finishing will be carried out as well.

ACKNOWLEDGMENTS

The authors wish to thank Saint-Gobain Weber Portugal for furnishing materials for the tests and workmanship to build the rigs. The authors also emphasize and thank Eng. Luís Silva, Eng. Vasco Pereira, Eng. Pedro Sequeira e Eng. Nuno Vieira, from Weber Portugal, for the interesting discussions that contributed to this work.

REFERENCES

Collina, A.; Lignola, G. P. 2010, “The External Thermal Insulation Composites System (ETICS) – More than comfort and energy saving” APFAC 2010, 3º Congresso Português de Argamassas de Construção. Lisboa, LNEC, 18 e 19 Março.

European Organization for Technical Approvals (EOTA) 2000. “Guideline for European Technical Approval of External Thermal Insulation Composite Systems with Rendering”. EOTA, Brussels, March. ETAG 004.

Instituto Português da Qualidade (IPQ) 1996, “Ladrilhos cerâmicos – Parte 8: Determinação da dilatação térmica linear”. Lisboa, IPQ. NP EN 10547-8.

Instituto Português da Qualidade (IPQ) 1997 “Produtos de isolamento térmico para aplicação em edifícios. Determinação das propriedades de transmissão ao vapor de água”. Lisboa, IPQ, NP EN 12086.

Lucas, J.; Abreu, M. 2005 “ Revestimentos cerâmicos colados. Descolamento”. Lisboa, LNEC. Informação Técnica de Edifícios ITPRC 4.

Magalhães, A. C. 2002 “Ficha de Ensaio de revestimentos de paredes FE Pa 39. Revestimentos de paredes. Ensaio absorção de água sob baixa pressão”. Lisboa: LNEC, Junho.

Morais, A.I. 2007 “Soluções de reabilitação de fachadas com revestimento em ladrilhos cerâmicos” Dissertação submetida para o grau de Mestre em Reabilitacao do Patrimonio Edificado. Porto, FEUP, Novembro.

RILEM 1980 “Water absorption under low pressure”. Pipe method. Test No. II.4, tentative recommendations. Paris, RILEM.

Veiga, M. R.; Pina dos Santos, C. 2009 "Revestimentos de isolamento térmico de fachada: eficiência, durabilidade e comprovação de qualidade". Construção Magazine, nº 32, Julho, págs. 12-18.

Veiga, M. R.; Velosa, A.; Magalhães, A. C. 2009 "Experimental Applications of mortars with pozzolanic additions. Characterization and performance evaluation". Construction and Building Materials, 23, pp. 318-327. January.

Veiga, M. R.; Malanho, S. 2010 "Sistemas Compósitos de Isolamento Térmico pelo Exterior (ETICS): Comportamento global e influência dos componentes". APFAC 2010 - 3º Congresso Português de Argamassas de Construção. Lisboa: LNEC, 18 e 19 Março.

XII DBMC
International Conference on Durability of Building Materials and Components
PORTO - PORTUGAL, April 12th-15th, 2011

Biocide Tolerance in Microorganisms with Respect to Durability of Building Coatings

Wolfgang Hofbauer [1]
Nicole Krueger [2]
Florian Mayer [3]
Klaus Breuer [4]

ABSTRACT

Present state of the art does not allow guaranteeing the exemption of unwanted biological growth on building coatings under all circumstances without the use of biocides. Currently only a limited range of active substances against façade microorganisms are available. In order to achieve an appropriate and ecological use of biocides in building coatings it is important to know about possible tolerances of the target organisms. Due to known efficiency gaps of different biocides it is already common use to apply adjusted combinations. Aerophytical microorganisms, like façade algae may be capable to follow different survival strategies to avoid or tolerate biocidal ingredients. Different features of aerophytical microorganisms and the biological effects against the target organisms of typical biocides are discussed. Based on current knowledge actual demands on the modern and responsible use of biocides in building coatings shall be shown in order to stimulate the discussion among experts. Important questions are a safe use of biocidal substances on one hand and durability and energy consumption on the other. Is it possible to keep building surfaces free from microorganisms at all?

KEYWORDS

Biocides, Biocide tolerance, Algae, Fungi, Coatings.

[1] Fraunhofer-Institute for Building Physics (IBP), Holzkirchen, GERMANY, wolfgang.hofbauer@ibp.fraunhofer.de
[2] Fraunhofer-Institute for Building Physics (IBP), Holzkirchen, GERMANY, nicole.krueger@ibp.fraunhofer.de
[3] Fraunhofer-Institute for Building Physics (IBP), Holzkirchen, GERMANY, florian.mayer@ibp.fraunhofer.de
[4] Fraunhofer-Institute for Building Physics (IBP), Holzkirchen, GERMANY, klaus.breuer@ibp.fraunhofer.de

1 INTRODUCTION

Biological infestation of building surfaces is an extensive and growing problem. While some materials like metals, for instance, can suffer severe damage caused by biodegradation and bio-fouling [e.g. Rège von, Sand 1996] growth on façades usually is mainly a visual problem. But if optical degradation of a surface by excessive soiling or microbial growth happens soon after the application of a coating this is regarded as damage and may lead to claim for recourse. Since it is not possible guaranteeing the exemption of unwanted biological growth on building coatings under all circumstances the use of biocides is present state of the art [Lindner 2005]. Different regulations such as the Biocidal Product Directive (BPD) in Europe control the use of biocides in coatings. Due to regulations big efforts are demanded for the licensing of new substances. Therefore currently only a limited range of active substances against façade microorganisms is available.

Unwanted biological staining of building surfaces may consist of quite different organisms, as there are algae, fungi, lichens and bryophytes [Hofbauer at al. 2003]. Bacteria are also involved, but usually they do not form visible growth patterns on modern building surfaces. The durability of biocidal products is dependant on different influences like climate (day course and year course) and material and construction properties. Apart from this also biocide tolerance of microorganisms and biodegradation of biocides are important factors. The contribution of bacterial degradation to the degradation of biocides may be significant [Cook & Dickinson 2004]. For Iodopropynylbutyl-carbamate (IPBC) it was already shown, that some wild isolates of bacteria from treated wood are more effective and more resistant to the compound than other strains [Cook & Dickinson 2004]. Fungicidal compounds may have gaps in their action spectrum. It is already known, that in case of Carbendazime some fungi, like *Alternaria* spp., *Ulocladium* spp., and other, show an increased tolerance (e.g. [Bollen et al. 1983], [Hassal 1990], [Deising et al. 2008]).

Because of the biological diversity at infested façades and known efficiency gaps of different biocides it is already common use to apply adjusted combinations. Aerophytical microorganisms, like façade algae may be capable to follow different survival strategies to avoid or tolerate biocidal ingredients. In the following the finding of new biocide tolerant algal strains is presented and different features of aerophytical microorganisms and the biological effects against the target organisms of typical biocides are discussed.

2 METHOD

In an interdisciplinary project the effectiveness and durability of biocides in coatings was investigated. In a four years outdoor study special designed specimens with the same structure as an external thermal insulation composite system (ETICS), finished with different coatings (a plaster or a plaster covered with paint) were employed. Fife different kinds of plaster (a lime cement plaster, a silicate plaster and three plasters with organic binders based on styrene acrylate, terpolymer and silicone resin) and three different paints (a dispersion type silicate paint, an emulsion paint and a silicon resin based paint) were used. The surface coatings only were supplied with different biocidal mixtures (four different biocide combinations), or without for comparison purposes. Every biocidal mixture consisted of three active ingredients: Terbutryne, Octylisothiazolinone (OIT) and a third compound which was either Carbendazime, Dichloro-Octylisothiazolinone (DCOIT), IPBC or Zinc-pyrithione.

Apart from chemical and physical measurements the development of biological growth on biocidal surfaces in comparison to non biocidal surfaces of the same kind was assessed by different methods. In addition to a permanent control of the visual condition of the surfaces of the specimens that were exposed to the natural environment facing west, according to Hofbauer et al. [2003], and regularly microbiological exploration of the surfaces by dilution plating and direct plating, according to Hofbauer [2007], also eco-physiological investigations were performed.

The biocide tolerance of unialgal isolates of algae that were recovered from biocidal surfaces was measured in comparison to standard test algae. Batch cultures of new algae isolates from biocidal surfaces and common green algal test strains from "Sammlung von Algenkulturen Göttingen" (SAG, Collection of Algae Cultures Göttingen) in a mixture, *Stichococcus bacillaris* SAG 379-1a and *Klebsormidium flaccidum* SAG 335-5, were grown in Bold´s Basalmedium modified after Bischoff & Bold [1963], [Ettl & Gärtner 1995], and maintained at 16°C, with light supplied by cool-white fluorescent tubes (Osram, Munich, Germany) on a 12:12 hours light:dark cycle. Room temperature Chlorophyll a (Chl a) fluorescence was measured under vivo conditions at 23±2°C using a pulse-amplitude-modulated fluorometer (Walz, Effeltrich, Germany). Non-photochemical Quenching was calculated as described in Cousins et al. [2002].

3 RESULTS

Continuous visual investigations of the different surfaces revealed a general efficiency of all tested biocide combinations but different patterns of starting growth processes according to different biocide combinations and different coating systems. Qualitative and quantitative microbiological investigations of the surface of the coatings showed different developments at the different coating systems with characteristic groups of organisms. Whereas on non biocidal variants for comparison growth started much earlier and showed a much higher biodiversity, growth on biocidal coatings was rather sparse and showed only limited biodiversity. In this paper selected peculiar results of the investigations shall be communicated.

Very frequently found on non biocidal variants are species of the fungal genus *Cladosporium* and *Epicoccum purpurascens*. Also *Alternaria alternata* appears quite often, but not dominantly. Apart from the most frequent and dominant species a broad range of different pioneer species can be found. On surfaces of the biocidal variants much fewer species could be isolated. It is conspicuous that on biocidal surfaces that are equipped with a biocide combination containing Carbendazime as second fungicide after gross reduction of OIT the fungal genera *Alternaria* und *Ulocladium* become predominant in the otherwise very sparse surface flora. These fungi are already known for their higher tolerance to Carbendazime. A further quite abundant species on these surfaces is also *Phoma glomerata*, which also can be assumed quite tolerant to Carbendazime according to our results. Further potentially new tolerances of fungi can be assumed and shall be presented elsewhere.

Apart from numerous different species of fungi after comparable short time non biocidal variants also show a quite high diversity in algal species. On biocidal surfaces, if there was any algal activity measurable within the course of the project, there were only found strains of the green algal genus Diplosphaera. This was interpreted as a potential tolerance of these algal strains against the algicide Terbutryne. Therefore measurements of room temperature Chl a fluorescence under in vivo conditions using a pulse-amplitude-modulated fluorometer were performed. Relative efficiency of non-photochemical Quenching (Fig 1) shows that the new isolates (*Diplosphaera*) are much less affected by biocidal action of Terbutryne. This result shows that these isolates seem to be quite tolerant against Terbutryne, a commonly used algicide in coatings.

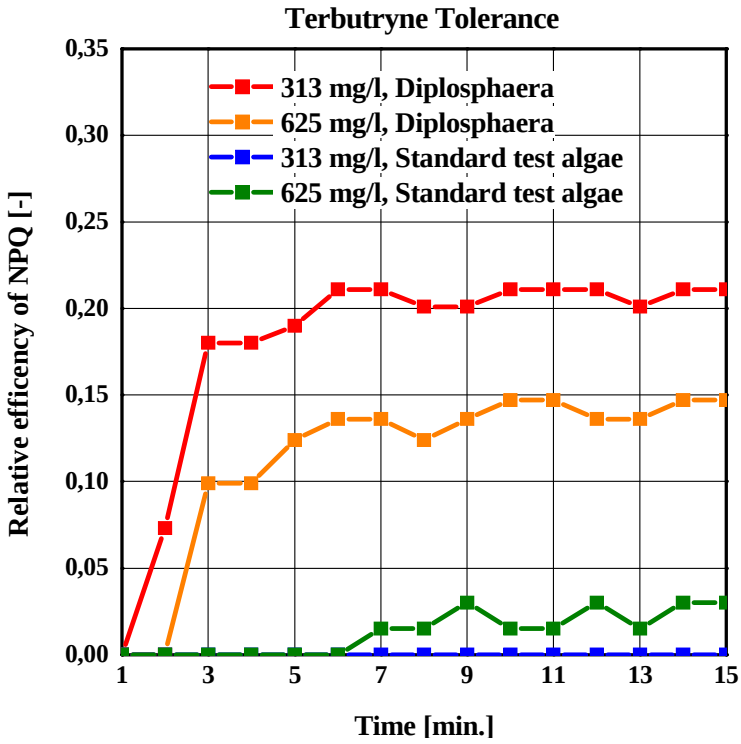

Figure 1. Comparison of the relative efficiency of the non-photochemical quenching shows that photosynthesis of an isolate of *Diplosphaera* sp. from a biocidal surface is much less affected by different concentrations of terbutryne than standard test algae.

4 DISCUSSION

While bacteria are hardly recognised for visual disfigurement of modern building surfaces they are well known for developing resistances against various bactericidal compounds. The so called “super bug”, a multi resistant pathogen germ is spreading in hospitals all over the world, for instance [Kumarasamy et al. 2010]. For coatings bacteria are mainly a problem in pot conservation and less for film conservation of building coatings.

In Central Europe mainly eukaryotic algae dominate biological stains on modern façades (e.g. Barberousse et al. [2007], Hofbauer [2007]). Therefore it is not surprising, that the primary algal colonization that was found by our investigations in this project comprises almost only (eukaryotic) green algae. But it was a surprise that in early algal colonization of biocidal surfaces only strains of *Diplosphaera* could be found. Since the only biocide against algae that was employed in the project was Terbutryne it seems obvious that this alga might have a higher tolerance against this compound. This could be confirmed by first overview measurements. Further detailed measurements are planned and will be completed by the analysis of further strains of this algal genus from further surface analyses.

Terbutryne comprises a chemical measure against unwanted growth of algae that has a general detrimental effect on photosynthesis and does have impact on all photosynthetic active organisms (e.g. Moreland et al. [1959], Shimabukuro [1967]). Previously documented tolerances of algae against algicides were only known from laboratory experiments with artificially produced resistances or from aquatic environments (e.g. Riemer & Trout [1980], Collier et al. [1990], Hassal [1990], Varsano et al. [1992], Lindner [2005]). The data shown reveal for the first time that a higher tolerance against algicides can also be developed by aerophytical alga that might colonize building surfaces. Since biocidal action means a high evolutional pressure it is to be assumed that these algal forms might spread in the future.

In order to achieve an appropriate and ecological use of biocides in building coatings it is important to know about possible tolerances of the target organisms. Due to known efficiency gaps of different biocides it is already common use to apply adjusted combinations. Aerophytical microorganisms, like façade algae may be capable to follow different survival strategies to avoid or tolerate biocidal ingredients.

The above discussed tolerances of algae against biocides are direct resistances on the basis of biochemical changes within the cells. But algae and fungi do have some other possibilities to escape the action of biocides. Many algae produce mucopolysaccharides that cover their cells or filaments. For some organisms it is already known that their surrounding mucilage can prevent toxic substances from reaching the cells. In some fungi, for instance, their elevated tolerance to heavy metals is connected to secretion of mucopolysaccharides and melanin production (e.g. Caesar-Tonthat et al. [1995], Martino et al. [2000]). Similar processes are also thinkable for biocides, but not yet confirmed and should be a topic for further studies.

Another possibility is the reduction of biocides by biodegradation. It is already known that growth of algae may be stimulated by co culture with bacteria, even in presence of toxic compounds [Safonova et al. 1999]. It is possible, even desirable in the sense of eco-toxicological aspects, that biocides may be degraded by bacteria. If algae and fungi live together with bacteria of this special kind in a symbiosis this may effectively reduce the biocidal content in their immediate surrounding.

An additional process that can be recognised in the field is not connected to special biological processes. Many plasters and renders that are used today do contain structure kernels that shall give the finished surface a pleasant structure. Structure kernels are usually made from natural rocks. If these kernels are weathered out at the surface they might be a place where growth could start if conditions otherwise would be favourable.

In the future it will be a great challenge to consider all demands on biocides that are used for building coatings. An appropriate and ecological use of biocides shall result in a more specific and responsible employment of eco-toxicologically bearable concentrations. Current regulations make efforts for the development of new chemicals that are active against the target organisms quite expensive. But emerging tolerances of target organisms against biocides used demand an increase in concentration or a change in compounds. It will not be possible to keep building surfaces free from unwanted growth of microorganisms at all for all time by chemical methods, if not completely new approaches are developed.

ACKNOWLEDGEMENTS

The research presented is sponsored by the Bundesministerium für Wirtschaft und Technologie on account of a decision of the German Bundestag, Projektträger Jülich and partners from industry.

REFERENCES

Bischoff, W.W. & Bold, H.C. 1963, ‘Phycological Studies IV. Some soil algae from Enchanted Rock and related algal species’, *Univ. Texas Publ*. **6318**, pp. 1-95.

Bollen, G.J., Hoeven van der, E.P., Lamers, J.G., Schoonen, M.P.M. 1983, ‘Effect of benomyl on soil fungi associated with rye. 2. Effect on fungi of culm bases and roots.’, *Neth. J. Pl. Path*. **89**, pp. 55-66.

Caesar-Tonthat, T.-C., Van Ommen Kloeke, F., Geesey, G.G., Henson, J.M. 1995, 'Melanin Production by Filamentous Soil Fungus in Response to Copper and Localization of Copper Sulfide by Sulfide-Silver Staining', *Applied And Environmental Microbiology* **61**(5), pp 1968-1975.

Collier, P.J., Ramsey, A.J., Austin, P., Gilbert, P. 1990, 'Growth inhibitory and biocidal activity of some isothiazolinone biocides', *Journal of Applied Bacteriology* **69**, pp. 569-577.

Cook, S.R. & Dickinson, D.J. 2004, 'Studies on the Toxicity of IPBC and Other Biocides to Bacteria', Proc. 35th Annual Meeting Ljubljana, Slovenia 6-10 June 2004, The International Research Group On Woos Preservation, Section 1 Biology, IRG/WP 04-10544, pp. 1-20.

Cousins, A.B., Adam, N.R., Wall, G.W., Kimball, B.A., Pinter JR, P.J., Ottman, M.J., Leavitt, S.W., Webber, A.N. 2002, 'Photosystem II energy use, non-photochemical quenching and the xanthophyll cycle in *Sorghum bicolor* grown under drought and free-air CO_2 enrichment (FACE) conditions', *Plant, Cell and Environment* **25**, pp. 1551-1559.

Deising, H.B., Reimann, S., Pascholati, S.F. 2008, 'Mechanism and significance of fungicide resistance', *Brazilian Journal of Microbiology* **39**, pp. 286-295.

Ettl, H. & Gärtner, G. 1995, *Syllabus der Boden- Luft- und Flechtenalgen*. Gustav Fischer, Stuttgart, Jena, New York.

Hassal, K.A. 1990, *The Biochemistry and uses of Pesticides. Structure, metabolism, Mode of Action and Uses in Crop Protection*. Second Edition. VCH, Weinheim, New York, Basel, Cambridge.

Hofbauer, W. 2007, *Aerophytische Organismen an Bauteiloberflächen*, Ph.D. Thesis, Innsbruck University (Austria).

Hofbauer, W., Breuer, K., Sedlbauer, K. 2003, 'Algen, Flechten, Moose und Farne auf Fassaden', *Bauphysik* **25**(6), pp. 383-396.

Kumarasamy, K.K., Toleman, M.A., Walsh, T.R., Bagaria, J., Butt, F., Balakrishnan, R., Chaudhary, U., Doumith, M., Giske, C.G., Irfan, S., Krishnan, P., Kumar, A.V., Maharjan, S., Mushraq, S., Noorie, T., Paterson, D.L., Pearson, A., Perry, C., Pike, R., Rao, B., Ray, U., Sarma, J.B., Sharma, M., Sheridan, E., Thirunarayan, M.A., Turton, J., Upadhyay, S., Warner, M., Weifare, W., Livermore, D.M., Woodford, N. 2010, 'Emergence of a new antibiotic resistance mechanism in India, Pakistan, and the UK: a molecular, biological, and epidemiological study', *The Lancet Infectious Diseases* **10**(9), pp. 597-602.

Lindner, W. 2005, '5.14 Surface coatings', in 'Directory of Microbiocides for the Protection of Materials', ed. W. Paulus, Springer, New York, pp. 347-376.

Martino, E., Turnau, K., Girlanda, M., Bonfante, P., Perotto, S. 2000, 'Ericoid mycorrhizal fungi from heavy metal polluted soils: their identification and growth in the presence of zinc ions', *Mycological Research* **104**(3), pp. 338-344.

Moreland, D.E., Gentner, W.A., Hilton, J.L., Hill, K.L. 1959, 'Studies on the mechanism of herbicidal action of 2-Chloro-4,6-bis(etylamino)-s-triazine', *Plant Physiol*. **34,** pp. 432-435.

Rège von, H., Sand, W. 1996: 'Mikrobielle Werkstoffzerstörung - Biofilm und Biofouling. Simulation mikrobiell beeinflußter Metallkorrosion (MIC) zur Prüfung von Gegenmaßnahmen', *Materials and Corrosion* **47**, pp. 486-494.

Riemer, D.N., Trout, J.R. 1980, 'Effects of Low Concentration of Terbutryn on *Myriophyllum* and *Cabomba*', *J. Aquat. Plant Manage*. **18**, pp. 6-9.

Safonova, E.T., Dmitrieva. I.A. Kvitko K.V**.** 1999, 'The interaction of algae with alcanotrophic bacteria in black oil decomposition', *Resources, Conservation and Recycling* **27**(1-2), pp. 193-201.

Shimabukuro, R.H. 1967, 'Atrazine Metabolism and Herbicidal Selectivity', *Plant Physiol*. **42**, pp. 1269-1276.

Varsano, R., Rabinowitch, H.D., Rubun, B. 1992, 'Mode of Action of Piperonyl Butoxide as Herbicide Synergist of Atrazine and Terbutryn in Maize.' *Pesticide Biochemistry and Physiology* **44**, pp. 174-192.

XII DBMC
International Conference on Durability of Building Materials and Components
PORTO - PORTUGAL, April 12th-15th, 2011

Movement Provisions in Exterior Cladding Systems: History and Evolution of Details and Materials

Edward Gerns[1]
Matthew Farmer[2]

ABSTRACT

All building cladding materials expand and contract as a result of environmental variations and material properties. Fired clay products, such as brick and terra cotta, expand as they absorb atmospheric moisture in the first years of service. Concrete products, such as concrete block, cast stone, and reinforced concrete, shrink as they cure. Thermal movements are proportional to the coefficients of thermal expansion of the materials and can vary dramatically. Structural systems, particularly reinforced concrete, also shrink or shorten over time as a result of sustained loading. Cladding systems are a complex assemblage of various components, systems and materials which are all subjected to various movements resulting from material properties, thermal cycles and structural behavior. These factors result in a complex multi-dimensional interaction, which if not properly accommodated can cause significant distress and deterioration in exterior cladding systems. These movements have historically been addressed both passively through subtleties in the details and actively with the incorporation of expansion joints. However, the materials used and the details themselves often lacked adequate movement capabilities and had limited long term effectiveness.

This paper will review the historical development of expansion provisions in cladding systems in the United States and will be divided between detailing considerations and materials. Various specific case studies will be included to demonstrate the historical evolution of movement detailing, materials, and specific detailing and design of movement provisions.

KEYWORDS

Expansion joints, Movement joints, Movement provisions.

---

[1] Principal, Wiss, Janney, Elstner Associates
10 South LaSalle, Suite 2600, Chicago, Illinois 60603 USA , egerns@wje.com
[2] Principal, Wiss, Janney, Elstner Associates
2751 Prosperity Avenue, Suite 450, Fairfax, Virginia 22031 USA, mfarmer@wje.com

1 INTRODUCTION

All buildings are exposed to natural environmental forces including wind, moisture in various forms and temperature variations. Over time, these forces begin to reduce the durability of building systems and materials. While building materials and typologies vary based on region, historical precedent, culture and function, building systems must interact and respond to these forces. Buildings have also become larger and more complex. Technologies and tastes change and evolve, yet at their basic essence, a building provides enclosure and protection from environmental forces. As building technologies have advanced, materials and systems have been combined in new and different combinations with increased complexity. A major ramification of this evolution of technologies and materials is a lag in the understanding of how various materials and systems can be combined to perform effectively and remain durable. Different material and physical properties introduce the need to allow the materials and systems to remain serviceable. Expansion joints are one of the methods which are incorporated into building systems to accommodate differential and anticipated and unanticipated movements. This paper will present a brief overview of the need for and development of expansion joints. Case studies will be introduced which exemplify atypical situations.

2 WALL ASSEMBLY MATERIALS AND SYSTEM MOVEMENTS

2.1 Expansion/Contraction Due to Thermal Changes

All materials increase in volume when heated, and decrease in volume when cooled; in summer months a typical wall will be greater in length and height than in winter months. All materials are susceptible to seasonal changes as well as daily changes in temperature from night to day. The amount of volume change that occurs is a function of the temperature change, and the material's coefficient of thermal expansion. Masonry has a unique and less understood property which is the irreversible nature of this process overtime. When a masonry system consisting of masonry units and mortar in between undergoes contraction, the individual masonry units contract as well, creating minute separations between the masonry units and the mortar binder. Fine debris collects in these separations, preventing the units from fully re-engaging with the mortar during an expansion cycle, wedging the materials apart. These small displacements accumulate over the length of the masonry section, resulting in net expansion of the masonry system over time.

2.2. Expansion/Contraction Due to Moisture Absorption

Another unique characteristic of clay-based masonry units is that they are the smallest they will ever be when leaving the kiln after the firing process due to the virtual absence of moisture in the units. As the units are exposed to the normal in-service environment, they absorb atmospheric moisture and expand in volume. Once the masonry unit's moisture content reaches equilibrium with the environment, the unit volume stabilizes, with only minor increases over time and some cyclic changes in volume due to seasonal fluctuations in environmental moisture.

2.3 Differential Volume Changes in Construction Materials

Variations in thermal coefficients result in adjacent materials expanding and contracting different amounts. Other physical properties such as reaction to moisture can create differential volume changes. If materials in contact expand or contract at different rates, then stresses can develop between the two as the material with a smaller volume changes restrains the one with a larger volume change. If these distinctly different materials were rigidly connected the expanding material develops compression forces because it

is restrained by the shrinking material. Conversely, the shrinking material tends to crack or pull apart due to tensile stresses that result as it is "dragged" by the expanding material.

2.4 Structural Frame Shrinkage

A condition unique to some structures is the impact of irreversible shrinkage and creep over time on materials such as concrete and wood. As the structural frame loses moisture it reduces in volume, resulting in a shortening effect on the structure. Typically the large majority of shrinkage occurs in the first few years of service but can continue for several years after, depending upon the exposure of the materials to environmental conditions, until it reaches equilibrium with the surrounding atmosphere. This type of volume change results in a vertical shortening of the structural frame that is in conflict with materials that remain constant or increase in volume over time.

2.5 Structural Frame Creep

When load is applied to structure and sustained, it will initially deflect but then continue to deform over time. This long-term change in volume due to application of load or stress is referred to as creep. Creep typically results in a continual vertical shortening of the structural frame due to the sustained application of dead load. Similarly to shrinkage, the majority of creep will impact a structure shortly after loading, but can continue to have a modest effect throughout the life of the structure.

2.6 Movement due to Lateral, Seismic and Gravity Loads

Whenever load is applied to a structural element, it undergoes displacement. The amount of displacement is dependent on the magnitude of the load, the direction of the load, and the physical properties of the structural element. All wall systems are exposed to lateral loads from either wind or seismic events, as well as gravity loads in the form of both dead (self weight, and permanent applied loads) and live loads (transient, occupancy-based loads). These loads can either affect the wall system directly, or cause deflections of the back-up structure supporting the materials that is then translated to the cladding material through the connections or supports securing it to the structure. The deflections resulting from the application of these loads need to be accommodated to limit cracking and damage where the stresses exceed the tensile capacity of the material.

3 WALL SYSTEM EVOLUTION

Wall systems undergo movements for many reasons. As our understanding of construction materials increased, so did the recognition that these movements need to be accommodated to prevent damage to the wall structure. This accommodation was accomplished by the introduction of expansion joints.

To understand the development of expansion joints into building construction, it is necessary to understand how building construction has evolved. For purposes of discussion, the evolution of building construction can be divided into four general time periods: the period before the Industrial Revolution (before 1870), the period of the Industrial Revolution through the beginning of 20th Century, the period between 1900 and World War II and the period beginning around 1950 through today.

3.1 Pre-Industrial Revolution (before 1870)

Buildings constructed prior to the Industrial Revolution were generally smaller, simple structures built from local materials, based on historical precedent, and of vernacular style. Structural systems were usually simple consisting of bearing walls and timber roofs. The walls served the dual purpose of

providing weather protection and structural support. Mass monolithic masonry walls function by absorbing moisture and holding the moisture within the masonry until it evaporates. Expansion joints were not explicitly included in these buildings. Building movements were accommodated by the materials and construction systems which had sufficient ductility and flexibility to accommodate such movements. Even masonry structures, normally considered rigid and brittle, were constructed with lime putty mortars which allowed for some movement without compromising the integrity of the structure.

Personal comfort and expectations prior to the Industrial Revolution were also much different than today. Non-uniform and varied temperatures were expected since the primary source of heat was fire places. Cross ventilation and air circulation were the only methods available for cooling. Thus, building movements which were unaccomodated and resulted in breaches in the envelope systems were often not considered a significant issue or were resolved on an as-needed basis through routine repair and maintenance. Building typologies were heavily influenced by the weather, available materials and historically proven precedents.

It should be noted that during this period, and even dating back to the previous century, the need to accommodate expansion and differential movement in bridges and other large civil structures was well understood and incorporated into designs. For masonry and concrete structures, the approach was to control cracking and distress since moisture infiltration was not as significant an issue for such structures. The introduction of metal in bridge construction and the much higher coefficient of thermal expansion of cast iron (double) and steel further necessitated the need for expansion joints.

3.2 Hybrid Curtain Wall Period (1870 to 1900)

The Industrial Revolution marked a dramatic shift both culturally and technologically. Cities were growing rapidly. The combination of economics and demand made the development of larger and taller buildings inevitable. High-rise buildings would not have been possible without the invention of the elevator and the development of the skeleton steel frame structural system. Elevators allowed building occupants to easily access upper floors of taller buildings which prior to that time actually had the lowest rents. Development of the skeleton frame structural system enabled the exterior walls of buildings to no longer be a part of the main structural system. Thus, window openings could be larger and the exterior skin of the buildings only had to provide enclosure. This type of wall system began to be referred to as a 'curtain wall' because the cladding system could be relative light and independent of the building's structural system. While supported at each floor, these wall systems were more of a hybrid wall system since the mass of the wall remained the primary means of resisting environmental forces. Larger and taller building walls were now comprised of multiple materials, resulting in challenges from the more the complex interactions.

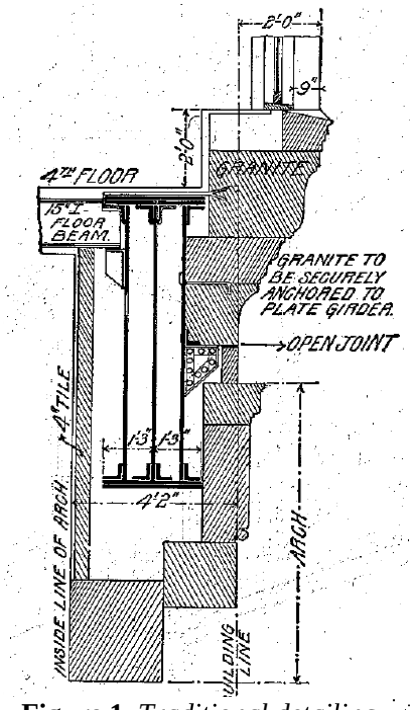

Figure 1. *Traditional detailing of masonry clad curtain wall systems.*

Some of these issues were understood from the beginning of this period and others were only understood after the early buildings of this period had been in service for some years. Building movement, and accommodating these movements, is one of the most significant of these issues. A review of construction details [Frietag 1895], reference books and buildings from this period reveals that there was an understanding of the need to accommodate these movements but there was not a complete understanding of the extent and magnitude of the movements (Fig.1). Cracking was generally attributed to differential

settlement or incorporation of wood members within the wall plane. Period literature suggests the use of a 'slip sill' [Kidder 1911] which does not extend into the adjacent pier as a method to reduce cracks at sills. The general approach of the detailing during this period for larger masonry units such as stone and terra cotta was to allow for individual units to move without binding against adjacent units thereby accommodating small movements related to thermal changes and expansion (Fig. 2). Joints below larger projecting units were often left open to allow the members to deflect or rotate slightly without coming into contact with the units below.

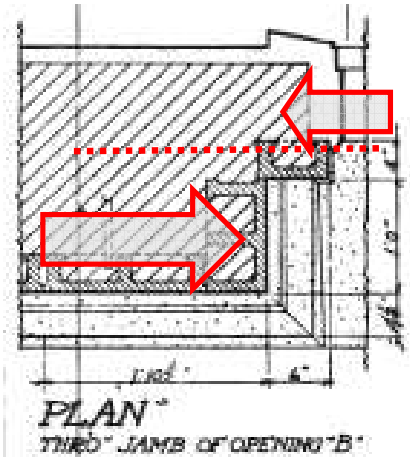

Figure 2. *Representative slip plane detail*

Vertical expansion joints were very rarely explicitly incorporated into building facades. Horizontal movements were often accommodated by the detailing of the wall cladding which would be created by layered planes of materials sliding parallel to each other without transferring load to the adjacent plane. Some technical literature of the time refers to these joints as 'slip joints' [Kidder 1911]. This practice was common below the roof areas, but less common at roof elements such as parapets, cornices and water tables. As a result, many of these elements frequently now exhibit movement and shifting consistent with unaccomodated expansion and contraction--particularly at corners [National Terra Cotta Society 1927].

Horizontal expansion joints were rarely incorporated into hybrid cladding systems. This tends to indicate that the exterior walls, while supported at each floor were still being considered mass/bearing walls in many respects. While the outer wythe was typically supported at each floor, the backup wall system was typically set directly on the floor slab. The position and configuration of shelf angles which support the cladding are typically shown extending less than half the depth of the cladding material. The remaining portion of the unit, not bearing on the steel, was filled with mortar. This seems to be an indication that the load of the cladding between floors was not intended to be completely transferred at each floor. Rather, some compression may have been intended to be imparted on the cladding to minimize cracking by essentially preloading the masonry.

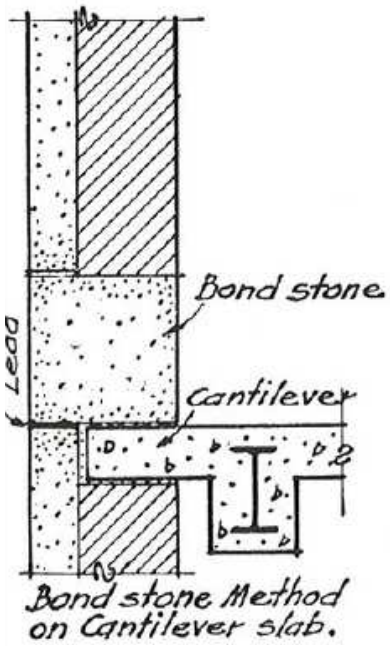

Figure 3. *Expansion provision in masonry curtain wall*

The need to accommodate cracking and shrinkage in concrete was well understood during this period. Numerous references exist in the literature of the time regarding the need to accommodate the shrinkage of concrete as it cured to minimize and control cracking [Newman 1894].

Also understood at the time was the differential movement of the curtain wall relative to the structural frame. As stated by Viollet-le-Duc:

> *If, therefore, we undertake to encase an iron structure with a shell of masonry, that shell must be regarded only as an envelope, having no function other than supporting itself, without lending any support to the iron, or receiving any from it. Whenever an attempt has been made to mingle the two systems, mischief has resulted in the shape of dislocations and unequal settlements.*[Violette-le-Duc 1877]

By 1894, lateral movement in curtain wall construction was actually being studied and analyzed. For example, lateral movements of steel-framed buildings in Chicago, including the seventeen-story Monadnock Building and the fourteen-story Pontiac Building, were documented under high wind loads [Stebbing 1894].

3.3. High Rise Masonry Curtain Walls Period (1900 to 1940)

The use of masonry bearing walls was pushed to its practical extreme by the early 1890s. Beginning around 1900, architects and engineers began to push the masonry curtain wall technology to its limits. Prior to 1900, high-rise curtain wall buildings were typically between 15 and 20 stories tall. Between 1900 and 1930 buildings in major cities throughout the United States gradually increased in height, routinely reaching more than 40 stories [Dupre 1996]. In 1900, the tallest building was roughly 122 m (400 ft). By 1930, the tallest building had exceeded 365 m (1200 ft) [Dupre 1996].

Horizontal expansion joints became more commonly incorporated, but were frequently undersized or inadequately spaced. Details of the period show a compressible material below support components. Commonly used materials included lead and various petroleum or linseed oil based materials (Fig. 3). Over time, these materials would age, become brittle and no longer accommodate movement. Taller buildings introduced a new behavior which, prior to this period, had not represented a significant issue--specifically, frame shrinkage. Moisture expansion, thermal expansion and differential coefficients of thermal expansion were known and understood, but frame shrinkage was a lesser understood phenomena and often knowledge of the issue did not bridge between the engineers and architect. The combination of expansion of the cladding system and shrinkage of the support frame could impart significant unintended loads and stresses into the cladding system. Later, additional stresses were imparted on the cladding as corrosion of the cladding support system occurred and the accumulation and confinement of corrosion scale occurred. Therefore, even if the various movements had originally been properly accommodated additional capacity for movement was required as the building aged but rarely provided.

The exterior cladding is exposed to temperature changes and consequent temperature-related movements, while the embedded frame is protected. Structural frames shorten under dead load and material creep. Conversely, masonry curtain walls expand due to the intake of moisture. Early curtain walls were not built to accommodate these differential movements resulting in the introduction of unanticipated stresses into the curtain wall and frame. This problem came to be understood as evidenced by displacement measurements that were performed during construction of the Empire State building in 1931:

> *The horizontal deflection of the top of the Empire State Building was monitored by the American Institute of Steel Construction. Measurements were also made to determine exactly how much lower the various floors are than their theoretical position. These measurements showed that the 85th floor was 6 1/4 in. below its theoretical elevation during construction.* [Balcom 1931]

An example of distress from this displacement includes the bowing of the face masonry between shelf angles. To address this differential movement, a lead pressure-relieving joint ("cowing") was developed by the 1930s [Ross 1925]. Cowing was typically laid horizontally at mid-span in every story of the highrise masonry facade. This form of pressure relief was used in masonry envelopes until the 1960s. This type of joint has been superseded by soft joints beneath masonry shelf angles, as commonly used in construction today.

The change in style from Classicisms to Art Deco continued to make the notion of layered planes of materials desirable, and allowed the detailing of the wall cladding to continue to accommodate horizontal movements (by the incorporation of slip planes). However, the explicit incorporation of vertical expansion joints into building facades continued to be rare, though some references to placing vertical joints between 7.5 m and 15 m (25 and 50 feet) are made [Ross 1919]. Further, the wedding cake massing

emblematic of Art Deco buildings both complicated and exacerbated accommodating horizontal movements with continuous vertical joints.

It was well understood that portions of buildings of different heights needed to be separated such that each section could move independently. The separation was achieved by creating slip planes between the building sections. During the construction process, the edge of a completed section of wall was treated with combinations of bitumens and felts to maintain a waterproof joint and allow for differential vertical movements.

3.4 Post War Period (1945 to 2000)

Following World War II building construction dramatically changed again. The desire for even taller buildings constructed rapidly and with standardized components resulted in a dramatic change in architectural expression and the development of the glass and metal curtain wall system. The curtain wall systems incorporated numerous building materials including various metals, stones, and clay masonry products, as well as cast-in-place and precast concrete. As buildings continued to increase in height, the desire to further reduce the weight of the exterior cladding and advancements in technologies resulted in gradual reduction of the thickness of the curtain wall systems. Wall systems prior to the 1940s were generally at least 300 mm (12 in) thick. In the decades following the 1940s the wall systems continued to get thinner culminating in claddings which were often less than 50 mm (2 in) supported by the stick framing of the metal curtain wall. By this period, the need to accommodate expansion and contraction in buildings was well understood and recognized within the construction industry.

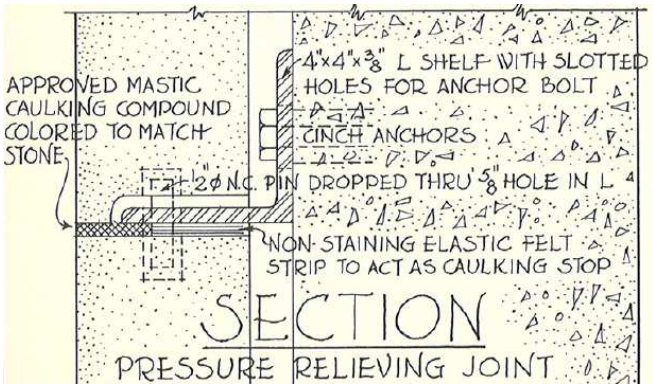

Figure 4. *Expansion joint detailing, circa 1949 exerted from Indiana Limestone Institute publication*

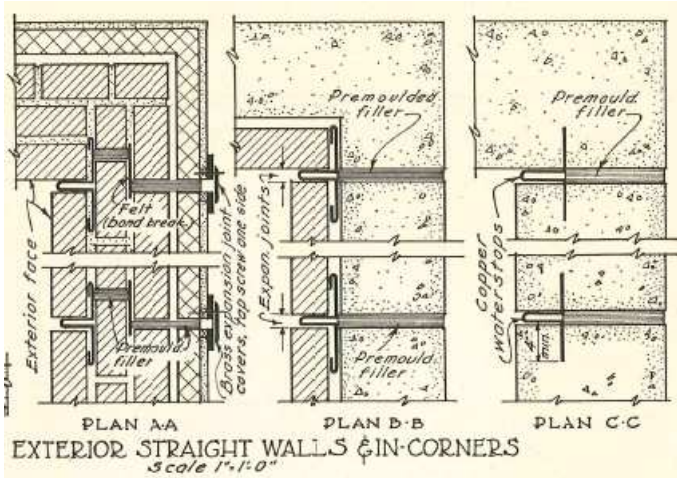

Figure 5. *Expansion joint detailing, circa 1950s*

A review of details from industry sources beginning in the 1940s reveals a greater emphasis on the incorporation of provisions to accommodate expansion and other building movements [ILI 1949]. Vertical and horizontal expansion joints are shown in typical details throughout the various publications being produced within the masonry and fenestration industries, Fig. 4.

A review of Architectural Graphic Standards, beginning with the first edition printed in 1932 and continuing through the fourth edition in 1951, revealed that a transition in recognition and design of expansion joints occurs between the third edition (1941) and fourth edition (1951) [Ramsey 1932, 1941 and 1951]. Virtually no mention of expansion joints relative to exterior cladding systems is made until the fourth edition, where the full implementation of expansion joints into exterior wall construction is

discussed (Fig. 5). It is also interesting to note that the need for expansion accommodation in concrete structures and roofing systems is acknowledged in these texts dating back to 1932, and in other references from previous decades.
Earlier references also identify the issue of both thermal and moisture expansion of masonry materials as well as the interaction of the embedded steel structure and the differential movement between the structural frame and the adjacent masonry. These conditions are acknowledged, but no suggestions are made for accommodating these phenomena. The larger issue seemed to be related to durability of the material due to moisture infiltration and subsequent freeze-thaw damage rather than the more global issues of cracking and macro movements of the wall systems.

A 1941 reference states '*expansion joints are expensive and in some cases difficult to maintain. They are, therefore, to be avoided if possible. In heated buildings joints can be spaced further apart than in unheated buildings. Also, where the outside walls are of brick or of stone ashlar backed with brick or where otherwise insulated, the joints can be farther apart than with exterior wall of lower insulting value.*' The reference goes on to state that in some instances buildings as long as 215 m (700 ft) long have been built without expansion joints. Joints were recommended at junctions in L-, T- and U-shaped building, at large openings in the floor construction. The joints were recommended to extend from the footing to the roof with doubled columns and girders [Huntington 1941].

Another significant development which began in the 1960s was the introduction of panelized and unitized cladding systems. This was an inevitable progression from hand setting of individual units: labor now represented a much greater percentage of the cost of construction and speed became an even greater necessity. Prefabrication of larger cladding components, which could be installed rapidly, was desirable to achieve greater quality control, consistency and productivity. Examples of these systems include clad and un-clad precast concrete panels, clad steel trusses and steel strong-back systems. Joints were critical to accommodate movement between larger facade components and to accommodate construction and structural tolerances (Fig. 6).

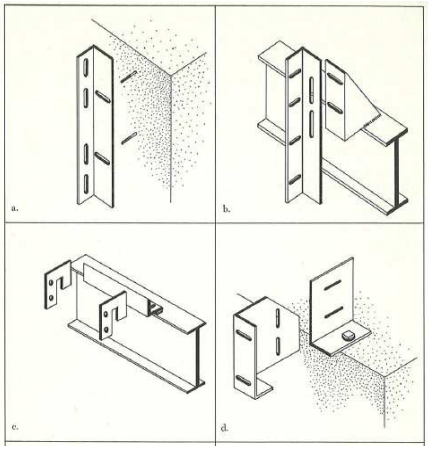

Figure 6. *Expansion/movement provision in anchorage for curtain wall*

4 CONCLUSION

Over the centuries, wall systems have became thinner, lighter, and less redundant. The effect of the environment and the inter-relationship of wall system components became more acute. All wall systems are dynamic in nature. A lack of understanding or recognition of actual wall system behavior, both historically and today, leads to physical damage, water leakage, and increased maintenance costs. In response to these concerns, there is and always been a constant effort to understand the physical properties of construction materials to better predict and accommodate the interaction between wall components. The introduction of expansion joints was a direct result of this desire to control and accommodate material movement due to material properties and exposure to the environment.

REFERENCES

Balcom, H. G., "New York's Tallest Skyscraper," *Civil Engineering* 1 (No 6, March 1931)

Dupre, J., "A History of the World's Most Famous and Important Skyscrapers", Black Dog & Leventhal, New York, NY, 1996, p. 120.
Freitag, J., "Architectural Engineering", Wiley & Sons Inc., New York, NY, 1895, p. 94.
Huntington, Whitney C., Building Construction, Materials and Types of Construction, 2nd Edition, John Wiley & Sons, Inc., New York, 1941, pp. 469-470.

Kidder, F. E., Building Construction and Superintendence; Masonry Work, 1911, p. 366.

"A Portfolio of Detail Plates ad General Information", Indiana Limestone Institute, 1949, Plate No. 18.

National Terra Cotta Society, "Terra Cotta, Standard Construction", New York, NY, 1927, Plate No. 9.
Newman, J. "Notes on Concrete and Works in Concrete", Spon & Chamberlain, 1894, p. 134.
Ramsey, C. G., Harold Sleeper, "Architectural Graphic Standards", 3rd and 5th edition, Wiley & Sons, Inc., New York, NY, 1941 and 1951, pp. 135-138.
Ross, W., Ralph Genry, "Architectural Construction; An Analysis of Design and Construction of American Buildings", John Wiley and Sons Inc., New York, NY, 1925, pp 414-419.
Ross, J., Waterproofing Engineering for Engineers, Architects, Builders, Roofers and Waterproofers, 1919, p. 127.

Stebbing, *Engineering News*, March 1, 1894, p. 471.

Viollet-le-Duc, Eugene-Emmanuel, *Lectures on Architecture*, Volume II (New York, New York: Dover Publications, Inc., 1987; first published in 1877), Lecture 11, 2.

XII DBMC
International Conference on Durability of Building Materials and Components
PORTO - PORTUGAL, April 12th-15th, 2011

Estimate of the Durability of Masonry Walls for Moisture Absorption Properties of Material Constituents

Niubis Luperon Mustelier [1]
Janaide Cavalcante Rocha [2]
Malik Cheriaf [3]

ABSTRACT

Water penetration in walls can damage the structure of the construction and it can also damage its appearance by causing stains and deterioration of the interior parts. The analysis of the phenomena that intervene in the transference of moisture in the interior of the building materials has a big importance for the characterization of his behaviour in what refers to the durability.

The present work proposed the evaluation of the hygro-physical property of the constituent elements of walls (mortar of coating, blocks) that influence in the transport of moisture with the objective of introduce new parameters of characterization that contribute in the understanding about the performance to the water penetration required for service life of walls of building. In this study was carried out the characterization of the property of the constituent material as: water absorption by capillarity for six kinds of mortars with bottom ashes and with air-entraining agent; the absorption of free water to the long one of the time analysing to sorptivity in case of two concrete blocks kinds with density different.

As results were obtained the correlation of the hygro-physical parameters of the mortars of coating and of the block as well as the importance of the diverse phenomena in the water migration with the water penetration essay in the walls, contributing for estimate of the durability of the walls it will be practiced and to the service life.

KEYWORDS

Durability, Mortar, Bottom ashes, Air-entraining agent, Moisture, Hygro-physical.

[1] Faculty of Engineering of the University of Porto (FEUP), Porto, PORTUGAL, niubis@fe.up.pt
[2] Department of Civil Engineering, Federal University of Santa Catarina, Florianópolis, BRAZIL, ecv1jcr@ecv.ufsc.br
[3] Department of Civil Engineering, Federal University of Santa Catarina, Florianópolis, BRAZIL, malik@ecv.ufsc.br

1 INTRODUCTION

The walls of buildings are composed of porous materials that are constantly subjected to various physical phenomena and combinations of agents causing deterioration; for example:

- Infiltration of rainwater followed by simultaneous evaporation and redistribution;
- Capillary absorption of water into the walls and foundations;
- Interstitial condensation of water in interior walls,
- Adsorption and desorption of atmospheric moisture under the hygrothermal conditions;
- Changes in water phase inside the walls due to variations in temperature and vapour pressure causing evaporation vapour diffusion, condensation or freezing, which can modify the thermal transmittance of the wall [Merouni, 1987].

From an understanding of mechanisms governing the transfer of moisture, theoretical models of combined transfer of heat and humidity were developed based on fluid mechanics using the laws of mass diffusion (e.g., liquid phase - Darcy's law and vapour - Fick's law) and diffusion of heat (Fourier's law). Among phenomenological models describing heat and mass transfer across porous materials are the models proposed by Glaser [1959], by Vos [1969] and by De Vries [1957]. These macroscopic and phenomenological models are in fact a generalization of Darcy's Law (for flow) and an extension to porous media of Fick's Law (for a gaseous diffusion). From a physical point of view, one can predict three moisture transfer mechanisms: adsorption, condensation and capillary action. Knowledge of these mechanisms helps explain, in many cases, the variation in moisture content in porous building materials [Resende & Demarzo 2000; Freitas *et al.* 1996]. Knowledge of the mechanisms for moisture transfer, and the hygrothermal behaviour of materials that make up the walls, is an important requirement to help establish strategies to mitigate the problems of degradation of materials due to moisture uptake and transfer, in addition to improving conditions of comfort and hygiene of the users.

This works focuses on, moisture absorption of building materials; in fact, this is one of the physical phenomena that must be strictly controlled in order to optimize the mechanical performances and to prevent the occurrence, for example, of cracks leading to irreversible deterioration processes. Water suction in masonry units represents a restrained water movement affected by capillary forces, chemical binding forces and physical adsorption forces. Whereas Philip [1957] developed the theory of sorptivity to describe water absorption by soil materials, Hall [1977], Gummerson *et al.* [1980], Hall *et al*. [1983] and Hall [1989] successfully applied the principles of water sorptivity to different porous building materials. Based on the work of Philip [1957], Gummerson [1981] estimated the cumulative volume of water absorbed per unit volume (*i*) can be expressed as a function of the moisture content θ, the saturation moisture content θ_1 and the absorption time *(t)* according to the relation given in equation 1:

$$i = t^{1/2} \int_{\theta_i}^{\theta_1} \phi(\theta)\, d\theta \qquad [1]$$

Philip [1957] defined the integral part of Equation [1] as the sorptivity S, from which:

$$i = S\, t^{1/2} \qquad [2]$$

From equation (2), a one-dimensional water absorption relation is linearly related to the square root of time. Therefore, before saturation of masonry units, the right volume of water absorbed per unit area of the suction surface versus the square root of the absorption time should be linear. The slope of the line defines the sorptivity of the material.

The objective of this study was to estimate the life cycle of masonry walls based on the moisture absorption properties of the constituent materials: mortars made with contents of 0, 50 and 100% by volume of bottom ash as a replacement for natural aggregate, with and without air-entraining agent.

Bottom ash was chosen because it is a residue of great availability in southern Brazil and its equilibrium moisture content is higher than that of sand, reflecting its porous nature. In relation to admixtures to cement-based materials, air-entraining agents deserve some prominence because they increase the disconnection of the capillary network and decrease the specific gravity. In this study the characterization of the property of the constituent material was determined and included: water absorption by capillarity for six kinds of mortars containing bottom ash and including air-entraining agent: the initial rate of absorption, the absorption of free water to the long one of the time analysing to sorptivity in case of two concrete blocks kinds having different densities.

2. EXPERIMENTAL PROCEDURE

2.1 Building Component Elements

Six different mortar coatings were used. The mix composition selected were based on studies developed by SANTOS *et al*. [2004] and produced from a formulation (mix proportion base) by volume composed of 10.91% of cement, 30.64% lime and 58.45% sand. From the base formulation were produced mortars with the substitution of sand by volume in bottom ash in the following percentages: 0, 50 and 100%, where the bottom ash that was incorporated was dried, the drying taking place in a ventilated greenhouse marinated at a temperature of 105ºC over 24 h. For each of the percentages of substitution of sand by bottom ash were prepared mortars with and without air-entraining agent. Due to the nature of the bottom ash, the water/cement ratio (w /c) was 2.29 for all mortars.

For those mortars in which additives were used, the amount of additive was 0.03% compared to the total weight of dry material. Two densities of hollow structural concrete block masonry (dimensions of 39 cm x 19 cm x 14cm) were produced on an industrial scale using a vibro-pressing process. . The blocks were designated as series D_1 for the case of the denser block and D_2 for the less dense masonry block series.

2.3. Sample Preparation and Testing

The samples of mortars used for testing were obtained from the pilot coating systems based mounting of small panels with dry joint and locking system peripheral, each panel being mounted horizontally and with six concrete blocks of dimensions 140mm x 190mm x 390mm in their composition; application of each type of mortar on the specific substrate to reach a coating thickness (30mm), separation of the blocks by wire-cutting steel through the dry joint blocks; monitoring the setting of the mortar; after the end of setting, each system was wrapped in plastic waterproof and maintaining in this way, conditioned until 28 days, when were cut the samples of mortar and substrate: 03 cylindrical samples of 5cm x 3cm for the assessment of capillary absorption of water.

After extraction, samples obtained of the pilot coating systems the substrate and the mortar had been dry in an oven at a temperature of 50° C until constant mass was achieved. The samples were then cooled and wrapped in waterproof plastic films until they underwent testing.

In the test for determination of the amount of capillary water absorbed was monitored using a graduated Mariotte bottle (hydraulic gradient of zero). In capillary absorption was employed distilled and deionised water. The apparatus used is illustrated in Figure 1.

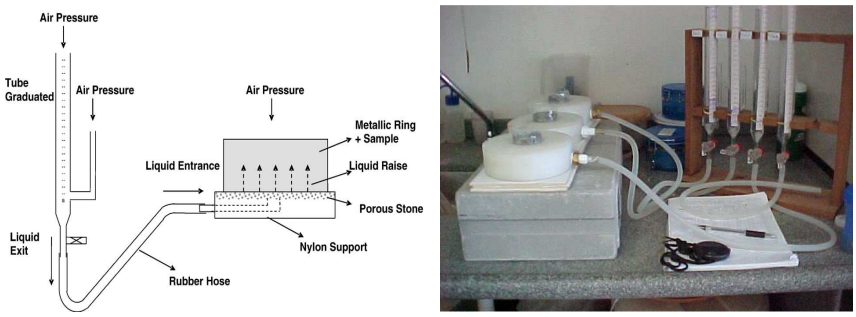

Figure 1. Test apparatus for capillary absorption.

The experimental program for blocks included the tests: Absorption over a prolonged period of up to 7 hours. To help ensure that the variation in average value for water absorption determined from tests did not exceed 15%, 270 blocks were tested for each series of concrete of block. All samples were numbered, weighed initially and dried for 24 hours at a temperature of 110ºC and thereafter, cooled for 24 hours in Styrofoam boxes in which silica gel had been placed to prevent absorption of atmospheric moisture. The blocks were again weighed and packed in plastic bags until the tests were conducted; just prior to testing and once unpacked, they were again weighed.

ASTM C 67 – 86 was the basis on which testing of the water absorption over a prolonged period of 7 hours was completed. Whereas the sorptivity was determined in accordance with procedures given in ASTM draft [1996] The amount of water absorbed in the absorption test conducted over a prolonged test period was determined by the gain in mass recorded at intervals of time, in minutes, of: 5, 10, 15, 20, 25, 30, 35, 50, 65, 80, 95, 110, 135, 180, 240, 300, 360, and 420.

3 RESULTS AND DISCUSSION

3.1 Capillarity Absorption – Sorptivity

3.1.1 Blocks

The sorptivity of the blocks was obtained from a review the of the free water absorption curve (absorption over a prolonged period of time), being obtained by the slope of the straight line traced from the point of intersection with the sorptivity function given as $i \times t^{1/2}$, as shown in Figure 2.

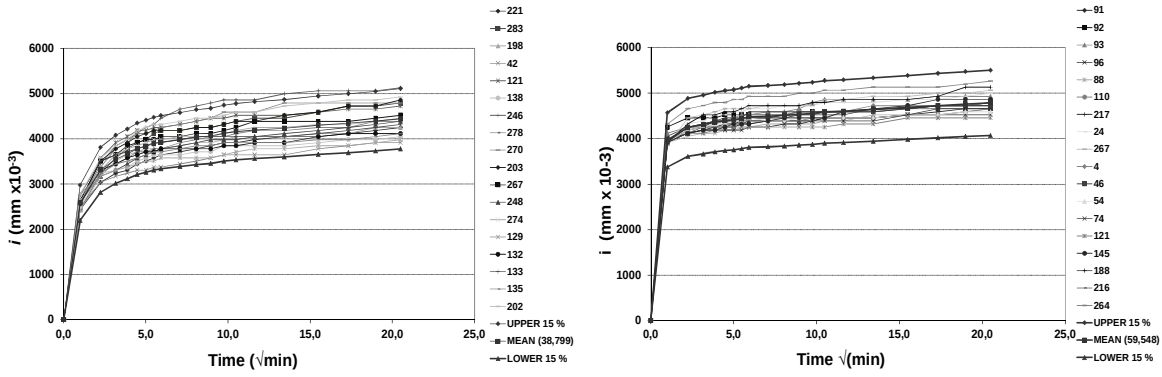

III_D$_1$ **III_D$_2$**

Figure 2. Suction behaviour of concrete blocks of on both series.

The curve was obtained by extraction of data ranging between the first five minutes to 25 minutes, as suggested in the ASTM standard [1996]. Regression analysis was performed for each block and the correlation coefficient (R^2) determined for each regression analysis; these results are provided in Table 2.

Table 2. Average and coefficient of variation (CV) of sorptivity test results.

BLOCKS	*SERIE D_1*				*SERIE D_2*			
	G I -Low	*G II - Medium*	*G III - High*	*Average*	*G I -Low*	*G II - Medium*	*G III - High*	*Average*
S ($mm/min^{1/2}$)x10^{-3}	220,80	242,99	203,16	222,32	121,76	87,94	57,27	88,99
CV (%)	12,76	16,67	23,46	17,63	27,15	38,77	35,62	33,85
R^2	0,99	0,97	0,96	0,97	0,94	0,89	0,82	0,88

***N= 90 blocks x groups** **Sd: standard deviation.**

In accordance with the results the greater sorptivity is attributed to concrete blocks D_1, being that the concrete blocks D_2 excessively absorbed water in the initial minute and quickly became saturated and maintained values of constant absorption over the prolonged test period contrarily to that of concrete blocks D_1. Concrete blocks D_1 absorbed water uniformly over the prolonged test period until reaching saturation. [Mustelier, 2008] According to the information provided in the ASTM standard [1996], when the correlation coefficient (r) is less than 0.98 ($r^2 < 0.96$) then the relation is considered not to be sufficiently linear and the sorptivity of the specimen should not be determined from the data.

Therefore, the low results for the regression coefficients obtained for concrete blocks D_2 indicated a deviation from the relationship once the sample was saturated and this suggested that flow during the saturation process was violated [Taha, 2001]. Thus, considering requirements to apply the theory of sorptivity, in the case of concrete blocks D_2 this theory could not be applied. Thus the absorption characteristics of this less dense material is one that has an abrupt absorption in the first minutes of contact with water causing saturation of the material following 35 minutes of initiation of the test.

3.2.2 Mortars

In the Figure 3 is shown the sorptivity coefficient of the different mortars in a time interval of 2 to 120 minutes, for mortars having 0% CZP with and without IA, and between 10 minutes and 240 minutes for the remaining mortars. These respective intervals were adopted such that, for all the mortars the relation between "X" and the square root of time were linear. It is important to point out, that the samples analysed had been extracted of the pilot coating systems, having a height of 30mm, in the case of mortars 0% CZP with and without AI, the top was reached in the early hours.

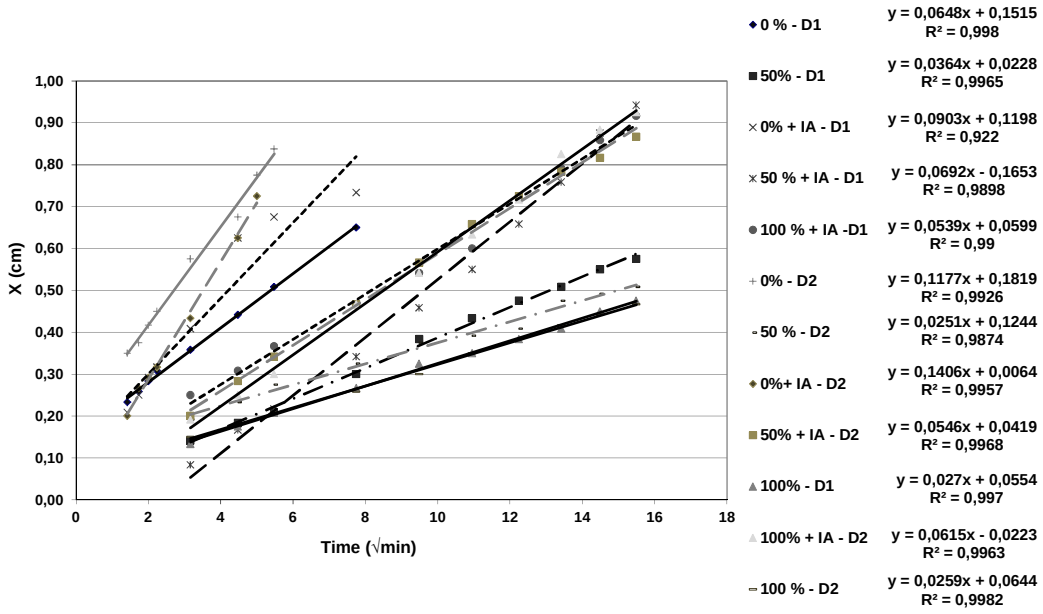

Figure 3. Volume of liquid absorbed as a function of square root of time.

It can be seen from observing the process of liquid water ingress into the porous material, the progression of the meniscus in the capillary (X) is proportional, in part, to the square root of time (√t).

The speed of advance of the wetting front decreases in relation 1/√t when testing over prolonged periods. On the other hand, the rate of ingress is proportional to the square root of the pore radius, since the largest pores are more quickly filled as compared to the finest pores [Mustelier, 2008].

In Table 3 are shown sorptivity coefficients obtained from the graphs given in Figure 3. From this information it can be seen that, for all mortars, the sorptivity of mortars containing bottom ash was much bigger, except in the case of mortar with 50% CZP and without IA D_2, where it did not have this tendency. This can be decurrent of the refinement of the pores of the mortars with bottom ash, therefore to CZP, in function of its thinness it promotes filler effects, beyond offering pozzolanic activity.

Table 3. Sorptivity coefficient (S) of the mortars.

Sorptivity (cmxmin$^{1/2}$)x10^{-2}		
Mortars	*Blocks*	
	D1	*D2*
0%CZP	6,48	11,77
50% CZP	3,64	2,51
100%CZP	2,7	2,59
0%CZP+IA	9,03	14,06
50%CZP+IA	6,92	5,46
100%CZP+IA	5,39	6,15

For the same percentages of ash, when one compares the mortars with and without IA for the two blocks, had a same tendency of behaviour. The presence of additives in the mortars, in general, produced an increase in the sorptivity coefficient. This increase can be attributed to the presence of permeable pores in the mortars that are a result of the use of air entraining additives, which cause the advance of liquid fronts in the porous media.

3.4 Estimate of the Durability of Masonry Walls

From the results of the capillarity absorption tests on the mortar and blocks, after 7 hours of testing it was observed that for walls built with the mortars and with the blocks of the each series, the water would not reach to another one face of the walls, as it can be conferred in Table 4, which illustrate the values of the position of wet front by capillarity and infiltration. These results were obtained from the Washburn relationship [1921] and Barbare *et al.* [2003], in which the position of the wet front by capillarity is given by:

$$: X_1(t) = \frac{m(t)}{\rho.A} \qquad [3]$$

Infiltration: $X_2(t) = \frac{m(t)}{2\rho.A.n}$ [4]

Table 4. Determination of the position of moisture front and infiltration.

BLOCKS	*Mortars*	*7 hours test*			
		Blocks (mmx10^{-3})		*Mortars (cm)*	
		XB_1	*XB_2*	*XM_1*	*XM_2*
D1	0%	4148,81	31913,93	0,99	3,47
	50%	4477,81	34444,68	0,79	2,66
	100%	3099,94	23845,73	0,62	1,95
	0 % + IA	3638,54	27988,79	0,88	2,39
	50 %+ IA	3888,77	29913,62	1,17	3,08
	100 % +IA	3346,83	25744,84	1,20	3,73
D2	0%	4957,64	26092,84	0,98	2,84
	50%	5023,24	26438,12	0,66	2,20
	100%	3861,90	20325,78	0,63	2,04
	0 % + IA	4502,17	23695,65	0,93	2,17
	50 %+ IA	4056,83	21351,74	1,06	3,03
	100 % +IA	4191,22	22059,06	1,10	2,66

Using those portions of the graph the equations of the straight lines obtained from the points of intersection of the graph $i \times t^{1/2}$ of the free water absorption curve to the prolonged test period ,a prediction was made of the time needed for water to completely traverse the wall, the speed of infiltration; the results obtained are shown in Table 5.

Table 5. Estimated time and speed of water infiltration through the walls.

Blocks	*Mortars*	*Time (days)*			*Infiltration velocity (cm/min)*		
		Mortar (22 cm)	*Block (20 cm)*	*Mortar+Block (2cm +20 cm)*	*Mortar (22 cm)*	*Block (20 cm)*	*Mortar+Block (2cm +20 cm)*
D1	0% CZP	80	6259	6260	1,93E-04	2,20E-02	2,45E-06
	50% CZP	255	1484	1486	5,95E-05	9,27E-02	1,02E-05
	100%CZP	41	5196	5198	3,33E-05	2,65E-02	2,96E-06
	0%CZP+IA	72	13196	13197	3,72E-04	1,04E-02	1,16E-06
	50%CZP+IA	116	2809	2809	2,10E-04	4,90E-02	5,37E-06
	100%CZP+IA	24	2190	2191	1,29E-04	6,28E-02	6,83E-06
D2	0%CZP	532	42261	42261	6,28E-04	3,26E-03	3,58E-07
	50% CZP	17	12829	12831	2,83E-05	1,07E-02	1,17E-06
	100%CZP	113	17630	17633	3,00E-05	7,82E-03	8,56E-07
	0%CZP+IA	463	42115	42115	8,77E-04	3,27E-03	3,57E-07
	50%CZP+IA	90	24348	24349	1,33E-04	5,66E-03	6,18E-07
	100%CZP+IA	502	27907	27908	1,68E-04	4,94E-03	5,40E-07

It was determined on the basis of the properties obtained from the prolonged water absorption test and by the sorptivity of blocks and mortar, that the water would not traverse the opposite side of the wall during the development of leakage test for all constructed walls. It was estimated that it would take days and perhaps years for the water to permeate to the opposite face of the wall; this was considering that gravitational forces were neglected, and that there exists perfect hydraulic continuity between the mortars of coating.

4 CONCLUSIONS

Was estimated by the properties of water absorption over time and the sorptivity blocks and mortar, the water could not cross the other side of the opposite side during the test development for all the walls with such material because it would take days and even years for the water to be present in said face, that neglecting gravitational forces, as well as other phenomena at interfaces, whereas there is hydraulic continuity between the mortars coating and settlement.

The results showed that with such elements of construction would be possible to fabricate walls over time presented as durable walls. Of particular interest to the walls built with mortar with coal ash which were the least likely to absorb water. In the evolution of water absorption of the mortars, was observed curves lowest absorption in the case of mortars with 100% addition of ash, with or without incorporation agent, evidenced by lower values of sorptivity, this allows the conclusion that walls made of mortar would be for said watertight over time, contributing to a longer service life and greater durability.

ACKNOWLEDGMENTS

The financial support was provided by the National Council of Scientific and Technological Development (CNPq) and the Brazilian Innovation Agency FINEP.

REFERENCES

American Society for Testing and Materials**.** C 67. 1986,: *Standards test methods of sampling and testing brick and structural clay tile*, p. 37-67. Philadelphia.

American Society for Testing and Materials. ASTM C1585 *draft # 9*, 1996. *Standard Test Method for Measurement of Initial Rate of Absorption of Hydraulic Cement Mortars and Concretes*. 8 p.

Barbare, N., Shukla, A., Bose, A. 2003, Uptake and Loss of Water in a Cenosphere–Concrete Composite Material□, *Cement and Concrete Research*, v. 33, n. 10, pp. 1681-1686.

Freitas, V.P., Abrantes, V., Crausse, P. 1996, Moisture Migration in Building Walls -Analysis of the Interface Phenomena, *Building and Environment*, v. 31, n. 2, pp. 99-108.

Gummerson, R. J., Hall, C. Hoff, W. D. 1980, Water Movement in Porous Building Materials - II. Hydraulic Suction and Sorptivity of Brick and Other Masonry Materials. *Building and Environment.* V.15, n. 2, p. 101-108.

Hall, C., 1977, "Water Movement in Porous Building Materials - I. Unsaturated Flow Theory and its Applications", *Building and Environment*, Vol. 12, pp. 117-125.

Hall, C., (1989), "Water Sorptivity of Mortars and Concretes: A Review", *Magazine of Concrete Research*, Vol.41, No.147, pp.51-61.

Hall, C., Hoff, W. D., and Skeldon, M. 1983, "The Sorptivity of Brick: Dependence on the Initial Water Content", *Journal of Physics, D: Applied Physics*, Vol. 16, pp. 1875 - 1880.

Hall, C. and Yau, M.H.R.1987, "Water Movement in Porous Building Materials -IX. The Water Absorption and Sorptivity of Concretes", *Building and Environment*, Vol.22, No.1, pp.77-82.

Merouani, L. 1987, *Phénomènes de Sorption et de Transfert d´Humidité dans des Matériaux du Bâtiment. Étude Expérimentale Comparative dún Mortier de Ciment et d´un Enduit de Façade*, *Thèse Docteur*, 3 Cycle, Institut National Polytechnique de Grenoble, France,.

Mustelier, L.N. 2008, *Estimativa do Comportamento de Paredes no Ensaio de Penetração de Água de Chuva através das Propriedades de Transferência de Umidade dos Materiais Constituintes*. Tese (Doutorado em Engenharia Civil) – Universidade Federal de Santa Catarina. Florianópolis.

Philip J.R., D. De Vries A. 1957, Moisture movement in porous materials under temperature gradients. *Transactions of American Geophysical Union*. V.38, p 222–232.

Resende, Z. de Sá.; Demarzo, M ª . 2000, "Processo de fluxo eletrocinético na secagem de paredes com umidade". In: *Congresso Internacional sobre o comportamento de estruturas danificadas*. 2º. Niterói. 8p.

Safiuddin, M.D., Hearn, N. 2005, Comparison of ASTM Saturation Techniques for Measuring the Permeable Porosity of Concrete, *Cement and Concrete Research*, v. 35, n. 5, pp. 1008-1013.

Santos, F.I.G., Lenzi, E.J., Rocha, J.C., Cheriaf, M. 2004, Avaliação de Resíduos para uso em Argamassas - Estudo com Cinza Pesada□, In: *I Conferência Latino-Americana de Construção Sustentável/ ENTAC04 - 10 Encontro Nacional de Tecnologia do Ambiente Construído*, São Paulo.

Taha Reda et *al*. 2001, Sorptivity: A Surface Absorption Criterion for Brick Units: A Proposal for the Canadian Masonry Standard. .In:: *Canadian Masonry Symposium*. 9th. Fredericton. Proceedings. Fredericton University of New Brunswick. Canadá. 2001. Disponível em: www.reda-taha.com/Publications/Fredericton-1-2001.PDF.

XII DBMC
International Conference on Durability of Building Materials and Components
PORTO - PORTUGAL, April 12th-15th, 2011

Durability Assessment to Water of Masonry Walls with Ashes of Mineral Coal

Niubis Luperon Mustelier [1]
Janaide Cavalcante Rocha [2]
Malik Cheriaf [3]

ABSTRACT

Rain penetration in masonry walls is an important performance consideration associated with utility, durability and aesthetics. The present study aims to expose a testing procedure for evaluation of the blocks and mortars as regards water penetration and leakage. An experimental prototype was developed for the testing program, in accordance with ASTM E514-90 "Standard Test Method for Water Penetration and Leakage through Masonry". The study materials included ashes of mineral coal obtained as a waste from the thermoelectric processes, besides the conventional components (cement, sand, lime and water). Masonry walls, particularly, those including new materials intended to be used in construction cannot be exempt from a thorough scientific research. That is, when these materials emerge as alternatives, they should come with technical information that will allow specialists to decide whether or not they may be adopted in the several areas of construction. The results evidenced that panels with coating and masonry mortars including coal ashes performed better relatively to conventional ones, in respect to time of appearance of dampness and time of appearance of first visible water on back of specimen. Although masonry with coal ashes presents the biggest final absorption, it was the best in terms of area of dampness, remarking that this is measured on back wall at the end of 7 h test period.

KEYWORDS

Testing, Water penetration, Masonry, Mineral coal ashes.

[1] Faculty of Engineering of the University of Porto (FEUP), Porto, PORTUGAL, niubis@fe.up.pt
[2] Department of Civil Engineering, Federal University of Santa Catarina, Florianópolis, BRAZIL, janaide@ecv.ufsc.br
[3] Department of Civil Engineering, Federal University of Santa Catarina, Florianópolis, BRAZIL, malik@ecv.ufsc.br

1 INTRODUCTION

Rain penetration in masonry walls is an important performance consideration associated with utility, durability and aesthetics. Owners, builders, designers and researchers have expended many years of considerable effort in field investigations and laboratory research to help solve problems associated with water penetration of masonry wall assemblies.

The panels, walls and other component elements of the façade should prevent penetration of rain water, or other sources of moisture, water needs to be managed since a wall cannot ever be sealed absolutely watertight; hence the need for limiting values on water penetration, in order to ensure their long-term performance and as well, facilitate their maintenance. Such preventatives measures help contribute to maintaining the building free from the effects of prolonged exposure to high levels of humidity. The penetration of water in masonry wall assemblies nonetheless still occurs too frequently in spite of on-going technological advancements. It is of or use well known that water penetration in walls can damage the structure and can also damage its appearance by causing stains and deterioration of the interior finishes.

This paper aims to describe a testing procedure for evaluation of the water penetration and leakage performance of masonry block and mortar wall assemblies. The procedure was used to determine the relative water penetration resistance between conventional block masonry wall assemblies in relation to that of a hollow block masonry assembly, in which the block includes mineral coal ash obtained as a waste material of the thermoelectric processes.

2 HISTORIC OF TESTING

It is important to carry out water-tightness testing to ensure satisfactory permeance performance of masonry structures during its service life. Laboratory tests are used for design evaluations of prototype assemblies whereas field tests are essential to evaluate workmanship issues. There are a variety of tests to analyse masonry wall systems in reference to levels of water penetration. The following group of tests differs in terms of costs and ease of application, but they are some of the methods currently used for testing wall assemblies.

2.1 Method of Testing: Centre Scientifique et Technique du Bâtiment (CSTB)

The method is characterized by the pulverization of water and pressure of constant air on the external face of a wall. The testing is accomplished in a chamber, in a test specimens of minimum dimensions of 1, 50 m x 1, 50 m. [CSTB, 1999] The characteristics of the method are: the flow rate of 24 l/m/h, pressure of constant air is equal to 100 Pa, inside the chamber; time of execution is equal to 24 hours. The main observations and measures are: weigh of the wall before and after the end of the test (verification of the absorption of water), observation of the time and place of appearance of the leak of water on the back of the specimen that received the incidence of jets of water and measurement of the amount of water that it was infiltrated and slipped for the face interns of the wall.

2.2 Method of Testing by British Standard Institution - BSI.

The testing is accomplished in a laboratory where a test specimen, within a square steel frame, is mounted to an appropriate test chamber test [BSI-4315 1987]. A lime coating applied to the backside of the specimen (i.e. interior face not exposed to water spray) is helps detect the presence wetting over the course of the test. Water is applied to the surface of the specimens at a flow rate of 25 ml/min for every 10 mm width of wall; the test is conducted over 48 continuous hours of water spray. The minimum dimensions of the test area are 1.0 m x 10 m in. A constant air pressure of 500 Pa is applied to the face of the test specimen. The test chamber is comprised of systems to supply air and water as required for the tests.

2.3 Method of the NRC-IRC's Building Envelope and Structure program, Canada.

IRC's Building Envelope and Structure research program has a unique test facility that incorporates a computer automated testing apparatus to assess the watertightness performance of full-scale wall assemblies (2.43 m x 2.43 m), referred to as the Dynamic Wind and Wall Test facility (DWTF) [Lacasse et al. 2003]. It can simulate conditions of wind driven rain through the use of a metered and flow adjustable water spray rack (up to 8 L/min-m^2) and computer controlled pressure differences up to 2kPa. Dynamic pressure fluctuations can also be obtained by displacement of a sealed 2.4-m diameter piston that upon movement causes the varying air pressure difference across the specimen. The movement of the piston can be programmed to produce sinusoidal, triangular or square waveforms of air pressure at frequencies ranging from 0.1 to 10Hz and amplitudes up to or exceeding 2KPa. A secondary blower generates the steady-state component of air pressure. The apparatus also contains sensors to measure pressure difference, water collection rates, and moisture content in materials. It has been used to benchmark the water entry of different wall assemblies, to evaluate the watertightness of the wall-window interface and to assess the water penetration of different cladding types.

2.4 Method of the Institute of Technological Researches of the State of São Paulo - IPT.

Two methods exist to evaluate the watertightness of wall assemblies: Water resistance: (i) a laboratory method using simulation rain and wind conditions occurring for a determined period of time.[Thomaz &Ranieri, 1998]; (ii)"in situ" watertightness performance assessment of the permeability to water of façades. The test consists of submitting a wall specimen to water spray under constant air pressure differential this being achieved by affixing the specimen to a chamber in which the air pressure can be maintained and are located the water deposition devices. In the case of the of the water penetration test at least two test specimens are used to obtain results; the minimum dimensions of these specimens is 105 cm in width and in length, 135 cm, there being no restrictions on the thickness of the specimen . The rate of deposition of water on and the air pressure difference across the specimen are 3.0 ± 0.3 L/min and 30 ± 0.5 MPa respectively. These conditions should be maintained for 7 hours.

2.5 Method by American Society Testing and Materials - ASTM.

ASTM E 514-90 is the test method specified for laboratory investigations for evaluating the effect of differences materials, coatings, construction details and workmanship on water penetration resistance of masonry. This method consists of placing a test specimen (dimensions 1.20 m by 0.90 m) to the test chamber and afterwards spraying water on the specimen at a rate of 138 L/m^2-hour and simultaneously applying air pressure of air of 500 Pa during 7 hours. After 7 hours the sample remains in observation to verify wetting and the first visible signs of water.

3. EXPERIMENTAL PROCEDURE AND MATERIALS

An experimental prototype was developed for the testing program, in accordance with ASTM E514-90 “Standard Test Method for Water Penetration and Leakage through Masonry”. Some parameters of the IPT - São Paulo, Brazil [1998], regarding minimal criteria for performance of social residential units, were also considered. To complete the testing program, water spray rate deposited on and pressure differential across the test specimen must be specified and these depend on the expected exposure conditions for a given location. In Brazil, the determination of these test conditions is based on that standardized by the IPT [1998]; the wind speed and rate of application of water are indicated in Table 1 and Figure 1. Thus, when submitted to those conditions, the wall specimens, representative of building facades, should stay air and watertight, without leakage, water flow or the formation of water droplets on the internal finished surfaces.

In these tests, the time to the appearance of dampness, the first visible free water, and the extent of damp patches on the back of the specimen as well as the quantity of water leakage were recorded.

Table 1 – Test conditions for water penetration test of masonry walls (IPT, 1998).

Area of Brasil	*Conditions of test of walls*	
	Static pessure (mmca)	*Rate of application of water ($dm^3/m^2/min$)*
I	10	30
II	20	
III	30	
IV	40	
V	50	

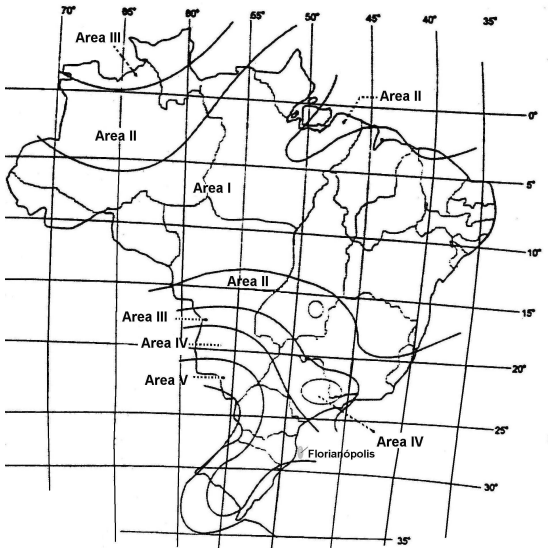

Figure 1. Area of Brazil for assessment of water penetration and leakage of masonry walls – the basic speed of wind of NB 599, 1987. [IPT, 1998].

The test chamber was adjusted so that it had a water flow rate of $3L/m^2$-min. and a pressure difference of 400 Pa (40 mmca) across the test assembly; these conditions are referenced to the city of Florianópolis, Santa Catarina, Brazil. This city is located in area IV (Figure 1), in accordance with the values of wind speed and rainfall rate presented previously. The testing also took into consideration the temperature and humidity; air temperature in the laboratory was maintained at 28^oC and relative humidity at 78%.

This study was developed to assess the durability of new masonry materials in a wall system. These new masonry materials are blocks and mortar incorporating mineral coal ash obtained from the thermoelectric processes. Mineral coal ash is waste material that originates from the combustion of mineral coal. From the ash, three main waste products are generated: fly ash, bottom ash and slag. Of the waste derived from the combustion of the coal consumed in the world, 30% is added to concrete products and cement production. This is a positive factor since the use of this waste also potentially decreases the environmental impacts caused by the generation of CO_2 in the production of cement.



Figure 2. Experimental test for leakage and water penetration.

Due to the increased availability of fly ash around the world, this artificial pozzolanic material is used in great amounts in the production of Portland cement as partial substitution for clinker. As well, it is used in the production of concrete and mortar as a partial substitution for cement [Silva *et al*, 1997]. Bottom ash is frequently used as a low-cost substitute for sand aggregate used in the production of concrete blocks and in many countries it is also used in the construction of roadways. **[**Ranganath *et al*. 1998; Possobon, 1999]

The wall assembly system composed of masonry block and mortar incorporating ash and used in this study were developed by the authors [Lenzi 2001; Silveira 2001]. The blocks had dimensions of 14 x 19 x 39 cm and the mortar consisted of a cement: lime: sand composition, in proportions, by volume, of: 1: 2: 9. In this formulation, the percent substitution, by volume, was: 30% fly ash substitution for cement and 50% bottom ash substitution for sand.

To undertake the water penetration and leakage testing, the prototypes wall assemblies were fabricated having dimensions of 1000 mm in width by 1200 mm in height and with a mortar covering of 20 mm in thickness. Six prototype wall assemblies were constructed, three of which included the modified blocks and mortar that incorporated fly ash and bottom ash in the block and mortar respectively and three wall assemblies constructed with conventional block and mortar. The water penetration tests were started after sixty days of cure of the covering mortar; the assemblies were cured in laboratory conditions (i.e. 28°C and 78% RH).

4 RESULTS AND DISCUSSION

Although three test specimens were fabricated for each mortar type, one specimen of each type suffered cracks during their respective move from the fabrication location to the location of the test facility.. For this reason these assemblies were not incorporate in the results, since it was not possible to complete the testing of these specimens. The remaining “good” specimens were tested over a 7 hour period, in which observations of the “interior” face of the test specimen was accomplishing every 30 minutes. The results obtained for each of the specimens are shown in Table 2.

Having made a detailed analysis of each test parameter described in Table 2 and reviewing the results provided in Figure 3, one can reasonably conclude that in relation to the time of appearance of the first visible water and of dampness, similar behaviours were apparent for each mortar type tested.

Table 2. Comparisons of results derived from water tightness testing of conventional masonry wall assemblies to assemblies with -masonry-coal ash components.

Test performed	*Panels block/mortar-conventional*			*Panels with block/mortar coal ashes*		
	P1	P2	P3	P4	P5	P6
Time first dampness, hrs	03:15	03:25	X	04:20	03:30	X
Time first visible water, hrs	04:30	05:30	X	06:30	05:00	X
Área of dampness the on end of test (m^2)	0,03	0,035	X	0,015	0,025	X
Initial water of entrance (m^3)	1,26	1,26	X	1,26	1,26	X
Total water collected at the end of the period (m3)	1,214	1,208	X	1,203	1,194	X
Absorption of the samples at the end of the period (%)	3,65	4,13	X	4,52	5,24	X
Percentage of the sum of the areas of dampness on the back in relation to the total area of the specimen submitted to the aspersion of water in the end of the test	3,00	3,50	X	1,50	2,50	X

(X) Test specimens that suffered cracks during displacement.

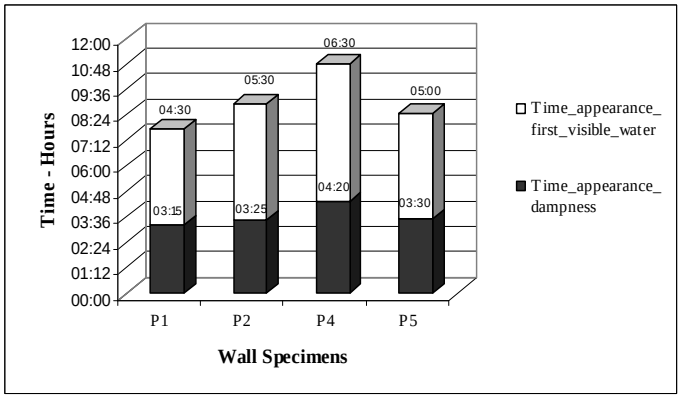

Figure 3. Time of appearance of dampness and first visible water.

The mortars that incorporate ash presented a greater time for the appearance of moisture and as well, visible water as compared to walls made of conventional materials; typical wetting patterns for both types of walls are shown in figure 4a and 4b for walls made of conventional materials and in Figure 4c and 4d for walls made of ash-based materials.

As shown in Figure 4, the locations and patterns of wetting occurred differently for walls of conventional mortar materials as compared to those incorporated ash-based materials. In the case of walls made with conventional mortar, wetting occurred at the edges of the specimen, the wetting front moving forward until the opposite face was likewise moistened. In addition, it was observed that along the lateral face of the specimen, water migrated towards the opposite face firstly through the block and after the joints.

For the prototype specimens made of ash-based materials, the first visible signs of wetting were smaller in size as compared to those observed of walls made of conventional materials (Figure 4), the progress of the wetting being through the joint and thereafter to the edges of the specimen. As well, the values for the area of dampness were greater for wall specimens having conventional mortars as compared to walls having mortar that incorporated ash as can be observed in Figure 5.

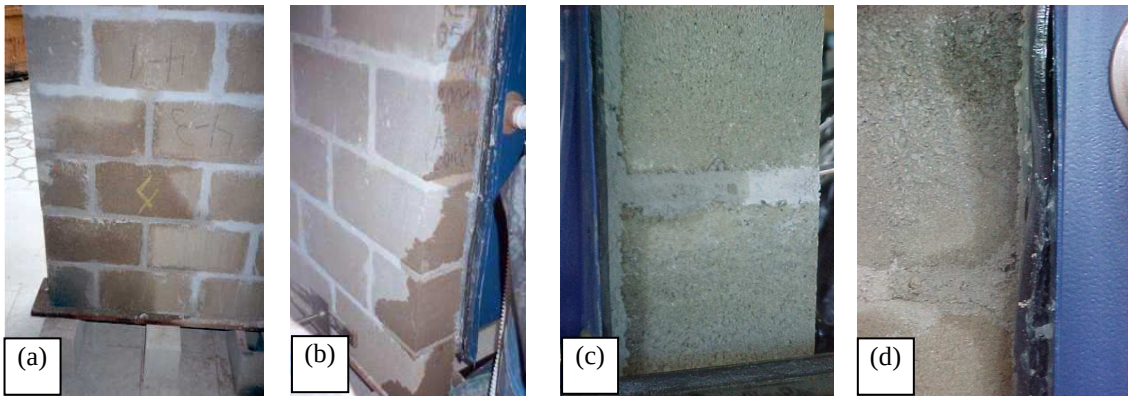

Figure 4. Area of dampness on back of wall at end of test.
(a) – (b) conventional mortar (c) – (d) coal ash mortar

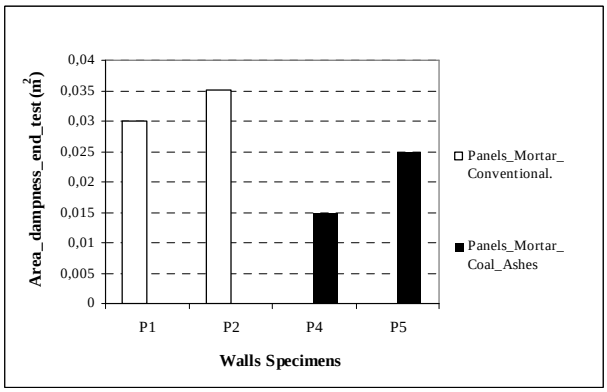

Figure 5. Area of dampness at end of test.

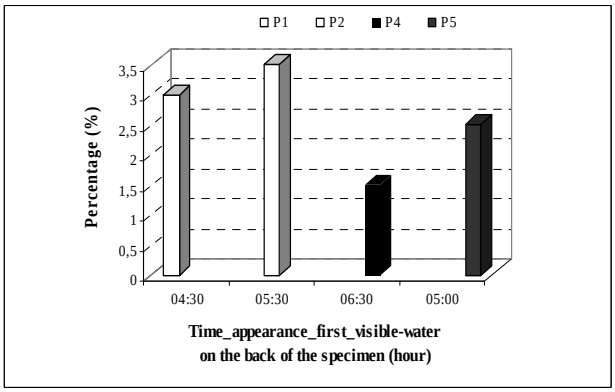

Figure 6. Percentage of dampness area.

In the two cases the value of the first visible water was below the limiting threshold value given in Table 3 for superior performance**.** It can be concluded that all specimens passed the minimum performance values given that minimum times achieved in the tests exceeded those provided in the standard provided in Table 3For the case of specimens made of conventional materials the percentage of dampness area (Figure 6) was 3 and 3.5% and for the specimens that incorporated ash this was 1.5 and 2.5%.

Table 3. Expected minimum levels of performance for leakage and water penetration.

Level of performance	*Minimum time of appearance of first visible water on the back of the*	*Percentage maximum of the sum of the areas of dampness on the back in relation to the total area of the specimen submitted to the aspersion of water in the end of the test*
Minimum	3 hours	0%
Superior	5 hours	5%
High	7 hours	10%

(CAIXA ECONÔMICA FEDERAL. Projeto 02:136.01.004)

The absorption of water by specimens over the course of the test period is given in Figure 7; specimens made with conventional mortar materials had a smaller degree of absorption than specimens made with mortar incorporating ash. Considering that the specimens made with conventional mortar materials were constituted of blocks having a smaller degree of absorption in comparison with the specimens made of ash-based mortar, and that presented smaller absorption, could be considered that the absorption of the blocks has influence on this property.

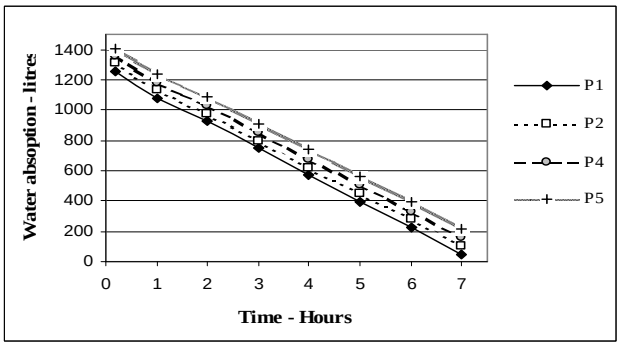

Figure 7. Water absorption of specimens over the test period.

5 CONCLUSIONS

The test results have shown that specimens fabricated with block masonry and mortar that included coal ash performed better relative to conventional brick and mortar masonry assemblies, in respect to the time of appearance of dampness and time of appearance of first visible water on the back of the specimen. Although masonry incorporating coal ash provided the largest final absorption, it nonetheless offered the least area of dampness following a 7 h test period, as compared to specimens made of conventional materials. As well, the dampness areas were also smaller, the one that allowed reach a smaller percentage of the humidity area in the opposite face of the panels, although the final absorption for the water penetration was larger when compared to the conventional panels. It is worth to point out that in spite of this the values of the final absorption were inferior to the 10% to you limit when submitted wind driven rain. It was observed that water penetration occurred, as might be expected, at the block-mortar interface and as well, through the blocks themselves.

REFERENCES

American Society for Testing and Materials. E 514**:** *Standards test method for water penetration and leakage through masonry,* ASTM, Baltimore, 1990 (reapproved 1996).

British Standards Institution. BS-4315. 1990: *Methods of test for resistance to air and water penetration. Part 2: Permeable walling constructions* (Water penetration). London.

Caixa Econômica Federal**. Projeto 02: 136.01.004, 2001**, Desempenho de edifícios habitacionais de até 4 pavimentos – Parte 4: Fachadas. São Paulo.

Cahier du Centre Scientifique et Technique du Bâtiment. 1959, *La resistance dês murs à la penetration de l´ eau de pluie*, (39).

Lacasse, M.A.; O'Connor, T.; Nunes, S.C.; Beaulieu, P. (2003), Report from Task 6 of MEWS Project: Experimental Assessment of Water Penetration and Entry into Wood-Frame Wall Specimens - Final Report Research Report, NRC Institute for Research in Construction, 133, pp.

Thomaz, E.; Ranieri C. G. **IPT, 1998**, *Critérios mínimos de desempenho para habitações térreas de interesse social*. São Paulo.

Silva, N. I. W. J. R., Chies F., Zwonok O. Uso de Cinzas de Carvão na Construção Civil. I *Encontro Nacional Sobre Edificações E Comunidades Sustentáveis*, Anais. Canela – RS, 1997. p. 15-20.

Pozzobon, C. E. 1999, *Aplicações Tecnológicas para a Cinza do Carvão Mineral Produzido no Complexo Termelétrico Jorge Lacerda***.**. Dissertação de Mestrado - Faculdade de Engenharia Civil - UFSC. Florianópolis.

Lenzi, E.J. 2001, *Influencia do uso de cinzas da combustão de carvão mineral em argamassa de revestimento*. Dissertação de Mestrado - Faculdade de Engenharia Civil - UFSC. Florianópolis.

Silveira. J.A. 2001, *Aproveitamento de cinzas volantes e pesadas para a produção de concretos usinados e de blocos e pavimentos de concreto.* Relatório - Cnpq.

XII DBMC
International Conference on Durability of Building Materials and Components
PORTO - PORTUGAL, April 12th-15th, 2011

Effectiveness and Durability of Biocides in Building Coatings – Biological Aspects

Nicole Krueger [1]
Wolfgang Hofbauer [2]
Martin Krus [3]
Cornelia Fitz [4]
Florian Mayer [5]
Klaus Breuer [6]

ABSTRACT

In 2004 an interdisciplinary publicly funded project on the effectiveness and durability of biocides in building coatings was started at the Fraunhofer-Institute for Building Physics in Holzkirchen, Germany. Material components, building coatings and biocide combinations were chosen and samples for outdoor weathering experiments were also designed, all in cooperation with partners from the industry. About 350 biocide-equipped samples together with control specimens without biocide were exposed to real climatic conditions at two locations in Germany. Emerging microbiological growth on the samples was assessed, according to a self-developed special scale. The periodic assessment took place in monthly/two monthly (first location) and half-year cycles (second location), respectively. For different samples of the same type the measurements were averaged and graphically evaluated in the course of the biological development on the surfaces. On most control specimens without biocide a wave like increase of the biological colonization could be detected. Whereas the conditions in Germany for growth on outdoor surfaces are best in the autumn, they stagnate or diminish in the dry seasons, winter and summer. All biocide equipped coatings showed, as expected, a retarded growth. However, some characteristic differences could be recognized which could be assigned to different features of the coatings and to different combinations of biocides.

KEYWORDS

Biocides, Biological colonisation, Retarded growth.

[1] Fraunhofer Institute for Building Physics, Holzkirchen Branch (IBP), Valley, Germany, Nicole.Krueger@ibp.fraunhofer.de
[2] Fraunhofer Institute for Building Physics, Holzkirchen Branch (IBP), Valley, Germany, Wolfgang.Hofbauer@ibp.fraunhofer.de
[3] Fraunhofer Institute for Building Physics, Holzkirchen Branch (IBP), Valley, Germany, Martin.Krus@ibp.fraunhofer.de
[4] Fraunhofer Institute for Building Physics, Holzkirchen Branch (IBP), Valley, Germany, Cornelia.Fitz@ibp.fraunhofer.de
[5] Fraunhofer Institute for Building Physics, Holzkirchen Branch (IBP), Valley, Germany, Florian.Mayer@ibp.fraunhofer.de
[6] Fraunhofer Institute for Building Physics, Holzkirchen Branch (IBP), Valley, Germany, Klaus.Breuer@ibp.fraunhofer.de

1 INTRODUCTION

Unwanted emergence of microorganisms on building surfaces, especially on the surface of external thermal insulation composite systems (ETICS), is a growing problem. According to current literature and public understanding, the influencing variables can be classified in the following groups: Global climate change, air pollution, geographical location, exposition of a building, construction details and the choice of materials. Not all of these factors can be influenced by building techniques. Present state of the art does not allow guaranteeing the exemption of unwanted biological growth on building coatings under all circumstances, without the use of biocides [Lindner 2008]. In order to be effective against the target organisms, an active compound has to be water soluble. Otherwise it could not be incorporated in the living cells of the target organisms and would be ineffective. This water solubility does, however, limit the durability of biocides for the film conservation in coatings for façades that are exposed to rain or condensate. In order to achieve an appropriate and ecological use of biocides in building coatings, knowledge about their durability and effectiveness in combination with different matrices (binders) is of importance.

In Germany the warranty for facades being without complaints is at least five years. In Europe the Biocidal Product Directive (BPD) insists on minimising (as far as possible) the amount of biocides which are allowed to enter the environment. Until now there were only limited data available on the long-term field performance of biocidal coatings. Therefore, the industry showed great interest in having products tested with regard to performance in a long term investigation.

An interdisciplinary publicly funded project on effectiveness and durability of biocides in building coatings was therefore started in 2004 at the Fraunhofer-Institute for Building Physics. In cooperation with partners from industry, material components, building coatings and biocide combinations were chosen, whilst samples for outdoor weathering experiments were also designed.

2 MATERIAL AND METHODS

The investigations presented are part of a four year outdoor study. Special specimens with the structure of an external thermal insulation composite system (ETICS), finished with different coatings (plaster or plaster covered with paint) were designed [see also Hofbauer et al. 2006]. Plaster finish was carried out as a structured render with structure grain at a size of 2 mm. Therefore the surfaces were not smooth but somewhat rough. The investigated surfaces of the specimens were of the dimension 30x30 cm² and the polystyrene insulation in each case was 5cm thick. Five different kinds of plaster and three different types of paint were used, as shown in Table 1.

Table 1. Tested coatings.

Plasters		*Paints*
With inorganic binder	Lime cement plaster	Dispersion type silicate paint
	Silicate plaster	Styrene acrylate based emulsion paint
With organic binder	Styrene acrylate based	Silicon resin based paint
	Terpolymer based	
	Silicone resin based	

The final rendering thickness was about 0.5 cm. Four different biocide combinations were added to the surface coatings. Every biocidal mixture consisted of three active ingredients. Two ingredients were always consistent in all combinations, a third ingredient was added from a selection of four (see Table 2). The biocide combinations were added in concentrations of 0.5 mass-% to the plasters and 1.0 mass-% to the paints.

Approximately 350 test specimens based on ETICS structure were exposed to real climatic conditions at two locations in Germany, most of them in Holzkirchen (Fig. 1) in Upper Bavaria, north of the Alps. The

climate is characterized by three main factors: heavy driving rain, temperatures below zero for long periods during winter and high daily differences in temperature, caused by radiation and occasional warm winds from the south (Foehn).

Table 2. Tested biocide mixtures.

Obligate compounds	*Variable compounds*
Terbutryne	Carbendazim
	Dichloro-Octylisothiazolinone (DCOIT)
Octylisothiazolinone (OIT)	Iodopropynylbutylcarbamate (IPBC)
	Zinc-pyrithione



Figure 1. Outdoor exposition of the specimen in Holzkirchen.

Apart from chemical and physical measurements, the development of biological growth on biocidal surfaces in comparison to non biocidal surfaces of the same kind, was assessed by different methods. The composition and development of the biological processes were recorded regularly. A visual characterisation of the pattern of the infection with microorganisms and succession was performed. The assessment took place in a monthly/two monthly (first location) and half-year cycle (second location), respectively, under the use of a semi quantitative assessment scale according to Hofbauer et al. [2003], see Table 3. The lower categories of this rating scale provide a minute resolution of the first colonization, whereas the upper categories follow the percentage of coverage by growth. A rating between 0 and 3 can hardly be recognised by an untrained person, because there is very little growth. A rating from 6 to 10 is also recognizable as disfigurement by laymen and would cause complaints and rating 4 and 5 form a transition position where complaints might occur.

Additional developing growth was further recorded by a specially developed visual-optical raster scan, and also documented by photographs. The growth recorded was also categorised if consisting of fungi, algae or both.

In addition to the methodology specified, further measurements were made, the results of which are presented elsewhere. Biological measurements for instance, were completed by physiological investigations (efficacy-test) and a complex quantitative and taxonomical analysis of the microorganisms colonizing the different coating-systems. Furthermore, an ecological analysis and a resistance-test also accomplished the results of the visual observations.

Table 3. Rating scale for the assessment of surface growth on the specimen according to Hofbauer et al. [2003], simplified. White table lines indicate minor growth intensity that would not lead to complaints; bright green is used in a transition area where complaints may start. The intense green colour marks growth intensities that would most certainly provoke complaints.

Rating	*Microbiological growth covering examined area on an average of*
10	87,5% - 100%
9	75% - 87%
8	62,5% - 75%
7	50% - 62,5%
6	37,5% - 50%
5	25% - 37,5%
4	5% - 25%
3	less than 5 %
2	few single spots (less than 5 %)
1	1-3 single spots
0	0 % - no spots

3 RESULTS

As shown in previous studies [Hofbauer et al. 2006]; [Hofbauer 2007], development of growth followed cyclic fluctuations (Fig. 3). During humid periods of the year (autumn, in Central Europe for example) a more intense development of growth is recognized whereas during dry and warm or dry and cold periods (in Central Europe during mid summer and late winter), a stagnation or even reduction of growth occurs. Once growth is present, it rarely disappears completely again. During the next convenient climate phase the development will recommence at a higher level. Figure 3 shows a scheme of a typical cyclic fluctuation of growth development with a wavelike increase.

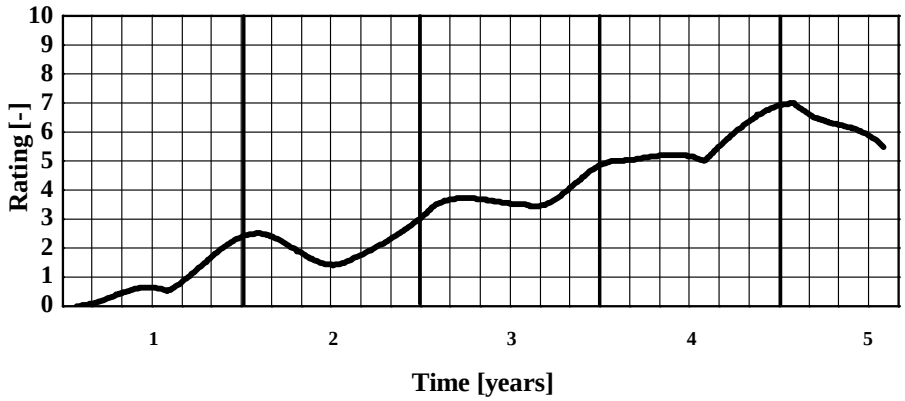

Figure 3. Typical growth development in phases as measured on a non biocidal surface during the project.

In general the efficiency of the biocide-mixtures used is confirmed, the growth development on all of the biocidal equipped coating systems is clearly retarded. Even after four years of exposition, the growth of some biocidal variants has to be rated as inconsiderable or stagnating. Some variants, on which only fungal growth occurred until the end of the project, are optically conspicuous, due to the presence of demaciaceous fungi (mould fungi with dark pigmentation).

A correlation between the effectiveness of biocides and the type of binding agent used can be observed. In the course of time, surface growth may occur earlier and more intensely on specimens with a high total measurable biocide content, in comparison to variants with a lower content over the same duration. This

effect could be a result of a different withholding capacity for biocides or a different release, respectively.

Specimens with silicon resin based variants turned out to be quite durable against microbiological growth, as shown in Figure 4. By observation completion, growth intensity on samples of all biocide combinations had to be rated as inconsiderable, they were rated below 3. Even on the specimen without biocide, the critical rating of 3 was not reached until after two years of exposition.

The ratings outlined in figure 4 comprise of approximate-curves based on geometric mean values from the measurements. The rating of the growth intensity is shown through the ordinate, the numbers on the abscissa show the number of months elapsed.

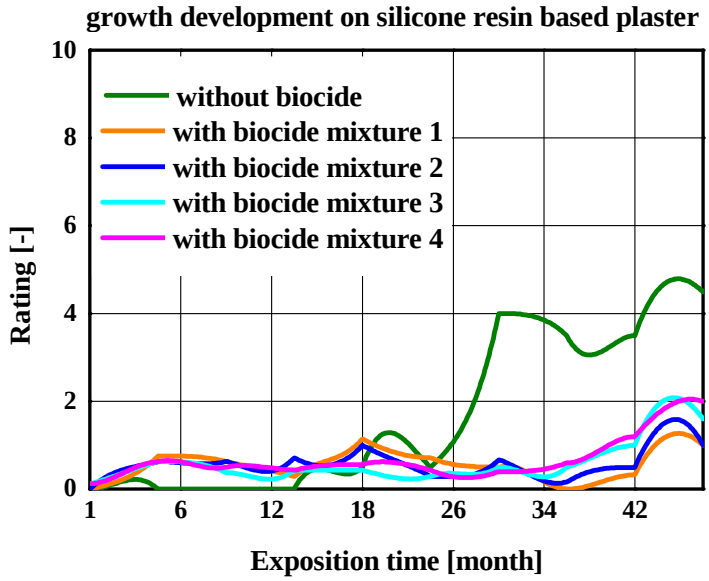

Figure 4. Observed growth on silicon resin variants.

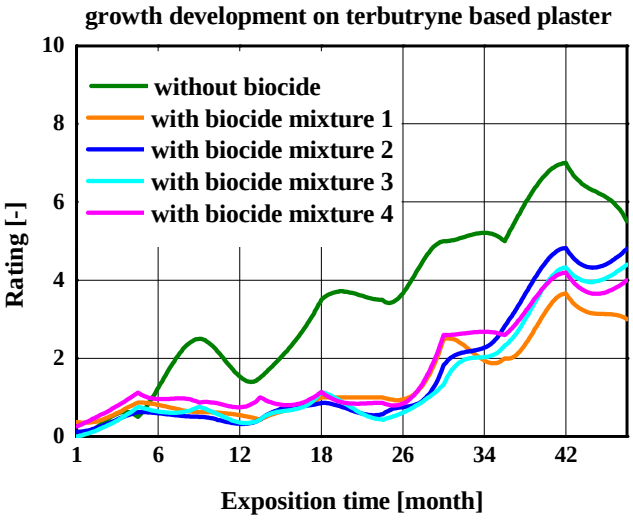

Figure 5. Observed growth on terpolymer variants.

Unlike the previous variants, the specimen with plaster coating based on terpolymer already showed significant growth earlier, on both biocidal equipped and non equipped variants, as shown in Figure 5. Within the measured period the “critical” rating of 3 was even reached by all biocidal equipped systems.

The lime cement plaster could not be rated conclusively, because the biocidal effect was overlaid by other effects, for instance by chalking and weathering because of heavy driving rain or hail.

While in some coating systems all active biocidal components show a similar effect, in some coating systems special biocidal combinations performed better than others. In general, systems with paint coating showed better results than systems without paint coating. The paint coatings were equipped with twice as much concentration of active compounds than the render. However, due to the substantially lower thickness of the paint coatings, the total content of active compounds is less than in renders.

4. DISCUSSION

The results show, that the concentrations of active compounds in a coating do not allow direct assessment of the effectiveness against biological growth. The interaction between the type of biocidal composition, the type of coating (binder) and the physical building conditions is of essential importance. Coatings upon which microorganism colonization is generally less because of their chemical constitution are protected by lower total amounts of active compounds. It is important to supply the immediate coating surface with effective concentrations of biocides. Therefore, coating systems with a pronounced withholding capacity for biocides may lead to an undersupply at the surface.

Depending on the chemical character of the biocides used (e.g. Terbutryne, IPBC), the formation of even more active transformation products from the biocidal agents, is possible. Transformation may be due to effects caused by temperature, oxidation, hydrolysation, sunlight, etc. These processes could cause an initial decrease in the concentration of the biocidal compounds primarily used, whilst, at the same time, the protection of the façade is still ensured through the potentially longer lasting biocidal effective transformation products.

The additional taxonomical and ecological analysis of the microorganism species found in the early stages of colonization on the surfaces confirmed that, according to the various biocidal compositions and coating systems, different ecological groups of organisms are present. Gaps in the efficiency spectrum of the other biocidal compounds became obvious, in the case of a decrease or loss of an active compound, by the appearance of typical species. For example; *Alternaria* spp., *Ulocladium* spp., are already known for an increased tolerance against Carbendazim (e.g. [Bollen et al. 1983], [Hassal 1990], [Deising et al. 2008]). Therefore, specimens equipped with a biocidal combination comprising of Terbutryne, OIT and Carbendazim were earlier colonised by the fungi listed, because OIT diminished faster than other biocides.

The results of the study presented show that biocidal equipped paints are very effective in the protection of building coatings against unwanted growth of microorganisms. If only the paint finish is equipped with biocides but not the underlying render, the total amount of biocides necessary may be reduced significantly.

ACKNOWLEDGMENTS

The research presented is sponsored by the Bundesministerium für Wirtschaft und Technologie based on a decision of the Bundestag of Germany, Federal Republic of Germany, Projektträger Jülich and partners from industry.

REFERENCES

Bollen, G.J., Hoeven van der, E.P., Lamers, J.G., Schoonen, M.P.M. 1983, ‘Effect of benomyl on soil fungi associated with rye. 2. Effect on fungi of culm bases and roots.’, *Neth. J. Pl. Path.* **89**, pp. 55-66.

Deising, H.B., Reimann, S., Pascholati, S.F. 2008, 'Mechanism and significance of fungicide resistance', *Brazilian Journal of Microbiology* **39**, pp. 286-295.

Hassal, K.A. 1990, *The Biochemistry and uses of Pesticides. Structure, metabolism, Mode of Action and Uses in Crop Protection*. Second Edition. VCH, Weinheim, New York, Basel, Cambridge.

Hofbauer, W. 2007, *Aerophytische Organismen an Bauteiloberflächen*, Ph.D. Thesis, Innsbruck University (Austria).

Hofbauer, W., Breuer, K., Sedlbauer, K. 2003, 'Algen, Flechten, Moose und Farne auf Fassaden', *Bauphysik* **25**(6), pp. 383-396.

Hofbauer, W., Fitz, C., Krus, M., Sedlbauer, K., Breuer, K. 2006, *Prognoseverfahren zum biologischen Befall durch Algen, Pilze und Flechten an Bauteiloberflächen auf der Basis bauphysikalischer und mikrobieller Untersuchungen*, Bauforschung für die Praxis Vol. 77, Fraunhofer IRB Verlag, Stuttgart, Germany.

Lindner, W. 2005, '5.14 Surface coatings', in 'Directory of Microbiocides for the Protection of Materials', editor W. Paulus, Springer, New York, pp. 347-376.

XII DBMC
International Conference on Durability of Building Materials and Components
PORTO - PORTUGAL, April 12th-15th, 2011

Detailed Investigation of Modulus of Elasticity in Linseed Oil-impregnated Mature Norway Spruce Sapwood

Thomas Ulvcrona [1]

ABSTRACT

Various techniques and preservatives are used in wood preservation, some of which are toxic. Hence, there is a need for further development (and use) of non-toxic alternatives, such as linseed oil impregnation by the Linotech process, especially for wood such as mature sapwood from Norway spruce (*Picea abies* L. Karst.) with anatomical features that make it difficult to impregnate with preservatives by currently applied industrial processes. In the study reported here we examined the modulus of elasticity (MOE) of sub-samples of mature Norway spruce sapwood impregnated by this process to evaluate its effects, caused by possible structural damage, on the wood's short-term mechanical properties. Two sets of process settings were applied, "low" and "high" with treatment times, pressures and temperatures of 2 and 3 h, 0.8 and 1.4 MPa, 60 and 140˚C, respectively. The treatments resulted in 30-50% mass increases in the specimens. MOE was generally slightly lower in control (unimpregnated) specimens than in specimens impregnated at low and high settings (9976, 10663 and 10528 MPa, respectively). The results indicate that the Linotech process does not cause more structural damage than drying without impregnation, and that determination of short-term mechanical properties followed by basic statistical analysis provides a convenient means for detailed evaluations of effects of varying process settings.

KEYWORDS

Short-term mechanical properties, Hydrophobic oil, Method development.

[1] Swedish University of Agricultural Sciences Unit for Field-based Research Svartberget Fieldstation SE-922 91,Vindeln SWEDEN, Thomas.Ulvcrona@esf.slu.se

1 INTRODUCTION

Right now there is worldwide a constant evaluation of possible sustainable processes that could substitute many of the environmentally adverse preservation techniques currently used. As one of many potential processes, impregnation of wood with hydrophobic oils has already been extensively evaluated for many years.

Potential sustainable alternatives to many currently used environmentally adverse preservation techniques are being intensively sought. One of many potential processes, impregnation of wood with hydrophobic oils, has been known for many years, but further evaluation and development of the process is still required. Previous studies have shown that it is possible to successfully impregnate even recalcitrant types of wood, such as mature sapwood from Norway spruce (*Picea abies* L. Karst), with the linseed oil product Linogard® using the Linotech process [Ulvcrona *et al.* 2006, Ulvcrona & Bergsten 2007]. In this process the linseed oil does not enter the cell wall structure, but the moisture uptake of the resulting wood-based material is retarded by the formation of a hydrophobic layer within the wood [Fredriksson *et al.* in press]. Thus, it probably does not affect the chemical (and hence structural) contents of the cell walls. However, the temperatures that may be used in the process are relatively high (60-140 °C) and external pressure may also be applied [Ulvcrona *et al.* 2006, Ulvcrona & Bergsten 2007], so it could potentially cause structural changes resulting in alterations of short-term mechanical properties. Accordingly, Wang [2007] has reported that impregnation with oils can have structural effects that might restrict use of impregnated materials in constructions. Thus, clarifying the effects of hydrophobic oil impregnation on wood's short-term strength properties is an important first step towards elucidating the potential range of uses for wood treated with hydrophobic oil.

Thus, in the presented study the Modulus of Elasticity (MOE) of mature Norway spruce sapwood impregnated by the Linotech process with two sets of process settings was investigated.

2 MATERIALS AND METHODS

2.1 Samples

In total, 15 Norway spruce (*Picea abies* L. Karst) trees from three stands in a mixed coniferous forest in northern Sweden (64°10'N, 160-320 m above sea level) were selected, from each of which in all more than 60 samples (500*25*25 mm) were sawn from the mature sapwood. A third of the samples (controls) were dried, but not impregnated, a third were impregnated by the Linotech process with "low" settings (2 h treatment at 0. 8 MPa and 60-140˚C) and the other third by the process with "high" settings (3 h treatment at 1.4 MPa and 140˚C). The moisture content of the wood (percentage of wood dry mass) before impregnation was calculated according to standard method EN 384 [1995]. The impregnation resulted in 30-50% increases in the mass of the mature sapwood specimens, and their linseed oil contents were calculated as a percentage of wood dry mass. For further details of these procedures, see Ulvcrona *et al.* [2006].

2.2 Modulus of Elasticity and Macroscopic Cracks

Forty impregnated mature sapwood samples were randomly chosen to test their MOE, as a general indicator of their mechanical properties, and eight unimpregnated mature sapwood samples were randomly chosen as controls. The top half of each sample was cut longitudinally with a band saw to form nine specimens of equal size (219*6*6 mm) with standing annual rings according to Fig. 1, then specimens representing each treatment, and control specimens, were randomly selected for the MOE measurements according to Table 1. In addition, material properties of the samples (moisture content and density) prior to impregnation, and their oil contents post-impregnation, were determined to assess possible correlations between these variables and the specimen's MOE values.

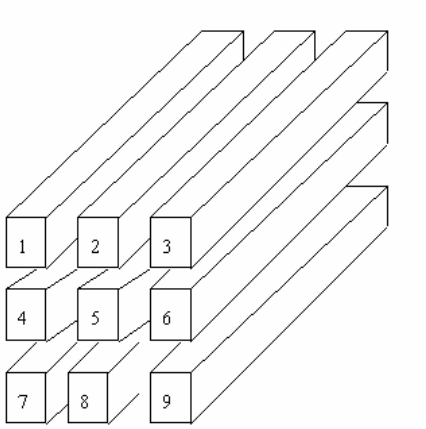

Figure 1. Sketch showing the sawing pattern of specimens from the samples.

Tests were performed using an Instron Universal, 10 kN testing machine with standard equipment for 3-P bending. All specimens were loaded until failure, using a crosshead speed of 4 mm minute^{-1}. Displacement of the crosshead was recorded and used to calculate the strain. Thus, the absolute flexural modulus values are not entirely correct, but are still useful for comparisons between reference and impregnated specimens. Specimens were conditioned and tested at 23°C with 50% humidity.

The elastic flexural strain, ε_{fl}, on the bottom surface was calculated as:

(1) $\varepsilon_{fl} = 6w_0h/l^2$

where w_0 is the measured deflection, and h is the thickness of the specimen.

Flexural stress, σ_{fl}, was calculated as:

(2) $\sigma_{fl} = 3Pl / 2h^2b$

where P is the applied load, and b is the width.

The flexural modulus, E_{fl}, was calculated, in MPa, as:

(3) $E_{fl} = \sigma_{fl} / \varepsilon_{fl}$

with measurements of applied load taken between 0.01 – 0.05 kN chosen for calculations.

The shear factor was neglected in the calculations of flexural modulus because the l/h ratio (26.7) made it insignificant [Kollman & Cote, 1984].

The bending strength, f_m, was calculated, in MPa, as:

(4) $f_m = aF_{max} / 2W$

according to standard method EN 408 [1995].

Macroscopic crack development was measured with the naked eye and a caliper across the whole ($25*25mm^2$) surface in the middle of samples before further sawing into specimens.

2.3 Statistical Analysis

All statistical calculations were performed using MINITAB software [Anon., 1999]. The data were tested for normality and heteroscedasticity, and the results indicated that no transformations were needed. To test for differences in mean values related to the treatments One-way Anova was used.

3 RESULTS AND DISCUSSION

There were no easily interpretable general trends concerning effects of process settings on the Modulus of Elasticity (MOE) values of the mature Norway spruce sapwood specimens impregnated by the Linotech process [Table 1], although they were slightly lower for untreated specimens than for impregnated specimens [Table 1]. However, MOE values of untreated specimens were not significantly lower than those of specimens impregnated with high settings [Table 1]. The standard deviation of the MOE values was also slightly lower for the unimpregnated specimens [Table 1].

Table 1. Mean (and standard deviation), minimum and maximum Modulus of Elasticity (MOE) values of samples following the applied treatments (numbers of investigated specimens in brackets).

Treatment	Mean MOE (MPa)	Standard Deviation	Variance	MOE Minimum (MPa)	MOE Maximum (MPa)
Untreated	9976[a] (48)	1330	1556	6643	13666
Low settings	10663[b] (107)	1556	1568	5593	14255
High settings	10528[ab] (95)	1568	1330	7983	14480

Note, superscript letters indicate significant differences between treatments according to Tukey's tests at the 0.05 probability level.

This tallies to some degree with findings reported by Megnis *et al.* [2002], who also discuss the possibility that hydraulic effects of oil present in the cavities may increase the wood's stiffness in compression , which in turn affects its MOE and strength. However, the levels of uptake in the investigated samples seem to have been insufficient to significantly alter the short-term mechanical properties of the impregnated wood. There appears to have been no more structural damage after impregnation than after drying without further treatment. Among the examined specimens, there were no significant differences between impregnation treatments regarding linseed oil uptake; the mean values of oil uptake were 25.4% of wood dry mass for both impregnation treatments (not further presented). No significant differences in macroscopic crack development were found either following the investigated impregnation treatments; mean values of macroscopic crack development were 6.6 and 5.8 mm, in treatments with "low" and "high" settings respectively (not further presented).

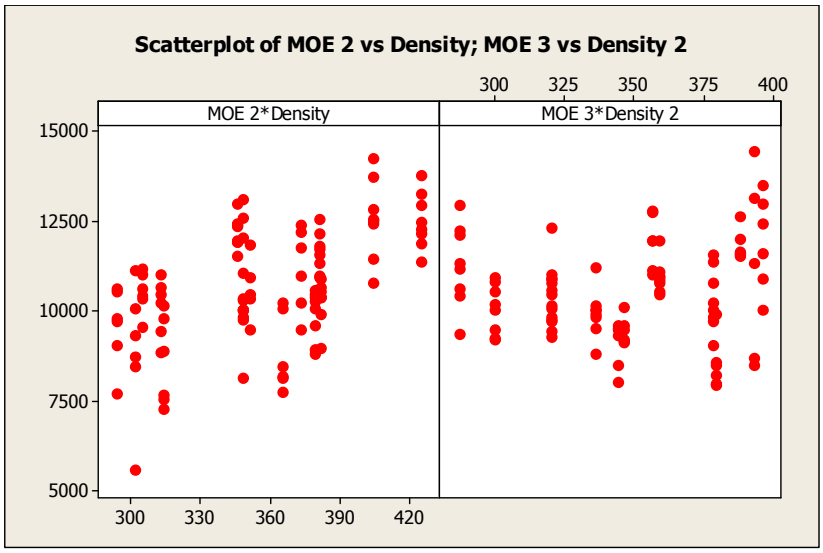

Figure 2. MOE of specimens impregnated by the Linotech process with "low" (MOE 2) and "high" (MOE 3) Linotech settings in relation to the samples' wood density (kg/ m^3) before impregnation.

There were also no significant differences between treatments regarding wood density before impregnation in the investigated samples [Fig. 2].

Wood density is generally quite strongly correlated with MOE in samples with otherwise similar variables. There were weak indications of this correlation in the specimens subjected to the Linotech process with "low" settings, but no such indications in the specimens subjected to the process with "high" settings [Fig. 2].

There were also no significant differences between treatments regarding wood moisture content before impregnation in the investigated samples [Fig. 3].

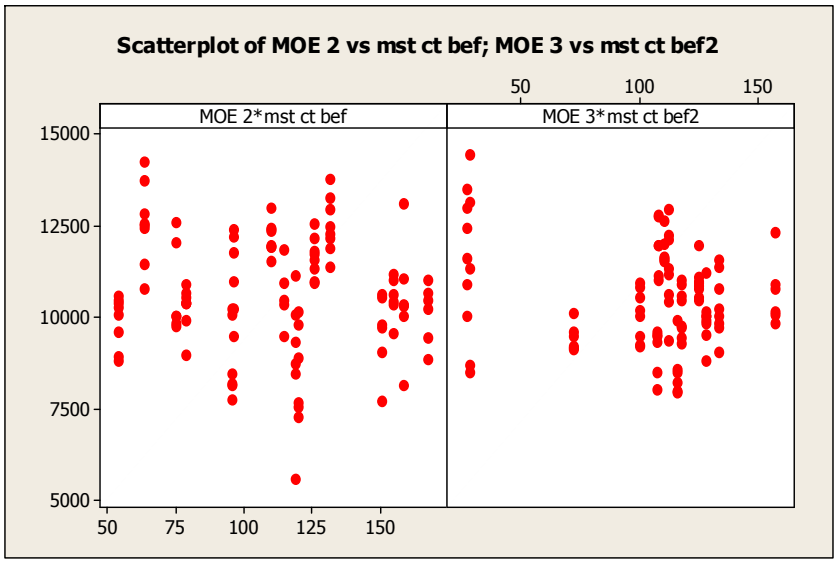

Figure 3. MOE of specimens impregnated by the Linotech process with "low" (MOE 2) and "high" (MOE 3) settings in relation to their wood moisture content (%) before impregnation.

Previous studies have shown that the wood moisture content (expressed as water-filled porosity) is positively correlated with uptake of oil in the Linotech process [Ulvcrona *et al.* 2006, Ulvcrona & Bergsten 2007]. However, the moisture content before impregnation of the samples examined here did not have any apparent effect on the MOE of the impregnated wood material [Fig. 3].

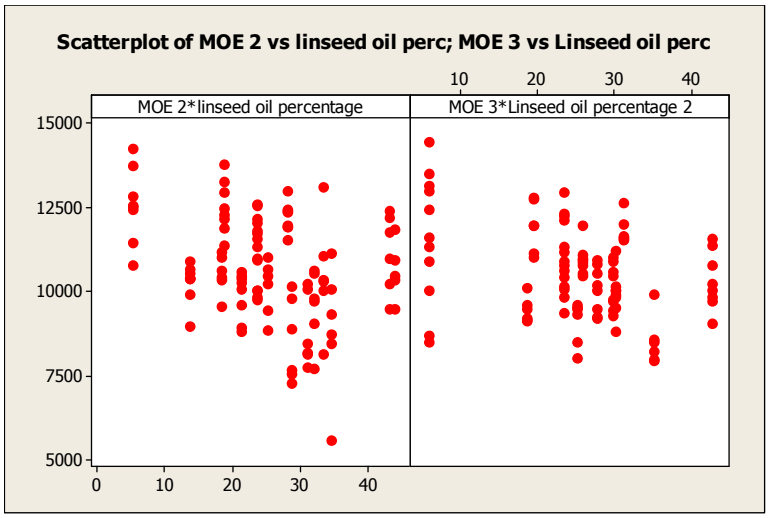

Figure 4. MOE of specimens impregnated by the Linotech process with "low" (MOE 2) and "high" (MOE 3) settings in relation to the samples' linseed oil percentage (%).

In addition, there were no significant differences between treatments regarding uptake of oil, expressed as linseed oil percentage of wood dry mass before impregnation in the investigated samples [Fig. 4].

Wang [2007] has reported that impregnation with oils can cause structural changes in impregnated materials that might restrict their use in constructions. However, we found no clear trends regarding effects of linseed oil uptake on the MOE of the resulting wood material [Fig. 4]. It should be noted the levels of oil uptake were generally similar following impregnation by the process with both sets of settings [Fig. 4]. Therefore, it is difficult to draw conclusions regarding possible effects of all levels of oil uptake. However, this study provides information about effects of impregnation to levels likely to be applied in commercial practice.

This study shows that the presented methodology can be used to study, in detail, the effects of variations in process settings on the short-term mechanical properties of impregnated wood, providing a convenient approach for optimizing parts of the process in screening studies before progressing to large-scale studies of short-term mechanical properties in full-scale products. Further, use of highly characterized raw wood materials allowed much of the natural variability present in wood from whole trees to be excluded, providing opportunities to highlight effects of separate parts of the process.

In addition, the study indicates that impregnation with linseed oil in the Linotech-process does not have major effects on the MOE of mature Norway spruce sapwood. Possible hydraulic effects in the wood are not significant when samples are divided into specimens. Neither do any of the investigated material properties have any obvious effect on MOE in the investigated samples.

Finally, the absence of clear negative effects of the investigated impregnation process on MOE indicates that further investigations of its effects on both the short-term and long-term mechanical properties of full-scale products are warranted. However, such investigations should be done in parallel with studies like this, allowing effects of specific process settings to be identified.

ACKNOWLEDGEMENTS

The author thanks The Swedish University of Agricultural Sciences theme research program “Future Forests” for financial support and Sees-Editing for professional editing.

REFERENCES

Anon. EN 384. 1995. *Structural timber – determination of characteristic values of mechanical properties and density,* European standard 384. European Committee for Standardization. 1-8.

Anon. EN 408. 1995. *Timber structures – Structural timber and glued laminated timber – Determination of some physical and mechanical properties,* European standard 408. European Committee for Standardization, 1-19.

Anon. 1999. *Minitab Statistical Software Release 13 for Windows.*

Fredriksson, M. Ulvcrona, T. & Wadsö, L. 2010. ´Swelling and moisture sorption of Norway spruce (*Picea abies* L. Karst.) impregnated with linseed oil´, *Wood Material Science and Engineering*. In press.

Megnis M., Olsson T. Varna J. & Lindberg H. 2002. `Mechanical performance of linseed oil impregnated pine as correlated to the take-up level`, Wood *Science and Technology*, **36**[1], 1-18.

Kollman, F.F.P. & Cote, W.A. 1984. Principles *of Wood Science and Technology, Vol. 1 Solid Wood*, Springer Verlag, Berlin.

Ulvcrona, T. Lindberg, H. & Bergsten, U. 2006. ´Impregnation of Norway spruce (*Picea abies* L. Karst) wood by hydrophobic oil and dispersion patterns in different tissues`, *Forestry*, **79**[1], 123-134.

Ulvcrona, T. & Bergsten, U. 2006. `Possibilities for compositional tailoring of Norway spruce (*Picea abies* L. Karst.) wood using a hydrophobic oil impregnation process`, *Holz als Roh- und Werkstoff*, **65**[2], 167-169.

Wang, J. 2007. *Initiating evaluation of thermal-oil treatment for post-MPB lodgepole pine*, Forintek Canada Corp., Vancouver BC, Canada.

XII DBMC
International Conference on Durability of Building Materials and Components
PORTO - PORTUGAL, April 12th-15th, 2011

The Durability of Carbon Fiber/Epoxy Composites under Hydrothermal Ageing

G. Alaimo [1]
S. Alessi [2]
D. Enea [3]
G. Pitarresi [4]
G. Przybytniak[5]
G. Spadaro [6]
D. Tumino [7]

ABSTRACT

Studies on fibre reinforced composites are now receiving greater attention. Industrial applications have been successful in areas like aerospace, automobile, marine, construction and sporting goods. The first generation of epoxy resins for use in carbon fibre composites are able to achieve optimized high stiffness modules and high heat resistance by a high crosslink density, reached through thermal curing. However, these formulations can be very toxic and brittle with low crack resistance, which was a major disadvantage for structural applications. In the last years the use of ionizing radiation as alternative to thermal curing has been proposed as an environmentally friendly process. Furthermore, in order to enhance toughness mechanical requirements for their applications, the formulation generally consists of blends of epoxy resins and engineering thermoplastics. In terms of durability (service life and reliability), in these materials it depends on different environmental conditions (temperature, moisture, etc.), and it is very important to know how their properties are modified after the exposure to different temperature and moisture absorption cycles. In this work carbon fibre composites produced by ionizing radiation induced curing of the epoxy based matrices have been subjected to thermal and moisture absorption ageing and the influence of these treatments on the thermal and mechanical properties has been investigated through dynamic mechanical thermal analysis and mechanical fracture toughness tests.

KEYWORDS

Durability, Carbon fiber composites, Hydrothermal ageing, Fracture toughness.

[1] Dipartimento di Progetto e Costruzione Edilizia (DPCE), Università degli Studi di Palermo, 90128, Palermo, ITALY (alaimo@unipa.it)
[2] Dipartimento di Ingegneria Industriale, Università degli Studi di Palermo, 90128, Palermo, ITALY (alessi@dicpm.unipa.it)
[3] Dipartimento di Progetto e Costruzione Edilizia (DPCE), Università degli Studi di Palermo, 90128, Palermo, ITALY (alaimo@unipa.it)
[4] Dipartimento di Ingegneria Industriale, Università degli Studi di Palermo, 90128, Palermo, ITALY (pitarresi@dima.unipa.it)
[5] Institute of Nuclear Chemistry and Technology, Dorodna 16, 03-195, Warsaw, POLAND (g.przybytniak@ichtj.waw.pl)
[6] Dipartimento di Ingegneria Industriale, Università degli Studi di Palermo, 90128, Palermo, ITALY (spadaro@dicpm.unipa.it)
[7] Facoltà di Ingegneria e Architettura, Università degli Studi di Enna Kore, Cittadella Universitaria, 94100, Enna, ITALY (tumino@dima.unipa.it)

1 INTRODUCTION

Fibre reinforced composites are receiving more and more interest, due to their industrial applications in several areas, like aerospace, automobile, marine, constructions etc... Composites are usually used when high performance and light weight are needed. Among all the polymer based composites, epoxy resin/carbon fibre systems present the best performances in term of mechanical properties and thermal resistance. They are used in particular for aerospace and advanced automotive applications [Feraboli & Masini 2004; Hufenbach et al.2011].

The first generation of epoxy resins for use in carbon fibre composites optimized high modulus and high heat resistance by a high crosslink density reached through thermal curing. However, these formulations can be very toxic. In the last years the use of ionizing radiation as alternative to thermal curing has been proposed as an environmentally friendly process. In fact radiation process allows to perform curing at mild temperatures with reduced emission of organic volatile substances and the obtained materials are characterized by the absence of thermally induced mechanical stresses [Lopata et al. 1999; Goodman & Palmese 2002].

A significant drawback in the use of cross-linked epoxy resins as polymer matrices is that the material is very brittle with low crack resistance. In order to achieve the mechanical requirements in term of toughening, the used formulations generally consist of blends of epoxy resins and engineering thermoplastics [Mimura et al. 2000].

The structures made of composites materials, in general, work in more or less aggressive environments, like temperature, humidity, chemical exposition, corrosive environments, UV and ionizing radiation. Consequently, it is very important to know how their properties are modified after the exposure to these different aggressive factors.

In this work carbon fibre composites produced by the ionizing radiation induced curing of the epoxy based matrices have been subjected to thermal and moisture absorption ageing. The influence of these treatments on the thermal and mechanical properties has been investigated through dynamic mechanical thermal analysis and mechanical fracture toughness tests.

2 EXPERIMENTAL

The epoxy monomer was 2,2-bis[4-(glycidyloxy)phenyl]propane, also named diglycidyl ether of bisphenol A (DGEBA), by aldrich and the toughening agent for the epoxy resin was an engineering thermoplastic, polyether sulfone (PES), produced by Sumitomo Chemicals. The initiator was an iodonium salt cumyltolyliodonium tetra(pentafluorophenil) borate rh 2047 (Rh), supplied by Rhodia Silicones.

The carbon fibers were sika unidirectional, high modulus, carbon fibers, Sikawrap 400c midmod nw, having a density: of 1.81 g/cm^3 and longitudinal young's modulus E_l of 390 GPa.

Two composite laminate panels have been prepared with two different resin blends with zero and 10 phr (per hundred of resin) of toughening agent:

DGEBA- Rh-carbon fibers (0PES)
DGEBA- 10PES-Rh-carbon fibers (10 PES)

The 0PES system has been prepared through the following procedure. A blend from DGEBF and initiator (Rh) was prepared at 60°C. First the resin was heated in an oil bath, then the initiator was added in small portions. The amount of initiator for this system was established to be 0.1 phr (per hundred resin). The blend was mixed for about 30 minutes until the initiator dissolves in the resin

then it was cooled down to the room temperature. The 10PES system has been prepared through the following procedure.

The blend was prepared at 80°C. First the resin was heated at 80°C, then the toughening agent was added in order to be dissolved. After 2 hours mixing a homogeneous but unclear blend was obtained. Rising the temperature step by step it was found that 130°C is the optimal temperature for the complete dissolution of the thermoplastic in the resin. As in the previous blend, the initiator is added after cooling down to 60°C.

The impregnation of unidirectional carbon fibers was done with a hand lay-up technique, and the final laminate lay-up is unidirectional comprised 8 laminas, $[0°]_8$. An aluminum foil strip was placed between the 4th and 5th laminas in order to introduce a delamination front. The strip orientation and dimensions were such to allow the cutting of samples for the "Double-Cantilever Beam" (DCB) test, with a delamination crack length of 50 mm. After impregnation the prepared composite was inserted between two aluminum plates, pressed by clamps in order to create an uniform thickness. The dimensions of the system were 20x25x0.4 cm.

The e-beam irradiation of the blends has been realized using the LAE 10 MeV linear, pulsed accelerator located in the laboratory of the ICHTJ (Inst. of Nuclear Chemistry and Technology) of Warsaw. The previously prepared uncured composites have been positioned in a horizontal position in the front of the pulsed beam. The temperature of the sample during the irradiation is a very important factor and it can affect the properties of the material. In order to monitor the sample's temperature a thermo-resistor was inserted in the blend and during the irradiation a thermal profile was registered. Due to the different reactivity, 0.5phr and 1phr of initiator has been used for 0PES and10PES respectively. The curing reaction has been followed by monitoring the temperature during the irradiation. After e-beam curing, the material was characterized by means of thermal and morphological analysis.

Radiation cured composites have been subjected to hydrothermal ageing by immersion of the samples in distilled water at 70 °C for two periods, 1 week and 1 month respectively. After reaching the desired ageing time, all materials have been characterized. The samples have been kept in water at room temperature until characterization tests, which were performed within few days from the end of hydrothermal treatments.

Thermal properties of both not-aged and aged materials have been determined through Dynamic Mechanical Thermal Analysis using a Rheometrics DMTA V instrument, single cantilever bending method. The test has been done in temperature swift mode, between 25-250 °C and a heating rate of 2 °C/min. The frequency was set to 1.8 Hz and the strain was 0.02 %. The storage modulus (E') and loss factor (tan δ) versus temperature (T) were recorded. The glass transition temperature was determined by tan δ peak.

Two types of beams samples were analyzed with DMTA, the first with the unidirectional fibre direction aligned with the beam axis, $[0°]_8$, and the second with the fibres direction oriented orthogonally to the beam axis, $[90°]_8$.

The laminate material has been also tested in order to evaluate its delamination fracture toughness in Mode I crack opening on DCB ("Double Cantilever Beam") samples [Reeder 1992]; this resulted in the evaluation of the critical Strain Energy Release Rate, G_{IC}, i.e. the value at which crack propagation in the material is started. The DCB samples (shown in Figure 1) had dimensions complying with the standard [ASTM D5528], and in particular: B = 20 mm, $2h$ = 4 mm, L > 125 mm, a_0 = 35 mm.

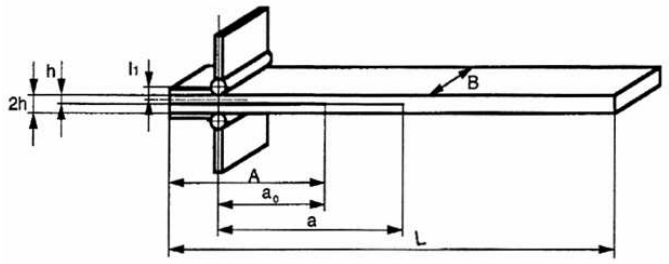

Figure 1. Scheme of a DCB test for delamination fracture toughness characterisation.

The initial crack length, obtained with the embedded thin aluminium foil, has length *A*, and is placed at the middle panel thickness. Two hinges are bonded at the far end of the delaminated fronts by using a bi-component cyanoacrilate adhesive applied, after the adhered surfaces were grinded with thin emery paper and cleaned and degreased with an opportune solvent. A white paint was applied upon the thickness surface on one side of each DCB sample in order to enhance the visual contrast with vertical lines drawn with a marker pen at one mm distance. This drawn scale is used to monitor the crack length changes during the crack propagation (see Figure 2).

The DCB samples where then mounted on the loading machine by gripping the free wing of the hinges on common wedge grips employed for tensile tests. The testing machine employed was an electric Instron 3367 rig equipped with a 1 kN load cell and controlled with the Instron Blue Hill software which allowed the synchronous measure of the load *P* and the crosshead displacement which is also the separating displacement between the two delamination fronts at the hinge location, *d*. The load versus displacement curve is measured by running each test in displacement control, i.e. at a given fixed crosshead rate. The length of the growing crack *a* is measured manually by the operator by locating the crack tip on the zoomed images of the sample painted side, taken with a digital video camera. Images where captured at determined displacement values, monitored by means of the testing machine software, in order to synchronise the crack length measurements with the corresponding load and displacement values.

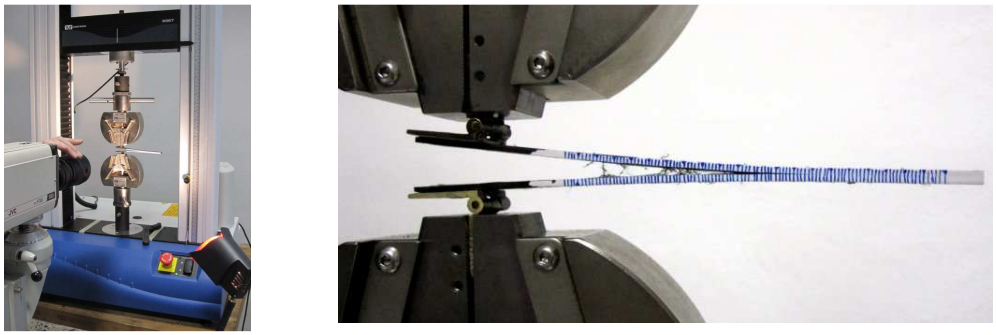

Figure 2. Images of the DCB test set-up and of a DCB sample during propagation of the delamination.

3 RESULTS AND DISCUSSION

As it is well known, e-beam curing can be considered a “cold” process because it does not need thermal activation, but during irradiation the temperature can significantly increase due to different thermal effects [Alessi et al. 2005]. For this reason the temperature of the irradiated sample is recorded during irradiation.

The thermal profiles, i.e. the temperature values as function of the irradiated dose, (here not reported) are very similar for both 0PES and 10PES systems and do not pass over 70 °C during the whole

curing process. In these irradiation conditions the influence of the temperature is minimal and the curing is realized mainly by the e-beam process.

3.1 DMTA Tests

The dynamic mechanical thermal behaviour has been studied for all e-beam cured carbon fiber composites (0PES and 10PES), considering both longitudinal and transversal samples. In the comparison between the samples differently cut it has to be taken into account that in the longitudinal samples the main response comes from fibers (high modulus) while for perpendicular samples the response is mainly generated by the epoxy matrix and the matrix-fiber interface.

In Figure. 3 DMTA curves for 0PES and 10PES samples produced by irradiation and transversally cut are reported. Similar qualitative behaviour are presented by longitudinally cut samples.

In all cases two main relaxation peaks in tanδ/T curves have been observed, with a broader extension for the peak at low temperature. The presence of two relaxation peaks can be attributed to the formation of a "not uniform" structure, consisting of portions having different cross-linking densities, which relax at different temperatures. This behaviour has been already observed for radiation cured epoxy matrices and is related to vitrification effects of the polymerizing resin due to the low process temperature [Alessi et al. 2005, 2007-a, 2007-b]. In fact when radiation curing is performed at mild temperature, as in this case, the glass transition temperature of the material soon approximates the cure temperature and the cure reactions become controlled by diffusion processes.

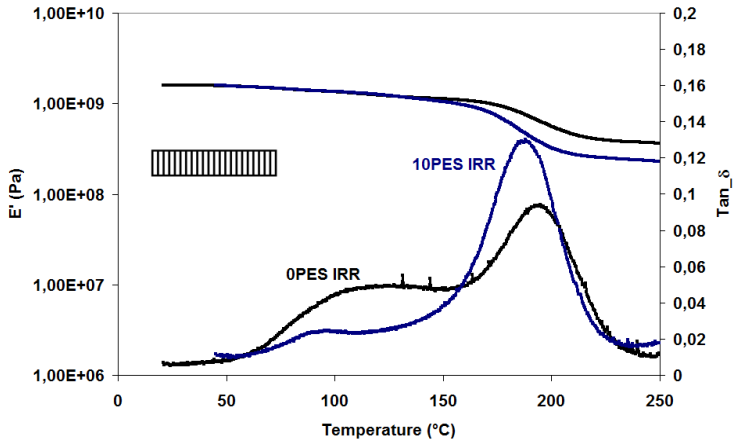

Figure 3. Tan δ and storage modulus vs temperature for 0PES and 10PES transversal, only irradiated.

In Table 1 the water uptake values of the irradiated samples are reported as M_t, with $M_t = (m_t - m_0)*100/m_0$, where m_t was the weight at immersion time t and m_0 that one before immersion.

Table 1. Water uptake for irradiated systems as $M_t = (m_t - m_0)*100/m_0$.

Systems	1 week hydrothermal ageing	1 month hydrothermal ageing
0 PES	1 %	1.5 %
10 PES	3 %	5 %

In Figure. 4 DMTA curves are presented for 0PES e-beam cured carbon fiber/epoxy transversal composites, after performing hydrothermal ageing for 1 week All the other DMTA curves, for 10 PES and for longitudinally and transversally cut samples, show similar qualitative behaviour.

After 1 week hydrothermal ageing the systems show only one relaxation peak at an intermediate temperature between the initial peaks. This effect is similar to that already observed in epoxy matrices hydrothermally aged after e-beam curing [Alessi et al. 2010]. It can be interpreted by the occurring of a combined effects of plasticization and degradation of the matrix, responsible of the decrease of the peak from high temperature, and a thermal post-curing which causes an increase of the peak from low temperature [Colombini et al. 2002], [Zhou and Lucas 1999].

After 1 month ageing DMTA curves show a further decrease of the relaxation temperatures even if with a minor extension compared to that observed after 1 week.

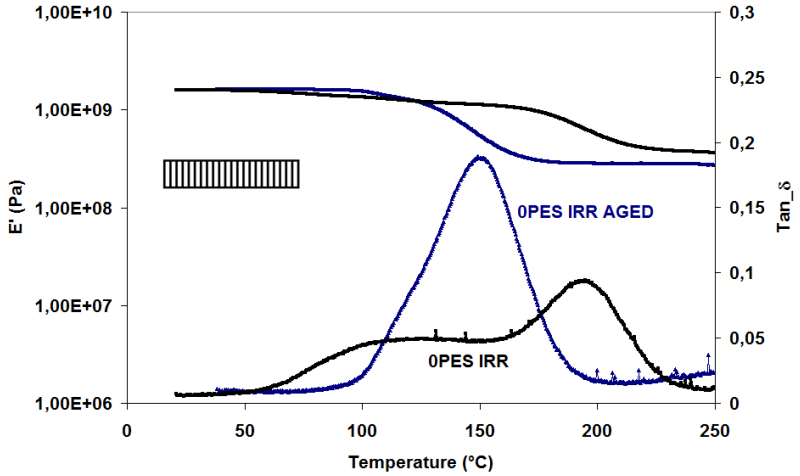

Figure 4. Tan δ and storage modulus vs temperature for 0PES transversal irradiated and 1 week aged.

In Table 2 a summary of the relaxation temperatures for all studied samples is presented. In general, after hydrothermal ageing, a more marked effect is observed for longitudinal samples than transversal ones, probably due to a strong decrease of interaction between fiber and matrix. In this respect it is worth to note that fiber sizing of the used fibers was designed for thermal curing and then the optimization for radiation curing should be considered in order to reach better hydrothermal ageing resistance.

Table 2. Glass transition temperatures for 0PES and 10PES.

Systems	Cure conditions	Sample type	Relaxation temperatures (not aged) [°C]	Relaxation temperature (after 1 week ageing) [°C]	Relaxation temperature (after 1 month ageing) [°C]
0 PES	Irradiated	Transv.	120, 195	152	150
		Long.	109, 200	150	145
10 PES	Irradiated	Transv.	95, 188	156	145
		Long.	125, 198	144	140

3.2 DCB Tests

Figure 5 shows the load vs displacement curves from Double Cantilever Beam tests on not aged samples. Although several tests were carried out for each beam type and aging condition, only one curve for each sample is reported for clarity.

In the case of untoughened samples (i.e. CFRP laminates adopting the untoughened resin batch) it is observed (see Figure. 5(a)) that after the first pseudo-linear stage the curve decreases with a rather irregular trend. This is probably caused by a non uniform and gradual crack growth accompanying the hinges displacement.

The same rough trend is still observable and even more marked in toughened samples (see Figure. 5(b)). One possible explanation is given the presence of PES agglomerates dispersed within the matrix, and observed by means of SEM micrographs. The tougher behaviour of this clustered PES rich phases act as an obstacle to a continuous smooth crack propagation. This determines the mechanical energy to accumulate, e.g. when the crack front reaches a PES reach area, as suggested by the load/displacement curve growing again after crack propagation onset. As soon as enough mechanical energy is stored then this is suddenly released generating a crack pop-in mechanism of crack growth (see Figure. 5(b)). When enough energy is accumulated the sudden crack pop-in releases the load very rapidly. By post-processing the measured load, displacement and crack growth data for the DCB geometry it is possible to evaluate the delamination crack resistance R-Curve of the material for the different analysed conditions. Figure 6 shows the curves of the energy G versus the crack length a.

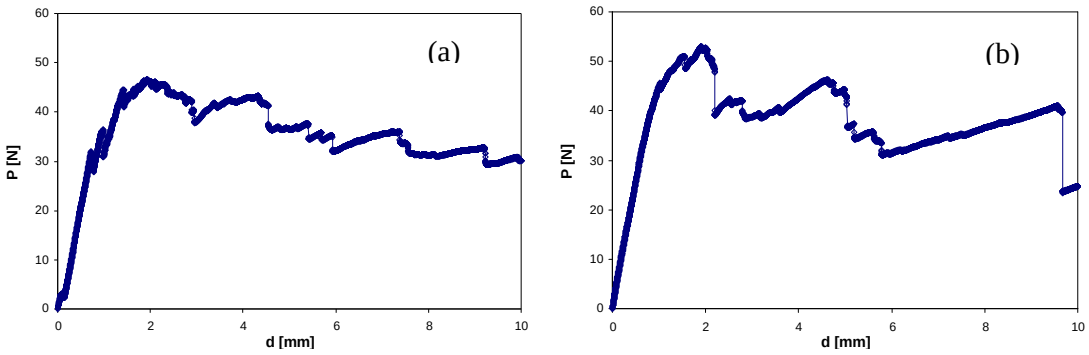

Figure 5. DCB test: load *vs* displ. curves for unaged DGEBA (a) and DGEBA+10phr PES (b) based composites.

In particular Figure 6(a) compares all curves from untoughened samples with different aging periods; it is noticed that this curves have a rather irregular but clearly growing trend. It seems that the curves become smoother at longer aging times, and this might be due to plasticizing phenomena induced in the resin matrix as aging is prolonged.

In Figure 6(b) the toughened material is considered. Again the curves evidence a general growing trend. Irregularity is now more marked then the untoughened material but it decreases significantly as the aging period is longer.

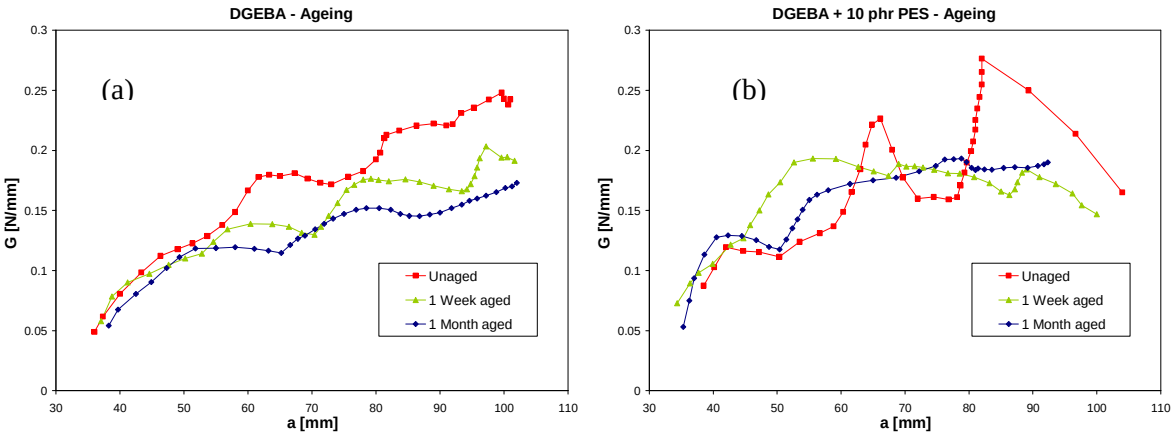

Figure 6. DCB test: resistance curves for DGEBA (a) and DGEBA+10phr PES (b) based composites.

Values of fracture toughness G_{IC} at crack propagation onset (i.e. at $a=a_0$) are summarised in Figure 7. This diagram shows that for the same aging time the toughened material has a higher delamination resistance than the untoughened one. The results obtained in this work show also that for the same

material the implemented aging procedure has not determined a meaningful variation of the initial crack resistance, i.e. of the critical fracture toughness.

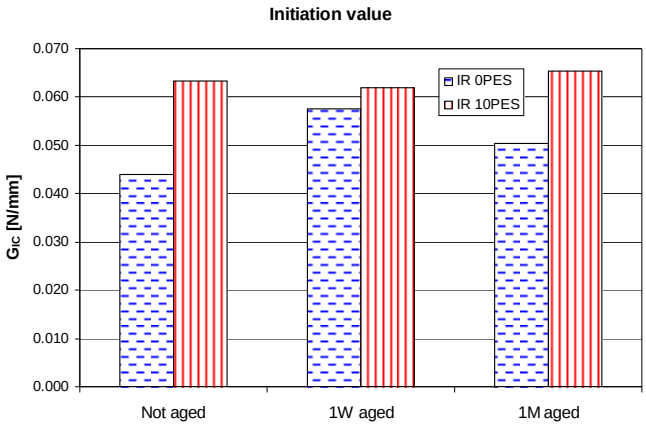

Figure 7. DCB test: initiation values of crack resistance.

4 CONCLUSIONS

In this work CFRP panels with a unidirectional fibre stacking sequence have been characterised after conditioning with different aging conditions. The tested material in particular uses a resin formulation suitable for radiation curing and has been manufacture by hand lay-up and cured with an e-beam accelerator. Two resin formulations have also been adopted, an untoughned DGEBA system and a toughened system obtained by mixing DGEBA with 10 phr of a PES monomer. Characterisation has been carried out through DMTA tests and mechanical delamination tests on DCB samples for fracture propagation in mode I. The aging influence on toughened and untoughened systems was then studied by characterising the materials glass transition temperature Tg, the critical initial fracture toughness at delamination and the crack resistance curve.

In general it was observed that dispersion of PES rich phases can have a strong influence on the crack propagation behaviour. The use of a toughened resin seems to promote an increase in the critical fracture toughness while this value was not significantly affected by the ageing procedure.

REFERENCES

Alessi S., Calderaro E., Parlato A., Fuochi P., Lavalle M., Corda U., Dispenza C., Spadaro G. 2005, 'Ionizing radiation induced curing of epoxy resin for advanced composites matrices.', *Nuclear Instruments and Methods in Physics Research B*, **236**, 55-60.

Alessi S., Parlato A., Dispenza C., De Maria M., Spadaro G. 2007, 'The influence of the processing temperature on gamma curing of epoxy resins for the production of advanced composites', *Radiat. Phys. and Chem.***76,** 1347-1350.a

Alessi, S., Dispenza, C., Spadaro, G. 2007 , 'Thermal properties of e-beam cured epoxy/thermoplastic matrices for advanced composite materials', *Macromolecular Symposia* **247,** 238-243. b

Alessi S., Conduruta D., Pitarresi G., Dispenza C., Spadaro G., 2010, 'Hydrothermal ageing of radiation cured epoxy resin-polyether sulfone blends as matrices for structural composites', *Polymer Degradation and Stability* **95**, 677-683.

ASTM Standard D5528-01, 'Standard Test Method for Mode I Interlaminar Fracture Toughness of Unidirectional FiberReinforced Polymer Matrix Composites'. USA, 2001.

Colombini D., Martinez-Vega J.J., Merle G., 2002, 'Dynamic mechanical investigations of the effects of water sorption and physical ageing on an epoxy resin system', *Polymer* **43**, 4479-4485.

Feraboli P., Masini A., 2004, 'Development of carbon/epoxy structural components for a high performance vehicle'**,** Composites: Part B, **35,** 323–330.

Goodman, D. L. & Palmese, G. R., 2002, 'Curing and Bonding of Composites using Electron Beam', in *Handbook of polymer blends & composites*, Kulshreshtha, A. K. and Vasile, C. vol. 1, ch. 11, RAPRA Technology Ltd, Shropshire, UK.

Hufenbach W., Böhm R., Thieme M., Winkler A., Mäder E., Rausch J., Schade M., 2011, Polypropylene/glass fibre 3D-textile reinforced composites for automotive applications', *Materials and Design* **32**, 1468–1476.

Lopata, V., Saunders, C.B., Singh, A., Janke J.C., Wrenn**,** G.E., Havens, S.J.,1999, 'Electron-beam curable epoxy resins for the manufacture of high-performance composites', *Radiation Physics and Chemistry*, **56**, 405-415.

Mimura, K., Ito, H., Fujioka, H., 2000, ' Improvement of thermal and mechanical properties by control of morphologies in PES-modified epoxy resins', *Polymer*, **41**, 4451-4459.

Reeder, JR., 1992, 'An evaluation of mixed-Mode delamination failure criteria', Technical Memorandum-1992-104210, NASA Langley Research Center.

Zhou J., Lucas J.P., 1999, 'Hygrothermal effects of epoxy resin. Part II: variations of glass transition temperature', *Polymer* **40**, 5513-5522.

XII DBMC
International Conference on Durability of Building Materials and Components
PORTO - PORTUGAL, April 12th-15th, 2011

Durability Test Designed for Double Glazing Units with Interjacent Light-deflecting System

Andreas Zegowitz [1]
Hartwig M. Künzel [2]

ABSTRACT

For double glazing units with a light-deflecting system in the cavity between the glass panes, a service life of at least 20 years should be expected. The durability of such a unit depends on the resistance of the glass itself, the unit's edge sealing system and the light-deflecting system against the environmental loads acting upon the glazing unit, when installed as a translucent roof element in the building. To verify the durability of the edge seal and of the solar reflectivity of the light-deflecting system factory-made samples of the glazing units, mostly with original dimensions, were exposed to alternating and constant hygrothermal loads. This included different ambient temperatures and humidity conditions on both sides of the units as well as exposure to artificial sunlight. For the evaluation of the test results the experience with standard tests on insulating glazing systems served as a basis. Thermal transmittance, total energy transmittance, light transmission, adhesion of the sealants and diffusion resistance of the sealants used at the glass edge, gas content und dew point temperatures of the gas in the gap between the glass panes, moisture content of the drying agent in the spacer, temperature resistance of the light deflection system, linear expansion of the deflection system and thickness changes of the gap between the panes were considered. The knowledge gained from these tests led to the optimization of the manufacturing process, the edge sealing and the glazing unit.

KEYWORDS

Double glazing unit, Light-deflecting system, Durability, Sealant, Gas content, Dew point temperature, Translucent roof.

[1] Fraunhofer Institute for Building Physics (IBP), Stuttgart, GERMANY, andreas.zegowitz@ibp.fraunhofer.de
[2] Fraunhofer Institute for Building Physics (IBP), Holzkirchen, GERMANY, hartwig.kuenzel@ibp.fraunhofer.de

1 INTRODUCTION

The Fraunhofer Institute for Building Physics in Stuttgart was mandated to test double glazing units with solar control and an anti-glare system in the gap between the glass panes to determine the operational reliability and serviceability of the system. The double glazing units with a solar control system were to be integrated into the glass roof of a museum to achieve indirect and glare-free lighting of the objects exhibited there. The system was a new development and so far only once integrated into a building. Investigations were to be conducted on test specimens with original dimensions, if possible, to achieve maximum safety concerning the actual performance of the glazing system with the light-deflecting system. The investigations included the quality of the edge bond, i.e. tightness, temperature resistance, adhesion, behaviour of the solar control and anti-glare system in the gap between the glass panes under temperature and moisture load and artificial sunlight as well as standard glazing parameters, e.g. thermal transmittance, total energy transmittance and light transmission coefficients.

2 INVESTIGATIONS

2.1 Investigated Glazing Units and the Light-deflecting System

The double glazing units to be investigated with solar control and anti-glare system in the gap between the glass panes were at first designed with one low-E layer and argon, then with two low-E layers and krypton in the gap between the glass panes as described in the following (see Fig. 1):

8 mm toughened safety glass, white glass with heat soak test (HST), with black screen printing on the edges and low-E layer on Pos 2,
24 mm gap between the glass panes with light-deflecting system of aluminium-coated plastic and krypton filling, Thiokol edge sealing,
14 mm laminated safety glass with 2 x partially tempered glass, white glass and 3.04 mm PVB film, with black screen printing on the edges and low-E coating on Pos 3.

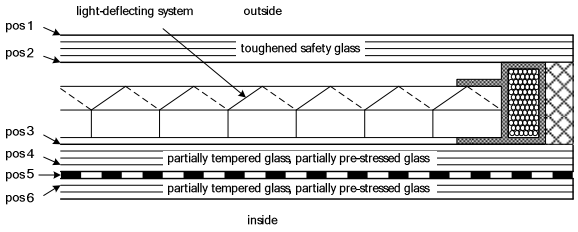

Figure 1. Cross section of the glazing unit with solar control and an anti-glare system in the gap between the glass panes.

2.2 Test Plan

Operational reliability and durability of the glazing system with a light-deflecting system is achieved if characteristics like thermal transmittance, total energy transmittance, light transmission coefficient, anti-glare control, condensation control in the gap between the glass panes, durability of the glass, durability of the glass edge bond and plastic inlays, as well as the required optical appearance are guaranteed for a period of at least 20 years. The standards EN 1279-1 to EN 1279-6 contain tests and guidelines for insulating glazing units, which are assumed to predict the serviceability of the glasses over a period of use of more than 20 years. Practical experience shows that the majority of glasses really fulfil the requirements of functionality over more than a period of 20 years. The question was whether the investigated double glazing unit with the light-deflecting system would also pass these standard tests. Another question was whether the durabilty of the integrated light-deflecting system

will match the predicted service life of the whole unit. To answer these questions the following investigations were conducted:

- Determination by measurement of the thermal transmittance according to DIN EN 674
- Checking of the moisture absorption of the drying agent through the glass edge bond according to DIN EN 1279-2: 2003-06 with the following test sequence:
  - Determination of the gas contents of the new and the artificially weathered glazing units,
  - Optical testing of the glazing surfaces and of the glass edge bond as well as of the light-deflecting system for damage,
  - Compliance check of the linear expansion of the light-deflecting system in the tested temperature range and of the edge distances,
  - Checking of the thickness change of the glazing and the dilatation of the light deflecting system,
  - Adhesion of the sealant/spacers.
- Fogging test
- Total energy transmittance at various angles of solar radiation
- Light transmission coefficient at various angles of solar radiation
- Testing of the durability and determination of the maximum temperatures to be expected in the gap between the glass panes under solar radiation.

2.3 Thermal Transmittance

First of all, thermal transmittance according to EN 674 was determined at samples of the glazing with the interjacent light-deflecting system. The result of 1.4 W/m²K was clearly less favourable than the required value of 1.1 W/m²K. The reason was that the thermal conductivity of the interjacent light-deflecting system made of plastics decreases the R-value.

Then, the following modifications of the system were carried out: argon was replaced by krypton as gas fill, and another low-E layer was added on Pos. 3 (Pos. 2 already had a low-E coating). The test of the thermal transmittance of the modefied glazing units showed a considerable improvement of the U-value to Ug = 0,98 W/(m²K) [IBP 2009, Prüfbericht P1-036/2009].

2.4 Tests under Alternating and Constant Hygrothermal Loads

To test the moisture diffusion through the glass edge sealing and to check the behaviour of the inlay under alternating thermal loads, the test plan according to DIN EN 1279-2: 2002 was chosen. In contrast to the standard test with small samples, test specimens with original dimensions were horizontally stored and exposed to alternating thermal loads in the climate chamber (Fig. 2) [IBP 2009, Prüfbericht P17-035/2009].

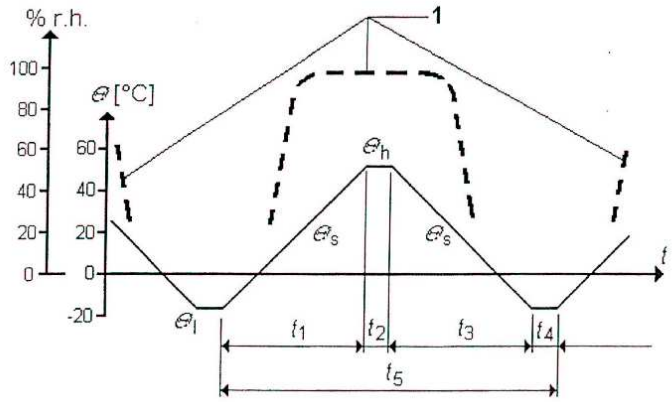

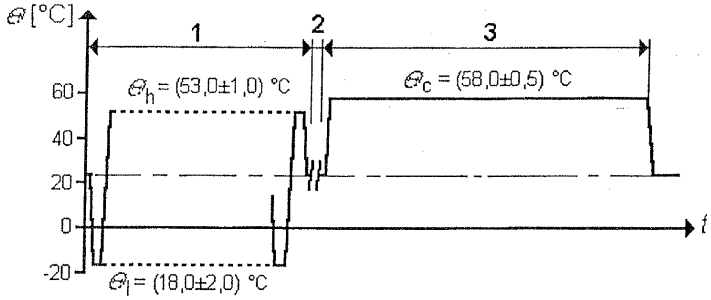

Figure 2. Test phase A (top figure and lower figure phase 1):

56 thermal cycles of 12 hours each according to DIN EN 1279-2: 2002 with temperatures between -18 °C and 53 °C and relative humidities of up to 100 % r. h.
Explanatory notes for the draft:
t 1 = 5 h, t 2 = 1 h, t 3 = 5 h, t 4 = 1 h, t 5 = 12 h.
Test phase B (lower figure phase 3):
7 weeks of constant load with a constant temperature of approx. 58 °C and a relative humidity of ≥ 95 % r. h. according to DIN EN 1279-2: 2002.



Figure 3. Photo of the test glazing units at a temperature lower than 0 °C in the climate chamber. Ice formation is clearly visible on the surfaces of the glazing units.

2.4.1 Test procedure

In a first step, three glazing units with light-deflecting systems according to test phase A (Fig. 1) were exposed to temperatures between 53 °C and -18 °C over a period of 4 weeks (56 thermal cycles) with simultaneous humidification of the samples in the positive temperature range at approx. 95 % r. h. In two further test cycles the samples were exposed to alternating thermal loads according to test phase A as well as according to test phase B with additional constant climatization at 58 °C and at least 95 % humidity over a period of 7 weeks.

2.4.2 Gas contents

After a first thermal cycle the gas content of the krypton filling in the gaps from 51 % to 83 % krypton (rest oxygen) of the samples was identified by the Institute of Materials Testing in Darmstadt [MPA 2008, Untersuchungsbericht B 08 1593] with gas chromatography (GC) and oxygen Analyser whereby the unloaded reference specimens also had gas contents below the specified value of 90 %. The reason was that manufacturing difficulties occurred when putting gas into the glazing units with interjacent inlay, since the inlay complicated the filling and the period of filling was significantly longer. Measurements of the gas content after the second test cycle showed similar problems. After the third cycle the problems were solved.

2.4.3 Moisture loading of the drying agent in the spacer

The determination of the moisture loading of the desiccant in the spacers showed that the desiccant of the four investigated glazing units had moisture contents from 14 % to 15 % with an increasing total absorption capacity of approximately 20 %. For the initial moisture loading of the desiccant a value of ≤ 3 % is specified as a requirement for the manufacturer according to DIN EN 1279-6: 2002-10. The reason for the high moisture contents was, and this was only identified by additional investigations, that the inlay, made of plastics, emitted humidity into the gap between the glass panes and thus loaded the desiccant in the spacers with humidity far beyond the value of 3 %. A strong moisture absorption through the edge sealing by alternating thermal loads could not be identified due to the approximately equal loading of the desiccant for the new as well as artificially weathered glazing units.

2.4.4 Expansion of the light-deflecting system

The determination of the linear expansion of the inlay and the thickness reduction of the gap between the glass panes showed that there was sufficient space left for expansion in length, width and thickness for the inlay.

2.4.5 Adhesion of the sealant on the upper surface of the spacer

When dismantling the glazing units at the Institute of Materials Testing in Darmstadt it was observed that while stripping the sealant from the upper surface of the spacer an adhesion crack occurred instead of a cohesion crack (Fig. 4) although the sealant tests according DIN EN 1279-6 has been passed. This was, however not considered to be the cause for the high moisture loading of the desiccant and not a result of the accelerated aging as we found out later.

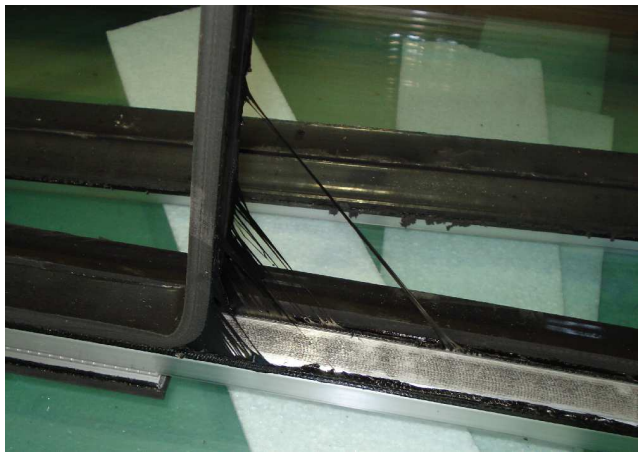

Figure 4. Photo taken while stripping the sealant from the upper surface of the spacer.

2.5 Consequences from the Tests with Alternating and Constant Hygrothermal Loads

By controlled and documented pre-drying of the inlays before integration in the gap between the glass panes, as well as the application of a double quantity of desiccant in the spacer, humidity input through the inlay into the desiccant of the spacer was reduced and the moisture absorption capacity of the desiccant was doubled. Relocating manufacturing to another company for probe filling achieved gas contents of more than 80%. Thicker sealants achieved higher safety of adhesion and diffusion resistance in the edge bonding. Stricter quality controls during the manufacturing process in combination with external controls by testing institutions should secure a permanently high quality in manufacturing.

2.6 Behaviour under Solar Radiation

2.6.1 Radiation parameters

To determine the behaviour under solar radiation the total energy transmittance (g-value) and light transmittance at various elevation angles of the sun were measured. The g-values were determined by calorimetry and amounted to approximately from 0.1 to 0.23 according to the respective elevation angle. The hemispheric (diffuse) light transmission amounted to 0.15 [ISE 2009, Bericht TAG3-UA-0901-E01].

2.6.2 Fogging-Test

To check whether a chemical precipitate occurs on the surfaces of the glazing units at an elevated temperature due to solar radiation the fogging test was conducted according to DIN EN 1276-6, but at an elevated temperature of 80 °C in contrast to the standard method. No chemical precipitate occurred on the surfaces of the glazing units.

2.6.3 Long-term exposure to sunlight

To investigate the durability and service life of the glass and light-deflecting system two test specimens were exposed to cyclic artificial sunlight on parts of the surfaces by a bank of lamps according to DIN EN ISO 12543-4: 1998-08 under summer and winter thermal boundary conditions over a period of 4 weeks. The duration of the exposure to artificial sunlight of e.g. 2,000 hours as required in DIN EN ISO 12543-4: 1998-08 was not possible due to the limitations imposed by the client. The intensity of radiation was adjusted to 600 W/m², deliberately not at a maximum value to be expected. Fig. 5 shows the test of long-term exposure to sunlight in the climate simulator [IBP 2009, Prüfbericht P17-035/2009].



Figure 5. Photos of the test under cyclic long-term exposure to sunlight.

2.6.4 Determination of the maximum temperature in the gap between the glass panes

To determine the expected maximum temperatures in the gap between the glass panes the Fraunhofer Institute for Solar Energy Systems conducted tests of exposure to sunlight in the g-value test facility with exposure intensities of approximately 1,000 W/m² and approximately 1,200 W/m² [ISE 2009, Bericht TAG3-UA-0905-E06]. Temperatures in the gap between the glass panes of more than 90 °C led to the assumption that failure of the aluminium-coated plastic inlay with a permissible maximum temperature of approximately 95 °C could not be completely excluded under the expected maximum solar radiation of approximately 1,050 W/m².

3 SUMMARY

To check the durability of a new glazing system with interjacent light-deflecting system the test specimens were exposed to alternating and constant hygrothermal loads, long-term exposure to sunlight by medium radiation intensity and short-term exposure by maximum radiation intensity, and relevant physical parameters were determined.

The results showed that modifications to the system were necessary e.g. a second reflecting glass coating, krypton instead of argon in the gap between the glass panes, widening of the sealing of the glass edge and the doubling of the drying agent in the spacer. Moreover, quality control measures were taken such as more detailed quality monitoring with pre-drying and gas-tight packaging of the plastic inlay as well as external control of the manufacturing processes of the glazing systems within short periods of time. The problem that the temperatures in the gap between the glass panes could reach the maximum permissible temperature of the plastic material used for the light-deflecting system under an unfavourable angle of the sunlight remains to be solved. The most obvious solution would be the selection of a plastic material with a higher temperature resistance.

REFERENCES

DIN EN 1279-2: 2003-06: Mehrscheiben-Isolierglas, Langzeitprüfverfahren und Anforderungen bezüglich Feuchtigkeitsaufnahme. (DIN EN 1279-2:2003-06: Glass in building - Insulating glass units - Part2: Long term test method and requirements for moisture penetration; German version EN 1279-2:2002)

IBP 2009, Prüfbericht P1-036/2009: *Bestimmung des Wärmedurchgangskoeffizienten nach DIN EN 674 an Zweischeiben-Isolierverglasung mit Sonnen- und Blendschutzsystem* des Fraunhofer-Instituts für Bauphysik (IBP), Jan Sigmund, Andreas Zegowitz, Stuttgart vom Februar 2009.

(IBP 2009; Test report P1-036/2009: Determination of thermal transmittance (U value) of a double glazing unit with interjacent light deflecting system).

IBP 2009, Prüfbericht P17-035/2009: *Funktionsprüfungen an Zweischeibenisolierverglasungen mit Sonnenschutz- und Blendschutzraster im Scheibenzwischenraum*, des Fraunhofer-Instituts für Bauphysik (IBP), Andreas Zegowitz, Hartwig Künzel, Stuttgart vom März 2009. (IBP 2009; Test report P17-035/2009: Functional testing at a double glazing unit with interjacent light deflecting system).

MPA 2008, Untersuchungsbericht B 08 1593: *Funktionsprüfung an Zweischeiben-Isolierverglasung mit Sonnenschutzsystem im Scheibenzwischenraum (SZR),* der Staatlichen Materialprüfungsanstalt Darmstadt (MPA), Hans-Jürgen Hosemann, B. Kaiser, vom 15.10.2008. (MPA 2008, Test report B 08 1593: Functional testing at a double glazing unit with interjacent light deflecting system).

DIN EN 1279-6: 2002-10: Mehrscheiben-Isolierglas, Werkseigene Produktionskontrolle und Auditprüfungen. (DIN EN 1279-6: 2002-10: Glass in building-Insulating glass units - Part 6: Factory production control and periodic tests; German version EN 1279-6:2002).

ISE, 2009, Bericht TAG3-UA-0901-E01: *Prüfung der Transmission und des g-Wertes* des Fraunhofer-Institut für Solare Energiesysteme (ISE), Ulrich Amann, Tilmann Kuhn, Freiburg vom Januar 2009. (ISE, 2009, Test Report TAG3-UA-0901-E01: Test of transmission and total engery transmission).

DIN EN ISO 12543-4: 1998-08: Verbundglas und Verbund-Sicherheitsglas, Teil 4, Verfahren zur Prüfung der Beständigkeit. (DIN EN ISO 12543-4:1998-08: Glass in Building - Laminated glass and laminated saftey glass – Part 4: Test methods for durability).

ISE 2009, Bericht TAG3-UA-0905-E06: *Prüfung der Temperaturen im Scheibenzwischenraum von Verglasungen*, Bonn des Fraunhofer-Institut für Solare Energiesysteme (ISE), Ulrich Amann, Tilmann Kuhn, Freiburg vom Mai 2009.
(ISE 2009, Test report TAG3-UA-0905-E06: Test of temperatures between glass panes.).

XII DBMC
International Conference on Durability of Building Materials and Components
PORTO - PORTUGAL, April 12th-15th, 2011

Durability of the Reaction to Fire Performance for FRT Wood Products in Different End Use Applications – A Ten Years Report

Birgit A.-L. Östman [1]
Lazaros D. Tsantaridis [2]

ABSTRACT

A long term experimental study on the maintained reaction to fire performance of fire retardant treated (FRT) wood products over time is presented. It is performed according to a Nordic system and includes accelerated ageing according to different procedures and natural weathering up to ten years. Main conclusions are:

- The hygroscopic properties are unchanged compared to untreated wood for most FRT wood products

- The reaction to fire properties of FRT wood may be maintained after accelerated and natural ageing if the retention levels are high enough

- Several FRT wood products loose most of the improved reaction to fire properties during weathering

- Paint systems contribute considerably to maintain of the fire performance at exterior application

KEYWORDS

Durability, Hygroscopicity, Reaction to fire, Weathering, Wood products.

[1] SP Trätek / Wood Technology, Stockholm, SWEDEN, birgit.ostman@sp.se
[2] SP Trätek / Wood Technology, Stockholm, SWEDEN, lazaros.tsantaridis@sp.se

1 DURABILITY CLASSES FOR FIRE PERFORMANCE - PRINCIPLES AND METHODS

Fire retardant treatments (FRT) may considerably improve the reaction to fire properties of wood-based products and the highest fire classifications for combustible products can be reached, but the maintained reaction to fire performance e g in exterior applications needs to be addressed in order to form a basis for new and reliable wood products with improved fire performance.

Requirements on the durability of fire retardant treatments are not yet mentioned in most national building codes. This is partly caused by unawareness of the problem and new procedures have to be implemented in order to increase the reliability and confidence of fire retardant wood products.

1.1 Interior and Exterior Durability of the Reaction to Fire Performance

Two cases of durability of the fire retardant treatment of wood-based products can be identified. One is the risk for high moisture content and migration of the fire retardant chemicals within the wood product and salt crystallisation on the product surface. These hygroscopic properties of the treated wood-based product can be evaluated by exposure to high relative humidity.

The other case is the risk for decreased fire performance due to loss of the fire retardant chemicals by leaching or other mechanisms. This case is mainly for exterior applications, e g as façade claddings. Maintained fire performance over time has to be verified. Some background information on these cases has been published [Östman *et al.* 2001]. A US study on exterior exposure in ten years is also available [LeVan & Holmes 1986].

A Nordic system with Durability of Reaction to Fire performance (DRF) classes has been developed in order to guide the potential users to find suitable FRT wood products, see Table 1. The new system has been developed upon Nordic initiatives from industry and research [Östman *et al.* 2002]. It consists of a classification system for the properties over time of FRT wood [NT FIRE 054] and suitable test procedures [NT BUILD 504], [NT FIRE 053], all published as Nordtest methods. A draft European standard prEN 15912 [2009] has been on enquiry within CEN.

Table 1. Requirements for DRF (Durability of Reaction to Fire performance) classes of FRT wood products in interior and exterior end use applications according to NT Fire 054.

DRF class		*Existing fire requirements*	*Additional performance requirements at different end use of fire retardant wood-based products* [a]	
	Intended use	*Reaction to fire class, initial*	*Hygroscopic properties*	*Reaction to fire performance after weather exposure*
0	Short term	Relevant fire class	-	-
Int 	Interior applications	- " -	- Moisture content < 30 % - No visible salt at surface - No exudation of liquid	-
Ext 	Exterior applications	- " -	- " -	Maintained reaction to fire performance [b] after - Accelerated ageing or - Natural weathering or - Other referenced ageing method

a) To be fulfilled using material produced using the same manufacturing process and having a similar retention level as for the reaction to fire performance.

b) Criteria for fire testing according to ISO 5660 after weather exposure: RHR ≤ 100 kW/m^2 during 1200 s testing time or THR_{1200s} not increased more than 20 % compared to testing before weather exposure.

The test methods [NT BUILD 504], [NT FIRE 053] to verify the DRF classes are based on ASTM standards [ASTM D 32014], [ASTM D 2898]. The relevant fire class should be tested according to EN or IMO systems [EN 13501-1 2002], [IMO FTP Code]. The problems with maintained reaction to fire performance over time have been known for a long time in the US and the UK.

1.2 Fire Performance

Main fire test method has been the Cone Calorimeter [2002]. In most cases, duplicate tests have been run, since the repeatability has been very good. The time to flashover in the room corner test has been predicted [Östman and Tsantaridis 1994].

1.3 Hygroscopic Properties

The hygroscopic properties of wood products have been determined according to NT Build 504. The method includes the calculation of equilibrium moisture content at two climates, 50 % RH at 23 ^{o}C and 90 % RH at 27 ^{o}C. The requirement for DRF class Int is moisture content below 30 % in the humid climate. Ordinary untreated wood has moisture content below 20 % in the same climate. In addition, possible salt crystallisation at the wood surface and exudation of liquid in the wet climate is observed.

1.4 Accelerated and Natural Weathering

For DRF class Ext, the durability of the fire performance at exterior applications has been studied by accelerated ageing according to NT Fire 053. Both Method A, i e exposure to 12 one-week cycles of simulated rain and drying and Method B which also includes UV radiation have been used.

Natural field exposure is being performed with wood panels facing south, both at vertical (90º) and at 45º slope. In both cases the rear sides of the panels were open. The test field is in the Stockholm area, Sweden. Results are presented for 1, 2, 3, 5 and 10 years.

1.5 Mass Loss During Accelerated and Natural Weathering

The weight of the FRT wood panels has been measured after conditioning at 50 % RH at 23 ^{o}C, both initially and after the weathering procedures. The mass loss during weathering has been calculated as percentage of the total panel weight.

2 WOOD PRODUCTS TESTED

The wood products tested are all wood panelling products, mainly spruce, vacuum pressure impregnated with different fire retardant chemicals. Untreated wood panelling has been used as reference. The initial reaction to fire performance has been determined and estimated to be equivalent to class B or C according to the Euroclass system [EN 13501-1] for the FRT wood products. Untreated wood i Euroclass D. These data have been used as reference for the fire performance after weathering.

Two sets of wood products have been studied, one set of commercial FRT wood products, X, Y and Z, intended for exterior application, a former commercial product, VF, and another set of development products [Östman *et al.* 2006]. All are wood panels impregnated with fire retardants to different levels of retention, see Tables 2 and 3.

The size of the specimen for ageing may have some influence on the effects of ageing due to edge effects. 800 mm long specimen were found to be superior to shorter specimen in a pre-study and have then been used together with edge seals both at accelerated and natural exposure. After the exposures the panels have been cut in a systematic way (with test pieces at the same position from the panels to secure consistency) and used for fire and other tests.

Table 2. Commercial FRT wood products.

FR ID	*Mean FR kg/m^3*	*Thick-ness mm*	*Width mm*	*Approximate initial density kg/m^3*	*Type of panel*
0	-				Tongue and groove with notched rear side
X	25-60	20	135	540	-"-
Y	45-110	20	135	510	-"-
ZA	95-190	22	130	690	Tongue and groove
ZG	170	22	130	660	Tongue and groove, factory primed
VF	70-140	20	135	520	Tongue and groove with notched rear side

Table 3. Development FRT wood products.

FR ID	*FR kg/m^3 **	*Thickness mm*	*Width mm*	*Approximate initial density kg/m^3*	*Type of panel*
-	-	20	100	540	Panel with straight edges
BS	107-347	20	100	640-830	-"-
FP	71-228	20	100	570-670	-"-
DQ	89-290	20	100	570-875	-"-
BH	87-236	20	100	635-790	-"-
MA	216	20	100	585	-"-
SI	84-368	20	100	625-850	-"-
FF	92-169	20	100	647-657	-"-
PhF	413-667	20	100	826-1007	-"-
BZ-15	78- 282	20	100	470-520	-"-
BZ-40	67-191	20	100	469-558	-"-
BZ-30	75-229	20	100	531-544	-"-
NF	115-206	20	100	541-711	-"-
AF	120-251	20	100	560-677	-"-
DF	125-556	20	100	629-1152	-"-
LG	114-536	20	100	614-673	-"-
NS	139-619	20	100	549-680	-"-

* Three retention levels per FR chemical, the range is given in the table

2.1 Paint Systems

Paint systems are usually needed to maintain the fire performance properties of FRT wood products for exterior applications. Four different paint systems have been used, see Table 4. The panels for weathering were 800 mm long and edge sealed, first with an alkyd solvent borne primer and then with a thick coat of a silicone sealer.

Table 4. Paint systems used.

Paint number	*Paint type*	*Number of coats*	*Total amount g/m^2*	*Comments*
1	Alkyd	4 *	530-650 **	1 coat primer oil, 1 coat alkyd primer, 2 alkyd top coats (all products solvent borne)
3	Red paint	1	200	Swedish red paint (water based)
4	Linseed oil	3	400-550 **	2 coats with diluted paint, 30 and 15 % resp, 1 top coat of undiluted paint
6	Wood oil	2	180-200 **	Pigmented oil

* only 2 top coats on factory primed panel, total amount 250 g/m^2;
** the higher amount on panel type Z

3 HYGROSCOPIC PROPERTIES

The hygroscopic properties of FR treatments as a function of the retention level are illustrated in Figure 1. The moisture content is unchanged compared to untreated wood for several FRT wood products.

It is evident from the test data that the moisture content may increase with increased amount of fire retardant chemical added. It is thus important to optimise the FR content not only from an economical point of view, but also to reach the intended fire performance with a safety margin to maintain the fire performance during service life of the product but not jeopardizing the moisture resistance.

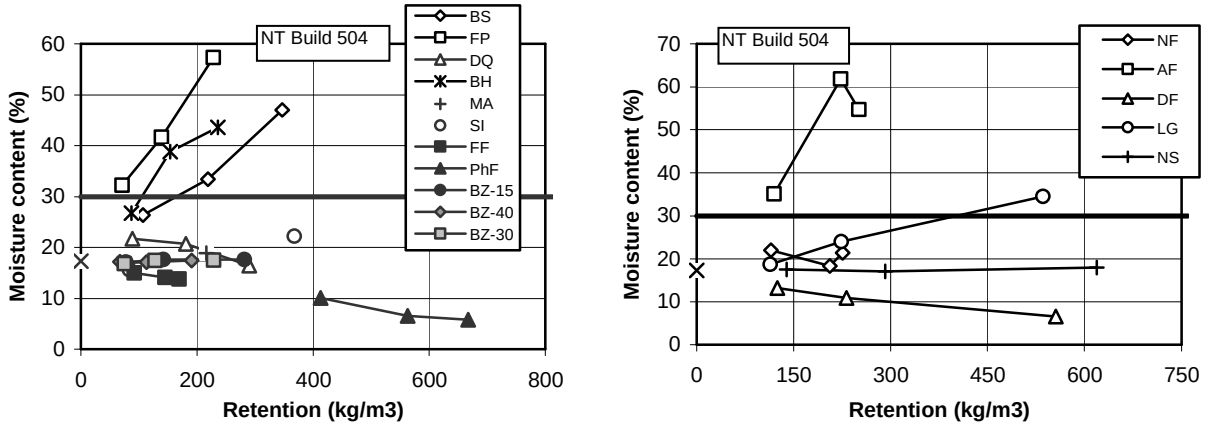

Figure 1. Moisture content at high RH vs retention for FR chemicals and for untreated pine sapwood.

4 COMPARISONS OF REACTION TO FIRE PERFORMANCE

The reaction to fire performance has been determined in the cone calorimeter at 50 kW/m^2. All results for the initial reaction to fire performance and after accelerated ageing and natural weathering are summarised and compared in Figure 2. The comparison is based on predicted time to flashover [Östman and Tsantaridis 1994]. Several products exhibit high initial reaction to fire performance, but it may be reduced over time during both accelerated and natural weathering.

Comparison of weathering exposures at vertical (90º) and at 45º slope is presented in Figure 3. No major difference can be observed.

5 DURABILITY OF THE REACTION TO FIRE PERFORMANCE

The reaction to fire performance is reduced both after accelerated ageing and natural field exposure for most of the FRT products. Only a few FRT products maintain a high fire performance after accelerated and natural exposures. The best performance is found at high retention levels and for FRT products with paint as a protective surface coat. Among the paints, the linseed oil paint and the factory primed product were found to exhibit a full maintenance of the reaction to fire performance. The other FRT products were more or less degraded during the weathering exposure, regardless of a protective coat or not. For products with low retention of FR chemicals and low initial fire class, the maintenance of the fire performance could not be evaluated.

The accelerated ageing according to NT Fire 053 seems to be equivalent to maximum 5 years natural field exposure. However, it should be noticed that the field exposure includes also a certain degree of acceleration. The 45° exposure was intended to include some acceleration, but no major difference to the vertical (90°) orientations was found, see Figure 3. One of the products, ZG, indicates instead a

more severe degradation at the vertical orientation. This may be explained by the lack of protection on the rear side of the vertical panels, which were open to the weather exposure. On the other hand, the panels at 45° slope, were at least partly protected on the rear side from direct influence of rainfall and snow. In a real end use, e.g. as a facade cladding, the rear side is totally protected. Such conditions have to be studied further before a more clear guidance on the accelerating factors can be established.

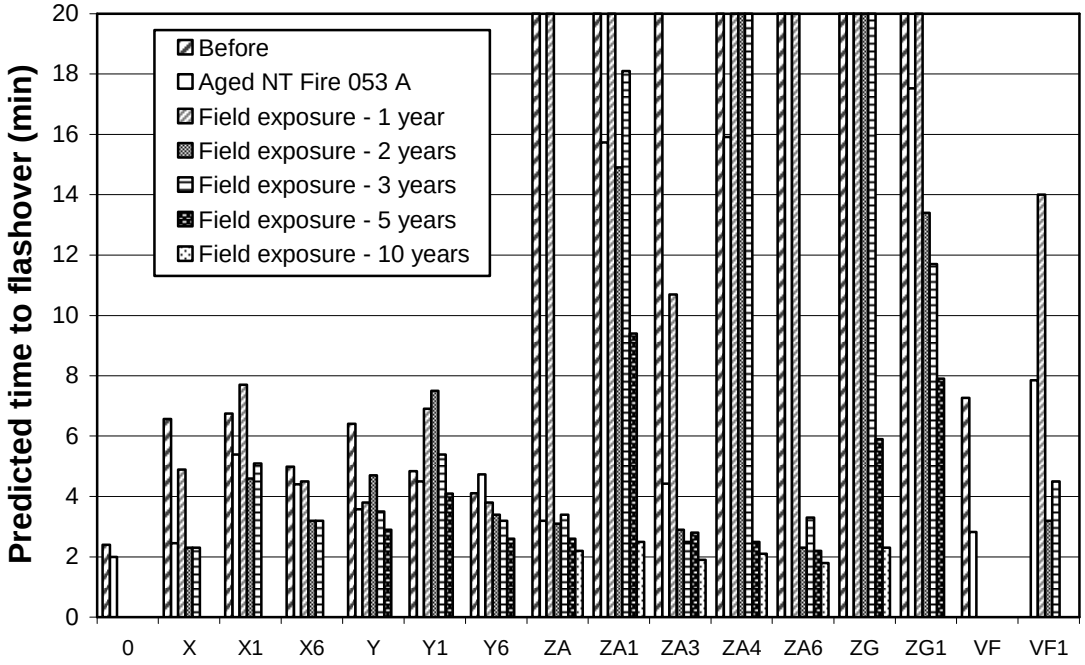

Figure 2. Reaction to fire performance (as predicted time to flashover) before and after accelerated ageing according to NT FIRE 053 Method A and after natural weathering at 45º slope during up to 10 years. Untreated spruce (0) and FR treated (X, Y, ZA, ZG and VF) spruce. Surface coatings with paints nr 1, 3, 4 and 6 are included.

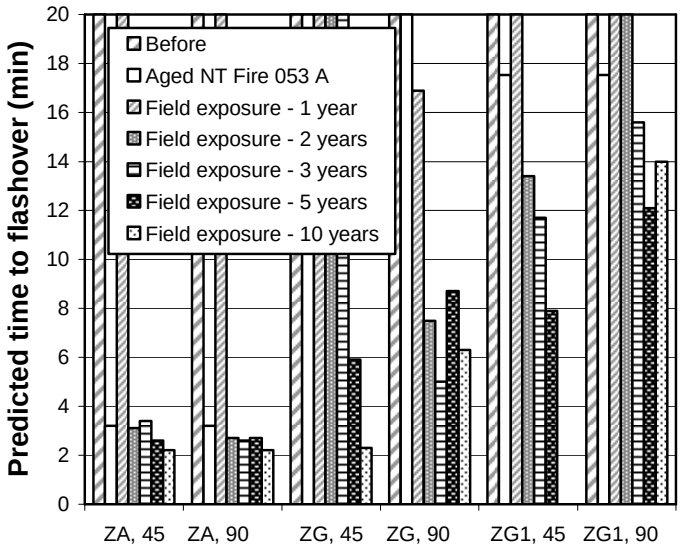

Figure 3. Comparison of reaction to fire performance after natural field exposure during up to 10 years with wood panels vertical (90º) and at 45º slope.

6 MASS LOSS DURING WEATHERING

The mass loss during accelerated aging and natural weathering may be used as an indicator of the maintained reaction to fire performance over time. Some data are presented in Figures 4-5.

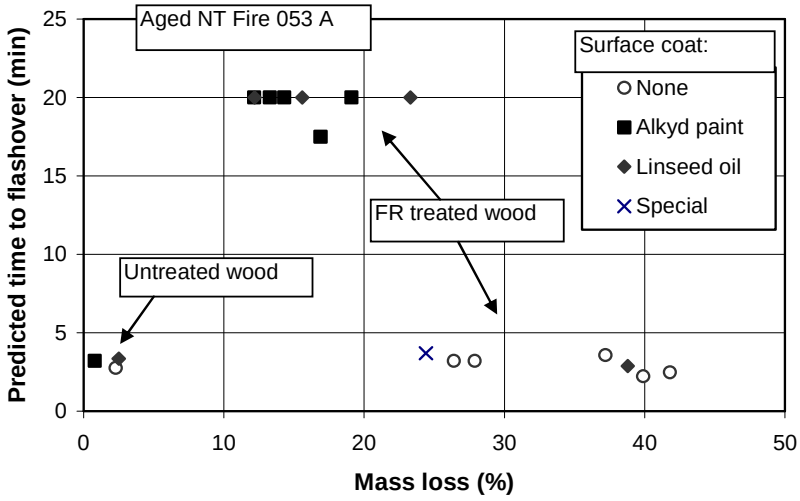

Figure 4. Reaction to fire performance (as predicted time to flashover) vs mass loss during accelerated ageing of FRT and untreated wood according to NT Fire 053 Method A.

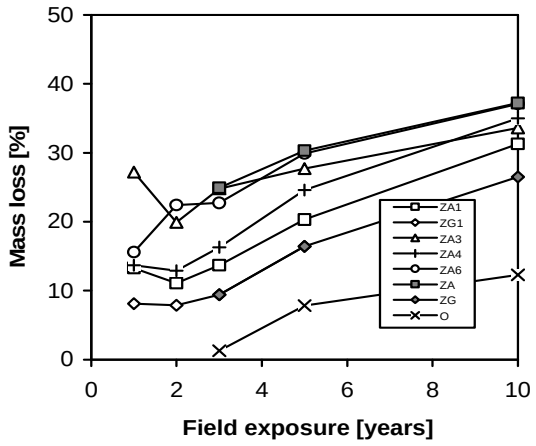

Figure 5. Mass loss during natural weathering of FRT and untreated wood up to ten years.

7 CONCLUSIONS AND SUGGESTIONS FOR FURTHER WORK

Main conclusions are:

- A system with Durability of Reaction to Fire performance (DRF) classes to evaluate the fire performance of FRT wood over time at humid and exterior conditions has been developed. It provides a supplement to requirements on the fire performance in national building codes and enables to guide potential users to find suitable FRT wood products.
- The hygroscopicity of sufficiently durable FRT wood is about the same as for untreated wood, but much higher for simple inorganic salts.
- The fire properties of FRT wood may be maintained after accelerated ageing and natural weathering if the retention levels are high enough.
- Several FRT wood products loose most of the improved reaction to fire properties during weathering.
- Paint systems contribute considerably to maintain of the fire performance at exterior applications.
- The mass loss during accelerated aging and natural weathering may be used as an indicator of the maintained reaction to fire performance over time.
- More experience with correlation of natural field testing and accelerated ageing methods is needed.

REFERENCES

Östman B, Voss A, Hughes A, Hovde PJ, Grexa O, 2001, Durability of fire retardant treated wood at humid and exterior conditions. Review of literature. Fire and Materials, vol 25, 95-104.

LeVan S, Holmes C A, 1986, Effectiveness of fire-retardant treatments for shingles after 10 years of outdoor weathering. Research Paper FPL 474.

Östman B, Tsantarids L, Mikkola E, Hakkarainen T, Nilsen T-N, Evans F, Grexa O, 2002, Durability of fire retardant wood - New test methods and round robin. Nordtest project 1527-01. Trätek Swedish Institute for Wood Technology Research, Report P 0211040.

Nordtest method NT FIRE 054. 2006, Durability of Reaction to Fire - Performance classes of fire-retardant treated wood-based products in interior and exterior end use applications.

Nordtest method NT BUILD 504, 2003, Hygroscopic properties of fire-retardant treated wood and wood-based products.

Nordtest method NT FIRE 053, 2003, Accelerated weathering of fire-retardant treated wood for fire testing.

prEN 15912, 2009, Durability of reaction to fire performances – Classes of fire retardant treated wood-based product in interior and exterior end use applications.

EN 13501-1, 2002, Fire classification of construction products and building elements – Part 1: Classification using test data from reaction to fire tests.

IMO FTP Code (MSC 61/67), International Code for Application of Fire Test Procedures.

ASTM D 3201, Standard Test Method for Hygroscopic properties of fire-retardant treated wood and wood-based products. American Society for Testing and Materials.

ASTM D 2898, Standard Methods for Accelerated weathering of fire-retardant-treated wood for fire testing. American Society for Testing and Materials.

ISO 5660-1, 2002, Fire tests – Reaction to fire – Part 1: Rate of heat release from building products.

Östman B A-L, Tsantaridis L D, 1994, Correlation between cone calorimeter and time to flashover in the room fire test, Fire and Materials, vol 18, 205-209.

Östman, Tsantaridis, Mikkola, Hakkarainen, Belloni, Brumer and Piispanen, 2006, Innovative eco-efficient high fire performance wood products for demanding applications. Final report for Vinnova-Tekes project InnoFireWood. SP Technical Research Institute of Sweden, SP Report 2006:30.

XII DBMC
International Conference on Durability of Building Materials and Components
PORTO - PORTUGAL, April 12th-15th, 2011

Low Energy Renovation of Buildings Using Prefabricated Systems

Helena Corvacho [1]
Joana Sousa [2]
Luís Pedro Pereira [3]
Marisa Quintela [4]

ABSTRACT

In the scope of IEA ECBCS Annex 50 *Prefabricated Systems for Low Energy Renovation of Residential Buildings*, the development of an integrated modular concept for the renovation of building envelopes was performed. The design of innovative facade retrofit modules was carried out.

In order to evaluate the application potential of these facade modules, national building stock was characterized and repair needs were identified. A detailed analysis of a sample of 132 buildings was then performed to define the current morphology of the facades to be renovated.

For the particular case of social housing which is now the object of a large retrofit campaign, different scenarios of retrofit design were considered and studied, identifying the main difficulties and discussing the possible solutions. The design of the facade retrofit solution for seven social housing neighbourhoods using facade modules was performed and evaluated.

In this paper, some of the results of these tasks are reported and discussed. It was concluded that there is an opportunity for the application of the integrated modular concept for a low-energy renovation of buildings in Portugal but it is very important to optimize the solutions in economical, technical and environmental terms for the guarantee of their sustainability.

KEYWORDS

Low energy renovation, Prefabricated systems, Sustainability.

[1] University of Porto, Faculty of Engineering, Building Physics Laboratory (FEUP), Porto, PORTUGAL, corvacho@fe.up.pt
[2] University of Porto, Faculty of Engineering (FEUP), Porto, PORTUGAL, ec09311@fe.up.pt
[3] University of Porto, Faculty of Engineering (FEUP), Porto, PORTUGAL , ec05121@fe.up.pt
[4] University of Porto, Faculty of Engineering, Building Physics Laboratory (FEUP), Porto, PORTUGAL, marisa@fe.up.pt

1 INTRODUCTION

The aim of the international project IEA ECBCS Annex 50 *Prefabricated Systems for Low Energy Renovation of Residential Buildings* was to develop a new concept of integrated low energy retrofit of a whole building using prefabricated solutions. The development of prefabricated modules for the retrofit of facades was performed within the scope of the definition of advanced retrofit strategies.

"A building strategy determines which investment should be made for a certain period of the building's service life. Today, a long-term building strategy is often lacking. Retrofit measures are often only tackled when they are unavoidable. This leads to uncoordinated, partial renovations that eventually result in additional costs. An advanced retrofit strategy aims at establishing a holistic building approach for the entire remaining life cycle of the building. The ultimate option in the building strategy is to construct a new building in replacement. An advanced retrofit strategy determines whether a building reaches this condition in five, twenty-five, or one hundred or more years. Intermediate objectives of an advanced retrofit strategy can be building maintenance, partial renovation or comprehensive renovation" [Schwehr, P. et als 2010].

The definition of these retrofit strategies must rely upon some important actions, namely, the market potential evaluation (considering the main parties: owners, tenants, contractors, construction products manufacturers and providers, public authorities), the retrofit needs evaluation, the analysis of the buildings and the target agreement (through an added value checklist).

For the Portuguese situation, retrofit needs were evaluated and an analysis of the morphology of buildings was performed in order to estimate the potential of application of prefab solutions. The focus was on facades retrofit. This study was carried out having in mind the type of retrofit prefabricated modules developed within the scope of IEA ECBCS Annex 50 (figure 1).

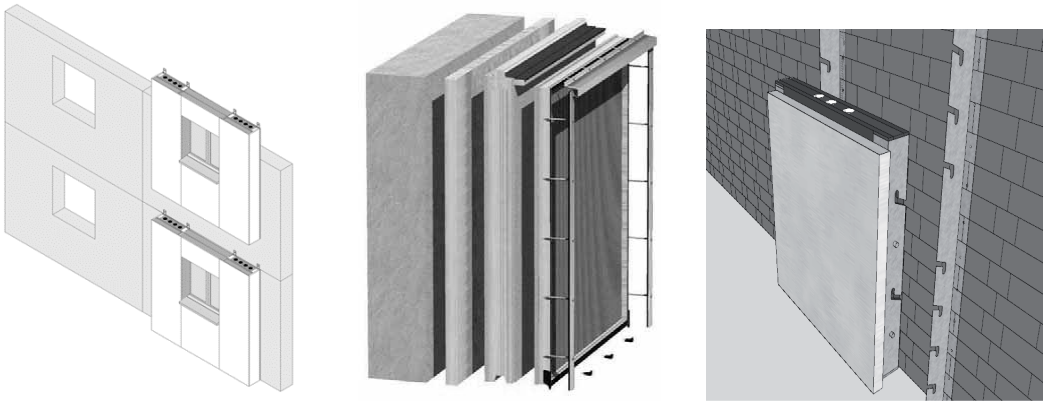

Swiss module Austrian module Portuguese module

Figure 1. Some prefab modules developed by IEA ECBCS Annex 50 [Geier, S. et als 2010].

A thorough study of the Portuguese housing stock was carried out. In the most recent statistics, there were 3,160,043 buildings in Portugal mainland and islands. However not all buildings were considered. The present study was focused on residential buildings so every non-residential building was disregarded. Furthermore, for reasons that will be explained below, a target group was defined: residential buildings built between 1919 and 1990, with 2 to 6 floors and presenting some repair needs in their exterior walls and windows.

In this context, around 600 000 buildings were estimated as having potentially favourable conditions for retrofit using prefabricated facade panels. However determining the number of potential targets for

buildings retrofit is not enough by itself to get an idea of the applicability of this technique. Other issues must be addressed, like architectural, technical, environmental and economical evaluations.

In architectural terms, the choice of a particular panel depends first on the morphology of the facades and the shape of their openings. Since there is no statistical information regarding these elements in Portugal, a study was carried out *in-situ* by observing and coding openings of 132 buildings chosen randomly in a geographical area as broad as possible, but with significant urban characteristics.

In parallel, it was evaluated what could be the possible application of the prefabricated modules proposed by the international project ECBCS IEA Annex 50 in the specific case of social housing. This housing stock was chosen due to its homogenous and repetitive typologies. Some neighbourhoods were selected so as to obtain a significant sample with a large number of buildings with clearly defined characteristics and types. This study lead to an exercise on geometrical features through the study of architectural elevations of facades, taking into account the various singularities that compose them (like recessions, projections, number and size of openings, size of spans, etc.).

In this work, a reflection was made on the choice of materials which is fundamental for the durability of the solution. Beyond mechanical resistance, there are still a number of other requirements that panels should ensure which are associated with a long service life. They must comply with requirements of safety (structural, fire risk), tightness (water, air), comfort (acoustic, thermal, luminous) and, at the same time, present cleaning and maintenance needs that are easy to undertake and within a reasonable cost. The expected durability of the solution with routine maintenance actions must be enough to justify the investment in the retrofit.

2 APPLICATION POTENTIAL OF PREFABRICATED MODULES FOR THE RETROFIT OF FACADES IN PORTUGAL

2.1 The Portuguese Housing Stock

2.1.1 State of the existing buildings

Within the housing stock, three major groups of buildings were described: those with no repair needs, those needing some repair actions and those that are highly degraded. Figure 2 shows the percentage distribution that characterizes the state of the existing buildings in what concerns external walls and windows.

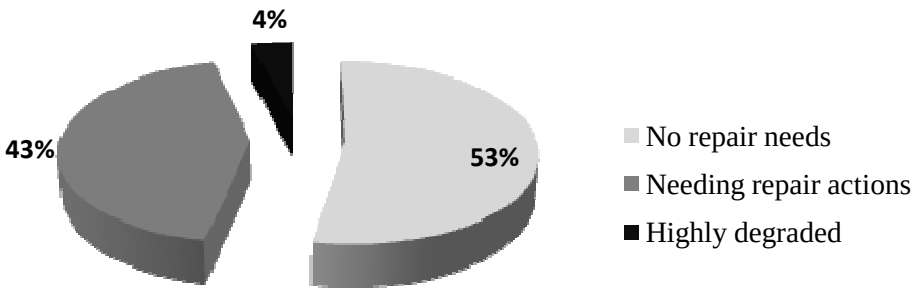

Figure 2. State of the existing buildings – external walls and windows.

2.1.2 Number of Floors

As seen in Figure 3, about 44% of the residential buildings have two floors and 42% just one floor. The sum of the remaining buildings which have more than two floors represents 14% of the total number of residential buildings.

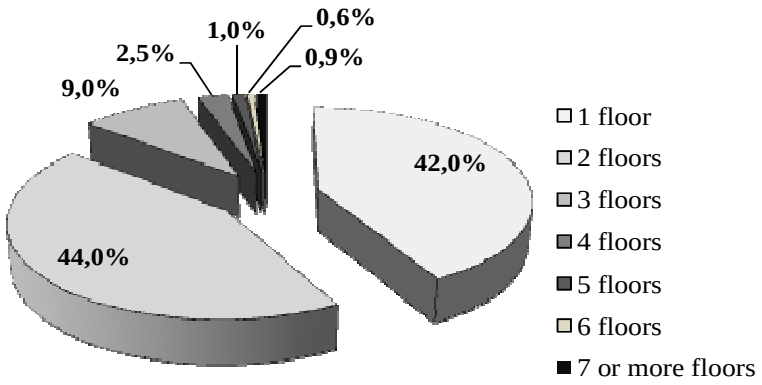

Figure 3. Percentage distribution of buildings per number of floors.

2.1.3 Date of Construction

The date of construction is also an important parameter to be considered. In the twentieth century, the time in which there was a higher production of buildings in Portugal was the period from 1981 to 1990, as it can be seen in Figure 4.

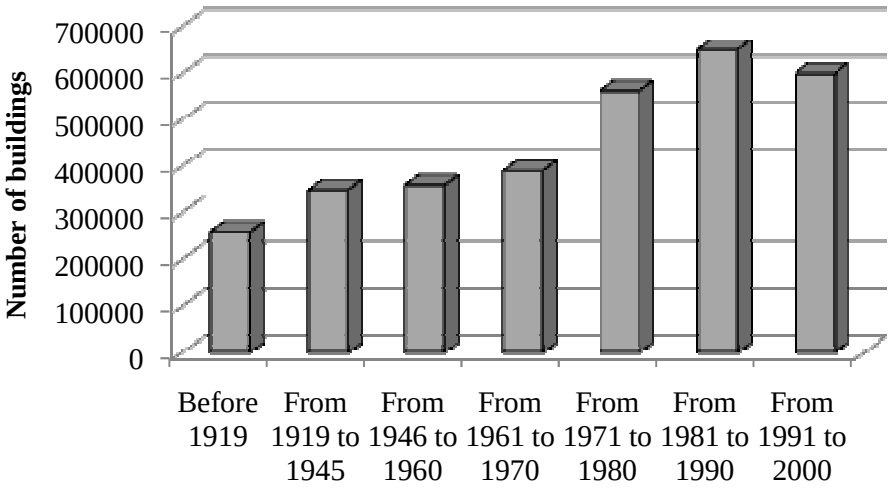

Figure 4. Number of new buildings per period of construction.

2.2 Definition of a Target Group of Buildings

A target group of buildings was defined based on the study of the housing stock. First, it was considered that only the buildings with some need of repair actions in external walls and/or windows would be possible objects for the application of the prefab modules. The need for repair is certainly not a necessary condition for the renovation of a building but it is undoubtedly a major argument for it. It is quite probable that, in those circumstances, a major renovation is better understood and accepted by the inhabitants.

It was decided to exclude buildings that have only one floor as well as buildings with seven or more floors. The exclusion of buildings with only one floor is related to the great architectural variability of the facades of those buildings, making it difficult to apply standardized solutions even if flexible and versatile. Furthermore, an integrated prefabricated system would be too expensive for small buildings because it would be impossible to implement a certain kind of large scale saving. It must be pointed out that this exclusion represents about 42% of the households in the country which is quite significant.

Buildings with seven or more floors were also excluded due to the difficulty of lifting large-scaled components, requiring exceptional and expensive means.

In what concerns the age of the buildings, the aim was to exclude the too old and the too recent buildings. Those that were built after 1990 had already to comply with the thermal regulation in force since then and although in many cases there is still some margin to improve their energy efficiency, those buildings were considered out of the main target group. All buildings built before 1919 were also not included in this study. The period of time considered was then from 1919 to 1990. However, in the group of buildings built between 1919 and 1960, there is certainly a high probability that a major low-energy renovation is not technically possible or economically justifiable. So, within the target group, a sub-group was identified, the one for buildings constructed from 1961 to 1990 which will constitute the main field of application of the retrofit strategies under analysis.

2.3 Characterization of the Morphology of Facades and Evaluation of Prefab Modules Applicability

2.3.1 Analysis of a random sample of 132 buildings

The determination of the potential applicability of prefabricated facade modules in buildings of the target group was performed by the observation *in-situ* of a considerable number of facades in order to identify their usual morphologies. Focusing on the number and type of openings in the facades of the buildings a coded classification was developed based on the following parameters: type of opening (cod.1- window; cod.2 - window behind balcony; cod.3 - door behind balcony), vertical alignment of openings (cod.1 - aligned openings, cod.2 - openings non aligned) and horizontal position of openings (cod.1- openings in a short distance from each other; cod.2 - openings in an intermediate position; cod.3 – openings in a large distance from each other; cod.4 - openings near to an adjoining building; cod.5 – projected openings; cod.6 - openings along the side of a projection of the building; cod.7 – openings in a recessed wall of the building; cod. 8 - openings in a projected wall of the building; cod. 9 – enclosed balconies, cod .10 - openings along the side of a balcony; cod.11 – openings between balconies).

A detailed presentation of this analysis was included in [Sousa, J. 2010]. In Table 1 the part of the openings classification that concerns their horizontal position is shown.

As said before, a sample of 132 buildings was analyzed. In a first step, 1282 openings in 93 buildings were characterized. In a second step, 508 openings in 39 buildings were added. With this two step analysis it was possible to find a similar percentage distribution of the different types of openings. The characterization of the facades morphology allowed an estimation of the potential use of different types of prefabricated modules.

Table 1. Characterization of facades morphology – horizontal position of openings [Sousa, J. 2010].

Cod. 1 *Openings in a short distance from each other*	***Cod. 2*** *Openings in an intermediate position*	***Cod. 3*** *Openings in a large distance from each other*	***Cod. 4*** *Openings near to an adjoining building*
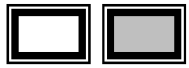			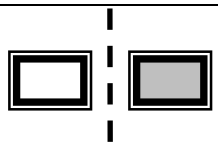
Cod. 5 *Projected openings*	***Cod. 6*** *Openings along the side of a projection of the building*	***Cod.7*** *Openings in a recessed wall*	***Cod. 8*** *Openings in a projected wall*
			

Cod.9 *Enclosed balconies*	***Cod.10*** *Openings along the side of a balcony*	***Cod.11*** *Openings between balconies*
		

2.3.2 The case of social housing

2.3.2.1 Sample characterization

A sample of seven social housing neighbourhoods, in Porto and Vila Nova de Gaia, in sum 107 buildings with a total of 2808 dwellings were chosen so that it had some statistical significance. As explained before, these buildings were chosen because of their homogeneous and repetitive typologies (as it can be observed in Figure 5), however, in each selected neighbourhood, all the buildings with different characteristics were picked up to better identify all potential problems in applying prefabricated solutions for the retrofit of facades. This analysis was carried out in the scope of the work presented in [Pereira, L. P. 2010].

For each of the seven neighbourhoods beyond the generic features like designation, location, date of construction, number of buildings, number of entrances, number of floors, number of dwellings, etc., more specific characteristics were carefully analyzed, some of them essential for the choice of the prefab panels to be used: type of structure, location of the structural elements (essential for the determination of the fixations of the retrofit system), floor to floor height, number and size of spans, number and types of openings (see classification above), type of usage, drainage system pipes along the facades (evaluation of their integration in the retrofit modules), etc..

2.3.2.2 Evaluation of the applicability of panels

The "puzzle" of the panels was designed for the facades of the different buildings under analysis (examples in Figure 5). The position of the structural elements (slabs, beams and columns), since these are the points where panels must be fixed, served as reference lines. The location of downpipes was also taken into account in order to integrate them in special voids created within the prefabricated modules. Ventilation pipes or other installations were also to be integrated.

The dimensions of the modules were defined in such a way that they were not too low that they compromised the advantages of the system nor too high that they demanded high costs of transport and placement. The maximum dimensions of the panels were 3.0 x 3.0 metres.

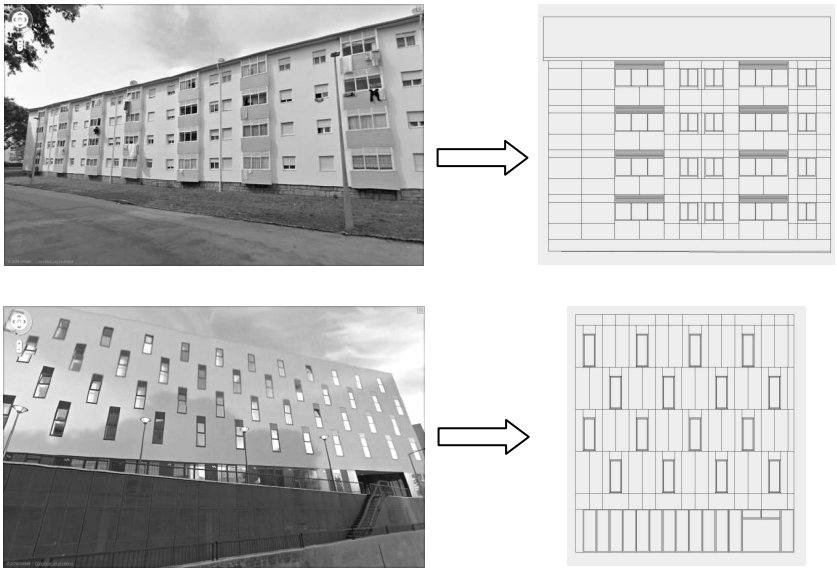

Figura 5. Examples of application of facade modules.

3 DISCUSSIONS

In architectural terms this study proved that there is a considerable potential for the application of retrofit prefabricated façade modules among a target group of buildings that includes the more "standardized" buildings of social housing estates.

In technical terms, the prefabrication is an old but renewed challenge. The panels that have been developed within the scope of Annex 50 express a new integrated retrofit concept resulting from an holistic approach to the buildings. Furthermore three fundamental guidelines were taken: the modules are standardized in construction, layers and joints; the modules are flexible in architecture, form and cladding; the modules can be combined with each other and with non-prefabricated (conventional) retrofit options [Schwehret als 2010].

In [Abreu et als 2010] the new technological challenges in the low-energy retrofit of external walls of buildings were discussed having in mind the economical and technical environment of the country. As it was mentioned, a significant part of the Portuguese housing stock presents repair needs. This should be looked at as an opportunity to re-qualify the buildings, making them more energy-efficient and more comfortable. The prefabrication, which has always been considered unsuitable for the small Portuguese market of buildings and also not compatible with the small size of the great majority of the companies in the construction sector, should be able to present solutions that provide innovative functions (integrating pipes, ventilation, etc.), that are flexible enough to allow for a great diversity of facades and a great variation in mounting conditions (different companies, different sites), that are not closed systems, i. e., that can be combined with other options and that represents a strong contribution for a low-energy running of the building (through integrated passive systems, for instance). All this must be reached at a reasonable and competitive cost.

In economical terms, one can argue that in a small country large-scale savings are not easy to achieve. However, there is also an important argument in favour of the prefabrication solutions that is the fact

that a long service life is more easily ensured due to the more demanding quality control in production and also because it is easier to plan a rational maintenance along its service life.

4 CONCLUSION

Portugal presents a significant part of its housing stock in need of repair actions. This should be considered as an opportunity for a low-energy renovation of the buildings. In the scope of the work of International Energy Agency ECBCS Annex 50, prefabricated modules for the retrofit of facades have been developed (and will be tested and monitored). The potential for their application in Portugal was evaluated and it was concluded that around 600 000 buildings have favourable conditions for retrofit using prefabricated facade panels. For this to be effective, careful technical, environmental and economical evaluations are needed.

ACKNOWLEDGMENTS

The participation of the first author in the work of the International Energy Agency ECBCS Annex 50 - *Prefabricated Systems for Low Energy Renovation of Residential Buildings* was undertaken in the scope of the project PTDC/ECM/67373/2006 'Reabilitação Energética de Edifícios' *(Low Energy Retrofit of Buildings)* funded by Portuguese Foundation for Science and Technology (FCT), from February 2008 to end of January 2011.

REFERENCES

Abreu, I. & Corvacho, H., 2010, 'Os Novos Desafios Tecnológicos na Reabilitação Energética de Paredes Exteriores de Edifícios' (*The New Technological Challenges in the Low Energy Retrofit of External Walls of Buildings*), in *Construção Magazine*, nº 35, Publindústria, pp 23 - 28.

Geier, S., Höfler, K., Cousin, S., Silva, P., Kobler, R., 2010 (draft) 'Retrofit Module Design Guide', IEA ECBCS Annex 50, *Prefabricated Systems for the Low Energy Renovation of Residential Buildings*, 133 pp., Swiss Federal Laboratories for Materials Testing and Research, Switzerland.

Pereira, L. P. 2010, 'Reabilitação Térmica de Fachadas. O Exemplo dos Bairros Sociais' (*Low Energy Retrofit of Facades. The Example of Social Houses*), Ms. Sc. Thesis, 81 pp, Faculty of Engineering of the University of Porto, Portugal.

Schwehr, P., Fischer, R., Geier, S. & Höfler, K. 2010 (draft) 'Retrofit Strategies Design Guide. Advanced Retrofit Strategies & 10 Steps to a Prefab Module', IEA ECBCS Annex 50, *Prefabricated Systems for the Low Energy Renovation of Residential Buildings*, 112 pp., Swiss Federal Laboratories for Materials Testing and Research, Switzerland.

Sousa, J. 2010, 'Potencial da Aplicação de Sistemas Pré-fabricados na Reabilitação Térmica de Fachadas' (*Application Potential of Prefabricated Systems for the Retrofit of Facades*), Ms. Sc. Thesis, 118 pp, Faculty of Engineering of the University of Porto, Portugal.

XII DBMC
International Conference on Durability of Building Materials and Components
PORTO - PORTUGAL, April 12th-15th, 2011

Increase of Durability of Carbonate Stones Consolidated with Nanoparticles of $Ca(OH)_2$

Paula López-Arce [1]
Ainara Zornoza Indart [2]
Luz Gómez-Villalba [3]
Rafael Fort [4]

ABSTRACT

Nanotechnology offers the use of innovative products to consolidate porous stones prone to decay due to the exposure to weathering agents. Calcium hydroxide ($Ca(OH)_2$ nanoparticles are considered a good compatible consolidation materials to increase the durability of carbonate stones, where the relative humidity (RH) of the environment during the consolidation process plays an important role in the modification of the physical properties of these stones in a short and in a long term.

The durability assessment of carbonate stones (dolostone), typically used in historical buildings from Madrid (Spain) has been determined just after their consolidation with these nanoparticles at 20ºC under a dry (33%RH) and a humid environment (75%RH), and after 18 months later under room temperature and humidity conditions (20ºC±5 and 50±10% RH). The increase of durability of this dolostone is shown through the combination of non-destructive techniques (Environmental Scanning Electron Microscopy, spectrophotometry, water absorption under vacuum and capillarity, ultrasounds velocity and Optical Surface Roughness analyses) together with destructive techniques (mercury intrusion porosimetry and microdriling resistance measurement) also necessary for a better accuracy determination of pore structure and resistance modifications. Consolidation process under both humid and dry environment gives rise to an increase in the durability of dolostone specimens. However, the humid environment favors the consolidation in a short and in a long term, being this condition necessary to take into account when $Ca(OH)_2$ nanoparticles are used to consolidate carbonate stones.

KEYWORDS

Consolidation, Calcium hydroxide nanoparticles, Carbonate stone, Durability.

[1] Instituto de Geología Económica/Instituto de Geociencias (CSIC-UCM), Madrid, Spain, plopezar@geo.ucm.es
[2] Instituto de Geología Económica/Instituto de Geociencias (CSIC-UCM), Madrid, Spain, ainarazornoza@pdi.ucm.es
[3] Instituto de Geología Económica/Instituto de Geociencias (CSIC-UCM), Madrid, Spain, luzgomez@geo.ucm.es
[4] Instituto de Geología Económica/Instituto de Geociencias (CSIC-UCM), Madrid, Spain, rafort@geo.ucm.es

1 INTRODUCTION

Carbonate rocks have been extensively used along history as building stones, due to their abundance, availability, easy workability and beauty. However, most of this type of rocks are prone to decay due to intrinsic and extrinsic factors that determine their durability, such as porosity or composition, which makes them susceptible to physical and chemical attack, together with the environment in which they are placed which contribute in a different way to the degradation of monuments. The durability of building stone is a measure of its ability to resist weathering and so retain its original size, shape, strength, and appearance over an extensive period of time [Bell 1993].

Stone preservation involves the use of chemical treatments that prolong the life of a stone, either by preventing or retarding the progress of stone decay or by restoring the physical integrity of the decayed stone. Calcium hydroxide ($Ca(OH)_2$) is broadly known from the past for being one of the most compatible products to perform consolidation of calcareous materials such as stone sculptures, monuments or wall paintings [Ashurst & Dimes 1990].

In the search of compatible materials to increase durability of carbonates stones, nanotechnology has become an opportunity to be applied in stone preservation. The nanotechnology and nanomaterials boom have given rise to the development of $Ca(OH)_2$ nanoparticles to be used as a consolidating product for carbonatone stones, solving some of the drawbacks of conventional $Ca(OH)_2$, such as the incomplete conversion of calcium hydroxide into calcium carbonate, post treatment chromatic alterations and the little penetration depth [Daniele *et al.* 2008]. The use of $Ca(OH)_2$ nanoparticles is funded by the fact that the specific surface area of a solid increases exponentially with the decrease of its volume, having the nanoparticles a much superior surface area available to react, and a better ability to penetrate in the stone pores net [Sequeira *et al.* 2006]. The use of alcohols as a substitute for water solvent in $Ca(OH)_2$ treatments also improves the consolidation process [Giorgi *et al.* 2000], since colloidal dispersions of these nanoparticles show a slower rate of agglomeration reducing the tendency of a white film to form on surfaces to be consolidated [Hansen *et al.* 2003].

In terms of durability, the selection of stone for building purposes has conventionally been based on its performance in the past and the results of standard tests [Bell 1993]. Previous research works carried out by Dei & Salvadori [2006], Daniele *et al.* [2008] or López-Arce *et al* [2010] have shown the use of different analytical techniques to characterize these nanoparticles and to evaluate the effect on the consolidation of carbonate stones.

The aim of this research was to show the durability assessment of carbonate stones (dolostone), typically used in historical buildings from Madrid (Spain) through characterization analyses using a combination of non-destructive techniques (NDT) together with destructive techniques, also necessary for a better accuracy determination of pore structure and resistance modifications. The increase in durability of dolostone has been determined just after 20 days of consolidation with these nanoparticles under a dry and a humid environment, and after 18 months later under room temperature and humidity conditions.

2 MATERIALS AND METHODS

2.1 Materials and Sample Preparation

The $Ca(OH)_2$ dispersion used in this study is a commercial product (Nanorestore®) developed at the University of Florence (CSGI Consortium) [Dei & Salvadori 2006]. It is based on a colloidal suspension of nanoparticles of slaked lime ($Ca(OH)_2$) dispersed in isopropyl alcohol (5 g/l). The nanoparticles were exposed to 33% and 75% relative humidity (RH) at 20ºC during 20 days and then left in the laboratory during 18 months under room temperature (RT) and RH conditions (20ºC±5 and 50±10% RH). The room CO_2 concentration can oscillate in the laboratory between 500 and 800 ppm. The equilibrium relative humidity (RHeq) of specific supersaturated salt solutions inside closed

desiccators used as climatic chambers was used to keep the humidity constant at 20ºC: NaCl (RHeq 75%) to simulate a humid environment and $MgCl_2$ (RHeq 33%) to simulate a drier environment. Inside the chambers there was no additional CO_2 flux and no air in circulation.

Additionally, ($Ca(OH)_2$) nanoparticles were applied as a direct preventive treatment to a cream color dolostone of a high open porosity and prone to decay. One specimen was a fresh sample (33RH) that came from an ancient quarry (Redueña) where in the past the stone had been extracted to be broadly used in the construction of several historical buildings located in Madrid (Spain). The other specimen (75RH) also came from the same quarry, but it was submitted to freezing–thawing cycles by artificially accelerated aging tests [Fort *et al.* 2008]. These two dolostone specimens (2.5 x 2.5 x 1.5 cm) were impregnated with the Nanorestore® product with no dilution drop-by-drop through a capillary tube (1.3 ml) in two applications within an interval of five days. These stone specimens were analyzed before and after being placed inside the climatic chambers for 20 days of consolidation at 33%RH (specimen 33RH-20d) and 75% RH (specimen 75RH-20d). A detailed description of the NDT used in their characterization and the results obtained were reported in a previous work [López-Arce *et al.* 2010]. These stone specimens were again analyzed 18 months later (specimen 33RH-18m and 75RH-18m) after being exposed to room temperature (RT) and RH conditions (20ºC±5 and 50±10% RH) and using some of the same NDT methods as were previously used combined with some destructive techniques.

2.2 Analytical Techniques and Experimental Procedure

The characterization of the ($Ca(OH)_2$) nanoparticles exposed to 33% and 75% relative humidity (RH) has been studied by Environmental Scanning Electron Microscopy (ESEM) and X-ray Diffraction (XRD) after 20 days exposure to these RH conditions and as well, after 18 months of exposure under room T and RH conditions. ESEM was performed to study the morphology, size and distribution of the particles disposed on plastic cups using a Quanta 200 FEI microscope. XRD were performed to determine the mineralogy and crystallinity of the product. XRD patterns were recorded in an X'Pert Pro MPD Panalytical X´Celerator diffractometer.

The stone specimens incorporating the consolidating product and exposed at 33% RH and 75%RH were analyzed with several NDT, before, after 20 days and after 18 months treatment, in the following order: spectrophotometry, mobile Optical Surface Roughness (OSR) analyses, propagation of ultrasound velocity and determination of water absorption under vacuum and by capillarity at atmospheric pressure. Spectrophotometry was used to measure the chromatic parameters on the surface of the stone specimens, by means of a spectrophotometer (MINOLTA CM-700d) using the Lab color space or CIELAB. The Standard illuminant was D65 and observer 10º and the measured parameters were L*, which accounts for luminosity, a* and b* coordinates (a* being the red-green parameter and b* the blue-yellow) and YI for yellow index (measured according to ASTM 313-73). The total color difference ΔE^* is given by the formula $\Delta E^* = ((\Delta L^*)^2 + (\Delta a^*)^2 + (\Delta b^*)^2)^{1/2}$ and the total chroma difference ΔC^* is provided by the formula $\Delta C^* = (\Delta a^*)^2 + (\Delta b^*)^2)^{1/2}$. OSR analyses were performed on the surface of the specimens to evaluate the change in surface roughness. The equipment used was a contact-free surface profilometer (white light), TRACEiT, patented by Innowep GmbH. The OSR analyses included 3D-topography maps (25 mm^2) and some surface roughness profiles (5mm length, ±1mm height) displaying the average roughness parameters according to the DIN EN ISO 4287 standard: Ra (arithmetic mean of the absolute values of profile deviations from the mean line) and Rz (sum of the vertical distances between the five highest peaks and the five deepest valleys within the sampling length). The cut off □(λc) used for calculations is 0.80 mm.

Propagation of ultrasound velocity was measured to evaluate the increase in effective porosity and the distribution of the consolidating product that is related to the durability. P-wave propagation time was measured to a precision of 0.1μs with a PUNDIT CNS Electronics instrument. Standard recommendations were followed according to the Spanish and European standard UNE-EN 14579 [2005]. The frequency of the transducers used was 1 MHz. Measurements were taken in direct

transmission/reception mode, across opposite parallel sides of the cubic specimens in the three spatial directions. Water absorption by capillarity was carried out to study the hydric behavior through the stone using a continuous data-recording ACUASOR. The balance device was linked to a computer which automatically records weight gain in the tested specimen at specified intervals (every (1/f) seconds$^{1/2}$, in the current study f=2). Water absorption under vacuum was performed to determine the bulk density, open porosity and to quantify the amount of water absorbed by the specimens once they reach saturation, as described in the Spanish and European standard UNE-EN 1936 [1999].

The stone specimens were also analyzed through destructive and micro-destructive techniques. Mercury Intrusion porosimetry (MIP) was applied to asses sample pore structure, i.e., total porosity (P) and pore size distribution (PSD). Readings were taken in pore diameters of 0.005 to 400 µm under measuring conditions ranging from atmospheric pressure to 60,000 psia (228 MPa) with a Micromeritics Autopore IV 9500 MIP. Drilling resistance measurement (DRMS-Sint Technology) was used to measure the penetration depth of the consolidating product and to determine if this resistance increases in the treated samples. The measurements were done with a hard widia drill bit with 5mm diameter and the drilling conditions used in this study were: penetration depth, 15 mm (the thickness of the specimen); penetration speed, 10 mm/min and speed rotation, 400 rpm.

3 RESULTS AND DISCUSSION

3.1 Characterization of Nanoparticles

The results of the ESEM and XRD analyses of the particles exposed to 75% RH and 33% RH after 20 days and 18 months are shown in 'Fig.1'. As a result of the respective RH conditioning several differences in the crystallinity, agglomeration and mineralogy of the particles are observed. When nanoparticles were exposed to 75% RH, after 20 days ('Fig 1a') needle-like habits of vaterite microcrystal (1.98-6µm) are observed. The XRD pattern ('Fig 1c') confirms the carbonation process with the presence of vaterite, calcite and traces of monohydrocalcite. After 18 months ('Fig 1b'), these microparticles (3-5µm and 8-10 µm) of vaterite and aragonite are associated to calcite (2.5-3.5µm) which is confirmed by XRD ('Fig 1c').

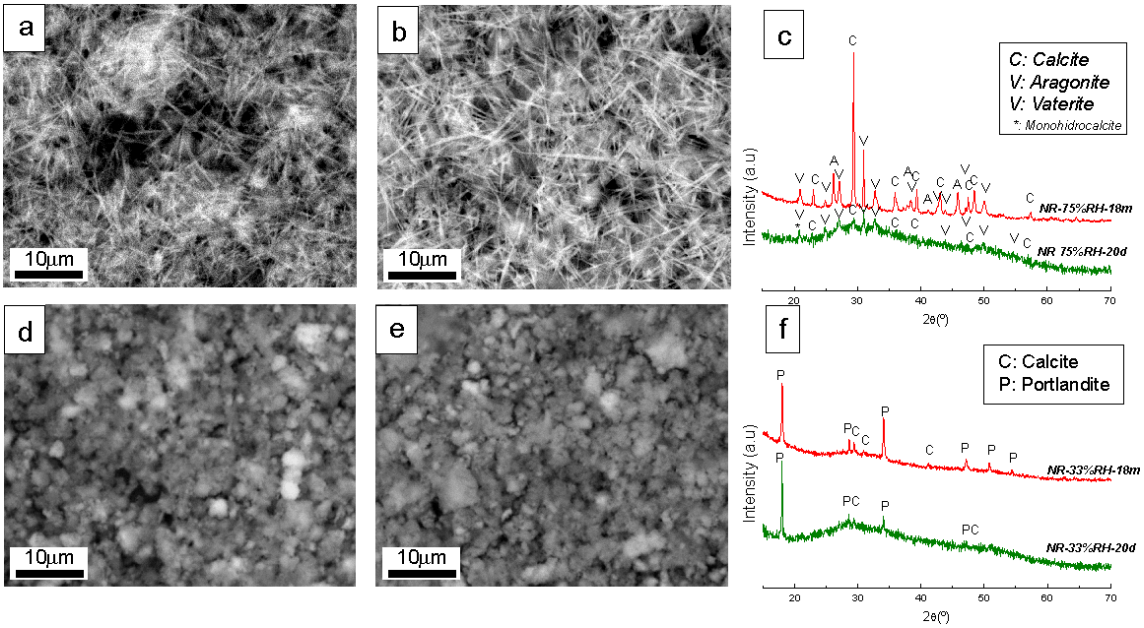

Figure 1. ESEM images and XRD patterns of nanoparticles: (a) ESEM after 20 days exposed to 75%RH; (b) same sample after 18 months exposed to room T and RH conditions; (c) XRD patterns of both samples (NR-75RH-20d and NR-75RH-18m); (d) ESEM after 20 days exposed to 33%RH; (e) same sample after 18 months; (f) XRD patterns of both samples (NR-33RH-20d and NR-33RH-18m).

The sample exposed to 33%RH after 20 days is shown in the ESEM image ('Fig 1d') where submicron clusters of portlandite with poor crystallinity (540nm to 5.16µm) can be observed. The XRD pattern ('Fig 1f') confirms the portlandite phase and displays a small signal of calcite. After 18 months, the carbonation process has not yet been completed, as is shown in the XRD ('Fig 1f') indicating the presence of portlandite and traces of calcite. The ESEM image ('Fig 1e') only reveals an increase in the particle size reaching values up to 8µm.

3.2 Characterization of Stone Specimens

3.2.1 Spectrophotometry

The results of spectrophotometric measurements are shown in Table 1. Color variations stabilized after 18 months of consolidation, being the differences between the fresh samples and the treated samples after 18 months smaller than the differences between the fresh samples and the samples after 20 days treatment. The greatest differences in color variation was for the 33RH-18m specimen, especially for values of ΔC*, ΔE* and ΔYI. On both specimens there is an increase of the chroma difference (ΔC*), this difference being greater for the 33RH-18m specimen due to the larger yellowing (ΔYI) effect.

Table 1. Color variation promoted on dolostone specimens after 20 days (75RH-20d and 33RH-20d) and 18 months (75RH-18m and 33RH-18m) treatment with Nanorestore®.

Specimen	Δ*L**	Δ*a**	Δ*b**	Δ*C**	Δ*E**	Δ*YI*
75RH-20d	1.81	-0.65	-1.77	1.89	2.61	-4.57
75RH-18m	1.01	0.05	-0.31	0.31	1.06	-0.75
33RH-20d	1.33	-1.53	-3.99	4.27	4.48	-9.36
33RH-18m	-1.68	-0.25	1.49	1.51	2.26	2.63

However, most of the chromatic parameters decrease after 18 months reaching much lower values than those obtained after 20 days treatment. The 75RH-18m specimen has a lower total color difference (ΔE*) as compared to the 33RH-18m specimen and this ΔE* also becomes lower after 18 months. Therefore, in both specimens the consolidating product does not significantly affect the color parameters of the stone after 20 days and even less so after 18 months; this result is based on considering the criteria for compatibility indicators that are available in the literature. When, for example, Δ*E** (total color difference) is less than 3 the risk of incompatibility is 0 and when Δ*E** is between 3 and 5 the risk is 5 (on a 5 to 10 scale) [Benavente *et al*. 2003, Delgado *et al*. 2007, Grossi *et al*. 2007]. Since ΔE* is lower than 3 for specimen 75RH and between 3 and 5 for specimen 33RH, the consolidation product does not affect stone color.

3.2.2 Optical Surface Roughness (OSR)

The results from OSR measurement are shown in Table 2. In specimen 75RH, values of Ra and Rz decrease after 20 days and 18 months. The decrease in Rz parameter is much greater after 18 months and this may be due to the penetration of nanoparticles through the pore network reducing the pore sizes and hence the depth of surface roughness giving rise to a shorter distance between the highest and lowest peaks of the roughness profiles ('Fig. 4a'). The decrease in Rz value could also be explained due to changes and transformations of the vaterite polymorph, increasing the density of the consolidating product during its transformation into calcite as is observed in 'Fig.1a-c'.

On other hand, in specimen 33RH, the roughness parameters increase slightly (Table 2). This may be because in a reduced humidity and drier environment the $Ca(OH)_2$ nanoparticles tend to agglomerate without penetrating the pores, thus covering the surface of the specimens and giving rise to longer distances between the highest and lowest peaks of roughness profiles, and thereby increasing the Rz parameter ('Fig. 4a'). This change is greater in the specimen after 20 days, since after 18 months it decreases slightly, whereas Ra increases slightly. Even although, the transformations of $Ca(OH)_2$

nanoparticles are less important in this latter specimen as observed in 'Fig.1d-f', these produce a greater increase in Ra parameter with time as compared to the other specimen.

Table 2. Optical Surface Roughness parameters: variation promoted on the dolostone specimens before consolidation (75RH-0d and 33RH-0d), after 20 days (75RH-20d and 33RH-20d) and 18 months (75RH-18m and 33RH-18m) treatment with Nanorestore®.

Specimen	75RH-0d	75RH-20d	75RH-18m	33RH-0d *	33RH-20d *	33RH-18m
Ra (µm)	7.95±2.08	7.89±2.07	7.32±2.10	6.61±1.63	6.64±1.76	6.76±1.67
Δ Ra (%)		-0.86/-0.7	-12.45/-6.48		-2/1.9	2.16/2.25
Rz (µm)	32.24±7.74	31.98±7.54	28.85±7.66	28.17±6.30	28.47±6.68	28.03±6.10
Δ Rz (%)		-0.25/-1.16	-15.62/-9.5		-0.3/1.93	0.27/-1

3.2.3 Propagation of ultrasound velocity (UV)

The propagation of UV of the specimens is shown in Table 3. In both specimens there is an increase in UV, but this increase is greater in specimen 75RH as compared to 33RH. In the former specimen, after 20 days of consolidation there is a significant increase (15%) and after 18 months this is stabilized, thus slightly decreasing in value, although reaching values above of those obtained in the specimen before treatment (6%). In specimen 33RH the increase in UV values after 20 days is lower than in the other specimen (2.5%) and after 18 months it reaches a similar value than that before consolidation.

3.2.4 Hydric behavior

The results of hydric tests are shown in Table 3. These results show that both the open porosity and water absorption saturation under vacuum slightly change after consolidation in both specimens. However, the most significant result corresponds to the capillarity coefficient (C). In the case of specimen 75RH, the value of C decreases (38%) after 20 days and this decrease continues up to 58% in the specimen after 18 months. In specimen 33RH, the value of C also decreases (16%). However, after 18 months this value shows a slight decrease to 7%.

The nanoparticles introduced in the pore system of the specimens, gave rise to a "nano-roughness" that in turn made capillary water absorption difficult. Calcite has a greater degree of water repellency as compared to dolomite and this could be one of the reasons for the reduction of the value of the C coefficient that was even higher in specimen 75RH in which all the portlandite was transformed into calcite, especially after 18 months. In specimen 33RH the penetration of nanoparticles inside the pore system was less significant; there was also reduced transformation of portlandite into calcite as shown by the decrease in C value and lower than in the other specimen. In this latter specimen after 18 months, the nanoparticles increased in size but did not totally transform into calcite.

Table 3. Values of ultrasound velocity (Vp), water absorption under vacuum and by capillarity for dolostone specimens before consolidation (75RH-0d and 33RH-0d), after 20 days (75RH-20d and 33RH-20d) and 18 months (75RH-18m and 33RH-18m).

Specimen	*Average Vp for 3 axes (m/s)*	*ΔVp (%)*	*Saturation (S) (%)*	*ΔS (%)*	*Open porosity (Op)(%)*	*ΔOp (%)*	*Capillary coefficient (C) ($g/m^2s^{0.5}$)*	*ΔC (%)*
75RH-0d	2187±91		8.30		18.95		172.5±4.6	
75RH-20d	2585±145	15.33	7.95	-0.35	18.20	-0.75	124.9±2.5	−38
75RH-18m	2336±58	6.42	8.24	-0.06	18.88	-0.07	72.06±0.3	−58
33RH-0d	2674±113		7.06		16.60		148.02±3.9	
33RH-20d	2747±163	2.55	6.91	-0.15	16.30	-0.3	123.9±1.3	−16
33RH-18m	2659±220	-0.5	7.01	-0.05	16.55	-0.05	137.43±3.3	−7

3.2.5 Mercury Intrusion porosimetry (MIP)

The MIP results are shown in Table 4. These show that both total porosity and pore size distribution changed slightly in specimen 33RH. There is also a slight decrease in the total porosity and a slight increase of pore diameters in the range between 1 and 100 µm ('Fig. 4b').

Table 4. Surface area, total porosity and pore size distribution of samples treated with $Ca(OH)_2$ nanoparticles as obtained by mercury intrusion porosimetry.

Specimen		*75RH-0d*	*75RH-18m*	*33RH-0d*	*33RH-18m*
Specific surface area (m^2/g)		0.30±0.02	0.26±0.05	0.37±0.05	0.27±0.01
Total connected porosity (%)		17.65±3.43	13.04±2.46	14.63±2.55	13.62±0.19
Pore size distribution (%)	*< 0.01 µm*	0.00	0.00	0.00	0.00
	0.01 - 0.1 µm	1.30	1.63	2.49	1.59
	0.1 - 1 µm	18.05	21.26	23.45	22.29
	1-10 µm	62.61	62.81	66.15	67.77
	10 - 100 µm	14.13	12.08	4.76	5.75
	>100 µm	3.90	2.23	3.15	2.58

The modification of the pore system in specimen 75RH is much greater. This is observed by the greater decrease in total porosity and a decrease of pore diameters in the range between 10 and 100 µm and an increase in diameters for the 1 to 10 µmpore size range (Table 4 and 'Fig.2b').

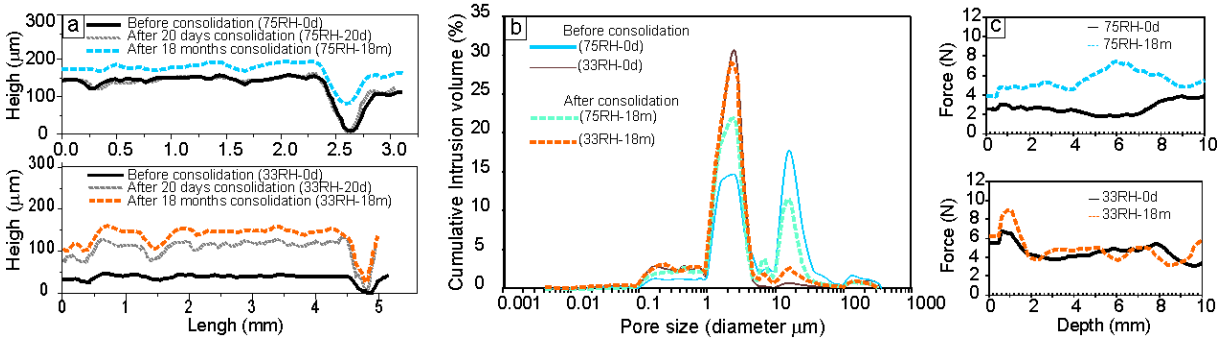

Figure 2. (a) OSR profiles before and after 20 days and 18 months consolidation at 33%RH and 75%RH; (b) Pore size distribution curves obtained with MIP in these stone specimens; (c) Drilling resistance graphs of same samples; drilling conditions: 10mm depth, 15 mm/min and 400 rpm.

3.2.6 Drilling resistance measurement (DRMS)

The results of the drilling resistance measurements ('Fig.4c') show that before consolidation the stone specimens display lower resistance values compared to the specimens after 18 months consolidation. Initially, in the specimens before consolidation the value for drilling resistance is slightly lower in the stone specimen 75RH-0d (3.98±2.00N) compared to the stone specimen 33RH-0d (4.11±1.08N). However, the increase in this value after 18 months consolidation is higher in the former specimen (75RH-18m), reaching values of 5.70±1.07N that are above the values attained by specimen 33RH-18m (4.74±1.47N). The highest increase in 33RH-18m is produced in the first 2 mm which is in agreement with the greatest number of particles located at the surface of this specimen as determined by ESEM and OSR analysis.

4 CONCLUSIONS

According to the results obtained in this study, the resistance to weathering effects of dolostone treated with $Ca(OH)_2$ nanoparticles increases, and this is greater, both in the short and long term, when the treatment is applied at higher RH (75%) as compared to an application at a lower RH (33%). For treatments at the higher RH, a complete transformation from portlandite ($Ca(OH)_2$) to calcite ($CaCO_3$) is achieved, giving rise to lower color variations, greater reduction in surface roughness and

a higher increase in the propagation of ultrasound velocity as compared to treatments at the lower RH. This is explained by a greater depth of penetration of the nanoparticle´s product and the total carbonation of the particles and their transformation from nano to micron-scale within the pore system. this effectively reduced pore sizes as was reflected by a corresponding reduction in the capillarity coefficient, and increased drilling resistance, thus providing a higher resistance to water penetration and hence, a greater resistance of dolostone to the effects of weathering agents.

ACKNOWLEDGMENTS

This study was funded by GEOMATERIALES (S2009/MAT-1629) and CONSOLIDERTCP (CSD2007-0058). Thanks also to the JAE CSIC Programme and to the UCM Research Group "Alteración y Conservación de los Materiales Pétreos del Patrimonio" (ref. 921349).

REFERENCES

Ashurst, J. & Dimes, F.G. 1990, 'The cleaning and treatment of limestone by the lime method' in *Conservation of Building and Decorative Stone,* Vol 2, pp. 169-184.

Bell, F.G. 1993, 'Durability of carbonate rock as building Stone with comments on its preservation', *Environmental Geology*, 21, 187-200.

Benavente, D., Martínez-Verdú, F., Bernabeu, A., Vigueira, V., Fort, R., García del Cura, M. A., Ilueca, C., Ordoñez, S. 2003, 'Influence of surface roughness on color changes in building stones', *Color Research and Application*, **28**[5], 343-351

Daniele, V., Taglieri, G., Quaresima, R. 2008, 'The nanolimes in cultural heritage conservation: characterisation and analysis of the carbonatation process', *J. Cult. Heritage*, **9**[3], 294–301.

Dei, L. & Salvadori, B. 2006, 'Nanotechnology in cultural heritage conservation: nanometric slaked lime saves architectonic and artistic surfaces from decay', *J. Cult. Heritage*, **7**[2],110–115.

Delgado, J. & Grossi, A. 2007, 'Indicators and rating for the compatibility asessment of conservation actions', *J. Cult. Heritage*, 8, 32-43

DIN EN ISO: 4287. Surface roughness—terminology: Part 1. Surface and its parameters.

Fort, R., Fernández-Revuelta, B., Varas, M.J., Alvarez de Buergo, M., Taborda-Duarte, M. 2008. 'Influence of anisotropy on the durability of Madrid-region Cretaceous dolostone exposed to salt crystallization processes', *Materiales de Construccion*, **58**[289–290], 161–78.

Giorgi, R., Dei, L., Baglioni, P. 2000, 'A new method for consolidating wall paintings based on dispersions of lime in alcohol', *Studies in Conservation*, 45, 154–161.

Grossi, C. M., Brimblecombe, P., Esbert, R. M., Alonso, F. J. 2007, 'Color Changes in Architectural Limestones from Pollution and Clearing', *Color Research and Application*, **32**[4], 320-331.

Hansen, E., Doehne, E., Fidler, J., et al. 2003, 'A review of selected inorganic consolidants and protective treatments for porous calcareous materials' *Reviews in Conservation*, 4,13–25.

López-Arce, P., Gómez, L.S., Pinho, L., Fernández-Valle, M.E., Álvarez de Buergo, M., Fort, R. 2010, 'Influence of porosity and relative humidity in the consolidation of dolostone with calcium hydroxide nanoparticles: assessment of consolidation effectiveness with non destructive techniques', *Materials Characterization*, **61**[2], 168-184.

Sequeira, S., Casanova, C., Cabrita, E.J. 2006, 'Deacidification of paper using dispersions of $Ca(OH)_2$ nanoparticles in isopropanol. Study of efficiency', *J. Cult. Heritage*, **7**[4], 264–272.

UNE-EN 14579:2005. Natural stone test methods. Determination of sound speed propagation.

UNE-EN 1936:1999. Natural stone test methods. Determination of real density and apparent density, and of total and open porosity.

XII DBMC
International Conference on Durability of Building Materials and Components
PORTO - PORTUGAL, April 12th-15th, 2011

The Resistance of Completely Recyclable Concrete to Carbonation, Chloride Penetration and Freeze-thaw Attack with De-icing Agents

Mieke De Schepper [1]
Philip Van den Heede [2]
Christophe Windels [3]
Nele De Belie [4]

ABSTRACT

As the construction sector uses 50% of the earth's raw material and produces 50% of its waste, the development of more durable and sustainable building products is crucial. Since Construction and Demolition Waste (CDW) is mostly inert material, it is nowadays used as recycled aggregates, but only in low-value concrete applications. On the other hand, the general trend today for the cement industries is the use of alternative raw materials for the production of cement clinker. Considering these aspects and the aim for high-value recycling of CDW, the concept of Completely Recyclable Concrete (CRC) has been developed. After demolition of a construction, the material's life cycle is closed as the CRC-rubble is given a second life as raw material for cement production, without need for adjustments. Therefore, the concrete mixture is designed to be chemically equivalent to raw material for cement production by adequately incorporating limestone aggregates, different types of cement and industrial by-products. For environment friendly building products, not only the closure of the material's life cycle, but also the quality of the product is of great importance. Therefore, three durability aspects were investigated for two types of CRC: the resistance to carbonation, chloride penetration and freeze-thaw attack with de-icing agents.

KEYWORDS

Completely Recyclable Concrete, Carbonation, Chloride penetration, Freeze-thaw attack with de-icing agents.

[1] Faculty of Engineering of Ghent University, Laboratory Magnel for Concrete Research, Ghent, BELGIUM
midschep.deschepper@ugent.be
[2] Faculty of Engineering of Ghent University, Laboratory Magnel for Concrete Research, Ghent, BELGIUM
philip.vandenheede@ugent.be
[3] Faculty of Engineering of Ghent University, Laboratory Magnel for Concrete Research, Ghent, BELGIUM
[4] Faculty of Engineering of Ghent University, Laboratory Magnel for Concrete Research, Ghent, BELGIUM
nele.debelie@ugent.be

1 INTRODUCTION

For every human being on earth, the construction industry produces approximately one ton of concrete per year [Huntzinger and Eatmon 2009]. As a consequence, the environmental impact of concrete is prominent. A first point of interest is the concrete rubble produced by the construction sector. Concrete accounts for 40% to 67% by weight [De Belie and Robeyst 2007; ISO 2005] of the around 850 million tons of construction and demolition waste (CDW) yearly produced in the EU, CDW representing 31% of the total waste generation [Fischer and Werge 2009]. The concrete rubble produced by demolishing concrete constructions is today mainly used in inferior applications, e.g. as aggregates in granular base or sub-base application, for embankment construction and earth construction works [Marinkovic *et al.* 2010]. The reason for such a situation is that the quality of recycled concrete aggregates is usually lower than the quality of natural aggregate. Due to higher water absorption of these recycled aggregates, the produced concrete might be less durable and has therefore restricted possibilities as construction material.

A second point of interest, after the waste production, are the high emissions of CO_2 in the construction sector and their related contribution to the greenhouse effect. Within the production process of Portland clinker, the basic ingredient of Ordinary Portland Cement (OPC), a lot of lime is decarbonated and because of a high energy demand (since clinker is produced at around 1450 °C), a lot of fuels are combusted. Both of the processes lead towards the high emission of CO_2 by clinker manufacturing. Worldwide, cement production accounts for more than 1.6 billion tons of CO_2 – over 8% of total CO_2 emission from human activities [ISO 2005].

The development of a concrete completely recyclable into cement (Completely Recyclable Concrete or CRC) addresses both issues. The design of CRC, as presented in De Schepper *et al.* [2010], reduces the production of waste on the one hand and the emission of CO_2 on the other hand, both leading towards a more sustainable construction. The emission of CO_2 in case of CRC is mainly reduced by using industrial by-products, such as fly ash and blast furnace slag, as cement replacement. Also the exploitation of natural resources in clinker production is reduced, as CRC can be used within cement manufacturing without need for adjustments. Essentially, the concept of CRC is straightforward. Because cement and concrete have mutual raw materials, CRC can be designed as raw material for clinker production. A necessary condition is that CRC is chemically the same as a raw meal for clinker manufacturing.

Obviously, the concept of CRC would not be meaningful if CRC is too small or greater extent less durable than traditional concrete. This paper presents the first results regarding three durability aspects of two designed CRCs: carbonation, chloride penetration and freeze-thaw attacks with de-icing agents. Their durability performance will be compared to that of concrete prescribed by NBN EN 206-1 (2000) and NBN B15-001 (2004).

2 MATERIALS & METHODS

2.1 Materials

2.1.1 Design for reincarnation

From a predesign state, CRC is intended to be recycled as raw material within the cement production. This makes it necessary to aim for a chemical composition of CRC similar to the one of a cement raw meal, of which the requirements are well known. More information regarding the design can be found in De Schepper *et al.* [2010].

2.1.2 Mix design of CRC

In this study the accurate chemical composition of two CRCs is achieved by using limestone aggregates as a source of CaO, the most important oxide within a cement raw meal, and fly ash as source of SiO_2 and Al_2O_3, other crucial oxides for cement manufacturing. CRC 1 is produced with

CEM I 52.5 N, and CRC 2 with CEM III/A 42.5 N LA, this with the intention to study the possibility of using both cement types within CRC. To achieve the most accurate chemical composition for CRC 2, it was necessary to add limestone filler as an additional CaO source and some copper slag as Fe_2O_3 source. Fe_2O_3 is another oxide needed for cement manufacturing, but most of the time sufficiently present as minor component in raw materials providing CaO, SiO_2 and Al_2O_3.

Table 1. Concrete mixture proportions and basic properties
FA/B = fly ash to binder ratio; W/B : water to binder ratio.

Concrete materials	**CRC 1**	**CRC 2**	**T(0.50)**	**T(0.45)**	**T(0.45)A**
Limestone sand 0/4 [kg/m³]	614.2	790.1	-	-	-
Copper slag 0/4 [kg/m³]	-	32.9	-	-	-
Limestone aggregate 2/8 [kg/m³]	378.0	493.8	-	-	-
Limestone aggregate 8/16 [kg/m³]	666.5	329.2	-	-	-
Siliceous sand 0/4 [kg/m³]	-	-	714.0	715.0	715.0
Round gravel 2/8 [kg/m³]	-	-	515.0	515.0	515.0
Round gravel 8/16 [kg/m³]	-	-	671.0	671.0	671.0
Limestone filler	-	50.0	-	-	-
CEM I 52.5 N [kg/m³]	292.5	-	320.0	340.0	340.0
CEM III/A 42.5 N LA [kg/m²]	-	292.5	-	-	-
Fly ash [kg/m³]	191.4	157.5	-	-	-
Water [kg/m³]	180.0	180.0	160.0	153.0	153.0
Air entraining agent [ml/kg B]	2.00	2.00	-	-	2.24
Superplasticizer [ml/ kg B]	5.78	8.89	-	4.90	4.90
FA/B [-]	0.40	0.35	-	-	-
W/B [-]	0.37	0.40	0.50	0.45	0.45
Slump [mm][a]	68	-	70	60	130
Slump flow [mm][b]	-	620	-	-	-
Flow [mm][c]	-	-	165	153	126
Air content [v%][d]	4.0	6.6	2.6	2.8	6.6
Density of fresh concrete [kg/m³][e]	2319	2738	2369	2400	2256
Compressive strength [N/mm²][f]	60.38	52.75	57.85	69.28	53.23

Tested according to: [a] NBN EN 12350-2 (1999); [b] NBN EN 12350-8;
[c] NBN EN 12350-5 (1999); [d] NBN EN 12350-7 (2000);
[e] NBN EN 12350-6 (1999); [f] NBN EN 12390-3 (2002) (28 days)

The reference mixtures are designed according to the exposure classes and their corresponding concrete types defined in NBN EN 206-1 (2000) and NBN B15-001 (2004). The reference mixtures for testing the resistance against carbonation, chloride penetration and freeze-thaw attacks with de-icing agents are T(0.50), T(0.45) and T(0.45)A, respectively. All these reference mixtures are produced with CEM I 52.5 N as only binder and the water-to-binder ratio (W/B) is mentioned between the brackets. The use of an air entraining agent for the production of T(0.45)A is indicated by A. The mixture proportions, fresh concrete properties and compressive strength at 28 days of the produced concretes are presented in Table 1. All concrete specimens are produced and cured according to NBN B 15-001 (2004). The properties of the aggregates used are shown in Table 2.

Table 2. Characteristics of the aggregates used.

Property	LS 0/4	LA 2/8	LA 8/16	CS 0/4	SS 0/4	RG 2/8	RG 8/16
Shape	---------- Angular ----------				------ Round ------		
d10 [mm]	0.30	2.4	8.4	0.35	0.27	3.5	8.0
d50 [mm]	1.2	4.9	14	1.2	0.73	5.8	11
d90 [mm]	2.9	7.4	16	3.1	3.1	7.8	15
Water absorption [%]	0.86	1.64	0.93	-	0.87	1.25	0.88

LS = Limestone Sand; LA = Limestone Aggregate; CS = Copper Slag; SS = Siliceous Sand; RG = Round Gravel

2.2 Methods

2.2.1 Carbonation

The most severe exposure class concerning carbonation is according to NBN EN 206-1 (2000) a cyclic wet and dry environment (XC4), which is simulated in the laboratory. The specimens (100x100x100mm³) are successively placed under water for one week and in a climate chamber (20±2 °C, RH 60±5%, 10 % CO_2) for the other week. Five surfaces of each concrete cube are coated to ensure a unidirectional CO_2 ingress. After every two cycles (2 weeks under water and 2 weeks in the climate room) the carbonation ingress is measured with phenolphthalein.

2.2.2 Chloride penetration

To evaluate the chloride penetration, a tidal zone is simulated by putting cylindrical specimens (d 230 mm, h 70 mm) on a rotating horizontal shaft. In one hour, the specimens rotate one time around their axis. The bottom of the specimen is immersed in a salt solution (NaCl, 3.5%). The TAP apparatus used for this test was developed at the Magnel Laboratory for Concrete Research [De Belie *et al.* 2002] and is shown in Figure 1on the left. After three, six and ten weeks, the chloride ingress is measured by sprinkling a 0.1 M $AgNO_3$ solution on six cross sections. These cross sections are produced by splitting the specimens into three likewise parts.

2.2.3 Freeze-thaw attack with de-icing agents

The resistance against freeze-thaw attack with de-icing agents is tested according to appendix D of NBN EN 1339 (2003). A concrete test specimen with a salt solution (NaCl, 3%) on top (see Figure 1 on the right) was subjected to 28 freeze-thaw cycles. After every 7 cycles, the scaled material is collected, dried for at least 24h at 105±5 °C and weighed.



Figure 1. *left:* The apparatus used for cyclic immersion. TAP – 'Toestel voor versnelde AantastingsProeven' (Apparatus for accelerated Deterioration Tests); *right:* Test specimen for freeze-thaw attack with de-icing salts. [1 Test surface; 2 cover of the test surface; 3 salt solution (NaCl, 3%); 4 Concrete specimen; 5 PVC encapsulation; 6 Thermal insulation; 7 sealing]

3 RESULTS & DISCUSSION

3.1 Carbonation

The mechanism of carbonation consists of gaseous diffusion combined with chemical reaction. The carbonation reaction of CO_2 from the atmosphere with $Ca(OH)_2$, a cement hydration product which

buffers the pH, plays the most important role in the de-passivating phenomena causing rebar corrosion [Sisomphon and Franke 2007].

To achieve an accurate chemical composition for CRC, the replacement of cement by fly ash is necessary. The effect of such pozzolanic replacements is known to reduce the carbonation resistance of concrete. On the one hand, the quantity of $Ca(OH)_2$ will be significantly reduced since there is less cement present and the pozzolanic fly ash reaction consumes the $Ca(OH)_2$. On the other hand, the slow rate of the pozzolanic reaction results in a higher porosity at early age, although a reduced porosity may be expected at later age. Since it is not clear which mechanism prevails, the carbonation resistance of CRC containing high volumes of fly ash should be verified.

The rate of carbonation decreases in function of time, and is usually considered as proportional to the square root of the exposure period. According to this theory, the depth of carbonation x can be considered to be related to the exposure duration, t, in accordance with the second law of Fick as shown in the following equation:

$$x = k\sqrt{t} \tag{1}$$

This formula is based on the steady-state condition, with a constant carbonation coefficient. However, in reality, the carbonation reaction itself blocks the air pores in concrete, and causes a reduction in gas diffusivity. For this reason, the carbonation coefficient k should decrease with time. Simplifying the relation by still keeping k as a constant, the relation of carbonation rate with respect to time can be written as follows: $x=k \cdot t^n$, where n is the exponent value which is less than 0.5. The empirical exponent n was chosen to be 0.4 according to Sisomphon and Franke [2007].

The carbonation test described in 2.2.1 was performed after 1 month and 3 months curing. The results obtained for T(0.50) will not be discussed since no carbonation was detected at all. In Figure 2, the k-value for both CRCs is shown. It is clearly seen for CRC 2 that a prolonged curing time decreases the k-value. This decrease is probably caused by the slow pozzolanic reaction that causes a decrease of porosity between one and three months, hindering the diffusion of CO_2 in the concrete. Also for CRC 1 the k-value is lower after a curing time of 3 months, but not significantly.

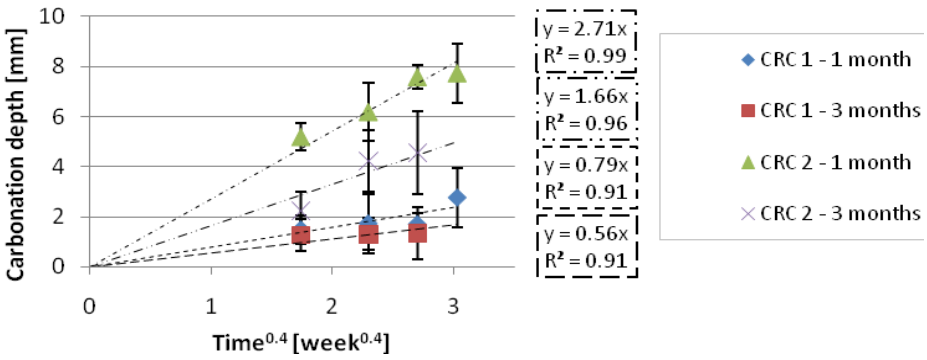

Figure 2. Determination of the carbonation coefficient *k*.

To predict the carbonation depth under field conditions, results from the accelerated carbonation test were used. According to Sisomphon and Franke [2007] k_{env} , the k-value under environmental conditions, can be calculated as followed:

$$\frac{k_{acc}}{k_{env}} = \frac{\sqrt{c_{acc}}}{\sqrt{c_{env}}} \tag{2}$$

with k_{acc} the k-value under test conditions and c_{acc} and c_{env} the CO_2 concentrations during the accelerated test and under environmental conditions. The CO_2 concentration in normal conditions, an urban area or an industrial zone is respectively 0.03%, 0.3% or 1% [Audenaert 2006]. To take into account the worst case, the simulation of carbonation depth in time in Figure 3 was performed for an environment with 1% CO_2.

With this model, it is possible to calculate the service life of reinforced concrete regarding carbonation. The end of service is defined as the moment that the carbonation depth exceeds the cover thickness of the steel rebars. According to Eurocode 2 (2005), the minimal cover thickness for both CRCs in exposure class XC4 is 25 mm, or 35 mm for a service life of 100 years. It is seen that for CRC 1 and CRC 2 a service life of 50 or even 100 years is no problem as the carbonation depth does not exceed 25 mm, based on the curves of CRC cured for three months. The higher carbonation rate during the first 3 months, probably caused by a lower porosity, is considered negligible within a service life of 50 or 100 years. Nevertheless, the use of CRC 1 is preferable to CRC 2 as its carbonation resistance is significantly better. The author also wants to note that the estimations made above are based on cyclic wet conditions with a temperature of 20 °C and a relative humidity of 60%, which does not take into account the variations in the real environment.

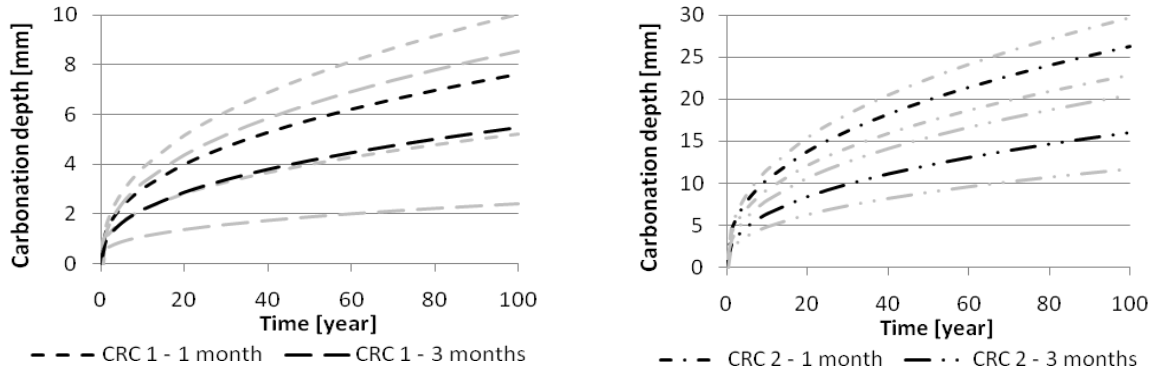

Figure 3. Model of carbonation depth in an environment with 1% CO_2: $x = k_{env} \cdot t^{0.4}$
The 95% confidence intervals (grey lines) do not take into account uncertainties concerning conversion factors.

3.2 Chloride Penetration

With the TAP apparatus, tides are simulated and chlorides can penetrate in the concrete through capillary sorption and diffusion, resulting in penetration depths x_{cap} and x_{dif} respectively. According to Audenaert [2006] the chloride ingress x_{tot} is time-dependent and can be described by the following equation:

$$x_{tot} = x_{cap} + x_{dif} = S\sqrt{t} + A\sqrt{t} = H\sqrt{t} \quad (3)$$

where S is the capillary sorption coefficient, A is the chloride diffusion coefficient and H is the chloride penetration coefficient. However, looking at the results in Figure 4, it is seen that all the results do not vary significantly from each other, and thus seem not to be time-dependent. For this reason it can be concluded that cyclic immersion of concrete in a chloride solution can not be theoretically approached by the summation of chloride penetration due to capillary sorption and diffusion. After all by doing so, the drying period is not taken into account. The succession of wet and dry periods, results in a sort of mean value around which the chloride ingress fluctuates.

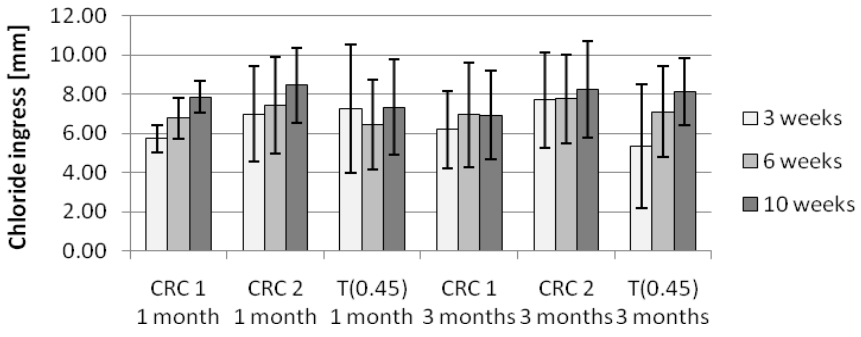

Figure 4. Chloride ingress after 3, 6 or 10 weeks cyclic immersion in a NaCl solution.

A possible explanation for the existence of a mean value is that during a drying period, the free chlorides are drawn back to the surface with the water front. For this reason chlorides need to travel the same distance every time. Therefore the chloride ingress does not increase in time, certainly not within the limited timeframe of the test. Of course, this phenomenon needs to be studied in more detail. More tests should be carried out for longer exposure periods and with slower and faster immersion cycli. Another interesting point to investigate is why the mean values do not seem to differ for the different concrete types, which for sure have different pore structures influencing capillary sorption and diffusion.

3.3 Freeze-thaw Attack with De-icing Agents

The amount of scaled off material after 28 freeze-thaw cycles is shown in Figure 5. It is seen that CRC 1 exceeds the limit of 1kg/m² scaled material and CRC 2 fulfils the requirements of NBN EN 1339 (2003). The better performance of CRC 2 compared to CRC 1 regarding freeze-thaw attack with de-icing agents is probably due to the higher air content of the fresh concrete (Table 1). The air content of CRC 1, namely 4.0%, just passes the lower limit of the European standard NBN EN 206-1 (2000) and the Belgian standard NBN B 15-001 (2004) being 4% for a nominal maximum aggregate size of 20 mm. The air content of CRC 2, namely 6.6%, on the other hand meets even the more strict American standard ACI 201.2R (2008) which requires an air content of 6-7%.

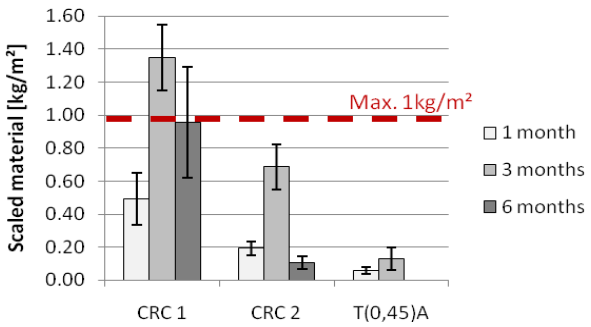

Figure 5. Scaling of concrete surfaces after 28 freeze-thaw cycles with de-icing salts, after curing for 1, 3 and 6 months.

Remarkable is that all CRC samples have the lowest resistance against freeze-thaw attacks with de-icing salts after curing for three months. Depending on the concrete type, it performs best after one or six months curing. Trying to understand the above results, namely scaling of CRC being worst after 3 months curing, a hypothesis is made based on the findings of Valenza Ii and Scherer [2007]. When a solution freezes on a concrete surface, an ice/concrete bi-material composite is formed. When the temperature is then reduced further below the melting point of the solution, the ice layer tends to contract 5 times as much as the underlying concrete. Subsequently the cracks appearing in the ice layer will propagate into the cement paste causing the scaling of the concrete surface.
The different results could then possibly be explained by the microstructure of the cement paste, which in case of concrete with fly ash (and thus in case of CRC) still develops significantly during the first 6 months. At the age of one month, the fly ash is not fully hydrated yet. Therefore, cracks in the cement paste, following the path with the lowest resistance, will stay just below the concrete surface and the amount of scaled material will be minimal. Then after curing for a longer period, the strength and microstructure of the cement paste develops and the surface layer will either be just not strong enough to resist the cracking resulting in deeper cracks and more scaled material is collected during the test (3 months curing). Or the surface layer is strong enough to resist the cracking, explaining the lower amount of scaled material after 6 months curing. Obviously this hypothesis should be verified by additional testing, as it is based on a limited series of tests and vague assumptions. Additional tests to be used could be e.g. air void analysis and microscopic analysis on thin sections of the concrete near its surface.

4 CONCLUSIONS

The main conclusion from this study is that a durable CRC can be designed. Within an environment with high risk of rebar corrosion caused by carbonation, it is better to use CRC 1. This concrete contains fly ash and CEM I 52.5 N and has a better carbonation resistance in comparison with CRC 2 with fly ash and CEM III/A 42.5 N LA. Regarding freeze-thaw resistance, CRC 2, with a higher air content, fulfils the requirements in NBN EN 1339 (2003). The resistance of CRC 1 against freeze-thaw attack with de-icing agents could probably be improved by using more air entraining agent. The results of the chloride ingress test were inconclusive and this phenomenon should be approached with a different test, e.g. an accelerated chloride penetration test according to NT BUILD 443 for a permanently wet environment (XS2). This test should also make it possible to predict the service life.
In the end, this paper proves that the extra parameter within the design of CRC, namely its chemical composition, should not limit its applicability and probably numerous other compositions can be designed depending on the availability of raw materials, which is depending on geography. Of course, for each type of CRC designed, its durability aspects should be verified. Nevertheless, thinking about sustainability, the development of Completely Recyclable Concrete could be important within the evolution towards a more sustainable construction. As CRC is designed to be recycled, CRC rubble is not a waste material, but instead a valuable material for the cement production.

ACKNOWLEDGMENTS

The author wants to thank the Institute for the Promotion of Innovation through Science and Technology in Flanders (IWT-Vlaanderen) for financial support.

REFERENCES

Audenaert, K. (2006). Transportmechanismen in zelfverdicthend beton in relatie met carbonatatie en chloridepenetratie. Department of structural engineering. Ghent, Ghent university. PhD Thesis

De Belie, N., J. Monteny and L. Taerwe 2002, 'Apparatus for accelerated degradation testing of concrete specimens', Materials and Structures, 35[251], 427-433.

De Belie, N. and N. Robeyst 2007, 'Recycling of construction materials', in Environment-conscious construction materials and systems. State of the art report of TC 192-ECM, eds N. Kashino, D. Van Gemert and K. Imamoto, RILEM Publications S.A.R.L., Bagneux, pp. 11-23.

De Schepper, M., P. Van den Heede and N. De Belie 2010, 'The Use of Fly Ash in Completely Recyclable Concrete', Proc. International RILEM Conference on Material Science (MatSci), Aachen, 2010, pp. 35-43.

Fischer, C. and M. Werge (2009) "EU as a Recycling Society." ETC/SCP working paper 2/2009.
Huntzinger, D. N. and T. D. Eatmon 2009, 'A life-cycle assessment of Portland cement manufacturing: comparing the traditional process with alternative technologies', Journal of Cleaner Production, 17[7], 668-675.

ISO (2005) "Business Plan." ISO/TC 71 Concrete, Reinforced Concrete and Prestressed Concrete.

Marinkovic, S., V. Radonjanin, M. Malesev and I. Ignjatovic 2010, 'Comparative environmental assessment of natural and recycled aggregate concrete', Waste Management, 30[11], 2255-2264.

Sisomphon, K. and L. Franke 2007, 'Carbonation rates of concretes containing high volume of pozzolanic materials', Cement and Concrete Research, 37[12], 1647-1653.

Valenza Ii, J. J. and G. W. Scherer 2007, 'A review of salt scaling: II. Mechanisms', Cement and Concrete Rese*arch*, **37**[7], 1022-1034.

XII DBMC
International Conference on Durability of Building Materials and Components
PORTO - PORTUGAL, April 12th-15th, 2011

Tailored Precipitated Silica Adsorbents for the Built Environment

Ebenezer Twumasi [1]
Peter Norberg [2]
Christer Sjöström [3]

ABSTRACT

The paper provides a review of the synthesis and adsorptive properties of a novel class of precipitated silica materials. To enhance or tailor the adsorption efficiency, various trapping chemicals (potassium hydroxide, potassium permanganate) or co-adsorbents (coconut activated carbon) are incorporated in the structure of the substrate material. Further, it discusses the applicability and performance over time of the material as adsorbents for removal of hydrogen sulphide, sulphur dioxide and toluene contaminants which are potentially hazardous to sensitive equipment and more importantly, human health. Chemical substances in the air are an unavoidable by-product of most human endeavours within industry and transportation. The need for adsorbents to combat Airborne Molecular Contamination (AMC) follows from the continued intensification of the global environmental movement as well as the rapid industrialisation of developing countries. The removal performance of modified precipitated silica adsorbent shows that the new adsorbent can be tailored to remove low concentrations of sulphur dioxide, hydrogen sulphide and toluene contaminants at indoor environment conditions. The results further shows that the new precipitated silica adsorbent impregnated with 8 wt% KOH shows better performance than commercial alumina impregnated with 8 wt% $KMnO_4$.The adsorbent material may find interesting and efficient uses as passive sinks for pollutants incorporated into more traditional building products such as acoustic baffles or as ingredients in various coatings. The filter material is environmentally friendly and consists of benign chemicals that are abundant worldwide. Performance over time aspects, re-use and recycling of exhausted filter materials are key issues.

KEYWORDS

Precipitated silica, Adsorbents, Molecular filtration, Indoor air quality, Performance over time.

[1] Materials Technology, KTH Research School, University of Gävle, Sweden, ebenezer.twumasi@hig.se
[2] Materials Technology, KTH Research School, University of Gävle, Sweden, peter.norberg@hig.se
[3] Materials Technology, KTH Research School, University of Gävle, Sweden, christer.sjöström@hig.se

1 INTRODUCTION

The lifestyles (work and leisure activities) of people living in industrialized nations mean they spend more than 90 percent of their time indoors [CPSC Document #455 1994]. The necessary ventilation of buildings means we are increasingly exposed to gas contaminants in the external air. Exposure to air contaminants in the indoor environment have been associated with health symptoms such headaches, itchy eyes, reduced work efficiency, and others that have generally been referred to as Sick Building Syndrome (SBS). Whether in museums or microelectronics production units even trace levels of pollutant gases can do irreversible damage [Sucha *et al*.1991 and Muller 2002]. Therefore it may be more economical to clean the indoor air and recycle a certain portion of it as compared to heating (or cooling) and eventually humidify or dehumidify the fresh air from the outside [John 2000]. The methods used to remove contaminating gas in the built environment are known but only adsorption has found widespread use [Schweitzer 1979]. The performance of the adsorption process depends on the quality of the adsorbent. The most generic adsorbents used commercially are activated carbon, activated alumina, molecular sieve and silica gel [Yang 2003]. Considering the global environmental movement for clean air as well as rapid growth of developing countries, the development of new and better sorbents will not only make major advances in gas adsorption technology, but also help meet the new challenges that cannot be met with the currently commercially available sorbents. Herein we present the synthesis of a new sorbent material that can be used as filter medium to remove contaminating gases. The adsorptive property of the prepared sorbent has been studied by the use of nitrogen gas adsorption. To enhance it adsorption performance various impregnate chemicals (KOH and $KMnO_4$) or co-adsorbents (coconut activated carbon) were incorporated in the structure of this sorbent material. The dynamic adsorption performance over time of the modified sorbents was tested by subjecting them to an air stream containing sulphur dioxide, hydrogen sulphide or toluene contaminants. These contaminating gases have been chosen because they are commonly found in the built environment at low concentration levels.

2 EXPERIMENTAL

2.1 Adsorbent Synthesis

The synthesis was based on the method published by Norberg et al., 2006. In this specific laboratory preparation 30g (22ml) of waterglass (SiO_2:Na_2O = 3.35) as silica source was diluted with 78ml of deionised water. A salt solution was prepared from 60g of $MgCl_2 \cdot 6H_2O$; 20g of $CaCl_2 \cdot 2H_2O$ and 930ml of deionised water. The salt solution (500ml) was added to the silicate solution (500ml) while being under vigorous stirring at room temperature. The resulting white precipitated silica slurry was allowed to settle. The slurry was then washed to remove soluble salts. Finally the slurry was dewatered by vacuum filtering until a coagulum holding 85% of water was obtained. From here activated coconut carbon and different impregnate chemicals were added to the coagulum. The detailed synthesis procedure has been described elsewhere [Twumasi *et al*. 2010]. The adsorbent with 16 wt% activated carbon added is denoted PSC(I)-16, with 8 wt% KOH addition named PSS-KOH whereas 8 wt% and 13 wt % $KMnO_4$ is denoted as PSS(I)-8 and PSS(I)-13 respectively.

2.2 Nitrogen Physisorption

The nitrogen adsorption/desorption isotherms were measured by a Micromeritics ASAP 2010 volumetric adsorption analyser. The samples were degassed at 150°C in vacuum for 20 hrs. The BET (Brunauer-Emmet-Teller) standard equation was used to calculate the surface area (S_{BET}) from adsorption data obtained in the relative pressure (p/p_o) range of 0.03 to 0.3. The micropore surface area S_{mic} and micropore volume V_{mic} were obtained via thickness method (t-method) [Rouquerol *et al*. 1996]. The total pore volume (V_{tot}) was calculated from the amount of gas adsorbed at $p/p^o \approx 0.99$. Pore size distribution (PSD) was derived using the density functional theory method (DFT) assuming cylindrical pores, oxide surface model and cylindrical pore geometry. These were performed with the software provided with the Micromeritics apparatus.

2.3 Dynamic Adsorption of H_2S, SO_2 and Toluene

The most common concentration range for pollutant gases emitted in the indoor environment are very low and by far the principles of dynamic adsorption has been employed for removal of these contaminant gases [John 2000]. Therefore the performance of tailored silica adsorbents for purification of contaminated gases has been done using a dynamic challenge test at indoor conditions in other to mimic a real life scenario.

The analysis was performed in a system similar to the setup described in ASHRAE 145.1 [Ashrae 2008] but with four parallel columns. Air with controlled temperature and humidity is fed from a large supply chamber and the selected challenge gas (i.e. H_2S; SO_2; toluene) is injected from a pressurised gas cylinder by means of a computer controlled mass flow valve. The H_2S is measured by a Thermo Environmental 43 C UV fluorescence instrument with a TE 340 H_2S converter. Four parallel samples of ~50 g each were loaded into the four columns forming 52 mm high beds. The flow was 0.9 m^3/h and 0.4 s contact time. The challenge upstream concentrations were ~12000 ppb H_2S and 3100 ppb SO_2 at 23 °C and 50% RH. In adsorption of SO_2, flow rate was 1.8 m^3/h, contact time of 0.1s and bed height of 26mm. The downstream concentrations with time as well as removal efficiency [%] in relation to adsorbed amount in grams were recorded.

3 RESULTS AND DISCUSSIONS

3.1 Surface Area and Pore Structure

Nitrogen adsorption isotherms and pore size distribution for pure PSS, PSC-16 and impregnated PSS samples are presented in Fig.1 and the corresponding physicochemical parameters are summarized in Table 1. Pure PSS substrate exhibits type IIb isotherm. The incorporation of impregnate chemicals or carbon into the PSS substrate did not change the shape of the isotherm. However, in the PSC (I)-16 isotherm a high nitrogen uptake in the p/p^o range of 0.003-0.3 was observed which is typical of micropore structure. The PSC (I)-16 shows an increase in S_{BET} area, micropore surface area and exhibits a higher micropore volume than pure PSS. When compared with pure PSS a 46% increase in micropore surface area was observed in PSC(I)-16. The presence of micropores in the samples prepared is confirmed by the fact that the linear region of the *t*-plot intercepts the y-axis in these plots (Fig.1B).

Table 1. Textural properties of new silica sorbent with various impregnates or activated carbon.

Samples	S_{BET} (m^2/g)	S_{mic} (m^2/g)	Smes (m^2/g)	V_{tot} (cm^3/g)	V_{mic} (cm^3/g)	V_{mes} (cm^3/g)	dmic (nm)	dmes (nm)
PSS pure	373	45	328	0.65	0.021	0.625	1.41	5.4
PSC(1)-16	511	82	429	0.70	0.042	0.658	1.39	5.4
PSS-KOH	312	30	282	0.59	0.012	0.578	1.41	5.4
PSS(I)-8	320	10	310	0.493	0.003	0.490	1.41	5.4
PSS(I)-13	260	8.4	252	0.399	0.002	0.397	1.41	5.4

SBET - BET specific surface area, Smic – t-plot micropore surface area, Smes – mesopore surface area, Vtot – total pore volume, Vmic – micropores volume, Vmes – mesopores volume, dmic, dmes – micro-and mesopore maxima peaks in DFT pore size distribution

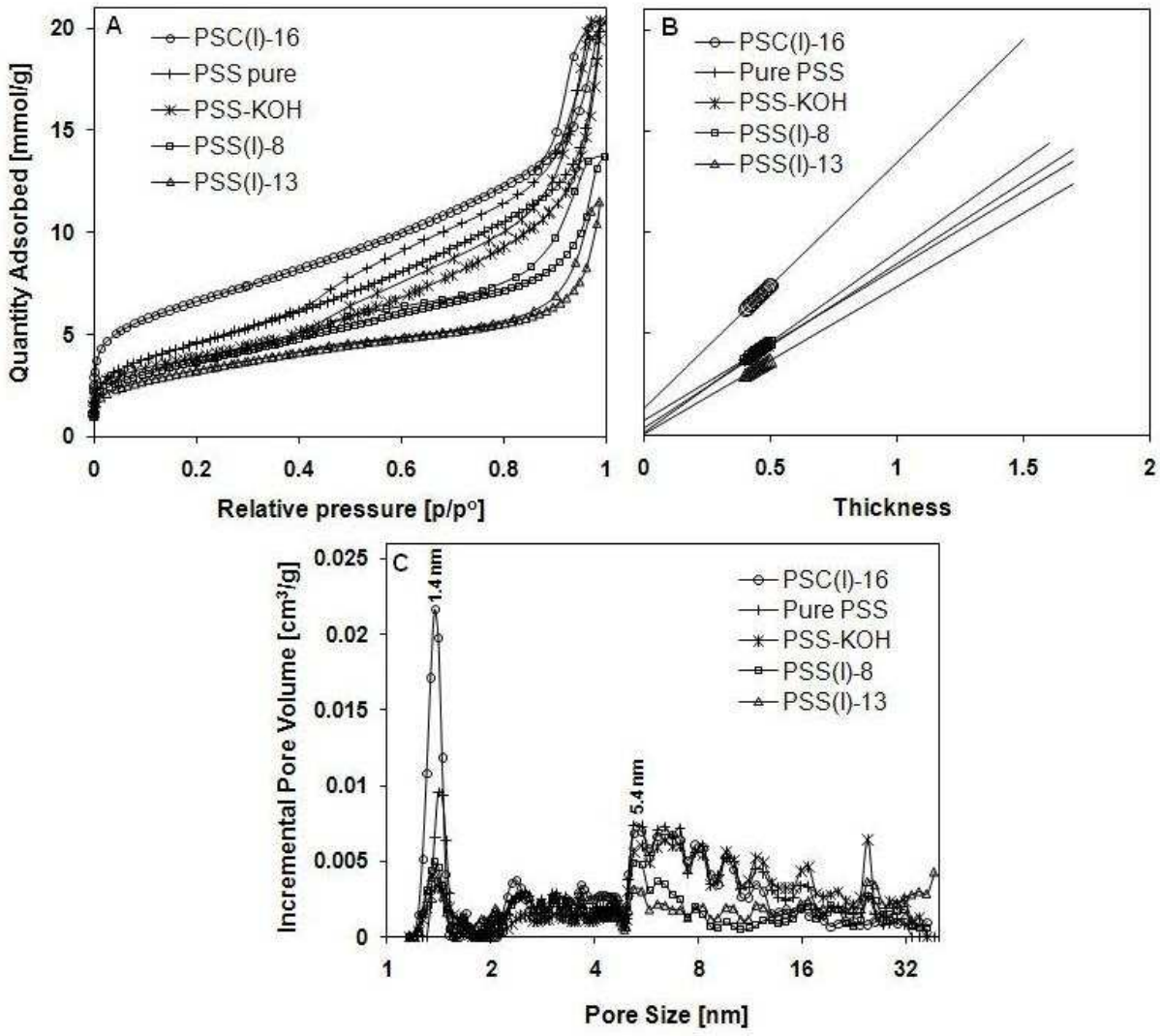

Figure 1. (A) Nitrogen adsorption isotherm, (B) t-plot and (C) pore size distribution of pure PSS and samples (PSS(I)-8,PSS(I)-13 and PSS-KOH) modified with doped chemicals and PSC(I)-16 with activated carbon.

A decrease in total pore volume and S_{BET} surface area were however observed for all impregnated materials in comparison to the corresponding pure PSS and PSC (I)-16, indicating the location of the impregnates into the pore systems of the PSS. The total pore volume, micro- and mesopore volumes and areas also decrease with increasing impregnate amount (Table 1).

The decrease of micro porosity with impregnation indicates that some deposition took place in the micropores; however when comparing the difference in micropore volume and mesopore volume reduction it turns out that the amount of e.g. permanganate deposited in mesopores pores was higher than that deposited in the micropores. This was further proven by the large reduction in incremental pore volume in the mesopore region of pore size distribution (Fig. 1C). The decrease was more pronounced for material (PSS (I) -13) obtained by 13 wt % $KMnO_4$ impregnation.

The maximum peaks from the PSDs of all the samples are identified in Fig. 1b and were about 1.4 nm in the micropore region and 5.4 nm in the mesopore region. Regardless of the impregnate chemical or activated carbon incorporated in the structure of the pure PSS, the complete pore size distribution (PSD) remained even if the incremental pore volume was changed. In the case of PSC (I)-16, an increase in incremental pore volume was observed in the micropore size region which confirmed also an increase in micropore volume. The samples treated with impregnate chemicals however show a

decrease in peak height of the distribution. This can be explained by that fact that the impregnated chemicals did not block pore entrance but rather are sited within and on the surface of the pore walls and volume of the silica substrate. The isotherms (Fig.1A) and pore size distribution (Fig.1C) for samples incorporating impregnation chemicals did not show any significant changes when compared to the starting substrate. These findings indicate that the porous structure of the new silica adsorbent do not significantly change when a chemical impregnant is added.

3.2 Dynamic Adsorption Performance of H_2S, SO_2 and Toluene

3.2.1 Toluene adsorption performance of pure PSS and PSC (I)-16

The uptake performance together with RH data of pure PSS substrate versus PSS incorporating 16 wt% activated carbon (PSC(I)-16) is shown in Fig.2A. The downstream concentration of pure PSS traces the upstream concentration thus no adsorption occurs at 3-9 ppm level of toluene. The plot of efficiency versus adsorbed amount (grams of toluene/grams of PSC (I)-16) as shown in Fig.2B, further confirms the poor performance of pure PSS by a sudden drop of its efficiency towards zero adsorbed amounts. In comparison, The PSC(I)-16 sample exhibits a much lower downstream concentration despite the variation in upstream concentration and humidity that depend on experimental errors. If the adsorbed amounts are compared at 65% efficiency and by this avoiding the concentration and humidity variation after 36 hours the uptake in (wt %) of the carbon content is 8.9 wt %. If the sample would have consisted of 100% carbon the uptake at 65% efficiency would have been in the range of 16-18(wt %) depending on the granule size 2-7 mm [Lindahl, 2010]. This indicates that the carbon pore system is accessible to a great extent even if the composite composition may be further improved.

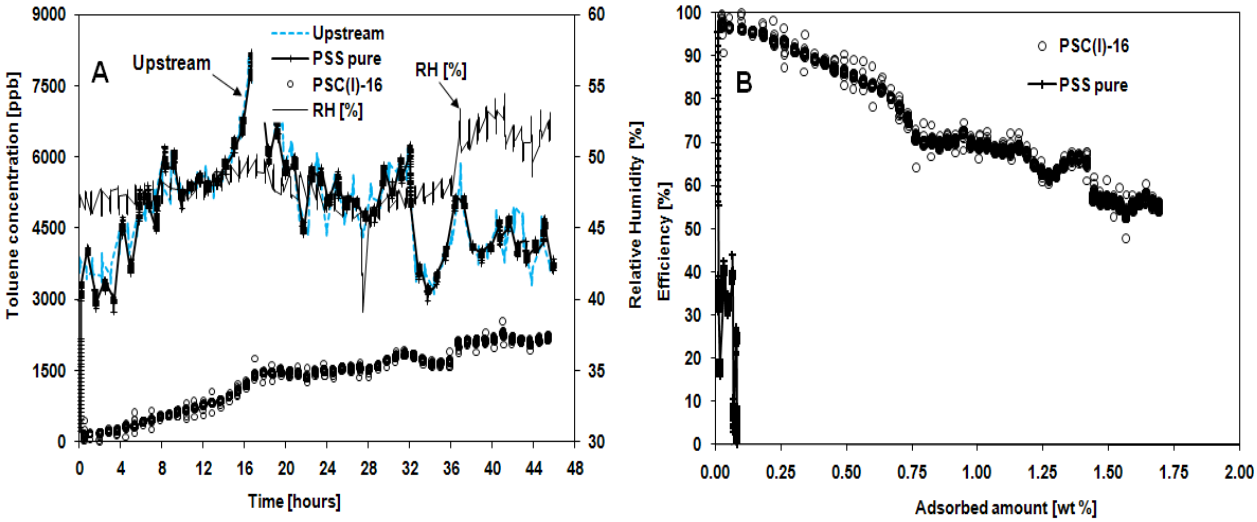

Figure 2. (A) Decrease of toluene inlet concentration with time and (B) efficiency vs. adsorbed amount (grams of toluene /grams of samples).

3.2.2 Desulfurization performance of the impregnate PSS

Figure 3 shows the desulphurization performance of the PSS doped with 8 wt % $KMnO_4$ (PSS (I)-8) versus PSS doped with 13 wt % $KMnO_4$, (PSS(I)-13). Table 1 shows the hydrogen sulphide uptake capacity (grams of sulphur/grams of doped PSS). The adsorbed amounts of hydrogen sulphide were compared at the time of 50% breakthrough (i.e. at 50% efficiency). The PSS(I)-13 shows a better performance over the PSS(I)-8 sample. This is evident from Fig.3A where downstream concentration of PSS(I)-8 traces the upstream concentration thus no adsorption occurs after ~60 hours while even lower downstream concentration was observed for materials impregnated with 13 wt% $KMnO_4$ after 120 hours. Fig.3A also indicate the immediate drop of PSS(I)-8 efficiency towards zero adsorbed amount while that of PSS(I)-13 shows gradual decline of performance over a wide period of time. It can be concluded that H_2S uptake performance occurred via chemical adsorption and relates to the

amount of $KMnO_4$ in the PSS substrate. Nevertheless, the use of $KMnO_4$ poses health hazards for human and environmental challenges when it comes to reuse or recycle of the worn out doped materials. In line with this, an alternative effective and yet environmental friendly impregnate chemical, potassium hydroxide (KOH), has been used as option for SO_2 removal.

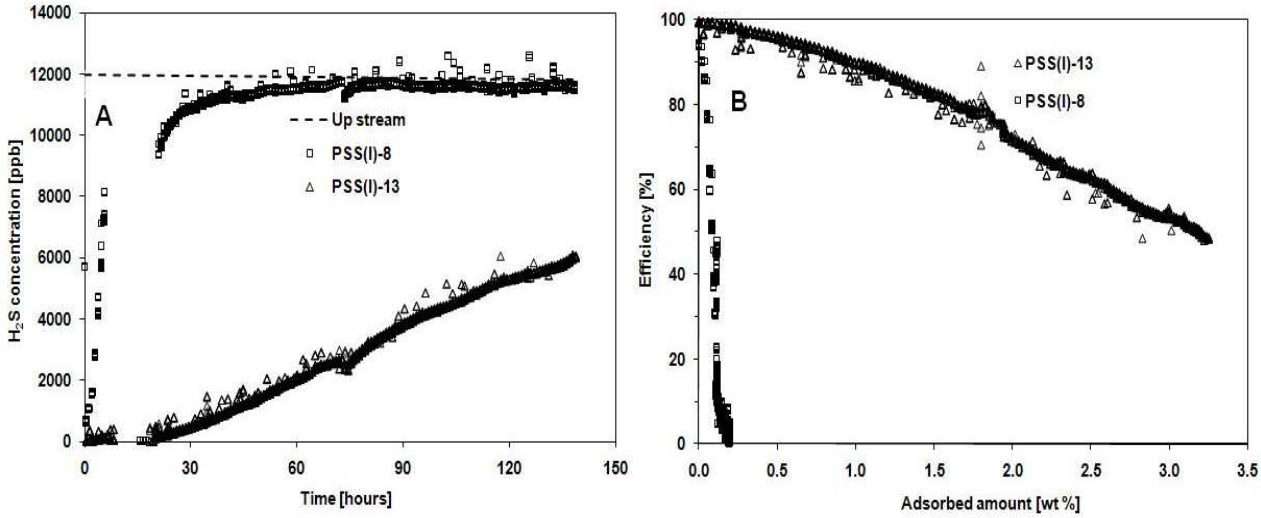

Figure 3. (A) Decrease of H_2S upstream concentration with time and (B) efficiency vs. adsorbed amount (grams of H_2S /grams of samples).

Figure 4 shows the performance of PSS substrate impregnated with 8 wt% KOH versus commercially available alumina impregnated with 8 wt% $KMnO_4$. The PSS-KOH sorbent has shown a better performance over commercial alumina-$KMnO_4$ material. This is evident from Fig.4A where downstream concentration of alumina impregnated with $KMnO_4$ traces the upstream concentration while lower downstream concentration was observed for PSS-KOH even after 250 hours. From Fig.4A if the sulphur dioxide uptake capacity (wt %, grams of SO_2/grams of sorbent) is compared at the 50% breakthrough (i.e. at 50% efficiency), the uptake in (wt %) are for PSS-KOH: 1.7 (wt %) and 0.49 (wt %) for alumina-$KMnO_4$. This indicates that the KOH impregnate in the PSS pore system is accessible to a great extent and possess high reactivity.

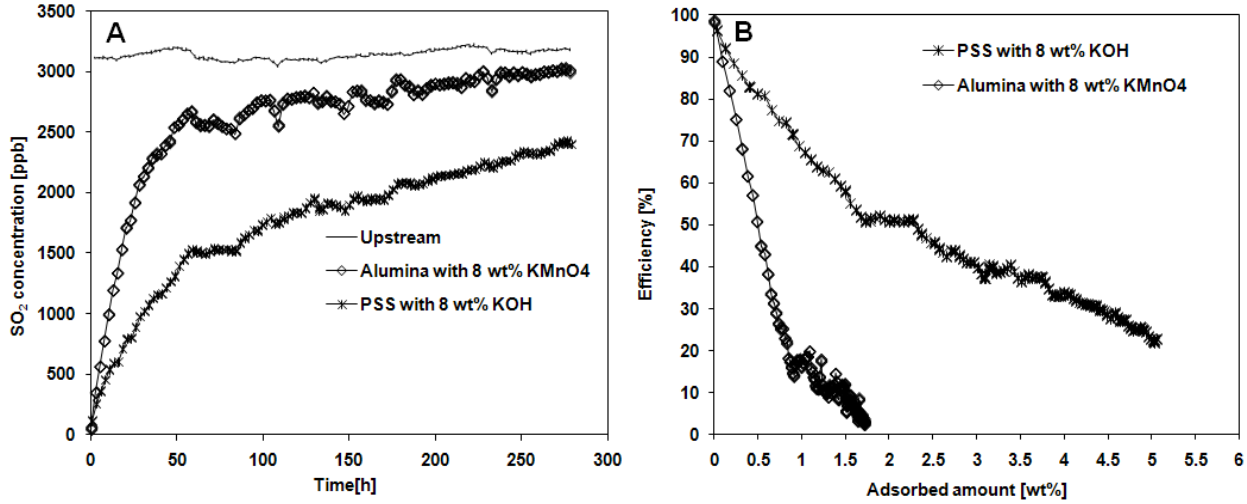

Figure 4. Comparative performance of PSS impregnate with 8wt% KOH vs. commercial alumina impregnated with 8 wt% $KMnO_4$.

3.3 Service Life and Re-use of the Tailored Silica Adsorbent

The assessment of the acceptable performance of adsorbents used in e.g. cleaning of air in the process industry may be performed by sampling of filter media from the filter cassettes. However, the most common approach is based on experience, i.e. with knowledge of the contaminant loading over time the filter media is exchanged well before the filter bed is completely used. Surveillance of filters by use of sensor technologies is less common. The used filter media is normally deposited, and reuse or recycling of filter media is today largely unusual. The environmental burden of this approach is evident, especially if considering that a significant amount of the deposited filter media may still contain active impregnate chemicals.

For cleaning of air also in indoor built environment applications, the service life of adsorbents will depend on the concentration of contaminants. Given the variability in the concentration of contaminants, the temperature and humidity, it will always be challenging to estimate the service life of an adsorbent material in a specific built environment condition. There are several complicating factors in determining the service life. The performance and prediction of lifetime of the tailored silica adsorbents have been determined and compared under carefully controlled conditions of flow velocity, temperature, relative humidity, challenge gas composition and concentration, among other factors. A performance standard ASHRAE 145.1 has been used to test the performance and estimate the service life of the tailored silica adsorbent under controlled conditions. Expressed generically, the time that the tailored silica adsorbent can remain in service depends on the amount of impregnate chemical or, as in the case of the silica/carbon composite, the composition of carbon in the adsorbent. Therefore the performance can be improved by altering the composition of impregnate chemicals or carbon with due concern at the same time not to negatively affect the porous system.

There is in general a pronounced need to further develop the reuse and recycling properties of filter media. Re-use means in this context that a used filter medium is gassed off under controlled conditions and then again may serve as a filter. This normally implies that the filtering process is predominantly physical adsorption in the porous system of the filter media. When the contaminants are chemisorbed within the adsorbents, and when no longer posing any risk, the used silica filter media may effectively serve as an ingredient material in other material matrixes. Examples may be based on using the effective porous system for insulation purposes, or just simply as a fertilizer together with e.g. other compounds rich in phosphor and/or nitrogen.

4 CONCLUSIONS

A new silica adsorbent has been prepared using sodium silicate and precipitated with magnesium and calcium salts. Their adsorptive properties; specific surface area, total pore volume and pore size distribution have been determined by nitrogen gas adsorption/desorption. The removal performance of sulphur dioxide, hydrogen sulphide and toluene has been tested by dynamic adsorption.

The adsorptive properties of a PSS adsorbent incorporating the co-adsorbent activated carbon shows an increase in surface area and total porous volume, whereas chemical impregnate incorporation results in a relative decrease in surface area and pore volume. However, the porous structure of the modified sorbent does not significantly change when carbon or chemical impregnate is added.

The removal performance of the precipitated silica adsorbent shows that the new sorbent can be tailored to remove low concentrations of sulphur dioxide, hydrogen sulphide and toluene contaminants at indoor environment conditions. The results further show that the new precipitated silica adsorbent impregnated with 8 wt% KOH provides better performance than commercially available alumina impregnated with 8 wt% $KMnO_4$.

Besides the use of KOH as an impregnate chemical, a search for other environmentally friendly and yet effective impregnate chemicals compatible with this new silica adsorbent is ongoing. In cases where contaminates are chemisorbed on the adsorbent and does not pose any risk, the material can be used in insulation panels or as fertilizer with other compounds rich in phosphorus and nitrogen.

ACKNOWLEDGMENTS

Svenska Aerogel AB is acknowledged for providing materials and contribution to synthesis technologies.

REFERENCES

Ashrae Standard I45.I 2008, *Laboratory Test Method for Assessing the Performance of Gas-Phase Air-Cleaning Systems: Loose Granular Media*.

Consumer Product Safety Commission, American Medical Association, Environmental Protection Agency and the American Lung Association. 1994, *Indoor Air Pollution. An Introduction for Health Professionals*, CPSC Document #455 pp.1.

John, D., McCarthy, F. Samet, J., Jonathan, M. 2000, *Indoor Air Quality Handbook*, McGraw-Hill, New York, pp. 271.

Lindahl, C. 2010, Camfil AB, personal communication.

Muller, C. 2002, *Implementation and evaluation of AMC control programs at a Dram and a Disk Drive manufacturing facility*, SEMICON Taiwan.

Norberg S.P., Lindahl L.G., Abrahamsson, J. 2007, *Agglomerates of precipitated silica, method for their preparation and their use as filter medium in gas filtration.* Swedish Patent SE 529160 C2.

Rouquerol, F. Rouquerol, J. Sing, K. 1996, *Adsorption by powders & porous solids principles, methodology and applications*, Academic press, pp.174.

Schweitzer, P.A. 1979, *Handbook of separation techniques for chemical engineers*, James Peter Associates, Inc. McGrawHill pp. 238.

Sucha S. P., Grosjean D. 1991, *Sorbent removal of air pollutants from museum display cases*, Environment International, Vol.17, pp. 39-50.

Twumasi E., Forslund M., Norberg P. Sjöström C. 2010, *Textural and adsorption properties of a carbon-silica composite adsorbent for air filtration.* World Journal of Engineering (accepted).

Yang R.T., 2003, *Sorbents: Fundamental and Applications*, John Wiley & Sons, Inc., Hoboken pp.3-7.

XII DBMC
International Conference on Durability of Building Materials and Components
PORTO - PORTUGAL, April 12th-15th, 2011

Development of Building Materials through Alkaline Activation of Construction and Demolition Waste (CDW) – Resistance to High Temperatures

Joana Gonçalves Rapazote [1]
Cristovão Laginhas [2]
Amândio Teixeira-Pinto [3]

ABSTRACT

Present work is dedicated to the development of a new building material obtained by the alkaline activation of construction and demolition waste (CDW). The proposed process is cement free. Raw materials for binder and aggregate compounds are exclusively made from CDW, used additions are also by-products from industry.

CDW are the goal of this work because they are not being currently recycled; they are inert and aluminosilicates are their major constituents.

Common CDW consists of two major fractions: concrete products and ceramic products. The major constituent of the first are SiO2 and CaO along with minor concentrations of Al2O3 and Fe2O3, mostly crystalline. The main constituent of the latter are SiO2 and Al2O3 and comprises crystalline and glassy constituents as well.

Aluminosilicates of both fractions will actively participate in the reaction and for the obtaining of ASH gel (A= Al2O3, S = SiO2, H = H2O) that is the main binding phase. Any deficiency in chemical constituents is compensated by the addition of suitable material.

Final products are a very hard ceramic like product with civil engineering potential applications such as pavement blocks, precast concrete blocks, retaining walls, in general the same use as plain concrete.

KEYWORDS

Construction and demolition waste recycling, Alkaline activation, Building materials, Durability.

[1] Trás-os-Montes e Alto Douro University (UTAD), Vila Real, PORTUGAL, joanarapazote@gmail.com
[2] Trás-os-Montes e Alto Douro University (UTAD), Vila Real, PORTUGAL, cristovaolg@yahoo.com
[3] Trás-os-Montes e Alto Douro University (UTAD), Vila Real, PORTUGAL, yrache@utad.pt

1 INTRODUCTION

Environmental issues dominates political, economical and research schedules all over the world.

In response to those concerns new challenges are arising everyday in the science community with respect to waste management, to the reduction of carbon dioxide emission, to natural resources demand and to landfill disposal. Construction is one of the most important activities and it is seen as a real threath to sustainable development considering the permanent use of limited resources and the disposal of huge quantities of debris [Symonds Group 1999;European Environment Agency 2001].

This study pretends to be a contribute to the waste management and in general to favour the sustainability of construction industry since the basic goal is to use exclusively construction and demolition waste to get new building materials with no Ordinary Portland Cement addition [Rapazote et al, 2008].

Alkaline activation is the used technique that is playing a promising role in the construction industry [Duxson et al 2007; van Deventer 2007; Teixeira Pinto 2002; Komnitsas and Zaharaki 2007; Xu and van Deventer 2002]. It is widely accepted that geopolymers (or alkali activated products) have better environmental performance than Ordinary Portland Cement (OPC) ones that can be an alternative with great potential. Nevertheless mores studies are needed to get real applications and to establish it as a viable technology.

Tiles, bricks and ceramic waste (named herein A), concrete products and stone masonry (named herein B) are the two major fractions of CDW commonly produced and are the raw material used in this research. Those materials are inert, which is an interesting characteristic to be mentioned (being not harmful to humans, animals or environment). In fact they have, as their major constituents, the most common minerals of the Earth crust, aluminosilicates. Another advantage of these materials is that they usually appear in different times on the construction process, so they can be easily separated and collected.

A good mechanical performance (already achieved) is not enough to announce a new kind of building materials, durability experiments are the following step that should be performed according to potential applications designed for them. Lixiviation tests have to be made in order to prove their stability and inoquity. Other particular properties must be studied if we want to promote special applications. Many author have noted that geopolymers present good behaviour at high temperature situations [Davidovits 1994; Teixeira Pinto et al 2002; Kong and Sanjayan 2008]. Present study evaluates the effect of high temperatures exposure (900ºC for 2 hours) on mechanical behaviour. High temperatures exposure during fire is responsible for a wide range of damages in concrete structures that implicate economical costs and risk for human life. New approaches in construction materials research are needed to get superior fire resistance.

2 EXPERIMENTAL

2.1 Classification of Materials

The first step of experimental work was collecting waste (considering that hazardous substances were previously excluded) according to the following:

- A: Ceramic products (including bricks, roof and floor tiles and sanitary ware);
- B: Concrete products (mainly cement blocks);
- AB: Mixture of A and B.

Their classification according to the European Waste Catalogue and Hazardous Waste List (established in European Comission Decision 2000/532/EC) is shown in Table 1 below.

Table 1. Classification of prime materials according to European Waste Catalogue.

Material	Code	Waste included in each category
-	17 00 00	Construction and demolition waste
-	17 01	Concrete, bricks tiles and ceramics
B	17 01 01	Concrete
A	17 01 02	Bricks
A	17 01 03	Tiles and ceramics
-	17 01 06(*)	Mixtures of, or separate fractions of concrete, bricks, tiles and ceramics containing dangerous substances
AB	17 01 07	Mixture of concrete, tiles, ceramics other than those mentioned in 17 01 06

Specimens made exclusively from CDW and water treatment plant sludge rich in aluminiun (as a chemical correction addition) were prepared. The binder and the aggregates were mixed with a liquid alkaline activator, conformed in 4x4x16cm3 moulds, vibrated and cured. After a certain curing time all samples were submitted to strength mechanical tests and durability experiments. In order to get comparable results probes of Ordinary Portland Cement 32.5 class were made with a water/cement ratio of 0.4 and a binder binder/aggregate of 0.5. Finally they were subjected to the same test conditions as CDW ones. Water treatment plant sludge, the used addition, was previously calcined and milled.

2.2 Preparation of Binders and Aggregates

From an initial amount of 800 kg of A and B raw materials respectively, aggregates were crushed below 4,75 mm, maximum size particle considering the dimension of the moulds. To prepare binders, powders were collected from A and B materials after crushing and then milled with a metal ball mill RETSCH S100 and sieved below 250µm. A thermal treatment for 2 hours at 750ºC was applied to material B to increase its reactivity for alkaline activation by dismantling its crystalline structure and increasing the amount of amorphous phases. The thermal history of ceramic products (A) favours the direct use without that treatment.

The specific weight of materials (LNEC E64 – 1979 specs), was 2700 kg/m³ for A and 2725 kg/m³ for B, water was used for the determination with picnometer. The sludge from the water treatment plant, herein named L, was used as supplementary alumina source to binder A in accordance with Portuguese patent nº 104535 from 2009 [Teixeira Pinto and Tavares], after being submitted to a thermal treatment of 2 hours at 750ºC, milled and sieved below 250µm. After that the new material was named binder AL. The binder ALB (after AL and B) was obtained by mixing 50% of each AL and B binders. Homogenization of the mixture of binders and additives was performed in the ball mill for 1 hour to get the final binders AL and ALB. Binder B, with no additive, was ready to use after manual homogenization.

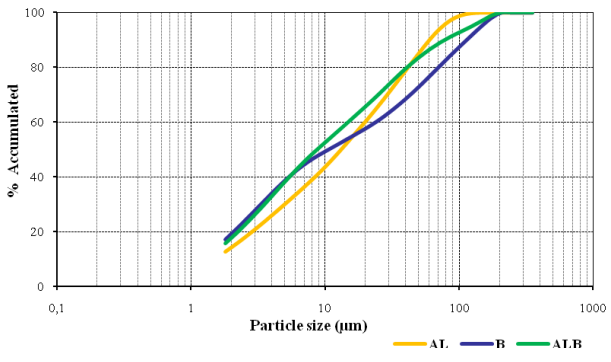

Figure 1. Particle size distribution of AL, B and ALB binders.

To determine the particle size of binders AL, B and ALB a Sympatec Helos laser difraction equipment was used. The binder particle size distribution for AL particles (Figure 1) showed more than 90% were below 125μm and 50% were below 31,08μm. For B binder, 90% of particles were below 85,81μm and 50% were below 6,52μm. The particle size distribution of ALB was comprised of 90% below 72μm and 50% below 8,6μm.

The chemical compositions and loss of ignition of materials before and after preparation were determined by X-Ray fluorescence on Siemens SRS3000 equipment and presented in Table 2.

Table 2. Chemical composition and loss of ignition of materials by XRF.

Type	SiO_2	Al_2O_3	CaO	Fe_2O_3	K_2O	MgO	TiO_2	Na_2O	LOI
A	66,37	21,62	3,13	2,56	2,96	0,78	0,61	0,64	0,82
L	29,98	49,17	0,56	6,16	1,44	0,56	0,16	0,21	10,24
AL	52,76	31,92	2,57	4,78	2,31	0,69	0,46	0,46	3,16
B	41,88	1,74	34,18	0,41	0,45	0,29	0,02	0	20,39
ALB	47,21	16,77	18,66	2,46	1,37	0,49	0,23	0,14	11,98

2.3 Activator (Liquid Phase)

Alkaline activator was obtained by mixing 1 part of sodium hydroxide solution (at 15 molal to binder AL and ALB and 12,5 molal to binder B) and 2 parts of sodium silicate solution (commercial brand Solvay D40), and was left to cool to ambient temperature before use. Solutions of sodium hydroxide were prepared from dissolution of pearls of NaOH with 99% of purity and then were left to cool to room temperature before mixing with sodium silicate.

2.4 Compositions

Better compositions achieved for each category (ceramics waste, concrete waste and mixture of concrete and ceramics wastes) were performed according the information on Table 3. To evaluate and select the optimal compositions the influence of the following parameters was considered: workability of pastes, needs of liquid phase (expressed on activator/binder ratio), setting process, strength results.

Table 3. Characteristics of optimal compositions achieved with CDW.

Code	Materials	Binders (with additives)	Aggregates	Ratio*
17 01 02 and 17 01 03	A	0,7A+0,3L	2A	0,8
17 01 01	B	1B	2B	0,6
17 01 07	AB	0,35A + 0,5B+0,15L	1A+1B	0,7

* Activator/Binder

2.5 Preparation of Probes

After mixing in a small lab batcher, the paste was conformed in steel prismatic moulds of 4x4x16cm3 and compacted on a vibration table. Samples were cured at 65ºC for 48 hours at 98% relative humidity. Thermal curing occurred at climatic chamber WEISS WK11340/40.

2.6 Mechanical Strength

Mechanical strength tests were performed according to EN196-1:2006 in a Form-Test model Mega 10-250-15D hydraulic press equipment as is shown in Fig. 2. Flexural strength was determined with centre point loading.

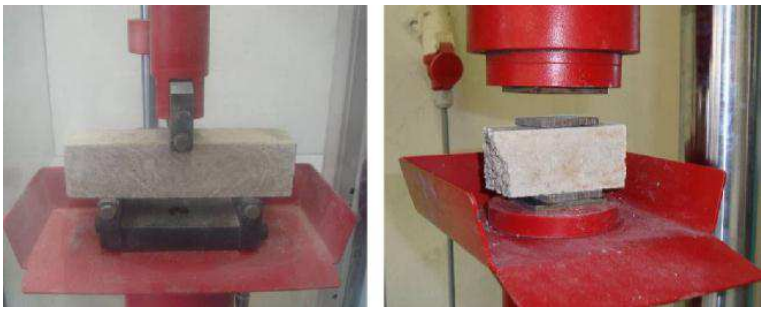

Figure 2. Flexural and compressive strength tests.

2.7 Resistance to High Temperature

All specimens, 3 for each material, AL, B, ALB and OPC, were placed inside the furnace at room temperature and were heated until 900ºC according to blue heating curve presented in „Fig. 3" measured [Osório, 2007]. The heating curve of a furnace in comparison to a standard heating curve of a fire (ISO834) grows slowly, which means that to reach target temperature it"s necessary approximately the double time of exposure. After reaching the target temperature they were left for two hours at 900ºC before shutting down the furnace and were left inside for 24 hours to cool down. Finally they were observed and subjected to compressive and flexural strength tests.

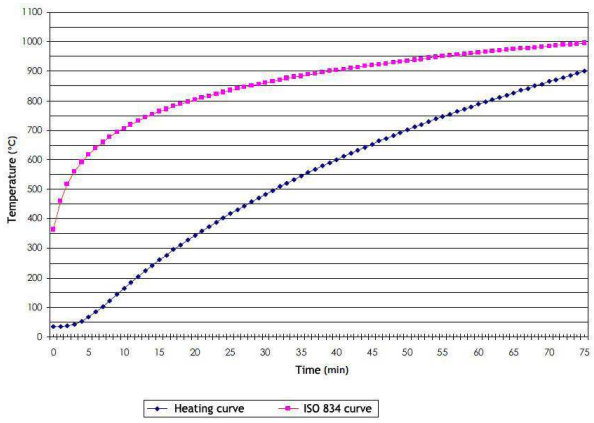

Figure 3. Heating curve of furnace in comparison to the heating curve of fire ISO 834.

3 RESULTS

It has been reported by authors [Rapazote et al, 2008 and 2010] that geopolymers made from CDW, as a control conditon, showed compresssive strength results of 43,8MPa to AL, 20,6 MPa to B and 42,9MPa to ALB and OPC mortar got 40,6 MPa after 28 days of cure (Figure 4).

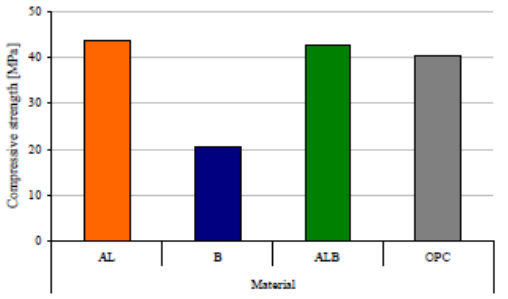

Figure 4: Compressive strength of AL, ALB, B and OPC in control conditions

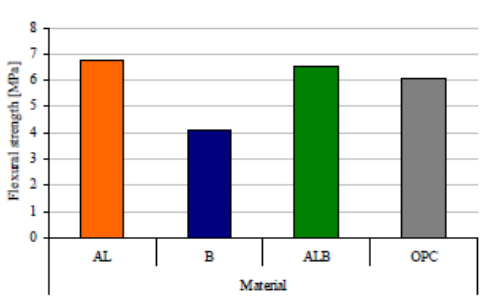

Figure 5: Flexural strength of AL, ALB, B and OPC in control conditions

Figure 5 shows the reported results for flexural strength in control conditions - 6,8MPa to AL, 4,10MPa to B, 6,6MPa to ALB and 6,0MPa to OPC probes.

Authors already noticed that in normal conditions better mechanical performance is presented for AL and ALB material when compared with OPC mortar and that material B presents a mechanical performance lower than all of OPC, AL or ALB materials [Rapazote et al 2010].

After being submmited to 900ºC for 2 hours, the visual inspection of probes showed that all OPC probes were destroyed without any cohesion, while AL, ALB and B probes were apparently stable in spite of some cracking. Color changes were also observed in all probes. Appearance of AL and ALB probes was very good when compared to B that seemed quite fragile and to OPC probes that were totally disintegrated, as is shown in Figure 6.



Figure 6. Samples inside furnace after temperature test and aspect of AL, ALB, B and OPC samples.

Final mechanical compressive resistance ranged from 18,0 MPa (AL) to 4,77 MPa (B) while OPC had no remaining strength. These results are presented in Figure 7 and they are indicative of the higher fire resistance of geopolymers. The flexural strength results ranged from 3,9MPa for AL to 1,63MPa for B as shown in Figure 8.

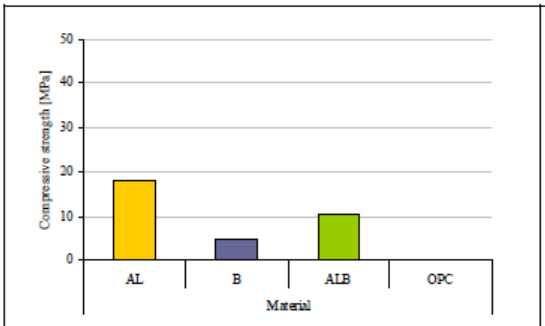

Figure 7: Compressive performance of AL, ALB, B and OPC after high temperature exposure

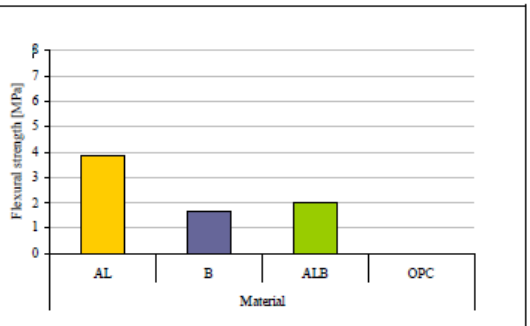

Figure 8: Flexural strength of AL, ALB, B and OPC after high temperature exposure

The remaining compressive strength, in percentage, after exposure to high temperature is shown in Figure 9. AL presented more than 40% remaining compressive strength when compared to control conditions and B and ALB showed more than 20% of the initial mechanical resistance against 0% to OPC as a consequence of non-remaining integrity. It is curious to verify that flexural strength was less affected than compressive strength and AL reached almost 60%, B 40% and ALB 30 % of the control resistances as is shown in Figure 10.

4 CONCLUSIONS

Results achieved indicate that AL and ALB materials have a better performance than Ordinary Portland Cement (OPC) in normal conditions, as previously documented [Rapazote et. al 2010] while in high temperature durability tests performed all AL, B and ALB samples made exclusively from construction and demolition waste (CDW) present better results than OPC.

It is remarkable the behaviour of the CDW materials after exposure to high temperatures, keeping reasonably high mechanical resistances unlike OPC which became completely desintegrated after the lost of constitution water, under the same conditions.

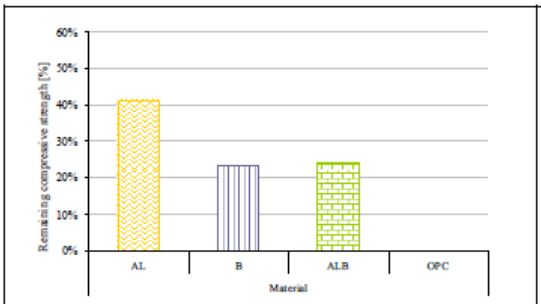

Figure 9: Remaining compressive strength of AL, ALB, B and OPC after high temperature exposure

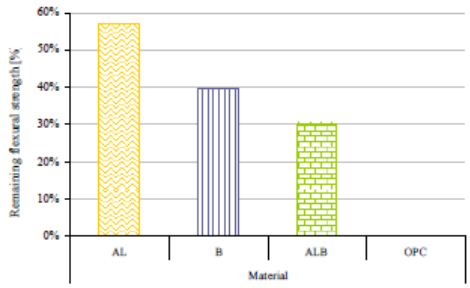

Figure 10: Remaining flexural strength of AL, ALB, B and OPC after high temperature exposure

The observed effect on geopolymers at very high temperature exposure, 900ºC for 2 hours, is in accordance with literature that refers that thermal resistance properties of geopolymers significantly exceed those of OPC in many instances [in Duxson et al 2007]. The superior resistance to those conditions confirms the great potential of CDW geopolymers to be used as building materials, as already reported by authors, mainly where the risk of fire is great. In fire situations OPC could collapse with severe consequences when compared with this new material with a significant remaining mechanical performance that itself represents an important advantage.

Considering environmental problems placed by CDW stream this research constitutes a contribute to get new building materials in a sustainable way. Recycling waste from construction activities to be used as raw material reduces energy, reduces natural resources deplection and also landfill disposal of CDW.

REFERENCES

Symonds Group, *Construction and demolition waste, management practices and their economic impacts*, Report to DGXI – European Commission. 1999.203p.

European Environment Agency: Environment *Signals 2001 (Chapter Waste), Environmental Assessment Report Nº 8* .2001. p 99-104.

Rapazote J., Laginhas C., Teixeira Pinto A. 2008. *A Reciclagem da fracção inerte de RCD pelo processo de activação alcalina*, in 5ºCLME proceedings, Mozambique, ref. 23A005.

Duxson P., Fernández-Giménez A., Provis J.L., Lukey G.C., Palomo A., van Deventer J.SJ.. 2007. *Geopolymer technology:the current state of the art*. Journal of Materials Science 42. p.2917-2933.

Duxson P., Provis J.L., Lukey G.C., van Deventer J.S.J.. 2007.*The role of inorganicc polymer technology in the development of green concrete*'. Cement and Concrete Research Vol. 37 p. 1590-1597.

van Deventer J.S.J., Provis J.L., Duxson P. Lukey G.C. 2007. *Reaction mechanisms in the geopolymeric conversion of inorganic waste to useful products*. Journal of hazardous materials A 139 p. 506-513.

Teixeira Pinto A.. 2002. *Novos sistemas ligantes obtidos por activação alcalina" in* Construção Magazine, nº 3.

Komnitsas K., Zaharaki D., 2007 . *Geopoyimerisation: A review and prospects for the minerals industry*. Minerals Engineering Vol. 20, p. 1261-1277.

Xu H., van Deventer J.S.J.. 2002. *Geopolymerisation of multiple minerals*. Minerals Engineering, Vol. 15, p.1131-1139.

Pacheco-Torgal F., Castro-Gomes J., Jalali S..2008.*Alkali activated binders: A review.Part2. About materials and binders manufacture.* Construction and Building Materials, Vol. 22, p. 1315-1322.

Davidovits J.. *Properties of geopolymer cements*. First Conference on alkaline cements and concretes, scientific research, Kiev, Ukraine, 1994, p131-149.

Teixeira Pinto A., Fernades, A., Jalali, S, 2002. *Geopolymer Manufacture and Application – Main Problems When Using Concrete Technology*" Geopolymer Conference proceedings, Melbourne, Austrália.

Teixeira-Pinto, A., Varela, B., Shroti, K., Panandiker, R.S. – "*Geopolymer-jute composite; a novel environmentally friendly composite with fire resistant properties*", Cocoa Beach International Conference, 2006.

Kong D., Sanjayan J. 2008 *Damage behavior of geopolymer composites exposed to elevated temperatures. Cement and Concrete composites.*doc. 10.1016/j.cemconcomp.2008.08.001.

Teixeira-Pinto A. and Tavares P.. *Portuguese Patent N.º 104535* (2009).

Rapazote J.G. , Laginhas C., Teixeira-Pinto A., 2010, *Development of building materials through alkaline activation of construction and demolition waste (CDW) – Resistance to acid attack.* Advances in Science and Technology, 69, 156-163 (doi:10.4028/www.scientific.net/AST.69.156).

Rapazote J.G. , Laginhas C., Teixeira-Pinto A., *Reciclagem de resíduos de construção e demolição (RCD) por Activação alcalina – Desempenho Mecânico*". Oral presentation nº70 on ENMEC. 2010, Porto Portugal.

Osório P., "Dissertação de Mestrado em Engenharia Civil: *Concepção de um saferoom anti-tornado em betão geopolimérico*", Universidade do Minho, 2007, Portugal.

XII DBMC
International Conference on Durability of Building Materials and Components
PORTO - PORTUGAL, April 12th-15th, 2011

Mix Design for Durable Recycled Concretes

Marco Viviani [1]

ABSTRACT

The production of recycled aggregate concrete presents a possible alternative to using construction materials from building demolition as landfill. Although this potential use is welcomed from a sustainable development perspective, it finds less acceptance in the ready-mix concrete market because of negative experiences in terms of the cost and durability of recycled concrete. We suggest some practical rules that can be applied to produce a recycled concrete that offers the required performance without additional costs.

KEYWORDS

Recycled aggregate, Recycled concrete, Rheology, Durability, New materials.

[1] HEIG-VD University of Applied Science of the Canton Vaud, Switzerland, marco.viviani@heig-vd.ch

1 INTRODUCTION

The crushing and use of concrete as recycled aggregate is one of the most promising actions taken to reduce the amount of materials from building demolition used as landfill. Concrete is the most widely used construction material in the world, because its basic components are available worldwide and are made with abundant materials (primarily limestone and clay). These characteristics make concrete a truly global material and one of the less polluting ones.

If the material "concrete" is global by composition, it is local by use and markets. In some markets, importing materials is necessary to overcome the shortage of natural aggregate. This is true for certain zones of Switzerland; see Table 1 [Vaud, 2007].

Table 1. Production and importation of rock between the year 2001 and 2006, (values in m^3).

Year	*Local aggregate (m^3)*	*Lake gravel and sand (m^3)*	*Imported aggregates (m^3)*	*Rock (various types (m^3)*	*Total (m^3)*
2001	852000	316000	320000	927000	**2415000**
2002	712000	308000	327000	792000	**2139000**
2003	760000	300000	290000	800000	**2150000**
2004	775000	260000	380000	752000	**2167000**
2005	944000	340000	353000	838000	**2475000**
Average	866000	308000	326000	834000	**2334000**

The use of recycled aggregate (RA) can make construction more sustainable. The benefits of using RA in concrete include:

1. the preservation of resources (for instance, by substituting 30% of natural aggregate with recycled aggregate in an ordinary concrete, the lifespan of the aggregate source is extended by 30%);
2. the reduction of landfill with all its connected costs (logistic, environmental and economic); and
3. the achievement of "green" label requirements in terms of reduced impact of construction and energy efficiency.

These objectives clearly imply the production and use of recycled concrete (BR) that possesses the same characteristics in terms of price and performance as common concrete. The term "recycled aggregate" (RA) encompasses several types of demolished and crushed materials (including concrete, bricks and plaster). Of these, the most interesting RA for structural application is recycled concrete aggregate (RCA), i.e. concrete that has been crushed. Although RCA is currently used in much construction and many building codes consider this "new" material, many structural engineers are hesitant to accept RCA because of some uncertainties in the relationships between the mechanical characteristics, durability parameters and the stress–strain behaviour of the BR. Furthermore, as RCA is composed of material collected from a variety of old demolished structures, there is the concern that this aggregate may not be suitable for producing concretes with stable performance.

The goals of the present research are: to detect the extent to which the quality of the concrete used to produce RCA influences the properties of the BR; and to determine which parameters enable a normal concrete to be converted into a BR with similar slump, mechanical properties and permeability without increasing costs.

2 STATE OF THE ART

The vast research on BR mostly focuses on the variation in the properties of concrete when the proportion of RCA is increased. Generally, a BR is a commercial concrete in which part of the (natural) aggregate has been replaced by an artificial aggregate obtained by crushing blocks of one or more materials collected from the demolition or deconstruction of buildings at the end of their life cycle. Research on RCA has focused primarily on the effect of various crushing methods on the physical properties and on the differences between RCA and the most common natural aggregates. Padmini *et al.* [2009] studied the effect of different types of RCA on the physical properties of concrete; they found that when the parent concrete (PC) strength increases, the water demand increases (PC is the concrete from which RCA is obtained). Furthermore, the same authors found that the strength and elastic modulus of PC are generally higher than those of BR.

Exteberria *et al*. [2007] obtained a BR that had the prescribed (effective) water to cement ratio (w/c) by systematically controlling the moisture state of the recycled coarse aggregate prior to mixing. The absorption of the RCA can easily be as high as 6–10% and this must be considered in the concrete production process. RCA water absorption depends also on the PC crushing methods used and on RCA selection after crushing: if the lower fractions (fines) are removed, the strength of the parent concrete is low and the crushing method is intense, less mortar will adhere to the aggregate particles and therefore the RCA absorption rate will be closer to that of the aggregates used for the PC rather than to that of the PC. Adherent mortar plays a role both in the properties of RCA and in the mix design: Abbas *et al.* [2007] found that controlling the total effective volume of paste made it easier to design a durable concrete.

Rheology is fundamental for every concrete: only a stable workability permits correct placement and compaction of concrete. RA has an effect on rheology and this must be taken into account when a substitution of aggregates is made in a well-known mix design. For instance, Poon *et al*. [2004] found a higher initial slump and quicker slump loss in BR made using oven-dried RCA.

The optimal rate of RCA substitution is one of the most debated topics within the scientific community. Most codes require a minimum of 25% RCA to denominate a concrete as recycled and attempts to produce concretes with 100% RCA have been made. High rates of aggregate substitution have been found to cause a drop in the mechanical and rheological properties of BR, and low rates of substitution affect mostly the strength and elastic modulus.

Elastic modulus is one of the greatest concerns when BR is used as a structural material because designers are used to calculating the elastic modulus of ordinary concrete with formulas including parameters such as the average compressive strength [SIA 262/2003]. The fact that BR has a different elastic modulus–strength relationship is discomforting for many engineers, even though models [Evangelista and De Brito, 2007] and codes are available.

Xiao *et al.* [2005] investigated the fundamental stress–strain curve of BR under compression. They found interesting differences from ordinary concrete, and Wirquim *et al.* [2000] conducted a series of tests on the relationship between the water absorption and durability of BR. Although both research groups interpreted their findings with caution, these two studies are of interest because they add to our knowledge and help designers to be more certain in their work.

3 MATERIALS AND METHODS

3.1 Materials

All the materials used in this research are available on the local market. The concrete used as a base concrete (labelled BASE) is a best seller in the region – a good, regular structural concrete used in

large quantities for slabs, walls and foundations. The mix design of the BASE concrete is shown in Table 2.

Aggregates (sand and gravels) were supplied in three fractions. They were all dug from a lake and prepared (washed, sieved, tested and classified) in an automatic plant. The particle size distribution is shown in Fig. 1.

Table 2. Mix design of BASE 1-3 concretes.

Component	*Kg/m^3*
Cement - CEM II/A-LL 42.5N	340.0
Aggregates (total)	1945.0
0-4	816.9
8-16	427.9
16-32	700.2
Water (effective)	164.0
W/C	0.48
Superplasticizer	0.6%

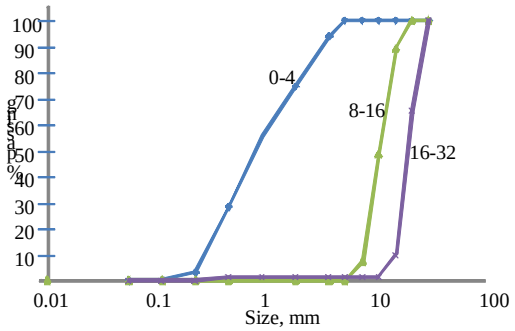

Figure 1. Particle size distribution of used natural aggregates.

The cement used is a commonly available CEM II/A-LL 42.5N with a limestone content of about 15%. It was acquired from a single production lot and was identified and tested for conformity by the producer. The superplasticizer used is a common polycarboxylate sold in the area; its solid content was tested at about 30%. A 150 L mixer was used for batching the BASE concrete that was ultimately tested for fresh concrete properties. BASE 2 and BASE 3 concretes were produced using the mix design given in Table 2, except that water was added at the end of the mixing phase in sufficient quantity to bring the effective w/c ratios to 0.55 and 0.65, respectively (see Table 3). This was done for a simple reason: the commercially available concretes are very often similar but their aspect and mechanical properties suggest that water is added in the field (especially for workability reasons or for retempering).

Table 3. W/C ratio of concrete BASE 1-3 and water added.

Concrete	*W/C (effective)*	*Added water l/m^3*
BASE 1	0.48	0
BASE 2	0.55	22
BASE 3	0.65	57

From the data in Table 4, it is apparent that the added water influences the fresh concrete properties of the BASE concretes.

Table 4. Tests of fresh concrete.

Concrete	*Temperature, °C*	*Slump, mm*	*Density, Kg/m^3*
BASE 1	12.5 °C	205	2406
BASE 2	25 °C	215	-
BASE 3	20 °C	235	2385

As expected, the strength and elastic modulus of the BASE concretes decrease as the effective w/c ratio increases (see Figs 2 and 3).

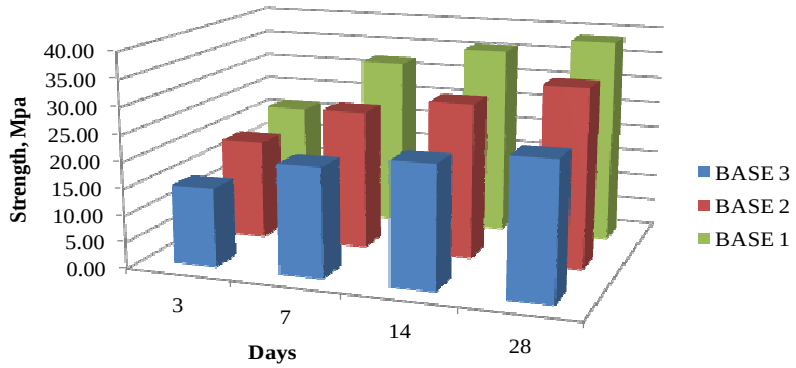

Figure 2. Compressive strength of BASE concretes.

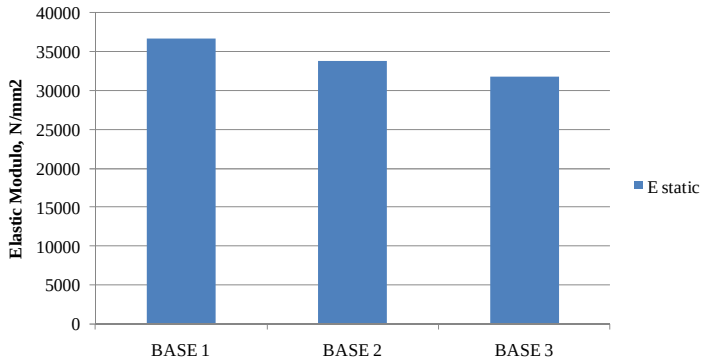

Figure 3. Static elastic modulus of BASE 1-3 concretes.

Once a suitable quantity was obtained, the concretes BASE 1 to 3 were tested and crushed using a laboratory jaw crusher and three recycled aggregates were obtained (RCA 1–3). They were of even aspects; the granulometry of each is presented in Fig. 4. BASE 1 and 2 made evenly size-distributed RCAs, but the particle size distribution of BASE 3 differed slightly from the other two.

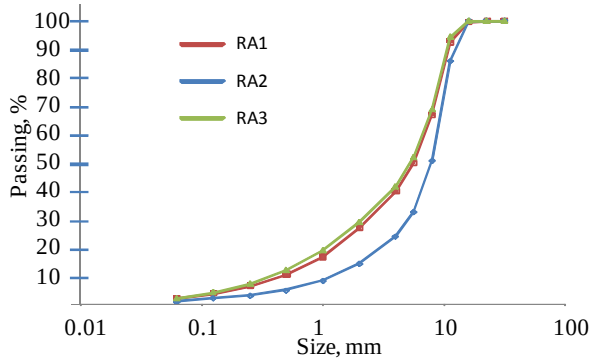

Figure 4. Particle size distributions of used recycled aggregate (RA).

Norm SN EN 206 indicates the optimal quantity of powders that should be found in a concrete (kg/m^3 of powders with size less than 0.125 mm). The optimal powder quantity depends on the aggregates' maximum size, in our case 350 kg/m^3 and 32 mm, respectively. The powder quantity affects the rheology and the permeability of the concrete. As Table 5 shows, there is a significant difference between the powder quantity found in the RCAs and that in the sand used for the tests. Furthermore, the BASE concrete contained 380 kg of fines per m^3 against an optimum of 350 kg/m^3.

Table 5. Powder in the aggregates.

Aggregate	*Average powder quantity(<0.125 mm) in %*
RCA1	3.47
RCA2	2.44
RCA3	3.65
0-4	4.76

The methods for determining the water absorption of fine and coarse aggregates differ; for this reason, each RCA was separated into fine and coarse fractions and the fractions tested appropriately. It is apparent from Table 6 that the RCA absorption values are consistent with the values found in the literature for jaw-crushed concrete.

Table 6. Absorption of recycled concrete aggregates.

Aggregate	*Water absorption %*
RCA1 (>4 mm)	5.38
RCA2 (>4 mm)	5.70
RCA3 (>4 mm)	6.50

The fraction 0–4 of the RCAs was also tested; a coefficient of about 1.1% was found for all fine fractions. An interesting correlation can be found by comparing the data in Tables 6 and 7: values for RCA water absorption and of BASE concretes water penetration appear linked.

Table 7. Water penetration under pressure for BASE concretes.

Concrete	*Depth of water penetration at 28 days*
BASE 1	29 mm
BASE 2	51.7 mm
BASE 3	150 mm

3.2 Mix Proportions

Proportioning of the mix for BR had the following constraints:

1) at least 25% of recycled aggregate was required in the mix;
2) the minimum possible modifications of the mix design and overall cost were required; and
3) workability and strength were required to be similar to base concrete.

The approach for the mix design was quite classical except for two parameters: the decision to keep the total (fresh) paste volume constant and the rheology. Paste is the medium in which the gravel is carried. It has a large effect on the strength of concrete in medium-strength classes. Because the original mix had a small excess of paste, the eventual extra paste required because of the shape of the aggregate was already present. Surprisingly, the supply of sand used for the BASE concretes was unusually rich in powder and thus the recycled aggregate did not have sufficient powder (380 kg/m^3). The Fuller–Bolomey relation was used to proportion the concrete skeleton, which now had four components. The mix proportions are shown in Table 8.

From the data in Table 8, it is apparent that the BR and BASE 1 mixes have two differences: part of the sand was substituted with RCAs and 7.5 kg/m^3 of limestone powder was added to equalize the overall paste content.

Table 8. Mix design of recycled concretes.

Component	*BR1 (Kg/m^3)*	*BR2 (Kg/m^3)*	*BR3 (Kg/m^3)*
Cement - CEM II/A-LL			
42.5N	340.0	340.0	340.0
Aggregates (total)	1945.0	1945.0	1945.0
0-4	330.7	330.7	330.7
8-16	427.9	427.9	427.9
16-32	700.2	700.2	700.2
RCA1	486.3		
RCA2		486.3	
RCA3			486.3
Limestone powder	7.5	7.5	7.5
Water (effective)	164.0	164.0	164.0
W/C	0.48	0.48	0.48
Superplasticizer	0.6%	0.6%	0.6%

3.3 Preparation of the Specimens

We used a 150 L planetary mixer. Cube moulds were 15 × 15 × 15 cm plastic moulds and each cube was vibrated with a poker vibrator. Specimens were kept covered by a plastic lid until they were demoulded and transferred to a water tank kept at standard temperature conditions. Cubes were rectified if required and no specimens had a dimension outside the norms.

4 TEST RESULTS

The results for the fresh concrete properties for the BRs confirm that the paste is the controlling factor for the slump (see Table 9). All the concretes remained in slump class S4, even though a small slump loss was observed.

Table 9. Tests of fresh recycled concrete.

Concrete	*Temperature, °C*	*Slump, mm*	*Density, Kg/m^3*
BR 1	23 °C	180	2463
BR 2	23.5 °C	180	2434
BR 3	24 °C	200	2406

The results of the mechanical tests on the BRs are reported in Figs 5 and 6: the strength of specimens matured for at least 14 days is similar for all concretes and, surprisingly, slightly higher for the BRs. A possible partial explanation for the lower performance of the BASE 1 concrete at this early age could be the lower initial temperature at batching, as apparent from Tables 5 and 9.

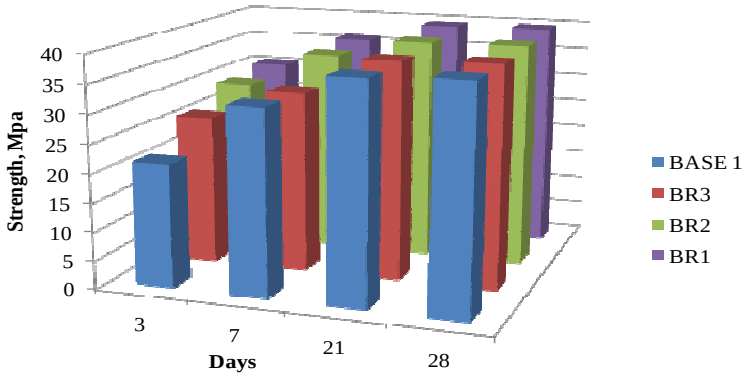

Figure 5. Compressive strength of recycled concretes and BASE concrete.

Elastic modulus values were similar to the BASE 1 concrete for all BRs, with a slight decrease in value for BR 2 and BR 3. In this series of tests it is interesting to observe that the quality of the RCA seems to have a limited effect on the elastic modulus and none on the compressive strength.

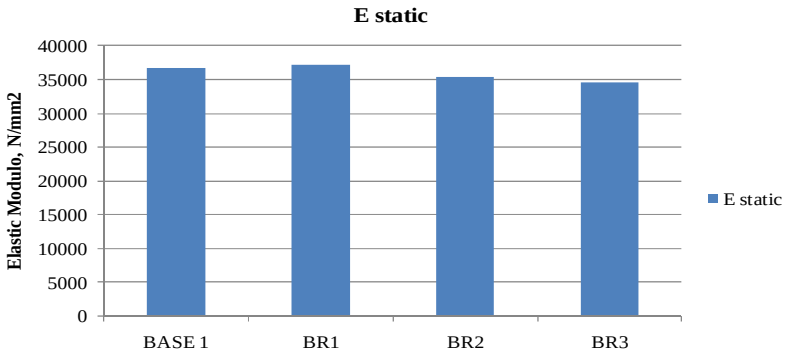

Figure 6. Static elastic modulus of Recycled concretes and BASE 1.

Water penetration under pressure confirmed the findings in Fig. 5 for compressive strength. Table 10 shows the permeability of BRs: all of them are very close to BASE 1 concrete with a slightly higher value for BR 1, of which one specimen (out of three) had a much lower performance than the other two.

Table 10. permeability of RCA concretes.

Concrete	*Depth of water penetration at 28 days*
BR 1	38 mm
BR 2	33.7 mm
BR 3	28 mm

Table 10 shows also that the permeability of the BRs can be considered comparable to that of a common concrete. External sulphate attack is a concern, especially for foundations. In the testing programme, engineers requested a test of sulfate attack. The test demonstrated that there are no concerns for external sulfate attack.

5 CONCLUSIONS

Based on the limited number of tests presented in this article, it is possible to draw the following conclusions.

- A good structural recycled concrete can be produced using RCA.
- Fresh concrete properties, notably slump, are controlled by the paste volume and quality, at least for low proportions of recycled aggregate.
- Strength and elastic modulus are not compromised by the addition of 25% recycled aggregate.
- Water penetration under pressure has approximately the same magnitude in recycled concrete and in ordinary concrete.

Further testing is necessary to confirm that these results can be extended to higher rates of recycled aggregates.

ACKNOWLEDGMENTS

This research has been conducted in the frame of a larger research project financed by the RCSO, the research commission of the HES-SO, Colas SA and ESM SA that are gratefully acknowledged.

REFERENCES

Abbas, A., Fathifazl, G., Isgor, O.B., Razaqpur, A.G., Fournier, B., & Foo, S., 2009 'Durability of Recycled Aggregate Concrete Designed with Equivalent Mortar Volume Method' *Cement and Concrete Composites*, 31, 555-563.

Etxeberria M., Vázquez E., Marí A. & Barra M., 2007 'Influence of amount of recycled coarse aggregate and production process on properties of recycled aggregates concrete', *Cement and concrete research*, 37, 735-742.

Evangelista, L. & De Brito, J. 2007, 'Mechanical Behaviour of Concrete Made with Fine Recycled Concrete Aggregates', *Cement & Concrete Composites*, 29, 397-401.

Padmini, A.K., Mathews, M.S., & Ramamurthy, K., 2009, 'Influence of parent concrete on the properties of recycled aggregate concrete', *Construction and Building Materials*, 23, 829–836.

Poon C.S., Kou S.C. & Lam L., 2002 'Use of recycled aggregates in molded concrete bricks and blocks', *Construction Building Materials,* 16**,** 281–289.

Sagoe-Crentsil, K., Brown T., & Taylor AH. 2001 'Performance of Concrete Made with Commercially Produced Coarse Recycled Concrete Aggregate'. *Cement and Concrete Research*, 31, 707-712.

SIA 262, 2003 Construction en béton www.sia.ch, last access November 2010.

Vaud 2007, Canton de Vaud, Département de la sécurité et de l'environnement (DSE), 2007 'Recyclage des déchets minéraux de chantier dans le canton de Vaud', http://www.vd.ch/, in french, last access October 2010.

Wirquin E., Hadjieva-Zaharieva R. & Buyle-Bodin F., 2000 'Utilisation de l'absorption d'eau des bétons comme critères de leur durabilité-application aux bétons de granulats recyclés' (in french), *Matererials and Structures* 33, 403–408.

Xiao J., Li J. & Zhang C., 2005 'Mechanical Properties of Recycled Aggregate Concrete Under Uniaxial Loading' *Cement and Concrete Research* 35, 1187-1194.

XII DBMC
International Conference on Durability of Building Materials and Components
PORTO - PORTUGAL, April 12th-15th, 2011

Sustainable Smart ECO-Buildings

Christer Sjöström [1]
Gurvinder Singh Virk [2]
Wolfram Trinius [3]
Alexandra Lebert [4]
Stefano Saldinini [5]
Hywel Davies [6]

ABSTRACT

The paper reports the main observations of the European project "Smart-ECO", which concluded in mid 2010. Smart-ECO was a Specific Support Action project funded by EU FP6, established to create and anchor a generic vision framework for Sustainable and Smart ECO-buildings in the period 2010 - 2030, to determine what innovations (technical and non-technical) that could be useful for realising this vision, and to identify those elements that have the highest potential impact, all while anchoring the work and the findings with a carefully selected wide ranging group of expert stakeholders involved in various aspects of the built sector. The defined Vision and Requirements has been met with great interest. The life cycle aspects of buildings were ranked as having the highest potential in achieving the vision of sustainable smart ECO-buildings, followed by miniming energy consumption, detailed monitoring the operational aspects of buildings, providing good user manuals of the buildings and their systems, flexibitlity of the buildings in being able to be adaptable to local and regional conditions. The paper focuses on the life cycle issues and the requirements resulting from a vision of sustainable and smart buildings.

KEYWORDS

Sustainability, ECO-buildings, Life Cycle, Vision, Requirements, Innovations.

[1] Materials Technology, KTH Research School, University of Gävle, Gävle, SWEDEN, christer.sjostrom@hig.se
[2] Endoenergy Systems ltd, Sheffield, UK, gsvirk@endoenergy.com
[3] Ingenieurbüro Trinius, Hamburg, GERMANY, trinius@trinius.de
[4] CSTB, Grenoble, FRANCE, alexandra.lebert@cstb.fr
[5] MACE, London, UK, Stefano.saldini@macegroup.com
[6] Hywel Davies Consultancy, Bedford, UK, hywel@hyweldc.co.ukn

1 INTRODUCTION

Smart-ECO is the short name for the EU-FP6-project "Sustainable Smart Eco-Buildings in the EU". The project started in October 2007, was conducted by a project consortium consisting of 12 partners, and led by the Center for Built Environment at the University of Gävle in Sweden. The project concluded in July 2010.

The Smart-ECO objectives were to establish a Vision with its resulting Requirements for sustainable smart ECO-buildings over the time perspective 2010 – 2030, and to evaluate Technical and non-Technical Innovations together with their potential to contribute to acheiving this Vision. Such innovations will only be successful if the potential to implement and apply the new solutions are sufficiently promising. Combining the overal criteria, the innovations were deemed to have good potential if they satisfied the following:

- they contributed to developments which were in-line with the vision for sustainable building
- they met the desired performance requirements arising from the vision
- they were perceived as being feasible in having high potential by a wide range of stakeholders

Figure 1 describes how the Smart-ECO is structured in its work plan.



Figure 1. Overall structure of the Smart-ECO project.

The first essential project step was to identify the Vision for sustainable and smart ECO-buildings, discuss and anchor this with a relevant panel of stakeholders which were chosen to be wide enough to represent all legitimate views on sustainable development in the building and construction sector.

A group of some 230 potential expert stakeholders was formed to contribute to the establishment of the vision, to help evaluate and to provide legitimacy to the key reference points of the project.

The project's starting point was the current position regarding sustainable building as described by established practice, current policies, existing standards and current EU-directives. An analysis of recently completed as well as ongoing research and development projects provided indications of the short- and mid-term drivers for the current developments in the built sector. Strategies and policies addressing other closely related sectors, especially energy and transport, have also been considered as they often address aspects that are relevant to the building sector.

A vision is usually a rather descriptive and qualitative presentation of an overarching ambition but it is important that specific and measurable requirements and metrics are included to quantify progress towards realising the global goals aime for in the vision. The potential of technical and non-technical innovations to contribute to the realisation of such developments can then be discussed and assessed against the requirements.

This evaluation of innovation has applied these metrics, after discussion and agreement with the stakeholder group and this stakeholder perspective is a core novelty of the Smart-ECO approach. The implementation of such an evaluation routine can itself be interpreted as a non-technical innovation aiming at enhanced sustainability within the building sector. Likewise the application of formalised assessment methodologies as part of the evaluation of building sector products and services can be perceived as innovative inits own right. The project therefore applies a cycle of self-evaluation involving assessment methodologies such as Environmental Life Cycle Assessment (LCA), Economic Life Cycle Assessment (Life Cycle Costing LCC), Service Life Planning (SLP), Life Cycle Management Systems (LMS) or the concept of Performance-Based Building (PBB).

A summary report (CIB, 2010) presenting predominantly the Smart-ECO work on the Vision, the Innovations supporting the Vision, and the work on processing results with the Stakeholder Group was published by CIB (partner of Smart-ECO) towards the end of the project and released at the CIB World Building Congress 2010. The report is freely downloadable from http://cibworld.xs4all.nl/dl/publications/pub332.pdf or www.smart-eco.eu.

2 THE VISION ON SUSTAINABLE SMART ECO-BUILDINGS 2010 - 2030

As the building sector is strongly interlinked with other sectors of the economy (i.e. the energy sector, transport, and labour development and deployment), the perspective applied when establishing the vision needed to be extensive and all-inclusive. The project vision used as far as possible the current status of sustainable construction within the EU (including the major outputs of previous related EU projects and thematic networks) as the starting point and to set out an ambitious yet realistic roadmap of development.

The Smart-ECO Vision has had an early impact on policy and standards development. This is because the Smart-ECO Vision document was adopted by ISO as the foundation for further standardisation on sustainable building. In the development of a procurement handbook for sustainable building by the UN SUN initiative the Smart-ECO Vision was used as the fundamental document defining sustainable building.

For the Smart-Eco project, it was essential to establish a vision expressed in generic terms and complemented with clear targets. Only if so, the targets contained in the vision can be communicated and applied by the various concerned stakeholders. Additionally, clear and unambiguously expressed targets are needed to monitor progress and to assess options with.

Furthermore, the vision must be ambitious in order to point towards the ultimate target, and realistic enough to function as a motivator and enabler. This "carrot and rabbit" concept implies that the vision has a clear temporal anchor and that significant improvements of the building and construction sector in its progress towards sustainability and stronger regulatory requirements will lead to the situation

that the vision needs to be revised and targets need to be sharpened over time. The earlier the vision and the associated targets are appreciated as being outdated, the better!

Separating the general issues of the Vision from specified targets it is expected that the Vision may be adapted to such developments. An example of such a development is e.g. the European forthcoming Construction Products Regulation with its inclusion of sustainable use of resources. Addressing the life cycle of the building, and the total energy demand throughout the life cycle and aiming at "near zero energy buidlings" will push new construction significantly into the direction of the Smart-Eco vision.

2.1 The "ten commandments" of the Smart-ECO Vision

A key statement by ISO (ISO 15392:2008) was, after rigorous discussions, adopted as the following guiding principle:

Buildings contribute to sustainable development when designed and operated to match the appropriate fitness for use, with minimum adverse environmental impacts, while encouraging improvements in economic, social and cultural aspects at local, regional and global levels.

With this as a corner stone and within an iterative process with the stakeholder group, the Vision was elaborated, and is presented next in a condensed short-version. The full Vision and Requirements report (Chevalier, J-L, et al, 2010) is freely downloadable from www.smart-eco.eu.

The Vision of Sustainable Smart ECO-buildings should be the following:

- apply the general principles of sustainability
- be designed to meet the needs individually and collectively
- be integrated into a local/regional strategy
- encompass Life Cycle perspective in Design / Refurbishment
- deliver minimized adverse environmental impact over life cycle
- deliver economic value over time
- provide social and cultural value over time
- be healthy, comfortable and safe for users
- be user friendly, simple and cost efficient in operation, and have measurable performance
- be adaptable throughout service life, and have an end of life strategy.

3 INNOVATIVE SOLUTIONS

The work on analysing the market and research literature on possible technical and non-technical innovations that could support reaching the Vision has been extensive. The full resulting report (Saldini, et al, 2009) is freely down-loadable from www.smart-eco.eu. For reason of available space only some hints of the results can be given here. The accounting of the stakeholders views and rankings of the various innovation categories presented in the next section also only gives a tiny flavour of the full results obtained.

The work on innovation was basically structured on the following aspects:

- Holistic design approaches applying innovative technologies

This includes a life cycle approach considering that a building's long-term impacts on the environment have to be seriously considered if advances in building design are to become sustainable. To reach the ambitious goal of the Smart-ECO Vision requires an Integrated Design Process. Such an approach to the design is radically different to the common approaches of the 20th century and today, which typically distinguish the architectural design and the engineering completion and detailing,

hence loosing the important integration asepcts and the opportunities of reaching the desired target, i.e. sustainablity. Among specific innovation areas declared as having the most interesting characteristics appears to be advanced tools like Building Smart (BIM), and Life Cycle Management approaches.

- Innovative technologies and solutions, including both energy saving and energy generation and distribution

The focus of energy saving came out to be advances and improvments in thermal insulation, cladding materials, glazing, thermal storage in the building fabric, natural ventilation for comfort, overheating controls, and generally better control systems. As regards lighting the focus should be on natural lighting and shading, and innovations on artificial lighting.
The main area of energy generation and distribution – in the Smart-ECO case with a specific focus on renewable sources – focused both at the building level, the non-building or regional area levels, and considering issues like integrated generation of energy.

- Building construction and operation

The work towards solution in this area focused on materials sourcing and the manufacture of components and systems, site assembly and logistics, and demolition and recycling. The stakeholders stated that construction is not as critical as design and operation in meeting the requirements of the Smart-ECO vision, although innovations in, for example, materials production would reduce waste, increase the efficiency of processes, and improve performances and sustainability aspects throughout the supply chain.

- Ways to meeting future requirements

This focussed the identification of changes that will affect the building sector in the near future. Adaptation strategies and other relevant aspects are considered to illustrate how Smart-ECO buildings, over their service life, could meet these future requirements and the stakeholders identified the following areas to be most critical:

Energy and environment:This includes mitigation and adaptation for climate change, integration of buildings in the energy networks, and using building strategies to reduce depletion of resources

Changing requirementsand use: This calls for sustainable design processes, which requires that service life considerations are integrated into the design process. The design for flexibility and adaptability are key criteria which allow buildings to be continued to be used even when changes need to be made.

Depletion of resources: The use of building materials should be reduced considerably to improve efficiency of resources. The revised and up-dated European Construction Products Directive/Construction Products Regulations will in the future demand proof of the environmental impact of building materials in accordance with full life cycle assessments. The extension of materials life-cycle could be obtained by promoting the extension of the life expectancy in buildings, i.e. by means of conversion / transformation of existing buildings instead of going for new constructions.

4 THE STAKEHOLDER PROCESS AND SOME RESULTS

At the start of the Smart-ECO project a stakeholder group was established, and a plan for their involvement in the project was set up. The following categories of experts were established:

1. Technical experts, comprising researchers, engineers, scientists, etc, all with vested interest in developing innovations for a sustainable construction sector
2. Industrialist involved in manufacturing and commercialising products for construction
3. Devolopers involved in real estate development and planning
4. Materials specialist to support the variety of matarials needed in construction

5. Architects involved in design of green and eco-friendly buildings in particular
6. Builders, ranging from domestic house builders to construction companies involved in building large commercial structures
7. Occupants of various categories, to give feedback from a general viewpoint on the acceptability of innovations being considered for adoption
8. Educationalists involved in traning and education of different types of stakeholders in the construction sector
9. Authorities, ranging from governmantal bodies to professional organisations involved in developing policy and having activities related to the construction area.

For the Stakeholder Group, a list of 238 contacts were created from the Smart-ECO consortium from the above mentioned wide range of sectors. From these contacts, a Stakeholder Group of 66 experts was created. The report for the Stakeholders Group describes the activities carried out in setting up the group and formulating the questionnaires to engage the Stakeholders with the Smart-ECO project and the work being carried out in 1) formulating the vision for sustainable construction, 2) identifying the innovations needed to realise the vision, and 3) evaluating the innovations for monitoring success. Three questionnaires have been formulated to distribute initial drafts of the work carried out within Smart-ECO in these three areas and responses from the Stakeholder group passed back to the Smart-ECO partnership for prioritising the details of the work in each of the tasks being carried out. The details of these questionnaires, and the results obtained, are presented in the Stakeholder Group report (Virk, G S, et al, 2010) which can be downloaded from www.smart-eco.eu. Following on from this work a market perspective on eco-buildings is created and also presented in the report but short summaries are presented next for convenience.

4.1 The Way of Working and Stakeholders Ranking of Eco-Efficient Measures and Innovations

The first Smart-ECO questionnaire (Q1) focused on ensuring the Vision comprised the most important elements and that the ranking of each component was appropriate as assessed by the Stakeholder Group. A total of 58 Q1 questionnaires were completed and the most important issues that should be included in the Smart-ECO vision (in ranked order) have been assessed to be as follows:

1. Lifecycle of building
2. Minimum energy consumption
3. Monitoring of building
4. Building user manuals
5. Building adaptability
6. Local issues
7. Dismantling building phase
8. Setting up building phase

The second Smart-ECO questionnaire (Q2) focussed on identifying the innovations (technical and non-technical) that had the potential to contribute to realizing the Smart-ECO Vision. A total of 51 Q2 questionnaires were completed with the questions aimed at assessing a variety of issues; the most important of these related to the innovations are summarised here.

Areas where innovations have the most potential for achieving the Smart-ECO Vision (in ranked order) are:	The energy saving and efficient technologies with high potential to impact Smart-ECO buildings (in ranked order) are:
1. Renewable energy generation	1. Insulation
2. Passive design measures	2. Passive cooling
3. Operation of building	3. Passive solar
4. Finance and incentives	4. Lighting
5. New materials	5. Orientation

6. Management and processes 7. Education 8. Policies 9. Recycling 10. Communications 11. Water conservation	6. Innovative material 7. Water conservation and storage

The renewable energy technologies with high potential to impact Smart-ECO buildings (in ranked order) are: 1. Solar thermal 2. Co-generation 3. Earth energy 4. PVs 5. Biomass 6. Wind related technologies 7. Fuel cells	The most important operational innovations with high potential to impact Smart-ECO buildings (in ranked order) are: 1. Building management systems 2. Automation for energy saving 3. Robustness to user behaviour 4. Post occupancy monitoring 5. Waste management plan 6. Intelligent lighting 7. Air quality control 8. Daylight dependent control systems

The third Smart-ECO questionnaire (Q3) focussed on evaluating the innovations identified in Q2 and their potential for realizing the Vision aims from Q1. A total of 18 Q3 questionnaires were completed with the questions aimed at assessing the various innovations via different evaluation criteria and the results are summarised here. From a holistic viewpoint the most important issues in ranked order are:

1. Technical performance
2. Economic
3. Sustainable
4. Regional pre-conditions
5. Social

Some of these criteria have been further assessed. For example the main issues that should be included in the regional pre-conditions (in ranked order) are: 1) climatic conditions, 2) local building regulations and local policies (equal second), and 4) geographical features; and the main issues to be included in the performing the technical evaluations (in ranked order) are: 1) requirements are met, 2) reliability, 3) robustness, and 4) maintainability. The economic evaluations should include (in ranked order): 1) cost-benefit analysis, 2) the set up costs, 3) the operational costs, and 4) service life time.

The various innovations have been assessed from different viewpoints such as minimising energy consumption, being easy to use, reliant on local issues, being adaptable, easy to set up, easy to dismantle, taking into account life cycle aspects and the increasing awareness of the user.

The market potentials of the various innovations have also been assessed by the Stakeholders. For example the market potential of the energy saving innovations (in ranked order) are:

1. Insulation products (with average score of 4.4 and market take up potential of 84% by 2030)
2. Lighting products (with average score of 4.1 and market take up potential of 69% by 2030)
3. Passive solar products (with average score of 3.2 and market take up potential of 52% by 2030)
4. Passive cooling products (with average score of 2.8 and market take up potential of 38% by 2030)
5. Building orientation (with average score of 2.7 and market take up potential of 32% by 2030).

Also, the market potentials of the renewable energy innovations have been assessed (in ranked order) as:

1. Co-generation products (with average score of 3.6 and market take up potential of 46% by 2030)
2. Solar thermal products (with average score of 3.5 and market take up potential of 54% by 2030)
3. Photovoltaic products (with average score of 3.4 and market take up potential of 42% by 2030)

4. Biomass products (with average score of 2.5 and market take up potential of 36% by 2030)
5. Earth energy products (with average score of 2.5 and market take up potential of 27% by 2030).

5 CONCLUSIONS AND DISCUSSION

The paper has presented the Smart-ECO project and outlined the main findings from the project in how the built sector community wishes to move towards becoming more sustainable within 2010-2030. This is a huge issue for us all and the built sector being a major consumer of energy and natural resources, needs to be more active in adopting sustainable approaches. It was the aim of the Smart-ECO project to develop a viable Roadmap for realising sustainable building community where holistic methods are used in designing, building, operating, maintaining and finally re-cycling constructions. To do this Smart-ECO has created a Vision that is properly grounded with the wider stakeholder community and has idenified the innovations (both technical and non-technical) which have the most potential in achieving the Vision. How the success of the community (or not) in realising a sustainable built sector has also been investigated and the most important metrics that should be used have been identified. The work carried out within the projet in these areas has been throughly assessed and various options put forward have been ranked by a wide range of experts who agreed to act as the Stakeholder Group for the project. This feedback from the wider community has been invaluable and ensures that we maximise our gains early by adopting the measures having maximum potential and then as new innovations emerge we can make even larger steps towards becoming a sustaianable society.

ACKNOWLEDGEMENTS

The hard work and considerable efforts of the Smart-ECO partners are all appreciated in completing this complicated and important project. The European Commission and DG TREN is acknowledged for the funding and the additional support in carrying the project through.

REFERENCES

CIB, 2010, *Towards Sustainable and Smart-ECO Buildings*, CIB Publication 332, ISBN: 978-90-6363-064-5, CIB; International Council for Research and Innovation in Building and Construction, Rotterdam, the Netherlands.

Chevalier, J-L, Lebert, A, Trinius, W, Davies, H, Liias, R, Biernatzki, R, Buschert, D, Sjöström, C, 2010, *Vision of a Sustainable Smart-ECO Building in 2030 and Requirements*, Smart-ECO project, Work Package 2 “Vision & Requirements”, Deliverable D2 and 3, FP6-2005-TREN4-038699, April 27, 2010.

Saldini, S, and WP3 partners, 2009, *Innovation supporting the Vision on Sustainable Building*, Smart-ECO project, Work Package 3 “Innovation”, Deliverable D4, FP6-2005-TREN4-038699, December 14, 2009.

Virk, G. S., and WP5 partners, 2010, *Market Perspectives on Eco-Buildings & Stakeholders*, Smart-ECO project, Work Package 5 “Stakeholders”, Deliverable D6, FP6-2005-TREN4-038699, September 12, 2010.

XII DBMC
International Conference on Durability of Building Materials and Components
PORTO - PORTUGAL, April 12th-15th, 2011

Influence of Durability on a Modular Building Life Cycle

Estibaliz Pérez Iribarren [1]
Luis A. Del Portillo Valdés [2]
José María Sala Lizarraga [3]
Jon Terés Zubiaga [4]

ABSTRACT

Sustainable development in the residential sector includes the achievement of social, economic and environmental sustainability. A major durability involves an increase in user's satisfaction, a decrease of the cost- due to the fact that the cost of maintenance is lower than of demolition and reconstruction- and an improvement in environmental results.

Use phase, which is closely related to durability term, is the most harmful phase of the building life cycle. It is estimated that this phase is responsible of 66-80% of energy consumption and of 80-90% of greenhouse gas emissions, depending on the type of building, its location and its installations.

In this paper a modular building element has been analyzed, supposing different values of service life, with the aim of obtaining the environmental hazard associated with the use phase for each case. Moreover, the influence of rehabilitation systems on durability of buildings has been considered. The present study has been developed by LCA methodology.

KEYWORDS

Sustainable development, Durability, Life Cycle Assessment, Environmental Impact, Rehabilitation.

[1] The University of The Basque Country (UPV), Thermal Engineering Department, SPAIN. estibalizpi@gmail.com (This authors have been given a grant by the Basque Government, in its "Formation Program of Research" of "Education, University and Research" department.)
[2] The University of The Basque Country (UPV), Thermal Engineering Department, SPAIN. luis.delportillo@ehu.es
[3] The University of The Basque Country (UPV), Thermal Engineering Department, SPAIN. josemariapedro.sala@ehu.es
[4] The University of The Basque Country (UPV), Thermal Engineering Department, SPAIN. jonteres@gmail.com (This authors have been given a grant by the Basque Government, in its "Formation Program of Research" of "Education, University and Research" department.)

1 INTRODUCTION

During the XX century overall energy consumption has been increased principally in the developed countries, generating higher resource consumption. As far as the construction sector is concerned, it has turned into a great consumer of energetic resources, being responsible of 41% of the primary energy consumed within the European Union and one of the major generators of GEG (Greenhouse Effect Gases) with a contribution of 35% [CIEMAT, 2006].

The Energy Efficiency mandate approved by the European Council in March, 2007, reveals that the European Union promises to diminish by the year 2020 its consumption of energy by 20%, the GEG emitted by 20% with respect to the year 1990 (14% with respect to 2005), and to increase by 20% the contribution of the renewable energies. This commitment which concerns 3 principal sectors - Industry, Transport and Residential Building- receives a major importance in dwellings due to the opportunities that it offers on having been in an initial phase in environmental improvements. The fulfilment of the European commitment 20-20-20 means that the existing buildings in the year 2005 will reduce its consumption by 20%, allowing an energetic saving of 140Mtep/year, being 700Mtep/year the energy consumption of buildings in Europe. Therefore, the new buildings constructed in the period 2005-2020 will have a saving of approximately 25 Mtep/year. On the other hand, both the new buildings and the existing buildings must include approximately 40/50 additional Mtep/year of renewable energies [CEC, 2008]. As it can be observed, the existing buildings have a wide range of improvement, having the rehabilitation of the buildings a great importance in energetic issues.

The law which establishes the need to insulate buildings came into effect in 1980 in Spain. Before this date all of the dwellings constructed were designed with low thermal requirements and most of them without using thermal insulation. The majority of the existing buildings in Basque Country, in particular the residential ones, are far away from actual scenario and are responsible for a significant energy consumption. These constructions represent the 80% of dwelling in the Basque Country. For this reason principal objective with regard to Energy Efficiency is to decrease the energy losses in this kind of buildings, due to their energy saving potential.

The benefits provided by rehabilitation or new construction are not easily estimated. The mainly aim of this paper is to determine the benefits of each case considering environmental criteria. Life Cycle Assessment constitutes an excellent tool to compare different construction scenarios including energy and environmental issues. Thus, it can be determined in which cases each scenario turns out to be more suitable. Blengini [2010] analyzed the behaviour of low energy buildings by a life cycle perspective, to reduce the energy consumption and the carbon footprint.

2 METHODOLOGY

2.1 Goal and Scope of the Study

Due to the challenge that implies the rehabilitation in the reduction of emissions and energy consumption in existing buildings for the mitigation of the climate change, different rehabilitation systems applied to a characteristic brick facade of the Basque Country dwellings have been analysed in this study. First the existing facade is supposed to have a lifetime of 50 years. After its usage phase two scenarios have been established. The first scenario includes the thermal rehabilitation of the existing facade. In the second scenario the facade is considered to be demolished and be constructed again supposing a current modular construction system.

Further to LCA of construction products, several studies have demonstrated that the energy use during the usage phase for a building is very large compared to the embodied energy of the components in the building products [Paulsen & Borg 2003]. According to the results of these researches the operating energy has the major share (80–90%), followed by embodied energy (10–20%), whereas demolition

and other process energy has negligible or little share [Ramesh *et al*. 2010]. Out of the energy consumed during the usage phase of a construction product, approximately 50–60% corresponds to heating, the rest to hot water supply and lighting [Zöld & Szalay 2007].

According to Balaras *et al.* [2007], to improve thermal building performance and indoor thermal comfort conditions, one of the most attractive measures is the addition of thermal insulation on exposed external walls. This measure allows an energy saving of about 49% on the whole energy consumption. In concordance with this, the energy consumption of heating related to the facade has been analyzed, i.e. the consumption that is associated with the losses across the enclosures. Only the heat losses across the North facade have been analyzed, for being the most unfavourable orientation in terms of energy performance. No other consumptions have been considered during the use phase. Furthermore, in this research neither the transport of the different components nor the demolition has been taken into account. Due to the low contribution of these phases, in several studies, these have been not considered [Kellenberger & Althaus 2009], [Zabalza *et al.* 2009].

This study focuses on determining the primary energy consumed and the GEG emission in both the components fabrication and service life of each considered scenario. To develop the LCA it is necessary to adopt a functional unit to which all the inputs and outputs will be referred to. In this case the functional unit is a facade integrated into a building located in Bilbao, with 1m² area and variable service life, understanding the losses of heating energy of the dwelling during the winter period. To be able to determine the GEG emissions during the usage period a natural gas heating has been supposed.

2.2 Description of Scenarios

As mentioned above, in this study the energy rehabilitation systems have been assessed for a characteristic facade located in a large number of buildings in the city of Bilbao. For this, it is considered an existing brick façade which was constructed before 1980, without insulating, and two different scenarios after its usage phase. As it can be seen in the fig. 1 below, the first scenario analysed in the current paper is the energy rehabilitation of the initial facade and afterwards a new usage period. The second scenario considers the demolition of the brick facade and then a new construction using an actual industrialized construction system and its service life. Jhonstone [1995] compared a rehabilitation model and a new construction system in order to improve the economic performance in dwelling.

Since no reliable data on the life span of buildings are available, in the LCA studies a wide range of buildings lifespan is considered, from 22 years in [Seo & Hwang 2001] to 100 years in [Gajda et al 2001], depending on the building service and on typology. In this case, the results can be calculated for a steady service period or a variable lifetime. A sensibility analysis of the usage period allows to evaluate the variation of its contribution to the entire life cycle when changing parameters as the lifetime period or the rehabilitation systems have been used [Verbeeck & Hens 2010]. In this paper the usage periods for both scenarios are 15, 30 and 50 years to establish the usage period for which rehabilitation systems are more suitable than the new construction.

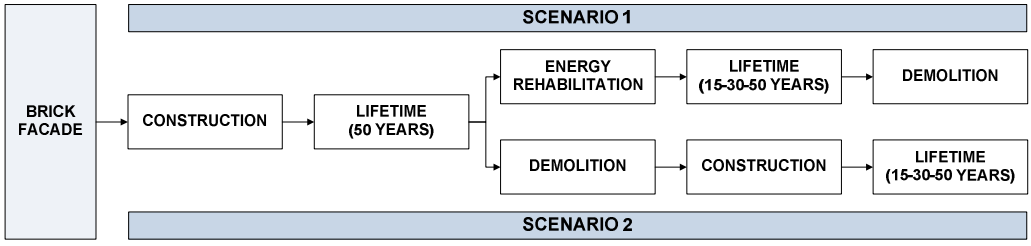

Figure 1. Scenarios before brick facade rehabilitation or demolition.

The sections of the initial brick facade, of the external and internal rehabilitation systems, and of the industrialized wall are shown in the following figure.

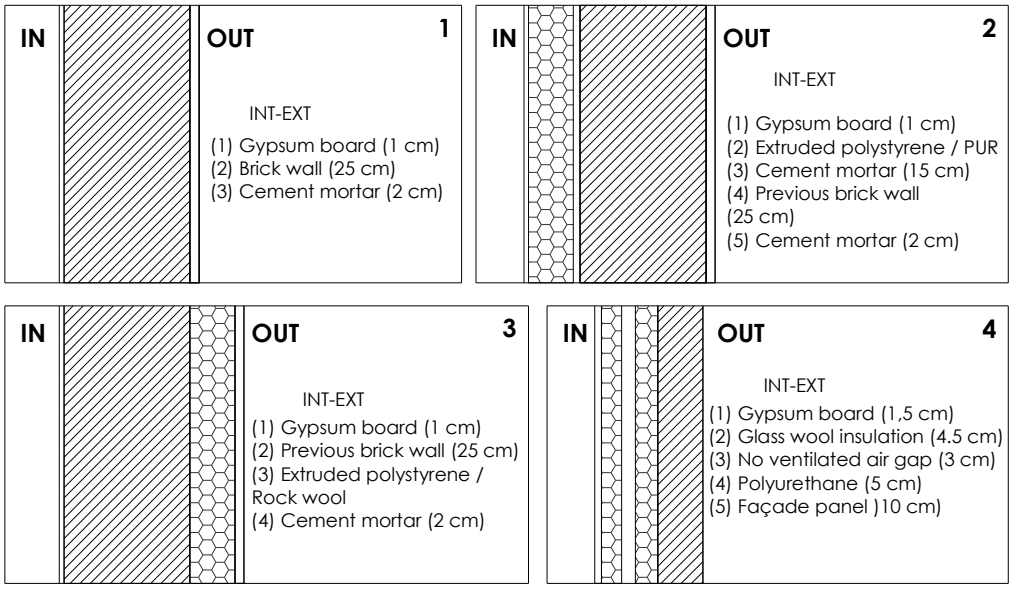

Figure 2. Initial brick facade (1). Internal rehabilitation (2). External rehabilitation (3). Industrialized facade (4).

The actual life span of a building is dependent on the durability of its materials and construction. In the present study, all the options considered are assumed to have a useful life span of 50 years, without significant energy consumption for maintenance. The assumption of a 50 year useful life for all configurations is based on limited data, so it is difficult to quantify the amounts of energy which would be required for their maintenance during this period [Huberman & Pearlmutter 2008]. In this paper, different durability is assumed for the materials used. Thus, the gypsum plasterboard is replaced after 25 years [Utama *et al*, 2009]. For the rest of materials no replacement or maintenance is calculated.

The durability of the insulations is not warranted over time [Mohammad & Al-Homoud, 2005]. For this reason, the variation of insulation performance over time has been taken into account. The R-value of rock wool and glass wool diminishes by the effect of the material compression, retaining 98% of their initial R-value over a fifteen year period. Furthermore, the R-value of polyurethane and extruded polystyrene decreases steadily over time. According to Kumaran & Bomberg [1990], the reduction of polyurethane thermal performance is due to the diffusion of the gases contained in the insulation cells (chlorofluorocarbons CFC or hydrochlorofluorocarbons HFC) and their replacement by air. In this paper, this R-value reduction is fixed in a value of 35% during the two first years and is stabilized after this period [Bomberg & Kumaran, 1999]. Extruded polystyrene is assumed to retain 75% of its R-value over a five year period [Tobiasson *et al*, 1987].

2.2.1 Scenario 1

In the first scenario external and internal energy rehabilitation systems have been taken into account. The External Thermal Insulation (ETI) is based on the external application of extruded polystyrene or rock wool; on the other hand, the Internal Thermal Insulation (ITI) focuses on the application of extruded polystyrene or polyurethane. The thermal transmittance of the rehabilitation solutions is calculated for insulation thicknesses of 3, 5, 8 and 10 centimetres. These values are shown in the fig.3. Moreover, the thermal transmittance after a period of fifteen years is calculated and represented by an asterisk in the fig.3. The initial value represents the thermal transmittance of the facade before the rehabilitation which decreases as the insulation thickness increases.

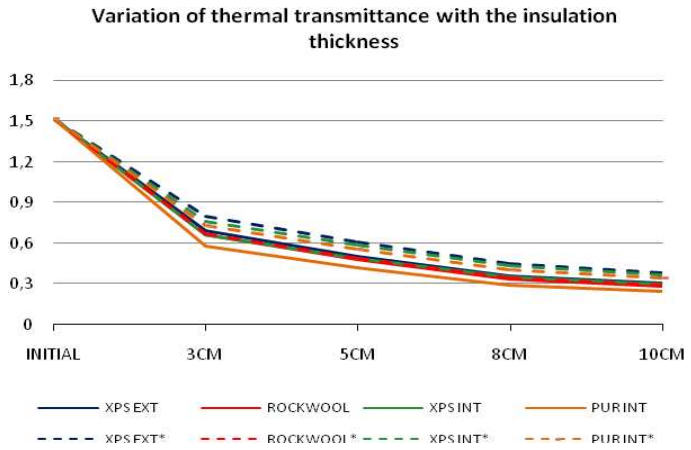

Figure 3. Thermal transmittance variation with the insulation thickness.

2.2.2 Scenario 2

The second scenario analyzed in the current paper is an industrialized facade placed in the Basque Country. The project which has been developed by the company Visesa (Housing and Soil in the Basque Country) includes structure and closures fabricated with elements of precast concrete. This facade is supposed to be constructed in the same location of the demolished facade. No assumptions of other modular facades have been made. The modular facade fulfils the new Spanish Technical Building Code and its thermal transmittance value is 0,308 W/m ² K. In the other hand, this value decreases over time by the R-value reduction of insulations. The thermal transmittance value is 0,366 after a two years period.

2.3 Methodology

The aim of this study is to determine the energy contained in the constructive element and the GEG emitted along its life cycle. For this reason the Midpoint methodologies "Cumulative Energy Demand" (CED) and "CML Baseline" have been used, to determine the primary energy consumption and greenhouse gases emissions respectively. CED method exposes the whole demand valued as primary energy and determines all the information about the energy resources consumption by means of an indicator measured in MJ-equivalent. CML Baseline method has been mainly used to determine the impact generated on the category of climate change. The impact category is characterised by means of IPCC (Intergovernmental Panel on), GWP 100 (Global Warming Potential), which is expressed as the potential of global warming for a period of 100 years in kg of carbon dioxide / kg of emission. Energy demand of buildings depends, among other factors, on its design, on the thermal behaviour of its enclosures and on the climatic conditions.

In this study the software SimaPro in its version 7.6.1 has been used to develop the life cycle assessment. The database Ecoinvent 2.0 has been used, which provides an updated wide and generic inventory that includes materials of construction, transport, different sources of generation and consumption of energy and waste scenario. The building simulation to determine the energy demand corresponding to the losses across $1m^2$ wall area, has been carried out with Trnsys v16 thermal simulation software. The climatic information for the façade location has been taken from the meteorological database Meteonorm.

3 RESULTS AND DISCUSSION

In this paper the results for the two analysed scenarios of the facade are presented. The hazard of 50 years lifetime of the brick facade before rehabilitation or demolition is not considered. Fig.4, Fig.5 and Fig.6 show the energy content in terms of primary energy in MJ_{eq}/m^2 for a usage period of 15, 30 and 50 years, respectively. The industrialized facade is represented by a horizontal line, since only one

section has been supposed. The intersection between rehabilitation systems and industrialized one highlights the insulation thickness for which the rehabilitation systems have less energy consumption than the new construction system considered. According to the results, this value increases with the increase of the usage period. For a usage period of 15 years the minimum insulation thickness needed is 6,3cm in the case of internal and external application of extruded polystyrene, and 6,4cm and 4,1cm whether polyurethane and rock wool are used, respectively. Nevertheless, for 30 years the insulation thicknesses that make the rehabilitation competitive are about 8,0cm in the case of external and interior application of extruded polystyrene, 7,8cm in the case of the polyurethane and 5,4cm in the rock wool solution; whereas for 50 years are 8,9cm when extruded polystyrene is externally or internally applied, 8,2cm for the polyurethane and 6,2cm for rock wool system.

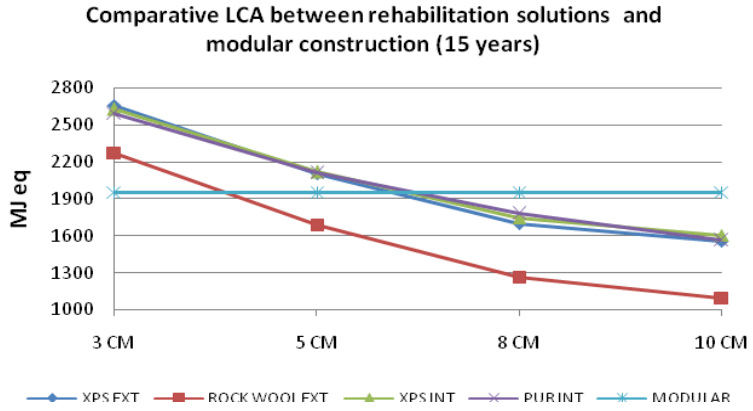

Figure 4. Comparative between rehabilitation solutions and modular system for 15 years lifetime.

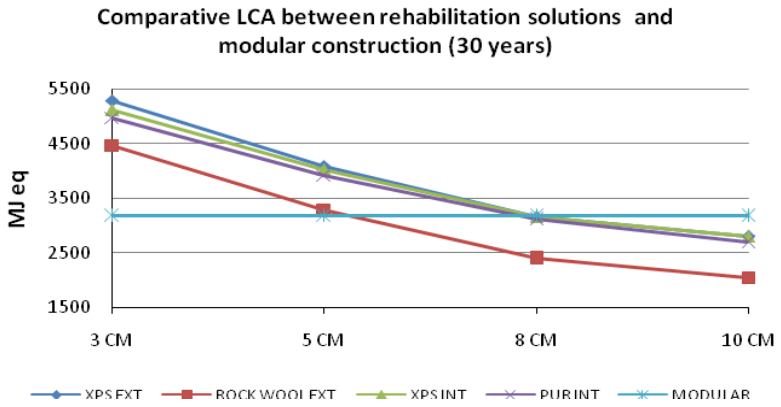

Figure 5. Comparative between rehabilitation solutions and modular system for 30 years lifetime.

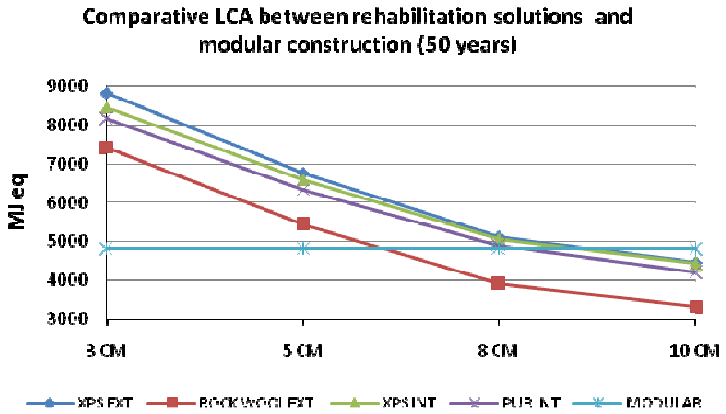

Figure 6. Comparative between rehabilitation solutions and modular system for 50 years lifetime.

Analyzing the overall results of the energy content in the life cycle of the rehabilitation and modular systems, 8cm and 10cm insulation thicknesses in rehabilitation would set better results than modular solution regarding to energy content depending on the usage period considered and would be a suitable solution to obtain most energy efficient facades, avoiding the facade demolition and the new construction. According to the Table.1 the embodied energy of the components constitute the rehabilitated or the modular facade is less in the case of the first system for 8cm and 10cm insulation thickness. Thus, it can be said that the embodied energy is greater in the modular system because of the high energy content of the precast concrete panel. The studies [Ortiz *et al.* 2009] [Xing *et al*. 2008] concluded that concrete had the highest embodied energy in the house at 61%. Furthermore, the polyurethane fabrication is more energy consuming than extruded polystyrene or rock wool.

Nevertheless, the energy consumption during the useful life in the modular solution is considerably less than the most of rehabilitation systems whether the thickness is 8cm, except in the case of rock wool which presents fewer values for all considered usage periods. Obviously, due to the less embodied energy of the rock wool rehabilitation, it presents a fewer value of energy content than the modular system along the entire life cycle. When the industrialized facade is comparing with the thermal rehabilitation systems for 10cm thickness it is observed that the energy consumption of the modular facade is greater for all service periods. The maintenance is responsible of less than 2% of the total energy consumption for a life span of 30 years and less than 1% for 50 years, in all solutions analyzed.

Table 1. Embodied energy and consumption in terms of primary energy.

SCENARIO	*MODULAR*	*INSULATION THICKNESS 8 cm*				*INSULATION THICKNESS 10 cm*			
		XPS EXT	*ROCK WOOL*	*XPS INT*	*PUR*	*XPS EXT*	*ROCK WOOL*	*XPS INT*	*PUR*
EMBODIED MJ_{eq}/m^2	766	328	142	415	503	402	168	488	598
MAINTENANCE MJ_{eq}/m^2	71	48	48	48	48	48	48	48	48
CONSUMPTION 15 MJ_{eq}/m^2	1955	1698	1265	1746	1781	1556	1097	1603	1564
CONSUMPTION 30 MJ_{eq}/m^2	3172	3160	2395	3163	3108	2798	2043	2811	2686
CONSUMPTION 50 MJ_{eq}/m^2	4796	5110	3901	5053	4877	4454	3304	4421	4183

The embodied energy of the construction materials, in particular of the plastic insulations, is really high. In contrast, their use contributes to the energy saving during the usage period, which is the most harmful phase. To determine the energy payback is necessary to calculate the annual energy saving respect to the initial brick facade. Energy payback has only been calculated for 10cm insulation thicknesses, since in this case all rehabilitation systems of the current paper are energetically profitable. The results highlight that the energy payback is about 0.9 years for the rock wool solution, 2.4 years for extruded polystyrene, 3.1 years for polyurethane and 4.1 years for modular solution.

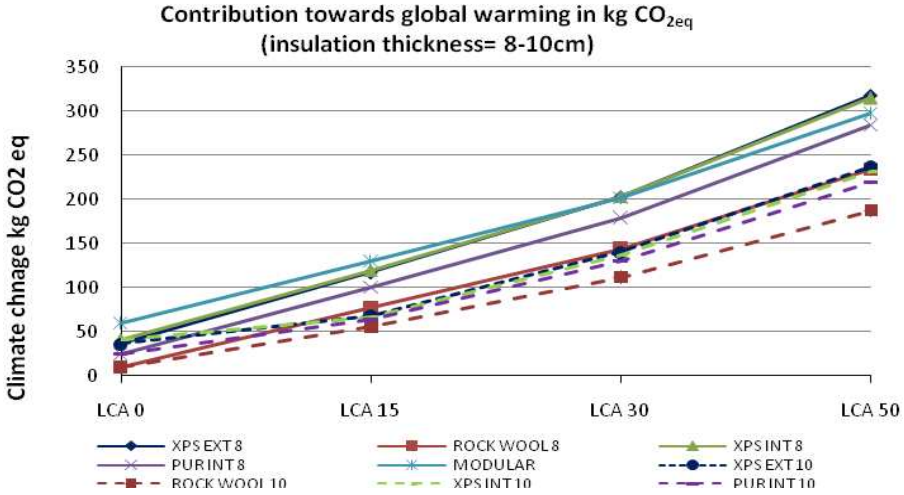

Figure 7. GWP 100 for modular system and 8-10cm insulation thickness rehabilitation solutions.

Finally, the greenhouse gasses emissions have been calculated. In the Fig.7 the emission of greenhouse gases in kg CO_{2eq} is shown for a usage periods of 15, 30 and 50 years. The intersection between the line of modular construction and extruded polystyrene rehabilitations represents the lifetime for which industrialized facade generates fewer greenhouse gases than extruded polystyrene solutions. This value is approximately 30 years for 8cm thickness of external and internal application of extruded polystyrene. In the case of both polyurethane and rock wool rehabilitation systems, the greenhouse gases emitted are fewer than the emissions of the new construction system for a lifetime of 15, 30 and 50 years. On the other hand, where a 10cm insulation thickness is considered, the industrialized solution is the most harmful to global warming for all of the usage periods considered.

4 CONCLUSIONS

In this research LCA methodology has been used in order to compare different construction scenarios with the aim of reducing the energy consumption and greenhouse emissions for an existing facade located in Bilbao. The results highlight that ETI and ITI rehabilitation solutions can be a suitable option, in opposition to the considered current modular construction system, provided the insulation thickness is greater than 8cm for a service period of 15, 30 and 50 years. No relevant differences have been found between ETI and ITI rehabilitation systems. Nevertheless, rock wool solution presents greater energy saving and fewer greenhouse emissions than polyurethane and extruded polystyrene rehabilitation whether both ETI and ITI system are considered. The results show that some rehabilitation solutions of facades allow increasing their durability and, in addition, reducing the energy consumption and GEG emissions during the useful life span.

According to the obtained results the usage period constitutes the most harmful phase of the LCA of a facade, due to its duration and the high consumption of fossil fuels. Nevertheless, the LCA cannot only focus on this phase. As it has been mentioned in this paper, the embodied energy of facade components, which is closely related to the fabrication phase, contributes to the whole energy consumption in 33%, however, when European Energy Efficiency Rules is applied the contribution of the usage phase can decrease and the energy embodied contribution increase. Therefore, greater energy embodied of the modular facade causes that the energy content along its entire life cycle is higher than 8cm polyurethane solution, though presenting less energy consumption during the usage phase.

REFERENCES

Balaras C & Gaglia A, 2007, European residential buildings and empirical assessment of the Hellenic building stock, energy consumption, emissions and potential energy savings, *Energy and Buildings*, 42, pp. 1298-1314.

Blengini G.A & Di Carlo T, 2010, The changing role of life cycle phases, subsystems and materials in the LCA of low energy buildings, *Energy and Buildings*, 42, pp. 869-880.

Bomberg M.T & Kumaran M.K, 1999, Use of Field-Applied Polyurethane Foams in Buildings, *Construction Technology Update*, 32.

CIEMAT, 2006, *Consumos de energía por sectores en la Unión Europea*.

Commission of the European Communities (CEC), 2008, *Directive of the European Parliament and of the Council on the energy performance of buildings.*

Gajda J, Van Geem MG & Marceau ML, 2001, Environmental Life-Cycle Inventory of Single-Family Housing, Sustainable Buildings III. *National Institute of Building Science*.

Huberman N & Pearlmutter D, 2008, A Life-Cycle Energy Analysis of Building Materials in the Negev Desert. *Energy and Buildings*, vol. 40, pp. 837-848.

Johnstone I. M, 1995, An actuarial model of rehabilitation versus new construction of housing, *Journal of Property Finance*, 6, pp. 7-26.

Kellenberger, Althaus, 2009, Relevance of simplifications in LCA of building components, *Building and Environment* 44, 818–825.

Kumaran M.K & Bomberg M.T , 1990. Thermal Performance of Sprayed Polyurethane Foam Insulation with Alternative Blowing Agents. *Journal of Thermal Insulation*, 14, pp 43-57.

Mohammad S. & Al-Homoud, 2005. Performance characteristics and practical applications of common building thermal insulation materials, *Building and Environment*, vol. 40, pp. 353-366.

Ortiz O., Bonnet C., Bruno J.C & Castells F. 2009, Sustainability based on LCM of residential dwellings: A case study in Catalonia, Spain. *Building and Environment* 44 584– 594.

Paulsen J. & Borg M, 2003, A Building Sector Related Procedure to Assess the Relevance of the Usage Phase, *Int J LCA*, 8, 142 – 150.

Ramesh T, Prakash R, Shukla K, 2010, Life cycle energy analysis of buildings: An overview, *Energy and Buildings* 42, 1592–1600.

SEO S. & Hwang Y., 2001, Estimation of CO2 Emissions in Life Cycle of Residential Buildings. *Journal of Construction Engineering and Management ASCE*., vol. 127. pp. 414–8.

Tobiasson, Greatorex A., & Van Pelt D. (CRRLE), 1987, Wetting of Polystyrene and Urethane Roof Insulation in the Laboratory and on a Protected Membrane Roof.

Utama A., Shabbir H. & Gheewala, 2009, Indonesian residential high rise buildings: A life cycle energy assessment. *Energy and Buildings*, 41, 1263–1268.

Verbeeck G. & Hens H., 2010, Life Cycle Inventory of Buildings: A Calculation Method. *Building and Environment*, vol. 45, pp. 1037-1041.

Xing, Su; Xu, Zhangand & Jun, Gao, 2008, Inventory Analysis of LCA on Steel- and Concrete-Construction Office Buildings, *Energy and Buildings*, vol. 40, pp. 1188-1193.

Zabalza Bribián, I. ; Aranda Usón, A & Scarpellini, 2009, Life Cycle Assessment in Buildings: State-of-the-Art and Simplified LCA Methodology as a Complement for Building Certification. *Building and Environment*, vol. 44, pp. 2510-2520.

Zöld A., Szalay Zs, 2007, What is missing from the concept of the new European Building Directive, *Building and Environment*, 42, 1761–1769.

XII DBMC
International Conference on Durability of Building Materials and Components
PORTO - PORTUGAL, April 12th-15th, 2011

Investigating of the Effects on Building Energy Consumption and Life Cycle Cost of Building Envelope Alternatives

Sibel Macka [1]
Yalcın Yasar [2]
Asiye Pehlevan [3]

ABSTRACT

With worldwide energy consumption and energy cost rising significantly in the building sector, there has been a pressing need to reduce energy consumption. Energy consumption for heating and cooling purposes in buildings can be reduced using appropriate building envelope components in terms of thermo-physical-optical and dimensional properties (total heat transmission coefficient of wall and window elements, coefficient of absorption, reflection and transmission, window - wall ratio and time lag and amplitude diminishing factor of opaque elements) according to climate conditions in early design stage.

This study investigates the influence of building energy performance and building economy of wall base layer changed in various wall construction alternatives in hypothetical building model in Trabzon. Turkey, having moderate-humid climate by employing EnergyPlus, detailed building heat transfer simulation software according to different window-wall ratios. During investigations, brick (inner leaf, outer leaf) and concrete (heavyweight, lightweight, medium and aerated) base layers are used in the wall constructions with and without insulation. Yearly and monthly net energy flows of these wall constructions is determined according to reference-opaque and %15, %30, %45, %60 of window wall ratio building models. Finally, all of the investigated alternatives are compared with reference-opaque building model and appropriate building envelope alternatives in terms of energy and economic efficiency according to local climatic conditions are offered designer in early design stage.

KEYWORDS

Window-wall ratio, Energy consumption, Life cycle cost, Energy simulation, EnergyPlus.

[1] Faculty of Architecture of the Karadeniz Technical University (KTU), Trabzon, Turkey, sibelmacka@ktu.edu.tr
[2] Faculty of Architecture of the Karadeniz Technical University (KTU), Trabzon, Turkey, yyasar@ktu.edu.tr
[3] Faculty of Architecture of the Karadeniz Technical University (KTU), Trabzon, Turkey, apehlevan@ktu.edu.tr

1 INTRODUCTION

Energy consumption worldwide is increasing due to increasing population, migration to large cities and improvement in standard of living. To maintain the standard of living in industrialized countries and to improve the situation in developing countries, energy can be used much more efficiently and also more use of renewable energy made. The most important of the energy strategy of a country is energy saving. Because of the limited energy-sources and environmental pollution coming from using the fuels, energy saving has become compulsory.

Turkey is one of the world's fastest growing energy markets. Its energy demand has grown rapidly almost every year and is expected to continue growing. On the other hand, meeting energy demand is of high importance in Turkey. Energy cost saving is vital for Turkey which imports most of the energy it uses. 66% and 73% of the total energy demand were imported in 2000 and 2010 respectively, it is suggested that 77% of the total energy demand will be imported in 2020 in Turkey [Sözen.2005]. It is estimated that the building sector consumes about 30 - 40% of total energy in Turkey, which is comparable to that of the transport sector and that of the industrial sector [Keskin.2008]. Therefore, considerable attention is currently been paid on reducing the energy demand for heating and cooling purposes in buildings. There are many parameters affecting heating and cooling loads in buildings which can be grouped into two main categories: (1) the optical (solar radiation transmittance) and thermal properties of the building envelope components; and (2) the meteorological data [Shariah et al. 1997]. Building envelope components -external wall, windows- are the interface between its interior and the outdoor environment and these components should be designed according to the outside environmental conditions and indoor thermal comfort requirements to reduce space heating and cooling, energy use and costs.

Calculations of heating and cooling loads in the building envelope have been the subject of many researchers. Takeda [Takeda.1979] investigated the characteristics of heating and cooling loads in apartments in Japan. Bruna et al. [Bruno et al.1979] discussed various methods of determining the heating and cooling requirements of buildings. Shariah et al. [Shariah et al. 1996] calculated cooling and heating loads for air-conditioned and heated buildings for three different cities in Jordan. They were analysed insulation effect of buildings for four combinations of wall and ceiling insulation. Lam et al. [Lam et al.2005] investigated energy performance of the building envelopes in terms of the overall thermal transfer value-OTTV. Lindberg et al. [Lindberg et al.2003] gathered 5-year measured data for analyses of building energy consumption and thermal performance of exterior walls. They were uses these data in calculated heating and cooling loads of six identical test buildings, having exterior walls that are constructed of different building materials. Energy conservation measures in various types of building and their economics have been studied by several authors. Ouyang et al. [Ouyang et al. 2009] used an urban existing residential building in China and analysed the economic benefits of certain energy-saving renovation measures through the simplified Life Cycle Cost method. Their study was based on the energy-saving effects of those measures calculated by thermal simulation, which they finally revised by applying the actual heating and cooling loads of the subject building. Nikolaidis et al. [Nikolaidis et al. 2009] investigated economic analysis and evaluation of various energy saving measures in the building sector, focusing on a domestic detached house in Greece.Ucar et al. [Ucar et al. 2010] calculated optimum insulation thickness of the external wall for four cities from four climate zones of Turkey, energy saving over a lifetime of 10 years and payback periods for the five different energy types and four different insulation materials applied externally on walls.

The present study deals with the determination of the effect on building energy performance and building economy of wall base layer changed in various wall construction alternatives used in a hypothetical building model in the moderate-humid climate regions of Turkey.

2 METHOD

For this study, five one storey hypothetical building models were conceived. These building models were to be subjected to the climate of Trabzon, Turkey (Climate Region II), a moderate-humid climate. the models had respectively reference-opaque window wall ratio of 15%, 30%, 45%, 60%. Each model (10 m x 10 m x 3 m) was simulated by means of the EnergyPlus simulation software using various wall construction alternatives having either a brick (inner leaf, outer leaf) or concrete (heavyweight, lightweight, medium and aerated) base layer. In these models, the net energy flows (heat gain/loss) from the HVAC system, infiltration, occupancy, lighting and power devices were ignored. The simulation model only considered the net energy flows through building elements. Data related to energy flows from interior conditions were later determined in these models. To investigate the effect of the various wall constructions and window wall ratios on the total net energy flows, all parameters except the base layer of wall were kept constant. In all of these buildings models, the widows were consider to be double-glazed unit having a clear glass and the void between glass panes filled with air. The total net energy flow through these wall constructions was calculated on a monthly and well as a yearly basis by means of the software. For each building model, a total twelve simulation outputs were obtained for the different wall construction alternatives that either had or did not have insulation. Next, the initial capital investment of each wall construction alternative was calculated according to the unit price per square meter. The life cycle cost (LCC) was determined for the reference-opaque building model by summing the initial capital investment to the present value of energy costs of the wall construction alternatives. In Turkey, since costs related to maintenance, repair, and replacement are not determined by institutions or firms, these costs were the same for all of the wall construction alternatives. Finally, the energy and economic efficiency of the wall construction alternatives were discussed according to window wall ratio.

2.1 EnergyPlus Simulation Software

As a dynamic building energy model, EnergyPlus can predict heating and cooling energy loads and indoor environmental conditions by using the heat balance method in which is solved a one-dimensional dynamic heat conduction equation that is used to model heat transfer through the envelope and partition elements [Crawley et al. 2008]. Details in respect to the use, applicability and operation of the EnergyPlus building systems simulation module can be found in Crawley et al. [2008] and Fumo et al. [2010]. In this study, only yearly and monthly net energy flows –(negative values are heating load, positive values are cooling load) through the building envelope are calculated, and other parameters such as heating and cooling system and plant sizing, occupancy comfort are not included. There are several studies that have been performed by using EnergyPlus simulation software, some examples of which include those reported by Eskin and Türkmen [2007], Chan et al. [2008] and Macka et al [2010].

2.2 Building Location and Meteorological Data

Trabzon (pop. of 975,137) is located in the Black Sea region (39.72^0 N latitude and 41^0 E longitude) and in Turkey is referred to as being in Climate Region II which is a moderate-humid climate [Online 1]. Meteorological data for Climate Region II are given in Table 1. This climate zone is spread over an area of 4685 km^2, and Trabzon itself is 30 m above the mean sea level.

Table 1. Meteorological data for Climate Region II [Online 2].

	JAN	FEB	MAR	APR	MAY	JUN	JUL	AUG	SEP	OCT	NOV	DEC
Dry bulb temp (^{0}C)	5,7	4,8	7,2	12,2	16,7	21,6	24,0	24,2	20,8	16,4	11,3	7,8
Dew-point temp. (^{0}C)	2,3	-0,6	3,0	5,8	11,4	14,3	17,9	19,2	13,7	10,5	6,9	5,0
Wind speed (m^2/s)	4,7	5,4	4,1	4,1	4,3	3,9	5,7	5,6	4,9	4,2	4,0	5,5
Wind direction	130,6	172,0	150,7	152,4	128,7	126,6	54,8	80,2	76,1	102,0	166,0	103,0
Atmos. pressure (Pa)	101,9	101,2	101,4	100,7	101,1	100,9	100,7	101,0	101,1	101,2	101,5	101,8
Direct normal radiation (W/m^2)	39,7	30,2	40,7	70,7	104,3	132,0	158,8	135,2	117,6	65,0	38,9	21,2
Horiz. diffuse radiation (W/m^2)	32,1	42,5	68,1	82,8	96,5	95,0	85,8	80,6	63,0	53,8	36,4	30,5

2.3 Hypothetical Building Model Details

The dimensions of the five single storey hypothetical building models used for the purpose of determining energy costs, was 10 m x 10 m with height of 3 m. For simplicity, it was supposed that these model plans had a thermal zone of 100 m^2 of unconditioned space; a summary of these different models and their associated window-wall ratios (WWR) are given in Figure 1.

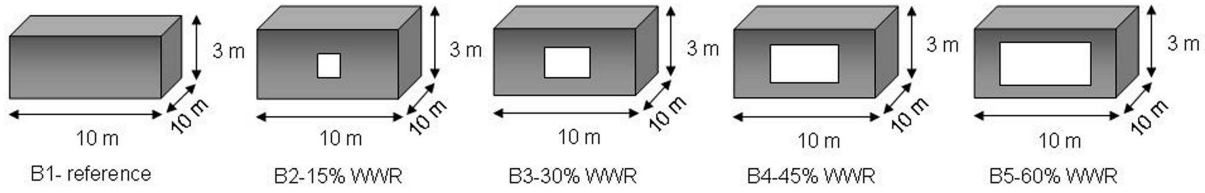

Figure 1. Five building models investigated.

Two types of wall construction alternatives were investigated: those with and those without insulation. The exterior walls without insulation consisted of three layers of material: a 240 mm base layer, on each side of which was a 20 mm thick plaster layer. The exterior walls with insulation consisted of four layers of material: a 190 mm base layer on either side of which was a 20 mm thick plaster layer, , and a 50-mm-thick insulation layer located on the outer surface of the wall. Hence, the overall thickness of both types of wall construction alternatives was the same. For all wall types, the plaster and heat insulation layers were gypsum and expanded polystyrene (EPS) respectively [Manioğlu.2002]. In this study, six wall construction alternatives were investigated according to the type of "base layer" of each of the respective wall construction types; these were: WB1, WB2, WC1, WC2, WC3 and WC4. The respective thermo-physical and dimensional properties of the various wall construction alternatives investigated in this study are given Table 2. The values of heat transmittance coefficient (U-value) for walls WB1, WB2, WC1, WC2, WC3 and WC4 and in which insulation is used are, respectively: 0.54, 0.57, 0.61, 0.39, 0.52 and 0.43 W/m^2K [Online 2]. Since it was the effects of the different wall construction alternatives on building energy performance that was of interest, the selection of types and number of windows, as well as the type of floor and roof constructions used in all of the building models were kept constant; values for thermo-physical and dimensional properties of these components are likewise given in Table 2.

2.4 Life Cycle Cost Analysis

The life cycle cost (LCC) is the total cost of ownership of machinery and equipment, including the cost of maintenance, repair, replacement, and operation. As such the LCC is a summation of cost estimates from inception to disposal of both the equipment and their operation over the life of the building, accrued annually, with consideration given to the time value of money [Barringer.2003]. For the evaluation of a unit in terms of LCC, all future costs during the unit life were discounted to the present value, except for the initial capital investment of the project [Manioğlu.2002]. The following formula was used to calculate yearly heating and cooling energy consumption costs of a wall.

$$C_{enr} = Q_{h,c}/COP_{h,c} \text{ x } C_{ng,el} \quad (1)$$

Where Q_h or Q_c are heating and cooling load, COP_h or COP_c is the coefficient of performance of heating or cooling system and C_{ng} or C_{el} are the cost of natural gas and electricity in TL/kWh. The present value of the cost of energy consumption over a life time of n years is determined using the present worth factor (PWF) defined as [Dombaycı et al, Bolatürk. 2006].

$$PWF = 1/r \text{ x } (1- 1/(1+r)^n) \quad (2)$$
$$LCC = (C_{enr} \text{ x } PWF) + C_i \quad (3)$$

Where C_i is the initial capital investment of a wall construction. The alternative with the lowest LCC is the most economic alternative. Factors used in the LCC analysis in this study are given in Table 3.

Table 2. Thermo-physical and dimensional properties of the building model components[Online 2].

Building components		Wall construction code	Materials (layers)	Thickness (mm)	Thermal conductivity (W/mK)	Specific heat capacity (J/kg K)	Density (kg/m^3)
External wall		WB1	[3]Brickwork (inner leaf)	190	0,62	800	1700
		WB2	[3]Brickwork (outer leaf)	190	0,84	800	1700
without insulation 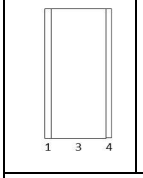	with insulation 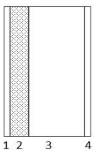	WC1	[3]Concrete (heavyweight)	190	1,63	1000	2300
		WC2	[3]Concrete (lightweight)	190	0,19	1000	600
		WC3	[3]Concrete (medium)	190	0,51	1000	1400
		WC4	[3]Aerated concrete	190	0,24	1000	750
		Common material	[2]Expanded Polystyrene-EPS	50	0,04	1400	15
		Common material	[1,4] Gypsum Plaster	20	0,4	1000	1000
Windows		2,7	Clear glass	6	1	750	2500
			Air gap	12	2,49	1008	1232
			Vinyl, PVC frame	20	0,17	900	1390
Floor		1,347	Carpet/textile flooring	20	0,06	1300	200
			Mortar	40	0,88	896	2800
			Concrete, Medium density	140	1,35	1000	1800
			Gypsum plaster	20	0,4	1000	1000
Roof		0,382	Bitumen, felt/sheet	20	0,23	1000	1100
			MV Stone wool	50	0,035	840	150
			Plaster/dense	20	0,5	1000	1300
			Concrete /aerated	140	0,16	840	500
			Gypsum plastering	20	40	1000	1000

3 RESULTS AND DISCUSSION

For the building models investigated in this study and which are located in Trabzon (TR), , the net monthly energy flows through walls, windows, floors and roofs were obtained from simulation. Evaluations related to the results obtained were performed in consideration of monthly net energy flows through the different wall construction alternatives and in accordance to the respective window-wall ratios. Finally, the calculated LCC of each wall construction alternative with insulation were compared in relation to the building model B1 (reference wall) by using the method described in Section 2.4.

Figure 2 shows that only cooling loads occur for wall construction alternatives with and without insulation in reference building B1; insulation contributes to heating energy savings during the heating period. In terms of cooling energy savings, wall constructions with lightweight, aerated and medium concrete (WC2, WC4, WC3) respectively provide 46%, 39% and 20% more energy savings than heavyweight concrete (WC1-reference wall construction) in alternatives without insulation. In alternatives with insulation, alternatives WC2, WC4 and WC3 provide 21%, 16% and 7% more energy savings than WB2, the reference wall construction.

In contrast to B1, only heating loads occur in wall construction alternative B2 - 15% WWR (Table 4) without and with insulation. They contribute cooling energy savings during the cooling period. In terms of heating energy savings, concrete wall constructions with lightweight, aerated and medium concrete (WC2, WC4, WC3) respectively provided 50%, 43% and 23% more energy savings than the heavyweight concrete construction (WC1- reference wall) in alternatives without insulation. In alternatives with insulation, WC2, WC4 and WC3 provided 55%, 51% and 28% more energy savings than WC1, the reference wall construction.

For the wall construction alternative B3- 30% WWR (Table 4) without and with insulation, again, only heating loads occurred. These contributed to cooling energy savings during the cooling period. In terms of heating energy savings, concrete wall constructions having lightweight, aerated and

Table 3. Factors used in the life cycle cost analysis.

Analysis type	General LCC analysis-non-federal, no taxes,
Beginning date for LCC	2010
Study period	30 years
Planning/Construction period	2 years
Service date	2012
Discount rate	8% [Daouas. 2010]
Life of walls	60 years
Fuel type	Natural gas, electricity
The unit cost of natural gas	0,07368 TL/kWh (for 2009)
The unit cost of electricity	0,1983 TL/kWh (for 2009)
Cooling system performance coefficient	2,93 [Daouas. 2010]

*Current Exchange rate (2010); 1TL=US$0.6811

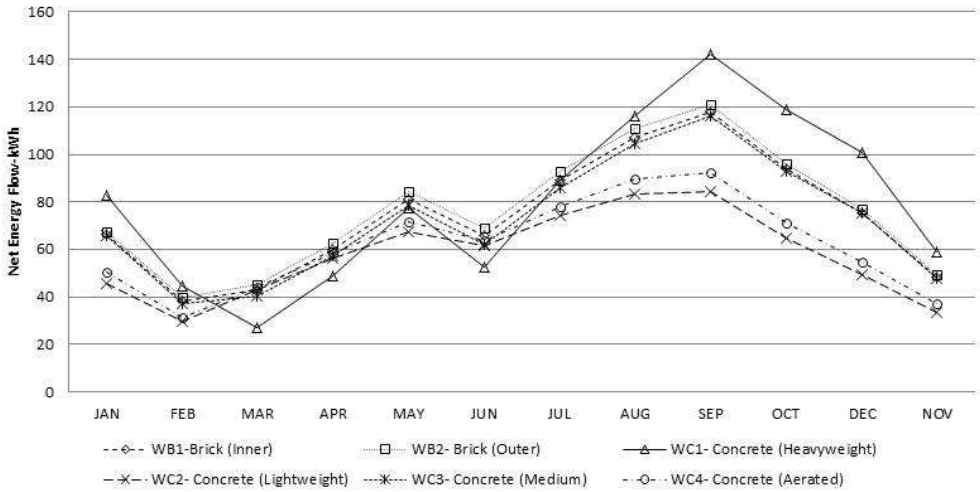

Figure 2. Monthly net energy flows of wall construction alternatives without and with insulation in reference building (B1) – kWh [Online 2].

medium concrete construction (WC2, WC4, WC3) respectively provided 55%, 48% and 26% more energy savings than heavyweight concrete construction (WC1-reference wall construction) in alternatives without insulation. In alternatives with insulation (i.e. WC2, WC4 and WC3) 18%, 14% and 9% more energy savings were provides as compared to WB2, the reference wall construction.

As was the case for B3, only heating load occurred for wall construction alternative B4 - 45% WWR building (Table 4) either with or without insulation and these likewise contribute cooling energy during the cooling period. In terms of heating energy savings, concrete wall constructions with lightweight, aerated and medium concrete (i.e. WC2, WC4, WC3) respectively provided 59%, 52% and 29% more energy savings than the reference wall construction of heavyweight concrete (WC1) in alternatives without insulation. In alternatives with insulation (WC2, WC4 and WC3) 23%, 18% and 8% more energy saving were provided as compared to WB2, the reference wall construction.

As was evident for B2 and B3, for construction alternative B5- 60% WWR (Table 4) without or with insulation only heating loads were evident thus contributing to cooling energy savings during the cooling period. In terms of heating energy savings, wall constructions with lightweight, aerated and medium concrete construction (WC2, WC4, WC3) provided 62%, 55% and 32% more energy saving respectively than the reference wall construction of heavyweight concrete (WC1) in alternatives without insulation. In alternatives with insulation, WC2, WC4 and WC3 provided 24%, 19% and 8% more energy savings than WB2 the reference wall construction.

In all of the investigated building models without and with insulation, walls with concrete construction (WC2, WC3, WC4) owing to their low thermal conductivity were shown to have a better energy performance than walls with brick construction (WB1, WB2). Only, WC1 (heavyweight concrete) due to its high thermal conductivity was generally lower in energy performance than brick construction (WB1, WB2). However it is evident from the information provided in Table 4 (and Fig. 2) that WC1 nonetheless provided the highest energy performance for a few months during the heating period in wall construction alternatives having insulation. As well, for all alternative wall constructions (B2, B3, B4, and B5), as might be expected, the net energy flows of wall alternatives with insulation are lower than alternatives without insulation.

In Table 4, the percentage of energy performance (%) and yearly net heating and cooling loads (kWh) of wall construction alternatives without and with insulation using building models are given. Whereas cooling loads only occurred for building model B1, heating loads occurred in building B2, B3, B4 and B5. The total wall area of building models affected yearly heating and cooling loads. Figure 7 shows the variation in yearly heating and cooling loads of wall construction alternatives with insulation in relation to the total wall area of the building. In B1 (reference building) without windows (wall area = 120 m^2) the yearly heating load is not evident. By decreasing wall area (from 120 m^2 to 102, 84 and 66 m^2), yearly heating loads increased in buildings B2, B3, B4 in which window wall ratios ranged between 15% and 45%. This study has shown that the window area in building models not surprisingly change the yearly heating loads. When the wall area of a building model (B5-60%WWR) is smaller than 50 m^2, the yearly heating loads decrease and differ from other building models (B2, B3, B4).

Table 4. Comparing the percentage of energy performance (%) and yearly net heating and cooling loads (kWh) of wall construction alternatives using building models [Online 2].

Building model		Wall construction alternative											
		Without insulation						With insulation					
		WC2	WC4	WC3	WB1	WB2	WC1	WC2	WC4	WC3	WB1	WB2	WC1
Ref.	B1(%)	46	39	20	15	9	*	21	16	7	4	*	3
	B1(kWh)	736	826	1092	1154	1238	1362	428	453	505	522	541	527
15%WWR	B2(%)	50	43	23	16	7	*	55	51	28	28	27	*
	B2(kWh)	-77	-87	-118	-129	-143	-153	-40	-44	-64	-64	-65	-88
30%WWR	B3(%)	55	48	26	20	12	*	18	14	9	4	*	4
	B3(kWh)	-329	-378	-539	-582	-642	-731	-166	-175	-185	-194	-203	-194
45%WWR	B4(%)	59	52	29	23	14	*	23	18	8	4	*	7
	B4(kWh)	-405	-470	-695	-756	-842	-983	-206	-219	-244	-254	-266	-248
60%WWR	B5(%)	62	55	32	26	16	*	24	19	8	5	*	4
	B5(kWh)	-361	-423	-644	-705	-794	-948	-182	-195	-220	-229	-240	-230

***** Reference wall construction alternatives

NOTE: positive values (+) refer yearly cooling load, negative values (-) refer yearly heating load

3.1 The Life Cycle Costs Of Wall Construction Alternatives with Insulation

The LCC of each wall construction alternative for the reference-opaque building model with insulation is calculated using values in the Table 3 according to equation 1, 2 and 3. Unit prices Turkish Lira) per m^2 of the wall construction for the alternatives evaluated in this study were obtained from the Ministry of Public Works and Settlement (Turkey). In accordance with the total wall area in the reference building, a total of six initial capital investments were calculated. The unit supply prices for wall construction alternatives are given in Table 5 as are the total initial capital investment of the reference wall, yearly energy costs, discounted value of energy, and present value of such costs.

Data related to maintenance/repair and replacements are not presently available from the Republic of Turkey Ministry of Public Works and Settlement. Thus, these data are ignored in the LCC, and only the initial capital investment and energy costs are used. In Table 5, the yearly energy costs calculated for the reference building using net energy flows calculated in the Section 3.1 and according to equation 1 and 2 are also given.

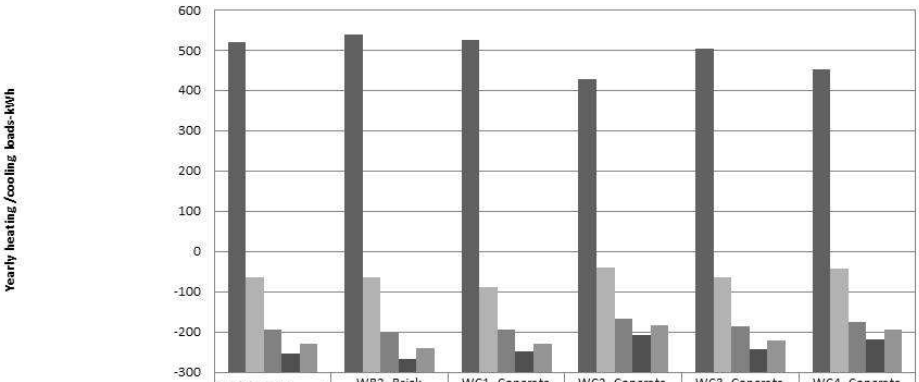

	WB1-Brick (Inner)	WB2- Brick (Outer)	WC1- Concrete (Heavyweight)	WC2- Concrete (Lightweight)	WC3- Concrete (Medium)	WC4- Concrete (Aerated)
B1-ref., wall area =120m2	521,51	540,65	526,52	427,55	504,92	453,19
B2-15%WWR, wall area=102m2	-63,53	-64,62	-88,45	-40,18	-63,64	-43,59
B3-30%WWR, wall area=84m2	-194,26	-203,38	-193,54	-166,45	-185,48	-175,37
B4-45%WWR, wall area=66 m2	-254,42	-266,18	-247,59	-206,19	-243,97	-219,49
B5-60%WWR, wall area=48m2	-229,51	-240,38	-229,9	-181,94	-220,12	-194,74

Figure 3. Variation in yearly heating and cooling loads of wall construction alternatives with insulation according to building model's total wall area [Online 2].

Table 5. Cost of wall construction alternatives units/m^2 (TL) [Material unit price, 2010].

Wall construction alternative-with insulation	Supply price /m^2 (TL)	Total initial capital investment*	Yearly energy costs* /m^2	Present value of energy cost* /m^2
WB1	69,63	8355	35,23	396,69
WB2	71,63	8595	36,53	411,26
WC1	65,51	7861	35,57	400,42
WC2	100,58	12069	28,89	325,24
WC3	94,32	11318	34,11	384,05
WC4	96,61	11593	30,62	344,74

* for wall construction alternatives with insulation used in the reference-opaque building model-B1

The present value of yearly energy costs given in Table 5 are based on a present worth factor =11.25 (Equation 3). By summing present values of energy costs and the initial capital investment for wall construction alternatives with insulation, the LCC of each wall construction alternative is determined as shown in Figure 4. The fact that the lowest LCC is the most economically efficient alternative was accepted in the evaluation of LCC. As shown in Figure 4, WC1, WB1, WB2, WC3 and WC4 provided 33%, 29%, 27 %, 6% and 4 % more cost savings, respectively, as compared to WC2, the reference building model-B1. As well, although operational costs of energy efficient alternatives are lower than other alternatives, their LCC are high because of great difference among initial capital investments.

In Table 6 a comparison is given of results from both the energy and economic performance of wall construction alternatives with insulation investigated of this study as compared to the reference building model-B1. As is evident, the lightweight concrete wall construction alternative (WC2) is an energy efficient performance alternative but having the lowest performance in terms of economic efficiency. If considering both energy and economic efficiency, the medium concrete wall construction (WC) provides good overall performance.

4 CONCLUSIONS

With energy consumption rising significantly in the building sector in Turkey, building owners and designers at the early design stage are forced take measures to minimize energy usage in buildings. In this context, building authorities should know those building envelope alternatives that cause a significant part of energy consumption for a building according to climate conditions. The method

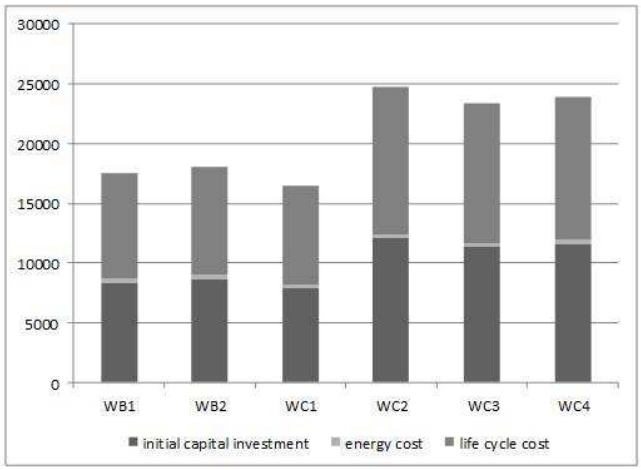

Figure 4. Life Cycle Costs of wall construction alternatives with insulation in reference-opaque building model-B1.

Table 6. Comparing of energy and economic efficiency performance of investigated wall construction alternatives with insulation in reference building model-B1.

Wall construction alternatives	Energy Efficient Performance	Economy Efficient Performance
WB1	•••	•••••
WB2	•	••••
WC1	••	••••••
WC2	••••••	•
WC3	••••	•••
WC4	•••••	••

•••••• denotes: best performance, demotes:• poorest performance

presented in this study provides the yearly heating and cooling loads for alternative sets of construction types that included: different window wall ratios, various brick and concrete wall construction alternatives without and with insulation. The different model construction types were subjected moderate-humid climate conditions of typical of the Trabzon region in Turkey. The energy usage was calculated only for those wall construction alternatives having insulation and the LCC of these were compared to a reference building. Using this method, a designer and building owner in the early design stage can determine energy and economic efficient alternatives among various wall constructions types that might be used in such a climate region. It was determined on the basis of the result from this study that concrete wall construction alternatives (WC2, WC4, WC3), with the exception of the heavyweight concrete wall construction (WC1), were more energy efficient than brick wall construction (WB1, WB2). However, in respect to the LCC analysis, it appeared that heavyweight concrete wall (WC1) and brick wall constructions (WB1, WB2) were more economically efficient than concrete walls WC2, WC4 and WC3. Since all evaluations were performed on a limited area (100 m^2), it should be understood that values of energy consumption and LCC in larger buildings will change depending on expected heating and cooling loads.

REFERENCES

Barringer, H.P. 2003, *"A life cycle cost summary, international conference of maintenance societies"*, ICOMS-2003, 20-23 May, Australia.

Bruno, R., Brombach,U. & Steinmuller, B. 1979, *"On calculating heating and cooling requirements"*, Energy Buildings, 2, 197-210.

Chan, A.L.S., Chow,K.F., Fong,K.F. & Lin,Z. 2009, *"Investigation on energy performance of double skin facade in Hong Kong"*, Energy and Buildings, 41, 1135–1142.

Crawley, D.B., Hand, J.W., Kummert, M. & Griffith, B.T. 2008, *"Contrasting the capabilities of building energy performance simulation programs"*, Building and Environment, 43, 661–673.

Daouas, N., Hassen, Z. & Aissia, H.B. 2010, *"Analytical periodic solution for the study of thermal performance and optimum insulation thickness of building walls in Tunisia"*, Applied Thermal Engineering, 30, 319-326.

EnergyPlus Energy Simulation Software [Online 2], Available: http : // apps1. eere. energy. gov / buildings / energyplus / cfm / Weather _ data . cfm.

Eskin, N & Türkmen, H. 2007, "Analysis of annual heating and cooling energy requirements for office buildings in different climates in Turkey", Energy and Buildings, 40, 763–773.

Fumo,N., Mago,P. & Luck, R. 2010, *"Methodology to estimate building energy consumption using EnergyPlus Benchmark Models"*, Energy and Buildings, 42, 2331–2337.

Giritli,H. 2001, *"Project and construction management methods of economic evaluation in construction"*, Lecture Document, Istanbul Technical University, Istanbul, Turkey.

Keskin,T. 2008, *"Energy Management in Building Sector: Turkish experience"*, ENERGAİA Montpellier 2008: an Intl. Renewable Energies Exhibition and Conference, 10-12 December, France.

Lam, J.C., Tsang, C.L., Danny, H.W. & Cheung, S.O. 2005, *" Residential building envelope heat gain and cooling energy requirements"*, Energy, 30, 933-951.

Lindberg, R., Binamu, A. & Teikari,M. 2004, *"Five-year data of measured weather, energy consumption, and time-dependent temperature variations within different exterior wall structures"*, Energy and Buildings, 36, 495-501.

Macka, S. & Yasar,Y. 2010, *"The effects of window alternatives on energy efficiency and building economy in high-rise residential buildings in cold climates"*, International Sustainable Buildings Symposium-ISBS,26-28 May, Ankara, Turkey.

Manioglu, G. 2002, *"An Approach for the determination of building envelope and operation period og heating system according to energy conservation and life cycle cost"*, pHD Thesis, Natural and Applied Science Institute, Istanbul Technical University, Istanbul, Turkey.

Nikolaidis, Y., Pilavachi, P.A. & Chletsis, A. 2009, *"Economic eveluation of energy saving measures in a common type of Greek building"*, Applied Energy, 86, 2550-2559.

Ouyang, J., Ge, J. & Hokao, K. 2009, "*Economic analysis of energy saving renovation measures for urban existing residential buildings in China based on thermal simulation and site investigation*", Energy Policy, 37, 140-149.

Republic of Turkey, Prime Ministry of Public Works and Settlement. 2010, *"List of material unit price"*

Shariah, A., Tashtoush, B. & Roussan, A. 1997, *"Cooling and heating loads in residential buildings in Jordan"*, Energy and Building, 26,137-143.

Sözen, A., Arçaklıoğlu, E. & Özkaymak,M. 2005, *"Turkey's net energy consumption"*, Applied Energy, 81, 209–221.

Sözer, H. 2010, "*Improving energy efficiency through the design of the building envelope"*, Building and Environment, 45, 2581-2593

Takeda, H. 1979, *"Characteristics of heating and cooling loads in apartments"*, Energy Building, 2, 9-15.

"The geographical structure and climatic features of Trabzon", [Online 1], Available: http://www.trabzonkulturturizm.gov.tr.

Ucar, A. & Balo, F. 2010, *"Determination of the energy saving and the optimum insulation thickness in the four different insulated exterior walls"*, Renewable Energy, 35, 88-94.

XII DBMC
International Conference on Durability of Building Materials and Components
PORTO - PORTUGAL, April 12th-15th, 2011

Bioclimatic Architecture Potential in Buildings Durability and in their Thermal and Environmental Performance

Nuno Serafim Cruz [1]
M. Isabel M. Torres [2]
J. A. Raimundo Mendes da Silva [3]

ABSTRACT

Bioclimatic architecture increases the comfort of a building in any season while reducing the need for heating, cooling, lighting and ventilation, which in turn leads to an accentuated decrease in energy costs. The implementation of these assumptions in a building does not involve increased investment in construction nor the installation of specific domotic systems.

The Regulation of the Characteristics of Thermal Performance of Buildings (RCCTE) was reviewed and the National Energy Certification Buildings was created in an attempt to overcome environmental and energy problems. They establish new rules and methods for improving the indoor comfort and health conditions of buildings and for changing the philosophy of current building to a more sustainable level. Dissemination of knowledge of and the capital gains from bioclimatic architecture combined with sustainable building is now an urgent matter, so that these new approaches can be implemented effectively.

Buildings designed based on bioclimatic architecture are more sustainable have a healthier indoor environment, are more comfortable and have improved energy efficiency, which ultimately leads to lower energy costs.

One of the issues this study will examine is the historical evolution of buildings on an energy and environmental level and explain the methods and strategies used in bioclimatic architecture. Their effects and results will be analysed carefully and several examples and a practical case study will be given.

KEYWORDS

Bioclimatic architecture, Thermal performance, Durability, Sustainability, Comfort.

[1] Coimbra Viva SRU, Sociedade de Reabilitação Urbana S.A., Coimbra, PORTUGAL, nuno.cruz@cm-coimbra.pt
[2] Faculdade de Ciências e Tecnologia da Universidade de Coimbra (FCTUC), Coimbra, PORTUGAL, itorres@dec.uc.pt
[3] Faculdade de Ciências e Tecnologia da Universidade de Coimbra (FCTUC), Coimbra, PORTUGAL, raimundo@dec.uc.pt

1 INTRODUCTION

1.1 Vernacular Buildings

Vernacular buildings have come from a history of good construction practices and traditional social and technological knowledge developments acquired from experience over time. Vernacular architecture (which is undoubtedly bioclimatic) originated in empiricism, dictated by our forebears' rules of good building. It arose at a time when there was no technology to answer the needs of HVAC and lighting, and this led to efficient construction optimized for the the building's location within the surrounding environment, using local materials. Vernacular buildings use simple techniques to provide comfort both in winter and summer:

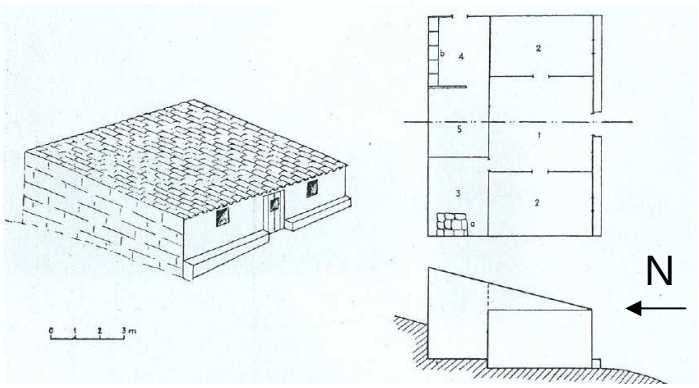

Figure 1. Isolated house in the hills of Monchique, mud: Perspective, cutting and elevation (according to a note by Ivo Castro Pereira).

In the Alentejo (Portugal) buildings used to be built in rows along narrow streets to provide more shade. Thick, white-painted walls were used to increase the thermal inertia and to reduce the absorption of solar radiation.

In northern countries houses have steep-sloped roofs so that snow does not stay on them for a long time. These are examples where the thermal comfort in both winter and summer can be improved with very simple steps. However, with the fascination for technical innovations, aid from industry, and belief in inexhaustible natural resources, the "best practices" evident in ancient and vernacular buildings were gradually abandoned and forgotten, because it was thought (and sometimes still is) that technology has magical solutions for everything.

2 BIOCLIMATIC ARCHITECTURE

Bioclimatic architecture is an integrated architecture, adapted to its physical, socio-economic and cultural environment. It is the kind of architecture that takes into account the analysis of the climate and environmental characteristics where the building is situated, promoting improved comfort and a reduction in energy consumption.

Its aim is to maximize interior environmental comfort, (thermal comfort, light, sound, etc..) using only the design elements and architectural forms available.

General Characteristics:

- It has very primitive roots in traditional or vernacular architecture, which are based on empiricism and the subsequent ancestral building arts;
- It seeks to give a practical response to the measures identified to achieve sustainability in construction;

- Its quest is to achieve conceptual and constructive integration with the environmental, thermal, climatic and biological context;
- It allows a "healthy balance" to be maintained in the building, rationalizing both the resources and waste.

Bioclimatic architecture is inseparable from passive solar design (which deals only with energy gained from sunlight), active building (which studies the mechanical low-energy means, usually associated with the use of renewable energy, eg solar panels, etc) and sustainable building (which deals with the environmental impact of all processes involved in building) since these concepts all work toward similar objectives and concerns.

2.1 Bioclimatic Building Techniques

The adoption of strategies in the design of a bioclimatic building significantly influence its performance in terms of thermal comfort and also leads to a reduction in energy consumption. During the project and building deployment, several aspects should be taken into account, such as:

- The local climate characteristics;
- The location that best fits its effective use in terms of human comfort;
- Technical factors associated with aspects like building orientation, the orientation of glazed façades, the building's shape, ventilation and air movements, the environment (heat gains and losses) and the internal and external temperatures;
- The effects of surrounding buildings in terms of sunlight and wind exposure;
- The solar radiation exposure during the year.

2.2 Passive Solar Architecture

Passive solar design refers to devices embedded in a building’s construction with the purpose of contributing to its natural heating or cooling.
During the cold season (heating), these systems aim to maximize the winter sun captured, through well-targeted and well-scaled glazing, which can be associated with mass elements, allowing the storage of solar energy and its use later on. In hot weather (cooling), one aim is to take advantage of sources of cold such as the soil or the outside air, which at certain periods of day will help cool the building.

2.2.1 Passive Heating Systems (Cold Season)

In passive heating systems, the glazed area to the south or southeast-southwest quadrant should be taken into account, in order to capture solar radiation and thermal mass for heat absorption, storage and distribution.

2.2.1.1 Direct Gain Systems – Glazing

Direct solar gain is the simplest way to take advantage of passive solar energy. It simply consists of opening oriented glazing in order to maximize the impact of radiation (S, SE, SO) and storing it in the surrounding thermal masses, thereby achieving substantial solar gain in winter.

2.2.1.2 Indirect or Lagged Gain Systems

In indirect gain systems, the system’s thermal mass is installed between the gain surface and the space to be heated. The thermal mass absorbs the incident solar energy, transferring it into the space later. The most popular systems are Trombe walls, storage walls and water walls and columns. Indirect gain systems must include mobile shading devices to turn them off during the summer, thus avoiding overheating conditions.

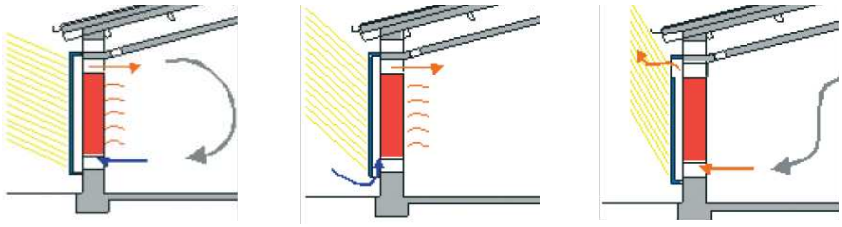

Figure 2. Trombe wall operation diagram.

A. Immediately transfers the incident energy into the space to be heated through natural ventilation via the existing holes. In this case, the space will be heated by a stream of natural convection between the interior space and the "greenhouse" space;
B. Preheats the outside air in mid-season (spring or autumn), requiring a hole between the outer and the "greenhouse" space.
C. Does not have natural ventilation between the wall and the glass, allowing the incident "energy" to gradually accumulate in the wall and be transferred (by conduction) to the interior of the space to be heated up. The amount of time this takes depends on the thickness of the wall - Storage Wall.

2.2.1.3 Isolated Gain Systems - Greenhouses
Greenhouse spaces can combine the effects of direct and indirect gain. Solar energy is transmitted to the adjacent greenhouse space by conduction through the separating storage wall and also by convection, when there are holes allowing air circulation.

This system should also provide a way of shading during summer.

2.2.2 Passive Cooling Systems (Hot Season)
These systems aim to considerably reduce the cooling requirements and improve thermal comfort without resorting to a conventional air conditioning system. Some of the strategies to take into account for passive cooling systems are:

- Solutions for preventing and mitigating heat gain, to reduce the uptake of solar radiation through shading, insulation and thermal mass;
- Solutions using the existing sources of cold in order to reduce the temperature inside the buildings;

The strategy of prevention or protection from solar gains can be considered in all buildings through different architectural options. We must bear in mind the following aspects:

- The choice of low-emissivity glass to reduce solar gains;
- The shading of glazing to reduce radiation entering the buildings;
- The insulation of the building surroundings (preferably on the outside) to restrict the gains by conduction;
- The increase in the thermal mass of the building to increase its capacity to store heat and reduce the peak cooling loads;
- The implementation of strategies for heat dissipation (passive or natural cooling), by providing environments acting as sources of cold, which allow significant processes of heat transfer, such as soil, exterior air during the night and morning or water.

3 EXAMPLES OF BIOCLIMATIC SOLUTIONS

3.1 Example 1 – Implementation of a Shading System in an Historical Building

In this example a shading system was implemented to prevent and mitigate heat gains in an old building. This is a solution that fits into the building without the neutering or amending its image instead of installing a solution on the 1st floor, which distorts building's lines and the reading one gets of it. The shading system adopted on the ground floor is very versatile (Figure 3). During the cooling season, it prevents the sun's rays from hitting the glass by lowering the screens, and in the heating season it allows the sunlight to enter through the glazing, by raising the screens.

3.2 Example 2 – Example 2 – Thermal Rehabilitation of Old Buildings (Altering Frames)

In this building, instead of replacing the existing window frames, which always looks out of place on the existing façade, a system of double frames was implemented by reshaping the existing portals and installing plain glass. A second portal was implemented to improve the frame's thermal/acoustic performance (Figure 4).

This measure preserves the overall image and the building's exterior lines and is therefore one of the most appropriate methodologies for these cases. This is an example of success that is recommended as it greatly increases a building's comfort and endows it with better thermal / acoustic properties.



Figure 3. View of shading system.



Figure 4. Double frame system.

3.3 Example 3 – Placement of Passive Solar System

This is a bad example of the implementation of photovoltaic and solar panels with disproportionate impact, without any care or rationale, which should never occur. The implementation of these systems should always done in a way that integrates them into the building and its surroundings. It is up to the municipalities to coordinate, regulate and monitor the implementation of these technologies through their municipal regulations. However, companies that sell these systems also have an added responsibility in that the solutions they provide to their customers must include studies performed by trained technicians about how to integrate the systems.



Figure 5. Wrong implementation of solar systems.

3.4 Example 4 – Solar Control using Glazing / Shades

In this example a shading system was implemented in a hospital, to prevent and mitigate heat gains during the cooling season. The results were satisfactory since it is an effective shading system that does not compromise the gains required during the heating season. In the cooling season this system also has the advantage of allowing you to enjoy the natural lighting and the views during the period in which the solar rays are strongest as it occludes the system without the need to occlude the openings.



Figure 6. Glazoing / Shades Solar Control.

4 CASE STUDY

The case study is about the group of houses that won the DGE 2003 Prize. The choice was made because this was a success case that can contribute to the dissemination of this type of architecture.

4.1 Case Study 1 - DGE 2003 Prize "Energy Efficiency in Buildings" - Winner in the "Residential Building" category, houses in Janas (Sintra - Portugal)

The houses in Janas, in the countryside around Sintra, consist of three detached row-houses. The location is slightly inclined with a southern-facing slope that facilitated the integration of the concept of harnessing solar energy.

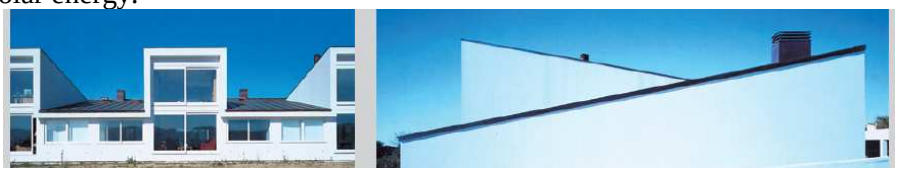

Figure 7. Photos from the South and West facade.

Project Strategy

The strategy of the project took into account the fact that the buildings have an east-west axis and took advantage of the excellent solar orientation of the southern façade. The building is also protected from the prevailing winds from the northwest quadrant, through the placement of vegetation at the north and west of the land. The complex is rectangular in shape (30x11 m), with two floors in the main body of each villa. The north façade is nearly opaque and has a small window and the entrance door, while the east and west façades are completely opaque. The service areas (kitchen and toilet facilities) are located in the northern part of the building, serving as a thermal buffer for the residential areas located in the south area. Thus each dwelling unit is organized from the nuclear space of each family's living room from which you access the other areas in the house. A mezzanine in the room will give the shape of the building its alternative profile of pitched roofs.

On the south façade we have extensive glazing to capture solar radiation (25 m2 of glazing for a total floor area of 110 m2). These openings are the fundamental elements of this project's strategy of passive use, together with the inertial mass of the building. The building features natural cross ventilation, which is an important element in controlling the temperature inside.

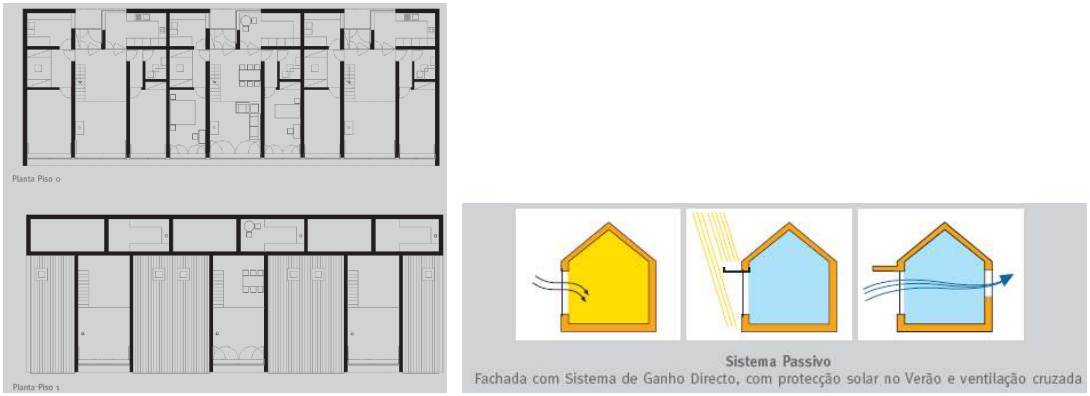

Figure 8. Floor 0 and floor 1 Plan / bioclimatic strategies used in these buildings.

In each house the living room and bedrooms are face south, enjoying the winter sunlight, whereas the kitchen and bathrooms are face North. The first floor (mezzanine) develops from the living room and is a working space, facing South.



Figure 9. Photos of the buildings.

Constructive Characteristics

The building has a portico structure of pillar, beam and slabs of reinforced concrete, with the slab floor installed over a ventilated air chamber insulated with extruded polystyrene. The exterior walls are simple masonry (20 cm), insulated from the outside with a 6 cm polystyrene system (Dryvit), totally eliminating thermal bridges. The slabs are massive and insulated from the outside by extruded polystyrene. The base slab has a 4 cm insulation layer over a ventilated chamber and the cover slab has a 10 cm layer of insulation covered with copper foil.

The separating walls of the houses are solid in order to increase the effect of the building's inertia and soundproofing of the adjoining spaces. The other interior walls of each house are made of clay brick rendered with plaster. The windows are colorless double-glazed with wooden frames and wooden interior shutters to provide shade and improve the insulation of the building at night. The openings have structural visor shades at ground level and exterior canvas awnings were considered on the upper level, for better shade in the summer.



Figure 10. Thermal conductivity coefficient of walls and glazing.

Energy Analysis

The RCCTE check gives excellent ratings for winter and summer with the canvas awnings down. The thermal behavior of the building is excellent and users approved of the overall thermal comfort of the houses. Neither west nor central house users (the only ones occupied) has used any auxiliary heating. In the summer cross-ventilation and shading of the openings have proved capable of coping with the specificity of local climate.

5 CONCLUSIONS

- The main objective of bioclimatic architecture is to achieve sustainability in construction, reflected in the improvement of energy efficiency parameters, reducing the need for lighting, ventilation and artificial air conditioning, replacing conventional energy consumption with a renewable one and reducing the construction "ecological footprint";

- Bioclimatic Architecture allows substantial energy savings, making the building comfortable in any season through renewable sources without additional costs;

- Buildings designed based on bioclimatic architecture are more energy efficient, have a healthier indoor environment and have good levels of comfort;

- The vast combinations of bioclimatic solutions can be implemented in new projects, historic settlements, rehabilitation or recovery of buildings;

- The methods of bioclimatic architecture can and should be complemented with active measures to retain solar energy through solar panels, photovoltaic panels or mini wind turbines;

- Bioclimatic techniques should be studied, weighted, designed and integrated so that their placement is an asset to the formal composition and architecture of the building and not something strange and crumbled that is applied later;

- The placement of solar or photovoltaic panels should be included in the plans of buildings' roofs, attics and façades either in rehabilitation or in new constructions;

- On the rehabilitation of historic buildings there should be particular care taken regarding the placement of exterior shading or other mechanisms on window frames, so as not to hurt the building's architecture and historical integrity.

REFERENCES

Appleton, João; - *Reabilitação de edifícios antigos, Patologias e Tecnologias de intervenção,* Lisboa, Edições Orion, 2003.

Nascimento, Carlos e Gonçalves, Hélder – *Prémio DGE 2003 – Eficiência Energética em Edifícios, Lisboa, DGGE – IP-3E 200.*

Lobão, Ricardo - *Modelo simplificado de previsão do comportamento térmico de edifícios,* Universidade do Minho, 2004.

Santos, C.A. Pina; Matias, Luis - *ITE 50 Coeficientes de transmissão térmica de elementos da envolvente de edifícios*, Lisboa, LNEC, 2007.

XII DBMC
International Conference on Durability of Building Materials and Components
PORTO - PORTUGAL, April 12th-15th, 2011

Selection of Construction Solutions and Materials to Optimize the Indoor Environmental Quality of Buildings

Sandra Monteiro da Silva [1]
Manuela Guedes de Almeida [2]

ABSTRACT

To achieve an adequate quality of buildings it is necessary to consider a set of aspects that are interconnected and influence each other, not always in a favourable way. The selection of the most suitable construction solution and materials for the building elements must consider its contribution for the thermal and acoustic comfort, the daylight conditions and the indoor air quality inside the buildings, its energy efficiency, but also the weight of the solution and its effect on the structural project of the building.

The solutions adopted in buildings, usually, only optimize no more than one of the necessary comfort requirements. In many cases, the best solutions to accomplish different comfort requirements are not compatible, especially in what concerns natural ventilation and lighting strategies and the acoustic and thermal performance.

Thus, it is necessary to provide designers with methodologies with an integrated approach, that allow them to take into account, since an early stage of the design phase, all of the, sometimes incompatible, comfort requirements, to ensure the best overall behaviour of the buildings.

In this work the use of a multi-criteria analysis, to balance all these aspects on the design phase, in order to assist the designer in the selection of construction solutions and materials will be presented.

The criteria selected are related to the most important characteristics of the indoor environmental quality, the thermal and acoustic comfort, it is possible to define them in an early stage of the design phase, in a non subjective way, are under the designer scope and are the issues that are also the most valued by the users of the buildings.

KEYWORDS

Thermal behavior, Acoustic performance, Energy efficiency, Multi-criteria analysis.

[1] School of Engineering of the University of Minho (UM), Guimarães, PORTUGAL, sms@civil.uminho.pt
[2] School of Engineering of the University of Minho (UM), Guimarães, PORTUGAL L, malmeida@civil.uminho.pt

1 INTRODUCTION

Energy efficiency and indoor environmental quality of buildings are nowadays major concerns as European Union (EU) buildings account for 40% of the total energy consumption and Men spend about 90% of their time inside closed spaces [Directive 2010/31/EU]. Thus, it is mandatory to control the energy consumption in the building sector, while maintaining, or even improving, the indoor environmental quality (IEQ) to reduce these needs and, consequently, reduce the EU energy dependency as well as the greenhouse gas emissions, in accordance with what is prescribed in the Energy Efficiency in Buildings Directive (EPBD) and reinforced with the "EPBD-recast" [Directive 2002/91/EC, Directive 2010/31/EU].

But, as buildings are complex systems, where all aspects are interconnected and influence each other, an integrated and comprehensive approach to the buildings design that enhance indoor health and comfort besides the energy efficiency should be followed. However, these goals are often in conflict and there is not a unique criterion that describes the consequences of each alternative solution adequately and there is not a single solution that optimizes all criteria.

Therefore, thermal quality, acoustic behaviour and energy reduction strategies should be meshed at an early stage with the other requirements to ensure the buildings overall comfort conditions and energy efficiency. To do so, it is necessary to select the correct materials, and construction solutions, among a large number of options, on the design phase, to improve the occupants overall comfort and, at the same time, reduce the energy costs. Furthermore, to make a conscious selection of the possible alternatives, it is necessary to balance the positive and negative aspects of each solution into the global behaviour of the building. The number of solutions is also increasing rapidly and a correct comparison becomes a challenging and difficult assignment as the behaviour of some are affected by imprecision and it is also necessary to take into account the constraints of the project and the decision maker point of view.

Multi-criteria decision analysis (MCDA) is, in this way, an important tool in such problems, since it employs mathematical models that evaluate alternative scenarios, taking into account both their objective characteristics (acoustic insulation, U-Value, embodied energy, hygroscopic inertia) and the preferences of the decision makers regarding the objectives and constraints of each project.

The aim of this study was to investigate the viability of the use of a MCDA method to assist the designer in the selection of construction solutions and materials in the an early stage of design phase. A simple case study was studied to demonstrate the feasibility of the approach using the MCDA method Electre III [Roy 1978].

2 METHODOLOGY

To achieve an adequate behaviour of the buildings it is necessary to consider either the indoor environmental quality as well as energy efficiency. It is then essential to optimize the building envelope, by improving construction solutions and insulation levels, glazing type, optimizing the thermal and acoustic behaviour, the natural ventilation and daylighting techniques through an appropriate design and selecting materials with low embodied energy. But the solutions adopted in buildings, usually, only optimize no more than one of the necessary comfort requirements. In many cases, the best solutions to accomplish different comfort requirements are not compatible, especially in what concerns natural ventilation and lighting strategies and the acoustic and thermal performance.

The design phase is the ideal moment to mesh and implement all these principals as it is still possible to implement modifications on the project. So, it is during the design phase that the sustainable, energy efficient and comfortable building concepts should be applied, by a judicious selection of materials, technologies and construction methods to be used. To test this integrated approach, two

floors and four rooms, were studied, estimating the thermal quality of the vertical envelope (U-value), the acoustic behaviour of the envelope (airbourne sound insulation), the embodied energy, the weight and the thickness of the construction solution.

The analysis considered the factors that have influence on the behaviour of the buildings, must be selected in an early stage of the design phase and are under the designer scope, such as glazing type, construction solutions and materials, weight (associated with thermal inertia, acoustic insulation and to the building structure) and embodied energy.

2.1 Prediction Tools

The prediction of the building thermal behaviour, related to thermal comfort and energy efficiency, was done using the U-value, determined using the publication ITE50 – U-Values of Building Envelope Elements [Pina dos Santos & Matias 2006]. All the solutions selected respect the minimum requirements defined in the Portuguese Thermal Regulation [RCCTE 2006]. The acoustic behaviour was considered estimating the weighted normalized airborne sound insulation index of the façade, measured at 2m from them ($D_{2m,\,nT,\,W}$), according the to the EN 12354 standard, using the Acoubat Sound Program [RRAE 2008; EN 12354-1 2002]. The embodied energy was assessed using Cumulative Energy Demand 1.04 [Frischknecht & Jungbluth 2007, Asif et al 2001].

2.2 Room Characteristics

To estimate the acoustic behaviour of the building, using Acoubat Sound Program, a geometry with two rooms (3m x 4m x 2.5m) was defined. The area of the windows, 1.2m x 1.2m, was maintained constant. The area of the windows was defined to optimize the solar gains during winter and the daylight availability and minimize the unwanted solar gains during summer, according to the Illuminating Engineering Society of North America (IESNA) recommendations, corresponding to a Window - Wall Ratio of about 20% [IESNA RP5-99 1999; IESNA 2000].

2.3 Construction Solutions Characteristics

The construction solutions analyzed are shown in Fig. 1, for the different types of elements of the building. The construction solutions selected, single and double pane walls (hollow concrete blocks, brick and hollow brick), cover a wide range of situations. The study was done for two insulation materials (expanded extruded polystyrene, XPS, and mineral wool, MW). The insulation could be placed in the exterior or in the interior of the single pane walls and in the air cavity of the double pane walls.

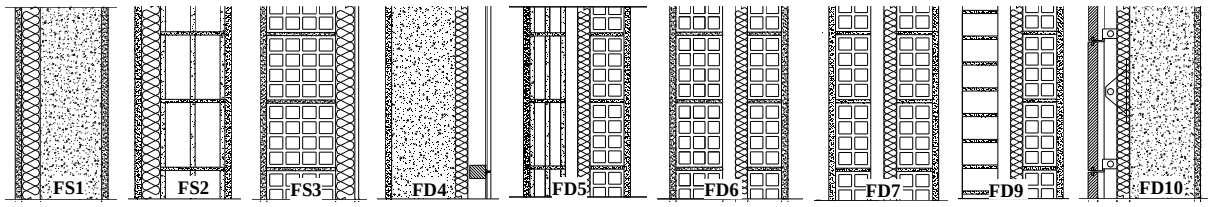

Figure 1. Vertical cross-section of the different walls considered on the study.

Different glazing types and frames were selected for the windows considering the existence of PVC roller shutters or air inlets in the windows frames. The air inlets were introduced to improve the air change rate and the indoor air quality. The roller shutters were selected as they are the most used shading devices in Portugal and they also allow controlling daylight. Roller shutters are also the most penalizing systems in what concerns thermal and acoustic behaviour of the façade (when comparing with the venetian blinds and shutters, for example) due to the existence of the roller shutters boxes.

2.4 Multi-criteria Analysis

The multi-criteria decision analysis (MCDA) defines flexible approach models to help the decision maker, and/or the design team, selecting the most adequate solutions to optimize the building IEQ and energy efficiency among a large number of options and possibilities. The MCDA methods can be applied when there are several decision agents, each one with different objectives and criteria, some times with opposite visions. The problem of the decision makers is a multi-objective optimization problem [Ehrgott & Wiecek 2005] characterized by the existence of multiple, and in several cases competitive, objectives that should be optimized, taking into account a set of parameters (criteria) and constraints.

This kind of analysis is able to reflect the objectives and limitations of each one of the alternatives to be studied, but it is necessary to be thorough on selecting the criteria that should be exhaustive but not redundant (is recomended to use no more than 12, which represents an acceptable compromise between feasibility and detailed description) and must be coherent (which are the criteria to be maximized and to be minimized) [Roy & Bouysson 1993, Roulet et al, 2002].

The multi-criteria methodology selected in this work to help the decision maker selecting the most adequate solutions to optimize the building indoor environmental quality, was the Electre III model as it may be considered as a decision-aid technique suited to the appraisal of complex civil engineering projects [Papadopoulos & Karagiannidis 2008].

2.4.1 The Electre III method

Electre III is a multi-criteria decision analysis method [Roy 1978] that takes into account the uncertainty and imprecision, which are usually inherent in data produced by predictions and estimations. The construction of an outranking relation amounts at validating or invalidating, for any pair of alternatives (a, b), the assertion "**a** is at least as good as **b**". This comparison is grounded on the evaluation vectors of both alternatives and on additional information concerning the decision maker's preferences, accounting for two conditions: concordance and non-discordance.

The Electre III method is based on the axiom of partial comparability according to which preferences are simulated with the use of four binary relations: I, indifference; P, heavy preference; Q, light preference and R, non-comparability. Furthermore, the thresholds of preference (p), indifference (q) and veto (v) have been introduced, so that relations are not expressed mistakenly due to differences that are less important [Roy 1978].

The indifference threshold (q) defines the value beneath which the decision maker is indifferent to two option valuations, the preference threshold (p) defines the value above which the decision maker shows a clear strict preference of one option over the other, and the veto threshold (v) where a ‘discordant’ difference in favour of one option greater than this value will require the decision maker to negate any possible outranking relationship indicated by the other criteria. The indifference (q) and preference (p) thresholds of any criterion can also be interpreted as the minimum imprecision and the maximum margin of error respectively [Maystre et al. 1994].

The Electre III method does not allow for compensation, which may occur when using methodologies based on performance indexes, due to the use of the veto threshold. Using this method, an option which shows too poor results in one criterion cannot be ranked in a higher position [Roulet et al 1999]. The model permits a general ordering of alternatives, even when individual pairs of options remain incomparable or when there is insufficient information to distinguish between them [Rogers 2000]. Also, the technique is capable of dealing with the use of different units, the mix of both quantitative and qualitative information and when some aspects are “the higher the better” and others are “the lower the better”.

3 RESULTS

In the study performed, the Electre III method was applied to the evaluation of several alternative solutions for the façade walls, on the basis of five criteria: thermal and acoustic insulation, embodied energy, weight and thickness. Table 1 lists the different criteria, thresholds and criteria weights that are needed to use the Electre III method. The criteria weights and thresholds presented here are just an example and shoud be defined by the design team according to the objectives and constraints of the project.

Table 1. Criteria, criteria weighting and thresholds (criteria to: ↓ - minimize; ↑ - maximize).

Category (Criteria)	*Units*		*Criteria Weight*	*Threshold*		
				Preference	*Indifference*	*Veto*
Thermal Insulation (U-Value)	$W/(m^2{}^oC)$	↓	25	0.25	0.10	0.50
Acoustic Insulation ($D_{2m, nT, W}$)	dB	↑	25	5	2	10
Embodied Energy (EE)	MJ/m^2	↓	20	220	80	460
Weight	kg/m^2	↓	15	80	30	160
Thickness	cm	↓	15	7	3	15

The criteria selected are related to the most important characteristics of the IEQ, the thermal and acoustic comfort. These criteria were also selected because it is possible to define them in a non subjective way, it is possible to predict them in an early stage of the design phase, are under the designer scope and are the issues that are also the most valued by the users of the buildings. The minimum thermal and acoustic insulation values are also defined in the Portuguese thermal and acoustic regulation and are mandatory. The weight and the thickness of the solutions are also relevant as they affect the structural design (and the thermal inertia) of the building and their useful area.

The definition of criteria weights and thresholds must take into account the objectives and constraints of the project and capture the points of view of the decision makers. Thus, to select them, a sensitivity analysis was performed and the visualization of the outcome impacts was assessed. The criteria weights were defined taking into account the relative importance of each one of the criteria. The criteria weighting established for the thermal and acoustic insulation criteria, associated to the thermal and acoustic comfort, was defined according to the relative importance of each one to the occupants based on studies performed in Portugal and according to literature [Rohles et al 1987; Kim et al 2005; Monteiro Silva 2009]. These studies showed that the thermal and acoustic comfort are the most valued criteria, as they are linked to thermal and acoustic comfort inside the buildings. The embodied energy, the weight an thickness of the solutions are essencially a concern of the designer.

The thresholds were defined according to the criteria characteristics, for example a 2 dB difference is the threshold at which human beings can perceive differences in noise levels and 5 dB is the noise difference at which clear preference can be expressed for one option over another [Rogers & Bruen 1998].

3.1 Façade Wall

The construction solutions analyzed for the façade walls are shown in Fig. 1 and listed in Table 2 (F - façade wall, S - single wall with insulation on the outside and D - double pane wall with insulation placed in the air cavity). Several options were defined for the opaque part of the façades walls and for the windows (frame and glazing type) and the existence, or not, of roller shutter boxes and air inlets.
Table 3 lists the results of the prediction of the façade walls behaviour according to the five criteria selected to outrank the design alternatives. The U-Value, embodied energy and the weight of the solution are weighted averaged values taking into account the opaque, the glazing part of the façade and the roller shutter box.

Table 2. Construction solutions studied for the façade (as represented in Figure 1).

Option	Wall	*Frame*	*Glazing*	*Roller box*	*Air inlets*
FS1	Single pane concrete wall with 20cm with 4cm of XPS	Aluminium	6+12+4	No	Yes
FS2	Single pane hollow concrete block wall, 20cm, with 4cm of XPS	wood	4+12+4	No	No
FS3	Single pane hollow brick wall with 22cm with 4cm of XPS	Aluminium	4+12+6	Yes	Yes
FD4	Double pane wall, concrete wall with 20cm and plasterboard wall with 1.3cm with 6cm of MW	PVC	4+12+6	No	Yes
FD5	Double pane wall, hollow brick (11cm) and hollow concrete block (12cm) with 5cm of MW	Wood	6+8+6	No	Yes
FD6	Double pane wall, hollow brick with 15cm and hollow brick with 11cm with 6cm of MW	PVC	4+8+6	Yes	Yes
FD7	Double pane wall, hollow brick with 11cm and hollow brick with 11cm with 6cm of MW	Wood	6+12+6	Yes	No
FD8	Double pane wall, brick with 15cm and hollow brick with 15cm with 6cm of MW	Aluminium	4+12+4	Yes	No
FD9	Double pane wall, brick with 11cm and hollow brick with 15cm with 6cm of MW	PVC	4+12+4	No	No
FD10	Ventilated wall, stone with 5cm and concrete wall with 22cm with 6cm of MW	Aluminium	4+12+6	No	Yes

Table 3. Criteria for the different design alternatives studied for the façade.

Options	*U-Value (weighted averaged values)* [W/(m^2°C)]	$D_{2m,nT,W}$ [dB]	*EE* [MJ/m^2]	*Weight* [kg/m^2]	*Thickness* [cm]
FS1	1.21	39	1768	464	27.5
FS2	1.02	42	699	265	27.5
FS3	1.11	34	1864	208	29.5
FD4	1.07	34	1378	395	29.3
FD5	0.96	34	907	355	32.5
FD6	0.78	34	1534	227	35.5
FD7	0.82	40	1004	226	31.5
FD8	0.84	44	2850	268	33.5
FD9	0.86	42	2162	296	37.5
FD10	1.24	41	3360	489	38.5

The results of the outranking using Electre III method are presented in Table 4. The single pane hollow concrete block wall, option FS2, was ranked as the best action, this solution has the second higher acoustic insulation. The double wall with hollow brick with 11cm and hollow concrete block with 12cm was ranked second. The best ranked options are the one with lower embodied energy.

Table 4. Credibility degrees matrix for the alternative solutions selected for the façade walls.

											Non-Dom		*Ranking*
Options	FS1	FS2	FS3	FD4	FD5	FD6	FD7	FD8	FD9	FD10	A	μ(A)	Options
FS1	-	0.00	0.00	0.22	0.00	0.00	0.00	0.00	0.00	1.00	FS1	0.02	FS2
FS2	0.77	-	0.67	0.75	0.75	0.73	0.97	1.00	1.00	0.8	FS2	1.16	FD5
FS3	0.98	0.00	-	0.00	0.00	0.80	1.00	1.00	1.00	0.95	FS3	0.33	FS3
FD4	0.93	0.00	0.00	-	0.00	0.00	0.00	0.85	0.85	0.88	FD4	0.02	FD6
FD5	0.68	0.59	0.53	0.98	-	0.85	0.85	0.85	0.91	0.75	FD5	0.84	FD4
FD6	0.42	0.00	0.64	0.52	0.00	-	0.96	1.00	1.00	0.48	FD6	0.15	FS1
FD7	0.00	0.00	0.00	0.00	0.00	0.00	-	0.00	0.00	0.00	FD7	0	FD10, FD9, FD8, FD7
FD8	0.00	0.00	0.00	0.00	0.00	0.00	0.80	-	0.00	0.67	FD8	0	
FD9	0.13	0.00	0.00	0.00	0.00	0.00	0.77	0.96	-	0.75	FD9	0	
FD10	0.00	0.00	0.00	0.00	0.00	0.00	0.00	0.00	0.00	-	FD10	0	

4 CONCLUSION

This methodology allows, in an easy and quick way, to outrank construction solutions options according to a set of criteria pre-established and based on criteria weights and thresholds assigned to each one. The design team has the possibility to change the criteria, criteria weights and thresholds according to the objectives and constraints of the project which enable the use of this methodology to a vast set of possibilities (selection of materials, construction solutions, design alternatives, rehabilitation scenarios, etc.), based on different criteria, (U-value, acoustic insulation, embodied energy, useful area, glazing area, heating and cooling needs, etc.). This methodology is not specific to a country and can be used in an early stage of the design phase, when not all the building characteristics are defined.

This method does not allow for compensation, allows a general ordering of alternatives (even if individual pairs of options are incomparable or when there is insufficient information to distinguish between them), is able to deal with the use of different units, quantitative and qualitative information and aspects that must be maximize with others that should be minimized.

The disadvantages of the methodology are the need to compare a large set of alternatives, to be able to select the best one, because it is difficult to select a representative set of alternatives and if a limited number of such solutions have been defined, there is no guarantee that the solution finally reached is the optimal, the necessity to determine the different solutions characteristics (thermal and acoustic insulation, embodied energy, etc.) and also the time needed to perform this detailed analysis.

The need to define criteria weights and thresholds that must consider the objectives and constrains of the project and also take into acount the points of view of the decision makers in the selection process, is a strength and also a weakness as may introduce some subjective inputs but allows the method to be easily adaptad to each situation and location.

The example here presented allows a robust analysis of the building elements as it comprise a broad study of each alternative through a detailed analysis of the main factors that affect the IEQ, based on the thermal and acoustic insulation levels and the embodied energy of the construction solutions.

Throughout the multi-criteria analysis performed, it was possible to verify that there are a large number of construction solutions that, when adequately used, will assure the all the needs, being only necessary to integrate the exigencies of all the different requirements.

REFERENCES

Asif, M., Davidson, A. & Muneer, T. 2001, 'Embodied energy analysis of aluminium-clad windows', *Building Services Engineering Research and Technology*, 22 (3), 195-199.

CEN, European Standard EN 12354-1 2002: *Building acoustics - Estimation of acoustic performance of buildings from the performance of elements - Airborne sound insulation between rooms*, Belgium.

Decree-Law nº 80/2006 - *Portuguese Building Thermal Legislation*, RCCTE 2006, Lisbon.

Decree-Law nº 96/2008 - *Portuguese Building Acoustics Legislation*, RRAE 2008, Lisbon.

Directive 2002/91/EC - *Directive of the European Parliament and of the Council from 16 of Decembe*r, 2002 *on the Energy Performance of Buildings*, EPBD.

Directive 2010/31/EU - *Directive of the European Parliament and of the Council, on the Energy Performance of Buildings (recast)*, from 10 of May, 2010, EPBD-recast.

Ehrgott, M. & Wiecek, M. 2005, 'Multiobjective programming' in *Multiple Criteria Decision Analysis: State of the Art Surveys*, eds Figueira J., Greco S. & Ehrgott M., Springer, New York, 667-722.

Frischknecht, R. & Jungbluth, N., 2007, *Implementation of Life Cycle Impact Assessment Methods*. Swiss Centre for Life Cycle Inventories, ecoinvent report No. 3, Dübendorf, December.

IESNA, 1999, *RP5-99 - Recommended Practice of Daylighting*, Illuminating Engineering Society of North America. New York.

IESNA, 2000. *Lighting Handbook*, Illuminating Engineering Society of North America. New York.

Maystre, M., Pictet, J. & Simos, J., 1994. *Methodes muhicriteres ELECTRE*. EPFL Presses Polytechniques et Universitaires Romandes, Lausanne.

Monteiro Silva, S. 2009, *Building sustainability and Comfort*. University of Minho, Guimarães.

Papadopoulos, A. & Karagiannidis, A. 2008, 'Application of the multi-criteria analysis method Electre III for the optimisation of decentralised energy systems', *Omega - The International Journal of Management Science*, 36, 766-776.

Pina dos Santos, C. & Matias, L. 2006, *U-Values of Building Envelope Elements*, LNEC, Lisbon.

Rogers, M. & Bruen M., 1998. 'Choosing realistic values of indifference, preference and veto thresholds for use with environmental criteria within ELECTRE'. *European Journal of Operational Research*. 107, 542-551.

Rogers, M. 2000. 'Using Electre III to aid the choice of housing construction process within structural engineering', *Construction Management and Economics*, 18: 3, 333-342.

Rohles, F. H., Woods, J. E. & Morey, P. E. 1987, 'Occupant Perception of the Work Environment', *Human Factors and Ergonomics Society Annual Meeting Proceedings*, 31[10], 105-1108.

Roulet, C., Flourentzou, F., Labben, H., Santamouris, M., Koronki, I. & Richalet, V., 1999, *ORME: Office Building Rating Methodology for Europe*, Office Project Report, University of Athens, Athens.

Roulet, C.-A., Flourentzou, F., Labben, H. H., Santamouris, M., Koronaki, I., Dascalaki, E. & Richalet, V. 2002, 'ORME: A multicriteria rating methodology for buildings'. *Building and Environment*, 37, 579-586.

Roy, B. 1978, *'Electre III - Algorithme de classement base sur une représentation floue des préférences en présence de critères multiples', Cahiers de CERO*, 20[1], 3-24.

Roy, B. & Bouysson, D. 1993, *Aid multiple a la decision: methods et cas*. Económica, Paris.

Kim, S., Yang, I., Yeo, M. & Kim, K. 2005, 'Development of a housing performance evaluation model for multi-family residential buildings in Korea', *Building and Environment*, 40, 1103-1116.

XII DBMC
International Conference on Durability of Building Materials and Components
PORTO - PORTUGAL, April 12th-15th, 2011

Influence of Degradation and Service Life of Construction Materials on the Embodied Energy and the Energy Requirements of Buildings

Carol Monticelli [1]
Fulvio Re Cecconi [2]
Giorgio Pansa [3]
Andrea Giovanni Mainini [4]

ABSTRACT

The construction of buildings and their operation have extensive direct and indirect impacts on the environment during the life cycle. Designers and builders face a unique challenge in attempting to meet the requirements of either new and renovated facilities that provide accessibility and security but also offer a healthy and productive working environment whilst minimizing their environmental impact. Methods to evaluate the environmental sustainability of buildings and those to measure operational energy efficiency often do not take into account the decay in performance of building materials over time. Results of ongoing research conducted at the Politecnico di Milano, Dept. BEST, are presented on the influence of the degradation of construction materials and their service life on the energy performance over the building life cycle. Focus was made on determining the embodied energy (ISO 14040) of building construction practices and maintenance, and the energy requirement (ISO 13790) for both heating and cooling. Studies were conducted on two different types of building: a 16 storey tower and a single-unit dwelling. Six types of building envelope were considered: five typical Italian brick masonry walls and one light-weight solution. For each of these wall systems and building types, standard methods were used to calculate the embodied energy for the selected solutions and the energy requirements over a building service life of 60 years. Monte-Carlo simulation was used to take into account the degradation of the thermal insulation over time, and thus to determine if and how building type and building envelope technology were sensitive to this degradation.

KEYWORDS

Life Cycle Assessment, Energy performance, Thermal insulation degradation.

[1] Dept. of Building, Environment, Science and Technology of the Politecnico di Milano, Milano, ITALY, carol.monticelli@polimi.it
[2] Dept. of Building, Environment, Science and Technology (BEST) of the Politecnico di Milano, Milano, ITALY, fulvio.rececconi@polimi.it
[3] Dept. of Building, Environment, Science and Technology (BEST) of the Politecnico di Milano, Milano, ITALY, giorgio.pansa@mail.polimi.it
[4] Dept. of Building, Environment, Science and Technology (BEST) of the Politecnico di Milano, Milano, ITALY, andreagiovanni.mainini@mail.polimi.it

1 INTRODUCTION

An important goal for the building sector is to design sustainable buildings, considering not only the construction process, but also the operational, maintenance and disposal phases. Durability of building materials and components should be considered from the first phases of the design, since their selection directly affects the environmental impact of the construction.

Total energy use during the life cycle of buildings is a growing research field, on one hand, and the aging and degradation processes of building components are object of theoretical and experimental studies, in order to define the durability of building materials and components, on the other hand. Researches on the environmental performance of building materials show how material choice may affect embodied energy in houses with a defined life time [Thormark 2006, Gustavsson et al. 2006, Monticelli 2006] and how the service life of materials affects the results [Junnila and Horvarth 2003]. There are also various studies focusing on the environmental impact of whole buildings: Scheuer et al. [2003] assessed a six-storey-building with a life time of 75 years, using LCA; Peuportier [2001] compared the life cycle analysis of three single-family houses with a service life of 80 years; Ortiz et al. [2009] apply the LCA approach to a typical Spanish house with a projected 50-year life span. Adalberth [1997] tried to propose a method about the calculation of energy use during life cycle of buildings taking into account energy associated to maintenance works. To summarize, lot of studies evaluate the environmental impact of buildings, from cradle to grave, considering the energy burdens and, in few cases [Thormark 2006], also the recycling potential of materials. Only the study of Haapio and Viitaniemi [2008] shows how durability of building components affects service life of buildings and how components and building service life together affect the environmental impact in a life cycle analysis. The Building Envelope Life Cycle Assessment Management Project tried to define a technique to predict the remaining service life of building envelope components and a procedure to optimize their maintenance [Lacasse et al. 1997]. In order to predict maintenance scheduling results from studies about building materials performance over time are very important because they give useful indication in order to quantify the maintenance cycles and their impacts in the LCA.

2 AIM OF THE STUDY

In order to evaluate the environmental compatibility of buildings and to measure operational energy efficiency, taking into account the maintenance and the durability, exist different methods, but often they do not take into account performance decay of building materials over time. The aim of this study was to investigate how different building envelope solutions and different building types affect environmental assessment over the whole building life cycle. In addition, the influence of the degradation of construction materials and of their service life on the energy performance over the building life cycle was analyzed. Focus was made on determining the embodied energy of building construction and maintenance (following the standard series for the LCA ISO 14040:2006), and the energy requirement for both heating and cooling (following the standard ISO 13790:2008).

3 REFERENCE CASES

Two different types of buildings were analyzed: 1. a single-family house (the shape factor defined as Gross Area of Heat Loss Elements / Gross Building Conditioned Volume A/V is 0.90), 2. a 16 storey tower (A/V = 0.375). Both analyzed building have the same type of basement system, roof system, windows, heating and cooling plants. The differences are related to the different solutions of building envelope investigated (for both types of buildings): five typical Italian brick masonry walls and one light weight solution. Totally 12 case studies were analyzed. The external walls' covering types, designed to have the same thermal transmittance (U-value =0,33 W/(m^2K)), are: A. external thermal insulation render system on single leaf brickwork cavity wall; B. cement rendered lightweight brickwork outer leaf, insulation, gypsum rendered brickwork inner leaf; C. dense solid brickwork outer leaf, insulation, gypsum rendered brickwork inner leaf; D. ventilated wall, an external thermal insulation brick masonry wall externally covered in brick hollow flat blocks, and assembled by means

of suspension devices and mechanical style fixings; E. single leaf brickwork cavity wall with cement rendering; F. dry assembled light weight solution with thermal insulation and external aluminum slabs. The thermal insulation material used was mineral wool. The walls' thickness is different, consequently each conditioned area of the case studies is different. In the evaluation of the embodied energy of buildings the input of the main structural system, of the internal walls and, for the tower, of the 16 floors were omitted: structure, foundations and floors surely would generate a big difference of the involved embodied energy between the single houses and the towers types, but they do not affect the comparison of different envelope technologies on the same building.

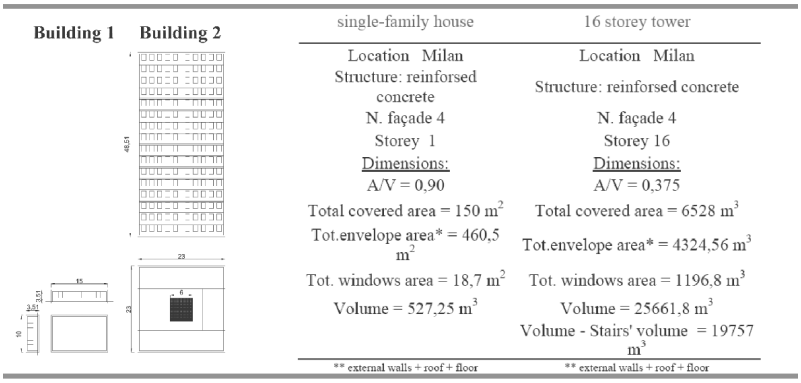

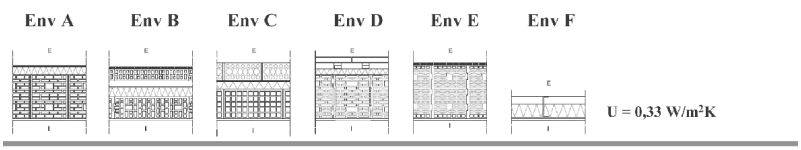

37,5	37	40	43,1	39,3	17,2	Wall thickness (cm)
30	15 + 8	20 + 12	30	36,5	-	Brickwork leaf (cm)
5	6	5	4	-	9	Insulation thickness (cm)
309,3	258,07	348,50	351,28	341,5	42,87	mass of wall (kg/m^2)

Figure 1. The 12 case studies: two buildings with six different external wall types.

The system limits of the energy computation in the life cycle analysis were the production phase and the operational phase, considering the maintenance cycles. Contributions of transportation from the industry to the building site, building site itself and end-of-life phase were excluded. In order to compare easily the environmental impact of the pre-operational phase with that of the service life, the synthetic indicator "Energy consumption" were used: a. Embodied Energy EE (MJ/kg) in order to quantify the energy for building materials and component production (including all working processes, from extraction of raw materials up to the packaging ready to leave the factory, and feedstock); b. "Non renewable Energy" required for the heating and cooling of the building, for the maintenance in the service life.

4 METHOD

The total embodied energy of building construction practices and maintenance, over the life cycle, was calculated and compared with the total energy requirement for both heating and cooling. The method used for the energy life cycle analysis follows the procedures in accordance with standardization ISO 14040. The assumed life time was 60 years. At first, the dimensions of the two buildings, the structure of the six external walls' covering types, than the quantities of the used building materials and also their thermal proprieties, in order to quantify the buildings' energy requirement during the operation, were calculated. The second step dealt with the quantification of the embodied energy of each building subsystem (basement, external walls, windows and roof were considered); their addition has generated the amount of total embodied energy of the case studies. The mass of materials and component (kg/m^2) and the areas of the buildings' systems were necessary in order to define the total embodied energy of the buildings. Practically the embodied energy was

defined on one square meter of each building system at first, then multiplied by their areas and normalized on the square meters of the usable floor area. Data on embodied energy (MJ/kg) were collected from the English database *ICE – Version 1.6a* [2008]. The third step dealt with the calculation of the energy need for heating (Q_H) and for cooling (Q_C) to maintain the intended temperature conditions (20°C in winter, 26°C in summer) in each building during the year. The energy for operation was calculated using the procedure of the national standard UNI/TS 11300-1:2008 (the Italian version of ISO 13790:2008). Buildings were located in Milan, considering climatic data from UNI 10349:1994. The dispersion due to ventilation and the solar heat gains through windows, optical properties of the glazing, shading effects from awnings and internal heating from other sources were considered in this evaluation. The infrared radiation's contribution to the wall thermal exchange was taken into account, together with solar heat gains over opaque elements (considering a solar absorption coefficient across of 0,6). Thermal bridges in the buildings were calculated according to ISO 14683:2007: those between pillars and those related to internal walls have been neglected. The contribution of the ground has been defined according to ISO 13370:2007 and the thermal capacity according to ISO 13786:2007 (calculating internal areal heat capacity for each building element). In both buildings, following thermal transmittances were considered: slab-on-ground U-value = 0,204 W/(m^2K) for single-family house and 0,183 W/(m^2K) for 16 storey house, roof U-value = 0,30 W/(m^2K), windows U-value = 1,685 W/(m^2K), external walls U-value = 0,33 W/(m^2K). The efficiency of the technical building system for heating (gas methane) and for cooling (electrical heat pump) were also taken into consideration to easily evaluate the delivered energy. The first resulted in a value of energy efficiency η = 0,79, and the second in a value of performance coefficient COP= 2,5. In order to evaluate the primary energy consumptions, total primary energy factors have been assumed: 1 for the fossil fuel (heating season) and 2,18 for the electrical carrier (summer season). The relative consumption of lighting and hot water production was not taken into consideration. The results have been related to the conditioned area, in terms of energy performance indicator [kWh/m^2].

The fourth step involved the investigation on the maintenance, calculated for each material and component as embodied energy time's interval/60 years. Maintenance intervals were assigned to each component in the six types of building envelope and based on the maintenance codes obtained from English data into HAPM [1996]. Two main kind of maintenance actions were assumed: standard operation on the façade component and replacement. The replacement is scheduled as follow: every 15 years the internal plaster of all different envelopes is replaced; every 15 years for the Env. A (replacement of external thermal insulation render system); every 40 years for the Env. B (replacement of the external plaster, in this case the insulation is not substituted over the period of analisys, being between the brick leafs); no other replacement for Env. C; every 40 years for the Env. D (replacement of the brick hollow flat blocks, the insulation layer, the suspension devices and mechanical style fixings); every 40 years for the Env. E (replacement of external plaster); every 15 years (replacement of the external aluminum composite panels), every 30 years (replacement of the plasterboards) and every 40 years (replacement of the whole building component) for the Env. F. The data for the embodied energy of the new materials were extracted from ICE again. It has to be underlined that the performance of the building materials was considered constant in this phase, neglecting the materials' aging and thermal degradation. After these four steps the obtained results allowed the comparison between the embodied energies of the different life cycle phases of the two buildings, in order to demonstrate their incidence on the total energy amount.

The last step was the investigation of the influence of degradation on embodied energy. Building components and materials degradation influences the environmental assessment of building because it changes both energy demands for winter heating and summer cooling over time and energy for maintenance phase. In order to take into account the influence of degradation on energy demands some simplifying assumptions were made, the most important are:

- degradation was taken into account only for façade; although this may not seem realistic, the choice is due to the fact that research focused on façade components and not on roofs or windows;

- degradation of thermal resistance happens only on the insulation layer of façade components; although this is not true, it has to be considered that in components under analysis more than 90% of thermal resistance is due to the thermal resistance of the insulation layer.

Energy demands were calculated according to these simplifying assumptions taking into account also the influence of degradation and of actual humidity and temperature of the insulation layer using the equation (1) in ISO 10456. The ISO equation was adapted to the case studies as follows:

$$\lambda_2 = \lambda_1 \, e^{0.0048(T_2-T_1)} \, e^{4(\psi_2-\psi_1)} \, e^{0.0123577A}$$

Where: λ_1 is the design value of thermal conductivity;

λ_2 is the actual value of thermal conductivity;

$e^{0.0048(T_2-T_1)}$ takes into account temperature difference between test condition when λ_1 is measured and the actual in use temperature (T in Celsius degrees);

$e^{4(\psi_2-\psi_1)}$ takes into account humidity difference between test condition when λ_1 is measured and the actual in use humidity (ψ in kg/kg of air);

$e^{0.0123577A}$ takes into account the degradation over time (A in years).

Assumption of different values of temperature T_2 and humidity ψ_2 were made according to the different position of the insulation layer in the façade component: for example the inner the layer the lower the temperature T_2 due to the lower effect of solar radiation. Both T_2 and ψ_2 were assumed constant during the heating or cooling period.

The influence of degradation on energy for the maintenance phase was also simplified by the assumption that degradation will only change the frequencies of maintenance operations and not the type. Service life of façade components was estimated using the factor method (ISO 15686-1) starting from reference service life used in step four.

At the end of step five a Monte Carlo simulation was carried out in order to measure possible errors in thermal conductivity calculations and in service life estimations.

5 RESULTS OF THE ENERGY ASSESSMENT OF BUILDINGS

5.1 Pre-construction Phase and Embodied Energy of Buildings

The embodied energy EE for each of six external wall types has been compared: the envelope solution F shows the highest EE value (1410,07 MJ for a envelope m^2), due to the external surface system (aluminium has an high EE value), and the solution B has the lowest EE value (820,28 MJ for a m^2 of envelope). Solution B involves less quantities of materials than the other brick wall type. The differences in both groups of cases studies are between the EE starting values of the envelope types, because the EE values of the other building systems is constant. The great difference between the EE results of the two building types (normalized on a m^2 of the conditionated area) is due to the form factor A/V: the tower has a more compact shape than the single family house, so its EE/m^2 of conditioned space is lower than the second one.

5.2 Operational Phase

The amount of total primary energy for heating and cooling during the year in the single family houses is in the range of 103 and 113 kWh/m^2y; the one in the towers is in the range of 69 and 78 kWh/m^2y. The differences of results between the tower and the single family houses are due to the shape factor. Although they have the same external wall solutions, the lower A/V ratio determines a thermal losses reduction. In both groups of cases strong differences in conductive thermal losses are also influenced by thermal bridges that, in accordance with UNI EN ISO 14683:2008, depends on

building external wall type. The percentage of thermal bridges influence on thermal losses varies from 8 to 27%. In every group of case, from A to F, of the single family house and the storey tower, the conditioned area are are different, even if the external dimension of the building are the same for every case in both groups, because of the use of different external walls type with different tickness. In the figure 2 emerges the amount of the energy involved in the pre-operational phase and the energy demand for heating and cooling.

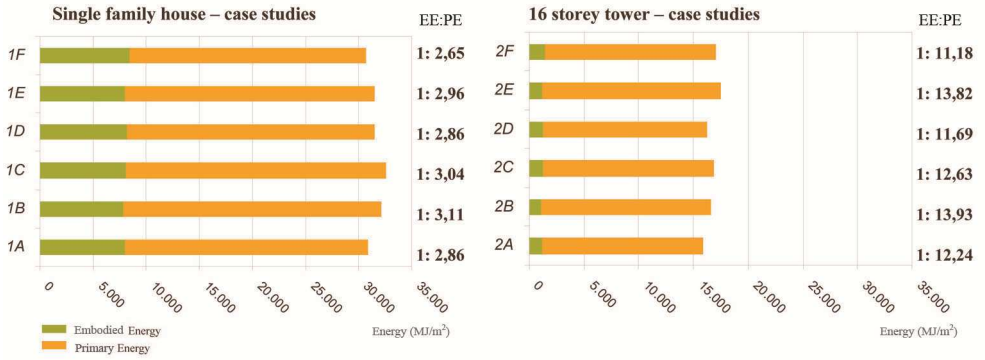

Figure 2. Case studies: comparison and ratio (e.g. 1:2,86 for the 1A) between the values of embodied energy EE and primary energy PE requirement in 60 years, normalized by the net usable floor area.

Comparing both groups of case studies and taking into account the maintenance contribution, the calculated energy needs are totally different in the whole life cycle. Both of building types assume the highest value of energy with the solution F, during a lifetime of 60 years, (fig. 3), just the opposite scenario than the previous phase: the durability of the components, and besides the maintenance with components' substitution, affect the results. The lightweight solution F has an high EE value and it allows a lower energy requirement for heating and cooling in buildings than other solutions, thanks to the thickness of the insulation slab. Considering the materials' service life, this solution needs more scheduled maitenance than the other solutions over the 60 years. The EE for the maitenance defines the final high energy amount (fig. 3). An other consideration: if only the pre-operational phase is considered, both of building types with the solution B have the lowest EE, because of the lower EE of the involved materials (compared with the other brick work walls). If the operational phase is taken into account, the single family house with the solution F consumes less energy than the other ones, just as the solution A between the 16 storey tower case studies. At least if the maintenance phase is taken into account, the single family house with the solution E has totally the less energy consumption than the other ones, just as solution A between the 16 storey tower case studies.

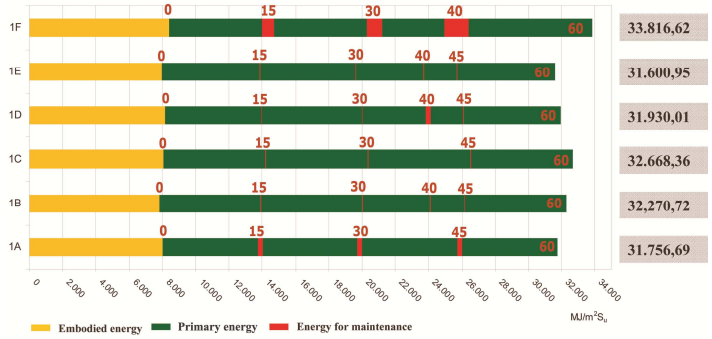

Figure 3. Affection of maintenance schedules in a life time of 60 years of the single family house.

Taking into account the difference of energy consumption between the most efficient case (in terms of energy) and the worst one, the envelope type choice affects the results and the energy consumption. For example, in the single family house the choice of the solution E generates an energy consumption of 31.600,95 MJ/m^2, equivalent to 8778,042 kWh/m^2 and to 146 kWh/m^{2}y. In the same building type the solution F generates a consumption of 33.816,62 MJ/m^2, equivalent to 9393,5 kWh/m^2 and to 156,5 kWh/m^{2}y. The difference of 10,5 kWh/m^{2}y is quite comparable to the primary energy heating demand of a class A new house (in Milan).

Table 1. Results of the energy assessment of the houses 1 and of the towers 2 (life exp. of 60 years).

LCA phases	*Unit*	*1A*	*1B*	*1C*	*1D*	*1E*	*1F*
EE $_{production}$	MJ/m^{2}S$_u$	7.993,56	7.809,93	8.066,31	8.176,21	7.954,82	8.401,51
Operational E	MJ/m^{2}S$_u$	22.891,13	24.327,25	24.499,02	23.347,74	23.513,19	22.298,62
EE $_{maintenance}$	MJ/m^{2}S$_u$	871,99	133,54	103,03	406,05	132,93	3.116,50
Tot. Energy/60	MJ/m^{2}S$_u$	31.756,69	32.270,72	32.668,36	31.930,01	31.600,95	33.816,62
LCA phases	*Unit*	*2A*	*2B*	*2C*	*2D*	*2E*	*2F*
EE $_{production}$	MJ/m^{2}S$_u$	1.199,71	1.113,03	1.236,60	1.277,20	1.181,26	1.399,62
Operational E	MJ/m^{2}S$_u$	14.678,81	15.503,04	15.612,86	15.051,72	16.321,02	15.650,88
EE $_{maintenance}$	MJ/m^{2}S$_u$	360,70	54,59	43,10	164,14	54,81	1.333,06
Tot. Energy/60	MJ/m^{2}S$_u$	16.239,22	16.670,67	16.892,56	16.493,06	17.557,09	18.383,55

5.3 Influence of Building Components and Material Degradation on Environmental Assessment

As an example of the analysis done on all façade components, the case 1A single family house is presented. The Monte Carlo simulation was performed using the following input values for conversion of thermal conductivity (ISO 10456): f_t = GaussNormal(0.0048; 0.0005333), f_ψ = GaussNormal(4;1) , f_a = GaussNormal(0.0123577; 0.0041192). The estimated service life of the external insulation layer was cumputed using the following equation:

$$\text{ESL} = \text{GaussNormal}(15;\ 5) \times 1 \times 1 \times \text{GaussNormal}(1;\ 0.133) \times 1 \times \text{GaussNormal}(1;\ 0.133) \times \text{GaussNormal}(1;\ 0.133) \times 1$$

This means that RSl, C, E and F factors were assumed as probability density functions in order to take into account possible errors in estimating their value.
Results of the simulation are presented in Table 2, where it is readable the minimum value, maximum value and mean value of the probability distribution function of total energy.

Table 2. Results of the MC simulation – Total energy [MJ/m^2] - case 1A - single family house.

Min	Max	Mean	%tile																		
			5%	10%	15%	20%	25%	30%	35%	40%	45%	50%	55%	60%	65%	70%	75%	80%	85%	90%	95%
23862	30960	24333	24045	24077	24101	24123	24141	24157	24172	24191	24209	24227	24248	24270	24295	24327	24363	24409	24469	24579	24893

6 CONCLUSION

The six building envelopes in the two different building typologies affect results of total energy computation over the life cycle. Differences in results (fig. 4) between the two groups of case studies are directly related with the shape factor, while differences into each group are related to building envelopes type because some technical solutions are more sensitive than others to aging and to environmental conditions, i.e. humidity and temperature.

Further are the continuous line (result of the effect of the degradation of materials on the total energy computation) and the corresponding dotted line (deterministic evaluation result of the total energy without the aging of materials), more important is the consideration of the materials aging in the energy demand computation over the service life. In addition, more inclinated is the continuous line, more these solutions are subjected to a possibility of error in the aging effects' evaluation. This is especially true for some envelope solutions. For example, the light weight solution F, with a thicker insulation layer than the others, and the solution A, with the external thermal insulation render system, are more subjected to aging effects and to humidity and temperature variations.

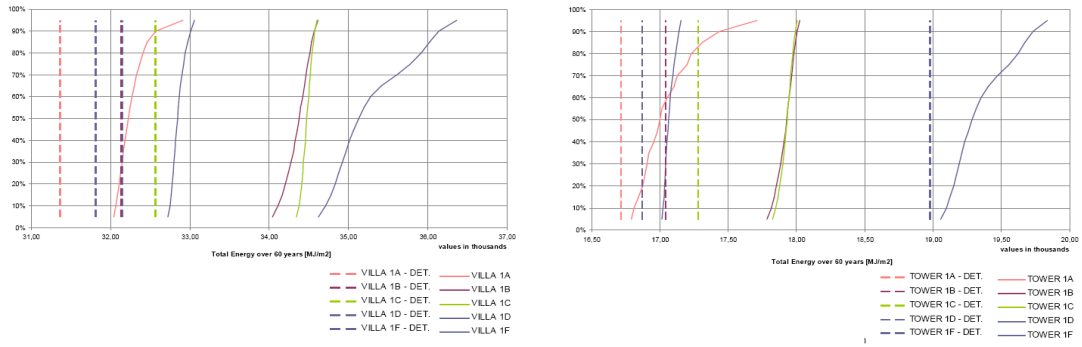

Figure 4. Results of the total energy consumption scenario with the Monte Carlo analysis.

ACKNOWLEDGMENTS

The framework of the present work is the research "Energy to build, energy to live. Energetically and environmental optimization of brick work envelope types" coordinated by prof. A. Campioli, dept. BEST, funded by ANDIL, the Italian Brick Development Association.

REFERENCES

Adalberth, K. 1997, "Energy use during the Life Cycle of Buildings: a Method", *Building and Environment*, **32**[4], pp. 317-20.

Gustavsson, L. & Sathre, R. 2006, *Variability in energy and carbon dioxide balances of wood and concrete building materials*, Building and Environment, **41**[7], pp. 940-51.

Hammond, G.P., Jones, C.I. 2008, *Inventory of Carbon & Energy (ICE) – Version 1.6a*, Sustainable Energy Research Team (SERT), Dept. of mechanical Engineering, University of Bath.

Haapio, A. & Viitaniema, P. 2008, "Environmental effect of structural solutions and building materials to a building", *Environmental Impact Assessment Review*, 28, pp. 587-600.

HAPM (Housing Association Property Mutual) 1996, *Component Life Manual* (4th edition), E & F.N. Spon, London,

Junnila, S., Horvarth, A. 2003, Life cycle environmental effects of an office building, *Journal of Infrastructurel systems*, **9**[4], pp. 157-66.

Lacasse, M.A., Vanier, D.J. & Kyle B.R. 1997, *Towards integration of service life and asset management tools for building envelope systems*, in Proc. 7th Conference on Building Science and Technology: Durability of buildings Design, Maintenance, Codes and Practice, Toronto, 20-12 may 1997, pp. 153-57.

Monticelli, C. 2006, *Environmental profile and Building Process. LCA application to experimental dry external wall Construction System*, in Proc. 23rd Int. Conference on Passive and Low Energy Architecture PLEA 2006, Swiss, Geneva, 12-15 september 2006, vol.2, pp. 1023-28.

Peuportier, B. 2001, "Life cycle assessment applied to the comparative evaluation of single family houses in the French context", *Energy and Buildings*, **33**[5], pp.443-50.

Scheuer, C., Keoleian, GA., Reppe, P. 2003, "Life cycle energy and environmental performance of a new university building: modelling challenges and design implications", *International Journal for Energy and Buildings*, **35**[10], pp.1049-64.

Thormark, C. 2006, "The effect of material choice on the total energy need and recycling potential of a building", *Building and Environment*, 41, 1019-26.

XII DBMC
International Conference on Durability of Building Materials and Components
PORTO - PORTUGAL, April 12th-15th, 2011

Some Considerations Regarding the Thermal Rehabilitation of Mass Dwellings

Ana-Maria Dabija [1]

ABSTRACT

According to the census of 2002, in Romania there are over 8.1 million dwellings, over 50% of them in cities. The buildings that accommodate these dwellings are a little over 4.8 million, out of which 23.5% are in the urban area. Around 25% of them are over 55 years old and only 10% were built in the last twenty years.

These figures bring us to the fact that the most important percentage of buildings is, from many points of view, outdated.

Based on the European Energy Performance of Buildings Directive, Romania adopted a Law on energy performance and a corresponding methodology of intervention on the stock of mass dwellings built between 1950 and 1990. As in the case of most European countries, the Romanian government is involved in the rehabilitation of outdated buildings. We have a national programme for thermal rehabilitation and the funds allocated to back up this programme.

However, after having finished the first lot of buildings, we are able to evaluate the results, not only in terms of energy performance but also with respect to other aspects that define a building.

The paper presents a (critical) approach to the means to improve the thermal behaviour of mass dwellings. It presents the situation of the buildings in Romania, although – probably – some of the problems that are presented may be found in similar approaches to other countries as well.

KEYWORDS

Outdated mass dwellings, Thermal insulation, Refurbishment solutions.

[1] 'Ion Mincu' University of Architecture and Urbanism, Bucharest, Romania, am.dabija@iaim.ro

1 INTRODUCTION. EUROPEAN CONTEXT

In recent years global preoccupations for saving the planetary environment have greatly increased. Many authorized voices claim that we are on the point of exhausting natural resources and therefore should focus on alternative sources for producing energy.

According to the Directive 2010/31/EU of the European Parliament and of the Council of 19 May 2010 on the Energy Performance of Buildings (recast) [published in the Official Journal of the European Union, L 153/13] 'Buildings account for 40 % of total energy consumption in the Union. The sector is expanding, which is bound to increase its energy consumption. Therefore, reduction of energy consumption and the use of energy from renewable sources in the buildings sector constitute important measures needed to reduce the Union's energy dependency and greenhouse gas emissions'. This document amended the Directive 2002/91/EC of the European Parliament and of the Council of 16 December 2002 on the energy performance of buildings (EPBD) and reiterated the corresponding other official documents adopted between 2002 and 2010.

The clauses of the recast EPBD take into consideration the context of the building: 'Measures to improve further the energy performance of buildings should take into account climatic and local conditions as well as indoor climate environment' (Clause 8) and 'Major renovations of existing buildings, regardless of their size, provide an opportunity to take cost-effective measures to enhance energy performance' (Clause 16). The methodology for calculating energy performance of the building 'includes, in addition to thermal characteristics, other factors that play an increasingly important role such as heating and air-conditioning installations, application of energy from renewable sources, passive heating and cooling elements, shading, indoor air-quality, adequate natural light and design of the building' (Clause 9).

Finally, Article 7 refers to existing buildings and stipulates a very important aspect: 'when buildings undergo major renovation, the energy performance of the building or the renovated part thereof is upgraded in order to meet minimum energy performance requirements set in accordance with Article 4 insofar as this is technically, functionally and economically feasible'.

We have quoted these Clauses and Articles as a preamble to the following critical approach.

Being a European country, Romania assumes the requests and commitments that stipulate that, prior to 2020, the energy consumption resulting from the use of traditional fuels and greenhouse effect shall decrease by 20% and the use of alternative energy sources shall increase accordingly.

2 THERMAL REHABILITATION OF MASS DWELLINGS IN ROMANIA

Everywhere the stock of existing buildings faces specialists with several dilemmas: to demolish or to refurbish? What is the predictable service life of a refurbished building, compared with the one of a new building? Is the performance of a refurbished building worth the costs of the intervention? And - most importantly - do the interventions on the building really improve its efficiency or, by having its hygrothermal behaviour improved, the building develops a new pathology?

Scientific research that aimed to improve the thermal behaviour of mass buildings in Romania has been carried out for a long time. Even during the communist regime there were research programmes that focused on producing more efficient windows or that analysed the behaviour of building envelopes in different climatic areas of Romania. They remained mostly on paper, but were an experience / exercise for research in more recent years. The specialists did not start from scratch these last years, but had previous experience in the specific research on the compliance or upgrade of the building.

However, unlike in other countries, in Romania the research and the interventions focused either on the unit (apartment) or the building envelope, leaving some items in a 'no man's land'. It may be, in principle, a matter of ownership, as each apartment is owned by a different individual. It is the case of the common parts of the building (the entrance, the staircase, the elevator, the garbage evacuation). It is also a lack of civic spirit, as most apartment owners feel connected to the property that begins (or ends) at the door of their apartment and not on the staircase or in the elevator.

Although the solution is a holistic approach to the envelope of the building, previous individual interventions and the funding problem have not allowed for an overall intervention to be taken.
One question may arise: from the owners' point of view, who does the façade of the building belong to? Who do the windows belong to? Whose are the balconies? As the (communist) state took no measures to improve the comfort conditions, people closed their balconies, changed the windows and in some cases provided a thermal protection as well. This is the reason why today, more than thirty years after the first individual interventions on the envelopes were carried out, we are still faced with the same problem, namely the heterogeneous aspect of the blocks of flats: my house, my façade, my windows.

The mass building rehabilitation programmes carried out in the nineties in Germany - for instance - included, along with the improvement of the thermal protection of the building (both the opaque and glazed envelope component), changing the equipment and installation systems within the building (elevators, heating and sanitation systems), as well as the rehabilitation of the entrances (according to Knut Höller & Britta Schmigotzki).

Thus the intervention for the rehabilitation of mass dwelling buildings is a holistic one, all building components that use energy in a dwelling being attacked and updated. More recent approaches include the use of alternative energy sources.

2.1 The Romanian Legislation

Based on the European EPBD, Romania adopted Law 372/2005. It was followed by the Methodological Norms regarding the increase of the energy performance of the blocks of flats, in 2009.

A National Programme aiming to accomplish the task of reducing energy consumption in mass buildings is also being carried out.

A first important issue in the approach is that, unlike most European countries, Romania is a country with an important seismic hazard. During the last century, buildings withstood four important earthquakes (after the two major quakes measuring over 7 on the Richter scale, in 1940 and 1977, resulted in about 3,000 dead and many more injured). In fact, the main problem of the stock of outdated buildings should not be the thermal rehabilitation but the seismic rehabilitation, much more difficult to achieve due, among others, to the fact that people actually live in these buildings and have nowhere else to go.

The legislation that the Methodology associated with the Romanian Energy Performance Law refers to in terms of seismic protection is outdated: on 1 January 2010 a new Code for Seismic design came into force. In comparison with the previous Norm (that is referred to in the Methodology), the technical expertise is much more elaborated. Prior to the thermal rehabilitation, a technical expertise should be carried out and, considering the state of the buildings, most of them should be consolidated.

The thermal 'blanket' that should be placed on the façades would only hide the deterioration of the buildings.

There is little to be done about reorganizing the internal space (by demolishing or changing the position of the partitions), as it is happening in other European countries, due to the seismic hazard. During the communist years, the room surface was rather small. After the refurbishment, in most cases (although there are some situations where the engineer accepted to cut an opening for a door in a wall), the rooms remain as small as they were prior to the intervention.

Therefore we believe that a thermal rehabilitation should be carried out as part of an overall rehabilitation – the structural intervention being the most important and the most expensive one.

The current European Directive deals with this aspect – not in terms of seismicity, but in terms of general repairs – changing the perspective into a more realistic one: the interventions for improving the thermal protection should be made within a more complex intervention. As mentioned before, a seismic rehabilitation implies costs far greater than a thermal rehabilitation – not to mention that many individuals have already replaced the old windows with new, efficient ones – and the modernization of the building can be included in the general costs of the interventions.

Another major difference is that, unlike other European Methodologies, the Romanian legislation does not include the use of alternative energy in the rehabilitation policy. The only important matter seems to be the quantity of saved energy, irrespective of how it was produced. There are other laws that try to arouse the interest of home owners in alternative energies but the current form of the Methodology is indifferent to the source of energy.

2.2 The Romanian Mass Dwellings

A survey of the architecture of Romanian mass dwellings will emphasize two main types: individual houses (which were built either before the war or after 1990) and blocks of flats, built throughout the 20th century.

A focus on the apartment buildings will – again – show an interesting aspect: each decade the style changes: during the thirties in Romania a genuine modernist style was crystallized (Figure 1).



Figure 1. Two apartment buildings on the Magheru Boulevard, one of the most important thoroughfares, cut in the thirties.

In the forties no buildings were built. In the fifties the Soviet apartment buildings were ‘imported’ and introduced (Figure 2).

The sixties came with long horizontals for the lines of the balconies and loggias, as well as for the windows. These apartments have a lot of light, the windows stretching from one end of the room to the other (Figure 3). Brick cladding and precious plaster with mica and marble are the usual exterior finishing.



Figure 2. The 'Soviet' apartment buildings are low-rise building (3 – 4 stories high) organized around an inner courtyard. The façades have some plaster decorations. The windows are rather small. The entrance to the courtyard is normally through an arcade or a colonnade (like in the case of the façade decorations, there is an intention of vague monumentality, deriving from the style of the time).



Figure 3. Clear horizontals of the loggias and window line. Unfortunately, more recent interventions of closing the balconies / loggias altered the character of the building.



Figure 4. Common blocks of flats of the seventies, in Bucharest.

The seventies brought coloured ceramics on the façades and a slimmer volumetry. The windows are still large. Towards the end of the decade, systems of prefabricated walls were developed. The window areas decreased, according to the structural possibilities of the prefabricated wall. As it behaved very well during the earthquake, the system went on to be used in the next decade as well. Simple panels were used for blocks facing inner courtyards or ensembles located on the outskirts.

The eighties came with some kind of post-modern influence, so the great boulevards are guarded by apartment buildings with highly decorated columns, attics and balustrades (Figure 5) or at least with precious finishing (brick or decorative exterior plaster).



Figure 5. The eighties, on the former Socialist Victory Boulevard, in Bucharest, which was built by destroying part of the old city.

The apartment buildings built after 1990 follow a less restrictive legislation, therefore the space is wider and the envelope offers better thermal protection.

3 INTERVENTIONS ON EXISTING BUILDINGS

3.1 The National Programme of Thermal Rehabilitation. Intentions

The National Programme of Thermal Rehabilitation [in The Thermal Rehabilitation Programme The Ministry of Regional Development and Tourism, http://www.mie.ro/index.php?p=1034] carried out in Romania (and applicable for the blocks built between 1950 and 1990) is rather generous and, in theory, aims to:

- improve hygiene and thermal comfort conditions;
- reduce heat loss and energy consumption;
- reduce maintenance costs for heating and hot water for consumption;
- reduce pollutant emissions generated by energy production, transport and consumption.

The Programme also mentions that ‘depending on the results of the technical expert’s report and the energy audit carried out on the building, the following can be added to these works:

- repairs to the construction elements which pose potential danger of detachment and / or affect the functionality of the housing block;
- intervention works on the distribution installation of the thermal agent for heating the common parts of the housing block.’

The Programme is based on Law 372 of 13/12/2005, which transposes the Directive no. 2002/91/CE of the European Parliament and Council, regarding the energy Performance of the Buildings,

published in the Official Journal of the European Communities (OJEC) L 001 on 4 January 2003, p. 0065-0071.

There are provisions requesting safe behaviour, according to the Romanian legislation, concerning the 'mechanical resistance and stability' and 'fire safety' criteria (requirements A and B in the European Directive 89/106 CEE regarding Construction Products).

The costs of thermal rehabilitation are covered as follows: 50% are covered by the Ministry of Regional Development and Tourism, 30% are covered by the local budget and 20% by the owners' associations. In some districts of Bucharest, the local budget takes over the 20% of the owners' associations, as it is know that many owners are relatively poor people (retirees, young people with modest salaries).

The intentions are obvious: to decrease the energy consumption in the building, **not** to promote the use of alternative energy sources. For alternative energy aspects there is another programme, 'The Green House'. Considering the funds and the needs, the solutions that are adopted are the least expensive, in order to ensure the largest number of rehabilitated apartments.

3.2 The National Programme of Thermal Rehabilitation. Results

The solution that is generally adopted consists of the following interventions:

- wrapping the vertical building envelope in (about) 10cm of polystyrene boards, covered with exterior thin coatings,
- changing the double glazed windows with IG units, plus closing the balconies
- insulating (in many cases with an expanding foam) the basement ceiling,
- adding a polystyrene thermal insulation on the roof (and the corresponding layers) and replacing the waterproof membrane.

And this is when the problems begin…
The solution for improving thermal protection in Romania is, unfortunately, always the same, as the cost of placing a coating system over a thermal insulation layer is the lowest. Therefore, if nothing will change, in the future we will have one type of building finishing for all the refurbished buildings, with the only difference that will be… the colour.

Furthermore, as the cost of expanded polystyrene is the lowest, this is the thermal insulation which is used for wrapping most buildings, although the wall structure may recommend the use of other type of insulation.

In other European countries, even if the main goal of the intervention is to improve the thermal behaviour, solutions with more precious finishing systems have been adopted, according to the position of the building within the city or against the thoroughfare.

At least a differentiation according to the location of the building (facing a major boulevard or building, inside an anonymous courtyard, in the centre or at the outskirts of a city) should be made and thus different solutions, with different levels of preciousness, should be adopted.

The National Programme for Thermal Rehabilitation has a specific provision regarding the windows: 'replacement of the windows of the block and of the existent exterior doors with qualitatively superior ones, which will better insulate each room'. Again, the intentions are honourable. However, many of the owners dealt with the problem of heat loss long before the National Programme came into being. In fact this was a problem that had to be solved during the eighties. And it was solved, individually, according to the means, the relations, the craftsmen and eventually the imagination of each owner (or tenant sometimes, at that time). From sealing the gaps between the windows and walls or between the window elements, to adding an extra glass pane to the existing window; from adding an extra window

(inside the room), to closing the balcony altogether with a line of windows, the desperate Romanian population had to invent means to survive the cold winters of the eighties [according to Dabija, 2005]. Therefore the current type of intervention only completes the previous ones, taking into consideration - and in many cases preserving - what was found on site (especially as the owner needs to approve the intervention).

During the last two decades, most users have at least changed the window, with PVC ones, not necessarily efficient, but very airtight (generating a set of humidity problems inside the apartments).

The original architecture – good or bad – is therefore distorted and has been so for the last three decades, the result being the creation or perpetuation of very heterogeneous – and sometimes hilarious – façades [Dabija, 2010).



part of a building (right). As it can be seen, each balcony was closed using a different 'pattern', through previous, independent, individual interventions.

4 CONCLUSIONS

The interventions that are proposed today do not deal with the building as a whole and concentrate only on the façades. The concern to restore the building to the original architecture does not exist either. The building is approached as if it were split into a multitude of properties, each with its own window architecture and closed – or open- balconies. Consequently, the result is of poor architectural quality.

Therefore, maybe an architectural audit should also be carried out, along with the energetic audit, in order to make sure that the proposed solution maintains the original features of the buildings, at least in those parts of the cities where they make a difference.

REFERENCES

Directive 2010/31/EU of the European Parliament and of the Council of 19 May 2010 on the energy performance of buildings (recast), Official Journal of the European Union, L 153/13 – 21.

Ministry of Regional Development and Tourism, The Thermal Rehabilitation Programme
See: http://www.mie.ro/index.php?p=1034

Dabija, A-M, 'A Bridge Between Old and New. Thermal Refurbishment of the Windows in Existing Dwellings', in Proceedings to the 10 Durability of Building Materials and Components, France 2005.

Dabija, A-M 'Rehabilitation of Mass Dwellings in Romania. A Critical Approach' in World Energy System Conference, Targoviste, Romania, 2010.

Höller, K, Schmigotzki,B, IWO e.V., Berlin / Germany "Strategies and Instruments Supporting Energy Efficient Refurbishment (EER) in Germany" in Tallinn, 29. November 2006.

XII DBMC
International Conference on Durability of Building Materials and Components
PORTO - PORTUGAL, April 12th-15th, 2011

Durable and Robust Vacuum Insulation Technology for Buildings

Kjartan Gudmundsson [1]
Christer Sjöström [2]
Peter Norberg [3]
Wolfram Trinius [4]
Ebenezer Twumasi [5]

ABSTRACT

Vacuum insulation panels (VIPs) provide unprecedented opportunities for obtaining excellent thermal insulation with light and slender constructions. This article discusses the performance over time of VIPs, and the possibilities to overcome the current problems related to fragility and limited durability.

Aerogels are together with fumed silica among the most competitive core materials for VIP's. The use of classical aerogels, as produced in autoclaves is, however, limited due to the high production costs. The fumed silica on the other hand requires vacuum levels that are difficult to maintain with the currently available vacuum envelopes. A material with comparatively smaller pores will on the other hand allow obtaining low thermal conductivity at higher pressure (less vacuum) and will therefore reduce the pressure difference over the envelope. There is therefore much to be gained by reducing the pore size. New cost and performance efficient silica aerogels offers opportunities to enhance the properties of the panels by customizing the pore structure and pore size distribution. Building technologies and how the panels are applied in a manner that improves the structural, thermal and hygroscopic performances of vacuum insulated constructions have been studied and are discussed.

KEYWORDS

Vacuum insulation technologies, Performance over time, Building technology, Aerogel, Core materials.

[1] School of Civil and Architectural Engineering, KTH, Stockholm, SWEDEN, kjartan.Gudmundsson@byv.kth.se
[2] Materials Technology, KTH Research School, University of Gävle, Gävle, SWEDEN, christer.sjostrom@hig.se
[3] Peter.Norberg@hig.se
[4] Ingenieurbüro Trinius, Hamburg, GERMANY, Trinius@Trinius.de
[5] Ebenezer_Twumasi/hig@hig.se

1 INTRODUCTION

1.1 Energy and the Climatic Envelope

Space heating constitutes a large part of the energy used in Sweden and the European Union (about 40%). About half of that can be related to the thermal losses through the climatic envelopes of buildings. This presents an economical problem as well as a threat to our local and global environment. The technical solution of the problem is complex, but will essentially involve severe reduction of heat losses through the walls, floors and roofs of the buildings. With traditional insulation materials this will lead to a significant increase in the thickness of the climatic envelope. A house in Sweden that is to meet the passive house standards would thus have an insulation thickness of some 335 mm in the wall and 500 mm in the roof in order to meet a U-value of 0,10 and 0,066 W/(m².K), respectively.

1.2 New Opportunities with VIPs

Today's requirements on energy savings demand vast insulation thicknesses if traditional insulation materials are to be used in the construction of residential buildings. As a result, significant living space area may be lost and restrictions are put on architectural expression. Regarding the refurbishment of the existing building stock there is often too little space available for adequate additional insulation on the inside of the building and the application of external insulation may endanger the architectural values of the facades. The excellent insulations properties of VIPs may however provide a solution since only a fraction of the insulation thickness is required.

A conventional vacuum insulation panel consists of a gas-tight envelope surrounding a porous core from which the air has been evacuated. The combination of pore size and low pressure prevents thermal transport through convection of the gases within the core. Conduction through the collision of gas molecules is eliminated by using core material with pore size less than the mean free path of the gas molecules, which in turn depends on the extent of evacuation. Consequently the gas pressure that has to be obtained within the envelope in order to reach a certain value of thermal conductivity in the VIPs depends on the pore structure of the material applied in the core. Fumed silica, for instance, maintains a constant thermal conductivity of about 0,004 $Wm^{-1}K^{-1}$ up to a gas pressure of about 10 mbar, the value being the double for a tenfold pressure of 100 mbar. Material with coarser pores, however, such as polyurethane, polystyrene or fiber glass will only maintain a comparable constant level up to a pressure just above 0,1mbar with a fourfold thermal conductivity at a pressure of 10 mbar (Fricke et al, 2006; vip-bau.de, 2009). The relationship between core pressure and the thermal conductivity of several different core materials is shown in figure 1.

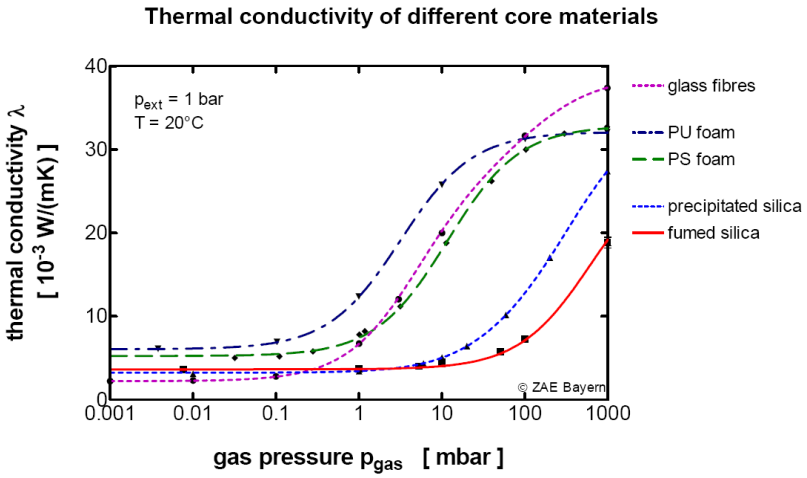

Figure 1. Core pressure and thermal conductivity of different core materials(IEA, Annex 39, 2005a).

Consequently a core material with coarser pores will require a greater degree of vacuum in order to obtain the same thermal insulation, other things being equal.

Conduction through the solid matrix of the core is limited by using materials with geometric structures that minimize the area of contact between the particles while the radiative heat exchange between the interior surfaces of the core material is determined by the temperatures as well as the geometries and surface properties, the latter which can be improved by the use of additives.

A regular VIP panel consists of a metalized polyester film with a core of fumed silica a picture of which is shown in figure 2. There are, however, vast possibilities of combining different core materials and envelopes in different typologies as described in the literature (Cremers, 2005).

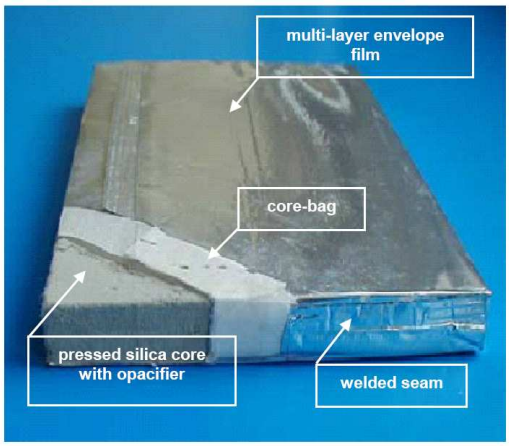

Figure 2. A regular VIP panel with a fumed silica core (IEA, Annex 39, 2005a).

The application of VIPs has been limited to a small number of buildings. An account of their applications is to be found in the report of the International Energy Agency (2005b) as well as in Ghazi Wakili et al. (2005), Schwab et al. (2005) and Binz and Steinke (2005). Batens et al. (2010) have done a review of VIPs in building applications.

1.3 Durability and Service Life of VIPs

The service life time of a VIP can be defined as the time at which the required thermal conductivity has been surpassed. A further account is given in ISO 15686-2 (2001).

The most important aging mechanism of VIPs with fumed silica cores and a metalized polymer film envelope is the permeation of gas through the envelope. This effect may be enhanced at higher temperatures and humidity and is further increased at the edges due to a higher defect density of wrinkles and at the seal of the foil (Simmler and Brunner, 2005).The edge effect will get greater with the ratio of edge length over area of the panel (Schwab et. al, 2005) As can been seen in figure 1, the thermal conductivity of the fumed silica core will increase by a factor of about 5, when going from a pressure of 1 mbar to standard atmospheric pressure.

Short term measurements of Vacuum insulation panels can be used to predict the service life of vacuum insulation panels. Based on the measured gas transmission rates or measurements of pressure increase (Caps et. al., 2008) and water vapor transmission rates of the VIPs, the service life can be predicted thorugh an analytical model that relates the gas pressure, vapour pressure and water content to the thermal conductivity of the panel (Simmler and Brunner, 2005; Annex 39, 2005a)

A commonly used method for securing or prolonging the service life of panels is to put getters or desiccants in the core material in order to adsorb or entrap residual gas or moisture (Thorsell, 2006).

With current technology the gas pressure increase of a 20mm thick VIP with metallized high barrier envelope is around 1 mbar a year giving a lifetime of 10-25 years depending on the required performance of the panel (Caps et al. 2008) and initial pressure that can asssumed to be in the range of 1-5 mbar at delivery (Microtherm, 2010).

While the problem of gas diffusion through the envelope may be solved by using virtually impermeable metal films with a thickness of 10 µm or more it has been shown that this may give lead to thermal losses that are of the same magnitude as the heat flow through the panel (Ghazi et al, 2004). One must bear in mind, however, that a VIP panel might even fail due to failures caused by imperfect production or through mechanical damages during installation.

2 VIP OPPORTUNITIES

The in situ performance of VIP panels depends of the properties of the panels and the manner in which they are applied. Our work is concerned with studies of how the prestanda of the panels may be improved by changing the material of the core and the possibilites of enhancing the robustness, performance and durability of the panels through an appropriate building technology. The relevance of these measures can be measured in terms of economical and environmental benefits.

2.1 Robust Building Technology

The superior thermal properties of the panels are somewhat diminished by the thermal bridges at the edges. Tenpierik and Cauberg have presented analytical models for calculating this thermal edge effect for thin high barrier laminates around VIPs (Tenpierik and Cauberg, 2007) while Thorsell and Källebrink studied the effects of applying a serpentine edge on a metal panel (Thorsell and Källebrink, 2005). Other researchers have investigated the different thermal bridges that arise when VIPs are applied in different constructions and various building details (Schwab et al., 2005; Ghazi Wakili et al, 2005; Nussbaumer et al, 2006, Platzer, 2007).

Our work is concerned with building technology that adresses the issue of thermal bridges while at the same time overcoming the fragility and limited durability of the VIPs. Previous and ongoing parametric studies show that the thermal edge loss can be compensated with an adjacent layer of thermal conductivity in the range of traditional insulation materials (Gudmundsson, 2009).

The left side of figure 3 shows a section where two VIPs meet with a gap of 2 mm at the joint. The VIP panel is assumed to have a λ-value of 0,005 $Wm^{-1}K^{-1}$ while that of the sealant in the gap is 0,02 $Wm^{-1}K^{-1}$. The figure on the right shows the thermal loss at the joint for different thermal conductivities of the adjacent insulation as compared the heat flow through an unbroken VIP. The results were obtained with COMSOL Multiphysics®.

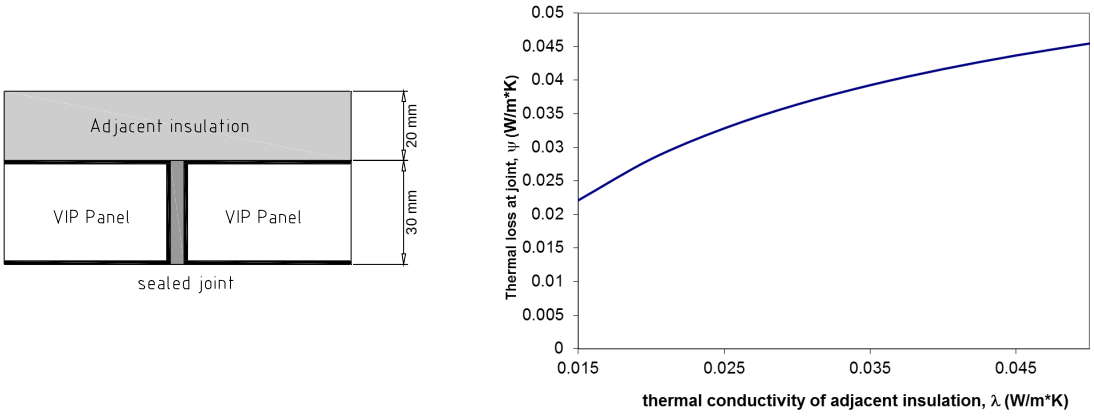

Figure 3. A section where two VIPs meet and a diagram that shows the additional linear thermal loss at the joint for different thermal conductivities of the adjacent insulation.

Based on our findings we therefore propose a solution where the panels and their edges of the panels are covered with an adjacent insulation material that breaks the thermal bridges while protecting the panels and providing acarrier for the rendering of the façade.

The effect of using an exterior insulation with low thermal conductivity is positive in terms of reducing the thermal bridge while much is to be gained by increasing the size of the panels and thus the length of the joints per square meter of VIP. The exterior application of VIPs is also favourable in terms of the risk of condensation and high relative humidities.

2.2 Improving the Core Material

Aerogels are together with fumed silica among the most competitive core materials for VIP's. The use of classical aerogels as produced in autoclaves is, however, limited due to the high production costs. The fumed silica on the other hand requires vacuum levels that are difficult to maintain with the currently available vacuum envelopes. A material with comparatively smaller pores will on the other hand allow us to obtain low thermal conductivity at higher pressure (less vacuum) and will therefore reduce the pressure difference over the envelope. Consequently there is much to be gained by reducing the pore size of the core material. It will be of particular interest to investigate the margin of improvement in terms of the environmental impact when substituting fumed silica with aerogel and to compare it with the results for traditional insulation materials. A study by Mukhopadhyaya et al. (2009) shows that fiber-powder composites have promising potential to be used as core materials for the construction of high-performance VIPs.

2.3 Economics and Durability

The use of VIPs can in some instances be motivated by the gain of living space area. The economic effect of increasing the service life of VIP panels in can be illustrated within that context. Assuming a VIP panel with a given thickness, thermal conductivity and price per sqm we can calculate the net cost of using vacuum insulation instead of EPS with the same thermal performance, given a certain rate of interest rate and inflation (Gudmundsson, 2009). The figure below illustrates the net cost as a function of net income per sqm and shows what is to be gained with an increased lifetime of the panels, through which the panels are assumed to have a constant thermal resistance.

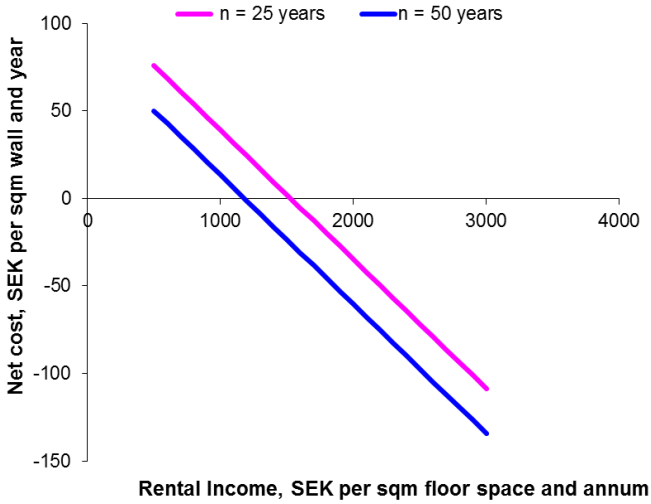

Figure 4. The net cost and net income per sqm. Assuming 30 mm thick VIP panel with a thermal conductivity of 0,004 $Wm^{-1}K^{-1}$ and a price of 1800 SEK/m^2. The real interest rate is assumed to be 5%.

Another way of approaching the problem is to look at the break even price for a given net income and a durability of a given period of time. The results are that for a lifetime of 25 years and an annual income corresponding to the average rental income in Sweden there will be a break even for an investment cost for VIPs of about 1250 SEK per sqm wall area. This prices is beneath the current price levels which means that with current lifetime the prices have to go down if VIPs are to be able to be fully economically competitive.

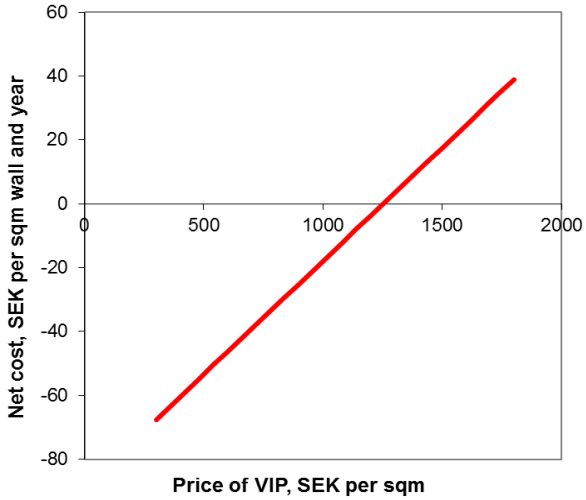

Figure 5. Price of VIP vs net cost for an average annual rental income of 1000 SEK/m^2. A lifetime of 25 years is assumed.

2.4 Life Cycle Impact of VIPs and Potential for Improvement

There are reasons and possibilites for improving the technical and economic aspects of VIPs. Together with the aspects of building technology and durability it is plausible to assume some advantages in terms of sustainability, that need to be analysed and verified in accordance to the relevant ISO standards.

Besides the discussion of the technical and economic possibilities, the quantification of environmental impacts, through the life cycle of a VIP panel is a necessity when evaluating the potential effects of altering their design. A Type III environmental product declaration (EPD) according to ISO 14025 and in line with the forthcoming European Standard prEN 15804 has to be carried out. The manufacturing processes have to be monitored in order to provide the necessary data. Complementary to the production process, the environmental declaration will include the “cradle to gate” stages in terms of environmental LCA (ISO 14040 and 14044), as well as the end-of-life stage. Aspects related to the use-stage of construction products can usually not be ascribed to the product itself, hence this stage is not a part of the declaration. Instead, key technical properties of the product will be presented, enabling the reader to put the presented data into the overall performance context of a building.

Ultimately, the forthcoming life cycle assessment will generate a strictly product related EPD presenting the quantified environmental impact according to the relevant standards, and in line with the detailed product category rules applicable to the VIP panels. The discussion of the environmental pro’s and con’s will include the application of the material in a building, focusing on the contribution of the material to the overall building performance. For such an assessment, either a reference-comparison with a building with the same technical properties but different materials must be set up, or the effect of changing from a given design to a design incorporating the presented materials must be set up.A direct raw comparison of the EPD data of this product with competing products is of limited use. Mainly the weaknesses and improvement potentials may be determined, but a fair comparison will necessarily need to be conducted in the application context of the products.

Previous work indicates that the greatest potential of improvement is replacing the fumed silica in the core since it is currently a by-product of the production for electronic chips. The common precursor silicon tetrachloride is highly energy intensive and dominates the results of the ecobalance to over 60% (IEA, Annex 39, 2005b).

3 CONCLUSIONS AND DISCUSSION

While vacuum insulation panels have superior thermal properties the fragility and limited durability pose a threat to the lifetime of the panels and hence the economy of their application.

The economical benefits of prolonging the lifetime of the panels are clear and the issue of fragility may be overcome by a applying an appropiate building technology such as panels with a protective layer that may also be used to reduce the thermal bridge at the joints of the panels.

Further improvements of the panels may be reached by replacing the fumed silica core with a material with comparatively smaller pores, thus reducing the pressure difference over the envelope and extending the service life of the panels.

We are currently working on a solution with an aerogel as a core material. Previous work indicates a potential for environmental benefits due to the prolonged lifetime and ultimately due to the production process of the core. A quantification of environmental impacts will be neccesary in order to quantify any advantages in terms of sustainability, however. This can be done according to the previously mentioned ISO standards and European Norms. Such work will demand the manufacturing process to be monitored in order to provide the necessary data.

ACKNOWLEDGEMENT
Anders Lundström, CEO of Svenska Aerogel AB, is acknowledged for contributions in personal communications.

REFERENCES

Baetens, R., Jelle, B.P., Thue, J.V, Tenpierik, M.J., Grynning, S., Uvsløkk, S. & Gustavsen A. 2010, Vacuum insulation panels for building applications: A review and beyond , *Energy and Buildings*, Vol. 42, Issue 2, pp 147-172.

Binz A. & Steinke G. 2005, Applications of Vacuum Insulation in the Building Sector, 7th International Vacuum Insulation Symposium 2005, Zürich.

Caps, R., Beyrichen, H., Kraus, D. & Weismann, S. 2008, 'Quality control of vacuum insulation panels: methods of measuring gas pressure', *Vacuum*, 82, 691–699.

Cremers, J. M. 2005, 'Typology of Applications for Opaque and Translucent VIP in the Building Envelope and their Potential for Temporary Thermal Insulation', 7th International Vacuum Insulation Symposium 2005, Zürich.

Fricke, J., Schwab, H. & Heinemann, U. 2006, 'Vacuum insulation panels-exciting thermal properties and most challenging applications', *International Journal of Thermophysics*, Vol. 27, No. 4, pp. 1123-1139.

Ghazi Wakili, K. , Bundi, R. and Binder, B. 2004, 'Effective thermal conductivity of vacuum insulation panels', *Building Research & Information*, 32:4, 293-299.

Ghazi Wakili, K., Nussbaumer, T., Bundi, R. 2005, 'Thermal Performance of VIP Assemblies in Building Constructions', 7th International Vacuum Insulation Symposium 2005, Zürich.

Gudmundsson, K. 2009, 'A parametric study of a metal sandwich VIP', 9th International Vacuum Insulation Symposium 2009, London.

IEA/ECBS Annex 39. 2005, 'High Performance Thermal Insulation, Vacuum Insulation Paneles-Study on VIP-components and Panels for Service Life Prediction of VIP in Building Applications (Subtask A)', http://www.ecbcs.org/docs/Annex_39_Report_Subtask-A.pdf (Accessed 27/10/2010).

IEA/ECBS Annex 39. 2005, 'High Performance Thermal Insulation, Vacuum Insulation in the Building Sector, Systems and applications (Subtask B)', http://www.ecbcs.org/docs/Annex_39_Report_Subtask-B.pdf (Accessed 21/09/2010).

ISO 15686-2, 2001. (E), '*Building and Constructed Assets – Service Life Planning – Part 2: Service Life Prediction Procedures*'.

Microtherm, 2010. 'Vacuum Insulation - Microtherm® SlimVac - Product characteristics and properties', http://www.microtherm.be/EXEN/site/vip-characteristics.aspx, (Accessed 21/10/2010).

Mukhopadhyaya, P., Kumaran, M.K., Normandin, N. & van Reenen, D. 2009, 'Fibre-powder composite as a core material for vacuum', 9th International Vacuum Insulation Symposium 2009, London.

Nussbaumer, T., Ghazi Wakili, K., Tanner, Ch. 2006, 'Experimental and numerical investigation of the thermal performance of a protected vacuuminsulation system applied to a concrete wall', *Applied Energy*, 83, pp. 841–855.

Platzer W. 2007, 'Optimisation and testing of an VIP exterior thermal insulation composite system (ETICS)', 8th International Vacuum Insulation Symposium 2007.

Schwab, H., Heinemann, U., Beck, A., Ebert, H.P., Fricke, J. 2005, 'Permeation of different gases through foils used as envelopes for vacuum insulation panels', *Journal of Thermal Envelope and Building Science*, Vol. 28, No. 4, 293–318.

Schwab H., Stark C., Wachtel J., Ebert H.-P. and Fricke J., Thermal Bridges in Vacuum-insulated Building Facades, Journal of thermal env. & bldg. sci.,Vol. 28, No. 4, 2005, pp. 345-355.

Simmler, H. & Brunner, S. 2005, 'Vacuum insulation panels for building application: Basic properties, aging mechanisms and service life', *Energy and Buildings*, Vol 37, Issue 11, November 2005,pp 1122-1131.

Tenpierik, M.J. & Cauberg, J.J.M. 2007, 'Analytical Models for Calculating Thermal Bridge Effects Caused by Thin High Barrier Envelopes around Vacuum Insulation Panels', J*ournal of Building Physics*, 30 (3), 2007, pp. 185-215.

Thorsell, T. 2006, '*Vacuum insulation in buildings, means to prolong service life*', Licentiate thesis, Kungliga Tekniska Högskolan, Stockholm, 2006.

Thorsell, T. and Källebrink, I. 2005, 'Edge loss minimization in vacuum insulation panels', Proceedings of the 7th Symposium on Building Physics in the Nordic Countries, The Icelandic Building Research Institute, Reykjavik, 13-15 June 2005, pp. 945-52.

Vip-bau.de. 2010, http://www.vip-bau.de/e_pages/technology/vip/howtheywork.htm (Accessed 21/09/2010).

XII DBMC
International Conference on Durability of Building Materials and Components
PORTO - PORTUGAL, April 12th-15th, 2011

FMEA Software for Building Products

Manuel Bazzana [1]
Julien Hans [2]
Gérard Sauce [3]

ABSTRACT

Risk analysis, and particularly Failure Mode and Effect Analysis (FMEA), has proved to be an interesting approach for durability assessment of building products. On the one hand FMEA allows identification of the potential failure modes of a product; on the other hand this method is known to be difficult to carry out, especially in the building and construction context. This paper describes the second version of a software developed by CSTB to support FMEA of building products with emphasis on automation and knowledge sharing. The purpose of the tool is to help product experts to lead FMEA on building products using information from previous cases. It relies on an ad hoc product model based upon functional modelling. This model, through fine-grained descriptions of structure and functions, allows representing faulty as well as normal behaviour of products based on a common set of functions and environmental agents. Functional and structural descriptions of products and product's components are made reusable. Cases studies have been conducted in order to assess both model and tool capacity to represent the wide range of building products and degradations phenomenon as well as the tool main functionalities.

KEYWORDS

Durability, FMEA, Product model.

[1] Centre Scientifique et Technique du Bâtiment, Grenoble, FRANCE, manuel.bazzana@cstb.fr
[2] Centre Scientifique et Technique du Bâtiment, Grenoble, FRANCE, julien.hans@cstb.fr
[3] Université de Savoie, Le Bourget-du-Lac, FRANCE, gerard.sauce@univ-savoie.fr

1 INTRODUCTION

Failure Mode and Effect Analysis (FMEA) is a reliability method that aims to identify the combination of events that might lead to the failure of a product or process. It is now widely used in the manufacturing industries and several quality related standards require FMEA to be conducted in different steps of a product's life cycle. Previous works have shown that this approach is of interest for the durability assessment of building systems [Talon, 2006]. According to Hans *et al.* [2007a], the fact that FMEA is based on knowledge at the material and component scale rather than knowledge at the product scale makes it usable for durability assessment of innovative products. However the common FMEA workflow shows several drawbacks that restrain its widespread use. Among the different drawbacks is often mentioned the fact that it is a time consuming task to complete. Furthermore, product experts involved in assessing durability usually do not tend to render explicit their knowledge on a products' failure modes, thus making the results derived from the implementation of FMEA difficult to reuse.

To date, several attempts to ease the use or even automate FMEA have been successfully completed in different product domains and even some have even been integrated into commercial tools [Bell *et al.* 2007]. Whereas, similar tools that have been developed for building components lack functionalities with respect to automation and knowledge sharing. The purpose of this work is to develop a product modelling framework to automate the FMEA process and that would serve as a basis for future software development.

2 BRIEF REVIEW

2.1 FMECA Automation

Most of the research related to FMEA automation has focused on developing tools and methods to help designers detect potential failure modes of and their effects on products. According to Bell *et al.* [2007] complete automation involves two main steps:

- Simulation of the system behaviour;
- Interpretation the simulation results.

Thus, identifying a proper modelling framework is the first step this work is focused on. Several modelling paradigms have been evaluated for FMEA automation. Even though reviewing these models may be beyond the scope of this paper, it is worth noting that several authors already indicated that qualitative models are suitable for FMEA [Struss, 2008] [Bell, 2006]. Among qualitative models, those derived from qualitative physics or functional modelling are usually preferred as they both allow product representation without numerical details. For example, in the field of building sciences, the use of a model based on qualitative physics for simulating degradation mechanisms has been addressed by Lair [2000]. From results it was apparent that developing a modelling framework based on qualitative physics and able to encompass a range of products, behaviours and degradation phenomena related to the building and construction field was not realistic. According to Teoh and Case [2004], in the field of functional modelling, a common approach is to see systems as a "black box" and their functions as relations between input and outputs of flows of material, energy and information. Function can be further broke down into sub-functions as shown in Figure 1.
Several sets of functions and flows already exist such as the "Functional Basis", which is a reconciliation of the main functions and flow sets used in conceptual design [Hirtz *et al.*, 2002]. The different types of flows and functions are usually organised as a classification of concepts by a supertype-subtype relationships (also known as parent-child relationships). For instance, in the case of flows, *liquid* is a subtype of material, *Energy* is a supertype of *thermal Energy* and *Mechanical energy* and so one. This type of classification of concepts is usually referred to as taxonomy.

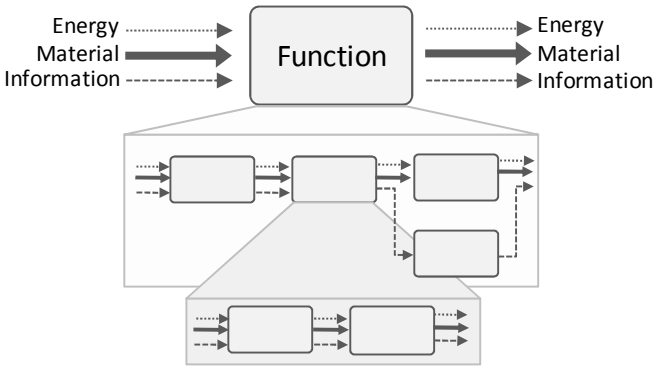

Figure 1. Relation between functions and sub-functions.

2.2 FMECA for Building Products

In literature is offered several approaches in which are presented guidelines for FMEA integration to the building sector as well as a number of related case studies [Talon *et al.*, 2006]. From a practical point of view Hans *et al.* [2007b] describe both method and results obtained from a common FMEA workflow involving products and FMEA experts on several building systems.

Talon *et al.* [2008] developed a prototype tool based on an ontological model that served as a basis for the development of software referred to as CPAO[1] (unpublished work). The objective of this work was to allow product experts to undertake a FMEA without the guidance of FMEA experts as well as permit a certain degree of reusability of knowledge derived in the process of conducting the FMEA. Cases studies revealed that the underlying product model could be further improved on several aspects including its capacity to take into account a wide range of products and degradation phenomena. This leads to the conclusion that a modelling framework based on more generic functional representation, as for example, the one described by Hirtz *et al.* [2002], could indeed be developed.

3 DEVELOPMENT OF A MODELLING FRAMEWORK

3.1 Main Concepts

The main purpose of this modelling framework is to derive the possible failure modes from a simple description of a product, failures modes being described in a generic fashion at the material and component scale. As pointed out before, a representation of the product behaviour is necessary. One particular aspects of our problem is that it should encompass a wide range of systems, behaviour and failure modes.

As a starting point this work used a modified version of the "Functional Basis" flow taxonomy as well as a limited set of functions to describe the product (see Fig. 2a). Our goal is not only to represent the functional structure, but also to detect potential degradation modes from a products' description. A common approach is to consider that most product degradations are caused to some extent by environmental agents, such as those described in ISO 6241 [ISO, 1984]. Each environmental agent has been classified into the proper class of the flow taxonomy (e.g. *water* as a subtype of *liquid*).

Products are modelled as network of interconnected components that represent physical parts of the system – some of them being in contact with sets of flows representing environmental constraints. Each component has a number of specific interfaces, called ports, through which it is brought into

[1] CPAO is a French acronym for "Computer Assisted Durable Design".

contact with another system's components (see Fig. 2b). Within a component, functions define the behaviour from one port to another with respect to flows. The flow and function formalism is designed to enable a simplified and qualitative description of a wide range of physical (e.g. mechanical, thermal, electrical) phenomena. Furthermore, components have additional properties, such as one or more constituent materials.

The system behaviour with respect to flows can be deduced from the behaviour of its components. A flow from outside the system will be processed by a succession of components based on their functions. Processing of all flows through a system can be seen as a *functional simulation*. As environmental agents are related to flows (e.g. *high temperature* is related to the flow type *thermal energy*) it is thus possible to compare component properties (e.g. constitutive materials) to the set of flows in contact with them in order to detect potential failure modes. Additional information regarding this approach can be found in [Bazzana *et al*, 2010].

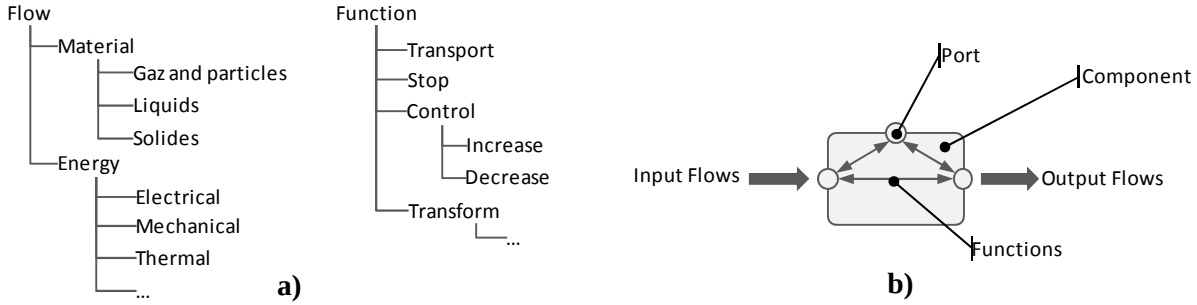

Figure 2. a) Extract from the functions and flows taxonomies and **b)** graphical representation of a component model.

3.2 Nominal and Faulty Behaviour of Products

The "correct" behaviour of a product model is assessed though flow propagation. This step may require modification of the model and of the set of flows involved in the propagation. The goal being to achieve a representation of the nominal behaviour of the system, i.e. the reference operating mode to which the effects of degradation will be compared.

The number of flows involved in a study may be important. Thus identifying those related to the product's main functions is necessary to ensure that critical failure modes will be easily identified. This can be simply done by marking the main functions of critical components. This is a way of identifying the main functions of a system and to alert a user if a change of the model behaviour with respect to the function occurs. It then remains to consider the evolution of the product model as a result of degradation modes. Three different types of degradation modes can be distinguished, according to their causes:

- Degradation caused by one or more flow types;
- Degradation caused by an incompatibility between constitutive materials of two adjacent components;
- Degradation caused by a process or design default described at a component or material scale.

The effects of degradation are expressed in terms of modification of a component's functions. In other words, when a degradation mode is applied to a component model, the new function replaces one or more of the component current functions.

The effects of degradation can then be reflected at the system level by propagating the flows according to the new function; the flow may then further spread into the system and eventually trigger new degradations.

3.3 State Graph and Fault Tree Construction

Degradation modes traditionally revealed by FMEA are usually presented as a spreadsheet or graphs, the latter making it easier to exploit results. In our approach, generic and specific failure modes are taken from a database and each applied failure mode modifies the system model. Furthermore, combinations of degradations are systematically taken into account, which is not usually the case when implementing traditional FMEA. This results in series of degradation sequences that can be seen as a state graph, nodes representing a system state and edges representing degradation modes. The first node represents the system in its nominal state and final nodes are either caused by degradations affecting a marked function or a steady state, i.e. failure modes derived from the available databases or user's knowledge can no longer be applied to the current product model. The construction of the state graph can be described by an algorithm, or more conveniently as a scheme (see Figure 3a).

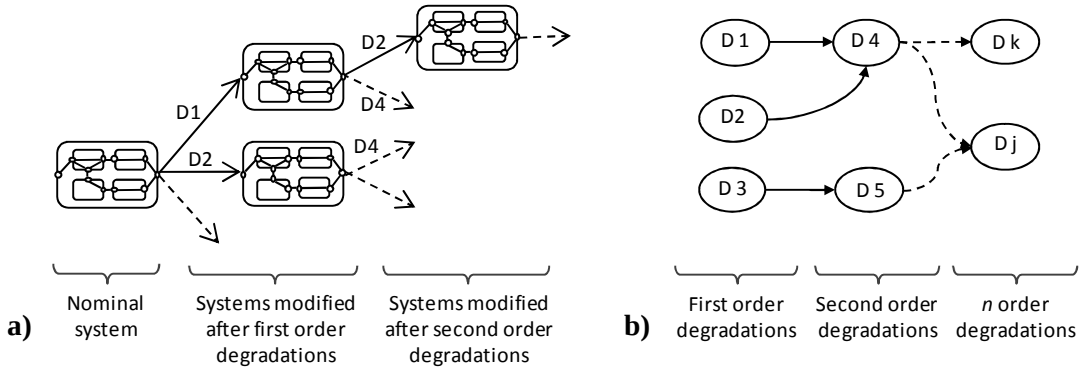

Figure 3. a) State graph and **b)** corresponding failure graph after criticality ranking.

State graphs represent an exhaustive representation of all combination of possible degradation modes. These should be further processed in order to highlight the most critical combination of events that affect the system (see Figure 3b). This process is usually carried out through criticality analysis. For building products, Talon [2006] and Lair [2000] have shown that temporal data of degradation modes (e.g. the duration of degradation phenomena or occurrence probability) play an important role in criticality ranking. It appears that exploitation of such an approach can only be achieved through the use of a computer tool. The prototype of such a tool has been developed and its functionalities are discussed in the next section.

4 PROTOTYPE TOOL

The primary modelling framework concepts have been implemented under Teexma®, a technical knowledge management platform [Teexma, 2010]. Functionalities of the resulting prototype are summarised in Figure 4. The databases within the prototype tool have been enriched with data taken from previous tools developed by CSTB [HANS *et al.* 2007a], as well as literature and literature [Offenstein, 1988] [Wright 2001] [Addleson & Rice, 1991] . To date, results are presented as text logs describing sequences of product model states and degradation phenomenon leading to them.

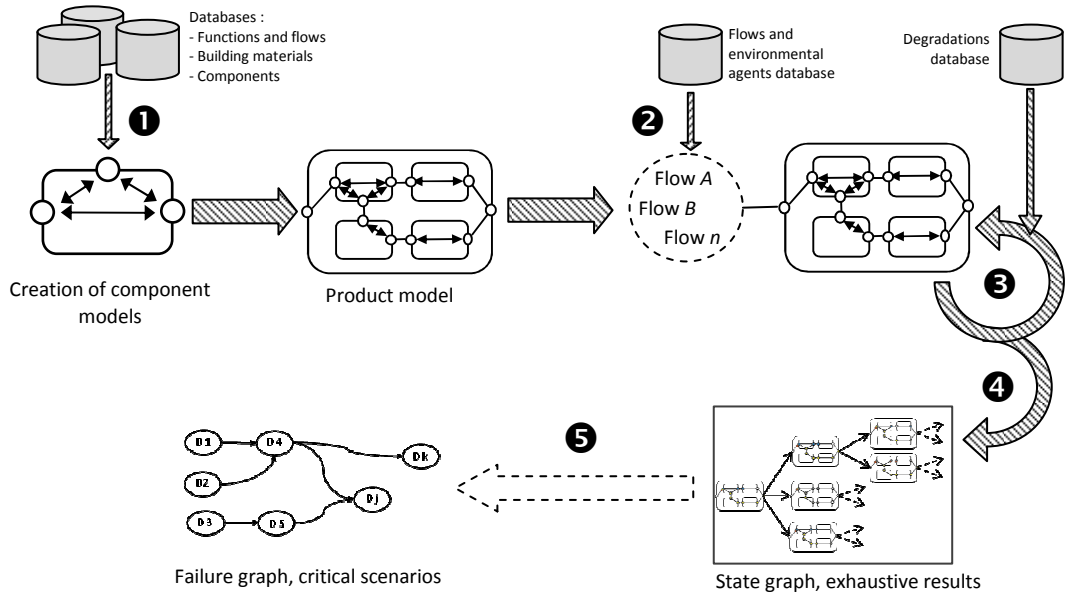

❶ Product modelling using existing knowledge: materials and components databases, functions and flows lists. Creation of new component models if needed.

❷ Description of environmental conditions as a set of flows (environmental agents).

❸ Automated search for relevant degradation types, modification of product model according to effects of degradation and flow propagation through the system.

This process is iterative and ends when labeled functions (main product functions) are affected by degradation types, or until no more degradation types are identified.

❹ Exhaustive results overview represented as a state graph: nodes represent system configurations and edges degradation phenomena.

❺ Most relevant results: Identification of critical degradation modes from the state graph and construction of a failure graph. *This step is not implemented yet.*

Figure 4. Current Prototype Tool (steps 1 to 4) and expected features (step 5).

5 CASE STUDIES AND INITIAL RESULTS

Case studies have been conducted in order to assess both the tool and the ability of the modelling framework to represent and simulate a product's nominal and faulty behaviour as well as suggest relevant failure modes from the degradation database. The very first step involved modelling a known product, namely a photovoltaic panel. Previous FMEA reports [HANS *et al.* 2007b] of this specific product served as a guideline for model description as well as benchmark for an analysis of the results. As well, a more systematic testing and evaluation procedure has been set up.

5.1 Product Modelling and Nominal Behaviour

The product has been modelled according to an existing FMEA report [HANS *et al.* 2007b] and the resulting structural decomposition has been implemented under the prototype tool (see Figure 5a). Each component model has then been further defined with respect to the function and flow taxonomies. Three environments, namely *external environment*, *fastening system* and *domestic electric network*, allow the representation of external constraints (model inputs flows) and system behaviour (model output flows).

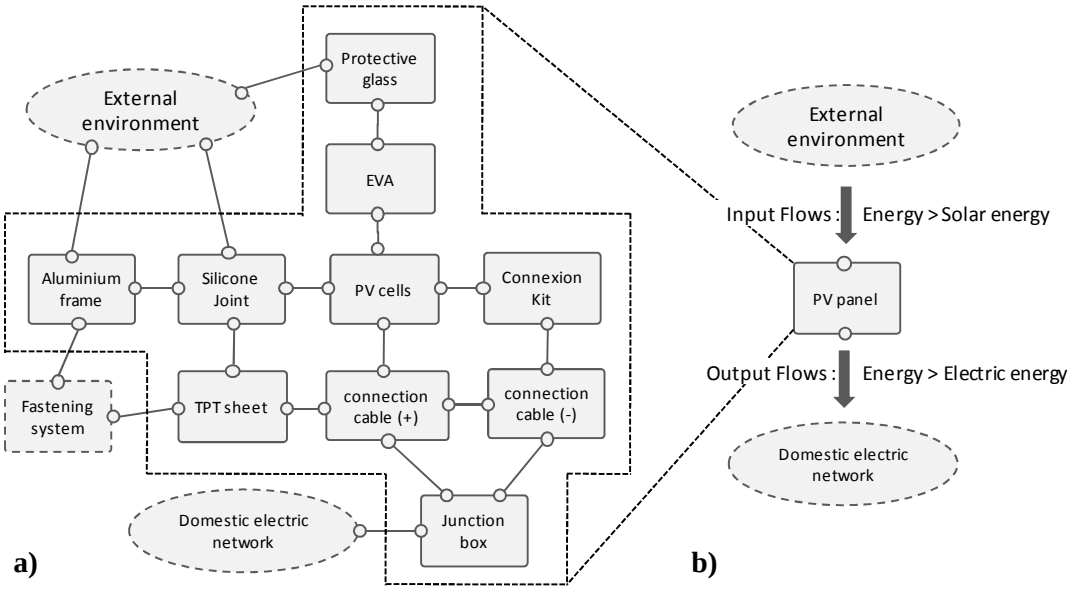

Figure 5. a) Simplified representation of a product model of a photovoltaic panel and **b)** representation of the expected behaviour of the entire product.

Flow propagations shown that the product model behaves according to expectations for most of the flow types, including *solar* and *electrical energy* which are related to the product's primary function as shown in Figure 5b. In some cases, however, results were inconsistent thus leading to a modification of the product model or revealing limitations of the modelling framework. These latter issues are briefly discussed in section 5.3.

5.2 Faulty Behaviour

The known failure modes of the photovoltaic component as well as the generic degradation modes (such as corrosion or photo-oxidation of polymers) have been implemented in the degradation database. Due to technical limitations, the study was discontinued after third order degradations were identified thus preventing the building of an exhaustive state graph. In this first step, thirty one distinct degradations modes have been identified, from mechanical deformation of the entire panel to process errors occurring during the fabrication process of the photovoltaic cells.

The model revealed that several of these degradations phenomena already affect main product functions, ether by limiting the flow of solar energy reaching the cell or by creating short circuits. In addition, several generic degradation modes related to constitutive materials of the product components are taken into account. The comparison of these results with the previous FMEA report [HANS *et al.* 2007b] also shows that the prototype automatically identified relevant degradation modes but sometimes fails to take their effects into account.

6 DISCUSSION AND CONCLUSIONS

A new functional modelling framework for FMEA of building products has been developed and has been implemented into a prototype software tool. An initial case study on a photovoltaic panel has shown that most of the relevant failure modes can be automatically identified using this tool as well as some of the failure mode combinations. As some of the degradation effects were not taken into account in a relevant way, the automatic construction of a state graph was only partially satisfactory.

This study also revealed some limitations that are inherent to the modelling framework. In some cases the function and flow formalism is limited with respect to the representation of some physical

phenomena, such as heat transfer or mechanical deformation. This is due to the qualitative nature of this formalism and the nature of studied systems. It does not necessarily prevent identifying relevant degradation modes but this particular aspect should be further explored. Further development is required in order to assess the impact of these limitations on the results. To date, the results are displayed as a state graph, in which an exhaustive representation of degradation combinations is provided. However the simplification of results as a failure tree remains to be done through the process of criticality ranking.

REFERENCES

Addleson, L. & Rice, C. 1991, 'Performance of Materials in Buildings: A Study of the Principles and Agencies of Change', First edition. Butterworth-Heinemann Ltd.

Bazzana, M., Sauce, G., Hans, J., Laé, L., & Mehl, C. 2010, 'Development of a product model for FMEA support of building products', Proc. CIB2010 Building a Better World Congress.

Bell, J. 2006, 'Interpretation of simulation for model-based design analysis of engineered systems', Thesis (PhD), University of Wales, Aberystwyth.

Bell, J., Snooke, N. & Price, C. 2007, 'A language for functional interpretation of model based simulation', *Advanced Engineering Informatics*, vol. 21.

Hans, J., Chorier, J., Morlot, R., Boddaert, S. Proisy B, & Boulanger, B. 2007b, 'Durabilité des équipements énergétiques et de composants d'enveloppe du bâtiment', CSTB – Internal report.

Hans, J., Joffre C., Boilève C. & Fies B., 2007a, 'FMEA Software to enhance innovation in building', Proc. of the 2007 CIB Construction Research Congress.

Hirtz, J., Stone, R.B., Mcadams, D.A., Szykman, S. & Wood, K.L., 2002 , 'A Functional Basis for Engineering Design: Reconciling and Evolving Previous Effort', *Research in Engineering Design*, Vol. 13, No. 2., pp. 65-82.

ISO – International Standard Organization, 1984, 'Performance standards in building. Principles for their preparation and factors to be considered', ISO 6241:1984.

Lair, J. 2000, 'Évaluation de la durabilité des systèmes constructifs du bâtiment', 2000. Thesis (PhD), University Blaise Pascal Clermont II.

Offenstein, F. 1988, 'Compatibles, incompatibles: ou comment associer les matériaux de construction', Edition du Moniteur. Paris.

Price, C.J. & Taylor, N.S. 2002, 'Automated multiple failure FMEA', in *Reliability Engineering & System Safety*, vol. 76. No. 1, pp. 1-10.

Struss, P. 2008, 'Model-based Problem Solving', in *Handbook of Knowledge Representation*, vol. 3, eds. van Harmelen, F., Vladimir Lifschitz, Bruce Porter, Elsevier p. 395-465.
Talon, A., 2006, 'Évaluation des scénarii de dégradation des produits de construction', Thesis (PhD), University Blaise Pascal Clermont II.

Talon, A., Boissier, D., Hans, J., Lacasse, M. A., Chorier, C., 2008, 'FMECA and management of building components', 11DBMC International Conference on Durability of Building Materials and Components Istanbul, Turkey.

Talon, A., Chevalier J.L., Hans J. 2006, 'Failure Modes Effects and Criticality Analysis Research for and Application to the Building Domain', Publication CIB n° 310. Working commission 80, 246 p.
Teexma® 2010, BASSETTI, [online] Software description available at <http://www.bassetti.fr/> last accessed on 01-31-2011.

Teoh, P.C. & Case, K. 2004, 'Modelling and reasoning for failure modes and effects analysis generation', Journal of Engineering Manufacture, vol. 218. No. 3., pp. 289-300.

Wright, D. 2001, 'Failure of plastics and rubber products: causes, effects, and case studies involving degradation'. Ed. William Andrew, 416p.

XII DBMC
International Conference on Durability of Building Materials and Components
PORTO - PORTUGAL, April 12th-15th, 2011

Building Maintenance Activity Supported in Virtual Interactive Models: Façades and Interior Walls

Alcínia Zita Sampaio [1]
Augusto M. Gomes [2]
Ana Rita Gomes [3]
Daniel P. Rosário [4]

ABSTRACT

A Virtual Reality model was created in order to help in the maintenance of exterior closures and interior finishes of walls in a building. It allows the visual and interactive transmission of information related to the physical behaviour of the elements, defined as a function of the time variable. To this end, the basic knowledge of material most often used in walls, anomaly surveillance, techniques of rehabilitation, and inspection planning were studied. This information was included in a database that supports the periodic inspection needed in a program of preventive maintenance. The results are obtained interactively and visualized in the virtual environment itself. This work brings an innovative contribution to the field of maintenance supported by emergent technology.

KEYWORDS

Construction, Maintenance, Cooperative visualization, Virtual reality, Decision-making.

[1] TU Lisbon, Dep. Civil Engineering and Architecture, Lisbon, PORTUGAL, zita@civil.ist.utl.pt
[2] TU Lisbon, Dep. Civil Engineering and Architecture, Lisbon, PORTUGAL, agomes@civil.ist.utl.pt
[3] TU Lisbon, Dep. Civil Engineering and Architecture, Lisbon, PORTUGAL, ritagomes05@hotmail.com
[4] TU Lisbon, Dep. Civil Engineering and Architecture, Lisbon, PORTUGAL, derosario@gmail.com

1 INTRODUCTION

The main aim of a research project, now in progress at the Department of Civil Engineering of the Technical University of Lisbon, is to develop virtual models as tools to support decision-making in the planning of **construction management** and **maintenance**. A first prototype concerning the lighting system has already been completed [Sampaio et al., 2009]. A second prototype concerning the maintenance of the closure of walls, both interior walls and façades, is now being developed. This paper describes this part of the project.

The interactive model integrates **Virtual Reality** (VR) technology, the EON system [EON, 2010], and an application implemented in Visual Basic (VB) language. The model allows interaction with the 3D geometric model of a building, visualizing components for each construction. It is linked to a database of the corresponding technical information concerned with the maintenance of the materials used as exterior closures and interior finishes. The principal objective of the interactive VR prototype is to support decision-making in the maintenance domain.

The present project aims to bring important contributions to this domain, through the implementation of virtual models able to relate the behaviour of materials, their characteristics, anomalies and repair work to each other. During this work the basic knowledge of the topics involved, such as aspects related to the materials, the techniques of rehabilitation and conservation and the planning of maintenance is outlined and discussed. In addition, methods of interconnecting this knowledge with the virtual model are explored.

The prototype for walls was trialled in a concrete project. This kind of building element has a continuous degradation, so requires the study of preventive maintenance (the planning of periodic local inspections) and of corrective maintenance with repair activity analysis. The model facilitates the visual and interactive access to results, supporting the definition of inspection reports. It will be possible in the future to apply this to other building situations whether in new constructions or those needing rehabilitation.

2 INTERACTIVE AND COLLABORATIVE MODELS

Virtual Reality technology can support the management of data that is normally generated and transformed or replaced throughout the lifecycle of a building. This technology becomes an important support in the management of buildings allowing interaction and data visualization. At present, the management of building planning can be presented in a 3D form and various materials can be assigned to the fixtures and furnishing enabling the user to be placed in the virtual building and view it from inside as well as outside. This study contemplates the incorporation of the 4th dimension, that is, time, into the concept of visualization. The focus of the work is on travelling through time: the ability to view a product or its components at different points in time throughout their life. It is envisaged that the incorporation of the time dimension into 3D visualization will enable the designer/user to make more objective decisions about the choice of the constituent components of the building. In maintenance the time variable is related to the progressive deterioration of the materials throughout the building's lifecycle.

The present prototype incorporates interactive techniques and input devices to perform visual exploration tasks. To support this system a database was created which included a bibliographic research support made in regard to the closure materials used in the interior and exterior walls of a building, anomalies concerning different kinds of covering material, and corrective maintenance. Repair activities were also studied. The programming skills of those involved in the project had to be enhanced so that they could achieve the integration of the different kinds of databases needed in the creation of the interactive model.

The 3D model linked to a database concerning maintenance produces a collaborative virtual environment, that is, one that can be manipulated by partners interested in creating, transforming and analyzing data in order to obtain results and to make decisions. For example, inspection reports can be defined and consulted by different collaborators. The process of developing the prototype interface considers these purposes. The developed prototype associates the characteristics of the coating component of the **exterior** and **interior walls** to activities concerning the maintenance of buildings (Fig. 1).

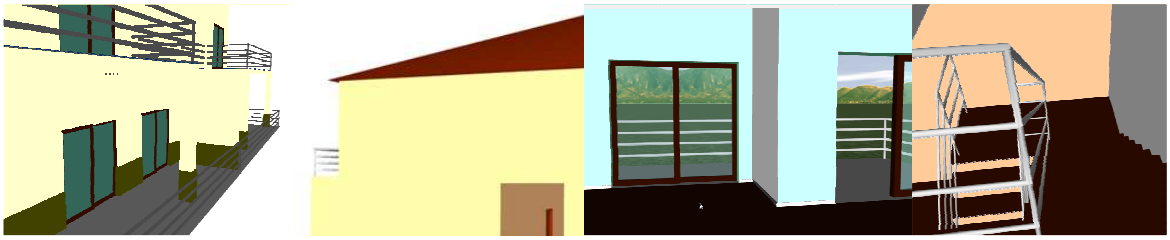

Figure 1. 3D model of the house: coating elements of exterior and interior walls.

3 WALL MAINTENANCE PROTOTYPE

Façade coatings play an important role in the durability of buildings, since they constitute the exterior layer that ensures the protection of the wall against the aggressive actions of physical, chemical or biological nature. Naturally, they should also give the façade the required decorative effect. Since this building component is exposed to bad atmospheric conditions it frequently shows an evident degree of deterioration, requiring maintenance interventions. It is recommended that prior to performing maintenance activities, a survey of failures in the building should be conducted in order to arrive at the best solution for repair and maintenance.

In order to better understand the operation of façade coating, bibliographic research of materials usually applied to façade coatings was carried out and a table of characteristics of these was drawn up. Subsequently, a survey was made of anomalies, probable causes, solutions and methods of repair for each of the coatings studied.

The visualization of the maintenance data of a building and the impact of time on the performance of these **exterior closure** materials require an understanding of their characteristics [Gomes and Pinto 2009]:

- **Types** of material: painted surfaces, natural stone panels and ceramic wall tiles;
- **Application processes**: stones (panel, support devices, adherent products, …); ceramic tiles (fixing mechanism, procedures, …); painted surfaces (types of paint products, prime and paint scheme surface, exterior emulsion paints, application processes);
- **Anomalies**: dust and dirt, lasting lotus leaf effect, covering power, insufficient resistance to air permeability or weatherproof isolation, damaged stones or ceramic tiles, alkali and smear effect, efflorescence, fractures and fissures;
- **Repair** works: surface cleaning, wire truss reinforcing, cleaning and pointing of stonework joints, removing and replacement of ceramic wall tiles, removing damaged paint and paint surface, preparing and refinishing stone panels.

3.1 Characteristics of the Materials Used in Façades

Depending on the role that the façade coatings play on the wall as a whole they can be classified as finishing, sealing or thermal insulation. The most frequent materials used as coating finishes are paint, tiling and sealed coating of the natural stone (Fig. 2):

- **Paint** coating contributes to the aesthetic quality of the building and its environment and also protects the surface of the exterior wall against corrosion, deterioration and penetration of aggressive agents [Lopes 2008]. In order to obtain a good performance as an exterior coating, several aspects must be considered, such as covering opacity degree and resistance to water, sunlight, chemical products and to the development of micro organisms;

- The ceramic coating consists essentially of **tiling panels**, cement and adhesive and the joints between the slabs. The application of ceramic tiling to building façades has considerable advantages particularly as some degree of waterproofing is afforded by the glazed surface along with a great resistance to acids, alkalis and vapour. Other advantages are that it does not need painting and that it can be easily applied or substituted during repair work [Ferreira et al. 2009];

- The use of **natural stone** in the coating of façade surfaces is a good solution both technically and aesthetically. The stone coating is composed of slabs of stone attached to the wall by a support system. The principal characteristics of the stones are: reduced water absorption, sufficient mechanical resistance to bending and impact, abrasion and shearing parallel to the face of the slabs [Veiga and Malanho 2009].



Figure 2. Different types of materials applied as façade coatings.

3.2 The Database

The most frequent anomalies that occur in the coated façades were analysed in order to create a database linked to the virtual model that could support planning of inspections and maintenance strategies in buildings. The database contains the identification of anomalies that can be found in each type of material used in façades and the corresponding probable cause. For each kind of anomaly the most adequate repair solutions are also selected and included in the database. The following example concerning deficiencies in tiles presents the methodology implemented in this virtual application (Table 1).

The characteristics related to anomalies, causes, repair solutions and rehabilitation tasks were included in a database of each type of material and linked to the 3D model of the building. Thus, the virtual model gives users the ability to transmit, visually and interactively, information related to the closure properties of exterior walls, allows them to analyse the anomalies observed in an inspection of the real building and to predict the corresponding repair work. The 3D virtual model can be seen, therefore, as an important tool for **anomaly surveillance** in structures and for supporting decision-making based on the visual analysis of alternative repair solutions.

Table 1. Example of anomalies and the associated repair solution.

Anomaly	Specification of the anomaly	Repair solution	Repair methodology
Detachment 	Fall in areas with deterioration of support	Replacement of the coat (with use of a repair stand as necessary)	1º Removal of the tiles by cutting grinder with the aid of a hammer and chisel; 2º Timely repair of the support in areas where the detachment includes material constituent with it; 3º Digitizing layer of settlement; 4º Re-settlement layer and the tiles.
Cracking / Fracturing 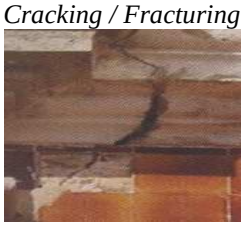	Failure of the support (wide cracks with well defined orientation)	Replacement of the coat (with repair of cracks in the support)	1º Removal of the tiles by cutting grinder; 2º Removal of material adjustment in the environment and along the joint; 3º Repair of cracks, clogging with adhesive material (mastic); 4º Settlement layer made with cement in two layers interspersed with glass fibre; 5º Re-settlement layer and the tiles.

3.3 The Interface

The implementation of the prototype system makes use of graphical software programming, *Visual Basic 6.0 Microsoft*, software to establish an adequate database, *Microsoft Office Access*, graphical drawing system, *AutoCAD Autodesk* and VR technology based software, *EON Studio*.

Human perception and cognitive capabilities were taken into account when designing this visualization tool so the model is easy to use and does not require sophisticated computer skills: many potential users are not computer experts. It uses an interactive 3D visualization system based on the selection of elements directly within the virtual 3D world. Furthermore, associated with each component, there are integrated databases, allowing the consultation of the required data at any point in time. The interface is composed of a display window allowing users to interact with the virtual model, and a set of buttons for inputting data and displaying results (Fig. 3). For each new building to be monitored the characteristics of the environment (exposure to rain and sea) and the identification of each element of the façades must be defined. The data associated to each element are the building orientation, the type of exterior wall (double or single), and the area and type of coating.

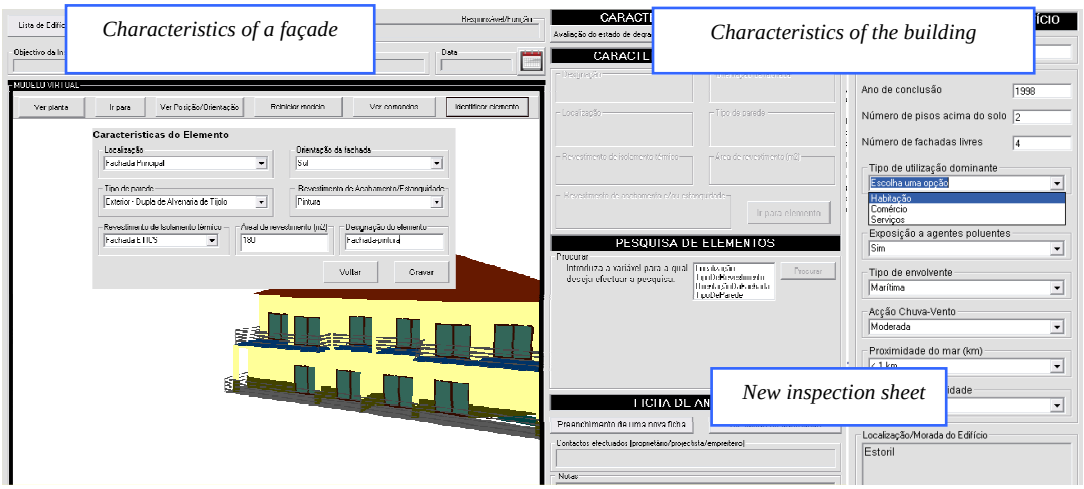

Figure 3. The main interface of the interactive application.

Once each monitored element has been characterized, several inspection reports can be defined and recorded and thereafter consulted when needed. An inspection sheet is accessed by the main interface (Fig. 4). Using the drop-down menus of the interface, the user can associate the characteristics of the observed anomaly to: a façade element; the type of anomaly, the specification, details and the probable cause of the anomaly, an adequate repair solution and pictures taken in the building. After completing all fields relating to an anomaly, the user can present the report as a *pdf* file.

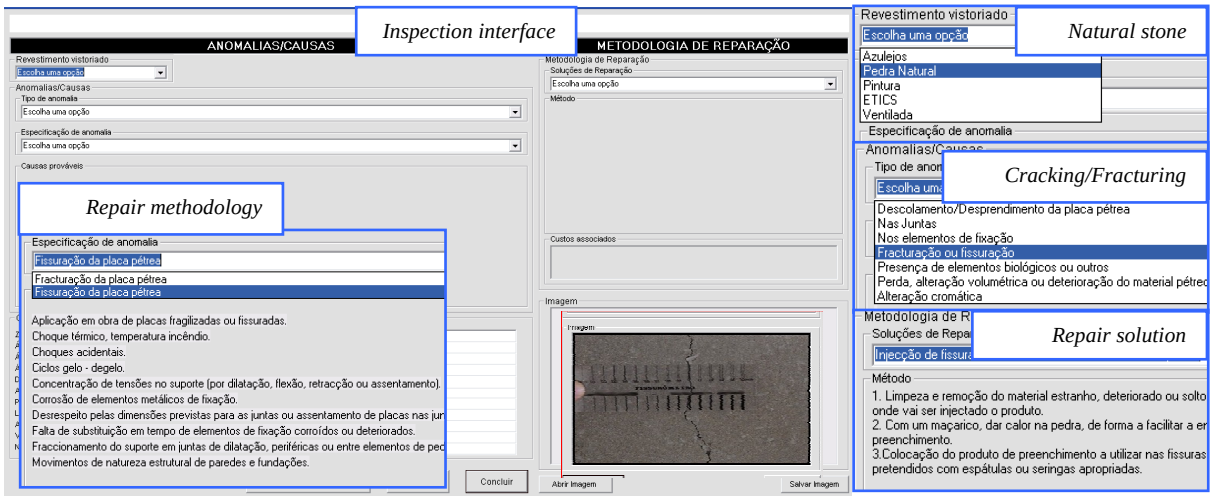

Figure 4. Inspection sheet interface.

3.4 The Case Study

First, the 3D geometric model of a building case was created (Fig. 5). The building consists of a ground-floor, a 1st floor and an attic with dwelling space shown. The coating elements of the walls were then modelled as independent geometric objects. In this way, each element can then support characterization data of the applied material and different kinds of information related to maintenance.

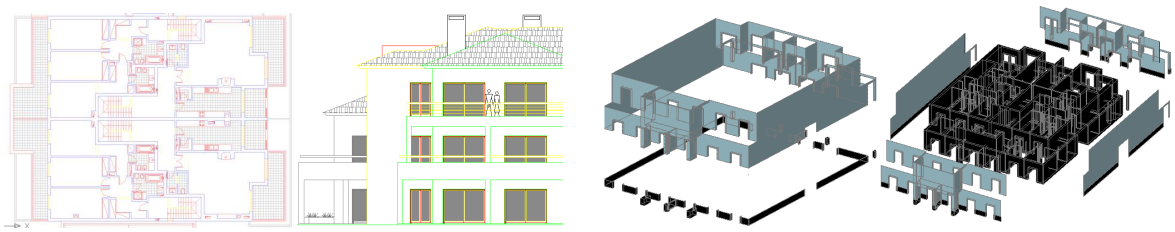

Figure 5. Steps of the geometric modelling process.

All coatings studied were considered in this case-study. Thus it was assumed that the main façade is covered with tile and the remaining façades are painted while hall façades are of natural stone. Figure 6 shows how to identify a façade in the virtual model of the building. The figure also includes the inspection report of a anomaly considered in a façade. The developed software is easy to handle and transport for on- site inspections and comprises information of the causes, solutions and methods for repairing.

4 THE INTERIOR WALLS

An identical analysis of the characteristics, anomalies and repair works concerning the **interior** finish materials was carried out. With this information a database was created. Another inspection interface was defined for the painted surfaces of interior walls, also associated to repair solutions and corresponding methodologies of rehabilitation (Fig. 7).



Figure 6. Identification of a façade element and an inspection sheet report.

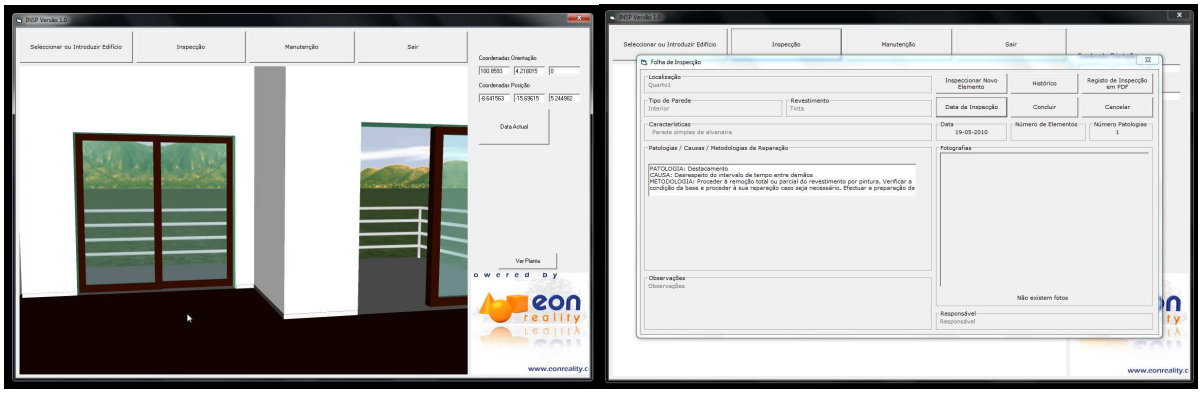

Figure 7. Painted coating of interior walls of the building and the inspection interface.

In addition the model identifies the period of time between the application of new paint and the predicted time when the next paint will be needed. The **colour changes** between white (new) and red (when an area needs to be painted again).

The data of periodic on-site inspections included in preventive maintenance is taken into account for each monitored element of the interior wall. Thus, when the date of interaction with the prototype is compared with the date predicted for the new paint application, the correspondent RGB (red, green and blue) values are calculated. Different RGB values generate different colour, using this virtual model. Therefore, by using data visualization supported by this VR technology, it is possible to estimate if the wall needs painting immediately or not (Fig. 8).

4 CONCLUSIONS

A VR model to support the maintenance of walls in a building was developed within a research project. It enables the visual and interactive transmission of information related to the physical behaviour of the elements, defined as functions of time. The model shows the characteristics of each element of the building in the model and the information related to inspection, anomalies and repair works. As the 3D model is linked to a database in an interactive environment and has a friendly interface to deal with this knowledge, it allows a collaborative system. The work is still in progress. With this application the user may fully interact with the program referring to the virtual model at any stage of the maintenance process and analyse the best solution for repair work. It can also support the planning of maintenance strategies.

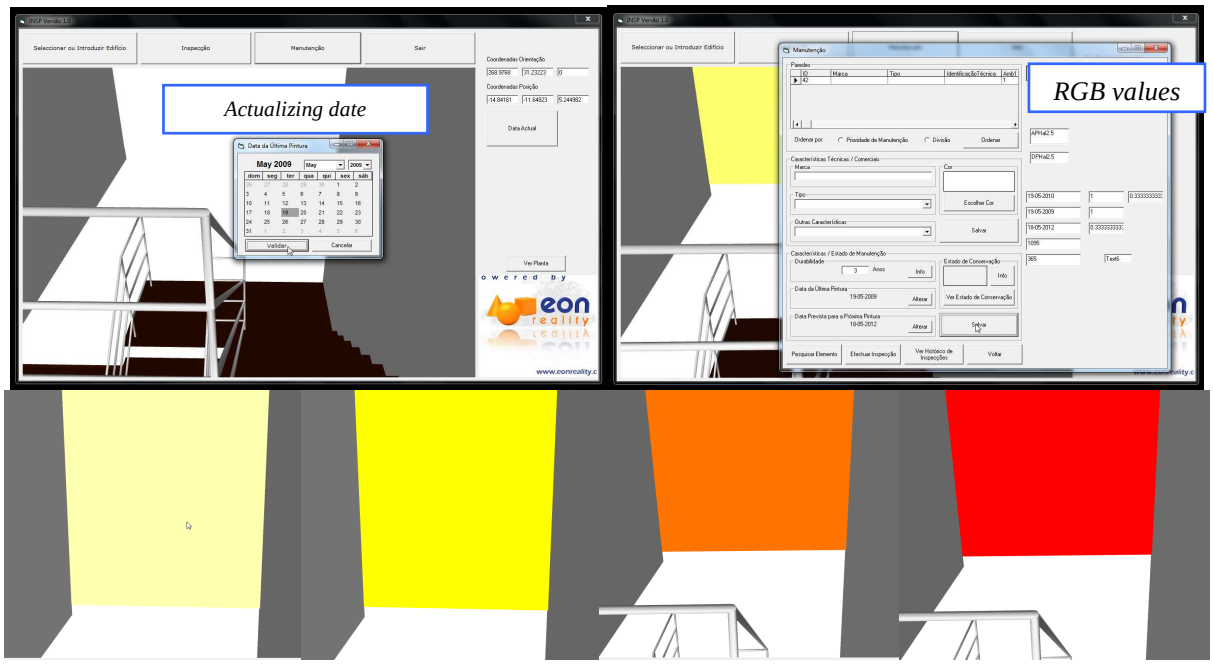

Figure 8. Changing colours related to the maintenance of the painted interior wall.

ACKNOWLEDGMENTS

The authors gratefully acknowledge the financial support of the Foundation for Science and Technology, a Governmental Organization for the research project PTDC/ ECM/67748/ 2006, now in progress.

REFERENCES

Ferreira, L., Coroado, J., Freitas, V. & Maguregui, I., 2009 'Causas da queda de azulejos aplicados em exteriores de edifícios: Azulejaria de padrão em edifícios de 1850-1920', Conf. Patorreb, 3º Encontro sobre Patologia e Reabilitação de Edifícios, FEUP, Porto, Portugal, March 18 - 20.

Gomes, A.M. & Pinto, A.P. 2009 'Didactic text of construction materials', Technical University of Lisbon, IST, Lisbon, Portugal, 2009.

Gomes, A.R. 2010 'Virtual Reality technology applied to the maintenance of façades', Integrated Master Degree Thesis in Construction, TU Lisbon, Portugal.

Introduction to working in EON Studio. EON Reality, Inc. http://www.eonreality.com/ [Accessed May 03, 2010].

Lopes, C. 2008 'Anomalias da cor em revestimentos por pintura em paredes exteriores'. Master Degree Thesis in Cosntrction Civil Engineering, TU Lisbon, Portugal de Mestrado em Construção, IST, Lisboa, Julho de 2008.

Sampaio, A.Z., Ferreira, M.M. & Rosário, D.P. 2009 'Interactive virtual application on building maintenance: The lighting component', Proc. IRF2009, 3rd International Conference on Integrity, Reliability and Failure: Challenges and Opportunities, Symposium Visualization and human-Computer Interaction, Porto, Portugal, July 20-24, abstract pp. 221-222, paper 11 pgs.

Veiga, M. & Malanho, S., 2009 'Revestimentos de pedra natural: Metodologia de diagnóstico e reparação de anomalias'. Conf. Patorreb, 3º Encontro sobre Patologia e Reabilitação de Edifícios, FEUP, Porto, Portugal, March 18 - 20.

XII DBMC
International Conference on Durability of Building Materials and Components
PORTO - PORTUGAL, April 12th-15th, 2011

From Building Pathology to Durability Via GIS

Ekaterini T. Delegou [1]
Ekaterini Sandri [2]
John Marakakis [3]
John Sayas [4]
Antonia Moropoulou [5]

ABSTRACT

In this paper, it is demonstrated how GIS modeling and analysis operations can be used as a methodological tool for the representation of building pathology, and in parallel for the control of building materials durability. GIS thematic maps were developed presenting the façade of the historic building of National Archaeological Museum in Athens Greece, and a marble surface of the historic building, where the representative decay pattern of black-grey crust existed and pilot conservation interventions took place. Attribute databases consisting of data of physical-chemical characteristics were elaborated and linked with the internal database of the specially designed GIS decay/conservation mapping/conservation planning projects. After the application of the pilot conservation interventions and since the attribute database is enriched by the new evidence regarding the assessment of the critical performance characteristics of the conservation interventions, and utilizing the GIS geoprocessing procedure, scientists have the opportunity of monitoring the preservation state of the investigated surface, and building material durability. Thus, the use of a GIS platform can create an information-decision management system where datasets concerning building pathology and conservation interventions are recorded, correlated, distributed and attributed to space, during different time periods, contributing decisively to durability control of building materials and strategic planning of periodical conservation interventions.

KEYWORDS

GIS, Relational database, Building pathology, Durability.

[1] School of Chemical Engineering, National Technical University of Athens (NTUA), Athens, Greece, edelegou@central.ntua.gr
[2] School of Chemical Engineering, National Technical University of Athens, (NTUA), Athens, Greece, ksandris@hotmail.com
[3] School of Rural and Surveying Engineering, National Technical University of Athens, (NTUA), Athens, Greece, imarak@eranet.gr
[4] School of Rural and Surveying Engineering, National Technical University of Athens, (NTUA), Athens, Greece, isayas@central.ntua.gr
[5] School of Chemical Engineering, National Technical University of Athens (NTUA), Athens, Greece, amoropul@central.ntua.gr

1 INTRODUCTION

The classification and representation of monuments pathology aims to control the decay progress and to improve planning of conservation interventions. This can be accomplished through the recording and presentation of building materials, developed decay patterns and their extent, on architectural drawings [Fitzner *et al.* 1992]. The use of electronic means and their special tools can achieve, in a modern and effective way, control of building pathology and its life cycle, cost analysis, pointing towards building protection through prediction and prevention [Warke *et al.* 2003]. Therefore, GIS modeling and analysis operations are frequently used for the above mentioned purposes, due to their special capabilities regarding the processing of different background data which incorporate spatial and attribute (descriptive) data sets. Thus, within the framework of building pathology representation and building preservation, several scientific projects have investigated GIS potential i.e. Salonia & Negri [2002]; Inkpen *et al.* [2001].

In the present work, GIS is utilized for developing decay/pilot conservation interventions/conservation planning thematic maps for a representative investigation of the marble surface on the western façade of the historic building of National Archaeological Museum, Athens, Greece (Figs. 1a and 1b). Decay diagnosis and pilot conservation intervention results along with GIS capabilities of recording, rouping, managing and analysing large volumes of spatially referenced data, were used for the elaboration of data-bases and spatial data transformation and spatial analysis. The aim of this work was the development of a methodology planning for monitoring the durability control of the marble surfaces of the building studied.

The historic building of National Archaeological Museum (NAM) is located in Athens centre, a city of polluted urban atmosphere. Its construction started in 1866 based on the drawings of the German architect Ludwig Lange, and ended in 1889 under the supervision of another German architect, Ernest Ziller, who made major modifications to Lange's initial drawings. National Archaeological Museum western façade consists of several types of plasters and pentelic marble surfaces. Due to its historic and architectural importance, this building is a high priority for strategic planning of periodical conservation interventions.



Figure 1. (a) The Historic building of National Archaeological Museum and (b) the representative investigation area of capital.

2 RESULTS & DISCUSSION

2.1 Methodological Approach

In order to perform characterisation of building materials and decay diagnosis, non destructive testing and evaluation (NDT & E) techniques in situ, and analytical ones in lab after sampling, are applied on representative investigation areas which are selected, during building inspection. This procedure constitutes the first part of the diagnosis protocol as presented by Moropoulou *et al.* [2005]. The proposed protocol concluded to building pathology representation through materials and decay mapping using GIS (Fig. 2), as well as incorporating data of structural analysis, architectural study, and geometric documentation.

The demands of sustainability for rational use of resources, brings to the foreground the urgent need of building materials durability control and buildings' life-cycle assessments (LCA). Several difficulties arise with monitoring of buildings, like different methodological approaches usually derived for different materials and components, different building uses, extended periods of LCA, different state priorities, lack of funds, etc. Therefore, the use of GIS, as a methodological and analysis tool, for monitoring selected representative surfaces where decay diagnosis and pilot conservation interventions take place, is proposed. In simple words, rather than monitoring a whole building, better economy of scale, management and durability control can be accomplished if carefully selected representative areas of the investigated building are periodically examined, whereby examination results are incorporated into a GIS platform. This will facilitate and possibly optimize the targeted and early evaluation of decay process, identifying and understanding decay mechanisms, in a rather focused scale in the field; aiding, in parallel, integrated assessment of pilot conservation interventions, in terms of real incorporation of durability criterion. Even though exclusively laboratory-derived measures of durability, like accelerating ageing tests, can not and must not be underestimated, the suggested GIS-based methodology (Fig. 3) is a tool for durability control in different building scales, which in addition can embody (through relational database elaboration) lab results of different studies, during different time periods. Thorough decay mapping and monitoring of selected representative surfaces, will assist in developing a robust plan for monitoring of building material durability and building life-cycle assessment. The above analysis does not diminish the importance and the usefulness of building pathology representation via GIS and durability control potential of an investigated building as a whole; it actually acts complementary and it enhances several issues concerning better time and fund management, permitting different approaches for the in-field investigation which depend on working-scale selection.

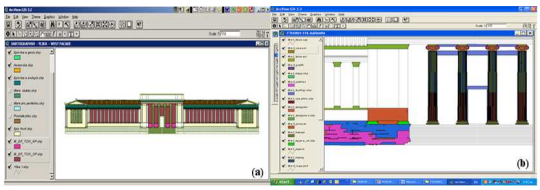

Figure 2. (a) Thematic map of building materials for NAM façade, (b) decay thematic map for marble surfaces on NAM façade.

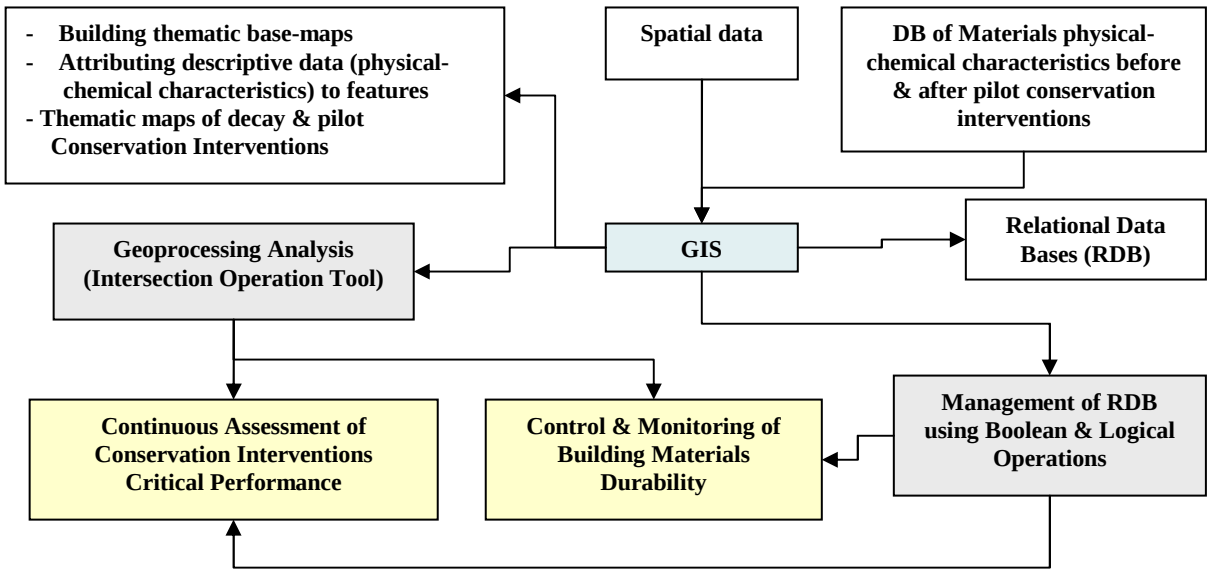

Figure 3. Methodological approach.

Within the context of the above methodological approach, four representative marble surfaces of the NAM, in addition to those in the thematic maps of Fig. 2, were selected to act as GIS pilot projects for

durability control and monitoring, one of which is hereby presented. In neoclassical buildings like NAM, marble is used as facings or load-bearing structures, presenting smooth or relief finishes. Marble surfaces are of high priority regarding strategic planning of periodical conservation interventions, since even partially reconstruction is out of question and sampling is rather limited not to say restricted. Therefore, the representative marble surface of the capital was selected due to its high artistic value as a sculptured surface and the arising challenges on conservation issues for the preservation of relief surfaces.

The capital under investigation is located on the first (from North) column of the propylon, has an eastern orientation, and is totally protected from rain-wash. During building inspection, it was observed macroscopically that the capital surface presented the characteristic decay pattern of black-grey crusts: gypsum ($CaSO_4 \cdot 2H_2O$) produced by sulphur dioxide (SO_2) attack to marble calcite ($CaCO_3$), along with black particles, soot, iron oxides, and alumino-silicates [Moropoulou *et al.* 2008].

The GIS thematic maps of the capital marble surface were elaborated in ArcMap/ArcInfo 9.2, using the CAD architectural drawing of the capital as the blueprint for the GIS base-map development.

In parallel, during diagnostic study, NDT&E techniques were applied in situ, whereas analytical and NDT&E techniques were used in lab after sampling, resulting in decay diagnosis for the investigated surface. The NDT&E techniques applied in situ were fibre optics microscopy and colorimetry; whereas the analytical techniques used in lab after sampling were optical microscopy (OM) and scanning electron microscopy with energy dispersion by X-ray analysis (SEM-EDS). The NDT&E techniques used in lab in the selected samples were the laser profilometry (LP) and the digital image processing (DIP) of SEM images.

Decay diagnosis results confirmed the presence of black-grey crust that was observed macroscopically, as well as the historic evidence that the building material of the capital is pentelic marble. The pilot conservation interventions that were applied consisted of different cleaning methods like AB57 poultice, poultice of ion exchange resin with deionized water, ion exchange resin with 10% w/v $(NH_4)_2CO_3$ solution, and a wet micro-blasting method of spherical calcium carbonate particles with diameter less than 100μm. After the pilot cleaning applications and during the study of pilot conservation interventions assessment, the same NDT&E and analytical techniques took place in situ and in lab after sampling. More information on the techniques used as well as on the cleaning assessment criteria for marble surfaces presenting black-grey crusts can be found in Moropoulou *et al.* [2008].

Assessment of the cleaning interventions focused on the sustained performance of the cleaned surfaces relative to chemical and mineralogical composition, texture roughness, fracturing and colour. Therefore, SEM-EDS was used to assess the chemical and mineralogical composition of the cleaned surfaces, LP was used for the texture roughness assessment, Digital Image Processing (DIP) of SEM images is utilized for the measurement of surface fracturing and colorimetry evaluates colour modifications of the cleaned surfaces.

These physical-chemical characteristics are describing the preservation state of the building material before cleaning, whereas their modification after cleaning, indicate the chemical, microstructural and aesthetical transformation of the investigated surface, depending though on the applied pilot cleaning intervention. These data are considered to be the monitoring indexes for durability control of the investigated marble surface and their modification through time will demonstrate decay processing, achieving integrated assessment of the different cleaning methods in a focused scale in the field. These monitoring indexes of the investigated sculptured surface are representative and corresponding to the ones that the other three capital surfaces of eastern orientation in NAM propylon would have presented if decay diagnosis and pilot conservation interventions had been performed on them. Thus, strategic planning of periodical conservation interventions on sculptured marble surfaces, incorporating durability, can be successfully accomplished.

Decay and cleaning interventions data, comprised the attribute data sets which describe the corresponding thematic maps features. Moreover, physical-chemical data derived by the above mentioned techniques, before and after pilot conservation interventions, were used for building the relational data-bases, in order to store the attribute data of each thematic map feature.

2.2 Development of Decay – Pilot Conservation Interventions Thematic Maps and Databases

Decay and pilot conservation interventions data comprised the attribute data sets which describe the characteristics of the recorded spatial entities of the investigated surface. Therefore, ascribing the decay and conservation intervention results of the physical-chemical study to the features of the GIS base map, during building topology, led to the development of the thematic maps of decay and pilot conservation interventions (Figs. 4 and 5). During spatial data input in ArcMap/ArcInfo, the process of topology building is of high importance. Topology building, in addition to building spatial relationships among features which configure a layer, is directly related to the recording and storing of the corresponding attribute data sets that describe real world entities or conditions [Padmanabhan *et al.* 2002].

In decay thematic mapping each layer was classified and recorded according to its spatial properties and physical-chemical characteristics, before cleaning treatments. The sculptured surface of anthemia present front and side relief surfaces for which decay diagnosis results had indicated different physical-chemical characteristics like gypsum layer width, roughness, surface area, fracture density, etc. Therefore, two different layers were elaborated, one for each relief surface (front and side), which were displayed by different colours, light and dark brown respectively (Fig. 4).

Furthermore, accordingly to the decay thematic map, two different layers were elaborated in the pilot conservation interventions thematic map, one for each relief surface (front and side), whereas the areas of the pilot applications of the different cleaning methods were elaborated as features and displayed by different colours (Fig. 5).

Moreover, attribute databases consisting of physical-chemical characteristics data were elaborated and linked to the attribute table of the corresponding GIS decay/pilot conservation interventions mapping project of capital surface, thus resulting in relational databases (RDBs). In particular, the GIS attribute tables, which include topological characteristics like perimeter, area, adjacency info etc were linked with external databases where data regarding petrography, chemical and mineralogical composition and stratification, total crust width, macro-crystalline gypsum layer width, and micro-crystalline gypsum layer width (results of OM and SEM-EDS), roughness Rq and surface area (LP results), fracture density and friability index (DIP of SEM images results), luminosity L, difference in red-green a*, difference in blue-yellow b*, and total colour difference ΔE (colorimetry results in CIELab colour space) were stored and classified. The databases were built using text and numerical elements as type of entries; whereas the data fragmentation permits the user to interrelate data regarding decay diagnosis and pilot cleaning interventions with the vector data, locating the info in a geometrically exact point or area, respecting the topological relationships among the various parts of the investigated surface [Padmanabhan *et al.* 2002]. This is possible since the first field of the above mentioned databases is flagged with the same identification code as the topological element to which the descriptive data refer to and the user can view the information, whenever the corresponding themes are active.

Data retrieval is accomplished by the use of the relational operators that the GIS platform provides in order to compare values associated with spatial data. Boolean operations (logical combinations of data, involving union, intersection, complement and exclusion), as well as logical operations (like equal to, greater than, etc) were used for different entities and attributes access, manipulation and analysis. As shown in figure 6a of the decay thematic map the geometric entities that comply with the combined expression of logical and Boolean operations of “black-grey crust total width *greater than or equal to* 80μm *AND* fracture density *greater than or equal to* 35.3” are highlighted on the map and

on the database with light blue colour. Furthermore it is demonstrated, by the database highlighting, that only one feature of the investigated surface (central area of the anthemia relief), satisfy the defined logical and relational criteria, a fact that reflects the dynamic and direct interrelation of the database to the vector data.

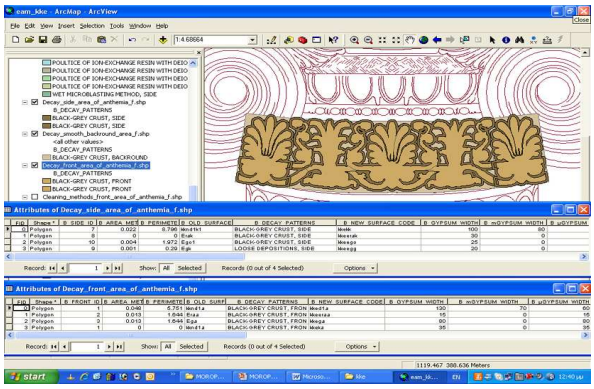

Figure 4. Decay thematic map for the capital surface, along with RDBs for both front & side anthemia surfaces.

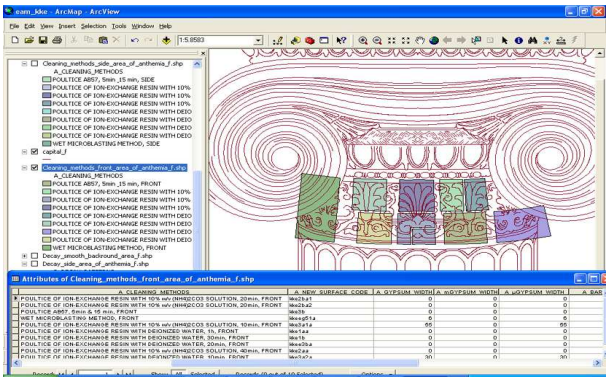

Figure 5. Pilot conservation interventions' thematic map for the capital surface, along with the RDB of the front anthemia surface.

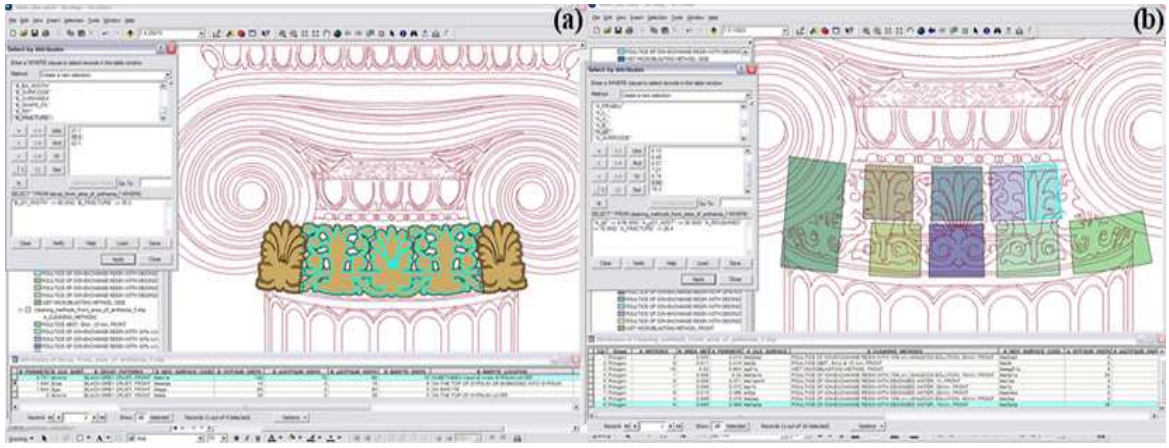

Figure 6. GIS analysis using Boolean and logical operations on (a) decay thematic map for the capital surface, and (b) pilot conservation interventions thematic map for the capital surface.

In accordance, as shown in Fig. 6b of the pilot conservation interventions thematic map the geometric entity that comply with the combined expression of logical and Boolean operations of "total colour difference ΔE *less than* 9.56, *AND* micro-crystalline gypsum width *greater than or equal to* 30, *AND* roughness *less than or equal to* 15, *AND* fracture density *less than or equal to* 26.4" is highlighted on the map and on the database with light blue colour. The only feature of the investigated surface that satisfies the defined logical and relational criteria, which in parallel are considered as accepted threshold values of the cleaning assessment criteria, is the cleaning method of ion exchange resin with deionized water applied for 10 minutes.

2.3 Development of Conservation Planning Thematic Map

Using geoprocessing procedure and in particular the intersection operation tool for both decay and pilot conservation interventions thematic maps, the resulting output theme is the conservation planning thematic map. This output theme includes features with attribute data from both input and overlay themes (decay and pilot conservation interventions themes respectively). Therefore, the new thematic map of conservation planning contains combined spatial information and the aggregation of the attribute data of both decay and pilot conservation intervention thematic maps.

Data retrieval is also accomplished in the conservation planning thematic map by the use of the relational operators that the GIS platform provides in order to access, manipulate and analyse different entities and attributes. As shown in Fig. 7 the geometric entities that comply with the combined expression of logical and Boolean operations of "micro-crystalline gypsum width before cleaning *less than or equal to* 60, *AND* micro-crystalline gypsum width after cleanig *greater than or equal to* 30, *AND* fracture density *less than or equal to* 26.4" are highlighted on the map and on the database with light blue colour. The features of the investigated surface that satisfy the defined logical and relational criteria are the cleaning methods of ion exchange resin with deionized water applied for 10 minutes and the ion exchange resin with 10% w/v $(NH_4)_2CO_3$ solution applied for 10 minutes.

Furthermore, comparative diagrams of selected attribute data sets can be elaborated, whereas features holding the selected attributes are highlighted on the vector data. In Fig. 8 the comparative diagram of fracture density (FD) for two different areas, presents the shift of the FD attribute values before and after cleaning for the features where ion exchange resin with deionised water for 10 and 20 minutes respectively were applied. The diagram demonstrates the increase of FD value in the area that ion exchange resin with deionised water for 20 minutes was applied, whereas accepted threshold value decrease for the FD attribute took place in the area of ion exchange resin with deionised water for 10 minutes application.

It is clear that when a new conservation assessment study takes place in the future using the same NDTE and analytical techniques, the attribute database will be enriched by the new evidence regarding the critical performance characteristics of the applied cleaning methods. Utilizing in parallel the GIS geoprocessing procedure, scientists will gain the opportunity of monitoring the selected physical-chemical indexes of the investigated sculptured marble surface in relation to environmental parameters on real scale, deciding the best one incorporating the durability criterion. Moreover, planning of conservation interventions for all the capital surfaces of eastern orientation in the NAM propylon, can be successfully accomplished.

3 CONCLUSIONS

Diagnostic study results concerning building material and decay data, as well as pilot conservation interventions study results were recorded and attributed to spatial entities of the representative investigated pilot surface of the capital, resulting in the development of GIS thematic maps, which after the use of GIS operational analysis provide valuable info regarding: (a) the presented decay and its physical-chemical characteristics, as they resulted by the application of NDT&E techniques, and of analytical techniques after sampling, and (b) how these physical-chemical characteristics altered after the application of pilot conservation interventions. The application of geoprocessing procedure on the above mentioned thematic maps, led to the conservation planning thematic map. This final map incorporated spatial and attribute data regarding decay and pilot conservation interventions, contributing to the planning of conservation interventions of the investigating surface.

The potential of the methodological approach using GIS to monitor selected representative surfaces, in order to continuously assess the critical performance of conservation interventions, and to control building materials durability, was demonstrated in practice.

It is concluded that the use of a GIS platform can create an information-decision management system where datasets concerning building pathology and conservation interventions are recorded, correlated, distributed and attributed to space in different working-scales, during different time periods, contributing decisively to durability control of building materials and strategic planning of periodical conservation interventions.

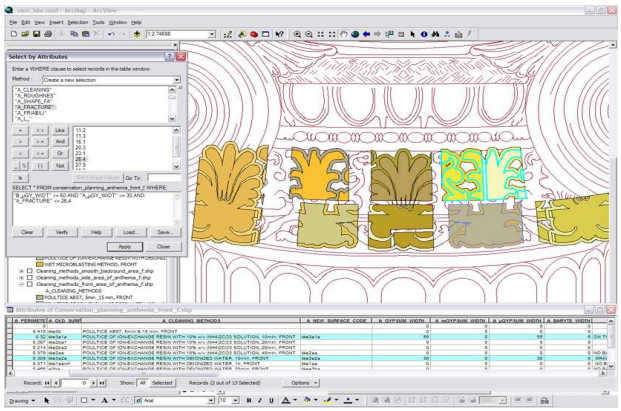

Figure 7. GIS analysis using Boolean and logical operations on conservation planning thematic map for the capital surface.

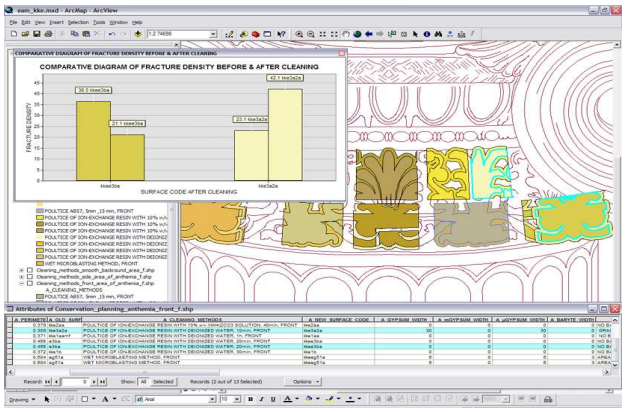

Figure 8. Comparative diagram of fracture density before and after cleaning for two highlighted areas, using GIS analysis operations on conservation planning thematic map for the capital surface.

REFERENCES

Fitzner B., Heinrichs K., Kownatzki R., 1992, 'Classification and mapping of weathering forms', in Proc. of the 7th International Congress on Deterioration and Conservation of Stone, vol. 2, 15-18 June, Lisbon, p. 957-968.

Warke P.A., Curran J.M., Turkington A.V., Smith B.J., 2003, 'Condition assessment for building stone conservation: a staging system approach', *Building and Environment*, 38, p. 1113-1123.

Salonia P., Negri A., 2002, 'Historical buildings and their decay: Data recording, analyzing and transferring in an ITC environment', The International Archives of the Photogrammetry, Remote Sensing and spatial Information Sciences, Vol. XXXIV, Part 5/W12, p.302-306.

Inkpen R.J., Fontana D., Collier P., 2001, 'Mapping decay: Integrating scales of weathering within GIS', Earth Surfaces Processes and Landforms, 26, 885-900.

Moropoulou A., Delegou E.T., Avdelidis N.P., Athanasiadou A., 2005, 'Integrated diagnostics using advanced in situ measuring technology', 10th International Conference on Durability of Building Materials and Components, Lyon, 1116-1123.

Moropoulou A., Delegou E.T., Konstadinidou M., Kiranoudis C. 2008, 'Decision making about cleaning interventions on marble surfaces using a fuzzy logic approach', 11th International Conference on Durability of Building Materials and Components, Istanbul, Vol. 3, 1275-1285.

Padmanabhan G., Leipnik M.R., Yoon J., 2002, 'A Glossary of GIS Terminology', NCGIA, (National Center for Geographic Information and Analysis), USA.

XII DBMC
International Conference on Durability of Building Materials and Components
PORTO - PORTUGAL, April 12th-15th, 2011

A GIS Tool for Accessing Climate Data Relevant to Building Practitioners

Brian R. Kyle [1]
Michael A. Lacasse [2]
Heather Auld [3]
Stephan G. Mainville [4]
Khaled Abdulghani [5]

ABSTRACT

Maintenance of building façades and related systems should be an on-going process. Nonetheless, maintenance prioritisation issues are often neglected due to the lack of available tools to assess vulnerability to climatic effects and susceptibility to deterioration. How is climatic information currently accessed and used and what are the existing means to assess climate loading effects? A Geographic Information System (GIS) platform [ESRI ArcGIS 9.3] was proposed as an appropriate tool to integrate climatic design information and other analyzed climate data in a geographical context and allow users ready access to climate information pertinent to building practitioners. On the basis of this effort climatic design data used for building codes and standards, such as degree days, 15 minute, one day and annual rainfall, driving rain wind pressure and related loads were made available in the GIS platform. This climatic design data provides basic information from which derivative climate parameters can be developed and from which relevant climate load projections can be extracted for use by building designers, practitioners and maintenance experts.

KEYWORDS

GIS, Climate design data, Building systems, Design and maintenance.

[1] XTN Sustainable Life-cycle Asset Management Consulting, CANADA, brian.kyle@xtn-slam.com
[2] National Research Council Canada, CANADA, Michael.Lacasse@nrc-cnrc.gc.ca
[3] Heather Auld, Environment Canada, CANADA, Heather.Auld@ec.gc.ca
[4] Public Works and Government Services Canada, CANADA, stephan.g.mainville@tpsgc-pwgsc.gc.ca
[5] National Research Council Canada, CANADA, Khaled.Abdulghani@nrc-cnrc.gc.ca

1 INTRODUCTION

Maintenance of building façades and related systems should be an on-going process. Nonetheless, maintenance prioritisation issues are often neglected due to the lack of available tools to assess vulnerability to climatic effects and susceptibility to deterioration. What are the current means employed to access climate information? Key components of the building systems that are most in need of maintenance interventions ought to be identified to prevent premature catastrophic failure, to sustain the health and safety of the occupants, and to maintain the serviceability of the system over its service life. Maintenance prioritisation ensures effective deployment of limited or insufficient funds.

1.1 The Need

The design and sizing of mechanical, heating, ventilation and air-conditioning systems is influenced directly by expected loads upon the systems, occupant functional requirements as well as legal and building operational regulations and frameworks. Amongst the climatic loadings, temperature and humidity are of primary concern having significant impact upon the required capacity of heating and cooling systems. Wind loads affect the efficiency of air-intake and handling units; potentially altering building pressurisation and effective operation of functional services such as elevators.

Buildings are making an ever-increasing use of weather-driven renewable energy sources such as integrated wind turbines, solar panels and enhanced day lighting techniques. The design, maintenance and longer-term performance and broader adoption of these technologies depend upon the availability of reliable climate information including temperature data, solar radiation exposure and cloud-cover information, as well as wind intensity projections.

Data on wind, solar radiation, temperature, moisture and precipitation is essential to properly evaluate the design and effects of maintenance on all building envelope components. This is significant when considering the expected performance of “green” walls and roofs since implied seasonal loadings may be drastically different from those expected with more conventional configurations.

Knowledge of the combined effects of wind, moisture and thermal loads on façade systems permits the determination of the response of the wall including the hygrothermal performance, dilation at the panel joints, susceptibility to water penetration or the product of combined responses that act to deteriorate the façade system. Hence, evaluating climatic effects in combination with wall response permits establishing the most severe combinations most likely to deteriorate the façade and thus provides a basis for prioritising maintenance programs for high-rise buildings. The process can be used to establish risk of deterioration from climatic effects among the different walls for a given building façade, between the level of risk among different buildings in a given climate, or for comparing the relative effects of similar façades exposed to different climate loadings.

The effects of moisture and other climate parameters on the deterioration of façade components are well known; spalling of masonry caused by freeze-thaw action, spalling and degradation caused by salt migration, damage due to expansion of materials or components; loss of adhesion or rupture of jointing products from joint movement. Likewise, water penetration of the façade from wind-driven rain to the interior causes failure of interior finishes, damage to gypsum plasters, mould or mildew growth and degradation of the thermal performance of insulation.

1.2 Background

Over the past 20 years the geo-information field , once a highly specialized niche domain, has evolved to a technology having a broad effect on society and its interaction with nature. Geographic Information Systems (GIS) applications range from simple navigation to critical and extremely

complex tasks, such as infrastructure risk management, prediction and mitigation of the effects of natural disasters.

This broadened GIS use is partially due to the increased availability of Geographic Positioning Systems (GPS) and greater access to georeferenced data. In North America most levels of government provide some level of "free-of-charge" access to geospatial data [e.g. GeoGratis, 2010,USGS National Map, 2010]. Historically, access to GIS data in Europe has been restricted by financial or legal barriers and as a result, European data often originated from U.S. based systems.

Various GIS initiatives have evaluated the interface of the natural and built environments, usually focusing upon a specific material or degradation processes [Inkpen *et al.*,2001, 2008,Cole *et al*., 1999, 2003a-c, 2004] with the intent of identifying geographically susceptible regions for the occurrence of the particular phenomenon. These works demonstrate the inherent capabilities as well as the ever increasing computational capabilities of GIS.

Numerous climate datasets and buildings related design tools have been developed [Hui and Cheung, 1997, ASHRAE, 2009, RETScreen, 2010]. An integral, and obviously required, characteristic of these tools is georeferenced climate data. Despite this potential direct linkage to GIS-based systems, to-date there have been relatively few initiatives to create GIS enabled climate data sets [Agnew and Palutikof, 2000, Mitchell *et al*., 2004,] and equally as few efforts specifically focused upon implementing GIS relative to building-level data [Kyle *et al.*, 2008, Hallberg *et al.*, 2008].

1.3 Continually Altered Context

The rising perception of the significance of climate change and the potential impacts upon infrastructure and buildings has resulted in several initiatives to monitor the impacts of future climate effects and to project potential longer-term changes [DEFRA, 2010, Environment Canada, 2008, IPCC, 2007, NASA, 2010]. The outputs of these efforts, while not explicitly aimed at assisting with the development of climate design data, if properly considered will contribute to the design and construction of more durable and climatically responsive buildings.

1.4 Approach

The intent of the work described herein was to create a tool that put Canadian climate design data in a GIS context. The GIS platform that was used to integrate climate information in a geographical context is ESRI ArcGIS 9.3. The ArcGIS database was populated with all necessary climate information as obtained from the National Building Code of Canada [NBCC, 2010], to provide basic information from which derivative climate parameters can be developed and from which relevant climate data can be extracted for building designers, practitioners and maintenance experts.

The remainder of this paper describes the nature of the dataset, the preparation and processing required to migrate the data to the GIS context, as well as the results of the exercise.

2 NATIONAL BUILDING CODE OF CANADA 2010 DATASET

Appendix C of the National Building Code of Canada [NBCC, 2010] provides recommended design data for a number of locations throughout Canada. This document acknowledges the yearly and seasonal variability in climate loadings and the potential long-term shift in climate regimes. Table 1 lists the climatic parameters used in the developed tool and includes a short description of the parameter as well as the number of weather stations sampled.

Table 1. Composition of the NBCC 2010 Climatic Data Subset as Implemented.

Climatic Parameter	*# of weather stations sampled*	*Description and (units)*
Heating degree-days	1030	Degree-days below 18 °C
15 min. rain 1/10	485	Annual maximum 15 min. rainfall – 10 year return period (mm)
One-day rainfall	3500+	Annual maximum one-day rainfall- 50 year return period (mm)
Annual rainfall	2051	Total annual rainfall (mm)
Annual precipitation	2051	Total annual precipitation (mm)
Driving Rain	2051	Driving rain wind pressure - 5 year return period (Pa)
Snow Load Ss	2000+	Total annual snow load - 50 year return period (KPa)
Snow Load Sr	2000+	Total annual snowload (rain-on-snow) - 50 year return period (KPa)
Hourly wind pressure 1/10	400+.	Average hourly wind pressure – 10 year return period (KPa)
Hourly wind pressure 1/50	400+.	Average hourly wind pressure – 50 year return period (KPa)

This national model dataset is representative of the nature of the raw data sampled as well as the statistical analysis employed and traditional historically-based probablistic assessment. The final determination of the content of the document is made via consultation with various domain experts, and the document is, as such, consensus driven. The current, 2010, version of the climatic design data has directly considered climate change effects in the determination of distributions for various design parameters, most notable being the intensity of precipitation events.

3 GIS TOOL AND DATASET PREPARATION

The principal software package used for this work was ESRI ArcGIS Desktop 9.3 from Environmental Systems Research Institute, Inc [ESRI, 2010]. Two additional tools, Spatial Analyst and ArcReader, were used during the development to add specific funtionality and ease-of-use.

ArcGIS Desktop is a collection of products that runs on desktop computers and is used to create, import, edit, query, map, analyze and publish geographic information. It allows examination of various data relationships, permits testing of predictions. ArcGIS Desktop includes ArcView, ArcEditor and ArcInfo; providing progressively greater GIS functionality.

Spatial Analyst is an extension to ArcGIS Desktop , providing tools for comprehensive, raster-based spatial modeling and analysis. This tool permits the derivation of new information from existing data, spatial relationship analysis, development of spatial models and complex raster operations.

ArcReader is a free, easy-to-use desktop mapping application that allows users to view, explore and print maps and globes. Users of ArcReader can view high-quality interactive maps authored by higher-level ArcGIS Desktop products and published with the ArcGIS Publisher extension. The availability and quality of the data typically represent significant limitations to GIS implementation. In this particular case, the datasets had been pre-processed for representation and required only a minor verification for consistencies and/or anomalies. The project approach used was to interpolate the dataset with various weather station locations. Within the ArcGIS framework there are various interpolation methods available. For this initiative, and as is commonly the case in other climate data analysis, Iverse Distance Weighting (IDW) was used. IDW is a multivariate interpolative process whereby values are assigned to unknown datapoints by using values from scattered set of known

datapoints. IDW is well suited for this type of analysis since the data is very predictable and consistent across the country. IDW is able to represent the data and interpolate a smooth distribution of unknown points. The control values for the interpolation analysis were chosen primarily by trial and error, aimed at generating results with adequate cartographic appeal to the audience and users. This process required considerable computing time and fine tuning . Once the results are complete, the whole mid-level product is packaged to be viewed using ArcReader.

The data manipulation process used for the migration of\the design dataset to the ArcGIS context is presented in Fig. 1. A basic description of the steps taken to reach the final products is as follows:

- **Interpolation** - Iverse Distance Weighting is used to estimate data values at locations without data, based upon the distances to populated datapoints;
- **Reclassification** – the interpolated dataset is transferred to a rastor file while maintaining the original raw data;
- **Conversion** - the raster file is converted to a polygon file containing specific attributes; and
- **Clipping** – limits the displayed map to a specified desire border, e.g. to the map of Canada.

The mapping capabilities of the ArcGIS system permit various layer selections and further combination of loads and effects; the colour selection and control over the ramping gradation.

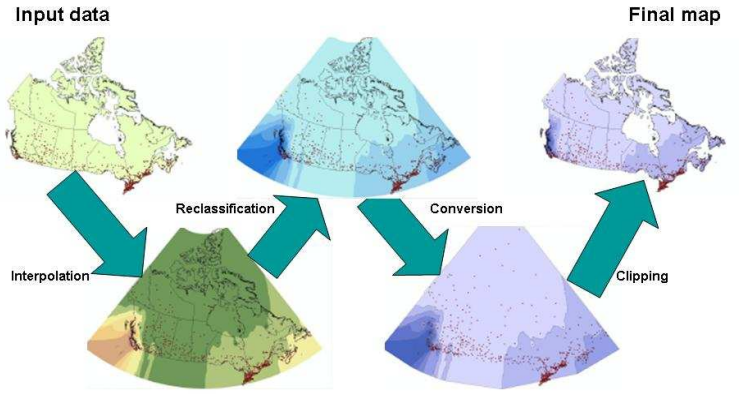

Figure 1. Process diagram for the dataset preparation and migration in ArcGIS 9.3.

4 RESULTS

The procedure described in Section 3 was applied to each of the design parameter datasets listed in Table 1 of Section 2. Figures. 2 to 4 present results for a sampling of these parameters.

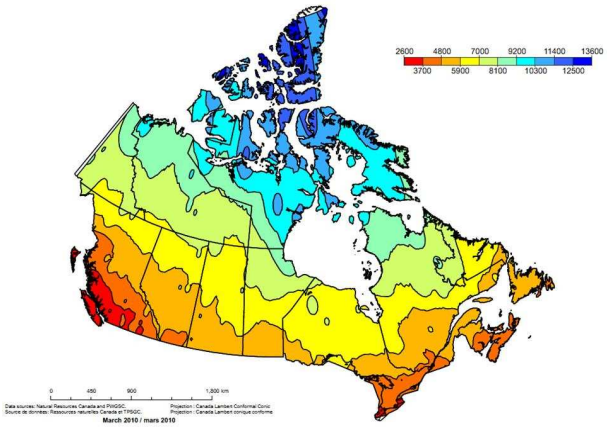

Figure 2. Canadian design data for degree-days below 18 °C.

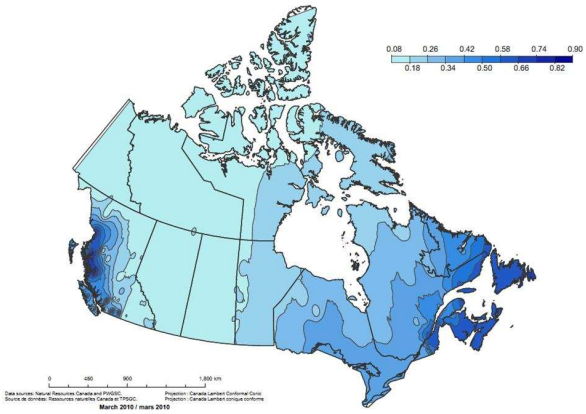

Figure 3. Canadian design data for annual snowload (rain-on-snow) - 50 year return period (KPa).

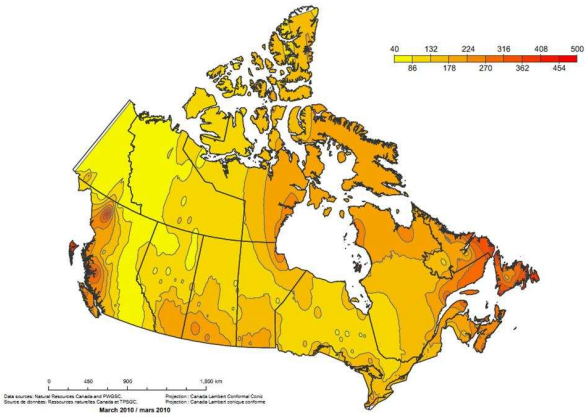

Figure 4. Canadian design data for driving rain wind pressure - 5 year return period (Pa).

5 DISCUSSION

This system provides National Building Code of Canada climate design data, a consensus-based dataset borne from recent climatic observations as well as historical weather records and tendencies. As such, it fulfills the minimum data requirements for typical building climate design considerations in Canada.

At the highest level, this system offers a visualization of the macroclimate of any particular region in Canada, and at the lowest level, it provides climate information on a meso (building) scale and basic information needed to determine the microclimate loads on a building, its façade and systems.

Many observers believe that climate change is having a greater, and more rapidly occurring, impact upon many design parameters than originally predicted. In some regions of Canada, long-standing design and construction practices are no longer perceived to adequately address climatic conditions and loadings and the usefulness of design data that is based, even in-part, on historical climate records is being questioned.[PIEVC, 2008, Auld and MacIver 2007].

With traditional approaches, the validity of such a stance (or climate design data itself) can only be substantiated with long-term data collection and comparisons of climate and weather observations relative to the climate design data that had been used. If the effects of climate change are as pressing as suggested, the time requirements to project and validate climate design data must be shortened. In the interim, if there are concerns about the adequacy of any projected climate loadings, at any stage

of a building's service life, designs should meet requirements beyond the limits of datasets comparable to that described in this paper. Climate design databases, in conjunction with GIS interfaces, provide basic information from which derivative climate parameters can be developed and relevant climate load projections can be extracted for use by building designers, practitioners and maintenance experts. Regardless of the basis of the databases, there will be an increasing role for GIS-based systems to provide building practitioners with current, historical and projection information on climate loadings.

6 SUMMARY

An ESRI ArcGIS 9.3 Geographic Information System (GIS) platform was proposed as an appropriate tool to integrate climatic design information and other analyzed climate data in a geographical context and allow ready access to climate information pertinent to building practitioners. On the basis of this effort climatic design data used for building codes and standards, such as degree days, 15 minute, one day and annual rainfall, driving rain wind pressure and related loads were made available in the GIS platform. This climatic design data provides basic information from which derivative climate parameters can be developed and from which relevant climate load projections can be extracted for use by building designers, practitioners and maintenance experts.

ACKNOWLEDGMENTS

The support of this work by the Program for Energy Research and Development (PERD) administered by Natural Resources Canada is gratefully acknowledged.

REFERENCES

Agnew, M.D., Palutikof, J.P. 2000, GIS-based construction of baseline climatologies for the Mediterranean using terrain variables, CLIMATE RESEARCH Vol. 14: 115–127.

American Society of Heating, Refrigerating, and Air-conditioning Engineers (ASHRAE) 2009, Handbook of Fundamentals, Chapter 14 – Climatic Design Information, Atlanta GA, 2009.

Auld, H., MacIver, D. 2007, Changing Weather Patterns, Uncertainty and Infrastructure Risks: Emerging Adaptation Requirements, Adaptation and Impacts Research Division, Environment Canada,Occasional Paper 9, 4905 Dufferin Street, Toronto, Canada.

Cole, I.S., King,, G.A., Trinidad, G.S., Chan, W.Y., Paterson D.A. 1999, 'An Australia-wide map of corrosivity: a GIS approach', 8th Int. Conf. On Durability of Building materials and Components, Vancouver, Canada, 30 May to 3 June 1999.

Cole, I.S., Chan, W.Y., Trinidad, G.S., Paterson D.A. 2004, An Holistic Model for Atmospheric Corrosion: Part 4 — A geographic information system for predicting airborne salinity Corrosion Engineering, Science and Technology, 200 4, vol. 39, no. 1.

Cole, I.S., Ganther, W.D., Paterson, D.A., King, G.A., Furman, S.A., Lau, D. 2003a. A Holistic Model for Atmospheric Corrosion: Part 2 — Experimental Measurement of Deposition of Marine Salts in a Number of Long-range Studies, Corrosion Engineering, Science and Technology, 2003, vol. 38, no. 4.

Cole, I.S., Paterson, D.A., Ganther, W.D. 2003b. A Holistic Model for Atmospheric Corrosion: Part 1 — Theoretical Framework for the production, Transportation and Deposition of Marine Salts. Corrosion Engineering, Science and Technology, 1 June 2003, vol. 38, no. 2, pp. 129-134(6).

Cole, I.S., Paterson, D.A., Ganther, W.D., Hinton, B., McAdam, G., Chotimongkol, L., Bhamornsut, C, Hue, N.V., Purwadaria, S. 2003c. A Holistic Model for Atmospheric Corrosion: Part 3 — Effect of Natural and Man-made Landforms on Deposition of Marine Salts in Australia and South East Asia, Corrosion Engineering, Science and Technology, 2003, vol. 38, no. 4.

Department of Environment, Food and Rural Affairs, United Kingdon (DEFRA), 2010, UK Climate Projections, 2010, http://ukclimateprojections.defra.gov.uk/

Engineers Canada, Public Infrstructure Engineering Vulnerability Committee (PIEVC) 2008, Adapting to Climate Change, Canada's First National Engineering Vulnerability Assessment, Appendix B-6, Thermosyphon Foundations, Northwest Territories and Yukon, Ottawa, Canada, April 2008, http://www.pievc.ca/e/Appendix_B.6_Northwest_Territories_Thermosyphon_Foundations.pdf

Environment Canada, 2008, Climate Trends and Variation Bulletin: Annual, 2008.

Environmental Systems Research Institute, Inc , (ESRI) 2010, http://www.esricanada.com

Hallberg, D., Akander, J., Stojanović, B., Kedbäck, M., 2008, Life Cycle Management System – A Planning Tool Supporting Long-Term Based Design and Maintenance Planning, 11th International Conference on Durability of Building Materials and Components, Istanbul Turkey, May 11-14, 2008.

Hui, S. C. M. and Cheung, K. P., 1997. Climatic data for building energy design in Hong Kong and Mainland China, In *Proc. of the CIBSE National Conference 1997*, 5-7 October 1997, London (paper for CIBSE Virtual Conference 1997).

Inkpen, R.J., Fontana, D., Collier, P., Mapping Decay: Integrating Scales of Weathering within a GIS, Earth Surface Processes and Landforms; Earth Surf. Process. Landforms **26**, 885–900 (2001).

Inkpen, R., Duane, B., Burdett, J., Yates, T. 2008, Assessing stone degradation using an integrated database and geographical information system (GIS), Environ. Geol. **56**:789–801, Springer-Verlag.

Intergovernmental Panel on Climate Change (IPCC), 2007, Climate Change 2007: The Physical Science Basis.Contribution of Working Group I to the Fourth Assessment Report of the Intergovernmental Panel on Climate Change. S. Solomon, D. Qin, M. Manning, Z. Chen, M. Marquis, K.B. Averyt, M. Tignor and H.L. Miller (Eds.). Cambridge University Press, Cambridge, United Kingdom and New York, NY, USA, 996 pp., 2007.

National Aeronautics and Space Administration, Goddard Institute for Space Studies (NASA), 2010, Common Sense Climate Index, http://data.giss.nasa.gov/csci/

National Building Code of Canada, (NBCC), 2010, Appendix C - Climatic and Seismic Information for Building Design in Canada, Ottawa,Canada, 2010.

GeoGratis 2010, Natural Resources Canada, http://geogratis.gc.ca/geogratis/en/index.html;jsessionid=3C4FFD51E9954D9DE09FFB6CA3D837FA

RETScreen International (RETScreen), 2010, Software & Data, Natural Resources Canada, http://www.retscreen.net/ang/version4.php

Kyle, B., Lacasse, M.A., Cornick, S.M., Richard, D., Abdulghani, K., Hilly, T., 2008, A GIS-Based Framework for the Evaluation of Building Façade Performance and Maintenance Prioritization, 11th International Conference on Durability of Building Materials and Components, Istanbul Turkey, May 11-14, 2008

Mitchell, T. D., Carter, T. R., Jones, P. D., Hulme, M., and New, M. 2004, A comprehensive set of high-resolution grids of monthly climate for Europe and the globe: the observed record (1901–2000) and 16 scenarios (2001–2100). Tyndall Centre Working Paper 55, Norwich, United Kingdom, 30 pp. URL: http://www.cru.uea.ac.uk/cru/data/hrg.htm

USGS (United States Geological Survey) National Map (2010). WWW document, http://nationalmap.gov/index.html

XII DBMC
International Conference on Durability of Building Materials and Components
PORTO - PORTUGAL, April 12th-15th, 2011

Handling Uncertainties in Visual Examination Procedure in Building Diagnostics

Gergely Molnárka [1]

ABSTRACT

The first step of each building diagnostic analysis is a detailed visual check of deteriorations of building elements. During this process the identification of touched components and the circumstances of the given failure are discussed. A properly completed survey determines the way of further analyses and interventions to be done. Thus the visual check may support indirectly the decisions which deal with the life cycle of the examined building or its part.

In the case of ad hoc and independent surveys the decision-supporting ability of the traditional visual examination procedures prove to be inconsiderable, if the subjects of the surveys belong to the same property. Due to several subjective factors the evaluation of these surveys and their comparative analysis are almost impossible.

It is supposable that the application of fuzzy expert system proposed in this article may solve the problem mentioned above, owing to the peculiarities of this professional field.

This paper sketches out the uncertainties of the visual examination procedure in building diagnostics, then describes the architecture and components of the fuzzy expert system in building diagnostics. Thereafter, the operation of this method is illustrated through several examinations on site.

KEYWORDS

Building diagnostics, Visual examinations, Fuzzy expert system.

[1] Department of Architecture and Building Construction, Széchenyi István University, Győr HUNGARY, mgergo@sze.hu

1 INTRODUCTION

The word ‘diagnostics’ roots from the Greek phrase of ’διά’ and ’γνωσις‘ (‘dia’ and ‘gnosis’ means: ‘through cognition’). The goal of each building diagnostics examination is to observe the relations between causes and consequences which may happen while one gets to know the mechanism of deterioration – ‘through cognition’.

In a process of building pathology this observation is added with recommendations, proposals for renovation, and other calculations. However the building pathology arises from the building diagnostics procedure.

The first step of each survey of building failures on site is a visual examination of the touched building constructions and other elements. In practice, the majority of these examinations on site end with the statements of this visual examination. Beside the fact that the non-destructive examinations came into view due to the more and more effective devices (ultrasensitive diagnostics cameras, crack spaciousness measurers, etc.), economic and other causes may also result in the consideration that no further examinations are necessary.

Thus the role of the expert who examines the failures on site becomes more and more important – his or her statements support decisions in investment strategies. However the experts’ evaluations have to be incontestable and clear, due to some attributes of the visual examination the final reports miss the core of reliability: the comparability. This comparability is even more important in the case of a Facility Management system, where the relative priorities of needful interventions in different buildings have to be ascertained. In the decision-making procedure an objective evaluation of the state of the buildings is more than necessary.

This fact means that the surveys by experts may be useful only for understanding the examined phenomenon itself, even in well-constructed and properly operated facilities. In addition, experts may be faced with infinite constellations of cause and effect linkages beyond the comprehension and knowledge of a single individual.

This domain of questions directed our research in the methods of building diagnostics: the development of an objective and comprehensive decision support system was defined. To develop this tool, the peculiarities of professional building diagnostics, and specially, the features of on-site visual examination on site had to be taken into consideration.

2 DIVERGENCES AMONG BUILDING DIAGNOSTICS SURVEYS

2.1 The General Process of Visual Examination

To determine the major problems of visual examinations and their results it is valuable to skecth procedures used. Regardless of the main purpose for the given examination (judicial, depreciation, responsibility statement, etc.), the sequence of steps is the same in every case. Although there are frameworks that provide direction (e.g. guide booklet series of National Building Scientific Committee [Kelemen, 1984]) neither national nor international standards exist focusing on visual examinations in building diagnostics. These fundamental steps can be described in the following text. For an overview see ‘Fig. 1’.

Description of concerned building elements. After the localization of failure the description of affected building and its parts is the next step. The first important task is to observe and properly identify the building components.

Observation of relationship between causes and consequences. The description of supposed causes and consequences can be based on these steps mentioned above. It is advisable to decide on the depth

of the observation of failure mechanism: with full knowledge of the given task, the analysis can be limited to the required level. If the given failure or the goal of the examination demands further analyses, it is necessary to specify the next steps (localization and methods of sampling, lab work, etc.).

Conclusion. On the basis of the observations, conclusions may be drawn. These statements may give a global overview about the severity of the given failure and contain the steps of required interventions.

Further tasks. Generally experts are required to give recommendations to recover from failures, and estimate the cost of repair or the amount of loss of value.

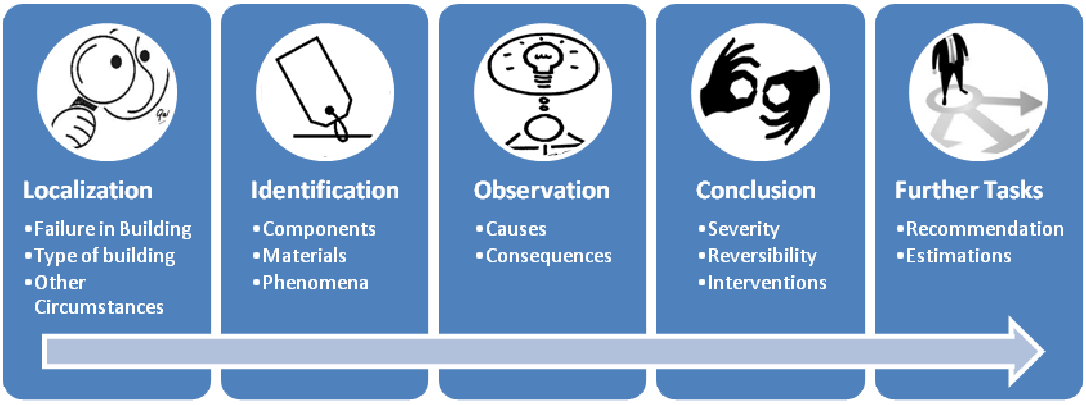

Figure 1. Consecutive Steps of the Visual Examination on Site.

2.2 The Origin of Alteration in the Process of Examinations

In an intermediate phase of an ongoing project, several surveys of building diagnostics analyses were evaluated. The evaluation is based on 117 diagnostic analyses, conducted between 1976 and 1996, on buildings owned by the Department of Building Construction, Technical University of Budapest.

This evaluation examined the revisions of surveys. The distribution of the amount of analyses by the number of revisions is provided in 'Fig.2'. In the majority of the available reports, at least three different conclusions were done on the same case. These conclusions do not correspond to each other from the step of identification.

The differences amongst conclusions were examined, and the root causes of the divergences were defined and are presented below.

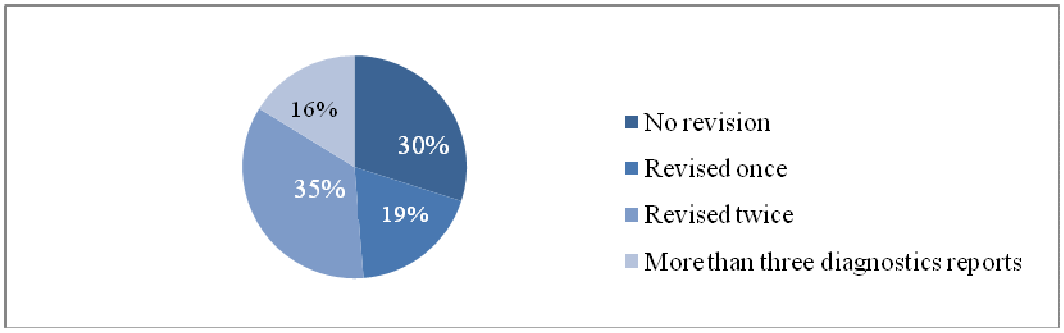

Figure 2. The Distribution of Diagnostics Reports of Examined Failures by Number of Revisions.

Cause No. 1: the used terminologies. In the process of identification, the use of bad determinations and inexact terminologies may drive the expert to wrong way. While the failure is described the experienced phenomena has to be described particularly – with the use of suitable expressions.

Cause No. 2: uneven knowledge and emotion in evaluation. On the field of building diagnostics discipline the basis of the expert's knowledge is the experience which may be common (based on guide books, lectures, etc.) or personal. It is the expert's own right how he or she wants to interpret his or her conclusions about the examined phenomenon. However, while such colorfulness of the visual examination gives a kind of beauty to this professional area, it diminishes the effectiveness of the examination.

Therefore the core of divergences is dual, namely the vocabulary and the uncertainty in evaluations. Generally we can state that the strength and the weakness of the expert's diagnostics procedure are the same: the human factors. The human thinking gives creative approach to the problem in each step – nevertheless it may also mislead us in that it predetermines the direction of analysis.

3 SOLUTIONS FOR HANDLING HUMAN FACTORS

The problem of human factors in examinations is a long recognized issue in the building science field.

The question of classification of terminologies used on building science area preoccupies research teams internationally. The first experiments [Kunszt, 1975] focused on synchronization and sharing the results within the network of CIB. Although this research ended without concrete results, the method and the approach proved to be useful in information systematization. With the expansion of IT technologies several solutions became available for creating systems in such a professional glossary. Despite this not being a recent question and a significant time-wasting attribute, there is not any international tool put order amongst the words used for visual examinations.

IT technologies also offer reasonable answers for handling the uneven and narrow knowledge and experience of experts on this field. In other disciplines successful tools have been developed to determine relations among causes and consequences (c.f. medical diagnostics, safety engineering, and vehicle diagnostics) [Moser, 2004]. Managing uncertainties in evaluations was targeted in several studies. According to [Zhang, 2005], the importance of uncertainty analysis cannot be neglected in any kind of decision support tool where the human being is an important factor. In her study, the adaptability of Markov chain model was presented.

4 PROPOSALS

The research approach of this topic has its roots in the State-of-the-Arts report of CIB W086 Committee. As Croce [1993] states, the results of soft-computing methods are applicable in building diagnostics analyses via the expert system.

The ongoing project at our institute focuses on the possibilities of creating a common database of gathered information and experiences collected by the society of building diagnostics experts. Besides the collection and classification of information, this tool is multipurpose devoted to: supporting analyses, giving statistical data for the building industry – and the most important – assuring the comparability among surveys.

The fuzzy expert system, a tool of IT techniques, gives a reliable solution for this goal. The method is able to keep the uncertainty of human thinking in sight, yet, it is based on the management of, and expressly supports the use of linguistic variables [Kandel, 1992]. The fuzzy expert system used for this subject is depicted in 'Fig 3'. The fuzzy expert system has two important units: the knowledge base and the database, linked by an inference engine. In our case, the knowledge base embodies the 'Damage Atlas' (expression from EC [1998]); that has a systematized dataset of information obtained from former reliable examinations. The frame of systematization is a complex unit of thesauri of building elements, materials and phenomena [Molnarka, 2007].

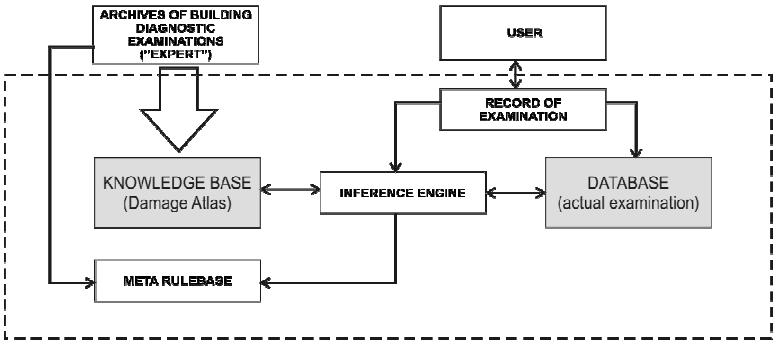

Figure 3. Diagram of Fuzzy expert system in building diagnostics.

According to de Oliveira Pedro et al.[2008], categories of defects can be establsihed; and via comparison with experiences of similar failures, the given defect can be classified. Tthis score may be weighted based on personal consideration and the result may be compared in a total examination. This kind of checklist is popular even in traditional visual examination procedures; several former directives propose its application.

The utilization of crisp values in evaluations may mislead the assessment, the exact judgment of the expert possibly not being reflected by the small number of categories. By increasing the number of categories, the effectiveness may decrease due to the enhanced reliance on decision. This fact led us to consider a fuzzy logic solution. The hazy contours of sets provided another kind of access: the value that was ordered to the experienced failure showed the degree of membership to the given set (instead of judging the failure as 'Medium' or 'Severe').

Taking into account the manageability of rule base, the number of input variables was narrowed down to three. The input variables were chosen to consider every failure effect while the importance of intervention as an output variable is defined. The relations among the input and output variables are based on "if-then" type rules. The accessible input variables (three variables) and their partitions (5;5;3 partitions by each variable) create a rule base consisting of 5 x 5 x 3 = 75 rules. Based on this condition, the input variables focus particularly on the examined building, experienced phenomena and economic questions: thus the main aspects will be evaluated independently from each other.

Note: in the present state of the recommended fuzzy expert system – in favour of simplifying the calculations – fuzzy membership functions decomposable into linear spans (triangular and trapezoidal) are applied, which form Ruspini partitions. According to this, the aggregate of function parameter of sets is 1 for every element of basic set; so the locations of the maximum of membership functions (which represent several partitions) correspond to the minimum of membership functions of both sides; in the intersection point the function parameter is always 0.5.

4.1 The Life and Property Protection (LPP) – The Aspect of Insurance

The „Life and Property Protection" (LPP) input variable estimates the seriousness of deterioration. The rate or types of failures produce different disadvantageous consequences in human or/and material relations. The five categories determined by linguistic variables are shown on 'Fig. 4'.

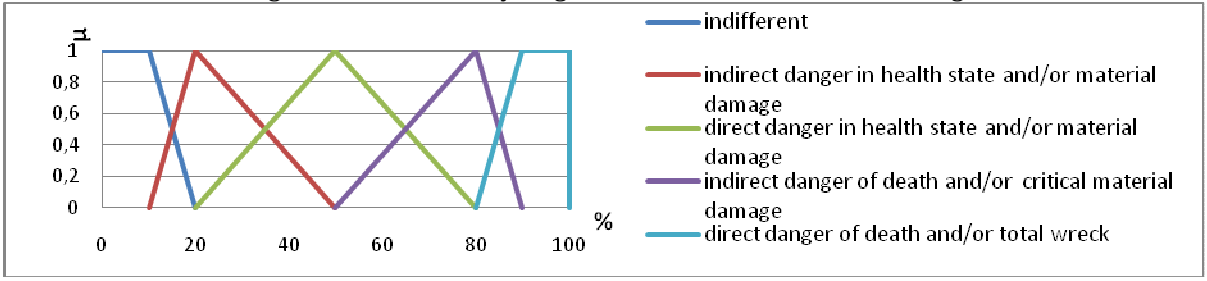

Figure 4. Fuzzy Sets of 'Life and Property Protection' Input Variable (LPP).

4.2 The Returns (Rs) – The Financial Aspect

The repair of deformations and the termination of existing failures are the basic interest of the owner, the operator or the facility management. The „Returns" (Rs) input variable takes the financial relation of failure and its maintenance into consideration: e.g. compares operational costs before and after the renovation, the reproduction costs of building components, etc. The five financial categories determined by linguistic variables are shown on 'Fig 5'.

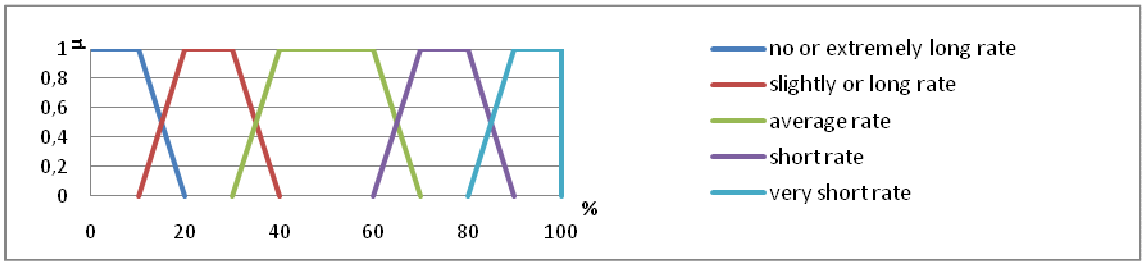

Figure 5. Fuzzy Sets of 'Returns' Input Variable (Rs).

4.3 The Architectural Value (AV) – The Architectural Aspect

The architectural value of a given building, its functional effectiveness and its synchrony with the applied technology are equally hardly measurable values, which may influence the intervention. Respecting this aspect, in the fuzzy evaluation process the „Architectural Value" (AV) input variable was created: this variable globally represents the non-technical and non-economic considerations. The three architectural categories determined by linguistic variables are shown on 'Fig 6'.

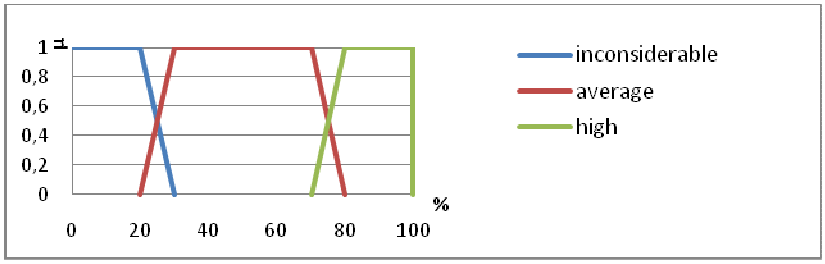

Figure 6. Fuzzy Sets of 'Architectural Value' input variable (AV).

4.4 Output Variable, Evaluation and Defuzzification

As the output variable of the analysis the Importance of the Intervention was found. Its categories define how important the maintenance is (keeping each point of view in sight). In the process of examined case studies the Mamdani-method was applied [Mamdani and Assilian, 1975] where the minimums of conjunction were taken into account. The fuzzy inference which resulted from the fuzzy expert system may be adequate for evaluating the surveys and for further examinations, but the comparison of independent phenomena was aimed. Therefore the fuzzy value of inference engine was turned into crisp value: the COG method was applied for defuzzification [Kóczy and Tikk, 2000].

5 CASE STUDIES

The mentioned 117 building diagnostics reports owned by the TUB, Hungary, were evaluated with the system outlined above. In addition to the main purpose, that the priority of intervention be ascertained, the evaluations resulted in improvement of specific elements of the knowledge base: the mapping of relations among construction – material – phenomenon thesauri.

A typical case from these evaluations is used to show the main features of the system. In this case, a mould problem is discussed; its repair may cause a periodic break in the operation of the given factory (see Table 1). Although this case (mould on the exterior wall of a bakery) was previously reported, with the background of thesaurus based dataset the terminologies were synchronized to other surveys. This harmonization helped ranking the experienced deteriorations by the 'importance of intervention'.

Table 1. Evaluation of a failure with the support of the fuzzy expert system.

General information	*Bakery; 1974*	Building Construction	*exterior partition wall*
Material	*reinforced concrete*	Phenomena	*moulding*

Expert's Statements*: Humid interior air; not operating ventilation. Free-mounted pipes and cables, visible pollution on low-temperature surfaces.*

Degree of Membership	Input Variable	Value	Set 1: Degree (No.)	Set 2: Degree (No.)
	LPP	*45%*	*0.17 (2)*	*0.83*
	Rs	*64%*	*0.60 (3)*	*0.40*
	AV	*28%*	*0.20 (1)*	*0.80*

Evaluation (Mamdani method)

Shooting Rules	LPP	Rs	AV	Evaluation		Area of Reasoning		Centre of Gravity	
22	*2*	*3*	*1*	$\omega_{min\,(22)}$	*0.17*	$\omega_{(22)}^{*}$	*3.05*	$y_{(22)}^{*}$	*35*
23	*2*	*3*	*2*	$\omega_{min\,(23)}$	*0.17*	$\omega_{(23)}^{*}$	*3.05*	$y_{(23)}^{*}$	*35*
25	*2*	*4*	*1*	$\omega_{min\,(25)}$	*0.17*	$\omega_{(25)}^{*}$	*3.05*	$y_{(25)}^{*}$	*35*
26	*2*	*4*	*2*	$\omega_{min\,(26)}$	*0.17*	$\omega_{(26)}^{*}$	*3.05*	$y_{(26)}^{*}$	*45*
37	*3*	*3*	*1*	$\omega_{min\,(37)}$	*0.20*	$\omega_{(37)}^{*}$	*3.6*	$y_{(37)}^{*}$	*45*
38	*3*	*3*	*2*	$\omega_{min\,(38)}$	*0.60*	$\omega_{(38)}^{*}$	*8.4*	$y_{(38)}^{*}$	*45*
40	*3*	*4*	*1*	$\omega_{min\,(40)}$	*0.20*	$\omega_{(40)}^{*}$	*3.6*	$y_{(40)}^{*}$	*55*
41	*3*	*4*	*2*	$\omega_{min\,(41)}$	*0.40*	$\omega_{(41)}^{*}$	*6.4*	$y_{(41)}^{*}$	*55*

Defuzzification (COG)

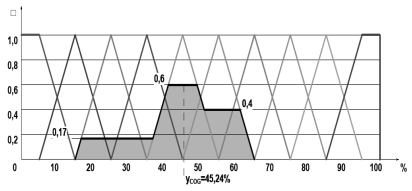

$$y_{COG} = \frac{\sum_{i=1}^{r} y_i^* \times \omega_i^*}{\sum_{i=1}^{r} \omega_i^*} = 45.24\% \rightarrow$$

„Worthy of consideration" *(27.6-62.5)*

6 CONCLUSIONS

In the present economic conditions in Hungary and around the world, questions arise about global development. Avoiding analyzing the circumstances, social and other problems generated a possible response in the political leadership in Hungary. Contrary to the efforts of last twenty years, when strengthening the private ownership was essential (due to the regime changing in 1989), the engagement of government on economics fields has been increased/ forced.

From the view of building maintenance this trend may be justified, since the state of the private housing stock in Hungary has been getting worse in the last twenty years. The tendency is worrisome; as owners cannot sustain their built environment alone. A global directive on the social tenement flat program is to be outlined in the near future in the country. The long-lasting quality and environment-friendly buildings require smart and effective facility management, with fast and low-cost maintenance. In such a maintenance regime, the presented diagnostics tool may help even in the management of a large quantity of buildings. Whenever the state-owned building project materializes, a well functioning decision support tool has to be present within the governmental FM system.

The research project on the global support tool for visual examination is currently underway. Its present state, the system and some details have been outlined; several analyses of existing reports were performed which helped refining the initial concepts. As further steps, more data mining and input has to be done. Contrary to the assertion of the cited State-of-the-Art Report of CIB No. 155, this task is realizable (due to the existence of available smart software and reasonable hardware) and is not an 'l'art pour l'art' action. In order to enhance effectiveness the development of the tool, must include the examination of real case situations.

REFERENCES

Van Balen, K., 1996, 'Expert System for Evaluation of Deterioration of Ancient Brick Masonry Structures' *The Science of Total Environment*, pp. 247-257.

Croce, S. 1993, *CIB W086 State-of-the-Art Report (publication No. 155)* CIB W086.

European Commission, 1998, *Damage Atlas - Classification and Analyses of Damage Patterns Found in Brick Masonry, Protection and Conservation of European Cultural Heritage* (Vol. 2). Fraunhofer IRB Verlag.

Kandel, A. ed. 1992, *Fuzzy Expert Systems.* CRC Press, Tampa, Florida, USA.

Kelemen, L. ed 1984, *Épülethibák szemrevételezéses épületdiagnosztikai vizsgálata,* ÉVM 5. sz. CPB, ÉTK, Budapest

Kunszt, Gy. 1975, *A tudományos kutatás logikai modellezése és tematikai irányítása.* Akadémiai Kiadó, Budapest

Kóczy T., L., & Tikk, D. 2000, *Fuzzy rendszerek.* Typotext, Budapest.

Mamdani, A., & Assilian, S. 1975, 'An experiment in linguistic synthesis with a fuzzy logic controller' *International Journal of Man-Machine Studies* , pp.1-13.

Molnárka, G. 2007, *The Construction of the Knowledge Base of Fuzzy Expert System in Building Pathology - From a Functional Access,* proc. CIB World Building Congress. Cape Town, South Africa, 23 May 2007. pp. 1406-1417.

Moser, I. 2004. *Engineering Design Methods for Service Life Prediction* CIB W80 / RILEM 175 – SLM Rotterdam: CIB. pp. 1-51.

Oliveira Pedro, C. B. , J. A de, Vasconelos de Paiva J. A.,., & Damaso Santos Matos Vilhena, A. J. 2008, 'Portuguese Method for Building Condition Assessment' *Emerald , Vol. 26.*, 322-335.

Zhang, Y. 2005, *Uncertainty Analysis in Using Markov Chain Model to Predict Roof Life Cycle Performance,* proc. 10 DBMC International Conference on Durability of Building Materials and Components, Lyon. France, April 2005, pp. 710-717.